

Comprehensive Coordination Chemistry II

FROM BIOLOGY TO NANOTECHNOLOGY

EDITORS-IN-CHIEF

**Jon A McCleverty
Thomas J Meyer**

**Edited by
M.D. Ward**

**Volume 9
Applications of Coordination Chemistry**

Introduction to Volume 9

This volume aims to give as complete a coverage of the real and possible applications of coordination complexes as is possible in a single volume. It is far more wide-ranging in its coverage than the related volume on ‘applications’ in the first edition of CCC (1987).

The chapters cover the following areas: (i) use of coordination complexes in all types of catalysis (Chapters 1–11); (ii) applications related to the optical properties of coordination complexes, which covers fields as diverse as solar cells, nonlinear optics, display devices, pigments and dyes, and optical data storage (Chapters 12–16); (iii) hydrometallurgical extraction (Chapter 17); (iv) medicinal and biomedical applications of coordination complexes, including both imaging and therapy (Chapters 18–22); and (v) use of coordination complexes as precursors to semiconductor films and nanoparticles (Chapter 23). As such, the material in this volume ranges from solid-state physics to biochemistry.

There are a few points to make about the extent and depth of the coverage of material in this volume. First, the sheer quantity of material involved necessarily limits the depth of the coverage. To take a single example, the use of metal complexes as catalysts for carbonylation reactions is a subject worth a large book in its own right, and covering it in a few tens of pages means that the focus is on recent examples which illustrate the scope of the subject rather than covering encyclopedically all of the many thousands of references on the subject which have appeared since CCC (1987) was published. Accordingly the general emphasis of this volume is on breadth rather than depth, with all major areas in which coordination complexes have practical applications being touched on, and extensive citations to more detailed and larger reviews, monographs, and books where appropriate.

Secondly, many of the chapters contain material which – if a strict definition is applied – is not coordination chemistry, but whose inclusion is necessary to allow a proper picture of the field to be given. A great deal of license has been taken with the division between “coordination” and “organometallic” complexes; the formal distinction for the purposes of this series is that if more than 50% of the bonds are metal–carbon bonds then the compound is organometallic. However, during a catalytic cycle the numbers of metal–carbon and metal–(other ligand) bonds changes from step to step, and it often happens that a catalyst precursor is a “coordination complex” (e.g., palladium(II) phosphine halides, to take a simple example) even when the important steps in the catalytic cycle involve formation and cleavage of M–C bonds. Likewise, many of the volatile molecules described in Chapter 23 as volatile precursors for MOCVD are organometallic metal alkyls; but they can be purified via formation of adducts with ligands such as bipyridine or diphosphines, and it would be artificial to exclude them and cover only “proper” coordination complexes such as diketonates and dithiocarbamates. In other fields, Chapter 15, which describes the use of phosphors in display devices, includes a substantial amount of solid-state chemistry (of doped mixed-metal oxides, sulfides, and the like) as well as coordination chemistry; Chapter 13 describes how a CD-R optical disk functions as a prelude to describing the metal complexes used as dyes for recording the information. So, some of the material in the volume is peripheral to coordination chemistry; but all of it is material that will be of interest to coordination chemists.

Thirdly, some obvious applications of coordination chemistry are omitted from this volume if they are better treated elsewhere. This is the case when a specific application is heavily associated with one particular element or group of elements, to the extent that the application is more appropriately discussed in the section on that element. Essentially all of the coordination chemistry of technetium, for example, relates to its use in radioimmunoimaging; inclusion of this in Chapter 20 of this volume would have left the chapter on technetium in Volume 5 almost empty. For the same reason, the applications of actinide coordination complexes to purification, recovery,

and extraction processes involving nuclear fuel are covered in Volume 2, as this constitutes a major part of the coordination chemistry of the actinides.

In conclusion, it is hoped that this volume will be a stimulating and valuable resource for readers who are interested to see just how wide is the range of applications to which coordination chemistry can be put. If nothing else it will help to provide an answer to the eternally irritating question which academics get asked at parties when they reveal what they do for a living: “But what’s it *for*?”

M D Ward
Bristol, UK
February 2003



ELSEVIER



COMPREHENSIVE COORDINATION CHEMISTRY II

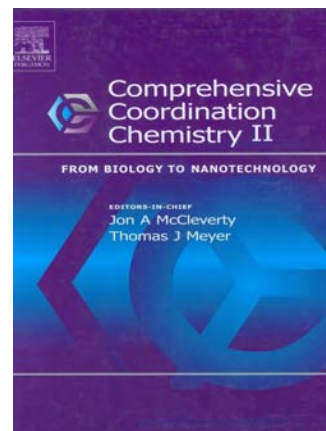
From Biology to Nanotechnology

Second Edition

Edited by

J.A. McCleverty, University of Bristol, UK

T.J. Meyer, Los Alamos National Laboratory, Los Alamos, USA



Description

This is the sequel of what has become a classic in the field, Comprehensive Coordination Chemistry. The first edition, CCC-I, appeared in 1987 under the editorship of Sir Geoffrey Wilkinson (Editor-in-Chief), Robert D. Gillard and Jon A. McCleverty (Executive Editors). It was intended to give a contemporary overview of the field, providing both a convenient first source of information and a vehicle to stimulate further advances in the field. The second edition, CCC-II, builds on the first and will survey developments since 1980 authoritatively and critically with a greater emphasis on current trends in biology, materials science and other areas of contemporary scientific interest. Since the 1980s, an astonishing growth and specialisation of knowledge within coordination chemistry, including the rapid development of interdisciplinary fields has made it impossible to provide a totally comprehensive review. CCC-II provides its readers with reliable and informative background information in particular areas based on key primary and secondary references. It gives a clear overview of the state-of-the-art research findings in those areas that the International Advisory Board, the Volume Editors, and the Editors-in-Chief believed to be especially important to the field. CCC-II will provide researchers at all levels of sophistication, from academia, industry and national labs, with an unparalleled depth of coverage.

Bibliographic Information

10-Volume Set - Comprehensive Coordination Chemistry II

Hardbound, ISBN: 0-08-043748-6, 9500 pages

Imprint: ELSEVIER

Price:

USD 5,975

EUR 6,274 Books and electronic products are priced in US dollars (USD) and euro (EUR). USD prices apply world-wide except in Europe and Japan. EUR prices apply in Europe and Japan. See also information about conditions of sale & ordering procedures -<http://www.elsevier.com/wps/find/bookconditionsofsale>.

[cws_home/622954/conditionsofsale](http://www.elsevier.com/wps/find/cws_home/622954/conditionsofsale), and links to our regional sales offices http://www.elsevier.com/wps/find/contact.cws_home/regional

GBP 4,182.50

030/301

Last update: 10 Sep 2005

Volumes

Volume 1: Fundamentals: Ligands, Complexes, Synthesis, Purification, and Structure

Volume 2: Fundamentals: Physical Methods, Theoretical Analysis, and Case Studies

Volume 3: Coordination Chemistry of the s, p, and f Metals

Volume 4: Transition Metal Groups 3 - 6

Volume 5: Transition Metal Groups 7 and 8

Volume 6: Transition Metal Groups 9 - 12

Volume 7: From the Molecular to the Nanoscale: Synthesis, Structure, and Properties

Volume 8: Bio-coordination Chemistry

Volume 9: Applications of Coordination Chemistry

Volume 10: Cumulative Subject Index

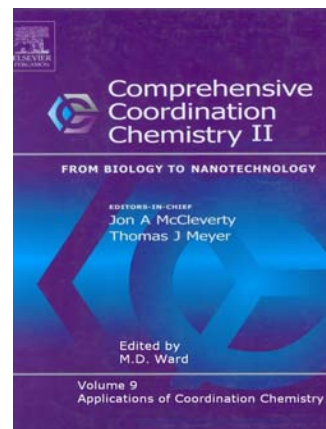
10-Volume Set: Comprehensive Coordination Chemistry II



COMPREHENSIVE COORDINATION CHEMISTRY II

Volume 9: Applications of Coordination Chemistry

Edited by
M.D. Ward



Contents

- Metal complexes as catalysts for polymerization reactions (V. Gibson, E.L. Marshall)
- Metal complexes as hydrogenation catalysts (C. Pettinari, D. Martini, F. Marchetti)
- Metal complexes as catalysts for addition of carbon monoxide (P.W.N. M. van Leeuwen, C. Claver)
- Metal complexes as catalysts for oxygen, nitrogen and carbon-atom transfer reactions (Tsutomu Katsuki)
- Metal complexes as catalysts for H-X (X = B,CN, Si, N, P) addition to CC multiple bonds (M. Whittlesey)
- Metal complexes as catalysts for C-C cross-coupling reactions (I. Beletskaya, A.V. Cheprakov)
- Metal complexes as catalysts for carbon-heteroatom cross-coupling reactions (J.F. Hartwig)
- Metal complexes as Lewis acid catalysts in organic synthesis (S. Kobayashi et al.)
- Supported metal complexes as catalysts (A. Choplin, F. Quignard)
- Electrochemical reactions catalyzed by transition metal complexes (A. Deronzier, J-C. Moutet)
- Combinatorial methods in catalysis by metal complexes (M.T. Reetz)
- Metal complexes as speciality dyes and pigments (P. Gregory)
- Metal complexes as dyes for optical data storage and electrochromic materials (R.J. Mortimer, N.M. Rowley)
- Non-linear optical properties of metal complexes (B. Coe)
- Metal compounds as phosphors (J. Silver)

Conversion and storage of solar energy using dye-sensitized nanocrystalline TiO₂ cells (M. Gratzel, Md.K. Nazeeruddin)

Metal complexes for hydrometallurgy and extraction (P.A. Tasker et al.)

Metal complexes as drugs and chemotherapeutic agents (N. Farrell)

Metal complexes as MRI contrast enhancement agents (A.E. Merbach et al.)

Radioactive metals in imaging and therapy (S. Jurisson et al.)

Fluorescent complexes for biomedical applications (S. Faulkner, J. Matthews)

Metal complexes for photodynamic therapy (R. Bonnett)

Coordination complexes as precursors for semiconductor films and nanoparticles (P.O'Brien, N.Pickett)

9.1

Metal Complexes as Catalysts for Polymerization Reactions

V. C. GIBSON and E. L. MARSHALL

Imperial College, London, UK

9.1.1	INTRODUCTION	2
9.1.2	OLEFIN POLYMERIZATION	2
9.1.2.1	Introduction	2
9.1.2.2	Catalyst Survey	3
9.1.2.2.1	Group 4 metallocene catalysts	3
9.1.2.2.2	Group 4 non-metallocenes	6
9.1.2.2.3	Group 3 and rare earth metal catalysts	11
9.1.2.2.4	Group 5 metal catalysts	12
9.1.2.2.5	Group 6 metal catalysts	13
9.1.2.2.6	Group 8 metal catalysts	14
9.1.2.2.7	Group 9 metal catalysts	15
9.1.2.2.8	Group 10 metal catalysts	15
9.1.2.2.9	Main group metal catalysts	17
9.1.3	POLYMERIZATION OF STYRENES	18
9.1.3.1	Introduction	18
9.1.3.2	Coordinative Polymerization of Styrenes	18
9.1.3.3	Atom Transfer Radical Polymerization of Styrenes	20
9.1.4	POLYMERIZATION OF ACRYLATES	23
9.1.4.1	Introduction	23
9.1.4.2	Anionic Initiators of the group 1, 2, and 3 Metals	23
9.1.4.3	Well-defined Magnesium and Aluminum Initiators	24
9.1.4.4	Lanthanide Initiators	26
9.1.4.5	Early Transition Metal Initiators	27
9.1.4.6	Atom Transfer Radical Polymerization	29
9.1.5	RING-OPENING METATHESIS POLYMERIZATION OF CYCLIC ALKENES	29
9.1.5.1	Introduction	29
9.1.5.2	Titanacyclobutanes	29
9.1.5.3	Group 6 Metal Initiators	30
9.1.5.4	Ruthenium Initiators	33
9.1.5.5	Acyclic Diene Metathesis	36
9.1.6	RING-OPENING POLYMERIZATION OF CYCLIC ESTERS	36
9.1.6.1	Introduction	36
9.1.6.2	General Features of Lactone Polymerization	37
9.1.6.3	Aluminum-based Initiators	37
9.1.6.4	Zinc–Aluminum Oxo-alkoxide Initiators	42
9.1.6.5	Magnesium and Zinc Initiators	42
9.1.6.6	Calcium Initiators	43
9.1.6.7	Tin Initiators	44
9.1.6.8	Iron Initiators	45
9.1.6.9	Yttrium and Rare-earth Initiators	46
9.1.6.10	Titanium and Zirconium Initiators	51
9.1.7	RING-OPENING POLYMERIZATION OF EPOXIDES	52
9.1.7.1	Introduction	52
9.1.7.2	Tetraphenylporphyrin Aluminum and Zinc Initiators	52
9.1.7.3	Non-porphyrinato Aluminum Initiators	54

9.1.7.4 Copolymerization of Epoxides and Carbon Dioxide	54
9.1.7.5 Copolymerization of Epoxides and Aziridines with Carbon Monoxide	57
9.1.8 OTHER LIVING COORDINATION POLYMERIZATIONS	58
9.1.8.1 ROP of N-carboxyanhydrides and β -lactams	58
9.1.8.2 Polymerization of Isocyanates and Guanidines	58
9.1.9 REFERENCES	59

9.1.1 INTRODUCTION

The period since the mid 1980s has seen a tremendous growth in the use of coordination complexes to catalyze chain growth polymerization processes. One of the main advances has been a move away from ill-defined catalysts, where relatively little is understood about the influence of the metal coordination environment on monomer insertion, to precisely defined single-site catalysts where macromolecular parameters such as molecular weight and molecular weight distribution, and microstructural features such as tacticity and monomer placement, can be controlled through the nature of the ligand donor atoms and their attendant substituents.

For many metal-mediated polymerization reactions it has proved possible to control the kinetics of chain propagation vs. chain transfer or chain termination to an extent that “living” polymerizations can be achieved. This has made accessible a plethora of new materials with novel topologies and micro- and macro-structural architectures. The following sections outline the important advances in polymerization catalyst technology for a number of polymerization mechanisms and polymer types.

Where the emphasis is placed on stereoselective polymerizations, the *r* and *m* notation is employed. Two adjacent stereocenters of the same configuration are said to form a *meso* (or *m*) dyad, whereas a *racemic*, *r* dyad contains two centers of opposing stereochemistries. If a polymer contains all *m* junctions, i.e., -RRRRR- or -SSSSS-, then it is termed isotactic, whereas a perfectly syndiotactic polymer possesses all *r* dyads, i.e., -RSRSRS-. Different tacticities are often distinguishable by NMR spectroscopy, with the level of detail dependent upon the polymer type.

9.1.2 OLEFIN POLYMERIZATION

9.1.2.1 Introduction

The transition metal catalyzed polymerization of ethylene was first reported by Ziegler in 1955 using a mixture of TiCl_4 and Et_2AlCl ^{1,2} and was quickly followed by Natta's discovery of the stereoselective polymerization of propylene.^{3,4} Polyolefins have since become the most widely produced family of synthetic polymers, the vast majority being produced using heterogeneous Ziegler systems, e.g., $\text{TiCl}_4/\text{MgCl}_2/\text{Et}_3\text{Al}$. However, during the 1980s interest grew in the use of well-defined homogeneous catalysts, largely stimulated by the discovery that group 4 metallocenes, in combination with methylaluminoxane (MAO) cocatalyst, afford exceptionally high activities and long-lived polymerization systems. More recently, attention has turned towards non-metallocene polymerization catalysts, partly to avoid the growing patent minefield in group 4 cyclopentadienyl systems, but also to harness the potential of other metals to polymerize ethylene on its own and with other monomers. A number of reviews have outlined the key developments in molecular olefin polymerization catalyst systems.⁵⁻¹⁵

Due to the importance of group 4 metallocenes to the development of the field, we include here a brief outline of some of their key features. The majority of this section, however, is devoted to advances in non-metallocene catalyst systems. Where necessary, catalyst activities have been converted into the units $\text{g mmol}^{-1} \text{h}^{-1} \text{bar}^{-1}$ for gaseous monomers such as ethylene and propylene, and $\text{g mmol}^{-1} \text{h}^{-1}$ for reactions carried out in liquid α -olefins such as 1-hexene. Activities are classified as very high (>1,000), high (1,000–100), moderate (100–10), low (10–1) and very low (<1).⁸

9.1.2.2 Catalyst Survey

9.1.2.2.1 Group 4 metallocene catalysts

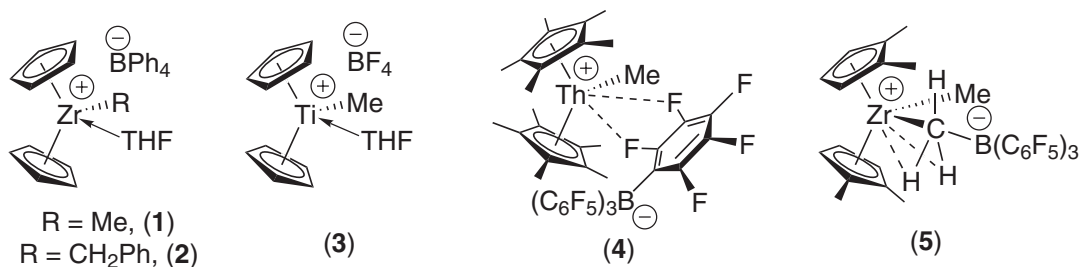
(i) Ethylene polymerization

In the mid 1950s both Breslow and Natta reported moderate ethylene polymerization activities for mixtures of Cp_2TiCl_2 and Et_2AlCl .^{16–18} Although Ziegler catalysts are very moisture-sensitive, trace quantities of water were later found to increase significantly the rate of olefin consumption. This was attributed to the formation of aluminoxanes resulting from the partial hydrolysis of the alkylaluminum cocatalyst^{19,20} and shortly thereafter it was shown that the addition of water to an inactive mixture of $\text{Cp}_2\text{ZrMe}_2/\text{Me}_3\text{Al}$ afforded a highly active ethylene polymerization catalyst.^{13,21} The direct synthesis of methylaluminumoxane, MAO, and its use as an activator (with typical Al:Zr ratios of 10^3 – 10^4) followed.²²

Generally, zirconocene catalysts are more active towards ethylene polymerization than analogous Ti and Hf complexes.²³ Activity generally increases as the metallocene fragment becomes more electron-donating, but steric bulk tends to reduce the activity.^{24–26} Polymer molecular weights are influenced by a variety of factors including substituents on the cyclopentadienyl rings, the reaction temperature^{27,28} and the catalyst concentration.^{29,30} M_w/M_n values for polyethylene, PE, produced by zirconocene catalysts are typically ca. 2.0–2.3.

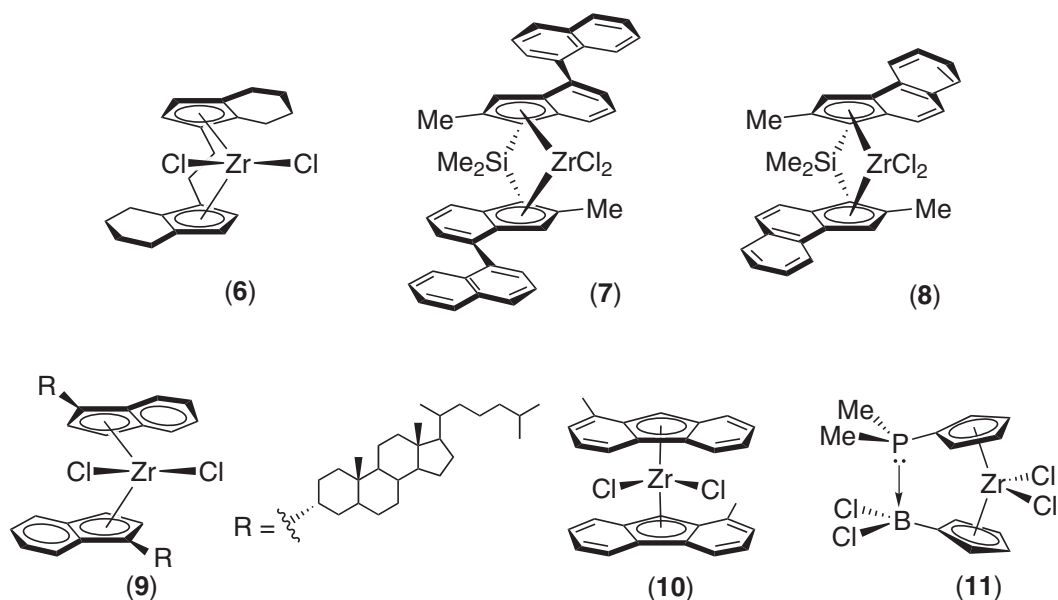
The polymerization of ethylene by group 4 metallocenes is widely recognized to proceed via 14-electron cationic intermediates.^{31,32} Cationic zirconocene^{33–35} and titanocene^{36–38} complexes, (1–3), were first isolated in 1986 by Jordan and Bochmann, respectively. Both (1) and (2) are active for ethylene polymerization in the absence of a cocatalyst.³⁴

In attempts to generate base-free cationic species, $[\text{Cp}_2\text{MR}]^+$, increasingly non-coordinating anions have been employed. Perfluorotetraphenylborate has been used to good effect as a counteranion, but even this may exhibit a non-innocent role as shown by the X-ray structural determination of complex (4).³⁹ Nonetheless, this compound displays an ethylene polymerization activity approximately 3,500 times greater than its BPh_4^- counterpart. $\text{B}(\text{C}_6\text{F}_5)_3$ has been employed as an alkyl abstracting agent; zwitterionic complexes such as (5) have been synthesized in this way.^{40,41} The development of boron-based activators and their use with metallocene catalysts has been recently reviewed.^{42,43}

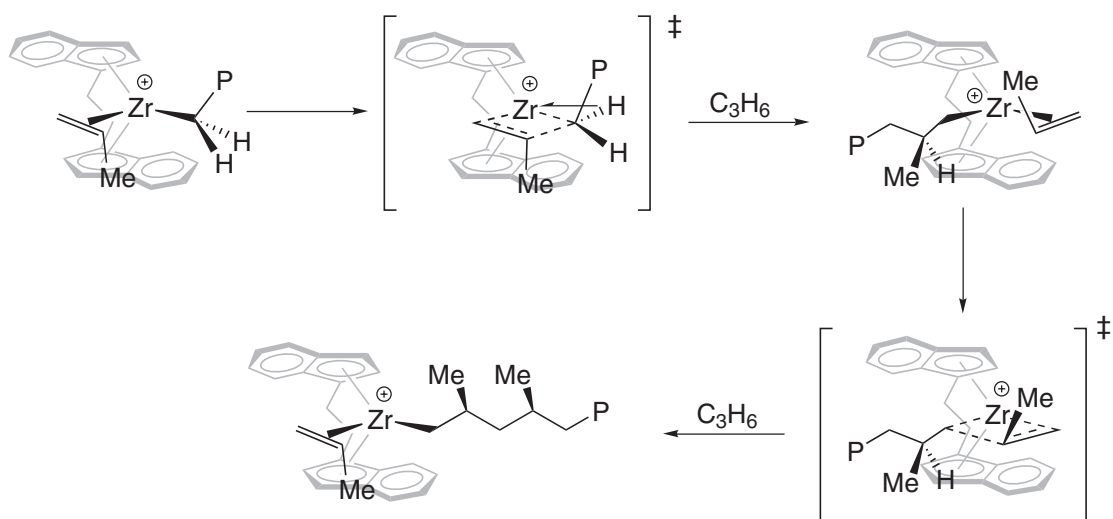


(ii) Isospecific propylene polymerization

One of the most important uses of group 4 metallocene polymerization catalysts has been in the stereoselective polymerization of propylene.⁴⁴ In 1984 it was reported that $\text{Cp}_2\text{TiPh}_2/\text{MAO}$ gave isotactic poly(propylene), i-PP, (73% mm triad content at -45°C) via a chain-end controlled mechanism.⁴⁵ Subsequently, the *ansa*-metallocenes, first introduced by Brintzinger, were shown to afford stereoselective polymerizations of propylene via enantiomorphic site control. Typically i-PP is prepared using C_2 -symmetric complexes such as (*rac*)-(6)/MAO, which affords 95% mm PP.⁴⁶ Subsequent studies showed that many other C_2 -symmetric *ansa*-metallocenes may be used to catalyze the formation of i-PP,^{47–50} and in the case of (7) and (8), high isoselectivity may be combined with exceptionally high activities.^{51–53} The non-bridged complexes (9)⁵⁴ and (10)⁵⁵ have also been used to prepare i-PP, as has (11) which contains a donor–acceptor interaction between the two cyclopentadienyl ligands.⁵⁶



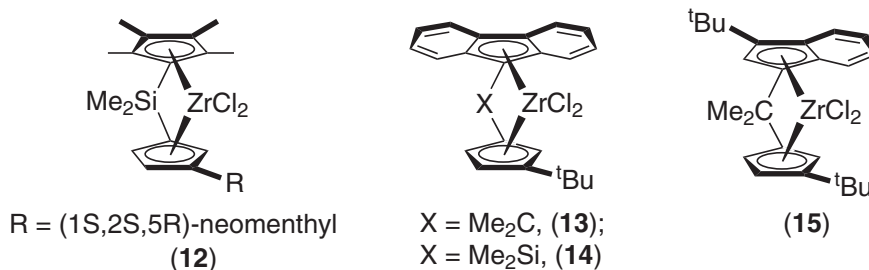
The origin of high isotacticity is generally attributed to a high level of enantiofacial selectivity governing the propylene insertion.^{44,57} The propagating PP chain occupies the sterically most open region of the metallocene and the incoming monomer adopts an orientation which minimizes steric interactions with the metallocene and the growing polymer chain.^{58–62} The transition state is rendered conformationally more rigid by α -agostic interactions between the metal center and the PP chain,^{63–65} as shown in the mechanism outlined in (Scheme 1). Stereoerrors could in principle occur via the insertion of the incorrect enantioface of the olefin. However, there is considerable evidence that epimerization of the propagating chain end is more likely to be responsible for stereoerrors.^{66–71} Site migration (i.e., without olefin insertion) should not introduce stereochemical defects since both of the active site enantiomers select the same monomer enantioface.



Scheme 1

Several isospecific C_1 -symmetry catalysts have also been described including (12–15). When activated with $[\text{Ph}_3\text{C}]^+[\text{B}(\text{C}_6\text{F}_5)_4]^-$, (12) affords highly regioregular i-PP (mmmm = 95%) with the stereochemical defects predominantly being isolated rr triads, consistent with a self-correcting enantiomorphic site-control pathway.^{72,73} The isospecificity was therefore explained by a mechanism

in which olefin insertion occurs with high facial selectivity and is rapidly followed by site isomerization. Molecular modeling studies support a similar insertionless migration mechanism using **(13)** (which produces 95% mmmm PP at 30 °C).^{74,75} Even higher selectivity is observed with **(15)** which generates >98% mmmm i-PP even at 60 °C.⁷⁶



(iii) Syndiospecific propylene polymerization

By contrast, the synthesis of syndiotactic PP, s-PP, is generally catalyzed by C_s-symmetry *ansa*-metallocenes. For example, **(16)**/MAO affords PP with a pentad (rrrr) content of 86% at 25 °C.⁷⁷ The stereoselectivity is highly sensitive to ligand variation. For example, substitution at the 3-position of the Cp ring with a methyl group affords heterotactic PP,⁷⁸ whilst the tBu analog favors i-PP production.^{50,75,79}

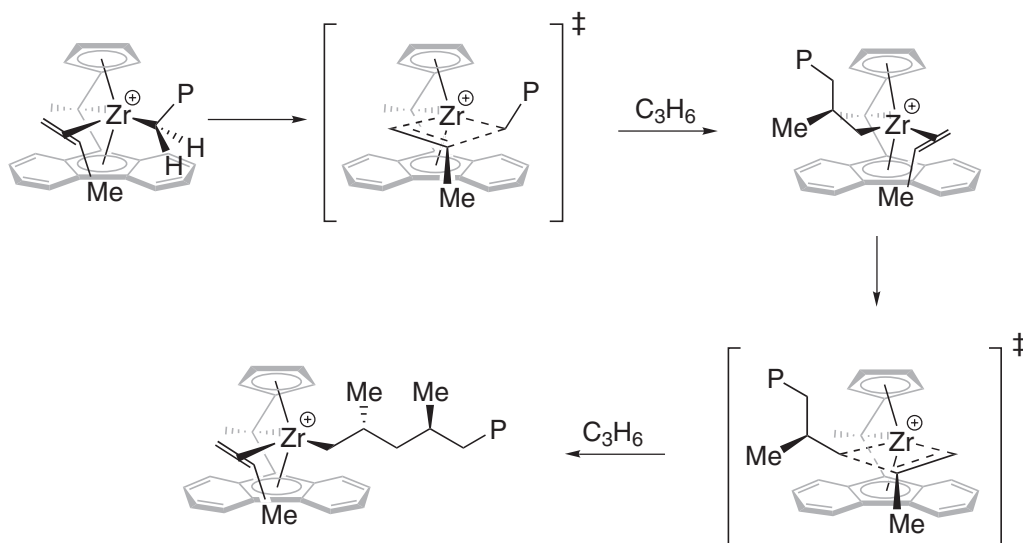
As shown in (Scheme 2), syndiospecificity is thought to arise from the insertion of the α-olefin at alternating sides of the metallocene center,⁸⁰ with the propylene methyl directed towards the open space between the two benzo substituents.⁸¹ Modifications of complex **(16)** have typically examined the effect of different bridging groups^{82–86} and substituents on the fluorenyl ring.^{87–93} Most of these have resulted in less syndioselective catalysts. Derivatization of the smaller cyclopentadienyl ring has recently been investigated and several examples of C₁-symmetric catalysts capable of producing elastomeric polypropylene with an isotactic–hemiisotactic structure have been discovered, such as **(17–19)**.⁹⁴

In order to mimic the steric accommodation afforded to the α-olefin by the fluorenyl ligand, a series of doubly bridged C_s-symmetric zirconocenes has been designed in which isopropyl substituents are positioned to the sides of the metallocene binding wedge.^{81,95} When activated with MAO complexes **(20–23)** are all highly syndiospecific for propylene polymerization. At 0 °C **(21)** produces s-PP with an rrrr pentad content of 98.9%, although this decreases to 38.8% at 25 °C. The same catalyst also polymerizes 1-pentene with very high syndioselectivity.⁹⁶ C₁-symmetric analogs such as **(24)** and **(25)** have also been prepared. Complex **(24)** behaves similarly to **(21)** (producing 83.1% rrrr PP at 0 °C). However, **(25)** exhibits an unusual stereospecific dependence on monomer concentration, switching from isoselective to syndioselective with increasing propylene pressure.⁹⁷ This behavior has been rationalized in terms of chain propagation competing with site epimerization. At higher reaction temperatures site epimerization again becomes competitive; hence, **(25)** generates 41.8% rrrr PP at 0 °C and 61.2% mmmm PP at 25 °C.⁸¹

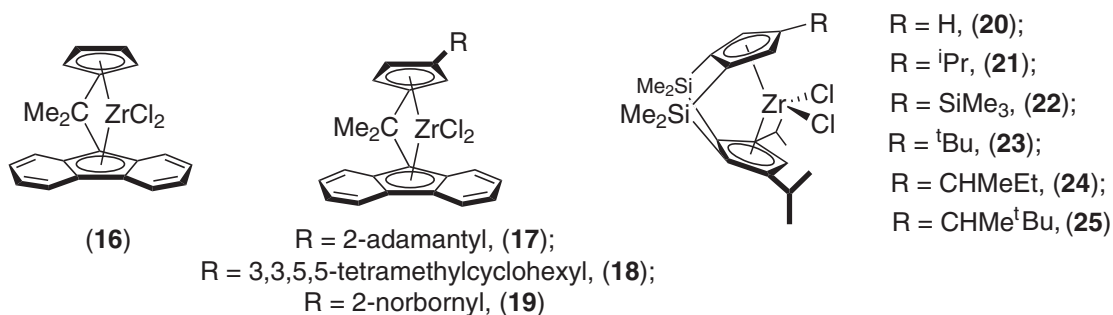
(iv) Elastomeric poly(propylene)

PP synthesized using TiCl₄/Et₃Al is mostly isotactic, but two minor fractions are also produced. One is a soluble, atactic PP, whilst the other fraction is a partially crystalline, elastomeric stereoblock of iso- and a-tactic PP sequences.⁹⁸ Elastomeric PP may also be prepared using the *ansa*-titanocene complex, **(26)**, (although this catalyst does undergo rapid deactivation).⁹⁹ Stereoblock formation was attributed to an equilibrium mixture of slowly interconverting isospecific and aspecific catalyst sites. Other stereoblock PP materials have been prepared via chain transfer between two catalysts of different stereoselectivities.^{101,102}

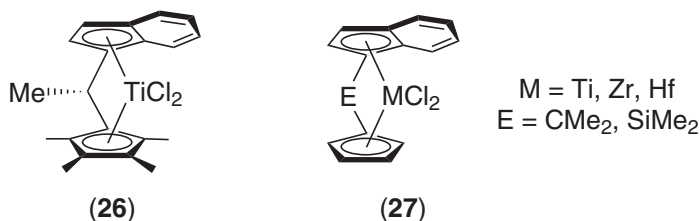
Elastomeric PP has also been synthesized using Ti, Zr and Hf *ansa*-metallocenes, **(27)**. An alternative explanation for stereoblock formation was proposed, in which epimerization between isospecific and aspecific sites is rapid, affording predominantly atactic PP with short isotactic-rich sequences.^{103–105}



Scheme 2



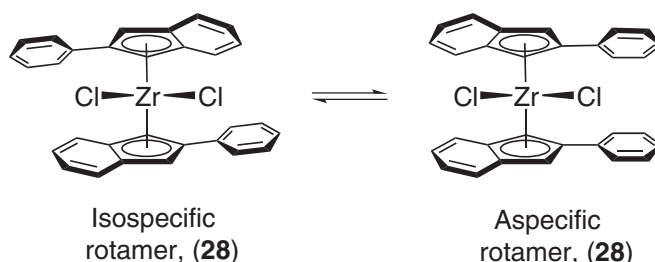
An alternative route to elastomeric PP, based upon ligand isomerization (rather than site epimerization) has also been described, using the equilibrium between isospecific and aspecific rotamers of (28).^{106,107} The relative rate of propagation and isomerization again determines the block lengths, but in addition the rotamer interconversion may be controlled by the reaction conditions. This allows much larger isotactic blocks to be prepared than using either (26) or (27), affording elastomeric PP with a higher melting point. Recent NMR studies suggest that the oscillation mechanism is more complex than originally thought. The stereoirregular portions are rich in *meso* dyads, and are believed to arise from equilibration between the two enantiomorphous forms of the *rac* rotamer.¹⁰⁸



9.1.2.2.2 Group 4 non-metallocenes

(i) Constrained geometry catalysts

The most successful examples of commercialized non-metallocene catalysts are the constrained geometry complexes such as (29) developed at Dow and Exxon.^{109–112} The open nature of the titanium center favors co-monomer uptake. Hence, α -olefins such as propene, 1-butene, 1-hexene

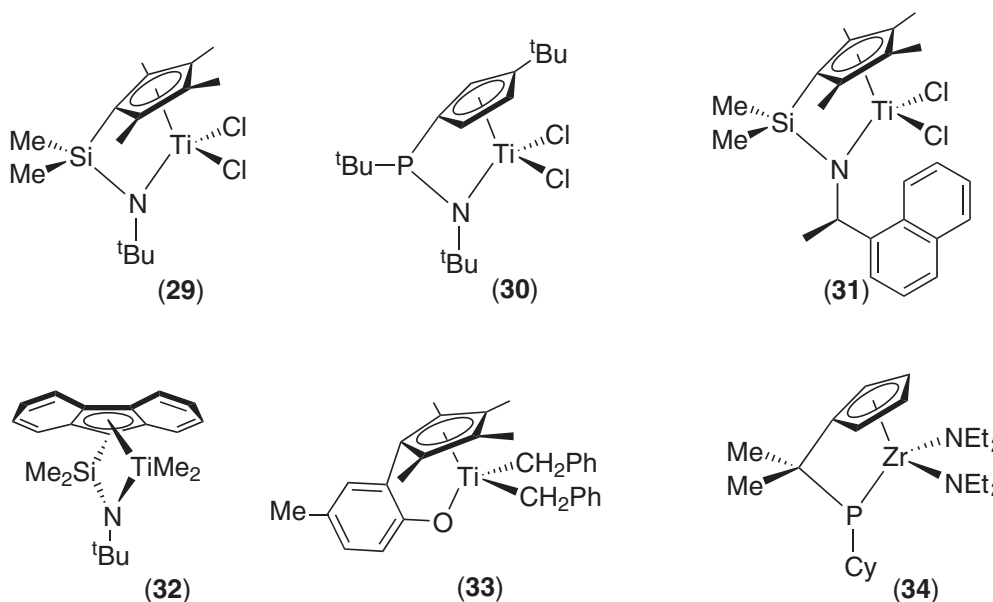


and 1-octene may all be copolymerized with ethylene to afford low-density materials.^{14,113} In the absence of co-monomers, PE with small amounts of long chain branches (≈ 3 chains per 1,000 carbons) is generated; β -H elimination of growing chains creates vinyl-terminated macromonomers which re-insert into other propagating chains.¹¹⁴ Incorporation of α,ω -dienes¹¹⁵ and α,ω -functionalized alkenes such as 10-undecen-1-ol¹¹⁶ has also been reported.

Many variants of complex (29) have been described, including hydrocarbyl bridged analogs^{117–123} and amido-fluorenyl complexes.¹²⁴ Examples of alkyl-substituted phosphorus bridges have also been reported. For example, complex (30) produces linear PE with an activity of $100 \text{ g mmol}^{-1} \text{ h}^{-1} \text{ bar}^{-1}$.¹²⁵

Variation in the substituents at the nitrogen donor atom has also been examined,¹²⁶ and in one case isoselective polymerization of propylene was described (mmmm pentad = 56% using (31)).¹²⁷ Syndioselective propylene polymerization with an rr triad content of 63% has been reported using (32)/MAO, although residual Me_3Al must be removed from the MAO in order to suppress chain transfer to aluminum.¹²⁸

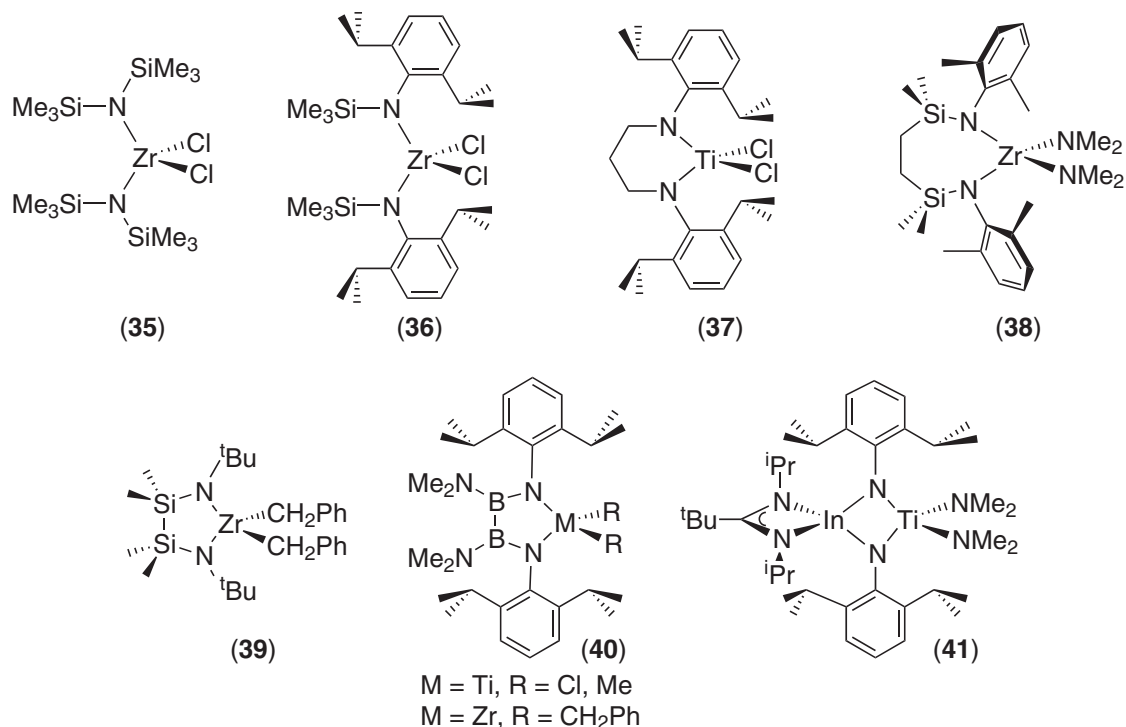
Constrained geometry catalysts with alkoxide^{129,130} and phosphide¹²⁵ donor arms have also been reported. The most active examples include complex (33), which polymerizes ethylene with an activity of $2,100 \text{ g mmol}^{-1} \text{ h}^{-1} \text{ bar}^{-1}$ ¹³¹ and (34), which exhibits an activity of $2,240 \text{ g mmol}^{-1} \text{ h}^{-1} \text{ bar}^{-1}$ for the copolymerization of ethylene with 1-octene.¹³²



(ii) Nitrogen-based ligands

Zirconium bis(amides) such as (35) and (36) display moderate ethylene polymerization activities.^{133,134} Complex (37) containing a chelating diamide ligand has been shown to initiate the living polymerization of α -olefins such as 1-hexene ($M_w/M_n = 1.05\text{--}1.08$) with activities up to $750 \text{ g mmol}^{-1} \text{ h}^{-1}$.^{135–137} The living polymerization of propylene using this system activated with

dried MAO has also recently been reported;¹³⁸ M_n data increase linearly with monomer conversion and M_w/M_n values lie in the range 1.1–1.4. When trialkylaluminum cocatalysts are used with (37) atactic-PP is produced, but when $[\text{Ph}_3\text{C}][\text{B}(\text{C}_6\text{F}_5)_4]$ is employed highly isotactic PP is generated.¹³⁹ The seven-membered chelate ring analog, (38), has been reported to be a highly active catalyst for the polymerization of ethylene ($990 \text{ g mmol}^{-1} \text{ h}^{-1} \text{ bar}^{-1}$),¹⁴⁰ whilst (39) activated with $[\text{Ph}_3\text{C}][\text{B}(\text{C}_6\text{F}_5)_4]$ is a highly active ethylene oligomerization catalyst.¹⁴¹ High-molecular-weight poly(ethylene-co-1-octene) has been reported using both (40) and (41); however, activities are not high and broad polydispersities suggest the existence of several different active sites.^{142,143} Activities of up to $300 \text{ g mmol}^{-1} \text{ h}^{-1} \text{ bar}^{-1}$ have also been recorded for a series of zirconium complexes of 1,8-naphthalene diamide.¹⁴⁴

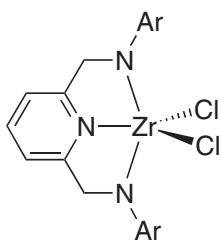
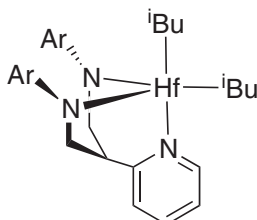
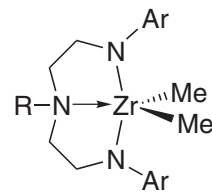


Dianionic bis(amide) ligands bearing additional donor atoms have been described by several researchers. High activities for ethylene polymerization are observed for pyridyldiamido zirconium complexes such as (42) ($1,500 \text{ g mmol}^{-1} \text{ bar}^{-1} \text{ h}^{-1}$),¹⁴⁵ although the corresponding titanium complex is much less active.¹⁴⁶

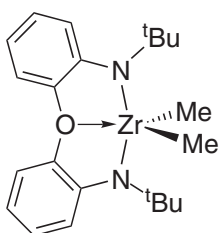
Bis(amide) ligands containing amine, ether and thioether donors have also been investigated. For example, the hafnium complex (44) polymerizes 1-hexene in a living manner ($M_w/M_n = 1.02$ – 1.05).¹⁴⁷ By contrast, the use of zirconium analogs is complicated by β -hydride elimination and the formation of inactive side-products.¹⁴⁸ A similar chain termination mechanism has been observed using (45), reflected by slightly higher polydispersities than expected for a truly living polymerization ($M_w/M_n = 1.2$ – 1.5).¹⁴⁹

Complex (46) also initiates the living polymerization of 1-hexene at 0°C .¹⁵⁰ Molecular weight (M_n) data closely parallel theoretical values and M_w/M_n values are typically below 1.10. Reducing the size of the N-substituent to ⁱPr or Cy affords far less active oligomerization catalysts.¹⁵¹ Similarly, the thioether complexes (47) only oligomerize 1-hexene, decomposing over 3 h at -10°C .¹⁵² Catalyst family (48) and complex (49) have also been used to polymerize 1-hexene; the latter is particularly active, consuming 30 equivalents of the α -olefin within a few minutes at 0°C .^{153–155} It has been suggested that too many donor heteroatoms in the bis(amide) framework substantially reduces activity. Hence, complex (50) displays only moderate activity towards ethylene at 50°C when activated with MAO,¹⁵⁶ whilst complex (51) is inactive.¹⁵⁷

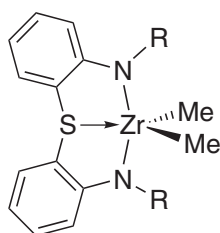
In general, Group 4 benzamidinates show poor activities as olefin polymerization catalysts.^{158–162} However, bis(benzamidinate) complex (52) affords isotactic PP ($\geq 95\%$ mmmm) at ≥ 7 atm propylene pressure;¹⁶³ at ambient pressure atactic PP is produced.¹⁶⁴ An unsymmetrical tris(benzamidinate) zirconium complex has also been shown to afford highly isotactic PP.¹⁶⁵

Ar = 2,6-Me₂C₆H₃, (42);Ar = 2,6-ⁱPr₂C₆H₃, (43)Ar = 2,4,6-Me₃C₆H₂, (44)

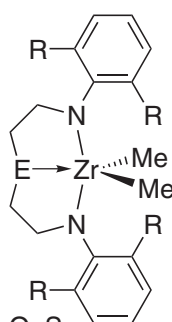
R = H, Me

Ar = 2,4,6-Me₃C₆H₂, (45)

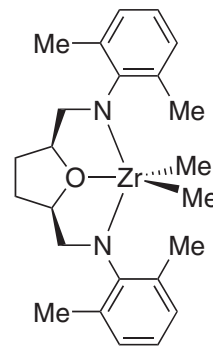
(46)

R = ^tBu, ⁱPr

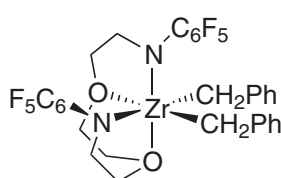
(47)



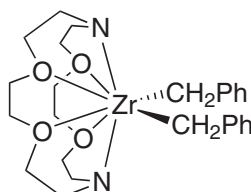
E = O, S

R = Me, ⁱPr (48)

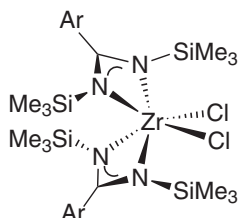
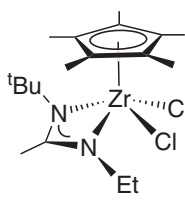
(49)



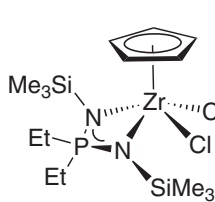
(50)



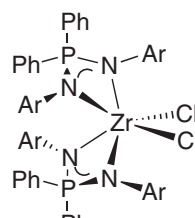
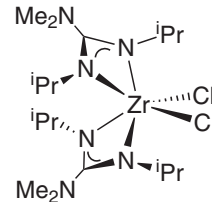
(51)

Ar = 4-MeC₆H₄, (52)

(53)



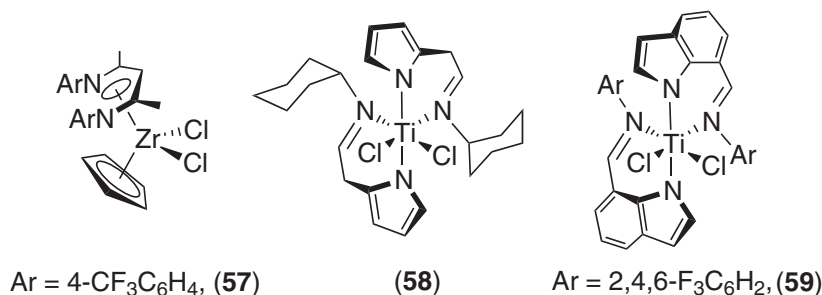
(54)

Ar = 4-MeC₆H₄, (55)

(56)

Half-sandwich zirconium complexes of unsymmetrically substituted amidinates such as (53) exhibit moderate activities for the polymerization of 1-hexene (110 g mmol⁻¹ h⁻¹ at 25 °C); at -10 °C the system displays living character ($M_w/M_n < 1.10$) and is stereospecific, affording isotactic (>95% mmmm) poly(1-hexene).¹⁶⁶ The isospecific, living polymerization of vinylcyclohexane has also been reported.¹⁶⁷ The related iminophosphonamide complexes (54) and (55) are highly active ethylene polymerization catalysts with activities up to 1,400 g mmol⁻¹ h⁻¹ bar⁻¹.¹⁶⁸ High activities have also been reported for a family of titanium phosphinimide catalysts.¹⁶⁹⁻¹⁷¹ Guanidinate complexes such as (56) also exhibit a higher ethylene polymerization activity (340 g mmol⁻¹ h⁻¹ bar⁻¹) than related amidinate catalysts.¹⁷²

The only reported example of a group 4 β -diketiminate complex which exhibits an activity for ethylene polymerization in excess of $100 \text{ g mmol}^{-1} \text{ h}^{-1} \text{ bar}^{-1}$ is complex (57), in which the normally bidentate ancillary ligand adopts an unusual η^5 coordination mode.^{173,174} Bis(iminopyrrolide)s, such as (58), polymerize ethylene to very high molecular weight with high activities ($14,000 \text{ g mmol}^{-1} \text{ h}^{-1} \text{ bar}^{-1}$).¹⁷⁵ This complex is also highly active for the living copolymerization of ethylene with norbornene ($M_w/M_n = 1.16$).¹⁷⁶ The same researchers have also reported that MAO-activated bis(iminoindolide) (59) polymerizes ethylene with an activity of $288 \text{ g mmol}^{-1} \text{ h}^{-1} \text{ bar}^{-1}$ in a living fashion ($M_w/M_n = 1.11$ at 25°C).^{177,178}

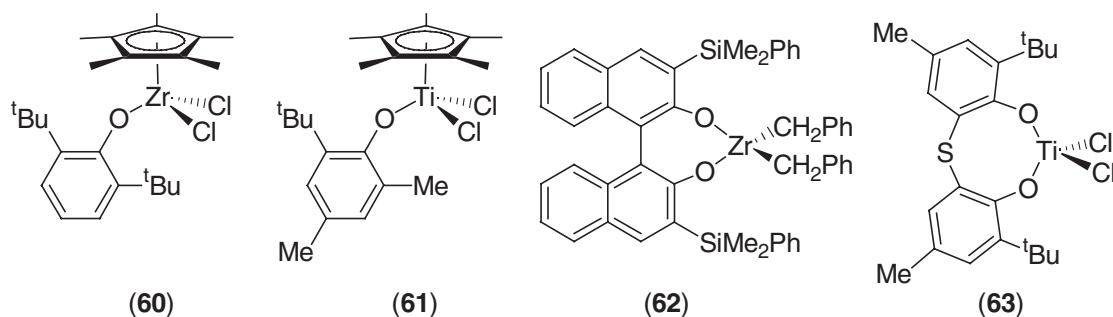


Other anionic nitrogen-containing ligands which have been examined in the search for new non-metallocene catalysts include macrocyclic porphyrins¹⁷⁹ and tetraazaannulenes.¹⁸⁰ However, activities with these catalysts are low.

(iii) Oxygen based ligands

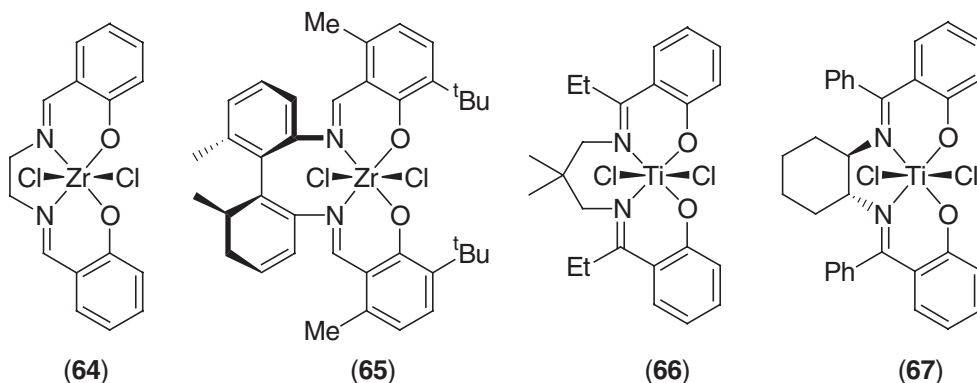
Certain half-sandwich phenoxides have been shown to be highly active olefin polymerization catalysts. For example, the zirconium complex (60) polymerizes ethylene with an activity of $1,220 \text{ g mmol}^{-1} \text{ h}^{-1} \text{ bar}^{-1}$.¹⁸¹ A similar titanium complex (61) displays an activity of $560 \text{ g mmol}^{-1} \text{ h}^{-1} \text{ bar}^{-1}$ at 60°C .¹⁸²⁻¹⁸⁹ Comparable activities were also recorded for the copolymerization of ethylene with 1-butene and 1-hexene.

A variety of substituted binaphthol and bisphenol complexes of titanium and zirconium have also been investigated as ethylene polymerization initiators. Of note, (62) and (63) exhibit activities of $350 \text{ g mmol}^{-1} \text{ h}^{-1} \text{ bar}^{-1}$ and $1,580 \text{ g mmol}^{-1} \text{ h}^{-1} \text{ bar}^{-1}$.¹⁹⁰⁻¹⁹²

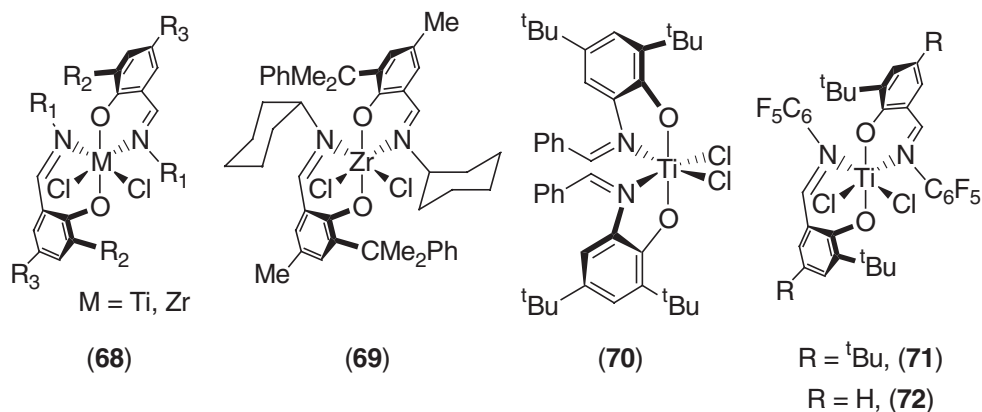


The highest ethylene polymerization activity for a tetradentate salen-type group 4 complex was reported for silica supported (64) ($600 \text{ g mmol}^{-1} \text{ h}^{-1} \text{ bar}^{-1}$).¹⁹³ Activities for a range of related zirconium and titanium complexes such as (65)–(67) are typically an order of magnitude lower.¹⁹⁴⁻¹⁹⁶

Much improved activities are obtained using bidentate salicylaldiminato ligands, as used in a family of catalysts of the type (68).¹⁹⁷⁻²⁰⁰ Activities rise with increasing bulk of the alkyl substituent *ortho* to the phenoxide bond. Thus, complex (69) activated with MAO exhibits an activity of $4,315 \text{ g mmol}^{-1} \text{ h}^{-1} \text{ bar}^{-1}$.²⁰⁰ Increasing the imino substituent has a twofold effect; steric congestion in such close proximity to the active site serves to reduce both the rate of polymerization and the rate of β -hydride transfer. As a result, higher molecular weight polymer is produced, but at a slower rate.²⁰¹ The structurally similar bis(iminophenoxide) complex (70) shows only moderate reactivity towards ethylene when activated with MAO, but much higher reactivity when ${}^t\text{Bu}_3\text{Al}/[\text{Ph}_3\text{C}][\text{B}(\text{C}_6\text{F}_5)_4]$ is used ($5,784 \text{ g mmol}^{-1} \text{ h}^{-1} \text{ bar}^{-1}$).²⁰²



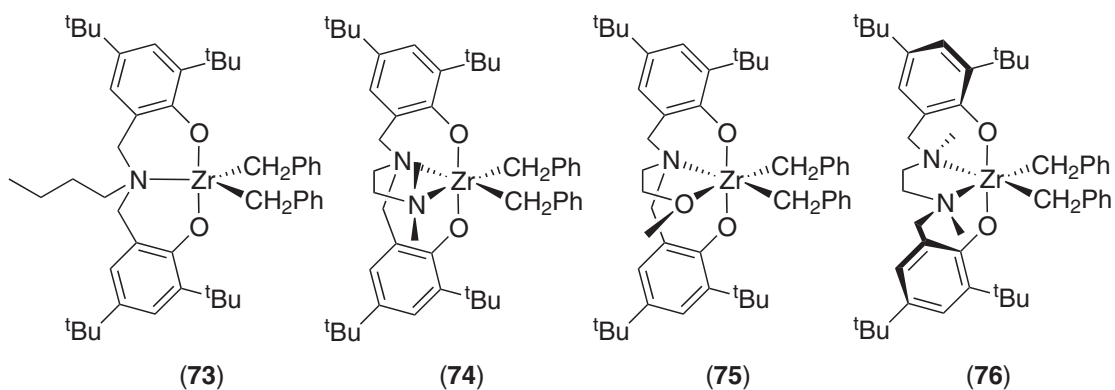
Fluorinated bis(salicylaldiminato) titanium complexes have also been examined and complex (71) produces highly syndiotactic PP ($r_{rrr} = 96\%$) at 0°C in a living manner ($M_w/M_n = 1.1$ up to M_n values of 10^5 with no terminal olefinic groups detected).^{203,204} Unlike C_s -symmetric zirconocenes, the polymerization occurs via 2,1-insertion of propylene.^{205,206} Low-molecular-weight oligomers of propylene prepared using (72) are also highly syndiotactic; however, PP samples of higher molecular weight are less stereoregular ($r_{rrr} = 76\%$) than those prepared using (71). The living nature of (71) and (72) allow well-defined ethylene/propylene diblocks to be prepared.^{204,207–209}



A variety of group 4 olefin polymerization catalysts featuring aminebis(phenoxide) ligands have been examined.²¹⁰ Although tridentate ligands result in poor activities (e.g., (73)), tetradentate-ligated complexes such as (74) are highly active 1-hexene polymerization catalysts ($15,500 \text{ g mmol}^{-1} \text{ h}^{-1}$).²¹¹ The titanium analog of (74) is less active but initiates the living polymerization of 1-hexene when activated with $\text{B}(\text{C}_6\text{F}_5)_3$.²¹² Incorporation of an additional oxygen donor, as in (75), affords another catalyst for the living polymerization of 1-hexene; this system is remarkable as it remains active for 31 hours allowing high-molecular-weight, monodisperse material to be prepared.^{213,214} Altering the connectivity of the bis(phenolate) ligand allows C_2 -symmetric analogs of *ansa*-metallocenes to be synthesized. As a result, complex (76) polymerizes 1-hexene in a living, isoselective ($>95\%$) manner.²¹⁵

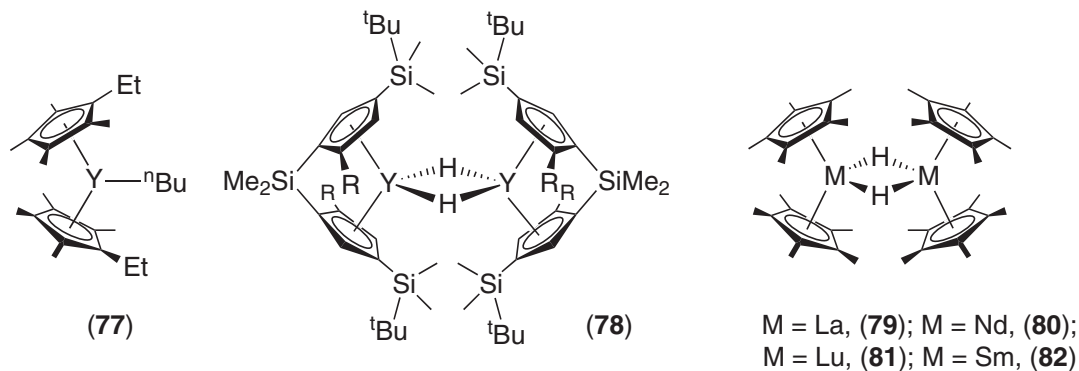
9.1.2.2.3 Group 3 and rare earth metal catalysts

Since group 3 metallocene alkyls are isoelectronic with the cationic alkyls of group 4 catalysts they may be used as olefin polymerization initiators without the need for cocatalysts. The neutral metal center typically results in much lower activities, and detailed mechanistic studies on the insertion process have therefore proved possible.^{216–220} Among the first group 3 catalysts reported to show moderate activities ($42 \text{ g mmol}^{-1} \text{ h}^{-1} \text{ bar}^{-1}$) was the ytrocene complex (77).²²¹



Ansa-metallocene analogs were later described by Bercaw and Yasuda, with ethylene activity figures of $584 \text{ g mmol}^{-1} \text{ h}^{-1} \text{ bar}^{-1}$ recorded for (78).^{222–224} Such complexes may also be used as isospecific α -olefin polymerization catalysts.²²⁵

A range of rare earth metal complexes were subsequently shown to catalyze ethylene polymerization and, on occasion, living characteristics have been reported.^{226–228} Dimeric hydrides such as (79)–(82) are extremely active with turnover numbers $>1800 \text{ s}^{-1}$ recorded for (79) at room temperature. The samarium hydride (82) also effects the block copolymerization of methyl methacrylate (MMA) and ethylene,²²⁹ further discussion may be found in Section 9.1.4.4.



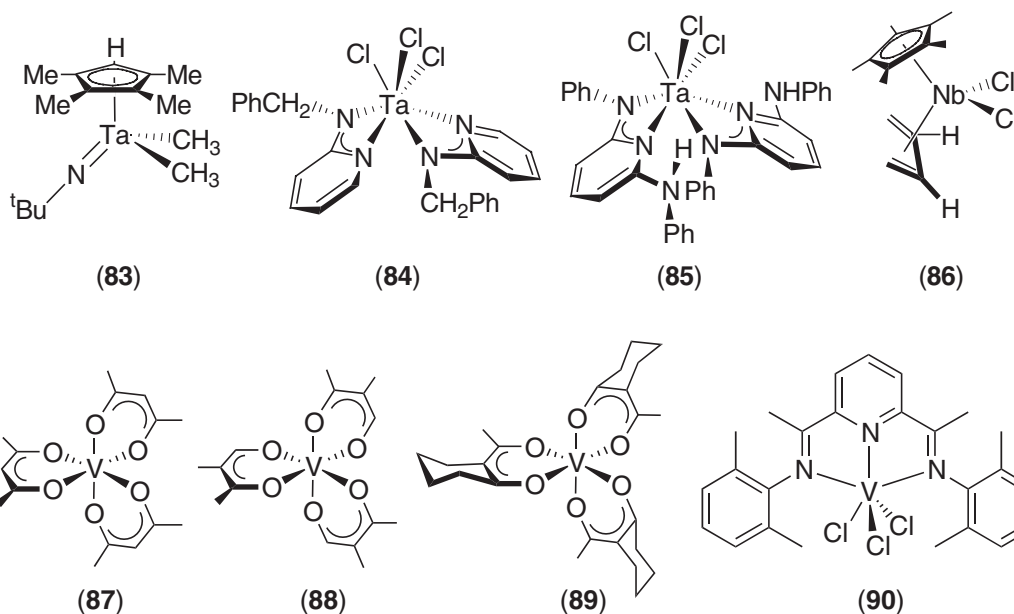
9.1.2.2.4 Group 5 metal catalysts

The isolobal relationship between the mono-anionic Cp-ligand and dianionic fragments,²³⁰ such as imido ligands, has been exploited to generate metallocene-related analogs of group 4 metal catalysts, with high valent, cationic 14-electron alkyls as the proposed active species.^{231–234} Some of the more active systems include (83) which copolymerizes ethylene and 1-octene with an activity of $1,206 \text{ g mmol}^{-1} \text{ h}^{-1} \text{ bar}^{-1}$ when activated with $[\text{HNMe}(\text{C}_{18}\text{H}_{37})_2][\{(\text{C}_6\text{F}_5)_3\text{Al}\}_2\text{C}_3\text{H}_3\text{N}_2]$.^{235,236} Other tantalum complexes which show high activity for ethylene polymerization include (84) and (85); at 80°C and 5 bar pressure activities approaching $5,000 \text{ g mmol}^{-1} \text{ h}^{-1} \text{ bar}^{-1}$ have been reported.²³⁷ Active niobium catalysts are less common, although (86) affords high molecular weight PE of narrow polydispersities with moderate activity ($39 \text{ g mmol}^{-1} \text{ h}^{-1} \text{ bar}^{-1}$).^{238–240}

When mixed with Et_2AlCl , the vanadium(III) complex (87) polymerizes propylene at -78°C in a living manner.^{241,242} Poor initiator efficiency ($\approx 4\%$) and low activities were improved by employing complex (88); activities of $100 \text{ g mmol}^{-1} \text{ h}^{-1} \text{ bar}^{-1}$ were reported and the polymerization of propylene remained living ($M_w/M_n = 1.2–1.4$) up to -40°C .^{243,244} The synthesis of end-functionalized PP and PP copolymers has also been achieved using these initiators.

More recently, (89)/ Et_2AlCl was shown to exhibit even higher activities ($584 \text{ g mmol}^{-1} \text{ h}^{-1} \text{ bar}^{-1}$).²⁴⁵ Vanadium(III) complexes such as (90) are also active for ethylene

polymerization ($325 \text{ g mmol}^{-1} \text{ h}^{-1} \text{ bar}^{-1}$).²⁴⁶ Several other vanadium catalysts for α -olefin polymerization have been detailed in a recent review.¹²



9.1.2.2.5 Group 6 metal catalysts

(i) Cyclopentadienyl systems

Silica-supported heterogenous Cr systems, such as the Phillips^{247,248} and Union Carbide catalysts,^{249,250} are used in the commercial production of polyethylene. The active sites are widely agreed to contain low-valent Cr centers. The relatively ill-defined nature of these catalysts has led to considerable efforts to synthesize well-defined homogeneous Cr-based catalysts.

Among the most highly active examples of molecular Cr-based olefin polymerization catalysts are a family of amine-functionalized half-sandwich complexes.²⁵¹ The activity increases for substituted cyclopentadienyl rings, such as tetramethyl or fluorenyl analogs. For example, complex (91) ($X = \text{Me}$) displays an ethylene polymerization activity of $5,240 \text{ g mmol}^{-1} \text{ h}^{-1} \text{ bar}^{-1}$, rising to $25,375 \text{ g mmol}^{-1} \text{ h}^{-1} \text{ bar}^{-1}$ at 80°C ($X = \text{Cl}$).²⁵² These catalysts require remarkably little MAO for activation; typically 100 equivalents are used. Even higher activities are obtained if activation is performed with 20 equivalents of Me_3Al . The active species is believed to be a cationic methyl complex.²⁵³

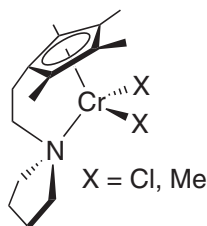
For phosphinoalkyl-substituted analogs (92) the phosphine substituents are key to determining the molecular weight of the resultant PE, with small groups giving oligomers (83.6% C_4 , 13.0% C_6 for $\text{R} = \text{Me}$) and more bulky alkyls favoring linear PE formation (96.9% PE for $\text{R} = \text{}^i\text{Pr}$, Cy).^{254,255} However, the larger alkyl groups display lower activities ($2,310 \text{ g mmol}^{-1} \text{ h}^{-1} \text{ bar}^{-1}$ for $\text{R} = \text{Me}$ vs. $295 \text{ g mmol}^{-1} \text{ h}^{-1} \text{ bar}^{-1}$ for $\text{R} = \text{}^t\text{Bu}$).

Other half-sandwich Cr complexes which show good activities for olefin polymerization include those with ether and thioether pendant arms (93) and (94) which show activities of $1,435 \text{ g mmol}^{-1} \text{ h}^{-1} \text{ bar}^{-1}$ and $2,010 \text{ g mmol}^{-1} \text{ h}^{-1} \text{ bar}^{-1}$ respectively.²⁵² The half-sandwich phosphine complex (95) affords α -olefins arising from chain transfer to aluminum,^{256,257} while the related boratabenzene chromium(III) complex (96) generates linear PE.^{258,259} Cationic species have also been investigated, and (97) polymerizes ethylene with an activity of $56 \text{ g mmol}^{-1} \text{ h}^{-1} \text{ bar}^{-1}$.^{260–263}

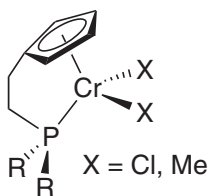
(ii) Nitrogen- and oxygen-based ligands

The complexation of a range of tridentate monoanionic ligands has been examined across the transition metal series and (98) was shown to catalyze the polymerization of ethylene with an activity of $500 \text{ g mmol}^{-1} \text{ h}^{-1} \text{ bar}^{-1}$.²⁶⁴ Bis(iminopyrrolide) complexes, such as (99),²⁶⁵ display moderate ethylene polymerization activities ($70 \text{ g mmol}^{-1} \text{ h}^{-1} \text{ bar}^{-1}$), as does the β -diketiminate complex (100).²⁶⁶

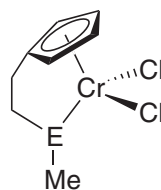
Salicylaldiminato ligands have also been studied and the bis(chelate) complex (**101**) has been reported to produce high molecular weight PE with an activity of $96 \text{ g mmol}^{-1} \text{ h}^{-1} \text{ bar}^{-1}$.²⁶⁷



(91)

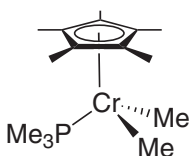


(92)

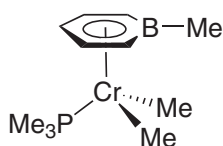


E = O, (93);

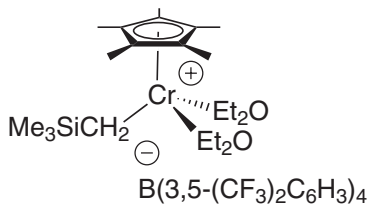
E = S, (94)



(95)



(96)

B(3,5-(CF₃)₂C₆H₃)₄

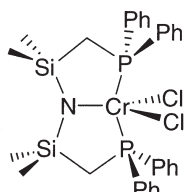
(97)

Monochelate analogs are accessible if the phenoxide ortho position contains a suitably bulky substituent, such as an anthracenyl group.²⁶⁸ High-throughput screening of a ligand library identified (**102**) as a particularly potent catalyst, capable of producing low molecular weight PE ($M_n = 600$) with an activity of $6,970 \text{ g mmol}^{-1} \text{ h}^{-1} \text{ bar}^{-1}$ at 50°C and 4 atm pressure.

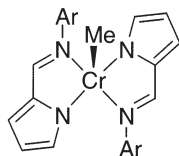
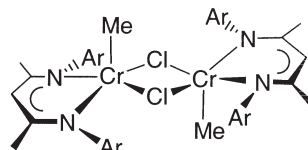
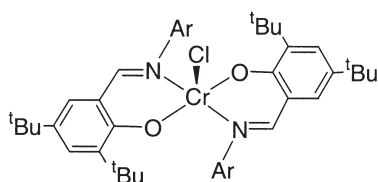
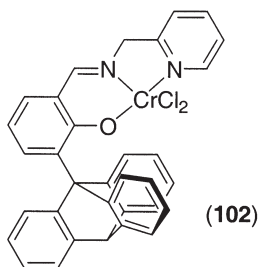
Another highly active chromium-based catalyst family is the triazacyclohexane series (**103**).²⁶⁹ Activities are dependent upon the length of the alkyl substituents attached to the nitrogen donors, reaching $717 \text{ g mmol}^{-1} \text{ h}^{-1} \text{ bar}^{-1}$ for R = n-dodecyl. With higher α -olefins, or when branched R substituents such as 3-propyl-heptyl are employed, these compounds behave as trimerization catalysts.^{270,271}

9.1.2.2.6 Group 8 metal catalysts

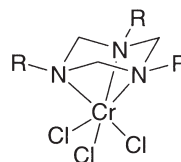
Highly active catalysts based on the bis(imino)pyridine family of complexes (**104**)–(**107**) were discovered independently in 1998 by Bennett, Brookhart and Gibson, and their co-workers.^{272–275}



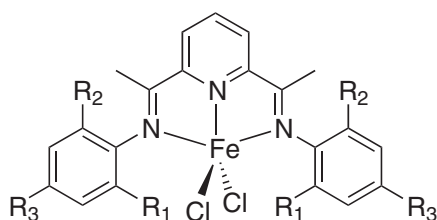
(98)

Ar = 2,6-ⁱPr₂C₆H₃, (99)Ar = 2,6-ⁱPr₂C₆H₃, (100)Ar = 2,6-ⁱPr₂C₆H₃, (101)

(102)



(103)



$R_1 = R_2 = iPr, R_3 = H$, (**104**);

$R_1 = R_2 = Me, R_3 = H$, (**105**);

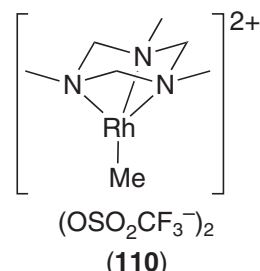
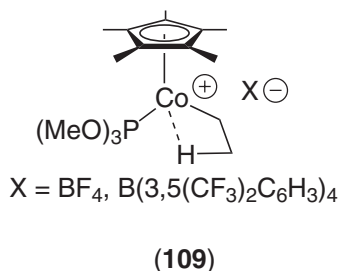
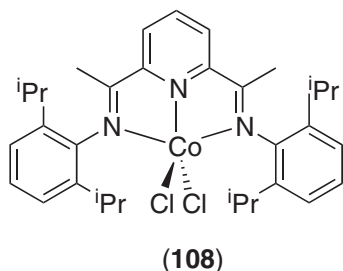
$R_1 = R_2 = R_3 = Me$, (**106**);

$R_1 = R_3 = H, R_2 = tBu$, (**107**)

In the presence of MAO, the ketimine catalysts show remarkably high activities for ethylene polymerization (comparable to the most active zirconocenes) with PE molecular weights highly dependent upon the aryl substitution pattern. The presence of only one small ortho substituent results in highly active oligomerization catalysts which exhibit high selectivity for linear α -olefins. High molecular weight PE is obtained for derivatives containing two ortho substituents, or a single ortho tBu group, on the imino aryl unit. Modifications to the original bis(imino)pyridine ligand framework have been examined extensively, but activities of the resultant catalysts rarely exceed those found for the parent system. These catalysts are also active for propylene polymerization. A chain end controlled [2,1] insertion mechanism affords isotactic-rich PP (mmmm = 55–67%) at $-20^\circ C$, with exclusive formation of propenyl end groups.^{276,277}

9.1.2.2.7 Group 9 metal catalysts

The Co analogs of iron complexes (**104**)–(**107**) are the most active catalysts amongst the group 9 metals, though they are considerably less active than their iron(II) relatives. With an activity of $460 \text{ g PE mmol}^{-1} \text{ h}^{-1} \text{ bar}^{-1}$, complex (**108**) is approximately one order of magnitude less active than (**104**), and produces much lower molecular weight PE.^{272,274,278} The cobalt analogues of (**106**) and (**107**) are more active than (**108**), with activities $>1700 \text{ g mmol}^{-1} \text{ h}^{-1} \text{ bar}^{-1}$.²⁷⁵ Another widely studied Co catalyst is the β -agostic d^6 cobalt(III) complex (**109**) which converts ethylene into high molecular weight polymer of narrow polydispersity.^{279–282} Stable, isolable cations are generated when non-coordinating anions are used²⁸³ and polymerizations initiated by such complexes are particularly well-controlled ($M_w/M_n = 1.1–1.3$), allowing end-group functionalized PE to be prepared.²⁸⁴ There are very few other group 9 catalysts of notable activity, although the slow *in aquo* polymerization of ethylene using complex (**110**) has been described.^{285,286}

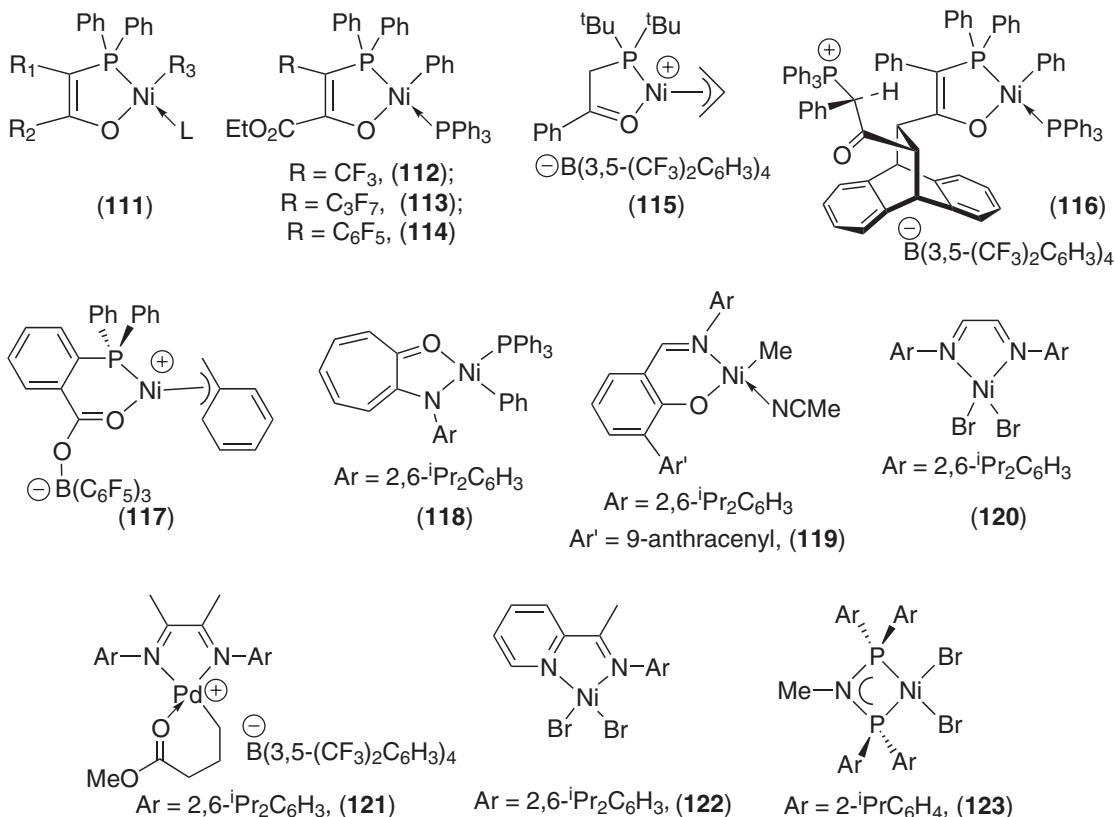


9.1.2.2.8 Group 10 metal catalysts

Nickel(II) compounds, of general formula (**111**), bearing monoanionic PO chelate ligands, are used industrially in the Shell higher olefin process (SHOP) for the production of linear α -olefins ($C_6–C_{20}$). If removal of the neutral ligand L (often PPh_3) is facilitated, then these complexes also polymerize ethylene.^{287–295} Particularly active examples include the fluorinated complexes (**112**)–(**114**) which afford low molecular weight linear PE ($M_w \approx 5,000$) with <1 branch per 1,000 carbons.²⁹⁶ These catalysts have also been used in aqueous emulsion polymerizations, although activities are substantially lower.²⁹⁷

Sterically bulky P,O-donor ligands have been used to prepare highly active catalysts, many of which are also capable of incorporating polar co-monomers. For example, complex (**115**) has

been shown to copolymerize ethylene with methyl-10-undecenoate.²⁹⁸ A very high activity ($8,720 \text{ g mmol}^{-1} \text{ h}^{-1} \text{ bar}^{-1}$) has been recorded for the polymerization of ethylene using complex **(116)**.²⁹⁹ It also copolymerizes ethylene with methyl methacrylate to give end-functionalized PE; insertion of MMA into a propagating PE chain results in immediate termination via β -hydrogen transfer.³⁰⁰



Oligomerization activities may be increased by forming cationic nickel catalysts via the addition of $\text{B}(\text{C}_6\text{F}_5)_3$ to a phosphinocarboxylate complex. This results in carbonyl coordination, which reduces the electron density at the nickel center.^{301,302} For example, complex **(117)** selectively dimerizes ethylene to 1-butene at 0°C and 1 atm, but higher olefins are produced at higher temperature and pressure. Such complexes have been used in conjunction with constrained geometry titanium catalysts to afford highly branched PE, with the level of branching a function of the Ni:Ti ratio.³⁰³ A similar strategy has been used to activate iminocarboxylate ligands attached to nickel.³⁰⁴

Complexes containing monoanionic N,O-donor chelates as alternatives to the P,O-donor ligands described above have also been investigated. The anilinoironate complex **(118)** produces high molecular weight PE with moderate activity.³⁰⁵ Salicylaldiminato ligands have been investigated extensively; derivatives such as **(119)** containing bulky substituents disfavor the formation of inactive bis(chelate) species and aid dissociation of the monodentate L donor ligand. **(119)** produces PE with a notably low branching content, and is tolerant of heteroatom-containing additives, including water.³⁰⁶ In the absence of any cocatalyst this complex appears to have an indefinite polymerization lifetime with activities up to $6,400 \text{ g mmol}^{-1} \text{ h}^{-1}$ at 100 psi ethylene pressure. It also catalyses the copolymerization of ethylene with norbornene and with ω -functionalized α -olefins. Less bulky, polymer-supported variants have also been described,³⁰⁷ as has the use of salicylaldiminato nickel(II) catalysts in the aqueous polymerization of ethylene.^{308,309}

The first examples of highly active olefin polymerization catalysts based on late transition metals were nickel and palladium complexes containing bulky diimine ligands.³¹⁰⁻³¹² For example, complex **(120)** was found to polymerize ethylene with an activity of $11,000 \text{ g mmol}^{-1} \text{ h}^{-1} \text{ bar}^{-1}$. A range of PE materials with molecular weights up to 10^6 and

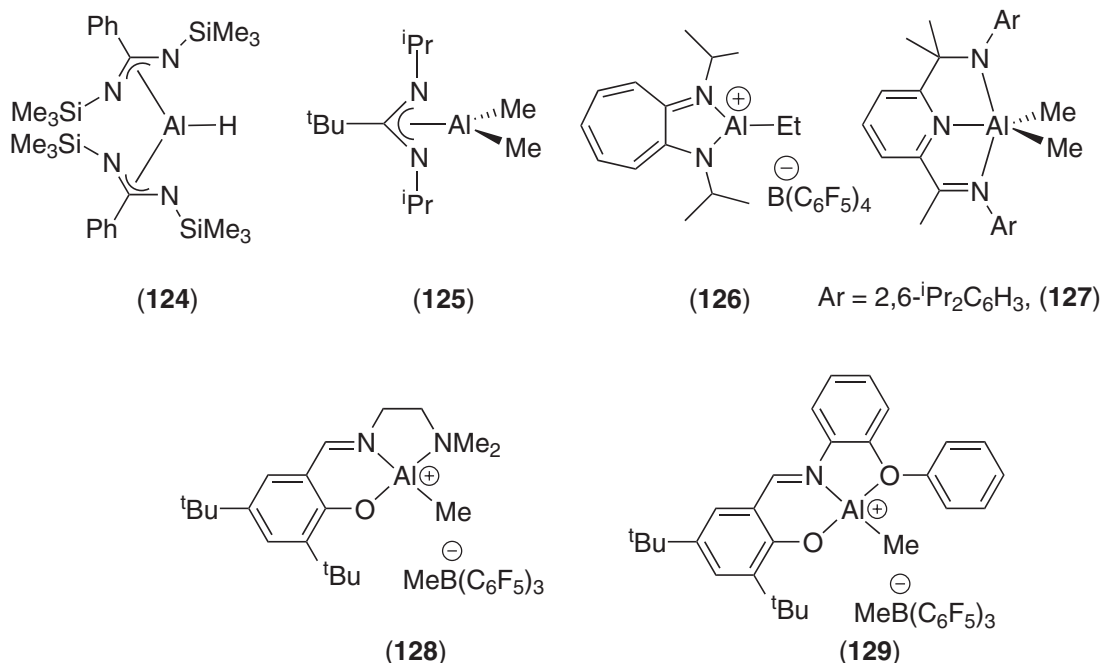
morphologies varying between linear and highly branched are accessible by altering reaction conditions and by modifying the diimine ligand architecture.³¹³ At low temperature the polymerization of ethylene is living and block copolymers with other α -olefins have been prepared.^{314,315} Furthermore, syndio-rich PP may be prepared via a chain-end controlled mechanism.^{316,317}

The diimine palladium compounds are less active than their nickel analogs, producing highly branched (e.g., 100 branches per 1,000 carbons) PE. However, they may be used for the copolymerization of α -olefins with polar co-monomers such as methyl acrylate.^{318,319} Cationic derivatives, such as (**121**), have been reported to initiate the living polymerization of ethylene at 5 °C and 100–400 psi.³²⁰ The catalyst is long-lived under these conditions and monodisperse PE ($M_w/M_n = 1.05$ – 1.08) may be prepared with a linear increase in M_n vs. time.

When less bulky ancillary ligands are used β -hydride elimination leads to the formation of α -olefins. As a consequence iminopyridine complexes are typically much less active than the diimine catalysts and afford lower-molecular-weight PE.^{321–324} For example, MAO/(**122**) polymerizes ethylene to branched oligomers with $M_n < 600$, and ≈ 240 branches per 1,000 carbons.³²⁵ Complex (**123**), is highly active for ethylene polymerization ($820 \text{ g mmol}^{-1} \text{ h}^{-1} \text{ bar}^{-1}$).³²⁶ As with the diimine systems, reduction in the steric bulk of the ligand substituents results in reduced activity and lower-molecular-weight products.

9.1.2.2.9 Main group metal catalysts

It is only relatively recently that ethylene polymerizations using molecular aluminum catalysts have been reported, though polymerization activities are generally low. Examples include the bis(benzamidinate) complex (**124**),³²⁷ and the mono-amidinate (**125**) which afford activities up to $3 \text{ g mmol}^{-1} \text{ h}^{-1} \text{ bar}^{-1}$.³²⁸ Aminotroponimate complexes such as (**126**) display similar activities.³²⁹ Activities of $0.12 \text{ g mmol}^{-1} \text{ h}^{-1} \text{ bar}^{-1}$ have been reported for the imino-amidopyridine species (**127**) when activated with $\text{B}(\text{C}_6\text{F}_5)_3$.³³⁰



In general, activation of these catalysts is typically performed using borane-mediated dealkylation, but the intermediacy of simple cationic alkyls has been questioned.^{331–333} It has also been shown that compounds similar to (**125**) may react with Lewis acids to give complex product mixtures, suggesting that the active component is not a single species.³³⁴ In non-coordinating solvents, bidentate salicylaldiminato aluminum dialkyls also do not react cleanly with $\text{B}(\text{C}_6\text{F}_5)_3$,³³⁵ but tridentate Schiff-base analogs yield stable cationic alkyls such as (**128**) and (**129**), which polymerize ethylene with very low activities.^{336,337}

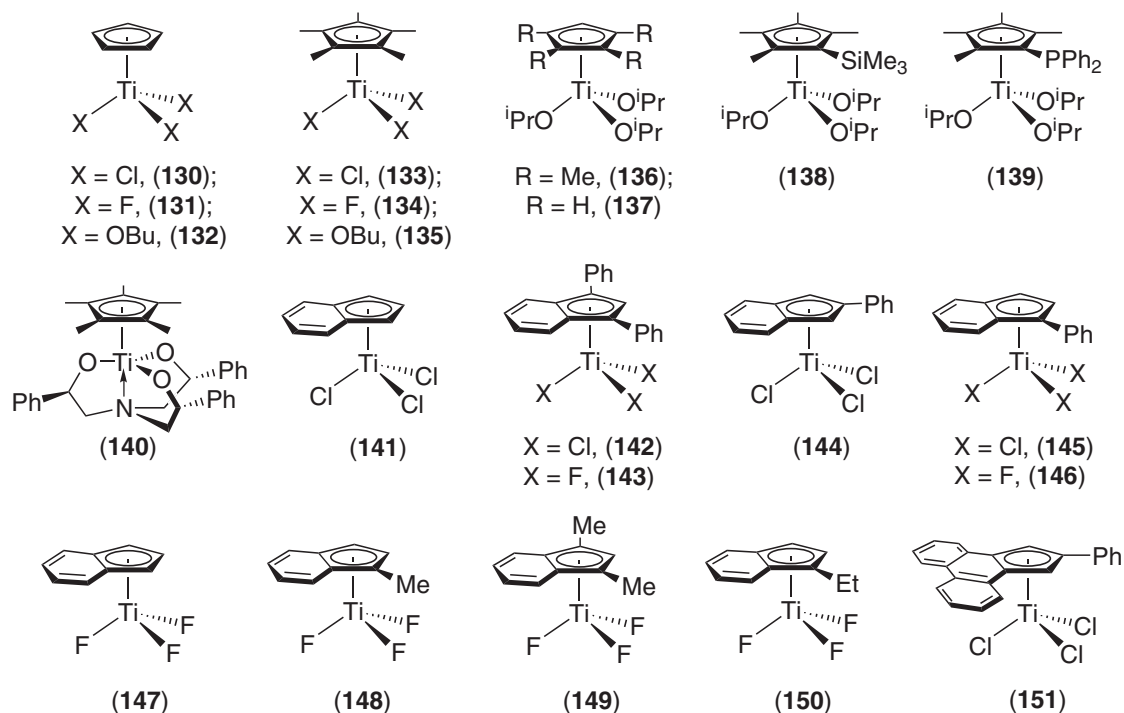
9.1.3 POLYMERIZATION OF STYRENES

9.1.3.1 Introduction

Coordination initiators for polystyrene synthesis have attracted interest due to their ability to control tacticity. Isotactic polystyrene was first prepared in 1955 using classical Ziegler–Natta type catalysts ($\text{TiCl}_4/\text{AlEt}_3$).^{338,339} More recently, syndiotactic polystyrene has proved accessible using a range of group 4 metal catalysts. Its high crystallinity and high melting temperature (270°C), combined with its good resistance to common organic solvents, give rise to a material with potential as an engineering thermoplastic.³⁴⁰ Another area where coordination complexes have found increased use is in the Atom Transfer Radical Polymerization (ATRP) of styrene, a versatile and robust methodology for controlled polystyrene assembly.

9.1.3.2 Coordinative Polymerization of Styrenes

Highly syndiotactic polystyrene, s-PS, was first synthesized in 1986 using an undisclosed catalyst formulation consisting of titanium and aluminum species.³⁴¹ Shortly afterwards, $\text{Ti}(\text{CH}_2\text{Ph})_4/\text{MAO}$ was also shown to catalyze the syndioselective polymerization of styrene.^{342–344} This system produces s-PS with an rr triad content $>98\%$, but exhibits a low initiator efficiency, with just 1.7% of the Ti centers catalyzing syndiotactic growth (17% promote atactic propagation).³⁴⁵ Much higher activities have been reported for monocyclopentadienyl titanium complexes such as $\text{CpTiCl}_3/\text{MAO}$,³⁴⁶ which polymerizes styrene at 50°C with an activity $>1,000\text{ g mmol}^{-1}\text{ h}^{-1}$.³⁴⁷ Zirconium analogs are far less active, with CpZrCl_3 reported to be 80 times less active than (130).³⁴⁸ In addition, both zirconocenes and titanocenes are poor initiators.³⁴⁹ Complex (130) may also be used to polymerize a variety of alkyl- and halo-substituted styrenes.³⁴⁸ In each case highly syndiotactic polymers were reported with melting points significantly higher than their isotactic analogs. Electron-withdrawing groups severely reduce the rate of polymerization; even sterically bulky *para*-^tbutylstyrene is consumed considerably faster than *meta*- or *para*-halostyrenes.



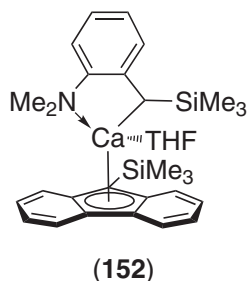
Subsequent studies revealed that a variety of cyclopentadienyl-based titanium complexes may be used to catalyze the production of s-PS and this area has been extensively reviewed.^{350–353} Indeed, most complexes of the general formula $(\text{Cp}')\text{TiX}_3$ generate s-PS when activated with a

large excess of MAO ($\text{Cp}' = \text{C}_5\text{R}_5$ or indenyl ligands). In addition to halide pre-catalysts, alkoxide^{344,345,354} and alkyl species have been employed. The alkoxides are activated with MAO, whereas the alkyl analogs require pretreatment with equimolar amounts of $\text{B}(\text{C}_6\text{F}_5)_3$, $[\text{Ph}_3\text{C}^+][\text{B}(\text{C}_6\text{F}_5)_4^-]$, or $[\text{PhNHMe}_2^+][\text{B}(\text{C}_6\text{F}_5)_4^-]$.

The size of the cyclopentadienyl ligand affects activity, syndiotactic content and molecular weight. However, the other ligands at the titanium center also play a key role. For example, CpTiF_3 (**131**) is more active than (**130**), typically affording $3,000 \text{ g mmol}^{-1} \text{ h}^{-1}$;^{347,354} intermediate activities have been observed using the tris(alkoxide) (**132**). A similar order of reactivity is observed for the pentamethyl analogs (**133**)–(**135**), although these are significantly less active than (**130**)–(**132**).^{347,355} By contrast, the tetramethyl complex (**136**) has been reported to be more active than the unsubstituted (**137**).³⁵⁶ The yet more bulky (**138**) produces polystyrene of similar syndiotacticity and molecular weight to (**136**), but is an order of magnitude less active. Complex (**139**) is almost totally inactive. A family of titanatrane complexes have also been investigated as catalysts. All are highly syndioselective^{357,358} and the sterically bulky complex (**140**) is particularly noteworthy as it generates high-molecular-weight s-PS at 30°C ($M_n = 443,000$; $M_w/M_n = 1.97$).³⁵⁹

Some of the most active catalyst systems for the production of s-PS are indenyl titanium complexes. The parent compound (**141**), when activated with MAO, is at least 50–100% more active than (**130**)/MAO.³⁶⁰ Phenyl substitution of the indenyl ring leads to significantly higher activities, with activity increasing in the order (**142**) < (**144**) < (**145**) (although the yield of s-PS displays the opposite trend). In accord with previous reports³⁴⁷ it was found that fluorides are consistently much more active than their chloride analogs.³⁶¹ Complex (**147**) was reported to be ≈ 4 times more active than (**131**), exhibiting an activity of $12,500 \text{ g mmol}^{-1} \text{ h}^{-1}$. Substitution of the indenyl ring with small alkyl or phenyl groups generated similarly active catalyst systems. Hence, the fluorides (**148,149,150,143,146**) all display activities $>10,000 \text{ g mmol}^{-1} \text{ h}^{-1}$. The bulk of the indenyl substituent also determines the stereocontrol, with (**150,143,146**) all giving slightly more atactic PS than (**147,148,149**). If the indenyl substituent is a larger alkyl, such as ^iPr , ^tBu or Me_3Si , then the activity and the s-PS content both decrease dramatically. One of the most active initiators reported to date is the cyclopenta[1]phenanthrene species (**151**) which exhibits its highest activity at 75°C when activated with MAO.³⁶²

In an attempt to combine the syndioselectivity of half-sandwich titanium catalysts with the living characteristics of anionic polymerization initiators, the use of half-sandwich calcium-based catalysts has been described.^{363,364} In neat styrene complex (**152**) affords 76% rr triad PS. However, polydispersities are still quite high ($M_w/M_n > 2.2$)

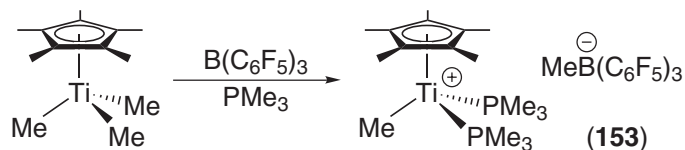


The mechanism responsible for the syndiotactic polymerization of styrene from such a range of precatalysts is not yet fully understood, although certain key components have been elucidated. It is believed that several different active sites are present, since the s-PS is nearly always produced alongside a small quantity of atactic material. In addition, attempts to copolymerize styrene with ethylene using these catalysts tend to result in the production of both PE and s-PS homopolymers, as well as various copolymers. The presence of multiple active sites could also explain why polydispersities are often >2.5 . ESR studies on systems such as $\text{Ti}(\text{CH}_2\text{Ph})_4/\text{MAO}$ ³⁶⁵ and $(\text{C}_5\text{Me}_5)\text{TiMe}_3/\text{B}(\text{C}_6\text{F}_5)_3$ ^{366,367} suggest that the predominant catalytic site is a cationic titanium(III) species, although this has been questioned.^{368,369} In accord with this proposition, studies have shown that the reduction of Ti^{IV} to Ti^{III} centers is accelerated upon the addition of styrene.^{366,370}

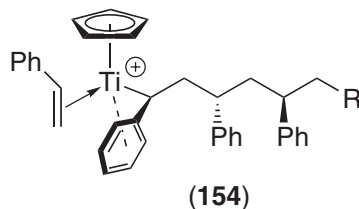
Further evidence for a Ti^{III} -centered pathway has been provided from model studies comparing the activity of analogous Ti^{IV} and Ti^{III} precatalysts; for example, $(\text{C}_5\text{Me}_5)\text{Ti}(\text{OMe})_2/\text{MAO}$ was reported to be more active than $(\text{C}_5\text{Me}_5)\text{Ti}(\text{OMe})_3/\text{MAO}$.³⁷¹ More recently it has been shown that Ti^{IV} catalysts only produce atactic-PS when the polymerization is performed in the absence of

light.³⁷² When used in the presence of light, however, they produce s-PS of similar molecular weight to a Ti^{III} catalyst, $(\text{C}_5\text{Me}_5)\text{Ti}(\eta^3\text{-C}_3\text{H}_5)_2$ used in the dark, suggesting that similar Ti^{III} active sites are involved.

The cationic titanium center is thought to retain the η^5 -cyclopentadienyl ligand during propagation.^{373–375} NMR analysis of s-PS produced with $\text{CpTi}(\text{C}_5\text{Me}_5)_3$ further shows that one of the alkyl ligands is incorporated as a $-\text{CH}(\text{Ph})\text{CH}_2^{13}\text{CH}_3$ end group.³⁷⁶ This implies a [2,1] secondary insertion mode in which the phenyl-substituted olefinic carbon becomes directly bonded to the titanium center.³⁷⁷ These observations suggest that the initiating species is a cationic monoalkyl species, $[\text{Cp}^*\text{TiR}]^+$. Such species have not been isolated, although the phosphine adduct (**153**) has been described.³⁶⁷ When treated with MAO, complex (**153**) also catalyzes the formation of s-PS.



The propagating species is generally believed to be (**154**), a pseudo-tetrahedral cation in which the electron-deficient metal center is stabilized by interactions with the α -phenyl of the propagating PS chain and with an incoming molecule of monomer. The precise origin of the stereoselectivity has not yet been determined, although a chain-end controlled process in which the orientation of the incoming monomer is determined by the binding nature of the α -phenyl is plausible. In this respect, labeling experiments have shown that, using $\text{Ti}(\text{CH}_2\text{Ph})_4/\text{MAO}$, the insertion occurs via *cis*-addition of the styrene to the $\text{M}-\text{CH}(\text{Ph})$ bond.³⁷⁸ The main termination step is thought to be β -hydrogen transfer.³⁷⁹



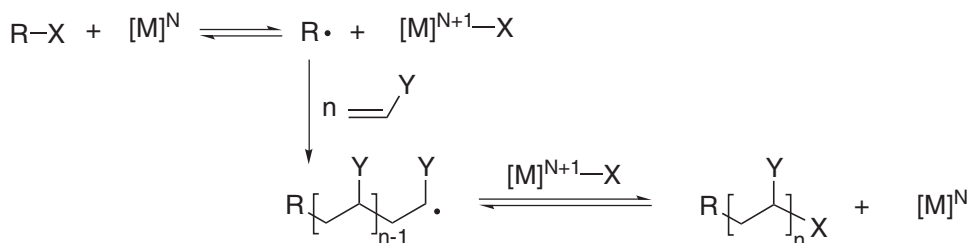
9.1.3.3 Atom Transfer Radical Polymerization of Styrenes

Atom transfer radical polymerization, ATRP, is a controlled radical process which affords polymers of narrow molecular weight distributions. Strictly this is not a coordinative polymerization, but its dependency upon suitable coordination complexes warrants a brief discussion here.

Like all controlled radical polymerization processes, ATRP relies on a rapid equilibration between a very small concentration of active radical sites and a much larger concentration of dormant species, in order to reduce the potential for bimolecular termination (Scheme 3). The radicals are generated via a reversible process catalyzed by a transition metal complex with a suitable redox manifold. An organic initiator (many initiators have been used but halides are the most common), homolytically transfers its halogen atom to the metal center, thereby raising its oxidation state. The radical species thus formed may then undergo addition to one or more vinyl monomer units before the halide is transferred back from the metal. The reader is directed to several comprehensive reviews of this field for more detailed information.^{380–382}

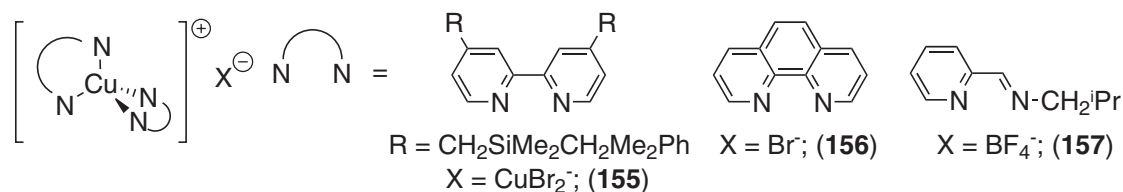
Several classes of vinyl monomer are suitable for ATRP including styrenes³⁸³ and methacrylates.³⁸⁴ Many of the studies have been performed using copper,^{385,386} iron,³⁸⁷ ruthenium,³⁸⁸ and rhenium systems.³⁸⁹ The most common catalysts for the ATRP of styrenes are heterogenous mixtures of a copper(I) halide and a neutral chelating amine, imine or pyridine ligand, often 2,2'-bipyridine or 1,10-phenanthroline.³⁸⁵ In order to increase the solubility of the copper catalyst, long-chain substituents on the ligand have been examined, and this in turn leads to increased catalyst efficiency.^{390–392} The addition of DMF may also serve to make the polymerization homogenous, but polydispersities are broadened (1.4–1.8).³⁹³ Most copper catalysts require temperatures of 110–130 °C,³⁹⁴ but lower temperatures (e.g., 90 °C) may be used if a particularly

efficient catalyst, such as CuBr/*N,N,N',N',N''*-pentamethyl-diethylenetriamine, is employed.³⁹⁵ The lower reaction temperatures often result in narrower molecular weight distributions due, it is believed, to a lower likelihood of thermal self-initiation.³⁹⁶

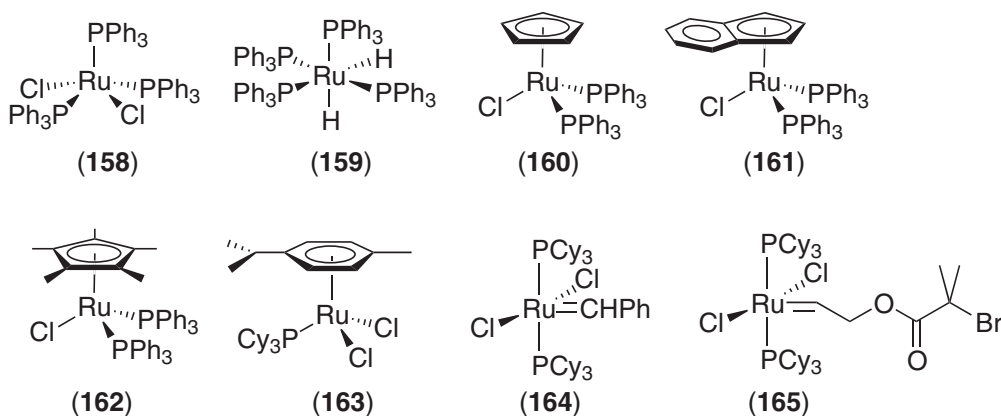


Scheme 3

Despite numerous studies involving copper catalysts, only a few isolated copper complexes have been examined, including complexes (155)–(157). Bipyridine,³⁹⁷ phenanthroline,³⁹⁸ and pyridylimine cationic complexes³⁹⁹ all exhibit tetrahedral geometries, in which the copper center is bound to two ligands.

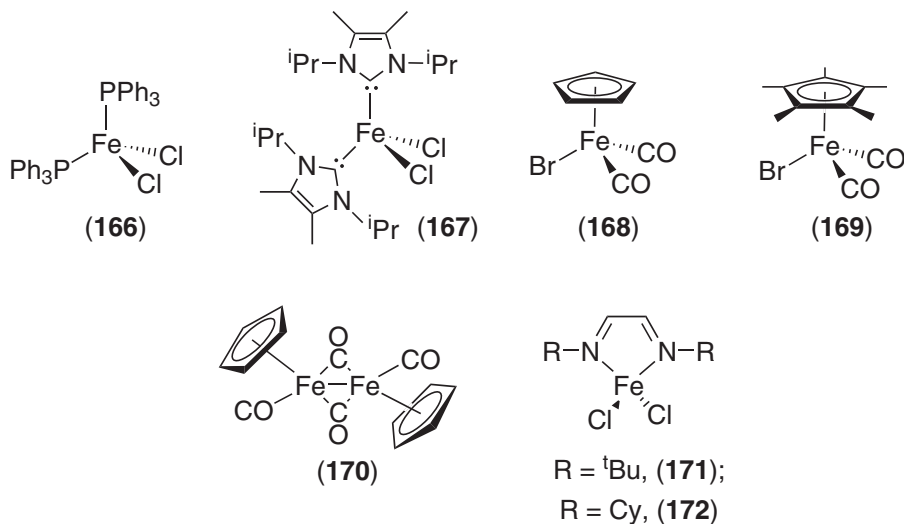


By contrast, much of the work performed using ruthenium-based catalysts has employed well-defined complexes. These have mostly been studied in the ATRP of MMA, and include complexes (158)–(165).^{400–405} Recent studies with (158) have shown the importance of amine additives which afford faster, more controlled polymerization.⁴⁰⁶ A fast polymerization has also been reported with a dimethylaminoindenyl analog of (161).⁴⁰⁷ The Grubbs-type metathesis initiator (165) polymerizes MMA without the need for an organic initiator, and may therefore be used to prepare block copolymers of MMA and 1,5-cyclooctadiene.⁴⁰⁵ Hydrogenation of this product yields PE-*b*-PMMA. *N*-heterocyclic carbene analogs of (164) have also been used to catalyze the free radical polymerization of both MMA and styrene.⁴⁰⁸

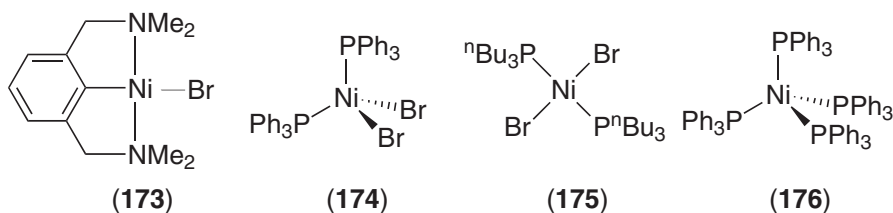


Iron catalysts such as (166)–(172) are generally more active than their ruthenium analogs, and in view of the lower cost and low bio-toxicity of this metal, are gaining increasing attention.^{409–413} For example, (166) polymerizes MMA in a well-controlled manner, and is faster than (158), although it is inactive for styrene polymerization.⁴⁰⁹ Complex (167) has been used to polymerize both MMA and styrene. Molecular weight distributions are narrow (1.1–1.3) and decrease upon addition of FeCl₃ (*M*_w/*M*_n = 1.1), although this slows the polymerization.⁴¹⁰ Compounds (168)

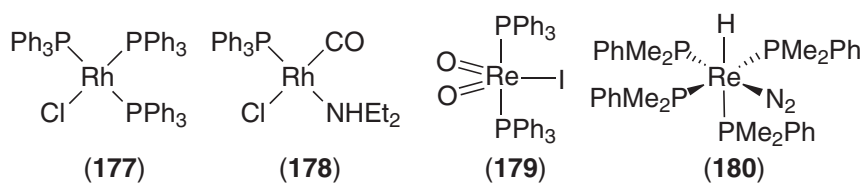
and (169) have been used to catalyze the radical polymerization of acrylates and styrene in aqueous media.⁴¹⁴ The living polymerization of styrene has also been described using dinuclear iron(I) complexes such as (170).⁴¹² In a recent study, well-defined iron(II) diimine compounds including (171) and (172) were examined.⁴¹³ The alkyl-substituted diimines were found to support the well-controlled ATRP of styrene, whilst aryl-substituted counterparts gave rise to β -hydrogen chain transfer processes. Iron(III) complexes may also be used in the “reverse” ATRP process.⁴¹⁵



Several nickel(II) complexes (e.g., (173)–(176)) have successfully been used to catalyze ATRP, especially when coupled with bromo-initiators, although activities are usually lower than with copper, ruthenium or iron systems.^{416–419} The alkylphosphine complex (175) is thermally more stable than (174) and has been used to polymerize a variety of acrylate monomers between 60 °C and 120 °C.⁴¹⁸ Complex (176) is an unusual example of a well-defined zerovalent ATRP catalyst; it displays similar activities to the Ni^{II} complexes, although molecular weight distributions (1.2–1.4) are higher.⁴¹⁹ Pd(PPh₃)₄ has also been investigated and was reported to be less controlled than (176).⁴²⁰



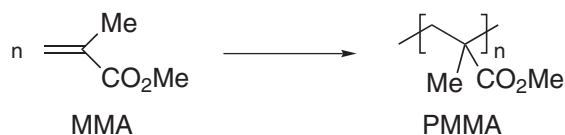
Several rhodium(I) complexes have also been employed as ATRP catalysts, including Wilkinson’s catalyst, (177),^{391,421,422} and complex (178).⁴²³ However, polymerizations with both compounds are not as well-controlled as the examples discussed above. In conjunction with an alkyl iodide initiator, the rhenium(V) complex (179) has been used to polymerize styrene in a living manner ($M_w/M_n < 1.2$).³⁸⁹ At 100 °C this catalyst is significantly faster than (160), and remains active even at 30 °C. A rhenium(I) catalyst has also been reported (180) which polymerizes MMA and styrene at 50 °C in 1,2-dichloroethane.⁴²⁴



9.1.4 POLYMERIZATION OF ACRYLATES

9.1.4.1 Introduction

Several poly(acrylates) and poly(alkylacrylates) are commercially manufactured commodity polymers, one of the most important being poly(methylmethacrylate), PMMA (Scheme 4). Renowned for its high optical clarity and good weatherability, PMMA forms the basis of the Perspex, Plexiglass, or Lucite families of materials.⁴²⁵ These polymers are traditionally prepared using free-radical polymerization technology, but such methods usually offer little control over molecular weight or tacticity. The commercial significance of PMMA has therefore encouraged the development of a variety of living anionic and coordinative polymerization catalysts. For brevity, alkyl-substituted monomers are abbreviated as MA for methacrylates and A for acrylates; e.g., EtA = ethyl acrylate and ⁱPrMA = *iso*-propyl methacrylate.



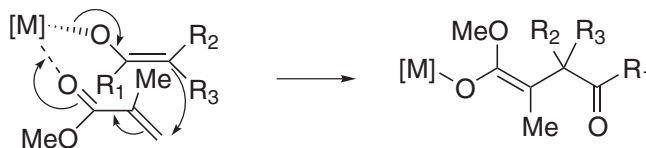
Scheme 4

PMMA can exist in two simple stereoregular forms, isotactic and syndiotactic, but commercially available samples—prepared via free-radical initiators—tend to have tacticities lying in the range 60–70% syndiotactic triad content, the exact content depending upon the reaction temperature.⁴²⁶ Several terminating side reactions have been identified, the most important of which is intramolecular cyclization leading to methoxide formation, as shown in Scheme 5.⁴²⁷



Scheme 5

Main group organometallic polymerization catalysts, particularly of groups 1 and 2, generally operate via anionic mechanisms, but the similarities with truly coordinative initiators justify their inclusion here. Both anionic and coordinative polymerization mechanisms are believed to involve enolate active sites, (Scheme 6), with the propagation step akin to a 1,4-Michael addition reaction.



Scheme 6

9.1.4.2 Anionic Initiators of the group 1, 2, and 3 Metals

A large number of group 1–3 metal compounds have been shown to polymerize MMA, especially lithium, magnesium, and aluminum species.^{426,427} These initiators generally give isotactic-biased PMMA when performed in toluene, and syndiotactic polymer when conducted in THF.^{428,429} However, most ill-defined main group catalysts generally initiate non-living polymerizations at ambient temperature, and afford little control over chain length. Molecular weight distributions are typically broad, consistent with multiple propagating species. Certain organolithium and

organomagnesium initiators do exhibit living-like behavior at low temperatures, but identification of the active site is complicated by processes such as aggregation and ligand exchange.

The most studied catalyst family of this type are lithium alkyls. With relatively non-bulky substituents, for example ${}^n\text{BuLi}$, the polymerization of MMA is complicated by side reactions.⁴³⁰ These may be suppressed if bulkier initiators such as 1,1-diphenylhexyllithium are used,⁴³¹ especially at low temperature (typically $-78\text{ }^\circ\text{C}$), allowing the synthesis of block copolymers.^{432,433} The addition of bulky lithium alkoxides to alkyl lithium initiators also retards the rate of intramolecular cyclization, thus allowing the polymerization temperature to be raised.⁴²⁷ LiCl has been used to similar effect, allowing monodisperse PMMA ($M_w/M_n = 1.2$) to be prepared at $-20\text{ }^\circ\text{C}$.⁴³⁴ Sterically hindered lithium aluminum alkyls have been used at ambient (or higher) temperature to polymerize MMA in a controlled way.⁴³⁵ This process has been termed “screened anionic polymerization” since the bulky alkyl substituents screen the propagating terminus from side reactions.

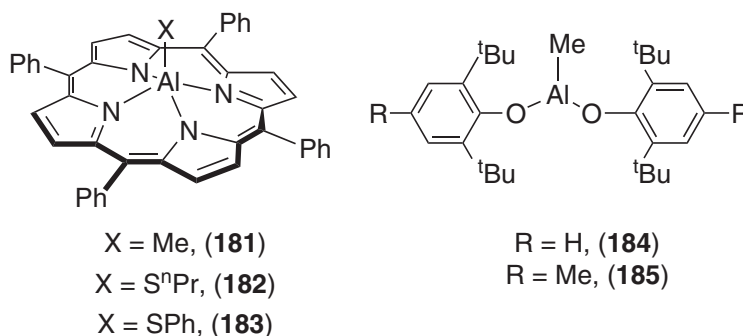
Stereoregular acrylate polymerizations have been reported using Grignard reagents at very low temperatures (Table 1). For example, ${}^t\text{BuMgBr}$ polymerizes MMA with almost 100% initiator efficiency at $-78\text{ }^\circ\text{C}$ in toluene, affording isotactic PMMA ($>95\%$ mm triad).⁴³⁶ The preparation of syndiotactic PMMA is more challenging, but is recognized as an important technological objective since the syndio-rich polymer possesses a higher T_g than the other forms of PMMA. Initiators affording high syndiotacticities include bulky alkylolithiums and certain Grignard reagents in THF, organocalcium species and several aluminum-based systems including amides and phosphine adducts; however, all require very low temperatures and are therefore not commercially attractive.

9.1.4.3 Well-defined Magnesium and Aluminum Initiators

The use of single-site initiators for the polymerization of acrylates is attractive, since steric protection of the metal center should eliminate the unwanted side reactions described above, allowing living polymerization systems to be developed. Further, stereocontrol may be achievable by appropriate ligand selection.

Upon irradiation, the tetraphenylporphyrinato (TPP) aluminum alkyl species (**181**) initiates a slow but well-controlled polymerization of MMA; in the dark the system is inactive.⁴⁴¹ The polymerization exhibits living characteristics and ${}^1\text{H}$ NMR analysis of the living oligomers generated upon ${}^t\text{BuMA}$ polymerization demonstrates that the propagating species is an oxygen-metallated enolate.^{441,442} The di-block copolymerization of MMA with ${}^n\text{BuMA}$ ⁴⁴¹ and of MMA with epoxides⁴⁴³ is further testament to the living nature of this system.

The rate of polymerization may be dramatically accelerated upon addition of a bulky Lewis acid. For example, addition of (**184**) to a sample of living PMMA generated by irradiation of (**181**)/MMA causes an increase in polymerization rate by a factor of $>45,000$.⁴⁴⁴ The dual-component systems (**181**)/(**184**), and (**181**)/(**185**), have been used to prepare monodisperse, ultra-high-molecular-weight samples of PMMA ($M_n > 10^6$, $M_w/M_n = 1.2$).⁴⁴⁵



The thiolate species (**182**) and (**183**) do not require photo excitation in order to initiate polymerization; (**182**) consumes 200 equivalents MMA in 18 h at $35\text{ }^\circ\text{C}$ ($M_n = 22,000$, $M_n(\text{calc}) = 20,000$, $M_w/M_n = 1.12$).⁴⁴⁶ The propagating species is again believed to be an enolate.⁴⁴⁷ Propagation is accelerated upon addition of (**185**), with 100 equivalents of MMA requiring just 90 seconds for full conversion. The steric bulk of the Lewis acid prevents scrambling of the propagating enolate between the two aluminum centers.⁴⁴⁸ Hence, for aluminum diphenolates, ortho substitution is essential, whilst smaller Lewis acids such as Me_3Al may only be used successfully at low temperatures, e.g., $-40\text{ }^\circ\text{C}$.

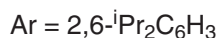
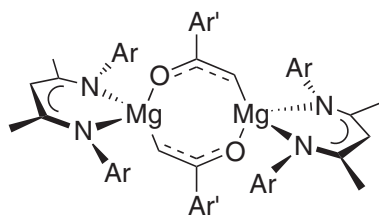
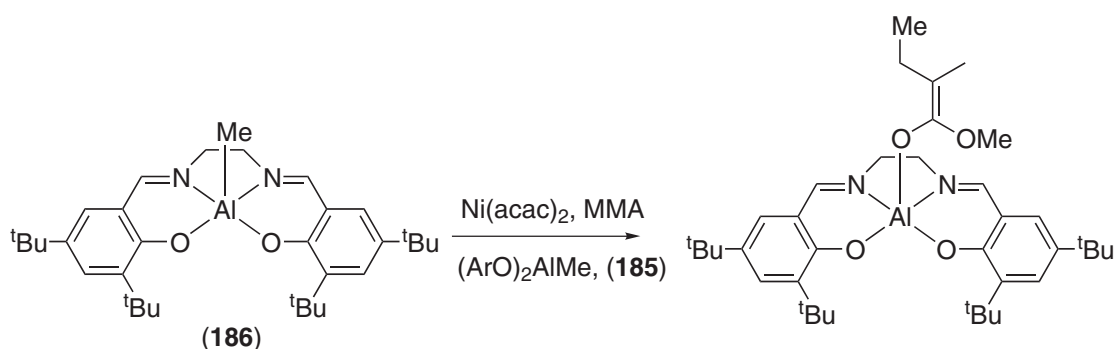
Table 1 Stereoregular polymerization of MMA

Initiator	Conditions	Tacticity	M_w/M_n	References
^t BuMgBr	Toluene, -78 °C	95–97% mm	1.2–1.3	436
Me(CH ₂) ₄ CPh ₂ Li	THF, -78 °C	84% rr	1.18	437
Et ₃ Al/TiCl ₄	Toluene, -78 °C	90% rr	4.58	438
(Ph ₃ C)CaCl	DME, -63 °C	95% rr	3.3	439
Et ₃ Al/PPh ₃	Toluene, -78 °C	90% rr	1.96	426
EtAl(NPh ₂) ₂	Toluene, -78 °C	86% rr	Multi-modal	426
m-vinylbenzyl magnesium chloride	THF, -110 °C	97% rr	1.19	440

Complexes (**181**)–(**183**) may also be used to polymerize acrylates⁴⁴⁹ and methacrylonitrile⁴⁵⁰ in a living manner, although (**181**) again requires photoinitiation. Acrylates such as ^tBuA polymerize faster than methacrylates. The rate of propagation of methacrylonitrile is much slower than methacrylates, although in the presence of (**185**), 100 equivalents are consumed within 3 hours.

Although Al(salen) complexes are readily accessible and are potentially attractive as initiators for acrylate polymerization, it is only recently that they have been opened to investigation, largely due to difficulties in accessing the active enolate species—the Al(salen) precursors are not amenable to UV activation, nor do thiolate derivatives act as suitable precursors. The solution to forming the enolate initiator in Al(salen) systems lies in a nickel-catalyzed rearrangement of MMA.⁴⁵¹ A three-component system comprising (**186**), Ni(acac)₂ and (**185**), polymerizes 200 equivalents of MMA within 2 minutes at room temperature ($M_n = 24,700$, $M_n \text{ calc} = 20,000$, $M_w/M_n = 1.17$). The resultant PMMA displays a slightly higher syndiotacticity than free radical generated samples, with rr = 68–72%; at -20 °C this rises to 84% rr. The living nature of the system is demonstrated by a linear dependence of M_n upon monomer conversion, and the synthesis of a PMMA-*b*-PⁿBuMA diblock by sequential monomer addition. The bulky Lewis acid (**185**) serves two functions, one of which is activation of the monomer as described for the porphyrinato aluminum initiators.⁴⁴⁴ In addition, it is believed to react with Ni(acac)₂ to afford a Ni–methyl species which then inserts MMA. The resultant enolate is then transferred onto the aluminum center to give the initiating species.

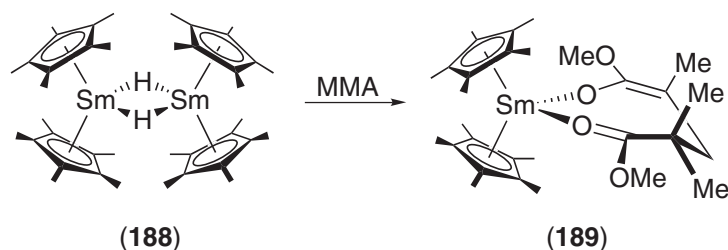
The well-defined single-site magnesium enolate initiator (**187**) initiates the living polymerization of MMA at -30 °C.⁴⁵² M_w/M_n values are typically 1.07–1.11, and M_n increases linearly both with



conversion and with the $[M]_0/[I]_0$ ratio. The polymer is highly syndiotactic, with an rr triad content of 92%, a level of stereocontrol not previously attainable with other polymerization systems at such a high reaction temperature.

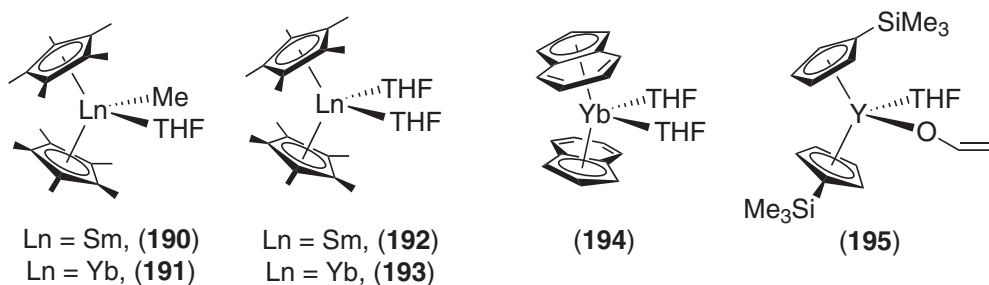
9.1.4.4 Lanthanide Initiators

$[\text{Cp}^*_2\text{Sm}(\mu\text{-H})_2]$, (**188**), affords very high-molecular-weight PMMA with very low polydispersities (typically ≤ 1.05).^{453–456} At -95°C the polymer formed is highly syndiotactic (95% rr triad). Isolation and X-ray analysis of (**189**), the 1:2 complex of (**188**) and MMA, provides strong support for the participation of a metal–enolate as the active site. (**189**) behaves in an identical manner to the hydride precursor, converting 100 equivalents MMA to polymer with $M_n = 11,000$ and $M_w/M_n = 1.03$.⁴⁵⁷ The successful structural characterization of (**189**) provides support for intermediates proposed earlier.^{458,459}



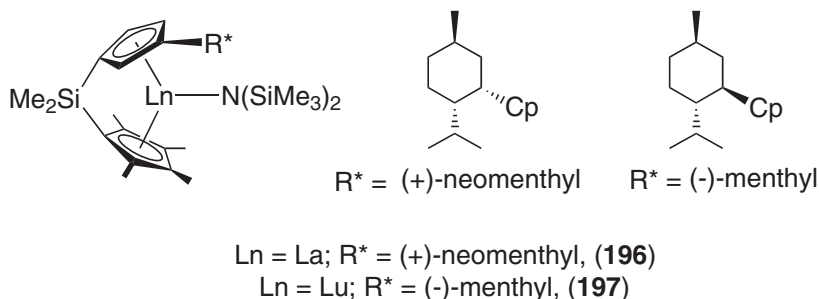
The lanthanocene alkyls (**190**) and (**191**) are also highly active initiators for MMA polymerization. These too are syndioselective, producing 82–85% rr PMMA at 0°C with high initiator efficiencies and narrow molecular weight distributions. Ln^{II} complexes such as (**192**)–(**194**) also generate syndiotactic PMMA, but exhibit much lower efficiencies (30–40%).

The lanthanocene initiators also polymerize EtMA, ⁱPrMA and ^tBuMA in a well-controlled manner, although syndiotacticity decreases as the bulk of alkyl substituent increases. Reactivity also decreases in the order $\text{MMA} \approx \text{EtMA} > \text{}^i\text{PrMA} > \text{}^t\text{BuMA}$. Chain transfer to provide shorter polymer chains is accomplished by addition of ketones and thiols.⁴⁶⁰ The alkyl complexes (**190**) and (**191**) also rapidly polymerize acrylate monomers at 0°C .^{461,462} Both initiators deliver monodisperse poly(acrylic esters) (M_w/M_n 1.07). An enolate is again believed to be the active propagating species since the model complex (**195**) was also shown to initiate the polymerization of MA.



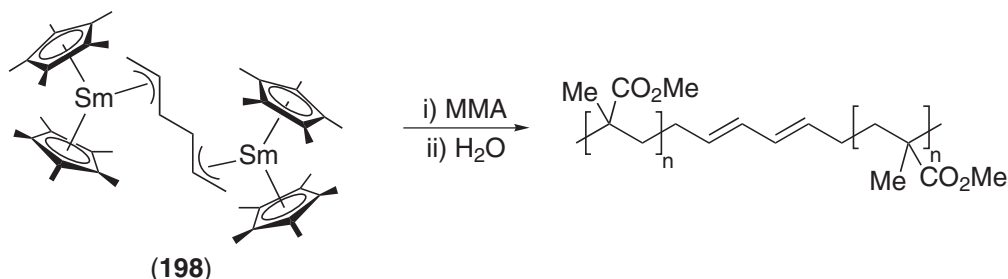
The polymerization of MMA has been shown to be subject to enantiomorphic site control when the C_1 -symmetric *ansa*-lanthanocene complexes (**196**) and (**197**) are employed as initiators.⁴⁶³ When the (+)-neomenthyl catalyst (**196**) is used, highly isotactic PMMA is produced (94% mm at -35°C), whereas the (-)-menthyl derived (**197**) affords syndiorich PMMA (73% rr at 25°C). NMR statistical analysis suggests that conjugate addition of monomer competes with enolate isomerization processes, and the relative rate of the two pathways determines the tacticity.

Many other lanthanide-based initiators have been shown to polymerize MMA, including lanthanocene amides,^{464–468} alkoxides,⁴⁶⁹ substituted indenyl and fluorenyl bivalent ytterbocenes,^{470,471} hexamethylphosphoric triamide thiolates,⁴⁷² and allyl, azaallyl, and diazapentadienyl complexes.⁴⁷³



As described in Section 9.1.2.2.3, several lanthanocene alkyls are known to be ethylene polymerization catalysts.^{221,226–229} Both (188) and (190) have been reported to catalyze the block copolymerization of ethylene with MMA (as well as with other polar monomers including MA, EA and lactones).²²⁹ The reaction is only successful if the olefin is polymerized first; reversing the order of monomer addition, i.e., polymerizing MMA first, then adding ethylene only affords PMMA homopolymer. In order to keep the PE block soluble the M_n of the prepolymer is restricted to $\leq 12,000$. Several other lanthanide complexes have also been reported to catalyze the preparation of PE-*b*-PMMA,^{474–476} as well as the copolymer of MMA with higher olefins such as 1-hexene.⁴⁷⁷

Initiation of MMA polymerization by complexes such as (192) was shown to proceed via a bimetallic bis(enolate) intermediate, arising from the dimerization of a radical anion.^{478–480} Such a mechanism^{481,482} explains why efficiencies with such initiators (calculated from polymer molecular weights) are always $\leq 50\%$. Using a similar methodology, the bimetallic bisallyl complex (198) was shown to polymerize MMA in a living fashion ($M_w/M_n \approx 1.1$) and triblock copolymers with methacrylate and acrylate segments have been prepared.

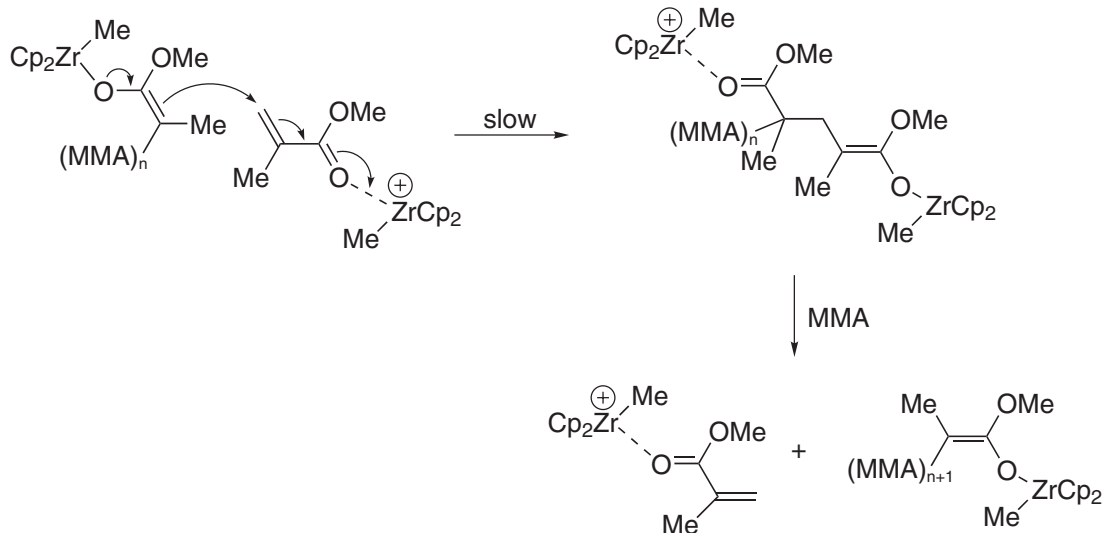


9.1.4.5 Early Transition Metal Initiators

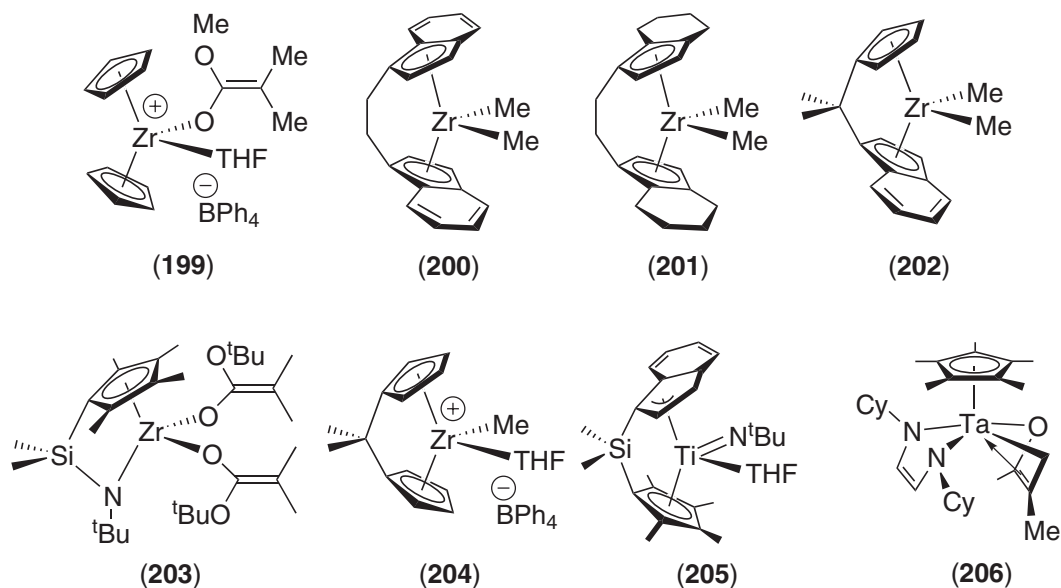
The polymerization of MMA using a group 4 metallocene initiator was first reported in the late 1960s.⁴⁸³ Some years later it was shown that an equimolar mixture of the cationic alkyl complex, $[\text{Cp}_2\text{ZrMe}(\text{THF})]^+[\text{BPh}_4]^-$, and the neutral dialkyl species, Cp_2ZrMe_2 , generates low polydispersity PMMA ($M_w/M_n = 1.2\text{--}1.4$) with a syndiotactic bias (80% *r* diad).⁴⁸⁴ Initially the active species was thought to be a cationic enolate complex, but this was refuted when (199) was shown to be a poor initiator.⁴⁸⁵ However, the addition of (199) to Cp_2ZrMe_2 does generate an active initiator system, shown to be a 1:1 mixture of $[\text{Cp}_2\text{ZrMe}(\text{THF})]^+[\text{BPh}_4]^-$ and the neutral alkyl enolate, $[\text{Cp}_2\text{ZrMe}(\text{OC}(\text{OMe})=\text{CMe}_2)]$. This mixture displays first order kinetics in both Zr species (the polymerization is zero order in MMA). A bimetallic mechanism (Scheme 7) was therefore proposed, the rate-limiting step of which involves intermolecular Michael addition of the propagating enolate to activated monomer.⁴⁸⁶ This system is very moisture-sensitive and trialkylaluminum compounds have been used *in situ* to remove traces of water. However, chain transfer to the Al center may occur unless the alkyl substituents are sufficiently bulky, e.g., $^i\text{Bu}_3\text{Al}$.

It has since been shown that if less coordinating anions are used, then cationic zirconocene alkyls may serve as highly active single-component catalysts. Hence, treatment of Cp_2ZrMe_2 with

$B(C_6F_5)_3$ to give $[Cp_2ZrMe]^+[MeB(C_6F_5)_3]$ prior to addition of MMA results in a rapid and controlled polymerization.⁴⁸⁷ Syndio-rich PMMA results with an rr content in the range 63–70% depending upon the solvent used. A variety of metallocene ligands were studied under these conditions and high levels of isotacticity (95% mm) were afforded by *rac* ansa-bis(indenyl) zirconium complex, (**200**), in accord with previous observations.^{488,489} Highly isotactic PMMA has also been reported using pre-catalysts (**201**)–(**203**).^{485,487,490–492}



Scheme 7



Attempts to prepare highly syndiotactic PMMA using zirconocene catalysts have met with little success, despite the initial observation of *rac* dyad selectivity with Cp_2ZrMe_2 . A notable exception is complex (**204**), which produces 89% rr PMMA at $-45^\circ C$ with $M_w/M_n = 1.31$,⁴⁹³ although several other initiators have been reported to generate syndiotacticities of 60–70% rr.^{487,494–496} An rr triad content of 88% has been recorded for PMMA initiated by the neutral ansa-titanocene imido complex (**205**) at $-78^\circ C$, but molecular weight control is poor ($M_w/M_n = 2.4$).⁴⁹⁷ The observation that $Al(C_6F_5)_3$ -derived anions favor syndiorich PMMA (rr 60%) has allowed the synthesis of a stereoblock material by exchanging counteranions mid-polymerization.⁴⁹⁸

The block copolymerization of MMA with ethylene was recently described using (202)/B(C₆F₅)₃.⁴⁹⁹ The olefin must be polymerized first (as observed with (188) and (190)) and the diblock nature of the product was inferred from solubility behavior.

Several group 5 complexes have also been examined as MMA polymerization initiators. A series of 1,4-diaza-1,3-diene tantalum complexes have been investigated and a mixture of (206)/Me₃Al was found to polymerize MMA in a living manner at -30 °C (rr = 78%).^{500,501} Cp₂TaMe₃ also polymerizes MMA when activated with two equivalents AlMe₃.²³⁵ However, initiator efficiencies are low and molecular weight distributions are broad.

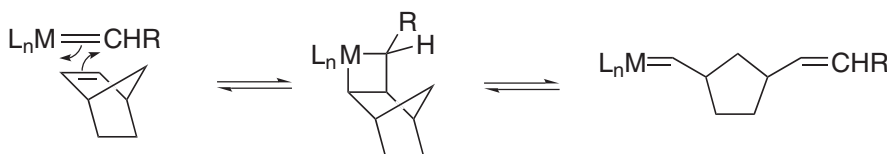
9.1.4.6 Atom Transfer Radical Polymerization

Acrylate monomers may also be polymerized by atom transfer radical polymerization (ATRP). The reader is referred to Section 9.1.3.3 for an overview of catalyst systems.

9.1.5 RING-OPENING METATHESIS POLYMERIZATION OF CYCLIC ALKENES

9.1.5.1 Introduction

The first example of the olefin metathesis reaction was the ring-opening metathesis polymerization, ROMP, of norbornene using TiCl₄/EtMgBr.⁵⁰² In 1970 Chauvin and Hérisson proposed the widely accepted mechanism for olefin metathesis based upon a [2_π + 2_π] cycloaddition of an olefinic bond to a metal-carbene (Scheme 8).⁵⁰³ Ring-opening of the intermediate metallacycle then proceeds either productively to give a new metal carbene (the propagating species in ROMP), or degeneratively to reform the starting materials. If the olefinic bond is part of a cyclic molecule then productive metathesis affords a propagating carbene, and subsequent monomer insertion yields a propagating polymer chain.



Scheme 8

Metallacyclobutanes and metal carbenes are energetically similar,⁵⁰⁴ and on occasion both may be observed simultaneously during a metathesis reaction.⁵⁰⁵⁻⁵⁰⁷ Each stage of the mechanism is, in principle, reversible. Therefore, most ROMP studies tend to focus on strained monomers, especially norbornenes, where the release of ring strain drives the reaction forward to the kinetic polymer product. For monocyclic substrates, the thermodynamics of ROMP are finely balanced and polymerizability is strongly influenced by factors such as ring substitution and reaction conditions.^{508,509}

Until the mid-1980s most ROMP initiators were ill-defined multi-component systems, typically containing an early- to mid-transition metal halide and a Lewis acid cocatalyst.⁵⁰⁸ In such mixtures, the active metal-carbene is formed in low concentration and hence identification of the active site(s) is difficult. Low levels of initiator efficiency also hamper reproducibility. Furthermore, the use of strong Lewis acid cocatalysts generally makes such catalysts incompatible with organic functionalities. Since the mid-1980s, a range of well-defined single-site initiators has been introduced which allow controlled, living polymerizations of cyclic olefins. The following sections outline the major advances that have occurred in the design and applications of well-defined ROMP initiators.

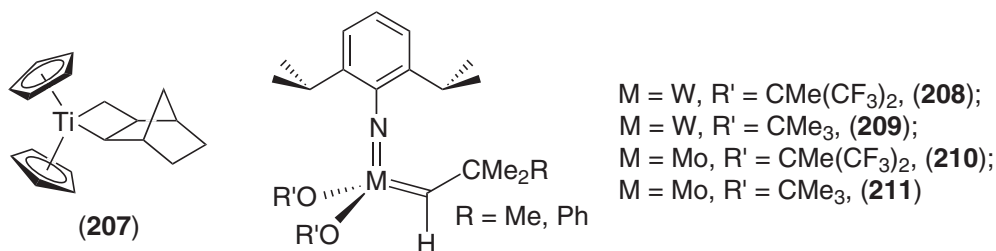
9.1.5.2 Titanacyclobutanes

The first documented example of the living ROMP of a cycloolefin was the polymerization of norbornene using titanacyclobutane complexes such as (207).⁵¹⁰⁻⁵¹² Subsequent studies described the synthesis of di- and tri-block copolymers of norbornenes and dicyclopentadiene.⁵¹³ However, functionalized monomers are generally incompatible with the highly electrophilic *d*⁰ metal center.

9.1.5.3 Group 6 Metal Initiators

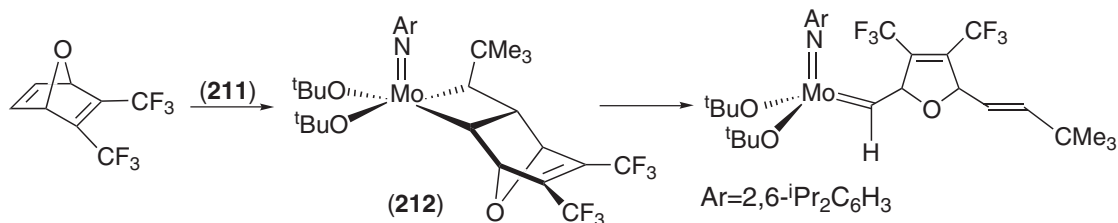
The development of well-defined molybdenum and tungsten ROMP initiators of the general formula $M(\text{NAr})(=\text{CHR})(\text{OR}')_2$ has been chronicled in several reviews.^{514–517} Initial studies revealed the ability of discrete tungsten alkylidenes to metathesize internal olefins in the presence of Lewis acids such as AlCl_3 .^{518,519} The tungsten(VI) complex (**208**) was then found to catalyze olefin metathesis without the need for a Lewis acid activator.^{520,521} This complex also initiates the living ROMP of norbornene, but secondary metathesis (“backbiting”) on double bonds contained within the propagating chains occurs, leading to a broadening in the molecular weight distribution and a decrease in the polymer *cis* content.⁵²² Replacement of the fluorinated alkoxide ligands with less electron-withdrawing *t*-butoxide ligands results in a less electron-deficient metal center; consequently (**209**) is inactive for the metathesis of *cis*-2-pentene, and when used to polymerize norbornene monodisperse polymer is produced ($M_w/M_n = 1.03–1.07$). The polymerization may be terminated in a Wittig-like reaction with PhCHO to afford metathesis-inactive $\text{W}(\text{NAr})(\text{O})(\text{O}^t\text{Bu})_2$ and a benzylidene chain terminus. The influence of the alkoxide substituents on the activity and selectivity of these initiators is a recurring theme throughout this work (*vide infra*).^{523,524}

Although the tungsten initiators allow a variety of functionalized monomers to be studied, the analogous molybdenum complexes show an even greater tolerance of functional groups.^{525,526} The synthetic route developed for $\text{Mo}(\text{NAr})(\text{CHR})(\text{OR}')_2$ allows for a wide variety of imido, alkoxide and alkylidene substituents to be prepared, and several (e.g., (**210**) and (**211**)) are commercially available.^{527–530}

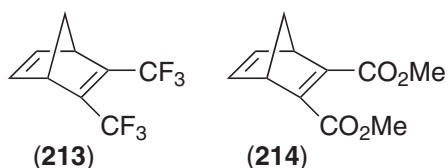


The range of functional groups compatible with the molybdenum initiators includes fluoroalkyls, esters, acetals and maleimides.^{531,532} However, protic functionalities such as alcohols and acids are not tolerated, and aldehydes terminate the polymerization.

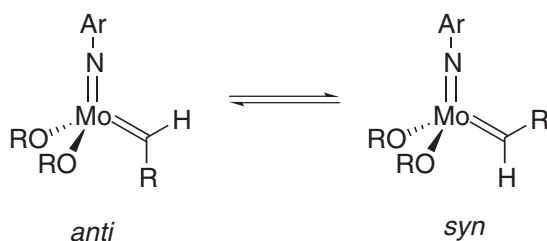
Confirmation that the polymerizations proceed via metallacyclic intermediates was obtained by studying the ROMP of functionalized 7-oxanorbornadienes. These polymerize slower than their norbornene analogs, allowing NMR identification of the metallacyclobutane resonances and subsequent monitoring of ring opening to the first insertion product. In addition, the X-ray crystallographic structure of complex (**212**) has been reported.⁵³³



Stereoselective ROMP has been reported with monomer (**213**). Initiator (**211**) affords highly stereoregular polymer with $>98\%$ *trans* C=C bonds in the polymer backbone.⁵³⁴ However, when (**210**) is used, $>98\%$ *cis*-poly-(**213**) is obtained.⁵³⁵ A similar situation occurs for the diester monomer (**214**). Furthermore, a rapidly equilibrating mixture of (**210**) and (**211**) can be used to allow intermediate *cis/trans* contents to be manipulated by the stoichiometry of the initiator mixture. ^{13}C NMR⁵³⁶ and dielectric analyses⁵³⁷ suggested that *trans*-poly-(**213**) is highly syndiotactic (92% *r* dyad content). The ROMP of other fluorinated olefins has been recently reviewed.⁵³⁸

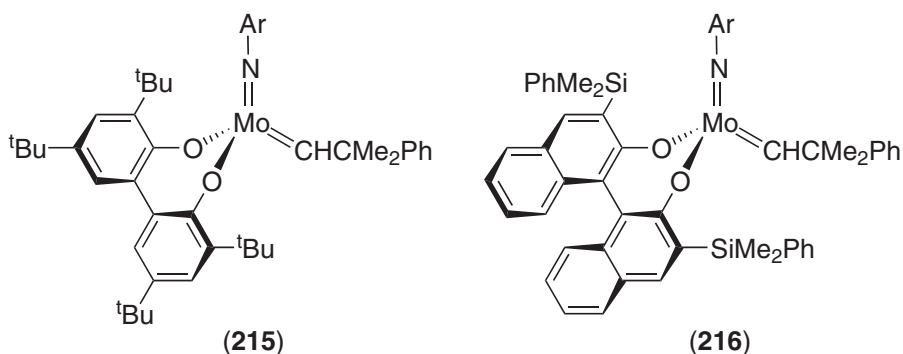


The four-coordinate molybdenum initiators exist in solution as an interconverting mixture of *syn* and *anti* rotamers, assigned according to the orientation of the alkylidene with respect to the imido ligand (Scheme 9).^{539,540} The rate of rotamer interconversion slows considerably as the alkoxide ligands become more electron-withdrawing.^{541,542} Furthermore, the *anti* rotamer, though present in trace quantities, is at least two orders of magnitude more reactive towards metathesis than its *syn* counterpart, and ring opening of the monomer via the *anti* rotamer affords a *trans* double bond in the polymer backbone. Therefore, (211), which has a relatively fast rate of *syn/anti* interconversion, consumes monomer (213) almost exclusively via its *anti* form to afford a highly *trans* polymer. Initiator (210) polymerizes via its *syn* rotamer to generate *cis*-poly-(213) since the rate of conversion to the *anti* form is much slower than the rate of propagation. Further studies revealed the potential to influence *syn/anti* interconversion rates, and thus *cis/trans* contents by performing polymerizations at different temperatures.⁵⁴³



Scheme 9

The ROMP of (213) and (214) using chiral Mo initiators, (215) and (216) affords >99% *cis* and >99% tactic polymers.⁵⁴⁴ The polymerization of enantiomerically pure chiral norbornadiene diesters also gives stereospecific polymers with (215) and (216), and COSY NMR experiments indicate that the *cis* polymers possess an isotactic structure.^{545,546} Imido alkylidene complexes featuring a variety of chelating C₂-symmetric diolate ligands have since been developed⁵⁴⁷⁻⁵⁴⁹ and have been used to develop asymmetric ring-closing metathesis chemistry.⁵⁵⁰⁻⁵⁵²

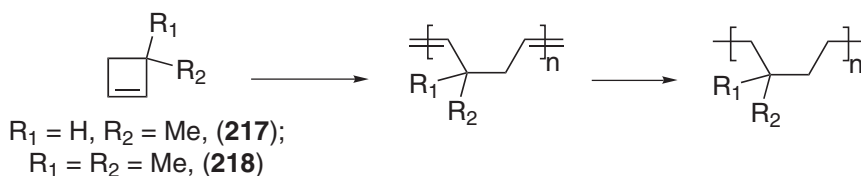


The molybdenum initiators also allow for functionalization of the polymer end groups. The use of appropriately substituted alkylidene ligands^{553,554} and functionalized termination agents⁵⁵⁵ have both been described. A more convenient approach using chain transfer agents has also been developed, initially with substituted cyclopentenes,⁵⁰⁹ and then with 1,3-dienes and styrenes.⁵⁵⁶

The facility to introduce well-defined chain ends has been used to prepare star polymers⁵⁵⁷ and diblocks via reaction with macromolecular aldehydes.⁵⁵⁸ The synthesis of amphiphilic star block copolymers has also been described using a cross-linking agent.^{559,560} A similar strategy has recently

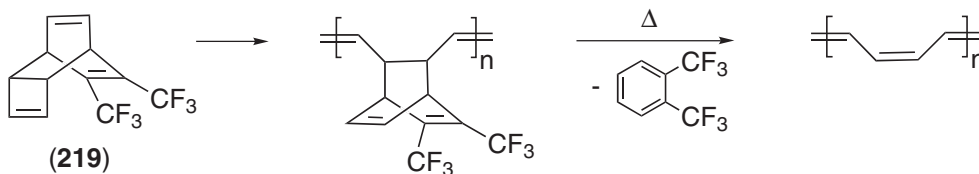
been reported in the preparation of functionalized polymer supports.^{561–563} The ROMP of macro-monomers to form comb-like structures has been reported by several research groups.^{564–569}

The synthesis of poly(alkenamers) via the ROMP of cycloalkenes has also received significant attention,^{509,570} as has their subsequent reduction to monodisperse polyethylene-like materials.^{557,571–573} The alternating copolymers poly(ethylene-alt-propylene) and poly(ethylene-alt-isobutylene) were prepared in analogous fashion from the (211)-initiated polymerization of 3-methylcyclobutene, (217), and 3,3-dimethylcyclobutene, (218), respectively (Scheme 10).⁵⁷⁴ Although the monoalkyl substituted monomer polymerizes in a regioirregular manner, the analogous dimethyl polymer is >98% head-tail (and >99% *trans*). Hydroxytelechelic polybutadiene was also synthesized via the ROMP of 1,5-cyclooctadiene using the TBS-ether of *cis*-1,4-butenediol as a chain transfer agent.⁵⁷⁵



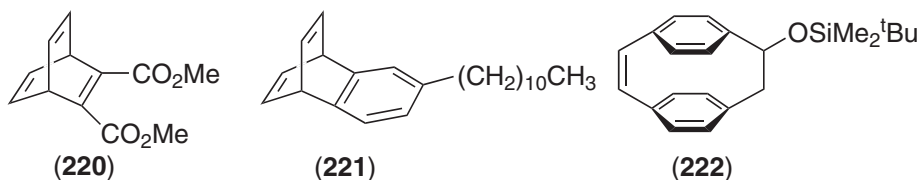
Scheme 10

A route to processible polyacetylene, devised initially using classical initiators (Scheme 11),^{576–578} has been developed using well-defined molybdenum initiators to prepare conjugated polymers.^{579–585} They have also been employed to prepare polyacetylene via the polymerization of cyclooctatetraene, COT,⁵⁸⁶ and by the isomerization of poly(benzvalene).^{587,588} Substituted, and hence soluble, polyacetylene derivatives may be synthesized by polymerizing monosubstituted COT substrates.^{589–591}



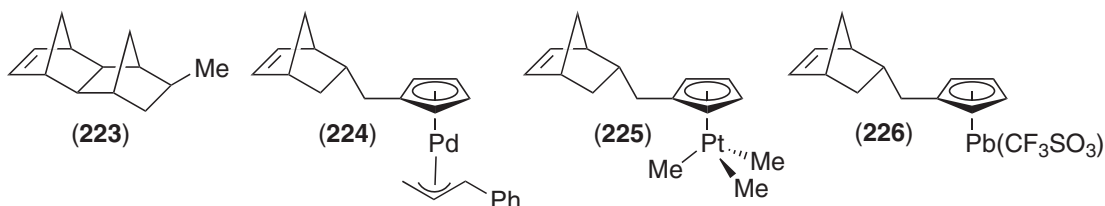
Scheme 11

A related precursor route to poly(1,4-phenylene vinylene), PPV, has also been reported.⁵⁹² Soluble, functionalized PPV may be directly prepared via the ROMP of barrelene monomers such as (220).⁵⁹³ This method has been modified to synthesize red-orange electroluminescent poly(naphthalene-vinylene)s from benzobarrelene substrates, such as (221).^{594–596} Non-conjugated poly(chromophores) have been synthesized via the ROMP of [2.2] paracyclophan-1-ene and substituted derivatives, (222).^{597–599} Blue light-emitting polymers have also been prepared via a metathesis strategy.^{600,601} In addition, the construction of light-emitting devices in which ROMP materials are also used for the construction of both electron- and hole-transport layers has been described.⁶⁰²

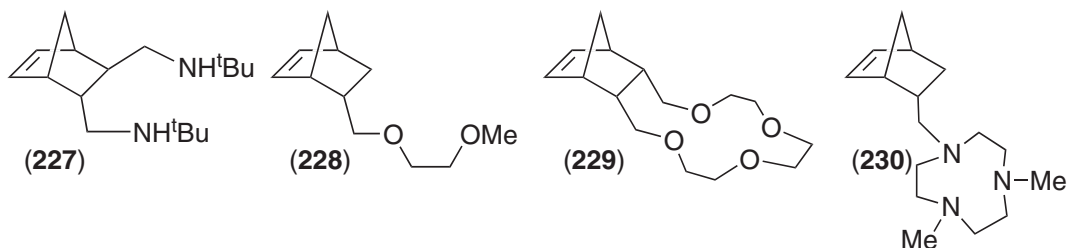


Norbornenes bearing 4-methoxy biphenyl groups (separated from the bicyclic framework by a long alkyl spacer unit) have been investigated as liquid crystalline polymers.^{603,604} Several other mesogens have also been studied, including 4-cyanobiphenyls^{605,606} and bis[(alkoxybenzoyl)oxy]-phenyls.⁶⁰⁷ Redox-active polymers may be prepared via the ROMP of norbornenes bearing ferrocene or phenothiazine substituents.^{608,609} Further, ferrocenyl end groups have been introduced by using an appropriately functionalized alkylidene initiator.⁵⁵⁴

Well-defined nanoclusters ($\approx 10\text{--}100$ Å diameter) of several metals have been prepared via the polymerization of metal-containing monomers. The synthetic approach involves the block copolymerization of a metallated norbornene with a hydrocarbon co-monomer which is used to form an inert matrix. Subsequent decomposition of the confined metal complex affords small clusters of metal atoms. For example, palladium and platinum nanoclusters may be generated from the block copolymerization of methyl tetracyclododecane (**223**) with monomers (**224**) and (**225**) respectively.^{610,611} Clusters of PbS have also been prepared by treating the block copolymer of (**223**) and (**226**) with H₂S.⁶¹² A similar approach was adopted to synthesize embedded clusters of Zn and ZnS.^{613,614}



Alternatively a non-metallated chelating monomer such as (**227**) or (**228**) may be copolymerized with (**223**) and the metal introduced post-polymerization. Using this strategy nanoclusters of silver,⁶¹⁵ gold,⁶¹⁶ ZnS⁶¹⁷ and CdS⁶¹⁸ have been prepared. A related approach has recently been adopted with the ROMP of norbornenes functionalized with crown ether, (**229**),⁶¹⁹ and triazacyclononane, (**230**),⁶²⁰ substituents.



Molybdenum initiators have also been successfully used to polymerize monomers bearing substituents such as amino esters (protected amino acids),^{621–623} peptide esters⁶²⁴ and acetal-protected sugars.⁶²⁵ However, the synthesis of biologically useful materials using these initiators is restricted by the prevalence of protic functionalities within naturally occurring macromolecules. For monomers bearing hydroxyl or carboxylic acid substituents, the ruthenium initiators detailed in the following section are more applicable.

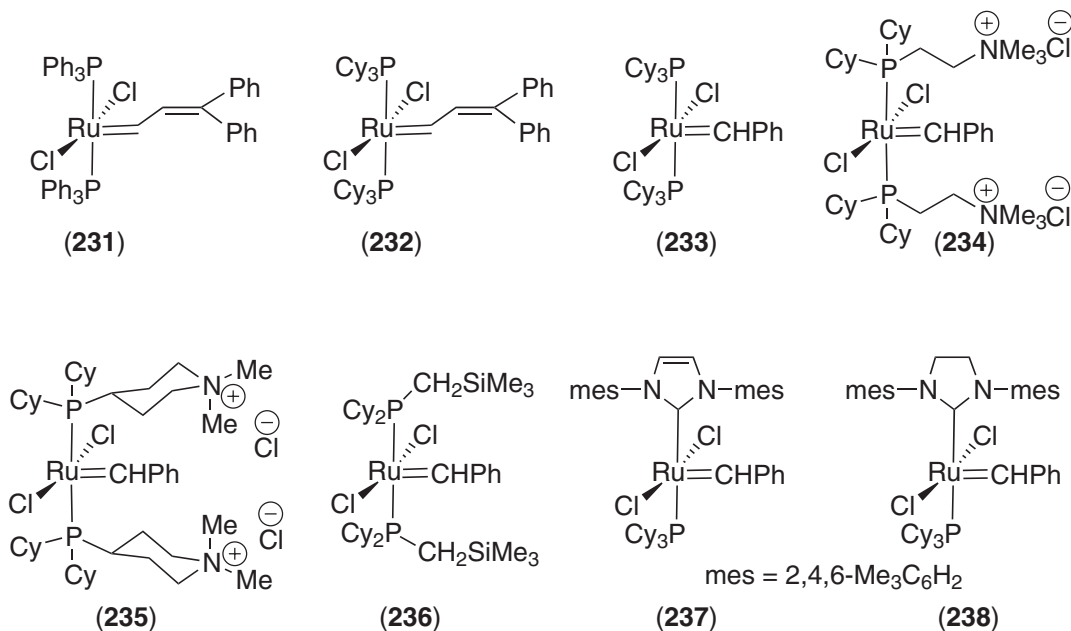
9.1.5.4 Ruthenium Initiators

The limited tolerance of functional groups exhibited by early transition metal catalysts arises from their high electropositivity, electrophilicity and oxophilicity. On traversing the transition metal series these properties diminish and tolerance towards polar and protic functionalities increases. As long ago as 1965 the ability of ruthenium complexes to initiate the ROMP of norbornene in protic media (EtOH) was established.⁶²⁶ In the late 1980s RuCl₃ was reinvestigated and it was found that 7-oxa-norbornenes were polymerized in EtOH after long (≈ 24 h) initiation times.⁶²⁷ The induction period is reduced by a factor of $\approx 5,000$ by performing the reactions in water under air. Polymerization is rapid, consuming 750–1,000 equivalents of monomer per minute, and the catalyst may be recycled many times with no discernible drop in activity. Subsequent reports revealed that [Ru(H₂O)₆](OTs)₂ was even more active and may be used to polymerize less strained cycloalkenes such as cyclooctene.^{628–631}

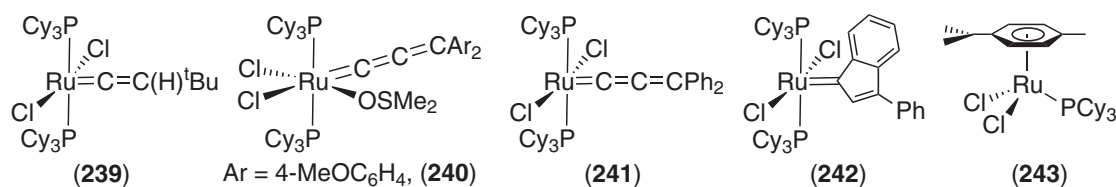
The first well-defined Ru alkylidene metathesis initiator, (**231**), was reported by Grubbs *et al.* in 1992.⁶³² This complex initiates the ROMP of norbornene and other highly strained monomers such as bicyclo[3.2.0]hept-6-ene.⁶³³ Examination of alternative ligands^{634–636} led to the development of more active initiators, in particular (**232**)⁶³⁷ and (**233**).^{638–640}

Initiator (**233**), and a polymer-supported analog,⁶⁴¹ are commercially available and have found widespread use in the ring-closing metathesis (RCM) and ROMP of functionalized substrates. In addition, water-soluble variants such as (**234**) and (**235**) have been synthesized using aliphatic ionic phosphines and employed in aqueous media.^{642–645}

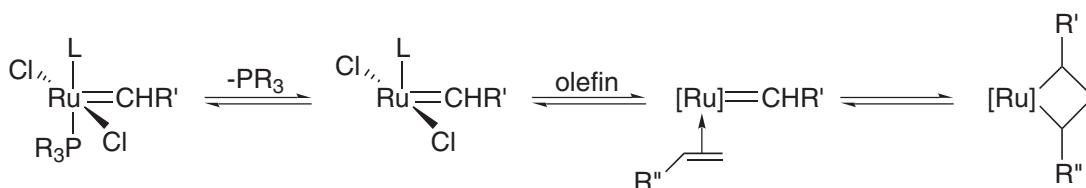
The ruthenium initiator family offers enhanced air stability and greater tolerance of protic functionalities than the molybdenum initiators (**210**) and (**211**). However, the polydispersities of polymers prepared from (**233**) are typically higher due to propagation rates being substantially faster than initiation. A simple modification using $\text{PCy}_2\text{CH}_2\text{SiMe}_3$ ligands (**236**) results in more favorable initiation kinetics and M_w/M_n values of 1.05–1.11 have been reported.⁶⁴⁶ The ruthenium initiators are also less active than the molybdenum systems, and attempts to overcome this have recently led to the development of “second generation” initiators featuring N-heterocyclic carbene ligands.^{647–654} Complexes (**237**) and (**238**) are much more reactive than (**233**) with metathesis activities almost comparable to (**210**) and (**211**). In addition, they are more thermally robust. To date they have mostly been used in olefin metathesis^{655,656} and RCM reactions,^{649,657} with few reports describing their use as ROMP initiators. The polymerization of low-strain cyclic olefins using (**238**) has been described but polydispersities are broad ($M_w/M_n > 2$) due to secondary metathesis (backbiting) reactions.⁶⁵⁸ Similar effects have been noted using (**237**).^{659,660}



Many other ruthenium alkylidene metathesis initiators have been reported in the literature, but the ROMP activity and control rarely approach the levels shown by (**233**). Ancillary ligands examined include tris(pyrazolyl)borates,^{661–663} bidentate salicylimines⁶⁶⁴ and bis(amino)pyridines.⁶⁶⁵ More active olefin metathesis initiators have recently been reported using electron-rich carbene complexes.^{666,667} Although ROMP initiation with such complexes has not been explored at the time of writing, a preliminary report on the ring-opening of cyclohexene using ester-carbenes has appeared.⁶⁶⁸ Several vinylidene ($[\text{Ru}]=\text{C}=\text{CR}_2$) and allenylidene ($\text{Ru}=\text{C}=\text{C}=\text{CR}_2$) initiators have also been investigated. For example, (**239**) polymerizes ester-functionalized norbornenes, but chain length control is poor ($M_w/M_n > 2$).⁶⁶⁹ Somewhat better control is afforded using (**240**), which produces polynorbornene with $M_w/M_n = 1.61$.⁶⁷⁰ A reported synthesis of the allenylidene complex (**241**)⁶⁷¹ has since been shown to be erroneous, the sequential addition of diphenylpropargyl alcohol and PCy_3 to $\text{RuCl}_2(\text{PPh}_3)_3$ actually yielding (**242**).⁶⁷² Interestingly, (**242**) possesses similar reactivity to (**233**), whereas (**241**), synthesized by an alternative route, displays no appreciable catalytic activity.⁶⁷³ In general, the vinylidene catalysts (and to a lesser extent the allenylidenes) are better suited to catalyzing RCM reactions.^{674–676} Ruthenium arene complexes⁶⁷⁷ such as (**243**), display good activity for the ROMP of norbornenes and cyclooctenes, especially in the presence of an added diazo compound⁶⁷⁸ or when irradiated.⁶⁷⁹



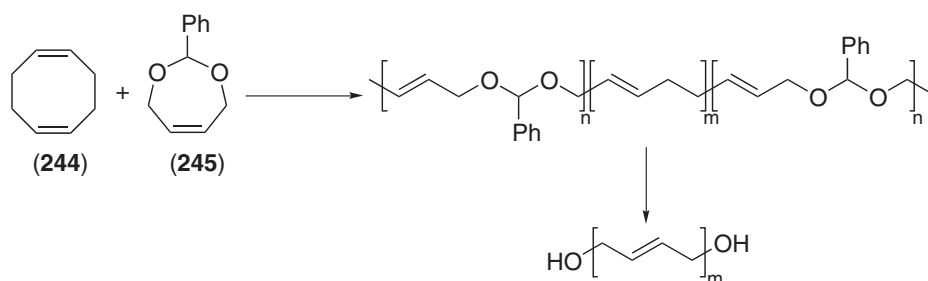
Key elements of the mechanism using initiators such as (233) and (238) have been elucidated (Scheme 12).⁶⁸⁰ Initiation commences with dissociation of a phosphine ligand; although the proposed 14-electron intermediate has never been observed, evidence for the stability of related complexes has been reported.⁶⁸¹ The olefinic substrate then coordinates to the metal center, followed by cycloaddition to afford the metallacyclobutane. The N-heterocyclic carbene initiators (237)–(238) are more active than (233) because, although initial dissociation of phosphine is slower than from (233),⁶⁸² their selectivity for subsequent olefin binding is four orders of magnitude greater than for reassociation of the phosphine. For (233), a phosphine ligand is lost quite readily, but its recoordination competes with binding of the monomer. A significant implication of this has recently been reported: if extra phosphine is added to (233) the rate of propagation, k_p , of a cyclic alkene is decreased. As a result, a more favorable k_p/k_i ratio (k_i = rate of initiation) and narrower molecular weight distributions may be obtained.⁶⁸³ Several reports of Ru initiators with chelating diphosphine ligands have appeared,^{684–687} it is currently unclear how relevant the phosphine dissociation mechanism described above is to such complexes.



Scheme 12

Most ruthenium-initiated ROMP studies have been performed using (233) and strained cycloolefinic monomers such as norbornene⁶⁸⁸ and cyclobutenes,⁶⁸⁹ although several reports on the polymerization of 8-membered rings have also appeared.^{690–692} A wide range of functionalities are tolerated, including ethers, esters, amines, amides, alcohols, carboxylic acids, and ketones.

The production of telechelic 1,4-polybutadiene and, via subsequent hydrogenation, telechelic polyethylene, has been achieved by the copolymerization of 1,5-cyclooctadiene, (244), with 4,7-dihydro-2-phenyl-1,3-dioxepin (245).⁶⁹³ Degradation of the acetal junctions affords hydroxyl end groups. (244) may also be polymerized by (232), (233), (237), or (238) in the presence of allylic difunctionalized chain transfer agents. The products are again readily converted into hydroxy telechelic polybutadiene.^{694,695} This approach has been modified to include cross-linking sites,⁶⁹⁶ amino end groups⁶⁹⁷ and polynorbornenes.^{698,699} Vinyl ethers have also been used as chain transfer agents in order to prepare ATRP macroinitiators.⁷⁰⁰



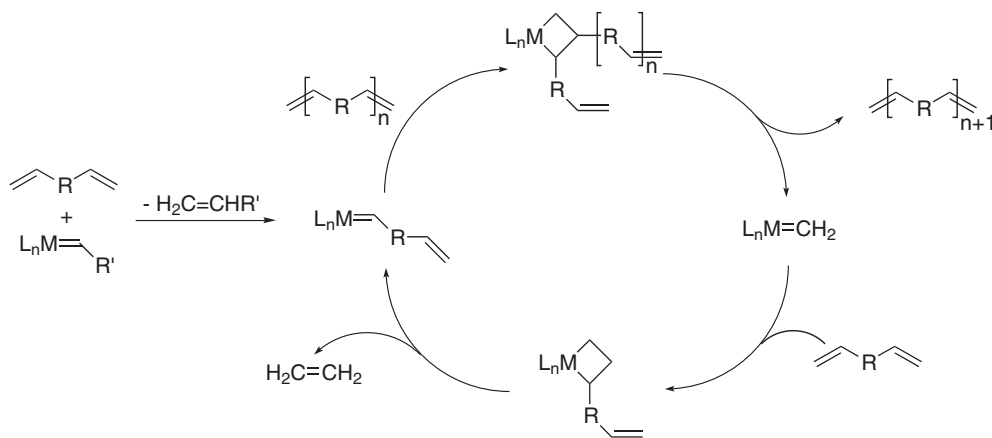
The synthesis of technologically interesting ROMP materials using (233) includes the preparation of molecular wires,⁷⁰¹ liquid-crystal polymers,^{702,703} chiral supports for catalysis,⁷⁰⁴ redox-active macromolecules,⁷⁰⁵ photochromic materials⁷⁰⁶ and embedded clusters of CdSe.⁷⁰⁷ Polymers

bearing inorganic functionalities have also been prepared, including metalloporphyrazines,⁷⁰⁸ phthalocyanine complexes,⁷⁰⁹ and phosphazenes.^{710,711}

The range of biologically relevant functionalities appended to cyclic alkene monomers includes amino acids,⁷¹² β -amino acid esters,⁷¹³ oligopeptides such as RGD sequences for cell wall binding,^{714,715} nucleotide bases,^{716,717} penicillin,⁷¹⁸ vancomycin,⁷¹⁹ and sulfonamides.⁷²⁰ Several reports have also described the polymerization of sugar-based substituents. In particular, Kiessling and co-workers have polymerized several monomers bearing mono-^{721–724} and di-⁷²⁵ saccharides and used the neoglycopolymer products as scaffolds for lectin assembly.⁷²⁶ Other sugar-based systems studied include glucose-functionalized norbornenes,⁷²⁷ and the preparation of a polymer similar in structure to β -D(-)-ribose.⁷²⁸

9.1.5.5 Acyclic Diene Metathesis

Acyclic diene metathesis (ADMET) is a step-growth polycondensation reaction for the polymerization of α,ω -dienes.⁷²⁹ The process is catalyzed by the same metal alkylidene initiators used for ROMP, and is driven by the removal of ethylene from the system (Scheme 13). Both molybdenum and ruthenium-based initiators have been used to prepare a variety of materials including functionalized polyethylenes,^{730–732} liquid crystalline macromolecules^{733,734} and amino acid-based chiral polymers.⁷³⁵

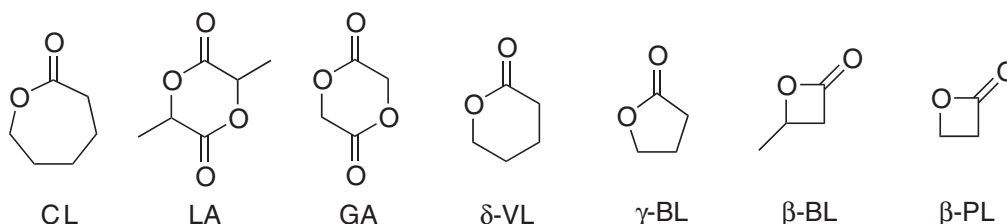


Scheme 13

9.1.6 RING-OPENING POLYMERIZATION OF CYCLIC ESTERS

9.1.6.1 Introduction

The high level of interest in the ring-opening polymerization (ROP) of cyclic esters (lactones) stems from the biocompatibility and biodegradability of their polymers. Resorbable aliphatic

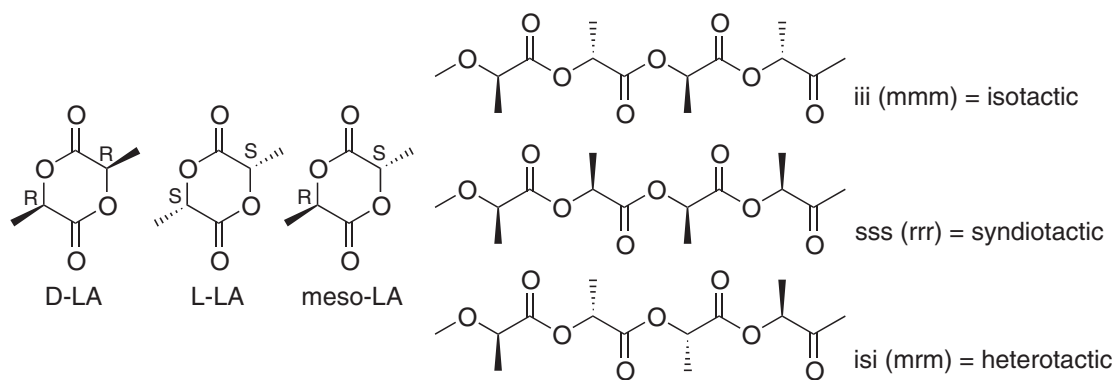


Scheme 14

CL : ϵ -caprolactone, LA = lactide, GA = glycolide, δ -VL = δ -valerolactone, γ -BL = γ -butyrolactone, β -BL = β -butyrolactone, β -PL = β -propiolactone

polyesters are usually tolerated well by mammalian tissue, making them good candidates for the construction of *in vivo* medical devices,⁷³⁶ while materials based on polylactic acid (PLA) are derivable from biosustainable resources such as corn starch and dairy products, which provide attractive feedstocks for the production of biodegradable films and fibers. Traditionally, such polymers were synthesized via high-temperature polycondensation reactions of appropriate α -hydroxy acids,⁷³⁷ but this step-growth method is accompanied by poor chain length control and low molecular weights. By contrast, the ROP of lactones is a chain-growth process, and advances in catalyst technology have led to high levels of control over molecular weight and polymer stereochemistry.^{738,739}

Lactide (LA), the cyclic diester of lactic acid, has two stereogenic centers and hence exists as three stereoisomers: L-lactide (S,S), D-lactide (R,R), and *meso*-lactide (R,S). In addition, *rac*-lactide, a commercially available racemic mixture of the (R,R) and (S,S) forms, is also frequently studied. PLA may exhibit several stereoregular architectures (in addition to the non-stereoregular atactic form), namely isotactic, syndiotactic, and heterotactic (Scheme 15). The purely isotactic form may be readily prepared from the ROP of L-LA (or D-LA), assuming that epimerization does not occur during ring opening. The physical properties, and hence medical uses, of the different stereoisomers of PLA and their copolymers vary widely and the reader is directed to several recent reviews for more information.^{736,740–743}



Scheme 15

9.1.6.2 General Features of Lactone Polymerization

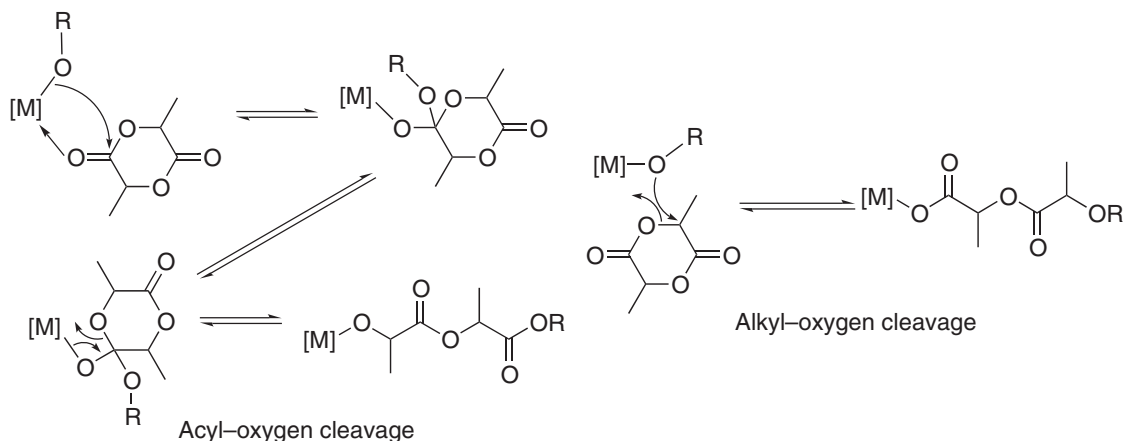
Initiators for the coordination–insertion polymerization of lactones are generally metal alkoxides, although carboxylates, amides, and other nucleophilic ligands have also been used. Initiation occurs via nucleophilic attack at the carbonyl carbon of the monomer, followed by acyl–oxygen bond cleavage (Scheme 16). Although most lactones appear to undergo ROP according to the acyl–oxygen route,⁷⁴⁴ examples are known in which the ring breaks at the alkyl–oxygen bond.⁷⁴⁵ In such cases the propagating species is a metal carboxylate.

Deviation from truly living behavior occurs primarily via transesterification side reactions (Scheme 17). Intramolecular transesterification (“backbiting”) affords cyclic oligomers, whereas its intermolecular counterpart results in a redistribution in the lengths of the living chains. Both forms of transesterification lead to a broadening of the molecular weight distribution and a loss of control over the target molecular weight. Transesterification is typically more problematic with highly active initiators, especially when alkali metal alkoxides are used to polymerize lactones.⁷⁴⁶

9.1.6.3 Aluminum-based Initiators

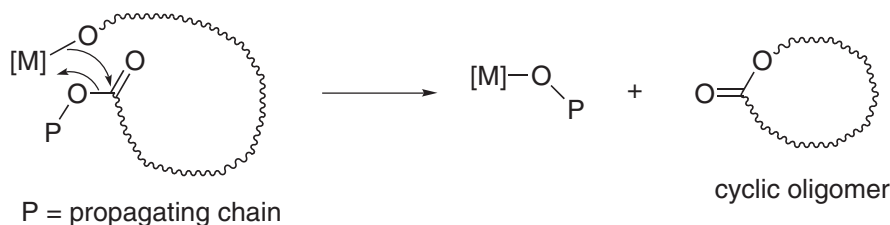
The most widely studied aluminum-based initiator for the ROP of lactones is $\text{Al}(\text{O}^i\text{Pr})_3$, (**246**), which has been used to initiate the living polymerization of a variety of cyclic esters including CL,^{747–749} LA,^{750,751} GA,⁷⁵² β -BL,⁷⁴⁵ and cyclic anhydrides.^{753,754} Polymerizations initiated by (**246**) are normally well controlled and often display living characteristics.⁷⁵⁵ For example, CL undergoes ROP in toluene solution at 25 °C to give a polymer of narrow polydispersity ($M_w/M_n \approx 1.1$). The ROP of LA at 70 °C is also well behaved up to M_n values of 90,000 (M_w/M_n

typically 1.25) and molecular weights indicate that each aluminum center generates three polymer chains. At higher monomer:initiator ratios, and also at higher temperatures, both inter- and intramolecular transesterification occur leading to a broadening of the molecular weight distribution ($M_w/M_n \approx 1.5$).⁷⁵⁶

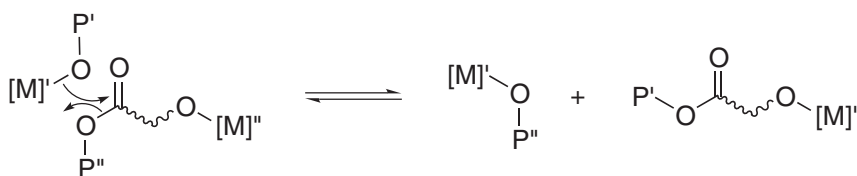


Scheme 16

Intramolecular transesterification:



Intermolecular transesterification:

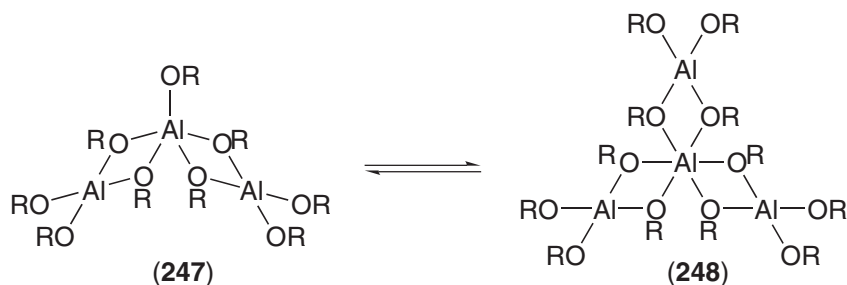


Scheme 17

The relative rates of polymerization of a series of substituted ϵ -caprolactones initiated by (**246**) demonstrate that methyl groups, particularly adjacent to the acyl oxygen, retard polymerization.⁷⁵⁷ In addition, the rate of polymerization of the parent unsubstituted CL at 25 °C was found to be 4×10^2 times greater than L-LA at 70 °C. The slower propagation of LA is usually attributed to coordination of the nearest inserted carbonyl of the polymer chain to the Al center, leading to formation of a stable 5-membered chelate, which hinders monomer uptake.⁷⁵⁸

For some years it was erroneously believed that, whilst every Al center generated three chains of PLA, the polymerization of CL proceeded via only one of the alkoxides. In fact (**246**) exists in toluene solution as a mixture of trimeric (**247**) and tetrameric (**248**) aggregates; (**248**) is the dominant component,^{759–762} but (**247**) is much more active towards lactones.^{763–765} An induction period prior to initiation (40 min at 70 °C for LA but just 4 min at 0 °C for CL⁷⁶⁶) arises from the conversion of the aggregated trimer into a non-aggregated six-coordinate mononuclear species, postulated to be $\text{Al}(\text{O}^i\text{Pr})_3(\text{monomer})_3$.^{767,768} The yttrium analog, $\text{YCl}_3(\text{CL})_3$, has been structurally characterized.⁷⁶⁹ CL quickly breaks up the structure of (**247**), but does not disrupt the structure of the more stable tetrameric (**248**). Hence, when pure trimeric (**247**) is employed,

molecular weights imply that each Al center initiates three PCL chains.²⁸ At the higher temperatures required for the ROP of LA the interconversion of (248) into (247) is more rapid and all of the aluminum centers are dissociated by monomer coordination.⁷⁷⁰



When a mixture of LA and CL is copolymerized using $\text{Al}(\text{O}^i\text{Pr})_3$, LA is incorporated preferentially ($r_{\text{LA}} = 17.9$, $r_{\text{CL}} = 0.58$).⁷⁵⁷ The propagating species derived from LA are 2.5×10^5 less reactive to CL than CL-derived species are towards LA.^{758,771} In line with these observations, the corresponding diblock copolymer has only been prepared by polymerizing CL first.

In order to effect stereocontrol over the ROP of lactones, several research groups have examined monoalkoxide aluminum initiators of the general formula $\text{L}_n\text{M}(\text{OR})$. Preliminary studies indicated that dialkylaluminum alkoxides, e.g., $\text{Et}_2\text{Al}(\text{OR})$, initiate the controlled ROP of lactones.⁷⁷²⁻⁷⁷⁵

Some of the first examples of single-site initiators for CL and LA polymerization were reported by Inoue and co-workers using tetraphenylporphyrin (TPP) aluminum initiators.^{776,777} The polymerizations are slow but display living characteristics such as a linear increase of M_n with monomer conversion and narrow polydispersities. The bulk of the TPP ancillary ligand, and the lack of a suitable binding-site *cis* to the propagating alkoxide, greatly reduces transesterification reactions. For example, (249) polymerizes 94 equivalents of D-LA over 96 h at 100 °C to give a polymer with M_n 16,400 (M_n calc = 13,500) and $M_w/M_n = 1.12$.⁷⁷⁸ The alkoxide (250) displays similar behavior and ring-opens D-LA exclusively at the acyl-oxygen bond. However, the corresponding chlorides, alkyls, and carboxylates, (251)–(253), are inactive for the ROP of LA, CL, and δ -VL.⁷⁷⁹

These initiators may be used in the presence of protic sources such as MeOH.⁷⁸⁰ The rapid and reversible exchange of propagating alkoxides with alcohol leads to a narrow molecular weight distribution (for example, $M_w/M_n < 1.15$ for oligomeric PCL), with the number of polymer molecules closely approaching the sum of the number of molecules of initiator and alcohol. In the absence of alcohol, the polymerization of CL is less well behaved with $M_w/M_n = 1.5$, presumably a consequence of unfavorable initiation and propagation rates.

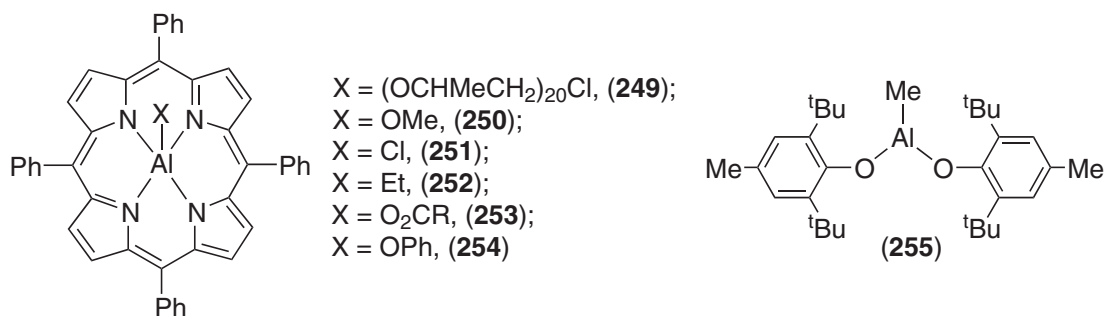
The metalloporphyrin system has also been used to initiate the ROP of the four-membered rings β -propiolactone, β -PL, and β -butyrolactone, β -BL. These may both be polymerized in a living manner by (251); the mechanism proceeds via alkyl-oxygen cleavage (following initial attack of the halide at the carbon adjacent to the ester oxygen).⁷⁴⁵ The propagating species is a carboxylate; thus (253) ($\text{R} = \text{CH}_2\text{CH}_2\text{Cl}$) also serves as an effective initiator ($M_w/M_n = 1.06$ – 1.20). Furthermore, a carboxylic acid may be used with (251) as a rapid chain transfer reagent in the ROP of β -BL.⁷⁸¹ Although alkoxides such as (250) display very low activity as initiators for the ROP of β -PL, the phenoxide (254) is active (again operating via alkyl-oxygen scission).⁷⁷⁹ However, (254) fails to polymerize larger lactones such as CL.

Block copolymers of β -PL and β -BL have been synthesized using (251), although reaction times of several weeks are required.⁷⁸² Since (TPP)Al-based carboxylates are also known to polymerize epoxides (see Section 9.1.7.2), the sequential addition of β -BL and propylene oxide (PO) results in formation of a p(β -BL- β -PO) diblock.⁷⁸² However, reversing the order of addition fails to produce the block copolymer since the propagating alkoxide $(\text{TPP})\text{Al}(\text{OCHMeCH}_2)_n\text{Cl}$ does not initiate the ROP of β -BL.

The polymerization of δ -VL using (250) as an initiator is also living but very slow; 200 equivalents of monomer in the absence of solvent attain a conversion of 86% after 580 h at 50 °C ($M_n = 12,000$, $M_w/M_n = 1.12$).⁷⁸³ ^1H NMR spectroscopy confirms that ring opening proceeds at the acyl-oxygen bond. The scope for tuning the catalyst activity by using substituted tetraphenylporphyrin ligands has been examined and *ortho*-Cl and *ortho*-OMe groups have been shown to give higher activities.⁷⁸⁴ However, polymerizations initiated with (250) are much more

dramatically accelerated by the addition of a bulky Lewis acid, such as **(251)**. For example, using a ratio of 1:1:200 of **(250)**:(**251**): δ -VL, 51% conversion was observed after just 1.3 h at 50 °C (cf. 53% after 320 h in the absence of **(251)**). The rate enhancement is due to activation of the lactone towards nucleophilic attack by binding to the Lewis acidic center of **(251)**.

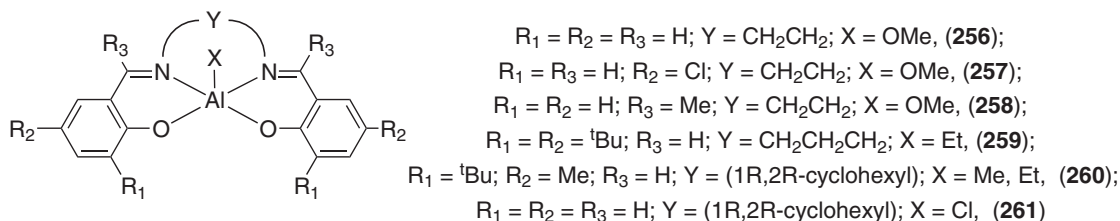
Other Lewis acids, such as methyl aluminum diphenolates, have also been shown to be good activators.⁷⁸⁵ For example, when **(255)**, MAD, is added to a mixture of CL and **(250)** at 50 °C, the rate is approximately 700 times greater than in the absence of the diphenolate.⁷⁸⁶ MAD also accelerates the ROP of δ -VL by a factor of 2,100 at 50 °C.⁷⁸⁵



The (TPP)AIX family of initiators has been used to initiate the polymerization of a range of other monomer classes including epoxides, episulfides, and methacrylates.⁷⁷⁶ In the latter case the propagating species is an aluminum enolate and this too may initiate the ROP of lactones, such as δ -VL, albeit slowly. In this way a block copolymer P(δ -VL)-b-PMMA of narrow molecular weight distribution ($M_w/M_n = 1.11$) has been prepared.⁷⁸⁷

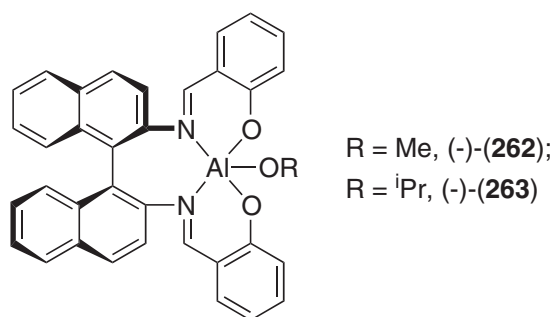
A range of tetradentate Schiff-base ligands have also been employed to prepare discrete aluminum alkoxides. The most widely studied system is the unsubstituted parent system **(256)**, which initiates the controlled ROP of *rac*-LA at 70 °C in toluene. The polymerization displays certain features characteristic of a living process (e.g., narrow M_w/M_n), but is only well behaved to approximately 60–70% conversion; thereafter transesterification causes the polydispersity to broaden.⁷⁸⁸ MALDI–TOF mass spectroscopy has been used to show that even at low conversions the polymer chains contain both even and odd numbers of lactic acid repeat units, implying that transesterification occurs in parallel with polymerization in this system.⁷⁸⁹

The more Lewis acidic, and hence more active, analog **(257)** polymerizes lactide in CH₂Cl₂ at room temperature.⁷⁹⁰ A linear relationship between M_n and monomer conversion for both L-LA and *rac*-LA was observed and M_w/M_n values were typically between 1.10 and 1.20. A similar increase in activity has been noted when using the methyl–ketimine salen complex **(258)**.⁷⁹¹ Rate enhancements due to *ortho*-phenyl substitution, and by the use of a trimethylene ligand backbone (e.g., **(259)**) have also been communicated.⁷⁹² The ROP of other lactones using salen-based Al initiators has received less attention; the ROP of CL using **(260)** has been briefly described⁷⁹³ and **(261)** oligomerizes β -BL via alkyl–oxygen cleavage.^{794,795}



By studying mixtures of L- and D-LA of varying composition, Spassky *et al.* have demonstrated that **(256)** yields PLA containing long isotactic sequences, with a ratio of homo:cross propagation of 2.8.⁷⁹⁶ Hence, an 80/20 L:D mixture when polymerized to 70% conversion displayed an optical purity of 87%. Even at the relatively low optical purity of 65/35 L:D, isotactic block lengths of >12 repeat units were reported. Achiral **(259)** converts *rac*-LA into highly isotactic PLA; a T_m of 192 °C indicates that the chains of P(L-LA) and P(D-LA) form a stereocomplex.^{792,797–799}

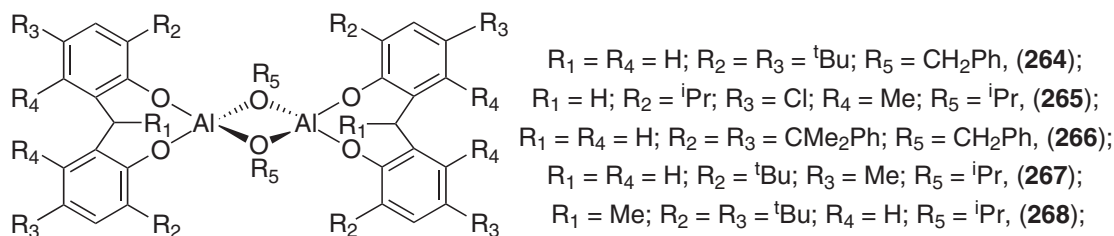
Good stereoselectivity is also exhibited by chiral binaphthyl-derived Schiff-base complexes (**262**) and (**263**). These initiators display slightly higher activities than the parent salen initiator and transesterification is much less of a problem (e.g., $M_w/M_n = 1.3$ at 97.5% conversion).⁸⁰⁰ Enantiopure (**262**) polymerizes *rac*-LA with a preference for the incorporation of the D enantiomer, with $k_D/k_L \approx 20$. At low conversions the PLA displays high optical purity (>88% e.e. at 19% monomer conversion), and after just 60% monomer conversion, only L-LA remains. As the content of L-LA in the monomer feed increases its incorporation becomes more favorable. The optical activity of the polymer therefore diminishes as the level of conversion increases. The tapered stereoblock thus formed possesses a $T_m > 185^\circ\text{C}$, significantly higher than the T_m value of isotactic P(L-LA) due to stereocomplex formation. Initiator (**262**) has also been used to polymerize *rac*- β -BL.⁸⁰¹ The process is living (410 equivalents of β -BL are consumed over 96 h at 20°C to give $M_n = 33,600$, $M_n(\text{calc}) = 35,000$, $M_w/M_n = 1.10$), although stereoselectivity is much less pronounced with $k_D/k_L = 1.3$.



The enantiomorphic site selectivity of (R)-(-)-(**263**) allows highly syndiotactic PLA to be prepared via the polymerization of *meso*-LA ($M_n = 12,030$, $M_n(\text{calc}) = 13,540$, $M_w/M_n = 1.05$).⁸⁰² The ring opening of *meso*-LA by (R)-(-)-(**263**) occurs to produce a syndiotactic propagating chain bound to the metal via an (S)-lactic acid unit.⁸⁰³ Attempts to produce syndiotactic PLA via the ROP of *meso*-LA using *rac*-(\pm)-(**263**) instead afforded heterotactic-biased material.

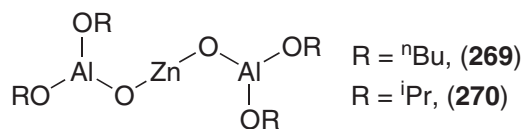
The racemic initiator (\pm)-(**263**) converts *rac*-LA into highly isotactic PLA. DSC analysis and X-ray diffraction supports the formation of a stereocomplex between the two isotactic homopolymers of p(D-LA) and p(L-LA) ($T_m = 191^\circ\text{C}$).⁸⁰⁴ Detailed analysis of the ¹H NMR spectrum of the product suggests that low levels of stereochemical impurities in the predominantly isotactic chains do not arise from occasional incorporation of the “wrong” LA enantiomer, but rather originate from the exchange of polymer chains between the different enantiomers of the metal centers.^{803,805} Average isotactic sequences of 11 lactide repeat units have been determined by NMR, and the observed T_m was thus explained as arising from the co-crystallization of enantiomeric segments within the polymer chains.

A series of bis(phenoxide) aluminum alkoxides have also been reported as lactone ROP initiators. Complexes (**264**)–(**266**) all initiate the well-controlled ROP of CL, δ -VL,^{806,807} and L-LA.⁸⁰⁸ Block copolymers have been prepared by sequential monomer addition, and resumption experiments (addition of a second aliquot of monomer to a living chain) support a living mechanism. The polymerizations are characterized by narrow polydispersities (1.20) and molecular weights close to calculated values. However, other researchers using closely related (**267**) have reported M_w/M_n values of 1.50 and proposed that an equilibrium between dimeric and monomeric initiator molecules was responsible for an efficiency of 0.36.⁸⁰⁹ In addition, the polymerization of LA using (**268**) only achieved a conversion of 15% after 5 days at 80°C ($M_n = 21,070$, $M_n(\text{calc}) = 2,010$, $M_w/M_n = 1.46$).⁸¹⁰



9.1.6.4 Zinc–Aluminum Oxo-alkoxide Initiators

Prior to the development of the aluminum initiators described above, a series of bimetallic μ -oxo alkoxides, such as (269) and (270) were examined as lactone polymerization initiators.^{811,812} At 10 °C, (269) polymerizes CL in a moderately controlled manner (60 equivalents, $t_{1/2} = 23$ min), as shown by a linear DP vs. $[M]_0/[I]_0$ plot and M_w/M_n values between 1.3 and 1.5. M_n data is consistent with only one of the terminal alkoxides initiating the ring opening, although in the presence of ⁿBuOH, which is known to dissociate (269), all four alkoxides are active.



Further studies have shown that the degree of aggregation, and hence the number of active sites, is a function of the alkoxide substituent.⁸¹³ For example, in (270) one of the *iso*-propoxide groups bridges two aluminum centers; the other three are terminal ligands and all three initiate the ROP of CL. Less aggregated species such as (270) generally exhibit simple first order kinetics.

The use of these initiators to polymerize LA⁸¹⁴ and methylglycolide⁸¹⁵ has been reported to proceed in a well-controlled fashion. Block copolymers such as PCL-*b*-PLA have also been prepared. Elimination of ⁱPrOH from the reaction of (270) with preformed hydroxyl terminated polymers, followed by lactone polymerization, yields diblocks of CL with polystyrene or polybutadiene.⁸¹⁶ The preparation of an ABA triblock has also been reported (A = CL, B = LA); since propagating chains of PLA do not initiate CL ring opening, (270) was pretreated with hydroxy terminated (PCL-*b*-PLA)-OH.⁸¹⁴

9.1.6.5 Magnesium and Zinc Initiators

Early reports document the use of $\text{Zn}(\text{OR})_2$ and $\text{EtZn}(\text{OR})$, ($\text{R} = \text{CH}_2\text{Br}$, $\text{CH}_2\text{CH}_2\text{CH}=\text{CH}_2$, $\text{CH}_2\text{CH}_2\text{NEt}_2$)⁸¹⁷ for well-controlled polymerizations of CL. Subsequently, the use of zinc(II) lactate and related carboxylates was described.^{818,819} For simple magnesium derivatives, low activities and epimerization are generally observed.⁸²⁰ In more recent years, research in this field has been directed towards the development of single-site initiators.

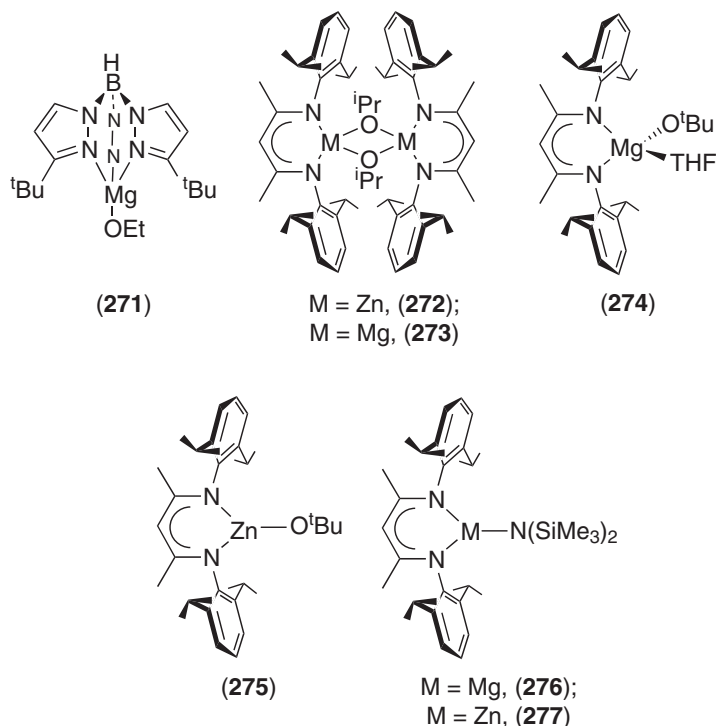
The polymerization of LA using (271) affords a linear relationship between M_n and lactide conversion, coupled with low polydispersities ($M_w/M_n = 1.10$ – 1.25).⁸²¹ ¹H NMR spectroscopy was used to confirm an acyl–oxygen scission pathway. A range of related Mg and Zn complexes have since been examined.⁸²² The zinc complexes are less active than their magnesium analogs. For example, at room temperature, (271) consumes 500 equivalents *rac*-LA in 60 min in CH_2Cl_2 (90% conversion), whereas the zinc analog requires 6 days to bring about the same conversion under identical conditions.

A more active zinc catalyst has been developed containing a β -diketiminato ancillary ligand.⁸²³ Complex (272) converts 200 equivalents *rac*-LA in less than 20 min at room temperature to highly heterotactic PLA (the probability of a racemic junction between monomer units, $P_R = 0.90$ at 25 °C and 0.94 at 0 °C) of narrow polydispersity ($M_n = 37,900$, M_n calc = 28,800, $M_w/M_n = 1.10$). Kinetic studies reveal that the zinc initiators display a fractional rate law order (1.56 ± 0.06). In accord with the observation that $k_{R/SS} \gg k_{R/RR}$ (or $k_{S/RR} \gg k_{S/SS}$), the polymerization of L-LA proceeds significantly slower than *rac*-LA (k_{app} L-LA = 0.031 min^{-1} ; k_{app} *rac*-LA = 0.22 min^{-1}).⁸²⁴

The substituents on the β -diketiminato ligand play a major role in controlling the monomer enchainment. For example, changing the ⁱPr groups to ⁿPr or Et leads to a drop in heterotacticity to $P_R = 0.76$ and $P_R = 0.79$ respectively at 25 °C. (272) also polymerizes *meso*-LA to syndiotactic PLA, although the stereoregularity is less than that observed when the chiral Schiff-base aluminum complex (R)-(-)-(263) is employed ($P_R = 0.76$ vs. $P_R = 0.96$). Reducing the size of the *ortho* substituents on the ancillary ligand again leads to a decrease in the stereoselectivity (e.g., for Et groups, $P_R = 0.37$) in this chain-end controlled process.

The analogous magnesium alkoxide dimer, (273), is more active than (272), although polydispersities are generally higher (ca.1.5), a result of transesterification side reactions.⁸²⁴ An increased level of control may be acquired by the addition of 1 equivalent of ⁱPrOH (M_w/M_n

values typically 1.25–1.3). Related monomeric Mg and Zn complexes (**274**) and (**275**) have also been examined.⁸²⁵ The Mg systems are again more active; for example, (**274**) polymerizes 100 equivalents of *rac*-LA in CH₂Cl₂ in just 2 min at 25 °C (98% conversion), while base-free (**275**) requires 10 min (95%).⁸²⁶ The relative reactivity of the two metals has been demonstrated by the addition of 1 equivalent LA to a 1:1 mixture of (**276**) and (**277**); close to 100% of (**276**) reacts whilst the zinc analog is largely unconsumed. Detailed analysis of the PLA derived from (**274**) reveals small levels of triads which can only arise from transesterification, thus explaining the broad molecular weight distribution observed using (**273**).



The magnesium initiators (**273**) and (**274**) do not display the same stereocontrol as their zinc analogs over the ROP of *rac*-LA in either CH₂Cl₂ or benzene. However, in THF highly heterotactic PLA is produced.⁸²⁶ In non-coordinating solvents the Mg and Zn initiators are believed to adopt dimeric and monomeric resting states respectively, whereas both exist as monomeric forms in THF and hence give rise to similar stereoselectivity.

9.1.6.6 Calcium Initiators

Early studies using calcium oxide, carbonate, and carboxylates reported low activities for the polymerization of LA, even in bulk at 120–180 °C.^{827,828} PolyGA and copolymers of GA with CL and L-LA have been prepared using Ca(acac)₂, but again high temperatures (150–200 °C) are required.⁸²⁹ Under these conditions transesterification occurs, although to a lesser extent than in analogous Sn(Oct)₂-initiated polymerizations.

Activities using calcium alkoxides are somewhat higher. Commercially available Ca(OMe)₂ polymerizes both CL and LA in bulk at 120 °C.⁸³⁰ In both cases M_w/M_n values imply a significant degree of control (1.25 for PCL, 1.43 for PLA), although racemization of the lactide stereogenic centers is also observed. Molecular weight data are also higher than calculated values, and this has been attributed to aggregation of the active species, rendering some of the alkoxides inactive.⁸³¹

Higher activities may be obtained if the bis(alkoxide) is generated *in situ*. For example, addition of 100 equivalents L-LA to a 1:2 mixture of Ca(NTMS₂)₂ and MeOH in THF generates PLA to 97% conversion in 18 min at room temperature (c.f. 66% conversion after 90 min in bulk at 120 °C using commercial Ca(OMe)₂).⁸³⁰ Furthermore, no epimerization is observed. Polydispersities are narrow (1.1), with M_n values slightly higher than those predicted from the monomer:initiator

ratios. Initiator efficiency may be improved by adding excess MeOH which promotes rapid, reversible transfer between dormant and active species.

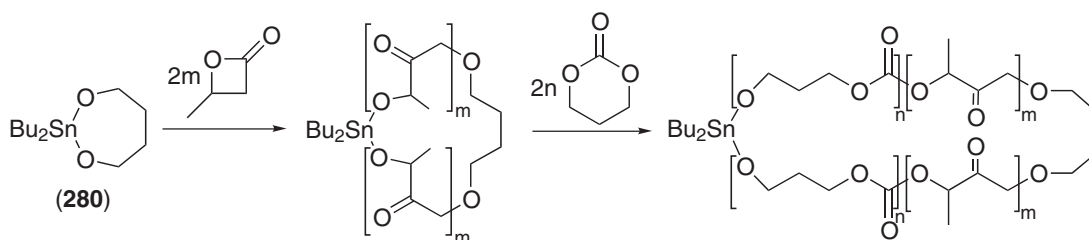
Bulkier alcohols provide improved levels of control.⁸³² For instance, $\text{Ca}(\text{NTMS}_2)_2 \cdot \text{THF}_2 / 2^i\text{PrOH}$ consumes 100 equivalents L-LA in 35 min at 25 °C ($M_n = 6,900$, $M_n \text{ calc} = 7,200$, $M_w/M_n = 1.05$). Chain lengths determined by NMR spectroscopy agree closely with GPC data; NMR spectra also confirm that only the isopropoxide groups initiate polymerization since no silylamide end-groups are detected. The absence of an induction period suggests that *in situ* formation of calcium alkoxides suppresses aggregation; a similar effect using *in situ*-generated yttrium alkoxides has also been observed.^{833,834}

If mono-hydroxyl functionalized poly(ethylene glycol), HO-PEG, is added to $\text{Ca}(\text{NTMS}_2)_2 \cdot \text{THF}_2$, then addition of LA affords the diblock PEG-*b*-PLA ($M_n = 15,500$, $M_n \text{ calc} = 15,500$, $M_w/M_n = 1.03$).⁸³² Using a similar strategy the reaction of CaH_2 with telechelic diol HO-(PEG)-OH, followed by polymerization of L-LA results in a triblock structure, PLA-*b*-PEG-*b*-PLA of narrow polydispersity (1.02–1.08).^{835,836} Triblock copolymers of morpholine-2,5-diones with PEO have also been prepared in this manner.⁸³⁷

9.1.6.7 Tin Initiators

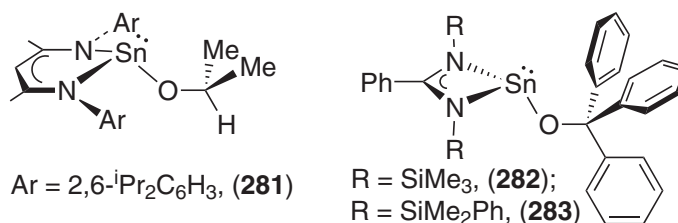
The most widely used industrial initiator for the ROP of lactide is tin(II) 2-ethylhexanoate, (**278**), since it is inexpensive and affords good yields of high molecular weight PLA without racemization. However, the mechanism of initiation using (**278**) is not clearly understood, with several studies reaching conflicting conclusions.^{838–843} The most widely accepted view involves formation of a Sn alkoxide moiety, followed by the standard acyl–oxygen scission coordination–insertion mechanism. The origin of the alkoxide ligand is ambiguous, but proposed sources include moisture (commercial supplies are $\approx 95\%$ pure with $\approx 4.6\%$ ethylhexanoic acid, 0.3–0.5% water and traces of a stabilizer, *t*-butylcatechol),⁸⁴⁴ or acidic impurities in the monomer feedstock. In most cases benzyl alcohol is added to control M_n ,⁸³⁹ and presumably it too aids alkoxide formation. Tin(II) carboxylates have been successfully used to polymerize several other monomers including CL,⁸⁴⁵ GA,⁸⁴⁶ morpholinediones,⁸⁴⁷ and cyclic carbonates.^{848,849}

Detailed studies have been performed on the simple homoleptic compound $\text{Sn}(\text{O}^i\text{Bu})_2$, (**279**), and under certain conditions it initiates well-behaved polymerizations.^{850,851} Believed to be dimeric in solution,⁸⁵² (**279**) initiates the rapid ROP of L-LA and CL in THF at 80 °C. M_n values for PLA samples strongly suggest that each Sn center generates two propagating chains, each capped with *n*-butyl-ester end groups as detected by ¹H NMR. Polydispersities are ≤ 1.25 for short (5 min) reaction times, increasing to 1.3–1.8 for >30 min experiments. Several groups have employed Sn^{IV} cyclic (and spirocyclic⁸⁵³) alkoxides such as (**280**) to polymerize lactones^{854,855} and cyclic carbonates.⁸⁵⁶ Such initiators may be readily used to prepare telechelic block copolymers (Scheme 18).



Scheme 18

Recent findings on the ROP of lactides by Ar_3SnX species ($\text{X} = \text{O}^i\text{Bu}$, NMe_2) suggest that even in seemingly simple tin initiator systems, mechanistic insight is complicated by ligand exchange and chain transfer.⁸⁵⁷ The use of bulky ancillary ligands to suppress such processes was first described for a β -diketiminato tin(II) alkoxide, (**281**),⁸⁵⁷ related to the zinc and magnesium initiators (**272**)–(**275**). This complex initiates the ROP of *rac*-LA with a slight heterotactic bias in a well-controlled, living manner. One hundred equivalents of monomer require several days at room temperature, but at 60 °C the polymerization time is lowered to 4 hours (85%). Polydispersities are typically < 1.10 and M_n increases linearly with monomer conversion.

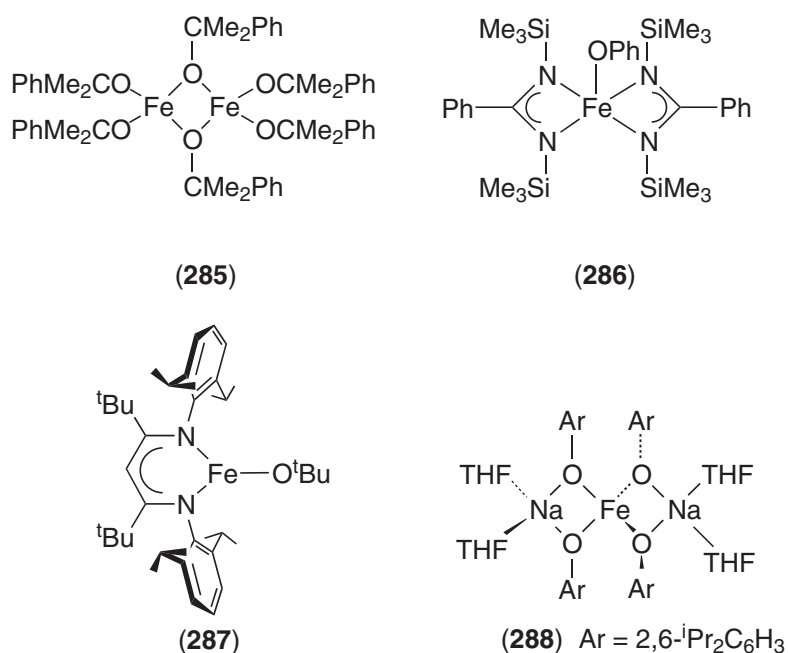


Mononuclear amidinate tin(II) alkoxides, (**282**) and (**283**), have also been examined; the latter consumes 92 equivalents *rac*-LA over 165 min in toluene at 80 °C (M_n calc = 28,900, M_n calc = 14400, $M_w/M_n = 1.18$).⁸⁵⁹ Reproducibility of the polymer chain length is problematic, but the addition of 1 equivalent of an alcohol serves to deliver greater control. Kinetic studies reveal that the rate law is $0.33 (\pm 0.02)$ in $[\text{Sn}]$, suggesting that aggregation of the active species may occur.

9.1.6.8 Iron Initiators

Low activity has been reported for several simple iron-based initiators including oxides,⁸²⁷ porphyrins,⁸⁶⁰ carboxylates^{861–863} and alkoxides.^{864–866} However, the ferric cluster $[\text{Fe}_3(\mu_5\text{-O})(\text{OEt})_{13}]$, (**284**), is a highly active initiator for the polymerization of LA;⁸⁶⁷ 97% conversion of 450 equivalents is achieved in just 21 min at 70 °C in toluene. Polydispersities are typically between 1.15 and 1.30, even at monomer loadings of 1,000 equivalents.

The binuclear complex (**285**) displays similar activities towards LA, although PDI values are notably higher (1.5–1.6). This compound polymerizes CL in a more controlled manner with M_w/M_n values typically ≤ 1.2 . ¹H NMR analysis indicates chain lengths consistent with three propagating chains per Fe center. A single-site bis(benzamidinate) Fe^{III} alkoxide, (**286**) has also been described.⁸⁶⁸ With CL this complex is an order of magnitude less active than the binuclear (**285**) and the polymerization is also less well controlled. PDI values are typically 1.4–2.0 and ¹H NMR studies indicate that only about one-half of the available iron–alkoxide bonds effect initiation. This is attributed to an equilibrium between inactive aggregates and the active mononuclear species, as evidenced by a fractional rate law order for the Fe complex (0.55 ± 0.02). More recently, two Fe^{II} complexes have been reported to polymerize lactide. The β -diketiminato (**287**) is particularly active, consuming lactide at a rate comparable to (**272**).⁸⁶⁹ Anionic Fe^{II} compounds such as (**288**) have also been examined.⁸⁷⁰



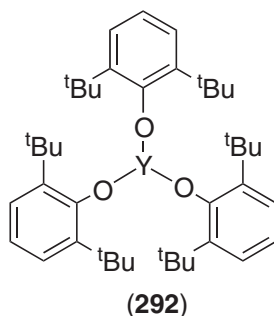
9.1.6.9 Yttrium and Rare-earth Initiators

The interest in lanthanide-based initiators stems mostly from a series of patents in the early 1990s.⁸⁷¹ A wide range of lanthanide alkoxides were studied and certain yttrium (and to a lesser extent samarium) complexes, such as $\text{Y}(\text{OCH}_2\text{CH}_2\text{NMe}_2)_3$, (**289**), and $\text{Y}(\text{OCH}_2\text{CH}_2\text{OEt})_3$, (**290**), were found to be highly active initiators for the ROP of CL (and LA and δ -VL) in a rapid yet controlled manner. In general, lanthanide initiators are extremely active for polymerizations of CL. However, the high activity is usually accompanied by transesterification side reactions; indeed, lanthanide alkoxides have been used as transesterification catalysts in organic synthesis.⁸⁷²

One of the most widely studied initiators is commercially available yttrium iso-propoxide, (**291**), which exists as an oxo-alkoxide cluster of the formula $\text{Y}_5(\mu_5\text{-O})(\mu_2\text{-O}^i\text{Pr})_4(\mu_3\text{-O}^i\text{Pr})_4(\text{O}^i\text{Pr})_5$, usually abbreviated to $\text{Y}_5(\mu_5\text{-O})(\text{O}^i\text{Pr})_{13}$.⁸⁷³ The ROP of *rac*-LA using several $\text{Ln}_5(\mu_5\text{-O})(\text{O}^i\text{Pr})_{13}$ complexes ($\text{Ln} = \text{La, Sm, Y}$ and Yb) has been reported;⁸⁷⁴ in all cases polymerization occurs at room temperature with rates $\text{La} \gg \text{Sm} > \text{Y} \gg \text{Yb}$. The polymerizations appear to be living with M_w/M_n values typically ≤ 1.30 . Transesterification occurs to a minor extent with the Sm, Y, and Yb initiators, even during the early stages of polymerization,⁸⁷⁵ but the La-catalyzed system is particularly prone, with $M_w/M_n > 2$ at longer reaction times (although $\text{La}(\text{O}^i\text{Pr})_3$ has since been used to polymerize a variety of lactones and cyclic carbonates^{876,877}). Determination of average polymer chain length by ^1H NMR spectroscopy indicates that, for Y and La, all 13 O^iPr groups initiate the polymerization, whereas for Sm and Yb the number of active sites is somewhat less.

When (**291**) is used as an initiator the rate law is not first order in initiator for the ROP of either CL⁸³⁴ or L-LA,⁸³³ suggesting that species of different activities are present in solution. An induction period occurs before propagation commences and UV studies suggest that CL coordination to the yttrium centers occurs prior to initiation. For both CL and LA the polymerization is controlled ($M_w/M_n = 1.15$) with a linear correlation between DP and $[\text{M}]_0/[\text{I}]_0$, the gradient of which confirms that 13 propagating chains arise per 5 yttrium centers. Ring opening occurs via an acyl-oxygen cleavage and the living nature of the process allows diblock copolymers to be prepared of narrow polydispersity (1.2–1.3).⁸⁷⁸ Initiator (**291**) has also been used to polymerize a macrolactone: 150 equivalents of ω -pentadecalactone are polymerized within 30 min at 60–100 °C in the bulk to give a product with M_n 16,000 (M_n calc. 14,000) and $M_w/M_n = 1.6$.⁸⁷⁹

In order to circumvent the mechanistic complications arising from cluster formation, Feijen and co-workers have developed a two-component initiating system comprising $\text{Y}(\text{O}-2,6\text{-}^t\text{Bu}_2\text{C}_6\text{H}_3)_3$, (**292**), and 3 equivalents $^i\text{PrOH}$.⁸⁸⁰ In the absence of alcohol, (**292**) only slowly polymerizes lactones and exerts poor levels of control, with broad polydispersities observed. Furthermore, NMR analysis has failed to identify end-groups suggesting that the initiating species is not a phenoxide. However, when alcohol is added, ligand exchange occurs rapidly, followed by rapid initiation. The initiating end-groups have been identified as iso-propyl esters and the polymerization is first order in yttrium. The polymerizations are rapid; for example, the rate of propagation for CL at 25 °C is $1.65 \text{ L mol}^{-1} \text{ min}^{-1}$ (c.f. $0.5 \text{ L mol}^{-1} \text{ min}^{-1}$ for $\text{Al}(\text{O}^i\text{Pr})_3$ at 25 °C). M_n closely parallels calculated values, and polydispersities are 1.1–1.2.



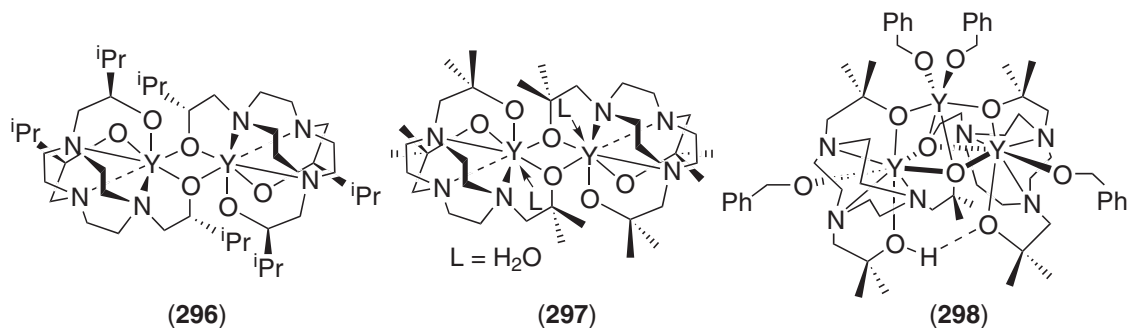
A similar *in situ* approach to alkoxide formation employs the readily accessible tris(amide)- $\text{Y}(\text{NTMS}_2)_3$, (**293**), and $^i\text{PrOH}$.⁸⁸¹ In the absence of alcohol the polymerization of CL is fast but not controlled ($M_w/M_n > 3$). However, upon addition of alcohol, a controlled living system with polydispersities 1.1–1.2 results. At least 50 equivalents of $^i\text{PrOH}$ may be added (the excess effects rapid chain transfer) with molecular weights in good agreement with theoretical values. Similar results have been reported using $\text{Nd}(\text{NTMS}_2)_3$, (**294**), and $^i\text{PrOH}$.⁸⁸² The reactions of $^i\text{PrOH}$ with (**292**) and (**293**) have both been studied by NMR, and in both cases $\text{Y}_5(\mu_5\text{-O})(\text{O}^i\text{Pr})_{13}$ is not

formed. The nature of the actual product remains to be established, but is independent of excess alcohol, and is stable in solution for several days.

The tris(alkoxides) $Y(OCH_2CH_2OR)_3$ have also been reported to be extremely active initiators.⁸⁸³ For example, β -BL is polymerized in a controlled and relatively rapid manner by $Y(OCH_2CH_2OMe)_3$, (**295**) (M_n determined by NMR = 48,000, M_n calc = 46,700, $M_w/M_n = 1.18$).⁸⁸⁴ Linear relationships between DP and conversion, and between DP and $[M]_0/[I]_0$, indicate a living polymerization. Ring opening was shown to occur at the acyl–oxygen bond, generating a metal–alkoxide which has been used to synthesize the diblock copolymer P(β -BL)-b-PLA with a M_w/M_n of 1.17. The block copolymers of CL and LA, and of LA with trimethylene carbonate, have also been prepared using this class of initiator.⁸⁸⁵

A series of structurally characterized di-yttrium(III) complexes bearing alkoxy-derivatized triazacyclononane ligands have been examined as initiators for lactone ROP.⁸⁸⁶ Both (**296**) and (**297**) are active for the polymerization of *rac*-LA at RT, but little control is afforded over molecular weights. Chain length distributions are broad, ($M_w/M_n = 1.5$ – 2.2) and attempts to identify the initiating group via end-group analysis have not been successful.

Improved control was observed, however, upon addition of benzyl alcohol to the dinuclear complexes.⁸⁸⁷ X-ray crystallography revealed that whereas (**296**) simply binds the alcohol, (**297**) reacts to form a trinuclear species bearing four terminal alkoxides. The resultant cluster, (**298**), polymerizes *rac*-LA in a relatively controlled manner ($M_w/M_n = 1.15$) up to 70% conversion; thereafter GPC traces become bimodal as transesterification becomes increasingly prevalent. NMR spectroscopy demonstrates that the PLA bears BnO end-groups and the number of active sites was determined to be 2.5 ± 0.2 . When CL is initiated by (**298**) only 1.5 alkoxides are active and kinetic analysis suggests that the propagation mechanisms for the two monomers are different, the rate law being first order in LA, but zero order in CL.

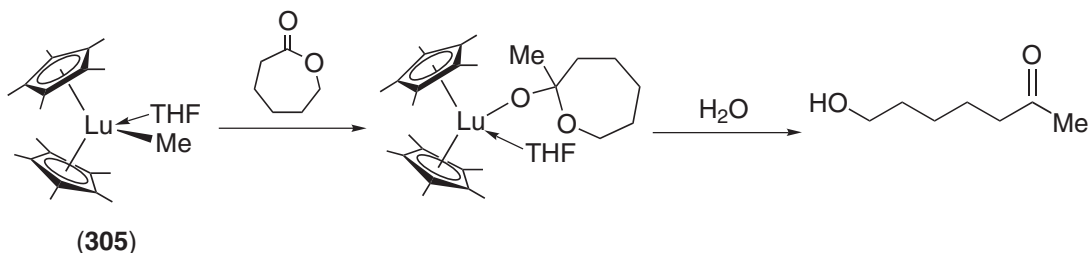
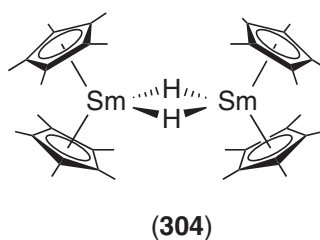
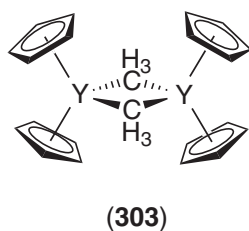
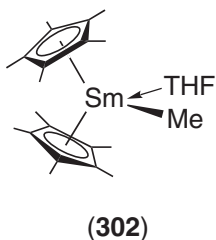
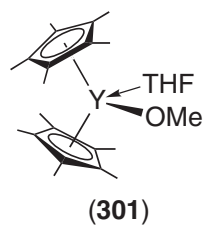
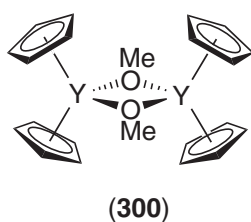
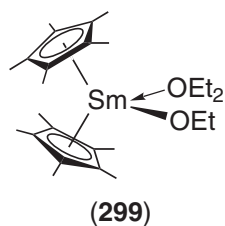


As described previously for aluminum, in order to obviate the kinetic complexity arising from aggregation, several groups have examined potentially less complicated single-site monoalkoxides. For example, complexes (**299**)–(**301**) are active for the ROP of CL, δ -VL and even β -PL at 0°C.⁸⁸⁸ Polydispersities are low (<1.10) even up to 90% conversion and M_n increases linearly with conversion for CL, although initiator efficiencies are typically 50–60%. Lanthanocene alkyls, such as (**302**) and (**303**), and hydrides, (**304**), exhibit almost identical reactivity for the polymerization of CL and δ -VL to the alkoxides (**299**)–(**301**) (although no activity for β -PL was observed).

Analysis of the hydrolysis products of the 1:1 stoichiometric reactions of (**304**) with δ -VL and with CL suggests that the initiation process involves reduction of the lactone carbonyls to form $[(Cp^*)_2Sm-O-(CH_2)_n-O-Sm(Cp^*)_2]$ ($n = 5, 6$). Initiation via the alkyl complexes has been analyzed by 1H NMR spectroscopy using (**305**) (a diamagnetic analog of (**302**)) and CL; the product is a cyclic acetal arising from the attack of the methyl ligand at the carbonyl carbon atom. Hydrolysis produces ring-opened 7-hydroxy-2-heptanone, suggesting that propagation occurs via acyl–oxygen cleavage. A methyl ketone end-group has also been detected by MALDI–TOF mass spectrometry.⁸⁸⁹

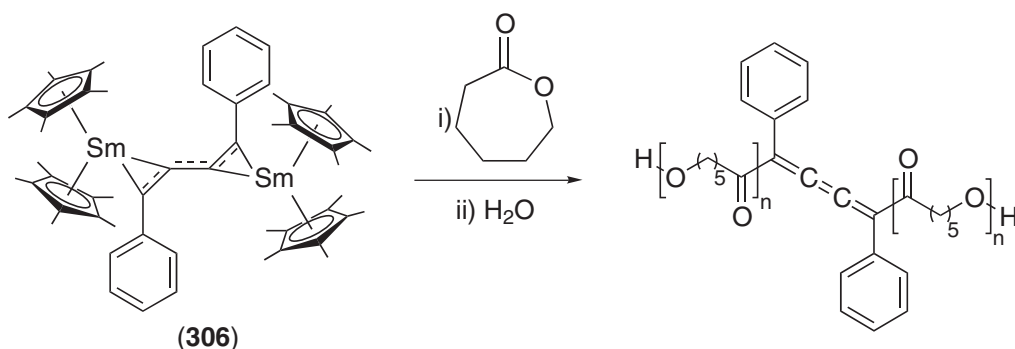
NMR studies on the alkoxide initiators confirm that all the lactones polymerize via an acyl–oxygen scission, including β -PL (which, by contrast, opens at the alkyl–oxygen bond with (**251**)). Monomer coordination and subsequent ring opening may be observed by 1H NMR spectroscopy. Coordination is also observed with γ -BL and γ -VL, although these adducts are stable to insertion and polymerization does not proceed.

The lanthanocene systems have been extended to cover a range of monomers including LA,⁸⁹⁰ cyclic carbonates⁸⁹¹ and even MMA.⁴⁵⁴ Block copolymers of MMA and lactones, with $M_w/M_n = 1.11$ – 1.23 , may be prepared but only if the vinyl monomer is polymerized first. The



lanthanocene hydrides and alkyls can also polymerize ethylene, and may be used to form block copolymers of the polyolefin with δ -VL and CL.²²⁹ Reverse addition (i.e., lactone followed by olefin) only produces the homopolyesters. In addition, the use of (304) to polymerize ethylene generates $[(Cp^*)_2Sm(CH_2CH_2)_nSm(Cp^*)_2]$, which has been used to generate the triblock copolymer PCL-b-PE-b-PCL.⁴⁷⁵

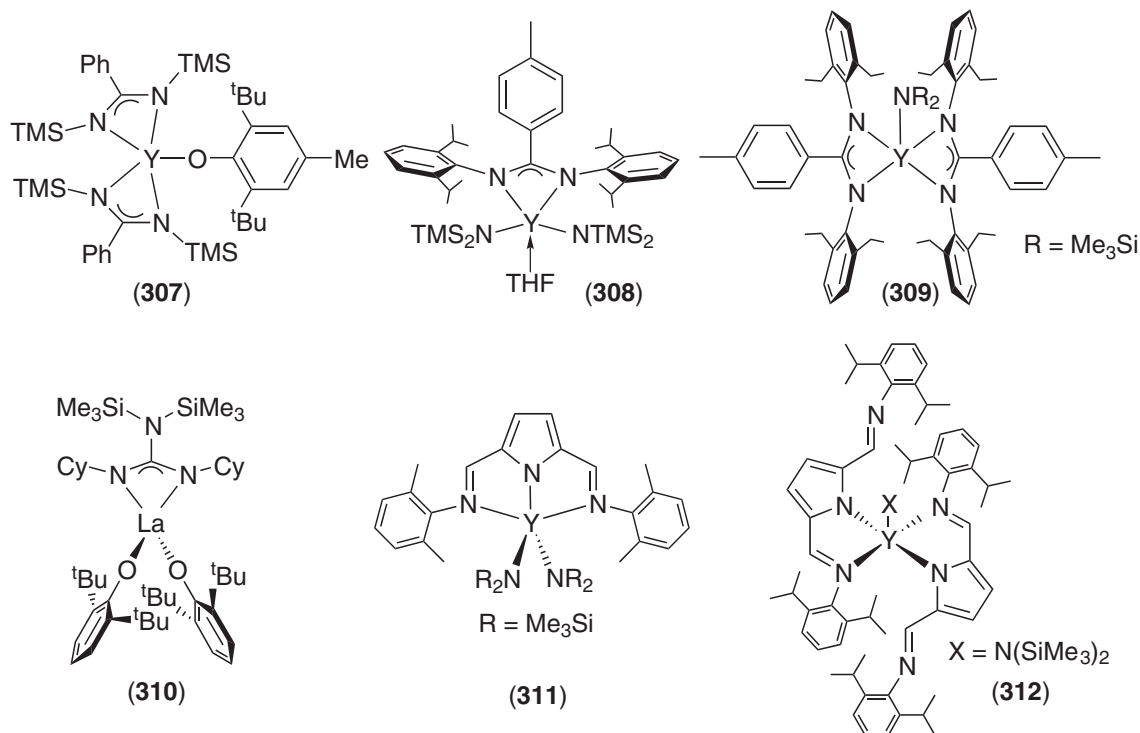
Initiators such as (306) initiate the ROP of CL to form telechelic triblock diols.⁴⁷⁸ Molecular weights approach theoretical values with polydispersities ≤ 1.3 and no significant level of transesterification was detected at up to 95% conversions. Alternative bimetallic samarium initiators have been used to synthesize aromatic, cumulene and amine/imine link-functionalized poly(lactones).⁴⁷⁹



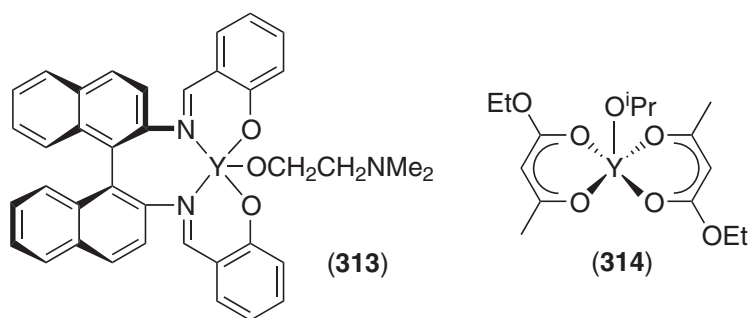
Non-cyclopentadienyl single-site lanthanide alkoxides mostly feature N-donor-based ancillary ligands. Examples include bulky bis(arylamidinate)-yttrium(III) alkoxides, phenoxides and amides such as complexes (307)–(309), which initiate the ROP of LA.⁸⁹² However, control over molecular weight is poor and polydispersities are broad (typically > 1.5), with the exception of (309) in the presence of exogenous benzyl alcohol.

The guanidinate complex (310) polymerizes LA at RT.⁸⁹³ M_n values increase with M_0/I_0 ratios, but control is only moderate, with M_w/M_n typically > 1.5 . Transesterification occurs to a large extent as shown by NMR studies on the isolated PLA. Potentially tridentate 2,5-bis(N-arylimino-methyl)pyrroles have been explored as ancillary ligands for yttrium.⁸⁹⁴ Their reactions with

$Y(NTMS_2)_3$ give products whose structures are dependent upon the size of the aryl substituents, as shown, for example, by (311) and (312). Both complexes rapidly polymerize CL (100 equivalents in 10 min at 25 °C), but the monoamide (312) is more controlled ($M_w/M_n = 1.3$ cf. 2.0 for (311)), although both initiators give M_n values greater than expected (e.g., for (312) $M_n = 58,000$, M_n calc = 11,400). The $N(TMS)_2$ ligand was detected as the PCL end-group suggesting that initiation involves nucleophilic attack of the amide at the monomer carbonyl unit.



Tetradentate N,O-donor ligands have also been investigated. The yttrium complex (–)(313) does not effect stereocontrol over the ROP of *rac*- or *meso*-LA, in contrast to related Al initiators (262) and (263).⁸⁰³ Polymerization is also slower than for most lanthanide initiators with 100 equivalents *meso*-LA requiring 14 h at 70 °C to attain near-quantitative conversion (97%).



Bis(ethylacetoacetate)-lanthanide(III) alkoxides, represented by structure (314), also initiate the well-controlled ROP of CL.⁸⁹⁵ M_n increases linearly with conversion (with $M_w/M_n < 1.10$ throughout), and increasing $[M]_0/[I]_0$. Kinetic analysis implies a first order dependence on the lanthanide initiator, consistent with a non-aggregated active site. Block copolymers with moderately narrow polydispersities (1.25–1.45) have also been prepared using these initiators. NMR spectroscopy confirms well-controlled block sequences suggesting that these initiators are less susceptible to transesterification than other lanthanide alkoxides. Initiation occurs exclusively at the alkoxide bond, and the tris(ethylacetoacetate) analogs are inactive under the same conditions.

Several other lanthanide complexes have been tested for ROP activity with varying degrees of success. Some of these are summarized in Table 2.

Table 2 Ring-opening polymerization of lactones initiated by lanthanide complexes (CL = ϵ -caprolactone; LA = lactide; TMC = trimethylene carbonate).

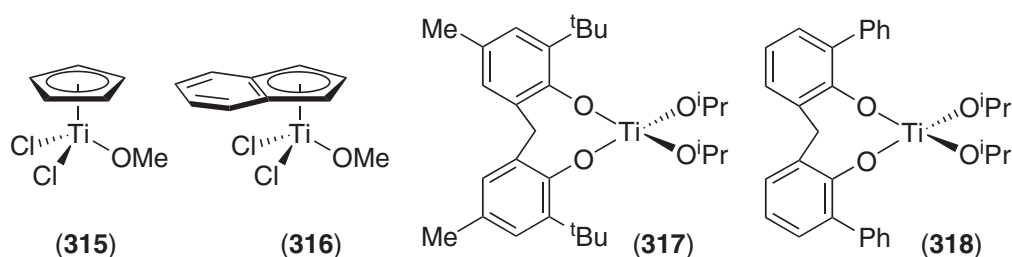
<i>Initiator</i>	<i>Monomer (equiv)</i>	<i>Conditions</i>	<i>Conversion</i>	<i>M_n</i>	<i>M_w/M_n</i>	<i>Comments</i>	<i>References</i>
Ln(OAc) ₃ , Ln = La	LA (100)	160 °C, 30 min	29%	15,900	1.84	Ln = La, Y, Nd, Sm	896, 897
LnCl ₃ + propylene oxide	CL (2500) + TMC (2500)	100 °C, 3 h	98%	82,100	1.19	Ln = La, Pr, Nd, Eu, Gd, Dy, Er, Yb	896–898
Ln = La Y [PhC(N(TMS) ₂) ₃] ₃	CL (450)	25 °C, 1 min, toluene	100%	95,000	3		896
LnPh ₃ , Ln = Y [Yb(NPPPh ₃) ₃] ₂	CL (100) CL (75)	60 °C, 30 min 20 °C, 3 min, toluene	86% 98%	65,000 12,690	1.37	Ln = Y, Nd, Sm	896–898 896
SmI ₂	CL (34)	25 °C, 14 h, THF	99%	27,400	1.58	Cp ₂ Sm and SmBr ₂ also studied	896
Sm(OAr) ₂ (THF) ₃	CL (100)	20 °C, 2 min	100%	34,000	1.52		896
[Sm(N(TMS) ₂) ₂ (μ -Cl)THF] ₂	CL (150)	20 °C, 20 min	98%	11,000	1.91	δ -VL also studied	896
Cp* ₂ Sm(THF) ₂	L-LA (100)	25 °C, 6 h, toluene	70%	27,000	1.55		891
Cp* ₂ Sm(Me)THF	L-LA (100)	80 °C, 24 h, toluene	74%	20,900	1.48	Cyclic carbonate and CL also studied	890
(ⁱ PrC ₅ H ₄) ₂ SmI(O ^t Bu)THF	CL (200)	20 °C, 15 min, toluene	95%	30,000	1.28		896
(ⁱ PrC ₅ H ₄) ₂ Sm(O ^t Bu)	CL (200)	20 °C, 10 min, toluene	80%	26,000	1.28		909
(MeC ₅ H ₄) ₂ Er(N ⁱ Pr) ₂ THF	CL (500)	20 °C, 4 h, toluene	66%	117,500	1.14	Y and Yb analogs also studied	896
	CL (90)	25 °C, 1.5 h, CH ₂ Cl ₂	78%	34,000	1.6		896
	L-LA (122)	25 °C, 2 h, CH ₂ Cl ₂	33%	15,600	1.2		896
	CL (600)	25 °C, 2 h, toluene	53%	43,800	1.85		467

9.1.6.10 Titanium and Zirconium Initiators

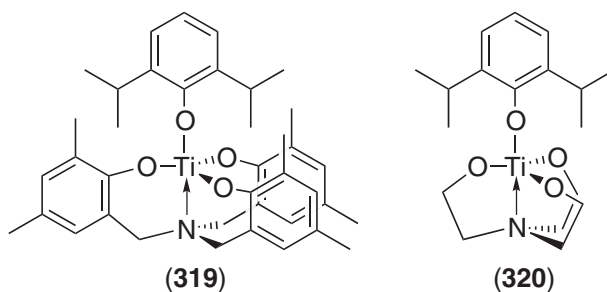
Although group 4 metallocenes display high activities as catalysts for the polymerization of α -olefins, methacrylates and styrenes, to date very few reports have appeared examining their use as lactone ROP initiators. $Zr(OR)_4$ and $Ti(OR)_4$ ($R = {}^iPr, {}^tBu$) have been briefly investigated for the polymerization of CL and LA,^{744,913} but high temperatures (100–150 °C) are required. Less control is afforded by $Zr(acac)_2$ ^{914,915} or $ZrCl_4$.⁹¹⁶

$[(Cp)TiCl_2(OMe)]$, (**315**), has been reported to polymerize CL in a living manner, although high temperatures (several hours at 110 °C) are required.⁹¹⁷ Molecular weight distributions are narrow at low conversion (1.04 at 12%), but rise to >1.4 at 80%. Electron-donating Cp ligands generally enhance the activity, although the highest activity was observed for indenyl (**316**).⁹¹⁸

Bulky bis(phenolate) titanium(IV) alkoxides have also been found to polymerize CL. Unlike the monocyclopentadienyl systems, these are active at ambient temperature and transesterification is much less of a problem.⁹¹⁹ Complex (**317**) consumes 100 equivalents CL in 5 hours at 25 °C (100% conversion, $M_n = 6,500$, $M_n \text{ calc} = 5,700$, $M_w/M_n = 1.15$) with each metal center generating two propagating chains. Narrower polydispersities (but slower kinetics) are observed for the ortho-phenyl substituted analog (**318**) (67% conversion after 24 h). NMR and UV studies confirm that the O^iPr ligands are the active initiating groups, with no phenolate residue detected in the polymer chains. Both (**317**) and (**318**) are inactive towards the ROP of epoxides, but the analogous dichlorides are active, and hence block copolymers such as PCL-b-PPO may be formed if the epoxide is polymerized first. The dichloride analog of (**317**) has also been used to polymerize cyclic carbonates to give narrow molecular weight distributions, whereas the bis(alkoxide) gives a bimodal distribution of chain lengths.^{920,921}



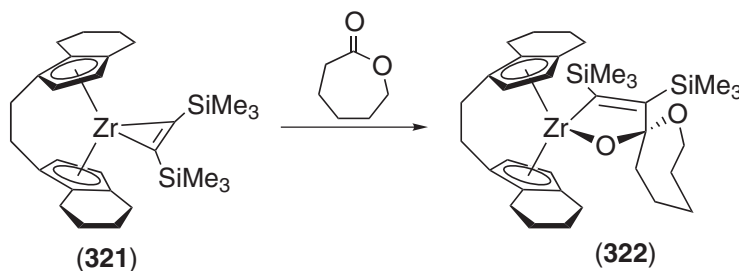
Titanatranes such as (**319**) and (**320**) polymerize 300 equivalents of L-LA or *rac*-LA to 70–100% conversion within 24h at 130 °C.⁹²² 1H NMR studies show that the polymer bears the bulky di-*iso*-propylphenolate end-group, indicating that initiation occurs in a controlled manner. However, molecular weight distributions are relatively broad (1.4–2.0), due in part to transesterification.



Some of the most active group 4 initiators for lactone polymerization are cationic zirconocene alkyls, which fully consume 100 equivalents CL within 2 hours at room temperature.⁹²³ Despite delivering very low polydispersities (<1.10), chain lengths are much longer than expected, due to low initiator efficiencies (typically 30%). Identical behavior was recorded for a cationic Hf complex, but the Ti analog is inactive at room temperature. Initiator efficiencies and reaction times depend upon the nature of the ancillary Cp ligands. For example, $[(Cp^*)(Cp)ZrMe_2]/[Ph_3C][B(C_6F_5)_4]$ polymerizes CL with 100% efficiency, but requires 22 hours to fully polymerize 100 equivalents of monomer; $M_n = 10,000$, $M_n \text{ calc} = 11,400$, $M_w/M_n = 1.29$.

The use of group 4 metallocene alkyne complexes⁹²⁴ and bimetallic aluminum derivatives⁹²⁵ as CL polymerization initiators has also been described. These catalysts generally exhibit poor control with M_n values much lower than expected and $M_w/M_n = 1.4$ –2.6. End groups have not

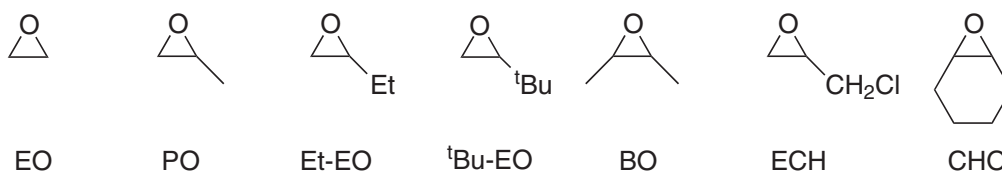
been identified, but the product resulting from the 1:1 reaction of *rac*-(**321**) and CL has been characterized by X-ray crystallography.⁹²⁶ The spiroacetal complex (**322**) thus formed is similar to the acetal proposed in the lanthanocene alkyl initiated polymerization of lactones.⁸⁸⁸



9.1.7 RING-OPENING POLYMERIZATION OF EPOXIDES

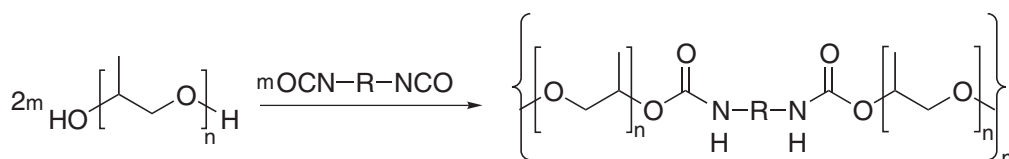
9.1.7.1 Introduction

Polyethers produced via the ROP of epoxides have many commercial uses, and are especially important as precursors to polyurethanes (Scheme 20).^{927–929} Although a wide variety of reagents can effect the cationic or anionic ROP of epoxides, low molecular weight polyols are generally prepared using potassium or sodium hydroxide.^{930,931}



EO = ethylene oxide, PO = propylene oxide, Et-EO = 1,2-epoxybutane, ^tBu-EO = ^tbutylethylene oxide, BO = 2,3-epoxybutane, ECH = epichlorohydrin, CHO = cyclohexene oxide

Scheme 19



Scheme 20

Higher molecular weight materials are typically prepared using coordination catalysts, such as the calcium amide–alkoxide system developed by Union Carbide,⁹³² and double metal cyanide initiators, e.g., [Zn(Fe(CN)₆)].⁹³³ The nature of the active sites in these catalysts is not well understood and only a few studies have been published outside the patent literature.^{810,934,935}

9.1.7.2 Tetraphenylporphyrin Aluminum and Zinc Initiators

One of the most widely studied systems for the polymerization of cyclic ethers is the tetraphenylporphyrinato aluminum system, (TPP)AlX. Most investigations have focused on the chloride complex, (**251**), which initiates the living ROP of EO, PO, and Et-EO.⁹³⁶ For example, 400 equivalents of EO require 3 hours in CH₂Cl₂ at 25 °C to reach 80% conversion. M_n values increase linearly with monomer conversion, with polydispersities typically ≤1.10, and chain lengths controlled by the initial monomer:initiator ratio.

The initiation mechanism comprises nucleophilic attack of the metal chloride at the least-hindered carbon. Thus hydrolysis of the 1:1 reaction product of (**251**) with PO yields 1-chloropropan-2-ol.⁹³⁷

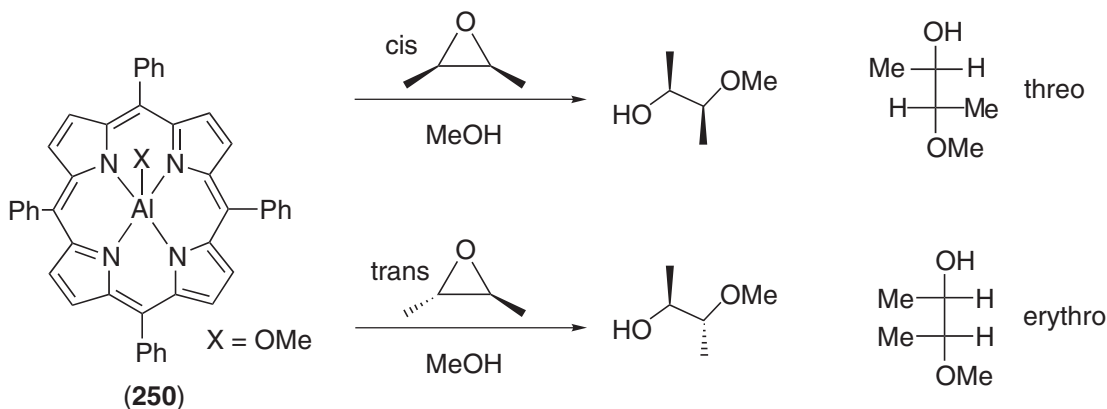
NMR analysis of hydroxyl-terminated oligomers reveals that the initiating Cl resides at a terminal methylene unit, and the OH is bonded to a methine group. As a result, samples of PPO prepared using (251) are highly regioregular (i.e., predominantly head–tail).⁹³⁸ Similar studies with EO suggest that for both monomers the propagating species is an Al–alkoxide.

The rate of polymerization is heavily dependent upon the size of the epoxide substituents. Consequently, Et-EO polymerizes slower than either PO or EO,⁹³⁶ and (TPP)AlCl inserts only one molecule of ^tBu-EO over a period of 5 days. Reactivity follows the order EO > PO > Et-EO ≈ *cis*-BO > ECH > ^tBu-EO. Further, in a 1:1 mixture of *cis*- and *trans*-BO, the *cis* monomer is opened preferentially, possibly because coordination of the monomer to the metal center occurs prior to ring cleavage. It has also been shown that the 1° alkoxide derived from the ring-opening of EO is much more reactive than the 2° alkoxide resulting from PO.

The living nature of the system has been utilized to prepare a range of block copolymers, including PEO-*b*-PPO,^{938,939} P(Et-EO)-*b*-PEO, P(Et-EO)-*b*-PPO and the triblock P(Et-EO)-*b*-PEO-*b*-PPO.⁹³⁶ Random copolymerization of EO and PO also affords narrow molecular weight distributions.⁹⁴⁰ However, for the copolymerization of PO with slower monomers, such as ECH, the more active PO incorporates preferentially to afford block-like materials.

Analogous alkoxides, phenoxides, and carboxylates will also initiate the ROP of epoxides, all forming propagating alkoxide species.⁷⁷⁹ Block copolymers of epoxides with β-butyrolactone have been prepared via the addition of EO or PO to living poly(ester) chains.⁷⁸² The oxygen-bound enolate of living PMMA will also react with epoxides to yield diblocks such as PEO-*b*-PMMA and PPO-*b*-PMMA ($M_n = 12,800$, $M_w/M_n = 1.16$).⁷⁸⁷

Much of the work on the living ROP of epoxides parallels developments made using the same system with lactones. For example, chain transfer has been performed using excess MeOH.⁹⁴¹ Exchange of propagating alkoxide chains with alcohol is estimated to occur ten times faster than propagation.⁷⁸¹ As a result, low molecular weight polyethers of very narrow polydispersities may be prepared, although the polymerization is significantly slowed down when a high concentration of the chain transfer agent is employed. This may be circumvented by addition of a Lewis acidic accelerant such as (255).⁹⁴² Further evidence for a bimetallic mechanism is provided from a study examining the stereochemistry of the ring opening of *cis*- and *trans*-BO at the (TPP)Al centers.⁹⁴³ With the methoxide species (250) in the presence of excess MeOH, *cis*-BO opens to form *threo*-3-methoxy-2-butanol exclusively, whereas *trans*-BO generates the *erythro*-isomer (Scheme 21). It therefore follows that inversion of configuration occurs at the carbon atom where the ring is opened, consistent with a bimetallic, “backside attack” mechanism.

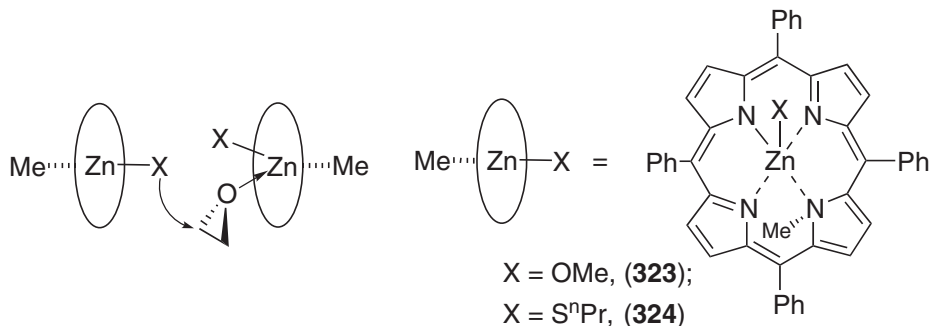


Scheme 21

A related N-methylated zinc methoxide (323) also polymerizes *cis*- and *trans*-BO with inversion of stereochemistry. In this case, coordination of the monomer *trans* to the axial alkoxide is hindered by the N–Me group, so a modified mechanism has been proposed based on *cis*-coordination of the monomer, but which still involves the simultaneous participation of two metal centers.

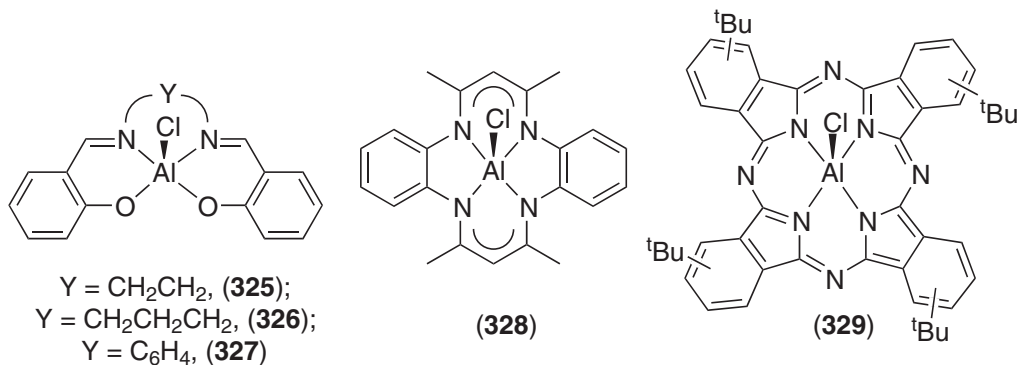
The corresponding thiolate (324) will also polymerize epoxides following photoinitiation.⁹⁴⁴ For example, using 190 equivalents of EO, a conversion of <2% was observed after 205 min in the dark. However, this rises to 97% if the system is irradiated for 80 min ($M_n = 8,700$, $M_n \text{ calc} = 8,100$, $M_w/M_n = 1.05$). ¹H NMR studies confirm that the propagating species is a metal–alkoxide and as a result, if irradiation is stopped once initiation has occurred, the polymerization will persist, although

at a slower rate than if the irradiation is continued. An application of this system has been reported for the copolymerization of EO with propylene sulfide, PS.⁹⁴⁵ In the dark, (324) will preferentially polymerize PS, so that at 80% PS conversion, >80% of the EO remains unpolymerized. However, if the reaction is repeated and irradiated, a more random copolymer is produced.



9.1.7.3 Non-porphyrinato Aluminum Initiators

The dramatic acceleration observed for the ROP of epoxides when (255) is present has also been observed with several other aluminum-based initiators, including salen- (325)–(327), tetraazaanulene- (328) and phthalocyanine- (329) ligated systems.⁹⁴⁶ For example, (325) polymerizes PO extremely slowly at room temperature (4% conversion of 50 equivalents over 8 days), but in the presence of MAD (255), 200 equivalents require just 70min to attain 43% conversion.^{794,795,947} Complex (328) shows a similar increase in activity upon addition of MAD; 200 equivalents PO reach 74% conversion within 90 seconds; in the absence of MAD such a yield requires several days.



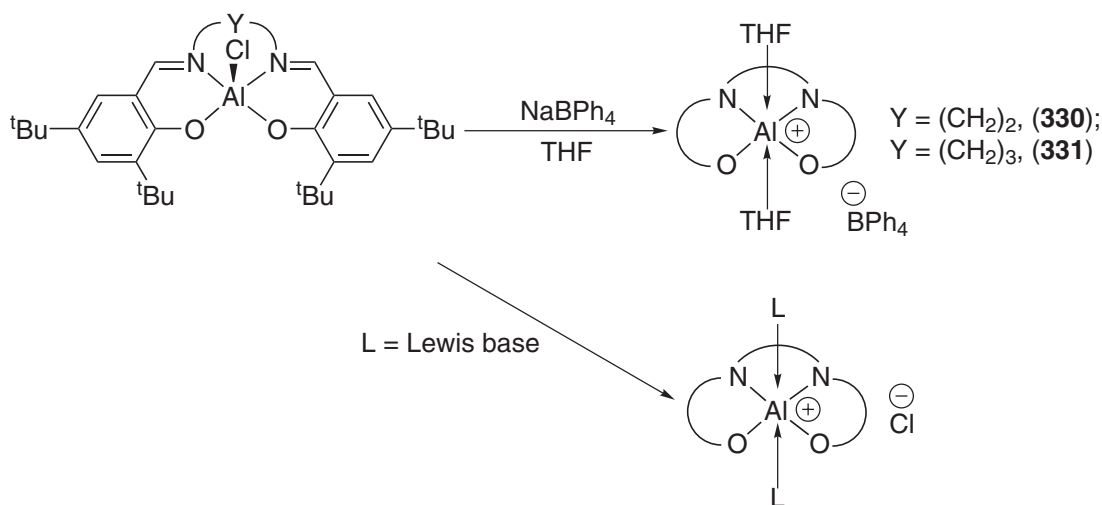
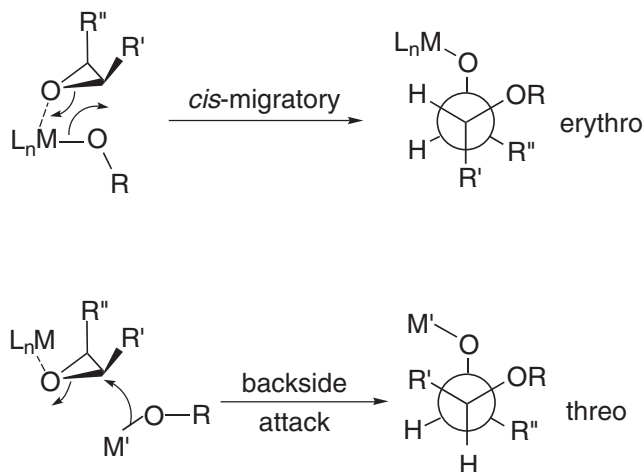
Several aluminum biphenolate complexes have been investigated as initiators for the ROP of PO.^{810,935} Unlike the TPP and salen-based systems, a *cis* coordination site is realistically accessible and in theory an alternative “*cis*-migratory” mechanism to the backside attack pathway might operate. However, NMR analyses on the resultant PPO show that stereochemical inversion still occurs when the biphenolate initiators are used (Scheme 22). It has also been confirmed that the same process occurs with the Union Carbide calcium alkoxide–amide initiator for both PO and CHO.⁸¹⁰

Several other Al-based initiators have been described, including ill-defined aluminophosphates for the ROP of PO and ECH,⁹⁴⁸ and a diamidoamine chloride complex, which displays low activity for the ROP of PO.⁹⁴⁹ A variety of cationic 5- and 6-coordinated aluminum(III)–salen species⁹⁵⁰ have also been investigated; molecular weights of 4×10^6 ($M_w/M_n = 1.32$) and 1.8×10^6 ($M_w/M_n = 1.16$) are achievable using (330) and (331), respectively.^{951,952} The ease with which the chloride complexes dissociate when in the presence of Lewis bases has also been noted, leading to the suggestion that PO may cause a similar effect, and therefore the catalytically active species in all Schiff-base Al^{III} complexes may be cationic.⁹⁵³

9.1.7.4 Copolymerization of Epoxides and Carbon Dioxide

The synthesis of polycarbonates from the alternating copolymerization of epoxides with CO₂ was first reported in 1969 using a ZnEt₂/H₂O mixture.⁹⁵⁴ Subsequent studies have focused upon a

range of alkylzinc and alkylaluminum compounds, and several complexes were found to catalyze the coupling of epoxides and CO₂ to monomeric cyclic carbonates.⁹⁵⁵ On occasion they would produce varying quantities of the polycarbonate. However, these systems require very high pressure, and usually exhibit low activities.

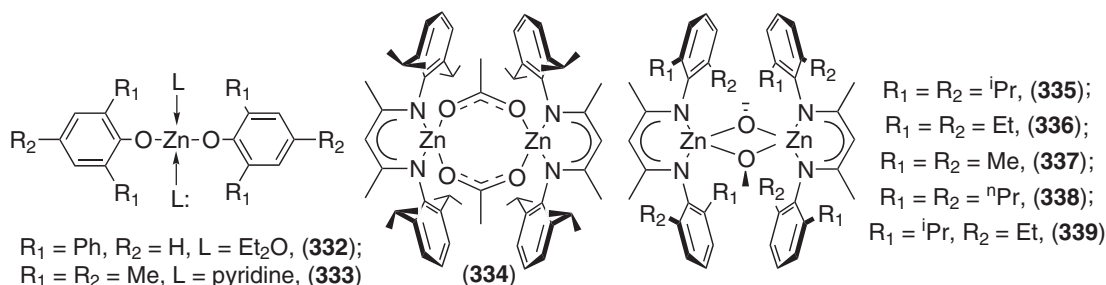


More active zinc phenoxide initiators of the type [Zn(OAr)₂(Et₂O)₂]⁹⁵⁶ were found to catalyze both the copolymerization of CHO with CO₂ and the terpolymerization of CHO, PO, and CO₂; attempts to copolymerize PO and CO₂ yielded predominantly cyclic carbonates. For example, (332) copolymerizes CHO and CO₂ at 80 °C and 800 psi to give a copolymer containing 91% syndiotactic polycarbonate linkages (and 9% polyether junctions due to the non-insertion of CO₂) with good activity (>350g polymer/g [Zn] in 69 h).⁹⁵⁷ However, the polymerization is not well-controlled ($M_w/M_n > 2.5$). Variation of the phenoxide ligands revealed that (333) is ≈ 4 times more active.⁹⁵⁸

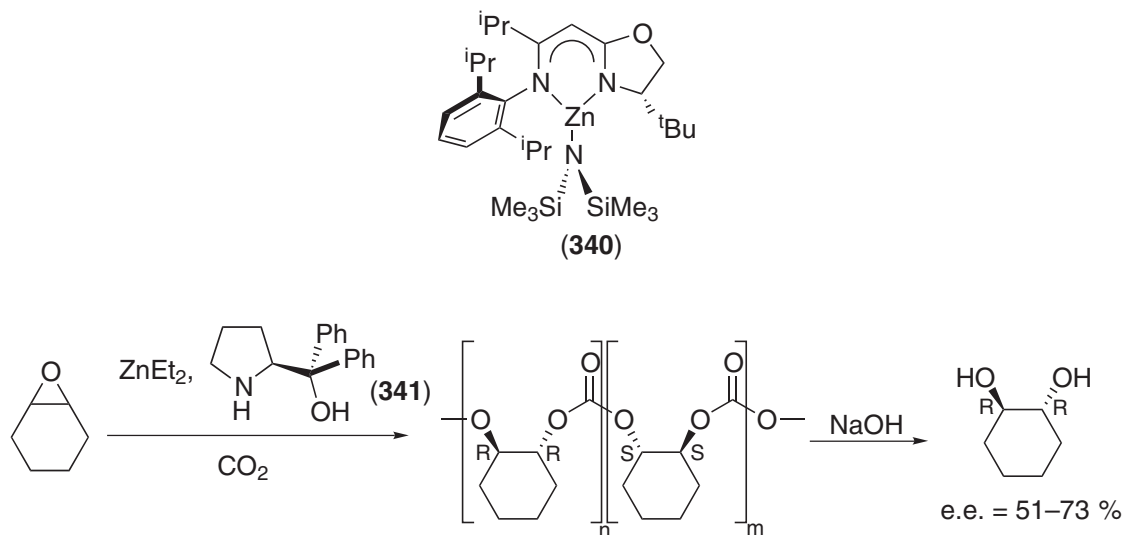
Several other zinc catalysts for this reaction have since been reported, but activities are significantly lower than for (332) or (333).^{959–962} More recently the zinc carboxylate (334), featuring a bulky β -diketiminate ancillary ligand, was shown to catalyze the highly alternating copolymerization of CHO and CO₂, with activities significantly higher than any previously reported.⁹⁶³ Furthermore, (334) operates under much milder conditions (100 psi, 20–80 °C). The polycarbonates produced exhibit narrow molecular weight distributions (<1.20), are atactic, and contain only *trans* cyclohexane junctions, consistent with backside attack on the epoxide monomer.

Related alkoxides, such as (272), and the amide (277) display a similar activity to the acetate,⁹⁶⁴ suggesting that both alkoxide and carbonate intermediates are formed during the reaction. ¹H NMR spectroscopy has been used to demonstrate that (334) reacts reversibly with CHO to generate an alkoxide intermediate which subsequently inserts CO₂. The amide complex initiates the copolymerization by first inserting CO₂ into the Zn–N bond and subsequent elimination of trimethylsilyl isocyanate.⁹⁶⁵

The substituents on the ancillary β -diketiminate ligand play a crucial role in determining the activity of these catalysts. Hence, although (335) and (336) are highly active, the less bulky (337) and (338) are inactive. The most active example reported is (339) which produces 558 g polymer/g [Zn]/h.



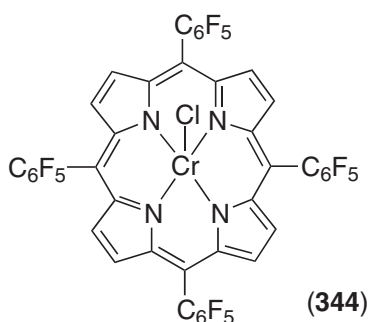
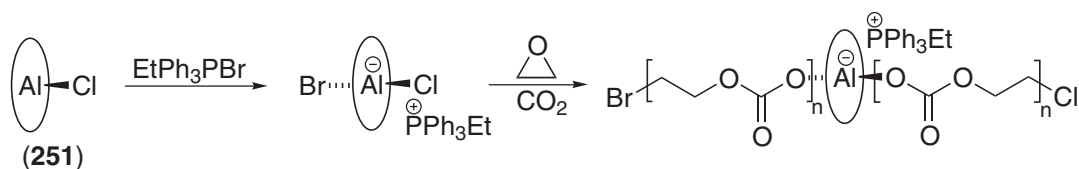
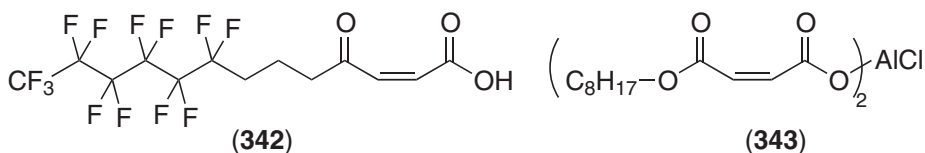
A related enantiomerically pure zinc amide initiator, (340), has also been described.⁹⁶⁶ This complex catalyzes the alternating copolymerization of CHO and CO₂ to yield isotactic material (RR:SS = 86:14). Similar enantiomeric excesses have been achieved using a mixture of Et₂Zn and the chiral amino alcohol (341).⁹⁶⁷ Molecular weight distributions are much broader than using catalyst (340), but this protocol is still a convenient way to prepare optically pure diols (Scheme 23).



The formation of relatively ill-defined catalysts for epoxide/CO₂ copolymerization catalysts, arising from the treatment of ZnO with acid anhydrides or monoesters of dicarboxylic acids, has been described in a patent disclosure.⁹⁶⁸ Employing the perfluoroalkyl ester acid (342) renders the catalyst soluble in supercritical CO₂.⁹⁶⁹ At 110 °C and 2,000 psi this catalyst mixture performs similarly to the zinc bisphenolates, producing a 96:4 ratio of polycarbonate:polyether linkages, with a turnover of 440 g polymer/g [Zn] and a broad polydispersity ($M_w/M_n > 4$). Related aluminum complexes have also been studied and (343) was found to be particularly active. However, selectivity is poor, with a ratio of 1:3.6 polycarbonate:polyether.⁹⁷⁰

Under ambient pressures, the Al^{III}-porphyrinato-alkoxide complex (250) traps CO₂^{971,972} and subsequent addition of EO affords the cyclic carbonate.⁹⁷³ However, at higher pressures (50 kg cm⁻²) (TPP)AlX complexes initiate the copolymerization of PO and CO₂, although activities are

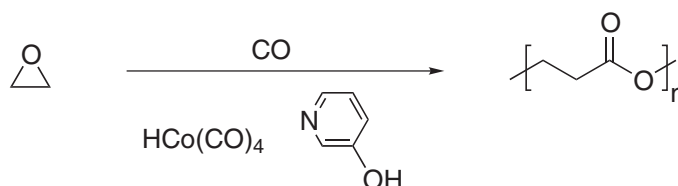
poor and the reaction affords only moderate polycarbonate content.^{974–976} Polycarbonates with no discernible polyether content may be prepared using a mixture of (251) and a quaternary ammonium or phosphonium salt.⁹⁷⁷ Copolymers of CO₂ with EO, PO, and CHO have all been reported with M_w/M_n values of 1.06–1.14, although this process is extremely slow (several weeks). The addition of EtPh₃PBr (or Et₄NBr) generates a bifunctional initiator^{978,979} which allows chain growth to proceed simultaneously on both sides of the porphyrin plane. Evidence for such a mechanism includes molecular weights which are approximately half the calculated values based upon [M]₀/[I]₀ ratios.



More recently, a CO₂-soluble chromium(III)–porphyrin catalyst, (344), has been reported to initiate the copolymerization of CO₂ with CHO.⁹⁸⁰ Carbonate linkages of >90% are observed and M_w/M_n values are consistently low (1.1–1.4). Complex (344) is highly active, producing 3,900 g polymer/g [Cr] over 18 hours; even higher activities have been achieved by supporting the catalyst on polymer beads.⁹⁸¹

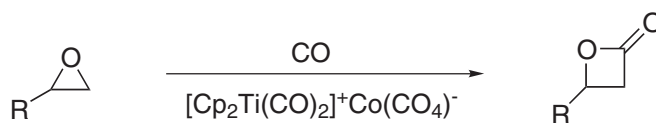
9.1.7.5 Copolymerization of Epoxides and Aziridines with Carbon Monoxide

A 1992 patent describes the carbonylation of EO to yield β-propiolactone using a mixture of Co₂(CO)₈ and 3-hydroxypyridine.⁹⁸² A recent re-investigation of this system has indicated that the major product is the alternating copolymer, a polyester, catalyzed by the [Co(CO)₄][−] anion (Scheme 24).⁹⁸³ The synthesis of lactones via this methodology has successfully been achieved using Lewis acidic counter-cations (Scheme 25),^{984,985} a similar strategy allows β-lactams to be

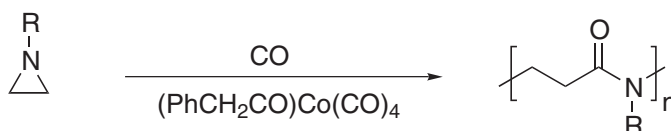


Scheme 24

prepared via the carbonylation of aziridines.⁹⁸⁶ The living copolymerization of carbon monoxide with aziridines to afford polyamides has also recently been described (Scheme 26).^{987,988}



Scheme 25

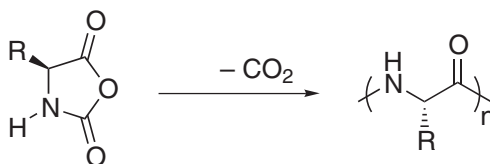


Scheme 26

9.1.8 OTHER LIVING COORDINATION POLYMERIZATIONS

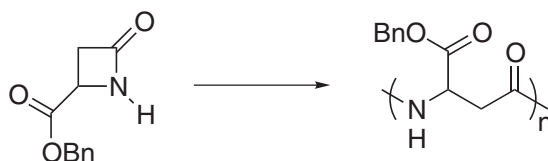
9.1.8.1 ROP of N-carboxyanhydrides and β -lactams

The synthesis of high molecular weight polypeptides can be accomplished by the ROP of α -amino acid-N-carboxyanhydrides (α -NCAs) as shown in (Scheme 27).⁹⁸⁹ Traditional catalysts for this process include group 1 alkoxides and organic amines.⁹⁹⁰ More recently, zerovalent late transition metals, such as (bipy)Ni(COD)^{991,992} and Co(PMe₃)₄,⁹⁹³ have been shown to initiate the living polymerizations of α -NCAs. High molecular weight, low polydispersity ($M_w/M_n < 1.20$) poly(α -peptide)s, and block copolymers may therefore be prepared as detailed in recent review articles.^{994,995}



Scheme 27

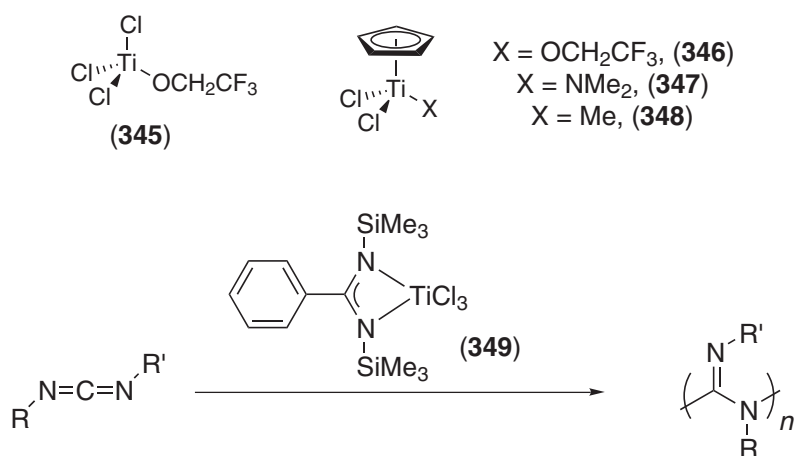
Low molecular weight poly(β -peptide)s may be synthesized in an analogous manner via the ROP of β -amino acid-N-carboxyanhydrides.⁹⁹⁶ Longer chain materials may be prepared by the ROP of β -lactams (Scheme 28). This polymerization is initiated by a range of metal amides, of which Sc[N(TMS)₂]₃ offers particularly high levels of control.⁹⁹⁷



Scheme 28

9.1.8.2 Polymerization of Isocyanates and Guanidines

The anionic polymerization of isocyanates using NaCN as an initiator was first reported in 1960.⁹⁹⁸ The living coordinative polymerization of *n*-hexylisocyanate has been described using the titanium(IV) complexes (345)–(348).^{999–1001} A trifunctional initiator has also been used to prepare star polyisocyanates.¹⁰⁰²



Scheme 29

Structurally related complexes are also active initiators for the living polymerization of carbodiimides (which are isoelectronic to isocyanates).¹⁰⁰³ The proposed intermediate for this polymerization process is a metal amidinate (Scheme 29), and the model complex (349) has been reported to be a highly efficient catalyst, polymerizing 500 equivalents of di-*n*-hexylcarbodiimide in less than 10 s. A more hydrolytically robust series of initiators has also been developed, based upon copper(I) and copper(II) amidinates.¹⁰⁰⁴

9.1.9 REFERENCES

- Ziegler, K.; Holzcamp, E.; Breil, H.; Martin, H. *Angew. Chem.* **1955**, *67*, 541.
- Ziegler, K. *Angew. Chem.* **1964**, *76*, 545.
- Natta, G. *Angew. Chem.* **1956**, *68*, 393.
- Natta, G. *Angew. Chem.* **1964**, *76*, 553.
- Kaminsky, W. *Adv. Catal.* **2001**, *46*, 89.
- Kaminsky, W. *J. Chem. Soc. Dalton Trans.* **1998**, 1413.
- Coates, G. W.; Hustad, P. D.; Reinartz, S. *Angew. Chem., Int. Ed. Engl.* **2002**, *41*, 2236.
- Britovsek, G. J. P.; Gibson, V. C.; Wass, D. F. *Angew. Chem., Int. Ed. Engl.* **1999**, *38*, 428.
- Coates, G. W. *J. Chem. Soc. Dalton Trans.* **2002**, 467.
- Coates, G. W. *Chem. Rev.* **2000**, *100*, 1223.
- Gibson, V. C.; Spitzmesser, S. *Chem. Rev.* **2003**, *103*, 283.
- Hagen, H.; Boersma, J.; van Koten, G. *Chem. Soc. Rev.* **2002**, *31*, 357.
- Sinn, H.; Kaminsky, W. *Adv. Organomet. Chem.* **1980**, *18*, 99.
- Soga, K.; Shiono, T. *Prog. Polym. Sci.* **1997**, *22*, 1503.
- Alt, H. G.; Köppl, A. *Chem. Rev.* **2000**, *100*, 1205.
- Breslow, D. S.; Newburg, N. R. *J. Am. Chem. Soc.* **1959**, *81*, 81.
- Breslow, D. S.; Newburg, N. R. *J. Am. Chem. Soc.* **1957**, *79*, 5072.
- Natta, G.; Pino, P.; Mazzanti, G.; Giannini, U. *J. Am. Chem. Soc.* **1957**, *79*, 2975.
- Reichert, K. H.; Meyer, K. R. *Makromol. Chem.* **1973**, *169*, 163.
- Long, W. P.; Breslow, D. S. *Liebigs Ann. Chem.* **1975**, 463.
- Andresen, A.; Cordes, H. G.; Herwig, J.; Kaminsky, W.; Merck, A.; Mottweiler, R.; Pein, J.; Sinn, H.; Vollmer, H. J. *Angew. Chem., Int. Ed. Engl.* **1976**, *15*, 630.
- Sinn, H.; Kaminsky, W.; Vollmer, H. J.; Woldt, R. *Angew. Chem., Int. Ed. Engl.* **1980**, *19*, 390.
- Herwig, J.; Kaminsky, W. *Polym. Bull.* **1983**, *9*, 464.
- Möhrling, P. C.; Coville, N. J. *J. Organomet. Chem.* **1994**, *479*, 1.
- Alt, H. G.; Milius, W.; Palackal, S. J. *J. Organomet. Chem.* **1994**, *472*, 113.
- Naga, N.; Mizunuma, K. *Macromol. Chem. Phys.* **1998**, *199*, 113.
- Kaminsky, W.; Luker, H. *Macromol. Chem. Rapid Commun.* **1989**, *5*, 225.
- Blom, R.; Dahl, I. M. *Macromol. Chem. Phys.* **1999**, *200*, 442.
- Chien, J. C. W.; Wang, B. P., *J. Polym. Sci., A Polym. Chem.* **1990**, *28*, 15.
- Frauenrath, H.; Keul, H.; Höcker, H. *Macromol. Chem. Phys.* **2001**, *202*, 3543.
- Dyachkovskii, F. S.; Shilova, A. K.; Shilov, A. E. *J. Polym. Sci. C.* **1967**, *16*, 2333.
- Eisch, J. J.; Piotrowski, A. M.; Brownstein, S. K.; Gabe, E. J.; Lee, F. L. *J. Am. Chem. Soc.* **1985**, *107*, 7219.
- Jordan, R. F.; Bajgur, C. S.; Willett, R.; Scott, B. *J. Am. Chem. Soc.* **1986**, *108*, 7410.
- Jordan, R. F.; LaPointe, R. E.; Bajgur, C. S.; Echols, S. F.; Willett, R. *J. Am. Chem. Soc.* **1987**, *109*, 4111.
- Jordan, R. F. *Adv. Organomet. Chem.* **1991**, *32*, 325.

36. Bochmann, M.; Wilson, L. M. *Chem. Commun.* **1986**, 1610.
37. Bochmann, M.; Wilson, L. M.; Hursthouse, M. B.; Short, R. L. *Organometallics* **1987**, *6*, 2556.
38. Bochmann, M. *J. Chem. Soc. Dalton Trans.* **1996**, 255.
39. Yang, X.; Stern, C. L.; Marks, T. J. *Organometallics* **1991**, *10*, 840.
40. Yang, X.; Stern, C. L.; Marks, T. J. *J. Am. Chem. Soc.* **1991**, *113*, 3623.
41. Yang, X.; Stern, C. L.; Marks, T. J. *J. Am. Chem. Soc.* **1994**, *116*, 10015.
42. Chen, E. Y. X.; Marks, T. J. *Chem. Rev.* **2000**, *100*, 1391.
43. Piers, W. E.; Chivers, T. *Chem. Soc. Rev.* **1997**, *26*, 345.
44. Brintzinger, H. H.; Fischer, D.; Mülhaupt, R.; Rieger, B.; Waymouth, R. M. *Angew. Chem., Int. Ed. Engl.* **1995**, *34*, 1143.
45. Ewen, J. A. *J. Am. Chem. Soc.* **1984**, *106*, 6355.
46. Kaminsky, W.; Külper, K.; Brintzinger, H. H.; Wild, F. R. W. P. *Angew. Chem., Int. Ed. Engl.* **1985**, *24*, 507.
47. Ewen, J. A.; Haspelslach, L.; Atwood, J. L.; Zhang, H. J. *J. Am. Chem. Soc.* **1987**, *109*, 6544.
48. Mise, T.; Miya, S.; Yamazaki, H. *Chem. Lett.* **1989**, 1853.
49. Röhl, W.; Brintzinger, H. H.; Rieger, B.; Zolk, R. *Angew. Chem., Int. Ed. Engl.* **1990**, *29*, 279.
50. Spaleck, W.; Aulbach, M.; Bachmann, B.; Küber, F.; Winter, A. *Macromol. Symp.* **1995**, *89*, 237.
51. Spaleck, W.; Antberg, M.; Rohrmann, J.; Winter, A.; Bachmann, B.; Kiprof, P.; Behm, J.; Herrmann, W. A. *Angew. Chem., Int. Ed. Engl.* **1992**, *31*, 1347.
52. Spaleck, W.; Küber, F.; Winter, A.; Rohrmann, J.; Bachmann, B.; Antberg, M.; Dolle, V.; Paulus, E. F. *Organometallics* **1994**, *13*, 954.
53. Stehling, U.; Diebold, J.; Kirsten, R.; Röhl, W.; Brintzinger, H. H.; Jüngling, S.; Mülhaupt, R.; Langhauser, F. *Organometallics* **1994**, *13*, 964.
54. Erker, G.; Temme, B. *J. Am. Chem. Soc.* **1992**, *114*, 4004.
55. Ravazi, A.; Atwood, J. L. *J. Am. Chem. Soc.* **1993**, *115*, 7529.
56. Starzewski, K. A. O.; Kelly, W. M.; Stumpf, A.; Freitag, D. *Angew. Chem., Int. Ed. Engl.* **1999**, *38*, 2439.
57. Resconi, L.; Cavallo, L.; Fait, A.; Piemontesi, F. *Chem. Rev.* **2000**, *100*, 1253.
58. Corradini, P.; Guerra, G. *Prog. Polym. Sci.* **1991**, *16*, 239.
59. Longo, P.; Grassi, A.; Pellecchia, C.; Zambelli, A. *Macromolecules* **1987**, *20*, 1015.
60. Sacchi, M. C.; Barsties, E.; Tritto, I.; Locatelli, P.; Brintzinger, H. H.; Stehling, U. *Macromolecules* **1997**, *30*, 3955.
61. Pino, P.; Cioni, P.; Wei, J. *J. Am. Chem. Soc.* **1987**, *109*, 6189.
62. Kaminsky, W.; Ahlers, A.; Möller-Lindenhof, N. *Angew. Chem., Int. Ed. Engl.* **1989**, *28*, 1216.
63. Piers, W. E.; Bercaw, J. E. *J. Am. Chem. Soc.* **1990**, *112*, 9406.
64. Krauledat, H.; Brintzinger, H. H. *Angew. Chem., Int. Ed. Engl.* **1990**, *29*, 1412.
65. Leclerc, M. K.; Brintzinger, H. H. *J. Am. Chem. Soc.* **1995**, *117*, 1651.
66. Busico, V.; Cipullo, R. *J. Am. Chem. Soc.* **1994**, *116*, 9329.
67. Busico, V.; Caporaso, L.; Cipullo, R.; Landriani, L.; Angelini, G.; Margonelli, A.; Segre, A. L. *J. Am. Chem. Soc.* **1996**, *118*, 2105.
68. Leclerc, M. K.; Brintzinger, H. H. *J. Am. Chem. Soc.* **1996**, *118*, 9024.
69. Resconi, L.; Fait, A.; Piemontesi, F.; Colonna, M.; Rychlicki, H.; Ziegler, R. *Macromolecules* **1995**, *28*, 6667.
70. Yoder, J. C.; Bercaw, J. E. *J. Am. Chem. Soc.* **2002**, *124*, 2548.
71. Busico, V.; Cipullo, R.; Caporaso, L.; Angelini, G.; Segre, A. L. *J. Mol. Cat. A Chem.* **1998**, *128*, 53.
72. Giardello, M. A.; Eisen, M. S.; Stern, C. L.; Marks, T. J. *J. Am. Chem. Soc.* **1993**, *115*, 3326.
73. Giardello, M. A.; Eisen, M. S.; Stern, C. L.; Marks, T. J. *J. Am. Chem. Soc.* **1995**, *117*, 12114.
74. Kaminsky, W.; Rabe, O.; Schauwienold, A. M.; Schupfner, G. U.; Hanss, J.; Kopf, J. *J. Organomet. Chem.* **1995**, *497*, 181.
75. Ewen, J. A. *Macromol. Symp.* **1995**, *89*, 181.
76. Miyake, S.; Okumura, Y.; Inazawa, S. *Macromolecules* **1995**, *28*, 3074.
77. Ewen, J. A.; Jones, R. L.; Ravazi, A.; Ferrara, J. D. *J. Am. Chem. Soc.* **1988**, *110*, 6255.
78. Farina, M.; Di Silvestro, G.; Sozzani, P. *Macromolecules* **1993**, *26*, 946.
79. Ewen, J. A. *J. Mol. Cat. A Chem.* **1998**, *128*, 103.
80. Cavallo, L.; Guerra, G.; Vacatello, M.; Corradini, P. *Macromolecules* **1991**, *24*, 1784.
81. Herzog, T. A.; Zubris, D. L.; Bercaw, J. E. *J. Am. Chem. Soc.* **1996**, *118*, 11988.
82. Ravazi, A.; Atwood, J. L. *J. Organomet. Chem.* **1993**, *459*, 117.
83. Chen, Y. X.; Rausch, M. D.; Chien, J. C. W. *J. Organomet. Chem.* **1995**, *497*, 1.
84. Patsidis, K.; Alt, H. G.; Milius, W.; Palackal, S. J. *J. Organomet. Chem.* **1996**, *509*, 63.
85. Lee, M. H.; Park, J. W.; Hong, C. S.; Woo, S. I.; Do, Y. *J. Organomet. Chem.* **1998**, *561*, 37.
86. Schaverien, C. J.; Ernst, R.; Terlouw, W.; Schut, P.; Sudmeijer, O.; Budzelaar, P. H. M. *J. Mol. Cat. A Chem.* **1998**, *128*, 245.
87. Ravazi, A.; Atwood, J. L. *J. Organomet. Chem.* **1995**, *497*, 105.
88. Alt, H. G.; Zenk, R.; Milius, W. *J. Organomet. Chem.* **1996**, *514*, 257.
89. Alt, H. G.; Zenk, R. *J. Organomet. Chem.* **1996**, *526*, 295.
90. Alt, H. G.; Zenk, R. *J. Organomet. Chem.* **1996**, *522*, 39.
91. Alt, H. G.; Zenk, R. *J. Organomet. Chem.* **1996**, *522*, 177.
92. Peifer, B.; Milius, W.; Alt, H. G. *J. Organomet. Chem.* **1998**, *553*, 205.
93. Alt, H. G.; Samuel, E. *Chem. Soc. Rev.* **1998**, *27*, 323.
94. Miller, S. A.; Bercaw, J. E. *Organometallics* **2002**, *21*, 934.
95. Miyake, S.; Bercaw, J. E. *J. Mol. Cat. A Chem.* **1998**, *128*, 29.
96. Veghini, D.; Day, M. W.; Bercaw, J. E. *Inorg. Chim. Acta.* **1998**, *280*, 226.
97. Veghini, D.; Henling, L. M.; Burkhardt, T. J.; Bercaw, J. E. *J. Am. Chem. Soc.* **1999**, *121*, 564.
98. Natta, G. *J. Polym. Sci.* **1959**, *34*, 531.
99. Mallin, D. T.; Rausch, M. D.; Lin, Y. G.; Dong, S.; Chien, J. C. W. *J. Am. Chem. Soc.* **1990**, *112*, 2030.
100. Chien, J. C. W.; Llinas, G. H.; Rausch, M. D.; Lin, G. Y.; Winter, H. H.; Atwood, J. L.; Bott, S. G. *J. Am. Chem. Soc.* **1991**, *113*, 8569.

101. Chien, J. C. W.; Iwamoto, Y.; Rausch, M. D.; Wedler, W.; Winter, H. H. *Macromolecules* **1997**, *30*, 3447.
102. Chien, J. C. W.; Iwamoto, Y.; Rausch, M. D. *J. Polym. Sci. A Polym. Chem.* **1999**, *37*, 2439.
103. Gauthier, W. J.; Corrigan, J. F.; Taylor, N. J.; Collins, S. *Macromolecules* **1995**, *28*, 3771.
104. Gauthier, W. J.; Collins, S. *Macromolecules* **1995**, *28*, 3779.
105. Bravakis, A. M.; Bailey, L. E.; Pigeon, M.; Collins, S. *Macromolecules* **1998**, *31*, 1000.
106. Coates, G. W.; Waymouth, R. M. *Science* **1995**, *267*, 217.
107. Lin, S.; Waymouth, R. M. *Acc. Chem. Res.* **2002**, *35*, 765.
108. Busico, V.; Cipullo, R.; Kretschmer, W.P.; Talarico, G.; Vacatello, M.; Van Axel Castelli, V. *Angew. Chem., Int. Ed. Engl.* **2002**, *41*, 505.
109. Canich, J. M.; Hlatky, G. G.; Turner, H. PCT Appl. WO92-00333, 1992.
110. Stevens, J. C.; Timmers, F. J.; Wilson, D. R.; Schmidt, G. F.; Nickias, P. N.; Rosen, R. K.; Knight, G. W.; Lai, S. Eur. Pat. Appl. EP 416,815-A2, 1991.
111. Okuda, J. *Chem. Ber.* **1990**, *123*, 1649.
112. McKnight, A. L.; Waymouth, R. M. *Chem. Rev.* **1998**, *98*, 2587.
113. Chen, Y. X.; Marks, T. J. *Organometallics* **1997**, *16*, 3649.
114. Imanishi, Y.; Naga, N. *Prog. Polym. Sci.* **2001**, *26*, 1147.
115. Santos, J. M.; Ribiero, M. R.; Portela, M. F.; Cramail, H.; Deffieux, A.; Antiñolo, A.; Otero, A.; Prashar, S. *Macromol. Chem. Phys.* **2002**, *203*, 139.
116. Marques, M. M.; Correia, S. G.; Ascenso, J. R.; Ribiero, A. F. G.; Gomes, P. T.; Dias, A. R.; Foster, P.; Rausch, M. D.; Chien, J. C. W. *J. Polym. Sci. Polym. Chem.* **1999**, *37*, 2457.
117. Gomes, P. T.; Green, M. L. H.; Martins, A. M.; Mountford, P. *J. Organomet. Chem.* **1997**, *541*, 121.
118. Gomes, P. T.; Green, M. L. H.; Martins, A. M. *J. Organomet. Chem.* **1998**, *551*, 133.
119. Sinnema, P. J.; van der Veen, L.; Spek, A. L.; Veldman, N.; Teuben, J. H. *Organometallics* **1997**, *16*, 4245.
120. van Leusen, D.; Beetstra, D. J.; Hessen, B.; Teuben, J. H. *Organometallics* **2000**, *19*, 4084.
121. Duda, L.; Erker, G.; Fröhlich, R.; Zippel, F. *Eur. J. Inorg. Chem.* **1998**, 1153.
122. Kunz, K.; Erker, G.; Döring, S.; Bredeau, S.; Kehr, G.; Fröhlich, R. *Organometallics* **2002**, *21*, 1031.
123. Sinnema, P. J.; Liekelema, K.; Staal, O. K. B.; Hessen, B.; Teuben, J. H. *J. Mol. Catal. A Chem.* **1998**, *128*, 143.
124. Okuda, J.; Schattenmann, F. J.; Wocaldo, S.; Massa, W. *Organometallics* **1995**, *14*, 789.
125. Kotov, V. V.; Avtomonov, E. V.; Sundermeyer, J.; Harms, K.; Lemenovskii, D. A. *Eur. J. Inorg. Chem.* **2002**, 678.
126. Rhodes, B.; Chien, J. C. W.; Wood, J. S.; Chandrasekaran, A.; Rausch, M. D. *Appl. Organomet. Chem.* **2002**, *16*, 323.
127. Kleinschmidt, R.; Griebenow, Y.; Fink, G. *J. Mol. Catal. A Chem.* **2000**, *157*, 83.
128. Hasan, T.; Ioku, A.; Nishii, K.; Shiono, T.; Ikeda, T. *Macromolecules* **2001**, *34*, 3142.
129. Gielen, E. E. C. G.; Tiesnitsch, J. Y.; Hessen, B.; Teuben, J. H. *Organometallics* **1998**, *17*, 1652.
130. Rieger, B. *J. Organomet. Chem.* **1991**, *420*, C17.
131. Chen, Y. X.; Fu, P. F.; Stern, C. L.; Marks, T. J. *Organometallics* **1997**, *16*, 5958.
132. Kunz, K.; Erker, G.; Döring, S.; Fröhlich, R.; Kehr, G. *J. Am. Chem. Soc.* **2001**, *123*, 6181.
133. Canich, J. A. M. U. S. Pat. 5,026,798, 1990.
134. Shah, S. A. A.; Dorn, H.; Voigt, A.; Roesky, H. W.; Parisini, E.; Schmidt, H.G.; Noltemeyer, M. *Organometallics* **1996**, *15*, 3176.
135. Scollard, J. D.; McConville, D. H. *J. Am. Chem. Soc.* **1996**, *118*, 10008.
136. Scollard, J. D.; McConville, D. H.; Payne, N.C.; Vittal, J. J. *Macromolecules* **1996**, *29*, 5241.
137. Scollard, J. D.; McConville, D. H.; Vittal, J. J. *Organometallics* **1997**, *16*, 4415.
138. Hagimoto, H.; Shiono, T.; Ikeda, T. *Macromol. Chem. Rapid Commun.* **2002**, *23*, 73.
139. Jin, J.; Tsubaki, S.; Uozumi, T.; Sano, T.; Soga, K. *Macromol. Chem. Rapid Commun.* **1998**, *19*, 597.
140. Gibson, V. C.; Kimberley, B. S.; White, A. J. P.; Williams, D. J.; Howard, P. *Chem. Commun.* **1998**, 313.
141. Horton, A. D.; von Hebel, K. L.; de With, J. *Macromol. Symp.* **2001**, *173*, 123.
142. Patton, J. T.; Bokota, M. M.; Abboud, K. A. *Organometallics* **2002**, *21*, 2145.
143. Patton, J. T.; Feng, S. G.; Abboud, K. A. *Organometallics* **2001**, *20*, 3399.
144. Lee, C. H.; La, Y. H.; Park, J. W. *Organometallics* **2000**, *19*, 344.
145. Guérin, F.; McConville, D. H.; Vittal, J. J. *Organometallics* **1996**, *15*, 5586.
146. Guérin, F.; McConville, D. H.; Payne, N. C. *Organometallics* **1996**, *15*, 5085.
147. Mehrkhodavandi, P.; Schrock, R. R. *J. Am. Chem. Soc.* **2001**, *123*, 10746.
148. Mehrkhodavandi, P.; Bonitatebus, P. J.; Schrock, R. R. *J. Am. Chem. Soc.* **2000**, *122*, 7841.
149. Liang, L. C.; Schrock, R. R.; Davis, W. M.; McConville, D. H. *J. Am. Chem. Soc.* **1999**, *121*, 5797.
150. Baumann, R.; Davis, W. M.; Schrock, R. R. *J. Am. Chem. Soc.* **1997**, *119*, 3830.
151. Baumann, R.; Stumpf, R.; Davis, W. M.; Liang, L. C.; Schrock, R. R. *J. Am. Chem. Soc.* **1999**, *121*, 7822.
152. Graf, D. D.; Schrock, R. R.; Davis, W. M.; Stumpf, R. *Organometallics* **1999**, *18*, 843.
153. Flores, M. A.; Manzoni, M. R.; Baumann, R.; Davis, W. M.; Schrock, R. R. *Organometallics* **1999**, *18*, 3220.
154. Aizenberg, M.; Turculet, L.; Davis, W. M.; Schattenmann, F.; Schrock, R. R. *Organometallics* **1998**, *17*, 4795.
155. Schrock, R. R.; Schattenmann, F.; Aizenberg, M.; Davis, W. M. *Chem. Commun.* **1998**, 199.
156. O'Connor, P. E.; Morrison, D. J.; Steeves, S.; Burrage, K.; Berg, D. J. *Organometallics* **2001**, *20*, 1153.
157. Lee, L.; Berg, D. J.; Bushnell, G. W. *Organometallics* **1997**, *16*, 2556.
158. Gómez, R.; Green, M. L. H.; Haggitt, J. L. *Chem. Commun.* **1994**, 2607.
159. Herskovics-Korine, D.; Eisen, M. S. *J. Organomet. Chem.* **1995**, *503*, 307.
160. Walthers, D.; Fischer, R.; Görls, H.; Koch, J.; Schweder, B. *J. Organomet. Chem.* **1996**, *508*, 13.
161. Littke, A.; Sleiman, N.; Bensimon, C.; Richeson, D. S.; Yap, G. P. A.; Brown, S. J. *Organometallics* **1998**, *17*, 446.
162. Hagadorn, J. R.; Arnold, J. *J. Chem. Soc. Dalton Trans.* **1997**, 3087.
163. Volkis, V.; Shmulinson, M.; Averbuj, C.; Lisoovskii, A.; Edelman, F. T.; Eisen, M. S. *Organometallics* **1998**, *17*, 3155.
164. Richter, J.; Edelman, F. T.; Noltemeyer, M.; Schmidt, H. G.; Shmulinson, M.; Eisen, M. S. *J. Mol. Catal. A Chem.* **1998**, *130*, 149.
165. Averbuj, C.; Tish, E.; Eisen, M. S. *J. Am. Chem. Soc.* **1998**, *120*, 8640.
166. Jayaratne, K. C.; Sita, L. R. *J. Am. Chem. Soc.* **2000**, *122*, 958.
167. Keaton, R. J.; Jayaratne, K. C.; Henningsen, D. A.; Koterwas, L. A.; Sita, L. R. *J. Am. Chem. Soc.* **2001**, *123*, 6197.

168. Vollmerhaus, R.; Shao, P.; Taylor, N. J.; Collins, S. *Organometallics* **1999**, *18*, 2731.
169. Stephan, D. W.; Guérin, F.; Spence, R. E. v.H.; Koch, L.; Gao, X.; Brown, S. J.; Swabey, J. W.; Wang, Q.; Xu, W.; Zoricak, P.; Harrison, D. G. *Organometallics* **1999**, *18*, 2046.
170. Stephan, D. W.; Stewart, J. C.; Guérin, F.; Spence, R. E. v.H.; Xu, W.; Harrison, D. G. *Organometallics* **1999**, *18*, 1116.
171. Yue, N. L. S.; Stephan, D. W. *Organometallics* **2001**, *20*, 2303.
172. Duncan, A. P.; Mullins, S. M.; Arnold, J.; Bergman, R. G. *Organometallics* **2001**, *20*, 1808.
173. Vollmerhaus, R.; Rahim, M.; Tomaszewski, R.; Xin, S. X.; Taylor, N. J.; Collins, S. *Organometallics* **2000**, *19*, 2161.
174. Rahim, M.; Taylor, N. J.; Xin, S.; Collins, S. *Organometallics* **1998**, *17*, 1315.
175. Yoshida, Y.; Matsui, S.; Takagi, Y.; Mitani, M.; Nakano, T.; Tanaka, H.; Kashiwa, N.; Fujita, T. *Organometallics* **2001**, *20*, 4793.
176. Yoshida, Y.; Saito, J.; Mitani, M.; Takagi, Y.; Matsui, S.; Ishii, S.; Nakano, T.; Kashiwa, N.; Fujita, T. *Chem. Commun.* **2002**, 1298.
177. Matsugi, T.; Matsui, S.; Kojoh, S.; Takagi, Y.; Inoue, Y.; Fujita, T.; Kashiwa, N. *Chem. Lett.* **2001**, 566.
178. Matsugi, T.; Matsui, S.; Kojoh, S.; Takagi, Y.; Inoue, Y.; Nakano, T.; Fujita, T.; Kashiwa, N. *Macromolecules* **2002**, *35*, 4880.
179. Brand, H.; Capriotti, J. A.; Arnold, J. *Organometallics* **1994**, *13*, 4469.
180. Uhrhammer, R.; Black, D. G.; Gardner, T. G.; Olsen, J. D.; Jordan, R. F. *J. Am. Chem. Soc.* **1993**, *115*, 8493.
181. Antiñolo, A.; Carrillo-Hermosilla, F.; Corrochano, A.; Fernández-Baeza, J.; Lara-Sanchez, A.; Ribiero, M. R.; Lanfranchi, M.; Otero, A.; Pellinghelli, M. A.; Portela, M. F.; Santos, J. V. *Organometallics* **2000**, *19*, 2837.
182. Nomura, K.; Naga, N.; Miki, M.; Yanagi, K.; Imai, A. *Organometallics* **1998**, *17*, 2152.
183. Nomura, K.; Naga, N.; Miki, M.; Yanagi, K. *Macromolecules* **1998**, *31*, 7588.
184. Nomura, K.; Komatsu, T.; Nakamura, M.; Imanishi, Y. *J. Mol. Catal. A Chem.* **2000**, *164*, 131.
185. Nomura, K.; Komatsu, T.; Imanishi, Y. *Macromolecules* **2000**, *33*, 8122.
186. Nomura, K.; Komatsu, T.; Imanishi, Y. *J. Mol. Catal. A Chem.* **2000**, *152*, 249.
187. Nomura, K.; Komatsu, T.; Imanishi, Y. *J. Mol. Catal. A Chem.* **2000**, *159*, 127.
188. Nomura, K.; Oya, K.; Imanishi, Y. *J. Mol. Catal. A Chem.* **2001**, *174*, 127.
189. Nomura, K.; Oya, K.; Komatsu, T.; Imanishi, Y. *Macromolecules* **2000**, *33*, 3187.
190. van der Linden, A.; Schaverien, C. J.; Meijboom, N.; Ganter, C.; Orpen, A. G. *J. Am. Chem. Soc.* **1995**, *117*, 3008.
191. Miyatake, T.; Mizunuma, K.; Seki, Y.; Kakugo, M. *Macromol. Chem. Rapid Commun.* **1989**, *10*, 349.
192. Miyatake, T.; Mizunuma, K.; Kakugo, M. *Macromol. Symp.* **1993**, *66*, 203.
193. Repo, T.; Klinga, M.; Pietikäinen, P.; Leskelä, M.; Uusitalo, A. M.; Pakkanen, T.; Hakala, K.; Aaltonen, P.; Löfgren, B. *Macromolecules* **1997**, *30*, 171.
194. Knight, P. D.; Clarke, A. J.; Kimberley, B. S.; Jackson, R. A.; Scott, P. *Chem. Commun.* **2002**, 352.
195. Corden, J. P.; Errington, W.; Moore, P.; Wallbridge, M. G. H. *Chem. Commun.* **1999**, 323.
196. Huang, J.; Lian, B.; Yong, L. Qian, Y. *Inorg. Chem. Commun.* **2001**, *4*, 392.
197. Matsui, S.; Tohi, Y.; Mitani, M.; Saito, J.; Makio, H.; Tanaka, H.; Nitabaru, M.; Nakano, T.; Fujita, T. *Chem. Lett.* **1999**, 1065.
198. Matsui, S.; Mitani, M.; Saito, J.; Tohi, Y.; Makio, H.; Tanaka, H.; Fujita, T. *Chem. Lett.* **1999**, 1263.
199. Matsui, S.; Mitani, M.; Saito, J.; Matsukawa, N.; Tanaka, H.; Nakano, T.; Fujita, T. *Chem. Lett.* **2000**, 554.
200. Matsui, S.; Mitani, M.; Saito, J.; Tohi, Y.; Makio, H.; Matsukawa, N.; Takagi, Y.; Tsuru, K.; Nitabaru, M.; Nakano, T.; Tanaka, H.; Kashiwa, N.; Fujita, T. *J. Am. Chem. Soc.* **2001**, *123*, 6847.
201. Matsui, S.; Fujita, T. *Catal. Today* **2001**, *66*, 61.
202. Suzuki, Y.; Kashiwa, N.; Fujita, T. *Chem. Lett.* **2002**, 358.
203. Tian, J.; Coates, G. W. *Angew. Chem., Int. Ed. Engl.* **2000**, *39*, 3626.
204. Tian, J.; Hustad, P. D.; Coates, G. W. *J. Am. Chem. Soc.* **2001**, *123*, 5134.
205. Hustad, P. D.; Tian, J.; Coates, G. W. *J. Am. Chem. Soc.* **2002**, *124*, 3614.
206. Saito, J.; Mitani, M.; Onda, M.; Mohri, J. I.; Ishii, S. I.; Yoshida, Y.; Nakano, T.; Tanaka, H.; Matsugi, T.; Kojoh, S. I.; Kashiwa, N.; Fujita, T. *Macromol. Chem. Rapid Commun.* **2001**, *22*, 1072.
207. Saito, J.; Mitani, M.; Mohri, J.; Ishii, S.; Yoshida, Y.; Matsugi, T.; Kojoh, S.; Kashiwa, N.; Fujita, T. *Chem. Lett.* **2001**, 576.
208. Saito, J.; Mitani, M.; Mohri, J.; Yoshida, Y.; Matsui, S.; Ishii, S.; Kojoh, S.; Kashiwa, N.; Fujita, T. *Angew. Chem., Int. Ed. Engl.* **2001**, *40*, 2918.
209. Mitani, M.; Mohri, J.; Yoshida, Y.; Saito, J.; Ishii, S.; Tsuru, K.; Matsui, S.; Furuyama, R.; Nakano, T.; Tanaka, H.; Kojoh, S.; Matsugi, T.; Kashiwa, N.; Fujita, T. *J. Am. Chem. Soc.* **2002**, *124*, 3327.
210. Tshuva, E. Y.; Versano, M.; Goldberg, I.; Kol, M.; Weitman, H.; Goldschmidt, Z. *Inorg. Chem. Commun.* **1999**, *2*, 371.
211. Tshuva, E. Y.; Goldberg, I.; Kol, M.; Weitman, H.; Goldschmidt, Z. *Chem. Commun.* **2000**, 379.
212. Tshuva, E. Y.; Goldberg, I.; Kol, M.; Goldschmidt, Z. *Inorg. Chem. Commun.* **2000**, *3*, 611.
213. Tshuva, E. Y.; Goldberg, I.; Kol, M.; Goldschmidt, Z. *Chem. Commun.* **2001**, 2120.
214. Tshuva, E. Y.; Groysman, S.; Goldberg, I.; Kol, M.; Goldschmidt, Z. *Organometallics* **2002**, *21*, 662.
215. Tshuva, E. Y.; Goldberg, I.; Kol, M. *J. Am. Chem. Soc.* **2000**, *122*, 10706.
216. Shapiro, P. J.; Cotter, W. D.; Schaefer, W. P.; Labinger, J. A.; Bercaw, J. E. *J. Am. Chem. Soc.* **1994**, *116*, 4623.
217. Shapiro, P. J.; Bunel, E. E.; Schaefer, W. P.; Bercaw, J. E. *Organometallics* **1990**, *9*, 867.
218. Burger, B. J.; Thompson, M. E.; Cotter, W. D.; Bercaw, J. E. *J. Am. Chem. Soc.* **1990**, *112*, 1566.
219. Hajela, S.; Bercaw, J. E. *Organometallics* **1994**, *13*, 1147.
220. Piers, W. E.; Shapiro, P. J.; Bunel, E. E.; Bercaw, J. E. *Synlett* **1990**, 74.
221. Ballard, D. G. H.; Curtis, A.; Holton, J.; McMeeking, J.; Pearce, R. *J. Chem. Soc. Chem. Commun.* **1978**, 994.
222. Mitchell, J. P.; Hajela, S.; Brookhart, S. K.; Hardcastle, K. I.; Henling, L. M.; Bercaw, J. E. *J. Am. Chem. Soc.* **1996**, *118*, 1045.
223. Yasuda, H.; Ihara, E. *Tetrahedron* **1995**, *51*, 4563.
224. Yasuda, H.; Ihara, E.; Morimoto, M.; Nodono, M.; Yoshioka, S.; Furo, M. *Macromol. Symp.* **1995**, *95*, 203.
225. Coughlin, E. B.; Bercaw, J. E. *J. Am. Chem. Soc.* **1992**, *114*, 7606.
226. Jeske, G.; Lauke, H.; Mauer mann, H.; Swepston, P. N.; Schumann, H.; Marks, T. J. *J. Am. Chem. Soc.* **1985**, *107*, 8091.

227. Watson, P. L.; Parshall, G. W. *Acc. Chem. Res.* **1985**, *18*, 51.
228. Watson, P. L. *J. Am. Chem. Soc.* **1982**, *104*, 337.
229. Yasuda, H.; Furo, M.; Yamamoto, H.; Nakamura, A.; Miyake, S.; Kibino, N. *Macromolecules* **1992**, *25*, 5115.
230. Gibson, V. C. *J. Chem. Soc. Dalton Trans.* **1994**, 1607.
231. Coles, M. P.; Gibson, V. C. *Polym. Bull.* **1994**, *33*, 529.
232. Coles, M. P.; Dalby, C. I.; Gibson, V. C.; Little, I. R.; Marshall, E. L.; da Costa, M. H. R.; Mastroianni, S. *J. Organomet. Chem.* **1999**, *591*, 78.
233. Nomura, K.; Sagara, A.; Imanishi, Y. *Chem. Lett.* **2001**, 36.
234. Antonelli, D. M.; Leins, A.; Stryker, J. M. *Organometallics* **1997**, *16*, 2500.
235. Feng, S.; Roof, G. R.; Chen, E. Y. X. *Organometallics* **2002**, *21*, 832.
236. LaPointe, R. E.; Roof, G. R.; Abboud, K. A.; Klosin, J. *J. Am. Chem. Soc.* **2000**, *122*, 9560.
237. Hakala, K.; Löfgren, B.; Polamo, M.; Leskelä, M., *Macromol. Rapid Commun.* **1997**, *18*, 635.
238. Mashima, K.; Fujikawa, S.; Tanaka, Y.; Urata, H.; Oshiki, T.; Tanaka, E.; Nakamura, A. *Organometallics* **1995**, *14*, 2633.
239. Mashima, K.; Fujikawa, S.; Urata, H.; Tanaka, E.; Nakamura, A. *Chem. Commun.* **1994**, 1623.
240. Mashima, K.; Fujikawa, S.; Nakamura, A. *J. Am. Chem. Soc.* **1993**, *115*, 10990.
241. Doi, Y.; Ueki, S.; Keii, T. *Macromolecules* **1979**, *12*, 814.
242. Doi, Y.; Ueki, S.; Keii, T. *Macromol. Chem. Phys.* **1979**, *180*, 1359.
243. Doi, Y.; Suzuki, S.; Soga, K. *Macromol. Chem. Rapid Commun.* **1985**, *6*, 639.
244. Doi, Y.; Suzuki, S.; Soga, K. *Macromolecules* **1986**, *19*, 2896.
245. May, Y.; Reardon, D.; Gambarotta, S.; Yap, G.; Zahalka, H.; Lemay, C. *Organometallics* **1999**, *18*, 2773.
246. Reardon, D.; Conan, F.; Gambarotta, S.; Yap, G.; Wang, Q. *J. Am. Chem. Soc.* **1999**, *121*, 9318.
247. Hogan, J. P. Banks, US Pat. 2,825,721, 1958.
248. Hogan, J. P. *J. Polym. Sci. A* **1970**, *8*, 2637.
249. Karapinka, G. L. US Pat. 3,709,853, 1973.
250. Karol, F. J.; Karapinka, G. L.; Wu, C.; Dow, A. W.; Johnson, R. N.; Garrick, W. L. *J. Polym. Sci. A* **1972**, *10*, 2621.
251. Emrich, R.; Heinemann, O.; Jolly, P. W.; Krüger, C.; Verhovnik, G. P. *J. Organometallics* **1997**, *16*, 1511.
252. Döhring, A.; Göhre, J.; Jolly, P. W.; Kryger, B.; Rust, J.; Verhovnik, G. P. *J. Organometallics* **2000**, *19*, 388.
253. Jensen, V. R.; Angermund, K.; Jolly, P. W.; Børve, K. J. *Organometallics* **2000**, *19*, 403.
254. Döhring, A.; Jensen, V. R.; Jolly, P. W.; Thiel, W.; Weber, J. C. *Organometallics* **2001**, *20*, 2234.
255. Döhring, A.; Jensen, V. R.; Jolly, P. W.; Thiel, W.; Weber, J. C. *Macromol. Symp.* **2001**, *173*, 117.
256. Rogers, J. S.; Bazan, G. C. *Chem. Commun.* **2000**, 1209.
257. Bazan, G. C.; Rogers, J. S.; Fang, C. C. *Organometallics* **2001**, *20*, 2059.
258. Rogers, J. S.; Bu, X.; Bazan, G. C. *Organometallics* **2000**, *19*, 3948.
259. Rogers, J. S.; Bu, X.; Bazan, G. C. *J. Am. Chem. Soc.* **2000**, *122*, 730.
260. Bhandari, G.; Kim, Y.; McFarland, J. M.; Rheingold, A. L.; Theopold, K. H. *Organometallics* **1995**, *14*, 7385.
261. Thomas, B. J.; Theopold, K. H. *J. Am. Chem. Soc.* **1988**, *110*, 5902.
262. White, P. A.; Calabrese, J.; Theopold, K. H. *Organometallics* **1996**, *15*, 5473.
263. Theopold, K. H. *Eur. J. Inorg. Chem.* **1998**, 15.
264. Matsunaga, P. T. Patent WO9,957,159, 1999.
265. Gibson, V. C.; Maddox, P. J.; Newton, C.; Redshaw, C.; Solan, G. A.; White, A. J. P.; Williams, D. J. *Chem. Commun.* **1998**, 1651.
266. Gibson, V. C.; Newton, C.; Redshaw, C.; Solan, G. A.; White, A. J. P.; Williams, D. J. *Eur. J. Inorg. Chem.* **2001**, 1895.
267. Gibson, V. C.; Mastroianni, S.; Newton, C.; Redshaw, C.; Solan, G. A.; White, A. J. P.; Williams, D. J. *J. Chem. Soc. Dalton Trans.* **2000**, 1969.
268. Jones, D. J.; Gibson, V. C.; Green, S. M.; Maddox, P. J. *Chem. Commun.* **2002**, 1038.
269. Köhn, R. D.; Haufe, M.; Mihan, S.; Lilge, D. *Chem. Commun.* **2000**, 1927.
270. Köhn, R. D.; Haufe, M.; Kociok-Köhn, G.; Grimm, S.; Wasserscheid, P.; Keim, W. *Angew. Chem., Int. Ed. Engl.* **2000**, *39*, 4337.
271. Wasserscheid, P.; Grimm, S.; Köhn, R. D.; Haufe, M. *Adv. Synth. Cat.* **2001**, *343*, 814.
272. Small, B. L.; Brookhart, M.; Bennett, A. M. A. *J. Am. Chem. Soc.* **1998**, *120*, 4049.
273. Small, B. L.; Brookhart, M. *J. Am. Chem. Soc.* **1998**, *120*, 7143.
274. Britovsek, G. J. P.; Gibson, V. C.; Kimberley, B. S.; Maddox, P. J.; McTavish, S. J.; Solan, G. A.; White, A. J. P.; Williams, D. J. *Chem. Commun.* **1998**, 849.
275. Britovsek, G. J. P.; Bruce, M.; Gibson, V. C.; Kimberley, B. S.; Maddox, P. J.; Mastroianni, S.; McTavish, S. J.; Redshaw, C.; Solan, G. A.; Stromberg, S.; White, A. J. P.; Williams, D. J. *J. Am. Chem. Soc.* **1999**, *121*, 8728.
276. Small, B. L.; Brookhart, M. *Macromolecules* **1999**, *32*, 2120.
277. Pellecchia, C.; Mazzeo, M.; Pappalardo, D. *Macromol. Rapid Commun.* **1998**, *19*, 651.
278. Gibson, V. C.; Humphries, M. J.; Tellmann, K. P.; Wass, D. F.; White, A. J. P.; Williams, D. J. *Chem. Commun.* **2001**, 2252.
279. Schmidt, G. F.; Brookhart, M. *J. Am. Chem. Soc.* **1985**, *107*, 1443.
280. Tanner, M. J.; Brookhart, M.; DeSimone, J. M. *J. Am. Chem. Soc.* **1997**, *119*, 7617.
281. Brookhart, M.; Lincoln, D. M. *J. Am. Chem. Soc.* **1988**, *110*, 8719.
282. Brookhart, M.; Volpe, A. F.; Lincoln, D. M.; Horvath, I. T.; Millar, J. M. *J. Am. Chem. Soc.* **1990**, *112*, 5634.
283. Brookhart, M.; Grant, B.; Volpe, A. F. *Organometallics* **1992**, *11*, 3920.
284. Brookhart, M.; DeSimone, J. M.; Grant, B. E.; Tanner, M. J. *Macromolecules* **1995**, *28*, 5378.
285. Wang, L.; Flood, T. C. *J. Am. Chem. Soc.* **1992**, *114*, 3169.
286. Wang, L.; Lu, R. S.; Bau, R.; Flood, T. C. *J. Am. Chem. Soc.* **1993**, *115*, 6999.
287. Braca, G.; Raspolli Galletti, A. M.; Di Girolamo, M.; Sbrana, G.; Silla, R.; Ferrarini, P. *J. Mol. Catal. A. Chem.* **1995**, *96*, 203.
288. Klabunde, U.; Ittel, S. D. *J. Mol. Catal.* **1987**, *41*, 123.
289. Klabunde, U.; Mülhaupt, R.; Herskovitz, T.; Janowicz, A. H.; Calabrese, J.; Ittel, S. D. *J. Polym. Sci.* **1987**, *25*, 1989.

290. Keim, W.; Howaldt, F. H.; Goddard, R.; Krüger, C. *Angew. Chem., Int. Ed. Engl.* **1978**, *17*, 466.
291. Wilke, G. *Angew. Chem., Int. Ed. Engl.* **1988**, *27*, 185.
292. Keim, W.; Appel, R.; Storeck, A.; Krüger, C.; Goddard, R. *Angew. Chem., Int. Ed. Engl.* **1981**, *20*, 116.
293. Keim, W.; Appel, R.; Gruppe, S.; Knoch, F. *Angew. Chem., Int. Ed. Engl.* **1987**, *26*, 1012.
294. Ostoja Starzewski, K. A.; Witte, J. *Angew. Chem., Int. Ed. Engl.* **1985**, *24*, 599.
295. Heinicke, J.; Koesling, M.; Brüll, R.; Keim, W.; Pritzkow, H. *Eur. J. Inorg. Chem.* **2000**, 299.
296. Soula, R.; Broyer, J. P.; Llauro, M. F.; Tomov, A.; Spitz, R.; Claverie, J.; Drujon, X.; Malinge, J.; Saudemont, T. *Macromolecules* **2001**, *34*, 2438.
297. Soula, R.; Novat, C.; Tomov, A.; Spitz, R.; Claverie, J.; Drujon, X.; Malinge, J.; Saudemont, T. *Macromolecules* **2001**, *34*, 2022.
298. Liu, W.; Malinoski, J. M.; Brookhart, M. *Organometallics* **2002**, *21*, 2836.
299. Gibson, V. C.; Tomov, A.; White, A. J. P.; Williams, D. J. *Chem. Commun.* **2001**, 719.
300. Gibson, V. C.; Tomov, A. *Chem. Commun.* **2001**, 1964.
301. Komon, Z. J. A.; Bu, X.; Bazan, G. C. *J. Am. Chem. Soc.* **2000**, *122*, 1830.
302. Komon, Z. J. A.; Bu, X.; Bazan, G. C. *J. Am. Chem. Soc.* **2000**, *122*, 12379.
303. Komon, Z. J. A.; Bazan, G. C. *Macromol. Rapid Commun.* **2001**, *22*, 467.
304. Lee, B. Y.; Bazan, G. C.; Vela, J.; Komon, Z. J. A.; Bu, X. *J. Am. Chem. Soc.* **2001**, *123*, 5532.
305. Hicks, F. A.; Brookhart, M. *Organometallics* **2001**, *20*, 3217.
306. Younkin, T. R.; Connor, E. F.; Henderson, J. I.; Friedrich, S. K.; Grubbs, R. H.; Bansleben, D. A. *Science*, **2000**, *287*, 460.
307. Zhang, D.; Jin, G. X.; Hu, N. H. *Chem. Commun.* **2002**, 574.
308. Bauers, F. M.; Mecking, S. *Macromolecules* **2001**, *34*, 1165.
309. Bauers, F. M.; Mecking, S. *Angew. Chem., Int. Ed. Engl.* **2001**, *40*, 3020.
310. Johnson, L. K.; Killian, C. M.; Brookhart, M. *J. Am. Chem. Soc.* **1995**, *117*, 6414.
311. Tempel, D. J.; Johnson, L. K.; Huff, R. L.; White, P. S.; Brookhart, M. *J. Am. Chem. Soc.* **2000**, *122*, 6686.
312. Svedja, S. A.; Johnson, L. K.; Brookhart, M. *J. Am. Chem. Soc.* **1999**, *121*, 10634.
313. Killian, C. M.; Johnson, L. K.; Brookhart, M. *Organometallics* **1997**, *16*, 2005.
314. Killian, C. K.; Tempel, D. J.; Johnson, L. K.; Brookhart, M. *J. Am. Chem. Soc.* **1996**, *118*, 11664.
315. Gates, D. P.; Svejda, S. A.; Oñate, E.; Killian, C. M.; Johnson, L. K.; White, P. S.; Brookhart, M. *Macromolecules* **2000**, *33*, 2320.
316. Pellecchia, C.; Zambelli, A.; Oliva, L.; Pappalardo, D. *Macromolecules* **1996**, *29*, 6990.
317. Milano, G.; Guerra, G.; Pellecchia, C.; Cavallo, L. *Organometallics* **2000**, *19*, 1343.
318. Johnson, L. K.; Mecking, S.; Brookhart, M. *J. Am. Chem. Soc.* **1996**, *118*, 267.
319. Mecking, S.; Johnson, L. K.; Wang, L.; Brookhart, M. *J. Am. Chem. Soc.* **1998**, *120*, 888.
320. Gottfried, A. C.; Brookhart, M. *Macromolecules* **2001**, *34*, 1140.
321. Laine, T. V.; Lappalainen, K.; Liimatta, J.; Aitola, E.; Löfgren, B.; Leskelä, M. *Macromol. Rapid Commun.* **1999**, *20*, 487.
322. Laine, T. V.; Klinga, M.; Leskelä, M. *Eur. J. Inorg. Chem.* **1999**, 959.
323. Laine, T. V.; Piironen, U.; Lappalainen, K.; Klinga, M.; Aitola, E.; Leskelä, M. *J. Organomet. Chem.* **2000**, *606*, 112.
324. Meneghetti, S. P.; Lutz, P. J.; Kress, J. *Organometallics* **1999**, *18*, 2734.
325. Köppl, A.; Alt, H. G. *J. Mol. Catal. A Chem.* **2000**, *154*, 45.
326. Cooley, N. A.; Green, S. M.; Wass, D. F.; Heslop, K.; Orpen, A. G.; Pringle, P. G. *Organometallics* **2001**, *20*, 4769.
327. Duchateau, R.; Meetsma, A.; Teuben, J. H. *Chem. Commun.* **1996**, 223.
328. Coles, M. P.; Jordan, R. F. *J. Am. Chem. Soc.* **1997**, *119*, 8125.
329. Ihara, E.; Young, V. G.; Jordan, R. F. *J. Am. Chem. Soc.* **1998**, *120*, 8277.
330. Bruce, M.; Gibson, V. C.; Redshaw, C.; Solan, G. A.; White, A. J. P.; Williams, D. J. *Chem. Commun.* **1998**, 2523.
331. Talarico, G.; Busico, V.; Budzelaar, P. H. M. *Organometallics* **2001**, *20*, 4721.
332. Talarico, G.; Budzelaar, P. H. M. *Organometallics* **2000**, *19*, 5691.
333. Talarico, G.; Budzelaar, P. H. M. *Organometallics* **2002**, *21*, 34.
334. Dagonne, S.; Guzei, I. A.; Coles, M. P.; Jordan, R. F. *J. Am. Chem. Soc.* **2000**, *122*, 274.
335. Cameron, P. A.; Gibson, V. C.; Redshaw, C.; Segal, J. A.; Solan, G. A.; White, A. J. P.; Williams, D. J. *Dalton. Trans.* **2001**, 1472.
336. Cameron, P. A.; Gibson, V. C.; Redshaw, C.; Segal, J. A.; Bruce, M. D.; White, A. J. P.; Williams, D. J. *Chem. Commun.* **1999**, 1883.
337. Cameron, P. A.; Gibson, V. C.; Redshaw, C.; Segal, J. A.; White, A. J. P.; Williams, D. J. *Dalton. Trans.* **2002**, 415.
338. Natta, G.; Pino, P.; Corradini, P.; Danusso, F.; Mantica, E.; Mazzanti, G.; Moraglio, G. *J. Am. Chem. Soc.* **1955**, *77*, 1708.
339. Natta, G.; Pino, P.; Mantica, E.; Danusso, F.; Mazzanti, G.; Peraldo, M. *Chim. Ind.* **1956**, *38*, 124.
340. Malanga, M. *Adv. Mater.* **2000**, *12*, 1869.
341. Ishihara, N.; Seimiya, T.; Kuramoto, M.; Uoi, M. *Macromolecules* **1986**, *19*, 2464.
342. Pellecchia, C.; Longo, P.; Grassi, A.; Ammendola, P.; Zambelli, A. *Makromol. Chem. Rapid Commun.* **1987**, *8*, 277.
343. Zambelli, A.; Longo, P.; Pellecchia, C.; Grassi, A. *Macromolecules* **1987**, *20*, 2035.
344. Zambelli, A.; Oliva, L.; Pellecchia, C. *Macromolecules* **1989**, *22*, 2129.
345. Chien, J. C. W.; Salajka, Z. *J. Polym. Sci. A.* **1991**, *29*, 1243.
346. Ishihara, N.; Kuramoto, M.; Uoi, M. *Macromolecules* **1988**, *21*, 3356.
347. Kaminsky, W.; Lenk, S.; Scholz, V.; Roesky, H. W.; Herzog, A. *Macromolecules* **1997**, *30*, 7647.
348. Longo, P.; Proto, A.; Oliva, L. *Macromol. Rapid Commun.* **1994**, *15*, 151.
349. Ricci, G.; Bosisio, C.; Porri, L. *Macromol. Rapid Commun.* **1996**, *17*, 781.
350. Tomotsu, N.; Ishihara, N.; Newman, T. H.; Malanga, M. T. *J. Mol. Catal. A: Chem.* **1988**, *128*, 167.
351. Po, R.; Cardi, N. *Prog. Polym. Sci.* **1996**, *21*, 47.
352. Zambelli, A.; Pellecchia, C.; Proto, A. *Macromol. Symp.* **1995**, *89*, 373.
353. Ishihara, N. *Macromol. Symp.* **1995**, *89*, 553.
354. Chien, J. C. W.; Salajka, Z. *J. Polym. Sci. A.* **1991**, *29*, 1253.

355. Campbell, R. E.; Newman, T. H.; Malanga, M. T. *Macromol. Symp.* **1995**, *97*, 151.
356. Kucht, A.; Kucht, H.; Barry, S.; Chien, J. C. W.; Rausch, M. D. *Organometallics* **1993**, *12*, 3075.
357. Kim, Y.; Hong, E.; Lee, M. H.; Kim, J.; Han, Y.; Do, Y. *Organometallics* **1999**, *18*, 36.
358. Kim, Y.; Han, Y.; Hwang, J. W.; Kim, M. W.; Do, Y. *Organometallics* **2002**, *21*, 1127.
359. Kim, Y.; Do, Y. *J. Organomet. Chem.* **2002**, *655*, 186.
360. Foster, P.; Chien, J. C. W.; Rausch, M. D. *Organometallics* **1996**, *15*, 2404.
361. Xu, G. X.; Ruckenstein, E. *J. Polym. Sci. Part A: Polym. Chem.* **1999**, *37*, 2481.
362. Schneider, N.; Proscenc, M. H.; Brintzinger, H. H. *J. Organomet. Chem.* **1997**, *545-546*, 291.
363. Harder, S.; Feil, F.; Knoll, K. *Angew. Chem., Int. Ed. Engl.* **2001**, *40*, 4261.
364. Harder, S.; Feil, F. *Organometallics* **2002**, *21*, 2268.
365. Chien, J. C. W.; Salajka, Z.; Dong, S. *Macromolecules* **1992**, *25*, 3199.
366. Grassi, A.; Zambelli, A.; Laschi, F. *Organometallics* **1996**, *15*, 480.
367. Grassi, A.; Saccheo, S.; Zambelli, A.; Laschi, F. *Macromolecules* **1998**, *31*, 5588.
368. Quyoum, R.; Wang, Q.; Tudoret, M. J.; Baird, M. C.; Gillis, D. J. *J. Am. Chem. Soc.* **1994**, *116*, 6435.
369. Ready, T. E.; Gurge, R.; Chien, J. C. W.; Rausch, M. D. *Organometallics* **1998**, *17*, 5236.
370. Xu, G. *Macromolecules* **1998**, *31*, 586.
371. Newman, T. H.; Malanga, M. T. *J. Macromol. Sci. Pure Appl. Chem.* **1997**, *A34*, 1921.
372. Mahanthappa, M. K.; Waymouth, R. M. *J. Am. Chem. Soc.* **2001**, *121*, 12093.
373. Zambelli, A.; Pellicchia, C.; Oliva, L.; Longo, P.; Grassi, A. *Makromol. Chem.* **1991**, *192*, 223.
374. Minieri, G.; Corradini, P.; Zambelli, A.; Guerra, G.; Cavallo, L. *Macromolecules* **2001**, *34*, 2459.
375. Minieri, G.; Corradini, P.; Guerra, G.; Zambelli, A.; Cavallo, L. *Macromolecules* **2001**, *34*, 5379.
376. Ammendola, P.; Tancredi, T.; Zambelli, A. *Macromolecules* **1986**, *19*, 307.
377. Pellicchia, C.; Pappalardo, D.; Oliva, L.; Zambelli, A. *J. Am. Chem. Soc.* **1995**, *117*, 6593.
378. Longo, P.; Grassi, A.; Proto, A.; Ammendola, P. *Macromolecules* **1988**, *21*, 24.
379. Duncalf, D. J.; Wade, H. J.; Waterson, C.; Derrick, P. J.; Haddleton, D. M.; McCamley, A. *Macromolecules* **1996**, *29*, 6399.
380. Matyjaszewski, K.; Xia, J. *Chem. Rev.* **2001**, *101*, 2921.
381. Matyjaszewski, K. *Macromol. Symp.* **2002**, *182*, 209.
382. Kamigaito, M.; Ando, T.; Sawamoto, M. *Chem. Rev.* **2001**, *101*, 3689.
383. Qiu, J.; Matyjaszewski, K. *Macromolecules* **1997**, *30*, 5643.
384. Kato, M.; Kamigaito, M.; Sawamoto, M.; Higashimura, T. *Macromolecules* **1995**, *28*, 1721.
385. Wang, J. S.; Matyjaszewski, K. *Macromolecules* **1995**, *28*, 7901.
386. Percec, V.; Barboiu, B. *Macromolecules* **1995**, *28*, 7970.
387. Matyjaszewski, K.; Wei, M.; Xia, J.; McDermott, N. E. *Macromolecules* **1997**, *30*, 8161.
388. Kotani, Y.; Kamigaito, M.; Sawamoto, M. *Macromolecules* **2000**, *33*, 6746.
389. Kotani, Y.; Kamigaito, M.; Sawamoto, M. *Macromolecules* **1999**, *32*, 2420.
390. Patten, T. E.; Xia, J.; Abernathy, T.; Matyjaszewski, K. *Science* **1996**, *272*, 866.
391. Percec, V.; Barboiu, B.; Neumann, A.; Ronda, J. C.; Zhao, M. *Macromolecules* **1996**, *29*, 3665.
392. Collins, J. E.; Fraser, C. L. *Macromolecules* **1998**, *31*, 6715.
393. Pascual, S.; Coutin, B.; Tardi, M.; Polton, A.; Vairon, J. P. *Macromolecules* **1999**, *32*, 1432.
394. Matyjaszewski, K.; Patten, T. E.; Xia, J. *J. Am. Chem. Soc.* **1997**, *119*, 674.
395. Xia, J.; Matyjaszewski, K. *Macromolecules* **1997**, *30*, 7697.
396. Matyjaszewski, K. *Macromol. Symp.* **1998**, *134*, 105.
397. Levy, A. T.; Olmstead, M. M.; Patten, T. E. *Inorg. Chem.* **2000**, *39*, 1628.
398. Cheng, G. L.; Hu, C. P.; Ying, S. K. *Macromol. Rapid Commun.* **1999**, *20*, 303.
399. Haddleton, D. M.; Duncalf, D. J.; Kukulj, D.; Crossman, M. C.; Jackson, S. G.; Bon, S. A. F.; Clark, A. J.; Shooter, A. J. *Eur. J. Inorg. Chem.* **1998**, 1799.
400. Complex **159**: Takahashi, H.; Ando, T.; Kamigaito, M.; Sawamoto, M. *Macromolecules* **1999**, *32*, 6461.
401. Complexes **160-162**: Takahashi, H.; Ando, T.; Kamigaito, M.; Sawamoto, M. *Macromolecules* **1999**, *32*, 3820.
402. Complex **162**: Watanabe, Y.; Ando, T.; Kamigaito, M.; Sawamoto, M. *Macromolecules* **2001**, *34*, 4370.
403. Complex **163**: Simal, F.; Demonceau, A.; Noels, A. F. *Angew. Chem., Int. Ed. Engl.* **1999**, *38*, 538.
404. Complex **164**: Simal, F.; Demonceau, A.; Noels, A. F. *Tet. Lett.* **1999**, *40*, 5689.
405. Complex **165**: Bielawski, C. W.; Louie, J.; Grubbs, R. H. *J. Am. Chem. Soc.* **2000**, *122*, 12872.
406. Hamasaki, S.; Kamigaito, M.; Sawamoto, M. *Macromolecules* **2002**, *35*, 2934.
407. Kamigaito, M.; Watanabe, Y.; Ando, T.; Sawamoto, M. *J. Am. Chem. Soc.* **2002**, *124*, 9994.
408. Simal, F.; Delfosse, S.; Demonceau, A.; Noels, A. F.; Denk, K.; Kohl, F. J.; Weskamp, T.; Herrmann, W. A. *Chem. Eur. J.* **2002**, *8*, 3047.
409. Complex **166**: Ando, T.; Kamigaito, M.; Sawamoto, M. *Macromolecules* **1997**, *30*, 4507.
410. Complex **167**: Louie, J.; Grubbs, R. H. *Chem. Commun.* **2000**, 1479.
411. Complex **168-169**: Kotani, Y.; Kamigaito, M.; Sawamoto, M. *Macromolecules* **1999**, *32*, 6877.
412. Complex **168-170**: Kotani, Y.; Kamigaito, M.; Sawamoto, M. *Macromolecules* **2000**, *33*, 3543.
413. Complex **171-172**: Gibson, V. C.; O'Reilly, R. K.; Reed, W.; Wass, D. F.; White, A. J. P.; Williams, D. J. *Chem. Commun.* **2002**, 1850.
414. Fujii, Y.; Ando, T.; Kamigaito, M.; Sawamoto, M. *Macromolecules* **2002**, *35*, 2949.
415. Moineau, G.; Dubois, Ph.; Jérôme, R.; Senninger, T.; Teyssié, Ph. *Macromolecules* **1998**, *31*, 545.
416. Complex **173**: Granel, C.; Dubois, Ph.; Jérôme, R.; Teyssié, Ph. *Macromolecules* **1996**, *29*, 8576.
417. Complex **174**: Moineau, G.; Minet, M.; Dubois, Ph.; Teyssié, Ph.; Senninger, T.; Jérôme, R. *Macromolecules* **1999**, *32*, 27.
418. Complex **175**: Uegaki, H.; Kotani, Y.; Kamigaito, M.; Sawamoto, M. *Macromolecules* **1998**, *31*, 6756.
419. Complex **176**: Uegaki, H.; Kamigaito, M.; Sawamoto, M. *J. Polym. Sci. A Polym. Chem.* **1999**, *37*, 3003.
420. Lecomte, Ph.; Drapier, I.; Dubois, Ph.; Teyssié, Ph.; Jérôme, R. *Macromolecules* **1997**, *30*, 7631.
421. Moineau, G.; Granel, C.; Dubois, Ph.; Jérôme, R.; Teyssié, Ph. *Macromolecules* **1998**, *31*, 542.
422. Hawker, C. J.; Hedrick, J. L.; Malmström, E. E.; Trollsås, M.; Mecerreyes, D.; Moineau, G.; Dubois, Ph.; Jérôme, R. *Macromolecules* **1998**, *31*, 213.

423. Petrucci, M. G. L.; Lebuis, A. M.; Kakkar, A. K. *Organometallics* **1998**, *17*, 4966.
424. Komiya, S.; Chigira, T.; Suzuki, T.; Hirano, M. *Chem. Lett.* **1999**, 347.
425. Chisholm, M. *Chem. Br. April* **1998**, 33.
426. Hatada, K.; Kitayama, T.; Ute, K. *Prog. Polym. Sci.* **1988**, *13*, 189.
427. Davis, T. P.; Haddleton, D. M.; Richards, S. N.; J. *Macromol. Sci. Rev. Macromol. Chem. Phys.* **1994**, *C34*, 243.
428. Glusker, D. L.; Galluccio, R. A.; Evans, R. A. *J. Am. Chem. Soc.* **1964**, *86*, 187.
429. Yuki, H.; Hatada, K. *Adv. Polym. Sci.* **1979**, *31*, 1.
430. Bywater, S. *Adv. Polym. Sci.* **1965**, *4*, 66.
431. Quirk, R. P.; Yoo, T.; Lee, Y.; Kim, J.; Lee, B. *Adv. Polym. Sci.* **2000**, *153*, 67.
432. Anderson, B. C.; Andrews, D. G.; Arthur, P.; Jacobson, H. W.; Melby, L. R.; Playtis, A. J.; Sharkey, W. H. *Macromolecules* **1981**, *14*, 1599.
433. Lutz, P.; Masson, P. Beinert, G.; Rempp, P. *Polym. Bull.* **1984**, *12*, 79.
434. Fayt, R.; Forte, R.; Jacobs, C.; Jérôme, R.; Ouhadi, T.; Teyssié, Ph.; Varshney, S. K. *Macromolecules* **1987**, *20*, 1442.
435. Ballard, D. G. H.; Bowles, R. J.; Haddleton, D. M.; Richards, S. N.; Sellens, R.; Twose, D. L. *Macromolecules* **1992**, *25*, 5907.
436. Hatada, K.; Ute, K.; Tanaka, K.; Okamoto, Y.; Kitayama, T. *Polym. J.* **1986**, *18*, 1037.
437. Cao, Z. K.; Okamoto, Y.; Hatada, K. *Kobunshi Ronbunshu* **1986**, *43*, 857.
438. Matsuzaki, K.; Kanai, T.; Ichijo, C.; Yuzawa, M. *Makromol. Chem.* **1984**, *185*, 2291.
439. Allen, K. A.; Grownlock, B. J.; Lindsell, W. E. *J. Polym. Sci. Chem. Ed.* **1974**, *12*, 1131.
440. Hatada, K.; Nakanishi, H.; Ute, K.; Kitayama, T. *Polym. J.* **1986**, *18*, 581.
441. Kuroki, M.; Aida, T.; Inoue, S. *J. Am. Chem. Soc.* **1987**, *109*, 4737.
442. Murayama, H.; Inoue, S. *Chem. Lett.* **1985**, 1377.
443. Kuroki, M.; Nashimoto, S.; Aida, T.; Inoue, S. *Macromolecules* **1988**, *21*, 3114.
444. Kuroki, M.; Watanabe, T.; Aida, T.; Inoue, S. *J. Am. Chem. Soc.* **1991**, *113*, 5903.
445. Adachi, T.; Sugimoto, H.; Aida, T.; Inoue, S. *Macromolecules* **1992**, *25*, 2280.
446. Adachi, T.; Sugimoto, H.; Aida, T.; Inoue, S. *Macromolecules*, **1993**, *26*, 1238.
447. Arai, T.; Sato, Y.; Inoue, S. *Chem. Lett.* **1990**, 1167.
448. Sugimoto, H.; Kuroki, M.; Watanabe, T.; Kawamura, C.; Aida, T.; Inoue, S. *Macromolecules* **1993**, *26*, 3403.
449. Hosokawa, Y.; Kuroki, M.; Aida, T.; Inoue, S. *Macromolecules* **1991**, *24*, 824.
450. Sugimoto, H.; Saika, M.; Hosokawa, Y.; Aida, T.; Inoue, S. *Macromolecules* **1996**, *29*, 3359.
451. Cameron, P. A.; Gibson, V. C.; Irvine, D. J. *Angew. Chem., Int. Ed. Engl.* **2000**, *39*, 2141.
452. Dove, A. P.; Gibson, V. C.; Marshall, E. L.; White, A. J. P.; Williams, D. J. *Chem. Commun.* **2002**, 1208.
453. Yasuda, H.; Yamamoto, H.; Yokota, K.; Miyake, S.; Nakamura, A. *J. Am. Chem. Soc.* **1992**, *114*, 4908.
454. Yasuda, H.; Ihara, E. *Macromol. Chem. Phys.* **1995**, *196*, 2417.
455. Yasuda, H. *J. Polym. Sci. Polym. Chem.* **2001**, *39*, 1955.
456. Yasuda, H. *J. Organomet. Chem.* **2002**, *647*, 128.
457. Yasuda, H.; Yamamoto, H.; Yamashita, M.; Yokota, K.; Nakamura, A.; Miyake, S.; Kai, Y.; Kanehisa, N. *Macromolecules* **1993**, *26*, 7134.
458. Cram, D. J.; Kopecky, K. R. *J. Am. Chem. Soc.* **1959**, *81*, 2748.
459. Bawn, C. E. H.; Ledwith, A. *Quart. Rev. Chem. Soc.* **1962**, *16*, 361.
460. Nodono, M.; Tokimitsu, T.; Tone, S.; Makino, T.; Yanagase, A. *Macromol. Chem. Phys.* **2000**, *201*, 2282.
461. Ihara, E.; Morimoto, M.; Yasuda, H. *Macromolecules* **1995**, *28*, 7886.
462. Kawaguchi, Y.; Yasuda, H. *J. Appl. Polym. Sci.* **2001**, *80*, 432.
463. Giardello, M. A.; Yamamoto, Y.; Brard, L.; Marks, T. J. *J. Am. Chem. Soc.* **1995**, *117*, 3276.
464. Mao, L.; Shen, Q.; Sun, J. *J. Organomet. Chem.* **1998**, *566*, 9.
465. Mao, L.; Shen, Q. *J. Polym. Sci. Polym. Chem.* **1998**, *36*, 1593.
466. Lee, M. H.; Hwang, J. W.; Kim, Y.; Kim, J.; Han, Y.; Do, Y. *Organometallics*, **1999**, *18*, 5124.
467. Qian, C.; Nie, W.; Chen, Y.; Sun, J. *J. Organomet. Chem.* **2002**, *645*, 82.
468. Shen, Q.; Wang, Y.; Zhang, K.; Yao, Y. *J. Polym. Sci. Polym. Chem.* **2002**, *40*, 612.
469. Gromada, J.; Fougá, C.; Chenal, T.; Mortreux, A.; Carpentier, J. F. *Macromol. Chem. Phys.* **2002**, *203*, 550.
470. Knjazhanski, S. Y.; Elizalde, L.; Cadenas, G.; Bulychev, B. M. *J. Polym. Sci. Polym. Chem.* **1998**, *36*, 1599.
471. Knjazhanski, S. Y.; Elizalde, L.; Cadenas, G.; Bulychev, B. M. *J. Organomet. Chem.* **1998**, *568*, 33.
472. Nakayama, Y.; Shibahara, T.; Fukumoto, H.; Nakamura, A.; Mashima, K. *Macromolecules* **1996**, *29*, 8014.
473. Ihara, E.; Koyama, K.; Yasuda, H.; Kanehisa, N.; Kai, Y. *J. Organomet. Chem.* **1999**, *574*, 40.
474. Tanaka, K.; Furo, M.; Ihara, E.; Yasuda, H. *J. Polym. Sci. Polym. Chem.* **2001**, *39*, 1382.
475. Desurmont, G.; Tanaka, M.; Li, Y.; Yasuda, H.; Tokimitsu, T.; Tone, S.; Yanagase, A. *J. Polym. Sci.; Polym. Chem.* **2000**, *38*, 4095.
476. Gromada, J.; Chenal, T.; Mortreux, A.; Leising, F.; Carpentier, J. F. *J. Mol. Cat. A. Chem.* **2002**, *182–183*, 525.
477. Desurmont, G. Tokimitsu, T.; Yasuda, H. *Macromolecules* **2000**, *33*, 7679.
478. Boffa, L. S.; Novak, B. M. *Macromolecules* **1994**, *27*, 6993.
479. Boffa, L. S.; Novak, B. M. *Macromolecules* **1997**, *30*, 3494.
480. Boffa, L. S.; Novak, B. M. *Tetrahedron*, **1997**, *53*, 15367.
481. Evans, W. J.; Keyer, R. A.; Rabe, G. W.; Drummond, D. K.; Ziller, J. W. *Organometallics* **1993**, *12*, 4664.
482. Evans, W. J.; Gonzales, S. L.; Ziller, J. W. *J. Am. Chem. Soc.* **1994**, *116*, 2600.
483. Benedek, I.; Simionescu, C.; Asandei, N.; Ungureanu, C. *Eur. Polym. J.* **1969**, *5*, 449.
484. Collins, S.; Ward, D. G. *J. Am. Chem. Soc.* **1992**, *114*, 5460.
485. Collins, S.; Ward, D. G.; Suddaby, K. H. *Macromolecules* **1994**, *27*, 7222.
486. Li, Y.; Ward, D. G.; Reddy, S. S.; Collins, S. *Macromolecules* **1997**, *30*, 1875.
487. Cameron, P. A.; Gibson, V. C.; Graham, A. J. *Macromolecules* **2000**, *33*, 4329.
488. Soga, K.; Deng, H.; Yano, T.; Shiono, T. *Macromolecules* **1994**, *27*, 7938.
489. Deng, H.; Shiono, T.; Soga, K. *Macromolecules* **1995**, *28*, 3067.
490. Stuhldreier, T.; Keul, H.; Höcker, H. *Macromol. Rapid Commun.* **2000**, *21*, 1093.
491. Hölscher, M.; Keul, H.; Höcker, H. *Chem. Eur. J.* **2001**, *7*, 5419.

492. Nguyen, H.; Jarvis, A. P.; Lesley, M. J. G.; Kelly, W. M.; Reddy, S. S.; Taylor, N. J.; Collins, S. *Macromolecules* **2000**, *33*, 1508.
493. Frauenrath, H.; Keul, H.; Höcker, H. *Macromolecules* **2001**, *34*, 14.
494. Hong, E.; Kim, Y.; Do, Y. *Organometallics* **1998**, *17*, 2933.
495. Shiono, T.; Saito, T.; Saegusa, N.; Hagihara, H.; Ikeda, T.; Deng, H.; Soga, K. *Macromol. Chem. Phys.* **1998**, *199*, 1573.
496. Bolig, A. D.; Chen, E. Y. X. *J. Am. Chem. Soc.* **2001**, *123*, 7943.
497. Jin, J.; Chen, E. Y. X. *Organometallics* **2002**, *21*, 13.
498. Bolig, A. D.; Chen, E. Y. X. *J. Am. Chem. Soc.* **2002**, *124*, 5612.
499. Frauenrath, H.; Balk, S.; Keul, H.; Höcker, H. *Macromol. Rapid Commun.* **2001**, *22*, 1147.
500. Matsuo, Y.; Mashima, K.; Tani, K. *Angew. Chem., Int. Ed. Engl.* **2001**, *40*, 960.
501. Mashima, K. *Macromol. Symp.* **2000**, *159*, 69.
502. Anderson, A. W.; Meckling, N. G. US Pat. 2721189, 1955.
503. Hérisson, J. L.; Chauvin, Y. *Makromol. Chem.* **1970**, *141*, 161.
504. Rappé, A. K.; Goddard, W. A. *J. Am. Chem. Soc.* **1982**, *104*, 448.
505. Kress, J.; Osborn, J. A.; Ivin, K. J. *Chem. Commun.* **1989**, 1234.
506. Kress, J.; Osborn, J. A.; Greene, R. M. E.; Ivin, K. J.; Rooney, J. J. *J. Am. Chem. Soc.* **1987**, *109*, 899.
507. Kress, J.; Osborn, J. A.; Amir-Ebrahimi, V.; Ivin, K. J.; Rooney, J. J. *Chem. Commun.* **1988**, 1164.
508. Ivin, K. J.; Mol, J. C. *Olefin Metathesis and Metathesis Polymerization*; Academic Press; San Diego, 1997.
509. Schrock, R. R.; Yap, K. B.; Yang, D. C.; Sitzmann, H.; Sita, L. R.; Bazan, G. C. *Macromolecules* **1989**, *22*, 3191.
510. Gilliom, L. R.; Grubbs, R. H. *J. Am. Chem. Soc.* **1986**, *108*, 733.
511. Grubbs, R. H.; Tumas, W. *Science* **1989**, *243*, 907.
512. Cannizzo, L. F.; Grubbs, R. H. *Macromolecules* **1987**, *20*, 1488.
513. Cannizzo, L. F.; Grubbs, R. H. *Macromolecules* **1988**, *21*, 1961.
514. Schrock, R. R. *Acc. Chem. Res.* **1990**, *23*, 158.
515. Schrock, R. R. *J. Organomet. Chem.* **1986**, *300*, 249.
516. Feldman, J.; Schrock, R. R. *Prog. Inorg. Chem.* **1991**, *39*, 1.
517. Schrock, R. R. *Chem. Rev.* **2002**, *102*, 145.
518. Kress, J.; Wesolek, M.; Osborn, J. A. *Chem. Commun.* **1982**, 514.
519. Wengrovius, J. H.; Schrock, R. R.; Churchill, M. R.; Missert, J. R.; Youngs, W. J. *J. Am. Chem. Soc.* **1980**, *102*, 4515.
520. Schaverien, C. J.; Dewan, J. C.; Schrock, R. R. *J. Am. Chem. Soc.* **1986**, *108*, 2771.
521. Schrock, R. R.; DePue, R. T.; Feldman, J.; Yap, K. B.; Yang, D. C.; Davis, W. M.; Park, L.; DiMare, M.; Schofield, M.; Anhaus, J.; Walborsky, E.; Evitt, E.; Krüger, C.; Betz, P. *Organometallics* **1990**, *9*, 2262.
522. Schrock, R. R.; Feldman, J.; Canizzo, L. F.; Grubbs, R. H. *Macromolecules* **1987**, *20*, 1169.
523. Schrock, R. R.; DePue, R. T.; Feldman, J.; Schaverien, C. J.; Dewan, J. C.; Liu, A. H. *J. Am. Chem. Soc.* **1988**, *110*, 1423.
524. Schrock, R. R. *Polyhedron* **1995**, *14*, 3177.
525. Murdzek, J. S.; Schrock, R. R. *Organometallics* **1987**, *6*, 1373.
526. Schrock, R. R.; Murdzek, J. S.; Bazan, G. C.; Robbins, J.; DiMare, M.; O'Regan, M. *J. Am. Chem. Soc.* **1990**, *112*, 3875.
527. Fox, H. H.; Yap, K. B.; Robbins, J.; Cai, S.; Schrock, R. R. *Inorg. Chem.* **1992**, *31*, 2287.
528. Oskam, J. H.; Fox, H. H.; Yap, K. B.; McConville, D. H.; O'Dell, R.; Lichtenstein, B. J.; Schrock, R. R. *J. Organomet. Chem.* **1993**, *459*, 185.
529. Schoettel, G.; Kress, J.; Osborn, J. A. *Chem. Commun.* **1989**, 1062.
530. Bell, A.; Clegg, W.; Dyer, P. W.; Elsegood, M. R. J.; Gibson, V. C.; Marshall, E. L. *Chem. Commun.* **1994**, 2547.
531. Bazan, G. C.; Schrock, R. R.; Khosravi, E.; Feast, W. J.; Gibson, V. C.; O'Regan, M. B.; Thomas, J. K.; Davis, W. M. *J. Am. Chem. Soc.* **1990**, *112*, 8378.
532. Bazan, G. C.; Schrock, R. R.; Cho, H. N.; Gibson, V. C. *Macromolecules* **1991**, *24*, 4495.
533. Bazan, G. C.; Oskam, J. H.; Cho, H. N.; Park, L. Y.; Schrock, R. R. *J. Am. Chem. Soc.* **1991**, *113*, 6899.
534. Bazan, G. C.; Khosravi, E.; Schrock, R. R.; Feast, W. J.; Gibson, V. C. *Polymer Commun.* **1989**, *30*, 258.
535. Feast, W. J.; Gibson, V. C.; Marshall, E. L. *Chem. Commun.* **1992**, 1157.
536. Davies, G. R.; Feast, W. J.; Gibson, V. C.; Hubbard, H. V. S.; Ivin, K. J.; Kenwright, A. M.; Khosravi, E.; Marshall, E. L.; Mitchell, J. P.; Ward, I. M.; Wilson, B. *Makromol. Chem. Macromol. Symp.* **1992**, *66*, 289.
537. Davies, G. R.; Hubbard, H. V. S.; Ward, I. M.; Feast, W. J.; Gibson, V. C.; Khosravi, E.; Marshall, E. L. *Polymer* **1995**, *36*, 235.
538. Feast, W. J.; Khosravi, E. *J. Fluorine Chem.* **1999**, *100*, 117.
539. Schrock, R. R.; Crowe, W. E.; Bazan, G. C.; DiMare, M.; O'Regan, M. B.; Schofield, M. H. *Organometallics* **1991**, *10*, 1832.
540. Fox, H. H.; Schofield, M. H.; Schrock, R. R. *Organometallics* **1994**, *13*, 2804.
541. Oskam, J. H.; Schrock, R. R. *J. Am. Chem. Soc.* **1992**, *114*, 7588.
542. Oskam, J. H.; Schrock, R. R. *J. Am. Chem. Soc.* **1993**, *115*, 11831.
543. Schrock, R. R.; Lee, J. K.; O'Dell, R.; Oskam, J. H. *Macromolecules* **1995**, *28*, 5933.
544. McConville, D. H.; Wolf, J. R.; Schrock, R. R. *J. Am. Chem. Soc.* **1993**, *115*, 4413.
545. O'Dell, R.; McConville, D. H.; Hofmeister, G. E.; Schrock, R. R. *J. Am. Chem. Soc.* **1994**, *116*, 3414.
546. Totland, K. M.; Boyd, T. J.; Lavoie, G. G.; Davis, W. M.; Schrock, R. R. *Macromolecules* **1996**, *29*, 6114.
547. Jamieson, J. Y.; Schrock, R. R.; Davis, W. M.; Bonitatebus, P. J.; Zhu, S. S.; Hoveyda, A. H. *Organometallics* **2000**, *19*, 925.
548. Alexander, J. B.; Schrock, R. R.; Davis, W. M.; Hultsch, K. C.; Hoveyda, A. H.; Houser, J. H. *Organometallics* **2000**, *19*, 3700.
549. Fujimura, O.; de la Mata, F. J.; Grubbs, R. H. *Organometallics* **1996**, *15*, 1865.
550. Schrock, R. R. *Tetrahedron* **1999**, *55*, 8141.

551. Weatherhead, G. S.; Ford, J. G.; Alexanian, E. J.; Schrock, R. R.; Hoveyda, A. H. *J. Am. Chem. Soc.* **2000**, *122*, 1828.
552. La, D. S.; Ford, J. G.; Sattely, E. S.; Bonitatebus, P. J.; Schrock, R. R.; Hoveyda, A. H. *J. Am. Chem. Soc.* **1999**, *121*, 11603.
553. Fox, H. H.; Lee, J. K.; Park, L. Y.; Schrock, R. R. *Organometallics* **1993**, *12*, 759.
554. Albagli, D.; Bazan, G. C.; Wrighton, M. S.; Schrock, R. R. *J. Am. Chem. Soc.* **1992**, *114*, 4150.
555. Mitchell, J. P.; Gibson, V. C.; Schrock, R. R. *Macromolecules* **1991**, *24*, 1220.
556. Crowe, W. E.; Mitchell, J. P.; Gibson, V. C.; Schrock, R. R. *Macromolecules* **1990**, *23*, 3534.
557. Dounis, P.; Feast, W. J. *Polymer* **1996**, *37*, 2547.
558. Notestein, J. M.; Lee, L. B. W.; Register, R. A. *Macromolecules* **2002**, *35*, 1985.
559. Bazan, G. C.; Schrock, R. R. *Macromolecules* **1991**, *24*, 817.
560. Saunders, R. S.; Cohen, R. E.; Wong, S. J.; Schrock, R. R. *Macromolecules* **1992**, *25*, 2055.
561. Buchmeiser, M. R.; Atzl, N.; Bonn, G. K. *J. Am. Chem. Soc.* **1997**, *119*, 9166.
562. Sinner, F.; Buchmeiser, M. R.; Tessadri, R.; Mupa, M.; Wurst, K.; Bonn, G. K. *J. Am. Chem. Soc.* **1998**, *120*, 2790.
563. Buchmeiser, M. R.; Kröll, R.; Wurst, K.; Schareina, Th.; Kempe, R.; Eschbaumer, Ch.; Schubert, U. S. *Macromol. Symp.* **2001**, *164*, 187.
564. Feast, W. J.; Gibson, V. C.; Johnson, A. F.; Khosravi, E.; Mohsin, M. A. *Polymer* **1994**, *35*, 3542.
565. Rizmi, A. C. M.; Khosravi, E.; Feast, W. J.; Mohsin, M. A.; Johnson, A. F. *Polymer* **1998**, *39*, 6605.
566. Nomura, K.; Takahashi, S.; Imanishi, Y. *Polymer* **2000**, *41*, 4345.
567. Nomura, K.; Takahashi, S.; Imanishi, Y. *Macromolecules* **2001**, *34*, 4712.
568. Héroguez, V.; Gnanou, Y.; Fontanille, M. *Macromol. Rapid Commun.* **1996**, *17*, 137.
569. Héroguez, V.; Amédro, E.; Grande, D.; Fontanille, M.; Gnanou, Y. *Macromolecules* **2000**, *33*, 7241.
570. Dounis, P.; Feast, W. J.; Kenwright, A. M. *Polymer* **1995**, *36*, 2787.
571. Wu, Z.; Wheeler, D. R.; Grubbs, R. H. *J. Am. Chem. Soc.* **1992**, *114*, 146.
572. Wu, Z.; Grubbs, R. H. *Macromolecules* **1994**, *27*, 6700.
573. Trzaska, S. T.; Lee, L. B. W.; Register, R. A. *Macromolecules* **2000**, *33*, 9215.
574. Wu, Z.; Grubbs, R. H. *Macromolecules* **1995**, *28*, 3502.
575. Hillmyer, M. A.; Grubbs, R. H. *Macromolecules* **1993**, *26*, 872.
576. Edwards, J. H.; Feast, W. J. *Polymer* **1980**, *21*, 595.
577. Edwards, J. H.; Feast, W. J.; Bott, D. C. *Polymer* **1984**, *25*, 395.
578. Feast, W. J.; Winter, J. N. *Chem. Commun.* **1985**, 202.
579. Knoll, K.; Krouse, S. A.; Schrock, R. R. *J. Am. Chem. Soc.* **1988**, *110*, 4424.
580. Knoll, K.; Schrock, R. R. *J. Am. Chem. Soc.* **1989**, *111*, 7989.
581. Krouse, S. A.; Schrock, R. R. *Macromolecules* **1988**, *21*, 1885.
582. Park, L. Y.; Schrock, R. R.; Stieglitz, S. G.; Crowe, W. E. *Macromolecules* **1991**, *24*, 3489.
583. Saunders, R. S.; Cohen, R. E.; Schrock, R. R. *Macromolecules* **1991**, *24*, 5599.
584. Craig, G. S. W.; Cohen, R. E.; Schrock, R. R.; Esser, A.; Schrof, W. *Macromolecules* **1995**, *28*, 2512.
585. Feast, W. J.; Tsiabouklis, J.; Pouwer, K. L.; Groenendaal, L.; Meijer, E. W. *Polymer* **1996**, *37*, 5017.
586. Klavetter, F. L.; Grubbs, R. H. *J. Am. Chem. Soc.* **1988**, *110*, 7807.
587. Swager, T. M.; Dougherty, D. A.; Grubbs, R. H. *J. Am. Chem. Soc.* **1988**, *110*, 2973.
588. Swager, T. M.; Grubbs, R. H. *J. Am. Chem. Soc.* **1989**, *111*, 4413.
589. Ginsburg, E. J.; Gorman, C. B.; Marder, S. R.; Grubbs, R. H. *J. Am. Chem. Soc.* **1989**, *111*, 7621.
590. Moore, J. S.; Gorman, C. B.; Grubbs, R. H. *J. Am. Chem. Soc.* **1991**, *113*, 1704.
591. Gorman, C. B.; Ginsburg, E. J.; Grubbs, R. H. *J. Am. Chem. Soc.* **1993**, *115*, 1397.
592. Conticello, V. P.; Gin, D. L.; Grubbs, R. H. *J. Am. Chem. Soc.* **1992**, *114*, 9708.
593. Wagaman, M. W.; Grubbs, R. H. *Macromolecules* **1997**, *30*, 3978.
594. Wagaman, M. W.; Grubbs, R. H. *Synth. Metals* **1997**, *84*, 327.
595. Pu, L.; Wagaman, M. W.; Grubbs, R. H. *Macromolecules* **1996**, *29*, 1138.
596. Tasch, S.; Graupner, W.; Leising, G.; Pu, L.; Wagaman, M. W.; Grubbs, R. H. *Adv. Mater.* **1995**, *7*, 903.
597. Miao, Y. J.; Bazan, G. C. *Macromolecules* **1994**, *27*, 1063.
598. Miao, Y. J.; Bazan, G. C. *J. Am. Chem. Soc.* **1994**, *116*, 9379.
599. Miao, Y. J.; Herkstroeter, W. G.; Sun, B. J.; Wong-Foy, A. G.; Bazan, G. C. *J. Am. Chem. Soc.* **1995**, *117*, 11407.
600. Lee, J. K.; Schrock, R. R.; Baigent, D. R.; Friend, R. H. *Macromolecules* **1995**, *28*, 1966.
601. Boyd, T. J.; Geerts, Y.; Lee, J. K.; Fogg, D. E.; Lavoie, G. G.; Schrock, R. R.; Rubner, M. F. *Macromolecules* **1997**, *30*, 3553.
602. Boyd, T. J.; Schrock, R. R. *Macromolecules* **1999**, *32*, 6608.
603. Komiya, Z.; Pugh, C.; Schrock, R. R. *Macromolecules* **1992**, *25*, 3609.
604. Komiya, Z.; Pugh, C.; Schrock, R. R. *Macromolecules* **1992**, *25*, 6586.
605. Komiya, Z.; Schrock, R. R. *Macromolecules* **1993**, *26*, 1393.
606. Gangadhara, Campistron, I.; Thomas, M.; Reyx, D. *J. Polym. Sci. Polym. Chem.* **1998**, *36*, 2807.
607. Pugh, C.; Schrock, R. R. *Macromolecules* **1992**, *25*, 6593.
608. Albagli, D.; Bazan, G. C.; Schrock, R. R.; Wrighton, M. S. *J. Am. Chem. Soc.* **1993**, *115*, 7328.
609. Albagli, D.; Bazan, G. C.; Schrock, R. R.; Wrighton, M. S. *J. Phys. Chem.* **1993**, *97*, 10211.
610. Chany, Y. N. C.; Craig, G. S. W.; Schrock, R. R.; Cohen, R. E. *Chem. Mat.* **1992**, *4*, 885.
611. Chan, Y. N. C.; Schrock, R. R. *Chem. Mat.* **1993**, *5*, 566.
612. Tassoni, R.; Schrock, R. R. *Chem. Mat.* **1994**, *6*, 744.
613. Sankaran, V.; Yue, J.; Cohen, R. E.; Schrock, R. R.; Silbey, R. J. *Chem. Mat.* **1993**, *5*, 1133.
614. Cummins, C. C.; Beachy, M. D.; Schrock, R. R.; Vale, M. G.; Sankaran, V.; Cohen, R. E. *Chem. Mat.* **1991**, *3*, 1153.
615. Chan, Y. N. C.; Schrock, R. R.; Cohen, R. E. *J. Am. Chem. Soc.* **1992**, *114*, 7295.
616. Chan, Y. N. C.; Schrock, R. R.; Cohen, R. E. *Chem. Mat.* **1992**, *4*, 24.
617. Cummins, C. C.; Schrock, R. R.; Cohen, R. R. *Chem. Mat.* **1992**, *4*, 27.
618. Fogg, D. E.; Radzilowski, L. H.; Blanski, R.; Schrock, R. R.; Thomas, E. L. *Macromolecules* **1997**, *30*, 417.
619. Eder, E.; Preishuber-Pflügl, P.; Stelzer, F. *J. Mol. Cat. A. Chem.* **2000**, *160*, 63.

620. Grenz, A.; Ceccarelli, S.; Bolm, C. *Chem. Commun.* **2001**, 1726.
621. Coles, M. P.; Gibson, V. C.; Mazzariol, L.; North, M.; Teasdale, W. G.; Williams, C. M.; Zamuner, D. *Chem. Commun.* **1994**, 2505.
622. Biagini, S. C. G.; Coles, M. P.; Gibson, V. C.; Giles, M. R.; Marshall, E. L.; North, M. *Polymer* **1998**, *39*, 1007.
623. Buchmeiser, M. R.; Sinner, F.; Mupa, M.; Wurst, K. *Macromolecules* **2000**, *33*, 32.
624. Biagini, S. C. G.; Davies, R. G.; Gibson, V. C.; Giles, M. R.; Marshall, E. L.; North, M.; Robson, D. A. *Chem. Commun.* **1999**, 235.
625. Nomura, K.; Schrock, R. R. *Macromolecules* **1996**, *29*, 540.
626. Michelotti, F. W.; Keavney, W. P. *J. Polym. Sci.* **1965**, *A3*, 895.
627. Novak, B. M.; Grubbs, R. H. *J. Am. Chem. Soc.* **1988**, *110*, 7542.
628. McGrath, D. V.; Grubbs, R. H.; Ziller, J. W. *J. Am. Chem. Soc.* **1991**, *113*, 3611.
629. France, M. B.; Grubbs, R. H.; McGrath, D. V.; Paciello, R. A. *Macromolecules* **1993**, *26*, 4742.
630. Hillmyer, M. A.; Lepetit, C.; McGrath, D. V.; Novak, B. M.; Grubbs, R. H. *Macromolecules* **1992**, *25*, 3345.
631. France, M. B.; Paciello, R. A.; Grubbs, R. H. *Macromolecules* **1993**, *26*, 4739.
632. Nguyen, S. T.; Johnson, L. K.; Grubbs, R. H. Ziller, J. W. *J. Am. Chem. Soc.* **1992**, *114*, 3974.
633. Wu, Z.; Benedicto, A. D.; Grubbs, R. H. *Macromolecules* **1993**, *26*, 4975.
634. Trnka, T. M.; Grubbs, R. H. *Acc. Chem. Res.* **2001**, *34*, 18.
635. Wu, Z.; Nguyen, S. T.; Grubbs, R. H.; Ziller, J. W. *J. Am. Chem. Soc.* **1995**, *117*, 5503.
636. Schwab, P.; Grubbs, R. H.; Ziller, J. W. *J. Am. Chem. Soc.* **1996**, *118*, 100.
637. Nguyen, S. T.; Grubbs, R. H.; Ziller, J. W. *J. Am. Chem. Soc.* **1993**, *115*, 9858.
638. Schwab, P.; France, M. B.; Ziller, J. W.; Grubbs, R. H. *Angew. Chem., Int. Ed. Engl.* **1995**, *34*, 2039.
639. Wilhelm, T. E.; Belderrain, T. R.; Brown, S. N.; Grubbs, R. H. *Organometallics* **1997**, *16*, 3867.
640. Belderrain, T. R.; Grubbs, R. H. *Organometallics* **1997**, *16*, 4001.
641. Nguyen, S. T.; Grubbs, R. H. *J. Organomet. Chem.* **1995**, *497*, 195.
642. Mohr, B.; Lynn, D. M.; Grubbs, R. H. *Organometallics* **1996**, *15*, 4317.
643. Lynn, D. M.; Mohr, B.; Grubbs, R. H. *J. Am. Chem. Soc.* **1998**, *120*, 1627.
644. Lynn, D. M.; Mohr, B.; Grubbs, R. H.; Henling, L. M.; Day, M. W. *J. Am. Chem. Soc.* **2000**, *122*, 6601.
645. Lynn, D. M.; Grubbs, R. H. *J. Am. Chem. Soc.* **2001**, *123*, 3187.
646. Robson, D. A.; Gibson, V. C.; Davies, R. G.; North, M. *Macromolecules* **1999**, *32*, 6371.
647. Weskamp, T.; Schattenmann, W. C.; Spiegler, M.; Herrmann, W. A. *Angew. Chem., Int. Ed. Engl.* **1998**, *37*, 2490.
648. Huang, J.; Stevens, E. D.; Nolan, S. P.; Petersen, J. L. *J. Am. Chem. Soc.* **1999**, *121*, 2674.
649. Scholl, M.; Trnka, T. M.; Morgan, J. P.; Grubbs, R. H. *Tet. Lett.* **1999**, *40*, 2247.
650. Jafarpour, L.; Hillier, A. C.; Nolan, S. P. *Organometallics* **2002**, *21*, 442.
651. Scholl, M.; Ding, S.; Lee, C. W.; Grubbs, R. H. *Org. Lett.* **1999**, *1*, 953.
652. Morgan, J. P.; Grubbs, R. H. *Org. Lett.* **2000**, *2*, 3153.
653. Ackermann, L.; Fürstner, A.; Weskamp, T.; Kohl, F. J.; Herrmann, W. A. *Tet. Lett.* **1999**, *40*, 4787.
654. Herrmann, W. A.; Köcher, C. *Angew. Chem., Int. Ed. Engl.* **1997**, *36*, 2163.
655. Chatterjee, A. K.; Grubbs, R. H. *Org. Lett.* **1999**, *1*, 1751.
656. Chatterjee, A. K.; Morgan, J. P.; Scholl, M.; Grubbs, R. H. *J. Am. Chem. Soc.* **2000**, *122*, 3783.
657. Spagnol, G.; Heck, M. P.; Nolan, S. P.; Mioskowski, C. *Org. Lett.* **2002**, *4*, 1767.
658. Bielawski, C. W.; Grubbs, R. H. *Angew. Chem., Int. Ed. Engl.* **2000**, *39*, 2903.
659. Frenzel, U.; Weskamp, T.; Kohl, F. J.; Schattenmann, W. C.; Nuyken, O.; Herrmann, W. A. *J. Organomet. Chem.* **1999**, *586*, 263.
660. Huang, J.; Schanz, H. J.; Stevens, E. D.; Nolan, S. P. *Organometallics* **1999**, *18*, 5375.
661. Sanford, M. S.; Valdez, M. R.; Grubbs, R. H. *Organometallics* **2001**, *20*, 5455.
662. Sanford, M. S.; Henling, L. M.; Grubbs, R. H. *Organometallics* **1998**, *17*, 5384.
663. Katayama, H.; Yoshida, T.; Ozawa, F. *J. Organomet. Chem.* **1998**, *562*, 203.
664. Chang, S.; Jones, L.; Wang, C.; Henling, L. M.; Grubbs, R. H. *Organometallics* **1998**, *17*, 3460.
665. del Río, I.; van Koten, G. *Tet. Lett.* **1999**, *40*, 1401.
666. van der Schaaf, P. A.; Kolly, R.; Kirner, H. J.; Rime, F.; Mühlebach, A.; Hafner, A. *J. Organomet. Chem.* **2000**, *606*, 65.
667. Louie, J.; Grubbs, R. H. *Organometallics* **2002**, *21*, 2153.
668. Ulman, M.; Belderrain, T. R.; Grubbs, R. H. *Tet. Lett.* **2000**, *41*, 4689.
669. Katayama, H.; Ozawa, F. *Chem. Lett.* **1998**, 67.
670. Abdallaoui, I. A.; Sémeril, D.; Dixneuf, P. H. *J. Mol. Cat.; A. Chem.* **2002**, *182–183*, 577.
671. Harlow, K. J.; Hill, A. F.; Wilton-Ely, J. D. E. T. *J. Chem. Soc., Dalton Trans.* **1999**, 285.
672. Jafarpour, L.; Schanz, H. J.; Stevens, E. D.; Nolan, S. P. *Organometallics* **1999**, *18*, 5416.
673. Schanz, H. J.; Jafarpour, L.; Stevens, E. D.; Nolan, S. P. *Organometallics* **1999**, *18*, 5187.
674. Sémeril, D.; Olivier-Bourbigou, H.; Bruneau, C.; Dixneuf, P. H. *Chem. Commun.* **2002**, 146.
675. Sémeril, D.; Bruneau, C.; Dixneuf, P. H. *Adv. Synth. Catal.* **2002**, *344*, 585.
676. Bruneau, C.; Dixneuf, P. H. *Acc. Chem. Res.* **1999**, *32*, 311.
677. Delaude, L.; Jan, D.; Simal, F.; Demonceau, A.; Noels, A. F. *Macromol. Symp.* **2000**, *153*, 133.
678. Stumpf, A. W.; Saive, E.; Demonceau, A.; Noels, A. F. *Chem. Commun.* **1995**, 1127.
679. Hafner, A.; Mühlebach, A.; van der Schaaf, P. A. *Angew. Chem., Int. Ed. Engl.* **1997**, *36*, 2121.
680. Sanford, M. S.; Love, J. A.; Grubbs, R. H. *J. Am. Chem. Soc.* **2001**, *123*, 6543.
681. Sanford, M. S.; Henling, L. M.; Day, M. W.; Grubbs, R. H. *Angew. Chem., Int. Ed. Engl.* **2000**, *39*, 3451.
682. Sanford, M. S.; Ulman, M.; Grubbs, R. H. *J. Am. Chem. Soc.* **2001**, *123*, 749.
683. Bielawski, C. W.; Grubbs, R. H. *Macromolecules* **2001**, *34*, 8838.
684. Hansen, S. M.; Rominger, F.; Metz, M.; Hofmann, P. *Chem. Eur. J.* **1999**, *5*, 557.
685. Amoroso, D.; Fogg, D. E. *Macromolecules* **2000**, *33*, 2815.
686. Hansen, S. M.; Volland, M. A. O.; Rominger, F.; Eisenträger, F.; Hofmann, P. *Angew. Chem., Int. Ed. Engl.* **1999**, *38*, 1273.
687. Six, C.; Beck, K.; Wegner, A.; Leitner, W. *Organometallics* **2000**, *19*, 4639.

688. Kanaoka, S.; Grubbs, R. H. *Macromolecules* **1995**, *28*, 4707.
689. Maughon, B. R.; Grubbs, R. H. *Macromolecules* **1997**, *30*, 3459.
690. Maughon, B. R.; Grubbs, R. H. *Macromolecules* **1996**, *29*, 5765.
691. Hillmyer, M. A.; Laredo, W. R.; Grubbs, R. H. *Macromolecules* **1995**, *28*, 6311.
692. Scherman, O. A.; Grubbs, R. H. *Syn. Met.* **2001**, *124*, 431.
693. Fraser, C.; Hillmyer, M. A.; Gutierrez, E.; Grubbs, R. H. *Macromolecules* **1995**, *28*, 7256.
694. Hillmyer, M. A.; Nguyen, S. T.; Grubbs, R. H. *Macromolecules* **1997**, *30*, 718.
695. Bielawski, C. W.; Scherman, O. A.; Grubbs, R. H. *Polymer* **2001**, *42*, 4939.
696. Maughon, B. R.; Morita, T.; Bielawski, C. W.; Grubbs, R. H. *Macromolecules* **2000**, *33*, 1929.
697. Morita, T.; Maughon, B. R.; Bielawski, C. W.; Grubbs, R. H. *Macromolecules* **2000**, *33*, 6621.
698. Gibson, V. C.; Okada, T. *Macromolecules* **2000**, *33*, 655.
699. Bielawski, C. W.; Benitez, D.; Morita, T.; Grubbs, R. H. *Macromolecules* **2001**, *34*, 8610.
700. Katayama, H.; Yonezawa, F.; Nagao, M.; Ozawa, F. *Macromolecules* **2002**, *35*, 1133.
701. Weck, M.; Jackiw, J. J.; Rossi, R. R.; Weiss, P. S.; Grubbs, R. H. *J. Am. Chem. Soc.* **1999**, *121*, 4088.
702. Maughon, B. R.; Weck, M.; Mohr, B.; Grubbs, R. H. *Macromolecules* **1997**, *30*, 257.
703. Weck, M.; Mohr, B.; Maughon, B. R.; Grubbs, R. H. *Macromolecules* **1997**, *30*, 6430.
704. Bolm, C.; Dinter, C. L.; Seger, A.; Höcker, H.; Brozio, J. *J. Org. Chem.* **1999**, *64*, 5730.
705. Watson, K. J.; Nguyen, S. T.; Mirkin, C. A. *J. Organomet. Chem.* **2000**, *606*, 79.
706. Myles, A. J.; Zhang, Z.; Liu, G.; Branda, N. R. *Org. Lett.* **2000**, *2*, 2749.
707. Skaff, H.; Ilker, M. F.; Coughlin, E. B.; Emrich, T. *J. Am. Chem. Soc.* **2002**, *124*, 5729.
708. Montalban, A. G.; Steinke, J. H. G.; Anderson, M. E.; Barrett, A. G. M.; Hoffman, B. M. *Tet. Lett.* **1999**, *40*, 8151.
709. Kimura, M.; Wada, K.; Ohta, K.; Hanabusa, K.; Shirai, H.; Kobayashi, N. *Macromolecules* **2001**, *34*, 4706.
710. Allcock, H. R.; de Denu, C. R.; Prange, R.; Laredo, W. R. *Macromolecules* **2001**, *34*, 2757.
711. Allcock, H. R.; Laredo, W. R.; Kellam, E. C.; Morford, R. V. *Macromolecules* **2001**, *34*, 787.
712. Biagini, S. C. G.; Davies, R. G.; Gibson, V. C.; Giles, M. R.; Marshall, E. L.; North, M. *Polymer* **2001**, *42*, 6669.
713. Bolm, C.; Dinter, C. L.; Schiffers, I.; Defrère, L. *Synlett*, **2001**, 1875.
714. Maynard, H. D.; Okada, S. Y.; Grubbs, R. H. *Macromolecules* **2000**, *33*, 6239.
715. Maynard, H. D.; Okada, S. Y.; Grubbs, R. H. *J. Am. Chem. Soc.* **2001**, *123*, 1275.
716. Gibson, V. C.; Marshall, E. L.; North, M.; Robson, D. A.; Williams, P. J. *Chem. Commun.* **1997**, 1095.
717. Davies, R. G.; Gibson, V. C.; Hursthouse, M. B.; Light, M. E.; Marshall, E. L.; North, M.; Robson, D. A.; Thompson, I.; White, A. J. P.; Williams, D. J.; Williams, P. J. *J. Chem. Soc., Perkin Trans. 1* **2001**, 3365.
718. Biagini, S. C. G.; Gibson, V. C.; Giles, M. R.; Marshall, E. L.; North, M. *Chem. Commun.* **1997**, 1097.
719. Arimoto, H.; Nishimura, K.; Kimuni, T.; Hayakawa, I.; Uemura, D. *Chem. Commun.* **1999**, 1361.
720. Wanner, J.; Harmed, A. M.; Probst, D. A.; Poon, K. W. C.; Klein, T. A.; Snelgrove, K. A.; Hanson, P. R. *Tet. Lett.* **2002**, *43*, 917.
721. Kanai, M.; Mortell, K. H.; Kiessling, L. L. *J. Am. Chem. Soc.* **1997**, *119*, 9931.
722. Strong, L. E.; Kiessling, L. L. *J. Am. Chem. Soc.* **1999**, *121*, 6193.
723. Manning, D. D.; Hu, X.; Beck, P.; Kiessling, L. L. *J. Am. Chem. Soc.* **1997**, *119*, 3161.
724. Manning, D. D.; Strong, L. E.; Hu, X.; Beck, P. J.; Kiessling, L. L. *Tetrahedron* **1997**, *53*, 11937.
725. Pohl, N. L.; Kiessling, L. L. *Synthesis* **1999**, 1515.
726. Gestwicki, J. E.; Strong, L. E.; Cairo, C. W.; Boehm, F. J.; Kiessling, L. L. *Chem. Biol.* **2002**, *9*, 163.
727. Fraser, C.; Grubbs, R. H. *Macromolecules* **1995**, *28*, 7248.
728. Meier, S.; Reisinger, H.; Haag, R.; Mecking, S.; Mülhaupt, R.; Stelzer, F. *Chem. Commun.* **2001**, 855.
729. Schwendeman, J. E.; Church, A. C.; Wagener, K. B. *Adv. Synth. Catal.* **2002**, *344*, 597.
730. Watson, M. D.; Wagener, K. B. *Macromolecules* **2000**, *33*, 8963.
731. Watson, M. D.; Wagener, K. B. *Macromolecules* **2000**, *33*, 5411.
732. Watson, M. D.; Wagener, K. B. *Macromolecules* **2000**, *33*, 3196.
733. Walba, D. M.; Keller, P.; Shao, R.; Clark, N. A.; Hillmyer, M.; Grubbs, R. H. *J. Am. Chem. Soc.* **1996**, *118*, 2740.
734. Joo, S. H.; Yun, Y. K.; Jin, J. I.; Kim, D. C.; Zin, W. C. *Macromolecules* **2000**, *33*, 6704.
735. Hopkins, T. E.; Pawlow, J. H.; Koren, D. L.; Deters, K. S.; Solivan, S. M.; Davis, J. A.; Gómez, F. J.; Wagener, K. B. *Macromolecules* **2001**, *34*, 7920.
736. Middleton, J. C.; Tipton, A. J. *Biomaterials* **2000**, *21*, 2335.
737. Gilding, D. K.; Reed, A. M. *Polymer* **1979**, *20*, 1459.
738. O'Keefe, B. J.; Hillmyer, M. A.; Tolman, W. B. *J. Chem. Soc., Dalton Trans.* **2001**, 2215.
739. Okada, M. *Prog. Polym. Sci.* **2002**, *27*, 87.
740. Södergård, A.; Stolt, M. *Prog. Polym. Sci.* **2002**, *27*, 1123.
741. Drumright, R. E.; Gruber, P. R.; Henton, D. E. *Adv. Mater.* **2000**, *12*, 1841.
742. Spinu, M.; Jackson, C.; Keating, M. Y.; Gardner, K. H. *J. Macromol. Sci. Pure Appl. Chem.* **1996**, *A33*, 1497.
743. Kumar, N.; Ravikumar, M. N. V.; Domb, A. J. *Adv. Drug. Delivery Rev.* **2001**, *53*, 23.
744. Kricheldorf, H. R.; Berl, M.; Scharnagl, N. *Macromolecules*, **1988**, *21*, 286.
745. Yasuda, T.; Aida, T.; Inoue, S. *Macromolecules*, **1983**, *16*, 1792.
746. Lofgren, A.; Albertsson, A.-C.; Dubois, Ph.; Jérôme, R. *J. Macromol. Sci. Rev. Macromol. Chem. Phys.* **1995**, *C35*, 379.
747. Ouhadi, T.; Stevens, C.; Teyssié, Ph. *Makromol. Chem. Supp.* **1975**, *1*, 191.
748. Dubois, Ph.; Jérôme, R.; Teyssié, Ph. *Polym. Bull.* **1989**, *22*, 475.
749. Tian, D.; Dubois, Ph.; Jérôme, R. *Macromolecules* **1997**, *30*, 2575.
750. Dubois, P.; Jacobs, C. Jérôme, R.; Teyssié, Ph. *Macromolecules* **1991**, *24*, 2266.
751. Yui, N.; Dijkstra, P. J.; Feijen, J. *Makromol. Chem.* **1990**, *191*, 481.
752. Barakat, I.; Dubois, Ph.; Grandfils, Ch.; Jérôme, R. *J. Polym. Sci. Polym. Chem.* **2001**, *39*, 294.
753. Ropson, N.; Dubois, Ph.; Jérôme, R.; Teyssié, Ph. *Macromolecules*, **1992**, *25*, 3820.
754. Ropson, N.; Dubois, Ph.; Jérôme, R.; Teyssié, Ph. *J. Polym. Sci. Poly. Chem.* **1997**, *35*, 183.
755. Mecerreyes, D.; Jérôme, R. *Macromol. Chem. Phys.* **1999**, *200*, 2581.
756. Dubois, Ph.; Barakat, I.; Jérôme, R.; Teyssié, Ph. *Macromolecules* **1993**, *26*, 4407.

757. Vion, J.-M.; Jérôme, R.; Teyssié, Ph.; Aubin, M.; Prud'homme, R. E. *Macromolecules*, **1986**, *19*, 1828.
758. Vanhoorne, P.; Dubois, Ph.; Jérôme, R.; Teyssié, Ph. *Macromolecules*, **1992**, *25*, 37.
759. Shiner, V. J.; Whittaker, D.; Fernandez, V. P. *J. Am. Chem. Soc.* **1963**, *85*, 2318.
760. Oliver, J. G.; Phillips, P. K.; Worrall, I. J. *J. Inorg. Nucl. Chem.* **1969**, *31*, 1609.
761. Turova, N. Y.; Fozunov, V. A.; Yanovskii, A. I.; Bokii, N. G.; Struchkov, T.; Tarnopolskii, B. L. *J. Inorg. Nucl. Chem.* **1979**, *41*, 5.
762. Foltling, K.; Streib, W. E.; Caulton, K. G.; Poncelet, O.; Hubert-Pfalzgraf, L. G. *Polyhedron* **1991**, *10*, 1639.
763. Duda, A.; Penczek, S. *Macromol. Rapid Commun.* **1995**, *16*, 67.
764. Duda, A.; Penczek, S. *Macromolecules* **1995**, *28*, 5981.
765. Duda, A. *Macromolecules* **1996**, *29*, 1399.
766. Ropson, N.; Dubois, Ph.; Jérôme, R.; Teyssié, Ph. *Macromolecules* **1995**, *28*, 7589.
767. Ropson, N.; Dubois, Ph.; Jérôme, R.; Teyssié, Ph. *Macromolecules* **1993**, *26*, 6378.
768. Ropson, N.; Dubois, Ph.; Jérôme, R.; Teyssié, Ph. *Macromolecules* **1994**, *27*, 5950.
769. Evans, W. J.; Shreeve, J. L.; Doedens, R. J. *Inorg. Chem.* **1993**, *32*, 245.
770. Kowalski, A.; Duda, A.; Penczek, S. *Macromolecules* **1998**, *31*, 2114.
771. Jacobs, C.; Dubois, Ph.; Jérôme, R.; Teyssié, Ph. *Macromolecules* **1991**, *24*, 3027.
772. Duda, A.; Florjanczyk, Z.; Hofman, A.; Slomkowski, S.; Penczek, S. *Macromolecules* **1990**, *23*, 1640.
773. Duda, A.; Penczek, S. *Makromol. Rapid Commun.* **1994**, *15*, 559.
774. Tian, D.; Dubois, Ph.; Jérôme, R.; Teyssié, Ph. *Macromolecules* **1994**, *27*, 4134.
775. Reeve, M. S.; McCarthy, S. P.; Gross, R. A. *Macromolecules* **1993**, *26*, 888.
776. Aida, T.; Inoue, S. *Acc. Chem. Res.* **1996**, *29*, 39.
777. Inoue, S. *J. Polym. Sci. Polym. Chem.* **2000**, *38*, 2861.
778. Trofimoff, L.; Aida, T.; Inoue, S. *Chem. Lett.* **1987**, 991.
779. Yasuda, T.; Aida, T.; Inoue, S. *Bull. Chem. Soc. Jpn.* **1986**, *59*, 3931.
780. Endo, M.; Aida, T.; Inoue, S. *Macromolecules*, **1987**, *20*, 2982.
781. Aida, T.; Maekawa, Y.; Asano, S.; Inoue, S. *Macromolecules* **1988**, *21*, 1195.
782. Yasuda, T.; Aida, T.; Inoue, S. *Macromolecules*, **1984**, *17*, 2217.
783. Shimasaki, K.; Aida, T.; Inoue, S. *Macromolecules*, **1987**, *20*, 3076.
784. Sugimoto, H.; Aida, T.; Inoue, S. *Macromolecules* **1990**, *23*, 2869.
785. Isoda, M.; Sugimoto, H.; Aida, T.; Inoue, S. *Macromolecules*, **1997**, *30*, 57.
786. Inoue, S.; Aida, T. *Makromol. Chem. Macromol. Symp.* **1993**, *73*, 27.
787. Kuroki, M.; Nashimoto, S.; Aida, T.; Inoue, S. *Macromolecules* **1988**, *21*, 3114.
788. LeBorgne, A.; Wisniewski, M.; Spassky, N. *Polym. Prep. Div. Polym. Sci. Am. Chem. Soc.* **1995**, *36*, 217.
789. Montaudo, G.; Montaudo, M. S.; Puglisi, C.; Samperi, F.; Spassky, N.; LeBorgne, A.; Wisniewski, M. *Macromolecules* **1996**, *29*, 6461.
790. Cameron, P. A.; Jhurry, D.; Gibson, V. C.; White, A. J. P.; Williams, D. J.; Williams, S. *Macromol. Rapid Commun.* **1999**, *20*, 616.
791. Bhaw-Luximon, A.; Jhurry, D.; Spassky, N. *Polym. Bull.* **2000**, *44*, 31.
792. Nomura, N.; Ishii, R.; Akakura, M.; Aoi, K. *J. Am. Chem. Soc.* **2002**, *124*, 5938.
793. Taden, I.; Kang, H. C.; Massa, W.; Okuda, J. *J. Organomet. Chem.* **1997**, *540*, 189.
794. Vincens, V.; LeBorgne, A.; Spassky, N. *Macromol. Symp.* **1991**, *47*, 285.
795. LeBorgne, A.; Vincens, V.; Jouglard, M.; Spassky, N. *Macromol. Symp.* **1993**, *73*, 37.
796. Wisniewski, M.; Le Borgne, A.; Spassky, N. *Macromol. Chem. Phys.* **1997**, *198*, 1227.
797. Ikada, Y.; Jamshidi, K.; Tsuji, H.; Hyon, S. H. *Macromolecules* **1987**, *20*, 904.
798. Tsuji, H.; Horii, H.; Hyon, S. H.; Ikada, Y. *Macromolecules* **1991**, *24*, 2719.
799. Brizzolara, D.; Cantow, H. J.; Diederichs, K.; Keller, E.; Domb, A. J. *Macromolecules* **1996**, *29*, 191.
800. Spassky, N.; Wisniewski, M.; Pluta, C.; Le Borgne, A. *Macromol. Chem. Phys.* **1996**, *197*, 2627.
801. Spassky, N.; Pluta, C.; Simic, V.; Thiam, M.; Wisniewski, M. *Macromol. Symp.* **1998**, *128*, 39.
802. Ovitt, T. M.; Coates, G. W. *J. Am. Chem. Soc.* **1999**, *121*, 4072.
803. Ovitt, T. M.; Coates, G. W. *J. Am. Chem. Soc.* **2002**, *124*, 1316.
804. Radano, C. P.; Baker, G. L.; Smith, M. R. *J. Am. Chem. Soc.* **2000**, *122*, 1552.
805. Ovitt, T. M.; Coates, G. W. *J. Polym. Sci. Polym. Chem.* **2000**, *38*, 4686.
806. Ko, B. T.; Lin, C. C. *Macromolecules* **1999**, *32*, 8296.
807. Chen, H. L.; Ko, B. T.; Huang, B. H.; Lin, C. C. *Organometallics* **2001**, *20*, 5076.
808. Liu, Y. C.; Ko, B. T.; Lin, C. C. *Macromolecules* **2001**, *34*, 6196.
809. Taden, I.; Kang, H. C.; Massa, W.; Spaniol, T. P.; Okuda, J. *Eur. J. Inorg. Chem.* **2000**, 441.
810. Chisholm, M. H.; Navarro-Llobet, D.; Simonsick, W. J. *Macromolecules* **2001**, *34*, 8851.
811. Hamitou, A.; Jérôme, R.; Hubert, A. J.; Teyssié, Ph. *Macromolecules* **1973**, *6*, 651.
812. Ouhadi, T.; Bioul, J. P.; Stevens, R.; Hocks, W. L.; Teyssié, Ph. *Inorg. Chim. Acta.* **1976**, *19*, 203.
813. Ouhadi, T.; Hamitou, A.; Jérôme, R.; Teyssié, Ph. *Macromolecules* **1976**, *9*, 927.
814. Song, C. X.; Feng, X. D. *Macromolecules* **1984**, *17*, 2764.
815. Dong, C. M.; Qiu, K. Y.; Gu, Z. W.; Feng, X. D. *J. Polym. Sci. Polym. Chem.* **2001**, *39*, 357.
816. Heuschen, J.; Jérôme, R.; Teyssié, Ph. *Macromolecules* **1981**, *14*, 242.
817. Barakat, I.; Dubois, Ph.; Jérôme, R.; Teyssié, Ph. *Macromolecules* **1991**, *24*, 6542.
818. Kreiser-Saunders, I.; Kricheldorf, H. R. *Macromol. Chem. Phys.* **1998**, *199*, 1081.
819. Kricheldorf, H. R.; Damrau, D. O. *Macromol. Chem. Phys.* **1998**, *199*, 1089.
820. Kricheldorf, H. R.; Lee, S. R. *Polymer* **1995**, *36*, 2995.
821. Chisholm, M. H.; Eilerts, N. W. *Chem. Commun.* **1996**, 853.
822. Chisholm, M. H.; Eilerts, N. W.; Huffman, J. C.; Iyer, S. S.; Pacold, M.; Phomphrai, K. *J. Am. Chem. Soc.* **2000**, *122*, 11845.
823. Cheng, M.; Attygalle, A. B.; Lobkovsky, E. B.; Coates, G. W. *J. Am. Chem. Soc.* **1999**, *121*, 11583.
824. Chamberlain, B. M.; Cheng, M.; Moore, D. R.; Ovitt, T. M.; Lobkovsky, E. B.; Coates, G. W. *J. Am. Chem. Soc.* **2001**, *123*, 3229; Dove, A.P.; Gibson, V.C.; Marshall, E.L. WO 0238 574, 2002 [Chem. Abstr., **2002**, *136*, 386482].

825. Chisholm, M. H.; Huffman, J. C.; Phomphrai, K. *J. Chem. Soc. Dalton Trans.* **2001**, 222.
826. Chisholm, M. H.; Gallucci, J.; Phomphrai, K. *Inorg. Chem.* **2002**, *41*, 2785.
827. Kricheldorf, H. R.; Serra, A. *Polym. Bull.* **1985**, *14*, 497.
828. Kricheldorf, H. R.; Damrau, D.-O. *J. Macromol. Sci. Pure Appl. Chem.* **1998**, *A35*, 1875.
829. Dobrzynski, P.; Kasperczyk, J.; Bero, M. *Macromolecules* **1999**, *32*, 4735.
830. Zhong, Z.; Ankoné, M. J. K.; Dijkstra, P. J.; Birg, C.; Westerhausen, M.; Feijen, J. *Polym. Bull.* **2001**, *46*, 51.
831. Tesh, K. F.; Hanusa, T. P.; Huffman, J. C.; Huffman, C. J. *Inorg. Chem.* **1992**, *31*, 5572.
832. Zhong, Z.; Dijkstra, P. J.; Birg, C.; Westerhausen, M.; Feijen, J. *Macromolecules* **2001**, *34*, 3863.
833. Stevels, W. M.; Ankoné, M. J. K.; Dijkstra, P. J.; Feijen, J. *Macromolecules* **1996**, *29*, 6132.
834. Stevels, W. M.; Ankoné, M. J. K.; Dijkstra, P. J.; Feijen, J. *Macromolecules* **1996**, *29*, 8296.
835. Rashkov, I.; Manolova, N.; Li, S. M.; Espartero, J. L.; Vert, M. *Macromolecules* **1996**, *29*, 50.
836. Li, S. M.; Rashkov, I.; Espartero, J. L.; Manolova, N.; Vert, M. *Macromolecules* **1996**, *29*, 57.
837. Feng, Y.; Klee, D.; Höcker, H. *Macromol. Chem. Phys.* **2001**, *202*, 3120.
838. Nijenhuis, A. J.; Grijsma, D. W.; Pennings, A. J. *Macromolecules* **1992**, *25*, 6419.
839. Kricheldorf, H. R.; Kreiser-Saunders, I.; Boettcher, C. *Polymer* **1995**, *36*, 1253.
840. Schwach, G.; Coudane, J.; Engel, R.; Vert, M. *J. Polym. Sci. Polym. Chem.* **1997**, *35*, 3431.
841. Kowalski, A.; Duda, A.; Penczek, S. *Macromolecules* **2000**, *33*, 689.
842. Kricheldorf, H. R. *Macromol. Symp.* **2000**, *153*, 55.
843. Ryner, M.; Stridsberg, K.; Albertsson, A. C.; von Schenck, H.; Svensson, M. *Macromolecules* **2001**, *34*, 3877.
844. Witzke, D. R.; Narayan, R.; Kolstad, J. J. *Macromolecules* **1997**, *30*, 7075.
845. Kricheldorf, H. R.; Stricker, A.; Langanke, D. *Macromol. Chem. Phys.* **2001**, *202*, 2963.
846. Bero, M.; Czaplá, B.; Dobrzynski, P.; Janeczek, H.; Kasperczyk, J. *Macromol. Chem. Phys.* **1999**, *200*, 911.
847. Jörres, V.; Keul, H.; Höcker, H. *Macromol. Chem. Phys.* **1998**, *199*, 835.
848. Kricheldorf, H. R.; Stricker, A. *Polymer* **2000**, *41*, 7311.
849. Kricheldorf, H. R.; Mahler, A. *Polymer* **1996**, *37*, 4383.
850. Kowalski, A.; Libiszowski, J.; Duda, A.; Penczek, S. *Macromolecules* **2000**, *33*, 1964.
851. Duda, A.; Penczek, S.; Kowalski, A.; Libiszowski, J. *Macromol. Symp.* **2000**, *153*, 41.
852. Gsell, R.; Zeldin, M. J. *Inorg. Nucl. Chem.* **1975**, *37*, 1133.
853. Kricheldorf, H. R.; Lee, S. R. *Macromolecules* **1996**, *29*, 8689.
854. Stridsberg, K.; Albertsson, A. C. *J. Polym. Sci. Polym. Chem.* **1999**, *37*, 3407.
855. Kricheldorf, H. R.; Stricker, A.; Langanke, D. *Macromol. Chem. Phys.* **2001**, *202*, 2525.
856. Kricheldorf, H. R.; Stricker, A. *Macromol. Chem. Phys.* **1999**, *200*, 1726.
857. Chisholm, M. H.; Delbridge, E. E. *Chem. Commun.* **2001**, 1308.
858. Dove, A. P.; Gibson, V. C.; Marshall, E. L.; White, A. J. P.; Williams, D. J. *Chem. Commun.* **2001**, 283.
859. Aubrecht, K. B.; Hillmyer, M. A.; Tolman, W. B. *Macromolecules* **2002**, *35*, 644.
860. Kricheldorf, H. R.; Boettcher, C. *Makromol. Chem.* **1993**, *194*, 463.
861. Kricheldorf, H. R.; Damrau, D. O. *Makromol. Chem. Phys.* **1997**, *198*, 1767.
862. Stolt, M.; Södergård, A. *Macromol. Symp.* **1998**, *130*, 393.
863. Stolt, M.; Södergård, A. *Macromolecules* **1999**, *32*, 6412.
864. Penczek, S.; Duda, A.; Szymanski, R.; Biela, T. *Macromol. Symp.* **2000**, *153*, 1.
865. Penczek, S.; Duda, A.; Szymanski, R. *Macromol. Symp.* **1998**, *132*, 441.
866. Baran, J.; Duda, A.; Kowalski, A.; Szymanski, R.; Penczek, S. *Macromol. Symp.* **1998**, *123*, 93.
867. O'Keefe, B. J.; Monnier, S. M.; Hillmyer, M. A.; Tolman, W. B. *J. Am. Chem. Soc.* **2001**, *123*, 339.
868. O'Keefe, B. J.; Breyfogle, L. E.; Hillmyer, M. A.; Tolman, W. B. *J. Am. Chem. Soc.* **2002**, *124*, 4384.
869. Gibson, V. C.; Marshall, E. L.; Navarro-Llobet, D.; White, A. J. P.; Williams, D. J. *Dalton Trans.* **2002**, 4321.
870. Gibson, V. C.; McGuinness, D. J. *Polym. Sci. Polym. Chem.* Submitted.
871. McLain, S. J.; Drysdale, N. E. US Pat. 5,028,667, 1991.
872. Okano, T.; Hayashizaki, Y.; Kiji, J. *Bull. Chem. Soc. Jpn.* **1993**, *66*, 1863.
873. Poncelet, O.; Sartain, W. J.; Hubert-Pfalzgraf, L. G.; Folting, K.; Caulton, K. G. *Inorg. Chem.* **1989**, *28*, 263.
874. Simic, V.; Spassky, N.; Hubert-Pfalzgraf, L. G. *Macromolecules* **1997**, *30*, 7338.
875. Spassky, N.; Simic, V.; Montaudo, M. S.; Hubert-Pfalzgraf, L. G. *Macromol. Chem. Phys.* **2000**, *201*, 2432.
876. Save, M.; Schappacher, M.; Soum, A. *Macromol. Chem. Phys.* **2002**, *203*, 889.
877. Schappacher, M.; Fabre, T.; Mingotaud, A. F.; Soum, A. *Biomaterials* **2001**, *22*, 2849.
878. Stevels, W. M.; Ankoné, M. J. K.; Dijkstra, P. J.; Feijen, J. *Macromol. Chem. Phys.* **1995**, *196*, 1153.
879. Zhong, Z.; Dijkstra, P. J.; Feijen, J. *Macromol. Chem. Phys.* **2000**, *201*, 1329.
880. Stevels, W. M.; Ankoné, M. J. K.; Dijkstra, P. J.; Feijen, J. *Macromolecules* **1996**, *29*, 3332.
881. Martin, E.; Dubois, Ph.; Jérôme, R. *Macromolecules* **2000**, *33*, 1530.
882. Tortosa, K.; Hamaide, T.; Boisson, C.; Spitz, R. *Macromol. Chem. Phys.* **2001**, *202*, 1156.
883. Simic, V.; Girardon, V.; Spassky, N.; Hubert-Pfalzgraf, L. G.; Duda, A. *Polymer Degrad. Stab.* **1998**, *59*, 227.
884. LeBorgne, A.; Pluta, C.; Spassky, N. *Macromol. Rapid Commun.* **1994**, *15*, 955.
885. Simic, V.; Pensec, S.; Spassky, N. *Macromol. Symp.* **2000**, *153*, 109.
886. Chamberlain, B. M.; Sun, Y.; Hagadorn, J. R.; Hemmesch, E. W.; Young, V. G.; Pink, M.; Hillmyer, M. A.; Tolman, W. B. *Macromolecules* **1999**, *32*, 2400.
887. Chamberlain, B. M.; Jazdzewski, B. A.; Pink, M.; Hillmyer, M. A.; Tolman, W. B. *Macromolecules* **2000**, *33*, 3970.
888. Yamashita, M.; Takemoto, Y.; Ihara, E.; Yasuda, H. *Macromolecules* **1996**, *29*, 1798.
889. Ihara, E.; Tanabe, M.; Nakayama, Y.; Nakamura, A.; Yasuda, H. *Macromol. Chem. Phys.* **1999**, *200*, 758.
890. Tsutsumi, C.; Yasuda, H. *J. Polym. Sci. Polym. Chem.* **2001**, *39*, 3916.
891. Yasuda, H.; Aludin, M. S.; Kitamura, N.; Tanabe, M.; Sirahama, H. *Macromolecules* **1999**, *32*, 6047.
892. Aubrecht, K. B.; Chang, K.; Hillmyer, M. A.; Tolman, W. B. *J. Polym. Sci., Polym. Chem.* **2001**, *39*, 284.
893. Giesbrecht, G. R.; Whitener, G. D.; Arnold, J. J. *J. Chem. Soc. Dalton Trans.* **2001**, 923.
894. Matsuo, Y.; Mashima, K.; Tani, K. *Organometallics* **2001**, *20*, 3510.
895. Shen, Y.; Shen, Z.; Zhang, Y.; Yao, K. *Macromolecules* **1996**, *29*, 8289.
896. Deng, X. M.; Yuan, M. L.; Xiong, C. D.; Li, X. H. *J. Appl. Polym. Sci.*, **1999**, *71*, 1941.

897. Zhang, J.; Gan, Z.; Zhong, Z.; Jing, X. *Polym. Int.* **1998**, *45*, 60.
898. Shen, Y.; Shen, Z.; Zhang, Y.; Huang, Q.; Shen, L.; Yuan, H. *J. Appl. Polym. Sci.* **1997**, *64*, 2131.
899. Shen, Y.; Shen, Z.; Shen, J.; Zhang, Y.; Yao, K. *Macromolecules* **1996**, *29*, 3441.
900. Shen, Y.; Shen, Z.; Shen, J.; Zhang, Y.; Hang, Q. *J. Polym. Sci. Polym. Chem.* **1997**, *35*, 1339.
901. Barbier-Baudry, D.; Bouazza, A.; Brachais, C. H.; Dormond, A.; Visseaux, M. *Macromol. Rapid Commun.* **2000**, *21*, 213.
902. Deng, X. M.; Yuan, M. L.; Xiong, C. D.; Li, X. H. *J. Appl. Polym. Sci.* **1998**, *73*, 1401.
903. Deng, X. M.; Yuan, M. L.; Li, X. H.; Xiong, C. D. *Eur. Polym. J.* **2000**, *36*, 1151.
904. Yuan, M. L.; Li, X. H.; Xiong, C. D.; Deng, X. M. *Eur. Polym. J.* **1999**, *35*, 2131.
905. Ravi, P.; Gröb, T.; Dehnicke, K.; Greiner, A. *Macromol. Chem. Phys.* **2001**, *202*, 2641.
906. Agarwal, S.; Brandukova-Szmikowski, N. E.; Greiner, A. *Macromol. Rapid Commun.* **1999**, *20*, 274.
907. Nishiura, M.; Hou, Z.; Koizumi, T.; Imamoto, T.; Wakatsuki, Y. *Macromolecules* **1999**, *32*, 8245.
908. Agarwal, S.; Karl, M.; Dehnicke, K.; Seybert, G.; Massa, W.; Greiner, A. *J. Appl. Polym. Sci.* **1999**, *73*, 1669.
909. Barbier-Baudry, D.; Heiner, S.; Kubicki, M. M.; Vigier, E.; Visseaux, M.; Hafid, A. *Organometallics* **2001**, *20*, 4207.
910. Shen, Q.; Yao, Y. *J. Organomet. Chem.* **2002**, *647*, 180.
911. Hultsch, K. C.; Spaniol, T. P.; Okuda, J. *Organometallics* **1997**, 4845.
912. Beckerle, K.; Hultsch, K. C.; Okuda, J. *Macromol. Chem. Phys.* **1999**, *200*, 1702.
913. Miola-Delaite, C.; Hamaide, T.; Spitz, R. *Macromol. Chem. Phys.* **1999**, *200*, 1771.
914. Bero, M.; Dobrzynski, P.; Kasperczyk, J. *Polym. Bull.* **1999**, *42*, 131.
915. Dobrzynski, P.; Kasperczyk, J.; Janeczek, H.; Bero, M. *Macromolecules* **2001**, *34*, 5090.
916. Dobrzynski, P. *J. Polym. Sci. Polym. Chem.* **2002**, *40*, 1379.
917. Okuda, J.; Rushkin, I. L. *Macromolecules* **1993**, *26*, 5530.
918. Okuda, J.; König, P.; Rushkin, I. L.; Kang, H. C.; Massa, W. *J. Organomet. Chem.* **1995**, *501*, 37.
919. Takeuchi, D.; Nakamura, T.; Aida, T. *Macromolecules* **2000**, *33*, 725.
920. Takeuchi, D.; Aida, T.; Endo, T. *Macromol. Rapid Commun.* **1999**, *20*, 182.
921. Takeuchi, D.; Aida, T.; Endo, T. *Macromol. Chem. Phys.* **2000**, *201*, 2267.
922. Kim, Y.; Verkade, J. G. *Organometallics* **2002**, *21*, 2395.
923. Mukaiyama, T.; Hayakawa, M.; Oouchi, K.; Mitani, M.; Yamada, T. *Chem. Lett.* **1995**, 737.
924. Arndt, P.; Thomas, D.; Rosenthal, U. *Tet. Lett.* **1997**, *38*, 5467.
925. Arndt, P.; Spannenberg, A.; Baumann, W.; Becke, S.; Rosenthal, U. *Eur. J. Inorg. Chem.* **2001**, 2885.
926. Thomas, D.; Arndt, P.; Peulecke, N.; Spannenberg, A.; Kempe, R.; Rosenthal, U. *Eur. J. Inorg. Chem.* **1998**, 1351.
927. Owens, K.; Kyllingstad, V. L.; *Kirk-Othmer Encyclopaedia of Chemical Technology*, 4th Edition; Wiley: New York, p 1079.
928. Back, D. M.; Clark, E. M.; Ramachandran, R. *Kirk-Othmer Encyclopaedia of Chemical Technology*, 4th Edition; Wiley: New York, p 701.
929. Gagnon, S. D. *Kirk-Othmer Encyclopaedia of Chemical Technology*, 4th Edition; Wiley: New York, p 722.
930. Gee, G.; Higginson, W. C. E.; Levesley, P.; Taylor, K. J. *J. Chem. Soc.* **1959**, 1339.
931. Gee, G.; Higginson, W. C. E.; Merrall, G. T. *J. Chem. Soc.* **1959**, 1345.
932. Goeke, G. L.; Karol, F. J. US Pat. 4,193,892, 1980.
933. Le-Khac, B. US Pat. 5,482,908, 1996.
934. Huang, Y. J.; Qi, G. R.; Wang, Y. H. *J. Polym. Sci. Polym. Chem.* **2002**, *40*, 1142.
935. Antelmann, B.; Chisholm, M. H.; Iyer, S. S.; Huffman, J. C.; Navarro-Llobet, D.; Pagel, M.; Simonsick, W. J.; Zhong, W. *Macromolecules* **2001**, *34*, 3159.
936. Aida, T.; Inoue, S. *Macromolecules* **1981**, *14*, 1162.
937. Aida, T.; Mizuta, R.; Yoshida, Y.; Inoue, S. *Makromol. Chem.* **1981**, *182*, 1073.
938. Aida, T.; Inoue, S. *Macromolecules* **1981**, *14*, 1166.
939. Aida, T.; Inoue, S. *Makromol. Chem. Rapid Commun.* **1980**, *1*, 677.
940. Aida, T.; Wada, K.; Inoue, S. *Macromolecules* **1987**, *20*, 237.
941. Asano, S.; Aida, T.; Inoue, S. *Chem. Commun.* **1985**, 1148.
942. Akatsuka, M.; Aida, T.; Inoue, S. *Macromolecules* **1994**, *27*, 2820.
943. Watanabe, Y.; Yasuda, T.; Aida, T.; Inoue, S. *Macromolecules* **1992**, *25*, 1396.
944. Watanabe, Y.; Aida, T.; Inoue, S. *Macromolecules* **1990**, *23*, 2612.
945. Watanabe, Y.; Aida, T.; Inoue, S. *Macromolecules* **1991**, *24*, 3970.
946. Sugimoto, H.; Kawamura, C.; Kuroki, M.; Aida, T.; Inoue, S. *Macromolecules* **1994**, *27*, 2013.
947. Vincens, V.; LeBorgne, A.; Spassky, N. *Makromol. Chem. Rapid. Commun.* **1989**, *10*, 623.
948. Mason, M. R.; Perkins, A. M. *J. Organomet. Chem.* **2000**, *599*, 200.
949. Emig, N.; Nguyen, H.; Krautscheid, H.; Réau, R.; Cazaux, J. B.; Bertrand, G. *Organometallics* **1998**, *17*, 3599.
950. Munoz-Hernandez, M. A.; McKee, M. L.; Keizer, T. S.; Yearwood, B. C.; Atwood, D. A. *J. Chem. Soc. Dalton Trans.* **2002**, 410.
951. Atwood, D. A.; Jegier, J. A.; Rutherford, D. *J. Am. Chem. Soc.* **1995**, *117*, 6779.
952. Muñoz-Hernández, M. A.; Sannigrahi, B.; Atwood, D. A. *J. Am. Chem. Soc.* **1999**, *121*, 6747.
953. Atwood, D. A.; Jegier, J. A.; Rutherford, D. *Inorg. Chem.* **1996**, *35*, 63.
954. Inoue, S.; Koinuma, H.; Tsuruta, T. *J. Polym. Sci.* **1969**, *B7*, 287.
955. Rokicki, A.; Kuran, W. *J. Macromol. Sci. Rev. Macromol. Chem.* **1981**, *C21*, 135.
956. Darnesbourg, D. J.; Holtcamp, M. W. *Macromolecules* **1995**, *28*, 7577.
957. Koning, C.; Wildeson, J.; Parton, R.; Plum, B.; Steeman, P.; Darnesbourg, D. J. *Polymer* **2001**, *42*, 3995.
958. Darnesbourg, D. J.; Holtcamp, M. W.; Struck, G. E.; Zimmer, M. S.; Niezgodna, S. A.; Rainey, P.; Robertson, J. B.; Draper, J. D.; Reibenspies, J. H. *J. Am. Chem. Soc.* **1999**, *121*, 107.
959. Darnesbourg, D. J.; Rainey, P.; Yarbrough, J. *Inorg. Chem.* **2001**, *40*, 986.
960. Dinger, M. B.; Scott, M. J. *Inorg. Chem.* **2001**, *40*, 1029.
961. Darnesbourg, D. J.; Zimmer, M. S. *Macromolecules* **1999**, *32*, 2137.
962. Darnesbourg, D. J.; Wildeson, J. R.; Yarbrough, J. C. *Inorg. Chem.* **2002**, *41*, 973.
963. Cheng, M.; Lobkovsky, E. B.; Coates, G. W. *J. Am. Chem. Soc.* **1998**, *120*, 11018.

964. Cheng, M.; Moore, D. R.; Reczek, J. J.; Chamberlain, B. M.; Lobkovsky, E. B.; Coates, G. W. *J. Am. Chem. Soc.* **2001**, *123*, 8738.
965. Sita, L. R.; Babcock, J. R.; Xi, R. *J. Am. Chem. Soc.* **1996**, *118*, 10912.
966. Cheng, M.; Darling, N. A.; Lobkovsky, E. B.; Coates, G. W. *Chem. Commun.* **2000**, 2007.
967. Nozaki, K.; Nakano, K.; Hiyama, T. *J. Am. Chem. Soc.* **1999**, *121*, 11008.
968. Sun, H. N. US Pat. 4,783,445, 1988.
969. Super, M.; Berluche, E.; Costello, C.; Beckman, E. *Macromolecules* **1997**, *30*, 368.
970. Sârbu, T.; Beckman, E. J. *Macromolecules* **1999**, *32*, 6904.
971. Takeda, N.; Inoue, S. *Bull. Chem. Soc. Jpn.* **1978**, *51*, 3564.
972. Kasuga, K.; Nagao, S.; Fukumoto, T.; Handa, M. *Polyhedron* **1996**, *15*, 69.
973. Aida, T.; Inoue, S. *J. Am. Chem. Soc.* **1983**, *105*, 1304.
974. Aida, T.; Inoue, S. *Macromolecules* **1982**, *15*, 682.
975. Koinuma, H.; Hirai, H. *Makromol. Chem.* **1977**, *178*, 1283.
976. Takeda, N.; Inoue, S. *Makromol. Chem.* **1978**, *179*, 1377.
977. Aida, T.; Ishikawa, M.; Inoue, S. *Macromolecules* **1986**, *19*, 8.
978. Aida, T.; Inoue, S. *J. Am. Chem. Soc.* **1985**, *107*, 1358.
979. Aida, T.; Sanuki, K.; Inoue, S. *Macromolecules* **1985**, *18*, 1049.
980. Mang, S.; Cooper, A. I.; Colclough, M. E.; Chauhan, N.; Holmes, A. B. *Macromolecules* **2000**, *33*, 303.
981. Stamp, L. M.; Mang, S. A.; Holmes, A. B.; Knights, K. A.; de Miguel, Y. R.; McConvey, I. F. *Chem. Commun.* **2001**, 2502.
982. Drent, E.; Kragwijk, E. Eur. Pat. EP577206, 1994.
983. Allmendinger, M.; Eberhardt, R.; Luinstra, G.; Rieger, B. *J. Am. Chem. Soc.* **2002**, *124*, 5646.
984. Getzler, Y. D. Y. L.; Mahadevan, V.; Lobkovsky, E. B.; Coates, G. W. *J. Am. Chem. Soc.* **2002**, *124*, 1174.
985. Lee, J. T.; Thomas, P. J.; Alper, H. *J. Org. Chem.* **2001**, *66*, 5424.
986. Mahadevan, V.; Getzler, Y. D. Y. L.; Coates, G. W. *Angew. Chem., Int. Ed. Engl.* **2002**, *41*, 2781.
987. Jia, L.; Sun, H.; Shay, J. T.; Allgeier, A. M.; Hanton, S. D. *J. Am. Chem. Soc.* **2002**, *124*, 7282.
988. Jia, L.; Ding, E.; Anderson, W. R. *Chem. Commun.* **2001**, 1436.
989. Woodward, R. B.; Schramm, C. H. *J. Am. Chem. Soc.* **1947**, *69*, 1551.
990. Kricheldorf, H. R. *α -Amino Acid-N-Carboxyanhydrides and Related Materials*; Springer: New York, 1987.
991. Deming, T. J. *Nature* **1997**, *390*, 386.
992. Deming, T. J. *J. Am. Chem. Soc.* **1998**, *120*, 4240.
993. Deming, T. J. *Macromolecules* **1999**, *32*, 4500.
994. Deming, T. J. *Adv. Drug Delivery Rev.* **2002**, *54*, 1145.
995. Deming, T. J. *J. Polym. Sci., Polym. Chem.* **2000**, *38*, 3011.
996. Cheng, J.; Deming, T. J. *Macromolecules* **2001**, *34*, 5169.
997. Cheng, J.; Deming, T. J. *J. Am. Chem. Soc.* **2001**, *123*, 9457.
998. Shashoua, V. E.; Sweeny, W.; Tietz, R. *J. Am. Chem. Soc.* **1960**, *82*, 866.
999. Patten, T. E.; Novak, B. M. *J. Am. Chem. Soc.* **1991**, *113*, 5065.
1000. Patten, T. E.; Novak, B. M. *Macromolecules* **1993**, *26*, 436.
1001. Patten, T. E.; Novak, B. M. *J. Am. Chem. Soc.* **1996**, *118*, 1906.
1002. Hoff Goodson, S.; Novak, B. M. *Macromolecules* **2001**, *34*, 3849.
1003. Schlitzer, D. S.; Novak, B. M. *J. Am. Chem. Soc.* **1998**, *120*, 2196.
1004. Shibayama, K.; Seidel, S. W.; Novak, B. M. *Macromolecules* **1997**, *30*, 3159.

9.2

Metal Complexes as Hydrogenation Catalysts

C. PETTINARI, F. MARCHETTI, and D. MARTINI

Università degli Studi, Camerino, Italy

9.2.1	INTRODUCTION	75
9.2.2	HISTORICAL BACKGROUND	76
9.2.3	HOMOGENEOUS HYDROGENATION	76
9.2.3.1	Metal Monohydride Mechanism	77
9.2.3.2	Metal Dihydride Mechanism	80
9.2.3.3	Asymmetric Hydrogenation Mechanisms	82
9.2.4	HOMOGENEOUS TRANSFER HYDROGENATION	92
9.2.4.1	Direct Hydrogen Transfer Mechanism	93
9.2.4.2	Metal Monohydride Mechanism	93
9.2.4.3	Metal Dihydride Mechanism	95
9.2.4.4	Metal–Ligand Bifunctional Concerted Mechanism	95
9.2.4.5	Mechanism of Aerobic Alcohol Oxidation	96
9.2.5	HOMOGENEOUS HYDROGENOLYSIS	98
9.2.5.1	Hydrodesulfurization	99
9.2.5.2	Hydrodenitrogenation	105
9.2.6	NEW DEVELOPMENTS IN HYDROGENATION	110
9.2.6.1	Hydrogenation in Aqueous Systems	110
9.2.6.1.1	<i>Water-soluble hydrogenation catalysts</i>	111
9.2.6.1.2	<i>Immobilization on solids</i>	114
9.2.6.1.3	<i>Immobilization via biphasic catalysis</i>	117
9.2.6.1.4	<i>Microheterogenization on organized amphiphiles in the colloidal or nanoscale dimension</i>	118
9.2.6.1.5	<i>Enantioselective hydrogenation in aqueous systems</i>	120
9.2.6.1.6	<i>Transfer hydrogenation and hydrogenolysis in aqueous systems</i>	121
9.2.6.1.7	<i>Hydrogenations with CO/H₂O mixtures</i>	121
9.2.6.2	Hydrogenation in Supercritical Carbon Dioxide	122
9.2.6.3	Hydrogenation by Cluster Catalysis	125
9.2.7	HYDROGENATION IN BIOLOGICAL SYSTEMS	129
9.2.8	REFERENCES	133

9.2.1 INTRODUCTION

Hydrogenation plays a key role in chemical synthesis. Homogeneous hydrogenation has become increasingly important in recent decades, mainly due to its application in the industrial production of specialty chemicals.^{1–6} Homogeneous hydrogenation is a chemical transformation during which one or more H atoms are incorporated into the product of the reaction, by the action of an active catalyst present in the same phase of the reactants.

Hydrogen (H₂) is the simplest molecule and its properties are fully understood. Because this clean resource is available in abundance at a very low cost, catalytic hydrogenation is a core technology in both research and industry.

The term “homogeneous hydrogenation” is generally referred to homogeneous catalyzed addition of H_2 to unsaturated organic substrates; however, also the processes “transfer hydrogenation” and “hydrogenolysis” must be taken into account.⁵ The former comprises all catalyzed hydrogen transfer reactions where hydrogen donors (DH_2) other than simple molecular hydrogen are involved as reactants in hydrogen addition, while the latter indicates those reactions, subsequent to hydrogenation by H_2 or DH_2 , in which the original substrate undergoes fragmentation leading to new products. However, hydrogenation involving activation and addition of H_2 constitutes, without doubt, the main field of homogeneous hydrogenation where the wider number of studies and examples of catalysts can be found.

Molecular hydrogen is rather unreactive at ambient conditions, but many transition and lanthanide metal ions are able to bind and therefore activate H_2 , which results in transformation into H^- (hydride) $H\cdot$ (hydrogen radical) or H^+ (proton), and subsequent transfer of these forms of hydrogen to the substrate.^{7,8} In this context, not only metal hydride but also dihydrogen complexes of transition metal ions, play a key role,^{9,10} especially since the first structural characterization of one of these species in 1984 by Kubas.¹¹

At present, the economic impact of industrial homogeneous hydrogenation is rapidly growing. Some hydrogenation reactions are very useful in practical applications in organic synthesis on the laboratory scale and more recently some enantioselective hydrogenation reactions have become very important in the industrial manufacture of fine chemicals and pharmaceuticals. The expanding interest in this area and the resulting increased knowledge in the field of asymmetric catalysis resulted in the award of the 2001 Nobel Prize in Chemistry to three prominent scientists, among whom William S. Knowles¹² and Ryoji Noyori¹³ were honored for their work on asymmetric catalytic hydrogenation.

The last decades have witnessed a continually increasing effort into the study of homogeneous hydrogenation,^{1–6} mainly because activation and addition of H_2 has proven to be amenable for detailed investigations under gentle conditions, with respect to more unreactive small molecules such as, for example, CO or N_2 ; and also because the characterization of the product distribution of alkene hydrogenation requires cheaper and simpler spectroscopic techniques compared to reactions carried out under high pressure and high temperature. In addition, knowledge of the mechanisms can be very important for the growing field of heterogeneous hydrogenation, and for biological studies on the structure–activity relationship of several naturally occurring hydrogenase enzymes.

Here we focus on the most representative aspects of the catalytic mechanisms so far elucidated and the catalytic systems developed, without covering all the literature; recent reviews are cited where appropriate.

9.2.2 HISTORICAL BACKGROUND

Homogeneous catalytic hydrogenation was first discovered in 1938.^{14,15} Interestingly, the discovery of the Meerwin–Ponndorf–Verley hydrogen transfer reaction, in which a ketone is reduced by an alcohol in the presence of an aluminum alkoxide, is still older, dating to 1925.^{16–18} Subsequent research in this field did not result in any important progress until the discovery of the catalytic properties of $[RhCl(PPh_3)_3]$, commonly known as “Wilkinson’s catalyst,”^{19,20} which marked the start of modern homogeneous catalysis.²¹ Subsequently, Schrock and Osborn reported new catalytic systems based on cationic Rh and Ir phosphine complexes,^{22–25} and laid the foundations for the development of asymmetric hydrogenation of prochiral substrates using catalysts containing chiral diphosphine ligands.^{26,27} Knowles and co-workers developed the concept of chiral catalysts by introduction into the metal coordination sphere of chiral diphosphines, in order to obtain significant ee (enantiomeric excess) in the hydrogenation of functionalized olefinic substrates.²⁸

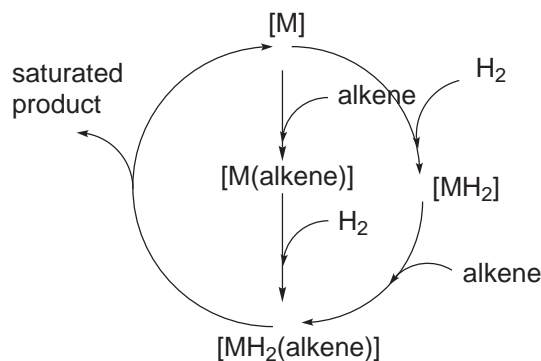
The most important progress in the last decade has been in the design and synthesis of $[RuCl_2(\text{diphosphine})(1,2\text{-diamine})]$ catalysts exploiting the “metal–ligand bifunctional concept” developed by Noyori and co-workers.^{29–31} The Noyori catalysts seem to possess all of the desired properties, such as high turnover number (TON), high turnover frequency (TOF), and operationally simple, safe, and environmentally friendly reaction conditions.

9.2.3 HOMOGENEOUS HYDROGENATION

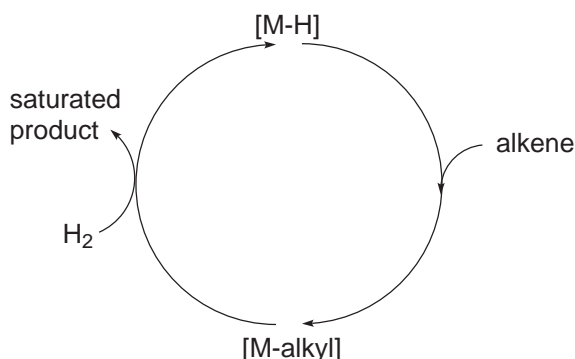
Since the first reports on Wilkinson’s catalyst,^{19,20} many transition-metal-based catalytic systems for hydrogenation of unsaturated organic molecules have been developed. Two major pathways seem to occur, one involving monohydride ($M-H$) species, and the other, dihydride (MH_2)

species. Elucidation of the mechanisms has required detailed kinetic and spectroscopic measurements of as many of the individual steps as possible, with analytical tools (IR, UV and particularly conventional NMR spectroscopy, but also new methods such as parahydrogen-induced nuclear polarization (PHIP)^{32–37}). Additionally, the isolation and/or independent syntheses of stable intermediates or model compounds, and theoretical calculations, have provided detailed mechanisms for the catalytic cycles.

In [Scheme 1](#) is represented an idealized picture of the two possibilities for the hydrogenation of alkenes by metal complexes not containing an M–H bond. One possibility involves initial coordination of the alkene followed by activation of H₂ (alkene route). The other (more general) possibility is the hydride route, which involves initial reaction with H₂ followed by coordination of the alkene. The second general mechanism, usually adopted by catalysts containing an M–H bond, is shown in [Scheme 2](#).



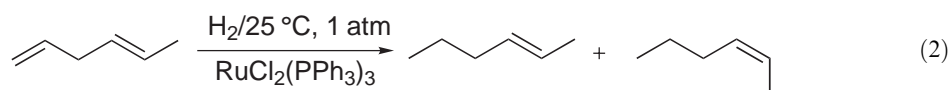
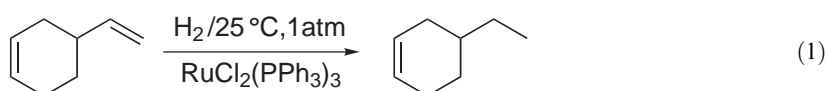
Scheme 1

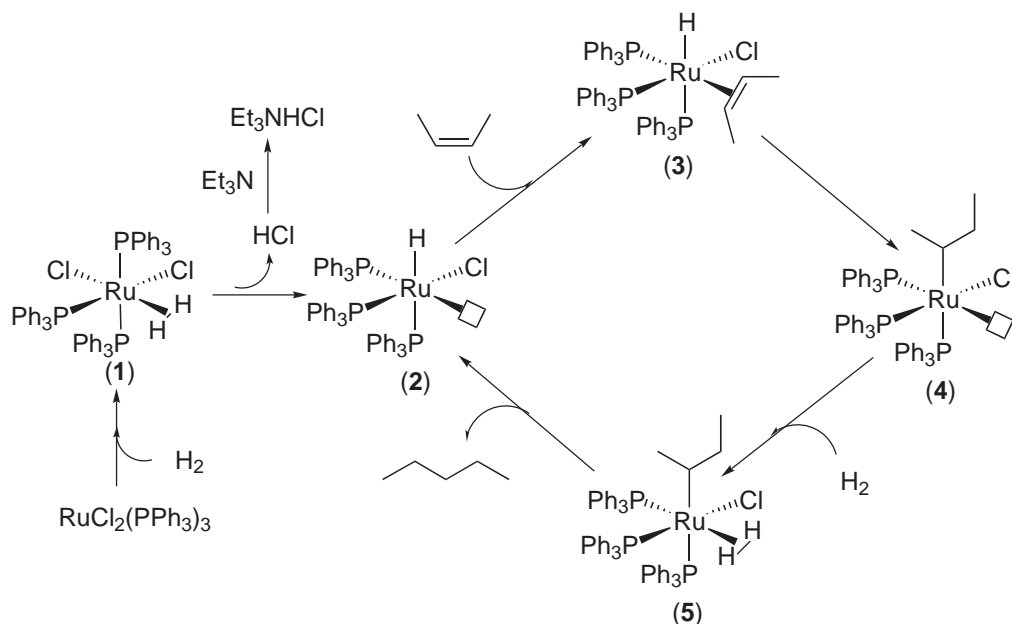


Scheme 2

9.2.3.1 Metal Monohydride Mechanism

One of the most famous catalysts, which operates through a mechanism involving formation of a mono-hydride (M–H), is [RuCl₂(PPh₃)₃].^{38–40} In the catalytic hydrogenation of alkenes ([Equations \(1\) and \(2\)](#)) it shows very high selectivity for hydrogenation of terminal rather than internal C=C bonds.





Scheme 3

Subsequent studies⁴¹ have shown that the active species is probably the 16-electron monohydride species $[\text{RuHCl}(\text{PPh}_3)_3]$ (2) which forms from the dihydrogen complex (1) in the presence of Et_3N . Complex (2), having a vacant site, interacts with the alkene to give (3), which undergoes 1,2-insertion to form the alkyl-Ru complex (4). Finally, heterolytic cleavage with H_2 ((4) \rightarrow (5) \rightarrow (2)) regenerates the active catalyst and gives the alkane (Scheme 3).

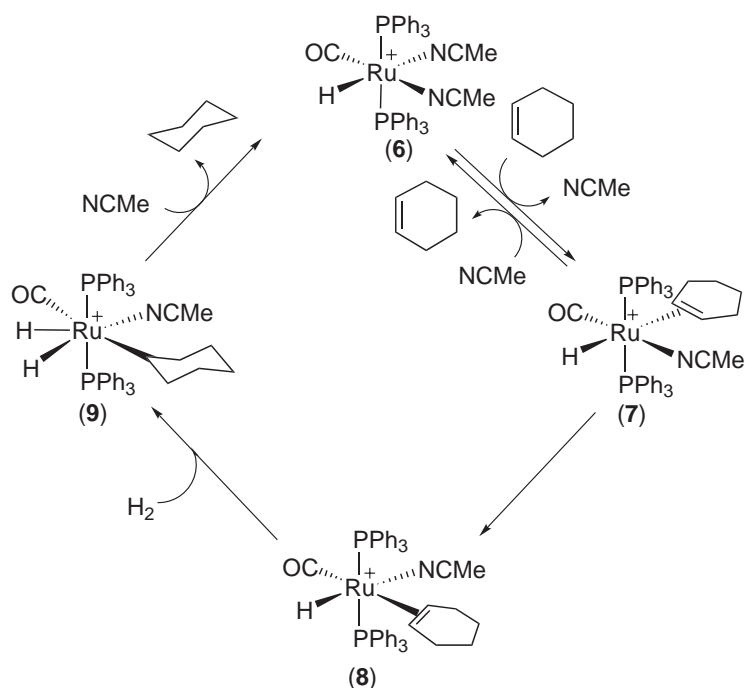
Recently, two other kinetic and mechanistic studies of the hydrogenation of cyclohexene with modified neutral and cationic ruthenium catalysts have been reported involving a monohydride intermediate. Sanchez-Delgado and co-workers employed $[\text{RuCl}_2(4\text{-Bu}^t\text{-py})_2(\text{PPh}_3)_2]$ which, after dissociation of one N-donor, forms an unsaturated monohydride which is the active catalyst, the steps of the mechanism being analogous to those of $[\text{RuHCl}(\text{PPh}_3)_3]$.⁴²

Probably more interesting is the examination of the catalytic cycle of hydrogenation studied by Rosales and co-workers⁴³ which used $[\text{RuH}(\text{CO})(\text{NCMe})_2(\text{PPh}_3)_2]\text{BF}_4$ as catalyst (species (6)).⁴⁴ The reversible displacement of the MeCN ligand trans to the hydride by cyclohexene is followed by an isomerization prior to rate-determining addition of hydrogen ((7) \rightarrow (8) \rightarrow (9)) (Scheme 4).

Other interesting examples of catalyzed hydrogenation proceeding through a monohydride intermediate are the so called "Zaragoza-Wurzburg catalysts," developed by extended cooperation between Oro and Werner.^{45,46} The complexes $[\text{OsHCl}(\text{CO})(\text{PR}_3)_2]$ ($\text{PR}_3 = \text{PPr}^i_3, \text{PMeBu}^t_2$) are selective catalysts for the sequential hydrogenation of phenylacetylene to styrene in 2-propanol solution with selectivity close to 100%. Mechanistic studies⁴⁷⁻⁴⁹ suggest the catalytic cycle in Scheme 5.

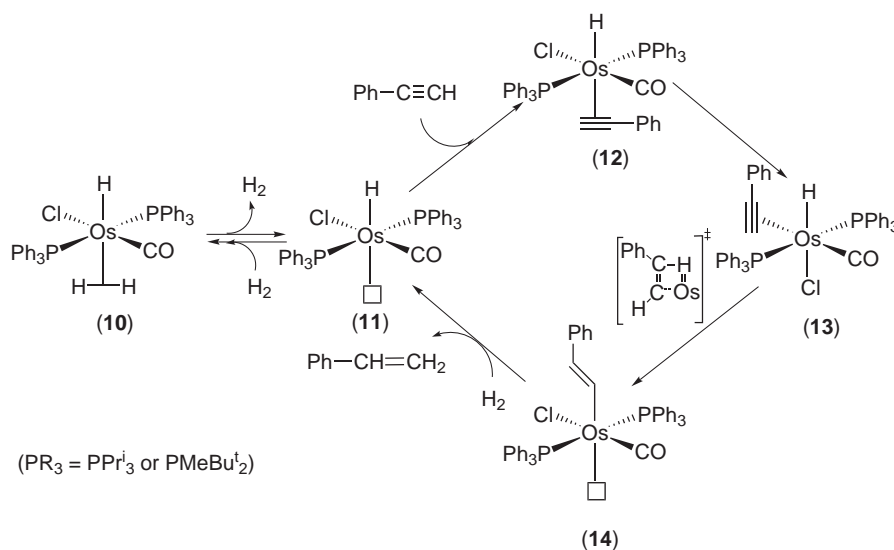
The monohydride (11) reacts rapidly with H_2 , giving the dihydrogen-hydride complex (10), and also with phenylacetylene initially through coordination of the triple bond to Os (12), followed by isomerization to (13), in which alkyne and hydride are mutually in *cis* positions, well suited for subsequent insertion of $\text{C}\equiv\text{C}$ into the $\text{M}-\text{H}$ bond and formation of the vinyl derivative (14). The slow step is the reaction of the vinyl intermediate with H_2 to yield styrene and regenerate the starting hydride. The dihydride $[\text{OsH}_2(\text{CO})(\text{PPr}^i_3)_2]$ catalyzes hydrogenation of styrene, methylstyrene, cyclohexene, cyclooctene, and the $\text{C}=\text{C}$ bond of α,β -unsaturated ketones.⁴⁷⁻⁴⁹

Another example of selective $\text{C}\equiv\text{C}$ bond hydrogenation has arisen from mechanistic studies on an iron *cis*-hydride dihydrogen complex, $[\text{Fe}(\text{PP}_3)(\text{H})(\text{H}_2)](\text{BF}_4)$ [$\text{PP}_3 = \text{P}(\text{CH}_2\text{CH}_2\text{PPh}_2)_3$], a catalyst inactive with alkene substrates. Scheme 6 shows that no decoordination of dihydrogen is required in any step of the cycle and that the vacant site is created by unfastening of one of the P-donor atoms (species (16)).⁵⁰ Extensive studies on catalytic alkene hydrogenation by analogous tripodal (polyphosphine) Rh, Os, and Ir complexes have been carried by Bianchini and co-workers.^{51,52}

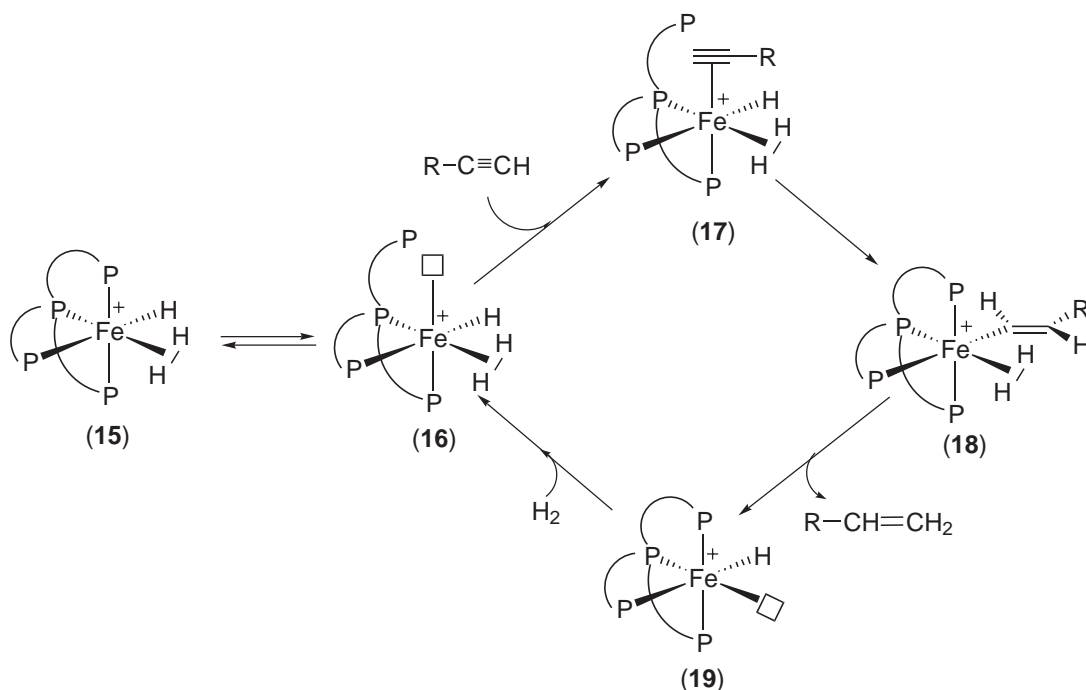


Scheme 4

Marks and co-workers have reported several organo-lanthanide complexes of formula $[(Cp')_2MH]_2$ ($Cp' = \eta^5-C_5Me_5$, $M = La, Nd, Sm, Lu$) and $[(Me_2SiCp'')_2MH]_2$ ($Cp'' = \eta^5-C_5Me_4$, $M = Nd, Sm, Lu$), very active as catalysts in olefinic hydrogenation under very mild conditions (25 °C and 1 atm H_2).⁵³ In Scheme 7, the proposed mechanism for the catalytic cycle shows that these hydrido-complexes (20) undergo hydrogenation through a mechanism involving close coupling of olefin/hydride insertion ((21) \rightarrow (22) \rightarrow (23)) followed by a four-center hydrogenolysis (24), rather than via classical oxidative addition/reductive elimination sequences.



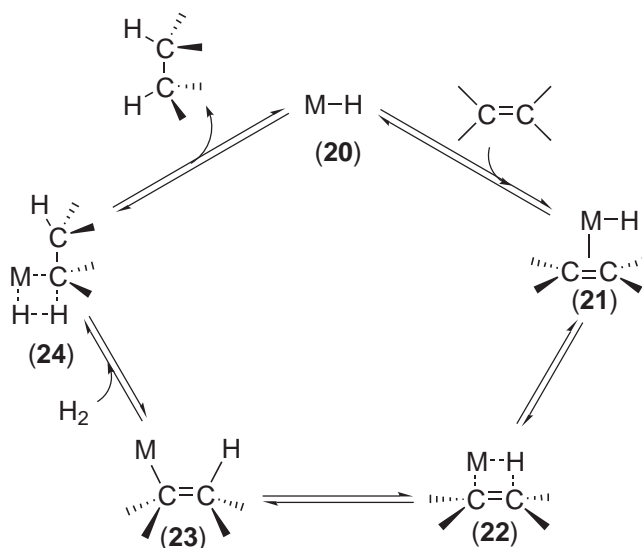
Scheme 5



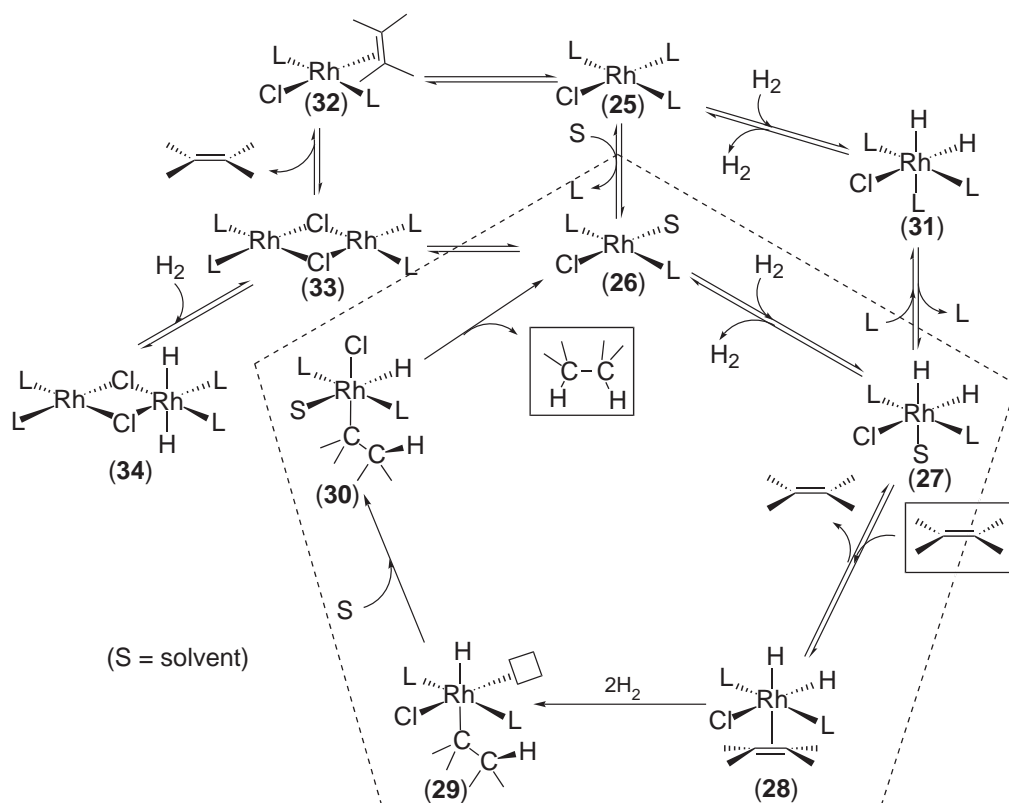
Scheme 6

9.2.3.2 Metal Dihydride Mechanism

One of the most well-studied and synthetically useful catalysts involving a dihydride (MH_2) intermediate is Wilkinson's catalyst, $[\text{RhCl}(\text{PPh}_3)_3]$.^{19–21} After molecular orbital calculations performed by Morokuma,⁵⁴ the following mechanism (Scheme 8) is generally accepted. The pre-catalyst (25) dissociates into the 14-electron species (26), which adds H_2 with a rate about 10,000 times greater than (25). Then the dihydride species (27) coordinates the alkene (species (28)), which undergoes 1,2-insertion into an $\text{M}-\text{H}$ bond affording the alkyl species (29). This intermediate contains the alkyl group in the *trans* position with respect to remaining hydride, but for the subsequent step (reductive elimination) these two ligands must be situated *cis* with



Scheme 7



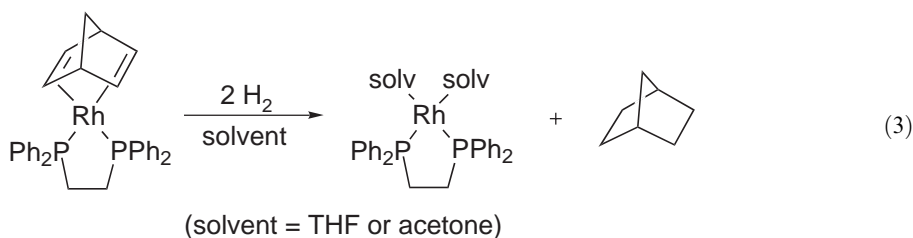
Scheme 8

respect to each other. This requires an isomerization, and theoretical calculations predict sequential hydride and chloride migration both with low activation barriers. The species (30) has now the correct geometry to undergo reductive elimination easily, yielding the alkane and regenerating the active catalyst (26).

This catalytic cycle shows other side cycles not proceeding with appreciable rates. In particular, the species (31)–(34), while detectable and isolable, are not responsible for the catalytic process; in fact their presence during hydrogenation may even slow down the overall reaction.

This is a valuable lesson for chemists trying to determine a catalytic mechanism: compounds readily isolable are probably not true intermediates. Instead, they can be seen as “labile reservoirs” to catalytic intermediates that usually do not accumulate in sufficient concentrations to be detected. It is important to bear in mind that this mechanism or any other catalytic process could be different dependent on the nature of the alkene, solvent, and phosphine ligands.

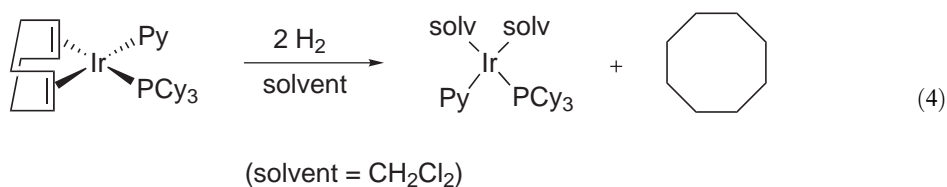
Many cationic Rh- or Ir-based hydrogenation catalysts were subsequently developed. Members of the Rh series were prepared according to Equation (3).^{22–25}



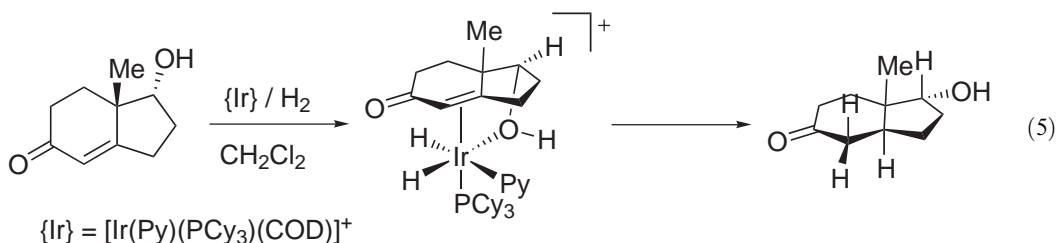
In catalytic reaction conditions (H_2 pressure), by interaction of a solvent such as THF or acetone, the 16-electron cationic $[Rh(\text{diphos})(\text{NBD})]^+$ affords a 12-electron unsaturated diphosphine intermediate, which is the real active species. The catalytic cycle begins with alkene binding, followed by oxidative addition of H_2 . These cationic catalysts can reduce alkenes to

alkanes, can convert alkynes to *cis*-alkenes, and also transform ketones to alcohols, their most important function being, however, the promotion of asymmetric hydrogenation of olefins.

The iridium analog of Wilkinson's catalyst, $[\text{IrCl}(\text{PPh}_3)_3]$, is not effective in reducing $\text{C}=\text{C}$ bonds because the phosphines are more strongly bound to Ir than to Rh, thereby preventing phosphine dissociation to give the active species $[\text{IrCl}(\text{PPh}_3)_2]$. In contrast, cationic catalysts $[\text{Ir}(\text{L})(\text{L}')(\text{COD})]^+$, developed mainly by Crabtree,⁵⁵ are even more active than Wilkinson's catalyst; they can promote saturation of even tetra-substituted $\text{C}=\text{C}$ bonds almost as fast as mono- and di-substituted double bonds. In the presence of CH_2Cl_2 and H_2 , an active and very reactive 12-electron species forms, similar to that formed by cationic Rh catalysts (Equation (4)). This active species is a relatively hard Lewis acid, able to bind not only alkene and hydrogen, but also polar ligands such as alcohol and carbonyl oxygen.



The stereoselectivity obtained in hydrogenation of an enone can be due to the formation of an intermediate in which alkene, hydrogen, and alcohol groups bind simultaneously to the metal (Equation (5)). This kind of stereoselectivity is typical in catalytic reactions where a polar group resides near to a $\text{C}=\text{C}$ bond.

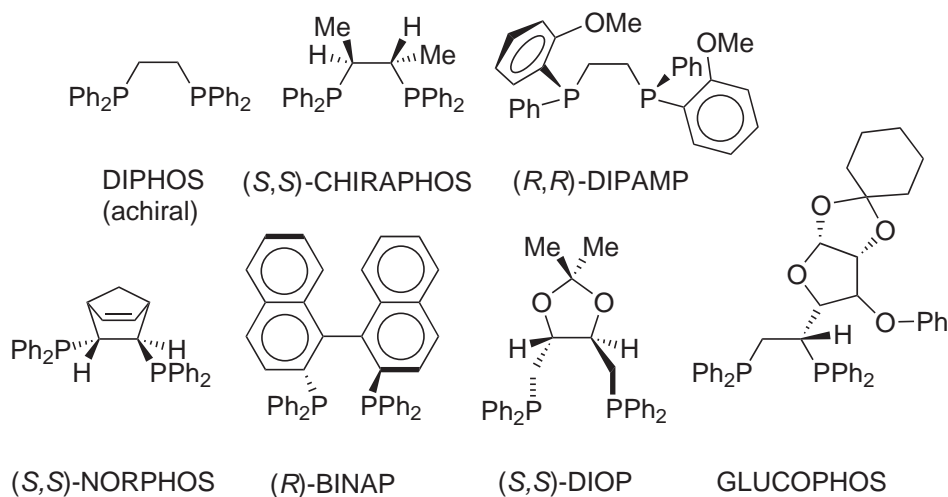


The hydrogenation of arenes also has attracted interest, but until recently only a few catalytic systems have been found effective.^{56–60} The catalytic activity of $[\text{Rh}(\text{MeOH})_2(\text{diphos})]\text{X}$ and of $[\text{RuH}_2(\text{H}_2)(\text{PPh}_3)_3]$ in the hydrogenation of 9-trifluoroacetylanthracene and 9-methylantracene has been explored.^{61,62}

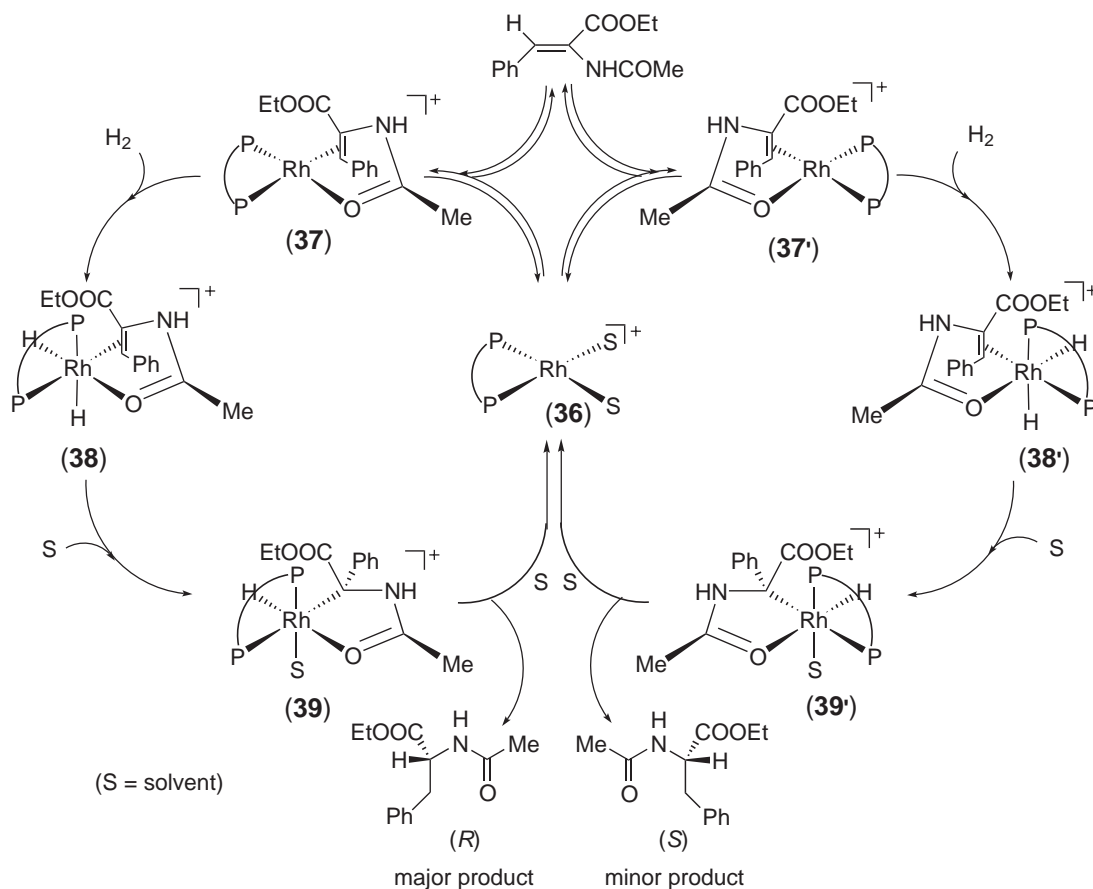
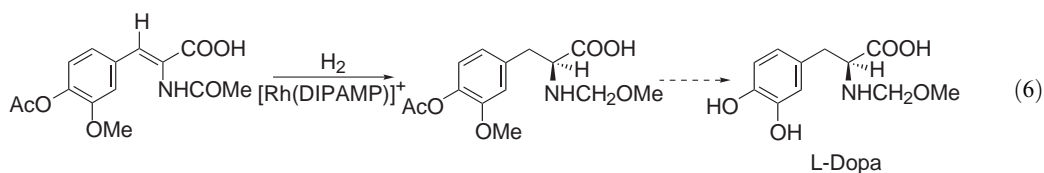
9.2.3.3 Asymmetric Hydrogenation Mechanisms

Enantioselective catalysis is rapidly becoming very important in the areas of pharmaceuticals, agrochemicals, flavors, and fragrances that require high degrees of chemical precision in their syntheses. Transition metal catalysts in some cases are highly stereoselective. Many metal catalysts have been developed containing chiral diphosphines such as those shown in Scheme 9, which provide a chiral environment around the metal center during the catalytic cycle.^{63–65} One of the best-known cases of stereoselectivity is the asymmetric hydrogenation in the synthesis of L-Dopa, where a Rh^{I} complex catalyses the enantioselective addition of H_2 across an unsymmetrical $\text{C}=\text{C}$ bond. This is a key step in the industrial-scale synthesis of this drug, developed by Monsanto in 1974, which is used to treat Parkinson's disease (Equation (6)).^{28,66}

The reduction proceeds with remarkable stereoselectivity, producing the *S* enantiomer in 94% ee. Thanks to the work of Halpern,⁶⁷ we have now a good understanding of the mechanism of this asymmetric hydrogenation, which is the prototype of many others. In Scheme 10 is reported the catalytic cycle for hydrogenation of ethyl (*Z*)-1-acetamidocinnamate (EAC) using a cationic Rh^{I} -DIPAMP complex as the catalyst. The catalyst (36) can bind the EAC through either $\text{C}=\text{C}$ and $\text{C}=\text{O}$ via a π and a σ interaction, respectively (37), and then undergoes H_2 oxidative addition (38). The dihydride Rh^{III} intermediate (38) undergoes hydride migration onto the $\text{C}=\text{C}$ unit, with formation of a M -alkyl σ bond (39). Subsequently, the reduced product is released and the



Scheme 9

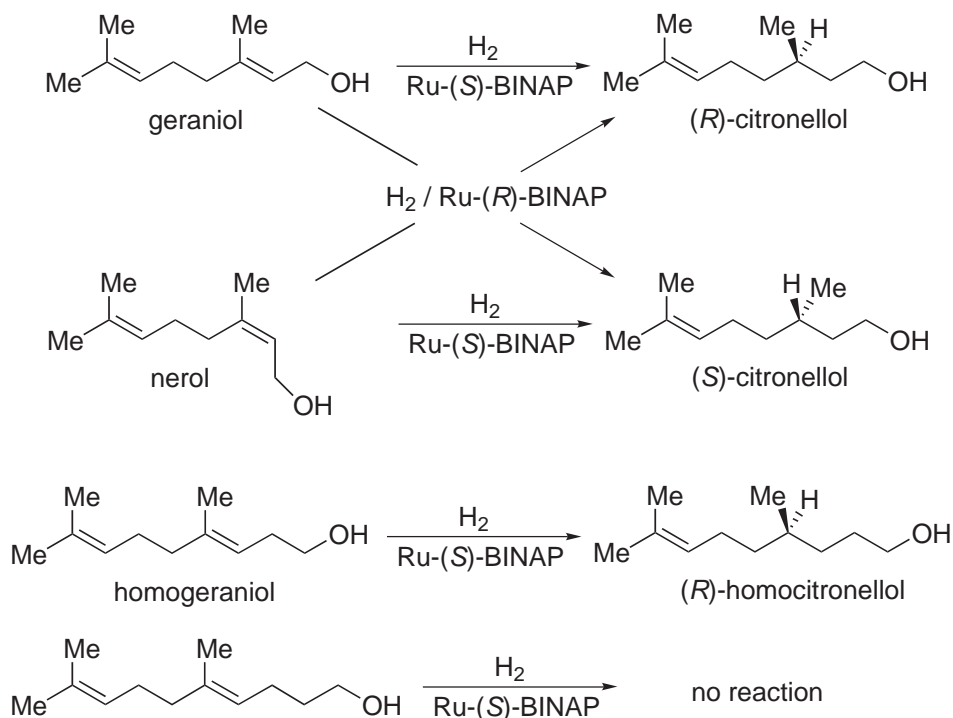


Scheme 10

catalyst regenerated. The presence of a chiral ligand such as CHIRAPHOS complicates the cycle because there are two parallel pathways that are diastereomerically different. Halpern was able to isolate (37') and obtain its crystal structure, but if hydrogen adds to (37'), then the final hydrogenation product should be the (*S*) enantiomer of *N*-acetylphenyl-alanine ethyl ester, in accordance with the mechanism in Scheme 10.

On the basis that the major product in the presence of Rh^I-CHIRAPHOS is the *R*-enantiomer, Halpern deduced that (37) and (37') form an equilibrium mixture rapidly and reversibly from reaction of EAC and the catalyst. Although the complex (37') is more stable than (37), the former reacts much faster during rate-determining oxidative addition of H₂, leading to the *R*-amino acid. Later, Halpern conducted the same experiments using a Rh^I-DIPAMP complex to catalyze hydrogenation of methyl-(*Z*)-1-acetamido-cinnamate (MAC) and the results were entirely analogous to the CHIRAPHOS system.⁶⁸ The conclusion was that “*it is not the preferred mode of the initial binding of the prochiral olefinic substrate to the chiral catalyst, but rather differences in the rates of the subsequent reactions of the diastereomeric catalyst–substrate adducts that determine the enantioselectivity in the asymmetric catalytic hydrogenation of prochiral olefinic substrates.*”⁶⁹ This interpretation also explains the inverse dependence of the optical yield on the H₂ partial pressure, observed for many asymmetric catalyzed hydrogenations. The reversibility of the initial catalyst–olefin adduct formation should be reduced by increasing the rate of the subsequent H₂ oxidative addition step, i.e., by increasing the H₂ concentration. This study further supports that, also in the mechanism for asymmetric hydrogenation, isolable intermediates are typically not the active species involved in the catalytic cycle, but rather labile “reservoirs” for the real catalytic intermediates. This means that it is necessary to have another group attached to the C=C bond which can also bind to the metal (like the amide carbonyl group in EAC), in order to obtain an efficient catalysis. This secondary binding helps to lock the C=C bond in a rigid conformation in the presence of the chiral diphosphine ligand, thus enabling stereoselection to occur. In fact, common unsymmetrical alkenes having only alkyl groups as substituents close to C=C undergo hydrogenation with much less stereoselectivity.

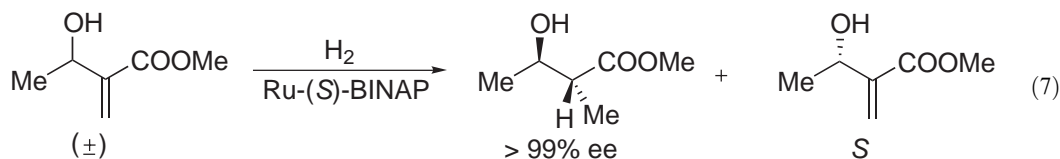
Allylic and homoallylic alcohols can be hydrogenated in the presence of [Ru(OOCCF₃)₂-(BINAP)] catalyst, which shows high specificity. For example, both enantiomers of citronellol are produced with high ee, starting from either geraniol or nerol, depending on whether (*S*)- or (*R*)-BINAP is used (Scheme 11).⁷⁰ The reaction shows C=C face selectivity, since the same catalyst, Ru-(*S*)-BINAP, transforms geraniol into (*R*)-citronellol and nerol into (*S*)-citronellol



Scheme 11

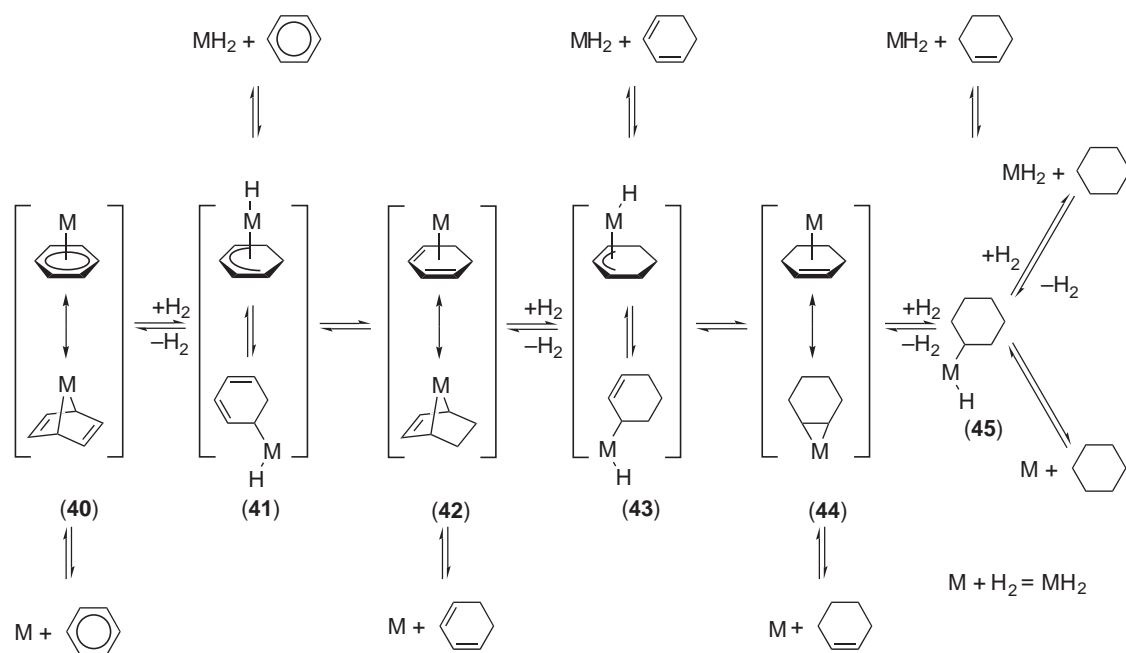
(Scheme 11). This kind of catalyst is regioselective, the remote C=C being unaffected, thus indicating that the allylic alcohol group provides a necessary secondary coordination during the cycle. Further confirmation comes from the evidence that extension of the carbon chain by just one more carbon, with respect to homoallylic alcohols, results in no reaction.

The great selectivity of Ru-BINAP species is also evident when they are used in kinetic resolution of enantiomers. When a racemic allylic alcohol reacts with H₂ in the presence of Ru-(S)-BINAP, the (R)-alcohol reacts preferentially, thus leaving the (S)-enantiomer unreacted (Equation (7)).⁷¹



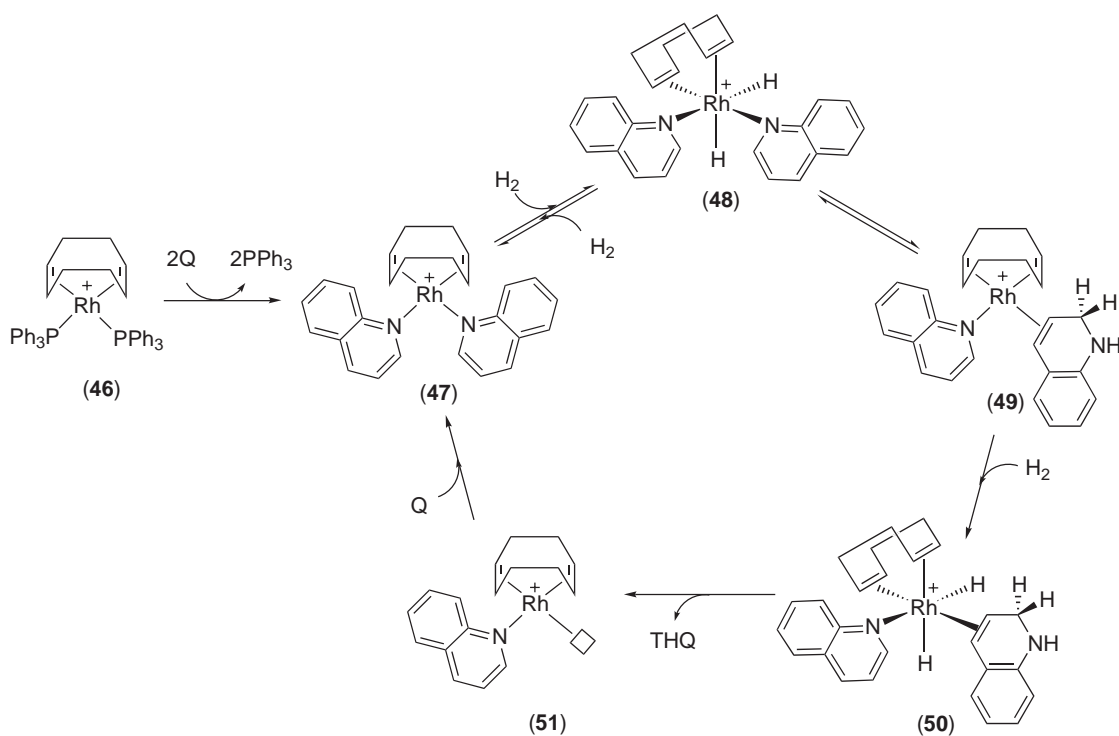
Conversion of benzene to cyclohexene by partial catalytic hydrogenation is a very important industrial process, since it provides a new route to cyclohexanol, a precursor of nylon, when combined with hydration of cyclohexene. For example, Asahi Chemical Company of Japan developed a selective bilayer catalytic system including a Ru catalyst, ZrO₂ and ZnSO₄ under 50 atm of H₂ pressure, a process affording the olefin with up to 60% selectivity after 90% conversion of benzene.⁷²

Various niobium and tantalum aryloxides are able to carry out regio- and stereoselective hydrogenation of aromatic substrates.^{73–76} Recent studies on species of general formula [Nb(OAr)₂R₂] and [Ta(OAr)_{5-x}(H)_x(PR₃)_n] (OAr = O-2,5-Prⁱ-C₆H₃; x = 2, 3; n = 1 or 2) give a better insight into the overall mechanism of arene hydrogenation by these catalysts.^{77,78} In Scheme 12 the hydrogenation mechanism of benzene, 1,3-cyclohexadiene and cyclohexene by a metal dihydride species is reported. The η⁴-cyclohexadiene species (40), formed by transfer of the two hydrides to benzene, is known to have structural parameters consistent with a metallonorbornene bonding description.⁷⁸ Successive H₂ additions and hydride transfers ((41) → (42) → (43) → (44)) afford a hydride cyclohexyl intermediate (45), which finally releases cyclohexane.



Scheme 12

Hydrogenation of heteroaromatic compounds also attracts much interest, mainly because it is regarded as a key step in industrially important hydrodenitrogenation (HDN) and hydrodesulfurization (HDS) processes. Several homogeneous Ru, Os, Rh, and Ir complexes are able to catalyze the regioselective hydrogenation of N-containing rings in quinoline, isoquinoline, indole, and benzoquinolines.^{79–84} Mechanistic studies on hydrogenation of quinoline (Q) to 1,2,3,4-tetrahydroquinoline (THQ) catalyzed by $[\text{Rh}(\text{COD})(\text{PPh}_3)_2](\text{PF}_6)$ are in accordance with a cycle like the one depicted in **Scheme 13**. Substitution of two phosphines by two Q units affords the active species, which undergoes rapid and reversible oxidative addition of H_2 , and hydrogenation of one coordinated Q to dihydroquinoline (DHQ), followed by rate-determining reduction of the DHQ intermediate to yield THQ.⁸⁵

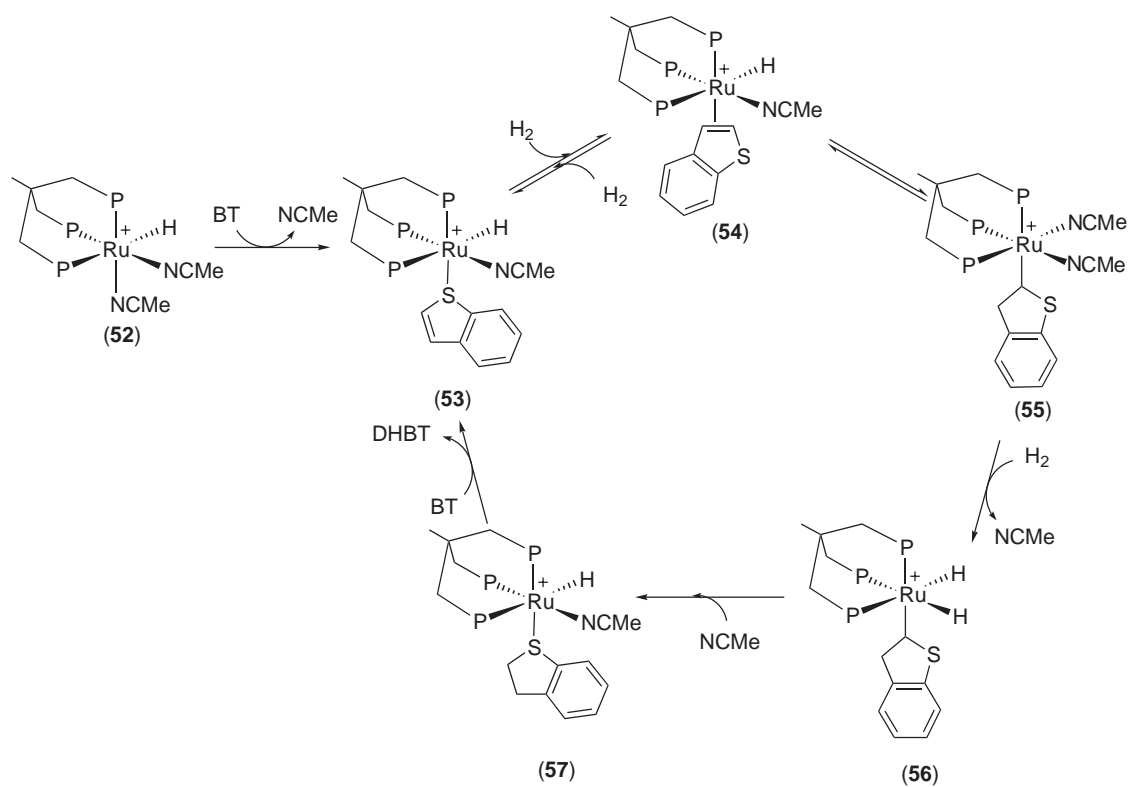


Scheme 13

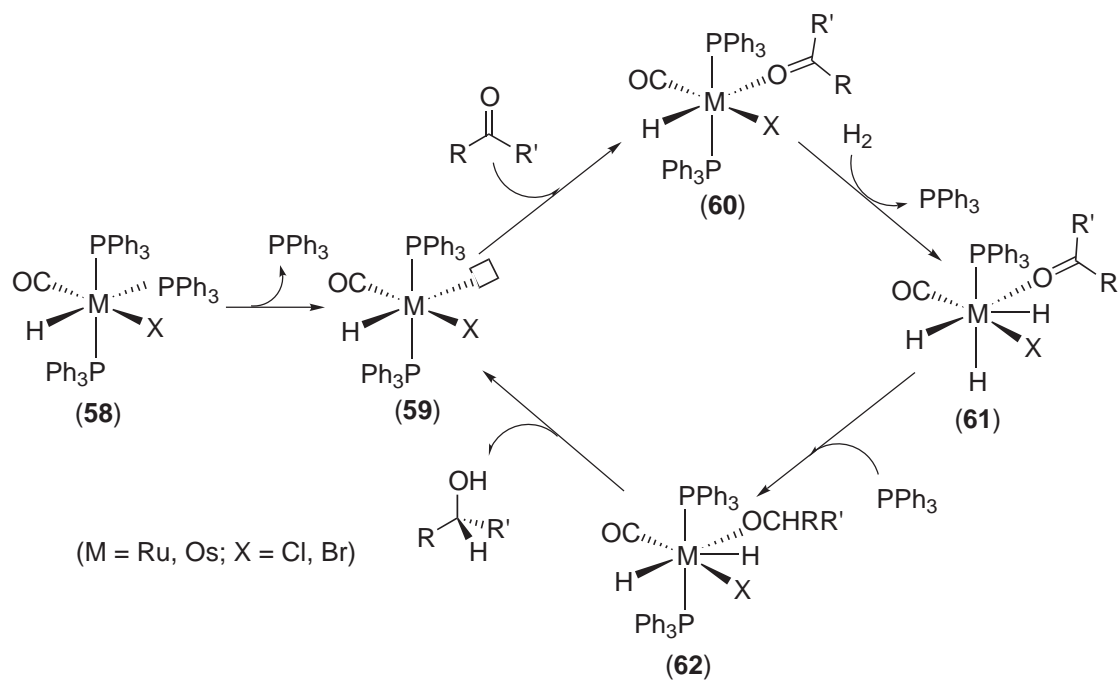
With regard to S-aromatic compounds, Sanchez-Delgado and Bianchini have elucidated the mechanism of hydrogenation of benzothiophene (BT) to 2,3-dihydrobenzothiophene (DHBT) catalyzed by $[\text{M}(\text{COD})(\text{PPh}_3)_2](\text{PF}_6)$ ($\text{M} = \text{Rh}$ or Ir).^{86,87} The same authors have designed a much more active catalyst precursor for hydrogenation of BT, of the form $[\text{Ru}(\text{TRIPHOS})(\text{NC-Me})_3](\text{BF}_4)$ [$\text{TRIPHOS} = \text{CH}_3\text{C}(\text{CH}_2\text{CH}_2\text{PPh}_2)_3$] operating in THF.⁸⁸ The mechanism proposed, shown in **Scheme 14**, involves a zero-order dependence on substrate concentration, and a rate-limiting hydride transfer to coordinated BT. Otherwise, the elementary steps which compose the cycle are very similar to those in BT hydrogenation mechanisms for previously mentioned $[\text{M}(\text{COD})(\text{PPh}_3)_2](\text{PF}_6)$ ($\text{M} = \text{Rh}$ or Ir).^{86,87}

Recent developments in asymmetric hydrogenation have witnessed the increasing employment of Ru^{II} catalysts, mainly in the enantioselective reduction of compounds containing $\text{C}=\text{O}$ or $\text{C}=\text{N}$ bonds. Hydrogenation by use of the complexes $[\text{MHX}(\text{CO})(\text{PPh}_3)_3]$ ($\text{M} = \text{Ru}, \text{Os}$; $\text{X} = \text{Cl}, \text{Br}$) has been extensively studied by Sanchez-Delgado and co-workers.⁸⁸ In **Scheme 15** is shown a cycle involving these catalysts in hydrogenation of aldehydes, where a vacant site of the metal (**59**) serves to coordinate the carbonylic oxygen (**60**). Subsequent H_2 oxidative addition, hydride migrations to carbonylic carbon and then to the oxygen ($(\text{61}) \rightarrow (\text{62}) \rightarrow (\text{59})$), afford the alcohol and regenerate the catalyst.^{89–91}

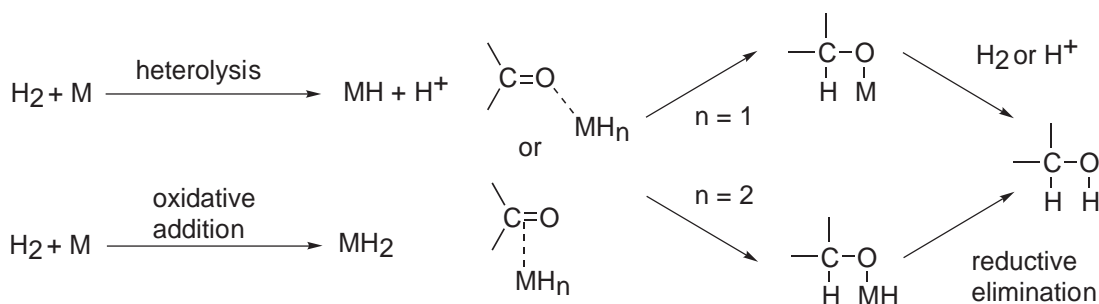
The generally accepted mechanism of homogeneous hydrogenation of simple ketones seems to occur by a $[\pi 2 + \sigma 2]$ pathway as depicted in **Scheme 16**.



Scheme 14

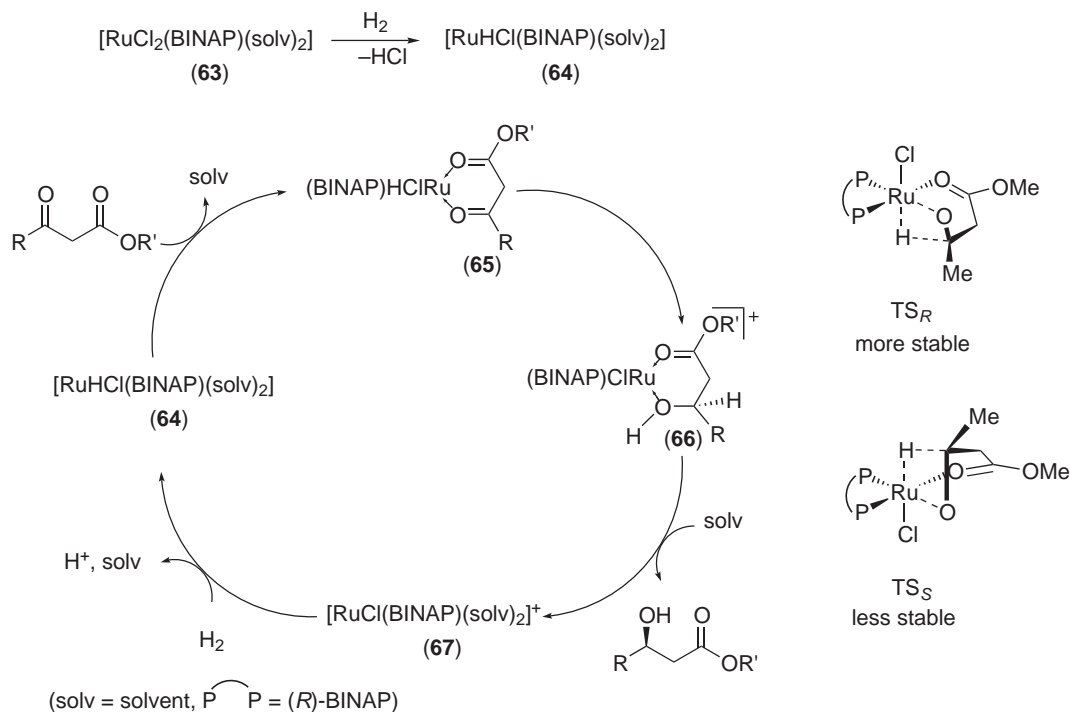


Scheme 15



Scheme 16

In early 1990, Ru^{II} complexes of chiral diphosphines were found to effect highly enantioselective hydrogenation of various β -ketoesters to chiral β -hydroxy esters.^{92–94} Noyori's work helped in elucidation of the mechanism of (*R*)-BINAP-Ru catalyzed hydrogenation of β -keto esters (Scheme 17).⁹⁵ The catalytic cycle probably proceeds through a monohydride Ru^{II} species (**64**) formed by the heterolysis of H₂ on Ru^{II} precatalyst (**63**). The hydride interacts reversibly with the substrate affording the chelate complex (**65**). Protonation of the keto oxygen increases the electrophilicity of the carbonyl carbon.

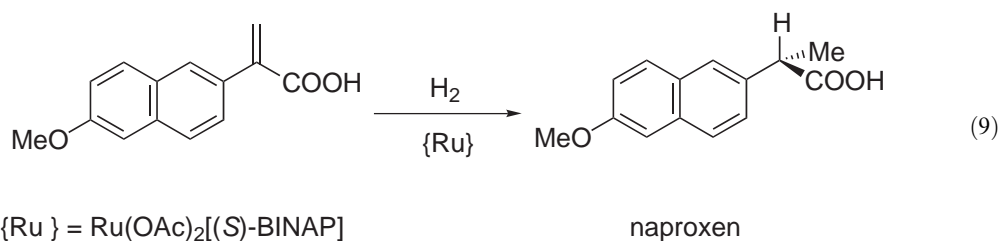
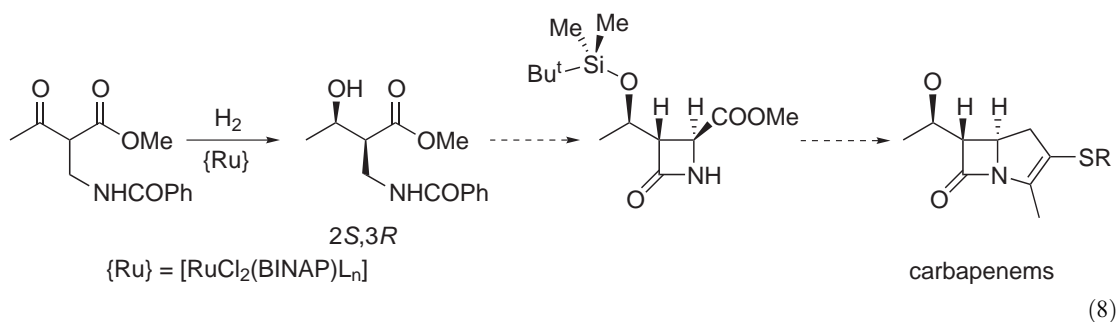


Scheme 17

This facilitates intramolecular hydride transfer resulting in a Ru–hydroxy ester complex (**66**) which readily releases the chiral product. When an (*R*)-BINAP-Ru catalyst is used, the *R* enantiomer is obtained in >99% ee. The chirality of the BINAP ligand accounts for the difference in energy between the possible transition states TS_R and TS_S .

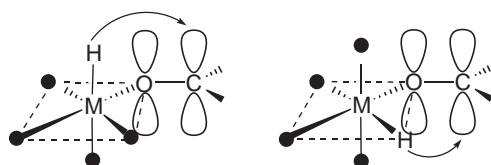
Takasago International Co. commercialized this hydrogenation method for the production of a chiral intermediate for the synthesis of *carbapenem* antibiotics (Equation (8)).²⁹

The use of an analogous (*S*)-BINAP-Ru-diacetate catalyst with axial chirality has led to important industrial applications, such as the synthesis developed by Monsanto where the asymmetric hydrogenation is involved in the last step to yield naproxen, a widely prescribed, non-steroidal, anti-inflammatory drug (Equation (9)).⁹⁶

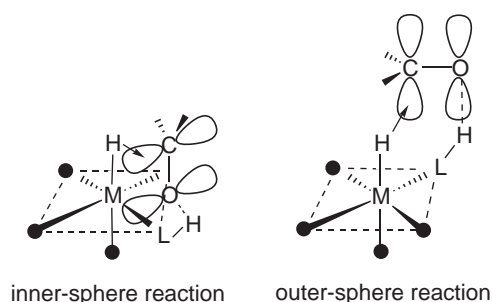


The hydrogenation of simple ketones without additional functionality close to the carbonyl group has been the object of many extensive studies. However, apart from some Ru catalysts designed by Schrock and Osborn,⁹⁷ and Rh catalysts by Tani and Otsuka,^{98–101} this field was open until a few years ago, when Noyori developed a new conceptual turning point: the “metal–ligand cooperation in molecular functions”. The lack of reactivity of simple ketones in the presence of conventional Ru^{II}–diphosphine complexes is probably due to the absence of coordinating heteroatoms near to the carbonyl group, since the H₂ is readily activated by ruthenium. Since electrophilic metals like ruthenium tend to form σ complexes rather than π complexes with carbonyl ligands, the relative locations of the nucleophile and carbonyl carbon are inappropriate for reactions involving a M–H species (Scheme 18a). The delivery of hydride from the metal to the carbonyl carbon is therefore difficult for geometric reasons. Noyori hypothesized that the presence of a protic LH ligand in the metal complex could be useful to form a L–H \cdots O=C hydrogen bond, thus facilitating the interaction between the M–H and the π face of the C=O unit. Scheme 18b illustrates a possible H-bond-assisted hydride transfer from the metal to the carbonyl carbon. The alcohol product may form in either the inner or outer coordination sphere of the MH species. Based on the above concept, Noyori and co-workers designed new stable ruthenium pre-catalysts of the form *trans*-[RuCl₂(phosphine)₂(1,2-diamine)] able to perform an even more rapid and productive hydrogenation of ketones.¹⁰² Also chemo-selective hydrogenation of C=O in the presence of an additional olefinic linkage in the substrate has been achieved. The complex [RuCl₂(PPh₃)₃] is an excellent catalyst for hydrogenation of terminal olefins, as stated previously,^{38–41} but very inactive for reduction of carbonyl compounds. However, addition of ethylenediamine and KOH to [RuCl₂(PPh₃)₃] in a 1:2:1 ratio completely reverses the selectivity, with the hydrogenation being therefore applicable to a variety of carbonyl compounds containing a C=C bond.¹⁰³

(a) difficult pathways

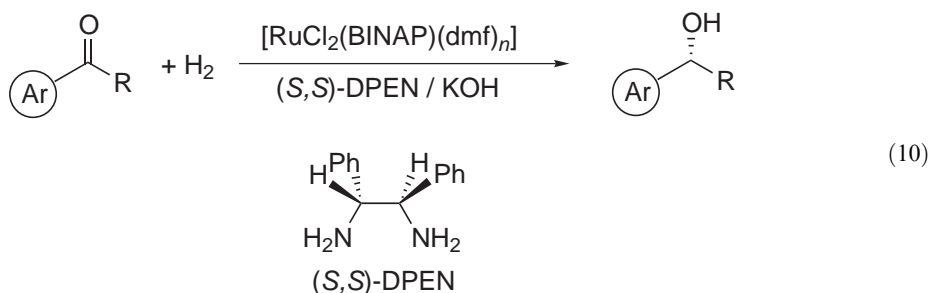


(b) pathways assisted by hydrogen bond

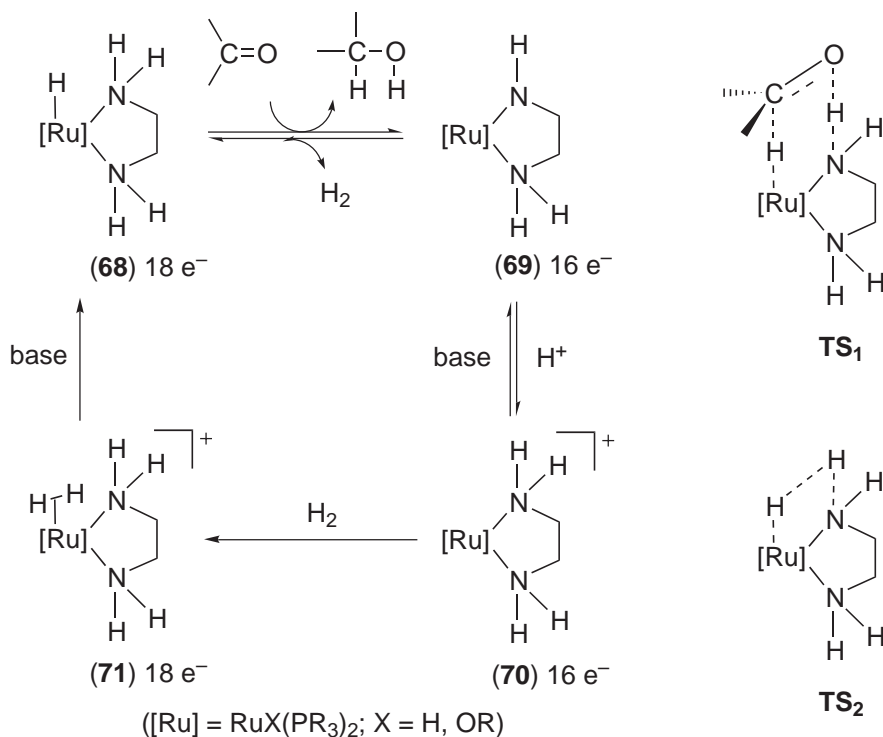


Scheme 18

In enantioselective hydrogenation of aromatic ketones, a catalytic system consisting of $[\text{RuCl}_2(\text{BINAP})(\text{dmf})_n]$, a chiral diamine such as (S,S) -DPEN and KOH in a 1:1:2 ratio, affords the *R* alcohol with 97% ee and quantitative yield (Equation (10)):¹⁰⁴



The high degree of enantioselectivity is a result of the synergistic effects of the chiral diphosphine and diamine. Other useful applications of these metal–ligand difunctional catalysts involve selective $\text{C}=\text{O}$ hydrogenation of heteroaromatic ketones, cyclopropyl ketones, amino ketones, α -alkoxy ketones, and olefinic ketones.⁹⁵ The mechanism of action of this new generation of catalysts is depicted in Scheme 19. First, the pre-catalyst is converted into an active hydride species by H_2 , where KOH neutralizes the HCl thus formed. The cycle involves two ground-state components, (68) and (69), which are linked by transition states TS_1 and TS_2 . The NH proton in (68) is important in hydrogen delivery to ketones, while the amide nitrogen in (69) cleaves H_2 . The high turnover efficiency relies on the universal functions of the complexes (68) and (69), in which the metal centers and the ligands directly cooperate in the bond-breaking and -forming reactions.

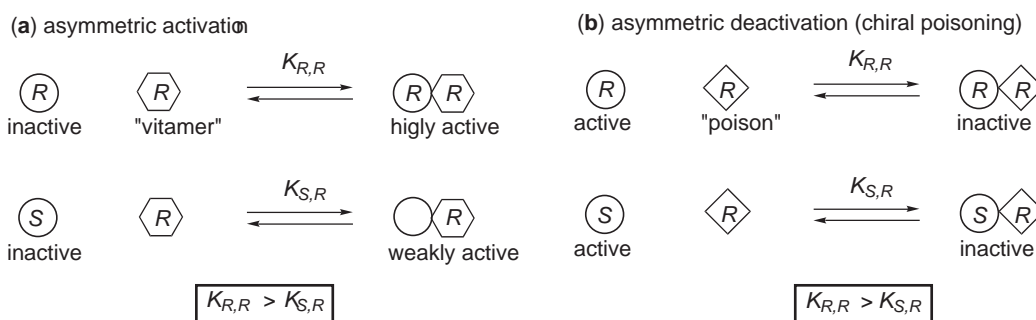


Scheme 19

Recent developments in chirality induced by ligands, and in efficient synthetic methods for ligands such as diphosphines, chiral diamines, amino-phosphine-phosphinites, phosphino-oxazolines and diimino-diphosphines, are available in the literature.^{105–107}

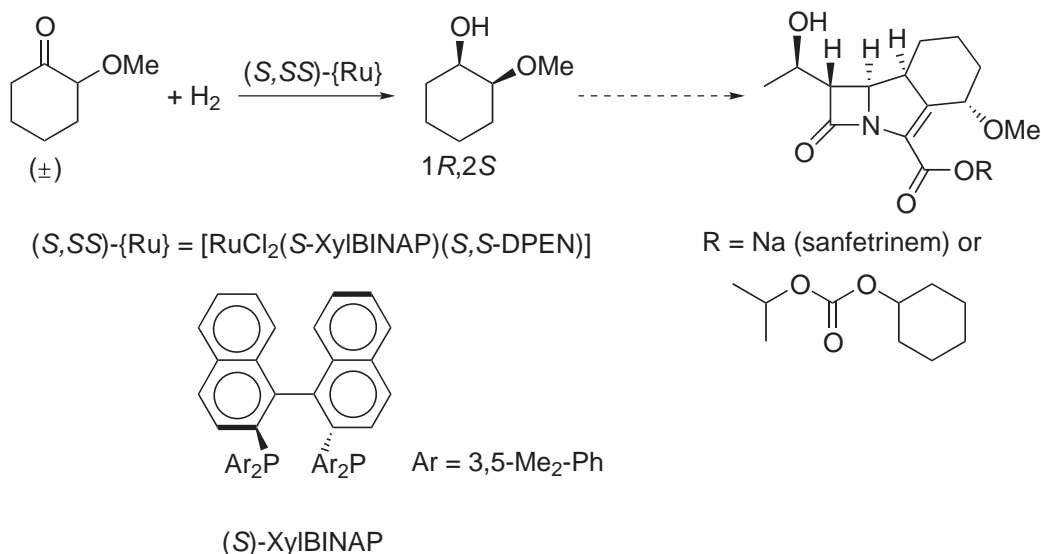
These “new generation” catalysts have been applied to the asymmetric activation of an inactive racemic metal compound by a non-racemic enantiopure ligand, called a “vitamer” (Scheme 20a). In contrast, a racemic catalyst can interact with an enantiopure “chiral poison” (asymmetric

deactivation, Scheme 20b), such that asymmetric catalysis is achieved only by the remaining enantiomer. In fact, diastereomeric interactions lead to unique stabilities and reactivities of the associates, resulting in unique chemical consequences.^{6,29} Thus, enantiomeric selective activation of racemic metal complexes by a chiral “vitamer” is becoming a viable approach for practical asymmetric catalysis when enantiomerically pure ligands are not available.



Scheme 20

Another application of the metal–ligand difunctional concept is the dynamic kinetic discrimination of stereoisomers.²⁹ This methodology has been applied to the production of sanfetrinem by Glaxo Wellcome and its metabolically labile ester which possesses high antibacterial activity (Scheme 21), the key step being the hydrogenation of racemic 2-methoxycyclohexanone with the catalyst [Ru(*S*-XylBINAP)(*S,S*-DPEN)] which affords (1*R*,2*S*)-2-methoxycyclohexanol.^{29,108,109}



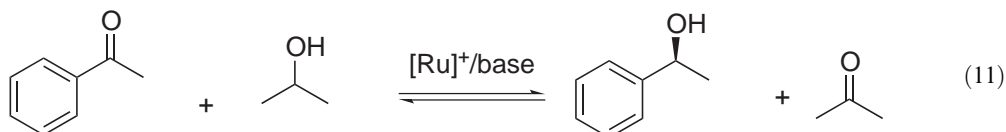
Scheme 21

Asymmetric catalysis is “four-dimensional chemistry” as stated by Noyori,⁶ because high efficiency can only be achieved through the coordination of both an ideal three-dimensional structure (x , y , z) and suitable kinetics (t). Recently developed metal–ligand difunctional catalysts really provide a new basis for developing efficient catalytic reactions.

The catalytic hydrogenation of the C=N bond of imines has attracted considerable attention, and a useful review covering the literature until 1996 has been reported by James.¹¹⁰ Chiral *ansa*-titanocene [(Cp'₂)TiCl₂] (Cp'₂ = ethylene(bis-tetrahydroindenyl)) and cationic [Ir(H₂)(PPh₃)₂(solvent)₂]⁺ catalysts for imine hydrogenation have been kinetically explored. This area is notably less developed than the reduction of C=O bonds.^{88,110}

9.2.4 HOMOGENEOUS TRANSFER HYDROGENATION

Hydrogen transfer reactions from an organic hydrogen source to another organic substrate constitute an alternative method of direct hydrogenation. The hydrogen is supplied by a donor molecule DH_2 , which itself undergoes dehydrogenation during the course of the reaction, to an acceptor molecule A (Equation (11)):



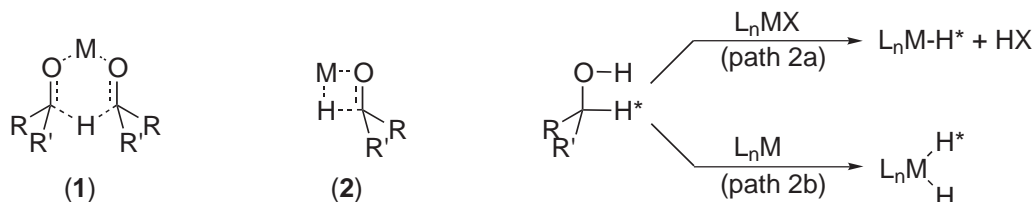
The donor molecules are generally organic compounds also employed as solvents, able to donate hydrogen. Suitable donors include alcohols, glycols, aldehydes, amides, ethers, amines, and even aromatic hydrocarbons, whereas acceptors are unsaturated organic molecules such as alkenes, alkynes, carbonyl compounds, nitriles, imines, azo- or nitro-compounds.⁵ However, the most investigated fields involve asymmetric reduction from secondary alcohols or aldehydes of $C=O$ and $C=N$ forming chiral alcohols and amines, respectively, and our discussion will be limited to this kind of hydrogen transfer reaction.³¹ Extensive reviews on systems catalyzing other hydrogen transfer reactions involving simple hydrocarbons or heteroatom-containing hydrocarbons as donors can be found in the literature.^{5,112}

Apart from the Meerwin–Ponndorf–Verley (MPV) reaction,^{16–18} catalytic asymmetric transfer hydrogenation has remained quite primitive,^{111,112} with successful examples of reduction of activated olefins, using alcohols or formic acid as hydrogen source, being reported only recently.^{113,114}

The generally accepted essential features for a catalyzed hydrogen transfer reaction are quite severe: (a) the DH_2 molecule must bind to a metal; transfer hydrogen to it; and must be released from the metal environment before back-transfer takes place; (b) the A molecule must be stable to hydrogen abstraction under the reaction conditions employed.

Recent studies on Ru catalysts bearing an arene and a secondary diamine or ethanolamine as ancillary ligands, in the presence of a base such as KOH as co-catalyst, seem, however, to contradict statement (a), suggesting a mechanism where substrate/metal complexation is not essential for alcohol \rightarrow $C=X$ ($X=O$ and N) hydrogen transfer to occur.^{30,115}

From a mechanistic point of view, two very general pathways can be envisaged for hydrogen transfer: direct hydrogenation transfer, consisting of a concerted process that involves a six-membered cyclic transition state in which both the hydrogen donor and the acceptor are coordinated to the metal (1 in Scheme 22) and a hydridic route (2 in Scheme 22).¹¹⁶



Scheme 22

In this latter hydridic route for hydrogen transfer from alcohols to ketones, two additional possibilities can be considered: one involving a metal hydride arising purely from a $C-H$ (path 2a), and another in which it may originate from both the $O-H$ and $C-H$ (path 2b); in this case any of the hydrides on the metal may add to the carbonyl carbon.

Suitable catalytic systems for secondary alcohols as donor (2-propanol is the widest employed, being the best hydrogen-donating alcohol), and aldehydes or ketones as acceptors, include Co,¹¹⁷ Rh,¹¹⁸ Ir,¹¹⁹ Fe,¹²⁰ Ru,¹²¹ Os,¹²² and Sm¹²³ complexes with π -acceptor ligands such as phosphines, thiophenes, N_2 -chelating ligands, or arenes, which are able to stabilize low oxidation states of the metal and prevent its decomposition under reducing conditions.⁵ Recent studies indicate path 2a for many Rh, Ir, and Ru catalysts bearing ligands such as PPh_3 , DIPHOS, bipy,

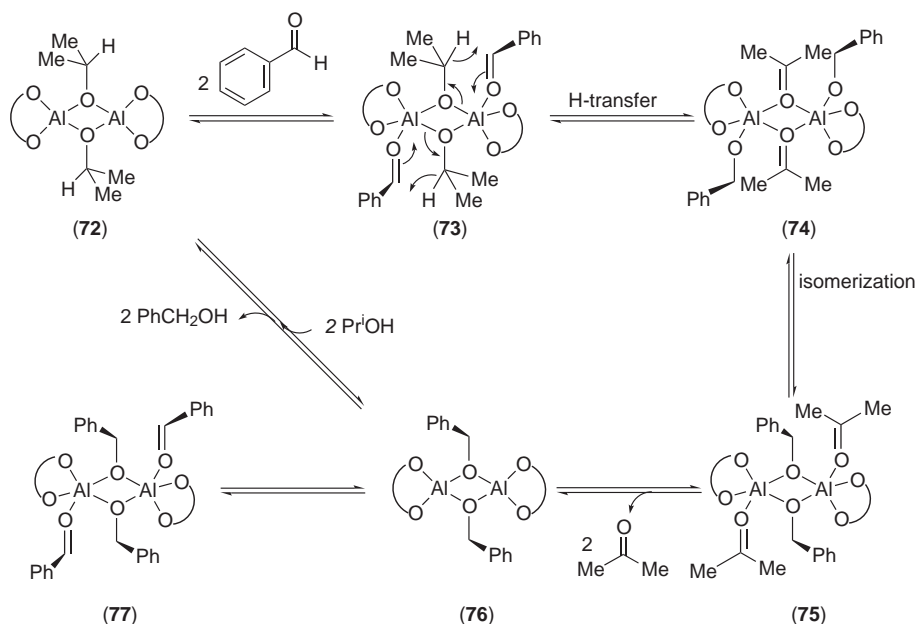
thiophenes,¹¹⁶ whereas path 2b is more likely for Ru and Rh catalysts containing secondary diamine ligands.^{116,124} For some Al, Co, and Sm catalytic systems a direct hydrogen transfer with a cyclic transition state seems more likely, although the involvement of a radical-based mechanism cannot be excluded.^{117,125}

As with hydrogenation, hydrogen transfer of imines is a poorly developed field.^{126–130} However, recent arene-Ru^{II} systems bearing chiral 1,2-diamine co-ligands have been found to be excellent catalysts for asymmetric reduction of imines with formic acid as donor.^{31,131–134}

An important aspect of hydrogen transfer equilibrium reactions is their application to a variety of oxidative transformations of alcohols to aldehydes and ketones using ruthenium catalysts.⁷² An extension of these studies is the aerobic oxidation of alcohols performed with a catalytic amount of hydrogen acceptor under O₂ atmosphere by a multistep electron-transfer process.^{132–134}

9.2.4.1 Direct Hydrogen Transfer Mechanism

Beside the well-known Al(OPrⁱ)₃ catalyst,^{16–18,135} Lin and co-workers have recently developed a new and highly effective aluminum alkoxide catalyst for MPV hydrogen transfer reactions.¹³⁶ Isolation of some intermediates suggests the mechanism shown in Scheme 23. The aldehyde molecules coordinate to aluminum centers forming the pentacoordinate intermediate (73); this is followed by H-transfer from the alcoholate to the C=O via a six-membered transition state to give the bridging ketone (74). Because acetone is a much weaker donor than bridging alkoxide, rapid isomerization and release of acetone occurs ((74) → (75) → (76)). The four-coordinate (76) can react with another aldehyde (→ (77)) or with 2-propanol to regenerate the catalyst.



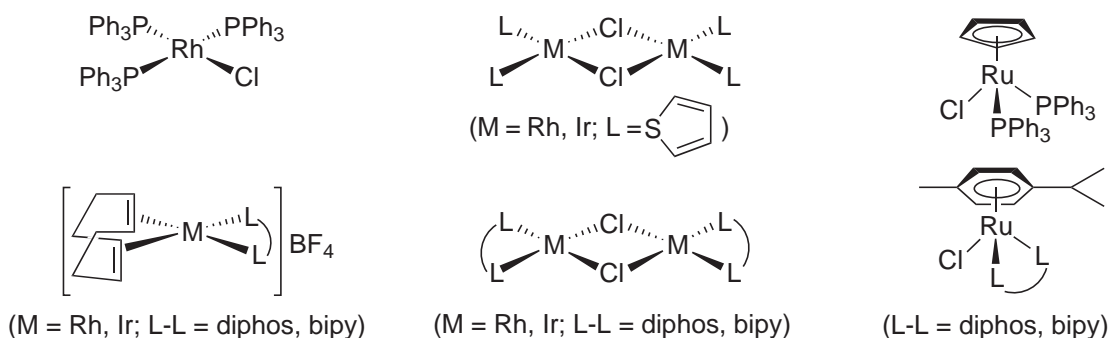
Scheme 23

9.2.4.2 Metal Monohydride Mechanism

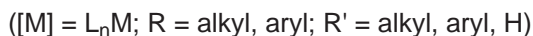
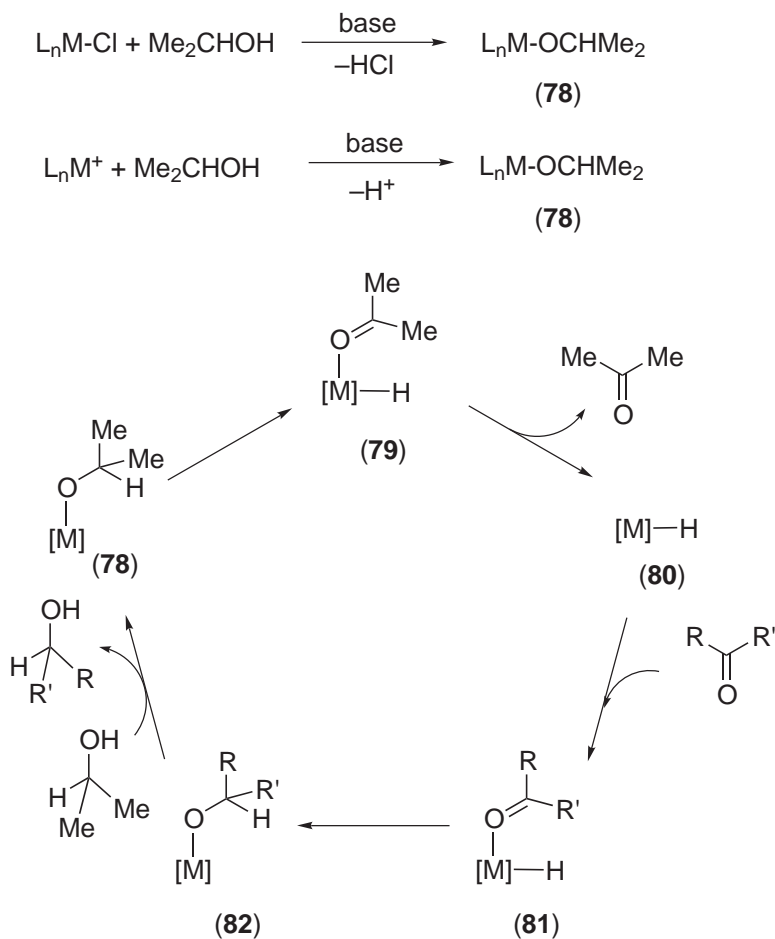
Several Rh, Ir, and Ru complexes follow the well-established hydrogen-transfer mechanism via a metal alkoxide intermediate and β -elimination.¹¹⁶

Examples of these catalysts are reported in Scheme 24, and a general catalytic cycle involving an M–H species is shown in Scheme 25.

Most of these reactions are promoted with an inorganic base such as KOH, NaOH, or K₂CO₃ as an essential co-catalyst. For reaction without alkaline bases see Mizushima *et al.*¹³⁷ Many of these complexes contain a chloride ligand, which is easily displaced by an alkoxide displacement/ β -hydride elimination sequence in the presence of a base to remove HCl formed (Scheme 25). In contrast, cationic L_nM⁺ systems add the alcohol by formation of M–O bond, with the base



Scheme 24

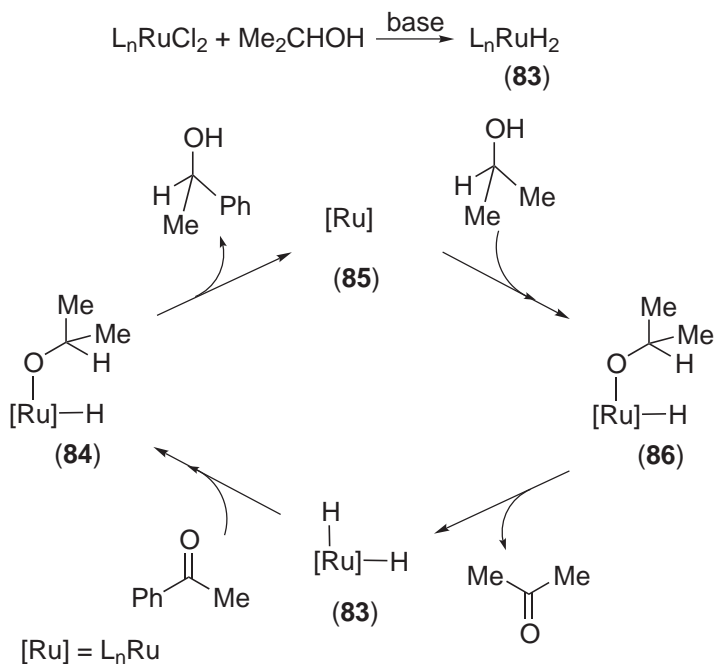


Scheme 25

deprotonating the alcohol (Scheme 25). In both cases the α -C—H of the alcohol is the origin of the M—H hydride (80) (and based on the principle of microscopic reversibility, the M—H adds exclusively to the carbonyl carbon of the C=O). Subsequent insertion of the ketone (or aldehyde) into the M—H bond results in the formation of the alkoxide intermediate (82). Finally, ligand exchange between this intermediate and alcohol results in the final product and the active metal-alkoxide species (78).^{112,116}

9.2.4.3 Metal Dihydride Mechanism

Ruthenium dichloride-based catalysts $[\text{RuCl}_2(\text{PPh}_3)_3]$ and $[\text{RuCl}_2(\text{PPh}_3)_2(\text{ethylenediamine})]$ ⁷² probably catalyze transfer hydrogenation by a dihydride mechanism (Scheme 26).¹¹⁶ The pre-catalyst is transformed under hydrogen transfer reaction conditions, and in the presence of a base, to an active dihydride species (**83**), through a mechanism in which both O—H and α -C—H hydrogen atoms of the alcohol are transferred to metal (Scheme 26).¹³⁸

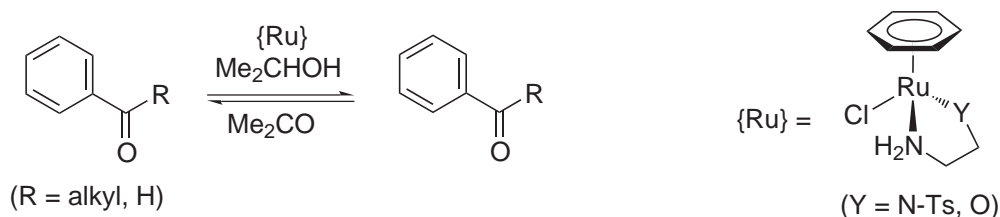


Scheme 26

This species adds a ketone yielding the alkoxide complex (**84**) which, after reductive elimination of the corresponding alcohol, generates the 16-electron species (**85**). This intermediate undergoes oxidative addition of 2-propanol (species (**86**)) and subsequent reductive elimination of acetone, regenerating the hydride complex (**83**).

9.2.4.4 Metal-Ligand Bifunctional Concerted Mechanism

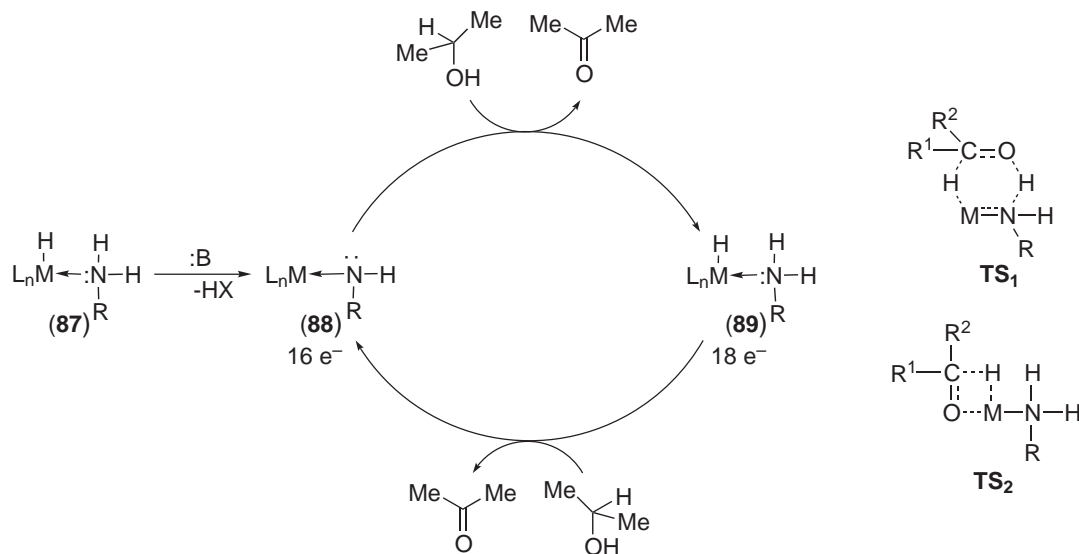
Among the most active catalysts for the asymmetric transfer hydrogenation of prochiral ketones and imines to chiral alcohols and amines are arene-ruthenium(II) amino-alcohol (or primary/secondary 1,2-diamine)-based systems, with an inorganic base as co-catalyst, developed by Noyori^{139–141} and further explored by others (Scheme 27).^{142–145}



Scheme 27

A monohydride mechanism is not operating in reactions catalyzed by these complexes. Noyori observed that the presence of an NH or NH₂ in the auxiliary ligands was crucial for catalytic activity, the corresponding dialkylamino analogs being totally ineffective. These findings indicate a novel metal-ligand bifunctional cycle (Scheme 28): KOH reacts with the pre-catalyst (**87**)

affording a 16-electron amide intermediate (**88**) which binds 2-propanol, oxidizing it and reducing itself to the 18-electron hydride (**89**). Subsequent saturation of a C=O function with (**89**) takes place via a six-membered pericyclic transition state **TS₁**, utilizing an “NH effect” instead of $\pi^2 + \sigma^2$ insertion of the C=O bond into the M—H linkage via a transition state like **TS₂**. The 18-electron hydride species (**89**) is regenerated by dehydrogenation of 2-propanol with the 16-electron Ru amide (**88**) via a similar cyclic transition state.^{30,115}



Scheme 28

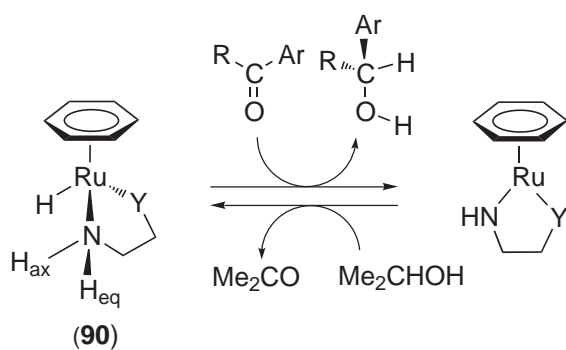
During this non-classical mechanism neither a carbonyl oxygen atom nor an alcoholic oxygen interacts with the metal throughout the hydrogen transfer process, the carbonyl reduction occurring in an outer sphere of the metal hydride complex, with the direct participation of the metal and the surrounding ligand in H-bond forming and breaking steps of the dehydrogenative and hydrogenative processes.^{30,115}

The kinetic asymmetric bias is generated by the combination of several steric and electronic factors, where also the arene ligand on ruthenium plays an important role. Theoretical structural studies¹⁴¹ suggest (Scheme 29) that Ru hydride (**90**) reacts with the carbonyl substrates preferentially through the “sterically congested” transition state **TS₁**, rather than the uncrowded **TS₂**. The reverse process occurs via the same TS. In addition to the chiral geometry of the five-membered chelate ring provided by the auxiliary ligand, the enantioselectivity originates from the C—H/ π attractive interaction between the η^6 -arene ligand and aryl substituents in ketone or aldehyde substrates (Scheme 29). Other theoretical studies on Rh^I complexes bearing chiral secondary diamines as auxiliary ligands confirm the above concerted mechanism for the transfer of both the hydride and an amine proton from the hydride–Rh complex to the C=O of the substrate.¹⁴⁶

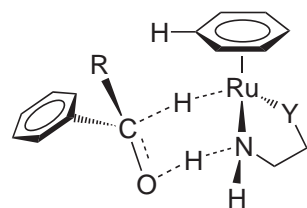
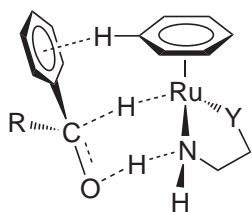
An interesting dinuclear Ru–hydride complex (structure **(91)** in Scheme 30) bearing CO ligands, known as “Shvo’s catalyst”, has recently attracted interest;^{147,148} it can catalyze the reduction of aldehydes and ketones, and also the kinetic resolution of secondary alcohols.^{149–152} A feature of **(91)** is that no addition of external base is needed as co-catalyst, since it dissociates into **(92)** and in a coordinatively unsaturated dienone dicarbonyl mononuclear fragment **(93)**, where one of the coordinating sites of the ligand acts as a basic center. Theoretical and kinetic studies^{116,148} indicate formation of a Ru^{II} intermediate **(92)** via a concerted transfer of both hydrogens from the alcohol through a six-membered transition state **(94)** as depicted in Scheme 30. The reduction of the substrate follows a similar transition state **(95)**.¹¹⁶

9.2.4.5 Mechanism of Aerobic Alcohol Oxidation

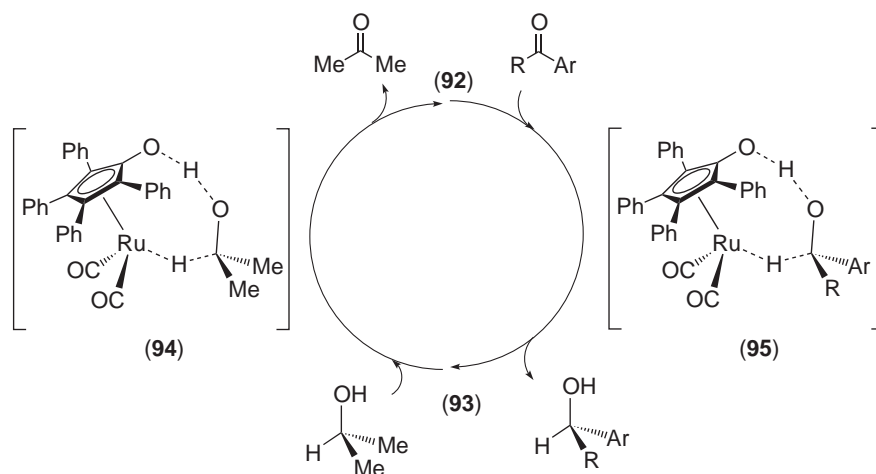
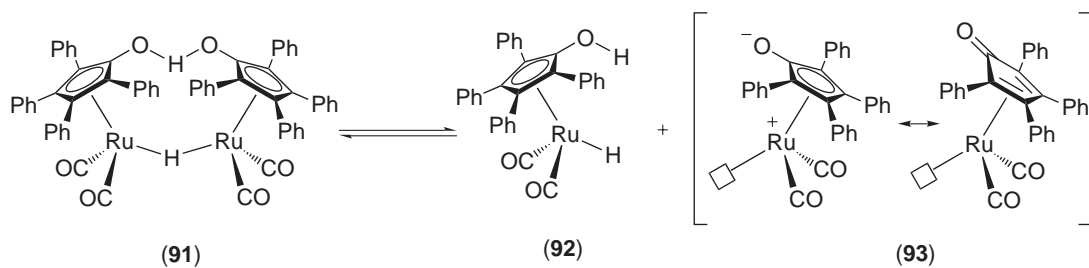
The principle of hydrogen transfer reactions has been applied to a variety of oxidative transformations of alcohols with Ru^{II} catalysts.⁷² Among them, one interesting application is the aerobic oxidation of alcohols developed by Bäckvall,^{153–157} which can be performed with a catalytic



R = alkyl or H
Y = O or N-Ts

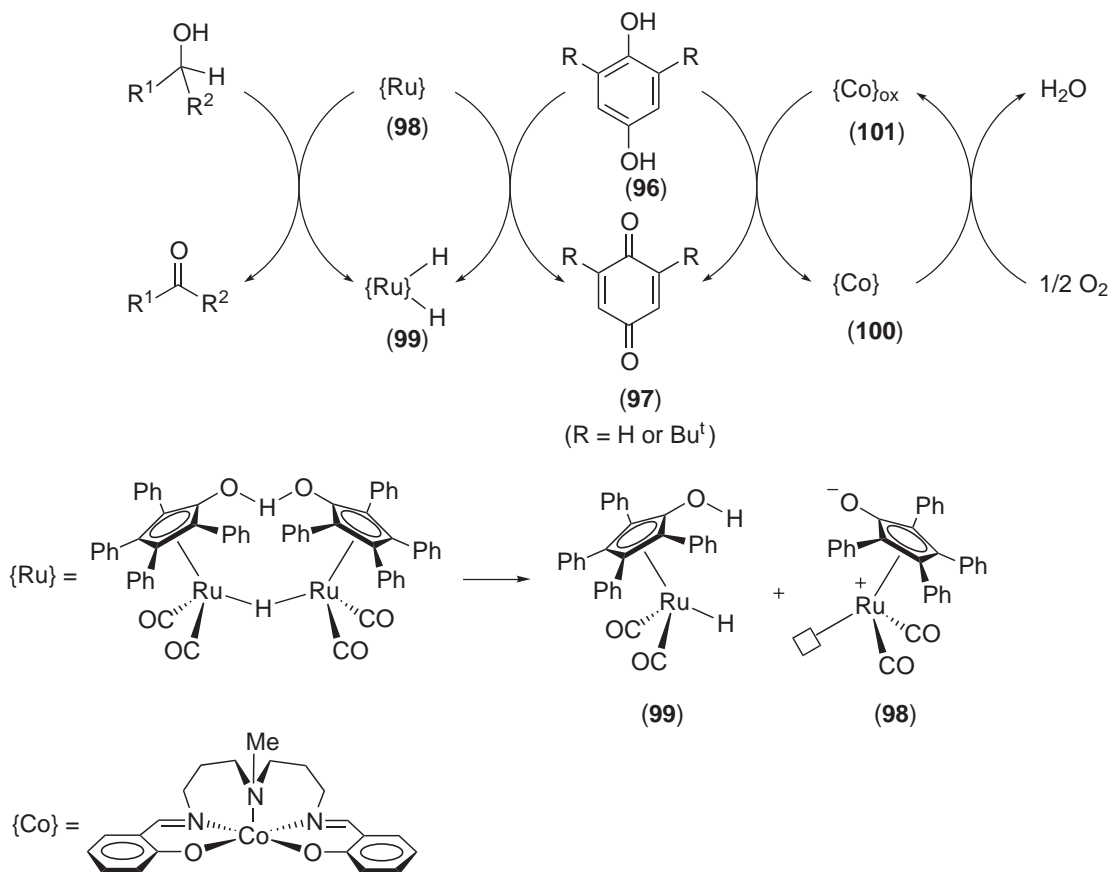


Scheme 29



Scheme 30

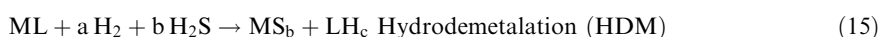
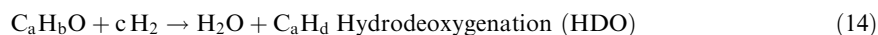
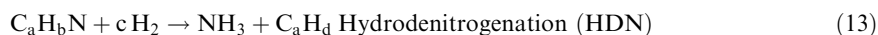
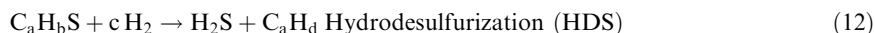
amount of a hydrogen acceptor under an O_2 atmosphere by a multistep electron-transfer process (Scheme 31). A variety of Ru complexes (for example, $[RuH_2(PPh_3)_3]$, $[RuCl_2(PPh_3)_3]$, and the Shvo catalyst (91)) can catalyze this reaction, coupled with a quinone acceptor (96) and a Co^{II} complex such as (100) which act as redox mediators. The Ru-dihydride species (99) formed during the hydrogen transfer can be regenerated by a multistep electron-transfer process including hydroquinone (97), metal complexes, and molecular oxygen (Scheme 31). When the Shvo catalyst is employed, it divides into two parts which constitute the hydrogen acceptor (98) and the hydrogen donor (99) (Scheme 31).¹⁵⁵



Scheme 31

9.2.5 HOMOGENEOUS HYDROGENOLYSIS

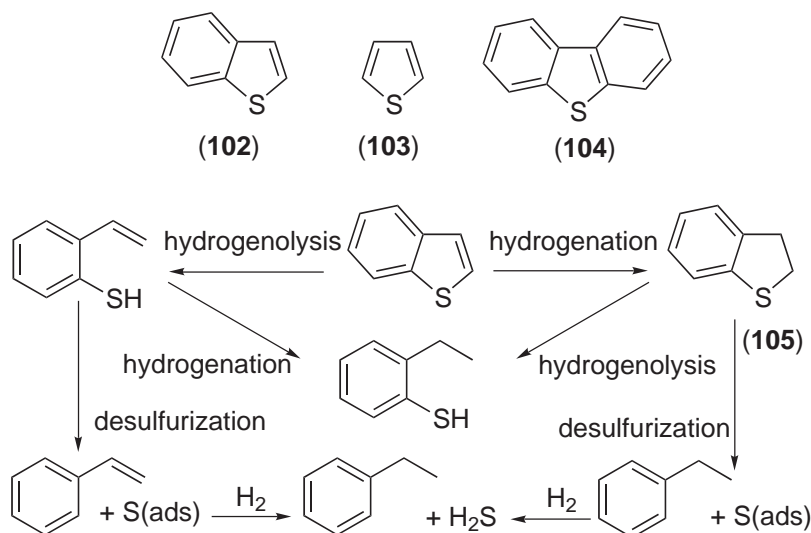
The discovery of heavy oil reservoirs world-wide, and the growing use of coal and oil shale for the production of fuels contaminated by variable amounts of organic compounds containing sulfur, nitrogen, oxygen, and metal ions, are pushing the petrochemical industry to invest an increasing amount of resources in the development of more efficient catalysts for removing heteroatoms from fossil fuels. This purification is currently carried out under hydrotreating conditions in the presence of heterogeneous catalysts and involves four main chemical processes: hydrodesulfurization (HDS), hydrodenitrogenation (HDN), hydrodeoxygenation (HDO) and hydrodemetalation (HDM) (Equations (12), (13), (14), (15)).¹⁵⁸⁻¹⁶⁹



The importance of heteroatom removal from crude oil feedstocks has therefore directed most of the R&D investments toward the design of more efficient heterogeneous catalysts for the reactions in Equations (12), (13), (14), (15). A considerable contribution to a better understanding of the HDS and HDN mechanism has been provided by homogeneous studies involving soluble metal complexes.^{161,162}

9.2.5.1 Hydrodesulfurization

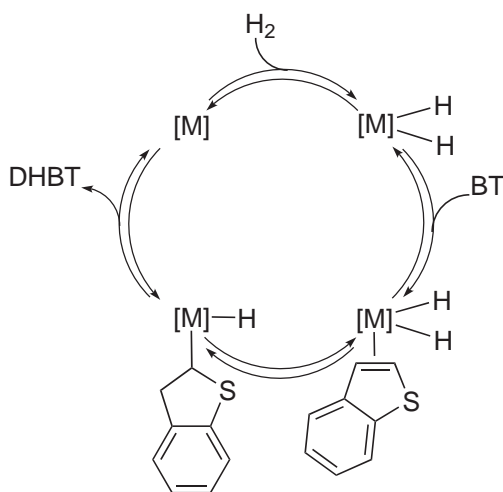
Of the four heterogeneous reactions outlined above, HDS has received, and is still receiving, the greatest attention. This is because sulfur, contained in thiols, sulfides, disulfides, and thiophenic molecules, is actually the most abundant heteroatom in fossil fuels and is also the element with the highest environmental impact. Furthermore, sulfur compounds are largely responsible for the poisoning of the hydrotreating catalysts.^{163–175} In the search for heterogeneous HDS catalysts with improved efficiency, homogeneous modeling studies have substantially contributed to a better understanding of fundamental aspects related to the interactions with transition metals of thiophenic substrates and of the sulfur compounds derived from them (e.g., thiols, sulfides). Many types of reaction between discrete organometallic complexes and thiophenes occur also on the surface of heterogeneous catalysts and the mechanistic understanding obtained in solution can be applied to elucidate surface phenomena.^{163–175} The hydrogenation to thioethers and the hydrogenolysis to thiols represent the preliminary and mechanistically crucial steps of the HDS of (102) (Scheme 32) as well as other thiophenic substrates (103–104). Whether the hydrogenation and hydrogenolysis paths are parallel, alternative, or competitive under HDS conditions, is the subject of a heated debate among heterogeneous and organometallic chemists. Indeed, understanding this mechanistic aspect, which is strictly related to the electronic nature of the surface metal atoms and to the preparation and pretreatment of the catalytic material, is of crucial importance for the development of catalysts specifically tailored for the HDS of thiophenes via the energetically favored hydrogenolysis mechanism. Of the three thiophenes generally employed in homogeneous studies, benzo[*b*]thiophene (102) is the most easily hydrogenated to the corresponding thioether, dihydrobenzo[*b*]thiophene (105).^{176–185}



Scheme 32

The high reactivity of (102) has been attributed to the more pronounced “olefinic” character of the C₂=C₃ double bond as compared to thiophene (103) and to its reduced aromatic character compared with dibenzo[*b,d*]thiophene (104), for which no example of hydrogenation to either tetrahydrodibenzothiophene or hexahydrodibenzothiophene has been reported so far. The regioselective hydrogenation of (102) to (105) is catalyzed by several metals, all of them belonging to the class of *promoters* (Ru, Os, Rh, and Ir),^{176–185} under reaction conditions that may be as mild as 40 °C and subambient H₂ pressure.^{180,181} The catalytic rates are generally low. A hydrogenation mechanism proposed on the basis of deuterium labeling experiments,¹⁸⁶ kinetic studies

applying gas uptake techniques,^{180,181} and theoretical methods,¹⁸¹ comprises the following steps: oxidative addition of H₂; coordination of (**102**) via the double bond; hydride migration to give 2- or 3-dihydrobenzothieryl; reductive coupling of hydride and dihydrobenzothieryl ligands; and displacement of (**105**) by the substrate (Scheme 33).

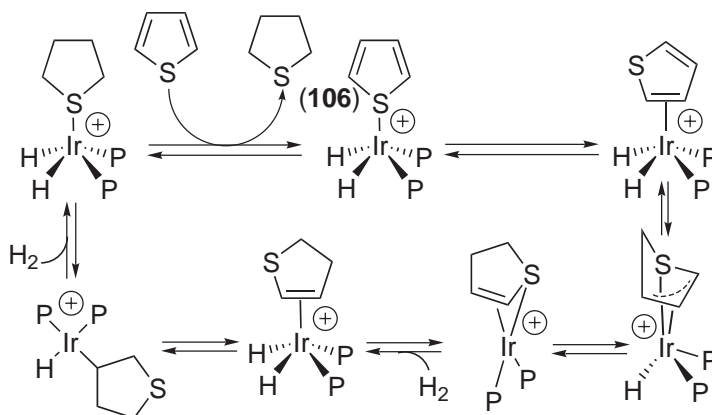


Scheme 33

The mechanistic features of the hydrogenation of (**102**) have been elucidated using [Cp**Rh*(CH₃CN)₃](BF₄)₂ (Cp* = pentamethylcyclopentadienyl) as a catalyst precursor (which suggested the reversibility of the first hydride migration step, and possible η⁶-coordination of DHTB);¹⁷⁶ and by Sánchez-Delgado using [Rh(COD)(PPh₃)₂](PF₆) (which showed that the reaction rate is determined by the hydride migration that gives the dihydrobenzothieryl intermediate).¹⁸¹ On the basis of a comparative study of the catalytic activities of [Rh(COD)(PPh₃)₂](PF₆) and [Ir(COD)(PPh₃)₂](PF₆) in different solvents (THF, 2-methoxyethanol, and 1,2-dichloroethane), Sánchez-Delgado and Bianchini have shown that the hydrogenation reactions proceed with the same mechanism but may be retarded (Rh) or even inhibited (Ir) depending on the coordinating properties of the solvent.^{180,181}

A quite efficient homogeneous catalyst for the regioselective hydrogenation of (**102**) to (**105**) has recently been developed using the Ru^{II} complex [(triphos)Ru(CH₃CN)₃]²⁺ in THF [triphos = MeC(CH₂PPh₂)₃] as precatalyst.¹⁸⁶ In an attempt to apply aqueous biphasic catalysis to the HDS process, particularly to the purification of naphtha, various water-soluble catalysts capable of catalyzing the hydrogenation of (**102**) to (**105**) in a 1:1 water/decalin mixture were recently designed.^{187,188} The catalysts are generated *in situ* by reaction of sulfonated phosphines with various Ru^{II} or Ru^{III} precursors. The catalytic rates are generally low (at 69 bar of H₂ and 130 °C, TOF = 2.5), but they increase significantly in the presence of quinoline or aniline cocatalysts. It was suggested that these nitrogen bases have several beneficial effects on the reaction rate by leading to faster formation and better stabilization of the catalytically active species and to more efficient emulsions as well. Also, if (**103**) forms η²-(C,C) adducts using the double bond adjacent to sulfur,^{189,190} its hydrogenation to tetrahydrothiophene (**106**) is a rare reaction, the only example being a reaction catalyzed by the precursor [Ir(H)₂(η¹-(S)-(**103**))₂(PPh₃)₂](PF₆) in 1,2-dichloroethane.¹⁹¹ This hydrogenation reaction is a stepwise process that involves the intermediacy of 2,3-dihydrothiophene in accordance with several reactor studies with commercial HDS catalysts (Scheme 34).^{158–160} The overall mechanism for the formation of (**106**) is not too different from that proposed for (**102**) in Scheme 33. A major difference, however, may be seen in the first hydride migration step which gives a thioallyl ligand (stereoselective *endo* migration to the C₂ carbon atom of η²-(C,C)-(**103**)). The poor catalytic activity has been attributed to the good σ-donor properties of (**103**). The thioallyl ligand is not easily displaced by (**103**) and traps all the catalytically active species as the bis-(**106**) complex [Ir(H)₂(η¹-S-(**106**))₂(PPh₃)₂](PF₆) which, in fact, is the termination metal product of the catalysis.¹⁹¹

In the design of a homogeneous catalyst for the plain hydrogenation of thiophenes it is necessary to take into account that, unlike simple alkenes, (**102**) and (**103**) are polyfunctional ligands which can bind metal centers in a variety of bonding modes, often in a rapid equilibrium with each other.^{166–172,192} Among the possible coordination modes, the η¹-(S) and the η²-(C,C)



Scheme 34

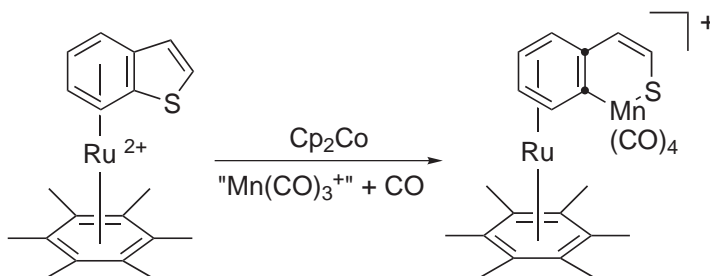
ones are the most common and also the most important to direct the following reactivity of the coordinated thiophene toward H_2 . The η^2 -(C,C) bonding mode is more sterically demanding than the η^1 -S bonding mode (the immediate precursor to C—S bond cleavage)^{193,194} even in the absence of substituents in the thiophene. No example of homogeneous hydrogenation of substituted thiophenes has ever been reported, this reaction being thwarted.^{158–160} Bulky metal fragments are poor hydrogenation catalysts, although they may be effective catalysts for the hydrogenolysis of thiophenes.^{184,185,195–198} In a similar way, a high basicity at the metal center is not required for an effective hydrogenation catalyst as it may favor C—S bond cleavage (hence hydrogenolysis pathways) via transfer of electron density from a filled metal orbital of appropriate symmetry into a σ^* C—S orbital (generally the C_2 —S).^{163–175,193,194} The most critical feature for a successful hydrogenation catalyst is a low thiophilicity to disfavor both η^1 -S coordination of the incoming thiophene and the formation of stable adducts with the thioether products. Ideal candidates are Ru^{II} fragments with moderate steric crowding.

The hydrogenolysis of thiophenes to thiols is a relevant reaction in the HDS process (Equation (16)).



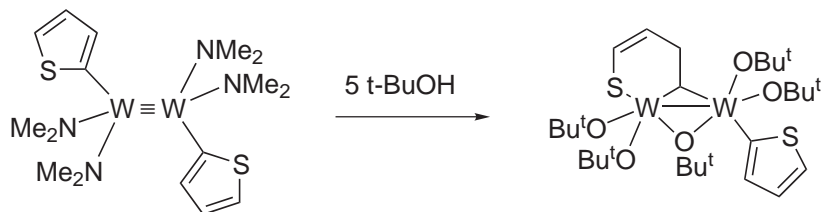
In particular, the thiols, like the thioethers, can efficiently be desulfurized over conventional catalysts under milder reaction conditions than those required to accomplish the HDS of the thiophene precursors.^{158,159}

Ring opening of thiophenes can be achieved in several different ways that have extensively been reviewed.^{163–175} Most common procedures involve either the direct interaction of electron-rich metal fragments with the desired thiophene (e.g., [(triphos)MH] (M = Rh, Ir),^{184,185,195–204} [$\text{Cp}^*\text{Rh}(\text{PMe}_3)_3$],^{193,194,205–207} [$\text{Pt}(\text{PEt}_3)_3$],^{208,209} [$\text{Fe}(\text{dmpe})_2$],²¹⁰ [$\text{Ir}(\text{PMe}_3)_3$],²¹¹ [Cp_2W],²¹² or [$\text{Tp}^*\text{Rh}(\text{PMe}_3)_3$]²¹³) or the addition of nucleophiles^{214–216} or electrophiles^{217–219} to η^4 - and η^5 -thiophene complexes. Alternative strategies for C—S bond scission have recently been reported by Sweigart^{220,221} and Chisholm.²²² The activation of the carbocyclic ring of (102) by an appropriate metal fragment (e.g., [$\text{Mn}(\text{CO})_3$]⁺ or [$\text{Ru}(\text{C}_6\text{Me}_6)$]²⁺) can favor the regioselective insertion of an electron-rich fragment (e.g., $\text{Mn}(\text{CO})_4$) into the S—C_{aryl} bond (Scheme 35),^{220,221} which is a



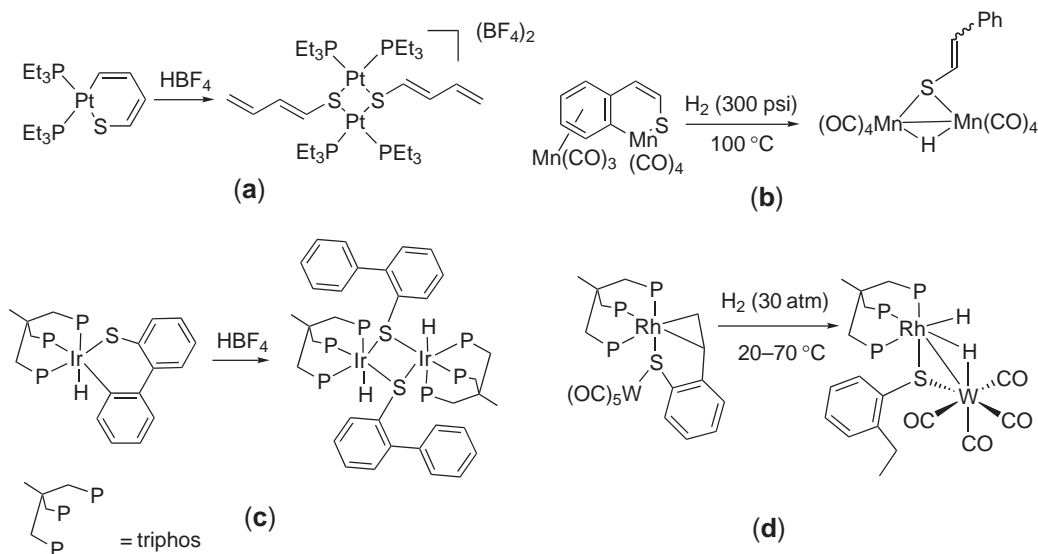
Scheme 35

quite unusual reaction unless (**102**) is substituted in the 2-position,²⁰⁶ whereas the cooperation of two metal centers can promote the opening of 2-thienyl ligands (but not of 3-thienyl ligands) in such a way that the carbon atom of the C—S inserted thiophene bridges two metal centers (Scheme 36).²²²



Scheme 36

Unlike C—S insertion, the conversion of metallathiacycles to thiolato complexes via M—C bond cleavage, followed eventually by the formation of free thiols, is a quite rare reaction occurring both stoichiometrically and catalytically. Stoichiometric reactions proceed via either protonolysis^{208,209,223} or hydrogenation of metallathiacycles.^{221,224,225,226–228} Selected examples are illustrated in Scheme 37 for (**103**),²⁰⁸ (**102**),^{221,224,225} and (**104**).²²³

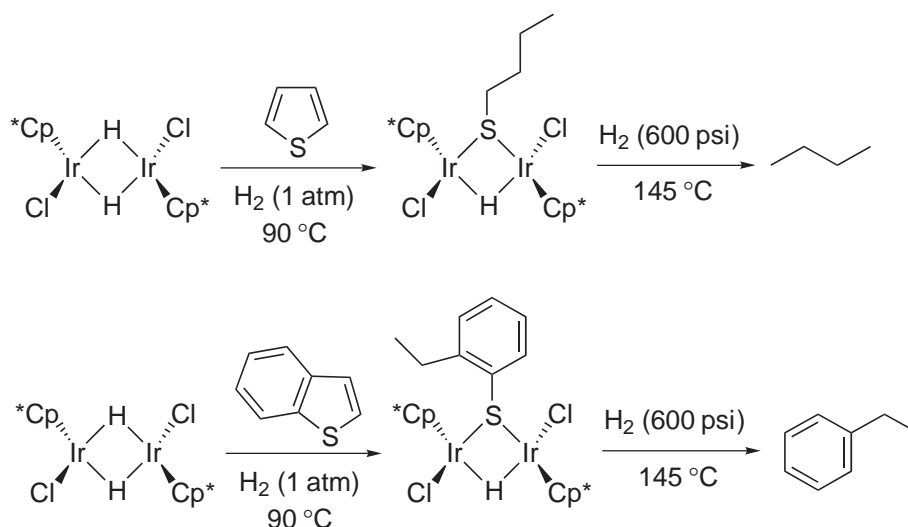


Scheme 37

One-pot hydrogenolysis, followed by desulfurization, has recently been observed by Vicic and Jones using the dimer $[\{\text{Cp}^*\text{IrHCl}\}_2]$, which reacts with (**103**) and (**102**) in the presence of H_2 to give $[\{\text{Cp}^*\text{IrCl}\}_2(\mu\text{-H})(\mu\text{-SC}_4\text{H}_9)]$ and $[\{\text{Cp}^*\text{IrCl}\}_2(\mu\text{-H})\{\mu\text{-S}(\text{C}_6\text{H}_4)\text{CH}_2\text{CH}_3\}]$, respectively (Scheme 38).²³¹ A mechanism has been proposed in which both the C—S bond cleavage of the thiophene and the hydrogenation of the unsaturated thiolate is brought about by a mononuclear species derived from the fragmentation of $[\{\text{Cp}^*\text{IrHCl}\}_2]$. The remaining Ir fragment, $[\text{Cp}^*\text{IrH}(\text{Cl})]$, stabilizes the hydrogenolysis products and ultimately contributes to form the dimers which can be desulfurized upon thermolysis under a high pressure of H_2 .

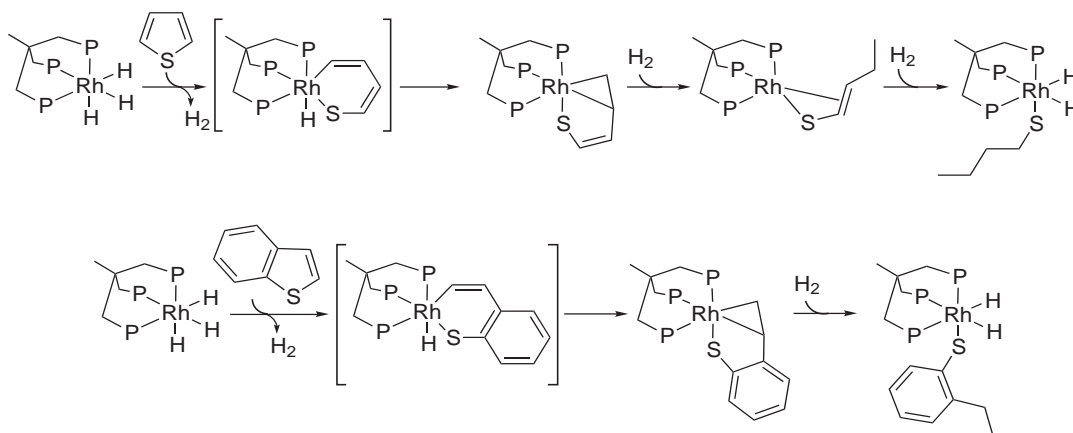
Catalytic examples of hydrogenolysis of thiophenic substrates are known exclusively for the $16e^-$ species $[(\text{triphos})\text{MH}]$ ($\text{M} = \text{Rh}$ ^{184,185,195,196} and Ir ¹⁹⁷) generated *in situ* by either thermolysis of appropriate precursors^{177,197} or base-assisted heterolytic splitting of H_2 (e.g., $[\text{M}]^{n+} + \text{H}_2 + \text{base}^- \rightarrow [\text{M-H}]^{(n-1)+} + \text{baseH}$).^{185,195,196} For kinetic reasons, the Rh fragment is more active than the Ir analog and effectively catalyzes the hydrogenolysis of (**103**),¹⁹⁵ (**102**),^{184,185,195} (**104**),¹⁹⁵ and dinaphtho[2,1-*b*:1',2'-*d*]thiophene¹⁹⁶ to the corresponding thiols in common organic solvents under relatively drastic conditions (160 °C, 30 atm of H_2).

The capability of triphos complexes to tolerate reaction temperatures as high as 200 °C with no substantial decomposition, and the high energy of the $16e^-$ fragments $[(\text{triphos})\text{MH}]$, are

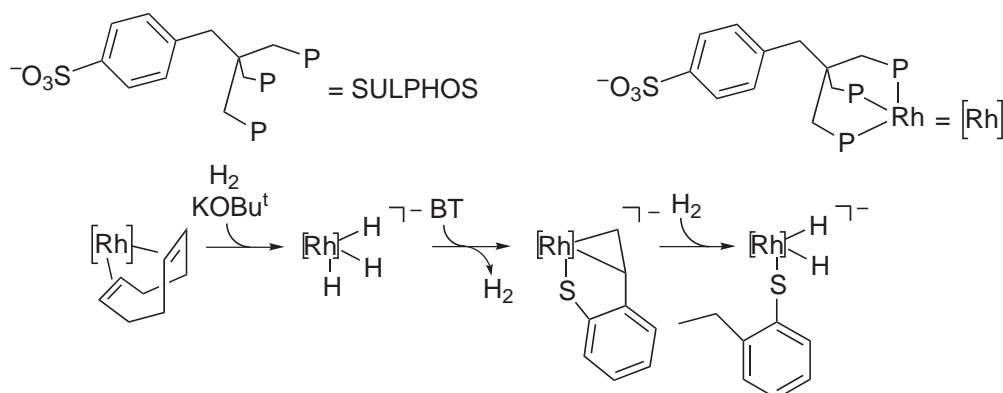


Scheme 38

important factors in ensuring catalytic activity. Typical reaction sequences that transform thiophenes into thiolate ligands by action of [(triphos)RhH] and H₂ are shown in Scheme 39. A sulfonated phosphine in combination with a strong Brønsted base has allowed the hydrogenolysis of (102) to 2-ethylthiophenol (ETP) using rhodium catalysts in liquid biphasic systems comprising *n*-heptane as hydrocarbon phase and water or methanol as polar phases (Scheme 40).¹⁸⁴



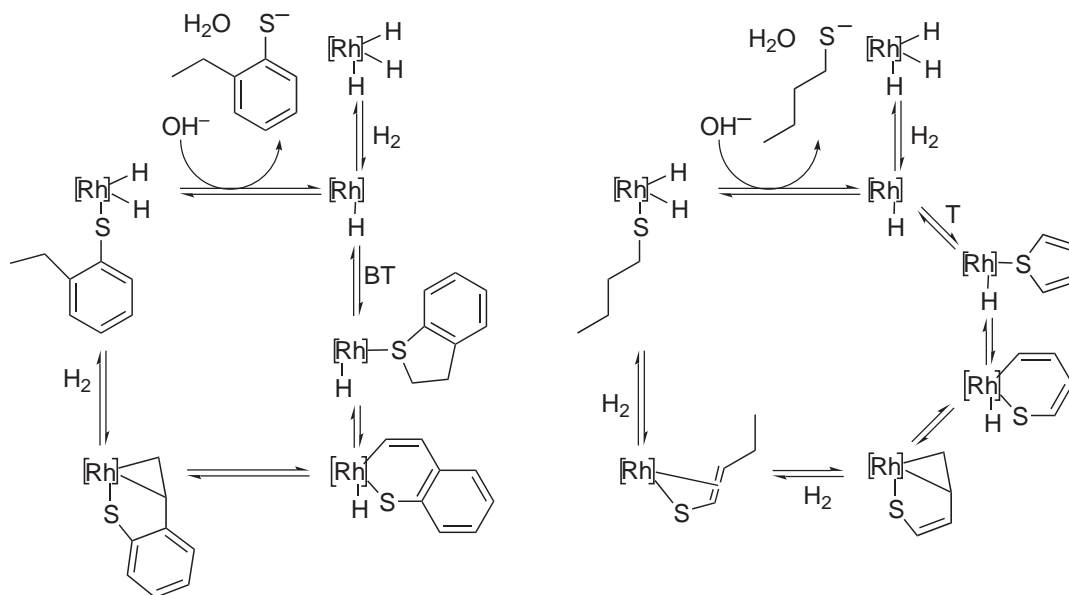
Scheme 39



Scheme 40

In the base-assisted reactions, the hydrogenolysis products are recovered as sodium or potassium thiolates which can either be converted to thiols by acidification with protic acids, or be oxidized to disulfides by exposure to air.^{184,195} In turn, all of the Rh catalyst of the aqueous biphasic reactions remains in the polar phase for use in a further catalytic run after the thiolate product is extracted as thiol.

The combined information gathered from kinetic studies,¹⁸⁴ *in situ* high-pressure NMR experiments,^{184,185,195} and the isolation of intermediates related to catalysis, leads to a common mechanism for all the hydrogenolysis reactions of (102)–(104) and other thiophenes catalyzed by triphos- or SULPHOS-rhodium complexes in conjunction with strong Brønsted bases. This mechanism (Scheme 41) involves the usual steps of C–S insertion, hydrogenation of the C–S inserted thiophene to the corresponding thiolate, and base-assisted reductive elimination of the thiol to complete the cycle.^{184,185,195–198}

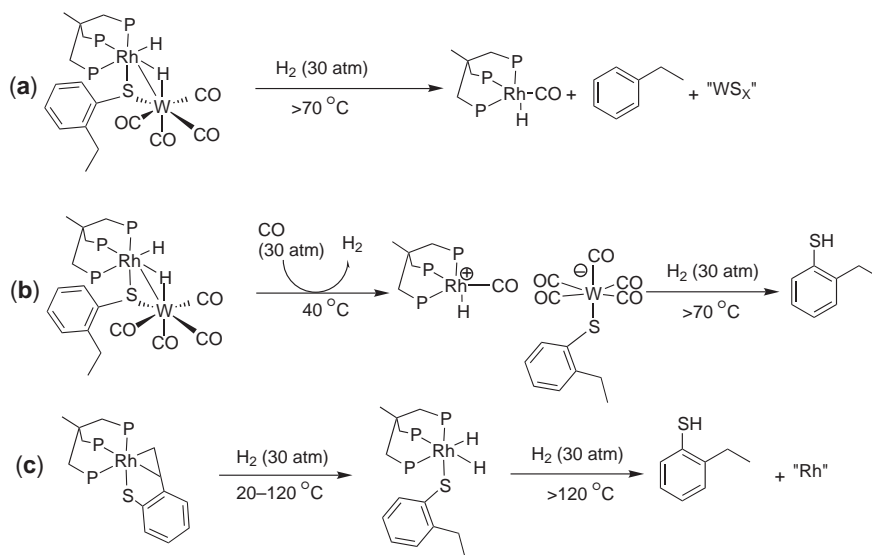


Scheme 41

The overall degradation of (103) assisted by the cluster [(Cp')₂Mo₂Co₂S₃(CO)₄] (Cp' = CH₃C₅H₄) is the model reaction that best resembles the heterogeneous counterparts, particularly those classified as “Co/Mo/S” phase,¹⁵⁸ in terms of both structural motif and HDS activity.²²⁹ Moreover, the Co/Mo/S cluster has successfully been employed to show that the C–S bond scission in the desulfurization of aromatic and aliphatic thiols occurs in homolytic fashion at 35 °C and that thiolate and sulfido groups can move over the face of the cluster as they are supposed to do over the surface of heterogeneous catalysts.²³⁰

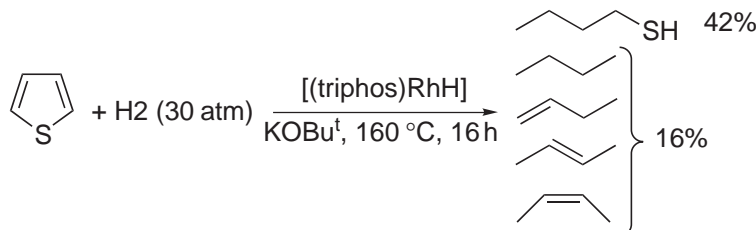
The mechanism proposed involves hydrogenation of the C₂–C₃ double bond, formation of 2-vinylthiophenol by an E₂ elimination, and hydrocarbon elimination by homolysis of the S–C_{aryl} bond. This pathway rationalizes the primary formation of (104) observed in some HDS reactions of (102) over “Co/Mo/S” catalysts, as well as the kinetic evidence that the rate-determining step on real catalysts is the removal of surface sulfur.^{158–160}

Both the cooperation of *component* and *promoter* metals in the desulfurization step of (102) to ethylbenzene and the walking of thiolate groups from one metal to another have recently been observed to take place in the reactions of the (102)-derived heterometal dimer [(triphos)RhH(μ-H){μ-*o*-S(C₆H₄)CH₂CH₃}W(CO)₄] with H₂ and CO, respectively (Scheme 42a, 42b)^{224,225} Most importantly, in the absence of the W *component*, [(triphos)Rh{η³-S(C₆H₄)CH=CH₂}] reacts with H₂ under comparable conditions undergoing M–C cleavage but not S–C cleavage (Scheme 42c),¹⁸⁵ while in the absence of the Rh *promoter*, [W(CO)₄{S(C₆H₄)CH₂CH₃}]⁻ undergoes M–S cleavage but not S–C cleavage (Scheme 42b).²²⁴ In light of these findings, it was concluded that the major activity of promoted catalysts in the HDS of (102) might also be due to the ability of *promoter* metals to favor hydrogenolysis pathways due to the lower energy barrier to C–S insertion as compared to *component* metals.



Scheme 42

In contrast to hydrogenation and hydrogenolysis, no catalytic desulfurization reaction of thiophenes by soluble metal complexes has ever been shown to take place through a clear and unambiguous homogeneous process. It has been found the C—S insertion product [(triphos)IrH(η^2 -(C,S)-(104))] reacts in THF with (104) under 30 atm of H₂ at 160 °C to give biphenyl and H₂S in excess of the stoichiometric amounts.¹⁹⁷ More recently, catalytic production of butane, butenes, and H₂S has been observed upon hydrogenation (30 atm of H₂) of (103) in the presence of the [(triphos)RhH] catalyst (generated *in situ*) and a strong base (Scheme 43).¹⁹⁵



Scheme 43

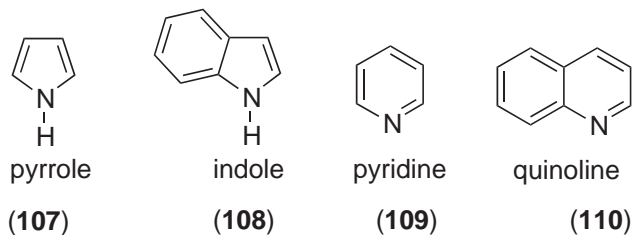
The great stability of the M=S and M—S—M' moieties toward the elimination of S as H₂S probably explains the lack of success of polynuclear species in assisting a catalytic reaction. The first example of hydrogenation of M=S to M(H)SH in a discrete homogeneous metal system was reported only in 1997 by Bergman and co-workers for [(Cp)*₂TiS(pyridine)].²³¹

9.2.5.2 Hydrodenitrogenation

The increasing interest for HDN reaction is due to environmental push and business pull. The degradation of nitrogen compounds to ammonia and hydrocarbons consumes more hydrogen than any other hydrotreating reaction, and therefore any improvement in the efficiency of HDN catalysis would produce an immediate business advantage.

Nitrogen in petroleum and coal is contained in various organic compounds, which include five- and six-membered heterocycles, aliphatic and aromatic amines and nitriles. Amines and nitriles are less abundant and their degradation is efficiently performed under hydrotreating conditions applying commercial catalysts. The HDN of the aromatic heterocycles, generally pyrroles (107), indoles (108), pyridines (109) and quinolines (110) (Scheme 44) is much more difficult to accomplish, even more than the HDS of fused-ring thiophenes. Moreover, HDN of the aromatic N-heterocycles requires a greater amount of H₂ than HDS of thiophenes, as the latter does not necessarily involve

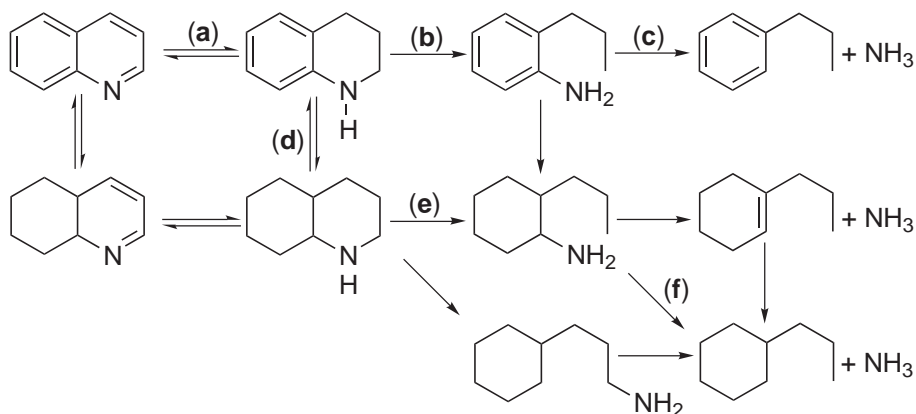
the saturation of the heterocyclic ring prior to hydrogenolysis.^{232–236} HDN model studies in solution are essentially based on four relevant issues: modes of bonding between N-heterocycles and metal centers; reactivity of coordinated N-heterocycles; elementary steps of metal-catalyzed hydrogenation of N-heterocycles; and insertion of metal centers into C–N bonds. A common strategy in HDN modeling is the reaction between mononuclear or polynuclear metal complexes, containing either coordination vacancies or weakly bound ligands, and N-heterocycles. The model substrates may be divided into two main categories according to the donor properties of the nitrogen atom. In **(107)** ($pK_a=0.4$) and **(108)** ($pK_a=-3.6$), the nitrogen lone pair is delocalized over the five-membered ring and is not available for interaction with electrophiles. In contrast, the nitrogen atom in **(109)** ($pK_a=5.2$) or **(110)** ($pK_a=4.9$) is a good nucleophile susceptible to attack by various electrophilic metal fragments. This greatly influences their interaction with the heterogeneous catalyst surface and, consequently, the mechanisms for their reduction.



Scheme 44

Although the intimate mechanism of metal-catalyzed HDN is still far from being understood completely, heterogeneous studies have provided data on product distribution, kinetics, and selectivity, whereas the homogeneous ones have contributed to the explanation of the binding of the nitrogen substrates to metal centers and the mechanisms of fundamental steps such as the hydrogen transfer from metal to coordinated substrate and the C–N bond scission. It has been experimentally demonstrated that aromatic nitrogen molecules undergo HDN via preliminary hydrogenation of the heterocyclic ring, followed by C–N bond scission (hydrogenolysis). The hydrogenation of the heterocyclic ring is necessary to reduce the high energy required to cleave the carbon–nitrogen bond that, in a typical N-heterocycle, is close to that of a C=N double bond.^{237–241} Since the hydrogenation of the heterocycle to a saturated amine occurs prior to C–N bond cleavage, the position of the hydrogenation equilibrium actually controls the removal of the nitrogen atom, mainly when the hydrogenolysis rate is much slower than the hydrogenation rate. Unfavorable hydrogenation equilibria would result in a low concentration of saturated amine with the consequent decrease of the overall HDN rate. Then, high pressures of H₂ are required for efficient HDN. Kinetic modeling of the HDN process indicates that dehydrogenation of partially hydrogenated substrates such as tetrahydroquinoline can be competitive with C–N bond cleavage, even in the presence of H₂.^{237–241}

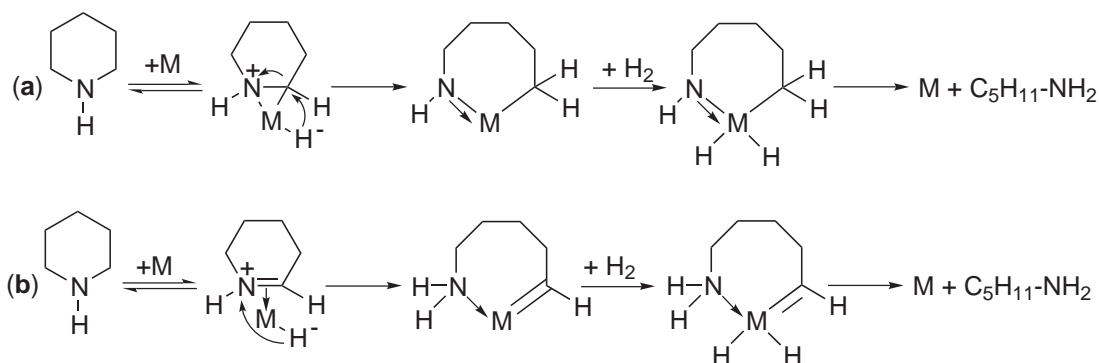
The principal reaction pathways proposed for the heterogeneous HDN of the model substrate **(110)**^{232–242} are shown in Scheme 45. A similar sequence of steps has also been suggested to occur for the HDN of **(107)**.



Scheme 45

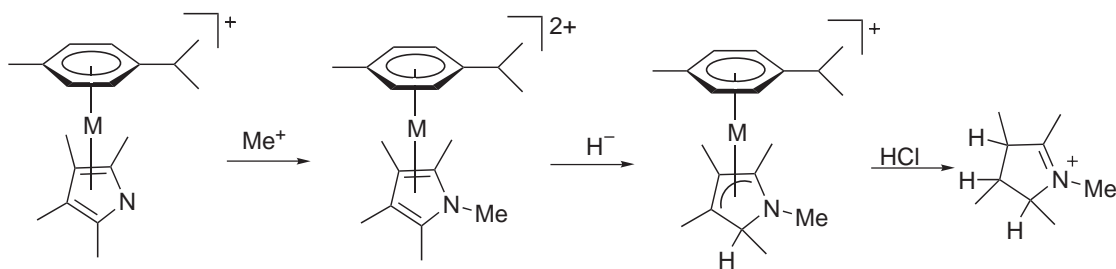
The most efficient and selective HDN of (**110**) likely occurs via the reaction sequence **a**→**b**→**c**, which does not involve the hydrogenation of the carbocyclic ring. However, most of the derivatives of (**110**) undergo HDN via the alternative sequence **a**→**d**→**e**→**f** that involves the hydrogenation of both rings and therefore consumes twice the amount of H₂, yielding propylcyclohexane. It was proposed that the hydrogenation of N-heterocycles to saturated cyclic amines involves the formation of metal π -adducts, followed by a reductive π → σ shift once the two consecutive hydrogen transfers have occurred from vicinal N—H groups.^{243,244}

The interaction of the surface metal atoms with saturated N-heterocycles has been the object of model studies by Laine and co-workers, which suggest that the C—N scission in saturated heterocycles may not require acidic sites, but rather metal centers.^{245,246} Two possible pathways have been proposed for the HDN of piperidine involving a metal alkyl (**a**) or a metal alkylidene intermediate (**b**) (Scheme 46). In either case, the first step has been suggested to involve the oxidative addition of the C—H bond adjacent to the nitrogen atom to give a metal–hydride species. The subsequent migration of the hydride from the metal to either the C_α atom or the N atom of an η^2 -piperidinyl ligand determines the nature of the intermediate that is ultimately hydrogenated to a primary amine.



Scheme 46

The η^5 -pyrrolyl complexes [(*p*-cymene)M(NC₄Me₄)](OTf) (M = Ru, Os) are readily converted into the corresponding η^5 -(**107**) by selective alkylation at the nitrogen atom (Scheme 47). Interestingly, the η^5 -(**107**) ligand in [(*p*-cymene)M(MeNC₄Me₄)](OTf)₂ undergoes regio- and stereoselective hydride addition to an α -carbon atom to give a η^4 -MeNC₄Me₄H derivative. This compound reacts with protic acids, leading to further (**107**) reduction and dissociation from the metal as an iminium salt.²⁴⁷

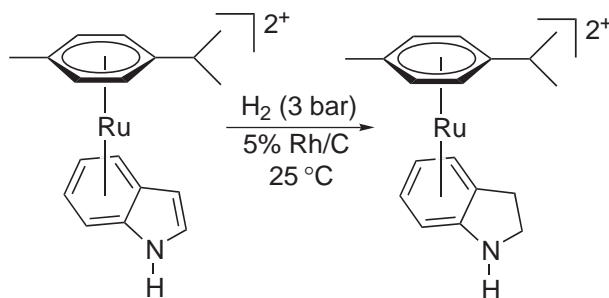


Scheme 47

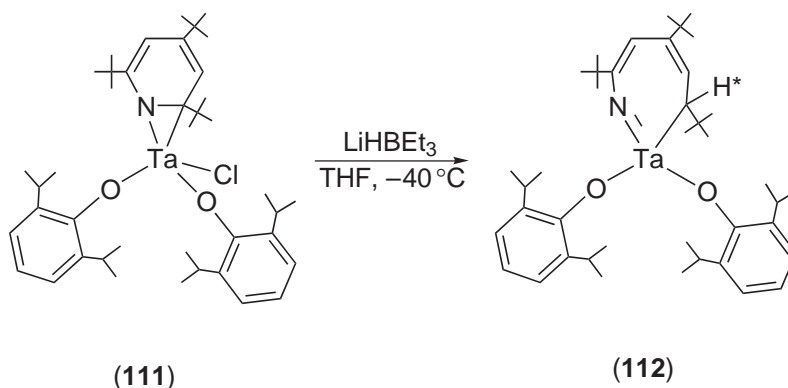
η^6 -(**108**) complexes are activated toward nucleophilic substitution at the carbocyclic ring,^{248–250} as well as reduction of the heterocyclic ring.²⁴⁸ The η^6 -coordination through the carbocyclic ring of (**108**) promotes the hydrogenation of the heterocyclic portion of the molecule to give an η^6 -indoline complex (Scheme 48).

In the dihapto mode the pyridine ring can be protonated intermolecularly at nitrogen, or even intramolecularly deprotonated at carbon. The first evidence for metal C—N insertion is the reaction of the metallaaziridine complex (**111**) with homogeneity: LiHBET₃ in THF at low temperature that yields (**112**) (Scheme 49).^{251–254} Experiments with carbon nucleophiles (RMgCl, MeLi) in place of LiHBET₃ have provided valuable information to allow discrimination between

the two possible pathways (*exo*-attack vs. *endo*-attack) to (**109**) C—N scission (Scheme 49).²⁵⁸ It has been established that the reaction occurs via an intramolecular *endo*-attack of the hydride that migrates to the (**109**) C $_{\alpha}$ atom as a σ -nucleophile.

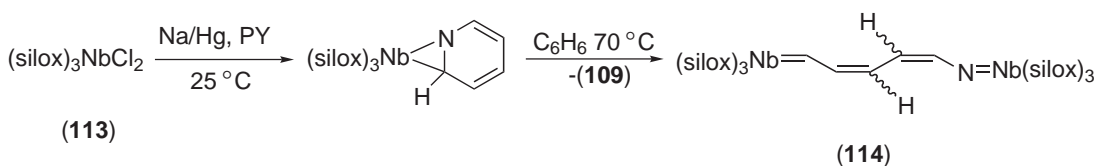


Scheme 48



Scheme 49

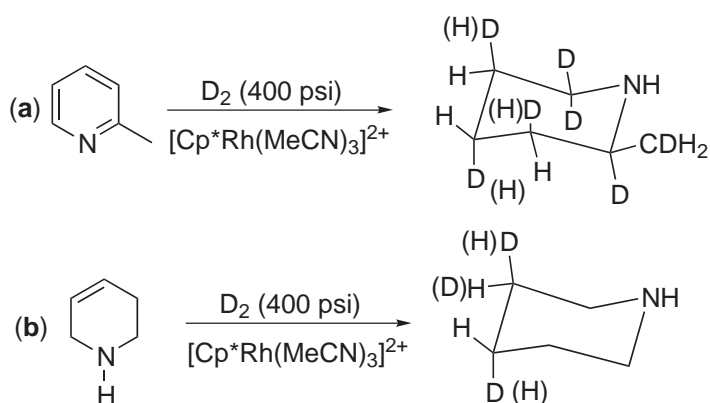
An interesting case of metal-assisted ring opening of (**109**) has been described by Wolczanski using the low-valent (silox) $_3$ Nb fragment that binds (**109**) in the η^2 (N,C) mode (Scheme 50). Derivative (**113**) undergoes C—N insertion by thermolysis in benzene at 70 °C only. The reaction gives 0.5 equiv. of (**109**) and 0.5 equiv. of (**114**) as a thermodynamic mixture of *cis,cis*-, *trans,cis*-, *trans,trans*- and *cis,trans*-isomers.^{255–257}



Scheme 50

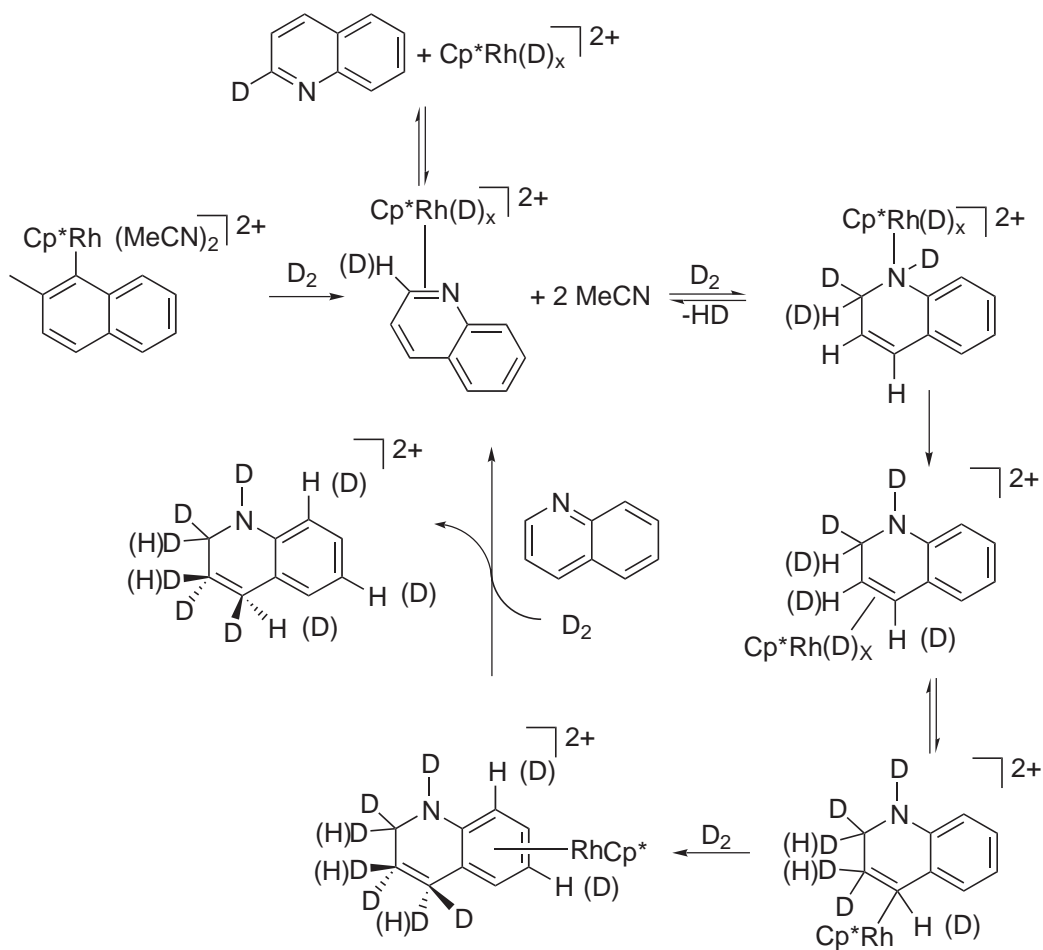
Fish and co-workers investigated the hydrogenation of 2-methylpyridine to 2-methylpiperidine catalyzed by [Cp* $\text{Rh}(\text{MeCN})_3$] $^{2+}$ with an in-depth study.²⁵⁸ On the basis of the deuteration pattern it was concluded that the reductions of the C=N and C=C bonds are reversible (Scheme 51). The initial C=N bond hydrogenation, which disrupts the aromaticity of the molecule, is the most critical hydrogenation step in the overall reduction process. Six-membered mononuclear N-heterocycles such as (**109**) are much less prone to undergo hydrogenation than bi- and trinuclear N-ring compounds (e.g., quinolines, benzoquinolines, acridines) due to their higher resonance stabilization energy.

Several Rh I , Ru II and Ir I catalysts containing tris(pyrazolyl)borate ligands (Tp) have been tested for the hydrogenation of (**110**), with Rh I complexes being the most active catalysts. The activity was found to increase with the ease of formation of Tp complexes, while the presence of ligands capable of competing with (**110**) for coordination decreased the hydrogenation rate (e.g., cyclo-octene and ethylene undergo competitive metal insertion into sp^2 C—H bonds).²⁵⁹



Scheme 51

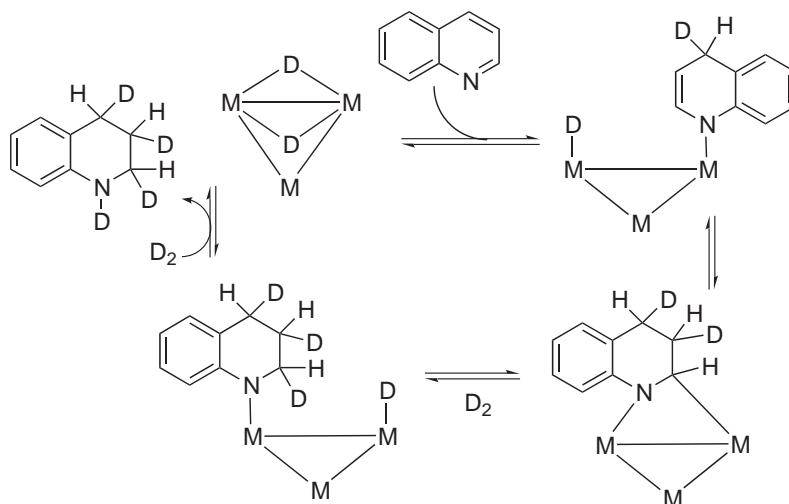
Scheme 52 explains the $[(Cp^*)Rh(MeCN)_3]^{2+}$ -assisted regioselective hydrogenation of pyridines, benzoquinolines, acridines as well as indoles and benzothiophene.²⁵⁸ The relative hydrogenation rates were attributed to both electronic and steric effects, the rate generally decreasing with increasing basicity and steric hindrance at the nitrogen atom.



Scheme 52

The deuteration pattern of the tetrahydroquinoline (Scheme 53)²⁵⁸ is rather similar to that reported by Laine for the hydrogenation of (110) with the clusters $H_2Os_3(CO)_{10}$ and $Os_3(CO)_{12}$,²⁶⁰ as well as with sulfide/Co-Mo/ γ - Al_2O_3 heterogeneous catalysts.^{248,249} The

differences in the deuteration pattern have been explained in terms of the oxidative addition of the Os cluster to C—H bonds in (**110**) and to the occurrence of 1,4-hydrogenation as well.



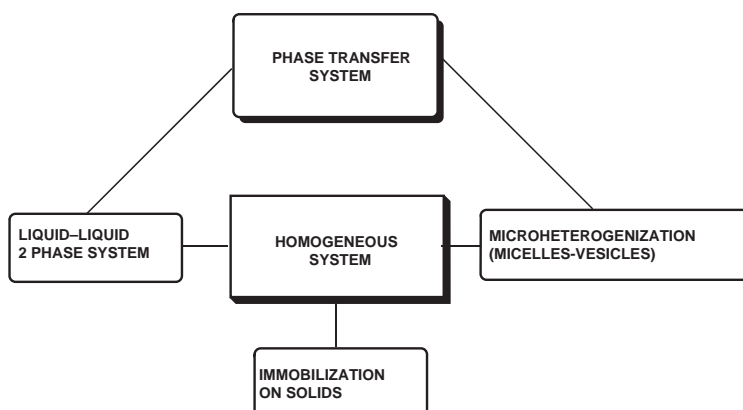
Scheme 53

9.2.6 NEW DEVELOPMENTS IN HYDROGENATION

9.2.6.1 Hydrogenation in Aqueous Systems

Water-soluble complexes able to catalyze hydrogenation reactions were generally regarded as curiosities, water being generally described as a medium which should be strictly avoided. $[\text{HCo}(\text{CO})_4]$ and $[\text{HCo}(\text{CN})_5]^{3-}$ were reported as water-soluble hydrogenation catalysts in 1980,²⁶¹ but until 1990 few examples of water-soluble complexes were described in the literature, because most of the substrates to be hydrogenated were not water soluble. Interest in this area increased dramatically in the 1990s, due to ever-increasing demand for complete recovery of precious-metal catalysts in industrial processes.

In particular, the impetus in the area of water-soluble catalysts derives from the well-known advantages (high activity, selectivity, and reproducibility under relatively mild conditions) and disadvantages (separation and recycling problems) of homogeneous with respect to heterogeneous hydrogenation catalytic processes. Several methods have been developed to combine the benefits of homogeneous and heterogeneous catalysis, the basic concept being to transfer a homogeneous catalyst into a multiphase system according to Scheme 54.



Scheme 54

One possibility is to bind the homogenous system to a solid support, to give a liquid–solid system. A second possibility is a liquid–liquid phase transfer system, and a third consists of microheterogenization of the catalytic system on organized amphiphiles in the colloidal or nanoscale regime. In the last of these cases, compounds and additives may form micelles, liposomes, or a lyotropic liquid crystalline phase, where hydrogenation occurs under the direct influence of the close environment. On an industrial scale only the first two methods are generally used. A number of examples have been reported of hydrogenation reactions resulting from combination of homogeneous organometallic and phase transfer catalysis (PTC), and from coupling of a metal-complex-catalyzed hydrogenation with simple enzymatic transformation (in order to model more complicated enzyme-catalyzed reactions).

An aqueous system is defined a homogeneous aqueous solution or a mixture of an aqueous and a water-immiscible organic solution in which the catalytic hydrogenation occurs. In the former case catalytic hydrogenation can proceed in either (or both) phases(s) or at the liquid/liquid interface, the transfer of reactant across the interface being in some cases facilitated by appropriate phase transfer agents. Water may also act as a reactant both in purely aqueous solution and in wet organic solvents, so it is not easy to distinguish between its molecular and bulk effects. Water is able to form strong hydrogen bonds to itself and to solutes, thereby exerting a significant influence on the final outcome of catalytic hydrogenations. All kinds of unsaturated functionalities can be reduced in aqueous systems, with high regio-, stereo-, and enantioselectivity being generally observed. Another advantage of aqueous media for hydrogen transfer reactions is that water-soluble donors such as ascorbate or EDTA can be employed as the hydrogen sources.

9.2.6.1.1 Water-soluble hydrogenation catalysts

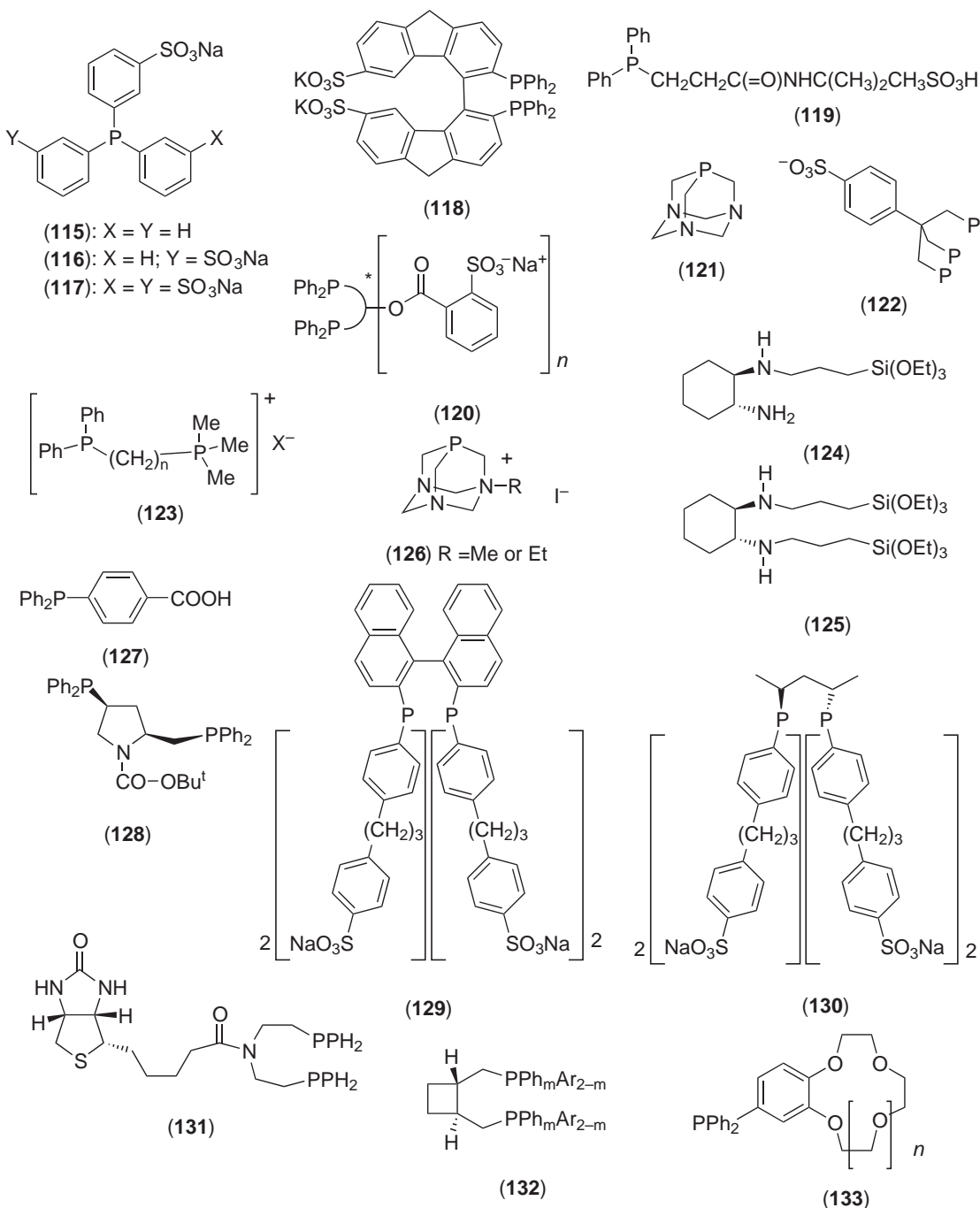
(i) Ligands

Solubility of a metal complex in water can be provided by appropriate ligands having ionic or polar substituents. The most important ligands are sulfonated phosphines, quaternary ammonium phosphines, and ligands containing carboxylate groups; but any ligand (halide, cyclopentadienyl, carbonyl) which stabilizes a lower-oxidation-state metal ion in an aqueous environment, retaining a net charge on the complex ion, could be employed. In the preparation of water-soluble ligands, direct functionalization can pose serious problems with respect to the precise control of the number and position of the substituents. For example, sulfonation is by far the most widely used method, but the reaction of PPh_3 with fuming sulfuric acid needs to be monitored and strictly controlled to achieve one of the possible products (**115**)–(**117**).

The most important development in direct functionalization is the method proposed by Hermann for the sulfonation of arylphosphines and arylphospholes in a superacidic medium made up from orthoboric acid and anhydrous sulfuric acid.^{262,263} Steltzer and co-workers have developed a general method for the synthesis of 4-sulfonphenylphosphines based on the reaction of 4-fluorobenzenesulfonates with PH_3 , primary or secondary phosphines in strongly basic solutions.²⁶⁴ Sulfonated and non-sulfonated forms of otherwise identical phosphines only show small differences in their complexation properties, the main ones being found in the number of coordinated phosphine ligands. Steric requirements for the bulky SO_3^- substituent and the electronic repulsion of the charged ligands generally contribute to the decrease in the number of coordinated phosphines. It is not very simple to rationalize the effects: kinetic studies showed a stabilizing effect against dissociation in *cis*- $[\text{Mo}(\text{CO})_4(\text{PPh}_3)_2]$ when PPh_3 was replaced by (**117**),²⁶⁵ whereas in the case of rhodium complexes there is often a large tendency to undergo hydrolysis even in non-alkaline solution.²⁶⁶ Scheme 55 contains some relevant examples of ligands generally employed in the synthesis of catalysts for aqueous hydrogenation.

(ii) Catalysts in homogeneous aqueous systems

Hydrogenation was one of the first organometallic catalytic processes observed in aqueous solution. The results obtained prior to 1994 have been summarized by Oro and co-workers.⁵ Recent studies are devoted to understanding the changes in reaction rates and selectivities which, in most cases, have been investigated in comparison with analogous non-aqueous hydrogenation reactions. We report here only selected examples useful to the reader for the choice of the catalytic system, showing the ways in which different metals can be employed.

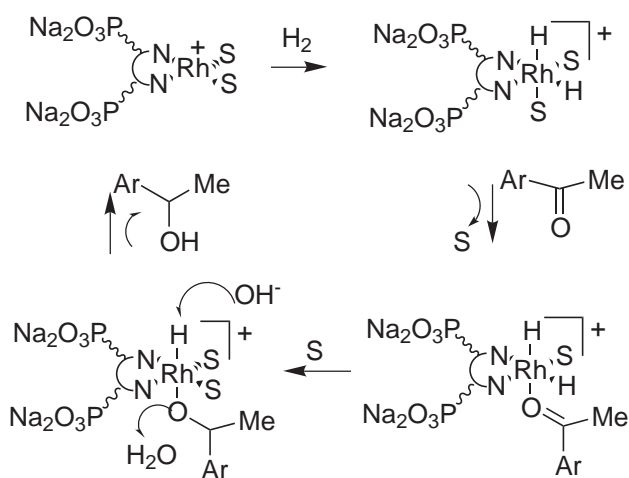


Scheme 55

When H_2 or NaBH_4 was added to a mixture of an aqueous solution of $(\text{NH}_4)_2[\text{PdCl}_4]$ containing the water-soluble chelating ligand polyvinylpyrrolidinone, a highly active catalyst for hydrogenation of alkenes and alkynes was obtained.²⁶⁷ A series of water-soluble cationic Rh complexes with pendant quaternary ammonium groups, able to carry out highly efficient hydrogenation of acetamidoacrylic acid derivatives in aqueous media, has been reported by Yan; but the enantioselectivities of these reactions in neat aqueous media are generally lower than in organic media.²⁶⁸ The ruthenium-catalyzed reduction of aromatic ketones using an enantiomerically pure catalyst derived from water-soluble analogs of Noyori's (1*S*,2*S*)-*N*-(*p*-tolylsulfonyl)-1,2-diphenylethylenediamine and Knochel's ligands (1*R*,2*R*)-*N*-(*p*-tolylsulfonyl)-1,2-diaminocyclohexane, and

[{RuCl₂(p-cymene)}₂], has been investigated; high enantioselectivity and moderate activity were observed in the 2-propanol/base system. Addition of water is necessary to stabilize the catalyst.²⁶⁹ The organometallic aqua complex [(Cp*)Ir(H₂O)₃]²⁺ is a pH-selective catalyst precursor for the transfer hydrogenation of carbonyl groups by HCOONa in water,²⁷⁰ acting as catalyst precursor for hydrogenation of water-soluble carbonyl compounds and alkenes in water over a pH range of about -1 to 4 under H₂ at pressure 0.1–0.7 MPa. The aqueous hydrogenation shows unique pH selectivity, governed by the following factors: (i) pH-dependent structural change of the catalyst precursor, which is deprotonated to form a catalytically inactive dinuclear complex [(Cp*Ir)₂(μ-OH)₃]⁺ above pH 4; (ii) stability of a putative iridium hydride active catalyst depending upon pH; (iii) difference in the proton affinity of the substrates, i.e., Lewis basicity of the carbonyl oxygen atoms of the carbonyl compounds and the C=C moieties of the alkenes. Turnover frequencies of the hydrogenations are also discussed on the basis of Lewis acidity of the carbocations that accept a hydride ion from the active catalyst.²⁷¹ A catalytic system containing [Rh(acac)(CO)₂] and a water-soluble phosphine was recently used for the hydrogenation of C4 unsaturated alcohols.²⁷² Formation and characterization of water-soluble rhodium and ruthenium complexes and their activity in hydrogenation of CO₂ and HCO₃⁻ in aqueous solution under mild conditions is reported by Joó and co-workers.²⁷³ By using water-soluble Ru^{II}-phosphine complexes, the initial turnover frequency of the reduction increases with increasing H₂ pressure. High pressure FT-IR can be used to find evidence for the formation of the catalytically active ruthenium hydride species.^{274,275} Homogenous catalysis using a water-soluble Ru complex of (117) is suitable for the combined hydrolysis and hydrogenation of inulin, a polysaccharide containing one D-glucose and 10 to 50 D-fructose units; the selectivity to D-mannitol in the hydrogenation of inulin is higher than expected, particularly at higher pH.²⁷⁶ Both enantiomers of ligand (118) are used in the ruthenium-catalyzed hydrogenation of methyl acetoacetate and (Z)-acetamidocinnamic acid in methanol and water. With (118) in water, a slight drop in the ee of the products is observed. When a small amount of acid was added, a fast reaction and high asymmetric induction was found.²⁷⁷

The catalyst precursor prepared *in situ* from rhodium dimer [{Rh(COD)Cl}₂] and the water-soluble phosphine (119) is an effective olefin hydrogenation catalyst. Catalytic hydrogenation reactions have been tested in either two phases: aqueous catalyst/insoluble olefin or methanolic catalyst/olefin systems. The observed reaction rates were higher for terminal than for internal olefins. The system has also been used in the form of a supported aqueous phase catalyst.²⁷⁸ Water-soluble rhodium and iridium complexes of 2,2'-bipyridine derivatives, functionalized with —PO₃Na₂ groups, show very good catalytic activities in the reduction of various substituted acetophenones under hydrogen pressure in basic aqueous media. No significant loss of catalyst is observed after one use. The effect of NaOH in the catalytic site of Rh-catalyzed hydrogenation of ketones in water under hydrogen pressure is proposed in Scheme 56.²⁷⁹



Scheme 56

Rhodium complexes based on the chiral ligand (120) have been used in the asymmetric hydrogenation of functionalized chelating olefins in methanol and water. The results are compared to those obtained using the corresponding non-sulfonated catalysts; in water all sulfonated

complexes are superior.²⁸⁰ A detailed study of hydrogenations in aqueous solution was carried out with $[\text{RhCl}(\mathbf{121})_3]$. The complex is an active catalyst for reduction of olefinic and oxo-acids, as well as of allyl alcohol and sulfostyrene. Mechanistic investigations were done with crotonic acid and allyl alcohol substrates. Pronounced maxima in the rates of hydrogenation of both substrates were found at pH 4.7. In these processes $[\text{HRh}(\mathbf{121})_3]$ has been proposed as the catalytically active species, formed by dehydrochlorination of the primary product of H_2 oxidative addition.²⁸¹ $[\text{RhCl}(\mathbf{121})_3]$ is able to catalyze hydrogen transfer from aqueous formate to α,β -unsaturated aldehydes.²⁸² $[\text{RhCl}(\mathbf{121})_3]$, in contrast to $[\text{RuCl}_2(\mathbf{121})_4]$,²⁸³ showed marked selectivity towards the reduction of the $\text{C}=\text{C}$ bond and can be recycled in the aqueous phase. $[\text{RuCl}_2(\mathbf{121})_4]$ is catalytically quite active for the conversion of unsaturated aldehydes to unsaturated alcohols using a biphasic aqueous/organic medium with formate as the source of hydrogen. Under similar conditions $[\text{RhCl}(\mathbf{121})_3]$ is a very active catalyst for olefin hydrogenation. Water-soluble analogs of Vaska's complex, *trans*- $[\text{IrCl}(\text{CO})(\text{PPh}_3)_2]$, have been prepared using the water-soluble phosphine ligands (**115**) and (**121**). The solution behavior of $[\text{IrCl}(\text{CO})(\mathbf{115})_2]$ in water is markedly different from that of the Vaska's complex in organic solvents, its reaction with O_2 and H_2 being irreversible due to formation of the strongly hydrated proton and chloride ions produced. $[\text{IrCl}(\text{CO})(\mathbf{115})_2]$ has been shown to be an active catalyst for the hydrogenation of olefinic double bonds in short-chain unsaturated acids in aqueous solution. The turnover frequency for the hydrogenation of maleic acid in water was significantly greater with $[\text{IrCl}(\text{CO})(\mathbf{115})_2]$ as a catalyst than the comparable process using Vaska's complex in dimethylacetamide at a much higher temperature.²⁸⁴ Rhodium complexes containing a series of phosphonium phosphines (**122**), described by Baird and co-workers, are very active olefin hydrogenation catalysts in aqueous and aqueous-organic biphasic media.²⁸⁵

9.2.6.1.2 Immobilization on solids

Immobilization of catalysts is an important process design feature (see Chapter 9.9). A recent example of catalyst immobilization is the biphasic approach which seems superior to immobilization on solids, as successfully proven in the Ruhrchemie/Rhone Poulenc process for the hydroformylation of olefins.²⁸⁶ Supported liquid phase catalysis was devised as a method for the immobilization of homogeneous catalysts on solids. When the liquid phase is water, a water-soluble catalyst may be physically bound to the solid.

The supports used for metal complexes are very different. Initially, several researchers investigated conventional polymers such as polystyrene, bearing functional groups for metal coordination. Silica and other metal oxides, which are inexpensive, easily functionalized, and thermally and mechanically stable, were generally employed. In soluble polymer-bound catalysts the attached ligand groups have little effect on physical properties of the polymer.²⁸⁷ Attachment of chiral catalysts to soluble polymeric ligands including dendritic polymers combines the advantages of catalysis in a homogeneous phase with facile separation by ultrafiltration in a membrane reactor. Several types of polymer have been used as ligands supports for water-soluble catalysts. They include poly(ethylene oxide),²⁸⁸ poly(acrylic acids),²⁸⁹ poly(*N*-alkylacrylamide),²⁹⁰ and derivatives of polyamines.²⁹¹ Catalysts for reduction of simple alkenes supported on phosphinated polystyrene including $[\text{RhCl}(\text{PPh}_3)_3]$ and $[\text{RuCl}_2(\text{PPh}_3)_3]$ have been also described.²⁹² Polystyrene functionalized with bipyridyl units has been coordinated to Pd^{II} to give a catalyst for alkene reduction.²⁹³ Pd^{II} has been supported also on poly(vinylpyridine)s and used as catalyst for reduction of unsaturated aldehydes, alcohols, and carboxylic acids.²⁹⁴ Rhodium or platinum complexes immobilized on acrylate polymers are good catalysts for reduction of alkenes, dienes, arenes, and nitroarenes.²⁹⁵ Radiation-induced copolymerization of *cis*- $[\text{PdCl}_2\{\text{CNMe}_2\text{OC}(\text{O})\text{CH}=\text{CH}_2\}_2]$ with acrylamides gave a terpolymer which catalyzed reduction of phenylethylene, styrene, or nitrobenzene under ambient conditions.²⁹⁶ Palladium supported on a polymer obtained by photochemical grafting of 4-vinylpyridine onto polyethene showed good selectivity for reduction of nitroarenes to anilines.¹⁵⁶ Nickel derivatives supported on polyethyleneimine catalyzed stereospecific reduction of alkynes to *cis*-alkenes.²⁹⁷ Chiral metal complexes can be immobilized on organic polymers and inorganic oxides as well as encapsulation in zeolites, mesoporous silicates, and polydimethylsiloxane membranes. Zeolites offer the possibility not only to immobilize metal complexes but also to influence reaction selectivity based on the size of pores, which give access to the intrazeolitic space.²⁹⁸

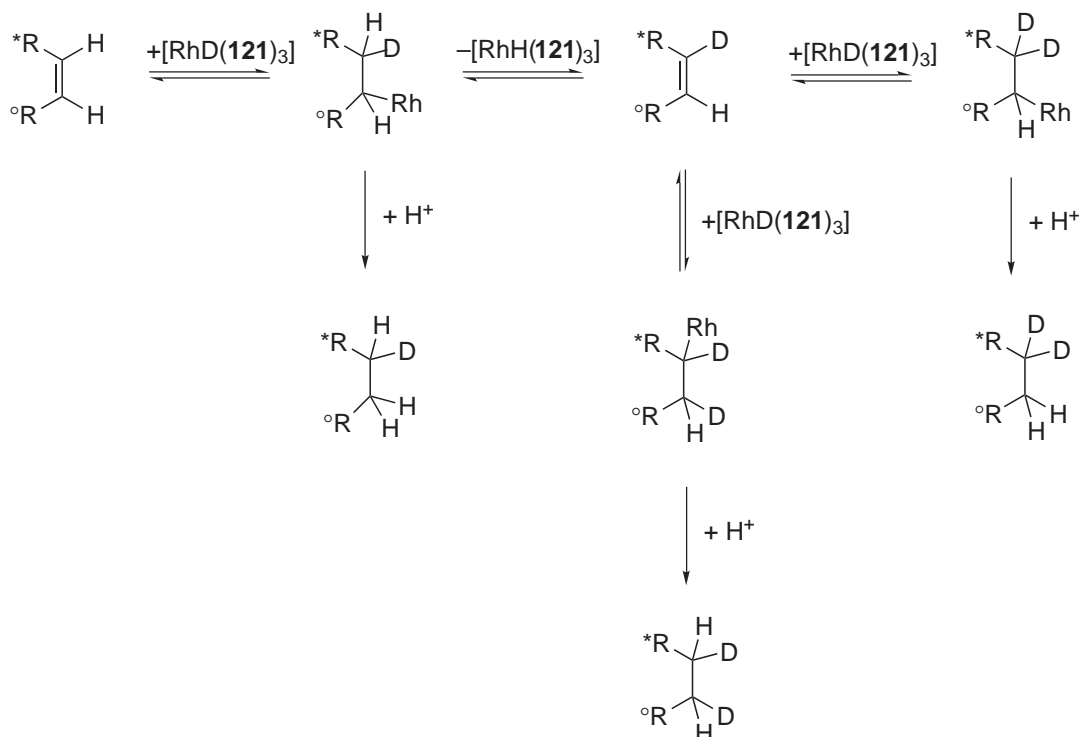
Catalysts for hydrogenation can be also supported on ion exchange resins. For example, rhodium(III) chloride, attached to a 3-carboxy-butenolic acid/DVB cation exchange resin with

a macromolecular structure, showed selectivity in alkene reduction similar to a homogeneous analog.²⁹⁹ Allyl benzene was reduced to propyl benzene using rhodium complexes attached to silica which had been modified with $\{\equiv\text{Si}(\text{CH}_2)_3\text{NHR}\}$ side-chains;³⁰⁰ both alkenes and dienes reacted in the presence of rhodium derivatives of $\text{SiO}_2/(\text{EtO})_3\text{Si}(\text{CH}_2)_n\text{PPh}_2$.³⁰¹ Catalysts supported on clays have been also employed. The adjustment of interlayer spacing by the introduction of substituents, pillaring, or solvent swelling, and the Lewis acidity nature of the interlamellar regions can also give usefully altered selectivity. As an example, $[\text{Rh}(\text{Me}_2\text{CO})_n(\text{NBD})](\text{ClO}_4)$ supported on polygorskite or montmorillonite is active for 1-hexene reduction but only after a substantial induction period.³⁰² Supported metal complexes are active also toward enantioselective reaction. For example, dehydroaminoacids were reduced in the presence of a rhodium complex on a derivatized silica gel.³⁰³ Bianchini and co-workers showed that both $[\text{Rh}(\text{COD})(\mathbf{122})]$ and $[\text{Rh}(\text{CO})_2(\mathbf{122})]$ can be grafted onto a high-surface-area silica with an immobilization procedure based on the capability of the sulfonate tail of (**122**) to link the silanol units of the support via hydrogen bonding.³⁰⁴ The catalysts obtained with this technique are denoted supported hydrogen bonded (SHB) catalysts. A similar heterogenization strategy has been previously employed for the preparation of supported transition metal oxide catalysts.³⁰⁵ The grafted $[\text{Rh}(\text{COD})(\mathbf{122})]/\text{SiO}_2$ is active for the hydrogenations of alkenes in either flow reactors (ethene, propene) or batch reactors (styrene) in hydrocarbon solvents.

The effects of catalyst site accessibility on the activities of supported olefin hydrogenation catalysts have been defined using rhodium complexes of phosphonium–phosphine ligands (**123**) tethered to a cation exchange resin via the tetra-alkylphosphonium moieties of the coordinated ligands. The most active catalysts are those containing the longer chain ligands, where the catalyst sites are farthest from the resin surface.³⁰⁶

Complexation of (**124**) and (**125**) with $[\{\text{Rh}(\text{COD})\text{Cl}\}_2]$ in the presence of $\text{Si}(\text{OEt})_4$, followed by sol–gel hydrolysis condensation, afforded new catalytic chiral hybrid material. The catalytic activities and selectivities of these solid materials have been studied in the asymmetric hydrogen-transfer reduction of prochiral ketones and compared to that of the homogeneous rhodium complexes containing the same ligands (**124**) and (**125**).³⁰⁷

Water-soluble rhodium(I) and ruthenium(II) complexes containing ligands (**115**) or (**121**) have been shown to catalyze the hydrogenation of aqueous HCO_3^- and HCO_2^- under mild conditions. No amine additive is needed for good turnovers. CO_2 accelerates the reactions with $[\text{RhCl}(\mathbf{115})_3]$, whereas it slightly inhibits the reductions catalyzed by $[\text{RuCl}_2(\mathbf{115})_2]$. Bicarbonate formed in the

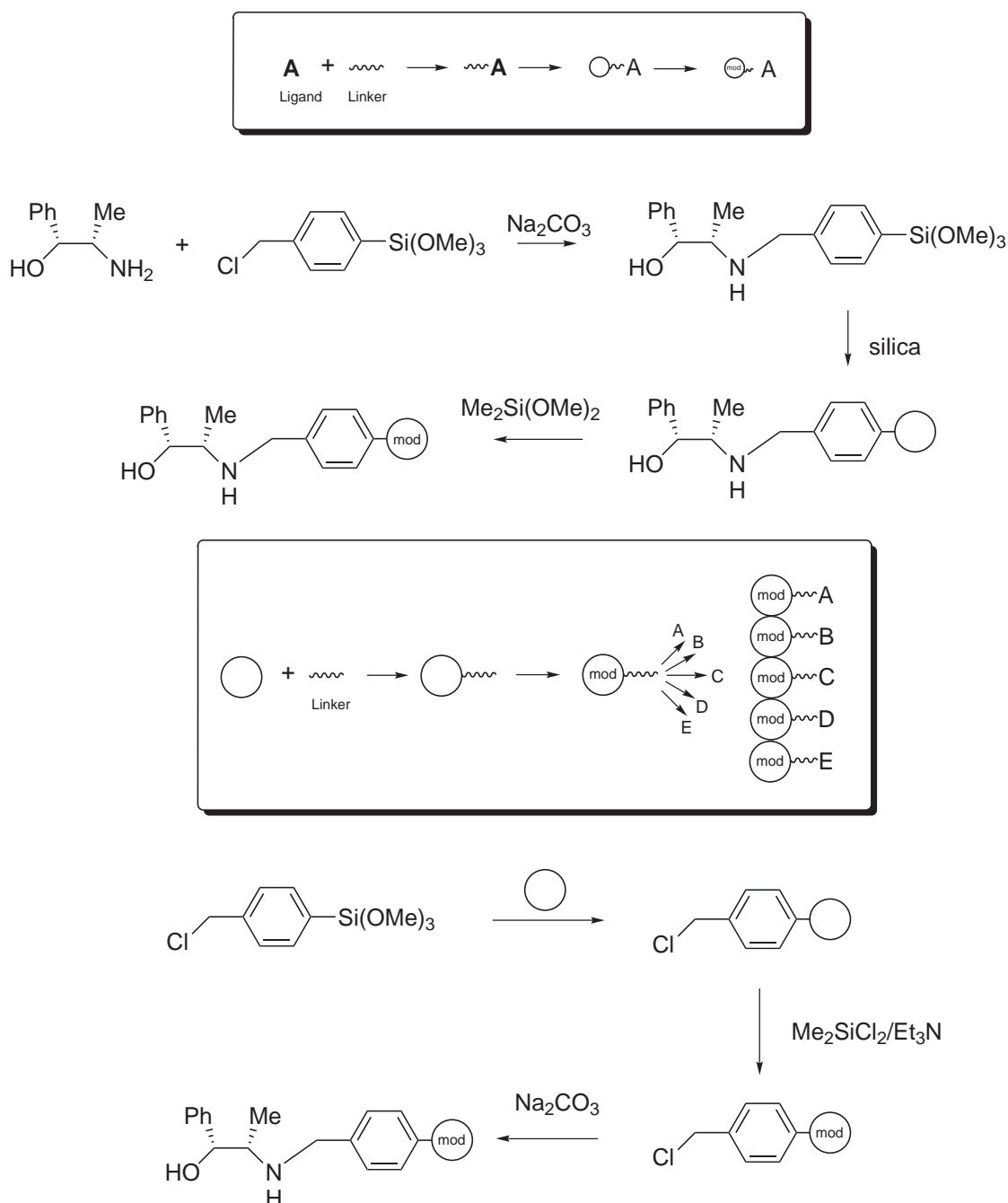


Scheme 57

reaction of limestone with aqueous CO_2 can also be used as starting material for the formate production.³⁰⁸ The water-soluble complex $[\text{RhCl}(\mathbf{121})_3]$ was also successfully employed for hydrogenation on phospholipid liposomes as model membranes in aqueous media under mild conditions; the highest conversion was achieved at pH 4.7. Formation of asymmetrically deuterated lipids, together with results from isomerization and kinetic experiments, revealed the important role of reversible formation of an alkyl-rhodium intermediate in the mechanism (Scheme 57).³⁰⁹ The solid-phase synthesis of a new asymmetric transfer hydrogenation catalyst and the use of these silica-supported systems in batch and flow reactors is described by Sandee.³¹⁰

The ruthenium complex of NH-benzyl-(1*R*,2*S*)-norephedrine covalently tethered to silica showed a high activity and enantioselectivity in the reduction of acetophenone.³¹⁰

Synthetic approaches to silica-immobilized aminoalcohol ligands are reported in Scheme 58.³¹⁰



Scheme 58

9.2.6.1.3 Immobilization via biphasic catalysis

One of the most documented applications of biphasic catalysis relates to the selective hydrogenation of unsaturated organic molecules, from the simple reduction of olefins³¹¹ and heteroaromatics³¹² to the controlled transformation of lipids in biomembranes and living cells.³¹³ At the present time the main efforts in this area are directed to the synthesis of new water-soluble ligands and to the development of mass transfer promoters to permit the reaction of water-insoluble substrates. Water-soluble $[\text{RuCl}_2(\text{DMSO})_4]$ is an active catalyst precursor for 1-hexene hydrogenation in water/organic solvent biphasic systems, giving 98% total conversion (400 psi H_2 , 80 °C, 6 h), with n-hexane as the principal product and 2-hexene isomers produced as by-products by isomerization of the substrate. $[\text{RuCl}_2(\text{DMSO})_4]$ is very sensitive to O_2 dissolved in water, and decomposes when halide salts or alcohols are added. It is also active in an alcoholic homogeneous phase, but less so than in the biphasic system, giving a greater extent of isomerization of the substrate instead of reduction.⁵

An investigation of different organic solvents, buffer, surfactants, and organorhodium compounds established that the catalytic reduction of tetralin using $[\{\text{Rh}(1,5\text{-hexadiene})\text{Cl}\}_2]$ proceeds with high efficiency at high substrate-to-catalyst ratios. The reaction occurs at r. t. and 1 atm. pressure in a biphasic mixture of hexane and an aqueous buffer containing a low concentration of a surfactant which stabilizes the catalysts.³¹⁴

Páez reported the hydrogenation of *trans*-cinnamaldehyde using as catalyst precursor the complexes $[\text{MCl}_2(\text{CH}_3\text{CN})_4]$ ($\text{M} = \text{Ru}^{\text{II}}$ and Os^{II}), stabilized with the water-soluble ligand (**115**).³¹⁵ The results are compared with those found for hydrogenations of *trans*-cinnamaldehyde carried out by other water-soluble organometallic complexes (Table 1).

Monflier and co-workers recently described a new approach based on the use of chemically modified β -cyclodextrins to perform efficiently the functionalization of water-insoluble olefins in a two-phase system. These compounds behave as inverse phase transfer catalysis, i.e., they transfer olefins into the aqueous phase via the formation of inclusion complexes.³²²

The ion-pairs formed in solution by group 8–10 metal halides and quaternary ammonium salts with long chain substituents can be extracted into nonpolar organic solvents, where they catalyze a range of reactions (isomerization, hydrogenation, dehydrogenation). The catalytically active species are not always well characterized, and the formation of stabilized metal colloids and halide and/or hydroxide bridged polynuclear complexes cannot be excluded. One of the best studied of these catalysts is the $\text{RhCl}_3 \cdot 3\text{H}_2\text{O}/\text{Aliquat-336}$ system, containing the $[(\text{C}_8\text{H}_{17})_3\text{N}(\text{CH}_3)]^+[\text{RhCl}_4(\text{H}_2\text{O})_2]^-$ ion pair which hydrogenates arenes in water/ $\text{ClCH}_2\text{CH}_2\text{Cl}$ at 30 °C and 1 bar total pressure.³²³ Dehydropeptides have been reduced in a two-phase system using $[\{\text{Rh}(\text{cod})\text{Cl}\}_2]$ associated with chiral water-soluble ligands; diastereoselectivities of up to 87% were obtained.³²⁴ Ellis reported the use of water-soluble ruthenium clusters

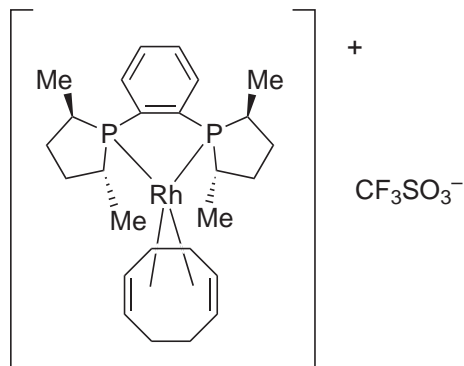
Table 1 Hydrogenation of *trans*-cinnamaldehyde using water-soluble organometallic complexes.

Catalyst precursor	Time (h)	Temperature (°C)	$P(\text{H}_2)$ (bar)	% Conversion	% Selectivity	References
$\text{RuCl}_3 \cdot 3\text{H}_2\text{O} + 6$ moles of (115)	3	100	30.1	100	90	312
$\text{RuCl}_3 \cdot 3\text{H}_2\text{O} + 6$ moles of (117)	3	100	30.1	100	95	316
$\text{RuCl}_3 \cdot 3\text{H}_2\text{O} + 5$ moles of (117)	3	35	20	99	98	317
$\text{RuCl}_3 \cdot 3\text{H}_2 + 5$ moles of (117)	3	40	20	100	96	316
$[\text{RuCl}_2(\text{115})_2]$	5	80	NaO_2CH	98	92	318
$[\{\text{RuCl}_2(\text{115})_2\}_2]$	3	100	30.1	100	83	319
$[\{\text{RuHCl}_2(\text{115})_2\}_2]$	3	100	30.1	100	54	319
$[\text{RuHCl}(\text{CO})(\text{115})_3]$	8	100	17	90	23	320
$[\text{RuHCl}(\text{CO})(\text{117})_3]$	8	100	17	87	30	320
$[\textit{cis}\text{-RuCl}_2(\text{121})_4]$	3	80	NaO_2CH	21	100	321
$[\{\text{RuCl}(\mu\text{-Cl})(\text{117})_2\}_2]$	3	40	20	100	91	316,319
$[\text{RuH}(\text{Cl})(\text{117})_3]$	3	40	20	100	96	316
$[\text{RuH}_2(\text{117})_4]$	3	40	20	100	95	316
$[\text{RuH}(\text{OAc})(\text{117})_3]$	3	40	20	100	96	316

[Ru₃(CO)₁₂(**117**)₃] and [H₄Ru₄(CO)₁₁(**117**)] as catalyst precursors in the hydrogenation of non-activated alkenes under biphasic conditions. Each cluster displays activity under moderate conditions, ca. 60 atm. H₂ at 60 °C with catalytic turnovers up to ca. 500. The trinuclear clusters undergo transformations during reaction but can be used repeatedly without loss of activity.³²⁵

[(PPh₃)₃Ru(H)Cl] and [(PrⁱP)₂Ir(H)Cl₂] react with H₂ (1 atm, 20 °C) in a 50% NaOH/benzene two-phase system in the presence of triethylbenzylammonium chloride as a PTC to form polyhydride complexes [(Ph₃P)₃Ru(H₂)(H)₂] and [(PrⁱP)₂IrH₅].³²⁶ [(Cy₃P)₂Rh(H)Cl₂] is an effective catalyst precursor for the hydrogenation of the double bond of α,β-unsaturated aldehydes and ketones under mild and biphasic conditions. Water or 0.5 M NaOH are necessary to promote the generation of the catalytically active species.³²⁷ Some rhodium hydride complexes containing the ligand (**126**) are efficient catalysts for hydrogenation of C=C bonds in two-phase catalytic systems.³²⁸ Water-soluble Ir and Rh complexes with tris(hydroxymethyl)phosphine catalyze the selective hydrogenation of the C=O bond of cinnamaldehyde under biphasic conditions.³²⁹ Two Rh complexes containing the carboxylated phosphine (**127**) were found to be effective catalysts for hydrogenation of olefins and polybutadiene in aqueous and aqueous/organic biphasic media. With these catalysts, terminal olefins were hydrogenated much faster than internal olefins, but an unusually enhanced hydrogenation rate was found for hydrogenation of the internal double bonds in 2-pentene and 3-pentenitriles. The catalysts show selectivity for the hydrogenation of 1,2 (vinyl) sites over 1,4 (internal) sites in the polybutadiene.³³⁰

Hydrogenation of nitrobenzene can be catalyzed by the water-soluble catalyst [PdCl₂(**117**)₂] under normal pressure at 65 °C in an H₂O/toluene biphasic solvent system. The water-soluble bimetallic catalyst system [PdCl₂(**117**)₂]-H₂PtCl₆ exhibits higher catalytic activity and selectivity than [PdCl₂(**117**)₂] and H₂PtCl₆ alone for the hydrogenation of aromatic nitrocompounds. The transmission electron micrographs demonstrate that the monometallic catalyst is composed of ultrafine palladium particles of almost uniform size while the particles of the bimetallic catalyst are more widely distributed in size than those of the monometallic ones.³³¹ A new chiral heterogeneous catalytic system obtained by occlusion of a Rh complex (Scheme 59) in polydimethylsiloxane was tested in the asymmetric hydrogenation of methyl-2-acetamidoacrylate in aqueous medium.³³²



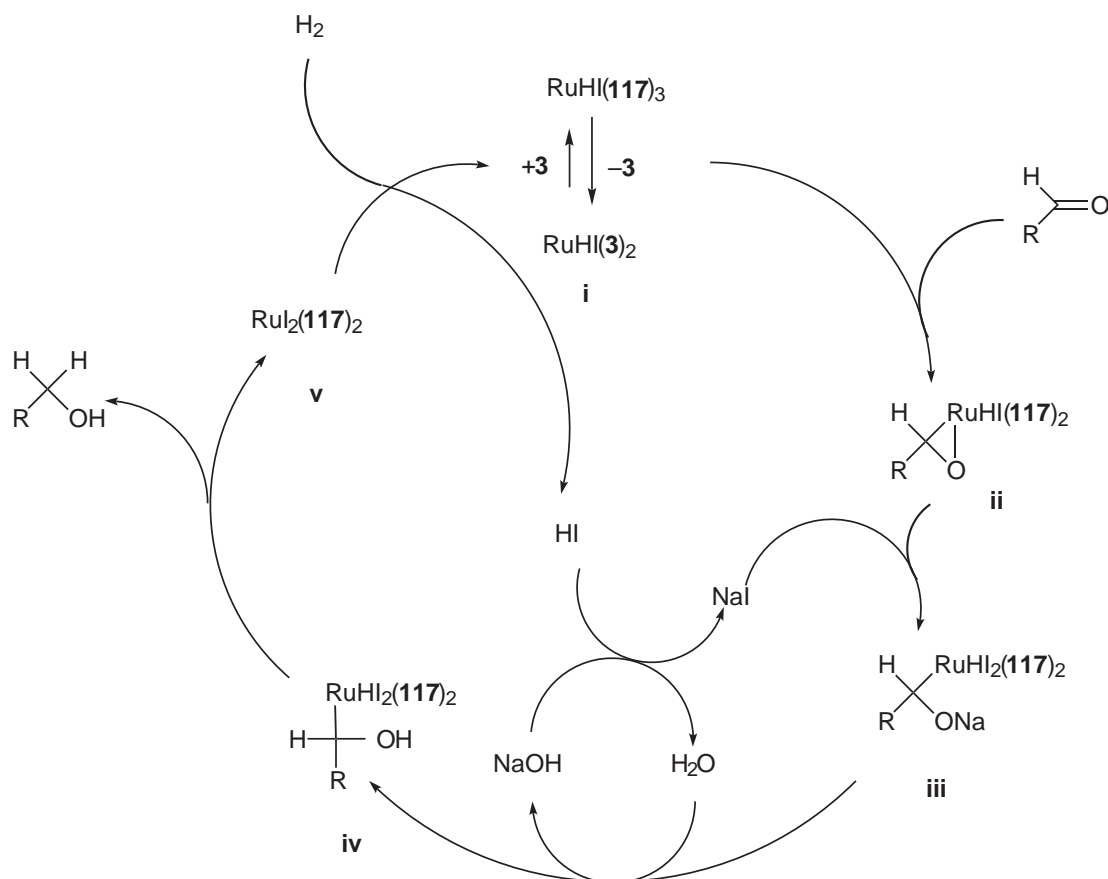
Scheme 59

9.2.6.1.4 Microheterogenization on organized amphiphiles in the colloidal or nanoscale dimension

The use of aqueous phase catalysis relies on highly water-soluble ligands to keep the catalytically active metal in the aqueous phase. Ligand modification has led to the use of tenside or amphiphilic ligands. Micelles derive from amphiphiles with one polar headgroup and one hydrophobic chain, whereas in most cases vesicles can be obtained from two amphiphiles with two chains per headgroup. The geometric shape of phosphine amphiphiles limits the way in which they may aggregate in micelles or vesicles. Amphiphilic phosphines serve not only as solubilizers for substrates in the aqueous phase, but also form micelle-like aggregates and in some case also vesicles. In addition to tenside ligands, surfactants may be added to water-soluble catalysts with the aim of increasing or altering the reaction selectivity.

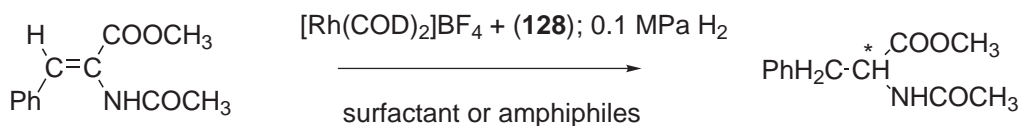
The effect of surfactant on enantioselective hydrogenation has been thoroughly investigated. Rhodium complexes of phosphinated glucopyranosides were used for hydrogenation of prochiral dehydroaminoacid derivatives in aqueous systems in the presence of sodium dodecylsulfate (SDS)

at 25 °C and 1 atm H₂. Addition of SDS generally increases both the rate and enantioselectivity of hydrogenations.³³³ Water-soluble Ru^{II} complexes containing the sulfonated ligand (**117**) exhibit, in the presence of various salts, an extremely high catalytic activity for the hydrogenation of aldehydes. Mechanistic studies indicate clearly that the salt effect occurs both via the cation and the anion in the catalytic cycle; the electrophilic cation favors an unusual type of aldehyde coordination, and the anion modifies the coordination sphere around the ruthenium atom (Scheme 60),³³⁴ both of which influence the mechanism.



Scheme 60

Ohme and co-workers investigated³³⁵ in an aqueous micellar system the asymmetric hydrogenation of α -amino acid precursors using optically active rhodium–phosphine complexes. Surfactants of different types significantly enhance both activity and enantioselectivity provided that the concentration of the surfactants is above the critical micelle concentration. The application of amphiphilized polymers and polymerized micelles as surfactants facilitates the phase separation after the reaction. Table 2 shows selected hydrogenation results with and without amphiphiles and with amphiphilized polymers for the reaction in Scheme 61.³³⁵



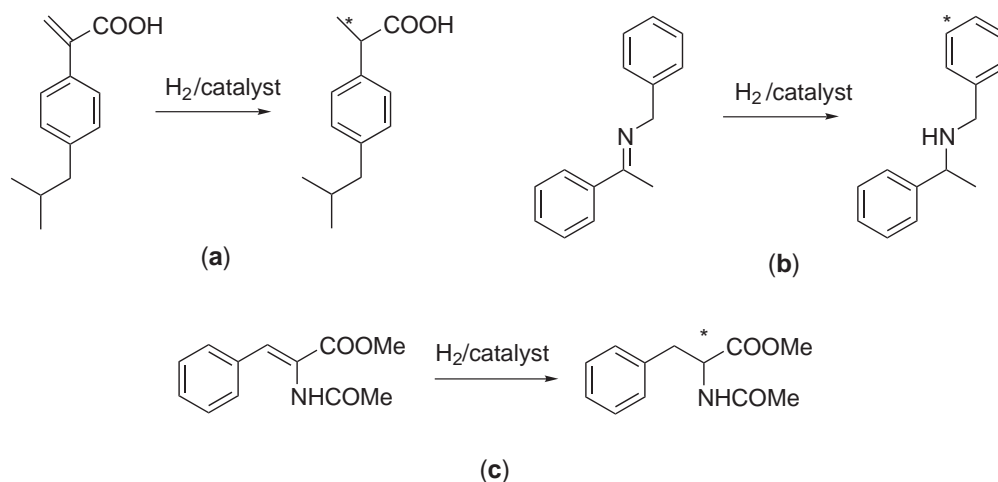
Scheme 61

Ruthenium complexes of (**129**) and (**130**)³³⁶ were investigated for the asymmetric hydrogenation of prochiral 2-*R*-propenoic acids (Scheme 62a); rhodium complexes of these ligands were used for hydrogenation of acetoamido–cinnamic acid methyl ester (Scheme 62c) and hydrogenation of acetophenone–benzylamine (Scheme 62b). The results obtained with these

Table 2 Selected hydrogenation results with and without amphiphiles and with amphiphilized polymers for the reaction in Scheme 61.

Surfactant	Rh:surfactant:substrate	t/2 (min)	Optical yield (%ee R)
None in water (methanol)	1:20:100	90 (2)	78 (90)
Anionic Sodium dodecylsulfate (SDS)	1:20:100	6	94
Cationic Cetyltrimethylammonium hydrogen sulfate (CTA HSO ₄)	1:20:100	5	95
Zwitterionic N-dodecyl-N,N'-dimethyl-3-ammonio- 1-propanesulfonate	1:20:100	5	93
Nonionic Polyoxyethylene(10)hexadecylether (Brij 56)	1:20:100	7	95
Amphiphiles	Rh:amphiphiles		
Silica ion exchanger 0.63 mmol g ⁻¹	1:20	11	92
Silica bound amphiphile 0.31 mmol g ⁻¹	1:20	24	93
Alumina adsorbed SDS 0.25 mmol g ⁻¹	1:20	7.5	90

catalysts have been compared with those obtained with BINAP as ligand. Amphiphilic water-soluble phosphines in aqueous biphasic catalysis lead to improved reaction rates with substrates that are poorly water soluble; the amphiphilic ligands (**129**) and (**130**), for example, aggregate in aqueous solution and there is evidence that these ligand aggregates solubilize the substrate in the aqueous phase.

**Scheme 62**

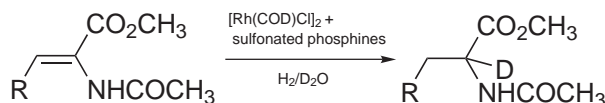
Rhodium-catalyzed enantioselective hydrogenation of acetamido-cinnamic in water was also achieved using pyrphos bound to poly-acrylic acid as ligand.³³⁷ Roucoux described some Rh⁰ nanoparticles which function as reusable hydrogenation catalyst for arene derivatives in a biphasic water-liquid system.³³⁸

9.2.6.1.5 Enantioselective hydrogenation in aqueous systems

Excellent enantioselectivities have been observed for hydrogenations both in homogeneous solutions (alcohols in water) and in biphasic systems. The effect of water on enantioselectivity varies from system to system; in some cases the ee value increases with increasing water concentration—

for example, in hydrogenation of 2-ethanamido-propenoic acid with water-soluble complexes³³⁹—whereas no change was found in the enantioselectivity of the hydrogenation of *Z*-2-ethanamido-3-phenylpropenoic acid catalyzed by a Rh complex in ethanol or ethanol:water mixtures.³⁴⁰

Rhodium complexes containing disulfonated phosphines can be used for enantioselective hydrogenation of enamides (<88% ee) and phenylethanone (28%).³²⁴ The hydrogenation of propenoic acid derivatives in ethanoate/D₂O mixtures catalyzed by Rh^I complexes containing sulfonated phosphines resulted in selective monodeuteration at the position α to the ethanamide and the ester groups (Scheme 63).³⁴¹



Scheme 63

Prochiral imines can be hydrogenated to the corresponding amines with extremely high enantioselectivities in H₂O/ethyl ethanoate biphasic systems, using Rh^I complexes of sulfonated phosphines.³⁴² The cationic rhodium complex [Rh(NBD)(**131**)]⁺ was an active catalyst for hydrogenation of 2-ethanamido-propenoic acid in aqueous solution.³⁴³

9.2.6.1.6 Transfer hydrogenation and hydrogenolysis in aqueous systems

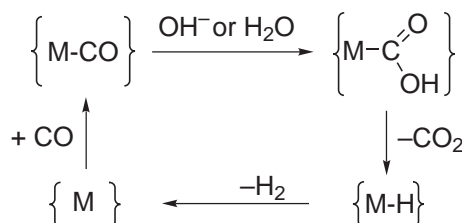
Methanoic acid and methanoates were amongst the most effective donors used for reduction of alkenes in aqueous solution, using Rh, Ru, Pt, and Pd complexes of (**115**), the most active catalyst being [RuCl₂(**115**)₂].³⁴⁴

Prochiral derivatives of propenoic acid were reduced by hydrogen transfer from aqueous solutions of M[HCOO] (M = K⁺, Na⁺ and [NH₄]⁺) catalyzed by Rh^I complexes of (**117**) or the tetrasulfonated cyclobutanediop (**132**).³⁴⁵ Aldehydes were reduced in a phase transfer catalytic system having [RuCl₂(PPh₃)₃] as the catalyst in the organic phase (for example chlorobenzene) and the hydrogen donor (Na-methanoate) in the aqueous phase.³⁴⁶

The complexes [PdCl₂(**133**)₂] catalyze the hydrogenolysis of 1-chloromethylnaphthalene with K[HCOO] or Na[HCOO]. Both the solid methanoates and their aqueous solutions could be used. Addition of [R₄N]⁺X⁻ phase transfer agents significantly accelerated the hydrogenolysis of aryl halides with methanoates.³⁴⁷

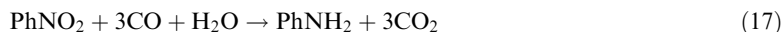
9.2.6.1.7 Hydrogenations with CO/H₂O mixtures

Several studies have reported the catalysis of the liquid-phase water gas shift reaction (WGSR). Actually, homogeneous catalysis of the WGSR is not competitive with its heterogeneous counterpart due to the limited rate, instability of the catalysts, and high costs. Scheme 64 shows the most important steps.



Scheme 64

Reduction of nitro compounds is a classic application of WGSR systems (Equation (17)).



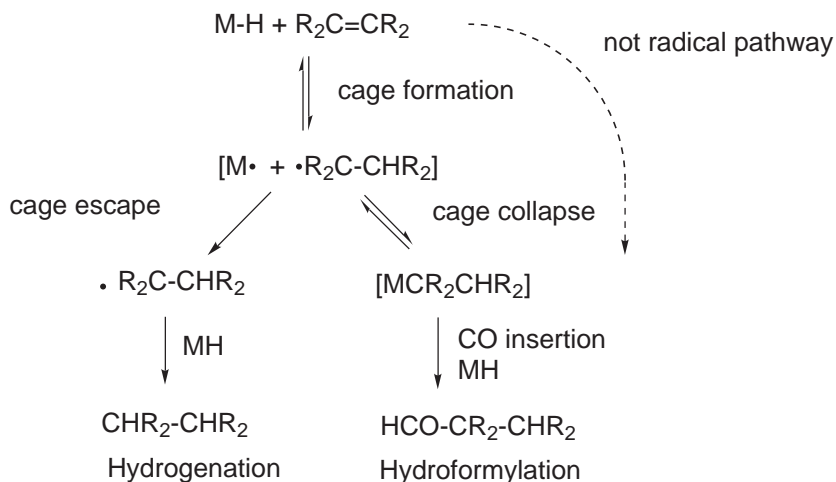
A good catalyst for this reaction is [FeH(CO)₄], produced by the reaction of [Fe(CO)₅] with OH⁻.³⁴⁸ Aldehydes were reduced by CO in 60:40 water: 2-ethoxy-ethanol mixtures under mild condition (30–80 °C, 20 bar CO) with a [Rh₆(CO)₁₆]/diamine catalyst system.³⁴⁹ In aqueous

methanol at 150 °C and 35 bar CO, $[\text{Fe}(\text{CO})_5]$ catalyzed the reduction of quinolines only at the aromatic ring; under identical conditions anthracene was reduced only stoichiometrically.

9.2.6.2 Hydrogenation in Supercritical Carbon Dioxide

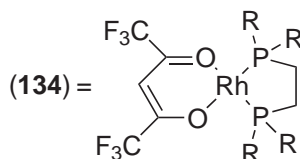
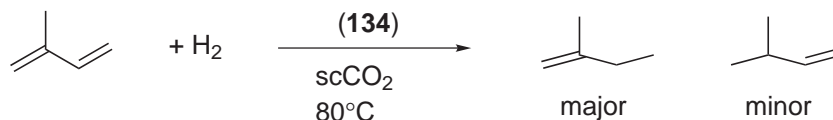
Supercritical carbon dioxide (scCO_2 ; $T_c = 31\text{ }^\circ\text{C}$, $p_c = 73.75\text{ bar}$, $d_c = 0.468\text{ g mL}^{-1}$) is considered as an ecologically benign and economically feasible reaction medium for metal catalyzed reactions with unique properties for chemical synthesis.³⁵⁰ The miscibility of scCO_2 with many gases, and the absence of a liquid/gas-phase boundary in the supercritical state, results in the maximum availability of gaseous reactants, avoiding potential problems of mass-transfer limitations.^{351,352} Beneficial effects can also arise from high compressibility of scCO_2 , allowing for selectivity changes by variation of the density with comparably small changes in the reaction conditions.³⁵³ The chemical interaction of CO_2 with functional groups of the substrate can lead to better compatibility with the employed catalysts (temporary protecting group). In favorable cases, the extractive properties of scCO_2 may allow simple separation of catalysts and products.

The first report of homogeneous hydrogenation of organic substrates in any supercritical fluid is probably a patent describing the hydrogenation of coal extracts in scH_2O .³⁵⁴ The first example using scCO_2 was the hydrogenation of a cyclopropene by $\text{MnH}(\text{CO})_5$ via the radical mechanism in Scheme 65.³⁵⁵



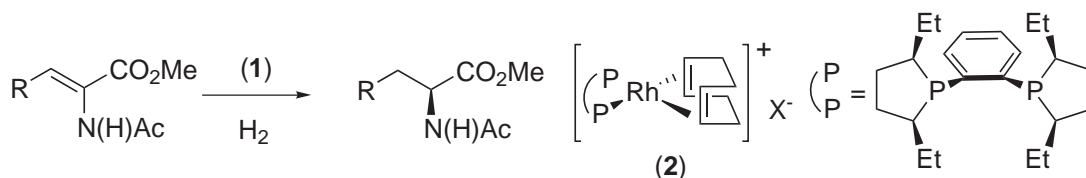
Scheme 65

This reaction can be performed catalytically or stoichiometrically. Carbonyl complexes such as $[\text{MnH}(\text{CO})_5]$ can hydrogenate or hydroformylate activated olefins; the selectivity for hydrogenation over hydroformylation is often used as a measure of the strength of the solvent cage. Complex (134), where $\text{R} = \text{C}_6\text{H}_4\text{-}m\text{-(CH}_2\text{)}_2\text{(CF}_2\text{)}_5\text{CF}_3$, catalyzes the hydrogenation of isoprene in scCO_2 (Scheme 66).³⁵⁶



Scheme 66

In addition to the practical advantage of a “solvent-free” reaction, the replacement of organic liquid solvents with scCO_2 can produce remarkable effects on the selectivity and rate of asymmetric hydrogenation processes. For example, Burk *et al.*³⁵⁷ reported significantly higher enantioselectivities in scCO_2 than in organic solvents during hydrogenation at β,β -disubstituted dehydroaminoacids using rhodium catalysts bearing chiral phosphinated ligands (Scheme 67).



Scheme 67

In a study by Leitner of the iridium-catalyzed hydrogenation of imines, a nearly 20-fold increase in catalytic efficiency was observed due to a different kinetic profile in scCO_2 as compared to methylene chloride.³⁵⁸ The change in rate and selectivity found in scCO_2 with respect to the other solvents can be related to the following major points:

- (i) Changes in the catalyst can result from adjusting the complex to the special properties of scCO_2 , e.g., by attaching “ CO_2 -philic” groups such as fluorocarbon chains.
- (ii) Changes in solvent polarity or other typical solvent parameters can influence the reaction.
- (iii) Changes in H_2 availability can result from the high miscibility of scCO_2 with gaseous reagents. Mass transfer limitations, which can have effects not only on rates but also on selectivities, are avoided under single phase conditions.
- (iv) Subtle changes in the reaction mechanism, such as variations in rates and equilibria of the individual transformations of a multistep catalytic cycle, may result from changes in solvation and/or stabilization of transition state and intermediates in a complex reaction pathway.
- (v) Major changes in the reaction mechanism can result from chemical interaction of the CO_2 molecule with reactive intermediates of the catalytic cycle. The generally accepted pathway for asymmetric hydrogenation reactions often involve solvato-complexes, and proceed always via metal hydride intermediates; CO_2 can directly interfere with such intermediates by acting as a ligand or by reversible insertion into the $\text{M}-\text{H}$ bond.

Recent research has demonstrated enhanced reaction rates in the ruthenium-catalyzed hydrogenation of CO_2 to formic acid and its derivatives.^{359,360} The highly enantioselective hydrogenation of $\text{C}=\text{C}$ double bonds has been demonstrated with prochiral α,β -unsaturated carboxylic acids as substrates.^{361,362}

A new “ CO_2 -philic” chiral rhodium diphosphinite complex was synthesized and applied as catalyst precursor in the asymmetric hydrogenation of dimethyl itaconate in scCO_2 , scC_2H_6 , and various liquid organic solvents.³⁶³ A water-soluble ruthenium(II) complex bearing tris(hydroxymethyl)phosphine is highly effective for the catalytic hydrogenation of supercritical carbon dioxide (scCO_2) under scCO_2 - H_2O multi-phasic conditions.³⁶⁴

Enantiopure phosphinodihydrooxazoles were used in the Ir-catalyzed enantioselective hydrogenation of imines in CH_2Cl_2 . Leitner reported that it is possible to replace the organic solvents with scCO_2 without loss of enantioselectivity, if these Ir catalysts are suitably tailored to the specific properties of the reaction medium by careful choice of the substituents on the chiral ligands and in the anion.³⁶⁵

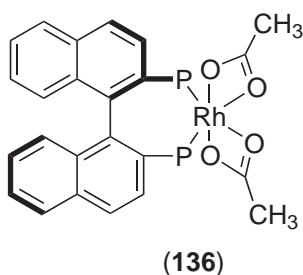
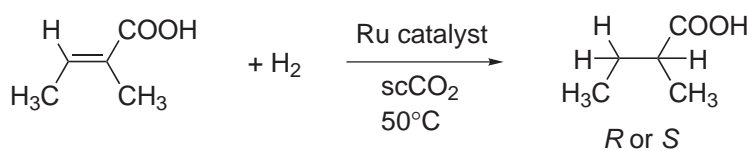
Hydrogenation of cinnamaldehyde was performed in scCO_2 -water biphasic catalyst system, which eliminates gas-liquid-liquid mass transfer and gives better activity and selectivity.³⁶⁶ The combined use of scCO_2 as a reaction medium, and water-soluble metal complexes for easy recycling of the catalyst, afford a truly environmentally friendly process. This eliminates the use of organic solvents and also gives easy catalyst/product separation and catalyst recycling. Table 3 summarizes the results for hydrogenation of cinnamaldehyde using several catalyst systems.²²²

Hydrogenation of tiglic acid in scCO_2 catalyzed by a chiral complex such as (136) (Scheme 68) proceeds cleanly with *cis* stereochemistry to afford 2-methylbutanoic acid in up to 89% ee and over 99% yield.³⁶⁷ These studies revealed a different influence of H_2 pressure on the selectivity between liquid solvents and scCO_2 .

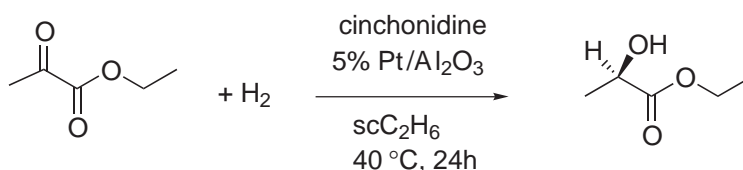
Table 3 Hydrogenation of cinnamaldehyde using various catalyst systems.^a

Reaction type	Catalyst		Solvent system	Pressure	Pressure	Conversion (%)	Selectivity	Selectivity
	precursor	Ligand		(MPa) scCO ₂	(MPa) H ₂		(%) UOL ^c	(%) SAL ^d
Homogeneous	RuCl ₃	PPh ₃	toluene		40	29	92	8
Homogeneous	RuCl ₃	PPh ₃	scCO ₂	140	40	1.5	89	11
Biphasic	RuCl ₃	(115)	toluene/water		40	11	92	8
Biphasic	RuCl ₃	(115)	scCO ₂ /water	140	40	38	99	0.5
Biphasic	RhCl ₃	(115)	scCO ₂ /water	140	40	35		100
Biphasic	Pd(OAc) ₂	(115)	scCO ₂ /water	140	40	22		100
SAPC ^b	RuCl ₃	(115)	toluene/water		40	13	93	7
SAPC	RuCl ₃	(115)	scCO ₂ /water	140	40	44	96	4

^a Reaction conditions: Catalyst precursor: 0.012 mmol; ligand/Ru: 8; T = 40 °C; cinnamaldehyde: 7.8 mmol; toluene: 25 cm³; time: 2 h; water = 0.5 cm³. ^b Gas-liquid-liquid on solid support (silica: 1.5 g). ^c UOL: unsaturated alcohol; ^d SAL: saturated aldehyde.

**Scheme 68**

Heterogeneously catalyzed hydrogenations have also been investigated.³⁶⁸ The enantioselectivity of the hydrogenations of ethylpyruvate using cinchonidine-modified Pt on alumina in scC₂H₆ was equal to that in toluene and greater than in ethanol (Scheme 69).³⁶⁹

**Scheme 69**

Hydrogenation of CO₂ using H₂ is strongly dependent on the conditions and catalysts employed.³⁷⁰ High-temperature hydrogenation conditions, usually with heterogenous catalysis, produce CO, CH₃OH, or CH₄, whereas mild conditions usually yield formic acid or related compounds. Noyori's group showed that reacting N(C₂H₅)₃, 0.0006 eq. [RuH₂{P(CH₃)₃}₄] and 85 atm of H₂ in 50 ml of scCO₂ (50 °C) leads to rapid production of formic acid. At higher temperature the preferred catalyst precursor is [RuCl₂{P(CH₃)₃}₄] due to its greater stability.^{371–374}

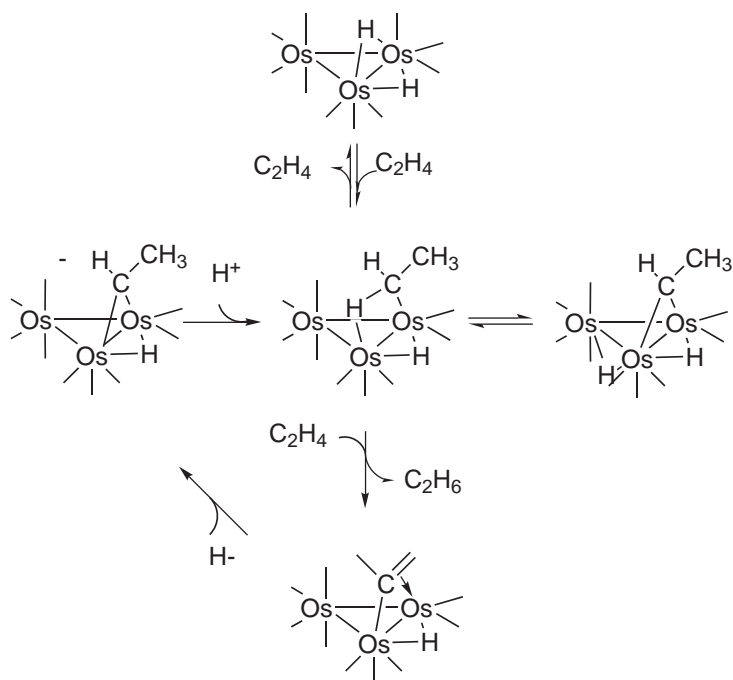
Mono- or dialkyl-formamides can be obtained in turnover numbers up to 420,000 when primary or secondary amines were hydrogenated at 100 °C in scCO₂ using [RuCl₂{P(CH₃)₃}₄] as catalyst precursor.^{373,374} A heterogenized analog of [RuCl₂{P(CH₃)₃}₄], supported by a sol-gel-derived silica matrix, was also very active for the synthesis of DMF,³⁷⁵ [RuCl₂(dppe)] is an even better catalyst, showing higher rates of reaction.³⁷⁶

9.2.6.3 Hydrogenation by Cluster Catalysis

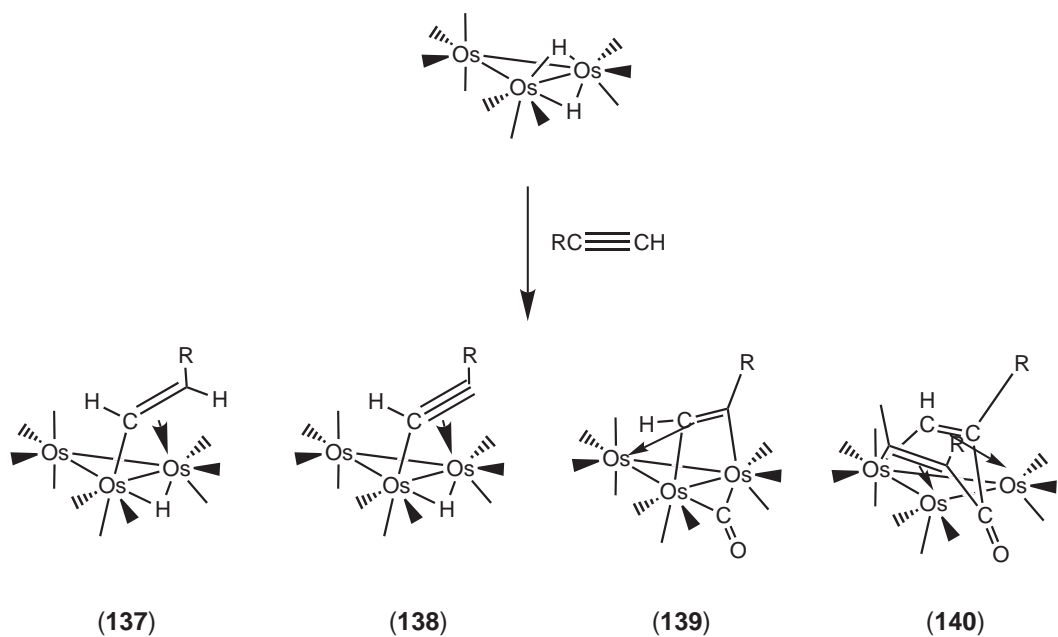
A metal cluster can be considered as a polynuclear compound which contains at least one metal-metal bond. A better definition of cluster catalysis is a reaction in which at least one site of the cluster molecule is mechanistically necessary. Theoretically, homogeneous clusters should be capable of multiple-site catalysis. Many heterogeneous catalytic reactions require multiple-site catalysis and for these reasons discrete molecular metal clusters are often proposed as models of metal surfaces in the processes of chemisorption and catalysis. The use of carbonyl clusters as catalysts for hydrogenation reactions has been the subject of a number of papers, an important question actually being whether the cluster itself is the species responsible for the hydrogenation. Often the cluster is recovered from the catalytic reaction, or is the only species spectroscopically observed under catalytic conditions. These data have been taken as evidence for cluster catalysis.

For homogeneous hydrogenation reactions catalyzed by clusters, three different mechanisms have been proposed. Shapley³⁷⁷ and Bassett³⁷⁸ suggested that the hydrogenation of alkenes catalyzed by $[\text{Os}_3\text{H}_2(\text{CO})_{10}]$ or by the silica-supported cluster $[\text{Os}_3(\text{CO})_{10}(\mu\text{-H})(\mu\text{-OSi}\equiv)]$ proceeds via a multiple-site mechanism (Scheme 70). In contrast, when $[\text{Ru}_4\text{H}_4(\text{CO})_{12}]$ was employed as catalyst, only one site seems mechanistically necessary.³⁷⁹ Cluster fragmentation has been hypothesized in the hydrogenation of styrene catalyzed, for example, by $[\text{Os}_4\text{H}_2(\text{CO})_{12}]^-$.³⁸⁰

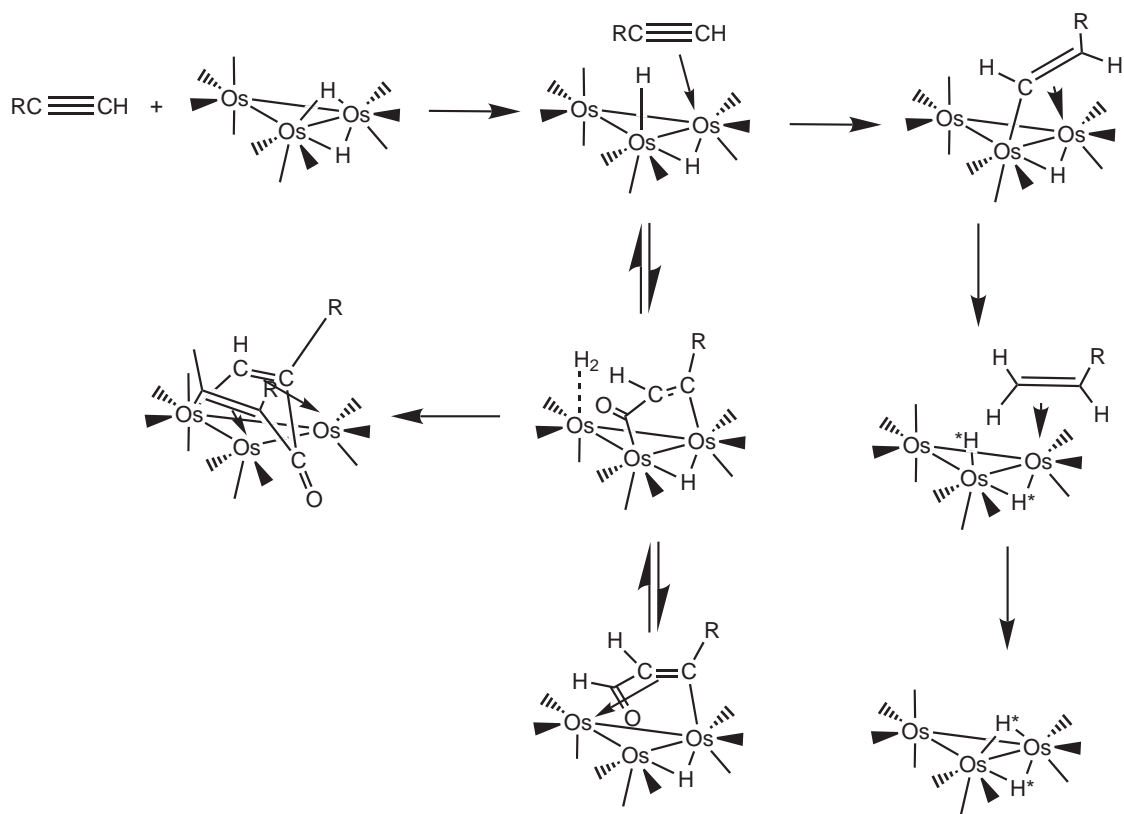
Duckett³⁸¹ reported on the use of parahydrogen-induced polarization (PHIP) to delineate the pathways involved in the catalytic hydrogenation of alkenes and alkynes by $[\text{Ru}_3(\text{CO})_{12-x}(\text{PPh}_3)_x]$ ($x = 1$ or 2) and showed that the mechanism is highly dependent on the solvent. Bassett and co-workers³⁷⁸ also found the silica-supported cluster $[\text{Os}(\text{CO})_{10}(\mu\text{-H})(\mu\text{-OSi}\equiv)]$ to be an efficient catalyst for the gas-solid hydrogenation of ethylene. The reaction was found to be zero-order in ethylene and first-order in hydrogen. The kinetic results together with volumetric and IR measurements on this system and on the soluble analog $[\text{Os}_3(\text{CO})_{10}(\mu\text{-H})(\mu\text{-OPh})]$ led to a mechanism involving the intact triosmium framework in all the steps, confirming the catalytic cycle. Sánchez-Delgado and co-workers reported that a number of tri- and tetranuclear osmium clusters can serve as catalyst precursor for hydrogenation of alkynes.³⁸⁰ The reaction of $[\text{Os}_3\text{H}_2(\text{CO})_{10}]$ with alkynes is more complex than with olefins. In the case of terminal alkynes the four products reported in Scheme 71 are formed. Only the σ - π -vinyl complex (**137**) goes on to yield alkene and the starting $[\text{Os}_3\text{H}_2(\text{CO})_{10}]$. The proposed mechanism for the reaction of terminal alkynes with $[\text{Os}_3\text{H}_2(\text{CO})_{10}]$ and para-hydrogen at -60°C in CDCl_3 is reported in Scheme 72.³⁸²



Scheme 70

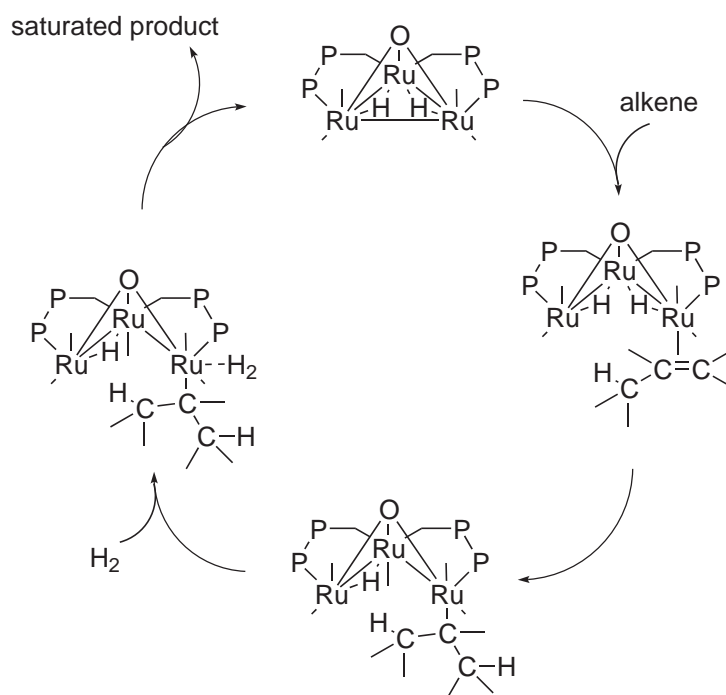


Scheme 71



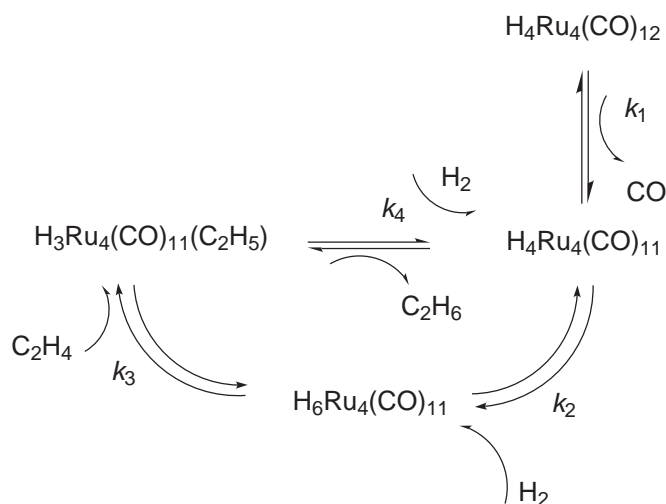
Scheme 72

The trinuclear cluster $[(\mu\text{-H})_2\text{Ru}_3(\mu_3\text{-O})(\text{CO})_5(\text{DPPM})_2]$ is also an efficient catalyst for alkene hydrogenation reaction, for which Bergounhou proposed the catalytic [Scheme 73](#).³⁸³



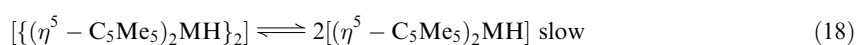
Scheme 73

Doi and co-workers³⁷⁹ carried out kinetic and mechanistic studies for the hydrogenation of ethylene with [H₄Ru(CO)₁₂] as the precatalyst. The hydrogenation rate is first-order with respect to cluster concentration, and increased to constant values with increasing ethylene and hydrogen pressure. An inverse dependence of the reaction rate on CO pressure was also observed. The mechanism proposed is in accordance with a cluster-catalyzed reaction (Scheme 74).

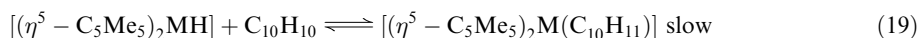


Scheme 74

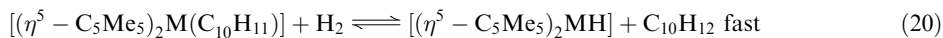
Hydrogenation catalysts from non-platinum group have been also reported. For example, some organolanthanides of formula $[\{\eta^5\text{-C}_5\text{Me}_5\}_2\text{MH}]_2$ are active catalyst for alkene hydrogenation.³⁸⁴ It has been proposed on the basis of kinetic studies that first the dimer dissociates according to (Equation (18)),



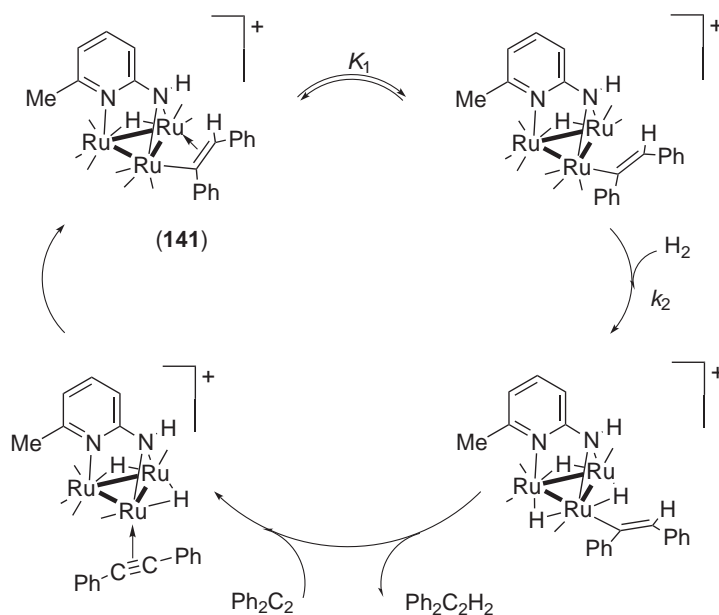
The addition of the lanthanide hydride to the cyclohexene double bond is the rate-limiting step (Equation (19)),



followed by fast reaction with H_2 (Equation (20)):



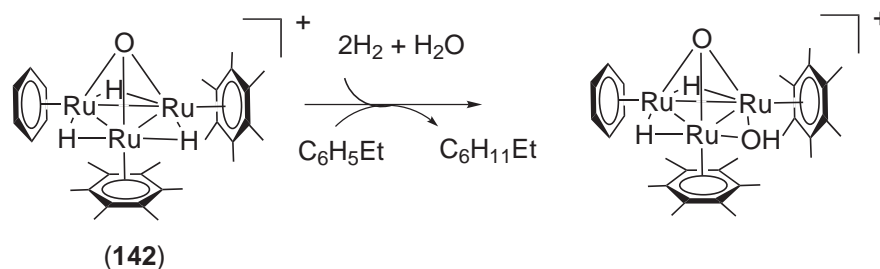
Hydrogenation reactions of 1-hexene with $[\text{Ru}_3(\text{CO})_{12}]$ and $[\text{Ru}_3(\text{CO})_9(\text{PPh}_3)_3]$ were recently compared. It has been reported that at H_2 pressures of 32 psi and 48 psi, $[\text{Ru}_3(\text{CO})_{12}]$ was more active in hydrogenation, but at 16 psi $[\text{Ru}_3(\text{CO})_9(\text{PPh}_3)_3]$ was the better catalyst. The catalytic activity of these clusters is diminished by an excess of PPh_3 .³⁸⁵ Homo- and heterometallic ruthenium-containing carbonyl clusters catalyze the hydrogenation of alkynes³⁸⁶ and of cyclic dienes;³⁸⁷ substitution of phosphine ligands for carbonyls in some cases increases the catalytic activity.³⁸⁸ Thus, the phosphine-substituted clusters $[\text{Ru}_3(\text{CO})_9(\text{PR}_3)_3]$ are active homogeneous catalysts for the hydrogenation of diphenylacetylene. In the catalytic reaction involving $[\text{Ru}_3(\text{CO})_9(\text{PEt}_3)_3]$, formation of $[\text{Ru}_3(\text{CO})_9(\text{PEt}_3)_2]$, which shows a hydrogenating activity greater than $[\text{Ru}_3(\text{CO})_9(\text{PEt}_3)_3]$, has been observed.³⁸⁹ Cabeza and co-workers reported a systematic investigation of homogeneous alkyne hydrogenations promoted by alkenyltriruthenium clusters,³⁹⁰ as an example, the cationic cluster (**141**) promotes homogeneous catalytic hydrogenation of diphenylacetylene to *cis*- and *trans*-stilbene under very mild conditions (333 K, $p(\text{H}_2) < 1$ atm). Reactivity, spectroscopic and kinetic studies support a hydrogenation mechanism in which the catalytic intermediates are cationic trinuclear complexes (Scheme 75).³⁹¹



Scheme 75

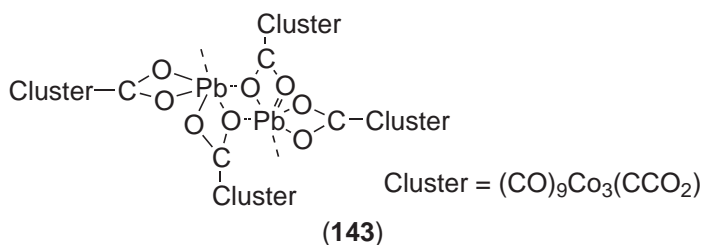
Catalytic hydrogenation of aromatics under biphasic conditions has been carried out with the water-soluble cluster cation $[(\eta^6\text{-C}_6\text{Me}_6)_2(\eta^6\text{-C}_6\text{H}_6)\text{Ru}_3(\mu_2\text{-H})_2(\mu_2\text{-OH})(\mu_3\text{-O})]^+$, the catalytic activity of which depends markedly on the substrates, with extremely high activity observed for ethylbenzene.³⁹² The water-soluble organometallic cluster cation (**142**), prepared by reaction of $[(\eta^6\text{-C}_6\text{H}_6)\text{Ru}(\text{H}_2\text{O})_3]^{2+}$ with $[(\eta^6\text{-C}_6\text{Me}_6)_2\text{Ru}_2(\mu_2\text{-H})_3]^+$ in aqueous solution, was found to catalyze the hydrogenation of aromatic substrates under biphasic conditions (Scheme 76).^{393,394} The water-soluble and air-stable triruthenium carbonyl cluster $[\text{Ru}_3(\text{CO})_9(\mathbf{115})_3]$ was an effective catalyst precursor for hydrogenation of acrylic acid and phenylethylene in good yield.³⁹⁵

The use of chemically assembled multicusters as precursors to solids with metastable porous microstructures constitutes a new approach to the preparation of heterogeneous hydrogenation



Scheme 76

catalysts. Fehlner and co-workers prepared an extended cluster lead(II) carboxylate $[\text{Pb}\{(\text{CO})_9\text{Co}_3(\mu_3\text{-CCO}_2)\}_2]_n$ (143) which, converted on pyrolysis into two metastable forms of solid material, was tested for hydrogenation of 2-butenal. The core metals play a direct chemical role in the activity of the catalyst which is a “clusters of clusters.”³⁹⁶ Fehlner also described a Ti/Co “cluster of clusters”-based catalyst for the selective hydrogenation of α,β -unsaturated aldehydes.³⁹⁷



Nagashima reported the hydrogenation of di-, tri- and tetranuclear ruthenium complexes bearing azulenes below 100 °C revealed that only the triruthenium compounds reacted with H_2 via triruthenium dihydride intermediates.³⁹⁸ This indicates that there exists a reaction pathway to achieve facile activation of dihydrogen on the face of a triruthenium carbonyl moiety.³⁹⁹

Complexes $[\text{HRu}_3(\text{CO})_9(\text{C}_2\text{Bu}^t)]$ and $[\text{Fe}_3(\text{CO})_9(\mu\text{-RC}_2\text{R}')] (R = R' = \text{Ph, Et}; R = \text{Me, R}' = \text{Ph})$, containing respectively an acetylide and an alkyne unit, catalyze hydrogenation of alkynes and 1,4-cyclohexadiene under homogeneous conditions. Cluster catalysis is probably occurring; evidence for partial fragmentation of the cluster has been also found.^{400,401} The hydrogenation of aromatic nitriles by $[\text{Fe}_3(\text{CO})_9]$ cluster has been described by Vahrenkamp.⁴⁰²

Four tetranuclear ruthenium carbonyl hydride clusters containing chiral diphosphine ligands catalyze asymmetric hydrogenation of *trans*-2-methyl-2-butenic acid with high conversion rates under relatively mild reaction conditions. The predominant enantiomeric form of the hydrogenated product, dependent on the configuration of the diphosphine, indicates strong chiral induction.⁴⁰³ Wang described a cyclometalation reaction of *N*-(3-methyl-2-thienylmethylidene)aniline with $[\text{Fe}_2(\text{CO})_9]$ that induces not only methyl migration and imido complex formation, but also hydrogenation.⁴⁰⁴ The catalytic hydrogenation of various benzene derivatives using $[(\eta^6\text{-C}_6\text{H}_6)_2\text{Ru}_2\text{Cl}_4]$ in aqueous solution as the catalyst precursor has been reported by Fidalgo.⁴⁰⁵ A theoretical study of the potential energy surface has been recently carried out for the catalytic cycle of ethylene hydrogenation by a Pd_2 cluster.⁴⁰⁶

Using functionalized polystyrenes and $[\text{Rh}_6(\text{CO})_{16}]$, polymer-bound Rh-cluster complexes were obtained in the presence of CO and H_2O , which exhibited high catalytic activities for hydrogenation of aldehydes to alcohols.^{407,408}

9.2.7 HYDROGENATION IN BIOLOGICAL SYSTEMS

Molecular hydrogen is an important intermediate in the degradation of organic matter by microorganisms in anoxic habitats such as freshwater and marine sediments, wet land soils, and the gastrointestinal tract of animals. In these particular conditions H_2 is produced during fermentation of carbohydrates, lipids, nucleic acids, and proteins by anaerobic bacteria and,

depending on the particular habitat, also some anaerobic protozoa, anaerobic fungi, anaerobically adapted algae, and/or anaerobic archaea may also be involved.

Some microorganisms are able to produce or consume molecular hydrogen through particular enzymes generally named “hydrogenases,” which catalyze the forward and reverse reactions in (Equation (21)):



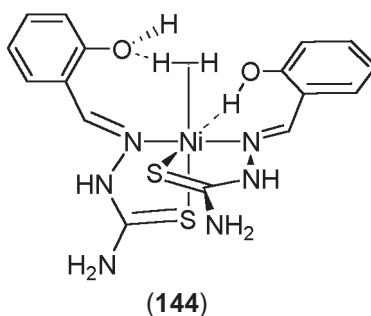
Other transformations supplied by these enzymes are *para-ortho*-hydrogen conversion, and the exchange reaction between H_2 and protons of water.^{409–412} The hydrogenase enzymes found in various microorganisms are very different in their protein structure and in the types of electron carrier they use.

In 1980 the role of nickel in certain hydrogenases as active catalytic center was definitely proved.^{413,414} Electrons produced by the oxidation of molecular hydrogen, or required for reduction of protons, are transported between the enzyme and the other components of the cell by primary electron carriers such as quinones, ferredoxin, rubredoxin, cytochrome c_3 , etc. The hydrogenase reducing power gives to the cell the possibility of transforming a wide number of terminal acceptors such as CO_2 , *E*-2-butene-diolate or inorganic ions such as SO_4^{2-} and NO_3^- . Hydrogenases assist the maintenance of energy balance of the cell, energy being supplied, for example, by reduction of CO_2 to CH_4 or by reduction of O_2 to H_2O .⁴¹⁵ Almost all hydrogenase enzymes are iron–sulfur proteins, $\{\text{Fe}_4\text{S}_4\}$ clusters being always present and bonded to the protein by S-coordination of the cysteine residues, apart from some new examples of purely organic hydrogenases.⁴¹⁵ In some enzymes $\{\text{Fe}_3\text{S}_4\}$ clusters and/or selenium have also been detected.

The metal-based hydrogenase enzymes known can be subdivided into three main groups:

- (i) [Fe] hydrogenases. These contain only iron–sulfur centers, in particular two $\{\text{Fe}_4\text{S}_4\}$ clusters, and a third site with two iron atoms which are believed to be the active site of H_2 oxidation and H^+ reduction.
- (ii) [NiFe] hydrogenases. These contain various iron–sulfur centers such as $\{\text{Fe}_4\text{S}_4\}$ and $\{\text{Fe}_3\text{S}_4\}$ clusters, and also a nickel–iron site.
- (iii) [NiFeSe] hydrogenases. These contain equivalent amounts of Ni and Se (the latter probably replacing some sulfur atoms in the coordination environment of the Ni), and two $\{\text{Fe}_4\text{S}_4\}$ clusters.

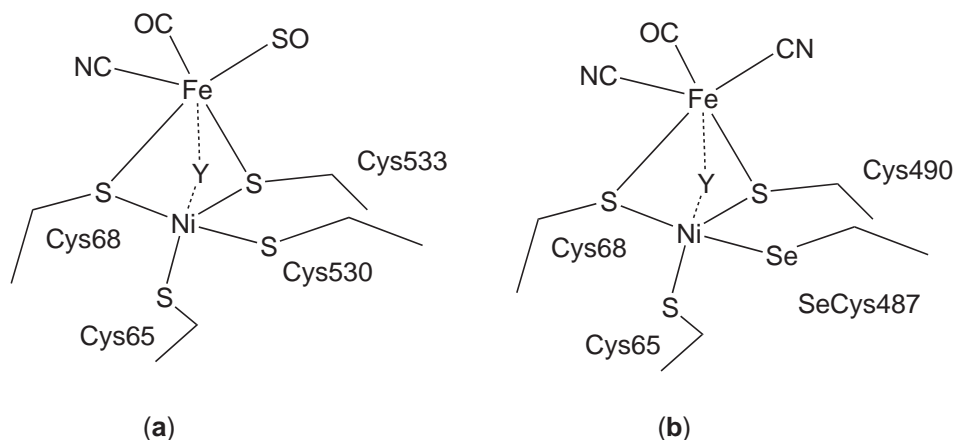
Because of the different kinds of enzyme, several synthetic models have been proposed which can be evaluated with regard to their composition and structure or to particular features of the enzymatic function. One of the most successful, proposed by Crabtree and co-workers some years ago,⁴¹⁶ involves the ionic complex $[\text{NiL}_2]\text{Cl}_2$ (**144**; $\text{L} = 2\text{-HOC}_6\text{H}_4\text{CH}=\text{N-NHC}(\text{S})\text{NH}_2$).



This system, rather stable in air, can be reduced electrochemically or with NaBH_4 , affording a Ni^{I} compound. Moreover, it catalyzes the D_2/H exchange with EtOH at 25°C and 1 bar pressure of D_2 , in the presence of promoters such as HI or HBF_4 . Because of the evidence that in solution the phenolic OH group is not coordinated to Ni, it has been suggested that hydrogen bonding between the Ni-coordinated H_2 and free OH groups in the ligand L could promote the activation of molecular hydrogen.

The structures of all three types of enzyme have been recently resolved.^{417–421} The first was the structure of the [NiFe] enzyme from *Desulfovibrio gigas*,⁴²² which revealed an active site containing a Ni center coordinated by γ -S of a cysteine (Cys 530) in an apical position and by three

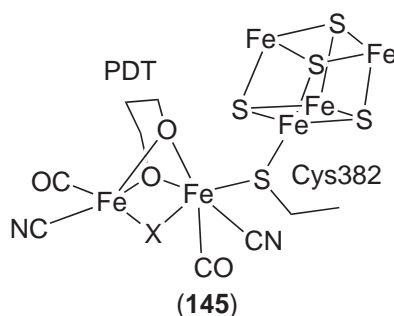
equatorial γ -S of cysteine ligands (Cys 65, Cys, 68, Cys 533) (Scheme 77a). An iron atom is less than 3 Å away from the nickel atom, and bound by γ -S of Cys 68 and Cys 533, the latter bridging the two metals, and by three diatomic molecules, recently identified as one CN^- , one CO, and one SO. ^{423,424} The Ni coordination site labeled Y, which is also a coordination position for the iron, is not occupied by any protein ligand, and could be a binding site for H_2 .



Scheme 77

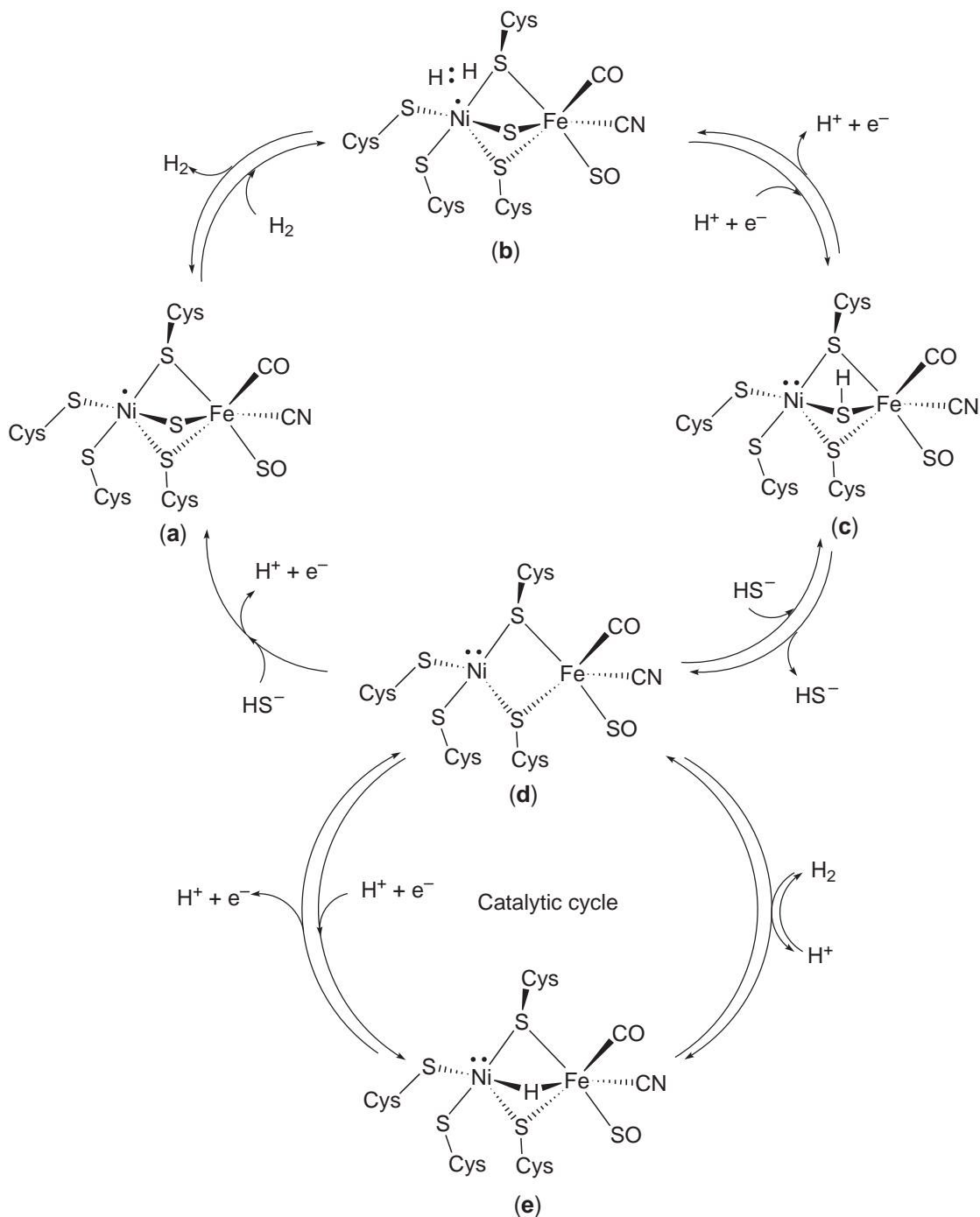
In the structure of the [NiFeSe] enzyme from *Desulfomicrobium baculatum*, one of the four cysteines involved in Ni coordination, one sulfur cysteine is replaced by a selenocysteine (Scheme 77b). ^{409,419}

In the [Fe] hydrogenase structure, the active site seems to consist of a typical $\{\text{Fe}_4\text{S}_4\}$ cluster bridged through Cys382 to an unusual Fe binuclear center (145). The two Fe are bridged by a small molecule which could be 1,3-propanediol (PDT) and, in addition, are coordinated by (probably) CN^- and CO ligands as well as a monoanionic bridging oxygen species (X). ⁴¹⁷



Many resolved crystal structures of enzymes are of inactive proteins obtained after aerobic purification, thus the active site might look quite different when the enzymes are active. ^{425,426} However, a recent example of crystal structure of the *Desulfomicrobium baculatum* [NiFeSe] hydrogenase was obtained by growing crystals anaerobically in a glove-box, from a hydrogen-treated protein solution, thus providing the first image of the active site in a reduced form. ⁴¹⁹

Recently, on the basis also of the resolved structures of a typical [NiFe] hydrogenase from *Desulfovibrio vulgaris*, a mechanism of action for the active site has been proposed (Scheme 78). ⁴¹⁹ The isolated hydrogenase contains a Ni^{II} center coordinated by five ligands, hence the sixth coordination site must be occupied by an unpaired electron (structure a), because the pentacoordinated Ni^{II} has a 17-electron configuration. Moreover, there are three Fe–S clusters, the proximal $\{\text{Fe}_4\text{S}_4\}$ (proximal the active Ni–Fe site), the distal $\{\text{Fe}_4\text{S}_4\}$ (distal to the active site) and $\{\text{Fe}_3\text{S}_4\}$ (located between the two $\{\text{Fe}_4\text{S}_4\}$ clusters). When H_2 is introduced to the enzyme in the presence of its electron carrier, H_2 will occupy the sixth coordination site (structure b). It undergoes heterolytic



Scheme 78

cleavage giving electrons to reduce Ni^{III} to Ni^{II}, which now has the sixth coordination site occupied by paired electrons (structure c). The other electron released may be consumed to reduce the {Fe₃S₄} cluster.^{427,428} Removal of HS⁻ from the reaction intermediate (c) produces the active enzyme (d), with the concomitant delivery of H₂S. The Fe atom is considered to be in a diamagnetic Fe^{II} state.⁴²⁹ At the moment of formation of (d), with unoccupied coordinating bridge site between Ni and Fe atoms, catalytic cycles including the coordination and heterolytic cleavage of H₂ proceed to supply electrons to reduce an externally added electron carrier.

9.2.8 REFERENCES

1. James, B. R. *Homogeneous Hydrogenation* **1973**, Wiley, New York.
2. James, B. R. Addition of Hydrogen and Hydrogen Cyanide to Carbon—Carbon Double and Triple Bonds. In Wilkinson, G.; Stone, F. B. A.; Abel, E. W., Eds., *Comprehensive Organometallic Chemistry*, Vol. 8, Pergamon, Oxford, 1982, Chapter 51.
3. Spencer, A. Catalytic Activation of Small Molecules. In Wilkinson, G.; Gillard, R. D.; McCleverty, J. A., Eds., *Comprehensive Coordination Chemistry*, Vol. 8, Pergamon, Oxford, 1987, Chapter 61.2.
4. Ojima, I.; Eguchi, M.; Tzamarioudaki, M. Transition Metal Hydrides: Hydrocarboxylation, Hydroformylation, and Asymmetric Hydrogenation. In Wilkinson, G.; Stone, F. B. A.; Abel, E. W., Eds., *Comprehensive Organometallic Chemistry* 2, Vol. 12, Pergamon, Oxford, 1995, Chapter 2.
5. Chaloner, P. A.; Esteruelas, M. A.; Jòo, F.; Oro, L. A. *Homogeneous Hydrogenation*, Kluwer Academic, Dordrecht, The Netherlands, 1994.
6. Noyori, R. *Asymmetric Catalysis in Organic Synthesis* **1994**, Wiley, New York.
7. Brothers, P. J. *Prog. Inorg. Chem.* **1981**, 28, 1–61.
8. Morris, R. H. *Can. J. Chem.* **1996**, 74, 1907–1915.
9. Kubas, G. J. *Acc. Chem. Res.* **1988**, 21, 120–128.
10. Crabtree, R. H. *Acc. Chem. Res.* **1990**, 23, 95–101.
11. Kubas, G. J.; Ryan, R. R.; Swanson, B. I.; Vergatini, P. J.; Wasserman, H. J. *J. Am. Chem. Soc.* **1984**, 106, 451–452.
12. Knowles, W. S. *Angew. Chem., Int. Ed. Engl.* **2002**, 41, 1998–2007.
13. Noyori, R. *Angew. Chem., Int. Ed. Engl.* **2002**, 41, 2008–2022.
14. Calvin, M. *Trans. Faraday Soc.* **1938**, 34, 1181–1191.
15. Calvin, M. J. *Am. Chem. Soc.* **1931**, 61, 2230–2234.
16. Meerwein, H.; Schmidt, R. *Justus Liebigs Ann. Chem.* **1925**, 444, 221–238.
17. Verley, A. *Bull. Soc. Chem. Fr.* **1925**, 37, 537–542.
18. Ponnendorf, W. *Angew. Chem.* **1926**, 39, 138–143.
19. Young, J. F.; Osborn, J. A.; Jardine, F. H.; Wilkinson, G. *J. Chem. Soc. Chem. Commun.* **1965**, 131–132.
20. Osborn, J. A.; Jardine, F. H.; Young, J. F.; Wilkinson, G. *J. Chem. Soc. A* **1966**, 1711–1732.
21. Jardine, F. H. *Prog. Inorg. Chem.* **1981**, 28, 63–202.
22. Schrock, R. R.; Osborn, J. A. *J. Am. Chem. Soc.* **1971**, 93, 2397–2407.
23. Schrock, R. R.; Osborn, J. A. *J. Am. Chem. Soc.* **1976**, 98, 2134–2143.
24. Schrock, R. R.; Osborn, J. A. *J. Am. Chem. Soc.* **1976**, 98, 2143–2147.
25. Schrock, R. R.; Osborn, J. A. *J. Am. Chem. Soc.* **1976**, 98, 4450–4455.
26. Noyori, R.; Takaya, H. *Acc. Chem. Res.* **1990**, 23, 345–350.
27. Whitesell, J. K. *Chem. Rev.* **1989**, 89, 1581–1590.
28. Knowles, W. S. *Acc. Chem. Res.* **1983**, 16, 106–112.
29. Noyori, R.; Ohkuma, T. *Angew. Chem., Int. Ed. Engl.* **2001**, 40, 40–73.
30. Noyori, R.; Yamakawa, M.; Hashiguchi, S. *J. Org. Chem.* **2001**, 66, 7931–7944.
31. Noyori, R.; Hashiguchi, S. *Acc. Chem. Res.* **1997**, 30, 97–102.
32. Stephan, M.; Kohlmann, O.; Niessen, H. G.; Eichhorn, A.; Bargon, J. *Magn. Reson. Chem.* **2002**, 40, 157–160.
33. Giernoth, R.; Heinrich, H.; Adams, N. J.; Deeth, R. J.; Bargon, J.; Brown, J. M. *J. Am. Chem. Soc.* **2000**, 122, 12381–12382.
34. Wildschütz, S.; Hübler, P.; Bargon, J. *Chem. Phys. Chem.* **2001**, 328–331.
35. Bowers, C. R.; Weitekamp, D. P. *Phys. Rev. Lett.* **1986**, 57, 2645–2648.
36. Bowers, C. R.; Weitekamp, D. P. *J. Am. Chem. Soc.* **1987**, 109, 5541–5542.
37. Hübler, P.; Giernoth, R.; Kümmerle, G.; Bargon, J. *J. Am. Chem. Soc.* **1999**, 121, 5311–5318.
38. Stephenson, T. A.; Wilkinson, G. *J. Inorg. Nucl. Chem.* **1966**, 28, 945–956.
39. Hallman, P. S.; Evans, D.; Osborn, J. A.; Wilkinson, G. *J. Chem. Soc. Chem. Commun.* **1967**, 305–306.
40. Hallman, P. S.; McGarvey, B. R.; Wilkinson, G. *J. Chem. Soc. A* **1968**, 3143–3150.
41. Crabtree, R. H.; Hamilton, D. G. *J. Am. Chem. Soc.* **1986**, 108, 3124–3125.
42. Argüello, E.; Bolanos, A.; Cuenu, F.; Navarro, M.; Herrera, V.; Fuentes, A.; Sanchez-Delgado, R. A. *Polyhedron* **1996**, 15, 909–915.
43. Rosales, M.; Alvarado, Y.; Gallardo, N.; Rubio, R. *Trans. Met. Chem.* **1995**, 20, 242–245.
44. Sanchez-Delgado, R. A.; Rosales, M.; Andriollo, A. *Inorg. Chem.* **1991**, 30, 1170–1173.
45. Andriollo, A.; Esteruelas, M. A.; Meyer, U.; Oro, L. A.; Sanchez-Delgado, R. A.; Sola, E.; Valero, C.; Werner, H. *J. Am. Chem. Soc.* **1989**, 111, 7431–7437.
46. Sanchez-Delgado, R. A.; Rosales, M.; Esteruelas, M. A.; Oro, L. A. *J. Mol. Catal. A: Chem.* **1995**, 96, 231–243.
47. Esteruelas, M. A.; Oro, L. A. *Chem. Rev.* **1998**, 98, 577–588.
48. Möhring, U.; Schäfer, M.; Kukla, F.; Schlaf, M.; Werner, H. *J. Mol. Catal. A: Chem.* **1995**, 99, 55–63.
49. Esteruelas, M. A.; Lopez, A. M.; Oro, L. A.; Perez, A.; Schulz, M.; Werner, H. *Organometallics* **1993**, 12, 1823–588.
50. Bianchini, C.; Meli, A.; Peruzzini, M.; Frediani, P.; Bohanna, C.; Esteruelas, M. A.; Oro, L. A. *Organometallics* **1992**, 11, 138–145.
51. Bianchini, C.; Linn, K.; Masi, D.; Peruzzini, M.; Polo, A.; Vacca, A.; Zanobini, F. *Inorg. Chem.* **1993**, 32, 2366–2376.
52. Bianchini, C.; Farnetti, E.; Graziani, M.; Kaspar, J.; Vizza, F. *J. Am. Chem. Soc.* **1993**, 115, 1753–1759 and references therein.
53. Jeske, G.; Lauke, H.; Mauermann, H.; Schumann, H.; Marks, T. J. *J. Am. Chem. Soc.* **1985**, 107, 8111–8118.
54. Daniel, C.; Koga, N.; Han, J.; Fu, X.Y.; Morokuma, K. *J. Am. Chem. Soc.* **1988**, 110, 3773–3787.
55. Crabtree, R. *Acc. Chem. Res.* **1979**, 12, 331–337.
56. Stuhl, L. S.; Rakowski Du Bois, M.; Hinsekorn, F. S.; Bleeke, J. R.; Stevens, A. R.; Muetterties, E. L. *J. Am. Chem. Soc.* **1978**, 100, 2405–2410.
57. Okano, T.; Tsukoyama, K.; Konishi, H.; Kiji, J. *Chem. Lett.* **1982**, 603–606.
58. Blum, J.; Amer, I.; Zoran, A.; Sasson, Y. *Tetrahedron Lett.* **1983**, 24, 4139–4142.
59. Januszklewicz, K. R.; Alper, H. *Organometallics* **1983**, 2, 1055–1057.

60. Amer, I.; Amer, H.; Blum, J. *J. Mol. Catal.* **1986**, *34*, 221–228.
61. Landis, C. R.; Halpern, J. *Organometallics* **1983**, *2*, 840–842.
62. Linn, D. E.; Halpern, J. *J. Am. Chem. Soc.* **1987**, *109*, 2969–2974.
63. Noyori, R.; Takaya, H. *Acc. Chem. Res.* **1990**, *23*, 345–350.
64. Hayashi, T. *Acc. Chem. Res.* **2000**, *33*, 354–362.
65. Burk, M. J. *Acc. Chem. Res.* **2000**, *33*, 363–372.
66. Knowles, W. S. *J. Chem. Ed.* **1986**, *63*, 222–225.
67. Halpern, J. *Science* **1982**, *217*, 401–407.
68. Landis, C. R.; Halpern, J. *J. Am. Chem. Soc.* **1987**, *109*, 1746–1754.
69. Halpern, J. *Inorg. Chim. Acta* **1981**, *50*, 11–19.
70. Takaya, H.; Noyori, R. *J. Am. Chem. Soc.* **1987**, *109*, 1596–1597.
71. Kitamura, M.; Kasahara, I.; Manabe, K.; Noyori, R.; Takaya, H. *J. Org. Chem.* **1988**, *53*, 708–710.
72. Naota, T.; Takaya, H.; Murahashi, S.-I. *Chem. Rev.* **1998**, *98*, 2599–2660.
73. Maitlis, P. M. *Acc. Chem. Res.* **1978**, *11*, 301–307.
74. Muetterties, E. L.; Bleeke, J. R. *Acc. Chem. Res.* **1979**, *12*, 324–331.
75. Fish, R. H.; Baralt, E.; Smith, S. J. *Organometallics* **1991**, *10*, 54–56.
76. Baralt, E.; Smith, S. J.; Hurwitz, J.; Horvath, I. T.; Fish, R. H. *J. Am. Chem. Soc.* **1992**, *114*, 5187–5196.
77. Parkin, B. C.; Clark, J. C.; Visciglio, V. M.; Fanwick, P. E.; Rothwell, I. P. *Organometallics* **1995**, *14*, 3002–3013.
78. Visciglio, V. M.; Clark, J. R.; Nguyen, M. T.; Mulford, D. R.; Fanwick, P. E.; Rothwell, J. P. *J. Am. Chem. Soc.* **1997**, *119*, 3490–3499.
79. Fish, R. H.; Tan, J. L.; Thormodsen, A. D. *J. Org. Chem.* **1984**, *49*, 4500–4505.
80. Sanchez-Delgado, R. A.; Gonzalez, E. *Polyhedron* **1989**, *8*, 1431–1436.
81. Chin, C. S.; Park, Y.; Lee, B. *Catal. Lett.* **1995**, *31*, 239–243.
82. Rosales, M.; Alvarado, Y.; Boves, M.; Rubio, R.; Soscun, H.; Sanchez-Delgado, R. A. *Transition Met. Chem.* **1995**, *20*, 246–251.
83. Rosales, M.; Navarro, J.; Sanchez, L.; Gonzalez, A.; Arvarado, Y.; Rubio, R.; De la Cruz, C.; Rajmankina, T. *Transition Met. Chem.* **1996**, *21I*, 11–15.
84. Rosales, M.; Boves, M.; Socun, H.; Ruetter, F. *J. Mol. Struct. Theochem.* **1998**, *433*, 319–328.
85. Sanchez-Delgado, R. A.; Rondon, D.; Andriollo, A.; Herrera, V.; Martin, G.; Chaudret, B. *Organometallics* **1993**, *12*, 4291–4296.
86. Sanchez-Delgado, R. A.; Herrera, V.; Rincon, L.; Andriollo, A.; Martin, G. *Organometallics* **1994**, *13*, 553–561.
87. Herrera, V.; Fuentes, A.; Rosales, M.; Sanchez-Delgado, R. A.; Bianchini, C.; Meli, A.; Vizza, F. *Organometallics* **1997**, *16*, 2465–2471.
88. Sanchez-Delgado, R. A.; Rosales, M. *Coord. Chem. Rev.* **2000**, *196*, 249–280, references therein.
89. Sanchez-Delgado, R. A.; Andriollo, A.; Valencia, N. *J. Chem. Soc. Chem. Commun.* **1983**, 444–445.
90. Sanchez-Delgado, R. A.; Andriollo, A.; Gonzalez, E.; Valencia, N.; Leon, V.; Espidel, J. *J. Chem. Soc. Dalton Trans.* **1985**, 1859–1863.
91. Sanchez-Delgado, R. A.; Valencia, N.; Marquez-Silva, R. L.; Andriollo, A.; Medina, M. *Inorg. Chem.* **1986**, *25*, 1106–1111.
92. Noyori, R.; Ohkuma, T.; Kitamura, M.; Takaya, H.; Sayo, N.; Kumobayashi, H.; Akutagawa, S. *J. Am. Chem. Soc.* **1987**, *109*, 5856–5858.
93. Noyori, R. *Chem. Soc. Rev.* **1989**, *18*, 187–208.
94. Noyori, R. *Science* **1990**, *248*, 1194–1199.
95. Noyori, R.; Ohkuma, T. *Angew. Chem., Int. Ed. Engl.* **2001**, *40*, 40–73, references therein.
96. Ohta, T.; Takaya, H.; Kitamura, M.; Nagai, K.; Noyori, R. *J. Org. Chem.* **1987**, *52*, 3174–3176.
97. Schrock, R. R.; Osborn, J. A. *J. Chem. Soc. Chem. Commun.* **1970**, 567–568.
98. Tani, K.; Suwa, K.; Tanigawa, E.; Yoshida, T.; Okano, T.; Otsuka, T. *Chem. Lett.* **1982**, 261–264.
99. Tani, K.; Tanigawa, E.; Tatsuno, S.; Otsuka, T. *J. Organomet. Chem.* **1985**, *279*, 87–101.
100. Burk, M. J.; Harpen, T. G. P.; Lee, J. R.; Kalberg, C. *Tetrahedron Lett.* **1994**, *35*, 4963–4966.
101. Lorkovic, I. M.; Duff, Jr., R.R.; Wrighton, M. S. *J. Am. Chem. Soc.* **1995**, *117*, 3617–3618.
102. Doucet, H.; Ohkuma, T.; Murata, K.; Yokozawa, T.; Kozawa, M.; Katayama, E.; England, A. F.; Ikariya, T.; Noyori, R. *Angew. Chem., Int. Ed. Engl.* **1998**, *37*, 1703–1707.
103. Ohkuma, T.; Ooka, H.; Ikariya, T.; Noyori, R. *J. Am. Chem. Soc.* **1995**, *117*, 10417–10418.
104. Ohkuma, T.; Ooka, H.; Ashiguki, S.; Ikariya, T.; Noyori, R. *J. Am. Chem. Soc.* **1995**, *117*, 2675–2676.
105. Gao, J.-X.; Zhang, H.; Yi, X.-D.; Xu, P.-P.; Tang, C.-L.; Wan, H.-L.; Tsai, K.-R.; Ikariya, T. *Chirality* **2000**, *12*, 383–388.
106. Helmchen, G.; Pfaltz, A. *Acc. Chem. Res.* **2000**, *33*, 336–345.
107. Agbossou, F.; Carpentier, J.-F.; Hapiot, F.; Suisse, I.; Mortreux, A. *Coord. Chem. Rev.* **1998**, *178–180*, 1615–1645.
108. Matsumoto, T.; Murayama, T.; Mitsuhashi, S.; Miura, T. *Tetrahedron Lett.* **1999**, *40*, 5043–5046.
109. Rossi, T.; Marchioro, C.; Paio, A.; Thomas, R. J.; Zarrantonello, P. *J. Org. Chem.* **1997**, *62*, 1653–1661.
110. James, B. R. *Catal. Today* **1997**, *37*, 209–221.
111. Matteoli, U.; Freudiani, P.; Binachi, M.; Botteghi, C.; Gladiali, S. *J. Mol. Catal.* **1981**, *12*, 263–319.
112. Zassinovich, G.; Mestroni, G.; Gladiali, S. *Chem. Rev.* **1992**, *92*, 1051–1069.
113. Leitner, W.; Brown, J. M.; Brunner, H. *J. Am. Chem. Soc.* **1993**, *115*, 152–159.
114. Saburi, M.; Ohnuki, M.; Ogasawara, M.; Takahashi, T.; Uchida, Y. *Tetrahedron Lett.* **1992**, *33*, 5783–5786.
115. Yamakawa, M.; Ito, H.; Noyori, R. *J. Am. Chem. Soc.* **2000**, *122*, 1466–1478.
116. Pamies, O.; Bäckvall, J.-E. *Chem. Eur. J.* **2001**, *7*, 5052–5058.
117. Gridnev, A. A.; Ittel, S. D.; Wayland, B. B.; Fryd, M. *Organometallics* **1996**, *15*, 5116–5126.
118. Gamez, P.; Fache, F.; Lemaire, M. *Tetrahedron: Asymmetry* **1995**, *6*, 705–718.
119. Müller, D.; Umbricht, G.; Weber, B.; Pfaltz, A. *Helv. Chim. Acta* **1991**, *74*, 232–240.
120. Jothimony, K.; Vamcheesan, S. *J. Mol. Catal.* **1989**, *52*, 301–304.
121. Genêt, J.-P.; Ratovelomanana-Vidal, V.; Pinel, C. *Synlett* **1993**, 478–480.
122. Esteruelas, M. A.; Valero, C.; Oro, L. A.; Meyer, U.; Werner, H. *Inorg. Chem.* **1991**, *30*, 1159–1160.

123. Evans, D. A.; Nelson, S. G.; Gagnè, M. R.; Muci, A. R. *J. Am. Chem. Soc.* **1993**, *115*, 9800–9801.
124. Guiral, V.; Delbecq, F.; Sautet, P. *Organometallics* **2001**, *20*, 2207–2214.
125. Ashby, E. C. *Acc. Chem. Res.* **1988**, *21*, 414–421.
126. Johansson, A. *Contemp. Org. Synth.* **1995**, 393–407.
127. James, B. R. *Chem. Ind.* **1995**, 62, 167–180.
128. Verdagner, X.; Lange, U. E. W.; Reding, M. T.; Buchwald, S. L. *J. Am. Chem. Soc.* **1996**, *118*, 6784–6785.
129. Buriak, J. M.; Osborn, J. A. *Organometallics* **1996**, *15*, 3161–3169.
130. Togni, A. *Angew. Chem., Int. Ed. Engl.* **1996**, *35*, 1475–1477.
131. Uematsu, N.; Fujii, A.; Hashiguchi, S.; Ikariya, T.; Noyori, R. *J. Am. Chem. Soc.* **1996**, *118*, 4916–4917.
132. Karlsson, U.; Wang, G.-Z.; Bäckvall, J.-F. *J. Org. Chem.* **1994**, *59*, 1196–1198.
133. Wang, G.-Z.; Andreasson, U.; Bäckvall, J.-F. *J. Chem. Soc. Chem. Commun.* **1994**, 1037–1038.
134. Bäckvall, J.-F.; Chowdhury, R. L.; Karlsson, U. *J. Chem. Soc. Chem. Commun.* **1991**, 473–475.
135. de Grauw, C. F.; Peters, J. A.; van Bekkum, H.; Huskens, J. *Synthesis* **1994**, 1007–1017.
136. Ko, B.-T.; Wu, C.-C.; Lin, C.-C. *Organometallics* **2000**, *19*, 1864–1869.
137. Mizushima, E.; Yamaguchi, M.; Yamagishi, T. *Chem. Lett.* **1997**, 237–238.
138. Aranyos, A.; Csjernyk, G.; Szabò, K. J.; Bäckvall, J. E. *J. Chem. Soc. Chem. Commun.* **1999**, 351–352.
139. Takehara, J.; Hashiguchi, S.; Fujii, A.; Shin-ichi, I.; Ikariya, T.; Noyori, R. *J. Chem. Soc. Chem. Commun.* **1996**, 233–234.
140. Yamakawa, M.; Ito, H.; Noyori, R. *J. Am. Chem. Soc.* **2000**, *122*, 1466–1478, references therein.
141. Noyori, R.; Yamakawa, M.; Hashiguchi, S. *J. Org. Chem.* **2001**, *66*, 7931–7944, references therein.
142. Palmer, M.; Walsgrove, T.; Wills, M. *J. Org. Chem.* **1997**, *62*, 5226–5228.
143. Alonso, D. A.; Brandt, P.; Nordin, S. J. M.; Andersson, P. G. *J. Am. Chem. Soc.* **1999**, *121*, 9580–9588.
144. Petra, D. G. I.; Kamer, P. C. J.; van Leuween, P. W. N. M.; Goubitz, K.; van Loon, A. M.; de Vries, J. G.; Shoemaker, H. E. *Eur. J. Inorg. Chem.* **1999**, 2335–2341.
145. Petra, D. G. I.; Reek, J. N. H.; Handgraaf, J.-W.; Meijer, E. J.; Dierkes, P.; Kamer, P. C. J.; Brussee, J.; Shoemaker, H. E.; van Leuween, P. W. N. M. *Chem. Eur. J.* **2000**, *6*, 2818–2829.
146. Guiral, V.; Delbecq, F.; Sautet, P. *Organometallics* **2001**, *20*, 2207–2214.
147. Shvo, Y.; Czarkie, D.; Rahamin, Y. *J. Am. Chem. Soc.* **1986**, *108*, 7400–7402.
148. Casey, C. P.; Singer, S. W.; Powell, D. R.; Hayashi, R. K.; Kavana, M. *J. Am. Chem. Soc.* **2001**, *123*, 1090–1100, references therein.
149. Menashe, N.; Shvo, Y. *Organometallics* **1991**, *10*, 3885–3891.
150. Menashe, N.; Salant, E.; Shvo, Y. *J. Organomet. Chem.* **1996**, *514*, 97–102.
151. Larsson, A. L. E.; Persson, B. A.; Bäckvall, J. E. *Angew. Chem., Int. Ed. Engl.* **1997**, *36*, 1211–1212.
152. Persson, B. A.; Larsson, A. L. E.; Le Ray, M.; Bäckvall, J. E. *J. Am. Chem. Soc.* **1999**, *121*, 1645–1650.
153. Bäckvall, J.-E.; Chowdhury, R. L.; Karlsson, U. *J. Chem. Soc. Chem. Commun.* **1991**, 473–475.
154. Wang, G.-Z.; Bäckvall, J.-E. *J. Chem. Soc. Chem. Commun.* **1992**, 337–339.
155. Wang, G.-Z.; Andreasson, U.; Bäckvall, J.-E. *J. Chem. Soc. Chem. Commun.* **1994**, 1037–1038.
156. Karlsson, U.; Wang, G.-Z.; Bäckvall, J.-E. *J. Org. Chem.* **1994**, *59*, 1196–1198.
157. Almeida, M. L. S.; Kocovsky, P.; Bäckvall, J.-E. *J. Org. Chem.* **1996**, *61*, 6587–6590.
158. Topsøe, H.; Clausen, B. S.; Massoth, F. E. *Hydrotreating Catalysis* **1996**, Springer-Verlag, Berlin Heidelberg.
159. Scherzer, J.; Gruia, A. *J. Hydrocracking Science* **1996**, Marcel Dekker, New York.
160. Satterfield, C. N. *Heterogeneous Catalysis in Industrial Practice* **1991**, McGraw-Hill, New York.
161. Bianchini, C.; Meli, A. *Acc. Chem. Res.* **1998**, *31*, 109–116.
162. Bianchini, C.; Meli, A.; Vizza, F. *Eur. J. Inorg. Chem.* **2001**, 43–68.
163. Angelici, R. J. In *Transition Metal Sulphides—Chemistry; Catalysis*, Weber, T.; Prins, R.; van Santen, A., Eds., Kluwer, Dordrecht, 1998, pp 89–127.
164. Angelici, R. J. *Polyhedron* **1997**, *16*, 3073–3088.
165. Angelici, R. J. *Bull. Soc. Chim. Belg.* **1995**, *104*, 265–282.
166. Angelici, R. J. In *Encyclopedia of Inorganic Chemistry*, King, R. B., Ed., John Wiley, New York, 1994, Vol. 3, pp 1433–1443.
167. Angelici, R. J. *Coord. Chem. Rev.* **1990**, *105*, 61–76.
168. Angelici, R. J. *Acc. Chem. Res.* **1988**, *21*, 387–394.
169. Rauchfuss, T. B. *Prog. Inorg. Chem.* **1991**, *39*, 259–329.
170. Bianchini, C.; Meli, A. In *Transition Metal Sulphides—Chemistry; Catalysis*, Weber, T.; Prins, R.; van Santen, R. A., Eds., Kluwer, Dordrecht, 1998, pp 129–154.
171. Bianchini, C.; Meli, A. *Acc. Chem. Res.* **1998**, *31*, 109–116.
172. Bianchini, C.; Meli, A. In *Aqueous-phase Organometallic Catalysis—Concepts; Applications*; Cornils, B.; Herrmann, W. A., Eds.; VCH, Weinheim, 1998, pp 477–485.
173. Bianchini, C.; Meli, A. In *Applied Homogeneous Catalysis with Organometallic Compounds*; Cornils, B.; Herrmann, W. A., Eds.; VCH, Weinheim, 1996, Vol. 2, pp 969–979.
174. Bianchini, C.; Meli, A. *J. Chem. Soc., Dalton Trans.* **1996**, 801–814.
175. Sánchez-Delgado, R. A. *J. Mol. Catal.* **1994**, *86*, 287–307.
176. Baralt, E.; Smith, S. J.; Hurwitz, I.; Horváth, I. T.; Fish, R. H. *J. Am. Chem. Soc.* **1992**, *114*, 5187–5196.
177. Fish, R. H.; Baralt, E.; Smith, S. J. *Organometallics* **1991**, *10*, 54–56.
178. Fish, R. H.; Tan, J. L.; Thormodsen, A. D. *Organometallics* **1985**, *4*, 1743–1747.
179. Fish, R. H.; Tan, J. L.; Thormodsen, A. D. *J. Org. Chem.* **1984**, *49*, 4500–4505.
180. Herrera, V.; Fuentes, A.; Rosales, M.; Sánchez-Delgado, R. A.; Bianchini, C.; Meli, A.; Vizza, F. *Organometallics* **1997**, *16*, 2465–2471.
181. Sánchez-Delgado, R. A.; Herrera, V.; Rincón, L.; Andriollo, A.; Martín, G. *Organometallics* **1994**, *13*, 553–561.
182. Sánchez-Delgado, R. A. In *Advances in Catalyst Design*, Graziani, M.; Rao, C. N. R., Eds., World Scientific Publishing, Singapore, 1991, pp 214–231.
183. Sánchez-Delgado, R. A.; González, E. *Polyhedron* **1989**, *8*, 1431–1436.
184. Bianchini, C.; Meli, A.; Patinec, V.; Sernau, V.; Vizza, F. *J. Am. Chem. Soc.* **1997**, *119*, 4945–4954.

185. Bianchini, C.; Herrera, V.; Jiménez, M. V.; Meli, A.; Sánchez-Delgado, R. A.; Vizza, F. *J. Am. Chem. Soc.* **1995**, *117*, 8567–8575.
186. Bianchini, C.; Meli, A.; Moneti, S.; Oberhauser, W.; Vizza, F.; Herrera, V.; Fuentes, A.; Sánchez-Delgado, R. A. *J. Am. Chem. Soc.* **1999**, *121*, 7071–7080.
187. INTEVEP S.A. (Páez, D. E.; Andriollo, A.; Sánchez-Delgado, R. A.; Valencia, N.; López-Linares, F.; Galiasso, R.) U.S. Patent 08/657.960, 1996.
188. INTEVEP S.A. (Páez, D. E.; Andriollo, A.; Sánchez-Delgado, R. A.; Valencia, N.; López-Linares, F.; Galiasso, R.) Sol. Patente Venezolana 96–1630, 1996.
189. Spera, M. L.; Harman, W. D. *Organometallics* **1995**, *14*, 1559–1561.
190. Cardone, R.; Harman, W. D.; Taube, H. *J. Am. Chem. Soc.* **1989**, *111*, 5969–5970.
191. Bianchini, C.; Meli, A.; Peruzzini, M.; Vizza, F.; Herrera, V.; Sánchez-Delgado, R. A. *Organometallics* **1994**, *13*, 721–730.
192. Bianchini, C.; Casares, J. A.; Osman, R.; Pattison, D. I.; Peruzzini, M.; Perutz, R. N.; Zanobini, F. *Organometallics* **1997**, *16*, 4611–4619.
193. Dong, L.; Duckett, S. B.; Ohman, K. F.; Jones, W. D. *J. Am. Chem. Soc.* **1992**, *114*, 151–160.
194. Jones, W. D.; Dong, L. *J. Am. Chem. Soc.* **1991**, *113*, 559–564.
195. Bianchini, C.; Casares, J. A.; Meli, A.; Sernau, V.; Vizza, F.; Sánchez-Delgado, R. A. *Polyhedron* **1997**, *16*, 3099–3114.
196. Bianchini, C.; Fabbri, D.; Gladiali, S.; Meli, A.; Pohl, W.; Vizza, F. *Organometallics* **1996**, *15*, 4604–4611.
197. Bianchini, C.; Jiménez, M. V.; Meli, A.; Moneti, S.; Vizza, F.; Herrera, V.; Sánchez-Delgado, R. A. *Organometallics* **1995**, *14*, 2342–2352.
198. Bianchini, C.; Meli, A.; Peruzzini, M.; Vizza, F.; Moneti, S.; Herrera, V.; Sánchez-Delgado, R. A. *J. Am. Chem. Soc.* **1994**, *116*, 4370–4381.
199. Bianchini, C.; Casares, J. A.; Masi, D.; Meli, A.; Pohl, W.; Vizza, F. *J. Organomet. Chem.* **1997**, *541*, 143–155.
200. Bianchini, C.; Meli, A.; Pohl, W.; Vizza, F.; Barbarella, G. *Organometallics* **1997**, *16*, 1517–1519.
201. Bianchini, C.; Jiménez, M. V.; Meli, A.; Moneti, S.; Vizza, F. *J. Organomet. Chem.* **1995**, *504*, 27–31.
202. Bianchini, C.; Frediani, P.; Herrera, V.; Jiménez, M. V.; Meli, A.; Rincón, L.; Sánchez-Delgado, R. A.; Vizza, F. *J. Am. Chem. Soc.* **1995**, *117*, 4333–4346.
203. Bianchini, C.; Jiménez, M. V.; Meli, A.; Vizza, F. *Organometallics* **1995**, *14*, 3196–3202.
204. Bianchini, C.; Meli, A.; Peruzzini, M.; Vizza, F.; Frediani, P.; Herrera, V.; Sánchez-Delgado, R. A. *J. Am. Chem. Soc.* **1993**, *115*, 2731–2742.
205. Myers, A. W.; Jones, W. D. *Organometallics* **1996**, *15*, 2905–2917.
206. Myers, A. W.; Jones, W. D.; McClements, S. M. *J. Am. Chem. Soc.* **1995**, *117*, 11704–11709.
207. Chin, R. M.; Jones, W. D. *Angew. Chem., Int. Ed. Engl.* **1992**, *31*, 357–358.
208. Garcia, J. J.; Arevalo, A.; Montiel, V.; Del Rio, F.; Quiroz, B.; Adams, H.; Maitlis, P. M. *Organometallics* **1997**, *16*, 3216–3220.
209. Garcia, J. J.; Mann, B. E.; Adams, H.; Bailey, N. A.; Maitlis, P. M. *J. Am. Chem. Soc.* **1995**, *117*, 2179–2186.
210. Buys, I. E.; Field, L. D.; Hambley, T. W.; McQueen, A. E. D. *J. Chem. Soc., Chem. Commun.* **1994**, 557–558.
211. Selnau, H. E.; Merola, J. S. *Organometallics* **1993**, *12*, 1583–1591.
212. Jones, W. D.; Chin, R. M.; Crane, T. W.; Baruch, D. M. *Organometallics* **1994**, *13*, 4448–4452.
213. Paneque, M.; Taboada, S.; Carmona, E. *Organometallics* **1996**, *15*, 2678–2679.
214. Feng, Q.; Rauchfuss, T. B.; Wilson, S. R. *Organometallics* **1995**, *14*, 2923–2930.
215. Krautscheid, H.; Feng, Q.; Rauchfuss, T. B. *Organometallics* **1993**, *12*, 3273–3281.
216. Chen, J.; Daniels, L. M.; Angelici, R. J. *J. Am. Chem. Soc.* **1990**, *112*, 199–204.
217. Bacchi, A.; Bianchini, C.; Herrera, V.; Jiménez, M. V.; Mealli, C.; Meli, A.; Moneti, S.; Peruzzini, M.; Sánchez-Delgado, R. A.; Vizza, F. *J. Chem. Soc., Chem. Commun.* **1995**, 921–922.
218. Dailey, K. M.; Rauchfuss, T. B.; Rheingold, A. L.; Yap, G. P. A. *J. Am. Chem. Soc.* **1995**, *117*, 6396–6397.
219. Luo, S.; Rauchfuss, T. B.; Gan, Z. *J. Am. Chem. Soc.* **1993**, *115*, 4943–4944.
220. Sun, S.; Dullaghan, C. A.; Sweigart, D. A. *J. Chem. Soc., Dalton Trans.* **1996**, 4493–4507.
221. Dullaghan, C. A.; Sun, S.; Carpenter, G. B.; Weldon, B.; Sweigart, D. A. *Angew. Chem., Int. Ed. Engl.* **1996**, *35*, 212–214.
222. Chisholm, M. H.; Haubrich, S. T.; Huffman, J. C.; Streib, W. E. *J. Am. Chem. Soc.* **1997**, *119*, 1634–1647.
223. Bianchini, C.; Casares, J. A.; Jiménez, M. V.; Meli, A.; Moneti, S.; Vizza, F.; Herrera, V.; Sánchez-Delgado, R. A. *Organometallics* **1995**, *14*, 4850–4857.
224. Bianchini, C.; Jiménez, M. V.; Meli, A.; Moneti, S.; Patinec, V.; Vizza, F. *Organometallics* **1997**, *16*, 5696–5705.
225. Bianchini, C.; Jiménez, M. V.; Mealli, C.; Meli, A.; Moneti, S.; Patinec, V.; Vizza, F. *Angew. Chem., Int. Ed. Engl.* **1996**, *35*, 1706–1708.
226. Vicić, D. A.; Jones, W. D. *Organometallics* **1997**, *16*, 1912–1919.
227. Jones, W. D.; Chin, R. M. *J. Am. Chem. Soc.* **1994**, *116*, 198–203.
228. Vicić, D. A.; Jones, W. D. *J. Am. Chem. Soc.* **1997**, *119*, 10855–10856.
229. Riaz, U.; Curnow, O. J.; Curtis, M. D. *J. Am. Chem. Soc.* **1994**, *116*, 4357–4363.
230. Curtis, M. D.; Druker, S. H. *J. Am. Chem. Soc.* **1997**, *119*, 1027–1036.
231. Sweeney, Z. K.; Polse, J. L.; Andersen, R. A.; Bergman, R. G.; Kubinec, M. G. *J. Am. Chem. Soc.* **1997**, *119*, 4543–4544.
232. Girgis, M. J.; Gates, B. C. *Ind. Eng. Chem. Res.* **1991**, *30*, 2031–2058.
233. Ho, T. C. *Catal. Rev.-Sci. Eng.* **1988**, *30*, 117–160.
234. Laine, R. M. *Catal. Rev.-Sci. Eng.* **1983**, *25*, 459–474.
235. Katzer, J. R.; Sivasubramanian, R. *Catal. Rev.-Sci. Eng.* **1979**, *20*, 155–208.
236. Gates, B. C.; Katzer, J. R.; Schuit, G. C. *A Chemistry of Catalytic Processes.*; McGraw-Hill: New York, 1979, Chapter 6.
237. Satterfield, C. N.; Smith, C. M.; Ingalis, M. *Ind. Eng. Chem. Process Des. Dev.* **1985**, *24*, 1000–1004.
238. Yang, S. H.; Satterfield, C. N. *Ind. Eng. Chem. Process Des. Dev.* **1984**, *23*, 20–28.
239. Yang, S. H.; Satterfield, C. N. *J. Catal.* **1983**, *81*, 168–173.
240. Satterfield, C. N.; Gülltekin, S. *Ind. Eng. Chem. Process Des. Dev.* **1981**, *20*, 62–68.

241. Satterfield, C. N.; Carter, D. L. *Ind. Eng. Chem. Process Des. Dev.* **1981**, *20*, 538–540.
242. Prins, R.; Jian, M.; Flechsenhar, M. *Polyhedron* **1997**, *16*, 3235–3246.
243. Kwart, H.; Katzer, J.; Horgan, J. J. *Phys. Chem.* **1982**, *86*, 2641–2648.
244. Kwart, H.; Schuit, G. C. A.; Gates, B. C. *J. Catal.* **1980**, *61*, 128–134.
245. Eisenstadt, A.; Giandomenico, C. M.; Frederick, M. F.; Laine, R. M. *Organometallics* **1985**, *4*, 2033–2039.
246. Laine, R. M. *J. Mol. Catal.* **1983**, *21*, 119–132.
247. Rakowski DuBois, M. *Coord. Chem. Rev.* **1998**, *174*, 191–205.
248. Chen, S.; Noll, B. C.; Peslherbe, L.; Rakowski DuBois, M. *Organometallics* **1997**, *16*, 1089–1092.
249. Johnson, T. J.; Aris, A. M.; Gladysz, J. A. *Organometallics* **1994**, *13*, 3182–3193.
250. Hegedus, L. S. *Angew. Chem., Int. Ed. Engl. Engl* **1988**, *27*, 1113–1126.
251. Weller, K. J.; Fox, P. A.; Gray, S. D.; Wigley, D. E. *Polyhedron* **1997**, *16*, 3139–3163.
252. Weller, K. J.; Gray, S. D.; Briggs, P.; Wigley, D. E. *Organometallics* **1995**, *14*, 5588–5597.
253. Gray, S. D.; Weller, K. J.; Bruck, M. A.; Briggs, P.; Wigley, D. E. *J. Am. Chem. Soc.* **1995**, *117*, 10678–10693.
254. Gray, S. D.; Smith, D. P.; Bruck, M. A.; Briggs, P.; Wigley, D. E. *J. Am. Chem. Soc.* **1992**, *114*, 5462–5463.
255. Kleckley, T. S.; Bennett, J. L.; Wolczanski, P. T.; Lobkowsky, E. B. *J. Am. Chem. Soc.* **1997**, *119*, 247–248.
256. Covert, K. J.; Neithamer, D. R.; Zonneville, M. C.; LaPointe, R. E.; Schaller, C.; Wolczanski, P. T. *Inorg. Chem.* **1991**, *30*, 2494–2508.
257. Neithamer, D. R.; Parkanyi, L.; Mitchell, J. F.; Wolczanski, P. T. *J. Am. Chem. Soc.* **1988**, *110*, 4421–4423.
258. Baralt, E.; Smith, S. J.; Hurwitz, J.; Horváth, I. T. Fish, R. H. *J. Am. Chem. Soc.* **1992**, *114*, 5187–5196.
259. Alvarado, Y.; Busolo, M.; López-Linares, F. *J. Mol. Catal. A* **1999**, *142*, 163–167.
260. Laine, R. M. *New J. Chem.* **1987**, *11*, 543–547.
261. Reger, D. L.; Habib, M. M.; Fauth, D. J. *J. Org. Chem.* **1980**, *45*, 3860–3865.
262. Herrmann, W. A.; Albanese, G. P.; Manetsberger, R. B.; Lappe, P.; Bahrmann, H. *Angew. Chem., Int. Ed. Engl. Engl* **1995**, *34*, 811–813.
263. Herd, O.; Langhans, K. P.; Steltzer, O.; Weferling, N.; Sheldrick, W. S. *Angew. Chem., Int. Ed. Engl.* **1993**, *32*, 1058–1059.
264. Bitterer, F.; Kucken, S.; Steltzer, O. *Chem. Ber.* **1995**, *128*, 275–279.
265. Darensbourg, D. J.; Bishoff, C. *J. Inorg. Chem.* **1993**, *32*, 47–53.
266. Herrmann, W. A.; Kulpe, J. A.; Kellner, J.; Riepl, H.; Bahrmann, H.; Konkol, W. *Angew. Chem., Int. Ed. Engl.* **1990**, *29*, 391–393.
267. Bayer, E.; Schumann, W. *J. Chem. Soc., Chem. Commun.* **1986**, 949–952.
268. Yan, Y. Y.; RayanBabu, T. V. *J. Org. Chem.* **2001**, *66*, 3277–3283.
269. Tubert, C.; Blacker, J.; Brown, S. M.; Crosby, J.; Fitzjohn, S.; Muxworthy, J. P.; Thorpe, T.; Williams, J. M. J. *Tetrahedron Lett.* **2001**, *42*, 4037–4039.
270. Ogo, S.; Makihara, N.; Watanabe, Y. *Organometallics* **1999**, *18*, 5470–5474.
271. Makihara, N.; Ogo, S.; Watanabe, Y. *Organometallics* **2001**, *20*, 497–500.
272. Mieczynska, E.; Trzeciak, A. M.; Ziolkowski, J. J. *J. Mol. Catal. A: Chem.* **1999**, *148*, 59–68.
273. Joó, F.; Laurency, G.; Karady, P.; Elek, J.; Nadasdi, L.; Roulet R., . *Appl. Organomet. Chem.* **2000**, *14*, 857–859.
274. Laurency, G.; Joó, F.; Nadasdi, L. *Inorg. Chem.* **2000**, *39*, 5083–5088.
275. Laurency, G.; Joo, F.; Nadasdi, L. *High Pressure Res.* **2000**, *18*, 251–255.
276. Heinen, A. W.; Papadogianakis, G.; Sheldon, R. A.; Peters, J. A.; van Bekkum, H. *J. Mol. Catal. A: Chem.* **1999**, *142*, 17–26.
277. Gelpke, A. E. S.; Kooijman, H.; Spek, A. L.; Hiemstra, H. *Chem. Eur. J.* **1999**, *5*, 2472–2482.
278. Grzybek, R. *React. Kinet. Catal. Lett.* **1996**, *58*, 315–322.
279. Penicaud, V.; Maillat, C.; Janvier, P.; Pipelier, M.; Bujoli, B. *Eur. J. Org. Chem.* **1999**, 1745–1748.
280. Trinkhaus, S.; Kadyrov, R.; Selke, R.; Holz, J.; Götz, L.; Börner, A. *J. Mol. Catal. A: Chem.* **1999**, *144*, 15–26.
281. Joó, F.; Nadasdi, L.; Bényei, A. Cs.; Darensbourg, D. J. *J. Organomet. Chem.* **1996**, *512*, 45–50.
282. Darensbourg, D. J.; Stafford, N. W.; Joó, F.; Reibenspies, J. H. *J. Organomet. Chem.* **1995**, *488*, 99–108.
283. Darensbourg, D. J.; Joó, F.; Kannisto, M.; Kathó, A.; Reibenspies, J. H. *Organometallics* **1992**, *11*, 1990–1993.
284. Kovacs, J.; Todd, T. D.; Reibenspies, J. H.; Joó, F. Darensbourg, D. J. *Organometallics* **2000**, *19*, 3963–3969.
285. Renaud, E.; Russell, R. B.; Fortier, S.; Brown, S. J.; Baird, M. C. *J. Organomet. Chem.* **1991**, *419*, 403–415.
286. Hermann, W. A.; Cornils, B. *Angew. Chem., Int. Ed. Engl. Engl.* **1997**, *36*, 1049–1067.
287. Doyle, M. P.; Eismont, M.; Bergbreiter, D. E.; Gray, H. N. *J. Org. Chem.* **1992**, *57*, 6103–6105.
288. Bergbreiter, D. E.; Caraway, J. W. *J. Am. Chem. Soc.* **1996**, *118*, 6092–6093.
289. Malmström, T.; Andersson, C. *Chem. Commun.* **1996**, 1135–1136.
290. Malmström, T.; Weigl, H.; Andersson, C. *Organometallics* **1995**, *14*, 2593–2596.
291. Joó, F.; Somsák, L.; Beck, M. T. *J. Mol. Catal.* **1984**, *24*, 71–75.
292. Clark, H. C.; Fyfe, C. A.; Hayes, P. J.; McMahon, I.; Davies, J. A.; Wasylishen, R. E. *J. Organomet. Chem.* **1987**, *322*, 393–404.
293. Newkome, G. R.; Yoneda, A.; Makromol, *Chem. Chem. Rapid Commun.* **1985**, *6*, 451–456.
294. Newkome, G. R.; Yoneda, A.; Makromol, *Chem. Chem. Rapid Commun.* **1985**, *6*, 77–84.
295. Karakhanov, E. A.; Loktev, A. S.; Pshezhetskii, V. S.; Dedov, A. G. Neftekhimiya, **1985**, *25*, 176; *Chem. Abstr.* 103, 104089x (1985).
296. Corain, B.; Zecca, M.; Sam, F. O.; Palua, G.; Lora, S. *Angew. Chem., Int. Ed. Engl. Engl.* **1990**, *29*, 384–385.
297. Pomogailo, A. D.; Klyuev, M. V. *Izv. Akad. Nauk. SSSR, Ser Khim.* **1985**, *8*, 1716–1721; *Chem. Abstr.*, *105*, 171933x (1986).
298. Andersen, J. A. M.; Currie, A. W. C. *J. Chem. Soc. Chem. Commun.* **1996**, 1543–1544.
299. Zheng, K.; Zang, M.; Lizi, M.; Jiaohuan Yu Xifu. *Chem. Abstr.* **1988**, *4*, 425;112, 121016z (1990).
300. Zbirovský, V.; Capka, M. *Coll. Czech. Chem. Commun.* **1986**, *51*, 836–841.
301. Dovganyuk, V. F.; Lafer, L. I.; Isaeva, V. I.; Dykh, Zh. L.; Yakerson, V. I.; Sharf, V. Z. *Bull. Acad. Sci. USSR, Div. Chem. Sci.* **1987**, *36*, 2465.
302. Choudary, B. M.; Mukkanti, K.; Subba Rao, Y. V. *J. Mol. Catal.* **1988**, *48*, 151–155.
303. Ishizuka, N.; Togashi, M.; Inoue, M.; Enomoto, S. *Chem. Pharm. Bull.* **1987**, *35*, 1686–1690.

304. Bianchini, C.; Burnaby, D. G.; Evans, J.; Frediani, P.; Meli, A.; Oberhauser, W.; Psaro, R.; Sordelli, L.; Vizza, F. *J. Am. Chem. Soc.* **1999**, *121*, 5961–5971.
305. Van der Voort, P.; Possemiers, K.; Vansant, E. F. *J. Chem. Soc. Faraday Trans.* **1996**, *92*, 843–848; references therein.
306. Renaud, E.; Baird, M. C. *J. Chem. Soc. Dalton Trans.* **1992**, 2905–2906.
307. Adima, A.; Moreau, J. J. E.; Wong Chi Man, M. *Chirality* **2000**, *12*, 411–420.
308. Joó, F.; Laurency, G.; Karády, P.; Elek, J.; Nadasdi, L.; Roulet, R. *Appl. Organomet. Chem.* **2000**, *14*, 857–859.
309. Joó, F.; Nadasdi, L. *Inorg. Chim. Acta* **1999**, *293*, 218–222.
310. Sandee, A. J.; Petra, D. G. I.; Reek, J. N. H.; Kamer, P. C. J.; van Leeuwen, P. W. N. M. *Chem. Eur. J.* **2001**, *7*, 1202–1208.
311. Toth, Z.; Joó, F.; Beck, M. T. *Inorg. Chim. Acta* **1980**, *42*, 153–161.
312. Páez, D. E.; Andriollo, A.; López-Linares, F.; Galiasso, R.; Revete, J. A.; Sánchez-Delgado, R.; Fuentes, A. Preprints of Symposia, Division of Inorganic Chemistry, 216th ACS National Meeting, August 22–27, 1998, Boston MA, pp 563–567.
313. Joó, F.; Balogh, N.; Horvath, L. I.; Filep, G.; Horvath, I.; Vigh, L. *Anal. Biochem.* **1991**, *194*, 34–40.
314. Yang, S.; Stock, L. M. *Energy & Fuels* **1998**, *12*, 644–648.
315. López-Linares, F.; Gonzalez, M. G.; Páez, D. E. *J. Mol. Catal. A: Chem.* **1999**, *145*, 61–68.
316. Kalck, P.; Hernandez, M. J. *Molec. Catal.* **1997**, *116*, 131–146.
317. Grosselin, J. M.; Mercier, C.; Allmang, G.; Grass, F. *Organometallics* **1991**, *10*, 2126–2133.
318. Joó, F.; Bényei, A. *J. Organomet. Chem.* **1989**, *363*, C19–C21.
319. Sánchez-Delgado, R. A.; Medina, M.; López-Linares, F.; Fuentes, A. *J. Molec. Catal.* **1997**, *116*, 167–177.
320. Páez, D. E.; Andriollo, A.; Carrasquel, J.; López-Linares, F.; Rojas, I.; Valencia, N. *J. Molec. Catal.* **1997**, *116*, 157–165.
321. Darensbourg, D. J.; Joó, F.; Kannisto, M.; Katho, A.; Reibenspies, J. H. *Organometallics* **1992**, *11*, 1990–1993.
322. Monflier, E.; Tilloy, S.; Castanet, Y.; Mortreux, A. *Tetrahedron Lett.*, **1998**, *39*, 2959–2960.
323. Blum, J.; Amer, I.; Vollhardt, K. P. C.; Schwarz, H.; Höhne, G. *J. Org. Chem.* **1987**, *52*, 2804–2813.
324. Laghmari, M.; Sinou, D.; Masdeu, A.; Claver, C. *J. Organomet. Chem.* **1992**, *438*, 213–216.
325. Ellis, D. J.; Dyson, P. J.; Parker, D. G.; Welton, T. *J. Molec. Catal. A: Chem.* **1999**, *150*, 71–75.
326. Grushin, V. V.; Vymenits, A. B.; Vol'pin, M. E. *J. Organomet. Chem.* **1990**, *382*, 185–189.
327. Grushin, V. V.; Alper, H. *Organometallics* **1991**, *10*, 831–833.
328. Pruchnik, F. P.; Smolenski, P.; Galdecka, E.; Galdecki, Z. *Inorg. Chim. Acta* **1999**, *293*, 110–114.
329. Fukuoka, A.; Kosugi, W.; Morishita, F.; Hirano, M.; McCaffrey, L.; Henderson, W.; Komiyama, S. *J. Chem. Soc. Chem. Commun.* **1999**, 489–490.
330. Chandrika Mudalige, D.; Rempel, G. L. *J. Mol. Catal. A: Chem.* **1997**, *116*, 309–316.
331. Jiang, H.; Xu, Y.; Liao, S.; Yu, D.; Chen, H.; Li, X. *J. Mol. Catal. A: Chem.* **1999**, *142*, 147–152.
332. Wolfson, A.; Janssens, S.; Vankelecom, I.; Geresh, S.; Gottlieb, M.; Herskowitz, M. *J. Chem. Soc. Chem. Commun.* **2002**, 388–389.
333. Kumar, A.; Oehme, G.; Roque, J. P.; Schwarze, M.; Selke, R. *Angew. Chem. Int. Ed. Engl.* **1994**, *33*, 2197–2199.
334. Fache, E.; Senocq, F.; Santini, C.; Bassett, J. M. *J. Chem. Soc. Chem. Commun.* **1990**, 1776–1778.
335. Oehme, G.; Grassert, I.; Paetzold, E.; Meisel, R.; Drexler, K.; Fuhrmann, H. *Coord. Chem. Rev.* **1999**, 185–186, 585–600.
336. Hanson, B. E. *Coord. Chem. Rev.* **1999**, 185–186, 795–807.
337. Malmstrom, T.; Andersson, C. J. *Mol. Catal. A: Chem.* **2000**, *157*, 79–92.
338. Schulz, J.; Roucoux, A.; Patin, H. *Chem. Eur. J.* **2000**, *6*, 618–624.
339. Hayashi, T.; Mise, T.; Mitachi, S.; Yamamoto, K.; Kumada, M. *Tetrahedron Lett.* **1976**, 1133–1134.
340. Brunner, H.; Pieronczyk, W. *Angew. Chem., Int. Ed. Engl.* **1979**, *18*, 620–621.
341. Laghmari, M.; Sinou, D. *J. Mol. Catal.* **1991**, *68*, L9.
342. Bakos, J.; Orosz, A.; Heil, B.; Laghmari, M.; Lhoste, P.; Sinou, D. *J. Chem. Soc. Chem. Commun.* **1991**, 1684–1685.
343. Wilson, M. E.; Nuzzo, R. G.; Whitesides, G. M. *J. Am. Chem. Soc.* **1978**, *100*, 2269–2270.
344. Chukhadjian, G. A.; Kukolev, V. P.; Matossian, V. A.; Balyushina, N. A. Proc. ISHC-5, Leningrad, 1984, p 138.
345. Sinou, D.; Saffi, M.; Claver, C.; Masdeu, A. *J. Mol. Catal.* **1991**, *68*, L9–L12.
346. Bar, R.; Bar, L. K.; Sasson, Y.; Blum, J. *J. Mol. Catal.* **1985**, *33*, 161–167.
347. Okano, T.; Iwahara, M.; Suzuki, K.; Konishi, H.; Kiji, J. *Chem. Lett.* **1986**, 1467–1470.
348. Cole, T.; Ramage, R.; Cann, K.; Pettit, R. *J. Am. Chem. Soc.* **1980**, *102*, 6182–6184.
349. Kaneda, K.; Yasumura, M.; Imanaka, T.; Teranishi, S. *J. Chem. Soc. Chem. Commun.* **1982**, 935–936.
350. Noyori, R. Supercritical fluids, (guest ed.). *Chem. Rev.* **1999**, *99*, 353–634.
351. Jessop, P. G.; Ikariya, T.; Noyori, R. *Nature* **1994**, *368*, 231–233.
352. Jessop, P. G.; Hsiao, Y.; Ikariya, T.; Noyori, R. *J. Am. Chem. Soc.* **1996**, *118*, 344–355.
353. Fürstner, A.; Koch, D.; Langemann, K.; Leitner, W.; Six, C. *Angew. Chem., Int. Ed. Engl.* **1997**, *36*, 2466–2469.
354. Coenen, H.; Hagen, R.; Kriegel, E. U.S. Patent, 4,485,003, **1984**.
355. Jessop, P. G.; Ikariya, T.; Noyori, R. *Organometallics* **1995**, *14*, 1510–1513.
356. Kainz, S.; Koch, D.; Leitner, W. In *Selective Reaction of Metal Activated Molecules*; Werner, H.; Schreier, W. Eds.; Vieweg: Wiesbaden, 1998.
357. Burk, M. J.; Feng, S.; Gross, M. F.; Tumas, W. *J. Am. Chem. Soc.* **1995**, *117*, 8277–8278.
358. Kainz, S.; Brinkmann, A.; Leitner, W.; Pfaltz, A. *J. Am. Chem. Soc.* **1999**, *121*, 6421–6429.
359. Jessop, P. G.; Ikariya, T.; Noyori, R. *Chem. Rev.* **1995**, *95*, 259–270.
360. Leitner, W. *Angew. Chem.* **1995**, *107*, 2391.
361. Xiao, J. L.; Nefkens, S. C. A.; Jessop, P. G.; Ikariya, T.; Noyori, R. *Tetrahedron Lett.* **1996**, *37*, 2813–2816.
362. Burk, M. J.; Feng, S.; Gross, M. F.; Tumas, W. *J. Am. Chem. Soc.* **1995**, *117*, 8277–8278.
363. Lange, S.; Brinkmann, A.; Trautner, P.; Woelk, K.; Bargon, J.; Leitner, W. *Chirality* **2000**, *12*, 450–457.
364. Kayaki, Y.; Suzuki, T.; Ikariya, T. *Chem. Lett.* **2001**, *10*, 1016–1017.
365. Kainz, S.; Brinkmann, A.; Leitner, W.; Pfaltz, A. *J. Am. Chem. Soc.* **1999**, *121*, 6421–6429.
366. Bhanage, B. M.; Ikushima, Y.; Shirai, M.; Arai, M. *Chem. Commun.* **1999**, *14*, 1277–1278.
367. Xiao, J. L.; Nefkens, S. C. A.; Jessop, P. G.; Ikariya, T.; Noyori, R. *Tetrahedron Lett.* **1996**, *37*, 2813–2816.

368. Hitzler, M. G.; Poliakov, M. *Chem. Commun.* **1997**, 1667–1668.
369. Minder, B.; Mallat, T.; Pickel, K. H.; Steiner, K.; Baiker, A. *Catal. Lett.* **1995**, *34*, 1–9.
370. Jessop, P. G.; Ikariya, T.; Noyori, R. *Chem. Rev.* **1995**, *95*, 259–272.
371. Jessop, P. G.; Ikariya, T.; Noyori, R. *Nature* **1994**, *368*, 231–233.
372. Ikariya, T.; Jessop, P. G.; Noyori, R. Japan Tokkai Patent, 5-274721, **1993**.
373. Jessop, P. G.; Hsiao, Y.; Ikariya, T.; Noyori, R. *J. Am. Chem. Soc.* **1996**, *118*, 344–355.
374. Ikariya, T.; Hsiao, Y.; Jessop, P. G.; Noyori, R. Eur. Patent Appl. Patent 0 652 202 A1, **1995**.
375. Kröcher, O.; Köppel, R. A.; Baiker, A. *Chem. Commun.* **1996**, 1497–1498.
376. Kröcher, O.; Köppel, R. A.; Baiker, A. *Chem. Commun.* **1997**, 453–454.
377. Cree-Uchiyama, M.; Shapley, J. R.; St. George, G. M. *J. Am. Chem. Soc.* **1986**, *108*, 1316–1317.
378. Choplin, A.; Besson, B.; D'Ornelas, L. D.; Sánchez-Delgado, R.; Bassett, J. M. *J. Am. Chem. Soc.* **1988**, *100*, 2783–2787.
379. Doi, Y.; Koshizuka, K.; Keii, T. *Inorg. Chem.* **1982**, *21*, 2732–2736.
380. Sánchez-Delgado, R.; Andriollo, A.; Puga, J.; Martín, G. *Inorg. Chem.* **1987**, *26*, 1867–1870.
381. Blazina, D.; Duckett, S. B.; Dyson, P. J.; Lohman, J. A. *Angew. Chem. Int. Ed. Engl.* **2001**, *40*, 3874–3877.
382. Gobetto, R.; Milone, L.; Reineri, F.; Salassa, L.; Viale, A. *Organometallics* **2002**, *21*, 1919–1924.
383. Bergounhou, G.; Fompegrine, P.; Commenges, G.; Bonnett, J. J. *J. Mol. Catal.* **1988**, *48*, 285–312.
384. Jeske, G.; Lauke, H.; Mauermann, H.; Schumann, H.; Marks, T. J. *J. Am. Chem. Soc.* **1985**, *107*, 8111–8118.
385. Dallmann, K.; Buffon, R. *J. Mol. Catal. A: Chem.* **2001**, *172*, 81–87.
386. Giordano, R.; Sappa, E. *J. Organomet. Chem.* **1993**, *448*, 157–166.
387. Castiglioni, M.; Giordano, R.; Sappa, E. *J. Organomet. Chem.* **1995**, *491*, 111–120.
388. Castiglioni, M.; Giordano, R.; Sappa, E. *J. Organomet. Chem.* **1988**, *342*, 111–127.
389. Gervasio, G.; Giordano, R.; Marabello, D.; Sappa, E. *J. Organomet. Chem.* **1999**, *588*, 83–91.
390. Cabeza, J. A.; Fernández-Colinas, J. M.; Llamazares, A.; Riera, V.; Garcia-Granda, S.; Van der Maelen, J. F. *Organometallics* **1994**, *13*, 4352–4359.
391. Cabeza, J. A.; del Río, I.; Fernández-Colinas, J. M.; Riera, V. *Organometallics* **1996**, *15*, 449–451.
392. Faure, M.; Vallina, A. T.; Stoeckli-Evans, H.; Süß-Fink, J. *J. Organomet. Chem.* **2001**, *621*, 103–108.
393. Süß-Fink, G.; Faure, M.; Ward, T. R. *Angew. Chem., Int. Ed. Engl.* **2002**, *41*, 99–101.
394. Faure, M.; Jahncke, M.; Neels, A.; Stoeckli-Evans, H.; Süß-Fink, G. *Polyhedron* **1999**, *18*, 2679–2685.
395. Gao, J. X.; Xu, P. P.; Yi, X. D.; Wan, H. L.; Tsai, K. R. *J. Mol. Catal. A: Chem.* **1999**, *147*, 99–104.
396. Lei, X.; Shang, M.; Patil, A.; Wolf, E. E.; Fehlner, T. P. *Inorg. Chem.* **1996**, *35*, 3217–3222.
397. LaNeve, M. C.; Lei, X. J.; Fehlner, T. P.; Wolf, E. E. *J. Catal.* **1998**, *177*, 11–21.
398. Nagashima, H.; Suzuki, A.; Nobata, M.; Aoki, K.; Itoh, K. *Bull. Chem. Soc. Jpn.* **1998**, *71*, 2441–2448.
399. Nagashima, H. *Monatsh. Chem.* **2000**, *131*, 1225–1239.
400. Campagnola, D.; Deabate, S.; Giordano, R.; Sappa, E. *J. Clust. Sci.* **1998**, *9*, 205–222.
401. Campagnola, D.; Giordano, R.; Sappa, E. *J. Clust. Sci.* **1998**, *9*, 487–504.
402. Kersting, B.; Suter, P.; Vahrenkamp, H. Z. *Anorg. Allg. Chem.* **1998**, *624*, 787–791.
403. Homanen, P.; Persson, R.; Haukka, M.; Pakkanen, T. A.; Nordlander, E. *Organometallics* **2000**, *19*, 5568–5574.
404. Wang, D. L.; Hwang, W. S.; Lee, L. S.; Chiang, M. Y. *J. Organomet. Chem.* **1999**, *579*, 211–216.
405. Fidalgo, E. G.; Plasseraud, L.; Süß-Fink, G. *J. Mol. Catal. A-Chem.* **1998**, *132*, 5–12.
406. Mamaev, V. M.; Gloriov, I. P.; Babin, Y. V.; Zernova, E. V. *Kinet. Catal. Engl. Tr.* **2001**, *42*, 511–519.
407. Kaneda, K.; Mizugaki, T. *Organometallics* **1996**, *15*, 3247–3249.
408. Mizugaki, T.; Ebitani, K.; Kaneda, K. *Appl. Surf. Sci.* **1997**, *121*, 360–365.
409. Albracht, S. P. J. *Biochim. Biophys. Acta* **1994**, *1088*, 167–204.
410. Cammack, R. *Nature* **1995**, *373*, 556–557.
411. Adams, M. W. W. *Biochim. Biophys. Acta* **1990**, *1020*, 115–145.
412. Berlier, Y.; Lespinat, P. A.; Dimon, B. *Anal. Biochem.* **1990**, *188*, 427–431.
413. Adams, M. W. W.; Mortenson, L. E.; Chen, J. S. *Biochim. Biophys. Acta* **1981**, *594*, 105–176.
414. Halcrow, M. A.; Christou, G. *Chem. Rev.* **1994**, *94*, 2421–2481.
415. Thauer, R. K.; Klein, A. R.; Hartmann, G. C. *Chem. Rev.* **1996**, *96*, 3031–3041.
416. Zimmer, M.; Sculte, G.; Luo, X. L.; Crabtree, R. H. *Angew. Chem., Int. Ed. Engl.* **1990**, *30*, 193–194.
417. Nicolet, Y.; Piras, C.; Legrand, P.; Hatchikian, C. E.; Fontecilla-Camps, J. C. *Structure* **1999**, *7*, 13–23.
418. Higuchi, Y.; Ogata, H.; Miki, K.; Yasuoka, N.; Yagi, T. *Structure* **1999**, *7*, 549–556.
419. Garcin, E.; Vernede, X.; Hatchikian, E. C.; Volbeda, A.; Frey, M.; Fontecilla-Camps, J. C. *Structure* **1999**, *7*, 557–566.
420. Volbeda, A.; Garcin, E.; Piras, C.; de Lacey, A. L.; Fernandez, V. M.; Hatchikian, E. C.; Frey, M.; Fontecilla-Camps, J. C. *J. Am. Chem. Soc.* **1996**, *118*, 12989–12996.
421. Higuchi, Y.; Yagi, T.; Yasuoka, N. *Structure* **1997**, *5*, 1671–1680.
422. Volbeda, A.; Charon, M.-H.; Piras, C.; Hatchikian, E. C.; Frey, M.; Fontecilla-Camps, J. C. *Nature* **1995**, *373*, 580–587.
423. Happe, R. P.; Roseboom, W.; Pierik, A. J.; Albracht, S. P. J.; Bagley, K. A. *Nature* **1997**, *385*, 126–126.
424. Higuchi, Y.; Toujou, F.; Tsukamoto, K.; Yagi, T. *J. Inorg. Biochem.* **2000**, *80*, 205–211.
425. Roberts, L. M.; Lindahl, P. A. *J. Am. Chem. Soc.* **1995**, *117*, 2565–2572.
426. Guigliarelli, B.; More, C.; Fournel, A.; Asso, M.; Hatchikian, E. C.; Williams, R.; Cammack, R.; Bertrand, P. *Biochemistry* **1995**, *34*, 4781–4790.
427. Asso, M.; Guigliarelli, B.; Yagi, T.; Bertrand, P. *Biochim. Biophys. Acta* **1992**, *1122*, 50–56.
428. Gebner, C.; Trofanchuk, O.; Kawagoe, K.; Higuchi, Y.; Yasuoka, N.; Lubitz, W. *Chem. Phys. Lett.* **1996**, *256*, 518–524.
429. Dole, F.; Fournel, A.; Magro, V.; Hatchikian, E. C.; Bertrand, P.; Guigliarelli, B. *Biochemistry* **1997**, *36*, 7847–7854.

9.3

Metal Complexes as Catalysts for Addition of Carbon Monoxide

P. W. N. M. VAN LEEUWEN

Universiteit van Amsterdam, The Netherlands

and

C. CLAVER

Universitat Rovira i Virgili, Tarragona, Spain

9.3.1	INTRODUCTION	142
9.3.2	CARBONYLATION OF METHANOL	142
9.3.2.1	Rhodium Catalysts	142
9.3.2.1.1	<i>Immobilization studies (see also Chapter 9.9)</i>	146
9.3.2.2	Iridium Catalysts	147
9.3.2.3	Palladium and Nickel Catalysts	147
9.3.2.4	Cobalt Catalysts	148
9.3.2.5	Miscellaneous	148
9.3.2.5.1	<i>Reductive carbonylation</i>	148
9.3.2.5.2	<i>Calculations</i>	149
9.3.3	HYDROFORMYLATION	149
9.3.3.1	Platinum	149
9.3.3.1.1	<i>Cis-PtCl₂(PPh₃)₂/SnCl₂ systems</i>	149
9.3.3.2	Palladium	153
9.3.3.3	Cobalt	154
9.3.3.4	Rhodium	155
9.3.3.4.1	<i>Introduction to phosphine catalysts</i>	155
9.3.3.4.2	<i>Introduction to phosphite catalysts</i>	158
9.3.3.5	Asymmetric Catalysis Using Platinum	166
9.3.3.5.1	<i>Chiral diphosphine ligands</i>	166
9.3.3.5.2	<i>Aminophosphine-phosphinite ligands</i>	169
9.3.3.5.3	<i>Diphosphite ligands</i>	169
9.3.3.5.4	<i>Miscellaneous</i>	170
9.3.3.6	Asymmetric Catalysis Using Rhodium	171
9.3.3.6.1	<i>Diphosphines as chiral ligands</i>	171
9.3.3.6.2	<i>Diphosphite ligands</i>	172
9.3.3.6.3	<i>Phosphine-phosphite ligands</i>	174
9.3.3.6.4	<i>Two-phase catalysis</i>	176
9.3.4	PALLADIUM-CATALYZED ALTERNATING COPOLYMERIZATION OF ALKENES AND CARBON MONOXIDE	179
9.3.5	REDUCTIVE CARBONYLATION OF NITRO COMPOUNDS	184
9.3.5.1	Introduction	184
9.3.5.2	Ruthenium catalysts	185
9.3.5.3	Palladium catalysts	185
9.3.5.4	Rhodium catalysts	186
9.3.5.5	Amidocarbonylation	186
9.3.5.5.1	<i>Palladium catalysts</i>	187
9.3.5.5.2	<i>Cobalt catalysts</i>	187

9.3.6	HYDROXYCARBONYLATION	188
9.3.6.1	Palladium/Phosphorus Complexes in Hydroxycarbonylation	189
9.3.6.2	Palladium Species Involved in the Hydroxycarbonylation Reaction	190
9.3.6.3	Methoxycarbonylation	191
9.3.6.3.1	Mechanistic studies	192
9.3.6.3.2	Palladium complexes involved in the methoxycarbonylation reaction	193
9.3.6.3.3	Phosphorus ligands in Pd methoxycarbonylation	193
9.3.6.3.4	Asymmetric methoxycarbonylation	194
9.3.7	REFERENCES	194

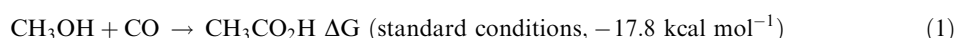
9.3.1 INTRODUCTION

Since 1985, several thousands of publications have appeared on complexes that are active as catalysts in the addition of carbon monoxide in reactions such as carbonylation of alcohols, hydroformylation, isocyanate formation, polyketone formation, etc. It will therefore be impossible within the scope of this chapter to review all these reports. In many instances we will refer to recent review articles and discuss only the results of the last few years. Second, we will focus on those reports that have made use explicitly of coordination complexes, rather than *in situ* prepared catalysts. Work not containing identified complexes but related to publications discussing well-defined complexes is often mentioned by their reference only. Metal salts used as precursors on inorganic supports are often less well defined and most reports on these will not be mentioned.

9.3.2 CARBONYLATION OF METHANOL

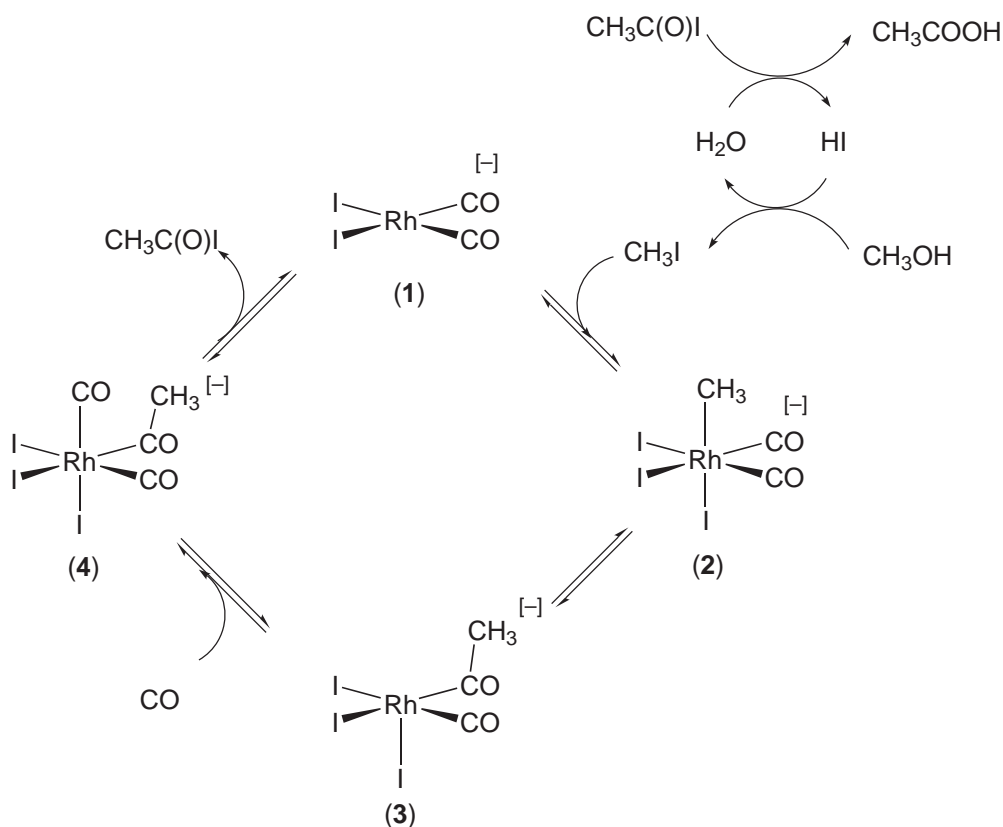
9.3.2.1 Rhodium Catalysts

The carbonylation of methanol was developed by Monsanto in the late 1960s. It is a large-scale operation employing a rhodium/iodide catalyst converting methanol and carbon monoxide into acetic acid. An older method involves the same carbonylation reaction carried out with a cobalt catalyst (see Section 9.3.2.4). For many years the Monsanto process has been the most attractive route for the preparation of acetic acid, but in recent years the iridium-based CATIVA process, developed by BP, has come on stream (see Section 9.3.2):



The rhodium catalyst has several distinct advantages over the cobalt catalyst; it is much faster and far more selective. The higher rate is in process terms translated into much lower pressures (the cobalt catalyst is operated at pressures of 700 bar). Nickel- and palladium-based catalysts have also been reported, but no applications have resulted from these. The mechanism for group 10 metals has not been studied (see Section 9.3.2.3).

The reaction sequence has been well established.¹⁻³ The two components of the Monsanto catalyst are rhodium and iodide, which can be added in many forms. Under the prevailing conditions, carbon monoxide and water reduce RhI_3 to monovalent rhodium. A large excess of iodide may be present, and both on a weight basis as well as on a molecular basis it would be fair to say that the catalyst is iodide and the promoter is a trace of rhodium; usually it is described the other way around. Under the reaction conditions, methanol and the iodide component form methyl iodide. Rhodium is present as the anionic species (**1**), $\text{RhI}_2(\text{CO})_2^-$. The first step of the catalytic cycle (see Scheme 1) is the oxidative addition of methyl iodide to this rhodium complex, to give (**2**) in the rate-determining step of the Monsanto process. The iodide enables the formation of a methyl rhodium complex; methanol is not sufficiently electrophilic to carry out this reaction. As for other nucleophiles, the reaction is much slower with methyl bromide or methyl chloride as the catalyst component. Migration of the methyl group gives an acetyl-rhodium complex. Carbon monoxide complexation and reductive elimination of acetyl iodide complete the cycle. Acetyl iodide hydrolyzes to give acetic acid and hydrogen iodide. The latter regenerates methyl iodide in a reaction with methanol.



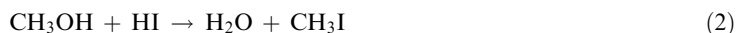
Scheme 1

A comprehensive kinetic, spectroscopic, and analysis study into the Rh-catalyzed carbonylation of ROH (R = Me, Et, Pr) has been reported.^{4,5} In all cases, the reaction rate is first order in both [Rh] and added [HI] and independent of CO pressure. The only Rh species observed under catalytic conditions was (1). The rates of carbonylation decreased in the stated order of R, with relative rates of 21:1:0.47, respectively at 170 °C. All the data are consistent with rate-determining nucleophilic attack by the Rh complex anion on the corresponding alkyl iodide.

The methyl-rhodium complex (2) was detected, at low concentration in neat CH₃I solution, by a combination of FTIR and NMR spectroscopy.⁶ The rate of the reaction (2) → (3) was measured between 5 °C and 35 °C. An Arrhenius plot yielded activation parameters of $\Delta H = 63 \text{ kJ mol}^{-1}$ and $\Delta S = -59 \text{ J mol}^{-1} \text{ K}^{-1}$ for the methyl migration step.

Rh K-edge EXAFS analysis⁷ showed that (3) exists in tetrahydrofuran (THF) at -20 °C, but fragments at temperatures >0 °C to give $[\text{Rh}(\text{COCH}_3)\text{I}_3(\text{CO})(\text{solvent})]^-$.

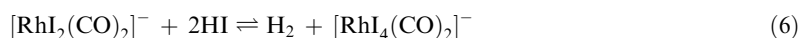
It is important that in the two “organic” equilibria involving iodide reaction (Equation (2)) shows complete conversion of methanol to methyl iodide, whereas the reaction with acetyl iodide shows complete conversion to acetic acid and hydrogen iodide (Equation (3)):



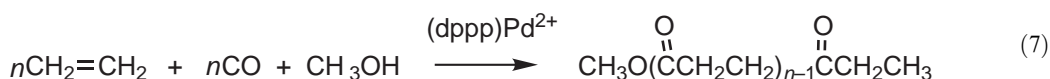
As a result of the kinetics and the equilibria mentioned above, all iodide in the system occurs as methyl iodide. The reaction in Equation (2) makes the rate of the catalytic process independent of the methanol concentration. Within the operation window of the process, the reaction rate is independent of the carbon monoxide pressure. The selectivity in methanol is in the high 90s but the selectivity in carbon monoxide may be as low as 90%. This is due to the water-gas shift reaction:



Thus, while water is an indispensable ingredient for the “organic” cycle (Equations (2) and (3)), a high concentration of water causes the major loss of one of the feedstocks. Water is also made *in situ* from methanol and acetic acid together with methyl acetate. In addition to water, HI is the cause of by-product formation:



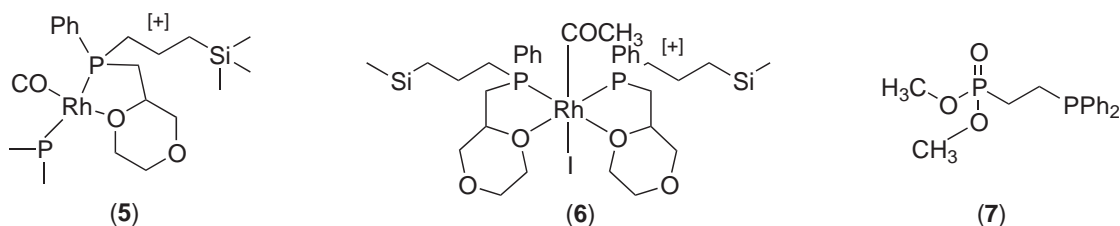
The reactions in Equations (5) and (6) involve oxidation of rhodium(I) to rhodium(III). Equations (6) can also be written as an oxidative addition of I_2 (formed thermally from 2 HI) to (1). Rhodium(III) iodides may precipitate from the reaction medium. They have to be converted to rhodium(I) again by water and carbon monoxide.



Other companies (e.g., Hoechst) have developed a slightly different process in which the water content is low in order to save CO feedstock. In the absence of water it turned out that the catalyst precipitates. Clearly, at low water concentrations the reduction of rhodium(III) back to rhodium(I) is much slower, but the formation of the trivalent rhodium species is reduced in the first place, because the HI content decreases with the water concentration. The water content is kept low by adding part of the methanol in the form of methyl acetate. Indeed, the shift reaction is now suppressed. Stabilization of the rhodium species and lowering of the HI content can be achieved by the addition of iodide salts. High reaction rates and low catalyst usage can be achieved at low reactor water concentration by the introduction of tertiary phosphine oxide additives.⁸ The kinetics of the title reaction with respect to $[\text{MeOH}]$ change if H_2O is used as a solvent instead of AcOH.⁹ Kinetic data for the Rh-catalyzed carbonylation of methanol have been critically analyzed. The discrepancy between the reaction rate constants is due to ignoring the effect of vapor–liquid equilibrium of the iodide promoter.¹⁰

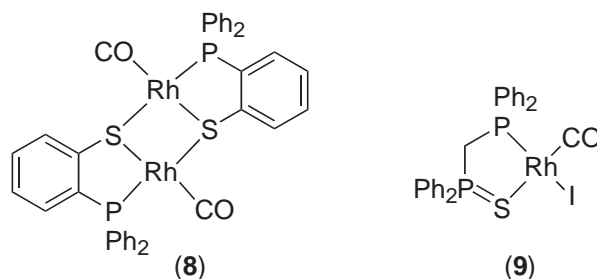
Iodide and acetate salts increase the rate of reaction of Li [1] with CH_3I at 25 °C in acetic acid. The effects of water, LiBF_4 , and other additives are also reported. Iodide salts also promote catalytic methanol carbonylation at low water concentrations. In the case of LiI promoter, lithium acetate is produced. The promotional effects of iodide and acetate on both the model and catalytic systems are rationalized in terms of iodide or acetate coordination to (1) to yield five-coordinate RhI anions as reactive intermediates for rate-determining reactions with CH_3I .¹¹

Complex (5) undergoes methyl migration after oxidative addition of CH_3I to afford the acyl complex (6) containing two Rh–O bonds. Heating (6) in the presence of CO results in the reductive elimination of AcI, which upon hydrolysis is transformed to AcOH.¹²



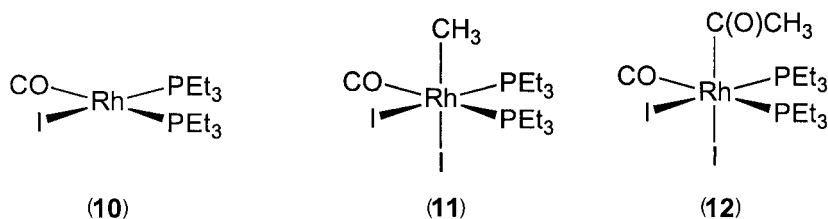
$[\text{Rh}(\text{CO})_2(\text{acac})(\text{dppp})]$ as a catalyst (where acac = acetylacetonate) gives high rates (100–200 turnovers h^{-1}) and selectivities in the reductive carbonylation of methanol to acetaldehyde comparable to the best Co catalysts, but at a much lower temperature (140 °C) and pressure

(70 bar). Addition of Ru to this catalyst results in the *in situ* hydrogenation of acetaldehyde and production of EtOH.¹³ The treatment of 2-(chloroethyl)phosphonic acid dimethylester with diphenylphosphine affords 2-(diphenylphosphino)ethylphosphonic acid dimethylester, (7), which can be used as a hemilabile complex ligand. Rhodium complexes of the type $(\text{MeO})_2\text{-P}(\text{O})\text{CH}_2\text{CH}_2\text{P}(\text{Ph})_2\text{RhL}_3$ were obtained and exhibit excellent catalytic properties in the carbonylation of methanol to acetic acid.¹⁴ Rhodium(I) carbonyl complexes containing phosphino-thiolate and -thioether ligands are four times as active in catalyzing the carbonylation of MeOH to AcOH as (1). The crystal structure of $[\text{Rh}(\text{SC}_6\text{H}_4\text{PPh}_2)(\text{CO})_2]$ (8) has been reported.¹⁵



The complex *cis*- $[\text{RhI}(\text{CO})(\text{Ph}_2\text{PCH}_2\text{P}(\text{S})\text{Ph}_2)]$ (9) is eight times more active than (1) for the carbonylation of methanol at 185 °C; the X-ray crystal structure of the analogous complex with chloride in place of iodide was reported together with *in situ* spectroscopic evidence in the catalytic cycle.¹⁶ A more detailed study of (9) showed that indeed oxidative addition is faster, but that in this instance due to a steric effect the migratory insertion was also accelerated.¹⁷

Under mild conditions (10), $[\text{RhI}(\text{CO})(\text{PEt}_3)_2]$, catalyzes the carbonylation of methanol in the presence of CH_3I and water at a rate 1.8 times that for (1) at 150 °C.^{18,19} The reaction is first order in $[\text{CH}_3\text{I}]$ and zero order in pCO. The phosphine complex degrades to (1) during the course of the reaction. Stoichiometric studies show that the rate of oxidative addition of CH_3I to (10) is 57 times faster than to (1) at 25 °C. Complex (11) can be isolated and characterized. In CH_2Cl_2 , (12) reductively eliminates CH_3COI . Complex (10) reacts with CO to give $[\text{RhI}(\text{CO})_2(\text{PEt}_3)_2]$. Catalyst degradation occurs via $[\text{RhHI}_2(\text{CO})(\text{PEt}_3)_2]$, formed by oxidative addition of HI to (10), which reacts further with HI to give $[\text{RhI}_3(\text{CO})(\text{PEt}_3)_2]$ from which $[\text{Et}_3\text{PI}]^+$ reductively eliminates and is hydrolyzed to give Et_3PO . In the presence of water, much less $[\text{RhI}_3(\text{CO})(\text{PEt}_3)_2]$ and Et_3PO are formed. The rate-determining step of the catalytic reaction in the presence of water is CH_3I oxidative addition to (10).



A series of square planar *cis*-dicarbonyl polymer-coordinated Rh complexes with uncoordinated donors near the central Rh atoms for carbonylation of MeOH to AcOH have been reported.²⁰ The work of the Sheffield group (UK),²¹ in developing a deeper understanding of the mechanism of the process, has been reviewed. The efficiency of methanol carbonylation arises primarily from rapid conversion of (2) into (3), leading to a low standing concentration of (2), and minimizing side reactions such as methane formation. By contrast, in the iridium-catalyzed carbonylation, for which similar cycles can be written, the migratory insertion reaction is rate determining. Model studies show that while $k(\text{Rh})/k(\text{Ir})$ is ca. 1:150 for the oxidative addition, it is ca. 10^5 – 10^6 :1 for migratory CO insertion. The migratory insertion for iridium can be substantially accelerated by adding either methanol or a Lewis acid (SnI_2); both appear to facilitate substitution of an iodide ligand by CO, resulting in easier methyl migration. The greater stability of $[\text{CH}_3\text{Ir}(\text{CO})_2\text{I}_3]^-$ compared with (2) accounts for the very different characters of the reactions catalyzed by the two metals.

Rh^{I} carbonyl complexes $[\text{Rh}(\text{CO})_2\text{CIL}]$ where $\text{L} = \text{Ph}_3\text{PO}$, Ph_3PS , and Ph_3PSe were synthesized and their catalytic activity was found to be higher than that of (1).²² A series of novel group 9

transition metal complexes, $[M_2L_2(CO)_2]$ and $[ML(CO)(PEt_3)]$ ($M = Rh, Ir$) containing the P,S-chelating ligand diphenylphosphino-*o*-carboranylthiol (LH) have been prepared. The bimetallic rhodium carbonyl complex was characterized by X-ray crystallography and is much more effective in the carbonylation of methanol than (1).²³ Rhodium complexes of unsymmetrical diphosphines of the type $Ph_2PCH_2CH_2PAR_2$, where $Ar = F$ -substituted Ph groups, are efficient catalysts for carbonylation of methanol and have extended service life compared with ligand-modified catalyst under temperatures of 150–200 °C and pressure of 10–60 bar.²⁴ Rhodium complexes of $[Rh(CO)_2Cl]_2$ with various ligands containing electron donors (amine, carboxy, pyridine, furan, etc.) were evaluated as catalysts in carbonylation of methanol to acetic acid.²⁵

Open-chain structures $[CIRh(COD)PPh_2-X-P(O)(OR)_2]$ ($COD =$ cyclooctadiene; $X = CH_2, CH_2CH_2, CH_2CH_2CH_2, p-C_6H_4$; $R = iso-Pr, Me$) were isolated and used to catalyze the carbonylation of methanol. FTIR investigations at temperatures between 150 °C and 250 °C suggest that the phosphonate–phosphane ligand stabilizes rhodium monocarbonyl species and allows the formation of free coordination sites to form dicarbonyl species, which is in accord with the proposed hemilabile behavior of the complexes.²⁶ The dimeric complex, $[(OC)_2Rh(\mu-Cl)_2Rh(CO)_2]$, undergoes a bridge splitting reaction with $Ph_2PCH_2CH_2SEt$ (P-S) to produce the chelated complex, $[Rh(CO)Cl(PS)]$ ($PS = \eta^2$ -coordinated P-S), which on oxidative addition with CH_3I and I_2 yields $[Rh(COCH_3)ICl(PS)]$ and $[Rh(CO)I_2Cl(PS)]$. As catalysts they were found to be faster than $[Rh(CO)Cl(PS)]$.²⁷

Evidence was shown for migration of an alkyl group in carbonyl insertion, and deinsertion steps between the methyl carbonyl rhodium complex $[\{\eta^5:\eta^1\text{-Indenyl-1-(CH}_2\text{)}_3\text{PPh}_2\}Rh(CO)\text{-Me}](BF_4)$ and the acetyl rhodium complex $[\{\eta^5:\eta^1\text{-Indenyl-1-(CH}_2\text{)}_3\text{PPh}_2\}RhI(COMe)]$ by crystallography as well as by 1H NMR spectroscopy.²⁸

9.3.2.1.1 Immobilization studies (see also Chapter 9.9)

In the carbonylation of MeOH in the presence of Rh-exchanged zeolites, the Rh^{III} ions are reduced to Rh^I ions, which lead to Rh-dicarbonyl and Rh-carbonyl-acetyl complexes.^{29–32} IrY and RhY zeolites catalyze the carbonylation of MeOH in the presence of a MeI promoter. The kinetics have been determined and IR spectra suggested that with the Ir catalyst the rate-determining step was the addition of MeOH to the active species followed by migration of a Me coordinated to Ir. With the Rh catalyst, oxidative addition of MeI was the rate-determining step.³³ A series of EXAFS measurements was made to determine the structural basis for the activity of transition metals exchanged into zeolite frameworks. Solutions of $[RhCl(NH_3)_5]Cl_2$ exchanged with NaX form a highly active catalyst (RhA) for MeOH carbonylation when used with an organic iodide promoter. Systems prepared from $RhCl_3$ are far less active. EXAFS spectroscopy from the Rh K-edge was used to follow the fate of the Rh species for the two preparation techniques. The former is a mobile aqua complex, while the nonactive catalyst is in the form of Rh_2O_3 crystallites.³⁴ Rh and Ir trivalent ions exchanged into faujasite-type zeolites undergo facile reduction to monovalent metal dicarbonyls. The chemistry of these complexes closely parallels the more familiar ones in solution.³⁵ Supported mixed bidentate rhodium and iridium complexes derived from phosphonate–phosphanes were studied for methanol carbonylation and hydroformylation of ethylene and propylene.³⁶ Metal-ion exchanged heteropoly acids of the general formula $M[W_{12}PO_{40}]$ ($M = Ir, Rh, Pd, Mn, Co, Ni, Fe$) supported on SiO_2 are excellent catalysts for the vapor phase carbonylation of MeOH or Me_2O to MeOAc at 225 °C and 1 atm total operating pressure.³⁷ In high-pressure gas phase conditions, methanol and syn-gas mixtures can be converted to acetic and higher carboxylic (C3–C5) acids on supported rhodium catalysts in presence of methyl iodide.³⁸ Rhodium catalysts supported on ZrO_2 , carbon, a cross-linked polystyrene with pendant Ph_2P groups, or PVP have been tested as catalysts for the heterogeneous carbonylation of methanol in the bulk liquid phase. In all cases, leaching of the catalyst into solution occurs.³⁹ For the carbonylation of MeOH to AcOH, the ionically supported complex (1) was equal in catalytic activity to the homogeneous complex, and leaching of the catalyst could be minimized by suitable choice of solvent and resin:Rh ratios. These experiments suggest a general application of anion-exchange resins as a mechanistic tool for detecting catalysis by anionic species in homogeneous processes.^{40,41}

The preparation, performance, and characterization of Cu-containing mordenite catalysts for carbonylation of MeOH under moderate conditions in the vapor phase and in the absence of halide promoter have been reported.⁴² The copolymer of 2-vinylpyridine and vinyl acetate coordinated with dicarbonyl-rhodium was used as a catalyst for carbonylation of methanol to acetic acid and acetic anhydride.⁴³ The kinetic study of carbonylation of a methanol–acetic acid mixture to acetic acid and acetic anhydride over (1) coordinated with the ethylene diacrylate cross-linked copolymer of Me acrylate and 2-vinylpyridine shows that the rate of reaction is zero order with respect to both reactants methanol and carbon monoxide, but first order in the concentrations of promoter CH_3I and rhodium.⁴⁴ Rhodium catalysts supported on a diphenylphosphinated copolymer of styrene and divinylbenzene (SDT) or poly(vinylpyrrolidone) (PVP) have been tested as catalysts for the heterogeneous carbonylation of methanol in continuous long-term vapor phase experiments under mild working conditions ($P = 80$ bar, $T = 180\text{--}190$ °C).⁴⁵ A novel Rh-containing diphenylphosphinated styrene-divinylbenzene copolymer was prepared, characterized, and used as a catalyst for MeOH carbonylation.⁴⁶ Porous C beads, prepared from poly(vinylidene chloride) (PVDC), were used as supports for Rh catalysts for carbonylation of MeOH. Transverse-electromagnetic (TEM) and scanning transmission microscopy (STM) show uniform pores spread over the surface of the beads. The optimum temperature for the pyrolysis of PVDC is 1,000 °C. The catalyst exhibits excellent activity and selectivity to MeOAc in MeOH carbonylation.⁴⁷ A catalyst derived from Linde 13X zeolite exchange with $[\text{Rh}(\text{NH}_3)_5\text{Cl}]\text{Cl}_2$ was active for MeOH carbonylation.⁴⁸

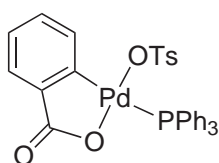
9.3.2.2 Iridium Catalysts

The use of Ir catalysis in the production of HOAc by carbonylation of MeOH has been discussed; advantages over Rh catalysis include less propionic acid by-product formation and very little generation of higher molecular weight derivatives of acetaldehyde.⁴⁹ There are three major catalyst systems for “acetyls” processes developed by BP. The first is the homogeneously promoted iridium methanol carbonylation system for acetic acid manufacturing recently commercialized-based in the USA and Korea (CATIVA). The second is a noncommercialized ruthenium-promoted rhodium system, also for methanol carbonylation. The third is a vapor-phase reaction of ethylene with acetic acid over silicotungstic acid supported on silica giving commercially viable activity and catalyst lifetimes for the manufacture of ethyl acetate. All three examples illustrate the importance of exploring process conditions to reveal the advantages of new catalyst systems, or transform known catalysts into commercial viability.⁵⁰ $[\text{Ir}(\text{CO})_2\text{I}_3\text{Me}]^-$ reacts with carboxylic acids, e.g., RCO_2H ($\text{R} = \text{Me}, \text{Et}$), or H (but not with mineral acids) at elevated temperature to cleave the $\text{Ir}^{\text{III}}\text{—Me}$ bond liberating methane; a cyclic transition state is proposed for the reactions with RCO_2H .⁵¹ Methanol carbonylation to acetic acid is catalyzed with high rates at low water concentrations using an iridium/iodide-based catalyst. The catalyst system exhibits high stability allowing a wide range of process conditions and compositions to be accessed without catalyst precipitation. Two distinct classes of promoters have been identified for the reaction: simple iodide complexes of zinc, cadmium, mercury, indium, and gallium, and carbonyl complexes of tungsten, rhenium, ruthenium, and osmium. The promoters exhibit a unique synergy with iodide salts, such as lithium iodide, under low water conditions. A rate maximum exists at low water conditions, and optimization of the process parameters gives acetic acid with a selectivity in excess of 99% based upon methanol. The levels of liquid by-products formed are a significant improvement over those achieved with the conventional high water rhodium-based catalyst systems and the quality of the product obtained under low water concentrations is exceptional.⁵² The rhodium-based Monsanto process, the CATIVA iridium catalyst for methanol carbonylation, purification, the environmental impact of CATIVA, and cost reduction were reviewed.⁵³

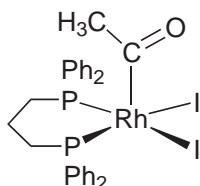
9.3.2.3 Palladium and Nickel Catalysts

Several nickel catalysts for the carbonylation of methanol have been reported,^{54–57} and an IR study has been described.⁵⁸ The carbonylation of MeOH to form MeOAc and HOAc was studied using phosphine-modified NiI_2 as the metal catalyst precursor. The reaction was monitored using a high-pressure, high-temperature, *in situ* Cylindrical Internal Reflectance FTIR reactor (CIR-REACTOR).

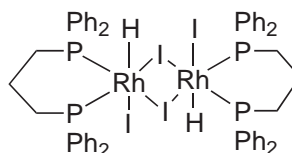
The reaction of alcohols with CO was catalyzed by Pd compounds, iodides and/or bromides, and amides (or thioamides). Thus, MeOH was carbonylated in the presence of Pd acetate, NiCl₂, *N*-methylpyrrolidone, MeI, and LiI to give HOAc.⁵⁹ AcOH is prepared by the reaction of MeOH with CO in the presence of a catalyst system comprising a Pd compound, an ionic Br or I compound other than HBr or HI, a sulfone or sulfoxide, and, in some cases, a Ni compound and a phosphine oxide or a phosphinic acid.⁶⁰ Palladium(II) salts catalyze the carbonylation of methyl iodide in methanol to methyl acetate in the presence of an excess of iodide, even without amine or phosphine co-ligands; platinum(II) salts are less effective.⁶¹ A novel Pd^{II} complex (**13**) is a highly efficient catalyst for the carbonylation of organic alcohols and alkenes to carboxylic acids/esters.⁶²



(13)



(14)



(15)

9.3.2.4 Cobalt Catalysts

The reduction steps on active Co sites are strongly affected by activated hydrogen transferred from promoter metal particles (Pt and Ru). Several indications for the existence and importance of hetero-bimetallic centers have been obtained.⁶³ [Cp*Co(CO)₂] in the presence of PEt₃ and MeI catalyzes the carbonylation of methanol with initial rates up to 44 mol L⁻¹ h⁻¹ before decaying to a second catalytic phase with rates of 3 mol L⁻¹ h⁻¹.⁶⁴ HOAc-AcOMe mixtures were prepared by reaction of MeOH with CO in the presence of Co(II) acetate, iodine, and additional Pt or Pd salts, e.g., [(Ph₃P)₂PdCl₂] at 120–80 °C and 160–250 atm.⁶⁵

9.3.2.5 Miscellaneous

Three equivalents of Me₂PR (L; R = (2-(1,4-dioxanyl)methyl, (2-tetrahydrofuryl)methyl, 2-methoxyethyl)) react with [Cl₂Ru(PPh₃)₃] to give *trans*-[Cl₂Ru(L-η¹-P)(L-η²-P,O)₂] which can be used for the carbonylation of methanol.⁶⁶ Carbonylation of MeOH to give AcOH catalyzed by Ru complexes such as *trans*-[Ru(CO)₂Cl₂(PPh₃)₂], *cis*-[Ru(CO)₂Cl₂(PPh₃)₂], and [H₂Ru(CO)(PPh₃)₃] was reported.⁶⁷

9.3.2.5.1 Reductive carbonylation

[Rh(CO)₂(acac)(dppp)] catalyst gives rates (100–200 turnovers h⁻¹) and selectivities (80–90%) in the reductive carbonylation of MeOH to acetaldehyde; this is comparable to the best Co-based catalysts, but requires a much lower temperature (140 °C) and pressure (70 bar). Addition of Ru to this catalyst results in the *in situ* hydrogenation of acetaldehyde and production of EtOH.⁶⁸

X-ray structure analyses of Rh(COCH₃)(I)₂(dppp) (**14**) and [Rh(H)(I)(μ-I)(dppp)]₂ (**15**), where dppp = 1,3-bis(diphenylphosphino) propane, were reported. Unsaturated complex (**14**) possesses a distorted five-coordinate geometry that is intermediate between sbp and tbp structures.⁶⁹ Under CO pressure, the rhodium/ionic-iodide system catalyzes either the reductive carbonylation of methyl formate into acetaldehyde or its homologation into methyl acetate. By using labeled methyl formate (H¹³CO₂CH₃) it was shown that the carbonyl group of acetaldehyde or methyl acetate does not result from that of methyl formate.⁷⁰

The cluster anion, [Os₃Ir(CO)₁₃]⁻, was prepared in 50% yield by reaction of Os₃(CO)₁₂ with [Ir(CO)₄]⁻. The single-crystal X-ray structure analysis shows it to consist of a tetrahedral metal core with one of the 13 carbonyl ligands bridging. The catalytic activity for carbonylation of

MeOH was studied. Using MeI as co-catalyst, catalytic turnover numbers of 1,800 were obtained within 14 h.⁷¹

Poly(*N*-vinyl-2-pyrrolidone)-Rh complex was used to catalyze the carbonylation of MeOH to MeOAc and AcOH in supercritical CO₂ at rates approximately 50% of those in liquid solution, but with minimal catalyst leaching.⁷²

9.3.2.5.2 Calculations

Quantum-mechanical calculations were carried out on the migratory insertion process (2) to (4) (both for Rh and Ir). The calculated free energies of activation are 27.7 kcal mol⁻¹ (Ir) and 17.2 kcal mol⁻¹ (Rh), which are in good agreement with the experimental estimates at 30.6 kcal mol⁻¹ (Ir) and 19.3 kcal mol⁻¹ (Rh). The higher barrier for Ir is attributed to a relativistic stabilization of the Ir—CH₃ bond.⁷³ The potential energy profile of the full catalytic cycle of MeOH carbonylation catalyzed by [Rh(CO)₂I₂]⁻ was explored computationally. The equilibrium structures of all isomers of the intermediates involved in the catalytic process were calculated. The rate-determining step of the reaction, CH₃I oxidative addition, proceeds via a back-side S_{N2} mechanism.⁷⁴ Experimental work has confirmed the existence of the *cis* forms of the active catalytic species, but they do not rule out the possibility of the *trans* isomers. The gas phase calculation results show that the *cis* isomer has 4.95 kcal mol⁻¹ lower free energy than the *trans* isomer. Conversion barriers for the isomers were calculated.⁷⁵ Density functional theory with hybrid B3LYP exchange and correlation functional has been used to investigate the first two catalytic reactions, the oxidative addition and migratory 1,1-insertion of the Monsanto and CATIVA processes. The calculated free energies of activation for the oxidative addition of methyl iodide to all isomers were calculated.⁷⁶

9.3.3 HYDROFORMYLATION

9.3.3.1 Platinum

Although most of the reports that have appeared since 1980 on hydroformylation of alkenes focus on rhodium catalysts, alkene hydroformylation catalyzed by Pt^{II} complexes in the presence of Sn^{II} halides has been the object of great interest and platinum can be considered as the second metal in hydroformylation.⁷⁷⁻⁷⁹

These systems based in Pt^{II} complexes with phosphorus ligands have been studied extensively mainly for the asymmetric hydroformylation of styrene, because until 1990, the platinum complexes provided the highest enantioselectivities in asymmetric hydroformylation.^{80,81} In the 1990s, however, several rhodium catalysts displayed higher enantioselectivity in asymmetric hydroformylation together with higher activity and regioselectivity than Pt–Sn catalysts. The catalytic systems based on Pt^{II}/SnCl₂ are in general less active and selective than rhodium catalysts, although they allow formation of high yields of straight-chain aldehydes from terminal alkenes.

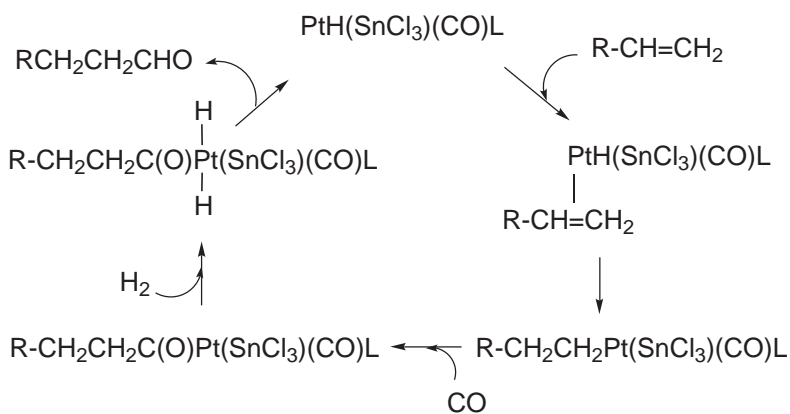
Phosphorus ligands are crucial for the stabilization of the systems and the complex *cis*-[PtCl₂(PPh₃)₂] (16) is most often employed, but complexes with chelating diphosphines also have been studied extensively. The stability of the related alkyl- and acylplatinum(II) complexes has favored extensive mechanistic investigations based on studies of the reactivity of model complexes.

9.3.3.1.1 *Cis*-PtCl₂(PPh₃)₂/SnCl₂ systems

(i) Studies on the mechanism of catalytic hydroformylation

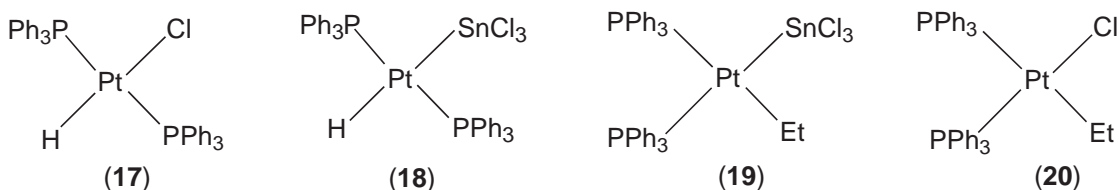
The isolation and molecular structures of complexes considered as intermediates in the *cis*-[PtCl₂(PPh₃)₂]/SnCl₂ catalyzed hydroformylation of alkenes have been reported in the last ten years. Other related Pt^{II} complexes derived from the studies of the reactivity of the species involved have also been described. Most of the studies deal with the hydroformylation of 1-alkenes, which are more reactive than internal alkenes. Hydrides such as alkyls such *trans*-[PtH(SnCl₃)(PPh₃)₂], alkyls such as *trans*-[PtR(SnCl₃)(PPh₃)₂], and acyls *trans*-[Pt(COR)(SnCl₃)(PPh₃)₂] have been suggested to

be involved in the catalytic process promoted by the *cis*-[PtCl₂(PPh₃)₂]/SnCl₂ system,⁸²⁻⁹¹ according to the catalytic cycle in Scheme 2.

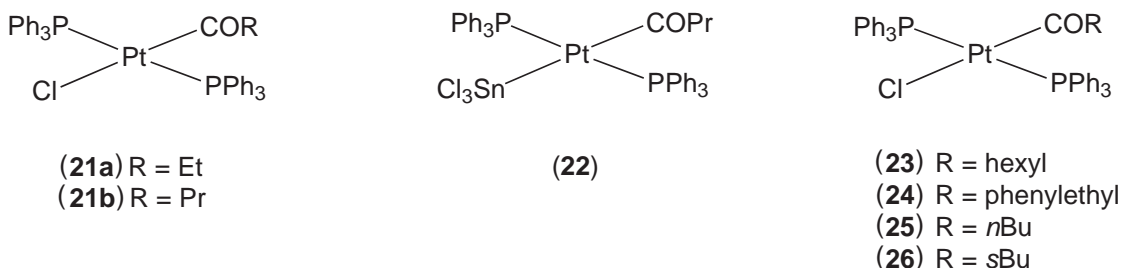


Scheme 2

Among the several hydrides formed when *trans*-[PtHClL₂] (L = PPh₃) (**17**) reacts with SnCl₂, only *trans*-[PtH(SnCl₃)L₂] (**18**) rapidly inserts ethylene at -80 °C to yield *cis*-[PtEt(SnCl₃)L₂] (**19**). At -10 °C, (**19**) irreversibly rearranges to the *trans* isomer, thus indicating that the *cis* isomer is the kinetically controlled species and that the *trans* isomer is thermodynamically more stable. At -50 °C, a mixture of (**17**) and (**18**) reacts with ethylene to give *cis*-[PtEtClL₂] (**20**) and (**19**).



CO promotes the *cis*-*trans* isomerization of (**19**), which occurs rapidly even at -80 °C. This rearrangement is followed by a slower reaction leading to the cationic complex *trans*-[PtEt(CO)L₂]⁺SnCl₃⁻. At -80 °C, this complex does not react further when kept at room temperature. Ethyl migration to coordinated CO takes place to give several acylplatinum complexes, i.e., *trans*-[PtCl(COEt)L₂], (**21a**) *trans*-[Pt(SnCl₃)(COEt)L₂], *trans*-[PtCl(COEt)L₂SnCl₂], and *trans*-[Pt(COEt)(CO)L₂]⁺SnCl₃⁻.⁹⁰ The isolation of *trans*-[PtCl(COPr)(PPh₃)₂] (**21b**) and *trans*-[Pt(SnCl₃)(COPr)(PPh₃)₂] (**22**) has also been reported.⁸² The crystal and molecular structures of several acyl complexes (**21b**),⁸² (**23**),⁸³ (**24**),⁸⁵ (**25**), and (**26**)⁸⁶ have been determined. The structures have approximately square planar geometry, the Pt atom is in a slightly distorted square-planar environment and shows no unusual dimensions.^{82,83,85,86}



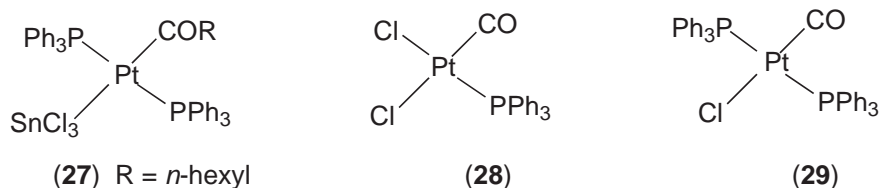
(**21a**) R = Et
(**21b**) R = Pr

(**22**)

(**23**) R = hexyl
(**24**) R = phenylethyl
(**25**) R = *n*Bu
(**26**) R = *s*Bu

The acyl complexes (25) and (26) have been characterized by IR, ^1H NMR and ^{13}C NMR spectroscopy. The formation of two isomers when 2-butene is used involves an isomerization process, which is likely to be limited to the alkyl precursor complexes. The reactivity of these acyl complexes has been tested in reactions with SnCl_2 , H_2 , HCl , and (17). From the reaction solutions, crystals of *cis*-[Pt(PPh_3) $_2\text{Cl}(\text{SnCl}_3)$] have been obtained and its molecular structure has been determined by XRD. The Pt atom has *cis* square planar coordination, with angular distortions due to steric factors. The strong *trans* influence of the SnCl_3 group is confirmed by the lengthening of the *trans* Pt–P distance.⁸⁶

The system (23)/ SnCl_2 , an active intermediate in the catalytic hydroformylation of 1-hexene, has been investigated by ^{31}P NMR spectroscopy and two species are observed at low temperature, in equilibrium with the starting Pt complex (23). One is complex (27), and the other is a species which does not show Sn–P coupling and which has been tentatively attributed to a complex having chloride ions bridging the Pt and Sn metal centers. Formation of the complex (27) does not occur when EtOH is added to the CD_2Cl_2 or acetone solutions.⁹¹



Stoichiometric model reactions in alkene hydroformylation by platinum–tin systems have been studied for the independent steps involved in the hydroformylation process, insertion of the alkene, insertion of CO, and hydrogenolysis, with use of Pt–Sn catalysts and 1-pentene as alkene at low pressure and temperature.⁹²

(ii) The role of the trichlorostannyl ligand in the Pt-catalyzed hydroformylation

The importance of the platinum–tin linkage in hydroformylation chemistry has promoted the publication of several articles dealing with this subject. ^{31}P , ^{119}Sn , ^{195}Pt , and ^{13}C NMR studies have been helpful in this aspect of the reaction.^{93–95}

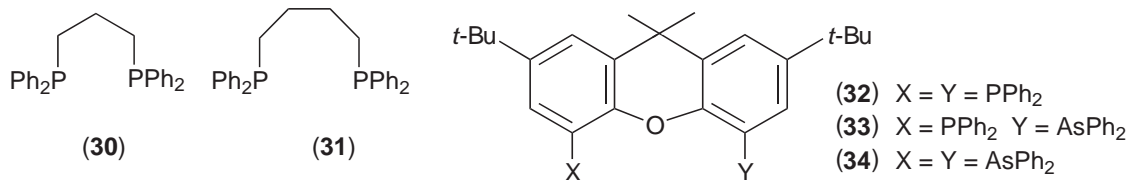
The reactions of *trans*-[PtCl(COR)(PPh_3) $_2$] (R = Ph, $\text{C}_6\text{H}_4\text{NO}_2$ -*p*, $\text{C}_6\text{H}_4\text{Me}$ -*p*, $\text{C}_6\text{H}_4\text{OMe}$ -*p*, Me, Et, Pr, hexyl, $\text{CH}_2\text{CH}_2\text{Ph}$, Me_3C) with SnCl_2 and SnCl_2 plus H_2 have been studied. The reactions with SnCl_2 alone afford a mixture of *trans*-[Pt(SnCl_3)(COR)(PPh_3) $_2$] and *trans*-[PtCl{C(OSnCl $_2$)R}(PPh_3) $_2$], with the last having a tin–oxygen bond. The ligand rearrangement reactions in the formation of an alkene hydroformylation catalyst precursor have been studied for the reaction of *cis*-[PtCl $_2$ (CO)(PR_3) $_2$] (28) with $\text{SnCl}_2 \cdot 2\text{H}_2\text{O}$. Complex (28) reacts with $\text{SnCl}_2 \cdot 2\text{H}_2\text{O}$ to give solutions active in catalytic hydroformylation. NMR studies including experiments using ^{13}CO , showed the formation of the cationic complex, *trans*-[PtCl(CO)(PPh_3) $_2$] $^+$ (29) and the anionic complexes, [Pt(SnCl_3) $_5$] $^{3-}$, *trans*-[PtCl(SnCl_3) $_2$ (CO)] $^-$, and *trans*-[PtCl(SnCl_3) $_2$ (PPh_3)] $^-$.⁹³

The catalytic system (16)/ SnCl_2 is also highly active for the regioselective of hydroformylation ethyl 3-butenolate. EtOH strongly inhibits the catalytic activity. In EtOH the catalytic precursor was recovered as the acyl complex, *trans*-[PtCl(COCH $_2$ CH $_2$ CH $_2$ CO $_2$ Et)(PPh_3) $_2$], which is also catalytically active.⁹⁶ Internal alkenes are hydroformylated to linear aldehydes in substantial amounts with the cationic Pt–Sn catalyst system (29)/ SnCl_2 . By altering the nature of the phosphine ligand, PR_3 (R = Bu, OPh, substituted Ph) as well as the reaction conditions the selectivity for terminal aldehyde production can be varied widely.⁹⁷ The activity of the catalytic system (16)/ SnCl_2 in the hydroformylation of alkenes (1-pentene, cyclopentene, cyclohexene, allylbenzene, styrene, methyl acrylate, vinyl acetate, and acrylonitrile) has been reported.⁹⁸

(iii) *Cis*-PtCl $_2$ (diphosphine)/ SnCl_2 systems

Mono and binuclear platinum(II) complexes with diphosphines have been reported as catalysts in the hydroformylation reaction. Dppp and related diphosphines are used as ligands in platinum/Sn systems for the hydroformylation of different substrates.^{99–107}

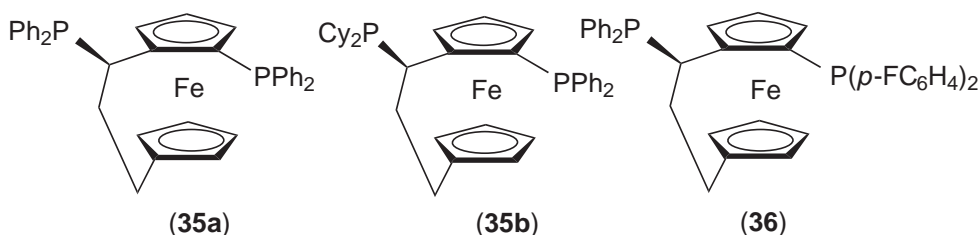
The complexes *cis*-[PtCl(Et)(diphosphine)], diphosphine = dppp (**30**) or dppb (**31**), were used as models for the hydroformylation of alkenes catalyzed by PtCl₂/diphosphine/SnCl₂. The reaction of (**30**) and (**31**) with SnCl₂ gives *cis*-[Pt(SnCl₃)(C₂H₅)(diphosphine)], which in the absence of free ethylene decomposes to form the species *cis*-[PtCl₂(diphosphine)], via an unstable hydrido species. Both the chloro- and trichlorostannate-alkyl complexes react with CO to give the acyl species *cis*-[PtX(COEt)(diphosphine)] (X = Cl, or SnCl₃).⁹⁹



Mechanistic studies using variable temperature HP NMR spectroscopy have been performed to establish the role of Pt–SnCl₃ bond in the CO insertion and hydrogenolysis steps of the Pt-diphosphine-catalyzed alkene hydroformylation reaction.^{108,109} The formation of the four-coordinate ionic complex *cis*-[Pt(Me)(CO){(*S,S*)-bdpp}]⁺X[−], where X = Cl, and X = SnCl₃, bdpp = (2*S*,4*S*)-2,4-bis(diphenylphosphino)pentane, has been observed through reaction with CO. The covalent acetyl [Pt(COMe)(Cl){(*S,S*)-bdpp}], and ionic acetyl compound [Pt(COMe)(CO){(*S,S*)-bdpp}]⁺SnCl₃[−], have been described.¹⁰⁸ The reactions of alkylplatinum–diphosphine complexes, [Pt(Me)(Cl)(bdpp)] and [Pt(Me)(SnCl₃)(bdpp)], as well as [Pt{CH(CO₂Et)CH₃}(Cl)(dppp)] with carbon monoxide have been studied and been observed through high-pressure NMR studies.¹⁰⁹

Large bite angle diphosphines derived from heteroatomic xanthene-type hydrocarbons have been used to form Pt–Sn catalyst systems. These xantphos ligands (**32**) combine the large bite angle with a rigid backbone and these catalysts show high regioselectivity for formation of the terminal aldehyde.¹¹⁰ Related amine, arsine and mixed phosphine–amine, and phosphine–arsine ligands based on xanthene backbones were synthesized. The coordination chemistry and the catalytic performance of these ligands were compared to those of the parent phosphine. Ligands (**33**) and (**34**) have been applied in the platinum/tin-catalyzed hydroformylation of 1-octene providing high activity and selectivity which is explained by its wide natural bite angle and the formation of *cis*-coordinated platinum complexes.¹¹¹

Platinum complexes [PtCl₂(diphosphine)] and [PtCl(SnCl₃)(diphosphine)] of the ferrocenyl diphosphine ligands (**35a**), (**35b**), and (**36**) have been synthesized. Complexes [PtCl₂(**35**)] and [PtCl₂(**36**)] have been structurally characterized by XRD. Both the preformed and the *in situ* catalysts have been used in the hydroformylation of styrene.¹¹²

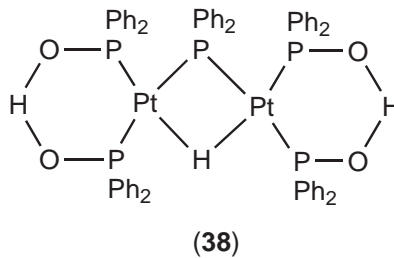
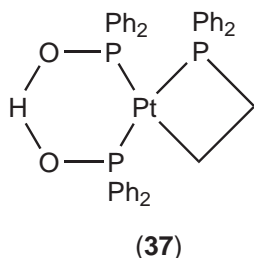


(iv) Miscellaneous

Mixed phosphines,¹¹³ phosphates,^{114,115} phosphinites (diphenylphosphine oxide) and related diphenylphosphine acids,^{116–119} phospholes,¹²⁰ and other phosphorus ligands^{121–123} have been used in Pt-catalyzed hydroformylation. [PtCl₂(COD)] has been used as starting material for the preparation of catalytic precursors.^{114,124–126}

A review on Pt-based catalysts containing phosphinous acid derivative ligands for the hydroformylation of alkenes has been published.¹¹⁶ Platinum complexes containing phosphinito ligands, Ph₂PO(H), afford active hydroformylation catalysts.¹¹⁷ Both 1- and 2-heptene were hydroformylated by [Pt(H)(Ph₂PO)(Ph₂POH)(PPh₃)] to give products of 90% and 60% linearity, respectively. Intermediate alkyl and acyl complexes, e.g., [Pt(COEt)(Ph₂PO)(Ph₂POH)(PPh₃)] were isolated

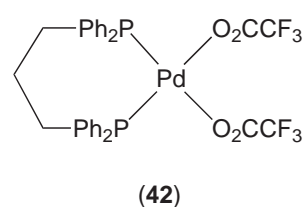
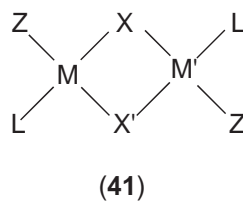
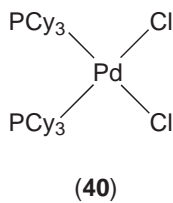
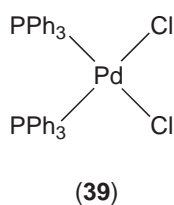
and characterized.¹¹⁸ The reactivity of $[(\text{Ph}_2\text{POHOPPh}_2)\text{Pt}(\text{H})(\text{L})]$, in particular the reactions related to hydroformylation, has been reported.¹¹⁹ Ligands L carrying alkenyl and alkynyl groups undergo intramolecular insertion into the adjacent Pt—H bond. Diphenylvinylphosphine initially gives a phosphaplatinacyclopropane, which rearranges to a phosphaplatinacyclobutane complex (37), for which the crystal structure has been determined. The crystal structure of a dimeric inactive complexes (38) containing a phosphido and a hydrido bridge has been determined.¹¹⁹



Thiolate-Pt^{II} complexes, in particular dinuclear thiolate and dithiolate bridged complexes, have been prepared and characterized a catalyst precursor in hydroformylation reactions for use as.^{127,128}

9.3.3.2 Palladium

Until recently, the hydroformylation using palladium had been scarcely explored as the activity of palladium stayed behind that of more active platinum complexes. The initiating reagents are often very similar to those of platinum, i.e., divalent palladium salts, which under the reaction conditions presumably form monohydrido complexes of palladium(II). A common precursor is (39). The mechanism for palladium catalysts is, therefore, thought to be the same as that for platinum. New cationic complexes of palladium that are highly active as hydroformylation catalysts were discovered by Drent and co-workers at Shell and commercial applications may be expected, involving replacement of cobalt catalysts.



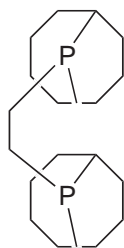
Bimetallic catalysts involving palladium and cobalt were developed¹²⁹ and reviewed by Ishii and Hidai.¹³⁰ Complex (39) in the presence of $\text{Co}_2(\text{CO})_8$ leads to a bimetallic catalyst effective for the carbonylation of ArI with CO/HSiEt_3 to give benzyl silyl ethers. Addition of NEt_3 to the reaction system changed the distribution of the carbonylation products to 1,2-diaryl-1,2-disiloxyethanes. The former reaction proceeds via the aldehyde intermediate, while a mechanism involving the aroylcobalt complex $[(\text{ArCO})\text{Co}(\text{CO})_3(\text{PPh}_3)]$ formed by way of a Pd–Co bimetallic complex is proposed for the latter reaction. $[\text{PdCl}_2(\text{PCy}_3)_2]$ (40) was found to work as a selective catalyst for the hydroformylation of internal alkynes to give the corresponding α,β -unsaturated aldehydes (150 °C, 6 h; 84% conversion, 83% yield), and the combined use of (40) and $\text{Co}_2(\text{CO})_8$ remarkably improved the catalytic activity with little change of the selectivity (150 °C, 1 h; 100% conversion, 95% yield).

A series of low oxidation state planar, triangular clusters containing palladium, including $[\text{Pd}_2\text{Mo}_2\text{Cp}_2(\text{CO})_6\text{L}_2]$, $[\text{Pd}_2\text{W}_2\text{Cp}_2(\text{CO})_6\text{L}_2]$, and $[\text{Pd}_2\text{Cr}_2\text{Cp}_2(\text{CO})_6\text{L}_2]$ (where $\text{Cp} = \eta^5\text{-C}_5\text{H}_5$ and $\text{L} = \text{PPh}_3$ or PEt_3) were studied as homogeneous catalysts in several reactions including the hydroformylation of 1-pentene.¹³¹

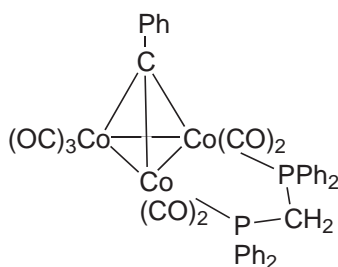
A review¹³¹ on the preparation, characterization, and reactivity of complexes (41) $[\text{MM}'(\mu\text{-X})(\mu\text{-X}')\text{Z}_2\text{L}_2]$ ($\text{M} = \text{M}' = \text{Pt}$ or Pd ; $\text{M} = \text{Pt}$, $\text{M}' = \text{Pd}$; $\text{X} = \text{X}' = \text{Cl}$, SR' ; $\text{X} = \text{Cl}$, $\text{X}' = \text{SR}'$; $\text{Z} = \text{Cl}$, SnCl_3 , R , $\text{L} =$ tertiary phosphine) has been published. The catalytic activity of some of these complexes in the presence of $\text{SnCl}_2 \cdot 2\text{H}_2\text{O}$ as co-catalyst in homogeneous hydroformylation has been described.

Fast hydroformylation reactions using palladium were reported by Drent^{133,134} in 1987. Complex (42), prepared *in situ* from palladium acetate, dppp and $\text{CF}_3\text{CO}_2\text{H}$, catalyzed the hydroformylation of 1-octene in diglyme (CO and H_2 68 bar, 100°C) to give 1-nonanal (71.9% linearity, 100% selectivity to nonanals) with a very low amount of alkane by-product. Using 1,3-(*di*-anisylphosphino)propane 76% nonanal was obtained.¹³⁵ Various carbonylation reactions¹³⁶ can be catalyzed by palladium complexes of the type PdX_2L_2 (where L_2 = mono- or bidentate phosphorus or nitrogen ligand, X = anion with low coordination ability). The chemoselectivity of the catalytic systems is influenced both by the ligand and the anion. Using styrene, ketones are the main product, even in the presence of hydrogen. Using 2-phenylpropene or (E)-1-phenylpropene only aldehyde formation was achieved. Aliphatic substrates give oligomeric ketones. Catalyst systems consisting of a palladium(II) diphosphine complex with weakly or noncoordinating counterions are efficient catalysts for the hydrocarbonylation.¹³⁷ Moreover, variations of ligand, anion, and/or solvent can be used to steer the reaction towards alcohols, aldehydes, ketones, or oligoketones. Noncoordinating anions and arylphosphine ligands produce primarily (oligo)ketones; increasing ligand basicity or anion coordination strength shifts selectivity towards aldehydes and alcohols. For the mechanisms of the aldehyde-producing step, Drent and Budzelaar proposed a heterolytic dihydrogen cleavage, assisted by the anion. At high electrophilicity of the palladium center, selective ketone formation is observed.

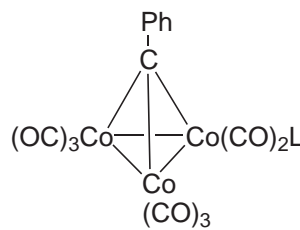
Structure (43) (QPCH₂CH₂PQ) (Q = mixture of 1,4- and 1,5-cyclooctanediyl) was reported to be a very effective ligand for the palladium catalyzed hydroformylation of internal and terminal alkenes using small amounts of NaCl or HCl as an additive in PhOMe or diglyme as the solvent.^{138–141}



(43)



(44)



(45)

9.3.3.3 Cobalt

Cobalt carbonyls are the oldest catalysts for hydroformylation and they have been used in industry for many years. They are used either as unmodified carbonyls, or modified with alkylphosphines (Shell process). For propene hydroformylation, they have been replaced by rhodium (Union Carbide, Mitsubishi, Ruhrchemie-Rhône Poulenc). For higher alkenes, cobalt is still the catalyst of choice. Internal alkenes can be used as the substrate as cobalt has a propensity for causing isomerization under a pressure of CO and high preference for the formation of linear aldehydes. Recently a new process was introduced for the hydroformylation of ethene oxide using a cobalt catalyst modified with a diphosphine. In the following we will focus on relevant complexes that have been identified and recently reported reactions of interest.

Reactions of $\text{Co}_2(\text{CO})_8$ with ferrocenylphosphine oligomers or polymers have been studied. Detailed IR and ³¹P NMR studies showed that the polymeric ligands chelate Co in a tridentate fashion when a high P/Co ratio is used. Use of such Co catalysts at $170\text{--}90^\circ\text{C}$ for 1-hexene hydroformylation showed reactivity and selectivity similar to those of Ph_3P . The observed tendency for tridentate chelation in these complexes inhibits the aldehyde-to-alcohol reduction step.¹⁴² Addition of (dppe) or $\text{Bu}_2\text{P}(\text{CH}_2)_4\text{PBu}_2$ to $\text{HCo}(\text{CO})_4$ or $\text{Co}_2(\text{CO})_8$ gave complexes containing stable five-membered and unstable seven-membered rings; these were catalytically inactive for hydroformylation of C_3H_6 . Under the action of the hydroformylation system, the seven-membered ring complex opened to give a catalyst of almost exactly the same activity as a catalyst modified with Bu_3P .¹⁴³ The hydroformylation, aminomethylation, and hydrocarbonylation of alkenes with $\text{Co}_2(\text{CO})_8$ and dppe using CO/ H_2O has been examined.¹⁴⁴ Reaction of $[(\mu_3\text{-CMe})\text{Co}_3(\text{CO})_9]$ with (dppm) gave the cluster $[(\mu_3\text{-CMe})\text{Co}_3(\text{CO})_7(\text{dppm})]$ (44) which was a catalyst for the hydroformylation of 1-pentene at 80 bar $\text{H}_2\text{-CO}$ and 110°C . The dppm bridging ligand stabilizes and activates the cluster for catalysis.¹⁴⁵

Density functional calculations have been carried out on the addition of H_2 to $[\text{CH}_3(\text{O})\text{CCo}(\text{CO})_3]$ as well as the product elimination step, in which AcH and $\text{HCo}(\text{CO})_3$ are formed.¹⁴⁶ Mono-substituted derivatives of phenylmethinyltricobalt enneacarbonyls $[\text{PhCCo}_3(\text{CO})_8\text{L}]$ ($\text{L} = \text{PPh}_3, \text{AsPh}_3, \text{SbPh}_3$) (**45**) were used as hydroformylation catalysts.¹⁴⁷

The stability of phosphine-substituted Co clusters derived from $\text{Co}_4(\text{CO})_{10}(\mu_4\text{-PPh})_2$ was examined under hydroformylation conditions using cylindrical internal reflectance (CIR) spectroscopy.¹⁴⁸ $[(\text{CO})_4\text{Fe}(\mu\text{-PtBu}_2)\text{Rh}(\text{CO})\text{L}]$, $\text{PPN}[(\text{CO})_3\text{Co}(\mu\text{-P}(\text{CMe}_3)_2)\text{Rh}(\text{CO})(\text{HP}(\text{CMe}_3)_2)]$, and $[(\text{CO})_2(\text{PPh}_3)\text{Co}(\mu\text{-H})(\mu\text{-P}(\text{CMe}_3)_2)\text{Rh}(\text{CO})(\text{HP}(\text{CMe}_3)_2)]$ were used as hydroformylation catalysts.¹⁴⁹ Cobalt–phosphine–carbonyl catalysts give hydroformylation catalytic activities in the following decreasing order: $\text{C}(\text{CH}_2\text{PPh}_2)_4 \approx \text{Ph}_2\text{P}(\text{CH}_2)_2\text{PPh}_2 > \text{Ph}_2\text{P}(\text{CH}_2)_3\text{PPh}_2 > \text{Ph}_2\text{PCH}_2\text{PPh}_2 > \text{Ph}_2\text{P}(\text{CH}_2)_4\text{PPh}_2$.¹⁵⁰ The complex $[\text{Co}_2(\text{CO})_6(\eta^2\text{-dppp})]$ is an efficient catalyst for hydroformylation because of its thermostability.¹⁵¹ A review on metal carbonyls from 1951 to 1993 on the preparation of more than 80 novel Co and Fe carbonyls and their application in catalytic alkene hydroformylation has been published.¹⁵² 1,3-Diols and 3-hydroxyaldehydes were prepared by the hydroformylation of 1,2-epoxides with Co carbonyl catalysts modified with ligand (**43**), also used for Pd-catalyzed hydroformylation.¹⁵³ The catalytic system $\text{Co}_2(\text{CO})_8/\text{diphos}/\text{THF-H}_2\text{O}$ was studied for simultaneous hydroxycarbonylation and hydroformylation of cyclohexene. Using this catalytic system, the cyclohexene reaction with CO and H_2O gives cyclohexene–carboxaldehyde and cyclohexenecarboxylic acid as the main reaction products and cyclohexyl–methanol as a by-product.¹⁵⁴ The rate of hydroformylation of cyclohexene to cyclohexanecarboxaldehyde in the presence of $\text{Co}_2(\text{CO})_8$ is strongly reduced by the presence of an additional gas, such as dinitrogen or argon, under very high pressure, other conditions being kept constant.¹⁵⁵ The rate of cobalt-catalyzed hydroformylation of cyclohexene to cyclohexanecarboxaldehyde is significantly reduced when xenon is added to the reaction mixture at a concentration similar to that of the alkene. These experiments suggest competitive coordination of xenon to the catalytically active cobalt species.¹⁵⁶ The equilibration reaction of $\text{Co}_2(\text{CO})_8$ with $\text{HCo}(\text{CO})_4$ in the presence of H_2 has been measured under semi-*in situ* conditions.¹⁵⁷ The two main equilibrium reactions involving $\text{Co}_2(\text{CO})_8$ have been studied. The first is the equilibrium reaction of $\text{Co}_2(\text{CO})_8$ with H_2 to yield $\text{HCo}(\text{CO})_4$. The second is the equilibrium decomposition of $\text{Co}_2(\text{CO})_8$ to $\text{Co}_4(\text{CO})_{12}$. The results were discussed as to their possible relevance and role in the mechanism of the hydroformylation reaction. Specifically, the formation of the trinuclear cobalt carbonyl hydride, $\text{HCo}_3(\text{CO})_9$, has been described.¹⁵⁸ Complexes of cobalt efficiently catalyze the hydroformylation of epoxides in the presence of hemilabile P–O chelating ligands to give β -hydroxyaldehydes in high selectivities and yields.¹⁵⁹ Time-resolved IR spectroscopic studies have been used to characterize the reactive intermediate $\text{CH}_3\text{C}(\text{O})\text{Co}(\text{CO})_2\text{-PPh}_3$, which is relevant to the mechanism of the catalysis of alkene hydroformylation by the phosphine-modified cobalt carbonyls.¹⁶⁰ Hydroformylation of internal alkynes is catalyzed by homogeneous Pd–Co bimetallic systems.¹⁶¹ Homogeneously catalyzed propylene hydroformylation in supercritical carbon dioxide using $\text{Co}_2(\text{CO})_8$ precatalyst was studied at temperatures of 66–108 °C and pressures of 90–194 bar; selectivity changes were explained.¹⁶² The homogeneous hydroformylation of 1-pentene under synthesis gas experimental conditions was studied using Wilkinson's catalyst and $\text{Co}_2(\text{CO})_8$ modified by different triarylstibines. The maximum yield of aldehydes was 85% with linear: branched ratio of 3.4 when the Co carbonyl and trimesityl stibine system was used.¹⁶³ Catalytically active complexes of Rh^{I} and Co^0 were used in the preparation of complexes of 3-pyridyldiphenylphosphine. $\text{Co}_2(\text{CO})_6(3\text{-PyPPh}_2)_2$ has been characterized. Activities of the prepared complexes were tested in hydroformylation reaction of 1-hexene.¹⁶⁴ The effects of temperature, concentrations of alkene and the catalyst $\text{Co}_2(\text{CO})_8$, and solvent nature on the rate and selectivity of hydroformylation of propylene dimers have been studied.¹⁶⁵ Toroid NMR probes have been employed to examine phosphine-substituted and unsubstituted cobalt carbonyl hydroformylation catalysts under catalytic and noncatalytic conditions in a variety of solvents.¹⁶⁶

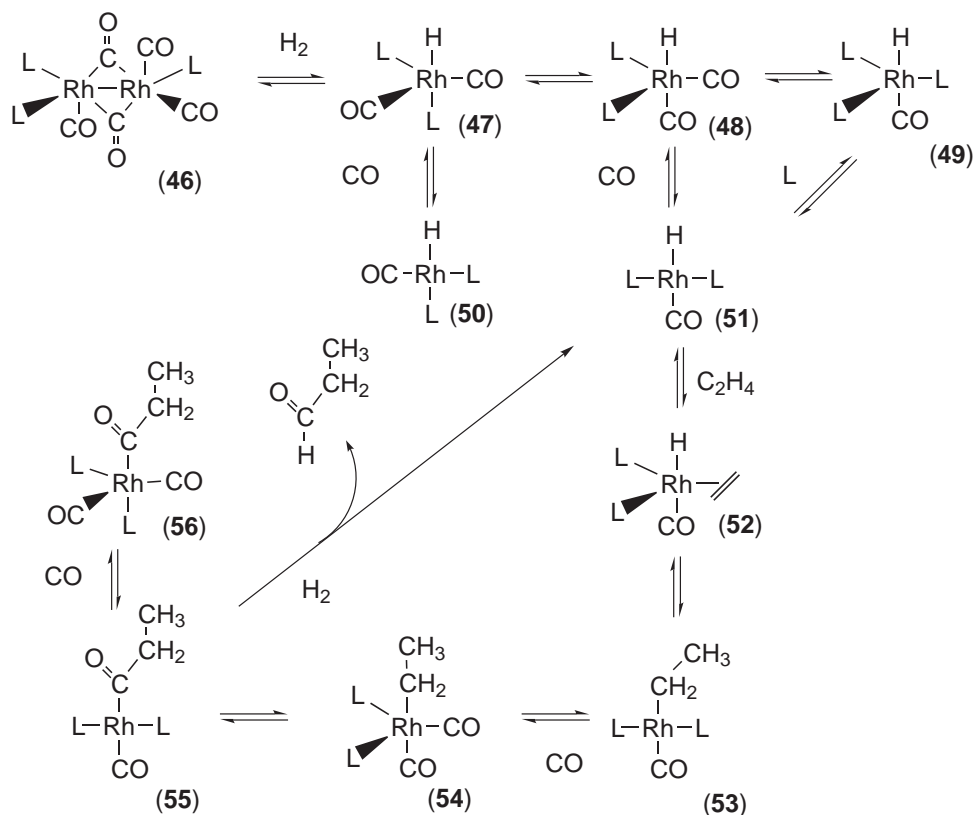
9.3.3.4 Rhodium

9.3.3.4.1 Introduction to phosphine catalysts

The best known rhodium catalyst precursor for hydroformylation is undoubtedly $\text{RhH}(\text{PPh}_3)_3\text{CO}$, first reported by Vaska in 1963,¹⁶⁷ but its activity for hydroformylation was discovered by Wilkinson and co-workers a few years later.^{168–171} The chemistry reported in the late 1960s and early 1970s is still

relevant for the hydroformylation studies of the 2000s. The chemistry and catalysis of $\text{Rh}^{\text{I}}\text{-PPh}_3$ systems has been reviewed many times.¹⁷²⁻¹⁷⁴ A review has been published on the synthesis and coordination chemistry of aminophosphine-phosphinites and closely related ligands.¹⁷⁵ A variety of ligands and complexes were discussed in a review by Trzeziak.¹⁷⁶ Hydroformylation was reviewed by Ungvary.⁷⁷⁻⁷⁹ Controlling stereoselectivity with the aid of a reagent-directing group was reviewed by Breit.¹⁷⁷ Catalysts for the hydroformylation of higher alkenes with emphasis on the work of Mitsubishi Kasei Company has been reviewed.¹⁷⁸ A book on Rh-catalyzed hydroformylation containing more than 600 references was published in 2000. It discusses catalysis with carbon monoxide ligands only, phosphite and phosphine ligands, enantioselective catalysis, applications in organic chemistry, two-phase catalysis, processes being applied and in development, catalyst preparation and decomposition, and future trends. The work focuses on the more common ligands and in spite of the many references even this work is far from comprehensive.¹⁷⁹

The mechanism accepted for Rh-catalyzed hydroformylation is the one proposed by Heck and Breslow for cobalt.¹⁸⁰ The so-called dissociative mechanism proposed by Wilkinson is depicted in Scheme 3. At low hydrogen pressures dimer (46) is formed. For $\text{L} = \text{PPh}_3$ the dimer has been characterized crystallographically.¹⁸¹ At high concentrations of ligand, species (49) forms. At moderate concentrations of the phosphine or phosphite ligand with respect to the concentration of CO, species (47) and (48) are formed containing two phosphorus ligands. These species can occur in bis-equatorial and equatorial-apical isomers. For the hydride and PPh_3 as the ligand the bis-equatorial isomer is the dominant one. In the acyl species (56) the two phosphine ligands occupy preferably one apical and one equatorial position.¹⁸²

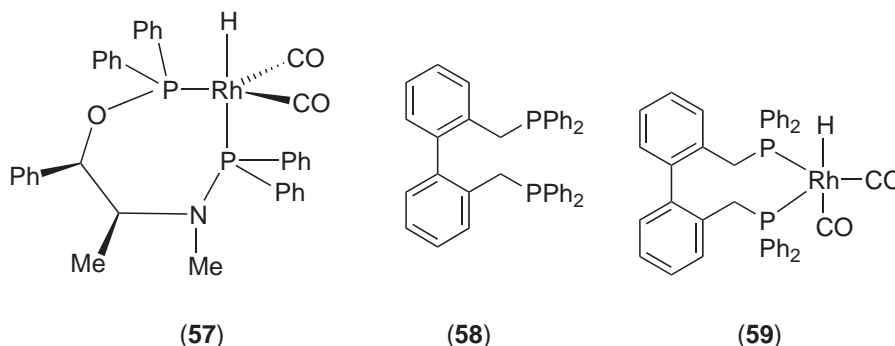


Scheme 3

Moser has studied complexes $[\text{RhH}(\text{CO})_2\text{L}_2]$ (47), (48), (54), (56) by *in situ* IR reflectance spectroscopy¹⁸³ during 1-hexene hydroformylation. Claver and van Leeuwen studied the system containing PPh_3 as the ligand during the hydroformylation of 1-octene using *in situ* IR transmission spectroscopy. They observed four bands, which were assigned to four CO stretching modes of the mixture of $[\text{RhH}(\text{CO})_2(\text{PPh}_3)_2]$ isomers (47) and (48) as reported in the NMR studies by Brown. Studies of the Rh catalyst systems $[\text{Rh}_2\{\mu\text{-S}(\text{CH}_2)_3\text{N}(\text{Me}_2)\}_2(\text{COD})_2]/\text{PR}_3$ ($\text{R} = \text{Ph}, \text{OPh}$),

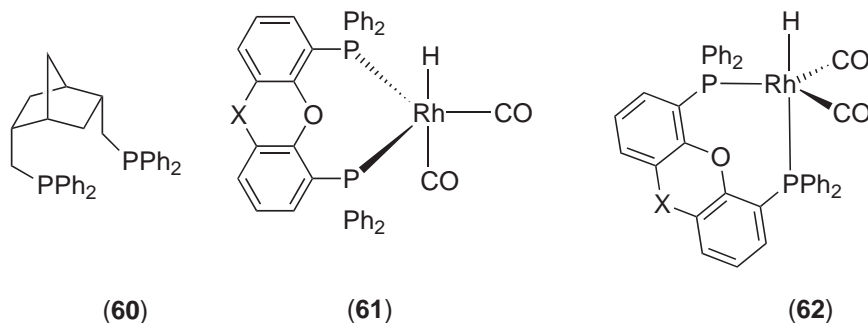
$[\text{Rh}_2\{\mu\text{-S}(\text{CH}_2)_2\text{S}\}(\text{COD})_2]/\text{PPh}_3$, $[\text{Rh}_2\{\mu\text{-S}(\text{CH}_2)_4\text{S}\}(\text{COD})_2]/\text{PPh}_3$, $[\text{Rh}_2\{\mu\text{-XANTOSS}\}(\text{COD})_2]/\text{PPh}_3$, and $[\text{Rh}(\text{Acac})(\text{CO})_2]/\text{PR}_3$ ($\text{R} = \text{Ph}, \text{OPh}$) revealed mononuclear Rh-hydride species under hydroformylation conditions (80°C , 5–30 bar). The activities and selectivities, obtained during the hydroformylation of 1-hexene using these systems as catalyst precursors, can be fully accounted for by the mononuclear species observed. Deuterioformylation experiments using dinuclear $[\text{Rh}_2\{\mu\text{-S}(\text{CH}_2)_3\text{N}(\text{Me}_2)\}_2(\text{COD})_2]/\text{PR}_3$ systems lent no support to a dinuclear mechanism.¹⁸⁴ Using the same ligand to metal ratios as in the IR studies above and pressures up to 4 bar, but significantly higher ligand concentrations, Oswald found in NMR studies that the predominant species is now the tris- PPh_3 complex (**49**).¹⁸⁵ Wilkinson and Andretta suggested that species (**49**), formed at high PPh_3 concentration, lead to higher linear aldehyde selectivity (1:b = 20:1).¹⁸⁶

Since the mid-1980s bidentate phosphines and phosphites have become very popular as ligands in hydroformylation and many compounds have been spectroscopically identified. The bidentate ligand $\text{PPh}_2\text{NMeCHMeCHPhOPPh}_2$ shown in (**57**), having two very distinct absorptions for the amido phosphorus and the phosphinite phosphorus nuclei, gives ^1H and ^{31}P spectra that are readily interpreted.¹⁸⁷



In 1987 Devon *et al.* from Texas Eastman reported a new diphosphine ligand, BISBI, (**58**) that shows a very high regioselectivity for the formation of linear aldehydes.^{188,189} Examination of molecular models of metal complexes of BISBI indicates that the chelate bite angle is much greater than 90° , the most common bite angle for bidentate ligands used in coordination chemistry and organometallic chemistry. Casey *et al.* have shown that ligands with wider bite angles form complexes in which the bidentate ligand occupies equatorial positions (**59**). Furthermore they found that the wider the bite angle is, the higher the selectivity for linear aldehyde.^{190,191}

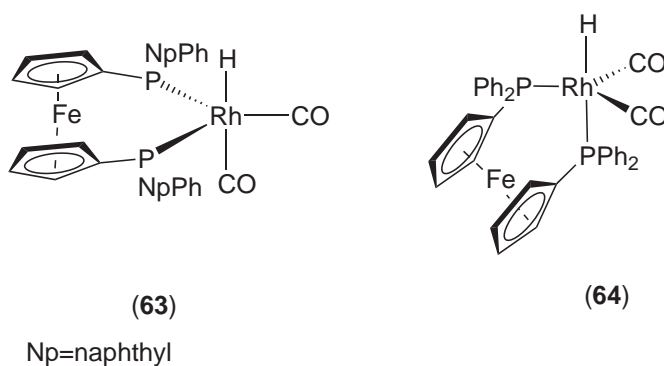
Ligand (**60**) forms an exception; Casey and Yamamoto reported a low selectivity for linear aldehyde even though the calculated bite angle is high (126°).^{192,193} Electronic effects have been investigated.^{194,195} The potential energy hypersurface for ethylene hydroformylation catalyzed by $[\text{HRh}(\text{PH}_3)_2(\text{CO})]$ was mapped out at the CCSD(T)//B3LYP and B3LYP//B3LYP levels of theory using effective core potentials.¹⁹⁶



A series of diphosphines (shown in complexes (**61**) and (**62**)) with a tunable bite angle were developed ($\text{X} = \text{PhP}, \text{Me}_2\text{Si}, \text{S}, \text{Me}_2\text{C}, \text{Me}_2\text{C}=\text{C}, \text{HN}, \text{PhN}$, etc.) covering a range of angles from 102° to 121° and applied in hydroformylation. Their complexes (**61**) and (**62**) were identified by *in situ* IR spectroscopy and NMR spectroscopy and the ratio of the two isomers depends on the bite angle. Electronic effects were also studied.^{197–199} Several MO studies on hydroformylation have

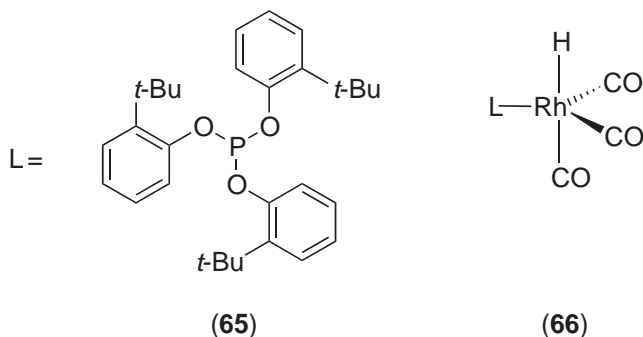
been published. DFT calculations including hybrid QM/MM calculations using the IMOMM method and hybrid QM/QM methods have shown that the origin of the selectivity for linear product is steric.^{200–203}

Dppf forms complexes (**64**) in preference to the bis-equatorial complexes (**63**) which are formed with related ligands, replacing one phenyl group at each phosphorus atom with a 1-naphthyl substituent leads to a wider bite angle and formation of (**63**) as the major species, and a higher selectivity for linear aldehyde than dppf. Its new electronically modified derivatives bearing methoxy and/or trifluoromethyl groups in *para* positions of the Ph rings were also studied. Depending on ligand basicity, HP NMR and IR characterization of the respective (diphosphine)-Rh(CO)₂ precursor complexes revealed subtle differences in the occupation of bis-equatorial (ee) and equatorial–apical (ea) coordination geometries.²⁰⁴



9.3.3.4.2 Introduction to phosphite catalysts

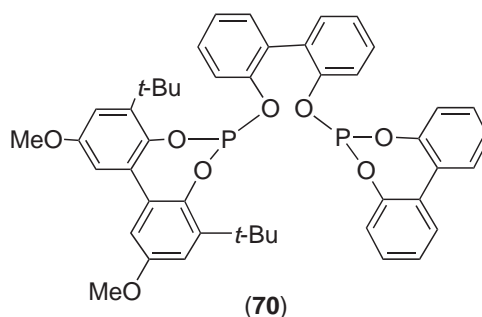
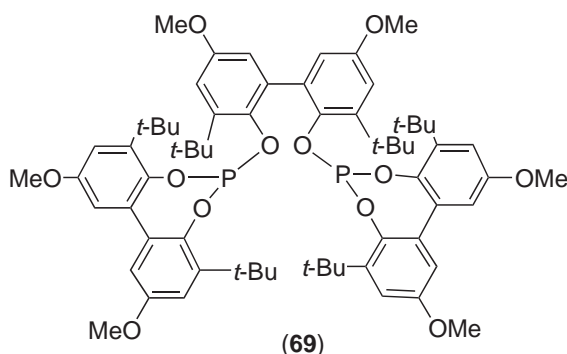
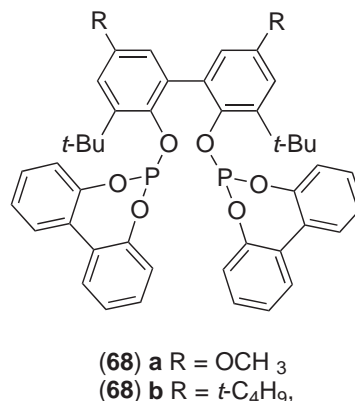
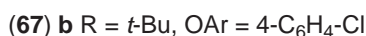
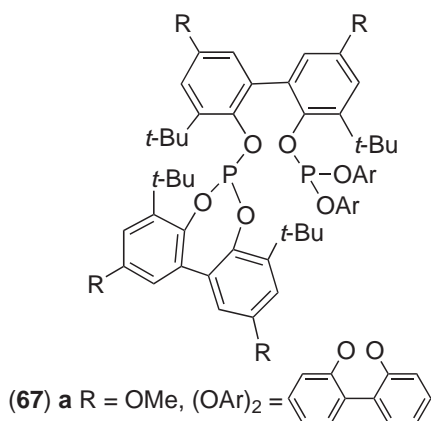
Phosphites have been used as ligands in Rh-catalyzed hydroformylation from the early days since their introduction in 1969.^{205,206} Identification of complexes occurred more recently. Ziolkowski and Trzeciak have studied extensively the use of phosphite ligands in the Rh-catalyzed hydroformylation of alkenes.^{207–210} The ligand tris(2-*tert*-butyl-4-methylphenyl) phosphite (**65**) leads to extremely fast catalysis and *in situ* spectroscopy showed that under the reaction conditions only a mono-ligated complex [Rh(H)(CO)₃(**65**)], (**66**), is formed due to the bulkiness of the ligand.^{211–213}



Remarkably, Claver *et al.* showed that in a square planar rhodium carbonyl chloride complex, two bulky phosphite ligands (**65**) were able to coordinate in a *trans* orientation.²¹⁴ Diphosphite ligands having a high selectivity for linear aldehyde were introduced by Bryant and co-workers. Typical examples are (**67**)–(**70**).^{215,216}

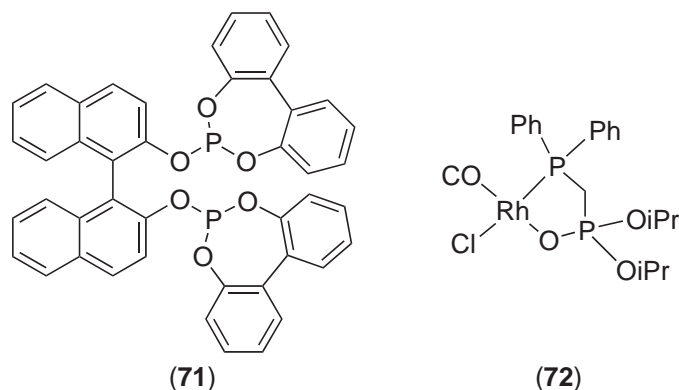
The selectivity was found to be dependent on the exact ligand structure. Structures of rhodium hydridodicarbonyls were shown to contain a bis-equatorial coordination mode for bisphenol backbones, 1,3- and 1,4 diol backbones, but apical–equatorial for 1,2-diol based backbones. The latter always lead to low selectivities.^{217–220} Dimer formation was observed.²²¹

The less bulky ligand (**71**) studied by Gladfelter leads to dimeric complexes [Rh₂(**71**)₂(CO)₂] and even tetramers.²²² Transformations of rhodium carbonyl complexes in alkene hydroformylation are discussed from the standpoint of the catalytic system self-control under the action of reaction



medium. The effect of the number of metal atoms in a cluster on the catalytic properties is considered.²²³ Several reports have appeared on hydroformylation in supercritical carbon dioxide using well-defined complexes [HRh(L)₃(CO)].^{224–226} The hydroformylation of 1-octene using [HRh(CO){P(*p*-CF₃C₆H₄)₃}]₃ in scCO₂ was investigated.²²⁷ A fluorinated catalyst, [HRh(CO){P(3,5-(CF₃)₂C₆H₃)₃}]₃, was found to be an extremely active catalyst in scCO₂ for hydroformylation of 1-octene.²²⁸ Several fluoroalkyl- and fluoroalkoxy-substituted tertiary arylphosphines 3,5-[(CF₃)₂C₆H₃]₃P, [4-CF₃C₆H₄]₃P, [3-CF₃C₆H₄]₃P, [4-CF₃OC₆H₄]₃P, and [4-F(CF₂)₄(CH₂)₃C₆H₄]₃P were studied in the homogeneous catalytic hydroformylation of 1-octene.²²⁹ A series of ponytail-appended arylphosphines P(C₆H₄-*m*-R)₃ (where *m* is 3 or 4, denoting *meta* or *para* substitution (*m* = 4, R = *n*-C₆F₁₃, *n*-CH₂CH₂C₆F₁₃, *n*-C₆H₁₃, *n*-C₁₀H₂₁, or *n*-C₁₆H₃₃; *m* = 3, R = *n*-C₆F₁₃) have been studied in the Rh-catalyzed hydroformylation of higher alkenes in scCO₂, with the perfluoroalkylated ligands exhibiting the highest and the alkylated one the lowest activities.²³⁰ The reaction rates and selectivities in the hydroformylation of various alkenes over [Rh(CO)₂(acac)] and P[C₆H₄CH₂CH₂(CF₂)₆F]₃ in supercritical CO₂ have been examined.²³¹ A continuous process for the selective hydroformylation of higher alkenes in supercritical carbon dioxide was presented; the rhodium complex of *N*-(3-trimethoxysilyl-*n*-propyl)-4,5-bis(diphenylphosphino)phenoxazine immobilized on silica as catalyst shows high selectivity and activity over several hours and no decrease in performance was observed over several days.²³²

P(OPh)₃, P(OC₆H₄-4-C₉H₁₉)₃, and Ph₂PCH₂CH(CO₂C₁₆H₃₃)CH₂CO₂C₁₆H₃₃ provide ligands for Rh₂(OAc)₄-based catalysts which are insoluble in supercritical CO₂ but which can show high activity and selectivity in the hydroformylation of 1-hexene; removing the products from the reaction by flushing them into a second autoclave and decompressing gives the aldehyde product.²³³ Rh^I complexes [Rh(acac)(CO)(PR₃)] with 1,3,5-triaza-7-phosphatricyclo[3.3.1.1^{3,7}]decane (tpa), tris(2-cyanoethyl)phosphine (cyep), tris(3-sodium sulfonatophenyl)phosphine (TPPTS), tris(*o*-methoxyphenyl)phosphine (ompp), tris(*p*-methoxyphenyl)phosphine (pmpp), tris(2,4,6-trimethoxyphenyl)phosphine (tmpp), PPh₂(pyl), PPh(pyl)₂ and P(pyl)₃ (pyl = 2-pyridyl) have been synthesized and characterized. They are efficient catalysts for hydroformylation of alkenes.²³⁴ 1-Aryl-phospholes [1-(2',4',6'-triisopropylphenyl)-3-methylphosphole, 1-(2',4',6'-tri-*tert*butylphenyl)-3-methyl-phosphole, and 1-(2',4'-di-*tert*butyl-6'-methylphenyl)-3-methylphosphole] were reacted with



$[\text{Rh}(\text{nbd})\text{Cl}]_2$ to give $[\text{Rh}(\text{nbd})(\text{phosphole})\text{Cl}]$ complexes. Both the conversion and the regioselectivity of Rh-catalyzed hydroformylation of styrene show strong dependence on the basicity of the phosphole ligand.²³⁵ 5,11,17,23-tetra-*tert*-butyl-25,26,27,28-tetrakis(2-diphenylphosphinoxy-ethoxy)calix[4]arene and 5,11,17,23-tetra-*tert*-butyl-25,26,27,28-tetrakis(2-diphenylphosphinoethoxy)calix[4]arene have been synthesized. High chemoselectivity was obtained in hydroformylation in the presence of rhodium-containing catalysts with both of the above calixarene-based phosphine and phosphinite ligands.²³⁶

Various bifunctional potentially hemilabile ligands (**72**) bearing phosphorus groups were prepared and their coordination to rhodium was studied. Their effect on the hydroformylation of styrene was assessed.²³⁷

SiO_2 -tethered Rh^{I} -thiolate complex catalysts $\text{Rh-S}/\text{SiO}_2$ and $\text{Rh-S-P}/\text{SiO}_2$ were prepared which exhibit high activity for 1-octene hydroformylation.²³⁸

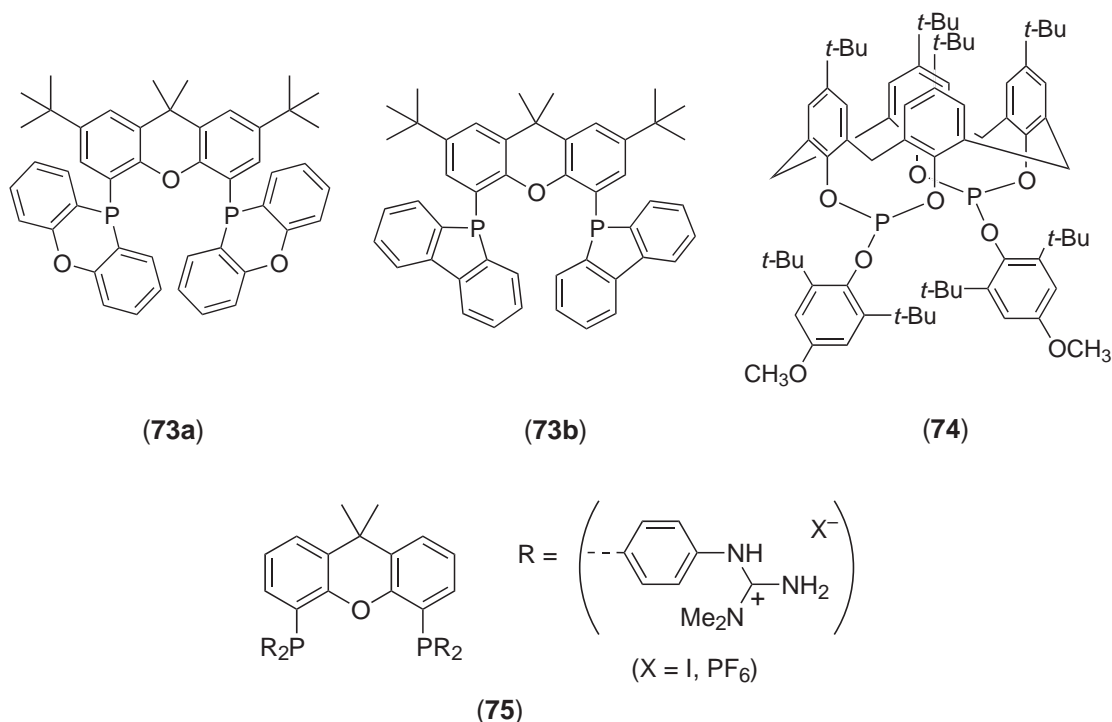
The solution structures of the dominant species present during the styrene hydroformylation using rhodium precursors $[\text{Rh}(\mu\text{-OMe})(\text{COD})]_2$ in the presence of bdpp have been determined. The high-pressure spectroscopic studies have revealed that the mononuclear complex $[\text{HRh}(\text{bdpp})(\text{CO})_2]$ is the predominant species during the hydroformylation process, but the dimeric species $[\text{Rh}(\text{bdpp})(\text{CO})_2]_2$ is also present.²³⁹ Dicarbonylsalicylaldoximato-rhodium $[\text{Rh}(\text{sox})(\text{CO})_2]$ combined with phosphorus ligands exhibits high activity for hydroformylation of alkenes under mild conditions.²⁴⁰ The hydroformylation of 1-decene was studied in the presence of the fluorosoluble $\text{P}[\text{CH}_2\text{CH}_2(\text{CF}_2)_5\text{CF}_3]_3$ -modified rhodium catalyst. HP NMR under 2.1–8.3 MPa of CO/H_2 (1:1) revealed that $\text{HRh}(\text{CO})_2\{\text{P}[\text{CH}_2\text{CH}_2(\text{CF}_2)_5\text{CF}_3]_3\}_2$ is formed.²⁴¹ Copolymers of 4- $\text{Ph}_2\text{PC}_6\text{H}_4\text{CH}:\text{CH}_2$ with $\text{F}_3\text{C}(\text{CF}_2)_7\text{CH}_2\text{CH}_2\text{O}_2\text{CCH}:\text{CH}_2$ in 1:5 or 1:9 ratio have been prepared and shown to be active and selective catalysts when combined with rhodium for the fluorosoluble biphasic hydroformylation of various alkenes.²⁴²

The effect of the bite angle has been reviewed.^{243,244} The ^{103}Rh chemical shifts of a series of hydridorhodiumbis(carbonyl)diphosphine compounds containing chelating bidentate P-ligands have been obtained by inverse HMQC detection sequences.²⁴⁵

The hydroformylation of acetylenic thiophenes is readily accomplished by using the zwitterionic rhodium catalyst $[(\eta^6\text{-C}_6\text{H}_5\text{BPh}_3^-)\text{-Rh}^+(1,5\text{-cod})]$ and triphenylphosphite in the presence of CO and H_2 .²⁴⁶ A hydroformylation catalyst covalently anchored to a silicate matrix by the sol-gel technique was prepared by simultaneous cocondensation of tetraalkoxysilane with functionalized trialkoxysilane, e.g., a diphosphanylphenoxazine derivative.²⁴⁷ Under the reaction conditions, the hydroformylation of 1-octene was studied using *in situ* IR spectroscopy. The intermediate complex is $[\text{HRh}(\text{CO})_x(\text{OPPh}_3)_y]$ ($x + y = 3$ or 4) when ligand OPPh_3 is added to the catalytic system, and dimers and multicarbonyl rhodium complexes are also detected.²⁴⁸ The structure and composition of rhodium dicarbonyl acetylacetonate complexes with the P-containing ligands etriol phosphite, triphenyl phosphite, and PPh_3 , were studied using ^{31}P NMR.²⁴⁹

Phosphacyclic diphosphines (**73a**) and (**73b**) with wide natural bite angles were synthesized and the effect of the phosphacyclic moieties on the coordination chemistry in the $[(\text{diphosphine})\text{Rh}(\text{CO})_2\text{H}]$ complexes was studied. Both NMR and IR spectroscopy showed that the phosphacyclic xantphos ligands exhibit an enhanced preference for diequatorial chelation compared to the diphenylphosphino-substituted parent compound. In the hydroformylation of 1-octene the introduction of the phosphacyclic moieties leads to higher reaction rates. The dibenzophospholy- and phenoxaphosphino-substituted xantphos ligands exhibit a high activity and selectivity in the hydroformylation of *trans*-2- and 4-octene to linear nonanal. CO dissociation rates from the

[(diphosphine)Rh(CO)₂H] complexes were determined using ¹³CO labeling in rapid-scan IR experiments.²⁵⁰



Ionic liquids such as 1-butyl-3-methylimidazolium hexafluorophosphate (BMIM(PF₆)) have been applied to hydroformylation of methyl 3-pentenoate.²⁵¹ The new guanidinium-modified diphosphine ligands (75) with a xanthene backbone show high overall activity and high regioselectivity in the biphasic hydroformylation of 1-octene using (BMIM(PF₆)) as solvent.²⁵² Sulfonated Xantphos ligands have also been applied in ionic liquids (BMI(PF₆)). Using 1-decene a linear branched ratio of 61:1 was obtained for the aldehyde product and a low isomerization was observed. Rates are much higher than in aqueous biphasic catalysis.²⁵³ The use of electron-poor phosphine-substituted cobaltocenium salts as ligands for the biphasic hydroformylation in ionic liquids has been studied. 1,1'-bis(diphenylphosphino)cobaltocenium nitrate, 1,1'-bis(diphenylphosphino)cobaltocenium hexafluorophosphate, and 1,1'-bis[1-methyl(1-diphenylphosphino)ethyl]cobaltocenium hexafluorophosphate were synthesized. 1,1'-bis(diphenylphosphino)cobaltocenium hexafluorophosphate, in particular, proved to be a very suitable ligand for the biphasic hydroformylation of 1-octene in BMIM(PF₆), enabling high catalyst activity and high selectivity to the linear product.²⁵⁴

Bayón and co-workers observed that constrained 1,2-diphosphines such as (3*R*,4*R*)-1-benzyl-3,4-bis(diphenylphosphino)pyrrolidine (deguphos) form dimeric complexes in addition to the expected monomeric complexes.²⁵⁵

Hydroformylation of 1-octene with [Rh(CO)₂(acac)] and ligands (74) as catalysts at 5–20 bar CO/H₂ showed a 99.5% regioselectivity for nonanal.²⁵⁶ The homogeneous hydroformylation of styrene catalyzed by the dihydridorhodium complex [RhH₂(Ph₂N₃)(PPh₃)₂] with synthesis gas (CO/H₂O = 1/1) was carried out in DMSO.²⁵⁷ The tetranuclear early–late heterobimetallic complexes [CpTi(μ₃-S)₃{Rh(diolef)}₃] (diolef = tfbb, cod) in the presence of P-donor ligands are active precursors in the hydroformylation of hex-1-ene and styrene.²⁵⁸

The heterogenization of the zwitterionic Rh^I catalysts [(sulfos)Rh(cod)] and [(sulfos)Rh(CO)₂] [sulfos = ⁻O₃S-*p*-(C₆H₄)CH₂C(CH₂PPh₂)₃; COD = cycloocta-1,5-diene] is performed by controlled adsorption on partially dehydroxylated high surface area silica.²⁵⁹ The reactions of rhodium(I) substrates with the ligands {4-(Ph₂PO)C₆H₄}₂X (I) (X = O, Me₂C, S) have been studied in order to obtain rhodium complexes useful as precatalysts in hydroformylation of alkenes. The results have been explained considering both the flexibility and the number of phosphorus atoms (considering each of them as a monodentate ligand) coordinated to each metal center in the trigonal bipyramidal hydridorhodium intermediates formed.²⁶⁰ Three hitherto unexplored classes of strong π-acceptor

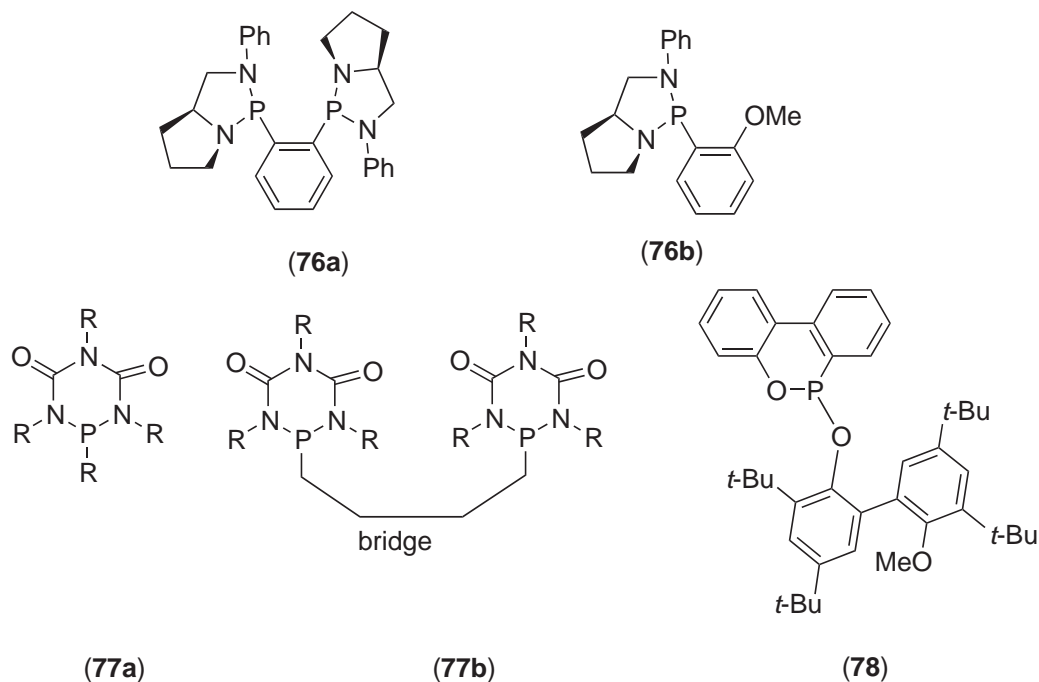
ligands for use in homogeneous catalysis: phospho- π -aromatic compounds, pyrrolyl phosphines, and phosphonium cations were evaluated for Rh catalyzed hydroformylation of styrene.²⁶¹

The novel rhodium complexes with the bidentate PO ligand ($\text{PO} = \text{OC}_6\text{H}_4\text{PPh}_2$) $[\text{Rh}(\text{PO})(\text{CO})\text{L}]$ ($\text{L} = \text{POH}$, PPh_3 , etc.) catalyzes hex-1-ene hydroformylation.²⁶² $\text{Zr}(\eta^5\text{-C}_5\text{H}_5)[\eta^5\text{-C}_5\text{H}_4\text{CMe}_2\text{-}\eta^5\text{-C}_{13}\text{H}_8\text{Rh}(\text{COD})]\text{Cl}_2$ has been used as a hydroformylation and cyclotrimerization catalyst.²⁶³ The preparation and coordinative properties of two upper-rim functionalized calixarenes, 5,17-bis(*tert*-butyl)-11,23-bis(diethoxyphosphinomethyl)-25,26,27,28-tetrakis(2-ethoxyethoxy)calix[4]arene and 5,17-bis(*tert*-butyl)-11,23-bis(diphenylphosphinomethyl)-25,26,27,28-tetrakis(2-ethoxyethoxy)calix[4]arene were reported. Their complexes catalyze the hydroformylation of styrene.²⁶⁴ A polyamine dendrimer containing a 1,4-diaminobutane core was prepared from acrylonitrile, treated with $\text{Ph}_2\text{PCH}_2\text{OH}$ to give diphenylphosphine end groups, and complexed with Pd, Ir, Rh, or Ni to give dendritic complexes. The rhodium complexes were useful as catalysts for hydroformylation.²⁶⁵

Polyamidoamine dendrimers, constructed on the surface of silica, were phosphonated by using diphenylphosphinomethanol, prepared *in situ*, and complexed to rhodium using $[\text{Rh}(\text{CO})_2\text{Cl}]_2$ and used in hydroformylation.²⁶⁶ Cyclodextrin monophosphinite was prepared from cyclodextrin and ClPPh_2 and combined with cyclooctadienylrhodium chloride dimer to give a catalyst that exhibits substrate selectivity in hydroformylation of C-8 and C-10 alkenes due to the inclusion of substrates in the cyclodextrin cavity.²⁶⁷ The reaction of dinuclear rhodium(I) derivatives of formula $[\text{Rh}(\text{DIOL})\text{X}]_2$ with the axially chiral phosphinyl-phosphane 2-(diphenylphosphinyl)-2'-(diphenylphosphanyl)-1,1'-binaphthalene (*S*)-BINAPO led to formation of cationic complexes $[(\text{BINAPO})\text{Rh}(\text{DIOL})]^+$ in which the ligand (*S*)-BINAPO consistently displays a P,O-chelate coordination. The mononuclear rhodium(I) complexes $[\text{Rh}(\text{S-BINAPO})(\text{cod})][\text{BF}_4]$ and $[\text{Rh}(\text{S-BINAPO})(\text{nbd})][\text{BF}_4]$ were isolated. These complexes are active catalysts for the hydroformylation of alkenes.²⁶⁸ Diphenylphosphine functionalized carbosilane dendrimers $\text{Si}((\text{CH}_2)_n\text{-Si}(\text{CH}_3)_2(\text{CH}_2\text{PPh}_2))_4$ ($n = 2, 3$; generation 1–3) and $\text{Si}((\text{CH}_2)_m\text{-Si}(\text{CH}_3)(\text{CH}_2\text{PPh}_2)_2)_4$ ($n = 2, 3$; generation 1–2) have been synthesized and used as ligands in the Rh-catalyzed hydroformylation of 1-octene. The activity of the system depends on the size and flexibility of the dendrimeric ligand.²⁶⁹ $[\text{Rh}(\text{acac})(\text{CO})_2]$ in combination with the bidentate ligand ESPHOS (**76a**) was applied to the asymmetric hydroformylation of vinyl acetate. Use of monodentate ligand SEMI-ESPHOS (**76b**) under the same conditions gave very low yields of essentially racemic product. ESPHOS and SEMI-ESPHOS were effective in styrene hydroformylation, but the product is essentially racemic.²⁷⁰ Three ligands were synthesized, of which the nucleophilicity is ordered as $\text{Ph}_2\text{P}(\text{CH}_2)_4\text{PPh}_2 > \text{Ph}_2\text{P}(\text{O})(\text{CH}_2)_4\text{PPh}_2 > \text{Ph}_2\text{P}(\text{O})(\text{CH}_2)_4\text{P}(\text{O})\text{Ph}_2$. When these ligands were used with $[\text{Rh}(\text{CH}_3\text{CO}_2)_2]_2$ precursor as catalysts in hydroformylation of mixed octenes, the catalytic activities and selectivities to isononylaldehydes reversed completely in the nucleophilicity order of synthesized ligands as mentioned above.²⁷¹ Results of linear alkene and styrene hydroformylation catalyzed by rhodium catalysts containing the ligand 1,4-bis(diphenylphosphino)benzene are reported. The catalyst is highly active and selective (branched product) for styrene.²⁷² Styrene hydroformylation over the rhodium $[\text{Rh}(\mu\text{-OMe})(\text{COD})]_2/\text{bdpp}$ system was studied. *In situ* IR and high-pressure (HP) NMR spectroscopic studies revealed the presence of different species as resting states, depending on the CO-H₂ total pressure.²⁷³ A novel catalyst consisting of encapsulated $[\text{HRh}(\text{CO})(\text{PPh}_3)_3]$ in NaY zeolite was synthesized and characterized using ICP, FTIR, powder XRD, SEM, and TEM methods. Its application to hydroformylation of alkenes (e.g., styrene and 1-hexene) has been demonstrated.²⁷⁴ Two carbene-Rh complexes are reported that are active hydroformylation catalysts, giving very high selectivities for the branched isomer (>95:5) when vinyl arenes were used as substrates. The carbene analog of Wilkinson's catalyst, $[\text{Rh}(\text{IMes})(\text{PPh}_3)_2\text{Cl}]$, ($\text{IMes} = 1,3\text{-dihydro-1,3-bis}(2,4,6\text{-trimethylphenyl})\text{-2H-imidazol-2-ylidene}$), and the related carbonyl complex $[\text{Rh}(\text{IMes})(\text{PPh}_3)(\text{CO})\text{Cl}]$, were both prepared.²⁷⁵

The Rh-catalyzed hydroformylation reaction of 1-octene with phosphorus diamide ligands (**77a**) and (**77b**) has been investigated. Four monodentate phosphorus diamide ligands and six bidentate phosphorus diamide ligands derived from a 1,3,5-trisubstituted biuret structure and various bridge structures have been synthesized. These types of ligand combine steric bulk with π -acidity. The rhodium complexes formed under CO/H₂ have been characterized by high-pressure spectroscopic techniques, which revealed that the monodentate ligands form mixtures of $[\text{HRhL}_2(\text{CO})_2]$ and $[\text{HRhL}(\text{CO})_3]$. The $\text{HRhL}_2(\text{CO})_2:\text{HRhL}(\text{CO})_3$ ratio depends on the ligand concentration and its bulkiness. The bidentate ligands form stable, well-defined catalysts with the structure $[\text{HRh}(\text{L-L})(\text{CO})_2]$ under hydroformylation conditions.²⁷⁶ The rhodium(I) complexes $[\text{HRh}(\text{CO})\{\text{Ph}_2\text{P}(\text{CH}_2)_x\text{Si}(\text{OMe})_3\}_3]$ [$a: x = 3$ or 6] were sol-gel processed with the bifunctional cocondensation agent $(\text{MeO})_3\text{Si}(\text{CH}_2)_6\text{Si}(\text{OMe})_3$ and in a separate reaction also with three

additional equivalents of the phosphine ligand $\text{Ph}_2\text{P}(\text{CH}_2)_x\text{Si}(\text{OMe})_3$. The resulting stationary phases show a relatively narrow particle size distribution.²⁷⁷

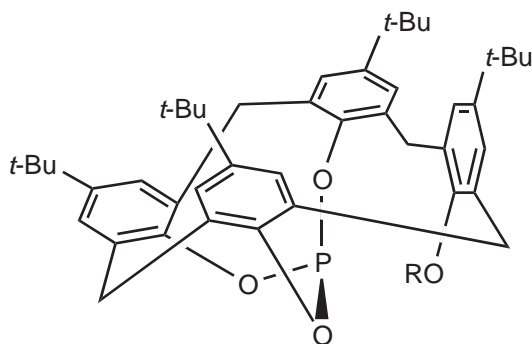


(*acac*)Rh(*cod*) and oxy-functionalized phosphonite ligands, **(78)**, catalyzed the hydroformylation of isomeric *n*-alkenes.²⁷⁸

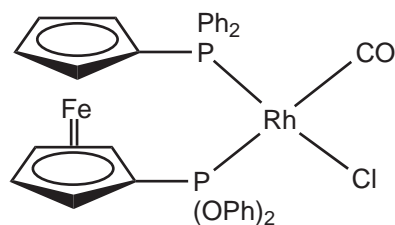
Eight monodentate phosphites **(79)** based on the calix[4]arene backbone were synthesized following two synthetic routes. Out of six conformations, only three were actually formed under the applied reaction conditions. X-ray analysis of two conformers provided insight into the three-dimensional structure of two of these conformations. The three conformations were characterized by NMR spectroscopy. NMR experiments showed that several of the phosphites were flexible showing fluxional behavior of the backbone in solution, but no interconversion between the different conformers was observed. The conformation of the product in the phosphite synthesis is determined at the point where the P atom is linked to two hydroxy groups of the calix[4]arene (P amidite). Such an intermediate P amidite was isolated. Several phosphites were tested in Rh-catalyzed hydroformylation.²⁷⁹ The monophosphites derived from calix[4]arene and *p*-*tert*-butylcalix[4]arene such as **(79)** react with $[\text{Rh}(\text{CO})_2(\text{piv})]$ ($\text{piv} = \text{Bu}^t\text{COCHCOBu}^t$) to give the mononuclear complexes $[\text{Rh}(\text{CO})(\text{L})(\text{piv})]$. The crystal structure of $[\text{Rh}(\text{CO})(\text{L})(\text{piv})]$ shows the calixarene conformation to have aryl groups in {down, out, up, up} orientations with one aryl blocking the axial site at the square planar metal. The rhodium complexes are very active and chemoselective catalysts for the hydroformylation of hexene but the regioselectivity is low.²⁸⁰

A variety of ferrocene-based 1-phosphonite-1'-phosphine ligands **(80)** have been prepared and their rhodium(II) complexes tested in hydroformylation reactions.²⁸¹ $(\text{Cp}-\text{PPh}_2)_2\text{ZrCl}_2$ reacts with dicarbonylrhodium chloride dimer to yield the triply bridged complex, $[\text{ClZr}(\mu\text{-Cp}-\text{PPh}_2)_2(\mu\text{-Cl})\text{Rh}(\text{CO})\text{Cl}]$. $[(\text{Cp}-\text{PPh}_2)_2\text{ZrMe}_2]$ reacts with $[\text{H}(\text{CO})\text{Rh}(\text{PPh}_3)_3]$ with loss of two PPh_3 ligands and instantaneous liberation of methane to form $[\text{CH}_3\text{Zr}(\mu\text{-Cp}-\text{PPh}_2)_2\text{Rh}(\text{CO})\text{PPh}_3]$ (Zr-Rh), which probably contains a metal-metal bond between the early and late transition metal. The latter complex is an active 1-hexene hydroformylation catalyst.²⁸²

Three generations of dendritic phosphines have been prepared from 3,5-diaminobenzoylglycine and 9-fluorenylmethoxycarbonyl-L-phenylalanine. The dendrimers were then attached to MBHA resin, treated with CH_2O and Ph_2PH_2 , and converted to their Rh complexes. The polymer-supported complexes are excellent catalysts for the hydroformylation of alkenes, which could be recycled.²⁸³ The bidentate diphosphine *N,N*-bis-(*P*-(phosphabicyclo[3.3.1]nonan) methyl)aniline was prepared by phosphanomethylation of aniline. It forms a Rh-complex which is a highly regioselective catalyst in the hydroformylation of citronellene.²⁸⁴



(79)



(81)

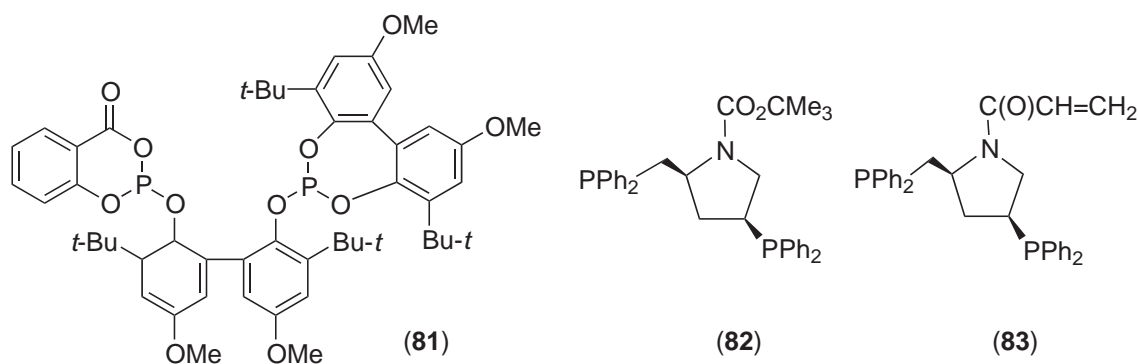
The new bifunctional ligand PhNHC(S)NHCH₂CH₂PPh₂ (Ptu), containing thiourea and the phosphine functions, and its Rh^I complexes [Rh(COD)(Ptu)]X (X = Cl or PF₆; and [Rh(cod)(Ptu)]₂[CoCl₄] were prepared. PtU behaves as a bidentate ligand forming seven-membered chelaten rings in a boat-like conformation. The related ligand (EtO)₃Si(CH₂)₃NHC(S)NHCH₂CH₂PPh₂ (SiPtU) was sol-gel processed giving xerogels. Anchored Rh^I complexes were active catalysts for the hydroformylation of styrene.²⁸⁵

The bite angle effect on rhodium diphosphine-catalyzed hydroformylation has been investigated. Xantphos-type ligands with natural bite angles ranging from 102° to 121° have been synthesized, and the effect of the natural bite angle on coordination chemistry and catalytic performance was studied. X-ray crystal structure determinations of the complexes [(nixantphos)Rh(CO)H(PPh₃)] and [(benzoxantphos)Rh(CO)H(PPh₃)] were obtained.²⁸⁶ The hydroformylation of 1-hexene with syngas (40 bar of 1:1 CO/H₂) in the presence of the catalyst precursor [RhH(CO)(PPh₃)₃] has been studied by HP NMR spectroscopy.²⁸⁷

First to fourth generation dendrimers were constructed on silica gel from acrylate and H₂N(CH₂)_nNH₂ [n = 2, 4, 6, 12]. The dendrimers were complexed with [Rh(CO)Cl]₂ and used to catalyze the hydroformylation of styrene and vinyl acetate.²⁸⁸ A tetramethoxy hemilabile N,P,N-ligand, and the corresponding amphiphilic tetrahydroxy ligand, have been synthesized via *ortho*-lithiation of *N,N*-bis(2-methoxyethyl)-benzenamine and *N,N*-bis[2-(methoxymethoxy)ethyl]-benzenamine, respectively. The rhodium complex of the former ligand was applied to hydroformylation of styrene and the complex of the latter ligand was evaluated in the hydrogenation of *trans*-cinnamaldehyde.²⁸⁹ Rhodium diphosphine systems, including chiral ones, were used as catalyst precursors for the hydroformylation of 2,5-dihydrofuran. The solution structures of the species present have been investigated spectroscopically through HP NMR experiments during the hydroformylation reaction.²⁹⁰ The compounds (C₆H₄O₂P)₂NN, (Ph₂P)₂NN, and (iPr₂P)₂NN (where NN = homopiperazine) prepared and in presence of Et₃N have been tested in Rh-catalyzed hydroformylation.²⁹¹ Phosphinine/rhodium catalysts for the hydroformylation of terminal and internal alkenes were presented. *Trans*-[(phosphabenzene)₂RhCl(CO)] complexes have been prepared. The hydroformylation of oct-1-ene has been used to identify optimal catalyst preformation and reaction conditions. Hydroformylation studies with 15 monophosphabenzene complexes have been performed. *In situ* pressure NMR experiments have been performed to identify the resting state of the catalyst. A monophosphabenzene complex [(phosphinine)Rh(CO)₃H] could be detected as the predominant catalyst resting state.²⁹² A rhodium complex containing a 16-membered chelated diphosphite, with the appropriate combination of stereogenic centers, produces ees above 70% in the hydroformylation of vinylarenes, while a related diastereoisomeric ligand renders very low ees because it does not form a chelated species.²⁹³ The geometry optimization for 1-phenyldibenzophosphole (PDBP) and triphenylphosphine were carried out using quantum chemical AM1 method.²⁹⁴

The results of unsymmetrical π-acid bidentate ligands, e.g., (81), have in the hydroformylation of *n*-octenes was described. The preparation of seven such ligands was described. Thus, [Rh(acac)(cod)]-catalyzed hydroformylation of *n*-octene in the presence of a phosphinite ligand gave 94% *n*-nonanal.²⁹⁵ A new upper-rim phosphacalix[4]arene 5,17-bis(diphenylphosphinomethyl)-25,26,27,28-tetrapropoxycalix[4]arene has been prepared. It reacted with [(cod)RhCl]₂ to give a dirhodium complex that is an active catalyst for the hydroformylation of 1-octene and styrene.²⁹⁶ Rhodium complexes of [1-propyl-3-methylimidazolium]⁺₂ [PhP(C₆H₄SO₃⁻)₂] dissolved in the

ionic liquid, BMIM (PF₆) catalyze the hydroformylation of 1-octene at a constant rate for >20 h in a continuous flow process in which the substrate, gases, and products are transported in and out of the reactor dissolved in scCO₂.²⁹⁷ Two new cationic rhodium(I) complexes with a hemilabile nitrogen-containing bis(phosphinite), PhN(CH₂CH₂OPPh₂)₂, or bis(phosphine), PhN(CH₂CH₂PPh₂)₂, ligand have been prepared. Phosphorus-31 NMR studies provide evidence that the ligands are coordinated to the metal in a P,P-bidentate mode, whereas for the *bis*(phosphine)-based ligand, a P,N,P-tridentate mode is also found at low temperatures. The complexes were applied to the hydroformylation of styrene and displayed a high chemoselectivity for aldehydes with a very good branched/linear ratio.²⁹⁸ Effects of *ortho*-alkyl substituents of TPP on the Rh-catalyzed hydroformylation have been investigated.²⁹⁹ Bisphosphines containing two electron-donating alkyl groups linked by a diamine backbone are extremely electron-rich σ -donor bidentate ligands and have been used, along with Ph- and catechol-substituted bis-phosphinoamines, to study hydroformylation reactions.³⁰⁰ A series of PPh₃ derivatives modified with different heteroatom groups in the *ortho* or *para* position of the Ph ring(s) were synthesized and tested for their catalytic behavior in the rhodium catalyzed hydroformylation of 1-hexene and propene. The ligands thus studied were [(2-methylthio)phenyl]diphenylphosphine, [(4-methylthio) phenyl]diphenylphosphine, 2-(diphenylphosphino) -*N,N*-dimethylbenzenamine, [(2-methylseleno) phenyl]diphenylphosphine, (2-methoxyphenyl)diphenylphosphine, diphenyl[2-(trifluoromethyl)-phenyl]phosphine, tris[2-(trifluoromethyl) phenyl]phosphine, and tris[4-(trifluoromethyl)phenyl] phosphine.³⁰¹



Cluster complexes [M₂Rh(μ -PCy₂)(μ -CO)₂(CO)₈] were used as hydroformylation catalysts.³⁰² The stepwise intramolecular hydroformylation reaction of allyldiphenylphosphine using a monodentate phosphorus diamide-based Rh catalyst was studied using NMR spectroscopy. Reaction of the Rh-hydride complex [HRhL₃(CO)] (L = triethylbiuretphenylphosphorus diamide) with allyldiphenylphosphine gave [HRhL₂(allylPPh₂)(CO)]. Hydride migration gives a cyclic Rh-alkyl complex. CO insertion occurs giving the cyclic Rh-acyl complex [Rh(COCH₂CH₂CH₂PPh₂)L(CO)₂]. Addition of H₂ completes the cycle forming the coordinated hydroformylated allyldiphenylphosphine ligand. The aldehyde-functionalized phosphine ligand is hydrogenated to the alcohol.³⁰³ The reaction of the amphiphilic ligand [4-[bis(diethylaminoethyl)aminomethyl]diphenyl]phosphine with zirconium phosphate, of intermediate surface area, provided a phosphine-functionalized support in which electrostatic interaction between ammonium groups on the ligand and de-protonated surface hydroxy groups on the support provided the binding force. When applied as catalyst in continuous gas-phase hydroformylation of propene, and in liquid phase hydroformylation of 1-hexene, the immobilized complex showed intermediate activity and regioselectivity.³⁰⁴ The synthesis and the effect of phosphite-phosphonate ligands in the Rh-catalyzed hydroformylation of styrene have been reported. The activity and selectivity of the catalyst are improved at low temperatures by increasing the bulk of both phosphite and phosphonate moieties.³⁰⁵ The mechanism of the Rh-catalyzed hydroformylation reaction using a monodentate P diamide ligand (1,3,5-triethyldihydro-2-phenyl-1,3,5,2-triazaphosphorine-4,6(1H,5H)-dione) was studied. Which step is rate determining depends strongly on the conditions used. The Rh hydride complex [HRhL₂(CO)₂] and several Rh-acyl complexes were observed during the hydroformylation reaction. The exchange rates of the equatorial and apical carbonyl ligands with dissolved CO differ significantly, the equatorial CO ligands being much more labile.³⁰⁶ The homogeneously catalyzed styrene hydroformylation in supercritical carbon dioxide was studied and it was shown that the reaction rate and the regioselectivity can be varied by changes in pressure at constant temperature.³⁰⁷

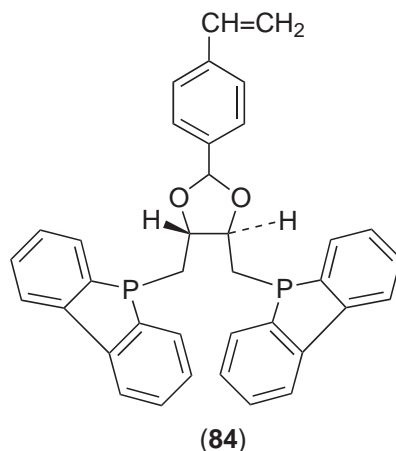
9.3.3.5 Asymmetric Catalysis Using Platinum

Platinum complexes with chiral phosphorus ligands have been extensively used in asymmetric hydroformylation. In most cases, styrene has been used as the substrate to evaluate the efficiency of the catalyst systems. In addition, styrene was of interest as a model intermediate in the synthesis of arylpropionic acids, a family of anti-inflammatory drugs.^{308,309} Until 1993 the best enantioselectivities in asymmetric hydroformylation were provided by platinum complexes, although the activities and regioselectivities were, in many cases, far from the obtained for rhodium catalysts. A report on asymmetric carbonylation was published in 1993.³¹⁰ Two reviews dedicated to asymmetric hydroformylation, which appeared in 1995, include the most important studies and results on platinum-catalyzed asymmetric hydroformylation.^{80,81} A report appeared in 1999 about hydrocarbonylation of carbon-carbon double bonds catalyzed by Pt^{II} complexes, including a proposal for a mechanism for this process.³¹¹

9.3.3.5.1 Chiral diphosphine ligands

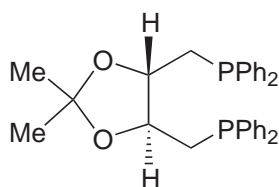
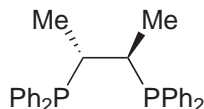
The *cis*-PtCl₂(diphosphine)/SnCl₂ constitutes the system mostly used in catalyzed hydroformylation of alkenes and many diphosphines have been tested. In the 1980s, Stille and co-workers reported on the preparation of platinum complexes with chiral diphosphines related to BPPM (**82**) and (**83**) and their activity in asymmetric hydroformylation of a variety of prochiral alkenes.^{312–314} Although the branched/normal ratios were low (0.5), ees in the range 70–80% were achieved in the hydroformylation of styrene and related substrates. When the hydroformylation of styrene, 2-ethenyl-6-methoxynaphthalene, and vinyl acetate with [(–)-BPPM]PtCl₂·SnCl₂ were carried out in the presence of triethyl orthoformate, enantiomerically pure acetals were obtained.

Chiral ligands, e.g., (**83**) and (**84**) were copolymerized with styrene (or with SDT). Hydroformylation in the presence of triethyl orthoformate could be carried out by using a catalyst containing the [(–)-BPPM]PtCl₂·SnCl₂ complex bound to 60 μm beads composed of cross-linked polystyrene.³¹² Hydroformylation utilizing the polymer-supported catalysts showed comparable rates, and gave nearly the same optical yields, as the homogeneous analogs although they had lower regioselectivities.³¹⁵

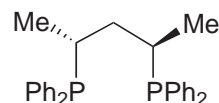


Platinum(II) complexes with diphosphines based on DIOP (**85**),^{315–321} CHIRAPHOS (**86**),^{316,320} and bdpp (**87**)^{322–325} backbones have been prepared to be used, in the presence of SnCl₂, as catalyst precursors in asymmetric hydroformylation of styrene and other alkenes.

1-Butene and styrene were hydroformylated with Pt catalysts using CHIRAPHOS (**86**) as the chiral ligand. The results were compared with those obtained when the chiral ligand is 4*R*,5*R*-DIOP.³¹⁶ [PtCl(SnCl₃){(*R,R*)-DIOP}] (**88**) was used in the asymmetric hydroformylation of butenes. Depending on the conditions, hydroformylation can be accompanied by extensive isomerization and hydrogenation of the substrate. Enantiomeric excess and regioselectivity depend on the extent of conversion, providing as best ee 46.7%.³¹⁷ Vinylidene esters such as CH₂=C(CO₂Me)CH₂CO₂Me are hydroformylated by (**88**), and (*R*)-OHCCH₂CH

(85) *S,S*-DIOP

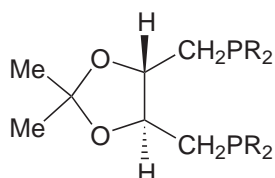
(86)

(87) *(R,R)* BDPP

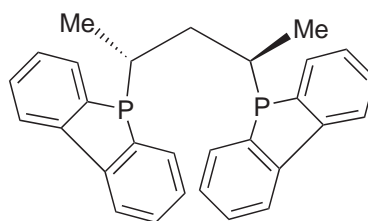
(CO₂Me)CH₂-CO₂Me was regioselectively prepared in >82% enantiomeric excess by homogeneous catalytic hydroformylation. For other vinylidene esters, the asymmetric induction was lower.³¹⁸

[Pt(CH₂)₂{(+)-DIOP}] (**89**), [PtCl₂{(+)-DIOP}] (**90**), or [PtCl₂{(±)-DIOP}] (**91**) were used as catalyst precursors for the hydroformylation of styrene and 1-hexene. A mixture of (**89**) and (**90**) hydroformylates styrene with 49% overall yield; the product contains 32.5% of linear aldehyde and the optical purity of the (*R*)-PhCHMeCHO was 28%. The hydroformylation of 1-hexene over the same catalyst gave Me(CH₂)₅CHO and (*R*)-Me(CH₂)₃CMeCHO in 64% overall yield; whereby the product contained 86.5% Me(CH₂)₅CHO and the optical purity of the (*R*)-Me(CH₂)₃CH₂CHO was 11%.

Alkylated diphosphines (*R,R*)-(**92**) and (**93**) were used as chiral ligands in the Pt-catalyzed hydroformylations of some alkenic substrates. These ligands bring about a loss of catalytic activity with respect to the corresponding diphenylphosphine homolog, particularly in the case of the platinum systems. The regioselectivity favors the straight-chain (or less branched) isomer in the case of terminal alkenes with the exception of styrene; the enantioselectivity is very low in all cases.³²⁰



(92) R = ethyl
(93) R = cyclohexyl

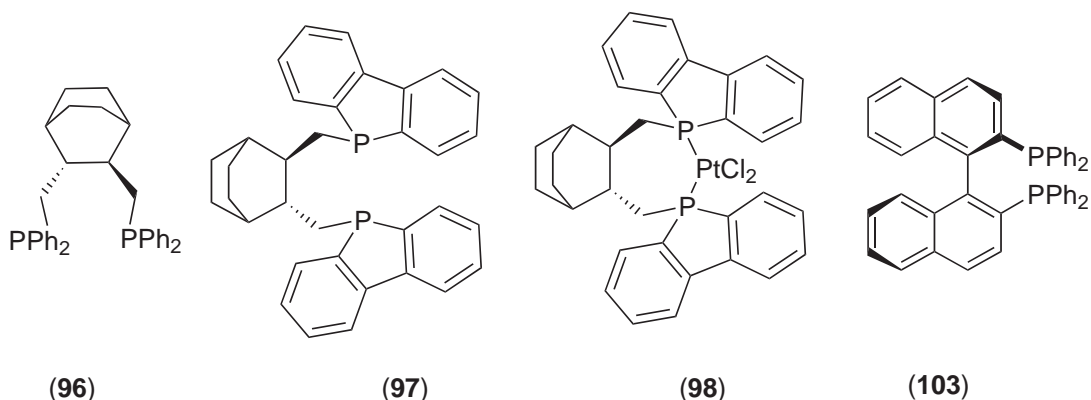


(94)

The platinum complexes *cis*-[PtCl₂(*S,S*)-(**87**)] and *cis*-[PtCl(SnCl₃)((*S,S*)-(**87**))] were prepared to be used as catalyst precursors in asymmetric hydroformylation.^{322–325} Tin(II) fluoride was used as co-catalyst with Pt(II) complexes containing (*S,S*)-(**87**) as chiral ligand giving a catalytic system of unusually high stability. Although the addition of 2-diphenylphosphinopyridine to the catalytic system strongly reduces the catalytic activity, the (*S,S*)-bdpp-2-diphenylphosphinopyridine “mixed-phosphine system” gave 86.7% ee.³²² Tin(II) triflate (or silver triflate) were also used as co-catalyst using the optically active Pt-(*S,S*)-(**87**) systems.³²⁵

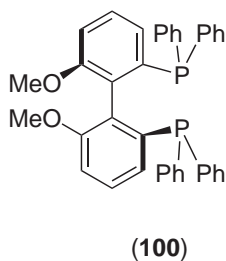
The reaction of PtCl₂(diphosphine) with mono- and bidentate phosphines has been investigated by NMR spectroscopy. [Pt(diphosphine)(PMe₃)₂]²⁺, [Pt(diphosphine)]₂²⁺, and [Pt((*S,S*)-(**87**))((*S,S*)-(**86**))]²⁺ cations have been characterized by ³¹P NMR. The presence of tin(II) chloride promotes the formation of the complex cations. Evidence for coordination of the diphosphine in monodentate mode has been obtained by NMR spectroscopy. The platinum species possessing a platinum–tin bond and ionic complexes with an SnCl₃[−] counterion can easily be distinguished by ¹¹⁹Sn Mossbauer spectroscopy. Asymmetric hydroformylation of styrene with [Pt((*S,S*)-(**87**))₂]²⁺(SnCl₃[−])₂ as catalyst precursor gave chemo-, regio-, and enantioselectivities different from those obtained with the covalent *cis*-[PtCl(SnCl₃)((*S,S*)-(**87**))] as catalyst precursor.³²³

Unlike bis(diphenyl)phosphine derivatives in general, (*2S,4S*)-pentane-2,4-diyl-bis(5*H*-dibenzo[b]phosphindole), (*S,S*)-BDBPP (**94**), gives a *trans* oligomeric compound. [PtCl₂(*S,S*-BDBPP)]_{*n*} (**95**), in reaction with precursors such as [PtCl₂(PhCN)₂], [PtCl₂(CH₃CN)₂], and [PtCl₂(COD)]. Compound (**95**), which could be readily isolated, slowly rearranges in solution to the expected *cis*-monomer. SnCl₂ adducts of both compounds, *trans*-[PtCl(SnCl₃)(*S,S*-BDBPP)]_{*n*}, and *cis*-[PtCl(SnCl₃)(*S,S*-BDBPP)], as well as (**95**), were tested as catalysts in the asymmetric hydroformylation of *p*-isobutylstyrene. The



(diphenyl)phosphine analogue provided up to 75% ee but only moderate yields of the chiral 2-(4-isobutylphenyl)-2-propanal. Compared to this, the regioselectivity to the branched aldehyde is remarkably increased, but the enantioselectivity is drastically decreased by the use of the dibenzophosphole derivatives. The X-ray crystal structure of *cis*-monomer shows a half-chair conformation for the chelate ring with a symmetric arrangement of dibenzophosphole groups.³²⁴

Platinum dichloride complexes containing the ligands (96) or (97) have been prepared for further reaction of the PtCl₂ with the corresponding ligands.^{326,327} Complexes such as (98) have been tested in the presence of SnCl₂ as catalyst precursors for the enantioselective hydroformylation of alkenes. The catalytic activity was high, and the capacity for enantioface discrimination was the highest reported for hydroformylation of styrene and 1-butene. Excellent regioselectivity in the case of styrene was achieved and asymmetric inductions up to 85% have been obtained.



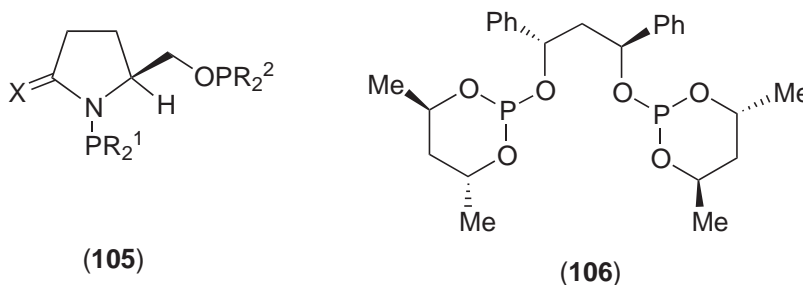
Asymmetric hydroformylation of styrene with PtCl₂(atropisomeric diphosphine)/SnCl₂ systems has been reported.^{328–330} The chiral complex [PtCl₂{(*S*)-(-)-MeOBIPHEP}] (99), where MeOBIPHEP is the atropisomeric diphosphine 2,2'-bis(diphenylphosphino)-6,6'-dimethoxy-1,1'-biphenyl (100), has been synthesized. In the presence of SnCl₂, this species is an efficient catalyst for the asymmetric hydroformylation of styrene. Asymmetric inductions are higher than those attainable using the system [PtCl₂{(*R*)-(+)-BINAP}]/SnCl₂, where BINAP is 2,2'-bis(diphenylphosphino)-1,1'-binaphthyl. The influence of CO and H₂ partial pressures on the catalytic activity of the (99)/SnCl₂ system has also been studied.³²⁸ Complexes [PtMeCl(P-P)] [(101), P-P = (*S*)-6,6'-(dimethoxybiphenyl)-2,2'-diylbis(diphenylphosphine) ((*S*)-MOBIPH); (102), P-P = (*R*)-BINAP; (103), P-P = (*S,S*)-(85)] in the presence of SnCl₂ catalyze the asymmetric hydroformylation of styrene to give the desired branched aldehyde with moderate regioselectivity. Enantioselectivities up to 75% were obtained using (102). The carbonylation of [PtMe(SnCl₃){(*S*)-MOBIPH}] has been studied. This reaction affords a mixture containing the cationic alkyl complex [PtMe(CO){(*S*)-MOBIPH}]⁺[SnCl₃]⁻ and the neutral acyl species [Pt(COCH₃)(SnCl₃){(*S*)-MOBIPH}]. The carbonylation of [PtMe(SnCl₃){(*R*)-BINAP}] proceeds in the same fashion to give [PtMe(CO){(*R*)-BINAP}]⁺[SnCl₃]⁻ and [Pt(COCH₃)(SnCl₃){(*R*)-BINAP}].³²⁹ Temperature dependence of the asymmetric induction in the [PtCl(SnCl₃){(-)-(*S,S*)-(87)}] and [PtCl₂{(*S*)-BINAP}]-catalyzed enantioselective hydroformylation reaction has been studied.^{330,331} The strong temperature dependence of the absolute configuration of the 2-phenylpropanal formed in hydroformylation of styrene catalyzed by [PtCl₂{(*S*)-BINAP}] is explained by the restricted rotation of the Ph rings on the basis of a dynamic NMR study.³³¹

9.3.3.5.2 Aminophosphine-phosphinite ligands

Aminophosphine phosphinite ligands are easily prepared from amino acid or amino alcohol precursors. These ligands are good auxiliary agents for asymmetric induction during several catalytic homogeneous reactions such as hydroformylation of alkenes with platinum complexes.^{332–335} The coordination chemistry and catalytic activity in homogeneous catalysis of the complexes containing these aminophosphine-phosphinite ligands have been reviewed.^{77–79,336,337}

Asymmetric hydroformylation of styrene using $\text{PtL}_2\text{Cl}_2\text{-SnCl}_2$ (L = aminophosphine-phosphinite ligands based on pyrrolidine, (*S*)-prolinol, and (*S*)-oxoprolinol) were synthesized and used as chiral auxiliaries for the platinum- and Rh-catalyzed enantioselective hydroformylations of styrene.^{335–337} The activities and selectivities depend on the nature of the ligand and the asymmetric inductions up to 48% have been obtained. A crystal structure of the complex [(*S*)-*N*-(2,2'-biphenoxyphosphino)-2-(2,2'-biphenoxyphosphinoxymethyl)pyrrolidine]dichloroplatinum(II) is described.³³⁵

The optically active complexes $[\text{PtCl}_2(\mathbf{105})]$ ($\mathbf{104a-g}$) ($\text{X} = \text{O}$, 2H; R^1 , $\text{R}^2 = \text{Ph}$, cyclohexyl, cyclopentyl) were prepared in high yields from the corresponding ligands (**105**) and $[\text{Pt}(\text{cod})\text{Cl}_2]$. The structure of (**104a**) was determined. The Pt atom has a *cis* square planar coordination, with angular distortions due to steric factors. ^1H , $^{13}\text{C}\{^1\text{H}\}$, and $^{31}\text{P}\{^1\text{H}\}$ NMR spectra of the complexes are also reported.³³⁴ Various branched/normal ratios (0.4–0.8) and enantiomeric excess values (40–56%) were obtained. Probably the catalytic activity of the complexes (**104**) is affected mainly by the aminophosphine moiety of the ligand (highest catalytic activities observed with *N*-diphenylphosphino substituents), whereas the enantioselectivity depends on the nature of the phosphinite part (best optical yields observed with (dicyclohexylphosphino)oxy substituents).³³⁴



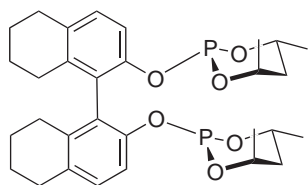
9.3.3.5.3 Diphosphite ligands

Several types of chiral diphosphite ligand have been synthesized and tested in Pt-catalyzed asymmetric hydroformylation.^{338–341}

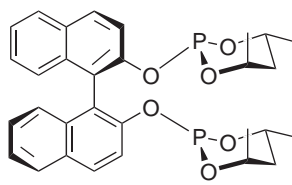
Diphosphite ligands containing six stereogenic centers, e.g., (**106**), were synthesized and tested in order to study chiral cooperativity in the Rh- and Pt-catalyzed asymmetric hydroformylation of styrene. The chirality was varied both in the chelate backbone and in the terminal groups of the ligands. In case of Pt-catalyzed hydroformylation, the stereogenic elements in the bridge were found to determine the product configuration with a cooperative effect from the terminal groups when the constellations were matched giving a maximum ee of 40%. Some coordination chemistry and the crystal structure determination of these ligands were also reported.³³⁴

Diastereomeric diphosphites (**107**)–(**110**) were prepared by the reaction of enantiomerically pure 2,2'-dihydroxy-5,5',6,6',7,7',8,8'-octahydro-1,1'-binaphthyl or 2,2'-dihydroxy-1,1'-binaphthyl with chlorophosphites. The structure of *R*-bis-(4*R*,6*R*)-(**107**) was determined by XRD. The diphosphites were tested in the Pt- and Rh-catalyzed asymmetric hydroformylation of styrene.

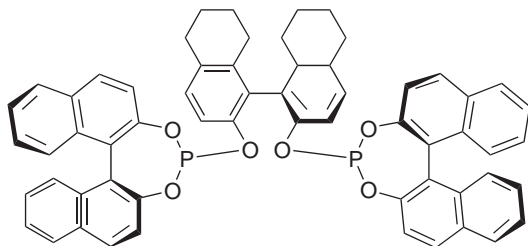
Systematic variation in chirality at both the chelate backbone and the terminal groups revealed a remarkable effect on the enantioselectivity of the catalysts. Ligand (**109**) generates chiral cooperativity between the backbone and the terminal moieties in Pt-catalyzed hydroformylation. The highest ee (65%) for 2-phenylpropanal was found for the ligand *R*-bis(*S*)-(**110**) in combination with Pt. The chemoselectivities with all ligands described in association with Pt were rather low. The comparative



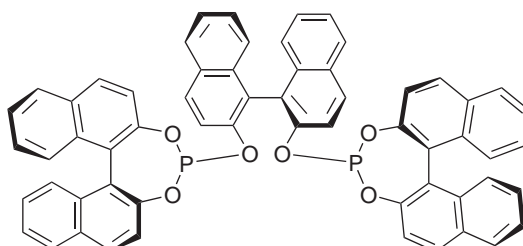
(107)



(109)



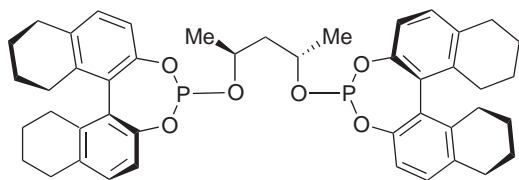
(108)



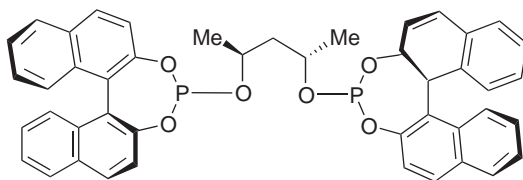
(110)

study clearly showed that the Pt complexes of diphosphites (107)–(110) gave higher enantioselectivities than the corresponding Rh complexes in the asymmetric hydroformylation of styrene.³³⁹

The influence of steric and electronic effects of diphosphites (111) and (112) have been studied with regard to their catalytic performance on the hydroformylation of styrene catalyzed by platinum complexes. The highest chemoselectivity to aldehyde (71%) and regioselectivity to branched aldehyde (85%), with an enantiomeric excess of 86%, was obtained with the platinum(II)–SnCl₂ catalytic system associated with ligand (2*S*,4*S*)-bis(*S*)-(111).³⁴⁰



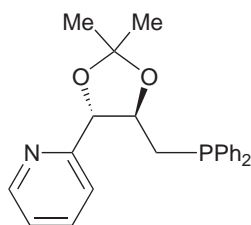
(111)



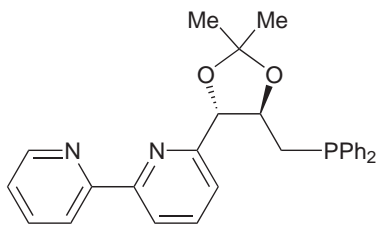
(112)

9.3.3.5.4 Miscellaneous

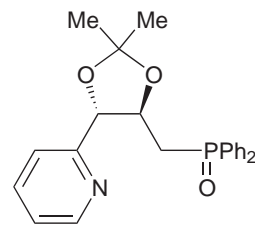
Homochiral pyridyl, bipyridyl, and phosphino derivatives of 2,2-dimethyl-1,3-dioxolane (113)–(115) were prepared from *L*-(+)-tartrate. These compounds were assessed in metal-catalyzed asymmetric hydroformylation of styrene; enantioselectivity was generally low.³⁴²



(113)

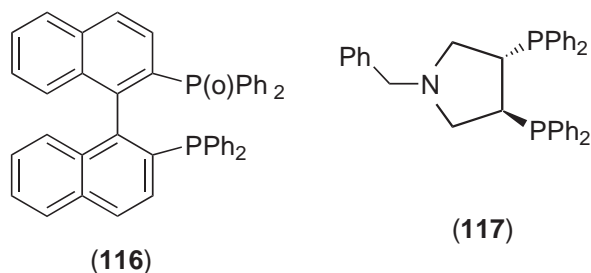


(114)



(115)

Platinum(II) complexes with ligand, the axially chiral P,O-heterodonor phosphinyl-phosphine ligand (*S*)-BINAPO (**116**) were prepared and their behavior in solution was studied by ^{31}P NMR spectroscopy. Reaction of $\text{PtCl}_2(\text{PhCN})_2$ with benzene gives a neutral complex, $[\text{PtCl}_2((S)\text{-BINAPO})]$ (**116**), which maintains the P,O-chelate coordination of the ligand even in solvents of low polarity. The hemilabile character of the ligand is apparent from the reactions with DMSO and carbon monoxide, which promote the cleavage of the chelate ring through displacement of the oxygenated arm. Insertion of tin(II) chloride into the Pt–Cl bond takes place readily at room temperature affording only one of the possible trichlorostannate derivatives $[\text{PtCl}(\text{SnCl}_3)((S)\text{-BINAPO})]$. In the presence of SnCl_2 , $[\text{PtCl}_2((S)\text{-BINAPO})]$ gives a hydroformylation catalyst that produces 30% ee, with the branched aldehyde as the prevalent product.³⁴³



Chiral bis-(binaphthophosphole) (bis(BNP)) ligands have been used in the asymmetric hydroformylation of styrene. In solution, the free diphospholes display fluxional behavior. Consistent with their structure, the reaction of the bis(BNP) compounds with platinum(II) derivatives gives either *cis* chelate mononuclear complexes or *trans* phosphorus-bridged polynuclear derivatives. Coordination to platinum enhances the conformational stability of bis(BNP)s and diastereomeric complexes can be detected in solution. In the presence of SnCl_2 , the platinum complexes give rise to catalysts that exhibit remarkable activity in the hydroformylation of styrene. Under optimum conditions, reaction takes place with high branched selectivity (80–85%) and moderate enantioselectivity (up to 45% ee).³⁴⁴

9.3.3.6 Asymmetric Catalysis Using Rhodium

Most of the reports on Rh-catalyzed asymmetric hydroformylation are concerned with asymmetric hydroformylation of vinyl aromatics, which are model substrates of interest to the pharmaceutical industry. In 1993 and 1995, reports were published describing the state of the art in hydroformylation with both rhodium and platinum systems.^{80,81,310} Two reports appeared in 1999 and 2000 on carbonylation and rhodium asymmetric hydroformylation respectively.^{311,345}

Modified rhodium systems show considerable activity in the hydroformylation of styrene to the branched aldehydes. Chiral diphosphines, diphosphites, and phosphine-phosphites have been the ligands most studied. Hydroformylation experiments have often been performed “*in situ*” but the characterization of intermediates has provided an interesting contribution to coordination chemistry.¹⁷⁹

9.3.3.6.1 Diphosphines as chiral ligands

Many chiral diphosphines have been used as ligands in rhodium systems for asymmetric hydroformylation. Although chiral diphosphine rhodium complexes lead to high activity and to high regioselectivity for branched aldehydes, chiral diphosphines providing high enantioselectivities in asymmetric hydrogenation lead to low enantioselectivity in hydroformylation. Stanley reported that a tetraphosphine ligand can be used to form a bimetallic complex and provide ees up to 85% using vinyl esters.³⁴⁶

CHIRAPHOS (**86**), bdpp (**87**), DIOP (**85**), deguphos (**117**), and related chiral diphosphines have been used as ligands in asymmetric hydroformylation of styrene and related substrates.^{255,347–349}

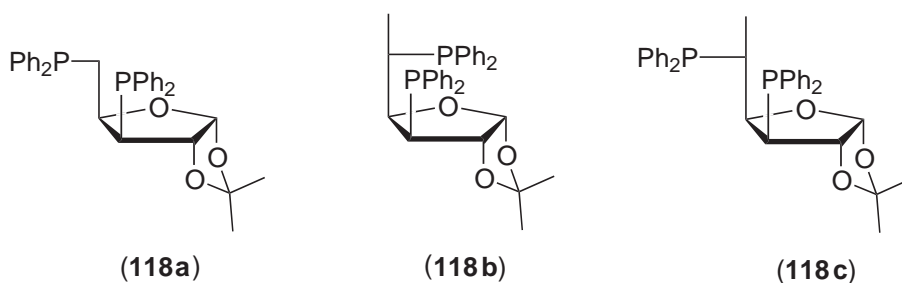
The hydroformylation of styrene using rhodium systems containing the four structurally related diphosphines dppe, dppp, (**86**), and (**87**) has been studied. A systematic analysis of the effect of the pressure, temperature, and the ligand:metal molar ratio shows that the five- and six-membered ring chelating diphosphines behave differently from one another.³⁴⁷ An analysis of the effect of pressure, temperature, and ligand:metal molar ratio on the selectivity of styrene hydroformylation catalyzed

by rhodium and (116) was carried out. An NMR study was performed in order to elucidate the species formed under catalytic reaction conditions.²⁵⁵ The highest enantioselectivities for these type of diphosphines in symmetric hydroformylation of styrene has been achieved using (+)-bdpp (87) as the chiral auxiliary ligand (ee 60%).³⁴⁸ HP NMR and *in situ* IR spectroscopic techniques have been used to study the species present in the hydroformylation of styrene by rhodium diphosphine systems. Rhodium precursors containing (87) and (86) as the chiral ligands were used.³⁴⁹

The use of a variety of chiral ferrocenylethyl diphosphines and a Rh^I precursor for the asymmetric hydroformylation of styrene has been described. Some of these catalysts yield chiral 2-phenylpropionic aldehyde with enantioselectivity up to 76% ee but at low conversion rates. The selectivity and activity of the catalysts are influenced by the substitution pattern of the phosphines.³⁵⁰ Zwitterionic rhodium catalysts have been applied as precursors in asymmetric hydroformylation for the preparation of several intermediates.^{351,352} The catalytic system consisting of a zwitterionic rhodium catalyst, [(nbd)Rh⁺(C₆H₅B-Ph₃⁻)], and (*S,S*)-bdpp, gave branched aldehydes with high regio- and stereoselectivity. The hydroformylated products are key intermediates in the synthesis of 1-methylcarbapenem antibiotics.³⁵² Rhodium and ruthenium complexes with enantiomerically pure BINAP and related 1,1'-binaphthyl chiral ligands have been used as precursors for asymmetric hydroformylation. The enantiomeric excesses obtained are in general low.³⁵³⁻³⁵⁵

[Rh(acac)(CO)₂] in combination with ESPHOS (76a) was applied in the asymmetric hydroformylation of vinyl acetate with excellent results. ESPHOS was effective in styrene hydroformylation, but the product is essentially racemic.²⁷⁰

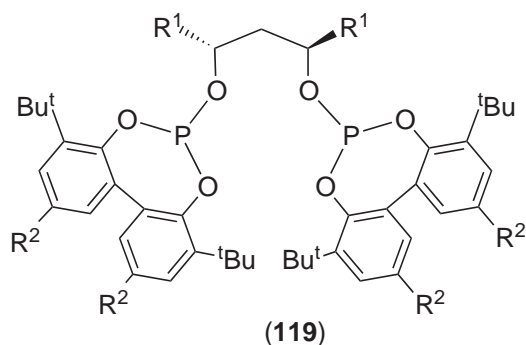
Rhodium complexes with diphosphines derived from carbohydrates as ligands have been studied as catalytic precursors in asymmetric hydroformylation. The chiral ligand 1,6-anhydro-2,4-bis(diphenylphosphino) β -D-(glucopyranose), prepared from D-glucose, was used to prepare a chiral rhodium catalyst. For vinyl acetate, the catalytic hydroformylation gave high enantioselectivity (92% ee), and high regioselectivity (b/n = 95/5). The high stereoselectivity in the hydroformylation of vinyl acetate was explained in terms of hydrogen bonding between the ligand and the carbonyl group of vinyl acetate.³⁵⁶ Chirality transfer by furanose diphosphines (118) was investigated in Rh-catalyzed asymmetric hydroformylation. In general, they induced high regioselectivities with branched aldehydes and moderate enantioselectivities of up to 58%. Improved activities were seen when a methyl substituent was introduced at C-5 of the sugar residue. Variation of the configuration at C-5 suggests that there is a cooperative effect between stereocenters, which results in a matched combination for the ligand with (*R*)-configuration at the C-5 stereogenic center.³⁵⁷



9.3.3.6.2 Diphosphite ligands

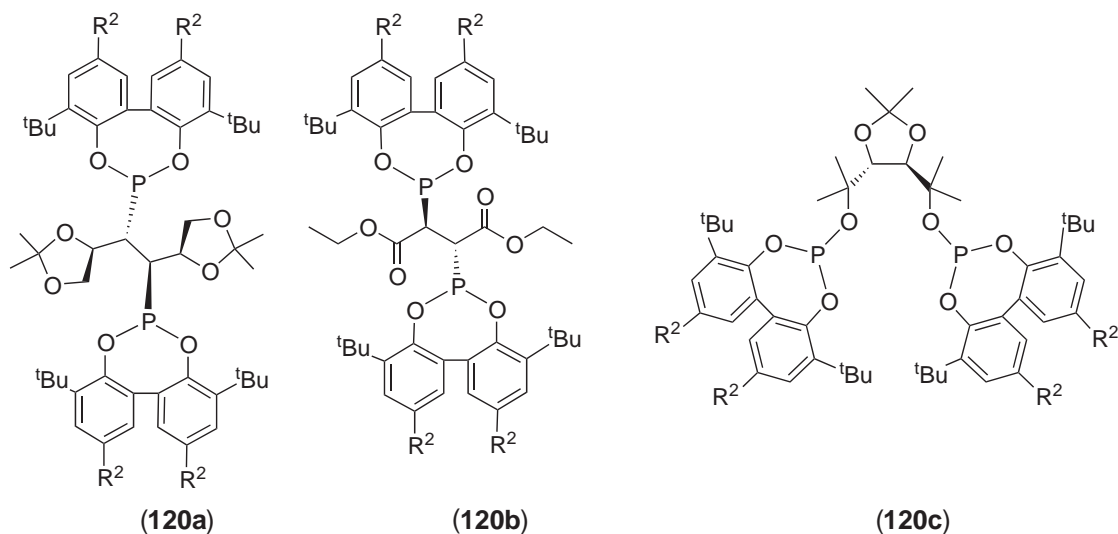
The first reports on asymmetric hydroformylation using diphosphite ligands revealed no asymmetric induction. In 1992, Takaya *et al.* published the results of the asymmetric hydroformylation of vinyl acetate (ee = 50%) with chiral diphosphites.³⁵⁸

In 1992, an important breakthrough appeared in the patent literature when Babin and Whiteker at Union Carbide reported the asymmetric hydroformylation of various alkenes with ees up to 90%, using bulky diphosphites derived from homochiral (2*R*,4*R*)-pentane-2,4-diol, UC-PP* (119).^{359,360} van Leeuwen *et al.* studied these systems extensively. The influence of the bridge length, of the bulky substituents and the cooperativity of chiral centers on the performance of the catalyst has been reported.^{217,218,221,361-363}



Chiral diphosphites based on (2*R*,3*R*)-butane-2,3-diol, (2*R*,4*R*)-pentane-2,4-diol, (2*S*,5*S*)-hexane-2,5-diol, (1*S*,3*S*)-diphenylpropane-1,3-diol, and *N*-benzyltartarimide as chiral bridges have been used in the Rh-catalyzed asymmetric hydroformylation of styrene. Enantioselectivities up to 76%, at 50% conversion, have been obtained with stable hydridorhodium diphosphite catalysts. The solution structures of [RhH(L)(CO)₂] complexes have been studied; NMR and IR spectroscopic data revealed fluxional behavior. Depending on the structure of the bridge, the diphosphite adopts equatorial–equatorial or equatorial–axial coordination to the rhodium. The structure and the stability of the catalysts play a role in the asymmetric induction.²¹⁸

The structures of hydridorhodium diphosphite dicarbonyl complexes [HRhL(LL)(CO)₂] have been studied. Diphosphites (LL) are based on C₂ symmetric (2*R*,3*R*)-butane-2,3-diol, (2*R*,3*R*)-diethyl tartrate, (2*R*,4*R*)-pentane-2,4-diol, and (2*S*,5*S*)-hexane-2,5-diol backbones substituted with 1,1'-biphenyl-2,2'-diyl- or (*S*)-(-)-1,1'-binaphthyl-2,2'-diylphosphoroxy derivatives (120). Variable-temperature ³¹P and ¹H NMR spectroscopy revealed fluxional behavior in the trigonal bipyramidal [HRhL(LL)(CO)₂] complexes of L∩L. Depending on the length of the bridge between the two phosphorus atoms in the diphosphite ligands, equatorial–axial or bis-equatorial coordination takes place. The enthalpies of activation increase with larger steric bulk of the coordinated diphosphite ligands.²²¹



Bakos *et al.* reported a series of diastereomeric diphosphites that were used in the Pt- and Rh-catalyzed asymmetric hydroformylation of styrene. Systematic variation in chirality at both the chelate backbone and the terminal groups revealed a remarkable effect on the enantioselectivity of the catalysts. These systems have been described in Section 9.3.3.5.^{338,339}

A chiral diphosphite based on binaphthol, coordinated with rhodium (I) forming a nine-membered ring, led to an efficient hydroformylation of vinylarenes, although moderate ees were obtained (up to 46%) at mild pressure and temperature reaction conditions.³⁶⁴ Chiral diphosphites and phosphinite-phosphites derived from spiro[4.4]nonane-1,6-diol were synthesized. Using these catalysts in the asymmetric hydroformylation of styrene, high regioselectivity (97%) and

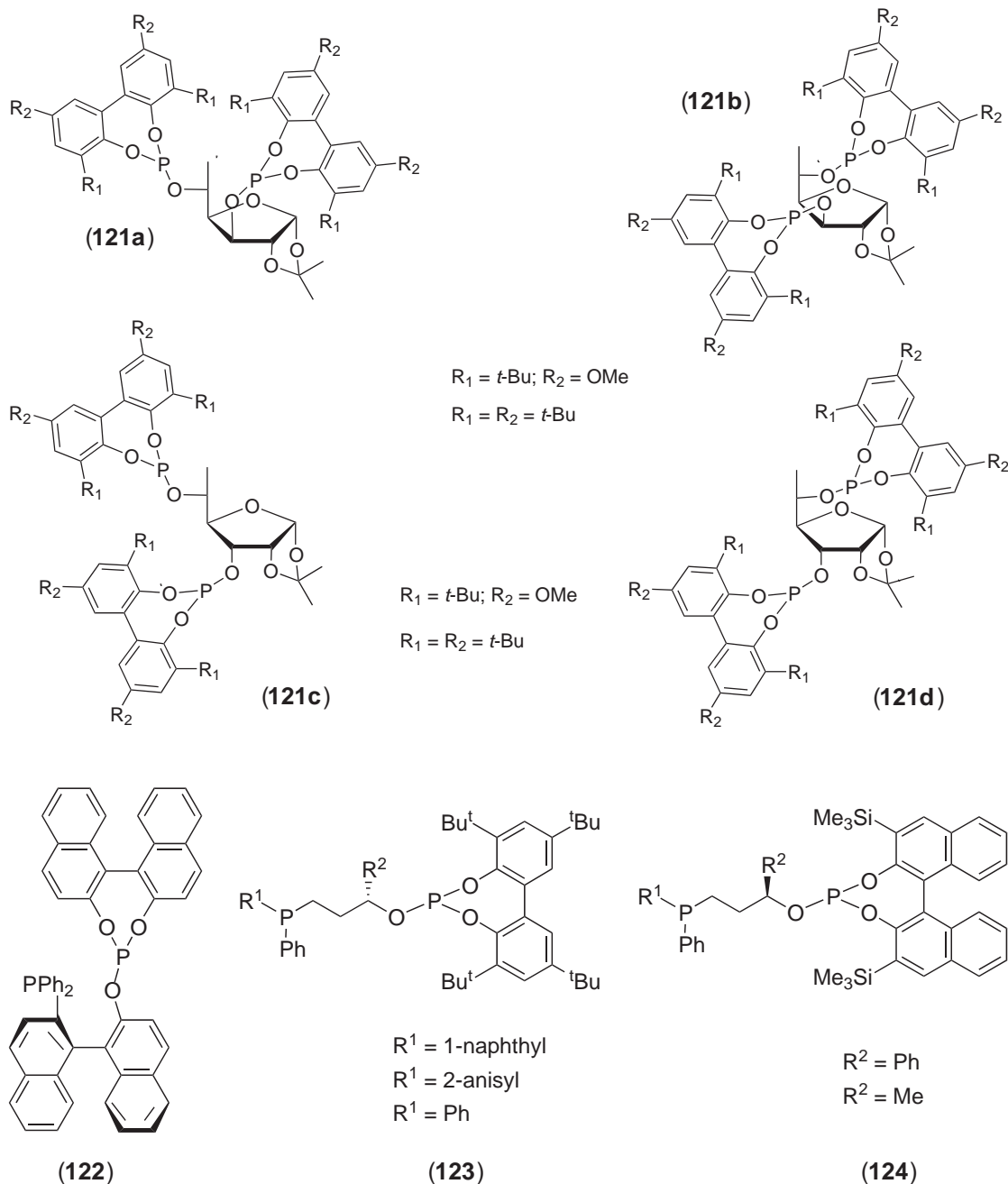
moderate enantioselectivity (65% ee) were obtained. Diphosphites bearing 1,1'-binaphthyl backbones were tested and the opposite configuration of the product indicates that the sense of enantioface selection is mainly dictated by the configuration of the terminal groups. The crystal structure of one complex has been reported.³⁶⁵ A rhodium complex containing a 16-membered chelated diphosphite with the appropriate combination of stereogenic centers produces ees above 70% in the hydroformylation of vinylarenes; a related diastereoisomeric ligand renders very low ees because it does not form a chelated species.²⁹³

The diphosphites derived from carbohydrates play an important role in the formation of rhodium complexes used for asymmetric hydroformylation. The synthesis of the 2,3-bis-phosphite derivatives of 4,6-O-benzylidene- β -D-glucopyranoside leads to chelating ligands. Their rhodium(I) complexes have been tested as catalysts for the asymmetric hydroformylation of vinyl acetate, allyl acetate, and *p*-methoxy-styrene. Enantioselectivities of only $\leq 36\%$ ee were found under mild reaction conditions.³⁶⁶ Chiral diphosphites prepared from xylose and ribofuranose have been used in the Rh-catalyzed asymmetric hydroformylation of styrene. Enantioselectivities up to 64% have been obtained with stable hydrido-rhodium diphosphite dicarbonyl catalysts [HRh(PP)(CO)₂]. High regioselectivities (up to 97%) to the branched aldehyde were found at relatively mild reaction conditions. The solution structures of [HRh(PP)(CO)₂] catalysts have been studied by ³¹P and ¹H NMR spectroscopy. Bidentate coordination of the diphosphite ligand to the rhodium center takes place in a bis-equatorial way. A relation between the trigonal bipyramidal structure and the enantioselectivity of the [HRh(PP)(CO)₂] complex is found.³⁶⁷ The Rh^I cationic complexes [M(cod)(PP)]BF₄ have been synthesized from diphosphite ligands derived from ribofuranose. Comparative experiments with the related epimer D-(+)-xylose derivatives showed that the configuration of the product is controlled by the absolute configuration of the stereogenic carbon atom C-3.³⁶⁸ Diphosphite ligands (**121**) derived from available D-(+)-glucose were used in the Rh-catalyzed hydroformylation of vinyl arenes, giving both excellent enantioselectivities (up to 91%) and regioselectivities (up to 98.8%). Their modular natures allow systematic variation in the configurations at the stereocenters [C-3, C-5] at the ligand bridge and in the biphenyl substituents. The absolute configuration of the product is governed by the configuration at the stereogenic center C-3, while the level of the enantioselectivity is influenced by a cooperative effect between stereocenters C-3 and C-5. Enantioselectivities were highest with ligands with a strong bis-equatorial coordination preference, while an equilibrium of species with bis-equatorial and equatorial-axial coordination modes considerably reduced the ees.^{369,370}

9.3.3.6.3 Phosphine-phosphite ligands

An important breakthrough in asymmetric-rhodium-catalyzed hydroformylation is the catalyst discovered by Takaya *et al.* using (*R,S*)BINAPHOS (**122**) a phosphine-phosphite ligand of C₁ symmetry. This rhodium catalyst has provided ees as high as 96% as well as total conversions and high regioselectivities.^{371,372} The origin of the stereodifferentiation in Rh-catalyzed hydroformylation has been discussed in theoretical reports.^{202,373} A review with 26 references has been published on the application of rhodium complexes with this type of chiral phosphine-phosphites in the hydroformylation of a variety of alkenes (aryl-substituted, alkyl-substituted, and heteroatom-substituted).³⁷⁴ The hydroformylation results show the high enantioselectivity obtained with these catalysts. A trigonal bipyramidal [RhH(CO)₂(phosphine-phosphite)] complex is suggested as the active species, in which the hydride and the phosphite moiety are located at the apical positions.^{374,375} Asymmetric hydroformylation of conjugated dienes, allylic alcohols, heterocyclic alkenes, and other substrates using rhodium complexes (**122**) and related ligands as catalysts gives high regio- and enantioselectivities.³⁷⁶⁻³⁸¹

The effects of CO and H₂ partial pressures on the reaction rate and selectivity of asymmetric hydroformylation of 1-hexene and styrene were examined using the (*R,S*)-BINAPHOS-Rh complex as a catalyst. For both substrates, the higher CO partial pressure inhibited the reaction, but the partial pressure of H₂ hardly affects the reaction rate. Deuterioformylation experiments prove that the regio- and enantioselectivity of the present hydroformylation should be controlled by the alkene-insertion step.³⁸² High enantioselectivity and unprecedented high regioselectivity for the BINAPHOS system are achieved in Rh-catalyzed asymmetric hydroformylation with a perfluoroalkyl-substituted BINAPHOS derivative bearing 2-F₃C(CF₂)₅CH₂CH₂C₆H₄ substituents in compressed CO₂.³⁸³

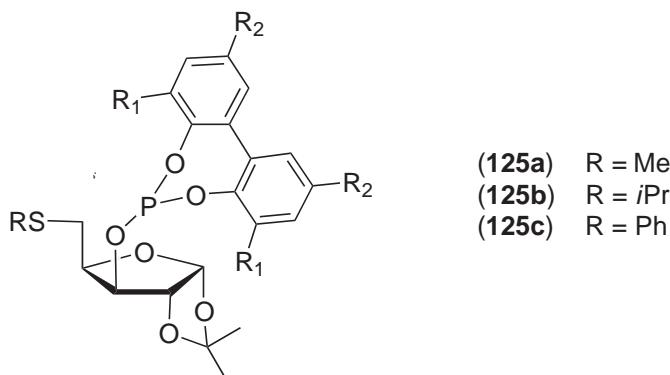


Asymmetric hydroformylation of alkenes using polymer-immobilized chiral phosphine-phosphite-Rh^I complexes has been reported. Mono-, di-, and trivinylBINAPHOS were synthesized. Recovery-reuse of the catalyst has been studied. Asymmetric hydroformylation of vinyl acetate, (*Z*)-2-butene, and 3,3,3-trifluoropropene was also successfully performed with the polymer-supported catalysts.^{384,385} Chiral phosphine-phosphite ligands (**123**), were used in Rh-catalyzed hydroformylation of styrene. The structures of the active catalysts, [HRh(L-L)(CO)₂] complexes where (L-L) = **1241**, were studied using HP NMR and IR spectroscopy. The obtained spectroscopic data showed that the ligands coordinate in an equatorial-apical fashion to the Rh center with the phosphine in the apical position. Variation in configuration of the stereo centers at both the ligand bridge and the phosphine moiety revealed a cooperative effect on the selectivity of the hydroformylation reaction. Spectroscopic data suggest that phosphine-phosphite ligands (L-L) containing the conformationally flexible and axially chiral biphenyl moiety exist predominantly as single atropisomers in the [HRh(L-L)(CO)₂] complexes.³⁸⁶

(i) Miscellaneous

Chiral thioureas have been synthesized and used as ligands for the asymmetric hydroformylation of styrene catalyzed by rhodium(I) complexes. The best results were obtained with *N*-phenyl-*N'*-(*S*)-(1-phenylethyl)thiourea associated with a cationic rhodium(I) precursor, and asymmetric induction of 40% was then achieved.^{387,388} Chiral polyether-phosphite ligands derived from (*S*)-binaphthol were prepared and combined with $[\text{Rh}(\text{cod})_2]\text{BF}_4$. These systems showed high activity, chemo- and regioselectivity for the catalytic enantioselective hydroformylation of styrene in thermoregulated phase-transfer conditions. *Ee* values of up to 25% were obtained and recycling was possible without loss of enantioselectivity.³⁸⁹

Chiral thioether-phosphite ligands (**125**) derived from 1,2-*O*-isopropylidenedxylofuranose have been synthesized. Reaction of these chiral ligands with $[\text{Rh}(\text{cod})_2]\text{BF}_4$ yielded $[\text{Rh}(\text{cod})(\mathbf{125})]\text{BF}_4$. These ligands were tested in the Rh-catalyzed hydroformylation of styrene. The hydroformylation results (*ee* values were insignificant) are discussed according to the solution structure of the species formed under hydroformylation conditions. HP NMR studies show that only the phosphite is coordinated during the catalytic reaction.³⁹⁰



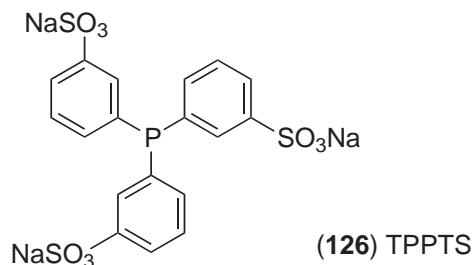
Rhodium complexes with chiral dithiolato and dithioether ligands have been studied in rhodium-catalyzed asymmetric hydroformylation. In all instances, enantioselectivities were low.^{391–393} Catalysis with compounds containing thiolate ligands has been reviewed.³⁹⁴

9.3.3.6.4 Two-phase catalysis

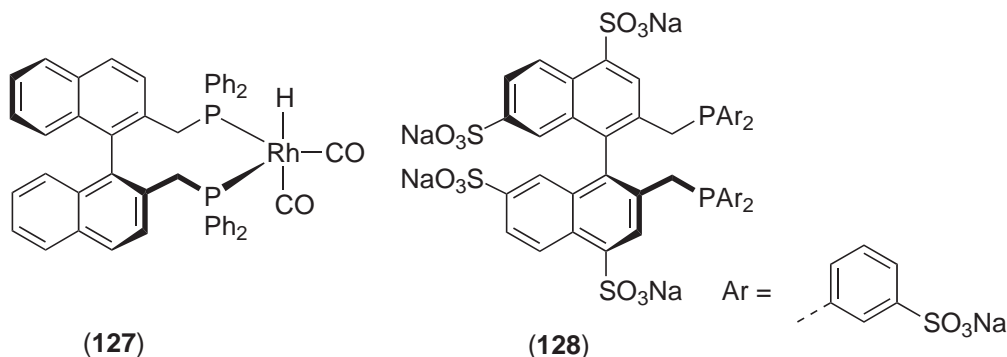
Hydroformylation in aqueous or biphasic catalysis has become very popular especially after the successful application of the initial invention of Kuntz at Ruhrchemie (later Hoechst, now Celanese) for the hydroformylation of propene and butene. Catalysis in water has been the topic of many reviews.^{77–79,395–402} Advances in hydroformylation of propylene via homogeneous catalysis for manufacture of *n*-butyraldehyde using aqueous, ligand-modified $[\text{RhH}(\text{CO})(\text{TPPTS})_3]$ were discussed where TPPTS = (**126**), with focus on interface reactions in the context of the RCH/RP [Ruhrchemie/Rhône-Poulenc] process. The main advantage of the catalyst system is the ease of separation of catalyst and product, which may find applicability beyond the proven hydroformylation process.⁴⁰³ A review concerning the environmental attractiveness of efficient organometallic catalysis in aqueous media has been published.⁴⁰⁴ Thermoregulated phase-transfer catalysis has been reviewed.⁴⁰⁵ One phase-catalysis followed by two-phase separation in the next step has also been reviewed.⁴⁰⁶ Kinetic studies for various reaction systems and the role of ligands, pH, co-solvents, and surfactants have been reviewed.⁴⁰⁷ A novel approach for determining interfacial kinetics by accurately excluding the mass transfer effect by numerical simulation of fluid flow and mass transfer in a chemical reactor has been presented.⁴⁰⁸

Relatively little work has been devoted to the characterization of complexes in water and generally it has been assumed that for Rh-catalyzed hydroformylation similar species are formed in water as inorganic solvents, i.e., $[\text{RhH}(\text{L})_2(\text{CO})_2]$ and $[\text{RhH}(\text{L})_3(\text{CO})]$ are the major species. Therefore, few references can be mentioned here which contain information about coordination complexes. In addition, a few, more recent, studies will be mentioned which do not report *in situ* coordination compounds. A HP NMR study of $[\text{RhH}(\text{TPPTS})_3(\text{CO})]$ has been reported. It was

found that the energy required for dissociation of TPPTS from the Rh centre is 10 kcal mol^{-1} higher than for dissociation of PPh_3 .⁴⁰⁹



A few sulfonated bidentate ligands have been used for which the coordination behavior has been well established for their nonsulfonated analogs; the sulfonated ligands showed a behavior that was very much the same as that of their parent ligands in organic solvents. NAPHOS as in rhodium complex (127) behaves the same as BISBI (58), as does its sulfonated analog BINAS (128), which was developed and extensively studied by Herrmann and co-workers.^{410–413} The catalytically active rhodium complexes $[\text{HRh}(\text{CO})_2(\text{P-P})]$ of NAPHOS and BINAS have been characterized by IR and NMR spectroscopy.⁴¹⁴



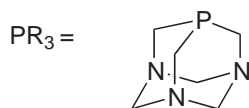
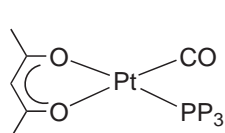
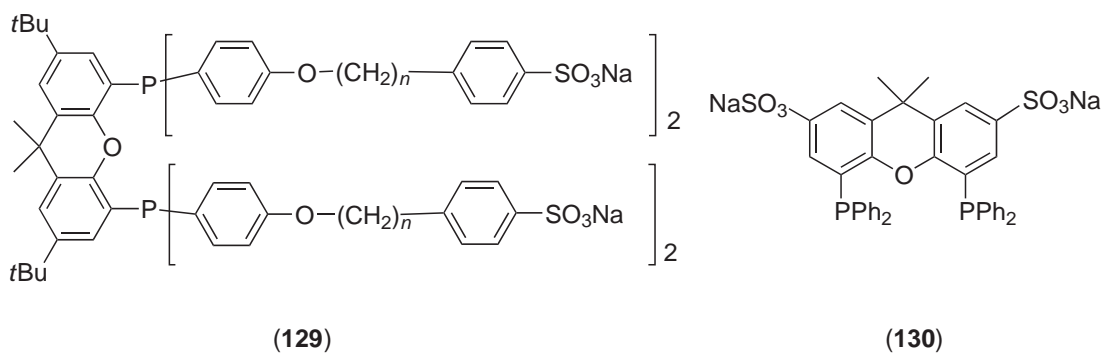
The xanthene-backbone derived diphosphines (129) also led to well-defined rhodium dicarbonyl hydride complexes. They were used in one-phase catalysis and two-phase separation after careful acidification of the system.⁴¹⁵

The synthesis, aggregation behavior, and catalytic activity of Rh complexes of Xantphos derivatives (129) with surface-active pendant groups have been described.⁴¹⁶ The complex $[\text{HRh}(\text{CO})(\text{TPPTS})_3]$ was used as a catalyst precursor in the hydroformylation of 1-butene, 1-octene, and styrene under biphasic reaction conditions.⁴¹⁷ The two-phase hydroformylation of buta-1,3-diene with $[\text{HRh}(\text{CO})(\text{TPPTS})_3]$, with excess TPPPS, gives high yields of C_5 -monoaldehydes.⁴¹⁸ The coordination behavior of the catalytic species $[\text{HRh}(\mathbf{130})(\text{CO})_2]$ was studied by HP NMR spectroscopy which showed the desired bis-equatorial coordination of the ligand to the rhodium center.⁴¹⁹

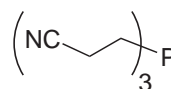
The monosulfonated PPh derivative, $\text{Ph}_2\text{P}(m\text{-C}_6\text{H}_4\text{SO}_3\text{K})$ (DPM) and its rhodium complex, $\text{HRh}(\text{CO})(\text{DPM})_3$ have been synthesized and characterized by IR and NMR spectroscopic techniques. The data showed that the structure was similar to $[\text{HRh}(\text{CO})(\text{PPh}_3)_3]$. The catalytic activity and selectivity of $[\text{HRh}(\text{CO})(\text{DPM})_3]$ in styrene hydroformylation were studied in biphasic catalytic systems.^{420,421} Rh^{I} complexes $[\text{Rh}(\text{acac})(\text{CO})(\text{PR}_3)]$ with tpa (131), cyep (132), (126), omp (133), pmpp (134), tmpp (135), $\text{PPh}_2(\text{pyl})$, $\text{PPh}(\text{pyl})_2$, and $\text{P}(\text{pyl})_3$ were characterized with NMR and IR spectra. Complexes with (131), (132), and (126) were catalysts for hydrogenation of C—C and C—O bonds, isomerization of alkenes, and hydroformylation of alkenes.⁴²² Asymmetric hydroformylation of styrene was performed using as catalyst precursor $[\text{Rh}(\mu\text{-OMe})(\text{COD})_2]$ associated with sodium salts of *m*-sulfonated diarylphosphines.⁴²³

The $[\text{HRh}(\text{CO})(\text{TPPTS})_3]$ precursor has opened a large area for the Supported-Aqueous-Phase (SAP) catalyzed functionalization of heavy substrates (see Chapter 9.9). Several ways to increase the efficiency of heavy alkene hydroformylation by $[\text{Rh}_2(\mu\text{-S-Bu})_2(\text{CO})_2(\text{TPPTS})_2]$ have been investigated.⁴²⁴

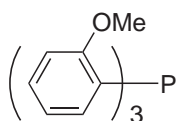
Ligand (136), an analog of PPh_3 with amphiphilic character, was used for making $[\text{Rh}(\text{CO})(\mathbf{136})(\text{acac})]$. The rhodium-based hydroformylation of 1-hexene using catalysts formed *in situ*



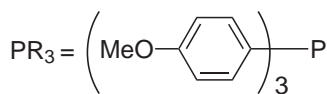
(131)



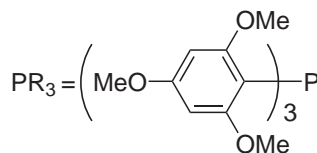
(132)



(133)

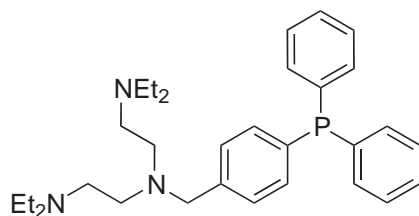


(134)



(135)

under biphasic conditions was also demonstrated.⁴²⁵ Higher terminal alkenes can be hydroformylated by using the catalyst precursor $[\text{Rh}_2(\mu\text{-S-Bu}^t)_2(\text{CO})_2(\text{TPPTS})_2]$ and β -cyclodextrin or its dimethylated form as phase-transfer agent.⁴²⁶



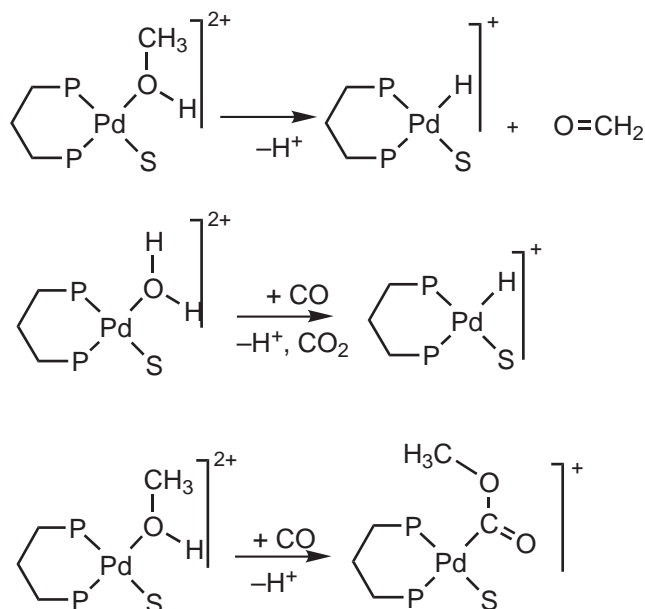
(136)

Efficient routes to phosphines modified with phosphonic acid groups have been developed. In the two-phase hydroformylation of propylene, some of the catalysts showed activities and regioselectivities similar to those of Rh/TPPTS. Amphiphilic Rh/phosphonate-phosphine catalysts were found to be superior to Rh/TPPTS in the hydroformylation of 1-octene.⁴²⁷ Well-defined core-shell particles of $[(\text{H})\text{Rh}(\text{CO})(\text{NaTPPTS})_3]$ on poly(diallyldimethylammonium chloride)-coated potassium *p*-styrenesulfonate-styrene copolymer microparticles were used as catalyst for hydroformylation of methyl acrylate.⁴²⁸ New rhodium(I) water-soluble complexes with 1-alkyl-1-azonia-3,5-diaza-7-phospha-adamantane iodides were active in the hydroformylation of alkenes.⁴²⁹ Complexes of 1-methyl-1-azonia-3,5-diaza-7-phospha-adamantane iodide (mtpa^+I^-) yielded square planar $[\text{RhI}(\text{CO})(\text{mtpa}^+\text{I}^-)_2]$ and trigonal-bipyramidal $[\text{RhI}(\text{CO})(\text{mtpa}^+\text{I}^-)_3]_4 \cdot \text{H}_2\text{O}$. The complexes catalyze the hydroformylation and the hydroxycarbonylation of alkenes and the hydrogenation of aldehydes and alkenes.⁴³⁰ Sol-gel processed rhodium(I) complexes $[\text{HRh}(\text{CO})\{\text{Ph}_2\text{P}(\text{CH}_2)_x\text{-Si}(\text{OMe})_3\}_3]$ were used as catalysts and identified by ³¹P CP/MAS NMR relaxation-time studies, 2D WISE NMR, and ²⁹Si CP/MAS NMR experiments.⁴³¹ The water-soluble tripodal phosphine ligand *cis,cis*-1,3,5-(PPh₂)₃-1,3,5-[CH₂(OCH₂CH₂)_xOCH₃]₃C₆H₆ ($x = 30\text{--}160$) has been reported. The catalytic activity of its Rh complex in the hydroformylation of 1-hexene was found comparable in a single-phase system (1-hexene/methanol) with that in the biphasic system (1-hexene/water).⁴³²

9.3.4 PALLADIUM-CATALYZED ALTERNATING COPOLYMERIZATION OF ALKENES AND CARBON MONOXIDE

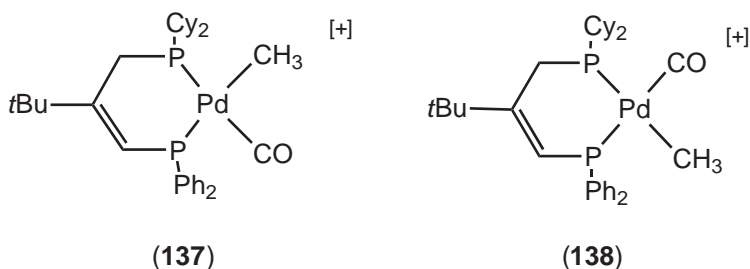
Thermoplastics with high-performance properties are in increasing demand.⁴³³ In recent years much effort has been devoted to the development of such high-performance plastics that might be produced at lower costs, such as ethene-CO copolymers. Coordination polymerization for ethene/CO was discovered by Reppe using nickel cyanide catalysts.⁴³⁴ The first palladium catalysts (phosphine complexes of PdCl₂) were reported in 1967.⁴³⁵⁻⁴³⁷ High molecular weights were achieved and the potential of the semicrystalline high-melting polymer was recognized. The polymers made, however, contained a considerable amount of catalyst (often as palladium black metal) and this was deleterious to the stability of the polymer during processing. Hence, considerably catalysts that are more active were needed.

Sen reported the use of well-defined, cationic [Pd(PPh₃)_n](BF₄)₂ species in acetonitrile as catalysts for the copolymerization of alkenes and CO.⁴³⁸⁻⁴⁴⁰ Drent discovered that cationic palladium complexes containing chelating bidentate diphosphine ligands (Scheme 4) produced polymers with 100% selectivity, high molecular weight, and yields up to several kilograms per gram of palladium per hour at much higher rates than monodentate ligand systems.⁴⁴¹⁻⁴⁴³ Key reviews concerning the developments in the decade 1982-1992 have been published.⁴⁴⁴⁻⁴⁴⁷ The mechanistic issues include the initiation modes of the reaction, the propagation mechanism, the perfect alternation of the polymerization reaction, chain termination reactions, and the combined result of initiation and termination as a process of chain transfer. The regio- and stereoselectivity has also been discussed. Most of the kinetic studies were carried out at temperatures of -40°C to 25°C, which is well below the temperature of the catalytic process. The polymerization reaction is efficiently catalyzed by complexes of the type PdX₂(L-L) (L-L is a chelating bidentate phosphorus or nitrogen ligand, coordinating in a *cis* fashion-, X is a weakly or noncoordinating anion) in methanol as the solvent. Suitable ligands are dppe, dppp, and dppb and both triflates and *p*-toluenesulfonic acid provide suitable anions. The catalyst can be made *in situ* by dissolving palladium acetate and adding ligand and a strong acid. When methanol is the solvent, there is no need to create an active palladium alkyl initiator. Alternatively, in aprotic solvents such as dichloromethane, palladium must be methylated with, for example, Sn(CH₃)₄ to provide an active catalyst.⁴⁴⁸ When carbon monoxide is bubbled through a solution of [(dppp)Pd(triflate)₂] a carbomethoxy-palladium species was formed.⁴⁴⁹ To ensure a clean formation of the carbomethoxy species, exclusion of water is a prerequisite. If during the preparation water was present, the formation of a palladium hydride complex [(dppp)PdH]⁺ was observed. Hydrides are also efficient initiators as their insertion reactions with alkenes are extremely fast. The initiation reactions are collected in Scheme 4.



Scheme 4

Migratory insertions of alkenes and CO have been studied by numerous authors.^{450–466} The mechanism was shown to contain a migratory step, rather than insertion, using the dissymmetric ligands (137) and (138).⁴⁶⁷ Detailed kinetic measurements and spectroscopic characterization have been carried out by Brookhart and co-workers. The polymerization reaction proceeds via a perfectly alternating sequence of carbon monoxide and alkene insertions in to palladium–carbon bonds. The insertion of CO is in many instances uphill thermodynamically. Insertion of CO is, therefore, always kinetically controlled. When an alkyl-palladium species has formed, the vacant site will be occupied by a coordinating CO molecule. Carbon monoxide coordinates more strongly to palladium than ethene. The acyl complex formed will, for the same reason, also preferentially coordinate to CO instead of ethene. Double insertions of CO do not occur because this is thermodynamically even more unfavorable, and, in addition, the migration of more electronegative groups to CO is usually slower (Scheme 5). An “occasional” coordination of ethene now leads to insertion of ethene and thus a perfect alternation of the two monomers occurs. After insertion of ethene, a very stable intermediate is formed as a result of the intramolecular coordination of the ketone group. Many intermediates of this structure have been isolated.

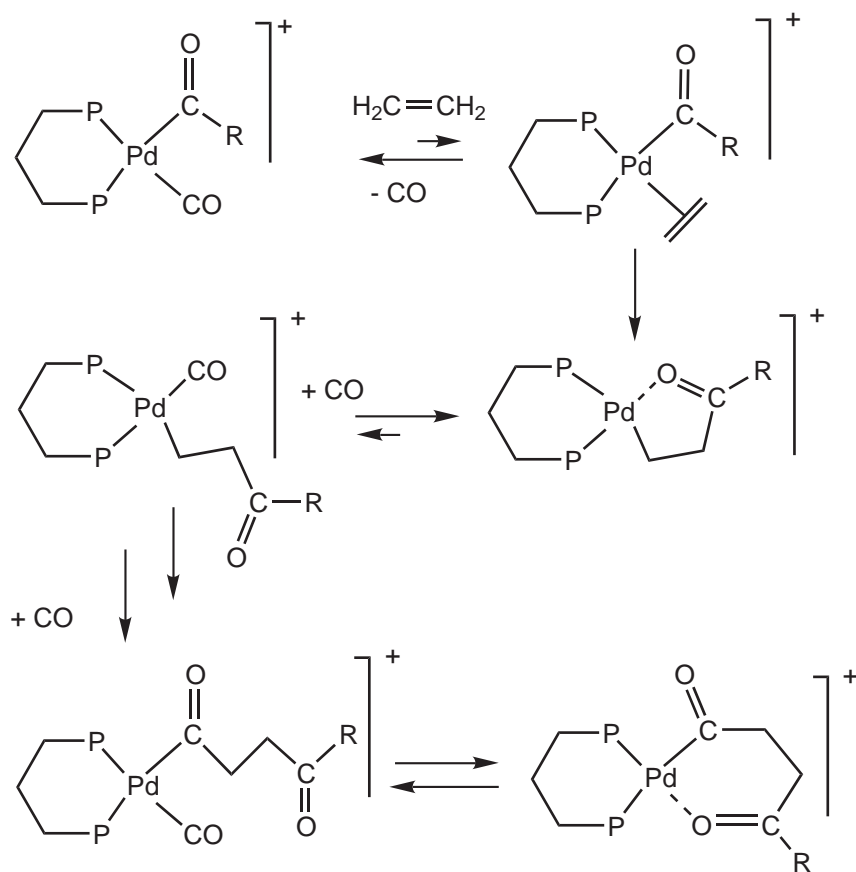


Chain termination has been discussed by Drent. At higher temperatures both ester and alkyl chain ends are formed, thus leading to polymer chains with two esters, two ketones, or one of each as end groups.⁴⁶⁸

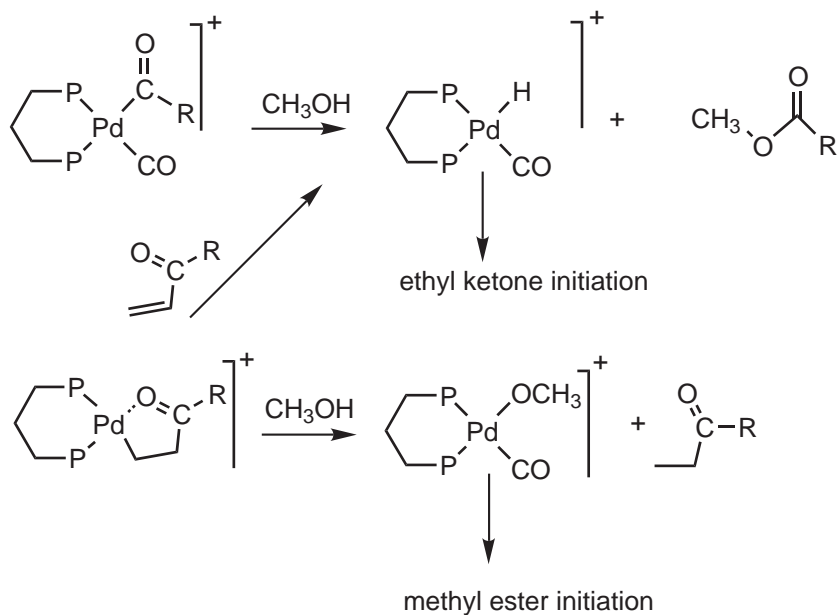
There are four basic reactions that terminate the polymerization (Scheme 6) are:

- (i) alcoholysis of an acylpalladium chain giving ester end groups,
- (ii) hydrolysis of an acylpalladium chain giving acid end groups,
- (iii) protonolysis of an alkylpalladium chain end giving ethyl ketone end-groups,
- (iv) β -elimination.

Dppp, bdpp, and 1,2-propanediyl-bis-(diisopropylphosphine) were compared as ligands in the regioselective polymerization of propene. The polymer obtained with 1,2-propanediyl-bis-(diisopropylphosphine) indicated perfect regioselectivity and good stereoselectivity.⁴⁶⁹ [(Bipy)Pd(Me)(NCMe)]⁺(Ar'₄B⁻) and [(phen)Pd(Me)(NCMe)]⁺(Ar'₄B⁻) (bipy = 2,2'-bipyridine, phen = 1,10-phenanthroline, Ar' = 3,5-(CF₃)₂C₆H₃) catalyze living alternating copolymerization of alkenes with CO in PhCl. Details of these polymerization reactions were illustrated using 4-*tert*butylstyrene in a living alternating copolymerization process. The catalyst resting state is the carbonyl acyl species [(bipy)Pd(CO)CO(CHRCH₂CO)_nMe]⁺.⁴⁷⁰ The presence of terminal CO₂Me groups primarily on the β carbon atom of styrene in CO copolymers indicates that it comes from the initiation step in the copolymerization. The presence of alkenyl aromatic groups and some branched ester groups shows that two processes occur to terminate the polymerization; either β -elimination, or esterification by MeOH used as the solvent.⁴⁷¹ [Pd(phen)(MeCN)₂](BF₄)₂ catalyzed the alternating copolymerization of styrene with CO to form syndiotactic copolymers with a strictly head-to-tail arrangement in the backbone.⁴⁷² Effects of the component ratio in the catalytic system Pd(C₅H₇O₂)₂-P(C₆H₅)₃-(*p*-CH₃C₆H₄SO₃H), and effects of monomer pressure, and preliminary heating of the catalytic system on the kinetics of copolymerization of CO with C₂H₄ in CH₃CO₂H were studied.^{472,473} Facile successive insertion of CO and strained alkenes has been observed for both neutral Pd(R)X(Ar-BIAN) and cationic [Pd(R)(MeCN)(Ar-BIAN)]-SO₃CF₃ complexes, i.e., complexes containing the rigid bidentate nitrogen ligands *bis*(arylimino)acenaphthene (Ar-BIAN; Ar = *p*-MeOC₆H₄ (*p*-An), *p*-MeC₆H₄ (*p*-Tol), *o,o'*-i-Pr₂C₆H₃), leading to the formation of new multiple insertion products of the type [PdCH(R')CH(R')C(O)CH(R')CH(R')C(O)R(X)] (Ar-BIAN). Insertion of norbornadiene, and dicyclopentadiene in the cationic acyl complexes [Pd(C(O)Me)(MeCN)(Ar-BIAN)]SO₃CF₃ was reported.⁴⁷⁵

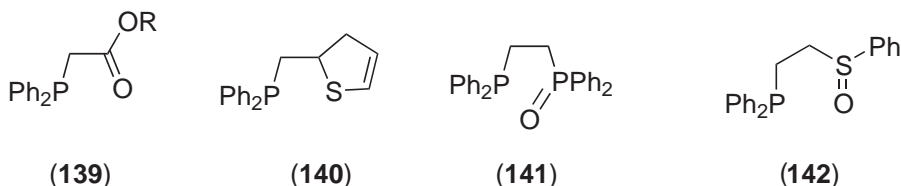


Scheme 5



Scheme 6

The hemilabile phosphino-ester and phosphino-thiophene ligands (139)–(142) behave like monodentate phosphine under catalytic conditions.⁴⁷⁶



Catalytic systems for synthesis of propionic acid and ketoacids $C_2H_5(COCH_2CH_3)_nCO_2H$ with $n = 1-3$ based on phosphine palladium complexes have been developed.⁴⁷⁷ The compound $[Pd(Me-DUPHOS)(MeCN)_2](BF_4)_2$, [Me-DUPHOS = 1,2-bis(2,5-dimethylphospholano) benzene], is an effective catalyst for the highly enantioselective, alternating copolymerization of aliphatic α -alkenes with CO to form optically active, isotactic polymers. This Pd compound was also a catalyst for the alternating isomerization cooligomerization of 2-butene with CO to form optically active, isotactic poly(1,5-ketone).⁴⁷⁸ Highly enantioselective alternating copolymerization of propene and carbon monoxide has been performed by use of a Pd^{II} complex of the chiral phosphine-phosphite (*R,S*)-BINAPHOS as a catalyst to afford isotactic poly(propene-alt-CO).⁴⁷⁹ Copolymerization of CO with diethyl-bicyclo[2.2.1]hepta-2,5-diene-2,3-dicarboxylate or diethyl-7-oxabicyclo[2.2.1]hepta-2,5-diene-2,3-dicarboxylate gave alternating copolymers.⁴⁸⁰ Various carbonylation reactions can be catalyzed by complexes PdX_2L_2 . The chemoselectivity is influenced both by the ligand and by the anion. Using styrene as the substrate, conditions were found that produce either (*E*)-1,5-diphenylpent-1-en-3-one or (*E*)-1,4-diphenylpent-1-en-3-one with high selectivity even in the presence of hydrogen.⁴⁸¹

Sol-gel bis-phosphine Pd^{II} complexes are catalytically active in the solvent-free CO-ethene copolymerization, producing polyketones with chain lengths comparable to those obtained with chelating diphosphine ligands.⁴⁸² Copolymerization of CO and ethylene was accomplished by the use of $[(dppp)Pd(OAc)_2]$ or $[(dppp)Pd\{C(O)Bu^t\}Cl]$ in the presence $[(Bu^t)AlO]_6$ as a co-catalyst. Terpolymers were obtained with 1-octene. No polymerization is observed for CO and either 1-octene or 4-phenyl-1-butene in the absence of ethylene.⁴⁸³ The catalytic activity of this system is highly dependent on the structure of the aluminoxane. A comparative study indicates the co-catalytic activity to be $[(Bu^t)Al(\mu_3-O)]_7 > [(Bu^t)Al(\mu_3-O)]_6 > [(Bu^t)Al(\mu_3-O)]_9 \sim [(Bu^t)_7Al_5(\mu_3-O)_3(\mu-OH)_2]$.⁴⁸⁴ Carbon monoxide and norbornene are copolymerized with $Pd(CH_3CO_2)_2$ and various ligands, with methanol and a protonic acid as co-initiators and chain-transfer agents respectively.⁴⁸⁵

Carbon monoxide and styrene alternating copolymer was prepared using a catalyst prepared from palladium acetate and 2,2'-bipyridyl.⁴⁸⁶ The microscopic steps catalyzed by 1, 10-phenanthroline (phen)-based Pd complexes were studied. Pd carbonylalkyl, carbonylacyl, ethylenealkyl, and ethyleneacyl complexes $[(phen)Pd(R)(L)]^+(Ar'_4B)^-$ ($Ar' = 3,5-(CF_3)_2C_6H_3$) and the β - and γ -keto chelate complexes $[(phen)PdCH_2CH_2C(O)CH_3]^+$ and $[(phen)PdC(O)CH_2CH_2C(O)CH_3]^+$ were prepared. The migratory insertion reaction rates were measured by low-temperature NMR techniques. The relative binding affinities of ethylene and CO to Pd Me, acyl, and chelate complexes were determined with relative equilibrium constants for ethene/CO binding between acyl and alkyl complexes. The catalyst resting state is a carbonyl acyl complex.⁴⁸⁷ Complexes of general formula $[Pd(dppp)(L-L)][PF_6]_2$ ($L-L = 2,2'$ -bipyridine (bipy), 4,4'-dimethyl-2,2'-bipyridine, phenanthroline, or 3,4,7,8-tetramethyl-1,10-phenanthroline) were active catalyst precursors in CO-alkene co- and terpolymerization.⁴⁸⁸ Polymerization of CO, styrene, and norbornene with $Pd(CH_3CO_2)_2$ in CH_3OH was studied.⁴⁸⁹

A nonlocal density functional study of the Pd^{II} -assisted copolymerization of ethylene and CO has been published.^{490,491}

Synthesis of stereoblock polyketones was accomplished by ligand exchange during polymerization. Copolymerization of 4-*tert*-butylstyrene/CO using $[(2,2-bis[2-[4(S)-methyl-1,3-oxazoliny]]-propane)PdCH_3(CH_3CN)]^+[BAR'_4]^-$ produces an isotactic block of the copolymer through enantiomorphic site control. Upon addition of 2,2'-bipyridine during the polymerization, the bis-oxazoline ligand is displaced from Pd without chain transfer, and through a chain-end control mechanism, a syndiotactic block is added to yield isotactic-block-syndiotactic block polymer.⁴⁹² The palladium-phosphine catalyst system $dppp/Pd(OAc)_2$ was studied using *in situ* ^{31}P NMR spectroscopy at elevated temperatures.⁴⁹³ Cationic palladium complexes containing coordinated phosphino(dihydro-oxazole) ligands were used for the production of alternating styrene-carbon

monoxide copolymers.⁴⁹⁴ The alternating copolymerization of functional alkenes, $\text{CH}_2\text{:CH}(\text{CH}_2)_x\text{OH}$ ($x=2, 3, 4, 9$), $\text{CH}_2\text{:CH}(\text{CH}_2)_x\text{CO}_2\text{H}$ ($x=1, 2, 4, 8$), and 4-allylanisole, with carbon monoxide was achieved by using $[\text{Pd}(\text{Me-DUPHOS})(\text{MeCN})_2](\text{BF}_4)_2$ as the catalyst. With most alkenes, the polymers had poly(1,4-ketone) and/or "regular" poly(spiroketal) (i.e., 1,6-dioxaspiro[4.4]nonane) enchainments. With 4-penten-1-ol and 3-buten-1-ol, the participation of the pendant hydroxy group in intra-chain reactions led to the formation of polycyclic repeating units in the backbone.⁴⁹⁵

The rate of alternating polymerization of ethene with CO was studied for the dppp system.⁴⁹⁶ The same catalyst was used for the copolymerization of CO and 4-vinylcyclohexene.⁴⁹⁷ Cyclo-copolymerization of 1,4-pentadiene with carbon monoxide gave polyketone in the presence of a Pd^{II} catalyst bearing (*R,S*)-BINAPHOS. In the repeating unit, exclusive formation of a cyclopentanone framework rather than cyclohexanone was revealed.⁴⁹⁸ Carbon monoxide was copolymerized with phenylacetylene using $[\text{Pd}(\text{CH}_3\text{CN})_4](\text{BF}_4)_2$.⁴⁹⁹ Carbon monoxide-styrene alternating copolymer was prepared by polymerization using (*S*)-2-[2-(diarylphosphino)phenyl]-4-benzyl-4,5-dihydro-oxazole-palladium compounds as catalysts.⁵⁰⁰

Two competing chain-transfer mechanisms in copolymerization of CO and ethene catalyzed by Pd^{II} acetate/dppp complexes were found. One involves termination via an isomerization into the enolate followed by protonation with methanol; the rate of this reaction should be independent of the concentration of the protic species. The second chain-transfer mechanism comprises termination via methanolysis of the acylpalladium species, and subsequent initiation by insertion of ethene into the palladium hydride bond.⁵⁰¹

Dppp-like ligands bearing different substituents on the carbon backbone and of their Pd^{II} complexes have been employed as catalyst precursors for the copolymerization of ethene and carbon monoxide. It has been found that the introduction of alkyl substituents in the C^2 -position of the carbon backbone of dppp does not significantly improve the performance of the corresponding catalyst precursors. The productivity increases when Me groups are introduced in both C^1 -positions of the diphosphine ligand, particularly with *R,S* (*S,R*) stereochemistry as in *meso*- $\text{CH}_2(\text{CH}_3\text{CHPPH}_2)_2$.⁵⁰²

The water-soluble diphosphine ($\text{NaO}_3\text{S}(\text{C}_6\text{H}_4)\text{CH}_2)_2\text{C}(\text{CH}_2\text{PPh}_2)_2$ (Na_2DPPPD) as the bis-trifluoroacetate Pd^{II} complex forms the most efficient catalyst system for the copolymerization of CO and ethene in water.⁵⁰³ Styrene has higher productivity than ethene during copolymerization with carbon monoxide using $[\text{Pd}(\text{CO-CH}_3)(\text{P}^*\text{N})(\text{solv})]\text{O}_3\text{SCF}_3$ (where P^*N is a phosphanyl-dihydro-oxazole ligand).⁵⁰⁴ The influence of CO and ethylene pressures on their copolymerization catalyzed by the precursor $[(\text{dppp})\text{Pd}(\text{H}_2\text{O})(\text{TsO})](\text{TsO})$ in MeOH was studied.⁵⁰⁵ Dicationic *N*-heterocyclic carbene chelates of formula $[\text{cis-CH}_2\{\text{N}(\text{H})\text{C}:\text{C}(\text{H})\text{N}(\text{R})\text{C}\}_2\text{Pd}(\text{NCCH}_3)_2]^{2+}$ ($\text{R} = \text{Me}, 2,4,6\text{-Me}_3\text{-C}_6\text{H}_2$) catalyze the copolymerization of ethene and CO under mild conditions and low pressures.⁵⁰⁶ The potentially hexadentate diphosphine ligands $(\text{ROCH}_2\text{CH}_2)_2\text{P}(\text{CH}_2)_3\text{P}(\text{CH}_2\text{CH}_2\text{OR})_2$ ($\text{R} = \text{Et}, \text{Bu}^n, \text{Bu}^t, \text{Cy}$) and palladium cations formed highly active catalysts for C^1 -symmetric copolymerization of alkenes with carbon monoxide.⁵⁰⁷ Carbon-1-symmetric chelate ligands containing the 3-phenyl-4-methoxymethyl-4,5-dihydrooxazole chiral moiety, and either *pyl* or 2-diphenylphosphinophenyl substituents, catalyze the copolymerization of styrene with carbon monoxide with either a prevailing syndiotactic or isotactic microstructure. This was interpreted on the basis of a site-selective coordination of the alkene before migratory insertion.⁵⁰⁸ A water-soluble Pd catalyst based on $\text{Pd}(\text{OAc})_2$ and the bidentate phosphine $(1,3\text{-C}_3\text{H}_6(\text{P}(\text{C}_6\text{H}_4\text{-}m\text{-SO}_3\text{Na})_2)_2)$ catalyzes the alternating copolymerization of CO and alkenes.⁵⁰⁹ Several bis-chelated Pd^{II} complexes, $[\text{Pd}(\text{P-P})(\text{N-N})_x](\text{PF}_6)_2$, containing binary combinations of diphosphine and dinitrogen ligands (dppp, *meso*-2,4-bis(diphenylphosphino)pentane, *rac*-2,4-bis(diphenylphosphino)pentane and 2,2'-bis(diphenylphosphinoethyl)pentane; dinitrogen ligands 2,2'-bipyridine or 1,8-naphthyridine) have been tested as catalyst precursors for the copolymerization of carbon monoxide and ethene.⁵¹⁰ A calixarene-based *syn*-diphosphite behaves as an exclusively *cis* coordinating ligand towards palladium(II) and it shows catalytic activity in the copolymerization of carbon monoxide and ethene. Hydrolysis of the acyl intermediate to a carboxylic acid is the most important chain-transfer mechanism.⁵¹¹ Complexes $[\text{Pd}(\eta_1, \eta_2\text{-C}_8\text{H}_{12}\text{OMe})(\text{bipy})]^+ \text{X}^-$ were characterized in solution by NMR spectroscopy. The catalytic activity of the complexes toward CO/styrene copolymerization was related to the type of counterion. The order of the catalytic activity of complexes is: $\text{BPh}_4^- \sim \text{CF}_3\text{SO}_3^- < \text{BF}_4^- < \text{PF}_6^- < \text{SbF}_6^- < \text{B}(3,5\text{-(CF}_3)_2\text{C}_6\text{H}_3)_4^-$.⁵¹² Palladium complexes with a hemilabile terdentate carbene ligand, 1,3-bis(*pyl*)imidazol-2-ylidene, were active toward the catalytic polymerization of CO/norbornylene.⁵¹³ Palladium complexes of *cis*-bidentate C_4 -bridged diphosphines *cis*- and *trans*-1,2-bis[(diphenylphosphino)methyl]cyclohexane, *endo,endo*-2,3-bis[(diphenylphosphino)methyl] norbornane,

and *exo,endo*-2,3-bis[(diphenylphosphino)methyl]norbornane were selective for the copolymerization of ethylene with CO, generating low molecular weight polymers. Catalyst systems formed from *exo,endo*-2,3-bis[(diphenylphosphino)methyl]norbornane were highly selective for the production of Me-propanoate.⁵¹⁴ Enantioselective, alternating copolymerizations of carbon monoxide with styrene, dicyclopentadiene, and methylcyclopentadiene were carried out with a palladium catalyst modified by 1,4-3,6-dianhydro-2,5-dideoxy-2,5-bis(display phosphino)-L-Iditol(DDPPI).⁵¹⁵ The neutral and cationic complexes of formula $[(CH_3)(X)Pd(P^*P(S))]$ and $[P^*P(S)=Ph_2PCH_2P(S)Ph_2$ and $Ph_2P(CH_2)_2P(S)Ph_2]$ were tested as catalysts in the alternating copolymerization of ethylene and carbon monoxide.⁵¹⁶ The enantioface discriminating copolymerization of styrene with carbon monoxide using palladium complexes $[(LL')Pd(S)_2](X)_2$ of the C_1 -symmetric ligands (*S,S*)-2-[2-(diphenylphosphino)phenyl]-3-phenyl-4-methoxymethyl-4,5-dihydrooxazole or (*S,S*)-2-(pyl)-3-phenyl-4-methoxymethyl-4,5-dihydrooxazole gives highly isotactic or syndiotactic poly(1-oxo-2-phenyl-1,3-propanediyl).⁵¹⁷ Palladium complexes of series of diphos ligands $CH_2(CH_2PR_2)_2$ ($R=(CH_2)_nOH$, $(CH_2)_nCH(CH_2OH)_2$, C_nH_{2n+1} , $CHMe_2$, $(CH_2)_2CHMe_2$, $(CH_2)_3CHMe_2$) proved to be highly active in the carbon monoxide/ethene copolymerization under biphasic conditions (water-toluene).⁵¹⁸ A chiral cationic palladium catalyst, modified with 1,2-bis(diarylphosphinomethyl)benzene ligands with different electronic properties, produced poly(propene-alt-CO) with essentially complete regioregularity and high isotacticity.⁵¹⁹ The CO/ethylene copolymerization catalyst $[(dppp)Pd(CH_3)(OTf)]$ was directly monitored by polarization modulation reflection absorption IR spectroscopy. During polymer growth, ethylene insertion into the Pd-acyl bond of a preformed 6-membered palladacycle was observed.⁵²⁰ Dppd, dppp and dppb catalysts were studied using EXAFS.⁵²¹ *In situ* NMR and IR studies have been reported on dppp-Pd-CF₃CO₂H catalysts.⁵²² The terpolymerization of ethylene, styrene, and carbon monoxide was prepared using two different palladium-based catalysts, i.e., a phosphine-based ligand system and a nitrogen-based ligand system.⁵²³ Enantioselective alternating copolymerization of carbon monoxide with propylene, 1-heptene, 1-octene, and styrene was carried out using a palladium catalyst modified by DDPPI. The pure poly(1,4-ketone)s were obtained by dissolving the copolymers containing spiroketal and 1,4-ketone units in 1,1,1,3,3,3-hexafluoro-2-propanol and reprecipitating with methanol. Highly optically active and isotactic alternating copolymers of propylene, 1-heptene, 1-octene, and styrene with CO have been prepared using $[(DDPPI)Pd(CH_3CN)_2](BF_4)_2$ as the catalyst.⁵²⁴⁻⁵²⁶

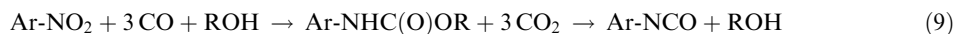
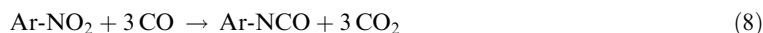
The kinetic behavior of the $[Pd(bdompp)(TFA)_2]$ catalyst (*bdompp* = 1,3-bis(*o*-methoxyphenyl)phosphino)propane) in the CO/ethylene copolymerization under slurry process conditions was studied by end-group analysis. Termination and initiation pathways of the reaction lead both to ester (E) and ketone (K) end-groups and therefore to EE, EK, and KK end-groups in the polymers. With increasing copolymer chain length, a transition of the running Pd-based catalyst species from the homogeneous into the heterogeneous phase was observed.⁵²⁷ Pd^{II} complexes of ligands of the type $Ar_2PCH_2-PAr_2$ and $Ar_2PN(Me)PAr_2$ ($Ar = ortho$ -substituted Ph group) are very efficient catalysts for copolymerization of CO and C₂H₄.⁵²⁸ C₂- and C₃-symmetric $[(PP)Pd(H_2O)_2](SO_3CF_3)_2$ complexes (where PP is either a *rac*- or a *meso*-diphosphine ligand) catalyzed the copolymerization of propylene and carbon monoxide to isotactic poly(1-methyl-2-oxo-1,3-propanediyl). The *meso* ligands are even more stereoselective than the racemic ligands and display much higher catalytic activity.⁵²⁹ New cationic Pd^{II} complexes, containing CS-symmetric nitrogen donor chelate ligands with pyrazolyl moieties, catalyze the copolymerization of styrene with CO under mild conditions, to produce a syndiotactic copolymer.⁵³⁰ Cationic Pd imine-phosphine complexes $[Pd(P-N)(CH_3)(CH_3CN)]^+$ catalyze the living block polymerization and copolymerization of alkenes and/or carbon monoxide.⁵³¹ PdMe complexes with a phosphine-imine bidentate ligand (*o*-Ph₂PC₆H₄ CH:NPh) were active in the insertion reaction with various alkenes as well as ethylene/CO cooligomerization.⁵³²

9.3.5 REDUCTIVE CARBONYLATION OF NITRO COMPOUNDS

9.3.5.1 Introduction

Reductive carbonylation of nitro compounds (in particular aromatic dinitro compounds) is an important target in industry for making diisocyanates, one of the starting materials for poly-carbamates. At present diisocyanates are made from diamines and phosgene. Direct synthesis of isocyanates from nitro compounds would avoid the reduction of nitro compounds to anilines, the

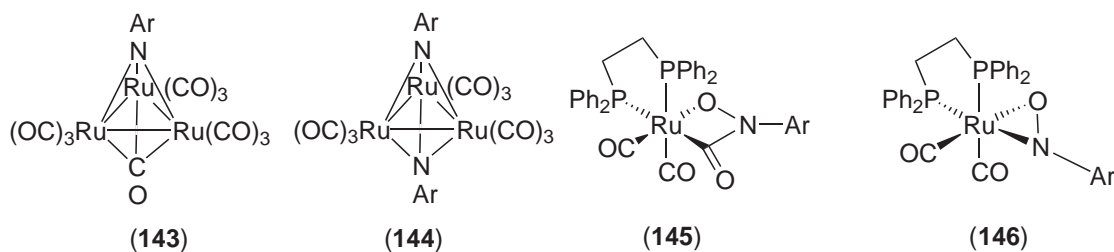
use of phosgene, and the regeneration of hydrogen chloride to chlorine. During the 1970s to 2000s a lot of research has been devoted to catalytic conversion of nitro compounds and carbon monoxide, be it either directly to isocyanates or to carbamates. The latter can be converted to isocyanates simply by heating under loss of alcohol:



Important by-products are urea derivatives (ArNHC(O)NHAr) and azo compounds (Ar-N=N-Ar). The reaction is highly exothermic ($-128 \text{ kcal mol}^{-1}$) and it is surprising that still such low rates are obtained (several hundred turnovers per hour) and high temperatures are required (130°C and 60 bar of CO) to obtain acceptable conversions.⁵³³ Up to 2002, no commercial application of the new catalysts has been announced. Therefore, it seems important to study the mechanism of this reaction in detail aiming at a catalyst that is sufficiently stable, selective, and active. Three catalysts have received a great deal of attention; those based on rhodium, ruthenium, and palladium. Many excellent reviews,⁵³⁴⁻⁵³⁷ have appeared and for the discussion of the mechanism and the older literature the reader is referred to those. Here we concentrate on the coordination compounds identified in relation to the catalytic studies.⁵³⁴⁻⁵³⁹

9.3.5.2 Ruthenium catalysts

Ruthenium cluster compounds (**143**) and (**144**) have been identified that may play a role in the catalysis when $\text{Ru}_3(\text{CO})_{12}$ was used as the precursor.⁵⁴⁰⁻⁵⁴³ The use of $[(\text{dppe})\text{Ru}(\text{CO})_3]$ as a catalyst including the intermediates (**145**) and (**146**) in the catalytic cycles, have been studied in detail by Gladfelter and co-workers.⁵⁴⁴⁻⁵⁵⁰



9.3.5.3 Palladium catalysts

Palladium compounds have been known as catalysts for the reductive carbonylation of nitro compounds to isocyanates since 1967. During the 1970s they were extensively studied by Nefedov and co-workers. Addition of Lewis acids such as FeCl_3 and pyridine derivatives accelerated the reaction, while 2,2'-bipyridine was reported to stop the reaction.⁵⁵¹ Palladium catalysts were studied by Schwetlick and co-workers in a series of papers also entirely concerned with isocyanate formation.⁵⁵² At the beginning of the 1980s the first papers appeared discussing the formation of carbamates using the same catalysts in methanol or ethanol. Rhodium and iridium PPh_3 complexes were used as new homogeneous catalysts for methyl-*N*-phenylcarbamate synthesis by the carbonylation of nitrobenzene in methanol.⁵⁵³⁻⁵⁵⁶

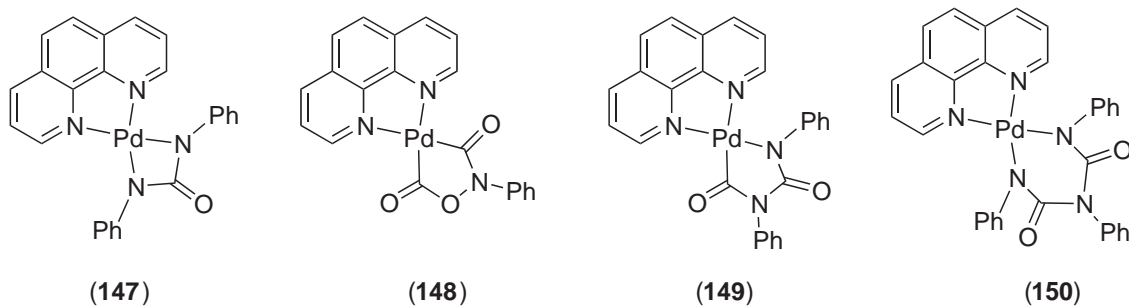
When noncoordinating anions were used, bidentate nitrogen ligands gave fast and selective catalysts.⁵⁵⁵ Addition of carboxylic acids to these systems led to very effective catalysts.⁵⁵⁷ Supported catalysts were found to be active.⁵⁵⁸ Ligand effects and various conditions have been studied with the aim of improving the efficiency of the system and to shed light on the nature of the catalyst.⁵⁵⁹⁻⁵⁶² 2,4,6-Trimethylbenzoic acid is a highly effective co-catalyst, which is also used for applications in organic syntheses.⁵⁶³

Effects of acid strength and anion concentration have been studied as well as the effect of monodentate amines.^{564,565} Phosphines, in particular dppp , have been used as favorable ligands,^{566,567} but it has been shown that dppp is oxidized by nitrobenzene under the prevailing conditions.⁵⁶⁸ Giant clusters and heteropolyanions have been used.^{569,570} The role of nitroso

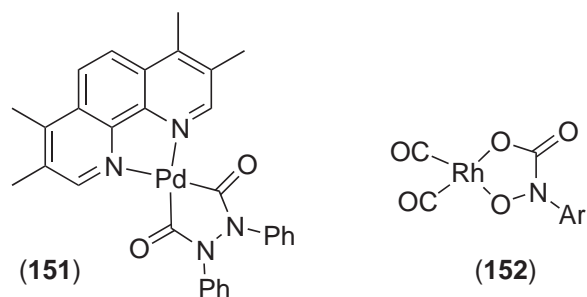
compounds has been studied.⁵⁷¹ Selectivity was optimized using the classic catalyst PdCl₂/pyridine/FeCl₃.^{572,573}

A metallacyclic complex has been isolated from the reaction of PhNO₂ with CO using the Pd^{II}-*o*-phenanthroline system known to produce PhNCO or carbamates catalytically. Reactions of this metallacycle have been studied and its role in the catalytic reaction discussed.⁵⁷⁴

The synthesis and characterization of a family of metallacyclic complexes (147)–(150) of Pd, were reported. The complexes were isolated during the catalytic carbonylation of nitroaromatics using Pd complexes and are probably intermediates in the catalytic process. A mechanistic pathway for the carbonylation process implicating metallacycle intermediates was proposed without intervention of a metal–imido intermediate. Thermal decomposition studies of the metallacycle were also presented.^{575,576}



During the reductive carbonylation of azoxybenzene to N-Ph urethane a possible key intermediate was isolated, i.e., (151).⁵⁷⁷



9.3.5.4 Rhodium catalysts

Rhodium compounds have also been used as catalysts since the late 1960s and mechanistic studies date from the 1970s.^{534,578–582} The binuclear rhodium complex [(Ph₃P)₄Rh₂(μ-OH)₂] was found to be an effective catalyst for the reductive carbonylation of nitrobenzenes to carbamate esters. Electron-withdrawing groups at the *para*-position enhance the reactivity of the substrate.⁵⁸³

Recent mechanistic studies were conducted by Ragaini *et al.* using tetracarbonyl rhodate complexes. Several potential intermediates such as (152) have been isolated.^{584,585} The catalytic system has been optimized and the influence of solvent was examined.⁵⁸⁶ 2-Hydroxypyridine has a large activating effect on the [PPN][Rh(CO)₄]-based catalytic system for the reductive carbonylation of nitrobenzene to Me phenylcarbamate.⁵⁸⁷

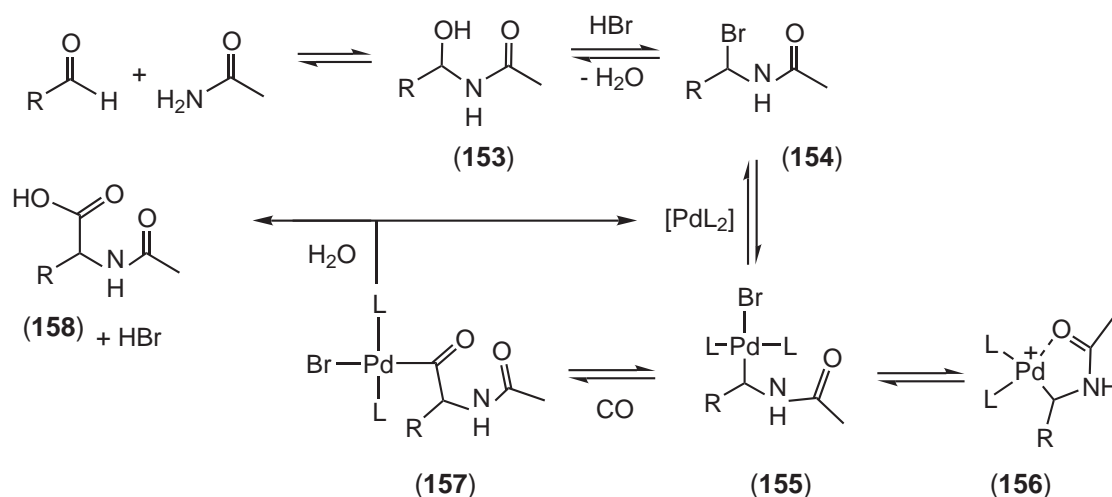
9.3.5.5 Amidocarbonylation

Amidocarbonylation converts aldehydes into amido-substituted amino acids, which have many important industrial applications ranging from pharmaceuticals to detergents and metal-chelating agents.⁵⁸⁸ Two catalyst systems have been developed, a cobalt-based system and, more recently a palladium-based system. In the cobalt system, alkenes can be used as the starting material, thus conducting alkene-hydroformylation, formation of hemi-amidal and carbonylation in one pot as

a cascade reaction. The reactions have been reviewed many times and reference is made to those reviews.^{589–596}

9.3.5.5.1 Palladium catalysts

In the 1990s palladium became the metal of choice for amidocarbonylation as it was much more active than cobalt. The first examples of effective palladium catalysts were reported by Jaegers and Koll who reacted $\text{Me}_2\text{CHCH}_2\text{CHO}$ and MeCONH_2 using $(\text{Ph}_3\text{P})_2\text{PdCl}_2$ and NaBr as the catalyst in *N*-methylpyrrolidone, with 120 bar CO at 120 °C to obtain 81.3% $\text{Me}_2\text{CHCH}_2\text{CH}(\text{CO}_2\text{H})\text{NHAc}$.⁵⁹⁷ Further modification by Beller *et al.* led to catalysts that are active at 80 °C and 30–60 bar of CO in the presence of palladium halides, protic acids, and lithium bromide. The reaction also proceeds in the absence of phosphines. Scheme 7 shows the proposed mechanism.⁵⁹⁸



Scheme 7

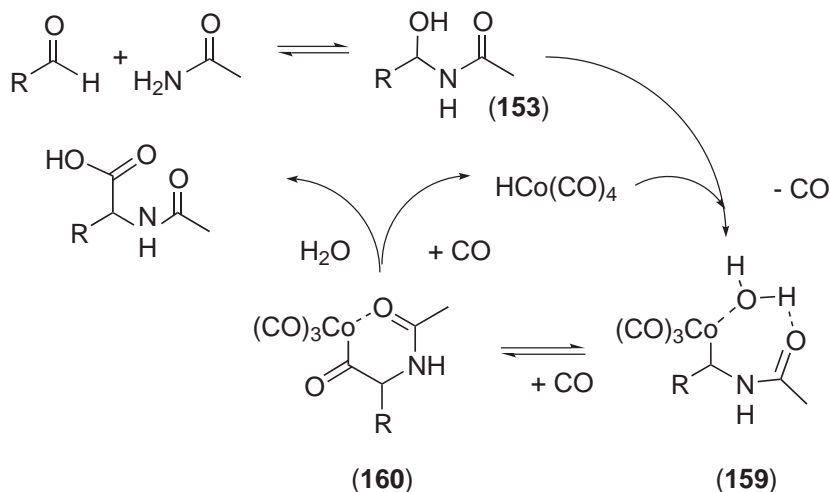
The mechanism differs from that of the cobalt-based reactions in that formation of an organic bromide (154) is assumed and an oxidative addition to Pd^0 is involved to give (155). The influence of solvent, temperature, pressure, co-catalysts, and substrates has been reported. The successful employment of acetals and various aldehydes as starting materials demonstrates the synthetic potential of this atom-economic process.⁵⁹⁹ The use of Pd/C as a catalyst has been demonstrated.⁶⁰⁰ An efficient one-pot synthesis of *N*-acyl α -amino acids by amidocarbonylation starting from aldehydes, nitriles, and CO in the presence of acid and Pd catalysts was described.⁶⁰¹ The putative intermediate (155) and (156) has been synthesized via insertion of imines into palladium acetyl bonds.^{602–606} It has been shown that enamides and *N*-acyl imines can be used as starting materials under amidocarbonylation conditions, although the reaction is markedly slower than the amidocarbonylation described above. These compounds were competent substrates resulting in the formation of *N*-acyl amino acids. The presence of water was found to be necessary and a mechanism in line with these new findings was presented.⁶⁰⁷ A theoretical study has been reported.⁶⁰⁷

Iridium, rhodium, and ruthenium complexes were found to be active for amidocarbonylation under similar conditions as palladium.⁶⁰⁹

9.3.5.5.2 Cobalt catalysts

Amidocarbonylation is derived from the findings by Wakamatsu. It has been extensively reviewed and many mechanistic studies were reported by Ojima.^{610,611}

Coordination of the amide carbonyl to the Co metal center bearing a H_2O molecule as a ligand in (159) is crucial for the suppression of hydrogenolysis as compared to hydrolysis even under a high pressure of H_2 . The mechanism is shown in Scheme 8.^{612,613}

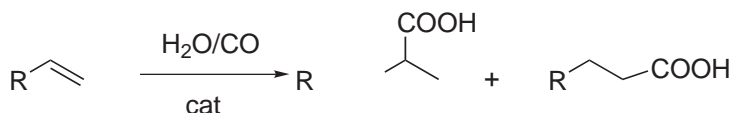


Scheme 8

The hydroformylation-amidocarbonylation of $\text{CF}_3\text{CH}=\text{CH}_2$ with AcNH_2 , CO , and H_2 catalyzed by a Co–Rh binary system gave $\text{CF}_3\text{CH}_2\text{CH}_2\text{CH}(\text{NHAc})\text{CO}_2\text{H}$ in a regiospecific manner.⁶¹⁴ Cobalt catalysts containing bidentate phosphine ligands $\text{Ph}_2\text{P}(\text{CH}_2)_n\text{PPh}_2$ ($n = 2, 3, 6$) have been reported; monophosphines were also used. The process proceeds via alkene hydroformylation and amidocarbonylation.^{615–618} The use of stibine ligands in amidocarbonylation of cyclohexene and 1-pentene catalyzed by $\text{Co}_2(\text{CO})_8$ not only enhances the activity of catalyst but also increases the selectivity in comparison to classical phosphinic ligands at 25 bar.⁶¹⁹ Mixed rhodium/cobalt systems have been reported.^{620,621} For benzylic starting materials for the preparation of *d*, *l*-phenylalanine via amidocarbonylation the use of chloride is required as alcohols give very low conversions.⁶²² Industrial applications include the synthesis of glufosinate.^{623,624}

9.3.6 HYDROXYCARBONYLATION

Hydroxycarbonylation and alkoxy carbonylation of alkenes catalyzed by metal catalyst have been studied for the synthesis of acids, esters, and related derivatives. Palladium systems in particular have been popular and their use in hydroxycarbonylation and alkoxy carbonylation reactions has been reviewed.^{625,626} The catalysts were mainly designed for the carbonylation of alkenes in the presence of alcohols in order to prepare carboxylic esters, but they also work well for synthesizing carboxylic acids or anhydrides.^{137,627} They have also been used as catalysts in many other carbonyl-based processes that are of interest to industry. The hydroxycarbonylation of butadiene, the dicarboxylation of alkenes, the carbonylation of alkenes, the carbonylation of benzyl- and aryl-halide compounds, and oxidative carbonylations have been reviewed.⁶²⁸ The Pd-catalyzed hydroxycarbonylation of alkenes has attracted considerable interest in recent years as a way of obtaining carboxylic acids. In general, in acidic media, palladium salts in the presence of mono- or bidentate phosphines afford a mixture of linear and branched acids (see Scheme 9).



Scheme 9

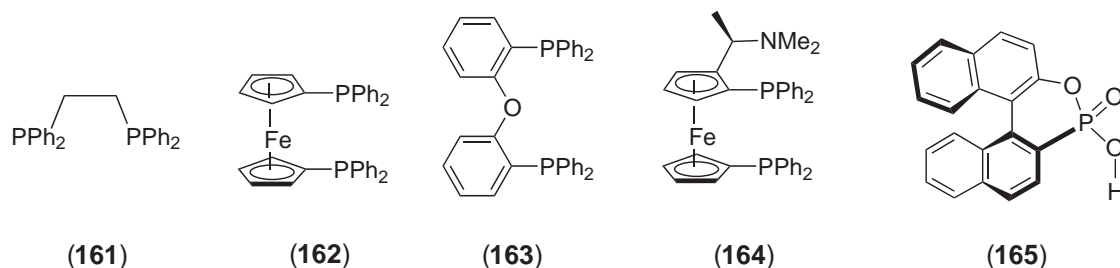
Several reports covering carbonylation and other aspects of homogeneous catalysis include the hydroxycarbonylation reaction with palladium systems.^{310,311,629} A review summarizing the results and findings about the mechanism has been published.⁶³⁰ The carbonylation of vinyl

aromatics is important for the syntheses of 2-phenylpropionic acids and esters, a class of nonsteroidal anti-inflammatory drugs.^{309,630} Also, the linear products 3-phenylpropionic acid and esters have found application as specialty chemicals. In view of the synthetic importance of the preparation of phenylpropionic acids, styrene has been selected as the model substrate in carbonylation studies. Several catalytic cycles have been proposed both for linear products as well as styrene hydroxycarbonylation.^{631–634}

9.3.6.1 Palladium/Phosphorus Complexes in Hydroxycarbonylation

Monophosphines and diphosphines have been the ligands mostly used in Pd-catalyzed processes. When monophosphines are used as ligands in the hydroxycarbonylation of styrene the major product is 2-phenylpropanoic acid with practically total regioselectivity. In contrast, the use of diphosphines as auxiliary ligands switches the regioselectivity to the linear product. Moreover, activity and regioselectivity in the hydroxycarbonylation of styrene are sensitive to the nature of the counter anion of the acid. The regioselectivities generally obtained for mono- and diphosphines depend strongly on the nature of the anion. In spite of several studies into the regioselectivity of the reaction, a satisfactory explanation for the regioselectivity is still lacking.⁶³¹ Highly regioselective hydroxycarbonylation of 4-methylstyrene to the branched α -(4-methylphenyl)propionic acid has been achieved with the system PdCl₂-CuCl₂-PPh₃, dissolved in a polar solvent. The effect of the mineral acids as additives in this reaction has been studied. Efficient hydroxycarbonylation reaction was achieved only after a halogen compound had been added; the addition of HCl improved the reaction rate significantly.⁶³⁵ Formic or oxalic acid have been used for the regioselective hydroxycarbonylation of alkenes and alkynes catalyzed by Pd and phosphine ligands. The reaction of mono- and disubstituted alkenes with formic acid, catalytic quantities of palladium acetate and dppb (**31**) in a carbon monoxide atmosphere, affords carboxylic acids in 45–98% yield. The reaction is regioselective, and in a number of cases, regiospecific for the straight chain acid. Control of the regioselectivity of the reaction depends, in part, on the effective bulk of the substituent group of the alkene; more hindered alkenes produce high yields of the linear acid.^{633,636,637} This system shows excellent functional group tolerance. For the Pd^{II} acetate/oxalic acid system a mechanism has been proposed. Monophosphines and diphosphines were used together in the hydroxycarbonylation of alkenes, PPh₃ was added to the [Pd(OAc)₂]/dppb system and this improved the yield and did not significantly affect the product distribution.^{633,638}

A systematic study of the hydroxycarbonylation reaction of styrene has been reported including the effects of the catalytic precursor and the reaction conditions. Several monophosphines (PPh₃, P(*p*-Tol)₃, P(*p*-C₆H₄OMe)₃, P(*p*-C₆H₄F)₃, PPh₂(*o*-Tol), PMe₃, and PCy₃) and diphosphines (dppb (**31**), dppe (**161**), dppp (**30**), dppf (**162**), Xantphos (**32**), DPEphos (**163**), bdpp (**87**), BINAP (**103**), BPPFA (**164**), and DIOP (**85**)) were applied to control the regioselectivity of the reaction. The effect of the bite angle of the diphosphines has been studied. Catalysts containing monophosphines as ligands give 2-phenylpropanoic acid as the major product; the 3-phenylpropanoic acid is obtained when diphosphines are used. Two catalytic cycles are proposed to explain the influence of the different palladium precursors with mono- and diphosphines.⁶³⁹



The critical role of the counter anion in the hydroxycarbonylation of styrene for different phosphorus-modified palladium systems has been reported. The regioselectivity can be controlled

by the phosphorus ligand and the counter anion.⁶⁴⁰ Hydroformylation of alkenes in a two-phase system using a water-soluble palladium complex of trisulfonated PPh₃ (TPPTS, (**126**)) as catalyst, and a Brønsted acid as promoter, has been reported. A catalytic cycle for the hydroxycarbonylation of alkenes in biphasic media has been proposed.⁶⁴¹ The application of a water-soluble diphosphine with a xanthene-type backbone in the biphasic Pd-catalyzed hydroxycarbonylation reaction of alkenes leads to the selective formation of carboxylic acids.⁶⁴² Asymmetric hydroxycarbonylation attracts considerable attention because of the biological activities of the acids that could be obtained. Unfortunately, however, as yet only a few cases of success have been reported.³¹¹ The synthesis of acids in high enantioselectivity (91%) using (**165**) for the Pd^{II}-catalyzed hydroxycarbonylation of 2-vinyl-6-methoxynaphthalene has been reported.⁶⁴³

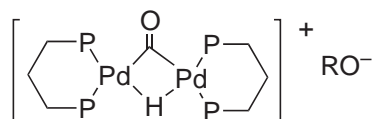
Several Pd^{II} complexes with thiolate or thioether derivative ligands have been studied to be applied in the hydroxycarbonylation reaction.³⁹⁴ Amino thiolate complexes of palladium with PPh₃ catalyze the conversion of styrene to 2-phenylpropionic acid in high yield and excellent regioselectivity.⁶⁴⁴ Under mild conditions and in the presence of a catalytic amount of an *S,N*-chelated palladium *ortho*-amino-arene thiolate complex, styrene reacts with CO and oxalic acid or water to selectively give 2-phenylpropanoic acid in high yield.⁶⁴⁵

9.3.6.2 Palladium Species Involved in the Hydroxycarbonylation Reaction

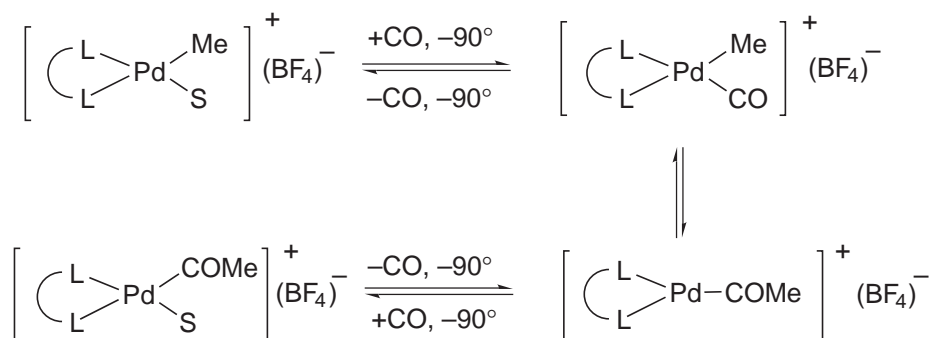
The reaction is shown in Scheme 9. A number of palladium complexes have been described through the study of the reactivity of the precursors of the hydroxycarbonylation reaction as well as in the determination of mechanisms and intermediates. Stable Pd⁰ complexes were generated *in situ* from a cationic Pd^{II} complex [Pd(PPh₃)₂](BF₄)₂, when water and PPh₃ were present in solution. PPh₃ was able to reduce the Pd^{II} metal center to Pd⁰, itself being oxidized to PPh₃=O. The reduction took place from a Pd^{II} complex in which the palladium ion was most likely ligated by a hydroxy group.^{646–649} The reduction of Pd^{II} to Pd⁰ was also investigated in the presence of both monodentate PPh₃ and bidentate dppp (**30**) phosphines. Phosphorus-31 NMR measurements showed that PPh₃ can reduce [Pd(OAc)₂] to Pd⁰ in toluene. Bidentate dppp is mainly responsible for the reduction in DMF, which results in dppp hemioxide and dppp dioxide.⁶⁵⁰ A Pd⁰ complex is spontaneously generated from Pd(OAc)₂ and a bidentate phosphine such as dppp, which is the reducing agent and is oxidized to the hemioxide (dpppO). A stable Pd⁰ complex is quantitatively formed in the presence of dppp, water, and a base.⁶⁵¹

Neutral palladium hydride complexes of the type [PdHCl(PPh₃)₂] can be synthesized by oxidative addition of strong acids, as in the oxidative addition of HCl to Pd⁰ complexes such as [Pd(CO)(PPh₃)₃] or [Pd(PPh₃)₄], and has been extensively studied.⁶³¹ With diphosphine ligands, the hydride complexes *cis*-[PdHCl(P-P)] seem highly unstable and numerous attempts to synthesize them failed, and cationic binuclear complexes of palladium [(P-P)₂Pd₂(μ-H)(μ-CO)]⁺ (**166**) form easily during carbonylation reactions. These binuclear complexes have been isolated, characterized, and the reactivity of them with alkenes under CO atmosphere has been studied. Apparently, it is important to stabilize the systems with CO and to create a bridging instead of a terminal hydride *trans* to phosphine.^{652–654} Benzyl palladium complexes *trans*-[Pd(CH₂Ph)Cl(PPh₃)₂] have been synthesized by the oxidative addition of benzyl chloride to Pd⁰ complexes as [Pd(PPh₃)₄].⁶⁵⁵ The structure of the arylpalladium complexes of the type *trans*-[Pd(Ph)X(PPh₃)₂] (X = F, Cl, Br, I) were studied by single-crystal XRD and the relative affinities of the halide anions for the metal center were studied using ³¹P NMR spectroscopy.⁶⁵⁶ Palladium η³-benzyl complexes have also been prepared by insertion of styrene into the Pd–Me bond of the solvated cation [PdMe(L-L)S]. This η³ coordination of the benzyl ligand has been elucidated by X-ray structure determination and NMR spectroscopy. NMR studies showed that the palladium η³-benzyl complexes undergo two dynamic processes in solution: the η³–η¹ coordination of the benzyl group and the ligand exchange of coordination sites.⁶⁵⁷ *In situ* IR spectroscopic studies were performed during the hydroxycarbonylation of ethene with [PdCl₂(PPh₃)₂] and the intermediate species [Pd(COEt)Cl(PPh₃)₂] was observed. A mechanism with Pd–H active species has been proposed.⁶⁵⁸ In favor of the participation of carbalkoxy palladium species the following two observations may be mentioned. Cationic complexes [(P-P)PdC(O)OCH₃(PPh₃)]⁺, where P-P = dppe, dppp, dppb, undergo slow insertion of reactive alkenes such as norbornadiene.^{468,659–661} Formation of diesters and polyketones with diester end-groups indicates that cationic species under anhydrous conditions may give insertion of alkenes into carbalkoxy palladium species.⁶⁶⁰ HP NMR spectroscopy was also used to identify the chiral ionic square planar [Pd(Me)(CO)((**87**)-2*S*,4*S*)]BF₄

compound (the *S,S* analog of **(87)** = (2*S*,4*S*)-2,4-bis(diphenylphosphino)pentane)) as an intermediate in the CO insertion into the Pd–Me bond. This compound was formed *in situ* by the reaction of the solvated [Pd(Me)S(bdpp)]BF₄ with ¹³CO in a HP NMR tube. Concomitant with the decomposition of [Pd(Me)(CO)(bdpp)]BF₄, the [Pd(COMe)(CO)(bdpp)]BF₄ complex was formed as shown in Scheme 10.



(166)



Scheme 10

Also, several experiments were carried out to investigate whether the methyl(carbonyl) complex was also an intermediate in the formation of the methoxycarbonyl compound [Pd(Me)(CO₂Me)(bdpp)], but this compound could not be obtained this way.⁶⁶² Phosphorus–nitrogen ligands were used for the insertion of carbon monoxide in both ionic and neutral complexes.⁶⁶³ In such complexes the preferred structures contain the methyl and acetyl group *cis* to the phosphine ligand, as one would expect according to the *trans* influence. As a result the insertion reaction for such P–N ligands is slower than those for either P–P or N–N ligands, because in the first instance migration leads to a less stable isomer containing the acetyl group *trans* to phosphorus.⁶⁶⁴

A similar involvement of palladium hydride, palladium alkyl, and palladium acyl complexes as intermediates in the catalytic cycle of the Pd-catalyzed hydroxycarbonylation of alkenes was reported for the aqueous-phase analogs. The cationic hydride [PdH(TPPTS)₃]⁺ was formed via the reduction of the Pd^{II} complex with CO and H₂O to [Pd(TPPTS)₃] and subsequent protonation in the acidic medium. The reaction of the hydride complex with ethene produced two new compounds, [Pd(Et)(TPPTS)₃]⁺ and [Pd(Et)(solvent)(TPPTS)₂]⁺. The sample containing the mixture of palladium alkyl complexes reacted readily with CO to afford *trans*-[Pd(C(O)Et)(TPPTS)₂]⁺.⁶⁶⁵

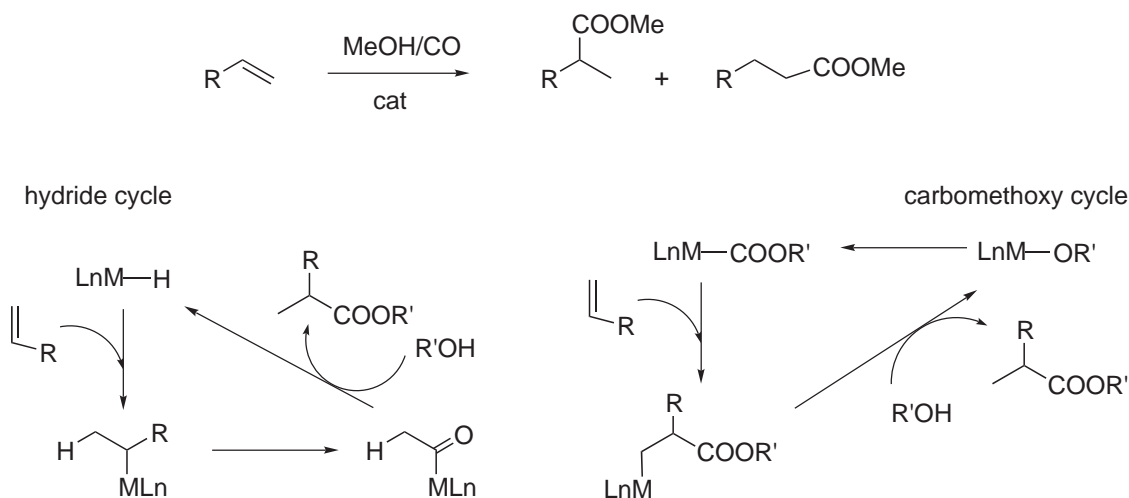
9.3.6.3 Methoxycarbonylation

As with carboxylic acids obtained by palladium hydroxycarbonylation, their derivatives esters, amides, anhydrides and acyl halides are synthesized from alkenes, CO and HX (X = OR⁻, NR₂⁻ etc.). The Pd-catalyzed methoxycarbonylation is one of the most studied reactions among this type of catalyzed carbonylations and has been reviewed and included in reports of homogeneous catalysis.^{625,626} The methoxycarbonylation has been applied to many different substrates to obtain intermediates in organic syntheses as well as specific products. For instance, the reaction has been applied for methoxycarbonylation of alkynes.⁶⁶⁶ Highly efficient homogeneous Pd cationic catalysts have been reported and the methoxycarbonylation of alkynes has been used to develop economically attractive and environmentally benign process for the production of methyl

methacrylate (MMA). The process is based on the highly efficient Pd-catalyzed methoxycarbonylation of propyne under mild, noncorrosive reaction conditions.⁶⁶⁷⁻⁶⁶⁹

9.3.6.3.1 Mechanistic studies

The mechanisms of the hydroxycarbonylation and methoxycarbonylation reactions are closely related and both mechanisms can be discussed in parallel (see Section 9.3.6).⁶³¹ This last reaction has been extensively studied. Two possibilities have been proposed. The first starts the cycle with a hydrido-metal complex.⁶⁷⁰ In this cycle, an alkene inserts into a Pd—H bond, and then migratory insertion of CO into an alkyl-metal bond produces an acyl-metal complex. Alcoholysis of the acyl-metal species reproduces the palladium hydride and yields the ester. In the second mechanism the crucial intermediate is a carbalkoxymetal complex. Here, the insertion of the alkene into a Pd—C bond of the carbalkoxymetal species is followed by alcoholysis to produce the ester and the alkoxymetal complex. The insertion of CO into the alkoxymetal species reproduces the carbalkoxymetal complex.⁶³⁰ Both proposed cycles have been depicted in Scheme 11.



Scheme 11

Most researchers currently agree that the hydrido mechanism is more common than the alkoxycarbonyl path in the alkoxycarbonylation of alkenes with palladium systems. However, carbalkoxy complexes are putative intermediates in carbonylation reactions giving succinates and polyketone diesters, with metals like Co, Rh, or Pd.¹³⁷

An *ab initio* MO study showed that hydrido-Pd species would be a preferable key intermediate instead of alkoxycarbonyl-Pd species in the Pd^{II} methoxycarbonylation of styrene. The unifying mechanistic theme of these diverse reactions may be the generation of a carbalkoxymetal intermediate, M—CO₂R.⁶⁷² Evidence for the hydride mechanism in the methoxycarbonylation of ethene catalyzed by palladium-PPh₃ complexes has been reported by using palladium PPh₃ complexes with a combination of HPLC and MS.⁶⁷³ The mechanism of styrene hydroesterification using [Pd(OTs)₂(PPh₃)₂] formed *in situ* from Pd(OAc)₂, PPh₃, and TsOH in MeOH was studied by isolation and characterization of catalytically active intermediates. Pd-hydridocarbonyl and Pd-acyl complexes were isolated and characterized from reaction mixtures, based on which a Pd hydride mechanism was proposed. Formation of Pd-hydride species was also confirmed by ³¹P NMR experiments.^{674,675} The catalytic pathways of the Pd(PPh₃)₂/SnCl₂ catalyzed alkoxycarbonylation of styrene have been studied using deuterium labeling and the different reaction products were detected by mass spectral analysis and NMR methods.⁶⁷⁶

The mechanism of the methoxycarbonylation of alkynes⁶⁶⁷⁻⁶⁶⁹ promoted by the Pd(OAc)₂/PPh₂(pyc)/CH₃SO₃H catalytic system has been reported. Experiments carried out using 1-alkynes and CH₃OD and ¹H NMR reveal that the catalyst also promotes the exchange of the terminal hydrogen of the alkyne with the deuterium of the alcohol.⁶⁷⁷

9.3.6.3.2 Palladium complexes involved in the methoxycarbonylation reaction

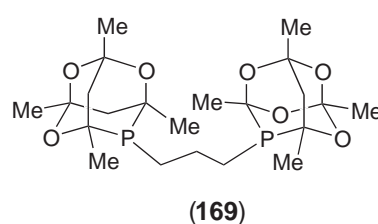
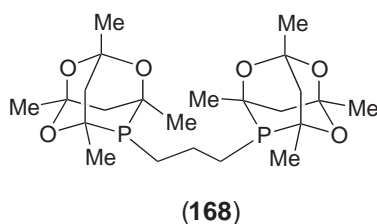
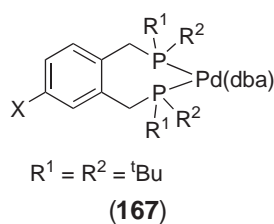
The synthesis and spectroscopic characterization of all the intermediates in the Pd-catalyzed methoxycarbonylation of ethane have been reported. The mechanism of the Pd-catalyzed methoxycarbonylation of C_2H_4 to give $EtCO_2Me$ involves a hydride rather than a methoxycarbonyl cycle. All the intermediates in this cycle were identified by multinuclear NMR spectroscopy and ^{13}C labeling. The complex $[Pd(L-L)(dba)]$ (**167**) (where $L-L = 1,2-(CH_2P^tBu)_2C_6H_4$ and $dba = trans,trans$ -dibenzylideneacetone) reacts in MeOH with HBF_4 or CF_3SO_3H to produce a new compound that can be formulated as either the neutral complex $[Pd(L-L)HX]$ or the solvated cation $[Pd(L-L)H(MeOH)]X$. This hydride complex reacts immediately with ethene to form the cationic $[Pd(L-L)Et(MeOH)]X$. On adding one equivalent of CO to the alkyl complex $[Pd(L-L)-(C(O)Et)(MeOH)]X$ is formed, and on addition of a trace of MeOH to the solution there is an immediate reaction to regenerate the palladium hydride complex with the formation of $EtCO_2Me$. It has to be noted that the palladium hydride complex is stable even in the presence of oxidants (benzoquinone or oxygen) under these conditions. There was no evidence of the formation of any carbomethoxy complex.⁶⁷⁸ For other systems formation of carbomethoxy-palladium species is a well documented process.^{679,680} It should be noted, however, that the formation of carbomethoxy complexes under these conditions requires anhydrous conditions, because, in the presence of traces of water, carbhydroxy-palladium forms which rapidly loses carbon dioxide to give palladium hydride.⁶⁸¹

In the case of the styrene, the mechanism of the methoxycarbonylation using *in situ* formed $[Pd(OTs)_2(PPh_3)_2]$ from $[Pd(OAc)_2]$, PPh_3 and $TsOH$ in methanol has been investigated by isolating and characterizing intermediates. From the reaction mixtures, palladium-hydridocarbonyl and palladium-acyl complexes were isolated and characterized, and in accordance with this, a palladium hydride mechanism has been proposed. After the catalyst precursor system $[Pd(OAc)_2]-4PPh_3-10TsOH$ was treated with CO at $75^\circ C$ for 30 min, the complex $[Pd(H)CO(PPh_3)_2](TsO)$ was characterized. When the methoxycarbonylation was performed with $PdCl_2$ as the catalyst precursor, the acyl complex *trans*- $[PdCl(COCH_2CH_2Ph)(PPh_3)_2]$ was isolated.⁶⁷⁴

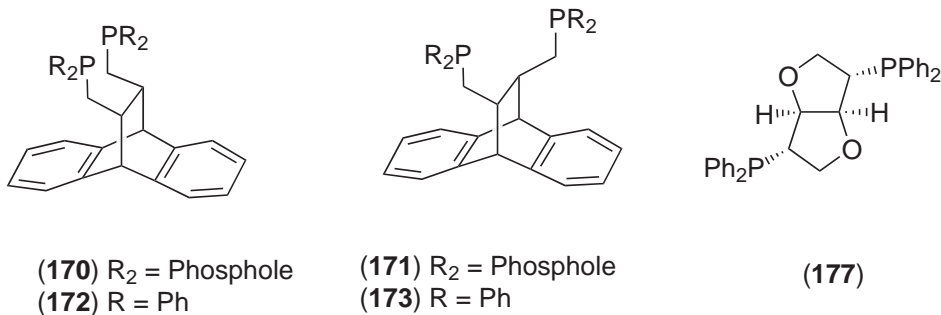
9.3.6.3.3 Phosphorus ligands in Pd methoxycarbonylation

Phosphorus ligands, mono- and diphosphines differently modified, have been used for palladium methoxycarbonylation of alkenes. A highly active and selective catalyst for the production of Me propanoate via the methoxycarbonylation of ethene is based on a zerovalent Pd complex (**167**).⁶⁸² The zerovalent complexes $[Pd(Ph_2Ppy)_3]$ and $[Pd(Ph_2Ppy)_2(dba)]$ ($Ph_2Ppy = diphenyl$ -pylphosphine) were synthesized and characterized. The complex $Pd(Ph_2Ppy)_3$ is found to catalyze the vinylation of Ph_2Ppy to the corresponding 2-propenylphosphonium trifluoromethanesulfonate.⁶⁸³ The cationic Pd^{II} complex $[Pd(MeCN)_2(PPh_3)_2](BF_4)_2$ was found to be an active catalyst for methoxycarbonylation of various alkenes under mild conditions. The system $Pd(OAc)_2-PPh_3-p$ -toluenesulfonic acid, which should give rise to cationic species "*in situ*," was effective in producing the branched ester regioselectively in the hydroesterification of styrene at ambient temperature.⁶⁸⁴ $Pd(OAc)_2$ in combination with tri(2-furyl)phosphine and methanesulfonic acid is an efficient catalyst for the alkoxy carbonylation of 1-alkynes. Moderate reaction rates are obtained under mild conditions with high regioselectivity (ca. 95%) towards the formation of 2-substituted acrylic ester.⁶⁸⁵

Fast, selective conversion of internal alkenes to linear esters is catalyzed by Pd^{II} complexes of chelating bis(phospha-adamanty)diphosphines, e.g., the *meso* (**168**) and racemic (**169**) isomers, and the catalysis is acutely sensitive to the ligand backbone and even to the diastereomer used; the results are compared with those for the P^tBu_2 analogous.⁶⁸⁶



The C₄-bridged phospholes 11,12-bis(2,3,4,5-tetramethylphospholylmethyl)-9,10-dihydro-9,10-ethano-anthracene (*cis*-(**170**); *trans*-(**171**)) and diphosphines 11,12-bis(diphenylphosphino-methyl)-9,10-dihydro-9,10-ethano-anthracene (*cis*-(**172**); *trans*-(**173**)) and their corresponding palladium complexes [(P-P)PdCl₂] have been prepared and characterized. Single-crystal X-ray analyses have been undertaken and they reveal that (**170**)–(**173**) coordinate in a bidentate manner forming seven-membered chelate rings with natural bite angles between 98.62° and 100.30°. The Pd-catalyzed carbonylation of ethylene has been studied using (**170**)–(**173**).⁶⁸⁷



The complexation of the mixed bidentate ligands 1-diphenylphosphino-1'-diphenylthiophosphinoferrocenyl and 1,2-bis(diphenylphosphino)ferrocenyl with palladium(II) species yield a range of palladium complexes. Their interest as possible catalysts for alkene alkoxycarbonylation has been reported.⁶⁸⁸ Palladium(II) phosphinothiolate complexes have been used as catalysts in the methoxycarbonylation of styrene. [PdCl(dppet)PPh₃] (**174**), [Pd(dppet)₂] (**175**), and [Pd₂Cl₂(dpppt-P, μ -S)₂] (**176**), where Hdppet = HSC₂H₄PPh₂, Hdpppt = HSC₃H₆PPh₂, have been synthesized and characterized. Complexes (**174**) and (**176**) catalyze the methoxycarbonylation of styrene at moderate temperatures.⁶⁸⁹

9.3.6.3.4 Asymmetric methoxycarbonylation

Although attempts have been made to achieve asymmetric methoxycarbonylation, only in a few cases has high enantioselectivity been reported.^{310,311} The cationic system Pd(OAc)₂-(chiral-diphosphine)-*p*-toluenesulfonic acid has been studied in the methoxycarbonylation of styrene and 6-methoxy-2-vinylnaphthalene. Enantioselectivities of 12–86% have been achieved, although in these systems with chelate ligands the regioselectivity in branched ester is not higher than 60%.⁶⁸⁴ Asymmetric induction up to 99% and good regioselectivities have been reported in the methoxycarbonylation of styrene in the presence of PdCl₂-CuCl₂ and chiral diphosphine (**177**). The formation of the branched ester in good yield and with high enantiomeric excess has been reported for this system. In this case, however, the rigid structure of the iditol derived ligand could lead to a nonchelating coordination being responsible of the high chiral induction. The monodentate coordination agrees with the high regioselectivity for the branched product.⁶⁹⁰

9.3.7 REFERENCES

- Forster, D.; Singleton, T. C. *J. Mol. Catal. A: Chem.* **1982**, *17*, 299–314.
- Marko, L. *Trans. Met. Chem.* **1992**, *17*, 587–592.
- Zoeller, J. R. *Chem. Ind.* **1993**, *49*, 35–51.
- Dekleva, T. W.; Forster, D. *J. Am. Chem. Soc.* **1985**, *107*, 3565–3567.
- Forster, D.; Dekleva, T. W. *J. Chem. Educ.* **1986**, *63*, 204–206.
- Haynes, A.; Mann, B. E.; Gulliver, D. J.; Morris, G. E.; Maitlis, P. M. *J. Am. Chem. Soc.* **1991**, *113*, 8567–8569.
- Cruise, N. A.; Evans, J. *J. Chem. Soc. Dalton* **1995**, 3089–3091.
- Hallinan, N.; Hinnenkamp, J. *Chem. Ind.* **2001**, *82*, 545–556.
- Dake, S. B.; Chaudhari, R. V. *J. Mol. Catal. A: Chem.* **1984**, *26*, 135–138.
- Nowicki, L.; Ledakowicz, S.; Zarzycki, R. *Ind. Eng. Chem. Res.* **1992**, *31*, 2472–2475.
- Murphy, M. A.; Smith, B. L.; Torrence, G. P.; Aguilo, A. *J. Organomet. Chem.* **1986**, *303*, 257–272.
- Lindner, E.; Glaser, E. *J. Organomet. Chem.* **1990**, *391*, C37–C40.
- Moloy, K. G.; Wegman, R. W. *Adv. Chem. Ser.* **1992**, *230*, 323–336.
- Freiberg, J.; Weigt, A.; Dilcher, H. *J. Prakt. Chem.* **1993**, *335*, 337–344.

15. Dilworth, J. R.; Miller, J. R.; Wheatley, N.; Baker, M. J.; Sunley, J. G. *J. Chem. Soc. Chem. Commun.* **1995**, 1579–1581.
16. Baker, M. J.; Giles, M. F.; Orpen, A. G.; Taylor, M. J.; Watt, R. J. *J. Chem. Soc. Chem. Commun.* **1995**, 197–198.
17. Gonsalvi, L.; Adams, H.; Sunley, G. J.; Ditzel, E.; Haynes, A. *J. Am. Chem. Soc.* **1999**, *121*, 11233–11234.
18. Rankin, J.; Poole, A. D.; Benyei, A. C.; Cole-Hamilton, D. J. *Chem. Commun.* **1997**, 1835–1836.
19. Rankin, J.; Benyei, A. C.; Poole, A. D.; Cole-Hamilton, D. J. *J. Chem. Soc. Dalton* **1999**, 3771–3782.
20. Jiang, H.; Pan, P.; Yuan, G.; Chen, X. *Sci. China Ser. B* **1999**, *42*, 311–315.
21. Maitlis, P. M.; Haynes, A.; Sunley, G. J.; Howard, M. J. *J. Chem. Soc. Dalton* **1996**, 2187–2196.
22. Das, P.; Konwar, D.; Sengupta, P.; Dutta, D. K. *Trans. Met. Chem.* **2000**, *25*, 426–429.
23. Lee, H.-S.; Bae, J.-Y.; Ko, J.; Kang, Y. S.; Kim, H. S.; Kang, S. O. *Chem. Lett.* **2000**, 602–603.
24. Carraz, C.-A.; Orpen, A. G.; Ellis, D. D.; Pringle, P. G.; Ditzel, E. J.; Sunley, G. J. *Chem. Commun.* **2000**, 1277–1278.
25. Jiang, H.; Diao, K.-S.; Pan, P.-L.; Zhang, S.-F.; Yuan, G.-Q. *Chin. J. Chem.* **2000**, *18*, 751–755.
26. Bischoff, S.; Weigt, A.; Miessner, H.; Luecke, B. *Energ Fuels* **1996**, *10*, 520–523.
27. Das, P.; Konwar, D.; Dutta, D. K. *Indian J. Chem. A* **2001**, *40*, 626–629.
28. Kataoka, Y.; Shibahara, A.; Yamagata, T.; Tani, K. *Organometallics* **2001**, *20*, 2431–2433.
29. Yamanis, J.; Yang, K. C. *J. Catal.* **1981**, *69*, 498–501.
30. Gelin, P.; Ben Taarit, Y.; Naccache, C. *Stud. Surf. Sci. Catal. Pt. B* **1981**, 898–910.
31. Yamanis, J.; Lien, C.; Caracotsios, M.; Powers, M. E. *Chem. Eng. Commun.* **1981**, *11*, 355–69.
32. Andersson, S.; Lars, T.; Scurrell, M. S. *J. Mol. Catal. A: Chem.* **1983**, *18*, 375–380.
33. Huang, T. N.; Schwartz, J.; Kitajima, N. *J. Mol. Catal. A: Chem.* **1984**, *22*, 389–393.
34. Denley, D. R.; Raymond, R. H.; Tang, S. C. *J. Catal. A: Chem.* **1984**, *87*, 414–423.
35. Lefebvre, F.; Gelin, P.; Elleuch, B.; Naccache, C.; Ben Taarit, Y. *B. Soc. Chim. Fr.* **1985**, *3*, 361–369.
36. Bischoff, S.; Weigt, A.; Kant, M.; Schuelke, U.; Luecke, B. *Catal. Today* **1997**, *36*, 273–284.
37. Wegman, R. W. *J. Chem. Soc. Chem. Commun.* **1994**, 947–948.
38. Chateau, L.; Hindermann, J. P.; Kiennemann, A.; Tempesti, E. *J. Mol. Catal. A: Chem.* **1996**, *107*, 367–378.
39. De Blasio, N.; Wright, M. R.; Tempesti, E.; Mazzocchia, C.; Cole-Hamilton, D. J. *J. Organomet. Chem.* **1998**, *551*, 229–234.
40. Hjortkjaer, J.; Chen, Y.; Heinrich, B. *Appl. Catal.* **1991**, *67*, 269–278.
41. Drago, R. S.; Nyberg, E. D.; El A'mma, A.; Zombeck, A. *Inorg. Chem.* **1981**, *20*, 641–644.
42. Ellis, B.; Howard, M. J.; Joyner, R. W.; Reddy, K. N.; Padley, M. B.; Smith, W. J. *Stud. Surf. Sci. Catal.* **1996**, *101*, 771–779.
43. Wang, X.; Liu, Z.; Pan, P.; Yuan, G. *Chin. J. Polym. Sci.* **1996**, *14*, 233–239.
44. Chen, Y. Y.; Yuan, G. Q.; Chen, R. Y. *Chin. J. Polym. Sci.* **1989**, *7*, 225–231.
45. De Blasio, N.; Tempesti, E.; Kaddouri, A.; Mazzocchia, C.; Cole-Hamilton, D. J. *J. Catal.* **1998**, *176*, 253–259.
46. Tempesti, E.; Kaddouri, A.; De Blasio, N. *J. Therm. Anal. Calorim.* **1998**, *53*, 177–187.
47. Jiang, H.; Liu, Z.; Pan, P.; Yuan, G. *J. Mol. Catal. A: Chem.* **1999**, *148*, 215–225.
48. Scurrell, M. S.; Howe, R. F. *J. Mol. Catal. A: Chem.* **1980**, *7*, 535–537.
49. Watson, D. J. *Prepr. Am. Chem. Soc., Div. Pet. Chem.* **1999**, *44*, 58–60.
50. Howard, M. J.; Sunley, G. J.; Poole, A. D.; Watt, R. J.; Sharma, B. K. *Stud. Surf. Sci. Catal.* **1999**, *121*, 61–68.
51. Ghaffar, T.; Charmant, J. P. H.; Sunley, G. J.; Morris, G. E.; Haynes, A.; Maitlis, P. M. *Inorg. Chem. Commun.* **2000**, *3*, 11–12.
52. Sunley, G. J.; Watson, D. J. *Catal. Today* **2000**, *58*, 293–307.
53. Jones, J. H. *Platinum Met. Rev.* **2000**, *44*, 94–105.
54. Inui, T.; Matsuda, H.; Takegami, Y. *J. Chem. Soc. Chem. Commun.* **1981**, 906–907.
55. Wang, X.; Jia, Z.; Wang, Z. *J. Nat. Gas Chem.* **1992**, *1*, 65–69.
56. Liu, T. C.; Chiu, S. J. *Ind. Eng. Chem. Res.* **1994**, *33*, 488–492.
57. Kelkar, A. A.; Ubale, R. S.; Deshpande, R. M.; Chaudhari, R. V. *J. Catal.* **1995**, *156*, 290–294.
58. Moser, W. R.; Marshik-Guerts, B. J.; Okrasinski, S. J. *J. Mol. Catal. A: Chem.* **1999**, *143*, 57–69.
59. Drent, E. *Chem. Abs.* **1985**, *102*, 78376.
60. van Leeuwen, P. W. N. M.; Roobeek, C. F. *Chem. Abs.* *102*, 205749.
61. Yang, J.; Haynes, A.; Maitlis, P. M. *Chem. Commun.* **1999**, 179–180.
62. Jayasree, S.; Seayad, A.; Chaudhari, R. V. *Org. Lett.* **2000**, *2*, 203–206.
63. Bischoff, S.; Weigt, A.; Fujimoto, K.; Lucke, B. *J. Mol. Catal. A: Chem.* **1995**, *95*, 259–268.
64. Marr, A. C.; Benyei, A. C.; Lightfoot, P.; Cole-Hamilton, D. J.; Ditzel, E. J. *Chem. Commun.* **1999**, 1379–1380.
65. von Kutepow, N.; Mueller, F. J. (BASF A.G.) DE 2303271. *Chem. Abs.* **1974**, *81*, 135473.
66. Lindner, E.; Karle, B. Z. *Naturforsch. B: Chem. Sci.* **1990**, *45*, 1108–1110.
67. Kelkar, A. A.; Kolhe, D. S.; Chaudhari, R. V. *J. Organomet. Chem.* **1992**, *430*, 111–116.
68. Moloy, K. G.; Wegman, R. W. *Adv. Chem. Ser.* **1992**, *230*, 323–336.
69. Moloy, K. G.; Petersen, J. L. *Organometallics* **1995**, *14*, 2931–2936.
70. Fontaine, M.; Castanet, Y.; Mortreux, A.; Petit, F. *J. Catal.* **1997**, *167*, 324–336.
71. Suss-Fink, G.; Haak, S.; Ferrand, V.; Stoekli-Evans, H. *J. Mol. Catal. A: Chem.* **1999**, *143*, 163–170.
72. Sowden, R. J.; Sellin, M. F.; de Blasio, N.; Cole-Hamilton, D. J. *Chem. Commun.* **1999**, 2511–2512.
73. Cheong, M.; Schmid, R.; Ziegler, T. *Organometallics* **2000**, *19*, 1973–1982.
74. Ivanova, E. A.; Gisdakis, P.; Nasluzov, V. A.; Rubailo, A. I.; Roesch, N. *Organometallics* **2001**, *20*, 1161–1174.
75. Kinnunen, T.; Laasonen, K. *J. Mol. Struct.-Theochem* **2001**, *540*, 91–100.
76. Kinnunen, T.; Laasonen, K. *J. Mol. Struct.-Theochem* **2001**, *542*, 273–288.
77. Ungvary, F. *Coord. Chem. Rev.* **2001**, *218*, 1–41.
78. Ungvary, F. *Coord. Chem. Rev.* **2001**, *213*, 1–50.
79. Frohning, C. D.; Kohlpaintner, C. W. *Applied Homogeneous Catalysis with Organometallic Compounds*; Cornils, B., Herrmann, W. A., Eds.; Springer-Verlag: New York, 1996; pp 29–90.
80. Agboussou, F.; Carpentier, J. F.; Mortreux, A. *Chem. Rev.* **1995**, *95*, 2485.
81. Gladiali, S.; Bayón, J. C.; Claver, C. *Tetrahedron: Asymmetry* **1995**, *6*, 1453.
82. Bardi, R.; Piazzesi, A. M.; Cavinato, G.; Cavoli, P.; Toniolo, L. *J. Organomet. Chem.* **1982**, *224*, 407–420.

83. Bardi, R.; Piazzesi, A. M.; Del Pra, A.; Cavinato, G.; Toniolo, L. *J. Organomet. Chem.* **1982**, *234*, 107–115.
84. Ruegg, H. J.; Pregosin, P. S.; Scrivanti, A.; Toniolo, L.; Botteghi, C. *J. Organomet. Chem.* **1986**, *316*, 233–241.
85. Graziani, R.; Cavinato, G.; Casellato, U.; Toniolo, L. *J. Organomet. Chem.* **1988**, *353*, 125–131.
86. Cavinato, G.; de Munno, G.; Lami, M.; Marchionna, M.; Toniolo, L.; Viterbo, D. *J. Organomet. Chem.* **1994**, *466*, 277–282.
87. Cavinato, G.; Toniolo, L. *J. Organomet. Chem.* **1983**, *241*, 275–279.
88. Anderson, G. K.; Clark, H. C.; Davies, J. A. *Organometallics* **1982**, *1*, 64.
89. Scrivanti, A.; Paganelli, S.; Matteoli, U.; Botteghi, C. *J. Organomet. Chem.* **1990**, *385*, 439–446.
90. Scrivanti, A.; Berton, A.; Toniolo, L.; Botteghi, C. *J. Organomet. Chem.* **1986**, *314*, 369–383.
91. Scrivanti, A.; Cavinato, G.; Toniolo, L.; Botteghi, C. *J. Organomet. Chem.* **1985**, *286*, 115–120.
92. Gomez, M.; Muller, G.; Sainz, D.; Sales, J.; Solans, X. *Organometallics* **1991**, *10*, 4036–4045.
93. Anderson, G. K.; Clark, H. C.; Davies, J. A. *Can. Inorg. Chem.* **1983**, *22*, 427–433.
94. Anderson, G. K.; Clark, H. C.; Davies, J. A. *Can. Inorg. Chem.* **1983**, *22*, 434–438.
95. Anderson, G. K.; Billard, C.; Clark, H. C.; Davies, J. A.; Wong, C. S. *Can. Inorg. Chem.* **1983**, *22*, 439–443.
96. Moretti, G.; Botteghi, C.; Toniolo, L. *J. Mol. Catal. A: Chem.* **1987**, *39*, 177–183.
97. Tang, S. C.; Kim, L. *J. Mol. Catal. A: Chem.* **1982**, *14*, 231–240.
98. Muller, G.; Sainz, D.; Sales, J. *J. Mol. Catal. A: Chem.* **1990**, *63*, 173–180.
99. Scrivanti, A.; Botteghi, C.; Toniolo, L.; Berton, A. *J. Organomet. Chem.* **1988**, *344*, 261–275.
100. Botteghi, C.; Paganelli, S. *J. Organomet. Chem.* **1991**, *417*, C41–C45.
101. Botteghi, C.; Paganelli, S.; Perosa, A.; Lazzaroni, R.; Uccello-Barretta, G. *J. Organomet. Chem.* **1993**, *447*, 153–157.
102. de O. Dias, A.; Augusti, R.; dos Santos, E. N.; Gusevskaya, E. V. *Tetrahedron Lett.* **1997**, *38*, 41–44.
103. Kollar, L.; Floris, B. *J. Organomet. Chem.* **1992**, *441*, 117–123.
104. Kollar, L.; Floris, B.; Pino, P. *Chimia* **1986**, *40*, 201–202.
105. Consiglio, G.; Morandini, F.; Haelg, P. L.; Pino, P. *J. Mol. Catal. A: Chem.* **1990**, *60*, 363–374.
106. Kollar, L.; Sandor, P.; Szalontai, G.; Heil, B. *J. Organomet. Chem.* **1990**, *393*, 153–158.
107. Botteghi, C.; Paganelli, S.; Matteoli, U.; Scrivanti, A.; Ciorciaro, R.; Venanzi, L. M. *Helv. Chim. Acta* **1990**, *73*, 284–287.
108. Toth, I.; Kegl, T.; Elsevier, C. J.; Kollar, L. *Inorg. Chem.* **1994**, *33*, 5708–5712.
109. Kegl, T.; Kollar, L.; Radics, L. *Inorg. Chim. Acta* **1997**, *65*, 249–254.
110. Meessen, P.; Vogt, D.; Keim, W. *J. Organomet. Chem.* **1998**, *551*, 165–170.
111. van der Veen, L. A.; Keeven, P. K.; Kamer, P. C. J.; van Leeuwen, P. W. N. M. *Dalton* **2000**, 2105–2112.
112. Sturm, T.; Weissensteiner, W.; Mereiter, K.; Kegl, T.; Jeges, G.; Petolz, G.; Kollar, L. *J. Organomet. Chem.* **2000**, *595*, 93–101.
113. Goel, A. B.; Goel, S. *Inorg. Chim. Acta* **1983**, *77*, L53–L55.
114. Ancillotti, F.; Lami, M.; Marchionna, M. *J. Mol. Catal. A: Chem.* **1991**, *66*, 37–50.
115. MacFarland, D. K.; Landis, C. R. *Organometallics* **1996**, *15*, 483–485.
116. van Leeuwen, P. W. N. M.; Roobeek, C. F. *Adv. Chem. Ser.* **1992**, *230*, 367–376.
117. van Leeuwen, P. W. N. M.; Roobeek, C. F. *New J. Chem.* **1990**, *14*, 487–493.
118. van Leeuwen, P. W. N. M.; Roobeek, C. F.; Wife, R. L.; Frijns, J. H. G. *Chem. Soc. Chem. Commun.* **1986**, 31–33.
119. van Leeuwen, P. W. N. M.; Roobeek, C. F.; Frijns, J. H. G.; Orpen, A. G. *Organometallics* **1990**, *9*, 1211–1222.
120. Csok, Z.; Keglevich, G.; Petocz, G.; Kollar, L. *J. Organomet. Chem.* **1999**, *586*, 79–84.
121. Ellis, D. D.; Harrison, G.; Orpen, A. G.; Phetmung, H.; Pringle, P. G.; deVries, J. G.; Oevering, H. *Dalton* **2000**, 671–675.
122. Janosi, L.; Kegl, T.; Hajba, L.; Berente, Z.; Kollar, L. *Inorg. Chim. Acta* **2001**, *316*, 135–139.
123. Karlsson, M.; Johansson, M.; Andersson, C. *J. Chem. Soc. Dalton* **1999**, 4187–4192.
124. Ancillotti, F.; Lami, M.; Marchionna, M. *J. Mol. Catal. A: Chem.* **1990**, *63*, 15–30.
125. Ancillotti, F.; Lami, M.; Marchionna, M. *J. Mol. Catal. A: Chem.* **1990**, *58*, 331–344.
126. Ancillotti, F.; Lami, M.; Marchionna, M. *J. Mol. Catal. A: Chem.* **1990**, *58*, 345–354.
127. Clark, H. C.; Jain, V. K.; Rao, G. S. *J. Organomet. Chem.* **1985**, *279*, 181–191.
128. Fornies-Camer, J.; Aaliti, A.; Ruiz, N.; Masdeu-Bultto, A. M.; Claver, C.; Cardin, C. *J. Organomet. Chem.* **1997**, *530*, 199–209.
129. Ishii, Y.; Miyashita, K.; Kamita, K.; Hidai, M. *J. Am. Chem. Soc.* **1997**, *119*, 6448–6449.
130. Ishii, Y.; Miyashita, K.; Kamita, K.; Hidai, M. *J. Am. Chem. Soc.* **1997**, *119*, 6448–6449.
131. Pittman, C. U., Jr.; Honnick, W.; Absi-Halabi, M.; Richmond, M. G.; Bender, R.; Braunstein, P. *J. Mol. Catal. A: Chem.* **1985**, *32*, 177–190.
132. Jain, V. K. In *Synthesis, Reactivity and Redistribution Reactions of Homo- and Heterobinuclear Palladium(II) and Platinum(II) Complexes*. Adv. Organomet. Proceedings Indo-Sov. Symp. Organomet. Chem., 1st. ed.; Jain, D. V. S., Ed.; Indian Natl. Sci. Acad: New Delhi, India 1989, 143–162.
133. Drent, E. *Chem. Abstr.* **1987**, *107*, 39199.
134. Arnoldy, P.; Bolinger, C. M.; Drent, E.; van Gogh, J.; van der Hulst, C. H. M.; Moene, R. *Chem. Abstr.* **2001**, *111*, 164823.
135. Drent, E. *Chem. Abstr.* **1993**, *118*, 212486.
136. Pisano, C.; Consiglio, G. *Gazz. Chim. Ital.* **1994**, *124*, 393–401.
137. Drent, E.; Budzelaar, P. H. M. *J. Organomet. Chem.* **2000**, *593–594*, 211–225.
138. Drent, E.; Pello, D. H. L.; Suykerbuyk, J. C. L. J.; van Gogh, J. *Chem. Abstr.* **1995**, *123*, 313386.
139. Arnoldy, P.; Bolinger, C. M.; Drent, E.; Keijsper, J. J. *Chem. Abstr.* **1999**, *130*, 268829.
140. Arnoldy, P.; Bolinger, C. M.; Mul, W. P. *Chem. Abstr.* **1999**, *130*, 224604.
141. Drent, E.; Jager, W. W. *Chem. Abstr.* **1998**, *129*, 137605.
142. Fellmann, J. D.; Garrou, P. E.; Withers, H. P.; Seyferth, D.; Traficante, D. D. *Organometallics* **1983**, *2*, 818–825.
143. Kagan, Y. B.; Butkova, O. L.; Korneeva, G. A.; Shishkina, M. V.; Zvezdkina, L. I.; Bashkirov, A. N. *Neftekhimiya* **1983**, *23*, 77–84.
144. Murata, K.; Matsuda, A.; Masuda, T. *J. Mol. Catal. A: Chem.* **1984**, *23*, 121–132.
145. Balavoine, G.; Collin, J.; Bonnet, J. J.; Lavigne, G. *J. Organomet. Chem.* **1985**, *280*, 429–439.

146. Versluis, L.; Ziegler, T. *Organometallics* **1990**, *9*, 2985–2992.
147. Wang, Y.; Lei, Z.; Feng, H.; Liu, Y. *Appl. Organomet. Chem.* **1991**, *5*, 517–519.
148. Don, M. J.; Richmond, M. G. *J. Mol. Catal. A: Chem.* **1992**, *73*, 181–189.
149. Walther, B.; Boettcher, H.-C.; Scheer, M.; Fischer, G.; Fenske, D.; Suess-Fink, G. *J. Organomet. Chem.* **1992**, *437*, 307–321.
150. Zhou, H.; Lu, Y.; Lu, S.; Zhen, Y.; Fu, H. *Fenzi Cuihua* **1994**, *8*, 99–104. *Chem. Abstr.* **1994**, *121*, 56961.
151. Lu, S.; Hang, F.; Zhou, H.; Zheng, Y.; Fu, H. *Fenzi Cuihua* **1994**, *8*, 320–324. *Chem. Abstr.* **1994**, *121*, 258458.
152. Marko, L.; Ungvary, F.; Palyi, Gy.; Sisak, A.; Vizi-Orosz, A. *Magy. Kem. Foly.* **1994**, *100*, 385–93.
153. Slaugh, L. H.; Weider, P. R.; Arhancet, J. P.; Lin, J.-J. *Chem. Abstr.* **1995**, *122*, 9490.
154. Cabrera, A.; Sharma, P.; Garcia, J. L.; Velasco, L.; Perez, F. J.; Arias, J. L.; Rosas, N. *J. Mol. Catal. A: Chem.* **1997**, *118*, 167–171.
155. Piacenti, F.; Calderazzo, F.; Bianchi, M.; Rosi, L.; Frediani, P. *Organometallics* **1997**, *16*, 4235–4236.
156. Rosi, L.; Piacenti, F.; Bianchi, M.; Frediani, P.; Salvini, A. *Eur. J. Inorg. Chem.* **1999**, 67–68.
157. Tannenbaum, R.; Dietler, U. K.; Bor, G.; Ungvary, F. *J. Organomet. Chem.* **1998**, *570*, 39–47.
158. Tannenbaum, R.; Bor, G. *J. Organomet. Chem.* **1999**, *586*, 18–22.
159. Weber, R.; Englert, U.; Ganter, B.; Keim, W.; Mothrath, M. *Chem. Commun.* **2000**, *15*, 1419–1420.
160. Massick, S. M.; Rabor, J. G.; Elbers, S.; Marhenke, J.; Bernhard, S.; Schoonover, J. R.; Ford, P. C. *Inorg. Chem.* **2000**, *39*, 3098–3106.
161. Ishii, Y.; Hidai, M. *Catal. Today* **2001**, *66*, 53–61.
162. Guo, Y.; Akgerman, A. *J. Supercrit. Fluid.* **1999**, *10*, 63–71.
163. Sharma, P.; Cabrera, A.; Arias, J. L.; Le Lagadec, R.; Manzo, R. L.; Sharma, M. *Main Group Met. Chem.* **1999**, *22*, 95–103.
164. Laitinen, R. H.; Soininen, J.; Suomalainen, P.; Pakkanen, T. A.; Ahlgren, M.; Pursiainen, J. *Acta Chem. Scand.* **1999**, *53*, 335–339.
165. Vigranenko, Y. T.; Katsnel'son, M. G. *Russ. J. Appl. Chem.* **1998**, *71*, 1779–1782.
166. Kramarz, K. W.; Klingler, R. J.; Fremgen, D. E.; Rathke, J. W. *Catal. Today* **1999**, *49*, 339–352.
167. Bath, S. S.; Vaska, L. *J. Am. Chem. Soc.* **1963**, *85*, 3500.
168. Evans, D.; Osborn, J. A.; Wilkinson, G. *J. Chem. Soc. A* **1968**, 3133.
169. Evans, D.; Yagupsky, G.; Wilkinson, G. *J. Chem. Soc. A* **1968**, 2660.
170. Brown, C. K.; Wilkinson, G. *J. Chem. Soc. A* **1970**, 2753.
171. Jardine, F. H. *Polyhedron* **1982**, *1*, 569.
172. Jardine, F. H.; Osborn, J. A.; Wilkinson, G.; Young, J. F. *Chem. Ind.* **1965**, 560.
173. Parshall, G. W.; Ittel, S. D. *Homogeneous Catalysis*, 2nd ed.; Wiley: New York, 1992.
174. Frohning, C. D.; Kohlpaintner, C. W. In *Applied Homogeneous Catalysis with Organometallic Compounds*; Cornils, B., Herrmann, W. A., Eds. VCH-Wiley: New York, 1996; Vol. 1, pp 3–25.
175. Agbossou, F.; Carpentier, J.-F.; Hapiot, F.; Suisse, I.; Mortreux, A. *Coord. Chem. Rev.* **1998**, *178–180*, 1615–1645.
176. Trzeciak, A. M.; Ziolkowski, J. J. *Coord. Chem. Rev.* **1999**, *190–192*, 883–900.
177. Breit, B. *Chem. Eur. J.* **2000**, *6*, 1519–1524.
178. Liu, C.; Mei, J.; Jin, Z. *Huagong Jinzhan* **2000**, *19*, 28–31. *Chem. Abstr.* **2000**, *132*, 153587.
179. van Leeuwen, P. W. N. M.; Claver, C.; Eds.; *Rhodium Catalyzed Hydroformylation*. In *Catal. Met. Complexes*, Vol. 22; Kluwer: Dordrecht, The Netherlands, 2000.
180. Heck, R. F. *Acc. Chem. Res.* **1969**, *2*, 10.
181. Chan, A. S. C.; Shieh, H. S.; Hill, J. R. *J. Chem. Soc. Chem. Commun.* **1983**, 688, 689.
182. Brown, J. M.; Kent, A. G. *J. Chem. Soc. Perkin Trans. II*, **1987**, 1597.
183. Moser, W. R.; Papite, C. J.; Brannon, D. A.; Duwell, R. A.; Weininger, S. J. *J. Mol. Catal.* **1987**, *41*, 271.
184. Diéguez, M.; Claver, C.; Masdeu-Bultó, A. M.; Ruiz, A.; van Leeuwen, P. W. N. M.; Schoemaker, G. C. *Organometallics* **1999**, *18*, 2107–2115.
185. Oswald, A. A.; Merola, J. S.; Mozeleski, E. J.; Kastrop, R. V.; Reisch, J. C. *Adv. Chem. Ser.* **1981**, *104*, 503.
186. Gregorio, G.; Montrasi, G.; Tampieri, M.; Cavalieri d'Oro, P.; Pagani, G.; Andreetta, A. *Chim. Ind.* **1980**, *62*, 389.
187. Pottier, Y.; Mortreux, A.; Petit, F. *J. Organomet. Chem.* **1989**, *370*, 333.
188. Devon, T. J.; Phillips, G. W.; Puckette, T. A.; Stavinoha, J. L.; Vanderbilt, J. J. U.S. Patent 4,694,109, 1987; *Chem. Abstr.* **1988**, *108*, 7890.
189. Devon, T. J.; Phillips, G. W.; Puckette, T. A.; Stavinoha, J. L.; Vanderbilt, J. J. (Texas Eastman) U.S. Patent 5,332,846, 1994; *Chem. Abstr.* **1994**, *121*, 280,879.
190. Casey, C. P.; Whiteker, G. T.; Melville, M. G.; Petrovich, L. M.; Gavney, J. A., Jr.; Powell, D. R. *J. Am. Chem. Soc.* **1992**, *114*, 5535.
191. Casey, C. P.; Petrovich, L. M. *J. Am. Chem. Soc.* **1995**, *117*, 6007.
192. Yamamoto, K.; Momose, S.; Funahashi, M.; Miyazawa, M. *Synlett.* **1990**, 711.
193. Casey, C. P.; Whiteker, G. T. *J. Org. Chem.* **1990**, *55*, 1394.
194. Casey, C. P.; Paulsen, E. L.; Beuttenmueller, E. W.; Proft, B. R.; Petrovich, L. M.; Matter, B. A.; Powell, D. R. *J. Am. Chem. Soc.* **1997**, *119*, 11817.
195. Casey, C. P.; Paulsen, E. L.; Beuttenmueller, E. W.; Proft, B. R.; Matter, B. A.; Powell, D. R. *J. Am. Chem. Soc.* **1999**, *21*, 63–70.
196. Decker, S. A.; Cundari, T. R. *Organometallics* **2001**, *20*, 2827–2841.
197. Kranenburg, M.; van der Burgt, Y. E. M.; Kamer, P. C. J.; van Leeuwen, P. W. N. M. *Organometallics* **1995**, *14*, 3081.
198. van der Veen, L. A.; Boele, M. D. K.; Bregman, F. R.; Kamer, P. C. J.; van Leeuwen, P. W. N. M.; Goubitz, K.; Fraanje, J.; Schenk, H.; Bo, C. *J. Am. Chem. Soc.* **1998**, *120*, 11616.
199. van der Veen, L. A.; Kamer, P. C. J.; van Leeuwen, P. W. N. M. *Angew. Chem. Int. Ed. Engl.* **1999**, *38*, 336.
200. Koga, N.; Qian Jin, S.; Morokuma, K. *J. Am. Chem. Soc.* **1988**, *110*, 3417.
201. Matsubara, T.; Koga, N.; Ding, Y.; Musaev, D. G.; Morokuma, K. *Organometallics* **1997**, *16*, 1065.
202. Gleich, D.; Schmid, R.; Herrmann, W. A. *Organometallics* **1998**, *17*, 4828.
203. Carbo, J. J.; Maseras, F.; Bo, C.; van Leeuwen, P. W. N. M. *J. Am. Chem. Soc.* **2001**, *123*, 7630–7637.

204. Nettekoven, U.; Kamer, P. C. J.; Widhalm, M.; van Leeuwen, P. W. N. M. *Organometallics* **2000**, *19*, 4596–4607.
205. Pruetz, R. L.; Smith, J. A. *J. Org. Chem.* **1969**, *34*, 327.
206. Pruetz, R. L.; Smith, J. A. S. African Patent 6,804,937, 1968 (to Union Carbide Corporation). *Chem. Abstr.* **1969**, *71*, 90819.
207. Trzeciak, A. M.; Ziolkowski, J. J.; Aygen, S.; van Eldik, R. J. *Mol. Catal. A: Chem.* **1986**, *34*, 337.
208. Trzeciak, A. M.; Ziolkowski, J. J. *Trans. Met. Chem.* **1987**, *12*, 408.
209. Trzeciak, A. M.; Ziolkowski, J. J. *J. Mol. Catal. A: Chem.* **1986**, *34*, 213.
210. Trzeciak, A. M.; Ziolkowski, J. J. *J. Mol. Catal. A: Chem.* **1987**, *43*, 13.
211. Jongsma, T.; Challa, G.; van Leeuwen, P. W. N. M. *J. Organometal. Chem.* **1991**, *421*, 121.
212. van Rooy, A.; Orij, E. N.; Kamer, P. C. J.; van den Aardweg, F.; van Leeuwen, P. W. N. M. *J. Chem. Soc. Chem. Commun.* **1991**, 1096.
213. van Rooy, A.; Orij, E. N.; Kamer, P. C. J.; van Leeuwen, P. W. N. M. *Organometallics* **1995**, *14*, 34.
214. Fernandez, E.; Claver, C.; Castillón, S.; Polo, A.; Piniella, J. F.; Alvarez-Larena, A. *Organometallics* **1998**, *17*, 2857.
215. Billig, E.; Abatjoglou, A. G.; Bryant, D. R. (Union Carbide) U. S. Pat. 4,668,651; Eur. Pat. Appl. 213,639, 1987; *Chem. Abstr.* **1987**, *107*, 7392.
216. Billig, E.; Abatjoglou, A. G.; Bryant, D. R.; Murray, R. E.; Maher, J. M. (Union Carbide) U.S. Pat. 4,599,206, 1986; *Chem. Abstr.* **1988**, *109*, 233177.
217. van Rooy, A.; Kamer, P. C. J.; van Leeuwen, P. W. N. M.; Goubitz, K.; Fraanje, J.; Veldman, N.; Spek, A. L. *Organometallics* **1996**, *15*, 835.
218. Buisman, G. J. H.; Vos, E.; Kamer, P. C. J.; van Leeuwen, P. W. N. M. *J. Chem. Soc. Dalton* **1995**, 409–417.
219. Moasser, B.; Gladfelter, W. L.; Roe, C. D. *Organometallics* **1995**, *14*, 3832.
220. van Rooy, A.; Kamer, P. C. J.; van Leeuwen, P. W. N. M.; Veldman, N.; Spek, A. L. *J. Organomet. Chem.* **1995**, *494*, C15–C18.
221. Buisman, G. J. H.; van der Veen, L. A.; Kamer, P. C. J.; van Leeuwen, P. W. N. M. *Organometallics* **1997**, *16*, 5681–5689.
222. Moasser, B.; Gladfelter, W. L. *Inorg. Chim. Acta* **1996**, *242*, 125.
223. Slivinskii, E. V.; Rozovskii, A. Ya.; Korneeva, G. A.; Kurkin, V. *Kinet. Catal.* **1998**, *39*, 764–774.
224. Koch, D.; Leitner, W. *J. Am. Chem. Soc.* **1998**, *120*, 13398–13404.
225. Palo, D. R.; Erkey, C. *Ind. Eng. Chem. Res.* **1998**, *37*, 4203–4206.
226. Bach, I. *Chem. Commun.* **1998**, 1463–1464.
227. Palo, D. R.; Erkey, C. *Ind. Eng. Chem. Res.* **1999**, *38*, 2163–2165, 3786–3792.
228. Davis, T.; Erkey, C. *Ind. Eng. Chem. Res.* **2000**, *39*, 3671–3678.
229. Palo, D. R.; Erkey, C. *Organometallics* **2000**, *19*, 81–86.
230. Banet Osuna, A. M.; Chen, W.; Hope, E. G.; Kemmitt, R. D. W.; Paige, D. R.; Stuart, A. M.; Xiao, J.; Xu, L. *J. Chem. Soc. Dalton* **2000**, *22*, 4052–4055.
231. Stemmer, H.; Leitner, W. *DGMK Tagungsber.* **2000**, *2000–2003*, 247–248.
232. Meehan, N. J.; Poliakoff, M.; Sandee, A. J.; Reek, J. N. H.; Kamer, P. C. J.; van Leeuwen, P. W. N. M. *Chem. Commun.* **2000**, 1497–1498.
233. Sellin, M. F.; Cole-Hamilton, D. J. *J. Chem. Soc. Dalton* **2000**, 1681–1683.
234. Pruchnik, F. P.; Smolenski, P.; Wajda-Hermanowicz, K. *J. Organomet. Chem.* **1998**, *570*, 63–69.
235. Csok, Z.; Keglevich, G.; Petocz, G.; Kollar, L. *J. Organomet. Chem.* **1999**, *586*, 79–84.
236. Csok, Z.; Szalontai, G.; Czira, G.; Kollar, L. *J. Organomet. Chem.* **1998**, *570*, 23–29.
237. Le Gall, I.; Laurent, P.; Soulier, E.; Salaun, J.-Y.; des Abbayes, H. *J. Organomet. Chem.* **1998**, *567*, 13–20.
238. Gao, H.; Angelici, R. J. *Organometallics* **1998**, *17*, 3063–3069.
239. Castellanos-Paez, A.; Castillon, S.; Claver, C.; van Leeuwen, P. W. N. M.; de Lange, W. G. J. *Organometallics* **1998**, *17*, 2543–2552.
240. Chen, W.; Xu, Y.; Liao, S. *J. Mol. Catal. A: Chem.* **1998**, *129*, 153–158.
241. Horvath, I. T.; Kiss, G.; Cook, R. A.; Bond, J. E.; Stevens, P. A.; Rabai, J.; Mozeleski, E. J. *J. Am. Chem. Soc.* **1998**, *120*, 3133–3143.
242. Chen, W.; Xu, L.; Xiao, J. *Chem. Commun.* **2000**, 839–840.
243. van Leeuwen, P. W. N. M.; Kamer, P. C. J.; Reek, J. N. H. *Pure Appl. Chem.* **1999**, *71*, 1443–1452.
244. van Leeuwen, P. W. N. M.; Kamer, P. C. J.; van der Veen, L. A.; Reek, J. N. H. *Chin. J. Chem.* **2001**, *19*, 1–8.
245. Bregman, F. R.; Ernsting, J. M.; Muller, F.; Boele, M. D. K.; van der Veen, L. A.; Elsevier, C. J. *J. Organomet. Chem.* **1999**, *592*, 306–311.
246. van den Hoven, B. G.; Alper, H. *J. Org. Chem.* **1999**, *64*, 9640–9645.
247. Sandee, A. J.; van der Veen, L. A.; Reek, J. N. H.; Kamer, P. C. J.; Lutz, M.; Spek, A. L.; van Leeuwen, P. W. N. M. *Angew. Chem. Int. Ed. Engl.* **1999**, *38*, 3231–3235.
248. Liu, C.-W.; Li, Y.-W.; He, D.-H.; Liu, J.-Y.; Zhu, Q.-M. *Tianranqi Huagong* **1999**, *24*, 8–13. *Chem. Abstr.* **1999**, *132*, 280839.
249. Teleshev, A. T.; Kolesnichenko, N. V.; Markova, N. A.; Terekhova, G. V.; Kurkin, V. I.; Slivinskii, E. V.; Nifantev, E. E. *Neftekhimiya* **1999**, *39*, 203–206. *Chem. Abstr.* **1999**, *131*, 338582.
250. van der Veen, L. A.; Kamer, P. C. J.; van Leeuwen, P. W. N. M. *Organometallics* **1999**, *18*, 4765–4777.
251. Keim, W.; Vogt, D.; Waffenschmidt, H.; Wasserscheid, P. *J. Catal.* **1999**, *186*, 481–484.
252. Wasserscheid, P.; Waffenschmidt, H.; Machnitzki, P.; Kottsieper, K. W.; Stelzer, O. *Chem. Commun.* **2001**, 451–452.
253. Dupont, J.; Silva, S. M.; de Souza, R. F. *Catal. Lett.* **2001**, *77*, 131–133.
254. Brasse, C. C.; Englert, U.; Salzer, A.; Waffenschmidt, H.; Wasserscheid, P. *Organometallics* **2000**, *19*, 3818–3823.
255. Freixa, Z.; Pereira, M. M.; Pais, A. A. C. C.; Bayón, J. C. *J. Chem. Soc. Dalton* **1999**, 3245–3251.
256. Paciello, R.; Siggel, L.; Roper, M. *Angew. Chem. Int. Ed. Engl.* **1999**, *38*, 1920–1923.
257. Kameda, N.; Yoneda, T. *Nippon Kagaku Kaishi* **1999**, *7*, 457–461. *Chem. Abstr.* **1999**, *131*, 144373.
258. Casado, M. A.; Perez-Torrente, J. J.; Ciriano, M. A.; Oro, L. A.; Orejon, A.; Claver, C. *Organometallics* **1999**, *18*, 3035–3044.
259. Bianchini, C.; Burnaby, D. G.; Evans, J.; Frediani, P.; Meli, A.; Oberhauser, W.; Psaro, R.; Sordelli, L.; Vizza, F. *J. Am. Chem. Soc.* **1999**, *121*, 5961–5971.

260. Arena, C. G.; Drago, D.; Faraone, F. *J. Mol. Catal. A: Chem.* **1999**, *144*, 379–388.
261. Breit, B. *J. Mol. Catal. A: Chem.* **1999**, *143*, 143–154.
262. Trzeciak, A. M.; Ziolkowski, J. J.; Lis, T.; Choukroun, R. *J. Organomet. Chem.* **1999**, *575*, 87–97.
263. Broussier, R.; Laly, M.; Perron, P.; Gautheron, B.; M'Koyan, S.; Kalck, P.; Wheatley, N. *J. Organomet. Chem.* **1999**, *574*, 267–275.
264. Bagatin, I. A.; Matt, D.; Thoennessen, H.; Jones, P. G. *Inorg. Chem.* **1999**, *38*, 1585–1591.
265. Reetz, M. T.; Lohmer, G.; Schwickardi, R. *Angew. Chem. Int. Ed. Engl.* **1997**, *36*, 1526–1529.
266. Bourque, S. C.; Maltais, F.; Xiao, W.-J.; Tardif, O.; Alper, H.; Arya, P.; Manzer, L. E. *J. Am. Chem. Soc.* **1999**, *121*, 3035–3038.
267. Deshpande, R. M.; Fukuoka, A.; Ichikawa, M. *Chem. Lett.* **1999**, *1*, 13–14.
268. Gladiali, S.; Medici, S.; K., T.; Kollar, L. *Monatsh. Chem.* **2000**, *131*, 1351–1361.
269. Groot, D. D.; Emmerink, P. G.; Coucke, C.; Reek, J. N. H.; Kamer, P. C. J.; van Leeuwen, P. W. N. M. *Inorg. Chem. Commun.* **2000**, *3*, 711–713.
270. Breeden, S.; Cole-Hamilton, D. J.; Foster, D. F.; Schwarz, G. J.; Wills, M. *Angew. Chem. Int. Ed. Engl.* **2000**, *39*, 4106–4108.
271. Liu, Y.; He, D.-H.; Li, C.-B.; Wang, T.-E.; Liu, J.-Y.; Zhu, Q.-M. *Fenzi Cuihua* **2000**, *14*, 337–340. *Chem. Abstr.* **2000**, *134*, 73224.
272. Li, Y.-Z.; Lai, Z.; Chen, H.; Chen, J.-R.; Cheng, P.-M.; Li, X.-J. *Fenzi Cuihua* **2000**, *14*, 332–336. *Chem. Abstr.* **2000**, *134*, 73223.
273. Del Rio, I.; Pamies, O.; van Leeuwen, P. W. N. M.; Claver, C. *J. Organomet. Chem.* **2000**, *608*, 115–121.
274. Mukhopadhyay, K.; Nair, V. S.; Chaudhari, R. V. *Stud. Surf. Sci. Catal. Pt C* **2000**, *130*, 2999–3003.
275. Chen, A. C.; Ren, L.; Decken, A.; Crudden, C. M. *Organometallics* **2000**, *19*, 3459–3461.
276. van der Slot, S. C.; Kamer, P. C. J.; van Leeuwen, P. W. N. M.; Fraanje, J.; Goubitz, K.; Lutz, M.; Spek, A. L. *Organometallics* **2000**, *19*, 2504–2515.
277. Lindner, E.; Auer, F.; Baumann, A.; Wegner, P.; Mayer, H. A.; Bertagnolli, H.; Reinohl, U.; Ertel, T. S.; Weber, A. *J. Mol. Catal. A: Chem.* **2000**, *157*, 97–109.
278. Selent, D.; Wiese, K.-D.; Rottger, D.; Borner, A. *Angew. Chem. Int. Ed. Engl.* **2000**, *39*, 1639–1641.
279. Parlevliet, F. J.; Kiener, C.; Fraanje, J.; Goubitz, K.; Lutz, M.; Spek, A. L.; Kamer, P. C. J.; van Leeuwen, P. W. N. M. *J. Chem. Soc. Dalton* **2000**, 1113–1122.
280. Cobley, C. J.; Ellis, D. D.; Orpen, A. G.; Pringle, P. G. *Dalton* **2000**, 1109–1112.
281. Laly, M.; Broussier, R.; Gautheron, B. *Tetrahedron Lett.* **2000**, *41*, 1183–1185.
282. Bosch, B. E.; Bruemmer, I.; Kunz, K.; Erker, G.; Froehlich, R.; Kotila, S. *Organometallics* **2000**, *19*, 1255–1261.
283. Arya, P.; Rao, N. V.; Singkhonrat, J.; Alper, H.; Bourque, S. C.; Manzer, L. E. *J. Org. Chem.* **2000**, *65*, 1881–1885.
284. Reetz, M. T.; Waldvogel, S. R.; Goddard, R. *Heterocycles* **2000**, *52*, 935–938.
285. Cauzzi, D.; Costa, M.; Cucci, N.; Graiff, C.; Grandi, F.; Predieri, G.; Tiripicchio, A.; Zaroni, R. *J. Organomet. Chem.* **2000**, *593–594*, 431–444.
286. van der Veen, L. A.; Keeven, P. H.; Schoemaker, G. C.; Reek, J. N. H.; Kamer, P. C. J.; van Leeuwen, P. W. N. M.; Lutz, M.; Spek, A. L. *Organometallics* **2000**, *19*, 872–883.
287. Bianchini, C.; Lee, H. M.; Meli, A.; Vizza, F. *Organometallics* **2000**, *19*, 849–853.
288. Bourque, S. C.; Alper, H.; Manzer, L. E.; Arya, P. *J. Am. Chem. Soc.* **2000**, *122*, 956–957.
289. Kostas, I. D. *J. Organomet. Chem.* **2001**, *634*, 90–98.
290. Del Rio, I.; van Leeuwen, P. W. N. M.; Claver, C. *Can. J. Chem.* **2001**, *79*, 560–565.
291. Izubiri, M. R.; Slawin, A. M. Z.; Cole-Hamilton, D.; Woollins, J. D. *Phosphorus Sulfur* **2001**, *168–169*, 441–444.
292. Breit, B.; Winde, R.; Mackewitz, T.; Paciello, R.; Harms, K. *Chem. Eur. J.* **2001**, *7*, 3106–3121.
293. Freixa, Z.; Bayon, J. C. *J. Chem. Soc. Dalton* **2001**, 2067–2068.
294. Zhang, J.-C.; Cao, W.-L.; Gao, W.; Wei, H.-L.; Yan, B.; Sun, F.-Q.; Li, J.-B. *Fenzi Cuihua* **2001**, *15*, 124–128. *Chem. Abstr.* **2001**, *135*, 197178.
295. Selent, D.; Hess, D.; Wiese, K.-D.; Rottger, D.; Kunze, C.; Boerner, A. *Angew. Chem. Int. Ed. Engl.* **2001**, *40*, 1696–1698.
296. Fang, X.; Scott, B. L.; Watkin, J. G.; Carter, C. A. G.; Kubas, G. J. *Inorg. Chim. Acta* **2001**, *317*, 276–281.
297. Sellin, M. F.; Webb, P. B.; Cole-Hamilton, D. J. *Chem. Commun.* **2001**, 781–782.
298. Kostas, I. D. *J. Organomet. Chem.* **2001**, *626*, 221–226.
299. Reinius, H. K.; Suomalainen, P.; Riihimaki, H.; Karvinen, E.; Pursiainen, J.; Krause, A. O. I. *J. Catal.* **2001**, *199*, 302–308.
300. Rodriguez i Zubiri, M.; Clarke, M. L.; Foster, D. F.; Cole-Hamilton, D. J.; Slawin, A. M. Z.; Woollins, J. D. *J. Chem. Soc. Dalton* **2001**, 969–971.
301. Suomalainen, P.; Reinius, H. K.; Riihimaki, H.; Laitinen, R. H.; Jaaskelainen, S.; Haukka, M.; Pursiainen, J. T.; Pakkanen, T. A.; Krause, A. O. I. *J. Mol. Catal. A: Chem.* **2001**, *169*, 67–78.
302. Haupt, H.-J.; Wittbecker, R.; Florke, U. *Z. Anorg. Allg. Chem.* **2001**, *627*, 472–484.
303. van der Slot, S. C.; Kamer, P. C. J.; van Leeuwen, P. W. N. M. *Organometallics* **2001**, *20*, 1079–1086.
304. Karlsson, M.; Andersson, C.; Hjortkjaer, J. *J. Mol. Catal. A: Chem.* **2001**, *166*, 337–343.
305. Roch-Neirey, C.; Le Bris, N.; Laurent, P.; Clement, J.-C.; des Abbayes, H. *Tetrahedron Lett.* **2001**, *42*, 643–645.
306. van der Slot, S. C.; Kamer, P. C. J.; van Leeuwen, P. W. N. M.; Iggo, J. A.; Heaton, B. T. *Organometallics* **2001**, *20*, 430–441.
307. Lin, B.; Akgerman, A. *Ind. Eng. Chem. Res.* **2001**, *40*, 1113–1118.
308. Sheldon, R. A. *Chem. Ind.* **1990**, 212.
309. Botteghi, C.; Paganelli, S.; Schionato, A.; Marchetti, M. *Chirality* **1991**, *3*, 355.
310. Consiglio, G. Asymmetric Carbonylation, in *Catalytic Asymmetric Syntheses*. In Ojima, I., Ed.; VCH Publishers, New York, **1993**, 273–302.
311. Nozaki, K. Hydrocarbonylation of Carbon-carbon Double Bonds. In *Comprehensive Asymmetric Catalysis*; Jacobsen, E. N.; Pfaltz, A.; Yamamoto, H. Eds.; Springer Heidelberg, 1999; Vol. I, pp 381–409.
312. Stille, J. K.; Parrinello, G. *J. Mol. Catal. A: Chem.* **1983**, *21*, 203–210.

313. Parrinello, G.; Stille, J. K. *J. Am. Chem. Soc.* **1987**, *109*, 7122–7127.
314. Stille, J. K.; Su, H.; Brechot, P.; Parrinello, G.; Hegedus, L. S. *Organometallics* **1991**, *10*, 1183–1189.
315. Parrinello, G.; Deschenaux, R.; Stille, J. K. *J. Org. Chem.* **1986**, *51*, 4189–4195.
316. Consiglio, G.; Morandini, F.; Scalone, M.; Pino, P. *J. Organomet. Chem.* **1985**, *279*, 193–202.
317. Haelg, P.; Consiglio, G.; Pino, P. *J. Organomet. Chem.* **1985**, *296*, 281–290.
318. Kollar, L.; Cosiglio, G.; Pino, P. *J. Organomet. Chem.* **1987**, *330*, 305–314.
319. Paganelli, S.; Matteoli, U.; Scrivanti, A. *J. Organomet. Chem.* **1990**, *397*, 119–125.
320. Consiglio, G.; Rama, F. *J. Mol. Catal. A: Chem.* **1991**, *66*, 1–5.
321. Kollar, L.; Farkas, E.; Batiu, J. *J. Mol. Catal. A: Chem.* **1997**, *115*, 283–288.
322. Kollar, L.; Kegl, T.; Bakos, J. *J. Organomet. Chem.* **1993**, *453*, 155–158.
323. Kegl, T.; Kollar, L.; Szalontai, G.; Kuzmann, E.; Vertes, A. *J. Organomet. Chem.* **1996**, *507*, 75–80.
324. Toth, I.; Elsevier, C. J.; de Vries, J. G.; Bakos, J.; Smeets, W. J. J.; Spek, A. L. *J. Organomet. Chem.* **1997**, *540*, 15–25.
325. Kegl, T.; Kollar, L. *J. Mol. Catal. A: Chem.* **1997**, *122*, 95–101.
326. Consiglio, G.; Nefkens, S. C. A. *Tetrahedron Asymmetry* **1990**, *1*, 417–420.
327. Consiglio, G.; Nefkens, S. C. A.; Borer, A. *Organometallics* **1991**, *10*, 2046–2051.
328. Scrivanti, A.; Zeggio, S.; Beghetto, V.; Matteoli, U. *J. Mol. Catal. A: Chem.* **1995**, *101*, 217–220.
329. Scrivanti, A.; Beghetto, V.; Bastianini, A.; Matteoli, U.; Menchi, G. *Organometallics* **1996**, *15*, 4687–4694.
330. Kollar, L. B. J.; Toth, I.; Heil, B. *J. Organomet. Chem.* **1988**, *350*, 277–284.
331. Kollar, L.; Sandor, P.; Szalontai, G. *J. Mol. Catal. A: Chem.* **1991**, *67*, 191–198.
332. Naili, S.; Suisse, I.; Mortreux, A.; Agbossou-Niedercorn, F.; Nowogrocki, G. *J. Organomet. Chem.* **2001**, *628*, 114–122.
333. Mutez, S.; Mortreux, A.; Petit, F. *Tetrahedron Lett.* **1988**, *29*, 1911–1914.
334. Naili, S.; Mortreux, A.; Agbossou, F. *Tetrahedron: Asymmetry* **1998**, *9*, 3421–3430.
335. Naili, S.; Carpentier, J.-F.; Agbossou, F.; Mortreux, A.; Nowogrocki, G.; Wignacourt, J.-P. *Organometallics* **1995**, *14*, 401–406.
336. Mortreux, A.; Petit, F.; Buono, G.; Peiffer, G. *B. Soc. Chim. Fr.* **1987**, *4*, 631–639.
337. Agbossou, F.; Carpentier, J.-F.; Hapiot, F.; Suisse, I.; Mortreux, A. *Coord. Chem. Rev.* **1998**, *178–180*, 1615–1645.
338. Cserepi-Szucs, S.; Toth, I. P. L.; Bakos, J. *Tetrahedron: Asymmetry* **1998**, *9*, 3135–3142.
339. Cserepi-Szucs, S.; Huttner, G.; Zsolnai, L.; Szolossy, A.; Hegedus, C.; Bakos, J. *Inorg. Chim. Acta* **1999**, *296*, 222–230.
340. Bakos, J.; Cserepi-Szucs, S.; Gomory, A.; Hegedus, C.; Marko, L.; Szolossy, A. *Can. J. Chem.* **2001**, *79*, 725–730.
341. Beghetto, V.; Scrivanti, A.; Matteoli, U. *Catal. Commun.* **2001**, *2*, 139–143.
342. Chelucci, G.; Cabras, M. A.; Botteghi, C.; Basoli, C.; Marchetti, M. *Tetrahedron: Asymmetry* **1996**, *7*, 885–895.
343. Gladiali, S.; Alberico, E.; Pulacchini, S.; Kollar, L. *J. Mol. Catal. A: Chem.* **1999**, *143*, 155–162.
344. Gladiali, S.; Fabbri, D.; Kollar, L. *J. Organomet. Chem.* **1995**, *491*, 91–96.
345. Claver, C.; van Leeuwen, P. W. N. M. Asymmetric Hydroformylation. In *Rhodium Catalyzed Hydroformylation*. van Leeuwen, P. W. N. M., Claver, C., Eds.; Catal. Met. Complexes, Vol. 22; Kluwer, Dordrecht, The Netherlands, 2000; Chapter 5, pp 107–144.
346. Stanley, G. G. *Catalysis of Organic Reactions*. In Scaros, M. G.; Prunier, M. L., Eds., Marcel Dekker: New York, 1995, p 363.
347. Dieguez, M.; Pereira, M. M.; Masdeu-Bulto, A. M.; Claver, C.; Bayon, J. C. *J. Mol. Catal. A: Chem.* **1999**, *143*, 111–122.
348. Masdeu-Bulto, A. M.; Orejon, A.; Castellanos, A.; Castillon, S.; Claver, C. *Tetrahedron: Asymmetry* **1996**, *7*, 1829–1834.
349. del Rio, I.; de Lange, W. G. J.; van Leeuwen, P. W. N. M.; Claver, C. *J. Chem. Soc. Dalton* **2001**, 1293–1300.
350. Rampf, F. A.; Herrmann, W. A. *J. Organomet. Chem.* **2000**, *601*, 138–141.
351. Lee, C. W.; Alper, H. *J. Org. Chem.* **1995**, *60*, 499–503.
352. Park, H. S.; Alberico, E.; Alper, H. *J. Am. Chem. Soc.* **1999**, *121*, 11697–11703.
353. Pamies, O.; Net, G.; Widhalm, M.; Ruiz, A.; Claver, C. *J. Organomet. Chem.* **1999**, *587*, 136–143.
354. Kockritz, A.; Bischoff, S.; Kant, M.; Siefken, R. *J. Mol. Catal. A: Chem.* **2001**, *174*, 119–126.
355. Kockritz, A.; Sonnenschein, H.; Bischoff, S.; Theil, F.; Gloede, J. *Phosphorus, Sulfur Silicon Relat. Elem.* **1998**, *132*, 15–19.
356. Lu, S.; Li, X.; Wang, A. *Catal. Today* **2000**, *63*, 531–536.
357. Dieguez, M.; Pamies, O.; Net, G.; Ruiz, A.; Claver, C. *Tetrahedron: Asymmetry* **2001**, *12*, 651–656.
358. Sakai, N.; Nozaki, K.; Mashima, K.; Takaya, H. *Tetrahedron: Asymmetry* **1992**, *3*, 583.
359. Babin, J. E.; Whiteker, G. T. (Union Carbide Chemicals and Plastics Technology Corporation, USA) Asymmetric syntheses using optically active metal-ligand complex catalysts. PCT Int. Appl. 1993, WO 93/03839; *Chem. Abstr.* **1993**, *119*, 159872.
360. U.S. Pat. 5,360,938, 1994; *Chem. Abstr.* **1995**, *122*, 186609.
361. Buisman, G. J. H.; Kamer, P. C. J.; van Leeuwen, P. W. N. M. *Tetrahedron: Asymmetry* **1993**, *4*, 1625.
362. Buisman, G. J. H.; van der Veen, L. A.; Klootwijk, A.; de Lange, W. G. J.; Kamer, P. C. J.; van Leeuwen, P. W. N. M.; Vogt, D. *Organometallics* **1997**, *16*, 2929.
363. van Leeuwen, P. W. N. M.; Buisman, G. J. H.; van Rooy, A.; Kamer, P. C. J. *Recl. Trav. Chim. Pays Bas* **1994**, *113*, 61.
364. Uriz, P.; Fernandez, E.; Ruiz, N.; Claver, C. *Inorg. Chem. Commun.* **2000**, *3*, 515–519.
365. Jiang, Y.; Xue, S.; Yu, K.; Li, Z.; Deng, J.; Mi, A.; Chan, A. S. C. *J. Organomet. Chem.* **1999**, *586*, 159–165.
366. Kadyrov, R.; Heller, D.; Selke, R. *Tetrahedron: Asymmetry* **1998**, *9*, 329–340.
367. Buisman, G. J. H.; Martin, M. E.; Vos, E. J.; Klootwijk, A.; Kamer, P. C. J.; van Leeuwen, P. W. N. M. *Tetrahedron: Asymmetry* **1995**, *6*, 719–738.
368. Pamies, O.; Net, G.; Ruiz, A.; Claver, C. *Tetrahedron: Asymmetry* **2000**, *11*, 1097–1108.
369. Dieguez, M.; Pamies, O.; Ruiz, A.; Claver, C.; Castillon, S. *Chem. Commun.* **2000**, *17*, 1607–1608.
370. Dieguez, M.; Pamies, O.; Ruiz, A.; Castillon, S.; Claver, C. *Chem. Eur. J.* **2001**, *7*, 3086–3094.
371. Sakai, N.; Mano, S.; Nozaki, K.; Takaya, H. *J. Am. Chem. Soc.* **1993**, *115*, 7033.
372. Nozaki, K.; Sakai, N.; Nanno, T.; Higashijima, T.; Mano, S.; Horiuchi, T.; Takaya, H. *J. Am. Chem. Soc.* **1997**, *119*, 4413.

373. Gleich, D.; Herrmann, W. A. *Organometallics* **1999**, *18*, 4354–4361.
374. Nozaki, K.; Takaya, H.; Hiyama, T. *Top. Catal.* **1998**, *4*, 175–185.
375. Nozaki, K.; Nanno, T.; Takaya, H. *J. Organomet. Chem.* **1997**, *527*, 103–108.
376. Nozaki, K.; Matsuo, T.; Shibahara, F.; Hiyama, T. *Adv. Synth. Cat.* **2001**, *343*, 61–63.
377. Horiuchi, T.; Ohta, T.; Nozaki, K.; Takaya, H. *Chem. Commun.* **1996**, 155–156.
378. Nozaki, K.; Li, W.; Horiuchi, T.; Takaya, H. *Tetrahedron Lett.* **1997**, *38*, 4611–4614.
379. Horiuchi, T.; Ohta, T.; Shirakawa, E.; Nozaki, K.; Takaya, H. *Tetrahedron* **1997**, *53*, 7795–7804.
380. Horiuchi, T.; Ohta, T.; Shirakawa, E.; Nozaki, K.; Takaya, H. *J. Org. Chem.* **1997**, *62*, 4285–4292.
381. Nozaki, K.; Kumobayashi, H.; Horiuchi, T.; Takaya, H.; Saito, T.; Yoshida, A.; Matsumura, K.; Kato, Y.; Imai, T.; Miura, T. *J. Org. Chem.* **1996**, *61*, 7658–7659.
382. Horiuchi, T.; Shirakawa, E.; Nozaki, K.; Takaya, H. *Organometallics* **1997**, *16*, 2981–2986.
383. Francio, G.; Leitner, W. *Chem. Commun.* **1999**, *17*, 1663–1664.
384. Nozaki, K.; Shibahara, F.; Itoi, Y.; Shirakawa, E.; Ohta, T.; Takaya, H.; Hiyama, T. *B. Chem. Soc. Jpn.* **1999**, *72*, 1911–1918.
385. Nozaki, K.; Itoi, Y.; Shibahara, F.; Shirakawa, E.; Ohta, T.; Takaya, H.; Hiyama, T. *J. Am. Chem. Soc.* **1998**, *120*, 4051–4052.
386. Deerenberg, S.; Kamer, P. C. J.; van Leeuwen, P. W. N. M. *Organometallics* **2000**, *19*, 2065–2072.
387. Breuzard, J. A.; Tommasino, M. L.; Bonnet, M. C.; Lemaire, M. C. *R. Acad. Sci., Ser. IIc: Chim.* **2000**, *3*, 557–561.
388. Breuzard, J. A. J.; Tommasino, M. L.; Touchard, F.; Lemaire, M.; Bonnet, M. C. *J. Mol. Catal. A: Chem.* **2000**, *156*, 223–232.
389. Breuzard, J. A.; Tommasino, M. L.; Bonnet, M. C.; Lemaire, M. *J. Organomet. Chem.* **2000**, *616*, 37–43.
390. Pamies, O.; Dieguez, M.; Net, G.; Ruiz, A.; Claver, C. *Organometallics* **2000**, *19*, 1488–1496.
391. Freixa, Z.; Martin, E.; Gladiali, S.; Bayon, J. C. *Appl. Organomet. Chem.* **2000**, *14*, 57–65.
392. Orejon, A.; Masdeu-Bulto, A. M.; Echarri, R.; Dieguez, M.; Fornies-Camer, J.; Claver, C.; Cardin, C. J. *J. Organomet. Chem.* **1998**, *559*, 23–29.
393. Ruiz, N.; Aaliti, A.; Fornies-Camer, J.; Ruiz, A.; Claver, C.; Cardin, C. J.; Fabbri, D.; Gladiali, S. *J. Organomet. Chem.* **1997**, *545–546*, 79–87.
394. Bayón, J. C.; Claver, C.; Masdeu-Bultó, A. M. *Coord. Chem. Rev.* **1999**, *193–195*, 73–145.
395. Cornils, B.; Herrmann, W. A. Eds. *Aqueous Phase Organometallic Catalysis*, Wiley-VCH, Weinheim, Germany, 1998.
396. Horváth, I. T.; Joó, F. Eds. *Aqueous Organometallic Chemistry and Catalysis*, NATO ASI Series, Kluwer, Dordrecht, The Netherlands, 1995.
397. Kuntz, E. G. *Chemtech* **1987**, *17*, 570–575.
398. Cornils, B.; Kuntz, E. G. *J. Organomet. Chem.* **1995**, *502*, 177–186.
399. Cornils, B.; Wiebus, E. *Recl. Trav. Chim. Pays Bas* **1996**, *115*, 2111–2215.
400. Cornils, B.; Wiebus, E. *Chemtech.* **1995**, January, 33–38.
401. Herwig, J.; Fischer, R. In *Catal. Met. Complexes*, Vol. 22; Kluwer, Dordrecht, The Netherlands, 2000.
402. van Leeuwen, P. W. N. M.; Kamer, P. C. J.; Reek, J. N. H. *CATTech*, **2000**, *6*, 164.
403. Wachsen, O.; Himmler, K.; Cornils, B. *Catal. Today* **1998**, *42*, 373–379.
404. Papadogianakis, G.; Sheldon, R. A. *New J. Chem.* **1996**, *20*, 175–185.
405. Jin, Z.-L.; Mei, J.-T.; Jiang, J.-Y. *Gaodeng Xuexiao Huaxue Xuebao* **2000**, *21*, 941–946.
406. Kamer, P. C. J.; van Leeuwen, P. W. N. M. The amphiphilic approach in aqueous-phase organometallic catalysis. In *Aqueous-Phase Organomet. Catal.* Cornils, B.; Herrmann, W. A., Eds.; Wiley-VCH Verlag, Weinheim, Germany, 1998, pp 564–576.
407. Chaudhari, R. V.; Bhanage, B. M. Kinetics of biphasic catalysis. In *Aqueous-Phase Organomet. Catal.* Cornils, B.; Herrmann, W. A., Eds., Wiley-VCH Verlag GmbH, Weinheim, Germany, **1998**, pp 283–294.
408. Zhang, Y.; Mao, Z.-S.; Chen, J. *Ind. Eng. Chem. Res.* **2001**, *40*, 4496–4505.
409. Horváth, I.; Kastrup, R. V.; Oswald, A. A.; Mozeleski, E. J. *Catal. Letters* **1989**, *2*, 85–90.
410. Herrmann, W. A.; Kohlpaintner, C. W.; Bahrmann, H.; Konkol, W. *J. Mol. Catal. A: Chem.* **1992**, *73*, 191.
411. Herrmann, W. A.; Kohlpaintner, C. W.; Manetsberger, R. B.; Bahrmann, H.; Kottmann, H. *J. Mol. Catal. A: Chem.* **1995**, *97*, 65–72.
412. Bahrmann, H.; Bach, H.; Frohning, C. D.; Kleiner, H. J.; Lappe, P.; Peters, D.; Regnat, D.; Herrmann, W. A. *J. Mol. Catal. A: Chem.* **1997**, *116*, 49.
413. Herrmann, W. A.; Kohlpaintner, C. W. *Angew. Chem. Int. Ed. Engl.* **1993**, *32*, 1524–1544.
414. Eckl, R. W.; Riermeier, T.; Herrmann, W. A. *J. Organomet. Chem.* **1997**, *532*, 243–249.
415. Buhling, A.; Kamer, P. C. J.; van Leeuwen, P. W. N. M.; Elgersma, J. W.; Goubitz, K.; Fraanje, J. *Organometallics* **1997**, *16*, 3027.
416. Schreuder Goedheijt, M.; Hanson, B. E.; Reek, J. N. H.; Kamer, P. C. J.; van Leeuwen, P. W. N. M. *J. Am. Chem. Soc.* **2000**, *122*, 1650–1657.
417. Wang, D.-B.; Yang, S.-Y.; Li, S.-B. *Shiyu Huagong* **2000**, *29*, 654–658. *Chem. Abstr.* **2000**, *133*, 363974.
418. Fell, B.; Hermanns, P.; Bahrmann, H. *J. Prakt. Chem./Chem.-Ztg.* **1998**, *340*, 459–467.
419. Schreuder Goedheijt, M.; Kamer, P. C. J.; van Leeuwen, P. W. N. M. *J. Mol. Catal. A: Chem.* **1998**, *134*, 243–249.
420. Yan, Y.-Y.; Zuo, H.-P.; Jin, Z.-L. *J. Nat. Gas Chem.* **1996**, *5*, 161–165.
421. Yan, Y.; Jiang, J.; Jin, Z. *Shiyu Huagong* **1996**, *25*, 89–91. *Chem. Abstr.* **1996**, *124*, 263962.
422. Pruchnik, F. P.; Smolenski, P.; Wajda-Hermanowicz, K. *J. Organomet. Chem.* **1998**, *570*, 63–69.
423. Miquel-Serrano, M. D.; Masdeu-Bulto, A. M.; Claver, C.; Sinou, D. *J. Mol. Catal. A: Chem.* **1999**, *143*, 49–55.
424. Kalck, P.; Miquel, L.; Dessoudeix, M. *Catal. Today* **1998**, *42*, 431–440.
425. Karlsson, M.; Johansson, M.; Andersson, C. *J. Chem. Soc. Dalton* **1999**, 4187–4192.
426. Dessoudeix, M.; Urrutigoity, M.; Kalck, P. *Eur. J. Inorg. Chem.* **2001**, 1797–1800.
427. Bischoff, S.; Kant, M. *Catal. Today* **2001**, *66*, 183–189.
428. Mecking, S.; Thomann, R. *Adv. Mater.* **2000**, *12*, 953–956.
429. Pruchnik, F. P.; Smolenski, P. *Appl. Organomet. Chem.* **1999**, *13*, 829–836.
430. Pruchnik, F. P.; Smolenski, P.; Galdecka, E.; Galdecki, Z. *New J. Chem.* **1998**, *22*, 1395–1398.

431. Lindner, E.; Auer, F.; Baumann, A.; Wegner, P.; Mayer, H. A.; Bertagnolli, H.; Reinohl, U.; Ertel, T. S.; Weber, A. *J. Mol. Catal. A: Chem.* **2000**, *157*, 97–109.
432. Stoessel, P.; Mayer, H. A.; Auer, F. *Eur. J. Inorg. Chem.* **1998**, 37–41.
433. Ash, C. E. *J. Mater. Educ.* **1994**, *16*, 1.
434. Reppe, W.; Magin, A. U.S. Patent 2,577,208. *Chem. Abstr.* **1952**, *46*, 6143.
435. Gough, A. Br. Pat. 1,081,304,1967. *Chem. Abstr.* **1967**, *67*, 10569.
436. Fenton, D. M. U.S. Patent 3,530,109, 1970. *Chem. Abstr.* **1970**, *73*, 110466.
437. Nozaki, K. U.S. Patent 3,689,460. *Chem. Abstr.* **1972**, *77*, 152860.
438. Sen, A.; Lai, T. W. *J. Am. Chem. Soc.* **1982**, *104*, 3520.
439. Lai, T. W.; Sen, A. *Organometallics* **1984**, *3*, 866.
440. Sen, A.; Brumbaugh, J. S. *J. Organomet. Chem.* **1985**, *279*, C5.
441. Drent, E. Eur. Pat. Appl. 121,965, 1984; *Chem. Abstr.* **1985**, *102*, 46423.
442. Drent, E. *Pure Appl. Chem.* **1990**, *62*, 661.
443. Drent, E. Eur. Pat. Appl. 229,408, 1986; *Chem. Abstr.* **1988**, *108*, 6617.
444. Drent, E.; Budzelaar, P. H. M. *Chem. Rev.* **1996**, *96*, 663.
445. Drent, E.; van Broekhoven, J. A. M.; Doyle, M. J.; Wong, P. K. Palladium Catalyzed Copolymerization of Carbon Monoxide with Alkenes to Alternating Polyketones and Polyspiroketals. Fink, G.; Muelhaupt, R.; Brintzinger, H. H. Eds.; *Ziegler Catal.* Springer, Berlin, 1995, pp 481–496.
446. Drent, E.; van Broekhoven, J. A. M.; Budzelaar, P. H. M. *Recl. Trav. Chim. Pays Bas* **1996**, *115*, 263–270.
447. Drent, E.; Jager, W. W. *Polym. Mater. Sci. Eng.* **1997**, *76*, 100–101.
448. van Leeuwen, P. W. N. M.; Roobeek, C. F. Catalysts for polymerization of carbon monoxide and alkenes. Eur. Pat. Appl. 380,162, 1990. *Chem. Abstr.* **1990**, *114*, 62975.
449. Dekker, G. P. C. M.; Elsevier, C. J.; Vrieze, K.; van Leeuwen, P. W. N. M. *J. Organomet. Chem.* **1992**, *430*, 357.
450. Lai, T. W.; Sen, A. *Organometallics* **1984**, *3*, 866.
451. Sen, A.; Brumbaugh, J. S. *J. Organomet. Chem.* **1985**, *279*, C5.
452. Vetter, W. M.; Sen, A. *J. Organomet. Chem.* **1989**, *378*, 485.
453. Rülke, R. E.; Han, I. M.; Elsevier, C. J.; Vrieze, K.; van Leeuwen, P. W. N. M.; Roobeek, C. F.; Zoutberg, M. C.; Wang, Y. F.; Stam, C. H. *Inorg. Chim. Acta* **1990**, *169*, 5.
454. de Graaf, W.; Boersma, J.; van Koten, G. *Organometallics* **1990**, *9*, 1479.
455. Markies, B. A.; Wijkens, P.; Boersma, J.; Spek, A. L.; van Koten, G. *Recl. Trav. Chim. Pays Bas* **1991**, *110*, 133.
456. Catellani, M.; Chiusoli, G. P.; Castagnoli, C. *J. Organomet. Chem.* **1991**, *407*, C30.
457. Li, C. S.; Cheng, C. H.; Liao, F. L.; Wang, S. L. *J. Chem. Soc., Chem. Commun.* **1991**, 710.
458. Ozawa, F.; Hayashi, T.; Koide, H.; Yamamoto, A. *J. Chem. Soc., Chem. Commun.* **1991**, 1469.
459. Brookhart, M.; Rix, F. C.; DeSimone, J. M.; Barborak, J. C. *J. Am. Chem. Soc.* **1992**, *114*, 5894.
460. Markies, B. A.; Rietveld, M. H. P.; Boersma, J.; Spek, A. L.; van Koten, G. *J. Organomet. Chem.* **1992**, *424*, C12.
461. Dekker, G. P. C. M.; Elsevier, C. J.; Vrieze, K.; van Leeuwen, P. W. N. M. *J. Organomet. Chem.* **1992**, *430*, 357.
462. Dekker, G. P. C. M.; Buijs, A.; Elsevier, C. J.; Vrieze, K.; van Leeuwen, P. W. N. M.; Smeets, W. J. J.; Spek, A. L.; Wang, Y. F.; Stam, C. *Organometallics* **1992**, *11*, 1937.
463. Dekker, G. P. C. M.; Elsevier, C. J.; Vrieze, K.; van Leeuwen, P. W. N. M. *Organometallics* **1992**, *11*, 1598.
464. Tóth, I.; Elsevier, C. J. *J. Am. Chem. Soc.* **1993**, *115*, 10388.
465. van Asselt, R.; Gielens, E. E. C. G.; Rülke, R. E.; Elsevier, C. J. *J. Chem. Soc. Chem. Commun.* **1993**, 1203.
466. *J. Am. Chem. Soc.* **1994**, *116*, 977.
467. van Leeuwen, P. W. N. M.; Roobeek, C. F. *Recl. Trav. Chim. Pays Bas* **1995**, *114*, 61.
468. Drent, E.; van Broekhoven, J. A. M.; Doyle, M. J. *J. Organomet. Chem.* **1991**, *417*, 235–251.
469. Batistini, A.; Consiglio, G.; Suter, U. W. *Angew. Chem. Int. Ed. Engl.* **1992**, *31*, 303–305.
470. Brookhart, M.; Rix, F. C.; DeSimone, J. M.; Barborak, J. C. *J. Am. Chem. Soc.* **1992**, *114*, 5894–5895.
471. Barsacchi, M.; Consiglio, G.; Suter, U. W. *Polym. Mater. Sci. Eng.* **1992**, *67*, 63–64.
472. Sen, A.; Jiang, Z. *Macromolecules* **1993**, *26*, 911–915.
473. Belov, G. P.; Chepaikin, E. G.; Bezruchenko, A. P.; Smirnov, V. I. *Vysokomol. Soedin. Ser. A* **1993**, *35*, 1585–1589. *Chem. Abstr.* **1994**, *120*, 107818.
474. Belov, G. P.; Golodkov, O. N.; Bzhabieva, Z. M. *Macromol. Symp.* **1995**, *89*, 455–464.
475. van Asselt, R.; Gielens, E. E. C. G.; Rülke, R. E.; Vrieze, K.; Elsevier, C. J. *J. Am. Chem. Soc.* **1994**, *116*, 977–985.
476. Keim, W.; Maas, H.; Mecking, S. Z. *Naturforsch., B: Chem. Sci.* **1995**, *50*, 430–438.
477. Chepaikin, E. G.; Bezruchenko, A. P.; Leshcheva, A. A.; Boiko, G. N. *Izv. Akad. Nauk Ser. Khim.* **1994**, *3*, 401–404. *Chem. Abstr.* **1995**, *122*, 315165.
478. Jiang, Z.; Sen, A. *J. Am. Chem. Soc.* **1995**, *117*, 4455–4467.
479. Nozaki, K.; Sato, N.; Takaya, H. *J. Am. Chem. Soc.* **1995**, *117*, 9911–9912.
480. Safir, A. L.; Novak, B. M. *Polym. Prepr. (Am. Chem. Soc., Div. Polym. Chem.)* **1995**, *36*, 227–228.
481. Pisano, C.; Consiglio, G. *Gazz. Chim. Ital.* **1994**, *124*, 393–401.
482. Lindner, E.; Schreiber, R.; Schneller, T.; Wegner, P.; Mayer, H. A.; Goepel, W.; Ziegler, C. *Inorg. Chem.* **1996**, *35*, 514–525.
483. Koide, Y.; Barron, A. R. *Macromolecules* **1996**, *29*, 1110–1118.
484. Koide, Y.; Bott, S. G.; Barron, A. R. *Organometallics* **1996**, *15*, 2213–2226.
485. Liaw, D.-J.; Lay, B.-F. *Polym. J. (Tokyo)* **1996**, *28*, 266–271.
486. Feng, Y.; Sun, J.; Zhu, Y. *Cuihua Xuebao* **1996**, *17*, 50–54. *Chem. Abstr.* **1996**, *124*, 233284.
487. Rix, F. C.; Brookhart, M.; White, P. S. *J. Am. Chem. Soc.* **1996**, *118*, 4746–4764.
488. Milani, B.; Vicentini, L.; Sommazzi, A.; Garbassi, F.; Chairparin, E.; Zangrando, E.; Mestroni, G. *J. Chem. Soc. Dalton* **1996**, 3139–3144.
489. Liaw, D.-J.; Tsai, J.-S.; Lay, B.-F. *Polym. J. (Tokyo)* **1996**, *28*, 608–612.
490. Margl, P.; Ziegler, T. *J. Am. Chem. Soc.* **1996**, *118*, 7337–7344.
491. Margl, P.; Ziegler, T. *Organometallics* **1996**, *15*, 5519–5523.
492. Brookhart, M.; Wagner, M. I. *J. Am. Chem. Soc.* **1996**, *118*, 7219–7220.
493. Luo, H.-K.; Li, D.-G. *Huaxue Xuebao* **1996**, *54*, 697–701. *Chem. Abstr.* **1996**, *125*, 168757.

494. Sperrle, M.; Aeby, A.; Consiglio, G.; Pfaltz, A. *Helv. Chim. Acta* **1996**, *79*, 1387–1392.
495. Kacker, S.; Jiang, Z.; Sen, A. *Macromolecules* **1996**, *29*, 5852–5858.
496. Golodkov, O. N.; Novikova, E. V.; Smirnov, V. I.; Gabutdinov, M. S.; Belov, G. P. *Zh. Prikl. Khim. (S.-Peterburg)* **1997**, *70*, 2000–2004. *Chem. Abstr.* **1998**, *128*, 205162.
497. Liaw, D.-J.; Tsai, J.-S. *J. Polym. Sci., Part A: Polym. Chem.* **1997**, *35*, 2759–2768.
498. Nozaki, K.; Sato, N.; Nakamoto, K.; Takaya, H. *B. Chem. Soc. Jpn.* **1997**, *70*, 659–664.
499. Liaw, D.-J.; Lay, B.-F. *J. Mol. Catal. A: Chem.* **1997**, *115*, 107–113.
500. Aeby, A.; Gsponer, A.; Consiglio, G. *J. Am. Chem. Soc.* **1998**, *120*, 11000–11001.
501. Zuideveld, M. A.; Kamer, P. C. J.; van Leeuwen, P. W. N. M.; Klusener, P. A. A.; Stil, H. A.; Roobeek, C. F. *J. Am. Chem. Soc.* **1998**, *120*, 7977–7978.
502. Bianchini, C.; Lee, H. M.; Meli, A.; Moneti, S.; Vizza, F.; Fontani, M.; Zanello, P. *Macromolecules* **1999**, *32*, 4183–4193.
503. Bianchini, C.; Lee, H. M.; Meli, A.; Moneti, S.; Patinec, V.; Petrucci, G.; Vizza, F. *Macromolecules* **1999**, *32*, 3859–3866.
504. Aeby, A.; Consiglio, G. *J. Chem. Soc. Dalton* **1999**, 655–656.
505. Fatutto, D.; Toniolo, L.; Chaudhari, R. V. *Catal. Today* **1999**, *48*, 49–56.
506. Gardiner, M. G.; Herrmann, W. A.; Reisinger, C.-P.; Schwarz, J.; Spiegler, M. *J. Organomet. Chem.* **1999**, *572*, 239–247.
507. Lindner, E.; Schmid, M.; Wegner, P.; Nachtigal, C.; Steimann, M.; Fawzi, R. *Inorg. Chim. Acta* **1999**, *296*, 103–113.
508. Aeby, A.; Consiglio, G. *Inorg. Chim. Acta* **1999**, *296*, 45–51.
509. Verspui, G.; Feiken, J.; Papadogianakis, G.; Sheldon, R. A. *J. Mol. Catal. A: Chem.* **1999**, *146*, 299–307.
510. Bianchini, C.; Man, L. H.; Barbaro, P.; Meli, A.; Moneti, S.; Vizza, F. *New J. Chem.* **1999**, *23*, 929–938.
511. Parlevliet, F. J.; Zuideveld, M. A.; Kiener, C.; Kooijman, H.; Spek, A. L.; Kamer, P. C. J.; van Leeuwen, P. W. N. M. *Organometallics* **1999**, *18*, 3394–3405.
512. Macchioni, A.; Bellachioma, G.; Cardaci, G.; Travaglia, M.; Zuccaccia, C.; Milani, B.; Corso, G.; Zangrando, E.; Mestroni, G.; Carfagna, C.; Formica, M. *Organometallics* **1999**, *18*, 3061–3069.
513. Chen, J. C. C.; Lin, I. J. B. *Organometallics* **2000**, *19*, 5113–5121.
514. Knight, J. G.; Doherty, S.; Harriman, A.; Robins, E. G.; Betham, M.; Eastham, G. R.; Tooze, R. P.; Elsegood, M. R. J.; Champkin, P.; Clegg, W. *Organometallics* **2000**, *19*, 4957–4967.
515. Yuan, J.-C.; Lu, S.-J. *J. Polym. Sci., Part A: Polym. Chem.* **2000**, *38*, 2919–2924.
516. Suranna, G. P.; Mastroilli, P.; Nobile, C. F.; Keim, W. *Inorg. Chim. Acta* **2000**, *305*, 151–156.
517. Aeby, A.; Gsponer, A.; Sperrle, M.; Consiglio, G. *J. Organomet. Chem.* **2000**, *603*, 122–127.
518. Lindner, E.; Schmid, M.; Wald, J.; Queisser, J. A.; Geprags, M.; Wegner, P.; Nachtigal, C. *J. Organomet. Chem.* **2000**, *602*, 173–187.
519. Sesto, B.; Consiglio, G. *Chem. Commun.* **2000**, 1011–1012.
520. Mul, W. P.; Oosterbeek, H.; Beitel, G. A.; Kramer, G.-J.; Drent, E. *Angew. Chem. Int. Ed.* **2000**, *39*, 1848–1851.
521. Luo, H.; Li, D.; Kou, Y. *Wuli Huaxue Xuebao* **2000**, *16*, 273–277. *Chem. Abstr.* **2000**, *132*, 334925.
522. Luo, H.-K.; Kou, Y.; Wang, X.-W.; Li, D.-G. *J. Mol. Catal. A: Chem.* **2000**, *151*, 91–113.
523. Kacker, S.; Sissano, J. A.; Schulz, D. N. *J. Polym. Sci., Part A: Polym. Chem.* **2000**, *38*, 752–757.
524. Yuan, J.-C.; Lu, S.-J. *Tetrahedron Lett.* **2001**, *42*, 4069–4073.
525. Yuan, J.-C.; Lu, S.-J. *Organometallics* **2001**, *20*, 2697–2703.
526. Yuan, J.-C.; Chen, M. D.; Zhang, Y. H.; Lu, S. J. *J. Polym. Sci., Part A: Polym. Chem.* **2001**, *39*, 2027–2036.
527. Mul, W. P.; Drent, E.; Jansens, P. J.; Kramer, A. H.; Sonnemans, M. H. W. *J. Am. Chem. Soc.* **2001**, *123*, 5350–5351.
528. Dossett, S. J.; Wass, D. F.; Jones, M. D.; Gillon, A.; Orpen, A. G.; Fleming, J. S.; Pringle, P. G. *Chem. Commun.* **2001**, 699–700.
529. Sesto, B.; Consiglio, G. *J. Am. Chem. Soc.* **2001**, *123*, 4097–4098.
530. Bastero, A.; Ruiz, A.; Reina, J. A.; Claver, C.; Guerrero, A. M.; Jalon, F. A.; Manzano, B. R. *J. Organomet. Chem.* **2001**, *619*, 287–292.
531. Chen, Y.-C.; Chen, C.-L.; Chen, J.-T.; Liu, S.-T. *Organometallics* **2001**, *20*, 1285–1286.
532. Reddy, K. R.; Surekha, K.; Lee, G.-H.; Peng, S.-M.; Chen, J.-T.; Liu, S.-T. *Organometallics* **2001**, *20*, 1292–1299.
533. Selivanov, V. D.; Konstatinov, I. I. *Russ. J. Phys. Chem.* **1975**, *49*, 620.
534. Cenini, S.; Ragaini, F. In *Reductive Carbonylation of Organic Nitro Compounds*, Catalysis by Metal Complexes, Ugo, R.; James, B. R., Eds.; Kluwer, Dordrecht, The Netherlands, 1997.
535. Tafesh, A. M.; Weiguny, J. *Chem. Rev.* **1996**, *96*, 2035.
536. Ragaini, F.; Cenini, S. *J. Mol. Catal. A: Chem.* **1996**, *109*, 1.
537. Cenini, S.; Crotti, C. In: Noëls, A. F.; Graziani, M.; Hubert, A. J., Eds., *Catalysis by Metal Complexes. Metal promoted selectivity in Organic Synthesis*, Vol. 12, Kluwer, Dordrecht, 1991, p 311.
538. Ikariya, T. *Catalysis* **1989**, *31*, 271.
539. Manov-Yuvenskii, V. I.; Nefedov, B. K. *Russ. Chem. Rev.* **1981**, *50*, 470.
540. Cenini, S.; Crotti, C.; Pizzotti, M.; Porta, F. *J. Org. Chem.* **1988**, *53*, 1243–1250.
541. Bhaduri, S.; Khwaja, H.; Sharma, K.; Jones, P. G. *J. Chem. Soc. Chem. Commun.* **1989**, 515–516.
542. Bhaduri, S.; Khwaja, H.; Sapre, N.; Sharma, K.; Basu, A.; Jones, P. G.; Carpenter, G. *J. Chem. Soc., Dalton* **1990**, 1313–1321.
543. Basu, A.; Bhaduri, S.; Khwaja, H. *J. Organomet. Chem.* **1987**, *319*, C28–C30.
544. Gargulak, J. D.; Berry, A. J.; Noirot, M. D.; Gladfelter, W. L. *J. Am. Chem. Soc.* **1992**, *114*, 8933–8945.
545. Gargulak, J. D.; Hoffman, R. D.; Gladfelter, W. L. *J. Mol. Catal. A: Chem.* **1991**, *68*, 289–293.
546. Gargulak, J. D.; Noirot, M. D.; Gladfelter, W. L. *J. Am. Chem. Soc.* **1991**, *113*, 1054–1055.
547. Kunin, A. J.; Noirot, M. D.; Gladfelter, W. L. *J. Am. Chem. Soc.* **1989**, *111*, 2739–2741.
548. Gargulak, J. D.; Gladfelter, W. L. *J. Am. Chem. Soc.* **1994**, *116*, 3792.
549. Skoog, S. J.; Campbell, J. P.; Gladfelter, W. L. *Organometallics* **1994**, *13*, 4137.
550. Skoog, S. J.; Gladfelter, W. L. *J. Am. Chem. Soc.* **1997**, *119*, 11049.
551. Nefedov, B. K.; Manov-Yuvenskii, V. I. *Izv. Akad. Nauk SSSR, Ser. Khim.* **1976**, 1905; **1977**, 2597–2598, **1979**, 585–589. *Chem. Abstr.* **1976**, *85*, 178014; **1978**, *88*, 62085; **1979**, *90*, 203604.
552. Tietz, H.; Unverferth, K.; Schwetlick, K. *Z. Chem.* **1980**, *20*, 295–296.

553. Gorbunova, L. V.; Knyazeva, I. L.; Nefedov, B. K.; Khoshdurdyev, Kh. O.; Manov-Yuvenskii, V. I. *Izv. Akad. Nauk SSSR, Ser. Khim.* **1981**, 1644–1645. *Chem. Abstr.* **1981**, 95, 115000.
554. Becker, R.; Rasp, C.; Stammann, G.; Grolig, J. (Bayer A.-G). Urethanes. Ger. Offen. 1981, DE 3009489. *Chem. Abstr.* **1981**, 95, 168838.
555. Drent, E.; van Leeuwen, P. W. N. M. (Shell International Research) Eur. Patent 86281 1981.
556. Manov-Yuvenskii, V. I.; Nefedov, B. K.; Khoshdurdyev, Kh. O. *Izv. Akad. Nauk SSSR Ser. Khim.* **1982**, 1320–1322. *Chem. Abstr.* **1982**, 97, 127211.
557. Alessio, E.; Mestroni, G. *J. Mol. Catal. A: Chem.* **1984**, 26, 337–340.
558. Alessio, E.; Mestroni, G. *J. Organomet. Chem.* **1985**, 291, 117–127.
559. Bontempi, A.; Alessio, E.; Chanos, G.; Mestroni, G. *J. Mol. Catal. A: Chem.* **1987**, 42, 67–80.
560. Wehman, P.; Kaasjager, V. E.; Hartl, F.; Kamer, P. C. J.; van Leeuwen, P. W. N. M.; Fraanje, J.; Goubitz, K. *Organometallics* **1995**, 14, 3751–3761.
561. Wehman, P.; Dol, G. C.; Moorman, E. R.; Kamer, P. C. J.; van Leeuwen, P. W. N. M.; Fraanje, J.; Goubitz, K. *Organometallics* **1994**, 13, 4856–4869.
562. Halligudi, S. B.; Khan, N. H.; Kureshy, R. I.; Suresh, E.; Venkatsubramanian, K. *J. Mol. Catal. A: Chem.* **1997**, 124, 147–154.
563. Tollari, S.; Cenini, S.; Crotti, C.; Gianella, E. *J. Mol. Catal. A: Chem.* **1994**, 87, 203–214.
564. Wehman, P.; Borst, L.; Kamer, P. C. J.; van Leeuwen, P. W. N. M. *J. Mol. Catal. A: Chem.* **1996**, 112, 23–36.
565. Halligudi, S. B.; Bhatt, K. N.; Khan, N. H.; Kurashy, R. I.; Venkatsubramanian, K. *Polyhedron* **1996**, 15, 2093–2101.
566. Reddy, N. P.; Masdeu, A. M.; El Ali, B.; Alper, H. *J. Chem. Soc. Chem. Commun.* **1994**, 863–864.
567. Lee, C. W. *Kongop Hwahak* **1999**, 10, 1079–1085. *Chem. Abstr.* **1999**, 132, 222323.
568. Wehman, P.; van Donge, H. M. A.; Hagos, A.; Kamer, P. C. J.; van Leeuwen, P. W. N. M. *J. Organomet. Chem.* **1997**, 535, 183–193.
569. Ragaini, F.; Macchi, M.; Cenini, S. *J. Mol. Catal. A: Chem.* **1997**, 127, 33–42.
570. Moiseev, I. I.; Stromnova, T. A.; Vargaftik, M. N.; Orlova, S. T.; Chernysheva, T. V.; Stolarov, I. P. *Catal. Today* **1999**, 51, 595–602.
571. Gallo, E.; Ragaini, F.; Cenini, S.; Demartin, F. *J. Organomet. Chem.* **1999**, 586, 190–195.
572. Pirozhkov, S. D.; Tonkonogov, B. P.; Lazarev, A. V.; Lapidus, A. L.; *Neftekhimiya* **2000**, 40, 103–107. *Chem. Abstr.* **2000**, 133, 192885.
573. Skupinska, J.; Karpinska, M. *J. Mol. Catal. A: Chem.* **2000**, 161, 69–73.
574. Leconte, P.; Metz, F.; Mortreux, A.; Osborn, J. A.; Paul, F.; Petit, F.; Pillot, A. *J. Chem. Soc. Chem. Commun.* **1990**, 1616–1617.
575. Paul, F.; Fischer, J.; Ochsenbein, P.; Osborn, J. A. *Organometallics* **1998**, 17, 2199–2206.
576. Santi, A. S. O.; Milani, B.; Mestroni, G.; Zangrando, E.; Randaccio, L. *J. Organomet. Chem.* **1997**, 545–546, 89–91.
577. Santi, A. S. O.; Milani, B.; Zangrando, E.; Mestroni, G. *Eur. J. Inorg. Chem.* **2000**, 11, 2351–2354.
578. Ottmann, G. F.; Schnabel, W. J.; Smith, E. (Olin Mathieson Chemical Corp.). Phenyl isocyanate and isocyanateno-trotoluenes, Fr. Pat.1, 556,876 1969; *Chem. Abstr.* **1969**, 71, 49523.
579. Unverferth, K.; Schwetlick, K. *React. Kinet. Catal. Lett.* **1977**, 6, 231–234.
580. Manov-Yuvenskii, V. I.; Smetanin, A. V.; Nefedov, B. K.; Chimishkyan, A. L. *Kinet. Katal.* **1980**, 21, 1335–1336.
581. Elleuch, B.; Taarit, Y. B.; Basset, J. M.; Kervennal, J. *Angew. Chem.* **1982**, 94, 722–723.
582. Lefebvre, F.; Gelin, P.; Elleuch, B.; Naccache, C.; Taarit, Y. B. *B. Soc. Chim. Fr.* **1985**, 361–369.
583. Mizuno, T.; Alper, H. *J. Mol. Catal. A: Chem.* **1997**, 121, 119–122.
584. Ragaini, F.; Cenini, S.; Demartin, F. *Organometallics* **1994**, 13, 1178–1189.
585. Ragaini, F.; Cenini, S.; Demartin, F. *J. Chem. Soc. Chem. Commun.* **1992**, 1467–1468.
586. Ragaini, F.; Cenini, S.; Fumagalli, A.; Crotti, C. *J. Organomet. Chem.* **1992**, 428, 401–408.
587. Ragaini, F.; Gallo, E.; Cenini, S. *J. Organomet. Chem.* **2000**, 593–594, 109–118.
588. Szmant, H. H. *Organic Building Blocks for the Chemical Industry*; **1989**, Wiley, New York.
589. Beller, M.; Eckert, M. *Angew. Chem., Int. Ed.* **2000**, 39, 1010–1027.
590. Kuehlehn, K.; Geissler, H. Amidocarbonylation; In *Transition Met. Org. Synth.* Beller, M.; Bolm, C., Eds.; Wiley-VCH Verlag, Weinheim, Germany, 1998, 1, 79–90.
591. Knifton, J. F. Amidocarbonylation. In *Appl. Homogeneous Catal. Organomet. Compd.* Cornils, B.; Herrmann, W. A., Eds.; VCH, Weinheim, Germany, 1996, 1, 159–168.
592. Knifton, J. F.; Lin, J. J.; Storm, D. A.; Wong, S. F. *Catal. Today* **1994**, 18, 355–384.
593. Lin, J. J.; Knifton, J. F. Amidocarbonylation. Catalyst Reaction Scope, and Industrial Application, In *Advances in Chemistry Series 230*; American Chemical Society: Washington, DC, 1992, 235–247.
594. Beller, M. *Med. Res. Rev.* **1999**, 19, 357–369.
595. Ojima, I.; Zhang, Z.; Korda, A.; Ingallina, P.; Clos, N. New Carbonylations Catalyzed by Transition Metal Complexes, In *Advances in Chemistry Series 230*; American Chemical Society, Washington, DC, 1992, 277–296.
596. Ojima, I. *Chem. Rev.* **1988**, 88, 1011.
597. Jaegers, E.; Koll, H. P. (Hoechst). Preparation of N-acylaminoacids from aldehydes carboxamides and carbonmonoxide. Ger. Offen. 1989, DE 3812737, EP 338330. *Chem. Abstr.* **1990**, 112, 77951.
598. Beller, M.; Eckert, M.; Vollmuller, F.; Bogdanovic, S.; Geissler, H. *Angew. Chem., Int. Edit.* **1997**, 36, 1494–1496.
599. Beller, M.; Eckert, M.; Vollmuller, F. *J. Mol. Catal. A: Chem.* **1998**, 135, 23–33.
600. Beller, M.; Moradi, W. A.; Eckert, M.; Neumann, H. *Tetrahedron Lett.* **1999**, 40, 4523–4526.
601. Beller, M.; Eckert, M.; Moradi, W. A. *Synlett.* **1999**, 108–110.
602. Dghaym, R. D.; Yaccato, K. J.; Arndtsen, B. A. *Organometallics* **1998**, 17, 4–6.
603. Kacker, S.; Kim, J. S.; Sen, A. *Angew. Chem. Int. Ed. Engl.* **1998**, 37, 1251.
604. Davis, J. L.; Arndtsen, B. A. *Organometallics* **2000**, 19, 4657.
605. Lafrance, D.; Davis, J. L.; Dhawan, R.; Arndtsen, B. A. *Organometallics* **2001**, 20, 1128.
606. Dghaym, R. D.; Dhawan, R.; Arndtsen, B. A. *Angew. Chem. Int. Ed. Engl.* **2001**, 40, 3228.
607. Freed, D. A.; Kozlowski, M. C. *Tetrahedron Lett.* **2001**, 42, 3403–3406.
608. Cavallo, L. *J. Am. Chem. Soc.* **1999**, 121, 4238.

609. Drauz, K.; Burkhardt, O.; Beller, M.; Eckert, M. (Degussa-Huels A.-G., Germany). Amidocarbonylation procedure and catalysts for the production of N-acylaminoacids from the reaction of carbon monoxide with aldehydes and amides or nitriles. Ger. Offen. 2000; DE 10012251. *Chem. Abstr.* **2000**, *134*, 56964.
610. Wakamatsu, H. *J. Chem. Soc. Chem. Commun.* **1971**, 1540.
611. Wakamatsu, H. *B. Chem. Soc. Jpn* **1971**, *44*, 288.
612. Ojima, I.; Zhang, Z. *Organometallics* **1990**, *9*, 3122–3127.
613. Ojima, I.; Zhang, Z. *J. Organomet. Chem.* **1991**, *417*, 253–276.
614. Ojima, I.; Hirai, K.; Fujita, M.; Fuchikami, T. *J. Organomet. Chem.* **1985**, *279*, 203–214.
615. Lin, J. J. (Texaco Development Corp.) Process for synthesis of amidoacids using a cobalt catalyst and a bidentate phosphine ligand Eur. Pat. Appl. 263,624 1988. *Chem. Abstr.* 1989, *110*, 154881.
616. Lin, J. J.; Knifton, J. F. *J. Organomet. Chem.* **1991**, *417*, 99–110.
617. Zhou, H.; Lu, S.; Sung, N.; Zhen, Y.; Fu, H. *Fenzi Cuihua* **1994**, *8*, 353–358. *Chem. Abstr.* **1995**, *122*, 56482.
618. Xu, P.; Lin, H.; Xu, C.; Zhang, F. *Xiamen Daxue Xuebao, Ziran Kexueban* 1996, *35*, 538–544. *Chem. Abstr.* 1997, *126*, 277744.
619. Gomez, R. M.; Sharma, P.; Arias, J. L.; Perez-Flores, J.; Velasco, L.; Cabrera, A. *J. Mol. Catal. A: Chem.* **2001**, *170*, 271–274.
620. Ojima, I.; Okabe, M.; Kato, K.; Kwon, H. B.; Horvath, I. T. *J. Am. Chem. Soc.* **1988**, *110*, 7–150.
621. Yuan, S. S.; Ajami, A. M. *J. Organomet. Chem.* **1986**, *302*, 8–255.
622. de Vries, J. G.; de Boer, R. P.; Hogeweg, M.; Gielens, E. E. C. G. *J. Org. Chem.* **1996**, *61*, 1842–1846.
623. Sakakura, T.; Huang, X. Y.; Tanaka, M. *B. Chem. Soc. Jpn* **1991**, *64*, 1707–1709.
624. Takigawa, S.; Shinke, S.; Tanaka, M. *Chem. Lett.* **1990**, 1415–1418.
625. Ali, B. E.; Alper, H. In *Transition Metals for Organic Synthesis*, Beller, M.; Bolm, C., Eds.; Wiley-VCH, Weinheim, Germany, 1998, Chapter 2.2.
626. Beller, M.; Tafesh, A. M. In *Applied Homogeneous Catalysis with Organometallic Compounds*; Cornils, B.; Herrmann, W. A., Eds; VCH: Weinheim, Germany, 1996; Chapter 2.1.2.6.
627. Drent, E.; Petrus, L.; van Langen, S. A. J. (Shell). EP 282 142, 1988.
628. Höhn, A. In *Applied Homogeneous Catalysis with Organometallic Compounds*, Cornils, B.; Herrmann, W. A., Eds.; VCH, Weinheim, Germany, 1996, Chapter 2.1.2.2.
629. van Leeuwen, P. W. N. M.; Kamer, P. C. J.; Reek, J. N. H.; Dierkes, P. *Chem. Rev.* **2000**, *100*, 2741–2769.
630. Rieu, J.-P.; Boucherle, A.; Cousse, H.; Mouzin, G. *Tetrahedron* **1986**, *42*, 4095.
631. del Río, I.; Claver, C.; van Leeuwen, P. W. N. M. *Eur. J. Inorg. Chem.* **2001**, 2719–2738.
632. Tilloy, S.; Monflier, E.; Bertoux, F.; Castanet, Y.; Mortreux, A. *New. J. Chem.* **1997**, *21*, 529.
633. Ali, B.; Alper, H. *J. Mol. Catal. A: Chem.* **1993**, *80*, 377.
634. Kron, T. A.; Noskov, Y. G.; Terekhova, M. I.; Petrov, T. S. *Zh. Fiz. Chim.* **1996**, *70*, 82–86.
635. Yoon, J.-Y.; Jang, E. J.; Lee, K. H.; Lee, J. S. *J. Mol. Catal.* **1997**, *118*, 181.
636. Ali, B. E.; Alper, H. *J. Mol. Catal. A: Chem.* **1992**, *77*, 7.
637. Zargarian, D.; Alper, H. *Organometallics* **1993**, *12*, 712.
638. Ali, B.; Alper, H. *J. Mol. Catal. A: Chem.* **1993**, *80*, 377.
639. del Río, I.; Ruiz, N.; Claver, C.; van der Veen, L. A.; van Leeuwen, P. W. N. M. *J. Mol. Catal. A: Chem.* **2000**, *161*, 39–48.
640. del Río, I.; Ruiz, N.; Claver, C. *Inorg. Chem. Commun.* **2000**, *3*, 166–168.
641. Tilloy, S.; Monflier, E.; Bertoux, F.; Castanet, Y.; Mortreux, A. *New. J. Chem.* **1997**, *21*, 529.
642. Goedheijt, M. S.; Reek, J. N. H.; Kamer, P. C. J.; van Leeuwen, P. W. N. M. *Chem. Commun.* **1998**, 2431–2432.
643. Alper, H.; Hamel, N. *J. Am. Chem. Soc.* **1990**, *112*, 2803–2804.
644. Real, J.; Pagé, M.; Polo, A.; Piniella, J.; Alvarez Larena, A. *Chem. Commun.* **1999**, 277.
645. Kruis, D.; Ruiz, N.; Janssen, M. D.; Boersma, J.; Claver, C.; van Koten, G. *Inorg. Chem. Comm.* **1998**, *1*, 295–298.
646. Amatore, C.; Jutand, A.; Medeiros, M. *New J. Chem.* **1996**, *20*, 1143.
647. Amatore, C.; Jutand, A.; Meyer, G.; Atmani, H.; Khalil, F.; Chahdi, F. O. *Organometallics* **1998**, *17*, 2958.
648. Amatore, C.; Carré, E.; Jutand, A.; M'Barki, M. A. *Organometallics* **1995**, *14*, 1818.
649. Ozawa, F.; Kubo, A.; Hayashi, T. *Chem. Lett.* **1992**, 2177.
650. Csáka, Z.; Skoda-Földes, R.; Kollár, L. *L. Inorg. Chim. Acta* **1999**, *286*, 93.
651. Amatore, C.; Jutand, A.; Thuilliez, A. *Organometallics* **2001**, *20*, 3241.
652. Tóth, I.; Elsevier, C. J. *Organometallics* **1994**, *13*, 2118.
653. Portnoy, M.; Milstein, D. *Organometallics* **1994**, *13*, 600.
654. Perez, P. J.; Calabrese, J. C.; Bunel, E. *Organometallics*, **2001**, *20*, 337.
655. Lin, Y.-S.; Yamamoto, A. *Organometallics*, **1998**, *17*, 3466.
656. Flemming, J. P.; Pilon, O. Y.; Borbulevitch, M. C.; Antipin, M. Y.; Grushin, V. V. *Inorg. Chim. Acta* **1998**, *280*, 87.
657. Gatti, G.; López, J. A.; Mealli, C.; Musco, A. *J. Organomet. Chem.* **1994**, 483–77.
658. Noskov, Y. G.; Terekhova, M. I.; Petrov, E. S. *Kinet. Katal.* **1993**, *34*, 1001.
659. Dekker, G. P. C. M.; Elsevier, C. J.; Vrieze, K.; van Leeuwen, P. W. N. M.; Roobeek, C. F. *J. Organomet. Chem.* **1992**, *430*, 357.
660. Nefkens, S. C. A.; Sperrle, M.; Consiglio, G. *Angew. Chem. Int. Edit.* **1993**, *32*, 1848.
661. Bianchini, C.; Mantovani, G.; Meli, A.; Oberhauser, W.; Brüggeller, P.; Stampfl, T. *J. Chem. Soc. Dalton* **2001**, 690.
662. Tóth, I.; Elsevier, C. J. *J. Am. Chem. Soc.* **1993**, *115*, 10388.
663. Dekker, G. P. C. M.; Buijs, A.; Elsevier, C. J.; Vrieze, K.; van Leeuwen, P. W. N. M.; Smeets, W. J. J.; Spek, A. L.; Wang, Y. F.; Stam, C. H. *Organometallics* **1992**, *11*, 1937.
664. van Leeuwen, P. W. N. M.; Roobeek, C. F.; van der Heijden, H. *J. Am. Chem. Soc.* **1994**, *116*, 12117.
665. Verspui, G.; Moiseev, I. I.; Sheldon, R. A. *J. Organomet. Chem.* **1999**, *586*, 196.
666. Vasilevsky, S. F.; Trofimov, B. A.; Malkina, A. G.; Brandsma, L. *Synth. Commun.* **1994**, *24*, 85–88.
667. Drent, E.; Arnoldy, P.; Budzelaar, P. H. M. *J. Organomet. Chem.* **1993**, *455*, 247–253.
668. Drent, E.; Arnoldy, P.; Budzelaar, P. H. M. *J. Organomet. Chem.* **1994**, *475*, 57–63.
669. Keijsper, J. J.; Arnoldy, P.; Doyle, M. J.; Drent, E. *Recl. Trav. Chim. Pays Bas* **1996**, *115*, 248–255.
670. Cavinato, G.; Toniolo, L. *J. Organomet. Chem.* **1990**, *398*, 187.

671. Milstein, D. *Acc. Chem. Res.* **1988**, *21*, 428.
672. Kawana, M.; Nakamura, S.; Watanabe, E.; Urata, H. *J. Organomet. Chem.* **1997**, *542*, 185–189.
673. Tooze, R. P.; Whiston, K.; Malyan, A. P.; Taylor, M. J.; Wilson, N. W. *J. Chem. Soc. Dalton* **2000**, 3441–3444.
674. Seayad, A.; Jayasree, S.; Damodaran, K.; Toniolo, L.; Chaudhari, R. V. *J. Organomet. Chem.* **2000**, *601*, 100–107.
675. Seayad, A.; Kelkar, A. A.; Toniolo, L.; Chaudhari, R. V. *J. Mol. Catal. A: Chemical* **2000**, *151*, 47–59.
676. Benedek, C.; Szalontai, G.; Gomory, A.; Toros, S.; Heil, B. *J. Organomet. Chem.* **1999**, *579*, 147–155.
677. Scrivanti, A.; Beghetto, V.; Campagna, E.; Zanato, M.; Matteoli, U. *Organometallics* **1998**, *17*, 630–635.
678. Eastham, G. R.; Tooze, R. P.; Heaton, B. T.; Iggo, J. A.; Whyman, R.; Zacchini, S. *Chem. Commun.* **2000**, 609–610.
679. Milstein, D. *J. Chem. Soc. Chem. Commun.* **1986**, 817.
680. Kim, K. Y. J.; Osakada, K.; Sugita, K.; Yamamoto, T.; Yamamoto, A. *Organometallics* **1988**, *7*, 2182.
681. Dekker, G. P. C. M.; Elsevier, C. J.; Vrieze, K.; van Leeuwen, P. W. N. M.; Roobeek, C. F. *J. Organomet. Chem.* **1992**, *430*, 357.
682. Clegg, W.; Elsegood, M. R. J.; Eastham, G. R.; Tooze, R. P.; Wang, X. L.; Whiston, K. *Chem. Commun.* **1999**, 1877–1878.
683. Dervisi, A.; Edwards, P. G.; Newman, P. D.; Tooze, R. P. *J. Chem. Soc. Dalton* **2000**, 523–528.
684. Oi, S.; Nomura, M.; Aiko, T.; Inoue, Y. *J. Mol. Catal. A: Chem.* **2000**, *115*, 289–295.
685. Scrivanti, A.; Beghetto, V.; Zanato, M.; Matteoli, U. *J. Mol. Catal. A: Chem.* **2000**, *160*, 331–336.
686. Pugh, R. I.; Pringle, P. G.; Drent, E. *Chem. Commun.* **2001**, 1476–1477.
687. Doherty, S.; Robins, E. G.; Knight, J. G.; Newman, C. R.; Rhodes, B.; Champkin, P. A.; Clegg, W. *J. Organomet. Chem.* **2001**, *640*, 182–196.
688. Broussier, R.; Bentabet, E.; Laly, M.; Richard, P.; Kuzmina, L. G.; Serp, P.; Wheatley, N.; Kalck, P.; Gautheron, B. *J. Organomet. Chem.* **2000**, *613*, 77–85.
689. Brugat, N.; Polo, A.; Alvarez-Larena, A.; Piniella, J. F.; Real, J. *Inorg. Chem.* **1999**, *38*, 4829.
690. Zhou, H.; Hou, J.; Cheng, J.; Lu, V.; Fu, H.; Wang, H. *J. Organomet. Chem.* **1997**, *543*, 227.

9.4

Metal Complexes as Catalysts for Oxygen, Nitrogen, and Carbon-atom Transfer Reactions

T. KATSUKI

Kyushu University, Fukuoka, Japan

9.4.1	INTRODUCTION	207
9.4.2	EPOXIDATION	207
9.4.2.1	Epoxidation of Allylic Alcohols	208
9.4.2.2	Epoxidation of Isolated Olefins	211
9.4.2.2.1	<i>Epoxidation using metalloporphyrin as catalysts</i>	211
9.4.2.2.2	<i>Epoxidation using metallocalen complexes as catalysts</i>	216
9.4.2.3	Epoxidation of Electron-deficient Olefins	223
9.4.3	OXIDATION OF ENOL ETHERS AND THEIR DERIVATIVES	225
9.4.4	ASYMMETRIC AZIRIDINATION	227
9.4.5	ASYMMETRIC DIHYDROXYLATION	231
9.4.5.1	General Features of Asymmetric Dihydroxylation	231
9.4.5.2	Mechanistic Considerations	235
9.4.5.3	Models for the Enantiodifferentiating Step in Dihydroxylation	238
9.4.5.4	Iron-mediated Dihydroxylation	238
9.4.6	ASYMMETRIC AMINOHYDROXYLATION	239
9.4.7	ASYMMETRIC CYCLOPROPANATION	243
9.4.7.1	Asymmetric Intermolecular Cyclopropanation	243
9.4.7.1.1	<i>Cu-catalyzed cyclopropanation</i>	243
9.4.7.1.2	<i>Rh-catalyzed cyclopropanation</i>	245
9.4.7.1.3	<i>Ru-catalyzed cyclopropanation</i>	248
9.4.7.1.4	<i>Co-catalyzed cyclopropanation</i>	250
9.4.7.2	Asymmetric Intramolecular Cyclopropanation	251
9.4.7.2.1	<i>Cu-catalyzed cyclopropanation</i>	251
9.4.7.2.2	<i>Rh-catalyzed cyclopropanation</i>	252
9.4.7.2.3	<i>Ru-catalyzed cyclopropanation</i>	253
9.4.7.2.4	<i>Co-catalyzed cyclopropanation</i>	254
9.4.7.3	Mechanism of Cyclopropanation	255
9.4.8	CONCLUSION	258
9.4.9	REFERENCES	259

9.4.1 INTRODUCTION

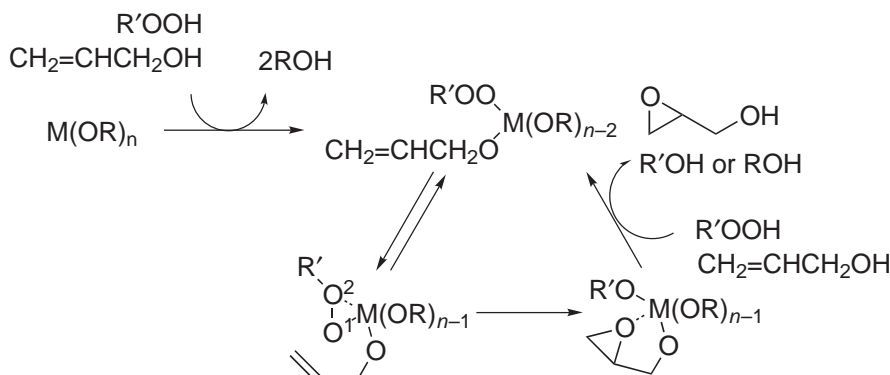
A π -bond can react with various active species, such as the electrophile oxene and its isoelectronic species (nitrenes and carbenes) and radicals. A π -bond can also react with a nucleophile, when it is conjugated with an electron-withdrawing group. In these reactions O, N, or C atom(s) are transferred from the active species to the olefins, forming two σ -bonds, such as C—O, C—N, and C—C, at the expense of the π -bond. If the π -bond is prochiral, chiral center(s) are

introduced as the σ -bond are formed. Thus, stereocontrolled reactions of the π -bond are of high synthetic value in the asymmetric synthesis of various useful compounds, such as pharmaceuticals and agrochemicals. Most active species are achiral and their reactions are nonstereoselective. However, many active species such as carbenes, nitrenes, oxenes, peroxides, etc. form complexes with various transition-metal ions without losing their reactivities.^{1,2} Sometimes the reactivity of the active species is enhanced by complexation (*vide infra*). Reactions of these complexes occur in the coordination spheres of the metal ions and, therefore, proceed in an enantioselective manner if the metal ions carry appropriate optically active ligand(s). Olefins are available in bulk from petroleum, and many conventional methods for olefin synthesis have been developed. Therefore, enantioselective atom-transfer reactions to olefins, their asymmetric functionalizations, are especially important from the synthetic viewpoint of useful optically active compounds. At the start of the twenty-first century, various well-designed optically active ligands have been introduced, and high enantioselectivity has been realized in many reactions.³ In this chapter, metal-mediated enantioselective O-, N-, and C-atom transfer reactions to olefins are dealt with: epoxidation,⁴⁻⁸ oxidation of enol ethers and their derivatives, dihydroxylation,⁹⁻¹² aminohydroxylation,^{13,14} aziridination,^{15,16} and cyclopropanation.¹⁷⁻²¹ Owing to limited space, emphasis is placed on highly enantioselective reactions. However, important pioneering studies that prompted the later development of asymmetric atom-transfer reactions are discussed, even though they are non- or poorly stereoselective. Heterogeneous reactions and the reactions of multiple bonds other than the C=C bond are beyond the scope of this chapter.

9.4.2 EPOXIDATION

9.4.2.1 Epoxidation of Allylic Alcohols

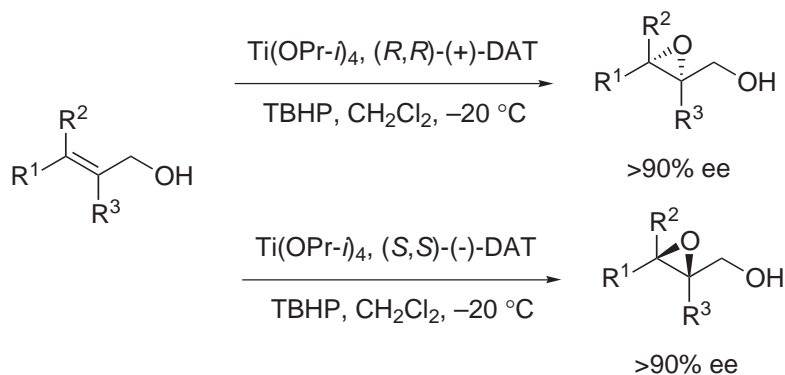
Metal alkoxides undergo alkoxide exchange with alcoholic compounds such as alcohols, hydroxamic acids, and alkyl hydroperoxides. Alkyl hydroperoxides themselves do not epoxidize olefins. However, hydroperoxides coordinated to a metal ion are activated by coordination of the distal oxygen (O^2) and undergo epoxidation (Scheme 1). When the olefin is an allylic alcohol, both hydroperoxide and olefin are coordinated to the metal ion and the epoxidation occurs swiftly in an intramolecular manner.²² Thus, the epoxidation of an allylic alcohol proceeds selectively in the presence of an isolated olefin.^{23,24} In this metal-mediated epoxidation of allylic alcohols, some alkoxide(s) ($-OR$) do not participate in the epoxidation. Therefore, if such "bystander" alkoxide(s) are replaced with optically active ones, the epoxidation is expected to be enantioselective. Indeed, Yamada *et al.*²⁵ and Sharpless *et al.*²⁶ independently reported the epoxidation of allylic alcohols using $MoO_2(acac)_2$ modified with *N*-methyl-ephedrine and $VO(acac)_2$ modified with an optically active hydroxamic acid as the catalyst, respectively, albeit with modest enantioselectivity.



Scheme 1

The scope of metal-mediated asymmetric epoxidation of allylic alcohols was remarkably enhanced by a new titanium system introduced by Katsuki and Sharpless: epoxidation of allylic alcohols using a titanium(IV) isopropoxide, dialkyl tartrate (DAT), and TBHP (TBHP = *tert*-butyl-hydroperoxide) proceeds with high enantioselectivity and good chemical yield, regardless of

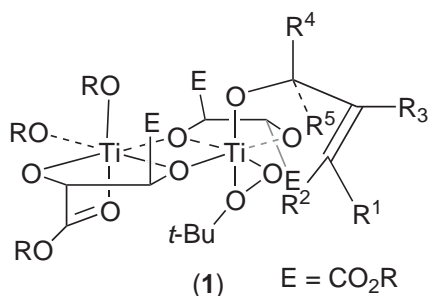
the substitution pattern of the allylic alcohol, except for some allylic alcohols possessing a bulky *Z*-substituent (R^2) or a coordinating group in the vicinity of the allylic hydroxyl group.²⁷ The stereochemistry of this reaction is determined by the chirality of the tartrate used and, therefore, is predictable from the empirical rule described in Scheme 2. Epoxidation with (*R,R*)- and (*S,S*)-DAT as the chiral auxiliary gives the 2*S*- and 2*R*-epoxide, respectively. There is no exception to this rule in the epoxidation of prochiral allylic alcohols.⁴ The epoxidation of allylic alcohols bearing a bulky *Z*-substituent shows substandard enantioselectivity, although its stereochemistry follows the empirical rule.²⁸



Scheme 2

The original titanium-mediated epoxidation is a stoichiometric reaction.²⁷ However, the epoxidation can be carried out with a catalytic amount (5–10 mol.%) of titanium–tartrate complex in the presence of molecular sieves.²⁹ The advantages of the catalytic procedure are ease of product isolation, increased yield, economy, and a high substrate concentration.

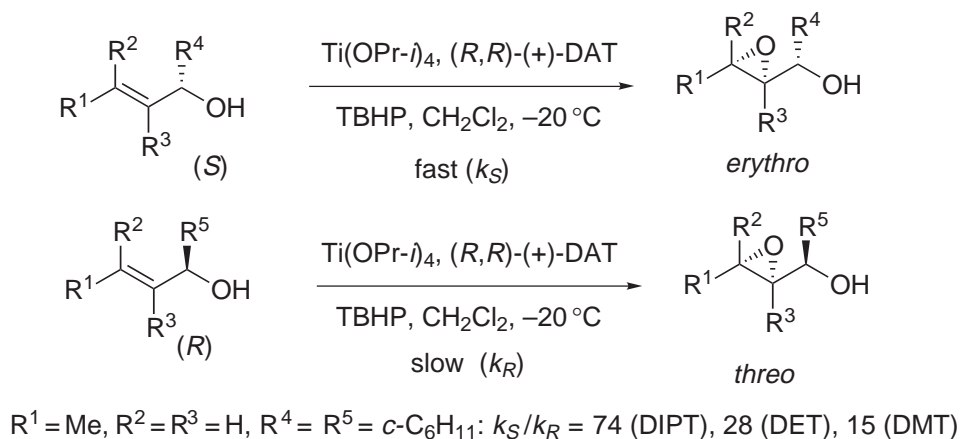
The transition-state model of this reaction has been proposed as (1), based on X-ray analyses of single crystals prepared from $\text{Ti(OPr}^i\text{)}_4$, (*R,R*)-diethyl tartrate (DET), and PhCON(OH)Ph ; and from $\text{Ti(OPr}^i\text{)}_4$, and (*R,R*)-*N,N'*-dibenzyltartramide.^{30–32} The *Z*-substituent (R^2), located close to the metal center, destabilizes the desired transition state and decreases enantioselectivity (*vide supra*). When the *Z*-substituent is chiral, face selection induced by the substituent strongly affects the stereochemistry of the epoxidation, and sometimes reversed face selectivity is observed.⁴ In contrast, the *E*-substituent (R^1) protrudes into an open space and *E*-allylic alcohols are generally good substrates for the epoxidation.



The proposed dinuclear transition-state model (1) has been supported by the observation of nonlinear relationship between enantiomeric excess (ee) of the epoxide and ee of DAT.³³ The use of simple diol instead of tartrate vitiates stereoselectivity of the reaction.^{34,35} The ester group of DAT is indispensable for the construction of the desired catalyst. It is noteworthy that 1,2-di(*o*-methoxyphenyl)ethylenediol is an efficient chiral auxiliary for titanium-mediated epoxidation, while 1,2-diphenylethylenediol is a poor one.³⁶

Model (1) further suggests that, if the substrate is a secondary allylic alcohol ($R^4 \neq \text{H}$, $R^5 = \text{H}$ or $R^4 = \text{H}$, $R^5 \neq \text{H}$), enantiomeric alcohols are epoxidized at different rates: when (*R,R*)-DAT is used as the chiral auxiliary, (*S*)-allylic alcohol ($R^4 \neq \text{H}$, $R^5 = \text{H}$) suffers less steric hindrance from the tartrate ligand and is oxidized faster than (*R*)-allylic alcohol ($R^4 = \text{H}$, $R^5 \neq \text{H}$).³⁷ As the ester alkyl group of DAT becomes bulkier, the hindrance becomes more intense and the relative

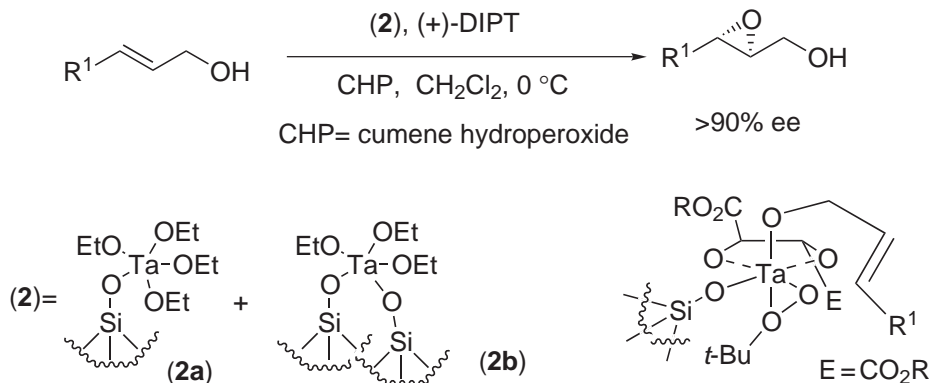
reaction ratio becomes larger. Thus, diisopropyl tartrate (DIPT) is better as a chiral auxiliary than DET which is, in turn, better than dimethyl tartrate (DMT) (Scheme 3). The relative reaction ratio (k_S/k_R) in the epoxidation of (*E*)-1-cyclohexyl-2-buten-1-ol decreases in the order DIPT, DET, and DMT. In general, secondary *E*-allylic alcohols are good substrates and good relative reaction ratios greater than 50 are observed when DIPT is used as the chiral auxiliary. When the conversion of starting material exceeds 60%, the unreacted alcohol becomes almost optically pure. The epoxidation of the fast-reacting enantiomer produces *erythro*-epoxide exclusively. In contrast, the kinetic resolution of *Z*-allylic alcohols is less efficient and the epoxidation of the fast isomers often produces *threo*-epoxide preferentially.⁴



Scheme 3

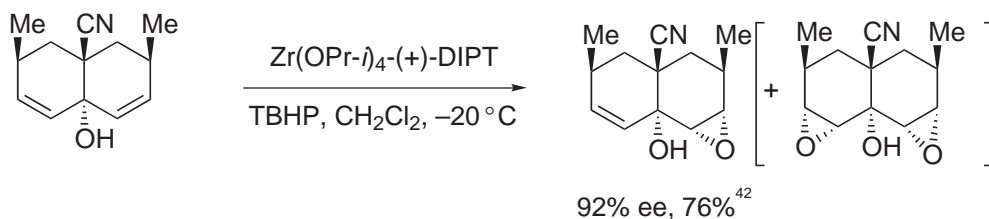
The original epoxidation with titanium–tartrate is homogeneous, but it can be carried out heterogeneously without diminishing enantioselectivity by using titanium-pillared montmorillonite catalyst (Ti-PILC) prepared from titanium isopropoxide, (+)-DAT, and Na^+ -montmorillonite.³⁸ Due to the limited spacing of Ti-PILC, the epoxidation becomes slower as the allylic alcohol gets bulkier.

A combination of DAT and a metal alkoxide other than titanium alkoxide serves as a poor catalyst for the epoxidation of allylic alcohols. However, the combination of DAT and silica-supported tantalum alkoxides (**2a**) and (**2b**) prepared from $\text{Ta}(=\text{CHCMe}_3)(\text{CH}_2\text{Cme}_3)_3$ and silica₍₅₀₀₎ shows high enantioselectivity in the epoxidation of *E*-allylic alcohols, though chemical yields are not very great (Scheme 4).³⁹



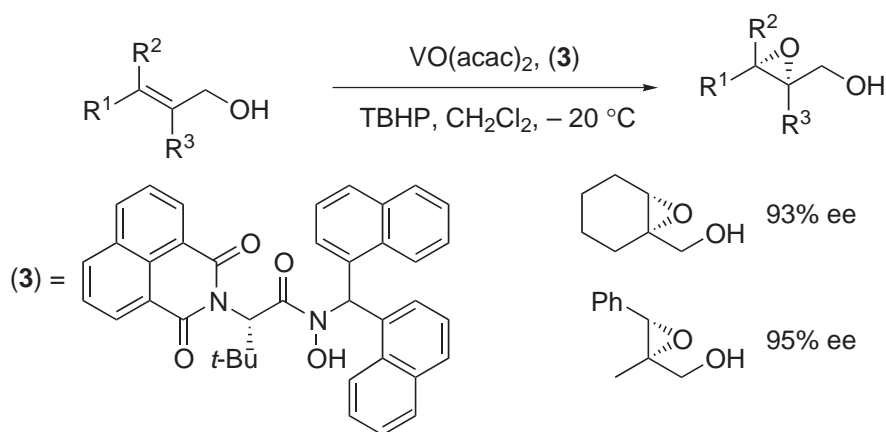
Scheme 4

Ti-DAT catalyst is not very efficient for the epoxidation of homoallylic alcohols⁴⁰ and *t*-allylic alcohols.^{4–8} The epoxidation of some of such substrates has been effected by using a Zr-tartramide⁴¹ or Zr-tartrate⁴² complex as catalyst (Scheme 5).



Scheme 5

Vanadium-catalyzed asymmetric epoxidation has recently been re-examined with a newly designed chiral hydroxamic acid (**3**).^{43–45} The hydroxamic acid (**3**) forms a 1:1 complex with vanadium ions and induces high enantioselectivity (Scheme 6).



Scheme 6

9.4.2.2 Epoxidation of Isolated Olefins

9.4.2.2.1 Epoxidation using metalloporphyrin as catalysts

Ti-mediated epoxidation is highly enantioselective, but its substrates are mostly limited to allylic alcohols. Various organic compounds, however, are known to be oxidized by oxidizing enzymes, irrespective of the presence or absence of a pre-coordinating group.¹ Of various oxidizing enzymes, the catalysis of cytochrome P-450s that carry an iron-porphyrin complex as their active site has been extensively studied, and the mechanism—that the iron(III) species is oxidized to active oxo-iron(IV) species and undergoes oxygen transfer—has been widely accepted (Figure 1).^{46,47} In 1979, Groves *et al.* disclosed that synthetic iron porphyrins were oxidized to oxo-iron(IV) species upon their treatment with iodosylbenzene and underwent epoxidation.^{48,49} Subsequently to this, they reported asymmetric epoxidation using an optically active iron-porphyrin complex (**4**) bearing chiral auxiliaries at its *meso*-carbons (Scheme 7).⁵⁰

These reports sparked off an extensive study of metalloporphyrin-catalyzed asymmetric epoxidation, and various optically active porphyrin ligands have been synthesized. Although porphyrin ligands can make complexes with many metal ions, mainly iron, manganese, and ruthenium complexes have been examined as the epoxidation catalysts. These chiral metalloporphyrins are classified into four groups, on the basis of the shape and the location of the chiral auxiliary. Class 1 are C_2 -symmetric metalloporphyrins bearing the chiral auxiliary at the

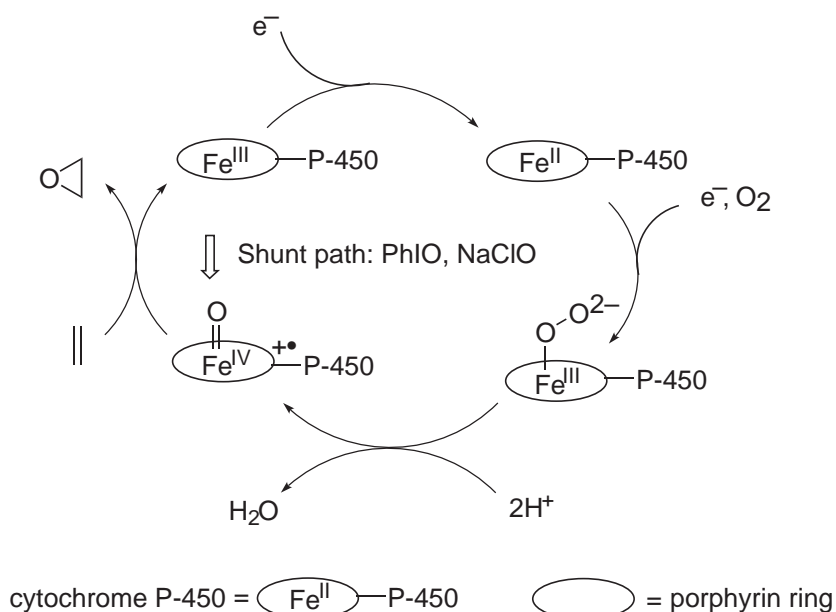
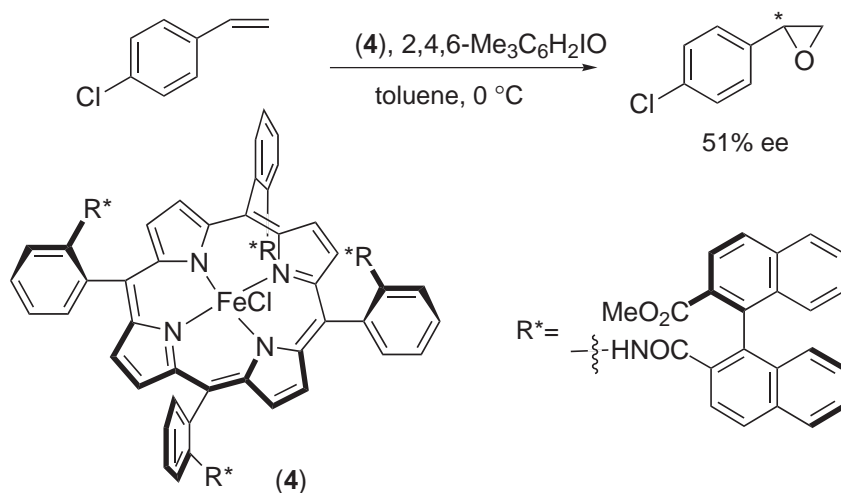


Figure 1 Proposed catalytic cycle of cytochrome P-450.

meso-carbons (Figure 2)^{51–62} class 2 are C_2 -symmetric metalloporphyrins bridged by chiral straps (Figure 3)^{63,64} class 3 are facially chiral metalloporphyrins bridged by a chiral strap (Figure 4);⁶⁵ while class 4 are facially chiral metalloporphyrins possessing a chiral bridge.^{66,67} Iodosylbenzene and sodium hypochlorite are usually used as the terminal oxidant for the epoxidation with iron or manganese porphyrins, while pyridine *N*-oxide derivatives⁶⁸ and iodosylbenzene are used for the oxidation with ruthenium porphyrins.



Epoxidation with chiral metalloporphyrins of class 1 has been extensively studied. However, good to high enantioselectivity is mostly limited to the epoxidation of styrene and its derivatives. In general, *trans*-olefins are poor substrates. This agrees with the proposal that the olefin approaches the metal-bound oxygen from its side and parallel to the porphyrin plane.⁴⁹ Some good results obtained with catalysts of class 1 are shown in Table 1. Complex (12) shows high enantioselectivity in the epoxidation of *o*-nitrostyrene, while the reaction of styrene is less selective.⁵⁹ It has been considered that the charge transfer interaction between the ligand and *o*-nitrostyrene plays an important role in the face selection of the former reaction. Metalloporphyrins such as (9), (10), and (14) show moderate to high enantioselectivity in the epoxidation

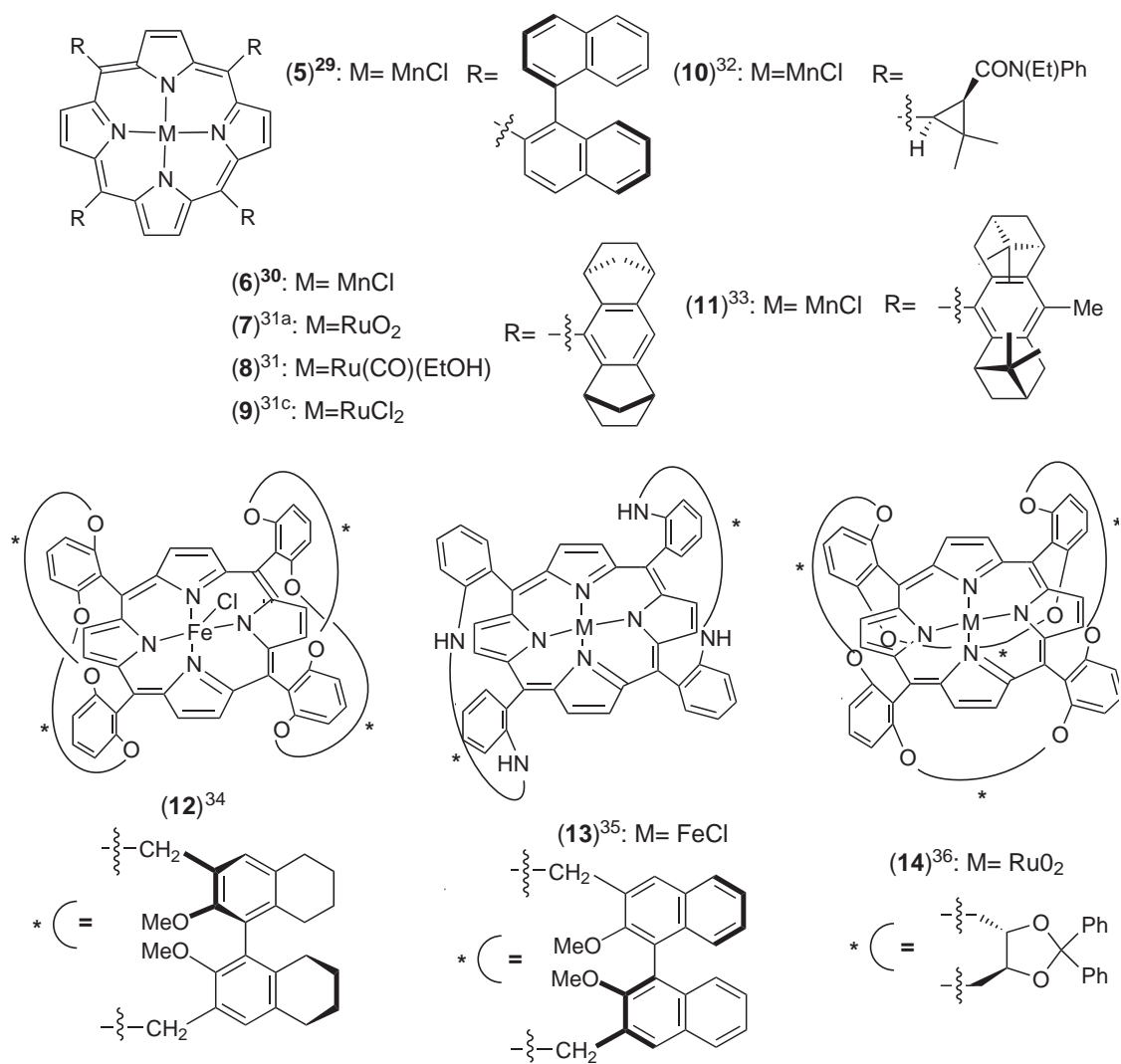


Figure 2 Metalloporphyrin complexes of class 1.

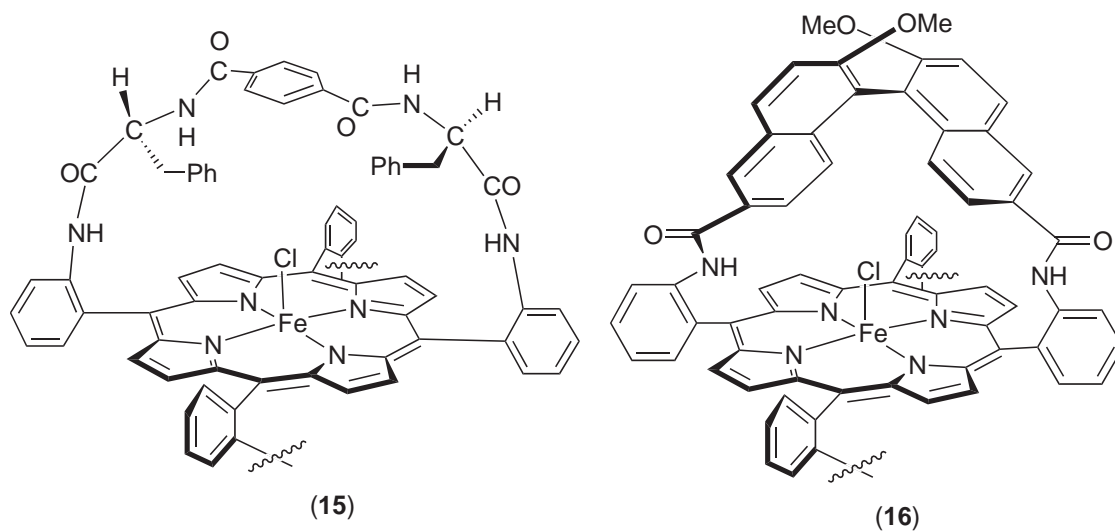


Figure 3 Metalloporphyrin complexes of class 2.

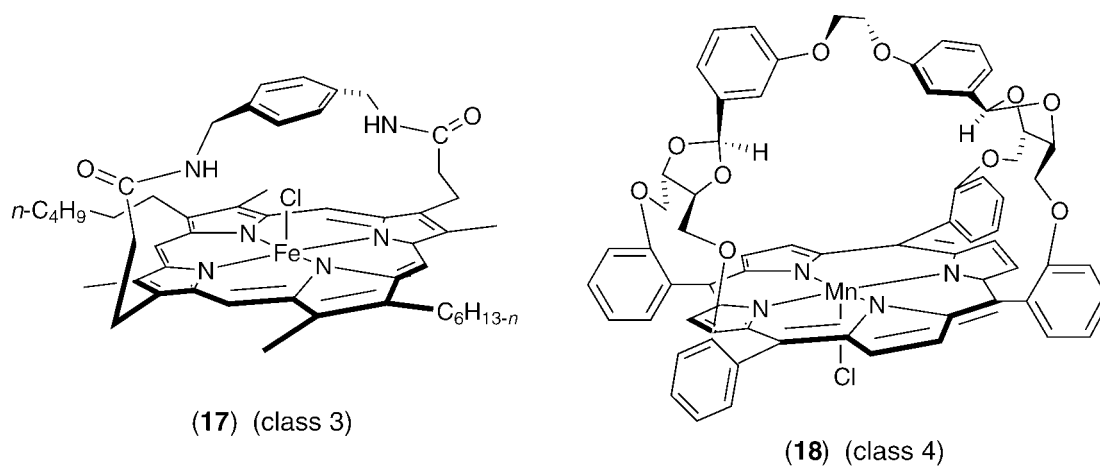


Figure 4 Metalloporphyrin complexes of classes 3 and 4.

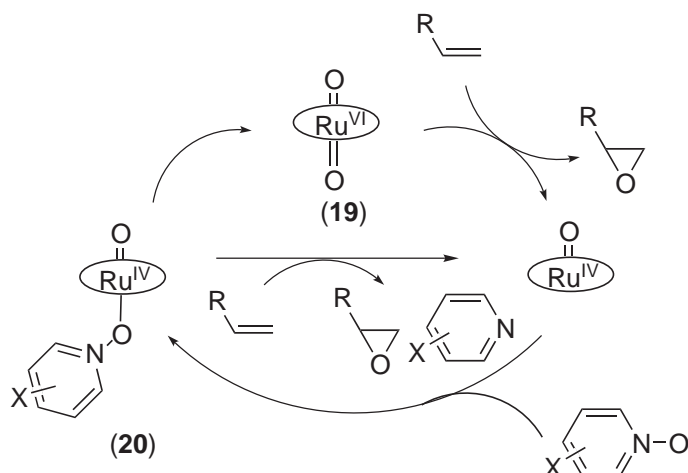
Table 1 Some examples of chiral metalloporphyrin-catalyzed epoxidation.

Entry	Catalyst	Substrate	% ee	References
1	(13)	styrene	83	60
2	(11)	styrene	70	57
3	(7)	styrene	70	54
4	(14)	styrene	75	61,62
5	(12)	styrene	56	58,59
6	(12)	<i>o</i> -nitrosyrene	89	58,59
7	(14)	<i>p</i> -chlorostyrene	80	61,62
8	(6)	<i>cis</i> - β -methylstyrene	76	52
9	(9)	<i>cis</i> - β -methylstyrene	68	55
10	(10)	dihydronaphthalene	86	56
11	(13)	dihydronaphthalene	55	60
12	(8)	dihydronaphthalene	77	53
13	(9)	dihydronaphthalene	80	55

of some cyclic olefins.^{55,56,61,62} It is also noteworthy that metalloporphyrins (e.g., (5), (6), (9), (11)) bearing *meso*-substituents which cannot contact with the metal oxo center are robust and show high turnover numbers.^{51,52,57} In contrast, one of the methoxynaphthalene units in the chiral straps of (13) is located close to the oxo metal center and is oxidized to the corresponding 2,6- or 2,8-naphthoquinone during the reaction. Interestingly, however, the oxidized complex shows better enantioselectivity than the parent (13).⁶⁰

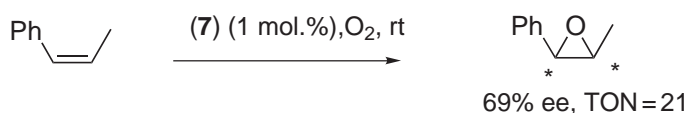
Asymmetric induction by metalloporphyrin is affected not only by the structure of the ligand, but also by other factors: the nature of the metal center, the oxidant used, and the donor ligand added.^{62,63} As shown in Figure 1, oxo-metalloporphyrins have been considered to be the active species in metalloporphyrin-catalyzed oxidation. In some oxidations, however, metal-oxidant adducts have been suggested as the real active species.

Dioxo-ruthenium porphyrin (19) undergoes epoxidation.⁶⁹ Alternatively, the complex (19) serves as the catalyst for epoxidation in the presence of pyridine *N*-oxide derivatives.⁶¹ It has been proposed that, under these conditions, a *trans*-*N*-oxide-coordinated (TMP)Ru(O) intermediate (20) is generated, and it rapidly epoxidizes olefins prior to its conversion to (19) (Scheme 8).⁶¹ In accordance with this proposal, the enantioselectivity of chiral dioxo ruthenium-catalyzed epoxidation is dependent on the oxidant used.^{55,61} In the iron porphyrin-catalyzed oxidation, an iron porphyrin-iodosylbenzene adduct has also been suggested as the active species.⁷⁰



Scheme 8

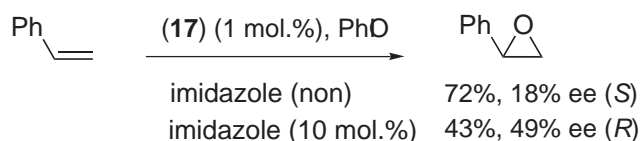
Oxidizing enzymes use molecular oxygen as the oxidant, but epoxidation with synthetic metalloporphyrins needs a chemical oxidant, except for one example: Groves and Quinn have reported that dioxo-ruthenium porphyrin (**19**) catalyzes epoxidation using molecular oxygen.⁶⁹ An asymmetric version of this aerobic epoxidation has been achieved by using complex (**7**) as the catalyst, albeit with moderate enantioselectivity (Scheme 9).⁵³



Scheme 9

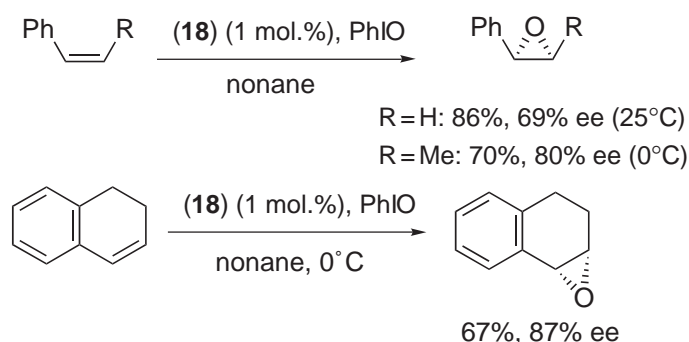
In the complexes of Class 1, chiral auxiliaries are attached outside the porphyrin ring and distant from the metal center. To avoid this problem, a new class of complexes ((**15**) and (**16**)) bridged by chiral straps above and below the metal center has been synthesized (Figure 3).^{63,64} Limited success, in terms of enantioselectivity (up to 72% ee), has been achieved with these complexes.

Complex (**17**) of Class 3 has no chiral auxiliary, but is endowed with facial chirality by the presence of a bridging strap (Figure 4).⁶⁵ Treatment of (**17**) with oxidant generates metal oxo bonds, preferentially on the sterically less hindered (nonbridged) side of the complex, and epoxidation with (**17**) is low in enantioselectivity (Scheme 10). However, the enantioselectivity is considerably improved by the addition of imidazole. The imidazole has been considered to coordinate the metal center from the nonbridged side and to force the formation of metal oxo bonds on the bridged (chiral) side, thus enhancing enantioselectivity.



Scheme 10

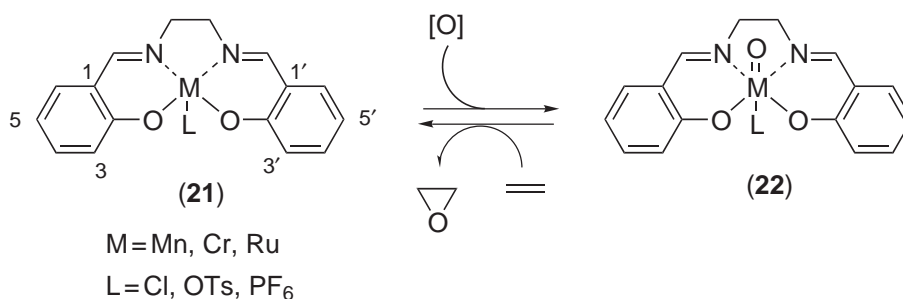
On the basis of the above result, the class 4 of chiral porphyrin complex (**18**) possessing a chiral strap, and facial chirality caused by it, has been introduced.^{66,67} Epoxidation with the complex (**18**) in the presence of 1,5-dicyclohexylimidazole, which blocks the nonbridged side of the complex, shows good to high enantioselectivity when the substrates are conjugated mono- and *cis*-di-substituted olefins (Scheme 11).



Scheme 11

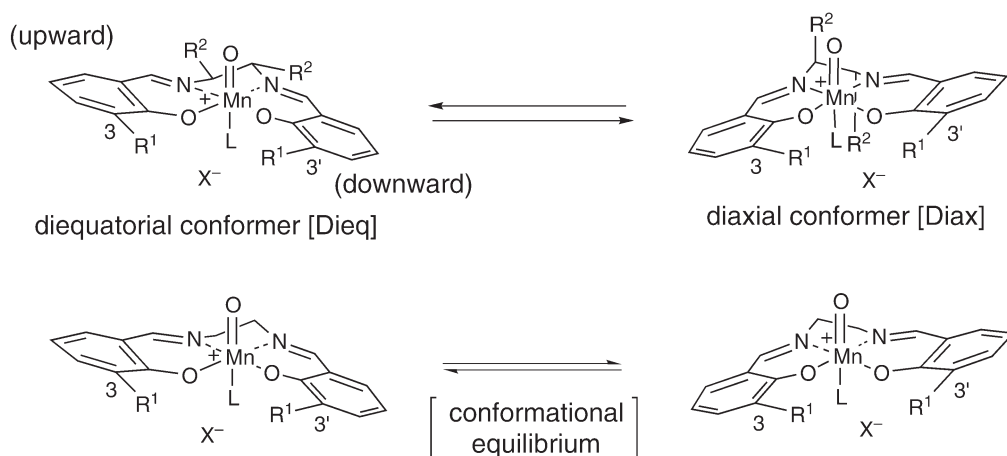
9.4.2.2.2 Epoxidation using metallosalen complexes as catalysts

Metal complexes (**21**) of *N,N'*-ethylenebis(salicyldeneaminato) ligands [hereafter denoted as metallosalens, M(salen)s] are structurally similar to metalloporphyrins, and both the complexes show similar catalyses. In 1985 and 1986, Kochi *et al.* reported Cr(salen)- and Mn(salen)-catalyzed epoxidation using isosylbenzene as the terminal oxidant, and proposed the mechanism via the corresponding oxo-M(salen)s (**22**) (M=Cr or Mn) for the epoxidation (Scheme 12).^{71,72} Actually, they isolated oxo-Cr(salen)s that underwent epoxidation, and determined their structures by X-ray analysis.⁷¹ Participation of oxo-Mn species in Mn(salen)-catalyzed epoxidation has also been proven by mass spectroscopic analysis.⁷³ Sodium hypochlorite, hydrogen peroxide, periodate, dioxirane, monopersulfate, and hypochlorite generated *in situ* by electro-oxidation⁷⁴ can also be used as terminal oxidants, especially for Mn(salen)-catalyzed epoxidation.^{6,8}



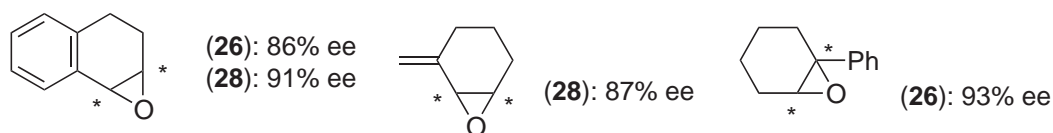
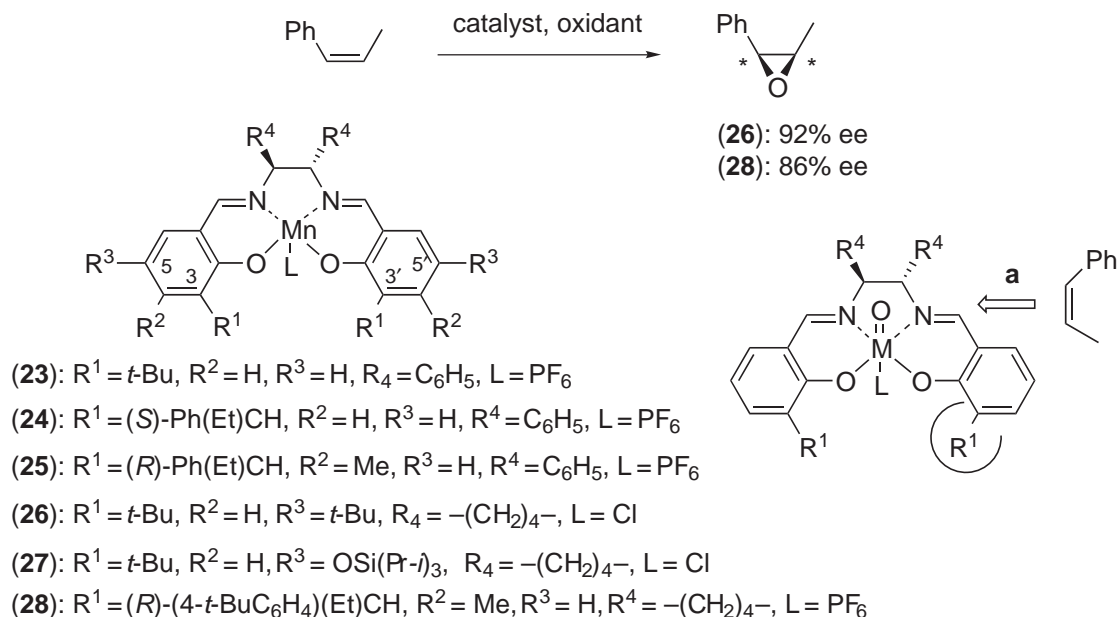
Scheme 12

The important structural features of salen ligands are: (i) the presence of the ethylene carbons; and (ii) the existence of a wide open space between the 3- and 3'-carbons. The presence of the ethylene carbons allows the introduction of chiral carbons near to the metal center. In addition, it endows metallosalens and oxo-metallosalens with conformational flexibility. The five-membered chelate ring formed between the metal ion and the ethylenediamine adopts the half-chair conformation, and makes the salen ligands nonplanar and chiral (Scheme 13).^{75,76} Some Mn^{III}(salen)s have been demonstrated to be nonplanar by their X-ray analyses⁷⁵, while structurally smaller Mn(salen)s have an almost planar structure.⁷⁷⁻⁷⁹ The nonplanar structure of the oxo-Mn(salen) species has been supported by calculation.⁸⁰⁻⁸² Of the two possible conformers, the conformer (Dieq) bearing equatorial substituents is considered to be more stable than the other conformer (Diax) bearing axial substituents, for steric reasons (Scheme 13).⁷⁶ Thus, the chirality of the basal salen ligand is dictated by the chirality of the ethylene carbons. In addition, the open space between the 3- and 3'-carbons allows the introduction of bulky and/or chiral substituents at the 3- and 3'-carbons. Accordingly, highly efficient asymmetric reaction sites can be constructed around the metal center by suitably designing the salen ligand.



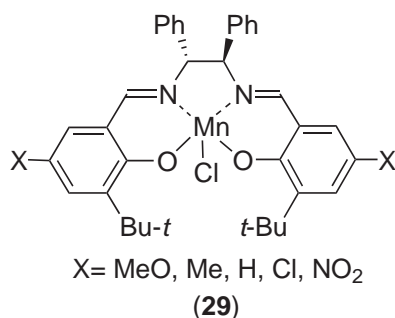
Scheme 13

In 1990 Jacobsen *et al.* and the present author and co-workers, independently synthesized chiral Mn(salen)s (**23**) and (**24**) as catalysts for asymmetric epoxidation, respectively.^{83–85} Complex (**23**) possesses a bulky *t*-butyl group at the 3- and 3'-carbons⁷⁰, and complex (**24**) has a bulky and chiral group at the carbons. These catalysts were designed on the hypothesis that olefins approach the metal oxo center from its side parallel to the salen ligand, directing their bulkier substituent away from the 3- or 3'-substituent (R^1) (approach via path **a**). Subsequently to this, several modified Mn(salen)s (**25**)–(**28**)^{86–88} have been introduced and, with these Mn(salen)s as catalysts, good to high enantioselectivity has been achieved in the epoxidation of conjugated *cis*-di-, tri- and some tetrasubstituted olefins (Scheme 14).⁸⁹ In order to explain the stereochemistry of these epoxidations, two other paths for the olefin's approach were proposed later (*vide infra*).



Scheme 14

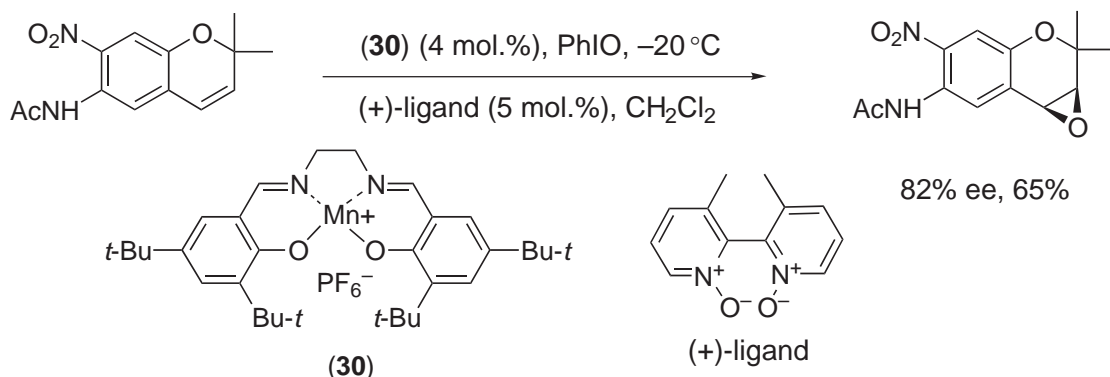
The enantioselectivity of Mn(salen)-catalyzed epoxidation depends not only on the salen ligand structure, but also on other factors. Substituents on the salen ligand affect the reactivity of oxo Mn(salen) species.⁷² With the complexes (**29**) as the catalysts, Jacobsen *et al.* systematically studied the effect of 5,5'-substituents (X) on enantioselectivity, and disclosed that enantioselectivity [$\log(\text{major enantiomer}/\text{minor enantiomer})$] linearly correlates with the σ -values of the substituents, proving that the effect of 5,5'-substituents is an electronic one:^{90,91} Introduction of an electron-donating group reduces the reactivity of oxo Mn(salen) species and enhances enantioselectivity. One exception has been reported: Mn(salen)s bearing an electron-withdrawing perfluoroalkyl group are good catalysts for the epoxidation of indene (93% ee) in fluoruous–organic two-phase systems, but the epoxidation of other substrates is less selective.⁹² The apical ligand (L) affects the coordination geometry of the metal ion,⁷¹ the ligand conformation,⁷⁵ and the reactivity⁹³ of oxo-Mn(salen); and addition of a donor ligand such as a pyridine *N*-oxide derivative generally improves enantioselectivity,^{94,95} as well as the yield of epoxide.⁹³



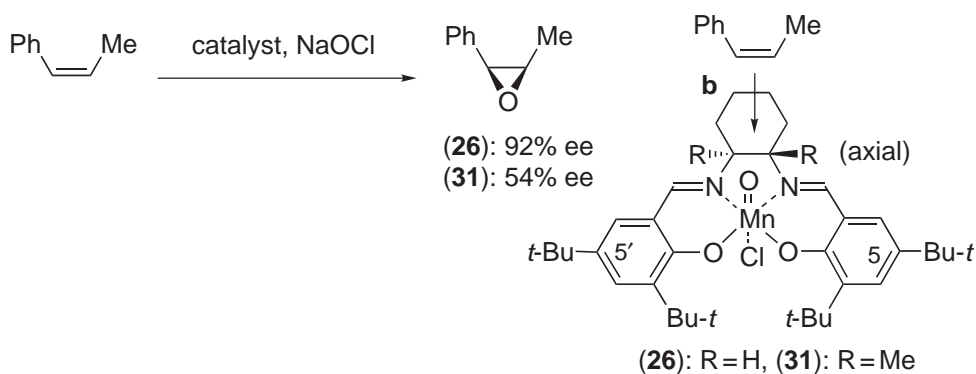
Asymmetric epoxidation with an achiral Mn(salen) as catalyst has been realized by using the effect of the apical ligand on the ligand conformation. As described in Scheme 13, the diequatorial conformer prevails over the diaxial conformer. However, if the substituents at the ethylene carbons are eliminated, the two conformers become enantiomeric. Thus, achiral oxo Mn(salen) bearing no substituent at the ethylene carbons exists in an equilibrium mixture of enantiomeric conformers that produce enantiomeric epoxides, respectively. However, if the ligand (L) coordinated to the manganese ion is chiral, the enantiomeric conformers become diastereomeric, and the equilibrium should lean toward the one diastereomer that produces enantiomerically enriched epoxide. Indeed, the epoxidation of 6-acetamido-7-nitro-2,2-dimethylchromene using achiral complex (**30**) in the presence of chiral bipyridine *N,N'*-dioxide [(+)-chiral ligand] showed a high enantioselectivity of 82% ee (Scheme 15).^{96,97} This is the first example of an asymmetric reaction with an achiral catalyst.

The sense of the enantioface selection of olefin in Mn(salen)-catalyzed epoxidation is determined by two factors: the olefin's approaching path, and its orientation.

As discussed above, olefins were initially proposed as approaching the oxo-Mn center along path **a**, with an orientation directing their bulkier substituent away from the C3(C3')-substituent (see Scheme 14). It is noteworthy that path **a** runs over the downwardly bent benzene ring. Later, Jacobsen *et al.* proposed path **b** for the epoxidation with (**26**) possessing *t*-butyl groups at C5 and



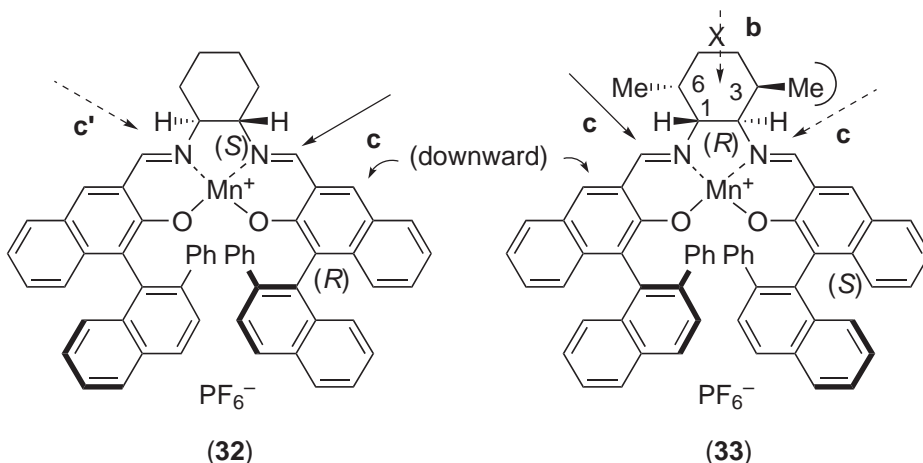
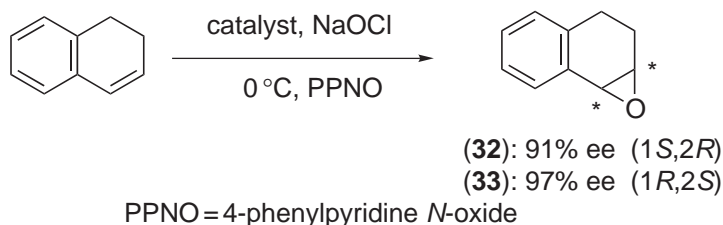
Scheme 15



Scheme 16

C5', on the assumption that the *t*-butyl groups would block path **a**.⁸⁶ The incoming olefin was considered as taking an orientation that directed its bulkier olefinic substituent away from the axial proton. However, the enantioselectivity diminishes when the axial proton is replaced with a methyl group (Scheme 16). From an analysis of the stereochemistry of many Mn(salen)-catalyzed epoxidations, the present author and co-workers have proposed path **c** (along the Mn—N bond), whereby the olefin approaches the oxo metal center with the bulkier substituent directed away from the 3(3')-substituent.⁹⁸ Path **c** runs near to the downwardly bent benzene ring of the salen ligand and, therefore, it is more readily approachable for the olefin than path **c'** along another Mn—N bond, leading to a wrong enantiomer.⁷⁵ Interestingly, asymmetric induction by complex (32) is enhanced by introducing methyl groups at the 3- and 6-carbons of the cyclohexanediamine unit (Scheme 17).⁹⁹ The C3-methyl group of (33) causes steric repulsion with the incoming olefin along **c'**, making the path **c'** more unfavorable. Thus, enantioselection by (33) is larger than that by (32) (note that the chiralities of the diamine parts in (32) and (33) are opposite to one another). Path **b** leads to a wrong enantiomer. In addition, Houk *et al.* have proposed a different path, with the olefin approaching between two oxygen atoms.¹⁰⁰

The orientation of incoming olefins along paths **a** and **c** is dictated mainly by the repulsion between the unsaturated substituent (R_u) and the 3(or 3')-substituent (Figure 5). Although bulky



Scheme 17

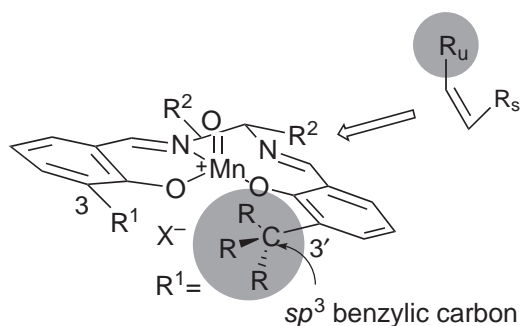


Figure 5 Steric repulsion between 3'-substituent and incoming olefin.

groups such as *t*-butyl and 1-phenylethyl were used as the 3(or 3')-substituents in the early Mn(salen)s ((23) to (28)), such groups are not ideal ones as the regulators of the olefin's orientation, because all the groups on the sp^3 benzylic carbon direct themselves away from incoming olefins. Any substituent that occupies the space close to the approaching path should be a desired one. Accordingly, the present author and co-workers designed a new type of Mn(salen), (34), bearing a 2''-phenylbinaphthyl substituent at C3 and C3', in which the 2''-phenyl group is expected to protrude into the desired space (Figure 6); an excellent level of enantioselectivity has been achieved in the epoxidation of conjugated *cis*-di- and trisubstituted olefins by using (34) as the catalyst.^{101,102}

In 2001, Ahn *et al.* introduced a Mn(salen) possessing a structurally related binaphthyl unit, and also achieved high enantioselectivity in the epoxidation of conjugated olefins.¹⁰³

The Mn(salen)-catalyzed epoxidation of conjugated olefins proceeds through a radical intermediate.^{72,84} Linde *et al.* have proposed, on the basis of calculations, that spin cross-over in the epoxidation pathway is related to the formation of a radical intermediate,¹⁰⁵ while Burt *et al.* have suggested, on the basis of DFT investigation, that the oxo-Mn species exists in different spin states, and participation of the oxo-Mn species of triplet state causes radical formation.¹⁰⁶ Although the details of the mechanism of Mn(salen)-catalyzed epoxidation are still controversial, participation of the radical species has been considered to be related to the high enantioselectivity observed in the epoxidation of conjugated olefins.^{91,104,107} However, the intervention of a radical intermediate causes geometric isomerization due to the rotation of the resulting C—C bond

(Scheme 18): epoxidation of acyclic *cis*-olefins usually gives a mixture of *cis*- and *trans*-epoxides.^{72,84} When the substrate is styrene (R = H), this isomerization generates the enantiomeric epoxide and diminishes enantioselectivity.⁹¹ Jacobsen *et al.* have found that the C—C bond rotation is delayed by reducing the reaction temperature. Indeed, a high enantioselectivity of 88% ee was realized in the epoxidation of styrene at -78°C using a *m*-CPBM–NMO system.¹⁰⁸

Interestingly, Jacobsen *et al.* have also reported that addition of a β -hydroxy ammonium salt to the reaction medium accelerates the isomerization: in the presence of an *N*-benzylated quinine salt; epoxidation of *cis*-stilbene with (27) gives *trans*-stilbene oxide with 90% ee as the major product (*trans*:*cis* =>96:4).¹⁰⁹ In 2000, Adam *et al.* reported that the isomerization ratio was related to the triplet-quintet energy gap of the radical intermediate which was affected by the

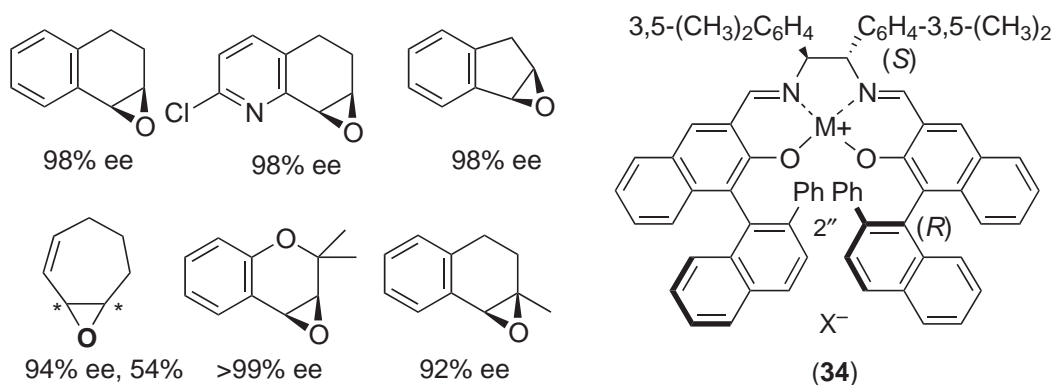
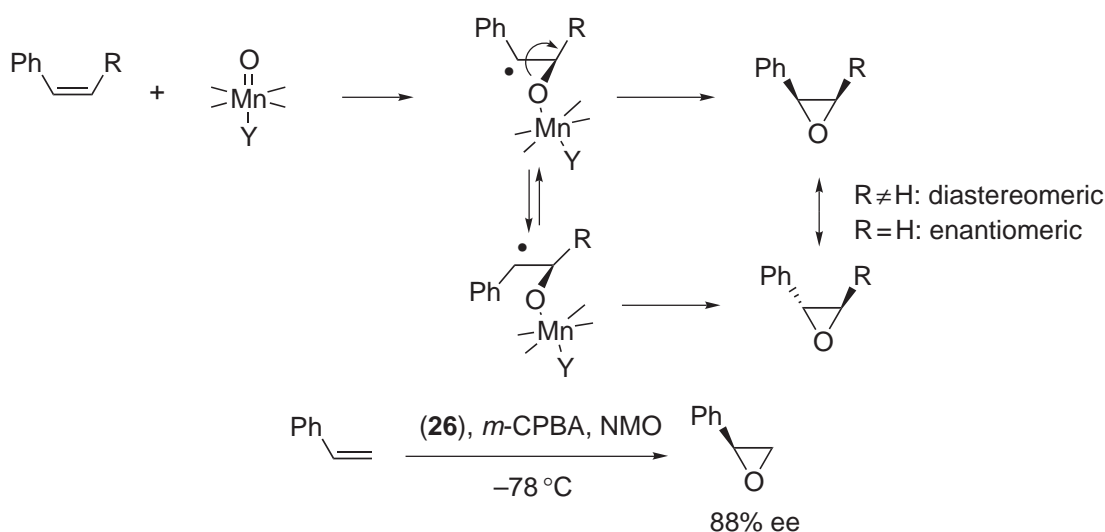


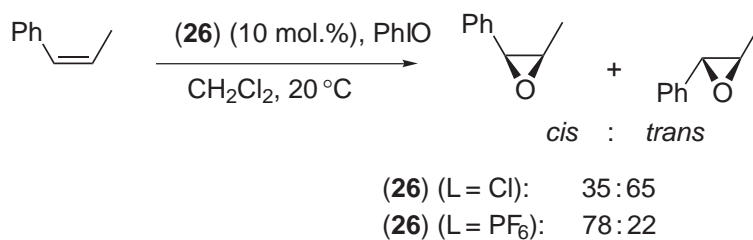
Figure 6 Newly designed Mn(salen) (34) and the epoxides obtained with it as catalyst.



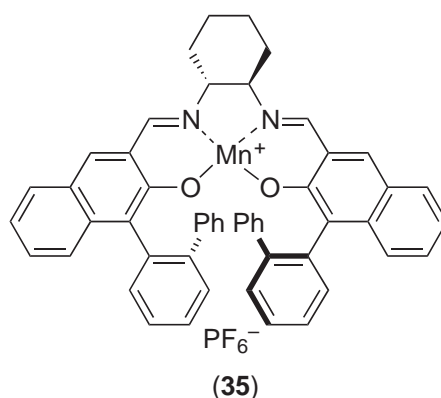
Scheme 18

presence or absence of an apical ligand, from the study of epoxidations with neutral and cationic complexes (**26**) ($\text{L} = \text{Cl}^-$ and $\text{L} = \text{PF}_6^-$, respectively) as the catalyst: the energy gap increases by a coordination of Cl^- and the lifetime of the radical intermediate becomes longer.¹¹⁰ Thus, extensive isomerization is observed in the epoxidation with a neutral complex, while less isomerization occurs in the reaction with a cationic complex (Scheme 19).

Most *trans*-olefins are still cumbersome substrates for metallosalen-catalyzed epoxidation, and only a few successful examples have been reported with Cr- or Mn(salen)s possessing nonplanar structures. Gilheany *et al.* reported that 3,3',5,5'-tetrafluorosubstituted Cr(salen) served as a good catalyst for the epoxidation of *trans*- β -methylstyrene.^{111,112} Jacobsen *et al.* also reported that the Mn complex bearing naphthyldiamine as its diamine unit catalyzed the epoxidation of *trans*- β -methylstyrene with high enantioselectivity.⁸ Mn(salen) (**35**) which has a deeply folded structure is also an efficient catalyst for the epoxidation of *trans*- β -substituted styrenes.¹¹³

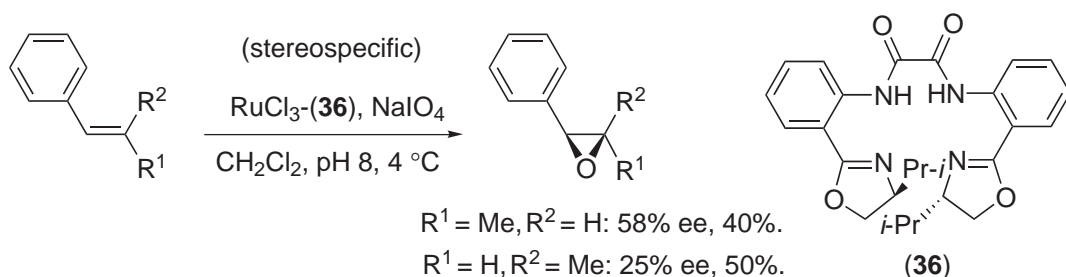


Scheme 19

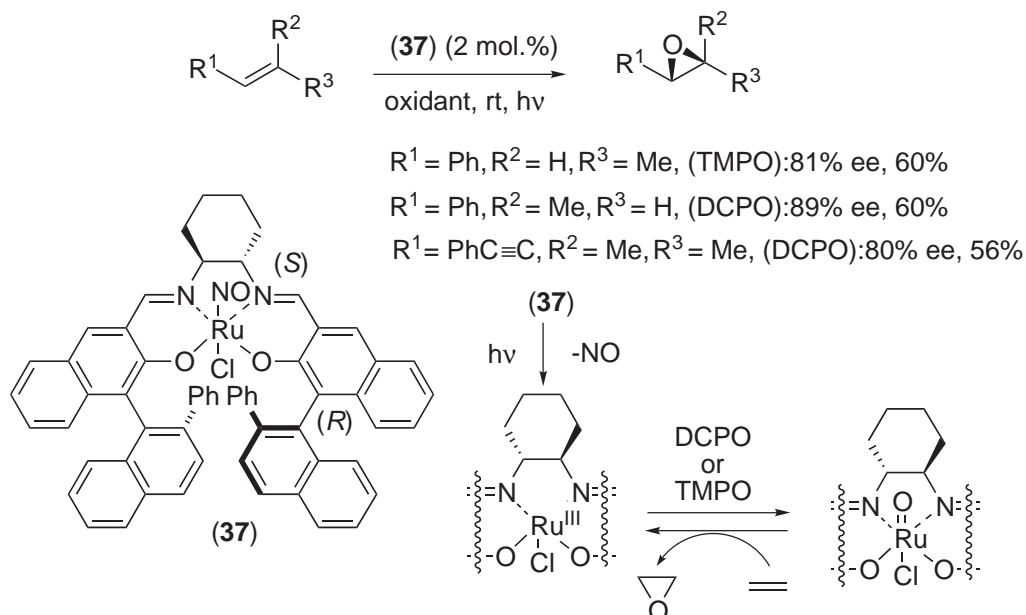


Besides ruthenium porphyrins (*vide supra*), several other ruthenium complexes were used as catalysts for asymmetric epoxidation and showed unique features;^{114,115} though enantioselectivity is moderate, some reactions are stereospecific and *trans*-olefins are better substrates for the epoxidation than are *cis*-olefins (Scheme 20).¹¹⁵ Epoxidation of conjugated olefins with the Ru (salen) (37) as catalyst was also found to proceed stereospecifically, with high enantioselectivity under photo-irradiation, irrespective of the olefinic substitution pattern (Scheme 21).^{116–118} Complex (37) itself is coordinatively saturated and catalytically inactive, but photo-irradiation promotes the dissociation of the apical nitrosyl ligand and makes the complex catalytically active. The wide scope of this epoxidation has been attributed to the unique structure of (37). Its salen ligand adopts a deeply folded and distorted conformation that allows the approach of an olefin of any substitution pattern to the intermediary oxo-Ru species.¹¹⁸ 2,6-Dichloropyridine *N*-oxide (DCPO) and tetramethylpyrazine *N,N'*-dioxide⁶⁸ (TMPO) are oxidants of choice for this epoxidation.

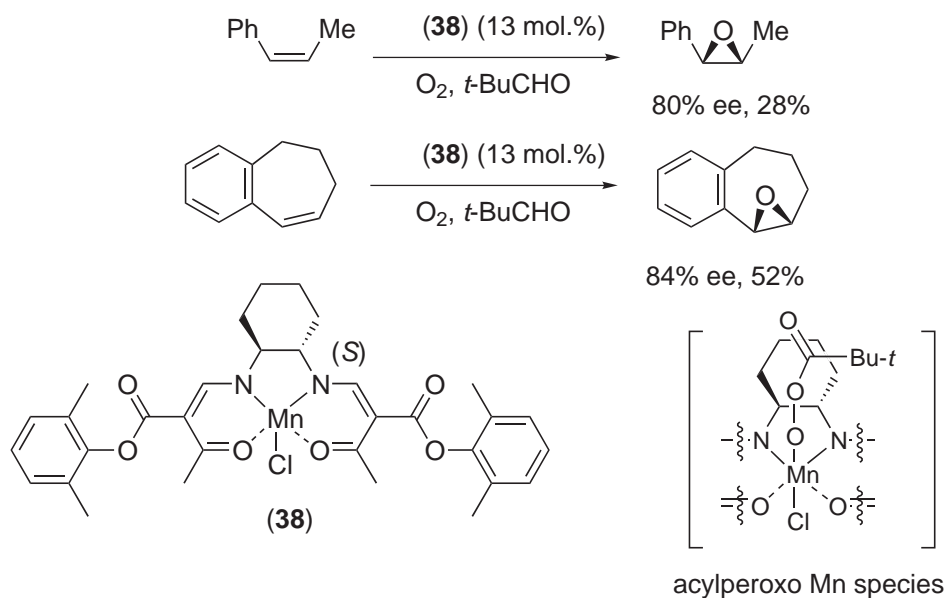
Mukaiyama and Yamada reported that molecular oxygen served as a terminal oxidant for metal-catalyzed epoxidation, in the presence of an aldehyde.¹¹⁹ This aerobic epoxidation was carried out in an enantioselective manner by using Mn(salen) catalyst (29) (X = Me).^{120,121} Subsequently, Mn(aldeiminato) complex (38) was found to be a better catalyst: good to high enantioselectivity has been achieved in the epoxidation of conjugated *cis*-olefins using it (Scheme 22).¹²² This epoxidation has been proposed to proceed via an acylperoxo-Mn species, based on the finding that the sense of the enantioselectivity is reversed with a change of oxidant from sodium hypochlorite, which generates the oxo-Mn species, to a molecular oxygen–aldehyde combination.



Scheme 20



Scheme 21



Scheme 22

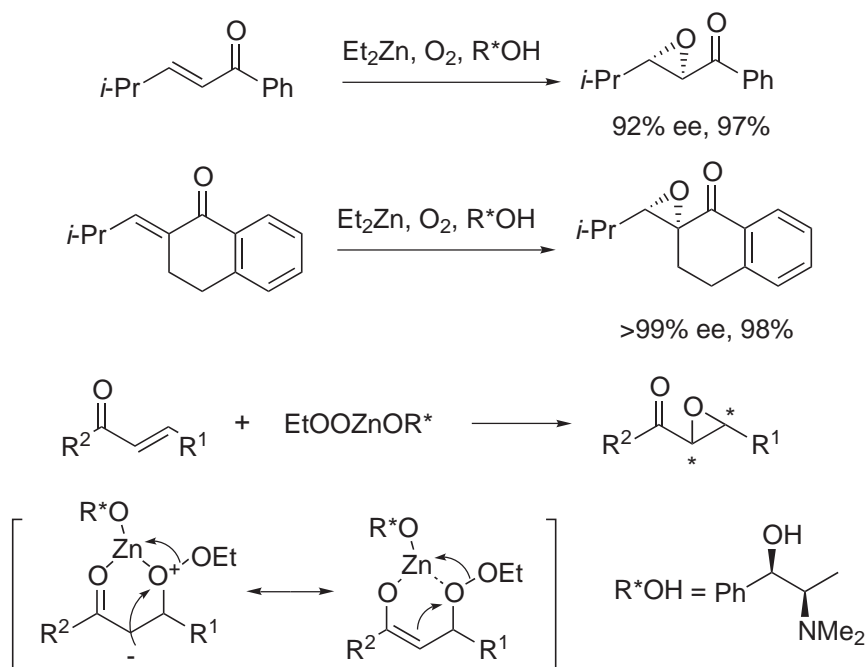
The epoxidation of nonconjugated olefins is slow^{123,124} and shows reduced enantioselectivity as compared with the epoxidation of conjugated olefins. For example, enantioselectivities from the epoxidation of (Z)-1-cyclohexyl-1-propene, 3,3-dimethyl-1-butene, and geranyl acetate are 82% (with (34)), 70% (with (34)),¹²³ and 53% (6,7-epoxide, with (26)),¹²⁴ respectively, and yields of the epoxides are modest.

9.4.2.3 Epoxidation of Electron-deficient Olefins

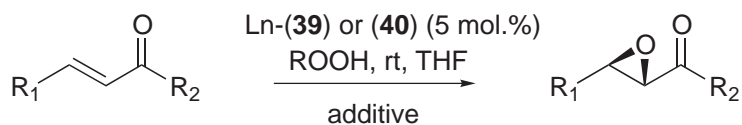
α,β -Epoxy ketones and esters are useful synthetic intermediates, and much effort has been directed toward the epoxidation of α,β -unsaturated ketones and esters. Some chiral phase-transfer reagents or polyamino acids serve as efficient catalysts for epoxidation of these electron-deficient olefins, but their scope has mostly been limited to chalcone and its derivatives.¹²⁵

The introduction of various metal-catalyzed reactions, however, remarkably expanded the scope of the epoxidation of α,β -unsaturated ketones. Enders *et al.* have reported that a combination of diethylzinc and *N*-methyl-pseudoephedrine epoxidizes various α,β -unsaturated ketones, under an oxygen atmosphere, with good to high enantioselectivity (Scheme 23).¹²⁶ In this reaction, diethylzinc first reacts with the chiral alcohol, and the resulting ethylzinc alkoxide is converted by oxygen to an ethylperoxo-zinc species that epoxidizes the α,β -unsaturated ketones enantioselectively. Although a stoichiometric chiral auxiliary is needed for this reaction, it can be recovered in almost quantitative yield.

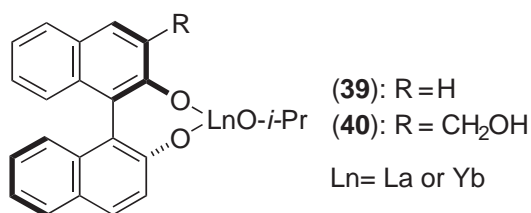
A breakthrough in this field was brought about by Shibasaki *et al.* They reported that lanthanide-BINOL (or its derivative) complex ((39) or (40)) catalyzed epoxidation of a wide range of α,β -unsaturated ketones with good to high enantioselectivity in the presence of alkyl hydroperoxide, especially when (40) is used as the catalyst (Scheme 24).^{127,128} The choice of metal and alkyl hydroperoxide depends on the nature of the substrate: epoxidation of aryl ketones is efficiently performed by a combination of La-(40)-CHP (cumene hydroperoxide), while that of alkyl ketones by a combination of Yb-(40)-TBHP. Nonlinearity between ee of epoxide and ee of BINOL observed in this epoxidation suggests that these lanthanide catalysts exist as oligomers, and the oligomerization affects enantioselectivity.¹²⁷ Shibasaki *et al.* have found that enantioselectivity of the reaction using a La-(39)-TBHP system is improved by adding water.¹²⁹ Inanaga *et al.* studied extensively the effect of additives on the lanthanide-BINOL system, and found that the addition of triphenylphosphine oxide (15–30 mol. %, 2–3 equivalents to the catalyst) considerably improved enantioselectivity.¹³⁰ The role of the additive has been attributed to deoligomerization of the lanthanide complex. Recently, Shibasaki *et al.* reported that triphenylarsine oxide showed the identical additive effect to triphenylphosphine oxide.¹³¹ The advantage of this additive



Scheme 23



	catalyst	oxidant	additive	
R ¹ = Ph, R ² = Ph	La-(40)	CHP	-	91% ee, 93%
R ¹ = Ph, R ² = Ph	La-(40)	TBHP	Ph ₃ As=O	97% ee, 95%
R ¹ = Ph, R ² = Me	Yb-(40)	TBHP	-	94% ee, 83%
R ¹ = Ph, R ² = Me	Yb-(39)	TBHP	H ₂ O	94% ee, 92%
R ¹ = Ph, R ² = Me	La-(39)	TBHP	Ph ₃ P=O	93% ee, 92%
R ¹ = Ph, R ² = Me	La-(39)	TBHP	Ph ₃ As=O	94% ee, 83%
R ¹ = Ph, R ² = <i>i</i> -Pr	La-(39)	TBHP	Ph ₃ P=O	96% ee, 67%
R ¹ = Ph, R ² = <i>i</i> -Pr	La-(39)	TBHP	Ph ₃ As=O	95% ee, 72%
R ¹ = PhCH ₂ CH ₂ , R ² = Me	Yb-(40)	TBHP	-	88% ee, 91%
R ¹ = PhCH ₂ CH ₂ , R ² = Me	La-(39)	TBHP	Ph ₃ P=O	87% ee, 92%
R ¹ = PhCH ₂ CH ₂ , R ² = Me	La-(39)	TBHP	Ph ₃ As=O	92% ee, 98%



Scheme 24

is that the addition of one equivalent of triphenylarsine oxide suffices for the reaction. Based on X-ray study and kinetic experiments, the reaction has been proposed to proceed via the La–BINOL–(Ph₃As=O) (1:1:1) complex (**41**) (Scheme 25).¹³¹

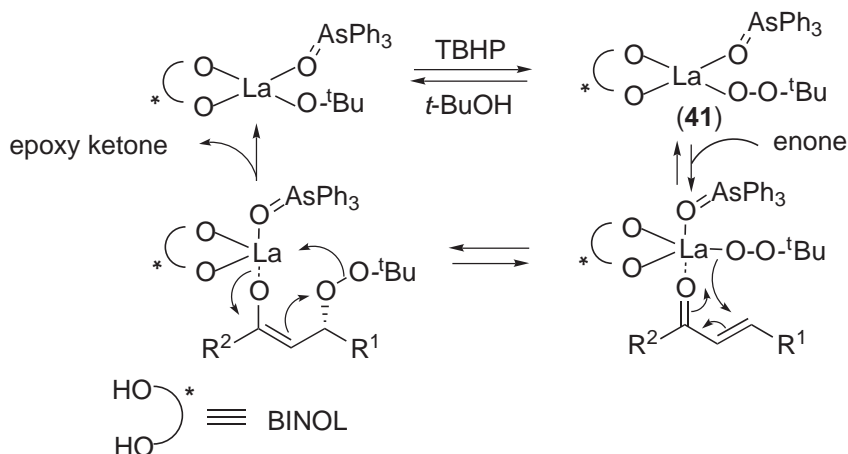
The epoxidation of electron-deficient olefins using a nucleophilic oxidant such as an alkyl hydroperoxide is generally nonstereospecific: epoxidation of both *cis*- and *trans*- α,β -unsaturated ketones gives the *trans*-epoxide preferentially. However, the epoxidation of *cis*- α,β -unsaturated ketones catalyzed by Yb-(**40**) gives *cis*-epoxides preferentially, with high enantioselectivity, because the oxidation occurs in the coordination sphere of the ytterbium ion (Scheme 26).¹³²

In contrast to the epoxidation of α,β -unsaturated ketones, the metal-catalyzed asymmetric epoxidations of α,β -unsaturated esters are much more limited in number. Epoxidation of ethyl *cis*-cinnamate with Mn(salen) (**26**) has been reported to give a mixture of the corresponding *cis*- (93% ee) and *trans*-epoxides in a ratio of 4:1.¹³³

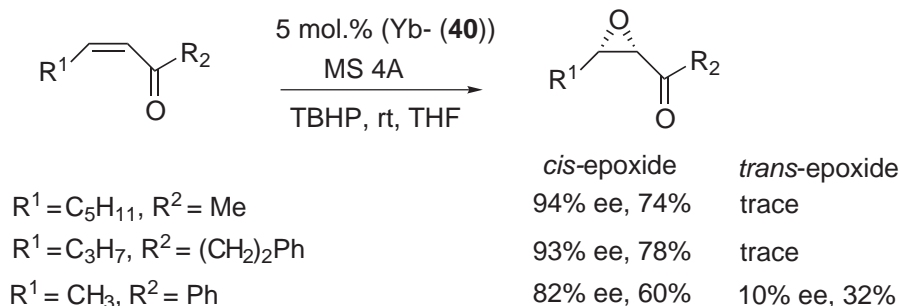
Shibasaki *et al.* have reported a new approach to α,β -epoxy esters: the epoxidation of α,β -unsaturated carboxylic acid imidazolides with a La(OPrⁱ)₃, BINOL, Ph₃As=O, and TBHP system provides epoxy-peroxy-esters (**41**), which are generated *in situ* from the intermediary epoxy acid imidazolide and converted to the corresponding methyl ester (**42**) upon treatment with methanol (Scheme 27).¹³⁴

9.4.3 OXIDATION OF ENOL ETHERS AND THEIR DERIVATIVES

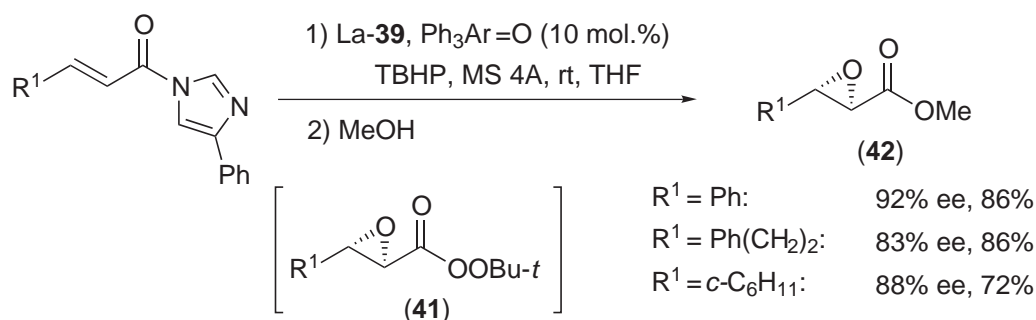
The oxidation of enol ethers and their derivatives is a useful method for the synthesis of α -hydroxy ketones or their derivatives, which are versatile building blocks for organic synthesis. Since enol ethers and esters are types of olefin, some asymmetric epoxidation and dihydroxylation reactions have been applied to their oxidation.



Scheme 25



Scheme 26

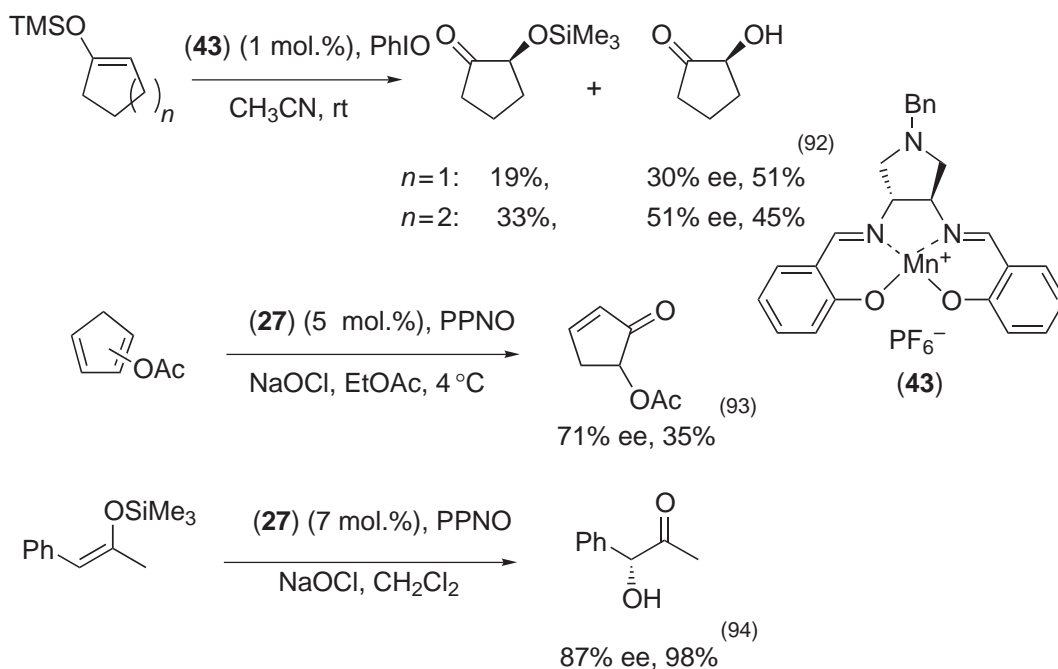


Scheme 27

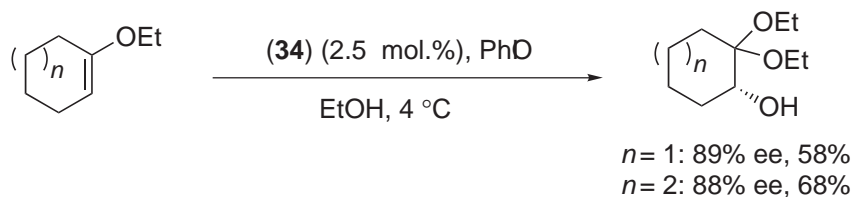
In 1992, Thornton *et al.* reported that Mn(salen) (**43**) catalyzed the asymmetric oxidation of silyl enol ethers to give a mixture of α -siloxy and α -hydroxy ketones, albeit with moderate enantioselectivity (Scheme 28).¹³⁵ Jacobsen *et al.* examined the oxidation of enol esters with Mn(salen) (**27**) and achieved good enantioselectivity.¹³⁶ Adam *et al.* also reported that the oxidation of enol ethers with (**27**) proceeded with moderate to high enantioselectivity.¹³⁷ Good substrates for these reactions are limited, however, to conjugated enol ethers and esters. Based on the analysis of the stereochemistry,¹³⁷ enol ethers have been proposed to approach the oxo-Mn center along the N—Mn bond axis (trajectory *c*, *vide supra*).

Katsuki *et al.* have reported that high enantioselectivity can be obtained in the oxidation of nonconjugated cyclic enol ethers by using Mn(salen) (**34**) as the catalyst.¹³⁸ The reactions were performed in an alcoholic solvent to obtain α -hydroxy acetals as the products, because α -hydroxy acetals are tolerant to a weak Lewis acid like Mn(salen) and do not racemize during the reaction and the isolation procedure (Scheme 29).

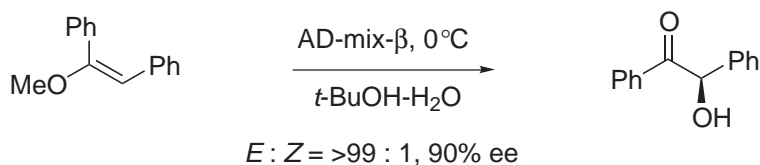
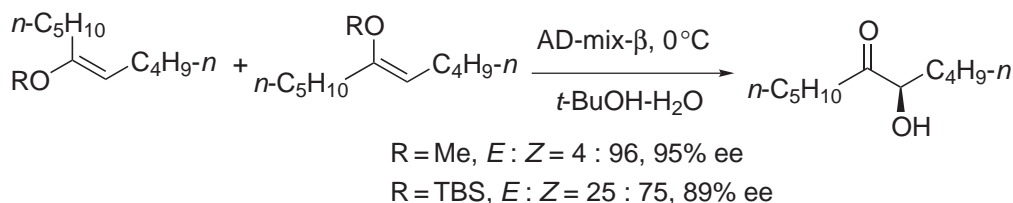
Another useful method for the asymmetric oxidation of enol derivatives is osmium-mediated dihydroxylation using cinchona alkaloid as the chiral auxiliary. The oxidation of enol ethers and enol silyl ethers proceeds with enantioselectivity as high as that of the corresponding dihydroxylation of olefins (*vide infra*) (Scheme 30).¹³⁹ It is noteworthy that the oxidation of *E*- and *Z*-enol ethers gives the same product, and the *E/Z* ratio of the substrates does not strongly affect the



Scheme 28



Scheme 29



AD-mix-β : pre-mixed dihydroxylation reagent containing $K_2OsO_2(OH)_4$, $(DHQD)_2PHAL$, K_2CO_3 , $K_3Fe(CN)_6$ (see, the Section 9.4.5.1 for dihydroxylation)

Scheme 30

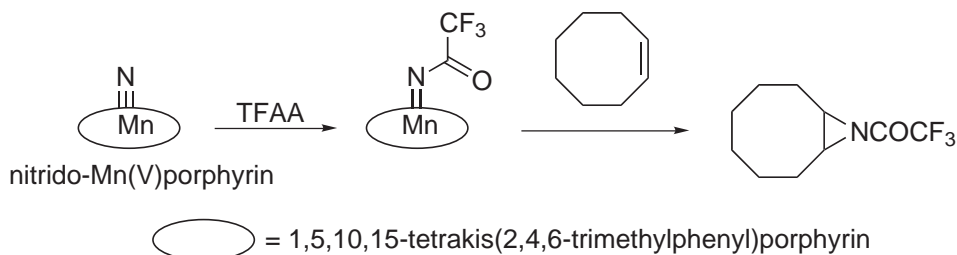
enantioselectivity of the oxidation. This reaction has also been applied to the asymmetric oxidation of cyclic ketene acetals to give an α -hydroxy lactone.¹⁴⁰

9.4.4 ASYMMETRIC AZIRIDINATION

Metal-oxenoid (oxo metal) species and metal-nitrenoid (imino metal) species are isoelectronic and show similar reactivity: both species can add to olefins and be inserted into C—H bonds. Naturally, the study of nitrene transfer reactions began with metalloporphyrins, which were originally used as the catalysts for oxene transfer reactions.

In 1983, Groves and Takahashi demonstrated that a nitrido-Mn^Vporphyrin underwent a nitrogen-transfer reaction via a *N*-trifluoroacetylnitrenoid species to give an aziridine, when it was treated with trifluoroacetic anhydride (TFAA) in the presence of olefins (Scheme 31).¹⁴¹

Later, Carreira *et al.* reported that nitrido-Mn^V(salen) also underwent a nitrogen-transfer reaction under similar reaction conditions.¹⁴² An asymmetric version of this reaction has been realized by using the chiral nitrido-Mn^V(salen) (44) (Scheme 32).¹⁴³ When trifluoroacetic acid



Scheme 31

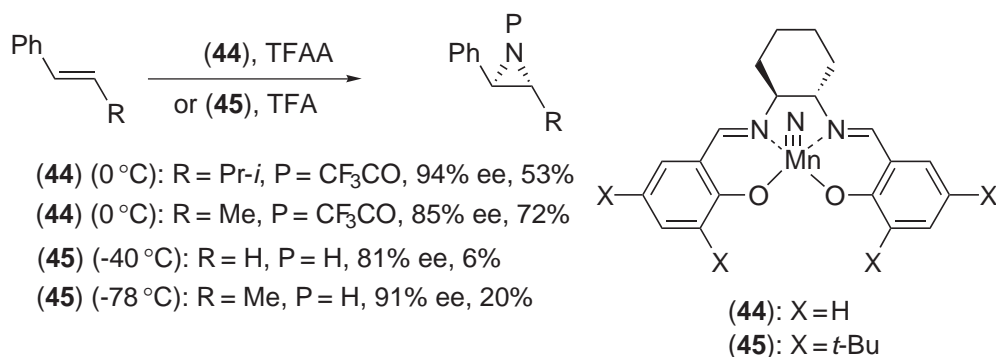
(TFA) was used in place of TFAA, non-*N*-protected aziridines were obtained as the products.¹⁴⁴ Although the reactions of conjugated *trans*-olefins show high enantioselectivity, a stoichiometric amount of the nitrido-Mn^V species is required.

However, Mansuy *et al.* reported that treatment of olefins with [*N*-(*p*-toluenesulfonyl)imino]phenyliodinane, PhI=NTs, in the presence of a Mn or Fe porphyrin, provided the corresponding aziridine or allylic sulfonamide, depending on the substrate and the catalyst used (Scheme 33).^{145–147} The reaction has been considered to proceed through a metal-*N*-toluenesulfonylnitrenoid species. Similarly to epoxidation via the oxo-Mn species, this aziridination is nonstereospecific, and the participation of a radical intermediate has been suggested.¹⁴⁶

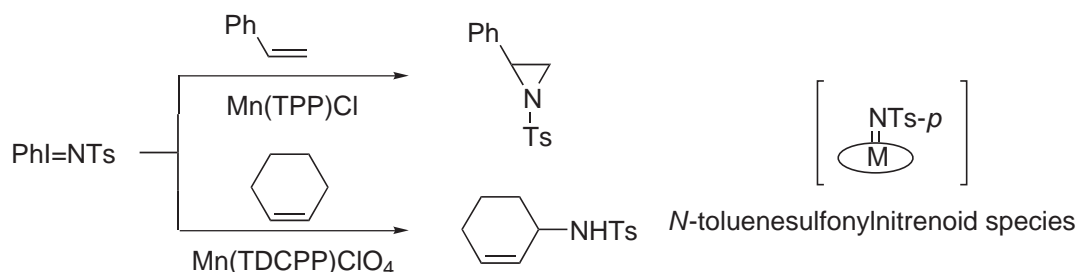
Subsequently to this, Evans *et al.* reported that Cu^I and Cu^{II} complexes also catalyzed aziridination using PhI=NTs.¹⁴⁸ Asymmetric aziridination has been examined by using bis(oxazoline) (46) as the chiral ligand: the aziridination of cinnamate esters is highly enantioselective, but that of simple olefins is less selective (Scheme 34).^{149,150} Use of [*N*-(*p*-methoxyphenylsulfonyl)imino]phenyliodinane (PhI=NA) or [*N*-(*p*-nitrophenylsulfonyl)imino]phenyliodinane (PhI=NN) in place of PhI=NTs somewhat improves the enantioselectivity.¹⁵¹ Masamune *et al.* have reported that the aziridination of styrene using (47) shows a high enantioselectivity of 88% ee,¹⁵² but Evans *et al.* have urged that Masamune's claim is not reproducible.¹⁵⁰ In 2001, Hutchings *et al.* reported that the heterogeneous aziridination of styrene using CuHY (copper-exchanged zeolite Y) as the copper ion source showed high enantioselectivity, especially when PhI=NNs was used as the nitrene precursor.¹⁵³ Improvement of the enantioselectivity has been attributed to the confinement of the catalyst within the micropores of the zeolite.

Jacobsen *et al.* reported that a different type of dinitrogen ligand (48), bis[(2,6-dichlorophenyl)methylideneamino]cyclohexane, was an efficient chiral ligand for copper-mediated asymmetric aziridination (Scheme 35).¹⁵⁴ The reactions of conjugated *cis*-olefins show high enantioselectivity with this catalyst, but enantioselectivity of the reactions of simple olefins such as styrene and indene is moderate.

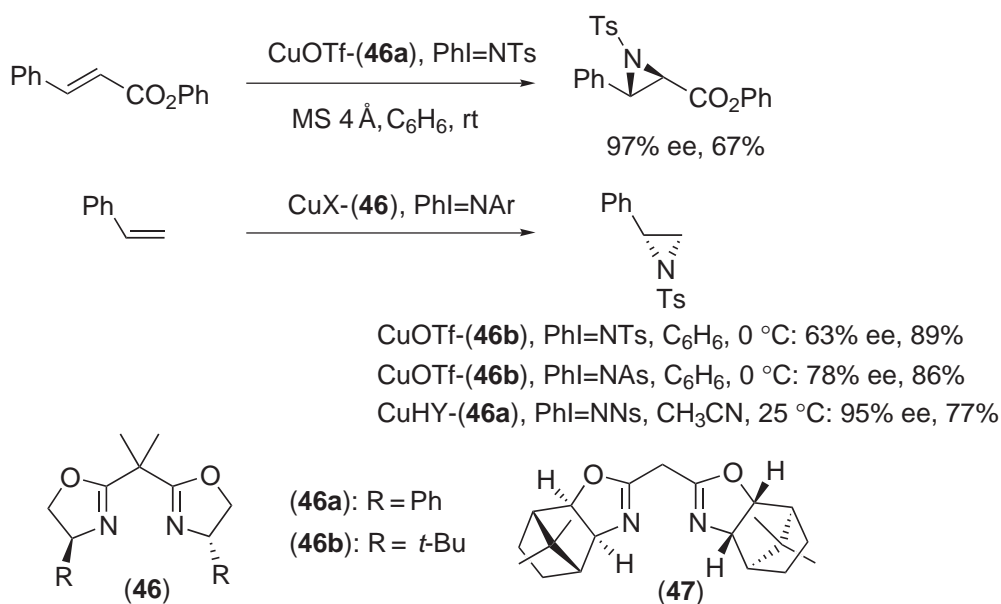
Two mechanisms are possible for the Cu-mediated aziridination using PhI=NTs as a nitrogen source: (i) aziridination via Cu–nitrenoid species (L*Cu=NTs); and (ii) aziridination via a L*(Cu–PhI=NTs) adduct, in which the Cu complex functions as a Lewis acid catalyst. Jacobsen *et al.* demonstrated that the enantioselectivity of the aziridination using (48) as the chiral auxiliary did not depend on the nitrogen precursors.¹⁵⁵ This supports the intermediacy of the Cu–nitrenoid



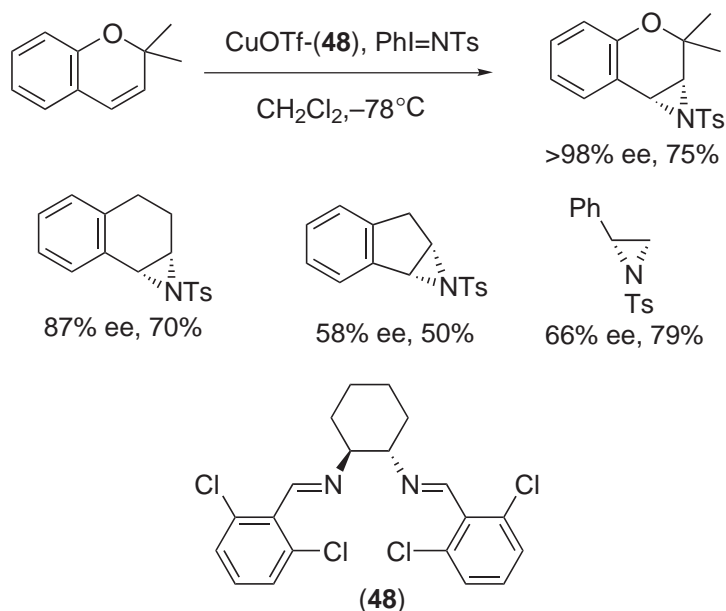
Scheme 32



Scheme 33



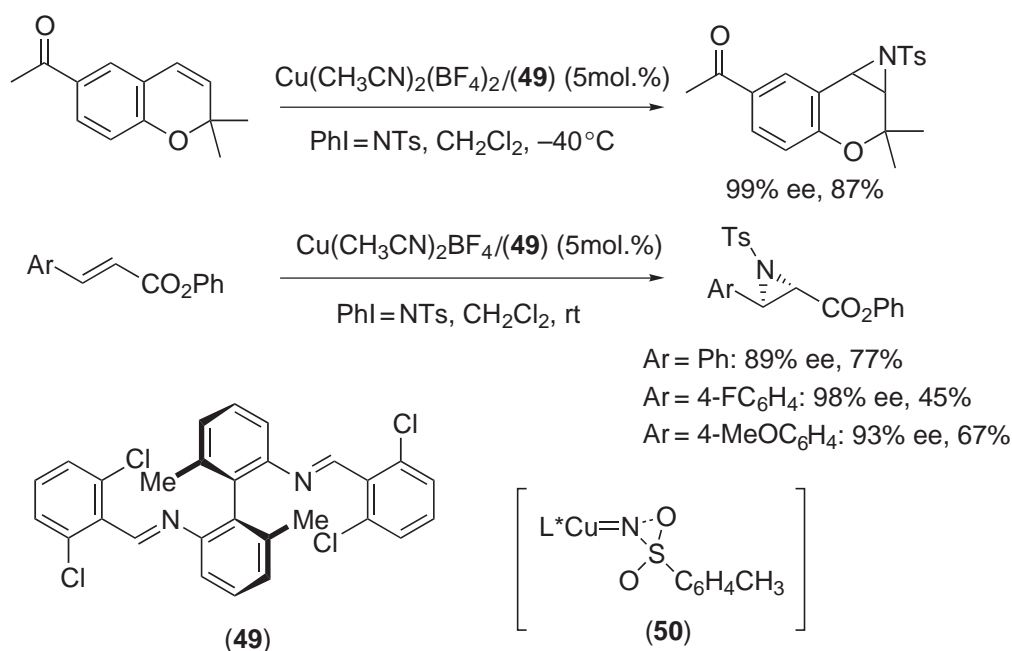
Scheme 34



Scheme 35

intermediate. A recent computational study has also suggested participation of a Cu–nitrenoid intermediate in which one of the oxygen atoms of the *N*-sulfonyl group is coordinated to the Cu ion.¹⁵⁶

Recently, Scott *et al.* have reported that a Cu complex bearing an axially chiral ligand (**49**) is an excellent catalyst for aziridination of 2,2-dimethylchromene and cinnamate esters (Scheme 36), though it is also less efficient for the reactions of simple olefins.^{157,158} On the basis of DFT investigation of the nitrenoid intermediate (**50**), one of the oxygen atoms of the *N*-sulfonyl group has been proposed to be interacting with the nitrene N-atom.¹⁵⁸



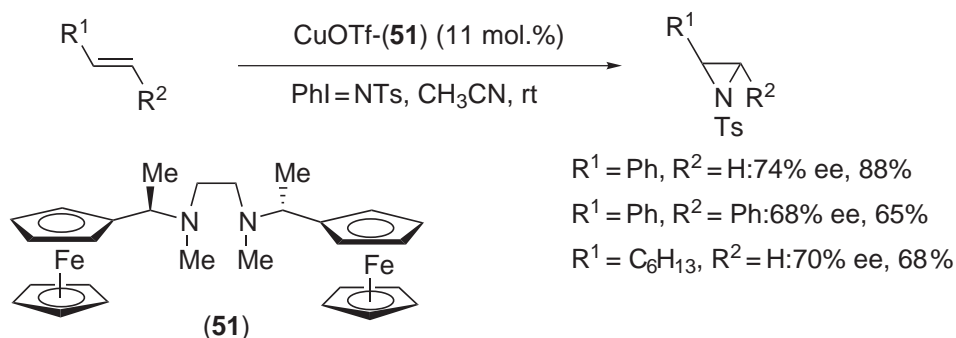
Scheme 36

Kim *et al.* have reported that the copper complex bearing the unique dinitrogen ligand (**51**) catalyzes the aziridination of conjugated as well as nonconjugated olefins with good enantioselectivity (Scheme 37).¹⁵⁹

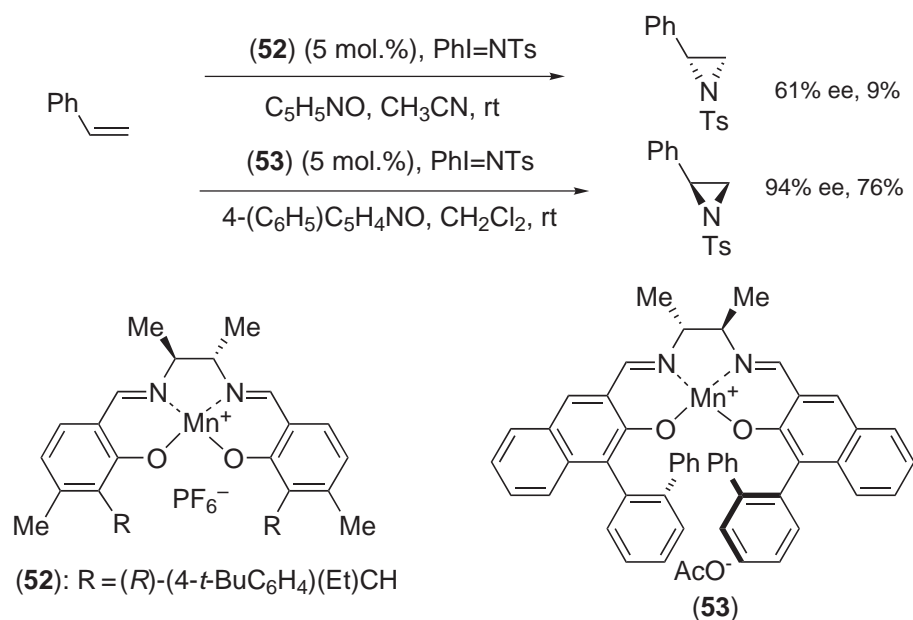
Burrow *et al.* examined aziridination with chiral Mn(salen) in the presence of PhI=NTs, but no enantioselectivity was observed.¹⁶⁰ However, Katsuki *et al.* reported that the aziridination of styrene with complex (**52**) showed moderate enantioselectivity, though the chemical yield was poor (Scheme 38).¹⁶¹ Remarkable improvements of both enantioselectivity (up to 94% ee) and chemical yield have been achieved by using a new type of Mn(salen) (**53**) as the catalyst.¹⁶²

Che *et al.* have reported that chiral Ru^{II}(salen)s (**54a**) and (**54b**) are efficient catalysts for aziridination of alkenes (up to 83% ee) and amidation of silyl enol ethers (up to 97% ee), respectively (Scheme 39).¹⁶³

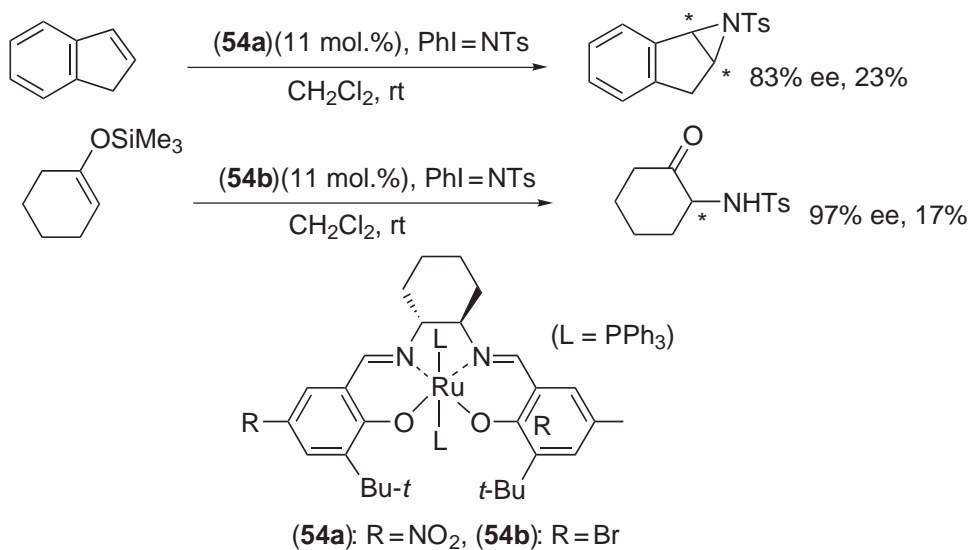
Chiral Mn^{III}porphyrin (**55**) catalyzes the aziridination of styrene derivatives in the presence of PhI=NTs. Though enantioselectivity is moderate, the turnover number of the catalyst is high (Scheme 40).¹⁶⁴ A Mn^{IV}-PhINTs adduct (**56**) has been proposed as the active intermediate for this reaction, on the basis of UV-vis and EPR analyses.



Scheme 37



Scheme 38

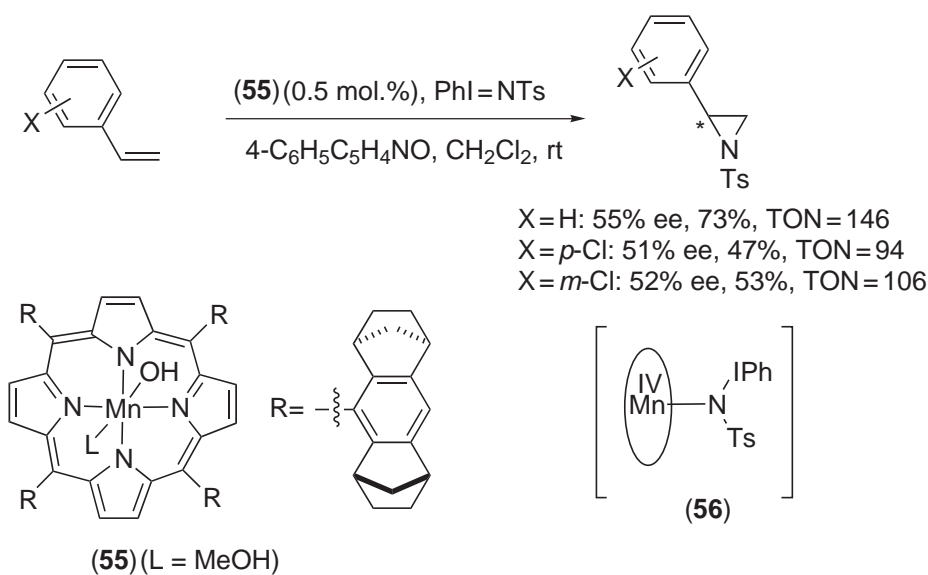


Scheme 39

9.4.5 ASYMMETRIC DIHYDROXYLATION

9.4.5.1 General Features of Asymmetric Dihydroxylation

Dihydroxylation of olefins is of high synthetic value because it introduces two vicinal hydroxy groups, endowing prochiral olefinic carbon(s) with chirality. Some oxo metal species of high valency, such as permanganate, ruthenium tetroxide, and osmium tetroxide undergo stereospecific *cis*-dihydroxylation. Among them, the osmium-mediated dihydroxylation is highly chemoselective and can be applied to a wide range of olefins. Thus, osmium-mediated asymmetric dihydroxylation has been extensively studied.⁹⁻¹²



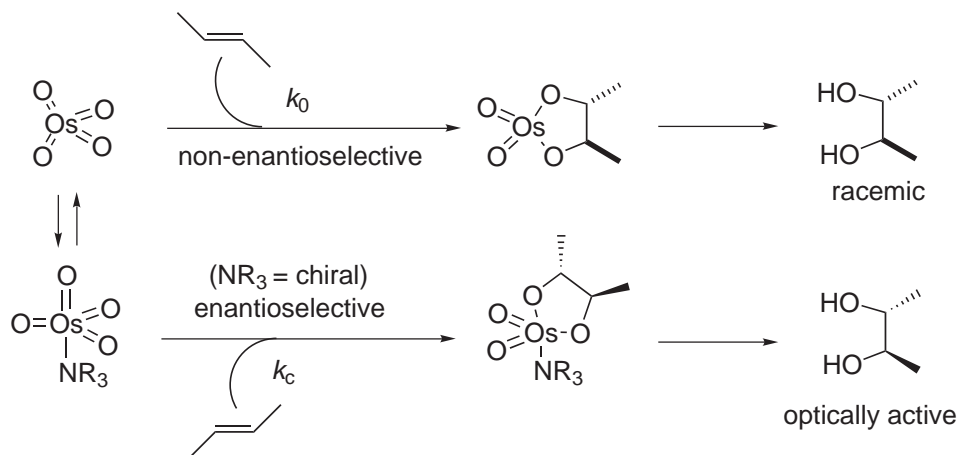
Scheme 40

More than sixty years ago, Criegee reported that the dihydroxylation of olefins by osmium tetroxide was accelerated by the addition of a tertiary amine.^{165,166} Later, this discovery prompted the study of asymmetric dihydroxylation, because the use of an optically active tertiary amine was expected to increase the reaction rate ($k_c > k_0$) and to induce asymmetry (Scheme 41).¹⁶⁷

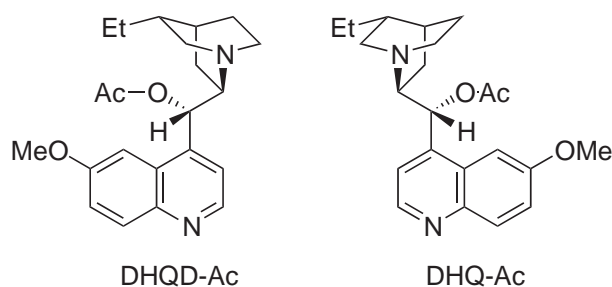
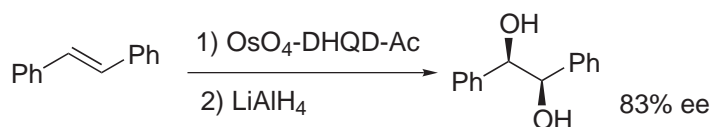
In 1980, Hengtges and Sharpless published a seminal report that dihydroxylation occurred in a good enantioselective manner when the reaction was carried out in the presence of a chiral amine, dihydroquinidine acetate (DHQD-Ac) or dihydroquinine acetate (DHQ-Ac). DHQD and DHQ are diastereomers to each other, but they behaved like enantiomers in this reaction (Scheme 42).¹⁶⁷

This report prompted further study of asymmetric dihydroxylation, and higher enantioselectivity has been realized with various C_2 - or quasi- C_2 -symmetric diamines as the chiral auxiliaries.¹⁶⁸⁻¹⁷⁴ One example reported by Tomioka and Koga is shown in Scheme 43.¹⁷⁰ Although the reaction is highly enantioselective, it needs the use of stoichiometric OsO_4 and chiral diamine, because the diamine coordinates Os^{VI} ion strongly and retards its reoxidation to Os^{VIII} ion.

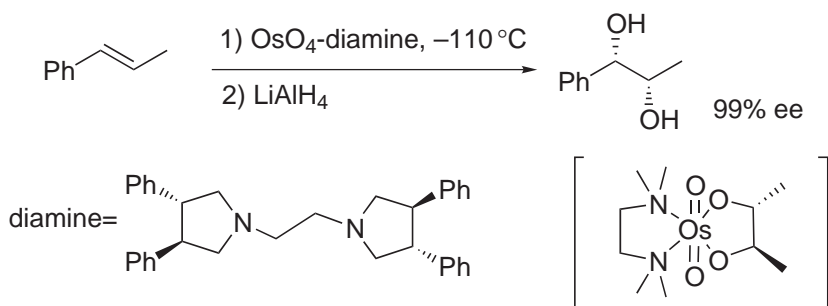
In 1988, Sharpless and co-workers reported that dihydroxylation was catalytically effected, with good enantioselectivity and remarkable ligand acceleration, when DHQD or DHQ *p*-chlorobenzoate



Scheme 41

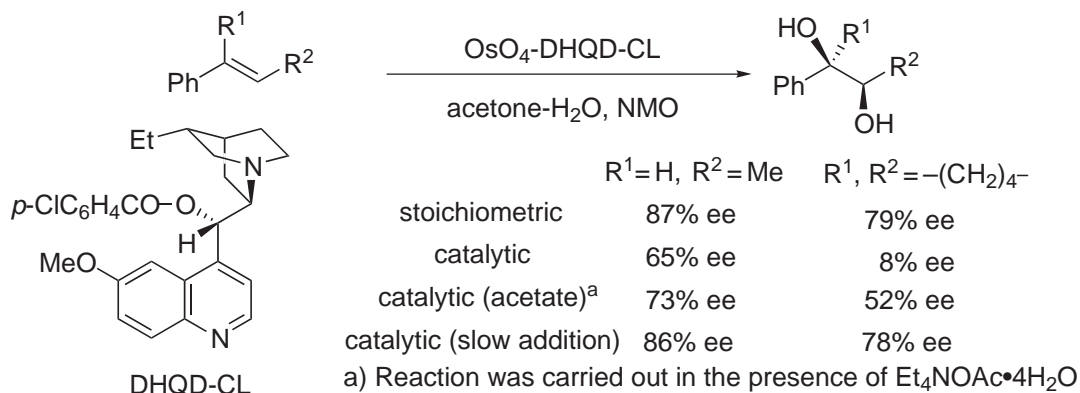


Scheme 42

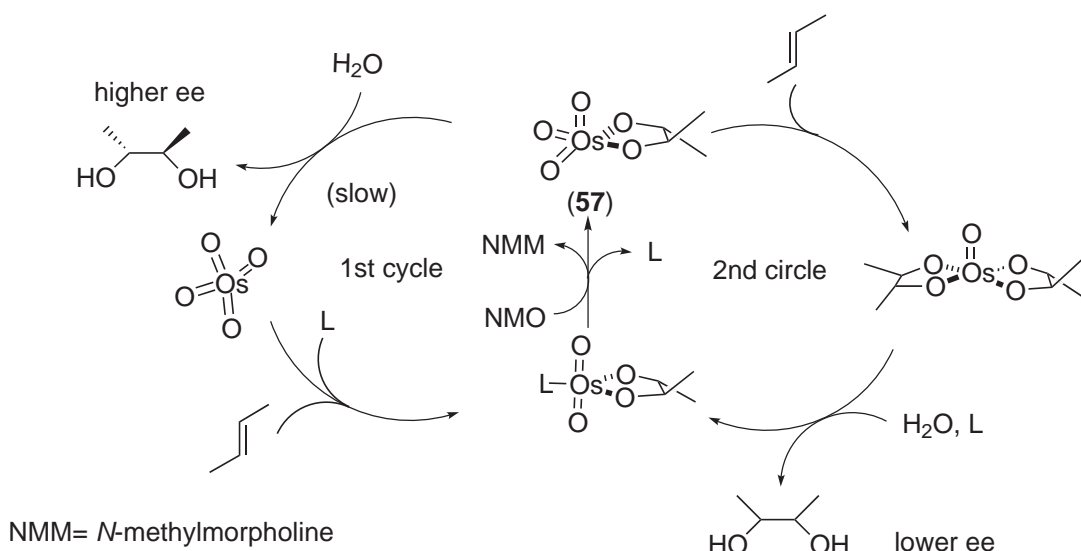


Scheme 43

(DHQD-CL or DHQ-CL) was used as the chiral auxiliary.^{175,176} However, the enantioselectivity observed under catalytic conditions was inferior to that observed under stoichiometric conditions. The addition of triethylammonium acetate, which increases the rate of hydrolysis of the Os^{VIII}-glycolate intermediate, improved enantioselectivity. A further improvement in enantioselectivity was brought about by the slow addition of substrates (Scheme 44).¹⁷⁷ These results indicated that the hydrolysis of the Os^{VIII}-glycolate intermediate (**57**) was slow under those conditions and (**57**) underwent low enantioselective dihydroxylation (second cycle). Thus, Sharpless *et al.* proposed a mechanism of the dihydroxylation including a second cycle (Scheme 45).¹⁷⁷ Slow addition reduces the amount of unreacted olefin in the reaction medium and suppresses the



Scheme 44

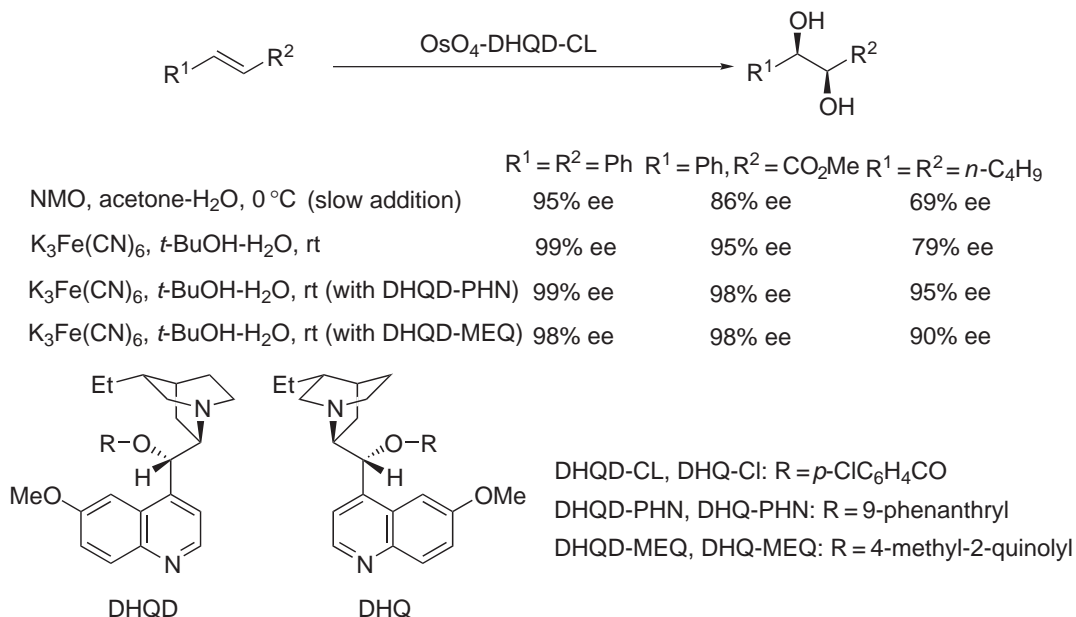


Scheme 45

second cycle. This scheme also suggests that acceleration of the hydrolysis of the Os^{VIII}-glycolate further improves the enantioselectivity of the reaction.

Tsuji *et al.* reported that osmium-catalyzed dihydroxylation was effected well by using potassium ferricyanide [K₃Fe(CN)₆] as a stoichiometric oxidant in *t*-butanol–water (1:1), especially in the presence of quinuclidine or DABCO.¹⁷⁸ Asymmetric dihydroxylation using this stoichiometric oxidant and solvent system exhibited far better enantioselectivity than that using the NMO system (Scheme 46).^{179,180} In this procedure, the Os^{VI} species [Os^{VI}O₂(OH)₄]²⁻ generated by the hydrolysis of the Os^{VI}-glycolate moves to the aqueous phases, and is reoxidized to [Os^{VIII}O₄(OH)₂]²⁻ which loses two water molecules and migrates back to the organic phase. Thus, the nonenantioselective second cycle is completely suppressed under these conditions.¹⁸⁰

The 9-*O*-substituent of the DHQD or DHQ ligand strongly influences both the enantioselectivity and the rate of the dihydroxylation reaction. Thus, enantioselectivity was further improved by introducing new chiral auxiliaries like DHQD-PHN and DHQD-MEQ (DHQ-PHN and



Scheme 46

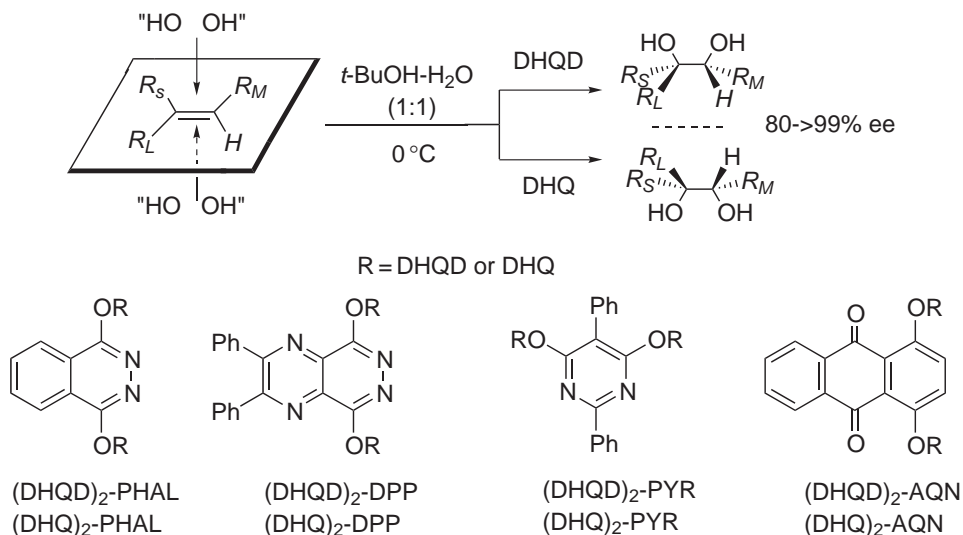
DHQ-MEQ) (Scheme 46).¹⁸¹ Finally, a remarkable improvement of both the enantioselectivity and the reaction rate was realized by conceptually new bis-cinchona ligands: 1,4-bis(dihydroquinidine)phthalazine ((DHQD)₂-PHAL) [1,4-bis(dihydroquinine)phthalazine ((DHQ)₂-PHAL),¹⁸² ((DHQD)₂-PYR [(DHQ)₂-PYR] (PYR = diphenylpyrimidine),¹⁸³ ((DHQD)₂-AQN [(DHQ)₂-AQN] (AQN = anthraquinone),¹⁸⁴ and ((DHQD)₂-DPP [(DHQ)₂-DPP] (DPP = diphenylpyrazinopyridazine)¹⁸⁵ (Scheme 47). Most olefins can be dihydroxylated with a high enantioselectivity of >80% ee, usually >90% ee, by choosing a suitable ligand.^{9-12,186} Dihydroxylation of aryl-substituted olefins is in general performed well with ((DHQD)₂-PHAL [(DHQ)₂-PHAL] or ((DHQD)₂-DPP [(DHQ)₂-DPP], allylically substituted terminal olefins with ((DHQD)₂-AQN [(DHQ)₂-AQN], monosubstituted aliphatic terminal olefins with ((DHQD)₂-PYR [(DHQ)₂-PYR], and branched aliphatic olefins with ((DHQD)₂-AQN [(DHQ)₂-AQN] (Table 2). The stereochemistry of the resulting diols is predictable from the empirical rule described in Scheme 47, although only a few reactions of substrates bearing pre-coordinating group(s) have been reported not to follow the rule.^{187,188} For the dihydroxylation of less reactive olefins, the addition of stoichiometric methanesulfonamide has been recommended.¹⁸⁹ In 1999/2000, Beller *et al.* reported that molecular oxygen could be used as the stoichiometric oxidant for the Sharpless dihydroxylation described above, albeit with somewhat reduced enantioselectivity.¹⁹⁰⁻¹⁹² When the resulting hydroxy group resides on a benzylic carbon, it is further oxidized under the aerobic conditions, reducing the selectivity of the reaction.

Ligand acceleration (the so-called Criegee effect) is the important feature of asymmetric dihydroxylation using cinchona ligands.¹⁹³ In particular, bis-cinchona ligands provide remarkable acceleration (Scheme 48). This enables high turnover rates of the osmium catalysts.

As discussed above (Scheme 45), the second cycle in osmium-mediated dihydroxylation is deleterious to enantioselectivity, and much effort has been put into suppressing the cycle. Recently, however, an effort to exploit the second cycle that starts with an osmium(VIII) ester for asymmetric dihydroxylation has been made.¹⁹⁴ To use the second cycle, an alcoholic ligand is required that is firmly anchored to the Os ion during the reaction, but that allows the rapid hydrolysis of the Os^{VI}-glycolate. Sulfonamides accelerate hydrolysis of the glycolate intermediate (*vide supra*). Thus, various *N*-sulfonyl-1,2-aminoalcohols have been examined as the ligand. Though enantioselectivity is moderate, a high turnover rate has been attained by using (58) as the chiral ligand (Scheme 49).

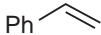
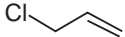
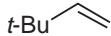
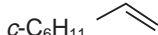
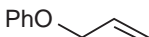
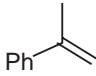
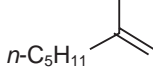
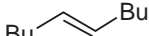
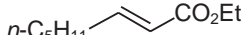
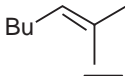
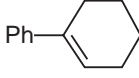
9.4.5.2 Mechanistic Considerations

Concerted [3 + 2] cycloaddition was proposed as the mechanism for dihydroxylation originally by Böesken¹⁹⁵ and Criegee¹⁶⁶ and reiterated in a refined manner by Corey.^{172,196,197} Another mechanism, stepwise [2 + 2] cycloaddition, has been proposed by Sharpless (Scheme 50).¹⁹⁸⁻²⁰⁰



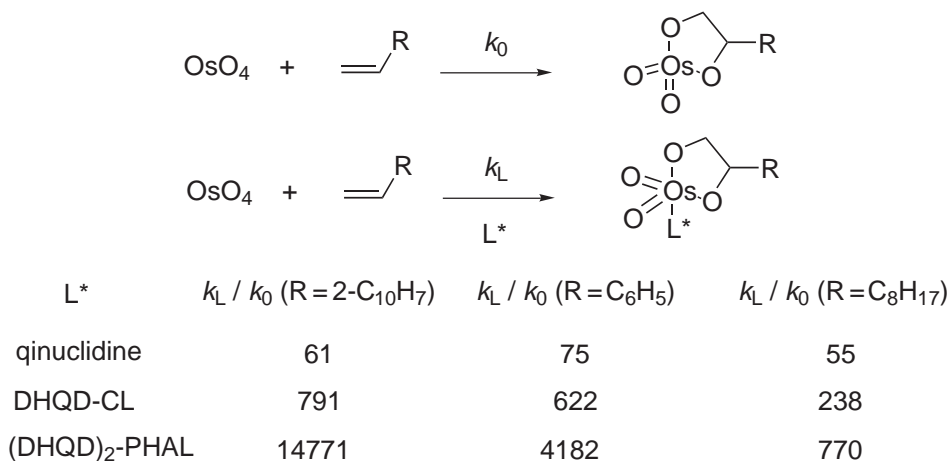
Scheme 47

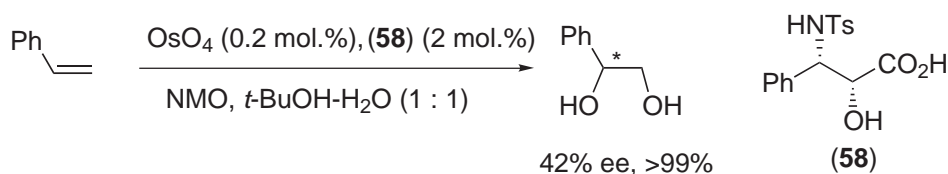
Table 2 Asymmetric dihydroxylation with bis-cinchona DHQD ligands.

Entry	Olefin	PHAL	DPP	PYR	AQN
<i>Monosubstituted olefins</i>					
1		97	99	80	89
2		63	68	70	90
3		64	59	92	
4		88	89	96	86
5		88			
<i>Disubstituted olefins</i>					
6		94	96	69	82
7		78	78		
8		97	96	88	98
9		99			99
<i>Trisubstituted olefins</i>					
10		98			
11		99			

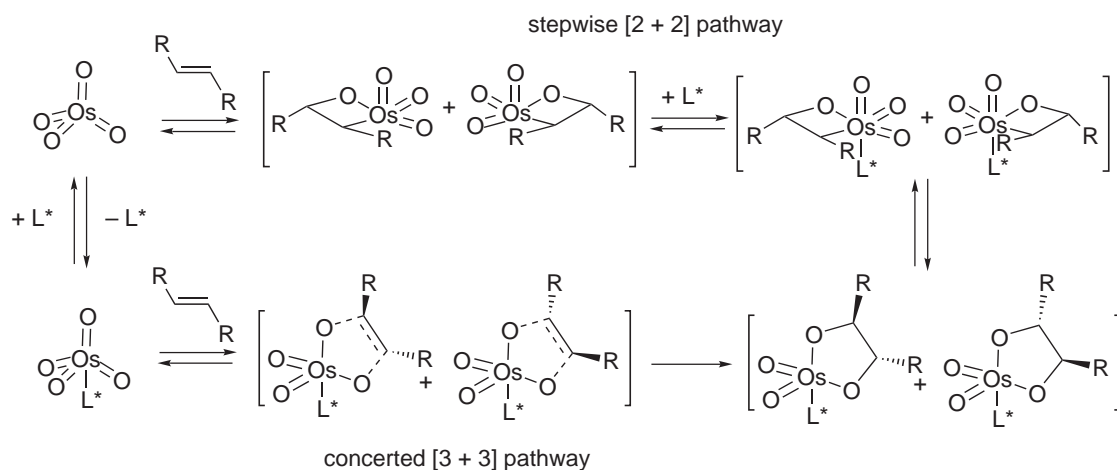
Extensive studies have been made of the mechanism of asymmetric dihydroxylation, but it is still difficult to conclusively determine the mechanism. Thus, the experimental data supporting each mechanism are highlighted below.

According to the Eyring equation [$\ln P = -\Delta\Delta H^\ddagger/RT + \Delta\Delta S^\ddagger/R$, where $P = k(\text{major diol})/k(\text{minor diol})$], an asymmetric reaction proceeding through a pair of diastereomeric transition states shows a linear temperature effect on the enantioselectivity. However, if the asymmetric

**Scheme 48**



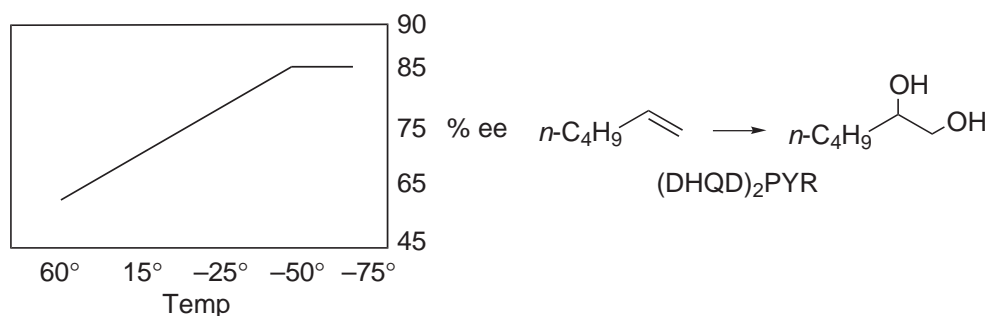
Scheme 49



Scheme 50

reaction proceeds through two diastereomeric transition states which are weighted differently at variable temperatures, a nonlinear temperature effect on the enantioselectivity can be observed.²⁰¹ Sharpless and co-workers discovered that asymmetric dihydroxylation reactions using a cinchona alkaloid ligand showed two linear areas (Scheme 51).²⁰² This observation is consistent with a stepwise [2 + 2] pathway which has two enantioselective steps: the coordination of the chiral ligand, and the rearrangement of the osmaoxetane to an Os^{VI} glycolate. Corey and Noe, however, have insisted that the olefin rapidly and reversibly forms a complex with the osmium tetroxide–ligand possessing a U-shape structure prior to dihydroxylation (*vide infra*) and its Michaelis–Menten kinetics explains the nonlinearity.¹⁹⁶ The substrate electronic effect in amine-accelerated osmylation has been extensively investigated by Sharpless' group.²⁰³ However, neither of the simple [2 + 2] or [2 + 3] pathways can provide a satisfactory explanation for the entire range of substrate electronic effects.

Corey *et al.* investigated the kinetic isotopic effect (KIE) in asymmetric dihydroxylation. ¹²C/¹³C KIE was measured for the dihydroxylation of styrene, *p*-nitrostyrene, and 4-methoxybenzoate (Figure 7).¹⁹⁷ The observed similar ¹²C/¹³C isotopic effect of two olefinic carbons



Scheme 51

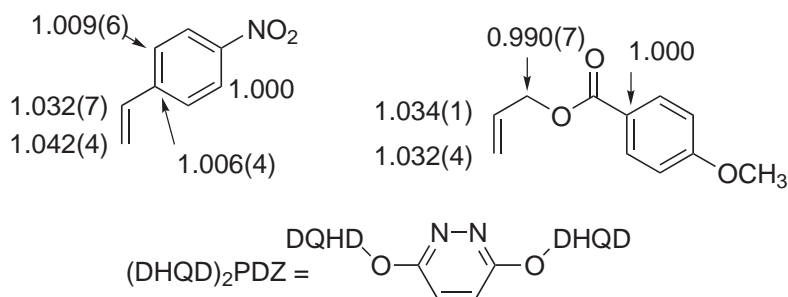


Figure 7 $^{12}\text{C}/^{13}\text{C}$ Kinetic isotopic effect in asymmetric dihydroxylation using $(\text{DHQD})_2\text{PDZ}$.

indicates a symmetrical transition state for asymmetric dihydroxylation. These results match with a [2 + 3] transition state.

Subsequent to this study, detailed H/D and $^{12}\text{C}/^{13}\text{C}$ KIE studies on asymmetric dihydroxylation using $(\text{DHPD})_2\text{-PHAL}$ as the chiral auxiliary have been carried out by using 3,3-dimethyl-1-pentene as the substrate, in order to avoid the regioselective problem in dihydroxylation. KIEs for [2 + 3] and [2 + 2] pathways were estimated by Becke 3LYP calculations on the model reaction, using trialkylamine instead of $(\text{DHPD})_2\text{-PHAL}$. The observed KIEs showed good consistency with the KIEs calculated for the [2 + 2] pathway.²⁰⁴

9.4.5.3 Models for the Enantiodifferentiating Step in Dihydroxylation

Two model structures ((**59**) and (**60**)) for the enantiodifferentiating step in the [2 + 2] and [2 + 3] pathways have been given by the Sharpless and Corey groups, respectively (Figure 8). Both models can explain the stereochemistry observed in asymmetric dihydroxylation.

In Sharpless' model (**59**), the ligand forms a chiral, L-shaped binding cleft that allows the olefinic substituent to have an attractive, face-to-face interaction with the phthalazine floor, and $\text{CH}-\pi$ (edge-to-face) interaction with the "bystander" aromatic group of the metalaoxetane intermediate.^{198–200} The ligand acceleration observed in asymmetric dihydroxylation has been attributed to ligand coordination to the intermediary osmaoxetane, which promotes its rearrangement to the Os^{VI} glycolate.¹⁹⁸

Corey *et al.* have proposed that the $(\text{DHQD})_2\text{PDZ} \cdot \text{OsO}_4$ adduct (**60**) has a U-shaped binding pocket, with favorable dimensions for the inclusion of the olefins and the acceleration of face-selective dihydroxylation by a proximate pentacoordinate OsO_4 .^{196,205} The free ligand $(\text{DHQD})_2\text{PDZ}$ (**61**) exists in a mixture of conformers, including the one drawn in Figure 8. However, its adipate-linked derivative (**62**) was confirmed by ^1H NMR analysis to have a restricted U-shape conformation. These two ligands, (**61**) and (**62**), behave identically in terms of rate acceleration and enantioselectivity, supporting the idea that (**60**) has the U-shaped binding pocket. The structure proposed for the adduct (**60**) also provides the following favorable characteristics: (i) the proximity of one apical oxygen and one equatorial oxygen of the complex unit to the olefinic carbons; and (ii) a minimum motion pathway for the [3 + 2] cycloaddition in an energetically favorable geometry. These features also explain the ligand acceleration and enantioselectivity in the dihydroxylation.^{196,205}

Based on the proposed ligand structure, Corey *et al.* designed a new ligand (**63**) bearing an anthracene ring instead of the bystander alkaloid moiety, and thus achieved highly efficient kinetic resolution of racemic allylic 4-methoxybenzoate (Scheme 52).¹⁹⁶ They also designed a new ligand (**64**), in which the U-shaped structure was capped with a benzoyl amide group. The adduct $\cdot \text{OsO}_4$ (**64**) catalyzes enantio- and position-selective dihydroxylation of the terminal isopropylidene group of polyisoprenoids.²⁰⁶

9.4.5.4 Iron-mediated Dihydroxylation

A germinal but interesting study on iron-mediated asymmetric dihydroxylation has recently been reported by Que *et al.*²⁰⁷ An iron complex bearing a chiral tetraaza ligand (Me-BPMCNC, **65b**) catalyzes the dihydroxylation of *trans*-olefins in the presence of hydrogen peroxide with good enantioselectivity to give *cis*-diols (Scheme 53). But the iron complex bearing a structurally related

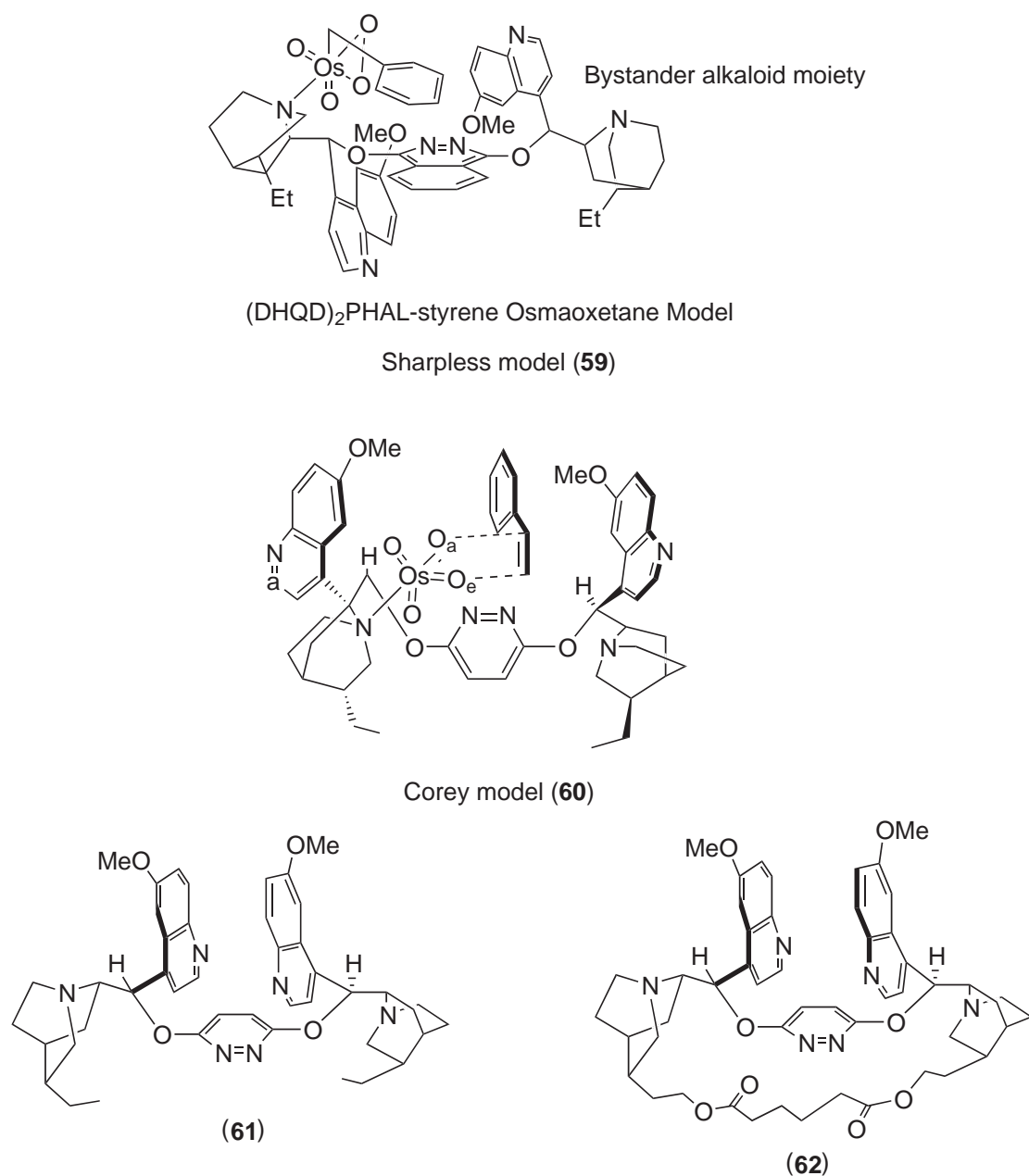
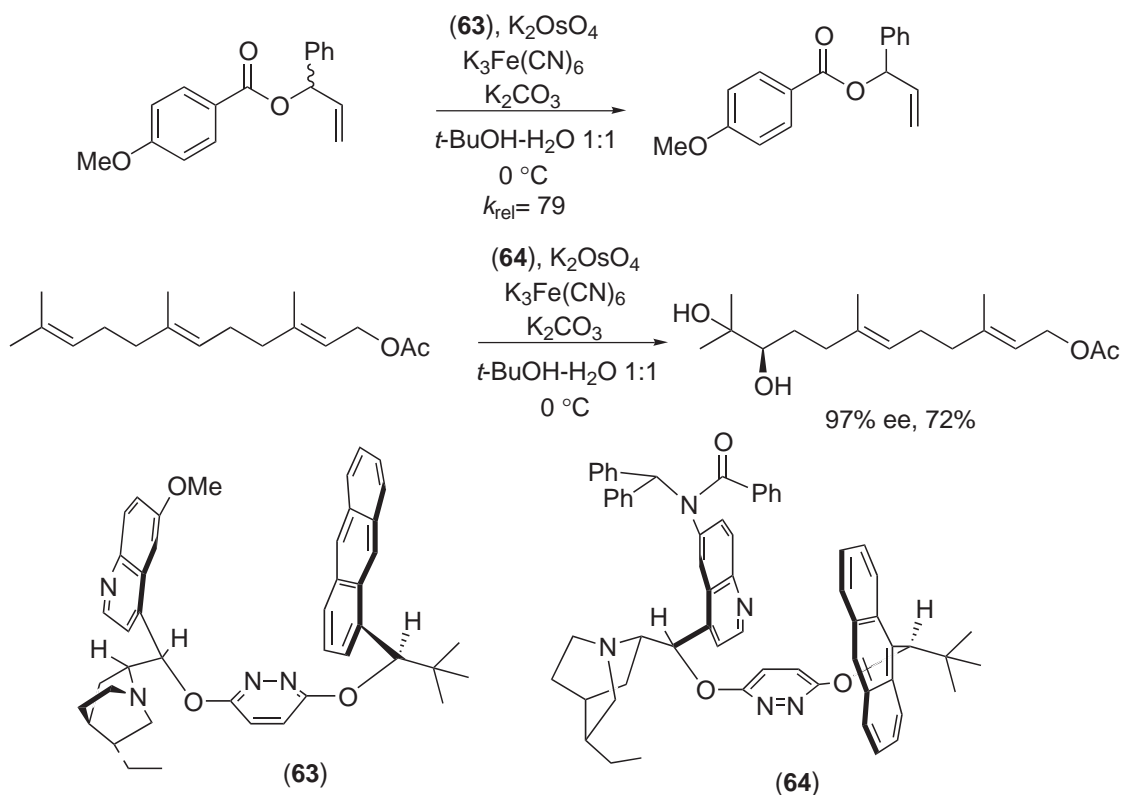


Figure 8 Sharpless and Corey models for the enantiodifferentiating step in dihydroxylation.

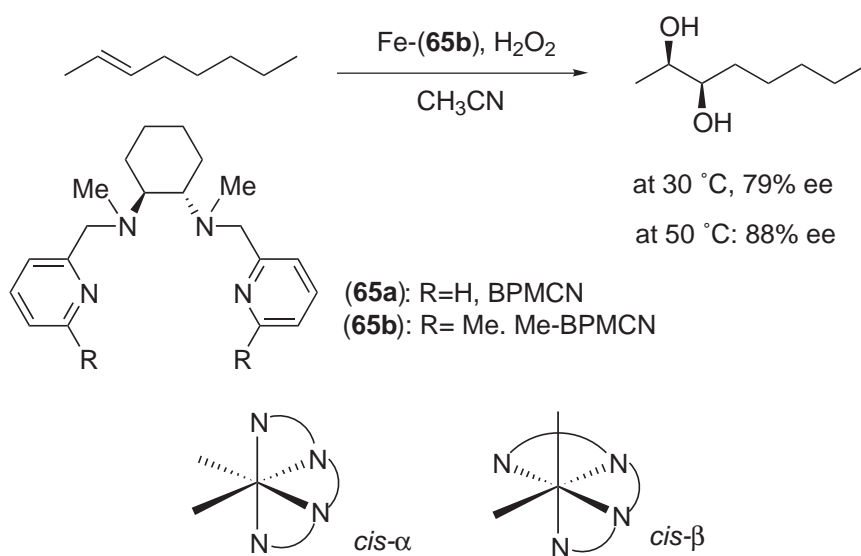
BPMCN ligand, (**65a**), catalyzes epoxidation preferentially with modest enantioselectivity. It is noteworthy that the complex of (**65b**) adopts a *cis*- β structure, while the complex of (**65a**) adopts a *cis*- α structure.

9.4.6 ASYMMETRIC AMINOHYDROXYLATION

In 1975, Sharpless *et al.* reported that imino-osmium trioxides underwent aminohydroxylation (Scheme 54).^{208,209} To perform aminohydroxylation with high efficiency, regio-, chemo-, and enantioselectivity must be addressed. This had made the practical realization of aminohydroxylation difficult. However, the development of asymmetric dihydroxylation, as described in the preceding section, propelled the study of asymmetric aminohydroxylation forward and, in 1996, Sharpless *et al.* reported a highly enantioselective version of catalytic aminohydroxylation

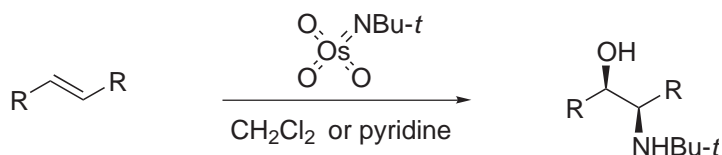


Scheme 52

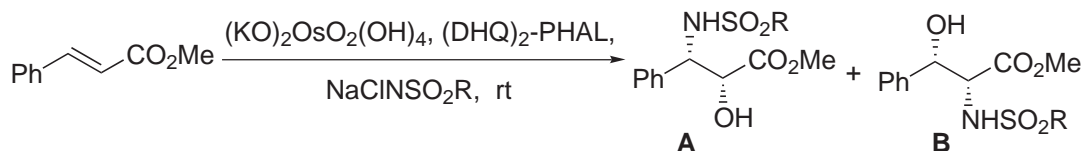


Scheme 53

by using bis(cinchona) ligands like (DHQ)₂-PHAL (Scheme 55).^{210,211} It is noteworthy that electron-deficient olefins such as dimethyl fumarate are good substrates for aminohydroxylation.²¹⁰ Another crucial factor for the success of aminohydroxylation was the use of much hydrated solvent, which allowed rapid hydrolysis of the Os^{VIII} intermediate to complete the catalytic cycle, and suppressed the poorly enantioselective second cycle (Figure 9).^{210,211} An appropriate combination of solvent, terminal oxidant (nitrogen source), and chiral auxiliary, which all influence



Scheme 54



R = *p*-CH₃C₆H₄, 81% ee, 64%, (A : B = 20: 1), CH₃CN-H₂O

R = *p*-CH₃C₆H₄, 89% ee, 51% (A), *t*-BuOH-H₂O

R = CH₃, 95% ee, 65% (A), *n*-PrOH-H₂O

Scheme 55

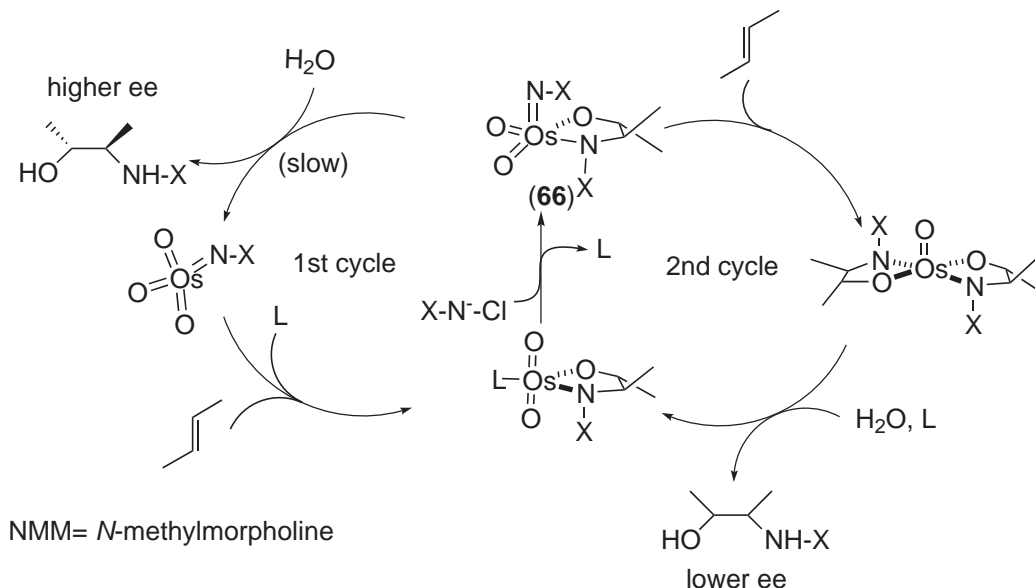


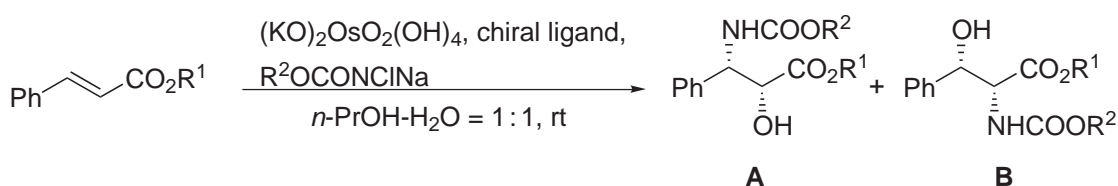
Figure 9 The proposed catalytic cycle of asymmetric aminohydroxylation.

the rate of hydrolysis of the azaglycolate intermediate (**66**), is necessary for achieving efficient aminohydroxylation.²¹¹ Three different classes of nitrogen source, *N*-halosulfonamides,^{210,211,212} *N*-halocarbamates,²¹³ and *N*-haloamides²¹⁴ have so far been developed by Sharpless' group.

The reactions with a combination of (DHQ)₂-PHAL [or (DHQD)₂-PHAL] and *N*-halosulfonamides can be successfully applied to *trans*-olefins. Especially when the substrates are α,β -unsaturated esters, high regioselectivity as well as good enantioselectivity is realized (Scheme 55).^{210,211} The use of an *N*-halosulfonamide bearing a smaller *N*-substituent increases the enantioselectivity.²¹¹ *n*-Propanol/water (1:1) is the solvent of choice. Aminohydroxylation of silyl enol ethers has been successfully performed with DHQD-CL or (DHQD)₂-PYR, to give the corresponding α -amino ketones.²¹²

The reactions with a combination of (DHQ)₂-PHAL [or (DHQD)₂-PHAL] and *N*-halocarbamates proceed with excellent enantioselectivity when the substrates are styrene derivatives and α,β -unsaturated esters.^{213,215} The required *N*-halocarbamates are easily synthesized by treatment of the corresponding carbamates with *t*-butyl hypochlorite. For large-scale experiments, the use of 1,3-dichloro-5,5-dimethyl hydantoin instead of *t*-butyl hypochlorite has been recommended.²¹⁶ It is noteworthy that the regioselectivity of the reaction is strongly affected by the cinchona ligands used.^{214,217} For example, the aminohydroxylation of cinnamate esters with a phthaladine (PHAL) ligand gives β -amino derivatives (**A**) preferentially; while the reaction with an anthraquinone (AQN) ligand gives α -amino derivatives (**B**) preferentially (Scheme 56). The reason for this reversal of regioselectivity is unknown.²¹⁷ Also noteworthy is that use of a sterically less demanding carbamate improves enantioselectivity, while a sterically more demanding carbamate inhibits the hydrolysis of the osmium(VI) azaglycolate (**66**) (Figure 9), thereby favoring the less enantioselective second cycle.²¹⁸ As a sterically less demanding carbamate, use of *N*-chloro-*N*-sodio-2-trimethylsilylethyl carbamate (TecC) has been recommended.²¹⁸

N-chloro carboxamides can also be used as nitrogen sources, but the reaction must be performed at 4 °C or below to avoid Hofmann degradation of the carboxamides. The regioselectivity of the reaction is dependent on the ligand and the solvent used: PHAL and AQN ligands again show opposite selectivity to each other (Scheme 57).²⁰⁴ The aminohydroxylation using

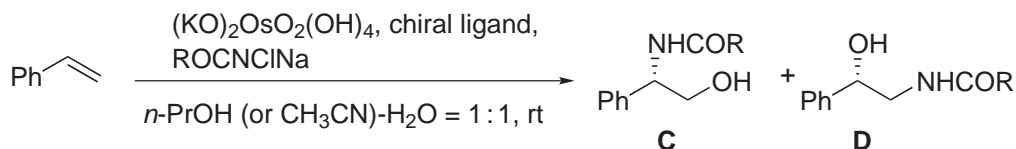


(DHQ)₂-PHAL, R¹ = Me; **A** : **B** (undetermined), **A** (R² = Bn) 94% ee, 65%

(DHQ)₂-PHAL, R¹ = Me; **A** : **B** (undetermined), **A** (R² = Et) 99% ee, 78%

(DHQ)₂-PHAL, R¹ = *i*-Pr; **A** : **B** (>98 : 2), **A** (R² = Tec) 99% ee, 70%

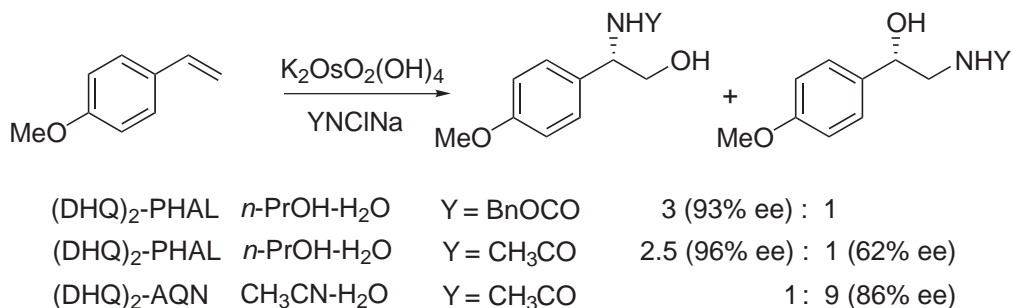
(DHQ)₂-AQN, R¹ = Me; **A** : **B** (21 : 79), **B** (R² = Bn) 95% ee, 58%



(DHQ)₂-PHAL (*n*-PrOH); **C** : **D** (55 : 45), **C** (R = OBn) 93% ee, 40%

(DHQ)₂-AQN (CH₃CN); **C** : **D** (1 : 13), **D** (R = CH₃) 88% ee, 36%

Scheme 56



Scheme 57

N-bromo-benzamide is a useful method for the synthesis of the side chain of paclitaxel (taxol) from isopropyl cinnamate.²¹⁹

9.4.7 ASYMMETRIC CYCLOPROPANATION

In 1966, Nozaki *et al.* reported that the decomposition of α -diazo-esters by a copper–chiral Schiff base complex in the presence of olefins gave optically active cyclopropanes (Scheme 58).^{220,221} Following this seminal discovery, Aratani *et al.* commenced an extensive study of the chiral salicylaldimine ligand and developed highly enantioselective and industrially useful cyclopropanation.^{222–224} Since then, various complexes have been prepared and applied to asymmetric cyclopropanation. In this section, however, only selected examples of cyclopropanations using diazo compounds are discussed. For a more detailed discussion of asymmetric cyclopropanation and related reactions, see reviews and books.^{17–21,225}

9.4.7.1 Asymmetric Intermolecular Cyclopropanation

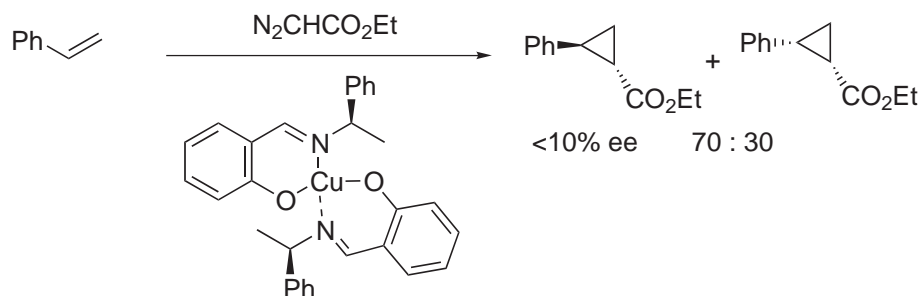
Intermolecular cyclopropanation of olefins poses two stereochemical problems: enantioface selection and diastereoselection (*trans*–*cis* selection). In general, for stereochemical reasons, the formation of *trans*-cyclopropane is kinetically more favored than that of *cis*-cyclopropane, and the asymmetric cyclopropanation so far developed is mostly *trans*-selective, except for a few examples. Copper, rhodium, ruthenium, and cobalt complexes have mainly been used as the catalysts for asymmetric intermolecular cyclopropanation.

9.4.7.1.1 Cu-catalyzed cyclopropanation

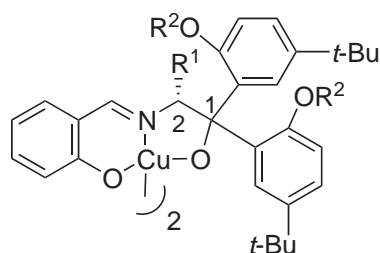
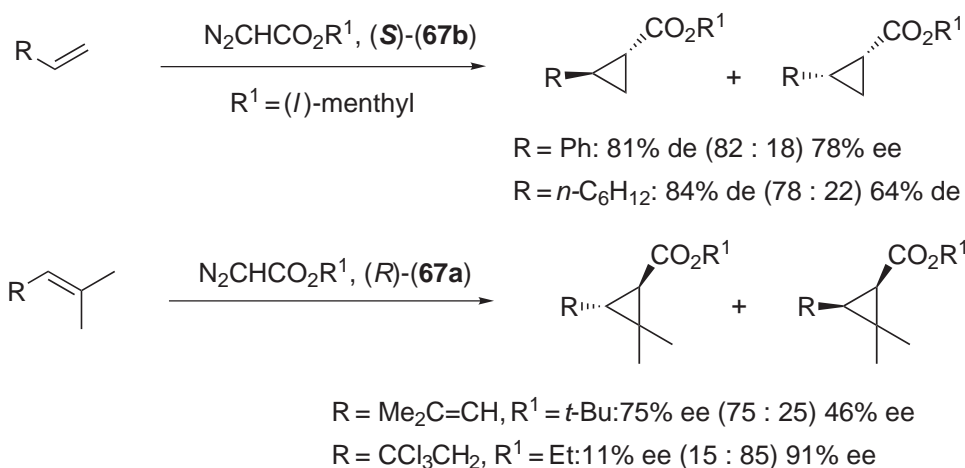
Highly enantioselective cyclopropanation was achieved for the first time by Aratani *et al.* After the systematic study of salicylaldimines, tridentate aldimines bearing two bulky geminal substituents at the C1 carbon were eventually found to be the chiral ligands of choice.^{222–224} Their copper(II) complexes (**67a**) and (**67b**) are reduced with diazo compound or phenylhydrazine, and the resulting copper(I) species catalyze the cyclopropanation of terminal, *trans*-disubstituted and trisubstituted olefins with good to high enantioselectivity, though diastereoselectivity was moderate (Scheme 59).^{224,226} It is noteworthy that the cyclopropanation of 1,1,1-trichloro-4-methyl-3-pentene provides the *cis*-product preferentially.²²⁴ The presence of a homoallylic halogen atom is essential for the occurrence of *cis*-selectivity.

In 1986, Pfaltz *et al.* introduced a new type of pseudo C_2 -symmetrical copper–semicorrin complex (**68**) as the catalyst (Scheme 60).^{227,228} The complexes (**68**) are reduced *in situ* by the diazo compound or by pretreatment with phenylhydrazine to give monomeric Cu^I species (**69**), which catalyze cyclopropanation. Of the semicorrin complexes, complex (**68a**) (R = CMe_2OH) showed the best enantioselectivity in the cyclopropanation of terminal and 1,2-disubstituted olefins.^{227,228,17} It is noteworthy that complex (**68a**) catalyzes cyclopropanation, using diazomethane as a carbene source, with good enantioselectivity (70–75% ee).¹⁷

Subsequently, bis(oxazoline) ligands ((**70**) and (**71**)), structurally related to the semicorrin ligand, were introduced and further expanded the scope of asymmetric cyclopropanation

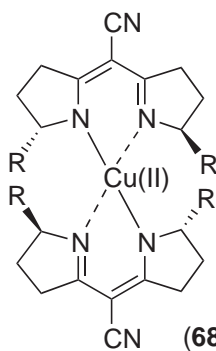
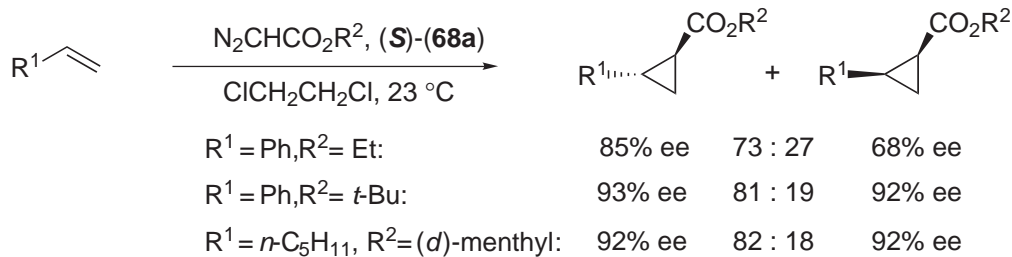


Scheme 58

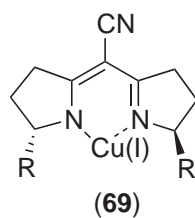


(R)-(67a): $R^1 = \text{Me}, R^2 = n\text{-octyl}$
(R)-(67b): $R^1 = \text{Bn}, R^2 = \text{butyl}$

Scheme 59



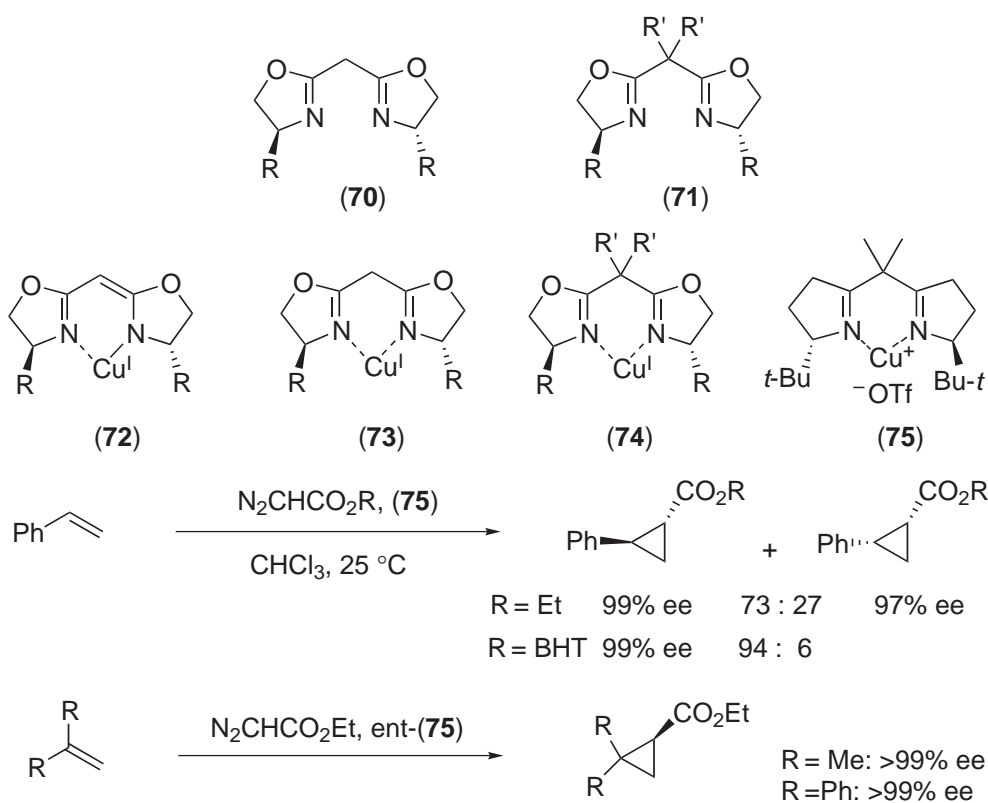
(68) **(68a):** $R = \text{C}(\text{Me})_2\text{OH}$



(69)

Scheme 60

(Scheme 61).^{22,149,150,152,229,230} The methylene-bridged bis(oxazoline)s (**70**) can afford either neutral copper complexes of the semicorrin type (**72**) or cationic copper complexes (**73**). Cyclopropanation with copper complexes of type (**70**) shows similar stereochemistry to that with the corresponding copper semicorrin complexes.^{229–231} Alternatively, bis(oxazoline) ligand (**71**), bearing



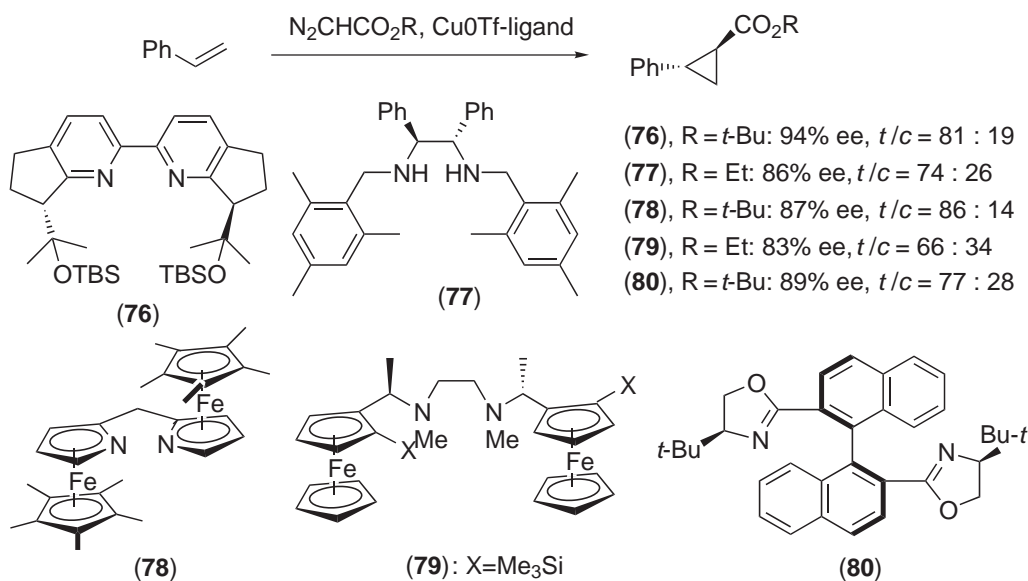
Scheme 61

a geminally substituted methylene bridge, affords only the cationic complex (74).^{149,150,230} Among the complexes of type (74), complex (75), bearing a bis(*t*-butyl oxazoline) ligand, shows excellent enantioselectivity in the cyclopropanation of terminal olefins, albeit with moderate diastereoselectivity.^{149,150} The enantioselectivity and diastereoselectivity generally increase as the ester group of the diazo compound becomes larger. The reaction of 2,6-di-*t*-butyl-4-methylphenyl (BHT) diazoacetate with styrene, for example, shows high *trans*-selectivity and excellent enantioselectivity.

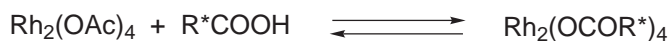
Later, several other copper catalysts bearing dinitrogen ligands [bipyridine derivatives (76),^{232,233} diamines (77),²³⁴ bis(azaferrocene) (78),²³⁵ bisferrocenyldiamine (79),¹⁵⁹ and bis(oxazolyl) binaphthyl (80)²³⁶] have been introduced (Scheme 62), but asymmetric induction by them does not exceed that by complex (75).

9.4.7.1.2 Rh-catalyzed cyclopropanation

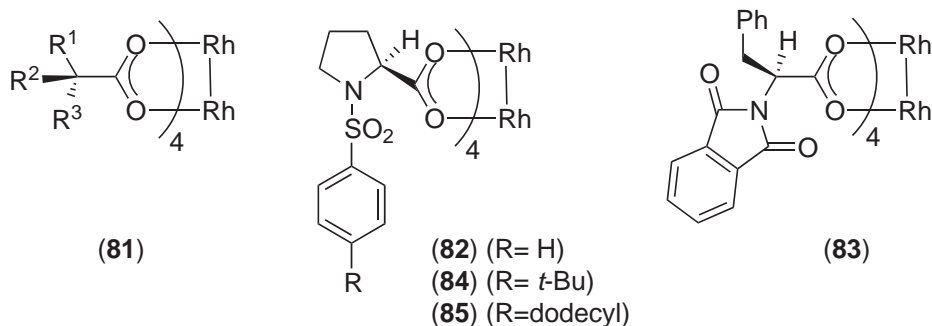
$\text{Rh}_2(\text{OCOR})_4$ compounds have been well studied as catalysts for cyclopropanation, and the electronic and steric natures of their carboxylates are known to affect the rate and the selectivity of the reaction.²³⁷ On the basis of this knowledge, Brunner,²³⁸ McKervey,²³⁹ and Hashimoto²⁴⁰ independently reported rhodium-mediated asymmetric cyclopropanation and C-H insertion reactions using an optically active acid or *N*-protected amino acid as the chiral auxiliary (Scheme 63). Since then, many chiral rhodium complexes have been reported.¹⁸ Of these complexes, (84) and (85) introduced by Davies *et al.* deserve comment. Due to the presence of *p*-alkyl substituents, they are soluble in nonpolar solvents such as pentane, and the reactions in such a nonpolar solvent show remarkably improved stereoselectivity.²⁴¹ The cyclopropanation of terminal olefins with α -vinyl- α -diazo esters in the presence of (84) or (85) proceeds with high enantioselectivity (>90% ee) and high diastereoselectivity (>40:1) (Scheme 64). Cyclopropanation with α -phenyl- α -diazo esters also proceeds with high enantio- and diastereoselectivity, especially when the substrates are 1,1-disubstituted terminal olefins. It is noteworthy that α -vinyl- α -diazo acid methyl esters are the best diazo compounds for these reactions, although diazo compounds bearing



Scheme 62



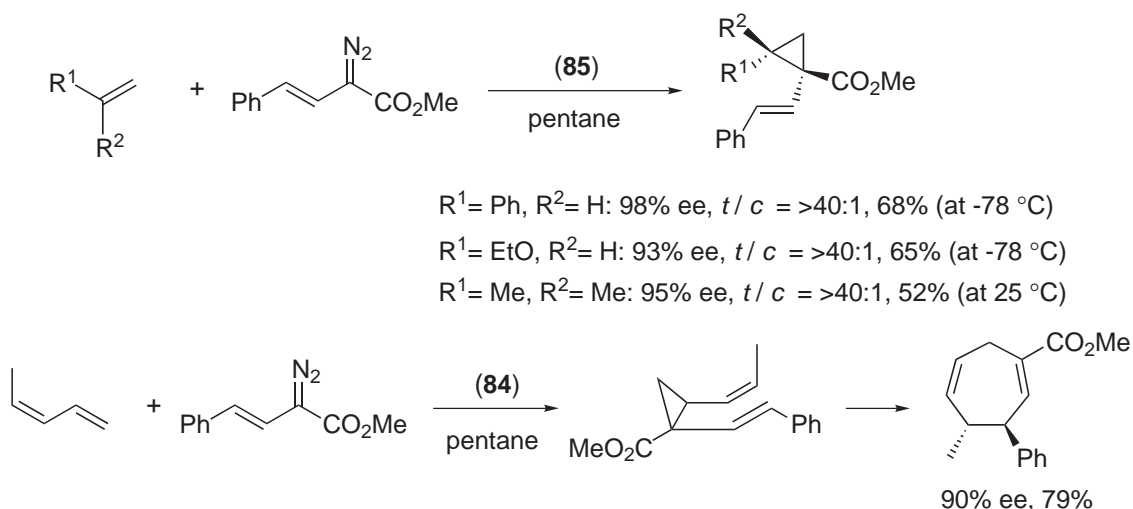
R*CO₂H = optically active acid



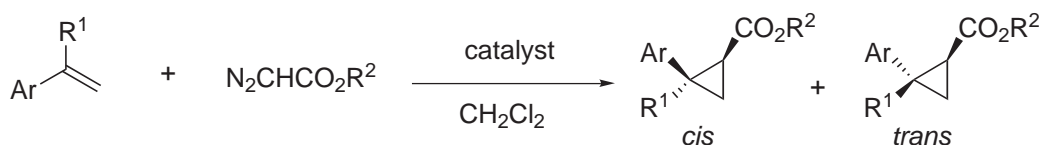
Scheme 63

bulkier ester alkyl group are in general better substrates for cyclopropanation (*vide supra*).²⁴² When the substrate is a diene, a tandem cyclopropanation/Cope rearrangement gives seven-membered carbocycles with high enantioselectivity.^{241,242}

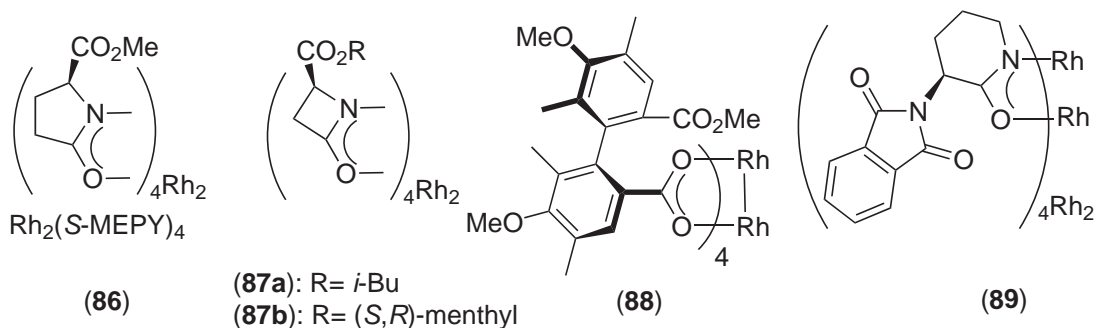
A new type of rhodium-carboamidate complexes (**86**), introduced by Doyle *et al.* make very efficient catalysts, especially for asymmetric intramolecular cyclization (*vide infra*).^{243,244} Although they are not very efficient for intermolecular cyclization, it is noteworthy that the rhodium-oxazetidine carboamidate complex (**87**) shows moderate *cis*-selectivity (Scheme 65). The enantioselectivity increased as the ester alkyl group became more bulky.²⁴⁵ Quite recently, use of (*S,R*)-menthyl oxazetidine carboxylate (**87b**) as the ligand was found to improve *cis*-selectivity in the cyclopropanation of substituted styrenes.²⁴⁶ Rhodium complex (**88**) bearing an axially chiral ligand has been reported to show *cis*-selectivity. Again, the enantioselectivity increased as the ester alkyl group became more bulky.²⁴⁷ Hashimoto *et al.* reported that dirhodium tetrakis[*N*-phthalimido-2-piperidinoate] (**89**) served as an efficient catalyst for the cyclopropanation of terminal olefins in ether.²⁴⁸ Excellent enantioselectivity was realized, albeit with modest *trans*-selectivity, when diisopropylmethyl diazoacetate was used as the diazo compound.



Scheme 64



- (86)**, Ar = Ph, R^1 = H, R^2 = *d*-menthyl: 88% de (43 : 57) 31% de
(87a), Ar = Ph, R^1 = H, R^2 = CH(*c*-C₆H₁₁)₂: 95% ee (66 : 34) 77% ee
(87a), Ar = Ph, R^1 = H, R^2 = Et: 73% ee (64 : 36) 47% ee
(87b), Ar = Ph, R^1 = H, R^2 = *t*-Bu: 94% ee (74 : 26) 71% ee
(87b), Ar = 2,4,6-Me₃C₆H₂, R^1 = H, R^2 = *t*-Bu: 97% ee (92 : 8) 76% ee
(88), Ar = Ph, R^1 = H, R^2 = *t*-Bu: 54% ee (69 : 31) 57% ee
(88), Ar = Ph, R^1 = H, R^2 = *d*-menthyl: 99% de (63 : 37) 45% de
(89), Ar = Ph, R^1 = H, R^2 = CH(*Pr-i*)₂: 96% ee (19 : 54) 98% ee
(89), Ar = Ph, R^1 = H, R^2 = Et: 49% ee (27 : 36) 51% ee
(89), Ar = Ph, R^1 = Me, R^2 = CH(*Pr-i*)₂: 95% ee (37 : 43) 94% ee



Scheme 65

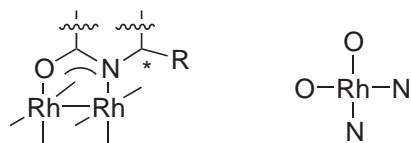
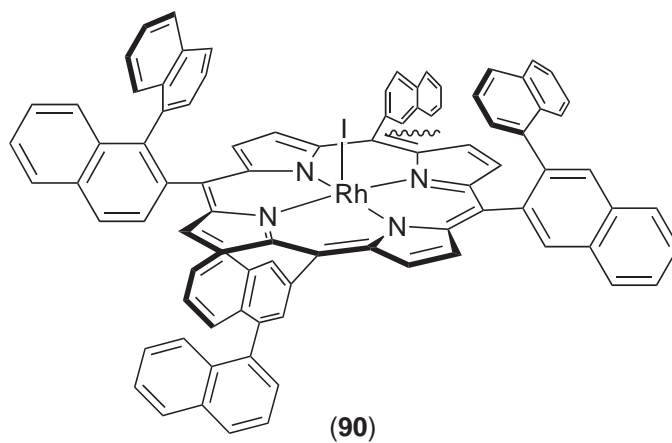


Figure 10 Coordination of carboxamidate ligand to rhodium ion.

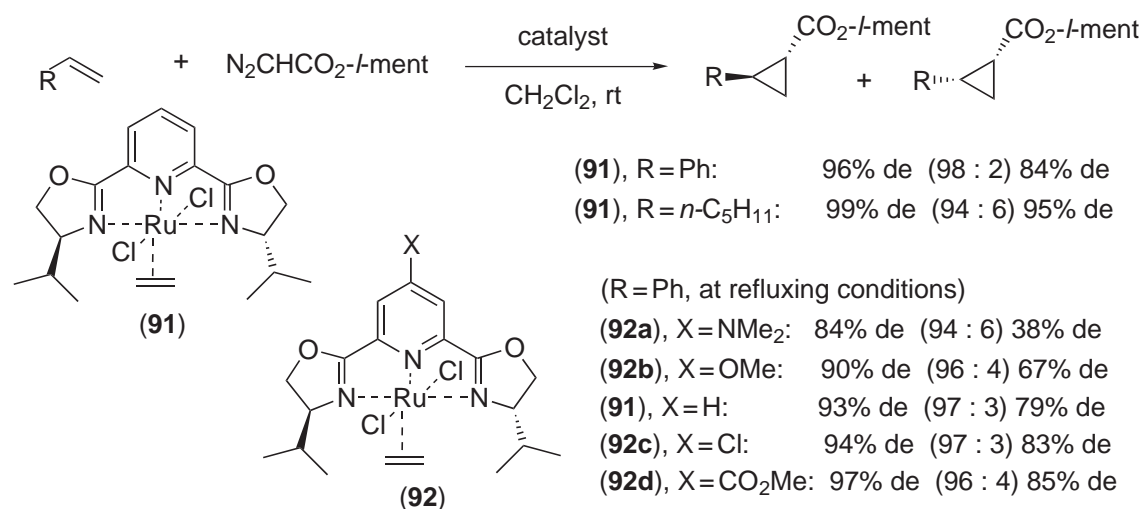
It is noteworthy that, in the carboxamidate-ligated dirhodium(II) complexes (**86**), (**87**), and (**89**), the rhodium core is coordinated by four ligands and two N and two O atoms are bound to each rhodium center, constituting a unique coordination sphere (Figure 10).²²⁵

The chiral rhodium porphyrin catalyst (**90**) shows a high turnover rate, though enantioselectivity is modest (less than 60% ee). It is, however, noteworthy that *cis*-selective cyclopropanation of simple olefins (*cis/trans* = 2–14.2/1) was realized for the first time with (**90**).^{249,250}



9.4.7.1.3 Ru-catalyzed cyclopropanation

Nishiyama *et al.* introduced a new catalyst, the chiral *trans*-RuCl₂(Pybox-*i*-Pr)(ethylene) complex (**91**), which showed for the first time both enantio- and diastereoselectivity (*trans*-selectivity) at excellent levels in the reactions of terminal olefins (Scheme 66).^{251–253} With 4-substituted Ru(Pybox-*i*-Pr) complexes (**92**), they studied the substituent effect on enantioselectivity



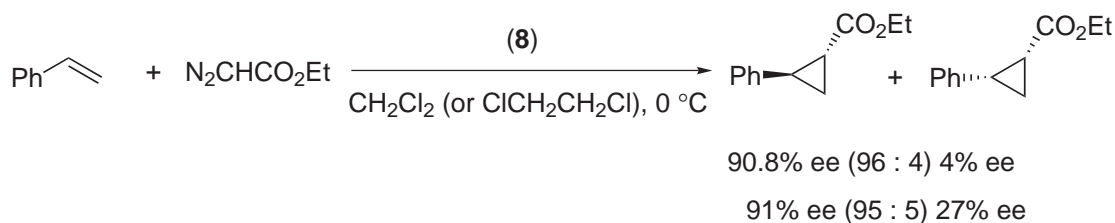
Scheme 66

and demonstrated that the presence of an electron-withdrawing group increased enantioface selectivity, though diastereoselectivity was little affected.²⁵³

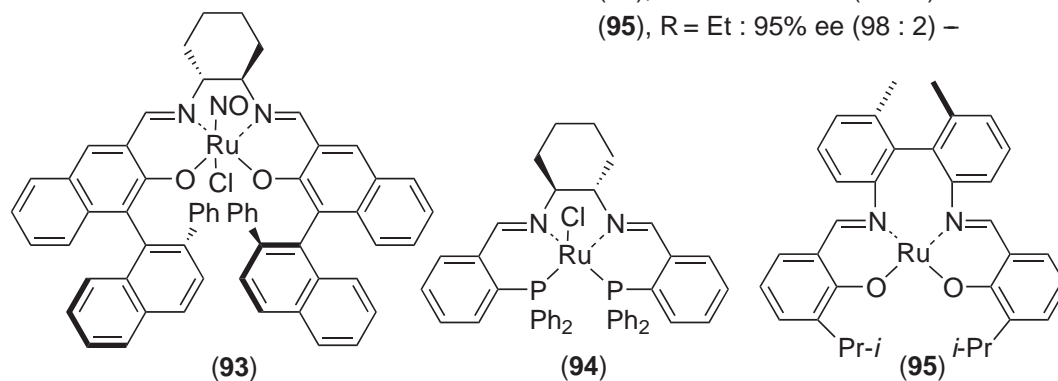
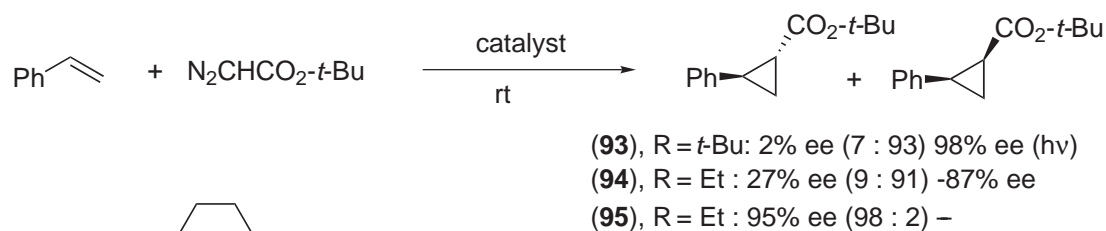
It has been widely accepted that the carbene-transfer reaction using a diazo compound and a transition metal complex proceeds via the corresponding metal carbenoid species. Nishiyama *et al.* characterized spectroscopically the structure of the carbenoid intermediate that underwent the desired cyclopropanation with high enantio- and diastereoselectivity, derived from **(91)**.^{254,255} They also isolated a stable dicarbonylcarbene complex and demonstrated by X-ray analysis that the carbene moiety of the complex was almost parallel in the Cl—Ru—Cl plane and perpendicular to the pybox plane (*vide infra*).²⁵⁵ These results suggest that the rate-determining step of metal-catalyzed cyclopropanation is not carbenoid formation, but the carbene-transfer reaction.²⁵⁴

Che *et al.* and Berkessel *et al.* independently reported that the cyclopropanation of mono- and disubstituted terminal olefins with the Ru-porphyrin complex **(8)** bearing Halterman's ligand proceeded with high enantio- and *trans*-selectivity (Scheme 67).^{256–258}

Katsuki *et al.* reported the first example of highly *cis*- and enantioselective cyclopropanation of simple terminal olefins by using Ru(salen) complex **(93)** as the catalyst under irradiation of visible light (Scheme 68).^{259,260} Similarly to **(37)**, complex **(93)** becomes coordinatively unsaturated upon photo-irradiation (see Scheme 21) and catalyzes the decomposition of diazo compounds. In 2001, Mezzetti *et al.* reported that cyclopropanation using the Ru(PNNP)Cl complex **(94)** also showed good *cis*-selectivity and high enantioselectivity.²⁶¹ However, the Ru^{II}-Schiff base complex **(95)** bearing a chiral biphenyl backbone catalyzes *trans*-selective cyclopropanation in a highly enantioselective manner.²⁶² It is worth noting that complex **(95)** adopts the *cis*- β structure, while complexes **(93)** and **(94)** have been considered to take square planar geometry.



Scheme 67



Scheme 68

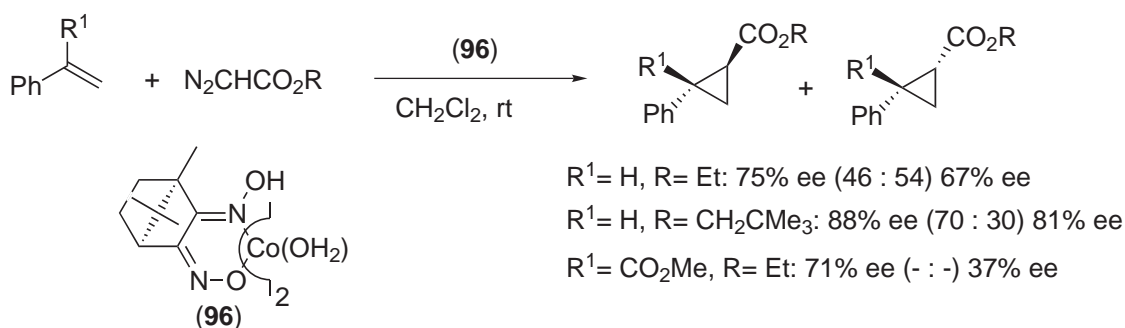
9.4.7.1.4 Co-catalyzed cyclopropanation

In 1974, Nakamura and Otsuka reported enantioselective cyclopropanation of terminal olefins, using bis[(1)-camphorquinone- α -dioximato]cobalt(II) complex (**96**) as the catalyst. Although diastereoselectivity was modest, good enantioselectivity was attained (Scheme 69).^{263–265} Cyclopropanation using Co^{II}(salen) as the catalyst was also examined, but the enantioselectivity was low.²⁶⁵

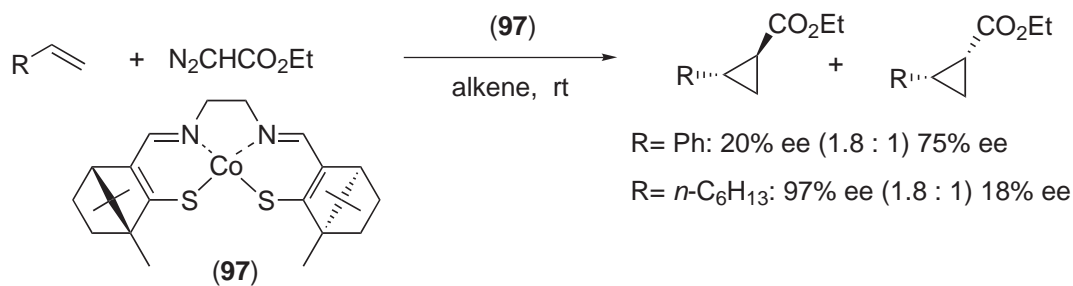
A quarter of a century later complex (**97**), structurally related to Co^{II}(salen), was prepared from camphor and used as the catalyst for cyclopropanation. Although diastereoselectivity was modest, good enantioselectivity was achieved in the reaction of 1-octene (Scheme 70).²⁶⁶

Katsuki *et al.* have reported that the Co^{III}(salen) ((**98**): X = I, Y = *t*-Bu) bearing an apical halide ligand shows high *trans*-selectivity in the cyclopropanation of styrene and its derivatives, albeit with moderate enantioselectivity (Scheme 71).²⁶⁷ The enantioselectivity is influenced, however, by the natures of the apical ligand and the 5,5'-substituents, and high enantio- and *trans*-selectivity has been realized by their appropriate tuning ((**98**): X = Br, Y = OMe).²⁶⁸ It is noteworthy that the Co^{III}(salen) complex bearing substituents at C3 and C3' shows no catalytic activity.

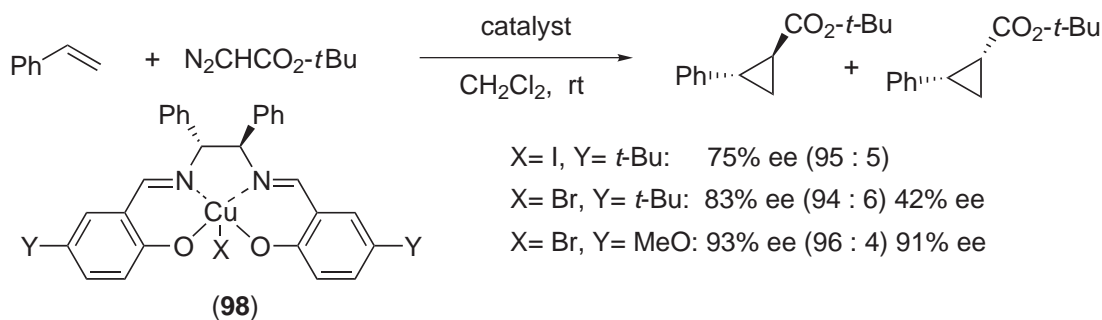
Yamada *et al.* reported that the β -ketoiminato cobalt(II) complex (**99**) was an efficient catalyst for the cyclopropanation of terminal olefins (Scheme 72).^{269–272} The addition of *N*-methylimidazole



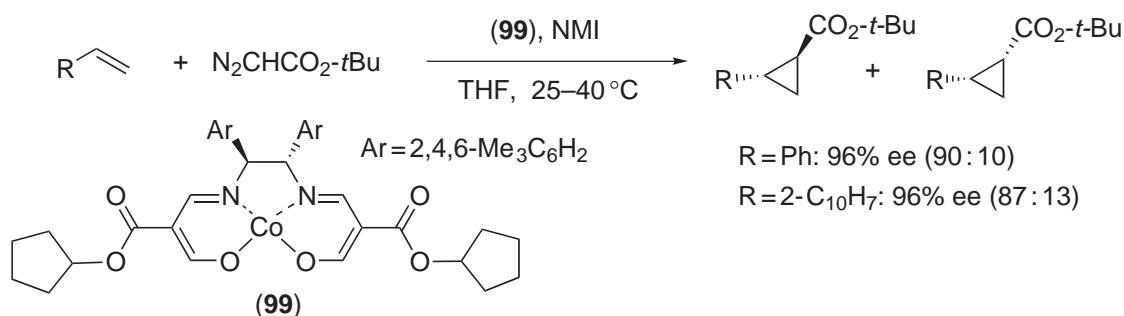
Scheme 69



Scheme 70



Scheme 71



Scheme 72

(NMI) improved both enantioselectivity (up to 97% ee) and chemical yield to a considerable extent. Use of methanol as the solvent also increased the enantioselectivity.

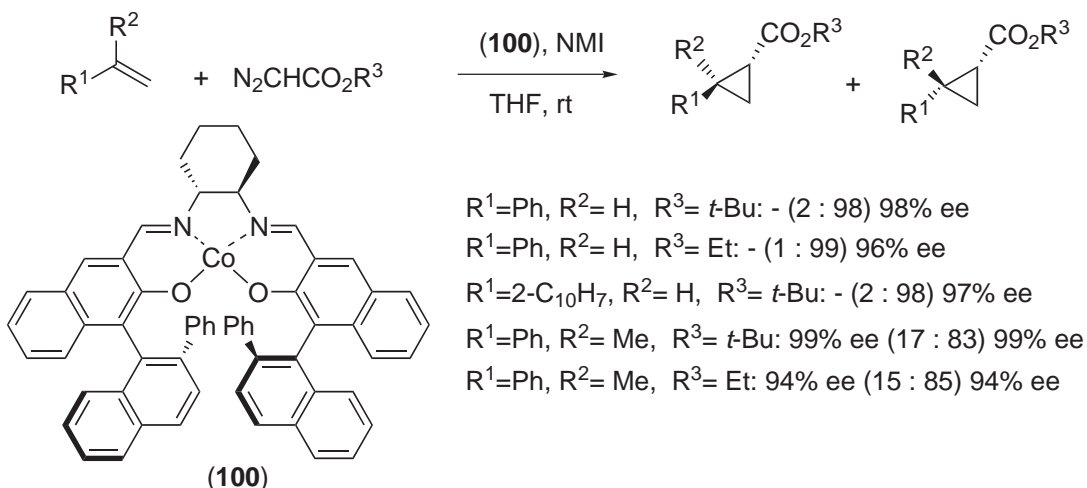
By contrast, Co^{II}(salen) (**100**), which has the same ligand as (**93**), catalyzes cyclopropanation with excellent *cis*- and enantioselectivity (Scheme 73).^{273,274} The addition of NMI also improves stereoselectivity. It is noteworthy, however, that the sense of enantioselection by (**100**) is opposite to that by (**93**). Reversal of the enantioselectivity has been attributed to differences in the substrate's approach to the carbenoid centers.²⁷⁴

9.4.7.2 Asymmetric Intramolecular Cyclopropanation

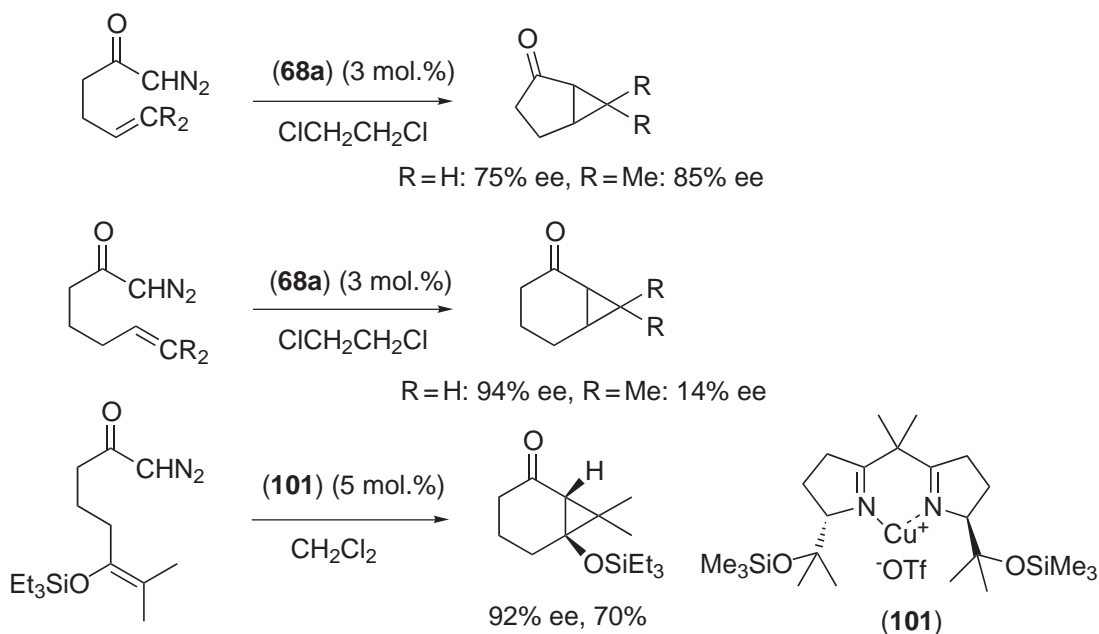
Intramolecular cyclopropanation is a useful method for construction of [n.1.0]-bicyclic compounds.^{17–21,225,275} As a matter of course, alkenyl and diazo groups of the substrate are connected by a linker and the transition-state conformation of intramolecular cyclization is influenced by the length and the shape of the linker. Thus, the enantioselectivity of the reaction often depends upon the substrates used. Use of a catalyst suitably designed for each reaction is essential for achieving high enantioselectivity.

9.4.7.2.1 Cu-catalyzed cyclopropanation

The Cu–semicorrin complex (**68a**) has been successfully used as the catalyst for cyclization of alkenyl diazoketones, though the reactions of some substrates showed modest enantioselectivity (Scheme 74).²⁷⁶ Shibasaki *et al.* have successfully used the cyclization of diazoketone with Cu–bis(oxazoline) (**101**) for the construction of the CD ring skeleton of phorbol.²⁷⁷



Scheme 73



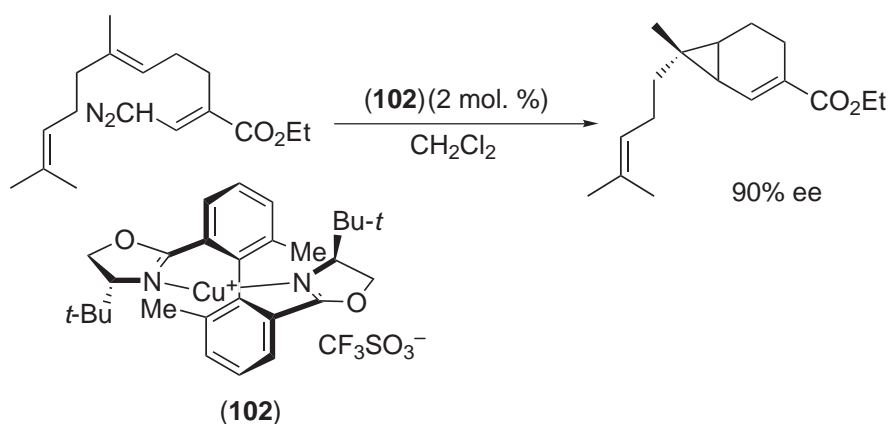
Scheme 74

For the cyclization of a vinylogue of diazo ester, the copper complex **(102)** bearing a biphenyl *bis*(oxazoline) ligand was found to be the catalyst of choice (Scheme 75).²⁷⁸

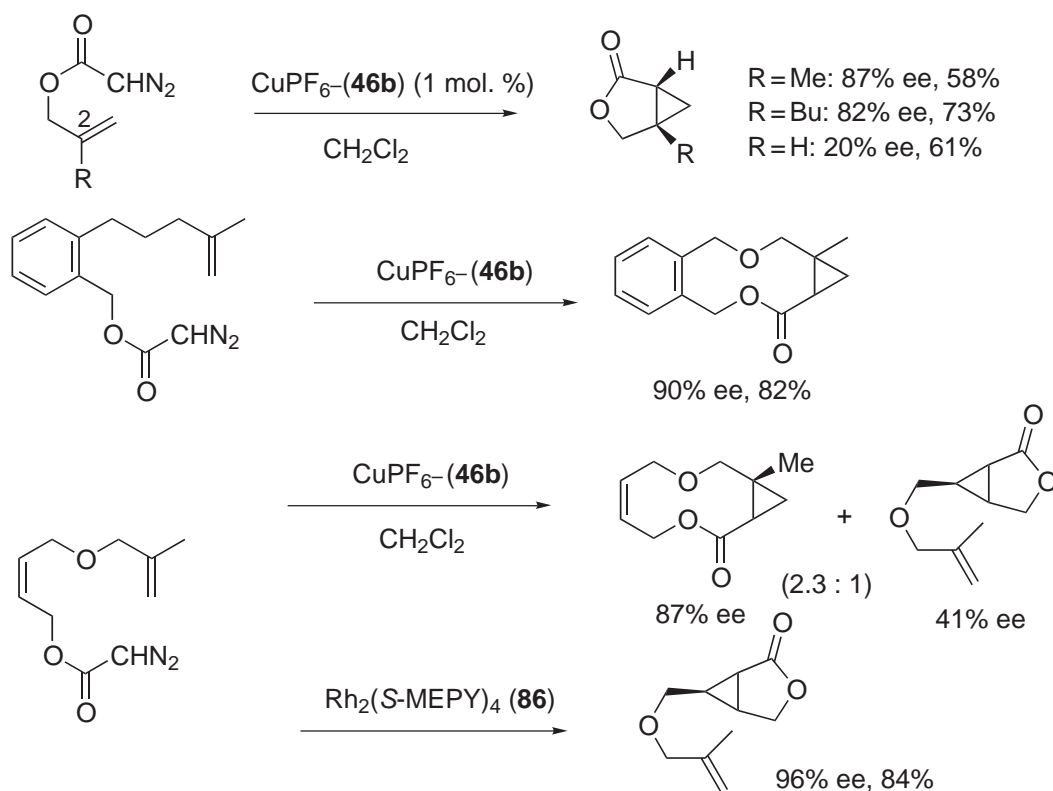
The cyclization of 2-alkenyl diazoacetates has also been examined with CuPF_6 –**(46b)** [*t*-butyloxazoline) ligand], but high enantioselectivity is observed only in the reactions of 2-substituted allyl diazoacetates (Scheme 76).²⁷⁹ Differing from the cyclization of 2-alkenyl diazoacetates, the macrocyclization of ω -alkenyl diazoacetate is effected well with CuPF_6 –**(46b)**.²⁸⁰ Macrocyclization seems to be favored by the catalyst of increasing electrophilicity, though the effect of the electrophilic nature of the ligand on enantioselectivity has not been examined.²⁸¹ It is noteworthy that, when the substrate has two double bonds, the reaction with CuPF_6 –**(46b)** preferentially gives the larger cyclic product, while the reaction with Rh_2 (*S*-MEPY)₄ **(86)** exclusively gives the smaller cyclic product.²⁸⁰

9.4.7.2.2 *Rh*-catalyzed cyclopropanation

Rh–carboxamide complexes **(86)**, **(103)**, and **(104)** introduced by Doyle *et al.* are by far the best catalysts for the cyclization of 2- and 3-alkenyl diazoesters and diazoamides, although the catalyst



Scheme 75



Scheme 76

of choice varies with the substrates used (Scheme 77).²⁸² Complex (86) has been successfully applied to the cyclization of *Z*- and trisubstituted allylic diazoacetate, while complex (103) is a better catalyst for the cyclization of *E*- and *gem*-disubstituted allylic diazoacetate.^{283–285} Rh–carboxamide complexes are also good catalysts for *N*-allyldiazoacetamides, but the catalyst of choice here again varies with the substrates used (Scheme 77).²⁸⁵ Furthermore, catalyst (104) can be successfully applied to the cyclization of allyl diazopropionate.²⁸⁶ Rh–carboxamide complexes are, however, less efficient as catalysts for the cyclization of alkenyl diazoketones.²⁸⁷ The low enantioselectivity has been attributed to the transition-state conformation of the cyclization, in which the alkenyl moiety approaches the carbenoid center from the side far from the enantiocontrolling ligand.

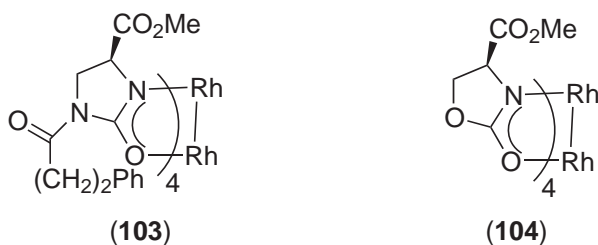
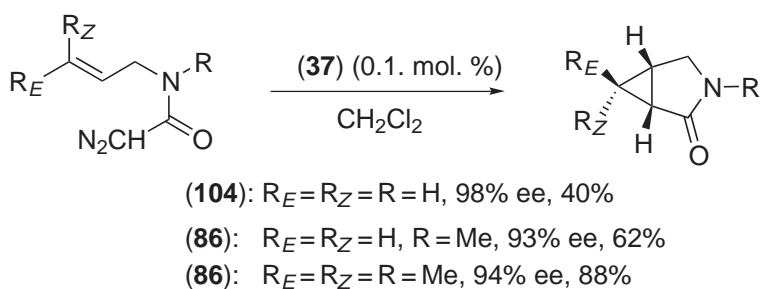
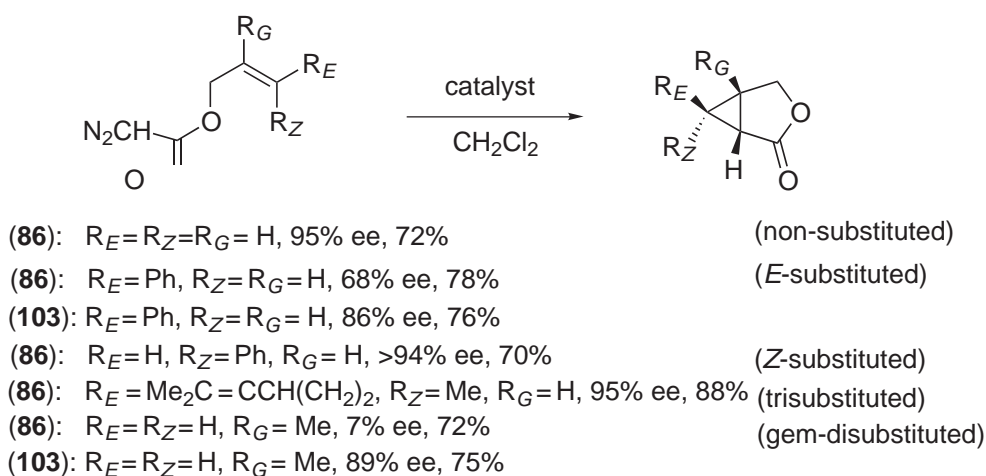
Pérez-Pietro *et al.* have introduced the dirhodium complex (105) with a unique *ortho*-metalated arylphosphine ligand. The complex is an efficient catalyst for the cyclization of alkenyl diazo ketones (Scheme 78).^{288,289}

Complex (85), an excellent catalyst for intermolecular cyclopropanation (*vide supra*), is also a good catalyst for the cyclization of allyl vinyl diazoacetates, though the enantioselectivity of the cyclization varies with the substrates used (Scheme 79).²⁹⁰

9.4.7.2.3 Ru-catalyzed cyclopropanation

The Ru(Pybox-*i*-Pr) complex (91), which induces high *trans*- and enantioselectivity in intermolecular cyclopropanation, has also been applied to the cyclization of allyl diazoacetates (Scheme 80).²⁵² The enantioselectivity observed depends largely on the substitution pattern of the allyl moiety.

The Ru–porphyrin complex (8) has also been used as a catalyst for the cyclization of allylic diazoacetates,²⁵⁸ albeit with limited success: only the cyclization of *E*-cinnamyl diazoacetate shows high enantioselectivity (Scheme 81). It is noteworthy that a carbenoid species prepared from allyl α -phenyl- α -diazoacetate and complex (8) has been isolated and subjected to X-ray diffraction analysis, though it does not undergo the desired cyclization. In the structure, the carbene plane lies almost halfway between the two adjacent Ru–N bonds.



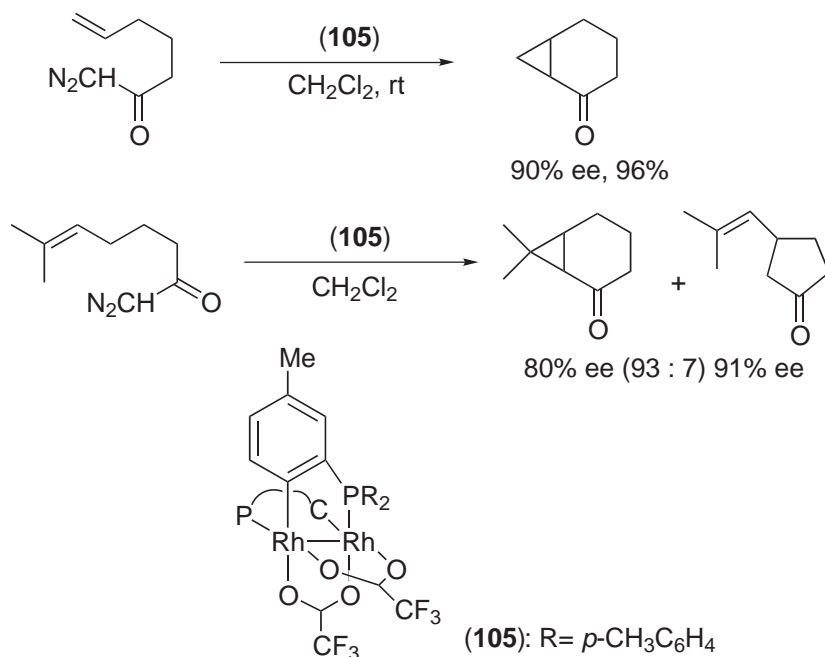
Scheme 77

Ru(salen)s complexes, **(106a)**, bearing a small 2''-substituent, and **(106b)**, lacking the 2''-substituent, catalyze the cyclization of *E*-2-alkenyl diazoacetates under photo-irradiation (Scheme 82).²⁹¹ Complex **(93)**, which is an efficient catalyst for intermolecular asymmetric cyclopropanation, is less efficient for this cyclization. It is noteworthy, however, that the complex **(93)** serves as a good catalyst for the cyclization of alkenyl diazoketones.²⁹² The effect of the presence or absence of the 2''-substituent has been considered to be related to the transition-state conformations of these cyclizations: the complex **(93)** bearing a bulky 2''-phenyl group is a good catalyst for the cyclization of alkenyl diazoketones, which has been proposed to occur at a distance from the enantiocontrolling ligand.²⁸⁷ Ru(salen)s catalyze the dimerization of diazoacetate. In order to avoid this undesired dimerization, slow addition of the substrates is required for these reactions.

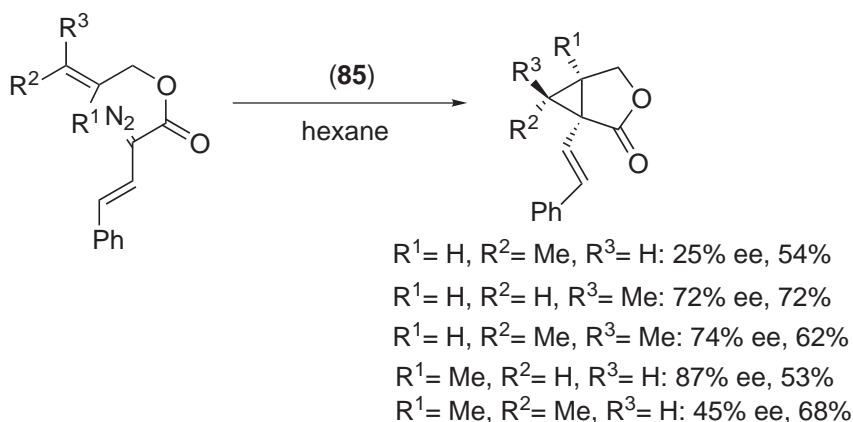
The Ru-Schiff base complex **(95)** with the *cis*- β structure serves as a good catalyst for the cyclization of *E*- and tri-substituted allyl diazoacetates (Scheme 83).²⁶²

9.4.7.2.4 Co-catalyzed cyclopropanation

Co(salen)s (**(107a)**) and (**(107b)**), which bear the same ligands as **(106a)** and **(106a)**, respectively, catalyze the cyclization of *E*- and tri-substituted allyl diazoacetates with good to high enantioselectivity.²⁹³



Scheme 78



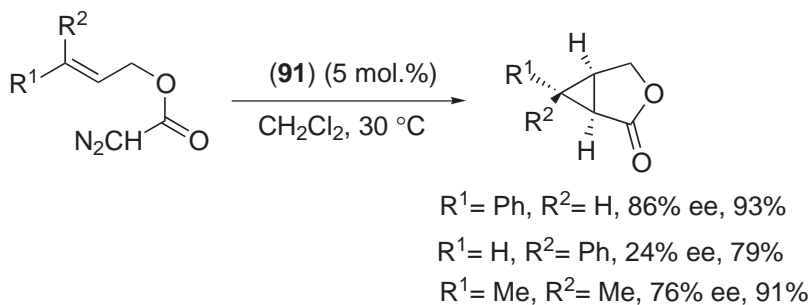
Scheme 79

Since Co(salen)s do not promote dimerization of diazoacetate, no high dilution condition is required for this reaction (Scheme 84).

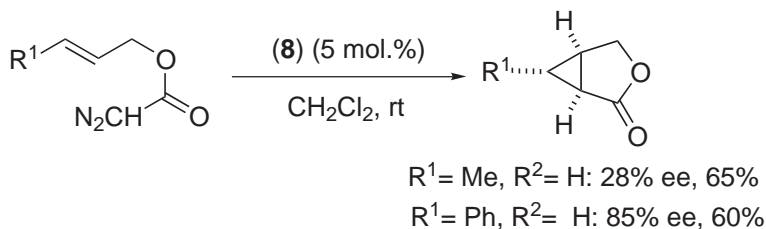
9.4.7.3 Mechanism of Cyclopropanation

The detailed mechanism of transition metal-catalyzed cyclopropanation using diazo compounds as a carbene source is still covered by clouds of controversy, but it is generally accepted that the reaction proceeds through metal-carbenoid complexes,^{17–21} and the valency of the metal ions (M) changes with carbenoid formation (Scheme 85).

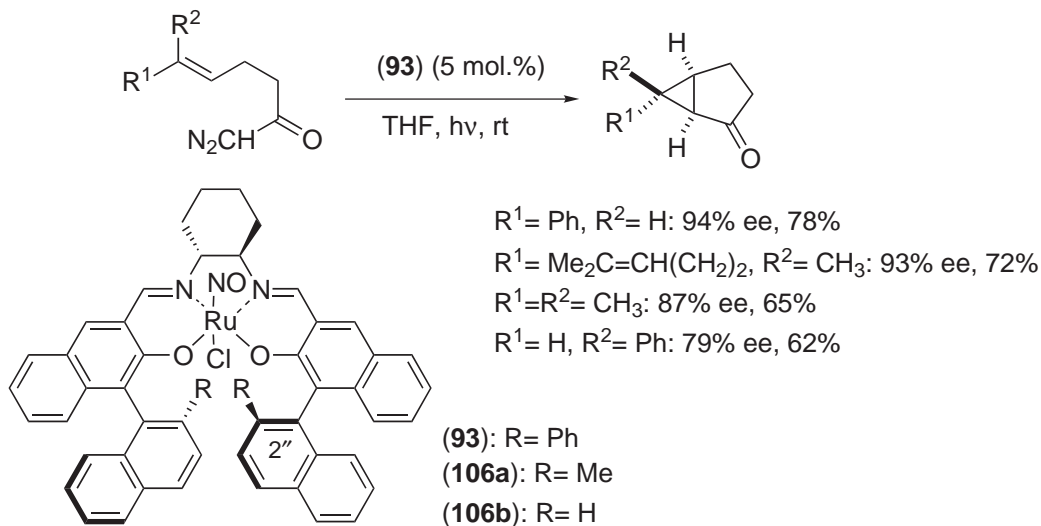
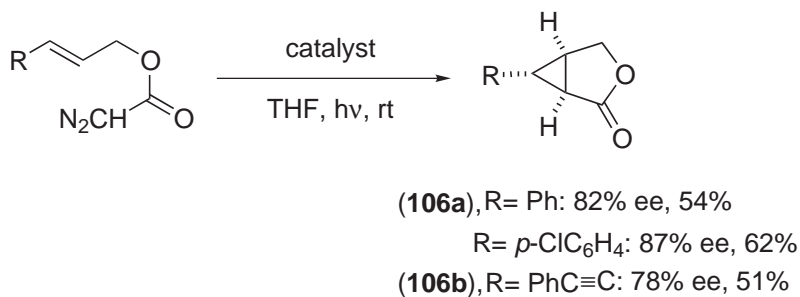
As described in Section 9.4.7.1, some Rh- and Ru-carbenoid intermediates that undergo cyclopropanation reactions have been spectroscopically identified.^{294,254} Less reactive metal-carbenoid intermediates (108) and (109) have been isolated and their structures have been determined unequivocally by X-ray analysis.^{255,258} The isolated carbenoid intermediate (108) undergoes cyclopropanation at high temperature (110 °C),²⁵⁵ and another intermediate (109) serves as the catalyst for asymmetric cyclopropanation (Figure 11).²⁵⁸



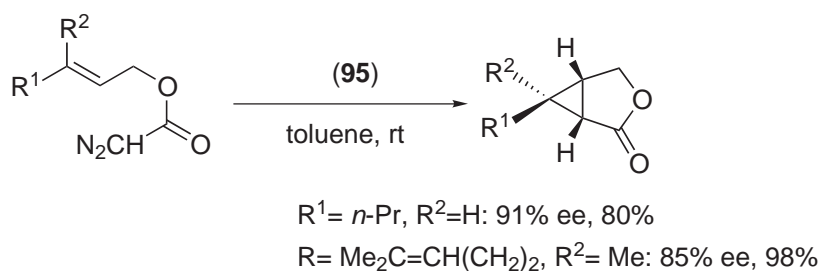
Scheme 80



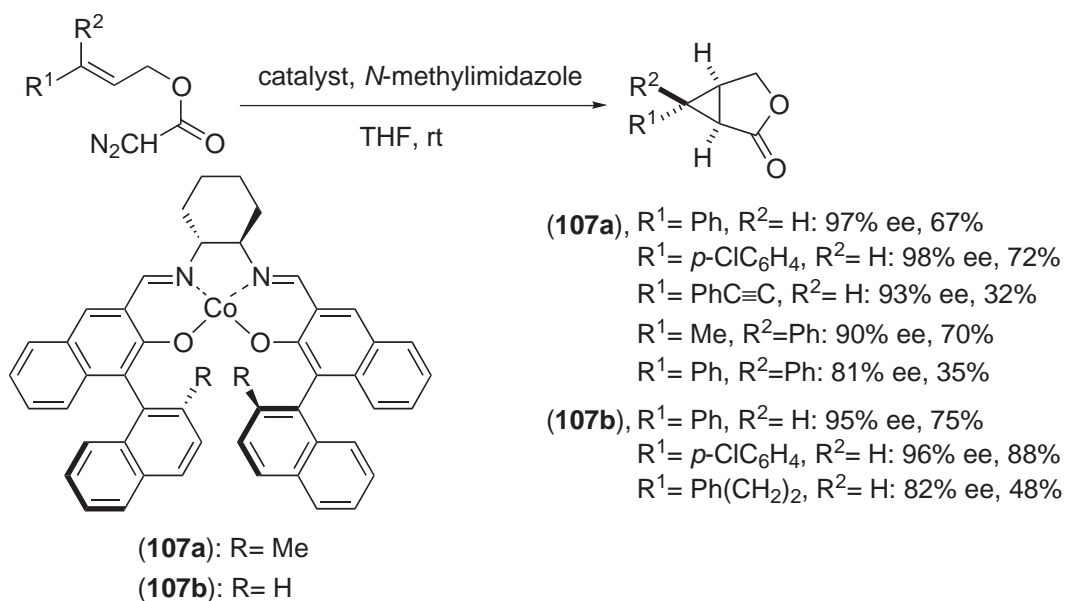
Scheme 81



Scheme 82

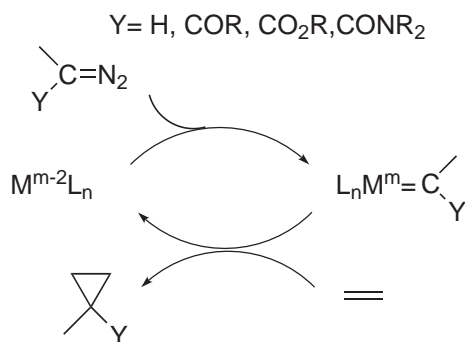


Scheme 83



Scheme 84

The metal-carbenoid intermediates, especially ones derived from α -diazocarbonyl compounds, are electrophilic, and electron-rich olefins in general react more easily with the carbenoid intermediates than electron-deficient olefins. For the interaction of metal-carbenoid and olefin, three different mechanisms have been proposed, based on the stereochemistry of the reactions and the reactivity of the substrates (Figure 12):^{17–21} (i) a nonconcerted, two-step process via a metallacyclobutane,^{226,264}



Scheme 85

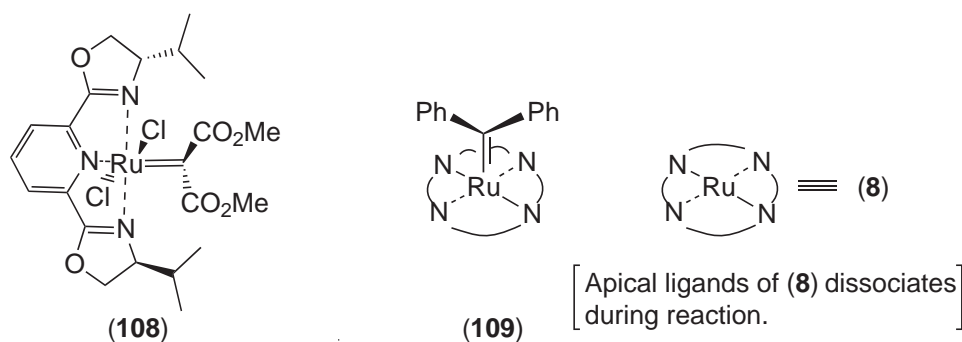


Figure 11 X-ray structures of metal-carbenoid species.

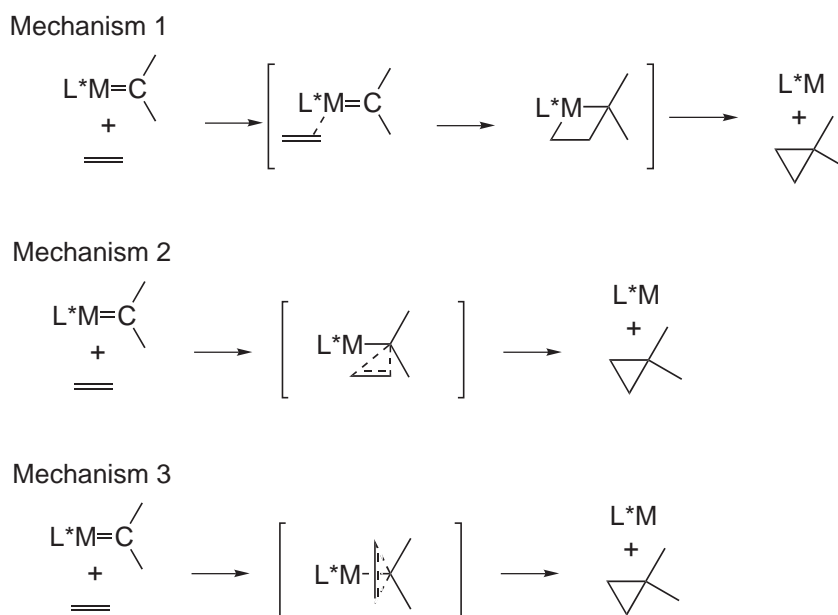


Figure 12 Proposed mechanisms for metal-mediated cyclopropanation.

(ii) a concerted process with the olefin's approach parallel to the metal–carbene bond,^{228,232,248,252,272} and (iii) a concerted process with the olefin's approach perpendicular or quasi-perpendicular to the metal–carbene bond.^{241,249,260,268,274,283–285} The mechanism of each reaction seems to depend on the nature of metal center, the electronic nature and the architecture of the ligand, and the substrates used.^{17–21} For example, the stereochemistry of inter- and intramolecular cyclopropanation reactions using **(8)** as the catalyst has been explained by assuming parallel and quasi-perpendicular approaches, respectively.²⁵⁸

Based on these mechanisms and ligand structures, various transition-state models to explain the stereochemistry of asymmetric cyclopropanation reactions have been proposed. For details, see the reviews^{17–21} and the references cited for **Figure 12**.

Recently, several mechanistic studies have been performed by means of calculations based on density functional theory.^{295–297} Pfaltz's model²²⁸ proposed for asymmetric cyclopropanation using copper-semicorrin or -bis(oxazolines) complex has been supported by calculation.²⁹⁵ Another calculation also supports the parallel approach.²⁹⁶

9.4.8 CONCLUSION

In this chapter, metal-mediated asymmetric oxygen-, nitrogen-, and carbon-atom transfer reactions were described. The substrates were limited to olefins. Owing to limited space, examples of the reactions were collected with the priority given to enantioselectivity, except for some germinal

reports. Reactions of low enantioselectivity were mostly omitted, even though they are important from the historical or mechanistic viewpoint. Asymmetric oxygen-, nitrogen-, and carbon-atom insertion reactions to C—H or C—C bonds are sister reactions to their transfer reactions to olefins. Naturally, some of the catalysts discussed in this chapter have been successfully applied to asymmetric C—H insertion reactions. For those who are interested in such reactions, see the appropriate books^{1,2} and special reviews.^{17–21,300}

9.4.9 REFERENCES

1. Trost, B. M., Ed.; *Comprehensive Organic Synthesis*; Pergamon: Oxford, UK, 1991; Vols. 4 and 7.
2. Helmchen, G.; Hoffmann, R. W.; Mulzer, J.; Schaumann, E., Eds.; *Stereoselective Synthesis*; Thieme: Stuttgart, Germany, 1996; Vols. 5 and 8.
3. Brunner, H.; Zettlmeier, W. *Handbook of Enantioselective Catalysis with Transition Metal Compounds*; VCH: Weinheim, Germany, 1993; Vols. I and II.
4. Katsuki, T.; Martin, V. S. *Org. React.* **1996**, *48*, 1–299.
5. Johnson, R. A.; Sharpless, K. B. In *Catalytic Asymmetric Synthesis*, 2nd ed.; Ojima, I. Ed.; Wiley-VCH: New York, 2000; Chapter 6A, pp 231–280.
6. Katsuki, T. In *Catalytic Asymmetric Synthesis*, 2nd ed.; Ojima, I. Ed.; Wiley-VCH: New York, 2000; Chapter 6B, pp 287–325.
7. Katsuki, T. In *Comprehensive Asymmetric Catalysis*; Jacobsen, E. N., Pfaltz, A., Yamamoto, H., Eds.; Springer: Berlin, 1999; Vol. II, Chapter 18.1, pp 621–648.
8. Jacobsen, E. N. In *Comprehensive Asymmetric Catalysis*; Jacobsen, E. N., Pfaltz, A., Yamamoto, H., Eds.; Springer: Berlin, 1999; Vol. II, Chapter 18.2, pp 649–677.
9. Johnson, R. A.; Sharpless, K. B. In *Catalytic Asymmetric Synthesis*, 2nd ed.; Ojima, I., Ed.; Wiley-VCH: New York, 2000; Chapter 6D, pp 357–398.
10. Bolm, C.; Hildebrand, J. P.; Muniz, K. In *Catalytic Asymmetric Synthesis*, 2nd ed.; Ojima, I., Ed.; Wiley-VCH, New York, 2000; Chapter 6E, pp 399–428.
11. Markó, I. E.; Svendsen, J. S. In *Comprehensive Asymmetric Catalysis*, Jacobsen, E. N.; Pfaltz, A.; Yamamoto, H., Ed.; Springer: Berlin, 1999; Vol. II, Chapter 20, pp 713–787.
12. Kolb, H. C.; Sharpless, K. B. In *Transition Metals for Organic Synthesis*, Beller, M., Bolm, C., Eds.; Wiley-VCH: Weinheim, Germany, 1998; Vol. 2, Chapter 2.5, pp 219–242.
13. Kolb, H. C.; Sharpless, K. B. In *Transition Metals for Organic Synthesis*, Beller, M., Bolm, C., Eds.; Wiley-VCH: Weinheim, Germany, 1998; Vol. 2, Chapter 2.6, pp 243–260.
14. Schlingloff, G.; Sharpless, K. B. In *Asymmetric Oxidation Reactions*, Katsuki, T., Ed.; Oxford University Press: Oxford, UK, 2001; Chapter 2.6, pp 104–114.
15. Faul, M. M.; Evans, D. A. In *Asymmetric Oxidation Reactions*, Katsuki, T., Ed.; Oxford University Press: Oxford, UK, 2001; Chapter 2.7, pp 115–128.
16. Jacobsen, E. N. In *Comprehensive Asymmetric Catalysis*, Jacobsen, E. N.; Pfaltz, A.; Yamamoto, H., Ed.; Springer: Berlin, 1999; Vol. II, Chapter 17, pp 607–618.
17. Pfaltz, A. In *Comprehensive Asymmetric Catalysis*, Jacobsen, E. N.; Pfaltz, A.; Yamamoto, H., Ed.; Springer: Berlin, 1999; Vol. II, Chapter 16.1, pp 513–538.
18. Lydon, K. M.; McKervy, M. N. In *Comprehensive Asymmetric Catalysis*; Jacobsen, E. N.; Pfaltz, A.; Yamamoto, H., Ed.; Springer: Berlin, 1999; Vol. II, Chapter 16.2, pp 539–580.
19. Charette, A. B.; Lebel, H. In *Comprehensive Asymmetric Catalysis*, Jacobsen, E. N.; Pfaltz, A.; Yamamoto, H., Ed.; Springer: Berlin, 1999; Vol. II, Chapter 16.3, pp 581–603.
20. Doyle, M. P. In *Catalytic Asymmetric Synthesis*, 2nd ed.; Ojima, I., Ed.; Wiley-VCH: New York, 2000; Chapter 5, pp 191–228.
21. Doyle, M. P.; McKervy, M. A.; Ye, T. *Modern Catalytic Methods for Organic Synthesis with Diazo Compounds*; Wiley: New York, 1998.
22. Sharpless, K. B.; Verhoeven, T. R. *Aldrichim. Acta* **1979**, *12*, 63–74.
23. Sheng, M. N.; Zajack, J. G. *J. Org. Chem.* **1970**, *35*, 1839–1843.
24. Sharpless, K. B.; Michaelson, R. C. *J. Am. Chem. Soc.* **1973**, *95*, 6136–6137.
25. Yamada, S.; Mashiko, M.; Terashima, S. *J. Am. Chem. Soc.* **1977**, *99*, 1988–1990.
26. Michaelson, R. C.; Parelmo, R. E.; Sharpless, K. B. *J. Am. Chem. Soc.* **1977**, *99*, 1990–1992.
27. Katsuki, T.; Sharpless, K. B. *J. Am. Chem. Soc.* **1980**, *102*, 5974–5976.
28. Schweiter, M. J.; Sharpless, K. B. *Tetrahedron Lett.*, **1985**, *26*, 2543.
29. Gao, Y.; Hanson, R. M.; Klunder, J. M.; Ko, S. Y.; Masamune, H.; Sharpless, K. B. *J. Am. Chem. Soc.* **1987**, *109*, 5765–5780.
30. Williams, I. D.; Pederson, S. F.; Sharpless, K. B.; Lippard, S. *J. Am. Chem. Soc.* **1984**, *106*, 6430–6431.
31. Sharpless, K. B. *Chem. Scr.* **1987**, *27*, 521–524.
32. Pederson, S. F.; Dewan, J. C.; Eckman, R. R.; Sharpless, K. B. *J. Am. Chem. Soc.* **1987**, *109*, 1279–1282.
33. Puchot, C.; Samuel, O.; Dunach, E.; Zhao, S.; Agami, C.; Kagan, H. B. *J. Am. Chem. Soc.* **1986**, *108*, 2353–2357.
34. Katsuki, T. *Kagaku-zokan* **1982**, *96*, 105–112.
35. Katsuki, T. *J. Synth. Org. Chem. Jpn.* **1991**, *49*, 340–345.
36. Yamamoto, K.; Ando, H.; Shuetake, T.; Chikamatsu, H. *J. Chem. Soc., Chem. Commun.* **1989**, 754–755.
37. Martin, V. S.; Woodard, S. S.; Katsuki, T.; Yamada, Y.; Ikeda, M.; Sharpless, K. B. *J. Am. Chem. Soc.*, **1981**, *103*, 6237–6240.
38. Choudary, B. M.; Valli, V. L. K.; Durga Prasad, A. *J. Chem. Soc., Chem. Commun.* **1990**, 1186–1187.
39. Meunier, D.; Piechaczyk, A.; Mallmann, A. *Angew. Chem., Int. Ed. Engl.* **1999**, *38*, 3540–3542.
40. Rossiter, B. E.; Sharpless, K. B. *J. Org. Chem.* **1984**, *49*, 3707–3711.

41. Ikegami, S.; Katsuki, T.; Yamaguchi, M. *Chem. Lett.* **1987**, 83–84.
42. Spivey, A. C.; Woodhead, S. J.; Weston, M.; Andrews, B. I. *Angew. Chem., Int. Ed.* **2001**, *40*, 769–771.
43. Murase, N.; Hoshino, Y.; Oishi, M.; Yamamoto, H. *J. Org. Chem.* **1999**, *64*, 338–339.
44. Hoshino, Y.; Murase, N.; Oishi, M.; Yamamoto, H. *Bull. Chem. Soc. Jpn.* **2000**, *73*, 1653–1658.
45. Hoshino, Y.; Yamamoto, H. *J. Am. Chem. Soc.* **2000**, *122*, 10452–10453.
46. Groves, J. T. *Adv. Inorg. Biochem.* **1979**, 119–145.
47. Ullrich, V. *Top. Curr. Chem.* **1979**, *83*, 67–104.
48. Groves, J. T.; Nemo, T. E.; Myers, R. S. *J. Am. Chem. Soc.*, **1979**, *101*, 1032–1033.
49. Groves, J. T.; Nemo, T. E. *J. Am. Chem. Soc.*, **1983**, *105*, 5786–5791.
50. Groves, J. T.; Myers, R. S. *J. Am. Chem. Soc.*, **1983**, *105*, 5791–5796.
51. O'Malley, S.; Kodadek, T. *J. Am. Chem. Soc.* **1889**, *111*, 9116–9117.
52. Halterman, R. L.; Jan, S. T. *J. Org. Chem.* **1991**, *56*, 5253–5254.
53. Lai, T. S.; Kwong, H. L.; Zhang, R.; Che, C. M. *J. Chem. Soc., Dalton Trans.* **1998**, 3559–3564.
54. Lai, T. S.; Zhang, R.; Cheung, K. K.; Kwong, H. L.; Che, C. M. *Chem. Commun.* **1998**, 1583–1584.
55. Zhang, R.; Yu, W. Y.; Wong, K. Y.; Che, C. H. *J. Org. Chem.* **2001**, *66*, 8145–8153.
56. Pérollier, C.; Pécaut, J.; Ramasseul, R.; Marchon, J.-C. *Inorg. Chem.* **1999**, *38*, 3758–3759.
57. Barry, J. F.; Campbell, L.; Smith, D. W.; Kodadek, T. *Tetrahedron* **1997**, *23*, 7753–7776.
58. Naruta, Y.; Tani, F.; Maruyama, K. *Chem. Lett.* **1989**, 1269–1272.
59. Naruta, Y.; Tani, F.; Ishihara, N.; Maruyama, K. *J. Am. Chem. Soc.* **1991**, *113*, 6865–6872.
60. Collman, J. P.; Wang, Z.; Straumanis, A.; Quelquejeu, M. *J. Am. Chem. Soc.* **1999**, *121*, 460–461.
61. Gross, Z.; Ini, S. *Inorg. Chem.* **1999**, *38*, 1446–1449.
62. Gross, Z.; Ini, S. *J. Org. Chem.* **1997**, *62*, 5514–5521.
63. Mansuy, D.; Battioni, P.; Renaud, J.-P.; Guerin, P. *J. Chem. Soc., Chem. Commun.* **1985**, 155–156.
64. Groves, J. T.; Viski, P. *J. Org. Chem.* **1990**, *55*, 3628–3634.
65. Konishi, K.; Oda, K.; Nishida, K.; Aida, T.; Inoue, S. *J. Am. Chem. Soc.*, **1992**, *114*, 1313–1317.
66. Collman, J. P.; Lee, V. J.; Kellen-Yuen, C. J.; Zhang, X.; Ibers, J. A.; Brauman, J. I. *J. Am. Chem. Soc.*, **1995**, *117*, 692–703.
67. Collman, J. P.; Lee, V. J.; Zhang, X.; Ibers, J. A.; Braumann, J. I. *J. Am. Chem. Soc.*, **1993**, *115*, 3834–3835.
68. Higuchi, T.; Ohtake, H.; Hirobe, M. *Tetrahedron Lett.* **1989**, *30*, 6545–6548.
69. Groves, J. T.; Quinn, R. *J. Am. Chem. Soc.*, **1985**, *107*, 5790–5792.
70. Collman, J. P.; Chien, A. S.; Eberspacher, T. A.; Brauman, J. I. *J. Am. Chem. Soc.* **2000**, *122*, 11098–11100.
71. Samsel, E. G.; Srinivasan, K.; Kochi, J. K. *J. Am. Chem. Soc.*, **1985**, *107*, 7606–7617.
72. Srinivasan, K.; Michaud, P.; Kochi, J. K. *J. Am. Chem. Soc.* **1986**, *108*, 2309–2320.
73. Feichtinger, D.; Plattner, D. A. *Angew. Chem., Int. Ed. Engl.* **1997**, *36*, 1718–1719.
74. Tanaka, H.; Kuroboshi, M.; Takeda, H.; Kanda, H.; Torii, S. *J. Electroanal. Chem.* **2001**, *507*, 75–81.
75. Hashihayata, T.; Punniyamurthy, T.; Irie, R.; Katsuki, T.; Akita, M.; Moro-oka, Y. *Tetrahedron* **1999**, *55*, 14599–14610.
76. Katsuki, T. *Adv. Synth. Catal.* **2002**, *34*, 131–147.
77. Rispens, M. T.; Meetsma, A.; Feringa, B. L. *Recl. Trav. Chim. Pays-Bas*, **1994**, *113*, 413–415.
78. Pospisil, P. J.; Carsten, D. H.; Jacobsen, E. N. *Chem. Eur. J.* **1996**, *2*, 974–980.
79. Finney, N. S.; Pospisil, P. J.; Chan, S.; Palucki, M.; Konsler, R. G.; Hansen, K. B.; Jacobsen, E. N. *Angew. Chem., Int. Ed. Engl.* **1997**, *36*, 1720–1723.
80. Strassner, T.; Houk, K. N. *Org. Lett.* **1999**, *3*, 419–421.
81. Jacobsen, H.; Cavallo, L. *Chem. Eur. J.* **2001**, *7*, 800–807.
82. El-Bahraoui, J.; Wiest, O.; Feichtinger, D.; Plattner, D. A. *Angew. Chem., Int. Ed. Engl.* **2001**, *40*, 2073–2076.
83. Zhang, W.; Loebach, J. L.; Wilson, S. R.; Jacobsen, E. N. *J. Am. Chem. Soc.* **1990**, *112*, 2801–2803.
84. Irie, R.; Noda, K.; Ito, Y.; Matsumoto, N.; Katsuki, T. *Tetrahedron Lett.* **1990**, *31*, 7345–7348.
85. Nakajima, K.; Kojima, M.; Fujita, J. *Chem. Lett.* **1986**, 1483–1486.
86. Jacobsen, E. N.; Zhang, W.; Muci, A. R.; Ecker, J. R.; Deng, Li. *J. Am. Chem. Soc.* **1991**, *113*, 7063–7064.
87. Chang, S.; Heid, R. M.; Jacobsen, E. N. *Tetrahedron Lett.* **1994**, *35*, 669–672.
88. Hosoya, N.; Irie, R.; Katsuki, T. *Synlett* **1993**, 261–263.
89. Katsuki, T. *J. Mol. Chem. A: Chem.* **1996**, *113*, 87–107.
90. Jacobsen, E. N.; Zhang, W.; Güler, M. L. *J. Am. Chem. Soc.* **1991**, *113*, 6703–6704.
91. Palucki, M.; Finney, N. S.; Pospisil, P. J.; Güler, M. L.; Ishida, T.; Jacobsen, E. N. *J. Am. Chem. Soc.* **1998**, *120*, 948–954.
92. Pozzi, G.; Cavazzini, M.; Cinato, F.; Montanari, F.; Quici, S. *Eur. J. Org. Chem.* **1999**, 1947–1955.
93. Sennayake, C. H.; Smith, G. B.; Ryan, K. M.; Fredenburgh, L. E.; Liu, J.; Roberts, F. E.; Hughes, D. L.; Larsen, R. D.; Verhoeven, T. R.; Reider, P. J. *Tetrahedron Lett.* **1996**, *37*, 3271–3274.
94. Irie, R.; Ito, Y.; Katsuki, T. *Synlett* **1991**, 265–266.
95. Irie, R.; Noda, K.; Ito, Y.; Matsumoto, N.; Katsuki, T. *Tetrahedron: Asymmetry* **1991**, *2*, 481–494.
96. Hashihayata, T.; Ito, Y.; Katsuki, T. *Synlett* **1996**, 1079–1081.
97. Miura, K.; Katsuki, T. *Synlett* **1999**, 783–785.
98. Hosoya, N.; Hatayama, A.; Yanai, K.; Fujii, H.; Irie, R.; Katsuki, T. *Synlett* **1993**, 641–645.
99. Kuroki, T.; Hamada, T.; Katsuki, T. *Chem. Lett.* **1995** (5), 339–340.
100. Houk, K. N.; DeMello, N. C.; Condroski, C.; Fennen, J.; Kasuga, T. In *Electronic Conference on Heterocyclic Chemistry, ECHT96*; Royal Society of Chemistry: London, June 24–July 22, 1996; Rzepa, H. S.; Snyder, J. P.; Leach, C., Eds; <http://www.ch.ic.ac.uk/ectoc/>.
101. Sasaki, H.; Irie, R.; Hamada, T.; Suzuki, K.; Katsuki, T. *Tetrahedron* **1994**, *50*, 11827–11838.
102. Fukuda, T.; Irie, R.; Katsuki, T. *Synlett* **1995**, 197–198.
103. Ahn, K. H.; Park, S. W.; Choi, S.; Kim, H. J.; Moon, C. *J. Tetrahedron Lett.* **2001**, *42*, 2485–2488.
104. Hamada, T.; Fukuda, T.; Imanishi, H.; Katsuki, T. *Tetrahedron* **1996**, *52*, 515–530.
105. Linde, Ch.; Akermark, B.; Norrby, P.-O.; Svensson, M. *J. Am. Chem. Soc.* **1999**, *121*, 5083–5084.
106. Abashkin, Y. G.; Collins, J. R.; Burt, S. K. *Inorg. Chem.* **2001**, *40*, 4040–4048.

107. Lee, N. H.; Jacobsen, E. N. *Tetrahedron Lett.* **1991**, 32, 6533–6536.
108. Palucki, M.; Pospicil, P. J.; Zhang, W.; Jacobsen, E. N. *J. Am. Chem. Soc.* **1994**, 116, 9333–9334.
109. Chang, S.; Galvin, J. M.; Jacobsen, E. N. *J. Am. Chem. Soc.*, **1994**, 116, 6937–6938.
110. Adams, W.; Roschmann, K. J.; Saha-Möller, C. R. *Eur. J. Org. Chem.* **2000**, 3519–3521.
111. Ryan, K. M.; Bousquet, C.; Gilheany, D. G. *Tetrahedron Lett.* **1999**, 40, 3613–3616.
112. O'Mahony, C. P.; McGarrigle, E. M.; Renehan, M. F.; Ryan, K. M.; Kerrigan, N. J.; Bousquet, C.; Gilheany, D. G. *Org. Lett.* **2001**, 3, 3435–3438.
113. Nishikori, H.; Ohta, C.; Katsuki, T. *Synlett* **2000**, 1557–1560.
114. Kureshy, R. I.; Khan, N. H.; Abdi, S. H. R. *J. Mol. Cat. A: Chem.* **1995**, 96, 117–122.
115. End, N.; Pfaltz, A. *Chem. Commun.* **1998**, 589–590.
116. Takeda, T.; Irie, R.; Shinoda, Y.; Katsuki, T. *Synlett* **1999**, 1157–1159.
117. Nakata, K.; Takeda, T.; Mihara, J.; Hamada, T.; Irie, R.; Katsuki, T. *Chem. Eur. J.*, **2001**, 7, 3776–3782.
118. Takeda, T.; Irie, R.; Katsuki, T. *Synlett* **1999**, 1166–1168.
119. Takai, T.; Hata, E.; Yamada, T.; Mukaiyama, T. *Bull. Chem. Soc. Jpn.* **1991**, 64, 2513–2518.
120. Yamada, T.; Imagawa, K.; Nagata, T.; Mukaiyama, T. *Chem. Lett.* **1992**, 2231–2234.
121. Imagawa, K.; Nagata, T.; Yamada, T.; Mukaiyama, T. *Chem. Lett.* **1994**, 527–530.
122. Nagata, T.; Imagawa, K.; Yamada, T.; Mukaiyama, T. *Bull. Chem. Soc. Jpn.* **1995**, 68, 1455–1465.
123. Mikame, D.; Hamada, T.; Irie, R.; Katsuki, T. *Synlett* **1995**, 827–828.
124. Garcia, M.-A.; Brun, P. *Synlett* **1996**, 1049–1050.
125. Porter, M.; Skidmore, J. *Chem. Commun.* **2000**, 1215–1225.
126. Enders, D.; Zhu, J.; Raabe, G. *Angew. Chemie. Int. Ed. Eng.* **1996**, 35, 1725–1728.
127. Bougachi, M.; Watanabe, S.; Arai, T.; Sasai, H.; Shibasaki, M. *J. Am. Chem. Soc.* **1997**, 119, 2329–2330.
128. Yamada, K.; Arai, T.; Sasai, H.; Shibasaki, M. *J. Org. Chem.* **1998**, 63, 3666–3672.
129. Watanabe, S.; Kobayashi, Y.; Arai, T.; Sasai, H.; Bougachi, M.; Shibasaki, M. *Tetrahedron Lett.* **1998**, 39, 7353–7356.
130. Daikai, K.; Kamaura, M.; Inanaga, J. *Tetrahedron Lett.* **1998**, 39, 7321–7322.
131. Nemoto, T.; Ohshima, T.; Yamaguchi, K.; Shibasaki, M. *J. Am. Chem. Soc.*, **2001**, 123, 2725–2732.
132. Watanabe, S.; Arai, T.; Sasai, H.; Bougachi, M.; Shibasaki, M. *J. Org. Chem.* **1998**, 63, 8090–8091.
133. Jacobsen, E. N.; Deng, L.; Furukawa, Y.; Martinez, L. E. *Tetrahedron* **1994**, 50, 4323–4334.
134. Nemoto, T.; Ohshima, T.; Shibasaki, M. *J. Am. Chem. Soc.* **2001**, 123, 9474–9475.
135. Reddeppa, R. D.; Thornton, E. R. *J. Chem. Soc., Chem. Commun.* **1992**, 172–173.
136. Chang, S.; Heid, R. M.; Jacobsen, E. N. *Tetrahedron Lett.* **1994**, 35, 669–672.
137. Adam, W.; Fell, R. T.; Stegmann, V. R.; Saha-Möller, C. R. *J. Am. Chem. Soc.* **1998**, 120, 708–714.
138. Fukuda, T.; Katsuki, T. *Tetrahedron Lett.* **1996**, 37, 4389–4392.
139. Hashiyama, T.; Morikawa, K.; Sharpless, K. B. *J. Org. Chem.* **1992**, 57, 5067–5068.
140. Upadhyya, T. T.; Gurunath, S.; Sudalai, A. *Tetrahedron: Asymmetry* **1999**, 10, 2899–2904.
141. Groves, J. T.; Takahashi, T. *J. Am. Chem. Soc.* **1983**, 105, 2073–2074.
142. Du Bois, J.; Hong, J.; Carreira, E. M.; Day, M. W. *J. Am. Chem. Soc.* **1996**, 118, 915–916.
143. Minakata, S.; Ando, T.; Nishimura, M.; Ryu, I.; Komatsu, M. *Angew. Chem., Int. Ed. Engl.* **1998**, 37, 3392–3394.
144. Ho, C. M.; Lau, T. C.; Kwong, H. L.; Wong, W. T. *J. Chem. Soc., Dalton, Trans.* **1999**, 2411–2413.
145. Mansuy, D.; Mahy, J.-P.; Dcureault, A.; Bedi, G.; Battioni, P. *J. Chem. Soc., Chem. Commun.* **1984**, 1161–1163.
146. Mahy, J.-P.; Bedi, G.; Battioni, P.; Mansuy, D. *J. Chem. Soc., Perkin, Trans. 2* **1988**, 1517–1524.
147. Breslow, R.; Gellman, S. H. *J. Chem. Soc., Chem. Commun.* **1982**, 1400–1401.
148. Evans, D. A.; Faul, M. M.; Bilodeau, M. T. *J. Org. Chem.* **1991**, 56, 6744–6746.
149. Evans, D. A.; Woerpel, K. A.; Hinman, N. M.; Faul, M. M. *J. Am. Chem. Soc.* **1991**, 113, 726–728.
150. Evans, D. A.; Faul, M. M.; Bilodeau, M. T.; Anderson, B. A.; Barnes, D. M. *J. Am. Chem. Soc.* **1993**, 115, 5328–5329.
151. Södergren, M. J.; Alonso, D. A.; Andersson, P. G. *Tetrahedron: Asymmetry* **1997**, 8, 3563–3565.
152. Lowenthal, R. E.; Masamune, S. *Tetrahedron Lett.* **1991**, 32, 7373–7376.
153. Tayler, S.; Gullick, J.; Memorn, P.; Bethell, D.; Page, P. C. B.; Hancock, F. E.; King, F.; Hutchings, G. J. *J. Chem. Soc., Perkin Trans. 2* **2001**, 1714–1723.
154. Li, Z.; Conser, K. R.; Jacobsen, E. N. *J. Am. Chem. Soc.* **1993**, 115, 5326–5327.
155. Li, Z.; Quan, R. W.; Jacobsen, E. N. *J. Am. Chem. Soc.* **1995**, 117, 5889–5890.
156. Brandt, P.; Södergren, M. J.; Andersson, P. G.; Norrby, P.-O. *J. Am. Chem. Soc.* **2000**, 122, 8013–8020.
157. Sanders, C. J.; Gillespie, K. M.; Bell, D.; Scott, P. *J. Am. Chem. Soc.* **2000**, 122, 7132–7133.
158. Gillespie, K. M.; Crust, E. J.; Deeth, R. J.; Scott, P. *Chem. Commun.* **2001**, 785–786.
159. Cho, D. J.; Jeon, S. J.; Kim, H. S.; Cho, C. S.; Shim, S. C.; Kim, T. J. *Tetrahedron: Asymmetry* **1999**, 10, 3833–3848.
160. O'Connor, K. J.; Wey, S. J.; Burrows, C. J. *Tetrahedron Lett.* **1992**, 33, 1001–1004.
161. Noda, K.; Hosoya, N.; Irie, R.; Ito, Y.; Katsuki, T. *Synlett* **1993**, 469–471.
162. Nishikori, H.; Katsuki, T. *Tetrahedron Lett.* **1996**, 37, 9245–9248.
163. Liang, J. L.; Yu, X. Q.; Che, C. M. *Chem. Commun.*, **2002**, 124–125.
164. Lai, T. S.; Kwong, H. L.; Che, C. M.; Peng, S. M. *Chem. Commun.* **1997**, 2373–2374.
165. Criegee, R.; Marchant, B.; Wannowius, H. *Liebig Ann. Chem.* **1942**, 550, 99–133.
166. Criegee, R. *Angew. Chem.* **1938**, 51, 519–520.
167. Hengtges, S. G.; Sharpless, K. B. *J. Am. Chem. Soc.* **1980**, 102, 4263–4265.
168. Yamada, T.; Narasaka, K. *Chem. Lett.* **1986**, 131–134.
169. Tokles, M.; Snyder, J. K. *Tetrahedron Lett.* **1986**, 27, 3951–3954.
170. Tomioka, K.; Nakajima, M.; Koga, K. *J. Am. Chem. Soc.* **1987**, 109, 6213–6215.
171. Oishi, T.; Hiram, M. *J. Org. Chem.* **1989**, 54, 5834–5835.
172. Corey, E. J.; Jardine, P. D.; Virgil, S.; Yuen, P. W.; Connell, R. D. *J. Am. Chem. Soc.* **1989**, 111, 9243–9244.
173. Fujii, K.; Tanaka, K.; Miyamoto, H. *Tetrahedron Lett.* **1992**, 4021–4024.
174. Hanessian, S.; Meffre, P.; Girard, M.; Beudoin, S.; Sancéau, J.-Y.; Bennani, Y. *J. Org. Chem.* **1993**, 58, 1991–1993.

175. Jacobsen, E. N.; Markó, I.; Mungall, W. S.; Schroder, G.; Sharpless, K. B. *J. Am. Chem. Soc.* **1988**, *110*, 1968–1970.
176. Jacobsen, E. N.; Markó, I.; France, M. B.; Svendsen, J. S.; Sharpless, K. B. *J. Am. Chem. Soc.* **1989**, *111*, 737–739.
177. Wai, J. S. M.; Markó, I.; Svendsen, J. S.; Finn, M. G.; Jacobsen, E. N.; Sharpless, K. B. *J. Am. Chem. Soc.* **1989**, *111*, 1123–1125.
178. Minato, M.; Yamamoto, K.; Tsuji, J. *J. Org. Chem.* **1990**, *55*, 766–768.
179. Kwong, H.-L.; Sorato, C.; Ogino, Y.; Chen, H.; Sharpless, K. B. *Tetrahedron Lett.* **1990**, *31*, 2999–3002.
180. Ogino, Y.; Kwong, H. L.; Chen, H.; Sharpless, K. B. *Tetrahedron Lett.* **1991**, *32*, 3965–3968.
181. Sharpless, K. B.; Amberg, W.; Beller, M.; Chen, H.; Hartung, J.; Kawanami, Y.; Lübben, D.; Manoury, E.; Ogino, Y.; Shibata, T.; Ukita, T. *J. Org. Chem.* **1991**, *56*, 4585–4588.
182. Sharpless, K. B.; Amberg, W.; Bennani, Y. L.; Crispino, G. A.; Hartung, J.; Jeong, K. Sung; K, Hoi L.; Morikawa, K.; Wang, Z. M.; Xu, D.; Zhang, X. L. *J. Org. Chem.* **1992**, 2768–2771.
183. Crispino, G. A.; Jeong, K. S.; Kolb, H. C.; Wang, Z. M.; Xu, D.; Sharpless, K. B. *J. Org. Chem.* **1993**, *58*, 3785–3786.
184. Becker, H.; Sharpless, K. B. *Angew. Chem., Int. Ed. Engl.* **1996**, *35*, 448–451.
185. Becker, H.; King, S. B.; Taniguchi, M.; Vanhessche, K. P. M.; Sharpless, K. B. *J. Org. Chem.* **1995**, *60*, 3940–3941.
186. Becker, H.; Sharpless, K. B. In *Asymmetric Oxidation Reactions*; Katsuki, T., Ed.; Oxford University Press: Oxford, UK, 2001; Chapter 2.5, pp 81–104.
187. Boger, D. L.; Mckie, J. A.; Nishi, T.; Ogiku, T. *J. Am. Chem. Soc.* **1996**, *118*, 2301–2302.
188. Salvadori, P.; Superchi, S.; Minutolo, F. *J. Org. Chem.* **1996**, *61*, 4190–4191.
189. Morikawa, K.; Park, J.; Andersson, P.; Hashiyama, T.; Sharpless, K. B. *J. Am. Chem. Soc.* **1993**, *115*, 8463–8464.
190. Döbler, C.; Mehlretter, G. M.; Beller, M. *Angew. Chem. Int. Ed.* **1999**, *38*, 3026–3028.
191. Döbler, C.; Mehlretter, G. M.; Sundermeier, U.; Beller, M. *J. Am. Chem. Soc.* **2000**, *122*, 10289–10297.
192. Krief, A.; Colaux-Castillo, C. *Tetrahedron Lett.* **1999**, *40*, 4189–4192.
193. Berrisford, D. J.; Bolm, C.; Sharpless, K. B. *Angew. Chem., Int. Ed. Engl.* **1995**, *34*, 1059–1070.
194. Andersson, M. A.; Epple, R.; Fokin, V. V.; Sharpless, K. B. *Angew. Chem., Int. Ed. Engl.* **2002**, *41*, 472–475.
195. Böseken, J.; de Graaff, C. *Rec. Trav. Chim. Pays-Bas*, **1922**, *41*, 199–207.
196. Corey, E. J.; Noe, M. C. *J. Am. Chem. Soc.* **1996**, *118*, 11038–11053.
197. Corey, E. J.; Noe, M. C.; Grogan, M. J. *Tetrahedron Lett.* **1996**, *37*, 4899–4902.
198. Norrby, P.-O.; Becker, H.; Sharpless, K. B. *J. Am. Chem. Soc.* **1996**, *118*, 35–42.
199. Norrby, P.-O.; Kolb, H. C.; Sharpless, K. B. *J. Am. Chem. Soc.* **1994**, *116*, 8470–8478.
200. Becker, H.; Ho, P. T.; Kolb, H. C.; Loren, S.; Norrby, P.-O.; Sharpless, K. B. *Tetrahedron Lett.* **1994**, *35*, 7315–7318.
201. Buschmann, H.; Scharf, H.-D.; Hoffmann, N.; Esser, P. *Angew. Chem. Int. Ed. Engl.* **1991**, *30*, 477–515.
202. Göbel, T.; Sharpless, K. B. *Angew. Chem. Int. Ed. Engl.*, **1993**, *32*, 1329–1331.
203. Nelson, D. W.; Gypser, A.; Ho, P. T.; Kolb, H. C.; Kondo, T.; Kwong, H. L.; McGrath, D. V.; Rubin, A. E.; Norrby, P.-O.; Gable, K. P.; Sharpless, K. B. *J. Am. Chem. Soc.* **1997**, *119*, 1840–1858.
204. Delmonte, A. J.; Haller, J.; Houk, K. N.; Sharpless, K. B.; Singleton, D. A.; Strassner, T.; Thomas, A. A. *J. Am. Chem. Soc.* **1997**, *119*, 9907–9908.
205. Corey, E. J.; Noe, M. C.; Sarshar, S. *Tetrahedron Lett.* **1994**, *35*, 2861–2864.
206. Corey, E. J.; Zhang, J. *Org. Lett.* **2001**, *3*, 3211–3214.
207. Costas, M.; Tipton, A. K.; Chen, K.; Jo, A. H.; Que, Jr. L. Q. *J. Am. Chem. Soc.* **2001**, *123*, 6722–6723.
208. Sharpless, K. B.; Patrick, D. W.; Truesdale, L. K.; Biller, S. A. *J. Am. Chem. Soc.* **1975**, *97*, 2305–2307.
209. Sharpless, K. B.; Chong, A. O.; Oshima, K. *J. Org. Chem.* **1976**, *41*, 177–179.
210. Li, G.; Chang, H. T.; Sharpless, K. B. *Angew. Chem., Int. Ed. Engl.* **1996**, *35*, 451–454.
211. Rudolph, J.; Sennhenn, P. C.; Vlaar, C. P.; Sharpless, K. B. *Angew. Chem.* **1996**, *35*, 2810–2813.
212. Phuka, P.; Sudalai, A. *Tetrahedron: Asymmetry* **1998**, *9*, 1001–1005.
213. Li, G.; Angert, H. H.; Sharpless, K. B. *Angew. Chem.* **1996**, *35*, 2813–2817.
214. Bruncko, M.; Schlingloff, G.; Sharpless, K. B. *Angew. Chem., Int. Ed. Engl.* **1997**, *36*, 1483–1486.
215. Reddy, K. L.; Sharpless, K. B. *J. Am. Chem. Soc.* **1998**, *120*, 1207–1217.
216. Barta, N. S.; Snider, D. R.; Somerville, K. B.; Weissman, S. A.; Larsen, R. D.; Reider, P. J. *Org. Lett.* **2000**, *2*, 2821–2824.
217. Tao, B.; Schlingloff, G.; Sharpless, K. B. *Tetrahedron Lett.* **1998**, *39*, 2507–2510.
218. Reddy, K. L.; Dress, K. R.; Sharpless, K. B. *Tetrahedron Lett.* **1998**, *39*, 3667–3670.
219. Song, C. E.; Oh, C. R.; Roh, E. J.; Lee, S. G.; Choi, J. H. *Tetrahedron: Asymmetry* **1999**, *10*, 671–674.
220. Nozaki, H.; Moriuchi, S.; Takaya, H.; Noyori, R. *Tetrahedron Lett.* **1966**, 5239–5244.
221. Nozaki, H.; Takaya, H.; Moriuchi, S.; Noyori, R. *Tetrahedron* **1968**, *24*, 3655–3669.
222. Aratani, T.; Yoneyoshi, Y.; Nagase, T. *Tetrahedron Lett.* **1975**, 1707–1710.
223. Aratani, T.; Yoneyoshi, Y.; Nagase, T. *Tetrahedron Lett.* **1977**, 2599–2602.
224. Aratani, T.; Yoneyoshi, Y.; Nagase, T. *Tetrahedron Lett.* **1982**, *23*, 685–688.
225. Doyle, M. P.; Protopopova, M. N. *Tetrahedron* **1998**, *54*, 7919–7946.
226. Aratani, T. *Pure & Appl. Chem.* **1985**, *57*, 1839–1844.
227. Fritschi, H.; Leutenegger, U.; Pfaltz, A. *Angew. Chem., Int. Ed. Engl.* **1986**, *25*, 1005–1006.
228. Fritschi, H.; Leutenegger, U.; Pfaltz, A. *Helv. Chim. Acta* **1988**, *71*, 1553–1565.
229. Lowenthal, R. E.; Abiko, A.; Masamune, S. *Tetrahedron Lett.* **1990**, *31*, 6005–6008.
230. Evans, D. A.; Woerpel, K. A.; Scott, M. J. *Angew. Chem., Int. Ed. Engl.* **1992**, *31*, 430–432.
231. Muller, D.; Umbrecht, G.; Weber, B.; Pfaltz, A. *Helv. Chim. Acta* **1991**, *74*, 232–240.
232. Ito, K.; Katsuki, T. *Tetrahedron Lett.* **1993**, *34*, 2661–2664.
233. Ito, K.; Yoshitake, M.; Katsuki, T. *Heterocycles* **1996**, *42*, 305–317.
234. Kanemasa, S.; Hamura, S.; Harada, E.; Yamamoto, H. *Tetrahedron Lett.* **1993**, *35*, 7985–7988.
235. Lo, M. M. C.; Fu, G. C. *J. Am. Chem. Soc.* **1998**, *120*, 10270–10271.
236. Uozumi, K.; Kyota, H.; Kishi, E.; Kitayama, K.; Hayashi, T. *Tetrahedron: Asymmetry* **1996**, *7*, 1603–1606.

237. Boyar, E. B.; Robinson, S. D. *Coord. Chem. Rev.* **1983**, *50*, 109–208.
238. Brunner, H.; Kluschanzoff, H.; Wurz, K. *Bull. Soc. Chim. Belg.* **1989**, *98*, 63–72.
239. Kennedy, M.; Mckervey, M. A.; Maguire, A. R.; Roos, G. H. P. *J. Chem. Soc. Chem. Commun.* **1990**, 361–362.
240. Hashimoto, S.; Watanabe, N.; Ikegami, S. *Tetrahedron Lett.* **1990**, *31*, 5173–5174.
241. Davies, H. M. L.; Bruzinski, P. R.; Lake, D. H.; Kong, N.; Fall, M. J. *J. Am. Chem. Soc.* **1996**, *118*, 6897–6907.
242. Davies, H. M. L.; Peng, Z. Q.; Hou, J. H. *Tetrahedron Lett.* **1994**, *35*, 8939–8942.
243. Doyle, M. P.; Winchester, W. R.; Hoorn, J. A. A.; Lynch, V.; Simonsen, S. H.; Ghosh, R. *J. Am. Chem. Soc.* **1993**, *115*, 9968–9978.
244. Doyle, M. P.; Winchester, W. R.; Protopopova, M. N.; Müller, P.; Bernardinelli, G.; Ene, D.; Motallebi, S. *Helv. Chim. Acta.* **1993**, *76*, 2227–2235.
245. Doyle, M. P.; Zhou, Q. L.; Simonsen, S. H.; Lynch, V. *Synlett* **1996**, 697–698.
246. Hu, W.; Timmons, D. J.; Doyle, M. P. *Org. Lett.* **2002**, 901–904.
247. Ishitani, H.; Achiwa, K. *Synlett* **1997**, 781–782.
248. Kitagaki, S.; Matsuda, H.; Watanabe, N.; Hashimoto, S. *Synlett* **1997**, 1171–1174.
249. Maxwell, J. L.; O'Malley, S.; Brown, K. C.; Kodadek, T. *Organometallics* **1992**, *11*, 645–652.
250. Brown, K. C.; Kodadek, T. *J. Am. Chem. Soc.* **1992**, *114*, 8336–8338.
251. Nishiyama, H.; Itoh, Y.; Matsumoto, H.; Park, S. B.; Itoh, K. *J. Am. Chem. Soc.* **1994**, *116*, 2223–2224.
252. Nishiyama, H.; Itoh, Y.; Sugiyama, Y.; Matsumoto, H.; Aoki, K.; Itoh, K. *Bull. Chem. Soc. Jpn.* **1995**, *68*, 1247–1262.
253. Park, S. B.; Murata, K.; Matsumoto, H.; Nishiyama, H. *Tetrahedron: Asymmetry* **1995**, *6*, 2487–2494.
254. Park, S. B.; Sakata, N.; Nishiyama, H. *Chem. Eur. J.* **1996**, *2*, 303–306.
255. Nishiyama, H.; Aoki, K.; Itoh, H.; Iwamura, T.; Sakata, N.; Kurihara, O.; Motoyama, Y. *Chem. Lett.* **1996**, 1071–1072.
256. Lo, W. C.; Che, C. M.; Cheng, K. F.; Mak, T. C. W. *J. Chem. Soc., Chem. Commun.* **1997**, 1205–1206.
257. Frauenkron, M.; Bekessel, A. *Tetrahedron Lett.* **1997**, *38*, 7175–7176.
258. Che, C. M.; Huang, J. S.; Lee, F. W.; Li, Y.; Lai, T. S.; Kwong, H. L.; Teng, P. F.; Lee, W. S.; Lo, W. C.; Peng, S. M.; Zhou, Z. Y. *J. Am. Chem. Soc.* **2001**, *123*, 4119–4129.
259. Uchida, T.; Irie, R.; Katsuki, T. *Synlett* **1999**, 1163–1165.
260. Uchida, T.; Irie, R.; Katsuki, T. *Tetrahedron* **2000**, *56*, 3501–3509.
261. Bachmann, S.; Furler, M.; Mezzetti, A. *Organometallics* **2001**, *20*, 2102–2108.
262. Munslow, I. J.; Gillespie, K. M.; Deeth, R. J.; Scott, P. *Chem. Commun.* **2001**, 1638–1639.
263. Tatsuno, Y.; Konishi, A.; Nakamura, A.; Otsuka, S. *J. Chem., Chem. Commun.* **1974**, 588–589.
264. Nakamura, A.; Konishi, A.; Tsujitani, R.; Kudo, M.-A.; Otsuka, S. *J. Am. Chem. Soc.* **1978**, *100*, 3449–3461.
265. Nakamura, A.; Konishi, A.; Tsujitani, R.; Tatsuno, Y.; Otsuka, S. *J. Am. Chem. Soc.* **1978**, *100*, 3443–3448.
266. Jommi, G.; Pagliarin, R.; Rizzi, G.; Sisti, M. *Synlett* **1993**, 833–834.
267. Fukuda, T.; Katsuki, T. *Synlett* **1995**, 825–826.
268. Fukuda, T.; Katsuki, T. *Tetrahedron* **1997**, *53*, 7201–7208.
269. Yamada, T.; Ikeno, T.; Sekino, H.; Sato, M. *Chem. Lett.* **1999**, 719–720.
270. Ikeno, T.; Sato, M.; Yamada, T. *Chem. Lett.* **1999**, 1345–1346.
271. Ikeno, T.; Nishizuku, A.; Sato, M.; Yamada, T. *Synlett* **2001**, 406–408.
272. Ikeno, T.; Sato, M.; Sekino, H.; Nishikazu, A.; Yamada, T. *Bull. Chem. Soc. Jpn.* **2001**, *74*, 2139–2150.
273. Niimi, T.; Uchida, T.; Irie, R.; Katsuki, T. *Tetrahedron Lett.* **2000**, *41*, 3647–3651.
274. Niimi, T.; Uchida, T.; Irie, R.; Katsuki, T. *Adv. Synth. Catal.* **2001**, *343*, 79–88.
275. Stork, G.; Ficini, J. *J. Am. Chem. Soc.* **1961**, *83*, 4678.
276. Piqué, C.; Fändrich, B.; Pfaltz, A. *Synlett* **1995**, 491–492.
277. Tokunoh, R.; Tomiyama, H.; Sodeoka, M.; Shibasaki, M. *Tetrahedron Lett.* **1996**, *37*, 2449–2452.
278. Gant, T. G.; Noe, M. G.; Corey, E. J. *Tetrahedron Lett.* **1995**, *36*, 8745–8748.
279. Doyle, M. P.; Peterson, C. S.; Zhou, Q. L.; Nishiyama, H. *J. Chem. Soc., Chem. Commun.* **1997**, 211–212.
280. Doyle, M. P.; Peterson, C. S.; Parker, Jr., D. L. *Angew. Chem., Int. Ed. Engl.* **1996**, *35*, 1334–1336.
281. Doyle, M. P.; Peterson, C. S.; Protopopova, M. N.; Marnett, A. B.; Parker, Jr., D. L.; Ene, D. G.; Lynch, V. *J. Am. Chem. Soc.* **1995**, *119*, 8826–8837.
282. Doyle, M. P.; Pieters, R. J.; Martin, S. F.; Austin, R. E.; Oalman, C. J.; Müller, P. *J. Am. Chem. Soc.* **1991**, *113*, 1423–1424.
283. Doyle, M. P.; Austin, R. E.; Bailey, A. S.; Dwyer, M. P.; Dyatkin, A. B.; Kalinin, A. V.; Kwan, M. M. Y.; Liras, S.; Oalman, C. J.; Pieters, R. J.; Protopopova, M. N.; Raab, C. E.; Roos, G. H. P.; Zhou, Q. L.; Martin, S. F. *J. Am. Chem. Soc.* **1995**, *117*, 5763–5775.
284. Doyle, M. P.; Zhou, Q. L.; Raab, C. E.; Roos, G. H. P.; Simonsen, S. H.; Lynch, V.; Doyle, Michael P.; Zhou, Q. L.; Raab, C. E.; Roos, G. H. P.; Simonsen, S. H.; Lynch, V. *Inorg. Chem.* **1996**, *35*, 6064–6073.
285. Doyle, M. P.; Kalinin, A. V. *J. Org. Chem.* **1996**, *61*, 2179–2184.
286. Doyle, M. P.; Zhou, Q. L. *Tetrahedron: Asymmetry* **1995**, *6*, 2157–2160.
287. Doyle, M. P.; Eismont, M. Y.; Zhou, Q. L. *Russ. Chem. Bull.* **1997**, *46*, 955–958.
288. Barberis, M.; Pérez-Prieto, J.; Stiriba, S.-E.; Lahuerta, P. *Org. Lett.* **2001**, *21*, 3317–3319.
289. Barberis, M.; Lahuerta, P.; Pérez-Prieto, J.; Sunau, M. *Chem. Commun.* **2001**, 439–440.
290. Davies, H. M. L.; Doan, B. D. *J. Org. Chem.* **1999**, *64*, 8501–8508.
291. Saha, B.; Uchida, T.; Katsuki, T. *Synlett* **2001**, 114–116.
292. Saha, B.; Uchida, T.; Katsuki, T. *Chem. Lett.* **2002**, 782–783.
293. Uchida, T.; Saha, B.; Katsuki, T. *Tetrahedron Lett.* **2001**, *42*, 2521–2524.
294. Bartley, D. W.; Kodadek, T. *J. Am. Chem. Soc.* **1993**, *115*, 1656–1660.
295. Fraile, J. M.; Garcia, J. I.; Martinez-merino, V.; Mayoral, J. A.; Salvatella, L. *J. Am. Chem. Soc.* **2001**, *123*, 7616–7625.
296. Ikeno, T.; Iwakura, I.; Yabushita, S.; Yamada, T. *Org. Lett.* **2002**, *4*, 517–520.
297. Bühl, M.; Terstegen, F.; Löffler, F.; Meynhardt, B.; Kierse, S.; Müller, M.; Näther, C.; Lüning, U. *Eur. J. Org. Chem.* **2001**, 2151–2160.

298. Katsuki, T. In *Comprehensive Asymmetric Catalysis*; Jacobsen, E. N., Pfaltz, A., Yamamoto, H., Eds.; Springer: Berlin, 1999; Vol. II, Chapter 21, pp 791–799.
299. Meunier, B. In *Transition Metals for Organic Synthesis*; Beller, M. Bolm, C., Eds.; Wiley-VCH; Weinheim, Germany, 1998; Vol. 2, Chapter 2.2, pp 173–192.
300. Schlingloff, G.; Bolm, C. In *Transition Metals for Organic Synthesis*; Beller, M., Bolm, C., Eds.; Wiley-VCH; Weinheim, Germany, 1998; Vol. 2, Chapter 2.2, pp 193–199.

9.5

Metal Complexes as Catalysts for H—X (X=B, CN, Si, N, P) Addition to CC Multiple Bonds

M. K. WHITTLESEY
University of Bath, UK

9.5.1	INTRODUCTION	265
9.5.2	HYDROBORATION	265
9.5.2.1	Developments Since CCC (1987)	265
9.5.2.2	Ligand Effects in Rhodium-catalyzed Hydroboration of Vinylarenes	269
9.5.2.3	Metal-catalyzed Hydroboration of Other C=C Bonds	270
9.5.2.4	Hydroboration of Substrates Containing C≡C Bonds: Enynes and Alkynes	270
9.5.2.5	Asymmetric Hydroboration	271
9.5.3	HYDROCYANATION	275
9.5.3.1	Reactions of Nonactivated Alkenes	276
9.5.3.2	Hydrocyanation of Activated Alkenes	277
9.5.4	HYDROSILYLATION	280
9.5.4.1	Developments in Achiral Catalytic Si-H Addition	280
9.5.4.2	Asymmetric Hydrosilylation	281
9.5.4.3	Enantioselective Hydrosilylation Employing Chiral Ferrocenyl Phosphine Ligands	285
9.5.4.4	Intramolecular Asymmetric Hydrosilylation	286
9.5.4.5	Enantioselective Hydrosilylation of C=O and C=N Bonds—A Brief Synopsis	288
9.5.5	HYDROAMINATION	288
9.5.5.1	Mechanism and Early Transition Metal/Lanthanide Catalysts	288
9.5.5.2	Rhodium and Iridium Catalysts	291
9.5.5.3	Palladium and Platinum Catalysts	294
9.5.6	HYDROPHOSPHINATION (AND HYDROPHOSPHORYLATION)	296
9.5.6.1	Hydrophosphination	297
9.5.6.2	Hydrophosphorylation and Hydrophosphinylation	298
9.5.7	REFERENCES	301

9.5.1 INTRODUCTION

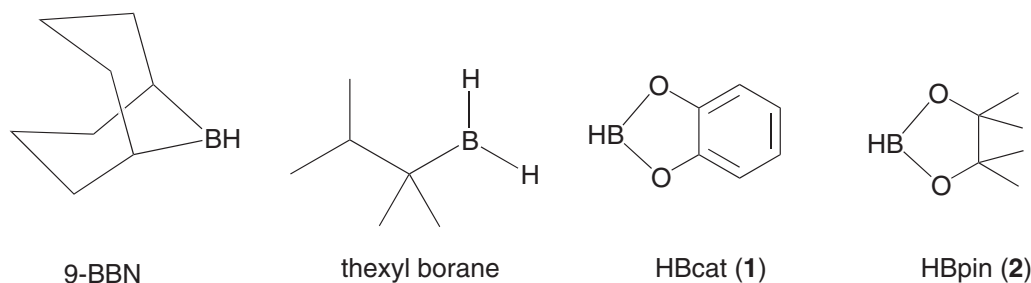
It is now virtually impossible to open the latest edition of any of the leading chemical research journals without finding at least one publication from inorganic or organic (or even a combination of the two) chemists detailing a new metal–ligand (M–L) combination for homogeneous catalysis. By combining a synthetic and computational approach to understanding reaction mechanisms, many M–L combinations can be rationalized leading to ever more active catalytic combinations. This chapter aims to survey the literature relating to catalytic hydroboration, hydrocyanation, hydrosilylation, hydroamination, and hydrophosphination of C=C and C≡C bonds since the early 1980s. Some of these areas are still in their infancy (hydroamination, hydrophosphination) in terms of industrially applicable reactions, while others (hydrocyanation being the prime example) follow directly from important commercial processes.

An overview of the catalytically active M—L systems is presented in terms of both achiral and chiral reactions. Where deemed appropriate, reference is also made to organometallic and organolanthanide catalysts, as well as (briefly) H—X addition to C=O.

9.5.2 HYDROBORATION

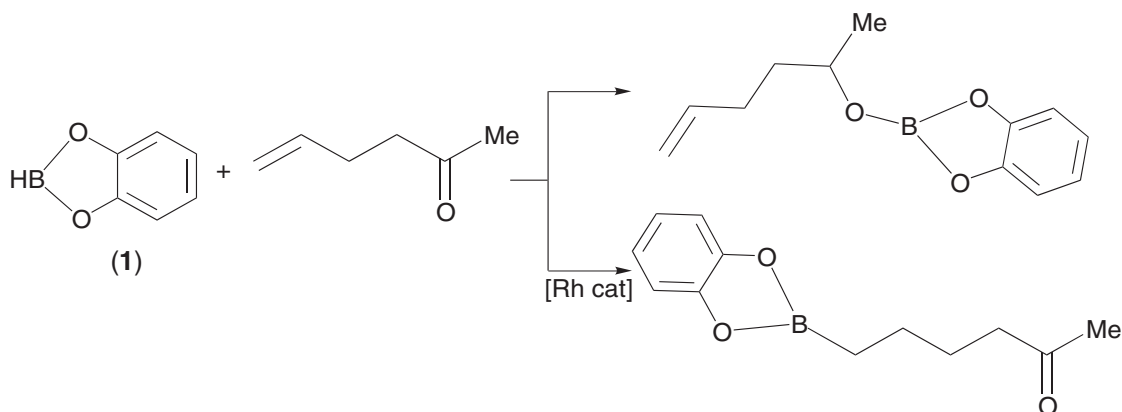
9.5.2.1 Developments Since CCC (1987)

The field of transition metal-catalyzed hydroboration has developed enormously over the last 20 years and is now one of the most powerful techniques for the transformation of C=C and C≡C bonds.^{1–3} While hydroboration is possible in the absence of a metal catalyst, some of the more common borane reagents attached to heteroatom groups (e.g., catecholborane or HBcat, **(1)**) react only very slowly at room temperature (Scheme 1); addition of a metal catalyst [M] accelerates the reaction. In addition, the ability to manipulate [M] through the judicious choice of ligands (both achiral and chiral) allows the regio-, chemo-, and enantioselectivity to be directed.



Scheme 1

Männig and Nöth reported the first example of rhodium-catalyzed hydroboration to C=C bonds in 1985.⁴ Catecholborane reacts at room temperature with 5-hexene-2-one at the carbonyl double bond; when the reaction was run in the presence of 5 mol.% Wilkinson's catalyst [Rh(PPh₃)₃Cl], addition of the B—H bond across the C=C double bond was observed affording the anti-Markovnikoff ketone as the major product (Scheme 2). Other rhodium complexes showed good catalytic properties ([Rh(COD)Cl₂]₂, [Rh(PPh₃)₂(CO)Cl], where COD = cyclooctadiene) not only for the ketone substrate, but also for terminal and cyclic unactivated alkenes (Table 1).

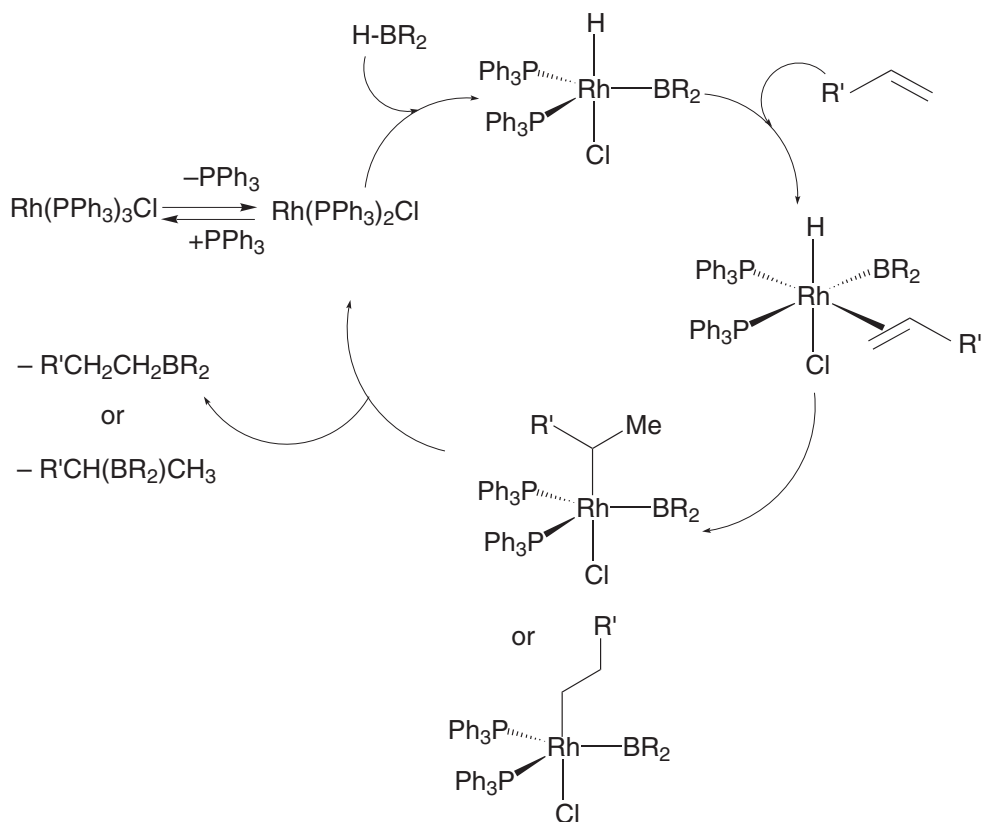


Scheme 2

The catalytic cycle for hydroboration is now widely accepted and direct examples of several intermediate species have been isolated and well characterized (Scheme 3).^{5–7} These now include σ -borane complexes, which have in some instances been found to be catalytic precursors for hydroboration.^{8–10} Oxidative addition of an H—B bond to a coordinatively unsaturated metal fragment

Table 1 Catalytic hydroboration using Rh(PPh₃)₃Cl/HBcat.

Substrate	% Yield of hydroborated product
1-octene	78
Cyclopentene	83
Cyclohexene	22
3-vinylcyclohexene	50 (vinyl group only)
1-hexyne	53

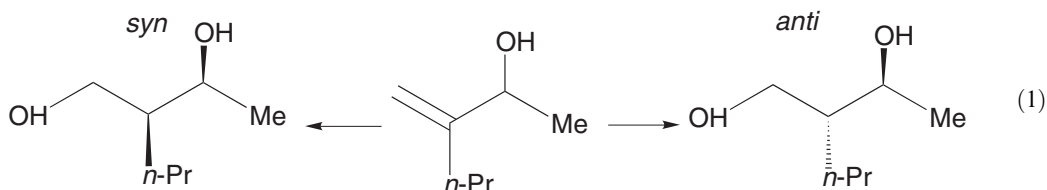
**Scheme 3**

proceeds by alkene coordination and subsequent migratory insertion to yield either linear or branched alkylboranes upon reductive elimination. A number of points of interest arise from the catalytic cycle:

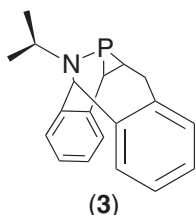
- Estimations of the reaction enthalpies for iridium-catalyzed hydroboration suggest that ethene insertion into an Ir–Bcat bond is 8 kcal mol^{-1} more exothermic than insertion into Ir–H, although the reductive elimination of alkylborane from an $\text{Ir}(\text{CH}_2\text{CH}_3)(\text{Bcat})$ unit is 8 kcal mol^{-1} more favorable than loss from an $\text{IrH}(\text{CH}_2\text{CH}_2\text{Bcat})$ unit.¹¹ Theoretical calculations support alkene insertion into both Rh–B and Rh–H bonds.^{12,13}
- Deuterium labeling studies have been reported to try and explain the regioselectivities observed in reactions of terminal alkenes,^{14,15} 1,1-dialkylalkenes,^{14–16} and styrene.¹⁵
- The reversibility (or otherwise) of steps in the catalytic cycle (alkene binding to H–M–BR₂) has been proposed as crucial to the diastereoselectivity observed in hydroboration of alkenes.^{14,15,17,18}

A wide range of catalysts is now known that will bring about B–H addition to simple terminal alkenes. For group 9 complexes, catalytic activity follows the order $[(\text{dppe})\text{Rh}(\text{nb})]^+ > [\text{Rh}(\text{PPh}_3)_3\text{Cl}] > [(\text{COD})\text{Ir}(\text{PCy}_3)(\text{C}_5\text{H}_5\text{N})]^+$ (where dppe = 2-bis(diphenylphosphino)ethane and nb = norbornadiene).¹⁹ Different facial selectivity is found for catalytic hydroboration reactions of these compounds with chiral alkenes (Equation (1)). Thus, $[(\text{dppe})\text{Rh}(\text{nb})]^+$ gives

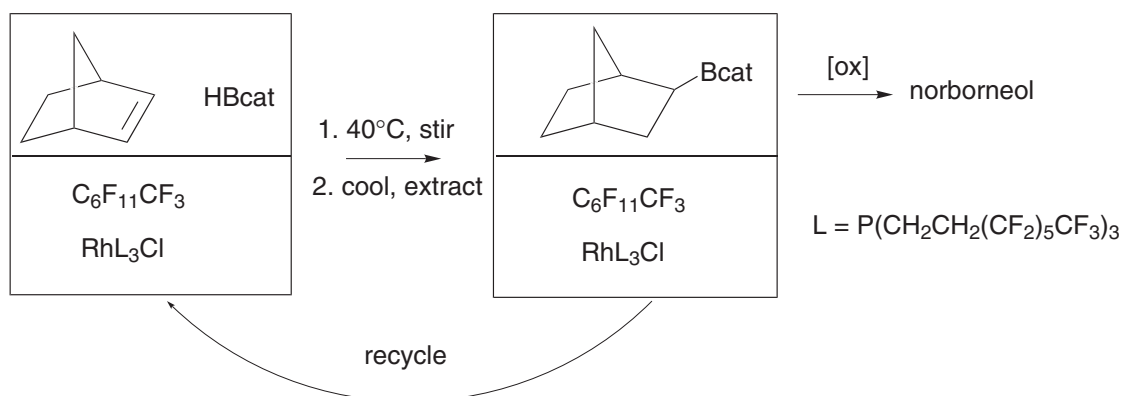
a *syn:anti* ratio of 50:50, while Wilkinson's catalyst favors the *syn* product 81:19. Studies using $[\text{Rh}(\text{COD})\text{Cl}]_2$ as the catalyst reveal that the electronic and steric characteristics of the substituent on the allylic oxygen dictates the stereoselectivity:²⁰



The development of new ligand sets has resulted in increases in regioselectivity and rates of reaction using small catalyst loadings. The phosphirane complex $[\text{Rh}(\text{iPrBABA}\text{R-Phos})_4]^+$ (BABA R-Phos , **(3)**) affords >98% of the anti-Markovnikov product corresponding to a turnover frequency of $>3 \times 10^5 \text{ h}^{-1}$ at 0.1 mol.% catalyst loading.²¹



The interest in catalyst recyclability has led to the development of biphasic catalysts for hydroboration.²² Derivatization of Wilkinson's catalyst with fluorocarbon "ponytails" affords $[\text{Rh}(\text{P}\{(\text{CH}_2)_2(\text{CF}_2)_5\text{CF}_3\}_3\text{Cl})]$ which catalyzes HBcat addition to norbornene in a mixture of $\text{C}_6\text{F}_{11}\text{CF}_3$ and tetrahydrofuran (THF) or toluene (alternatively a nonsolvent system can be used with just the fluorocarbon and norbornene) to give *exo*-norborneol in 76% yield with a turnover number up to 8,500 (Scheme 4). Mono-, di- and trisubstituted alkenes can all be reacted under these conditions. The catalyst can be readily recycled over three runs with no loss of activity.²³



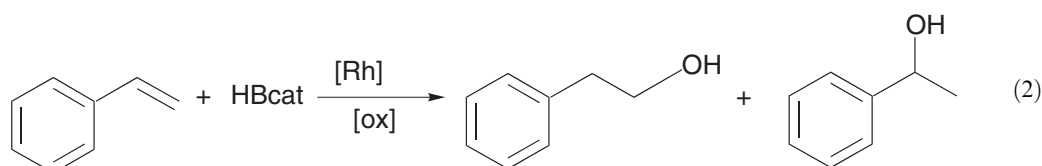
Scheme 4

Reactivity is not only associated with rhodium. As already shown,¹⁹ $[(\text{COD})\text{Ir}(\text{PCy}_3)(\text{C}_5\text{H}_5\text{N})]^+$ catalyzes HBcat addition to 1-heptene (98:2 anti-Markovnikov: Markovnikov regioselectivity), although this can be moderated by directing groups, such as amides.²⁴ Ruthenium complexes (e.g., $[\text{Ru}(\text{PPh}_3)_4\text{H}_2]$, $[\text{Ru}(\text{PPh}_3)_3\text{HCl}]$) have been shown to offer no improvements over the established rhodium systems for hydroboration of unhindered alkenes.²⁵ Simple lanthanide halides and alkoxides (e.g., LuI_3 , PrI_3 , $\text{Sm}(\text{iPrO})_3$) catalyze hydroboration of terminal alkenes such as 1-decene to give high yields of the primary alcohols upon oxidation.²⁶ With the highly reactive pinacolborane (HBpin, **(2)**) as the B—H source, $[\text{Rh}(\text{PPh}_3)_3\text{Cl}]$, $[\text{Rh}(\text{PPh}_3)_2(\text{CO})\text{Cl}]$, $[\text{CpNi}(\text{PPh}_3)\text{Cl}]$, and $[\text{Cp}_2\text{ZrHCl}]$ (Schwartz's reagent) will hydroborate alkenes.^{27,28} As expected, 1-octene afforded the anti-Markovnikov addition product, which was also found upon starting with *trans*-4-octene. For Zr, this was explained by operation

of a hydrozirconation/isomerization mechanism. With rhodium, formation of terminal products with HBpin (but not HBcat) was ascribed to the larger size of the former, which results in rapid β -hydride elimination and recombination, placing the rhodium on the least hindered carbon of the chain.

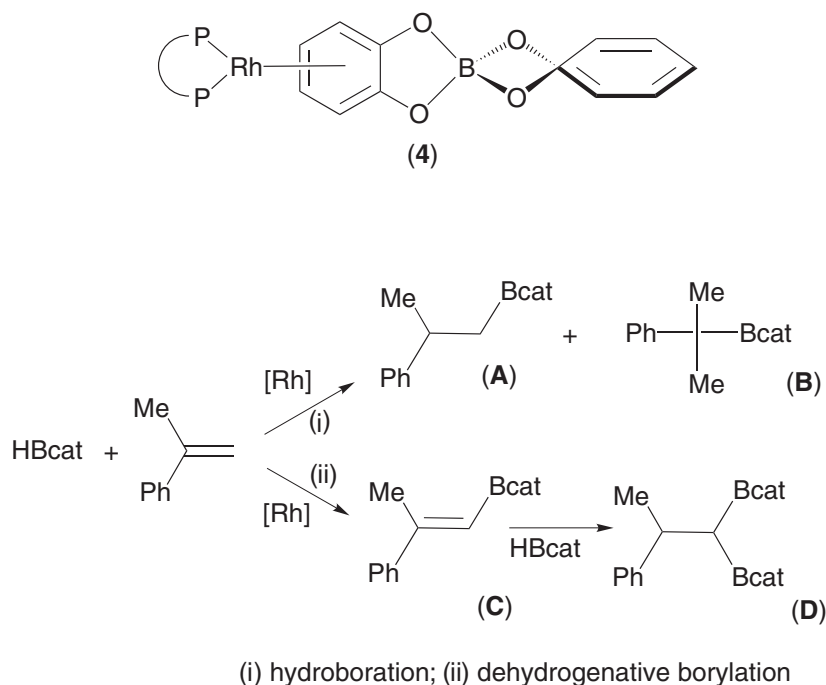
9.5.2.2 Ligand Effects in Rhodium-catalyzed Hydroboration of Vinylarenes

Attempts to utilize rhodium complexes for hydroboration of vinylarenes (Equation (2)) were somewhat complicated by discrepancies in the results from different research groups. Thus, it was found that $[\text{Rh}(\text{PPh}_3)_3\text{Cl}]$ catalyzed the addition of HBcat to styrene to afford a quantitative yield of the branched product:¹⁵



Other results suggested that $[\text{Rh}(\text{PPh}_3)_3\text{Cl}]$ gave the terminal alcohol after oxidation, while the cationic phosphine complexes $[(\text{L-L})\text{Rh}(\text{COD})]^+$ (where $\text{L-L} = (\text{PPh}_3)_2$, dppe, or 1,4-bis(diphenylphosphino)butane (dppb)) afforded the branched isomer (Equation (2)).^{29,30} Other reports also suggested that Wilkinson's catalyst gave the branched alcohol, while a mixture of $[\text{Rh}(\text{COD})_2]^+/4\text{PPh}_3$ gave 98% of the branched product, but with only two equivalents of phosphine present, the branched:terminal ratio changed to 59:41.³¹

Similarly, hydroboration of *p*-methoxystyrene with HBcat using zwitterionic $[(\text{P-P})\text{Rh}(\eta^6\text{-catBcat})]$ ((4), $\text{P-P} = \text{dppe}$, dippe) or $[(\text{dippe})\text{Rh}(\eta^3\text{-2-Me-allyl})]$ (dippe = 1,2-bis(diisopropylphosphine)ethane) gave 99% of the internal hydroboration product. Complications arose in studying reactions of hindered styrenes due to the appearance of not only the hydroboration products (A and B), but also the dehydrogenative borylation products C and D (Scheme 5).³² The ratio of products was found to be highly catalyst dependent (Table 2).³³



Scheme 5

The observed contradictions are down to variations in catalyst purity, the level of oxygen contamination, and compensatory effects from the presence of excess phosphine. Hence, freshly

Table 2 Ratios of hydroboration/dehydrogenative borylation products shown in Scheme 4 found with a range of rhodium catalysts.^{33,34}

Catalyst	% Yield of A	% Yield of B	% Yield of C	% Yield of D
[Rh(coe) ₂ Cl]/PPh ₃	98			
[(dppb)Rh(COD)] ⁺	30	70		
[(dppb)Rh(η^6 -catBcat)]	5	95		
[Rh(PPh ₃) ₃ Cl]	14	3	53	27
[Rh(PPh ₃) ₃ Cl]/10 \equiv PPh ₃	10	1	70	18
[Rh(PPh ₂ - <i>o</i> -Tol) ₂ Cl] ₂	15		76	8

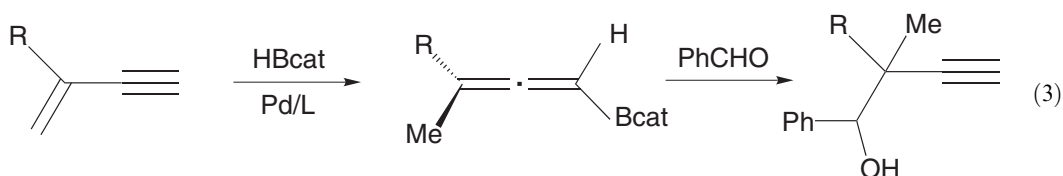
prepared [Rh(PPh₃)₃Cl] (handled under anaerobic conditions) catalyzes the addition of HBcat across styrene to give 99% regioselectivity for the branched isomer. In contrast, addition of oxygen changed this ratio to 60:40 branched:linear. Manipulation of Wilkinson's catalyst in air but in the presence of excess PPh₃ reverted this selectivity back to >99% branched.¹⁶ The role of phosphine-free cationic complexes in hydroboration reactions has also been discussed.³⁵

9.5.2.3 Metal-catalyzed Hydroboration of Other C=C Bonds

Wilkinson's catalyst has also been utilized for the hydroboration of other alkenes. Sulfone derivatives of allyl alcohol can be hydroborated with HBcat and subsequently oxidized to give the secondary rather than primary alcohol. This reactivity proves to be independent of substituents on the sulfur atom.³⁶ Similarly, thioalkenes undergo anti-Markovnikoff addition to afford α -thioboronate esters.³⁷ The benefits of metal-catalyzed reactions come to the fore in the hydroboration of bromoalkenes (higher yields, shorter reaction times), although the benefits were less clear for the corresponding chloroalkenes (Table 3).^{38,39} Dienes can be hydroborated using both rhodium and palladium catalysts; [Pd(PPh₃)₄] reacts readily with 1,3-dienes, but cyclic dienes are more active towards [Rh₄(CO)₁₂].⁴⁰

9.5.2.4 Hydroboration of Substrates Containing C \equiv C Bonds: Enynes and Alkynes

Palladium phosphine complexes prove active for the hydroboration of 1,3-enynes as a route to the homopropargyl alcohols (Equation (3)). For R = Me, the selectivity for forming allenylborane is dependent both on the nature of the phosphine and also on the Pd:L ratio. The yield increases on changing from L = PPh₃ to L = PPh₂(C₆F₅). With chelating phosphine ligands, 1,2-addition to the triple bond yields 1,3-dienylboranes as alternative products:⁴¹

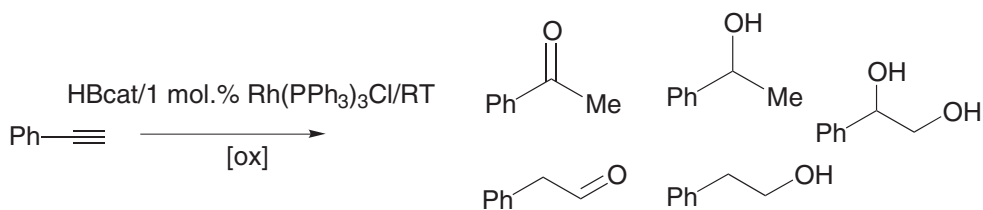


Hydroboration of alkynes is easier to achieve than B—H addition to alkenes. A mixture of alcohol, ketone, and diol products is produced upon [Rh(PPh₃)₃Cl] catalyzed hydroboration of

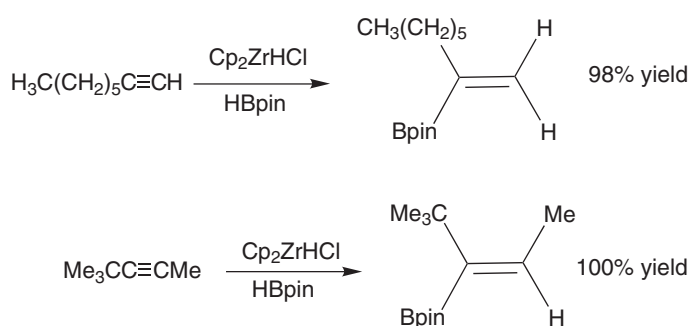
Table 3 Noncatalyzed and [Rh(PPh₃)₃Cl]-catalyzed hydroboration with HBcat of RR₁C=CHX to RR₁CH—CHX(Bcat) at 80–90 °C.

R	R ₁	X	Product yield (%)	Conditions
Me	H	Br	76	Uncatalyzed, 24 h
Me	H	Br	82	0.1 mol.%, 8 h
Me	Me	Cl	66	Uncatalyzed, 18 h
Me	Me	Cl	70	0.2 mol.%, 24 h

alkynes (Scheme 6). The product distribution reflects the stage of the reaction; at early time, carbonyl products are principally formed, while at later stages of the reaction, alcohols are the principal products.¹⁶ Pinacolborane adds readily across $\text{RC}\equiv\text{CR}'$ in the presence of 5 mol.% $[\text{Cp}_2\text{ZrHCl}]$ to give high yields of products with high *syn* selectivity (Scheme 7).⁴² The zirconocene dichloride $[\text{Cp}_2\text{ZrCl}_2]$ shows zero catalytic activity.

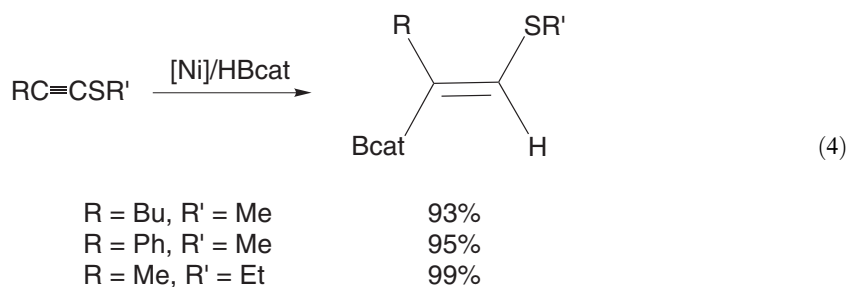


Scheme 6



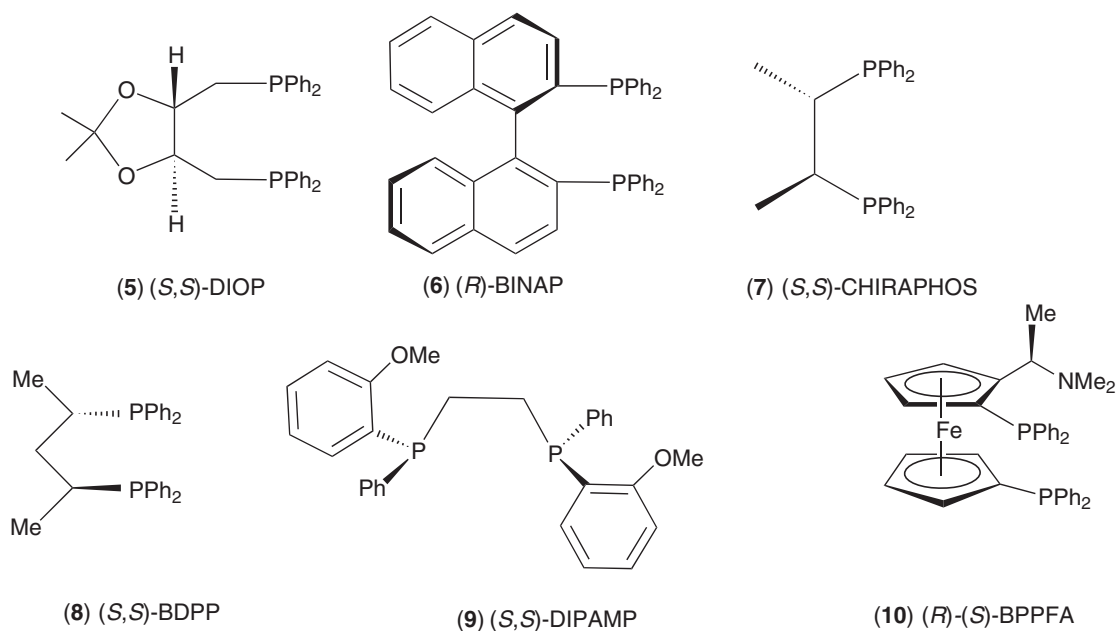
Scheme 7

Nickel complexes prove to be the most effective catalysts for hydroboration of thioalkynes. The bidentate phosphine systems $[(\text{P}-\text{P})\text{NiCl}_2]$ ($\text{P}-\text{P} = \text{dppf}$, 1,3-bis(diphenylphosphino)propane(dppp), dppe) all displayed high activity, even with bulky substituents on the alkyne (Equation (4)):^{43,44}



9.5.2.5 Asymmetric Hydroboration

Early work in the field of asymmetric hydroboration employed norbornene as a simple unsaturated substrate. A range of chiral-chelating phosphine ligands were probed (DIOP (5), 2,2'-bis(diphenylphosphino)-1,1'-binaphthyl (BINAP) (6), 2,3-bis(diphenylphosphino)butane (CHIRAPHOS) (7), 2,4-bis(diphenylphosphino)pentane (BDPP) (8), and 1,2-bis(*o*-methoxyphenyl)(phenyl)phosphino)ethane (DIPAMP) (9)) in combination with $[\text{Rh}(\text{COD})\text{Cl}]_2$ and catecholborane at room temperature (Scheme 8).⁴⁵ General observations were that enantioselectivities increased as the temperature was lowered below ambient, but that variations of solvent (THF, benzene, or toluene) had little impact.

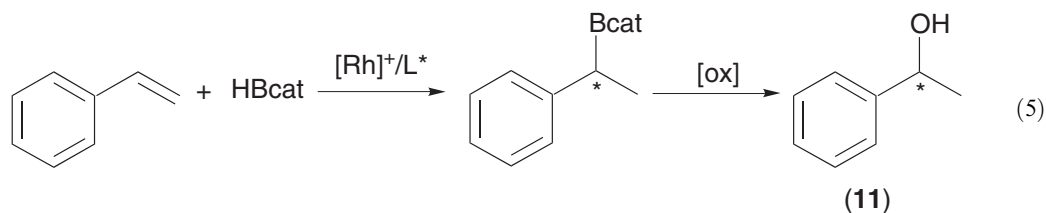


Scheme 8

The five-membered ring chelate ligands (CHIRAPHOS (7) and DIPAMP (9)) showed poor activity. DIOP (5) was found to be more effective than BINAP (6), while no real improvements in the levels of asymmetric induction were found by using cationic complexes $[\text{Rh}(\text{COD})(\text{L}-\text{L})]^+$ instead of neutral systems.

Subtle ligand changes have pronounced effects in hydroboration of 1,1-disubstituted alkenes. Addition of HBcat across the C=C bond in 2,3,3-trimethyl-1-butene is catalyzed by $[\text{Rh}(\text{COD})\text{Cl}]_2/\text{DIOP}$ at -5°C affording 2-*t*-butyl-1-propanol in 69% ee upon oxidation. In the case of 2-phenylpropene, $[\text{Rh}(\text{C}_2\text{H}_4)_2\text{Cl}]_2$ combines with either DIOP or BINAP to provide higher enantiomeric excesses than with $[\text{Rh}(\text{COD})\text{Cl}]_2$.⁴⁶

An extensive array of chiral phosphine ligands has been tested for the asymmetric rhodium-catalyzed hydroboration of aryl-substituted alkenes. It is well known that cationic Rh complexes bearing chelating phosphine ligands (e.g., dppf) result in Markovnikov addition of HBcat to vinylarenes to afford branched boryl compounds. These can then be oxidized through to the corresponding chiral alcohol (11) (Equation (5)):

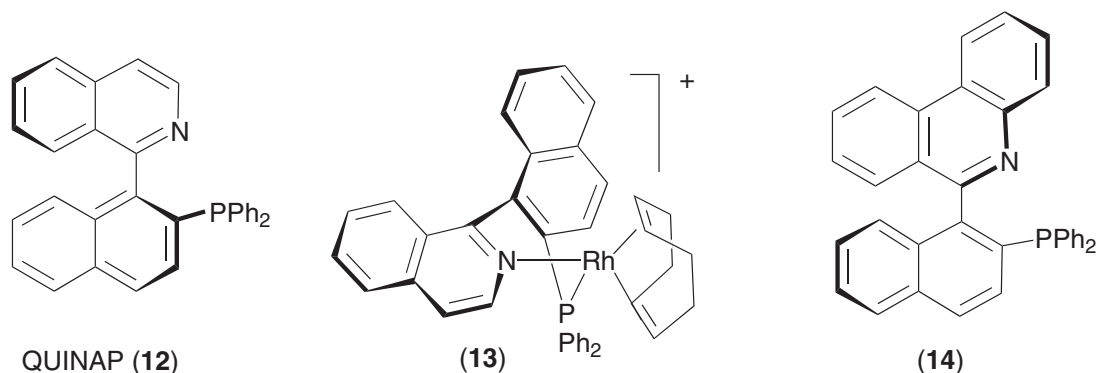


Some of the earlier studies in this area with chiral chelate phosphines identified a mixture of $[\text{Rh}(\text{COD})_2]^+$ with BINAP (1 or 2 mol.%) at low temperature (-78°C) in DME as highly effective. Thus B-H addition of HBcat to styrene in the presence of (R)-BINAP (6) gave 96% ee (R)-1-phenylethanol with a chemical yield of up to 91%. A number of general observations were made in this chemistry. For example, higher enantioselectivity is observed when the reactions are performed at low temperatures. In addition, high enantiomeric purity is observed in the product alcohols starting from styrenes substituted with both electron-donating and electron-withdrawing groups (somewhat lower selectivity is found with *ortho*-substituted styrenes) and other chiral phosphines (CHIRAPHOS (7), DIOP (5), [(1-dimethylamino)ethyl]-1,2'-bis(diphenylphosphino)-ferrocene (BPPFA)(10)) are less effective than BINAP (Table 4).^{29,47}

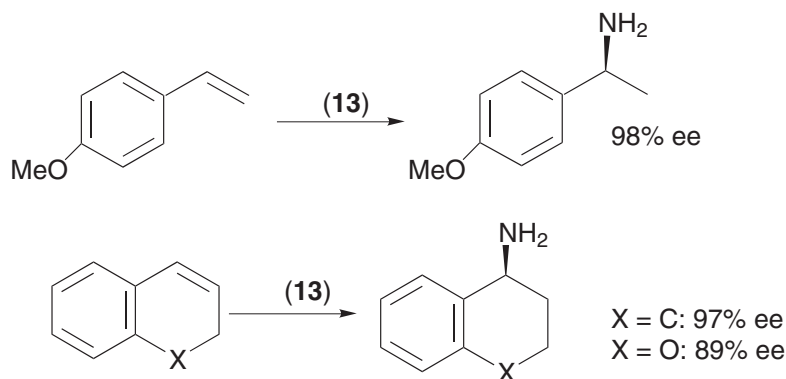
Table 4 Enantioselectivities for $[\text{Rh}(\text{COD})_2]^+/\text{L}^*$ catalyzed asymmetric hydroboration of styrene.

L^*	Conditions	Regioselectivity (branched:linear alcohol)	% ee
(<i>R</i>)-BINAP	−78 °C, DME	>99:1	96 (<i>R</i>)
(<i>R</i>)-BINAP	−30 °C, DME	>99:1	78 (<i>R</i>)
(<i>R</i>)-(<i>S</i>)-BPPFA	25 °C, THF	95:5	22 (<i>R</i>)
(<i>S</i> , <i>S</i>)-DIOP	25 °C, THF	>99:1	4 (<i>R</i>)

Other chelating ligands have been developed that afford catalysts with high reactivity for vinylarenes. Addition of the QUINAP ligand (**12**) (QUINAP = to $[\text{Rh}(\text{COD})(\text{acac})]^+$ (where acac = acetylacetonate) affords $[(\text{P}-\text{N})\text{Rh}(\text{COD})]^+$ (**13**) (Scheme 9), which catalyzes the hydroboration of styrene at room temperature to give 2-(phenyl)ethanol in 96% yield and 91% ee.^{48,49} The phenanthridyl analogue (**14**) shows no advantages for the rhodium-catalyzed hydroboration of styrene, but in the reaction of bulky alkenes (e.g., 1,2-dihydronaphthalene) higher ees are produced in comparison to (**12**).

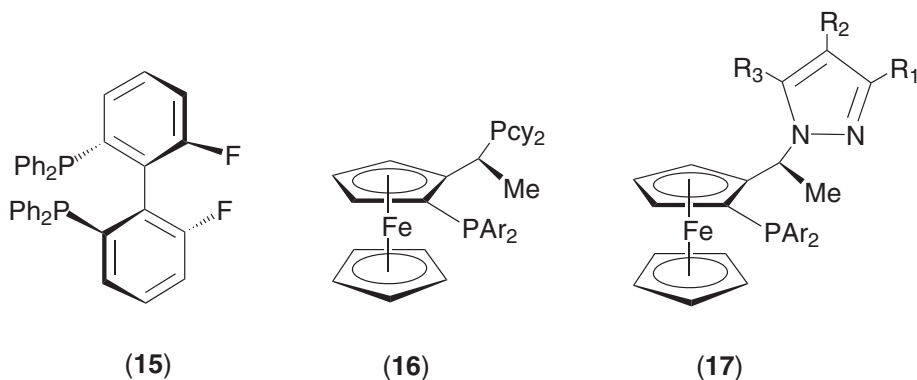
**Scheme 9**

The QUINAP ligands are highly active for reaction of *p*-substituted vinylarenes, thus, *p*-methoxystyrene gives the corresponding branched alcohol in 95% yield (57% ee) within 15 min at room temperature. Similarly, a combination of hydroboration/amination using (**13**) has allowed primary amines to be formed in a one-pot reaction of vinylarenes upon reaction of the B—H addition product with $\text{MeMgCl}/\text{H}_2\text{NOSO}_3\text{H}$ (Scheme 10).⁵⁰

**Scheme 10**

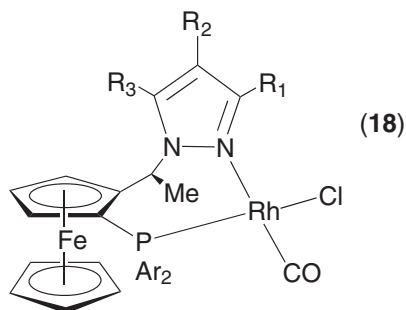
The electron-poor biphenyl diphosphine (**15**) displays poorer regioselectivity for hydroboration of styrene (78% chemical yield) but higher enantioselectivity (78%).⁵¹ The [1,2-(diphenylphosphino)ferrocenyl]ethylcyclohexylphosphine (JOSIPHOS) ligand⁵² (**16**) in combination with

$[\text{Rh}(\text{nbd})_2]^+$ catalyzes H—B addition to vinylarenes, affording >90% ee at low temperature (Scheme 11).⁵³



Scheme 11

Replacement of the phosphine group with a pyrazole at the stereogenic carbon has allowed a series of ligands (**17**) to be synthesized that are readily modulated in terms of both steric and electronic effects. The pyrazole derived ligands (**17**) can be utilized at room temperature to give (**11**) with high enantioselectivity, although the regioselectivity is not as impressive, giving the branched product in only ca. 60% yield.⁵⁴ Substituent effects produce changes in enantioselectivity induced by (**17**) which cover a wide range. With Ar = (*p*-MeO-C₆H₄), R₁ = R₃ = CF₃ and R₂ = H, only 5% ee is observed. Changing the characteristics of the phosphine and pyrazole completely with Ar = 3,5-(CF₃)₂C₆H₄, R₁ = R₃ = Me and R₂ = H gives 98% ee. Optimum enantioselectivities are, therefore, produced if the σ -donor characteristics and π -accepting properties of the phosphine are enhanced. Stoichiometric studies of neutral, spectroscopically and structurally characterized rhodium complexes (e.g., (**18**)) have helped to quantify these effects (Table 5).⁵⁵



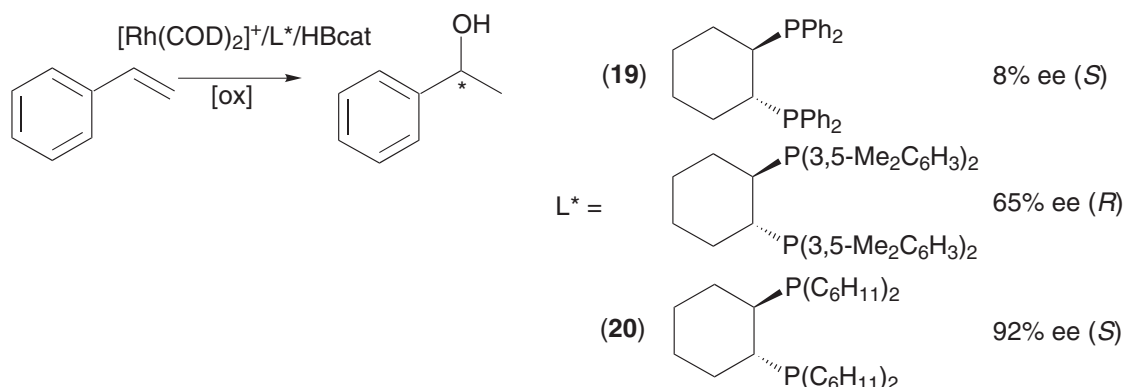
Chiral ruthenoceny phosphine ligands offer no great advantages for hydroboration of styrene relative to the ferrocenyl analogues.⁵⁶

Very recent investigations of styrene hydroboration with C₂-symmetrical 1,2-diphosphines give promising regio- and stereoselectivities. As with the other ligands described above, the electronic properties of the phosphorus substituents prove paramount in determining the reactivity (Scheme 12). Hence, the combination of (1*R*,2*R*)-1,2-bis(diphenylphosphino)cyclohexane (**19**) with $[\text{Rh}(\text{COD})_2]^+$

Table 5 Electronic effects of R and aryl groups on $\nu(\text{CO})$ of rhodium(I) carbonyl complex (**18**).

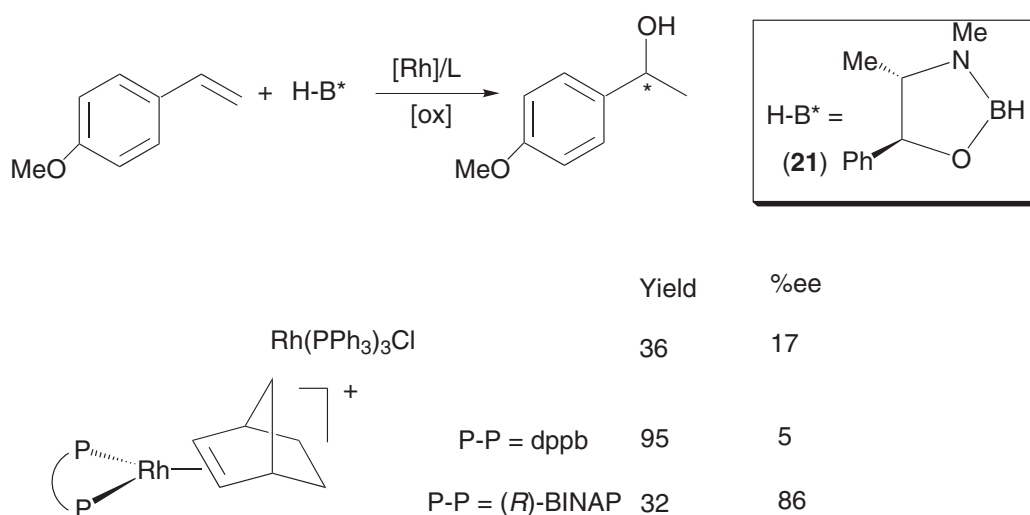
R_1	R_2	R_3	Ar	$\nu(\text{CO})(\text{cm}^{-1})$
Me	H	Me	C ₆ H ₅	1,989
CF ₃	H	CF ₃	C ₆ H ₅	2,000
C ₉ H ₃	H	Me	<i>p</i> -MeO-C ₆ H ₄	1,987
Me	H	Me	<i>p</i> -CF ₃ -C ₆ H ₄	2,006
Me	H	Me	3,5-(CF ₃) ₂ C ₆ H ₃	2,008

gives poor catalytic activity, whereas the very electron-rich (1*R*,2*R*)-1,2-bis(dicyclohexylphosphino)-cyclohexane ligand (**20**) shows >99:1 selectivity for secondary alcohol formation with over 90% ee. These reactions need to be performed at well-below room temperature, but the ligands show good activity for both *p*- and *o*-substituted styrenes.⁵⁷



Scheme 12

An alternative approach to hydroboration has utilized a chiral B—H source with either achiral or chiral rhodium complexes.⁵⁸ The enantiomerically pure reagent (**21**) is derived from ephedrine. Notably in the reactions with BINAP, a higher enantiomeric excess is produced from (*R*)-BINAP (**6**) compared to the *S*-form (Scheme 13).



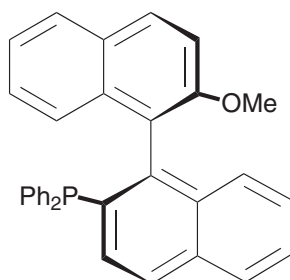
Scheme 13

The MOP series of ligands⁵⁹ (see Section 9.5.4.2) in conjunction with standard palladium precursors has been reported to catalyze the addition of HBcat to 1,3-enynes. With 1 mol.% catalyst produced by combination of $\text{Pd}_2(\text{dba})_3$ and the monodentate ligand (*S*)-MeO-MOP (**22**), axially chiral allenylboranes are formed (Equation (3)). Subsequent oxidation affords the corresponding alcohols with moderate ee values.⁶⁰

9.5.3 HYDROCYANATION

Hydrocyanation represents a reaction of considerable economic importance largely due to the value of the DuPont process involving HCN addition to butadiene to afford adiponitrile.^{61,62} The mechanism is well known, and involves (i) oxidative addition of H—CN to a coordinatively unsaturated metal complex, (ii) coordination of an alkene to the H—M—CN species, (iii) migratory

insertion of the alkene into M—H, and (iv) reductive elimination to afford the alkyl nitrile product.⁶³ In terms of developments in the well-established $[\text{Ni}(\text{P}(\text{O}-o\text{-tolyl})_3)_4]$ catalyzed hydrocyanation, work in the mid-1980s established that simple Lewis acids (AlCl_3 , ZnCl_2) behave as effective cocatalysts in accelerating hydrocyanation of alkenes.^{64,65} Similar effects were discussed for the hydrocyanation of butadiene; nickel phosphine catalysts (e.g., $[\text{Ni}(\text{DIOP})_2]$) were reported that showed improved performance over $[\text{Ni}(\text{P}(\text{O}-o\text{-tolyl})_3)_4]$ for the hydrocyanation of penta-1,4-diene.⁶⁶

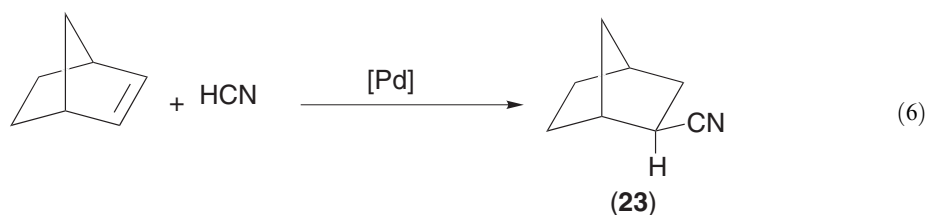


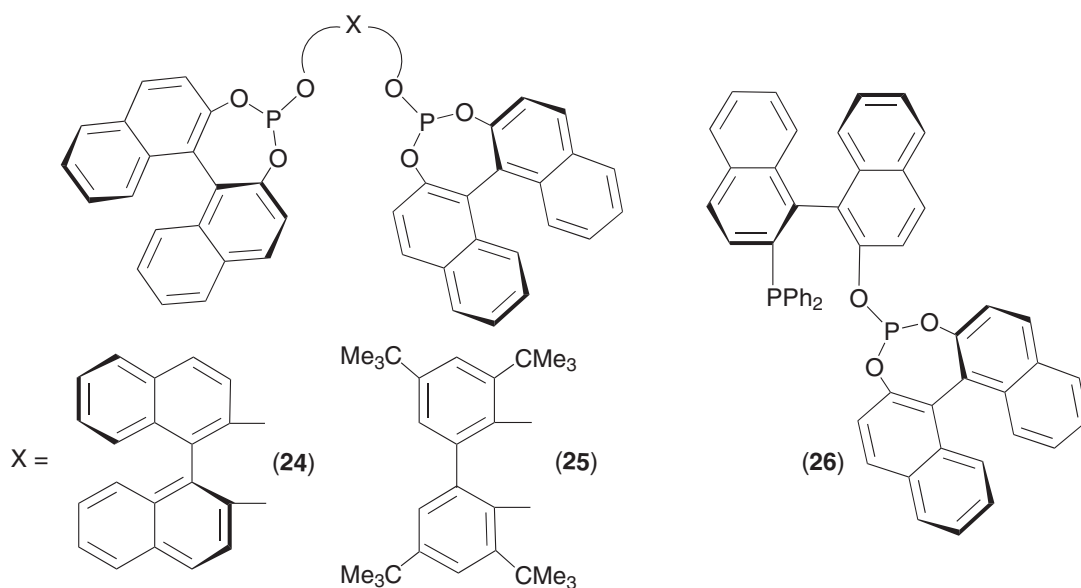
(*S*)-MeO-MOP (**22**)

Most of the major developments in homogeneous transition metal-catalyzed hydrocyanation since the early 1980s have been reviewed;^{62,67} considerable effort in this area has focused on enantioselective reactions.⁶⁸ In this regard, the emphasis has been on complexes of the group 10 metals (particularly Ni and Pd) incorporating new classes of phosphine, phosphite, and phosphinite ligands.

9.5.3.1 Reactions of Nonactivated Alkenes

Enantioselective hydrocyanation of nonactivated alkenes has largely focused on HCN addition to norbornene. Palladium complexes bearing chiral bidentate phosphines PdL_2 afford *exo*-5-cyanobicyclo[2.2.1]heptane (**23**) at 120 °C (Equation (6)), although the yield and degree of enantioselectivity is very dependent on the phosphine used.⁶⁹ While (*R,R*)- or (*S,S*)-DIOP (**5**) gave >60% chemical yields, ee's of only 10–20% are found; (*R*)-BINAP (**6**) affords the *exo* product in only 6% yield, but 40% ee. Chelating phosphines based on a steroid backbone give similar results.⁷⁰ CHIRAPHOS (**7**) and 1,2-bis(diphenylphosphino)propane (PROPHOS) give no catalytic activity.⁶⁹ Stoichiometric reactions indicate that alkene binding to a coordinatively unsaturated Pd center is followed by HCN addition.⁷¹ Thus the product selectivity can be explained by binding of the *exo*-face of norbornene to Pd, followed by the directed addition of HCN to the *exo* position. Whereas bidentate phosphite ligands such as (**24**) show no significant improvements relative to the phosphine systems,⁷² increase of the steric bulk from binaphthyl to a di-*t*-butyl-biphenyl to give (**25**) afforded 84% yield (55% ee).⁷³ Mixed phosphine–phosphite ligands (e.g., (*R,S*)-BINAPHOS, (**26**)) prove to have high activity (Scheme 14).⁷⁴ A catalytic mixture of $\text{Pd}_2(\text{dba})_3$ with one equivalent of (**26**) at 100 °C brings about the addition of H—CN (in the form of acetone cyanohydrin) to norbornene to give (**23**) in 52% yield (48% ee). Similar results are found using a mixture of $\text{Ni}(\text{COD})_2$ /**(26)**. In the Pd case, the presence of excess ligand, leads to suppression of the reaction, while in the case of Ni, the enantioselectivity increases with excess ligand present:

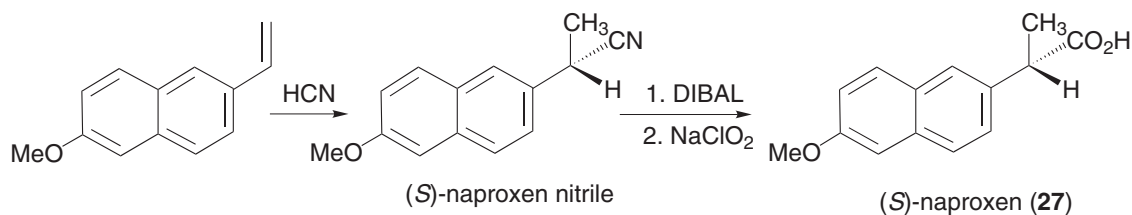




Scheme 14

9.5.3.2 Hydrocyanation of Activated Alkenes

Considerable effort has been directed towards the catalytic addition of HCN to vinylarenes since this represents a route to 2-arylpropionic acids, well-known anti-inflammatory agents.⁷⁵ High levels of asymmetric induction are required; (*R*)-naproxen has undesirable properties associated with it and only the (*S*)-form (**27**) is required (Scheme 15).



Scheme 15

The most successful ligands for Ni-catalyzed hydrocyanation of vinylarenes have proved to be bidentate phosphinite ligands (**28**) based on a carbohydrate skeleton (Equation (7)).^{76,77} Reactions were performed with 1–5 mol.% catalyst (prepared by reaction of $[\text{Ni}(\text{COD})_2]$ with one equivalent of ligand) at room temperature and result exclusively in Markovnikoff addition to afford the required branched aryl nitrile products.⁷⁸ Variation of the R groups at phosphorus shows that electron-withdrawing groups dramatically enhance enantioselectivity (Table 6), while a solvent effect was also noted with nonpolar solvents giving the highest ee values ($\text{C}_6\text{F}_6 \approx \text{hexane} > \text{benzene} > \text{THF}$). A general catalytic cycle for the reaction is shown in Scheme 16. The catalytic resting state $[\text{HNi}(\text{P}-\text{P})(\eta^2\text{-CHR}=\text{CH}_2)(\text{CN})]$ can be reached by either HCN oxidative addition or alkene coordination to $[\text{Ni}(\text{P}-\text{P})(\text{COD})]$ as the first step. Insertion then affords a (η^3 -benzyl)nickel-cyanide intermediate; a related intermediate in hydroamination reactions has since been characterized by other workers (see Section 9.5.5.3).

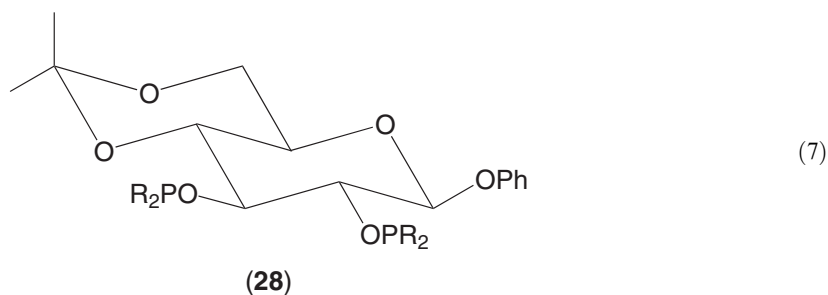
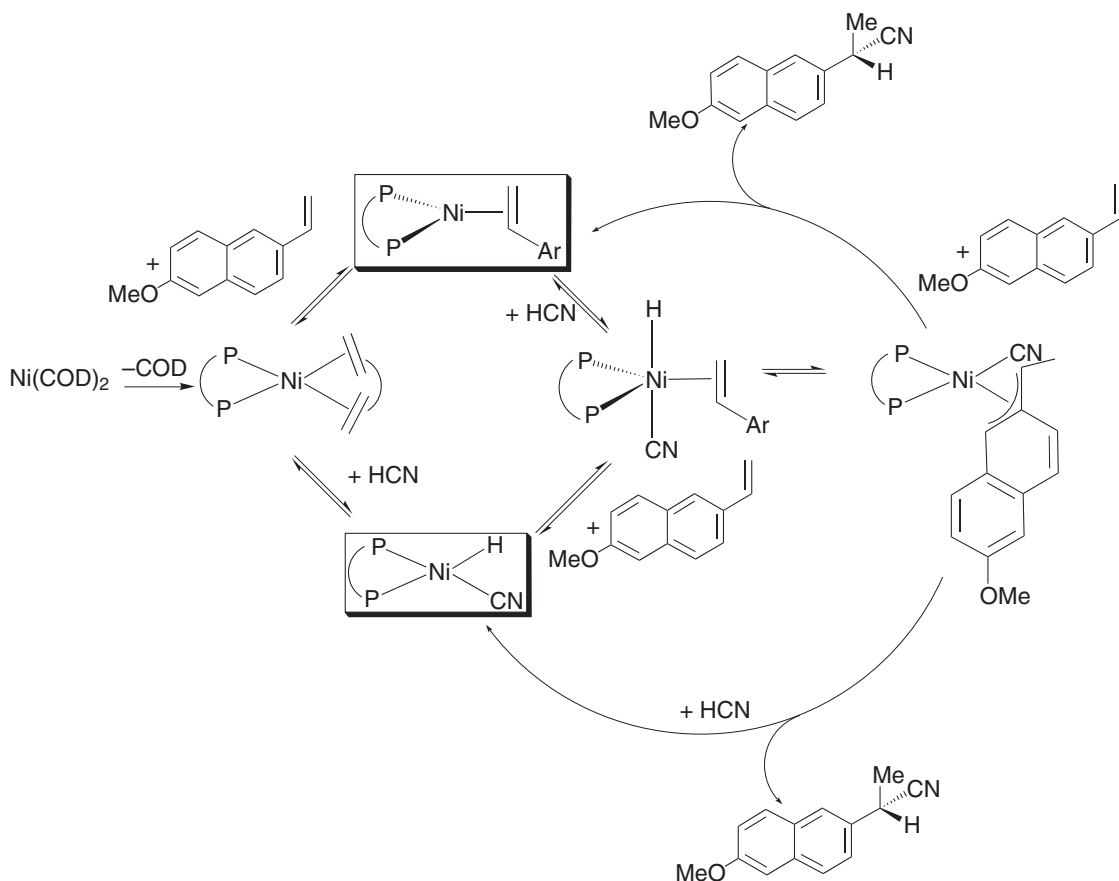


Table 6 The effect of substituents in carbohydrate phosphine (28) on the asymmetric hydrocyanation of 2-methoxy-6-vinylnaphthalene.

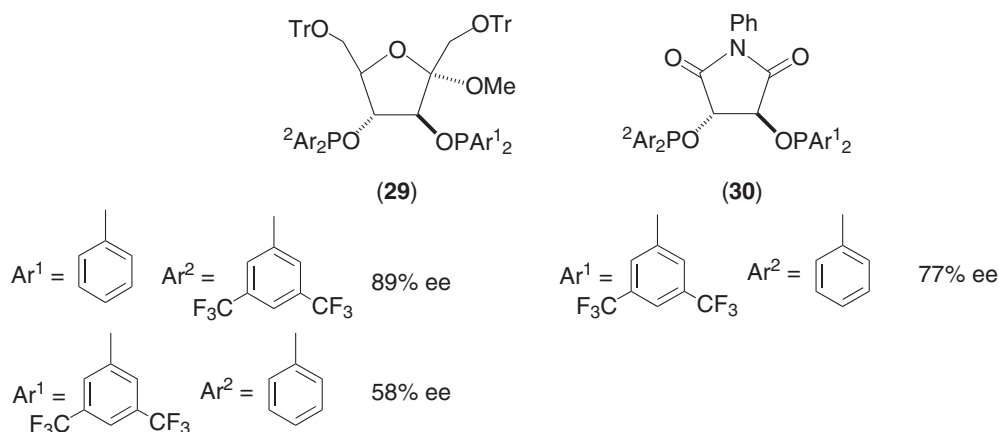
<i>R</i> group	% ee for (<i>S</i>)-naproxen nitrile
C ₆ H ₅	40
3,5-MeC ₆ H ₃	16
3,5-(CF ₃) ₂ C ₆ H ₃	76 (85–91 optimized)
3,5-C ₆ F ₂ H ₃	78
3,5-(CF ₃)MeC ₆ H ₃	75



Scheme 16

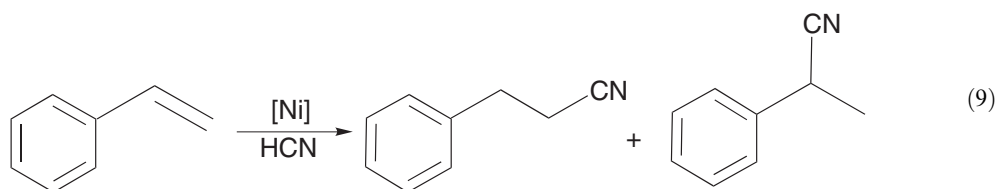
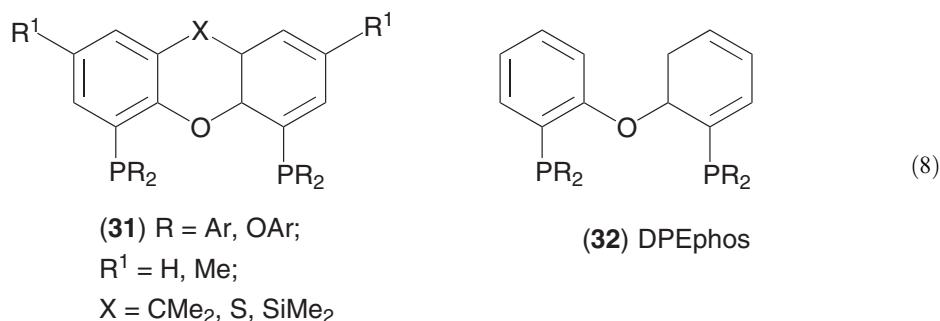
The introduction of electronic asymmetry into this class of bis(diaryl)phosphinites has been used to design catalysts that can afford both enantiomers of naproxen nitrile. If the carbohydrate scaffold is based on methyl α -D-fructofuranoside (29), (*R*)-naproxen nitrile is produced. In a similar manner to the results above, electron-donating aryl substituents on phosphorus afford

poor enantioselectivity. However, the combination of electron donating R at the C-3 position and an electron-withdrawing group at C-4 gives 89% ee. The level of chiral induction drops if the relative position of these groups is switched, implying that an electronic effect is responsible for the behavior. Diarylphosphinites derived from (*S,S*)-tartranil (**30**) show similar, though less impressive, substituent effects. While the C₂-symmetric phenyl and 3,5-bis(trifluoromethyl)phenyl derivatives give good levels of chiral induction (54 and 70% ee, respectively), this is increased in the mixed ligand (Scheme 17).⁷⁹

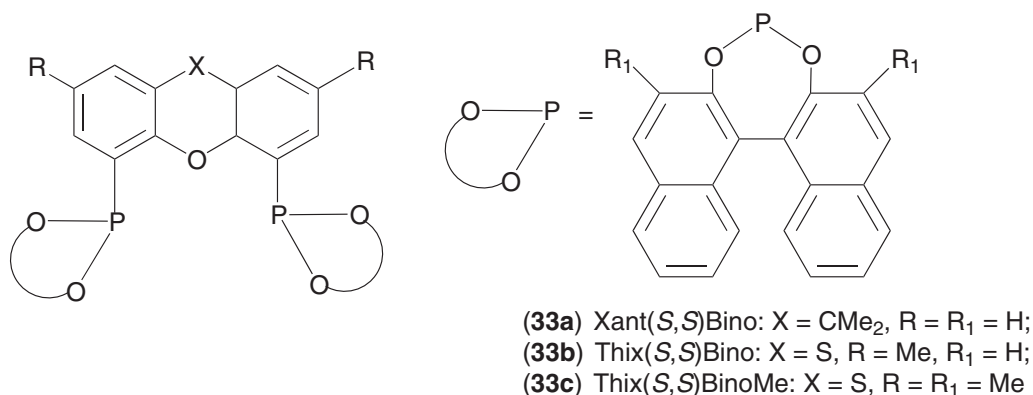


Scheme 17

An additional class of nickel catalyst that has proved highly active for both achiral and chiral hydrocyanation of vinylarenes incorporates chelating diphosphines based on xanthene-type polycyclic heteroarenes (Equation (8)).^{80,81} These so-called xantphos ligands (**31**) have a rigid backbone and a large bite angle; others have shown that a large bite angle favors the reductive elimination of nitriles from nickel diphosphine complexes.⁸² This group of ligands shows markedly improved activity compared to conventional diphosphines. Hence, Ni/L (L = PPh₃, dppe, dppp, or dppb) catalyzed hydrocyanation of styrene (Equation (9)) gives <10% conversion to products, DPEphos (**32**) produces ca. 35–40% while Sixantphos (**31**, R = Ph, R¹ = H, X = SiMe₂) and Thixantphos (**31**, R = Ph, R¹ = Me, X = S) afford yields of up to 95% with 99% selectivity for the branched product.^{83,84}



On the basis of this high reactivity, chiral xantphos diphosphinite ligands have been studied.^{85,86} Addition of HCN to a toluene solution of styrene containing $[\text{Ni}(\text{COD})_2]/(\mathbf{33a-c})$ (ratio 1:1.05) gave the branched nitrile as the major product with 99% regioselectivity. Ligands ($\mathbf{33a}$) and ($\mathbf{33b}$) give poor enantioselectivities, whereas ($\mathbf{33c}$) with methyl groups at the *ortho*-positions of the binaphthyl frame produces an ee of 42% (Scheme 18).



Scheme 18

This same trend is produced upon addition of HCN to 4-isobutylstyrene, but in the case of 6-methoxy-2-vinylnaphthalene, all three ligands afford ca. 30% enantiomeric excess.

9.5.4 HYDROSILYLATION

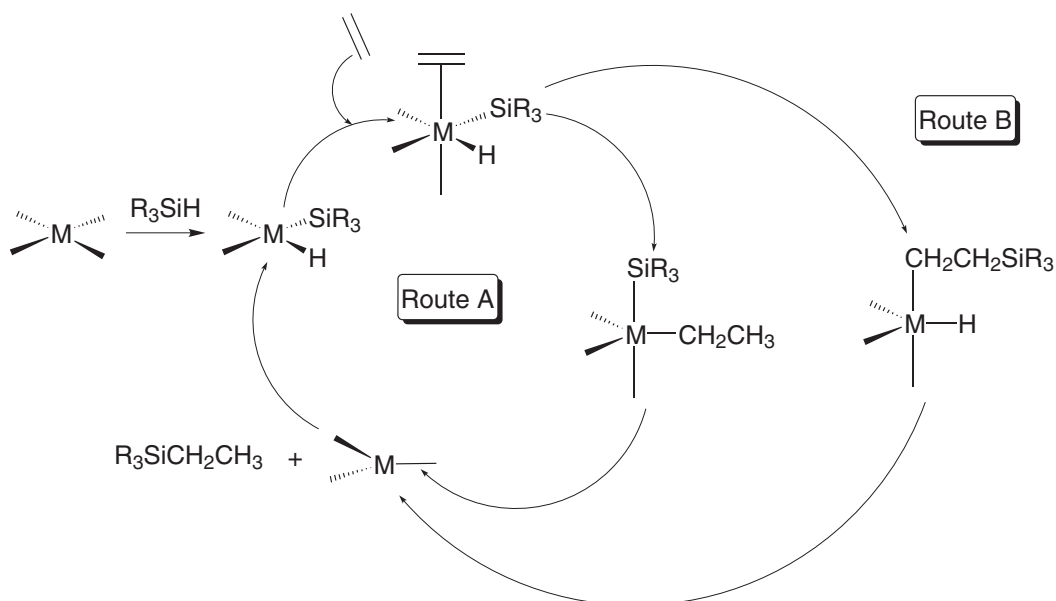
9.5.4.1 Developments in Achiral Catalytic Si—H Addition

The vast majority of studies of metal-catalyzed hydrosilylation reactions involve either rhodium, or more particularly, platinum catalysts.^{87,88} A widely accepted mechanism for alkene hydrosilylation is the Chalk–Harrod cycle (Scheme 19, route A).⁸⁹ Silicon–hydrogen bond oxidative addition to a coordinatively unsaturated metal fragment is followed by alkene coordination and migratory insertion of alkene into the M—H bond. Reductive elimination releases the alkylsilane. Subsequent experimental studies revealed the formation of dehydrogenative silylation products, which cannot be explained by this pathway. An alternative migratory insertion step was proposed (Scheme 19, route B), involving alkene (or alkyne) insertion into M—SiR₃ which allows for β -hydrogen elimination from the silylalkyl metal hydride intermediate.^{90–92} The operation of each specific route is likely to depend on both metal and the surrounding ligand set, although calculations have shown that at least in the case of HSiR₃ (R = H, Cl, Me) and ethene reacting with Pt(PH₃)₂, the standard Chalk–Harrod route is most favorable.⁹³

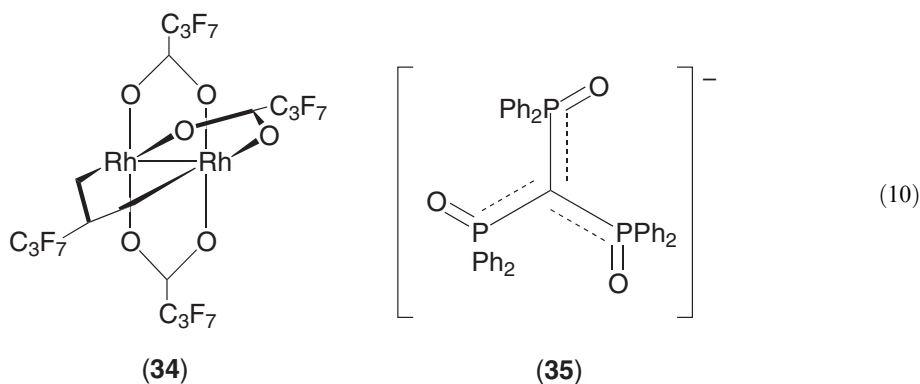
Recent developments in Pd-catalyzed asymmetric H—Si addition are described in Sections 9.5.4.2 and 9.5.4.3. Much of the platinum chemistry from 1982 to the early 1990s sits on the border of coordination and organometallic chemistry and will not be discussed in detail here. Definitive textbook reviews exist in these areas.^{89,90} The application of hydrosilylation from both inorganic and organic aspects has also been discussed in detail.^{94–98} Major developments in the well-established platinum metal salt-catalyzed hydrosilylation include the relevance of colloidal Pt and Rh as catalytically active species from metal halide precursors^{99–102} and a structural determination of Karstedt's catalyst.¹⁰³

Dirhodium tetraeperfluorobutyrate ($\mathbf{34}$) yields alkylsilanes with terminal silyl groups (i.e., normal or anti-Markovnikoff products) when alkene is added to silane; if silane is added to alkene, vinyl, or allylsilane products are formed (Equation (10)).¹⁰⁴ Similarly, these same catalysts will undertake hydrosilylation of alkynes with the formation of allylsilane or vinylsilane products depending upon the order of addition.¹⁰⁵ Iridium complexes capped by the anionic triso ligand ($\mathbf{35}$) (triso = tris(diphenylphosphoranyl)methanide) will hydrosilylate C₂H₄ at room temperature, but are unreactive for most other alkenes (styrene, 1-heptene, norbornene). Thus, $[(\mathbf{35})\text{Ir}(\eta^2\text{-C}_2\text{H}_4)_2]$, $[(\mathbf{35})\text{Ir}(\eta^2\text{-C}_2\text{H}_4)(\text{SiEt}_3)\text{H}]$, and $[(\mathbf{35})\text{Ir}(\text{SiEt}_3)_2\text{H}_2]$ catalyze Et₃SiH addition across

PhC≡CH to give the antiprodut from *cis*-addition. Prolonged contact of the reaction mixture with the catalyst affords the *trans* isomer.^{92,106,107}



Scheme 19



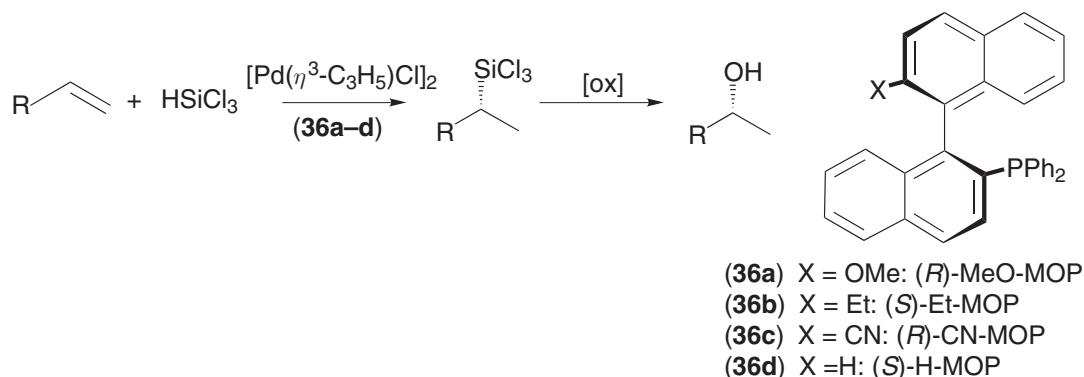
Wilkinson's catalyst brings about the hydrosilylation of a range of terminal alkenes (1-octene, trimethylvinylsilane) by 2-dimethylsilylpyridine with good regioselectivity for the anti-Markovnikoff product. Both 3-dimethylsilylpyridine and dimethylphenylsilane are less reactive sources of Si—H. In contrast, these two substrates are far more reactive than 2-dimethylsilylpyridine for the hydrosilylation of alkynes by [Pt(CH₂=CHSiMe₂)₂O]/PR₃ (R = Ph, Bu^t). This difference was explained to be due to the operation of the two different pathways for Si—H addition—the standard Chalk–Harrod pathway with platinum and the modified Chalk–Harrod pathway with rhodium.¹⁰⁸

9.5.4.2 Asymmetric Hydrosilylation

Catalytic asymmetric hydrosilylation is an important goal in synthetic organic chemistry. Incorporation of chiral ligands into the metal catalyst may result in the hydrosilylation reaction furnishing optically active alkylsilanes. The C—Si bond can then be oxidized (with retention of configuration at the stereogenic carbon center) to afford optically active alcohols. Much of the focus in ligand design to bring about such enantioselective hydrosilylation has involved chiral phosphine ligands.

The MOP range of ligands designed by Hayashi has proved remarkably useful for asymmetric hydrosilylation reactions.⁵⁹ MOP ligands are a series of enantiomerically pure monophosphine ligands whose chirality is due to 1,1'-binaphthyl axial chirality.

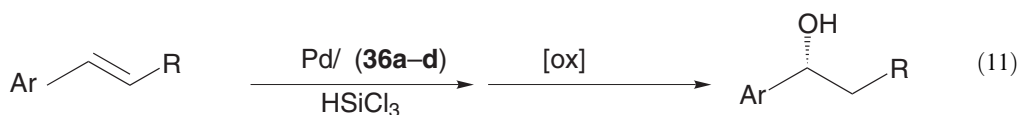
The silylation of simple terminal alkyl substituted alkenes $\text{CH}_2=\text{CHR}$ ($\text{R} = n\text{-C}_4\text{H}_9$, $n\text{-C}_6\text{H}_{13}$, $n\text{-C}_{10}\text{H}_{21}$, $\text{CH}_2\text{CH}_2\text{Ph}$, or C_6H_{11}) with trichlorosilane is catalyzed by a mixture of $[\text{Pd}(\eta^3\text{-C}_3\text{H}_5)\text{Cl}]_2$ and the chiral monodentate phosphine MOP ligands (**36a–d**) to give 1-alkanols with 94–97% ee (Scheme 20).¹⁰⁹



Scheme 20

These reactions can be performed at 40 °C with <0.1 mol.% of the generated palladium catalyst. Most notably, high regioselectivity for the branched product is found (e.g., (*S*)-MeO-MOP (**22**) yields a 2-octylsilane to 1-octylsilane product ratio of 93:7) and both this and the enantioselectivity are essentially invariant with the substituent on the alkene, indicating that steric bulk has little effect on the asymmetry in the reaction (Table 7).

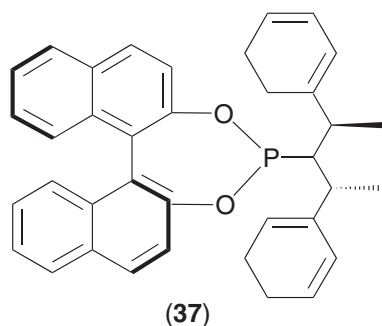
However, in the palladium-catalyzed addition of HSiCl_3 to β -substituted styrenes, the size of the substituent on the MOP ligand is crucial. While (*R*)-MeO-MOP/ $[\text{Pd}(\eta^3\text{-C}_3\text{H}_5)\text{Cl}]_2$ yielded (*R*)-phenylethanol with poor enantioselectivity (14% ee),¹¹⁰ replacement of the methoxy group with hydrogen (H-MOP, (**36d**)) affords the same product with 93% ee (Equation (11)).¹¹¹



Electronic effects cannot be used to explain this difference since X-MOP (X = HO, CO_2Me , CN, or Et) ligands containing both electron-donating and electron-withdrawing groups all show low reactivity, indicating that steric influence must be the dominant influence. Chiral phosphoramidite ligands show phenomenal activity for asymmetric hydrosilylation of substituted styrenes. Thus 1 mol.% of catalyst derived from $[\text{Pd}(\eta^3\text{-C}_3\text{H}_5)\text{Cl}]_2$ and (**37**) (Scheme 21) affords 100% yield and 99% ee (room temperature, 24 h) of 1-phenylethanol from styrene. This is the highest level of asymmetric induction found for the hydrosilylation of styrenes.¹¹²

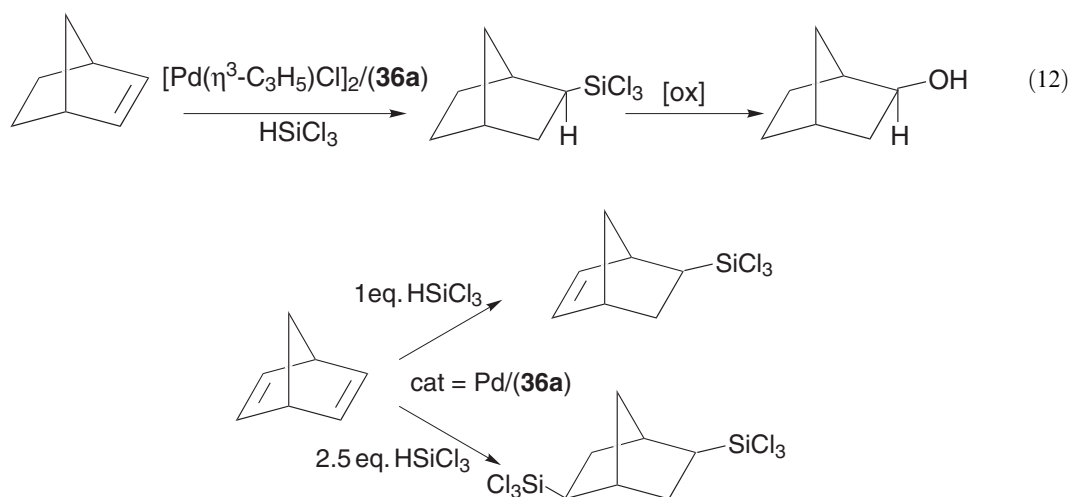
Table 7 Regio- and enantioselectivity for hydrosilylation of terminal alkenes with $\text{Pd}(\text{S})$ -/MeO-MOP (**22**).

Substrate	Regioselectivity (% branched:linear)	Enantioselectivity (% ee for branched alcohol)
$\text{C}_4\text{H}_9\text{CH}=\text{CH}_2$	89:11	94 (<i>R</i>)
$\text{C}_6\text{H}_{13}\text{CH}=\text{CH}_2$	93:7	95 (<i>R</i>)
$\text{C}_{10}\text{H}_{21}\text{CH}=\text{CH}_2$	94:6	95 (<i>R</i>)
$\text{C}_6\text{H}_5\text{CH}_2\text{CH}_2\text{CH}=\text{CH}_2$	81:19	97 (<i>S</i>)
$\text{C}_6\text{H}_{11}\text{CH}=\text{CH}_2$	66:43	96 (<i>R</i>)



Scheme 21

The Pd/MOP combination has proved active for the asymmetric hydrosilylation of cyclic alkenes and dienes. Thus treatment of norbornene with HSiCl_3 at 0°C for 24 h in the presence of 0.01 mol.% of MeO-MOP/ $[\text{Pd}(\eta^3\text{-C}_3\text{H}_5)\text{Cl}]_2$ gave quantitative yield of *exo*-2-(trichlorosilyl)norbornane; oxidation produced the corresponding alcohol in 93% ee (Equation (12)). Lowering the temperature (to -20°C) increased this to a 96% ee. Both mono- and difunctionalization of nbd has proved possible, depending upon the quantity of trichlorosilane used (Scheme 22). In both reactions, extremely good enantioselectivities are observed:¹¹³

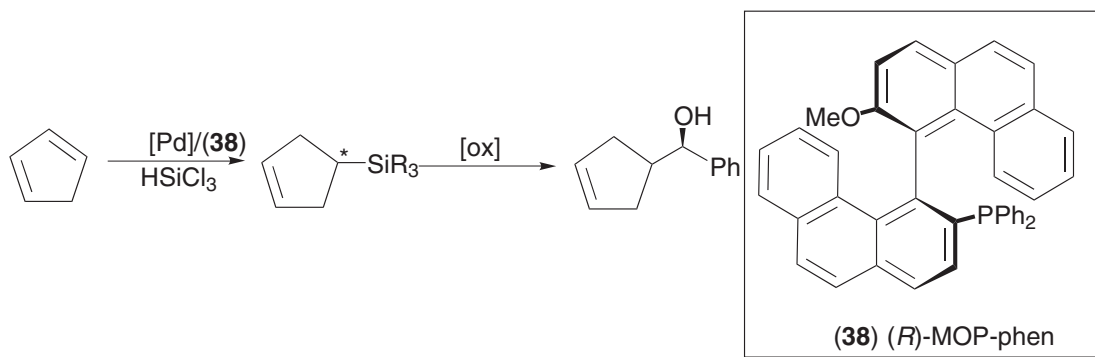


Scheme 22

The most active palladium catalyst system developed for the asymmetric hydrosilylation of cyclopentadiene (Scheme 23) involves the use of the (*R*)-MOP-phen ligand (**38**), which shows significant enhancement of enantioselectivity compared to (*R*)-MeO-MOP (80% ee from (**38**), 39% ee from (**36a**)).¹¹⁴ Other phosphine ligands that afford active palladium catalysts for the same transformation include the β -*N*-sulfonylaminoalkylphosphine (**39**) and phosphetane ligand (**40**) (Equation (13)).^{115–117} A comparison of the enantioselectivities of these ligands for the palladium-catalyzed hydrosilylation of cyclopentadiene is given in Table 8.

MOP ligands prove useful for the hydrosilylation of heteroatom-functionalized cyclic alkenes to give optically active alcohols with high enantioselectivities.¹¹⁸ Recently, a dual platinum/palladium system incorporating the electronically and sterically modified MOP ligand (**41**) has allowed the double asymmetric hydrosilylation of alkynes to 1,2-diols to be performed (Scheme 24).¹¹⁹ Reaction of 1-phenyl-ethyne with HSiCl_3 in the presence of $[\text{Pt}(\text{C}_2\text{H}_4)\text{Cl}]_2$ at room temperature gave the Markovnikov Si—H addition product in 97% yield. Subsequent addition of trichlorosilane and $[\text{Pd}(\eta^3\text{-C}_3\text{H}_5)\text{Cl}]_2$ /**(41)** resulted in a second Si—H addition. The MOP ligand (**41**) has also been shown to be active in the palladium-catalyzed hydrosilylation of styrene, where it is more active than (**36d**) and only slightly less than (**37**).¹²⁰ The relative reactivity of these MOP ligands has been rationalized due to the rates of

β -hydrogen elimination in an alkene hydride intermediate and the selectivity of the subsequent reductive elimination step from one of the diastereomeric intermediates.



Scheme 23

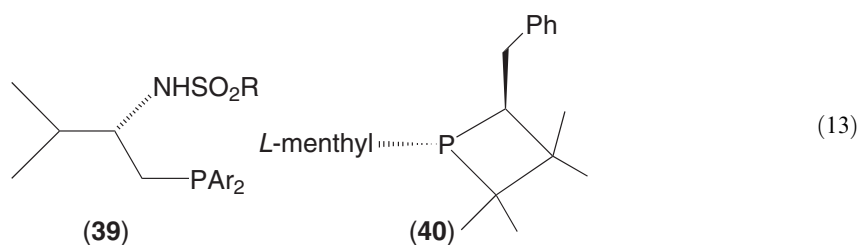
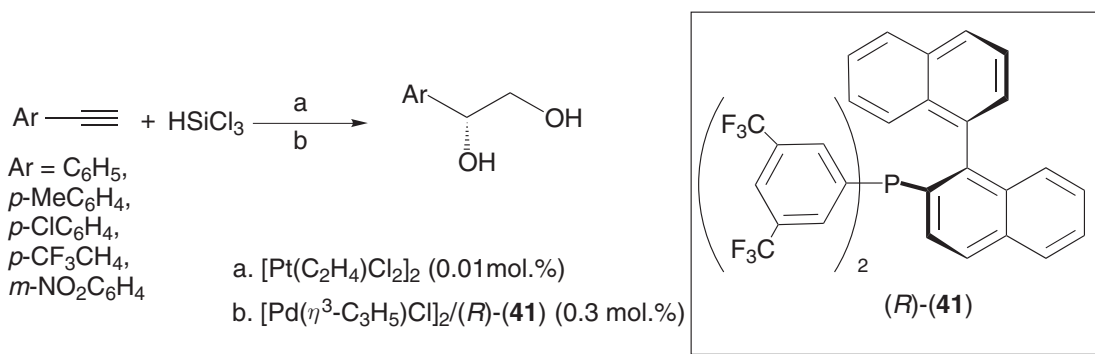


Table 8 Hydrosylation of cyclopentadiene by PdL*.

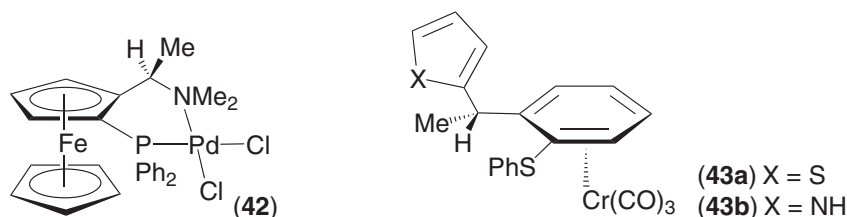
<i>PdL*</i>	<i>Conditions</i>	<i>% yield and % ee</i>
$\text{Pd}(\text{CH}_3\text{CN})_2\text{Cl}_2/$ (<i>S</i>)- (39) , R=Me, Ar = Ph	0.1 mol.%, -20°C	35, 71 (<i>S</i>)
$\text{Pd}(\text{PhCN})_2\text{Cl}_2/$ (40)	0.03 mol.%, 30°C , 2 h	70, 54 (<i>S</i>)
$[\text{Pd}(\eta^3\text{-C}_3\text{H}_5)\text{Cl}]_2/$ (38)	0.1 mol.%, 20°C , 120 h	99, 88 (<i>R</i>)
$[\text{Pd}(\eta^3\text{-C}_3\text{H}_5)\text{Cl}]_2/$ (36a)	0.1 mol.%, 20°C , 14 h	100, 39 (<i>R</i>)



Scheme 24

9.5.4.3 Enantioselective Hydrosilylation Employing Chiral Ferrocenyl Phosphine Ligands

As an alternative to the MOP ligands, chiral ferrocenyl phosphines have received attention in enantioselective hydrosilylation reactions (Scheme 25). The palladium(II) catalyst (**42**) incorporating the monodentate ferrocenylphosphine ligand (*R*)-(*S*)-*N,N*-dimethyl-1-[2-(diphenylphosphino)ferrocenyl]ethylamine (PPFA) was reported to give the hydrosilylation/oxidation product (*S*)-1-phenylethanol from styrene/ HSiCl_3 in 52% ee.¹²¹ Attachment to a polymer (cf Chapter 9.9) support gives a tethered catalyst, although the activity of the system was lowered.¹²² A related system¹²³ bearing the arene chromium tricarbonyl derived ligand (**43a**) gives (*S*)-1-phenylethanol in 92% ee at -50°C .



Scheme 25

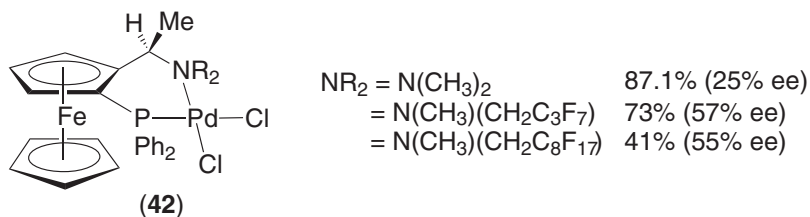
As with asymmetric hydroboration, the pyrazolyl substituted analogues of the PPFA ligand (**17**) react with $[\text{Pd}(\text{COD})\text{Cl}_2]$ to give a catalyst system that will hydrosilylate norbornene to give both *exo* and *endo* alcohols. The former is always the major product, although the degree of enantioselective induction can be directed by the substituents on the pyrazolyl arm of the phosphine and the R groups on the phosphorus center itself. Thus, the enantiomeric excess of (1*R*,2*R*,4*S*)-*exo*-2-norbornanol can be increased from 91% ee ($\text{R}_1 = \text{Ph}$, $\text{R}_2 = \text{H}$, and $\text{R}_3 = \text{mesityl}$ (Mes)) to >99.5% ee ($\text{R}_1 = 3,5\text{-(CF}_3)_2\text{C}_6\text{H}_3$, $\text{R}_2 = \text{H}$, $\text{R}_3 = \text{Mes}$).¹²⁴

A summary of the ligand effects of the palladium-catalyzed enantioselective hydrosilylation of styrene is given in Table 9.

Addition of HSiMeCl_2 to cyclopentadiene is catalyzed by (**42**) at room temperature at low catalyst loading (0.01 mol.%) to give the (*S*)-allylsilane in moderate ee.¹²⁵ This enantioselectivity can be enhanced dramatically with incorporation of perfluoroalkyl groups into the amine functionality (Scheme 26).¹²⁶

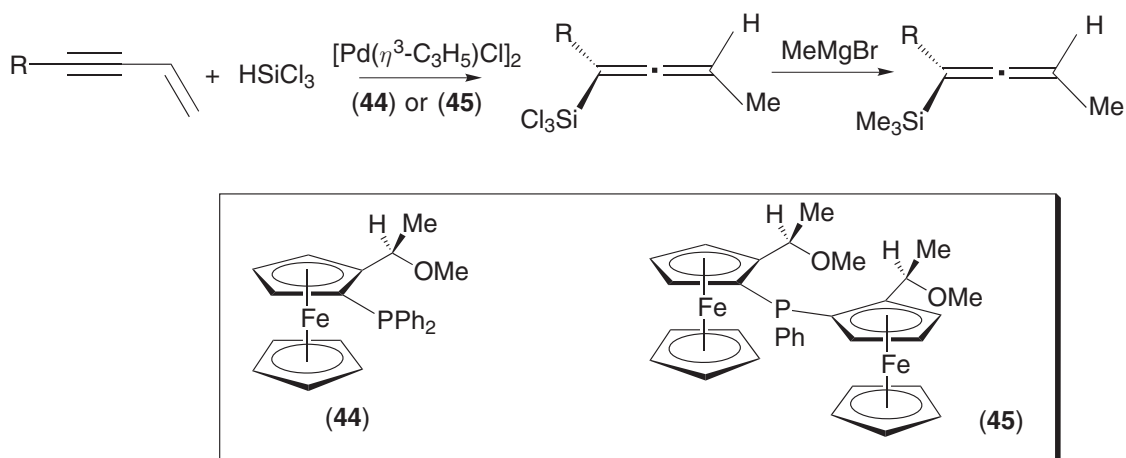
Table 9 Palladium-catalyzed asymmetric hydrosilylation of styrene.

Catalyst system	Conditions (% cat, temp/time, % conversion to silane)	% ee 1-phenyl ethanol	References
$\text{Pd}(\text{CH}_3\text{CN})_2\text{Cl}_2$ (39) (R = Me, Ar = C_6H_5)	0.1 mol.%, 20°C	65 (<i>S</i>)	115
$\text{Pd}(\text{CH}_3\text{CN})_2\text{Cl}_2$ (39) (R = Me, Ar = <i>p</i> - MeOC_6H_4)	0.1 mol.%, 20°C	52 (<i>S</i>)	115
$\text{Pd}(\text{CH}_3\text{CN})_2\text{Cl}_2$ (39) (R = C_6H_5 , Ar = C_6H_5)	0.1 mol.%, 20°C	51 (<i>S</i>)	115
$[\text{Pd}(\eta^3\text{-C}_3\text{H}_5)\text{Cl}]_2$ (36a)	0.1 mol.%, 0°C , 24 h, 100%	14 (<i>R</i>)	111
$[\text{Pd}(\eta^3\text{-C}_3\text{H}_5)\text{Cl}]_2$ (36b)	0.1 mol.%, 0°C , 12 h, 100%	18 (<i>R</i>)	111
$[\text{Pd}(\eta^3\text{-C}_3\text{H}_5)\text{Cl}]_2$ (36c)	0.1 mol.%, 0°C , 24 h, 100%	26 (<i>R</i>)	111
$[\text{Pd}(\eta^3\text{-C}_3\text{H}_5)\text{Cl}]_2$ (36d)	0.1 mol.%, -10°C , 32 h, 92%	94 (<i>R</i>)	111
$[\text{Pd}(\eta^3\text{-C}_3\text{H}_5)\text{Cl}]_2$ (37)	1 mol.%, 20°C , 100%	99 (<i>R</i>)	112
(42)	0.01 mol.%, 70°C ,	52 (<i>S</i>)	121



Scheme 26

Both the nature of the ligand and the silane have been shown to influence the efficiency of cyclohexadiene hydrosilylation.¹²⁷ Thus, replacement of the dialkylamino moiety in (10) by an acetate group gives a more active catalyst system; intriguingly, use of HSiF_2Ph produces higher ee values than recorded with HSiCl_3 . Both mono- and bisPPFA-derived ligands afford catalysts upon treatment with $[\text{Pd}(\eta^3\text{-C}_3\text{H}_5)\text{Cl}]_2$ that provide a pathway to axially chiral allenylsilanes (Scheme 27). In the presence of (*S*)-(*R*)-PPFOMe (44), >80% chemical yield of the hydrosilylated species is produced (subsequent methylation gives a 72% ee of trimethyl(allyl)silane). Changing the ligand to (*S*)-(*R*)-bisPPFOMe (45) results in enhanced enantioselectivity in the final methylated allenyl system (90% ee).¹²⁸



Scheme 27

9.5.4.4 Intramolecular Asymmetric Hydrosilylation

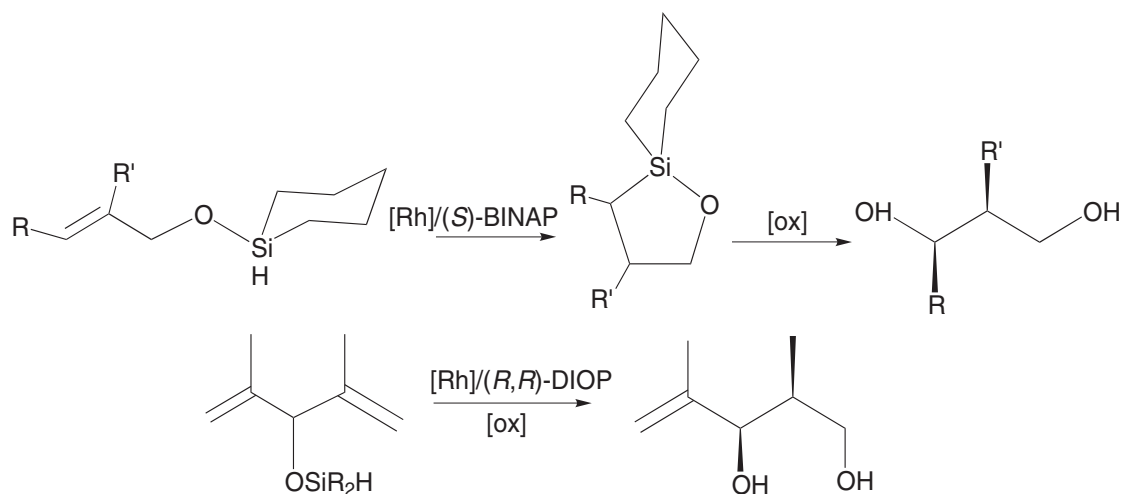
The rhodium-catalyzed intramolecular hydrosilylation of allylic alcohol derived silyl ethers has been described. Oxidative cleavage of the resulting cyclized hydrosilylation products affords a route to optically active diols (Scheme 28).^{129,130}

The catalyst system employed was the cationic rhodium solvent complex $[\text{Rh}(\text{P}-\text{P})\text{S}_2]^+$ (P–P = BINAP, CHIRAPHOS, S = solvent). The BINAP ligand enhances the activity of the complex (Table 10), although additional studies have revealed that both the solvent and the substituents on Si influence the levels of enantioselectivity (Scheme 29).^{131,132}

Deuterium-labeling studies pointed to the operation of a nonstandard Chalk–Harrod mechanism for these reactions involving a silyl-alkene insertion step.¹³³

Intramolecular hydrosilylation of the *bis*-alkenyl silane yields the chiral spirosilane with high diastereoselectivity (Scheme 30). With 0.3–0.5 mol.% of catalyst consisting of $[\text{Rh}(\text{hexadiene})\text{Cl}]_2$ and a range of chelating phosphines P–P (P–P = (*R*)-BINAP (6), (*R,R*)-DIOP (5)), a maximum chemical yield of spirosilane of 82% was found with 83% enantiomeric excess. These values were improved considerably by the use of the new ligand

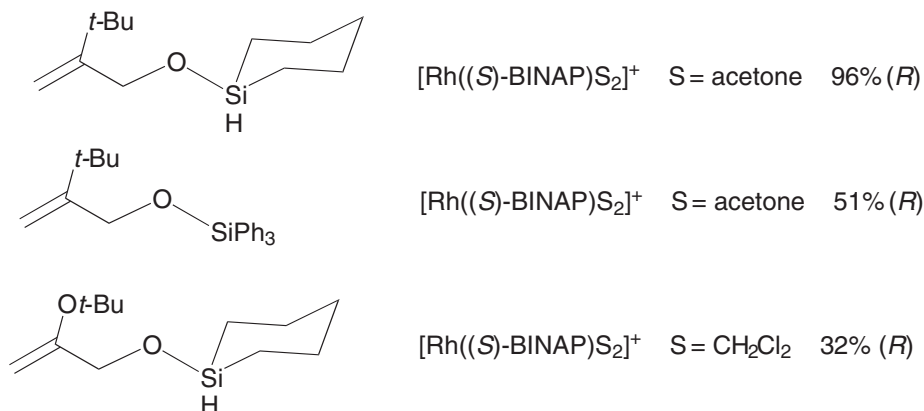
(2,3-bis(siloxy)-1,4-bis(diphenylphosphino)butane) (SILOP) (**46**). The presence of a bulky Bu^tMe_2 substituent on the siloxane backbone gave over 98% yield and 99% ee at -20°C .¹³⁴



Scheme 28

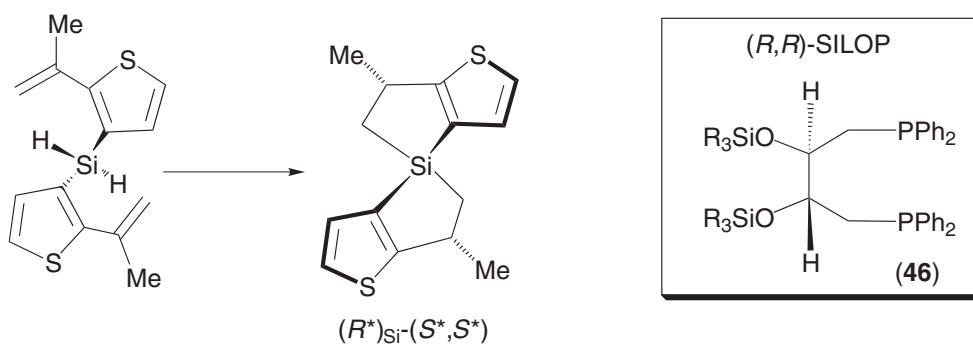
Table 10 Impact of the chelating phosphine on levels of enantioselectivity in rhodium-catalyzed intramolecular hydrosilylation with $[\text{Rh}(\text{P}-\text{P})(\text{acetone})_2]^+$.

Silyl ether substituents	% ee ($P-P = (S)$ -BINAP)	% ee ($P-P = (S,S)$ -CHIRAPHOS)
R = Ph, R' = H	96 (<i>R</i>)	74 (<i>R</i>)
R = naphthyl, R' = H	94 (<i>R</i>)	
R = Ph, R' = Me	90 (<i>R,R</i>)	0

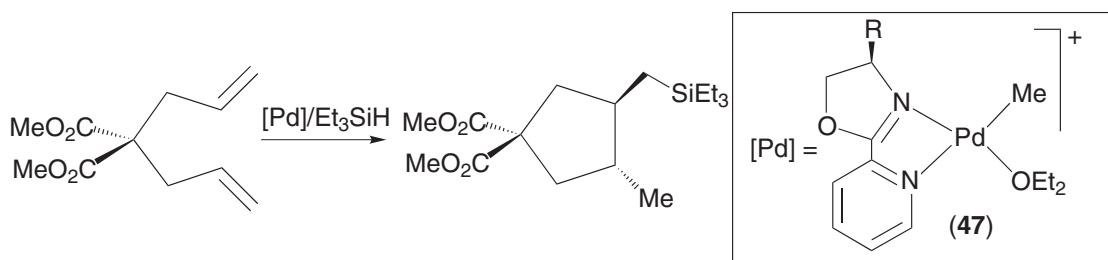


Scheme 29

Palladium oxazoline compounds (e.g., (**47**)) have been used to catalyze the cyclization/hydrosilylation of functionalized 1,6-dienes (Scheme 31). With $\text{R} = \text{Pr}^i$, >95% diastereomeric excess and 87% ee was achieved at low temperature. Changing the ligand bulk with $\text{R} = \text{Bu}^i$ gave a higher ee value, but poorer diastereoselectivity. A range of functional groups can be tolerated at both the allylic and terminal alkene positions.^{135–137}



Scheme 30



Scheme 31

9.5.4.5 Enantioselective Hydrosilylation of C=O and C=N Bonds—A Brief Synopsis

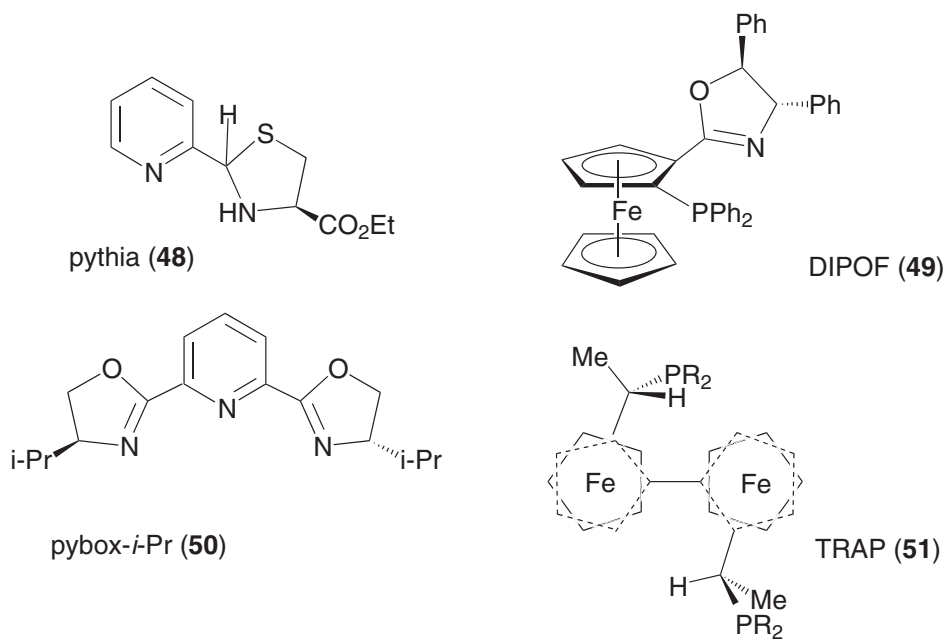
While it is beyond the scope of this chapter to cover the asymmetric hydrosilylation of ketones and imines in any detail, a number of the more catalytically active M–L combinations will be mentioned here. A full review of the area has recently appeared.¹³⁸ Asymmetric hydrosilylation of carbonyl groups is usually performed with rhodium or titanium catalysts bearing chelating N- or P-based ligands. Representative results for some of the most active Rh/L combinations (Scheme 32) for addition of Si–H to acetophenone are given in Table 11.

Among titanium compounds, many sit on the border of being organometallic/coordination compounds. One which is of interest in relation to the enhancing effects of F[−] (see Section 9.5.5.2) is the titanium fluoride complex (52), which is highly active for the hydrosilylation of imines (Scheme 33).¹⁴³

9.5.5 HYDROAMINATION

9.5.5.1 Mechanism and Early Transition Metal/Lanthanide Catalysts

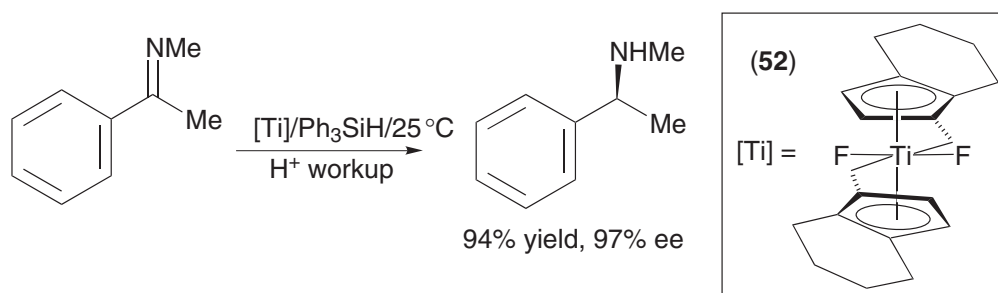
Hydroamination involves the addition of primary or secondary amines to alkenes to afford terminal or branched higher value substituted amines via anti-Markovnikoff or Markovnikoff addition.¹⁴⁴ Although the addition of RNH₂ to C=C is thermodynamically favorable (Equation (14)), there is a strong entropic factor disfavoring N–H addition which has to be overcome through use of a metal catalyst.



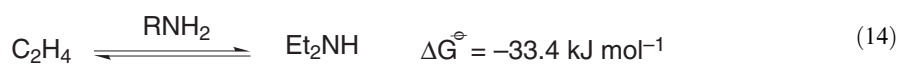
Scheme 32

Table 11 Asymmetric hydrosilylation of acetophenone with Ph_2SiH_2 .

<i>Rh</i> precursor	<i>L</i> *	Temp. (°C)	% Yield	% ee	References
$[\text{Rh}(\text{COD})\text{Cl}]_2$	(48)	−20	99	98	139
(49) RhCl_3		0	91	94	140
$[\text{Rh}(\text{COD})\text{Cl}]_2$	(50)	25	100	91	141
$[\text{Rh}(\text{COD})_2]^+$	(51), R = Bu ⁿ	−40	88	92	142



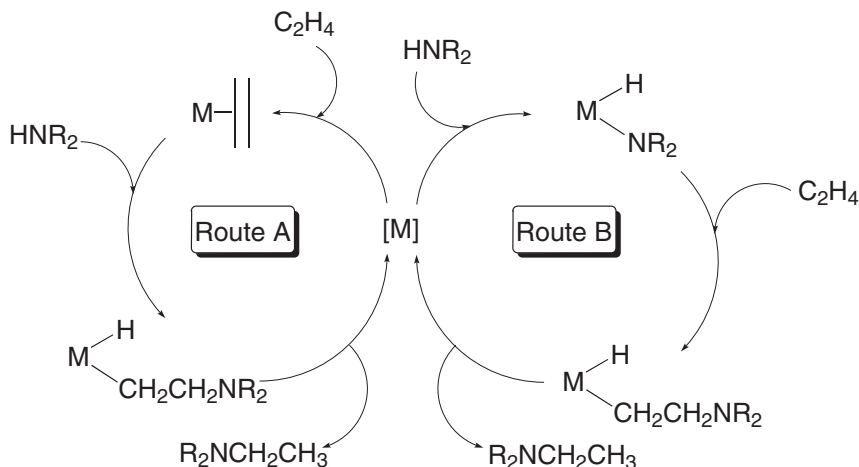
Scheme 33



Considerable effort has been directed at this problem utilizing both early and late transition metal coordination compounds, as well as lanthanide and actinide complexes. While progress has been made,^{145,146} hydroamination reactions are, in general, still characterized by their lack of applicability to many types of unsaturated substrates and paucity of catalytic systems with high enough turnover frequencies and appropriate levels of regioselectivity which are active at low levels of catalyst loading. Indeed, in 1993, an article in *Chemical and Engineering News* identified a route to anti-Markovnikoff addition of N—H to alkenes as one of the top 10 catalytic challenges to be overcome.¹⁴⁷ The progress made in transition metal and *f*-element-catalyzed hydroamination was comprehensively reviewed in 1998.¹⁴⁸ This section of the chapter will outline the major developments in the area up to that point and the significant number of catalytic processes described since then.

Two potential pathways exist for the addition of N—H across C=C bonds (Scheme 34):

- (i) Nucleophilic attack of an N—H bond on a metal-coordinated alkene (route A).
- (ii) Oxidative addition of N—H to a coordinatively unsaturated metal fragment [M], followed by alkene insertion into M—N (or M—H) and then reductive elimination (route B).



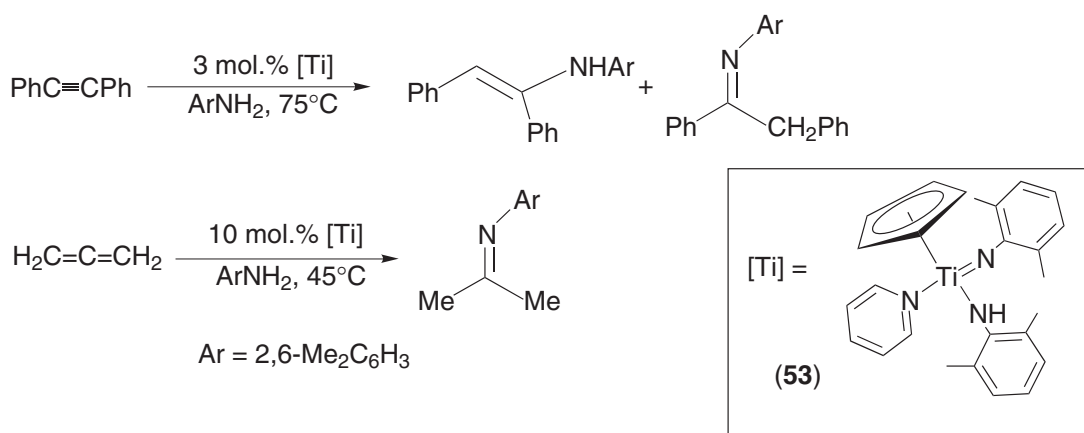
Scheme 34

Organometallic complexes of the *f*-elements have been reported that will perform both intra- and intermolecular hydroamination reactions of alkenes and alkynes, although these lie outside of the scope of this review.^{149–155} Early transition metal catalysts are not very common, although a number of organometallic systems exist.^{156–158} In these and other cases, the intermediacy of a metal imido complex $L_nM=NR$ was proposed.^{159,160} Such a species has recently been isolated (53) and used as a direct catalyst precursor for N—H addition to alkynes and allenes (Scheme 35).^{161,162}

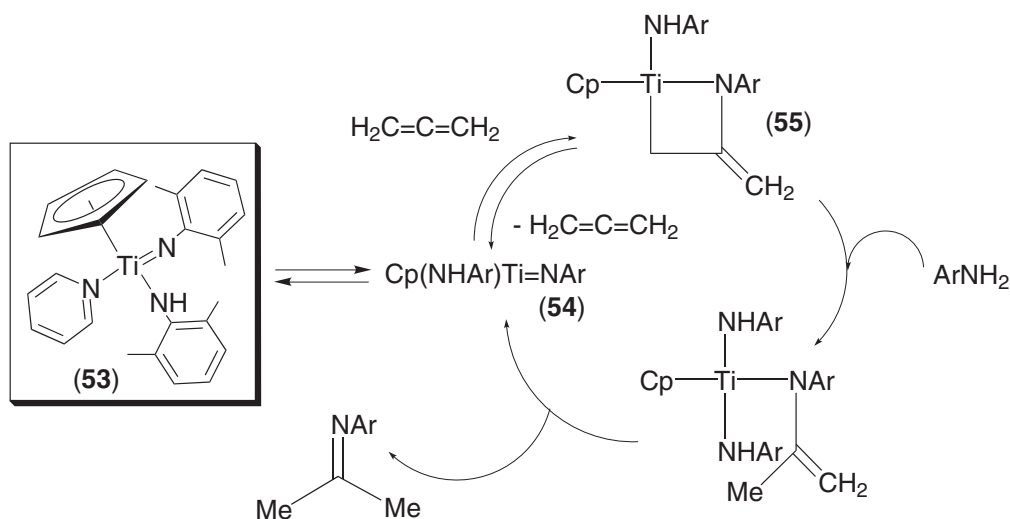
Kinetic measurements are consistent with the mechanism shown in Scheme 36.

Reversible pyridine dissociation yields the non-Lewis base stabilized imido complex $[Cp(NHAr)Ti=NAr]$ (54). This coordinatively unsaturated species undergoes a [2 + 2] cycloaddition reaction with allene to give an azatitanacyclobutane (55), which is then protonated to the trisamido complex. Elimination of enamine occurs followed by isomerization to the energetically more favorable imine.

Titanium amido complexes have been utilized in the hydroamination of alkynes using primary amines to afford predominantly branched (Markovnikoff) products. Both $PhNH_2$ and Bu^tNH_2 can be added across terminal and internal alkynes with 10 mol.% $Ti(NMe_2)_4$ at elevated temperature.¹⁶³ Aniline affords the highest yield of products, although the regioselectivity varies with alkyne (3:1 for $Bu^tC\equiv CH$, >100:1 $PhC\equiv CH$). The related complex $[Ti(NMe_2)_2(dpma)]$ ($dpma = di(\text{pyrrol-}\alpha\text{-methyl})\text{methylamine}$) gives higher selectivity for Markovnikoff addition.¹⁶⁴



Scheme 35



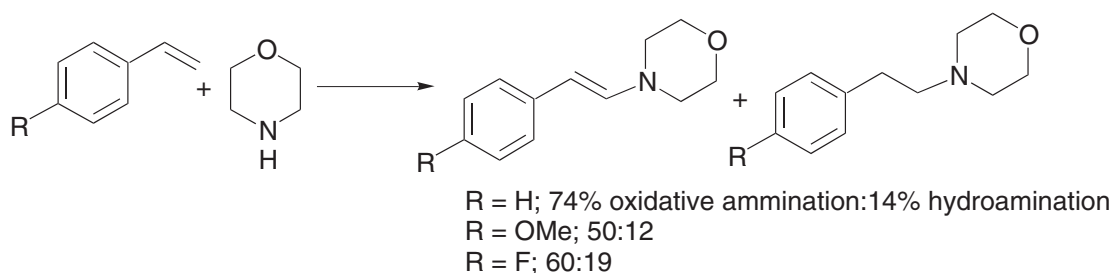
Scheme 36

9.5.5.2 Rhodium and Iridium Catalysts

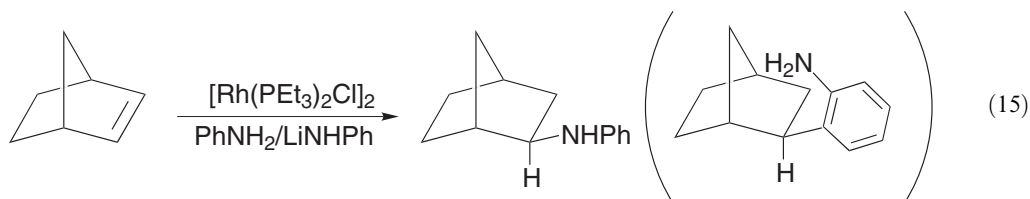
A range of rhodium complexes have been studied as hydroamination catalysts. Treatment of norbornene with a mixture of aniline and lithium anilide in the presence of [Rh(PEt₃)₂Cl]₂ at 70 °C for over 1 week yields the *exo* addition product in ca. 15% yield.¹⁶⁵

Some of the hydroarylation product is also observed; substituted anilines afford the two products to varying degrees (Equation (15)). The closely related rhodium complexes [Rh(PCy₃)₂Cl]₂, [Rh(dmpe)Cl]₂ (where dmpe = 1,2-bis(dimethylphosphino)ethane), and [Rh(C₈H₁₄)Cl]₂ show essentially no catalytic activity.¹⁶⁶ Application of [Rh(PEt₃)₂Cl]₂ to the reaction of aniline with styrene gives a mixture of hydroamination and oxidative amination products, the latter predominating.¹⁶⁷ Other related rhodium-catalyzed amination reactions (oxidative amination) have been reported.^{168,169}

The first example of anti-Markovnikoff hydroamination of aromatic alkenes has been demonstrated with cationic rhodium complexes.¹⁷⁰ A combination of [Rh(COD)₂]⁺/2PPh₃ in THF under reflux yields the N—H addition product as the minor species alongside that resulting from oxidative amination (Scheme 37). Hydrogenation products are also detected.

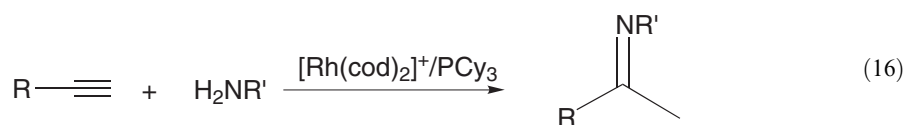


Scheme 37



If the more activated alkene 2-vinylpyridine is used in place of styrene with the same catalysts and the same range of substrates, anti-Markovnikov hydroamination is also found. Thus, *N*-[2-(2'-pyridyl)ethyl]piperidine was isolated in 53% yield from reaction of 2-vinylpyridine with piperidine in the presence of $[\text{Rh}(\text{COD})_2]^+/\text{2PPh}_3$ under reflux. N–H addition was observed with other amines, the remaining product in all cases being primarily that from oxidative amination (Table 12). When the catalytic reaction was run in the absence of phosphine, the yield of hydroamination product increased dramatically.¹⁷¹

Intermolecular hydroamination of 1-alkynes with anilines has recently been performed using $[\text{Rh}(\text{COD})_2]^+$ in combination with three equivalents of tricyclohexylphosphine (1.5 mol.% catalyst) at 50 °C to yield the corresponding imines (Equation (16)):¹⁷²



The scope of the reaction with other potential catalysts has been investigated; PPh_3 , $\text{P}(o\text{-tolyl})_3$ and $\text{P}(\text{Bu}^n)_3$ are active but less so than PCy_3 . Noncationic rhodium species (e.g., $[\text{Rh}(\text{COD})\text{Cl}]_2$, $[\text{Rh}(\text{PPh}_3)_3\text{Cl}]$) in combination with phosphines are completely inactive. Tests using 1-hexyne with a range of anilines RNH_2 ($R = o\text{-Me-C}_6\text{H}_4$, $m\text{-F-C}_6\text{H}_4$, or $p\text{-MeO-C}_6\text{H}_4$) show good yields in just about all cases (Table 13).

The cationic imidazolium rhodium complex (56) has been found to catalyze the intramolecular hydroamination of alkynes in refluxing THF. In the case of 2-ethynylaniline, indole is formed in 100% yield over 9 h at 55 °C (Scheme 38).¹⁷³ One of the earliest examples of late transition metal-catalyzed hydroamination involved the use of the iridium(I) complex $[\text{Ir}(\text{PEt}_3)_2(\text{C}_2\text{H}_4)\text{Cl}]$ as

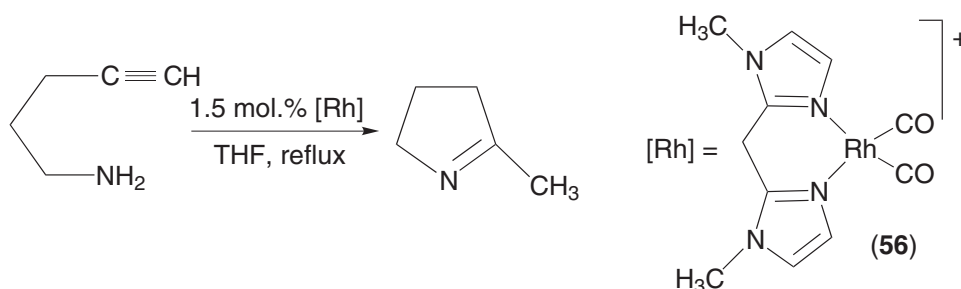
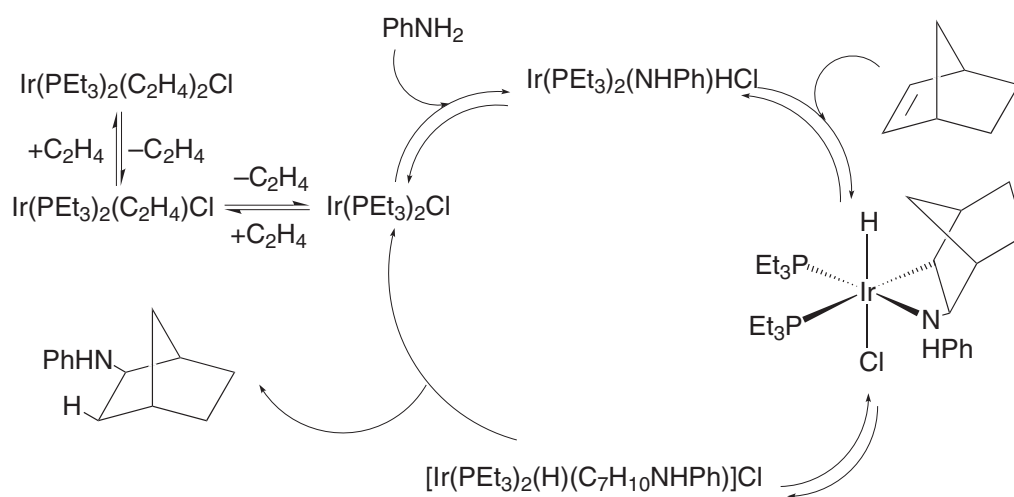
Table 12 $[\text{Rh}(\text{COD})_2]^+/\text{2PPh}_3$ -catalyzed hydroamination of 2-vinylpyridine.

Amine	% Yield of hydroamination product
Piperidine	53
Pyrrolidine	21
Morpholine	98
<i>n</i> -butylamine	<1

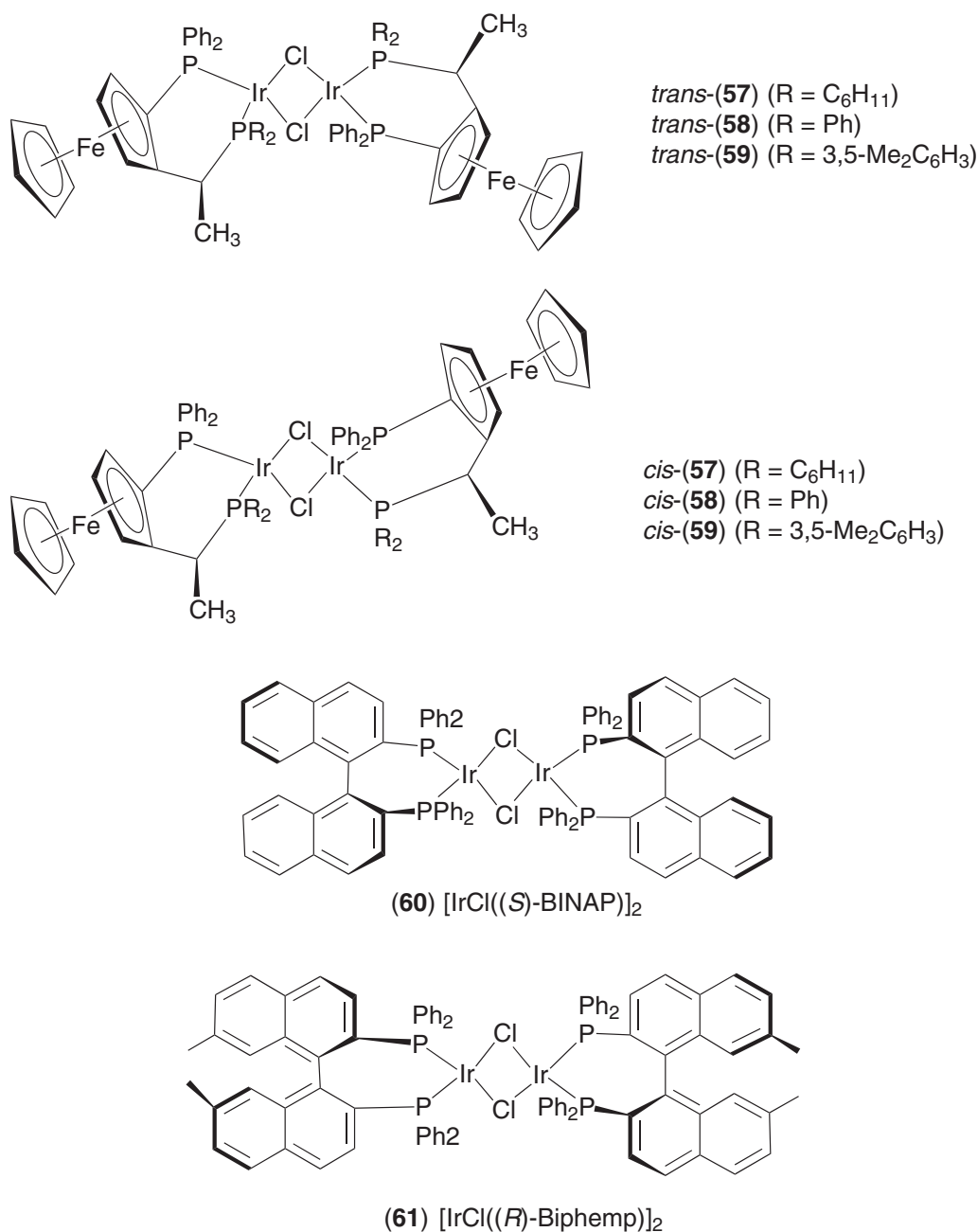
Table 13 Rhodium-catalyzed hydroamination of terminal alkynes with anilines (catalyst system = [Rh-(COD)₂]⁺/3PCy₃).

<i>R</i> group	<i>R'</i> group	Conditions	% Yield of product
<i>n</i> -hexyl	C ₆ H ₅	1.5 mol.% cat, 20 h	79
<i>n</i> -hexyl	<i>p</i> -MeO-C ₆ H ₄	1.5 mol.% cat, 20 h	63
<i>n</i> -butyl	<i>o</i> -Me-C ₆ H ₄	1.5 mol.% cat, 44 h	55
Ph	C ₆ H ₅	2.5 mol.% cat, 20 h	10

a catalyst precursor (Scheme 39).¹⁷⁴ In the presence of 0.2 equivalents of ZnCl₂, this system afforded up to six turnovers of *exo*-2-(phenylamino)norbornane after 2 days of reflux.

**Scheme 38****Scheme 39**

Based on this, asymmetric hydroamination was developed using [Ir(C₂H₄)₄Cl] or [Ir(coe)₂Cl]₂ (coe = cyclooctene) with chiral diphosphines to give complexes (57)–(61) (Scheme 40). While (57) afforded only a low yield and poor enantiomeric excess (51% 2*S*) of *exo*-2-(phenylamino)norbornane, addition of up to one equivalent of fluoride ion gave a six-fold increase in chemical yield (from 12% to 81%) and a reversal of enantioselectivity. In the case of (60), addition of four equivalents of fluoride led to an ee of 95%! The role of fluoride in these reactions has still not been explained satisfactorily.¹⁷⁵

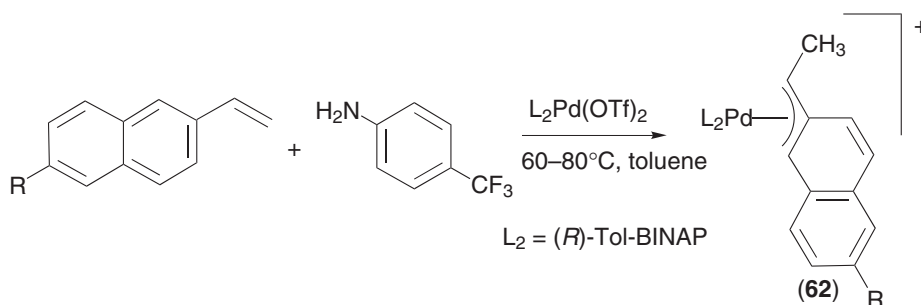


Scheme 40

9.5.5.3 Palladium and Platinum Catalysts

A number of examples have been reported documenting the use of palladium phosphine complexes as catalysts. The dialkyl species [PtL₂R₂] (L₂ = dmpe, dppe, (PMe₃)₂; R = Me, CH₂SiMe₃) catalyze the reaction of [PhNH₃]⁺ with activated alkenes (acrylonitrile, methyl acrylate, acrolein).¹⁷⁶ Unfunctionalized alkenes prove unreactive. The reaction mechanism is believed to proceed via protonation of Pt–R by the ammonium salt (generating PhNH₂ in turn) and the subsequent release of alkane to afford a vacant coordination site on the metal. Coordination of alkene then allows access into route A of the mechanism shown in Scheme 34. Protonation is also

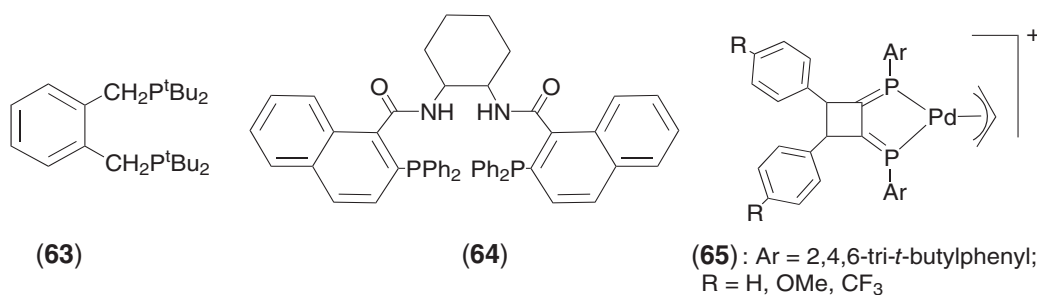
an important step in the hydroamination of vinylarenes using an *in situ* catalyst consisting of $\text{Pd}(\text{O}_2\text{CCF}_3)_2$ with four equivalents of PPh_3 and 20% TFA. In the absence of acid, reaction of styrene with aniline affords the Markovnikov product in 28% yield; with TFA present, this increases to 68%. Remarkably, a mixture consisting of 2% $\text{Pd}(\text{O}_2\text{CCF}_3)_2$, 3% 1,1'-bis(diphenylphosphino)ferrocene, and 20% triflic acid gave 90% conversion. Use of the isolated chiral phosphine complex $[\text{Pd}((R)\text{-BINAP})(\text{OTf})_2]$ led to asymmetric N—H addition to $p\text{-CF}_3\text{C}_6\text{H}_4\text{CH}=\text{CH}_2$ in 80% yield (81% ee) after 3 days at room temperature.¹⁷⁷ Follow up studies have identified an additional mechanism that operates in this chemistry (Scheme 41). The stoichiometric reaction of $[\text{Pd}((R)\text{-Tol-BINAP})(\text{OTf})_2]$ with vinylnaphthalene and trifluoromethylaniline led to the isolation of the η^3 -naphthylethyl complex (**62**), which was structurally characterized. This species was shown conclusively to be an intermediate on the pathway to catalytic hydroamination; the use of enantio- and diastereomerically pure (**62**) showed that the η^3 ligand is subject to nucleophilic attack by amine.¹⁷⁸

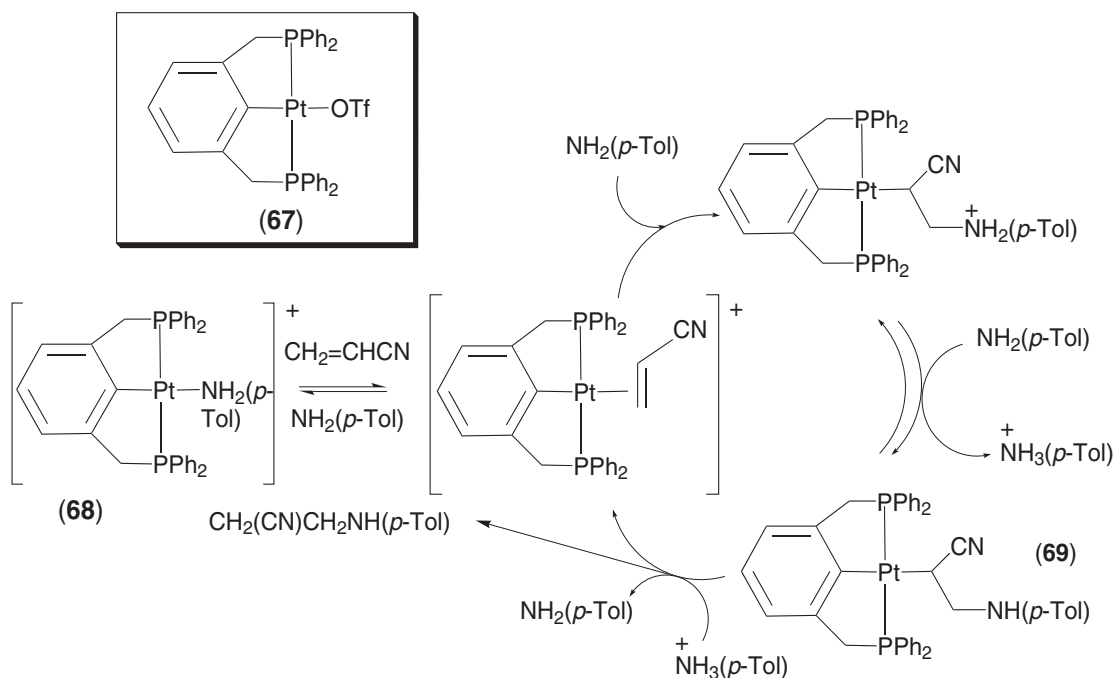


Scheme 41

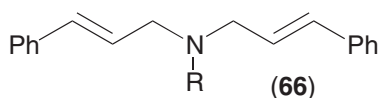
Using combinatorial methodology (see Chapter 9.11), a colorimetric assay has been devised to assess the activity of catalysts for hydroamination of activated alkenes. Thus, $\text{Pd}(\text{OAc})_2$, $\text{Pd}(\text{TFA})_2$, $[\text{Pd}(\eta^3\text{-C}_3\text{H}_5)\text{Cl}]_2$, $[(p\text{-cymene})\text{RuCl}_2]_2$, and $[\text{M}(\text{COD})_2]^+$ ($\text{M} = \text{Rh}, \text{Ir}$) (both in the presence and absence of phosphines) were assessed for addition of piperidine to methacrylonitrile. In general, Pd proved to be less active than Rh or Ir, which themselves were more active upon addition of phosphine (PPh_3 , dppe, BINAP). However, large variations were found for the catalysts best suited for a particular alkene/amine combination. The pincer ligand (**63**) with $\text{Pd}(\text{OAc})_2$ proved highly active for addition of aniline to methacrylonitrile.¹⁷⁹

The same high-throughput approach has revealed that 2 mol.% $[\text{Pd}(\text{PPh}_3)_4]$ with 10 mol.% TFA catalyzes aniline addition to cyclohexadiene and cycloheptadiene.¹⁸⁰ A range of electron-donating and electron-withdrawing substituents are tolerated on the amine, while the reactivity applies to many acyclic as well as cyclic dienes. Generation of a chiral PdP_4 analogue *in situ* from $[\text{Pd}(\eta^3\text{-C}_3\text{H}_5)\text{Cl}]_2$ and (**64**) allowed the asymmetric hydroamination of cyclohexadiene to proceed with 90% ee. Treatment of $[\text{Pd}(\eta^3\text{-C}_3\text{H}_5)\text{Cl}]_2$ with 1,2-diaryl-3,4-bis[(2,4,6-tri-*t*-butylphenyl)phosphinidene]cyclobutenes affords (**65**), which proves extremely reactive towards amines (e.g., reaction with diethylamine yields 3-(*N,N*-diethylamino)propene). The impact of the chelating ligand which contains sp^2 -hybridised phosphorus atoms with strong π -acceptor capabilities is seen in that $[\text{Pd}(\eta^3\text{-C}_3\text{H}_5)(\text{P-P})]^+$ ($\text{P-P} = \text{dppe}, \text{dppf}$) are completely inactive under identical conditions. Complex (**65**) is also catalytically active for addition of substituted anilines to 1,3-cyclohexadiene, and hydroamination of both aromatic and aliphatic dienes with aniline.¹⁸¹





Other Pd complexes are active for the addition of N—H bonds to alkynes and enynes. A combination of $[\text{Pd}(\text{PPh}_3)_4]$ and PhCO_2H (ratio 1:2) leads to the addition of dibenzylamine to terminal aromatic substituted alkynes (aliphatic alkynes are unreactive) to afford the (*E*)-alkene in 98% yield. Use of primary amines gives 2:1 adducts (**66**).¹⁸² An *in situ* catalyst made from $[\text{Pd}(\eta^3\text{-C}_3\text{H}_5)\text{Cl}]_2/\text{dppf}/\text{AcOH}$ in THF at 80 °C will doubly hydroaminate conjugated enynes, thus providing a route to unsymmetrical 1,4-diamines.¹⁸³ Both $[\text{Pd}(\text{triphos})]^{2+}$ and $[\text{Pd}(\text{CH}_3\text{CN})_4]^{2+}$, as well as $[\text{Cu}(\text{CH}_3\text{CN})_4]^+$ and $\text{Zn}(\text{OTf})_2$, perform intramolecular hydroamination of $\text{RC}\equiv\text{C}(\text{CH}_2)_n\text{NH}_2$ ($n=3$, R=H, Ph; $n=4$, R=H). For the palladium systems, the nature of the anion proves important for reactivity. The highest activity is associated with large, nonnucleophilic groups ($\text{OTf}^- \gg \text{ClO}_4^- > \text{BF}_4^- \approx \text{PF}_6^- \approx \text{NO}_3^- \gg \text{C}_6\text{H}_5\text{CO}_2^- > \text{Cl}^-$).¹⁸⁴ The platinum(II) complex (**67**) with the pincer phosphine ligand has been used as a precursor to catalyze the addition of *p*-tolylaniline across acrylonitrile (Scheme 42). The isolable cationic intermediate amine complex (**68**) has been shown to insert alkene to give the regioselective product (**69**). The subsequent reactivity of this to afford the hydroamination product is dependent of the $\text{p}K_a$ of the ammonium salt used in the reaction.¹⁸⁵

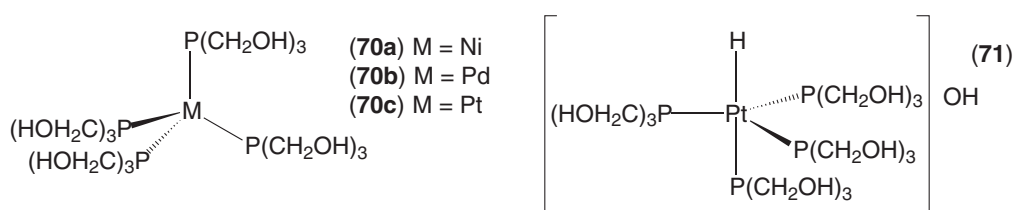


9.5.6 HYDROPHOSPHINATION (AND HYDROPHOSPHORYLATION)

In contrast to the other X—H additions surveyed in this chapter, there have been only a limited number of studies on the addition of P—H linkages across C—C (and C—O) multiple bonds. At the same time, there has been significant progress made in the development of catalytic systems for performing hydrophosphination and hydrophosphorylation compared to what was known pre-1982.

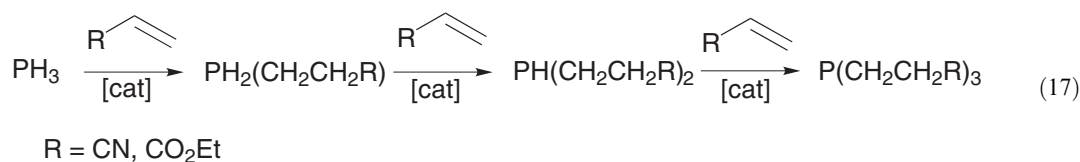
9.5.6.1 Hydrophosphination

All of the work that will be described involves group 10 metal complexes, primarily palladium- and platinum-catalyzed reactions. Early work from Pringle and co-workers showed that a range of nickel and palladium complexes bearing the water-soluble alkylphosphine *tris*(hydroxymethyl)phosphine (or THMP) $\text{P}(\text{CH}_2\text{OH})_3$ would bring about the addition of PH_3 to formaldehyde to generate THMP catalytically.¹⁸⁶ Thus, the zero-valent four-coordinate complexes $[\text{M}(\text{P}(\text{CH}_2\text{OH})_3)_4]$ (**70a,b**) and the cationic platinum hydride $[\text{HPt}(\text{P}(\text{CH}_2\text{OH})_3)_4][\text{OH}]$ (**71**) (formed upon dissolution of **70c** in water) prove highly efficient (Scheme 43).¹⁸⁷



Scheme 43

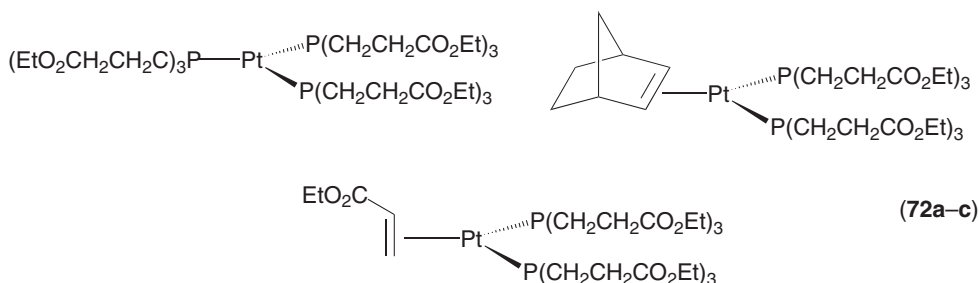
Building on from these results, catalytic hydrophosphination of activated alkenes was developed. Addition of PH_3 to acrylonitrile ($\text{R} = \text{CN}$, Equation (17)) at room temperature affords *tris*(cyanoethyl)phosphine in the presence of three-coordinate $[\text{Pt}(\text{P}\{\text{CH}_2\text{CH}_2\text{CN}\}_3)_3]$.¹⁸⁸



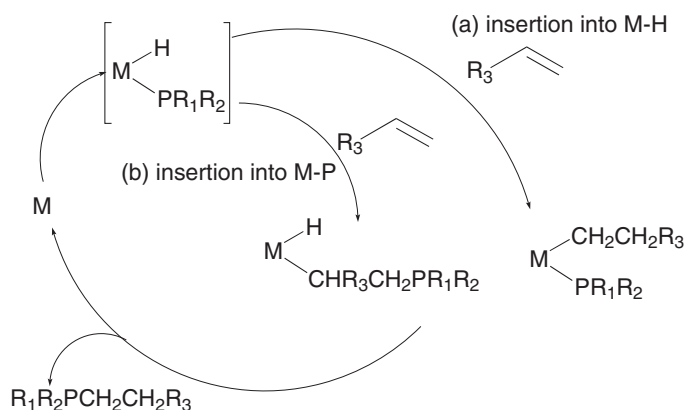
Mechanistic studies of the reaction were inhibited by the apparent involvement of three parallel reactions involving addition of $\text{PH}_3\text{R}_{3-x}$ to $\text{CH}_2=\text{CHCN}$. Later investigations of the catalytic activity of $[\text{M}(\text{P}\{\text{CH}_2\text{CH}_2\text{CN}\}_3)_3]$ ($\text{M} = \text{Ni}, \text{Pd}$, or Pt) and $[\text{MCl}(\text{P}\{\text{CH}_2\text{CH}_2\text{CN}\}_3)_3]$ ($\text{M} = \text{Rh}, \text{Ir}$) for the final step in Equation (17) led to an ordering of activity of $\text{Pt} > \text{Pd} \approx \text{Ir} > \text{Ni}$; the rhodium(I) catalyst $[\text{RhCl}(\text{P}\{\text{CH}_2\text{CH}_2\text{CN}\}_3)_3]$ failed to give beyond 50% conversion. A kinetic investigation underlined the original arguments on the complexity of the reaction, revealing a mononuclear complex catalyzed pathway at high concentrations of $\text{P}\{\text{CH}_2\text{CH}_2\text{CN}\}_3$ and a route catalyzed by a dinuclear complex at low phosphine concentration.¹⁸⁹

Hydrophosphination of ethyl acrylate using PH_3 ($\text{R} = \text{CO}_2\text{Me}$, Equation (17)) is catalyzed by a mixture of the zero-valent platinum complexes (**72a–c**), which are formed upon addition of $\text{P}\{\text{CH}_2\text{CH}_2\text{CO}_2\text{Et}\}_3$ to $[\text{Pt}(\text{norbornene})_3]$ (Scheme 44). Failure of these complexes to bring about P–H addition to $\text{CH}_2=\text{CHCF}_3$ indicates that Michael activation of the alkene through $-I$ and $-R$ effects of the substituents is crucial for catalytic activity in this class of metal complexes.¹⁹⁰

Platinum-catalyzed addition of the P–H bond in bulky primary and secondary phosphines has been probed in considerable detail through a series of elegant studies.^{191,192} The zero-valent acrylonitrile complexes $[\text{Pt}(\text{P–P})(\eta^2\text{-CH}_2\text{CHCN})]$ ($\text{P–P} = \text{Ph}_2\text{PCH}_2\text{CH}_2\text{PPh}_2$, $(\text{C}_6\text{H}_{11})_2\text{PCH}_2\text{CH}_2\text{P}(\text{C}_6\text{H}_{11})_2$) are catalytic precursors (10 mol.% catalyst, THF, 50 °C) for the addition of PH_2Ph and PH_2Mes^* ($\text{Mes}^* = 2,4,6\text{-}t\text{-Bu}_3\text{C}_6\text{H}_2$) or $\text{HPPh}(\text{R})$ ($\text{R} = 2,4,6\text{-Me}_3\text{C}_6\text{H}_2$, C_6H_5 , C_6H_{11} , or Me) to $\text{CH}_2=\text{CHCN}$ to give $\text{PPh}(\text{CH}_2\text{CH}_2\text{CN})_2$, $\text{HPMes}^*(\text{CH}_2\text{CH}_2\text{CN})$, and $\text{PPh}(\text{R})(\text{CH}_2\text{CH}_2\text{CN})$, respectively. Two possible mechanistic pathways were identified for the reaction, involving alkene insertion into either the M–H or M–P bond of a phosphido hydride intermediate (Scheme 45).



Scheme 44



Scheme 45

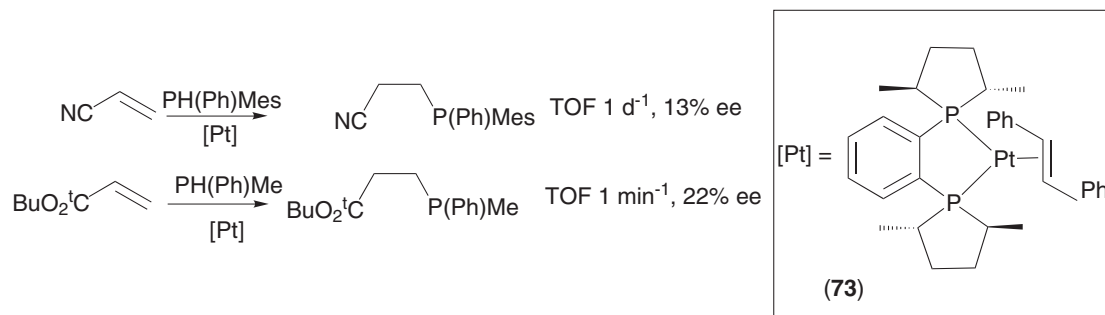
Synthesis and isolation of $[\text{Pt}(\text{dppe})(\text{PR}_1\text{R}_2)(\text{CH}_2\text{CH}_2\text{CN})]$ ($\text{R}_1 = \text{R}_2 = \text{Mes}$; $\text{R}_1 = \text{H}$, $\text{R}_2 = \text{Mes}^*$) shows that it is stable to reductive elimination of the P—C bond even upon heating. In contrast, $[\text{Pt}(\text{dcpe})\{\text{CH}(\text{CN})\text{CH}_2\text{PHMes}^*\}\text{H}]$ (where $\text{dcpe} = 1,2\text{-bis}(\text{dicyclohexylphosphino})\text{ethane}$) decomposes in the presence of acrylonitrile to yield $\text{HPMes}^*(\text{CH}_2\text{CH}_2\text{CN})$, demonstrating that the route to hydrophosphination involves path (b) in Scheme 45. The first example of catalytic P—H addition to styrene has recently been described.¹⁹³ Both $[\text{Ni}\{\text{P}(\text{OEt})_3\}_4]$ and $[\text{Pd}(\text{CH}_3\text{CN})_2\text{Cl}_2]$ prove highly active at high temperatures (90–130 °C) to give the anti-Markovnikoff product $\text{PhCH}_2\text{CH}_2\text{PPh}_2$ in good yields. Nickel(II) complexes such as $[\text{Ni}(\text{PPh}_3)_2\text{Br}_2]$ lead mainly to oxidative dimerization of the secondary phosphine rather than P—H addition to C=C. Nickel and palladium complexes have been utilized for the hydrophosphination of terminal alkynes at >80 °C.¹⁹⁴ A combination of $[\text{Ni}(\text{acac})_2]$ and $(\text{EtO})_2\text{P}(\text{O})\text{H}$ gave high selectivity for addition of the phosphorus atom of Ph_2PH to the substituted carbon atom in $\text{PhC}\equiv\text{CH}$. Different regioselectivity was observed in the case of $[\text{Pd}(\text{PPh}_3)_4]$, which gave phosphorus addition to the terminal carbon (95% yield, $E/Z = 10/90$).

Asymmetric hydrophosphination has been utilized as a route for preparing chiral phosphines. The Pt^0 complex $[(\text{Me-DUPHOS})\text{Pt}(\text{trans-PhCH}=\text{CHPh})]$ (**73**) brings about the catalytic P—H addition of bulky secondary phosphines to activated alkenes with modest enantioselectivity. The most promising substrate combinations for further development appear to be bulky alkenes and less bulky phosphines (Scheme 46).¹⁹⁵

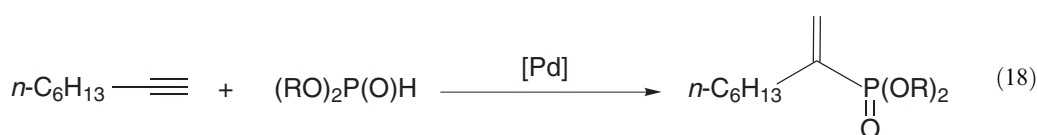
9.5.6.2 Hydrophosphorylation and Hydrophosphinylation

Addition of the P—H bond of hydrogen phosphonates $(\text{RO})_2\text{P}(\text{O})\text{H}$ across alkynes (hydrophosphorylation) may be catalyzed using both Pd^0 and Pd^{II} complexes.¹⁹⁶ Reaction of oct-1-yne with either $(\text{MeO})_2\text{P}(\text{O})\text{H}$ or $(\text{EtO})_2\text{P}(\text{O})\text{H}$ affords the Markovnikoff adduct (Equation (18)) as the

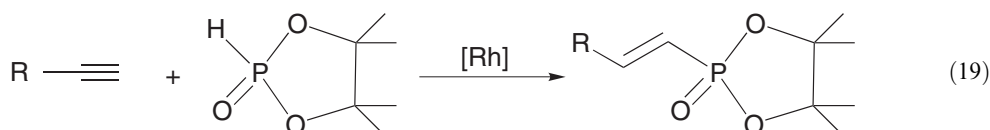
predominant product upon reflux with either $[\text{Pd}(\text{PPh}_3)_4]$, $[\text{Pd}(\text{PPh}_3)_2(\eta^2\text{-CH}_2=\text{CH}_2)]$, or *cis*- $[\text{Pd}(\text{PPh}_2\text{Me})_2\text{Me}_2]$. Palladium(II) complexes, including PdCl_2 and $\text{Pd}(\text{OAc})_2$, are completely inactive. Double hydrophosphorylation reactions are possible, while the reaction with 1-ethynyl-cyclohexene results in P—H addition across the triple bond only.¹⁹⁷



Scheme 46

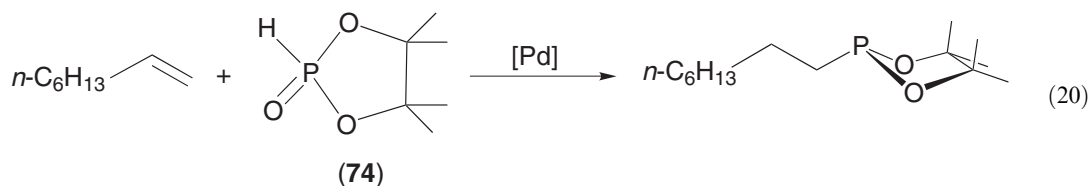


Hydrophosphorylation has recently been extended to rhodium catalysts as a route to anti-Markovnikoff products.¹⁹⁸ Thus, 3 mol.% $\text{Rh}(\text{PPh}_3)_3\text{Cl}$ affords the (*E*)-alkenylphosphonates ($\text{R} = \text{H}$, Ph , $n\text{-C}_6\text{H}_{13}$, $\text{CH}_2\text{CH}_2\text{CN}$, SiMe_3 , or cyclohexenyl) in high yields (>80%) at room temperature when 4,4,5,5-tetramethyl-1,3,2-dioxaphospholane-2-oxide (74) is used as the P—H source (Equation (19)).¹⁹⁹ The rate of reaction is highly solvent dependent ($\text{THF} < \text{CH}_2\text{Cl}_2 \approx \text{CH}_3\text{CN} < \text{acetone}$). The carbonyl complex $[\text{Rh}(\text{PPh}_3)_2(\text{CO})\text{Cl}]$ is active as a catalyst at elevated temperature, while $[\text{Rh}(\text{COD})\text{Cl}]_2$, $[\text{Rh}(\text{C}_2\text{H}_4)_2\text{Cl}]_2$, and $[\text{Rh}(\text{COD})_2]^+/\text{PPh}_3$ are all totally ineffective:

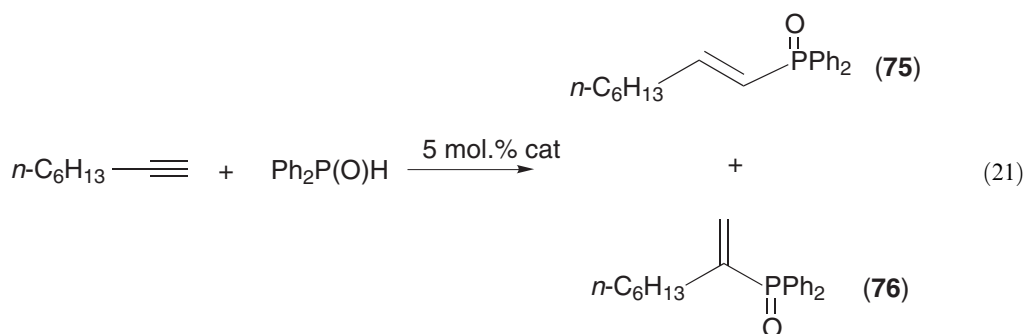


The first example of alkene hydrophosphorylation has been realized using the same five-membered hydrogen phosphonate P—H precursor (Equation (20)). The most active systems are Pd^{II} *bis*-phosphine complexes which give the β -substitution (anti-Markovnikoff) product; *cis*- $[\text{Pd}(\text{PPh}_2\text{Me})_2\text{Me}_2]$ proves highly active (63% yield of product with 5 mol.% catalyst, 110°C), while Wilkinson's catalyst and $[\text{Ni}(\text{PPh}_3)_4]$ also display moderate activity for reaction. The P—H source is vital since both noncyclic and cyclic six-membered ring hydrogen phosphonates gave none of the P—H addition product. The catalytic reaction can be readily applied to both aliphatic and aromatic alkenes, although substrates containing bulky R substituents $\text{RCH}=\text{CH}_2$ ($\text{R} = \text{Bu}^t$, Ph) gave mixtures of both α - and β -products. For example, the α -adduct 1,1-diphenylethane is

formed in 45% yield with styrene; yields of this could be increased up to 95% with *cis*-[Pd(PPh₂Cy)₂Me₂] as the catalyst:¹⁹⁹



Hydrophosphinylation of alkynes utilizing Ph₂P(O)H has been described using the same range of palladium catalysts (Table 14).²⁰⁰ Both [Pd(PPh₃)₄] and *cis*-Pd(PR₃)₂Me₂ (PR₃ = PPh₃, PPh₂Me, or PPhMe₂) yield the anti-Markovnikoff product through *cis* P—H addition. Remarkably, this regioselectivity can be reversed upon addition of traces of phosphinic acid Ph₂P(O)OH.²⁰¹ Thus, thermolysis (70 °C) of an equimolar mixture of 1-octyne and Ph₂P(O)H with a catalytic quantity of *cis*-[Pd(PPhMe₂)₂Me₂] gave products (75) and (76) in 75% total yield in ratio of 88:12 (Equation (21)). Repeat of the catalysis in the presence of 1 mol.% phosphinic acid gave a higher overall yield, but switched the regioselectivity discriminating in favor of the α-product (76):

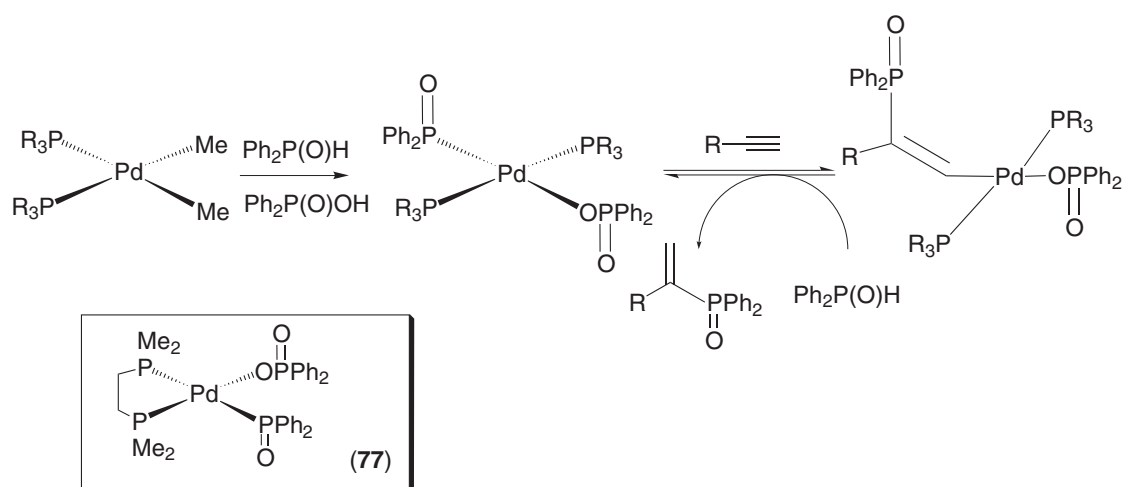


In the case of [Pd(dmpe)Me₂], the presence of phosphinic acid-induced catalytic activity. While dibutylphosphate and phosphoric acid also bring about the same changes in selectivity, hexamethylphosphoramide, acetic acid, and benzoic acid fail to do so. This can be explained by the mechanism shown in Scheme 47. Indeed the catalytic activity of the isolated adduct (77) proved to be identical to that formed upon combining [Pd(dmpe)Me₂] and Ph₂P(O)OH.

In the most recent developments in this area, organometallic lanthanide complexes have been utilized for hydrophosphination/cyclization reactions of phosphinoalkenes.^{202,203}

Table 14 Hydrophosphinylation of 1-octyne.

Catalyst	% Yield without Ph ₂ P(O)OH (75):(76)	% Yield with Ph ₂ P(O)OH (75):(76)
Pd(PPh ₃) ₄ (5 mol.%)	54 (92:8)	89 (33:67)
<i>cis</i> -Pd(PPh ₂ Me) ₂ Me ₂ (5 mol.%)	56 (90:10)	100 (16:84)
<i>cis</i> -Pd(PPhMe ₂) ₂ Me ₂ (1 mol.%)	75 (88:12)	92 (21:79)
(5 mol.%)		99 (5:95)
(10 mol.%)		96 (4:96)
Pd(dmpe)Me ₂ (5 mol.%)	0	93 (8:92)



Scheme 47

9.5.7 REFERENCES

- Burgess, K.; Ohlmeyer, M. J. *J. Chem. Rev.* **1991**, *91*, 1179–1191.
- Beletskaya, I.; Pelter, A. *Tetrahedron Lett.* **1997**, *53*, 4957–5026.
- Miyaura, N. Hydroboration, Diboration, Silylboration and Stannylboration. In *Catalytic Heterofunctionalization*; Togni, A., Grützmacher, H., Eds.; Wiley-VCH: Weinheim: 2001; pp 1–47.
- Männig, D.; Nöth, H. *Angew. Chem., Int. Ed. Engl.* **1985**, *24*, 878–879.
- Irvine, G. J.; Lesley, M. G. J.; Marder, T. B.; Norman, N. C.; Rice, C. R.; Robins, E. G.; Roper, W. R.; Whittell, G.; Wright, L. J. *J. Chem. Rev.* **1998**, *98*, 2685–2722.
- Wadepohl, H. *Angew. Chem., Int. Ed. Engl.* **1997**, *36*, 2441–2444.
- Braunschweig, H.; Colling, M. *Coord. Chem. Rev.* **2001**, *223*, 1–51.
- He, X.; Hartwig, J. F. *J. Am. Chem. Soc.* **1996**, *118*, 1696–1702.
- Smith, M. R., III. Advances in Metal Boryl Chemistry. In *Advances in Metal Boryl Chemistry*; Karlin, K. D., Ed.; Progress in Inorganic Chemistry Vol. 49; Wiley: Chichester, U.K., 1999; pp 505–569.
- Kubas, G. J. *Metal Dihydrogen and σ -Bond Complexes*; Kluwer: New York, 2001; Chapter 13, pp 417–437.
- Westcott, S. A.; Marder, T. B.; Baker, R. T.; Calabrese, J. C. *Can. J. Chem.* **1993**, *71*, 930–936.
- Musaev, D. G.; Mebel, A. M.; Morokuma, K. *J. Am. Chem. Soc.* **1994**, *116*, 10693–10702.
- Dorigo, A. E.; Schleyer, P. V. R. *Angew. Chem., Int. Ed. Engl.* **1995**, *34*, 115–118.
- Evans, D. A.; Fu, G. C.; Anderson, B. A. *J. Am. Chem. Soc.* **1992**, *114*, 6679–6685.
- Evans, D. A.; Fu, G. C. *J. Org. Chem.* **1990**, *55*, 2280–2282.
- Burgess, K.; van der Donk, W. A.; Westcott, S. A.; Marder, T. B.; Baker, R. T.; Calabrese, J. C. *J. Am. Chem. Soc.* **1992**, *114*, 9350–9359.
- Burgess, K.; Ohlmeyer, M. J. Stereocontrol in Catalysed and Uncatalysed Hydroborations. In *Homogeneous Transition Metal Catalyzed Reactions*; Moser, W. R.; Slocum, D. W., Eds.; Advances in Chemistry Series 230; American Chemical Society: Washington DC, 1992; pp 163–177.
- Matthews, J. L.; Steel, P. G. *Tetrahedron Lett.* **1994**, *35*, 1421–1424.
- Evans, D. A.; Fu, G. C.; Hoveyda, A. H. *J. Am. Chem. Soc.* **1992**, *114*, 6671–6679.
- Burgess, K.; Cassidy, J.; Ohlmeyer, M. J. *J. Org. Chem.* **1991**, *56*, 1020–1027.
- Liedtke, J.; Rügger, H.; Loss, S.; Grützmacher, H. *Angew. Chem., Int. Ed. Engl.* **2000**, *39*, 2478–2481.
- Horváth, I. T. *Acc. Chem. Res.* **1998**, *31*, 641–650.
- Juliette, J. J.; Horváth, I. T.; Gladysz, J. A. *Angew. Chem., Int. Ed. Engl.* **1997**, *36*, 1610–1612.
- Evans, D. A.; Fu, G. C. *J. Am. Chem. Soc.* **1991**, *113*, 4042–4043.
- Burgess, K.; Jaspars, M. *Organometallics* **1993**, *12*, 4197–4200.
- Evans, D. A.; Muci, A. R.; Stürmer, R. *J. Org. Chem.* **1993**, *58*, 5307–5309.
- Pereira, S.; Srebnik, M. *Tetrahedron Lett.* **1996**, *37*, 3283–3286.
- Pereira, S.; Srebnik, M. *J. Am. Chem. Soc.* **1996**, *118*, 909–910.
- Hayashi, T.; Matsumoto, Y.; Ito, Y. *Tetrahedron Asymmetry* **1991**, *2*, 601–612.
- Burgess, K.; van der Donk, W. A.; Kook, A. M. *J. Org. Chem.* **1991**, *56*, 2949–2951.
- Zhang, J.; Lou, B.; Guo, G.; Dai, L. *J. Org. Chem.* **1991**, *56*, 1670–1672.
- Marder, T. B.; Norman, N. C. *Topics in Catalysis* **1998**, *5*, 63–73.
- Westcott, S. A.; Marder, T. B.; Baker, R. T. *Organometallics* **1993**, *12*, 975–979.
- Westcott, S. A.; Blom, H. P.; Marder, T. B.; Baker, R. T. *J. Am. Chem. Soc.* **1992**, *114*, 8863–8869.
- Brown, J. M.; Lloyd-Jones, G. C. *J. Am. Chem. Soc.* **1994**, *116*, 866–878.
- Hou, X.-L.; Hong, D.-G.; Rong, G.-B.; Guo, Y.-L.; Dai, L.-X. *Tetrahedron Lett.* **1993**, *34*, 8513–8516.

37. Carter, C. A. G.; Vogels, C. M.; Harrison, D. J.; Gagnon, M. K. J.; Norman, D. W.; Langler, R. F.; Baker, R. T.; Westcott, S. A. *Organometallics* **2001**, *20*, 2130–2132.
38. Elgandy, S.; Patel, G.; Kakkar, V. V.; Claeson, G.; Green, D.; Skordalakes, E.; Baban, J. A.; Deadman, J. *Tetrahedron Lett.* **1994**, *15*, 2435–2436.
39. Elgandy, S.; Claeson, G.; Kakkar, V. V.; Green, D.; Patel, G.; Goodwin, C. A.; Baban, J. A.; Scully, M. F.; Deadman, J. *Tetrahedron* **1994**, *50*, 3803–3812.
40. Satoh, M.; Nomoto, Y.; Miyaura, N.; Suzuki, A. *Tetrahedron Lett.* **1989**, *30*, 3789–3792.
41. Matsumoto, Y.; Naito, M.; Hayashi, T. *Organometallics* **1992**, *11*, 2732–2734.
42. Pereira, S.; Srebnik, M. *Organometallics* **1995**, *14*, 3127–3128.
43. Gridnev, I. D.; Miyaura, N.; Suzuki, A. *Organometallics* **1993**, *12*, 589–592.
44. Gridnev, I. D.; Miyaura, N.; Suzuki, A. *J. Org. Chem.* **1993**, *58*, 5351–5354.
45. Burgess, K.; van der Donk, W. A.; Ohlmeyer, M. J. *Tetrahedron Asymmetry* **1991**, *2*, 613–621.
46. Burgess, K.; Ohlmeyer, M. J. *J. Org. Chem.* **1988**, *53*, 5178–5179.
47. Hayashi, T.; Matsumoto, Y.; Ito, Y. *J. Am. Chem. Soc.* **1989**, *111*, 3426–3428.
48. Brown, J. M.; Hulmes, D. I.; Layzell, T. P. *J. Chem. Soc., Chem. Commun.* **1993**, 1673–1674.
49. Valk, J. M.; Whitlock, G. A.; Layzell, T. P.; Brown, J. M. *Tetrahedron Asymmetry* **1995**, *6*, 2593–2596.
50. Fernandez, E.; Hooper, M. W.; Knight, F. I.; Brown, J. M. *Chem. Commun.* **1997**, 173–174.
51. Jendralla, H.; Li, C. H.; Paulus, E. *Tetrahedron Asymmetry* **1994**, *5*, 1297–1320.
52. Togni, A. New Chiral Ferrocenyl Ligands for Asymmetric Catalysis. In *Metalloenes*; Togni, A., Halterman, R. L., Eds.; VCH, Weinheim, 1998, Volume 2; pp 685–781.
53. Togni, A.; Breutel, C.; Schnyder, A.; Spindler, F.; Landert, H.; Tijani, A. *J. Am. Chem. Soc.* **1994**, *116*, 4062–4066.
54. Schnyder, A.; Hintermann, L.; Togni, A. *Angew. Chem., Int. Ed. Engl.* **1995**, *34*, 931–933.
55. Schnyder, A.; Togni, A.; Wiesli, U. *Organometallics* **1997**, *16*, 255–260.
56. Abbenhuis, H. C. L.; Burckhardt, U.; Gramlich, V.; Martellett, A.; Spencer, J.; Steiner, I.; Togni, A. *Organometallics* **1996**, *15*, 1614–1621.
57. Demay, S.; Volant, F.; Knochel, P. *Angew. Chem., Int. Ed. Engl.* **2001**, *40*, 1235–1238.
58. Brown, J. M.; Lloyd-Jones, G. C. *Tetrahedron Asymmetry* **1990**, *1*, 869–872.
59. Hayashi, T. *Acc. Chem. Res.* **2000**, *33*, 354–362.
60. Matsumoto, Y.; Naito, M.; Uozumi, Y.; Hayashi, T. *J. Chem. Soc., Chem. Commun.* **1993**, 1468–1469.
61. Parshall, G. W.; Ittel, S. D. *Homogeneous Catalysis*, 2nd ed.; Wiley: New York, 1992.
62. Huthmacher, K.; Krill, S. Reactions with Hydrogen Cyanide (Hydrocyanation). In *Applied Homogeneous Catalysis with Organometallic Compounds*; Cornils, B., Herrmann, W. A., Eds.; VCH: Weinheim, Germany, 1996; pp 465–486.
63. Tolman, C. A.; McKinney, R. J.; Seidel, W. C.; Druliner, J. D.; Stevens, W. R. Homogeneous Catalysed Olefin-hydrocyanation. In *Homogeneous Catalyzed Olefin Hydrocyanation*; Advances in Catalysis Series 33; Academic Press: New York, 1985, pp 1–46.
64. Tolman, C. A.; Seidel, W. C.; Druliner, J. D.; Domaille, P. C. *Organometallics* **1984**, *3*, 33–38.
65. McKinney, R. J.; Nugent, W. A. *Organometallics* **1989**, *8*, 2871–2875.
66. Campi, E. M.; Elmes, P. S.; Jackson, W. R.; Lovel, C. G.; Probert, M. K. S. *Aust. J. Chem.* **1987**, *40*, 1053–1061.
67. Bryndza, H. E.; Harrelson, J. A., Jr. Hydrocyanation. In *Aqueous-Phase Organometallic Catalysis*; Cornils, B., Herrmann, W. A., Eds.; VCH: Weinheim, Germany, 1998; pp 393–408.
68. RajanBabu, T. V.; Casalnuovo, A. L. Hydrocyanation of Carbon–Carbon Double Bonds. In *Comprehensive Asymmetric Catalysis*; Jacobsen, E. N., Pfaltz, A., Yamamoto, H., Eds.; Springer-Verlag: Berlin, 1999; pp 367–378.
69. Hodgson, M.; Parker, D.; Taylor, R. J.; Ferguson, G. *Organometallics* **1988**, *7*, 1761–1766.
70. Thomson, R. J.; Jackson, W. R.; Haarbarger, D.; Klabunovsky, E. I.; Pavlov, V. A. *Aust. J. Chem.* **1987**, *40*, 1083–1106.
71. Hodgson, M.; Parker, D.; Taylor, R. J.; Ferguson, G. *J. Chem. Soc., Chem. Commun.* **1987**, 1309–1310.
72. Baker, M. J.; Pringle, P. G. *J. Chem. Soc., Chem. Commun.* **1991**, 1292–1293.
73. Yan, M.; Xu, Q.-Y.; Chan, A. S. C. *Tetrahedron Asymmetry* **2000**, *11*, 845–849.
74. Horiuchi, T.; Shirakawa, E.; Nozaki, K.; Takaya, H. *Tetrahedron Asymmetry* **1997**, *8*, 57–63.
75. Nugent, W. A.; RajanBabu, T. V.; Burk, M. J. *Science* **1993**, *259*, 479–483.
76. RajanBabu, T. V.; Casalnuovo, A. L. *Pure Appl. Chem.* **1994**, *66*, 1535–1542.
77. RajanBabu, T. V.; Casalnuovo, A. L. *J. Am. Chem. Soc.* **1992**, *114*, 6265–6266.
78. Casalnuovo, A. L.; RajanBabu, T. V.; Ayers, T. A.; Warren, T. H. *J. Am. Chem. Soc.* **1994**, *116*, 9869–9882.
79. RajanBabu, T. V.; Casalnuovo, A. L. *J. Am. Chem. Soc.* **1996**, *118*, 6325–6326.
80. Kamer, P. C. J.; van Leeuwen, P. W. N. M.; Reek, J. N. H. *Acc. Chem. Res.* **2001**, *34*, 895–904.
81. van Leeuwen, P. W. N. M.; Kamer, P. C. J.; Reek, J. N. H.; Dierkes, P. *Chem. Rev.* **2000**, *100*, 2741–2769.
82. Marcone, J. E.; Moloy, K. G. *J. Am. Chem. Soc.* **1998**, *120*, 8527–8528.
83. Kranenburg, M.; Kamer, P. C. J.; van Leeuwen, P. W. N. M.; Vogt, D.; Keim, W. *J. Chem. Soc., Chem. Commun.* **1995**, 2177–2178.
84. Goertz, W.; Kamer, P. C. J.; van Leeuwen, P. W. N. M.; Vogt, D. *Chem. Commun.* **1997**, 1521–1522.
85. Goertz, W.; Keim, W.; Vogt, D.; Englert, U.; Boele, M. D. K.; van der Leen, L. A.; Kamer, P. C. J.; van Leeuwen, P. W. N. M. *J. Chem. Soc., Dalton Trans.* **1998**, 2981–2988.
86. Goertz, W.; Kamer, P. C. J.; van Leeuwen, P. W. N. M.; Vogt, D. *Chem. Eur. J.* **2001**, *7*, 1614–1618.
87. Ojima, I. The Hydrosilylation Mechanism. In *The Chemistry of Organic Silicon Compounds*, Part 2; Patai, S., Rappoport, Z., Eds.; Wiley: Chichester, U.K., 1989; Chapter 25, pp 1479–1526.
88. Marciniak, B., Ed.; *Comprehensive Handbook on Hydrosilylation*; Pergamon: Oxford, U.K., 1992.
89. Chalk, A. J.; Harrod, J. F. *J. Am. Chem. Soc.* **1965**, *87*, 16–21.
90. Randolph, C. L.; Wrighton, M. S. *J. Am. Chem. Soc.* **1986**, *108*, 3366–3374.
91. Duckett, S. B.; Perutz, R. N. *Organometallics* **1992**, *11*, 90–98.
92. Horn, K. A. *Chem. Rev.* **1995**, *95*, 1317–1350.
93. Sakaki, S.; Mizoe, N.; Sugimoto, M. *Organometallics* **1998**, *17*, 2510–2523.
94. Marciniak, B. *J. Organomet. Chem.* **1993**, *446*, 15–23.
95. Marciniak, B. Hydrosilylation and Related Reaction of Silicon Compounds. In *Applied Homogeneous Catalysis with Organometallic Compounds*; Cornils, B., Herrmann, W. A., Eds.; VCH: Weinheim, Germany, 1996; pp 487–506.

96. Hiyama, T.; Kusumoto, T. Hydrosilylation of $\text{H}-\text{C}=\text{C}$ and $\text{C}\equiv\text{C}$. In *Comprehensive Organic Synthesis*; Trost, B. M., Ed.; Pergamon: Oxford, U.K., 1991; Volume 8, pp 763–792.
97. Tanke, R. S.; Crabtree, R. H. *J. Am. Chem. Soc.* **1990**, *112*, 7984–7989.
98. Hayashi, T. Hydroboration of Carbon–Carbon Double Bonds. In *Comprehensive Asymmetric Catalysis*; Jacobsen, E. N., Pfaltz, A., Yamamoto, H., Eds.; Springer-Verlag: Berlin, Germany, 1999; pp 351–364.
99. Lewis, L. N.; Uriate, R. J.; Lewis, N. *J. Catal.* **1991**, *127*, 67–74.
100. Lewis, L. N.; Uriate, R. *J. Organometallics* **1990**, *9*, 621–625.
101. Lewis, L. N. *J. Am. Chem. Soc.* **1990**, *112*, 5998–6004.
102. Lewis, L. N.; Uriate, R. J.; Lewis, N. *J. Mol. Catal.* **1991**, *66*, 105–113.
103. Hitchcock, P. B.; Lappert, M. F.; Warhurst, N. J. W. *Angew. Chem., Int. Ed. Engl.* **1991**, *30*, 438–440.
104. Doyle, M. P.; Devora, G. A.; Nefedov, A. O.; High, K. G. *Organometallics* **1992**, *11*, 549–555.
105. Doyle, M. P.; High, K. G.; Nesloney, C. L.; Clayton, T. W., Jr.; Lin, J. *Organometallics* **1991**, *10*, 1225–1226.
106. Tanke, R. S.; Crabtree, R. H. *Organometallics* **1991**, *10*, 415–418.
107. Tanke, R. S.; Crabtree, R. H. *J. Chem. Soc., Chem. Commun.* **1991**, 1056–1057.
108. Itami, K.; Mitsudo, K.; Nishino, A.; Yoshida, J. *J. Org. Chem.* **1990**, *55*, 2645–2652.
109. Uozumi, Y.; Hayashi, T. *J. Am. Chem. Soc.* **1991**, *113*, 9887–9888.
110. Uozumi, Y.; Kitayama, K.; Hayashi, T. *Tetrahedron Asymmetry* **1993**, *4*, 2419–2422.
111. Kitayama, K.; Uozumi, Y.; Hayashi, T. *J. Chem. Soc., Chem. Commun.* **1995**, 1533–1534.
112. Jensen, J. F.; Svendsen, B. Y.; la Cour, T. V.; Pedersen, H. L.; Johannsen, M. *J. Am. Chem. Soc.* **2002**, *124*, 4558–4559.
113. Uozumi, Y.; Lee, S.-Y.; Hayashi, T. *Tetrahedron Lett.* **1992**, *33*, 7185–7188.
114. Kitayama, K.; Tsuji, H.; Uozumi, Y.; Hayashi, T. *Tetrahedron Lett.* **1996**, *37*, 4169–4172.
115. Okada, T.; Morimoto, T.; Achiwa, K. *Chem. Lett.* **1990**, 999–1002.
116. Marinetti, A. *Tetrahedron Lett.* **1994**, *35*, 5861–5864.
117. Marinetti, A.; Ricard, L. *Organometallics* **1994**, *13*, 3956–3962.
118. Uozumi, Y.; Hayashi, T. *Tetrahedron Lett.* **1993**, *34*, 2335–2338.
119. Shimada, T.; Mukaide, K.; Shinohara, A.; Han, J. W.; Hayashi, T. *J. Am. Chem. Soc.* **2002**, *124*, 1584–1585.
120. Hayashi, T.; Hirate, S.; Kitayama, K.; Tsuji, H.; Torri, A.; Uozumi, Y. *J. Org. Chem.* **2001**, *66*, 1441–1449.
121. Hayashi, T. *Pure Appl. Chem.* **1988**, *60*, 7–12.
122. Cullen, W. R.; Han, N. F. *J. Organomet. Chem.* **1987**, *333*, 269–280.
123. Weber, I.; Jones, G. B. *Tetrahedron Lett.* **2001**, *42*, 6983–6986.
124. Pioda, G.; Togni, A. *Tetrahedron Asymmetry* **1998**, *9*, 3903–3910.
125. Hayashi, T.; Kabeta, K.; Yamamoto, T.; Tamao, K.; Kumada, M. *Tetrahedron Lett.* **1983**, *24*, 5661–5664.
126. Hayashi, T.; Matsumoto, Y.; Morikawa, I.; Ito, Y. *Tetrahedron Asymmetry* **1990**, *1*, 151–154.
127. Ohmura, H.; Matsushashi, H.; Tanaka, M.; Kuroboshi, M.; Hiyama, T.; Hatanaka, Y.; Goda, K. *J. Organomet. Chem.* **1995**, *499*, 167–171.
128. Han, J. W.; Tokunaga, N.; Hayashi, T. *J. Am. Chem. Soc.* **2001**, *123*, 12915–12916.
129. Bosnich, B. *Acc. Chem. Res.* **1998**, *31*, 667–674.
130. Tamao, K.; Tohma, T.; Inui, N.; Nakayama, O.; Ito, Y. *Tetrahedron Lett.* **1994**, *35*, 7333–7336.
131. Bergens, S.; Noheda, P.; Whelan, J.; Bosnich, B. *J. Am. Chem. Soc.* **1992**, *114*, 2121–2128.
132. Wang, X.; Bosnich, B. *Organometallics* **1994**, *13*, 4131–4133.
133. Bergens, S.; Noheda, P.; Whelan, J.; Bosnich, B. *J. Am. Chem. Soc.* **1992**, *114*, 2128–2135.
134. Tamao, K.; Nakamura, K.; Ishii, H.; Yamaguchi, S.; Shiro, M. *J. Am. Chem. Soc.* **1996**, *118*, 12469–12470.
135. Perch, N.; Widenhoefer, R. A. *J. Am. Chem. Soc.* **1999**, *121*, 6960–6961.
136. Perch, N.; Pei, T.; Widenhoefer, R. A. *J. Org. Chem.* **2000**, *65*, 3836–3845.
137. Wang, X.; Stankovich, S. Z.; Widenhoefer, R. A. *Organometallics* **2002**, *21*, 901–905.
138. Nishiyama, H.; Itoh, K. Hydrosilylation of Carbonyl and Imino Groups. In *Catalytic Asymmetric Synthesis*, 2nd ed.; Ojima, I., Ed.; VCH: New York, 2000, pp 267–287.
139. Brunner, H.; Becker, R.; Riepl, G. *Organometallics* **1984**, *3*, 1354–1359.
140. Nishiyama, H.; Sakaguchi, H.; Nakamura, T.; Horihata, M.; Kondo, M.; Itoh, K. *Organometallics* **1989**, *8*, 846–848.
141. Nishibayashi, Y.; Segawa, K.; Ohe, K.; Uemura, S. *Organometallics* **1995**, *14*, 5486–5487.
142. Sawamura, M.; Kuwano, R.; Ito, Y. *Angew. Chem., Int. Ed. Engl.* **1994**, *33*, 111–113.
143. Verdager, X.; Lange, U. E. W.; Reding, M. T.; Buchwald, S. L. *J. Am. Chem. Soc.* **1996**, *118*, 6784–6785.
144. Brunet, J. J.; Neibecker, D. Catalytic Hydroamination of Unsaturated Carbon–Carbon Bonds. In *Catalytic Heterofunctionalization*; Togni, A., Grützmacher, H., Eds.; Wiley-VCH: Weinheim, 2001; pp 91–141.
145. Taube, R. Reaction with Nitrogen Compounds: Hydroamination. In *Applied Homogeneous Catalysis with Organometallic Compounds*; Cornils, B.; Herrmann, W. A., Eds.; VCH: Weinheim, Germany, 1996; pp 507–520.
146. Nobis, M.; Drieffen-Hölscher, B. *Angew. Chem., Int. Ed. Engl.* **2001**, *40*, 3983–3985.
147. Haggin, J. *Chem. Eng. News* **1993**, *71*, 6–7.
148. Müller, T. E.; Beller, M. *Chem. Rev.* **1998**, *98*, 675–703.
149. Gagné, M. R.; Marks, T. J. *J. Am. Chem. Soc.* **1989**, *111*, 4108–4109.
150. Gagné, M. R.; Nolan, S. P.; Marks, T. J. *Organometallics* **1990**, *9*, 1716–1718.
151. Li, Y.; Marks, T. J. *Organometallics* **1996**, *15*, 3770–3772.
152. Haskel, A.; Straub, T.; Eisen, M. S. *Organometallics* **1996**, *15*, 3773–3775.
153. Tian, S.; Arredondo, V. M.; Stern, C. L.; Marks, T. J. *Organometallics* **1999**, *18*, 2568–2570.
154. Arredondo, V. M.; McDonald, F. E.; Marks, T. J. *Organometallics* **1999**, *18*, 1949–1960.
155. Douglass, M. R.; Stern, C. L.; Marks, T. J. *J. Am. Chem. Soc.* **2001**, *123*, 10221–10238.
156. McGrange, P. L.; Jensen, M.; Livinghouse, T. *J. Am. Chem. Soc.* **1992**, *114*, 5459–5460.
157. Haak, E.; Bytschkov, I.; Doye, S. *Angew. Chem., Int. Ed. Engl.* **1999**, *38*, 3389–3391.
158. Haak, E.; Siebeneicher, H.; Doye, S. *Org. Lett.* **2000**, *2*, 1935–1937.
159. Walsh, P. J.; Baranger, A. M.; Bergman, R. G. *J. Am. Chem. Soc.* **1992**, *114*, 1708–1719.
160. Baranger, A. M.; Walsh, P. J.; Bergman, R. G. *J. Am. Chem. Soc.* **1993**, *115*, 2753–2763.
161. Johnson, J. S.; Bergman, R. G. *J. Am. Chem. Soc.* **2001**, *123*, 2923–2924.

162. Straub, B. F.; Bergman, R. G. *Angew. Chem., Int. Ed. Engl.* **2001**, *40*, 4632–4635.
163. Shi, Y.; Ciszewski, J. T.; Odom, A. L. *Organometallics* **2001**, *20*, 3967–3969.
164. Cao, C.; Ciszewski, J. T.; Odom, A. L. *Organometallics* **2001**, *20*, 5011–5014.
165. Brunet, J.-J.; Neibecker, D.; Philippot, K. *J. Chem. Soc., Chem. Commun.* **1992**, 1215–1216.
166. Brunet, J.-J.; Commenges, G.; Neibecker, D.; Philippot, K. *J. Organomet. Chem.* **1994**, *469*, 221–228.
167. Brunet, J.-J.; Neibecker, D.; Philippot, K. *Tetrahedron Lett.* **1993**, *34*, 3877–3880.
168. Beller, M.; Eichberger, M.; Trauthwein, H. *Angew. Chem., Int. Ed. Engl.* **1997**, *36*, 2225–2227.
169. Trauthwein, H.; Tillack, A.; Beller, M. *Chem. Commun.* **1999**, 2029–2030.
170. Beller, M.; Trauthwein, H.; Eichberger, M.; Breindl, C.; Herwig, J.; Müller, T. E.; Thiel, O. R. *Chem. Eur. J.* **1999**, *5*, 1306–1319.
171. Beller, M.; Trauthwein, H.; Eichberger, M.; Breindl, C.; Müller, T. E. *Eur. J. Inorg. Chem.* **1999**, 1121–1132.
172. Hartung, C. G.; Tillack, A.; Trauthwein, H.; Beller, M. *J. Org. Chem.* **2001**, *66*, 6339–6343.
173. Burling, S.; Field, L. D.; Messerle, B. A. *Organometallics* **2000**, *19*, 87–90.
174. Casalnuovo, A. L.; Calabrese, J. C.; Milstein, D. *J. Am. Chem. Soc.* **1988**, *110*, 6738–6744.
175. Dorta, R.; Egli, P.; Zürcher, F.; Togni, A. *J. Am. Chem. Soc.* **1997**, *119*, 10857–10858.
176. Seligson, A. L.; Trogler, W. C. *Organometallics* **1993**, *12*, 744–751.
177. Kawatsura, M.; Hartwig, J. F. *J. Am. Chem. Soc.* **2000**, *122*, 9546–9547.
178. Nettekoven, U.; Hartwig, J. F. *J. Am. Chem. Soc.* **2002**, *124*, 1166–1167.
179. Kawatsura, M.; Hartwig, J. F. *Organometallics* **2001**, *20*, 1960–1964.
180. Löber, O.; Kawatsura, M.; Hartwig, J. F. *J. Am. Chem. Soc.* **2001**, *123*, 4366–4367.
181. Minami, T.; Okamoto, H.; Ikeda, S.; Tanaka, R.; Ozawa, F.; Yoshifuji, M. *Angew. Chem., Int. Ed. Engl.* **2001**, *40*, 4501–4503.
182. Kadota, I.; Shibuya, A.; Lutete, L. M.; Yamamoto, Y. *J. Org. Chem.* **1999**, *64*, 4570–4571.
183. Radhakrishnan, U.; Al-Masum, M.; Yamamoto, Y. *Tetrahedron Lett.* **1998**, *39*, 1037–1040.
184. Müller, T. E.; Grosche, M.; Herdtweck, E.; Pleier, A.-K.; Walter, E.; Yan, Y.-K. *Organometallics* **2000**, *19*, 170–183.
185. Seul, J. M.; Park, S. *J. Chem. Soc., Dalton Trans.* **2002**, 1153–1158.
186. Harrison, K. N.; Hoye, P. A. T.; Orpen, A. G.; Pringle, P. G.; Smith, M. B. *J. Chem. Soc., Chem. Commun.* **1989**, 1096–1097.
187. Hoye, P. A. T.; Pringle, P. G.; Smith, M. B.; Worboys, K. *J. Chem. Soc., Dalton Trans.* **1993**, 269–274.
188. Pringle, P. G.; Smith, M. B. *J. Chem. Soc., Chem. Commun.* **1990**, 1701–1702.
189. Costa, E.; Pringle, P. G.; Smith, M. B.; Worboys, K. *J. Chem. Soc., Dalton Trans.* **1997**, 4277–4282.
190. Costa, E.; Pringle, P. G.; Worboys, K. *Chem. Commun.* **1998**, 49–50.
191. Wicht, D. K.; Kourkine, I. V.; Lew, B. M.; Nthenge, J. M.; Glueck, D. S. *J. Am. Chem. Soc.* **1997**, *119*, 5039–5040.
192. Wicht, D. K.; Kourkine, I. V.; Kovacic, I.; Glueck, D. S.; Concolino, T. E.; Yap, G. P. A.; Incarvito, C. D.; Rheingold, A. L. *Organometallics* **1999**, *18*, 5381–5394.
193. Shulyupin, M. O.; Kazankova, M. A.; Beletskaya, I. P. *Org. Lett.* **2002**, *4*, 761–763.
194. Kazankova, M. A.; Efimova, I. V.; Kochetkov, A. N.; Afanas'ev, V. V.; Beletskaya, I. P.; Dixneuf, P. H. *Synlett* **2001**, *4*, 497–500.
195. Kovacic, I.; Wicht, D. K.; Grewal, N. S.; Glueck, D. S.; Incarvito, C. D.; Guzei, I. A.; Rheingold, A. L. *Organometallics* **2000**, *19*, 950–953.
196. Han, L.-B.; Tanaka, M. *Chem. Commun.* **1999**, 395–402.
197. Han, L.-B.; Tanaka, M. *J. Am. Chem. Soc.* **1996**, *118*, 1571–1572.
198. Zhou, C.-Q.; Han, L.-B.; Goto, M.; Tanaka, M. *Angew. Chem. Int. Ed. Engl.* **2001**, *40*, 1929–1932.
199. Han, L.-B.; Mirzaei, F.; Zhao, C.-Q.; Tanaka, M. *J. Am. Chem. Soc.* **2000**, *122*, 5407–5408.
200. Han, L.-B.; Choi, N.; Tanaka, M. *Organometallics* **1996**, *15*, 3259–3261.
201. Han, L.-B.; Hua, R.; Tanaka, M. *Angew. Chem. Int. Ed. Engl.* **1998**, *37*, 94–96.
202. Douglass, M. R.; Ogasawara, M.; Hong, S.; Metz, M. V.; Marks, T. J. *Organometallics* **2002**, *21*, 283–292.
203. Wicht, D. K.; Glueck, D. S. Hydrophosphination and Related Reactions. In *Catalytic Heterofunctionalization*; Togni, A.; Grützmaier, H., Eds.; Wiley-VCH: Weinheim, 2001; pp 143–170.

9.6

Metal Complexes as Catalysts for C—C Cross-coupling Reactions

I. P. BELETSKAYA and A. V. CHEPRAKOV
Moscow State University, Russia

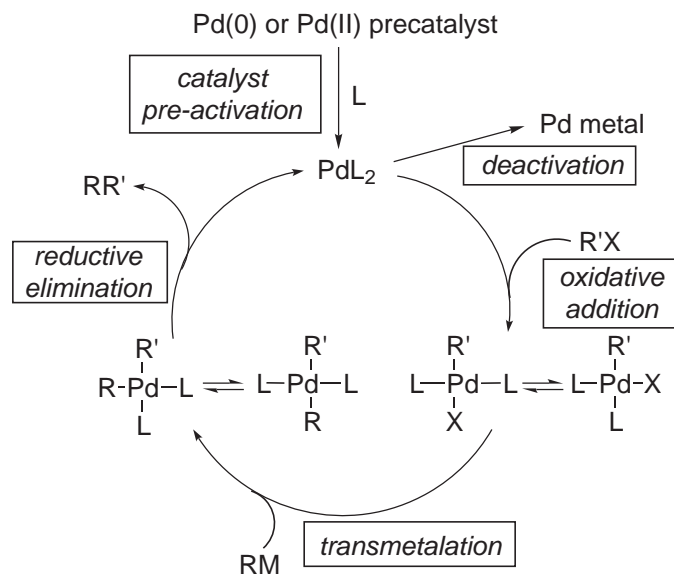
9.6.1	INTRODUCTION	306
9.6.1.1	Notation used in examples	307
9.6.2	MAJOR METHODS OF CROSS-COUPLING	307
9.6.2.1	Cross-coupling with Organoboron Compounds	308
9.6.2.2	Cross-coupling with Organotin Compounds	310
9.6.2.3	Cross-coupling with Organozinc Reagents	312
9.6.2.4	Cross-coupling with Organomagnesium and Organolithium Reagents	315
9.6.2.5	Cross-coupling with Terminal Acetylenes	316
9.6.3	THE DEVELOPMENT OF THE CROSS-COUPLING METHODOLOGY	318
9.6.3.1	Less Common Nucleophilic Reagents	319
9.6.3.1.1	<i>Less common organometallics</i>	319
9.6.3.1.2	<i>Electrochemical cross-coupling</i>	322
9.6.3.1.3	<i>CH-nucleophiles</i>	322
9.6.3.2	Activation of Cross-coupling Reactions	325
9.6.3.2.1	<i>Electrophilic catalysis</i>	325
9.6.3.2.2	<i>Activation of the nucleophilic reagent</i>	327
9.6.3.2.3	<i>Various activation methods in the cross-coupling of organosilicon compounds</i>	331
9.6.3.3	Leaving Groups	334
9.6.3.3.1	<i>Fluorides</i>	335
9.6.3.3.2	<i>Chlorides</i>	335
9.6.3.3.3	<i>Esters as electrophiles in cross-coupling reactions</i>	336
9.6.3.3.4	<i>Other neutral electrophiles</i>	338
9.6.3.3.5	<i>Diazonium salts</i>	341
9.6.3.3.6	<i>Iodonium salts</i>	341
9.6.3.4	Catalysts	341
9.6.3.4.1	<i>Monophosphine catalysis</i>	343
9.6.3.4.2	<i>Chelating ligands with both phosphine and nonphosphine binding sites</i>	343
9.6.3.4.3	<i>Bulky trialkyl- and dialkylphosphines</i>	345
9.6.3.4.4	<i>Bulky dialkylarylphosphines</i>	347
9.6.3.4.5	<i>Heterobimetallic complexes</i>	347
9.6.3.4.6	<i>Phosphorus ligands other than phosphines</i>	348
9.6.3.4.7	<i>Bidentate diphosphine ligands</i>	349
9.6.3.4.8	<i>Palladacycles</i>	351
9.6.3.4.9	<i>Nonphosphorus ligands</i>	352
9.6.3.4.10	<i>Heterocyclic carbene ligands</i>	353
9.6.3.4.11	<i>Palladium nanoparticles and “ligand-free” catalysis</i>	356
9.6.3.5	Technological Aspects of Cross-coupling Chemistry	356
9.6.3.5.1	<i>Microwave heating</i>	357
9.6.3.5.2	<i>Supported catalysts</i>	357
9.6.3.5.3	<i>Aqueous systems</i>	359
9.6.3.5.4	<i>Fluorous systems</i>	359
9.6.3.5.5	<i>Supercritical CO₂</i>	359
9.6.3.5.6	<i>Ionic liquids</i>	360
9.6.4	REFERENCES	360

9.6.1 INTRODUCTION

Cross-coupling is a name commonly ascribed to any exchange (σ -bond metathesis) reaction (Equation (1)), where RM is a nucleophilic reagent and R'X is an electrophilic reagent. While in many practical cases the cross-coupling reactions do not require a catalyst, the discovery of catalytic versions made them a general-purpose method of organic synthesis, principally because of their unprecedented versatility and extension of their scope to virtually all imaginable combinations of organic residues. The derivatives of two metals, Pd and Ni, have won a dominating position in synthetic cross-coupling chemistry, and this domination can hardly be challenged in future, though the development of new interesting catalytic procedures involving Cu, Rh, Pt, and some other metals is likely to gain in importance. This chapter is devoted entirely to the Pd- and Ni-catalyzed cross-coupling reactions involving σ -bonded organometallic reagents and intermediates. Therefore, reactions involving allylic and similar residues, which are believed to involve π -bonded intermediates, are omitted. Due to strict space limitations the discussion is devoted to the current state of the area, with references in most cases given not to the most important but rather to the most recent examples found in the literature, from which the key references can be backtracked:



The mechanism of a typical cross-coupling reaction catalyzed by Pd⁰ or Ni⁰ complexes can be represented by a standard catalytic cycle (Scheme 1, shown for Pd; ancillary ligands not given, for simplicity).



Scheme 1

The cycle involves the following key steps: (i) the oxidative addition to a zerovalent metal of an electrophile R'X to give an R'-Pd^{II}-X species; (ii) the metathesis of the resulting intermediate and the organometallic nucleophile RM (transmetalation) to give a diorganopalladium(II) intermediate R-Pd^{II}-R' (and MX); (iii) the reductive elimination of the cross-coupling product RR' with concomitant regeneration of the zerovalent metal. The Pd derivative introduced into the reaction mixtures is never the actual catalyst, but rather a precatalyst, requiring *in situ* transformation into the catalytically active form (preactivation). Both derivatives of Pd^{II} (various Pd salts and complexes; by far the most popular are Pd(OAc)₂ and PdCl₂(PPh₃)₂), and of Pd⁰ (usually Pd₂(dba)₃ or Pd(PPh₃)₄) can be used as precatalysts. Preactivation involves the reduction of Pd^{II} to the zerovalent state, and tuning of the coordination sphere to the requirements of a given implementation of the catalytic cycle. The reduction usually does not need to be performed explicitly, but is effected by the components of the reaction mixture: the organometallic reagent

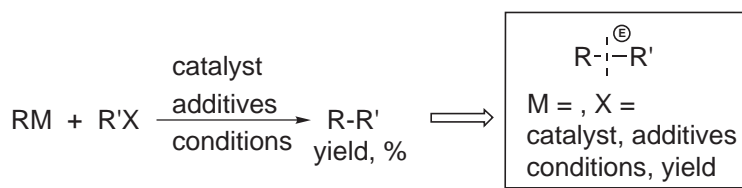
RM, phosphine ligands, or tertiary amine base. Some reactions, however, do benefit from the addition of special reducing agents, such as DIBAL-H or the like. Deactivation of the palladium catalyst often occurs via the formation of Pd metal sediments (Pd black), which often happens if the amount of supporting ligand is insufficient for full ligation of the Pd⁰ species. The alternative pathway for deactivation involves oxidation by oxygen. It should be noted that most likely it is not Pd⁰ itself which is targeted by oxidation, because: (i) Pd⁰ species are not easily oxidized by O₂ in the absence of helper co-oxidants such as Cu^{II} salts; and (ii) Pd⁰ is effectively regenerated under the conditions of cross-coupling reactions. The most likely targets of either direct or Pd-catalyzed oxidation are the phosphine ligands, which leads to the depletion of ligand and formation of Pd black. Air-tolerant, Pd-catalyzed cross-coupling processes are therefore not infrequent, and catalytic systems robust to unfavorable conditions (technical-grade solvents used without purification, air atmosphere, etc.) can be intentionally developed for large-scale implementation.

The catalytic cycle with Ni catalysts is generally similar. The essential difference is the deactivation process, which in this case occurs not via the formation of a precipitate of Ni⁰, but rather due to interception of the highly reactive Ni⁰ species by any fortuitous oxidant, such as oxygen. As Ni^{II} is not so easily reduced to Ni⁰ as Pd^{II} is to Pd⁰, Ni-catalyzed systems often require the addition of a stoichiometric reducing agent (Zn, DIBAL-H, other hydride transfer agents, BuLi, etc.).

Either oxidative addition or transmetalation can be the rate-limiting step in cross-coupling reactions. Generally, it is believed that in the vast majority of cross-coupling reactions the transmetalation is the rate-limiting step, although with less reactive electrophiles (aryl and vinyl chlorides, electron-rich aryl bromides, alkyl halides or sulfonates) the oxidative addition step can be slow. Cross-coupling reactions are generally highly stereospecific, involving the retention of configuration at both nucleophilic and electrophilic centers if *sp*²-carbons or cyclopropyl residues are involved. Both retention and inversion may occur in the case when an *sp*³-electrophile is used.¹

9.6.1.1 Notation used in examples

In order to conserve space and avoid redundancy in this chapter, we adopt wherever possible the following short notation for cross-coupling reactions: in place of a full equation only the product is given, with a dashed line showing the bond being formed. The electrophilic part is denoted by a circled E, and both leaving groups are given immediately below the structure with all other pertinent information. Scheme 2 shows a “template” for subsequent examples.



Scheme 2

9.6.2 MAJOR METHODS OF CROSS-COUPLING

Since the discovery of cross-coupling chemistry in the 1970s, five major methods have become predominant in synthetic applications, which are: cross-coupling with organoboron, organotin, organozinc, or organomagnesium compounds, or with terminal acetylenes. In spite of considerable success in the development of the cross-coupling with organosilicon compounds and the apparently huge potential of this reaction, its synthetic applications are rare. Each of the five major methods of cross-coupling now has a vast history of its own. Since each has been extensively reviewed (cf. ref. 2 for a full bibliography), here we give only a short enumeration of the major uses of each method. The synthetic potential of any given cross-coupling method depends on: (i) the variety of sources of the nucleophilic coupling partner (i.e., the organometallic compound); (ii) the number of different types of organic residue which can be combined; and (iii) tolerance to other functional groups in the coupling partners.

9.6.2.1 Cross-coupling with Organoboron Compounds

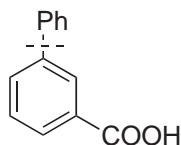
Cross-coupling with organoboron compounds (the Suzuki–Miyaura reaction) is by far the most popular and versatile method of cross-coupling, and has been extensively reviewed.^{3–5}

The sources of the required organoboron compounds are manifold. The most popular organoboron compounds for this method, boronic acids and their esters (boronates), can be obtained through:

- (i) transmetalation from organolithium or organomagnesium compounds using $B(OR)_3$, or by transmetalation from other organometallics, e.g., stannanes⁶ or silanes;^{7–9}
- (ii) haloboration of terminal alkynes with subsequent hydrolysis;¹⁰
- (iii) *syn*-hydroboration of double or triple bonds;
- (iv) Rh-catalyzed *syn*-hydroboration of double and triple bonds by catechol- or pinacolboranes,¹¹ (which by adjustment of the catalytic system can also be performed as a formal *anti*-addition);¹²
- (v) Rh-catalyzed dehydrogenative hydroboration of styrenes;¹³
- (vi) Pd-catalyzed C—B cross-coupling reaction of aryl halides with bis(pinacolato)diboron;¹⁴
- (vii) Pd catalyzed C—B cross-coupling of aryl halides or triflates with dialkoxyboranes;¹⁵
- (viii) Pt-catalyzed addition of bis(pinacolato)diboron to alkynes.¹⁶ The $B(OH)_2$ function is robust enough to endure modification of other parts of the molecule, e.g., by oxidation of electrophilic substitution reactions. Besides boronic acids, 9-BBN derivatives obtained by hydroboration are often used for $sp^3(B)$ – sp^2 cross-coupling.

The standard protocol of the Suzuki–Miyaura reaction uses $Pd(PPh_3)_4$ as a precatalyst, in the presence of an aqueous solution of base (Na_2CO_3 , $NaOH$, $LiOH$, etc.) in dioxane, THF, dimethoxyethane (DME), EtOH, benzene, and similar solvents, at reflux. The addition of base is necessary for cross-coupling with organoboron compounds, as only tetracoordinate, anionic boronates are nucleophilic enough to effect the transmetalation step. Nonaqueous conditions may be required in those cases where the organoboron compounds used are prone to protonolysis, and organic-soluble bases such as K_3PO_4 or Cs_2CO_3 are then used.

Catalysis by phosphine-free Pd derivatives, often realized in aqueous media, is an important modification of the Suzuki–Miyaura reaction.¹⁷ Although this protocol is largely limited to the reactions of aryl iodides and reactive aryl bromides, it has significant advantages: these are not only economic (cheaper catalytic system, ecologically and technologically superior media, high catalytic efficiency allowing use of less of the precious metal, etc.), but they also allow the avoidance of side reactions which occur in the presence of phosphine ligands due to the involvement of phosphine aryl groups in the reaction (aryl scrambling). Aqueous, phosphine-free reactions are often highly effective, allowing high turnover numbers to be obtained (**1**).¹⁷ Moreover, in phosphine-free reactions, lower initial concentrations of the Pd precatalyst are advantageous, as the growth of large Pd clusters leading to Pd-black precipitation is thus impaired. In the presence of a phase-transfer agent, $Pd(OAc)_2$ can be used for cross-coupling of activated aryl bromides even at room temperature.¹⁸ Alternatively, the reaction between aryl bromides and arylboronic acids can be facilitated simply by grinding.¹⁹ Simple Ni salts and phosphine-free complexes can also be used for the cross-coupling of aryl bromides with arylboronic acids in good yields.^{20,21}

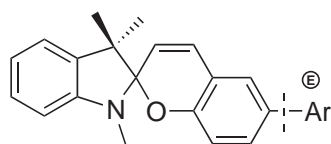


RM = Ph_4BNa , X = Br
 $PdCl_2$, Na_2CO_3 , H_2O
 reflux, TON = 250,000

(1)

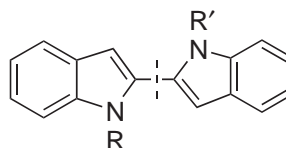
The scope of Suzuki–Miyaura reactions is extremely broad, covering practically all types of organic residues. The cross-coupling of arylboronic acids with aryl halides or triflates is the most

potent method for the synthesis of unsymmetrical biaryls (**2**),²² including all sorts of heterobiaryls (**3**).^{23,24} Either standard or aqueous phosphine-free protocols are usually applied. Sterically hindered biaryls may require the use of boronates in place of boronic acids, and anhydrous conditions, such as $\text{K}_3\text{PO}_4/\text{DMF}$ ²⁵ or PhONa/PhH to avoid protodeboronation (**4**).²⁶ Small amounts of water as, for example, in hydrated K_3PO_4 , may improve yields even in the case of sterically hindered biaryls.²⁷ The cross-coupling of alkenylboronic acids (boronates) with alkenyl or aryl halides or triflates is an important route to dienes, styrenes, and other conjugated olefins.⁴ Cross-coupling of cyclopropylboronic acids can be similarly carried out using standard protocols (**5**).^{28–30} Coupling with enantiomerically pure cyclopropylboronate, obtained by cyclopropanation of the respective vinylboronate, with a tartrate ester residue serving as chiral auxiliary, gives an example of an enantioselective cross-coupling reaction (**6**).³⁰



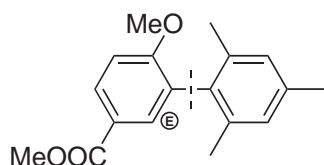
$\text{M} = \text{B}(\text{OH})_2$, $\text{X} = \text{I}$
 $\text{Pd}(\text{OAc})_2$, Na_2CO_3
 DMF , 80°C

(2)



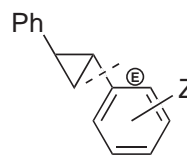
$\text{M} = \text{B}(\text{OMe})_2$, $\text{X} = \text{I}$
 $\text{Pd}(\text{PPh}_3)_4$, Na_2CO_3
 PhMe aq.
 R , $\text{R}' = \text{Me}$, MeOCH_2 etc.

(3)



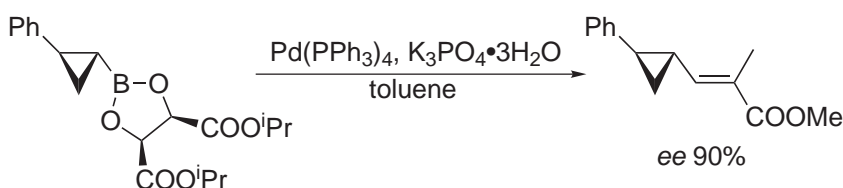
$\text{M} = \text{B}(\text{OCH}_2\text{CMe}_2\text{CH}_2\text{O})$, $\text{X} = \text{I}$
 $\text{Pd}(\text{PPh}_3)_4$, PhONa , PhH , reflux

(4)



$\text{M} = \text{B}(\text{OH})_2$, $\text{X} = \text{Br}$
 $\text{Pd}(\text{PPh}_3)_4$, K_3PO_4 , toluene
 $\text{Z} = \text{H}$, $p\text{-Ph}$, $o\text{-OMe}$, $m\text{-OMe}$,
 $o\text{-COOMe}$, $p\text{-COOMe}$, $p\text{-NO}_2$

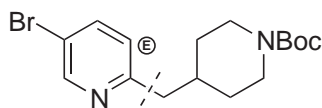
(5)



(6)

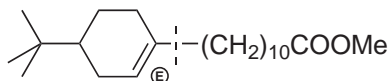
The cross-coupling of alkylboron compounds with alkenyl or aryl halides or triflates is a powerful method for the synthesis of complex molecules, through the use of terminal double bonds as the precursors of organoboron nucleophiles.^{31,32} The method has been reviewed.³³ Trialkylboranes are preferred nucleophiles in this reaction, by far the most convenient being the 9-alkyl-9-BBN compounds.³¹ In order to suppress possible β -hydride elimination, dppf (bis(diphenylphosphino)ferrocene, Section 9.6.3.4.7) is usually used as ligand, sometimes with other supporting ligands (**7**).³⁴ The use of triflates as electrophiles requires the same protocol (**8**).³⁵ Simple alkyl groups like ethyl can be introduced in this way, as in (**9**), with triflate as a leaving group, though in this case the highly effective Buchwald's ligand (Section 9.6.3.4.4) should be used.³⁶ This variety of cross-coupling reactions is useful for macrocyclizations, as in the syntheses

of various cyclophane molecules (**10**).^{37–42} Simple primary alkylboronic acids can be directly cross-coupled with aryl halides or triflates in the presence of a dppf complex of Pd.⁴³



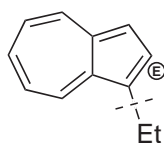
M = 9-BBN, X = I
PdCl₂(dppf)/Ph₃As, K₂CO₃
DMF-H₂O, 95%

(7)



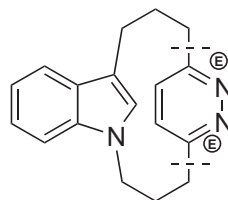
M = 9-BBN, X = OTf
PdCl₂(dppf), K₂CO₃
dioxane, 85 °C, 89%

(8)



M = 9-BBN or BEt₂, X = OTf
Pd(OAc)₂, (o-PhC₆H₄)PCy₂
Cs₂CO₃ or KF, THF, reflux

(9)



M = 9-BBN, X = I
PdCl₂(PPh₃)₂, Cs₂CO₃
THF, reflux; 30%

(10)

9.6.2.2 Cross-coupling with Organotin Compounds

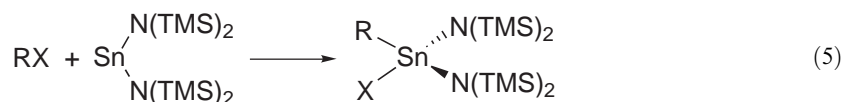
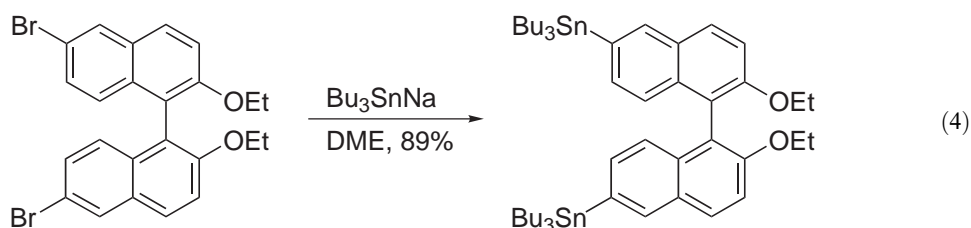
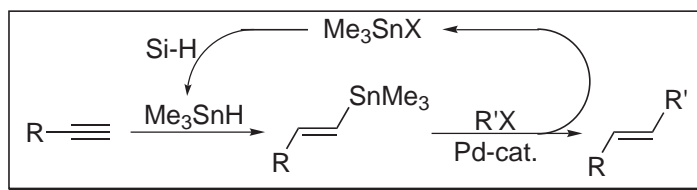
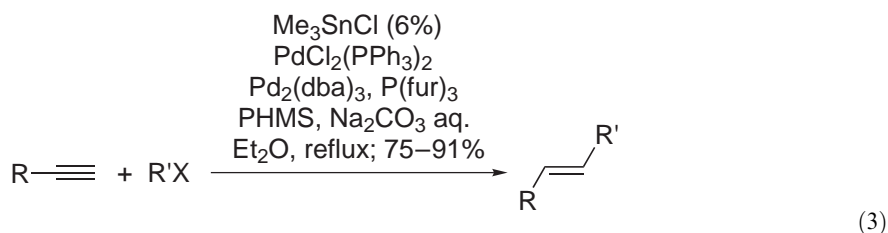
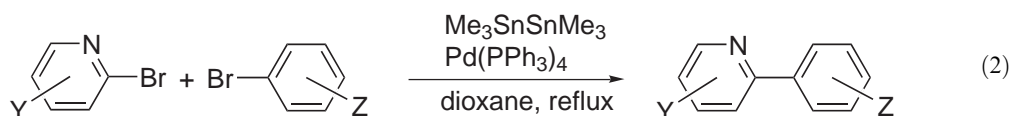
From the number of applications and reported body of examples, this method (usually referred to as the Stille, or Kosugi–Migita–Stille, reaction) comes second only to the Suzuki–Miyaura reaction, with the main reason for its lesser popularity being the high toxicity of organotin compounds. Unlike the cross-coupling with organoboron compounds, this method does not require the addition of strong bases, resulting in a significant simplification of the protocol which is essential for processing base-sensitive compounds.

Sources of the organotin compounds for this reaction are as follows:

- (i) transmetalation from organolithium or magnesium compounds, and more rarely from other organometallics, such as aluminum;⁴⁴
- (ii) Pd-catalyzed addition of Sn–Sn, Sn–silicon, and other Sn–M compounds to triple bonds;^{45–47}
- (iii) Pd-catalyzed addition of various stannanes (carbostannylation) to alkynes;^{48,49}
- (iv) Sn–C cross-coupling reaction of aryl or alkenyl halides (triflates) with Sn–Sn reagents. This is a powerful method, and avoids the severe limitations of the common transmetalation method; two cross-coupling reactions, with Sn–C and subsequent C–C bond formation, can be combined in one pot (Equation (2)).⁵⁰
- (v) hydrostannylation, both free-radical⁵¹ and transition-metal catalyzed.^{52–54} Pd-catalyzed *in situ* hydrostannylation has been used to perform one-pot transformation of terminal acetylenes to disubstituted alkenes.⁵⁵ This was further developed into a unique protocol, catalytic in tin (Equation (3)); PMHS stands for “polymeric hydrosiloxane,” used to recycle tin hydride).^{56–58} In the presence of Lewis acids (ZrCl₄ etc.) hydrostannylation of alkynes can be performed as an *anti*-addition, thus leading to (*Z*)-alkenylstannanes.⁵⁹
- (vi) The trialkylstannate anion, being a supernucleophile, can directly effect nucleophilic aromatic substitution to afford organotin compounds, as in the synthesis of stannylated binaphthyls, which are useful building blocks for the preparation of 1,1'-binaphthyl-based polymers (Equation (4)).⁶⁰

In the case of less reactive aryl halides, a photostimulated $S_{RN}1$ substitution can be applied.⁶¹

- (vii) Oxidative addition of Lappert's stannylene readily gives organotin species which are useful in cross-coupling reactions (Equation (5)).⁶²
 (viii) free-radical substitution of phenylsulfonyl group by SnBu_3 .^{63,64}

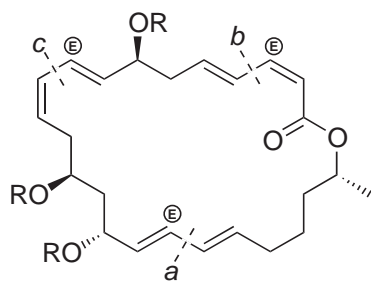


The standard protocol for organotin-based cross-couplings uses the common Pd precatalysts $\text{Pd(PPh}_3)_4$ or $\text{Pd(PPh}_3)_2\text{Cl}_2$; or Pd(OAc)_2 , $\text{Pd}_2(\text{dba})_3$, $\text{PdCl}_2(\text{MeCN})_2$ together with phosphine ligands. Since organotin compounds are moderately reactive nucleophiles, and in order to facilitate transmetalation, polar solvents (most frequently DMF) are preferentially used in this method, though ethereal solvents (dioxane, THF) are also useful.

The synthetic scope of the Stille cross-coupling is extremely wide, seemingly unlimited, with all sorts of coupling partners being involved. The cross-coupling of alkenylstannanes with alkenyl or aryl halides (triflates) is a general route to conjugated olefins of all kinds. The reactions with reactive alkenyl or aryl iodides are often best performed in phosphine-free catalytic systems. The stereo- and regiospecific assembly of complex molecules, including the formation of macrocycles, can be accomplished (11).⁶⁵

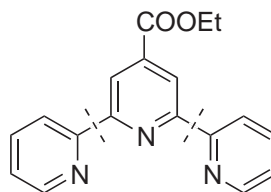
If the stannane bears substituents at the position geminal to tin, the reaction requires activation by Cu^I (Section 9.6.3.2.1). The cross-coupling of aryl (or heteroaryl) stannanes with aryl (or heteroaryl) halides or triflates is a general route to various biaryls and their analogues, particularly useful in those cases when the Suzuki–Miyaura reaction is less effective: for

example, in the introduction of pyridyl residues (**12**).⁶⁶ The cross-coupling of alkynylstannanes with aryl or alkenyl halides or triflates requires very soft reaction conditions and is tolerant to most functional groups; consequently this method works where other $sp-sp^2$ cross-coupling reactions fail, e.g., for heavily functionalized substrates (**13**),⁶⁷ or cross-coupling with bromoallenes (**14**).⁶⁸



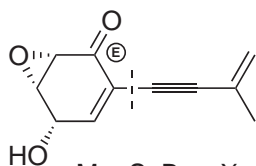
M = SnBu₃, X = I
 a, b: PdCl₂(MeCN)₂, DMF
 c: Pd₂(dba)₃, ⁱ-Pr₂NEt, DMF

(11)



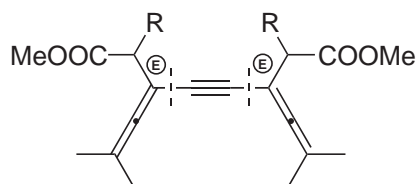
M = SnBu₃, X = Br
 Pd(PPh₃)₄, toluene, reflux

(12)



M = SnBu₃, X = I
 Pd(PPh₃)₂Cl₂, CuI
 THF, r.t., 74%

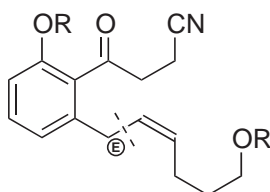
(13)



M = SnMe₃, X = Br
 Pd(PPh₃)₄
 NMP, r.t., 55–66%

(14)

The sp^3-sp^2 cross-coupling reactions of organotin compounds are quite rare. Me₄Sn is often used as the methylating agent, while other alkyltin reagents are not as useful. Vinyltin reagents can be cross-coupled with heavily substituted benzylic electrophiles, which are otherwise very poor substrates for cross-coupling reactions (**15**).^{69,70}



M = SnBu₃, X = Br
 Pd₂(dba)₃, AsPh₃, THF

(15)

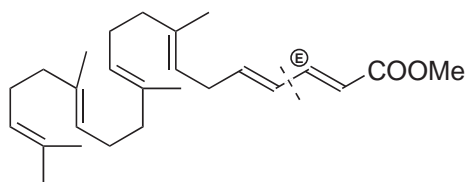
9.6.2.3 Cross-coupling with Organozinc Reagents

Organozinc compounds are more reactive nucleophiles requiring no activation for the transmetalation step, while allowing for much wider functionality to be present in the molecule than in organomagnesium compounds. However, organozinc compounds cannot be stored without special precautions, and therefore should be generated immediately prior to use, which makes

them much less convenient than organoboron and organotin compounds. Thus, the cross-coupling with organozinc compounds (commonly referred to as the Negishi reaction) is a more specialized method; it is, however, indispensable when the combination of high reactivity and maximal tolerance to functionality in the coupling partners is required.

Sources for the organozinc compounds are as follows:

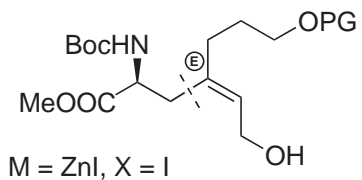
- (i) A common source of organozinc compounds for cross-coupling is the *in situ* transmetalation from RLi or RMgX, which essentially limits the scope of the method, although the recent discovery of methods for the generating of functionalized Grignard reagents allows the scope of this method to be extended (Section 9.6.2.4). Transmetalation from other organometallic compounds is also possible and may be much more tolerant of other functional groups. A very important protocol involves the *in situ* generation of organozinc compounds from organozirconium compounds, obtained by hydrozirconation of terminal acetylenes,^{71,72} as in (16);⁷³ this method has also been used in other natural product syntheses.^{73–77} Transmetalation from organoboron reagents obtained by hydroboration is a versatile route to various alkylzinc compounds,⁷⁸ and transmetalation from organotellurium reagents can also be a convenient route to alkenylzinc compounds.^{79,80}



M = ZnCl [via Zr(Cl)Cp₂], X = I
Pd(PPh₃)₄, THF, r.t.; 75%

(16)

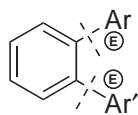
- (ii) Functionalized organozinc compounds can be obtained by the insertion of chemically or ultrasonically activated Zn metal into C—X (mostly C—I) bonds. One of the most widely used protocols employing this approach is Jackson's method⁸¹ for the synthesis of non-natural amino-acids using L-serine as common synthon (17).^{82–85} Other such organozinc reagents can also be used.⁸⁶



M = ZnI, X = I
Pd(PPh₃)₄, PhH-HMPA, 80 °C

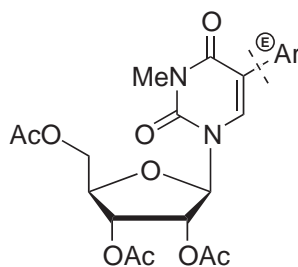
(17)

Ortho-phenylenedizinc easily generated by activated-Zn insertion into *o*-diiodobenzene or *o*-iodophenol triflate,^{87–89} undergoes the reaction with two equivalents of either aryl iodide or aryl chloride, giving disubstituted benzenes in good to high yields.⁸⁸ Stepwise substitutions with two different electrophiles can be perfectly chemoselective if an electron-rich phosphine with a larger cone angle is taken (18).⁹⁰ Formation and application of β -ethoxyvinylzinc by insertion of Zn/Ag into the respective bromide give another example of this synthetic paradigm.⁹¹ A wide range of valuable organozinc reagents can be generated by Zn insertion into iodinated nitrogen heterocycles, including nucleosides, and further used in cross-coupling reactions (19).⁹² Zn can be inserted into the C—I bond of iodo-cyclohexenones or their heteroanalogues.⁹³ Alkyl bromides and even some chlorides react with Zn activated by iodine in polar, aprotic solvents.⁹⁴ These examples clearly show the vast synthetic potential and outstanding tolerance of this method for the generation of organozinc reagents.



M = ZnI, X = I
 PdCl₂(MeCN)₂,
 P[2,4,6-C₆H₂(OMe)₃]₃
 TMU, 40 °C

(18)

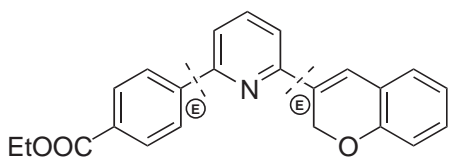


M = ZnI, X = I
 Pd₂(dba)₃, P(fur)₃
 THF, r.t., 58%

(19)

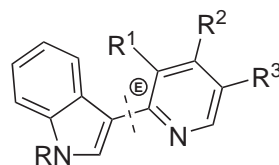
- (iii) Organozinc compounds, including aryl or heteroaryldizinc reagents, can be prepared by electrocatalysis using a sacrificial Zn anode.^{95–99}
- (iv) Halogen–zinc metathesis can be accomplished by the reaction of organic halides with simple dialkylzinc reagents.¹⁰⁰
- (v) Zirconocene dichloride and similar complexes catalyze carbozincation of alkenes and alkynes.^{101,102} Carbozincation of alkynes^{103,104} can also be performed with nickel catalysis. The methods of generation of functionalized organozinc reagents have been reviewed.¹⁰⁵

The scope of the Negishi reaction is roughly the same as that of the two other major methods of cross-coupling. Its strongest advantage, the possibility of running the reaction under milder conditions (often at room temperature) in shorter times without any additives—which additionally simplifies the product isolation procedure—makes this method the best choice for complex, product-oriented, synthetic tasks. Aryl–aryl coupling by this method has been used for the modification of calixarenes,¹⁰⁶ and heteroaryl–aryl and heteroaryl–alkenyl couplings were combined in the synthesis of chromene derivatives (20).¹⁰⁷ Heteroaryl–heteroaryl coupling using organozinc reagents is also well documented (21).¹⁰⁸ The Negishi reaction is very convenient for the synthesis of pyridine derivatives.¹⁰⁹



a: M = ZnBr, X = OTf; b: X = I
 Pd(PPh₃)₂Cl₂, THF–DME, 60 °C

(20)

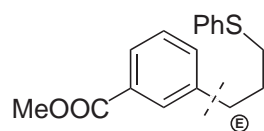


M = ZnCl, X = Cl or Br
 Pd(PPh₃)₂Cl₂, DIBAL–H
 THF, reflux

(21)

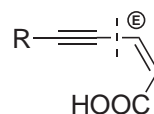
Cross-coupling reactions at *sp*³-centers are among the most valuable applications of organozinc reagents. Cross-coupling of arylzinc reagents with alkyl iodides is catalyzed by Ni(acac)₂ in the presence of some electron-deficient styrenes under very mild conditions (22).^{110,111} The same catalytic system can be applied to *sp*³–*sp*³ cross-coupling between alkylzincs and alkyl iodides.^{112,113} β-Branched alkylzinc reagents can be cross-coupled with various *sp*²-electrophiles in the presence of PdCl₂(dppp).¹⁰² Alkynyl–alkenyl or alkynyl–aryl coupling protocols have been described by Negishi (23).^{114,115}

Cross-coupling reactions with Zn acetylenides are the most convenient and selective routes to terminal acetylenes. In this reaction Zn is markedly superior to other metals, including Sn (24).¹¹⁶ The higher reactivity of Zn acetylides allowed assembly of hexaethynylbenzenes in two steps, with the last three groups introduced at the second stage by the Negishi reaction (25).¹¹⁷



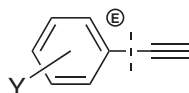
M = ZnBr, X = I
 Ni(acac)₂,
p-CF₃C₆H₄CH=CH₂
 THF, -15 °C, 75%

(22)



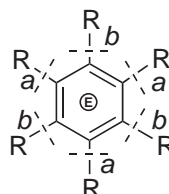
M = ZnBr, X = I
 Pd(PPh₃)₄
 THF, r.t., 92–98%
 R = Alk, Cy, Ph

(23)



M = ZnBr, X = I
 Pd(PPh₃)₄, THF, r.t.
 Y = NO₂, COOMe, Me, H, OMe *etc.*

(24)



R = C≡C-Ph

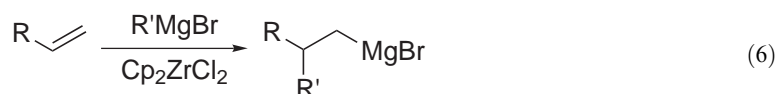
a: M = H, X = I
 Pd(PPh₃)₄, CuI, ⁱPr₂NH
 THF, reflux, 47%
b: M = ZnCl, X = Cl
 Pd(PPh₃)₄, THF, reflux, 83%

(25)

9.6.2.4 Cross-coupling with Organomagnesium and Organolithium Reagents

Organomagnesium compounds (mostly Grignard reagents) have been used for cross-couplings since the earliest history of this chemistry. The nickel-catalyzed reaction is referred to as the Kumada–Tamao–Corriu reaction. Later the palladium-catalyzed version of cross-coupling with Grignard reagents was developed by Murahashi and co-workers.¹¹⁸ Unlike RMgX compounds, organolithium compounds are not applicable in the nickel-catalyzed cross-coupling; however, they have been shown by Murahashi and co-workers to be useful in some Pd-catalyzed reactions.¹¹⁸

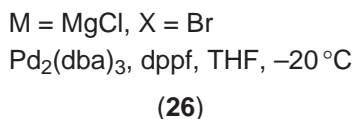
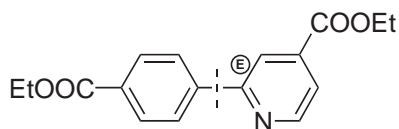
Besides the conventional Grignard reaction used for the generation of organomagnesium reagents, new methods have been proposed using the highly activated forms of Mg metal: Rieke's Mg,^{119–123} the Mg–anthracene complex,¹²⁴ vacuum-deposited Mg clusters,¹²⁵ and Mg nanoparticles.¹²⁶ Such methods allow the organomagnesium species to be obtained under very mild conditions not only from a wide range of organic halides, but also from other electrophilic species which are normally unreactive in common Grignard reactions. Recently, the scope of this reaction has been dramatically expanded, as a route to functionalized Grignard reagents bearing COOR, CN, and similar groups has been discovered, involving the transmetalation of aryl iodides with *i*Pr₂Mg or *i*PrMgBr,¹²⁷ or low-temperature insertion of Rieke's Mg.¹¹⁹ An alternative path to alkylmagnesium compounds is zirconocene-dichloride-catalyzed carbomagnesation of alkenes (Equation (6)),^{128–136} and transmetalation from boranes can lead to Grignard reagents from alkenes.¹³⁷



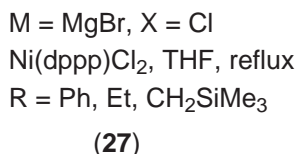
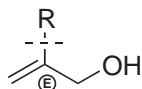
The scope of cross-couplings using Grignard reagents and organolithium compounds is much narrower than that of any of the other major methods. However, the easy availability and high reactivity of RMgX, and particularly RLi, species makes this method a welcome alternative when it can be used. Additionally, it should be noted that the reactions with RMgX are usually catalyzed by cheaper Ni complexes, an important feature for larger-scale applications. Due to the high reactivity

of Grignard reagents, cross-couplings with aryl or alkenyl chlorides can be realized in some cases without any special techniques, within the framework of the standard protocol.

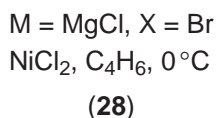
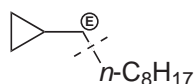
Aryl–aryl or Aryl–heteroaryl cross-coupling reactions can be performed with either Ni- or Pd-based catalysis. Due to the low reaction temperatures, substrates containing some additional functional groups are tolerated (26).¹³⁸



Aryl–alkenyl cross-coupling is straightforward. Simple alkylmagnesium reagents (Me, Et, CH₂SiMe₃, etc.) can be easily involved in Ni-catalyzed cross-coupling (27),^{139,140} while more complex alkyl halides—particularly branched ones prone to β-hydride elimination—require Pd catalysts with bidentate phosphines, such as dppf, to achieve good selectivity (Section 9.6.3.4.7).



The *sp*³–*sp*³ cross-coupling, one of the most challenging tasks among cross-coupling reactions, can be achieved by using Grignard reagents and nickel catalysts. Butadiene and other 1,3-dienes were noted to accelerate the reaction and enable the use of less reactive alkyl bromides and even tosylates, possibly through the *in situ* formation of a reactive complex of Ni with the diene (28).¹⁴¹

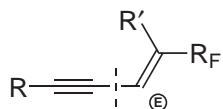


9.6.2.5 Cross-coupling with Terminal Acetylenes

Cross-coupling of terminal acetylenes used as nucleophiles with aryl or alkenyl halides (referred to as the Sonogashira–Hagihara, or SH, reaction) is a versatile method of synthesis for acetylenic compounds, which are rapidly gaining importance as advanced new materials and building blocks for implementing unusual molecular architectures.

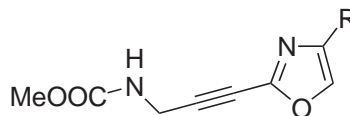
In the SH reaction acetylenes are used as they are, without the prior transformation into organometallic compounds which is required in other methods of *sp*(M)–*sp*^x coupling. The SH reaction commonly uses a standard protocol with Pd(PPh₃)₄ or similar Pd complexes used as precatalysts, a tertiary amine as base, and copper(I) salts as cocatalysts, in a number of media including ethers (THF, dioxane) and dipolar aprotic solvents. The combination of amine and cuprous salt is believed to effect the *in situ* transformation of the alkyne into a copper(I) acetylide, which is likely to serve as a coupling partner.¹⁴² This interpretation is not flawless, as it is well known that cross-coupling of aryl iodides with terminal acetylenes can be performed in the absence of cuprous cocatalyst, and other bases can be used in place of amines.

The scope of the SH reaction encompasses $sp-sp^2$ (alkenyl, aryl (29),¹⁴³ heteroaryl) and $sp-sp$ couplings (the modified Cadiot–Chodkiewicz reaction).¹⁴² Iodides are most frequently used as electrophilic coupling partners, though the use of bromides, triflates (30),¹⁴⁴ or even some reactive chlorides (31)¹⁴⁵ is also possible. Due to the low steric bulk of the acetylenic unit, as well as its exceptional ability in the transduction of electronic effects, the SH reaction is well suited for construction of new (e.g., star-like) molecular architectures through polysubstitution (32).¹⁴⁶



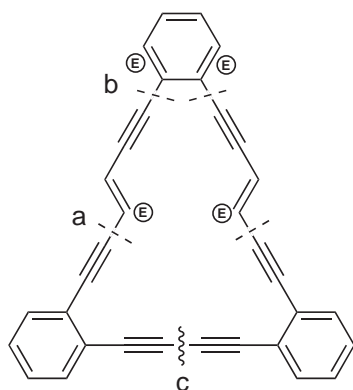
M = H, X = I
 PdCl₂(PPh₃)₂/CuI
 Et₃N, 40 °C

(29)



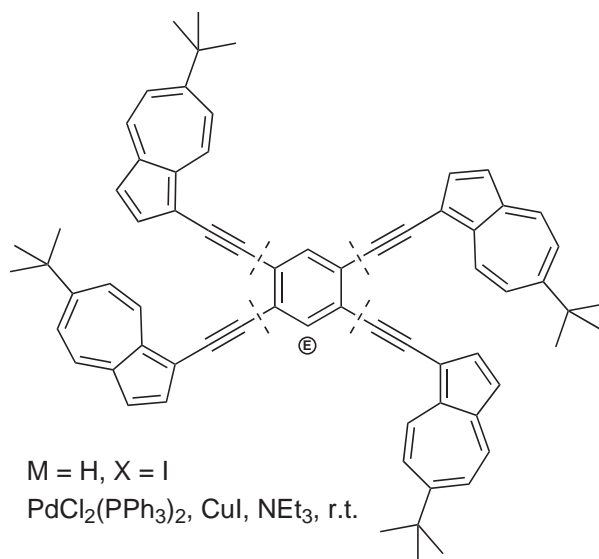
M = H, X = OTf
 Pd(PPh₃)₄, CuI, 2,6-lutidine, r.t.

(30)



a: M = H, X = Cl
 Pd(PPh₃)₄/CuI, Et₃N
 THF, 60 °C
 b: M = H, X = I
 PdCl₂(PPh₃)₂/CuI, Et₃N
 THF, 60 °C
 c: homocoupling:
 CuCl/Cu(OAc)₂, py

(31)

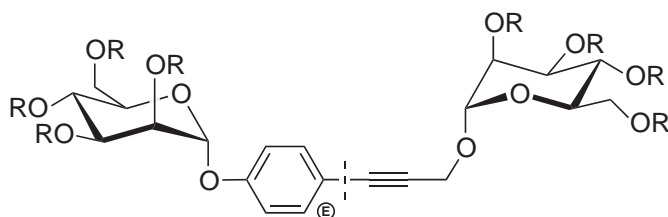


M = H, X = I
 PdCl₂(PPh₃)₂, CuI, NEt₃, r.t.

(32)

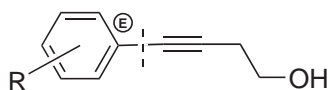
In spite of the common conception that Ni catalysts are useless in the Sonogashira reaction, NiCl₂(PPh₃) has been disclosed as being able to catalyze the cross-coupling of aryl iodides with terminal acetylenes in aqueous dioxane, in the presence of CuI.¹⁴⁷

The exclusion of copper from the Sonogashira reaction protocols is a desirable modification for several reasons. The essential simplification of the procedure is very important for large-scale applications. Copper salts also have a well-known ability to promote undesired homocoupling of acetylenes, giving rise to diacetylene by-products,¹⁴⁸ or intramolecular carbopalladation in the case of tethered acetylenes.¹⁴⁹ However, no general copper-free protocol has been developed, though occasionally the cross-coupling with terminal acetylenes is shown to proceed flawlessly in the absence of Cu^I salts. It has been reported that Pd(PPh₃)₄ as a precatalyst does not require CuI, while PdCl₂(PPh₃)₂ does.¹⁵⁰ Indeed, in copper-free procedures Pd(PPh₃)₄ is usually used in the presence of an amine base and an aryl iodide as electrophile, as in the synthesis of rod-like carbohydrate clusters (33);¹⁵¹ aryl bromides or triflates can also be used as the electrophile,¹⁵² albeit not as smoothly (34).¹⁵³ Symmetrical tolanses can be prepared in a Cu-free procedure using trimethylsilylacetylene as an acetylene synthon (35).¹⁵⁴ Silver oxide in conjunction with Bu₄NF serves in a copper- and amine-free procedure.¹⁵⁵ The other notable Cu-free procedure requires the use of a phase-transfer agent in aqueous MeCN solvent.¹⁵⁶



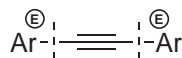
M = H, X = I
Pd(PPh₃)₄, Et₃N, DMF, 60 °C, 71–100%

(33)



M = H, X = Br
PdCl₂(PPh₃)₂, Et₃N, DMF, 80 °C

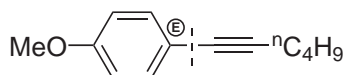
(34)



M = H and SiMe₃, X = I
Pd(PPh₃)₄, MeONa, MeOH
reflux, 63–91%

(35)

Apart from Cu^I, Zn^{II} salts or Zn metal were also shown to be effective, thus bringing forward an alternative efficient protocol (36) which may be useful for the applications in which the contamination of products by Cu cannot be tolerated. Such protocols can also be advantageous in cross-coupling with acetylenes bearing electron-withdrawing substituents, such as propiolate esters,¹¹⁵ which usually give unsatisfactory results under the standard conditions.



M = H, X = Br
Pd(PPh₃)₄,
ZnCl₂ or Zn dust, NaI, NEt₃, DBU
DMSO, 60 °C, 88–100%

(36)

9.6.3 THE DEVELOPMENT OF THE CROSS-COUPLING METHODOLOGY

The conventional methods of cross-coupling, though successfully applied to an overwhelming number of synthetic applications, leave unresolved a number of fundamental challenges, which

prompt the investigation of new advanced methods. The most important problems calling for the further development of cross-coupling methodology are:

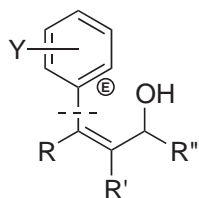
- (i) the need for softer and more selective procedures allowing the scope of method to be extended;
- (ii) an increase of reactivity and extension of the scope of electrophiles towards the less expensive chlorides, sulfonates, diazonium salts, etc.;
- (iii) minimizing the use of expensive Pd and ligands through (a) increasing catalytic efficiency, with a goal of obtaining more product per unit loading of precatalyst; (b) use of Ni in place of Pd; (c) design of new ligands (nonphosphine, cheap, recoverable, etc.); and (d) development of environmentally and technologically safer methods.

9.6.3.1 Less Common Nucleophilic Reagents

9.6.3.1.1 Less common organometallics

(i) Copper

The involvement of organocopper intermediates in various cross-coupling reactions carried out in the presence of Cu^{I} is often suggested, although in the majority of cases no experimental proof is provided, and the actual role of Cu^{I} may be different (Section 9.6.3.2.1). The potential of copper-mediated cross-coupling can be shown by the stereospecific reaction of 3-trimethylsilylallylic alcohols, which takes place via a prior transmetalation of Si to Cu (37).¹⁵⁷

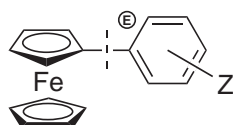


M = Cu (via SiMe_3), X = I
 Pd(PPh_3)₄, TBAF,
 THF- H_2O , r.t.

(37)

(ii) Mercury

Organomercuric compounds require nucleophilic assistance by soft iodide anions (cf. Section 9.6.3.2.2) for participation in cross-coupling reactions.¹⁵⁸ The reaction is useful for aryl–aryl cross-coupling in those cases in which the organomercury species are obtained by direct mercuriation of aromatic compounds (38).¹⁵⁹

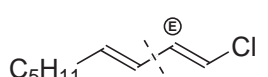


M = 1/2Hg, X = I
 PdCl₂(PPh_3)₂, NaI
 Me₂CO-THF, reflux

(38)

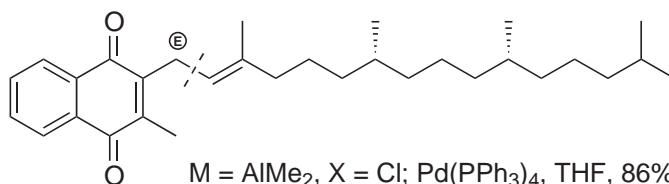
(iii) Aluminum

Although this metal was introduced to cross-coupling chemistry very early, for the synthesis of dienes by $sp^2(\text{Al})-sp^2(\text{I})$ cross-coupling using vinylaluminum compounds generated by hydroalumination of alkynes,¹⁶⁰ the development of more effective protocols has left the method so far almost unexplored. The lower reactivity of alkenylalanes requires their activation by Zn halides. The very high regioselectivity of cross-coupling of β,β -disubstituted alkenylalanes with alkenyl halides found a valuable application in simple syntheses of carotenoids.¹⁶¹ The sp^2-sp^2 cross-coupling can also be performed using Ni catalysts (39).¹⁶² Otherwise, Al has found only occasional use, e.g., for $sp^3(\text{Al})-sp^2$ cross-coupling.¹⁶³ Alkenylaluminum compounds, readily obtained through Zr-catalyzed carboalumination of terminal acetylenes, are good coupling partners for cross-couplings, e.g., with alkyl halides, as in the direct assembly of vitamin K without masking of the reactive naphthoquinone moiety (40).¹⁶⁴



M = Al(*i*Bu)₂, X = Cl
Ni(PPh₃)₄, PhH-Et₂O

(39)



M = AlMe₂, X = Cl; Pd(PPh₃)₄, THF, 86%

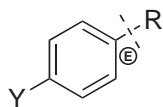
(40)

(iv) Gallium

This is a very rare metal in cross-coupling reactions. Direct comparison of similar methylating reagents derived from Al, Ga, and In showed that the Ga derivative is the least reactive.¹⁶⁵ Vinylgallium dichlorides underwent cross-coupling with aryl iodides in the presence of Pd catalysts with P(*o*-tol)₃; the reaction is moderately tolerant to acidic functional groups.¹⁶⁶

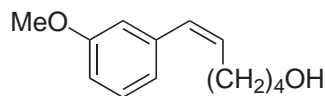
(v) Indium

Indium has been introduced very recently, and turns out to be an excellent metal for cross-coupling reactions. A very broad range of organoindium compounds including triaryl, trialkyl, trialkenyl, and trialkynylindium species were reactive in cross-coupling reactions with aryl iodides and triflates (41) and alkenyl triflates. All three organic residues in the R₃In component are transferred to the product, and no activation is required; even monoorganoindium compounds are reactive enough to effect transmetalation.^{167,168} Diorganoindium compounds can be employed in aqueous media.¹⁶⁹ The free-radical addition of indium hydride to alkynes gives the *anti*-adduct, a very rare outcome for hydrometalation reactions; the resulting alkenyl-indium species provides a convenient route to (*Z*)-alkenes (42).¹⁷⁰



M = InR₂, X = I, Br, OTf
PdCl₂(PPh₃)₂ or PdCl₂(dppf)
THF, reflux; 80–97%
Y = Me, Ac;
R = Ar, Alk, alkenyl, alkynyl

(41)



M = InCl₂, X = I
Pd₂(dba)₃, P(fur)₃
DMI/THF, 66 °C; 97%

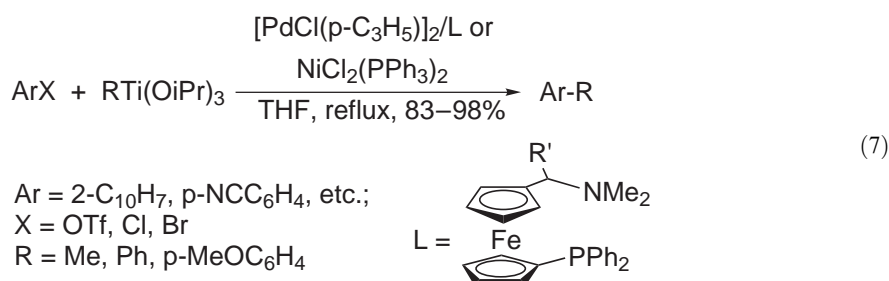
(42)

(vi) Germanium

Organogermanium compounds resemble their organosilicon analogues in their reactivity in cross-coupling reactions, and require nucleophilic activation (Section 9.6.3.2.2).

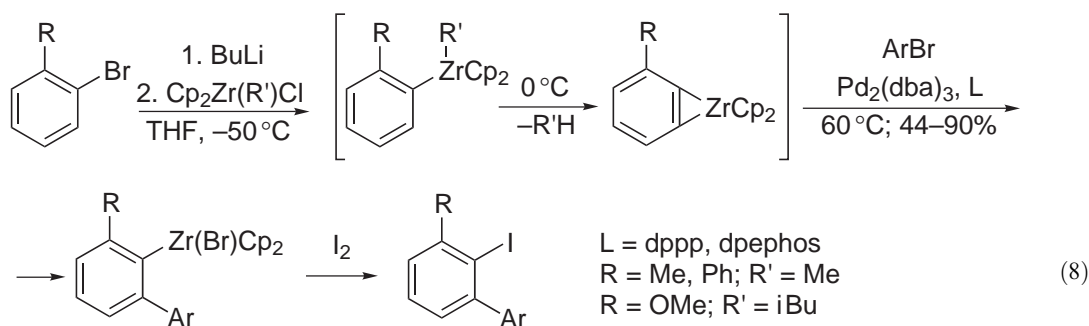
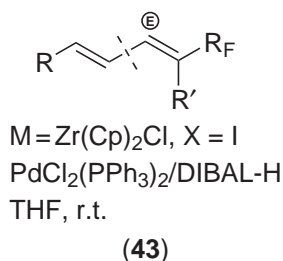
(vii) Titanium

Titanium derivatives were shown to serve as cross-coupling partners for aryl triflates, chlorides, or bromides, with better tolerance to functional groups than Grignard reagents, although specific, expensive N,P-chelating ligands are required (Equation (7)):¹⁷¹



(viii) Zirconium

Organozirconium derivatives, obtained by hydrozirconation of alkynes, usually possess insufficient reactivity for use in cross-couplings, most likely due to the bulkiness of the Cp₂Zr residue, but are very useful as intermediates for the generation of organozinc compounds (Section 9.6.2.3). In some cases, however, organozirconium compounds can be used directly, as in the reaction with highly reactive perfluoroalkylvinyl iodides (43).¹⁴³ Strained benzo[*b*]zirconacyclopropenes, obtained by spontaneous intramolecular metathesis from dicyclopentadienylalkylzirconobenzenes, are highly reactive in cross-coupling with aryl bromides in a regiospecific reaction. Due to differences in reactivity between C—Zr bonds, the σ-arylzirconium intermediate formed after the cleavage of the zirconacyclopropene ring is inert towards further cross-coupling, and is retained for further transformations (see equation (8) below).¹⁷² RCOZrClCp₂ can be cross-coupled with diaryliodonium salts under mild conditions.¹⁷³



(ix) *Bismuth*

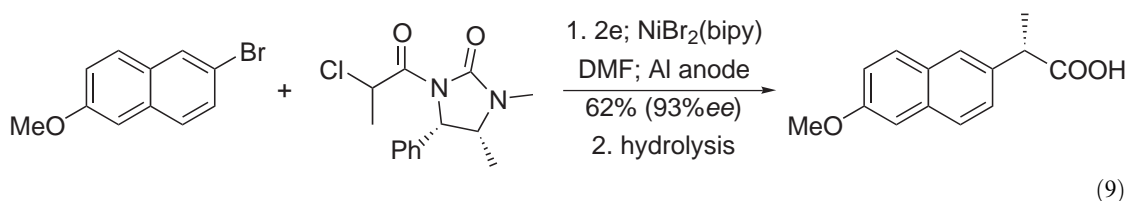
Triarylbi-muth compounds can be used in cross-coupling reactions with aryl iodides, bromides, or triflates in the presence of Pd(PPh₃)₄ and CsF or K₂CO₃.¹⁷⁴

(x) *Manganese*

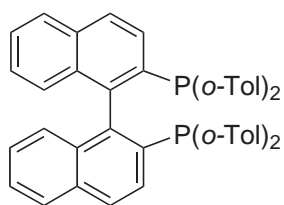
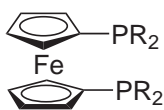
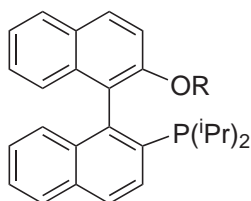
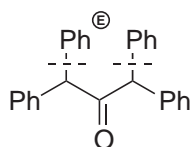
Benzylmanganese halides, prepared by the insertion of Rieke's manganese into benzylic halides, undergo cross-coupling with aryl iodides in the presence of Pd(PPh₃)₄.¹⁷⁵

9.6.3.1.2 *Electrochemical cross-coupling*

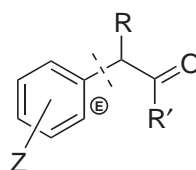
Coelectrolysis of two organic halides in the presence of Ni complexes such as NiX₂(bipy), with an inert cathode and a "sacrificial" metal anode which is dissolved during the reaction (Mg, Zn, Al, Fe), may give cross-coupling products. In this case Ni⁰ is generated through the electro-reduction of Ni^{II} to take part in oxidative addition with the more reactive halide. It remains questionable, however, what comes next, and how the transmetalation step is achieved. The most likely mechanism implies the participation of RNi^I complexes, which undergo a second oxidative addition to give RR'Ni^{III}X,^{176,177} although the involvement of nucleophilic organometallic species formed by the metal anode in a single-compartment electrochemical cell cannot be ruled out in some cases. In order to perform cross-coupling selectively, and avoid homocoupling, the organic halides should be different in nature—it is impossible to perform by this method the routine aryl–aryl or vinyl–vinyl cross-couplings, because the homocoupling prevails.¹⁷⁸ Instead, aryl or vinyl halides can be cross-coupled with activated alkyl halides (such as α -chloroketones, α -chloroesters, or allyl chlorides).^{179–181} A broader range of coupling partners, including (besides activated alkyl halides) some vinyl halides and aryl halides, are compatible with bromothiophenes and 2-halopyridines.^{182,183} The method can be applied to such sophisticated tasks as an enantioselective arylation of α -chloroesters, which can be realized in high chemical and optical yields, as exemplified by the synthesis of the anti-inflammatory drug (*S*)-naproxen (Equation (9)):¹⁸⁴

9.6.3.1.3 *CH-nucleophiles*

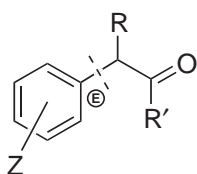
Pd-catalysed cross-coupling with the direct participation of CH-bonds (rather than C—M bonds) is feasible if either a sufficiently acidic CH group, or a sufficiently electron-rich aromatic compound, is used. The first case is dominated by the well-known Sonogashira–Hagihara reaction using terminal alkynes (Section 9.6.2.5). Apart from sporadic early examples,^{185–187} the application of cross-coupling methodology to other CH-acids, such as enolizable carbonyl compounds (ketones, esters) has not long been developed into dependable protocols. Thus, the Pd-catalyzed arylation of benzylketones by iodoarenes can be performed under phosphine-free conditions (44).¹⁸⁸ Polyarylation of alkylaromatic ketones, as well as vinylogous polyarylation of α,β -unsaturated carbonyl compounds, readily occurs in the presence of either PPh₃ or P^tBu₃ as ligands.¹⁸⁹ More general and selective methods, applicable to a wide range of ketones and similar enolizable compounds (esters, including protected aminoacids, nitriles, malonates, cyanoacetates, etc.), employ bulky bidentate ligands derived from binaphthyl (BINAP, TolBINAP (**L1**)) (45)^{190,191} or ferrocene scaffolds (dppf, dtpf (**L2**, R = *o*-tol), dtbpf (**L2**, R = ^tBu), **L3**); or the trialkylphosphines PCy₃ or P^tBu₃ (46),^{192,193} (47)^{194,195} (Section 9.6.3.4.3), or heterocyclic carbene ligands^{194,196} (Section 9.6.3.4.10). In many cases such ligands allow the use of aryl chlorides as the arylating agents. α,β -Unsaturated ketones can be arylated at the γ -position (48).¹⁹⁷

**L1****L2****L3****L4**

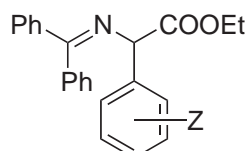
M = H, X = I
PdCl₂, Cs₂CO₃, LiCl,
DMF, 100 °C

(44)

M = H, X = Br
Pd₂(dba)₃, L, NaOtBu
THF, 70 °C, 54–93%
R, R' = Alk, Ar
Z = *o*-, *m*-, *p*-Me, OMe, Cl, CN etc
L = BINAP, TolBINAP

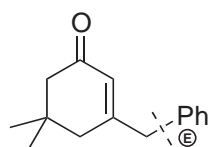
(45)

M = H, X = Br, Cl, OTs
Pd(dba)₂, L, NaOtBu
25–70 °C, 60–99%
R, R' = Alk, Ar or
R = COOEt, R' = OEt
Z = H; *o*-, *p*-Me; *m*-, *p*-OMe; etc
L = dtbpf, L3, P^tBu₃, PCy₃

(46)

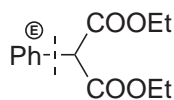
M = H, X = Cl, Br
Pd₂(dba)₃, P^tBu₃
K₃PO₄, toluene, 100 °C

(47)



M = H, X = Br
 Pd(OAc)₂, PPh₃
 Cs₂CO₃, DMF
 60 °C, 71%

(48)

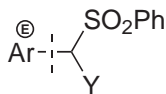


M = H, X = Cl, Br, I
 Na₂PdCl₄, Ba(OH)₂
 DMAc, 100 °C, 93–100%

(49)

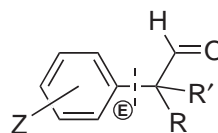
Although most of the methods for the arylation of enolizable compounds so far developed rely on special phosphine ligands, there is a report of an unusually mild and efficient phosphine-free procedure for the arylation of diethyl malonate, the key to success of which is announced to be the use of a heterogeneous base. In this procedure all three halobenzenes, including PhCl, showed practically identical reactivity (49).¹⁹⁸

Sulfones with an additional electron-withdrawing α -substituent can be smoothly arylated in the presence of PPh₃ as ligand (50).¹⁹⁹ Similar methods were developed for the α -arylation of nitrotoluene and alkylazines (51).²⁰⁰



M = H, X = Br, I, Cl
 Pd₂(dba)₃, PPh₃, NaH
 dioxane, 70 °C, 51–90%
 Y = SO₂Ph, COOEt, CN, NO₂
 Ar = C₆H₄Z (Z = *m*-, *p*-Me,
 OMe, F, CF₃, etc.); 1-C₁₀H₇;
 3-pyridyl; 3-quinolyl; etc.

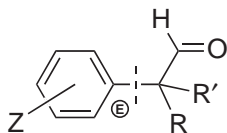
(50)



M = H, X = Br
 Pd(OAc)₂, P^tBu₃, Cs₂CO₃
 dioxane, 110 °C, 77–82%
 R, R' = H, Alk, Ar;
 Z = H, *p*-Me, OMe, Ph

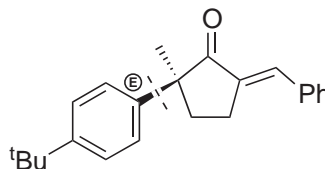
(51)

The use of P^tBu₃ as the ligand allowed the α -arylation of aldehydes (52).²⁰¹



M = H, X = Br
 Pd(OAc)₂, P^tBu₃, Cs₂CO₃
 dioxane, 110 °C, 77–82%
 R, R' = H, Alk, Ar;
 Z = H, *p*-Me, OMe, Ph

(52)



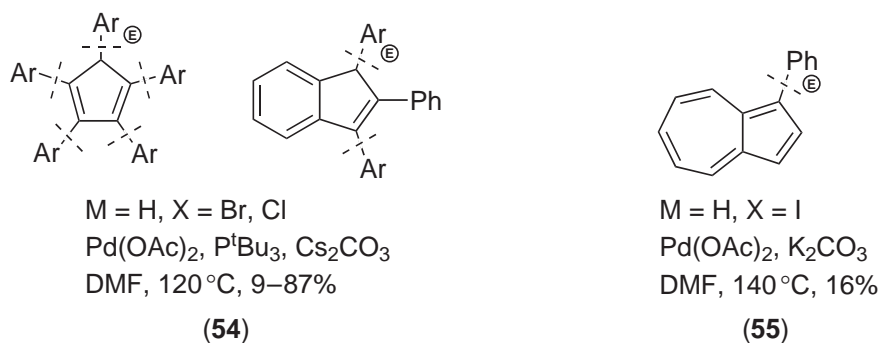
M = H, X = Br
 Pd(OAc)₂, (*S*)-BINAP,
 NaHMDS
 PhMe, 100 °C, 75% (98% ee)

(53)

Enantioselective arylation of ketones can be realized either with the standard BINAP ligand, which requires harsh conditions and a high loading of catalyst to produce high yields (53),²⁰² or with newer, MOP-type ligands (L4) (Section 9.6.3.4.2) under mild conditions and only one-tenth as much catalyst.^{203,204}

CH-acids such as cyclopentadiene and indene give no monoarylation products under the conditions of cross-coupling, but rather are transformed into the exhaustively polyarylated

derivatives. The reaction is best performed with P^tBu_3 as ligand, which additionally makes possible the use of aryl chlorides as arylating agents (54).²⁰⁵



The arylation of electron-rich arenes, such as azulene (55)²⁰⁶ and heteroarenes, has been sporadically described. Under similar conditions phenols undergo arylation, which is preferably directed at the *ortho*-positions, probably due to the involvement of palladium phenolate intermediates.^{188,207} Polysubstitution occurs readily.²⁰⁸ The *para*-position can be attacked only with the sterically hindered 2,6-di-*t*-butylphenol.²⁰⁹ Similar *ortho*-diarylation of arenes bearing carbonyl groups (acetophenone, anthrone, benzanilide, etc.) shows that the *ortho*-directing effect of the substituent is more important than its other electronic effects.¹⁸⁹

9.6.3.2 Activation of Cross-coupling Reactions

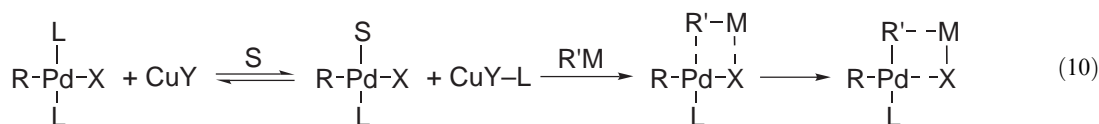
The reactivity of the organometallic reagent is of importance primarily for the transmetalation step of the catalytic cycle. Weakly nucleophilic and stable C—M bonds may inhibit this step, and thus impede the cross-coupling as a whole. This problem may be overcome by applying activation to either (i) increasing the electrophilicity of the species $R-Pd^{II}-X$ species; or (ii) increasing the nucleophilicity of the organometallic reagent $R'M$ by means common to organic/organometallic chemistry, namely, either electrophilic or nucleophilic catalysis.

9.6.3.2.1 Electrophilic catalysis

Metal cations can lend electrophilic assistance to weaken the Pd—X bonds in the intermediate $R-Pd^{II}-X$. Either full fission of this bond, leading to the realization of a polar mechanism, or partial polarization, might take place. Soft Lewis acids (the cations of Cu, Ag, Tl) are used most often (see Chapter 9.8 for a discussion of how metal ions act as Lewis-acid catalysts).

(i) Copper

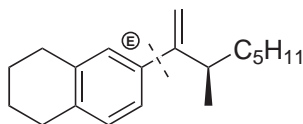
The well-known effect of copper salts on various cross-coupling reactions can be listed under this category, though the actual source of copper effect is poorly understood and may be manifold. For example, in cross-coupling reactions with organotin compounds, copper salts were proven to scavenge neutral ligands (phosphines) rather than halide ions,²¹⁰ which may help transmetalation by freeing a vacancy in the coordination sphere of Pd—necessary for the metathesis of ligands to take place (Equation (10)):



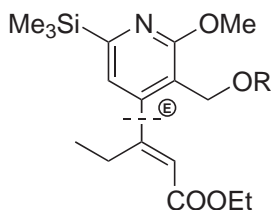
Alternatively, copper salts can themselves be engaged in transmetalation with a nucleophilic coupling partner to give organocopper intermediates, which then either enter the Pd-catalyzed

reaction, or may react with organic halides without the participation of palladium. The latter process is often thought to be the main driving force of the Sonogashira–Hagihara reaction (Section 9.6.2.5).

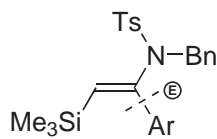
Copper salts have long been known to accelerate the Stille coupling.^{210,211} A huge positive influence of CuCl on both the yields and selectivity of cross-coupling with sterically hindered alkenyltin compounds has been noted (**56**),²¹² giving a very useful protocol for natural-product synthesis (e.g., (**57**)²¹³ and (**58**),⁴⁶ amongst others^{214–217}), although in some cases CuI is equally effective.²¹⁸ Cu^I salts are ineffective in cross-coupling reactions, while CuO can be used to improve yields in some reactions with stannylated, nitrogen-containing heterocycles.^{219–221}



M = SnBu₃, X = OTf
Pd(PPh₃)₄, CuCl, LiCl
DMSO, 60 °C, 95%
(56)

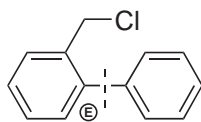


M = SnBu₃, X = OTf
Pd(PPh₃)₄, CuCl, LiCl
DMSO, 60 °C; 80%
(57)



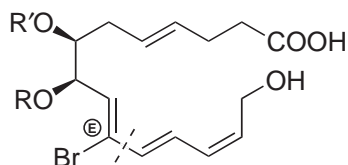
X = I, M = SnBu₃
Pd₂(dba)₃, AsPh₃
CuCl, THF, r.t.
(58)

In cross-coupling with arylboronic acids, some Cu^I carboxylates were found to provide a way to realize a very mild, base-free procedure, which is helpful in cases when added base can induce side reactions (**59**).²²²



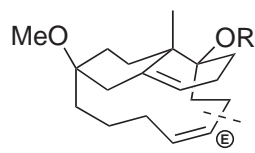
M = B(OH)₂, X = I
Pd(PPh₃)₄, CuOCOR
THF, r.t., 72%
(59)

Besides Cu^I promoters, the Ag^I and Tl^I derivatives are used as soft electrophilic catalysts in cross-coupling reactions, particularly the Suzuki–Miyaura reaction, where both (used as hydroxides, carbonates, or the like) can additionally provide base catalysis from the anion. The use of Tl-containing bases (TlOH²²³ or TlOEt²²⁴) is prescribed in the Suzuki–Miyaura reaction with sterically hindered coupling partners, in order to avoid the side reactions (protodeboration),²⁶ they are also used in cross-couplings with less reactive organoboron compounds.²²⁵ Also advantageous is the use of Tl-based bases to increase the yield and selectivity in cross-coupling of alkenylboronic acids with 1,1-dibromoalkenes, in which only the (E)-bromine is displaced (**60**),^{226,227} or (B-alkyl)-alkenyl coupling leading to a transannular macrocyclization (**61**).²²⁸ It should be noted, however, that the extreme toxicity of Tl compounds limits their use.



M = B(OH)₂, X = Br
 Pd(PPh₃)₄, TIOEt,
 THF, r.t., 83%

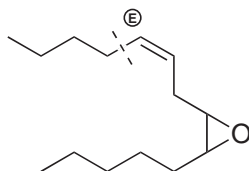
(60)



M = 9-BBN, X = I
 Pd(dppf)Cl₂, AsPh₃,
 TIOEt, THF, 46%

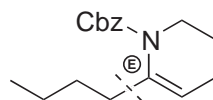
(61)

Silver oxide is used as the base in special cases of Suzuki–Miyaura cross-couplings as, for example, in reactions with *n*-alkylboronic acids ((62)²²⁹ and (63)²³⁰), including MeB(OH)^{231,232} — which have been considered as substrates of low nucleophilicity, giving low yields of cross-coupling products under standard conditions. It has been shown, however, that K₂CO₃ alone can be equally efficient as the base for cross-couplings with alkylboronic acids, though high loadings of the Pd(dppf)Cl₂ precatalyst are required in this case to achieve good yields (63).⁴³



M = B(OH)₂, X = I
 Pd(dppf)Cl₂, Ag₂O, K₂CO₃
 THF, 80 °C, 84%

(62)



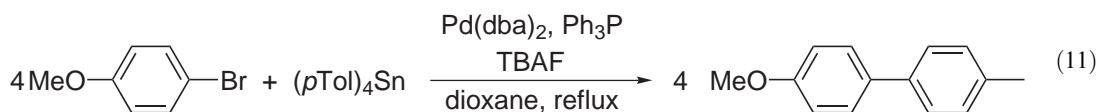
M = B(OH)₂, X = OTf
 PdCl₂(dppf), K₂CO₃, Ag₂O
 PhMe, 80 °C, 93%

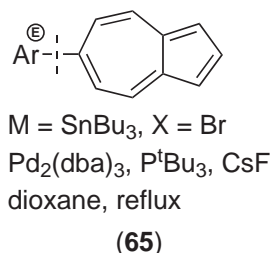
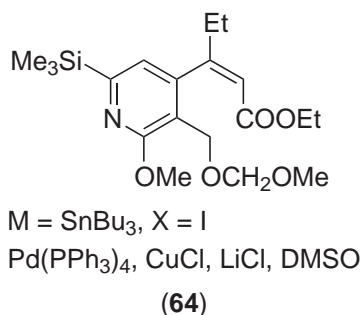
(63)

9.6.3.2.2 Activation of the nucleophilic reagent

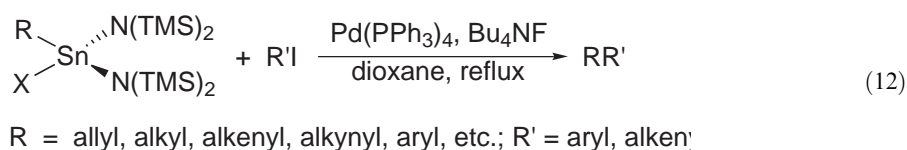
Alternatively, the transmetalation can be facilitated by increasing the nucleophilicity of the carbon nucleophile participating in the cross-coupling, which is most often done by increasing the electron density on the metal by coordination of extra anionic ligands. Two distinct approaches to nucleophilic activation are: (i) the addition of appropriate Lewis bases to the reaction mixture (nucleophilic catalysis); or (ii) the use of a preformed, electron-rich, organometallic reagent with enhanced nucleophilicity.

Nucleophilic catalysis is a common practice in cross-coupling reactions with less reactive organometallics. Organotin compounds are intermediate in nucleophilicity between B and Zn derivatives, in most cases requiring no explicit activation, but favoring mild assistance for transmetalation. The use of polar aprotic solvents such as DMF, DMSO, or HMPA, which are well-known Lewis bases, or the addition of LiCl in the Stille reaction, can be considered as examples of nucleophilic catalysis. Combined electrophilic and nucleophilic assistance—as, for example, in Corey's protocol²¹² using the Pd(PPh₃)₄/CuCl/LiCl system in DMSO solution—enables many hitherto-unsuccessful Stille couplings (64)²¹⁸ to be performed. Similarly, the so-called “tin scavengers,” such as Ph₂P(O)O[−]NR₄⁺ salts are, in fact, effective nucleophilic catalysts, which additionally help to remove tin as an insoluble salt Ph₂P(O)OSnBu₃.^{65,233,234} Coordination by the nitrogen donor atom is likely to account for the positive influence of amines on yields and selectivity in Stille reactions.²³⁵ A more vigorous activation can be provided by fluoride anions (65).^{236–238} The addition of TBAF allowed the use of the otherwise inert tin chloride reagents ArBu₂SnCl, as well as the use of all four aryl groups of tetraaryltin compounds (Equation (11)).²³⁹

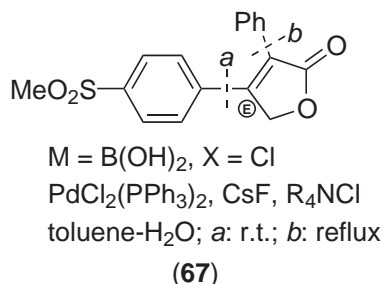
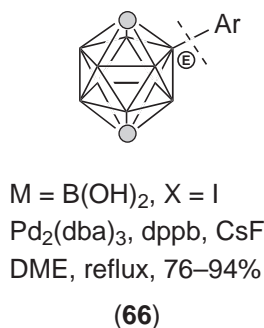




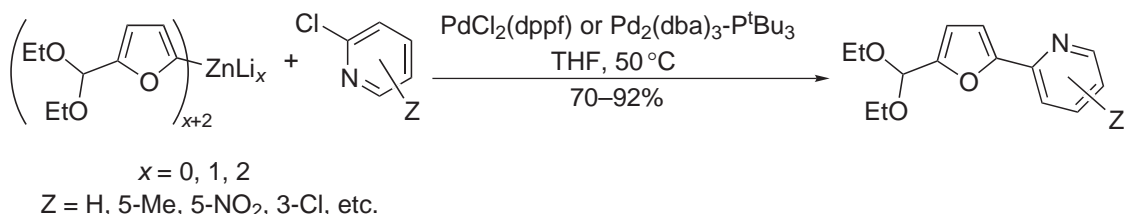
Fluoride-activated monoorganotin derivatives can be used in cross-coupling with aryl or vinyl iodides to transfer a very wide range of organic residues, including alkyls which are not normally reactive (Equation (12)).⁶²



Organoboron compounds cannot react without proper activation. The use of oxygen bases is inherent in the standard Suzuki–Miyaura cross-coupling method. Fluorides (usually CsF) can be used as alternative activating agents, which is particularly useful in cases when the reagents are incompatible with oxygen bases for the reactions run under anhydrous conditions,²⁴⁰ (66).²⁴¹ Fluoride activation can be effective, however, even under aqueous phase-transfer conditions (67).²⁴²

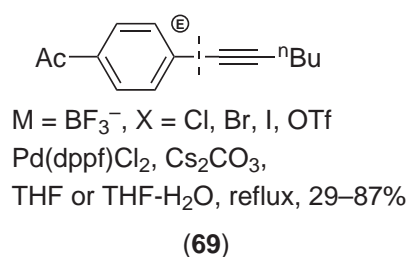
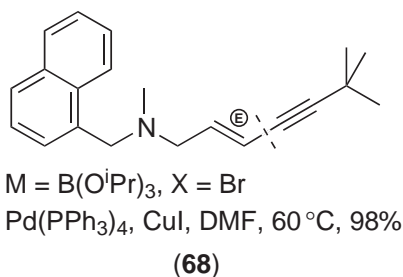


Organometallic reagents with enhanced nucleophilicity can be used to achieve acceleration of cross-coupling reactions. Although organozinc compounds do not generally require special activation, some advantages may be gained by varying their nucleophilicity. Thus diorganozinc compounds R₂Zn, for example, are more reactive than the commonly used RZnX reagents (Equation (13)). Besides R₂Zn, tri- and tetraorganozincates can be successfully used for cross-coupling, with all organic residues being transferred to the product; this can be essential for large-scale applications, where the minimization of the amount of transition metal is a separate, important task.²⁴³

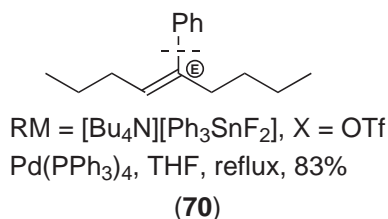


Anionic complexes of boron (boronates, borinates, etc.) have been introduced as convenient reagents in cross-coupling reactions of broad scope, particularly interesting for the transfer of alkynyl and primary alkyl residues, which cannot be accomplished using the standard protocols of the Suzuki–Miyaura reaction. Readily available Ph_4BNa can be used as a convenient reagent for phenylation in place of the much more expensive PhB(OH)_2 , and all four phenyl groups can be utilized when the reaction is carried out with a phosphine-free catalyst in aqueous solutions.²⁴⁴

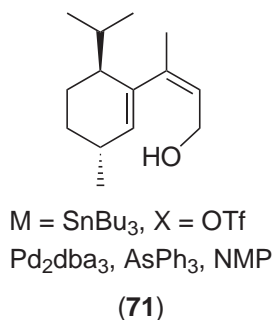
Ate-complexes of 9-MeO-9-BBN with alkali-metal organometallics were used to catalyze the transfer of alkynyl and simple alkyl groups.²⁴⁵ Similar reactions can be performed with *sec*-BuLi adducts of primary alkylboronates.²⁴⁶ More atom-economical reagents can be obtained from trialkoxyboronates, in the presence of fluoride salts or CuI (**68**)²⁴⁷ as additional activators. As trialkoxyboronates should be generated *in situ* and immediately used, more convenient are trifluoroboronates (alkyl, alkenyl, or alkynyl) which are stable, easily handled compounds useful in various cross-coupling reactions with aryl, hetero-aryl, alkyl, alkenyl, or alkynyl halides (Cl, Br, I) or triflates (**69**).^{248–250}



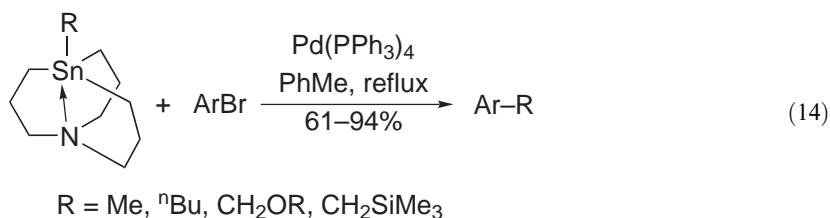
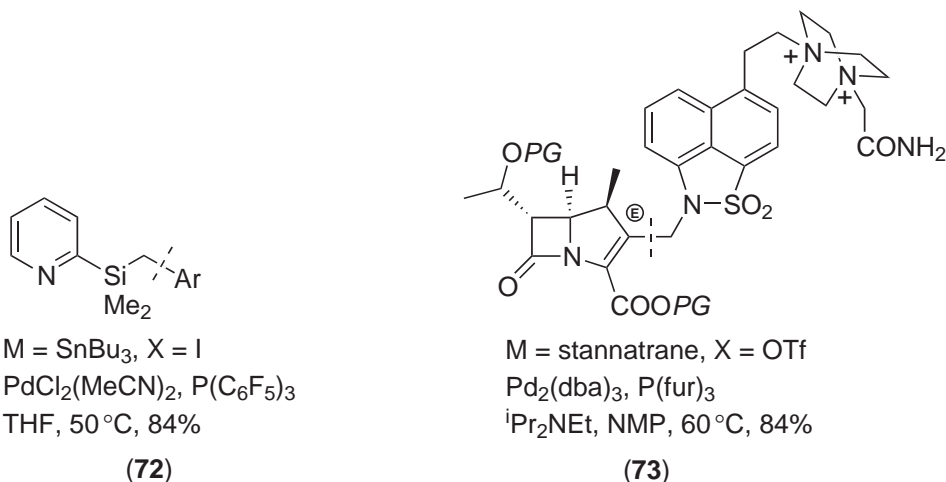
Pentacoordinate anionic complexes of tin possess enhanced reactivity in cross-coupling reactions. The complexes [Bu₄N][R₃SnF₂] (R = Ar, PhCH₂) can be used for cross-coupling with aryl triflates under milder conditions than those required by the standard protocols of the Stille reaction (**70**).²⁵¹ Normally unreactive trichlorostannanes, on treatment with aqueous alkali, turn into hydroxystannates, which are useful coupling partners in aqueous solutions.^{252,253} Tetra-alkynylaluminates transfer all four alkynyl residues in cross-coupling reactions with aryl or heteroaryl bromides.²⁵⁴



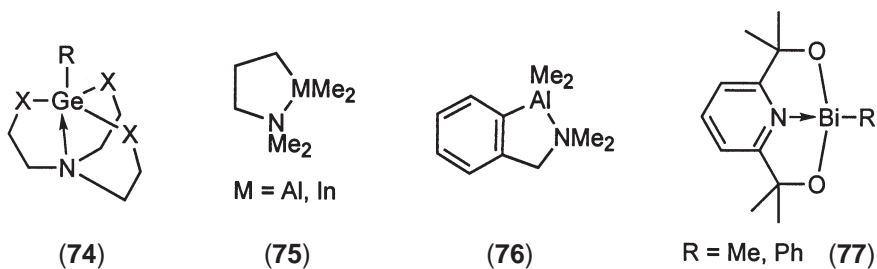
Intramolecular nucleophilic assistance is another distinct possibility for providing activation, and can be realized by coordination of the metal center by a heteroatom (O, N, etc.) within the ligand which transiently forms a chelate-like attachment to the metal. Such a mode of activation was supposed to account for the ease of reaction of vinyl triflates with (*Z*)-isomers of alkenylstannanes bearing OH groups in the proximity of the reaction center (**71**).²⁵⁵



Intramolecular activation by coordination with nitrogen donors is also documented. Better yields of cross-coupling products were obtained for substrates containing amino or amido groups at a distance from the reaction center suitable for chelation.^{235,256} Intramolecular coordination makes the 2-pyridyldimethylsilyl group very easily transferred (**72**) even in comparison to phenyl, in sharp contrast to other silylmethyl groups which are well known to be reluctant to be transferred in cross-coupling reactions.²⁵⁷ Stannatranes (**Equation (14)**) easily transfer such inert groups as simple alkyls etc.;²⁵⁸ this method has been applied to the synthesis of a new carbapenem (**73**), with a complex aminomethyl group being transferred in the cross-coupling.



Water-soluble stannatranes were announced as promising reagents for cross-coupling chemistry, with easy aqueous removal of tin-containing waste in the work-up.²⁵⁹ The first example, one of a very few, of a cross-coupling reaction with organogermanium compounds was reported for the geratrane ((**74**), X = CH₂).²⁶⁰ More readily accessible geratranes ((**74**), X = O) make good coupling partners for aryl iodides, being significantly more reactive than the respective trialkoxygermanes.²⁶¹

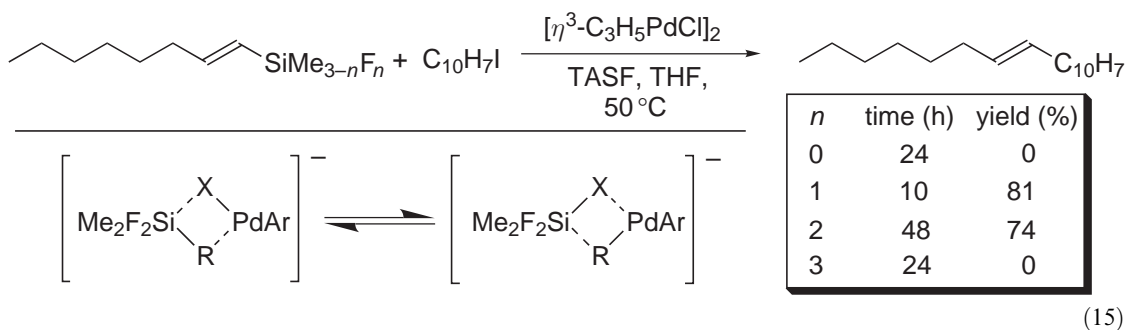


Intramolecularly coordinated Al and In compounds (e.g., (**75**), (**76**)) transfer the Me group in cross-coupling reactions with various aryl halides, including chlorides, catalyzed by Pd and Ni complexes.^{165,262–265} Monoorganobismuth compounds are reactive in cross-coupling reactions only if they contain an intramolecularly coordinating residue (**77**).^{266,267}

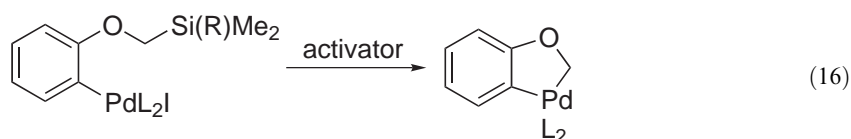
9.6.3.2.3 Various activation methods in the cross-coupling of organosilicon compounds

Organosilicon compounds cannot react in cross-coupling reactions without proper activation. Thus, this type of cross-coupling presents an exemplary study in activation methods. So far, the cross-coupling of organosilicon compounds (the Hiyama–Hatanaka reaction) cannot be counted as one of the major methods of cross-coupling chemistry—though the synthetic potential of this method is likely to be not far below that of the Suzuki–Miyaura reaction—because of the variety and versatility of the methods for the preparation of organosilicon reagents: tolerance of the reaction to functional groups; absence of toxic wastes, etc.). It should be noted also that organosilicon compounds, unlike the derivatives of B, Sn, and Zn, are widely used in the chemical industry. Apparently, further studies on refinement of the activation methods are needed to fully unleash the potential of this method, both for laboratory and industrial organic syntheses.

Activation with fluoride was the first activation method used for cross-couplings with organosilicon compounds, and became a standard protocol of the Hiyama–Hatanaka reaction,^{268–272} the sources of fluoride being usually easily soluble TBAF or TASF ((Et₂N)₃S⁺(Me₂SiF₂)⁻). The latter salt does not contain residual water, which cannot be completely removed from TBAF. Not all organosilicon compounds behave as cross-coupling partners under the conditions of fluoride activation, but only those prone to form hypervalent derivatives, which usually require electronegative groups attached to the Si atom to enhance its Lewis acidity. Standard coupling partners for fluoride-activated reactions are aryl and vinylsilanes bearing at least one chlorine or fluorine atom, RSiX_nR'_{3-n} (*n* = 1–3, X = F, Cl) (Equation (15)). Trifluorosilanes (*n* = 3, X = F) do not react, however, probably due to the easy binding of two equivalents of fluoride, thus blocking all coordination sites at Si and thereby preventing transmetalation (which requires a five-coordinate Si atom):



The necessity of an activator reagent has been explicitly revealed using arylpalladium complexes containing silanyl residues, which are stable in the absence of activator, but immediately undergo transmetalation upon addition of an activator (Equation (16)).²⁷³

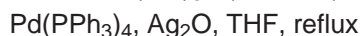
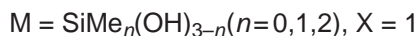
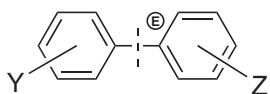


Further developments of this method were directed at broadening the range of organosilicon compounds capable of participation in cross-coupling, as well as at developing alternative (fluoride-free) activation methods.

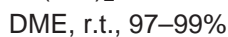
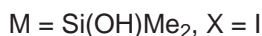
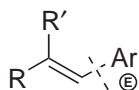
(i) Compounds with Si—O bonds

Arylsilanols, silanediols, and triols performed poorly under fluoride activation conditions, but instead required Ag₂O (78).²⁷⁴ However, the cross-coupling of arylsilanediols and similar organosilicon reagents (formed *in situ* from the respective halosilanes) can be achieved under very mild conditions, using phosphine-free catalysts in water in the absence of any organic cosolvents.²⁷⁵

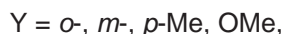
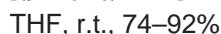
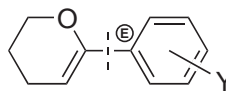
Alkenylsilanols have been shown to serve as activators themselves in the presence of strong base, opening a route to a highly effective, fluoride-free protocol ((79)²⁷⁶ and (80)²⁷⁷).



(78)

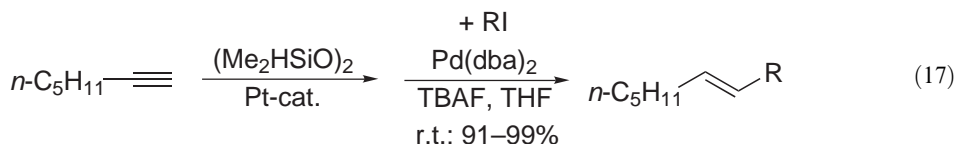


(79)

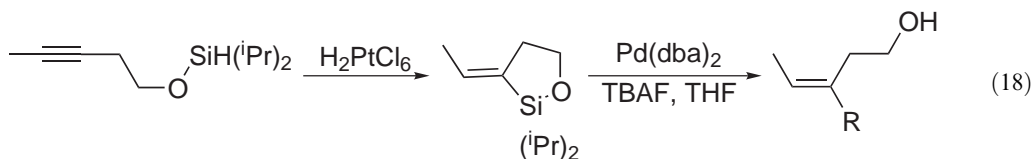


(80)

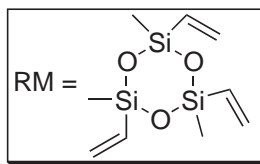
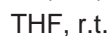
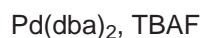
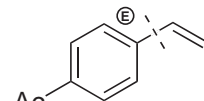
Alkenylsiloxanes take part in cross-couplings as well. Hydrosilylation and cross-coupling can be combined in one pot to give an effective method of hydrocarbation of a triple bond (Equation (17)).²⁷⁸



The formation of a cyclic siloxane obtained by intramolecular hydrosilylation has been used to control the stereochemistry of a cross-coupling reaction (Equation (18)).²⁷⁹

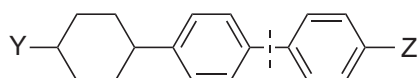


Among other organosilicon reagents used for cross-couplings, notable ones are commercial vinylsiloxanes, which are useful for vinyl–transfer reactions (81).²⁸⁰



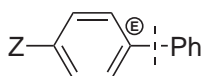
(81)

Readily available trialkoxysilanes constitute another major class of organosilicon derivatives for use in cross-coupling reactions.²⁸¹ Trimethoxysilanes react with aryl iodides and bromides in the presence of fluoride (82).²⁸² The fluoride-assisted cross-coupling with trialkoxysilanes was developed into a general protocol applicable to aryl bromides and iodides (83), as well as alkenyl bromides.²⁸³ Alkynylsilanolols make good cross-coupling partners in the presence of either TBAF or Ag_2O (84).²⁸⁴



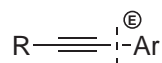
M = Si(OMe)₃, X = Br, I
 Pd(OAc)₂, PPh₃, TBAF
 toluene, reflux, 72–92%
 Y = alkyl; Z = CN, NO₂, Ac, etc.

(82)



M = Si(OMe)₃, X = Br, I
 Pd(dba)₂, TBAF
 DMF, 95 °C, 78–94%
 Z = Me, OMe, Cl, Ac, etc

(83)

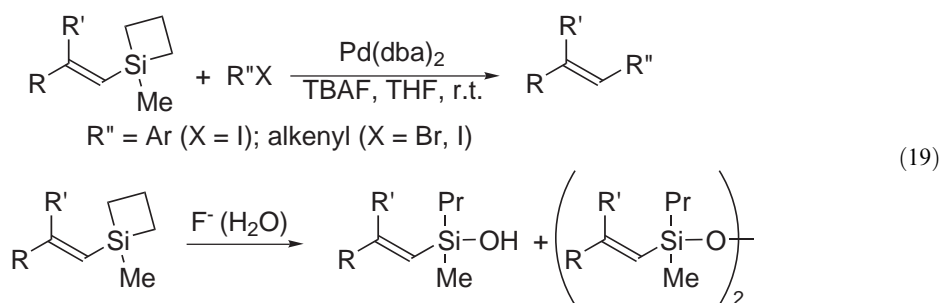


M = Si(OH)Me₂, X = I
 Pd(PPh₃)₄, TBAF or Ag₂O
 THF, 60 °C, 52–99%

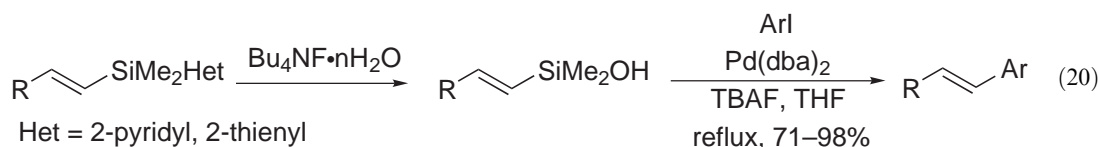
(84)

(ii) Tetraorganosilanes

These are not reactive enough for use in cross-couplings, although the first examples of the participation of organosilicon compounds in cross-coupling reactions were obtained with vinyl-trimethylsilane and similar reagents. However, these reactions are likely to proceed via a Heck-like mechanism, and thus cannot be regarded as true cross-couplings.^{285,286} The notable exclusions are sila-cyclobutanes possessing enhanced Lewis acidity, which have the ability to react under fluoride activation conditions—most likely due to steric strain which is effectively relieved upon increase of the coordination number of Si. Later it was shown, however, that in the presence of residual water, fluoride ion opens the four-membered cycle, leading to silanols or siloxanes (Equation (19)).²⁸⁷ Both alkenyl and arylcyclobutanes have been explored, the latter having lower reactivity and requiring such phosphine ligands as P^tBu₃ for success,²⁸⁸ whereas the former is reactive under phosphine-free conditions.²⁸⁹

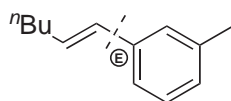


Silanes with heterocyclic residues were also found to be reactive (Equation (20)), although the most likely reason is the *in situ* cleavage of the heterocyclic residue in the presence of hydrated TBAF to form silanols.^{290–292} Similarly, among various arylgermanes, only those containing 2-furyl groups were reactive in cross-coupling reactions.²⁹³



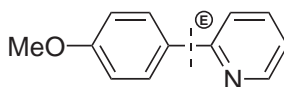
(iii) Nonfluoride activation

The application of bases other than fluoride for activation of organosilicon compounds to cross-coupling is documented. NaOH can replace fluoride in the cross-coupling of aryl and alkenyldichloroalkylsilanes with aryl halides, including chlorides. Apart from providing milder reaction conditions, the reaction in the presence of NaOH is applicable to a wider range of substrates ((85) and (86)).²⁹⁴



M = SiMeCl₂, X = Cl
Pd(PiPr₃)₂Cl₂, NaOH
PhH, reflux, 12h, 91%

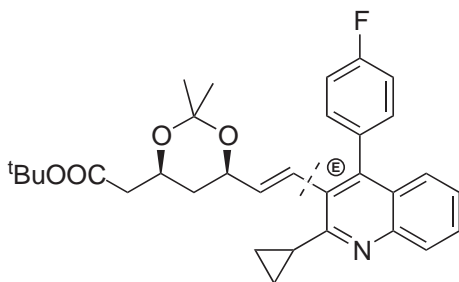
(85)



M = SiMeCl₂, X = Br
Pd(OAc)₂, PPh₃, NaOH
THF, reflux, 64%

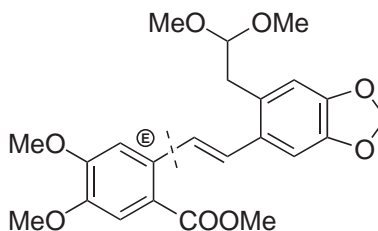
(86)

So far only a few examples of the uses of organosilicon compounds in cross-couplings have been published. Noteworthy is the smooth reaction with a sterically hindered substrate (87).²⁹⁵ The synthesis of the alkaloid nitidine included a cross-coupling step using an alkenylsilane (88),²⁹⁶ while the syntheses of some antitumor agents involved the alkenylation of unprotected iodouracils using alkenyl-silicon species.²⁹⁷



M = SiMe₂Cl, X = I
[η³-C₃H₅PdCl]₂, TBAF, THF, 60 °C

(87)

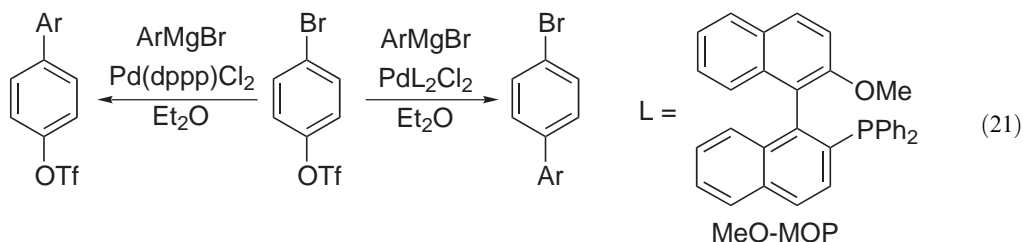


M = SiMe₂(OEt), X = I
[η³-C₃H₅PdCl]₂, P(OEt)₃, TBAF, THF, 60 °C

(88)

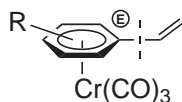
9.6.3.3 Leaving Groups

Among the three standard leaving groups (Br, I, OTf) in cross-coupling reactions, iodide is the most reactive, and organic iodides almost never pose any problems for oxidative addition. Phosphine-free catalysis may therefore be used in many cases, as the Pd⁰ species are effectively scavenged and supporting ligands are not required. The reactivities of the other two standard leaving groups (bromide and triflate) are comparable to one another, with that of Br being higher in most cases. The choice of ligands may in some cases invert this order of reactivity to allow for chemospecific partial substitution (Equation (21)).²⁹⁸



9.6.3.3.1 Fluorides

There are only a few examples of displacement of a fluorine atom in a cross-coupling reaction. With tricarbonylchromium complexes of fluoroarenes as substrates, cross-coupling with both boronic acids and vinylstannanes has been realized. Interestingly, only PMe_3 is effective as ligand in this reaction (89).²⁹⁹ See Section 9.6.3.4.10 for an example of the involvement of unactivated fluoroarenes in cross-coupling reactions.



$M = \text{SnBu}_3, X = \text{F}$

$\text{Pd}_2(\text{dba})_3, \text{PMe}_3, \text{CsF}$

DME, reflux, 37–52%

(89)

9.6.3.3.2 Chlorides

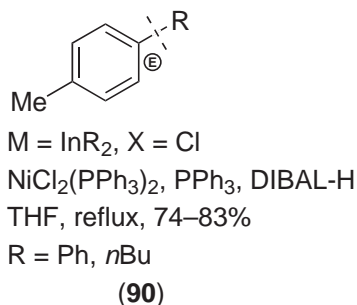
The involvement of organochlorine compounds in cross-coupling reactions was for a long while considered a challenge, but with the introduction of better catalytic systems (Section 9.6.3.4) chloride virtually became a fourth standard leaving group in laboratory-scale cross-coupling reactions. It should be noted, however, that one of the major reasons for seeking ways to process organochlorine compounds has always been the price of substrates, an important factor for large-scale synthesis. Effective, reliable, and inexpensive catalytic systems for the cross-coupling of organochlorine compounds have yet to be discovered. The use of organochlorine compounds gives other advantages besides low price of substrates; organochlorine compounds are less prone to give side products due to, e.g., transmetalation, protodehalogenation, and homocoupling (cf. ref. 300).

The reactivity of haloarenes towards oxidative addition in Pd-catalyzed reactions roughly parallels their reactivity in aromatic nucleophilic substitution. Thus, the activated substrates can usually be processed in cross-coupling reactions without special catalysts. The activation of C—Cl bonds in chloroarenes towards oxidative addition can be achieved through the complexation of the aryl moiety with $\text{Cr}(\text{CO})_3$ and similar organometallic pendant groups. These chloroarene complexes were estimated to be an order of magnitude more reactive than the respective uncomplexed iodoarenes, and thus usable in various cross-coupling reactions giving excellent yields.^{301–306} Although the organometallic pendant can be easily removed, a trivial use of this approach just to achieve the activation of the C—Cl bond is apparently impractical. This chemistry, however, has more specific applications for the construction of new materials, as well as for the synthesis of chiral biphenyls employing the planar chirality introduced by the pendant.³⁰⁷

There are many examples of reactions of chlorinated, electron-poor heterocycles (azines and their analogues). Chloropyridines, quinolines, and related heterocycles take part in cross-coupling reactions with arylboronic acids in the presence of $\text{PdCl}_2(\text{dppb})$ (rarely used in other cross-coupling reactions)³⁰⁸ or the common $\text{Pd}(\text{PPh}_3)_4$ complex.³⁰⁹ 1-Chloroisoquinoline is equally useful in the Suzuki–Miyaura reaction.³¹⁰ Both chlorine atoms in dichloro-1,3,5-triazines are readily displaced by phenyl groups in cross-coupling with phenylboronic acid.³¹¹ Chlorobenzenes with electron-withdrawing substituents can be cross-coupled with arylboronic acids in the presence of palladium complexes with various mono- and bidentate phosphines.³¹²

Nickel catalysts are more efficient in cross-couplings of aryl chlorides than are similar palladium catalysts. Several good systems have been proposed, based on simple Ni complexes with mono- and bidentate complexes. Nickel complexes $\text{NiCl}_2(\text{LL})$ or (in the order of activity for LL $\text{dppf} > \text{dppp} > \text{dppe} > \text{dppb} > 2\text{PPh}_3$) prereduced by BuLi or DIBAL-H are effective catalysts in dioxane or similar solvents in the presence of K_3PO_4 hydrate as the base.³¹³ In parallel work³¹⁴ it was shown that prereduction of the Ni catalyst is not required, and by a slight adjustment of reaction conditions the actual efficiency of the Ni complex can be essentially increased, so that high yields of cross-coupling products are achieved with as little as 1 mol.% of catalyst. Though common Ni catalysts usually do not tolerate water, the complex with a water-soluble monosulfonated

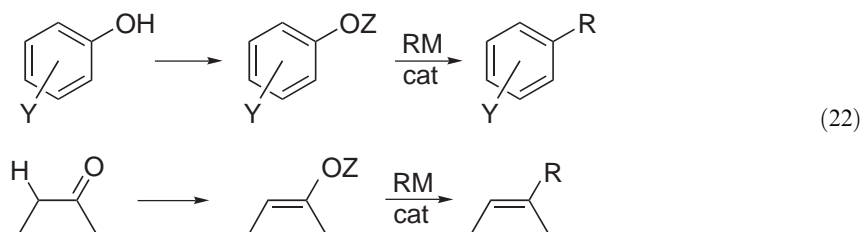
triphenylphosphine ligand turned out to be a good catalyst for the cross-coupling of aryl chlorides in aqueous dioxane, though a high loading of catalyst and ligand was required.³¹⁵ $\text{NiCl}_2(\text{PPh}_3)_2$ can be employed as catalyst for the cross-coupling of organostannanes with aryl chlorides.³¹⁶ Ni catalysts are also required for cross-coupling of organoindium compounds with chloroarenes (90).¹⁶⁸



The processing of unactivated organochlorine substrates requires the application of special ligands and will be treated in Section 9.6.3.4.

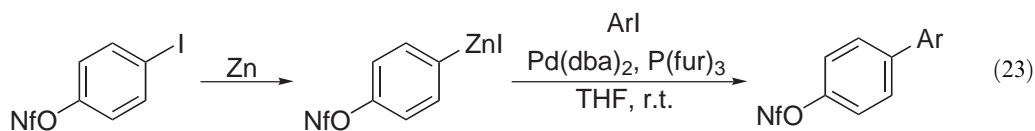
9.6.3.3 Esters as electrophiles in cross-coupling reactions

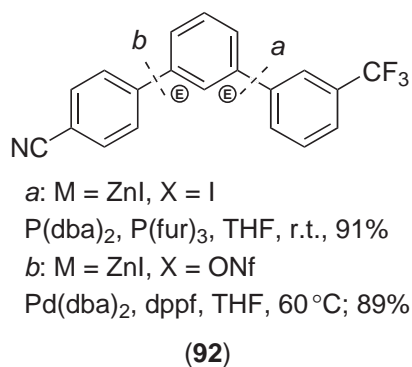
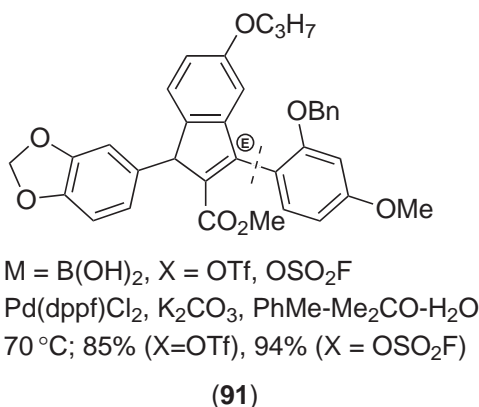
The use of enol- and phenol-esters in cross-coupling reactions is a valuable protocol, as it gives an indirect way to involve readily available phenols and carbonyl compounds as the electrophilic components of cross-couplings (Equation (22)):



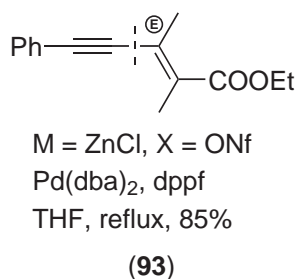
Various sulfonate and phosphate esters have been used, though only triflates proved to be universal for various types of cross-coupling reaction. The major disadvantages of triflates are inconvenient handling and high cost.

Besides the expensive triflates, cheaper fluorosulfonate esters have been proposed as electrophiles.³¹⁷ Fluorosulfonates possess practically the same reactivity as triflates (91),³¹⁸ but the necessity of using the highly toxic, aggressive, volatile anhydride $(\text{FSO}_2)_2\text{O}$ for the preparation of these compounds precludes their wider application. In spite of their higher molecular mass, nonaflates $\text{ROSO}_2\text{C}_4\text{F}_9$ present an interesting alternative to triflates, mainly because of their more convenient preparation and handling. In cross-coupling reactions, nonaflates showed marginally higher reactivity than the respective triflates.³¹⁹ In spite of this, nonaflates allow sequential, chemospecific cross-coupling reactions (as in (92)) to be performed cleanly,³¹⁹ while similar transformations with triflates give lower selectivity and yields.³²⁰ Arenes with both iodine and nonaflate substituents react with activated zinc only at the iodine site, to afford organozinc compounds with combined electrophilic and nucleophilic reactivity (Equation (23)), which can be further exploited in cross-coupling reactions.³¹⁹ A similar trick with triflates is impractical, because of the low selectivity of Zn insertion:

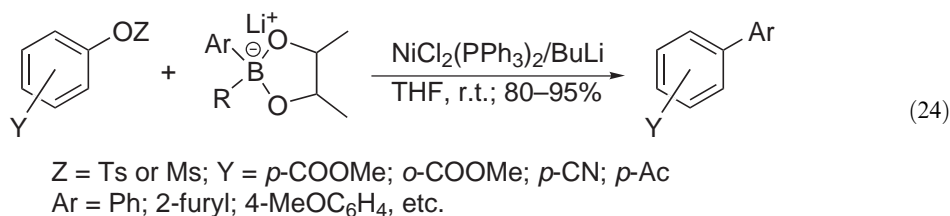




Nonaflates obtained from enolates of 1,3-diketones and β -ketoesters serve as easily available coupling partners (93).³²¹

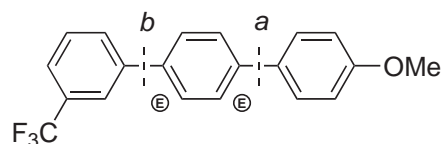


The development of methods allowing the use of cheaper sulfonates, such as mesylates or tosylates, is an important task. The reactivity of mesylates and tosylates is apparently similar to that of chlorides; therefore both require similar conditions to become involved in cross-coupling reactions. The cross-coupling of mesylates with organozinc or organomagnesium compounds, or arylboronic acids, in the presence of Ni complexes with PPh₃ and dppf ligands, has been reported; in contrast, cross-coupling with organotin compounds gave low yields.^{322,323} Both mesylates and tosylates bearing electron-withdrawing groups on the phenyl ring perform well in cross-couplings with anionic boronates under mild conditions (Equation (24)).^{324,325}



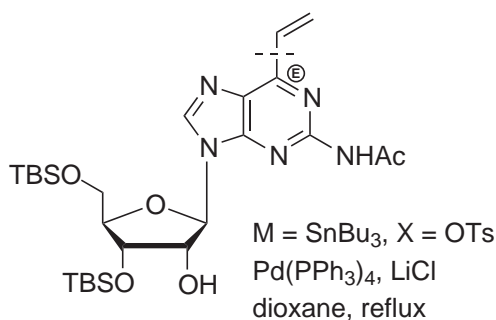
A Ni complex with PCy₃ ligands turned out to serve as a highly effective and stable catalyst for the cross-coupling of arylboronic acids with aryl tosylates (NiCl₂(PCy₃)₂, PCy₃, K₃PO₄, dioxane, 130 °C). The key to success of this catalyst is probably that it allows operation at high temperatures (130 °C), which are prohibitive for the more common Ni complexes with triarylphosphine or bidentate phosphine ligands.³²⁶ The different reactivity of Br and OTs as leaving groups makes possible effective one-pot sequential substitution (94).

The occasional use of tosylates for synthetic applications shows that the true synthetic potential of these simple derivatives is considerable. With more reactive heteroaryl or vinyl tosylates, palladium complexes are used as catalysts as, for example, in the modification of nucleosides (95).³²⁷ 4-Tosyloxycoumarins can be brought into cross-coupling reactions with acetylenes (96), organozinc derivatives,³²⁸ arylboronic acids,³²⁹ or organotin compounds, even for complex compounds containing a lot of vulnerable functional groups (97).³³⁰ The palladium-catalyzed cross-coupling of vinyltosylates with a wide range of organozinc reagents has been described (98).³³¹



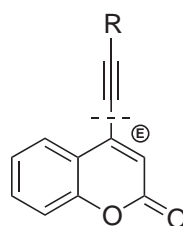
a: M = B(OH)₂, X = Br
 Pd(OAc)₂, K₃PO₄, 130 °C
b: M = B(OH)₂, X = OTs
 NiCl₂(PCy₃)₂, K₃PO₄, 130 °C

(94)



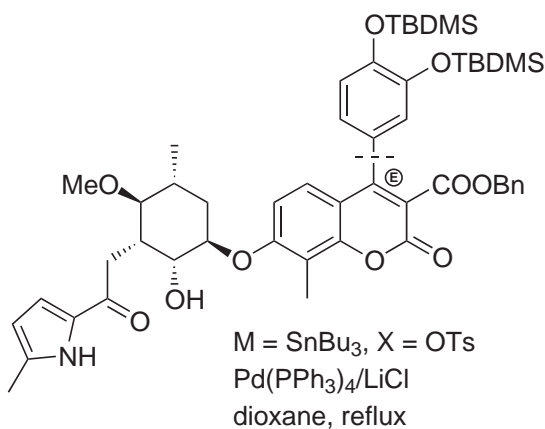
M = SnBu₃, X = OTs
 Pd(PPh₃)₄, LiCl
 dioxane, reflux

(95)



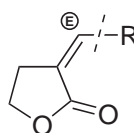
M = H, X = OTs
 PdCl₂(PPh₃)₂/CuI, ⁱPr₂NEt
 MeCN, 50–60 °C
 R = Ar, Alkyl, SiMe₃

(96)



M = SnBu₃, X = OTs
 Pd(PPh₃)₄/LiCl
 dioxane, reflux

(97)



M = ZnBr, X = OTs
 Pd(PPh₃)₄
 THF, reflux
 R = Ar, HetAr, Alkyl, C≡CR'

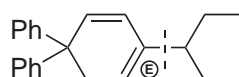
(98)

Yet another useful leaving group is phosphate. Cross-coupling reactions of enol phosphates with RMgX using a palladium (PdCl₂(PPh₃)₂, THF, reflux),³³² or Ni catalyst (**99**),³³³ as well as with RZnX (NiCl₂(dppe), benzene, r.t.)³³⁴ have been reported. Apart from esters, some ethers, e.g., aryloxy-substituted, electron-deficient heterocycles, can be also be utilized in Ni-catalyzed cross-couplings (**100**).³³⁵

9.6.3.3.4 Other neutral electrophiles

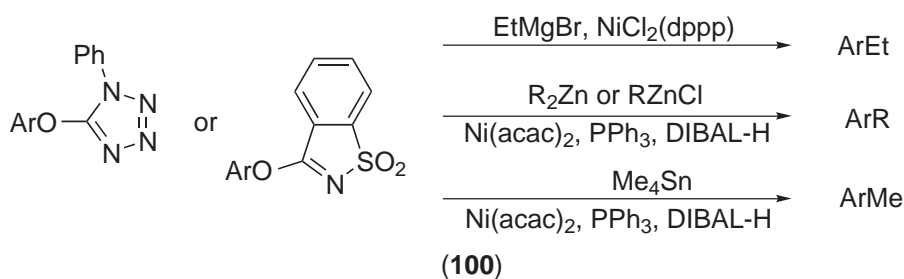
(i) Sulfur derivatives

As Pd⁰ and Ni⁰ are capable of oxidative addition by C—S bonds, organosulfur compounds can take part in cross-coupling reactions as electrophilic reagents. Due to the formation of stable Pd—S



M = MgBr, X = OP(O)(OPh)₂
NiCl₂(dppp), THF, 40 °C

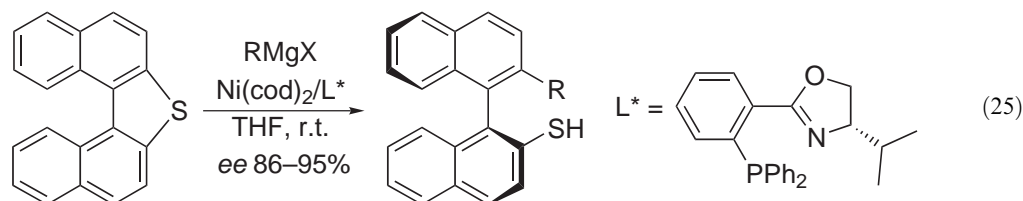
(99)



(100)

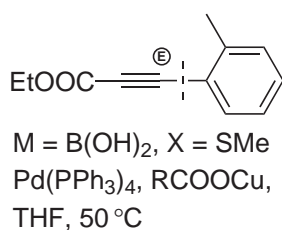
bonds in the intermediate complexes, the cross-coupling reactions with organosulfur electrophiles suffer from ineffective transmetalation, particularly with less reactive nucleophiles such as organotin or organoboron compounds. Therefore, either a careful design of the sulfur-containing leaving group, or the intervention of additional reagents lending electrophilic assistance, is required.

Aromatic and vinylic sulfides take part in cross-coupling reactions with Grignard reagents in the presence of Ni catalysts.^{336,337} This reaction has been applied to the enantioselective synthesis of binaphthyls using a standard chiral oxazoline ligand (Equation (25)):³³⁸

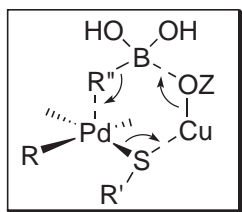


(25)

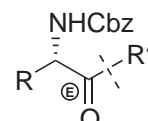
With other nucleophiles the reactivity of sulfides is low. Either specific, highly reactive substrates or activating additives are required. Thus, benzylzinc reagents were shown to react in the presence of a Pd catalyst with methylthiopyrimidines and similar, highly reactive MeS-substituted heterocycles.³³⁹ The reaction with boronic acids can take part in the presence of soluble carboxylates of Cu^I, such as 2-thiophenecarboxylate or 3-methylsalicylate. Apparently, the copper cation lends soft electrophilic assistance to enable transmetalation, while the carboxylate anion lends nucleophilic assistance to the organoboron reagent (101). This method has been successfully applied to acetylenic³⁴⁰ and heteroaromatic sulfides,^{341,342} and thiopseudoureas.³⁴³ Thiol esters can be transformed into ketones by reaction with alkylzinc compounds, as in the synthesis of aminoketones (102).^{344,345}



M = B(OH)₂, X = SMe
Pd(PPh₃)₄, RCOOCu,
THF, 50 °C



(101)

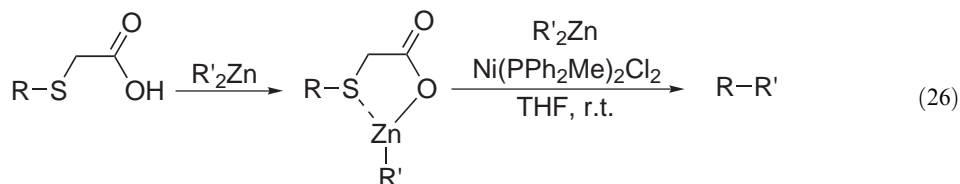


M = ZnI, X = SEt
PdCl₂(PPh₃)₂,
toluene, PhMe, r.t.

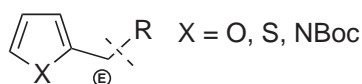
(102)

The Zn^{II} cation may lend soft electrophilic assistance for transmetalation. The most efficient such assistance is in the intramolecular chelating mode, which is exemplified by cross-coupling of

the derivatives of thioglycolic acid with organozinc reagents, occurring only in the presence of excess of Zn reagent (Equation (26)). This mechanism is thought to resemble what happens in some biocatalytic processes, e.g., in methanogenesis:³⁴⁶

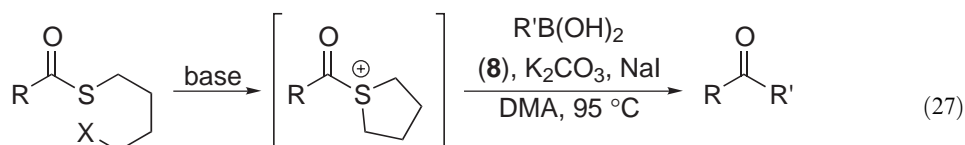


Neutral sulfides (R_2S) are much better leaving groups than thiolates, and consequently cross-coupling of sulfonium salts has been realized in several reactions. The use of tetrahydrothiophene as a leaving group allowed the cross-coupling of benzylic and heterobenzylic sulfonium salts with organotin compounds,²³⁴ arylboronic acids, and organozinc compounds (**103**)³⁴⁷ to be performed. Cross-coupling of thiol esters with boronic acids requires additional activation of the sulfur-containing leaving group by intramolecular alkylation (see equation (27) below).³⁴⁸



$\text{M} = \text{SnBu}_3, \text{X} = \text{S}^+(\text{CH}_2)_4$
 $\text{Pd}_2(\text{dba})_3, \text{P}(\text{OPh})_3, \text{CuI}$
 $\text{PhCH}_2\text{Me}_3\text{NO}(\text{O})\text{PPh}_2$
 NMP, r.t., 49–97%

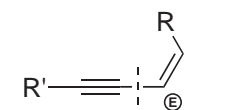
(103)



$\text{X} = \text{Br, I}; \text{R} = \text{Ph, Me, C}_{11}\text{H}_{23}; \text{R}' = \text{Ph, } m\text{-MeOC}_6\text{H}_4, 2\text{-naphthyl, et}$

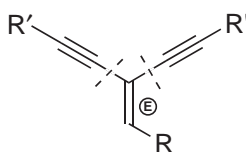
(ii) Se and Te derivatives

These can be used as electrophiles in cross-coupling reactions. Organotellurium(II) compounds participate in cross-coupling reactions with organozinc compounds, e.g., in $sp(\text{Zn})-sp^2$ (**104**)³⁴⁹ or $sp^3(\text{Zn})-sp^2$ cross-coupling reactions,³⁵⁰ as well as with terminal alkynes.³⁵¹ Divinylselenenides and tellurides take part in Pd- and Ni-catalyzed cross-coupling reactions with terminal acetylenes.^{351–353} Ketene telluroacetals in cross-coupling with terminal acetylenes provide easy access to enediynes (**105**).³⁵⁴ The use of vinylselenenides in Ni- or Pd-catalyzed cross-coupling with Grignard reagents has been also described.^{352,355}



$\text{M} = \text{ZnCl}, \text{X} = \text{TeBu}$
 $\text{Pd(PPh}_3)_4, \text{CuI}$
 THF-DMF, r.t.

(104)



$\text{M} = \text{H}, \text{X} = \text{TeBu}$
 $\text{PdCl}_2, \text{Et}_3\text{N}$
 MeOH, r.t., 75–91%

(105)

Besides Te^{II} derivatives, Te^{IV} compounds such as Ar_2TeCl_2 can be used in cross-coupling reactions,³⁵⁶ e.g., with arylboronic acids in aqueous DME in the presence of $\text{PdCl}_2(\text{PPh}_3)_2$, or with organotin compounds in MeCN in the presence of PdCl_2 .^{357,358} Mixed RTeCl_2Bu derivatives transfer sp^2 -groups (alkenyl, heteroaryl) in cross-couplings with terminal acetylenes.³⁵⁹

(iii) Organometallic compounds of main group metals

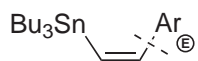
In higher oxidation states such as Tl^{III} , Pb^{IV} , Sb^{V} , Bi^{V} these compounds are well known as electrophiles in noncatalytic substitution reactions, in which they serve as sources of organic (usually, aryl) groups. Almost all have been already tried as electrophiles in Pd-catalyzed cross-coupling reactions. A common feature of these reactions is the need for Cu^{I} as a cocatalyst, which is supposed to suppress the concomitant homocoupling side reaction. Cross-coupling of organolead compounds $\text{ArPb}(\text{OAc})_3$ has been reported with organotin compounds,³⁶⁰ arylboronic acids,³⁶¹ and terminal acetylenes.³⁶² Organobismuth(V) compounds $\text{Ar}_3\text{Bi}(\text{OAc})_2$ behave similarly to arylplumbates, though in this case only one of three aryl groups is commonly transferred to products.³⁶³ Triarylantimony(V) diacetates take part in cross-coupling with trimethylsilylacetylenes in the presence of a phosphine-free catalyst and CuI ,³⁶⁴ or with organotin compounds under very mild conditions (room temperature, phosphine-free catalyst, absence of Cu cocatalyst), giving high yields of products.³⁶⁵ In cross-coupling with diaryliodonium salts (Section 9.6.3.3.6) the normally electrophilic organolead(IV), organobismuth(V) and organotellurium(IV) compounds reveal reversed reactivity and behave as nucleophiles.^{366–368}

9.6.3.3.5 Diazonium salts

Through the use of arenediazonium salts, the straightforward transformation of amines into cross-coupling products can be realized. Whenever the diazonium salts do not tolerate bases and strong nucleophiles (e.g., phosphines), base- and phosphine-free protocols have to be used. Heterocyclic carbene ligands serve well in cross-coupling of Aryl- and vinylboronic acids, or alkylboronates with arenediazonium salts.^{369,370} Several convenient phosphine-free protocols have been developed for the same purpose.^{371–373}

9.6.3.3.6 Iodonium salts

Diaryliodonium salts are proven, powerful electrophiles for various cross-coupling reactions, having an important advantage as compared to arenediazonium salts in being less prone to uncontrolled decomposition. The high reactivity of these electrophiles allows the reactions to be performed under very mild conditions using cheap, phosphine-free catalysts. Among the reactions investigated are cross-coupling with terminal alkynes,^{374,375} and derivatives of Zr,¹⁷³ Sn (106),^{376–378} B,^{379–381} and Si.^{382,383} The use of both diazonium and iodonium salts for a number of cross-coupling reactions in aqueous media has been described.¹⁷



M = SnBu₃, X = IPh

PdCl₂, DMF, r.t.

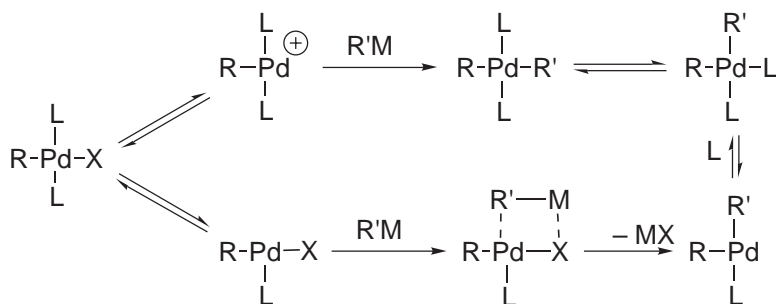
(106)

9.6.3.4 Catalysts

The ideal ligand for the cross-coupling reactions should satisfy the requirements of all stages of the catalytic cycle. In practice this is unlikely, as these requirements are not parallel. A careful compromise between various factors is necessary for any particular realization of cross-coupling chemistry. The path of reasoning should be similar for both Pd- and Ni-catalyzed processes; however, since very little information is available concerning Ni catalysis, only Pd catalysis will be discussed here.

The ligands must be strong enough to sustain zerovalent Pd during the catalytic cycle. Pd⁰ species are generated (i) during catalyst pre-activation, and (ii) at the reductive elimination step; they are consumed at the oxidative addition step. Thus, if the oxidative addition is a slow reaction, a build-up of Pd⁰ can ensue, which may lead to the formation of Pd metal sediments through the nucleation and growth of Pd clusters and then nanoparticles. Strong ligands tightly bound to Pd (chelating ligands, strong σ -donor monodentate ligands) are required to keep Pd⁰ in solution. But if the oxidative addition is fast, Pd⁰ is effectively scavenged by the electrophile and no deactivation of catalyst occurs, even in the absence of strongly bound ligands (phosphines).

Transmetalation, though, requires enhanced electrophilicity of the Pd. Additionally a free coordination site may be required, which may be freed by dissociation of either a neutral or an anionic ligand. The involvement of five-coordinate species and association–dissociation ligand-exchange mechanisms in the individual steps of Pd-catalyzed reactions also cannot be neglected (Scheme 3).³⁸⁴



Scheme 3

The demand for facile ligand exchange at the transmetalation step accounts for the high effectiveness of ligands with intermediate binding properties, neither too weak (which may result in fast deactivation of catalyst) nor too strong (leading to suppression of ligand exchange). Two such ligands, tris(2-furyl)phosphine (P(fur)₃) and triphenylarsine AsPh₃, are usually used in those cases when simpler ligands based on PPh₃ or P(o-Tol)₃ ligands fail.^{210,385}

Reductive elimination, though usually not a rate-limiting step, may seriously affect the reaction outcome, particularly in those cases when side reactions may occur in the intermediate complex, e.g., Pd hydride elimination in the case when alkyl groups are involved, leading to the loss of regioselectivity.

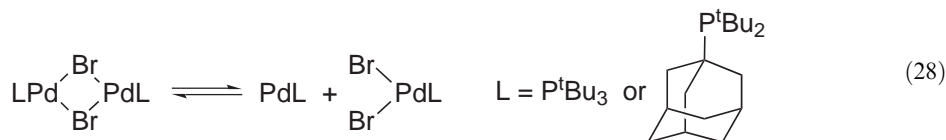
The efficiencies of different ligands/precatalysts cannot easily be compared, as in many cases the particular ligand/precatalyst requires careful adjustment of conditions (solvent, nature of promoter agents, temperature, aqueous or anhydrous mode, the ratio Pd/L), and if the optimal conditions were not found the performance of a given catalytic system may be underestimated. One of the best-known examples of this is the discovery of the outstanding properties of simple trialkylphosphines, P^tBu₃ and PCy₃. Both have been known since the very birth of transition-metal catalysis, and both have been occasionally tried in cross-coupling reactions and abandoned because the systems chosen were not specially optimized to these ligands, which gave appreciable but not remarkable performance.

The parameters of ligands which define their performance (cone angle; bite angle; thermodynamics of complexation; nature of species formed for different ratios metal/ligand; kinetic lability of ligands; electronic properties (σ -basicity and π -acidity); steric factors) are multiple. Unfortunately, the knowledge of these factors and their exact roles in the multistep catalytic cycle of cross-coupling is minimal, so that intentional design of new catalyst systems has been so far hardly possible. Rough estimation of activity can be done for a certain types of reaction. Thus, for cross-coupling reactions with chloroarenes and similar substrates reluctant to undergo oxidative addition, two parameters are critical: high steric bulk, estimated by cone angle, and high ligand σ -donicity.³⁸⁶ However, in general a separate optimization of each catalytic system is required to achieve the best results. Some of the most spectacular achievements have been made by a combinatorial approach using random high-throughput screening techniques, in which many ligands/precatalysts are applied in standardized set-up and reaction conditions. The use of combinatorial methods in catalysis is discussed in Chapter 9.11.

9.6.3.4.1 Monophosphine catalysis

During the catalytic cycle of Pd-catalyzed cross-coupling reactions, at least two coordination sites must be available for product-forming chemistry (oxidative addition, transmetalation, reductive elimination) to take place. Also, good ancillary ligands are required to sustain the Pd⁰ state and prevent deposition as Pd black. Moreover, it is well known that due to the *trans*-effect, ligands such as phosphines tend to form *trans*-complexes with the transition metals, which is the configuration unfavorable for catalysis, requiring the involvement of *cis*–*trans* isomerization. Thus, the best case would be a single, strongly bonded ligand which could perform all tasks involved in the catalytic cycle. It should be noted that, apart from special cases, such monophosphine systems cannot be directly prepared by mixing a Pd source with one equivalent of a phosphine, because the *trans*-effect often results in the binding constant for the second ligand being higher than for the first. This makes the desired monophosphine complex a minor constituent in an equilibrium which is shifted towards diphosphine complex and unligated Pd⁰ (which is prone to deactivation). However, bulky phosphines are very likely to form monophosphine complexes, e.g., in the systems derived from Pd(dba)₂ as precursor. This may account for a very high reactivity of 1:1 Pd(dba)₂/P^tBu₃ systems, as compared to the preformed Pd(P^tBu₃)₂ catalyst.³⁸⁷ Only one dba molecule is displaced by the bulky phosphine from the Pd coordination shell.³⁸⁸

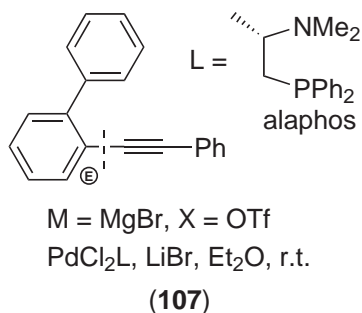
Generally, monophosphine complexes can be generated by decomposition of suitable precursors, among which the most notable are palladacycles (Section 9.6.3.4.7). A spectacular example makes use of spontaneous disproportionation of a dimeric complex of Pd^I with very bulky ligands to give one of the most reactive catalytic systems known so far, which catalyzes the fast cross-coupling of arylboronic acids with aryl chlorides and hindered aryl bromides at room temperature (Equation (28)).³⁸⁹



9.6.3.4.2 Chelating ligands with both phosphine and nonphosphine binding sites

Mixed-donor chelating ligands with one phosphine and one other binding site actually explore the same idea as monophosphine systems. The role of the nonphosphine binding site (nitrogen, oxygen, or even an unsaturated bond) is probably to serve as a temporary “placeholder” for the second coordination site. Being less strongly bonded than the P-center, such extra coordination sites are likely to be dechelated under the conditions of a given reaction (e.g., elevated temperatures) forming a monophosphine catalyst. However, as complexes of this type often serve as enantioselective catalysts, it is obvious that under mild conditions the coordination shell around Pd is conserved.

The cross-coupling of aryltriflates with alkynylmagnesium reagents is best carried out in the presence of the PN-ligand *alaphos* (**107**).³⁹⁰ The PO-ligand MeO—MOP has been used to control precisely the chemoselectivity of cross-coupling (cf. Section 9.6.3.3).²⁹⁸ An analogue of this ligand (**L4**) is useful in enantioselective cross-coupling with CH-acids (Section 9.6.3.1.3).

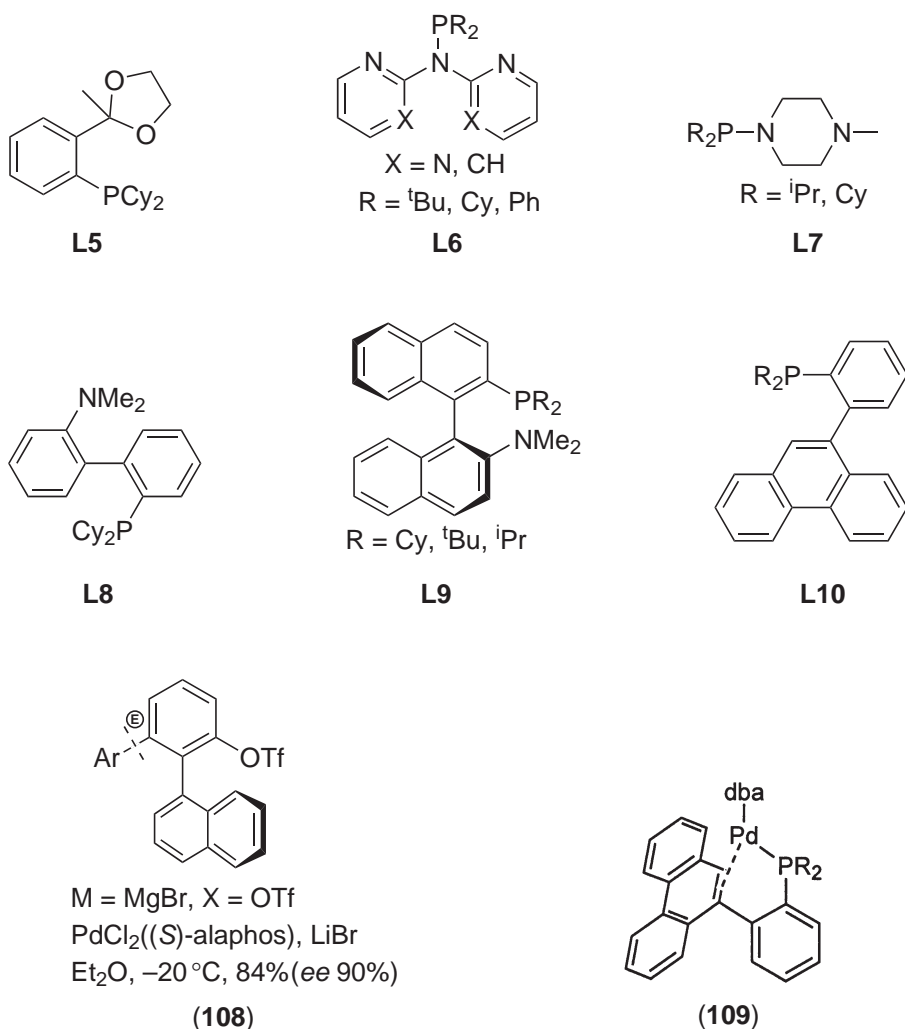


Various PX-ligands showed high efficiency in catalyzing cross-coupling reactions of aryl chlorides. The PO-ligand (**L5**) is used in the system (1% Pd(dba)₂–3L, CsF, toluene, reflux).³⁹¹

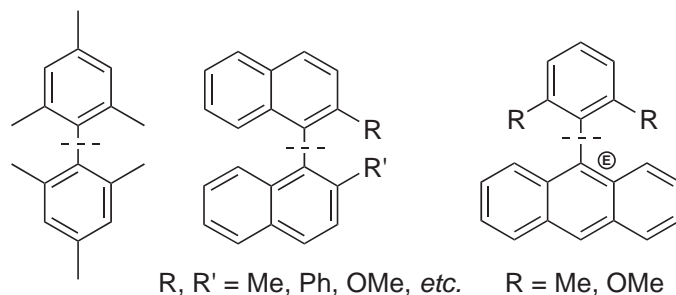
A large library of NP-ligands (**L6**) has been shown to be highly active in the cross-coupling of arylboronic acids with aryl chlorides ($\text{Pd}_2(\text{dba})_3\text{-L}$, K_3PO_4 , THF, 60°C), with the best activity shown by the ^tBu -containing aminophosphines.³⁹² The less bulky aminophosphine PN-ligands (**L7**) showed comparable activity in the same reaction ($\text{Pd}_2(\text{dba})_3/\text{L}$ (Pd:L = 1:2), CsF or K_3PO_4 , toluene, 90°C).³⁹³ PN-ligands derived from biphenyl (**L8**) are highly effective in cross-coupling of arylboronic acids or 9-alkyl-9-BBN with aryl chlorides and bromides ($\text{Pd}(\text{OAc})_2/1.5\text{L}$, CsF, r.t.– 100°C).³⁹⁴ Such ligands may actually establish P,C-donor rather than P,N-donor coordination in Pd complexes.³⁹⁵

PX-ligands have been employed in several rare examples of enantioselective cross-coupling, mostly in the syntheses of biphenyls and similar compounds with axial chirality, where the performance with such ligands (yields and stereoselectivity) were consistently markedly higher than that with common bidentate ligands such as BINAP. Thus, chiral *alaphos* was highly effective for enantioselective cross-coupling of aryl triflates with Grignard reagents, affording an atropisomeric product in high yield and optical purity (**108**).³⁹⁶ The use of chiral oxazoline ligands for a similar purpose has been described (Section 9.6.3.3.4).³³⁸ Enantioselective coupling with arylboronic acids leading to atropisomeric 1-arylnaphthalenes can be realized using binaphthyl analogues of Buchwald's *o*-aminobiphenyl PN-ligands (**L9**).³⁹⁷

Several new ligands have been designed for the cross-coupling of sterically hindered substrates.³⁹⁸ A delicate balance should be maintained between the reactivity furnished by substituents at the phosphorus atom and reasonable steric bulk. Due to overcrowding of the coordination sphere of Pd by the residues being cross-coupled, no more than a single coordination site should be occupied by the ligand. The ligands are bidentate, with the second coordination site being the olefinic bond of a phenanthrene residue (**L10**) forming a σ,π -bonded chelate (**109**).



These ligands afford high yields of cross-coupling products in the highly sterically burdened reactions of aryl bromides with arylboronic acids when both contain substituents in the *ortho*- (or equivalent) positions, although drastic reaction conditions are required (**110**).



M = B(OH)₂, X = Br

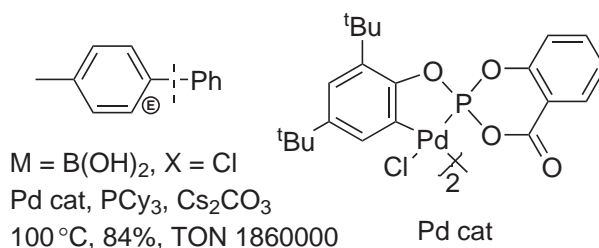
Pd₂(dba)₃, **L10**, K₃PO₄, PhMe, reflux, 70–93%

(110)

9.6.3.4.3 Bulky trialkyl- and dialkylphosphines

Until very recently trialkylphosphines had found only modest application in palladium-catalyzed reactions, though their ability to catalyze cross-coupling reactions with aryl chlorides—which require electron-rich Pd complexes to facilitate the oxidative addition step—was noticed long ago.³⁹⁹ In order to obtain high yields in reactions catalyzed by trialkylphosphine complexes, the conditions should be carefully optimized for each reaction, which requires experimental screening of conditions. Under optimized conditions, bulky trialkylphosphines are among the most effective ligands so far known. Tri-*t*-butylphosphine, the most useful ligand of this sort, is steadily acquiring the status of an indispensable ligand for cross-coupling of substrates which are reluctant to undergo oxidative addition (electron-rich aryl bromides, aryl chlorides). The cheaper and more readily available tricyclohexylphosphine PCy₃ apparently possesses a similar reactivity, although—probably because of its high sensitivity to the reaction conditions and the composition of catalytic system—the data on the use of this ligand in cross-coupling reactions is controversial. Air-stable salts of trialkylphosphines can be used in place of air-sensitive free phosphines whenever the latter are applicable.⁴⁰⁰

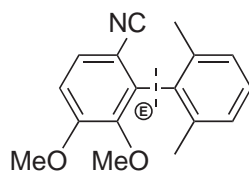
P^tBu₃ is useful in the cross-coupling of arylboronic acids with aryl bromides, iodides, and activated aryl chlorides at room temperature (Pd₂dba₃/P^tBu₃, Pd:L = 1, KF, THF, r.t.), or unactivated aryl chlorides at elevated temperatures (Pd:L = 1.5, 70–100 °C),³⁸⁷ while being ineffective for aryl triflates, for which PCy₃ should be used (Pd(OAc)₂/PCy₃, KF, THF, r.t.).³⁸⁷ Use of a different, more robust source of Pd, namely, the PO or PN palladacycles, also allows PCy₃ to be effective in cross-coupling of arylboronic acids with unactivated aryl chlorides (palladacycle/PCy₃, Pd:PCy₃ = 2:1, Cs₂CO₃, dioxane, 100 °C). The high stability of this catalytic system enables very low Pd loadings to be used, affording huge turnover numbers (**111**).^{401,402}



(111)

The cross-coupling of organotin compounds with aryl chlorides can be realized with either PCy₃ (Pd(OAc)₂/PCy₃, K₃PO₄, dioxane, reflux)⁴⁰² or P^tBu₃ (Pd₂dba₃/P^tBu₃, Pd:L = 1:2, CsF,

dioxane, reflux).⁴⁰³ The latter catalytic system can be used for room-temperature cross-coupling of aryl and vinyl bromides, including sterically hindered ones (**112**).⁴⁰³

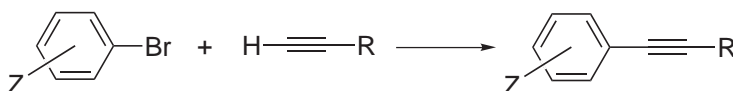


M = ZnCl, X = Cl
Pd(P^tBu₃)₂, THF-NMP
100 °C, 78%

(**112**)

Commercially available Pd(P^tBu₃)₂ is a unique, air-stable 14e Pd⁰ complex, an excellent catalyst for cross-coupling reactions of aryl chlorides. The ability of P^tBu₃ to stabilize such a coordinatively unsaturated, extremely reactive, and yet easily manageable form of Pd⁰ is one of the most amazing and fruitful recent findings in Pd-based catalysis. The cross-coupling of arylzinc reagents with aryl or vinyl chlorides can be readily accomplished with as little as 0.03% of this catalyst. Both electron-rich and sterically hindered substrates are welcome in this protocol.⁴⁰⁴

Very effective room-temperature systems for cross-coupling of aryl bromides with terminal acetylenes have been proposed, based on the ligands on P^tBu₃ and PCy₃ (Equation (29)). The first uses a 1:2 mixture of Pd₂(dba)₃ and PR₃ in neat Et₃N (i.e., a 1:1 Pd : ligand ratio),⁴⁰⁵ while the second uses a 1:2 mixture of Pd(PhCN)₂Cl₂ and P^tBu₃ in dioxane in the presence of CuI.⁴⁰⁶ Since one equivalent of phosphine is required for initial reduction of Pd^{II} to Pd⁰, the second system actually uses the same 1:1 Pd : phosphine stoichiometry as the first system. The activity of the second system is notably different, however. Although both systems operate at room temperature and allow reaction of the same range of substrates at comparable rates, the second system requires the addition of CuI as promoter and works only with P^tBu₃ as the ligand; while in the first system, P^tBu₃ and PCy₃ showed comparable activity. This difference clearly shows the importance of the proper choice of all parameters involved, including the nature of Pd precatalyst and solvent. The cross-coupling of unactivated aryl chlorides with terminal acetylenes still remains an unresolved challenge:



Method A

Pd₂(dba)₃-P^tBu₃ (Pd:L = 1:1)

Et₃N neat or Et₃N-THF

r.t., 20 h, 42–99%

Z = H; *p*-F, Cl, Me, OMe, COMe, *o*-Me

R = Ph, SiMe₃

Method B

Pd(PhCN)₂Cl₂-P^tBu₃ (Pd:L = 1:2)

iPr₂NH, dioxane

r.t., 0.5–15 h; 63–95%

Z = H, *p*-OMe, *p*-NMe₂, *p*-Ac, *o*-Me, 2,6-Me₂

R = Ph, SiMe₃, *n*-C₆H₁₃, C(OH)Me₂

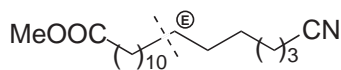
(29)

The cross-coupling of aryl or alkenylsilanes with aryl chlorides bearing electron-withdrawing substituents has been reported to require trialkylphosphine (P^tPr₃) ligands.⁴⁰⁷

Trialkylphosphines turned out to be excellent ligands for performing the cross-coupling with *sp*³-electrophiles, particularly those containing β-hydrogens, which are prone to causing PdH elimination and isomerization. PCy₃ is an excellent ligand for alkyl bromides, chlorides, and sulfonates, which are well known for their utmost reluctance to undergo oxidative addition. The reaction of Grignard reagents with alkyl chlorides can be realized in the system (Pd(OAc)₂/PCy₃, NMP, r.t.).⁴⁰⁸ 9-BBN derivatives can be cross-coupled with alkyl bromides at room temperature in the system (Pd(OAc)₂/PCy₃, THF, K₃PO₄, r.t.) (**113**),⁴⁰⁹ or alkyl chlorides under more stringent conditions in the system (Pd₂(dba)₃/PCy₃, dioxane, CsOH, 90 °C).⁴¹⁰ In the reaction of alkyl tosylates (Section 9.6.3.3.3) with 9-BBN derivatives, the phosphine PMe(^tBu)₂ works better (**114**).¹

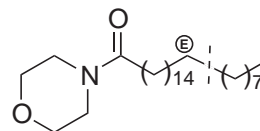
The same ligand allowed the cross-coupling of various boronic acids (aryl, alkenyl, alkyl) with alkyl bromides in the system (Pd(OAc)₂/PMe^tBu₂, ^tBuOK, ^tamyl alcohol, r.t.).⁴¹¹

The other use of the bulky trialkylphosphines is in the cases where PPh₃ or similar ligands can interfere with the cross-coupling reaction by forming by-products (**115**).⁴¹²



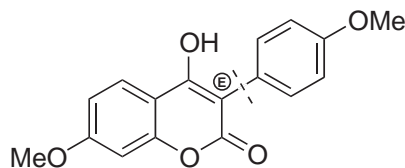
M = 9-BBN, X = Br
Pd(OAc)₂, PCy₃, K₃PO₄
THF, r.t., 81%

(113)



M = 9-BBN, X = OTs
(HP^tBu₂Me)BF₄, NaOH,
dioxane, 50 °C; 76%

(114)



M = B(OH)₂, X = IPh⁺
Pd(OAc)₂, P^tBu₃, LiOH
DME-H₂O, r.t., 85%

(115)

Bulky dialkylphosphines (HPR₂, where R = *t*-butyl, cyclohexyl, 1-adamantyl, 2-norbornyl, and the like) were used together with simple CO- and CN-palladacycles for cross-coupling of unactivated chloroarenes with arylboronic ligands (Pd:L = 1.5, K₃PO₄, dioxane, reflux),⁴¹³ thus apparently having a similar activity as trialkylphosphines.

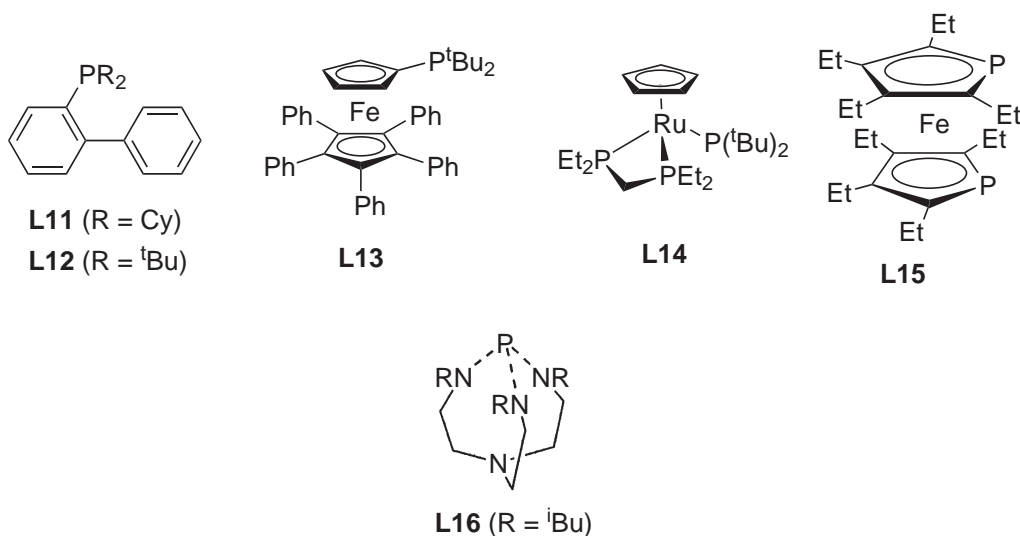
9.6.3.4.4 Bulky dialkylarylphosphines

Bulky *o*-dialkylphosphinobiphenyls constitute the other group of highly effective ligands for cross-coupling of substrates reluctant to undergo the oxidative addition step (*o*-Ph₂PR₂; R = Cy (**L11**), ^tBu (**L12**)). As the necessary steric bulk in these ligands is largely furnished by the *o*-biphenyl residue, the difference between cyclohexyl and *t*-butyl substituted ligands is not as evident as the difference between the respective trialkylphosphines. Both ligands form catalysts for cross-coupling of unactivated aryl bromides and chlorides in the system (Pd(OAc)₂/2L, K₃PO₄, toluene, 100 °C), giving high yields of coupling products and high turnover ratios (up to 20,000 for unactivated aryl bromides, and 2,000 for aryl chlorides). The ligand *o*-Ph₂PCy₂ (**L11**) is particularly effective in the one-pot borylation-coupling procedure allowing the linking together of two different aryl halides.⁴¹⁴

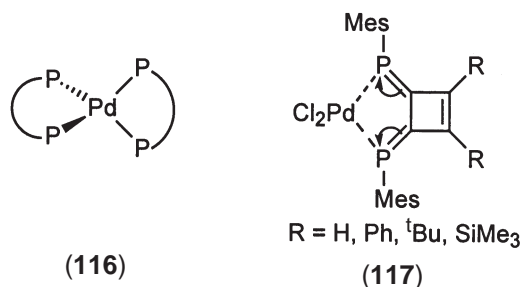
9.6.3.4.5 Heterobimetallic complexes

Several phosphine ligands containing bulky organometallic residues exploit essentially the same paradigm—an electron-rich dialkylphosphine center attached to a huge scaffold. An additional modulation of catalytic properties due to a second metal center can be suggested, although there is no unambiguous evidence in favor of this effect. Thus, the bulky ferrocene derivative (**L13**) is effective in the cross-coupling of arylboronic acids with unactivated aryl bromides at room temperature, and aryl chlorides at elevated temperature (system Pd(dba)₂/2L, CsF, THF).⁴¹⁵ A new approach to the design of ligands for cross-coupling reactions employs phosphide complexes of transition metals as ligands for palladium. Phosphide complexes of Re and Ru (**L14**) show high

catalytic activity, comparable to that of bulky trialkylphosphines.⁴¹⁶ Obviously, further development of such ligands may lead to the development of highly reactive, reusable, selective catalysts.

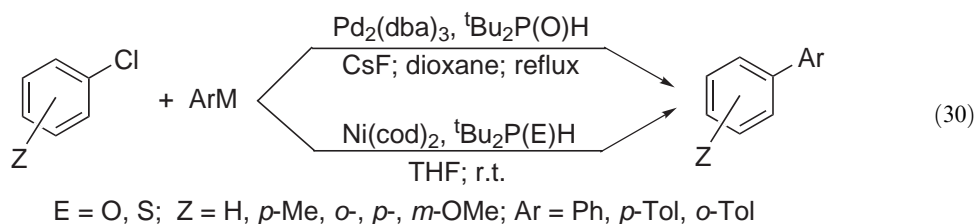


A diphospha-analogue of ferrocene (**L15**), modified with ethyl groups to enhance solubility, forms Pd⁰ complexes with an unusual tetrahedral coordination mode (**116**), which makes the complex labile towards dechelation. Therefore, at elevated temperatures such a ligand should behave as a bulky monophosphine donor, to afford a highly effective precatalyst in the cross-coupling of aryl bromides with arylboronic acids in refluxing toluene, showing very high turnover numbers up to 10⁶.⁴¹⁷



9.6.3.4.6 Phosphorus ligands other than phosphines

A series of heteroanalogues of phosphines, PR_nX_m, have been reported as ligands for cross-coupling reactions. The enhanced donicity of such ligands, particularly those with amino-groups or negatively charged oxygen donors, is accounted for by the “α-effect,” the repulsion of lone pairs at neighboring atoms. Phosphinous acids R₂P(OH) make excellent ligands for the cross-coupling of aryl chlorides with arylboronic acids (Pd catalysis) or Grignard reagents (Ni catalysis).^{418,419} In the presence of base, phosphinous acid is deprotonated to give a highly electron-rich ligand R₂PO[−], which should facilitate the oxidative addition of C—Cl bonds to the metal. The analogous sulfur derivatives turned out to be equally useful for Ni-catalyzed cross-coupling of aryl chlorides with Grignard reagents at room temperature (Equation (30)).⁴²⁰ Both of these ligands are air-stable and readily available.



Phosphites $\text{P}(\text{OR})_3$ are much weaker ligands for Pd, and are not capable of supporting Pd^0 species in solution for the reactions where oxidative addition is rate-limiting: therefore they are very rarely used in cross-coupling reactions. Phosphite-derived palladacycles, however, are among the most effective precatalysts (Section 9.6.3.4.8).

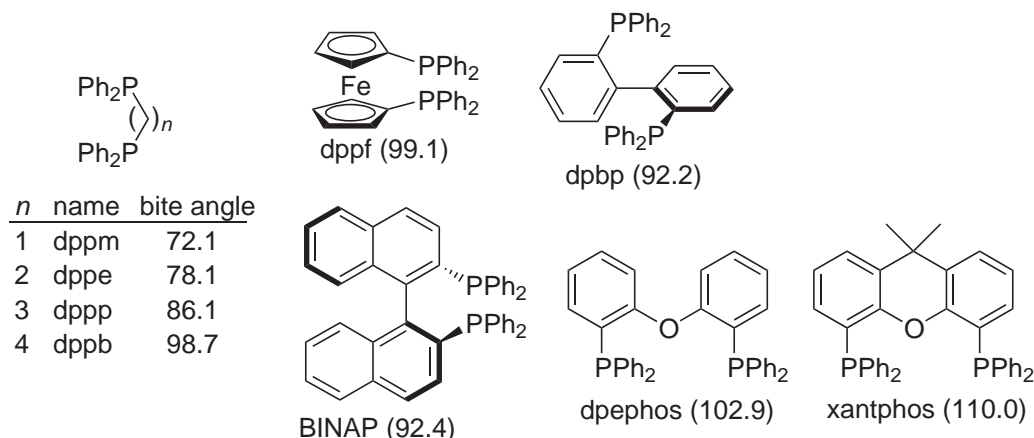
Amides of phosphorous acid (e.g., $\text{P}(\text{NMe}_2)_3$ and the bicyclic compound (**L16**)) are useful ligands for cross-coupling of arylboronic acids with aryl bromides and chlorides (system $\text{Pd}(\text{OAc})_2/2\text{L}$, Cs_2CO_3 , toluene, 80°C), the bicyclic amide being markedly more effective than simple acyclic ones.⁴²¹ Amides of phosphinous acids are also excellent bidentate ligands with PN coordination mode (**L6**, Section 9.6.3.4.2).

The series of wide-bite-angle, bulky ligands derived from a cyclobutene scaffold gave Pd complexes (**117**) showing appreciable activity in the cross-coupling of reactive aryl bromides with trimethylsilylacetylene. A considerable shift of electron density to the phosphorus atoms, probably arising from alternative aromatic canonical structures, may account for the ligand properties.⁴²²

9.6.3.4.7 Bidentate diphosphine ligands

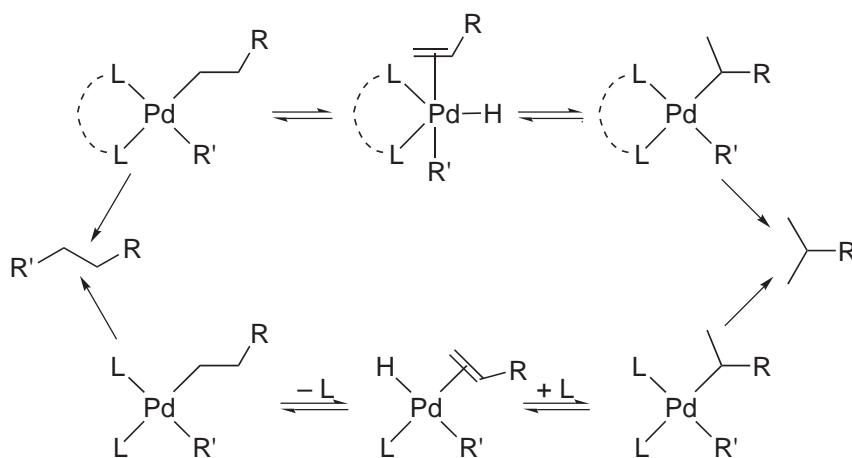
Bidentate diphosphine ligands find limited application in cross-coupling chemistry. Simple bidentate ligands tend to overpopulate the coordination shell of Pd due to easy formation of *bis*-chelates, thus forming catalytic systems with moderate or low activity. However, in the reactions with highly reactive nucleophiles, e.g., Grignard reagents, such ligands perform reasonably well. Chelating ligands which ensure a *cis*-configuration in the intermediates are believed to be advantageous in the cases when the reductive elimination step is likely to control the catalytic cycle; the larger the bite angle, the more facile is the reductive elimination believed to be.^{423,424}

The natural bite angle^{425,426} for bidentate ligands depends on the geometry of the free ligand. The closer this parameter is to the equilibrium geometry of the ligand in a given type of complex (90° for square planar, 120° for trigonal, etc.), the more stable should be the chelate and the less prone the ligand should be to dechelation. In estimating the stability of a given complex, the bite angle is not, however, a fully adequate parameter. Entropic contributions should also be taken into consideration: the more flexible the ligand, the more negative should be the entropy of chelation, and thus the more probable is the dechelation. Thus, although *dppb* and *dppf* ligands possess practically equal bite angles, the alkane tether of *dppb* allows for many more degrees of conformational freedom than does the rigid scaffold of *dppf*. Accordingly, the latter is well known to be a much more effective ligand in the processes where a better control of selectivity is required. Common bidentate ligands are listed in Scheme 4, along with their bite angles.



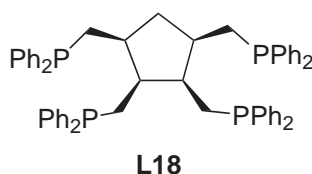
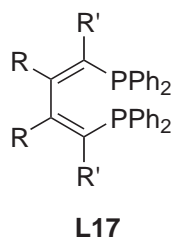
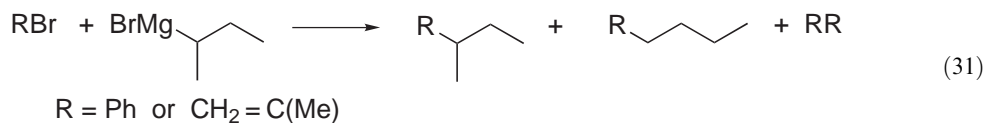
Scheme 4

The most important application of these wide-bite-angle bidentate ligands is for the control of selectivity in the cross-coupling reactions involving alkyl residues. In cross-couplings with the participation of *sec*-alkyl organometallics, rearrangement (isomerization) of the alkyl group is likely to occur, due to β -hydride elimination followed by reversible addition of PdH species to the double bond (Scheme 5).



Scheme 5

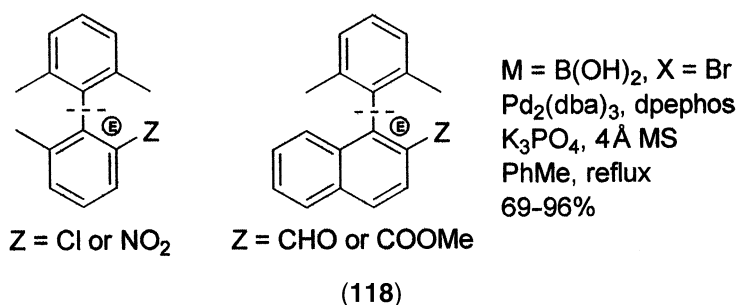
Optimal ligands for such reactions, e.g., for the cross-coupling of aryl or alkenyl bromides with *sec*-BuMgBr (Equation (31)), are those which form stable chelates with a bite angle slightly over the normal 90° , among which are dppf, dpephos,⁴²⁷ and dpbp,⁴²⁸ while those ligands with smaller or larger bite angles fail to control the selectivity effectively. However, the observation that the NUPHOS ligands (**L17**) (which have smaller bite angles, close to 90°) are as effective as dppf, and markedly more effective and selective than BINAP,⁴²⁹ makes unsafe any predictions using solely the bite-angle parameter.



Besides the control of regioselectivity, the use of bidentate or polydentate ligands may be helpful in those cases in which the stability of the catalyst is the issue, principally in the reactions which use a small loading of Pd catalyst precursor to achieve maximum catalytic efficiency under harsh conditions. Thus, the use of the tetrapodal ligand *tedicyp* (**L18**) allows turnover numbers of 10^5 – 10^6 catalytic cycles, and high yields, in cross-couplings with arylboronic acids.⁴³⁰ Under the same conditions, the standard bidentate ligand dppe also is capable of giving high yields and TONs of up to 10^4 – 10^5 , while Pd(PPh₃)₄ is much less effective. High TON values can be reached in the Suzuki–Miyaura reaction with NUPHOS ligands (**L17**).⁴²⁹

Bidentate ligands with very wide bite angles (like dpephos or xantphos, Scheme 4) are likely to form unstable chelates prone to dechelation at elevated temperatures, thus giving another route to monophosphine species. The application of such ligands to the cross-coupling of sterically hindered bromides and arylboronic acids under strictly anhydrous conditions enforced by the addition of molecular sieves has been shown to be advantageous (**118**).³⁹⁸

The use of chiral bidentate phosphines (such as BINAP) in enantioselective cross-coupling reactions has been described, though only modest stereoselectivity has been achieved.⁴³¹



9.6.3.4.8 Palladacycles

(i) PC–Palladacycles

Since the introduction of Herrmann's palladacycle (**119**) into Pd catalysis, the interest in these convenient Pd precatalysts has been steady.⁴³² Many Pd complexes containing at least one Pd—C bond have been tested in cross-coupling reactions and showed good promise. The palladacycles provide a bridge between phosphine-based and phosphine-free catalysis. It is indeed essential that very simple ligands, such as various nitrogen-containing compounds (themselves very poor ligands for Pd⁰) form very stable palladacycles, which were reported to show performance similar to, if not higher than, PC and PCP palladacycles in cross-coupling reactions with unactivated aryl halides. These results clearly show that phosphine-free Pd complexes may possess very high reactivity at all stages of the catalytic cycle. Therefore, it is not the presence of specific ligands in the coordination sphere that defines the performance of a catalytic system, but rather it is the relative rates of the individual steps of the catalytic cycle and catalyst-deactivation processes. A major disadvantage of robust palladacycles is the requirement for elevated temperatures, probably because the activation of such precatalysts involves full or partial disassembly of the palladacycle structure, which in the case of PC and PCP palladacycles is a route to highly reactive monophosphine species.

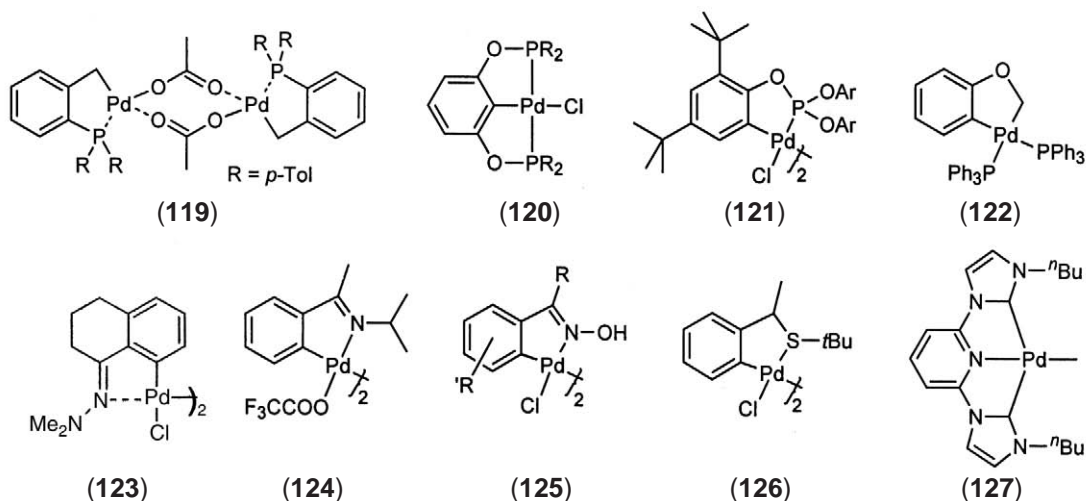
The now-classical Herrmann's palladacycle (**119**) has been applied to all major types of cross-coupling reactions. In cross-coupling with arylboronic acids, aryl bromides and activated aryl chlorides were found to give high yields of target products, though high temperatures (reflux in xylene) are required.⁴³² Cross-couplings of aryl bromides with organotin compounds, as well as cross-couplings of organozinc and organomagnesium compounds with aryl bromides and chlorides, have also been successfully realized.

The pincer-type palladacycle (**120**) (R = ⁱPr), which is actually a derivative of a dialkylphosphinous acid (themselves excellent ligands: see Section 9.6.3.4.6) was shown to allow the cross-coupling of aryl chlorides with terminal acetylenes ((**120**), ZnCl₂, Cs₂CO₃, dioxane, 160 °C). However the high reaction temperature may be prohibitive for the actual application of this catalytic system, as acetylenes are known to be thermally sensitive.⁴³³ The same palladacycle (R = Ph) is effective in the Suzuki–Miyaura reaction with aryl bromides and activated aryl chlorides (K₂CO₃, toluene, 130 °C).

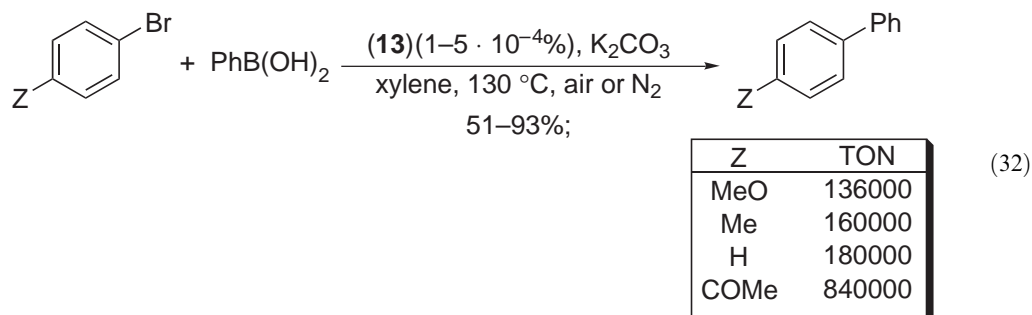
Phosphine precursors are not necessary to build effective palladacycle precursors, as a large group of such precatalysts can be made from nonphosphine ligands. The robust palladacycle (**121**), derived from readily available tris(2,4-di-*t*-butylphenyl)phosphite, showed a good catalytic activity in the cross-coupling of aryl bromides with phenylboronic acid and PhSnMe₃, giving high yields of cross-coupling products with both reactive *p*-bromoacetophenone and electron-rich *p*-bromoanisole. Huge TONs of the order of 10⁶ were reported for cross-couplings of *p*-bromoacetophenone in both the Suzuki and Stille reactions. Similarly to the reactions catalyzed by other palladacycles, elevated temperatures are required for (**121**) to show its best performance.^{434,435}

(ii) NC and OC–palladacycles

A vast series of palladacycles derived from simple nitrogen-, oxygen-, and sulfur-containing molecules provide a good library for investigation of catalytic properties. Although elevated temperatures above 100 °C are necessary to awaken the catalysis with such complexes, the easy



availability and convenience of handling of these complexes are so remarkable that their use as precatalysts, at least in routine reactions, may be advantageous. Some such palladacycles (**122**, **123**) have been tested as precatalysts for the cross-coupling of aryl iodides with vinyltributyltin and phenylboronic acid.⁴³⁶ The palladacycle (**124**), derived from a simple imine ligand, showed outstanding performance in cross-coupling reactions of aryl bromides with PhB(OH)_2 (Equation (32)); one of the highest TONs reported so far for the reactions with electron-rich bromoarenes has been reached with this precatalyst.⁴³⁷



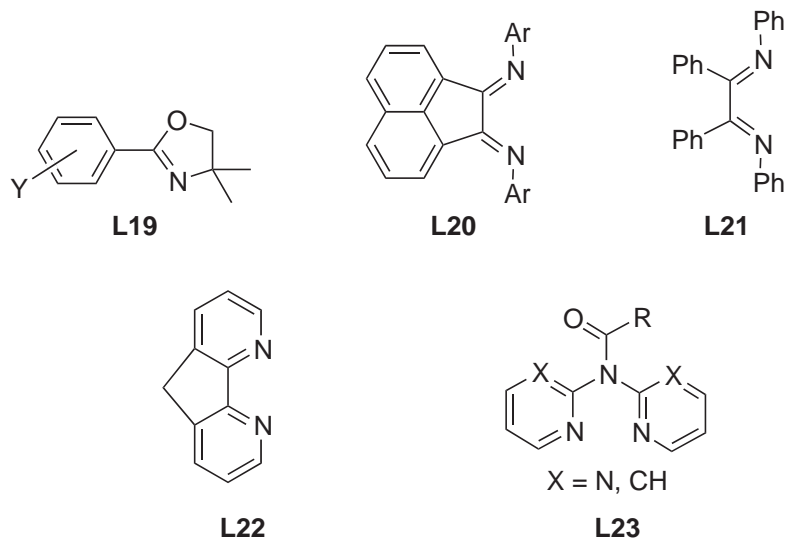
A similarly high performance has been reported for oxime-derived (**125**) and benzylsulfide-derived (**126**) palladacycles.⁴³⁸ These precatalysts are effective in the cross-coupling of arylboronic acids,^{438,439} organotin compounds,⁴⁴⁰ and terminal acetylenes⁴⁴¹ with aryl iodides and bromides, and of activated aryl chlorides. SC-palladacycles can effect the Suzuki–Miyaura reaction even at room temperature.

9.6.3.4.9 Nonphosphorus ligands

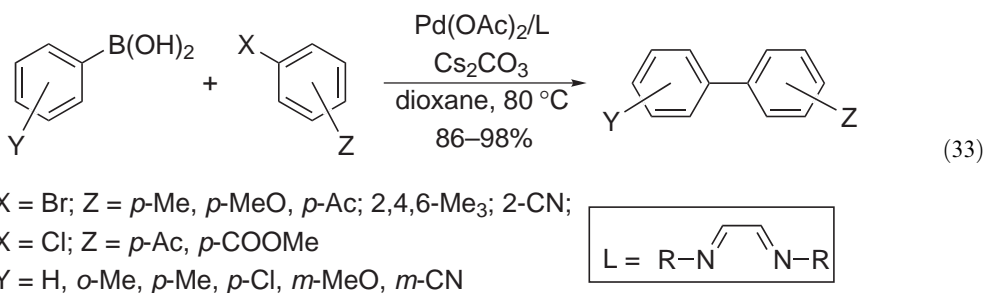
A variety of ligands which do not contain phosphorus have been revealed to be effective in cross-coupling reactions. Though inferior to the best phosphines, such ligands show great promise due to a better performance/cost ratio. Several such ligands have been discussed in the section devoted to palladacycles (Section 9.6.3.4.7). It should be stressed that the performance of such catalytic systems cannot be rationally predicted, as it depends on a fine interplay of the rates of individual stages of both the catalytic cycle and the deactivation reactions, and thus is heavily dependent on a particular implementation of the catalytic system (coupling partners, solvent, additives, etc.).

The readily available oxazolines (**L19**) are used in the cross-coupling of arylboronic acids with aryl bromides, including nonactivated ones in the system $(\text{Pd(OAc)}_2/\text{L})$, Cs_2CO_3 , dioxane, 80 °C). It is notable that the system works well at 1:1 Pd:L ratio.⁴⁴² A simple sulfide complex showed similar activity $(\text{PdCl}_2(\text{SEt}_2)_2)$, K_3PO_4 , DMF, 130 °C).¹⁸ A series of bidentate N,N-donor ligands

capable of forming *cis*-complexes with Pd was introduced (**L20–L22**). Such complexes were shown to serve as potent catalysts for cross-coupling reactions of organomagnesium, -tin, and -zinc compounds, showing reactivities comparable to those of common phosphine complexes. In the cross-coupling reaction of secondary benzyl halides, and similar substrates which present a special case due to their enhanced ability to yield homocoupled by-products, the dinitrogen ligands showed slightly better selectivity than phosphine-containing ligands.^{443–447}



The utility of similar ligands based on aromatic or aliphatic diimines of glyoxal (*N,N'*-disubstituted diazabutadienes, DAB-R ligands) for cross-coupling of arylboronic acids with aryl bromides and reactive aryl chlorides has been established (Equation (33)).⁴⁴⁸ The efficiency of the ligands depends on the nature of substituent R, the best being those with saturated residues (e.g., cyclohexyl), while those with aryl groups gave slightly lower yields.

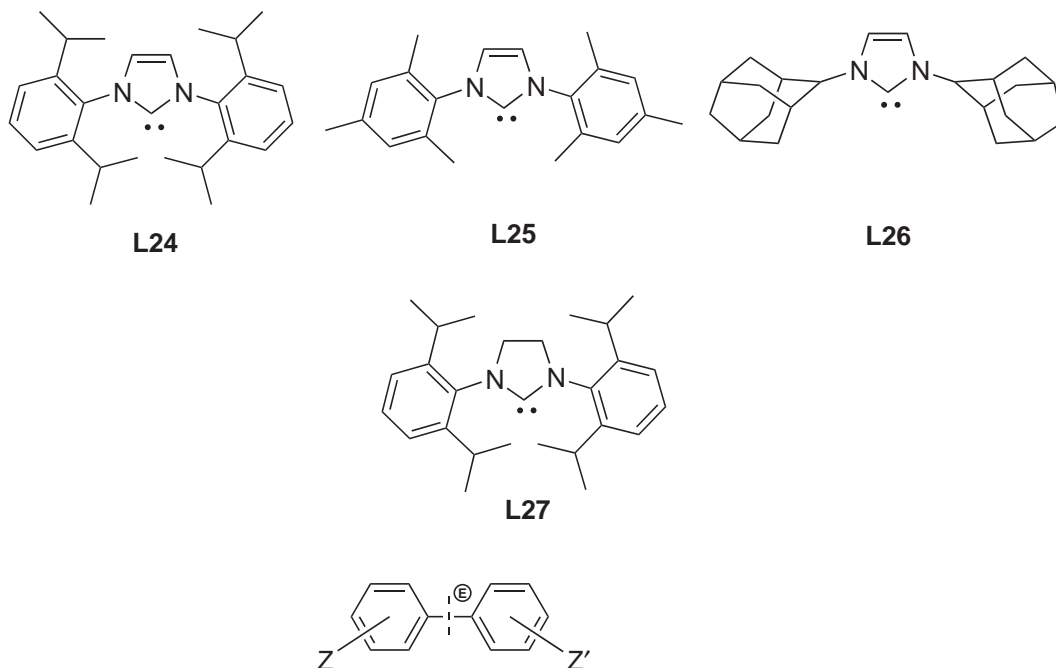


Simple bidentate ligands involving dipyridyl- or dipyrimidylamino fragment (**L23**) form Pd catalysts of moderate activity for the cross-coupling of terminal acetylenes (copper-free reaction) or arylboronic acids. Supported versions of such ligands were also reported (see Chapter 9.9 for more details about supported catalysts).^{449,450}

9.6.3.4.10 Heterocyclic carbene ligands

N,N'-disubstituted imidazol-2-ylidenes, stable carbenes capable of forming robust σ -complexes with a number of transition metals, resemble to a certain degree bulky, electron-rich phosphines.⁴⁵¹ Both mono- and bidentate carbene ligands of this sort have been described, as well as mixed-donor ligands with additional binding sites such as pyridine rings, including a tridentate pincer-type ligand (as in complex (**127**)) or a bidentate ligand with chiral oxazoline binding site.⁴⁵² Carbene complexes turned out to be highly active in cross-coupling reactions, allowing the successful use of chloroarenes and electron-rich bromoarenes as substrates in cross-coupling with arylboronic acids,^{453–459} organotin⁴⁵⁵ and organosilicon⁴⁶⁰ compounds, Grignard reagents,⁴⁶¹ and

terminal acetylenes,^{455,457,458} as well as the coupling of arenediazonium salts with arylboronic acids.³⁷⁰ So far, the most useful carbene ligands reported are (**L24**)–(**L26**), all of which bear bulky substituents. Such ligands can be used as their respective imidazolium salts, generating the carbenes *in situ*, to catalyze a broad range of cross-coupling reactions of aryl chlorides and bromides with arylboronic acids (**128a**),⁴⁶² Grignard reagents (example **128b**),⁴⁶¹ and phenyl and vinyltrimethoxysilane (**128c**).⁴⁶⁰ Cross-coupling with aryltrialkylstannanes requires activation by fluorides (**128d**), as also used for cross-couplings with analogous organosilicon reagents.²³⁷ The reaction with organotin compounds imposes the most stringent requirements on the catalytic system, as this is the only case when (**L25**) failed, and the bulkiest ligand of the series (**L26**), with adamantyl residues, was required to achieve the highest conversions. The latter ligand forms a homoleptic complex Pd(**L26**)₂, which catalyzes the room-temperature cross-coupling of arylboronic acids with aryl chlorides.⁴⁶³



a. $M = B(OH)_2$, $X = Cl$; $Z = H, \sigma\text{-Me}, p\text{-OMe}, \text{etc.}$; $Z' = H, p\text{-Me}, p\text{-OMe}, \text{etc.}$

$Pd_2(dba)_3$ (1.5%), 2**L25**•HCl; Cs_2CO_3 ; dioxane, 80 °C

b. $M = MgBr$, $X = Cl$; $Z = H, \sigma\text{-Me}, p\text{-Me}, o\text{-F}, 2,4,6\text{-Me}_3$;

$Z' = p\text{-Me}, p\text{-OMe}, p\text{-OH}, 2,6\text{-Me}_2, \text{etc.}$

$Pd_2(dba)_3$ (1%), 4**L24**•HCl; dioxane, 80 °C

c. $M = Si(OMe)_3$, $X = Cl$; $Z = H$; $Z' = p\text{-Me}, OMe, CN, COMe$

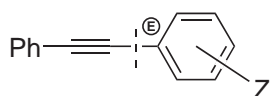
$Pd(OAc)_2$ (3%), **L24**•HCl; TBAF; dioxane, 60 °C

d. $M = SnMe_3$, $X = Cl, Br$; $Z = H$; $Z' = p\text{-Me}, p\text{-OMe}, p\text{-COMe}, 2,4,6\text{-Me}, \text{etc.}$

$Pd(OAc)_2$ (3%), **L24**•HCl; TBAF; dioxane, 80–100 °C

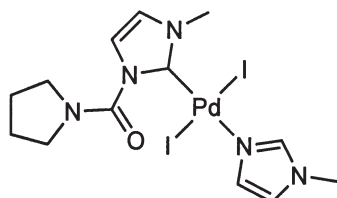
(128)

While the cross-coupling with terminal acetylenes in the presence of carbene complexes is rather nonselective and gives considerable amounts of diacetylene by-product,^{405,464} much better yields and selectivities can be reached if trimethylsilylphenylacetylene is used in place of phenylacetylene (**129**).⁴⁶⁵ The application of Pd complex (**130**) with mixed-donor imidazole–imidazolylidene ligands showed promising results in the cross-coupling of aryl iodides and bromides with terminal acetylenes, giving high yields of cross-coupling products under mild conditions (room temperature for ArI, 80 °C for ArBr) with a wide range of substrates including less reactive ones (**131**).⁴⁶⁶ The application of carbene–Pd catalysts has been extended to the arylation of ketones by aryl chlorides.⁴⁶⁷

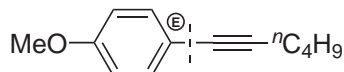


M = SiMe₃, X = Br, Cl
 Pd(OAc)₂, IMes HCl
 Cs₂CO₃; DMAc, 80 °C
 Z = H, *o*-Me, *p*-Me, *o*-OMe
p-OMe, 2,4,6-Me₃, etc.

(129)



(130)

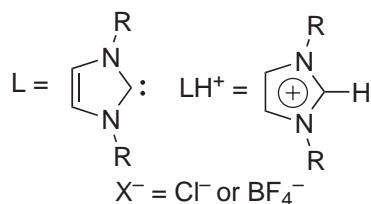
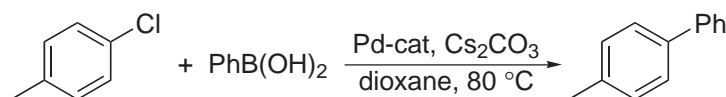


M = H, X = Br
 (17), PPh₃, CuI, Cs₂CO₃
 DMF, 80 °C, 74%

(131)

The mechanism of, and the nature of catalytic species in, the reactions catalyzed by carbene complexes are currently unknown, though it can be hypothesized that highly coordinatively unsaturated and therefore very reactive monocarbene complexes may be operating. A single carbene ligand should be strongly bonded and not allow further de-ligation, thereby preventing deactivation of “ligand-free” palladium by formation of Pd metal deposits. The formation of highly reactive monocarbene complexes is likely to be favored when: (i) a very bulky carbene ligand is used; (ii) a bidentate ligand with carbene and non-carbene binding sites (analogous to similar mixed phosphine–nonphosphine ligands: see Section 9.6.3.4.2) is used; and (iii) the catalyst is formed *in situ* from one equivalent of imidazolium salt by deprotonation. Indeed, the most active systems reported conform to these criteria. Thus, Pd–carbene catalysts are likely to behave similarly to monophosphine systems. In contrast, nonbulky imidazolylidene carbenes, as well as chelating bis-carbene analogues, show modest performance comparable to that of the common phosphine ligands.

The activity of catalytic systems based on imidazolylidene carbenes depends on many factors, among which the most important are likely to be the electronic effects of the ligand and the parameters of complexation. Therefore, the dependence of the performance of such systems on, e.g., the choice of precatalyst is not well understood, as in the following example (Equation (34)) in which two similar ligands behave in exactly the opposite way in the systems based on the presynthesized complex or *in situ* generation of the catalyst:⁴⁵⁴

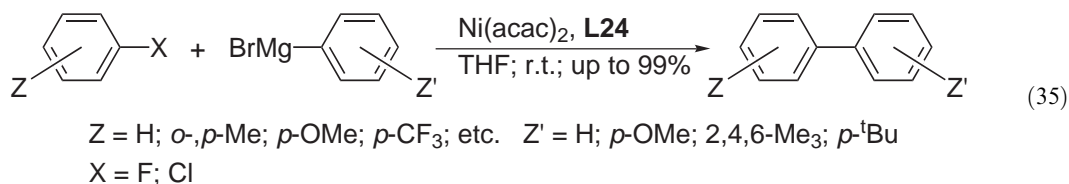


	R	
	^t Bu	Mes
PdL ₂	68	0
Pd ₂ (dba) ₃ /LH ⁺ X ⁻	0	93

(34)

Apart from imidazol-2-ylidene carbenes, other electron-rich carbenes such as (L27)—generated by deprotonation of a 4,5-dihydroimidazole—have been tested for cross-coupling reactions, but gave much poorer results. The only reported exception is in the cross-coupling of arenediazonium salts with arylboronic acids, in which (L27) (used as hydrochloride) proved to be efficient.³⁶⁹

Nickel complexes with imidazolylidene ligands also can be prepared and showed catalytic activity in cross-coupling reactions, such as the standard reaction of 4-bromoacetophenone with PhB(OH)_2 ,⁴⁵⁶ though their performance was inferior to that of the respective Pd complex. However, the Ni complex of (**L24**) has been shown to be highly active in cross-coupling with Grignard reagents (Equation (35)).⁴⁶⁸ Moreover, this catalyst allowed an unprecedented reaction of fluoroarenes with Grignard reagents—the only example of cross-coupling with participation of an unactivated C—F bond—to be performed easily.⁴⁶⁹ Both reactions run well under very mild conditions at room temperature, which is essential for controlling the selectivity:



9.6.3.4.11 Palladium nanoparticles and “ligand-free” catalysis

Simple Pd salts and complexes which contain neither phosphines nor any other deliberately added ligands are well known to provide catalytic activity in cross-coupling reactions. Such catalytic systems (often referred to as “ligand-free catalysts”) often require the use of water as a component of the reaction medium.¹⁷ In the majority of cases such systems are applicable to electrophiles easily undergoing the oxidative addition (aryl iodides and activated bromides), although there are examples of effective reactions with unactivated substrates (electron-rich aryl bromides, and some aryl chlorides).^{18,470}

In the absence of effective supporting ligands, Pd^0 should undergo aggregation into clusters and thence to inactive Pd black, as mentioned earlier. However, in some cases the aggregation may lead to Pd nanoparticles (sols), which retain some catalytic activity. The formation of sols is facilitated by: (i) low concentrations of Pd; (ii) the presence of nanoparticle stabilizing agents, such as phase-transfer agents, organic acids, or any other species with amphiphilic properties; and (iii) carrying out the reactions in microheterogeneous media, e.g., microemulsions.¹⁷ If the nanoparticles retain their reactivity towards oxidative addition their formation is reversible, and such sols may play a major role in the mechanism of the “ligand-free” catalysis.

The formation of Pd nanoparticles during the cross-coupling of aryl iodides with arylboronic acids, and in other Pd-catalyzed reactions, has been noted both in aqueous (PdCl_2 , K_2CO_3 , microemulsion media)¹⁷ and nonaqueous (Pd(OAc)_2 , NaHCO_3 , DMF, 130°C) media.⁴⁷¹ In both cases the sols showed reasonable catalytic activity. Specially prepared Pd sols with various stabilizing shells, such as polyvinylpyrrolidone or special ligands, were shown to have a high catalytic activity in various cross-coupling reactions, mostly the Suzuki–Miyaura reaction.^{472–474} A Pd sol stabilized by polyoxometalate anions effected the cross-coupling of arylboronic acids with even unactivated aryl bromides in high yields.⁴⁷⁵ Whereas the sol catalysts are commonly quite unstable, owing to uncontrollable dissolution/reprecipitation phenomena, a sophisticated nanomaterial constituted of nano-sized hollow spheres was shown to serve as a perfectly recyclable catalyst for cross-coupling reactions.⁴⁷⁶

9.6.3.5 Technological Aspects of Cross-coupling Chemistry

As with any other major method of synthesis, cross-coupling reactions are applied in two distinct ways: (i) complex, laboratory-scale organic synthesis, which is entirely product oriented, with little or no attention paid to the cost of chemicals; and (ii) large-scale, fine organic products synthesis for production of pharmaceuticals, agrochemicals, other specialty chemicals, and new advanced materials. In the latter case the minimization of costs is a high priority, along with environmental considerations. The technological implementation of processes involving homogeneous catalysis by precious metals necessitates the use of recyclable catalytic systems, both to minimize costs and to allow for effective recovery of the metal, minimization or exclusion of expensive and toxic phosphine ligands, and simplification of the preparative procedure.

Recyclability can be achieved by heterogenization of the reaction mixture, by binding the catalyst and products to different phases. This can be achieved by: (i) immobilization of the catalyst on a solid inorganic or polymeric support (solid–liquid protocols); or (ii) partitioning the catalyst and reagents/products in different liquid phases (liquid–liquid protocols) (see Chapter 9.9 for more details on supported catalysts).

9.6.3.5.1 Microwave heating

Microwave heating allows dramatic shortening of reaction times, and increased yields. Simple catalytic systems (e.g., phosphine-free catalysts, aqueous or solventless systems) can be effective under microwave heating, even with relatively unreactive substrates. Fast processing has a very important implication for phosphine-free reactions, since the deactivation of catalyst can be slower than the main catalytic reaction. The application of microwave heating to cross-couplings with terminal acetylenes, arylboronic acids, and organotin compounds (amongst others) has been described.^{477–480}

9.6.3.5.2 Supported catalysts

(i) Physical absorption on inorganic or similar supports

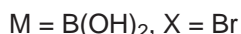
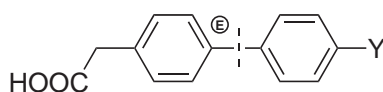
So far, no systematic work has been done on the use of recyclable, solid-phase catalysts in cross-coupling reactions. Most of the examples have been obtained for cross-couplings with either arylboronic acids or terminal acetylenes. It should be noted, however, that due care should be exercised when interpreting results on the cross-coupling of arylboronic acids with aryl iodides, as this extremely facile reaction can be catalyzed by practically any palladium-containing material, including trivial Pd black,⁴⁸¹ e.g., as a sediment on the reaction vessel. Therefore, this reaction cannot serve as a reliable test for comparison between different catalytic systems.

Among the solid supports already tested are virtually all materials popular in green chemistry research: alumina, various clays, controlled porosity glasses, mesoporous materials, etc. Palladium on porous glass works without supporting ligands or a copper promoter in cross-couplings with terminal acetylenes. The reaction is carried out at high temperature under microwave irradiation, and is applicable towards aryl iodides and reactive aryl bromides.⁴⁸² Palladium black mechanically mixed with KF/alumina catalyzes the cross-coupling of iodobenzene with aryl and vinylboronic acids in the absence of solvent and unsupported base,⁴⁸³ using either conventional or microwave heating.⁴⁸⁴ The same catalyst can be used in solvent-free cross-coupling of aryl iodides with terminal acetylenes, using microwave heating.⁴⁷⁹ A palladium sol, stabilized by polyoxometallate anions supported over alumina, turned out to be active enough to effect the cross-coupling of arylboronic acids with unactivated chloroarenes in the absence of solvent (Pd sol, KF, Al₂O₃, 130 °C).⁴⁷⁵ PdCl₂ co-intercalated on clay with Ph₄PBr showed moderate reactivity and recyclability in cross-coupling of aryl iodides and reactive bromides with arylboronic acids.⁴⁸⁵

(ii) Pd/C and Ni/C

The readily available hydrogenation catalyst Pd/C can also serve as a good catalyst for a number of cross-coupling reactions. In the cross-coupling of aryl iodides with arylboronic acid it showed a high efficiency,⁴⁸⁶ particularly in aqueous media using water-soluble reagents (**132**). Aryl bromides and chlorides can also be cross-coupled with arylboronic acids using Pd/C in aqueous dimethylacetamide.⁴⁸⁷ Pd/C has been successfully used for cross-coupling with terminal acetylenes.^{488,489}

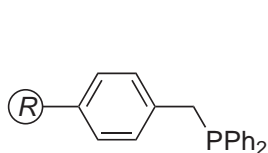
Nickel salts impregnated on charcoal after treatment by strong reducing agents make a highly active catalyst (Ni/C) for the cross-coupling of organozinc,⁴⁹⁰ organoaluminum,⁴⁹¹ and organomagnesium compounds,⁴⁹² and arylboronic acids,⁴⁹³ with aryl bromides and chlorides, although with aryl chlorides the addition of phosphine ligands is required.



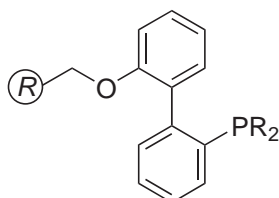
(132)

(iii) Polymer-immobilized catalysts

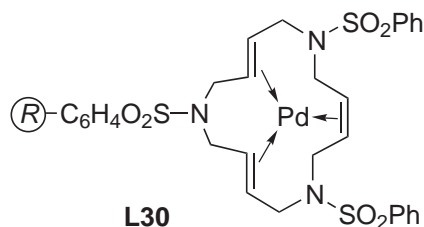
The simplest method of immobilization of the phosphine ligand (**L28**) is the direct attachment of the diphenylphosphino group to Merrifield's resin (chloromethylated, cross-linked polystyrene), which gives an air-stable, recyclable catalyst of moderate reactivity for the cross-coupling of $PhB(OH)_2$ with reactive bromoarenes.⁴⁹⁴ The immobilization of dialkylphosphinobiphenyl ($R = Cy$ or tBu) ligands (**L29**) (cf. Section 9.6.3.4.4) gave highly active, recyclable catalysts capable of catalyzing the Suzuki reaction with aryl iodides, bromides, and chlorides—including sterically encumbered ones—under mild conditions.⁴⁹⁵ An amphiphilic, triphenylphosphine-containing polymer was a good ligand for the cross-coupling of aryl iodides, bromides, and triflates with arylboronic acids in the absence of any other solvent except water, allowing for at least 10 reuses without noticeable loss of activity.⁴⁹⁶ The use of high-throughput testing techniques (see Chapter 9.11) allowed optimization of the reaction conditions for a series of catalysts which were immobilized on polyethylene-based fibers through pendant diphenylphosphine groups. This allowed the development of highly active catalysts for the room-temperature cross-coupling of arylboronic acids with aryl bromides and chlorides in aqueous media. For less reactive substrates, the activity can be additionally modulated by use of P^tBu_3 ligands.⁴⁹⁷



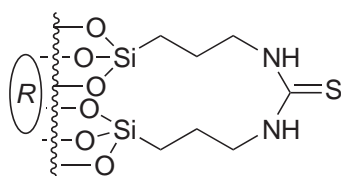
L28



L29



L30



L31

Catalysts can also be immobilized through nonphosphine ligands. A new type of immobilized Pd^0 complex with a macrocyclic triolefin ligand (**L30**) has been successfully used for simple cross-coupling reactions of aryl iodides and allyl bromide with arylboronic acids, in both aqueous and anhydrous media.⁴⁹⁸

A number of phosphine-free carriers which contain sulfur as the palladium-bonding element have been described to serve as highly persistent, air-stable catalysts, which bind the Pd very strongly. A palladium complex immobilized on silica via mercaptopropyl residues is active in cross-coupling with terminal acetylenes.⁴⁹⁹ The commercial, thiourea-containing polysiloxane resin (**L31**), routinely used for removing heavy metals from wastes, has been used (after charging with Pd) for cross-coupling between arylboronic acids and aryl iodides or activated aryl bromides in aqueous solvent.⁵⁰⁰

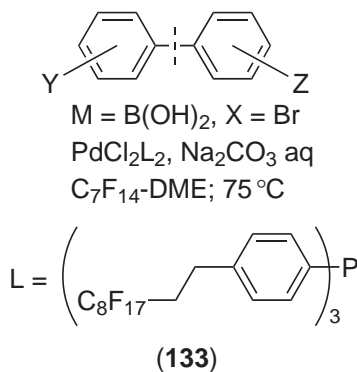
9.6.3.5.3 Aqueous systems

Almost all cross-coupling reactions, except those involving the most reactive organometallics (derivatives of Li, Mg, Zn), are compatible with water and can be performed in aqueous media. The use of water creates a number of important opportunities including: (i) the development of environmentally benign catalytic processes; (ii) the application of highly effective, phosphine-free protocols, particularly in the Suzuki–Miyaura reaction but also in cross-couplings with other organometallic compounds and terminal acetylenes; (iii) the design and implementation of biphasic catalytic systems with the recyclable catalyst bound in the aqueous phase. Reactions in homogeneous aqueous solutions can be carried out both with phosphine-free catalysts⁵⁰¹ (cf. Section 9.6.3.4.11), and also with hydrophilized phosphine ligands, the most important of which are the sulfonated triphenylphosphines TPPMS (sodium salt of monosulfonated triphenylphosphine), and TPPTS (trisodium salt of trisulfonated triphenylphosphine).⁵⁰² A microheterogeneous system of high solubilizing capacity, e.g., a microemulsion, can be used to perform reactions with water-insoluble reagents.⁵⁰¹

Recyclable systems require the use of hydrophilic phosphine ligands which keep Pd in the recyclable aqueous phase, with the reaction products being isolated from the water-immiscible organic phase. However, low reaction rates—due to ineffective mixing of the reacting species (reagents, additives, catalyst)—is a serious drawback of biphasic systems. Much better efficiency can be achieved using solvent systems possessing temperature-dependent miscibility, as in this case the process is run in a homogeneous environment (Sections 9.6.3.5.4 and 9.6.3.5.6) before changing the temperature to separate the catalyst-containing and product-containing phases. An alternative solution employs the immobilization of aqueous phase over solid supports, ensuring a high interfacial area (supported aqueous-phase (SAP) palladium catalysts: see Chapter 9.9).⁵⁰³

9.6.3.5.4 Fluorous systems

The application of so-called fluorous (a hybrid of *fluorine* + *aqueous*) systems towards designing environmentally friendly recyclable processes is rapidly gaining popularity. Perfluoroorganic liquids are miscible with common polar organic solvents at elevated temperatures, but separate into two immiscible phases on cooling. Therefore, unlike reactions in biphasic aqueous/organic systems, the reaction is run under homogeneous conditions, and there are no problems associated with restricted mass transfer across interfaces. The solubilization of catalyst is achieved through attaching highly fluorinated, long alkyl chains to the ligand, usually a phosphine. The use of highly fluorinated dialkylsulfides as ligands for cross-coupling reactions has been described, as has the use of a fluorous palladacycle.⁵⁰⁴ Fluorous systems have been applied to the cross-coupling of aryl bromides with arylboronic acids (**133**)⁵⁰⁵ and terminal acetylenes.⁵⁰⁶ Palladium nanoparticles stabilized by a fluorous ligand can be used as recyclable catalysts.⁴⁷⁴ In addition to allowing recovery of the catalyst, the fluorous technique also allows recycling of the organotin residue, if perfluorocarbon tails are attached to ligands on the tin atom.⁵⁰⁷



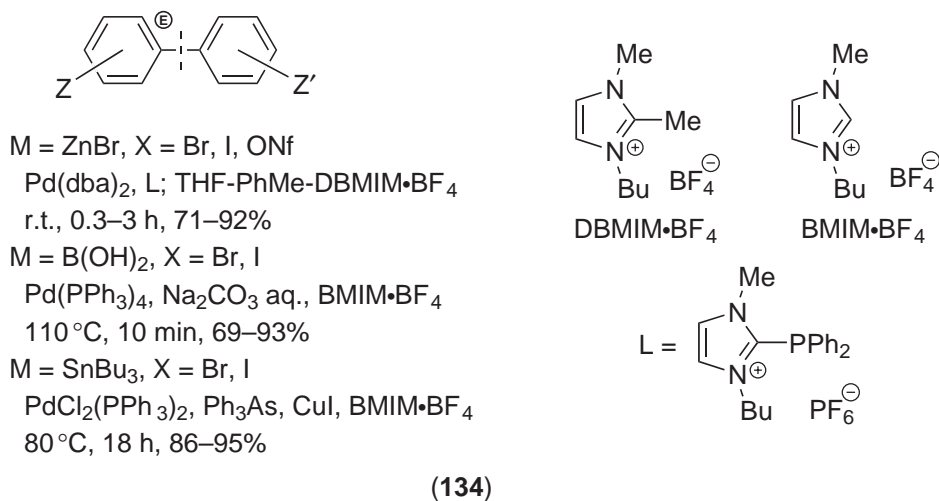
9.6.3.5.5 Supercritical CO₂

Supercritical CO₂ (scCO₂) is one of the most appealing easily recyclable solvents, allowing the design of environmentally safe processes. Supercritical CO₂ has properties similar to those of

fluoroorganic solvents, though the solubilization of catalysts in scCO_2 places less strict restrictions on the content of fluorine. Small fluorine-containing groups (even CF_3) are usually enough to increase the solubility in scCO_2 to reasonable levels; therefore trifluoromethyl-substituted triphenylphosphines, or even $\text{Pd}(\text{OCCF}_3)_2$, make good ligands/catalysts. Among the reactions tested in scCO_2 are cross-coupling with organotin compounds^{508–511} and boronic acids.⁵¹⁰ Apart from fluorine-containing ligands, P^tBu_3 has been shown to act as a good ligand for cross-coupling in scCO_2 .⁵¹² Further improvements can be achieved by using supported Pd catalysts in this solvent.⁵¹³

9.6.3.5.6 Ionic liquids

Recyclable systems can be prepared with so-called ionic liquids⁵¹⁴—salts which are liquid at the temperature of reaction, such as 1-butyl-3-methylimidazolium tetrafluoroborate (BMIM- BF_4) or related materials (134).⁵¹⁵ The products can be distilled off or extracted during postreaction work-up by common organic solvents, while the catalyst is retained in the ionic liquid phase. The lifetime of such systems is limited, however, due to accumulation of reaction wastes in the ionic liquid phase, although the inorganic salts can be partially extracted from the ionic liquid phase by water. Solvents of this type have been successfully applied to cross-couplings of aryl bromides and iodides with organotin compounds allowing up to five recyclings,⁵¹⁶ and with arylboronic acids allowing at least three recyclings,⁵¹⁷ and also to the reactions with polymer-immobilized reagents.⁵¹⁸ To improve the retention of the palladium catalyst in the ionic liquid phase, specific ligands having enhanced affinity to such media can be used, as in the cross-coupling of organozinc compounds with aryl halides and nonaflates.⁵¹⁹



Besides the advantage of recyclability, reactions in ionic liquids are generally faster and are run under milder conditions than reactions with conventional solvents. Further activation may come from ultrasonic agitation.⁵²⁰ Since the majority of ionic liquids used are imidazolium salts, the effect of these solvents can be at least partly attributed to the *in situ* formation of carbene complexes (Section 9.6.3.4.10).⁵²¹ Cross-coupling of $\text{ArB}(\text{OH})_2$ can also be efficiently performed in ionic liquids based on long-chain tetraalkylphosphonium salts, in which case aryl bromides and some aryl chlorides can be processed in the presence of the trivial ligand PPh_3 .⁵²²

9.6.4 REFERENCES

- Netherton, M. R.; Fu, G. C. *Angew. Chem., Int. Ed. Engl.* **2002**, *41*, 3910–3912.
- Negishi, E.-I., Ed., *Handbook of Organopalladium Chemistry*; Wiley Interscience: New York, 2002.
- Kotha, S.; Lahiri, K.; Kashinath, D. *Tetrahedron* **2002**, *58*, 9633–9695.
- Miyaura, N.; Suzuki, A. *Chem. Rev.* **1995**, *95*, 2457–2483.
- Stanforth, S. P. *Tetrahedron* **1998**, *54*, 263–303.
- Mandolesi, S. D.; Vaillard, S. E.; Podesta, J. C.; Rossi, R. A. *Organometallics* **2002**, *21*, 4886–4888.
- Babudri, F.; Farinola, G. M.; Naso, F.; Panessa, D. *J. Org. Chem.* **2000**, *65*, 1554–1557.

8. Babudri, F.; Farinola, G. M.; Fiandanese, V.; Mazzone, L.; Naso, F. *Tetrahedron* **1998**, *54*, 1085–1094.
9. Farinola, G. M.; Fiandanese, V.; Mazzone, L.; Naso, F. *J. Chem. Soc., Chem. Commun.* **1995**, 2523–2524.
10. Suzuki, A. *Rev. Heteroatom Chem.* **1997**, *17*, 271–314.
11. Beletskaya, I.; Pelter, A. *Tetrahedron* **1997**, *53*, 4957–5026.
12. Ohmura, T.; Yamamoto, Y.; Miyaura, N. *J. Am. Chem. Soc.* **2000**, *122*, 4990–4991.
13. Murata, M.; Kawakita, K.; Asana, T.; Watanabe, S.; Masuda, Y. *Bull. Chem. Soc. Jpn.* **2002**, *75*, 825–829.
14. Ishiyama, T.; Murata, M.; Miyaura, N. *J. Org. Chem.* **1995**, *60*, 7508–7510.
15. Murata, M.; Oyama, T.; Watanabe, S.; Masuda, Y. *J. Org. Chem.* **2000**, *65*, 164–168.
16. Ishiyama, T.; Matsuda, N.; Murata, M.; Ozawa, F.; Suzuki, A.; Miyaura, N. *Organometallics* **1996**, *15*, 713–720.
17. Beletskaya, I. P.; Cheprakov, A. V. In *Handbook of Organopalladium Chemistry*; Negishi, E.-I., Ed., Wiley Interscience: New York, 2002; Vol. 2, pp 2957–3006.
18. Zim, D.; Monteiro, A. L.; Dupont, J. *Tetrahedron Lett.* **2000**, *41*, 8199–8202.
19. Klingensmith, L. M.; Leadbeater, N. E. *Tetrahedron Lett.* **2003**, *44*, 765–768.
20. Leadbeater, N. E.; Resouly, S. M. *Tetrahedron* **1999**, *55*, 11889–11894.
21. Zim, D.; Monteiro, A. L. *Tetrahedron Lett.* **2002**, *43*, 4009–4011.
22. Lee, J. H.; Park, E. S.; Yoon, C. M. *Tetrahedron Lett.* **2001**, *42*, 8311–8314.
23. Merlic, C. A.; McInnes, D. M.; You, Y. *Tetrahedron Lett.* **1997**, *38*, 6787–6790.
24. Hassan, J.; Sevignon, M.; Gozzi, C.; Schulz, E.; Lemaire, M. *Chem. Rev.* **2002**, *102*, 1359–1469.
25. Watanabe, T.; Miyaura, N.; Suzuki, A. *Synlett* **1992**, 207–210.
26. Chaumeil, H.; Signorella, S.; Le Drian, C. *Tetrahedron* **2000**, *56*, 9655–9662.
27. Urawa, Y.; Naka, H.; Miyazawa, M.; Souda, S.; Ogura, K. *J. Organomet. Chem.* **2002**, *653*, 269–278.
28. Luthle, J. E. A.; Pietruszka, J. *J. Org. Chem.* **1999**, *64*, 8287–8297.
29. Charette, A. B.; Giroux, A. *J. Org. Chem.* **1996**, *61*, 8718–8719.
30. Zhou, S. M.; Deng, M. Z.; Xia, L. J.; Tang, M. H. *Angew. Chem., Int. Ed. Engl.* **1998**, *37*, 2845–2847.
31. Miyaura, N.; Ishiyama, T.; Ishikawa, M.; Suzuki, A. *Tetrahedron Lett.* **1986**, *27*, 6369–6372.
32. Miyaura, N.; Ishiyama, T.; Sasaki, H.; Ishikawa, M.; Satoh, M.; Suzuki, A. *J. Am. Chem. Soc.* **1989**, *111*, 314–321.
33. Chemler, S. R.; Trauner, D.; Danishefsky, S. J. *Angew. Chem., Int. Ed. Engl.* **2001**, *40*, 4544–4568.
34. Vice, S.; Bara, T.; Bauer, A.; Evans, C. A.; Ford, J.; Josien, H.; McCombie, S.; Miller, M.; Nazareno, D.; Palani, A.; Tagat, J. *J. Org. Chem.* **2001**, *66*, 2487–2492.
35. Oh-e, T.; Miyaura, N.; Suzuki, A. *J. Org. Chem.* **1993**, *58*, 2201–2208.
36. Kane, J. L.; Shea, K. M.; Crombie, A. L.; Danheiser, R. L. *Org. Lett.* **2001**, *3*, 1081–1084.
37. Bodwell, G. J.; Li, J. *Org. Lett.* **2002**, *4*, 127–130.
38. Bodwell, G. J.; Li, J. *Angew. Chem., Int. Ed. Engl.* **2002**, *41*, 3261–3262.
39. Smith, B. B.; Hill, D. E.; Cropp, T. A.; Walsh, R. D.; Cartrette, D.; Hipps, S.; Shachter, A. M.; Pennington, W. T.; Kwochka, W. R. *J. Org. Chem.* **2002**, *67*, 5333–5337.
40. Smith, B. B.; Kwochka, W. R.; Damrauer, R.; Swope, R. J.; Smyth, J. R. *J. Org. Chem.* **1997**, *62*, 8589–8590.
41. Kwochka, W. R.; Smith, B. B. *Abstr. Pap. Am. Chem. Soc.* **1997**, *213*, 421–ORGN.
42. Damrauer, R.; Kwochka, W. R. *Abstr. Pap. Am. Chem. Soc.* **1994**, *207*, 492–ORGN.
43. Molander, G. A.; Yun, C. S. *Tetrahedron* **2002**, *58*, 1465–1470.
44. Bellina, F.; Carpita, A.; Fontana, E. A.; Rossi, R. *Tetrahedron* **1994**, *50*, 5189–5202.
45. Lunot, S.; Thibonnet, J.; Duchene, A.; Parrain, J. L.; Abarbri, M. *Tetrahedron Lett.* **2000**, *41*, 8893–8896.
46. Timbart, L.; Cintrat, J. C. *Chem. Eur. J.* **2002**, *8*, 1637–1640.
47. Kang, S. K.; Baik, T. G.; Kulak, A. N.; Ha, Y. H.; Lim, Y.; Park, J. *J. Am. Chem. Soc.* **2000**, *122*, 11529–11530.
48. Yoshida, H.; Honda, Y.; Shirakawa, E.; Hiyama, T. *J. Chem. Soc., Chem. Commun.* **2001**, 1880–1881.
49. Shirakawa, E.; Hiyama, T. *Bull. Chem. Soc. Jpn.* **2002**, *75*, 1435–1450.
50. Zhang, N.; Thomas, L.; Wu, B. Q. *J. Org. Chem.* **2001**, *66*, 1500–1502.
51. Nozaki, K.; Oshima, K.; Utimoto, K. *J. Am. Chem. Soc.* **1987**, *109*, 2547–2549.
52. Alami, M.; Liron, F.; Gervais, M.; Peyrat, J. F.; Brion, J. D. *Angew. Chem., Int. Ed. Engl.* **2002**, *41*, 1578–1580.
53. Smith, N. D.; Mancuso, J.; Lautens, M. *Chem. Rev.* **2000**, *100*, 3257–3282.
54. Ichinose, Y.; Oda, H.; Oshima, K.; Utimoto, K. *Bull. Chem. Soc. Jpn.* **1987**, *60*, 3468–3470.
55. Maleczka, R. E.; Lavis, J. M.; Clark, D. H.; Gallagher, W. P. *Org. Lett.* **2000**, *2*, 3655–3658.
56. Gallagher, W. P.; Terstiege, I.; Maleczka, R. E. *J. Am. Chem. Soc.* **2001**, *123*, 3194–3204.
57. Maleczka, R. E.; Gallagher, W. P.; Terstiege, I. *J. Am. Chem. Soc.* **2000**, *122*, 384–385.
58. Maleczka, R. E.; Gallagher, W. P. *Org. Lett.* **2001**, *3*, 4173–4176.
59. Asao, N.; Liu, J. X.; Sudoh, T.; Yamamoto, Y. *J. Org. Chem.* **1996**, *61*, 4568–4571.
60. Ma, L.; White, P. S.; Lin, W. B. *J. Org. Chem.* **2002**, *67*, 7577–7586.
61. Corsico, E. F.; Rossi, R. A. *J. Org. Chem.* **2002**, *67*, 3311–3316.
62. Fouquet, E.; Pereyre, M.; Rodriguez, A. L. *J. Org. Chem.* **1997**, *62*, 5242–5243.
63. Shen, Y. C.; Wang, G. P. *Org. Lett.* **2002**, *4*, 2083–2085.
64. Jeong, I. H.; Park, Y. S.; Kim, B. T. *Tetrahedron Lett.* **2000**, *41*, 8917–8921.
65. Smith, A. B.; Ott, G. R. *J. Am. Chem. Soc.* **1998**, *120*, 3935–3948.
66. Ulrich, G.; Bedel, S.; Picard, C.; Tisnes, P. *Tetrahedron Lett.* **2001**, *42*, 6113–6115.
67. Graham, A. E.; McKerrecher, D.; Davies, D. H.; Taylor, R. J. K. *Tetrahedron Lett.* **1996**, *37*, 7445–7448.
68. Saalfrank, R. W.; Haubner, M.; Deutscher, C.; Bauer, W. *Eur. J. Org. Chem.* **1999**, 2367–2372.
69. Shen, R. C.; Lin, C. T.; Bowman, E. J.; Bowman, B. J.; Porco, J. A. *Org. Lett.* **2002**, *4*, 3103–3106.
70. Kamlage, S.; Sefkow, M.; Peter, M. G. *J. Org. Chem.* **1999**, *64*, 2938–2940.
71. Negishi, E.; Okukado, N.; King, A. O.; Vanhorn, D. E.; Spiegel, B. I. *J. Am. Chem. Soc.* **1978**, *100*, 2254–2256.
72. Wipf, P.; Kendall, C. *Chem. Eur. J.* **2002**, *8*, 1778–1784.
73. Lee, T. W.; Corey, E. J. *J. Am. Chem. Soc.* **2001**, *123*, 1872–1877.
74. Panek, J. S.; Hu, T. *J. Org. Chem.* **1997**, *62*, 4912–4913.
75. Hu, T.; Panek, J. S. *J. Org. Chem.* **1999**, *64*, 3000–3001.
76. Drouet, K. E.; Theodorakis, E. A. *Chem. Eur. J.* **2000**, *6*, 1987–2001.
77. Thompson, C. F.; Jamison, T. F.; Jacobsen, E. N. *J. Am. Chem. Soc.* **2000**, *122*, 10482–10483.

78. Hupe, E.; Calaza, M. I.; Knochel, P. *Tetrahedron Lett.* **2001**, *42*, 8829–8831.
79. Terao, J.; Kambe, N.; Sonoda, N. *Tetrahedron Lett.* **1996**, *37*, 4741–4744.
80. Studemann, T.; Gupta, V.; Engman, L.; Knochel, P. *Tetrahedron Lett.* **1997**, *38*, 1005–1008.
81. Jackson, R. F. W.; Wishart, N.; Wood, A.; James, K.; Wythes, M. J. *J. Org. Chem.* **1992**, *57*, 3397–3404.
82. Masaki, H.; Maeyama, J.; Kamada, K.; Esumi, T.; Iwabuchi, Y.; Hatakeyama, S. *J. Am. Chem. Soc.* **2000**, *122*, 5216–5217.
83. Masaki, H.; Mizozoe, T.; Esumi, T.; Iwabuchi, Y.; Hatakeyama, S. *Tetrahedron Lett.* **2000**, *41*, 4801–4804.
84. Liu, S. F.; Dockendorff, C.; Taylor, S. D. *Org. Lett.* **2001**, *3*, 1571–1574.
85. Jung, M. E.; Starkey, L. S. *Tetrahedron* **1997**, *53*, 8815–8824.
86. Dexter, C. S.; Hunter, C.; Jackson, R. F. W. *J. Org. Chem.* **2000**, *65*, 7417–7421.
87. Goedheijt, M. S.; Nijbacker, T.; Akkerman, O. S.; Bickelhaupt, F.; Veldman, N.; Spek, A. L. *Angew. Chem., Int. Ed. Engl.* **1996**, *35*, 1550–1552.
88. Takagi, K.; Shimoishi, Y.; Sasaki, K. *Chem. Lett.* **1994**, 2055–2058.
89. Amano, M.; Saiga, A.; Ikegami, R.; Ogata, T.; Takagi, K. *Tetrahedron Lett.* **1998**, *39*, 8667–8668.
90. Saiga, A.; Hossain, K. M.; Takagi, K. *Tetrahedron Lett.* **2000**, *41*, 4629–4632.
91. Shi, G. Q.; Huang, X. H.; Hong, F. *J. Org. Chem.* **1996**, *61*, 3200–3204.
92. Prasad, A. S. B.; Stevenson, T. M.; Citineni, J. R.; Nyzam, V.; Knochel, P. *Tetrahedron* **1997**, *53*, 7237–7254.
93. Prasad, A. S. B.; Knochel, P. *Tetrahedron* **1997**, *53*, 16711–16720.
94. Hou, S. *Org. Lett.* **2003**, *5*, 423–425.
95. Fillon, H.; Gosmini, C.; Nedelec, J. Y.; Perichon, J. *Tetrahedron Lett.* **2001**, *42*, 3843–3846.
96. Le Gall, E.; Gosmini, C.; Nedelec, J. Y.; Perichon, J. *Tetrahedron* **2001**, *57*, 1923–1927.
97. Mellah, M.; Labbe, E.; Nedelec, J. Y.; Perichon, J. *New J. Chem.* **2001**, *25*, 318–321.
98. Gosmini, C.; Rollin, Y.; Nedelec, J. Y.; Perichon, J. *J. Org. Chem.* **2000**, *65*, 6024–6026.
99. Gosmini, C.; Nedelec, J. Y.; Perichon, J. *Tetrahedron Lett.* **1997**, *38*, 1941–1942.
100. Micouin, L.; Knochel, P. *Synlett* **1997**, 327–328.
101. Negishi, E.; Vanhorn, D. E.; Yoshida, T.; Rand, C. L. *Organometallics* **1983**, *2*, 563–565.
102. Gagneur, S.; Montchamp, J. L.; Negishi, E. *Organometallics* **2000**, *19*, 2417–2419.
103. Studemann, T.; Knochel, P. *Angew. Chem., Int. Ed. Engl.* **1997**, *36*, 93–95.
104. Studemann, T.; Ibrahim-Ouali, M.; Knochel, P. *Tetrahedron* **1998**, *54*, 1299–1316.
105. Knochel, P.; Singer, R. D. *Chem. Rev.* **1993**, *93*, 2117–2188.
106. Larsen, M.; Jorgensen, M. *J. Org. Chem.* **1997**, *62*, 4171–4173.
107. Alami, M.; Peyrat, J. F.; Belachmi, L.; Brion, J. D. *Eur. J. Org. Chem.* **2001**, 4207–4212.
108. Amat, M.; Hadida, S.; Pshenichnyi, G.; Bosch, J. *J. Org. Chem.* **1997**, *62*, 3158–3175.
109. Nshimyumukiza, P.; Cahard, D.; Rouden, J.; Lasne, M. C.; Plaquevent, J. C. *Tetrahedron Lett.* **2001**, *42*, 7787–7790.
110. Giovannini, R.; Knochel, P. *J. Am. Chem. Soc.* **1998**, *120*, 11186–11187.
111. Jensen, A. E.; Dohle, W.; Knochel, P. *Tetrahedron* **2000**, *56*, 4197–4201.
112. Giovannini, R.; Studemann, T.; Dussin, G.; Knochel, P. *Angew. Chem., Int. Ed. Engl.* **1998**, *37*, 2387–2390.
113. Giovannini, R.; Studemann, T.; Devasagayraj, A.; Dussin, G.; Knochel, P. *J. Org. Chem.* **1999**, *64*, 3544–3553.
114. Anastasia, L.; Xu, C.; Negishi, E. *Tetrahedron Lett.* **2002**, *43*, 5673–5676.
115. Anastasia, L.; Negishi, E. *Org. Lett.* **2001**, *3*, 3111–3113.
116. Negishi, E.; Kotora, M.; Xu, C. D. *J. Org. Chem.* **1997**, *62*, 8957–8960.
117. Sonoda, M.; Inaba, A.; Itahashi, K.; Tobe, Y. *Org. Lett.* **2001**, *3*, 2419–2421.
118. Murahashi, S. I. *J. Organomet. Chem.* **2002**, *653*, 27–33.
119. Lee, J. S.; Velarde-Ortiz, R.; Guijarro, A.; Wurst, J. R.; Rieke, R. D. *J. Org. Chem.* **2000**, *65*, 5428–5430.
120. Rieke, R. D. *Aldrichimica Acta* **2000**, *33*, 52–60.
121. Guijarro, A.; Rosenberg, D. M.; Rieke, R. D. *J. Am. Chem. Soc.* **1999**, *121*, 4155–4167.
122. Rieke, R. D.; Kim, S. H.; Wu, X. M. *J. Org. Chem.* **1997**, *62*, 6921–6927.
123. Rieke, R. D.; Hanson, M. V. *Tetrahedron* **1997**, *53*, 1925–1956.
124. Bogdanovic, B. *Angew. Chem., Int. Ed. Engl.* **1985**, *24*, 262–273.
125. Tjurina, L. A.; Smirnov, V. V.; Barkovskii, G. B.; Nikolaev, E. N.; Esipov, S. E.; Beletskaya, I. P. *Organometallics* **2001**, *20*, 2449–2450.
126. Zhang, Y. K.; Liao, S. J.; Fan, Y. H.; Xu, J.; Wang, F. D. *J. Nanopart. Res.* **2001**, *3*, 23–26.
127. Abarbri, M.; Dehmel, F.; Knochel, P. *Tetrahedron Lett.* **1999**, *40*, 7449–7453.
128. Bell, L.; Brookings, D. C.; Dawson, G. J.; Whitby, R. J.; Raymond, V. H.; Michael, C. H. *Tetrahedron* **1998**, *54*, 14617–14634.
129. Dzhemilev, U. M. *Tetrahedron* **1995**, *51*, 4333–4346.
130. Hoveyda, A. H.; Morken, J. P. *J. Org. Chem.* **1993**, *58*, 4237–4244.
131. Houri, A. F.; Didiuk, M. T.; Xu, Z. M.; Horan, N. R.; Hoveyda, A. H. *J. Am. Chem. Soc.* **1993**, *115*, 6614–6624.
132. Hoveyda, A. H.; Morken, J. P.; Houri, A. F.; Xu, Z. M. *J. Am. Chem. Soc.* **1992**, *114*, 6692–6697.
133. Rousset, C. J.; Negishi, E. I.; Suzuki, N.; Takahashi, T. *Tetrahedron Lett.* **1992**, *33*, 1965–1968.
134. Lewis, D. P.; Muller, P. M.; Whitby, R. J.; Jones, R. V. H. *Tetrahedron Lett.* **1991**, *32*, 6797–6800.
135. Hoveyda, A. H.; Xu, Z. M. *J. Am. Chem. Soc.* **1991**, *113*, 5079–5080.
136. Dzhemilev, U. M.; Vostrikova, O. S. *J. Organomet. Chem.* **1985**, *285*, 43–51.
137. Kondo, K.; Murahashi, S. I. *Tetrahedron Lett.* **1979**, 1237–1240.
138. Bonnet, W.; Mongin, F.; Treccourt, F.; Queguiner, G.; Knochel, P. *Tetrahedron Lett.* **2001**, *42*, 5717–5719.
139. Organ, M. G.; Murray, A. P. *J. Org. Chem.* **1997**, *62*, 1523–1526.
140. Uenishi, J.; Kawahama, R.; Izaki, Y.; Yonemitsu, O. *Tetrahedron* **2000**, *56*, 3493–3500.
141. Terao, J.; Watanabe, H.; Ikumi, A.; Kuniyasu, H.; Kambe, N. *J. Am. Chem. Soc.* **2002**, *124*, 4222–4223.
142. Siemsen, P.; Livingston, R. C.; Diederich, F. *Angew. Chem., Int. Ed.* **2000**, *39*, 2633–2657.
143. Jennings, M. P.; Cork, E. A.; Ramachandran, P. V. *J. Org. Chem.* **2000**, *65*, 8763–8766.
144. Dakin, L. A.; Langille, N. F.; Panek, J. S. *J. Org. Chem.* **2002**, *67*, 6812–6815.
145. Wan, W. B.; Chiechi, R. C.; Weakley, T. J. R.; Haley, M. M. *Eur. J. Org. Chem.* **2001**, 3485–3490.
146. Elwahy, A. H. M.; Hafner, K. *Tetrahedron Lett.* **2000**, *41*, 4079–4083.

147. Beletskaya, I. P.; Latyshev, G. V.; Tsvetkov, A. V.; Lukashev, N. V. *Tetrahedron Lett.* **2003**, in print.
148. Lei, A.; Srivastava, M.; Zhang, X. *J. Org. Chem.* **2002**, *67*, 1969–1971.
149. Teply, F.; Stara, I. G.; Stary, I.; Kollarovic, A.; Saman, D.; Fiedler, P. *Tetrahedron* **2002**, *58*, 9007–9018.
150. Grosshenny, V.; Ziessel, R. *Tetrahedron Lett.* **1992**, *33*, 8075–8078.
151. Roy, R.; Das, S. K.; Santoyo-Gonzalez, F.; Hernandez-Mateo, F.; Dam, T. K.; Brewer, C. F. *Chem. Eur. J.* **2000**, *6*, 1757–1762.
152. Alami, M.; Ferri, F.; Linstrumelle, G. *Tetrahedron Lett.* **1993**, *34*, 6403–6406.
153. Pal, M.; Parasuraman, K.; Gupta, S.; Yeleswarapu, K. R. *Synlett* **2002**, 1976–1982.
154. Wu, M. J.; Wei, L. M.; Lin, C. F.; Leou, S. P.; Wei, L. L. *Tetrahedron* **2001**, *57*, 7839–7844.
155. Mori, A.; Kawashima, J.; Shimada, T.; Suguro, M.; Hirabayashi, K.; Nishihara, Y. *Org. Lett.* **2000**, *2*, 2935–2937.
156. Nguefack, J. F.; Bolitt, V.; Sinou, D. *Tetrahedron Lett.* **1996**, *37*, 5527–5530.
157. Taguchi, H.; Ghoroku, K.; Tadaki, M.; Tsubouchi, A.; Takeda, T. *J. Org. Chem.* **2002**, *67*, 8450–8456.
158. Beletskaya, I. P. *J. Organomet. Chem.* **1983**, *250*, 551–564.
159. Beletskaya, I. P.; Tsvetkov, A. V.; Latyshev, G. V.; Tafeenko, V. A.; Lukashev, N. V. *J. Organomet. Chem.* **2001**, *637*, 653–663.
160. Negishi, E.; Baba, S. *J. Chem. Soc., Chem. Commun.* **1976**, 596–597.
161. Zeng, F.; Negishi, E. *Org. Lett.* **2001**, *3*, 719–722.
162. Alami, M.; Peyrat, J. F.; Brion, J. D. *Tetrahedron Lett.* **2002**, *43*, 3007–3009.
163. Saulnier, M. G.; Kadou, J. F.; Tun, M. M.; Langley, D. R.; Vyas, D. M. *J. Am. Chem. Soc.* **1989**, *111*, 8320–8321.
164. Huo, S. Q.; Negishi, E. I. *Org. Lett.* **2001**, *3*, 3253–3256.
165. Gelman, D.; Schumann, H.; Blum, J. *Tetrahedron Lett.* **2000**, *41*, 7555–7558.
166. Mikami, S.; Yorimitsu, H.; Oshima, K. *Synlett* **2002**, 1137–1139.
167. Perez, I.; Sestelo, J. P.; Sarandeses, L. A. *Org. Lett.* **1999**, *1*, 1267–1269.
168. Perez, I.; Sestelo, J. P.; Sarandeses, L. A. *J. Am. Chem. Soc.* **2001**, *123*, 4155–4160.
169. Takami, K.; Yorimitsu, H.; Shinokubo, H.; Matsubara, S.; Oshima, K. *Org. Lett.* **2001**, *3*, 1997–1999.
170. Takami, K.; Yorimitsu, H.; Oshima, K. *Org. Lett.* **2002**, *4*, 2993–2995.
171. Han, J. W.; Tokunaga, N.; Hayashi, T. *Synlett* **2002**, 871–874.
172. Frid, M.; Perez, D.; Peat, A. J.; Buchwald, S. L. *J. Am. Chem. Soc.* **1999**, *121*, 9469–9470.
173. Kang, S. K.; Yoon, S. K. *J. Chem. Soc., Perkin Trans. 1* **2002**, 459–461.
174. Rao, M. L. N.; Yamazaki, O.; Shimada, S.; Tanaka, T.; Suzuki, Y.; Tanaka, M. *Org. Lett.* **2001**, *3*, 4103–4105.
175. Kim, S. H.; Rieke, R. D. *J. Org. Chem.* **2000**, *65*, 2322–2330.
176. Durandetti, M.; Devaud, M.; Perichon, J. *New J. Chem.* **1996**, *20*, 659–667.
177. Budnikova, Y. H.; Perichon, J.; Yakhvarov, D. G.; Kargin, Y. M.; Sinyashin, O. G. *J. Organomet. Chem.* **2001**, *630*, 185–192.
178. Cannes, C.; Labbe, E.; Durandetti, M.; Devaud, M.; Nedelec, J. Y. *J. Electroanal. Chem.* **1996**, *412*, 85–93.
179. Durandetti, M.; Sibille, J.; Nedelec, J. Y.; Perichon, J. *Synth. Commun.* **1994**, *24*, 145–151.
180. Durandetti, M.; Nedelec, J. Y.; Perichon, J. *J. Org. Chem.* **1996**, *61*, 1748–1755.
181. Cannes, C.; Condon, S.; Durandetti, M.; Perichon, J.; Nedelec, J. Y. *J. Org. Chem.* **2000**, *65*, 4575–4583.
182. Gosmini, C.; Lasry, S.; Nedelec, J. Y.; Perichon, J. *Tetrahedron* **1998**, *54*, 1289–1298.
183. Durandetti, M.; Perichon, J.; Nedelec, J. Y. *Tetrahedron Lett.* **1997**, *38*, 8683–8686.
184. Durandetti, M.; Perichon, J.; Nedelec, J. Y. *J. Org. Chem.* **1997**, *62*, 7914–7915.
185. Uno, M.; Seto, K.; Takahashi, S. *J. Chem. Soc., Chem. Commun.* **1984**, *14*, 932–933.
186. Ciufolini, M. A.; Browne, M. E. *Tetrahedron Lett.* **1987**, *28*, 171–174.
187. Ciufolini, M. A.; Qi, H.-B.; Browne, M. E. *J. Org. Chem.* **1988**, *53*, 4149–4151.
188. Satoh, T.; Kawamura, Y.; Miura, M.; Nomura, M. *Angew. Chem., Int. Ed. Engl.* **1997**, *36*, 1740–1742.
189. Satoh, T.; Miura, M.; Nomura, M. *J. Organomet. Chem.* **2002**, *653*, 161–166.
190. Palucki, M.; Buchwald, S. L. *J. Am. Chem. Soc.* **1997**, *119*, 11108–11109.
191. Culkin, D. A.; Hartwig, J. F. *J. Am. Chem. Soc.* **2002**, *124*, 9330–9331.
192. Hamann, B. C.; Hartwig, J. F. *J. Am. Chem. Soc.* **1997**, *119*, 12382–12383.
193. Kawatsura, M.; Hartwig, J. F. *J. Am. Chem. Soc.* **1999**, *121*, 1473–1478.
194. Lee, S.; Beare, N. A.; Hartwig, J. F. *J. Am. Chem. Soc.* **2001**, *123*, 8410–8411.
195. Beare, N. A.; Hartwig, J. F. *J. Org. Chem.* **2002**, *67*, 541–555.
196. Viciu, M. S.; Germaneau, R. F.; Nolan, S. P. *Org. Lett.* **2002**, *4*, 4053–4056.
197. Terao, Y.; Satoh, T.; Miura, M.; Nomura, M. *Tetrahedron Lett.* **1998**, *39*, 6203–6206.
198. Aramendia, M. A.; Borau, V.; Jimenez, C.; Marinas, J. M.; Ruiz, J. R.; Urbano, F. J. *Tetrahedron Lett.* **2002**, *43*, 2847–2849.
199. Kashin, A. N.; Mitin, A. V.; Beletskaya, I. P.; Wife, R. *Tetrahedron Lett.* **2002**, *43*, 2539–2542.
200. Inoh, J.-I.; Satoh, T.; Pivsa-Art, S.; Miura, M.; Nomura, M. *Tetrahedron Lett.* **1998**, *39*, 4673–4676.
201. Terao, Y.; Fukuoka, Y.; Satoh, T.; Miura, M.; Nomura, M. *Tetrahedron Lett.* **2002**, *43*, 101–104.
202. Ahman, J.; Wolfe, J. P.; Troutman, M. V.; Palucki, M.; Buchwald, S. L. *J. Am. Chem. Soc.* **1998**, *120*, 1918–1919.
203. Hamada, T.; Chieffi, A.; Ahman, J.; Buchwald, S. L. *J. Am. Chem. Soc.* **2002**, *124*, 1261–1268.
204. Hamada, T.; Buchwald, S. L. *Org. Lett.* **2002**, *4*, 999–1001.
205. Dyker, G.; Heiermann, J.; Miura, M.; Inoh, J. I.; Pivsa-Art, S.; Satoh, T.; Nomura, M. *Chem.-Eur. J.* **2000**, *6*, 3426–3433.
206. Dyker, G.; Borowski, S.; Heiermann, J.; Korning, J.; Opwis, K.; Henkel, G.; Kockerling, M. *J. Organomet. Chem.* **2000**, *606*, 108–111.
207. Satoh, T.; Inoh, J.-I.; Kawamura, Y.; Miura, M.; Nomura, M. *Bull. Soc. Chem. Jpn* **1998**, *71*, 2239–2246.
208. Kawamura, Y.; Satoh, T.; Miura, M.; Nomura, M. *Chem. Lett.* **1999**, 961–962.
209. Kawamura, Y.; Satoh, T.; Miura, M.; Nomura, M. *Chem. Lett.* **1998**, 931–932.
210. Farina, V. *Pure Appl. Chem.* **1996**, *68*, 73–78.
211. Liebeskind, L. S.; Fengl, R. W. *J. Org. Chem.* **1990**, *55*, 5359–5364.
212. Han, X. J.; Stoltz, B. M.; Corey, E. J. *J. Am. Chem. Soc.* **1999**, *121*, 7600–7605.
213. Gabarda, A. E.; Du, W.; Isarno, T.; Tangirala, R. S.; Curran, D. P. *Tetrahedron* **2002**, *58*, 6329–6341.

214. Wong, L. S. M.; Sharp, L. A.; Xavier, N. M. C.; Turner, P.; Sherburn, M. S. *Org. Lett.* **2002**, *4*, 1955–1957.
215. Sugiyama, H.; Yokokawa, F.; Shioiri, T. *Org. Lett.* **2000**, *2*, 2149–2152.
216. Minière, S.; Cintrat, J. C. *J. Org. Chem.* **2001**, *66*, 7385–7388.
217. Tivola, P. B.; Deagostino, A.; Prandi, C.; Venturello, P. *J. Chem. Soc., Perkin Trans. 1* **2001**, 437–441.
218. Lebsack, A. D.; Link, J. T.; Overman, L. E.; Stearns, B. A. *J. Am. Chem. Soc.* **2002**, *124*, 9008–9009.
219. Gronowitz, S.; Bjork, P.; Malm, J.; Hornfeldt, A. B. *J. Organomet. Chem.* **1993**, *460*, 127–129.
220. Clapham, B.; Sutherland, A. J. *J. Org. Chem.* **2001**, *66*, 9033–9037.
221. Larhed, M.; Hoshino, M.; Hadida, S.; Curran, D. P.; Hallberg, A. *J. Org. Chem.* **1997**, *62*, 5583–5587.
222. Savarin, C.; Liebeskind, L. S. *Org. Lett.* **2001**, *3*, 2149–2152.
223. Uenishi, J.; Beau, J. M.; Armstrong, R. W.; Kishi, Y. *J. Am. Chem. Soc.* **1987**, *109*, 4756–4758.
224. Frank, S. A.; Chen, H.; Kunz, R. K.; Schnaderbeck, M. J.; Roush, W. R. *Org. Lett.* **2000**, *2*, 2691–2694.
225. Sato, M.; Miyaura, N.; Suzuki, A. *Chem. Lett.* **1989**, 1405–1408.
226. Frank, S. A.; Roush, W. R. *J. Org. Chem.* **2002**, *67*, 4316–4324.
227. Evans, D. A.; Starr, J. T. *Angew. Chem., Int. Ed.* **2002**, *41*, 1787–1790.
228. Chemler, S. R.; Danishefsky, S. J. *Org. Lett.* **2000**, *2*, 2695–2698.
229. Zou, G.; Reddy, Y. K.; Falck, J. R. *Tetrahedron Lett.* **2001**, *42*, 7213–7215.
230. Occhiato, E. G.; Trabocchi, A.; Guarna, A. *J. Org. Chem.* **2001**, *66*, 2459–2465.
231. Mu, Y. Q.; Gibbs, R. A. *Tetrahedron Lett.* **1995**, *36*, 5669–5672.
232. Mu, Y. Q.; Eubanks, L. M.; Poulter, C. D.; Gibbs, R. A. *Bioorg. Med. Chem.* **2002**, *10*, 1207–1219.
233. Allred, G. D.; Liebeskind, L. S. *J. Am. Chem. Soc.* **1996**, *118*, 2748–2749.
234. Zhang, S. J.; Marshall, D.; Liebeskind, L. S. *J. Org. Chem.* **1999**, *64*, 2796–2804.
235. Barros, M. T.; Maycock, C. D.; Madureira, M. I.; Ventura, M. R. *J. Chem. Soc., Chem. Commun.* **2001**, 1662–1663.
236. Ito, S. J.; Okujima, T.; Morita, N. *J. Chem. Soc., Perkin Trans. 1* **2002**, 1896–1905.
237. Grasa, G. A.; Nolan, S. P. *Org. Lett.* **2001**, *3*, 119–122.
238. Littke, A. F.; Fu, G. C. *Angew. Chem., Int. Ed. Engl.* **1999**, *38*, 2411–2413.
239. Fugami, K.; Ohnuma, S.; Kameyama, M.; Saotome, T.; Kosugi, M. *Synlett* **1999**, 63–64.
240. Wright, S. W.; Hageman, D. L.; McClure, L. D. *J. Org. Chem.* **1994**, *59*, 6095–6097.
241. Eriksson, L.; Beletskaya, I. P.; Bregadze, V. I.; Sivaev, I. B.; Sjöberg, S. *J. Organomet. Chem.* **2002**, *657*, 267–272.
242. Zhang, J.; Blazevcka, P. G.; Belmont, D.; Davidson, J. G. *Org. Lett.* **2002**, *4*, 4559–4561.
243. Gauthier, D. R.; Szumigala, R. H.; Dormer, P. G.; Armstrong, J. D.; Volante, R. P.; Reider, P. J. *Org. Lett.* **2002**, *4*, 375–378.
244. Bykov, V. V.; Bumagin, N. A.; Beletskaya, I. P. *Dokl. Akad. Nauk* **1995**, *340*, 775–778.
245. Furstner, A.; Seidel, G. *Tetrahedron* **1995**, *51*, 11165–11176.
246. Zou, G.; Falck, J. R. *Tetrahedron Lett.* **2001**, *42*, 5817–5819.
247. Oh, C. H.; Jung, S. H. *Tetrahedron Lett.* **2000**, *41*, 8513–8516.
248. Molander, G. A.; Ito, T. *Org. Lett.* **2001**, *3*, 393–396.
249. Molander, G. A.; Rivero, M. R. *Org. Lett.* **2002**, *4*, 107–109.
250. Molander, G. A.; Katona, B. W.; Machrouhi, F. *J. Org. Chem.* **2002**, *67*, 8416–8423.
251. Martinez, A. G.; Barcina, J. O.; Heras, M. D. C.; Cerezo, A. D. *Organometallics* **2001**, *20*, 1020–1023.
252. Roshchin, A. I.; Bumagin, N. A.; Beletskaya, I. P. *Tetrahedron Lett.* **1995**, *36*, 125–128.
253. Rai, R.; Aubrecht, K. B.; Collum, D. B. *Tetrahedron Lett.* **1995**, *36*, 3111–3114.
254. Gelman, D.; Tsvetikhovskiy, D.; Molander, G. A.; Blum, J. *J. Org. Chem.* **2002**, *67*, 6287–6290.
255. Dominguez, B.; Pazos, Y.; de Lera, A. R. *J. Org. Chem.* **2000**, *65*, 5917–5925.
256. Brown, J. M.; Pearson, M.; Jastrzebski, J.; Vankoten, G. *J. Chem. Soc., Chem. Commun.* **1992**, 1440–1441.
257. Itami, K.; Kamei, T.; Yoshida, J. *J. Am. Chem. Soc.* **2001**, *123*, 8773–8779.
258. Vedejs, E.; Haight, A. R.; Moss, W. O. *J. Am. Chem. Soc.* **1992**, *114*, 6556–6558.
259. Han, X. J.; Hartmann, G. A.; Brazzale, A.; Gaston, R. D. *Tetrahedron Lett.* **2001**, *42*, 5837–5839.
260. Kosugi, M.; Tanji, T.; Tanaka, Y.; Yoshida, A.; Fugami, K.; Kameyama, K.; Migita, T. *J. Organomet. Chem.* **1996**, *508*, 255–257.
261. Faller, J. W.; Kultyshev, R. G.; Parr, J. *Tetrahedron Lett.* **2003**, *44*, 451–453.
262. Jaber, N.; Gelman, D.; Schumann, H.; Dechert, S.; Blum, J. *Eur. J. Org. Chem.* **2002**, 1628–1633.
263. Gelman, D.; Dechert, S.; Schumann, H.; Blum, J. *Inorg. Chim. Acta* **2002**, *334*, 149–158.
264. Gelman, D.; Hohne, G.; Schumann, H.; Blum, J. *Synthesis* **2001**, 591–594.
265. Blum, J.; Gelman, D.; Baidossi, W.; Shakh, E.; Rosenfeld, A.; Aizenshtat, Z.; Wassermann, B. C.; Frick, M.; Heymer, B.; Schutte, S.; Wernik, S.; Schumann, H. *J. Org. Chem.* **1997**, *62*, 8681–8686.
266. Rao, M. L. N.; Shimada, S.; Yamazaki, O.; Tanaka, M. *J. Organomet. Chem.* **2002**, *659*, 117–120.
267. Rao, M. L. N.; Shimada, S.; Tanaka, M. *Org. Lett.* **1999**, *1*, 1271–1273.
268. Hatanaka, Y.; Goda, K.; Okahara, Y.; Hiyama, T. *Tetrahedron* **1994**, *50*, 8301–8316.
269. Hatanaka, Y.; Goda, K.; Hiyama, T. *Tetrahedron Lett.* **1994**, *35*, 6511–6514.
270. Hatanaka, Y.; Goda, K.; Hiyama, T. *J. Organomet. Chem.* **1994**, *465*, 97–100.
271. Hatanaka, Y.; Goda, K.; Hiyama, T. *Tetrahedron Lett.* **1994**, *35*, 1279–1282.
272. Hiyama, T.; Hatanaka, Y. *Pure Appl. Chem.* **1994**, *66*, 1471–1478.
273. Mateo, C.; Fernandez-Rivas, C.; Cardenas, D. J.; Echavarren, A. M. *Organometallics* **1998**, *17*, 3661–3669.
274. Hirabayashi, E.; Mori, A.; Kawashima, J.; Suguro, M.; Nishihara, Y.; Hiyama, T. *J. Org. Chem.* **2000**, *65*, 5342–5349.
275. Huang, T. S.; Li, C. J. *Tetrahedron Lett.* **2002**, *43*, 403–405.
276. Denmark, S. E.; Sweis, R. F. *J. Am. Chem. Soc.* **2001**, *123*, 6439–6440.
277. Denmark, S. E.; Neuville, L. *Org. Lett.* **2000**, *2*, 3221–3224.
278. Denmark, S. E.; Wang, Z. G. *Org. Lett.* **2001**, *3*, 1073–1076.
279. Denmark, S. E.; Pan, W. T. *Org. Lett.* **2001**, *3*, 61–64.
280. Denmark, S. E.; Wang, Z. G. *J. Organomet. Chem.* **2001**, *624*, 372–375.
281. Tamao, K.; Kobayashi, K.; Ito, Y. *Tetrahedron Lett.* **1989**, *30*, 6051–6054.
282. Shibata, K.; Miyazawa, K.; Goto, Y. *J. Chem. Soc., Chem. Commun.* **1997**, 1309–1310.

283. Mowery, M. E.; DeShong, P. *J. Org. Chem.* **1999**, *64*, 1684–1688.
284. Chang, S.; Yang, S. H.; Lee, P. H. *Tetrahedron Lett.* **2001**, *42*, 4833–4835.
285. Yoshida, J.; Tamao, K.; Yamamoto, H.; Kakui, T.; Uchida, T.; Kumada, M. *Organometallics* **1982**, *1*, 542–549.
286. Hallberg, A.; Westerlund, C. *Chem. Lett.* **1982**, 1993–1994.
287. Denmark, S. E.; Wehrli, D.; Choi, J. Y. *Org. Lett.* **2000**, *2*, 2491–2494.
288. Denmark, S. E.; Wu, Z. C. *Org. Lett.* **1999**, *1*, 1495–1498.
289. Denmark, S. E.; Choi, J. Y. *J. Am. Chem. Soc.* **1999**, *121*, 5821–5822.
290. Itami, K.; Nokami, T.; Yoshida, J. *J. Am. Chem. Soc.* **2001**, *123*, 5600–5601.
291. Hosoi, K.; Nozaki, K.; Hiyama, T. *Chem. Lett.* **2002**, 138–139.
292. Itami, K.; Mineno, M.; Kamei, T.; Yoshida, J. *Org. Lett.* **2002**, *4*, 3635–3638.
293. Nakamura, T.; Kinoshita, H.; Shinokubo, H.; Oshima, K. *Org. Lett.* **2002**, *4*, 3165–3167.
294. Hagiwara, E.; Gouda, K.; Hatanaka, Y.; Hiyama, T. *Tetrahedron Lett.* **1997**, *38*, 439–442.
295. Takahashi, K.; Minami, T.; Ohara, Y.; Hiyama, T. *Bull. Chem. Soc. Jpn.* **1995**, *68*, 2649–2656.
296. Minami, T.; Nishimoto, A.; Hanaoka, M. *Tetrahedron Lett.* **1995**, *36*, 9505–9508.
297. Matsuhashi, H.; Hatanaka, Y.; Kuroboshi, M.; Hiyama, T. *Heterocycles* **1996**, *42*, 375–384.
298. Kamikawa, T.; Hayashi, T. *Tetrahedron Lett.* **1997**, *38*, 7087–7090.
299. Wilhelm, R.; Widdowson, D. A. *J. Chem. Soc., Perkin Trans. 1* **2000**, 3808–3813.
300. Herrmann, W. A.; Bohm, V. P. W.; Reisinger, C. P. *J. Organomet. Chem.* **1999**, *576*, 23–41.
301. Muller, T. J. J.; Ansorge, M.; Lindner, H. J. *Chem. Ber.-Recl.* **1996**, *129*, 1433–1440.
302. Muller, T. J. J.; Lindner, H. J. *Chem. Berichte* **1996**, *129*, 607–613.
303. Muller, T. J. J.; Ansorge, M. *Chem. Ber.-Recl.* **1997**, *130*, 1135–1139.
304. Uemura, M.; Miyake, R.; Nishimura, H.; Matsumoto, Y.; Hayashi, T. *Tetrahedron: Asymmetry* **1992**, *3*, 213–216.
305. Uemura, M.; Nishimura, H.; Hayashi, T. *Tetrahedron Lett.* **1993**, *34*, 107–110.
306. Uemura, M.; Nishimura, H.; Hayashi, T. *J. Organomet. Chem.* **1994**, *473*, 129–137.
307. Nelson, S. G.; Hilfiker, M. A. *Org. Lett.* **1999**, *1*, 1379–1382.
308. Mitchell, M. B.; Wallbank, P. J. *Tetrahedron Lett.* **1991**, *32*, 2273–2276.
309. Ali, N. M.; McKillop, A.; Mitchell, M. B.; Rebelo, R. A.; Wallbank, P. J. *Tetrahedron* **1992**, *48*, 8117–8126.
310. Alcock, N. W.; Brown, J. M.; Hulmes, D. I. *Tetrahedron: Asymmetry* **1993**, *4*, 743–756.
311. Janietz, D.; Bauer, M. *Synthesis* **1993**, 33–34.
312. Shen, W. *Tetrahedron Lett.* **1997**, *38*, 5575–5578.
313. Saito, S.; Ohtani, S.; Miyaura, N. *J. Org. Chem.* **1997**, *62*, 8024–8030.
314. Indolese, A. F. *Tetrahedron Lett.* **1997**, *38*, 3513–3516.
315. Galland, J. C.; Savignac, M.; Genet, J. P. *Tetrahedron Lett.* **1999**, *40*, 2323–2326.
316. Shirakawa, E.; Yamasaki, K.; Hiyama, T. *Synthesis* **1998**, 1544–1549.
317. Roth, G. P.; Fuller, C. E. *J. Org. Chem.* **1991**, *56*, 3493–3496.
318. Pridgen, L. N.; Huang, G. K. *Tetrahedron Lett.* **1998**, *39*, 8421–8424.
319. Rottlander, M.; Knochel, P. *J. Org. Chem.* **1998**, *63*, 203–208.
320. Rottlander, M.; Palmer, N.; Knochel, P. *Synlett* **1996**, 573–&.
321. Bellina, F.; Ciucci, D.; Rossi, R.; Vergamini, P. *Tetrahedron* **1999**, *55*, 2103–2112.
322. Percec, V.; Bae, J. Y.; Hill, D. H. *J. Org. Chem.* **1995**, *60*, 6895–6903.
323. Percec, V.; Bae, J. Y.; Hill, D. H. *J. Org. Chem.* **1995**, *60*, 1060–1065.
324. Kobayashi, Y.; Mizojiri, R. *Tetrahedron Lett.* **1996**, *37*, 8531–8534.
325. Kobayashi, Y.; William, A. D.; Mizojiri, R. *J. Organomet. Chem.* **2002**, *653*, 91–97.
326. Zim, D.; Lando, V. R.; Dupont, J.; Monteiro, A. L. *Org. Lett.* **2001**, *3*, 3049–3051.
327. Nagatsugi, F.; Uemura, K.; Nakashima, S.; Maeda, M.; Sasaki, S. *Tetrahedron Lett.* **1995**, *36*, 421–424.
328. Wu, J.; Liao, Y.; Yang, Z. *J. Org. Chem.* **2001**, *66*, 3642–3645.
329. Wu, J.; Wang, L.; Fathi, R.; Yang, Z. *Tetrahedron Lett.* **2002**, *43*, 4395–4397.
330. Schio, L.; Chatreaux, F.; Klich, M. *Tetrahedron Lett.* **2000**, *41*, 1543–1547.
331. Castulik, J.; Mazal, C. *Tetrahedron Lett.* **2000**, *41*, 2741–2744.
332. Miller, J. A. *Tetrahedron Lett.* **2002**, *43*, 7111–7114.
333. Sofia, A.; Karlstrom, E.; Itami, K.; Backvall, J. E. *J. Org. Chem.* **1999**, *64*, 1745–1749.
334. Wu, J.; Yang, Z. *J. Org. Chem.* **2001**, *66*, 7875–7878.
335. Brigas, A. F.; Johnstone, R. A. W. *J. Chem. Soc., Perkin Trans. 1* **2000**, *11*, 1735–1739.
336. Okamura, H.; Miura, M.; Takei, H. *Tetrahedron Lett.* **1979**, 43–46.
337. Fiandanese, V.; Marchese, G.; Naso, F.; Ronzini, L. *J. Chem. Soc., Chem. Commun.* **1982**, 647–649.
338. Shimada, T.; Cho, Y. H.; Hayashi, T. *J. Am. Chem. Soc.* **2002**, *124*, 13396–13397.
339. Angiolelli, M. E.; Casalnuovo, A. L.; Selby, T. P. *Synlett* **2000**, 905–907.
340. Savarin, C.; Srogl, J.; Liebeskind, L. S. *Org. Lett.* **2001**, *3*, 91–93.
341. Liebeskind, L. S.; Srogl, J. *Org. Lett.* **2002**, *4*, 979–981.
342. Alphonse, F. A.; Suzenet, F.; Keromnes, A.; Lebret, B.; Guillaumet, G. *Synlett* **2002**, 447–450.
343. Kusturin, C. L.; Liebeskind, L. S.; Neumann, W. L. *Org. Lett.* **2002**, *4*, 983–985.
344. Mori, Y.; Seki, M. *Heterocycles* **2002**, *58*, 125–127.
345. Tokuyama, H.; Yokoshima, S.; Yamashita, T.; Fukuyama, T. *Tetrahedron Lett.* **1998**, *39*, 3189–3192.
346. Srogl, J.; Liu, W. S.; Marshall, D.; Liebeskind, L. S. *J. Am. Chem. Soc.* **1999**, *121*, 9449–9450.
347. Srogl, J.; Allred, G. D.; Liebeskind, L. S. *J. Am. Chem. Soc.* **1997**, *119*, 12376–12377.
348. Savarin, C.; Srogl, J.; Liebeskind, L. S. *Org. Lett.* **2000**, *2*, 3229–3231.
349. Dabdoub, M. J.; Dabdoub, V. B.; Marino, J. P. *Tetrahedron Lett.* **2000**, *41*, 437–440.
350. Dabdoub, M. J.; Dabdoub, V. B.; Marino, J. P. *Tetrahedron Lett.* **2000**, *41*, 433–436.
351. Braga, A. L.; Vargas, F.; Zeni, G.; Silveira, C. C.; de Andrade, L. H. *Tetrahedron Lett.* **2002**, *43*, 4399–4402.
352. Silveira, C. C.; Santos, P. C. S.; Braga, A. L. *Tetrahedron Lett.* **2002**, *43*, 7517–7520.
353. Barrientos-Astigarraga, R. E.; Castalani, P.; Comasseto, J. V.; Formiga, H. B.; da Silva, N. C.; Sumida, C. Y.; Vieira, M. L. *J. Organomet. Chem.* **2001**, *623*, 43–47.
354. Zeni, G.; Perin, G.; Cella, R.; Jacob, R. G.; Braga, A. L.; Silveira, C. C.; Stefani, H. A. *Synlett* **2002**, 975–977.

355. Hevesi, L.; Hermans, B.; Allard, C. *Tetrahedron Lett.* **1994**, *35*, 6729–6730.
356. Ritter, K. *Synthesis* **1993**, 735–762.
357. Kang, S. K.; Hong, Y. T.; Kim, D. H.; Lee, S. H. *J. Chem. Res.—S* **2001**, 283–285.
358. Kang, S. K.; Lee, S. W.; Ryu, H. C. *J. Chem. Soc., Chem. Commun.* **1999**, 2117–2118.
359. Braga, A. L.; Luedtke, D. S.; Vargas, F.; Donato, R. K.; Silveira, C. C.; Stefanib, H. A.; Zenia, G. *Tetrahedron Lett.* **2003**, *44*, 1779–1781.
360. Kang, S. K.; Ryu, H. C.; Choi, S. C. *J. Chem. Soc., Chem. Commun.* **1998**, 1317–1318.
361. Kang, S. K.; Ryu, H. C.; Son, H. J. *Synlett* **1998**, 771–773.
362. Kang, S. K.; Ryu, H. C.; Lee, S. H. *Synth. Commun.* **2001**, *31*, 1059–1064.
363. Kang, S. K.; Ryu, H. C.; Lee, S. W. *Synth. Commun.* **2001**, *31*, 1027–1034.
364. Kang, S. K.; Ryu, H. C.; Hong, Y. T. *J. Chem. Soc., Perkin Trans. 1* **2001**, 736–739.
365. Kang, S. K.; Ryu, H. C.; Lee, S. W. *J. Organomet. Chem.* **2000**, *610*, 38–41.
366. Kang, S. K.; Ryu, H. C.; Kim, J. W. *Synth. Commun.* **2001**, *31*, 1021–1026.
367. Kang, S. K.; Lee, S. W.; Kim, M. S.; Kwon, H. S. *Synth. Commun.* **2001**, *31*, 1721–1725.
368. Kang, S. K.; Choi, S. C.; Baik, T. G. *Synth. Commun.* **1999**, *29*, 2493–2499.
369. Andrus, M. B.; Song, C. *Org. Lett.* **2001**, *3*, 3761–3764.
370. Selvakumar, K.; Zapf, A.; Spannenberg, A.; Beller, M. *Chem. Eur. J.* **2002**, *8*, 3901–3906.
371. Willis, D. M.; Strongin, R. M. *Tetrahedron Lett.* **2000**, *41*, 6271–6274.
372. Darses, S.; Michaud, G.; Genet, J. P. *Tetrahedron Lett.* **1998**, *39*, 5045–5048.
373. Darses, S.; Jeffery, T.; Brayer, J. L.; Demoute, J. P.; Genet, J. P. *Bull. Soc. Chim. Fr.* **1996**, *133*, 1095–1102.
374. Radhakrishnan, U.; Stang, P. J. *Org. Lett.* **2001**, *3*, 859–860.
375. Kang, S. K.; Lee, H. W.; Jang, S. B.; Ho, P. S. *J. Chem. Soc., Chem. Commun.* **1996**, 835–836.
376. Kang, S. K.; Lee, Y. T.; Lee, S. H. *Tetrahedron Lett.* **1999**, *40*, 3573–3576.
377. Kang, S. K.; Lee, H. W.; Jang, S. B.; Kim, T. H.; Kim, J. S. *Synth. Commun.* **1996**, *26*, 4311–4318.
378. Kang, S. K.; Lee, H. W.; Kim, J. S.; Choi, S. C. *Tetrahedron Lett.* **1996**, *37*, 3723–3726.
379. Kang, S. K.; Yoon, S. K.; Lim, K. H.; Son, H. J.; Baik, T. G. *Synth. Commun.* **1998**, *28*, 3645–3655.
380. Kang, S. K.; Yamaguchi, T.; Kim, T. H.; Ho, P. S. *J. Org. Chem.* **1996**, *61*, 9082–9083.
381. Kang, S. K.; Lee, H. W.; Jang, S. B.; Ho, P. S. *J. Org. Chem.* **1996**, *61*, 4720–4724.
382. Kang, S. K.; Yamaguchi, T.; Ho, P. S.; Kim, W. Y.; Yoon, S. K. *Tetrahedron Lett.* **1997**, *38*, 1947–1950.
383. Kang, S. K.; Yamaguchi, T.; Hong, R. K.; Kim, T. H.; Pyun, S. J. *Tetrahedron* **1997**, *53*, 3027–3034.
384. Casares, J. A.; Espinet, P.; Salas, G. *Chem. Eur. J.* **2002**, *8*, 4843–4853.
385. Andersen, N. G.; Keay, B. A. *Chem. Rev.* **2001**, *101*, 997–1030.
386. Pickett, T. E.; Roca, F. X.; Richards, C. J. *J. Org. Chem.* **2003**, *68*, 2592–2599.
387. Littke, A. F.; Dai, C. Y.; Fu, G. C. *J. Am. Chem. Soc.* **2000**, *122*, 4020–4028.
388. Stambuli, J. P.; Buhl, M.; Hartwig, J. F. *J. Am. Chem. Soc.* **2002**, *124*, 9346–9347.
389. Stambuli, J. P.; Kuwano, R.; Hartwig, J. F. *Angew. Chem. Intl. Ed. Engl.* **2002**, *41*, 4746–4748.
390. Kamikawa, T.; Hayashi, T. *J. Org. Chem.* **1998**, *63*, 8922–8925.
391. Bei, X. H.; Turner, H. W.; Weinberg, W. H.; Guram, A. S.; Petersen, J. L. *J. Org. Chem.* **1999**, *64*, 6797–6803.
392. Schareina, T.; Kempe, R. *Angew. Chem., Intl. Ed. Engl.* **2002**, *41*, 1521–1523.
393. Clarke, M. L.; Cole-Hamilton, D. J.; Woollins, J. D. *J. Chem. Soc., Dalton Trans.* **2001**, 2721–2723.
394. Old, D. W.; Wolfe, J. P.; Buchwald, S. L. *J. Am. Chem. Soc.* **1998**, *120*, 9722–9723.
395. Kocovsky, P.; Vyskocil, S.; Cisarova, I.; Sejbál, J.; Tislerova, I.; Smrcina, M.; Lloyd-Jones, G. C.; Stephen, S. C.; Butts, C. P.; Murray, M.; Langer, V. *J. Am. Chem. Soc.* **1999**, *121*, 7714–7715.
396. Kamikawa, T.; Uozumi, Y.; Hayashi, T. *Tetrahedron Lett.* **1996**, *37*, 3161–3164.
397. Yin, J. J.; Buchwald, S. L. *J. Am. Chem. Soc.* **2000**, *122*, 12051–12052.
398. Yin, J. J.; Rainka, M. P.; Zhang, X. X.; Buchwald, S. L. *J. Am. Chem. Soc.* **2002**, *124*, 1162–1163.
399. Grushin, V. V.; Alper, H. *J. Chem. Soc., Chem. Commun.* **1992**, 611.
400. Netherton, M. R.; Fu, G. C. *Org. Lett.* **2001**, *3*, 4295–4298.
401. Bedford, R. B.; Hazelwood, S. L.; Limmert, M. E. *J. Chem. Soc., Chem. Commun.* **2002**, 2610–2611.
402. Bedford, R. B.; Cazin, C. S. J.; Hazelwood, S. L. *J. Chem. Soc., Chem. Commun.* **2002**, 2608–2609.
403. Littke, A. F.; Schwarz, L.; Fu, G. C. *J. Am. Chem. Soc.* **2002**, *124*, 6343–6348.
404. Dai, C. Y.; Fu, G. C. *J. Am. Chem. Soc.* **2001**, *123*, 2719–2724.
405. Bohm, V. P. W.; Herrmann, W. A. *Eur. J. Org. Chem.* **2000**, 3679–3681.
406. Hundertmark, T.; Littke, A. F.; Buchwald, S. L.; Fu, G. C. *Org. Lett.* **2000**, *2*, 1729–1731.
407. Gouda, K.; Hagiwara, E.; Hatanaka, Y.; Hiyama, T. *J. Org. Chem.* **1996**, *61*, 7232–7233.
408. Frisch, A. C.; Shaikh, N.; Zapf, A.; Beller, M. *Angew. Chem., Int. Ed.* **2002**, *41*, 4056–4059.
409. Netherton, M. R.; Dai, C. Y.; Neuschütz, K.; Fu, G. C. *J. Am. Chem. Soc.* **2001**, *123*, 10099–10100.
410. Kirchhoff, J. H.; Dai, C. Y.; Fu, G. C. *Angew. Chem., Int. Ed. Engl.* **2002**, *41*, 1945–1947.
411. Kirchhoff, J. H.; Netherton, M. R.; Hills, I. D.; Fu, G. C. *J. Am. Chem. Soc.* **2002**, *124*, 13662–13663.
412. Zhu, Q.; Wu, J.; Fathi, R.; Yang, Z. *Org. Lett.* **2002**, *4*, 3333–3336.
413. Schnyder, A.; Indolese, A. E.; Studer, M.; Blaser, H. *Angew. Chem., Int. Ed. Engl.* **2002**, *41*, 3668–3671.
414. Baudoin, O.; Cesario, M.; Guenard, D.; Gueritte, F. *J. Org. Chem.* **2002**, *67*, 1199–1207.
415. Kataoka, N.; Shelby, Q.; Stambuli, J. P.; Hartwig, J. F. *J. Org. Chem.* **2002**, *67*, 5553–5566.
416. Planas, J. G.; Gladysz, J. A. *Inorg. Chem.* **2002**, *41*, 6947–6949.
417. Sava, X.; Ricard, L.; Mathey, F.; Le Floch, P. *Organometallics* **2000**, *19*, 4899–4903.
418. Li, G. Y.; Zheng, G.; Noonan, A. F. *J. Org. Chem.* **2001**, *66*, 8677–8681.
419. Li, G. Y. *Angew. Chem., Int. Ed. Engl.* **2001**, *40*, 1513–1516.
420. Li, G. Y.; Marshall, W. J. *Organometallics* **2002**, *21*, 590–591.
421. Urgaonkar, S.; Nagarajan, M.; Verkade, J. G. *Tetrahedron Lett.* **2002**, *43*, 8921–8924.
422. Toyota, K.; Masaki, K.; Abe, T.; Yoshifuji, M. *Chem. Lett.* **1995**, 221–222.
423. Kamer, P. C. J.; van Leeuwen, P. W. N.; Reek, J. N. H. *Acc. Chem. Res.* **2001**, *34*, 895–904.
424. van Leeuwen, P.; Kamer, P. C. J.; Reek, J. N. H.; Dierkes, P. *Chem. Rev.* **2000**, *100*, 2741–2769.
425. Casey, C. P.; Whiteker, G. T. *Isr. J. Chem.* **1990**, *30*, 299–304.

426. Dierkes, P.; van Leeuwen, P. *J. Chem. Soc., Dalton Trans.* **1999**, 1519–1529.
427. Kransenburg, M.; Kamer, P. C. J.; van Leeuwen, P. *Eur. J. Inorg. Chem.* **1998**, 155–157.
428. Ogasawara, M.; Yoshida, K.; Hayashi, T. *Organometallics* **2000**, *19*, 1567–1571.
429. Doherty, S.; Robins, E. G.; Nieuwenhuyzen, M.; Knight, J. G.; Champkin, P. A.; Clegg, W. *Organometallics* **2002**, *21*, 1383–1399.
430. Feuerstein, M.; Doucet, H.; Santelli, M. *Tetrahedron Lett.* **2001**, *42*, 5659–5662.
431. Castanet, A. S.; Colobert, F.; Broutin, P. E.; Obringier, M. *Tetrahedron: Asymmetry* **2002**, *13*, 659–665.
432. Beller, M.; Fischer, H.; Herrmann, W. A.; Ofele, K.; Brossmer, C. *Angew. Chem., Int. Ed. Engl.* **1995**, *34*, 1848–1849.
433. Eberhard, M. R.; Wang, Z. H.; Jensen, C. M. *J. Chem. Soc., Chem. Commun.* **2002**, 818–819.
434. Albisson, D. A.; Bedford, R. B.; Lawrence, S. E.; Scully, P. N. *J. Chem. Soc., Chem. Commun.* **1998**, 2095–2096.
435. Bedford, R. B.; Welch, S. L. *J. Chem. Soc., Chem. Commun.* **2001**, 129–130.
436. Munoz, M. P.; Martin-Matute, B.; Fernandez-Rivas, C.; Cardenas, D. J.; Echavarren, A. M. *Adv. Synth. Catal.* **2001**, *343*, 338–342.
437. Weissman, H.; Milstein, D. *J. Chem. Soc., Chem. Commun.* **1999**, 1901–1902.
438. Zim, D.; Gruber, A. S.; Ebeling, G.; Dupont, J.; Monteiro, A. L. *Org. Lett.* **2000**, *2*, 2881–2884.
439. Alonso, D. A.; Najera, C.; Pacheco, M. C. *J. Org. Chem.* **2002**, *67*, 5588–5594.
440. Alonso, D. A.; Najera, C.; Pacheco, M. C. *Org. Lett.* **2000**, *2*, 1823–1826.
441. Alonso, D. A.; Najera, C.; Pacheco, M. C. *Tetrahedron Lett.* **2002**, *43*, 9365–9368.
442. Tao, B.; Boykin, D. W. *Tetrahedron Lett.* **2002**, *43*, 4955–4957.
443. Vanasselt, R.; Elsevier, C. J.; Smeets, W. J. J.; Spek, A. L. *Inorg. Chem.* **1994**, *33*, 1521–1531.
444. Vanasselt, R.; Elsevier, C. J. *Organometallics* **1994**, *13*, 1972–1980.
445. Vanasselt, R.; Elsevier, C. J. *Tetrahedron* **1994**, *50*, 323–334.
446. Elsevier, C. J. *Coord. Chem. Rev.* **1999**, *186*, 809–822.
447. Dol, G. C.; Kamer, P. C. J.; van Leeuwen, P. *Eur. J. Org. Chem.* **1998**, 359–364.
448. Grasa, G. A.; Hillier, A. C.; Nolan, S. P. *Org. Lett.* **2001**, *3*, 1077–1080.
449. Buchmeiser, M. R. *Bioorg. Med. Chem. Lett.* **2002**, *12*, 1837–1840.
450. Buchmeiser, M. R.; Schareina, T.; Kempe, R.; Wurst, K. *J. Organomet. Chem.* **2001**, *634*, 39–46.
451. Herrmann, W. A.; Elison, M.; Fischer, J.; Kocher, C.; Artus, G. R. *J. Angew. Chem., Int. Ed. Engl.* **1995**, *34*, 2371–2374.
452. Cesar, V.; Bellemin-Lapponnaz, S.; Gade, L. H. *Organometallics* **2002**, *21*, 5204–5208.
453. Herrmann, W. A.; Reisinger, C. P.; Spiegler, M. *J. Organomet. Chem.* **1998**, *557*, 93–96.
454. Bohm, V. P. W.; Gstottmayr, C. W. K.; Weskamp, T.; Herrmann, W. A. *J. Organomet. Chem.* **2000**, *595*, 186–190.
455. Herrmann, W. A.; Bohm, V. P. W.; Gstottmayr, C. W. K.; Grosche, M.; Reisinger, C. P.; Weskamp, T. *J. Organomet. Chem.* **2001**, *617*, 616–628.
456. McGuinness, D. S.; Cavell, K. J.; Skelton, B. W.; White, A. H. *Organometallics* **1999**, *18*, 1596–1605.
457. McGuinness, D. S.; Cavell, K. J. *Organometallics* **2000**, *19*, 741–748.
458. Loch, J. A.; Albrecht, M.; Peris, E.; Mata, J.; Faller, J. W.; Crabtree, R. H. *Organometallics* **2002**, *21*, 700–706.
459. Zhang, C. M.; Trudell, M. L. *Tetrahedron Lett.* **2000**, *41*, 595–598.
460. Lee, H. M.; Nolan, S. P. *Org. Lett.* **2000**, *2*, 2053–2055.
461. Huang, J. K.; Nolan, S. P. *J. Am. Chem. Soc.* **1999**, *121*, 9889–9890.
462. Grasa, G. A.; Viciu, M. S.; Huang, J. K.; Zhang, C. M.; Trudell, M. L.; Nolan, S. P. *Organometallics* **2002**, *21*, 2866–2873.
463. Gstottmayr, C. W. K.; Bohm, V. P. W.; Herdtweck, E.; Grosche, M.; Herrmann, W. A. *Angew. Chem., Int. Ed. Engl.* **2002**, *41*, 1363–1365.
464. Yang, C. L.; Nolan, S. P. *J. Org. Chem.* **2002**, *67*, 591–593.
465. Yang, C. L.; Nolan, S. P. *Organometallics* **2002**, *21*, 1020–1022.
466. Batey, R. A.; Shen, M.; Lough, A. J. *Org. Lett.* **2002**, *4*, 1411–1414.
467. Viciu, M. S.; Germaneau, R. F.; Navarro-Fernandez, O.; Stevens, E. D.; Nolan, S. P. *Organometallics* **2002**, *21*, 5470–5472.
468. Bohm, V. P. W.; Weskamp, T.; Gstottmayr, C. W. K.; Herrmann, W. A. *Angew. Chem., Int. Ed. Engl.* **2000**, *39*, 1602–1604.
469. Bohm, V. P. W.; Gstottmayr, C. W. K.; Weskamp, T.; Herrmann, W. A. *Angew. Chem., Int. Ed. Engl.* **2001**, *40*, 3387–.
470. Deng, Y.; Gong, L.; Mi, A.; Liu, H.; Jiang, Y. *Synthesis* **2003**, 337–339.
471. Reetz, M. T.; Westermann, E. *Angew. Chem., Int. Ed. Engl.* **2000**, *39*, 165.
472. Li, Y.; Boone, E.; El-Sayed, M. A. *Langmuir* **2002**, *18*, 4921–4925.
473. Li, Y.; Hong, X. M.; Collard, D. M.; El-Sayed, M. A. *Org. Lett.* **2000**, *2*, 2385–2388.
474. Moreno-Manas, M.; Pleixats, R.; Villarroya, S. *Organometallics* **2001**, *20*, 4524–4528.
475. Kogan, V.; Aizenshtat, Z.; Popovitz-Biro, R.; Neumann, R. *Org. Lett.* **2002**, *4*, 3529–3532.
476. Kim, S. W.; Kim, M.; Lee, W. Y.; Hyeon, T. *J. Am. Chem. Soc.* **2002**, *124*, 7642–7643.
477. Erdelyi, M.; Gogoll, A. *J. Org. Chem.* **2001**, *66*, 4165–4169.
478. Nambodiri, V. V.; Varma, R. S. *Green Chem.* **2001**, *3*, 146–148.
479. Kabalka, G. W.; Wang, L.; Nambodiri, V.; Pagni, R. M. *Tetrahedron Lett.* **2000**, *41*, 5151–5154.
480. Villemin, D.; Caillot, F. *Tetrahedron Lett.* **2001**, *42*, 639–642.
481. Kabalka, G. W.; Nambodiri, V.; Wang, L. *J. Chem. Soc., Chem. Commun.* **2001**, 775–775.
482. Li, J. T.; Mau, A. W. H.; Strauss, C. R. *J. Chem. Soc., Chem. Commun.* **1997**, 1275–1276.
483. Kabalka, G. W.; Pagni, R. M.; Hair, C. M. *Org. Lett.* **1999**, *1*, 1423–1425.
484. Kabalka, G. W.; Pagni, R. M.; Wang, L.; Nambodiri, V.; Hair, C. M. *Green Chem.* **2000**, *2*, 120–122.
485. Varma, R. S.; Naicker, K. P. *Tetrahedron Lett.* **1999**, *40*, 439–442.
486. Marck, G.; Villiger, A.; Buchecker, R. *Tetrahedron Lett.* **1994**, *35*, 3277–3280.
487. LeBlond, C. R.; Andrews, A. T.; Sun, Y. K.; Sowa, J. R. *Org. Lett.* **2001**, *3*, 1555–1557.
488. Roth, G. P.; Farina, V.; Liebeskind, L. S.; Penacabrera, E. *Tetrahedron Lett.* **1995**, *36*, 2191–2194.
489. Heidenreich, R. G.; Kohler, K.; Krauter, J. G. E.; Pietsch, J. *Synlett* **2002**, 1118–1122.

490. Lipshutz, B. H.; Blomgren, P. A. *J. Am. Chem. Soc.* **1999**, *121*, 5819–5820.
491. Lipshutz, B. H.; Frieman, B.; Pfeiffer, S. S. *Synthesis* **2002**, 2110–2116.
492. Lipshutz, B. H.; Tasler, S.; Chrisman, W.; Spliethoff, B.; Tesche, B. *J. Org. Chem.* **2003**, *68*, 1177–1189.
493. Lipshutz, B. H.; Sclafani, J. A.; Blomgren, P. A. *Tetrahedron* **2000**, *56*, 2139–2144.
494. Fenger, I.; Le Drian, C. *Tetrahedron Lett.* **1998**, *39*, 4287–4290.
495. Parrish, C. A.; Buchwald, S. L. *J. Org. Chem.* **2001**, *66*, 3820–3827.
496. Yamada, Y. M. A.; Takeda, K.; Takahashi, H.; Ikegami, S. *Org. Lett.* **2002**, *4*, 3371–3374.
497. Colacot, T. J.; Gore, E. S.; Kuber, A. *Organometallics* **2002**, *21*, 3301–3304.
498. Cortes, J.; Moreno-Manas, M.; Pleixats, R. *Eur. J. Org. Chem.* **2000**, 239–243.
499. Cai, M. Z.; Song, C. S.; Huang, X. *Synth. Commun.* **1997**, *27*, 1935–1942.
500. Zhang, T. Y.; Allen, M. J. *Tetrahedron Lett.* **1999**, *40*, 5813–5816.
501. Beletskaya, I. P.; Cheprakov, A. V. In *Transition Metal Catalyzed Reactions*; Murahashi, S.-I., Davies, G., Eds.; Blackwell: Oxford, UK, 1999; pp 29–54.
502. Genet, J. P.; Savignac, M. *J. Organomet. Chem.* **1999**, *576*, 305–317.
503. Quignard, F.; Larbot, S.; Goutodier, S.; Choplin, A. *J. Chem. Soc., Dalton Trans.* **2002**, 1147–1152.
504. Rocaboy, C.; Gladysz, J. A. *Tetrahedron* **2002**, *58*, 4007–4014.
505. Schneider, S.; Bannwarth, W. *Helv. Chim. Acta* **2001**, *84*, 735–742.
506. Markert, C.; Bannwarth, W. *Helv. Chim. Acta* **2002**, *85*, 1877–1882.
507. Hoshino, M.; Degenkolb, P.; Curran, D. P. *J. Org. Chem.* **1997**, *62*, 8341–8349.
508. Morita, D. K.; Pesiri, D. R.; David, S. A.; Glaze, W. H.; Tumas, W. *J. Chem. Soc., Chem. Commun.* **1998**, 1397–1398.
509. Carroll, M. A.; Holmes, A. B. *J. Chem. Soc., Chem. Commun.* **1998**, 1395–1396.
510. Shezad, N.; Oakes, R. S.; Clifford, A. A.; Rayner, C. M. *Tetrahedron Lett.* **1999**, *40*, 2221–2224.
511. Osswald, T.; Schneider, S.; Wang, S.; Bannwarth, W. *Tetrahedron Lett.* **2001**, *42*, 2965–2967.
512. Early, T. R.; Gordon, R. S.; Carroll, M. A.; Holmes, A. B.; Shute, R. E.; McConvey, I. F. *J. Chem. Soc., Chem. Commun.* **2001**, 1966–1967.
513. Gordon, R. S.; Holmes, A. B. *J. Chem. Soc., Chem. Commun.* **2002**, 640–641.
514. Dupont, J.; de Souza, R. F.; Suarez, P. A. Z. *Chem. Rev.* **2002**, *102*, 3667–3691.
515. Gordon, C. M. *Appl. Catal. A-Gen.* **2001**, *222*, 101–117.
516. Handy, S. T.; Zhang, X. L. *Org. Lett.* **2001**, *3*, 233–236.
517. Mathews, C. J.; Smith, P. J.; Welton, T. *J. Chem. Soc., Chem. Commun.* **2000**, 1249–1250.
518. Revell, J. D.; Ganesan, A. *Org. Lett.* **2002**, *4*, 3071–3073.
519. Sirieix, J.; Ossberger, M.; Betzemeier, B.; Knochel, P. *Synlett* **2000**, 1613–1615.
520. Rajagopal, R.; Jarikote, D. V.; Srinivasan, K. V. *J. Chem. Soc., Chem. Commun.* **2002**, 616–617.
521. Mathews, C. J.; Smith, P. J.; Welton, T.; White, A. J. P.; Williams, D. J. *Organometallics* **2001**, *20*, 3848–3850.
522. McNulty, J.; Capretta, A.; Wilson, J.; Dyck, J.; Adjabeng, G.; Robertson, A. *J. Chem. Soc., Chem. Commun.* **2002**, 1986–1987.

9.7

Metal Complexes as Catalysts for Carbon-heteroatom Cross-coupling Reactions

J. F. HARTWIG

Yale University, New Haven, Connecticut, USA

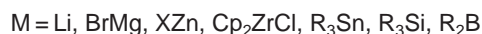
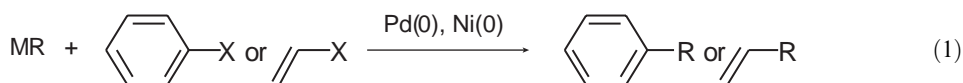
9.7.1	INTRODUCTION	369
9.7.2	EARLY EXAMPLES	371
9.7.3	SCOPE OF THE REACTIONS	372
9.7.3.1	Initial Intermolecular Tin-free Aminations of Aryl Halides	372
9.7.3.2	Second Generation Catalysts Bearing Aromatic Bisphosphines	372
9.7.3.2.1	<i>Amination of aryl halides</i>	372
9.7.3.2.2	<i>Amination of aryl triflates</i>	373
9.7.3.2.3	<i>Amination of heteroaromatic halides</i>	374
9.7.3.3	Third-generation Catalysts Bearing Alkylmonophosphines	374
9.7.3.3.1	<i>Sterically hindered bisphosphine ligands for aminations</i>	375
9.7.3.3.2	<i>P,N, P,O, and dialkylphosphinobiaryl ligands</i>	376
9.7.3.3.3	<i>Low-temperature reactions catalyzed by P(<i>t</i>-Bu)₃ complexes</i>	377
9.7.3.3.4	<i>Heterocyclic carbenes as ligands</i>	377
9.7.3.3.5	<i>Phosphine oxide ligands</i>	378
9.7.3.4	Heterogeneous Catalysts	378
9.7.4	AROMATIC C—N BOND FORMATION WITH RELATED SUBSTRATES	378
9.7.5	ETHERIFICATION	381
9.7.5.1	Initial Studies with Arylphosphines	382
9.7.5.2	Second-generation Catalysts Containing Sterically Hindered Alkylphosphines	382
9.7.6	CARBON—SULFUR AND CARBON—SELENIUM BOND-FORMING CROSS-COUPPLINGS	384
9.7.7	CARBON—PHOSPHORUS BOND-FORMING CROSS-COUPPLINGS	386
9.7.7.1	Coupling of Aryl and Vinyl Halides with Phosphorus(V) Reagents	386
9.7.7.2	Coupling of Aryl and Vinyl Halides with Phosphorus(V) Reagents	387
9.7.8	COUPLING OF ARYL HALIDES WITH SILANES, STANNANES, GERMANES, AND BORANES	388
9.7.8.1	Coupling with Silanes, Stannanes, and Germanes	388
9.7.8.2	Coupling with Boranes	389
9.7.9	INTERMEDIATES IN THE COUPLING CHEMISTRY	390
9.7.10	REFERENCES	394

9.7.1 INTRODUCTION

Direct aromatic substitution of unactivated aryl halides is slow and generally requires a catalyst to become a useful synthetic method. Copper reagents have been used in some cases in classical procedures for the formation of products from aromatic substitution. In many cases these copper-mediated reactions occur at high temperatures and are substrate dependent. Since the 1970s, transition metal catalysts have been developed for aromatic substitution. Most of the early effort toward developing metal-catalyzed aromatic substitution focused on the formation of

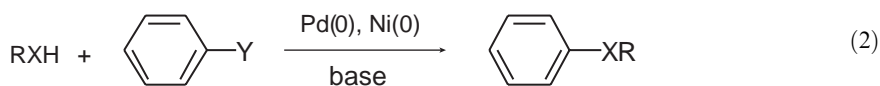
carbon-carbon bonds, and this research has now led to the widespread use of nickel and palladium catalysts for the formation of sp^2-sp , sp^2-sp^2 , and sp^2-sp^3 carbon-carbon linkages.¹⁻⁵ In some rare cases, sp^3-sp^3 couplings have been reported.⁶⁻⁹ This transition metal-catalyzed coupling, summarized in Equation (1), is generally called cross-coupling. Tin, silicon, zinc, zirconium, magnesium, lithium, bismuth, or boron reagents are generally combined with aryl halides, triflates, or in some cases tosylates or phosphates in these cross-coupling reactions. Some homocouplings have also been developed in which an aryl halide and a reducing agent produce symmetric biaryls:

Classic Coupling Chemistry



In contrast, intensive research toward developing transition metal-catalyzed aromatic substitution with heteroatom nucleophiles began only during the 1990s. Reagents that serve as a source of "heteroatom nucleophile" for metal-catalyzed cross-coupling include main group nitrogen, oxygen, sulfur, phosphorus, and selenium compounds or the combination of a base and a substrate with an NH, OH, SH, PH, or SeH bond (Equation (2)). Of course, most pharmaceuticals contain amine or ether substructures, and many of these substructures are aromatic amines and ethers. Aryl sulfides can also be found in biologically active molecules. In addition, aromatic amines, ethers, and sulfides are important in materials science. Important arylamine materials include triaryl amines that serve as hole-transport layers in light emitting diodes¹⁰⁻¹² and diarylamine polymers that are conductive when partially oxidized.¹³⁻¹⁵ Diaryl ether and diaryl sulfide polymers^{16,17} are useful engineering plastics. Finally, aromatic amines, ethers, and phosphines often comprise ligands for catalysts. Thus, the transition metal-catalyzed conversion of aryl halides to amines, ethers, sulfides, and phosphines has provided new methods for the synthesis of ligands:

Carbon-heteroatom Coupling

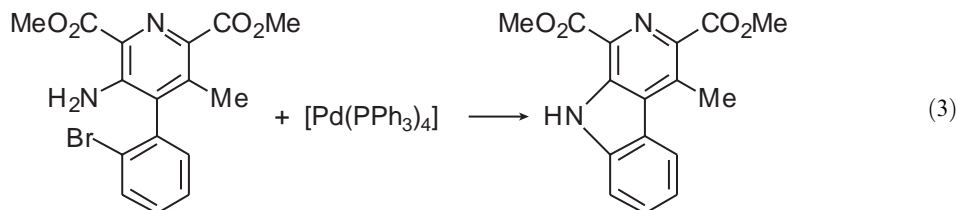


Palladium complexes have also been studied as catalysts for the coupling of aryl and vinyl halides and triflates with silyl, stannyl, germyl, and boryl groups. These reactions have most often been conducted with disilanes, distannanes, digermane, and diborane(4) reagents to form such carbon-element bonds. In some cases, bases or fluoride sources have been added to promote the E-E bond cleavage. Recent developments have allowed the coupling of aromatic electrophiles with silanes, stannanes, and boranes. These various couplings have provided a route to the arylsilane, arylstannane, and arylboronic ester reagents that are commonly used in cross-couplings to form biaryls.¹⁻⁵

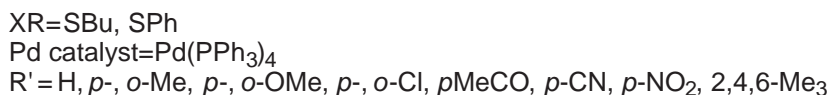
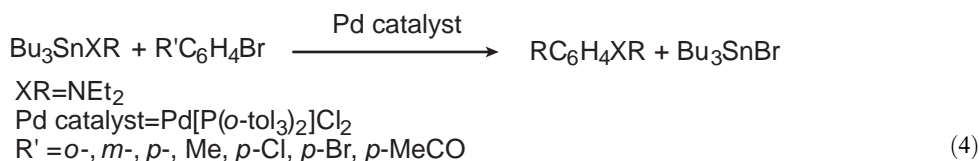
The transition-metal chemistry of the palladium and nickel-catalyzed cross-coupling reactions that form carbon-heteroatom bonds includes unusual classes of amido and alkoxo complexes and some new classes of elementary reactions. These complexes and their reactivity lie at the interface of organometallic and coordination chemistry. The reactions involve coupling of a ligand bound through a metal-carbon bond with a ligand bound through a metal-heteroatom bond. The supporting ligands for these reactions are generally phosphines; some of these phosphines bear nitrogen or oxygen substituents that may or may not bind to the metal during the catalytic cycle. This section will review the types of cross-coupling reactions that form carbon-heteroatom bonds with transition-metal catalysts. Several reviews on this topic have been published in recent years.¹⁸⁻²² This section will focus on the types of ligands used to generate catalysts for in these carbon-heteroatom bond-formations and the reactions that complexes of these ligands undergo during the catalytic process. One review on the reductive elimination chemistry of these complexes has been published elsewhere.²³

9.7.2 EARLY EXAMPLES

A few stoichiometric reactions that formed aromatic carbon nitrogen bonds in the presence of stoichiometric amounts of $\text{Pd}(\text{PPh}_3)_4$ had been reported by Boger and co-workers (Equation (3)).^{24–26} In the absence of base, the palladium(0) was apparently not regenerated. $\text{Pd}(\text{PPh}_3)_4$ failed to catalyze these reactions when used in a 1 mol.% quantity, but it did induce cyclization in good yield when it was used in stoichiometric amounts.^{24–26}



In many cases, the first examples of cross-coupling to form carbon–heteroatom bonds were conducted with main group reagents (Equation (4)). In 1983, Kosugi, Kameyama, and Migita reported the coupling of *N,N*-diethylaminotributyltin with aryl bromides in the presence of a palladium catalyst ligated by tri-*ortho*-tolylphosphine.²⁷ In a review article in 1983,²⁸ Beletskaya and co-workers reported the $[\text{Pd}(\text{PPh}_3)_2(\text{Ph})\text{I}]$ -catalyzed coupling of a distannyl sulfide with an aryl halide and a vinyl halide to form a symmetrical diaryl sulfide and a divinyl sulfide. In 1985, Kosugi and Migita showed that the cross-coupling of tin thiolates with aryl halides occurred in the presence of $\text{Pd}(\text{PPh}_3)_4$ as catalyst,²⁹ and others have reported selective reactions of vinyl halides with tin thiolates.³⁰ In 1986, Tunney and Stille reported the cross-coupling of stannyl and silylphosphides with aryl halides in the presence of PPh_3 -ligated palladium catalysts (Equation (5))³¹ to form a range of aryldiphenyl phosphines that contained esters, ketones, trifluoromethyl groups, and amides. Vinylphosphines have also been prepared from vinyl halides and silylphosphides catalyzed by palladium complexes:³²

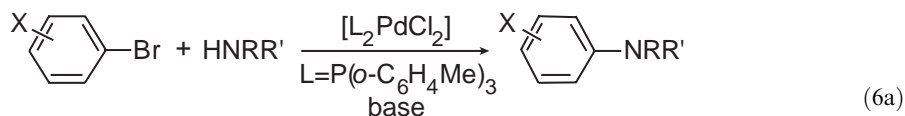


Tin and silicon reagents can provide greater tolerance of functional groups than the strong bases of subsequent chemistry, but tin and silicon amides, thiolates, and phosphides can be hydrolytically unstable and are, therefore, difficult to purify by chromatography. Many of the tin reagents have weak enough $\text{Sn}-\text{X}$ bonds that distillation of even low molecular weight derivatives can lead to decomposition, and the tin reagents are toxic and generate toxic byproducts. Thus, the carbon–heteroatom couplings became a commonly used synthetic method when procedures were developed for the reactions of amines, thiols, and phosphines in the presence of base. The remainder of the discussion of $\text{C}-\text{N}$, $\text{C}-\text{S}$, and $\text{C}-\text{P}$ bond formation will, therefore, focus on reactions of these protic reagents in the presence of base.

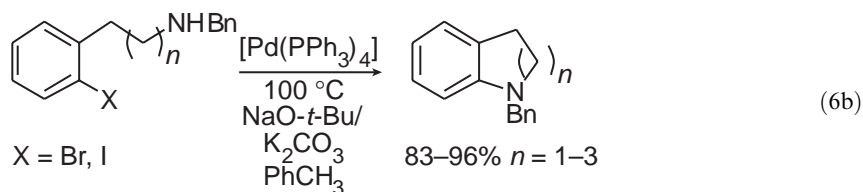
9.7.3 SCOPE OF THE REACTIONS

9.7.3.1 Initial Intermolecular Tin-free Aminations of Aryl Halides

In 1995, the first palladium-catalyzed reactions of aryl halides with amines and base were reported (Equation (6a)).^{33,34} These reactions were typically conducted between 80 °C and 100 °C in toluene solvent in the presence of catalytic amounts of {Pd[P(*o*-tol)₃]₂Cl₂}, {Pd[P(*o*-tol)₃]₂}, or a combination of [Pd₂(dba)₃] (dba = *trans*, *trans*-dibenzylidene acetone) and P(*o*-tol)₃. Reactions of secondary amines gave the coupled products in high yields, but the reactions of primary amines with electron-neutral aryl halides produced mostly arene. Intramolecular aryl halide aminations formed nitrogen heterocycles in the presence of a variety of palladium phosphine complexes, such as those containing P(*o*-tol)₃, PPh₃, Ph₂P(CH₂)_{*n*}PPh₂ (*n* = 2–4) or 1,1'-bis(diphenylphosphino)ferrocene (DPPF), and bases such as NaO-*t*-Bu and K₂CO₃ (Equation (6b)):^{34,35}



X = *o*, *m*, or *p*-alkyl, phenacyl, amino, alkoxy
base = NaO-*t*-Bu, or LiN(SiMe₃)₂

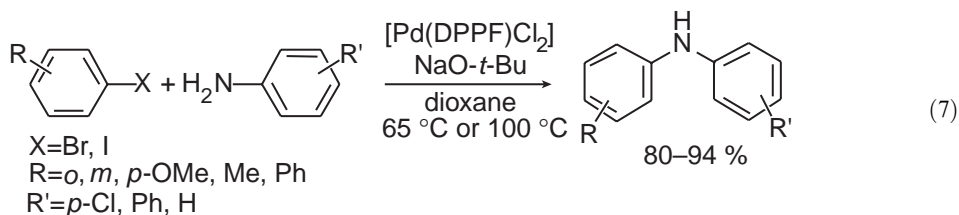


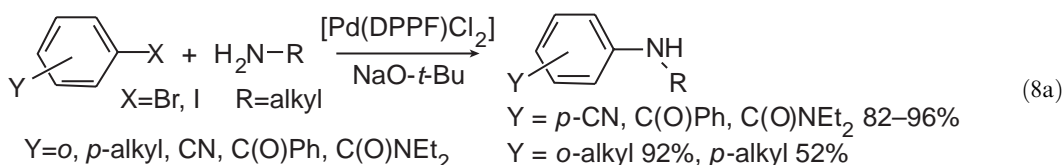
9.7.3.2 Second Generation Catalysts Bearing Aromatic Bisphosphines

9.7.3.2.1 Amination of aryl halides

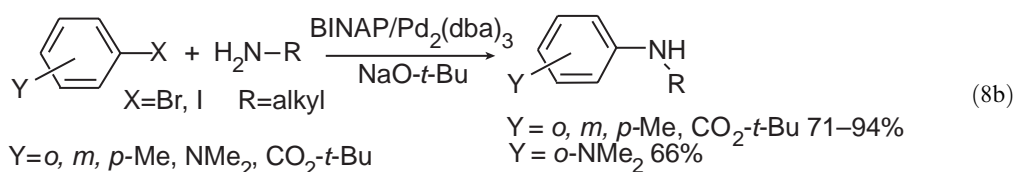
With the exception of intramolecular amination reactions, all of the early aryl halide aminations were catalyzed by palladium complexes containing the sterically hindered P(*o*-tol)₃. In papers published back-to-back in 1996, amination chemistry catalyzed by palladium complexes of DPPF and BINAP was reported.^{36,37} These catalysts allowed for the coupling of aryl bromides and iodides with primary alkyl amines, cyclic secondary amines, and anilines.

DPPF-ligated palladium provided nearly quantitative yields for amination of most electron-rich, electron-poor, hindered, or unhindered aryl bromides or iodides with anilines (Equation (7)). However, nitro haloarenes and aryl halides with carbonyl groups bearing enolizable hydrogens gave poor yields, and esters were converted to the *t*-butyl ester by the *t*-butoxide base. DPPF-ligated palladium also gave good yields of mixed alkyl arylamines with a variety of substrates (Equation (8a)):





The coupling of electron-neutral aryl halides with alkylamines occurred in higher yields when catalyzed by BINAP-ligated palladium than when catalyzed by DPPF-ligated palladium (Equation (8b)). The increased yields resulted in large part from the lack of diarylation products. In favorable cases, 0.05 mol.% catalyst could be used. A subtle but sometimes important advantage of chelating ligands is the coupling of amines that bear a stereocenter α to nitrogen without racemization.³⁸ These data imply that chelation of the phosphine prevents even reversible β -hydrogen elimination of the amido group. Reactions of secondary amines with aryl halides in the presence of BINAP-ligated palladium as the catalyst are less general; reactions of morpholine occurred in good yield, but reactions of piperidine or acyclic secondary amines occurred in low to modest yields:



At this time, many aromatic bisphosphines and aromatic phosphines with potentially hemilabile groups have been tested for activity in the amination chemistry. Some of these are valuable for certain aryl halide aminations (Figure 1). PHANEPHOS, in combination with a palladium precursor, catalyzed the amination of 2,2'-dibromo-[2,2]paracyclophane, and this amination was used to resolve the chiral dibromide reagent.³⁹ Palladium complexes ligated by DPEphos (bis-(2,2'-diphenylphosphino)diphenyl ether) catalyzed the formation of certain diarylamines in higher yield than did catalysts containing BINAP or DPPF.⁴⁰ Reactions of acyclic dialkylamines and reactions with milder bases first occurred in high yield in the presence of palladium and Kumada's ferrocenyl phosphinoether ligand.^{41,42} Related phosphines based on arene-chromium, instead of ferrocene, have been studied as ligands for the coupling of cyclic and acyclic secondary amines.⁴³ A sulfonated version of BISBI (2,2'-bis(diphenylphosphinomethyl)biphenyl)^{44,45} allowed aminations of electron-poor aryl halides to occur in a two-phase system containing water and alcohol or containing water, methanol, and toluene.⁴⁶

9.7.3.2.2 Amination of aryl triflates

Palladium complexes of DPPF and BINAP catalyzed the coupling of amines with aryl triflates (Equations (9)–(11)).^{47,48} The yields for formation of mixed diarylamines all exceeded 90%,⁴⁷ and reactions of electron-neutral aryl halides with alkylamines occurred in yields between 42% and 75% in the presence of catalysts bearing DPPF and between 54% and 77% in the presence of catalysts bearing BINAP or Tol-BINAP. The reactions of electron-poor aryl triflates were plagued by triflate cleavage to form phenol. Slow addition of the triflate²³ or the use of Cs_2CO_3 as base^{48,49} improved reactions of electron-poor triflates. In the presence of Cs_2CO_3 as base, primary and secondary amines reacted in high yields with electron-poor or electron-rich aryl triflates in the presence of BINAP-ligated palladium as catalyst. Reactions of aryl triflates with *N*-

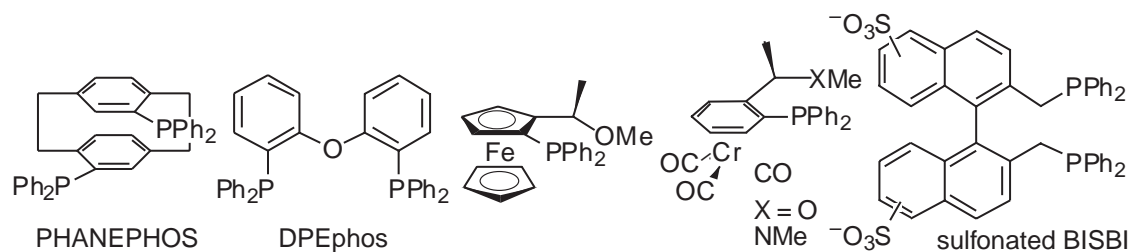
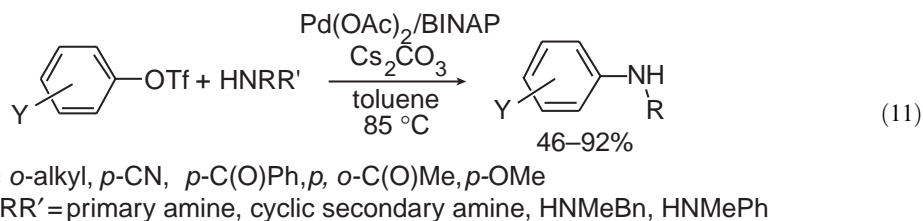
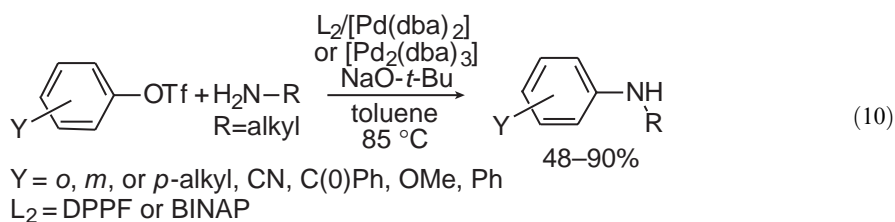
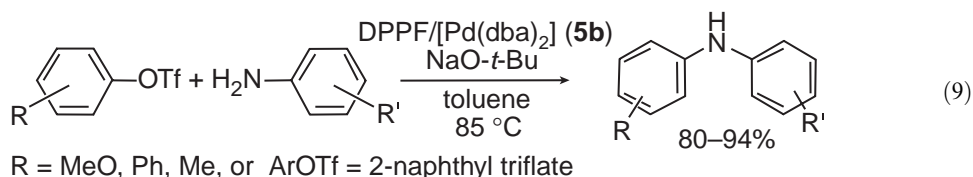


Figure 1 Chelating and hemilabile ligands used in palladium-catalyzed amination of aryl halides.

Boc piperazine conducted in the presence of Cs_2CO_3 as base and added 18-crown-6 occurred in higher yields and shorter reaction times than those conducted without added crown ether:⁵⁰



9.7.3.2.3 Amination of heteroaromatic halides

Because many nitrogen heterocycles act as ligands for late transition metals, coupling of heteroaromatic halides with basic nitrogens can be capricious. Indeed, pyridine displaces $\text{P}(o\text{-tol})_3$ from arylpalladium halide complexes to form the corresponding pyridine complexes.⁵¹ Obviously, chelation will prevent such ligand displacement, and the first aminations of pyridyl halides were catalyzed by palladium complexes of bisphosphines.⁵² The combination of $\text{Pd}(\text{OAc})_2$ or $\text{Pd}_2(\text{dba})_3$ and BINAP catalyzed the amination of pyridyl halides with either primary or secondary amines, except unbranched primary amines. The combination of these palladium precursors and DPPF (1,3-bis(diphenylphosphino)propane) catalyzed the coupling of pyridyl bromides with secondary amines or amines lacking hydrogens α to the nitrogen. Yet, neither combination of metal and ligand catalyzed in high yield reactions of acyclic secondary amines with pyridyl halides. Several reactions of pyridyl chlorides, bromides, and triflates occurred to generate *N*-pyridyl hydrazine derivatives in good yield.²²³ Reactions of 2-bromo- and chloropyridine with benzophenone hydrazone occurred in good yield in the presence of palladium catalysts ligated by BINAP, and *t*-butylcarbazate ($t\text{-BuOC}(\text{O})\text{NHNH}_2$) and di-*t*-butyl hydrazodiformate ($t\text{-BuOC}(\text{O})\text{NHNHC}(\text{O})\text{O-}t\text{-Bu}$) reacted with halopyridines in the presence of catalysts ligated by DPPF to give 45–85% yield of the coupled products. These reactions are surprising if one considers the potential for reduction of palladium by hydrazines. $\text{Pd}(\text{PPh}_3)_4$ is generally prepared by reduction of palladium(II) precursors by hydrazine.⁵³ Later studies have shown that chelation by the ligand is not necessary to observe aminations of pyridyl halides, and these results will be presented below.

9.7.3.3 Third-generation Catalysts Bearing Alkylmonophosphines

Complexes ligated by alkylphosphines had been used rarely as catalysts in cross-coupling chemistry, but several studies suggested that they could catalyze the amination of aryl halides with higher selectivity and activity than catalysts of arylphosphines. Steric hindrance promotes reductive elimination at the expense of β -hydrogen elimination.⁵⁴ Therefore, reactions of primary amines and, in

particular, acyclic secondary amines could be improved by catalysts bearing hindered *t*-butylphosphines. Moreover, the second arylation of a primary amine should be retarded by sterically hindered ligands.³⁷ Finally, oxidative addition of aryl halides to Pd[P(*o*-tolyl)₃]₂ was faster than it was to Pd(PPh₃)₄,⁵⁵ and, therefore, a larger and more electron-rich ligand may provide even faster addition.

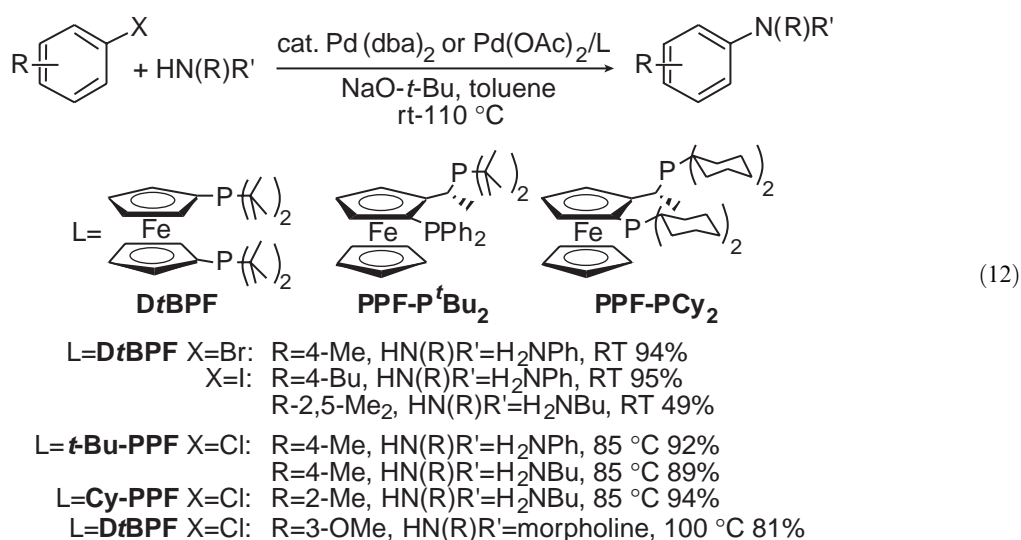
Indeed, palladium complexes ligated by P(*t*-Bu)₃ catalyzed the formation of aryl piperazines from aryl halides and piperazine in high yields with turnover numbers of 7,000 at 120 °C.⁵⁶ These complexes also catalyzed the formation of triaryl amines from aryl halides and diarylamines with turnovers of 4,000.⁵⁷

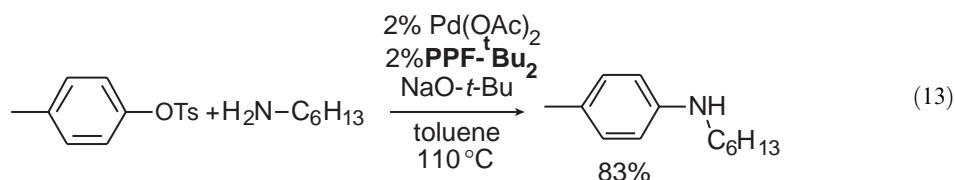
In addition, complexes of P(*t*-Bu)₃ have been shown to catalyze the formation of diaryl heteroarylamines from bromothiophenes.²²⁴ Aminations of five-membered heterocyclic halides such as furans and thiophenes are limited because their electron-rich character makes oxidative addition of the heteroaryl halide and reductive elimination of amine slower than it is for simple aryl halides. Reactions of diarylamines with 3-bromothiophenes occurred in higher yields than did reactions of 2-bromothiophene, but reactions of substituted bromothiophenes occurred in more variable yields. The yields for reactions of these substrates in the presence of catalysts bearing P(*t*-Bu)₃ as ligand were much higher than those in the presence of catalysts ligated by arylphosphines.

9.7.3.3.1 Sterically hindered bisphosphine ligands for aminations

Activated aryl chlorides, which are close in reactivity to unactivated aryl bromides, underwent reaction with the original P(*o*-tol)₃-ligated catalyst.⁵⁸ Nickel complexes, which catalyze classic C—C bond-forming cross-couplings of aryl chlorides,^{59–64} also catalyzed aminations of aryl chlorides under mild conditions.^{65,66} However, the nickel-catalyzed chemistry generally occurred with lower turnover numbers and with a narrower substrate scope than the most efficient palladium-catalyzed reactions.

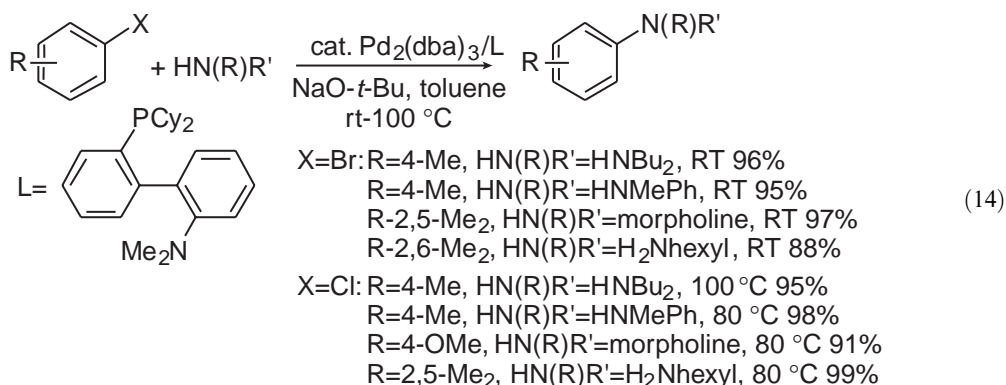
The first palladium complexes that catalyzed the aminations of unactivated aryl chlorides in high yield under mild conditions⁶⁷ were ligated by D^tBPF [1,1-bis(di-*t*-butylphosphino)ferrocene]^{68,69} and related sterically hindered bis-dialkylphosphinoferrocenes (Equation (12)).^{70–72} Reactions of unactivated aryl halides with either anilines or cyclic secondary amines occurred in high yields under mild conditions (80–100 °C) when catalyzed by complexes of D^tBPF. Reactions catalyzed by the more geometrically constrained ferrocenyl ligands (Equation (12)), which were first reported by Spindler, Togni, and Bläser, occurred in high yields with the most favorable selectivity for monoarylation over diarylation and amination over hydrodehalogenation that has been reported for a system that activates aryl chlorides under mild conditions. In addition, the complexes of *t*-Bu-PPF (1-diphenylphosphino-2-(1-di-*t*-butylphosphinoethyl)ferrocene)⁷² also catalyzed the amination of aryl tosylates, albeit at 110 °C (Equation (13)). This amination of *p*-tolyl tosylate is the first palladium-catalyzed coupling of an unactivated aryl tosylate:



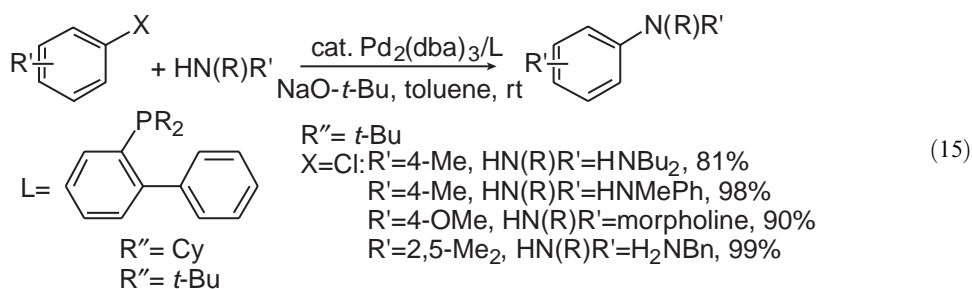


9.7.3.3.2 P,N, P,O, and dialkylphosphinobiaryl ligands

Complexes of the ferrocenylphosphinoether ligands that were originally developed by Kumada and Hayashi for enantioselective coupling catalyzed the coupling of aryl bromides and acyclic secondary amines in high yields.⁴¹ To generate related ligands for catalytic amination of aryl chlorides, cyclohexyl analogs of ligands related to Kocovsky's MAP (Equation (14)), Hayashi's MOP, and Noyori's BINAP were prepared.⁷³ These alkyl analogs of these arylphosphines generated catalysts for coupling of unhindered aryl bromides with secondary amines and of ortho-substituted aryl bromides with primary amines in high yield (Equation (14)). The amination of activated aryl chlorides occurred at room temperature, and the amination of unactivated aryl chlorides occurred at 80–100 °C in the presence of palladium complexes of these ligands. Reactions catalyzed by the cyclohexyl analog of MAP displayed the broadest scope of reactions catalyzed by complexes of these ligands:

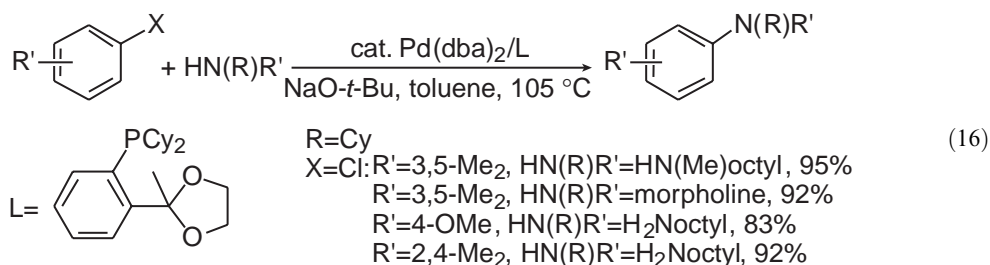


Although the P,O and P,N structures were chosen²⁰ because of the potential for hemilability, and a weak interaction between palladium and the ipso carbon of a ligand aminoaryl groups has, indeed, been observed,⁷⁴ the desamino di-alkylphosphino-2-biphenyl ligands in Equation (15) generated more active catalysts. The dicyclohexylphosphino-2-biphenyl and di-*t*-butylphosphino-2-biphenyl ligands, in combination with Pd₂(dba)₃, catalyzed the amination of unactivated aryl chlorides in selected cases at room temperature:



Combinations of palladium and related P,O and P,N ligands have been evaluated as catalysts for the amination chemistry. A dicyclohexylphosphinoarene containing a bulky ortho substituent, shown in Equation (16), gave high yields for the coupling of aryl chlorides with secondary amines at 105 °C.^{75,76} This ligand was selected from a phosphine library as a highly active ligand for the amination chemistry. Unactivated aryl chlorides reacted with secondary cyclic or acyclic amines

in the presence of catalysts containing this ligand in good yields, and unactivated ortho-substituted aryl chlorides reacted with primary aryl- or alkylamines in good yields. However, reactions of primary amines with unhindered aryl halides were not reported, and these ligands presumably generate the common side products from diarylation and hydrodehalogenation:



9.7.3.3.3 Low-temperature reactions catalyzed by $P(t\text{-Bu})_3$ complexes

Following work on the arylation of piperazine at high temperatures in the presence of a combination of $\text{Pd}(\text{OAc})_2$ and an excess of $P(t\text{-Bu})_3$ with respect to palladium, early stages of a kinetic study⁷⁷ showed that the aminations occurred under much milder conditions in the presence of the isolated palladium(0) complex as catalyst. Even milder conditions were required when the reaction was catalyzed by a 1:1 ratio of ligand to $\text{Pd}(\text{dba})_2$.⁷⁸ Reactions of secondary amines catalyzed by this combination of $P(t\text{-Bu})_3$ and $\text{Pd}(\text{dba})_2$ occurred in nearly quantitative yields in all cases tested. Aryl chlorides reacted with secondary amines or anilines at 70°C ,⁷⁸ and in some cases reactions of aryl chlorides occurred at room temperature. This ligand is more air sensitive than the biphenyl ligands discussed above, but is available as a 10% solution in hexanes in a Sure/Seal bottle and can be generated *in situ* from the air-stable H salt $[\text{HP}(t\text{-Bu})_3]\text{BF}_4$.⁷⁹

9.7.3.3.4 Heterocyclic carbenes as ligands

A large body of literature has emerged on the use of heterocyclic carbenes as ligands for many catalytic processes, and amination is no exception. These compounds can be made in a sterically hindered form, and they are strongly electron donating. Figure 2 shows several structures of heterocyclic carbene ligands that catalyze, in combination with palladium precursors, the amination of aryl halides. In general, these ligands are added to the reaction in their air-stable protonated form, and the stoichiometric base deprotonates the ligand precursor and generates the free carbene that binds to palladium. The 2,6-diisopropyl carbene with a saturated backbone generates the most active of the carbene-ligated catalysts shown for the amination of aryl halides.

Complexes ligated by the unsaturated carbene at the top right of Figure 2, catalyze the reaction of aryl chlorides with a variety of amines, including primary amines at 100°C and the reactions of aryl

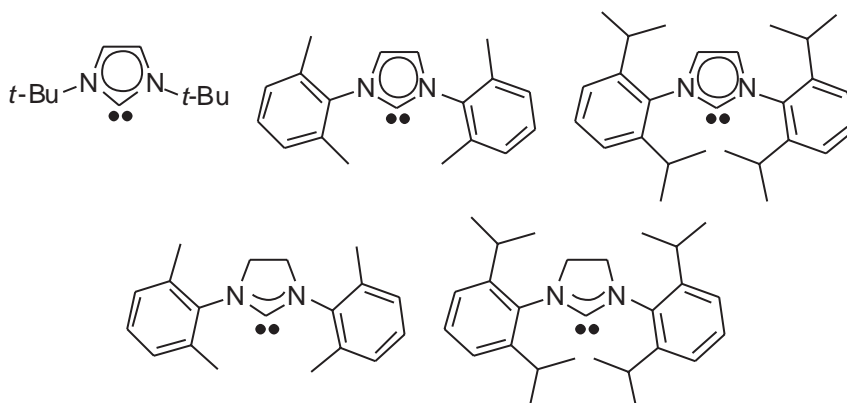
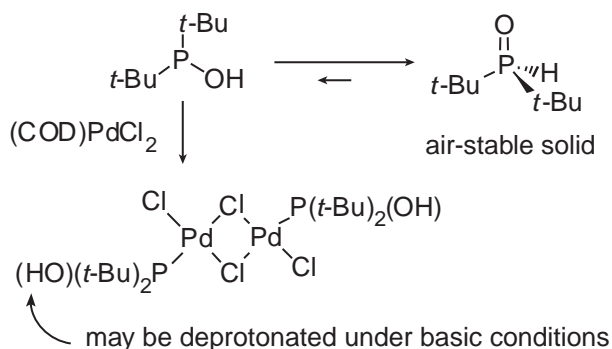


Figure 2 Carbenes that have been used, in combination with palladium, for the amination of aryl halides.

bromides and iodides at room temperature.^{80,81} These temperatures for reactions of aryl chlorides are higher than those of reactions catalyzed by complexes of $P(t\text{-Bu})_3$ or the 2-biphenyl di-*t*-butylphosphines, but reaction yields were high in the presence of 2 mol.% palladium. In contrast, the carbene precursor with 2,6-diisopropylphenyl groups and a saturated backbone at the bottom right of Figure 2 generated complexes that catalyzed the reactions of aryl chlorides at room temperature.⁸² Even reactions of electron-rich substrates, such as 4-chloroanisole, occurred in nearly quantitative yields. The high binding energy of these heterocyclic carbene ligands⁸³ apparently prevents displacement of the ligand in the active form of the catalyst by pyridine, and reactions of 2- and 3-chloropyridine occurred in high yield. In addition, catalyst loadings of only 0.02 mol.% led to full conversion and high yield in one case. Although mechanistic work on the aminations involving carbene ligands has not been conducted, bis-carbene complexes are likely resting states for the catalyst. The palladium(0) complex of 1,3-di-*N-tert*-butylimidazol-2-ylidne (see Figure 2) has been isolated.⁸⁴ It contains two carbene ligands and does catalyze the amination reactions, although at higher temperatures than the catalysts generated *in situ* from a 1:1 ratio of ligand and palladium precursor.

9.7.3.3.5 Phosphine oxide ligands

A strategy that makes use of phosphine oxides and their tautomeric phosphinous acid form has been reported.^{85,86} As shown in Scheme 1, di-*t*-butylphosphinous acid, which is air-stable, could be deprotonated when coordinated to the metal to generate a strongly electron-donating ligand. Complexes generated from the phosphinous acid catalyze a variety of cross-coupling reactions, including aryl halide amination. However, the scope of the amination chemistry was narrow, and several reactions that occur in high yield with catalysts bearing other ligands occurred in modest yield with catalysts bearing this ligand.



Scheme 1

9.7.3.4 Heterogeneous Catalysts

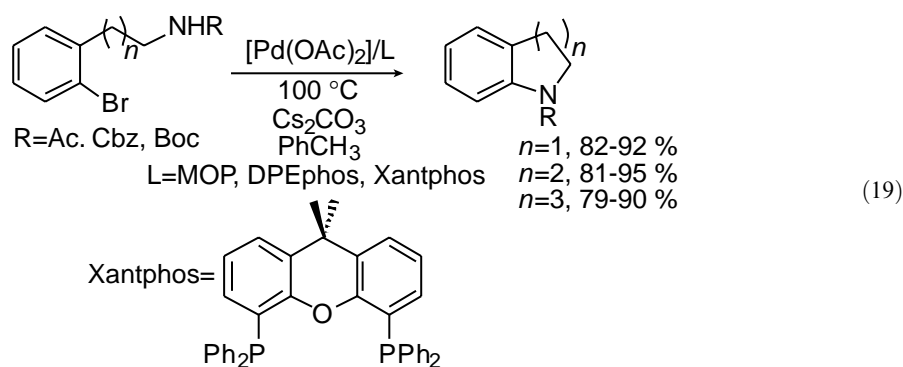
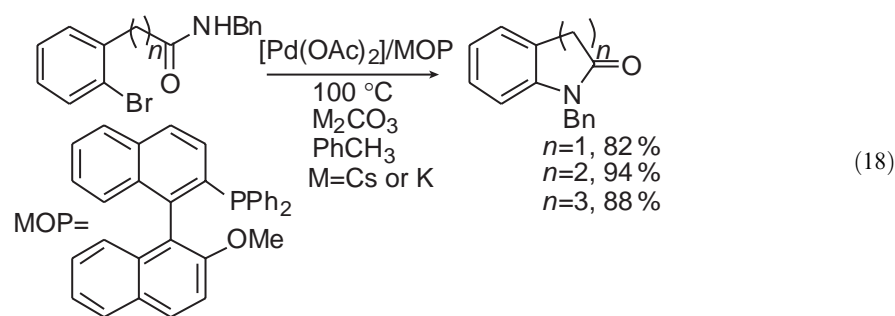
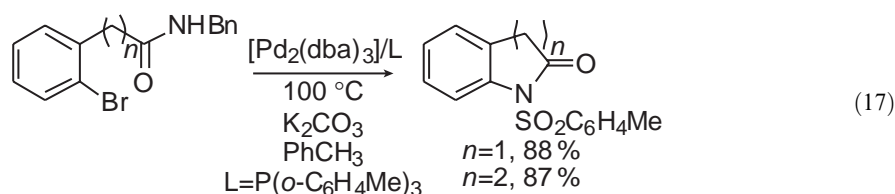
The amination chemistry has also been catalyzed by heterogeneous or supported homogeneous catalysts. The reaction has been conducted with palladium particles immobilized onto metal oxide supports, as well as palladium complexes contained in NaY zeolites.⁸⁷ In most cases these reactions were conducted at high temperatures, generally 135 °C. Nickel on carbon catalyzed the amination of aryl chlorides in the presence of an added phosphine ligand.⁸⁸ The scope of the process is similar to that of homogeneous nickel species, and recent data suggests that reaction occurs by a homogeneous catalyst.²²⁵ In addition, the dialkylphosphinobiphenyl ligands have been linked to Merrifield resin through a 2'-OH on the biphenyl group. The scope for reactions were similar to those of homogeneous catalysts bearing these types of ligands, and catalysts were recycled four times starting with 2 mol.% catalyst.

9.7.4 AROMATIC C—N BOND FORMATION WITH RELATED SUBSTRATES

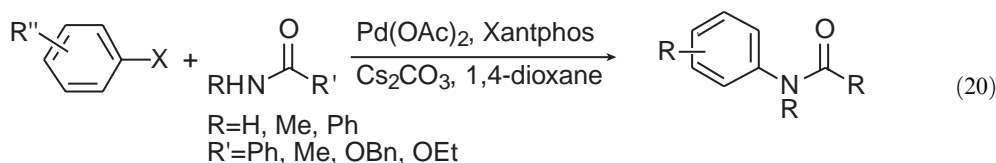
The scope of the aromatic C—N bond-forming reaction extends beyond amines. For example, selected imines, sulfoximines, hydrazines, lactams, azoles, amides, carbamates, and sulfonamides

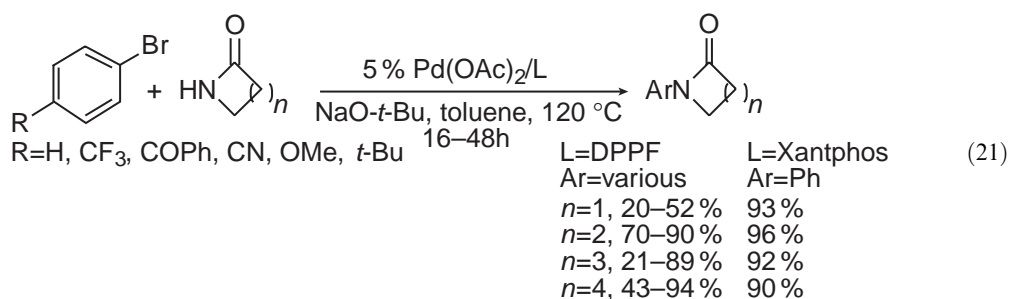
all react with aryl halides in the presence of a palladium catalyst and base to form useful products.

Amides and sulfonamides undergo intramolecular chemistry to form aryl amides and aryl sulfonamides (Equations (17)–(19)) in the presence of palladium catalysts ligated by arylphosphines.^{35,89} Initially, complexes of P(furyl)₃ and P(*o*-tol)₃ were most effective catalysts, but complexes of Hayashi's MOP and van Leeuwen's DPEphos and xantphos have lately been shown to be more active.⁹⁰ In the presence of catalysts containing one of these ligand systems, five-, six-, and seven-membered rings were formed from halogenated benzamides or from substrates containing an acetamide, an *N*-carbobenzyloxy, or a *t*-butylcarbamate substituent tethered to the aryl halide (Equations (18) and (19)):

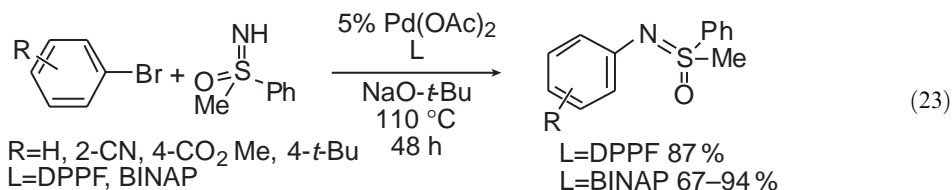
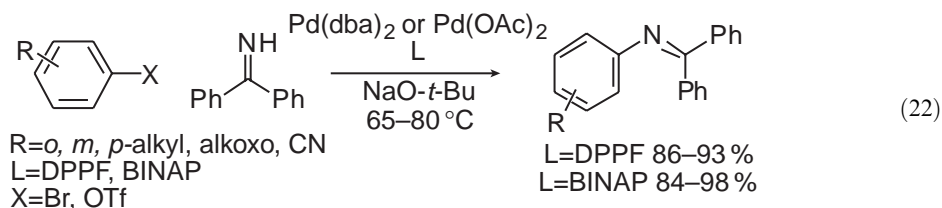


The intermolecular coupling of lactams and acyclic amides has also been reported. Reactions of carbamates with aryl halides occurred in the presence of catalysts ligated by P(*t*-Bu)₃.⁷⁸ Both carbamates and amides coupled with aryl halides in the presence of a catalyst bearing Xantphos.⁹⁰ In addition, the coupling of lactams with aryl halides has been successful. A combination of Pd(OAc)₂ and DPPF first formed *N*-aryl lactams in good yields from γ -lactams, but the arylation of amides was improved significantly by the use of Xantphos (Equations (20) and (21)).^{90,91} The reaction of aryl halides with vinylogous amides has also been reported.⁹²



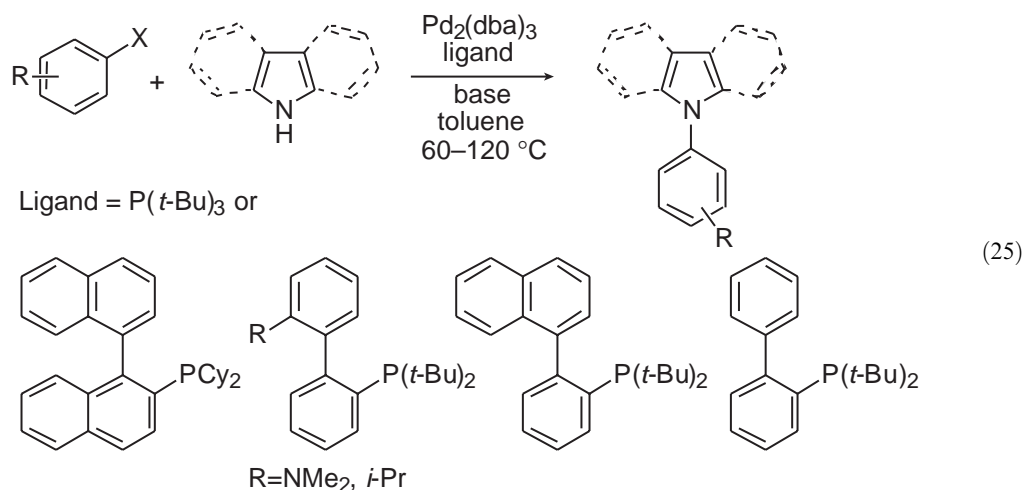
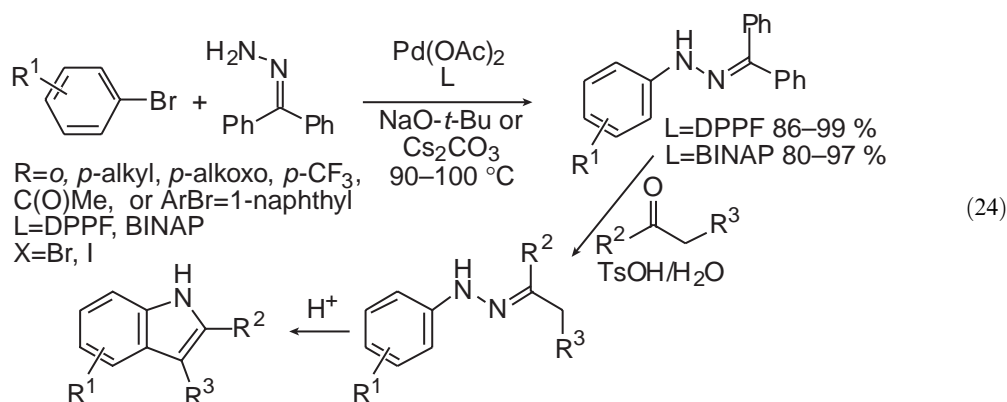


Benzophenone imine is commercially available and serves as an ammonia surrogate that reacts with aryl halides in high yields under standard palladium-catalyzed conditions (Equation (22)). Hydrolysis or hydrogenolysis of the *N*-aryl imine product provides the free aniline. Catalysts based on both DPPF- and BINAP-ligated palladium gave essentially quantitative yields for reactions of aryl bromides in the presence of either Cs₂CO₃ or NaO-*t*-Bu.^{93,94} Sulfoximines have also proven to be suitable substrates for palladium-catalyzed C–N bond formation, although reactions of this substrate are less general than those of benzophenone imine, (Equation (23)).^{95,96} Reaction times were long, but good yields were obtained from reactions of electron-deficient aryl halides with sulfoximines in the presence of palladium complexes of either BINAP or DPPF:



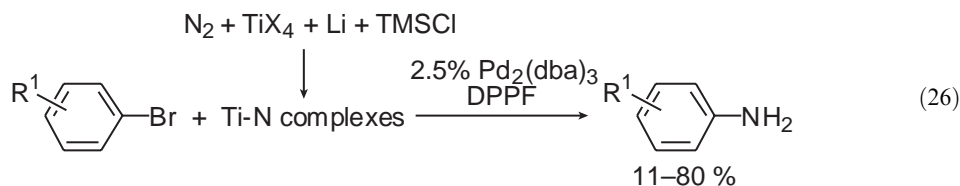
Benzophenone hydrazone is a particularly active substrate for palladium-catalyzed reactions, as summarized in (Equation (24)),^{97–99} and these products can serve as precursors to *N*-aryl hydrazines for pyrazole synthesis¹⁰⁰ or as precursors to substrates for the Fischer indole synthesis.⁹⁸ Reactions of benzophenone hydrazone with electron-rich or electron-poor, hindered or unhindered aryl bromides or iodides occurred in high yields in the presence of palladium complexes of either DPPF or BINAP. *t*-Butylcarbazate (H₂NNHBoc) can serve as an alternative protected hydrazine, and this substrate reacts with electron-deficient aryl halides in the presence of palladium catalysts ligated by DPPF, PPF-P(*t*-Bu)₂, or BINAP.¹⁰¹

Indoles, pyrroles, and carbazoles themselves are suitable substrates for palladium-catalyzed coupling with aryl halides. Initially, these reactions occurred readily with electron-poor aryl halides in the presence of palladium and DPPF, but reactions of unactivated aryl bromides were long, even at 120 °C. Complexes of sterically hindered alkylmonophosphines have been shown to be more active catalysts (Equation (25)).^{78,102,103} In the presence of these more active catalysts, reactions of electron-poor or electron-rich aryl bromides and electron-poor or electron-neutral aryl chlorides occurred at 60–120 °C. Reactions catalyzed by complexes of most of the *t*-butylphosphines generated a mixture of 1- and 3-substituted indoles. In addition, 2- and 7-substituted indoles reacted with unhindered aryl halides at both the N1 and C3 positions. The 2-naphthyl di-*t*-butylphosphinobenzene ligand in Equation (25), however, generated a catalyst that formed predominantly the product from *N*-arylation in these cases.



The reaction of benzotriazoles with aryl halides catalyzed by a mixture of $\text{Pd}(\text{dppe})\text{Cl}_2$ (DPPE = bis-(diphenylphosphino)ethane) or $\text{Pd}(\text{dppf})\text{Cl}_2$, copper(I)iodide or copper(II)carboxylates, and a phase-transfer catalyst has been shown to proceed in good yield in DMF solvent.¹⁰⁴ Both copper and palladium were required for these reactions to occur at the *N*-1 position in high yields. Similar results for the coupling of amines with arylidonium salts in aqueous solvent were observed.¹⁰⁵

A remarkable process was reported by Mori that forms aniline from dinitrogen (Equation (26)).¹⁰⁶ "Titanium nitrogen fixation complexes" were generated from reactions of titanium tetrachloride or tetraisopropoxide, lithium metal, TMS chloride, and dinitrogen. These complexes generated a mixture of aryl and diarylamines in yields as high as 80% when treated with aryl halide and a palladium catalyst containing DPPF:



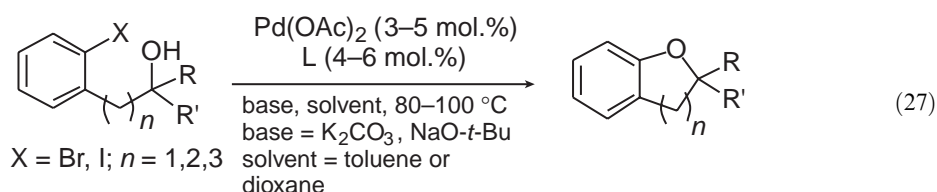
9.7.5 ETHERIFICATION

Palladium-catalyzed aromatic C—O bond formation is less developed than palladium-catalyzed aryl amination. Except when the aryl halide is strongly electron deficient,¹⁰⁷⁻¹¹⁰ catalysts ligated by the conventional aryl phosphines such as DPPF and BINAP are ineffective for coupling of

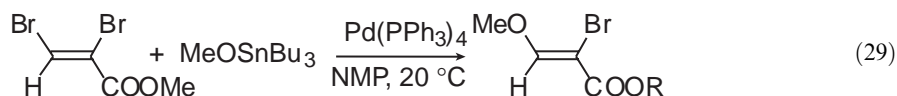
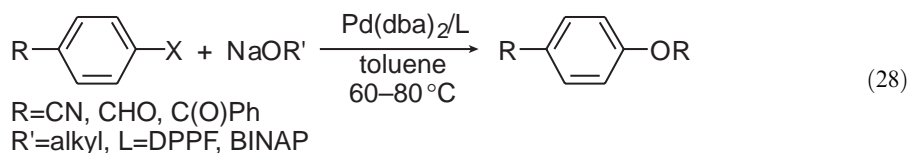
alkoxides with aryl halides. However, complexes bearing unusually hindered phosphines catalyzed the intramolecular formation of oxygen heterocycles,¹¹¹ and the intermolecular formation of *t*-butyl aryl ethers, *t*-butyldimethylsilyl aryl ethers,^{112,113} diaryl ethers,^{112–114} and of selected alkyl aryl ethers.

9.7.5.1 Initial Studies with Arylphosphines

The first palladium-catalyzed couplings to form aryl ethers (Equation (27)) were intramolecular reactions that formed oxygen heterocycles.¹¹¹ Reactions of aryl halides containing a pendant cyclohexanol occurred in good yield when catalyzed by palladium complexes ligated by DPPF and BINAP, but reactions of aryl halides containing pendant acyclic secondary alcohols occurred in low yields. Slightly lower loadings were required for reactions catalyzed by DPPF complexes, and cyclizations of substrates that could undergo β -hydrogen elimination were reported only with palladium catalysts containing DPPF as ligand:



The first palladium-catalyzed formation of aryl alkyl ethers in an intermolecular fashion occurred between activated aryl halides and alkoxides (Equation (28)), and the first formation of vinyl ethers occurred between activated vinyl halides and tin alkoxides (Equation (29)). Reactions of activated chloro- and bromoarenes with NaO-*t*-Bu to form *t*-butyl aryl ethers occurred in the presence of palladium and DPPF as catalyst,¹⁰⁷ while reactions of activated aryl halides with alcohols that could undergo β -hydrogen elimination occurred in the presence of palladium and BINAP as catalyst.¹¹⁰ Reactions of NaO-*t*-Bu with unactivated aryl halides gave only modest yields of ether when catalyzed by aromatic bisphosphines.¹¹⁰ Similar chemistry occurred in the presence of nickel catalysts. In fact, nickel catalysts produced higher yields of silyl aryl ethers than palladium catalysts.¹⁰⁸ The formation of diaryl ethers from activated aryl halides in the presence of palladium catalysts bearing DPPF or a CF₃-substituted DPPF was also reported.¹⁰⁹



9.7.5.2 Second-generation Catalysts Containing Sterically Hindered Alkylphosphines

The formation of aryl ethers from unactivated aryl halides has been improved dramatically by the development of catalysts that contain sterically hindered alkylphosphines. Palladium complexes bearing di-*t*-butylphosphinobiaryls and di-*t*-butylphosphinoferrrocenes as ligands provide good yields for certain types of aryl halide etherifications. Figure 3 shows the members of these ligand families that have generated active catalysts for etherification.

Reactions of aryl halides with phenoxides or phenols (Equation (30)) and base catalyzed by complexes of these ligands occurred in significantly higher yields than did the same reactions catalyzed by complexes of DPPF or BINAP. For example, a large number of diaryl ethers have

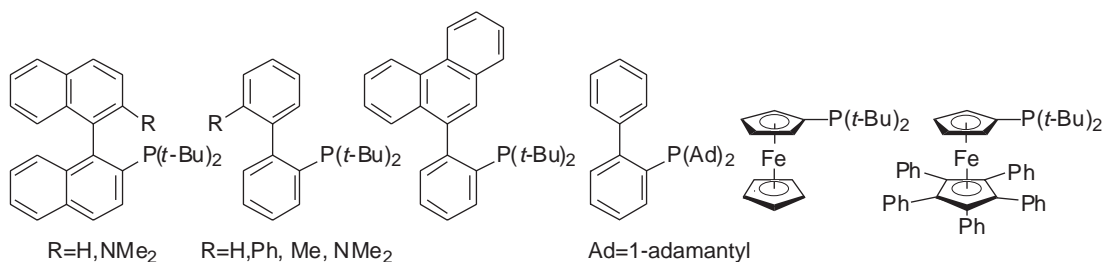
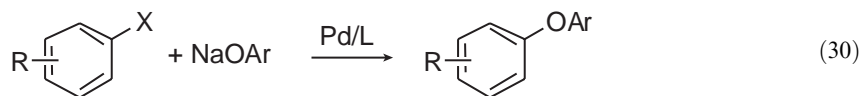
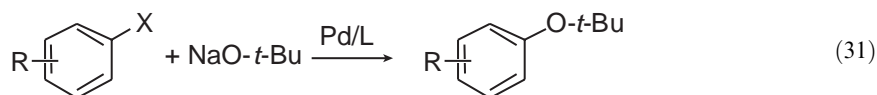


Figure 3 Monophosphine ligands for the etherification of aryl halides.

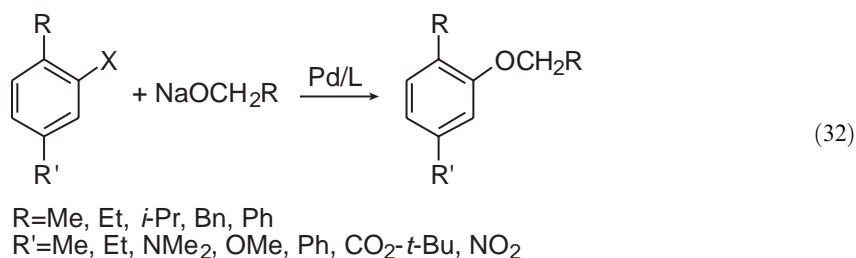
been formed from electron-deficient aryl halides and the combination of phenol and base in the presence of palladium acetate and the ligand in **Figure 3** that contains the parent biphenyl unit.¹¹⁴ Reactions of unactivated aryl halides with aryl alcohols and base occurred in the highest yields when one or both of the substrates contained at least one ortho substituent. These reactions occurred in the presence of a palladium catalyst bearing the parent di-*t*-butylphosphinobiphenyl or the dimethylamino-substituted binaphthyl ligand. When both substrates lacked ortho substituents, the 2'-phenyl-substituted biphenyl ligand or the diadamantylphosphinobiphenyl ligand was required. These reactions were conducted at 100–110 °C. Etherifications catalyzed by palladium complexes of the ferrocenyl ligands were unusual because the parent ferrocenyl ligand of **Figure 3**¹¹³ was converted to the pentaaryl ligand *in situ*.¹¹² Reactions catalyzed by a combination of Pd₂(dba)₃ and the pentaphenylferrocenyl ligand occurred with fast rates and even occurred at room temperature when coupling an electron-rich phenoxide with an unactivated aryl bromide.¹¹² Reactions to form diaryl ethers with this ligand, although rapid, were more limited in scope than reactions catalyzed by complexes of the biaryl di-*t*-butylphosphines:



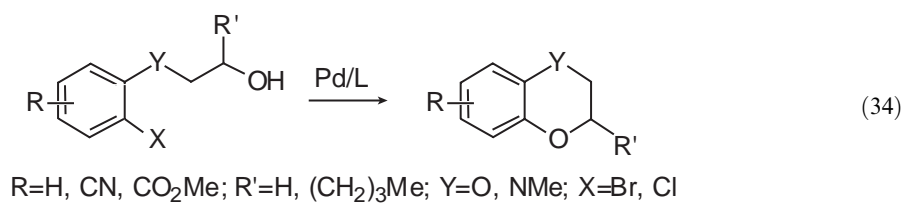
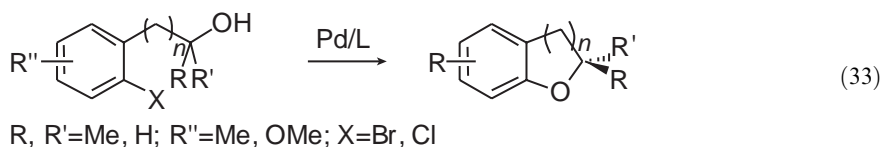
The intermolecular formation of alkyl aryl ethers was also improved by the use of hindered alkylphosphine ligands. The formation of *t*-butyl aryl ethers from *t*-butoxide and either aryl chlorides or aryl bromides (**Equation (31)**) catalyzed by complexes of *t*-butylphosphines occurred in a general fashion. Complexes containing the unsubstituted, methyl-substituted or dimethylamino-substituted di-*t*-butylphosphinobiaryl ligands catalyzed the formation of *t*-butyl aryl ethers from electron-rich and even ortho-substituted aryl bromides or chlorides.¹¹⁵ Reactions of aryl halides with *t*-butoxide catalyzed by complexes of the pentaphenylferrocenylphosphine occurred with similar scope, and reactions catalyzed by complexes of this ligand occurred at room temperature in most cases.¹¹² In addition, complexes of the most hindered of the biaryl dialkylphosphines, the binaphthyl di-*t*-butylphosphines, catalyzed the intermolecular formation of aryl ethers from aryl halides and primary alcohols (**Equation (32)**).¹¹⁶ Complexes of these two ligands catalyzed the formation of aryl ethers from electron-neutral, *ortho*-substituted aryl halides and primary alcohols in high yields, and from *n*-butyl or benzyl alcohols and unhindered electron-neutral or electron-poor aryl halides in modest yields. Thus, the scope of alcohol that can participate in these reactions is limited, and the aryl halide cannot be electron rich, but the formation of alkyl aryl ethers with catalysts bearing sterically hindered ligands occurs with substantially greater scope than it did with catalysts bearing arylphosphines:



In general, intramolecular palladium-catalyzed etherifications are easier to conduct than intermolecular etherifications. Thus, intramolecular reactions that are catalyzed by complexes of hindered alkylphosphines now provide useful methodology for the synthesis of oxygen heterocycles. For example, complexes of the pentaphenylferrocenylphosphine catalyzed the cyclizations in **Equation (33)** within minutes at room temperature.¹¹⁷ However, reactions of substrates that contained hydrogens α to the oxygen occurred in lower yields because of competing β -hydrogen

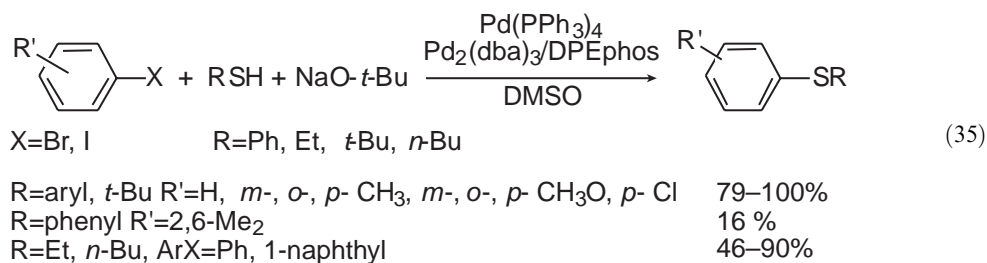


elimination. In these cases reactions catalyzed by complexes of the biaryldialkylphosphines occurred in high yields.¹¹⁷ Complexes of the biaryldialkylphosphines also catalyzed the cyclizations to form the heterocycles shown in Equation (34). In addition to the biaryl ligands that were used to conduct intermolecular reactions, the phenanthrene-containing ligand in Figure 3 was used to optimize reaction yields of the intramolecular chemistry:



9.7.6 CARBON-SULFUR AND CARBON-SELENIUM BOND-FORMING CROSS-COUPINGS

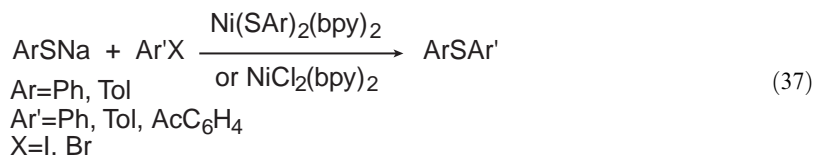
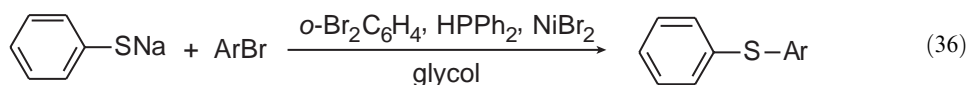
In 1978 and 1980 the coupling of aryl bromides and iodides with both aliphatic and aromatic thiols was first reported in the presence of NaO-*t*-Bu and Pd(PPh₃)₄ (Equation (35)).^{118,119} In contrast to aryl halide aminations and etherifications, the thiation reactions did not require unusual catalysts. Yet, reactions that form aryl alkyl sulfides from alkyl thiols occurred in modest yields in many cases:



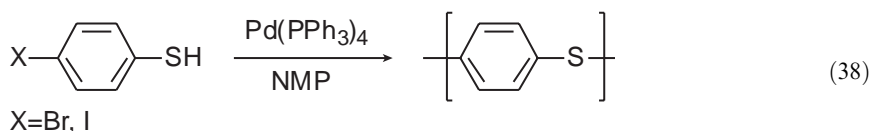
Several palladium catalysts for formation of aryl sulfides from aryl halides have been investigated more recently. A combination of Pd₂(dba)₃ and DPEphos catalyzed the formation of a broad range of diaryl sulfides in the presence of 1 mol.% palladium and NaO-*t*-Bu base in toluene solvent.¹²⁰ The highest yields of alkyl aryl sulfides were obtained from aryl triflates and *n*-butyl thiol catalyzed by a combination of palladium acetate and BINAP. However, these reactions contained 10 mol.% catalyst, were long, and required deactivated aryl triflates. A combination of Pd₂(dba)₃ and DPPF catalyzed the coupling of thiols with resin-bound aryl halides.¹²¹

Nickel complexes also catalyze the coupling of aryl halides with thiolates. In one case, the phosphine ligand on the catalyst was generated *in situ* from 1,2-dibromobenzene and diphenylphosphine

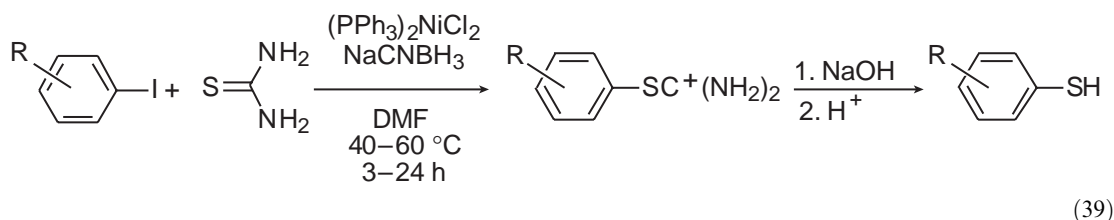
(Equation (36)).¹²² This process to form aryl sulfides occurred good yields, but required long times at 200 °C. At somewhat lower temperatures, the nickel complexes of bipyridine such as Ni(SAr)₂(bpy)₂ and NiCl₂(bpy)₂¹²³ or the combination of DPPF, NiBr₂, and zinc catalyzed the same type of coupling to form diaryl sulfides (Equation (37)).¹²⁴ Some reactions that form unsymmetrical diaryl sulfides also formed symmetrical sulfides. Oxidative addition of the C—S bond of the product diaryl sulfide, exchange of the resulting palladium thiolate with the free arenethiol, and reductive elimination accounts for the formation of the symmetrical sulfide:



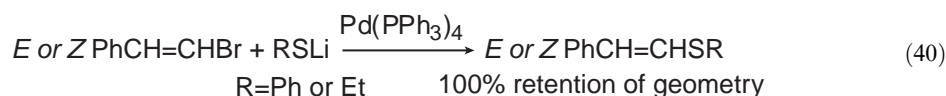
The palladium-catalyzed formation of sulfides can generate polyphenylene sulfide from a dithiol and a dibromoarene, or from 4-bromobenzenethiol (Equation (38)).¹⁷ In 1984 Asahi Glass obtained patents for the formation of this polymer in the presence of palladium and nickel catalysts.^{125,126} In addition, Gingras reported palladium-catalyzed couplings of aryl halides and thiols to form discrete phenylene sulfide oligomers.^{127,128} A number of polyphenylene sulfide wires, ranging from dimeric to pentameric structures, were prepared by the palladium coupling, albeit in modest yields:



Although not directly analogous to the coupling of thiols with aryl halides, the reaction of thiourea with an aryl halide in the presence of palladium catalyst, nevertheless, can be used to generate a thiophenol from an aryl halide after hydrolysis (Equation (39)).¹²⁹ This process occurred in greater than 90% yield with a variety of simple aryl halides:

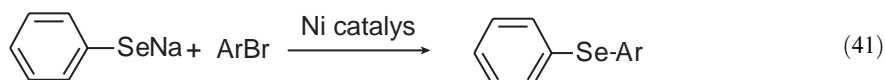


In 1979, the reaction of styrenyl and hexenyl halides with an alkali metal thiophenolate and ethanethiolate was reported (Equation (40)).¹³⁰ Reaction yields exceeded 90%, and the products retained the geometry of the starting olefin. In contrast to the stereospecificity of palladium-catalyzed couplings involving vinyl halides, nickel-catalyzed couplings of vinyl halides with thiolates gave mixtures of stereoisomeric products:¹³¹



The formation of aryl selenides from aryl halides and sodium benzeneselenoate occurs in the presence of nickel catalysts (Equation (41)).¹³² The trend in catalytic activity was shown to be

$[(bpy)_2NiBr_2] > [(phen)_2NiBr_2] = [C_6H_4(PPh_2)_2NiBr_2] = [Ni(acac)_2] > [(NH_2)_2C=S]_6NiBr_2$. Yields ranged from 74% to 94%:

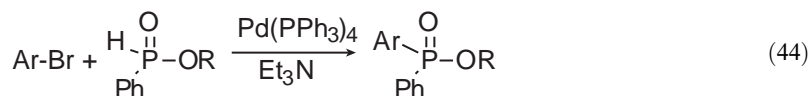
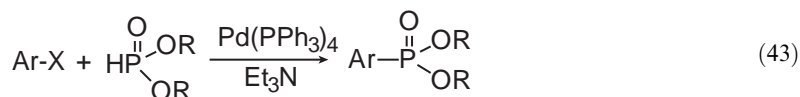
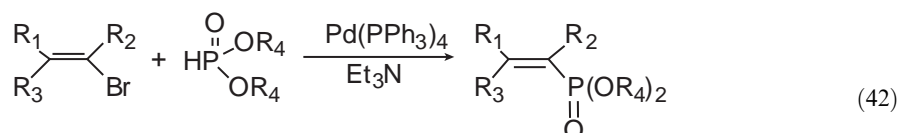


9.7.7 CARBON-PHOSPHORUS BOND-FORMING CROSS-COUPINGS

Nickel and palladium complexes also catalyze the formation of the carbon-phosphorus bonds in phosphorus(V) and phosphorus(III) compounds. Indeed, this chemistry has become a common way to prepare phosphine ligands by the catalytic formation of phosphine oxides and subsequent reduction, by the formation of phosphine boranes and subsequent decomplexation, or by the formation of phosphines directly. The catalytic formation of both aryl and vinyl carbon-phosphorus bonds has been accomplished.

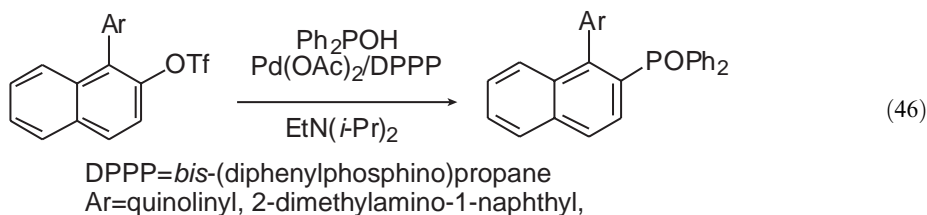
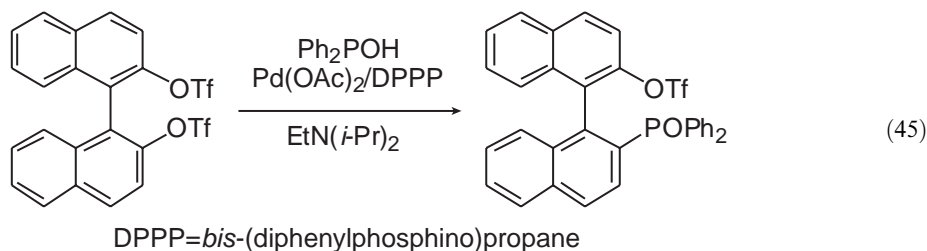
9.7.7.1 Coupling of Aryl and Vinyl Halides with Phosphorus(V) Reagents

The synthesis of vinyl dialkylphosphonates and aryl dialkylphosphonates from vinyl halides and dialkylphosphonates at 90 °C in the presence of triethylamine base and $Pd(PPh_3)_4$ as catalyst has been reported (Equations (42) and (43)).¹³³⁻¹³⁵ The stereochemistry of the alkene was preserved in the vinylation reactions. The formation of aryl phosphonates occurred with many aryl iodides and bromides, including those containing *p*-CH₃, *p*-Cl, *p*-H₃CO, *p*-O₂N, and *p*-NC substituents. Nucleic acid analogs have been generated by this type of P-C coupling. A thymidine dimer linked by a 5'-deoxy-5'-methylidene phosphonate was prepared by coupling of a nucleoside that contained a vinyl bromide and a phosphonate analog of a protected nucleoside.¹³⁶ Monoalkyl benzenephosphonites also coupled with aryl halides to form the unsymmetric alkyl diarylphosphinates (Equation (44)).¹³⁷



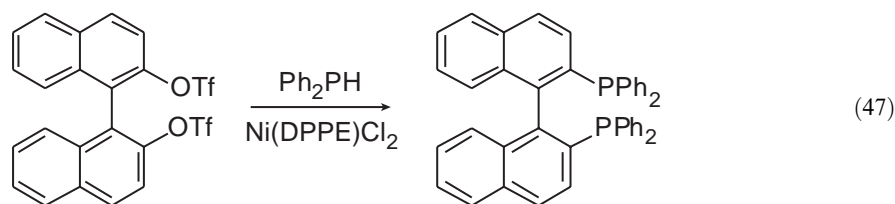
In other cases, palladium complexes of chelating ligands have catalyzed the formation of P-C bonds in phosphorus(V) products. For example, palladium complexes of DPPP catalyzed the coupling of Ph_2POH with (R)-(-)-1,1'-bi-2-naphthol triflate.¹³⁸ The product from monoaddition was obtained. This reaction has been used in the synthesis of a series of optically active 2-(diarylphosphino)-1,1'-binaphthyls.¹³⁹ The selective single addition generates an intermediate that can be used to prepare unsymmetrical, optically pure monophosphines from resolved binaphthol (Equation (45)). A related reaction has been used to generate amino analogs of these binaphthylmonophosphines from a binaphthyl monotriflate (Equation (46)).^{140,141}

1'-(2-(Diarylphosphino) 1-naphthyl)isoquinolines (Quinaps) have been generated by this procedure from the respective triflate,¹⁴² as have analogs of Quinap with different heterocyclic nitrogen donors (Equation (46)).¹⁴³

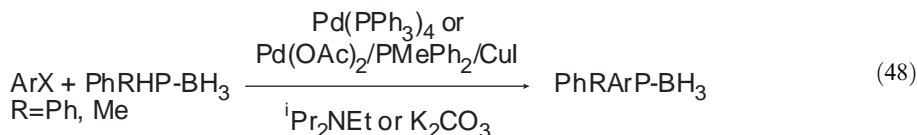


9.7.7.2 Coupling of Aryl and Vinyl Halides with Phosphorus(V) Reagents

Several phosphines have now been prepared by the coupling of phosphorus(III) reagents with aryl halides. BINAP has been prepared by double phosphorylation of the ditriflate of binaphthol, as shown in Equation (47).¹⁴⁴ NiCl₂(DPPE) was used as a catalyst because it was active enough to generate the product from double addition, and the DPPE ligand resisted displacement by the product phosphine. Water-soluble phosphines¹⁴⁵ and phosphine-containing amino acids^{146,147} have also been formed by palladium catalysts. In one case,¹⁴⁵ Pd(OAc)₂ alone was an effective precursor, presumably because a phosphine ligand is formed by the reaction. In other cases^{146,147} triphenylphosphine was present on the catalyst added to the reaction. Vinylphosphines have also been prepared by the reaction of vinyl halides with secondary phosphines in the presence of base. These vinyldiphenylphosphines have been prepared in the presence of conventional catalysts such as (PPh₃)₂PdCl₂:



Complexes of secondary phosphines with boranes are generally air stable and undergo reactions with aryl halides or triflates to form borane-protected phosphines (Equation (48)). Diphenylphosphine borane and aryl triflates or nonaflates (—OSO₂C₄F₉) coupled to form borane-protected triarylphosphine products in high yields in the presence of K₂CO₃ as base and Pd(PPh₃)₄ as catalyst.¹⁴⁸ Methylphenylphosphine borane coupled with various aryl halides and nonaflates in 50–97% yields at temperatures between 0 °C and 25 °C in the presence of Pd(OAc)₂, Ph₂MeP, and CuI as catalyst and ⁱPr₂NEt as base:¹⁴⁹



Although more hydrolytically sensitive than the phosphine boranes, diorganochlorophosphines can be more accessible than diorganophosphines and are not pyrophoric. Thus, the reaction of a chlorophosphine with an aryl halide or aryl triflate in the presence of zinc as a reducing agent and (DPPE)NiCl₂ as catalyst provides a convenient procedure for P–C coupling (Equation (49)).¹⁵⁰ A related nickel-catalyzed process driven by electrochemical reduction has also been reported:¹⁵¹



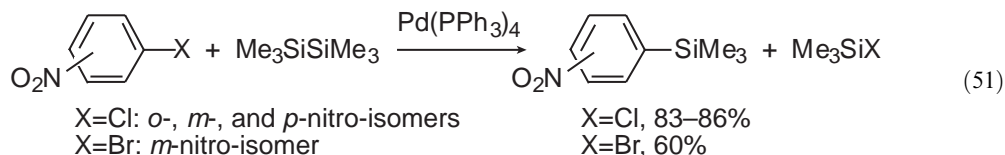
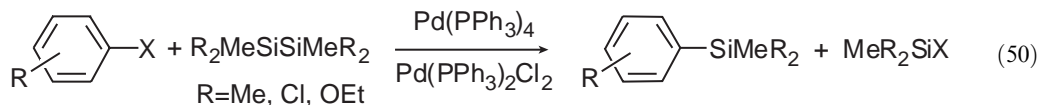
Triphenylphosphine itself has also been used as a reagent for phosphination. P–C cleavage of triarylphosphines is a common pathway for catalyst degradation, but a series of mixed triarylphosphines^{152,153} and atropisomeric *P,N*-ligands^{154–156} has been synthesized from PPh₃ by the P–C cleavage process. The reaction of an aryl halide with PPh₃ occurred in the presence of Pd(OAc)₂, Pd(PPh₃)₄, or palladium on charcoal¹⁵⁷ as catalyst. In only a few cases were the yields as high as those from reactions of aryl halides with secondary phosphines, phosphine oxides, phosphine boranes, or chlorophosphines, but PPh₃ is inexpensive and the use of P–C cleavage for synthesis is unusual.

Catalytic arsination has also been reported.²²⁶ The arsine analog of BINAP (BINAs) has been prepared from the reaction of diphenylarsine with the optically pure ditriflate that is generated from binaphthol. Triarylarisines themselves have been used like triphenyl phosphine, in this case as a reagent for the conversion of aryl triflates to mixed aryl diphenylarsines.

9.7.8 COUPLING OF ARYL HALIDES WITH SILANES, STANNANES, GERMANES, AND BORANES

9.7.8.1 Coupling with Silanes, Stannanes, and Germanes

A patent from 1973 and later manuscripts^{158–163} included reactions of disilane derivatives with organic halides in the presence of palladium complexes of triarylphosphines to give products containing a new silicon–carbon bond. Aryl halides were particularly effective electrophiles (Equation (50)). In general, Pd(PPh₃)₄, Pd(PPh₃)₂Cl₂, or complexes of closely related ligands catalyzed these reactions, albeit at 140–180 °C. Hexamethyldisilane, 1,1,2,2-tetramethyl-1,2-dichlorosilane, 1,2-dimethyl-1,1,2,2-tetrachlorosilane, and 1,2-dimethyl-1,1,2,2-tetraethoxydisilane were suitable silicon reagents. Vinylsilanes and vinylenes bis-silanes have been prepared from halosilanes and vinyl chlorides in modest yields and from halosilanes and vinyl bromides in good yields.¹⁶⁴ Most recently, aryl and alkenyl iodides have been shown to react with triethoxysilane, instead of a disilane, to form organosilanes at room temperature.^{165,166} These reactions were conducted in the presence of a base, such as ⁱPr₂EtN, and the combination of Pd₂(dba)₃ and P(*o*-tol)₃ as catalyst. The silylation of aryl halides provides a route to silanes bearing functional groups that are incompatible with aryl Grignard or lithium reagents.^{167,168} Some examples of this greater functional group tolerance for reactions of aryl halides with disilanes are given in Equation (51):



The coupling of disilanes with aryl halides was improved by adding tris(diethylamino)sulfonium difluoro(trimethyl)silicate (TASF) to generate from the disilane an anionic silyl species.^{169–171} These procedures are analogous to those for the activation of distannanes by added chloride noted below.¹⁷² Under these conditions (Equation (52)) hexamethyldisilane reacted with vinyl iodides in a mixture of THF and HMPA in the presence of Pd(PPh₃)₄ as catalyst to give 53–92% yields of vinylsilanes stereospecifically after only 10 min at room temperature. Reactions of vinyl bromides occurred in lower yields. Protection of esters and nitriles was not necessary, in contrast to the synthesis of organosilanes from organolithium or Grignard reagents:



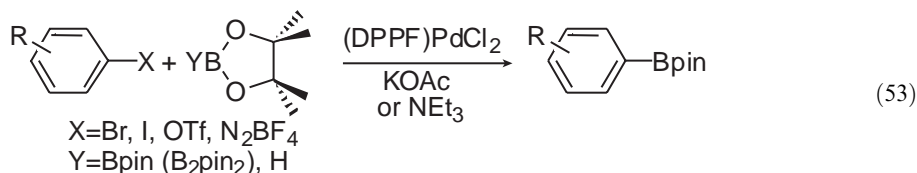
The analogous formation of aryl stannanes and aryl germanes from aryl halides occurs in the presence of catalytic amounts of palladium complexes of triphenylphosphine.^{160,161,172,173} Hexabutyl- and hexamethyldistannane reacted with some aryl bromides to give arylstannanes, but the yields were lower than they were for reactions of disilanes. Biaryl products formed in competition with arylstannanes. Reactions conducted with a 2:1 ratio of stannane to aryl halide formed less biaryl, and yields of arylstannane were higher. Analogous reactions of hexaethyldigermene occurred to form some aryl germane product, but biaryl compounds were, in this case, the major product. Reactions of mixed metal reagents such as Bu₃SnSiMe₃ formed exclusively aryl silane products.¹⁶¹ The addition of chloride sources improved yields.¹⁷² Coupling of tin hydrides with aryl halides in the presence of base and PdCl₂(PMePh₂)₂ as catalyst to form arylstannanes has also been reported.¹⁷⁴

These reactions to form aryl–tin bonds could occur by initial oxidative addition of the aryl halide or the distannane. The stoichiometric reaction between [(PPh₃)₂Pd(Ph)(I)] and Me₃SnSnMe₃ in the presence of chloride generated good yields of the aryltin product. This result suggests that the reactions occur by initial oxidative addition of aryl halide.

The stannylation and silylation of heteroaryl halides has also been studied. The stannylation of 4-iodo pyrimidine was conducted with hexamethyl and hexa-*n*-butyl ditin in the presence of fluoride ion and Pd(PPh₃)₂(OAc)₂ as catalyst. The stannylation of 5-bromopyrimidine occurred in the highest yields in the presence of the “ligandless catalyst” bis(π-allylpalladium chloride).¹⁷⁵ The silylation of bromopyridines, bromopyrimidines, and bromoquinolines also occurred after 96 h at 160 °C with Pd(PPh₃)₄ as catalyst in HMPT solvent.¹⁶²

9.7.8.2 Coupling with Boranes

Arylboronic acids have become one of the most important types of reagent for cross-coupling because of the many improvements and applications of the Suzuki–Miyaura reaction. In 1995, the cross coupling of haloarenes with alkoxydiboron compounds catalyzed by palladium complexes (Equation (53)) was reported.¹⁷⁶ Reactions of electron-rich aryl iodides occurred in higher yields than did reactions of the analogous bromides, but reactions of electron-neutral or electron-poor aryl bromides occurred in good yields. Sterically hindered haloarenes coupled in high yields, and *p*-dibromobenzene reacted cleanly to give the diboronic ester that is the unsubstituted version of diboronic esters that have been used in polyphenylene syntheses.^{177–180} Aryl triflates and aryl diazonium salts were also suitable substrates. Related reactions of chloroarenes catalyzed by palladium complexes of PCy₃ have been reported. The borylation of aryl halides has also been conducted with solid-supported aryl iodides.¹⁸¹

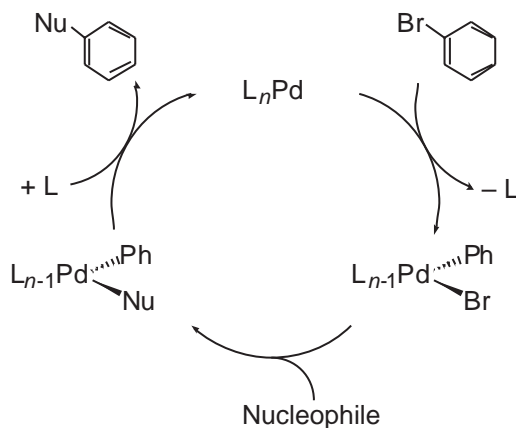


In addition, the reactions of dialkoxyboranes, such as pinacolborane, with aryl halides and base have been reported.^{182,183} The yields are lower for reactions of this reagent in some cases than they are for reactions of the diboron reagent, but good yields are obtained from aryl bromides in most cases. Dialkoxyboranes are less expensive than the analogous diboron compounds, but the diboron compound is very stable thermally and is stable in air.

Almost all of the couplings that form arylboronic esters from aryl bromides and iodides have been conducted in the presence of catalysts containing DPPF as ligand. Reactions catalyzed by (DPPF)PdCl₂ occurred in higher yields than did reactions catalyzed by palladium complexes of triaryl monophosphines. Of course, the palladium complexes used in the generation of arylboronic esters from the haloarenes are also catalysts for the cross-coupling of the resulting boron reagent with organic electrophiles. Thus, the choice of NaOAc as base was important to observe borylation of the aryl halides without formation of the symmetrical biaryl by coupling of the arylboronic ester product with the aryl halide reagent. Nevertheless, the dual activity of the catalyst does allow one to conduct a one-pot procedure to form the arylboronic ester and conduct a subsequent coupling with a second aryl halide.^{184,185}

9.7.9 INTERMEDIATES IN THE COUPLING CHEMISTRY

Cross-coupling to form carbon heteroatom bonds occurs by oxidative addition of an organic halide, generation of an aryl- or vinylpalladium amido, alkoxo, thiolato, phosphido, silyl, stannyl, germyl, or boryl complex, and reductive elimination (Scheme 2). The relative rates and thermodynamics of the individual steps and the precise structure of the intermediates depend on the substrate and catalyst. A full discussion of the mechanism for each type of substrate and each catalyst is beyond the scope of this review. However, a series of reviews and primary literature has begun to provide information on the overall catalytic process.^{18,19,22,23,77,186}



Scheme 2

A series of interesting coordination compounds is involved in the cross-coupling chemistry described in this section. Because some of these complexes are included in other sections of the compendium, only selected compounds directly related to the catalytic chemistry will be discussed here. For example, Pd(PPh₃)₄ is a classic palladium(0) complex and a common catalyst. Its catalytic reactions involve well-known arylpalladium halide complexes. Yet, the arylpalladium thiolate, amide, and alkoxide complexes ligated by even common arylphosphines, such as PPh₃, had not been prepared until recently. Moreover, isolated complexes containing ligands, such as the sterically hindered phosphines, that have been designed or selected to improve cross-coupling are less common. A few complexes containing these hindered ligands, such as Pd(P^{*t*}Bu₃)₂, are known,^{187–189} but arylpalladium halide complexes of most of the most hindered ligands have been prepared only recently.¹⁹⁰

Several new palladium(0) complexes of *t*-butylphosphine ligands, such as those in Figure 4, have been prepared. For example, the palladium(0) complexes of the parent ferrocenyl ligand¹¹³ and of a biarylphosphine¹⁹¹ that was present in Figure 3 have been characterized crystallographically. The palladium(0) complex of the pentaphenylferrocenyl ligand has been identified, but its structure has not been reported.¹¹²

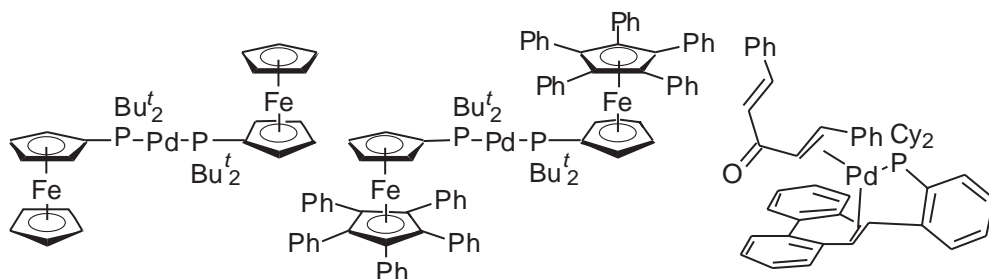
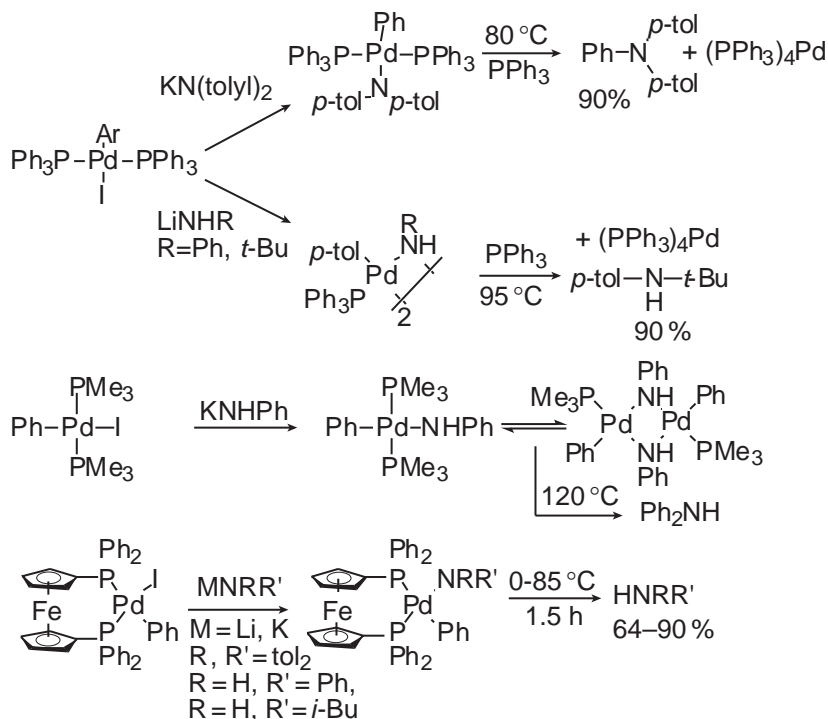


Figure 4 Isolated palladium(0) complexes of sterically hindered alkylphosphines used in C–X coupling.

The oxidative addition of aryl halides to almost all palladium(0) complexes generates stable arylpalladium halides. The mechanism of this reaction has been studied in detail because of its importance to all types of cross-coupling.^{55,77,186,192–202} However, the oxidative addition of aryl bromides and chlorides to $\text{Pd}(\text{P}^t\text{Bu}_3)_2$ has been shown to be thermodynamically unfavorable in some cases.²⁰³ This information does not preclude oxidative addition of aryl halides to $\text{Pd}(\text{P}^t\text{Bu}_3)_2$ in the mechanism of the amination because the thermodynamics are likely to be only mildly unfavorable. In fact, reaction of an excess of PI with a combination of $\text{Pd}(\text{dba})_2$ and P^tBu_3 or reaction of an excess of PhDr with $\text{Pd}(0)$ complexes of $\text{P}^t\text{Bu}_2(1\text{-adamantyl})$, $\text{P}^t\text{Bu}_2(1\text{-adamantyl})$, and $\text{Ph}_5\text{FcP}^t\text{Bu}_2$ have all been shown to form metastable arylpalladium halide complexes.¹⁹⁰ The structures of the arylpalladium halide complexes bearing these ligands are unusual examples of arylpalladium halide complexes containing a single dative ligand. A weak agostic $\text{M}-\text{H}-\text{C}$ interaction seems to contribute to the stability of these species.

During the cross-couplings to form C–N, C–O, C–S, and C–P bonds, the arylpalladium halide complexes are converted to arylpalladium amide, alkoxide, thiolate, and phosphide complexes. Examples of each type of complex have now been isolated, and the reductive elimination of the organic products has been studied. Although the reductive elimination to form carbon–hydrogen and carbon–carbon bonds is common, reductive elimination to form carbon–heteroatom bonds has been studied only recently. This reductive elimination chemistry has been reviewed.²³

Scheme 3 summarizes the reductive elimination chemistry of arylpalladium amides. Arylpalladium amido complexes containing PPh_3 as the dative ligand were stable enough to isolate, and

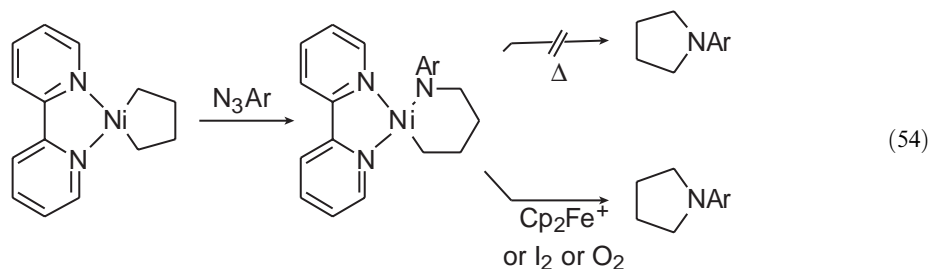


Scheme 3

they underwent reductive elimination of amine in high yield in the presence of PPh_3 .^{36,204,205} The added PPh_3 serves to generate a stable palladium(0) product. Arylpalladium amide complexes of PMe_3 also undergo reductive elimination. In this case the reductive elimination occurs in competition with the formation of dimeric amido complexes.²⁰⁶ Mechanistic studies of the reductive elimination of amine from the PPh_3 complexes^{204,205} showed that reductive elimination occurred by two concurrent pathways, one involving reductive elimination from a three-coordinate intermediate formed by dissociation of phosphine, and one involving reductive elimination from a four-coordinate complex that is presumably the *cis*-isomer of the starting *trans* complex. The dimeric complexes underwent reductive elimination after cleavage to form a three-coordinate, monomeric, monophosphine amido complex.

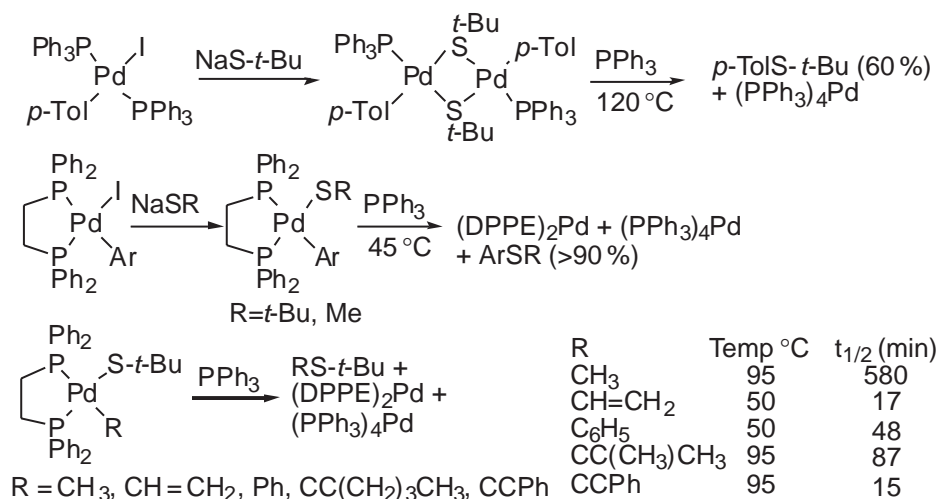
Arylpalladium amido complexes ligated by chelating phosphines have also been prepared, and these complexes also underwent reductive elimination.^{36,205} Studies of the complexes ligated by DPPF revealed important electronic effects on the rate of C—N bond-forming reductive elimination. Complexes with more electron-rich amido groups underwent reductive elimination faster than those with less electron-rich amido groups, and complexes with more electron-rich palladium-bound aryl groups underwent reductive elimination slower than those with less electron-rich palladium-bound aryl groups. Reductive eliminations of *N*-aryl azoles, *N*-aryl benzophenone imines, and *N*-aryl hydrazones from palladium(II) phosphine complexes also occurred. Complexes of azolyl groups⁹³ underwent reductive elimination slowly because these groups are less electron-donating than are amido groups, while complexes of diphenylmethylenimido ($-\text{N}=\text{CPh}_2$)⁹³ and η^1 -hydrazonato ($-\text{NHN}=\text{CPh}_2$)⁹⁹ ligands underwent reductive elimination at rates that were similar to those for reductive elimination of amines from arylpalladium anilido complexes because methyleneimido and hydrazonato ligands are about as electron-donating as arylamido groups.

Alkylnickel amido complexes ligated by bipyridine have been prepared that undergo reductive elimination of *N*-alkyl amines (Equation (54)).^{207,208} Unlike the phosphine-ligated palladium arylamides, these complexes underwent reductive elimination only after oxidation to nickel(III). Thermally induced reductive elimination of alkylamines from phosphine-ligated nickel complexes appears to occur after consumption of phosphine by arylazides:²⁰⁹



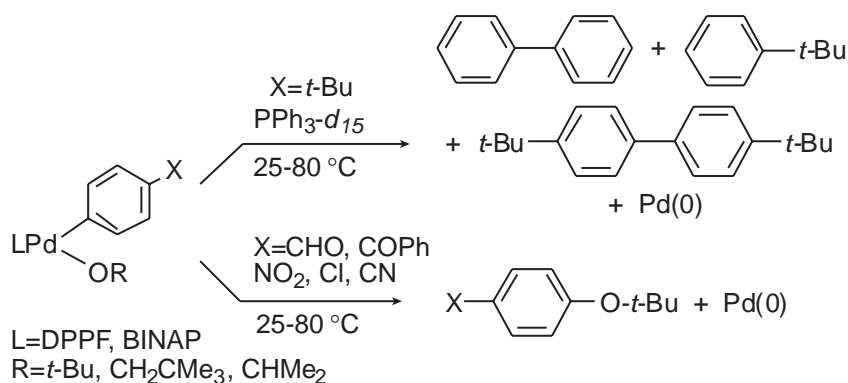
Arylpalladium and arylnickel thiolate complexes undergo reductive elimination of sulfides in high yields in many cases (Scheme 4).^{123,210–212} For example, $[(\text{bpy})_2\text{Ni}(\text{SR})_2]$ reacted with aryl halides to form aryl sulfide products, although an arylnickel thiolate complex was not observed directly as an intermediate.¹²³ Other work has focused on reductive elimination from isolated arylpalladium thiolates.^{210–212} PPh_3 -ligated arylpalladium thiolates are dimeric and underwent reductive elimination in modest yields at 120°C ,²¹² but isolated DPPE-ligated complexes are stable at room temperature in most cases and underwent reductive elimination of sulfide in high yields under mild conditions.²¹¹ Reductive elimination occurred directly from this four-coordinate complex containing DPPE. Electronic factors again influenced reaction rates, although in a less pronounced manner than they influenced reductive elimination from the amido complexes. Arylpalladium thiolate complexes with more electron-donating thiolate groups underwent reductive elimination faster than those with less electron-donating groups, and complexes with more electron-rich palladium-bound aryl groups underwent reductive elimination more slowly than those with more electron-poor palladium-bound aryl groups. Various hydrocarbylpalladium thiolate complexes were prepared to determine the influence of hybridization of the palladium-bound carbon on the rate of reductive elimination. The rates for reductive elimination followed the trend, vinyl > aryl > alkynyl > alkyl. These relative rates have been explained by a combination of the coordinating ability of the π -system of the hydrocarbyl group and the amount of distortion required for this coordination. This explanation for the relative rates was supported by

studies that revealed the effects of the steric properties of the thiolate and palladium-bound aryl group on reductive elimination.



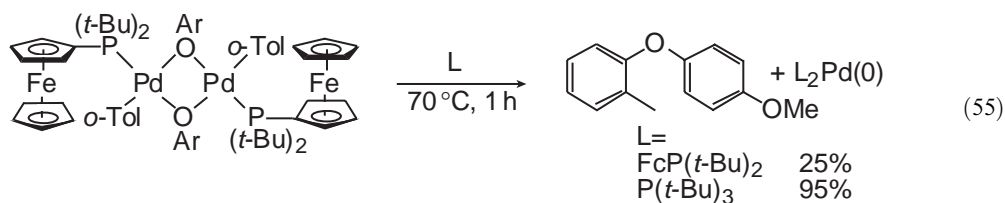
Scheme 4

The reductive elimination of ethers from arylpalladium alkoxide complexes has also been reported (Schemes 5 and 6).^{107,113,213,214} The effect of the electronic properties of ligands on the rate of reductive elimination of amines and sulfides suggests that the weaker electron-donating ability of the alkoxo ligand would make the reductive elimination of aryl ethers slow. Indeed, the first arylpalladium alkoxo complexes that underwent reductive elimination of ethers contained a strongly electron-withdrawing substituent on the palladium-bound aryl group (Scheme 5).¹⁰⁷ Subsequent studies showed that reductive elimination of aryl ethers occurred in good yields from DPPF and BINAP-ligated palladium complexes generated *in situ* when the complexes contained electron-poor, palladium-bound aryl groups.²¹⁴ BINAP-ligated arylpalladium alkoxo complexes underwent reductive elimination faster than analogous DPPF complexes. Complexes with more sterically hindered alkoxo groups underwent elimination faster than those with less hindered alkoxo groups.

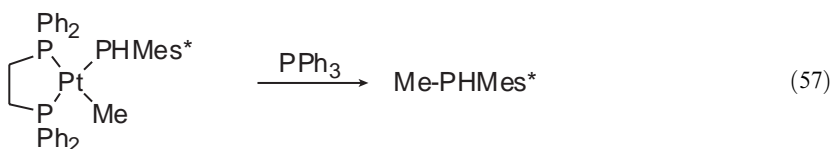
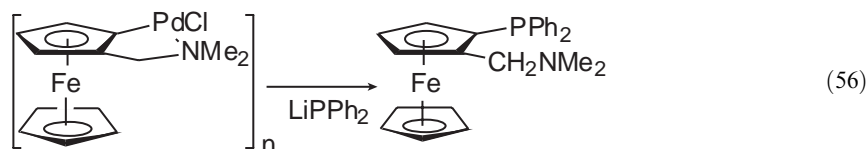


Scheme 5

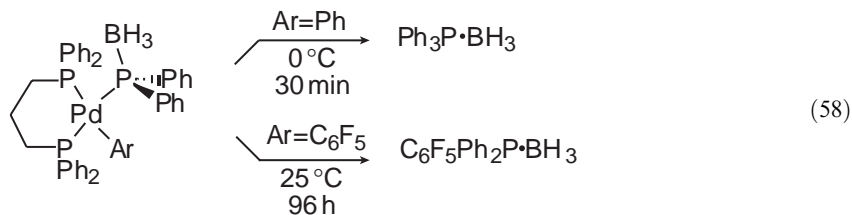
More recently, reductive elimination of aryl ethers has been reported from complexes that lack the activating substituent on the palladium-bound aryl group (Equation (55)). These complexes contain sterically hindered phosphine ligands, and these results demonstrate how steric effects of the dative ligand can overcome the electronic constraints of the reaction.^{112,113} Reductive elimination of oxygen heterocycles upon oxidation of nickel oxametallacycles has also been reported, but yields of the organic product were lower than they were for oxidatively induced reductive eliminations of alkylamines from nickel(II) mentioned above.²¹⁵⁻²¹⁷



Organometallic phosphido and phosphidoborane complexes undergo facile reductive elimination to form P—C bonds (Equations (56) and (57)). One of the first examples of P—C bond-forming reductive elimination was the formation of 1-diphenylphosphino-2-dimethylaminomethylferrocene from the ferrocenyl halide complex in Equation (56) and lithiumdiphenylphosphide.²¹⁸ A palladium phosphido complex was not detected during these studies, but a ferrocenylpalladium phosphide most likely forms the P—C bond by reductive elimination. Recent studies have shown that reductive elimination to form the P—C bond in phosphines occurs rapidly even from alkylpalladium or alkylplatinum phosphido complexes (Equation (57)).²¹⁹ Presumably, the strongly nucleophilicity and polarizability of the phosphido ligand causes these types of complexes to undergo fast reductive elimination. P—C bond-forming reductive elimination from phosphido complexes of metals outside of the nickel triad, such as tungsten²²⁰ and iridium, has also been observed.²²¹



Complexes of phosphidoboranes, instead of phosphides, have also been generated, and these complexes undergo rapid formation of triarylphosphineboranes (Equation (58)).²²² To generate a stable arylpalladium phosphido borane complex, a pentafluorophenylpalladium phosphidoborane complex was generated. This complex was stable enough at room temperature to be isolated and characterized crystallographically:



9.7.10 REFERENCES

- Diederich, F.; Stang, P. J., Eds. *Metal Catalyzed Cross-coupling Reactions*; Wiley-VCH: Weinheim, 1998.
- Miyaura, N.; Suzuki, A. *Chem. Rev.* **1995**, *95*, 2457–2483.
- Kumada, M. *Pure Appl. Chem.* **1980**, *52*, 669–679.
- Stanforth, S. P. *Tetrahedron* **1998**, *54*, 263–303.
- Suzuki, A. *J. Organomet. Chem.* **1999**, *576*, 147–168.
- Jensen, A. E.; Knochel, P. *J. Org. Chem.* **2002**, *67*, 79–85.
- Giovannini, R.; Studemann, T.; Devasagayaraj, A.; Dussin, G.; Knochel, P. *J. Org. Chem.* **1999**, *64*, 3544–3553.
- Giovannini, R.; Studemann, T.; Dussin, G.; Knochel, P. *Angew. Chem. Int. Ed. Engl.* **1998**, *37*, 2387–2390.

9. Netherton, M. R.; Dai, C. Y.; Neuschütz, K.; Fu, G. C. *J. Am. Chem. Soc.* **2001**, *123*, 10099–10100.
10. Strukelj, M.; Jordan, R. H.; Dodabalapur, A. *J. Am. Chem. Soc.* **1996**, *118*, 1213.
11. Bellmann, E.; Shaheen, S.; Thayumanavan, S.; Barlow, S.; Grubbs, R.; Marder, S.; Kippelen, B.; Peyghambarian, N. *Chem. Mater.* **1998**, *10*, 1668–1676.
12. Chen, J. P.; Klaerner, G.; Lee, J.-I.; Markiewicz, D.; Lee, V. Y.; Miller, R. D.; Scott, J. C. *Synth. Met.* **1999**, *107*, 129–135.
13. MacDiarmid, A. G. *Angew. Chem. Int. Ed. Engl. Int. Ed.* **2001**, *40*, 2581–2590.
14. MacDiarmid, A. G.; Epstein, A. J. *Faraday Discuss. Chem. Soc.* **1989**, *88*, 317–332.
15. MacDiarmid, A. G.; Epstein, A. J. In *Science and Applications of Conducting Polymers*; W. R. Salaneck.; D. T. Clark and E. J. Samuelsen, Ed.; Adam Hilger: New York, 1991; p 117.
16. Odian, G. In *Principles of Polymerization*; 3rd ed.; Wiley: New York, 1991; pp 152–155.
17. Cleary, J. W. *Polym. Sci. Technol.* **1985**, *31*, 187.
18. Hartwig, J. F. *Synlett* **1997**, 329–340.
19. Hartwig, J. F. *Angew. Chem. Int. Ed. Engl.* **1998**, *37*, 2046–2067.
20. Wolfe, J. P.; Wagaw, S.; Marcoux, J.-F.; Buchwald, S. L. *Acc. Chem. Res.* **1998**, *31*, 805–818.
21. Yang, B. H.; Buchwald, S. L. *J. Organomet. Chem.* **1999**, *576*, 125–146.
22. Hartwig, J. F. In *Modern Amination Methods*; A. Ricci, Ed.; Wiley-VCH: Weinheim, 2000.
23. Hartwig, J. F. *Acc. Chem. Res.* **1998**, *31*, 852–860.
24. Boger, D. L.; Panek, J. S. *Tetrahedron Lett.* **1984**, *25*, 3175–3178.
25. Boger, D. L.; Duff, S. R.; Panek, J. S.; Yasuda, M. *J. Org. Chem.* **1985**, *50*, 5782–5789.
26. Boger, D. L.; Duff, S. R.; Panek, J. S.; Yasuda, M. *J. Org. Chem.* **1985**, *50*, 5790–5795.
27. Kosugi, M.; Kameyama, M.; Migita, T. *Chem. Lett.* **1983**, 927–928.
28. Beletskaya, I. P. *J. Organomet. Chem.* **1983**, *250*, 551–564.
29. Kosugi, M.; Ogata, T.; Terada, M.; Sano, H.; Migita, T. *Bull. Chem. Soc. Jpn.* **1985**, *58*, 3657–3658.
30. Carpita, A.; Rossi, R.; Scamuzzi, B. *Tetrahedron Lett.* **1989**, *30*, 2699–2702.
31. Tunney, S. E.; Stille, J. K. *J. Org. Chem.* **1987**, *52*, 748–753.
32. Veits, Y. A.; Karlstedt, N. B.; Beletskaya, I. P. *Russ. J. Org. Chem.* **1994**, *30*, 70–73.
33. Louie, J.; Hartwig, J. F. *Tetrahedron Lett.* **1995**, *36*, 3609–3612.
34. Guram, A. S.; Rennels, R. A.; Buchwald, S. L. *Angew. Chem. Int. Ed. Engl.* **1995**, *34*, 1348–1350.
35. Wolfe, J. P.; Rennels, R. A.; Buchwald, S. L. *Tetrahedron* **1996**, *52*, 7525–7546.
36. Driver, M. S.; Hartwig, J. F. *J. Am. Chem. Soc.* **1996**, *118*, 7217–7218.
37. Wolfe, J. P.; Wagaw, S.; Buchwald, S. L. *J. Am. Chem. Soc.* **1996**, *118*, 7215–7216.
38. Wagaw, S.; Rennels, R. A.; Buchwald, S. L. *J. Am. Chem. Soc.* **1997**, *119*, 8451–8458.
39. Rossen, K.; Pye, P. J.; Maliakal, A.; Volante, R. P. *J. Org. Chem.* **1997**, *62*, 6462–6463.
40. Sadighi, J. P.; Harris, M. C.; Buchwald, S. L. *Tetrahedron Lett.* **1998**, *39*, 5327–5330.
41. Marcoux, J.-F.; Wagaw, S.; Buchwald, S. L. *J. Org. Chem.* **1997**, *62*, 1568–1569.
42. Wolfe, J. P.; Buchwald, S. L. *Tetrahedron Lett.* **1997**, *38*, 6359–6362.
43. Kamikawa, K.; Sugimoto, S.; Uemura, M. *J. Org. Chem.* **1998**, *63*, 8407–8410.
44. Devon, T. J.; Phillips, G. W.; Puckette, T. A.; Stavinoha, J. L.; Vanderbilt, J. J. **1987**, U.S. Patent 4694109.
45. Casey, C. P.; Whiteker, G. T.; Melville, M. G.; Petrovich, L. M.; Gavney, J. A., Jr.; Powell, D. R. *J. Am. Chem. Soc.* **1992**, *114*, 5535–5543.
46. Wullner, G.; Jansch, H.; Kannenberg, S.; Schubert, F.; Boche, G. *Chem. Commun.* **1998**, 1509–1510.
47. Louie, J.; Driver, M. S.; Hamann, B. C.; Hartwig, J. F. *J. Org. Chem.* **1997**, *62*, 1268–1273.
48. Wolfe, J. P.; Buchwald, S. L. *J. Org. Chem.* **1997**, *62*, 1264–1267.
49. Åhman, J.; Buchwald, S. L. *Tetrahedron Lett.* **1997**, *38*, 6363–6366.
50. Torisawa, Y.; Nishi, T.; Minamikawa, J. *Bioorg. Med. Chem. Lett.* **2000**, *10*, 2489–2491.
51. Paul, F.; Patt, J.; Hartwig, J. F. *Organometallics* **1995**, *14*, 3030–3039.
52. Wagaw, S.; Buchwald, S. L. *J. Org. Chem.* **1996**, *61*, 7240–7241.
53. Coulson, D. R. *Inorg. Synth.* **1990**, *28*, 107–109.
54. Hartwig, J. F.; Richards, S.; Barañano, D.; Paul, F. *J. Am. Chem. Soc.* **1996**, *118*, 3626–3633.
55. Hartwig, J. F.; Paul, F. *J. Am. Chem. Soc.* **1995**, *117*, 5373–5374.
56. Nishiyama, M.; Yamamoto, T.; Koie, Y. *Tetrahedron Lett.* **1998**, *39*, 617–620.
57. Yamamoto, T.; Nishiyama, M.; Koie, Y. *Tetrahedron Lett.* **1998**, *39*, 2367–2370.
58. Beller, M.; Reirmeier, T. H.; Reisinger, C.; Herrman, W. A. *Tetrahedron Lett.* **1997**, *38*, 2073–2074.
59. Saito, S.; Sakai, M.; Miyaura, N. *Tetrahedron Lett.* **1996**, *37*, 2993–2996.
60. Indolese, A. F. *Tetrahedron Lett.* **1997**, *38*, 3513–3516.
61. Saito, S.; Oh-tani, S.; Miyaura, N. *J. Org. Chem.* **1997**, *62*, 8024–8030.
62. Miller, J.; Farrell, R. *Tetrahedron Lett.* **1998**, 6441–6444.
63. Galland, J.-C.; Savignac, M.; Genet, J.-P. *Tetrahedron Lett.* **1999**, *40*, 2323–2326.
64. Lipshutz, B. H.; Blomgren, P. A. *J. Am. Chem. Soc.* **1999**, *121*, 5819–5820.
65. Brenner, E.; Fort, Y. *Tetrahedron Lett.* **1998**, *39*, 5359–5362.
66. Wolfe, J. P.; Buchwald, S. L. *J. Am. Chem. Soc.* **1997**, *119*, 6054–6058.
67. Hamann, B. C.; Hartwig, J. F. *J. Am. Chem. Soc.* **1998**, *120*, 7369–7370.
68. Butler, I. R.; Cullen, W. R.; Kim, T. J.; Rettig, S. J.; Trotter, J. *Organometallics* **1985**, *4*, 972–980.
69. Cullen, W. R.; Kim, T. J.; Einstein, F. W. B.; Jones, T. *Organometallics* **1983**, *2*, 714–719.
70. Blaser, H.; Spindler, F. *Chimia* **1997**, *51*, 297–299.
71. Togni, A.; Breutel, C.; Soares, M. C.; Zanetti, N.; Gerfin, T.; Gramlich, V.; Spindler, F.; Rihs, G. *Inorg. Chim. Acta* **1994**, *222*, 213–224.
72. Togni, A.; Breutel, C.; Schnyder, A.; Spindler, F.; Landert, H.; Tijani, A. *J. Am. Chem. Soc.* **1994**, *116*, 4062–4066.
73. Old, D. W.; Wolfe, J. P.; Buchwald, S. L. *J. Am. Chem. Soc.* **1998**, *120*, 9722–9723.
74. Kocovsky, P.; Vyskocil, S.; Cisarova, I.; Sejbál, J.; Tíclerová, I.; Smrcina, M.; Guy, C.; Lloyd-Jones; Stephen, S. C.; Butts, C. P.; Murray, M.; Langer, V. *J. Am. Chem. Soc.* **1999**, *121*, 7714–7715.
75. Bei, X.; Uno, T.; Norris, J.; Turner, H. W.; Weinberg, W. H.; Guram, A. S. *Organometallics* **1999**, *18*, 1840–1853.

76. Bei, X.; Guram, A. S.; Turner, H. W.; Weinberg, W. H. *Tetrahedron Lett.* **1999**, *40*, 1237–1240.
77. Alcazar-Roman, L. M.; Hartwig, J. F. *J. Am. Chem. Soc.* **2001**, *123*, 12905–12906.
78. Hartwig, J. F.; Kawatsura, M.; Hauck, S. I.; Shaughnessy, K. H.; Alcazar-Roman, L. M. *J. Org. Chem.* **1999**, *64*, 5575–5580.
79. Netherton, M. R.; Fu, G. C. *Org. Lett.* **2001**, *3*, 4295–4298.
80. Huang, J.; Grasa, G.; Nolan, S. P. *Org. Lett.* **1999**, *1*, 1307–1309.
81. Grasa, G. A.; Viciu, M. S.; Huang, J. K.; Nolan, S. P. *J. Org. Chem.* **2001**, *66*, 7729–7737.
82. Stauffer, S.; Hauck, S. I.; Lee, S.; Stambuli, J.; Hartwig, J. F. *Org. Lett.* **2000**, *2*, 1423–1426.
83. Huang, J. K.; Schanz, H. J.; Stevens, E. D.; Nolan, S. P. *Organometallics* **1999**, *18*, 2370–2375.
84. Caddick, S.; Cloke, F. G. N.; Clentsmith, G. K. B.; Hitchcock, P. B.; McKercher, D.; Titcomb, L. R.; Williams, M. R. V. *J. Organomet. Chem.* **2001**, *617–618*, 635–639.
85. Li, G. Y. *Angew. Chem. Int. Ed. Engl.* **2001**, *40*, 1513–1516.
86. Li, G. Y.; Zheng, G.; Noonan, A. F. *J. Org. Chem.* **2001**, *66*, 8677–8681.
87. Djakovitch, L.; Wagner, M.; Kohler, K. *J. Organomet. Chem.* **1999**, *592*, 225–234.
88. Lipshutz, B. H.; Ueda, H. *Angew. Chem. Int. Ed. Engl.* **2000**, *39*, 4492–4494.
89. Yang, B. H.; Buchwald, S. L. *Org. Lett.* **1999**, *1*, 35–37.
90. Yin, J.; Buchwald, S. L. *Org. Lett.* **2000**, *2*, 1101–1104.
91. Shakespeare, W. *Tetrahedron Lett.* **1999**, *40*, 2035–2038.
92. Edmondson, S. D.; Mastracchio, A.; Parmee, E. R. *Org. Lett.* **2000**, *2*, 1109–1112.
93. Mann, G.; Hartwig, J. F.; Driver, M. S.; Fernandez-Rivas, C. *J. Am. Chem. Soc.* **1998**, *120*, 827–828.
94. Wolfe, J. P.; Åhman, J.; Sadighi, J. P.; Singer, R. A.; Buchwald, S. L. *Tetrahedron Lett.* **1997**, *38*, 6367–6370.
95. Bolm, C.; Hildebrand, J. P. *J. Org. Chem.* **2000**, *65*, 169–175.
96. Bolm, C.; Hildebrand, J. P. *Tetrahedron Lett.* **1998**, *39*, 5731–5734.
97. Wagaw, S.; Yang, B. H.; Buchwald, S. L. *J. Am. Chem. Soc.* **1998**, *120*, 6621–6622.
98. Wagaw, S.; Yang, B.; Buchwald, S. L. *J. Am. Chem. Soc.* **1999**, *121*, 10251–10263.
99. Hartwig, J. F. *Angew. Chem. Int. Ed. Engl.* **1998**, *37*, 2090–2093.
100. Haddad, N.; Baron, J. *Tetrahedron Lett.* **2002**, *43*, 2171–2173.
101. Wang, Z.; Skerlj, R. T.; Bridger, G. J. *Tetrahedron Lett.* **1999**, *40*, 3543–3546.
102. Watanabe, M.; Nishiyama, M.; Yamamoto, T.; Koie, Y. *Tetrahedron Lett.* **2000**, *41*, 481–483.
103. Old, D. W.; Harris, M. C.; Buchwald, S. L. *Org. Lett.* **2000**, *2*, 1403–1406.
104. Beletskaya, I. P.; Davydov, D. V.; Morenomanas, M. *Tetrahedron Lett.* **1998**, *39*, 5617–5620.
105. Beletskaya, I. P.; Davydov, D. V.; Morenomanas, M. *Tetrahedron Lett.* **1998**, *39*, 5621–5622.
106. Hori, K.; Mori, M. *J. Am. Chem. Soc.* **1998**, *120*, 7651–7652.
107. Mann, G.; Hartwig, J. F. *J. Am. Chem. Soc.* **1996**, *118*, 13109–13110.
108. Mann, G.; Hartwig, J. F. *J. Org. Chem.* **1997**, *62*, 5413–5418.
109. Mann, G.; Hartwig, J. F. *Tetrahedron Lett.* **1997**, *38*, 8005–8008.
110. Palucki, M.; Wolfe, J. P.; Buchwald, S. L. *J. Am. Chem. Soc.* **1997**, *119*, 3395–3396.
111. Palucki, M.; Wolfe, J. P.; Buchwald, S. L. *J. Am. Chem. Soc.* **1996**, *118*, 10333–10334.
112. Shelby, Q.; Kataoka, N.; Mann, G.; Hartwig, J. F. *J. Am. Chem. Soc.* **2000**, *122*, 10718–10719.
113. Mann, G.; Incarvito, C.; Rheingold, A. L.; Hartwig, J. F. *J. Am. Chem. Soc.* **1999**, *121*, 3224–3225.
114. Aranyos, A.; Old, D. W.; Kiyomori, A.; Wolfe, J. P.; Sadighi, J. P.; Buchwald, S. L. *J. Am. Chem. Soc.* **1999**, *121*, 4369–4378.
115. Parrish, C. A.; Buchwald, S. L. *J. Org. Chem.* **2001**, *66*, 2498–2500.
116. Torraca, K. E.; Huang, X. H.; Parrish, C. A.; Buchwald, S. L. *J. Am. Chem. Soc.* **2001**, *123*, 10770–10771.
117. Kuwabe, S.; Torraca, K. E.; Buchwald, S. L. *J. Am. Chem. Soc.* **2001**, *123*, 12202–12206.
118. Kosugi, M.; Shimizu, T.; Migita, T. *Chem. Lett.* **1978**, 13–14.
119. Migita, T.; Shimizu, T.; Asami, Y.; Shiobara, J.; Kato, Y.; Kosugi, M. *Bull. Chem. Soc. Jpn.* **1980**, *53*, 1385–1389.
120. Schopfer, U.; Schlapbach, A. *Tetrahedron* **2001**, *57*, 3069–3073.
121. Wendeborn, S.; Berteina, S.; Brill, W. K. D.; Demesmaeker, A. *Synlett* **1998**, 671–675.
122. Cristau, H. J.; Chabaud, B.; Chêne, A.; Christol, H. *Synthesis* **1981**, 892–894.
123. Yamamoto, T.; Sekine, Y. *Inorg. Chim. Acta* **1984**, *83*, 47–53.
124. Takagi, K. *Chem. Lett.* **1987**, 2221–2224.
125. Asahi Glass, K. K. *Chem. Abstr.* **1984**, *100*, 192566s.
126. Asahi Glass, K. K. *Chem. Abstr.* **1984**, *100*, 192567t.
127. Pinchart, A.; Dallaire, C.; Gingras, M. *Tetrahedron Lett.* **1998**, *39*, 543–546.
128. Gingras, M.; Pinchart, A.; Dallaire, C. *Angew. Chem. Int. Ed. Engl.* **1998**, *37*, 3149–3151.
129. Takagi, K. *Chem. Lett.* **1985**, 1307.
130. Murahashi, S. I.; Yamamura, M.; Yanagisawa, K.; Mita, N.; Kondo, K. *J. Org. Chem.* **1979**, *44*, 2408–2417.
131. Cristau, H. J.; Chabaud, B.; Labaudiniere, R.; Christol, H. *J. Org. Chem.* **1986**, *51*, 875–878.
132. Cristau, H. J.; Chabaud, B.; Labaudiniere, R.; Christol, H. *Organometallics* **1985**, *4*, 657–661.
133. Hirao, T.; Masunaga, T.; Ohshiro, T.; Agawa, T. *Tetrahedron Lett.* **1980**, *21*, 3595–3598.
134. Hirao, T.; Masunaga, T.; Ohshiro, Y.; Agawa, T. *Synthesis* **1981**, 56–57.
135. Hirao, T.; Masunaga, T.; Yamada, N.; Ohshiro, Y.; Agawa, T. *Bull. Chem. Soc. Jpn.* **1982**, *55*, 909–913.
136. Abbas, S.; Hayes, C. J. *Synlett* **1999**, 1124–1126.
137. Xu, Y.; Li, Z.; Xia, J.; Guo, H.; Huang, Y. *Synthesis* **1983**, 377–378.
138. Kurz, L.; Lee, G.; Morgans, Jr., D.; Waldyke, M. J.; Ward, T. *Tetrahedron Lett.* **1990**, *31*, 6321–6324.
139. Uozumi, Y.; Tanahashi, A.; Lee, S.; Hayashi, T. *J. Org. Chem.* **1993**, *58*, 1945–1948.
140. Vyskocil, S.; Smrcina, M.; Hanus, V.; Polasek, M.; Kocovsky, P. *J. Org. Chem.* **1998**, *63*, 7738–7748.
141. Vyskocil, S.; Smrcina, M.; Kocovsky, P. *Tetrahedron Lett.* **1998**, *39*, 2989–2992.
142. Doucet, H.; Brown, J. M. *Tetrahedron: Asymmetry* **1997**, *8*, 3775–3784.
143. McCarthy, M.; Guiry, P. J. *Tetrahedron* **1999**, *55*, 3061–3070.
144. Cai, D.; Payack, J. F.; Bender, D. R.; Hughes, D. L.; Verhoeven, T. R.; Reider, P. J. *J. Org. Chem.* **1994**, *59*, 7180–7181.

145. Herd, O.; Hessler, A.; Hingst, M.; Tepper, M.; Stelzer, O. *J. Organomet. Chem.* **1996**, 522, 69–76.
146. Gilbertson, S. R.; Starkey, G. W. *J. Org. Chem.* **1996**, 61, 2922–2923.
147. Kraatz, H.-B.; Pletsch, A. *Tetrahedron: Asymmetry* **2000**, 11, 1617–1621.
148. Lipshutz, B. H.; Buzard, D. J.; Yun, C. S. *Tetrahedron Lett.* **1999**, 40, 201–204.
149. Al-Masum, M.; Livinghouse, T. *Tetrahedron Lett.* **1999**, 40, 7731–7734.
150. Ager, D. J.; East, M. B.; Eisenstadt, A.; Laneman, S. A. *Chem. Commun.* **1997**, 2359–2360.
151. Budnikova, Y.; Kargin, Y.; Nedelec, J.-Y.; Perichon, J. *J. Org. Chem.* **1999**, 575, 63–66.
152. Kwong, F. Y.; Lai, C. W.; Tian, Y.; Chan, K. S. *Tetrahedron Lett.* **2000**, 41, 10285–10289.
153. Kwong, F. Y.; Chan, K. S. *Chem. Commun.* **2000**, 1069–1070.
154. Kwong, F. Y.; Chan, K. S. *Organometallics* **2001**, 20, 2570–2578.
155. Kwong, F. Y.; Chan, A. S. C.; Chan, K. S. *Tetrahedron* **2000**, 56, 8893–8899.
156. Kwong, F. Y.; Chan, K. S. *Organometallics* **2000**, 19, 2058–2060.
157. Lai, C. W.; Kwong, F. Y.; Wang, Y. C.; Chan, K. S. *Tetrahedron Lett.* **2001**, 42, 4883–4885.
158. Atwell, W.; Bokerman, G. N. *U.S. Patent* **1973**, 3,772,347.
159. Matsumoto, H.; Nagashima, S.; Yoshihiro, K.; Nagai, Y. *J. Organomet. Chem.* **1975**, 85, C1–C3.
160. Azarian, D.; Dua, S.; Eaborn, C.; Walton, D. R. M. *J. Organomet. Chem.* **1976**, 117, C55–C57.
161. Azizian, H.; Eaborn, C.; Pidcock, A. *J. Organomet. Chem.* **1981**, 215, 49–58.
162. Babin, P.; Bennetau, B.; Dunoguès, J. *J. Organomet. Chem.* **1993**, 446, 135–138.
163. Cros, S.; Bennetau, B.; Dunoguès, J.; Babin, P. *J. Organomet. Chem.* **1994**, 468, 69–74.
164. Matsumoto, H.; Nagashima, S.; Kato, T.; Nagai, Y. *Angew. Chem. Int. Ed. Engl.* **1978**, 17, 279–280.
165. Murata, M.; Suzuki, K.; Watanabe, S.; Masuda, Y. *J. Org. Chem.* **1997**, 62, 8569–8571.
166. Murata, M.; Watanabe, S.; Masuda, Y. *Tetrahedron Lett.* **1999**, 40, 9255–9257.
167. Matsumoto, H.; Shono, K.; Natai, Y. *J. Organomet. Chem.* **1981**, 208, 145–152.
168. Matsumoto, H.; Yoshihiro, K.; Nagashima, S.; Watanabe, H.; Nagai, Y. *J. Organomet. Chem.* **1977**, 128, 409–413.
169. Hatanaka, Y.; Hiyama, T. *Tetrahedron Lett.* **1987**, 28, 4715–4718.
170. Hatanaka, Y.; Hiyama, T. *J. Synth. Org. Chem. Jpn* **1990**, 48, 834–843.
171. Hatanaka, Y.; Hiyama, T. *Synlett* **1991**, 845–853.
172. Kashin, A. N.; Bumagina, I. G.; Bumagin, N. A.; Beletskaya, I. P. *J. Org. Chem., USSR* **1981**, 17, 789–794.
173. Kosugi, M.; Shimizu, K.; Ohtani, A.; Migita, T. *Chem. Lett.* **1981**, 829–830.
174. Murata, M.; Watanabe, S.; Masuda, Y. *Synlett* **2000**, 1043–1045.
175. Majeed, A. J.; Antonsen, Ø.; Benneche, T.; Undneim, K. *Tetrahedron* **1989**, 45, 993–1006.
176. Ishiyama, T.; Murata, M.; Miyaura, N. *J. Org. Chem.* **1995**, 60, 7508–7510.
177. Wasgindt, M.; Klemm, E. *Synth. Commun.* **1999**, 29, 103–110.
178. Balanda, P. B.; Child, A. D.; Reynolds, J. R. *Polym. Prepr. Am. Chem. Soc., Div. Polym. Chem.* **1994**, 35, 257–258.
179. Rehahn, M.; Schlueter, A. D.; Wegner, G. *Makromol. Chem.* **1990**, 191, 1991–2003.
180. Kallitsis, J. K.; Rehahn, M.; Wegner, G. *Makromol. Chem.* **1992**, 193, 1021–1029.
181. Piettre, S. R.; Baltzer, S. *Tetrahedron Lett.* **1997**, 38, 1197–1200.
182. Murata, M.; Watanabe, S.; Masuda, Y. *Tetrahedron Lett.* **2000**, 41, 5877–5880.
183. Murata, M.; Watanabe, S.; Masuda, Y. *J. Org. Chem.* **1997**, 62, 6458–6459.
184. Giroux, A.; Han, Y. X.; Prasit, P. *Tetrahedron Lett.* **1997**, 38, 3841–3844.
185. Baudoin, O.; Guenard, D.; Gueritte, F. *J. Org. Chem.* **2000**, 65, 9268–9271.
186. Alcazar-Roman, L. M.; Hartwig, J. F.; Rheingold, A. L.; Liable-Sands, L. M.; Guzei, I. A. *J. Am. Chem. Soc.* **2000**, 122, 4618–4630.
187. Otsuka, S.; Yoshida, T.; Matsumoto, M.; Nakatsu, K. *J. Am. Chem. Soc.* **1976**, 98, 5850–5858.
188. Yoshida, T.; Otsuka, S. *J. Am. Chem. Soc.* **1977**, 99, 2134–2140.
189. Yoshida, T.; Otsuka, S. *Inorg. Synth.* **1985**, 28, 113.
190. Stambuli, J. P.; Bühl, M.; Hartwig, J. F. *J. Am. Chem. Soc.* **2002**, 124, 9346–9347.
191. Yin, J. J.; Rainka, M. P.; Zhang, X. X.; Buchwald, S. L. *J. Am. Chem. Soc.* **2002**, 124, 1162–1163.
192. Amatore, C.; Pfluger, F. *Organometallics* **1990**, 9, 2276–2282.
193. Amatore, C.; Jutand, A.; Suarez, A. *J. Am. Chem. Soc.* **1993**, 115, 9531–9541.
194. Stille, J. K.; Lau, K. S. Y. *Acc. Chem. Res.* **1977**, 10, 434–442.
195. Portnoy, M.; Milstein, D. *Organometallics* **1993**, 12, 1665–1673.
196. Jutand, A.; Mosleh, A. *Organometallics* **1995**, 14, 1810–1817.
197. Amatore, C.; Jutand, A.; Meyer, G. *Inorg. Chim. Acta* **1998**, 273, 76–84.
198. Amatore, C.; Jutand, A.; Meyer, G.; Atmani, H.; Khalil, F.; Chahdi, F. O. *Organometallics* **1998**, 17, 2958–2964.
199. Jutand, A. *J. Organomet. Chem.* **1999**, 576, 254–278.
200. Amatore, C.; Fuxa, A.; Jutand, A. *Chem. Eur. J.* **2000**, 6, 1474–1430.
201. Amatore, C.; Carré, E.; Jutand, A.; M'Barki, M.; Meyer, G. *Organometallics* **1995**, 14, 5605–5614.
202. Amatore, C.; Bucaille, A.; Fuxa, A.; Jutand, A.; Meyer, G.; Ntepe, A. N. *Chem. Eur. J.* **2001**, 7, 2134–2142.
203. Roy, A.; Hartwig, J. F. *J. Am. Chem. Soc.* **2001**, 123, 1232–1233.
204. Driver, M. S.; Hartwig, J. F. *J. Am. Chem. Soc.* **1995**, 117, 4708–4709.
205. Driver, M. S.; Hartwig, J. F. *J. Am. Chem. Soc.* **1997**, 119, 8232–8245.
206. Villanueva, L. A.; Abboud, K. A.; Boncella, J. M. *Organometallics* **1994**, 13, 3921–3931.
207. Matsunaga, P. T.; Hess, C. R.; Hillhouse, G. L. *J. Am. Chem. Soc.* **1994**, 116, 3665–3666.
208. Koo, K.; Hillhouse, G. L. *Organometallics* **1995**, 14, 4421–4423.
209. Koo, K.; Hillhouse, G. L. *Organometallics* **1996**, 15, 2669–2671.
210. Barañano, D.; Hartwig, J. F. *J. Am. Chem. Soc.* **1995**, 117, 2937–2938.
211. Mann, G.; Barañano, D.; Hartwig, J. F.; Rheingold, A. L.; Guzei, I. A. *J. Am. Chem. Soc.* **1998**, 120, 9205–9219.
212. Louie, J.; Hartwig, J. F. *J. Am. Chem. Soc.* **1995**, 117, 11598–11599.
213. Widenhoefer, R. A.; Buchwald, S. L. *J. Am. Chem. Soc.* **1998**, 120, 6504–6511.
214. Widenhoefer, R. A.; Zhong, H. A.; Buchwald, S. L. *J. Am. Chem. Soc.* **1997**, 119, 6787–6795.
215. Matsunaga, P. T.; Hillhouse, G. L.; Rheingold, A. L. *J. Am. Chem. Soc.* **1993**, 115, 2075–2077.
216. Matsunaga, P. T.; Mavropoulos, J. C.; Hillhouse, G. L. *Polyhedron* **1995**, 14, 175–185.

217. Han, R.; Hillhouse, G. L. *J. Am. Chem. Soc.* **1997**, *119*, 8135–8136.
218. Sokolov, V. I.; Troitskaya, L. L.; Reutov, O. A. *J. Organomet. Chem.* **1980**, *202*, C58–C60.
219. Wicht, D. K.; Paisner, S. N.; Lew, B. M.; Glueck, D. S.; Yap, G. P. A.; Liable-Sands, L. M.; Rheingold, A. L.; Haar, C. M.; Nolan, S. P. *Organometallics* **1998**, *17*, 652–660.
220. Geoffroy, G. L.; Rosenberg, S.; Shulman, P. M.; Whittle, R. R. *J. Am. Chem. Soc.* **1984**, *106*, 1519–1521.
221. Fryzuk, M. D.; Joshi, K.; Chadha, R. K.; Rettig, S. J. *J. Am. Chem. Soc.* **1991**, *113*, 8724–8736.
222. Gaumont, A. C.; Hursthouse, M. B.; Coles, S. J.; Brown, J. M. *Chem. Commun.* **1999**, 63–64.
223. Arterburn, J. B.; Rao, K. V.; Rancas, R.; Dible, B. R. *Org. Lett.* **2001**, *3*, 1351–1354.
224. Watanabe, M.; Yamamoto, T.; Nishiyama, M. *Chem. Commun.* **2000**, 133–134.
225. Lipshitz, B. H.; Tasler, S.; Chrisman, W.; Spliethoff, B.; Tesche, B. *J. Org. Chem.* **2003**, *68*, 1177–1189.
226. Kojima, A.; Boden, C. D. J.; Shibasaki, M. *Tetrahedron Lett.* **1997**, *38*, 3459–3460.

9.8

Metal Complexes as Lewis-acid Catalysts in Organic Synthesis

S. KOBAYASHI, Y. MORI, and Y. YAMASHITA

The University of Tokyo, Japan

9.8.1	INTRODUCTION	399
9.8.2	ALKALI METALS	399
9.8.3	MAGNESIUM	401
9.8.4	SCANDIUM AND LANTHANIDES	402
9.8.5	TITANIUM	405
9.8.6	ZIRCONIUM	415
9.8.7	HAFNIUM	416
9.8.8	COPPER	419
9.8.9	SILVER AND GOLD	421
9.8.10	ZINC	422
9.8.11	OTHER TRANSITION-METAL LEWIS ACIDS	424
9.8.12	BORON	426
9.8.13	ALUMINUM	429
9.8.14	SILICON	430
9.8.15	TIN	433
9.8.16	OTHERS	435
9.8.17	CONCLUSION/CLASSIFICATION OF LEWIS ACIDS	437
9.8.18	REFERENCES	439

9.8.1 INTRODUCTION

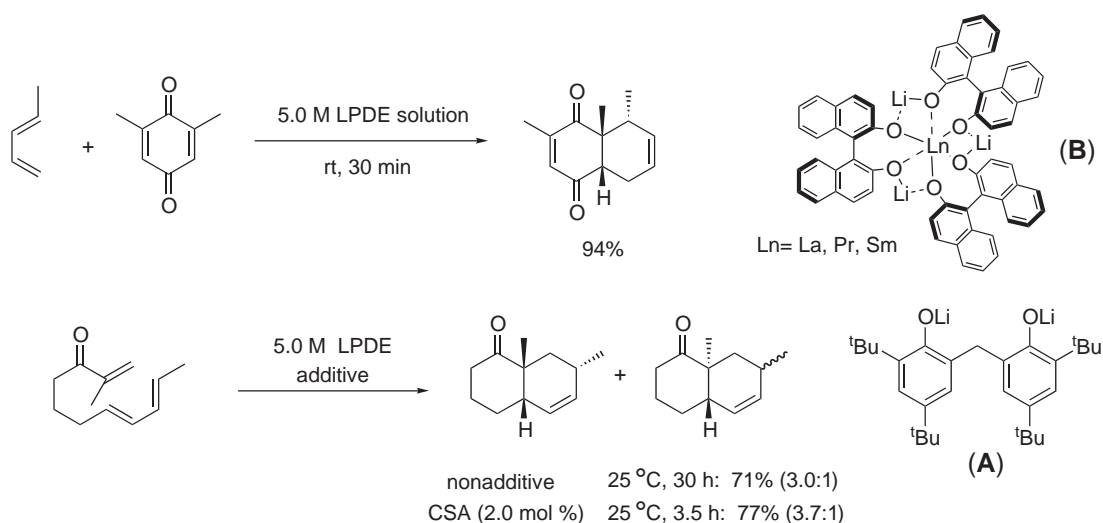
Lewis-acid-catalyzed reactions often occur with unique reactivity and selectivity, and the reactions proceed under mild conditions. Many Lewis-acid-mediated reactions are now used not only in laboratories but also in industry. This chapter summarizes these Lewis acid-mediated reactions successfully used in organic synthesis; they are organized mainly by the element of the Lewis-acid catalyst. Due to limitations of space, the focus is on more recent publications.¹⁻³

9.8.2 ALKALI METALS

Alkali-metal Lewis acids based on Li^{I} , Na^{I} , and K^{I} are new reagents as Lewis acids in organic reactions. Due to their lower Lewis acidity and limited scope for modification of counter anions, these Lewis acids are less well developed than those based on other metals. Alkali-metal ions, especially lithium, have an extensive coordination chemistry; many lithium compounds form complex aggregates, which show various interesting reactivities under different conditions. By controlling the degree of aggregation, the rates of Li-mediated reactions have been regulated, and several highly regio- and stereocontrolled organic reactions have been attained.⁴

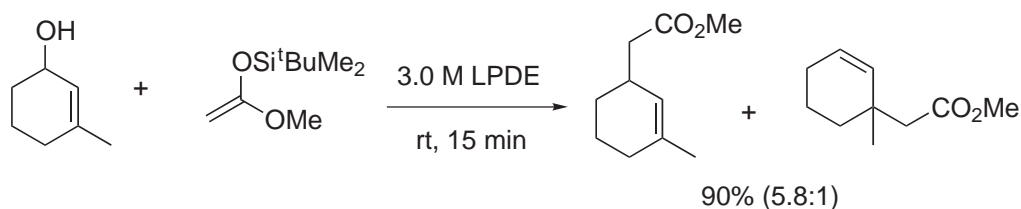
The most well-known and most employed alkali-metal Lewis acid is lithium perchlorate (LiClO_4).⁵ As mentioned above, the Lewis acidity of LiClO_4 is not very strong, but its mild acidity results in useful reactivity and selectivity in several synthetic reactions, especially in the presence of other reactive functional groups in the substrate(s). Diethyl ether (Et_2O) is known to be one of the best solvents for LiClO_4 ; a LiClO_4 solution of diethyl ether is known as LPDE.^{6–7} Highly concentrated solutions of LiClO_4 are often employed in several reactions to compensate for its low Lewis acidity.

The LPDE system is applied to several reactions in which the metal ions coordinate to the lone pairs of heteroatoms, thereby activating the substrate. Initially, the effectiveness was shown in Diels–Alder reactions (Scheme 1). In a highly concentrated (5.0 M) LPDE solution, Diels–Alder reactions proceeded smoothly.^{6–7} Generally, a catalytic amount of LiClO_4 is not effective in this reaction. In some cases, a catalytic amount of an additional Brønsted acid, such as camphorsulphonic acid (CSA), gives better results.⁸ An interesting double activation of carbonyl moieties by using dilithium compounds has been reported (compound (A) in Scheme 1).⁹ Furthermore, asymmetric Diels–Alder reactions have been developed in LPDE solutions or using hetero-bimetallic catalysts containing lithium ions (compound (B)).^{10–12}



Scheme 1

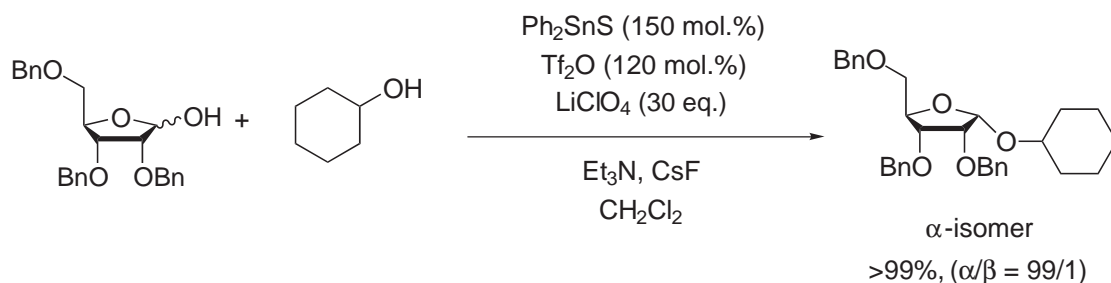
Allylic substitution reactions using LPDE have also been reported. The reaction of an allyl alcohol with several nucleophiles proceeds smoothly in a 3.0 M LPDE solution (Scheme 2).¹³ Moreover, a highly cationic lithium species has been developed, and a catalytic amount of this species promotes allylic substitution reactions efficiently.¹⁴



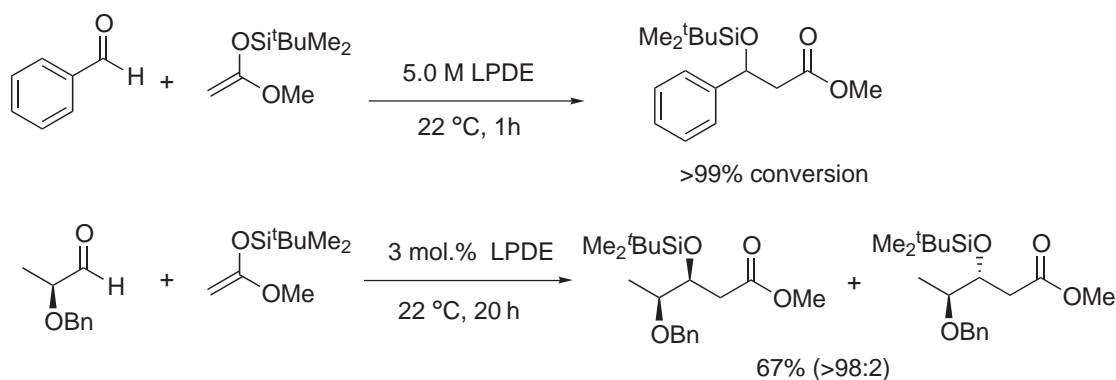
Scheme 2

A significant role of lithium in controlling stereochemistry in glycosylation reactions has been reported. In the presence of lithium perchlorate, glycosylation with alcohols proceeds with excellent α -selectivity (Scheme 3).¹⁵

Several reactions of carbonyl groups in an LPDE system have been examined. Mukaiyama aldol reactions are effectively promoted in an LPDE solution, and remarkable chelating effects of oxygen functional groups at the α -positions of aldehydes are observed (Scheme 4).^{16,17} Regarding



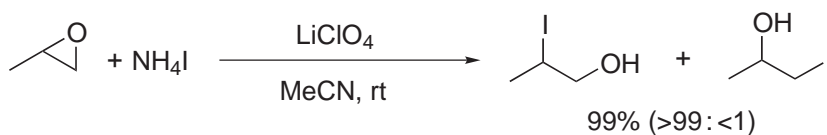
Scheme 3



Scheme 4

mechanistic aspects, an open-chain, transition-state model is suggested for the aldol reaction in an LPDE solution by crossover experiments of silyl groups of ketene silyl acetals.¹⁸ Beside this, carbonyl allylation,¹⁹ cyanation,¹⁷ Mukaiyama Michael reactions,¹⁷ and hetero Diels–Alder reactions²⁰ have been reported in LPDE solutions.

Ring-opening reactions of oxiranes in some alkali-metal solutions have been well investigated. Several nucleophiles, such as halide,²¹ azide,²² amine,²³ cyanide,²⁴ and enolate,²⁵ are employed in the reactions with epoxides; in all cases, LiClO_4 solutions gave good results, and high yields and high regioselectivities were obtained (Scheme 5).



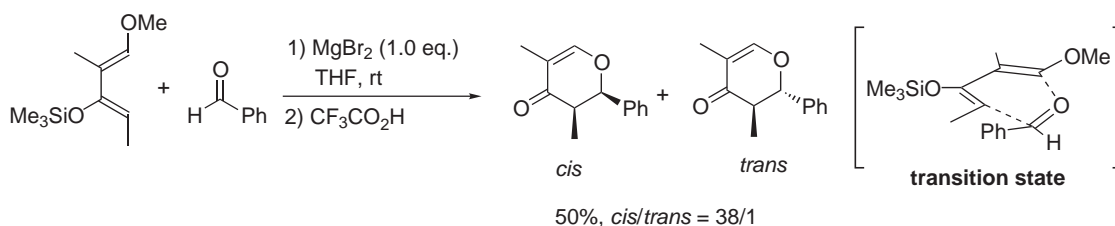
Scheme 5

9.8.3 MAGNESIUM

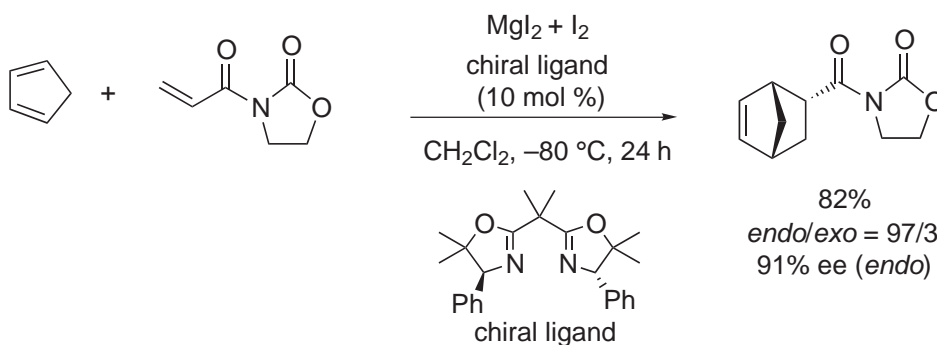
Magnesium(II) is a milder Lewis acid than traditionally used ones such as boron(III), aluminum(III), or titanium(IV). A characteristic feature of Mg^{II} is the presence of coordination sites which are occupied by Lewis bases other than counter anions. By using bidentate Lewis-basic ligands, it is therefore possible to form rigid stereochemical environments.

Mg^{II} is often employed in stereoselective reactions. In hetero Diels–Alder reactions of aldehydes with Danishefsky's diene, Mg^{II} results in good acceleration and stereoselection, and 2,3-*cis*-products are obtained exclusively (Scheme 6).²⁶ Milder Lewis acidity is necessary for obtaining higher yield and higher stereoselectivity in this reaction, which occurs through a cyclic transition state.

In catalytic enantioselective Diels–Alder reactions, Mg^{II} catalysts bearing chiral auxiliaries, such as chiral bidentate ligands containing oxazoline moieties,^{27–29} chiral diamines,³⁰ and



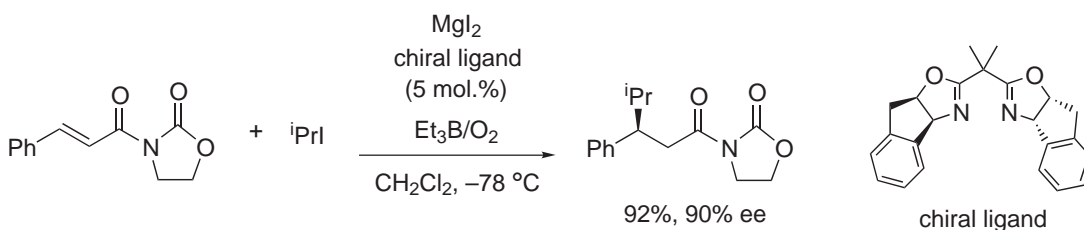
Scheme 6



Scheme 7

chiral bidentate sulfoxide ligands,³¹ are effective; high enantioselectivities are observed (Scheme 7). A small amount of water sometimes influences enantioselectivity, and inversion of enantioselection occurs in some reactions.³² These effects are explained by differences in coordination forms. In the absence of water, the metal complex forms a tetrahedral structure with a chiral bidentate ligand and a bidentate substrate. However, addition of water to the complex changes the structure to an octahedral form, and reverse enantioselectivity is observed.

Mg^{II} complexes are also effective for controlling asymmetric radical reactions.^{33,34} Moreover, enantioselective radical reactions using chiral Mg^{II} complexes have been studied, and high enantioselectivities have been realized in the presence of stoichiometric or catalytic amounts of chiral auxiliaries such as bis-oxazolines (Scheme 8).^{35–39} In most cases, substrates having bidentate chelating moieties are required.



Scheme 8

In addition to this, asymmetric 1,3-dipolar cyclization reactions of nitrones with olefins,^{40,41} catalytic enantioselective cyanation of aldehydes,⁴² catalytic enantioselective amination,⁴³ and aza-Michael reactions⁴⁴ have been reported, and high enantioselectivities are observed.

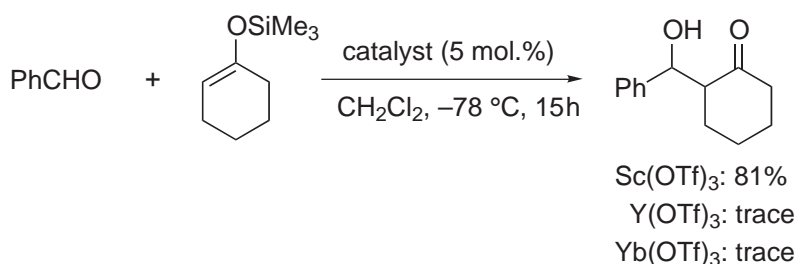
9.8.4 SCANDIUM AND LANTHANIDES

The element scandium (Sc) is in group 3 (above La and Y), and its radius is appreciably smaller than that of any other rare-earth element. Scandium is uncommon, probably because of both the

lack of rich sources and difficulties in its separation. Its chemical behavior is known to be intermediate between that of aluminum and lanthanides. Use of scandium in organic synthesis was rather limited before scandium trifluoromethanesulfonate ($\text{Sc}(\text{OTf})_3$) was first introduced as a promising Lewis acid in 1993.⁴⁵

$\text{Sc}(\text{OTf})_3$ is stable in water, and effectively activates carbonyl and related compounds as a Lewis acid in water. This is remarkable, because most Lewis acids react immediately with water rather than the substrates, and are decomposed or deactivated. It has already been found that lanthanide triflates $\text{Ln}(\text{OTf})_3$ ($\text{Ln} = \text{La}, \text{Ce}, \text{Pr}, \text{Nd}, \text{Sm}, \text{Eu}, \text{Gd}, \text{Tb}, \text{Dy}, \text{Ho}, \text{Er}, \text{Tm}, \text{Yb}, \text{Lu}$) and yttrium triflate $\text{Y}(\text{OTf})_3$ are stable in water, and can act as Lewis-acid catalysts in aqueous media.^{46–48} They are used catalytically in many reactions and can often be recovered and reused, because they are stable under the usual water-quenching conditions.

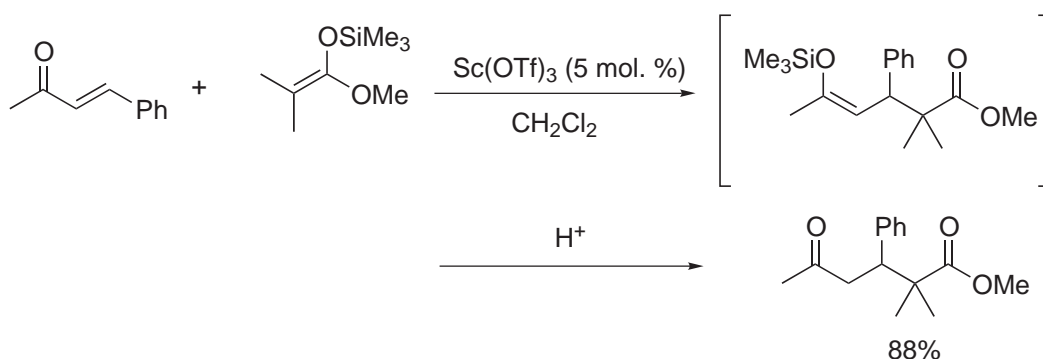
$\text{Sc}(\text{OTf})_3$ is an effective catalyst in aldol reactions of silyl enol ethers with aldehydes.⁴⁹ Compared with other typical rare-earth-metal (Y, Yb) triflates, $\text{Sc}(\text{OTf})_3$ has the strongest activity in the reaction of 1-trimethylsilyloxycyclohexane with benzaldehyde in dichloromethane. Although the reaction scarcely proceeded at -78°C in the presence of $\text{Y}(\text{OTf})_3$ or $\text{Yb}(\text{OTf})_3$, the aldol adduct was obtained in 81% yield in the presence of $\text{Sc}(\text{OTf})_3$ (Scheme 9).



Scheme 9

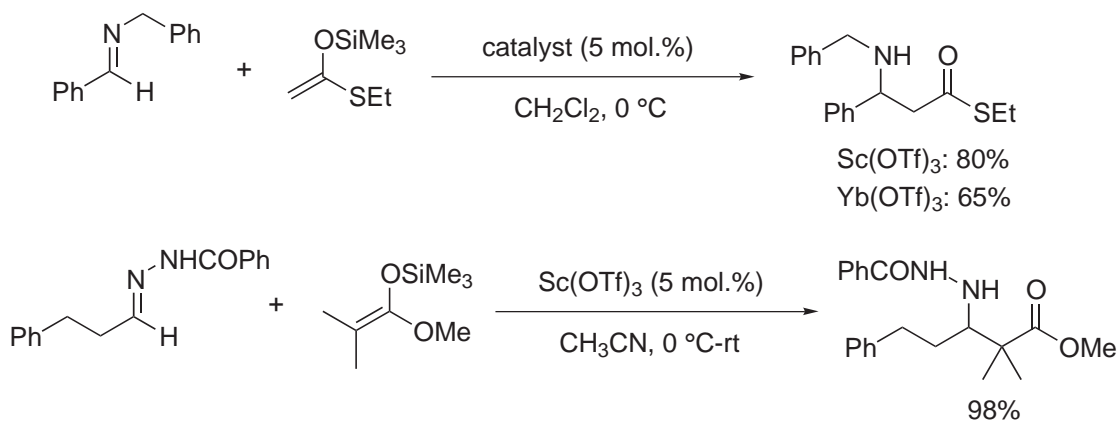
Silicon enolates derived from ketones, thioesters, and esters reacted smoothly with different types of aldehyde in the presence of 5 mol.% $\text{Sc}(\text{OTf})_3$ to afford the aldol adducts in high yields.

$\text{Sc}(\text{OTf})_3$ is effective for Mukaiyama–Michael reactions under extremely mild conditions to give the corresponding 1,5-dicarbonyl compounds in high yields after acidic work-up (Scheme 10).^{46–48} Silicon enolates derived from ketones, thioesters, and esters are applicable, and no 1,2-addition products are obtained.



Scheme 10

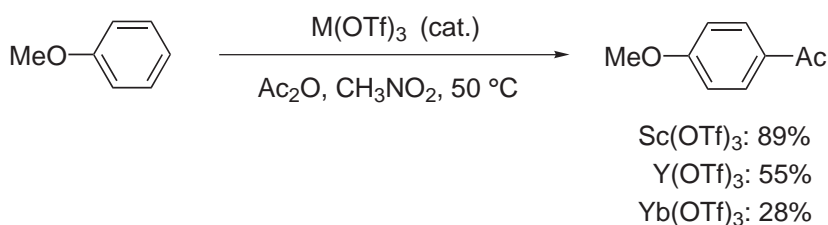
It was first observed that reactions of imines with ketene silyl acetals proceeded smoothly in the presence of 5 mol.% $\text{Yb}(\text{OTf})_3$ to afford the corresponding β -amino ester derivatives in moderate yields.⁵⁰ However, $\text{Sc}(\text{OTf})_3$ was found to be a more active catalyst in this reaction. Benzoylhydrazones also react with ketene silyl acetals in the presence of a catalytic amount of $\text{Sc}(\text{OTf})_3$ to afford the corresponding adducts in high yields (Scheme 11).⁵¹ In contrast, catalytic activation of benzoylhydrazones by use of a typical Lewis acid such as TiCl_4 , SnCl_4 , or $\text{BF}_3 \cdot \text{OEt}_2$, etc. is not effective.



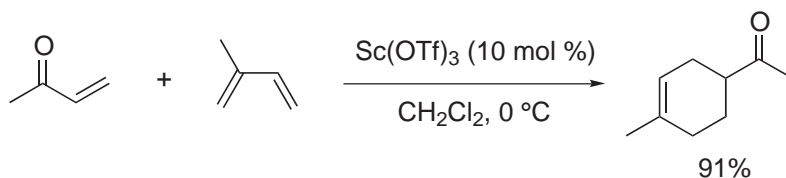
Scheme 11

Sc(OTf)₃ catalyzes Friedel–Crafts acylation reactions effectively (Scheme 12).⁵² While more than stoichiometric amounts of a Lewis acid such as AlCl₃ or BF₃·OEt₂ are needed because of consumption of the Lewis acid by coordination to products, a catalytic amount of Sc(OTf)₃ is enough to complete the reactions.

Rare-earth-metal triflates are efficient catalysts in Diels–Alder reactions, and Sc(OTf)₃ is clearly more effective than Ln(OTf)₃ as a catalyst.^{45,53–55} In the presence of 10 mol.% Y(OTf)₃ or Yb(OTf)₃, only a trace amount of the adduct was obtained in the Diels–Alder reaction of methyl vinyl ketone (MVK) with isoprene. In contrast, the reaction proceeded smoothly to give the adduct in 91% yield in the presence of 10 mol.% Sc(OTf)₃ (Scheme 13).⁴⁵ Sc(OTf)₃ has also proved to be an efficient catalyst for the Diels–Alder reaction of imines (aza Diels–Alder reactions).^{56,57}



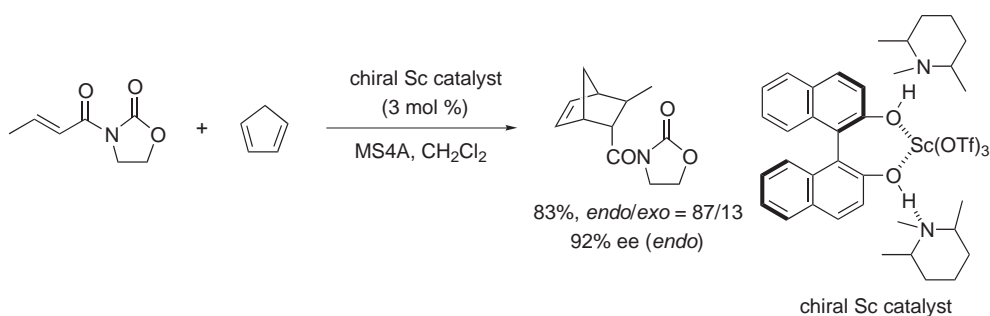
Scheme 12



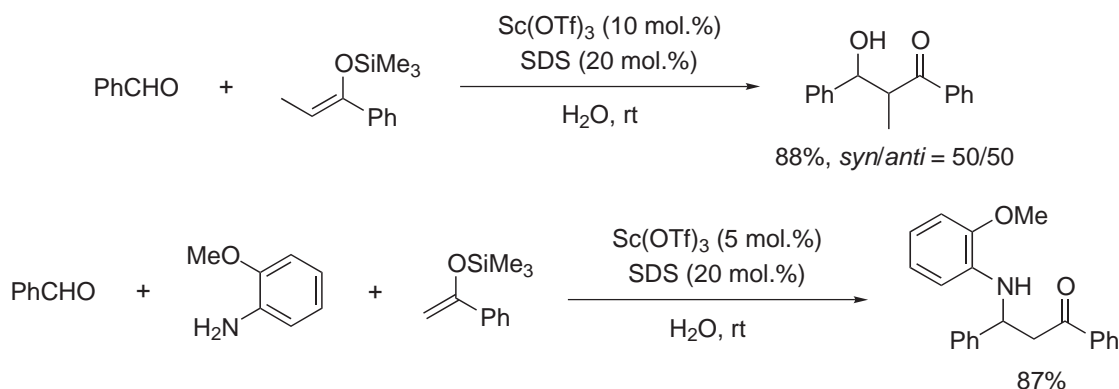
Scheme 13

Enantioselective Diels–Alder reactions proceed smoothly in the presence of a chiral Sc catalyst, prepared *in situ* from Sc(OTf)₃, (*R*)-(+)-1,1'-bi-2-naphthol [(*R*)-BINOL], and a tertiary amine in dichloromethane.⁵⁸ The catalyst is also effective in Diels–Alder reactions of an acrylic acid derivative with dienes (Scheme 14).

Sc(OTf)₃ is effective in aldol reactions in aqueous media (water–THF, Scheme 15).⁴⁹ Direct treatment of aqueous solutions of water-soluble formaldehyde and chloroacetaldehyde with silyl enol ethers affords the corresponding aldol adducts in good yields. Water-sensitive silicon enolates can be used in aqueous solutions in the presence of a catalytic amount of Sc(OTf)₃.



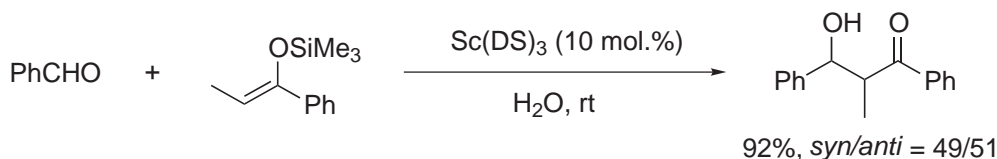
Scheme 14



Scheme 15

Sc(OTf)₃-catalyzed aldol reactions have been successfully performed in micellar systems (Scheme 15).⁵⁹ The catalyst activity is remarkably enhanced by adding a small amount of a surfactant. Allylation⁶⁰ and Mannich-type reactions⁶¹ also proceed smoothly in water in the presence of a catalytic amount of Sc(OTf)₃ and a surfactant.

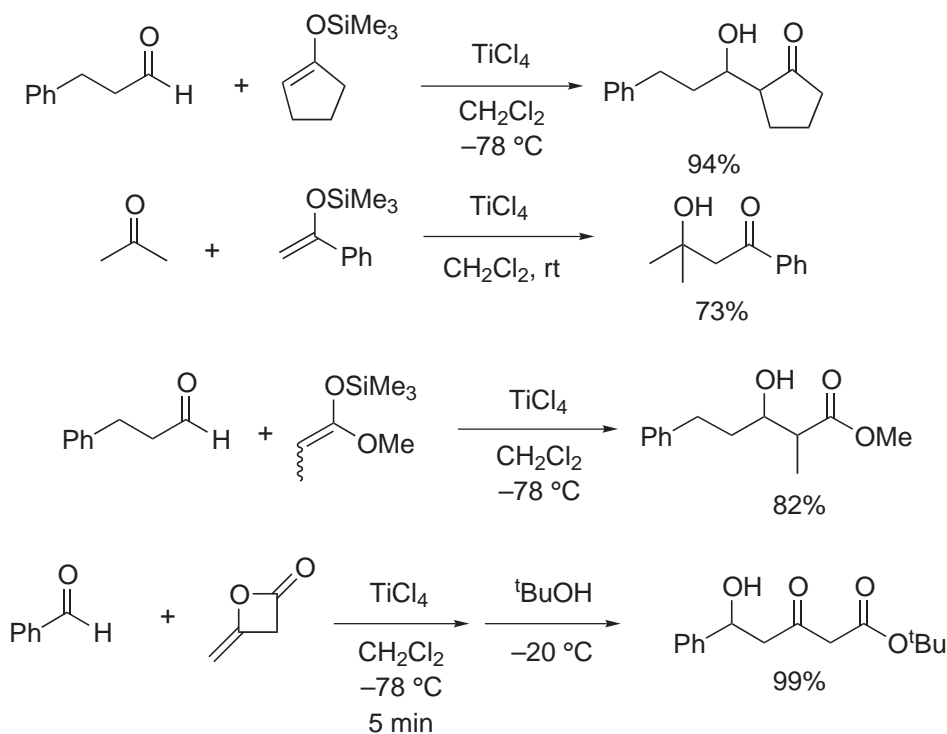
Moreover, a new type of catalyst, scandium tris(dodecyl sulfate) [Sc(O₃SOC₁₂H₂₅)₃, Sc(DS)₃] has been developed.^{62,63} The catalyst (a Lewis Acid–Surfactant Combined Catalyst, LASC) acts both as a catalyst and as a surfactant, and aldol reactions proceed smoothly in the presence of a catalytic amount of Sc(DS)₃ in water, without using any organic solvents (Scheme 16).



Scheme 16

9.8.5 TITANIUM

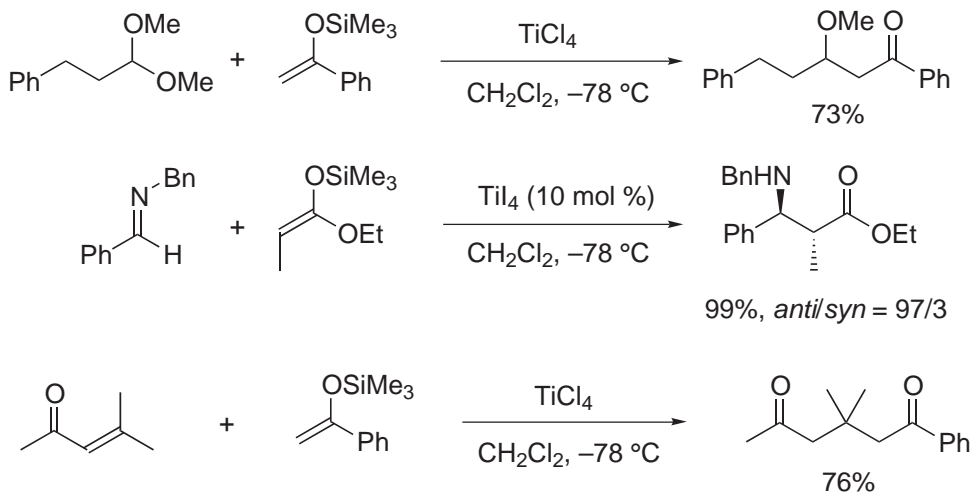
Titanium compounds are amongst the most important Lewis acids in organic chemistry. Titanium(IV) compounds TiX₄ (X = halide, alkoxide, etc.) are often employed as effective Lewis acids in organic syntheses, and most of them are easily available. The Lewis acidity of TiX₄ is controlled by the nature of the anionic groups, X. Among these, the tetrahalides show stronger Lewis acidity,⁶⁴ whereas the tetraalkoxides show milder Lewis acidity. The choice of anionic groups dramatically affects the reactivity and selectivity. Mixed-ligand systems such as TiX₂Y₂ can also be effectively used to control the Lewis acidity.



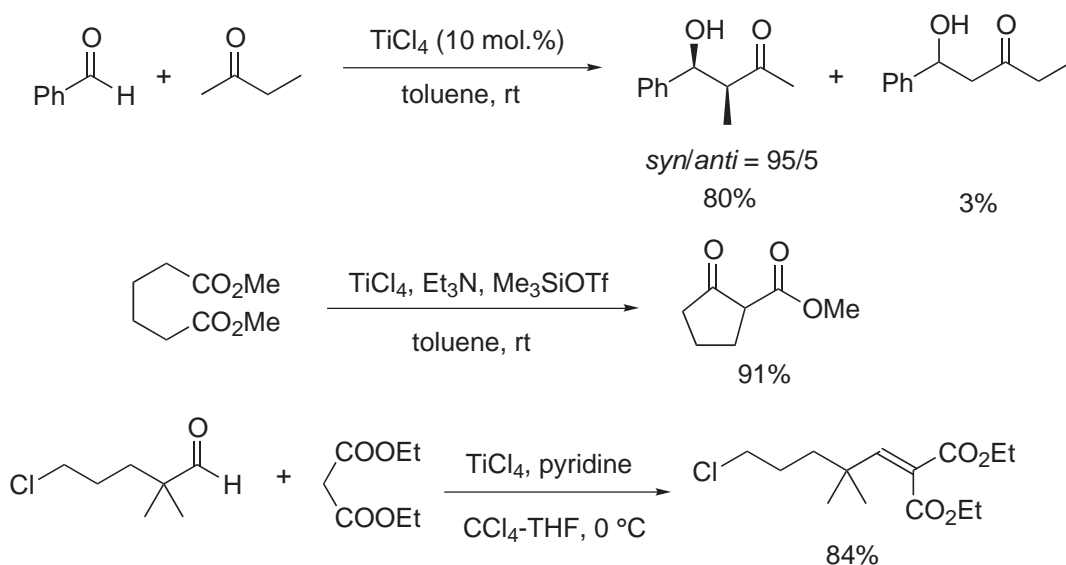
Scheme 17

In aldol reactions, especially Mukaiyama aldol reactions, Ti^{IV} compounds are widely employed as efficient promoters. The reactions of aldehydes or ketones with reactive enolates, such as silyl enol ethers derived from ketones, proceed smoothly to afford β -hydroxycarbonyl compounds in the presence of a stoichiometric amount of TiCl_4 (Scheme 17).^{65,66} Many examples have been reported; in addition to silyl enol ethers derived from ketones, ketene silyl acetals derived from ester derivatives and vinyl ethers can also serve as enolate components.⁶⁷⁻⁶⁹

Besides aldehydes and ketones, TiCl_4 activates acetals effectively for reaction with enolates (Scheme 18).^{70,71} The reactivity of acetals is higher than that of the corresponding aldehydes in



Scheme 18



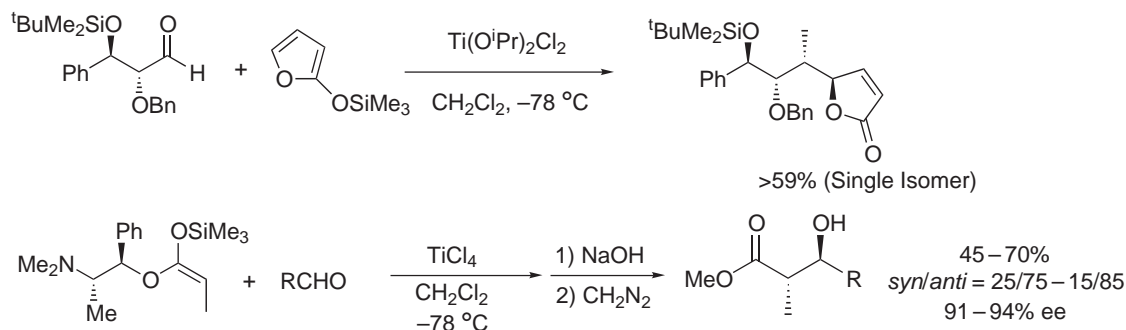
the presence of Ti^{IV} halides; imines and α,β -unsaturated carbonyl compounds are also activated for reaction with enolates in the same way (Scheme 18).^{72,73}

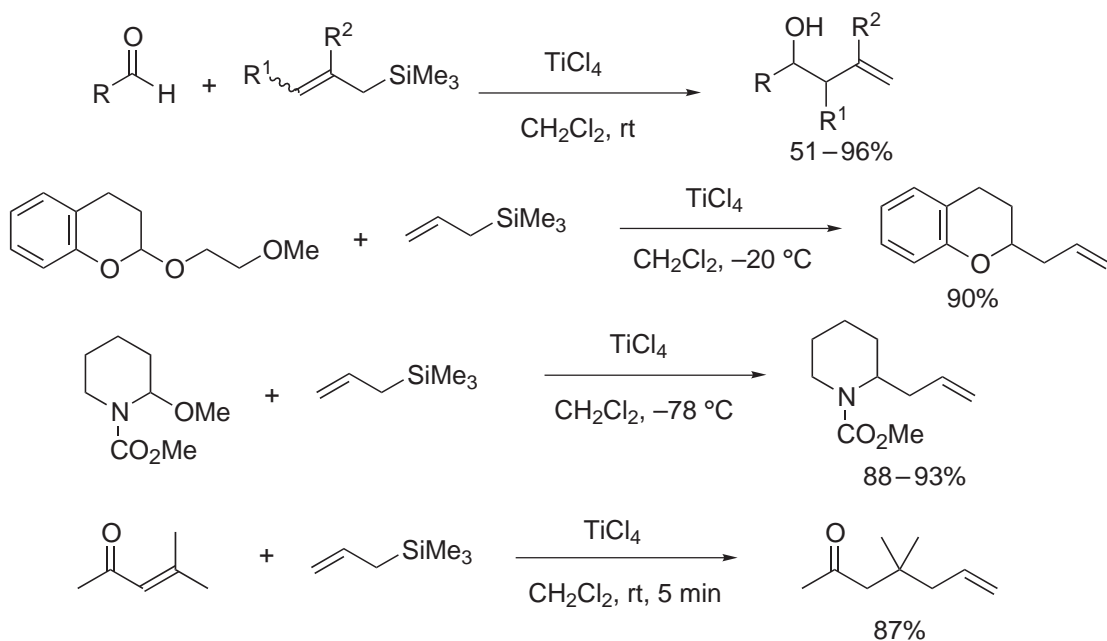
Ti^{IV} compounds also work well at promoting cross-aldol reactions between two different aldehydes and/or ketones without prior activation or protection (Scheme 19).⁷⁴ Claisen condensation and Knoevenagel condensation are promoted by TiX_4 , an amine, and trimethylsilyl triflate.^{75–77}

TiX_4 is employed as an effective promoter for asymmetric aldol reactions. A chiral aldehyde or a chiral enolate reacts to afford homochiral aldol adducts with high selectivity (Scheme 20).^{78,79}

Allylation of aldehydes or ketones using allylsilanes, known as the Hosomi–Sakurai reaction, is a useful method for obtaining homoallylic alcohols. Ti^{IV} compounds have been successfully applied to this reaction (Scheme 21).⁸⁰ Besides aldehydes and ketones, acylsilanes, O,O -acetals, and N,O -acetals can be employed.^{81–83} 1,4-Addition of an allyl group to an α,β -unsaturated ketone has been also reported.⁸⁴

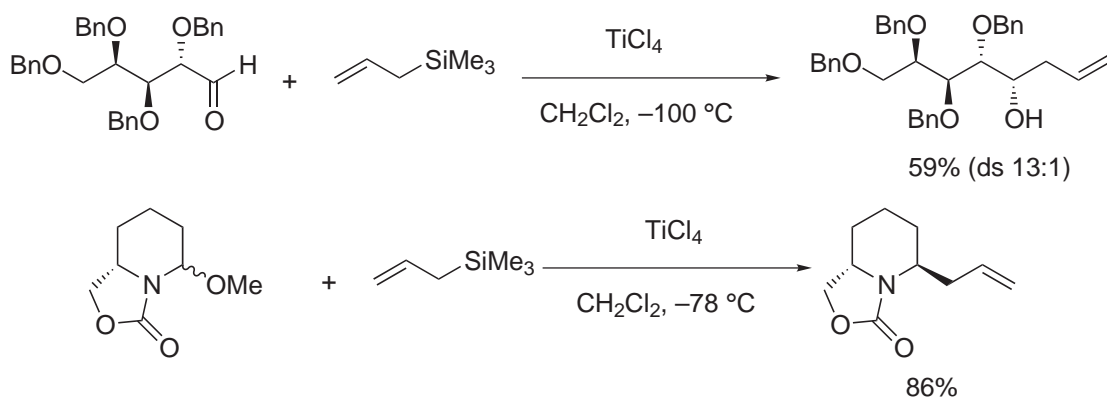
In reactions of chiral aldehydes, Ti^{IV} compounds work well as both activators and chelation control agents. α - or β -oxygenated chiral aldehydes react with allylsilanes to afford chiral homoallylic alcohols with high selectivity (Scheme 22).⁸⁵ These chiral alcohols are useful synthetic units for the synthesis of highly functionalized chiral compounds. Cyclic chiral O,O - and N,O -acetals react with allylsilanes in the same way.^{86,87} Allenylsilanes have also been reported as allylation agents.





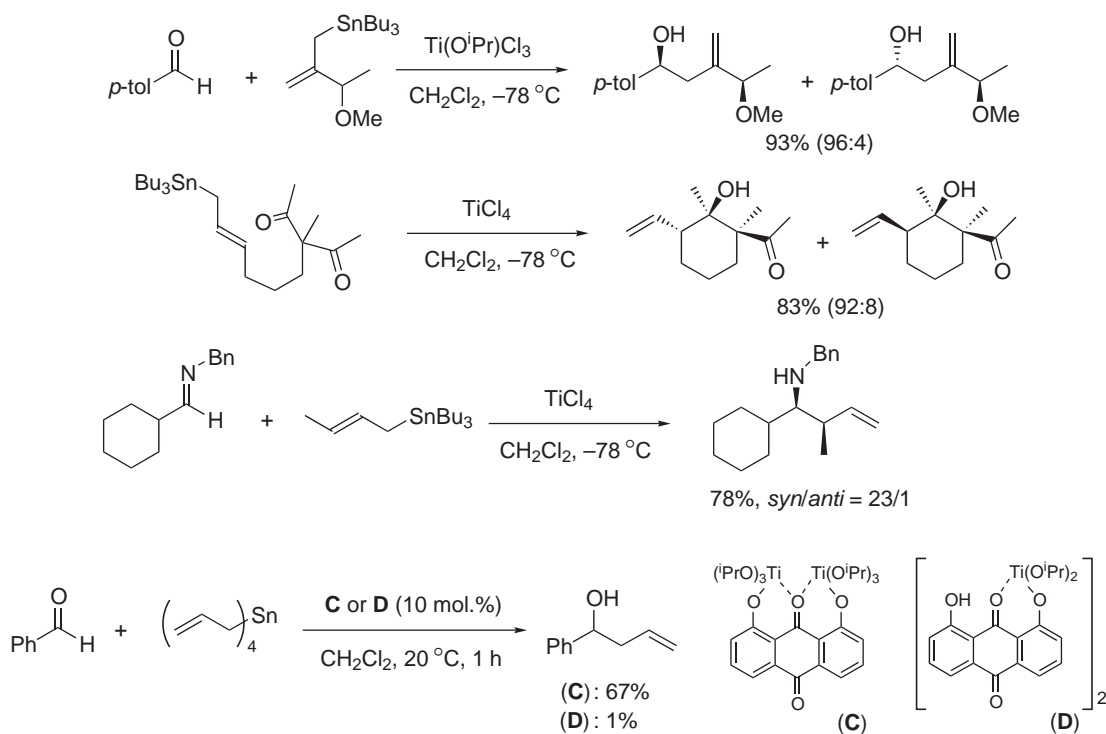
Scheme 21

Allyl–tin compounds are employed as more reactive allylating agents. Because of their high reactivity, less active catalysts (Ti^{IV} species having mild Lewis acidity) or less reactive substrates are often required (Scheme 23).^{88,89} In addition to carbonyl compounds as substrates, allylation reactions of imines have been also reported.⁹⁰ Also, a binuclear Ti^{IV} Lewis acid has been developed (compound (C) in Scheme 23), which shows higher catalytic activity than the mononuclear analogue (D) because of bidentate coordination to the carbonyl moiety of the substrate.⁹¹

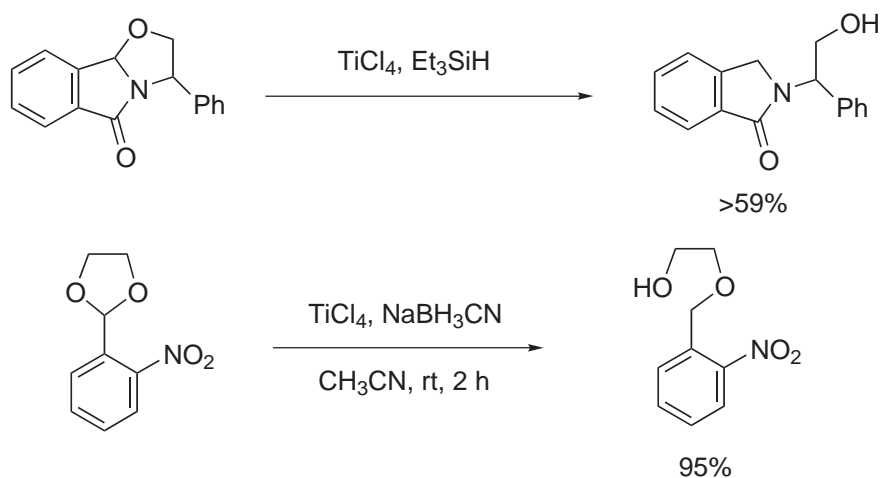


Scheme 22

TiCl_4 promotes reduction of carbonyl groups or acetals with R_3SiH or R_3SnH (Scheme 24).⁹² Other hydride sources are also effective.⁹³

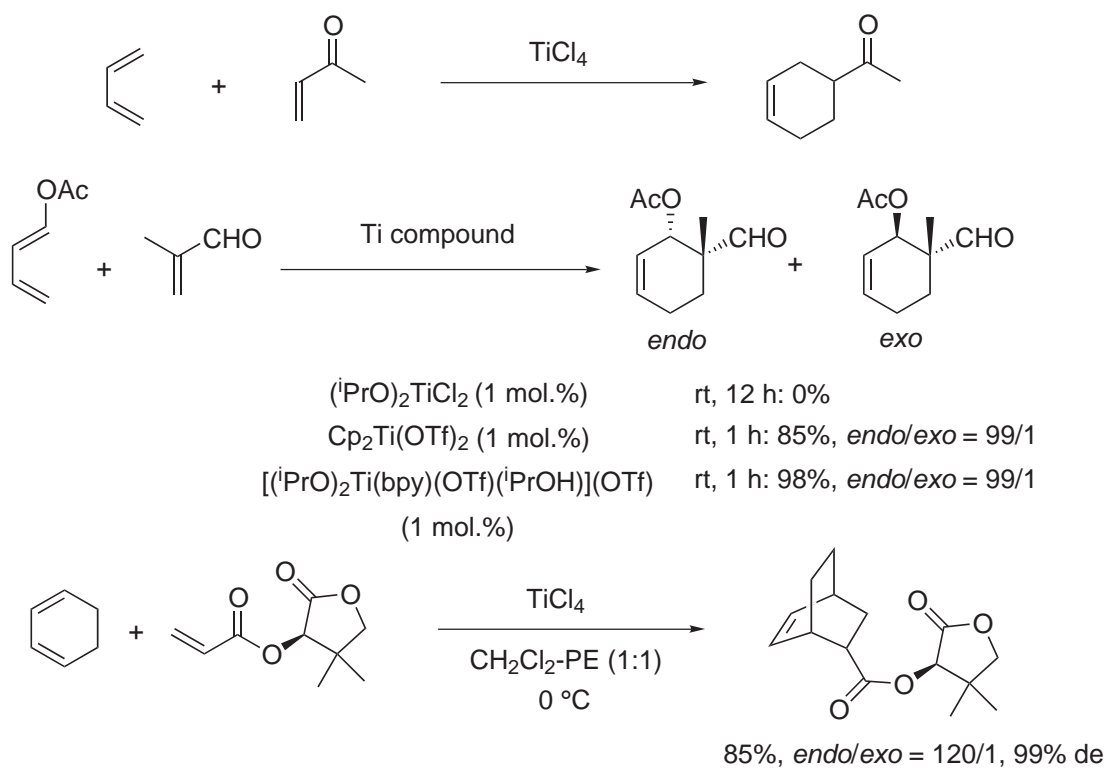


Scheme 23



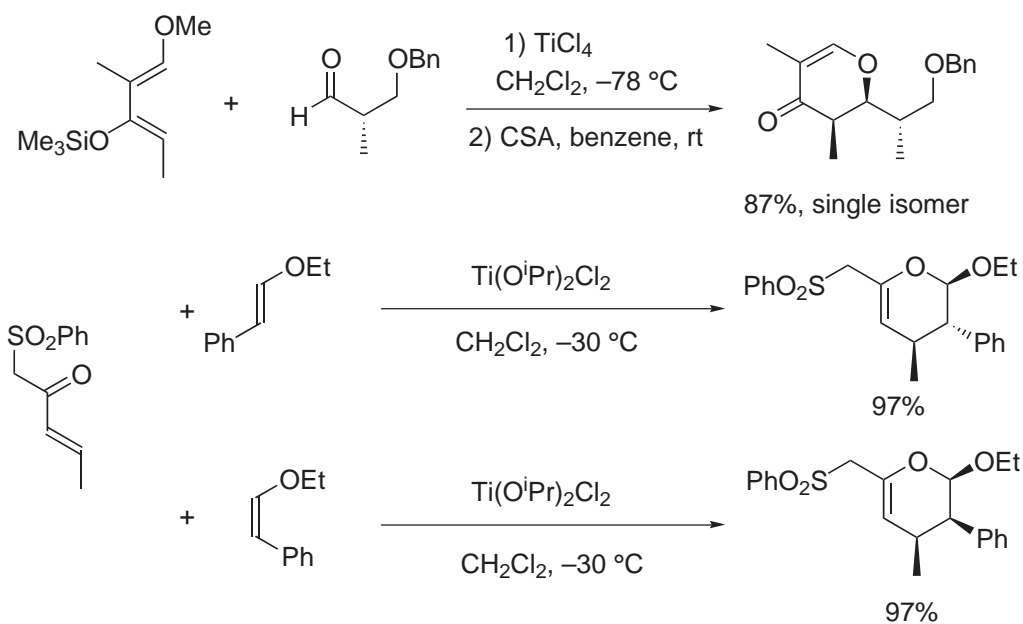
Scheme 24

Ti^{IV} -based Lewis acids are effective in ring-forming reactions such as Diels–Alder reactions (Scheme 25).⁹⁴ Besides the usual TiX_4 compounds ($\text{X} = \text{halide or alkoxide}$), $\text{Cp}_2\text{Ti(OTf)}_2$ is also a reactive catalyst for the Diels–Alder reaction,⁹⁵ and it has been reported that $[(^i\text{PrO})_2\text{Ti}(\text{bpy})(\text{OTf})]$ ($^i\text{PrOH}$)(OTf) is even more effective than $\text{Cp}_2\text{Ti(OTf)}_2$.⁹⁶ In asymmetric synthesis, reactions with chiral dienophiles have been widely investigated.⁹⁷



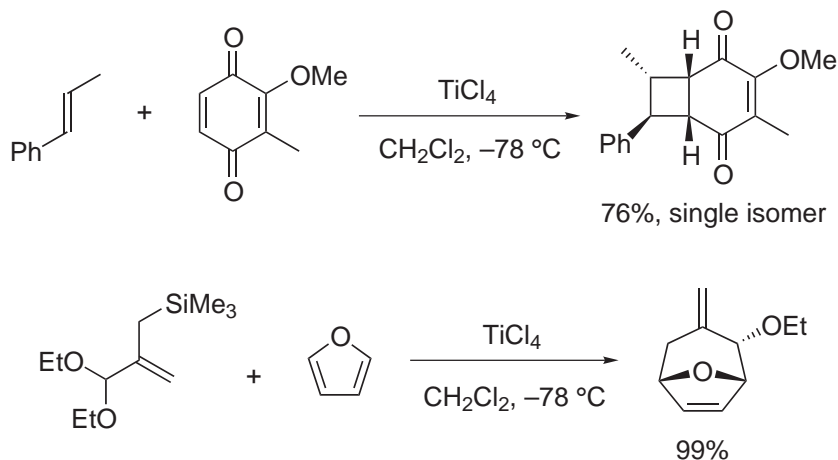
Scheme 25

The hetero Diels–Alder reaction is a useful method for constructing six-membered ring systems containing hetero-atoms. Ti^{IV} compounds with mild Lewis acidity promote the reactions well (Scheme 26);⁹⁸ it has been proposed that these reactions proceed via a concerted pathway.⁹⁹



Scheme 26

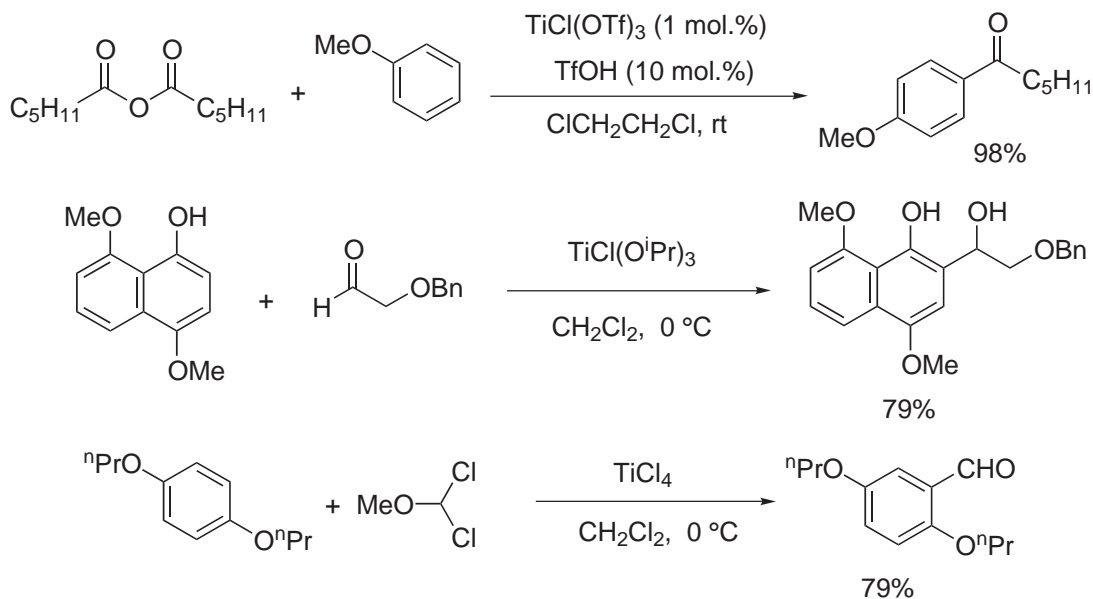
Other annulation reactions using Ti^{IV} -based Lewis acids have been also reported (Scheme 27); 1,3-dipolar cycloadditions,¹⁰⁰ [2+2] cycloadditions,¹⁰¹ the ene reaction,¹⁰² and [3+4] cycloadditions¹⁰³ are also promoted by Ti^{IV} compounds.



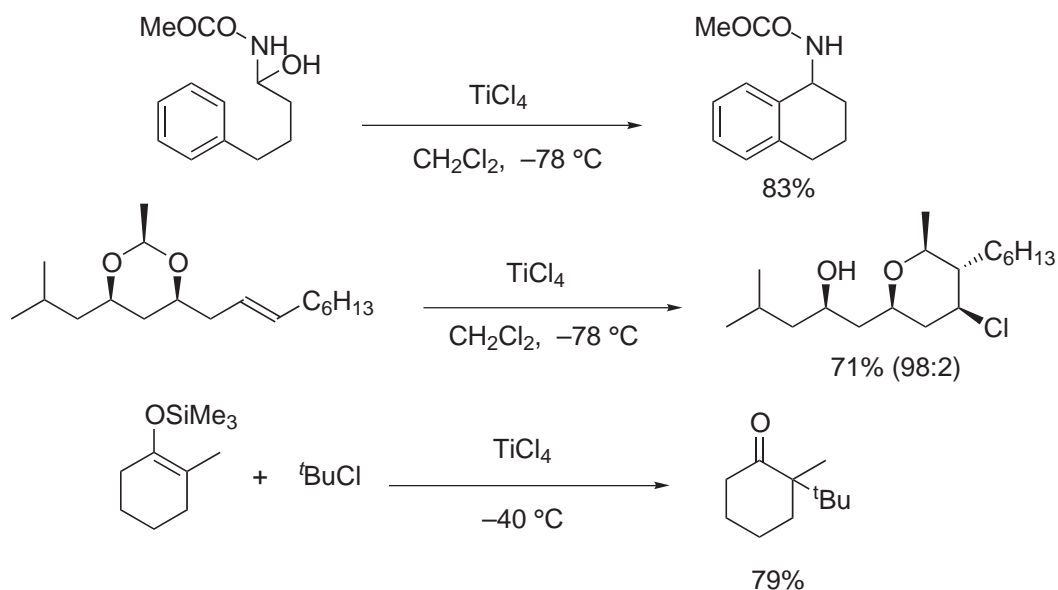
Scheme 27

Friedel–Crafts acylation reactions of aromatics are promoted by Ti^{IV} complexes.¹⁰⁴ In some cases, a catalytic amount of the titanium compound works well (Scheme 28). In addition to acyl halides or acid anhydrides, aldehydes, ketones, and acetals can serve as electrophile equivalents for this reaction.¹⁰⁵ The formylation of aromatic substrates in the presence of TiCl_4 is known as the Rieche–Gross formylation; metalated aromatics or olefins are also formylated under these conditions.¹⁰⁶

Titanium-mediated intramolecular Friedel–Crafts acylation and alkylation are important methods for construction of fused-ring systems (Scheme 29).¹⁰⁷ As well as aromatics, olefin units also react in the same way.¹⁰⁸ Alkylation of electron-rich olefins such as enol ethers or silyl enol ethers proceeds effectively in the presence of TiCl_4 .¹⁰⁹



Scheme 28



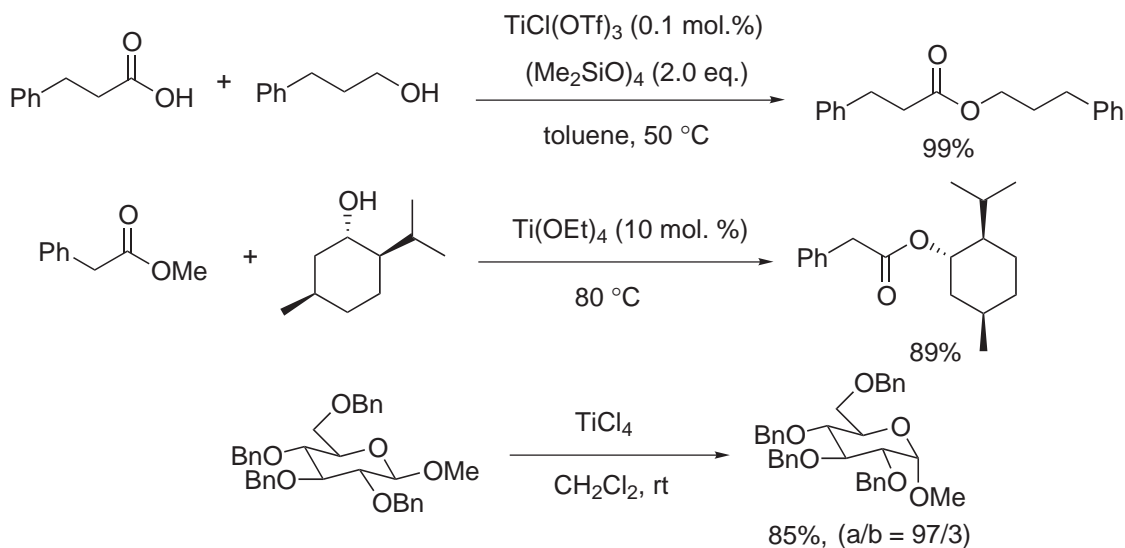
Scheme 29

Esterification and transesterification using Ti^{IV} compounds are useful methods for functionalization of ester moieties under mild conditions. In the transformation of carboxylic acids to esters, a catalytic amount of $\text{TiCl}(\text{OTf})_3$ is effective (Scheme 30).¹¹⁰ Titanium alkoxides, such as $\text{Ti}(\text{OEt})_4$ or $\text{Ti}(\text{O}^i\text{Pr})_4$, easily promote transesterification of alkoxy groups to other ones—even to more hindered groups.¹¹¹ Anomerization of glycosides to α -isomers using a Ti^{IV} -based Lewis acid is an important method for controlling the product structure.¹¹²

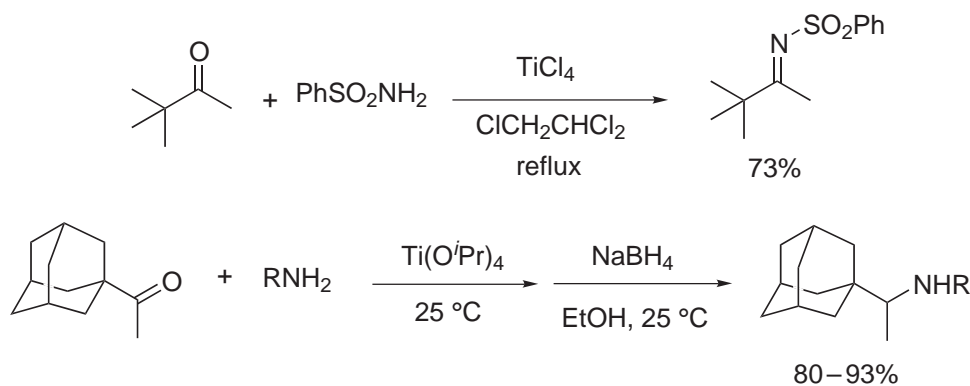
TiCl_4 also effectively promotes formation of imines and enamines from carbonyl compounds (Scheme 31). The combination of imine formation using TiCl_4 and reduction leads to reductive alkylation of an amine moiety.^{113,114}

Ti^{IV} compounds also promote epoxidation of olefins, mainly allyl alcohol moieties in the presence of peroxides (Scheme 32).¹¹⁵

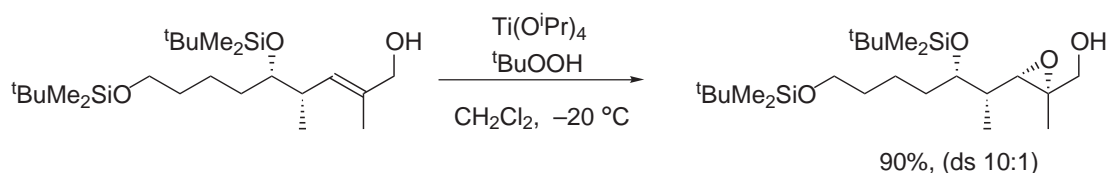
Regio- and stereoselective ring opening of epoxides is facilitated by Ti^{IV} complexes. The existence of hydroxy groups at the α -position of epoxides is quite important to the reactivity of



Scheme 30



Scheme 31

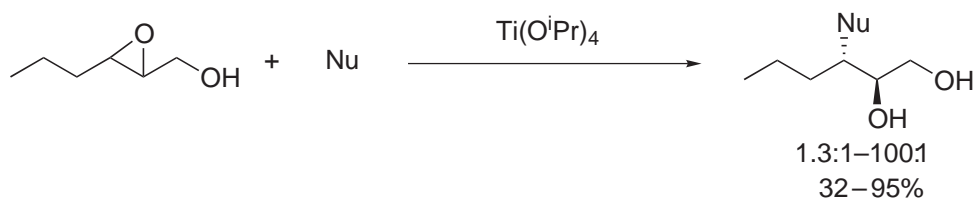


Scheme 32

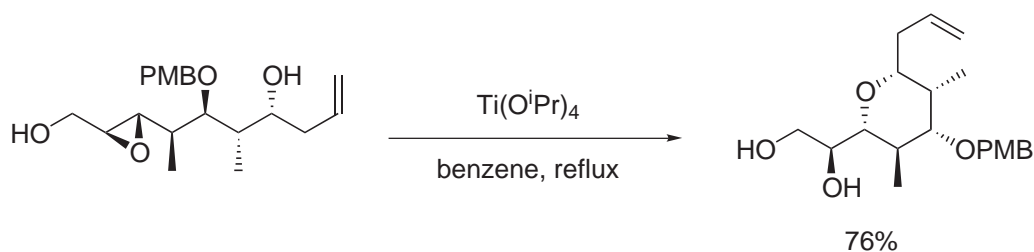
these reactions, which show good to excellent regioselectivity (Scheme 33).^{116,117} Several nucleophiles are available and many kinds of functionalized compound can be synthesized using this method.¹¹⁸

Ti^{IV} halides are useful for deprotection of functionalized groups, especially protecting groups on alcohols and phenols. For example, *t*-butyl groups, benzyl groups, methoxymethyl groups, and methoxyethoxymethyl groups are deprotected selectively using Ti^{IV} Lewis acids (Scheme 34).¹¹⁹

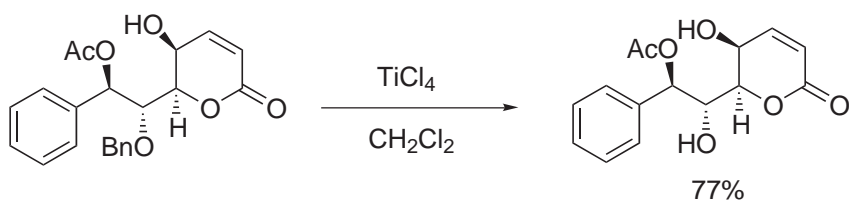
Chiral Ti^{IV} complexes are the most important and powerful tools in catalytic asymmetric reactions, and have been developed extensively since the early 1980s because of their high Lewis acidity and relatively short metal–ligand bond length. Enantioselective additions to carbonyl groups, especially aldehydes, have been intensively studied using chiral Ti catalysts bearing several chiral auxiliaries. In alkylation of dialkylzinc reagents,^{120–122} allylation,^{123,124} carbonyl-ene reactions,^{125,126} Diels–Alder reactions,^{127,128} hetero Diels–Alder reactions,^{129,130} [2 + 2] cycloaddition,^{131–133}



Nu : $^i\text{PrOH}$, PhSH , Me_3SiN_3 , Me_3SiCN , KCN , PhCO_2H etc.

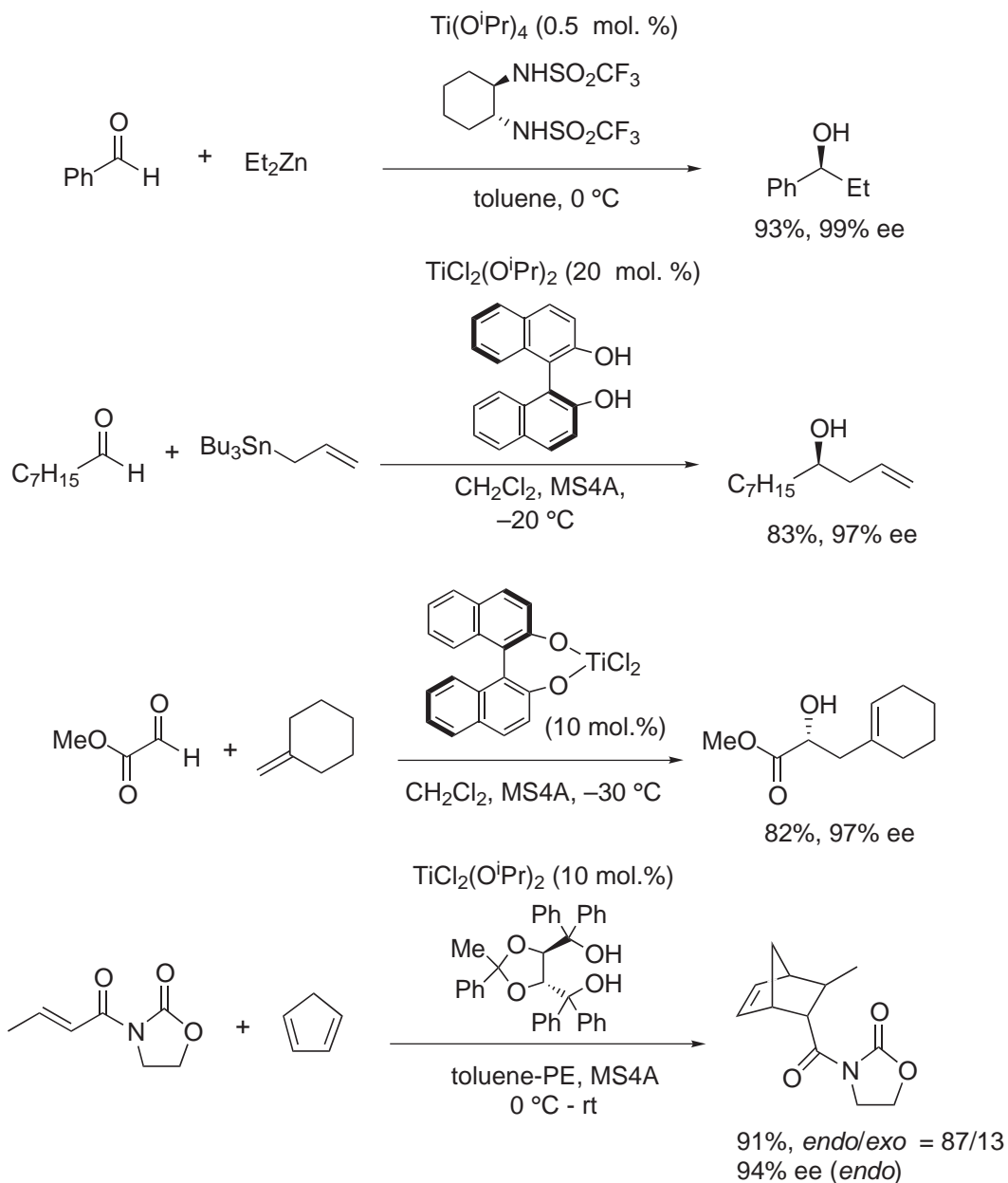


Scheme 33



Scheme 34

cyanation,¹³⁴ and Mukaiyama aldol reactions,¹³⁵ chiral titanium complexes work well and high levels of enantioselectivity have been achieved (Scheme 35). As chiral ligands for Ti^{IV} , BINOL derivatives, TADDOL derivatives, bis-sulfonamides, and Schiff bases have been employed in several transformations (Figure 1).



Scheme 35

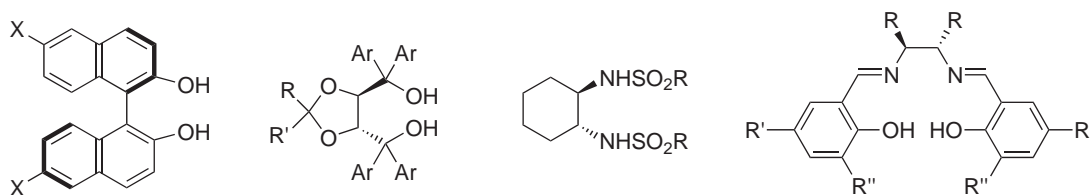


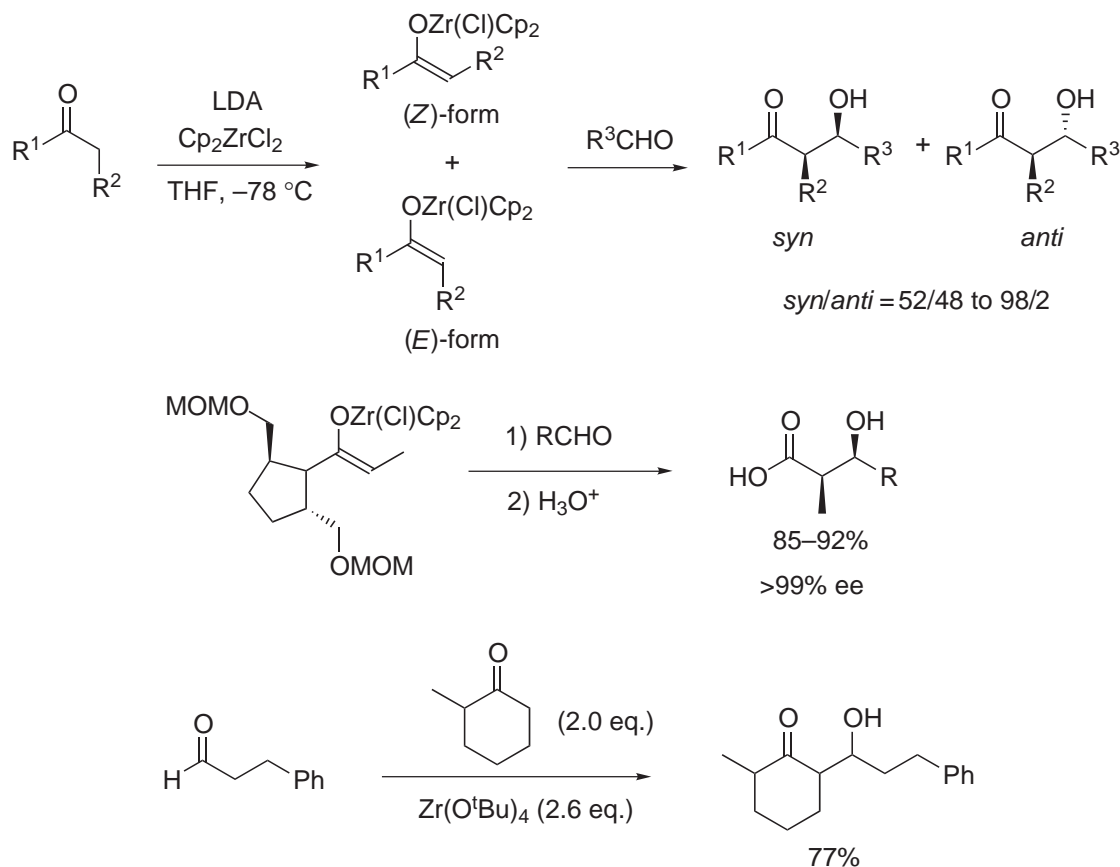
Figure 1 Chiral ligands for Ti^{IV} .

9.8.6 ZIRCONIUM

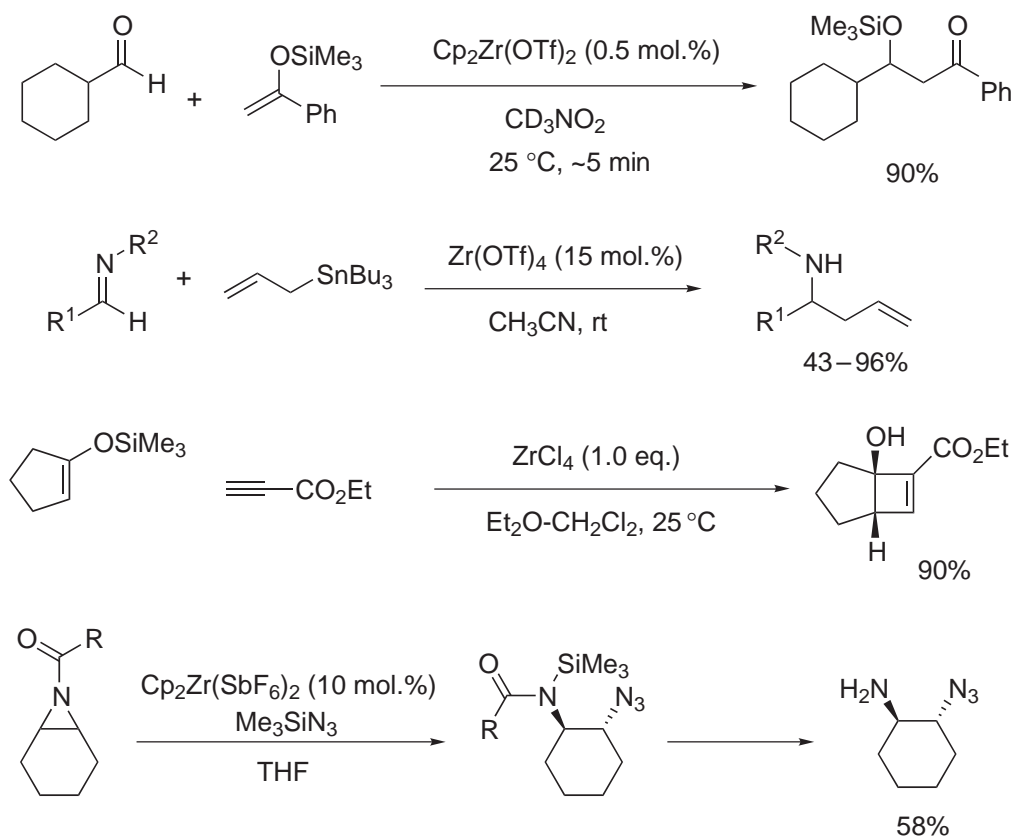
Zirconium(IV) complexes are milder Lewis acids than Ti^{IV} complexes, and they are employed in several stereo- and enantioselective reactions. They often show better selectivities than stronger Lewis acids.

Zirconium enolates are employed as good reactive reagents in aldol reactions. As shown in Scheme 36, the reactions of aldehydes with Cp_2ZrCl enolates prepared from lithium enolates of ketones show good *syn*-selectivity via cyclic transition states. Both *E*- and *Z*-enolates give the same *syn*-adducts selectively.^{136,137} Furthermore, Cp_2ZrCl enolates of amides bearing chiral auxiliaries react with aldehydes, and the desired aldol adducts are obtained with high enantioselectivities.^{138,139} In contrast, $\text{Zr}(\text{O}^t\text{Bu})_4$ acts as a base and deprotonates ketones at the α -position to form zirconium enolates. The enolates react with aldehydes to afford aldol adducts in moderate yields.¹⁴⁰

Several Zr^{IV} compounds are employed as Lewis-acid catalysts which activate carbonyl and imino groups effectively. Complexes such as Cp_2ZrX_2 or ZrX_4 promote Lewis acid-catalyzed reactions, especially carbon–carbon bond-forming reactions. Zr^{IV} -mediated Friedel–Crafts-type reactions,^{141–144} Mukaiyama aldol reactions,^{145,146} Mannich-type reactions,^{147–149} allylation of aldehydes^{150,151} and imines,¹⁵² Diels–Alder reactions,^{153,154} hetero Diels–Alder reactions,¹⁵⁵ and [2 + 2] cycloaddition reactions^{156,157} have all been investigated, and several effective reaction systems have been developed (Scheme 37). In addition, ring-opening addition to oxiranes^{158,159}



Scheme 36



Scheme 37

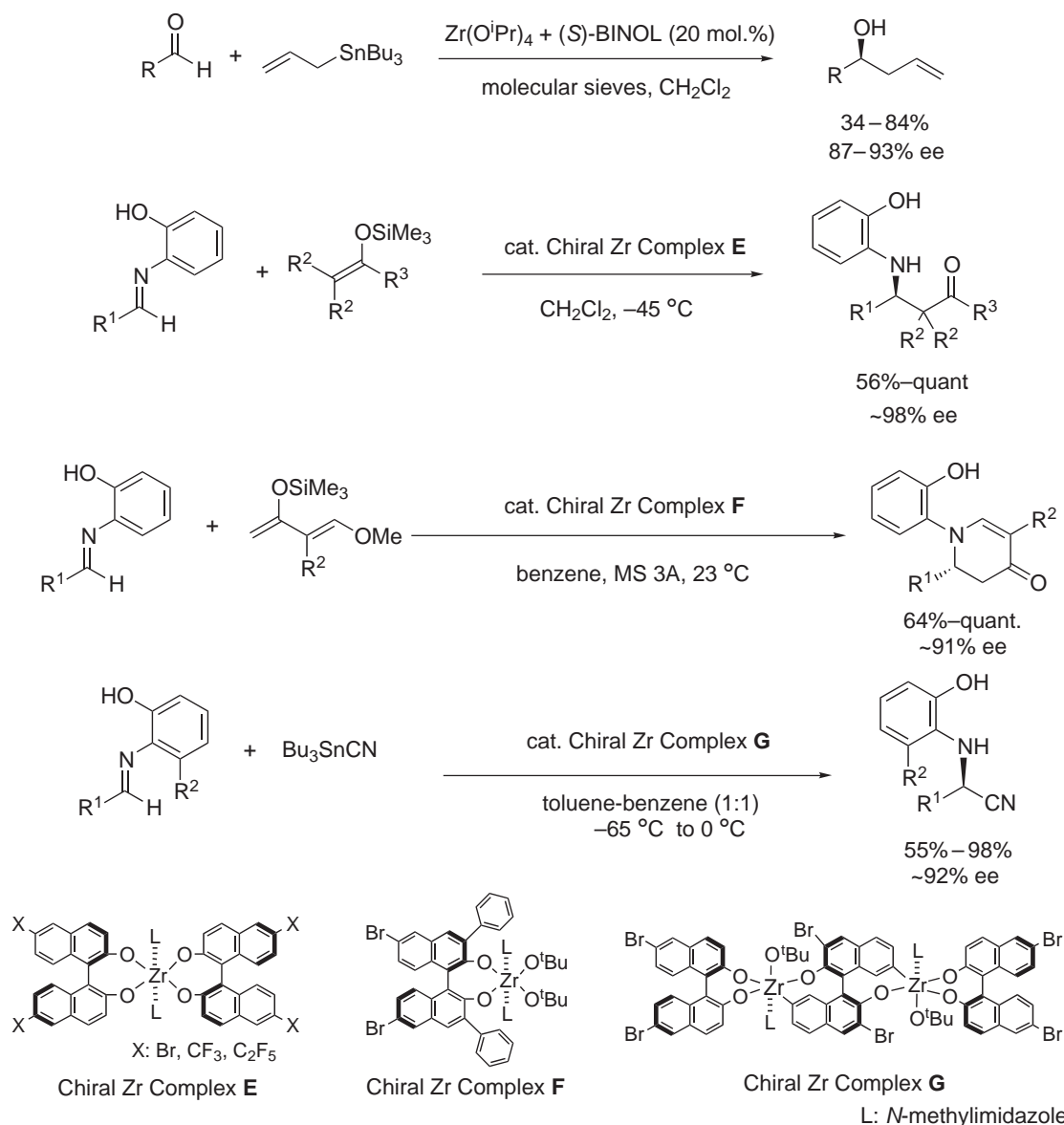
and aziridines,¹⁶⁰ and hydrometalation reactions^{161,162} mediated by zirconium compounds, have been also reported.

In catalytic asymmetric synthesis, chiral Zr^{IV} compounds play an important role as useful catalysts. Catalytic asymmetric allylation of aldehydes using chiral zirconium-BINOL complexes (e.g., compounds (E)–(G) in Scheme 38) has been studied, and high enantioselectivity has been achieved (Scheme 38).^{150,151} More importantly, it is reported that complexes prepared from zirconium alkoxides and BINOL derivatives are effective for the activation of azomethine compounds, and that catalytic asymmetric Mannich-type reactions,^{147–149} aza Diels–Alder reactions,^{163–165} Strecker reactions,¹⁶⁶ and imine allylations¹⁶⁷ proceed smoothly with high enantioselectivities. These complexes are also effective in Mukaiyama aldol reactions¹⁶⁸ and hetero Diels–Alder reactions.¹⁵⁵ In asymmetric ring-opening reactions of epoxides,^{158,159} catalysts containing chiral alcohols or amide ligands work well. Moreover, one-pot synthesis of β -cyanohydrins from olefins is reported using Zr^{IV} -TADDOL derivatives (Scheme 39).¹⁶⁹

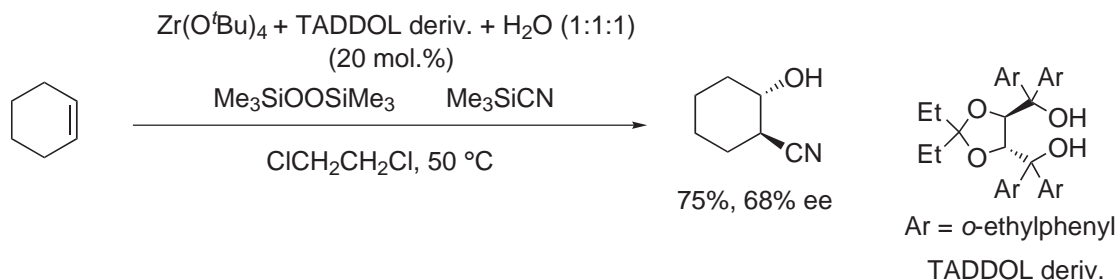
Zr compounds are also useful as Lewis acids for oxidation and reduction reactions. Cp_2ZrH_2 or $\text{Cp}_2\text{Zr}(\text{O}^i\text{Pr})_2$ catalyze the Meerwein–Ponndorf–Verley-type reduction and Oppenauer-type oxidation simultaneously in the presence of an allylic alcohol and benzaldehyde (Scheme 40).¹⁷⁰ $\text{Zr}(\text{O}^t\text{Bu})_4$ in the presence of excess 1-(4-dimethylaminophenyl) ethanol is also an effective catalyst for the Meerwein–Ponndorf–Verley-type reduction.¹⁷¹ Similarly, $\text{Zr}(\text{OR})_4$ catalyze Oppenauer-type oxidation from benzylic alcohols to aldehydes or ketones in the presence of hydroperoxide.^{172,173}

9.8.7 HAFNIUM

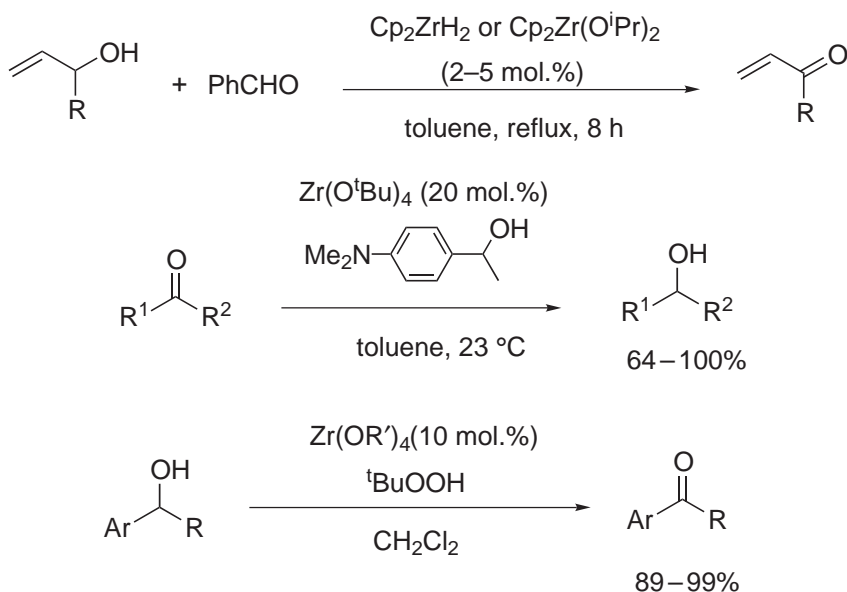
Hafnium-centered Lewis acid usage is limited in organic chemistry, because of its lower availability and its similarity to zirconium. There are some reactions, however, for which Hf^{IV} compounds are used as effective activators. Glycosylation of glycosyl fluorides using a combination



Scheme 38



Scheme 39

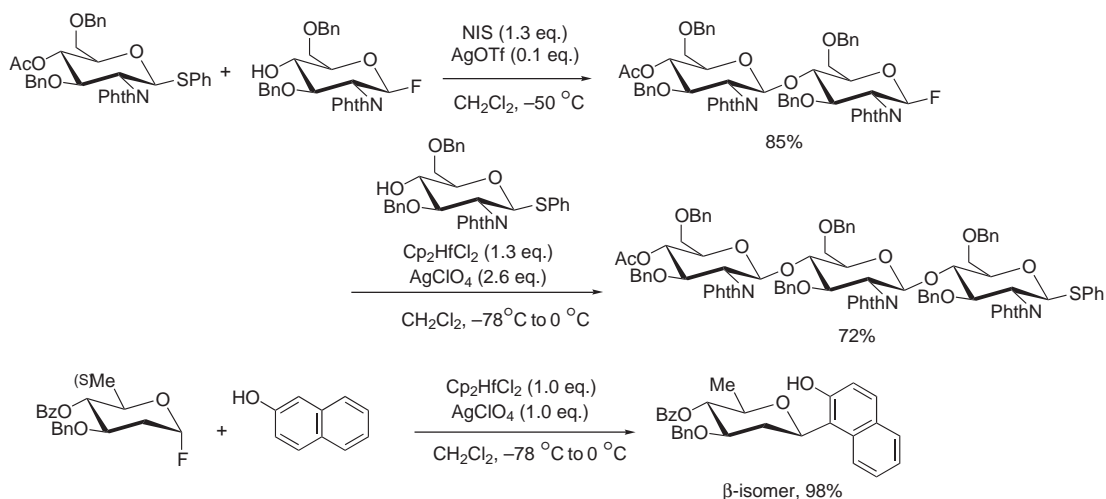


Scheme 40

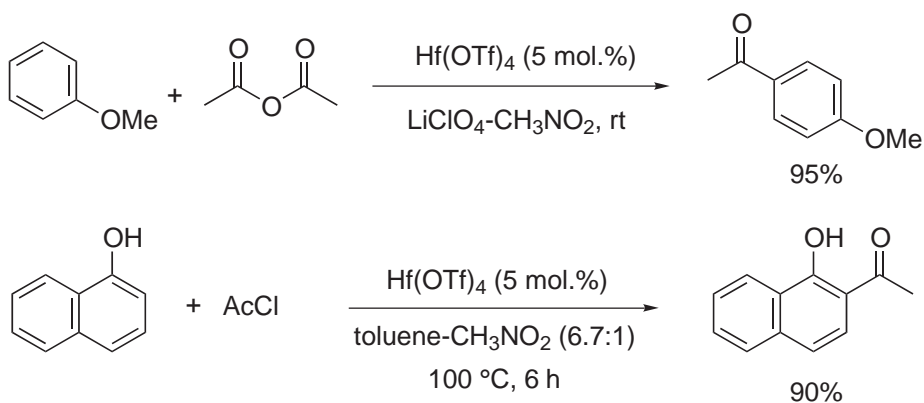
of Cp_2HfCl_2 and AgClO_4 is effective (Scheme 41). In oligosaccharide synthesis in both the liquid and the solid phase, selective activation of a thioglycoside with *N*-iodosuccinimide (NIS)- AgOTf and of a glycosyl fluoride with Cp_2HfCl_2 - AgClO_4 are important.¹⁷⁴ Other characteristic reactions using Cp_2HfCl_2 and AgClO_4 include synthesis of aryl C-glycoside compounds through the “O to C glycoside rearrangement.”¹⁷⁵ This reaction is important for the synthesis of antibiotics such as Vineomycine B2 and Gilvocarcin V.¹⁷⁵⁻¹⁷⁷

Catalytic amounts of HfCl_4 - AgClO_4 and $\text{Hf}(\text{OTf})_4$ are used for activation of acid halides and acid anhydrides for Friedel-Crafts acylation (Scheme 42);¹⁷⁸ the reactions of both reactive and unreactive aromatic substrates proceed smoothly in the presence of $\text{Hf}(\text{OTf})_4$. Furthermore, the Fries rearrangement^{179,180} and direct C-acylation of phenolic compounds^{181,182} take place using $\text{Hf}(\text{OTf})_4$. Formation of esters and Mannich-type reactions and allylation of imines have been also reported.¹⁵²

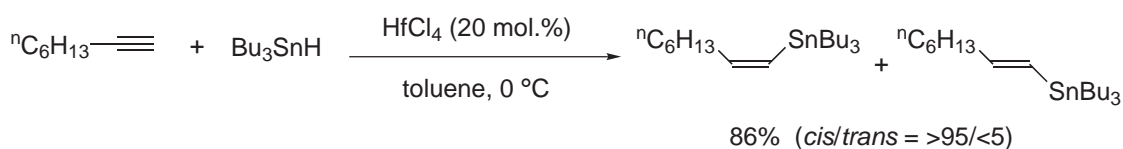
HfCl_4 -catalyzed hydro- and carbometalation have been investigated.¹⁸³ *trans*-Addition of tributyltin hydride or allyltrimethylsilane to alkynes occurs with high selectivities (Scheme 43).¹⁶² In α -olefin polymerization, the Hf -methylaluminumoxane (MAO) system also works well.¹⁸⁴



Scheme 41



Scheme 42



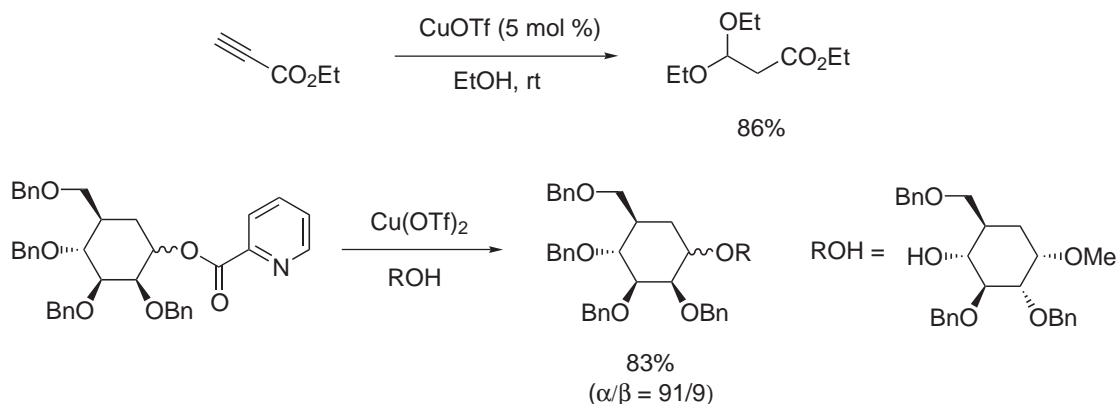
Scheme 43

9.8.8 COPPER

Copper-based Lewis acids have been widely used and many Lewis-acidic copper complexes have been developed. These are divided into two groups: Cu^{I} salts and Cu^{II} salts. Generally, Cu^{II} salts have stronger Lewis acidity than Cu^{I} . Copper fluoride and chloride are more Lewis acidic than bromide and iodide; other salts used include triflate, sulfate, perchlorate, tetrafluoroborate, and hexafluoroantimonate. Many of these are commercially available. Cu^{II} complexes usually adopt a square planar, square pyramidal, or trigonal bipyramidal geometry; Cu^{I} complexes usually adopt a tetrahedral geometry.

Copper-based Lewis acids can be applied to various kinds of reaction. While Cu^{I} complexes catalyze acetal formation (Scheme 44),¹⁸⁵ $\text{Cu}(\text{OTf})_2$ is used for formation of glycosyl bonds.^{186,187} Since the ability of $\text{Cu}(\text{OTf})_2$ to be chelated by the substrate is essential for the reaction, typical Lewis acids such as $\text{BF}_3\cdot\text{OEt}_2$ and Me_3SiOTf are ineffective.

Transesterification from thioesters to esters¹⁸⁸ or amides^{189,190} (lactams) are conducted by Cu^{I} - or Cu^{II} -based Lewis acids (Scheme 45). Addition of alcohols to isocyanates is accelerated by CuCl .¹⁹¹

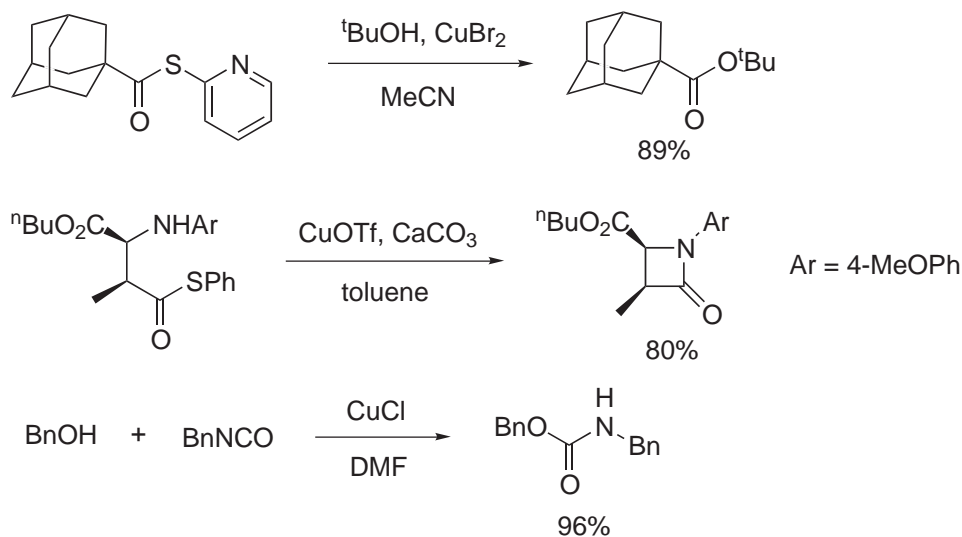


Scheme 44

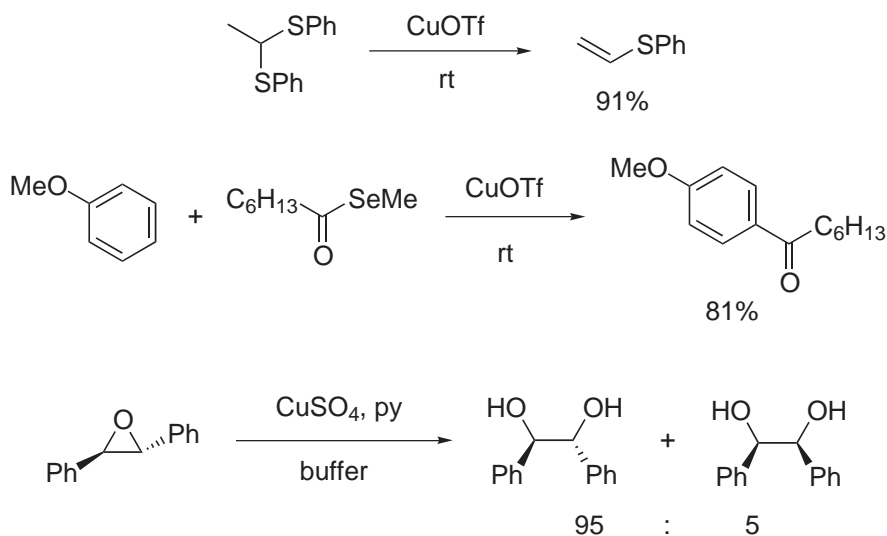
Thioacetals eliminate to vinylsulfides in the presence of CuOTf (Scheme 46).¹⁹² Cu^I and Cu^{II} triflates are mild Lewis acids for Friedel–Crafts acylation and alkylation reactions. CuOTf effectively catalyzes the reaction of anisole with selenoesters.^{193,194} Copper(II) sulfate promotes epoxide ring opening reactions in the presence of pyridine,¹⁹⁵ with retention of configuration being observed. Cu(OTf)₂ is a catalyst for the ring opening of aziridine by aniline.¹⁹⁶

Copper-based Lewis acids have some advantages for hydrolysis reactions: they are mild, nonacidic, and can control reactions due to chelation by the substrate to achieve high selectivity. CuSO₄ is effective for acetal deprotection (Scheme 47).¹⁹⁷ Thioacetals^{198,199} and selenoacetals^{200–202} are also hydrolyzed by copper Lewis acids, and dehydration is accelerated by Cu^{II} Lewis acids under mild conditions.²⁰³

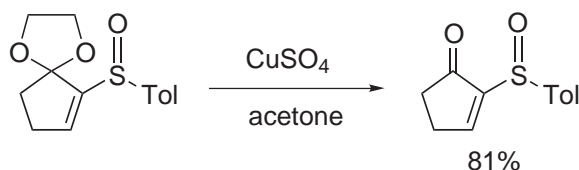
Many examples of asymmetric reactions catalyzed by copper complexes with chiral ligand systems have been reported. In particular, various copper–bis(oxazoline) catalysts (e.g., complexes **(H)** to **(L)**, Scheme 48) are effective for carbon–carbon bond-forming reactions such as aldol,²⁰⁴ Mukaiyama–Michael,²⁰⁵ Diels–Alder,²⁰⁶ hetero Diels–Alder,^{207,208} dipolar cycloaddition,^{209,210}



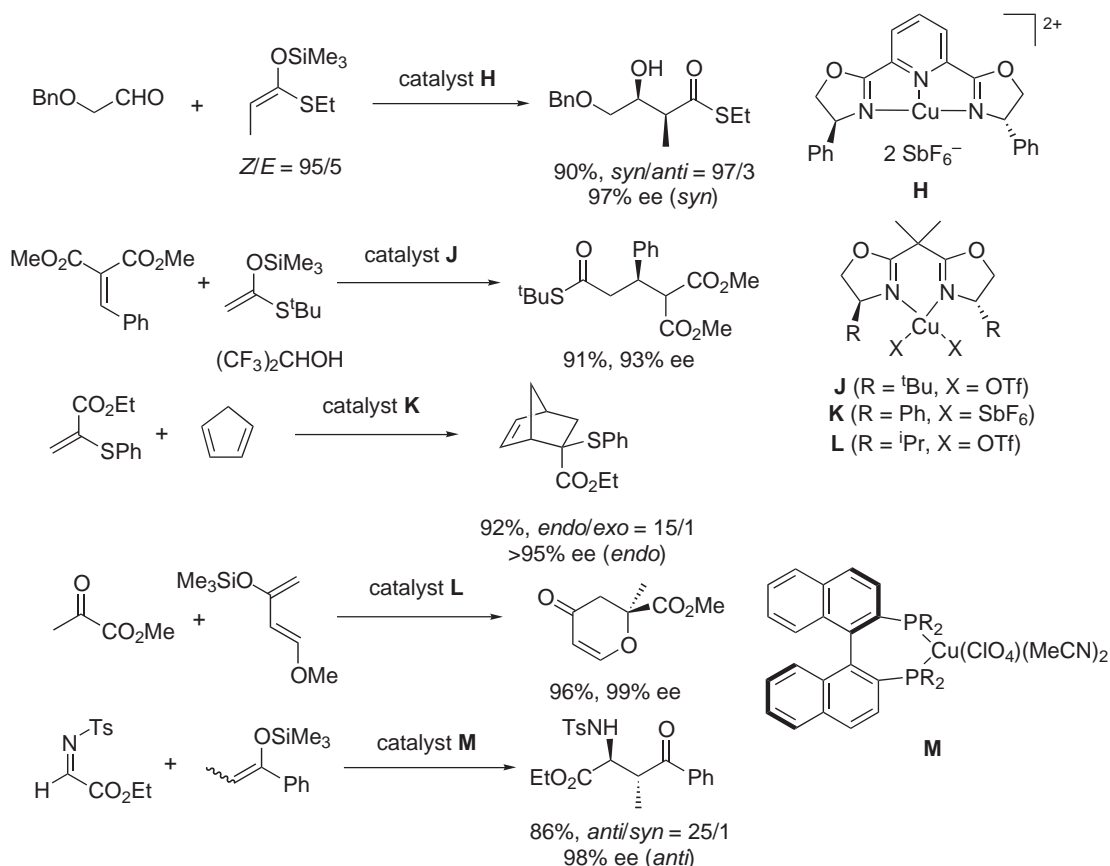
Scheme 45



Scheme 46



Scheme 47



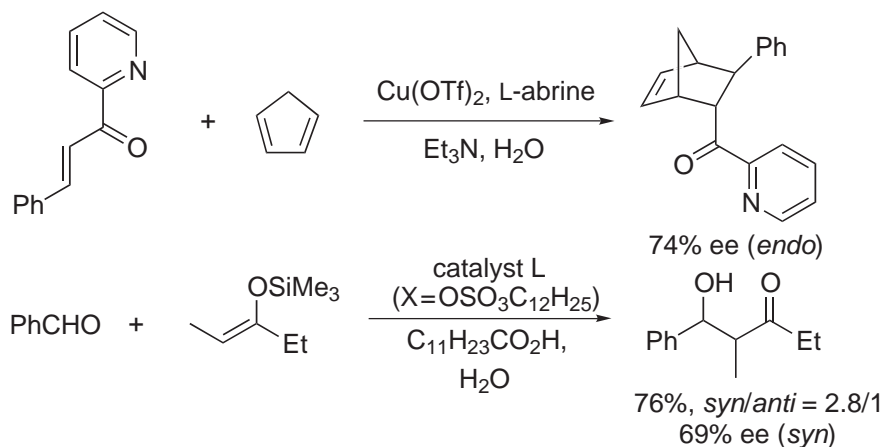
Scheme 48

and ene reactions²¹¹ (Scheme 48). Copper–phosphine complexes (e.g., compound (**M**)) have also been developed for imine activation.^{212,213}

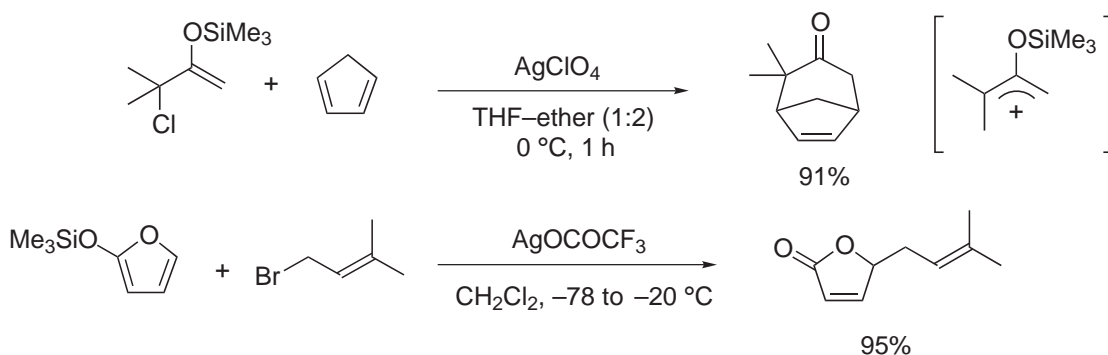
Asymmetric reactions using chiral copper Lewis acids are also performed in aqueous media. It has been reported that an asymmetric Diels–Alder reaction proceeds smoothly in water using Cu(OTf)₂ and abrine as a chiral ligand (Scheme 49).²¹⁴ The Cu^{II}–bis(oxazoline) system is effective in asymmetric aldol reactions in an aqueous solvent such as water/ethanol and even in pure water.²¹⁵

9.8.9 SILVER AND GOLD

Silver(I) salts have mild Lewis acidity and have been used as promoters and catalysts in organic synthesis. Among many salts, AgNO₃, AgClO₄, AgBF₄, and AgOTf are the most popular reagents. In contrast, gold compounds have attracted little attention as Lewis-acid catalysts for organic reactions. In reactions using silver salts as promoters, the special affinity of silver for



Scheme 49



Scheme 50

halide groups is exploited to produce carbocations, forming reactive intermediates in many cases; some cyclization and alkylation reactions proceed in good yields (Scheme 50).^{216–219}

In asymmetric reactions, chiral phosphine ligands such as BINAP derivatives are used as effective chiral ligands in silver complexes. In particular, an Ag^{I} -BINAP complex activates aldehydes and imines effectively; and asymmetric allylations,^{220–222} aldol reactions,²²³ and Mannich-type reactions²²⁴ proceed in high yield with high selectivity (Scheme 51).

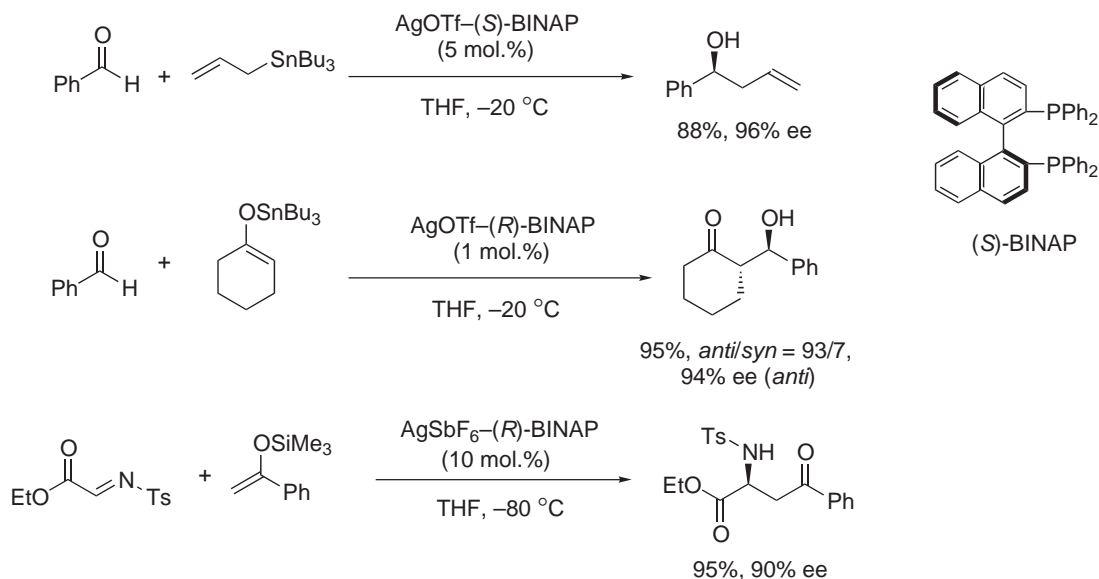
The gold(I) complex of a chiral ferrocenylphosphine complex promotes asymmetric aldol reactions of α -isocyanocarboxylates to form chiral oxazolines in high diastereo- and enantioselectivities (Scheme 52).^{225,226} In these reactions, the analogous silver(I) ferrocenylphosphine complex also works well.

Silver salts are also employed to create more effective chiral catalysts by exchange of counter anions. For example, in the Mizoroki–Heck reaction of alkenyl or aryl halides, silver salts are employed to form effective chiral Pd intermediates by abstracting a halide group from the Pd^{II} precursor species (Scheme 53).^{227,228}

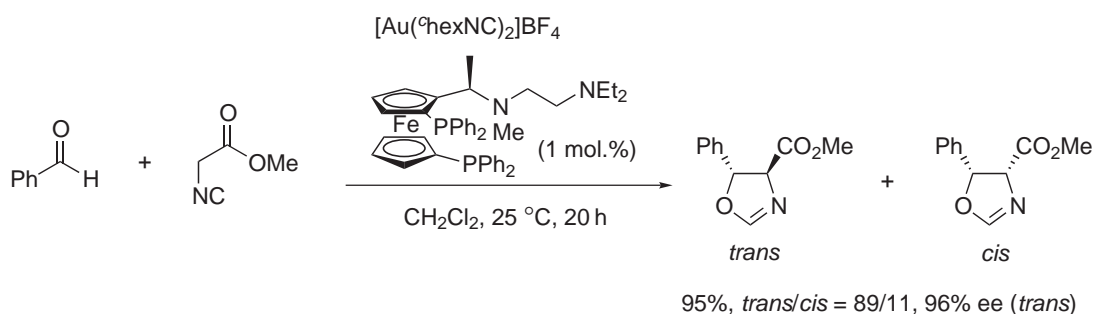
9.8.10 ZINC

The chemistry and utility of zinc-based Lewis acids are similar to those of their magnesium analogs. Their mild Lewis acidity promotes several synthetic reactions, such as Diels–Alder reactions, hetero Diels–Alder reactions,²²⁹ radical-mediated reactions,²³⁰ ene-type cyclization, and Simmons–Smith reactions.

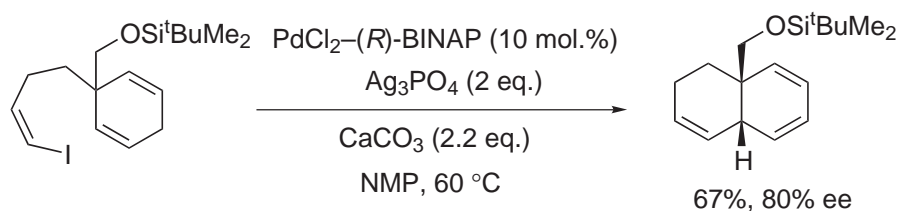
In stereoselective reactions, Zn^{II} Lewis acids work well to achieve high selectivities (Scheme 54). Chiral complexes of Zn^{II} with chiral bis(oxazoline) ligands act as effective catalysts in Diels–Alder reactions of reactive dienes with dienophiles having bidentate chelating moieties such as



Scheme 51



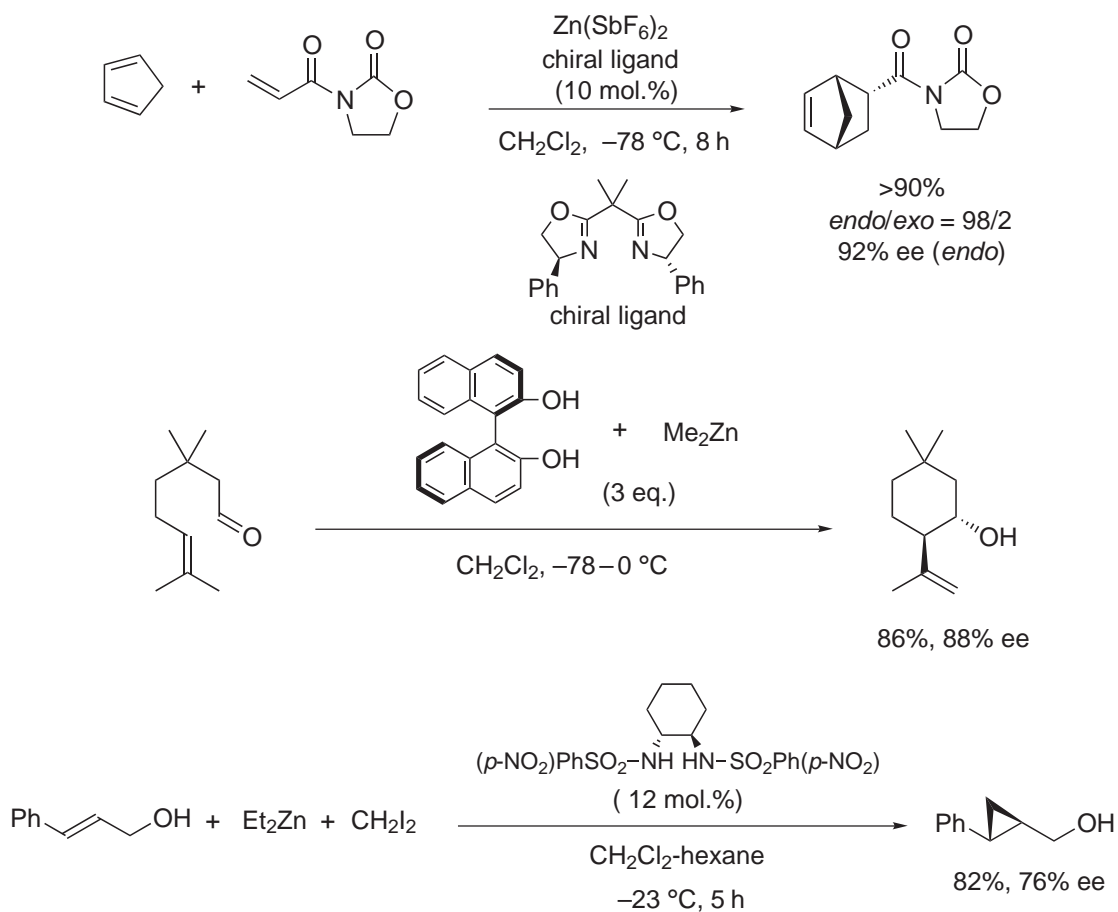
Scheme 52



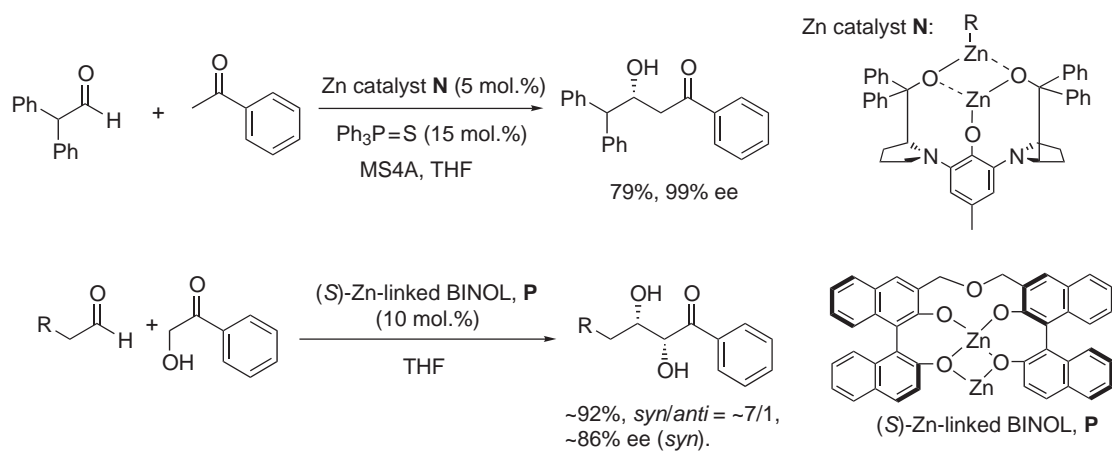
Scheme 53

3-acryloyloxazolidin-2-one.²⁸ In ene-type cyclization, zinc-1,1'-binaphthalene-2,2'-diol (BINOL) complex works well to afford *trans*-cyclohexanol in high diastereo- and enantioselectivity.²³¹ Simmons–Smith reactions of allylic alcohols are effectively promoted by a chiral Zn^{II} bis(sulfonamide) complex, and the desired cyclopropane derivatives are obtained in high yields with good enantioselectivity.²³²

Recently, novel bifunctionalized zinc catalysts have been developed (compounds **(N)** and **(P)**, Scheme 55). They have both Lewis-acid and Lewis-base centers in their complexes, and show remarkable catalytic activity in direct aldol reactions.^{233–236} A Zn^{II} chiral diamine complex effectively catalyzes Mannich-type reactions of acylhydrazones in aqueous media to afford the corresponding adducts in high yields and selectivities (Scheme 56).²³⁷ This is the first example of catalytic asymmetric Mannich-type reactions in aqueous media, and it is remarkable that this chiral Zn^{II} complex is stable in aqueous media.



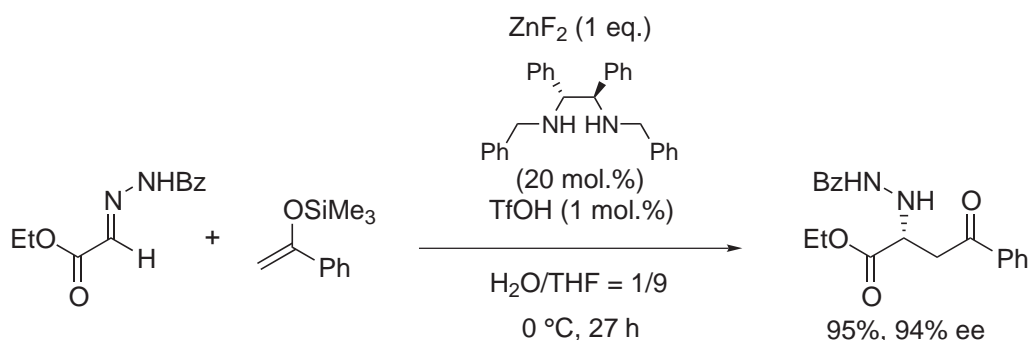
Scheme 54



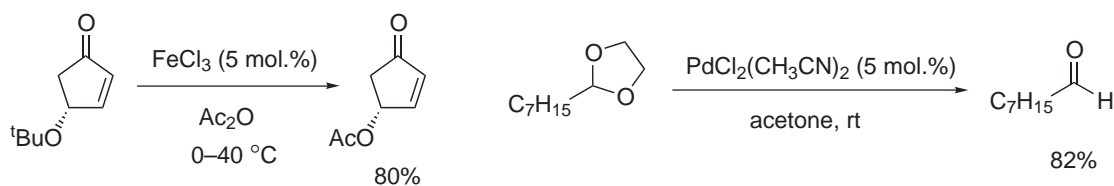
Scheme 55

9.8.11 OTHER TRANSITION-METAL LEWIS ACIDS

A variety of other transition-metal-based Lewis acids are used in organic transformations. Some of them are water tolerant and promising as sources of highly functionalized Lewis-acid catalysts.



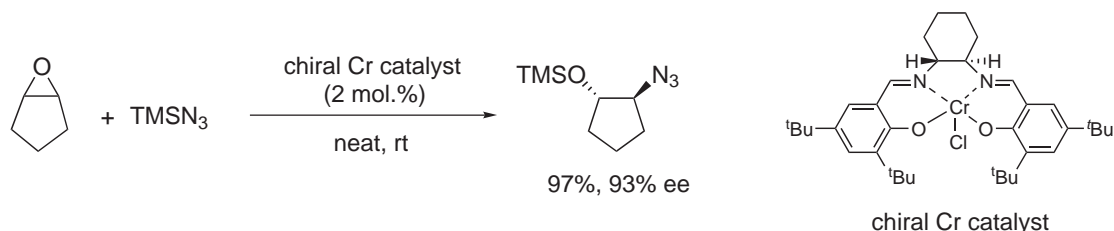
Scheme 56



Scheme 57

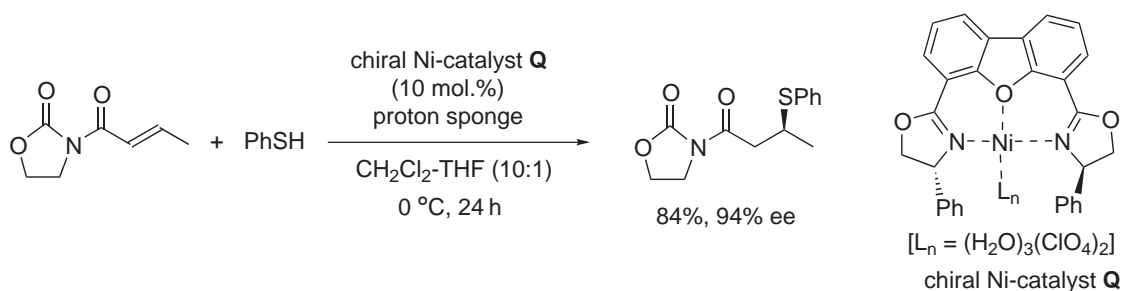
In reactions of functional groups containing ether-type oxygens, transition-metal chlorides work well. In ether cleavage reactions, FeCl_3 and its derivatives are efficient catalysts, and deprotection of ethers and acetals occurs easily to afford the corresponding alcohols in high yields in the presence of iron compounds (Scheme 57).^{238,239} Furthermore, direct conversion of protecting groups from alkyl ethers to esters is possible.²⁴⁰ Besides these, $[\text{PdCl}_2(\text{CH}_3\text{CN})_2]$, $[\text{Ru}(\text{CH}_3\text{CN})_3(\text{TRIPHOS})](\text{OTf})_2$, and WCl_6 are also employed in similar types of reaction, and some of them show milder activity,^{241–243} they also work well in acetal formation reactions.^{244,245} Further reactions with acetals are also developed well: cyanation and Mukaiyama aldol reactions of acetals proceed smoothly in the presence of NiCl_2 , CoCl_2 , and $[\{\text{Rh}(\text{COD})\text{Cl}\}_2]$.²⁴⁶

The development of ring-opening reactions of epoxides using Cr and Fe has been well studied, and some highly enantioselective catalysis is reported. An Fe^{III} -porphyrin complex catalyzes transformation of epoxides to carbonyls.²⁴⁷ A Cr^{III} -porphyrin complex also catalyzes formation of a cyclic carbonate from methyloxirane and CO_2 .²⁴⁸ Regio- and stereoselective opening reactions of terminal epoxides with several reagents proceed in good yield in the presence of a catalytic amount of FeCl_3 .²⁴⁹ In asymmetric ring opening reactions of *meso*-epoxides, chiral (salen)- Cr^{III} and (salen)- Co^{III} derivatives show higher turnover numbers and higher enantioselectivities (Scheme 58).^{250,251}



Scheme 58

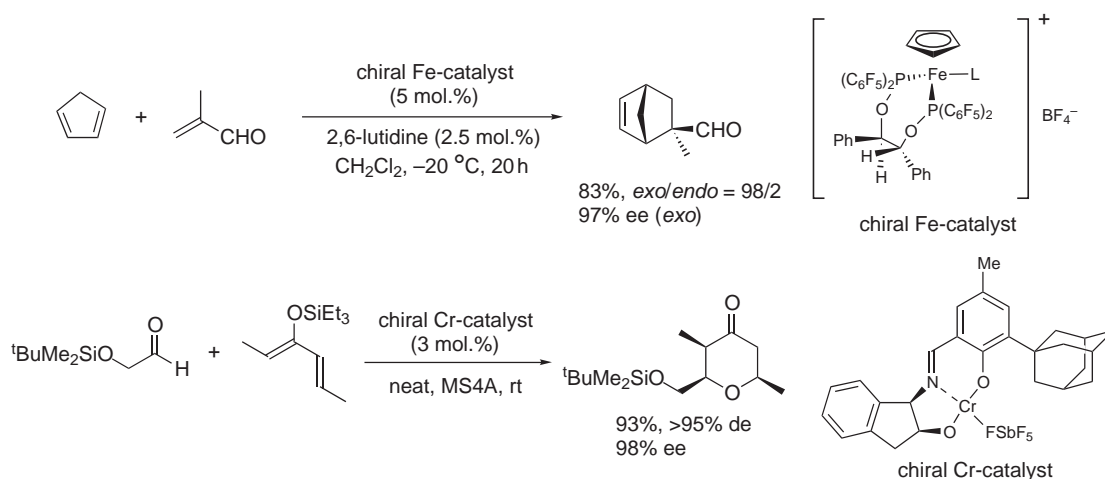
In addition, transition-metal Lewis acids also work well in reactions with carbonyl and imine groups and α,β -unsaturated carbonyl compounds. Some Rh^{III} catalysts, with chiral terdentate ether-pyrrolidine-pyridine or bis(oxazolonyl)phenyl ligands, have been developed for allylation reactions of aldehydes, and moderate selectivities are obtained.^{252,253} Mukaiyama aldol reactions are also catalyzed by other transition-metal Lewis acids including cationic organometallic Fe^{II} complexes; $[\text{Ru}(\text{salen})(\text{NO})(\text{H}_2\text{O})][\text{SbF}_6]$; tungsten-nitrosyl species such as $[(\text{Me}_3\text{P})(\text{NO})(\text{CO})_3\text{W}(\mu\text{-F})\text{SbF}_5]$; and 2,2'-biphenolate adducts of oxo-vanadium(IV).^{254–258} A chiral



Scheme 59

bis(oxazolyl)phenyl-Pt^{II} complex controls alkylation of imines in high selectivities.²⁵⁹ Conjugated addition to α,β -unsaturated carbonyl compounds is catalyzed by FeCl₃ and NbCl₅.^{260–263} It has been reported that a chiral Ni^{II} catalyst (Scheme 59, compound **Q**) shows high selectivities in the reaction with thiols.²⁶⁴ Nitrile groups are also activated by a variety of complexes, including dicationic Pd^{II} complexes with N- or N/P-donor ligands such as BINAP, terpyridyl, and bis(oxazolinyl)pyridines; Pt^{II} complexes of chiral P,C,P-donor ligands; Ru^{II} hydride–phosphine complexes such as [RuH₂(PPh₃)₄]; and Rh^I complexes of a *trans*-chelating chiral bis-phosphine. C–C bond-forming reactions have been achieved in high selectivities with these systems.^{265–270} [RuH₂(PPh₃)₄] also promotes the addition of water to nitrile groups.²⁷¹

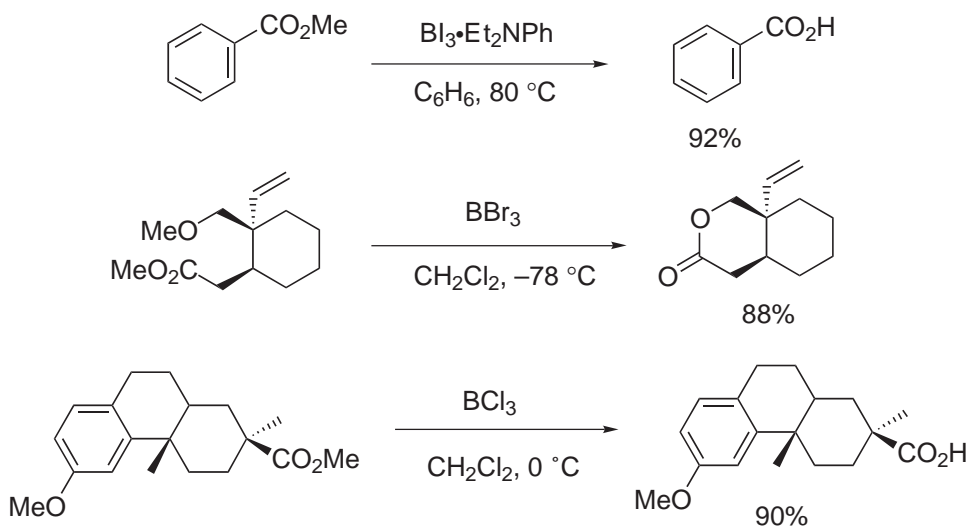
In concerted cycloaddition reactions, several chiral transition-metal catalyst systems have been developed. Among them, complexes of Fe^{II} and Fe^{III}, Ru^{II}, Ni^{II}, and Pd^{II} with various chiral C₂-symmetric ligands (bis-oxazolines and diphosphines for M^{II}; bis-sulfoxides for Fe^{III}) serve as effective Lewis acids in Diels–Alder reactions (Scheme 60).^{272–278} Furthermore, hetero Diels–Alder reactions also proceed under similar conditions using a chiral Cr^{III} catalyst (Scheme 60).^{279–282} 1,3-Dipolar cycloaddition reactions of nitrones with olefins are catalyzed by a chiral Ni^{II} or Pd^{II} catalyst.^{283,284}



Scheme 60

9.8.12 BORON

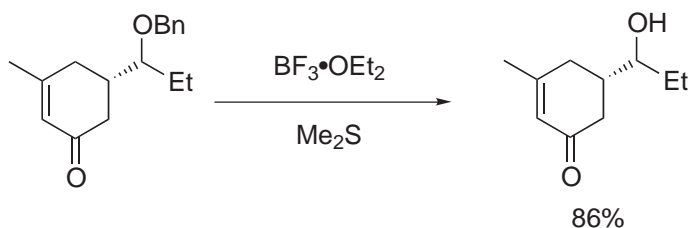
Boron-based Lewis acids are often used in organic syntheses. Since the boron atom has an empty *p*-orbital, many boron compounds can function as Lewis acids. Typical boron Lewis acids are boron trihalides, for which Lewis acidity increases according to the order of fluoride < chloride < bromide < iodide, the reason for this order being the relative abilities of the different halogens to act as π -donors to boron.



Scheme 61

BX_3 ($\text{X} = \text{Cl}, \text{Br}, \text{I}$) are mainly used for cleavage of ethers (Scheme 61). BI_3 is a powerful reagent²⁸⁵ for the cleavage of carbon–oxygen bonds in ethers, esters, and alcohols; BBr_3 also promotes carbon–oxygen bond cleavage.²⁸⁶ BBr_3 has been widely used to cleave ethers because the reaction proceeds completely under mild conditions.^{287,288} BCl_3 can be used for cleavage of hindered esters.²⁸⁹

BF_3 is also used for ether carbon–oxygen cleavage in the presence of sulfide or thiol (Scheme 62).²⁹⁰



Scheme 62

BF_3 is an effective reagent for various kinds of reaction such as Friedel–Crafts alkylation and acylation reactions (Scheme 63),²⁹¹ cyclization reactions, rearrangement,²⁹² Diels–Alder reactions,²⁹³ and aldol reactions.

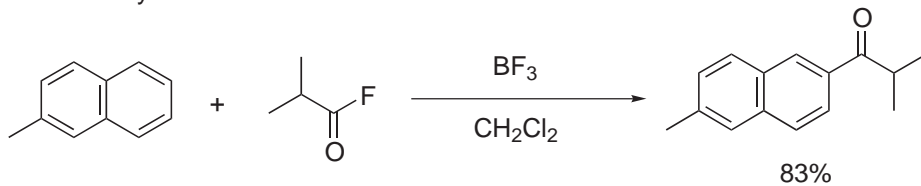
Recently, arylboron compounds have been developed as Lewis acids. For example, in the presence of a catalytic amount of $\text{B}(\text{C}_6\text{F}_5)_3$, several carbon–carbon bond-forming reactions proceed smoothly (Scheme 64).^{294–296}

Chiral boron Lewis-acid complexes have been successfully used in Diels–Alder and aldol reactions. Representative chiral Lewis-acidic boron compounds are shown in Figure 2.^{297–301}

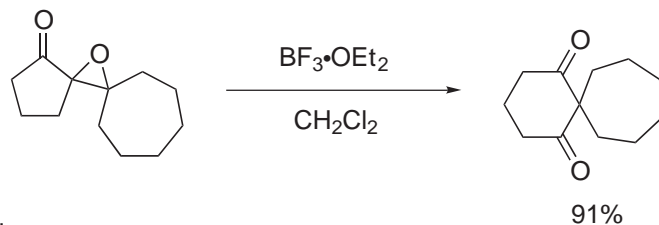
Boron enolates are often used for aldol reactions. Boron enolates are usually prepared from the corresponding carbonyl compounds, tertiary amine, and a boron source (e.g., dibutylboron triflates). The aldol reactions proceed via a six-membered transition state to give high diastereoselectivity which depends upon the geometry of the boron enolates.

In boron enolate-mediated aldol reactions, stoichiometric amounts of boron reagents are necessary. However, it has been reported that only a catalytic amount of a boron source is sufficient for boron enolate-mediated aldol reactions in water (Scheme 65).³⁰² It should be noted that even water-sensitive boron enolates can be successfully employed in water.

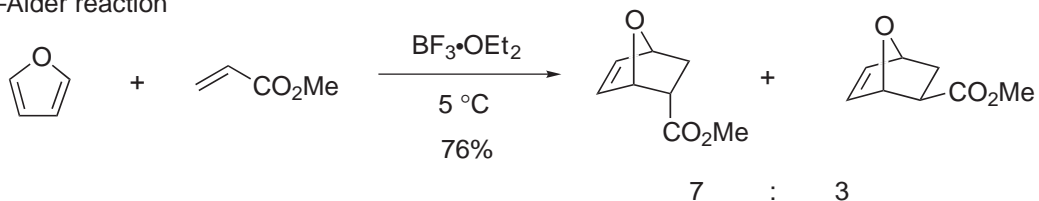
Friedel–Crafts acylation



Rearrangement

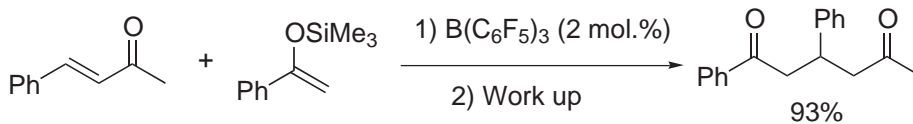


Diels–Alder reaction

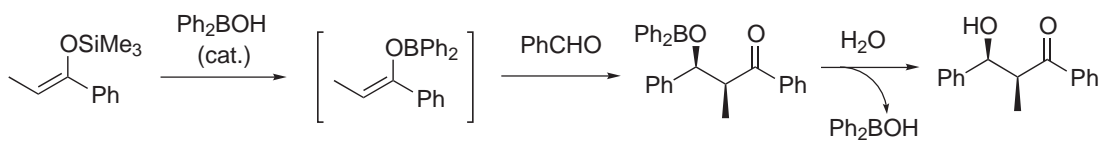


Scheme 63

Michael reaction



Scheme 64



Scheme 65

Chiral Boron Catalysts for Diels–Alder reaction

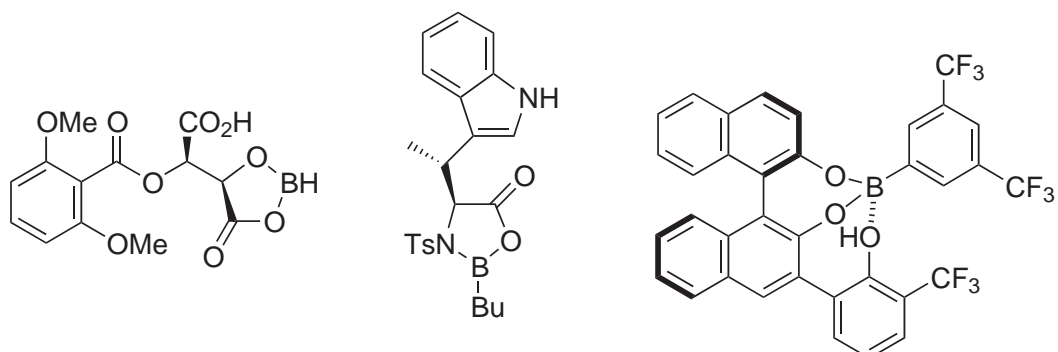
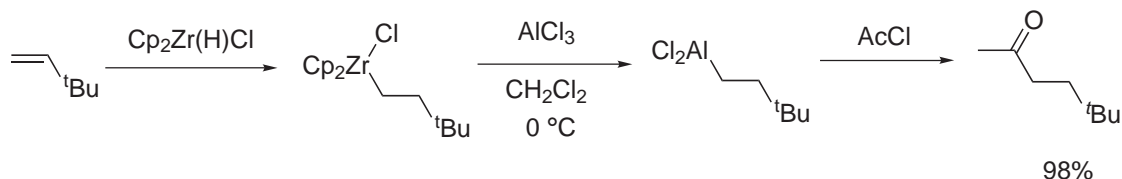


Figure 2 Chiral Lewis-acidic boron compounds.

9.8.13 ALUMINUM

Aluminum(III) complexes are amongst the most common Lewis acids. In particular, aluminum halide species (e.g., AlCl_3 , AlBr_3) are commercially available and are widely used for various reactions. Other types of Lewis acid such as aluminum alkoxides, alkylaluminum halides, and trialkylaluminum species are also used for many kinds of Lewis-acid-mediated reactions.

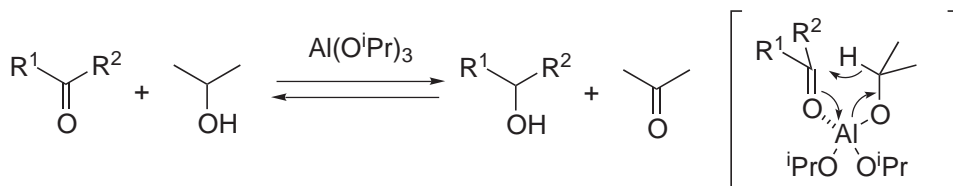
AlCl_3 is a moisture-sensitive and strong Lewis acid. It is a first choice for Friedel–Crafts-type reactions, which provide numerous important transformations in laboratory and industry. It can also be applied to the transformation of alkenes to ketones via alkylaluminum halides.³⁰³ Hydrozirconation of an olefin and subsequent transmetalation from zirconium to aluminum gives the corresponding alkylaluminum dichloride, and the subsequent acetylation by acetyl chloride affords the corresponding ketone in high yield (Scheme 66).



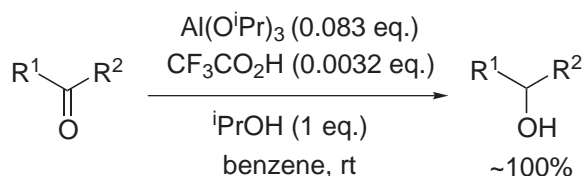
Scheme 66

The Meerwein–Ponndorf–Verley (MPV) reduction is generally mediated by aluminum triisopropoxide, $\text{Al}(\text{O}^i\text{Pr})_3$. In MPV reduction, reversible hydride transfer occurs via a six-membered transition state (Scheme 67). By removing acetone from the reaction system, the reversible reaction proceeds smoothly. The advantages of the reduction are the mildness of the reaction conditions, chemoselectivity, safety, operational simplicity, and its applicability to large-scale synthesis. It is reported that the addition of trifluoroacetic acid significantly accelerates the reduction (Scheme 68),^{304,305} in which case a catalytic amount of $\text{Al}(\text{O}^i\text{Pr})_3$ is enough to complete the reaction.

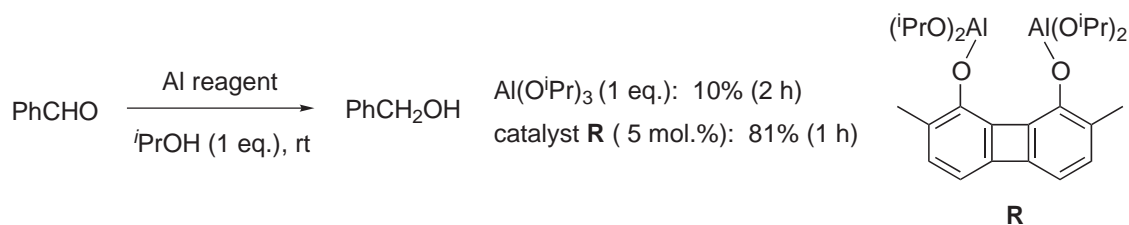
Binuclear Al^{III} complexes for MPV reduction have been developed. In the presence of 5 mol.% of the bidentate catalyst (Scheme 69, compound (**R**)), the reduction proceeds smoothly at room



Scheme 67



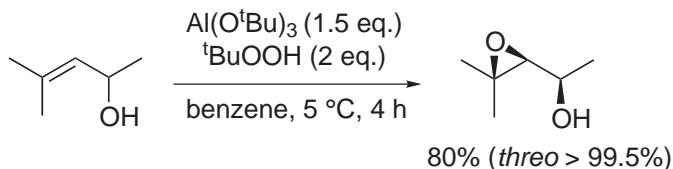
Scheme 68



Scheme 69

temperature to give the corresponding alcohols in high yields.³⁰⁶ Double carbonyl activation may cause the remarkable efficiency.

$\text{Al}(\text{O}^t\text{Bu})_3$ can be used for epoxidation of allylic alcohols in the presence of a stoichiometric amount of $^t\text{BuOOH}$ with high selectivity (Scheme 70).³⁰⁷



Scheme 70

Organoaluminum compounds have a strong Lewis acidity and react with oxygen in air. They have great affinity for various heteroatoms, especially oxygen. Organoaluminum compounds work as Lewis acids for many types of reactions (e.g., aldol, Diels–Alder, ene reactions, cyclization, and rearrangement, etc.; two examples are shown in Scheme 71).^{308,309}

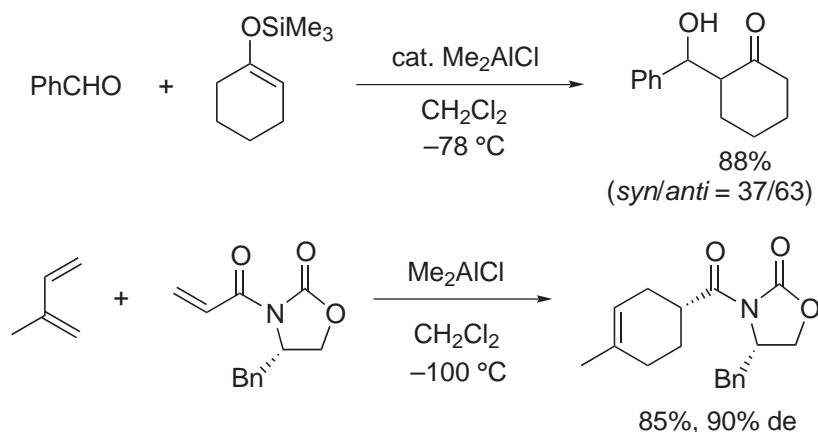
Several modifications have been made to organoaluminum-based catalysts. Methylaluminum bis(2,6-di-*tert*-butyl-4-alkylphenoxide) (MAD) shows high diastereofacial selectivity in carbonyl alkylation (Scheme 72).^{310,311} Aluminum tris(2,6-diphenylphenoxide) (ATPH) has been developed as a catalyst for conjugate addition reactions. Since a carbonyl group is stabilized by steric effect of ATPH, the 1,4-adduct is obtained selectively.³¹²

Numerous asymmetric reactions using chiral aluminum Lewis acids have been developed; some examples are shown in Scheme 73.^{313–315}

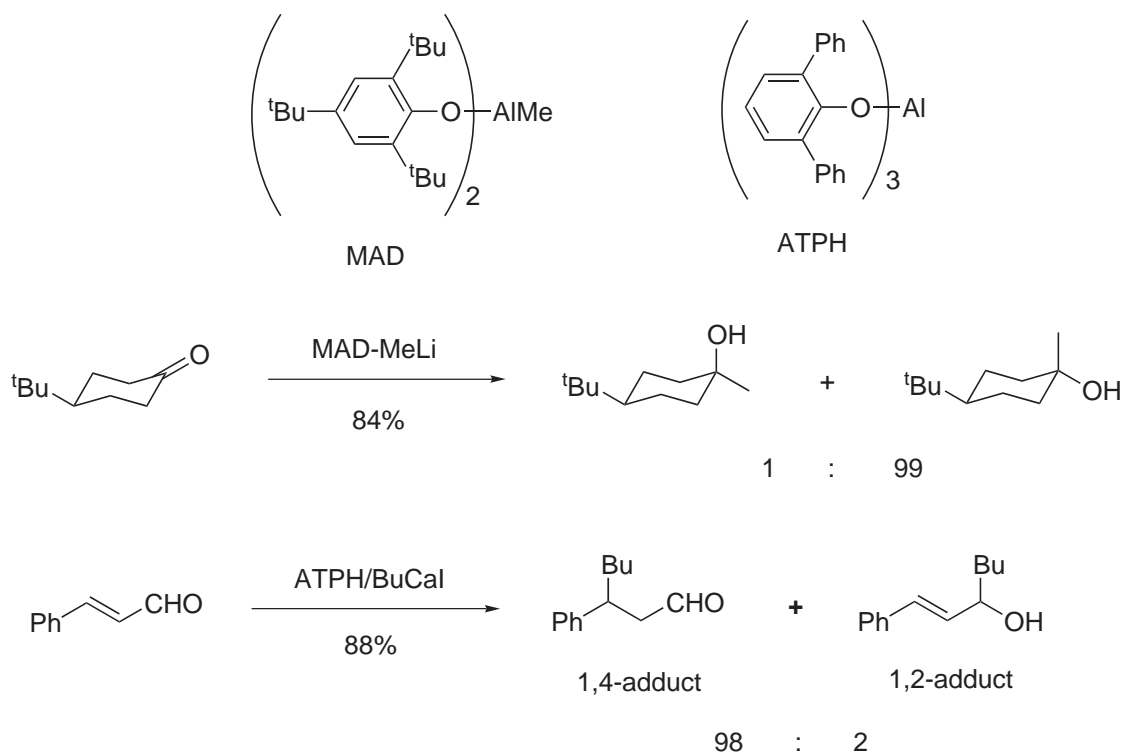
9.8.14 SILICON

Organosilicon compounds have been widely used as protecting groups for various protic functional groups, and they have been found to be versatile Lewis acids.^{316–318} One of the most well-known silicon Lewis acids is trimethylsilyl triflate, Me_3SiOTf , which can be applied to many Lewis-acid-mediated or -catalyzed reactions such as aldol, allylation, cyclization, rearrangement, and glycosylation reactions. Other silicon-based Lewis acids include iodotrimethylsilane, trimethylsilyl nonafluoromethanesulfonate (nonaflate), *tert*-butyldimethylsilyl triflate, and trimethylsilyl bis(trifluoromethanesulfonyl)imide. These compounds all contain three alkyl groups and one leaving group, and the latter is essential for their Lewis acidity.

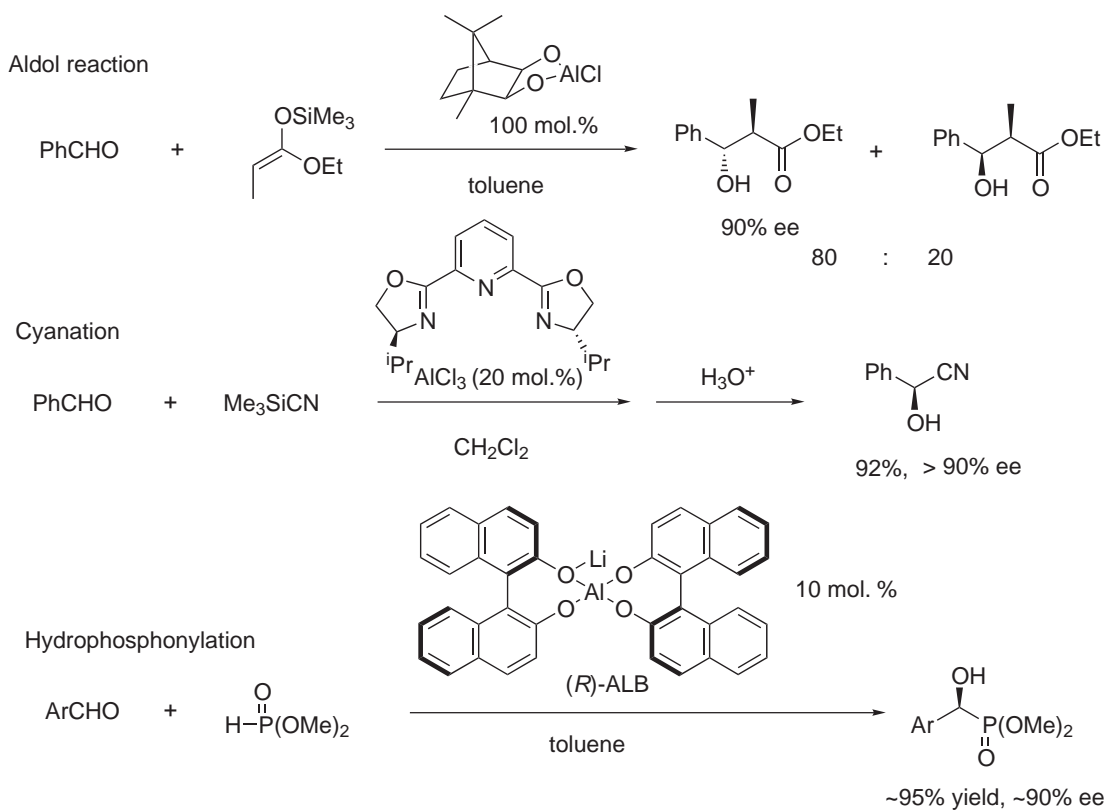
Mukaiyama aldol reactions of aldehydes with silyl enol ethers are amongst the most widely used Lewis-acid-mediated or -catalyzed reactions. However, trimethylsilyl triflate is not active enough to promote these reactions,⁶⁶ and more active silicon-based Lewis acids have been developed. One example is the species generated by mixing trimethylsilyl triflate (or chloride) and $\text{B}(\text{OTf})_3$,^{319,320} for which the formulation $\text{R}_3\text{Si}^+[\text{B}(\text{OTf})_4]^-$ is suggested by NMR experiments. Only a catalytic amount of this was needed to complete Mukaiyama aldol reactions of



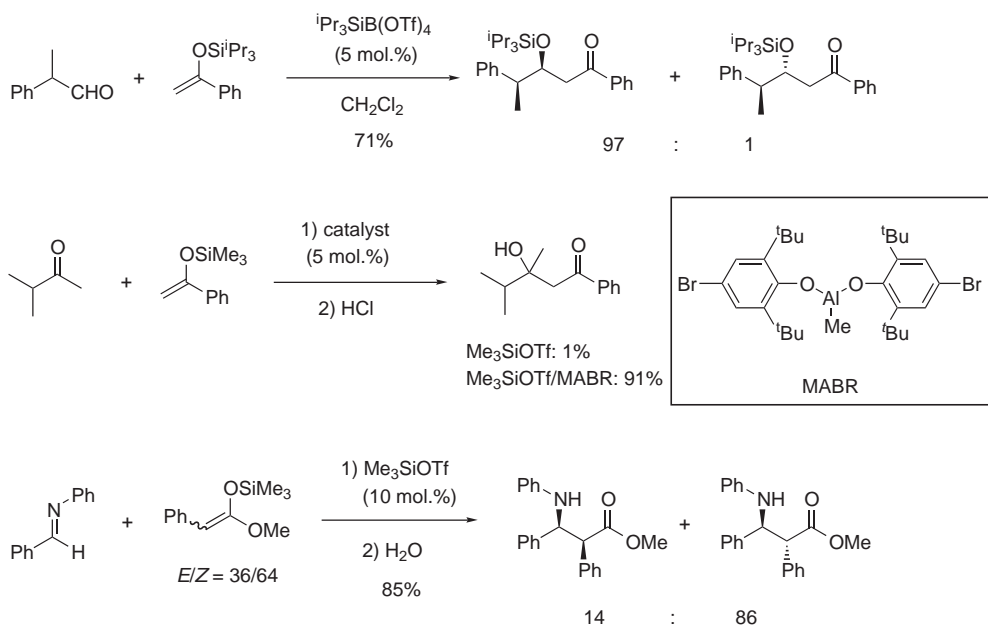
Scheme 71



Scheme 72



Scheme 73



Scheme 74

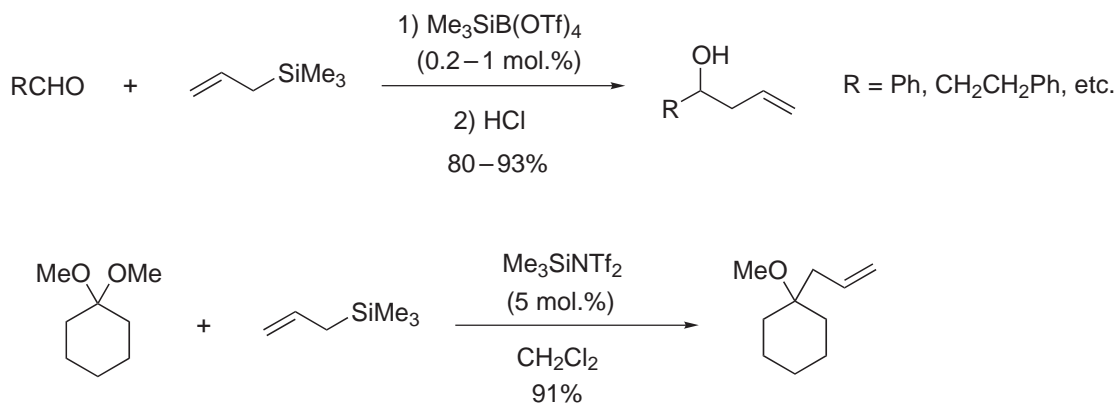
aldehydes with silyl enol ethers (Scheme 74). From NMR experiments, formation of $\text{R}_3\text{Si}^+[\text{B}(\text{OTf})_4]^-$ is suggested. Another active Lewis acid is formed by combination of trimethylsilyl triflate and a bulky Al^{III} -based Lewis acid; significant rate acceleration is observed by using aluminum co-catalysts in Mukaiyama aldol reactions.³²¹ Aldol-type reactions of acetals with silyl enol ethers are catalyzed by trimethylsilyl triflate,^{322,323} which also enhances Mannich-type reactions of imines with ketene silyl acetals.^{324,325}

Trimethylsilyl triflate itself can not promote allylation reactions of aldehydes with allyltrimethylsilane. By using the more highly reactive system $\text{Me}_3\text{SiB}(\text{OTf})_4$, the reactions proceed smoothly.³²⁶ A very small amount (0.2–1 mol.%) of $\text{Me}_3\text{SiB}(\text{OTf})_4$ is enough for the reactions (Scheme 75). Allylation of acetals can be promoted by trimethylsilyl bis(trifluoromethanesulfonyl)imide ($\text{Me}_3\text{SiNTf}_2$),³²⁷ which is also a reactive catalyst for Diels–Alder reactions.³²⁸

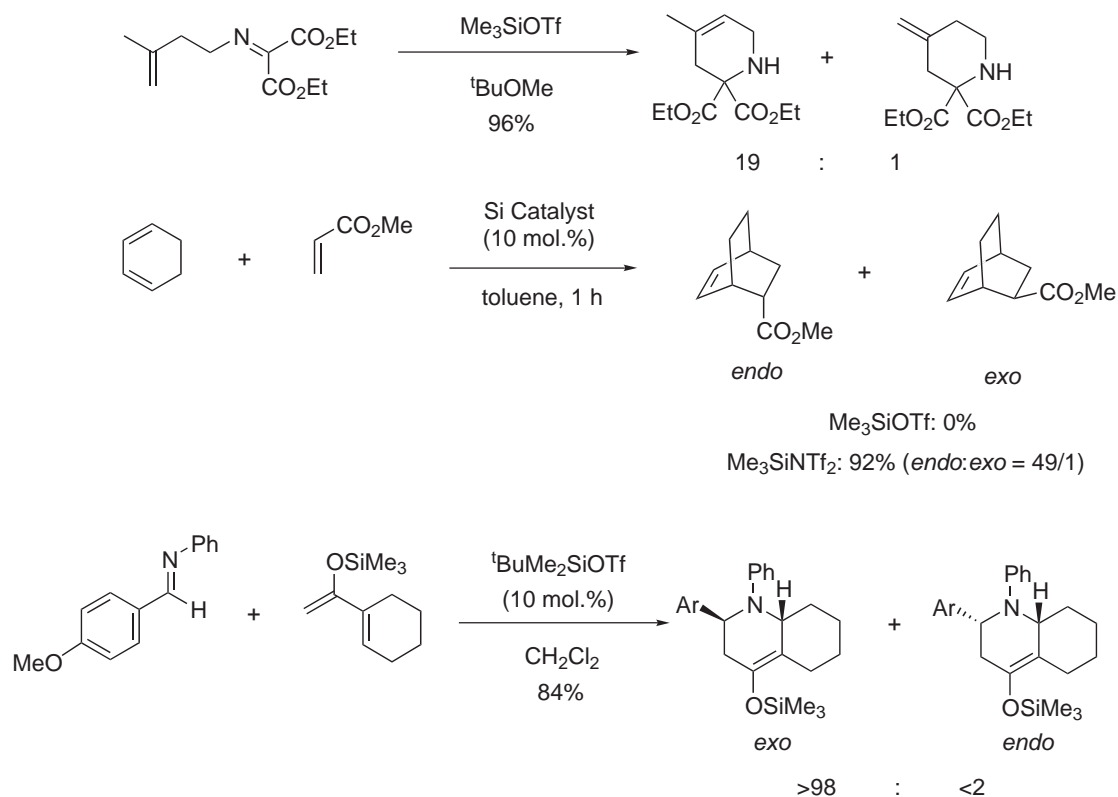
Selective cyclization of an alkenyl imine is catalyzed by trimethylsilyl triflate (Scheme 76).³²⁹ *t*-Butyldimethylsilyl triflate ($\text{tBuMe}_2\text{SiOTf}$) catalyzes imino Diels–Alder reactions of *N*-phenylaromatic aldimines to afford *exo* adducts preferentially.³³⁰ When AlCl_3 is used instead of $\text{tBuMe}_2\text{SiOTf}$, *endo* adducts are obtained predominantly.

Rearrangement reactions are also catalyzed by silicon Lewis acids; the example in Scheme 77 uses Me_3SiOTf ;³³¹ iodo- and bromotrimethylsilanes are also effective.

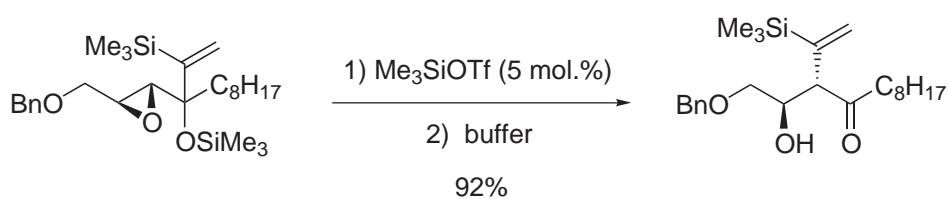
Effective glycosylation is often achieved using a silicon Lewis acid. In the presence of Me_3SiOTf , *N*-glycosylation reaction proceeds smoothly to give the desired products in high yields (Scheme 78).³³²



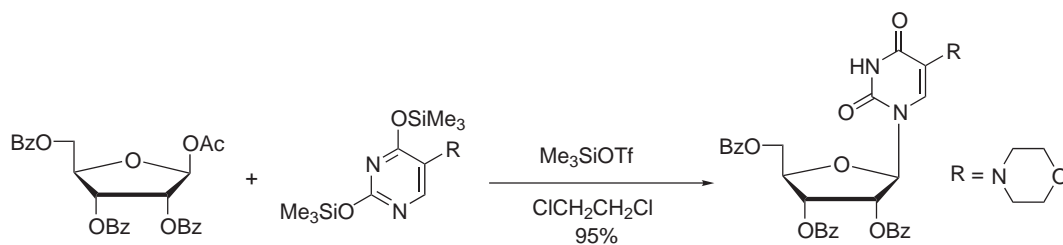
Scheme 75



Scheme 76



Scheme 77

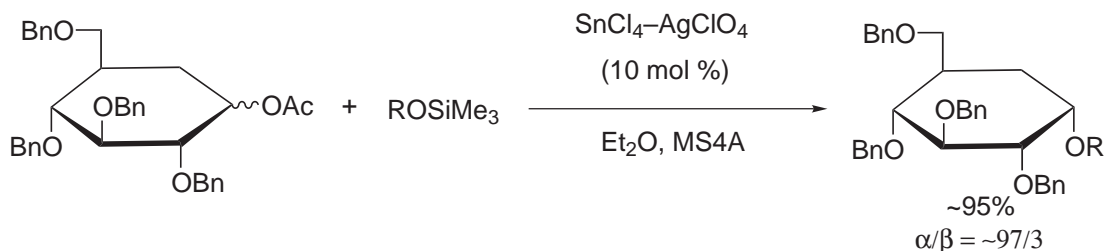


Scheme 78

9.8.15 TIN

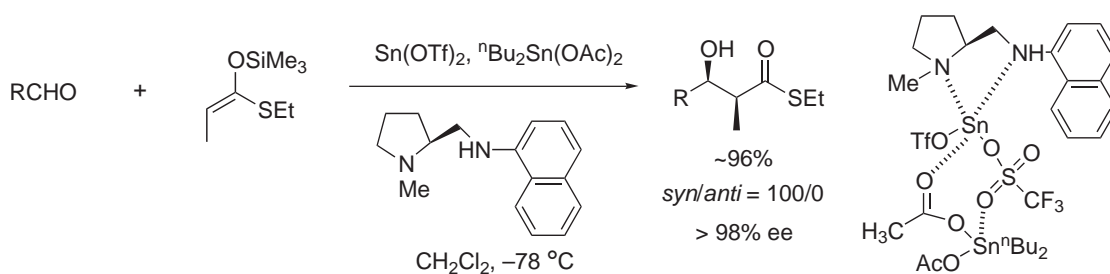
Tin-based Lewis acids can be divided into two groups, Sn^{II} and Sn^{IV} . Although Sn^{II} is more cationic than Sn^{IV} , the covalent and ionic radii of Sn^{II} (1.02 Å) are larger than those of Sn^{IV} (0.71 Å).³³³ Tin Lewis acids have been applied to many kinds of reactions, including several asymmetric versions.

Sn^{II} halides, Sn^{II} triflate, and Sn^{IV} halides are representative tin Lewis acids. Sn^{II} halides can be applied to various reactions, such as aldol reactions, allylations, Michael reactions, glycosylations, annulations, β -diketoester synthesis, and deprotections. In the presence of a combination of SnCl_2 and chlorotrimethylsilane (Me_3SiCl),³³⁴ or SnCl_2 and trityl chloride,³³⁵ silyl enol ethers react with various kinds of electrophile such as aldehydes, acetals, orthoesters, and enones. A combination of SnCl_4 and AgClO_4 is effective for stereoselective glycosylation (Scheme 79).^{337,338}



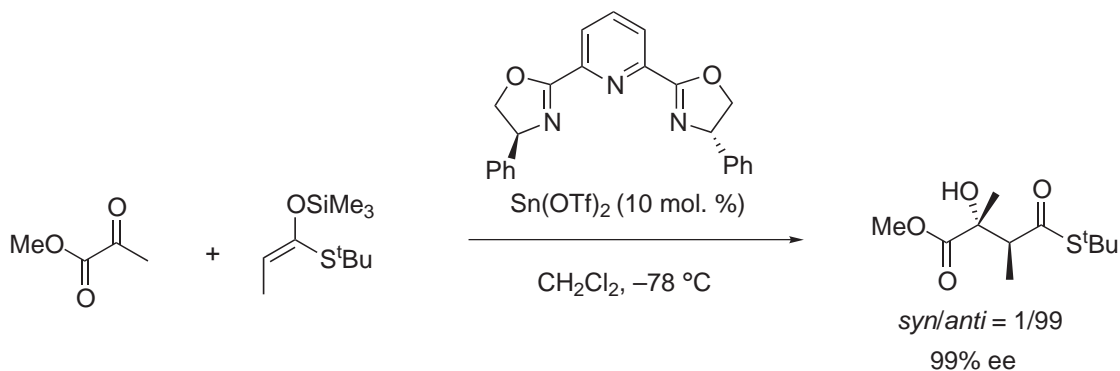
Scheme 79

$\text{Sn}(\text{OTf})_2$ can function as a catalyst for aldol reactions, allylations, and cyanations; asymmetric versions of these reactions have also been reported. Diastereoselective and enantioselective aldol reactions of aldehydes with silyl enol ethers using $\text{Sn}(\text{OTf})_2$ and a chiral amine have been reported (Scheme 80).^{338,339} A proposed active complex is shown in the scheme. Catalytic asymmetric aldol reactions using $\text{Sn}(\text{OTf})_2$, a chiral diamine, and tin(II) oxide have been developed.³⁴⁰ Tin(II) oxide is assumed to prevent achiral reaction pathway by weakening the Lewis acidity of Me_3SiOTf , which is formed during the reaction.



Scheme 80

Catalytic asymmetric aldol reactions of α -heterosubstituted substrates such as glyoxaldehyde, and methyl pyruvate have been reported (Scheme 81). High diastereo- and enantioselectivity have been obtained by using combined use of $\text{Sn}(\text{OTf})_2$ and bis(oxazoline) or pyridinebis(oxazoline) ligands.³⁴¹

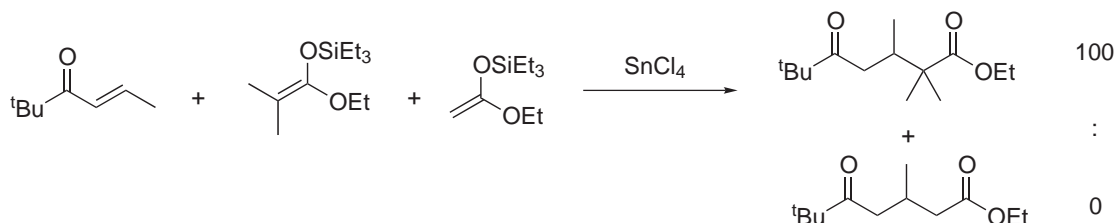


Scheme 81

SnCl_4 is a stronger Lewis acid and often used as a catalyst in organic syntheses. It is highly soluble in organic solvents, and relatively easy to handle. Various reactions such as allylations,

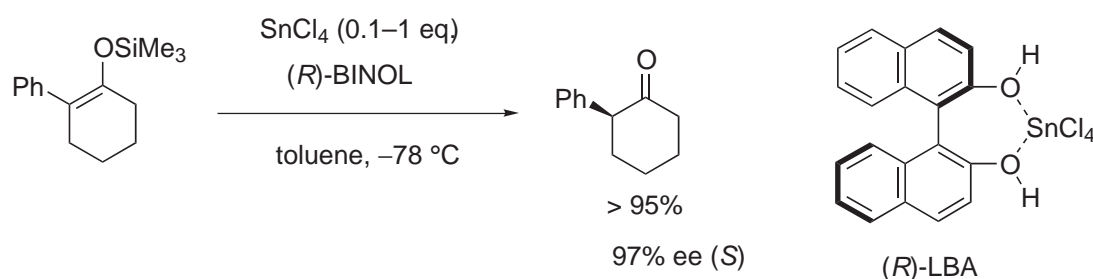
aldol reactions, Michael reactions, rearrangements, and cycloadditions can be promoted in the presence of SnCl_4 , and asymmetric reactions have also been reported.

In SiCl_4 -mediated Mukaiyama–Michael reactions, an electron-transfer mechanism is proposed for the case in which ketene silyl acetals bearing less hindered silyl substituent are used as substrates.^{342–344} As shown in Scheme 82, ketene silyl acetals having more substituents at the β -position are much more reactive.



Scheme 82

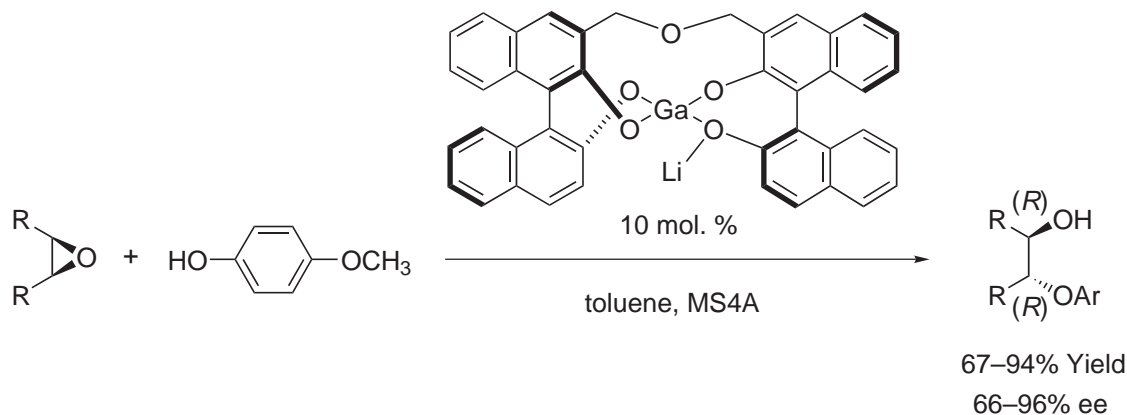
Enantioselective protonation of silyl enol ethers using a SnCl_4 –BINOL system has been developed (Scheme 83).³⁴⁵ This Lewis-acid-assisted chiral Brønsted acid (LBA) is a highly effective chiral proton donor. In further studies, combined use of a catalytic amount of SnCl_4 , a BINOL derivative, and a stoichiometric amount of an achiral proton source is found to be effective for the reaction.^{346,347}



Scheme 83

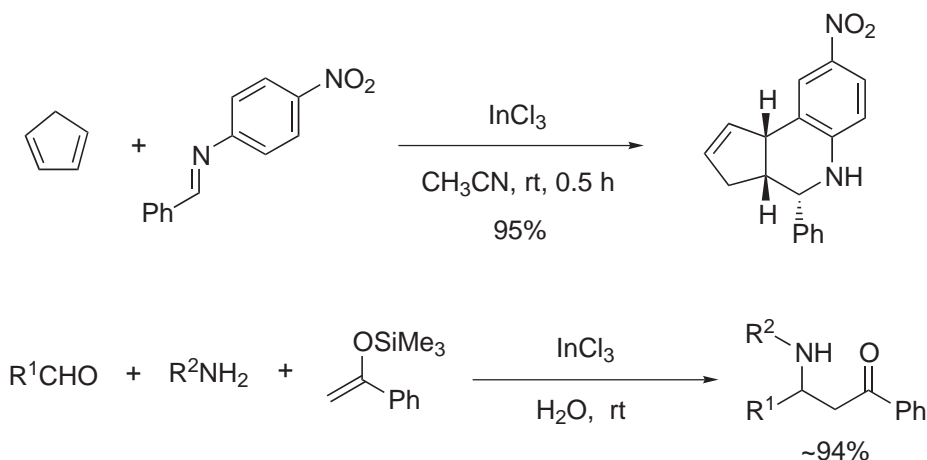
9.8.16 OTHERS

Complexes of other metals such as gallium, indium, lead, and antimony have also been used as Lewis acids. Catalytic enantioselective *meso*-epoxide ring-opening reactions using a chiral gallium(III) catalyst (Ga–Li-linked-BINOL) have been reported (Scheme 84).³⁴⁸ The chemical yields are much improved by linking two BINOL units.



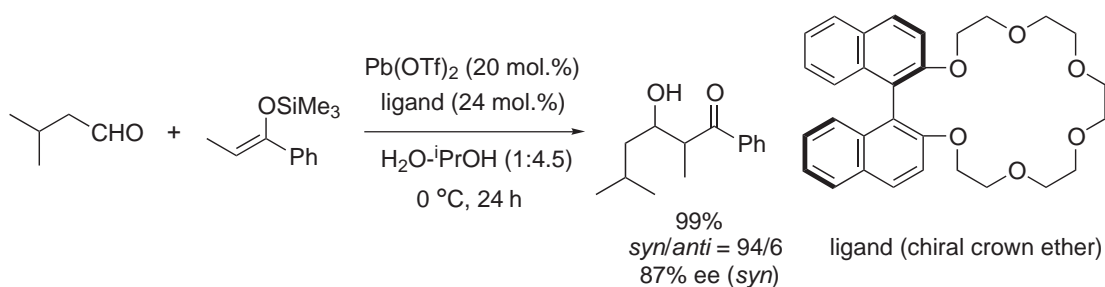
Scheme 84

Indium trichloride^{349–351} is a mild Lewis acid that is effective for various kinds of Lewis-acid-catalyzed reactions such as Diels–Alder reactions (Scheme 85), aldol reactions, and Friedel–Crafts reactions. Since indium trichloride is stable in water, several aqueous reactions have been investigated (Scheme 85); indium(III) triflate is also used as a Lewis acid.



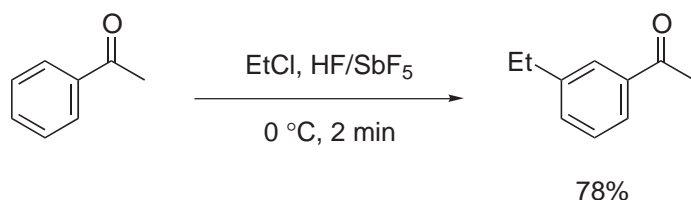
Scheme 85

A lead(II) triflate–crown ether complex functions as a chiral Lewis-acid catalyst for asymmetric aldol reactions in aqueous media (Scheme 86).³⁵² This is the first example of a chiral crown-based Lewis acid that can be successfully used in catalytic asymmetric reactions.



Scheme 86

Antimony pentachloride is a reactive Lewis acid that can be used for Friedel–Crafts reactions and some other Lewis-acid-catalyzed reactions. The HF–SbF₅ system is known as “magic acid,” and carbocations are stabilized in this medium.³⁵³ By using the HF–SbF₅ system, alkylation of acetophenone (a relatively unreactive aromatic compound) has been achieved (Scheme 87).



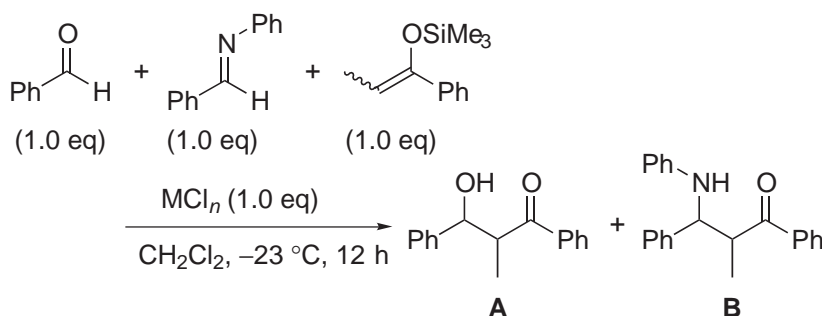
Scheme 87

9.8.17 CONCLUSION/CLASSIFICATION OF LEWIS ACIDS

In this chapter Lewis-acid-mediated reactions have been summarized. While more than stoichiometric amounts of the Lewis acids were employed in conventional reactions, many efforts have been made to reduce the amounts of Lewis acid needed, and many truly catalytic reactions have been developed. Chiral Lewis-acid catalysis has been of great interest in the 1990s and early 2000s, and various combinations of metals and ligands have been investigated. Importantly, the established understanding that Lewis acids are easily hydrolyzed in water has been exploded. Water-compatible Lewis acids are stable in air and moisture, and are easily recovered and reused in many cases. These Lewis acids may solve recent environmental issues, and will be used further in many reactions in future.

The Lewis-acid catalysts and mediators described, which have been employed in a wide variety of reactions, have been chosen by experimental trial and error. This is because the character of Lewis acids is only crudely understood on the basis of the expected periodic properties of the elements. Evidently, fundamental understandings and better classifications of Lewis acids are expected to give a solution to this problem; however, only limited examples have been reported in the literature. In a simple classification procedure, a number of Lewis acids have been classified into just two classes, "hard" and "soft."³⁵⁴ It was also reported that Lewis acidic activities followed the order $\text{BCl}_3 > \text{AlCl}_3 > \text{TiCl}_4 > \text{BF}_3 > \text{SnCl}_4 > \text{ZnCl}_2$ for the acylation of olefins.³⁵⁵ Lewis acids in the Friedel–Crafts alkylation reaction are more finely classified into five categories: very active; moderately active; weak; very weak; or inactive.³⁵⁶ Several trials to scale the strength of Lewis acidity based on nuclear magnetic resonance (NMR) data^{357,358} or theoretical methods^{359–362} have been reported. These efforts are focused only on "traditional" Lewis acids in most cases, even though many more esoteric types of Lewis acid, including complexes of late transition elements, are now used in modern chemistry.^{363–365} In addition, recent research efforts have revealed that use of strong Lewis acids does not necessarily promote reactions smoothly,^{47,366} and that selectivity—one of the most important issues in modern organic synthesis—is strongly dependent on the Lewis acids used.^{160,367–370}

In 2002 a novel classification of Lewis acids based on acidity and selectivity was reported.³⁷¹ Group 3–15 metal chlorides were classified on the basis of their activity, and aldehyde vs. aldimine selectivity in addition of a silyl enol ether (Scheme 88). Based on experimental results, Lewis-acidic metal chlorides are classified as follows: A, active; B, weak; C, inactive for the activation of the aldehyde and/or aldimines. Groups A and B are further divided into A-1 or B-1 (aldehyde-selective), A-2 or B-2 (aldimine-selective), and A-3 or B-3 (neutral). The final classification is as follows: A-1, BCl_3 , AlCl_3 , TiCl_4 , GaCl_3 , ZrCl_4 , SnCl_4 , SbCl_5 , SbCl_3 , HfCl_4 , ReCl_5 ; A-2, ScCl_3 , FeCl_3 , InCl_3 , BiCl_3 ; A-3, NbCl_5 , MoCl_3 , MoCl_5 , SnCl_2 , TaCl_5 , WCl_5 , WCl_6 , ReCl_3 , TiCl_3 ; B-1, None; B-2, SiCl_4 , FeCl_2 , CoCl_2 , CuCl , CuCl_2 , GeCl_4 , YCl_3 , OsCl_3 , PtCl_2 ; B-3, ZnCl_2 , RuCl_3 ; C, VCl_3 , CrCl_3 , MnCl_2 , NiCl_2 , RhCl_3 , PdCl_2 , AgCl , CdCl_2 , IrCl_3 , AuCl , HgCl_2 , HgCl , PbCl_2 (Schemes 89 and 90). This classification has revealed several new fundamental aspects of the properties of metal chlorides as Lewis acids.






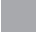
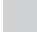
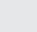
Scheme 88

Group A (active)	
A-1 (aldehyde-selective)	BCl₃ , AlCl ₃ , TiCl₄ , GaCl₃ , ZrCl₄ , SnCl ₄ , SbCl ₅ , SbCl ₃ , HfCl ₄ , ReCl ₅
A-2 (aldimine-selective)	ScCl₃ , FeCl ₃ , InCl ₃ , BiCl ₃
A-3 (neutral)	NbCl ₅ , MoCl ₅ , MoCl ₃ , SnCl ₂ , TaCl ₅ , WCl ₆ , WCl ₅ , ReCl ₃ , TiCl ₃
Group B (weak)	
B-1 (aldehyde-selective)	none
B-2 (aldimine-selective)	SiCl ₄ , ^b FeCl ₂ , CoCl₂ , CuCl₂ , CuCl , GeCl ₄ , YCl₃ , YbCl₃ , OsCl ₃ , PtCl ₂
B-3 (neutral)	ZnCl ₂ , RuCl ₃
Group C (inactive)	
PCl ₅ , ^b VCl ₃ , CrCl ₃ , MnCl ₂ , NiCl ₂ , RhCl ₃ , PdCl ₂ , AgCl, CdCl ₂ , IrCl ₃ , AuCl, HgCl ₂ , HgCl, PbCl ₂	

^aActive: Yield = >40% (-23 °C, 12 h). Weak or inactive: Yield = <40% (-23 °C, 12 h). Aldehyde-selective: **A/B** = >2/1. Aldimine-selective: **B/A** = >2/1. Bold: **A/B** = >9/1 or **B/A** = >9/1. ^bSee ref. 18.

Scheme 89

														13	14	15
														B ⁺³	C	N
														Al ⁺³	Si ⁺⁴	P ⁺⁵
	3	4	5	6	7	8	9	10	11	12						
	Sc ⁺³	Ti ⁺⁴	V ⁺³	Cr ⁺³	Mn ⁺²	Fe ⁺² / Fe ⁺³	Co ⁺²	Ni ⁺²	Cu ⁺¹ / Cu ⁺²	Zn ⁺²				Ga ⁺³	Ge ⁺⁴	As
	Y ⁺³	Zr ⁺⁴	Nb ⁺⁵	MO ⁺³ / Mo ⁺⁵	Tc	Ru ⁺³	Rh ⁺³	Pd ⁺²	Ag ⁺¹	Cd ⁺²				In ⁺³	Sn ⁺² / Sn ⁺⁴	Sb ⁺³ / Sb ⁺⁵
	Ln ⁺³	Hf ⁺⁴	Ta ⁺⁵	W ⁺⁵ / W ⁺⁶	Re ⁺³ / Re ⁺⁵	Os ⁺³	Ir ⁺³	Pt ⁺²	Au ⁺¹	Hg ⁺²				Tl ⁺³	Pb ⁺²	Bi ⁺³

	A-1		A-3		B-3
	A-2		B-2		C

Scheme 90

9.8.18 REFERENCES

- Schinger, D., Ed. *Selectivities in Lewis Acid Promoted Reactions* 1989, Kluwer Academic: Dordrecht, Netherlands.
- Yamamoto, H., Ed. *Lewis Acid Reagents* 1999, Oxford University Press: Oxford, UK.
- Yamamoto, H., Ed. *Lewis Acids in Organic Synthesis* 2000, Wiley-VCH: Weinheim, Germany.
- Trost, B. M.; Fleming, I., Eds.; *Comprehensive Organic Synthesis*; Pergamon Press: Oxford, UK, 1991; Vols. 1, 2, and 3.
- Ekelin, K.; Sillen, L. G. *Acta Chem. Scand* **1953**, *7*, 987–1000.
- Braun, R.; Sauer, J. *Chem. Ber.* **1986**, *119*, 1269–1274.
- Grieco, P. A.; Nunes, J. J.; Gaul, M. D. *J. Am. Chem. Soc.* **1990**, *112*, 4595–4596.
- Grieco, P. A.; Handy, S. T.; Beck, J. P. *Tetrahedron Lett.* **1994**, *35*, 2663–2666.
- Ooi, T.; Saito, A.; Maruoka, K. *Tetrahedron Lett.* **1998**, *39*, 3745–3748.
- Shibasaki, M.; Sasai, H.; Arai, T. *Angew. Chem. Int. Ed. Engl.* **1997**, *36*, 1236–1256.
- Morita, T.; Arai, T.; Sasai, H.; Shibasaki, M. *Tetrahedron Asymmetry* **1998**, *9*, 1445–1450.
- Arai, T.; Sasai, H.; Yamaguchi, K.; Shibasaki, M. *J. Am. Chem. Soc.* **1998**, *120*, 441–442.
- Grieco, P. A.; DuBay, W. J.; Todd, L. J. *Tetrahedron Lett.* **1996**, *37*, 8707–8710.
- Barbarich, T. J.; Handy, S. T.; Miller, S. M.; Anderson, O. P.; Grieco, P. A.; Strauss, S. H. *Organometallics* **1996**, *15*, 3776–3778.
- Mukaiyama, T.; Matsubara, K.; Suda, S. *Chem. Lett.* **1991**, 981–984.
- Reetz, M. T.; Raguse, B.; Marth, C. F.; Hügel, H. M.; Bach, T.; Fox, D. N. A. *Tetrahedron* **1992**, *48*, 5731–5742.
- Reetz, M. T.; Fox, D. N. A. *Tetrahedron Lett.* **1993**, *34*, 1119–1122.
- Carreira, E. M.; Singer, R. A. *Tetrahedron Lett.* **1994**, *35*, 4323–4326.
- Henry, Jr., K. J.; Grieco, P. A.; Jagoe, C. T. *Tetrahedron Lett.* **1992**, *33*, 1817–1820.
- Reetz, M. T.; Gansäuer, A. *Tetrahedron* **1993**, *49*, 6025–6030.
- Chini, M.; Crotti, P.; Gardelli, C.; Macchia, F. *Tetrahedron* **1992**, *48*, 3805–3812.
- Chini, M.; Crotti, P.; Macchia, F. *Tetrahedron Lett.* **1990**, *31*, 5641–5644.
- Chini, M.; Crotti, P.; Macchia, F. *Tetrahedron Lett.* **1990**, *31*, 4661–4664.
- Chini, M.; Crotti, P.; Favero, L.; Macchia, F. *Tetrahedron Lett.* **1991**, *32*, 4775–4778.
- Chini, M.; Crotti, P.; Favero, L.; Pineschi, M. *Tetrahedron, Lett.* **1991**, *32*, 7583–7586.
- Danishesky, S.; Pearson, W. H.; Harvey, D. F. *J. Am. Chem. Soc.* **1984**, *106*, 2456–2458.
- Corey, E. J.; Ishihara, K. *Tetrahedron Lett.* **1992**, *33*, 6807–6810.
- Evans, D. A.; Kozlowski, M. C.; Tedrow, J. S. *Tetrahedron Lett.* **1996**, *37*, 7481–7484.
- Ichiyanagi, T.; Shimizu, M.; Fujisawa, T. *J. Org. Chem.* **1997**, *62*, 7937–7941.
- Bromidge, S.; Wilson, P. C.; Whiting, A. *Tetrahedron Lett.* **1998**, *39*, 8905–8908.
- Ordóñez, M.; Guerrero-de la Rosa, V.; Labastida, V.; Llera, J. M. *Tetrahedron: Asymmetry* **1996**, *7*, 2675–2686.
- Desimoni, G.; Faita, G.; Righetti, P. P. *Tetrahedron Lett.* **1996**, *37*, 3027–3030.
- Sibi, M. P.; Ji, J. *Angew. Chem., Int. Ed. Engl.* **1996**, *35*, 190–192.
- Sibi, M. P.; Jasperse, C. P.; Ji, J. *J. Am. Chem. Soc.* **1995**, *117*, 10779–10780.
- Murakata, M.; Tsutsui, H.; Hoshino, O. *J. Chem. Soc., Chem. Commun.* **1995**, 481–482.
- Sibi, M. P.; Ji, J.; Wu, J. H.; Gürtler, S.; Porter, N. A. *J. Am. Chem. Soc.* **1996**, *118*, 9200–9201.
- Sibi, M. P.; Ji, J. *J. Org. Chem.* **1997**, *62*, 3800–3801.
- Wu, J. H.; Zhang, G.; Porter, N. A. *Tetrahedron Lett.* **1997**, *38*, 2067–2070.

39. Porter, N. A.; Wu, J. H.; Zhang, G.; Reed, A. D. *J. Org. Chem.* **1997**, *62*, 6702–6703.
40. Gothelf, K. V.; Hazell, R. G.; Jørgensen, K. A. *J. Org. Chem.* **1996**, *61*, 346–355.
41. Gothelf, K. V.; Hazell, R. G.; Jørgensen, K. A. *J. Org. Chem.* **1998**, *63*, 5483–5488.
42. Corey, E. J.; Wang, Z. *Tetrahedron Lett.* **1993**, *34*, 4001–4004.
43. Evans, D. A.; Nelson, S. G. *J. Am. Chem. Soc.* **1997**, *119*, 6452–6453.
44. Sibi, M. P.; Shay, J. J.; Liu, M.; Jasperse, C. P. *J. Am. Chem. Soc.* **1998**, *120*, 6615–6616.
45. Kobayashi, S.; Hachiya, I.; Araki, M.; Ishitani, H. *Tetrahedron Lett.* **1993**, *34*, 3755–3758.
46. Kobayashi, S. *Chem. Lett.* **1991**, 2187–2190.
47. Kobayashi, S. *Synlett* **1994**, 689–701.
48. Kobayashi, S. *Eur. J. Org. Chem.* **1998**, 15–27.
49. Kobayashi, S.; Hachiya, I.; Ishitani, H.; Araki, M. *Synlett* **1993**, 472–474.
50. Kobayashi, S.; Araki, M.; Ishitani, H.; Nagayama, S.; Hachiya, I. *Synlett* **1995**, 233–234.
51. Oyamada, H.; Kobayashi, S. *Synlett* **1998**, 249–250.
52. Kawada, A.; Mitamura, S.; Kobayashi, S. *Synlett* **1994**, 545–546.
53. Arseniyadis, S.; Rodriguez, R.; Yashunsky, D. V.; Camara, J.; Ourisson, G. *Tetrahedron Lett.* **1994**, *35*, 4843–4846.
54. Ishihara, K.; Kubota, M.; Kurihara, H.; Yamamoto, H. *J. Am. Chem. Soc.* **1995**, *117*, 4413–4414.
55. Sammakia, T.; Berliner, M. A. *J. Org. Chem.* **1995**, *60*, 6652–6653.
56. Kobayashi, S.; Ishitani, H.; Nagayama, S. *Chem. Lett.* **1995**, 423–424.
57. Kobayashi, S.; Ishitani, H.; Nagayama, S. *Synthesis* **1995**, 1195–1202.
58. Kobayashi, S.; Araki, M.; Hachiya, I. *J. Org. Chem.* **1994**, *59*, 3758–3759.
59. Kobayashi, S.; Wakabayashi, T.; Nagayama, S.; Oyamada, H. *Tetrahedron Lett.* **1997**, *38*, 4559–4562.
60. Kobayashi, S.; Wakabayashi, T.; Oyamada, H. *Chem. Lett.* **1997**, 831–832.
61. Kobayashi, S.; Busujima, T.; Nagayama, S. *Synlett* **1999**, 545–546.
62. Kobayashi, S.; Wakabayashi, T. *Tetrahedron Lett.* **1998**, *39*, 5389–5392.
63. Manabe, K.; Mori, Y.; Wakabayashi, T.; Nagayama, S.; Kobayashi, S. *J. Am. Chem. Soc.* **2000**, *122*, 7202–7207.
64. Mukaiyama, T. *Angew. Chem. Int. Ed. Engl.* **1977**, *16*, 817–826.
65. Mukaiyama, T.; Narasaka, K. In *Organic Syntheses*; Vedejs, E., Ed.; Wiley: New York, 1987; Vol. 65, pp 6–11.
66. Mukaiyama, T.; Banno, K.; Narasaka, K. *J. Am. Chem. Soc.* **1974**, *96*, 7503–7509.
67. Saigo, K.; Osaki, M.; Mukaiyama, T. *Chem. Lett.* **1975**, 989–990.
68. Izawa, T.; Mukaiyama, T. *Chem. Lett.* **1974**, 1189–1192.
69. Izawa, T.; Mukaiyama, T. *Chem. Lett.* **1975**, 161–164.
70. Mukaiyama, T.; Hayashi, M. *Chem. Lett.* **1974**, 15–16.
71. Murakami, M.; Mukaiyama, T. *Synthesis* **1987**, 1043–1054.
72. Shimizu, M.; Kume, K.; Fujisawa, T. *Chem. Lett.* **1996**, 545–546.
73. Narasaka, K.; Soai, K.; Aikawa, Y.; Mukaiyama, T. *Bull. Chem. Soc. Jpn.* **1976**, *49*, 779–783.
74. Mahrwald, R.; Gündogan, B. *J. Am. Chem. Soc.* **1998**, *120*, 413–414.
75. Yoshida, Y.; Hayashi, R.; Sumihara, H.; Tanabe, Y. *Tetrahedron Lett.* **1997**, *38*, 8727–8730.
76. Lehnert, W. *Tetrahedron* **1973**, *29*, 635–638.
77. Trost, B. M.; Fleitz, F. J.; Watkins, W. J. *J. Am. Chem. Soc.* **1996**, *118*, 5146–5147.
78. Mukai, C.; Hirai, S.; Kim, I. J.; Kido, M.; Hanaoka, M. *Tetrahedron* **1996**, *52*, 6547–6560.
79. Gennari, C.; Bernardi, A.; Colombo, L.; Scolastico, C. *J. Am. Chem. Soc.* **1985**, *107*, 5812–5813.
80. Hosomi, A.; Sakurai, H. *Tetrahedron Lett.* **1976**, 1295–1298.
81. Nishiyama, H.; Itoh, K. *J. Org. Chem.* **1982**, *47*, 2496–2498.
82. Tsirk, A.; Gronowitz, S.; Hörnfeldt, A.-B. *Tetrahedron* **1997**, *53*, 771–784.
83. Sadakane, M.; Vahle, R.; Schierle, K.; Kolter, D.; Steckhan, E. *Synlett* **1997**, 95–96.
84. Hosomi, A.; Sakurai, H. *J. Am. Chem. Soc.* **1977**, *99*, 1673–1675.
85. Longépé, J.; Prandi, J.; Beau, J.-M. *Angew. Chem. Int. Ed. Engl.* **1997**, *36*, 72–75.
86. David, M.; Dhiimane, H.; Vanucci-Bacqué, C.; Lhomme, G. *Synlett* **1998**, 206–208.
87. Heckmann, B.; Mioskowski, C.; Lumin, S.; Falck, J. R.; Wei, S.; Capdevila, J. H. *Tetrahedron Lett.* **1996**, *37*, 1425–1428.
88. Nishigaichi, Y.; Kuramoto, H.; Takuwa, A. *Tetrahedron Lett.* **1995**, *36*, 3353–3356.
89. Shimada, T.; Yamamoto, Y. *Tetrahedron Lett.* **1998**, *39*, 471–474.
90. Keck, G. E.; Enholm, E. J. *J. Org. Chem.* **1985**, *50*, 146–147.
91. Asao, N.; Kii, S.; Hanawa, H.; Maruoka, K. *Tetrahedron Lett.* **1998**, *39*, 3729–3732.
92. Fains, O.; Vernon, J. M. *Tetrahedron Lett.* **1997**, *38*, 8265–8266.
93. Peng, L.; Goeldner, M. *J. Org. Chem.* **1996**, *61*, 185–191.
94. Oppolzer, W. In *Comprehensive Organic Synthesis*; Trost, B. M.; Fleming, I., Eds.; Pergamon Press: Oxford, UK, 1991; Vol. 5, pp 315–399.
95. Hollis, T. K.; Robinson, N. P.; Bosnich, B. *Organometallics* **1992**, *11*, 2745–2748.
96. Motoyama, Y.; Tanaka, M.; Mikami, K. *Inorg. Chim. Acta* **1997**, *256*, 161–163.
97. Poll, T.; Abdel, Hady, A. F.; Karge, R.; Linz, G.; Weetman, J.; Helmchen, G. *Tetrahedron Lett.* **1989**, *30*, 5595–5598.
98. Meng, D.; Bertinato, P.; Balog, A.; Su, D.-S.; Kamenecka, T.; Sorensen, E. J.; Danishefsky, S. J. *J. Am. Chem. Soc.* **1997**, *119*, 10073–10092.
99. Wada, E.; Pei, W.; Yasuoka, H.; Chim, U.; Kanemasa, S. *Tetrahedron* **1996**, *52*, 1205–1220.
100. Jensen, K. B.; Gothelf, K. V.; Hazell, R. G.; Jørgensen, K. A. *J. Org. Chem.* **1997**, *62*, 2471–2477.
101. Engker, T. A.; Iyengar, R. *J. Org. Chem.* **1998**, *63*, 1929–1934.
102. Mikami, K.; Shimizu, M. *Chem. Rev.* **1992**, *92*, 1021–1050.
103. Harmata, M.; Jones, D. E. *J. Org. Chem.* **1997**, *62*, 1578–1579.
104. Izumi, J.; Mukaiyama, T. *Chem. Lett.* **1996**, 739–740.
105. Brimble, M. A.; Oppen, E. *Synth. Commun.* **1997**, *27*, 989–1007.
106. Stalmach, U.; Kolshorn, H.; Brehm, I.; Meier, H. *Liebigs Ann. Chem.* **1996**, 1449–1456.
107. DeNinno, M. P.; Eller, C. *Tetrahedron Lett.* **1997**, *38*, 6545–6548.
108. Hu, Y.; Skaltitzky, D. J.; Rychnovsky, S. D. *Tetrahedron Lett.* **1996**, *37*, 8679–8682.

109. Reetz, M. T. *Angew. Chem. Int. Ed. Engl.* **1982**, *21*, 96–108.
110. Izumi, J.; Shiina, I.; Mukaiyama, T. *Chem. Lett.* **1995**, 141–142.
111. Krasik, P. *Tetrahedron Lett.* **1998**, *39*, 4223–4226.
112. Mukaiyama, T.; Takeuchi, K.; Uchiro, H. *Chem. Lett.* **1997**, 625–626.
113. Sandrinelli, F.; Perrio, S.; Beslin, P. *J. Org. Chem.* **1997**, *62*, 8626–8627.
114. Bhattacharyya, S. *J. Chem. Soc. Perkin Trans 1* **1995**, 1845–1847.
115. Ishobe, M.; Kitamura, M.; Mio, S.; Goto, T. *Tetrahedron Lett.* **1982**, *23*, 221–224.
116. Caron, M.; Sharpless, K. B. *J. Org. Chem.* **1985**, *50*, 1557–1560.
117. Chong, J. M.; Sharpless, K. B. *J. Org. Chem.* **1985**, *50*, 1560–1563.
118. Ye, T.; Pattenden, G. *Tetrahedron Lett.* **1998**, *39*, 319–322.
119. Mukai, C.; Hirai, S.; Hanaoka, M. *J. Org. Chem.* **1997**, *62*, 6619–6626.
120. Noyori, R.; Kitamura, M. *Angew. Chem., Int. Ed. Engl.* **1991**, *30*, 49–69.
121. Soai, K.; Niwa, S. *Chem. Rev.* **1992**, *92*, 833–856.
122. Takahashi, H.; Kawakita, T.; Ohno, M.; Yoshioka, M.; Kobayashi, S. *Tetrahedron* **1992**, *48*, 5691–5700.
123. Cozzi, P. G.; Tagliavini, E.; Umami-Ronchi, A. *Gazz. Chim. It.* **1997**, *127*, 247–254.
124. Costa, A. L.; Piazza, M. G.; Tagliavini, E.; Trombini, C.; Umami-Ronchi, A. *J. Am. Chem. Soc.* **1993**, *115*, 7001–7002.
125. Mikami, K.; Terada, M. In *Comprehensive Asymmetric Catalysis*; Jacobsen, E. N.; Pfaltz, A.; Yamamoto, H., Eds.; Springer: Heidelberg, Germany, 1999; Vol. 3, pp 1143–1174.
126. Mikami, K. *Pure Appl. Chem.* **1996**, *68*, 639–644.
127. Dias, L. C. J. *Braz. Chem. Soc.* **1997**, *8*, 289–332.
128. Narasaka, K.; Iwasawa, N.; Inoue, M.; Yamada, T.; Nakashima, M.; Sugimori, J. *J. Am. Chem. Soc.* **1989**, *111*, 5340–5345.
129. Keck, G. E.; Li, X.-Y.; Krishnamurthy, D. *J. Org. Chem.* **1995**, *60*, 5998–5999.
130. Wang, B.; Feng, X.; Huang, Y.; Liu, H.; Cui, X.; Jiang, Y. *J. Org. Chem.* **2002**, *67*, 2175–2182.
131. Bellus, D.; Ernst, B. *Angew. Chem., Int. Ed. Engl.* **1988**, *27*, 797–827.
132. Engler, T. A.; Letavic, M. A.; Reddy, J. P. *J. Am. Chem. Soc.* **1991**, *113*, 5068–5070.
133. Narasaka, K.; Hayashi, Y.; Shimadzu, H.; Niihata, S. *J. Am. Chem. Soc.* **1992**, *114*, 8869–8885.
134. Effenberger, F. *Angew. Chem., Int. Ed. Engl.* **1994**, *33*, 1555–1564.
135. Nelson, S. G. *Tetrahedron: Asymmetry* **1998**, *9*, 357–389.
136. Evans, D. A.; McGee, L. R. *Tetrahedron Lett.* **1980**, *21*, 3975–3978.
137. Yamamoto, Y.; Maruyama, K. *Tetrahedron Lett.* **1980**, *21*, 4607–4610.
138. Evans, D. A.; McGee, L. R. *J. Am. Chem. Soc.* **1981**, *103*, 2876–2878.
139. Katsuki, T.; Yamaguchi, M. *Tetrahedron Lett.* **1985**, *47*, 5807–5810.
140. Sasai, H.; Kirio, Y.; Shibasaki, M. *J. Org. Chem.* **1990**, *55*, 5306–5308.
141. Heine, H. W.; Cottle, D. L.; van Matter, H. L. V. *J. Am. Chem. Soc.* **1946**, *68*, 524.
142. Gore, P. H.; Hoskins, J. A. *J. Chem. Soc.* **1964**, 5666–5674.
143. Segi, M.; Nakajima, T.; Suga, S. *Bull. Chem. Soc. Jpn.* **1980**, *53*, 1465–1466.
144. Hachiya, I.; Moriwaki, M.; Kobayashi, S. *Tetrahedron Lett.* **1995**, *36*, 409–412.
145. Hollis, T. K.; Robinson, N. P.; Bosnich, B. *Tetrahedron Lett.* **1992**, *33*, 6423–6426.
146. Lin, S.; Bondar, G. V.; Levy, C. J.; Collins, S. *J. Org. Chem.* **1998**, *63*, 1885–1892.
147. Kobayashi, S.; Ueno, M.; Ishitani, H. *J. Am. Chem. Soc.* **1998**, *120*, 431–432.
148. Ishitani, H.; Ueno, M.; Kobayashi, S. *J. Am. Chem. Soc.* **2000**, *122*, 8180–8186.
149. Kobayashi, S.; Hasegawa, Y.; Ishitani, H. *Chem. Lett.* **1998**, 1131–1132.
150. Bedeschi, P.; Casolari, S.; Costa, A. L.; Tagliavini, E.; Umami-Ronchi, A. *Tetrahedron Lett.* **1995**, *36*, 7897–7900.
151. Casolari, S.; Cozzi, P. G.; Orioli, P.; Tagliavini, E.; Umami-Ronchi, A. *Chem. Commun.* **1997**, 2123–2124.
152. Kobayashi, S.; Iwamoto, S.; Nagayama, S. *Synlett* **1997**, 1099–1101.
153. Wipf, P.; Xu, W. *Tetrahedron* **1995**, *51*, 4551–4562.
154. Jaquith, J. B.; Guan, J.; Wang, S.; Collins, S. *Organometallics* **1995**, *14*, 1079–1081.
155. Yamashita, Y.; Saito, S.; Ishitani, H.; Kobayashi, S. *Org. Lett.* **2002**, *4*, 1221–1223.
156. Franck-Neumann, M.; Miesch, M.; Gross, L. *Tetrahedron Lett.* **1990**, *31*, 5027–5030.
157. Franck-Neumann, M.; Miesch, M.; Gross, L. *Tetrahedron Lett.* **1992**, *33*, 3879–3882.
158. Nugent, W. A. *J. Am. Chem. Soc.* **1992**, *114*, 2768–2769.
159. Adolphsson, H.; Moberg, C. *Tetrahedron: Asymmetry* **1995**, *6*, 2023–2031.
160. Ferraris, D.; Drury III, W. J.; Cox, C.; Lectka, T. *J. Org. Chem.* **1998**, *63*, 4568–4569.
161. Sato, F.; Tomuro, Y.; Ishikawa, H.; Sato, M. *Chem. Lett.* **1980**, 99–102.
162. Asao, N.; Liu, J.-X.; Sudoh, T.; Yamamoto, Y. *J. Org. Chem.* **1996**, *61*, 4568–4571.
163. Kobayashi, S.; Komiyama, S.; Ishitani, H. *Angew. Chem. Int. Ed. Engl.* **1998**, *37*, 979–981.
164. Kobayashi, S.; Kusakabe, K.; Komiyama, S.; Ishitani, H. *J. Org. Chem.* **1999**, *64*, 4220–4221.
165. Kobayashi, S.; Kusakabe, K.; Ishitani, H. *Org. Lett.* **2000**, *2*, 1225–1227.
166. Ishitani, H.; Komiyama, S.; Hasegawa, Y.; Kobayashi, S. *J. Am. Chem. Soc.* **2000**, *122*, 762–766.
167. Gastner, T.; Ishitani, H.; Akiyama, R.; Kobayashi, S. *Angew. Chem. Int. Ed. Engl.* **2001**, *40*, 1896–1898.
168. Yamashita, Y.; Ishitani, H.; Shimizu, H.; Kobayashi, S. *J. Am. Chem. Soc.* **2002**, *124*, 3292–3302.
169. Yamasaki, S.; Kanai, M.; Shibasaki, M. *J. Am. Chem. Soc.* **2001**, *123*, 1256–1257.
170. Nakano, T.; Ishii, Y.; Ogawa, M. *J. Org. Chem.* **1987**, *52*, 4855–4859.
171. Knauer, B.; Krohn, K. *Liebigs Ann. Chem.* **1995**, 677–683.
172. Krohn, K.; Khanbabaee, K.; Rieger, H. *Chem. Ber.* **1990**, *123*, 1357–1364.
173. Krohn, K.; Vinke, I.; Adam, H. *J. Org. Chem.* **1996**, *61*, 1467–1472.
174. Kanie, O.; Ito, Y.; Ogawa, T. *J. Am. Chem. Soc.* **1994**, *116*, 12073–12074.
175. Matsumoto, T.; Katsuki, M.; Jona, H.; Suzuki, K. *J. Am. Chem. Soc.* **1991**, *113*, 6982–6992.
176. Suzuki, K.; Matsumoto, T. In *Recent Progress in the Chemical Synthesis of Antibiotics and Related Microbial Products*; Lukacs, G., Ed.; Springer: Berlin, 1993; Vol. 2, p 353.
177. Suzuki, K.; Matsumoto, T. In *Preparative Carbohydrate Chemistry*; Hanessian, S., Ed.; Marcel Dekker: New York, 1997; p 527.

178. Hachiya, I.; Moriwaki, M.; Kobayashi, S. *Bull. Chem. Soc. Jpn.* **1995**, *68*, 2053–2060.
179. Kobayashi, S.; Moriwaki, M.; Hachiya, I. *Tetrahedron Lett.* **1996**, *37*, 2053–2056.
180. Kobayashi, S.; Moriwaki, M.; Hachiya, I. *Bull. Chem. Soc. Jpn.* **1997**, *70*, 267–273.
181. Mukaiyama, T.; Shiina, I.; Miyashita, M. *Chem. Lett.* **1992**, 625–628.
182. Miyashita, M.; Shiina, I.; Miyoshi, S.; Mukaiyama, T. *Bull. Chem. Soc. Jpn.* **1993**, *66*, 1516–1527.
183. Knochel, P. In *Comprehensive Organic Synthesis*; Trost, B. M.; Fleming, I., Eds.; Pergamon: Oxford, 1991; Vol. 4, pp 865–911.
184. Kaminsky, W.; Arndt, M. *Adv. Polym. Sci.* **1997**, *127*, 143–187.
185. Bertz, S. H.; Dabbagh, G.; Cotte, P. *J. Org. Chem.* **1982**, *47*, 2216–2217.
186. Koide, I.; Ohno, M.; Kobayashi, S. *Tetrahedron Lett.* **1991**, *32*, 7065–7068.
187. Furukawa, H.; Koike, K.; Takao, K.-I.; Kobayashi, S. *Chem. Pharm. Bull.* **1998**, *46*, 1244–1247.
188. Kim, S.; Lee, J. I. *J. Org. Chem.* **1984**, *49*, 1712–1716.
189. Miyachi, N.; Kanda, F.; Shibasaki, M. *J. Org. Chem.* **1989**, *54*, 3511–3513.
190. Miyachi, N.; Shibasaki, M. *J. Org. Chem.* **1990**, *55*, 1975–1976.
191. Duggan, M. E.; Imagire, J. S. *Synthesis* **1989**, 131–132.
192. Cohen, T.; Herman, G.; Falck, J. R.; Mura, Jr., A. J. *J. Org. Chem.* **1975**, *40*, 812–813.
193. Kozikowski, A. P.; Ames, A. *J. Am. Chem. Soc.* **1980**, *102*, 860–862.
194. Kozikowski, A. P.; Ames, A. *Tetrahedron* **1985**, *41*, 4821–4834.
195. Imuta, M.; Ziffer, H. *J. Am. Chem. Soc.* **1979**, *101*, 3990–3991.
196. Sekar, G.; Singh, V. K. *J. Org. Chem.* **1999**, *64*, 2537–2539.
197. Hulce, M.; Mallomo, J. P.; Frye, L. L.; Kogan, T. P.; Posner, G. H. *Org. Syn. Coll. Vol.* **1990**, *7*, 495–500.
198. Narasaka, K.; Sakashita, T.; Mukaiyama, T. *Bull. Chem. Soc. Jpn.* **1972**, *45*, 3724–3724.
199. Mukaiyama, T.; Narasaka, K.; Furusato, M. *J. Am. Chem. Soc.* **1972**, *94*, 8641–8642.
200. Burton, A.; Hevesi, L.; Dumont, W.; Cravador, A.; Krief, A. *Synthesis* **1979**, 877–880.
201. Lucchetti, J.; Dumont, W.; Krief, A. *Tetrahedron Lett.* **1979**, 2695–2696.
202. Raucher, S.; Koolpe, G. A. *J. Org. Chem.* **1978**, *43*, 3794–3796.
203. Laali, K.; Gerzina, R. J.; Flajnik, C. M.; Geric, C. M.; Dombroski, A. M. *Helv. Chim. Acta* **1987**, *70*, 607–611.
204. Evans, D. A.; Murry, J. A.; Kozlowski, M. C. *J. Am. Chem. Soc.* **1996**, *118*, 5814–5815.
205. Evans, D. A.; Rovis, T.; Kozlowski, M. C.; Tedrow, J. S. *J. Am. Chem. Soc.* **1999**, *121*, 1994–1995.
206. Aggarwal, V. K.; Anderson, E. S.; Jones, D. E.; Obierey, K. B.; Giles, R. *Chem. Commun.* **1998**, 1985–1986.
207. Yao, S.; Johannsen, M.; Audrain, H.; Hazell, R. G.; Jørgensen, K. A. *J. Am. Chem. Soc.* **1998**, *120*, 8599–8605.
208. Thorhouge, J.; Johannsen, M.; Jørgensen, K. A. *Angew. Chem., Int. Ed. Engl.* **1998**, *37*, 2404–2406.
209. Jensen, K. B.; Hazell, R. G.; Jørgensen, K. A. *J. Org. Chem.* **1999**, *64*, 2353–2360.
210. Miura, M.; Enna, M.; Okuro, K.; Nomura, M. *J. Org. Chem.* **1995**, *60*, 4999–5004.
211. Evans, D. A.; Burgey, C. S.; Paras, N. A.; Vojkovsky, T.; Tregay, S. W. *J. Am. Chem. Soc.* **1998**, *120*, 5824–5825.
212. Ferraris, D.; Young, B.; Cox, C.; Drury, III, W. J.; Dudding, T.; Lectka, T. *J. Org. Chem.* **1998**, *63*, 6090–6091.
213. Ferraris, D.; Young, B.; Dudding, T.; Lectka, T. *J. Am. Chem. Soc.* **1998**, *120*, 4548–4549.
214. Otto, S.; Boccaletti, G.; Engberts, J. B. F. N. *J. Am. Chem. Soc.* **1998**, *120*, 4238–4239.
215. Kobayashi, S.; Nagayama, S.; Busujima, T. *Tetrahedron* **1999**, *55*, 8739–8746.
216. Shimizu, N.; Tanaka, M.; Tsuno, Y. *J. Am. Chem. Soc.* **1982**, *104*, 1330–1340.
217. Jefford, C. W.; Sledeski, A. W.; Boukouvalas, J. *Tetrahedron Lett.* **1987**, *28*, 949–950.
218. Jefford, C. W.; Sledeski, A. W.; Boukouvalas, J. *J. Chem. Soc. Chem. Commun.* **1988**, 364–365.
219. Jefford, C. W.; Sledeski, A. W.; Boukouvalas, J. *Helv. Chim. Acta* **1989**, *72*, 1362–1370.
220. Yanagisawa, A.; Nakashima, H.; Ishiba, A.; Yamamoto, H. *J. Am. Chem. Soc.* **1996**, *118*, 4723–4724.
221. Yanagisawa, A.; Ishiba, A.; Nakashima, H.; Yamamoto, H. *Synlett* **1997**, 88–90.
222. Yanagisawa, A.; Nakatsuka, Y.; Nakashima, H.; Yamamoto, H. *Synlett* **1997**, 933–934.
223. Yanagisawa, A.; Matsumoto, Y.; Nakashima, H.; Asakawa, K.; Yamamoto, H. *J. Am. Chem. Soc.* **1997**, *119*, 9319–9320.
224. Ferraris, D.; Young, B.; Cox, C.; Dudding, T.; Drury, W. J.; Ryzhkov, L.; Taggi, A. E.; Lectka, T. *J. Am. Chem. Soc.* **2002**, *124*, 67–77.
225. Ito, Y.; Sawanura, M.; Hayashi, T. *J. Am. Chem. Soc.* **1986**, *108*, 6405–6406.
226. Sawamura, M.; Ito, Y. *Chem. Rev.* **1992**, *92*, 857–871.
227. Sato, Y.; Sodeoka, M.; Shibasaki, M. *J. Org. Chem.* **1989**, *54*, 4738–4739.
228. Sato, Y.; Nukui, S.; Sodeoka, M.; Shibasaki, M. *Tetrahedron* **1994**, *50*, 371–382.
229. Danishefsky, S.; Larson, E. R.; Askin, D. *J. Am. Chem. Soc.* **1982**, *104*, 6457–6458.
230. Yamamoto, Y.; Onuki, S.; Yumoto, M.; Asao, N. *J. Am. Chem. Soc.* **1994**, *116*, 421–422.
231. Sakane, S.; Maruoka, K.; Yamamoto, H. *Tetrahedron* **1986**, *42*, 2203–2209.
232. Takahashi, H.; Yoshioka, M.; Shibasaki, M.; Ohno, M.; Imai, N.; Kobayashi, S. *Tetrahedron* **1995**, *51*, 12013–12026.
233. Trost, B. M.; Ito, H. *J. Am. Chem. Soc.* **2000**, *122*, 12003–12004.
234. Trost, B. M.; Ito, H.; Silcoff, E. R. *J. Am. Chem. Soc.* **2001**, *123*, 3367–3368.
235. Yoshikawa, N.; Kumagai, N.; Matsunaga, S.; Moll, G.; Ohshima, T.; Suzuki, T.; Shibasaki, M. *J. Am. Chem. Soc.* **2000**, *123*, 2466–2467.
236. Kumagai, N.; Matsunaga, S.; Yoshikawa, N.; Ohshima, T.; Shibasaki, M. *Org. Lett.* **2001**, *3*, 1539–1542.
237. Kobayashi, S.; Hamada, T.; Manabe, K. *J. Am. Chem. Soc.* **2002**, *124*, 5640–5641.
238. Dalla Cort, A. *Synth. Commun.* **1990**, *20*, 757–760.
239. Still, I. W. J.; Shi, Y. *Tetrahedron Lett.* **1987**, *28*, 2489–2490.
240. Eschler, B. M.; Haynes, R. K.; Ironside, M. D.; Kremmydas, S.; Ridley, D. D.; Hambley, T. W. *J. Org. Chem.* **1991**, *56*, 4760–4766.
241. Lipshutz, B. H.; Pollart, D.; Monforte, J.; Kotsuki, H. *Tetrahedron Lett.* **1985**, *26*, 705–708.
242. Ma, S.; Venanzi, L. M. *Tetrahedron Lett.* **1993**, *34*, 8071–8074.
243. Firouzabadi, H.; Iranpoor, N.; Karimi, B. *Synth. Commun.* **1999**, *29*, 2255–2263.
244. Li, T.-S.; Zhang, Z.-H.; Gao, Y.-J. *Synth. Commun.* **1998**, *28*, 4665–4671.
245. Ma, S.; Venanzi, L. M. *Synlett* **1993**, 751–752.

246. Soga, T.; Takenoshita, H.; Yamada, M.; Mukaiyama, T. *Bull. Chem. Soc. Jpn.* **1990**, *63*, 3122–3131.
247. Suda, K.; Baba, K.; Nakajima, S.; Takanami, T. *Tetrahedron Lett.* **1999**, *40*, 7243–7246.
248. Kruper, W. J.; Dellar, D. V. *J. Org. Chem.* **1995**, *60*, 725–727.
249. Iranpoor, N.; Tarrian, T.; Movahedi, Z. *Synthesis* **1996**, 1473–1476.
250. Martinez, L. E.; Leighton, J. L.; Carsten, D. H.; Jacobsen, E. N. *J. Am. Chem. Soc.* **1995**, *117*, 5897–5898.
251. Schaus, S. E.; Larrow, J. F.; Jacobsen, E. N. *J. Org. Chem.* **1997**, *62*, 4197–4199.
252. Shi, M.; Lei, G.-X.; Masaki, Y. *Tetrahedron: Asymmetry* **1999**, *10*, 2071–2074.
253. Motoyama, Y.; Narusawa, H.; Nishiyama, H. *Chem. Commun.* **1999**, 131–132.
254. Bach, T.; Fox, D. N. A.; Reetz, M. T. *J. Chem. Soc., Chem. Commun.* **1992**, 1634–1636.
255. Odenkirk, W.; Whelan, J.; Bosnich, B. *J. Tetrahedron Lett.* **1992**, *33*, 5729–5732.
256. Hollis, T. K.; Odenkirk, W.; Robinson, N. P.; Whelan, J.; Bosnich, B. *Tetrahedron* **1993**, *49*, 5415–5430.
257. Chen, C.-T.; Hon, S.-.; Weng, S.-S. *Synlett* **1999**, 816–818.
258. Bonnesen, P. V.; Puckett, C. L.; Honeychuck, R. V.; Hersh, W. H. *J. Am. Chem. Soc.* **1989**, *111*, 6070–6081.
259. Motoyama, Y.; Mikami, Y.; Kawakami, H.; Aoki, K.; Nishiyama, H. *Organometallics* **1999**, *18*, 3584–3588.
260. Cabral, J.; Laszlo, P.; Mahé, L.; Montaufer, M.-T.; Randriamahefa, S. L. *Tetrahedron Lett.* **1989**, *30*, 3969–3972.
261. Christoffers, J. *J. Chem. Soc., Perkin Trans 1* **1997**, 3141–3149.
262. Suzuki, K.; Hashimoto, T.; Maeta, H.; Matsumoto, T. *Synlett* **1992**, 125–128.
263. Hashimoto, T.; Maeta, H.; Matsumoto, T.; Morooka, M.; Ohba, S.; Suzuki, K. *Synlett* **1992**, 340–342.
264. Kanemasa, S.; Oderaotoshi, Y.; Wada, E. *J. Am. Chem. Soc.* **1999**, *121*, 8675–8676.
265. Nesper, R.; Pregosin, P. S.; Püntener, K.; Wörle, M. *Helv. Chim. Acta* **1993**, *76*, 2239–2249.
266. Gorla, F.; Togni, A.; Venanzi, L. M.; Albinati, A.; Lianza, F. *Organometallics* **1994**, *13*, 1607–1616.
267. Longmire, J. M.; Zhang, X.; Shang, M. *Organometallics* **1998**, *17*, 4374–4379.
268. Murahashi, S.-I.; Naota, T.; Taki, H.; Mizuno, M.; Takaya, H.; Komiya, S.; Mizuho, Y.; Oyasato, N.; Hiraoka, M.; Hirano, M.; Fukuoka, A. *J. Am. Chem. Soc.* **1995**, *117*, 12436–12425.
269. Kuwano, R.; Miyazaki, H.; Ito, Y. *Chem. Commun.* **1998**, 71–72.
270. Sawamura, M.; Hamashima, H.; Ito, Y. *Tetrahedron* **1994**, *50*, 4439–4454.
271. Murahashi, S.-I.; Sasao, S.; Saito, E.; Naota, T. *J. Org. Chem.* **1992**, *57*, 2521–2523.
272. Kanemasa, S.; Oderaotoshi, Y.; Sakaguchi, H.; Yamamoto, H.; Tanaka, J.; Wada, E.; Curran, D. P. *J. Am. Chem. Soc.* **1998**, *120*, 3074–3088.
273. Corey, E. J.; Imai, N.; Zhang, H.-Y. *J. Am. Chem. Soc.* **1991**, *113*, 728–729.
274. Khair, N.; Fernández, I.; Alcudia, F. *Tetrahedron Lett.* **1993**, *34*, 123–126.
275. Oi, S.; Kashiwagi, K.; Inoue, Y. *Tetrahedron Lett.* **1998**, *39*, 6253–6256.
276. Kündig, E. P.; Bourdin, B.; Bernardinelli, G. *Angew. Chem. Int. Ed. Engl.* **1994**, *33*, 1856–1858.
277. Bruin, M. E.; Kündig, E. P. *Chem. Commun.* **1998**, 2635–2636.
278. Kündig, E. P.; Saudan, C. M.; Bernardinelli, G. *Angew. Chem. Int. Ed. Engl.* **1999**, *38*, 1220–1223.
279. Hu, Y.-J.; Huang, X.-D.; Yao, Z.-J.; Wu, Y.-L. *J. Org. Chem.* **1998**, *63*, 2456–2461.
280. Saito, T.; Takakawa, K.; Takahashi, T. *Chem. Commun.* **1999**, 1001–1002.
281. Oi, S.; Terada, E.; Ohuchi, K.; Kato, T.; Tachibana, Y.; Inoue, Y. *J. Org. Chem.* **1999**, *64*, 8660–8667.
282. Dossetter, A. G.; Jamison, T. F.; Jacobsen, E. N. *Angew. Chem., Int. Ed. Engl.* **1999**, *38*, 2398–2400.
283. Kanemasa, S.; Oderaotoshi, Y.; Tanaka, J.; Wada, E. *J. Am. Chem. Soc.* **1998**, *120*, 12355–12356.
284. Hori, K.; Kodama, H.; Ohta, T.; Furukawa, I. *J. Org. Chem.* **1999**, *64*, 5017–5023.
285. Kobalka, G. W.; Narayana, C.; Reddy, N. K. *Synth. Commun.* **1992**, *22*, 1793–1798.
286. Benton, F.; Dillon, T. *J. Am. Chem. Soc.* **1942**, *64*, 1128–1129.
287. Grieco, P. A.; Hiroi, K.; Reap, J. J.; Noguez, J. A. *J. Org. Chem.* **1975**, *40*, 1450–1453.
288. Grieco, P. A.; Reap, J. J.; Noguez, J. A. *Synth. Commun.* **1975**, *5*, 155–159.
289. Manchand, P. S. *J. Chem. Soc., Chem. Commun.* **1991**, 667–667.
290. Danishefsky, S. J.; Pearson, W. H.; Harvey, D. F. *J. Am. Chem. Soc.* **1984**, *106*, 2455–2456.
291. Hyatt, J. A.; Reynolds, P. W. *J. Org. Chem.* **1984**, *49*, 384–385.
292. Bach, R. D.; Klix, R. C. *J. Org. Chem.* **1985**, *50*, 5438–5440.
293. Kotsuki, H.; Asao, K.; Ohnishi, H. *Bull. Chem. Soc. Jpn.* **1984**, *57*, 3339–3340.
294. Ishihara, K.; Hanaki, N.; Yamamoto, H. *Synlett* **1993**, 577–579.
295. Ishihara, K.; Funahashi, M.; Hanaki, N.; Miyata, M.; Yamamoto, H. *Synlett* **1994**, 963–964.
296. Ishihara, K.; Hanaki, N.; Funahashi, M.; Miyata, M.; Yamamoto, H. *J. Am. Chem. Soc. Jpn.* **1995**, *68*, 1721–1730.
297. Furuta, K.; Miwa, Y.; Iwanaga, K.; Yamamoto, H. *J. Am. Chem. Soc.* **1988**, *110*, 6254–6255.
298. Furuta, K.; Shimizu, S.; Miwa, Y.; Yamamoto, H. *J. Org. Chem.* **1989**, *54*, 1481–1483.
299. Corey, E. J.; Loh, T.-P. *Tetrahedron Lett.* **1993**, *34*, 3979–3982.
300. Ishihara, K.; Kurihara, H.; Yamamoto, H. *J. Am. Chem. Soc.* **1996**, *118*, 3049–3050.
301. Ishihara, K.; Kurihara, H.; Matsumoto, M.; Yamamoto, H. *J. Am. Chem. Soc.* **1996**, *120*, 6920–6930.
302. Mori, Y.; Manabe, K.; Kobayashi, S. *Angew. Chem. Int. Ed.* **2001**, *40*, 2815–2818.
303. Carr, D. B.; Schwartz, J. *J. Am. Chem. Soc.* **1977**, *99*, 638–640.
304. Akamanchi, K. G.; Varalakshmy, N. R. *Tetrahedron Lett.* **1995**, *36*, 3571–3572.
305. Akamanchi, K. G.; Varalakshmy, N. R. *Tetrahedron Lett.* **1995**, *36*, 5085–5088.
306. Ooi, T.; Miura, T.; Maruoka, K. *Angew. Chem. Int. Ed.* **1998**, *37*, 2347–2349.
307. Takai, K.; Oshima, K.; Nozaki, H. *Tetrahedron Lett.* **1980**, *21*, 1657–1660.
308. Naruse, Y.; Ukai, J.; Ikeda, N.; Yamamoto, H. *Chem. Lett.* **1985**, 1451–1452.
309. Evans, D. A.; Chapman, K. T.; Bisaha, J. *J. Am. Chem. Soc.* **1984**, *106*, 4261–4263.
310. Maruoka, K.; Itoh, T.; Yamamoto, H. **1985**, *J. Am. Chem. Soc.* *107*, 4573–4576.
311. Maruoka, K.; Itoh, T.; Sakurai, M.; Nonoshita, K.; Yamamoto, H. *J. Am. Chem. Soc.* **1988**, *110*, 3588–3597.
312. Maruoka, K.; Imoto, H.; Saito, S.; Yamamoto, H. *J. Am. Chem. Soc.* **1994**, *116*, 4131–4132.
313. Shimizu, M.; Kawamoto, M.; Yamamoto, Y.; Fujisawa, T. *Synlett* **1997**, 501–502.
314. Iovel, I.; Popelis, Y.; Fleisher, M.; Lukevics, E. *Tetrahedron Asymmetry* **1997**, *8*, 1279–1285.
315. Arai, T.; Bougauchi, M.; Sasai, H.; Shibasaki, M. *J. Org. Chem.* **1996**, *61*, 2926–2927.
316. Noyori, R.; Murata, S.; Suzuki, M. *Tetrahedron* **1981**, *37*, 3899–3910.

317. Emde, H.; Domsch, D.; Feger, H.; Frick, U.; Götz, A.; Hergott, H. H.; Hofmann, K.; Kober, W.; Krägeloh, K.; Oesterle, T.; Steppan, W.; West, W.; Simchen, G. *Synthesis* **1982**, 1–26.
318. Murata, S.; Suzuki, M.; Noyori, R. *Tetrahedron* **1988**, *44*, 4259–4275.
319. Davis, A. P.; Plunkett, S. J. *J. Chem. Soc., Chem. Commun.* **1995**, 2173–2174.
320. Davis, A. P.; Muir, J. E.; Plunkett, S. J. *Tetrahedron Lett.* **1996**, *37*, 9401–9402.
321. Oishi, M.; Aratake, S.; Yamamoto, H. *J. Am. Chem. Soc.* **1998**, *120*, 8271–8272.
322. Murata, S.; Suzuki, M.; Noyori, R. *J. Am. Chem. Soc.* **1980**, *102*, 3248–3249.
323. Murata, S.; Suzuki, M.; Noyori, R. *Tetrahedron Lett.* **1980**, *21*, 2527–2528.
324. Guanti, G.; Narisano, E.; Banfi, L. *Tetrahedron Lett.* **1987**, *28*, 4331–4334.
325. Pilli, R. A.; Russowsky, D. *J. Chem. Soc., Chem. Commun.* **1987**, 1053–1054.
326. Davis, A. P.; Jaspars, M. *Angew. Chem., Int. Ed. Engl.* **1992**, *31*, 470–471.
327. Ishii, A.; Kotera, O.; Saeki, T.; Mikami, K. *Synlett* **1997**, 1145–1146.
328. Mathieu, B.; Ghosez, L. *Tetrahedron Lett.* **1997**, *38*, 5497–5500.
329. Tietze, L. F.; Bratz, M.; Pretor, M. *Chem. Ber.* **1989**, *122*, 1955–1961.
330. Nogue, D.; Pauzam, R.; Wartski, L. *Tetrahedron Lett.* **1992**, *33*, 1265–1268.
331. Suzuki, K.; Miyazawa, M.; Tsuchihashi, G. *Tetrahedron Lett.* **1987**, *28*, 3515–3518.
332. Vorbrüggen, H.; Kroliekiewicz, K.; Bennua, B. *Chem. Ber.* **1981**, *114*, 1234–1255.
333. Ishihara, K. In *Lewis Acids in Organic Synthesis*; Yamamoto, H., Ed.; Wiley-VCH: Weinheim, Germany, 2000; Vol. 1, Chap. 9, p 395.
334. Iwasawa, N.; Mukaiyama, T. *Chem. Lett.* **1987**, 463–466.
335. Mukaiyama, T.; Kobayashi, S.; Tamura, M.; Sagawa, Y. *Chem. Lett.* **1987**, 491–494.
336. Mukaiyama, T.; Takashima, T.; Katsurada, M.; Aizawa, H. *Chem. Lett.* **1991**, 533–536.
337. Mukaiyama, T.; Katsurada, M.; Takashima, T. *Chem. Lett.* **1991**, 985–988.
338. Kobayashi, S.; Uchiro, H.; Fujishita, Y.; Shiina, I.; Mukaiyama, T. *J. Am. Chem. Soc.* **1991**, *113*, 4247–4252.
339. Mukaiyama, T.; Uchiro, H.; Kobayashi, S. *Chem. Lett.* **1989**, 1757–1760.
340. Mukaiyama, T.; Uchiro, H.; Kobayashi, S. *Chem. Lett.* **1990**, 1147–1150.
341. Evans, D. A.; MacMillan, W. C.; Campos, K. R. *J. Am. Chem. Soc.* **1997**, *119*, 10859–10860.
342. Sato, T.; Wakahara, Y.; Otera, J.; Nozaki, H.; Fukuzumi, S. *J. Am. Chem. Soc.* **1991**, *113*, 4028–4030.
343. Otera, J.; Fujita, Y.; Sakuta, N.; Fujita, M.; Fukuzumi, S. *J. Org. Chem.* **1996**, *61*, 2951–2962.
344. Fujita, Y.; Fukuzumi, S.; Otera, J. *Tetrahedron Lett.* **1997**, *38*, 2117–2120.
345. Ishihara, K.; Kaneeda, M.; Yamamoto, H. *J. Am. Chem. Soc.* **1994**, *116*, 11179–11180.
346. Ishihara, K.; Nakamura, S.; Kaneeda, M.; Yamamoto, H. *J. Am. Chem. Soc.* **1996**, *118*, 12854–12855.
347. Yanagisawa, A.; Ishihara, K.; Yamamoto, H. *Synlett* **1997**, 411–420.
348. Matsunaga, S.; Das, J.; Roels, J.; Vogl, E. M.; Yamamoto, N.; Iida, T.; Yamaguchi, K.; Shibasaki, M. *J. Am. Chem. Soc.* **2000**, *122*, 2252–2260.
349. Babu, G.; Perumal, P. T. *Tetrahedron Lett.* **1997**, *38*, 5025–5026.
350. Babu, G.; Nagarajan, R.; Natarajan, R.; Perumal, P. T. *Synthesis* **2000**, 661–666.
351. Loh, T. P.; Wei, L.-L. *Tetrahedron Lett.* **1998**, *39*, 323–326.
352. Nagayama, S.; Kobayashi, S. *J. Am. Chem. Soc.* **2000**, *122*, 11531–11532.
353. Yoneda, N.; Fukuhara, T.; Takahashi, Y.; Suzuki, A. *Chem. Lett.* **1979**, 1003–1006.
354. Pearson, R. G. *J. Am. Chem. Soc.* **1963**, *85*, 3533–3539.
355. House, H. O. *Modern Synthetic Reactions* **1972**, Benjamin: Menlo Park, CA.
356. Olah, G. A.; Kobayashi, S.; Tashiro, M. *J. Am. Chem. Soc.* **1972**, *94*, 7448–7461.
357. Deters, J. F.; Mccusker, P. A.; Pilger, Jr., R. C. *J. Am. Chem. Soc.* **1968**, *90*, 4583–4585.
358. Childs, R. F.; Mulholland, D. L.; Nixon, A. *Can. J. Chem.* **1982**, *60*, 801–808.
359. Satchell, D. P. N.; Satchell, R. S. *Chem. Rev.* **1969**, *69*, 251–278.
360. Laszlo, P.; Teston, M. *J. Am. Chem. Soc.* **1990**, *112*, 8750–8754.
361. Luo, Y.-R.; Benson, S. W. *Inorg. Chem.* **1991**, *30*, 1676–1677.
362. Corriu, R.; Dore, M.; Thomassin, R. *Tetrahedron Lett.* **1968**, *23*, 2759–2762.
363. Kündig, E. P.; Saudan, C. M.; Bernardinelli, G. *Angew. Chem., Int. Ed. Engl.* **1999**, *38*, 1219–1223.
364. Annis, D. A.; Jacobsen, E. N. *J. Am. Chem. Soc.* **1999**, *121*, 4147–4154.
365. Johnson, L. K.; Killian, C. M.; Brookhart, M. *J. Am. Chem. Soc.* **1995**, *117*, 6414–6415.
366. Engberts, J. B. F. N.; Feringa, B. L.; Keller, E.; Otto, S. *Recl. Trav. Chim. Pays-Bas* **1996**, *115*, 457–464.
367. Braga, A. L.; Dornelles, L.; Silveira, C. C.; Wessjohann, L. A. *Synthesis* **1999**, 562–564.
368. Sekar, G.; Singh, V. K. *J. Org. Chem.* **1999**, *64*, 2537–2539.
369. Mukaiyama, T.; Ohno, T.; Nishimura, T.; Han, J. S.; Kobayashi, S. *Bull. Chem. Soc. Jpn.* **1991**, *64*, 2524–2527.
370. Kobayashi, S.; Nagayama, S.; Busujima, T. *J. Am. Chem. Soc.* **1998**, *120*, 8287–8288.
371. Kobayashi, S.; Busujima, T.; Nagayama, S. *Chem. Eur. J.* **2002**, *6*, 3491–3494.

9.9

Supported Metal Complexes as Catalysts

F. QUIGNARD

Ecole Nationale Supérieure de Chimie, Montpellier, France

and

A. CHOPLIN

Institut de Recherches sur la Catalyse, Villeurbanne, France

9.9.1	INTRODUCTION	445
9.9.2	THE DIFFERENT PROCEDURES OF IMMOBILIZATION OF METAL COMPLEXES ON SOLID SUPPORTS	446
9.9.2.1	Introduction	446
9.9.2.2	Direct Reaction between the Solid Support and the Metal Complex	446
9.9.2.2.1	<i>Inorganic supports</i>	446
9.9.2.2.2	<i>Organic supports</i>	450
9.9.2.3	Immobilization by Copolymerization	452
9.9.2.3.1	<i>Inorganic matrices</i>	452
9.9.2.3.2	<i>Organic supports</i>	453
9.9.2.4	Supported Liquid Phase Catalysts (SLPC)	454
9.9.3	SOME REACTIONS CATALYZED BY SUPPORTED METAL COMPLEXES	456
9.9.3.1	Hydrogenation	456
9.9.3.2	Epoxidation	458
9.9.3.2.1	<i>Supported titanium-based catalysts</i>	458
9.9.3.2.2	<i>Supported salen-type complexes</i>	461
9.9.3.3	C—C Bond Formation by Cross Coupling	463
9.9.3.3.1	<i>Heck reaction</i>	463
9.9.3.3.2	<i>Trost–Tsuji allylic substitution</i>	465
9.9.3.4	Polymerization	466
9.9.4	CONCLUSION AND PERSPECTIVES	467
9.9.5	REFERENCES	467

9.9.1 INTRODUCTION

The procedures which allow for the immobilization of a metal complex on or in a solid are numerous and well described; they result from more than thirty years of continuous and imaginative efforts. More difficult, and consequently less successful, work has been described regarding the syntheses of efficient catalysts from these precursors. An immobilized complex must show high activity and selectivity for the target reaction, must be easily recovered intact, and must be stable towards metal leaching under the reaction conditions. These two latter requirements are particularly important where asymmetric catalysis is the goal, because the metal and the ligands

are generally expensive and the products (often used as pharmaceuticals) will not tolerate the presence of even trace amounts of metal contaminants. A quick survey of the area of synthesis and applications of supported catalysts shows significant progress during the last twenty years, which can be attributed to a multidisciplinary approach which takes simultaneously into account the recent developments in surface science, in coordination and organometallic chemistry, and in the understanding of the mechanisms of homogeneous and heterogeneous catalysis.

We will describe first the different methods of immobilization of catalysts, and highlight their advantages and disadvantages and their fields of application. We will then examine the properties of such supported complexes for the major classes of catalytic reactions. We will focus mainly on those studies where at least some characterization of the supported catalyst is given, unless the catalytic properties of the described system are outstanding: the review is therefore far from being exhaustive. Finally, where possible, we will mention tests of recyclability, which are essential for the supported complex to be as a potential industrial catalyst.

Two main classes of solid are used for the immobilization of complexes: inorganic oxides such as silica, alumina, magnesia, or zeolites; and organic polymers such as polystyrene, polydivinylbenzene, or nafion. Some other more exotic supports are considered which are relevant to specific goals: these include glycosides such as chitosan, cellulose, or even silk. References 1–14 give the surface properties of some of the inorganic supports, data which are necessary to understand the reactions involved in the immobilization processes. These solids are chosen for their high thermal and mechanical stability, their chemical surface properties (acid-base, redox, hydrophilicity), and their high specific surface area.^{1–14} Polymers—although less thermally stable—have the advantages of a wide variety of functional groups available for attaching catalysts, as well as swelling and gelling properties which may be explored. The choice of support will be most pertinent if the precursor complex, the support, and the method of immobilization are chosen in conjunction with a target catalytic reaction; the best results will be achieved when only one surface species is formed which is stable under the catalytic reaction conditions.

9.9.2 THE DIFFERENT PROCEDURES OF IMMOBILIZATION OF METAL COMPLEXES ON SOLID SUPPORTS

9.9.2.1 Introduction

Three main methods of synthesis of supported metal complex catalysts can be distinguished from the literature, which we will successively analyze:

- (i) the complex catalyst or a precursor is directly reacted with the solid support;
- (ii) the complex is copolymerized with monomeric precursors of the solid;
- (iii) the complex is immobilized in a liquid phase (i.e., in solution) on a solid: the interaction between the solvent and the solid is the driving force of heterogeneization.

With the two first methods, the complex (i.e., the homogeneous catalyst or a closely related analog) and the solid are either reacted together directly, or are first modified so as to be able to react with each other. With the third method, the complex must generally be modified so as to acquire a high solubility in the liquid solvent, which acts as the immobilizing agent. Each method of immobilization, and each type of solid support, can have specific advantages and disadvantages according to the nature of the catalyst and the target reaction.

9.9.2.2 Direct Reaction between the Solid Support and the Metal Complex

9.9.2.2.1 Inorganic supports

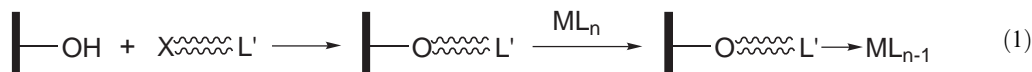
(i) Incorporation by ion exchange reactions

This method is certainly the oldest one described in the literature; the first example concerns the ion exchange of $[\text{Pt}(\text{NH}_3)_4]^{2+}$ and the surface of a sulfonated silica.¹⁵ Even now, the preparation of many heterogeneous catalysts (i.e., supported metal or oxide particles) involves as the first step the reaction of a coordination complex with the surface of an ionic solid such as alumina,

magnesia, zinc oxide and zeolites.^{16–18} The fundamental aspects of this approach were recently reviewed by J. F. Lambert *et al.*¹⁹ We shall not discuss this methodology further because the resulting supported complexes are most often reduced or oxidized into metallic or oxide particles.

When supported *complexes* are the catalysts, two types of ionic solid were used: zeolites and clays. The structures of these solids (microporous and lamellar respectively) help to improve the stability of the complex catalyst under the reaction conditions by preventing the catalytic species from undergoing dimerization or aggregation, both phenomena which are known to be deactivating. In some cases, the pore walls can tune the selectivity of the reaction by steric effects. The strong similarities of zeolites with the protein portion of natural enzymes was emphasized by Herron.²⁰ The protein protects the active site from side reactions, sieves the substrate molecules, and provides a stereochemically demanding void. Metal complexes have been encapsulated in zeolites, successfully mimicking metalloenzymes for oxidation reactions. Two methods of synthesis of such encapsulated/intercalated complexes have been tested, as follows.

- (i) *The cationic complex catalyst is directly exchanged with the charge compensating cation of the solid.* The synthesis of intercalated complexes is represented in Figure 1 and has been shown to be efficient with swelling clays, such as smectites. Thus, complexes such as $[\text{Rh}(\text{NBD})(\text{PPh}_3)]^{2+}$ (NBD = norbornadiene) or $[\text{Rh}(\text{dppe})(\text{NBD})]^+$ (dppe = 1,2-bis(diphenyl-diphosphino)ethane), $[\text{Rh}(\text{cod})-(S)\text{-BINAP}]^+$, and $[\text{Rh}(\text{cod})((S)\text{-R-BPPFA})]^+$, (cod = cyclooctadiene; BPPFA = *N,N*-dimethyl-1-[1',2-bis(diphenylphosphino)ferrocenyl]ethylamine) were intercalated in hectorite.^{21–23} Intercalation resulted in a significant increase of the interlayer spacing, as determined by XRD. These catalysts, when tested for reactions of hydrogenation of alkenes and alkynes, show a strong solvent effect which correlates with their swelling efficiency. Steric effects and surface chemical effects resulted in selectivities which were different from those of their homogeneous counterparts. In the case of asymmetric hydrogenation of α,β -unsaturated carboxylic acid esters, the dependence of the selectivity on the solvent and on the bulkiness of the ester group suggests that the interaction between the substrate and the active site increases in the interlayer space, thus enhancing the enantioselectivity.²³ Unfortunately, problems of metal leaching are frequently encountered with these systems; this implies that preliminary functionalization of the interlayer surface by Equation(1),²⁴ which would prevent leaching, is desirable.



Because the size of the interlayers can be easily varied by incorporation of complex moieties of different sizes, these clays (montmorillonite, hectorite) may nevertheless compete as catalyst supports with zeolites which have a rigid, predetermined cavity size.

- (ii) *The cationic exchange concerns a metal complex, having small, easily exchangeable ligands.* The first step of this type of encapsulation/intercalation is the introduction of the metal into the pores of the solid either via a cation exchange reaction or as a complex labile

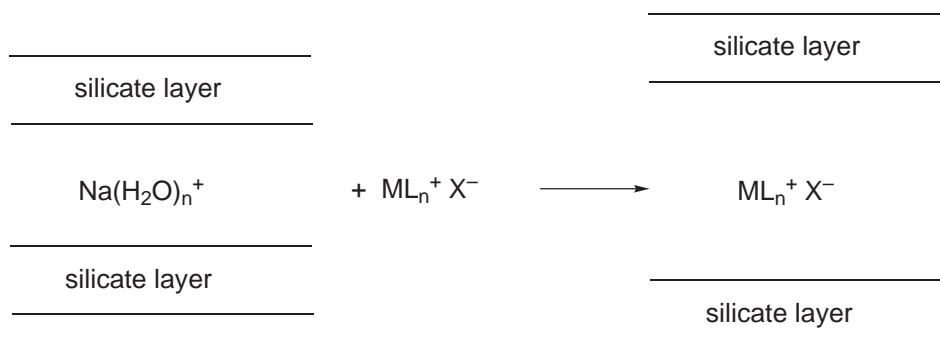


Figure 1 Synthesis of intercalated complexes.

towards ligand substitution. In the second step, the ligands necessary to make the actual complex catalyst (e.g., CO, PR_3 , 1,2-dicyanobenzene, N,N' -bis(salicylidene)ethylenediamine (H_2Salen), and more recently 5,7,12,14-tetramethyl-1,4,8,11-tetraazacyclotetradeca-4,6,11,13-tetraene (TMC)) are introduced under conditions which allow complex formation.

The induction of steric effects by the pore walls was first demonstrated with heterogeneous catalysts, prepared from metal carbonyl clusters such as $\text{Rh}_6(\text{CO})_{16}$, $\text{Ru}_3(\text{CO})_{12}$, or $\text{Ir}_4(\text{CO})_{12}$, which were synthesized *in situ* after a cation exchange process under CO in the large pores of zeolites such as HY, NaY, or 13X.^{25,26} The zeolite-entrapped carbonyl clusters are stable towards oxidation-reduction cycles; this is in sharp contrast to the behavior of the same clusters supported on non-porous inorganic oxides. At high temperatures these metal carbonyl clusters aggregate to small metal particles, whose size is restricted by the dimensions of the zeolitic framework. Moreover, for a number of reactions, the size of the pores controls the size of the products formed; thus a higher selectivity to the lower hydrocarbons has been reported for the Fischer–Tropsch reaction.

Two types of complex have been most studied, *viz.* the salen and the phthalocyanine (Pc) complexes, whose dimensions fit that of the large pores of available zeolites.²⁷ Thus, the aluminosilicate faujasites (X, Y, EMT) encapsulate Rh^{III} -salen, Co^{II} -salen, Mn^{III} -salen and Pd^{II} -Salen derivatives, as well as Fe^{II} Pc, Co^{II} Pc, and Fe^{II} -TMC.^{28–35} The aluminophosphate VPI-5 can accommodate FePc.³⁶ The ligand 1,2-dicyanobenzene enters easily the pores of these two zeolites, and the ligands H_2Salen and TMC—although larger—are also flexible enough to enter the pores (Figures 2 and 3).

In both cases, the complex formed is like a “ship in a bottle,” confined after formation in the super-cages of the zeolite: these catalysts are reported to show a greater stability than the same complexes in solution. No metal leaching has been reported as long as the complex is exclusively inside the pores. For most tested reactions, such as oxidation of alkanes or alkenes, and hydrogenation of alkenes, a high selectivity in competitive reactions is observed which is correlated to molecular sieving effects (reactant size selectivity effect); and a better regioselectivity is obtained when compared to the homogeneous system (the 2 position is favored over the 4 position in the oxidation of *n*-octane, for example).^{28,30,31,37} However, these good selectivities are associated with lower activities due to diffusion limitations.

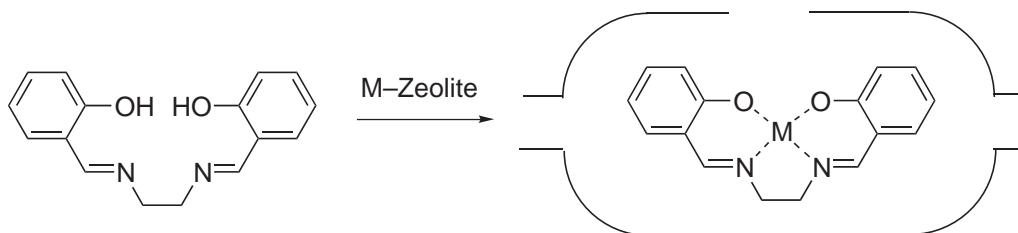


Figure 2 “Ship in a bottle” synthesis of encapsulated salen complexes.

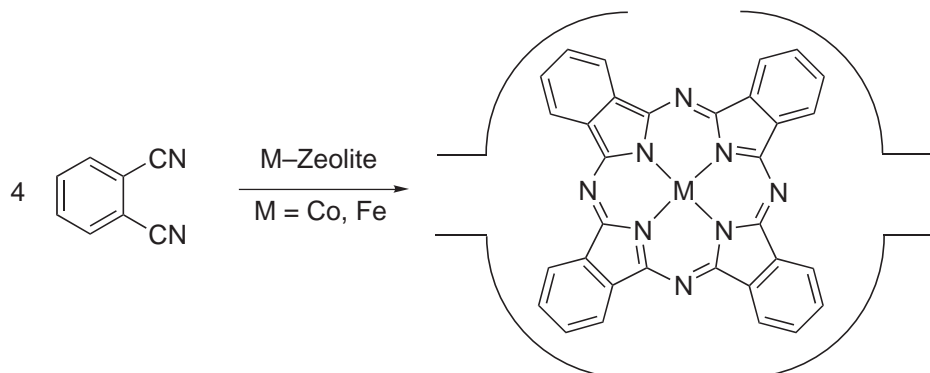
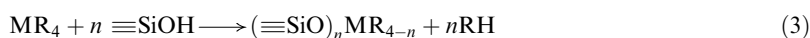


Figure 3 Synthesis of encapsulated phthalocyanine complexes.

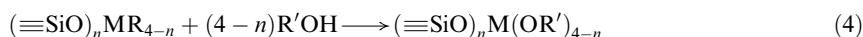
(ii) Incorporation by covalent anchoring

(a) *Formation of a bond between the solid and the metal center.* Most of the studies in this area concern the anchoring of organometallic complexes on the surface of inorganic oxides, and several reviews have been published up to 1993 to which the reader is referred.³⁸⁻⁴³ We will focus here on those systems which are based on supported *coordination* complexes. An organometallic complex is used as the source of well-dispersed mononuclear metal centers; these supported organometallic complexes are subsequently transformed into a coordination complex, active for the target reaction. The support is behaving as a ligand and, as such, influences the reactions via electronic and/or steric effects. Of course, the grafting bond must be stable under the conditions of synthesis and those of the catalytic reactions.

The synthesis of group 4 alkoxide complexes grafted on the surface of silica illustrates this approach.⁴⁴⁻⁴⁷ Two routes were considered, which are schematically represented in [Equation\(2\)](#) and [\(3\)](#); they differ in the nature of the precursor complex, which is either the tetra-alkoxide $M(OR)_4$ ([Equation\(2\)](#)), or the tetra-alkyl complex MR_4 , $M = Ti, Zr, Hf$ ([Equation\(3\)](#)):



The stoichiometry of these reactions can be controlled by modulating the concentration of hydroxyl groups on the surface of silica. When starting with the tetra-alkyl complex, subsequent reaction with an alcohol $R'OH$ ([Equation\(4\)](#)) is necessary; this generally occurs under conditions mild enough to maintain the anchoring bond $SiO-M$.



The second approach ([Equation\(3\)](#)) has a number of advantages over the first one ([Equation\(2\)](#)). The alkyl complexes are more reactive than the related alkoxides, the latter being for group 4 elements generally associated into dimers or trimers;⁴⁸ also, reaction (2) liberates an alcohol which may further react with the surface of silica, whereas the alkane ([Equation\(3\)](#)) is inert. It was demonstrated by various spectroscopic techniques and elemental analysis that with a silica dehydroxylated at 500 °C under vacuum, the stoichiometry of reaction (3) corresponds to $n = 1$.^{45,46} Moreover, a better control of the surface reaction was achieved with the procedure represented in [Equation\(3\)](#).

(b) *Formation of a bond between the solid and a ligand.* Two different approaches to this have been used. The first method ([Equation\(1\)](#)) consists of functionalization of the surface of silica with ligand sites L' by reaction between a bifunctional ligand, $X \approx L'$ and the surface silanols; attachment of the immobilised L' units to metal complex fragments is then performed. The X group of $X \approx L'$ is chosen so as to react easily with the silica hydroxyls; it is generally $Cl, SiCl_3, Si(OEt)_3, OH,$ or $SiR'_2(OR)$.⁴⁹ In most cases, L' is a phosphine, PR'_2R , the R alkyl or aryl substituent bearing the reactive X group, such that $X \approx L'$ is $X-(CH_2)_n PPh_2$ or $X-C_6H_4-PPh_2$. With $X = OH$ or $SiR'_2(OR)$, a better control of the surface reaction is generally claimed: the cross linking reactions are suppressed ([Figure 4](#)) and the stoichiometry of the anchoring reaction simple.⁵⁰

The length of the chain $(CH_2)_n$ must be optimized so as to allow for a certain mobility of the complex and a partial release of the steric hindrance induced by the support, but no catalyst

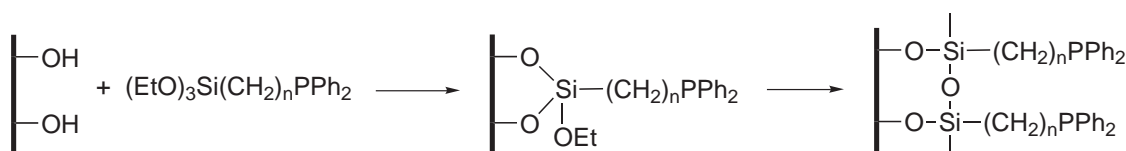
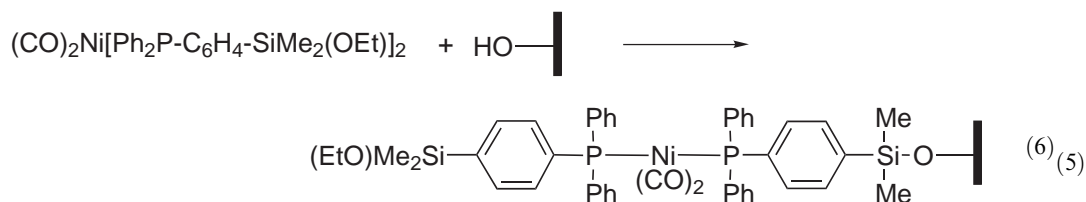
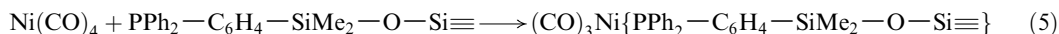


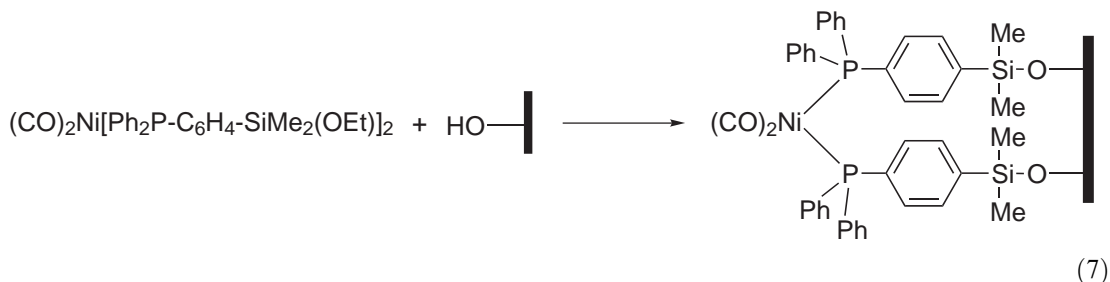
Figure 4 Possible cross linking surface reactions.

deactivation by dimerization of the active species. The complex ML_n of interest (L is typically CO or PR_3) is then grafted on the functionalized solid by a ligand exchange reaction with the surface ligands L' .

The second approach consists of synthesizing first the complex $ML_{n-1}(L' \approx X)$ with the desired ratio $(L')/(M)$; this complex bears the reactive fragment X which then reacts with the surface of the silica. This method is of limited interest, because the synthesis and isolation of these functionalized complexes is not straightforward. One of the successful examples concerns the synthesis of nickel carbonyl complexes anchored to the surface via two bonds in an attempt to increase the stability through a sort of "chelate" effect. Initial attempts to achieve this by the methods described in Equation(5) (initial functionalization of silica) and Equation(6) (initial functionalization of complex) failed, as demonstrated by ^{29}Si and ^{31}P CP MAS NMR spectroscopies.⁵¹



Only when the solution of the functionalized complex is added dropwise to silica is the desired di-anchored complex formed (Equation(7)).



These complexes anchored to a solid via a ligand have been tested for a number of reactions including the hydrogenation, hydroformylation, hydrosilylation, isomerization, dimerization, oligomerization, and polymerization of olefins; carbonylation of methanol; the water gas shift reaction; and various oxidation and hydrolysis reactions (see later for some examples). In most cases, the characterization of the supported entities is very limited; the surface reactions are often described on the basis of well-known chemistry, confirmed in some cases by spectroscopic data and elemental analysis.

9.9.2.2.2 Organic supports

(i) Incorporation by ion exchange reactions

Nafion, a perfluorinated sulfonated polymer, is a typical example of an ion-exchangeable resin with high promise as a catalyst support. Its properties are significantly different from those of common polymers (stability towards strong bases, and strong oxidizing and reducing acids; and thermal stability up to at least 120 °C if the counter ion is a proton, and up to 200–235 °C if it is a

metal). Its structure is described as consisting of hydrophilic clusters of 40–50 Å diameter separated by channels with a hydrophobic fluorocarbon matrix (Figure 5).^{52,53}

Nafion has been used as a metal complex support.⁵³ Examples include ion exchange with Hg^{II} for the hydration of alkynes,⁵⁴ with Cr^{III} and Ce^{VI} for the oxidation of alcohols by Bu^tO^oH,⁵⁵ and by Pd(PPh₃)₄ and [Pd(PPh₃)₃(CH₃CN)]²⁺ for the carbomethoxylation of alkenes.^{56,57} For this latter catalyst, Nafion seems to act as both a support and an acid promoter. Most of these studies must be considered as exploratory. Recently, however, a complete survey of the reaction of [Pd(1,10-phen)₂]²⁺ with Nafion highlighted the importance of the nature of the solvent, the degree of catalyst loading, the experimental conditions of synthesis, and the size of the solid particles.⁵⁸ The dispersion of Nafion is increased in the composite Nafion–silica, described recently⁵⁹ and tested as a support of a bis(oxazoline)–Cu^{II} complex.⁶⁰

(ii) Incorporating by covalent bonding

Three approaches have been tested, as already described above for inorganic supports. The first attempts concern the direct reaction of transition metal carbonyls with unmodified organic polymers like poly-2-vinyl-pyridine.^{61,62} However, this kind of anchoring is restricted to only a few complexes. Various polymers have been functionalized with donor groups,^{63–72} ligand displacement reactions using these afforded the corresponding immobilized complexes. Finally, tests with modified complexes and unmodified polymers are scarce because of the low stability of these complexes under the conditions of reactions.

A large variety of polymers has been considered. In the beginning, polystyrene and styrene/divinylbenzene copolymers (Merrifield resins) were by far the most used.⁷³ Then others were tested such as polyvinyls,^{47–50,61–64} polyacrylates,^{72,74,75} and cellulose.^{76,77} Most commonly, diphenylphosphane groups were grafted on the polymeric support, either directly or via one CH₂ group.

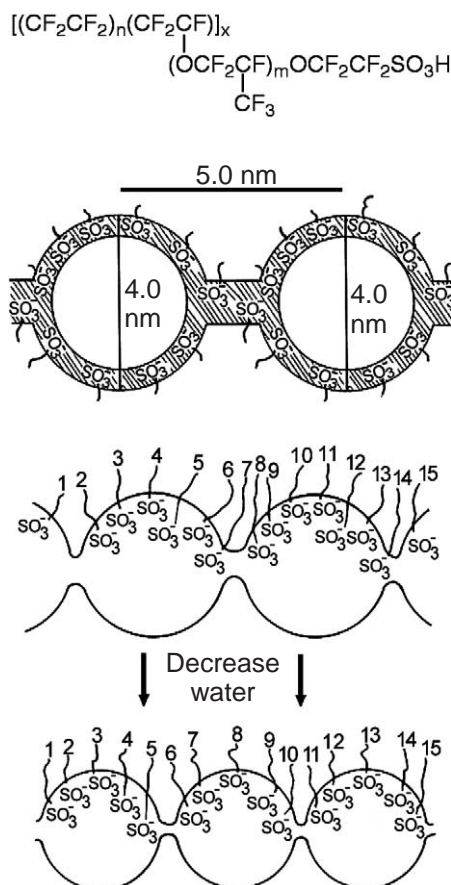


Figure 5 Chemical structure of Nafion (reproduced by permission of Elsevier from ref. 53).

The most well-developed recent examples of catalysis concern catalysts for oxidation reactions; these are essentially achiral or chiral metal–salen complexes. Taking into account a number of results suggesting the importance of a degree of mobility of the bound complex, Sherrington *et al.* synthesized a series of polymer-supported complexes in which [Mn(salen)Cl] units are immobilized in a pendant fashion by only one of the aromatic rings, to polystyrene or poly(methacrylate) resin beads of various morphology (Figure 6).^{78,79}

9.9.2.3 Immobilization by Copolymerization

In this approach the metal complexes are introduced directly in the mixture of the reactants used as components in the synthesis of the solid support. Work in this area was pioneered by Panster *et al.*⁸⁰

9.9.2.3.1 Inorganic matrices

The sol–gel processing of the functionalized complexes $(RO)_3Si \approx L/ML_n$ leads to a solid with metal entities homogeneously distributed through the whole material. The catalyst is trapped in the solid, but as the porosity and surface area can be easily tuned, access of the reactants to the metal center is possible. A detailed study of the catalytic properties of Wilkinson-type catalysts, homogeneous or heterogenized by different methods, shows that the catalysts obtained by the sol–gel method have higher stabilities but similar catalytic activities.⁸¹ A number of such entrapped catalysts were tested for catalytic isomerization, hydrogenation, and hydroformylation of olefins, and hydrogenation of α,β -unsaturated olefins; the results all confirm the superior stability of the sol–gel-based catalysts, and their reasonable activities when one considers that not all catalytic centers are accessible.^{24,82–84} Similarly, metal complexes can be mixed with the reactants for the hydrothermal synthesis of zeolites; they will thus be entrapped in the porous network of the zeolite.⁸⁵ In conclusion, the problems encountered with entrapped complexes clearly show the importance of finding new porous solids able to accommodate the metal complexes of interest, and allow for a good diffusion of the reactants and the products.

The simultaneous copolymerization of suitably modified hydrolyzable precursors of both the solid support and the coordination complexes allows modulation of the solid from rigid to highly

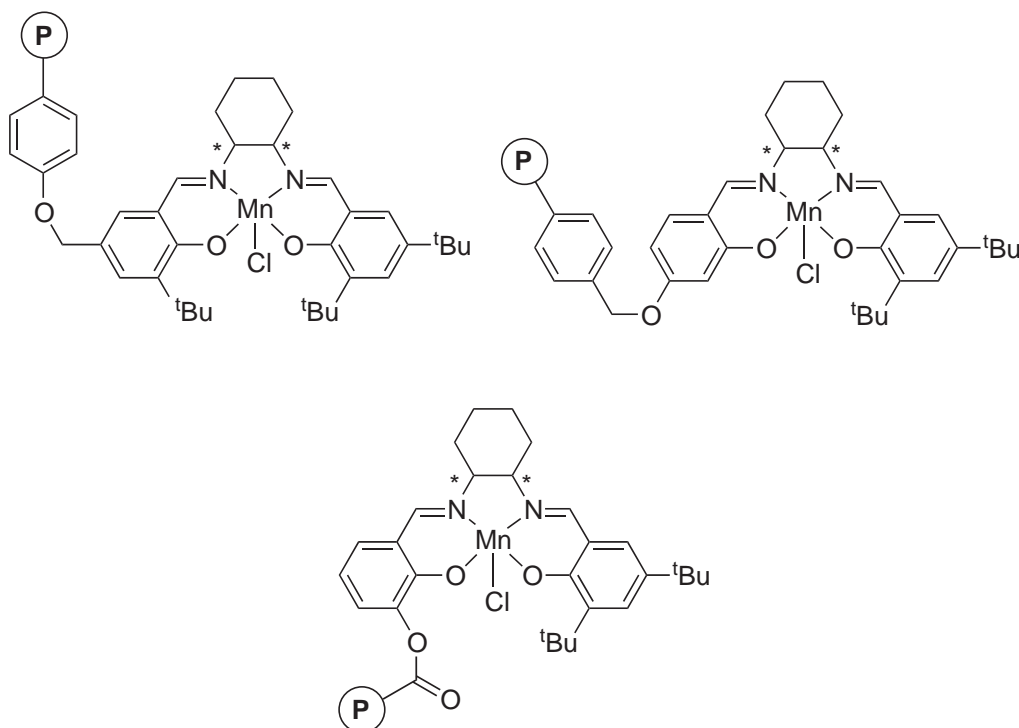


Figure 6 Immobilization of [Mn(salen)Cl] derivatives in a pendant fashion (**P** = polymer support).

flexible materials. Most of the studies concern alkyl-silyl functionalized metal complexes, with different alkoxy silanes and polysilsesquioxanes acting as network modifiers. Most of these solids have been characterized by IR, MAS NMR, EXAFS, and EDX spectroscopies, elemental analysis, and scanning electron microscopy.⁸⁶ Their porosity and swelling ability are both adjustable. The complex is linked to the matrix by a spacer which is generally a hydrocarbon chain, ensuring that it has sufficient mobility (Figure 7).⁸⁶

The limitations of the method come from the stability of the complexes under sol-gel conditions; however, even biocatalysts can be suitable for entrapment in sol-gel materials.⁸⁷

This type of solid was synthesized with complexes such as $[\text{HRh}(\text{CO})\{\text{PPh}_2(\text{CH}_2)_3\text{S}=\}_3]$ and $[\text{ClRuH}\{\text{P}(\text{O})(\text{CH}_2)_3\text{Si}=\}_3]$ (which were tested as catalysts for the hydrogenation and hydroformylation of tolan), and $[(\text{dba})\text{Pd}\{\text{P}(\text{O})(\text{CH}_2)_3\text{Si}=\}_2]$ (tested for copolymerization reactions).⁸⁸⁻⁹¹ The activity and the selectivity of these catalysts are in all cases solvent-dependent, a phenomenon explained by their swelling ability. The authors claim that no leaching is occurring.

9.9.2.3.2 Organic supports

With organic supports, the approach comprises a first step of copolymerization of a monomer and a potential ligand, with coordination of the target complex by a ligand-exchange reaction involving the polymer being the second step. Examples concern essentially chiral catalysts; this field was recently reviewed by Bianchini.⁹² Common procedures for the immobilization of chiral ligand/catalysts onto organic polymers involve radical polymerization of a chiral monomer in the presence of linkers and/or cross-linkers (styrene or divinylbenzene). All of the polymerization reactions leading to the polystyrene-immobilized catalysts have been carried out in the presence of a radical initiator such as AIBN (α, α' -azobis(*iso*-butyronitrile)) (used to obtain the (*R*)-salicylaldimine derivative: Scheme 8, polymer P1) or 2,2'-azobis(2,4-dimethylpentanenitrile) (used to obtain the (*R,S*)-vinyl-BINAPHOS derivatives: Figure 8, polymer P2). $\text{Ti}(\text{OiPr})_4$ associated to polymer P1 catalyzed the Mukaiyama condensation,⁹³ and polymer P2 was used in the asymmetric hydroformylation of styrene.⁹⁴

Seebach and co-workers copolymerized a dendritically modified TADDOL ligand with styrene (Figure 9). When associated with $\text{Ti}(\text{OiPr})_4$, the immobilized catalyst gave a very high ee (98%) for more than 20 runs in the enantioselective addition of diethylzinc to benzaldehyde.^{95,96}

Pu and co-workers incorporated atropisomeric binaphthols in polymer matrixes constituted of binaphthyl units, the macromolecular chiral ligands obtained being successfully used in numerous enantioselective metal-catalyzed reactions,⁹⁷⁻⁹⁹ such as asymmetric addition of dialkylzinc reagents to aldehydes.⁹⁹ Recently, they also synthesized a stereoregular polymeric BINAP ligand by a Suzuki coupling of the (*R*)-BINAP oxide, followed by a reduction with trichlorosilane (Figure 10).¹⁰⁰

This (*R*)-polyBINAP support, when treated with $[\text{Rh}(\text{cod})_2]\text{BF}_4$ or $[\{\text{RuCl}_2(\text{C}_6\text{H}_6)\}_2]$, afforded a heterogeneous asymmetric catalyst for hydrogenation of dehydroaminoacid derivatives and ketones.¹⁰⁰ As an extension, a copolymer with BINOL and BINAP units randomly distributed

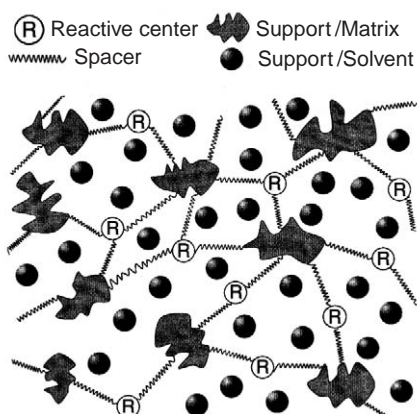


Figure 7 Schematic representation of an interphase (reproduced with the permission of Wiley-VCH from ref. 86).

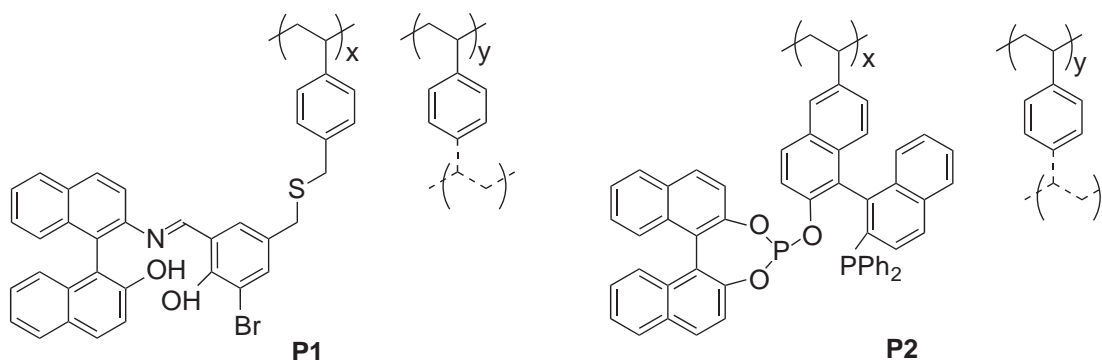


Figure 8 Immobilized chelating ligands obtained by radical polymerization.

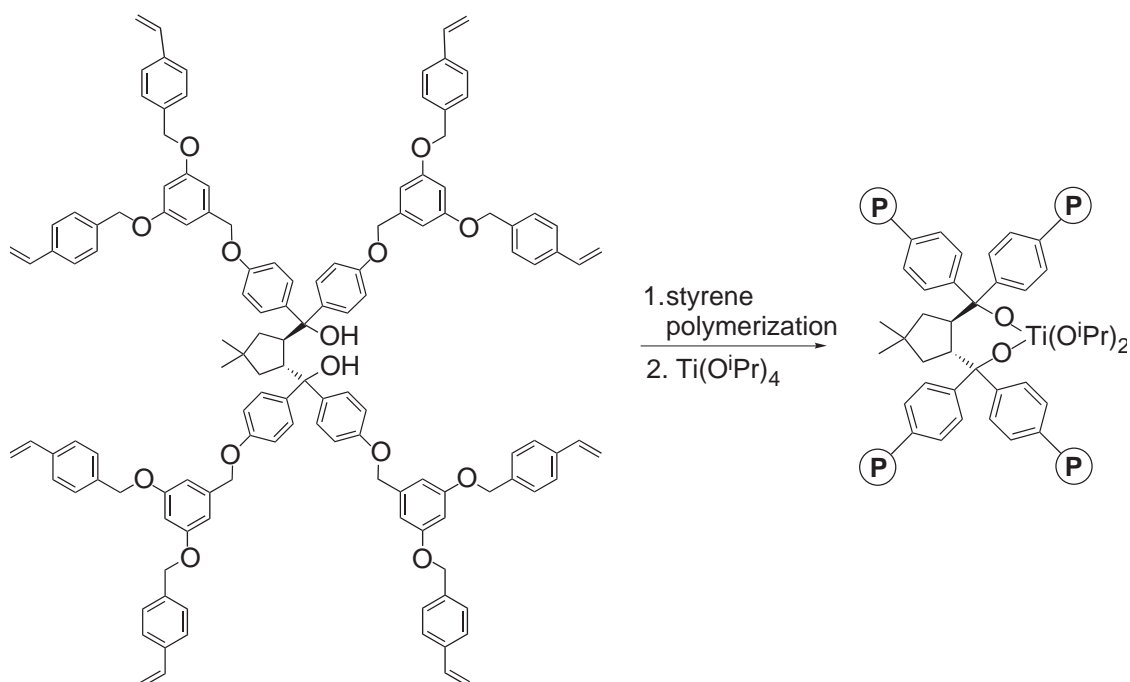


Figure 9 Supported Ti-TADDOLate catalyst for enantioselective addition of diethylzinc to benzaldehyde (**P** = polymer support).

along the polymer chain was synthesized;¹⁰¹ with $\{[\text{RuCl}_2(\text{C}_6\text{H}_6)]_2\}$ and 1,2-diphenylethylenediamine (DPEN), this BINOL–BINAP polymer afforded an efficient catalyst for the tandem asymmetric diethylzinc addition and hydrogenation of *p*-acetylbenzaldehyde.

An alternative method for the preparation of polymer-chained pendant ligands has been recently developed.¹⁰² The polymerization of the (*R*)-hydroxylpiperidinyl fragment was realized by ROMP of a bicyclic olefin with the commercially available Grubbs catalyst.

Spectacular achievements in catalytic asymmetric epoxidation of olefins using chiral Mn^{III} –salen complexes have stimulated a great deal of interest in designing polymeric analogs of these complexes and in their use as recyclable chiral catalysts. Techniques of copolymerization of appropriate functional monomers have been utilized to prepare these polymers, and both organic and inorganic polymers have been used as the carriers to immobilize these metal complexes.¹⁰³

9.9.2.4 Supported Liquid Phase Catalysts (SLPC)

Catalysis in biphasic media is one of the most elegant and efficient means to solve the problem of catalyst recovery. Many excellent reviews are available and industrial processes are currently running.^{104–107} This method is (like all others) not applicable for all situations, and is particularly

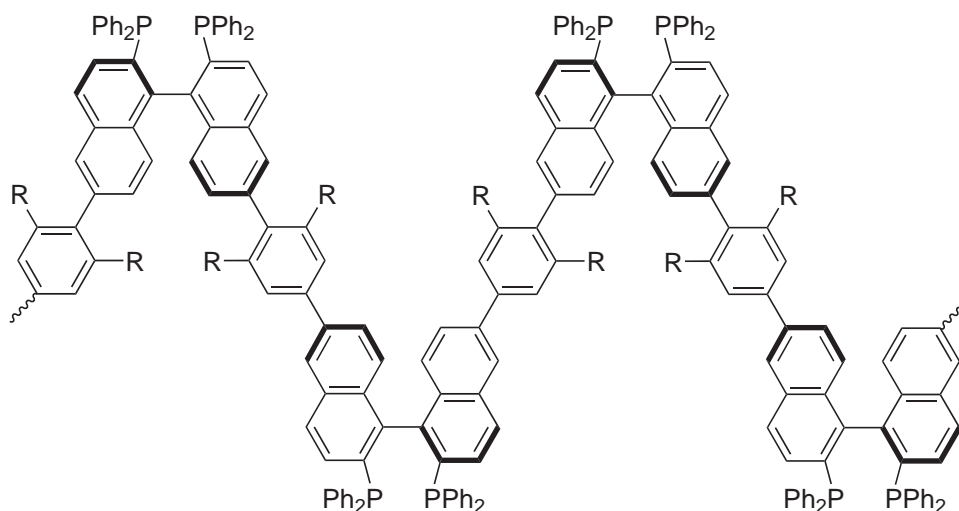


Figure 10 Optically active poly-BINAP.

unsuitable when the solubility of the reactants in the catalyst phase is too low: then the activity is confined to the interfacial surface, which is small. In these cases, supporting the catalyst in a thin film of liquid deposited on a solid of high specific surface area significantly improves the activity.

The synthesis of supported liquid phase catalysts was described for the first time in 1939.¹⁰⁸ Their domain of application and a first description of their mode of operation were later reported simultaneously by Acres *et al.*¹⁰⁹ and by Rony.^{110,111} The method, inspired by gas liquid chromatography, uses a catalyst deposited on the surface of a high-surface-area porous inorganic oxide in a thin film of a non-volatile solvent; reactants and products are in the gas phase. This technique was applied for the isomerization of 1-pentene catalyzed by RhCl_3 (in a thin film of ethylene glycol) and to the hydroformylation of propene catalyzed by $[(\text{Ph}_3\text{P})_2\text{Rh}(\text{CO})\text{Cl}]$ (in a film of benzylbutylphthalate). The amount of solvent must be large enough to constitute a small film on the solid, but low enough to avoid pore plugging that could restrict the diffusion of the reactants. The phosphine itself, molten under the reaction conditions, can serve as the solvent.^{112–115} This method seemed to be suitable only for gaseous reactants and products, since the presence of flowing organic liquids can draw the supported liquid out of the system. High reaction temperatures are, therefore, needed, which can also bring about the volatilization of the solvent involved in the liquid phase catalysts. To avoid this, membrane reactors were employed.¹¹⁶

Renewed interest in this method came recently from its adaptation to the immobilization of water/organic solvent biphasic catalysts, resulting in the so-called supported aqueous phase catalysts (SAPCs).¹¹⁷ The molecular catalyst is immobilized via water, which is hydrogen bonded to the surface silanol groups; reactants and products are in the organic phase (Figure 11)

Thus, $[\text{HRh}(\text{CO})(\text{TPPTS})_3]/\text{H}_2\text{O}/\text{silica}$ (TPPTS = sodium salt of tri(*m*-sulfophenyl)phosphine) catalyzes the hydroformylation of heavy and functionalized olefins,^{118–122} the selective hydrogenation of α,β -unsaturated aldehydes,⁸⁴ and the asymmetric hydrogenation of 2-(6'-methoxy-2'-naphthyl)acrylic acid (a precursor of naproxen).^{123,124} More recently, this methodology was tested for the palladium-catalyzed Trost–Tsuji (allylic substitution) and Heck (olefin arylation) reactions.^{125–127}

In most cases, the SAPCs are less active than their homogeneous counterparts, but more active than their liquid biphasic catalyst analogue, a phenomenon very simply interpreted as resulting from the increase of the interphase surface area which, in the case of the SAPCs, is similar to that of the silica support.

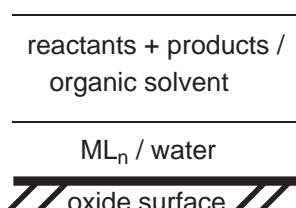


Figure 11 Principle of the SLPC catalysts.

An alternative to the supported liquid phase (SLP) method was recently proposed using the same type of solid: the supported hydrogen bonded (SHB) catalysts. First demonstrated with the zwitterionic Rh^{I} catalysts [(sulphos)Rh(cod)] (**1**) and [(sulphos)Rh(CO)₂] (**2**) (sulphos = ⁻O₃S(C₆H₄)CH₂C(CH₂PPh₂)₃), the immobilization procedure is based on the capability of the sulfonate tail of sulphos to link the silanol groups of the support via hydrogen bonds (Figure 12).

Experimental evidence of the —SO₃•••HOSi— interaction have been obtained from IR, Rh K-edge EXAFS, and CP MAS 31P NMR studies. These supported catalysts have been tested for the hydrogenation and hydroformylation of alkenes. No Rh leaching was observed.^{128–130} An extension to the immobilization of chiral metal complexes for asymmetric hydrogenation is reported below.

9.9.3 SOME REACTIONS CATALYZED BY SUPPORTED METAL COMPLEXES

A list of examples in this section is not exhaustive; rather, they have been chosen to illustrate the different approaches used for immobilization of the catalysts for important classes of organic reactions, namely hydrogenation, oxidation, and coupling reactions. Due to the major industrial importance of olefin polymerization (see Chapter 9.1), and although the objectives of immobilization of polymerization catalysts are rather different from the other examples, some references to this will also be given here.

9.9.3.1 Hydrogenation

Immobilization of homogeneous catalysts for hydrogenation reactions concerns essentially enantioselective hydrogenations, important for the synthesis of fine chemicals (see Chapter 9.2). The pioneering work of Pugin *et al.*¹³¹ concerns the synthesis of a rhodium-based catalyst, with a diphosphine–pyrrolidine-based ligand for the hydrogenation of methylacetamide cinnamate (Equation(8)).

The catalysts were prepared by the method described in Figure 2 above.

A number of Rh^{I} -diphosphine complexes were grafted on the surface of inorganic oxides such as zeolites¹³² or silica.¹³³ In the latter case, catalysts prepared by reaction of $[\text{Rh}(\text{COD})_2]\text{BF}_4$ with previously functionalized silicas give ee's up to 94.5% for this reaction.

These silica-supported catalysts (Figure 13) are, according to their authors, more advantageous because the functionalization is performed from the easily available linker, 3-isocyanato-propyl-

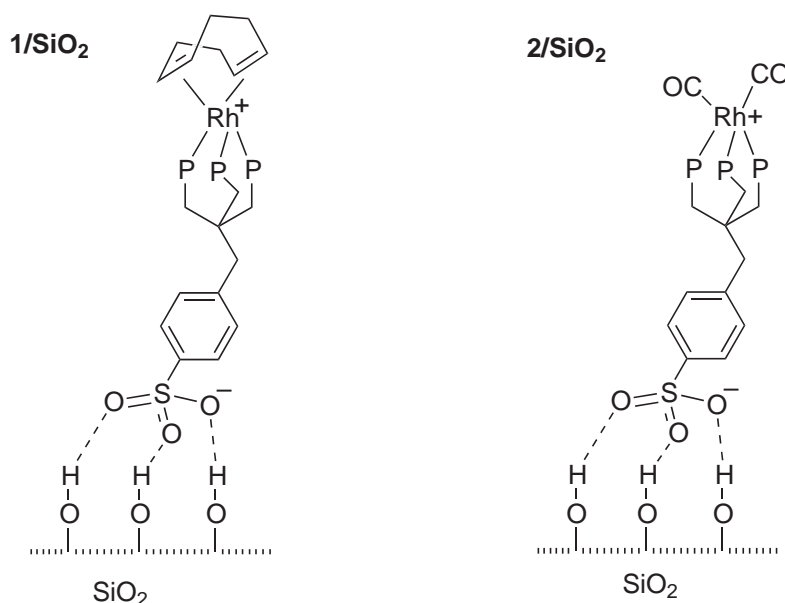


Figure 12 Principle of the SHB catalyst.

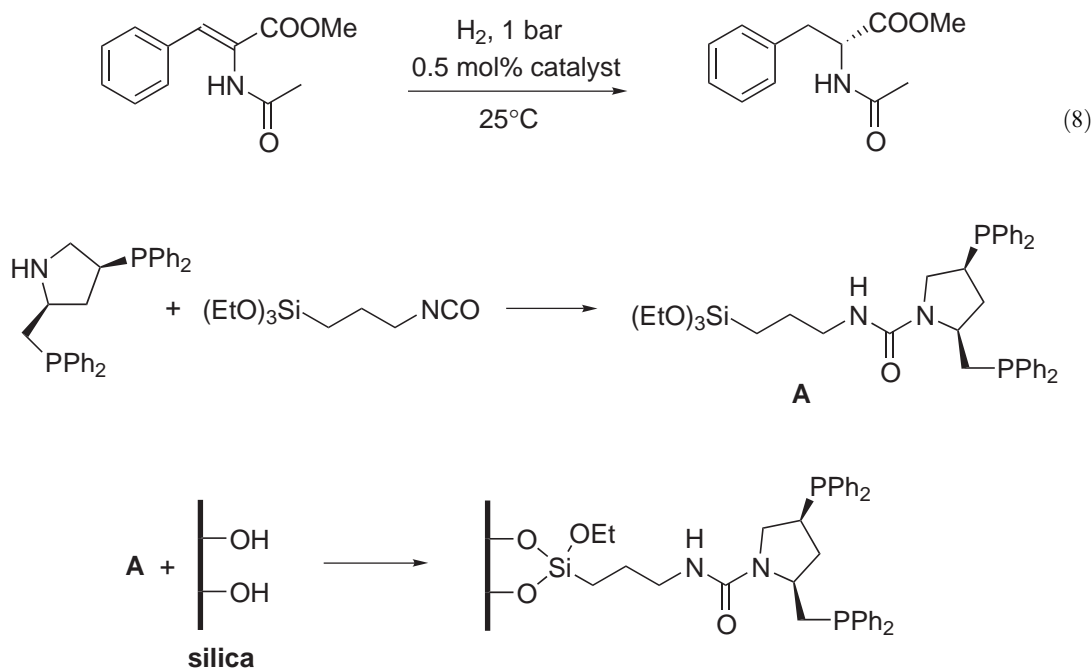


Figure 13 Method of synthesis of a silica-anchored asymmetric ligand according to Pugin.

triethoxysilane, $\text{OCN}(\text{CH}_2)_3\text{Si}(\text{OEt})_3$, and the catalysts are of low “molecular weight”. They are reportedly easy to separate and re-use. Interestingly, the catalysts obtained with these functionalized silicas from the neutral complexes $[\text{M}(\text{COD})\text{Cl}]_2$ ($\text{M} = \text{Rh}, \text{Ir}$) are as active as their homogeneous counterparts, but they show an activity drop with increasing metal loading. This effect is related to the formation of chloride-bridged Rh—or hydrogen-bridged Ir—dimers at higher metal loadings. As the authors point out, this phenomenon hampers any future industrial application of these catalysts because their productivity (expressed as volume substrate converted/volume catalysts) is too low and leads to severe handling problems.

Recently, a series of chiral diphosphines (*S,S*)-Me-Duphos, (*S,S*)-chiraphos, (*R,R*)-diop and (+)-Norphos were grafted after an ionic exchange onto Al-MCM-41;¹³⁴ complexes of the form $[\text{Rh}(\text{cod})(\text{diphosphine})]^+$ were tested for the hydrogenation of dimethylitaconate. The supported complex with (*S,S*)-methyl-Duphos reached an activity for the formation of dimethyl (*R*)-methylsuccinate as high as $\text{TON} = 4000$ with an ee close to 92%. Both (*R,R*)-diop and (*S,S*)-chiraphos give lower enantioselectivities (ee = 34% and 47% respectively). With (+)-Norphos, dimethyl-(*S*)-succinate is obtained with 47% ee. Good recyclability is claimed after four runs, and low leaching occurs (as deduced from the very low activity of the filtered solutions).

Polymerization of a BINAP derivative (Figure 14) followed by complexation with $[\{\text{RuCl}_2(\text{benzene})\}_2]$ afforded a catalyst showing high enantioselectivities for the hydrogenation of various substrates such as dehydroaminoacids, ketoesters, olefins, and ketones.¹³⁵ The catalyst may be re-used four times with negligible loss of enantioselectivity and activity.

Two different types of SHB chiral catalyst containing rhodium have been prepared so far: neutral complexes such as $[\text{Rh}(\text{nbdc})\{(R)-(R)\text{-BDPzPSO}_3\}]$, (BDPzPSO₃ = 3-(4-sulphonate)benzyl-2,4-bis(diphenylphosphino)pentane), and cationic complexes containing triflate counteranion such as $[\text{Rh}(\text{nbdc})(+)\text{-DIOP}]\text{OTf}$, $[\text{Rh}(\text{nbdc})(S)\text{-BINAP}]\text{OTf}$, and $[\text{Rh}(\text{cod})\{(R)-(R)\text{-Me-DuPHOS}\}]\text{OTf}$, (respectively **1**, **2–4** in Figure 15).^{136,137} The immobilization of the neutral complex implies a direct H-bonding interaction between the sulfonate group and the surface silanols, while the immobilization of the cationic complexes results from a electrostatic interaction with the triflate anion. Selected results for the enantioselective hydrogenation of prochiral olefins are given in the table in Figure 15; the immobilization of the complexes on silica has a beneficial effect both on conversion and enantioselectivity. No appreciable leaching of rhodium was observed, both activity and enantioselectivity being maintained within several consecutive runs.

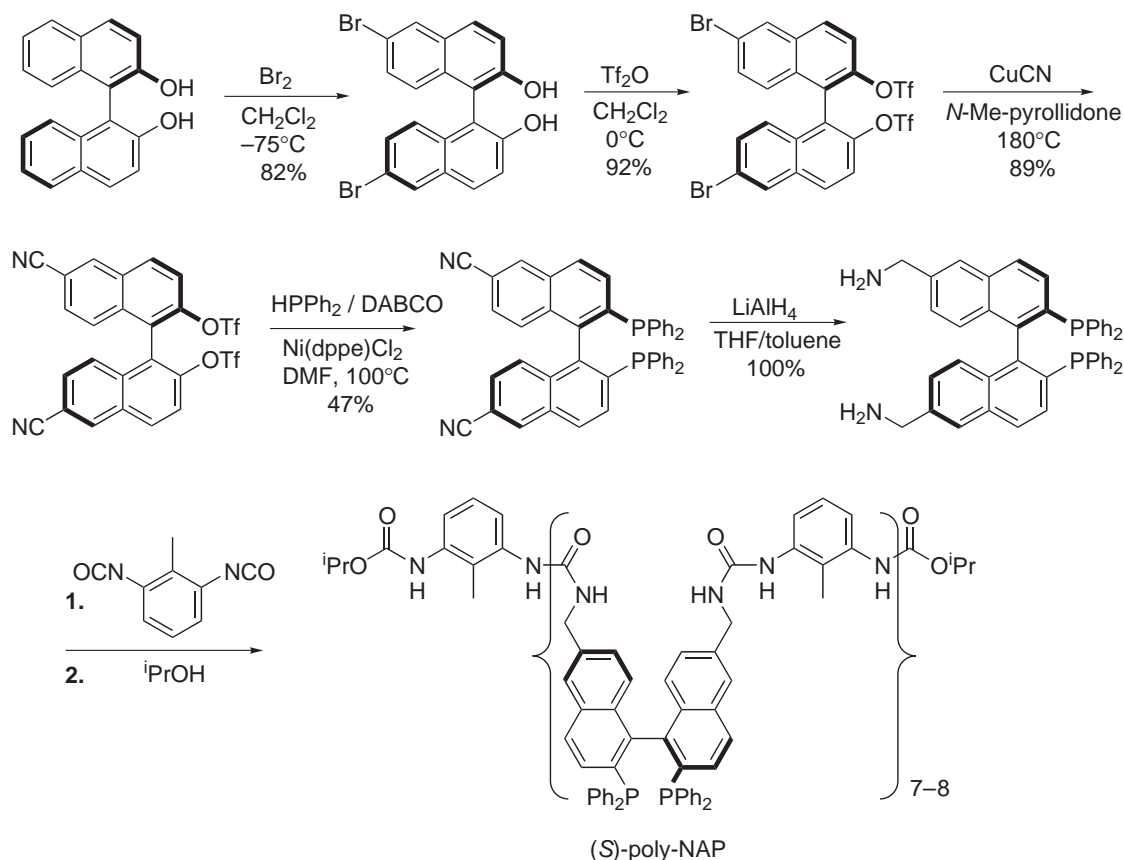


Figure 14 Synthesis of diam-BINAP and poly-BINAP.

9.9.3.2 Epoxidation

Two most remarkable systems described to perform the epoxidation of various olefins concern the heterogeneous TS-1, a titano-silicalite, and the homogeneous Mn^{III} -salen complex. The first is highly efficient for the epoxidation of small olefins by aqueous hydrogen peroxide, under mild conditions.^{138–141} However, applications of this system are restricted to small molecules, compatible with the size of the pores of the zeolite. The second type, among which the most famous are the so-called Katsuki¹⁴² and Jacobsen¹⁴³ catalysts (Figure 16), achieve the enantioselective epoxidation of simple olefins using an oxidant such as aqueous sodium hypochlorite or an organic peracid. This also required the presence of a co-oxidant such as *N*-methylmorpholine-*N*-oxide which is thought to prevent the formation of unreactive μ -oxo- Mn^{IV} dimers.

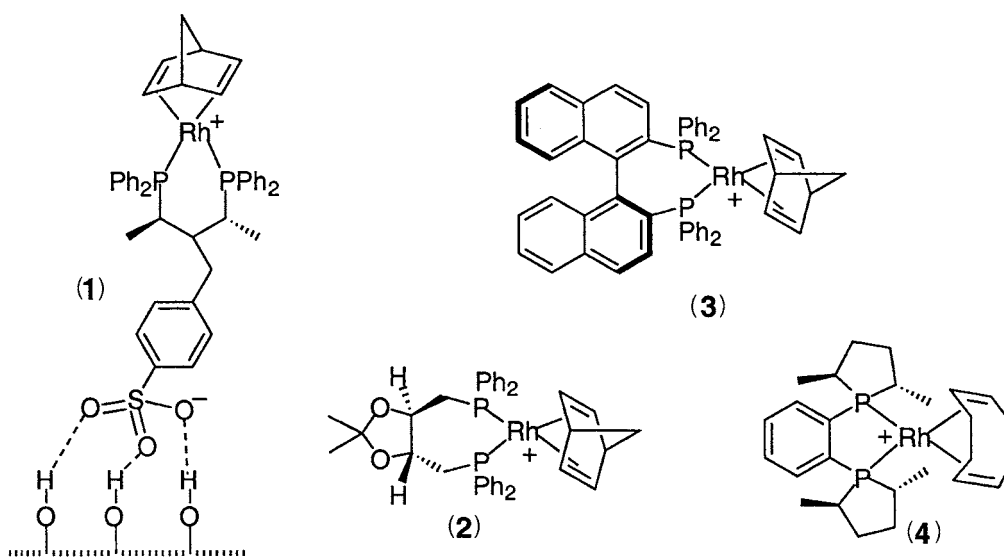
Yields up to 97% with an asymmetric induction as high as 98% ee could be achieved. Given the large range of metal-salen complexes, and reactions efficiently catalyzed by them, the study of their heterogeneous counterparts became very attractive. Although the first reports concerned essentially achiral complexes,¹⁴⁴ the most interesting and recent concern the chiral analogues.

9.9.3.2.1 Supported titanium-based catalysts

The first attempts concerned the grafting of TiCl_4 and $\text{Ti}(\text{OEt})_4$ onto the surface of silica;¹⁴⁵ this reaction was followed by an oxidation at 400°C . The surface complex is presumed to be a titanyl species in which a $\{\text{Ti}=\text{O}\}^{2+}$ unit is connected to the surface by two $\text{Si}-\text{O}-\text{Ti}$ linkages.

The performance of these catalysts is excellent, but only under anhydrous conditions, i.e., with Bu^tOOH as the oxidant. With aqueous hydrogen peroxide as oxidant, the catalytic activity drops sharply. The properties are considerably improved when the residual silanol groups are annealed by silanization.

The $\text{TiF}_4/\text{SiO}_2$ catalysts were reported as stable and efficient even with aqueous H_2O_2 as the oxidant.¹⁴⁶ Although the reasons for this are not fully understood, the authors suspect the



Precursor	T (°C)	t (h)	Substrate	Yield (%), ee (%)	
				Homogeneous ^a	Heterogeneous ^b
1	r.t.	24		100, 57(S)	100, 53(S)
2	60	4		24, 16(R)	56, 11(R)
3	60	4		9, 22(S)	41, 20(S)
3	r.t.	3		100, 25(S)	100, 30(S)
4	r.t.	0.5		>99, >99 ^c	>99, 99 ^c
4	r.t.	16		>99, 96 ^d	99, 98 ^c
4	r.t.	16		99, 96 ^e	>99, 98 ^e

^aH₂ pressure = 20 bar; solvent MeOH 20 ml, 350 rpm, substrate/Rh = 100. ^bH₂ pressure = 20 bar; solvent *n*-heptane 30 ml, 1,500 rpm, substrate/Rh = 100. ^cH₂ pressure = 8 psi.

^dH₂ pressure = 8 psi. ^eH₂ pressure = 90 psi.

Figure 15 Enantioselective SHB catalysts for hydrogenation reactions.

fluoride anion to be involved in the process of site isolation via the formation of surface SiF species, which may block any migration and/or dimerization of Ti species, even under oxidizing conditions.

The more hindered alkoxide Ti(OiPr)₄ was used as the precursor complex with surface silanols of an amorphous silica support; this reaction is reported to lead to the same environment of Ti as in TS-1, but only when the reaction is carried in cyclohexanol as the solvent. Epoxidation of octene, cyclohexenol, and norbornene with H₂O₂ in phenylethanol leads to 95–98% epoxide selectivity.¹⁴⁷

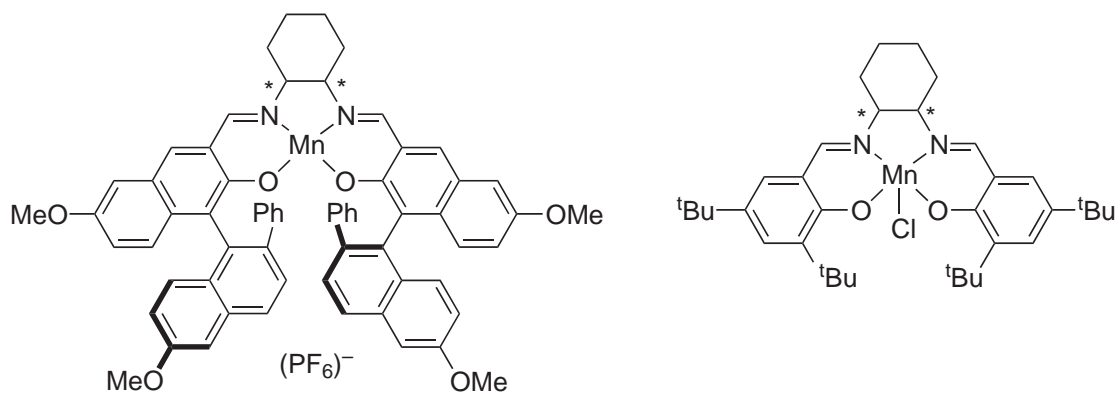


Figure 16 The Katsuki epoxidation catalysts.

For the $\text{Ti}(\text{OiPr})_4/\text{silica}$ system, the advantage of MCM-41 (a mesoporous silica) over an amorphous silica is not evident either in terms of activity or selectivity for the epoxidation of cyclohexene with H_2O_2 in *tert*-butyl-alcohol.¹⁴⁸ Nevertheless, deactivation of the catalysts seems slower, although the selectivity of the recovered catalysts is also lower (allylic oxidation:epoxidation = 1:1). Treatment of these solids with tartaric acid improves the properties of the Ti/silica system, but not of the Ti/MCM-41 system, although NMR,¹⁴⁹ EXAFS,¹⁵⁰ and IR¹⁵¹ data suggest that the same titanium species are present on both supports.

More recently, attempts to graft titanium sites onto various supports of high specific surface area and/or with more constrained environments have been described using an organometallic precursor; thus, TiCp_2R_2 is reacted with the mesoporous MCM-41 silica,¹⁵² and $\text{Ti}(\text{CH}_2\text{CMe}_3)_4$ with silica.⁴⁶ All authors claim the formation of isolated titanium sites, although the characterization of the final supported species is difficult to achieve fully and unambiguously. In particular, it is not easy to demonstrate the formation of small titanium oxide particles under the calcination conditions which lead to the catalytically active solid. The performance of these systems is very good, as long as Bu^tOOH is the oxidant (selectivity for the epoxide >95%). No direct comparison can be made between the different catalysts, the experimental conditions being too different to justify any extrapolation. It was demonstrated that catalyst leaching occurs in presence of water, due to easy hydrolysis of the Ti—O bonds.⁴⁶ A significant improvement is claimed when the surface of silica is partially silanized before the reaction with the organometallic complex.¹⁵³ These studies suggest that the epoxidation of olefins is a reaction highly sensitive to the presence of isolated sites, and much less to the hydrophilic/hydrophobic character of their immediate environment.

The zirconium alkoxides $\text{Zr}(\text{OR})_4$ are reported as inactive for the epoxidation of olefins under the conditions recommended with the titanium analogs. When synthesized by reaction of $\text{Zr}(\text{CH}_2\text{CMe}_3)_4$ with silica, followed by hydrolysis or calcination, a solid as active as the related Ti-based catalyst is obtained. The low selectivity for the formation of the epoxide is related to the fact that the same Zr centers catalyze both the formation and the decomposition of the epoxide.⁴⁶

Many catalysts generally described as mixed oxides $\text{SiO}_2\text{—TiO}_2$, but which are hoped to be in fact silica with some of the Si sites substituted by Ti, were synthesized by sol-gel procedures in order to obtain porous solids with easily accessible titanium sites. By varying the nature of the surfactant, the nature of the precursors, and the method of extraction, different solids were obtained.^{154–156} Most of these are active for the epoxidation of allylic alcohols and various olefins with alkylperoxides^{157,158} and some even with aqueous hydrogen peroxide.^{159,160} Addition of even a weak base such as NaHCO_3 led to significant improvement of their properties, in terms of both activity and selectivity,¹⁶¹ due to neutralization of the surface acid sites responsible for most of the side reactions. Introduction of amines such as $\text{R}_2\text{N—}(\text{CH}_2)_n\text{—Si}(\text{OMe})_3$ directly in the sol-gel reaction mixture further enhances the properties: the nature and concentration of the “solid” amine modifier are important parameters.¹⁶²

A solution of $\text{Ti}(\text{OiPr})_4$ in CHCl_3 was used to impregnate beads of poly(4-hydroxy-styrene-co-styrene-co-divinylbenzene) having various levels of cross-linking (Figure 17).¹⁶³ All of the resulting catalysts are better than the homogeneous one,¹⁶⁴ their activity for the epoxidation of cyclohexene with Bu^tOOH decreases with increasing cross linking in the polymer beads. Their recycling induces a sharp drop of the activity which becomes constant after the second run. Clearly, Ti is leached via exchange of the phenoxy ligand by Bu^tOOH .

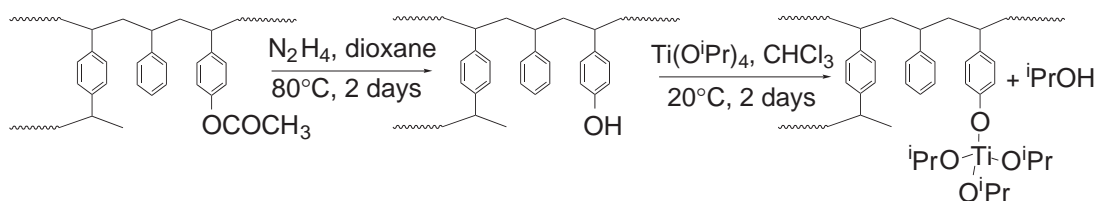


Figure 17 Preparation of a macroporous polymer-supported alkoxy-titanate.

9.9.3.2.2 Supported salen-type complexes

Essentially two types of inorganic support have been used for this: silica and zeolites. A chiral $[\text{Mn}^{\text{III}}(\text{salen})]^+$ derivative (based on *S,S*-1,2-diaminocyclohexane) was inserted into a hexagonal faujasite with EMT topology; the resulting solid showed good asymmetric inductions up to 88% ee for epoxidation of *cis-beta*-methylstyrene.¹⁶⁵ When encapsulated in a zeolite USY, a similar chiral Mn–salen complex exhibited catalytic activity similar to that of the homogeneous analog; 74% ee was obtained for the asymmetric epoxidation of ethyl cinnamate. Neither recycling nor leaching experiments were reported.¹⁶⁶

Finally, a Mn–salen derivative was grafted onto the mesoporous silica MCM-41.¹⁶⁷ Thiol-functionalized silica particles were prepared by condensing γ -mercaptopropyl-trimethoxysilane to commercially available LiChrospher-Si(100) silica gel; free radical coupling of this with a diolefin-difunctionalized Mn^{III}–salen complex led to the formation of the supported catalyst.¹⁶⁸ The modest enantioselectivity obtained for the asymmetric epoxidation of a number of olefins in the presence of MCPBA/NMO as the oxidant were explained by the fact that the complex is attached by two points, which would result in restricted mobility and unfavorable steric restriction for approach of the olefin to the catalytic sites. Anchoring of similar Mn–salen derivatives was thus carried out on siliceous MCM-41 modified with 3-aminopropyl-trimethoxysilane, through a single site linkage.¹⁶⁹ With styrene and α -methylstyrene as substrates, high chemical and enantiomeric yields (70%) for epoxidation were achieved using MCPBA/NMO as the oxidant system.

Because of the cationic nature of the Mn^{III}–salen catalysts, their heterogeneization by exchange was attempted using clays with an exchange capacity such as Na-bentonite, Na-K10, or laponite.¹⁷⁰ Both chiral and achiral salen complexes were directly exchanged; this reaction led to a homogeneous distribution of the catalyst in the clay support (Figure 18).¹⁶⁹

Depending on the size and amount of exchanged complex and the structure and surface area of the clays, the catalysts can show expanded basal spacings. A second method of synthesis consisted of the treatment of the Mn-exchanged clay with the salen ligand. All catalysts promote the epoxidation reactions with iodosylbenzene, reaching turnover numbers similar to or slightly higher than those obtained in solution with the corresponding homogeneous catalysts. However, the supported chiral catalysts give a slightly lower enantioselectivity. The recovery of the heterogeneous catalysts leads to a reduction of activity and enantioselectivity, which is not related to metal leaching but to ligand decomposition.

The synthesis of the first polymer-supported chiral Mn–salen derivatives was reported independently by Sivaram¹⁷¹ and Minutolo.^{171–173} Different monomeric Jacobsen-type units, containing two polymerizable vinyl groups, were copolymerized with styrene and divinylbenzene to yield the corresponding cross-linked polymers as a monolithic compact block.^{174–176} The less mobile system (Figure 19) with no spacer between the aromatic ring and the polymer backbone is less enantioselective.

Recently, as part of their continuing efforts on the synthesis of optically active polymer-supported epoxidation catalysts, Dhal *et al.*¹⁰³ synthesized new catalysts by copolymerizing complexes (Figure 20) with ethyleneglycol-dimethacrylate to obtain cross linked, macroporous polymer networks with high accessibility of the catalytic sites. Characterization was performed by various analytical techniques including scanning electron microscopy. The enantioselectivity for the epoxidation of asymmetric olefins with iodosylbenzene depends sharply upon the structure of the supported complex/polymer. Nevertheless, the activity of these solids is always much lower than their homogeneous analogs. However, these solids are recyclable without losing their activity and selectivity, whereas the homogeneous complex is deactivated by dimerization.

Sherrington *et al.* were the first to attempt the synthesis of chiral polymeric metal complexes by the chemical modification route,^{78,177,178} whereby the $[\text{Mn}(\text{salen})\text{Cl}]$ units are attached in a pendant fashion, by only one of the aromatic rings, to poly(styrene) or poly(methacrylate) resin beads of various morphology. Epoxidation of 1-phenylcyclohexene gave enantioselectivity values between 61% and 91%.

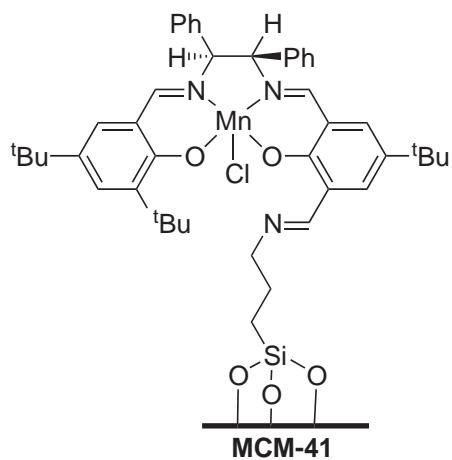


Figure 18 Heterogenized chiral salen catalyst on siliceous MCM-41 according to Kim (ref. 169).

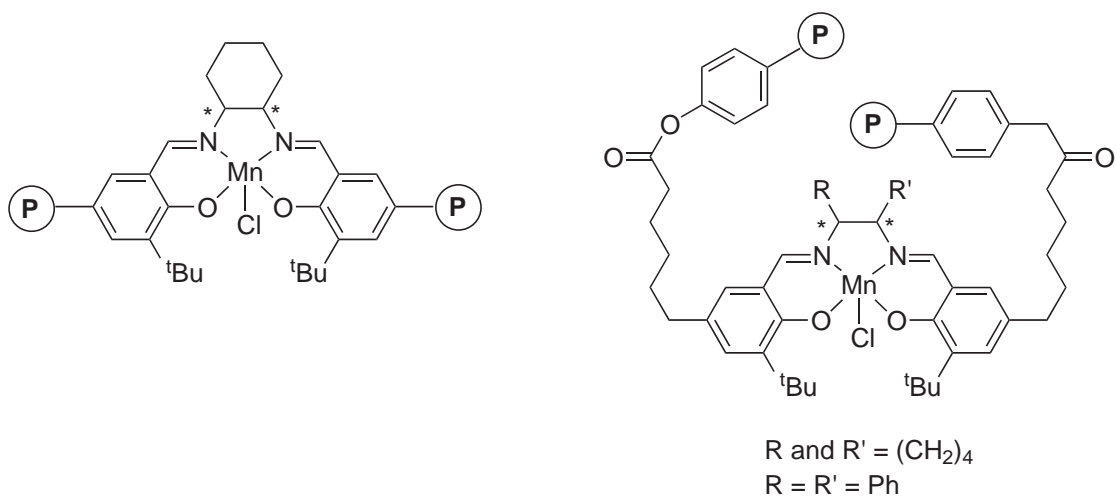


Figure 19 Polymer-supported chiral Mn(III)-salen complexes (**P** = polymer support).

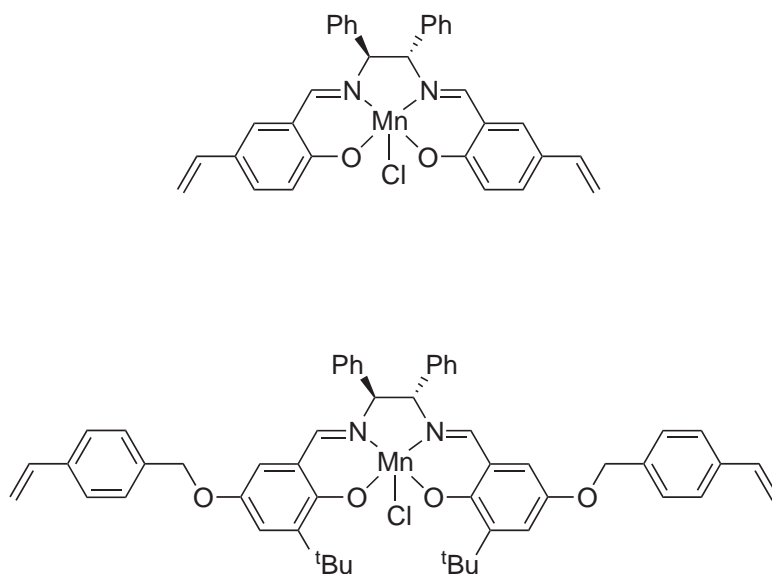


Figure 20 Chiral Mn(III)-salen monomers.

Kureshy developed a polymer-based chiral Mn–salen complex (Figure 21). Copolymerization of styrene, divinylbenzene, and 4-vinylpyridine generated highly cross-linked (50%) porous beads loaded with pyridine ligands at 3.8 mmol g^{-1} . Once the polymer was charged with the metal complex catalyst, enantioselective epoxidation of styrene derivatives was achieved with ee values in the range 16–46%.¹⁷⁹

Jacobsen proposed a related heterogeneous catalyst in which the complex is bound via an ester linkage to commercial hydroxymethylpolystyrene beads. Such catalysts are of value not only in large-scale processes, but also in the combinatorial automated synthesis of libraries of new compounds.¹⁸⁰

9.9.3.3 C—C Bond Formation by Cross Coupling

9.9.3.3.1 Heck reaction

Supported palladium catalysts for fine chemicals synthesis are generally based on metal particles. Nevertheless, a few examples are reported of the use of supported complexes as catalysts for the Heck reaction (see Chapter 9.6). Nearly all the possible immobilization methods have been tested for this reaction.

The vinylation of iodobenzene with methylacrylate was studied using palladium-based heterogeneous catalysts on modified silica by Kiviaho.¹⁸¹ All catalysts were of the type $\text{SiO}_2\text{-X-(NH)}_2\text{-Pd-L}_2$ where $\text{L} = \text{PPh}_3$ or PhCN , and $\text{X} = \text{Sn}$, Al , or Ti . The catalysts were stable and reused several times without appreciable loss in catalytic activity. The surface-bound catalytically active species arises from cleavage of two Pd-L bonds (Figure 22) and, importantly, is not just surface-bound metal particles. Both ESCA and FT-IR measurements were carried out to characterize the supported palladium complexes, and showed that the vinylation reaction had a modifying effect on the surface species (Figure 22).

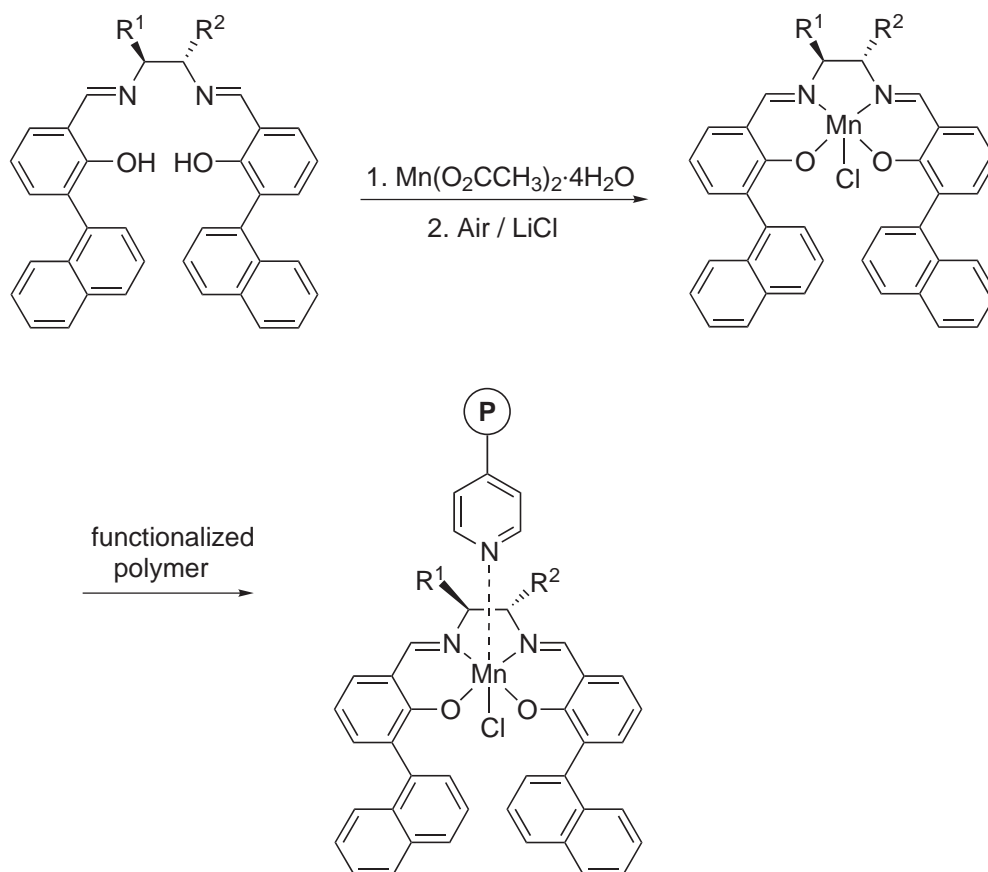


Figure 21 Kureshy's polymer-based Mn-salen complex.

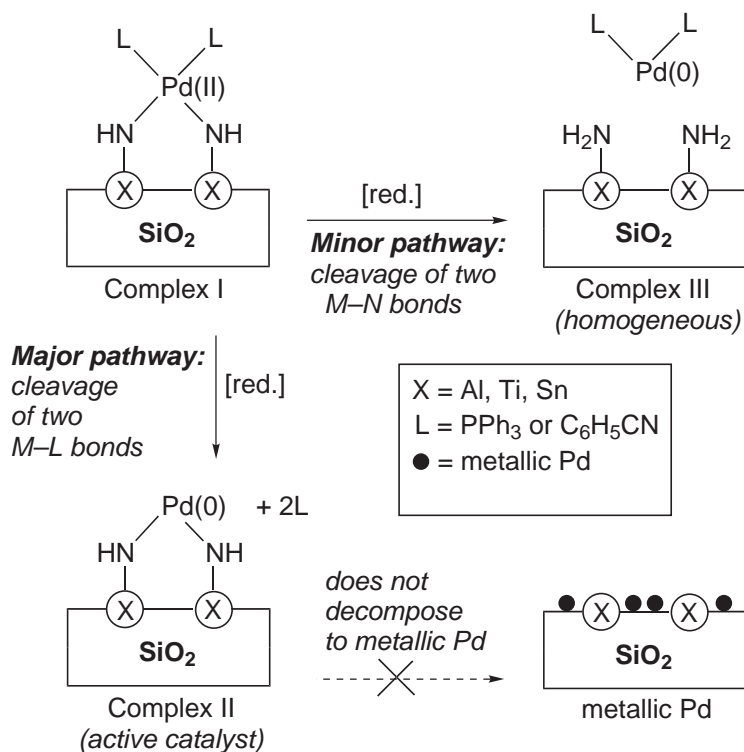


Figure 22 Proposed modification scheme for the surface complex during vinylation reaction.

The application of the supported aqueous phase catalyst method at high temperature is rather limited due to the deterioration of the water film. However, a similar concept was applied using ethylene glycol as catalyst phase. Tonks *et al.* have reported the preparation of palladium catalysts supported in ethylene glycol on glass beads, and their successful application to Heck reactions. The supported catalysts were prepared as described in Figure 23 and were tested for their ability to catalyze the Heck reaction between iodobenzene and methyl cinnamate. Other Heck reactions were examined in order to explore the scope of this methodology (Figure 23).¹²⁶

Depending on the palladium precursor (PdCl_2 or $\text{Pd}(\text{OAc})_2$) and the nature of the phosphine (TPPTS or TPPMS), Pd leaching varied from 0.2 ppm to 8.4 ppm. The use of an organic base like triethylamine, which has high affinity for coordination with Pd^{II} , may cause leaching in a significant quantity.

To overcome this drawback, a new heterogeneous catalytic system has been developed by Arai¹⁸² using Pd-TPPTS immobilized in an ethylene glycol film supported on silica, and an inorganic base instead of triethylamine. The overall reaction rate depended on several factors including solvent, inorganic base, catalyst-supporting phase, and catalyst precursor. KOAc and NaOAc were found to be suitable bases due to their high solubility in the catalyst-containing phase. Conversion of 80% was observed for coupling of iodobenzene and butyl acrylate; much lower conversion (28%) was obtained with bromobenzene, and no reaction occurred with chlorobenzene. The catalyst was recycled up to five times with freshly added KOAc, butyl acrylate, and iodobenzene. The TON is more than 200 mol product/mol Pd per cycle, and the catalyst was active for more than 1,200 turnovers without deactivation. Separation of salts formed during the reaction is the principal disadvantage of this catalytic system, as it is retained with reactants and products.

Phosphane-free ligands such as dipyriddy—amide-based systems incorporated into suitable monomers were used for the preparation of well-defined heterogeneous Heck systems via ring-opening metathesis polymerization (Figure 24).^{183,184}

The palladium-loaded chelating groups are located exclusively at the surface of the particle; they are accessible and there is no problem of diffusion. TONs of up to 210,000 were obtained for the vinylation of aryl iodides and aryl bromides. However, no recycling is reported and the authors did not exclude the participation of a dissolved (homogeneous) Pd species in the catalytic activity.

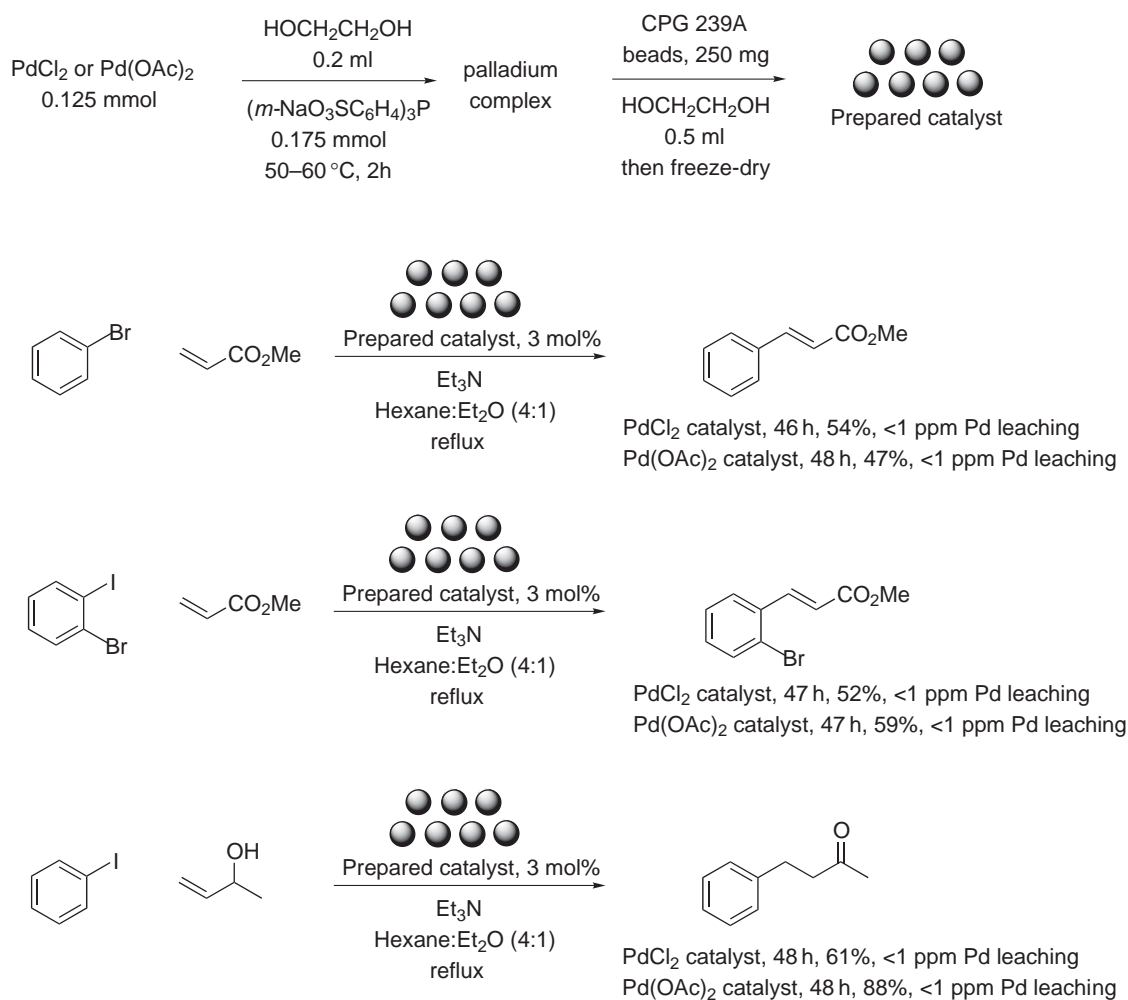
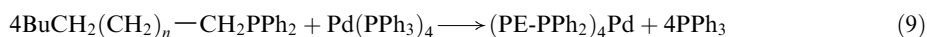


Figure 23 Preparation and activity in Heck reaction of glass bead/palladium catalysts.

9.9.3.3.2 Trost–Tsuji allylic substitution

The original catalyst for this reaction is $\text{Pd}(\text{PPh}_3)_4$. Heterogenization of this catalyst was attempted by grafting it onto functionalized polystyrene or modified silica gels,¹⁸⁵ which increased significantly the selectivity for the reaction of 3-acetoxy-5-carbomethoxy-1-cyclohexene with diphenylamine. Data concerning the stability of these solids are, however, not reported.

Bergbreiter took advantage of the temperature-dependent solubility of a polystyrene: the catalytic system is homogeneous at the temperature of reaction whereas it is heterogeneous at ambient temperature (Equation(9)).¹⁸⁶



This allows for easy reuse of the catalyst in the reaction of allylation of secondary amines like piperidine or morpholine for several runs. The leaching of palladium was less than 0.001% of the initial amount.

The supported aqueous phase methodology was applied to the system $\text{Pd}(\text{OAc})_2/5$ TPPTS, a catalytic precursor for the Trost–Tsuji reaction. The characterization of the solid by ^{31}P MAS NMR confirms the presence of $\text{Pd}^0(\text{TPPTS})_3$ as the main surface species. The catalytic properties of the solid were tested for the allylic substitution of E-cinnamylethylcarbonate by different nucleophiles such as ethyl acetoacetate, dimethyl malonate, morpholine, phenol, and 2-mercapto-pyridine. The absence of palladium leaching was demonstrated, and having solved the problem of water leaching from the solid to the organic phase, the SAP–Pd catalyst was successfully recycled several times without loss in its activity. It was used in a continuous flow experiment which

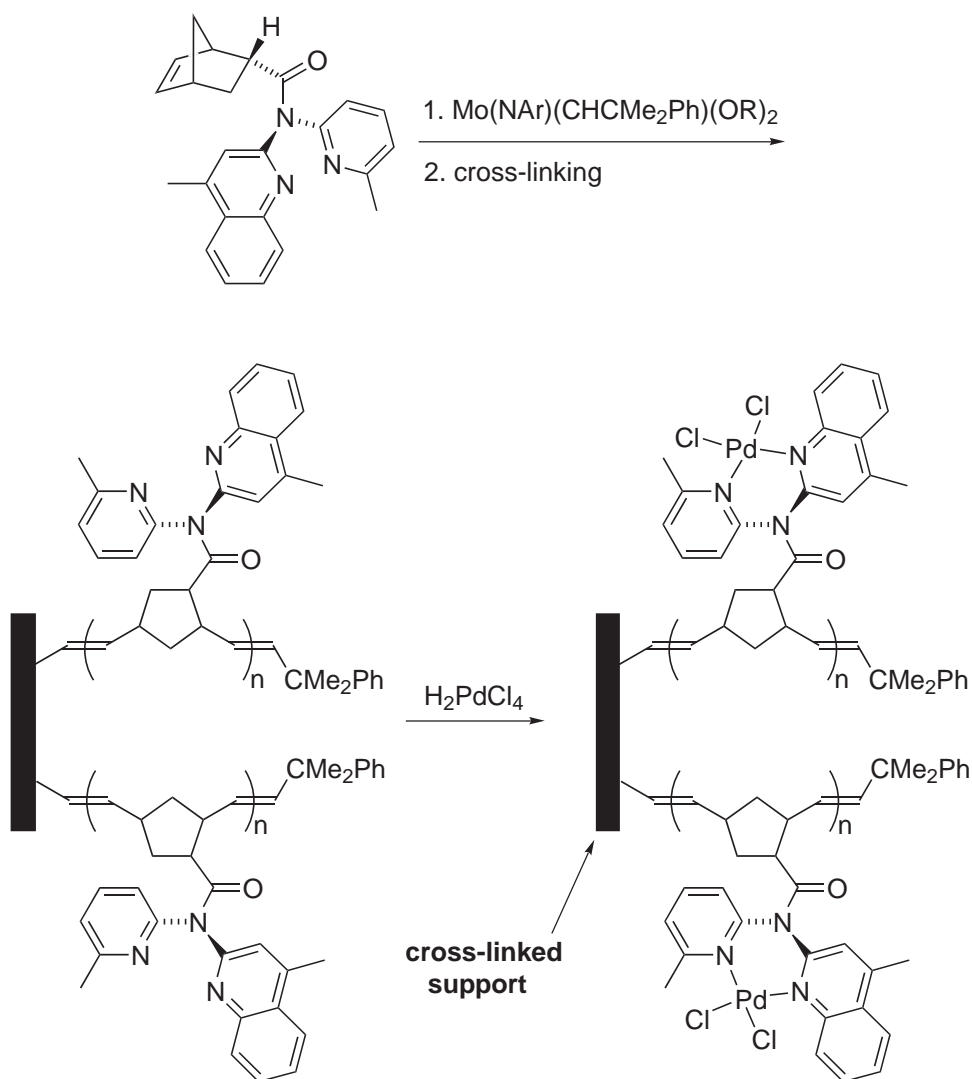


Figure 24 Synthesis of derivatized polymer beads based on substituted dipyrindyl amides via ROMP.

allowed it to reach a productivity of better than 2,200 moles of carbonate selectively converted per mole of palladium.¹⁸⁷

Some attempts to obtain a polymer-supported catalyst for chiral asymmetric allylic alkylation have been reported with some success in respect of catalyst recycling on activity, but with unsatisfactory results concerning enantioselectivity.^{188,189}

9.9.3.4 Polymerization

The heterogenization of catalysts for olefin polymerization has been extensively studied as demonstrated by the numerous publications and patents concerning this reaction, which is of major industrial importance. Polymerization differs from the other reactions in the field of heterogenization of catalysts in that recycling of the catalyst is not of interest. The major objective of the heterogenization process is to combine the advantages of the homogeneous metallocenes (polymer microstructure control, high activity) with the desirable properties of supported catalysts such as high powder density, no reactor fouling, and good morphology. A comprehensive survey of the subject was recently done by Hlatky¹⁹⁰ in a review with 326 references concerning heterogeneous single-site catalysts for olefin polymerization. Heterogenization introduces new parameters such as the nature of the support and the supporting method, which influenced the polymer structure and morphology, and Fink has analyzed how—and by which parameters—

polymerization kinetics, polymer growth, polymer morphology, and particle fragmentation are influenced by the properties of the support.^{191,192}

9.9.4 CONCLUSION AND PERSPECTIVES

Since the mid-1980s, there have been numerous attempts to heterogenize a large variety of catalysts. These efforts have so far been only partially rewarded. However, a large amount of knowledge has been accumulated, so that the synthesis of better-supported complex catalysts should be a less unpredictable matter.

Indeed, major progress has been made concerning the understanding of the mechanisms of homogeneous catalysis; the knowledge of the surface state of a number of potential supports, through spectroscopic studies and by computer modeling; and the knowledge of their surface chemistry (type, reactivity, accessibility, concentration, etc. of the surface sites). Most important is the reactivity of precursor complexes toward these sites on the supports, which follows the same general rules as those established in classical coordination or organometallic chemistry. Thus, all of the information is now in our hands to develop a more rational approach to the problem.

Particular attention is now given to the characterization of the supported species, and to the control of stability and recycling of the catalyst. The behavior of the supported catalyst under the reaction conditions (temperature, pressure, and nature of reactants and products) is certainly a less well-developed area, even though these data are valuable for the conception and development of a fully recyclable catalyst. Very few chemical engineering studies have been so far reported; they will become crucial if the objective is the synthesis of an industrial catalyst.

Most of the supports so far studied are conventional in the field of catalysis. Some new kinds of support have emerged including mesostructured materials,¹⁹³ dendrimers, organic-inorganic hybrids, and natural polymers such as polysaccharides or polyaminoacids. Nevertheless, at the moment, supported catalysts still suffer from relatively poor stability when compared to classical heterogeneous catalysts, and from limited activity when compared to homogeneous catalysts. The driving force for this research is thus to make up some of these deficits.

9.9.5 REFERENCES

1. Anderson, P. J.; Horlock, R. F.; Oliver, J. F. *Trans. Faraday. Soc.* **1965**, *61*, 2754–2762.
2. Peri, J. B. *J. Phys. Chem.* **1965**, *69*, 220–230.
3. Peri, J. B.; Hensley, A. L. J. *J. Phys. Chem.* **1968**, *72*, 2926–2933.
4. Knoezinger, H. *Adv. Catal.* **1976**, *25*, 184–271.
5. Zecchina, A.; Stone, F. S. *J. Chem. Soc. Faraday Trans. 1* **1978**, *74*, 2278–2292.
6. Maciel, G. E.; Sindorf, D. W. *J. Am. Chem. Soc.* **1980**, *102*, 7606–7607.
7. Scokart, P. O.; Rouxhet, P. G. *J. Colloid. Interface Sci.* **1982**, *86*, 96–104.
8. Boehm, H. P.; Knoezinger, H. In *Catalysis and Technology*, Vol. 4; Anderson, J. R., Boudart, M., Eds. Springer: Berlin, 1983.
9. Colbourn, E. A.; Mackrodt, W. C. *Surf. Sci.* **1984**, *143*, 391–410.
10. Garrone, E.; Stone, F. S. *Proceedings 8th International Congress in Catalysis, Berlin*. Verlag Chemie: 1984; Vol. 3.
11. Spitz, R.; Barton, J. E.; Barteau, M. A.; Staley, R. H.; Sleight, A. W. *J. Phys. Chem.* **1986**, *90*, 4067–4075.
12. Hsu, L. Y.; Shore, S. G.; d'Ornelas, L.; Choplin, A.; Basset, J. M. *Polyhedron* **1988**, *17*, 2399–2403.
13. Leonardelli, S.; Facchini, L.; Fretigny, C.; Tougne, P.; Legrand, A. P. *J. Am. Chem. Soc.* **1992**, *110*, 6412–6418.
14. Huggins, B. A.; Ellis, P. D. *J. Am. Chem. Soc.* **1992**, *114*, 2098–2108.
15. Haag, W. O.; Whitehurst, D. D. German Patent, 1 800 371 **1969**.
16. Stumm, W. *Process at the Mineral–Water Interface and Particle–Water Interface in Natural Systems*. Wiley: New York, 1992.
17. Brunelle, J. P. *Pure Appl. Chem.* **1978**, *50*, 1211–1229.
18. Che, M. *Stud. Surf. Sci. Catal.* **1993**, *75A*, 31–68.
19. Lambert, J. F.; Che, M. *J. Mol. Catal. A : Chem.* **2000**, *162*, 5–18.
20. Herron, N. *Chem. Tech.* **1989**, 542–548.
21. Pinnavaia, T. J.; Raythatha, R.; Guo-Shuh, J.; Halloran, L. J.; Hoffman, J. F. *J. Am. Chem. Soc.* **1979**, *101*, 6891–6897.
22. Raythatha, R.; Pinnavaia, T. J. *J. Catal.* **1983**, *80*, 47–55.
23. Blum, J.; Rosenfeld, A.; Polak, N.; Israelson, O.; Avnir, D.; Schumann, H. *J. Mol. Catal. A: Chem.* **1996**, *107*, 217–223.
24. Choudary, B. M.; Ravi Kumar, K.; Lakshmi Kantam, M. *J. Catal.* **1991**, *130*, 41–51.
25. Montavani, E.; Palladurio, N.; Zanotti, A. *J. Mol. Catal.* **1977**, *3*, 385–391.
26. Ichikawa, M. *Adv. Catal.* **1992**, *38*, 283–400.
27. Meier, W. M.; Olson, D. H. *Atlas of Zeolite Structure Types*. Butterworth-Heinemann: London, 1992.
28. Balkus, K. J.; Welch, A. A.; Guade, B. E. *Zeolites* **1990**, *10*, 722–729.

29. Herron, N.; Stucky, G. D.; Tolman, C. A. *J. Chem. Soc., Chem. Commun.* **1986**, 1521–1522.
30. Bowers, C.; Dutta, P. *J. Catal.* **1990**, *122*, 271–279.
31. Kowalak, S.; Weiss, R. C.; Balkus, K. J. Jr. *J. Chem. Soc., Chem. Commun.* **1991**, 57–58.
32. Herron, N. *Inorg. Chem.* **1986**, *25*, 4714–4717.
33. Thibault-Starzyk, F.; Parton, R. F.; Jacobs, P. A. *Stud. Surf. Sci. Catal.* **1994**, *84*, 1419–1424.
34. Ernst, S.; Traa, Y.; Deeg, U. *Stud. Surf. Sci. Catal.* **1994**, *84*, 925–932.
35. Paez-Mozo, E.; Medina, J. C.; Gabriunas, N. *J. Mol. Catal. A: Chem.* **1997**, *115*, 233–239.
36. Parton, R. F.; Bezoukhanova, C. P.; Thibault-Starzyk, F.; Reynders, R. A.; Grobet, P. J.; Jacobs, P. A. *Stud. Surf. Sci. Catal.*, **1994**, *84*, 813–820.
37. Bedioui, F.; De Boysson, E.; Devynck, J.; Balkus, Jr., K. J. *J. Chem. Soc., Faraday Trans.* **1991**, *87*, 3831–3834.
38. Yermakov, Y. I. *Catalysis by Supported Complexes*. Elsevier: Amsterdam, 1981.
39. Iwasawa, Y. *Tailor-made Catalysts*. Reidel: Dordrecht, The Netherlands, 1986.
40. Basset, J.-M.; Gates, B. C.; Candy, J. P.; Choplin, A.; Leconte, M.; Quignard, F.; Santini, C. C. *Surface Organometallic Chemistry: Molecular Approaches to Surface Catalysis*. Kluwer: Amsterdam, 1981.
41. Lamb, H. H.; Gates, B. C.; Knoezinger, H. *Angew. Chem., Int. Ed. Engl.* **1988**, *27*, 1162–1180.
42. Basset, J.-M.; Candy, J. P.; Choplin, A.; Nédéz, C.; Quignard, F.; Santini, C. C.; Théolier, A. *Mater. Chem. Phys.* **1991**, *29*, 5–20.
43. Choplin, A.; Quignard, F. *Trends Inorg. Chem.* **1993**, *3*, 463–478.
44. Ishii, Y.; Nakano, T.; Inada, A.; Kishigami, Y.; Sakurai, K.; Ogawa, M. *J. Org. Chem.* **1986**, *51*, 240–246.
45. Quignard, F.; Lecuyer, C.; Bougault, C.; Lefebvre, F.; Choplin, A.; Olivier, D.; Basset, J.-M. *Inorg. Chem.* **1992**, *31*, 928–830.
46. Holmes, S. A.; Quignard, F.; Choplin, A.; Teissier, R.; Kervennal, J. *J. Catal.* **1998**, *176*, 173–181.
47. Quignard, F.; Graziani, O.; Choplin, A. *Appl. Catal. A: General* **1999**, *182*, 29–40.
48. Greenwood, N. N.; Earnshaw, A. *Chemistry of the Elements*. Pergamon: Oxford, UK, 1984.
49. Hartley, F. R. *Supported Metal Complexes*. Reidel: Dordrecht, The Netherlands, 1985.
50. Behringer, K. D.; Blumel, J. *Inorg. Chem.* **1996**, *35*, 1814–1819.
51. Behringer, K. D.; Blumel, J. *Chem. Commun.* **1996**, 653–654.
52. Stinson, S. C. *Chem. Eng. News* **1982**, *60*, 22–25.
53. Seen, A. J. *J. Mol. Catal. A: Chem.* **2001**, *177*, 105–112.
54. Olah, A.; Meidar, D. *Synthesis* **1978**, 671–672.
55. Kanemoto, S.; Saimoto, H.; Oshima, Koichiro; Nozaki, H. *Tetrahedron Lett.* **1984**, *25*, 3317–3320.
56. Waller, F. J. *Brit. Polym. J.* **1984**, *16*, 239–242.
57. Chang, B.-H. *Inorg. Chim. Acta* **1988**, *150*, 245–247.
58. Seen, A. J.; Cavell, K. J.; Mau, A. W.-H.; Hodges, A. M. *J. Mol. Catal.* **1994**, *94*, 163–172.
59. Harmer, M. A.; Farneth, W. E.; Sun, Q. *J. Am. Chem. Soc.* **1996**, *118*, 7708–7715.
60. Fraile, J. M.; Garcia, J. I.; Mayoral, J. A.; Tarnai, T.; Harmer, M. A. *J. Catal.* **1999**, *186*, 214.
61. Moffat, A. J. *J. Catal.* **1970**, *18*, 193–199.
62. Moffat, A. J. *J. Catal.* **1970**, *19*, 322–329.
63. Rollmann, L. D. *Inorg. Chim. Acta* **1972**, *6*, 137–140.
64. Allum, G.; Hancock, R. D.; Howell, I. V.; McKenzie, S.; Pitkethly, R. C.; Robinson, P. J. *J. Organomet. Chem.* **1975**, *87*, 203–216.
65. Kraus, M. *Czech. Chem. Commun.* **1974**, *39*, 1318–1323.
66. Capka, M.; Czakoova, M.; Urbaniak, W.; Schubert, U. *J. Mol. Catal.* **1992**, *74*, 335–344.
67. Grubbs, R. H.; Gibbons, C.; Kroll, L. C.; Bonds, W. D., Jr.; Brubaker, C. H. Jr. *J. Am. Chem. Soc.* **1973**, *95*, 2373–2375.
68. Wild, F. R. W. P.; Gubitosa, G.; Brintzinger, H. H. *J. Organomet. Chem.* **1978**, *148*, 73–80.
69. Cermak, J.; Kviclova, M.; Blechta, V.; Capka, M.; Bastl, Z. *J. Organomet. Chem.* **1996**, *509*, 77–84.
70. Eisen, M.; Bernstein, T.; Blum, J.; Schumann, H. *J. Mol. Catal.* **1987**, *43*, 199–212.
71. Eisen, M.; Weitz, P.; Shtelzer, S.; Blum, J.; Schumann, H.; Gorella, B.; Görlitz, F. H. *Inorg. Chim. Acta* **1991**, *188*, 167–176.
72. Capka, M.; Svoboda, P.; Kraus, M.; Hettflejs, J. *Chem. Ind.* **1972**, *16*, 650–651.
73. Pomogailo, A. D.; Wohlrle, D. **1996**, 11–129.
74. Takaishi, N.; Imai, H.; Bertelo, C. A.; Stille, J. K. *J. Am. Chem. Soc.* **1976**, *98*, 5400–5402.
75. Takaishi, N.; Imai, H.; Bertelo, C. A.; Stille, J. K. *J. Am. Chem. Soc.* **1978**, *100*, 264–268.
76. Kaneda, K.; Imanaka, T. *Trends Org. Chem.* **1991**, *2*, 109–126.
77. Pracejus, H.; Bursian, M. East German patent 92031 **1972**.
78. Canali, L.; Cowan, E.; Deleuze, F.; Gibson, C. L.; Sherrington, D. C. *Chem. Commun.* **1998**, 2561–2562.
79. Sherrington, D. C.; Canali, L. *Chem. Soc. Rev.* **1999**, *28*, 85–93.
80. Deschler, U.; Kleinschmitt, P.; Panster, P. *Angew. Chem., Int. Ed. Engl.* **1986**, *25*, 237–253.
81. Schubert, U. *New J. Chem.* **1994**, *18*, 1049–1058.
82. Rosenfeld, A.; Avnir, D.; Blum, J. *J. Chem. Soc., Chem. Commun.* **1993**, 583–584.
83. Avnir, D. *Acc. Chem. Res.* **1995**, *28*, 328–338.
84. Fache, E.; Mercier, C.; Pagnier, N.; Despeyroux, B.; Panster, P. *J. Mol. Catal.* **1993**, *79*, 117–131.
85. Balkus, Jr., K. J.; Kowalak, S.; Ly, K. T.; Hargis, D. C. *Stud. Surf. Sci. Catal.* **1991**, *69*, 93–99.
86. Lindner, E.; Schneller, T.; Auer, F.; Mayer, H. A. *Angew. Chem., Int. Ed. Engl.* **1999**, *38*, 2154–2174.
87. Reetz, M. T. *Adv. Mater.* **1997**, *9*, 943–954.
88. Lindner, E.; Kemmler, M.; Mayer, H. A.; Wegner, P. *J. Am. Chem. Soc.* **1994**, *116*, 348–361.
89. Lindner, E.; Jäger, A.; Kemmler, M.; Auer, F.; Wegner, P.; Mayer, H. A.; Benez, A.; Plies, E. *Inorg. Chem.* **1997**, *36*, 862–866.
90. Lindner, E.; Jäger, A.; Auer, F.; Wegner, P.; Mayer, H. A.; Benez, A.; Adam, D.; Plies, E. *Chem. Mater.* **1998**, *10*, 217–225.
91. Lindner, E.; Jager, A.; Auer, F.; Wielandt, W.; Wegner, P. *J. Mol. Catal. A: Chem.* **1998**, *129*, 91–95.
92. Bianchini, C.; Barbaro, P. *Top. Catal.* **2002**, *19*, 17–32.

93. Mandoli, A.; Pini, D.; Orlandi, S.; Mazzini, F.; Salvadori, P. *Tetrahedron: Asymmetry* **1998**, *9*, 1479–1482.
94. Nozaki, K.; Itoi, Y.; Shilbahara, F.; Shirakawa, E.; Ohta, T.; Takaya, H.; Hiyama, T. *J. Am. Chem. Soc.* **1998**, *120*, 4051–4052.
95. Rheiner, P. B.; Sellner, H.; Seebach, D. *Helv. Chim. Acta* **1997**, *80*, 2027–2030.
96. Sellner, H.; Seebach, D. *Angew. Chem., Int. Ed. Engl.* **1999**, *38*, 1918–1920.
97. Pu, L. *Chem. Rev.* **1998**, *98*, 2405–2494.
98. Pu, L. *Chem. Eur. J.* **1999**, *5*, 2227–2232.
99. Huang, W.-S.; Hu, Q.-S.; Pu, L. *J. Org. Chem.* **1999**, *64*, 7940–7956.
100. Yu, H.-B.; Hu, Q.-S.; Pu, L. *Tetrahedron Lett.* **2000**, *41*, 1681–1685.
101. Yu, H.-B.; Hu, Q.-S.; Pu, L. *J. Am. Chem. Soc.* **2000**, *122*, 6500–6501.
102. Bolm, C.; Dinter, C. L.; Seger, A.; Hocker, H.; Brozio, J. *J. Org. Chem.* **1999**, *64*, 5730–5731.
103. Dhal, P. K.; De, B. B.; Sivaram, S. *J. Mol. Catal. A: Chem.* **2001**, *177*, 71–87.
104. Kuntz, E. G. *Chem. Tech.* **1987**, *17*, 570–575.
105. Kalck, P.; Monteil, F. *Adv. Organometal. Chem.* **1992**, *34*, 219–284.
106. Joo, F.; Katho, A. *J. Mol. Catal. A: Chem.* **1997**, *116*, 3–26.
107. Cornils, B.; Kuntz, E. G. *J. Organometal. Chem.* **1995**, *502*, 177–186.
108. Moravec, R. Z.; Schelling, W. T.; Oldershaw, C. F. *Br. Patent* **1939**, *511*, 556.
109. Acres, G. J. K.; Bond, G. C.; Cooper, B. J.; Dawson, J. A. *J. Catal.* **1966**, *6*, 139–141.
110. Rony, P. R. *Chem. Eng. Sci.* **1969**, *23*, 1021.
111. Rony, P. R. *J. Catal.* **1969**, *14*, 142–147.
112. Hjortkjaer, J.; Scurrell, M. S.; Simonsen, P. *J. Mol. Catal.* **1979**, *6*, 405–420.
113. Gerritsen, L. A.; Herman, J. M.; Scholten, J. J. F. *J. Mol. Catal.* **1980**, *9*, 241–256.
114. Eumatsu, T.; Kawakami, T.; Saitho, F.; Miura, M.; Hashimoto, H. *J. Mol. Catal.* **1981**, *12*, 11–26.
115. de Munck, N. A.; Verbruggen, M. W.; de Leur, J. E.; Scholten, J. J. F. *J. Mol. Catal.* **1981**, *11*, 331–342.
116. Kim, J. S.; Datta, R. *AichE J.* **1991**, *37*, 1657–1667.
117. Arhancet, J. P.; Davis, M. E.; Merola, J. S.; Hanson, B. E. *Nature* **1989**, *339*, 454–455.
118. Horvath, I. T. *Catal. Lett.* **1990**, *6*, 43–48.
119. Guo, I.; Hanson, Brian E.; Toth, I.; Davis, M. E. *J. Organomet. Chem.* **1991**, *403*, 221–227.
120. Guo, I.; Hanson, B. E.; Toth, I.; Davis, M. E. *J. Mol. Catal.* **1991**, *70*, 363–368.
121. Fremy, G.; Monflier, E.; Carpentier, J. F.; Castanet, Y.; Mortreux, A. *Angew. Chem., Int. Ed. Engl.* **1995**, *34*, 1474–1476.
122. Fremy, G.; Monflier, E.; Carpentier, J. F.; Castanet, Y.; Mortreux, A. *J. Catal.* **1996**, *162*, 339–348.
123. Wan, K. T.; Davis, M. E. *Nature* **1994**, *370*, 449–450.
124. Wan, K. T.; Davis, M. E. *J. Catal.* **1995**, *152*, 25–30.
125. Schneider, P.; Quignard, F.; Choplin, A.; Sinou, D. *New J. Chem.* **1996**, *20*, 545–547.
126. Tonks, L.; Anson, M. S.; Hellgardt, K.; Mirza, A. R.; Thompson, D. F.; Williams, J. M. J. *Tetrahedron Lett.* **1997**, *38*, 4319–4322.
127. dos Santos, S.; Tong, Y.; Quignard, F.; Choplin, A.; Sinou, D.; Dutasta, J. P. *Organometallics* **1998**, *17*, 78–89.
128. Bianchini, C.; Burnaby, D. G.; Evans, J.; Fradrani, P.; Meli, A.; Oberhauser, W.; Psaro, R.; Sordelli, L.; Vizza, F. *J. Am. Chem. Soc.* **1999**, *121*, 5961–5971.
129. Bianchini, C.; Dal Santo, V.; Meli, A.; Oberhauser, W.; Psaro, R.; Vizza, F. *Organometallics* **2000**, *19*, 2433–2444.
130. Bianchini, C.; Frediani, M.; Mantovani, G.; Vizza, F. *Organometallics* **2001**, *20*, 2660–2662.
131. Pugin, B.; Muller, M. *Stud. Surf. Sci. Catal.* **1993**, *78*, 107–114.
132. Corma, A.; Iglesias, M.; Mohino, F.; Sanchez, F. *J. Organomet. Chem.* **1997**, *544*, 147–156.
133. Pugin, B. *J. Mol. Catal. A: Chem.* **1996**, *107*, 273–279.
134. Holderich, W. F.; Wagner, H. H.; Valkenberg, M. H. In *Supported Catalysts and their Applications*. Sherrington, D. C., Kybett, A. P. (Eds.); Royal Society of Chemistry: London, 2001, pp 76–93.
135. ter Halle, R.; Schulz, E.; Spagnol, M.; Lemaire, M. *C. R. Acad. Sci. – Series IIC – Chemistry* **2000**, *3*, 553–556.
136. Bianchini, C.; Barbaro, P.; Dal Santo, V.; Gobetto, R.; Meli, A.; Oberhauser, W.; Psaro, R.; Vizza, F. *Adv. Synth. Catal.* **2001**, *343*, 41–45.
137. De Rege, F. M.; Morita, D. K.; Ott, K. C.; Tumas, W.; Broene, R. D. *Chem. Commun.* **2000**, 1797–1798.
138. Taramasso, M.; Perego, G.; Notari, B. U.S. Patent 4, 410, 501 **1983**.
139. Notari, B. *Stud. Surf. Sci. Catal.* **1988**, *37*, 413–426.
140. Perego, G.; Bellussi, G.; Corno, C.; Taramasso, M.; Buonomo, F. *Stud. Surf. Sci. Catal.* **1986**, *28*, 129–136.
141. Notari, B. *Stud. Surf. Sci. Catal.* **1991**, *60*, 243–256.
142. Katsuki, T. *J. Mol. Catal. A: Chem.* **1996**, *113*, 87–107.
143. Jacobsen, E. N. Transition Metal-catalyzed Oxidations: Asymmetric Epoxidation. In *Comprehensive Organometallic Chemistry II*; Abel, E. N.; Stone, F. G. A.; Wilkinson, E., Eds.; Pergamon: Oxford, UK, 1995; Vol. 12, Chapter 11.1, pp 1097–1135.
144. Bied-Charreton, C.; Frostin-Rio, M.; Pujol, D.; Gaudemer, A.; Audebert, R.; Idoux, J. P. *J. Mol. Catal.* **1982**, *16*, 335–348.
145. Sheldon, R. A. *J. Mol. Catal.* **1980**, *7*, 107–126.
146. Jorda, E.; Tuel, A.; Teissier, R.; Kervennal, J. *J. Chem. Soc., Chem. Commun.* **1995**, 1775–1776.
147. Capel-Sanchez, M. C.; Campos-Martin, J. M.; Fierro, J. L. G.; de Frustos, M. P.; Polo, P. *Chem. Commun.* **2000**, 855–856.
148. Fraile, J. M.; Garcia, J. I.; Mayoral, J. A.; Vispe, E.; Brown, D. R.; Naderi, M. I. *Chem. Commun.* **2001**, 1510–1511.
149. Fraile, J. M.; Garcia, J. L.; Mayoral, J. A.; de Menorval, L. C.; Rachdi, F. *J. Chem. Soc., Chem. Commun.* **1995**, 539–540.
150. Fraile, J. M.; Garcia, J. L.; Mayoral, J. A.; Proietti, M. G.; Sanchez, M. C. *J. Phys. Chem.* **1996**, *100*, 19484–19488.
151. Fraile, J. M.; Garcia, J. L.; Mayoral, J. A.; Vispe, E. *J. Catal.* **2000**, *189*, 40–51.
152. Maschenmeyer, T.; Rey, F.; Sankar, G.; Thomas, J. M. *Nature* **1995**, 159–160.
153. Holmes, S. A.; Quignard, F.; Choplin, A.; Teissier, R.; Kervennal, J. *J. Catal.* **1998**, *176*, 182–191.
154. Neumann, R.; Chava, M.; Levin, M. *J. Chem. Soc., Chem. Commun.* **1993**, 685–686.

155. Dutoit, D. C. M.; Schneider, M.; Baiker, A. *J. Catal.* **1995**, *153*, 165–176.
156. Klein, S.; Thorimbert, S.; Maier, W. F. *J. Catal.* **1996**, 476–487.
157. Hutter, R.; Mallat, T.; Baiker, A. *J. Catal.* **1995**, *153*, 177–189.
158. Dusi, M.; Mallat, T.; Baiker, A. *J. Mol. Catal.* **1999**, *138*, 15–23.
159. D'Amore, M. B.; Schwarz, S. *Chem. Commun.* **1999**, 121–122.
160. Kochkar, H.; Figueras, F. *J. Catal.* **1997**, *171*, 420–430.
161. Dusi, M.; Mallat, T. *J. Catal.* **1999**, *187*, 191–201.
162. Muller, C. A.; Schneider, M.; Mallat, T.; Baiker, A. *App. Catal. A: General* **2000**, *201*, 253–261.
163. Deleuze, H.; Schultze, X.; Sherrington, D. C. *J. Mol. Catal. A: Chem.* **2000**, *159*, 257–267.
164. Jorgensen, K. A. *Chem. Rev.* **1989**, *89*, 431–459.
165. Ogunwumi, S. B.; Bein, T. *Chem. Commun.* **1997**, 901–902.
166. Sabater, M. J.; Corma, A.; Domenech, A.; Fornés, V.; Garcia, H. *Chem. Commun.* **1997**, 1285–1286.
167. Sutra, P.; Brunel, D. *Chem. Commun.* **1996**, 2485–2486.
168. Pini, D.; Mandoli, A.; Orlandi, S.; Salvadori, P. *Tetrahedron: Asymmetry* **1999**, *10*, 3883–3886.
169. Kim, G.-J.; Shin, J.-H. *Tetrahedron Lett.* **1999**, *40*, 6827–6830.
170. Fraile, J. M.; Garcia, J. I.; Massam, J.; Mayoral, J. A. *J. Mol. Catal. A: Chem.* **1998**, *136*, 47–57.
171. De, B. B.; Lohray, B. B.; Sivaram, S.; Dhal, P. K. *Tetrahedron: Asymmetry* **1995**, *6*, 2105–2108.
172. Minutolo, F.; Pini, D.; Petri, A.; Salvadori, P. *Tetrahedron: Asymmetry* **1996**, *7*, 2293–2302.
173. Minutolo, F.; Pini, D.; Salvadori, P. *Tetrahedron Lett.* **1996**, *37*, 3375–3378.
174. Samsel, E. G.; Srinivasan, K.; Kochi, J. K. *J. Am. Chem. Soc.* **1985**, *107*, 7606–7617.
175. Wu, M. H.; Jacobsen, E. N. *Tetrahedron Lett.* **1997**, *38*, 1693–1696.
176. Schaus, S. E.; Branalt, J.; Jacobsen, E. N. *J. Org. Chem.* **1998**, *63*, 403–405.
177. Canali, L.; Sherrington, D. C.; Deleuze, H. *React. Funct. Polym.* **1999**, *40*, 155–168.
178. Canali, L.; Cowan, E.; Deleuze, H.; Gibson, C. L.; Sherrington, D. C. *J. Chem. Soc. Perkin Trans. 1* **2000**, 2055–2066.
179. Kureshy, R. I.; Khan, N. H.; Abdi, S. H. R.; Iyer, P. *React. Funct. Polym.* **1997**, *34*, 153–160.
180. Annis, D. A.; Jacobsen, E. N. *J. Am. Chem. Soc.* **1999**, *121*, 4147–4154.
181. Kiviaho, J.; Hanaoka, T.; Kubota, Y.; Sugi, Y. *J. Mol. Catal. A: Chem.* **1995**, *101*, 25–31.
182. Bhanage, B. M.; Shirai, M.; Arai, M. *J. Mol. Catal. A: Chem.* **1999**, *145*, 69–74.
183. Buchmeiser, M. R.; Kroll, R.; Wurst, K.; Schareina, T.; Kempe, R.; Eschbaumer, C.; Schubert, U. *Macromol. Symp.* **2001**, *164*, 187–196.
184. Buchmeiser, M. R.; Schareina, T.; Kempe, R.; Wurst, K. *J. Organomet. Chem.* **2001**, *634*, 39–46.
185. Trost, B. M.; Keinan, E. *J. Am. Chem. Soc.* **1978**, *100*, 7779–7782.
186. Bregbreiter, D. E.; Weatherford, D. *J. Org. Chem.* **1989**, *54*, 2726–2732.
187. dos Santos, S.; Quignard, F.; Sinou, D.; Choplin, A. *Top. Catal.* **2000**, *13*, 311–318.
188. Bao, M.; Nakamura, H.; Yamamoto, Y. *Tetrahedron Lett.* **2000**, *41*, 131–134.
189. Park, H.-J.; Han, J. W.; Seo, H.; Jang, H.-Y.; Chung, Y. K.; Suh, J. *J. Mol. Catal. A: Chem.* **2001**, *174*, 151–157.
190. Hlatky, G. G. *Chem. Rev.* **2000**, *100*, 1347–1376.
191. Fink, G.; Steinmetz, B.; Zechlin, J.; Przybyla, C.; Tesche, B. *Chem. Rev.* **2000**, *100*, 1377–1390.
192. Fink, G.; Tesche, B.; Korber, F.; Knoke, S. *Macromol. Symp.* **2001**, *173*, 77–87.
193. Trong On, D.; Desplandier-Giscard, D.; Danumah, C.; Kaliaguine, S. *Appl. Catal. A: General* **2001**, *222*, 299–357.

9.10

Electrochemical Reactions Catalyzed by Transition Metal Complexes

A. DERONZIER and J.-C. MOUTET

Université Joseph Fourier-CNRS, Grenoble, France

9.10.1	INTRODUCTION	472
9.10.2	BASIC PRINCIPLES	472
9.10.3	ELECTROCATALYTIC REDUCTION OF PROTONS AND HYDRIDE TRANSFER REACTIONS	473
9.10.3.1	Metal Hydride Complexes: Electrogenation and Electrocatalytic Dihydrogen Evolution	473
9.10.3.1.1	<i>Transition metal macrocycles</i>	474
9.10.3.1.2	<i>Polypyridyl complexes</i>	475
9.10.3.1.3	<i>Phosphine complexes</i>	476
9.10.3.1.4	<i>Miscellaneous complexes</i>	476
9.10.3.2	Electrochemically Driven Hydride Transfer Reactions	477
9.10.3.2.1	<i>Electrocatalytic regeneration of reduced nicotinamide cofactors</i>	477
9.10.3.2.2	<i>Electrocatalytic hydrogenation of organics</i>	477
9.10.4	ELECTROCATALYTIC REDUCTION OF CARBON DIOXIDE	478
9.10.4.1	Polypyridyl Metal Complexes	479
9.10.4.1.1	<i>Re(bpy)(CO)₃Cl and related complexes</i>	479
9.10.4.1.2	<i>[Ru(bpy)₂(CO)₂]²⁺ and related complexes</i>	480
9.10.4.1.3	<i>Other polypyridyl metal complexes</i>	481
9.10.4.2	Metal Complexes with Macrocycles	482
9.10.4.2.1	<i>Phthalocyanine complexes</i>	482
9.10.4.2.2	<i>Porphyrin complexes</i>	482
9.10.4.2.3	<i>Cyclam and other polyazamacrocyclic complexes</i>	483
9.10.4.3	Phosphine Complexes and Miscellaneous Complexes	484
9.10.4.3.1	<i>Phosphine complexes</i>	484
9.10.4.3.2	<i>Other complexes</i>	484
9.10.4.4	Carboxylation of Organic Substrates	484
9.10.5	ELECTROCATALYTIC REDUCTION OF ORGANIC HALIDES	485
9.10.5.1	Polypyridyl Complexes	485
9.10.5.1.1	<i>Reductive homo- and heterocoupling of organic halides</i>	485
9.10.5.1.2	<i>Carbonylation of organic halides</i>	486
9.10.5.2	Phosphine Complexes	486
9.10.5.2.1	<i>Electroreductive coupling of organic halides</i>	486
9.10.5.2.2	<i>Carbonylation and carboxylation of organic halides</i>	487
9.10.5.3	Schiff Bases and Macrocyclic Nickel and Cobalt Complexes	487
9.10.5.3.1	<i>Ni^{II} and Co^I Schiff base complexes</i>	487
9.10.5.3.2	<i>Ni^{II} complexes of cyclams and other tetradentate N-ligands</i>	488
9.10.5.3.3	<i>Vitamin B₁₂ derivatives and model complexes</i>	489
9.10.6	ELECTROCATALYTIC REDUCTION OF DINITROGEN AND NITROGEN OXIDES	490
9.10.6.1	Electrocatalytic Activation of Dinitrogen	490
9.10.6.2	Electrocatalytic Conversion of Nitrate to Ammonia	490
9.10.6.3	Electrocatalytic Reduction of Nitrite and Nitric Oxide	491
9.10.6.3.1	<i>Metal complexes of nitrogen macrocycles</i>	491
9.10.6.3.2	<i>Polypyridyl complexes</i>	492

9.10.6.3.3 Polyaminocarboxylate complexes	492
9.10.6.4 Electrochemical Sensors for Nitrite and Nitric Oxide Determination	492
9.10.7 ELECTROCATALYTIC REDUCTION AND ACTIVATION OF DIOXYGEN	493
9.10.7.1 Electrocatalytic Four-electron Reduction of Dioxygen	493
9.10.7.2 Electrocatalytic P-450 Model Systems	495
9.10.7.3 The Gif-Orsay System	496
9.10.8 ELECTROCATALYTIC OXIDATION OF WATER AND ORGANICS	497
9.10.8.1 Oxidation of Water	497
9.10.8.2 Oxidation of Organics	498
9.10.9 REFERENCES	500

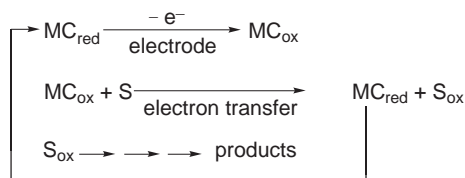
9.10.1 INTRODUCTION

Electrochemistry is a major technique for studying and understanding the redox chemistry of metal complexes. Most of the papers that have appeared in the literature since the early 1980s about new metal complexes contain a description of their electrochemical properties. Another important aspect of the electrochemistry of metal complexes is that the principles of metal complex catalysis can be transferred to the catalysis of electrochemical reactions. The electrode can replace oxidants or reductants to generate selectively low- or high-valent metal species, and active intermediates through coordination of substrates at a metal center. The objective of electrocatalysis is to drive highly efficient and selective oxidation or reduction of substrates, at modest potential and in mild, clean conditions. Studies on electrocatalysis with metal complexes are also of great interest for the understanding of catalytic redox processes, especially those involving model complexes of metalloenzymes.

The aim of this overview is first to present the general principles of electrocatalysis by metal complexes, followed by a series of selected examples published over the last 20 years illustrating the major electrochemical reactions catalyzed by metal complexes and their potential applications in synthetic and biomimetic processes, and also in the development of sensory devices. The area of metal complex catalysts in electrochemical reactions was reviewed in 1990.¹

9.10.2 BASIC PRINCIPLES

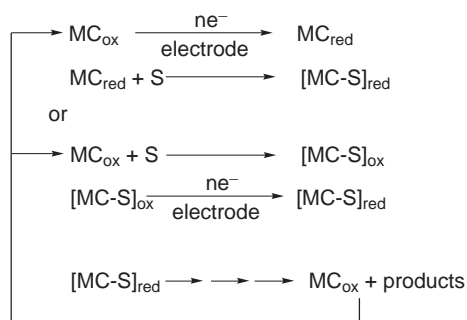
Indirect electrochemical processes combine a heterogeneous electron transfer reaction with a homogeneous process. The redox reagent formed at the electrode/electrolyte interface reacts with the substrate in a homogeneous reaction and can be subsequently regenerated at the electrode.² In principle electrocatalysts can be classified into two groups according to the reaction mechanism they undergo in the homogeneous step.³ When the redox reaction is a pure, outer-sphere electron transfer the process is called “redox catalysis.”³ This mechanism is depicted in [Scheme 1](#) for oxidation. In this process, the metal complex acts only as a shuttle to transfer electrons from the electrode to the substrate S. Basically the coordination sphere of the complex remains unchanged in the course of the catalysis (outer-sphere mechanism). The main interest of redox catalysis is to accelerate sluggish electrode reactions.²



Scheme 1

A more interesting situation is found when the homogeneous redox reaction is combined with a chemical reaction between the electrocatalyst and the substrate. In this case, the catalytic process is called “chemical catalysis.”³ This mechanism is depicted in [Scheme 2](#) for reduction. The coupling of the electron transfer and the chemical reaction takes place *via* an inner-sphere mechanism and involves the formation of a catalyst–substrate [MC–S] complex. Here the selectivity of the mechanism is determined by the chemical step. Metal complexes are ideal candidates

for such processes as compared to organic electrocatalysts. They possess the advantage of a great variation in their structure and reactivity by varying the central metal atom or the ligands. Furthermore, very active intermediates can be created through the coordination of substrates at the metal center.



Scheme 2

Homogeneous catalytic processes can be transformed to heterogeneous systems *via* the immobilization of transition metal catalysts onto an electrode surface by different surface derivatization techniques.^{4,5} From a general point of view, electrocatalysis using an electrode modified by a layer of catalyst has a number of obvious advantages over the homogeneous case, including faster regeneration of the active form of the catalyst, easier recovery of products and catalyst, and the use of much lower quantities of a catalyst highly concentrated in the reaction layer.^{4,5} The immobilization of the catalyst on the electrode surface can avoid solubility problems and can also provide some stabilization, thus allowing the turnover numbers to increase as compared to the analogous homogeneous system. Some selected examples of efficient metal complexes-based electrode materials for applications in electrosynthesis and in electrochemical sensing are also presented in this overview.

9.10.3 ELECTROCATALYTIC REDUCTION OF PROTONS AND HYDRIDE TRANSFER REACTIONS

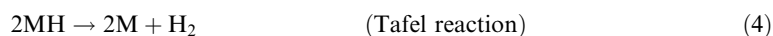
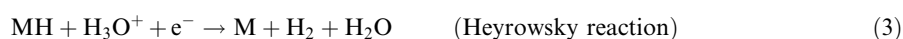
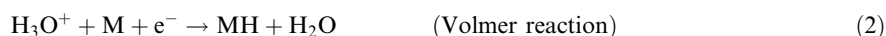
The reduction of protons is one of the most fundamental chemical redox reactions. Transition metal-catalyzed proton reduction was reviewed in 1992.⁶ The search for molecular electrocatalysts for this reaction is important for dihydrogen production, and also for the electrosynthesis of metal hydride complexes that are active intermediates in a number of electrocatalytic systems.

9.10.3.1 Metal Hydride Complexes: Electrogeneration and Electrocatalytic Dihydrogen Evolution

It is well accepted⁷ that the electroreduction of proton to dihydrogen (Equation (1)) at metal surfaces proceeds via the Volmer–Heyrowsky–Tafel reaction mechanism depicted in Equations (2)–(4).



Hydrogen electrosorbed at the metal (M) electrode surface (Equation (2)) is further desorbed electrochemically (Equation (3)) or chemically (Equation (4)).



Proton electroreduction catalyzed by metal complexes is different from reduction at a metal electrode. It definitely involves the formation of metal hydride species through protonation of electroreduced, low-oxidation-state metal complexes that function as Brønsted base (Equation (5)). From protonated

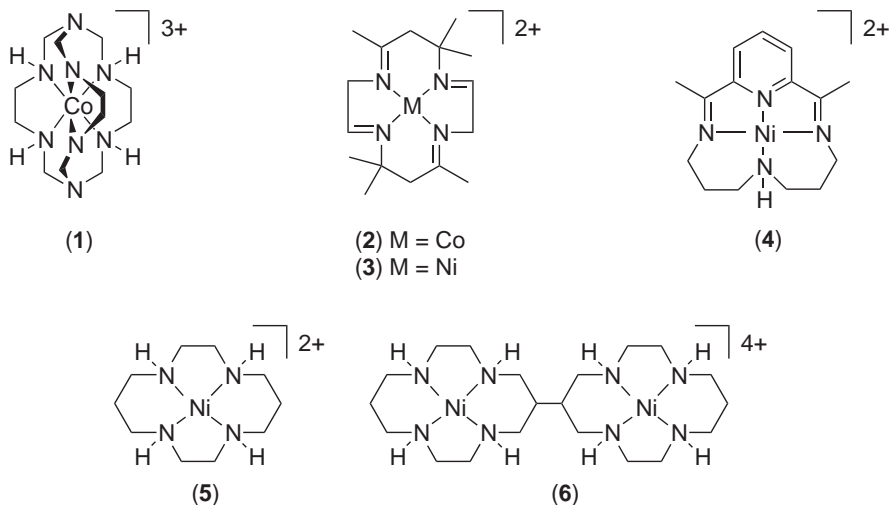
metal complexes, dihydrogen can be liberated in one of several possible ways. It could be generated homolytically by a bimolecular reaction (Equation (6)), or heterolytically through a proton hydride reaction (Equation (7)). In cases where hydride complexes are stable, dihydrogen evolution can be enforced by electroreduction (Equation (8)).



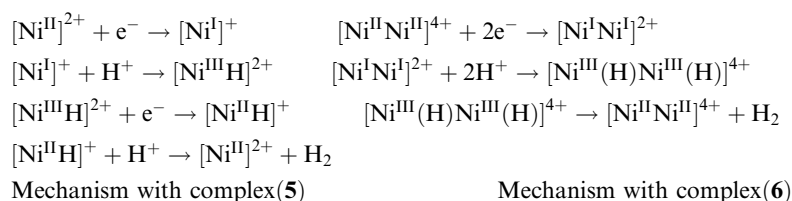
Only a limited number of true metal complex electrocatalysts have been proposed for proton reduction due to the difficulty inherent in the bi-electronic nature of this reaction. It is obvious that the design of such electrocatalysts must take into account the lowering of the overpotential for proton reduction, the stability of the catalytic system, and the regeneration of the starting complex.

9.10.3.1.1 Transition metal macrocycles

Cobalt(III) sepulchrate (**1**)⁸ and tetrazamacrocyclic complexes of cobalt(II) (**2**)⁹ and nickel(II) (**3**)–(**6**)^{9–11} catalyze the electroreduction of water to dihydrogen, at potentials ranging from -0.7 V (complex **1**) to -1.5 V (complexes **4**)–(**6**) vs. SCE in aqueous electrolytes, with current efficiencies as high as 95% for complex **4**.⁹ It is noteworthy that the binuclear nickel biscyclam complex (**6**) is 10 times more active (at pH 7) than the mononuclear nickel cyclam complex (**5**). This behavior tends to indicate that some cooperativity between the two metal centers occurs in complex **6**, as depicted in the possible reaction (Scheme 3) involving a dihydride intermediate.¹¹



A number of metal porphyrins have been examined as electrocatalysts for H_2O reduction to H_2 . Cobalt complexes of water soluble *meso*-tetrakis(*N*-methylpyridinium-4-yl)porphyrin chloride, *meso*-tetrakis(4-pyridyl)porphyrin, and *meso*-tetrakis(*N,N,N*-trimethylanilinium-4-yl)porphyrin chloride have been shown to catalyze H_2 production *via* controlled potential electrolysis at relatively low overpotential (-0.95 V vs. SCE at Hg pool in 0.1 M in fluoroacetic acid), with nearly 100% current efficiency.¹² Since the electrode kinetics appeared to be dominated by porphyrin adsorption at the electrode surface, H_2 -evolution catalysts have been examined at Co-porphyrin films on electrode surfaces.^{13,14} These catalytic systems appeared to be limited by slow electron transfer or poor stability.¹³ However, CoTPP incorporated into a Nafion[®] membrane coated on a Pt electrode shows high activity for H_2 production, and the catalysis takes place at the theoretical potential of H^+/H_2 .¹⁴

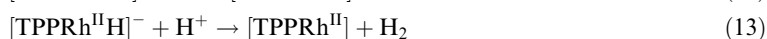
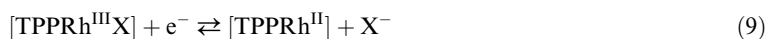


Scheme 3

The cobalt(II)¹⁵ and zinc(II)¹⁶ complexes of phthalocyanine(Pc), octacyano-Pc, and tetrasulfonato-Pc incorporated in poly(4-vinylpyridine-co-styrene) or Nafion[®] films coated on graphite have also been examined as catalytic devices for dihydrogen electrogeneration in phosphate buffer. These catalytic systems were strongly suggested to be dominated by the electron transfer within the polymer matrix. The best catalytic film is that constituted of the nonsubstituted Co^{II}-Pc complex in poly(4-vinylpyridine-co-styrene), giving a turnover number of $2 \times 10^5 \text{ h}^{-1}$ at an applied potential of $-0.90 \text{ V vs. Ag|Ag Cl}$.

Cofacial ruthenium and osmium bisporphyrins proved to be moderate catalysts (6–9 turnover h^{-1}) for the reduction of proton at mercury pool in THF.^{17,18} Two mechanisms of H₂ evolution have been proposed involving a dihydride or a dihydrogen complex. A wide range of reduction potentials (from -0.63 V to -1.24 V vs. SCE) has been obtained by varying the central metal and the carbon-based axial ligand. However, those catalysts with less negative reduction potentials needed the use of strong acids to carry out the catalysis. These catalysts appeared handicapped by slow reaction kinetics.

An iron porphyrin in the zero valent state, electrogenerated from [(TPP)Fe^{III}Cl], is a very efficient and persistent molecular catalyst of dihydrogen evolution in DMF containing Et₃NH⁺ Cl⁻ or CHF₂CO₂H as the acid.¹⁹ With reference to hydrogenases, the potential of this catalyst (-1.46 V vs. SCE) is far beyond biological potentials. The rate-limiting step in the proposed mechanism is the reaction with a second acid molecule of the Fe^{II}-H hydride intermediate, formed by protonation of the iron(0) porphyrin. This reaction is fast ($K = 4 \times 10^{-5} \text{ M}^{-1} \text{ s}^{-1}$) and H₂ evolution is in fact limited by the diffusion of H⁺ to the electrode surface. In the same way, a Rh^I porphyrin (electrogenerated from (TPP)Rh^{III}I, Equations (9) and (10)) reacts readily with organic acids in DMSO or butyronitrile to give Rh^{III}-hydride species (Equation (11)). Formation of hydride was demonstrated by UV-visible and FT-IR spectroelectrochemical studies. The Rh^{II}-hydride, formed at more negative potential (Equation (12)), catalyzes hydrogen evolution (Equation (13)).²⁰

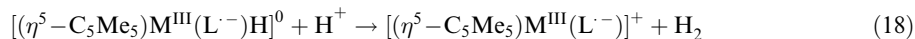
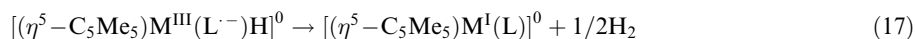
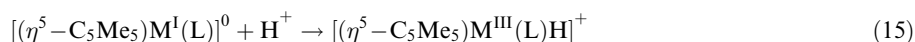
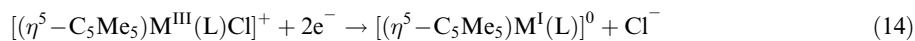


The introduction of triethylphosphine as axial ligand increases the hydride transfer activity of [TPPRh^{III}H] and changes the H₂ evolution mechanism, since it is then able to catalyze this reaction.²⁰

9.10.3.1.2 Polypyridyl complexes

In conjunction with polypyridinyl [2,2-bipyridine (bpy) and 1,10-phenanthroline (phen)] or biazinyl (3,3'-bipyrazine, 2,2'-bipyrazine, 2,2'-, and 4,4'-bipyrimidine) ligands, the C₅Me₅M (M = Ir, Rh^{21–29}) and C₆H₆M (M = Ru, Os²⁶) fragments have proven to be valuable for the electroreductive generation of hydrido complexes and the evolution of dihydrogen.

[(η^5 -C₅Me₅)Ir^{III}(L)Cl]⁺ complexes (L = bpy and phen derivatives) form stable hydrides upon oxidative addition of a proton to the doubly reduced [(η^5 -C₅Me₅)Ir(L)]⁰ intermediate (Equations (14) and (15)),^{23,24,26,28} which have been characterized by absorption spectroscopy and ¹H-NMR spectrometry. Additional electrochemical activation is thus required for efficient H₂ evolution, by either spontaneous decomposition (Equation (17)) or protonation (Equation (18)) of the reduced hydride complex (ECE mechanism):^{24,26,28}



$[(\eta^5-C_5Me_5)Rh^{III}(L)Cl]^+$ complexes present a similar electrocatalytic behavior.^{21,22,25,26,28,29} However, the corresponding Rh–H complex is less stable and could not be isolated, or even characterized, from spectroscopic experiments.

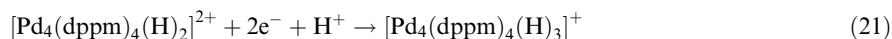
Polymeric films of $[(\eta^5-C_5Me_5)M(L)Cl]^+$ complexes (M = Ir, Rh; L = pyrrole-substituted bpy or phen) have been coated on an electrode by oxidative electropolymerization. The buildup of hydrido complexes in films is well known;^{27,28,30} the high electrocatalytic activity of these molecular electrode materials towards dihydrogen evolution in organic and aqueous electrolytes is also well known.^{25,31} For example, H₂ is evolved at –0.55 V vs. SCE at a poly $[(\eta^5-C_5Me_5)-Rh(bpy)Cl]^+$ film in pH 1 aqueous solution.³¹

Electroreductive generation in an organic electrolyte, containing H₂O or HCO₂H as proton source, of stable $[Rh^{III}(H)_2(PPh_2Et)_2(L)]^+$ dihydrido complexes (L = bpy derivatives) from $[Rh^{III}(X)(Cl)(PPh_2Et)_2(L)]^+$ complexes (X = Cl[–] or H[–]) has been demonstrated in homogeneous solution and in polymeric films.³² Polymer film-modified carbon electrodes are active for water reduction and dihydrogen evolution in basic (pH 10) aqueous solution.^{32,33} Similar behavior occurs with cathodes modified by polymer films derived from a number of transition metal complexes, including $[Rh^{III}(bpy)_2(Cl)_2]^+$,³⁴ $[Pd^{II}(bpy)_2]^{2+}$,³⁵ $[Rh^I(bpy)(1,5-cyclooctadiene)]^+$,³⁶ $[Pt^{II}(bpy)_2]^{2+}$,³⁷ $[Pt^{II}(terpy)Cl]^+$,³⁷ and $[Co^{II}(terpy)_2]^{2+}$ (terpy = 2,2',6',2'' terpyridyl).³⁸

9.10.3.1.3 Phosphine complexes

It is well recognized that protonated phosphine complexes such as $[M(dppe)(H)_2]^+$ (dppe = 2-bis(diphenylphosphine)ethane), M = Co, Ir),³⁹ $[Fe(dppe)(L)H]^+$,⁴⁰ or $[Pt(PEt_3)_3H]^+$ ⁴¹ catalyze proton reduction at very negative potentials, ~–2 V vs. SCE. In contrast, the protonated $[(\eta^5-C_5H_5)Co^{III}\{P(OMe)_3\}_2H]^+$ complex is a catalyst for hydrogen production at –1.15 V vs. SCE at a Hg-pool cathode in pH 5 aqueous buffer.⁴² Dihydrogen is evolved from the reduced $[(\eta^5-C_5H_5)Co^{III}-P(OMe)_3\}_2H]^0$ form of the complex, which decays to H₂ or reacts in a proton–hydride reaction.

The stable hydride cluster $[Pd_4(dppm)_4(H)_3]^+$ [dppm = bis(diphenylphosphino)methane] can be electrochemically generated from $[Pd_2(dppm)_2Cl_2]$ at –1.35 V vs. SCE in DMF containing HCO₂H (Equations (21) and (22)). Subsequent addition of proton under the same reducing conditions induces dihydrogen evolution.⁴³



9.10.3.1.4 Miscellaneous complexes

Square planar complexes $[M(mnt)_2]^{3-}$ (M = Rh, Co, mnt = dithiomalonitrile), generated by electroreduction of $[M(mnt)_2]^{2-}$, are protonated to form $[M(mnt)_2H]^{2-}$, from which dihydrogen is evolved at a mercury electrode at potentials more negative than those of the reversible $[M(mnt)_2]^{2-}/[M(mnt)_2H]^{2-}$ redox couple.⁴⁴

Iron(II), cobalt(II), and nickel(II) monothiocyanato complexes also catalyze evolution of hydrogen in aqueous buffer. The active intermediate is the protonated doubly reduced, zero-valent form of the complex.⁴⁵

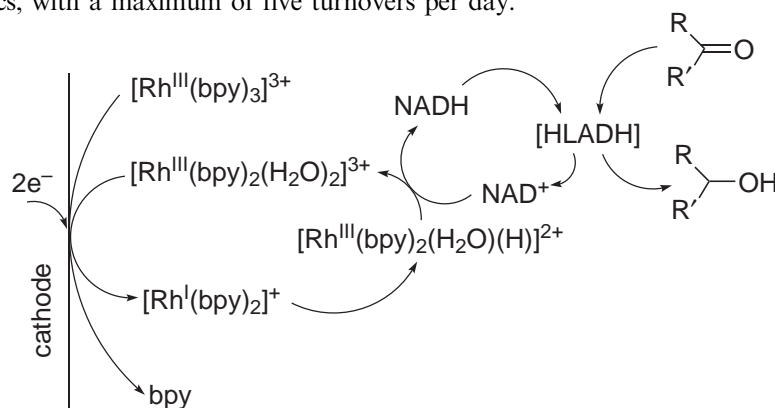
Efficient dihydrogen formation catalyzed by polynuclear metal–cyanide complexes, coated on the electrode, takes place in acidic aqueous solution. This was shown for Prussian white $(K_4[Fe_4^I Fe^II(CN)_6]_3)$ ⁴⁶ and ferric ruthenocyanide $(Fe_4^III[Ru^II(CN)_6]_3)$ ⁴⁷ materials.

9.10.3.2 Electrochemically Driven Hydride Transfer Reactions

9.10.3.2.1 Electrocatalytic regeneration of reduced nicotinamide cofactors

Nonenzymatic regeneration of NAD(P)H requires the regioselective transfer of two electrons and a proton to NAD(P)⁺. Various rhodium(III) complexes are effective electrocatalysts capable of mimicking hydrogenase enzymes.^{48–54}

[Rh^{III}(bpy)₃]³⁺ and its derivatives are able to reduce selectively NAD⁺ to 1,4-NADH in aqueous buffer.^{48–50} It is likely that a rhodium-hydride intermediate, e.g., [Rh^{III}(bpy)₂(H₂O)(H)]²⁺, acts as a hydride transfer agent in this catalytic process. This system has been coupled internally to the enzymatic reduction of carbonyl compounds using an alcohol dehydrogenase (HLADH) as an NADH-dependent enzyme (Scheme 4). The [Rh^{III}(bpy)₃]³⁺ derivative containing 2,2'-bipyridine-5-sulfonic acid as ligand gave the best results in terms of turnover number (46 turnovers for the metal catalyst, 101 for the cofactor), but was handicapped by slow reaction kinetics, with a maximum of five turnovers per day.⁵⁰



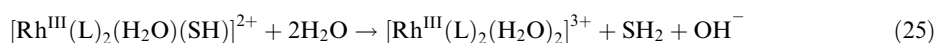
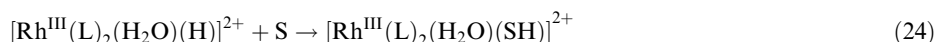
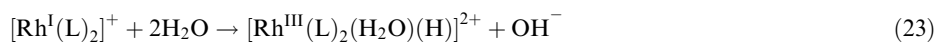
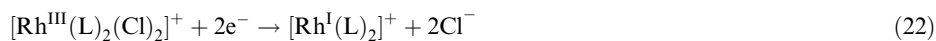
Scheme 4

The complex $[(\eta^5\text{-C}_5\text{Me}_5)\text{Rh}(\text{bpy})\text{Cl}]^+$ is a better electrocatalyst for NADH regeneration.^{51,52,54} Its catalytic activity is decreased by electron-withdrawing substituents on the 2,2'-bipyridine ligand and increased by electron-donating substituents, the rate-determining step being the formation of the active intermediate rhodium(III)-hydride.⁵² This electrocatalytic system has been coupled to the enzymatic reduction of pyruvate to D-lactate catalyzed by the redox enzyme D-LDH in *tris*-HCl buffer.⁵¹ The catalyst was regenerated at a rate of 5 turnover h⁻¹, and D-lactate was produced with good current yields (50–70%) and a high enantiomeric excess (93.5%). The same system for NADH regeneration has been coupled to a monooxygenase reaction, giving productivity rates at about 50% of the *in vitro* process with enzymatic regeneration of the coenzyme.⁵⁴

Electrocatalytic regeneration of NADH has also been performed at polymer-modified electrodes with pendent $[(\eta^5\text{-C}_5\text{Me}_5)\text{Rh}(\text{bpy})\text{Cl}]^+$ ^{55,56} and $[\text{Rh}(\text{terpy})_2]^{3+}$ ⁵⁷ complexes, and coupled to enzymatic reduction with alcohol dehydrogenase.^{55,57}

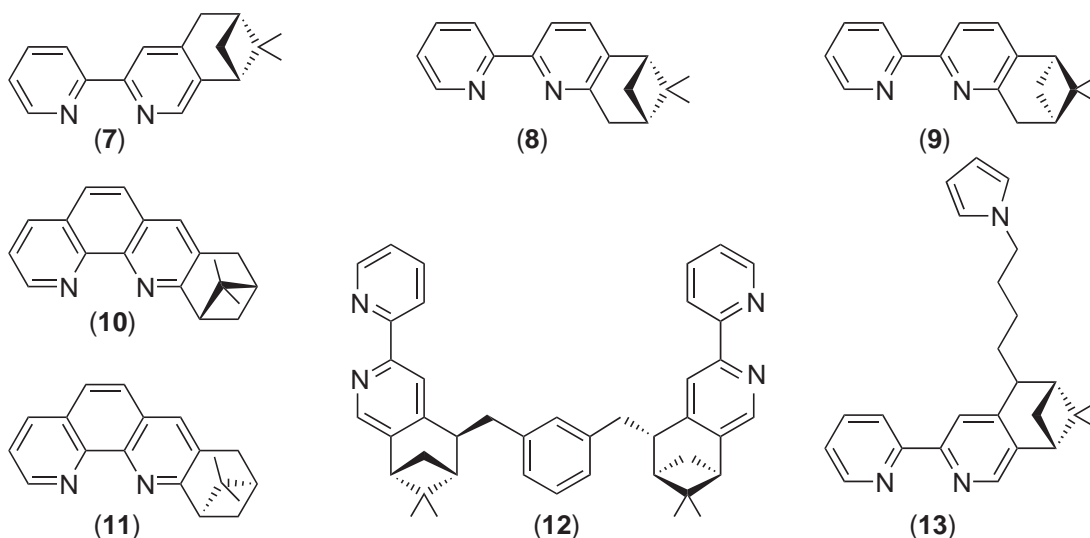
9.10.3.2.2 Electrocatalytic hydrogenation of organics

The electrocatalytic hydrogenation (ECH) of unsaturated organic compounds with transition metal complexes has been mainly performed at polymer film-modified electrodes.⁵⁸ The best results have been obtained using poly[Rh^{III}(L)₂(Cl)₂]⁺ films (L = bpy and phen derivatives). Such electrode materials are stable and very active for the hydrogenation of aliphatic or aromatic ketones and enones in aqueous electrolytes,^{34,59,60} giving turnovers as high as 5,000 in the course of the hydrogenation of millimolar amounts of substrates. By analogy with catalytic hydrogen transfer hydrogenation using 2-propanol or formic acid as hydrogen source, ECH is likely to take place *via* a rhodium hydride intermediate formed by the reaction with water of the electrogenerated Rh^I complex (Equation (23)). Hydride species react with the unsaturated substrate S (Equation (24)), to finally release the hydrogenated product SH₂ and a rhodium(III) complex (Equation (25)) that can enter in a new cycle.⁵⁹



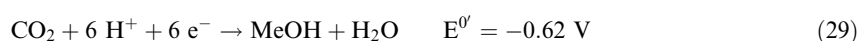
The participation of hydride species in this process is corroborated by the ability of complexes $[(\eta^5\text{-C}_5\text{Me}_5)\text{Rh}^{\text{III}}(\text{bpy})\text{Cl}]^+$ ($\text{M} = \text{Rh}$ or Ir)²⁸ and $[\text{Rh}^{\text{III}}(\text{bpy})(\text{PPh}_2\text{Et})_2(\text{Cl})_2]^+$ ³² in films to perform ECH of organics. Indeed, such complexes are readily transformed to hydride derivatives upon electroreduction in protic electrolytes (see Section 9.10.3.1.1). However, these complexes give more stable hydride species and are much less active than $[\text{Rh}(\text{bpy})_2(\text{Cl})_2]^+$ complexes.

Asymmetric ECH with $[\text{Rh}(\text{L})_2(\text{Cl})_2]^+$ complexes containing chiral polypyridyl ligands has been attempted, in homogeneous media ($\text{L} = (7)–(12)$) and at carbon electrodes coated with polymer films prepared by electropolymerization of $[\text{Rh}(13)_2(\text{Cl})_2]^+$.^{61,62} The latter catalytic system gave the best results in terms of turnover number (up to 4,750) and enantiomeric excess, (ee) when applied to the hydrogenation of acetophenone (ee: 18%) and 2-butanone (ee: 10%).⁶² Polymeric materials derived from the complexes $[\text{Rh}^{\text{I}}(\text{bpy})(\text{COD})]^+$ ³⁶ and $[\text{Pd}(\text{bpy})_2]^{2+}$ ³⁵ have also been applied to the ECH reaction.



9.10.4 ELECTROCATALYTIC REDUCTION OF CARBON DIOXIDE

The quantities of carbon dioxide stored in the terrestrial environment exceed those of fossil fuel. However, the industrial use of carbon dioxide or carbonates as a source of various organic compounds is actually limited.⁶³ This situation is expected to be changed if efficient catalytic systems for their reductive activation are available. Towards this objective, the electrochemical reduction of CO_2 appears as a promising long-term challenge. The redox potential of the one-electron reduction of CO_2 into $\text{CO}_2^{\cdot -}$ is -2.1 V (vs. SCE) making this process highly unfavorable. In contrast, proton-assisted multi-electron steps are much more favorable and the nature of the reduction product has a strong influence on its thermodynamic accessibility (Equations (26)–(30); pH 7 in aqueous solution vs. SCE).⁶⁴





The reduction of CO_2 can be driven electrochemically at metallic cathodes, however, it requires large overpotentials ($< -1.5 \text{ V}$) and electrode poisoning often occurs.⁶⁵ Those problems can be addressed by adding catalysts. Metal complexes are *a priori* good candidates as electrocatalysts. It is expected that their reduction will be accompanied by the appearance of a vacant coordination site able to bind CO_2 and thus activate its reduction in the metal coordination sphere.¹

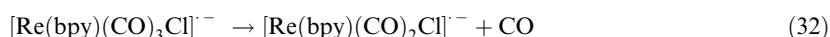
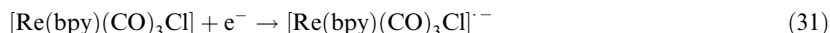
Numerous metal complexes have been proven to be active electrocatalysts for CO_2 reduction.^{1,66–68} These catalysts can be conveniently grouped into three main families: metal complexes with polypyridyl ligands, metal complexes with macrocyclic ligands, and metal complexes with phosphorus ligands.

9.10.4.1 Polypyridyl Metal Complexes

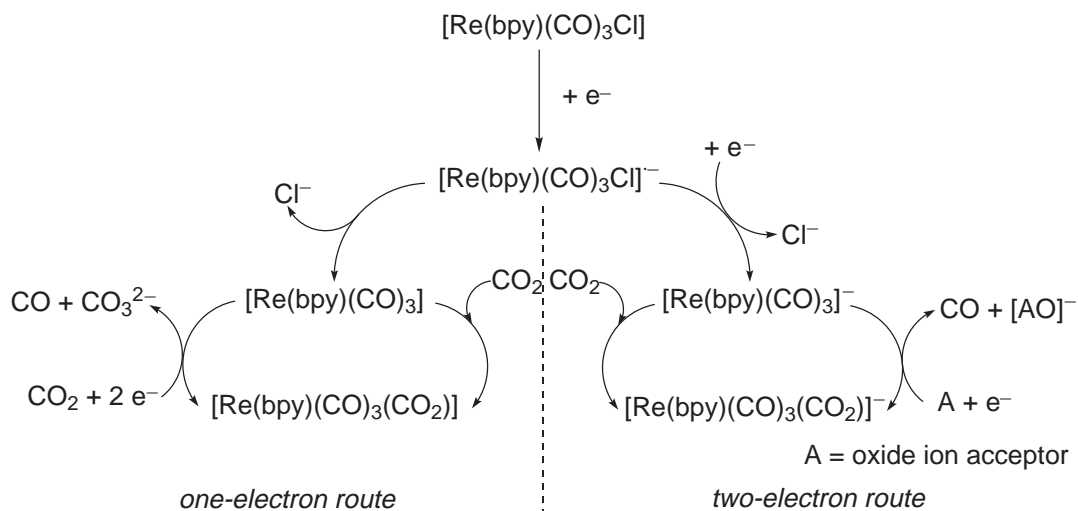
Many polypyridyl metallic complexes have been used successfully as electrocatalysts in homogeneous and heterogeneous systems and generally CO and HCOO^- are the main products of reduction. Among these, the two complexes, $[\text{Re}(\text{bpy})(\text{CO})_3\text{Cl}]$ and $[\text{Ru}(\text{bpy})_2(\text{CO})\text{X}]^{n+}$ ($\text{X} = \text{CO}, \text{Cl}, \text{H}$; $n = 2$ or 1), have attracted much attention because of their characteristic reactivity and their high efficiency and stability.

9.10.4.1.1 *Re(bpy)(CO)₃Cl and related complexes*

The first electrocatalytic system based on a bipyridyl complex was $[\text{Re}^{\text{I}}(\text{bpy})(\text{CO})_3\text{Cl}]$, a complex originally intended to serve as a photosensitizer.^{69,70} It has been found that the electrochemical reduction of CO_2 into CO catalyzed by $[\text{Re}(\text{bpy})(\text{CO})_3\text{Cl}]$ at -1.5 V vs. SCE in DMF–water (9:1) occurs with high faradaic yield ($\eta = 98\%$) and large catalyst turnover numbers (several hundred) without significant depletion of the complex. An excess of Cl^- as coordinating anion, and the presence of H_2O , both seem to be needed to improve the efficiency and selectivity of the systems. The authors suggested that the initially one-electron reduced form of the complex $[\text{Re}(\text{bpy})(\text{CO})_3\text{Cl}]^-$ (Equation (31)) loses a CO ligand to give a five-coordinate complex (Equation (32)) able to coordinate CO_2 and to activate its reduction.



Using the same complex or some related ones, other groups^{71–73} have studied the mechanism of this electrocatalysis in a strictly nonaqueous solvent (MeCN) in detail. In this solvent, it has been shown that CO is also produced by electrolysis at a fixed potential either at -1.5 V or -1.8 V vs. SCE following respectively a one- or a two-electron pathway (Scheme 5).



Scheme 5

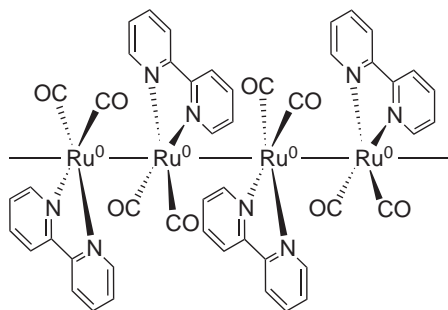
This mechanism differs from that initially proposed, as the one-electron reduced active species $[\text{Re}^0(\text{bpy})(\text{CO})_3]$ results here via loss of Cl^- instead of CO . Since these first results, the arguments concerning the reaction mechanisms have still continued.^{74–78} However, some recent IR spectroelectrochemical studies⁷⁹ have confirmed the occurrence of the CO_2 attack on both the one and two electron reduced forms $[\text{Re}(\text{bpy})(\text{CO})_3]$ and $[\text{Re}(\text{bpy})(\text{CO})_3]^-$.

Several technical arrangements have been used successfully to immobilize this catalyst on an electrode surface as thin films.^{80–85} In such arrangements the metal sites in films show a dramatic increase in reactivity and stability toward CO_2 reduction into CO . Moreover, this kind of modified electrode (for instance $[\text{Re}(\text{bpy})(\text{CO})_3\text{Br}]$ incorporated in Nafion[®] membrane) appeared as a good electrocatalyst in pure aqueous electrolyte.⁸⁶ However, in such systems both CO and HCOO^- are also produced, and the total current yield of CO_2 reduction is lowered by the concurrent H^+ reduction into H_2 .

9.10.4.1.2 $[\text{Ru}(\text{bpy})_2(\text{CO})_2]^{2+}$ and related complexes

Electrolysis performed in CO_2 -saturated aqueous DMF (10:90) at a potential of -1.5 V vs. SCE in the presence of $[\text{Ru}(\text{bpy})_2(\text{CO})_2]^{2+}$ or $[\text{Ru}(\text{bpy})(\text{CO})\text{Cl}]^+$ leads to variable amounts of CO , HCOO^- , and H_2 .^{87,88} The influence of several experimental factors (e.g., water content, pH, solvent) on the ratio of the products of reduction has been studied.^{89,90} It has been postulated that the active species is the two electron reduced form of the starting complex, i.e., $[\text{Ru}^0(\text{bpy})_2(\text{CO})]$. This pentacoordinated species may react with CO_2 to lead to a $\sigma\text{-CO}_2$ complex $[\text{Ru}(\text{bpy})_2(\text{CO})(\text{CO}_2)]$, which is the precursor of either CO or HCOO^- formation depending on the pH of the solution.

Furthermore, it has been demonstrated that the successful electrocatalytic reduction of CO_2 with $[\text{Ru}(\text{bpy})_2(\text{CO})_2]^{2+}$ in aqueous MeCN is mainly due to the formation of a polymeric electroactive film, which occurs during the reduction of the complex.⁹¹ This film is composed of an “open” cluster polymer $[\text{Ru}(\text{bpy})(\text{CO})_2]_n$ (Scheme 6) based upon extended $\text{Ru}^0\text{—Ru}^0$ bonds. Electropolymerization of $[\text{Ru}(\text{bpy})_2(\text{CO})_2]^{2+}$ results from the overall addition of two electrons per mole of $[\text{Ru}(\text{bpy})_2(\text{CO})_2]^{2+}$ and is associated with the decoordination of one bpy ligand (Equation (33)).



Scheme 6



The selective and almost quantitative electrocatalytic formation of CO is obtained when $[\text{Ru}(\text{bpy})_2(\text{CO})_2]^{2+}$ is used as electrocatalyst in aqueous acetonitrile (20:80) medium. In the absence of added water, formation of the $[\text{Ru}(\text{bpy})(\text{CO})_2]_n$ polymer is in competition with that of the hydride derivative $[\text{Ru}(\text{bpy})(\text{CO})\text{H}]^+$, the latter being the active catalyst as demonstrated in a separate experiment using an authentic sample of this hydrido-complex.⁹² In those conditions HCOO^- and H_2 are also formed besides CO .

Carbon electrodes modified by polymeric films of $[\text{Ru}(\text{bpy})(\text{CO})_2]_n$ appear to be efficient molecular cathodes for selective reduction of CO_2 into CO ($\eta > 95\%$) especially in pure aqueous electrolyte, at a moderate overpotential (-1.2 V vs. $\text{Ag}|\text{AgCl}$).⁹³ Strongly adherent thin films of $[\text{Ru}(\text{bpy})(\text{CO})_2]_n$ can also be easily prepared from the electroreduction of monobipyridyl mono- or binuclear complexes of Ru containing two leaving groups per Ru, such as $[\text{Ru}(\text{bpy})(\text{CO})_2\text{Cl}_2]$, $[\text{Ru}(\text{bpy})(\text{CO})_2(\text{MeCN})_2]^{2+}$, $[\text{Ru}(\text{bpy})(\text{CO})_2(\text{MeCN})_2]^{2+}$, and $[\text{Ru}(\text{bpy})(\text{CO})_2\text{Cl}_2]$.^{94–97}

With films based on a 2,2'-bipyridine ligand which is 4,4'-disubstituted with electron-withdrawing carboxyester groups the selectivity is drastically changed, since HCOO^- is obtained with a high yield ($\eta > 90\%$) at a very low overvoltage (-0.75 V vs. $\text{Ag}|\text{AgCl}$).⁹⁸ This difference was

attributed to the nature of the intermediates (hydroxycarbonyl or formate complex) formed during the electrocatalytic process.

Furthermore, the utilization of preformed films of polypyrrole functionalized by suitable monomeric ruthenium complexes allows the circumvention of problems due to the moderate stability of these complexes to aerial oxidation when free in solution. A similar CO/HCOO⁻ selectivity with regards to the substitution of the *N*-pyrrole-bpy ligand by an electron-withdrawing group is retained in those composite materials.⁹⁸ The related osmium-based redox-active polymer [Os⁰(bpy)(CO)₂]_{*n*} was prepared, and is also an excellent electrocatalyst for the reduction of CO₂ in aqueous media.⁹⁹ However, the selectivity toward CO vs. HCOO⁻ production is lower.

9.10.4.1.3 Other polypyridyl metal complexes

Several other polypyridyl metal complexes have been proposed as electrocatalysts for CO₂ reduction.^{100–108} For some of them HCOO⁻ appears as the dominant product of reduction. It has been shown for instance that the complexes [Rh^{III}(bpy)₂Cl₂]⁺ or [Rh^{III}(bpy)₂(CF₃SO₃)₂]⁺ catalyze the formation of HCOO⁻ in MeCN (at -1.55 V vs. SCE) with a current efficiency of up to 80%.^{100,103} The electrocatalytic process occurs *via* the initially electrogenerated species [Rh^I(bpy)₂]⁺, formed by two-electron reduction of the metal center, which is then reduced twice more (Rh^I/Rh⁰; Rh⁰/Rh⁻¹). The source of protons is apparently the supporting electrolyte cation, Bu₄N⁺ *via* the Hoffmann degradation (Equation (34)).

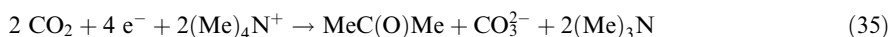


A similar result has been obtained with another Rh^{III} complex, [(η⁵-Me₅C₅)Rh(bpy)Cl]⁺. A current efficiency for HCOO⁻ production up to 50% has been obtained in MeCN containing water (20%) at -1.4 V vs. SCE.³⁰ In this case, it was demonstrated that the initial step of the electrocatalysis involves the formation of the corresponding hydrido complex [(η⁵-Me₅C₅)Rh(bpy)H]⁺. It appears also that the Rh^{III} complex is a better catalyst than the corresponding [(η⁵-Me₅C₅)Ir^{III}(bpy)Cl]⁺ complex as a consequence of the lower stability of the [(η⁵-Me₅C₅)Rh(bpy)H]⁰ vs. [(η⁵-Me₅C₅)Ir^{III}(bpy)Cl]⁰ one-electron reduced species.

Several oligopyridyl (terpyridyl, quaterpyridyl, etc.) complexes of Co^{II}, Ni^{II}, Fe^{II}, or Cr^{II} have been tested.^{109–114} Most of them exhibit some degree of electrocatalytic activity for the reduction of CO₂. In the case of electropolymerizable metal complexes, electrodeposited films exhibit a higher activity than the corresponding complexes in solution. With electropolymerized films of [Co(vterpy)₂]²⁺ (vterpy = 4'-vinyl-2,2':6',2''-terpyridine) in DMF at -1.20 V vs. SCE, HCO₂H is produced with a nearly quantitative yield.¹⁰⁹ A remarkable feature of these materials is that in water formaldehyde (HCOH), resulting from a four electron process, is obtained with a 39% yield at -1.10 V vs. SCE. Furthermore with a poly[Cr(vterpy)₂]²⁺ film the yield of formaldehyde reaches a 87% yield at the same overpotential.¹¹⁴

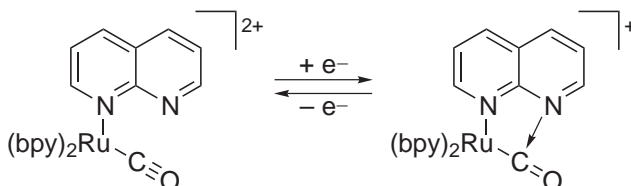
It is unusual for molecular catalysts to form reduction products that require more than two electrons. Besides the examples reported above, under certain conditions four- and six-electron reductions and C—C bond formation with some particular polypyridyl complexes have been observed. However, the catalytic rates and/or the selectivity for these more highly reduced products remain generally modest. The controlled potential electrolysis of [Ru(bpy)(terpy)(CO)]²⁺ complex at -1.75 V vs. Ag/Ag⁺ in CO₂-saturated C₂H₅OH/H₂O (8:2) medium at -20 °C produced HOCCO₂H and HOCH₂CO₂H in addition to CO, HCO₂H, HCHO, and MeOH.^{115,116} At room temperature the electrocatalysis gives only CO, HCO₂H, H₂, and traces of MeOH. In these conditions, the achievement of the multielectron reduction is ascribed to the stabilization of the protonated two-electron reduced form [Ru(bpy)(terpy)(CHO)]⁺, which is the key species. Further two-electron reduction affords HCOH or MeOH from the possible precursor [Ru(bpy)(terpy)(CH₂OH)]⁺. Concurrent carboxylation of [Ru(bpy)(terpy)(CHO)]⁺ and [Ru(bpy)(terpy)(CH₂OH)]⁺ possibly gives H(O)CCO₂H and HOCH₂CO₂H.

Efficient formation of ketones has been observed when the electrochemical reduction of CO₂ is catalyzed by [Ru(bpy)(napy)₂(CO)₂]²⁺ (napy = 1,8-naphthyridine) or [Ru(bpy)₂(qu)(CO)]²⁺ (qu = quinoline) complexes in a nonaqueous solvent in the presence of (Me)₄NBF₄ as electrolyte.^{117–121} (Me)₄N⁺ works not only as an electrolyte, but also as a methylation agent. The current efficiency of the reaction (Equation (35)) can reach 70% at 100 °C.



The selective formation of acetone is ascribed to the suppression of the reductive cleavage of the Ru—CO bond by the electroinduced metallacyclization (Scheme 7).

The same group has also shown that mono- or dinuclear trisbipyridine-like complexes containing the ligand 2,2'-bis(1-methyl-benzimidazol-2-yl)-4,4'-bipyridine instead of unsubstituted 2,2'-bipyridine catalyze the reduction of CO₂ to oxalate (C₂O₄²⁻) in anhydrous MeCN at -1.65 V and -1.55 V, respectively (vs. Ag|AgCl) with a good current yield ($\eta = 70\%$). In contrast, HCOO⁻ is then generated almost quantitatively in the presence of added H₂O.¹²²



Scheme 7

Finally, it has been reported that carbon electrodes modified with thin polymeric films of polypyridyl metal complexes containing a dispersion of metal particles (Rh⁰ or Pd⁰) can be used as electrocatalyst for reduction of CO₂ to hydrocarbons in MeCN. Apparently CH₄ is the dominant reduction product (up to 18% of faradaic efficiency).^{123,124} It should be noted that the product distribution is reminiscent of a Fischer–Tropsch process since C₂, C₃, and C₄ hydrocarbons are also formed.

9.10.4.2 Metal Complexes with Macrocycles

9.10.4.2.1 Phthalocyanine complexes

Several metallophthalocyanines have been reported to be active toward the electroreduction of CO₂ in aqueous electrolyte especially when immobilized on an electrode surface.^{125–127} CoPc and, to a lesser extent, NiPc appear to be the most active phthalocyanine complexes in this respect. Several techniques have been used for their immobilization.^{128,129} In a typical experiment, controlled potential electrolysis conducted with such modified electrodes at -1.0 vs. SCE (pH 5) leads to CO as the major reduction product ($\eta = 60\%$) besides H₂, although another study indicates that HCOO⁻ is mainly obtained.¹²⁹ It has been more recently shown that the reduction selectivity is improved when the CoPc is incorporated in a polyvinyl pyridine membrane (ratio of CO to H₂ around 6 at pH 5). This was ascribed to the nature of the membrane which is coordinative and weakly basic. The microenvironment around CoPc provided by partially protonated pyridine species was suggested to be important.^{130,131} The mechanism of CO₂ reduction on CoPc is thought to involve the initial formation of a hydride derivative followed by its reduction associated with the insertion of CO₂.¹²⁸

Interesting results have been obtained using metallophthalocyanines supported on porous carbon gas diffusion electrodes.^{132–136} In the case of CoPc and NiPc, CO is formed with a current efficiency of almost 100%.¹³⁵ With Sn, Pb, and In phthalocyanines, mainly HCO₂H is formed, while Cu and Ti phthalocyanines promote the formation of CH₄. The reason why some metal–Pc complexes give CO or CH₄, while others yield HCO₂H, has been interpreted in terms of the electron configuration in the metal.¹³⁷ A rather different type of reaction is the very recent demonstration of the simultaneous reduction of CO₂ and NO₂⁻ to give urea (NH₂)₂CO, which can be achieved with an efficiency up to 40% at similar gas-diffusion electrode devices with a NiPc supported catalyst.¹³⁸

9.10.4.2.2 Porphyrin complexes

Studies on the electrocatalytic activity of metal porphyrins are limited in comparison with those on other classes of macrocyclic metal complex. Among the few porphyrin complexes tested, cobalt porphyrins have been demonstrated to be efficient electrocatalysts for the reduction of CO₂ to CO

($\eta = 90\%$, $E = -1.1$ V vs. SCE) in aqueous solution when they are fixed on a glassy carbon electrode.^{138–142} The current efficiency becomes quantitative when the porphyrin is supported on a gas diffusion electrode under high pressure of CO_2 .¹⁴³ It has been suggested that the electrocatalysis occurs at the Co^{I} species.¹⁴⁴

In contrast, electrocatalysis in a nonaqueous solvent like dichloromethane with soluble palladium(II) and silver(II) porphyrins produces mainly oxalate.¹⁴⁵ However, demetallation rapidly deactivates the catalysts. In these cases the catalytic processes are interpreted in terms of reduced forms of the macrocyclic ligand, rather than by formation of Pd^{I} or Ag^{I} species following metal-centered reduction.

Iron porphyrins may also serve as electrocatalysts through the electrogenerated formal oxidation state iron(0) species in DMF. The main reaction product is CO, with HCOO^- as a side product. At room temperature, the catalysis efficiency is poor and the catalyst is rapidly destroyed. It has been shown that lowering the temperature, or addition of Mg^{2+} ions or of a weak Brønsted acid, dramatically improves the catalysis efficiency and the stability of the catalyst.^{146–150} Kinetic analysis of the reaction suggests a mechanism where the first step in the iron(0) porphyrin catalysis is the formation of a Fe-CO_2 adduct corresponding to a two-electron oxidative addition converting the Fe^0 complex into a Fe^{II} -carbene species.

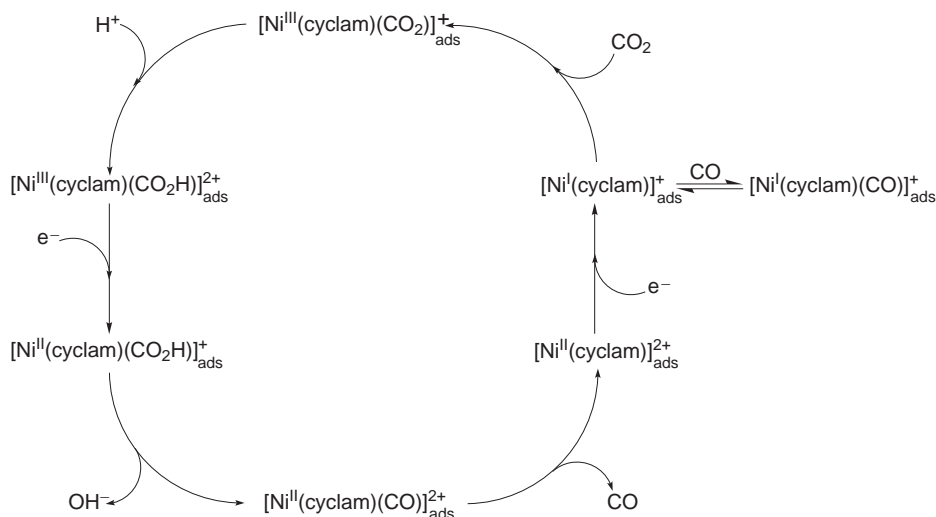
9.10.4.2.3 Cyclam and other polyazamacrocyclic complexes

It has been known since 1980 that polyazamacrocyclic complexes of Ni^{II} or Co^{II} are good candidates to catalyze electroreduction of CO_2 into CO even in aqueous electrolyte.^{9,151} The most extensively studied compound of this class of complexes is $[\text{Ni}(\text{cyclam})]^{2+}$ (**5**), which is a particularly effective and selective catalyst for the electrochemical reduction of CO_2 to CO at mercury electrodes in water at -1.4 V vs. SCE (pH 4).^{11,152,153} The main features of this system are the following:

- The catalyst is particularly chemically resistant and exhibits high turnover frequencies.
- The presence of the carbonylated complex $[\text{Ni}^{\text{I}}(\text{cyclam})(\text{CO})]^+$ during the reaction was clearly demonstrated. This compound results from the three-electron reduction product of $[\text{Ni}(\text{cyclam})]^{2+}$ and CO_2 (Equation (36)).



- In low water content DMF, HCOO^- is mainly obtained ($\eta = 75\%$) instead of CO.
- The active intermediate $[\text{Ni}(\text{cyclam})]^+$ —the initial electrogenerated species—is adsorbed on the surface of the mercury electrode.^{153–155} The catalytic activity is severely reduced in the presence of CO,¹⁵⁶ possibly due to formation of the insoluble complex $[\text{Ni}^0(\text{cyclam})(\text{CO})]^0$ following a two-electron reduction. Scheme 8 summarizes the mechanism for this catalysis.



Scheme 8

This mechanism has been probed by *ab initio* calculation.¹⁵⁷ Structural modifications of the cyclam framework can drastically affect the catalytic efficiency, as a consequence of the modification of the metal ability to interact with CO₂ or of the modification of the adsorption ability of the complex.^{157–163} For instance it has been found that the increase of *N*-methyl substitution of the cyclam increases the adsorption of the Ni^{II} complex on the mercury electrode, but decreases the stability of the Ni^I reduced form.¹⁶⁴

Modified electrodes containing cyclam derivatives have been prepared. The approach utilizing cyclam incorporated in Nafion[®] film on a carbon electrode shows that the catalytic efficiency of the system is much lower than observed when the catalyst is adsorbed on the mercury. With electrodes prepared following the Langmuir–Blodgett technique, only the electrode materials that allow the orientation of the monolayer so that the tail points to the substrate were found to be electrocatalytically active.¹⁶⁵

Other aza macrocyclic complexes, such as Schiff bases or tetraazaannulene derivatives, have been also used with some success for the electrocatalytic reduction of CO₂ in organic solvent in the presence of proton sources.^{166–168}

9.10.4.3 Phosphine Complexes and Miscellaneous Complexes

9.10.4.3.1 Phosphine complexes

Although numerous phosphine complexes are extensively used in organic homogeneous catalysis (e.g., hydrogenation, hydroformylation of alkenes), only a few transition metal phosphine complexes have been reported as catalysts for the reduction of CO₂.¹⁶⁹ The most extensively studied metal phosphine for this purpose are the [Pd(triphosphine)(solvent)]²⁺ complexes.^{170–177} Catalytic reduction of CO₂ into CO is generally observed in acidified MeCN or DMF with high selectivity, high rate, and low overpotential (–1.1V vs. SCE). However, turnover numbers are quite low as a consequence of catalyst decomposition. It has been suggested that the catalytic cycle involves first the one-electron reduction of the complex into the Pd^I species [Pd(triphosphine)(solvent)]⁺, followed by reaction with CO₂. The next two steps are protonation and a second one-electron transfer. It has been also shown that the utilization of water-soluble analogues of this complex allows this electrocatalytic process to be carried out in buffered aqueous solutions.¹⁷⁸

Some other phosphine complexes with late transition metals such as Rh, Ir, Ni, Cu, and Co have been reported to act as active electrocatalysts for reduction of CO₂ into CO and/or HCOO[–] in anhydrous conditions.^{179–182}

9.10.4.3.2 Other complexes

Some metal–sulfur clusters have been used in anhydrous organic solvents as CO₂ electrocatalysts. They lead mainly to HCOO[–],^{183–185} except when LiBF₄ is used as electrolyte, where oxalate formation is observed.^{186,187}

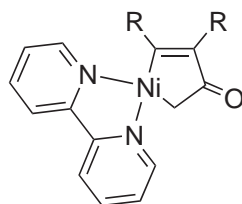
Although peripheral to the scope of this review, interesting systems based on modified electrodes with two-layered films containing an inorganic conductor (Prussian blue film) and a conducting polymer (polyaniline) doped (or not) with a metal complex (e.g., 1,8-dihydroxy-naphthalene-3,6-disulfonatoferrate) have been described. Electrolyses conducted at –0.8V vs. SCE gave with a total faradaic efficiency of 30% in a mixture of alcohols (MeOH, C₂H₅OH) and acids (HCO₂H, MeCO₂H, MeCH(OH)CO₂H).^{188–192} It is believed that the role of the polyaniline film and the metal complex is to render CO₂ chemically active by its chemical interaction with the amino group of the polyaniline and the metal of complex, while Prussian blue film provides catalytically active H_{ads} atoms. The activated CO₂ is then hydrogenated and converted to organic acids and alcohols.

9.10.4.4 Carboxylation of Organic Substrates

The fixation of carbon dioxide into organics may involve its activation by coordination to low-valent transition metal complexes. Carbon–carbon bonds can be thus formed by simultaneous activation at a metal center of both carbon dioxide and an organic substrate.

The electroreductive carbonylation and carboxylation of organic halides catalyzed by different metal complexes is summarized in Section 9.10.5. Electrogenerated Ni⁰ complexes containing bpy^{193–196} or pentamethyldiethylenetriamine^{196–199} ligands are effective catalysts for the electrosynthesis of

carboxylic acids by incorporation of CO₂ into alkynes,^{193,196,197} enynes,¹⁹⁹ 1,3-dienes,¹⁹⁵ or allenes.¹⁹⁶ Electrocatalytic reactions were performed in DMF using a consumable Mg anode. The cyclic organometallic intermediate (**14**) was isolated in the course of carboxylation of alkynes catalyzed by the Ni-bpy system.¹⁹⁴ Cleavage of this intermediate by magnesium ions is the key step of the catalysis.



(14)

[Ni(cyclam)]²⁺ was shown to be an efficient electrocatalyst for the intramolecular cyclization–carboxylation of allyl or propargyl-2-haloaryl ethers,²⁰⁰ and for the synthesis of cyclic carbonates from epoxides and carbon dioxide.²⁰¹

9.10.5 ELECTROCATALYTIC REDUCTION OF ORGANIC HALIDES

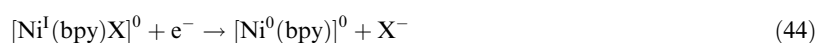
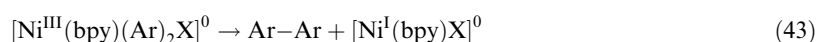
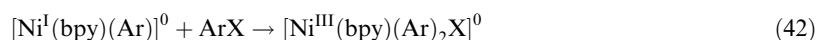
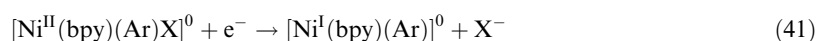
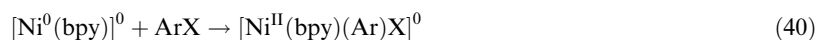
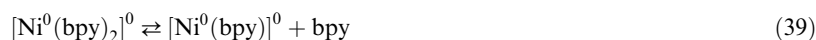
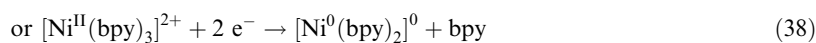
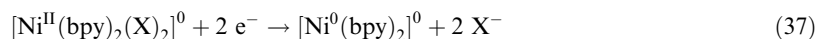
The reduction of organic halides is of practical importance for the treatment of effluents containing toxic organic halides and also for valuable synthetic applications. Direct electroreduction of alkyl and aryl halides is a kinetically slow process that requires high overpotentials. Their electrochemical activation is best achieved by use of electrochemically generated low-valent transition metal catalysts. Electrocatalytic coupling reactions of organic halides were reviewed in 1997.²⁰²

The main classes of metal complex that act as electrocatalysts for reduction of organic halides are polypyridyl, macrocyclic, and phosphine complexes.

9.10.5.1 Polypyridyl Complexes

9.10.5.1.1 Reductive homo- and heterocoupling of organic halides

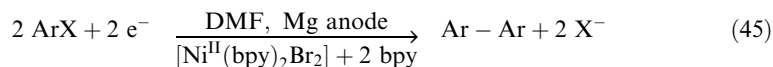
Alkyl, allyl, and aryl bromides are dehalogenated mainly with the formation of R–R dimers in the presence of polypyridyl complexes of the metals of Group VIII. It has been demonstrated that the complexes [Co(bpy)₃]²⁺,^{203,204} [Ni(bpy)₃]²⁺,²⁰⁵ and [Ni(phen)₃]²⁺²⁰⁶ catalyze the reductive dimerization of allyl and alkyl bromides in organic^{203,205,206} and aqueous micellar²⁰⁴ solution.



Low-valent nickel complexes of bpy are also efficient electrocatalysts in the reductive coupling reaction of aromatic halides.²⁰⁷ Detailed investigations are in agreement with a reaction mechanism involving the oxidative addition (Equation (40)) of the organic halide to a zero valent complex.^{208–210} Starting from [Ni^{II}(bpy)₂(X)₂]⁰ with excess bpy, or from [Ni^{II}(bpy)₃]²⁺, results in the [Ni⁰(bpy)₂]⁰ complex (Equations (37) and (38)). However, the reactive complex is the

low-ligated $[\text{Ni}^0(\text{bpy})]^0$ complex.^{208,210} After oxidative addition of the organic halide, reduction of the Ni^{II} -aryl intermediate (Equation (41)) is followed by oxidative addition of a second aryl halide (Equation (42)), leading to a Ni^{III} -diaryl species that decomposes to biaryl and a Ni^{I} complex (Equation (43)). Reduction of the latter complex regenerates the Ni^0 catalyst.

Electrocatalysis with nickel–bpy complexes has been shown useful for synthetic applications,^{202,211} especially when used in combination with the sacrificial anode process in an undivided cell (Equation (45)).^{207,211} Under these very simple experimental conditions, efficient nickel catalysts can be also generated in the presence of the cheap pyridine ligand.²¹²



Nickel–bpy and nickel–pyridine catalytic systems have been applied to numerous electroreductive reactions,²⁰² such as synthesis of ketones by heterocoupling of acyl and benzyl halides,^{210,213} addition of aryl bromides to activated alkenes,^{212,214} synthesis of conjugated dienes, unsaturated esters, ketones, and nitriles by homo- and cross-coupling involving alkenyl halides,²¹⁵ reductive polymerization of aromatic and heteroaromatic dibromides,^{216–221} or cleavage of the C–O bond in allyl ethers.²²²

Low-valent cobalt pyridine complexes, electrogenerated from CoCl_2 in DMF containing pyridine and associated with a sacrificial zinc anode, are also able to activate aryl halides to form arylzinc halides.²²³ This electrocatalytic system has also been applied to the addition of aryl bromides containing an electron-withdrawing group onto activated alkenes²²⁴ and to the synthesis of 4-phenylquinoline derivatives from phenyl halides and 4-chloroquinoline.²²⁵ Since the use of iron as anode appeared necessary, the role of iron ions in the catalytic system remains to be elucidated.

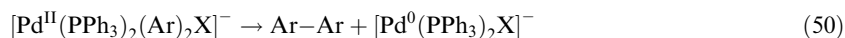
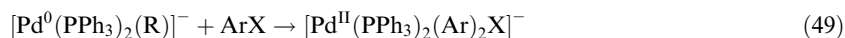
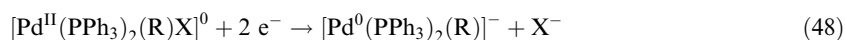
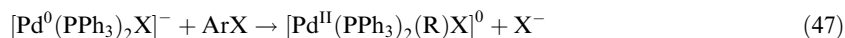
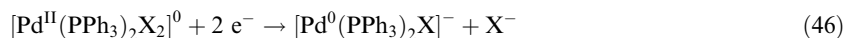
9.10.5.1.2 Carbonylation of organic halides

The complex $[\text{Ni}(\text{bpy})_2]^{2+}$ catalyzes the electroreductive coupling of organic halides and carbon monoxide into ketones under a CO atmosphere,²²⁶ or in the presence of a metal carbonyl,²²⁷ especially iron pentacarbonyl. Unsymmetrical ketones have been obtained from mixtures of two different organic halides.²²⁸ CO is very reactive towards reduced Ni^0 species to form the stable $[\text{Ni}^0(\text{bpy})(\text{CO})_2]^0$ complex, which probably evolves to a transient arylnickel $[\text{Ni}^{\text{II}}(\text{bpy})(\text{R})(\text{CO})\text{X}]^0$ complex in the presence of both ArX and $[\text{Ni}^0(\text{bpy})]^0$ species.^{229,230}

9.10.5.2 Phosphine Complexes

9.10.5.2.1 Electroreductive coupling of organic halides

Homocoupling of organic halides electrocatalyzed by $[\text{Ni}^{\text{II}}(\text{PPh}_3)_2(\text{MeCN})_4]^{2+}$,²³¹ $[\text{Ni}^{\text{II}}(\text{PPh}_3)_2\text{Cl}_2]^0$,²³² $[\text{Ni}^{\text{II}}(\text{dppe})\text{Cl}_2]^0$ (dppe = 2-bis(diphenylphosphino)ethane),²³³ $[\text{Pd}^0(\text{PPh}_3)_4]^0$, and $[\text{Pd}^{\text{II}}(\text{PPh}_3)_2\text{Cl}_2]^0$ ²³⁴ complexes is well established and has been reviewed.²³⁵ The detailed mechanisms for the synthesis of biaryls under catalytic conditions has been established for nickel–dppe,^{236,237} palladium– PPh_3 ²³⁸ and nickel– PPh_3 ²³⁹ complexes. The mechanism for nickel–phosphine complexes is similar to that for $[\text{Ni}(\text{bpy})_3]^{2+}$. It involves monoelectronic transfers and two sequential oxidative additions, i.e., between ArX and a Ni^0 complex, then between a second ArX and an aryl Ni^{I} intermediate. With palladium catalysts the reaction proceeds via bielectronic transfers:²³⁸

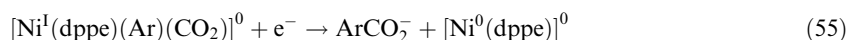
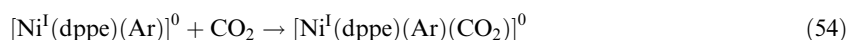
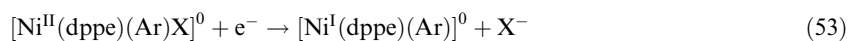
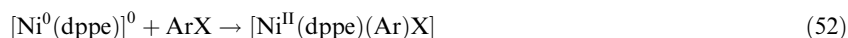
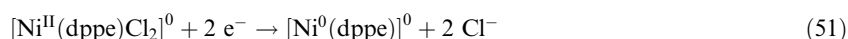


Efficient electrosynthesis of biaryls with $[\text{Pd}^{\text{II}}(\text{PPh}_3)_2\text{Cl}_2]^0$ has been performed starting from bromo- and iodoaromatic compounds,²³⁹ or even aryl triflates.^{240,241} The synthesis of biphenyls

from aryl chlorides has been carried out employing $[\text{Ni}^{\text{II}}(\text{dppb})_2\text{X}_2]^0$ as electrocatalyst (dppb = 1,2-bis(di-2-propylphosphino)benzene; $\text{X} = \text{Cl}^-$, Br^-), giving almost quantitative product and current yields using 2 mol% of catalyst.²⁴² In the binaphthyl series, efficient electroreductive coupling of 1-triflate derivatives was best achieved using $[\text{Ni}^{\text{II}}(\text{dppf})\text{Cl}_2]^0$ [dppf = 1,1'-bis(diphenylphosphino)ferrocene] or $\text{Pd}^{\text{II}} + 2,2'$ -bis(diphenylphosphino)-1,1'-binaphthyl as catalyst. The nickel–diphosphine system has also been employed for the reductive electropolymerization of various dihalides, including dichloro-²⁴² and dibromo aryls,^{243,244} and diiodoacetylene.²⁴⁵

9.10.5.2.2 Carbonylation and carboxylation of organic halides

$[\text{Ni}^{\text{II}}(\text{L})\text{Cl}_2]^0$ ($\text{L} = (\text{PPh}_3)_2$ or dppe),²⁴⁶ $[\text{Pd}(\text{PPh}_3)_2\text{Cl}_2]$, and/or $[\text{Pd}^0(\text{PPh}_3)_4]^0$ ²⁴⁷ as electrocatalytic systems have been applied to the carboxylation of aryl bromides,²⁴⁷ aryl iodides,^{246,247} vinylbromide,²⁴⁷ and allyl acetates²⁴⁷ with carbon dioxide. The nickel-catalyzed electrocarboxylation proceeds through a chain reaction (Equations (51)–(55)) involving reaction of a Ni^0 complex with carbon dioxide and the intermediate formation of a nickel(I) arenecarboxylate (Equation (54)).²⁴⁸ For the palladium-catalyzed reaction, the key carboxylation step definitely involves reaction of carbon dioxide with a free Ar^- anion produced by dissociation of a σ -arylpalladium(0) complex (“ $[\text{Pd}^0(\text{PPh}_3)_2(\text{Ar})]^-$ ”; see Equation (48)).²⁴⁹ This catalytic system has been also applied to the electrosynthesis of aldehydes by carbonylation of aryl iodides with carbon monoxide in the presence of formic acid as the proton source.²⁵⁰



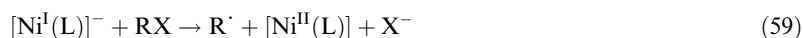
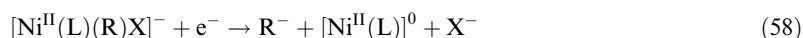
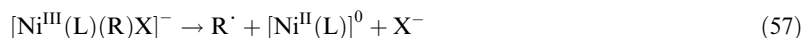
9.10.5.3 Schiff Bases and Macrocyclic Nickel and Cobalt Complexes

The third class of metal catalysts includes nickel and cobalt complexes of Schiff bases and nitrogen macrocyclic ligands, which can form on electroreduction cobalt(I) and nickel(I) reactive intermediates for the activation of organic halides.

9.10.5.3.1 Ni^{II} and Co^{I} Schiff base complexes

Electrogenerated nickel(I)²⁵¹ and cobalt(I)²⁵² complexes of Salen (Salen = bis(salicylidene)ethane-1,2-diamine) have displayed good catalytic properties in the cleavage of carbon–halogen bonds in a variety of organic compounds. Recent research in this field has been reviewed.²⁵³

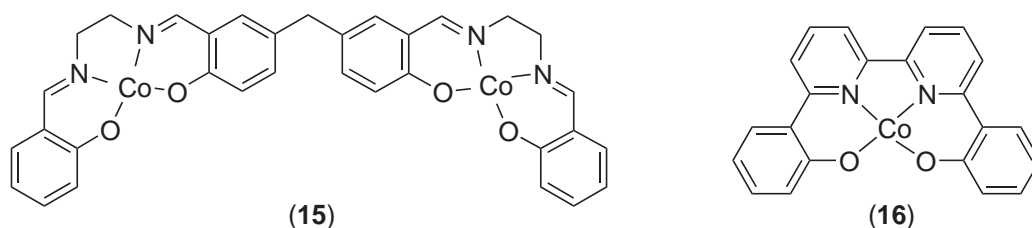
It was first suggested that the reaction of an alkyl halide with a nickel(I) Schiff base complex yields an alkylnickel(III) intermediate (Equation (56)). Homolytic cleavage of RBr to give an alkyl radical R^\cdot and a nickel(II) complex (Equation (57)) or, alternatively, one-electron dissociative reduction leading to R^- (Equation (58)) are possible pathways.²⁵⁴ A mechanism based on the formation of R^\cdot via dissociative electron transfer of Ni^{I} –salen to RX (Equation (59)) has also been proposed.²⁵⁵



Significant synthetic applications of the nickel–salen catalysts are the formation of cycloalkanes by reduction of α,ω -dihaloalkanes^{255,256} and unsaturated halides,^{257,258} the conversion of benzal chloride ($\text{C}_6\text{H}_5\text{CHCl}_2$) into a variety of dimeric products,²⁵⁹ the synthesis of 1,4-butanediol from 2-bromo- and 2-iodoethanol,²⁶⁰ or the reduction of acylhalides to aldehydes²⁶¹ and carboxylic acids.²⁶²

The electrochemistry of cobalt–salen complexes in the presence of alkyl halides has been studied thoroughly.^{252,263–266} The reaction mechanism is similar to that for the nickel complexes, with the intermediate formation of an alkylcobalt(III) complex. Co^I–salen reacts with 1,8-diiodooctane to afford an alkyl-bridged bis[Co^{III}(salen)] complex.²⁶⁷ Electrosynthetic applications of the cobalt–salen catalyst are homo- and heterocoupling reactions with mixtures of alkylchlorides and bromides,²⁶⁸ conversion of benzal chloride to stilbene with the intermediate formation of 1,2-dichloro-1,2-diphenylethane,²⁶⁹ reductive coupling of bromoalkanes with an activated alkenes,²⁷⁰ or carboxylation of benzylic and allylic chlorides by CO₂.^{271,272} Efficient electroreductive dimerization of benzyl bromide to bibenzyl is catalyzed by the dicobalt complex (15).²⁷³ The proposed mechanism involves an intermediate bis[alkylcobalt(III)] complex.

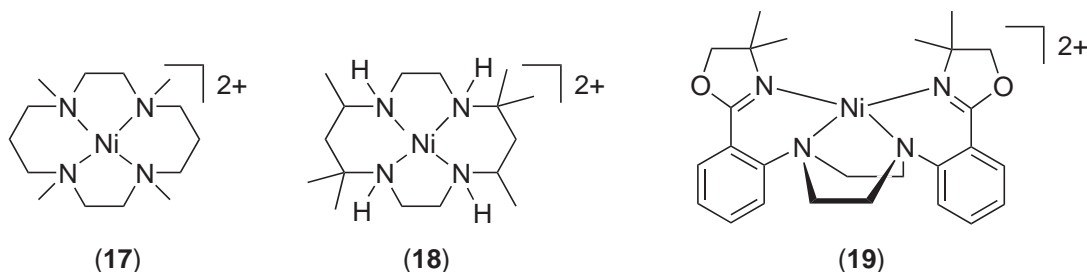
Complex (16), which has a similar structure to Co^{II}–salen, catalyzes the electrocarboxylation of arylmethyl chlorides.²⁷⁴ The enhancement of the catalytic life of (16) as compared to Co–salen may be due to the absence of imino bond in its ligand. The catalytic reduction of halogenated compounds has also been attempted at poly[M^{II}(salen)]-coated electrodes (M = Ni,²⁵³ Co²⁷⁵), which might have potential use for determination of organohalide pollutants.²⁷⁵



9.10.5.3.2 Ni^{II} complexes of cyclams and other tetradentate N-ligands

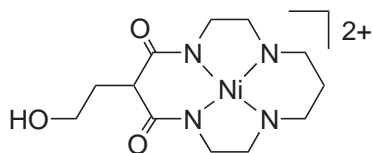
It is well-established that electroreduced nickel(I) complexes of cyclam and a variety of substituted cyclams add oxidatively to alkyl halides to give alkylnickel(III) complexes in organic solvents,^{251,276} the lifetime of the carbon–nickel bond governing the overall behavior of the system. However, it was shown that [Ni^I(tmc)]⁺ (one-electron reduced form of complex (17); tmc = 1,4,8,11-tetramethyl 1,4,8,11-tetraazacyclotetradecane) reacts with alkyl chlorides in aqueous alkaline solution in a one-electron process.^{277,278}

Nickel(I) species electrogenerated from [Ni(cyclam)]²⁺,^{258,279–284} [Ni(tmc)]²⁺ (complex (17),²⁷⁹ and [Ni(tet-a)]²⁺ (complex (18); tet a = 5,5,7,12,12,14-hexamethyl-1,4,8,11-tetraazacyclotetradecane)^{279,285–287} have been extensively used to perform radical cyclization of haloethers²⁷⁹ or haloallylethers,²²² allyl-2-halophenylesters,^{280,281,283} vinyl and aryl halides,^{258,282,284,286,287} and *N*-allylic and *N*-propargylbromoamides.²⁸⁵ This electrocatalytic system affords good yields of cyclized products under mild conditions. Other nickel complexes containing tetradentate nitrogen ligands, such as complexes (3),²⁷⁹ (4),²⁸⁵ and (19)²⁸⁸ have been used in electroreductive radical cyclization reactions. In contrast, application of electrogenerated Co^I-cyclam for the catalytic reduction of organic halides appears limited to one example.²⁸⁹



The catalytic activity of electrogenerated nickel–porphyrin anions toward MeI has been investigated for a series of nickel(II) porphyrins.²⁹⁰ As previously suggested,²⁹¹ results are in agreement with the presence of Ni^I in the singly reduced [nickel–porphyrin][−] anions.

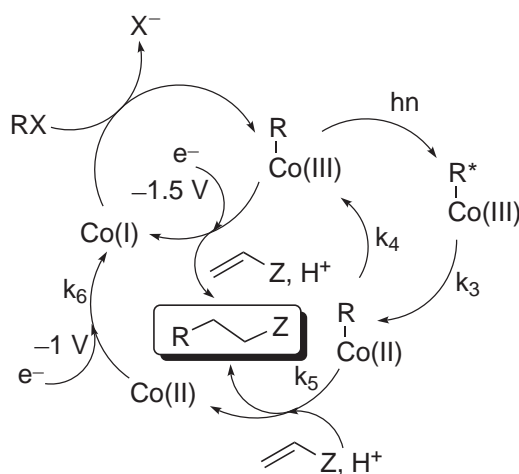
Electrocatalytic dehalogenation of organohalides has also been performed in heterogeneous conditions, at a graphite electrode coated by a poly(acrylic acid) film grafted with the nickel(II) tetra-azamacrocyclic complex (20).²⁹²



(20)

9.10.5.3.3 Vitamin B₁₂ derivatives and model complexes

The cobalt atom in cobalamins and cobinamides can exist under the formal reduced state Co^I, which is characterized by strong nucleophilic properties.²⁹³ Vitamin B₁₂ derivatives and cobalt(II) model complexes can thus catalyze the electrochemical reduction^{294–296} and the reductive coupling²⁹⁷ of alkyl halides. The rate-determining step is the nucleophilic attack of Co^I on the halide to form an alkyl-cobalt(III) complex,^{296,297} which is then reductively cleaved to yield reduced organic products. These electrocatalytic systems are relevant to biological catalytic systems, and are also of interest for analytical and synthetic applications. A striking example is the sun-powered photo-assisted electrosynthesis of the pheromone (±)-4-methyl-3-heptanone from ethylbromide and 2-methyl-1-penten-3-one, using vitamin B₁₂ as photo- and electrocatalyst (Scheme 9).²⁹⁸



Scheme 9

Vitamin B₁₂ derivatives are also effective catalysts for the electroreductive cyclization of bromoalkenes in conductive microemulsions,^{299,300} or for ring-expansion reactions in cyclic α -(bromomethyl)- β -keto esters in DMF.³⁰¹ Vitamin B₁₂ attached to an epoxy-polymer has been used in electrosynthesis of valeronitrile by reductive coupling of iodoethane and acrylonitrile.³⁰²

Potential applications of vitamin B₁₂ in electrocatalytic degradation of dibromide and α -haloacetic acid pollutants has been demonstrated in aqueous buffers^{303,304} and in surfactant-stabilized emulsions.³⁰⁵ Electroreductive dehalogenations in water and microemulsions were also efficiently catalyzed by a vitamin B₁₂ derivative grafted onto a polylysine-coated electrode.³⁰⁶

Cobaloxime(I) generated by the electrochemical reductions of cobaloxime(III), the most simple model of vitamin B₁₂, has been shown to catalyze radical cyclization of bromoacetals.³⁰⁷ Cobalt(I) species electrogenerated from [Co^{II}TPP] also catalyze the reductive cleavage of alkyl halides. This catalyst is much less stable than vitamin B₁₂ derivatives.²⁹⁶ It has, however, been applied in the carboxylation of benzyl chloride and butyl halides with CO₂.³⁰⁸ Heterogeneous catalysis of organohalides reduction has also been studied at cobalt porphyrin-film modified electrodes,^{275,309–311} which have potential application in the electrochemical sensing of pollutants.

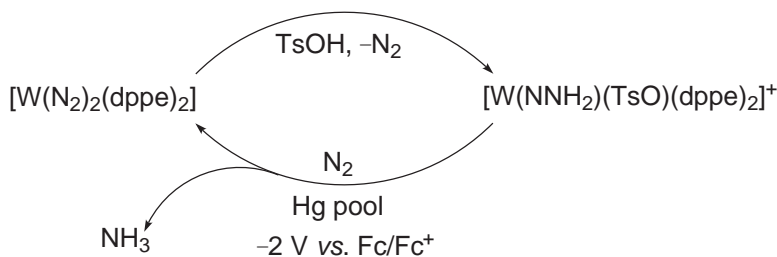
9.10.6 ELECTROCATALYTIC REDUCTION OF DINITROGEN AND NITROGEN OXIDES

9.10.6.1 Electrocatalytic Activation of Dinitrogen

The conversion of molecular nitrogen to ammonia constitutes a potentially useful energy-storage reaction utilizing abundant raw material. The interaction of molecular dinitrogen with metal centers has been studied in considerable depth. It has been shown that N₂ can be bound and reduced to NH₃ at Mo, W, V, or Fe centers, particularly where these metals are in a low oxidation state and have a tertiary phosphine environment.³¹²

Considerable attention has been paid to electrochemical reactions which lead to formation, transformation, or cleavage of (nitrogen–ligand)–metal bonds.^{313–315} The nitrogen ligand can be dinitrogen, but also cyanide, aminocarbide, nitrides, imides, amides, methyleneamide, hydrazides, diazoalkanes, or diazenides.³¹³ These electrochemical reactions may be relevant to biological nitrogen fixation and can provide routes from dinitrogen to ammonia and other nitrogen compounds.

An electrochemical cycle (Scheme 10) has been developed for the synthesis of ammonia using the dinitrogen complex *trans*-[W(N₂)₂(dppe)₂].^{316,317} Protonation with *p*-toluenesulfonic acid gives the hydrazido cation *trans*[W(NNH₂)(*p*-MeC₆H₄SO₃)(dppe)₂]⁺. Reduction of the latter at a mercury-pool cathode in tetrahydrofuran electrolyte under N₂ (1 atm) affords free ammonia in excellent yield (20–30% per mol of complex catalyst) with regeneration of the dinitrogen complex.³¹⁷ Successive electronation–protonation cycles could be performed in a single cathodic compartment to produce significant amounts of ammonia.



Scheme 10

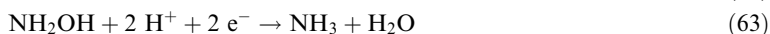
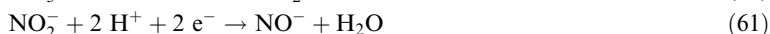
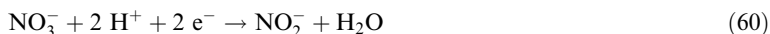
The electrocatalytic properties of several parent dinitrogen or hydrazido-containing molybdenum and tungsten complexes with dppe ligand have also been investigated. Each of these complexes yielded NH₃, in chemical yields which ranged from 1% to 36% per mole of complex.³¹⁸

Active catalysts for dinitrogen activation have been prepared by reduction at a mercury pool of MoCl₅ in basic methanolic solutions containing MgCl₂, phospholipids, and various tertiary phosphines.³¹⁹ The turnover number reached several hundreds per Mo center. Both ammonia and hydrazine were formed in a ratio of about 1:10.

Electroreduction of N₂ to NH₃ has also been examined using gas-diffusion electrodes modified by 14 different metal phthalocyanines.³²⁰ It was found that the Sn–Pc complex is the best catalyst in terms of current efficiency and stability of the electrode for the electrochemical dinitrogen activation.

9.10.6.2 Electrocatalytic Conversion of Nitrate to Ammonia

The reduction of NO₃[−] to NH₃ is an 8-electron process, which probably involves the intermediate formation of nitrite and hydroxylamine:



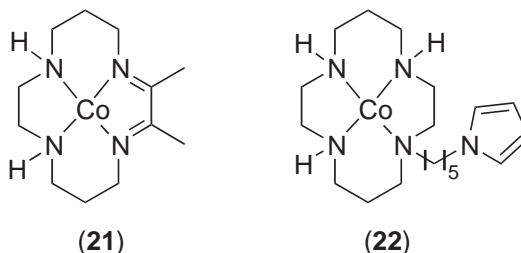
This process is of interest for the destruction of nitrate in water and nitrate electrocatalytic reduction offers a possible route to treat contaminated water.

This reduction has been performed in water at glassy carbon electrodes modified by the cluster [Mo₂Fe₆S₈(SC₆H₅)₉](*n*-Bu₄N)₃ by controlled-potential electrolysis at −1.25 V vs. SCE, with a

good current efficiency (80%) for the formation of NH_3 .³²¹ Nitrite and hydroxylamine were detected as reaction intermediates, but both of them are reduced to ammonia under the same conditions.

Co^{III} -cyclam^{322–324} and Ni^{II} -cyclam³²² catalyze the electroreduction of nitrate in aqueous electrolytes with good current efficiencies and turnover numbers, giving mixtures of ammonia, nitrite, and hydroxylamine at a variety of electrode materials. Mechanistic investigations suggested the adsorption of electroreduced Co^{I} - and Ni^{I} -cyclam onto the electrode surface,³²² and the formation of an oxo-metal bond via reduction of coordinated nitrate.³²³

Complex (21), a Co^{II} -cyclam analogue, is very active for the reduction of NO_2^- and NH_2OH intermediates and catalyzes the complex electrochemical conversion of NO_3^- to NH_3 .³²⁵ Gold electrodes modified with cobalt-cyclam incorporated in Nafion[®] films,³²⁴ or by electropolymerization of the pyrrole-substituted cobalt cyclam (22)³²⁶ have shown catalytic activity for the reduction of nitrate in strongly basic media.

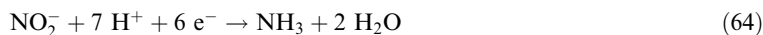


9.10.6.3 Electrocatalytic Reduction of Nitrite and Nitric Oxide

The first interest in the electroreduction of NO_2^- or NO catalyzed by metal complexes is to model the activity of nitrite reductase enzymes.³²⁷ There is also an extensive growth in studies related to the development of metal complex-based electrochemical sensors for NO determination in biological and environmental samples.^{328,329} Nitrate disproportionates to nitric oxide and nitrate in aqueous solution.

9.10.6.3.1 Metal complexes of nitrogen macrocycles

Water soluble iron porphyrins $[\text{Fe}^{\text{III}}(\text{TPPS})(\text{H}_2\text{O})_n]^{3+}$ ³³⁰ and $[\text{Fe}^{\text{III}}(\text{TMPyP})(\text{H}_2\text{O})_2]^{5+}$ ^{331,332} (TPPS = *meso*-tetrakis(*p*-sulfonatophenyl)porphyrin, TMPyP = *meso*-tetrakis(*N*-methyl-4-pyridinium)porphyrin³³¹ or *meso*-tetrakis(*N*-methyl-2-pyridinium)porphyrin³³² dications) act as effective electrocatalysts for the reduction of nitrite to ammonia in aqueous electrolytes (Equation (64)); $E_{1/2} = 0.103 \text{ V vs. SCE at pH } 7$, with NH_2OH or N_2O also appearing as products depending on the reaction conditions. Nitric oxide then ligates to the iron(III) porphyrin to form a nitrosyl complex $[\text{Fe}^{\text{II}}(\text{P})(\text{NO}^+)]$ (P = porphyrin) as intermediate.



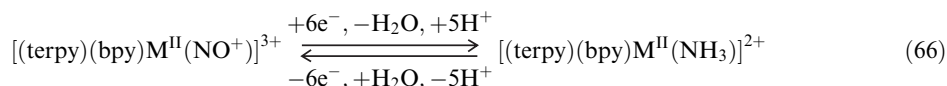
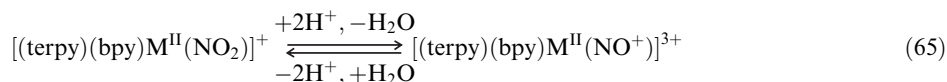
Reduction of the nitrosyl complex occurs by sequential electron steps.^{330–332} Although NH_3 is the ultimate reduction product at -0.9 V vs. SCE , NH_2OH appeared to be an intermediate and reduction at the first two-electron stage at a less negative potential (-0.63 V) gave increasing yields of N_2O .³³¹ Polymeric films synthesized at electrode surfaces by electropolymerization of an iron(III) (protoporphyrin-IX)-dimethylester catalyzes the electroreduction of NO_2^- or NO to N_2O , N_2 , NH_2OH , and NH_3 .³³³ The formation of dinitrogen as a major product is the most striking difference between the heterogeneous system and electrocatalysis with water-soluble iron porphyrins. It was suggested that the enhanced N–N coupling may be a consequence of the enforced proximity between the catalytic sites within the polymeric matrix.

The electroreduction of NO to NH_2OH and NH_3 in aqueous media is also catalyzed by Mn^{III} -TMPyP complexes.³³⁴ In contrast to the behavior found with iron porphyrin complexes, the reaction proceeds through an ECE mechanism, in which reduction of Mn^{III} to Mn^{II} is followed by NO coordination and then by electroreduction of $[\text{Mn}^{\text{II}}(\text{NO})(\text{TMPyP})]$.

Co^{III}-cyclam³²² and vitamin B₁₂³³⁵ catalyze the reduction of NO₂⁻ or NO to give NH₂OH and NH₃ as reaction products.

9.10.6.3.2 Polypyridyl complexes

Studies on the electrochemical reduction of [(terpy)(bpy)M^{II}(NO₂)⁺] complexes (M = Ru, Os) have relevance for the catalytic conversion of nitrite to ammonia:^{336,337}



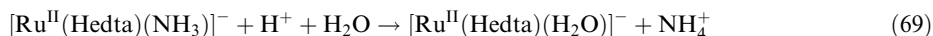
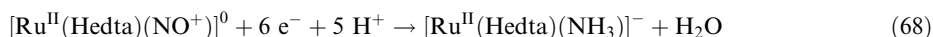
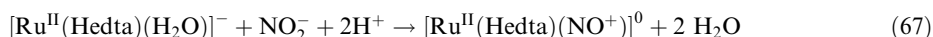
The key step is the acid–base interconversion of the nitrosyl [(terpy)(bpy)M^{II}(NO)]³⁺ complex (Equation (65)), which undergoes a series of stepwise, one-electron reductions associated with acid–base reactions (Equation (66)). Experimental evidence has been obtained for a series of intermediates formulated as [M^{IV}(NH)]²⁺, [M^V(N)]⁺, [M^{II}(NH₂OH)]²⁺, [M^{II}(NHO)]²⁺, and [M^{II}(NO·)]²⁺ [M = (terpy)(bpy)Ru or (terpy)(bpy)Os].³³⁷

The oxo complex *trans*-[Re^V(py)₄(O)]²⁺ catalyzes the reduction of NO₂⁻ to NH₃ through the Re^{III/II} redox couple.³³⁸

9.10.6.3.3 Polyaminocarboxylate complexes

[Ru^{II}(Hedta)(NO⁺)⁰] and [Fe^{II}(Hedta)(NO)]⁻ have been shown to be effective electrocatalysts for the reduction of NO₂⁻ in acidic aqueous media, to yield N₂O, N₂, NH₃OH⁺, or NH₄⁺.^{339,340} An element of selectivity is available by control of pH and applied potential. Steps involved in the typical six-electron reduction of nitrite to ammonia catalyzed by [Ru^{II}(Hedta)(NO⁺)⁰] are summarized in Equations (67)–(69). The mechanisms by which nitrite is reduced appeared to be similar to those identified for Fe–porphyrin³³¹ and Ru or Os–polypyridyl complexes.³³⁷

The iron complex (23) adsorbed on graphite electrode surfaces is an active catalyst for the electroreduction of both nitrite and nitric oxide to yield NH₂OH and NH₃, as demonstrated by rotating ring-disk electrode voltammetry experiments.³⁴¹

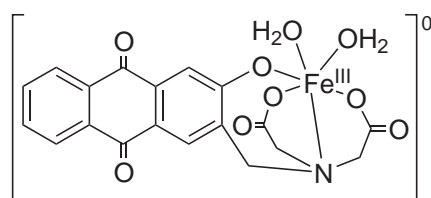


9.10.6.4 Electrochemical Sensors for Nitrite and Nitric Oxide Determination

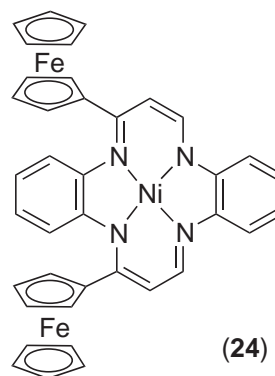
There is an increasing interest in the development of electrochemical sensors and microsensors for detecting and monitoring NO or NO₂⁻, due to their importance in clinical and environmental analysis. It has been suggested that transition metal electrocatalysts active for NO or NO₂⁻ coordination and reduction could be exploited for the development of metal-complex film electrodes for NO₂⁻ and NO sensing.^{333,342,343} However, most of the sensory devices reported so far in the literature are based on metal complexes able to catalyze NO oxidation through purely outer-sphere electron transfer. An exhaustive overview of the various attempts to develop microsensors for NO determination by catalytic oxidation has been published recently.³⁴⁴

Extensive work has been carried out on microsensors built from electropolymerized nickel porphyrin films.^{328,329} Films of Prussian blue (Fe₄[Fe(CN)₆]₃),³⁴⁵ metal–salen complexes (M = Co, Fe, Cu, Mn),³⁴⁶ or the ferrocene-containing Ni^{II}-tetraaza[14] annulene (24),³⁴⁷ also exhibit interesting activity for NO electrooxidation and sensing.

Films of [Os^{II}(bpy)₂(pvp)₁₀Cl]Cl³⁴⁸ and [Ru^{II}(bpy)₂(pvp)₁₀Cl]Cl³⁴⁹ (pvp = poly(4-vinylpyridine)) have been shown active for reductive and oxidative detection of nitrite, respectively.



(23)



(24)

9.10.7 ELECTROCATALYTIC REDUCTION AND ACTIVATION OF DIOXYGEN

9.10.7.1 Electrocatalytic Four-electron Reduction of Dioxygen

The four-electron reduction of dioxygen in water (Equation (70)) is an essential reaction carried out by aerobic organisms during the energy production cycle in the mitochondria.



The development of such a reaction proceeding under mild conditions is a technological challenge constituting one of the key points for the finalizing of efficient and low cost fuel cells. The catalytic properties of macrocyclic complexes like porphyrins and phthalocyanines for the reduction of molecular oxygen have been well known for four decades^{350,351} and numerous papers are devoted to this area. Here only some relevant and recent work in this field is described.

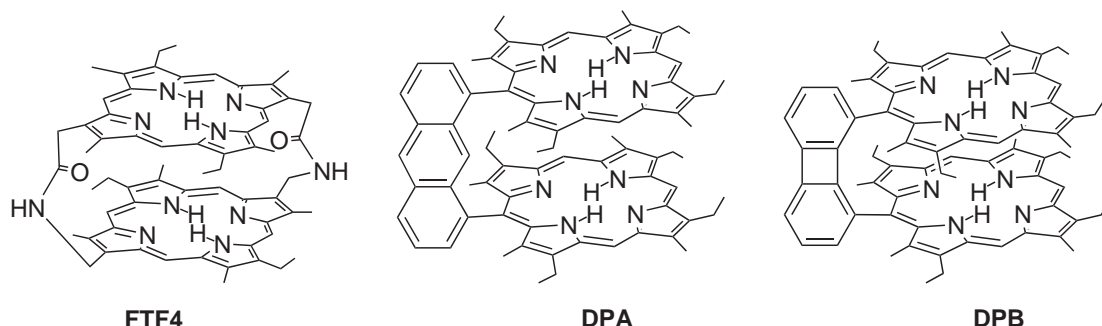
Most transition metal macrocyclic complexes catalyze the reduction of dioxygen following a two-electron process leading to H_2O_2 at relatively negative potentials.^{352,353} Alternatively, H_2O_2 rapidly destroys the catalyst. For a fuel cell application it is necessary to use catalysts capable of delivering four electrons, more or less simultaneously, to the dioxygen substrate at as positive a potential as possible (near the reversible potential 1.23 V vs. NHE).

Several strategies based on porphyrin derivatives have been developed to reach this objective. The first approach involves the utilization of dimeric cofacial metallic porphyrins adsorbed on the surface of an edge-plane graphite (EPG) electrode.¹⁸ An O_2 molecule was expected to be coordinated to form a $\mu\text{-O}_2$ bridge between the two metal centers allowing subsequent scission of the O—O bond by reductive activation, while the dimeric structure acts as a four-electron reservoir.

A large range of cofacial diporphyrins possessing different linking groups, containing different metal centers, and having diverse metal–metal separations has been synthesized and tested.^{354–369} Only a few examples promote the four-electron reduction to H_2O , most other cofacial metalloporphyrins catalyze mainly the two-electron reduction to H_2O_2 . The efficiency of the four-electron reduction of O_2 vs. the two-electron one has been evaluated by rotating ring-disk voltammetry experiments.

Best results were obtained with cofacial cobalt bisporphyrins using the ligands depicted in Scheme 11. For the bisporphyrins linked by two amide chains (FTF4) the increase of the length of the linkage chain decreases dramatically the efficiency of the H_2O production vs. the H_2O_2 formation, showing that the metal–metal distance is a crucial factor. A particular orientation of the two metal sites is necessary to stabilize intermediates and promote the four-electron reduction. For ligands having slipping flexibility (DPA and DPB, containing the anthracene and biphenylene bridges, respectively) the geometric requirement is less strict, this singly bridged ligand may be flexible enough to adopt an appropriate metal–metal distance. The distribution of two- and four-electron products is strongly dependent on the pH of the oxygenated electrolytic solution, since for pH 3.5 no H_2O_2 is detected while at pH above 4.5 H_2O_2 is the major product. It has been

suggested that the reduction process proceeds via the formation of a superoxo complex which is stabilized by interaction with Co^{III} ions. Replacement of one or two Co atoms by other metals (Cu, Mn, Pd, Al, amongst others) decreases dramatically the efficiency of the four-electron catalysis except when the second Co center is replaced by a metal cation having a strong Lewis acid character [Lu^{III} , Sc^{III}].³⁶⁶



Scheme 11

In addition, it has been shown that the performance of the four-electron O_2 reduction depends not only on the diporphyrin structure, but also on the electrode material upon which it is absorbed. Attempts to affix these catalysts onto electrode surfaces other than EPG, whilst preserving the four-electron catalytic activity, have been largely unsuccessful.¹⁸ One explanation is that some axial coordination of the porphyrin by the EPG electrode occurs which plays an important role.

The main problem arising from the utilization of cofacial bisporphyrins is the difficulty and the low yields of their synthesis. Some simpler strategies have been recently developed to immobilize a cofacial bisporphyrin-like structure on an electrode surface. Mixtures of water-soluble metalloporphyrins bearing positively (e.g., tetrakis(*N*-methyl-4-pyridinium)porphyrin) or negatively (e.g., tetrakis(4-sulphonatophenyl)porphyrin) charged peripheral units on the porphyrin ring are known to form stable ion-pair face-to-face bisporphyrins with a 1:1 molecular stoichiometry,^{370–372} the intermolecular distance between the porphyrin rings in this pair is small and close to that in covalently linked bisporphyrins. These ion-pair bisporphyrins can be easily immobilized on an electrode surface by adsorption or in Nafion[®] film. Although the ion pair Fe–Fe porphyrin gives only poor catalytic efficiency (12%) towards four-electron reduction of O_2 to H_2O ,³⁷⁰ a catalytic efficiency of >95% is reached with ion pair Co–Co or Co–Ru complexes.³⁷² Another alternative is to use an adsorbed μ -oxo Fe^{III} - or Mn^{III} -porphyrin dimer on an electrode surface.^{373–375} Electroreduction of the adsorbate in aqueous acid solution produces cofacially fixed M^{II} -porphyrin monomers able to reduce O_2 into H_2O with a yield >90%.³⁷⁵

It has been recently demonstrated that the simplest of the cobalt porphyrins (Co porphine) adsorbed on a pyrolytic graphite electrode is also an efficient electrocatalyst for reduction of O_2 into H_2O .³⁷⁶ The catalytic activity was attributed to the spontaneous aggregation of the complex on the electrode surface to produce a structure in which the cobalt–cobalt separation is small enough to bridge and activate O_2 molecules. The stability of the catalyst is quite poor and largely improved by using porphyrin rings with *meso*-substitution.^{377–380} However, as the size of the *meso*-substituents increases the four-electron reduction efficiency decreases.

A similar catalytic activity with a monomeric porphyrin of iridium has been observed when adsorbed on a graphite electrode.^{381–383} It is believed that the active catalyst on the surface is a dimeric species formed by electrochemical oxidation at the beginning of the cathodic scan, since cofacial bisporphyrins of iridium are known to be efficient electrocatalysts for the tetraelectronic reduction of O_2 . In addition, some polymeric porphyrin coatings on electrode surfaces have been also reported to be active electroactive catalysts for H_2O production, especially with adequately thick films or with a polypyrrole matrix.^{384–387}

A somewhat different approach has been explored in which the cobalt porphyrin molecules contain some coordinated metal complexes serving as electron donors attached to the periphery of the porphyrin ring.^{388–397} The idea is that molecules containing multiple redox active sites might be efficient catalysts for multiple electron-transfer reactions. A series of cobalt *meso*-tetrakis(4-pyridyl) and *meso*-tetrakis(4-cyanophenyl)porphyrins bound to $\{\text{Ru}(\text{NH}_3)_5\}^{2+}$ or $\{\text{Os}(\text{NH}_3)_5\}^{2+}$ fragments has been studied. The adsorbed complexes act as catalysts for the reduction of dioxygen, but at least two substituted metal complex groups are needed to ensure the four-electron reduction of O_2 instead of just a two-electron process. It has been demonstrated that this phenomenon is mainly due to π -back bonding interactions

between the Ru^{III} centers and the cobalt porphyrin, rather than to an intramolecular electron transfer process. Related systems in which the cobalt porphyrin is substituted by four $[(\mu_3\text{-O})\text{Ru}_3(\text{OAc})_6(\text{py})_2]^+$ clusters (py = pyridine) or by $\{\text{Ru}(\text{bpy})_2\text{Cl}\}^+$ groups have also been developed.^{398–403} The first system adsorbed on a glassy carbon electrode exhibits outstanding catalytic activity for the tetraelectronic reduction of O₂ to H₂O, while the second system has been employed for construction of efficient amperometric sensors for detection of NADH, dopamine,⁴⁰⁰ SO₂, or sulfite anion,^{402,403} for instance.

In contrast to Co–porphyrin complexes, the direct four-electron reduction of O₂ has been only very rarely claimed to be catalyzed by a cobalt phthalocyanine.^{404–407} In particular cofacial binuclear Co–Pc complexes immobilized on pyrolytic graphite catalyze only the two-electron electroreduction of O₂ to H₂O₂.^{408,409} However, recent work has established that an electropolymerized Co–Pc derivative provides a stable four-electron reduction pathway over a wide pH range.⁴¹⁰

In contrast to the porphyrin case, Fe–Pc appears to be a more promising candidate than Co–Pc for the electroreduction of O₂ to H₂O.^{126,411–413} A large number of papers has been published on this subject and some authors have attributed the four-electron reduction to give H₂O to the catalytic activity of the Fe–Pc in chemically decomposing electrogenerated H₂O₂ on the electrode surface.

To be a viable candidate as cathode electrocatalyst in fuel cell applications, a complex must have a good electrocatalytic stability. The beneficial effect of heat-treatment of N₄-macrocyclic metal complexes (porphyrin, phthalocyanines, and tetraazaannulene complexes, with metal = Fe or Co) adsorbed on carbon on their stability and efficiency as electrocatalysts, has been known for more than two decades.^{414,415} Many papers have focused on the transformation of N₄-macrocyclic metal complexes (adsorbed on high-area carbon), which occurs at high temperature (500–1,000 °C). However, there is still no agreement about the nature of the species formed during this treatment, and which of them are truly responsible for the improvement in catalytic performance.^{416–425} The best electrocatalytic activities have been shown to occur with a pyrolysis temperature of <700 °C; however, the resulting catalysts are only moderately stable.^{421,422} In these conditions the catalytic sites seem to be N₄-metal complexes bound to the carbon support. With higher pyrolysis temperatures (≥800 °C), the catalyst is more stable but shows lower catalytic activity.^{423,424} The catalytic site is no longer a simple N₄-metal complex but its exact structure has not yet been elucidated.⁴²⁵ Moreover, it has been shown that at these high pyrolysis temperatures, it is not even necessary to use a presynthesized metal–macrocyclic complex to obtain a good catalyst: a catalyst for O₂ reduction can be simply obtained by pyrolyzing a metal precursor (e.g., Fe or Co salt) and an N-donor ligand precursor coadsorbed on carbon.^{426,427}

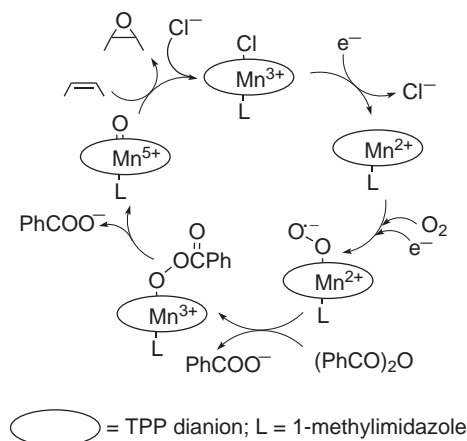
Another important aspect of the four-electron reduction of dioxygen is the design of molecules mimicking the active site of cytochrome *c* oxidase. This terminal enzyme of the respiratory chain performs the four-electron reduction of dioxygen to water in the mitochondria. This reaction is coupled to proton transport through the membrane, and the energy released is used to synthesize ATP from ADP. The active site has a structural motif in which a myoglobin-type iron center is associated with a *tris*-histidine copper center. A few synthetic models which combine a structural similarity to natural site with catalytic activity have been recently reported. These biomimetic models are constructed from a cobalt(II) or iron(II) picket-fence porphyrin covalently linked to a copper(I) site also coordinated by a triazamacrocyclic or by imidazole moieties.^{428–431} When adsorbed on an EPG electrode, these bimetallic complexes catalyze the four-electron reduction of O₂ at physiological pH (~7). Further studies have shown that the iron-only complex (without copper coordinated) is an efficient catalyst for the four-electron reduction of O₂.^{432–434} These results seem to indicate that an iron porphyrin adsorbed on an electrode is an intrinsically efficient catalyst for the reduction, and that the formation of a μ -peroxo intermediate between iron and copper centers is not necessary for O₂ activation in the enzyme site.

9.10.7.2 Electrocatalytic P-450 Model Systems

The cytochrome P-450 monooxygenase is a heme system which is capable of catalytic oxygenation of hydrocarbons, yielding alcohols from alkanes and epoxides from alkenes. Many chemical systems using synthetic metalloporphyrins and various oxygen sources have been proposed as models of the P-450 monooxygenase enzymatic system. As oxygen sources, the following compounds or systems have been utilized: iodosobenzene, hypochlorite, amine oxides, peroxycarboxylic acids, hydrogen peroxide, alkyl hydroperoxides, or molecular oxygen (in the presence of reducing agents such as sodium tetrahydroborate, hydrogen and colloidal platinum, or zinc powder and acetic acid), and potassium superoxide. In these models, the metal center of the porphyrins is reduced by electrons coming from chemical species generated during the reaction and the reduced porphyrin acts as a catalyst.

Considerably less work has been reported on an electrocatalytic approach to modeling cytochrome P-450 utilizing an electrochemically reduced metalloporphyrin (Fe or Mn) in the presence of

dioxygen.^{435–439} Nevertheless it has been demonstrated that epoxidation of alkenes can be achieved with a high selectivity following this approach. Scheme 12 describes the proposed electrocatalytic cycle involved using $[\text{Mn}^{\text{III}}(\text{TPP})\text{Cl}]$ as the electrocatalyst.⁴³⁶ The one-electron electrochemical reduction leads first to $[\text{Mn}^{\text{II}}(\text{TPP})]$ after loss of the chloride ligand, followed by strong dioxygen binding that promotes a second one-electron transfer to give a Mn^{II} -superoxo complex. This reacts with an acylating agent (for instance benzoic anhydride) added to the solution, to give a metalloacetylperoxy intermediate complex that undergoes O–O bond heterolysis to yield a high-valent oxo manganese porphyrin complex ($\text{Mn}^{\text{V}}=\text{O}$) which can transfer one oxygen atom to substrates. Addition of an extra ligand like 1-methylimidazole is also required to improve to stability of the catalyst.



Scheme 12

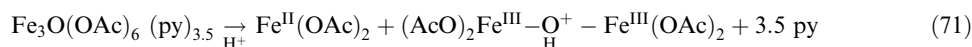
It has been found that this system is also able to oxidize alkanes to alcohols and ketones, and sulfides into sulfoxides and sulfones. Although the current efficiency of oxidation of the substrates is high (60–90%), the number of turnovers per molecule of catalyst is generally low. One limitation of such a system is the concurrent electrochemical reduction of the intermediate high-valent oxo-metal porphyrin complex. Several modifications of the system designed to improve the performance of the electrocatalysis have been investigated. One involves addition of a redox mediator (such as a viologen derivative) to increase the electron transfer rate from the electrode to the catalyst.⁴⁴⁰ A second approach is the use of an electrode covered by a polymeric film which is permeable to O_2 but acts as a transfer barrier to the porphyrin;⁴⁴¹ this prevents unproductive reduction of the oxo-metal porphyrin intermediate. In order to achieve rapid electron transfer to the enzyme model active site, the porphyrin complexes have been immobilized on the electrode surface,^{442–448} mainly as functionalized polypyrrole films. Comparison between homogeneous phase and supported phase electrocatalytic reactions shows that the confinement of the catalyst in a polymeric film on the electrode surface markedly improves its stability and dramatically improves turnover numbers.^{449,450}

Some similar electrocatalytic epoxidations have been carried out using Schiff base complexes instead of porphyrin complexes.^{451,452} However, the turnover per molecule of catalyst is lower due to the limited lifetime of the catalyst.

9.10.7.3 The Gif–Orsay System

The Gif system (dioxygen, acetic acid, pyridine, zinc powder, and an iron catalyst) is a very specific oxidizing system for oxidation of saturated hydrocarbons.⁴⁵³ It shows a selectivity different from other systems, especially those based on a biomimetic approach, in that it oxidizes saturated hydrocarbons mainly to ketones and gives only minor amounts of aldehydes. The yields of ketone (20–30%) are higher than those observed with comparable systems using molecular dioxygen. A convenient electrochemical equivalent of the Gif system, called the Gif–Orsay system, has been developed in parallel.^{454–457} Here a mercury pool cathode replaces the zinc powder as electron source and delivers electrons under well-controlled conditions ($E = -0.6$ V to -0.7 V vs. SCE). With a catalytic amount of the iron cluster $[\text{Fe}_3\text{O}(\text{OAc})_6(\text{py})_3]_3$ the yields of oxidation products and the regioselectivity are close to those observed in the chemical system. However, the advantage of the electrochemical oxidation method is that higher coulombic yields

are consistently reached than in the chemical system. Moreover, this coulombic yield tends to remain constant through the course of electrolysis, and better conversions could be achieved simply by prolonging the duration of electrolysis. It has been suggested that the real catalyst in the Gif-Orsay system is a protonated dimeric μ -oxo compound resulting from acidic decomposition of the initial iron cluster (Equation (71)):



The dimeric μ -oxo diferric complex is then reduced and reacts with HO_2 to produce a terminal oxo-iron(V) complex which oxidizes hydrocarbons.

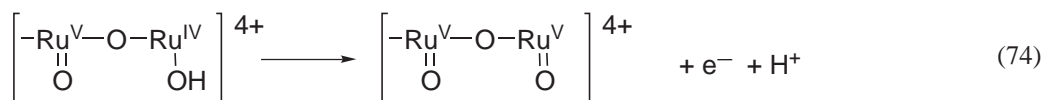
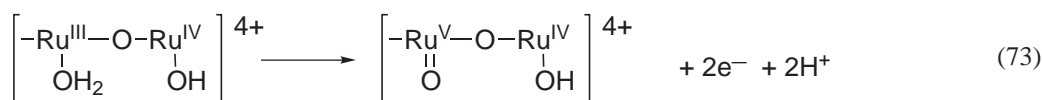
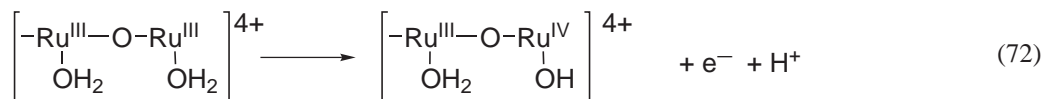
9.10.8 ELECTROCATALYTIC OXIDATION OF WATER AND ORGANICS

9.10.8.1 Oxidation of Water

Water oxidation has been the focus of intensive studies due its importance in photosynthesis and in designing devices for solar energy conversion.⁴⁵⁸ In the natural photosystem, a tetranuclear manganese cluster catalyzes evolution of oxygen by four-electron oxidation of water. Extensive efforts have been made to synthesize structural models of the water oxidation complex, but none of them act as an active catalyst for O_2 evolution without ambiguity. It was reported that $[\text{Mn}_2\text{O}_2(\text{bpy})_4]^{3+}$ works as a heterogeneous catalyst to evolve O_2 in aqueous suspension or when immobilized in a membrane deposited on an electrode surface.^{459,460} However, neither the reaction mechanism nor the nature of the catalytically active species has been elucidated. However, an electrochemical study of this complex in aqueous medium (bpy/bpyH⁺ buffer) has shown that it cannot act as a homogeneous electrocatalyst for H_2O oxidation,^{461,462} since the one-electron oxidized $\text{Mn}^{\text{IV}}-\text{Mn}^{\text{IV}}$ species is unstable and affords the stable tetranuclear complex $[\text{Mn}_4\text{O}_6(\text{bpy})_6]^{4+}$. Covalently linked Mn-porphyrin dimers were reported to electrochemically oxidize water in homogeneous solution, although it is far from a structural model of the water oxidation natural complex.⁴⁶³ The faradaic efficiency is modest (<2%) and the process occurs in MeCN containing 5% of H_2O at high anodic potential ($E = 1.8 \text{ V vs. Ag/Ag}^+$).

In contrast the oxo-ruthenium complex *cis,cis*- $[\{(\text{bpy})_2\text{Ru}^{\text{III}}(\text{OH}_2)_2(\mu\text{-O})\}]^{4+}$ and some of its derivatives are known to be active catalysts for the chemical or electrochemical oxidation of water to dioxygen.⁴⁶⁴⁻⁴⁷² Many studies have been reported⁴⁷³⁻⁴⁸¹ on the redox and structural chemistry of this complex for understanding the mechanism of water oxidation. Based on the results of pH-dependent electrochemical measurements, the basic structural unit is retained in the successive oxidation states from $\text{Ru}^{\text{III}}-\text{O}-\text{Ru}^{\text{III}}$ to $\text{Ru}^{\text{V}}-\text{O}-\text{Ru}^{\text{V}}$.⁴⁶⁶

A relatively low potential, one-electron oxidation is observed (Equation (72)), followed above pH 2.2 by a two-electron oxidation, two-proton step (Equation (73)) and a one-electron oxidation (Equation (74)). In more acidic solutions a direct three-electron oxidation occurs leading also to the $[\text{Ru}^{\text{V}}-\text{O}-\text{Ru}^{\text{V}}]^{4+}$ species. In various studies the $\text{Ru}^{\text{IV}}-\text{O}-\text{Ru}^{\text{IV}}$, $\text{Ru}^{\text{IV}}-\text{O}-\text{Ru}^{\text{V}}$, and $\text{Ru}^{\text{V}}-\text{O}-\text{Ru}^{\text{V}}$ species have been considered as the catalytically active form. Although these species have been characterized by resonance Raman and EPR spectroscopies,^{475,476,480} no definitive conclusion about the mechanism involved in the catalysis can be drawn and the question remains largely open.

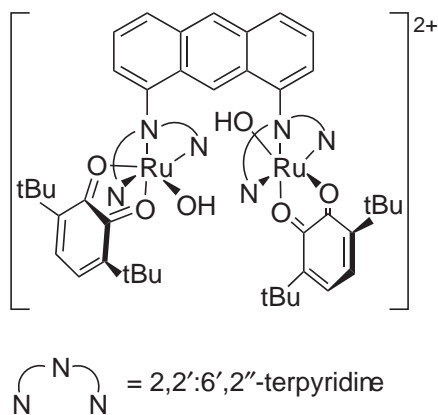


Bulk electrolysis studies have shown that for the parent μ -oxo complex $[\{(bpy)_2Ru^{III}(OH_2)\}_2(\mu-O)]^{4+}$ the current efficiency of oxygen evolution is quite low (19% at 1.30 V vs. SCE in 0.1 M CF_3SO_3H).⁴⁶⁶ This coulombic efficiency is dramatically improved ($\sim 90\%$ in 0.1 M H_3PO_4) by using an oxo complex containing a saturated alkyl bridge between bipyridines bound to each of the two ruthenium atoms.⁴⁷¹ Also it has been found that replacement of unsubstituted bpy in $[\{(bpy)_2Ru^{III}(OH_2)\}_2(\mu-O)]^{4+}$ by 4,4'- or 5,5'-dichloro-2,2'-bipyridine increases its stability,⁴⁷² while substitution of the bipyridine by CO_2H groups improves markedly the kinetics of the catalysis.^{467,468,470}

Several strategies to immobilize the μ -oxo catalysts on an electrode surface or in a membrane have been employed. However, no available data about their efficiency as modified electrodes for water oxidation have been given.⁴⁸²⁻⁴⁸⁶ It should be noted that $[\{(bpy)_2Ru^{III}(OH_2)\}_2(\mu-O)]^{4+}$ is also an excellent electrocatalyst for oxidation of chloride to chlorine (better than for the oxidation of H_2O into O_2) at 1.20 V vs. SCE in 0.05 M HCl solution,⁴⁸⁷ or at a modified electrode prepared by incorporation of the complex by ion-exchange into polystyrene sulfonate or Nafion[®] films.^{482,488}

The solution chemistry and water oxidation of a trinuclear complex $[(bpy)_2ORu^{III}(OH_2)(bpy)_2]^{6+}$ ⁴⁸⁹ and of a (nonisolated) binuclear Ru^{III} -terpyridine complex $[\{(terpy)(H_2O)_2Ru^{III}\}_2O]^{4+}$ ⁴⁹⁰ have also been reported. However, these complexes, as well as mononuclear $[Ru(bpy)_2(H_2O)_2]^{2+}$,⁴⁹¹ are not catalysts as a consequence of their fast decomposition.

Very recently a new kind of electrocatalyst has been propounded using the dinuclear quinone-containing complex of ruthenium (**25**).^{492,493} Controlled-potential electrolysis of the complex at 1.70 V vs. $Ag|AgCl$ in $H_2O + CF_3CH_2OH$ evolves dioxygen with a current efficiency of 91% (21 turnovers). The turnover number of O_2 evolution increases up to 33,500 when the electrolysis is carried out in water (pH 4.0) with an indium-tin oxide (ITO) electrode to which the complex is bound. It has been suggested that the four-electron oxidation of water is achieved by redox reactions of not only the two Ru^{II}/Ru^{III} couples, but also the two semiquinone/quinone couples of the molecule.

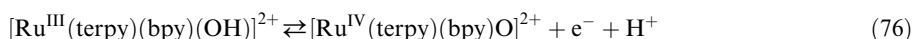
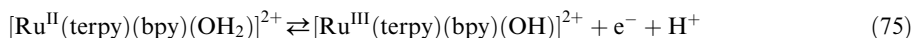


(25)

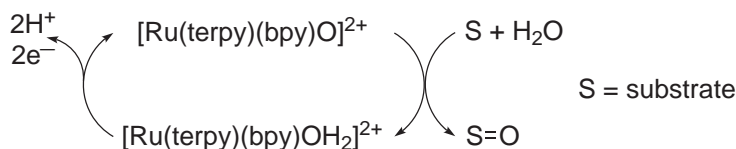
9.10.8.2 Oxidation of Organics

Many transition metal compounds with a high oxidation state are strong oxidants and are frequently used in synthetic organic chemistry. These principles of catalysis using such a class of metal complexes have been applied with success to the electrooxidation of organics, the electrode serving to regenerate the oxidant in the presence of substrates.

Among the metal complexes used in electrocatalytic oxidation of organic compounds, polypyridyl oxo-ruthenium complexes have attracted special attention,⁴⁹⁴⁻⁵⁰⁸ especially $[Ru^{IV}(terpy)(bpy)O]^{2+}$.^{495-497,499,500,502,504} This high oxidation state is reached from the corresponding Ru^{II} -aqua complex by sequential oxidation and proton loss (Equations (75) and (76)).



As an oxidant, the complex $[\text{Ru}(\text{terpy})(\text{bpy})\text{O}]^{2+}$ is coordinatively well-defined, chemically stable, and can be easily regenerated by the electrode according to the simplified Scheme 13.



Scheme 13

The organic compounds were dissolved or dispersed in an aqueous solution of the catalyst, with or without an organic cosolvent, and the net oxidations were carried out at applied potentials causing the oxidation of Ru^{II} to Ru^{IV} complex (0.6–0.8 V vs. SCE). It has been demonstrated that this electrocatalytic system is capable of providing a general and selective method for the oxidation of alcohols, aldehydes, cyclic ketones, and C—H bonds adjacent to alkeneic or aromatic groups.

Generally, primary aliphatic alcohols are oxidized to their respective aldehydes, secondary aliphatic and aromatic alcohols to the corresponding ketones, and allyl and benzyl alcohols to their carboxylic acid or carboxylate ions. For instance, 2-propanol, acetaldehyde, and methylbenzoate ions are oxidized quantitatively to acetone, acetate, and terephthalate ion respectively, while toluene is converted into benzoate ion with an 86% yield. Controlling the number of coulombs passed through the solution allows oxidation in good yield of benzyl alcohol to its aldehyde. For diols,⁵⁰² some excellent selectivity has been reached by changing the experimental conditions such as pH, number of coulombs, and temperature.

By using various polypyridyl oxo complexes a relationship between redox potentials ($E_{1/2}$) of the complexes and the efficiency and the selectivity of the electrocatalytic oxidation of alcohols and diols has been established.⁵⁰⁶ Higher $E_{1/2}$ gives higher reactivity. The best results, from the point of view of synthesis, were obtained with the complex *trans*- $[\text{Ru}^{\text{VI}}(\text{terpy})(\text{O})_2(\text{OH}_2)]^{2+}$ which is characterized by a high redox potential and a relatively high stability.

A number of mechanistic pathways have been identified for the oxidation, such as O-atom transfer to sulfides, electrophilic attack on phenols, hydride transfer from alcohols, and proton-coupled electron transfer from hydroquinone. Some kinetic studies indicate that the rate-determining step involves preassociation of the substrate with the catalyst.^{507,508} The electrocatalytic properties of polypyridyl oxo-ruthenium complexes have been also applied with success to DNA cleavage^{509,510} and sugar oxidation.⁵¹¹

Techniques for attaching such ruthenium electrocatalysts to the electrode surface, and thereby realizing some of the advantages of the modified electrode devices, have been developed.^{512–521} The electrocatalytic activity of these films have been evaluated and some preparative scale experiments performed. The modified electrodes are active and selective catalysts for oxidation of alcohols.^{516–521} However, the kinetics of the catalysis is markedly slower with films compared to bulk solution. This is a consequence of the slowness of the access to highest oxidation states of the complex and of the chemical reactions coupled with the electron transfer in films. In compensation, the stability of catalysts is dramatically improved in films, especially with complexes sensitive to bpy ligand loss like $[\text{Ru}(\text{bpy})_2(\text{O})_2]^{2+}$.^{517,519–521}

Another important class of catalysts and electrocatalysts for oxidation of organics is metalloporphyrin complexes. The majority of studies involving metalloporphyrin derivatives involves the reductive activation of oxygen (see Section 9.10.7). However, some interesting examples based on the direct electrooxidation of complexes in aqueous solution have been reported recently.^{522–527} The advantage of metalloporphyrin oxidation electrochemistry in aqueous solution is the possibility of selecting the appropriate oxidized form of the complex by adjusting the solution pH and the electrode potential. For instance, electrooxidation of the Fe^{III} complex of *meso*-tetrakis(3-sulfonatomesityl)porphyrin (TSMP) leads to high valent $[\text{O}=\text{Fe}^{\text{IV}}(\text{TSMP})]$, $[\text{O}=\text{Fe}^{\text{IV}}(\text{TSMP})]^+$, and $[\text{O}=\text{Fe}^{\text{IV}}(\text{TSMP})]^{2+}$ species corresponding to one-, two-, and three-electron oxidations, these species each exhibiting different activities for catalysis. $[\text{O}=\text{Fe}^{\text{IV}}(\text{TSMP})]$ slowly reacts with cyclopent-2-ene-1-acetic acid to form cyclopent-2-ene-4-one-1-acetic acid in the presence of dioxygen, whereas $[\text{O}=\text{Fe}^{\text{IV}}(\text{TSMP})]^+$ reacts rapidly to form cyclopent-2,3-diol-1-acetic acid in the absence of oxygen.^{524,526} In contrast, styrene oxidation by a high valent ruthenium porphyrin under electrochemical oxidation ($E = 1.24$ V in CH_2Cl_2) gives phenylacetaldehyde (96%) and benzaldehyde (4%).⁵²⁸

9.10.8.3 REFERENCES

1. Efimov, O. N.; Strelets, V. V. *Coord. Chem. Rev.* **1990**, *99*, 15–53.
2. Steckhan, E. *Angew. Chem., Int. Ed. Engl.* **1986**, *25*, 683–701.
3. Andrieux, C. P.; Dumas-Bouchiat, J.-M.; Savéant, J. M. *J. Electroanal. Chem.* **1978**, *87*, 39–53.
4. Merz, A. *Top. Curr. Chem.* **1990**, *152*, 49–90.
5. Deronzier, A.; Moutet, J.-C. *Coord. Chem. Rev.* **1996**, *147*, 339–371.
6. Koelle, U. *New J. Chem.* **1992**, *16*, 157–169.
7. Conway, B. E.; Tilak, B. V. *Adv. Catal.* **1992**, *38*, 1–147.
8. Houlding, V.; Geiger, T.; Koelle, U.; Graetzel, M. *J. Chem. Soc., Chem. Commun.* **1982**, 681–683.
9. Fisher, B.; Eisenberg, R. *J. Am. Chem. Soc.* **1980**, *102*, 7361–7363.
10. Efros, L. L.; Thorp, H. H.; Brudvig, G. W.; Crabtree, R. H. *Inorg. Chem.* **1992**, *31*, 1722–1724.
11. Collin, J.-P.; Jouaiti, A.; Sauvage, J.-P. *Inorg. Chem.* **1988**, *27*, 1986–1990.
12. Kellett, R. M.; Spiro, T. G. *Inorg. Chem.* **1985**, *24*, 2373–2377.
13. Kellett, R. M.; Spiro, T. G. *Inorg. Chem.* **1985**, *24*, 2378–2382.
14. Abe, T.; Taguchi, F.; Imaya, H.; Zhao, F.; Zhang, J.; Kaneko, M. *Polym. Adv. Technol.* **1998**, *9*, 559–562.
15. Zhao, F.; Zhang, J.; Abe, T.; Wöhrle, D.; Kaneko, M. *J. Mol. Catal. A: Chem.* **1999**, *145*, 245–256.
16. Zhao, F.; Zhang, J.; Wöhrle, D.; Kaneko, M. *J. Porphyrins Phthalocyanines* **2000**, *4*, 31–36.
17. Collman, J. P.; Ha, Y.; Wagenknecht, P. S.; Lopez, M. A.; Guillard, R. *J. Am. Chem. Soc.* **1993**, *115*, 9080–9088.
18. Collman, J. P.; Wagenknecht, P. S.; Hutchison, J. E. *Angew. Chem., Int. Ed. Engl.* **1994**, *33*, 1537–1554.
19. Bhugun, I.; Lexa, D.; Savéant, J.-M. *J. Am. Chem. Soc.* **1996**, *118*, 3982–3983.
20. Grass, V.; Lexa, D.; Savéant, J.-M. *J. Am. Chem. Soc.* **1997**, *119*, 7526–7532.
21. Koelle, U.; Graetzel, M. *Angew. Chem., Int. Ed. Engl.* **1987**, *26*, 567–570.
22. Koelle, U.; Kang, B.-S.; Infelta, P.; Comte, P.; Graetzel, M. *Chem. Ber.* **1989**, *122*, 1869–1880.
23. Ladwig, M.; Kaim, W. *J. Organomet. Chem.* **1992**, *439*, 79–90.
24. Caix, C.; Chardon-Noblat, S.; Deronzier, A.; Ziessel, R. *J. Electroanal. Chem.* **1993**, *362*, 301–304.
25. Chardon-Noblat, S.; Cosnier, S.; Deronzier, A.; Vlachopoulos, N. *J. Electroanal. Chem.* **1993**, *352*, 213–228.
26. Kaim, W.; Reinhardt, R.; Sieger, M. *Inorg. Chem.* **1994**, *33*, 4453–4459.
27. Caix, C.; Chardon-Noblat, S.; Deronzier, A.; Ziessel, R. *J. Electroanal. Chem.* **1996**, *403*, 189–202.
28. Caix, C.; Chardon-Noblat, S.; Deronzier, A.; Moutet, J.-C.; Tingry, S. *J. Organomet. Chem.* **1997**, *540*, 105–111.
29. Ladwig, M.; Kaim, W. *J. Organomet. Chem.* **1991**, *419*, 233–243.
30. Caix, C.; Chardon-Noblat, S.; Deronzier, A. *J. Electroanal. Chem.* **1997**, *434*, 163–170.
31. Cosnier, S.; Deronzier, A.; Vlachopoulos, N. *J. Chem. Soc., Chem. Commun.* **1989**, 1259–1261.
32. Cano-Yelo Bettega, H.; Moutet, J.-C.; Tingry, S. *J. Electroanal. Chem.* **1995**, *391*, 51–61.
33. Cano-Yelo Bettega, H.; Moutet, J.-C. *J. Electroanal. Chem.* **1994**, *364*, 271–275.
34. de Oliveira, I. M. F.; Moutet, J. C.; Vlachopoulos, N. *J. Electroanal. Chem.* **1990**, *291*, 243–249.
35. Deronzier, A.; Moutet, J. C.; Saint-Aman, E. *J. Electroanal. Chem.* **1992**, *327*, 147–158.
36. Hamar-Thibault, S.; Moutet, J.-C.; Tingry, S. *J. Organomet. Chem.* **1997**, *532*, 31–37.
37. Abe, T.; Hirano, K.; Shiraishi, Y.; Toshima, N.; Kaneko, M. *Eur. Polym. J.* **2001**, *37*, 753–761.
38. Abe, T.; Kaneko, M. *J. Mol. Catal. A: Chem.* **2001**, *169*, 177–183.
39. Schiavon, G.; Zecchin, S.; Pilloni, G.; Martelli, M. *J. Electroanal. Chem.* **1978**, *93*, 141–144.
40. Pilloni, G.; Zotti, G.; Mulazzani, Q. G.; Fuochi, P. G. *J. Electroanal. Chem.* **1982**, *137*, 89–102.
41. Fisher, J. R.; Compton, R. G.; Cole-Hamilton, D. J. *J. Chem. Soc., Chem. Commun.* **1983**, 555–556.
42. Koelle, U.; Ohst, S. *Inorg. Chem.* **1986**, *25*, 2689–2694.
43. Meilleur, D.; Rivard, D.; Harvey, P. D.; Lucas, D.; Mugnier, Y. *Inorg. Chem.* **2000**, *39*, 2909–2914.
44. Vlček, A., Jr.; Vlček, A. A. *Inorg. Chim. Acta* **1980**, *41*, 123–131.
45. Heyrovský, M. *Collect. Czech. Chem. Commun.* **2001**, *66*, 67–80.
46. Abe, T.; Taguchi, F.; Tokita, S.; Kaneko, M. *J. Mol. Catal. A: Chem.* **1997**, *126*, L89–L92.
47. Abe, T.; Toda, G.; Tajiri, A.; Kaneko, M. *J. Electroanal. Chem.* **2001**, *510*, 35–42.
48. Wienkamp, R.; Steckhan, E. *Angew. Chem., Int. Ed. Engl.* **1982**, *21*, 782–783.
49. Grammenudi, S.; Franke, M.; Voegtle, F.; Steckhan, E. *J. Incl. Phenom.* **1987**, *5*, 695–707.
50. Franke, M.; Steckhan, E. *Angew. Chem.* **1988**, *100*, 295–297.
51. Ruppert, R.; Herrmann, S.; Steckhan, E. *Tetrahedron Lett.* **1987**, *28*, 6583–6586.
52. Steckhan, E.; Herrmann, S.; Ruppert, R.; Dietz, E.; Frede, M.; Spika, E. *Organometallics* **1991**, *10*, 1568–1577.
53. Koelle, U.; Ryabov, A. D. *Mendeleev Commun.* **1995**, 187–189.
54. Hollmann, F.; Schmid, A.; Steckhan, E. *Angew. Chem., Int. Ed. Engl.* **2001**, *40*, 169–171.
55. Cosnier, S.; Gunther, H. *J. Electroanal. Chem.* **1991**, *315*, 307–312.
56. Hoefler, E.; Steckhan, E.; Ramos, B.; Heineman, W. R. *J. Electroanal. Chem.* **1996**, *402*, 115–122.
57. Beley, M.; Collin, J.-P. *J. Mol. Catal.* **1993**, *79*, 133–140.
58. Deronzier, A.; Moutet, J.-C. *Platinum Metals Rev.* **1998**, *42*, 60–68.
59. de Oliveira, I. M. F.; Moutet, J.-C. *J. Mol. Catal.* **1993**, *81*, L19–L24.
60. Chardon-Noblat, S.; de Oliveira, I. M. F.; Moutet, J.-C.; Tingry, S. *J. Mol. Catal. A: Chem.* **1995**, *99*, 13–21.
61. Moutet, J.-C.; Duboc-Toia, C.; Ménage, S.; Tingry, S. *Adv. Mater.* **1998**, *10*, 665–667.
62. Moutet, J.-C.; Yao Cho, L.; Duboc-Toia, C.; Ménage, S.; Riesgo, E. C.; Thummel, R. P. *New J. Chem.* **1999**, *23*, 939–944.
63. Arakawa, H.; Aresta, M.; Armor, J. N.; Barteau, M. A.; Beckman, E. J.; Bell, A. T.; Bercaw, J. E.; Creutz, C.; Dinjus, E.; Dixon, D. A.; Domen, K.; Du Bors, D. L.; Eckert, J.; Fujita, E.; Gibson, D. H.; Goddard, W. A.; Goodman, D. W.; Keller, J.; Kbas, G. J.; Kung, H. H.; Lyons, J. E.; Manzer, I. E.; Marks, T. J.; Morokumar, K.; Nicholas, K. M.; Periana, R.; Que, L.; Rostrup-Nielson, J.; Sachtler, W. M. H.; Schmidt, L. D.; Sen, A.; Somorjai, G. A.; Stair, P. C.; Stults, B. R. *Chem. Rev.* **2001**, *101*, 953–996.
64. Sullivan, B. P. *Platinum Metals Rev.* **1989**, *33*, 2–9 and references therein.
65. Augustynski, J.; Kedzierzawski, P.; Jermann, B. In *Advances in Chemical Conversions for Mitigating Carbon Dioxide*; Inui, T.; Anpo, M.; Izui, K.; Yanagida, S.; Yamaguchi, T. Eds.; Studies in Surface Science and Catalysis, Vol. 114; Elsevier: Amsterdam, 1998, pp 107–116.

66. Collin, J.-P.; Sauvage, J.-P. *Coord. Chem. Rev.* **1989**, *93*, 245–268.
67. Sullivan, B. P.; Bruce, M. R. M.; O'Toole, T. R.; Bolinger, C. M.; Megehee, E.; Thorp, H.; Meyer, T. J. Electro-catalytic Carbon Dioxide Reduction. In *Carbon Dioxide Activation by Metal Complexes*; Ayers, W. M., Ed., A. C. S. Symposium Series No 363; American Chemical Society: Washington, DC 1988; pp 52–90.
68. Keene, F. R.; Sullivan, B. P. In *Electrochemical and Electrocatalytic Reaction of Carbon Dioxide*; Sullivan, B. P., Krist, K.; Guard, H. E., Eds.; Elsevier: Amsterdam, **1993**, pp 118–145.
69. Hawecker, J.; Lehn, J.-M.; Ziessel, R. *J. Chem. Soc., Chem. Commun.* **1984**, 328–330.
70. Hawecker, J.; Lehn, J.-M.; Ziessel, R. *Helv. Chim. Acta.* **1986**, *69*, 1990–2012.
71. Sullivan, B. P.; Bolinger, C. M.; Conrad, D.; Vining, W. J.; Meyer, T. J. *J. Chem. Soc., Chem. Commun.* **1985**, 1414–1416.
72. Breikss, A. I.; Abruña, H. D. *J. Electroanal. Chem.* **1986**, *201*, 347–358.
73. Calzaferri, G.; Hädener, K.; Li, J. *J. Photochem. Photobiol. A: Chem.* **1992**, *64*, 259–262.
74. Christensen, P.; Hamnett, A.; Muir, A. V. G.; Timney, J. A. *J. Chem. Soc., Dalton Trans.* **1992**, 1455–1463.
75. Stor, G. J.; Hartl, F.; van Outersterp, J. W. M.; Stufkens D. J. *Organometallics* **1995**, *14*, 1115–1131.
76. Lee, Y. F.; Kirchhoff, J. R.; Berger, R. M.; Gosztola, D. *J. Chem. Soc., Dalton Trans.* **1995**, 3677–3682.
77. Scheiring, T.; Klein, A.; Kaim, W. *J. Chem. Soc., Perkin Trans. 2* **1997**, *2*, 2569–2571.
78. Wong, K.-Y.; Chung, W.-H.; Lau, C.-P. *J. Electroanal. Chem.* **1998**, *453*, 161–170.
79. Johnson, F. P. A.; George, M. W.; Hartl, F.; James, J. *J. Organometallics* **1996**, *15*, 3374–3387.
80. O'Toole, T. R.; Margerum, L. D.; Westmoreland, T. D.; Vining, W. J.; Murray, R. W.; Meyer, T. J. *J. Chem. Soc., Chem. Commun.* **1985**, 1416–1417.
81. O'Toole, T. R.; Sullivan, B. P.; Bruce, M. R.-M.; Margerum, L. D.; Murray, W. M.; Meyer, T. J. *J. Electroanal. Chem.* **1989**, *259*, 217–239.
82. Cosnier, S.; Deronzier, A.; Moutet, J.-C. *J. Electroanal. Chem.* **1986**, *207*, 315–321.
83. Cosnier, S.; Deronzier, A.; Moutet, J.-C. *J. Mol. Catal.* **1988**, *45*, 381–391.
84. Cosnier, S.; Deronzier, A.; Moutet, J.-C. *New J. Chem.* **1990**, *14*, 831–839.
85. Cabrera, C. R.; Abruña, H. D. *J. Electroanal. Chem.* **1986**, *2*, 09, 101–107.
86. Yoshida, T.; Tsutsumida, K.; Teratani, S.; Yasufuku, K.; Kaneko, M. *J. Chem. Soc., Chem. Commun.* **1993**, 631–633.
87. Ishida, H.; Tanaka, K.; Tanaka, T. *Chem. Lett.* **1985**, 405–406.
88. Ishida, H.; Tanaka, K.; Tanaka, T. *Organometallics* **1987**, *6*, 181–186.
89. Ishida, H.; Tanaka, H.; Tanaka, K.; Tanaka, T. *J. Chem. Soc., Chem. Commun.* **1987**, 131–132.
90. Ishida, H.; Fujiki, K.; Ohba, T.; Ohkubo, K.; Tanaka, K.; Tereda, T.; Tanaka, T. *J. Chem. Soc., Dalton Trans.* **1990**, 2155–2160.
91. Chardon-Noblat, S.; Collomb-Dunand-Sauthier, M.-N.; Deronzier, A.; Ziessel, R.; Zsoldos, D. *Inorg. Chem.* **1994**, *33*, 4410–4412.
92. Pugh, J. R.; Bruce, M. R. M.; Sullivan, B. P.; Meyer, T. J. *Inorg. Chem.* **1991**, *30*, 86–91.
93. Collomb-Dunand-Sauthier, M.-N.; Deronzier, A.; Ziessel, R. *J. Chem. Soc., Chem. Commun.* **1994**, 189–191.
94. Collomb-Dunand-Sauthier, M.-N.; Deronzier, A.; Ziessel, R. *Inorg. Chem.* **1994**, *33*, 2961–2967.
95. Chardon-Noblat, S.; Cripps, G. H.; Deronzier, A.; Field, J. S.; Gouws, S.; Haines, R. J.; Southway, F. *Organometallics* **2001**, *20*, 1668–1675.
96. Chardon-Noblat, S.; Deronzier, A.; Zsoldos, D.; Ziessel, R.; Haukka, M.; Pakkanen, T.; Venäläinen, T. *J. Chem. Soc., Dalton Trans.* **1996**, 2581–2583.
97. Chardon-Noblat, S.; Deronzier, A.; Ziessel, R. *Collect. Czech. Chem. Commun.* **2001**, *66*, 207–227.
98. Chardon-Noblat, S.; Deronzier, A.; Ziessel, R.; Zsoldos, D. *J. Electroanal. Chem.* **1998**, *444*, 253–260.
99. Chardon-Noblat, S.; Deronzier, A.; Hartl, F.; van Slagaren, J.; Mahabiersing, T. *Eur. J. Inorg. Chem.* **2001**, 613–617.
100. Bolinger, C. M.; Sullivan, B. P.; Conrad, D.; Gilbert, J. A.; Story, N.; Meyer, T. J. *J. Chem. Soc., Chem. Commun.* **1985**, 796–797.
101. Daniele, S.; Ugo, P.; Bontempelli, G.; Fiorani, M. *J. Electroanal. Chem.* **1987**, *219*, 259–271.
102. Garnier, L.; Rollin, Y.; Perichon, J. *New J. Chem.* **1989**, *13*, 53–59.
103. Simpson, T. C.; Durand, R. R., Jr. *Electrochim. Acta* **1988**, *33*, 581–583.
104. Bolinger, C. M.; Story, N.; Sullivan, B. P.; Meyer, T. J. *Inorg. Chem.* **1988**, *27*, 4582–4587.
105. Bruce, M. R. M.; Megehee, E.; Sullivan, B. P.; Thorp, H. H.; O'Toole, T. R.; Downard, A.; Meyer, T. J. *Organometallics* **1988**, *7*, 238–240.
106. Rasmussen, S. C.; Richter, M. M.; Yi, E.; Place, H.; Brewer, K. J. *Inorg. Chem.* **1990**, *29*, 3926–3932.
107. Bruce, M. R. M.; Megehee, E.; Sullivan, B. P.; Thorp, H. H.; O'Toole, T. R.; Downard, A.; Pugh, J. R.; Meyer, T. J. *Inorg. Chem.* **1992**, *31*, 4864–4873.
108. Mustafa Hossain, A. G. M.; Nagaoka, T.; Ogura, K. *Electrochim. Acta* **1996**, *41*, 2773–2780.
109. Hurrell, H. C.; Mogstad, A.-L.; Usifer, D. A.; Potts, K. T.; Abruña, H. D. *Inorg. Chem.* **1989**, *28*, 1080–1084.
110. Arana, C.; Yan, S.; Keshavarz-K, M.; Potts, K. T.; Abruña, H. D. *Inorg. Chem.* **1992**, *31*, 3680–3682.
111. Yoshida, T.; Iida, T. *J. Electroanal. Chem.* **1993**, *344*, 355–362.
112. Arana, C.; Keshavarz, M.; Potts, K. T.; Abruña, H. D. *Inorg. Chim. Acta.* **1994**, *225*, 285–295.
113. Lam, K.-M.; Wong, K.-Y.; Yang, S.-M.; Che, C.-M. *J. Chem. Soc., Dalton Trans.* **1995**, 1103–1107.
114. Ramos Sende, J. A.; Arana, C. R.; Hernández, L.; Potts, K. T.; Keshevarz-K, M.; Abruña, H. D. *Inorg. Chem.* **1995**, *34*, 3339–3348.
115. Nagao, H.; Mizukawa, T.; Tanaka, K. *Chem. Lett.* **1993**, 955–958.
116. Nagao, H.; Mizukawa, T.; Tanaka, K. *Inorg. Chem.* **1994**, *33*, 3415–3420.
117. Nakajima, H.; Mizukawa, T.; Nagao, H.; Tanaka, K. *Chem. Lett.* **1995**, 251–252.
118. Nakajima, H.; Kushi, Y.; Nagao, H.; Tanaka, K. *Organometallics* **1995**, *14*, 5093–5098.
119. Mizukawa, T.; Tsuge, K.; Nakajima, H.; Tanaka, K. *Angew. Chem., Int. Ed. Engl.* **1999**, *38*, 362–363.
120. Tanaka, K. *Bull. Chem. Soc. Jpn.* **1998**, *71*, 17–29.
121. Tanaka, K.; Mizukawa, T. *Appl. Organomet. Chem.* **2000**, *14*, 863–866.
122. Ali, Md.M.; Sato, H.; Mizukawa, T.; Tsuge, K.; Haga, M.-a.; Tanaka, T. *J. Chem. Soc., Chem. Commun.* **1998**, 249–250.
123. O'Toole, T. R.; Meyer, T. J.; Sullivan, B. P. *Chem. Mater.* **1989**, *1*, 574–576.

124. Bakir, M.; Sullivan, B. P.; MacKay, S. G.; Linton, R. W.; Meyer, T. J. *Chem. Mater.* **1996**, *8*, 2461–2467.
125. Costamagna, J.; Ferraudi, G.; Canales, J.; Vargas, J. *Coord. Chem. Rev.* **1996**, *148*, 221–248.
126. Zagal, J. H. *Coord. Chem. Rev.* **1992**, *119*, 89–136.
127. Vasudevan, P.; Phougat, N.; Shukla, A. K. *Appl. Organometal. Chem.* **1996**, *10*, 591–604.
128. Kapusta, S.; Hackerman, N. *J. Electrochem. Soc.* **1984**, *131*, 1511–1514.
129. Lieber, C. M.; Lewis, N. S. *J. Am. Chem. Soc.* **1984**, *106*, 5033–5034.
130. Yoshida, T.; Kamato, K.; Tsukamoto, M.; Iida, T.; Schlettwein, D.; Wöhrle, D.; Kaneko, M. *J. Electroanal. Chem.* **1995**, *385*, 209–225.
131. Abe, T.; Yoshida, T.; Tokita, S.; Taguchi, F.; Imaya, H.; Kaneko, M. *J. Electroanal. Chem.* **1996**, *412*, 125–132.
132. Mahmood, M. N.; Masheder, D.; Harty, C. J. *J. Appl. Electrochem.* **1987**, *17*, 1223–1227.
133. Masheder, D.; Williams, K. P. J. *J. Raman Spectrosc.* **1987**, *18*, 391–398.
134. Christensen, P. A.; Hamnett, A.; Muir, A. V. G. *J. Electroanal. Chem.* **1988**, *241*, 361–371.
135. Savinova, E. R.; Yashnik, S. A.; Savinov, E. N.; Parmon, V. N. *React. Kinet. Catal. Lett.* **1992**, *46*, 249–254.
136. Furuya, N.; Matsui, K. *J. Electroanal. Chem.* **1989**, *271*, 181–191.
137. Furuya, N.; Koide, S. *Electrochim. Acta* **1991**, *36*, 1309–1313.
138. Shibata, M.; Furuya, N. *J. Electroanal. Chem.* **2001**, *507*, 177–184.
139. Atoguchi, T.; Aramata, A.; Kazusaka, A.; Enyo, M. *J. Chem. Soc., Chem. Commun.* **1991**, 156–157.
140. Atoguchi, T.; Aramata, A.; Kazusaka, A.; Enyo, M. *J. Electroanal. Chem.* **1991**, *318*, 309–320.
141. Tanaka, H.; Aramata, A. *J. Electroanal. Chem.* **1997**, *437*, 29–35.
142. Aga, H.; Aramata, A.; Hisaeda, Y. *J. Electroanal. Chem.* **1997**, *437*, 111–118.
143. Sonoyama, N.; Kirii, M.; Sakata, T. *Electrochem. Commun.* **1999**, *1*, 213–216.
144. Behar, D.; Dhanasekaran, T.; Neta, P.; Hosten, C. M.; Ejeh, D.; Hambright, P.; Fujita, E. *J. Phys. Chem. A* **1998**, *102*, 2870–2877.
145. Becker, J. Y.; Vainas, B.; Eger-Levin, R.; Kaufman-Orenstein, L. *J. Chem. Soc., Chem. Commun.* **1985**, 1471–1472.
146. Hammouche, M.; Lexa, D.; Savéant, J.-M. *J. Electroanal. Chem.* **1988**, *249*, 347–351.
147. Hammouche, M.; Lexa, D.; Momenteau, M.; Savéant, J.-M. *J. Am. Chem. Soc.* **1991**, *113*, 8455–8466.
148. Bhugun, I.; Lexa, D.; Savéant, J.-M. *J. Am. Chem. Soc.* **1994**, *116*, 5015–5016.
149. Bhugun, I.; Lexa, D.; Savéant, J.-M. *J. Am. Chem. Soc.* **1996**, *118*, 1769–1776.
150. Bhugun, I.; Lexa, D.; Savéant, J.-M. *J. Phys. Chem.* **1996**, *100*, 19981–19985.
151. Tinnemans, A. H. A.; Koster, T. P. M.; Thewissen, D. H. M. W.; Mackor, A. *Recl. Trav. Chim. Pays-Bas* **1984**, *103*, 288–295.
152. Beley, M.; Collin, J.-P.; Ruppert, R.; Sauvage, J.-P. *J. Chem. Soc., Chem. Commun.* **1984**, 1315–1316.
153. Beley, M.; Collin, J.-P.; Ruppert, R.; Sauvage, J.-P. *J. Am. Chem. Soc.* **1986**, *108*, 7461–7467.
154. Fujihira, M.; Hirata, Y.; Suga, K. *J. Electroanal. Chem.* **1990**, *292*, 199–215.
155. Balazs, G. B.; Anson, F. C. *J. Electroanal. Chem.* **1992**, *322*, 325–345.
156. Balazs, G. B.; Anson, F. C. *J. Electroanal. Chem.* **1993**, *361*, 149–157.
157. Sakaki, S. *J. Am. Chem. Soc.* **1992**, *114*, 2055–2062.
158. Shionoya, M.; Kimura, E.; Itaka, Y. *J. Am. Chem. Soc.* **1990**, *112*, 9237–9245.
159. Smith, C. I.; Crayston, J. A.; Hay, R. W. *J. Chem. Soc. Dalton Trans.* **1993**, 3267–3269.
160. Abbà, F.; De Santis, G.; Fabbri, L.; Licchelli, M.; Manotti Lanfredi, A. M.; Pallavicini, P.; Poggi, A.; Ugozzoli, F. *Inorg. Chem.* **1994**, *33*, 1366–1375.
161. Fujita, E.; Haff, J.; Sanzenbacher, R.; Elias, H. *Inorg. Chem.* **1994**, *33*, 4627–4628.
162. Hay, R. W.; Kinsman, B.; Smith, C. I. *Polyhedron* **1995**, *14*, 1245–1249.
163. Hay, R. W.; Crayston, J. A.; Cromie, T. J.; Lightfoot, P.; de Alwis, D. C. L. *Polyhedron* **1997**, *16*, 3557–3563.
164. Bujno, K.; Bilewicz, R.; Siegfried, L.; Kaden, T. A. *J. Electroanal. Chem.* **1998**, *445*, 47–53.
165. Jarzebińska, A.; Rowiński, P.; Zawisza, I.; Bilewicz, R.; Siegfried, L.; Kaden, T. *Anal. Chim. Acta* **1999**, *396*, 1–12.
166. Pearce, D. J.; Pletcher, D. *J. Electroanal. Chem.* **1986**, *197*, 317–330.
167. Bailey, C. L.; Bereman, R. D.; Rillema, D. P.; Nowak, R. *Inorg. Chim. Acta* **1986**, *116*, L45–L47.
168. de Alwis, D.; Crayston, J. A.; Cromie, T.; Eisenblätter, T.; Hay, W. R.; Lampeka, Y. D.; Tsybal, L. V. *Electrochim. Acta* **2000**, *45*, 2061–2074.
169. Dubois, D. L. *Comm. Inorg. Chem.* **1997**, *19*, 307–325.
170. Dubois, D. L.; Miedaner, A. *J. Am. Chem. Soc.* **1987**, *109*, 113–117.
171. Dubois, D. L.; Miedaner, A.; Haltiwanger, R. C. *J. Am. Chem. Soc.* **1991**, *113*, 8753–8764.
172. Miedaner, A.; Curtis, C. J.; Barkley, R. M.; Dubois, D. L. *Inorg. Chem.* **1994**, *33*, 5482–5490.
173. Bernatis, P. R.; Miedaner, A.; Haltiwanger, R. C.; Dubois, D. L. *Organometallics* **1994**, *13*, 4835–4843.
174. Steffey, B. D.; Miedaner, A.; Maciejewski-Farmer, M. L.; Bernatis, P. R.; Herring, A. M.; Allured, V. S.; Carperos, V.; Dubois, D. L. *Organometallics* **1994**, *13*, 4844–4855.
175. Steffey, B. D.; Curtis, C. J.; Dubois, D. L. *Organometallics* **1995**, *14*, 4937–4943.
176. Wander, S. A.; Miedaner, A.; Noll, B. C.; Barkley, R. M.; Dubois, D. L. *Organometallics* **1996**, *15*, 3360–3373.
177. Miedaner, A.; Noll, B. C.; Dubois, D. L. *Organometallics* **1997**, *16*, 5779–5791.
178. Herring, A. M.; Steffey, B. D.; Miedaner, A.; Wander, S. A.; Dubois, D. L. *Inorg. Chem.* **1995**, *34*, 1100–1109.
179. Slater, S.; Wagenknecht, J. H. *J. Am. Chem. Soc.* **1984**, *106*, 5367–5368.
180. Szymaszek, A.; Pruchnik, F. P. *J. Organomet. Chem.* **1989**, *376*, 133–140.
181. Haines, R. J.; Wittrig, R. E.; Kubiak, C. P. *Inorg. Chem.* **1994**, *33*, 4723–4728.
182. Mostafa Hossain, A. G. M.; Nagaoka, T.; Ogura, K. *Electrochim. Acta* **1997**, *42*, 2577–2585.
183. Tezuka, M.; Yajima, T.; Tsuchiyana, A.; Matsumoto, Y.; Uchida, Y.; Hidai, M. *J. Am. Chem. Soc.* **1982**, *104*, 6834–6836.
184. Nakazawa, M.; Mizobe, Y.; Matsumoto, Y.; Uchida, Y.; Tezuka, M.; Hidai, M. *Bull. Chem. Soc. Jpn.* **1986**, *59*, 809–814.
185. Tomohiro, T.; Uoto, K.; Okuno, H. Y. *J. Chem. Soc., Chem. Commun.* **1990**, 194–195.
186. Kushi, Y.; Nagao, H.; Nishioka, T.; Isobe, K.; Tanaka, K. *Chem. Lett.* **1994**, 2175–2178.
187. Kushi, Y.; Nagao, H.; Nishioka, T.; Isobe, K.; Tanaka, K. *J. Chem. Soc., Chem. Commun.* **1995**, 1223–1224.
188. Ogura, K.; Sugihara, H.; Yano, J.; Higasa, M. *J. Electrochem. Soc.* **1994**, *141*, 419–424.

189. Ogura, K.; Endo, N.; Nakayama, M.; Ootsuka, H. *J. Electrochem. Soc.* **1995**, *142*, 4026–4032.
190. Ogura, K.; Nakayama, M.; Kusumoto, C. *J. Electrochem. Soc.* **1996**, *143*, 3606–3615.
191. Ogura, K.; Endo, N.; Nakayama, M. *J. Electrochem. Soc.* **1998**, *145*, 3801–3809.
192. Ogura, K.; Endo, N. *J. Electrochem. Soc.* **1999**, *146*, 3736–3740.
193. Duñach, E.; Perichon, J. *J. Organomet. Chem.* **1988**, *352*, 239–246.
194. Derien, S.; Duñach, E.; Perichon, J. *J. Am. Chem. Soc.* **1991**, *113*, 8447–8454.
195. Derien, S.; Clinet, J.-C.; Duñach, E.; Perichon, J. *J. Org. Chem.* **1993**, *58*, 2578–2588.
196. Derien, S.; Clinet, J.-C.; Duñach, E.; Perichon, J. *Synlett* **1990**, 361–364.
197. Duñach, E.; Perichon, J. *Synlett* **1990**, 143–145.
198. Derien, S.; Clinet, J.-C.; Duñach, E.; Perichon, J. *Tetrahedron* **1992**, *48*, 5235–5248.
199. Derien, S.; Clinet, J.-C.; Duñach, E.; Perichon, J. *J. Organomet. Chem.* **1992**, *424*, 213–224.
200. Olivero, S.; Duñach, E. *Eur. J. Org. Chem.* **1999**, 1885–1891.
201. Tascadda, P.; Duñach, E. *Heterocycl. Commun.* **1997**, *3*, 427–432.
202. Nedelec, J.-Y.; Perichon, J.; Troupel, M. *Top. Curr. Chem.* **1997**, *185*, 141–173.
203. Margel, S.; Anson, F. C. *J. Electrochem. Soc.* **1978**, *125*, 1232–1235.
204. Kamau, G. N.; Rusling, J. F. *J. Electroanal. Chem.* **1988**, *240*, 217–226.
205. Mabrouk, S.; Pellegrini, S.; Folest, J.-C.; Rollin, Y.; Perichon, J. *J. Organomet. Chem.* **1986**, *301*, 391–400.
206. Smith, W. H.; Kuo, Y.-M. *J. Electroanal. Chem.* **1985**, *188*, 189–202.
207. Rollin, Y.; Troupel, M.; Tuck, D. G.; Perichon, J. *J. Organomet. Chem.* **1986**, *303*, 131–137.
208. Durandetti, M.; Devaud, M.; Perichon, J. *New J. Chem.* **1996**, *20*, 659–667.
209. Yamamoto, T.; Wakabayashi, S.; Osakada, K. *J. Organomet. Chem.* **1992**, *428*, 223–237.
210. Amatore, C.; Jutand, A.; Perichon, J.; Rollin, Y. *Monatsh. Chem.* **2000**, *131*, 1293–1304.
211. Chaussard, J.; Folest, J.-C.; Nedelec, J.-Y.; Perichon, J.; Sibille, S.; Troupel, M. *Synthesis* **1990**, 369–381.
212. Condon-Gueugnot, S.; Leonel, E.; Nedelec, J.-Y.; Perichon, J. *J. Org. Chem.* **1995**, *60*, 7684–7686.
213. Marzouk, H.; Rollin, Y.; Folest, J.-C.; Nedelec, J.-Y.; Perichon, J. *J. Organomet. Chem.* **1989**, *369*, C47–C50.
214. Condon, S.; Dupre, D.; Falgayrac, G.; Nedelec, J.-Y. *Eur. J. Org. Chem.* **2002**, 105–111.
215. Cannes, C.; Condon, S.; Durandetti, M.; Perichon, J.; Nedelec, J.-Y. *J. Org. Chem.* **2000**, *65*, 4575–4583.
216. Schiavon, G.; Zotti, G.; Bontempelli, G.; Lo Coco, F. *Synth. Met.* **1988**, *25*, 365–373.
217. Schiavon, G.; Zotti, G.; Bontempelli, G.; Lo Coco, F. *J. Electroanal. Chem.* **1988**, *242*, 131–142.
218. Zotti, G.; Schiavon, G.; Comisso, N.; Berlin, A.; Pagani, G. *Synth. Met.* **1990**, *36*, 337–351.
219. Helary, G.; Chevrot, C.; Sauvet, G.; Siove, A. *Polym. Bull.* **1991**, *26*, 131–138.
220. Faid, K.; Ades, D.; Chevrot, C.; Siove, A. *Synth. Met.* **1993**, *55*, 845–850.
221. Chevrot, C.; Benazzi, T.; Barj, M. *Polymer* **1995**, *36*, 631–638.
222. Olivero, S.; Franco, D.; Clinet, J.-C.; Duñach, E. *Collect. Czech. Chem. Commun.* **2000**, *65*, 844–861.
223. Gosmini, C.; Rollin, Y.; Nedelec, J.-Y.; Perichon, J. *J. Org. Chem.* **2000**, *65*, 6024–6026.
224. Gomes, P.; Gosmini, C.; Nedelec, J.-Y.; Perichon, J. *Tetrahedron Lett.* **2000**, *41*, 3385–3388.
225. Le Gall, E.; Gosmini, C.; Nedelec, J.-Y.; Perichon, J. *Tetrahedron Lett.* **2001**, *42*, 267–269.
226. Oçafraïn, M.; Devaud, M.; Troupel, M.; Perichon, J. *J. Chem. Soc., Chem. Commun.* **1995**, 2331–2332.
227. Dolhem, E.; Oçafraïn, M.; Nedelec, J. Y.; Troupel, M. *Tetrahedron* **1997**, *53*, 17089–17096.
228. Dolhem, E.; Barhdadi, R.; Folest, J.-C.; Nedelec, J.-Y.; Troupel, M. *Tetrahedron* **2001**, *57*, 525–529.
229. Oçafraïn, M.; Devaud, M.; Nedelec, J. Y.; Troupel, M. *J. Organomet. Chem.* **1998**, *560*, 103–107.
230. Oçafraïn, M.; Dolhem, E.; Nedelec, J. Y.; Troupel, M. *J. Organomet. Chem.* **1998**, *571*, 37–42.
231. Schiavon, G.; Bontempelli, G.; Corain, B. *J. Chem. Soc., Dalton Trans.* **1981**, 1074–1081.
232. Troupel, M.; Rollin, Y.; Sibille, S.; Fauvarque, J.-F.; Perichon, J. *J. Chem. Res., Synop.* **1980**, 26–27.
233. Fauvarque, J.-F.; Petit, M. A.; Pfluger, F.; Jutand, A.; Chevrot, C.; Troupel, M. *Makromol. Chem., Rapid Commun.* **1983**, *4*, 455–457.
234. Torii, S.; Tanaka, H.; Morisaki, K. *Tetrahedron Lett.* **1985**, *26*, 1655–1658.
235. Bontempelli, G.; Fiorani, M. *Ann. Chim.* **1985**, *75*, 303–316.
236. Amatore, C.; Jutand, A. *Organometallics* **1988**, *7*, 2203–2214.
237. Amatore, C.; Jutand, A.; Mottier, L. *J. Electroanal. Chem.* **1991**, *306*, 125–140.
238. Amatore, C.; Carre, E.; Jutand, A.; Tanaka, H.; Ren, Q.; Torii, S. *Chem. Eur. J.* **1996**, *2*, 957–966.
239. Colon, I.; Kelsey, D. R. *J. Org. Chem.* **1986**, *51*, 2627–2637.
240. Jutand, A.; Negri, S.; Mosleh, A. *J. Chem. Soc., Chem. Commun.* **1992**, 1729–1730.
241. Jutand, A.; Mosleh, A. *J. Org. Chem.* **1997**, *62*, 261–274.
242. Fox, M. A.; Chandler, D. A.; Lee, C. *J. Org. Chem.* **1991**, *56*, 3246–3255.
243. Aboulkassim, A.; Chevrot, C. *Polymer* **1993**, *34*, 401–405.
244. Tomat, R.; Zecchin, S.; Schiavon, G.; Zotti, G. *J. Electroanal. Chem.* **1988**, *252*, 215–219.
245. Kijima, M.; Sakai, Y.; Shirakawa, H. *Synth. Met.* **1995**, *71*, 1837–1840.
246. Fauvarque, J.-F.; Chevrot, C.; Jutand, A.; Francois, M.; Perichon, J. *J. Organomet. Chem.* **1984**, *264*, 273–281.
247. Torii, S.; Tanaka, H.; Hamatani, T.; Morisaki, K.; Jutand, A.; Pfluger, F.; Fauvarque, J.-F. *Chem. Lett.* **1986**, 169–172.
248. Amatore, C.; Jutand, A. *J. Am. Chem. Soc.* **1991**, *113*, 2819–2825.
249. Amatore, C.; Jutand, A.; Khalil, F.; Nielsen, M. F. *J. Am. Chem. Soc.* **1992**, *114*, 7076–7085.
250. Carelli, I.; Chiarotto, I.; Cacchi, S.; Pace, P.; Amatore, C.; Jutand, A.; Meyer, G. *Eur. J. Org. Chem.* **1999**, 1471–1473.
251. Gosden, C.; Healy, K. P.; Pletcher, D. *J. Chem. Soc., Dalton Trans.* **1978**, 972–976.
252. Costa, G.; Puxeddu, A.; Reisenhofer, E. *J. Chem. Soc., Dalton Trans.* **1973**, 2034–2039.
253. Alleman, K. S.; Samide, M. J.; Peters, D. G.; Mubarak, M. S. *Curr. Top. Electrochem.* **1998**, *6*, 1–31.
254. Gosden, C.; Kerr, J. B.; Pletcher, D.; Rosas, R. *J. Electroanal. Chem.* **1981**, *117*, 101–107.
255. Mubarak, M. S.; Peters, D. G. *J. Electroanal. Chem.* **1995**, *388*, 195–198.
256. Dahm, C. E.; Peters, D. G. *J. Electroanal. Chem.* **1996**, *406*, 119–129.
257. Fang, D. M.; Peters, D. G.; Mubarak, M. S. *J. Electrochem. Soc.* **2001**, *148*, E464–467.
258. Duñach, E.; Esteves, A. P.; Freitas, A. M.; Medeiros, M. J.; Olivero, S. *Tetrahedron Lett.* **1999**, *40*, 8693–8696.

259. Fry, A. J.; Fry, P. F. *J. Org. Chem.* **1993**, *58*, 3496–3501.
260. Butler, A. L.; Peters, D. G. *J. Electrochem. Soc.* **1997**, *144*, 4212–4217.
261. Bhattacharya, D.; Samide, M. J.; Peters, D. G. *J. Electroanal. Chem.* **1998**, *441*, 103–107.
262. Gennaro, A.; Isse, A. A.; Maran, F. *J. Electroanal. Chem.* **2001**, *507*, 124–134.
263. Fry, A. J.; Sirisoma, U. N. *J. Org. Chem.* **1993**, *58*, 4919–4924.
264. Alleman, K. S.; Peters, D. G. *J. Electroanal. Chem.* **1998**, *451*, 121–128.
265. Isse, A. A.; Gennaro, A.; Vianello, E. *J. Electroanal. Chem.* **1998**, *444*, 241–245.
266. Pletcher, D.; Thompson, H. *J. Electroanal. Chem.* **1999**, *464*, 168–175.
267. Alleman, K. S.; Peters, D. G. *J. Electroanal. Chem.* **1999**, *460*, 207–213.
268. Dupriol, J.-M.; Bedioui, F.; Devynck, J.; Folest, J.-C.; Bied-Charreton, C. *J. Organomet. Chem.* **1985**, *286*, 77–90.
269. Fry, A. J.; Sirisoma, U. N.; Lee, A. S. *Tetrahedron Lett.* **1993**, *34*, 809–812.
270. Cannes, C.; Bedioui, F.; Condon-Gueugnot, S.; Nedelec, J.-Y.; Devynck, J. *New J. Chem.* **1999**, *23*, 489–494.
271. Folest, J.-C.; Dupriol, J.-M.; Perichon, J.; Robin, Y.; Devynck, J. *Tetrahedron Lett.* **1985**, *26*, 2633–2636.
272. Isse, A. A.; Gennaro, A.; Vianello, E. *J. Chem. Soc., Dalton Trans.* **1996**, 1613–1618.
273. Shimakoshi, H.; Ninomiya, W.; Hisaeda, Y. *J. Chem. Soc., Dalton Trans.* **2001**, 1971–1974.
274. Chung, W.-H.; Guo, P.; Wong, K.-Y.; Lau, C.-P. *J. Electroanal. Chem.* **2000**, *486*, 32–39.
275. Ordaz, A. A.; Rocha, J. M.; Aguilar, F. J. A.; Granados, S. G.; Bedioui, F. *Analisis* **2000**, *28*, 238–244.
276. Becker, J. Y.; Kerr, J. B.; Pletcher, D.; Rosas, R. *J. Electroanal. Chem.* **1981**, *117*, 87–99.
277. Bakac, A.; Espenson, J. H. *J. Am. Chem. Soc.* **1986**, *108*, 713–719.
278. Bakac, A.; Espenson, J. H. *J. Am. Chem. Soc.* **1986**, *108*, 719–723.
279. Ozaki, S.; Matsushita, H.; Ohmori, H. *J. Chem. Soc., Chem. Commun.* **1992**, 1120–1122.
280. Olivero, S.; Duñach, E. *Synlett* **1994**, 531–533.
281. Olivero, S.; Clinet, J.-C.; Duñach, E. *Tetrahedron Lett.* **1995**, *36*, 4429–4432.
282. Ihara, M.; Katsumata, A.; Setsu, F.; Tokunaga, Y.; Fukumoto, K. *J. Org. Chem.* **1996**, *61*, 677–684.
283. Olivero, S.; Rolland, J.-P.; Duñach, E. *Organometallics* **1998**, *17*, 3747–3753.
284. Esteves, A. P.; Freitas, A. M.; Medeiros, M. J.; Pletcher, D. *J. Electroanal. Chem.* **2001**, *499*, 95–102.
285. Ozaki, S.; Matsushita, H.; Ohmori, H. *J. Chem. Soc., Perkin Trans. 1* **1993**, 2339–2344.
286. Ozaki, S.; Horiguchi, I.; Matsushita, H.; Ohmori, H. *Tetrahedron Lett.* **1994**, *35*, 725–728.
287. Ozaki, S.; Matsui, E.; Waku, J.; Ohmori, H. *Tetrahedron Lett.* **1997**, *38*, 2705–2708.
288. Clinet, J.-C.; Duñach, E. *J. Organomet. Chem.* **1995**, *503*, C48–C50.
289. Semones, M. A.; Peters, D. G. *J. Electrochem. Soc.* **2000**, *147*, 260–265.
290. Kadish, K. M.; Franzen, M. M.; Han, B. C.; Araullo-McAdams, C.; Sazou, D. *Inorg. Chem.* **1992**, *31*, 4399–4403.
291. Lexa, D.; Savéant, J.-M.; Su, K. B.; Wang, D. L. *J. Am. Chem. Soc.* **1987**, *109*, 6464–6470.
292. Kashiwagi, Y.; Kikuchi, C.; Anzai, J.-I. *J. Electroanal. Chem.* **2002**, *518*, 51–55.
293. Lexa, D.; Savéant, J.-M. *Acc. Chem. Res.* **1983**, *16*, 235–243.
294. Williams, R. J. P.; Hill, H. A. O.; Pratt, J. M.; O’Riordan, M. P.; Williams, F. R. *J. Chem. Soc. A* **1971**, 18559–18562.
295. Walder, L.; Rytz, G.; Meier, K.; Scheffold, R. *Helv. Chim. Acta* **1978**, *61*, 3013–3017.
296. Lexa, D.; Savéant, J.-M.; Soufflet, J.-P. *J. Electroanal. Chem.* **1979**, *100*, 159–172.
297. Scheffold, R.; Dike, M.; Dike, S.; Herold, T.; Walder, L. *J. Am. Chem. Soc.* **1980**, *102*, 3642–3644.
298. Steiger, B.; Walder, L.; Scheffold, R. *Chimia* **1986**, *40*, 93–97.
299. Gao, J.; Rusling, J. F.; Zhou, D.-L. *J. Org. Chem.* **1996**, *61*, 5972–5977.
300. Gao, J.; Rusling, J. F. *J. Org. Chem.* **1998**, *63*, 218–219.
301. Hisaeda, Y.; Takenaka, J.; Murakami, Y. *Electrochim. Acta* **1997**, *42*, 2165–2172.
302. Ruhe, A.; Walder, L.; Scheffold, R. *Helv. Chim. Acta* **1985**, *68*, 1301–1311.
303. Connors, T. F.; Arena, J. V.; Rusling, J. F. *J. Phys. Chem.* **1988**, *92*, 2810–2816.
304. Rusling, J. F.; Miao, C. L.; Couture, E. C. *Inorg. Chem.* **1990**, *29*, 2025–2027.
305. Rusling, J. F.; Connors, T. F.; Owlia, A. *Anal. Chem.* **1987**, *59*, 2123–2127.
306. Zhou, D.-L.; Njue, C. K.; Rusling, J. F. *J. Am. Chem. Soc.* **1999**, *121*, 2909–2914.
307. Torii, S.; Inokuchi, T.; Yukawa, T. *J. Org. Chem.* **1985**, *50*, 5875–5877.
308. Zheng, G.; Stradiotto, M.; Li, L. *J. Electroanal. Chem.* **1998**, *453*, 79–88.
309. Rocklin, R. D.; Murray, R. W. *J. Phys. Chem.* **1981**, *85*, 2104–2112.
310. Vilchez-Aguado, F.; Gutierrez-Granados, S.; Sucar-Succar, S.; Bied-Charreton, C.; Bedioui, F. *New J. Chem.* **1997**, *21*, 1009–1013.
311. Demel, R.; Dotterl, E.; Merz, A. *Acta Chem. Scand.* **1999**, *53*, 1038–1042.
312. Richards, R. L. *Coord. Chem. Rev.* **1996**, *154*, 83–97.
313. Pickett, C. J.; Azametallic Electrochemistry. In *Molecular Electrochemistry of Inorganic, Bioinorganic and Organometallic Compounds*; Pombeiro, A. J. L. McCleverty, J. A. Eds., *NATO ASI Series C* **1993**, *385*, 357–380.
314. Alias, Y.; Ibrahim, S. K.; Queiros, M. A.; Fonseca, A.; Talarmin, J.; Volant, F.; Pickett, C. J. *J. Chem. Soc., Dalton Trans.* **1997**, 4807–4816.
315. Collman, J. P.; Hutchison, J. E.; Ennis, M. S.; Lopez, M. A.; Guillard, R. *J. Am. Chem. Soc.* **1992**, *114*, 8074–8080.
316. Pickett, C. J.; Talarmin, J. *Nature* **1985**, *317*, 652–653.
317. Pickett, C. J.; Ryder, K. S.; Talarmin, J. *J. Chem. Soc., Dalton Trans.* **1986**, 1453–1457.
318. Becker, J. Y.; Avraham, S. *J. Electroanal. Chem.* **1990**, *280*, 119–127.
319. Didenko, L. P.; Gavrilov, A. B.; Shilova, A. K.; Strelets, V. V.; Tsarev, V. N.; Shilov, A. E.; Makhaev, V. D.; Banerjee, A. K.; Pospisil, L. *Nouv. J. Chim.* **1986**, *10*, 583–588.
320. Furuya, N.; Yoshida, H. *J. Electroanal. Chem.* **1989**, *272*, 263–266.
321. Kuwabata, S.; Uezumi, S.; Tanaka, K.; Tanaka, T. *Inorg. Chem.* **1986**, *25*, 3018–3022.
322. Taniguchi, I.; Nakashima, N.; Matsushita, K.; Yasukouchi, K. *J. Electroanal. Chem.* **1987**, *224*, 199–209.
323. Li, H.-L.; Anderson, W. C.; Chambers, J. Q.; Hobbs, D. T. *Inorg. Chem.* **1989**, *28*, 863–868.
324. Ma, L.; Zhang, B.-Y.; Li, H.-L.; Chambers, J. Q. *J. Electroanal. Chem.* **1993**, *362*, 201–205.
325. Xiang, Y.; Zhou, D.-L.; Rusling, J. F. *J. Electroanal. Chem.* **1997**, *424*, 1–3.
326. Simon, E.; Sable, E.; Handel, H.; L’Her, M. *Electrochim. Acta* **1999**, *45*, 855–863.
327. Losada, M. *J. Mol. Catal.* **1975**, *1*, 245–264.

328. Malinski, T.; Taha, Z. *Nature* **1992**, *358*, 676–678.
329. Bedioui, F.; Trevin, S.; Devynck, J. *Electroanalysis* **1996**, *8*, 1085–1091.
330. Barley, M. H.; Takeuchi, K. J.; Meyer, T. J. *J. Am. Chem. Soc.* **1986**, *108*, 5876–5885.
331. Barley, M. H.; Rhodes, M. R.; Meyer, T. J. *Inorg. Chem.* **1987**, *26*, 1746–1750.
332. Chen, S. M.; Su, Y. O. *J. Electroanal. Chem.* **1990**, *280*, 189–194.
333. Younathan, J. N.; Wood, K. S.; Meyer, T. J. *Inorg. Chem.* **1992**, *31*, 3280–3285.
334. Yu, C.-H.; Su, Y. O. *J. Electroanal. Chem.* **1994**, *368*, 323–327.
335. Vilakazi, S. L.; Nyokong, T. *Electrochim. Acta* **2000**, *46*, 453–461.
336. Murphy, W. R. Jr.; Takeuchi, K. J.; Meyer, T. J. *J. Am. Chem. Soc.* **1982**, *104*, 5817–5819.
337. Murphy, W. R. Jr.; Takeuchi, K. J.; Barley, M. H.; Meyer, T. J. *Inorg. Chem.* **1986**, *25*, 1041–1053.
338. Rhodes, M. R.; Meyer, T. J. *Inorg. Chem.* **1988**, *27*, 4772–4774.
339. Pipes, D. W.; Meyer, T. J. *J. Am. Chem. Soc.* **1985**, *107*, 7201–7202.
340. Rhodes, M. R.; Barley, M. H.; Meyer, T. J. *Inorg. Chem.* **1991**, *30*, 629–635.
341. Zhang, J.; Lever, A. B. P.; Pietro, W. J. *Inorg. Chem.* **1994**, *33*, 1392–1398.
342. Hayon, J.; Raveh, A.; Bettelheim, A. *J. Electroanal. Chem.* **1993**, *359*, 209–221.
343. Hayon, J.; Ozer, D.; Rishpon, J.; Bettelheim, A. *J. Chem. Soc., Chem. Commun.* **1994**, 619–620.
344. Pontie, M.; Bedioui, F. *Analisis* **2000**, *28*, 465–469.
345. Pan, K.-C.; Chuang, C.-S.; Cheng, S.-H.; Su, Y. O. *J. Electroanal. Chem.* **2001**, *501*, 160–165.
346. Mao, L.; Yamamoto, K.; Zhou, W.; Jin, L. *Electroanalysis* **2000**, *12*, 72–77.
347. Casero, E.; Pariente, F.; Lorenzo, E.; Beyer, L.; Losada, J. *Electroanalysis* **2001**, *13*, 1411–1416.
348. Doherty, A. P.; Vos, J. G. *J. Chem. Soc., Faraday Trans.* **1992**, *88*, 2903–2907.
349. Doherty, A. P.; Stanley, M. A.; Leech, D.; Vos, J. G. *Anal. Chim. Acta* **1996**, *319*, 111–120.
350. Jasinski, R. *Nature* **1964**, *201*, 1212–1213.
351. Beck, F. *J. Appl. Electrochem.* **1977**, *7*, 239–245.
352. van den Brink, F.; Barendrecht, E.; Visscher, W. *Recl Trav. Chim. Pays-Bas* **1980**, *99*, 253–262.
353. Yeager, E. *Electrochim. Acta* **1984**, *29*, 1527–1537.
354. Collman, J. P.; Marrocco, M.; Denisevich, P.; Koval, C.; Anson, F. C. *J. Electroanal. Chem.* **1979**, *101*, 117–122.
355. Collman, J. P.; Denisevich, P.; Konai, Y.; Marrocco, M.; Koval, C.; Anson, F. C. *J. Am. Chem. Soc.* **1980**, *102*, 6027–6036.
356. Liu, H. Y.; Weaver, M. J.; Wang, C.-B.; Chang, C. K. *J. Electroanal. Chem.* **1983**, *145*, 439–447.
357. Durand, R. R. Jr.; Bencosme, C. S.; Collman, J. P.; Anson, F. C. *J. Am. Chem. Soc.* **1983**, *105*, 2710–2718.
358. Chang, C. J. K.; Liu, H. Y.; Abdalmuhdi, I. *J. Am. Chem. Soc.* **1984**, *106*, 2725–2726.
359. Liu, H.-Y.; Abdalmuhdi, I.; Chang, C. K.; Anson, F. C. *J. Phys. Chem.* **1985**, *89*, 665–670.
360. Ni, C.-L.; Abdalmuhdi, I.; Chang, C. K.; Anson, F. C. *J. Phys. Chem.* **1987**, *91*, 1158–1166.
361. Collman, J. P.; Hendricks, N. H.; Kim, K.; Bencosme, C. S. *J. Chem. Soc., Chem. Commun.* **1987**, 1537–1538.
362. Collman, J. P.; Hendricks, N. H.; Leidner, C. R.; Ngameni, E.; L'Her, M. *Inorg. Chem.* **1988**, *27*, 387–393.
363. Karaman, R.; Jeon, S.; Almarsson, Ö.; Bruice, T. C. *J. Am. Chem. Soc.* **1992**, *114*, 4899–4905.
364. Jeon, S.; Almarsson, Ö.; Karaman, R.; Blaskó, ; Bruice, T. C. *Inorg. Chem.* **1993**, *32*, 2562–2569.
365. Park, G. J.; Nakajima, S.; Osuka, A.; Kim, K. *Chem. Lett.* **1995**, 255–256.
366. Guillard, R.; Brandès, S.; Tardieux, C.; Tabard, A.; L'Her, M.; Miry, C.; Gouerec, P.; Knop, Y.; Collman, J. P. *J. Am. Chem. Soc.* **1995**, *117*, 11721–11729.
367. Le Mest, Y.; Inisan, C.; Laouénan, A.; L'Her, M.; Talarmin, J.; El Khalifa, M.; Saillard, J.-Y. *J. Am. Chem. Soc.* **1997**, *119*, 6095–6106.
368. Choi, Y.-K.; Jeon, S.; Park, J.-K.; Chjo, K.-H. *Electrochim. Acta* **1997**, *42*, 1287–1293.
369. Chang, C. J.; Deng, Y.; Shi, C.; Chang, C. K.; Anson, F. C.; Nocera, D. G. *J. Chem. Soc., Chem. Commun.* **2000**, 1355–1356.
370. Sawaguchi, T.; Matsue, T.; Itaya, K.; Uchida, I. *Electrochim. Acta* **1991**, *36*, 703–708.
371. D'Souza, F.; Hsieh, Y.-Y.; Deviprasad, G. R. *J. Chem. Soc., Chem. Commun.* **1998**, 1027–1028.
372. Imaoka, T.; Nakazawa, S.; Yamamoto, K. *Chem. Lett.* **2001**, 412–413.
373. Oyaizu, K.; Haryono, A.; Yonemaru, H.; Tsuchida, E. *J. Chem. Soc., Faraday Trans.* **1998**, *94*, 3393–3399.
374. Haryono, A.; Oyaizu, K.; Yamamoto, K.; Natori, J.; Tsuchida, E. *Chem. Lett.* **1998**, 233–234.
375. Oyaizu, K.; Haryono, A.; Natori, J.; Shinoda, H.; Tsuchida, E. *Bull. Chem. Soc. Jpn.* **2000**, *73*, 1153–1163.
376. Shi, C.; Steiger, B.; Yuasa, M.; Anson, F. C. *Inorg. Chem.* **1997**, *36*, 4294–4295.
377. Yuasa, M.; Steiger, B.; Anson, F. C. *J. Porphyrins Phthalocyanines* **1997**, *1*, 181–188.
378. Song, E.; Shi, C.; Anson, F. C. *Langmuir* **1998**, *14*, 4315–4321.
379. Shi, C.; Anson, F. C. *Inorg. Chem.* **1998**, *37*, 1037–1043.
380. Yuasa, M.; Nishihara, R.; Shi, C.; Anson, F. C. *Polym. Adv. Technol.* **2001**, *12*, 266–270.
381. Collman, J. P.; Kim, K. *J. Am. Chem. Soc.* **1986**, *108*, 7847–7849.
382. Shi, C.; Mak, K. W.; Chan, K. S.; Anson, F. C. *J. Electroanal. Chem.* **1995**, *397*, 321–324.
383. Collman, J. P.; Chng, L. L.; Tyvoll, D. A. *Inorg. Chem.* **1995**, *34*, 1311–1324.
384. Dong, S.; Jiang, R. *J. Mol. Catal.* **1987**, *42*, 37–50.
385. Bettelheim, A.; White, B. A.; Murray, R. W. *J. Electroanal. Chem.* **1987**, *217*, 271–286.
386. Bettelheim, A.; Ozer, D.; Harth, R.; Ydgar, R. *J. Electroanal. Chem.* **1990**, *281*, 147–161.
387. Dong, S.; Qiu, Q.; Guillard, R.; Tabard, A. *J. Electroanal. Chem.* **1994**, *372*, 171–184.
388. Shi, C.; Anson, F. C. *J. Am. Chem. Soc.* **1991**, *113*, 9564–9570.
389. Shi, C.; Anson, F. C. *Inorg. Chem.* **1992**, *31*, 5078–5083.
390. Steiger, B.; Shi, C.; Anson, F. C. *Inorg. Chem.* **1993**, *32*, 2107–2113.
391. Steiger, B.; Anson, F. C. *Inorg. Chem.* **1994**, *33*, 5767–5779.
392. Shi, C.; Anson, F. C. *Electrochim. Acta* **1994**, *39*, 1613–1619.
393. Shi, C.; Anson, F. C. *Inorg. Chem.* **1995**, *34*, 4554–4561.
394. Steiger, B.; Anson, F. C. *Inorg. Chem.* **1995**, *34*, 3355–3357.
395. Shi, C.; Anson, F. C. *Inorg. Chem.* **1996**, *35*, 7928–7931.
396. Steiger, B.; Anson, F. C. *Inorg. Chem.* **1997**, *36*, 4138–4140.
397. Anson, F. C.; Shi, C.; Steiger, B. *Acc. Chem. Res.* **1997**, *30*, 437–444.
398. Araki, K.; Dovidauskas, S.; Winnischofer, H.; Alexiou, A. D. P.; Toma, H. E. *J. Electroanal. Chem.* **2001**, *498*, 152–160.

399. Araki, K.; Angnes, L.; Azevedo, C. M. N.; Toma, H. E. *J. Electroanal. Chem.* **1995**, *397*, 205–210.
400. Angnes, L.; Azevedo, C. M. N.; Araki, K.; Toma, H. E. *Anal. Chim. Acta* **1996**, *329*, 91–96.
401. Azevedo, C. M. N.; Araki, K.; Angnes, L.; Toma, H. E. *Electroanalysis* **1998**, *10*, 467–471.
402. Azevedo, C. M. N.; Araki, K.; Toma, H. E.; Angnes, L. *Anal. Chim. Acta* **1999**, *387*, 175–180.
403. Rea, N.; Loock, B.; Lexa, D. *Inorg. Chim. Acta* **2001**, *312*, 53–66.
404. Osaka, T.; Naoi, K.; Hirabayashi, T.; Nakamura, S. *Bull. Chem. Soc. Jpn.* **1986**, *59*, 2717–2722.
405. Ikeda, O.; Itoh, S.; Yoneyama, H. *Bull. Chem. Soc. Jpn.* **1988**, *61*, 1428–1430.
406. Kobayashi, N.; Sudo, K.; Osa, T. *Bull. Chem. Soc. Jpn.* **1990**, *63*, 571–575.
407. Coutanceau, C.; Crouigneau, P.; Léger, J.-M.; Lamy, C. *J. Electroanal. Chem.* **1994**, *379*, 389–397.
408. Nevin, W. A.; Liu, W.; Greenberg, S.; Hempstead, M. R.; Marcuccio, S. M.; Melnik, M.; Leznoff, C. C.; Lever, A. B. P. *Inorg. Chem.* **1987**, *26*, 891–899.
409. Kobayashi, N.; Lam, H.; Nevin, W. A.; Janda, P.; Leznoff, C. C.; Lever, A. B. P. *Inorg. Chem.* **1990**, *29*, 3415–3425.
410. Tse, Y.-H.; Janda, P.; Lam, H.; Zhang, J.; Pietro, W. J.; Lever, A. B. P. *J. Porphyrins Phthalocyanines* **1997**, *1*, 3–16.
411. Coowar, F.; Contamin, O.; Savy, M.; Scarbeck, G. *J. Electroanal. Chem.* **1988**, *246*, 119–138.
412. El Hourch, A.; Belcadi, S.; Moisy, P.; Crouigneau, P.; Léger, J.-M.; Lamy, C. *J. Electroanal. Chem.* **1992**, *339*, 1–12.
413. Zagal, J.; Páez, M.; Tanaka, A. A.; dos Santos, J. R., Jr.; Linkous, C. A. *J. Electroanal. Chem.* **1992**, *339*, 13–30.
414. Jahnke, H.; Schonborn, M.; Zimmermann, G. *Top. Curr. Chem.* **1976**, *61*, 133–181.
415. Wiesener, K. *Electrochim. Acta* **1986**, *31*, 1073–1078.
416. Widelöf, A. *Electrochim. Acta* **1993**, *38*, 2493–2502.
417. Biloul, A.; Contamin, O.; Scarbeck, G.; Savy, M.; Palys, B.; Riga, J.; Verbist, J. *J. Electroanal. Chem.* **1994**, *365*, 239–246.
418. Gojković, S. Lj.; Gupta, S.; Savinell, R. F. *J. Electroanal. Chem.* **1999**, *462*, 63–72.
419. Gojković, S. Lj.; Gupta, S.; Savinell, R. F. *Electrochim. Acta* **1999**, *45*, 889–897.
420. Lefèvre, M.; Dodelet, J. P.; Bertrand, P. *J. Phys. Chem. B* **2000**, *104*, 11238–11247.
421. van Veen, J. A. R.; Colijn, H. A.; van Baar, J. F. *Electrochim. Acta* **1988**, *33*, 801–804.
422. Van Wingerden, B.; Van Veen, J. A. R.; Mensch, C. T. *J. Chem. Soc., Faraday Trans. 1* **1988**, *84*, 65–74.
423. Tamizhmani, G.; Dodelet, J. P.; Guay, D.; Lalonde, G. *J. Electrochem. Soc.* **1994**, *141*, 41–45.
424. Lalonde, G.; Côté, R.; Tamizhmani, G.; Guay, D.; Dodelet, J. P.; Dignard-Bailey, L.; Weng, L. T.; Bertrand, P. *Electrochim. Acta* **1995**, *40*, 2635–2646.
425. Bae, I. T.; Tryk, D. A.; Scherson, D. A. *J. Phys. Chem. B* **1998**, *102*, 4114–4147.
426. Wang, H.; Côté, R.; Faubert, G.; Guay, D.; Dodelet, J. P. *J. Phys. Chem. B* **1999**, *103*, 2042–2049.
427. Bouwkamp-Wijnoltz, A. L.; Visscher, W.; van Veen, J. A. R.; Tang, S. C. *Electrochim. Acta* **1999**, *45*, 379–386.
428. Collman, J. P.; Fu, L.; Herrmann, P. C.; Zhang, X. *Science* **1997**, *275*, 949–951.
429. Collman, J. P.; Fu, L.; Herrmann, P. C.; Wang, Z.; Rapta, M.; Bröring, M.; Schwenninger, R.; Boitrel, B. *Angew. Chem., Int. Ed. Engl.* **1998**, *37*, 3397–3400.
430. Collman, J. P.; Schwenninger, R.; Rapta, M.; Bröring, M.; Fu, L. *J. Chem. Soc., Chem. Commun.* **1999**, 137–138.
431. Collman, J. P.; Rapta, M.; Bröring, M.; Raptova, L.; Schwenninger, R.; Boitrel, B.; Fu, L.; L'Her, M. *J. Am. Chem. Soc.* **1999**, *121*, 1387–1388.
432. Ricard, D.; Andrioletti, B.; L'Her, M.; Boitrel, B. *J. Chem. Soc., Chem. Commun.* **1999**, 1523–1524.
433. Ricard, D.; Didier, A.; L'Her, M.; Boitrel, B. *Chem. Biochem.* **2001**, *2*, 144–148.
434. Ricard, D.; L'Her, M.; Richard, P.; Boitrel, B. *Chem. Eur. J.* **2001**, *7*, 3291–3297.
435. Khenkin, A. M.; Shteinman, A. A. *J. Chem. Soc., Chem. Commun.* **1984**, 1219–1220.
436. Creager, S. E.; Raybuck, S. A.; Murray, R. W. *J. Am. Chem. Soc.* **1986**, *108*, 4225–4227.
437. Leduc, P.; Battioni, P.; Bartoli, J.-F.; Mansuy, D. *Tetrahedron Lett.* **1988**, *29*, 205–208.
438. Ojima, F.; Kobayashi, N.; Osa, T. *Bull. Chem. Soc. Jpn.* **1990**, *63*, 1374–1380.
439. Michida, T.; Kasuya, Y.; Nishiyama, M.; Sayo, H. *Chem. Pharm. Bull.* **1994**, *42*, 1724–1729.
440. Suzuki, Y.; Koseki, Y.; Takahashi, K.; Matsui, S.; Komura, T. *Bull. Chem. Soc. Jpn.* **1994**, *67*, 847–853.
441. Nishihara, H.; Pressprich, K.; Murray, R. W.; Collman, J. P. *Inorg. Chem.* **1990**, *29*, 1000–1006.
442. Bedioui, F.; Bongars, C.; Devynck, J. *J. Electroanal. Chem.* **1986**, *207*, 87–99.
443. Khenkin, A. M.; Shilov, A. E. *React. Kinet. Catal. Lett.* **1987**, *33*, 125–130.
444. Moisy, P.; Bedioui, F.; Robin, Y.; Devynck, J. *J. Electroanal. Chem.* **1988**, *250*, 191–199.
445. Bedioui, F.; Moisy, P.; Devynck, J.; Salmon, L.; Bied-Charreton, C. *J. Mol. Catal.* **1989**, *56*, 267–275.
446. Bedioui, F.; Granados, S. G.; Devynck, J.; Bied-Charreton, C. *New J. Chem.* **1991**, *15*, 939–941.
447. Granados, S. G.; Bedioui, F.; Devynck, J. *Electrochim. Acta* **1993**, *38*, 1747–1751.
448. Cauquis, G.; Cosnier, S.; Deronzier, A.; Galland, B.; Limosin, D.; Moutet, J.-C.; Bizot, J.; Deprez, D.; Pulicani, J.-P. *J. Electroanal. Chem.* **1993**, *352*, 181–195.
449. Bedioui, F.; Devynck, J.; Bied-Charreton, C. *Acc. Chem. Res.* **1995**, *28*, 30–36.
450. Bedioui, F.; Devynck, J.; Bied-Charreton, C. *J. Mol. Catal. A: Chem.* **1996**, *113*, 3–11.
451. Horwitz, C. P.; Creager, S. E.; Murray, R. W. *Inorg. Chem.* **1990**, *29*, 1006–1011.
452. Moutet, J.-C.; Ourari, A. *Electrochim. Acta* **1997**, *42*, 2525–2531.
453. Barton, D. H. R. *Tetrahedron* **1998**, *54*, 5805–5817.
454. Balavoine, G.; Barton, D. H. R.; Boivin, J.; Gref, A.; Ozbalik, N.; Rivière, H. *Tetrahedron Lett.* **1986**, *27*, 2849–2852.
455. Balavoine, G.; Barton, D. H. R.; Boivin, J.; Gref, A.; Ozbalik, N.; Rivière, H. *J. Chem. Soc., Chem. Commun.* **1986**, 1727–1729.
456. Balavoine, G.; Barton, D. H. R.; Boivin, J.; Gref, A.; Le Coupance, P.; Ozbalik, N.; Pestana, J. A. X.; Rivière, H. *Tetrahedron* **1988**, *44*, 1091–1106.
457. Balavoine, G.; Barton, D. H. R.; Boivin, J.; Gref, A.; Hallery, I.; Ozbalik, N.; Pestana, J. A.; Rivière, H. *New J. Chem.* **1990**, *14*, 175–183.
458. Yagi, M.; Kaneko, M. *Chem. Rev.* **2001**, *101*, 21–35.
459. Ramaraj, R.; Kira, A.; Kaneko, M. *Angew. Chem., Int. Ed. Engl.* **1986**, *25*, 825–827.
460. Yao, G. Y.; Kira, A.; Kaneko, M. *J. Chem. Soc. Faraday Trans. 1* **1988**, *84*, 4451–4456.
461. Collomb-Dunand-Sauthier, M.-N.; Deronzier, A.; Pradon, X. *J. Am. Chem. Soc.* **1997**, *119*, 3173–3174.
462. Collomb-Dunand-Sauthier, M.-N.; Deronzier, A.; Piron, A.; Pradon, X.; Ménage, S. *J. Am. Chem. Soc.* **1998**, *120*, 5373–5380.
463. Naruta, Y.; Sasayama, M.-a.; Sasaki, T. *Angew. Chem., Int. Ed. Engl.* **1994**, *33*, 1839–1841.

464. Gersten, S. W.; Samuels, G. J.; Meyer, T. J. *J. Am. Chem. Soc.* **1982**, *104*, 4029–4030.
465. Honda, K.; Frank, A. J. *J. Chem. Soc., Chem. Commun.* **1984**, 1635–1636.
466. Gilbert, J. A.; Eggleston, D. S.; Murphy, W. R., Jr.; Geselowitz, D. A.; Gersten, S. W.; Hodgson, D. J.; Meyer, T. J. *J. Am. Chem. Soc.* **1985**, *107*, 3855–3864.
467. Rotzinger, F. P.; Munavalli, S.; Comte, P.; Hurst, J. K.; Graetzel, M.; Pern, F.-J.; Frank, A. J. *J. Am. Chem. Soc.* **1987**, *109*, 6619–6626.
468. Nazeeruddin, M. K.; Rotzinger, F. P.; Comte, P.; Graetzel, M. *J. Chem. Soc., Chem. Commun.* **1988**, 872–874.
469. Raven, S. J.; Meyer, T. J. *Inorg. Chem.* **1988**, *27*, 4478–4483.
470. Comte, P.; Nazeeruddin, M. K.; Rotzinger, F. P.; Frank, A. J.; Grätzel, M. *J. Mol. Catal.* **1989**, *52*, 63–64.
471. Petach, H. H.; Elliott, C. M. *J. Electrochem. Soc.* **1992**, *139*, 2217–2221.
472. Lai, Y.-K.; Wong, K.-Y. *J. Electroanal. Chem.* **1995**, *380*, 193–200.
473. Geselowitz, D.; Meyer, T. J. *Inorg. Chem.* **1990**, *29*, 3894–3896.
474. Hurst, J. K.; Zhou, J.; Lei, Y. *Inorg. Chem.* **1992**, *31*, 1010–1017.
475. Lei, Y.; Hurst, J. K. *Inorg. Chem.* **1994**, *33*, 4460–4467.
476. Schoonover, J. R.; Ni, J.-F.; Roecker, L.; White, P. S.; Meyer, T. J. *Inorg. Chem.* **1996**, *35*, 5885–5892.
477. Chronister, C. W.; Binstead, R. A.; Ni, J.; Meyer, T. J. *Inorg. Chem.* **1997**, *36*, 3814–3815.
478. Nagoshi, K.; Yamashita, S.; Yagi, M.; Kaneko, M. *J. Mol. Catal. A: Chem.* **1999**, *144*, 71–76.
479. Binstead, R. A.; Chronister, C. W.; Ni, J.; Hartshorn, C. M.; Meyer, T. J. *J. Am. Chem. Soc.* **2000**, *122*, 8464–8473.
480. Yamada, H.; Hurst, J. K. *J. Am. Chem. Soc.* **2000**, *122*, 5303–5311.
481. Yamada, H.; Koike, T.; Hurst, J. K. *J. Am. Chem. Soc.* **2001**, *123*, 12775–12780.
482. Vining, W. J.; Meyer, T. J. *Inorg. Chem.* **1986**, *25*, 2023–2033.
483. Ramaraj, R.; Kira, A.; Kaneko, M. *J. Chem. Soc., Faraday Trans.1* **1986**, *82*, 3515–3524.
484. Ramaraj, R.; Kira, A.; Kaneko, M. *J. Electroanal. Chem.* **1993**, *348*, 367–376.
485. Ramaraj, R.; Kira, A.; Kaneko, M. *Polym. Adv. Tech.* **1995**, *6*, 131–140.
486. Collomb-Dunand-Sauthier, M.-N.; Deronzier, A.; Navarro, M. *J. Chem. Soc., Chem. Commun.* **1996**, 2165–2166.
487. Ellis, C. D.; Gilbert, J. A.; Murphy, W. R. Jr.; Meyer, T. J. *J. Am. Chem. Soc.* **1983**, *105*, 4842–4843.
488. Vining, W. J.; Meyer, T. J. *J. Electroanal. Chem.* **1985**, *195*, 183–187.
489. Geselowitz, D. A.; Kutner, W.; Meyer, T. J. *Inorg. Chem.* **1986**, *25*, 2015–2023.
490. Lebeau, E. L.; Adeyemi, S. A.; Meyer, T. J. *Inorg. Chem.* **1998**, *37*, 6476–6484.
491. Collin, J.-P.; Sauvage, J.-P. *Inorg. Chem.* **1986**, *25*, 135–141.
492. Wada, T.; Tsuge, K.; Tanaka, K. *Angew. Chem., Int. Ed. Engl.* **2000**, *39*, 1479–1482.
493. Wada, T.; Tsuge, K.; Tanaka, K. *Inorg. Chem.* **2001**, *40*, 329–337.
494. Meyer, T. J. *J. Electrochem. Soc.* **1984**, *131*, 221C–228C.
495. Moyer, B. A.; Thompson, M. S.; Meyer, T. J. *J. Am. Chem. Soc.* **1980**, *102*, 2310–2312.
496. Thompson, M. S.; De Giovanni, W. F.; Moyer, B. A.; Meyer, T. J. *J. Org. Chem.* **1984**, *49*, 4972–4977.
497. Madurro, J. M.; Chiericato, G. Jr.; De Giovanni, W. F.; Romero, J. R. *Tetrahedron Lett.* **1988**, *29*, 765–768.
498. Che, C.-M.; Lee, W.-O. *J. Chem. Soc., Chem. Commun.* **1988**, 881–882.
499. Navarro, M.; De Giovanni, W. F.; Romero, J. R. *Synthetic Commun.* **1990**, *20*, 399–406.
500. Campos, J. L.; De Giovanni, W. F.; Romero, J. R. *Synthesis* **1990**, 597–599.
501. Wong, K.-Y.; Lee, W.-O.; Che, C.-M.; Anson, F. C. *J. Electroanal. Chem.* **1991**, *319*, 207–216.
502. Navarro, M.; De Giovanni, W. F.; Romero, J. R. *Tetrahedron* **1991**, *47*, 851–857.
503. Kelson, E. P.; Henling, L. M.; Schaefer, W. P.; Labinger, J. A.; Bercaw, J. E. *Inorg. Chem.* **1993**, *32*, 2863–2873.
504. Carrizo, R. M. C.; Romero, J. R. *Synth. Commun.* **1994**, *24*, 433–440.
505. Lima, E. C.; Fenga, P. G.; Romero, J. R.; De Giovanni, W. F. *Polyhedron* **1988**, *17*, 313–318.
506. Navarro, M.; De Giovanni, W. F.; Romero, J. R. *J. Mol. Catal. A: Chem.* **1998**, *135*, 249–256.
507. Catalano, V. J.; Heck, R. A.; Immoos, C. E.; Öhman, A.; Hill, M. G. *Inorg. Chem.* **1998**, *37*, 2150–2157.
508. Catalano, V. J.; Heck, R. A.; Öhman, A.; Hill, M. G. *Polyhedron* **2000**, *19*, 1049–1055.
509. Grover, N.; Thorp, H. H. *J. Am. Chem. Soc.* **1991**, *113*, 7030–7031.
510. Grover, N.; Gupta, N.; Singh, P.; Thorp, H. H. *Inorg. Chem.* **1992**, *31*, 2014–2020.
511. Gerli, A.; Reedijk, J. *J. Mol. Catal.* **1994**, *89*, 101–112.
512. Samuels, G. J.; Meyer, T. J. *J. Am. Chem. Soc.* **1981**, *103*, 307–312.
513. McHatton, R. C.; Anson, F. C. *Inorg. Chem.* **1984**, *23*, 3935–3942.
514. Kutner, W.; Meyer, T. J.; Murray, R. W. *J. Electroanal. Chem.* **1985**, *195*, 375–394.
515. Kutner, W. *J. Electroanal. Chem.* **1989**, *259*, 99–111.
516. Stoessel, S. J.; Elliott, C. M.; Stille, J. K. *Chem. Mater.* **1989**, *1*, 259–268.
517. De Giovanni, W. F.; Deronzier, A. *J. Chem. Soc., Chem. Commun.* **1992**, 1461–1463.
518. De Giovanni, W. F.; Deronzier, A. *J. Electroanal. Chem.* **1992**, *337*, 285–298.
519. Guadalupe, A. R.; Chen, X.; Sullivan, B. P.; Meyer, T. J. *Inorg. Chem.* **1993**, *32*, 5502–5512.
520. Collomb-Dunand-Sauthier, M.-N.; Deronzier, A.; Le Bozec, H.; Navarro, M. *J. Electroanal. Chem.* **1996**, *410*, 21–29.
521. Moss, J. A.; Leasure, R. M.; Meyer, T. J. *Inorg. Chem.* **2000**, *39*, 1052–1058.
522. Liu, M.-H.; Su, Y. O. *J. Chem. Soc., Chem. Commun.* **1994**, 971–972.
523. Lee, T.-S.; Su, Y. O. *J. Electroanal. Chem.* **1996**, *414*, 69–73.
524. Liu, M.-H.; Yeh, C.-Y.; Su, Y. O. *Chem. Commun.* **1996**, 1437–1438.
525. Liu, M.-H.; Su, Y. O. *J. Electroanal. Chem.* **1997**, *426*, 197–203.
526. Liu, M.-H.; Su, Y. O. *J. Electroanal. Chem.* **1998**, *452*, 113–125.
527. Chen, F.-C.; Cheng, S.-H.; Yu, C.-H.; Liu, M.-H.; Su, Y. O. *J. Electroanal. Chem.* **1999**, *474*, 52–59.
528. Chen, C.-Y.; Cheng, S.-H.; Su, Y. O. *J. Electroanal. Chem.* **2000**, *487*, 51–56.

9.11

Combinatorial Methods in Catalysis by Metal Complexes

M. T. REETZ

Max-Planck-Institut für Kohlenforschung, Mülheim/Ruhr, Germany

9.11.1	INTRODUCTION	509
9.11.2	ACHIRAL CATALYTIC PROCESSES	510
9.11.2.1	Hydrolysis Reactions	510
9.11.2.2	Hydrosilylation of Olefins and Imines	512
9.11.2.3	Heck Reactions	512
9.11.2.4	Hydroamination Reactions	514
9.11.2.5	Allylic Substitution	514
9.11.2.6	Annulation Reactions	516
9.11.2.7	Epoxidation Reactions	516
9.11.2.8	Ring-closing Olefin Metathesis	516
9.11.2.9	Reductive Aldol Addition	518
9.11.2.10	Olefin Polymerization	518
9.11.2.11	Novel Strategies in the Design of Ligand Libraries	522
9.11.3	ENANTIOSELECTIVE PROCESSES	523
9.11.3.1	High-throughput ee-Assays	524
9.11.3.2	Strategies Used in the Combinatorial Design and Preparation of Enantioselective Transition Metal Catalysts	535
9.11.4	CONCLUSIONS AND PERSPECTIVES	545
9.11.5	REFERENCES	546

9.11.1 INTRODUCTION

The combinatorial approach to the discovery of therapeutic drugs and agrochemicals has turned out to be successful, complementing traditional methods in the respective academic and industrial laboratories.¹⁻³ There is no doubt that it promises to produce more pharmaceuticals and plant-protecting agents per unit of time than ever before. More recently another area has profited from combinatorial methods, namely materials science.⁴ Parallel to this development catalysis has also entered the “combinatorial stage.”⁴⁻¹² Among the three types of catalysis, namely homogeneous and heterogeneous catalysis and biocatalysis, the latter was the first to embrace combinatorial aspects. Specifically, the concept of directed evolution of functional enzymes has emerged as a complementary and very powerful approach to transforming wild-type enzymes into mutants displaying improved catalytic properties such as higher activity and stability and/or enhanced enantioselectivity.¹³⁻¹⁶ The basic idea rests upon repeating cycles of gene mutagenesis and expression followed by screening. Since researchers in this endeavor were confronted with the problem of screening thousands of catalysts (mutant enzymes) in a given reaction of interest, high-throughput assays had to be developed. Whereas in the case of improving activity and stability rather simple assays sufficed (often on the basis of color tests), the development of high-throughput enantiomeric excess (ee)-assays for the directed evolution of enantioselective enzymes proved to be more demanding.¹⁶⁻¹⁸ However these assays, once developed,

turned out to be useful in the area of combinatorial asymmetric transition metal catalysis as well, which is the reason why they and other screening systems are reviewed in this chapter (see Section 9.11.3.1).

Returning to homogeneous and heterogeneous catalysis, the latter has had a more extensive and therefore impressive start in adapting combinatorial methods.^{4–10} In view of the chemistry inherently involved, this is not surprising. The purpose of the combinatorial process is the design and preparation of high-density catalyst libraries for exploring large numbers of structurally or compositionally diverse catalysts within a given time. In heterogeneous catalysis the preparation of large libraries of solid materials is readily possible using known methods such as vapor deposition and various solution methods such as sol–gel based syntheses. When allowing for several metals as well as different matrices and relative compositions in the synthesis of solid materials, huge diversity results in addition to the possibility of varying such parameters as temperature in the actual catalytic process which follows. Moreover, parallelized methods have been developed which are close to the conditions used in traditional heterogeneous catalysis.⁶ The (achiral) products which result from such methods can be screened quantitatively using a variety of techniques, mass spectrometry (MS) being commonly employed.

In the case of homogeneous catalysis, truly efficient combinatorial methods are more difficult to put into practice. Three different situations arise which result in diversity and therefore in the enhanced probability of finding hits:¹⁷ (i) using a known or a new transition metal complex while varying the conditions such as temperature and/or additives; (ii) using a synthetic strategy which allows for the preparation of large numbers of different ligands; or (iii) using a known or a new catalyst while varying the nature of the substrate undergoing reaction. Although all three points deserve consideration, the problem of developing synthetic strategies for the preparation of meaningful ligand libraries is perhaps most challenging. Intellectual input is also necessary when drawing conclusions upon screening a given catalyst library in the continuous effort to improve catalyst performance. Another crucial problem that calls for basic research concerns the development of high-throughput screening systems. Thus, the occasionally-voiced criticism regarding combinatorial methods in the area of homogeneous catalysis is really only psychological in nature. Moreover, the traditional one-catalyst-at-a-time approach and the combinatorial process are complementary, which means that one method will never displace the other.

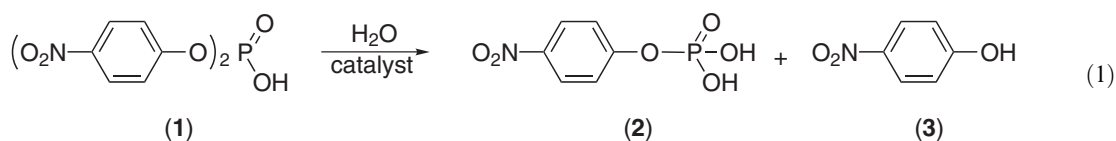
Strictly speaking the combinatorial approach to homogeneous transition metal catalysis involves split-pool synthesis. Theoretically this allows for very high numbers of catalysts, but screening is difficult because of the necessity to develop efficient deconvolution strategies. Due to this difficulty it is rarely applied in homogeneous catalysis. The alternative is parallel synthesis and screening in spatially addressable format. Although the libraries of catalysts are smaller, the parallel array permits rapid identification of hits. Parallel synthesis and screening has also been termed combinatorial catalysis, although only in a loose sense of the word. Indeed, the difference between running six catalytic reactions in traditional Schlenk tubes simultaneously around a magnetic stirrer and performing 96 such reactions on a microtiter plate is not fundamental.

Prior to the first reports of combinatorial homogeneous transition metal catalysis, several combinatorial approaches to metal binding ligands were described.^{19–28} For example, libraries of up to 10^5 peptide-modified macrocyclic cyclones were prepared and tested for selective metal binding.^{19,21} Although much can be learned from such studies, it must be remembered that screening binding properties is different from screening catalyst performance.

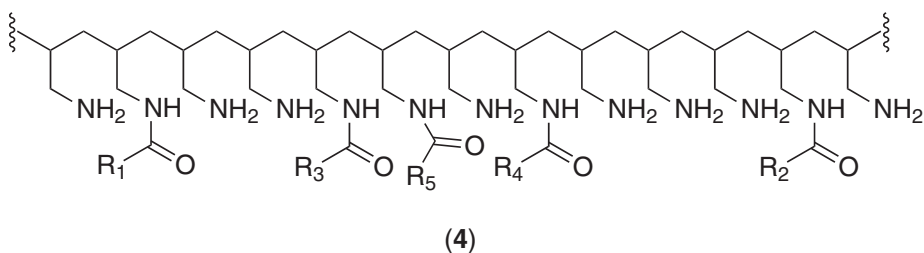
9.11.2 ACHIRAL CATALYTIC PROCESSES

9.11.2.1 Hydrolysis Reactions

An early example of a combinatorial approach to a reaction catalyzed by transition metal coordination compounds concerns phosphatase mimics, specifically in the hydrolysis of bis(*p*-nitrophenyl)phosphate (1) → (2) (Equation (1)):²⁹

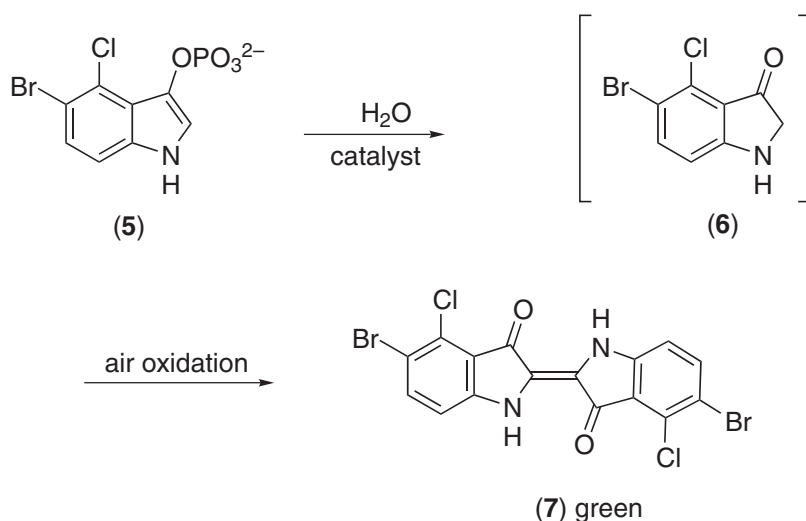


The basic idea was to randomly acylate polyallylamine (MW = 50,000–65,000) all at once with eight different activated carboxylic acids. The relative amounts of acids used in the process was defined experimentally. Since the positions of attack could not be controlled, a huge family of diverse polymers (**4**) was formed. In separate runs the mixtures were treated with varying amounts of transition metal salts and tested in the hydrolysis reaction (**1**) → (**2**) (Equation (1)). The best catalyst performance was achieved in a particular case involving Fe^{3+} , resulting in a rate acceleration of 1.5×10^5 . The weakness of this otherwise brilliant approach has to do with the fact that the optimal system is composed of many different Fe^{3+} complexes, and that deconvolution and therefore identification of the actual catalyst is not possible. A similar method has been described in other types of reaction.^{30,31}



In a different approach three different structurally defined aza-crown ethers were treated with 10 different metal salts in a spatially addressable format in a 96-well microtiter plate, producing 40 catalysts, which were tested in the hydrolysis of *p*-nitrophenol esters.³² A plate reader was used to assess catalyst activity. A cobalt complex turned out to be the best catalyst. Higher diversity is potentially possible, but this would require an efficient synthetic strategy. This research was extended to include lanthanide-based catalysts in the hydrolysis of phospho-esters of DNA.³³

An impressive strategy for putting the split-and-mix method into practice has been described.³⁴ A 625-member library of undecapeptides, attached to Tentagel beads, was prepared by split-and-mix protocols. Seven fixed and four randomized positions ensured the desired diversity. The ligands were mixed with various salts (Cu^{2+} , Zn^{2+} , Fe^{3+} , Co^{3+} , Eu^{3+} , Ce^{4+} , or Zr^{4+}). The actual catalytic reaction involved phosphate hydrolysis, compound (**5**) serving as the model compound (see Scheme 1). It allows for a simple color test, because catalytic hydrolysis affords the intermediate (**6**), which is then rapidly oxidized to the green-colored indigo dye (**7**). Due to its insolubility it precipitates rapidly on the beads bearing the most active catalyst, allowing for visual identification. Several Zr^{4+} complexes having certain amino acid sequences (determined by Edman degradation) in the peptide chain showed the highest degree of catalyst activity.³³ However, the actual structure of the zirconium complex (or complexes) has not been elucidated to date.

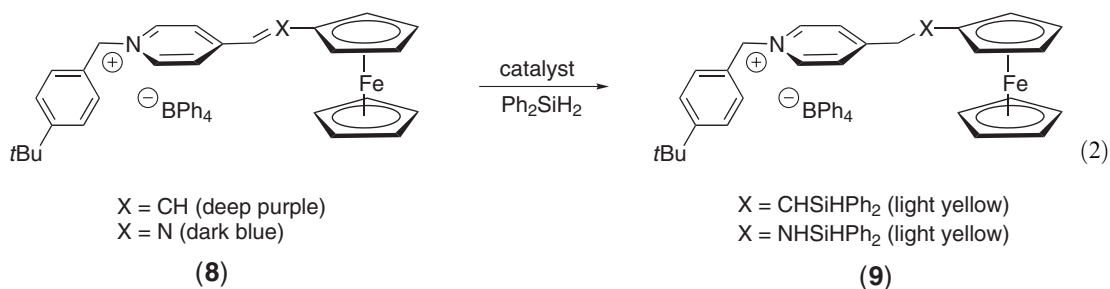


Scheme 1

In related work a library of 1,458 peptide ligands and various metal salts was tested in hydrolysis reactions of (*p*-nitrophenyl)phosphates.³⁵ An active substructure composed of polymer-bound histidine in combination with Eu^{3+} was identified by further dissecting the original hit structure. It needs to be pointed out that catalytically active polymer beads can also be tested for catalytic activity using IR-thermography. In a seminal paper this was demonstrated using 7,000 encoded polymer beads prepared by split-and-pool methods, specifically in the metal-free acylation of alcohols.³⁶

9.11.2.2 Hydrosilylation of Olefins and Imines

In rather different approaches to combinatorial methods to homogeneous transition metal catalysis, attention was paid to developing novel detection systems, the actual catalysts being known metal complexes. A prominent example concerns a simple and efficient colorimetric assay useful in the hydrosilylation of alkenes or imines.^{37,38} Several colored ferrocenyl-substituted alkenes and imines (**8**) having electron acceptor and donor moieties were prepared and used as model substrates in transition metal catalyzed hydrosilylation. Upon reaction (**8** → **9**) (Equation (2)) conjugation is interrupted, causing the color of the dye to be bleached. Thus, active catalysts can be identified qualitatively by eye, quantification being possible by a plate reader.

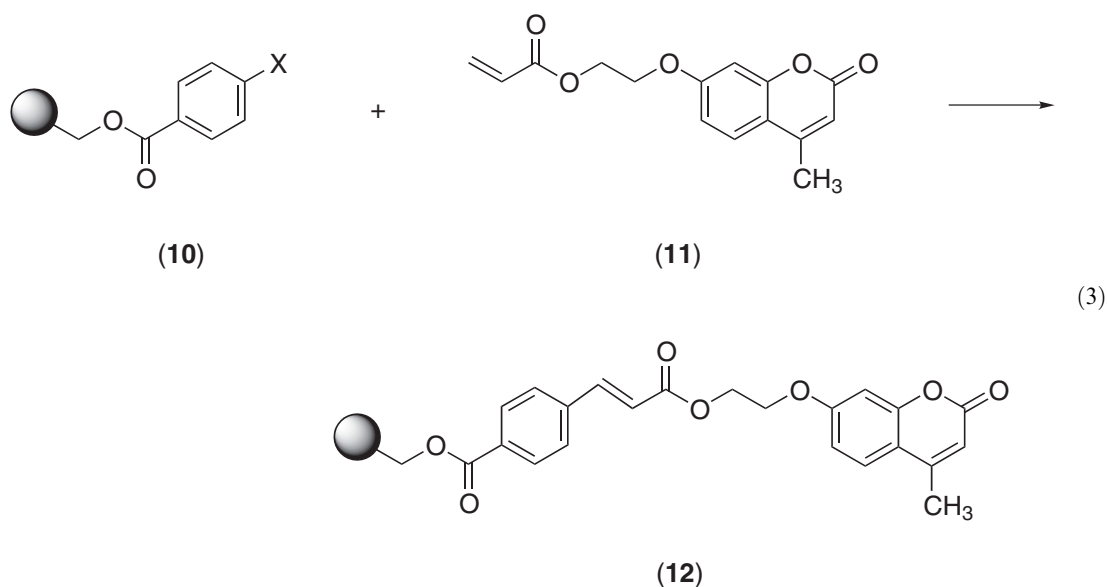


Although only a dozen known metal complexes were tested in this manner, proof of principle was demonstrated. The test revealed Wilkinson's catalyst to be the most active hydrosilylating agent, its use in this type of reaction being known. However, the study also led to the discovery that a palladacycle, $[\text{Pd}\{(o\text{-tolyl})_2\text{PC}_6\text{H}_4\}(\text{OAc})_2]$, which is usually considered to be potent in Heck reactions, is also an excellent hydrosilylation catalyst.^{37,38} Control experiments showed that the relative order of catalytic activity is the same when conventional substrates are used in place of the dyes (**8**).

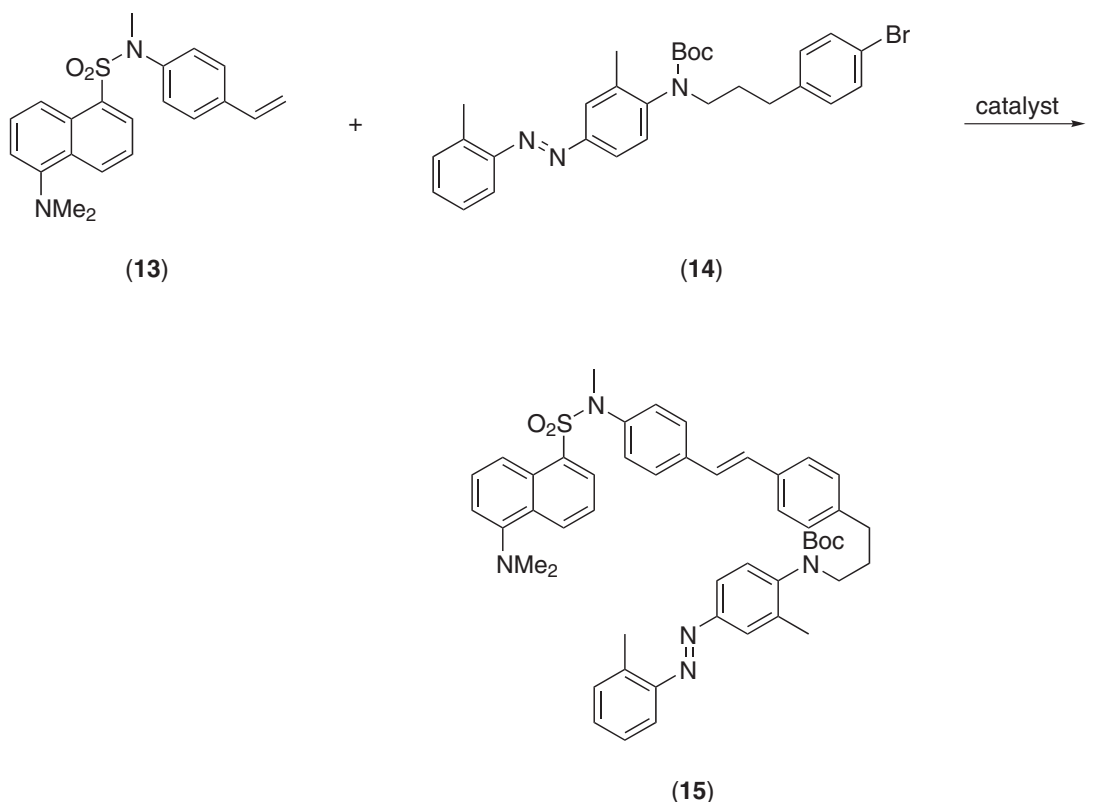
9.11.2.3 Heck Reactions

Another system in which the substrate was tagged in order to ensure emission of a signal upon reaction concerns the palladium-catalyzed Heck reaction of acrylates which bear a tethered fluorophore (**11**) (see Equation (3)).³⁹ Polymer-supported aryl halides (e.g., **10**) were coupled with (**11**) using palladium salts complexed by 45 different phosphines. Successful Heck coupling was signaled by the fluorescence of the respective solid support. Subsequently GC was used as a control to substantiate the assay. Two highly effective ligands for Heck reactions of aryl bromides and chlorides were revealed, namely di(*tert*-butylphosphino)ferrocene and tris(*tert*-butyl)-phosphine. These ligands had previously been discovered to be efficient ligands in palladium-catalyzed amination reactions. Thus the authors were guided by intuition when defining the library of ligands. Interestingly, they were discovered to be excellent ligands for Heck reactions by another researcher using the traditional one-catalyst-at-a-time approach.⁴⁰ Nevertheless, assays of this type allow for the high-throughput screening of much larger numbers of ligands/catalysts and therefore offer the opportunity for novel discoveries, provided that proper ligand libraries are constructed intelligently.

In an important extension of the above strategy, fluorescence resonance energy transfer (FRET) was used to screen room-temperature Heck reactions.⁴¹ FRET had previously been



used to measure binding constants and enzyme activity, the phenomenon occurring when the emission band of one molecule overlaps with an excitation band of a second molecule and when the two chromophores are within 20–80 Å of each other (see Chapter 9.21). Consequently, a catalytic reaction leading to a covalent bond can be quantified fluorimetrically simply by using an automated fluorescence plate reader, provided one reaction partner contains a fluorophore and the second one a quencher. This was accomplished in the Heck reaction involving the olefin (**13**) displaying strong fluorescence and the aryl bromide (**14**) having quencher properties (Equation (4)):



Therefore, a good catalyst leads to weak fluorescence in the Heck product (**15**). A relatively small library of 96 known phosphines was tested in the palladium-catalyzed Heck coupling. Several sterically hindered ligands led to high catalyst activity. Fluorescence tags have also been used in the combinatorial search for metal-free catalysts in other types of reaction.^{42,43}

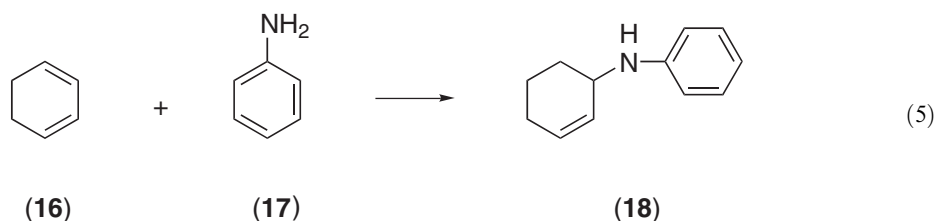
A very different approach to rapid screening of catalysts for Heck reactions (and for other processes as well) is based on reaction calorimetry.⁴⁴ The protocol offers a multidimensional kinetic and stability profile of a catalyst candidate in liquid and multiphase reactions. Moreover, "one-pot" screening of multiple catalyst candidates is possible, provided that there is no interaction between different catalyst species. Substrate screening⁴⁵ was also described.⁴⁴ This elegant method led to the discovery that palladium salts in the presence of certain nitrogen-based ligands are much more active than palladacycles. Several limitations need to be considered. The test reaction must exhibit a heat of reaction large enough and a reaction rate fast enough to trigger an appreciable heat flow signal. Possible side reactions must also be considered.

9.11.2.4 Hydroamination Reactions

The FRET-based approach described above should also work in appropriate cases of transition metal catalyzed Suzuki coupling, aryl halide amination and carbonylation, carbonyl α -arylation, and Hiyama coupling with silanes. In the case of palladium-catalyzed hydroamination of 1,3-dienes (**16**) + (**17**) \rightarrow (**18**) (Equation (5)), an alternative colorimetric assay had to be developed.⁴⁶ In doing so, the known observation that furfural undergoes an acid-catalyzed condensation and ring opening with aniline (but not with the allylic amine product) to form a red product was utilized. Therefore, addition of furfural and acid to the wells of a microtiter plate in which the hydroamination had occurred revealed the most active catalysts. Figure 1 shows a typical microtiter plate, a red color indicating nonreacted aniline and therefore a poor catalyst. Various phosphines in conjunction with palladium, rhodium, iridium, nickel, and ruthenium precursors were tested, $[\{\text{Pd}(\pi\text{-allyl})\text{Cl}\}_2(\text{PPh}_3)_2]$ turning out to be one of the best catalysts. Although only a limited number of ligands/metals were actually tested, this study shows that simple color tests as described in Feigl's classical monograph⁴⁷ can lead to efficient screening systems. A similar system has been devised for amine addition to acrylates.⁴⁸

9.11.2.5 Allylic Substitution

A somewhat different colorimetric assay had to be devised for testing transition metal catalysts in allylic substitution.⁴⁹ The underlying idea is to employ 1-naphthylallyl carbonate as the stoichiometric source of an allyl moiety needed in forming the intermediate π -allyl metal species (Scheme 2). Oxidative addition of the metal and decarboxylation generates 1-naphthol, which can undergo coupling with a diazonium salt forming a red-colored azo compound. A variety of transition metal salts and complexes in the presence of different ligands were tested as catalysts in model allylation reactions in the wells of a 96-format microtiter plate. The appearance of a red color indicated the presence of an active catalyst. A UV/Vis plate reader allowed for quantitative analysis of catalyst activity. The study revealed that not only traditional palladium catalysts are active, but also rhodium and iridium complexes. Here again the purpose of the research was proof of principle, rather than discovering new catalysts. In a different study a modular synthesis of phosphine-containing peptides was performed on a solid support for the purpose of studying palladium-catalyzed allylic substitution.⁵⁰ In a 96-member library a catalyst was identified which shows an ee-value of 80% in the allylation of cyclopentenyl acetate.



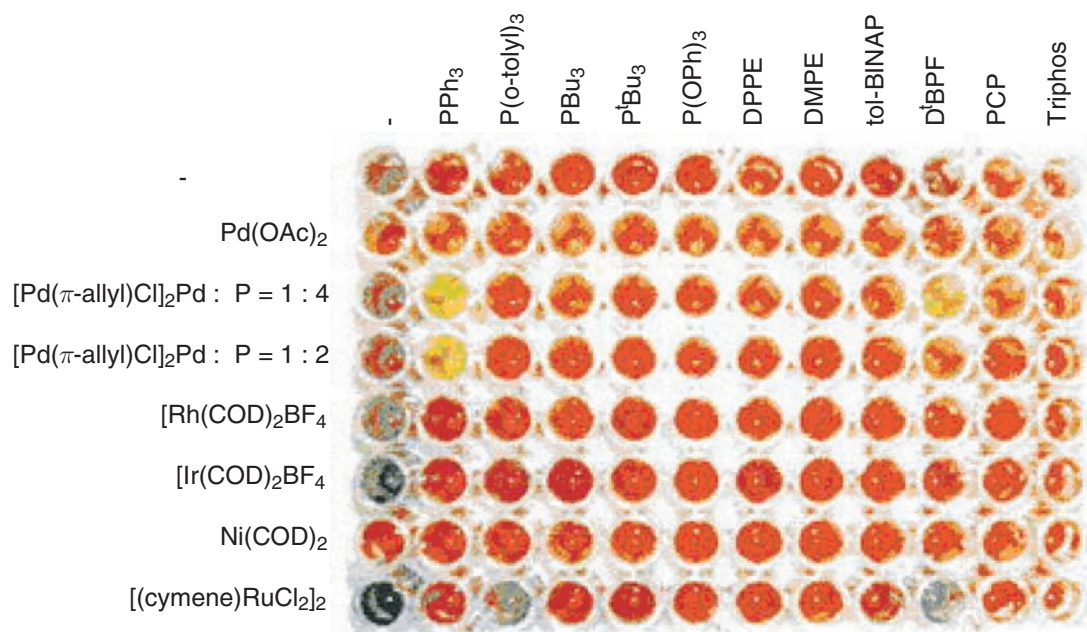
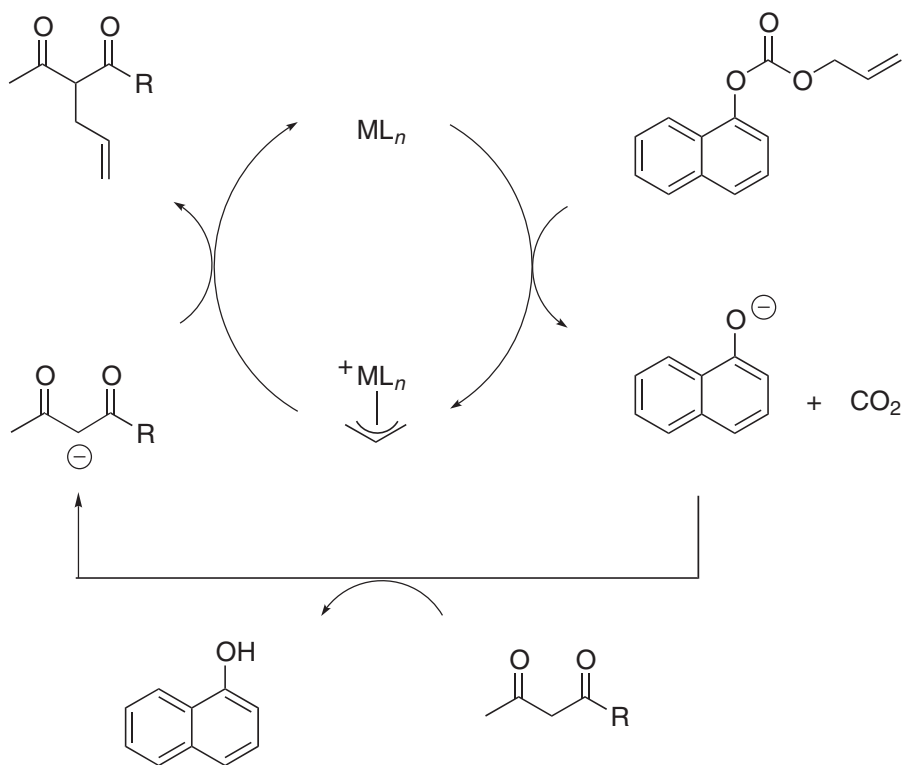


Figure 1 Use of a simple spot test to screen catalysts for the hydroamination of cyclohexadiene with aniline. A red color indicates remaining aniline reactant.⁴⁶

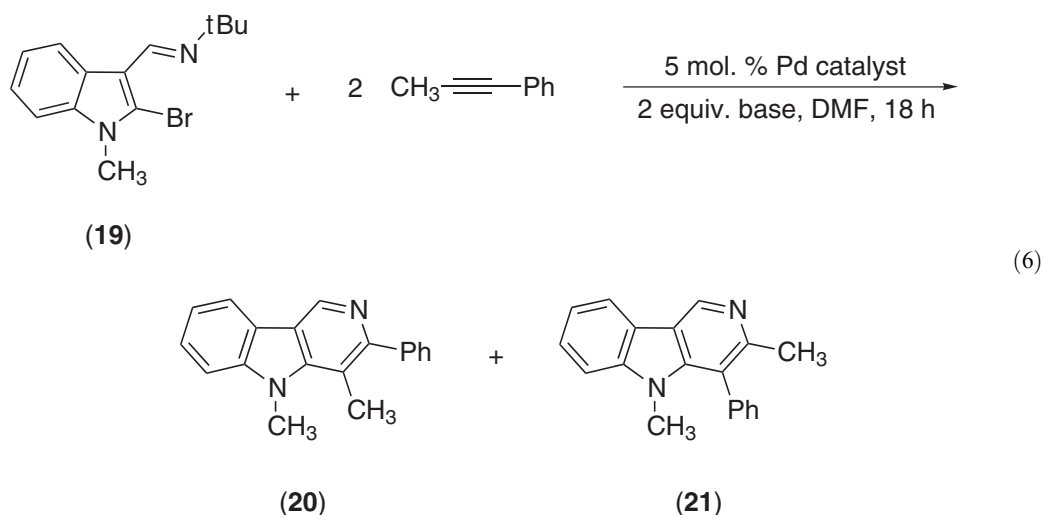


Scheme 2

9.11.2.6 Annulation Reactions

Capillary array electrophoresis (CAE), used in the Human Genome Project,^{51,52} can be adapted to handle typical organic compounds in nonaqueous media in an automated and high-throughput manner, rapid separation of achiral or chiral (see Section 9.11.3) products being possible. In an illustrative investigation a previously discovered palladium-catalyzed annulation reaction of the indole derivative (**19**) yielding two isomeric products (**20**) and (**21**) (Equation (6)), was optimized in a combinatorial manner.⁵³ Previous experience had shown that a number of parameters can affect the yield and product distribution, the optimum conditions being a matter of trial and error. In order to speed up discovery, various known palladium precursors, ligands, and bases were combined in parallel experiments, the yield and product ratio (**20**):(**21**) being detected by CAE. Although only 88 combinations were tested, several hits were identified. For example, the combination PdBr₂/2PPh₃/K₂CO₃ proved to be superior to the best reaction conditions originally reported in a traditional study, resulting in 96% conversion (but poor isomer selectivity). Other conditions led to some degree of isomer selectivity, but in this case conversion was poor.

Nevertheless, this study shows that CAE is a reliable detection system for rapid screening. It also suggests that larger libraries need to be prepared and screened.



9.11.2.7 Epoxidation Reactions

In an attempt to bridge the gap between heterogeneous and homogeneous catalysis, specifically concerning insoluble silica containing dispersed titanium-centers in its matrix, organic-inorganic hybrid compounds proved to be useful models.⁵⁴ When silsesquioxanes (**22**) are reacted with Ti(OiPr)₄, the hydroxy functions at silicon become titanated, forming soluble catalysts (**23**) useful in *tert*-butylhydroperoxide-mediated epoxidation of alkenes. The structure and performance of the catalyst depends upon the conditions used in their synthesis and the type of organic residue at silicon. These parameters were varied using high-speed experimentation techniques (which can be considered to be combinatorial-like). The results (Figure 2) are astounding and demonstrate the power of this approach. Even higher diversity can be envisioned upon using other Ti(OR)₄ reagents.

9.11.2.8 Ring-closing Olefin Metathesis

Following a report that enantioselectivity in homogeneous transitional metal reactions can be detected by IR-thermography⁵⁵ (see Section 9.11.3.1), it was shown that this method can also be applied to the screening of catalysts in ruthenium-catalyzed ring-closing olefin metathesis.⁵⁶ In this case high catalyst activity was indicated by “cold spots” in the IR-thermographic images. This unusual behavior is the result of several factors, including desolvation and heat of vaporization of ethylene, which is formed as a side-product.

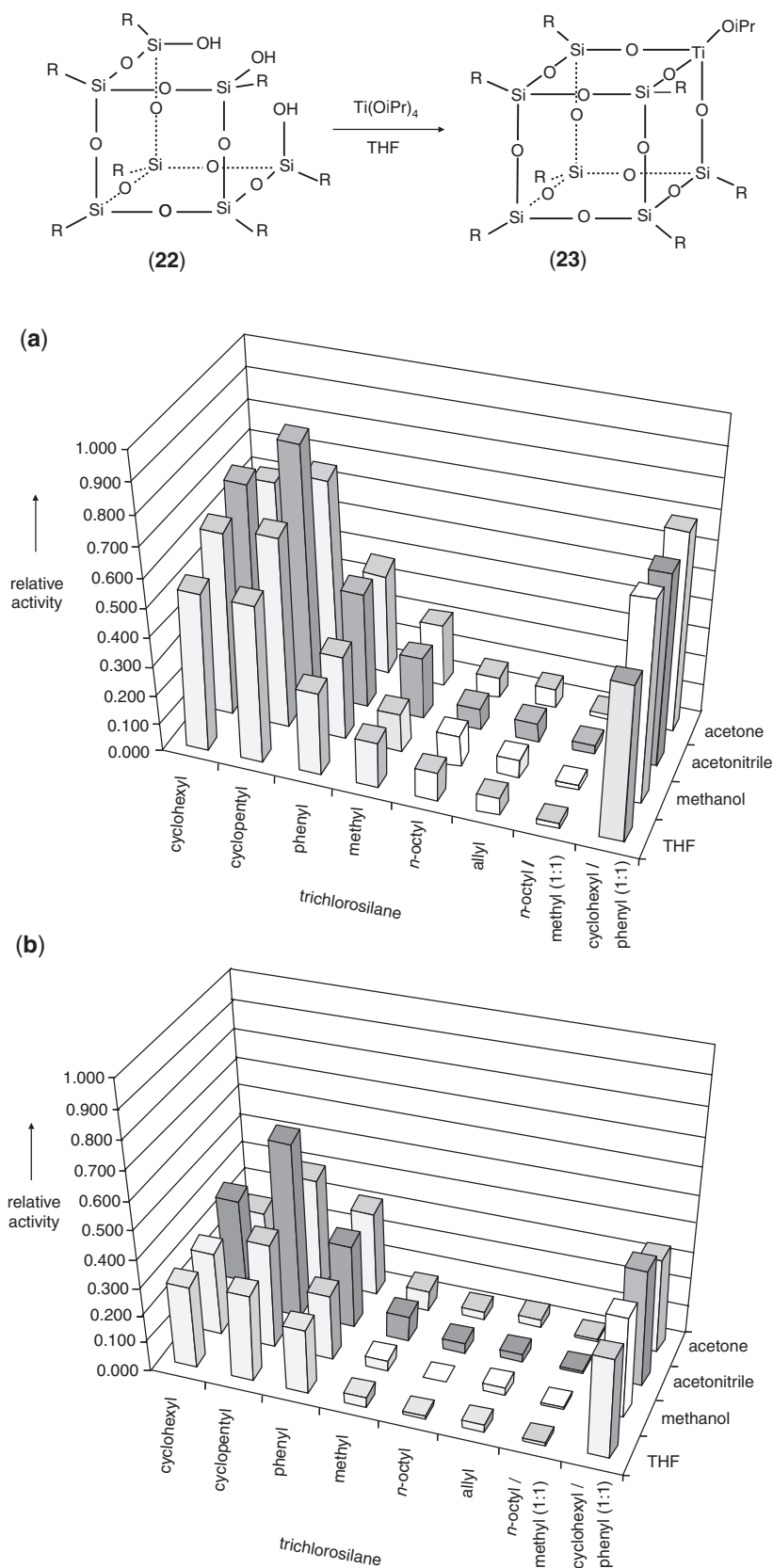


Figure 2 Activities of Ti-silsesquioxane catalyst (obtained by combining different trichlorosilanes and solvents, using water (a) or a 0.13 M HCl solution (b) as hydrolyzing agent) relative to Ti-cyclopentylsilsesquioxane (activity set at 1) in the epoxidation of 1-octene.⁵⁴

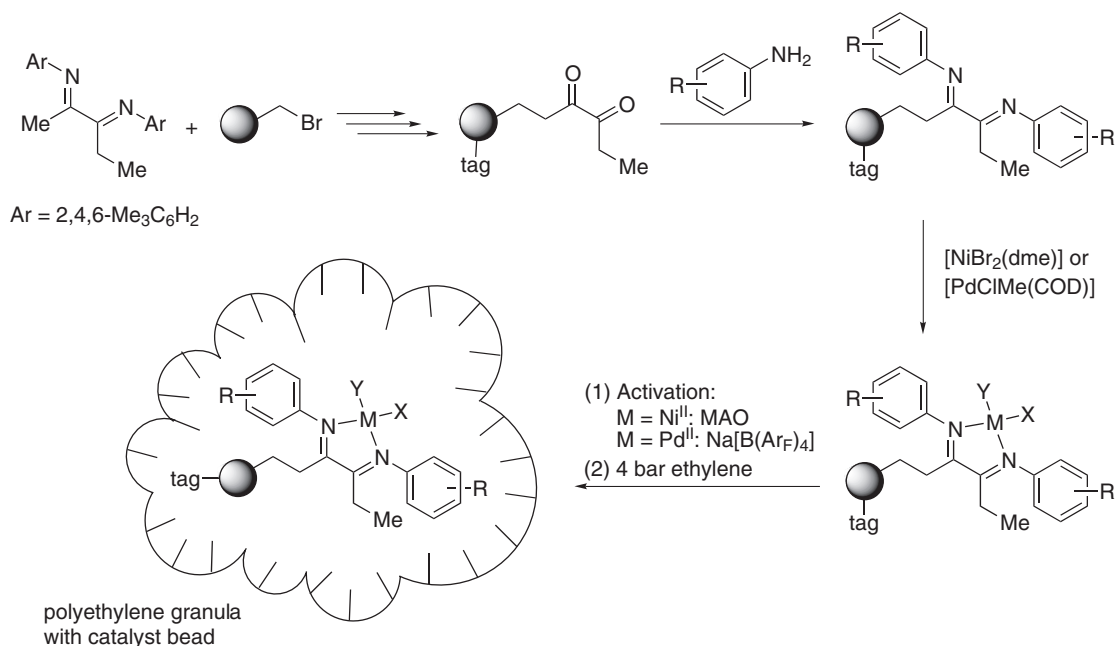
9.11.2.9 Reductive Aldol Addition

It is well known that acrylates undergo transition metal catalyzed reductive aldol reaction, the silanes R_3SiH first reacting in a 1,4 manner and the enolsilanes then participating in the actual aldol addition.^{57,58} A catalytic diastereoselective version was discovered by arrayed catalyst evaluation in which 192 independent catalytic systems were screened on 96-well microtiter plates.⁵⁹ Conventional GC was used as the assay. A Rh-DuPhos catalyst turned out to be highly diastereoselective, but enantioselectivity was poor.⁵⁹

9.11.2.10 Olefin Polymerization

Several combinatorial approaches to the discovery of transition metal based catalysts for olefin polymerization have been described. In one study Brookhart-type polymer-bound Ni- and Pd-(1,2-diimine) complexes were prepared and used in ethylene polymerization (Scheme 3).^{60,61} A resin-bound diketone was condensed with 48 commercially available aminoarenes having different steric properties. The library was then split into 48 nickel and 48 palladium complexes by reaction with $[NiBr_2(dme)]$ and $[PdClMe(COD)]$, respectively, all 96 pre-catalysts being spatially addressable.

The nickel and palladium complexes were activated with methylalumoxane (MAO) or tetrakis(3,5-bistrifluoromethyl)phenylborate, respectively. The 96-member catalyst library was then evaluated by carrying out ethylene polymerization in a custom built high-pressure parallel reactor with a modular series of 48 reaction chambers. These allowed for individual ethylene pressure control. Control experiments showed that the on-bead nickel catalysts have lower activities relative to the analogous free complexes in solution. In contrast, the opposite trend was observed in the case of the palladium complexes. It was assumed that catalyst performance is proportional to the growth of the polystyrene support beads (2–10 times relative to the initial diameter of 70 μm), so that visual inspection of the beads allowed the nickel and palladium catalysts to be distinguished. Chemical encoding/deconvolution using cleavable tertiary amine tags followed by HPLC analysis confirmed these conclusions. Of course, a truly new catalyst was not involved since the synthetic strategy limited diversity. Nevertheless, this study confirms the feasibility of combinatorial techniques, which include solid-phase preparation, on-bead screening, and encoding/deconvolution of pooled libraries of catalysts. It may be speculated that application of this type of strategy has in fact led to proprietary hits of industrial interest which were not published.



Scheme 3

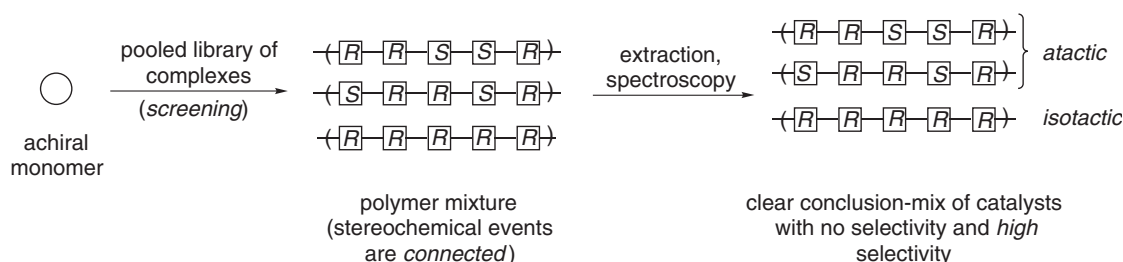
In a highly innovative and practical approach to combinatorial catalysis in olefin polymerization, rapid screening of catalyst libraries has been made possible on the basis of electrospray-ionization-tandem-mass-spectrometry.^{62,63} As a model reaction the ethylene polymerization catalyzed by Brookhart-type complexes was studied. Eight different ligands were prepared, treated with palladium salts and activated by AgOTf. Application of ESI-MS/MS allowed for the simultaneous and competitive screening of catalytic reactions. It appears that this powerful method can be used to evaluate more than 100 combinatorially prepared ligands within a short time. Moreover, intermediate palladium species, which are of mechanistic significance, are readily identified.^{62,63}

Following these developments two further combinatorial approaches to catalyst discovery in olefin polymerization were reported. In one study a mixture of transition metal catalysts (pooled library of complexes) in a given polymerization process (e.g., polypropylene) was used, rough screening being possible on the basis of solubility properties in a given solvent (Scheme 4).⁶⁴ The presence of a stereoregular polymer is revealed by its lower solubility relative to the atactic form. Of course, once a library has been identified to contain a hit, it needs to be systematically narrowed in order to pinpoint the specific catalyst responsible for the high stereoregularity (which may be time consuming!).

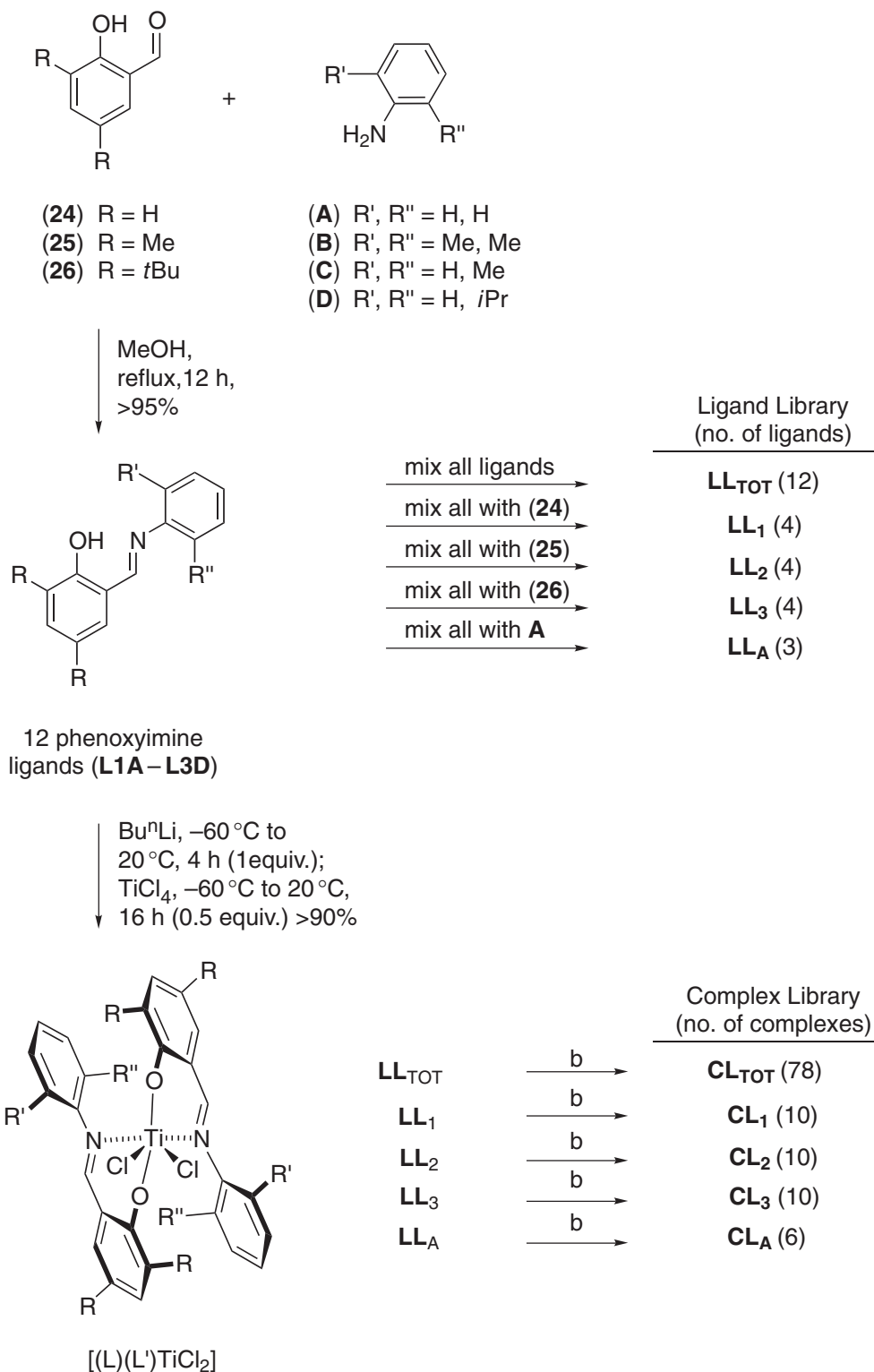
Starting from aldehydes (24)–(26) 12 different salicylaldiminato ligands were first prepared separately. The mixture was then subjected to pooled synthesis of 78 titanium complexes by reacting with *n*-butyllithium and TiCl₄ (Scheme 5). The complex library CL_{TOT} was activated with MAO in toluene and the resultant catalyst solution was exposed to propylene. As a result polypropylene (PP) was slowly formed with an activity of 480 g PP mol⁻¹ Ti h⁻¹. Whereas 90% of the polymeric mixture was soluble in refluxing diethyl ether, the remaining 10% was insoluble. Unexpectedly it turned out to be syndiotactic PP.⁶⁴

In order to identify the actual catalyst responsible for the formation of syndiotactic PP, the polymerization behavior of four sub-libraries of CL_{TOT} had to be studied.⁶⁴ A specific titanium complex [(L_{3A})₂TiCl₂] was shown to produce 8.8 kg PP mol⁻¹ Ti h⁻¹. Although the type of ligand had been known in titanium-catalyzed ethylene polymerization, the results are novel and unexpected because formally C₂-symmetric pre-catalysts are involved. Two possible explanations were offered, one being enchainment of the olefin by a secondary (2,1) mechanism, the other focusing on a ligand isomerization pathway. Although it is not clear how time-consuming encoding/deconvolution actually is, the method may well be applicable to other polymerization processes.⁶⁴

A different approach to genuine combinatorial catalysis is based on the use of tagged supports for the testing and direct comparison of silica- or polymer-supported catalysts for α -olefin polymerization.⁶⁵ Direct detection of the different product beads obtained by different catalysts is principally possible by fluorescence. The process begins with the tagging of different catalysts with fluorescent dyes which exhibit different emission wavelengths. The catalysts are then mixed and used in a single polymerization vessel. As polymerization proceeds, each catalyst particle forms a single product granule as a consequence of particle growth. In order to assign the different components of the product mixture to the catalyst used, the polymer products were exposed to UV light. Due to the different emissions of the labels on the beads, the resulting products could be identified directly, which means that manual separation and characterization are possible (Figure 3). Fluorescence microscopic images of polymer products obtained from the tagged catalysts served as a guide. In further experiments the products of copolymerization of ethylene/hexene were characterized by conventional GPC.⁶⁵



Scheme 4



Scheme 5

Due to their high chemical stability, their high tendency to physisorb on silica, and their high fluorescence quantum yields, rylene dyes (**27**) and (**28**) (Scheme 6) were chosen as tags for the catalysts.⁶⁵ They were shown not to influence the actual catalytic process. Known zirconium

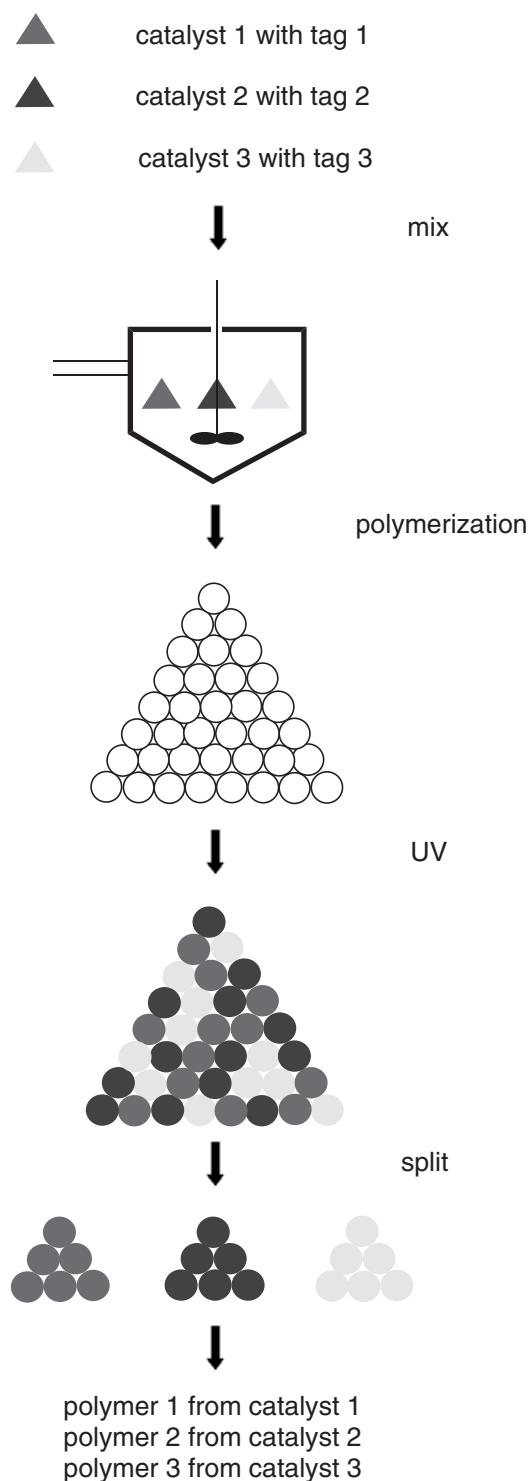
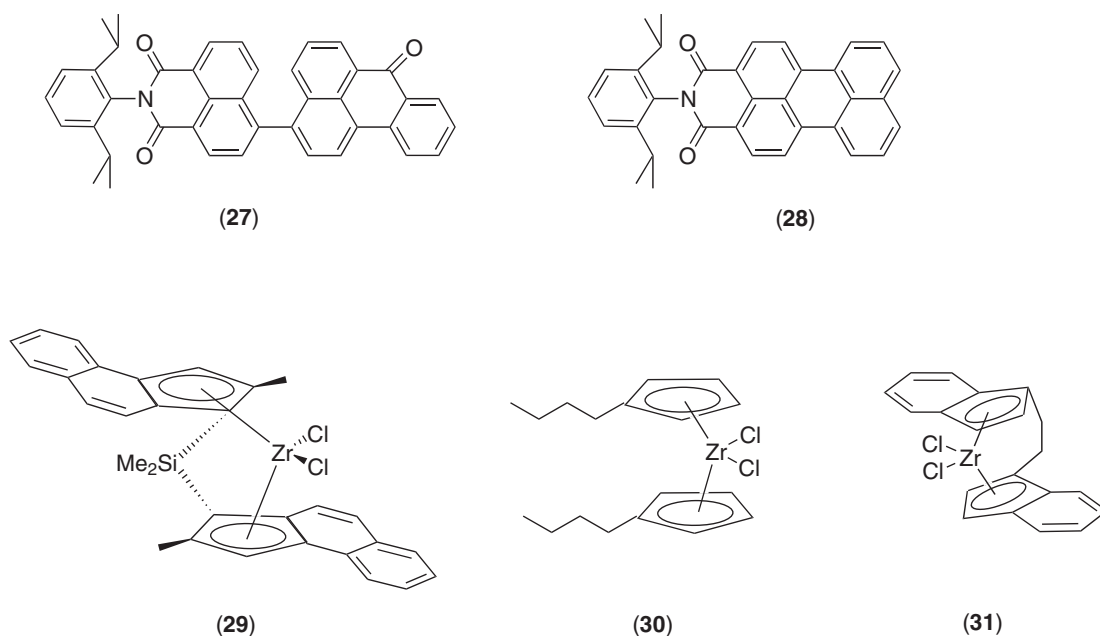


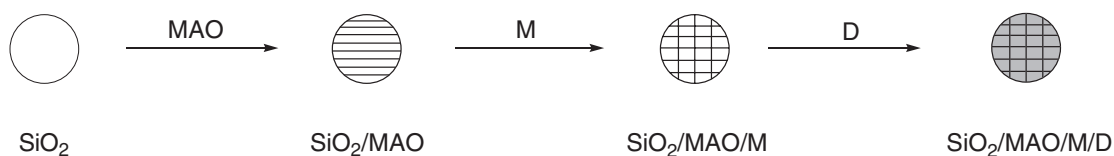
Figure 3 Combinatorial olefin polymerization catalysis.⁶⁵

catalysts of type (29)–(31) (Scheme 6) were immobilized on MAO-containing supports which were then tagged (Scheme 7: M = metallocene, D = dye, MAO = methylaluminoxane).⁶⁵

Although the library of catalysts was actually very small, this combinatorial approach was shown to work surprisingly well. It remains to be seen if truly high throughput can be put into practice, which would require on-line methods for the detection and characterization of the particles bearing the polymers.



Scheme 6



Scheme 7

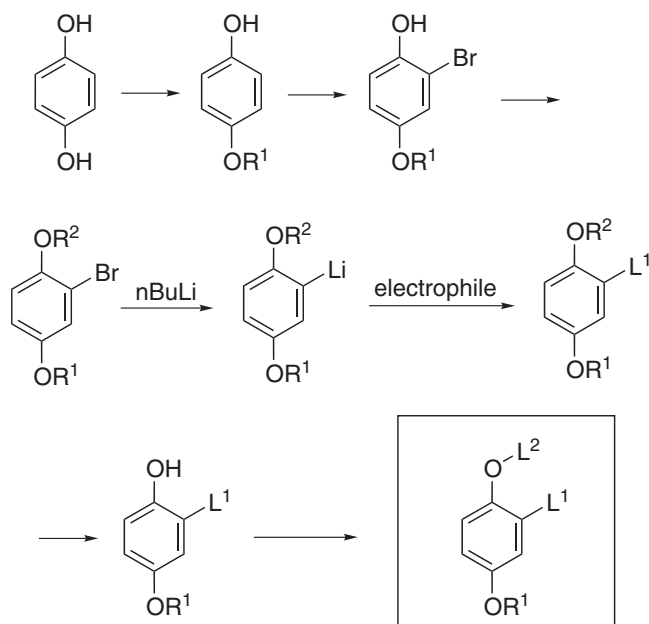
9.11.2.11 Novel Strategies in the Design of Ligand Libraries

With the notable exception of peptide libraries, which are by nature highly modular, most of the studies presented so far have focused on methodological aspects such as screening. However, if combinatorial chemistry is to become an integral part of transition metal catalysis, then methods need to be developed which allow for high diversity in ligand synthesis. A few approaches have already been described above, although truly high density was not always put into practice. Several groups have concentrated on modular ligand synthesis not involving peptides, this goal constituting a major challenge. One notable strategy begins with hydroquinone, which can be functionalized easily in a modular manner, making accessible a wide variety of chelating ligands (Scheme 8).⁶⁶ Such achiral or chiral ligands are of potential use in transition metal catalysis.

In preliminary studies various metal salts such as PdCl₂ were attached to the ligands and the complexes characterized by NMR spectroscopy and X-ray crystallography. Typical examples are the palladium complexes (32)–(44) (Scheme 9).⁶⁶ The catalytic profiles of these and other transition metal complexes prepared by this method still need to be defined. Moreover, solid-phase synthetic versions would be advantageous, and this may well be possible via the (protected) phenol function.

Two reports have appeared describing the first examples of the parallel solution- and solid-phase synthesis of substituted aminomethylphosphines of the type R¹R²PCHR³NR⁴R⁵, assembled in a multicomponent Mannich condensation.^{67,68} Since the components (R¹R²PH, R³CHO, and R⁴R⁵NH) can be varied widely, high diversity is possible. The solid-state strategy is particularly attractive.⁶⁸ Metal complexation and catalysis are in progress.

The Dupont method to prepare polymer-supported bidentate phosphorus-containing ligands makes use of Merrifield's resin (Scheme 10).⁶⁹



Scheme 8

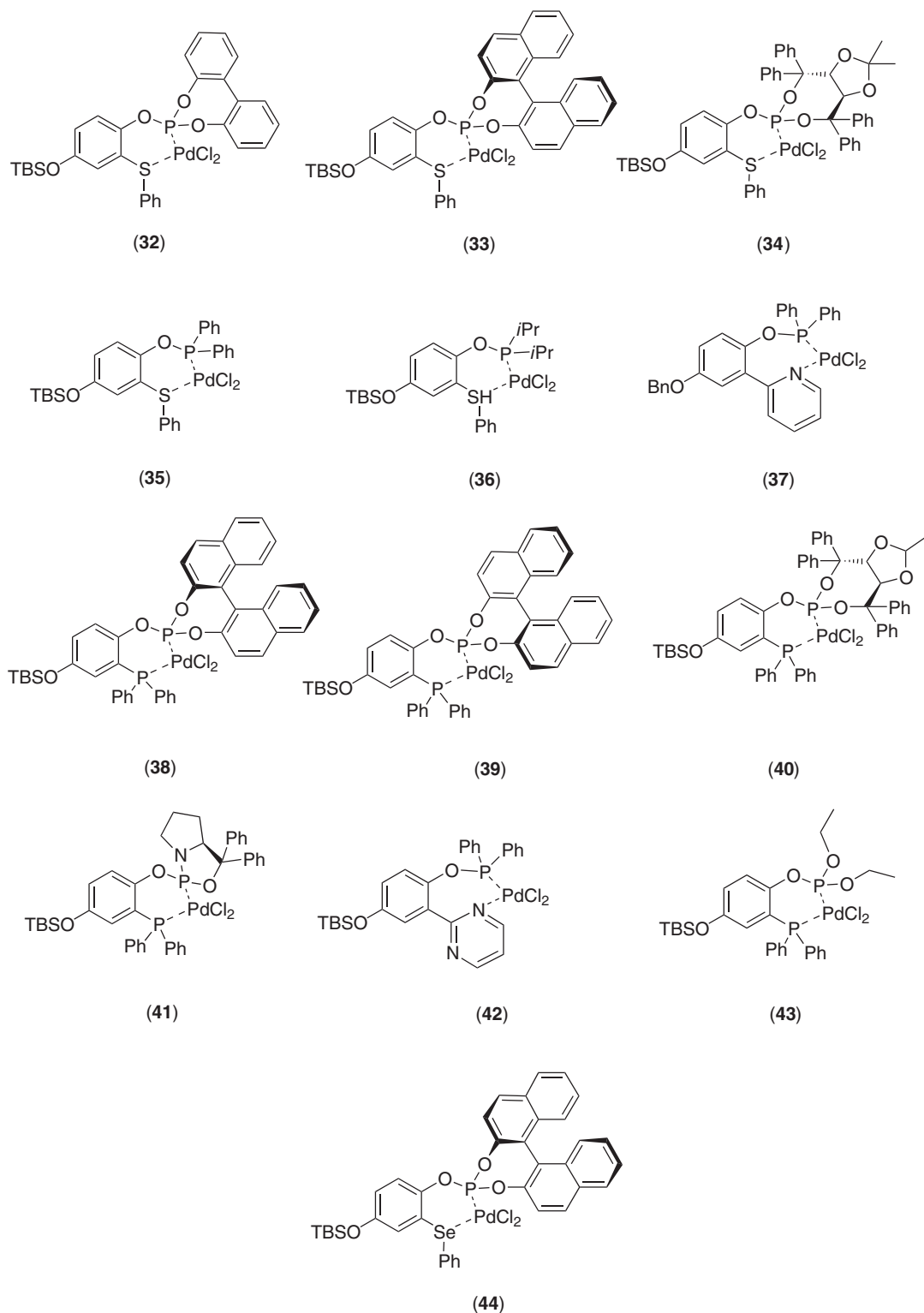
Several dozen P—P ligands have been prepared by this method. Importantly, they can be readily released from the resin by cleavage of the P—N bond, generating new derivatives in solution which can be further modified if so desired.⁶⁹

Finally, two other directions concerning combinatorial aspects in transition metal catalyzed reactions deserve mention. Rather than screening a library of catalysts in a given reaction of interest, it is also possible to screen a given transition metal catalyst for performance in a library of substrates.^{45,70} For this purpose multi-substrate screening approaches are necessary. One possibility is MS or adaptation of FT-IR spectroscopy, which has been used to analyze the gaseous products arising from certain reactions catalyzed by heterogeneous systems.⁷¹

The other direction concerns the use of immobilized transition metal catalysts in the synthesis of libraries of organic compounds of interest in therapeutic drug discovery. One such strategy uses immobilized catalysts (e.g., scandium complexes), leading to efficient library syntheses of quinolines, amino ketones, and amino acid esters.^{72,73}

9.11.3 ENANTIOSELECTIVE PROCESSES

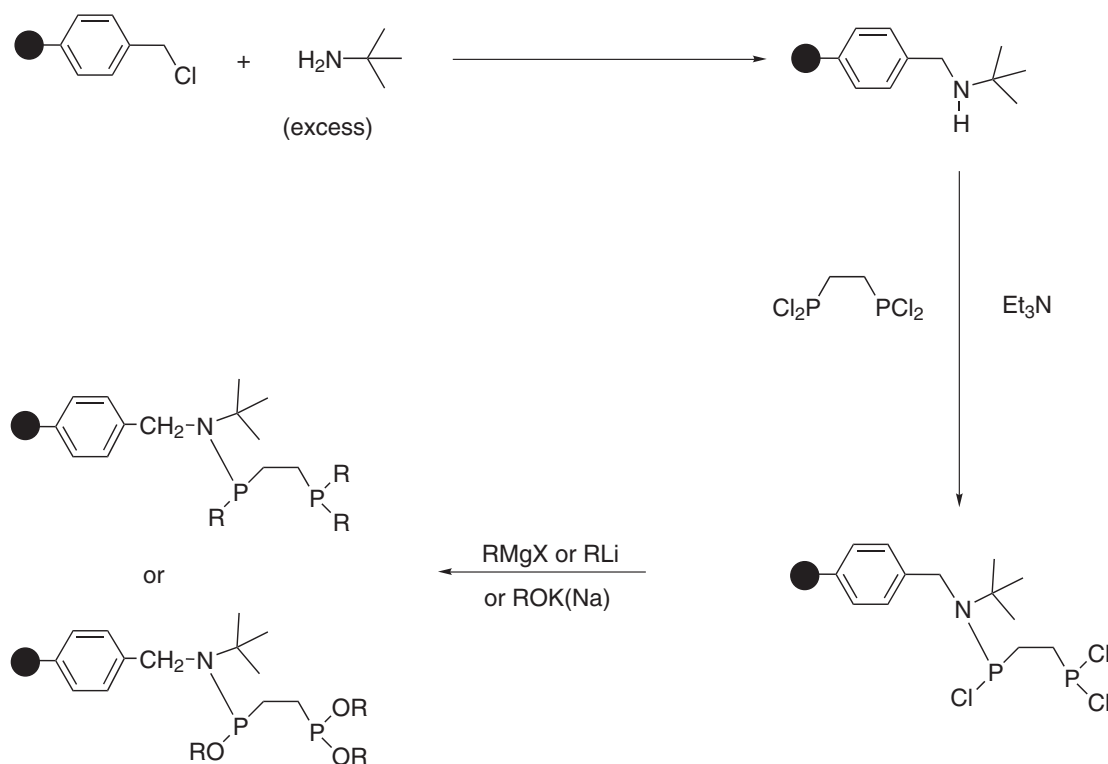
The importance of homogeneous transition metal-based asymmetric catalysis is undisputed, as evidenced, *inter alia*, by the award of the 2001 Nobel Prize for Chemistry to K. B. Sharpless, R. Noyori, and W. S. Knowles. At the heart of this research is ligand tuning, which is based on intuition, experience, knowledge of the reaction mechanism, molecular modeling, as well as some degree of trial and error. In the 1990s a new technique emerged which has been loosely called combinatorial asymmetric catalysis.^{17,74,75} This generally involves time-saving parallel synthesis and testing of large numbers of spatially addressable chiral catalysts. The problems in this interesting new area of asymmetric catalysis are twofold, centering around strategies for the modular synthesis of chiral ligands on the one hand, and on developing high-throughput assays for determining the ee on the other. So far the size of the catalyst libraries has usually been limited to less than a hundred or so catalysts, which are analyzed for ee conventionally. This means that the potential of combinatorial asymmetric catalysis has not been exploited to its full extent. Success in finding hits is likely to increase upon expanding the size of the libraries. However, when entering this realm, high-throughput ee-assays are needed.^{17,18} Since this is a crucial issue, it will be treated first, before dealing with strategies centering around the parallel synthesis of chiral ligands/catalysts.



Scheme 9

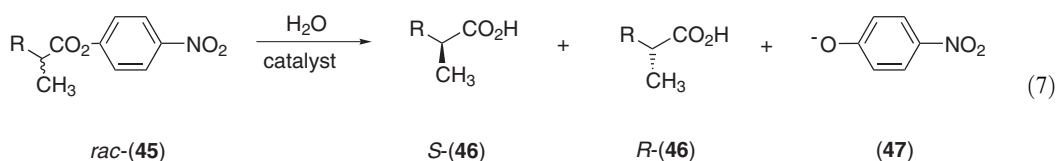
9.11.3.1 High-throughput ee-Assays

The first ee-assay designed to handle a reasonably large number of samples (400–700 ee-determinations per day) was a rather crude UV/Vis-based screening system for the lipase-catalyzed



Scheme 10

kinetic resolution of chiral *p*-nitrophenol esters of the type (45) (see Equation (7)).⁷⁶ However, the test is independent of the type of catalyst used and can in fact be employed in the asymmetric transition metal catalyzed kinetic resolution of chiral esters. It is therefore instructive to illuminate the underlying principle and to outline limitations.



The *p*-nitrophenol ester (45) rather than the methyl ester was used in the study because the appearance of the yellow-colored *p*-nitrophenolate (47) in buffered medium provides a simple means to monitor the reaction by measuring absorbance at 410 nm as a function of time.⁷⁶ Since the racemate would only afford kinetic information concerning total activity, the (*R*)- and (*S*)-esters (45) were synthesized and tested *separately* pairwise for each catalyst. Using a standard 96-well microtiter plate equipped with a plate reader, 48 catalysts could be screened within a few minutes. Two typical experimental plots are displayed in Figure 4. Figure 4a shows a catalyst with almost no stereoselectivity (in this case the wild-type enzyme) and Figure 4b indicates the improved enantioselectivity of the best mutant identified in a library of approximately 2,000 members. This ee-assay can also be used to screen chiral transition metal complexes. The disadvantage of the method has to do with the fact that enzyme or ligand optimization is directed towards the *p*-nitrophenol ester rather than an industrially more interesting substrate such as the corresponding methyl ester.

Several other color tests useful in the kinetic resolution of chiral compounds have been developed, most of them being based on the concept of testing *R*- and *S*-substrates separately as described above.^{77–80}

An unusual ee-screening system for enantioselective transition metal catalysts is based on IR-thermography,⁵⁵ which had previously been used in heterogeneous catalysis.^{36,81,82} Using an AIM-256² IR

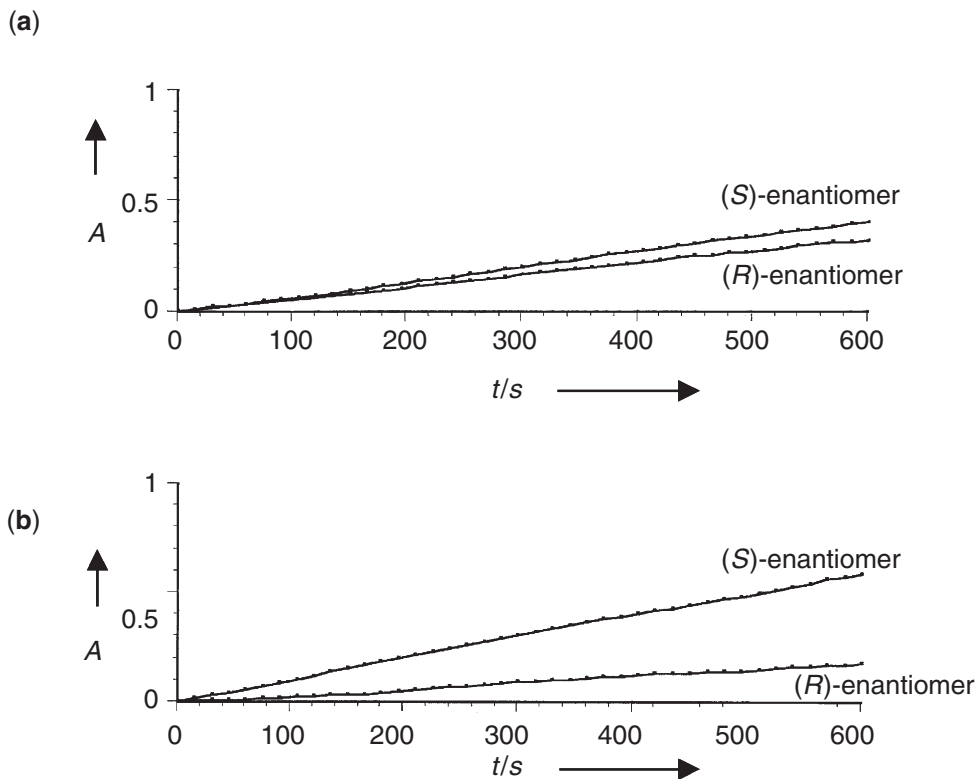
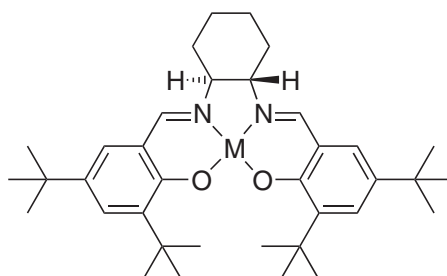
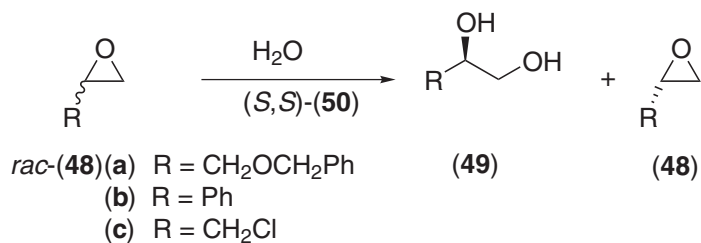


Figure 4 Course of the catalytic of the (*R*)- and (*S*)-ester (**45**) as a function of time. (a) Wildtype lipase from *P. aeruginosa*, (b) improved mutant in the first generation.⁷⁶

camera equipped with a PtSi-FPA detector and a germanium lens, it was not only shown that IR-thermography can be used to monitor reactions in solution catalyzed by homogeneous transition metal complexes, but also to detect enantioselectivity.⁵⁵ This was accomplished using the hydrolytic kinetic resolution of chiral epoxides (**48**) mediated by Jacobsen catalysts (**50**) (Equation (8)).



(**50**) (a) M = Mn (Cl)
 (b) M = Cr (Cl)
 (c) M = Co

(8)

A special microtiter plate which allows for efficient heat transfer and which can be shaken so as to ensure sufficient mixing was first developed. Accordingly, a commercially available Eppendorf

Thermomixer was modified such that the top was replaced by an aluminum plate. Holes were then drilled into the plate and cylindrical glass reaction vessels about 8 mm in diameter and 35 mm in height placed therein. Thus, the whole microtiter plate can be shaken so as to ensure agitation of the reaction contents in each well.⁵⁵

Since the use of a racemate would deliver information regarding only the overall catalyst activity, the *S*- and *R*-enantiomers were tested pairwise in separate wells of the microtiter plate. This is the same trick that was used in the original UV/Vis-based screening system for the kinetic resolution of chiral esters.⁷⁶ In the present case the racemate was also included. Following placement of moist toluene solutions of the *S,S*-catalysts (**50**) in the wells of the microtiter plate, *R*- and *S*-epichlorohydrin (**48c**) were added and the temperature calibrated in the range of 24–39 °C. The reaction was then initiated by the addition of water. After a specified amount of time shaking was interrupted for 10 s, 500 IR-thermographic pictures taken and the average of these printed out as an image. The time-resolved results (Figure 5) show for the first time that IR-thermography can be used to detect heat evolution caused by a reaction occurring in homogeneous solution, and that a highly enantioselective catalyst can indeed be identified.⁵⁵ The cobalt complex *S,S*-(**50c**) was found to exhibit the highest catalyst activity and selectivity; it reacts enantioselectively with the epoxide *S*-(**48c**). The chromium catalyst *S,S*-(**50b**) is also selective, although less active, whereas the manganese complex *S,S*-(**50a**) displays no significant activity. This is in line with results obtained by Jacobsen *et al.* using benzoic acid as the nucleophile in laboratory scale reactions. It was also seen that heat generation after 7 min was so pronounced in the case of the cobalt complex for the reaction of *S*-(**48c**) and *rac*-(**48c**) that no significant difference in visualization using the applied temperature window (1 °C) could be detected. Therefore, the temperature scale covered by the window was increased to a total of 10 °C, which resulted in the clear identification of the “hottest” reaction (compare Figures 5e and 5f).

Moreover, using the cobalt catalyst *S,S*-(**50c**) it was possible to perform substrate screening⁴⁵ so that the chiral epoxides (**48a–c**) could be studied in parallel.⁵⁵ It was found that *S*-(**48a**) is the most reactive substrate followed by *S*-(**48c**) and *R*-(**48b**). The relative reactivity of *R*-(**48b**) and *S*-(**48c**) corresponds to that reported in the literature for laboratory scale reactions,⁸³ whereas the reaction

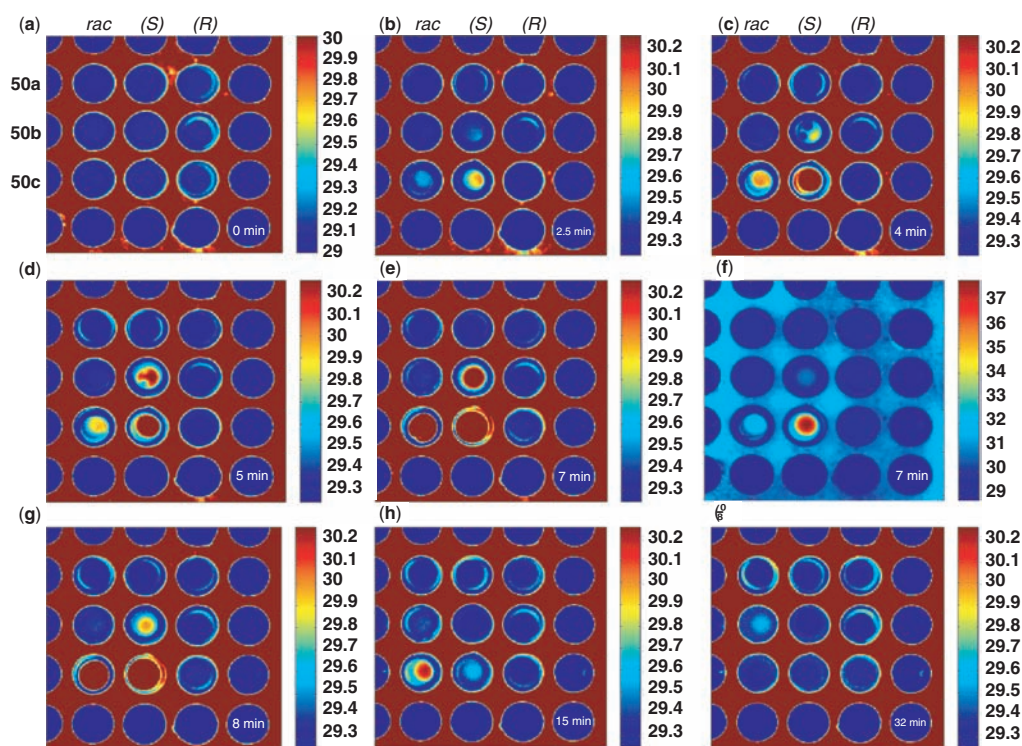


Figure 5 Time-resolved IR thermographic imaging of the enantioselective hydrolysis of epoxide (**48c**) catalyzed by *S,S*-(**50a–c**) after (a) 0, (b) 2.5, (c) 4, (d) 5, (e) 7, (g) 8, (h) 15, and (i) 32 min. In (f) the same images is shown as in (e), except that the temperature window ranges over 10 K. The bar on the far right of each image is the temperature/colour key of the temperature window used (°C).⁵⁵

of *S*-(**48a**), which is most rapid, had not been described in the literature previously. Thus, the IR thermographic images contain an interesting chemical prediction. In summary, IR-thermography is quite useful in the identification of highly enantioselective metal complexes used in kinetic resolution. This also applies to the screening of achiral homogeneous transition metal catalysts, the purpose being to identify highly active catalysts as, for example, in ruthenium-catalyzed ring-closing olefin-metathesis⁵⁶ (see Section 9.11.2). Quantification of heat development should be possible.

In principle it should be possible to use HPLC in the high-throughput determination of enantiomeric purity, provided that efficient separation of enantiomers by chirally modified columns is possible within a reasonable amount of time. Since rapid separation of this kind is a formidable challenge, an alternative approach is to use normal columns which simply separate the starting materials from the enantiomeric products, the ee of the mixture of enantiomers then being determined by circular dichroism (CD). Indeed, this principle was first established in the 1980s.^{84–86} More recently, it was shown that the method can be applied in the screening of combinatorially prepared enantioselective catalysts.^{87–89} It is based on the use of sensitive detectors for HPLC which determine in a parallel manner both the circular dichroism ($\Delta\varepsilon$) and the UV-absorption (ε) of a sample at a fixed wavelength in a flow-through system. The CD-signal depends only on the enantiomeric composition of the chiral products, whereas the absorption relates to their concentration. Thus, only short HPLC-columns are necessary. Upon normalizing the CD-value with respect to absorption, the so-called anisotropy factor *g* is obtained:

$$g = \frac{\Delta\varepsilon}{\varepsilon}$$

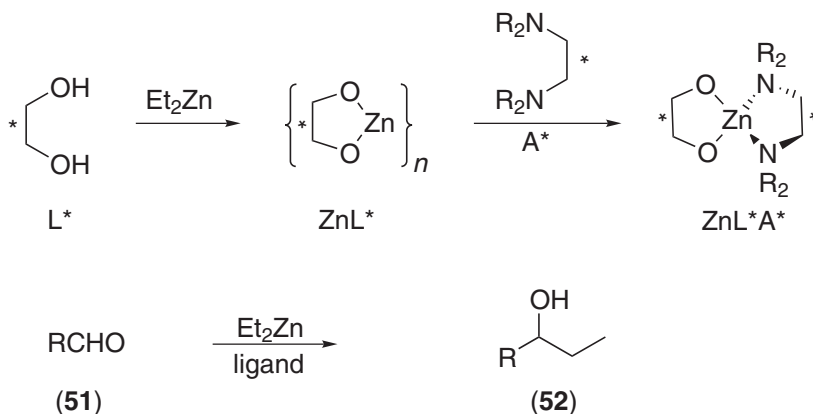
For a mixture of enantiomers it is thus possible to determine the ee-value without recourse to complicated calibration. The fact that the method is theoretically valid only if the *g* factor is independent of concentration and if it is linear with respect to ee has been emphasized repeatedly.^{84–89} However, it needs to be pointed out that these conditions may not hold if the chiral compounds form dimers or aggregates, because such enantiomeric or diastereomeric species would give rise to their own particular CD effects.⁸⁸ Although such cases have yet to be reported, it is mandatory that this possibility be checked in each new system under study.

In a seminal study various libraries of chiral ligands and activators in the addition of Et₂Zn to aldehydes (**51**) were investigated (Scheme 11).^{87,89}

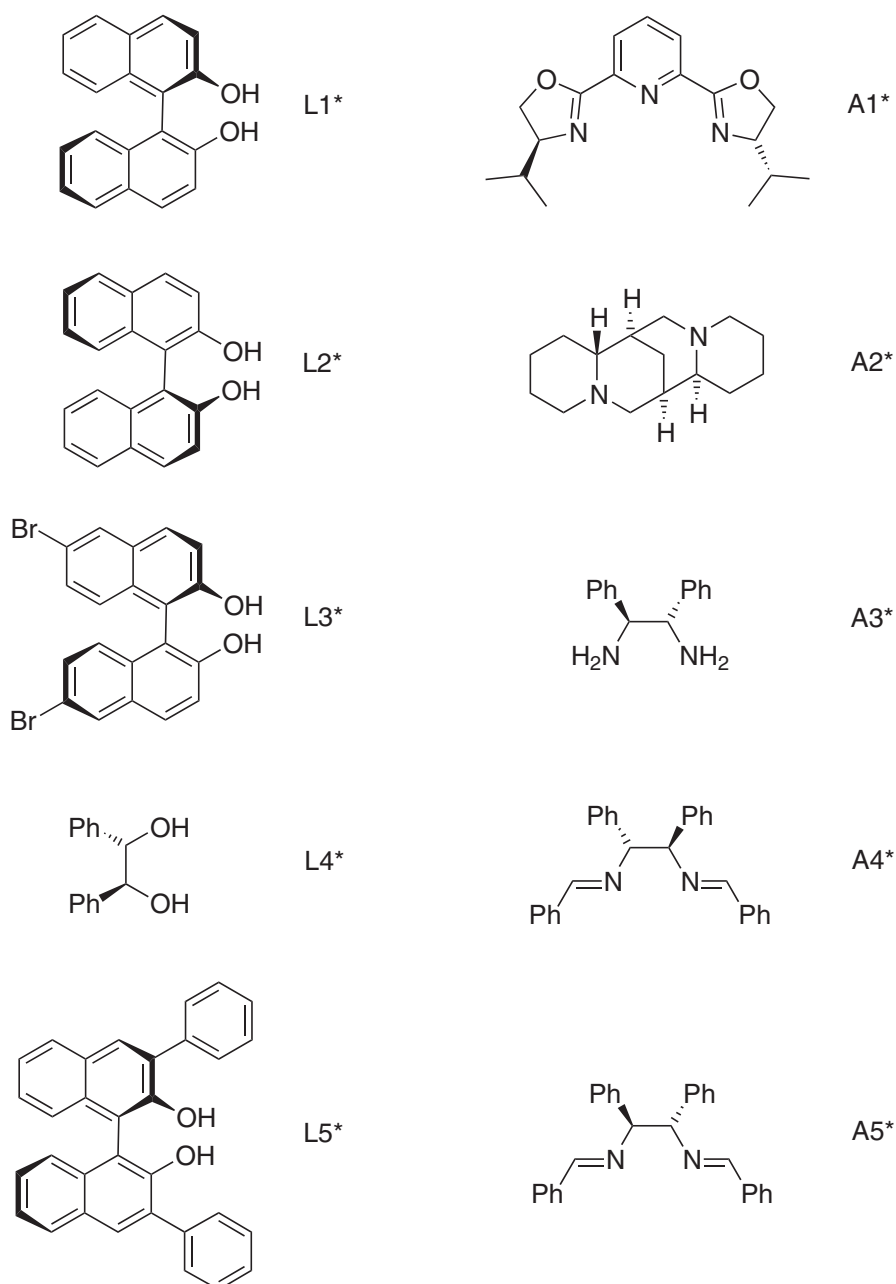
First the primary combinatorial library of chiral ligands L1*–L5* and chiral activators A1*–A5* (Scheme 12) were studied in order to optimize the lead structure of the next generation of chiral ligands and activators.^{87,89}

The best combinations were found to be L5*/A4* and L5*/A5*, ee-values of up to 65% being observed in the Et₂Zn addition to benzaldehyde with formation of (**51**). Based on these results a new library composed of chiral diimines as activators was scrutinized (Scheme 13).^{87,89}

The best combination turned out to be L5*/A9* (ee = 90% at room temperature and 99% at –78 °C with benzaldehydes and ee = 92–99% with other aldehydes).⁸⁷ Further improvements were reported later.⁸⁹ Although only a few dozen reactions were monitored by a JASCO-CD-995 instrument, the CD-based assay is amenable to high-throughput screening of enantioselective catalysts. The chemistry itself lends itself ideally to combinatorial asymmetric metal catalysis, since the principle of asymmetric activation is turning out to be very powerful.⁸⁹



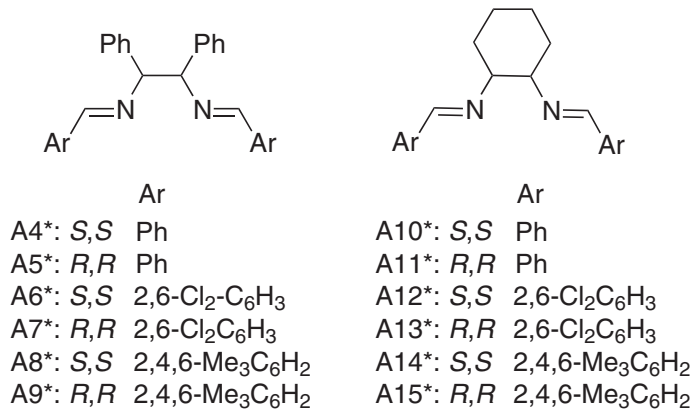
Scheme 11



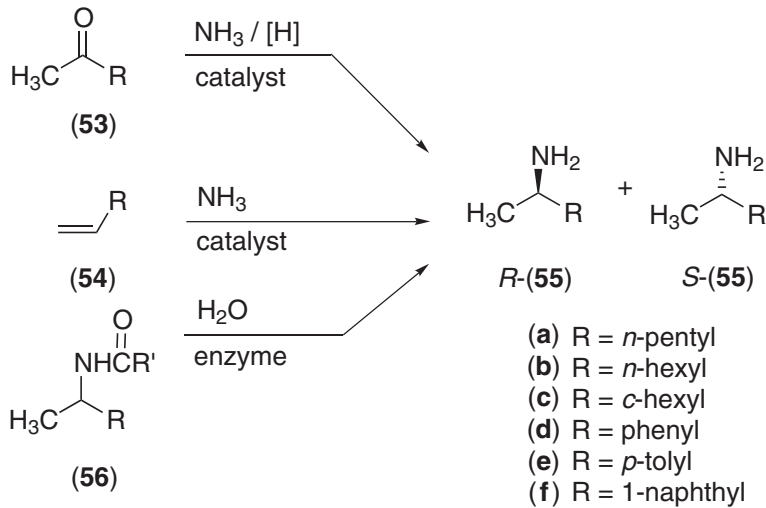
Scheme 12

In a different approach a super-high-throughput ee-assay was developed on the basis of chirally modified capillary array electrophoresis (CAE).⁹⁰ CAE was used in the Human Genome Project, and commercially available instruments have been developed which comprise a high number of capillaries in parallel, for example the 96-capillary unit MegaBACE consisting of 6 bundles of 16 capillaries.⁹¹ The system can address a 96-well microtiter plate. It was adapted to perform ee-determinations of chiral amines, which are potentially accessible by catalytic reductive amination of ketones, transition metal catalyzed Markovnikov addition of ammonia, or enzymatic hydrolysis of acetamides (Scheme 14).⁹⁰

The chiral amines (**55**) were first derivatized by conventional reaction with fluoresceine-isothiocyanate (**57**) leading to fluorescein-active compounds (**58**) (Equation (9)) that enable a sensitive detection system, specifically laser-induced fluorescence detection (LIF), to be used.⁹⁰ Although



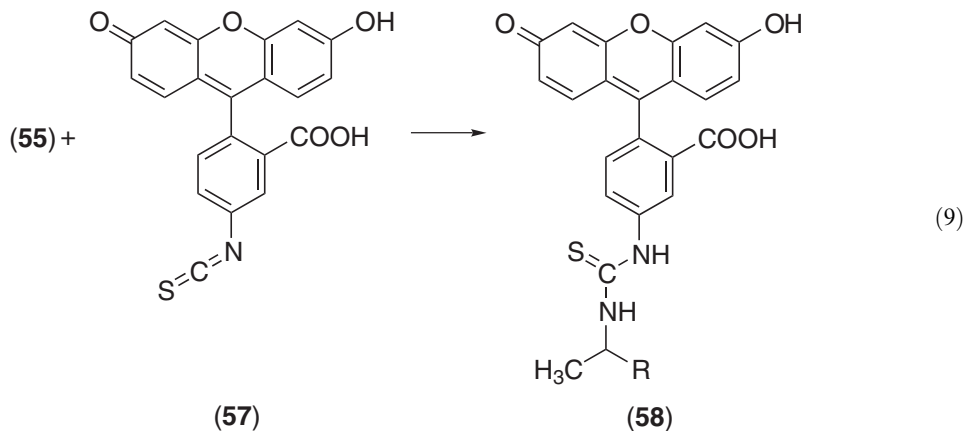
Scheme 13



Scheme 14

extensive optimization was not carried out (only six chiral selectors of the type cyclodextrins were tested), satisfactory baseline separation was accomplished in all cases.

Following these exploratory studies a super-high-throughput screening system was implemented, allowing for 7,000–30,000 ee-determinations per day.⁹⁰ Of course, in each new case of a chiral

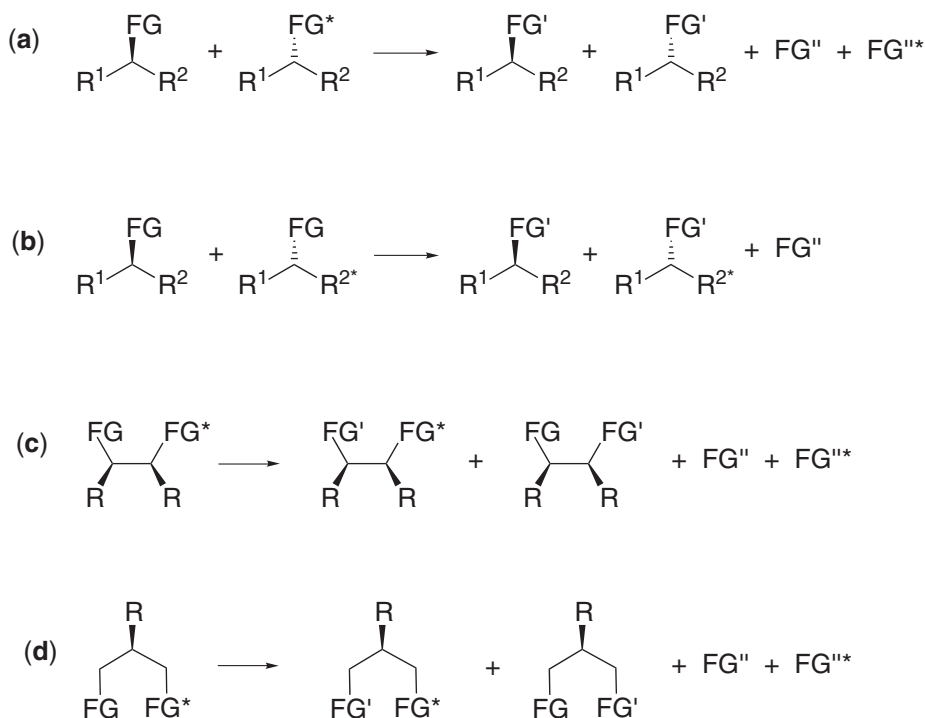


amine, optimization of the chiral selector and the conditions need to be optimized. This also applies to other classes of chiral compounds (e.g., alcohols).

Although such traditional separation techniques such as gas chromatography (GC) are usually considered to be slow (although very precise), it has been demonstrated that a special form of GC can in fact be adapted as a medium-throughput ee-assay (400–700 ee-determinations per day).⁹² It involves two chirally modified GC columns in two different ovens, one prep-and-load sample manager and one PC. Here again, generality cannot be claimed, but for many purposes medium-throughput suffices. The same applies to medium-throughput HPLC-based separation and detection of chiral compounds.⁹³

Whereas the MS-based detection of achiral products is easily parallelized,^{4,5} ee-determination by MS is not straightforward because the *R*- and *S*-forms of two enantiomers show identical mass spectra. Nevertheless, two screening systems have been developed which allow for high-throughput.^{94,95} In one case the underlying concept is to use deuterium-labeled *pseudo*-enantiomers or *pseudo* prochiral compounds bearing enantiotopic groups (Scheme 15, key: a, asymmetric transformation of a mixture of *pseudo*-enantiomers involving cleavage of the groups FG and labeled FG*; b, asymmetric transformation of a mixture of *pseudo*-enantiomers involving either cleavage or bond formation at the functional group FG; isotopic labeling at R² is indicated by the asterisk; c, asymmetric transformation of a *pseudo-meso* substrate involving cleavage of the functional groups FG and labeled FG*; d, asymmetric transformation of a *pseudo*-prochiral substrate involving cleavage of the functional groups FG and labeled FG*). The underlying idea is that deuterium-labeled enantiomers have different masses and can therefore be distinguished in the mass spectrum of a mixture. Integration of relevant peaks delivers the enantiopurity of a sample. In general electrospray ionization (ESI) is used, although MALDI also works.

If kinetic resolution is being studied, the ratio of *pseudo*-enantiomers can be measured by MS, allowing for the determination of ee-values (and/or of selectivity factors *E*). The same applies to the reaction of *pseudo* prochiral compounds. This system has been used successfully in the directed evolution of enantioselective enzymes. However, it should work equally well in the case of asymmetric transition metal catalyzed reactions. In the original version about 1,000 ee-determinations were possible per day (Figure 6).⁹⁴ The second-generation version based on an 8-channel multiplexed spray system enables about 10,000 samples to be handled per day, the sensitivity being $\pm 2\%$ ee.⁹⁶



Scheme 15

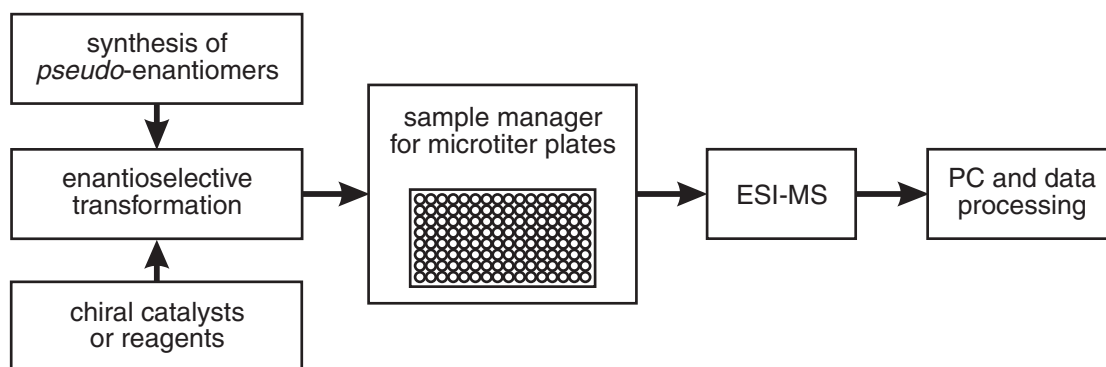


Figure 6 ESI-MS-based ee-screening system.⁹⁴

A different MS-based ee-assay makes use of a proline-derived mass-tagged acylating agent.⁹⁵ In the course of derivatization it is necessary that some degree of kinetic resolution comes about. The sensitivity of the method was reported to be $\pm 10\%$ ee. It can also be applied to the reaction of a prochiral compound lacking enantiotopic groups, as in the transformation of acetophenone to phenylethanol.

The concept of isotope labeling of *pseudo*-enantiomers and *pseudo* prochiral compounds also works well in conjunction with ^1H NMR spectroscopy as a detection system.⁹⁷ In this case ^{13}C -labeling of a CH_3 -group results in a doublet, whereas the nonlabeled enantiomer gives rise to a singlet. Integration of the signals affords ee-values of high precision ($\pm 2\%$), at least 1,400 samples being possible per day in a flow-through system. Parallel robotic derivatization using chiral reagents with formation of diastereomers followed by rapid ^1H NMR analysis is also possible.⁹⁷ Since NMR instrumentation is available in essentially all laboratories, this high-throughput and high-precision ee-assay has considerable practical value.

Several other new approaches to the high-throughput analysis of enantioselective catalysts have also been described. A novel technique makes use of DNA microarrays, a technology that previously had been used to determine relative gene expression levels on a genome-wide basis as measured by the ratio of fluorescent reporters.⁹⁸ In the newly developed ee-assay, the goal was to measure the enantiopurity of chiral amino acids.⁹⁹ One can imagine that such *R/S*-mixtures are produced by rhodium-catalyzed hydrogenation of the corresponding *N*-acyl amino acrylate using a library of combinatorially prepared catalysts. In the model study, mixtures of an *R/S* amino acid were first subjected to acylation at the amino function with formation of *N*-Boc protected derivatives. Samples were then covalently attached to amine-functionalized glass slides in a spatially arrayed manner (Figure 7). In a second step the uncoupled surface amino functions were acylated exhaustively. The third step involved complete deprotection to afford the free amino function of the amino acid. Finally, in a fourth step two *pseudo*-enantiomeric fluorescent probes were attached to the free amino groups on the surface of the array. An appreciable degree of parallel kinetic resolution in the process of amide coupling is a requirement for the success of the ee-assay, similar to the MS-based system previously described.⁹⁵ In the present case the ee-values are accessible by measuring the ratio of the relevant fluorescent intensities. It was reported that 8,000 ee-determinations are possible per day, precision amounting to $\pm 10\%$ of the actual value. It remains to be seen whether DNA microarray technology can be modified in an analogous manner in the case of other types of substrates.

Along a different line an enzymatic method for determining enantiomeric excess (EMD_{ee}) has been described.¹⁰⁰ It is based on the idea that an appropriate enzyme can be used to selectively process one enantiomer of a product from a catalytic reaction. The well-known catalytic addition of diethylzinc to benzaldehyde (**51**, R = Ph) was chosen as a test-bed for demonstrating EMD_{ee}. Various known chiral amines were used as pre-catalysts. The reaction product, 1-phenylpropanol (**59**), can be oxidized to ethyl phenyl ketone (**60**) using the alcohol dehydrogenase from *Thermoanaerobium sp.*, this process being completely *S*-selective (Scheme 16). It was possible to measure the rate of this enzymatic oxidation by monitoring the formation of NADPH by UV-spectroscopy at 340 nm.

Decisive for the success of the assay is the finding that the rate of oxidation constitutes a direct measure of the ee (Figure 8). High throughput was demonstrated by analyzing 100 samples in a 384-well format using a UV/fluorescence plate reader. Each sample contained 1 μmol of

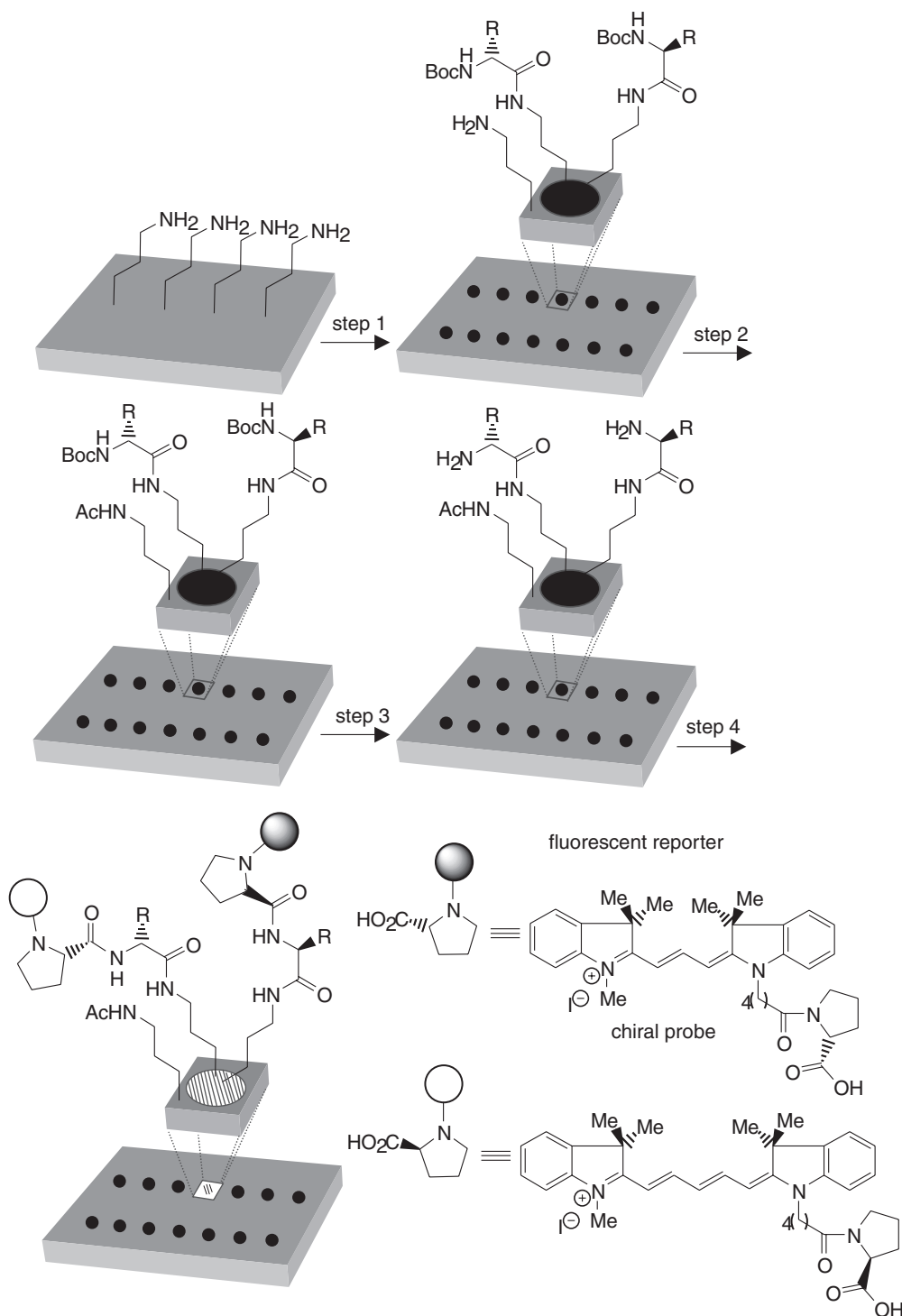
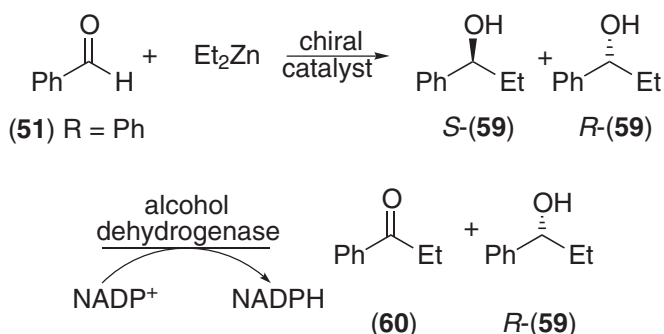


Figure 7 Reaction microarrays in high-throughput ee-determination. Reagents and conditions: step 1, BocHNCH(R)CO₂H, PyAOP, ¹Pr₂NEt, DMF; step 2, Ac₂O, pyridine; step 3, 10% CF₃CO₂H and 10% Et₃SiH in CH₂Cl₂, then 3% Et₃N in CH₂Cl₂; step 4, pentafluorophenyl diphenylphosphinate, ¹Pr₂NEt, 1:1 mixture of the two fluorescent proline derivatives, DMF, -20 °C.⁹⁹

1-phenylpropanol (**59**) in a volume of 100 μL. The accuracy in the ee-value amounts to ±10%, as checked by independent GC determinations.¹⁰⁰ About 100 samples can be processed in 30 minutes, which calculates to be 4,800 ee determinations per day.

EMD_{ee} does not distinguish between processes that proceed with low enantioselectivity but high conversion, and high enantioselectivity but low conversion. EMD_{ee} was therefore modified



Scheme 16

to provide information regarding both ee and conversion.¹⁰⁰ Accordingly, in a second set of assays the *R*-selective alcohol dehydrogenase from *Lactobacillus kefir* was used to quantify the amount of *R*-(60) present in the mixture. Since the amounts of *R*-(59) and *S*-(59) are known, conversion can be calculated.

The question arises as to the generality of the EMDee assay in the case of other chiral alcohols that do not show such high enantioselectivity in the alcohol dehydrogenase catalyzed oxidation. Theoretically, the test should still work, although accuracy in such cases would have to be demonstrated. It may be easier to use a different more selective alcohol dehydrogenase, and indeed a large number of such enzymes are commercially available. In summary, EMDee constitutes an interesting way to determine the ee of alcohols in a high-throughput manner using standard instrumentation. Of course, the assay has to be optimized in each new case of a chiral alcohol under study. A related assay in which the reaction product (ethanol) is also detected by an enzyme reaction has also been reported, although not yet in a chiral version.¹⁰¹

Another development concerns high-throughput screening of enantioselective catalysts by enzyme immunoassays,¹⁰² a technology that is routinely applied in biology and medicine. The new assay was illustrated by analyzing *R/S*-mixtures of mandelic acid (62) prepared by enantioselective ruthenium-catalyzed hydrogenation of benzoyl formic acid (61) (Equation (10)). By employing an antibody that binds both enantiomers (marked black in Equation (10)) it was possible to measure the concentration of the reaction product, thereby allowing the yield to be calculated. The use of an *S*-specific antibody (marked grey in Equation (10)) then makes the determination of ee possible.¹⁰²

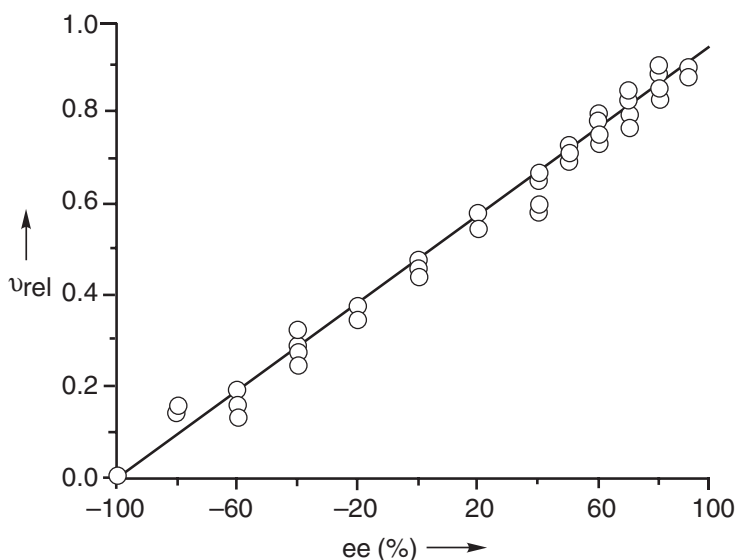
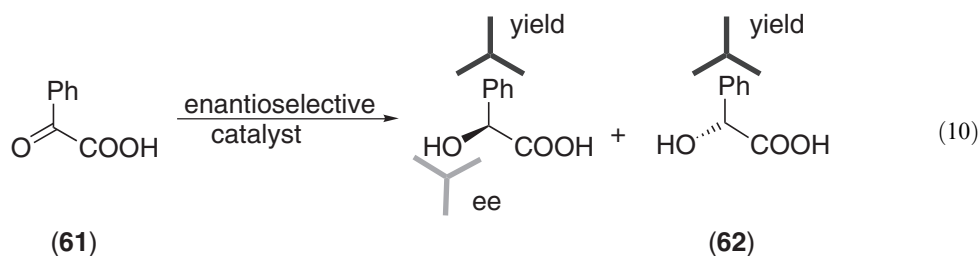


Figure 8 Plot of the initial rate of the enzyme-catalyzed oxidation of 1-phenylpropanol as a function of % ee. The solid line represents a fit of the data to the Michaelis–Menten formalism for competitive inhibition where $[S] = [S\text{-(60)}]$ and $[I] = [R\text{-(60)}]$. The total alcohol concentration was maintained constant at 10 mM.¹⁰⁰



Although this procedure may sound complicated to some organic chemists, and in fact details need to be consulted, antibodies can be raised to almost any compound of interest. Moreover, simple automated equipment comprising a plate washer and plate absorbance reader is all that is necessary. About 1,000 ee determinations are possible per day, precision amounting to $\pm 9\%$.¹⁰²

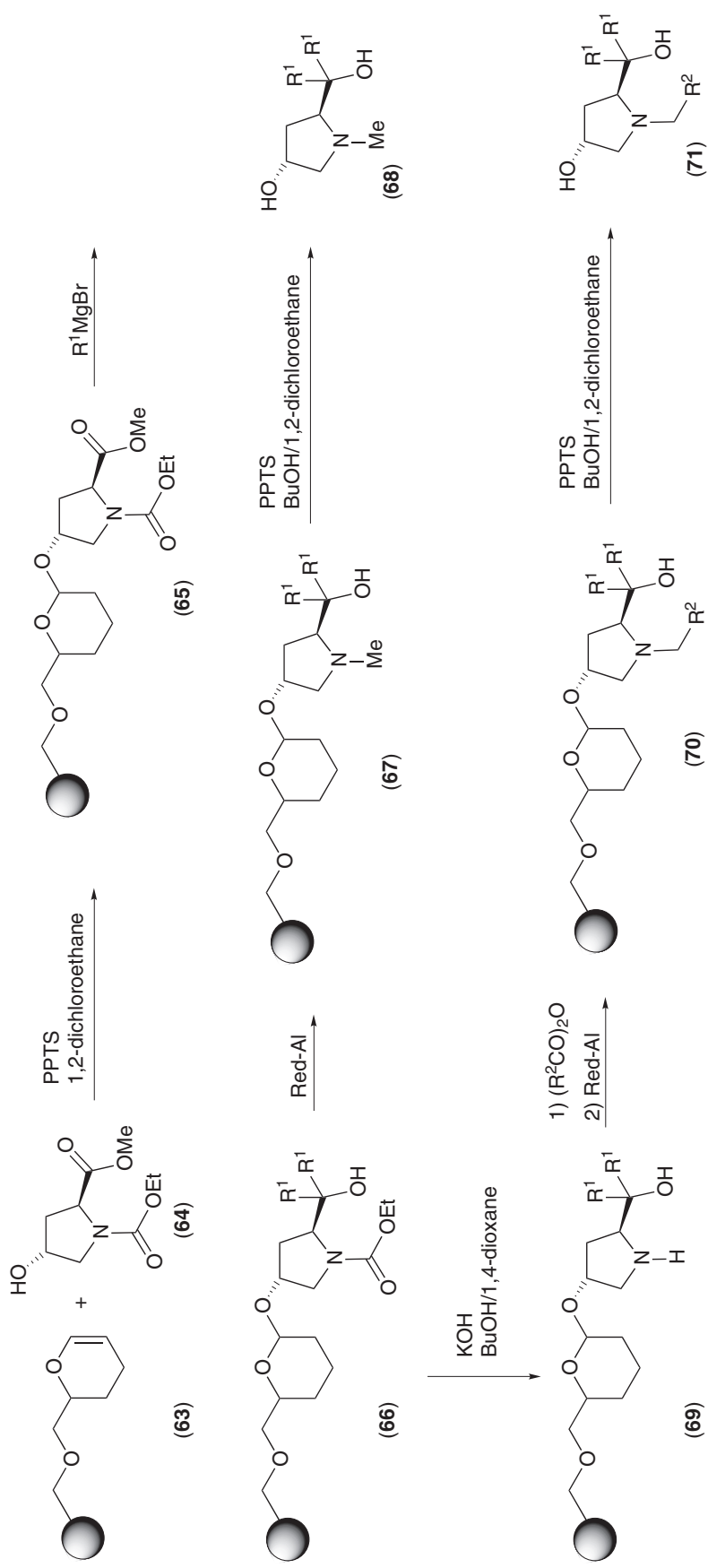
In summary, several medium-high- and super-high-throughput ee-assays are currently available. No single system is universally applicable. In most cases the publications deal with the establishment of the actual ee-assay, and not with real applications. The choice as to which system to use depends upon the particular problem at hand. Before embarking on a project concerning combinatorial asymmetric transition metal catalysis, it is important to remember that appropriate ee-assays need to be considered. Moreover, the ee-analysis is not the only instrumental aspect that requires automation. Robotics which handle of hundreds (or thousands) of catalysts and/or substrates as well as the actual catalytic reactions and the workup also need to be considered. Currently laboratory miniaturization and automation allow for about 100 catalytic reactions (e.g., hydrogenations) to be carried out simultaneously. It would be highly desirable to have machines that can perform 1,000–5,000 reactions per day. Combined with the existing high-throughput ee-assays the full power of combinatorial asymmetric transition metal catalysis could then be realized.

9.11.3.2 Strategies Used in the Combinatorial Design and Preparation of Enantioselective Transition Metal Catalysts

As outlined earlier, putting combinatorial asymmetric transition metal catalysis into genuine practice requires the availability of suitable ee-assays as well as the development of strategies for the preparation of large numbers of chiral transition metal complexes. Moreover, if thousands of catalytic reactions are to be carried out per day, the appropriate miniaturized reactors need to be developed. So far most researchers have focused on parallel synthesis of small libraries, rather than applying split-pool techniques. This has to do with the fact that spatially addressable formats in conjunction with medium- to high-throughput are easier to put into practice than methods based on split-and-pool approaches which require difficult deconvolution strategies.

Early studies concerning combinatorial methods in enantioselective transition metal catalysis resulted in the emergence of two basic approaches: (i) the preparation of analogues of known types of ligands, preferably using a modular building block strategy to incorporate diversity with respect to steric and electronic effects at the metal binding site; and (ii) optimization of reaction conditions in a given catalytic asymmetric transformation, including solvent, temperature, etc. in conjunction with known ligands. Since solid-phase chemistry has been shown to be ideal in the preparation of libraries of potential therapeutic drugs,^{1–3} the advantages involved also operate in the preparation of chiral ligands for asymmetric catalysis. Specifically, parallel synthesis, as opposed to the split-and-pool methodology, allows spatial access to each ligand, which means that catalysts can be screened individually. Theoretically this limits diversity and therefore the size of the libraries. This raises the question whether the method is only applicable to the optimization of known ligands, or whether new *types* of chiral ligand systems can also be discovered combinatorially by parallel synthesis. It is likely that the latter prediction holds.

Based on previous reports involving the use of chiral β -amino alcohols as catalytically active ligands in the enantioselective addition of Et_2Zn to aldehydes, the parallel solid-phase synthesis of a small library of substituted 2-pyrrolidine methanol derivatives (**68**) and (**71**) was reported (Scheme 17).¹⁰³ *trans*-4-Hydroxy-L-proline methyl ester (**64**) was first anchored onto a polystyrene (Merrifield) resin (**63**) via a cleavable tetrahydropyranol linker. Addition of various Grignard reagents followed by protective group manipulation at nitrogen afforded different immobilized ligands (**67**) and (**70**), which on an optional basis could be released from the resin by acid-induced hydrolytic cleavage to form (**68**) and (**71**), respectively. They were then tested one by one in the



Scheme 17

addition of Et_2Zn to various aldehydes using classical methods, including ee-determination by conventional GC on a chiral stationary phase. On-bead performance in the best cases (for aromatic and aliphatic aldehydes up to 94% and 85% ee, respectively) was also studied and turned out to be slightly inferior relative to enantioselectivity of the corresponding free ligand in solution. This early contribution demonstrates the feasibility of solid-phase parallel synthesis of new members of a specific ligand class, but it did not include any hint as to how high-throughput screening might be achieved in real applications. Indeed the authors did not claim that the concept of high-throughput preparation and screening of new enantioselective catalysts had been put into practice.¹⁰³ It is conceivable that the diversity of the library and therefore the probability of finding even better catalysts could be increased by using hundreds of different Grignard reagents and *N*-protective groups. Automation would make larger ligand libraries available within a short period of time.

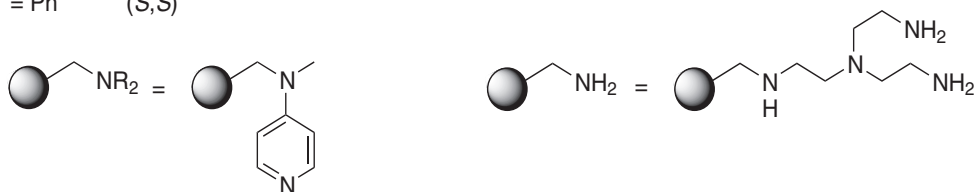
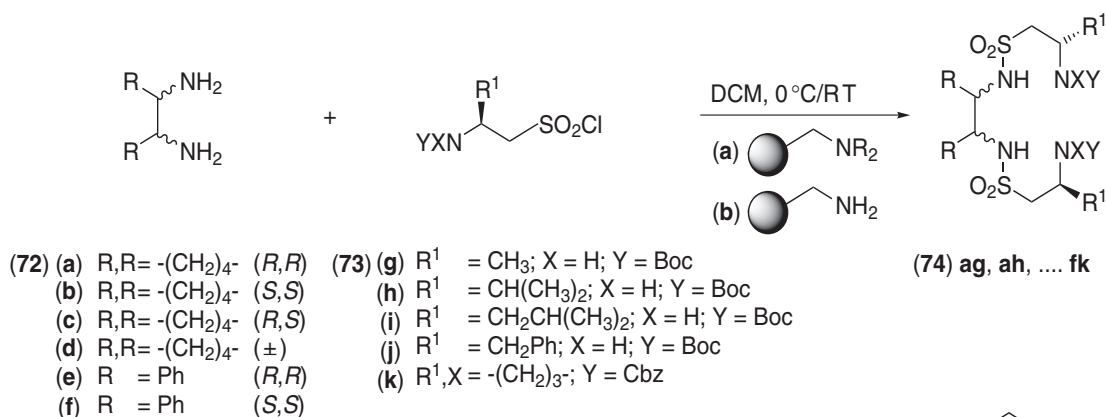
In another early effort the Geysen polyethylene pin technique was used to synthesize a 63-member library of phosphane-modified peptides as ligands in the enantioselective rhodium-catalyzed hydrogenation of methyl-2-acetamidoacrylate.¹⁰⁴ Individual on-bead screening in a parallel 24-vial reactor was performed conventionally using GC. Although the ee-values did not exceed 18%, correlations between peptide sequence and enantioselectivity were observed. The actual chemistry is novel, and it should be possible to prepare larger libraries of ligands. These aspects as well as the appropriate high-throughput screening systems were not considered. Nevertheless, this research is a noteworthy first step, because phosphanes constitute a very important class of ligands. Indeed, it remains a challenge to devise an efficient combinatorial approach to the preparation and use of chiral phosphanes. A similar strategy for optimizing palladium-catalysts for use in asymmetric allylic substitution (up to 85% ee) was also described.⁵⁰

One step further was then taken in developing new enantioselective catalysts via parallel synthesis, although again genuine high-throughput screening was not part of the effort. New members of a known family of chiral ligands based on sulfonamides were constructed in a modular manner using solid-phase extraction (SPE) techniques.¹⁰⁵ Vicinal diamines (**72**) were treated with an excess of sulfonyl chlorides (**73**) to ensure complete conversion (Scheme 18). To avoid laborious purification of the sulfonamide products (**74**), the reactions were run in DCM in the presence of polymer bound dimethylaminopyridine, which not only catalyzes the coupling reaction but also scavenges the liberated HCl. The excess sulfonyl chloride was then removed by reaction with solid-phase bound tris(2-aminoethyl)amine. Thus, modular preparation and smooth separation of the "side products" from the "pure" ligands were possible in a simple protocol.¹⁰⁵

The disulfonamide library was tested in the $\text{Ti}(\text{O}^i\text{Pr})_4$ -mediated addition of Et_2Zn to aldehydes, a known process using the bis-trifluoromethylsulfonamide of 1,2-diaminocyclohexane.¹⁰⁶ The tests were run in 30 different reaction vessels in parallel format. In order to increase throughput, each vessel was charged with four different aldehydes, and the enantioselectivities of the four reaction products were determined by conventional GC analysis of the crude mixtures. The idea of using a given catalyst to screen combinatorially the reactions of different substrates had previously been proposed but in a different context.⁴⁵ In the present case each mixture required about one hour to be screened, which means that about 96 ee-determinations of products (**52**) (Scheme 11) could be performed per day.¹⁰⁵ A total of 120 results were collected, the best ees being >90%.

Thereafter a similar approach based on solid-phase synthesis of a small library of peptidosulfonamides as chiral ligands for the same reaction (up to 66% ee) was described.¹⁰⁷ Again, about 96 ee-determinations per day were reported to be possible by GC, but only a few dozen were actually carried out. Nevertheless, it is the synthetic strategy that deserves attention at this stage. Certainly better results are to be expected upon generating larger libraries. Along related lines the copper-catalyzed conjugate addition of Et_2Zn nitroolefins was studied, leading to ees of up to 98%.¹⁰⁸ The value of this study has to do with the fact that it would have been difficult to find the optimal catalyst using traditional approaches.

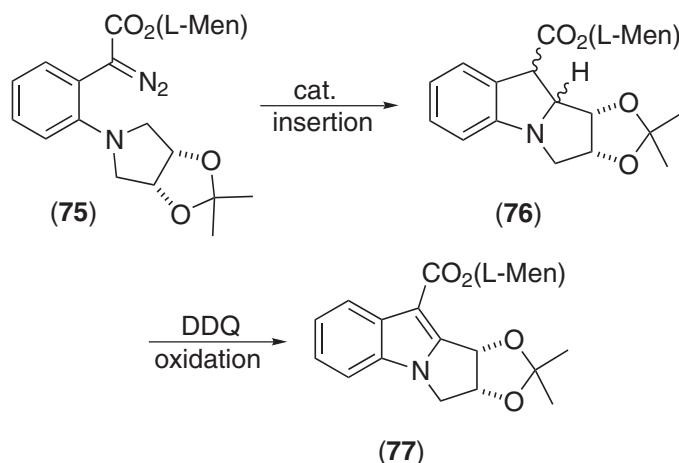
Using the results of an earlier study concerning enantioselective copper-catalyzed intramolecular C–H insertion of metal carbenoids,¹⁰⁹ an interesting system for optimizing the proper combination of ligand, transition metal, and solvent for the reaction of the diazo compound (**75**) was devised (see Scheme 19).¹¹⁰ The reaction parameters were varied systematically on a standard 96-well microtiter/filtration plate. A total of five different ligands, seven metal precursors, and four solvents were tested in an iterative optimization mode. Standard HPLC was used to monitor stereoselectivity following DDQ-induced oxidation. This type of catalyst search led to the



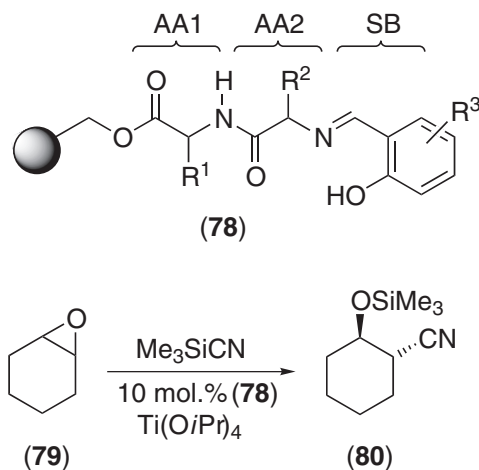
Scheme 18

discovery that silver(I) catalyzes the process, a finding that had no precedent in the literature. Moreover, by using a Pfaltz-type ligand¹¹¹ the diastereoselectivity in the formation of the final product (77) increased from the original 2.3:1 (at 64% yield) to 3.9:1 (at 75% conversion) or to 5.9:1 (at 23% conversion).¹¹⁰ Here again, it would be of interest to see if truly high-throughput screening of a much greater number of reactions would lead to even better results. Such proof of principle would really illustrate the power of combinatorial techniques relative to the traditional approach based on the sequential study of individual catalysts under different conditions.

The palladium-catalyzed asymmetric allylic substitution using seven different phosphano-oxazoline ligands at various ligand-to-metal ratios was also studied.¹¹² An aluminum block containing 27 wells was placed in a dry box in which the reactions were carried out in parallel. Analyses were performed by conventional chiral GC equipped with an autosampler. Such a setup allowed about 33 catalyst evaluations per day. Apparently, only a few dozen were carried out in the study, resulting in the identification of a catalyst showing an ee-value of 74% in the reaction of 4-acyloxy-2-pentene with malonate.¹¹² It is not clear whether further ligand diversification would lead to catalysts more selective than the record set in this case by the Trost-catalyst (92% ee).¹¹³



Scheme 19

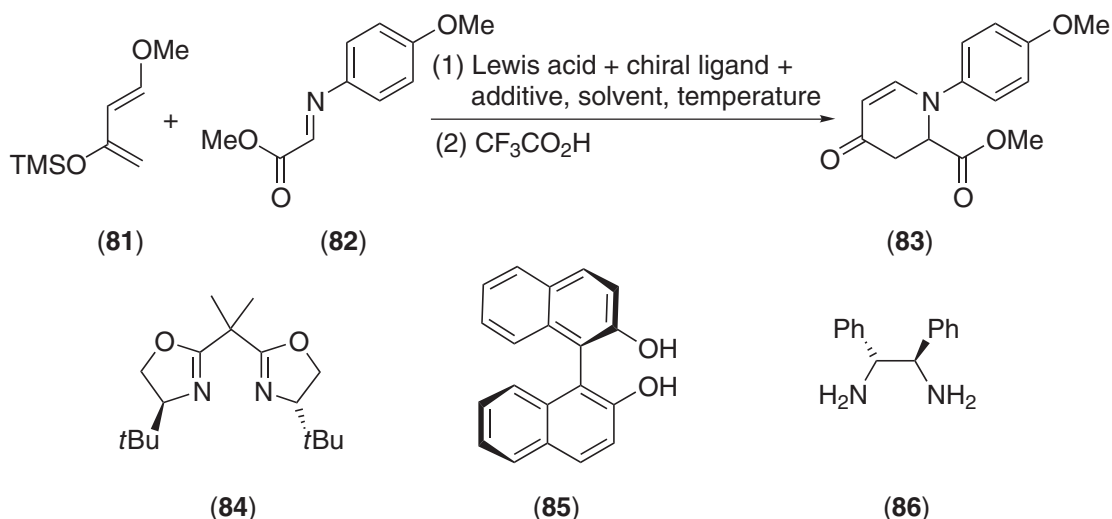


Scheme 20

Another important advancement concerning combinatorial optimization of asymmetric catalysts was described in 1996.¹¹⁴ Diversity-based procedures in the titanium-mediated enantioselective ring-opening reaction of *meso* epoxides such as (79) with cyanotrimethylsilane (TMSCN) leading to the formation of nitrile (80) (Scheme 20). Peptides composed of three independently variable subunits, namely Schiff base (SB), amino acid 1 (AA1), and amino acid 2 (AA2) were chosen as the catalysts. The modular nature of this system allows for high diversity and is therefore ideally suited for combinatorial catalyst research. A simple calculation shows that the use of 20 different aldehydes for the Schiff bases and 20 natural amino acids would give rise to 8,000 different chiral ligands. However, the lack of high-throughput screening systems at the time of this seminal study contributed to the decision *not* to generate such large libraries. Rather, only a small library of ligands was prepared. All of them were detached from the respective beads and screened in the titanium-catalyzed reaction of cyclohexene oxide (79) with TMSCN in solution, the assay system being conventional GC.¹¹⁴ Later a similar study was performed on the catalytically active beads themselves.¹¹⁵

A search strategy which makes possible the “identification of effective ligands without examination of all possibilities” was utilized.¹¹⁴ Accordingly, each of the three modular subunits was successively optimized while the other two subunits were kept constant. Of a total of only 60 catalysts, the best one was identified as inducing an enantioselectivity of 89% ee for the model reaction. Positional scanning of this type is based on the assumption that additivity but not cooperativity between the three subunits pertains. Although this assumption cannot be proven or disproven without scrutinizing larger libraries, it appears reasonable. A similar search strategy has been applied in the titanium-catalyzed enantioselective addition of cyanide to imines.^{116,117} Nevertheless, finding and optimizing modular catalyst systems that do show synergistic effects between subunits may be an intriguing goal for the future.

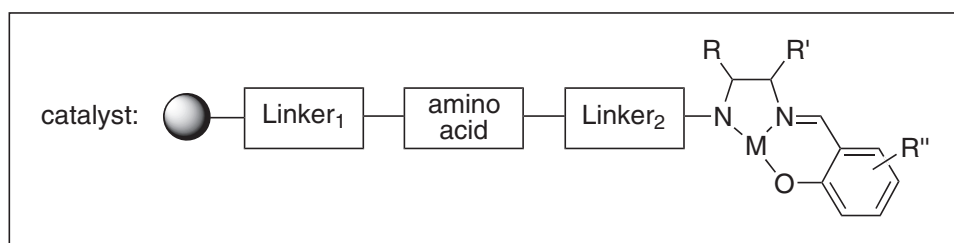
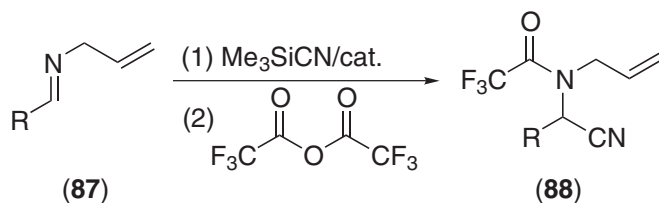
In the attempts to find optimal conditions for an enantioselective Lewis acid catalyzed aza-Diels–Alder reaction (81) + (82) \rightarrow (83) (Scheme 21), several parameters were varied in parallel.¹¹⁸ Good literature precedent for the potential catalyst was not available, although it was known that many different Lewis acids, including Yb(OTf)₃ catalyze Diels–Alder reactions. Three different chiral ligands (84)–(86) known in the literature were tested in conjunction with Yb(OTf)₃, Cu(OTf)₂, MgI₂, and FeCl₃ as Lewis acids, a limited number of additives and solvents also being evaluated. By using an autosampler and a conventional HPLC instrument equipped with a column having a chiral phase, 144 approximate yield and ee-values were obtained in about one week, which means that in this system approximately 20 evaluations of catalyst systems for a given reaction are possible per day. Four of the best hits were then applied in scaled-up reactions. The optimal catalyst consisted of Yb(OTf)₃/(86), resulting in cycloadduct (83) with 97% ee and in 64% yield (Scheme 21).¹¹⁸ Although quite successful in this particular case, it is not clear how effective this type of search really is, since ligand diversity is hardly considered. In principle, it can be expected that libraries composed of modular chiral ligands or of simple chiral ligands in conjunction with a high diversity of achiral additives are more meaningful in the combinatorial search for enantioselective catalysts.



Scheme 21

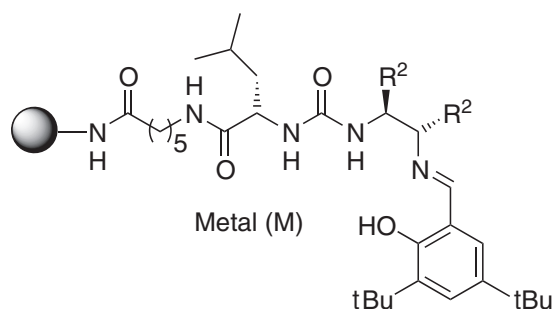
A seminal paper which demonstrated that a combinatorial diversity-based method leads to the discovery of highly enantioselective catalysts, not readily possible by the traditional one-at-a-time approach to catalyst optimization, was published in 1998.¹¹⁹ A strategy for the parallel synthesis of a certain class of modularly constructed ligands, specifically for use in the catalytic asymmetric Strecker reaction of imines (87) (Scheme 22) was described. The first step in the parallel preparation of a catalyst library is the selection of a ligand system amenable to solid-phase synthesis and systematic structural variation. In addition to the requirement of high-yield reactions in the modular construction of the ligands, an unobtrusive site for attachment to the solid support is necessary. A number of traditional C_2 -symmetric ligands would require several tedious synthetic steps. In contrast, tridentate Schiff base complexes, which are known to be ligands for a variety of catalytic reactions, are in fact suitable for solid-phase synthesis. These systems are normally comprised of three units, a chiral amino alcohol, a salicylaldehyde derivative, and a metal ion. In the above study the amino alcohol unit was replaced by chiral diamines, the two linkers also contributing to structural diversity (Scheme 22).¹¹⁹

A given ligand system was first prepared on the solid support, and a small collection of catalysts (library 1) generated by adding 11 different metals and in one case no metal (Scheme 23).¹¹⁹ It turned out that the best ee-value (19%) was in fact obtained in the *metal-free* system. Based on this



Scheme 22

Library 1



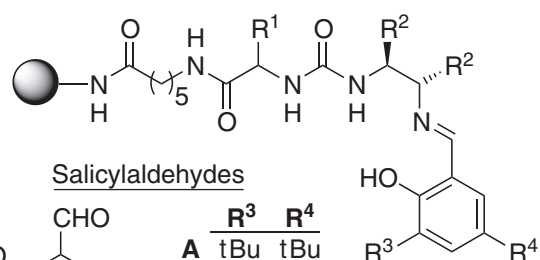
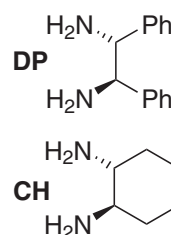
M	None	Ti	Mn	Fe	Ru	Co	Cu	Zn	Gd	Nf	Yb	Eu
ee (%)	19	4	5	10	13	0	9	1	2	3	0	5
conv. (%)	59	30	61	69	63	68	55	91	95	84	94	34

Library size: 12 compounds

Library 2

Amino acid
Leu, D-Leu, His
Phg (Phenylglycine)

Diamines

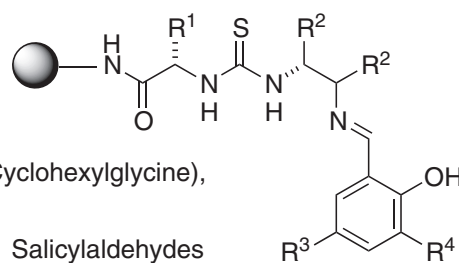
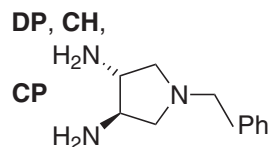


	R ³	R ⁴
A	tBu	tBu
B	tBu	H
C	H	tBu
D	tBu	OMe
E	Br	Br
F	tBu	NO ₂

Library size: 48 compounds

Library 3

L-Amino acids
Leu, Iie, Met, Phe,
Tyr (OtBu), **Val, Thr** (OtBu),
Nor (Norleucine), **Phg, Chg** (Cyclohexylglycine),
tLeu (*tert*-Leucine)

(R,R)-Diamines

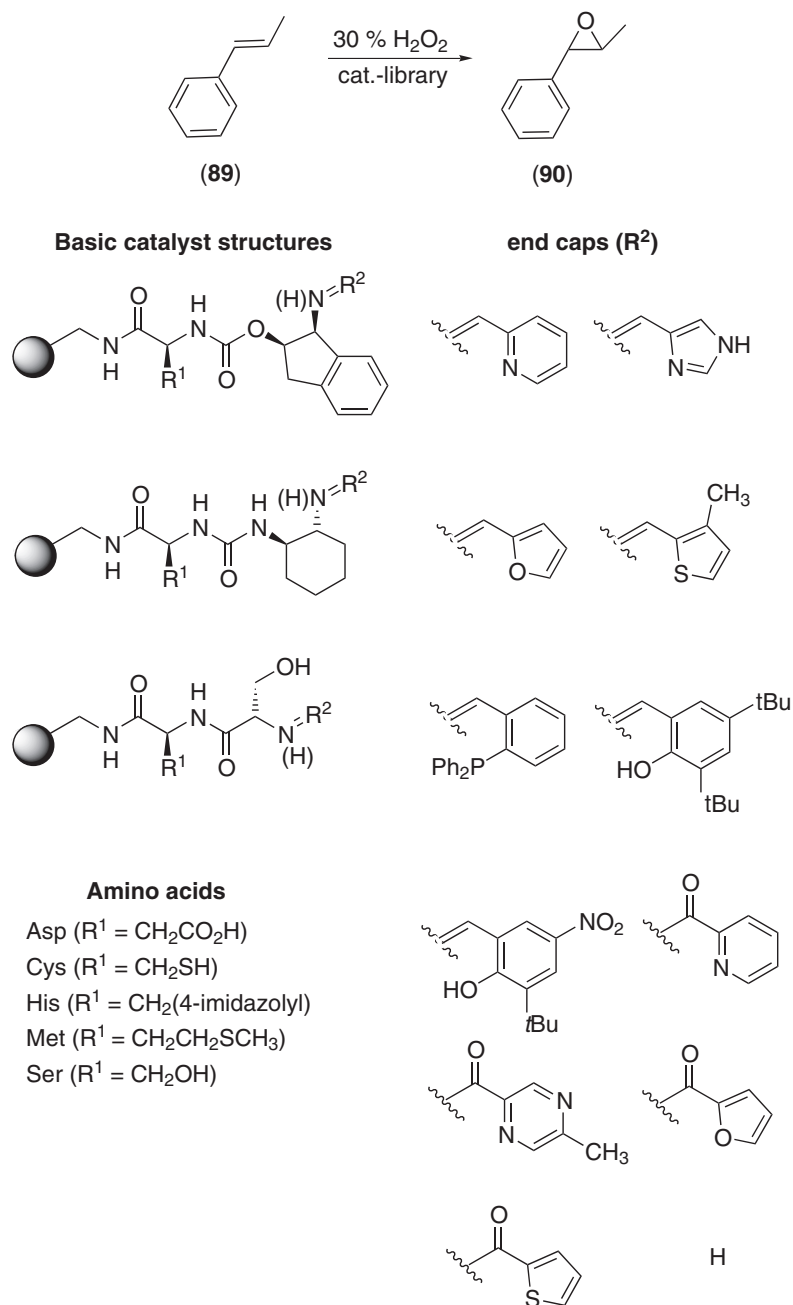
X
OMe
H
tBu
Br

Library size: 132 compounds

Scheme 23

observation, a parallel ligand library of 48 members (library 2) was prepared using two different chiral 1,2-diamines and a variety of amino acids and Schiff bases. The combination of L-leucine and *(R,R)*-diamine was shown to be optimal, the substitution pattern in the salicylaldehyde also playing a crucial role. Thereafter, the linker elements were optimized by a traditional one-catalyst-at-a-time

approach, resulting in the emergence of more selective catalysts having thiourea linkers. Finally, these results were used to prepare library 3 containing 132 thiourea derivatives (Scheme 23).¹¹⁹ The enantioselectivities in the addition of HCN to a variety of imines turned out to be greater than 80%, with the best case being 91% ee at -78°C in a laboratory scale experiment. The ee-determinations were performed using conventional chiral HPLC with a chiral stationary phase. The actual throughput, however, was not defined. Nevertheless, the importance of this contribution concerns the fact that it touches on the question of the complexity arising from interrelated variables in catalytic processes. Indeed, the diversity-based method led to synergistic effects between catalyst components which are unexpected and which do not correspond to “normal” intuition.¹¹⁹



Scheme 24

Another important conceptual advancement addressed the question as to whether combinatorial methods can be used to discover new *types* of chiral ligand.¹²⁰ In this case efforts concentrated on the combinatorial search for a chiral ligand/metal system that catalyzes the H₂O₂-mediated enantioselective epoxidation of *trans*- β -methylstyrene (**89**) (Scheme 24).¹²⁰ First, the solid-phase synthesis of modularly constructed ligands composed of (i) amino acids, (ii) 1-amino-2-indanol, *trans*-1,2-diaminocyclohexane or serine, and (iii) end-groups was performed on a Wang-resin. End-capped salicylamine was also attached to the Wang resin so as to include types of ligands known to be active in metal-catalyzed epoxidations. The combined library of 192 ligands was then treated with 30 different metal salts, theoretically resulting in 5,760 possible metal–ligand complexes. On the basis of earlier experience concerning the application of metal-binding combinatorial libraries for the identification of coordination complexes,²⁴ it was possible to show by visual color assays and by qualitative inorganic color tests that about 80% of the 5,760 possible metal–ligand complexes had been generated.¹²⁰

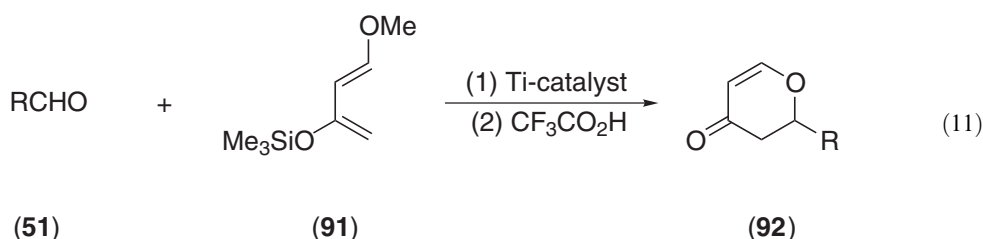
In order to identify the most active and stereoselective bead, a mixture of all 192 ligands was treated with a single metal source, and each group of catalysts was tested in the model epoxidation reaction.¹²⁰ Conventional GC analysis of these 30 experiments showed that the two groups derived from VOSO₄ and FeCl₂ are most active. Since it was observed that VOSO₄ alone is also catalytically quite active, the rest of the efforts focused on FeCl₂. Accordingly, 12 ligand libraries, each containing the 16 basic structures and one of the various end groups, were prepared and treated with FeCl₂. The usual screening procedure showed that the most active catalysts are those containing a pyridine-type end group. It was then logical to test the 16 ligands with the most active end groups. However, since an active catalyst might theoretically be overlooked by such a restrictive procedure, further encoding was not carried out. Rather, all FeCl₂ complexes of the original 192 ligands were screened for activity. Pyridine-capped ligands turned out to be most active. This small group was then assayed with respect to enantioselectivity, culminating in the identification of three FeCl₂/ligand complexes which led to ee-values of 15–20% for product (**90**) in the model reaction (see Scheme 24). Although the enantioselectivities are modest, this study shows for the first time that it is possible to discover new lead ligand structures for use in asymmetric catalysis.¹²⁰

The original concept of asymmetric activation of chiral alkoxyzinc catalysts by chiral nitrogen activators for dialkylzinc addition to aldehydes has been extended within the context of combinatorial catalysis, high-throughput screening again being performed by HPLC-CD/UV or HPLC-OR/RIU systems^{87,89} (Section 9.11.3.1, Scheme 11). The combination of such screening systems and asymmetric activation lends itself ideally to combinatorial enantioselective transition metal catalysis.

Finally, the discovery of exceptionally efficient catalysts for solvent-free enantioselective hetero-Diels–Alder reactions was made possible by a combinatorial approach.¹²¹ The object was to find a chiral titanium catalyst for the reaction of aldehydes (**51**) with Danishefsky's diene (**91**), with formation of cycloadduct (**92**) in >99% enantiopurity (Equation (11)).

In order to reach this goal, a combinatorial library of chiral metal complexes was generated by combining a diol ligand (L_m) with Ti(O^{*i*}Pr)₄ and an alternative diol ligand (L_n) in a parallel manner (Figure 9). Due to ligand diversity and the possibility of aggregation of titanium complexes, each member of the L_m /Ti/ L_n library is actually a mixture of species.¹²¹

Thirteen different chiral diol ligands were used (Scheme 25), leading to a catalyst library of 104 members.¹²¹ In a model reaction benzaldehyde (**51**), (R = Ph) was used as the carbonyl component, HPLC being used to ascertain the enantiopurity of (**92**). Initially 1 mol.% of catalyst was used. In the primary screening catalysts modified by L₄, L₅, L₆, and L₇ turned out to be excellent (77–96% ee; yields 63–100%). Thereafter the catalyst loading of L_m /Ti/ L_n ($m, n = 4-7$) was decreased to 0.1 mol.%, but this led to only trace amounts of product. Finally, the solvent was



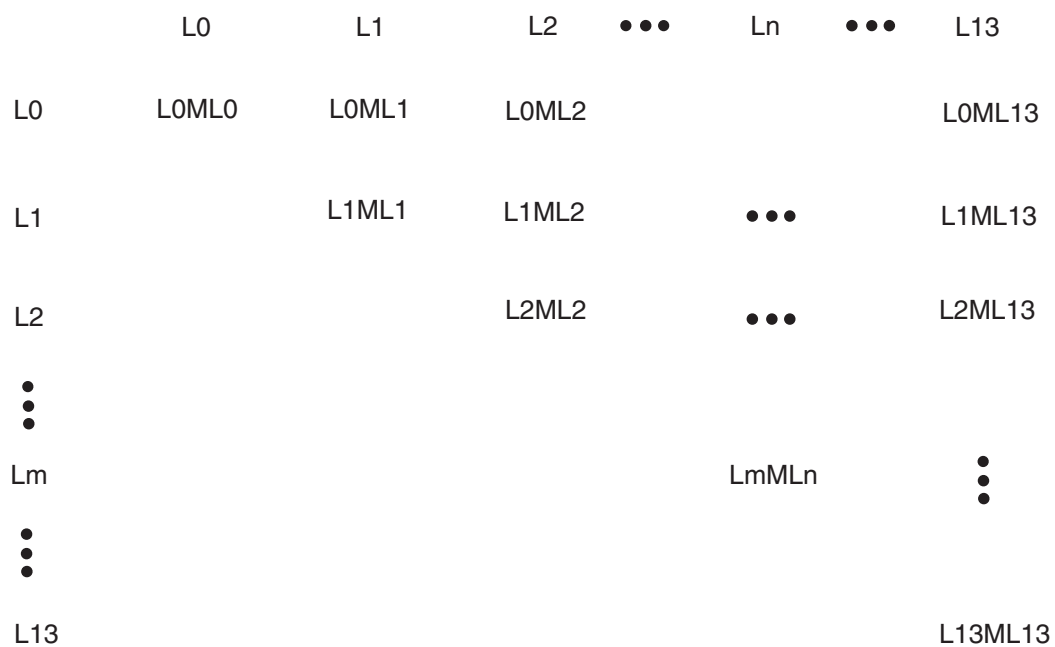
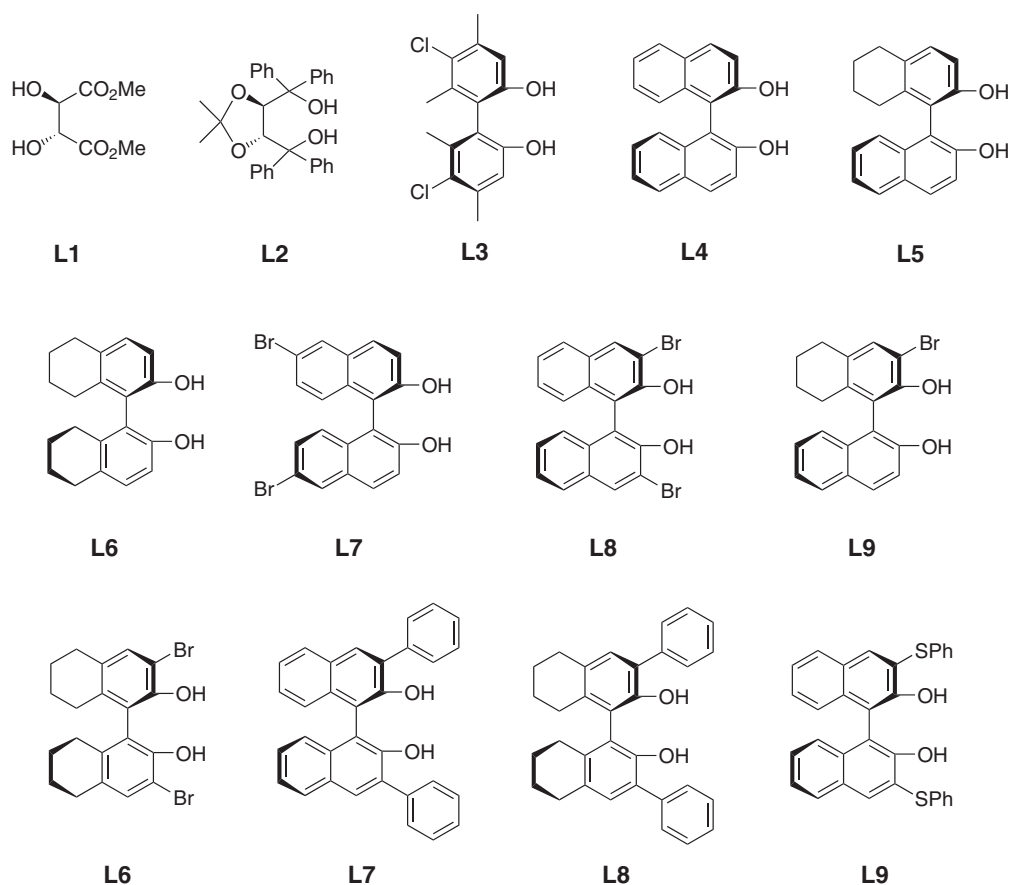


Figure 9 Parallel preparation of catalysts.¹²¹



Scheme 25

varied, toluene being better than ether. However, solvent-free conditions led to 100% yield and 99% ee, and catalyst loading could be reduced to 0.05–0.005! This is the lowest known catalyst loading in an asymmetric Lewis acid-catalyzed reaction.¹²¹ A number of other aldehydes reacted similarly, demonstrating the power of this combinatorial approach.

9.11.4 CONCLUSIONS AND PERSPECTIVES

Combinatorial homogeneous transition metal catalysis is in its infancy, but a number of trends are already visible. So far only relatively small libraries of achiral or chiral ligands have been generated and tested. With the establishment of high-throughput screening systems for achiral and chiral products, the stage is now set for real applications involving large libraries of catalysts and/or catalyst formulations. It is likely that many interesting catalysts will be created and identified by means of combinatorial methods, including those that would have been missed by using only traditional approaches. The creation of meaningful libraries requires chemical knowledge and intuition. The same applies to the process of drawing conclusions after identifying hits, specifically when further optimization is necessary.

There are certain catalyst systems which appear to be more amenable to combinatorial studies than others. For example, libraries of small peptides as ligands are particularly easy to prepare (e.g., on solid supports), and due to their modular nature high diversity is possible. High diversity is also readily achieved when using mixtures of two or more chiral monodentate ligands.¹²² This novel approach offers many perspectives.

Another novel way to approach extremely high ligand diversity involves the concept of directed evolution of hybrid catalysts.^{123,124} Accordingly, large libraries of mutant enzymes (typically 2,000–5,000 membered) are generated by gene mutagenesis and expression, which are then chemically modified at a cysteine function in the cavity of the relevant enzyme, resulting in the implantation of achiral ligand/metal centers (Figure 10).

Such a process creates thousands of potential catalysts, each differing only in the protein structure, i.e., in the microenvironment that gives rise to different catalyst performance (activity/selectivity). Upon identifying the best catalyst in a given reaction (e.g., hydrogenation, hydroformylation, olefin metathesis, allylic substitution, oxidation, etc.), further rounds of mutagenesis/chemical modification/screening allows for catalyst optimization on the basis of Darwinistic principles (Figure 11). This means that the methods of molecular biology^{13,14} are used to tune

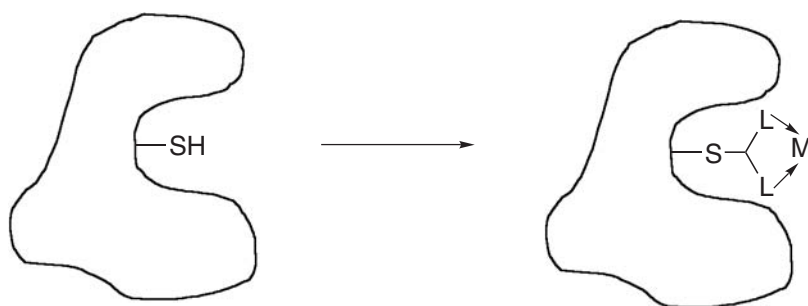


Figure 10 Implantation of ligand/metal centers in an enzyme.¹²³

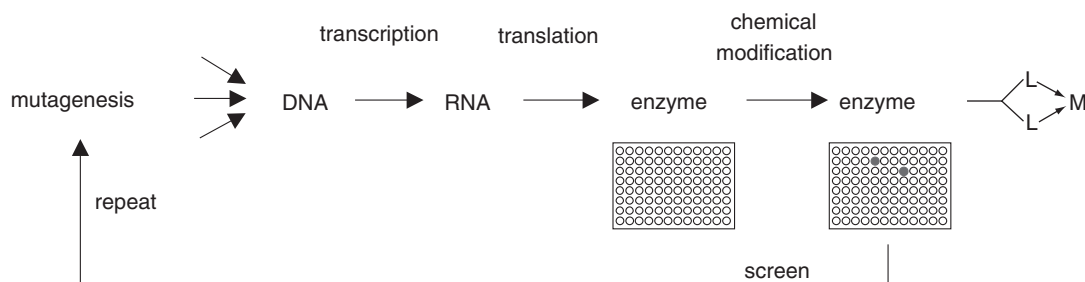


Figure 11 Directed evolution of hybrid catalysts.^{123,124}

the nature and the performance of a transition metal catalyst.^{123,124} Although ligand implantation has been achieved in exploratory experiments, a number of technical problems have to be solved before this type of combinatorial catalyst optimization can be realized on an industrial level.¹²⁴

9.11.5 REFERENCES

1. Balkenhohl, F.; von dem Bussche-Hünnefeld, C.; Lansky, A.; Zechel, C. *Angew. Chem. Int. Ed. Engl.* **1996**, *35*, 2288–2337.
2. *Chem. Rev.* **1997**, *97*, 347–510 (special issue on combinatorial chemistry).
3. Nicolaou, K. C.; Hanks, R.; Hartwig, W., Eds.; *Handbook of Combinatorial Chemistry*, Wiley-VCH: Weinheim, Germany, **2002**; Vols. 1 & 2.
4. Jandeleit, B.; Schaefer, D. J.; Powers, T. S.; Turner, H. W.; Weinberg, W. H. *Angew. Chem. Int. Ed.* **1999**, *38*, 2494–2532.
5. Senkan, S. *Angew. Chem. Int. Ed.* **2001**, *40*, 312–329.
6. Hoffmann, C.; Wolf, A.; Schüth, F. *Angew. Chem. Int. Ed.* **1999**, *38*, 2800–2803.
7. Maier, W. F. *Angew. Chem. Int. Ed.* **1999**, *38*, 1216–1218.
8. Schlögl, R. *Angew. Chem. Int. Ed.* **1998**, *37*, 2333–2336.
9. Bein, T. *Angew. Chem. Int. Ed.* **1999**, *38*, 323–326.
10. Archibald, B.; Brümmer, O.; Devenney, M.; Gorer, S.; Jandeleit, B.; Uno, T.; Weinberg, W. C. H.; Weskamp, T. *Combinatorial Methods in Catalysis*. In *Handbook of Combinatorial Chemistry*; Nicolaou, K. C., Hanks, R., Hartwig, W., Eds.; Wiley-VCH: Weinheim, Germany, **2002**, Vol. 2, pp 885–990.
11. Hoveyda, A. H. *Diversity-Based Identification of Efficient Homochiral Organometallic Catalysts for Enantioselective Synthesis*. In *Handbook of Combinatorial Chemistry*; Nicolaou, K. C., Hanks, R., Hartwig, W., Eds.; Wiley-VCH: Weinheim, Germany, **2002**, Vol. 2, pp 991–1016.
12. Dahmen, S.; Bräse, S. *Synthesis* **2001**, 1431–1449.
13. Arnold, F. H. *Nature (London)* **2001**, *409*, 253–257.
14. Powell, K. A.; Ramer, S. W.; del Cardayré, S. B.; Stemmer, W. P. C.; Tobin, M. B.; Longchamp, P. F.; Huisman, G. W. *Angew. Chem. Int. Ed.* **2001**, *40*, 3948–3959.
15. Reetz, M. T.; Jaeger, K.-E. *Chem. Eur. J.* **2000**, *6*, 407–412.
16. Reetz, M. T. *Pure Appl. Chem.* **2000**, *72*, 1615–1622.
17. Reetz, M. T. *Angew. Chem. Int. Ed.* **2001**, *40*, 284–310.
18. Reetz, M. T. *Angew. Chem. Int. Ed.* **2002**, *41*, 1335–1338.
19. Burger, M. T.; Still, W. C. *J. Org. Chem.* **1995**, *60*, 7382–7383.
20. Czarnik, A. T. W. *Curr. Opin. Chem. Biol.* **1997**, *1*, 60–66.
21. Singh, A.; Yao, Q.; Tong, L.; Still, W. C.; Sames, D. *Tetrahedron Lett.* **2000**, *41*, 9601–9605.
22. Shibata, N.; Baldwin, J. E.; Wood, M. E. *Bioorg. Med. Chem. Lett.* **1997**, *7*, 413–416.
23. Gao, C.; Brümmer, O.; Mao, S.; Janda, K. D. *J. Am. Chem. Soc.* **1999**, *121*, 6517–6518.
24. Francis, M. B.; Finney, N. S.; Jacobsen, E. N. *J. Am. Chem. Soc.* **1996**, *118*, 8983–8984.
25. Malin, R.; Steinbrecher, R.; Janssen, J.; Semmler, W.; Noll, B.; Johannsen, B.; Frömmel, C.; Höhne, W.; Schneider-Mergener, J. *J. Am. Chem. Soc.* **1995**, *117*, 11821–11822.
26. Pirrung, M. C.; Park, K. *Bioorg. Med. Chem. Lett.* **2000**, *10*, 2115–2118.
27. Szurdoki, F.; Ren, D.; Walt, D. R. *Anal. Chem.* **2000**, *72*, 5250–5257.
28. Bergbreiter, D. E.; Zaitsev, V. N.; Gorlova, E. Y.; Khodakovskiy, A. *Spec. Publ.–R. Soc. Chem.* **1999**, *235*, 353–360.
29. Menger, F. M.; Eliseev, A. V.; Migulin, V. A. *J. Org. Chem.* **1995**, *60*, 6666–6667.
30. Menger, F. M.; West, C. A.; Ding, J. *Chem. Commun., Cambridge, UK* **1997**, 633–634.
31. Menger, F. M.; Ding, J.; Barragan, V. *J. Org. Chem.* **1998**, *63*, 7578–7579.
32. Berg, T.; Vandersteen, A. M.; Janda, K. D. *Bioorg. Med. Chem. Lett.* **1998**, *8*, 1221–1224.
33. Berg, T.; Simeonov, A.; Janda, K. D. *J. Comb. Chem.* **1999**, *1*, 96–100.
34. Berkessel, A.; Héroult, D. A. *Angew. Chem. Int. Ed.* **1999**, *38*, 102–105.
35. Berkessel, A.; Riedl, R. *J. Comb. Chem.* **2000**, *2*, 215–219.
36. Taylor, S. J.; Morken, J. P. *Science (Washington, D.C.)* **1998**, *280*, 267–270.
37. Crabtree, R. H. *Chem. Commun., Cambridge, UK* **1999**, 1611–1616.
38. Loch, J. A.; Crabtree, R. H. *Pure Appl. Chem.* **2001**, *73*, 119–128.
39. Shaughnessy, K. H.; Kim, P.; Hartwig, J. F. *J. Am. Chem. Soc.* **1999**, *121*, 2123–2132.
40. Littke, A. F.; Fu, G. C. *J. Am. Chem. Soc.* **2001**, *123*, 6989–7000.
41. Stambuli, J. P.; Stauffer, S. R.; Shaughnessy, K. H.; Hartwig, J. F. *J. Am. Chem. Soc.* **2001**, *123*, 2677–2678.
42. Copeland, G. T.; Miller, S. J. *J. Am. Chem. Soc.* **1999**, *121*, 4306–4307.
43. Harris, R. F.; Nation, A. J.; Copeland, G. T.; Miller, S. J. *J. Am. Chem. Soc.* **2000**, *122*, 11270–11271.
44. Blackmond, D. G.; Rosner, T.; Pfaltz, A. *Org. Process Res. Dev.* **1999**, *3*, 275–280.
45. Kagan, H. B. *J. Organomet. Chem.* **1998**, *567*, 3–6.
46. Löber, O.; Kawatsura, M.; Hartwig, J. F. *J. Am. Chem. Soc.* **2001**, *123*, 4366–4367.
47. Feigl, F. *Qualitative Analysis by Spot Tests, Inorganic and Organic Applications* 3rd ed., Elsevier: New York, **1946**.
48. Kawasura, M.; Hartwig, J. F. *J. Organometallics* **2001**, *20*, 1960–1964.
49. Lavastre, O.; Morken, J. P. *Angew. Chem. Int. Ed.* **1999**, *38*, 3163–3165.
50. Gilbertson, S. R.; Collibee, S. E.; Agarkov, A. *J. Am. Chem. Soc.* **2000**, *122*, 6522–6523.
51. Chankvetadze, B. *Capillary Electrophoresis in Chiral Analysis*, Wiley: Chichester, UK, **1997**.
52. Blaschke, G.; Chankvetadze, B. *J. Chromatogr. A* **2000**, *875*, 3–25.
53. Zhang, Y.; Gong, X.; Zhang, H.; Larock, R. C.; Yeung, E. S. *J. Comb. Chem.* **2000**, *2*, 450–452.
54. Pescarmona, P. P.; van der Waal, J. C.; Maxwell, I. E.; Maschmeyer, T. *Angew. Chem. Int. Ed.* **2001**, *40*, 740–742.
55. Reetz, M. T.; Becker, M. H.; Kühling, K. M.; Holzwarth, A. *Angew. Chem. Int. Ed.* **1998**, *37*, 2647–2650.

56. Reetz, M. T.; Becker, M. H.; Liebl, M.; Fürstner, A. *Angew. Chem. Int. Ed.* **2000**, *39*, 1236–1239.
57. Revis, A.; Hilty, T. K. *Tetrahedron Lett.* **1987**, *28*, 4809–4812.
58. Kiyooka, S. I.; Shimizu, A.; Torri, S. *Tetrahedron Lett.* **1998**, *39*, 5237–5238.
59. Taylor, S. J.; Morken, J. P. *J. Am. Chem. Soc.* **1999**, *121*, 12202–12203.
60. Bousisie, T. R.; Murphy, V.; Hall, K. A.; Coutard, C.; Dales, C.; Petro, M.; Carlson, E.; Turner, H. W.; Powers, T. S. *Tetrahedron* **1999**, *55*, 11699–11710.
61. Bousisie, T. R.; Coutard, C.; Turner, H.; Murphy, V.; Powers, T. S. *Angew. Chem. Int. Ed.* **1998**, *37*, 3272–3275.
62. Hinderling, C.; Chen, P. *Angew. Chem. Int. Ed.* **1999**, *38*, 2253–2256.
63. Volland, M. A. O.; Adlhart, C.; Kiener, C. A.; Chen, P.; Hofmann, P. *Chem. Eur. J.* **2001**, *7*, 4621–4632.
64. Tian, J.; Coates, G. W. *Angew. Chem. Int. Ed.* **2000**, *39*, 3626–3629.
65. Stork, M.; Herrmann, A.; Nemnich, T.; Klapper, M.; Müllen, K. *Angew. Chem. Int. Ed.* **2000**, *39*, 4367–4368.
66. Kranich, R.; Eis, K.; Geis, O.; Mühle, S.; Bats, J. W.; Schmalz, H.-G. *Chem. Eur. J.* **2000**, *6*, 2874–2894.
67. LaPointe, A. M. *J. Comb. Chem.* **1999**, *1*, 101–104.
68. Ben-Aroya, B.B.-N.; Portnoy, M. *J. Comb. Chem.* **2001**, *3*, 524–527.
69. Li, G. Y.; Fagan, P. J.; Watson, P. L. *Angew. Chem. Int. Ed.* **2001**, *40*, 1106–1109.
70. Gennari, C.; Ceccarelli, S.; Piarulli, U.; Montalbetti, C. A. G. N.; Jackson, R. F. W. *J. Org. Chem.* **1998**, *63*, 5312–5313.
71. Snively, C. M.; Oskarsdottir, G.; Lauterbach, J. *Angew. Chem. Int. Ed.* **2001**, *40*, 3028–3030.
72. Kobayashi, S. *Curr. Opin. Chem. Biol.* **2000**, *4*, 338–345.
73. Kobayashi, S. *Combinatorial Library Synthesis Using Polymer-supported Catalysts*. In *Combinatorial Chemistry*; Fenniri, H., Ed.; Oxford University Press: Oxford, U.K., 2000; pp 421–432.
74. Burgess, K.; Lim, H.-J.; Porte, A. M.; Sulikowski, G. A. *Angew. Chem. Int. Ed. Engl.* **1996**, *35*, 220–222.
75. Cole, B. M.; Shimizu, K. D.; Krueger, C. A.; Harrity, J. P. A.; Snapper, M. L.; Hoveyda, A. H. *Angew. Chem. Int. Ed. Engl.* **1996**, *35*, 1668–1671.
76. Reetz, M. T.; Zonta, A.; Schimossek, K.; Liebeton, K.; Jaeger, K.-E. *Angew. Chem. Int. Ed. Engl.* **1997**, *36*, 2830–2832.
77. Janes, L. E.; Löwendahl, A. C.; Kazlauskas, R. J. *Chem. Eur. J.* **1998**, *4*, 2324–2331.
78. Zocher, F.; Enzelberger, M. M.; Bornscheuer, U. T.; Hauer, B.; Schmid, R. D. *Anal. Chim. Acta* **1999**, *391*, 345–351.
79. Moris-Varas, F.; Shah, A.; Aikens, J.; Nadkarni, N. P.; Rozzell, J. D.; Demirjian, D. C. *Bioorg. Med. Chem.* **1999**, *7*, 2183–2188.
80. Baumann, M.; Stürmer, R.; Bornscheuer, U. T. *Angew. Chem. Int. Ed.* **2001**, *40*, 4201–4204.
81. Moates, F. C.; Somani, M.; Annamalai, J.; Richardson, J. T.; Luss D.; Willson, R. C. *Ind. Eng. Chem. Res.* **1996**, *35*, 4801–4803.
82. Holzwarth, A.; Schmidt, H.-W.; Maier, W. F. *Angew. Chem. Int. Ed.* **1998**, *37*, 2644–2647.
83. Tokunaga, M.; Larrow, J. F.; Kakiuchi, F.; Jacobsen, E. N. *Science (Washington, D. C.)* **1997**, *277*, 936–938.
84. Drake, A. F.; Gould, J. M.; Mason, S. F. *J. Chromatogr.* **1980**, *202*, 239–245.
85. Salvadori, P.; Bertucci, C.; Rosini, C. *Chirality* **1991**, *3*, 376–385.
86. Manschreck, A. *Trends Anal. Chem.* **1993**, *12*, 220–225.
87. Ding, K.; Ishii, A.; Mikami, K. *Angew. Chem. Int. Ed.* **1999**, *38*, 497–501.
88. Reetz, M. T.; Kühling, M. K.; Hinrichs, H.; Deege, A. *Chirality* **2000**, *12*, 479–482.
89. Mikami, K.; Angelaud, R.; Ding, K.; Ishii, A.; Tanaka, A.; Sawada, N.; Kudo, K.; Senda, M. *Chem. Eur. J.* **2001**, *7*, 730–737.
90. Reetz, M. T.; Kühling, M. K.; Deege, A.; Hinrichs, H.; Belder, D. *Angew. Chem. Int. Ed.* **2000**, *39*, 3891–3893.
91. MegaBACE[®] is commercially available from Amersham Pharmacia Biotech (Freiburg, Germany).
92. Reetz, M. T.; Kühling, M. K.; Wilensek, S.; Husmann, H.; Häusig, U. W.; Hermes, M. *Catal. Today* **2001**, *67*, 389–396.
93. Reetz, M. T., *et. al.*, unpublished.
94. Reetz, M. T.; Becker, M. H.; Klein, H.-W.; Stöckigt, D. *Angew. Chem. Int. Ed.* **1999**, *38*, 1758–1761.
95. Guo, J.; Wu, J.; Siuzdak, G.; Finn, M. G. *Angew. Chem. Int. Ed.* **1999**, *38*, 1755–1758.
96. Schrader, W.; Eipper, A.; Pugh, D. J.; Reetz, M. T. *Can. J. Chem.* **2002**, *80*, 626–632.
97. Reetz, M. T.; Eipper, A.; Tielmann, P.; Mynott, R. *Adv. Synth. Catal.* **2002**, *344*, 1008–1016.
98. Phimister, B. *Nat. Genet. Suppl.* **1999**, *21*, 1.
99. Korb, G. A.; Lalic, G.; Shair, M. D. *J. Am. Chem. Soc.* **2001**, *123*, 361–362.
100. Abato, P.; Seto, C. T. *J. Am. Chem. Soc.* **2001**, *123*, 9206–9207.
101. Berkowitz, D. B.; Bose, M.; Choi, S. *Angew. Chem. Int. Ed.* **2002**, *41*, 1603–1607.
102. Taran, F.; Gauchet, C.; Mohar, B.; Meunier, S.; Valleix, A.; Renard, P. Y.; Créminon, C.; Grassi, J.; Wagner, A.; Mioskowski, C. *Angew. Chem. Int. Ed.* **2002**, *41*, 124–127.
103. Liu, G.; Ellman, J. A. *J. Org. Chem.* **1995**, *60*, 7712–7713.
104. Gilbertson, S. R.; Wang, X. *Tetrahedron* **1999**, *55*, 11609–11618.
105. Gennari, C.; Nestler, H. P.; Piarulli, U.; Salom, B. *Liebigs Ann./Recl.* **1997**, 637–647.
106. Takahashi, H.; Kawakita, T.; Ohno, M.; Yoshioka, M.; Kobayashi, A. *Tetrahedron* **1992**, *48*, 5691–5700.
107. Brouwer, A. J.; van der Linden, H. J.; Liskamp, R. M. J. *J. Org. Chem.* **2000**, *65*, 1750–1757.
108. Onger, S.; Piarulli, U.; Jackson, R. F. W.; Gennari, C. *Eur. J. Org. Chem.* **2001**, 803–807.
109. Lim, H.-J.; Sulikowski, G. A. *J. Org. Chem.* **1995**, *60*, 2326–2327.
110. Burgess, K.; Lim, H.-J.; Porte, A. M.; Sulikowski, G. A. *Angew. Chem. Int. Ed. Engl.* **1996**, *35*, 220–222.
111. Pfaltz, A. *J. Heterocycl. Chem.* **1999**, *36*, 1437–1451.
112. Burgess, K.; Porte, A. M. *Tetrahedron: Asymmetry* **1998**, *9*, 2465–2469.
113. Trost, B. M.; Krueger, A. C.; Bunt, R. C.; Zambrano, J. *J. Am. Chem. Soc.* **1996**, *118*, 6520–6521.
114. Cole, B. M.; Shimizu, K. D.; Krueger, C. A.; Harrity, J. P. A.; Snapper, M. L.; Hoveyda, A. H. *Angew. Chem. Int. Ed. Engl.* **1996**, *35*, 1668–1671.
115. Shimizu, K. D.; Cole, B. M.; Krueger, C. A.; Kuntz, K. W.; Snapper, M. L.; Hoveyda, A. H. *Angew. Chem. Int. Ed. Engl.* **1997**, *36*, 1704–1707.

116. Krueger, C. A.; Kuntz, K. W.; Dzierba, C. D.; Wirschun, W. G.; Gleason, J. D.; Snapper, M. L.; Hoveyda, A. H. *J. Am. Chem. Soc.* **1999**, *121*, 4284–4285.
117. Hoveyda, A. H. *Chem. Biol.* **1998**, *5*, R187–R191.
118. Bromidge, S.; Wilson, P. C.; Whiting, A. *Tetrahedron Lett.* **1998**, *39*, 8905–8908.
119. Sigman, M. S.; Jacobsen, E. N. *J. Am. Chem. Soc.* **1998**, *120*, 4901–4902.
120. Francis, M. B.; Jacobsen, E. N. *Angew. Chem. Int. Ed.* **1999**, *38*, 937–941.
121. Long, J.; Hu, J.; Shen, X.; Ji, B.; Ding, K. *J. Am. Chem. Soc.* **2002**, *124*, 10–11.
122. Reetz, M. T.; Sell, T.; Meiswinkel, A.; Mehlex, G. *Angew. Chem. Int. Ed.* **2003**, *42*, 790–793.
123. Reetz, M. T. *Tetrahedron* **2002**, *58*, 6595–6602.
124. Reetz, M. T. Pat. Appl. DE 101 29 187.6.

9.12

Metal Complexes as Speciality Dyes and Pigments

P. GREGORY

Avecia Ltd., Manchester, UK

9.12.1	INTRODUCTION	549
9.12.2	NATURE OF BONDING IN METAL COMPLEX AZO COLORANTS	551
9.12.2.1	Azo/Hydrazone Tautomerism	552
9.12.2.2	Nature of Azo-to-metal Bonding	553
9.12.3	EFFECT OF METALLIZATION ON PROPERTIES	555
9.12.3.1	Lightfastness	555
9.12.3.2	Color	556
9.12.4	TEXTILE AND RELATED APPLICATIONS	557
9.12.4.1	Azo Dyes	557
9.12.4.2	Azo Pigments	559
9.12.4.3	Phthalocyanine Dyes and Pigments	560
9.12.4.4	Formazan Dyes	561
9.12.4.5	Ortho-hydroxy Nitroso Dyes and Pigments	563
9.12.4.6	Others	563
9.12.5	ELECTROPHOTOGRAPHY (LASER PRINTING AND PHOTOCOPYING)	563
9.12.5.1	Laser Printing Process	563
9.12.5.2	Organic Photoconductors	564
9.12.5.3	Toners	566
9.12.6	INK JET PRINTING	567
9.12.6.1	Ink Jet Printing Process	568
9.12.6.2	Ink Jet Dyes and Pigments	569
9.12.7	INFRARED ABSORBERS	572
9.12.8	SILVER HALIDE PHOTOGRAPHY	574
9.12.9	MISCELLANEOUS APPLICATIONS	574
9.12.9.1	Dark Oxidation Catalysts	574
9.12.9.2	Singlet Oxygen Generators	575
9.12.9.3	Organic Semiconductors	576
9.12.10	TOXICOLOGICAL AND ECOTOXICOLOGICAL CONSIDERATIONS	576
9.12.11	REFERENCES	577

9.12.1 INTRODUCTION

Metallic compounds have figured prominently throughout mankind's history. The first known use of *any* colored compound was by Neanderthal man ~180,000 years ago. They collected red ochre, which is iron(III) oxide (Fe_2O_3), i.e., rust, from the riverbeds and daubed it on to their dead prior to burial.¹ Iron(III) oxide is an *inorganic pigment*. Inorganic pigments are the most stable and durable of all colorants and are used where high durability is required, such as in outdoor paints. Indeed, iron(III) oxide, CI Pigment Red 101 and 102, is still used today (where CI refers to the Color Index number of the dye²).

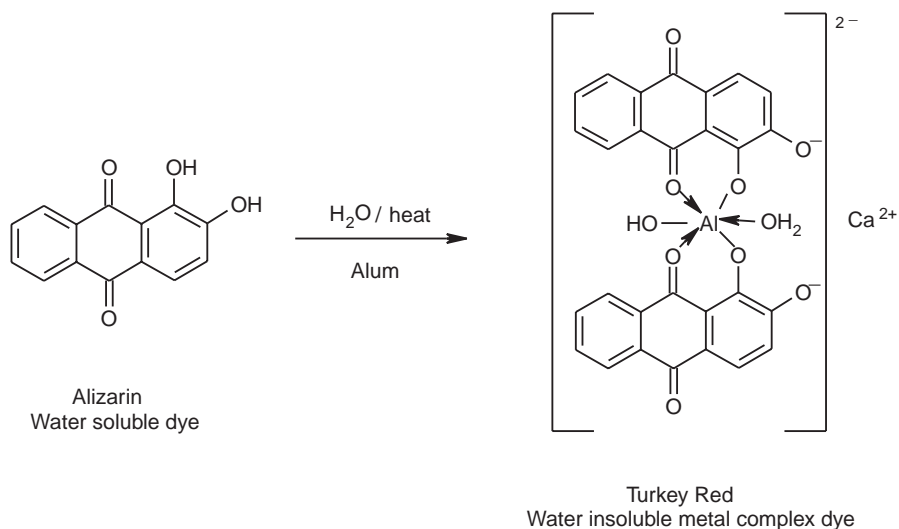
The first known use of an *organic colorant* was by the ancient Egyptians ~4,000 years ago. The blue dye indigo, used nowadays to color jeans and denims, was found in the wrappings in a mummy's tomb.³ Indigo, also known as woad, was a natural dye, i.e., a dye obtained from nature. Until Perkin's historic discovery of the world's first synthetic dye, mauveine in 1856, all the dyes used were natural dyes.³ A major problem with natural dyes was very poor durability. For example, they had poor fastness to washing (when clothes were washed much of the dye was removed from the fabric) and to light (the dyes faded quickly in sunlight).

A method was found to improve the durability of natural dyes to both washing and light. The method was *mordanting*. In a normal dyeing process, the cloth to be dyed is placed in a solution of the dye in hot or boiling water, whereupon most of the dye transfers from the aqueous phase to the cloth. However, it is only bound to the cloth, usually cotton (synthetic fibers weren't invented until the twentieth century)⁴ by weak forces such as hydrogen bonding and van der Waals forces. Consequently, it was easily removed. In the mordanting process, the cloth is placed in hot water and a soluble metallic salt, typically alum, a soluble aluminum salt, is added to the water. The alum dissolves and impregnates the cloth with aluminum ions (Al^{3+}). The impregnated cloth is then dyed normally. However, in this case, when the water-soluble dye enters the cloth it reacts with the aluminum ions to form a water insoluble complex within the cloth. This renders the dye much more waterfast (Scheme 1). In addition, complexation to the metal also increases the light fastness of the dye (see Section 9.12.3.1).

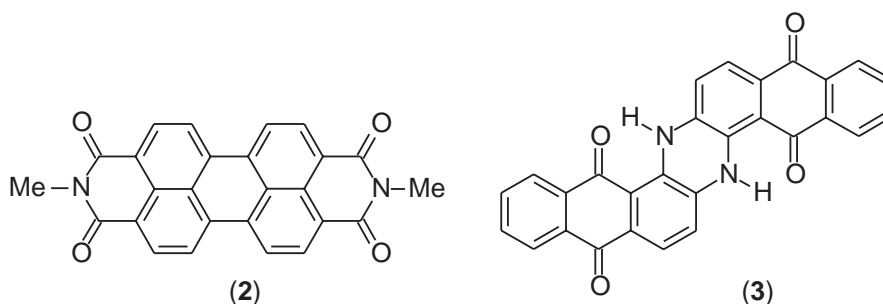
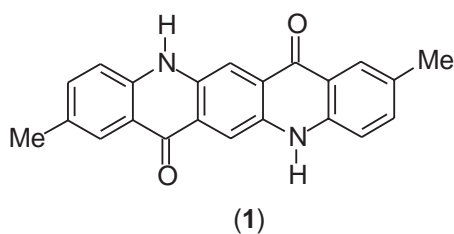
The use of the mordanting process with the natural red dye alizarin to form the metal complex dye Turkey Red (so-called because the color was like that found on a turkey's neck), was one of the first examples of the preparation and use of a *metal complex colorant*.

The many classes of synthetic dye that followed Perkin's discovery of mauveine were superior to the natural dyes and quickly replaced them in the marketplace.³ However, even synthetic dyes having high fastness to light were scarce and, once again, metal complex dyes were needed to achieve high lightfastness. In general, the dyes were metallized before application to the cloth (pre-metallized dyes), not during application, as is the case with mordant dyeing.

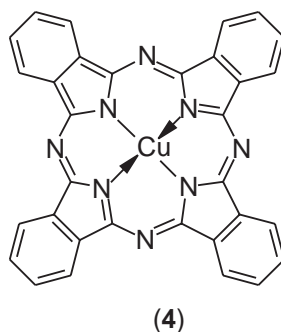
Organic pigments were discovered somewhat later than dyes, around the beginning of the twentieth century.⁵ Although there are others, the major difference between a pigment and a dye is solubility. A dye is a *soluble organic colorant* whereas a pigment is an *insoluble organic or inorganic colorant*. One significant consequence of the insolubility of pigments is enhanced lightfastness. Therefore, many pigments, particularly high performance pigments, have excellent lightfastness without the need for metal complexation. Typical examples include red pigments, such as quinacridones, CI Pigment Red 122 (1), and perylenes, CI Pigment Red 179 (2), and the blue pigment indanthrone, CI Pigment Blue 60 (3).



Scheme 1



However, there are metal complex pigments. Without doubt the most important metal complex pigment is copper phthalocyanine (4). The phthalocyanines were discovered by accident in 1928⁶ and now represent the second most important class of colorants after the azo colorants. Copper phthalocyanine itself exists in several polymorphic forms and gives beautiful blue and cyan colors with outstanding fastness properties.⁵⁻⁷ Halogenated copper phthalocyanines provide green pigments (see Section 9.12.4.3).

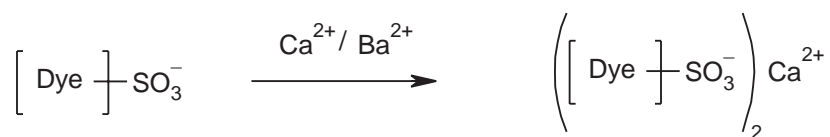


Another important class of pigment are the so-called “toner pigments.” These are water-soluble dyes containing sulfonic acid groups which are insolubilized by forming a salt with a divalent cation such as calcium and barium⁵ (Scheme 2). Until recently the toner pigments were perceived merely as insoluble salts but X-ray studies have shown them to exist as supramolecular metal complexes (see Section 9.12.4.2).

A more comprehensive historical account of metal complex dyes and pigments can be found in ref. 7.

9.12.2 NATURE OF BONDING IN METAL COMPLEX AZO COLORANTS

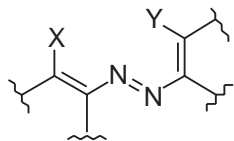
Azo dyes and azo pigments are the most important class of both non-metallized and metallized colorants. Therefore, this section is devoted entirely to metal complex azo dyes and pigments.



Scheme 2

There are two main factors to consider in order to understand the bonding and structures of metal complex azo colorants, namely (i) azo/hydrazone tautomerism and (ii) the nature of the azo-to-metal bonding.

To have sufficient stability for commercial application, chelating tridentate azo ligands (**5**) are required.⁷ The most important and widely used tridentate azo ligands are the *ortho,ortho'*-dihydroxy azo dyes, i.e., (**5**, X=Y=OH). Other tridentate azo ligands are *ortho*-carboxy-*ortho'*-hydroxyazo and *ortho*-hydroxy-*ortho'*-aminoazo.



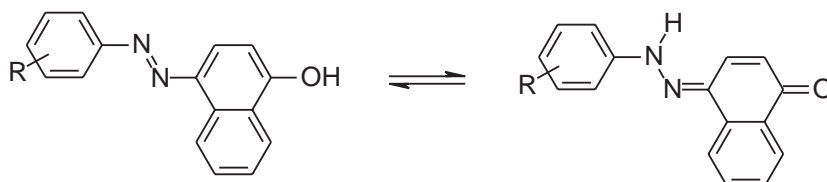
(5)

X	Y
OH	OH
CO ₂ H	OH
OH	NH ₂

9.12.2.1 Azo/Hydrazone Tautomerism

Hydroxyazo dyes fall into four main categories depending upon the nature of the coupling component used to make them, namely acyclics, phenols, heterocyclics, and naphthols. Those derived from naphthols comprise the largest and most important group commercially.

Dyes based on 4-phenylazo-1-naphthol (**6**) have been used extensively to study azo/hydrazone tautomerism since they exist as an equilibrium mixture of both the azo and hydrazone tautomers.⁸ However, they are of little use commercially and of no use whatsoever for metal complex azo dyes since the hydroxy group is not *ortho* to the azo group so these cannot act as chelating ligands.

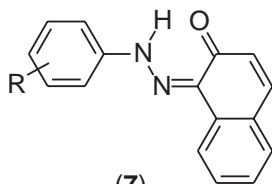


azo

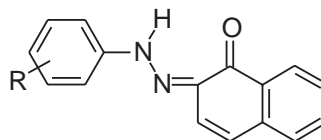
hydrazone

(6)

The 1-phenylazo-2-naphthol (**7**) and particularly the 2-phenylazo-1-naphthol (**8**) systems are used extensively, providing many of the commercial metal complex azo colorants. Azo pigments are derived from (**7**) whilst azo dyes are obtained from (**8**). Both these types of colorant exist predominantly, if not exclusively, in the hydrazone tautomeric form.^{8,9}



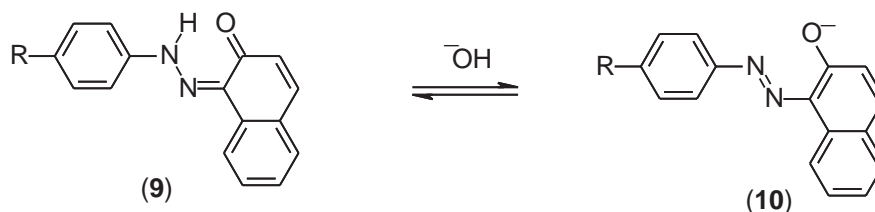
(7)



(8)

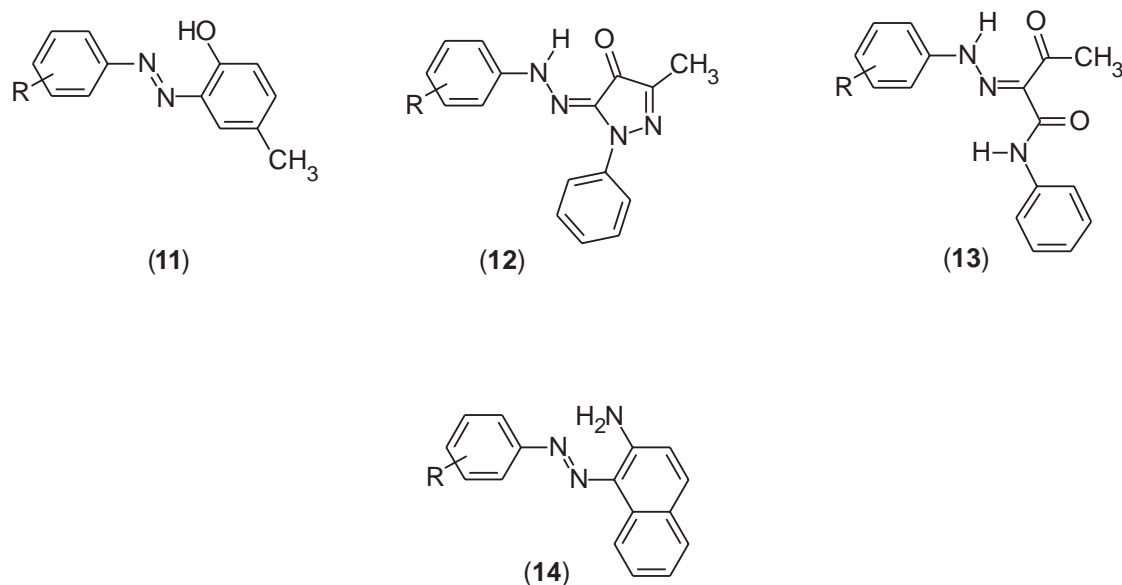
However, the ligand itself is the anionic dye formed by deprotonation of the hydroxy group(s). Anionic dyes, even from dyes shown to exist totally in the hydrazone tautomeric form, such as Orange II (**9**, R=SO₃H) and Para Red (**9**, R=NO₂), have been shown by resonance Raman spectroscopy to exist in the azo form (**10**).¹⁰ This isn't surprising: oxygen is

more electronegative than nitrogen and the negative charge resides preferentially on the most electronegative atom.



Therefore, it is reasonable to assume that the metal complex dyes formed from dye anions such as (10) also exist in the azo form, irrespective of the tautomeric form of the neutral dye. As is evident later, this assumption is confirmed by X-ray diffraction studies on the metal complex dyes.

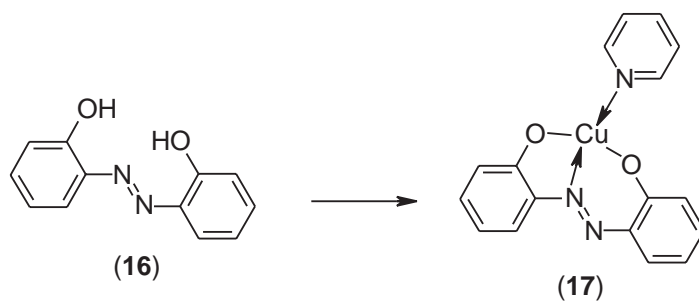
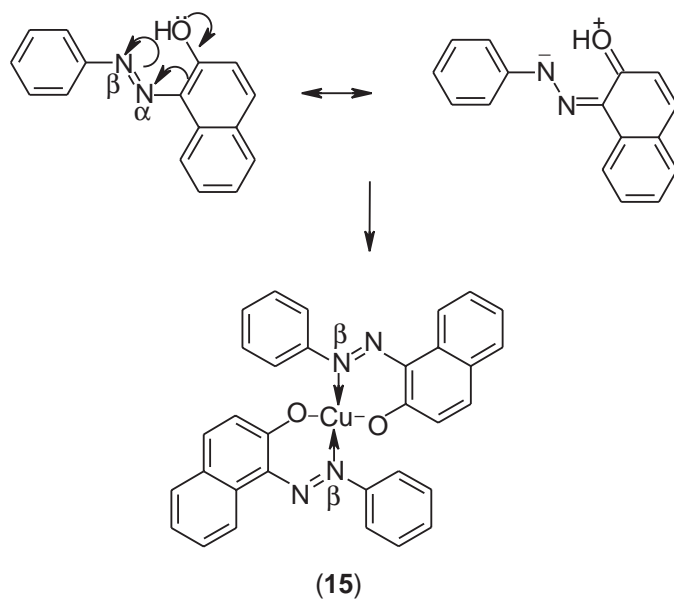
Dyes (11) from azophenols exist totally in the azo form⁸ whereas dyes (12) from heterocyclic couplers such as pyrazolones^{8,11} and acyclic couplers such as acetoacetanilides^{8,12} (13) exist totally in the hydrazone form. Dyes (14) derived from amino couplers exist in the azo form.⁸ However, as described above, all these dyes will exist predominantly in the azo form in the derived metal complexes.



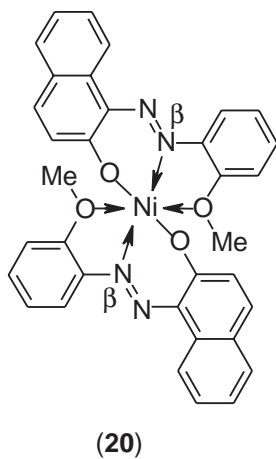
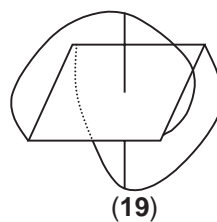
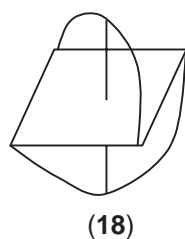
9.12.2.2 Nature of Azo-to-metal Bonding

In metal complex azo dyes, it is known from X-ray crystallographic data on 2:1 copper complex azo dyes such as (15), that the metal is bonded to the lone pair on one of the azo nitrogen atoms, not to the π -bond of the azo group.⁷ This is expected on both electronic and steric grounds. The β -azo nitrogen atom is electron-rich in the ground state since it is conjugated to the electron-donating hydroxy group of the naphthol. Furthermore, complexation with the β -azo nitrogen atom produces a stable six-membered chelate ring (although a five-membered ring is also stable).⁷

X-ray crystallographic data has become available on the commercially important 1:1 copper complex azo dyes. The symmetrical dihydroxyazo ligand (16) forms the 1:1 square planar complex (17).¹³ A pyridine molecule occupies the fourth coordination site since this complex facilitated the formation of crystals suitable for X-ray diffraction. The complex (17) actually exists as an unusual trimer which is held together by long bridging interactions between the copper atom in one molecule and one of the hydroxy oxygen atoms from the adjacent molecules.

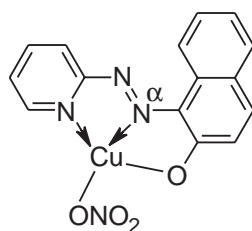


In addition to the 1:1 square planar Cu^{2+} complex azo dyes, 2:1 Cr^{3+} , Co^{3+} , and, to a lesser extent, Ni^{2+} complex azo dyes are important commercially. Such 2:1 octahedral complex azo dyes generally adopt the meridial (*mer*) stereochemical structure (18) rather than the facial (*fac*) structure (19).⁷

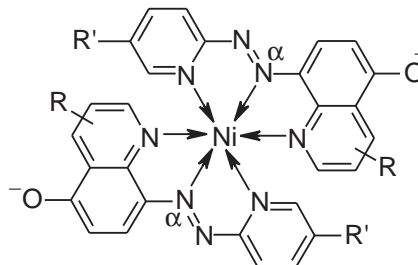


(The stereochemistry of 2:1 metal complex azo dyes is discussed fully in ref. 7 and is not repeated here). X-ray diffraction studies¹⁴ on such a 2:1 octahedral meridial nickel(II) complex azonaphthol dye (**20**) show that it is the β -azo nitrogen atom that is coordinated to the nickel atom. It is very likely that the commercially important 2:1 Cr^{3+} and Co^{3+} dye complexes bond in a similar way.

A ring nitrogen atom may replace hydroxy as the donor group in azo dye complexes. Replacing one hydroxy group produces a PAN (pyridylazonaphthol) dye (**21**), whilst replacing both hydroxy groups produces a PAQ (pyridylazoquinoline) dye (**22**).^{7,15,16}



(21)



(22)

R = H, Cl, CO_2H

R' = H, $\text{SO}_2\text{NHalkyl}$

X-ray diffraction studies¹³ on the 1:1 copper complex dye (**21**) show it to have a square planar structure. Unlike conventional metal complex azo dyes, it is the α -azo nitrogen atom that is coordinated to the copper atom, producing a stable 5:5 chelate ring system. (Coordination via the β -azo nitrogen atom would produce an unstable 4:6 ring system). Coordination to the α , rather than the β -azo nitrogen atom, will affect the properties of the dye, such as color and lightfastness. For example, it is known that in the first excited singlet state of an azo dye, the electron density is highest at the α -azo nitrogen atom.¹⁷ Coordination of this atom to a metal cation will stabilize the first excited state with the electron-withdrawing metal cation reducing the electron density on the α -azo nitrogen atom. Therefore, a bathochromic shift should be observed, as well as higher lightfastness. The copper complex dye (**21**) exists as a dimer in the solid state.¹³

9.12.3 EFFECT OF METALLIZATION ON PROPERTIES

9.12.3.1 Lightfastness

As mentioned earlier, mordant dyeing was used to improve both the wash fastness and lightfastness of dyes. Nowadays, wash fastness is generally achieved by other means so the prime reason for using metal complex dyes is to achieve high lightfastness. To understand why metal complex dyes exhibit high lightfastness, it is necessary to examine the principal causes of dye degradation with light.

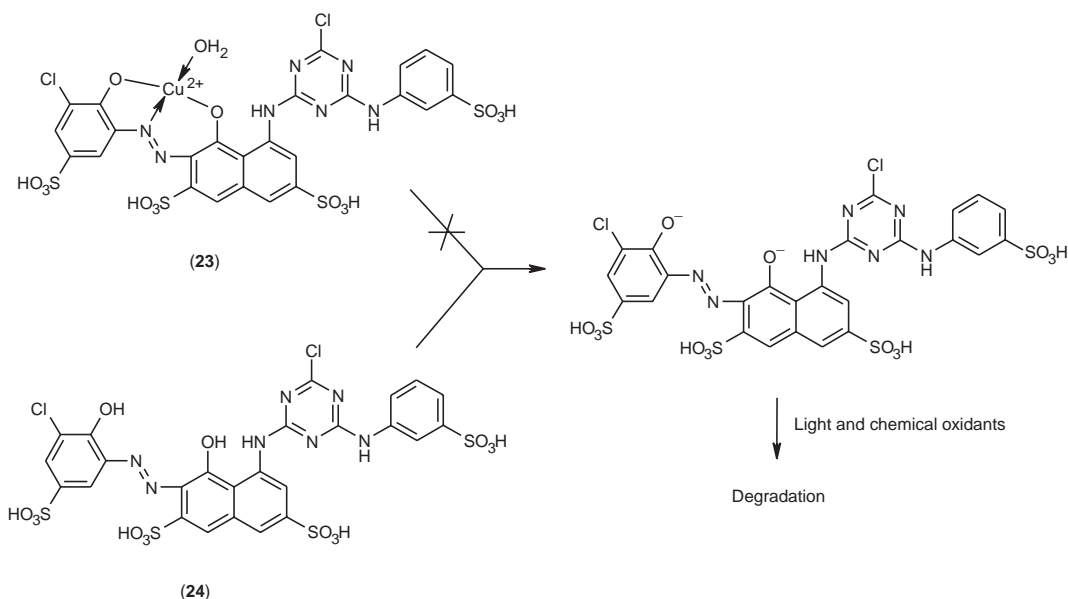
Photo-oxidation is the main photofading pathway for the majority of dyes.¹⁸ Oxygen, particularly singlet oxygen, and radicals such as hydroxyl and hydroperoxyl, are believed to be the major electrophilic species responsible for photodegradation. Attack normally occurs at or around the azo (or hydrazone) group and plausible mechanistic pathways for the photo-oxidation of hydroxyazo dyes have been proposed.^{18,19}

Studies of the chemical oxidation of azo dyes^{20,21} have also revealed similar mechanisms: these have led to structure-activity relationships regarding the stability of azo dyes to (photo)oxidation. A key finding is that it is the *dye anion* (formed by ionization of the hydroxy group) that is preferentially attacked, not the neutral dye (Scheme 3). This is eminently feasible since the ionized dye, with its delocalized negative charge, is much more electron-rich than the neutral dye and therefore more likely to be attacked by electrophiles such as singlet oxygen.

The $\text{p}K_a$ of the hydroxy group determines the ease of formation of the dye anion. For many hydroxyazo dyes, the $\text{p}K_a$ is typically 8–10.^{7,21} Therefore, pH values of 8–10, which are not uncommon in many applications, will form the dye anion. In contrast, provided it is stable under the usage conditions and does not undergo de-metallization, a metal complex azo dye cannot form a



Scheme 3



Scheme 4

dye anion and this is probably the main reason why they have high lightfastness. Other reasons include protection of the susceptible sites of attack around the azo group, both sterically and electronically (the positively charged metal cation hinders the approach of electrophiles and reduces the electron density at and around the azo group). For example, the copper complex azo dye CI Reactive Violet 1 (**23**) has very good fastness to light and chemical oxidants (e.g., bleaches), whereas the metal-free precursor dye (**24**) has very poor fastness (Scheme 4).

9.12.3.2 Color

Metallization of an azo dye changes its color. Generally, the metallized dye undergoes a bathochromic shift (i.e., it absorbs at longer wavelength, which is manifested as a change to a deeper color, such as from red to blue). In the majority of cases, metallization results in dullness. In dyes, dullness is associated with a broad absorption curve. In the case of 2:1 Cr^{3+} , Co^{3+} , and Ni^{2+} complex dyes, the absorption curve is shifted to longer wavelength and becomes broader (Figure 1). This is what is expected by correlation of the absorption curve with the observed properties. However, the 1:1 metal complex azo dyes (Cu^{2+} , Ni^{2+} , Cr^{3+} , and Co^{3+}) display different absorption curves from the 2:1 complex dyes: the curves are narrower than those of both the metal-free precursor dyes and the 2:1 metal complex dyes, but exhibit a long wavelength tail²² (Figure 2). It is this tail which is responsible for the blueness and dullness of the dyes. The narrower absorption curves are expected theoretically. Metallization increases the rigidity of the dye, thereby reducing the number of vibrational degrees of freedom. Consequently, the number of vibronic transitions is reduced resulting in a narrower absorption curve.

In the 2:1 complexes, bathochromicity increases in the order $\text{Ni}^{2+} < \text{Co}^{3+} < \text{Cr}^{3+}$. In contrast, the 1:1 Cu^{2+} , Ni^{2+} , Cr^{3+} , and Co^{3+} metal complexes exhibit similar spectral curves to one another, absorbing at shorter wavelength than the corresponding 2:1 complex dyes.²²

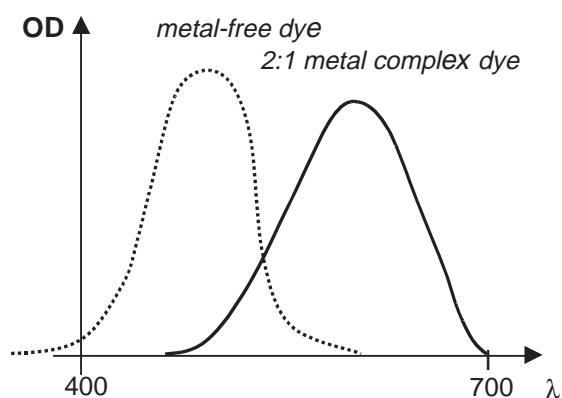


Figure 1 Spectral changes upon formation of a 2:1 metal complex azo dye.

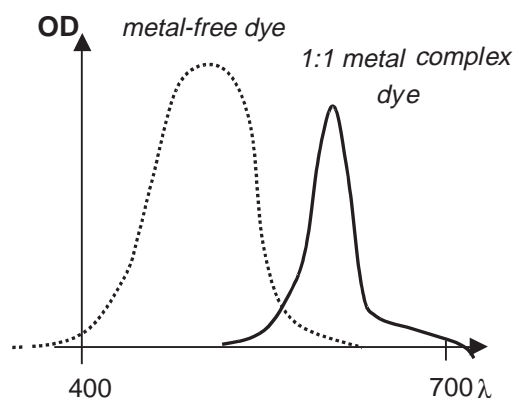


Figure 2 Spectral changes upon formation of a 1:1 metal complex azo dye.

9.12.4 TEXTILE AND RELATED APPLICATIONS

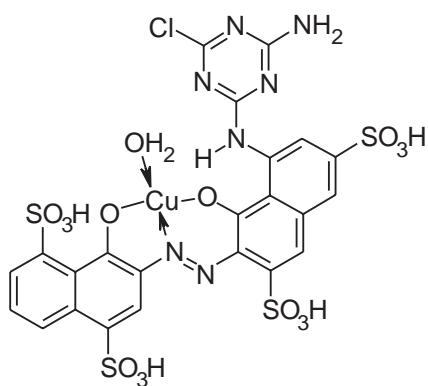
The use of metal complex dyes for textile and related applications has already been treated comprehensively.⁷ There have been few major advances since that review. Therefore, this section focuses on typical commercial metal complex dyes, key structure–property relationships, and some recent studies on metal complex azo pigments.

9.12.4.1 Azo Dyes

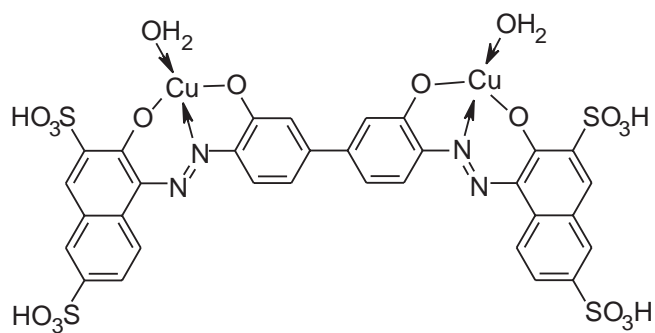
The most prevalent metal complex dyes for textile and related applications are metal complex azo dyes. Their colors span the entire spectrum although, as described earlier, they tend to give dull shades. They may be 1:1 dye:metal complexes or 2:1 complexes and contain mainly one (mono-azo) or two (disazo) azo groups.

The 1:1 copper complex azo dyes are used both as reactive dyes for cotton and as direct dyes for paper. (For definitions of reactive dyes, which form covalent linkages with the substrate, and direct dyes, which bind more weakly, see refs. 23 and 24, respectively.) Typical monoazo dyes are CI Reactive Violet 1 (**23**) and CI Reactive Blue 13 (**25**), and the bis-copper-ed dye, CI Direct Blue 80 (**26**). The navy blue dye, CI Reactive Blue 82 (**27**), is a typical disazo dye.

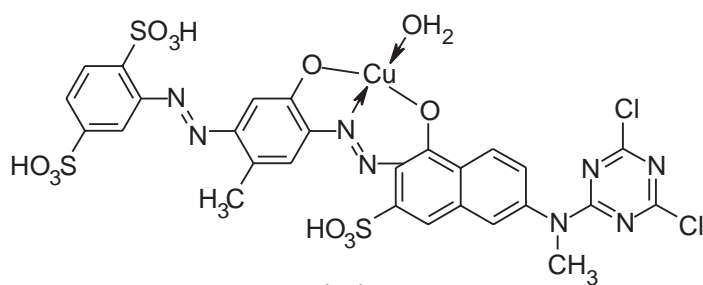
The most important 2:1 metal complex azo dyes are the 2:1 Cr^{3+} dyes. These may be symmetrical dyes, such as the water-soluble dye CI Reactive Brown 10 (**28**), and the solvent-soluble dye CI Solvent Yellow 21 (**29**), used in varnishes as a wood stain. They may also be unsymmetrical complexes, such as CI Acid Violet 121 (**30**), used for dyeing wool and nylon.



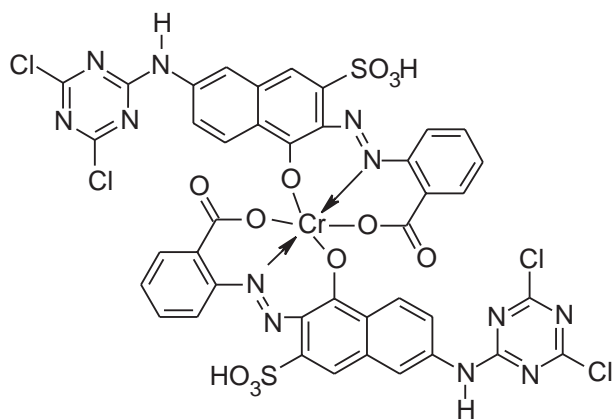
(25)



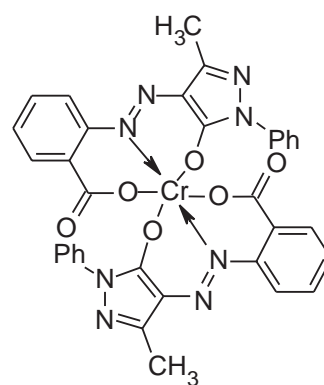
(26)



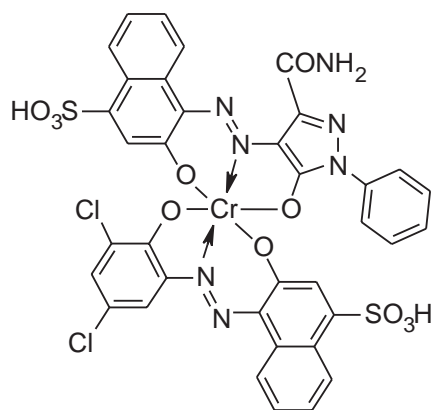
(27)



(28)

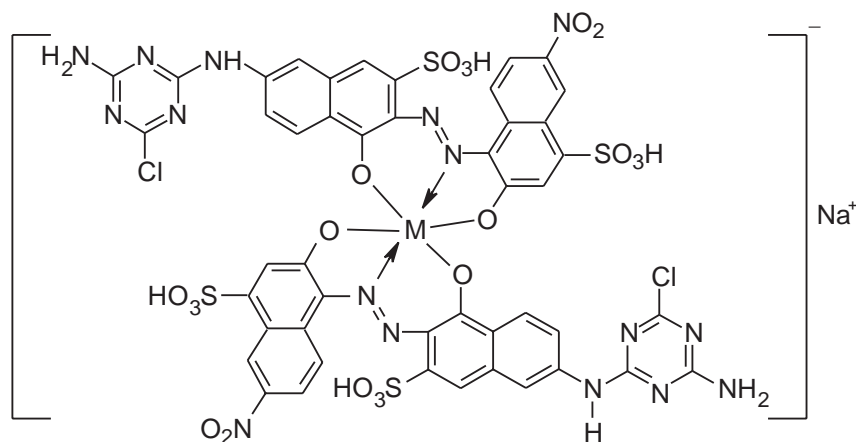


(29)



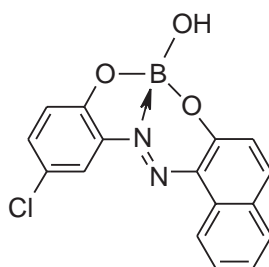
(30)

A mixture of Cr^{3+} and Co^{3+} is sometimes used to obtain the desired properties. The dye CI Reactive Black 1 (**31**) is a good example.



(31)

M = Cr/Co

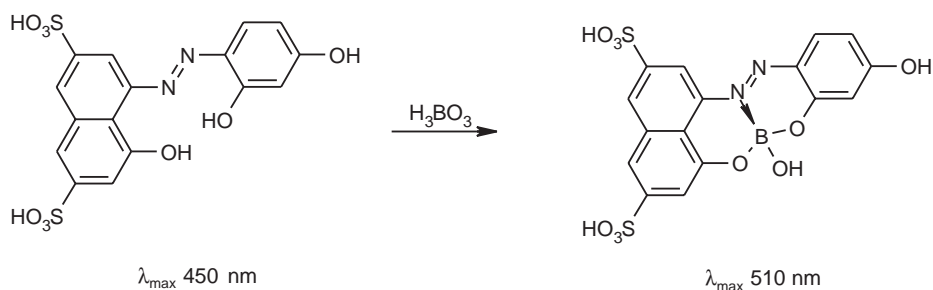


(32)

Boron complex azo dyes have also been reported. These include solvent soluble boron complexes, such as the red dye (**32**) used for dyeing polyester and coloring plastics^{25,26} and water-soluble dyes for the detection of boron (as boric acid) by a color change²⁷ (Scheme 5).

9.12.4.2 Azo Pigments

Azo toner pigments provide the standard worldwide process magenta colorants for printing inks. CI Pigment Red 57:1 (**33**), known as Calcium 4B toner, is one of the most important. These pigments were considered as insoluble calcium (or barium) salts of the sulfonated azo dye



Scheme 5

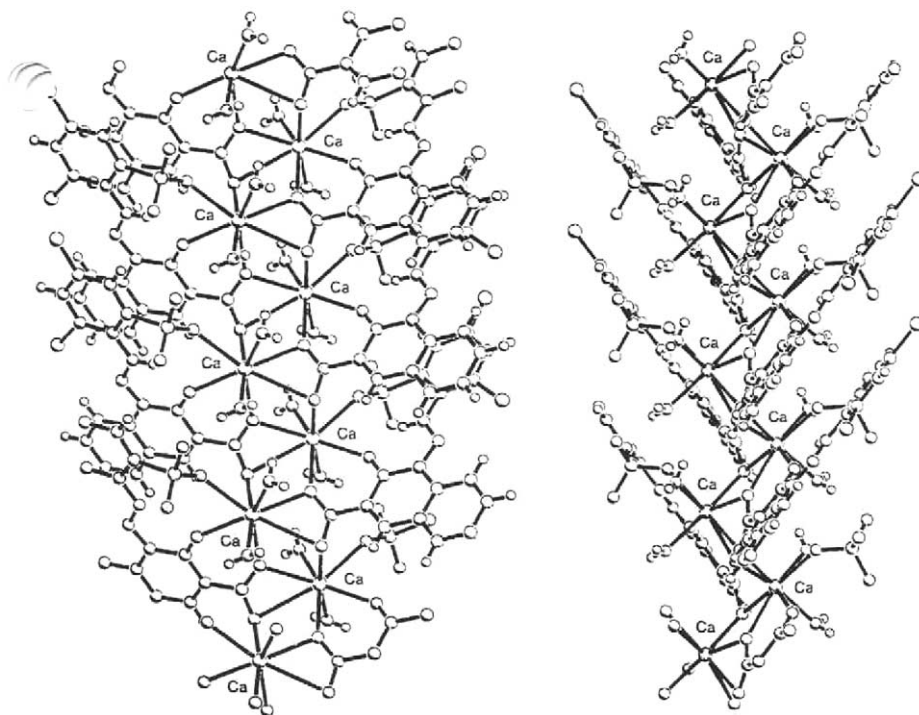
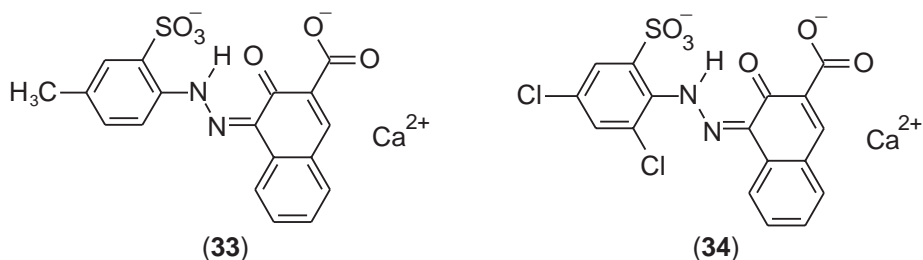


Figure 3 Two views of the polymeric structure of (34) as it extends along the *b* direction.

(Scheme 2). However, Kennedy²⁸ and co-workers succeeded in growing, by slow evaporation of a dimethyl formamide solution, small crystals of a dichloro analogue of (33), namely (34), suitable for characterization by synchrotron radiation. This pigment displays a complex, supramolecular structure (Figure 3) of a type not previously suspected for red azo pigments and is probably a suitable model structure for many other red azo pigments.

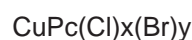
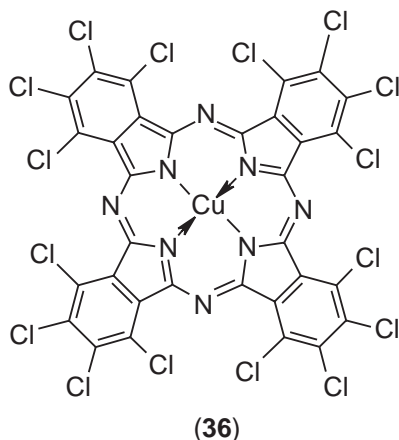
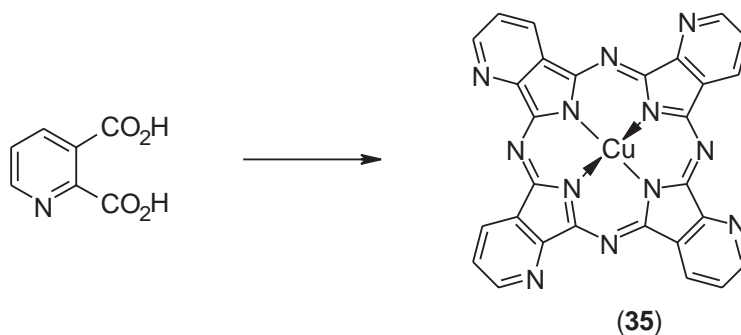


9.12.4.3 Phthalocyanine Dyes and Pigments

Copper phthalocyanine provides extremely important dyes and especially pigments (see also Chapter 9.13). CI Pigment Blue 15 (4) is the most widely used bright blue pigment on account of its outstanding fastness properties. The redder, metastable α -form is preferred for paint, whereas the greener, stable β -polymorph is used in printing inks.⁶ Aza phthalocyanines, such as (35), give an attractive blue pigment²⁹ having slightly inferior lightfastness to copper phthalocyanine. Because of its lower lightfastness, together with low yields in its synthesis, (35) has not been commercialized.

Halogenation produces excellent green pigments, such as CI Pigment Green 7 (36). Yellow green pigments, such as CI Pigment Green 36 (37), are obtained by replacing some of the chloro substituents with bromo substituents.

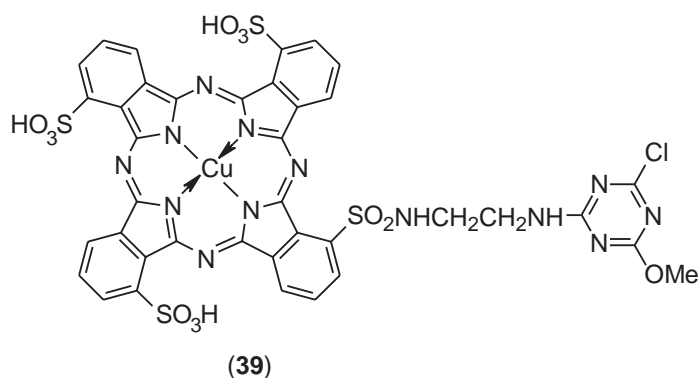
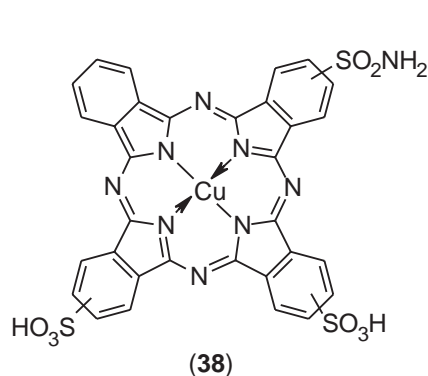
Water-soluble phthalocyanine dyes may contain only sulfonic acid groups but normally contain both sulfonic acid and sulfonamido groups. They are used as direct dyes for paper and as reactive dyes for cotton. Representative examples are CI Direct Blue 199 (38) and CI Reactive Blue 71 (39). These dyes are also used for the ink jet printing of textiles (see Section 9.12.6.2).



(37)

Pc = phthalocyanine nucleus

$x + y = \sim 15$



The reasons why copper and, rarely, other metal phthalocyanine dyes and pigments are used extensively is because of (i) their high stability and particularly (ii) their pure colors. In copper phthalocyanines, the Q-band in the visible region of the spectrum has λ_{max} at ~ 660 nm which produces a beautiful cyan color. Crucially, the Soret band lies completely in the ultraviolet and therefore doesn't affect the color. With other metal phthalocyanines, the Soret band tails into the visible region, producing a yellow component to the color³⁰ (Figure 4). Thus, the observed color is green rather than cyan (blue + yellow = green). However, this effect can be used to advantage if a green dye is required. Thus, the inherent green color of the nickel phthalocyanine dye is augmented by the covalent attachment of a yellow dye to produce an emerald green dye (40).

9.12.4.4 Formazan Dyes

There are bi-, tri-, and tetradentate formazan dyes⁷ but only the tetradentate copper complex formazan dyes have found use as commercial products. The dye CI Reactive Blue 160, of generic structure (41), is a representative example. Because of the intensity of their colors, the metal complex formazan dyes have also found application in analysis. Thus, the dye (42) detects zinc at a concentration of 1 part in 50 million.³¹

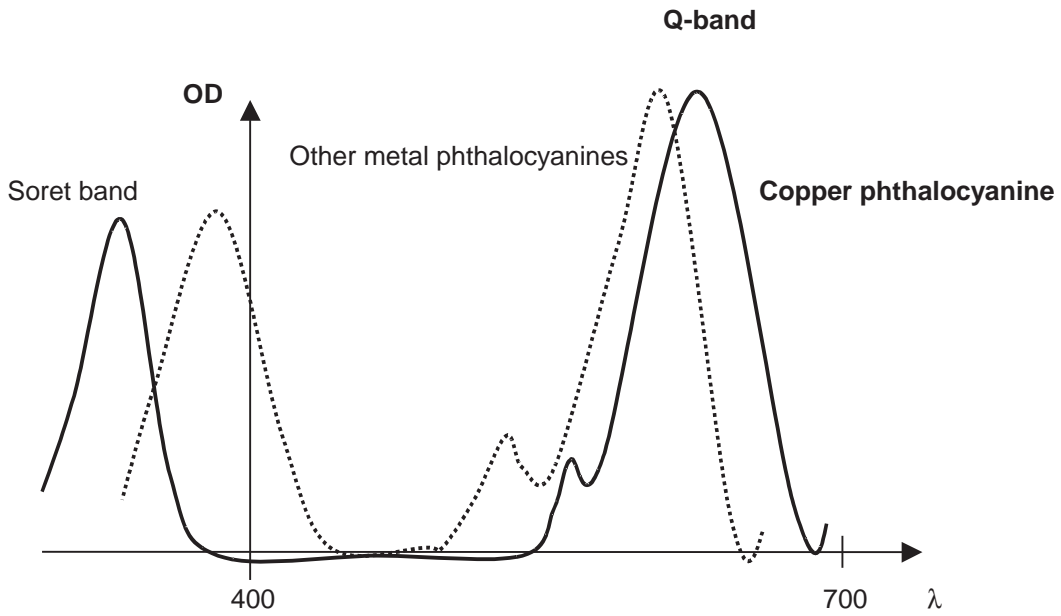
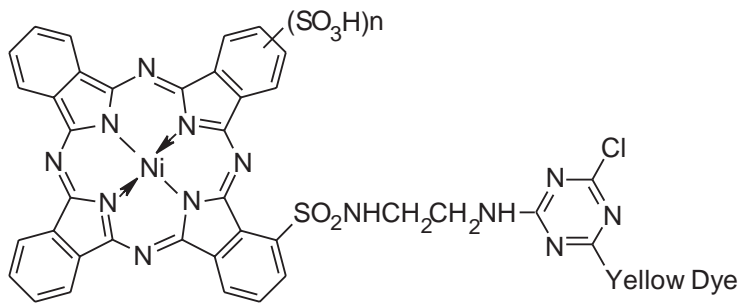
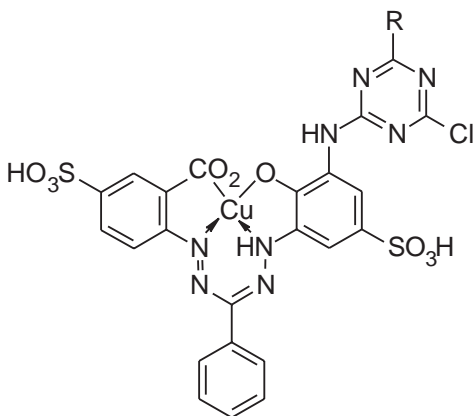


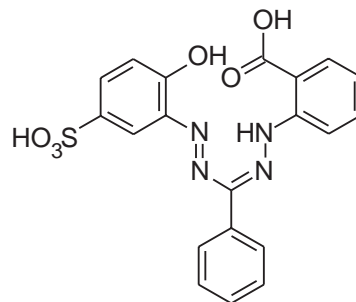
Figure 4 Absorption spectra of copper phthalocyanine and other metal phthalocyanines.



(40)



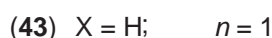
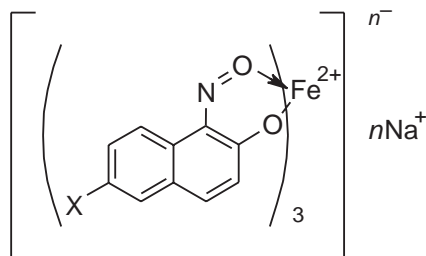
(41)



(42)

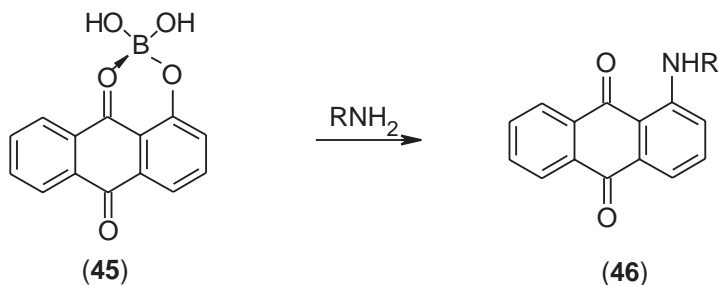
9.12.4.5 Ortho-hydroxy Nitroso Dyes and Pigments

These metal complex dyes and pigments are interesting since the iron complex of 1-nitroso-2-naphthol (CI Pigment Green 8) (**43**) is one of the oldest metal complex colorants, dating back to 1885.⁷ This pigment, together with the water-soluble dye CI Acid Green 1 (**44**), are the only nitroso colorants of commercial importance.³²



9.12.4.6 Others

The only other classes of metallized dyes that are, or have been, commercially significant are anthraquinones and azamethines. The classical forerunner of metallizable anthraquinone dyes was alizarin, which produced the aluminum complex dye Turkey Red by the mordanting process (Scheme 1). Commercial anthraquinone dyes have declined rapidly since the late 1980s and anthraquinone metal complex dyes are no longer of any commercial importance. However, boron complexes such as (**45**) are still used to facilitate manufacture of aminoanthraquinone dyes, particularly arylaminoanthraquinones such as (**46**).^{7,33} Metal complex azamethine dyes have been reported as having high lightfastness but are dull and tinctorially weak. Despite this, they have found limited use as yellow to brown pigments.⁷



9.12.5 ELECTROPHOTOGRAPHY (LASER PRINTING AND PHOTOCOPYING)

Since the 1960s, many technologies have attempted to take a large share of the imaging market, particularly the non-impact printing market.³⁴ From these technologies, two now dominate, namely laser printers and especially ink jet printers. The vital role of metal complex dyes and pigments in these two technologies is described. However, to understand their role requires a knowledge of the laser printing and ink jet printing processes.

9.12.5.1 Laser Printing Process

Laser printers and photocopiers use electricity and light to produce an image, hence the name electrophotography. The two main components are the photoconductor, now invariably an

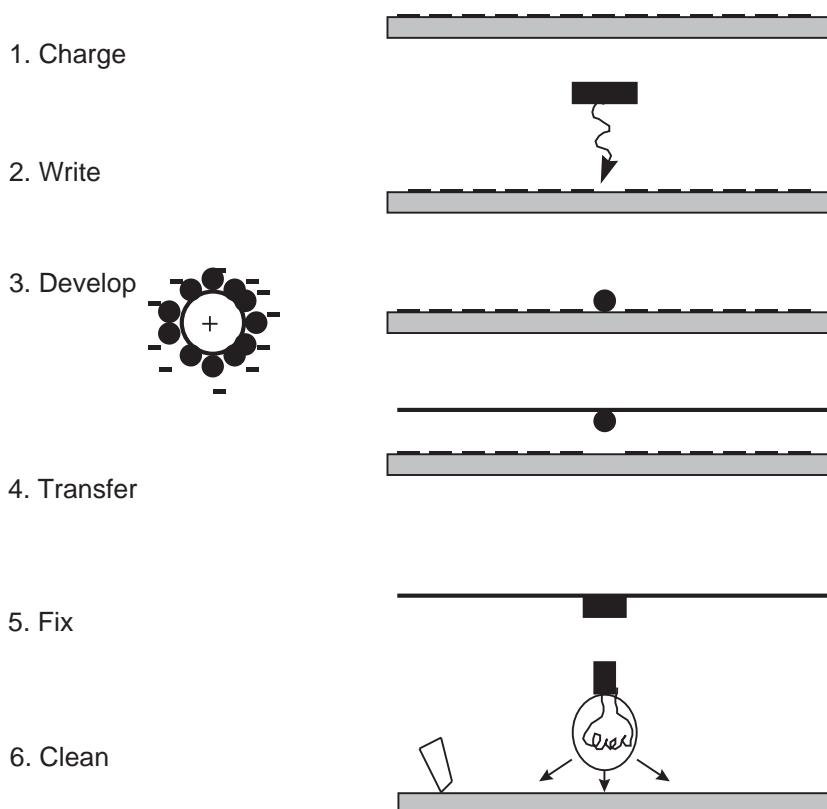


Figure 5 Laser printing process.

organic photoconductor (OPC), and a toner. The basic process, whether it is photocopying or the laser printing process described below, comprises six steps³⁵ (Figure 5).

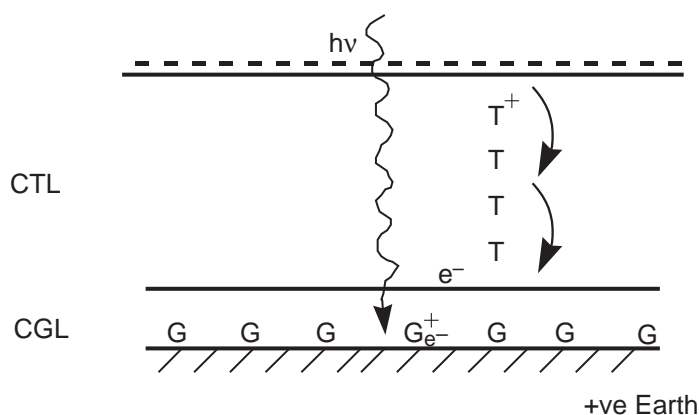
In the first step, the OPC drum or belt is given a uniform electrostatic potential of ~ 700 V. As the name implies, a photoconductor is a conductor of electricity in the presence of light but an insulator in the dark. In the second step, the imaging step, the laser, invariably a gallium-aluminum-arsenide semiconductor laser emitting at 780 or 830 nm, writes on the photoconductor and dissipates the electrostatic charge. This produces a latent electrostatic image on the photoconductor of an uncharged image and a charged background. The third step, the development step, consists of rendering this latent image visible by treating it with a toner. In laser printing, the toner particles have the same electrical charge (negative) as the background and are repelled into the uncharged image areas. The fourth and fifth steps simply involve the transfer and thermal fixation of the toner to the paper. This is the reason why prints/copies emerge warm from a laser printer or copier! The final step is simply a cleaning step to ensure the system is ready for the next print or copy.

Full color printing is essentially the same as for black and white but requires four steps, one each for the yellow, magenta, cyan, and black toners needed for full color reproduction.^{35,36} Consequently, color laser printers and color copiers are significantly more expensive than both monochrome laser printers and especially ink jet printers. Obviously, they are also slower than monochrome laser printers.

Metal complex dyes and pigments perform key functions in both the image generation step and the toner development step. It is the metal complex pigment that produces the positive hole in the organic photoconductor.

9.12.5.2 Organic Photoconductors

Organic photoconductors (OPCs) are dual layer devices comprising a thin (around 0.1–1.0 μm) charge generation layer (CGL) on top of which is a thicker (around 20 μm) charge transport layer (CTL)^{35,36} (Figure 6). Light passes through the transparent CTL and upon striking the CGL,



G = charge generating molecule

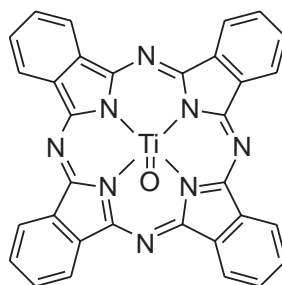
T = charge transport molecule

Figure 6 How an OPC works.

which contains a pigment, forms an ion-pair complex. The electron passes to earth leaving a positive hole, which is transported to the interface. Hence, the need for pigments of high crystallinity in the CGL to avoid crystal defects which can trap the positive holes and hinder their transport to the interface. The CTL contains highly electron-rich compounds which readily donate an electron to the positive hole, forming a positive hole in the CTL; this is attracted to the negatively charged surface by a hopping mechanism where it neutralizes the negative charge. Thus, the key chemicals in OPCs are the charge generation materials (CGMs) in the CGL and the charge transport materials (CTMs) in the CTL.

The charge generating materials in the charge generating layer are invariably pigments. A variety of organic pigments has been used for charge generation including polyazo, perylene tetracarboxydiimide, polycyclic quinone, phthalocyanine, and squarilium pigments.^{35,36} The pigments used as photoconductors must be extremely pure and possess the correct morphology, otherwise their performance is impaired. For example, traces of impurities can alter deleteriously the photoconductive characteristics of a compound. In some cases, the pigments are purified by sublimation whereas, in other cases, a less expensive crystallization treatment is possible. The crystallinity of a pigment and its particle size are often important parameters in determining OPC performance.

Almost without exception, all modern laser printers now use titanyloxy-phthalocyanine, type IV polymorph (47), as the CGM. Unlike copper phthalocyanine, which is planar (Figure 7) titanyloxy-phthalocyanine has a "shallow shuttlecock" shape (Figure 8). This has a subtle effect on the packing of the molecules, which contributes to its excellent performance as a CGM. Indeed, titanyloxy-phthalocyanine has the best combination of properties and is unlikely to be surpassed.³⁷



Titanyloxy phthalocyanine

(47)

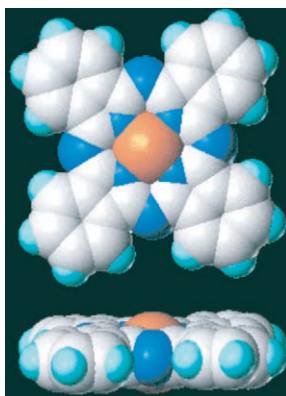


Figure 7 Molecular model of copper phthalocyanine.

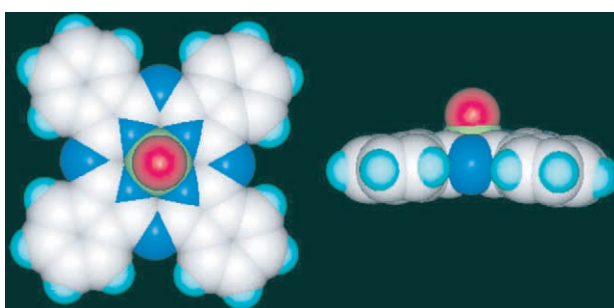


Figure 8 Molecular model of titanyloxy phthalocyanine.

9.12.5.3 Toners

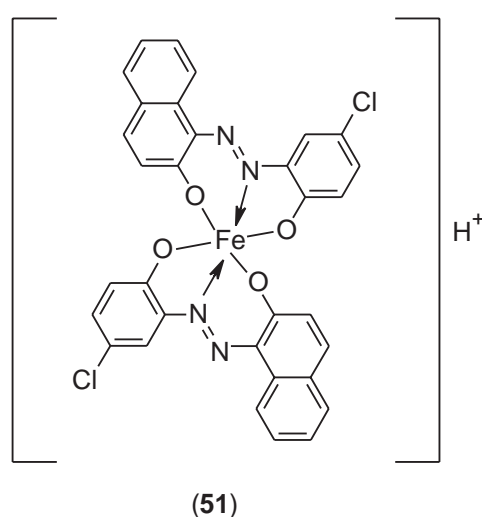
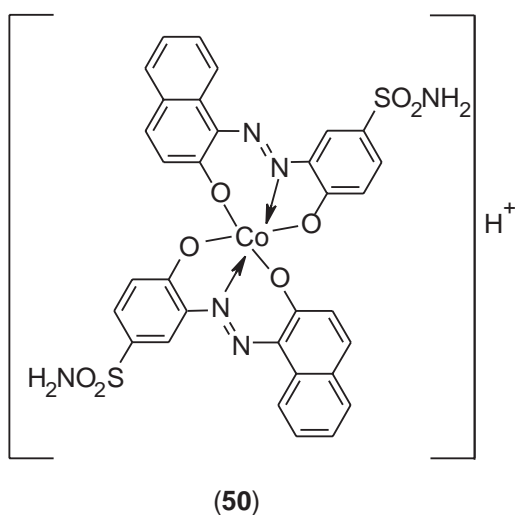
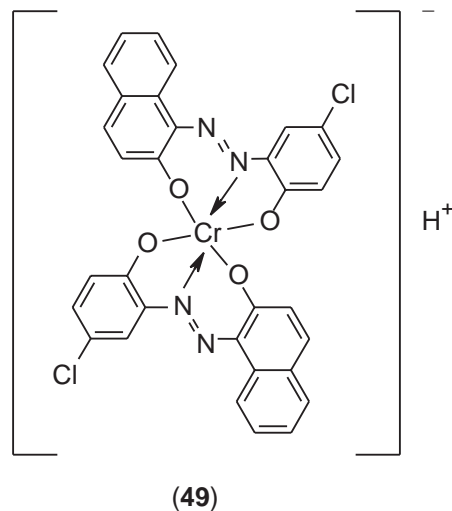
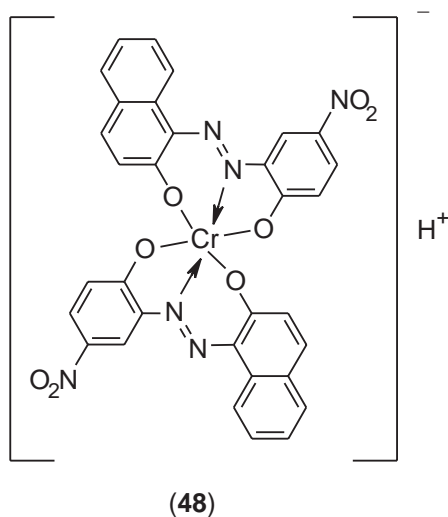
There are two types of colored molecule that are used in the toner, namely the colorant and the charge control agent (CCA). The colorant is used to impart color to the toner whereas the CCA is used to help impart and especially control the triboelectric charge on the toner particles.

Copper phthalocyanine, CI Pigment Blue 15:4 (**4**), is used as the cyan colorant on account of its beautiful cyan color and outstanding fastness properties, particularly to light and heat. Metal-free pigments are used for the yellow and magenta colorants. Examples include azo and isoindoline pigments for the yellow colorant, and dimethyl quinacridone, CI Pigment Red 122 (**1**), as the magenta colorant.^{35,36}

Charge control agents (CCAs) can be either colored or colorless and are mainly metal complex dyes rather than pigments. Colored CCAs are more effective than colorless CCAs but, because of their color, are restricted to black toners. Colorless CCAs are needed for yellow, magenta, and cyan toners.

CCAs that impart a negative charge to the toner are invariably metal complexes, particularly 2:1 Cr³⁺ azo dye complexes.³⁶ Orient Chemical Industries of Japan marketed the first CCA, BONTRON S31 (**48**). However, it was found to possess two major defects: (i) it was mutagenic (Ames positive)³⁸ and (ii) it had only borderline thermal stability. Therefore, it was withdrawn from the marketplace. The nitro group was implicated as the causative agent both for the thermal instability and the reported mutagenic activity.^{36,39} Subsequent dye-based CCAs were devoid of nitro groups. CCA 7 (**49**), marketed by Avecia, is a typical example. Cobalt complex dyes, such as CCA 5 (**50**), and iron complex dyes, such as T-77 (**51**), are also used, mainly because cobalt and especially iron are perceived as more environmentally friendly metals than chromium (see Section 9.12.10). However, they are generally inferior to the chromium complex CCAs and are little used nowadays.

Hodogaya adopted an alternative approach to circumvent the mutagenic and thermal instability problems associated with (**48**). Nitro groups impart excellent performance to a CCA. Therefore, in order to retain the nitro groups whilst minimizing their adverse effects on mutagenicity and thermal instability, they used a nitro-containing pigmentary CCA.



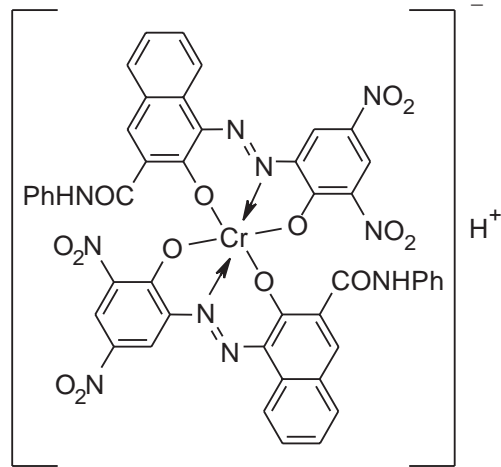
Pigments are generally more thermally stable than dyes and, because of their extreme insolubility, are usually non-mutagenic, even if they contain nitro groups.³⁶ Accordingly, Hodogaya's SPILON Black TRH (**52**) is a 2:1 chromium complex azo pigment containing four nitro groups based on a BON-acid anilide coupler. It is claimed to be non-mutagenic (Ames negative).⁴⁰

Good non-colored negative charging CCAs have been obtained by making non-colored analogues of the 2:1 chromium complex azo dyes. This is achieved by making the metal complex of an aromatic *ortho*-hydroxy carboxylic acid. Typical examples are the chromium, aluminum, and zinc complexes of di-*tert*-butyl salicylic acid, e.g., BONTRON E-81^{36,41} (**53**) and BON-acid^{36,41,42} e.g., BONTRON E-82 (**54**).

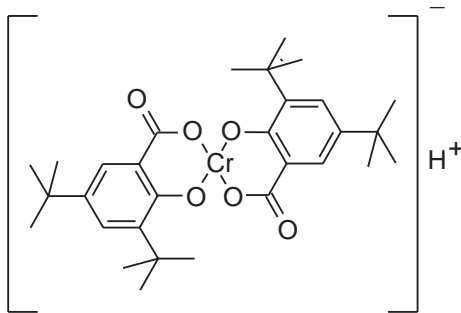
The less important positive CCAs are metal-free cationic molecules, such as the black dye nigrosine and the colorless quaternary compound cetyl pyridinium chloride.^{35,36}

9.12.6 INK JET PRINTING

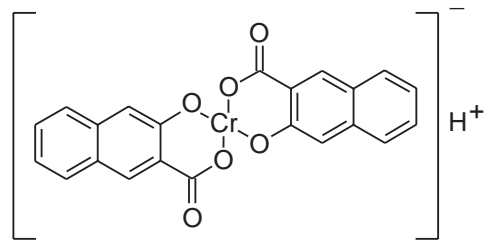
Ink jet printing is now the dominant non-impact printing technology. It has achieved this position from a platform of low cost, full color, very good (and ever improving) quality, and reasonable speed. For example, good quality color ink jet printers currently retail for ca. US\$70, whereas the cheapest color laser printer costs ca. US\$1,400 at the time of writing.⁴³



(52)



(53)



(54)

9.12.6.1 Ink Jet Printing Process

The main reason for the low cost of ink jet printers is their simplicity. Unlike electrophotography and thermal transfer (D2T2)⁴⁴ ink jet printing is a truly primary process. There are no intermediate steps involving photoconductors or transfer ribbons. In ink jet printing, a solution of a dye (an ink) is squirted through tiny nozzles and the resulting ink droplets impinge on the substrate, usually paper or special media, to form an image (Figure 9).

The simplicity associated with being a primary printing technology has enabled ink jet printing to be used in many areas. From its humble beginnings in the Small Office and Home Office (SOHO) market of the mid-1980s, ink jet has expanded into a diverse number of markets ranging from photorealistic, wide format, textiles, and industrial, to short-run printing and displays (e.g., printing of color filters for flat panel displays).

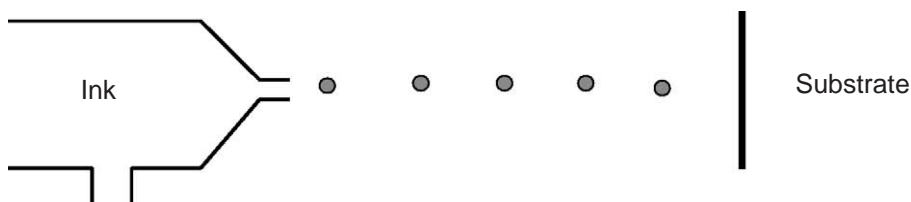
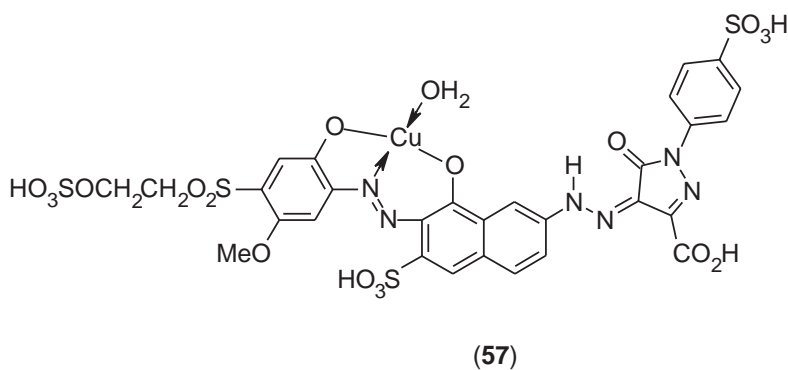
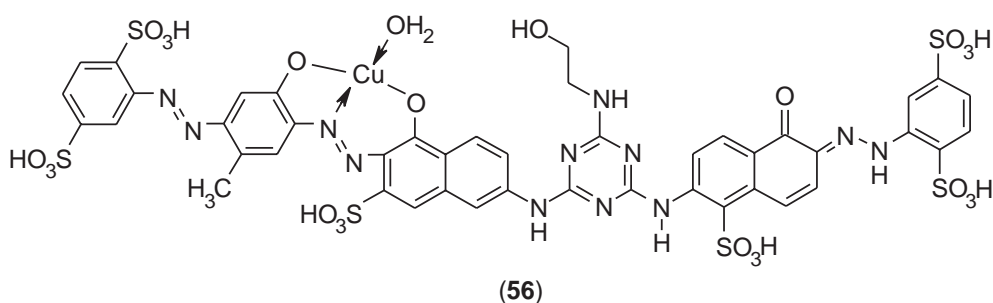
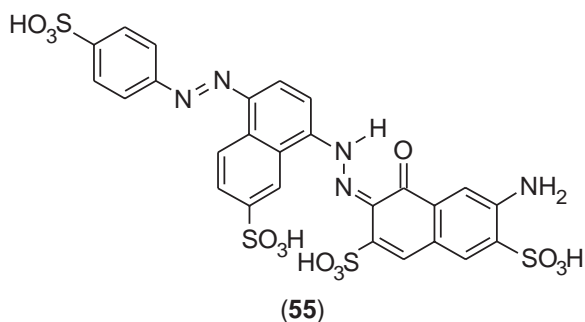


Figure 9 Principle of ink jet printing.

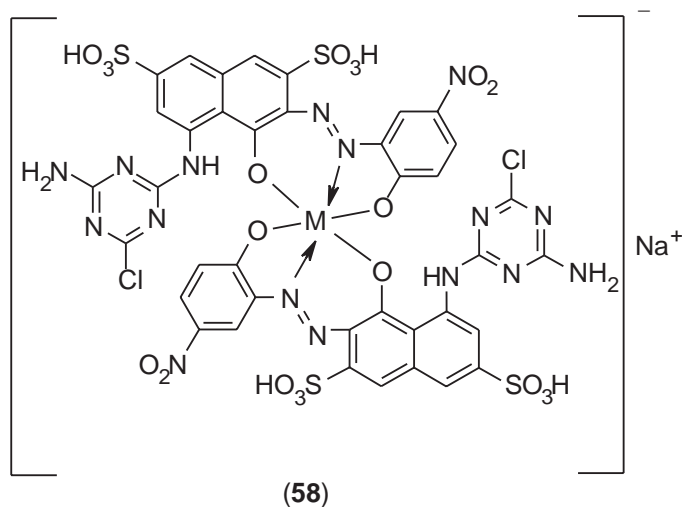
The predominant ink jet inks consist of water-soluble dyes in an aqueous vehicle. The substrates are many and varied but are conveniently divided into two basic types: (i) special media, and (ii) (plain) paper. Special media include photographic type media for photorealistic ink jet printing, vinyl type media for wide format, and overhead transparencies. All of these have in-built mechanisms to give high waterfastness. Hence, the main dye requirements are high optical density, high chroma (vividness) for the colors, and excellent lightfastness, especially for photorealistic applications. Because of the need for excellent lightfastness, metal complex dyes (and pigments) have become increasingly important.

9.12.6.2 Ink Jet Dyes and Pigments

Black is the most important color for ink jet printing because of the large amount of printed text. Therefore, black dyes and pigments are the most important ink jet colorants. All the early black colorants for ink jet printers were non-metallized polyazo dyes, particularly disazo dyes such as CI Food Black 2 (**55**). With the increased emphasis on excellent light fastness, metallized azo dyes have been studied. These include hybrid black dyes, such as (**56**), derived by covalently linking a navy blue metal complex dye to an orange dye⁴⁵ though none have been commercialized for ink jet use. However, the copper complex dye CI Reactive Black 31 (**57**) has been commercialized and is used in several ink jet printers.

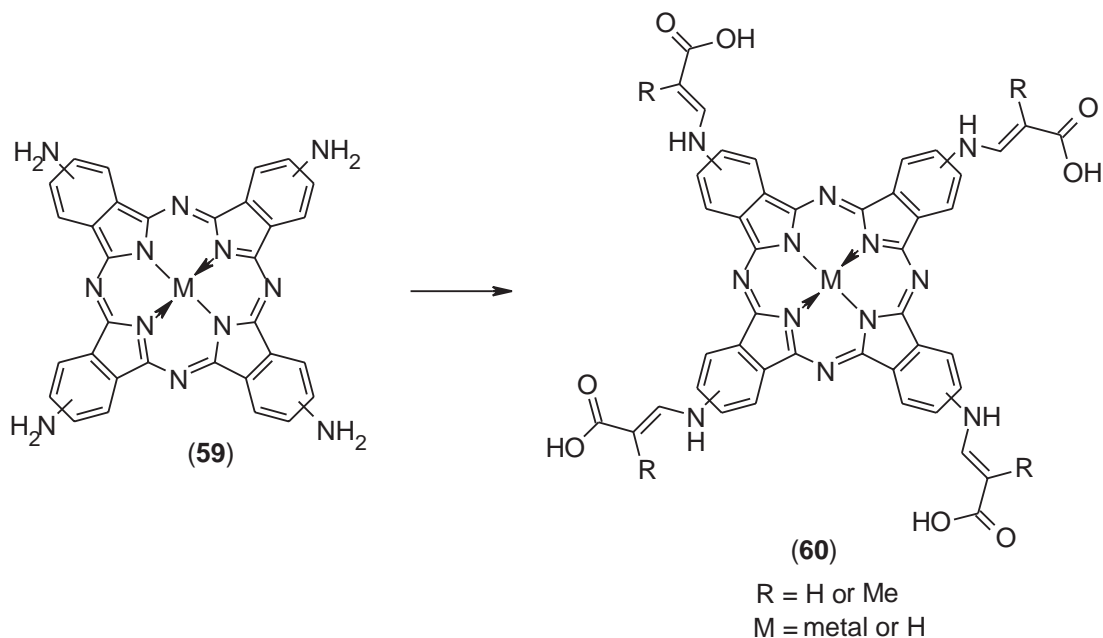


For textile ink jet printing, conventional 2:1 $\text{Cr}^{3+}/\text{Co}^{3+}$ azo dye complex blacks are used, such as CI Reactive Black 8 (**58**).⁴⁶



M = Cr/Co (70:30)

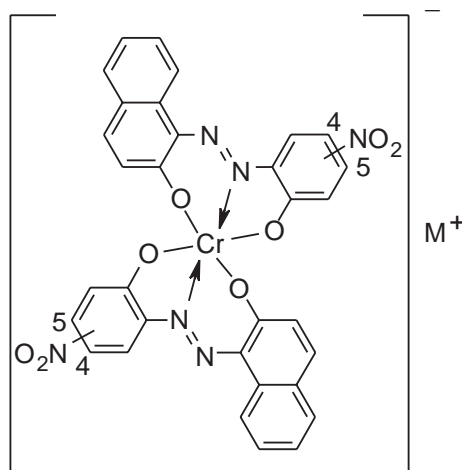
There have also been attempts to obtain a black phthalocyanine dye for ink jet printing. Thus, a patent⁴⁷ from Nippon Kayaku describes reacting the amino phthalocyanine (**59**) with acrylic or methacrylic acid to produce the black dyes (**60**).



Solvent-soluble metal complex azo black dyes are used in both industrial ink jet printing and hot melt ink jet printing. CI Solvent Black 35 (**61**) is a typical dye.⁴⁸

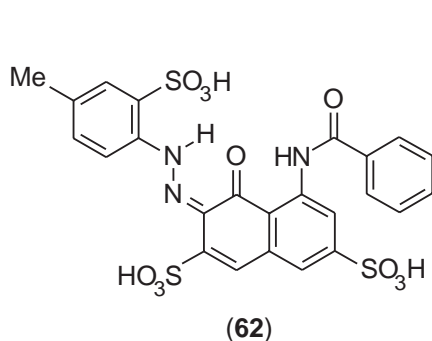
The yellow ink jet dyes (and pigments) are metal-free azo dyes, such as CI Direct Yellow 132 and CI Acid Yellow 23 (Tartrazine).^{48,49} Most of the magentas are azo dyes derived from H-acid (1-amino-8-naphthol-3,6-disulfonic acid), such as (**62**), and xanthenes, such as CI Acid Red 52 and CI Acid Red 289.^{48,49} Where high lightfastness is a requirement, a copper complex azo dye, CI Reactive Red 23 (**63**), is used. However, such dyes are dull (see Section 9.12.3.2). Nickel complex PAQ dyes, such as (**22**), are claimed to be brighter and to have similar high lightfastness

to (63), and are being evaluated for ink jet printers.¹⁶ The copper complex violet dye (23) has also been added to magenta dyes in order to improve their lightfastness (and to make them bluer in shade).

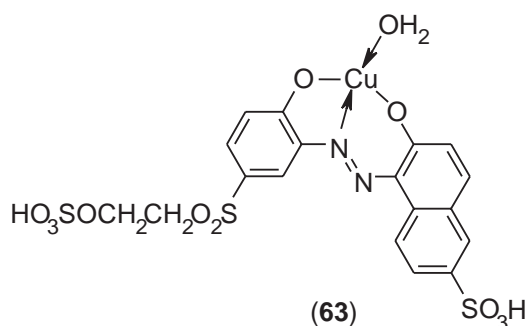


(61)

Mixture of 4- and 5-nitro

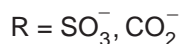
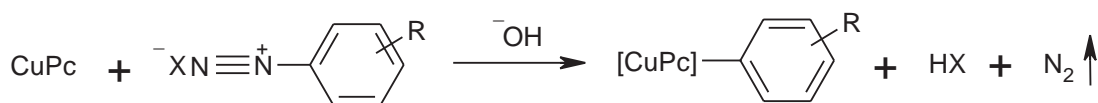


(62)



(63)

Copper phthalocyanine colorants reign supreme as cyans for ink jet printing. CI Direct Blue 199 (38) is typical of the cyan dyes whilst copper phthalocyanine itself (4) is used as the cyan pigment.^{48,49} Functionalized pigments, which are self-dispersing, have been commercialized by Cabot.⁵⁰ This is achieved by surface modification of the pigment using either cationic or, more usually, anionic groups covalently bound to the pigment. The covalent binding is achieved by the Gomberg–Hey reaction, whereby a diazonium salt, in the presence of alkali, loses nitrogen and the aryl radical becomes bound to the pigment (Scheme 6). For textile ink jet printing, conventional reactive dyes are used, such as CI Reactive Blue 71⁴⁶ (39).

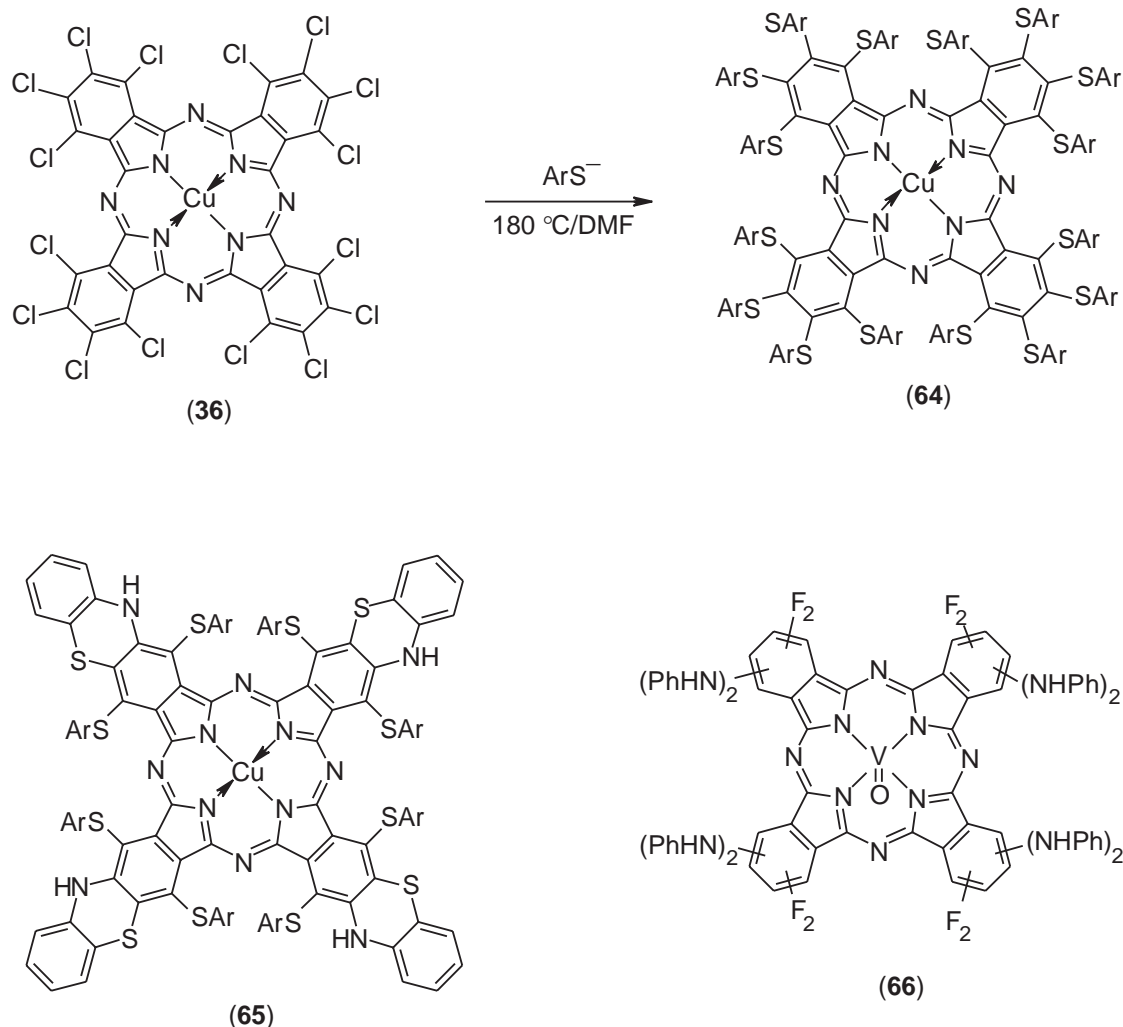


Scheme 6

Divalent metal cations such as Ca^{2+} are used in some ink jet media, such as coated paper and glossy photorealistic media, to fix the water-soluble dye and make it waterfast by forming an insoluble salt. However, cationic organic compounds are currently the preferred choice for this function.

9.12.7 INFRARED ABSORBERS

Phthalocyanines have many desirable attributes as colorants. For instance, the best blue and green pigments are copper phthalocyanines.⁶ The discovery⁵¹ that the fully chlorinated green pigment (**36**) could be transformed smoothly into infrared absorbers (**64**) having high solubility in organic solvents was a major breakthrough (see Chapter 9.13). Molecules such as (**64**) have narrow absorption curves at ~ 780 nm ($\epsilon_{\text{max}} \sim 180,000$) (Figure 10). Phthalocyanines containing amino donors, in combination with either thiols⁵² (**65**) or halogens⁵³ (**66**) give broader curves absorbing at longer wavelengths, typically around 900 nm.



The highest performance pigments are planar molecules: this facilitates intermolecular interactions, such as hydrogen bonding and van der Waals forces, producing a stable crystal lattice. Copper phthalocyanine pigments are the prime example: they are large macrocycles which are extremely planar (Figure 11). Conversion to the infrared absorber destroys this planarity, with eight of the sterically demanding thiophenol groups lying above the plane of the phthalocyanine ring and eight lying below (Figure 12). This is why molecules such as (**64**) are soluble in organic solvents.

Phthalocyanine infrared absorbers are used in a number of applications. For instance, they are used as a high-level security feature in currency^{54,55} and in computer-to-plate technology to

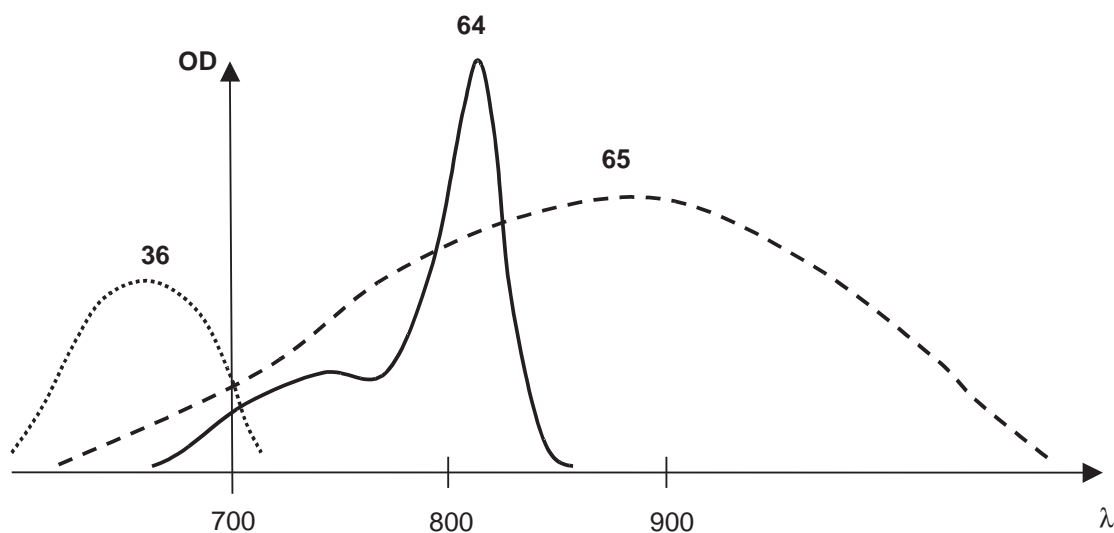


Figure 10 Absorption spectra of a phthalocyanine green pigment and phthalocyanine infrared absorbers.

convert the near infrared radiation into heat.^{56,57} Infrared absorbers with broad absorption curves, such as (65) and (66), are being evaluated as solar screens for use in car windscreens and the windows of buildings to let in daylight but to screen out the infrared radiation component which causes heat.⁵⁴ Although phthalocyanines are renowned for their durability, it is proving difficult to meet the demanding requirements of ca. 10 years lightfastness for cars and ca. 25 years for windows.

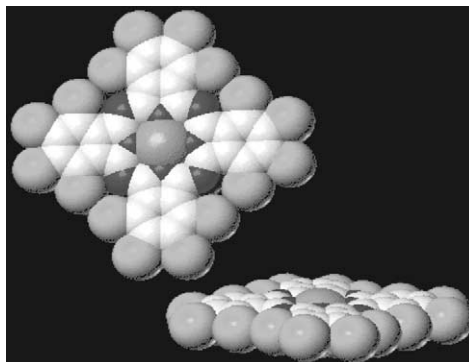


Figure 11 Molecular model of CuPc-Cl₁₆.

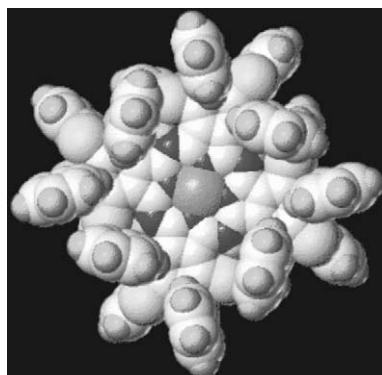
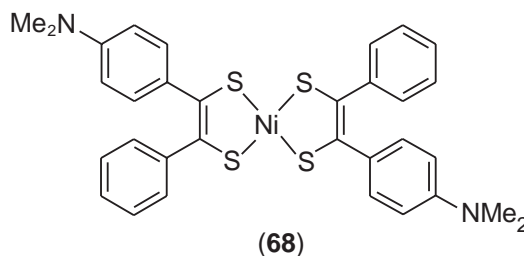
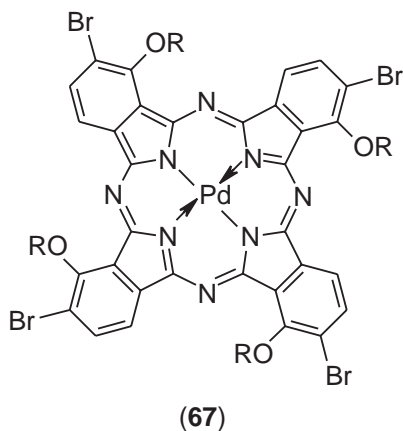


Figure 12 Molecular model of CuPc-(SPh)₁₆.

The palladium phthalocyanine (**67**), developed by Mitsui Toatsu and Ciba^{58,59} is one of the leading phthalocyanine infrared absorbers for CD-R (Compact Disk-Rewritable) (see Chapter 9.13). Bulky groups (R) reduce undesirable molecular aggregation, which lowers the extinction coefficient and hence the absorptivity and reflectivity. Partial bromination allows fine tuning of the film absorbance and improves reflectivity. The palladium atom influences the position of the absorption band, the photostability and the efficiency of the radiationless transition from the excited state.⁵⁸ It is marketed by Ciba as Supergreen.⁶⁰

Infrared absorbing nickel dithiolenes (**68**) are also used in certain applications (see Chapter 9.13). However, they are far less durable than the phthalocyanine infrared absorbers.⁶¹



9.12.8 SILVER HALIDE PHOTOGRAPHY

In the traditional silver halide “dye-forming” and “dye-bleach” processes, metal complex dyes are not normally used.^{62,63} However, metal complex azo dyes have been claimed¹⁵ for use in color diffusion transfer photography employing non-diffusible magenta dye-releasing dyes which, upon development of the silver halide layer, release a diffusible magenta dye (Scheme 7).

The nickel complex PAQ dye (**69**) is a typical dye for these purposes.¹⁵

Other types of metal complex azo dyes described for color diffusion transfer photography include pyridylazonaphthols⁶⁴ (**70**) and pyridylazo aminophenols⁶⁵ (**71**).

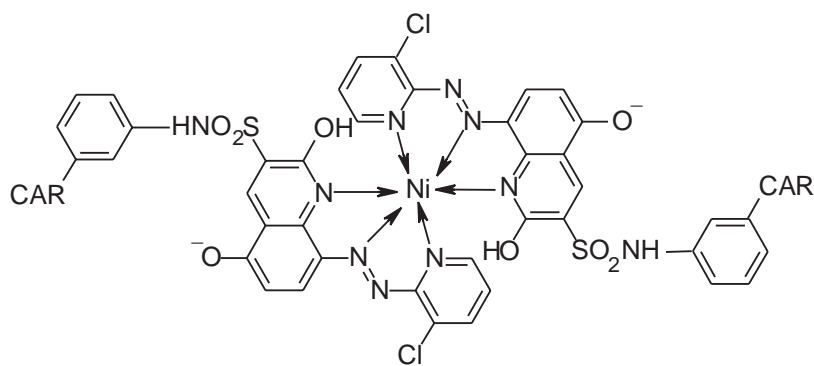
9.12.9 MISCELLANEOUS APPLICATIONS

9.12.9.1 Dark Oxidation Catalysts

Organometallic complexes based on transition metals having a number of available oxidation states, such as manganese, have been evaluated as dark oxidation catalysts.⁶⁶ For example, the manganese complex (**72**) was developed and marketed by Unilever^{67–69} and was the active ingredient in their Persil Power brand of washing powder. Whilst it removed the dirt and stains on clothes, it also destroyed the fabric.^{70,71} Consequently, it was quickly withdrawn from the marketplace. Proctor and Gamble, in collaboration with Zeneca, had also developed a similar dark oxidation catalyst, manganese phthalocyanine *tetra*-sulfonic acid (**73**)⁷² but, because of the adverse publicity caused by Persil Power^{70,71} it never reached the market. The public perception, fueled by television and newspapers, was that the “manganese accelerator” was the culprit in causing the fabrics to disintegrate. Because of this unfortunate effect, it is unlikely that dark oxidation catalysts will re-appear on the market in the near future.

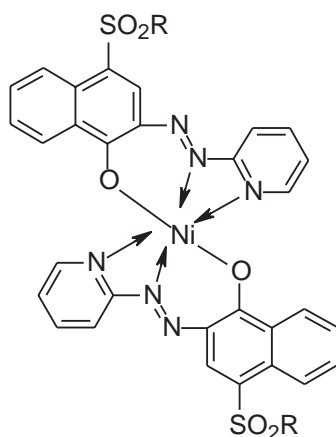


Scheme 7

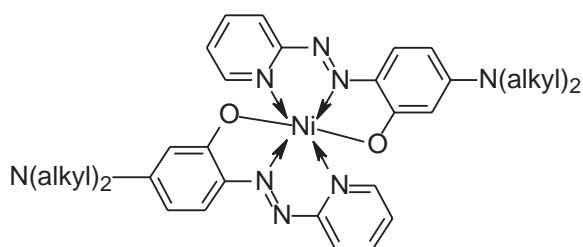


(69)

CAR = (Ballast–Carrier–Link)



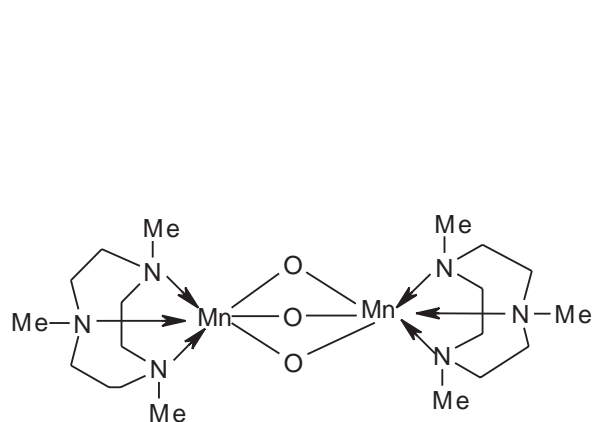
(70)



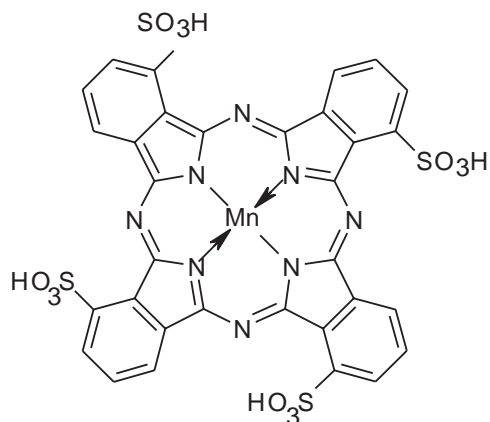
(71)

9.12.9.2 Singlet Oxygen Generators

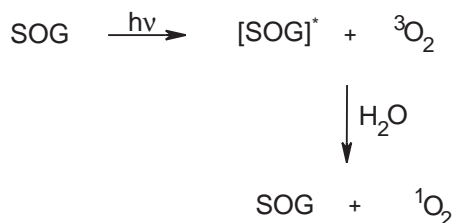
The most important application for singlet oxygen generators (SOGs), namely the anti-cancer treatment known as photodynamic therapy (PDT), is described elsewhere in this series (see Chapter 9.22). However, SOGs are also being evaluated in other areas, such as hard surface disinfectants, soaps and washing powders,⁷³ and insecticides.^{74,75}



(72)



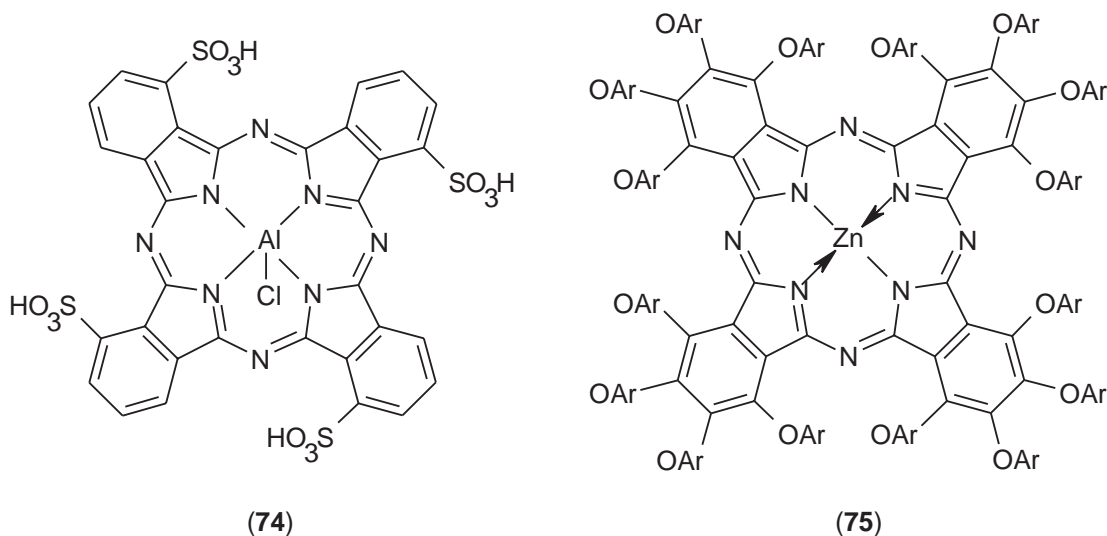
(73)



Scheme 8

SOGs are environmentally friendly photobleaches. In the presence of light they convert normal triplet oxygen (${}^3\text{O}_2$) into the highly reactive singlet oxygen (${}^1\text{O}_2$)⁷⁶ (Scheme 8). Just a few milligrams of a SOG could replace all the hypochlorite or perborate bleaches in a conventional washing powder. With an SOG, the stains aren't removed in the washing machine (because there is no light), but when the clothes are hung on the washing line. The process is relatively fast with the stains disappearing in a matter of minutes.

The blue aluminum phthalocyanine dye, Tinolux BBS (74), marketed by Ciba, is a commercial SOG.^{77,78} Zinc phthalocyanines, such as (75), which absorb in the near infrared at ~ 725 nm, are also very good SOGs.⁷³

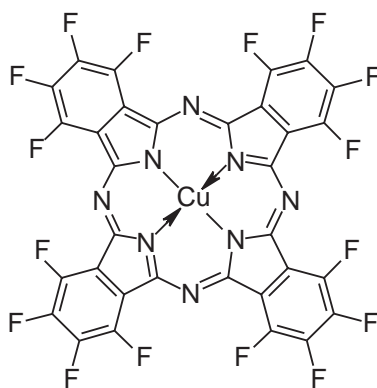


9.12.9.3 Organic Semiconductors

Organic semiconductors are becoming increasingly important in the fabrication of electronic devices. For electron transport, metal complex pigments, such as hexa-deca-fluoro copper phthalocyanine (76), are showing potential.⁷⁹

9.12.10 TOXICOLOGICAL AND ECOTOXICOLOGICAL CONSIDERATIONS

The toxicological and ecotoxicological profiles of *all* commercial chemicals are extremely important and are the subject of much debate and scrutiny. All novel chemicals must pass a battery of short-term (acute) and long-term (chronic) tests according to well defined protocols before they can be placed on to the market.⁸⁰ Metallic compounds, including metal complex dyes and pigments, are no exception. Indeed, because of the highly toxic nature of certain metals, metallic compounds may attract more attention. For instance, lead, cadmium, and mercury are poisons, and chromates are carcinogenic.^{81,82} For metal complex dyes and pigments, the role of the metal in toxicology and ecotoxicology depends upon the inherent toxicity of the metal, the stability of the metal-dye complex and the amount of free metal in the sample. Obviously, the last two are



(76)

related: the more stable the complex, the less the dissociation of the metal complex and the lower the free metal content.

Water-soluble dyes contain sulfonic acid and, to a lesser extent, carboxylic acid groups. These are generally present as salts, with alkali metals such as sodium and lithium being the favored cations. These alkali metals are regarded as having minimal toxicological issues. The “toner” pigments contain divalent metal cations. In the past barium, strontium, and calcium were used, but currently calcium is preferred, primarily on toxicological grounds.

Commercial metal complex dyes and pigments are based mainly on copper(II), chromium(III), and cobalt(III). Nickel(II) and iron(III) are also used but are much less common. Of these, chromium gives the most cause for concern. However, this is based mainly on the fact that compounds containing chromium(VI), such as chromates, have been shown to be carcinogenic.⁸² In metal complex colorants, chromium is present as chromium(III), which is not carcinogenic and is unlikely to be converted into the carcinogenic chromium(VI) under most usage conditions. Cobalt is viewed with a little less concern than chromium. Copper and nickel are seen as somewhat safer than cobalt and chromium but are still treated with caution. Where the copper (or nickel) is tightly bound to the dye or pigment, such as in copper phthalocyanines, it is considered less of a concern. Iron complexes are viewed as reasonably safe.

9.12.11 REFERENCES

1. *Color by Design: The Salters' Advanced Chemistry Project*. University of York: York, UK, 1992, p 1.
2. *Color Index*, Vol. 4, 3rd ed.; The Society of Dyers and Colorists: Bradford, UK, 1971.
3. Gordon, P. F.; Gregory, P. *Organic Chemistry in Color*; Springer-Verlag: Berlin, 1983; Chapter 1, pp 1–22.
4. Gordon, P. F.; Gregory, P. *Organic Chemistry in Color*; Springer-Verlag: Berlin, 1983; Chapter 6, pp 271–280.
5. Lenoir, J. *Organic Pigments. In The Chemistry of Synthetic Dyes*; Venkataraman, K., Ed.; Vol. V. Academic Press: New York, 1971, pp 313–474.
6. Gordon, P. F.; Gregory, P. *Organic Chemistry in Color*; Springer-Verlag: Berlin, 1983; Chapter 5, pp 219–226.
7. Price, R. *Dyes and Pigments. In Comprehensive Coordination Chemistry*; Wilkinson, G., Ed.; Pergamon Oxford U.K., 1987; pp 35–94.
8. Gordon, P. F.; Gregory, P. *Organic Chemistry in Color*; Springer-Verlag: Berlin, 1983; Chapter 3, pp 96–112.
9. Whitaker, A. Z. *Kristallogr. Kristallgeom. Kristallphys. Kristallchem.* **1978**, *147*(1), 99.
10. Barnes, A. J.; Majid, M. A.; Stuckey, M. A.; Gregory, P.; Stead, C. V. *Spectrochim. Acta* **1985**, *41*(4), 629–635.
11. Whitaker, A. *J. Soc. Dyers Colour.* **1995**, *111*(3), 66–72.
12. Chisholm, G.; Kennedy, A. R.; Wilson, S.; Teat, S. J. *Acta Crystallogr.* **2000**, *B56*, 1046–1053.
13. Adams, H.; Bucknall, R. M.; Fenton, D. E.; Garcia, M.; Oaks, J. *Polyhedron* **1998**, *17*(23–24), 4169–4177.
14. Choudhury, S. B.; Ray, D.; Chakravorty, A. *J. Chem. Soc., Dalton Trans.* **1992**, 107–112.
15. Evans, S.; Elwood, J. K. (Eastman Kodak Co.) Photographic Products and Processes Employing Novel Non-Diffusible Magenta Dye-releasing Compounds and Precursors Thereof. U.S. Patent 4,420,550, Dec. 13, 1983.
16. Evans, S.; Weber, H. Metal Complex for Ink Jet. U.S. Patent 6,001,161, Dec. 14 1999.
17. Gordon, P. F.; Gregory, P. *Organic Chemistry in Color*; Springer-Verlag: Berlin, 1983; Chapter 3, pp 136–140.
18. Gordon, P. F.; Gregory, P. *Organic Chemistry in Color*; Springer-Verlag: Berlin, 1983; Chapter 6, pp 282–297.
19. Griffiths, J.; Hawkins, C. *J. Chem. Soc., Perkin Trans. 2* **1977**, *6*, 747.
20. Gregory, P.; Stead, C. V. *J. Soc. Dyers Colour.* **1978**, 402.
21. Oakes, J.; Gratton, P. L. *Adv. Colour Sci. Technol.* **1998**, *1*(3), 73.
22. Gregory, P. Unpublished work.
23. Gordon, P. F.; Gregory, P. *Organic Chemistry in Color*; Springer-Verlag: Berlin, 1983; Chapter 1, pp 278–281.
24. Gordon, P. F.; Gregory, P. *Organic Chemistry in Color*; Springer-Verlag: Berlin, 1983; Chapter 6, pp 271–272.

25. Hohaus, E.; Wessendorf, K. Z. *Naturforsch. B: Inorg. Chem. Org. Chem.* **1980**, *35B*(3), 319.
26. Lewis C. E.; (American Cyanamid). Boron Complexes of o,o'-DiHydroxyPhenylAzoNaphthyl Dyes. U.S. Patent 3726,854, April 10 1973.
27. Motomizu, S.; Oshima, M.; Jun, Z. *Analyst* **1990**, *115*, 389–392.
28. Kennedy, A. R.; McNair, C.; Smith, W. E.; Chisholm, C.; Teat, S. J. *Angew. Chem., Int. Ed. Engl.* **2000**, *39*(3), 638–640.
29. Kudrevich, S. V.; Van Lier, J. E. *Coord. Chem. Rev.* **1996**, *156*, 163–182.
30. Gregory, P. J. *Porphyryns Phthalocyanines* **2000**, *4*, 432.
31. Roe, J. H.; Rush, R. M. *Anal. Chim. Acta* **1952**, *6*, 526–527.
32. Gordon, P. F.; Gregory, P. *Organic Chemistry in Color*; Springer-Verlag: Berlin, 1983; Chapter 5, pp 257–270.
33. Gordon, P. F.; Gregory, P. *Organic Chemistry in Color*; Springer-Verlag: Berlin, 1983; Chapter 2, pp 66–76.
34. Gregory, P. *Rev. Prog. Color. Relat. Top.* **1994**, *24*, 1.
35. Gairns, R. S. *Electrophotography*. In *Chemistry and Technology of Printing and Imaging Systems*; Gregory, P., Ed.; Blackie: London, 1996; pp 76–112.
36. Gregory, P. *High-Technology Applications of Organic Colorants*; Plenum: New York, 1991; Chapter 7, pp 59–122.
37. Koch-Yee Law. Organic photoconductor materials for xerographic photoreceptors (Advanced Tutorial A2). IS and T's Non-Impact Printing Conference 12, San Antonio, Texas, October 27, 1996.
38. Anon. *Pestic. Toxic Chem. News* **1984**, (Sept. 25), 6.
39. Birkett K. L.; Gregory, P. *Dyes Pigm.* **1986**, *7*, 341–350.
40. Hodogaya. Japanese Patents 58 111,649A and 58 185,635A, 1982.
41. Ishida, Y. K. Y.; Otsuka, K. I. M. (Orient Chemical Ind.). Electrostatic Image Toners. G. B. Patent Application 2,090,008A, 28 October, 1981; Japanese Patent 59 188,659A, 1983.
42. Ricoh. Japanese Patent 59 079,256A, 1982.
43. Gregory, P. *Chem. Br.* **2000**, *36*(8), 39–42.
44. Gregory, P. *Chem. Br.* **1989**, *25*(1), 47–50.
45. Baxter, A. G. W.; Bostock, S.; Greenwood, D. (ICI). Water-Soluble Phthalocyanine Black Dyes from Cellulose Reactive Groups and Suitable for Use in Inks. U.S. Patent 4,705,528, November 10, 1987.
46. Provost, J.; Gregory, P. (Avecia Ltd.). Multicolor Ink Jet Printing. U.S. Patent 6,336,721, January 8, 2002.
47. Nippon Kayaku. New Phthalocyanine Compounds Useful in Water-Based Inks are Prepared by Reacting Aminophthalocyanine Compounds with Methacrylic or Acrylic Acid. World Patent Application, 200064901A, 27 April, 1999.
48. Kenyon, R. W. Ink Jet Printing. In *Chemistry and Technology of Printing and Imaging Systems*; Gregory, P., Ed.; Blackie, London, 1996; pp 113–138.
49. Gregory, P. *High-Technology Applications of Organic Colorants*; Plenum: New York, 1991; Chapter 9, pp 175–206.
50. Johnson, J. E.; Belmont, J. A. (Cabot Corp.). Colored Pigment and Aqueous Compositions Containing The Same. U. S. Patent 5,837,045, November 17, 1998.
51. Duggan P. J.; Gordon, P. F. (ICI). Infrared Absorber. European Patent 155,780 March 28, 1990.
52. Stark, W. M. (ICI). Substituted Phthalocyanine. U.S. Patent 4,824,947, March 25, 1989.
53. Kaeida, O., et al. (Nippon Shokubai). Novel Phthalocyanine Compounds: Production Method Thereof: Near Infrared Ray Absorption Materials Containing the Same. European Patent 523,959, July 14, 1992.
54. Gregory, P. J. *Porphyryns Phthalocyanines* **1999**, *3*, 468–476.
55. Gregory, P. *High-Technology Applications of Organic Colorants*; Plenum: New York, 1991; Chapter 11, pp 215–254.
56. Haley, N. F.; Corbiere, S. L. Radiation-Sensitive Composition Containing a Resole Resin and a Novolac Resin and Use Thereof in Lithographic Printing Plates. U.S. Patent 5,372,907, December 13, 1994.
57. Haley, N. F.; Corbiere, S. L. Method of Making a Lithographic Printing Plate Containing a Resole Resin and a Novolac Resin in the Radiation Sensitive Layer. U.S. Patent 5,372,915, December 13, 1994.
58. Hurditch, R. Dyes for optical storage disc media. *Chemichromics '99*, New Orleans, January 27–29, 1999.
59. Wolleb, H. (Ciba-Geigy). Process for the Preparation of Brominated, Alkoxy-Substituted Metal Phthalocyanines. U.S. Patent 5,594,128, January 14, 1997.
60. Ciba, Supergreen Product Dossier, Issue 2.0, November 1999.
61. Matsuoka, M. *Infrared Absorbing Dyes*; Plenum: New York, 1990.
62. Gordon, P. F.; Gregory, P. Non-Textile Uses of Dyes. In *Developments in the Chemistry and Technology of Dyes*; Griffiths, J., Ed.; Critical Reports on Applied Chemistry, Vol. 7; Blackwell: Oxford, 1984; pp 67–77.
63. Bergthaller, P. W. Silver Halide Photography. In *Chemistry and Technology of Printing and Imaging Systems*; Gregory, P., Ed.; Blackie: London, 1996; pp 35–75.
64. Chapman, D.; E-Ming, W. (Eastman Kodak Co.). Photographic Products and Processes Employing Novel Nondiffusible Heterocyclazaphthol Dye-Releasing Compounds. U.S. Patent 4,207,104, June 10, 1980.
65. Anderson, et al. (Eastman Kodak Co.). U.S. Patent Application Serial No. 282,613, July 13, 1981.
66. Moser F. H.; Thomas, A. L. *Phthalocyanine Compounds*; Rheinhold: New York, 1963; pp 62, 109, 133, 134.
67. Akkermans, J. H. M., et al. (Unilever). Bleach Catalyst Composition in Form of Granules. WO Patent 9,421,777,29 September, 1994.
68. Hage, R.; Iburg, J. E.; Kerschener, J.; Koek, J. H.; Lempers, E. L. M.; Martens, R. J.; Racherla, U. S.; Russell, S. W.; Swarthoff, T.; Van Vliet, M. R. *Nature* **1994**, *369*(6482), 637–639.
69. Martens, R. J.; Swarthoff, T. (Unilever). Detergent Compositions Containing Dinuclear Manganese Complex as Bleach. Canadian Patent 2,083,661, 27 May, 1993.
70. Anon, *Daily Mail* **1994** (Monday June 6), 24.
71. Anon, *Daily Mail* **1994** (Tuesday June 7), 24–25.
72. Gregory, P.; Reynolds, S.; White, R.L. (Zeneca). Sulfonated Manganese Phthalocyanines and Compositions Thereof. US Patent 5484,915, January 16, 1996.
73. Gregory, P.; Thetford, D. (Zeneca). Poly-Substituted phthalocyanines. U S Patent 5486,274, January 23, 1996.
74. Service, R. F. *Science* **1995**, *268*, 806.
75. Anon. *Chem. Br.* **1995**, *31*(7), 518.
76. Wells, C. H. J. *Educ. Chem.* **1990**, (May), 77.
77. Tinolux BBS Trade Literature, Edition 1986; Ciba-Geigy, April, 1986.

78. Anon. *Chem. Ind.* **1995**, (April 17), 295.
79. Bao, Z. N.; Rogers, J. A.; Katz, H. E. *J. Mater. Chem.* **1999**, *9*, 1895–1904.
80. Gregory, P. *High-Technology Applications of Organic Colorants*; Plenum: New York, 1991; Chapter 12, pp 255–272.
81. *Color by Design: The Salters' Advanced Chemistry Project*. University of York: York, U.K., 1992; p 7.
82. Sax, N. I.; Lewis, R. J. *Dangerous Properties of Industrial Materials*; Van Nostrand, London, 1992.

9.13

Metal Complexes as Dyes for Optical Data Storage and Electrochromic Materials

R. J. MORTIMER

Loughborough University, UK

and

N. M. ROWLEY

The University of Birmingham, UK

9.13.1	ELECTROCHROMIC DYES	581
9.13.1.1	Introduction	581
9.13.1.2	Classes of Electrochromic Material	582
9.13.1.3	Electrochromism in Transition Metal Coordination Complexes	583
9.13.1.3.1	<i>Electrochromism of polypyridyl complexes</i>	583
9.13.1.3.2	<i>Electrochromism in metal phthalocyanines and porphyrins</i>	586
9.13.1.3.3	<i>Prussian blue systems</i>	591
9.13.1.3.4	<i>Near-infrared region electrochromic systems</i>	597
9.13.2	METAL COMPLEXES AS DYES FOR OPTICAL DATA STORAGE	602
9.13.2.1	Background	602
9.13.2.2	Optical Data Storage Categories	602
9.13.2.2.1	<i>Read only media</i>	602
9.13.2.2.2	<i>Write-once recordable media: CD-R and DVD-R</i>	605
9.13.2.2.3	<i>Rewritable media</i>	607
9.13.2.3	Optical Data Storage on Write-once Media	607
9.13.2.3.1	<i>Heat-mode recording</i>	607
9.13.2.3.2	<i>CD-R: Recording mechanism</i>	608
9.13.2.3.3	<i>Brief history of development of dyes for optical data storage</i>	608
9.13.2.3.4	<i>Specific requirements for dyes for optical disk recording</i>	609
9.13.2.3.5	<i>Phthalocyanines and related compounds</i>	610
9.13.2.3.6	<i>Metal complexes of azo dyes</i>	614
9.13.2.4	Future Developments	615
9.13.3	REFERENCES	615

9.13.1 ELECTROCHROMIC DYES

9.13.1.1 Introduction

Many chemical species exhibit different redox states with distinct electronic absorption spectra, usually in the UV/visible region of the electromagnetic spectrum. Where the switching of redox

states generates new or different electronic absorption bands, the material is said to be electrochromic.¹⁻⁷ While materials are considered electrochromic when they show marked visible color changes, recent interest in electrochromic devices (ECDs) for multispectral energy modulation by reflectance and absorbance has extended the definition.⁸ ECDs are now being studied for modulation of radiation in the near-infrared (NIR),⁹ thermal infrared and microwave regions, and “color” can mean response of detectors of these wavelengths, not just the human eye.⁸

Electrochromic materials are generally one of three types.¹ Type I materials are soluble in both redox states. Type II materials are soluble in their colorless redox state but form a colored solid on the surface of the electrode following electron transfer. Type III materials are solid in both redox states. “Color” changes are generally between a transparent (“bleached”) state, where the chromophore only absorbs in the UV region, and a colored state; or between two colored states. The color itself, when under illumination, results from either an intervalence optical charge transfer where there are two centers of differing valence or oxidation state, or a moderate-energy internal electronic excitation. In Type II and III electrochromic systems, once the redox state has been switched, no further charge injection is needed to retain the new color, in the so-called “memory effect.” For type I electrochromic systems, in contrast, diffusion of the soluble material away from the electrode occurs and it is necessary to keep current flowing until the whole solution has been electrolyzed. Where more than two redox states are electrochemically accessible in a given electrolyte solution, the electrochromic material may exhibit several colors and be termed polyelectrochromic. Whilst the term “colored” generally implies absorption in the visible region, metal coordination complexes that switch between a colorless state and a state with strong absorption in the NIR region have recently been receiving much attention.⁹

Proposed applications of electrochromic materials include anti-glare car rear-view mirrors, which have already been commercialized,^{3,6} controllable light-reflective or light-transmissive devices for optical information and storage, sunglasses, protective eyewear, controllable aircraft canopies, glare-reduction systems for offices, “smart windows” for use in cars and in buildings⁶ and in frozen-food monitoring.¹⁰ Other roles presently envisaged involve long-term display of information, such as at transport termini, re-usable price labels, and advertising boards. While a system showing only changes of color is technically electrochromic, one of the states evoked in most of these practical applications needs to be a colorless one, though a weak yellow often suffices. Polyelectrochromic systems could see applications in the field of electrochromic data displays. Until very recently, ECDs have been considered to have insufficiently fast response times. However, a new type of system overcomes this problem.^{11,12} Other miscellaneous applications include gasochromic (a term used to describe electrochromic devices where the electrons for the redox process come via a gas-phase reductant or oxidant) systems, where a range of electrochromic sensing devices have been studied, such as electrochromic strips as battery state-of-charge indicators, and electrochromic gels that change color in response to corrosion processes.

9.13.1.2 Classes of Electrochromic Material

There is a vast number of chemical species that show electrochromic properties.¹ In addition to the electrochromic metal coordination complexes described here (polypyridyl complexes, metal phthalocyanines and porphyrins, Prussian blue and its analogs, NIR systems), other materials such as metal oxides¹ (especially tungsten oxide^{1,2}), viologens¹ (4,4'-bipyridylium salts), and conducting polymers¹ (e.g., polyaniline, polypyrrole, and polythiophene) are also intensively studied for their electrochromic applications. Other classes of electrochromic material include Y, La, and Y/La alloys—which switch from a reflecting-mirror metallic state to a transparent semiconducting phase on hydride formation⁷—and metal deposition/stripping systems.¹

It is important, however, to realize that whilst many types of chemical species exhibit electrochromism, only those with favorable electrochromic performance parameters¹ are potentially useful in commercial applications. Thus, most applications require electrochromic materials with a high contrast ratio, coloration efficiency, cycle life, and write-erase efficiency.¹ Some performance parameters are application dependent; displays need low response times, whereas “smart windows” can tolerate response times of up to several minutes.

Electrochromic materials (either as an electroactive surface film or an electroactive solute) are generally first studied at a single working electrode, under potentiostatic or galvanostatic control, using three-electrode circuitry.¹ Traditional electrochemical techniques such as cyclic voltammetry (CV), coulometry, and chronoamperometry, all partnered by *in situ* spectroscopic measurements

as appropriate, are employed for characterization. For ECD investigations, a solid (often polymeric) or liquid electrolyte is sandwiched between two electrodes, in what is essentially a rechargeable electrochemical cell. In practical devices, in order to achieve high coloration efficiencies, the working and counter electrode reactions are *both* chosen to be electrochromic, with complementary color changes. The electrochromic electrode(s), which can work in the reflective or transmissive mode, generally consist of a glass substrate coated with an electrically conducting film such as indium-doped tin oxide (ITO), onto which is deposited the electrochromic material. Alternatively, if one or both redox states are soluble, the electrochromic material may be present dissolved in the electrolyte solution.

9.13.1.3 Electrochromism in Transition Metal Coordination Complexes

Transition metal coordination complexes are potentially useful as electrochromic materials because of their intense coloration and redox reactivity. Chromophoric properties arise from low-energy metal-to-ligand charge transfer (MLCT), intervalence CT, intraligand excitation, and related visible-region electronic transitions. Because these transitions involve valence electrons, chromophoric characteristics are altered or eliminated upon oxidation or reduction of the complex. A familiar example is the redox indicator ferroin, $[\text{Fe}(\text{phen})_3]^{2+}$, which has been employed in a solid-state ECD, the deep red color of which is lost on oxidation to the iron(III) form.¹³ Any colored metal complex susceptible to a redox change will in general undergo an accompanying color change, and will therefore be electrochromic to some extent.

While these spectroscopic and redox properties alone would be sufficient for direct use of transition metal complexes in solution-phase ECDs, polymeric systems based on coordination complex monomer units, which have potential use in all-solid-state systems, have also been investigated.

9.13.1.3.1 Electrochromism of polypyridyl complexes

(i) Polypyridyl complexes in solution

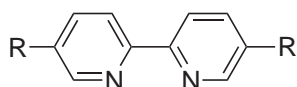
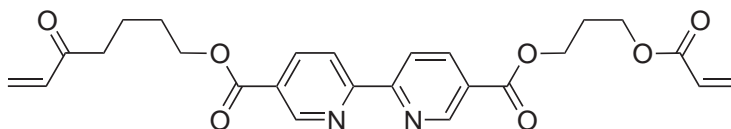
The complexes $[\text{M}(\text{bipy})_3]^{2+}$ ($\text{M} = \text{Fe}, \text{Ru}, \text{Os}$; $\text{bipy} = 2,2'$ -bipyridine) are respectively red, orange, and green, due to the presence of an intense MLCT absorption band.¹⁴ Electrochromicity results from loss of the MLCT absorption band on switching to the M^{III} redox state. Such complexes also exhibit a series of ligand-based redox processes, the first three of which are accessible in solvents such as acetonitrile and dimethylformamide (DMF).¹⁴ Attachment of electron-withdrawing substituents to the 2,2'-bipyridine ligands allows additional ligand-based redox processes to be observed, due to the anodic shift of the redox potentials induced by these substituents. Thus, Elliott and co-workers have shown that a series of colors is available with $[\text{M}(\text{bipy})_3]^{2+}$ derivatives when the 2,2'-bipyridine ligands have electron-withdrawing substituents at the 5,5' positions, Table 1.¹⁵ The electrochromic colors established by bulk electrolysis in acetonitrile are given in Table 1.

A surface-modified polymeric system can be obtained by spin coating or heating $[\text{Ru}(\text{L}^6)_3]^{2+}$ as its *p*-tosylate salt.¹⁶ The resulting film shows seven-color electrochromism whose colors cover the spectral range, which can be scanned in 250 ms.

Spectral modulation in the NIR region has been reported for the complex $[\text{Ru}(\text{L}^8)_3]^{2+}$ which undergoes six ligand-centered reductions, two per ligand.¹⁷ It initially shows no absorption

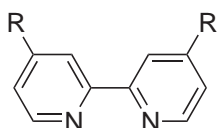
Table 1 Colors (established by bulk electrolysis in acetonitrile) of the ruthenium(II) tris-bipyridyl complexes of the ligands given below, in all accessible oxidation states.¹⁵

Charge on RuL_3 unit	L^1	L^2	L^3	L^4	L^5
+2	Orange	Orange	Orange	Red–orange	Red–orange
+1	Purple	Wine red	Gray-blue	Purple	Red–brown
0	Blue	Purple	Turquoise	Blue	Purple–brown
–1	Green	Blue	Green	Turquoise	Gray–blue
–2	Brown			Aquamarine	Green
–3	Red			Brown–green	Purple

L¹ R = CO₂EtL² R = CONEt₂L³ R = CON(Me)PhL⁴ R = CNL⁵ R = C(O)ⁿBuL⁶

between 700 and 2,100 nm. However, upon reduction by one electron a very broad pair of overlapping peaks appear with maxima at 1,210 nm ($\epsilon = 2,600 \text{ dm}^3 \text{ mol}^{-1} \text{ cm}^{-1}$) and 1,460 nm ($\epsilon = 3,400 \text{ dm}^3 \text{ mol}^{-1} \text{ cm}^{-1}$). Following the second one-electron reduction, the peaks shift to slightly lower energy (1,290 nm and 1,510 nm) and increase in intensity ($\epsilon = 6,000$ and $7,300 \text{ dm}^3 \text{ mol}^{-1} \text{ cm}^{-1}$ respectively). Following the third one-electron reduction, the two peaks coalesce into a broad absorption at 1,560 nm, which is again enhanced in intensity ($\epsilon = 12,000 \text{ dm}^3 \text{ mol}^{-1} \text{ cm}^{-1}$). Upon reduction by the fourth and subsequent electrons the peak intensity diminishes continuously to approximately zero for the six-electron reduction product. These NIR transitions are almost exclusively ligand-based.

An optically transparent thin-layer electrode (OTTLE) study¹⁸ revealed that the visible spectra of the reduced forms of $[\text{Ru}(\text{bipy})_3]^{2+}$ derivatives can be separated into two classes. Type A complexes, such as $[\text{Ru}(\text{bipy})_3]^{2+}$, $[\text{Ru}(\text{L}^7)_3]^{2+}$, and $[\text{Ru}(\text{L}^1)_3]^{2+}$ show spectra on reduction which contain low-intensity ($\epsilon < 2,500 \text{ dm}^3 \text{ mol}^{-1} \text{ cm}^{-1}$) bands; these spectra are similar to those of the reduced free ligand and are clearly associated with ligand radical anions. In contrast, type B complexes such as $[\text{Ru}(\text{L}^8)_3]^{2+}$ and $[\text{Ru}(\text{L}^9)_3]^{2+}$ on reduction exhibit spectra containing broad bands of greater intensity ($1,000 < \epsilon < 15,000 \text{ dm}^3 \text{ mol}^{-1} \text{ cm}^{-1}$).

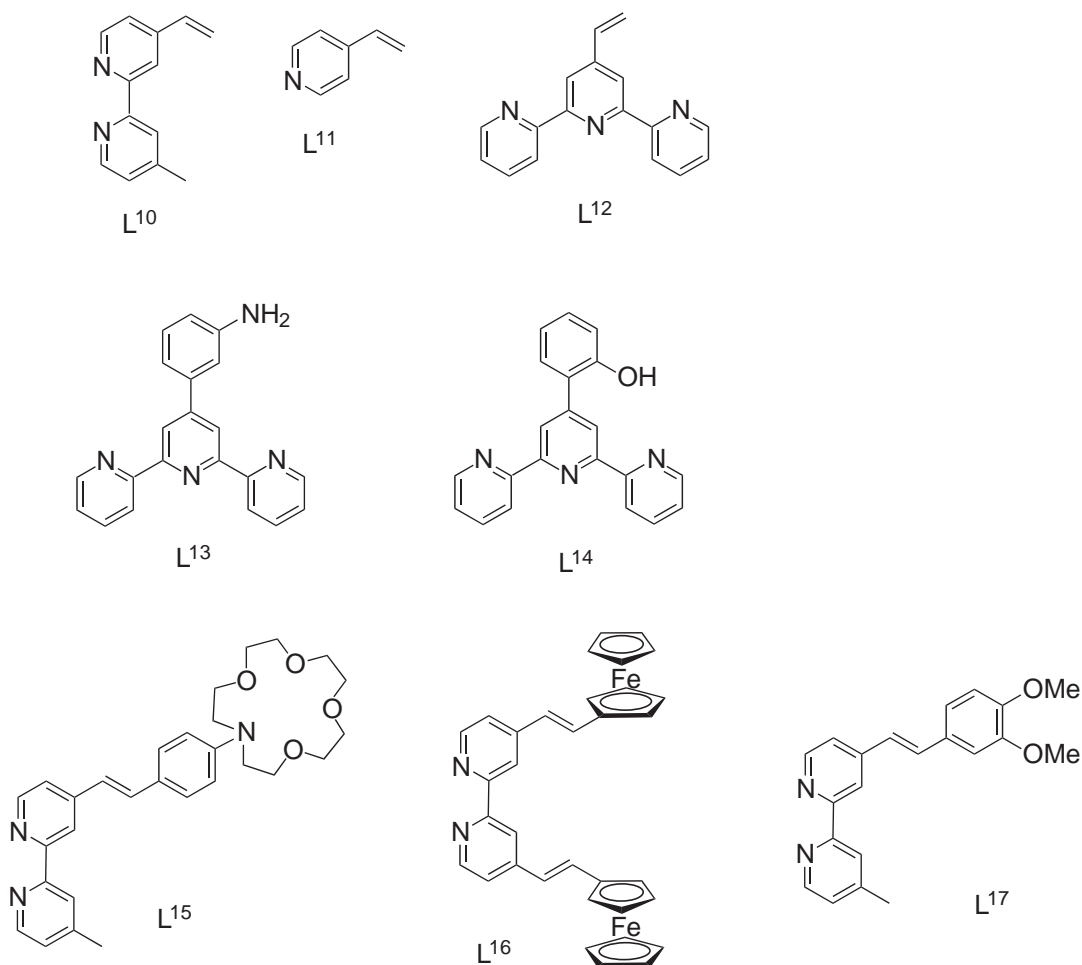
L⁷ R = MeL⁸ R = COOEtL⁹ R = CONEt₂

(ii) Reductive electropolymerization of polypyridyl complexes

The reductive electropolymerization technique relies on the ligand-centered nature of the three sequential reductions of complexes such as $[\text{Ru}(\text{L}^{10})_3]^{2+}$ ($\text{L}^{10} = 4\text{-vinyl-4'-methyl-2,2'-bipyridine}$), combined with the anionic polymerizability of suitable ligands.¹⁹ Vinyl-substituted pyridyl ligands such as $\text{L}^{10}\text{--L}^{12}$ are generally employed, although metallopolymers have also been formed from chloro-substituted pyridyl ligands, via electrochemically initiated carbon-halide bond cleavage. In either case, electrochemical reduction of their metal complexes generates radicals leading to carbon-carbon bond formation and oligomerization. Oligomers above a critical size are insoluble and thus thin films of the electroactive metallopolymer are produced on the electrode surface.

(iii) Oxidative electropolymerization of polypyridyl complexes

Oxidative electropolymerization has been described for iron(II) and ruthenium(II) complexes containing amino-²⁰ and pendant aniline-²¹ substituted 2,2'-bipyridyl ligands, and amino- and



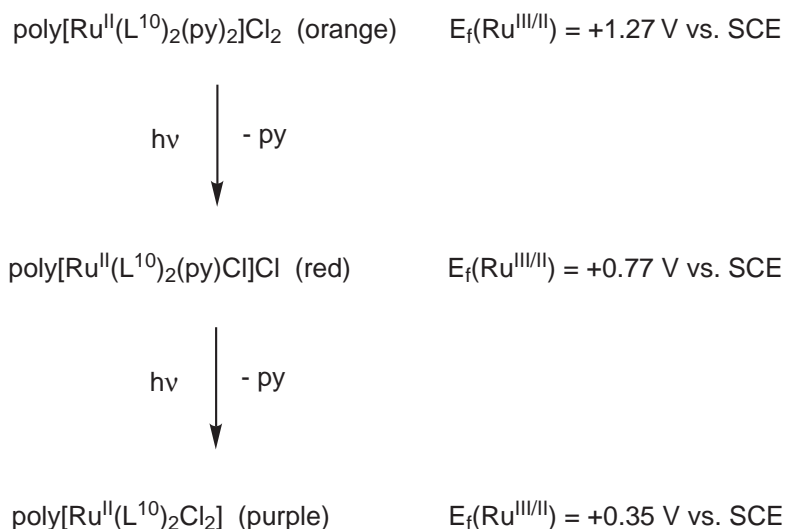
hydroxy- substituted 2,2':6',2''-terpyridinyl ligands.²² Analysis of IR spectra suggests that the electropolymerization of $[\text{Ru}(\text{L}^{13})_2]^{2+}$ via the pendant aminophenyl substituent proceeds by a reaction mechanism similar to that of aniline.²² The resulting modified electrode reversibly switched from purple to pale pink on oxidation of Fe^{II} to Fe^{III} . For polymeric films formed from $[\text{Ru}(\text{L}^{14})_2]^{2+}$ via polymerization of the pendant hydroxyphenyl group the color switch was from brown to dark yellow. The dark yellow color was attributed to an absorption band at 455 nm, probably due to quinone moieties in the polymer formed during electropolymerization. IR spectra confirmed the absence of hydroxyl groups in the initially deposited brown films.

Metallopolymer films have also been prepared by oxidative polymerization of complexes of the type $[\text{M}(\text{phen})_2(4,4'\text{-bipy})_2]^{2+}$ ($\text{M} = \text{Fe}, \text{Ru}, \text{or Os}$; phen = 1,10-phenanthroline, 4,4'-bipy = 4,4'-bipyridine).²³ Such films are both oxidatively and reductively electrochromic; reversible film-based reduction at potentials below -1 V lead to dark purple films,²³ the color and potential region being consistent with the viologen dication/radical cation electrochromic response. A purple state at high negative potentials has also been observed for polymeric films prepared from $[\text{Ru}(\text{L}^{15})_3]^{2+}$.²⁴ Electropolymerized films prepared from the complexes $[\text{Ru}(\text{L}^{16})\text{-(bipy)}_2][\text{PF}_6]_2$ ²⁵ and $[\text{Ru}(\text{L}^{17})_3][\text{PF}_6]_2$ ^{26,27} exhibit reversible orange/transparent electrochromic behavior associated with the $\text{Ru}^{\text{II}}/\text{Ru}^{\text{III}}$ interconversion.

(iv) *Spatial electrochromism of polymeric polypyridyl complexes*

Spatial electrochromism has been demonstrated in metallopolymeric films.²⁸ Photolysis of *poly*- $[\text{Ru}^{\text{II}}(\text{L}^{10})_2(\text{py})_2]\text{Cl}_2$ thin films on ITO glass in the presence of chloride ions leads to photochemical loss of the photolabile pyridine ligands, and sequential formation of *poly*- $[\text{Ru}^{\text{II}}(\text{L}^{10})_2(\text{py})\text{Cl}]\text{Cl}$ and *poly*- $[\text{Ru}^{\text{II}}(\text{L}^{10})_2\text{Cl}_2]$ (Scheme 1).

Contact lithography can be used to spatially control the photosubstitution process to form laterally resolved bicomponent films with image resolution below 10 μm . Dramatic changes occur in the colors and redox potentials of such ruthenium(II) complexes upon substitution of chloride for the pyridine ligands (Scheme 1). Striped patterns of variable colors are observed on addressing such films with a sequence of potentials.



Scheme 1

9.13.1.3.2 Electrochromism in metal phthalocyanines and porphyrins

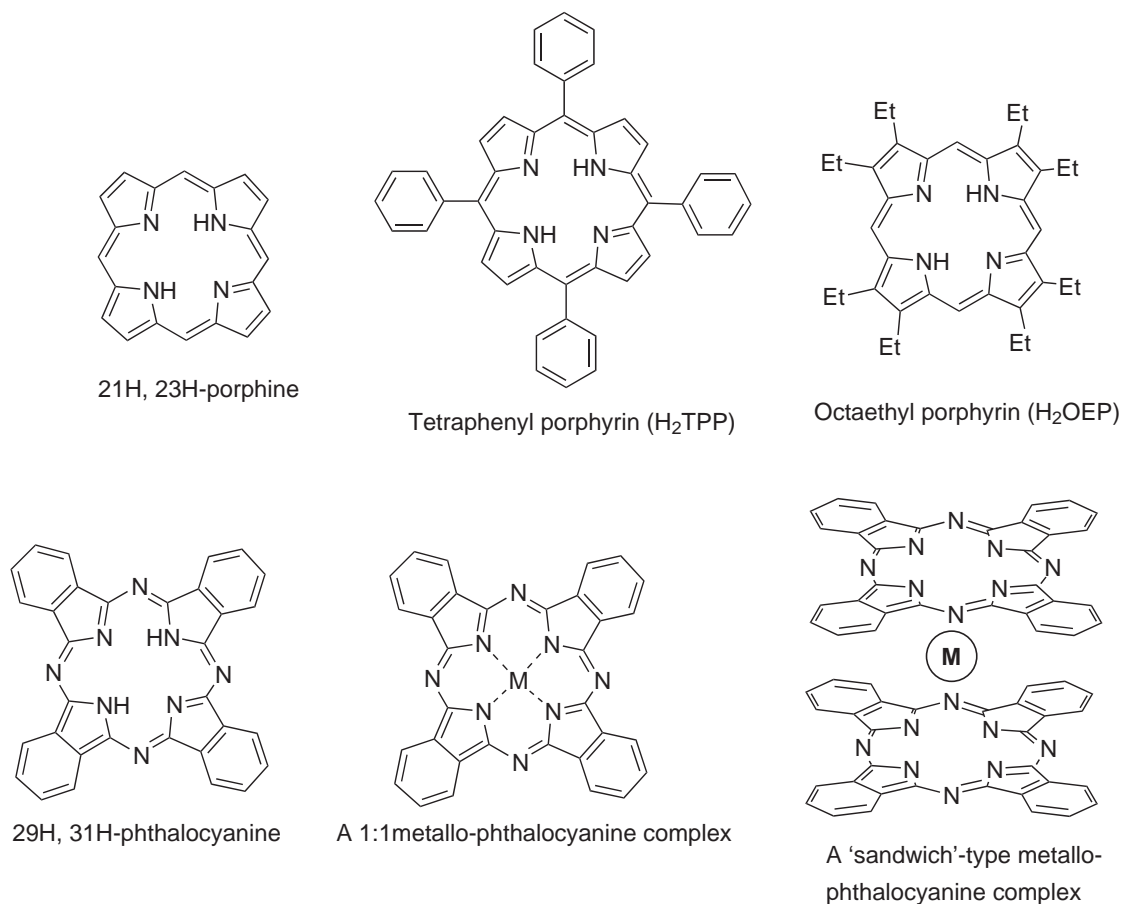
(i) Introduction to metal phthalocyanines and porphyrins

The porphyrins are a group of highly colored, naturally occurring pigments containing a tetrapyrrole porphine nucleus (Scheme 2) with substituents at the eight β positions of the pyrroles, and/or the four *meso* positions between the pyrrole rings.²⁹ The natural pigments themselves are metal chelate complexes of the porphyrins. Phthalocyanines (Scheme 2) are tetraazatetrabenzo derivatives of porphyrins with highly delocalized π -electron systems. Metallophthalocyanines are important industrial pigments, blue to green in color, used primarily in inks and for coloring plastics and metal surfaces (see Chapter 9.12).^{29,30} The water-soluble sulfonate derivatives are used as dyestuffs for clothing. In addition to these uses, the metallophthalocyanines have been extensively investigated in many fields including catalysis, liquid crystals, gas sensors, electronic conductivity, photosensitizers, non-linear optics, and electrochromism.³⁰ The purity and depth of the color of metallophthalocyanines arise from the unique property of having an isolated, single band located in the far-red end of the visible spectrum (near 670 nm), with ϵ often exceeding $10^5 \text{ dm}^3 \text{ mol}^{-1} \text{ cm}^{-1}$. The next most energetic set of transitions is generally much less intense, near 340 nm. Charge transfer transitions between a chosen metal and the phthalocyanine ring introduce additional bands around 500 nm, allowing tuning of the hue.³⁰

The metal ion in metallophthalocyanines lies either at the center of a single phthalocyanine (Pc = dianion of phthalocyanine), or between two rings in a sandwich-type complex (Scheme 2).³⁰ Phthalocyanine complexes of transition metals usually contain only a single Pc ring while lanthanide-containing species usually form bis(phthalocyanines), where the π -systems interact strongly with each other, resulting in characteristic features such as the semiconducting ($\kappa = 5 \times 10^{-5} \Omega^{-1} \text{ cm}^{-1}$) properties of thin films of bis(phthalocyaninato) lutetium(III) $[\text{Lu}(\text{Pc})_2]$.³¹

(ii) Sublimed bis(phthalocyaninato) lutetium(III) films

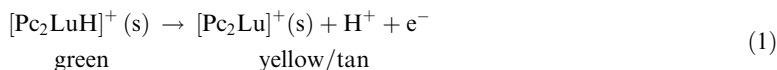
The electrochromism of the phthalocyanine ring-based redox processes of vacuum-sublimed thin films of $[\text{Lu}(\text{Pc})_2]$ was first reported in 1970,³² and since that time this complex has received most attention, although many other (mainly lanthanide) metallophthalocyanines have been investigated for their electrochromic properties.¹ $\text{Lu}(\text{Pc})_2$ has been studied extensively by Collins and Schiffrin^{33,34} and by



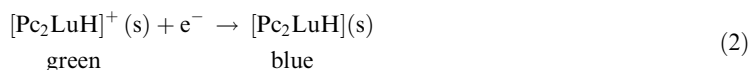
Scheme 2

Nicholson and Pizzarello.^{35–40} Collins and Schiffrin's Lu(Pc)₂ was initially studied as a film immersed in aqueous electrolyte, but hydroxide ion from water causes gradual film destruction, attacking nitrogens of the Pc ring.³³ Acidic solution allows a greater number of stable write–erase cycles, up to 5×10^6 cycles in sulfuric acid.³³ Lu(Pc)₂ films in ethylene glycol solution were found to be more stable.³⁴

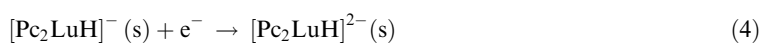
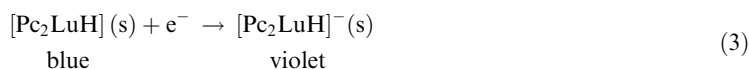
Fresh Lu(Pc)₂ films (likely to be singly protonated,⁴⁰ although this issue is contentious^{33,41}), which are brilliant green in color ($\lambda_{\max} = 605$ nm), are electro-oxidized to a yellow/tan form (Equation (1)).^{35,38,41} A further oxidation product is red,^{35,38,41} of unknown composition.



Electroreduction of Lu(Pc)₂ films gives a blue-colored film (Equation (2));⁴²



with further reduction yielding a violet–blue product (Equations (3) and (4)).³⁸



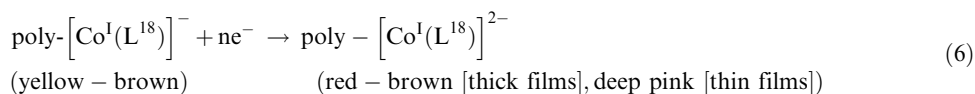
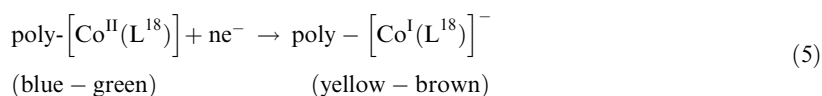
The lutetium bis(phthalocyanine) system is a truly polyelectrochromic one,³² but usually only the blue-to-green transition is used in ECDs. Although prototypes have been constructed,⁴³ no ECD incorporating Lu(Pc)₂ has yet been marketed, owing to experimental difficulties such as film disintegration caused by constant counteranion ingress/egress on color switching.³³ For this reason, larger anions are best avoided to minimize the mechanical stresses. A second, related handicap of metallophthalocyanine electrochromic devices is their relatively long response times. Nicholson and Pizzarello³⁹ investigated the kinetics of color reversal and found that small anions like chloride and bromide allow faster color switching. Sammells and Pujare overcame the problem of slow penetration of anions into solid lattices by using an ECD containing an electrochrome suspension in semi-solid polyAMPS (AMPS = 2-acrylamido-2-methyl-propanesulfonic acid) electrolyte.⁴³ While the response times are still somewhat long, the open-circuit lifetimes ("memory" times) of all colors were found to be very good.³⁹ Films in chloride, bromide, iodide, and sulfate-containing solutions were found to be especially stable in this respect.

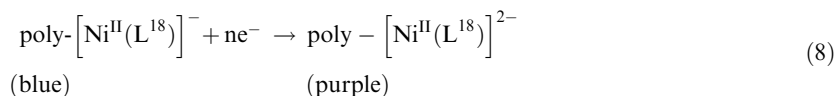
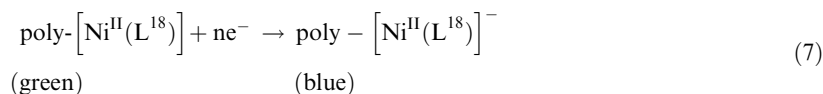
(iii) Other metal phthalocyanines

Moskalev *et al.* prepared the phthalocyanine complexes of neodymium, americium, europium, thorium, and gallium (the latter as the half acetate).⁴⁴ Collins and Schiffrin³³ have reported the electrochromic behavior of the phthalocyanine complexes CoPc, SnCl₂Pc, SnPc₂, MoPc, CuPc, and the metal-free H₂Pc. No electrochromism was observed for either the metal-free or for the copper phthalocyanines in the potential ranges employed; all of the other complexes showed limited electrochromism. Both SnCl₂Pc and SnPc₂ could be readily reduced, but showed no anodic electrochromism. Other molecular phthalocyanine electrochromes studied include complexes of aluminum,⁴⁵ copper,⁴⁶ chromium,^{45,47} erbium,⁴⁸ europium,⁴⁹ iron,⁵⁰ magnesium,⁵¹ manganese,^{47,51} titanium,⁵² uranium,⁵³ vanadium,⁵² ytterbium,^{54,55} zinc,⁵⁶ and zirconium.^{49,45,57} Mixed phthalocyanine systems have also been prepared by reacting mixed-metal precursors comprising the lanthanide metals dysprosium, holmium, erbium, thulium, ytterbium, lutetium, yttrium, and small amounts of others;⁵⁸ the response times for such mixtures are reportedly superior to those for single-component films. Walton *et al.* have compared the electrochemistry of lutetium and ytterbium bis(phthalocyanines), finding them to be essentially identical.⁵⁹ Both chromium and manganese mono-phthalocyanine complexes undergo metal-centered oxidation and reduction processes.⁴⁷ In contrast, the redox reactions of LuPc₂ occur on the ligand; electron transfer to the central lutetium causes molecular dissociation.⁶⁰ Lever and co-workers have studied cobalt phthalocyanine systems in which two or four Co(Pc) units are connected via chemical links.^{61–64} These workers have also studied tetrasulfonated cobalt and iron phthalocyanines.⁶⁵ Finally, polymeric ytterbium bis(phthalocyanine) has been studied^{66–68} using a plasma technique to effect the polymerization.

(iv) Electrochemical routes to metallophthalocyanine electrochromic films

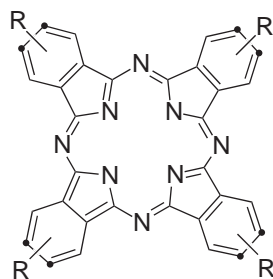
For complexes with pendant aniline and hydroxy-substituted ligands, oxidative electropolymerization is an alternative route to metallophthalocyanine electrochromic films. Although polymer films prepared from [Lu(L¹⁸)₂] monomer show loss of electroactivity on cycling to positive potentials, in dimethyl sulfoxide (DMSO) the electrochemical response at negative potentials is stable, with the observation of two broad quasi-reversible one-electron redox couples.⁶⁹ Spectroelectrochemical measurements revealed switching times of <2s for the observed green–gray–blue color transitions in this region. The oxidative electropolymerization technique using pendant aniline substituents has also been applied to monophthalocyaninato transition metal complexes;⁷⁰ the redox reactions and color changes of two of the examples studied are given in Equations (5)–(8).





The first reduction in the cobalt-based polymer is metal-centered, resulting in the appearance of a new MLCT transition, with the second reduction being ligand-centered. For the nickel-based polymer, in contrast, both redox processes are ligand-based.

Electrochromic polymer films have been prepared by oxidative electropolymerization of the monomer $[\text{Co}(\text{L}^{19})]$.⁷¹ The technique involved voltammetric cycling from -0.2 to $+1.2$ V vs. SCE at 100 mV s^{-1} in dry acetonitrile, resulting in the formation of a fine, green polymer. Cyclic voltammograms during polymer growth showed the irreversible phenol oxidation peak at $+0.58$ V and a reversible phthalocyanine ring oxidation peak at $+0.70$ V. Polymer-modified electrodes gave two distinct redox processes with half wave potentials at -0.35 $[\text{Co}^{\text{II}}/\text{Co}^{\text{I}}]$ and -0.87 V (reduction of the ring). Color switching was from transparent light green $[\text{Co}^{\text{II}}$ state] to yellowish green $[\text{Co}^{\text{I}}$ state] to dark yellow (reduced ring).



- L¹⁸ R = NH₂
 L¹⁹ R = O-(2-C₆H₄OH)
 L²⁰ R = CO₂-CH₂CH₂CMe₃

NB. These complexes exist as a mixture of isomers with the substituents attached at either of the positions labelled * on the benzyl rings.

(v) Langmuir–Blodgett metallophthalocyanine electrochromic films

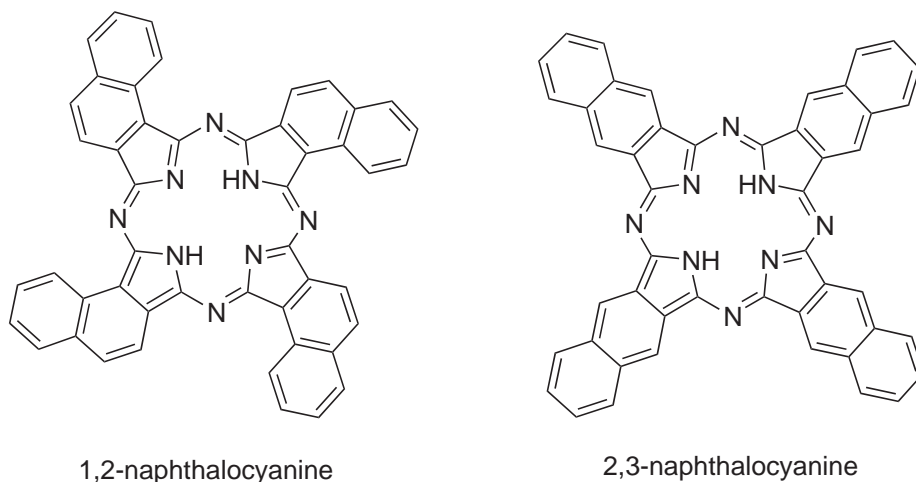
The electrochemical properties of a variety of metallophthalocyanines as multilayer Langmuir–Blodgett (LB) films have been studied. For example, LB films of alkyloxy-substituted $[\text{Lu}(\text{Pc})_2]$ exhibited a one-electron reversible reduction and a one-electron reversible oxidation corresponding to a transition from green to orange and blue forms respectively, with the electron transport through the multilayers being at least in part diffusion controlled.⁷² An explanation of the relatively facile redox reaction in such multilayers is that the Pc ring is large compared with the alkyl tail, and there is enough space and channels present in the LB films to allow ion transport. More recently, the structure, electrical conductivity, and electrochromism in thin films of substituted and unsubstituted lanthanide bis-phthalocyanine derivatives have been investigated with particular reference to the differences between unsubstituted and butoxy-substituted $[\text{Lu}(\text{Pc})_2]$ materials.⁷³ Scanning tunneling microscopy (STM) images on graphite reveals the differences in the two structures, and gives molecular dimensions of 1.5×1.0 nm and 2.8×1.1 nm respectively. The in-plane d.c. conductivity was studied as a function of film thickness and temperature, with unsubstituted $[\text{Lu}(\text{Pc})_2]$ being approximately 10^6 times more conductive than the substituted material. The green–red oxidative step is seen for both cases but the green–blue reductive step is absent in the butoxy-substituted material. High-quality LB films of $[\text{M}(\text{L}^{20})]$ ($\text{M} = \text{Cu}, \text{Ni}$) have also been reported.⁷⁴ Ellipsometric and polarized optical absorption measurements suggest that the Pc rings are oriented with their large faces perpendicular to the dipping direction and to the substrate plane.

The LB technique is amenable to the fabrication of ECDs as demonstrated by the report of a thin-film display based on bis(phthalocyaninato)praseodymium(III).⁷⁵ The electrochromic electrode in the display was fabricated by deposition of multilayers (10–20 layers, ≈ 100 – 200 Å) of the complex onto ITO-coated glass ($7 \times 4 \text{ cm}^2$) slides. The display exhibited blue–green–yellow–red polyelectrochromicity over a potential range of -2 to $+2$ V. After 10^5 cycles no significant

changes are observed in the spectra of these color states. The high stability of the device was ascribed to the preparation, by the LB technique, of well-ordered monolayers which allow better diffusion of the counter ions into the film, which improves reversibility.

(vi) *Species related to metal phthalocyanines*

Naphthalocyanine (nc) species (Scheme 3) are structurally similar to the simpler phthalocyanines described above and have two isomers, denoted here (2,3-nc) and (1,2-nc).



Scheme 3

Naphthalocyanines show an intense optical absorption at long wavelengths ($700 < \lambda < 900$ nm) owing to electronic processes within the extended conjugated system of the ligand.^{76,77} Thin-film $[\text{Co}(2,3\text{-nc})_2]$ is green and is readily oxidized to form a violet-colored species. Thin-film $[\text{Zn}(2,3\text{-nc})_2]$ is also green when neutral. A “triple-decker” naphthalocyanine compound $[(1,2\text{-nc})\text{-Lu}(1,2\text{-nc})\text{-Lu}(1,2\text{-nc})]$ has been reported.⁷⁸ Electrochromism in the pyridinoporphyrine system and its cobalt complex has also received some attention.⁷⁹ Here, the ligand is similar to a phthalocyanine but with quaternized pyridyl residues replacing all four fused benzo groups.

It is not only homoleptic phthalocyanine complexes that can form sandwich structures; recently a substantial number of heteroleptic sandwich-type metal complexes, with mixed phthalocyaninato and/or porphyrinato ligands, have been synthesized and are likely to show interesting electrochromic properties.⁸⁰ Although considerable progress has been made in this field, there is clearly much room for further investigation. By attaching functional groups or special moieties (donor or acceptor moieties) to these compounds, it may be possible to tune their electronic properties without altering the ring-to-ring separation. The properties associated with these units may also be imparted to the parent sandwich compounds. The electrochromic properties of some silicon–phthalocyanine thin films, in which a redox-active ferrocenecarboxylato unit is appended to the electrochromic centre, have been studied.⁸¹

(vii) *Electrochromic properties of porphyrins*

Early results suggest that an investigation into porphyrin electrochromism is warranted, although there has been little systematic study to date. Thus, the spectra of the chemical reduction products of $\text{Zn}(\text{TPP})$ have been reported,^{82,83} with colors changing between pink (parent complex), green (mononegative ion), and amber (dinegative ion).⁸² Felton and Linschitz⁸⁴ reported that the electrochemically produced monoanion spectrum is similar to that produced chemically. Fajer *et al.*⁸⁵ showed that $\text{Zn}(\text{TPP})$ changes color to green upon one-electron oxidation by controlled potential electrolysis. Felton *et al.*⁸⁶ reported that the electrolysis of $\text{Mg}(\text{OEP})$ yielded a blue–green solution. The recently reported⁸⁷ green/pink “electrochromism” of a porphyrin monomer appears to be a pH change-induced transformation of the J-aggregate (ordered molecular arrangement, excited state

spread over N molecules in 1-D) to the monomer, and is therefore not electrochromic, in the sense that it is not triggered by a redox process.

9.13.1.3.3 Prussian blue systems

(i) Prussian blue systems: history and bulk properties

Prussian blue (PB; ferric ferrocyanide, or iron(III) hexacyanoferrate(II)) was first made by Diesbach in Berlin in 1704.⁸⁸ It is extensively used as a pigment in the formulation of paints, lacquers, and printing inks.^{89,90} Since the first report⁹¹ in 1978 of the electrochemistry of PB films, numerous studies concerning the electrochemistry of PB and related analogs have been made,⁹² with proposed applications in electrochromism¹ and electrochemical sensing and catalysis.⁹³

PB is the prototype of numerous polynuclear transition metal hexacyanometallates, which form an important class of insoluble mixed-valence compounds.^{94–96} They have the general formula $M'_k[M''(\text{CN})_6]_l$ (k, l integral) where M' and M'' are transition metals with different formal oxidation numbers. These materials can contain ions of other metals and varying amounts of water. In PB the two transition metals in the formula are the two common oxidation states of iron, Fe^{III} and Fe^{II} . Preparation of PB can easily be demonstrated by mixing aqueous solutions of either a ferricyanide salt with a ferrous salt or a ferrocyanide salt with a ferric salt. In the PB chromophore, the distribution of oxidation states is $\text{Fe}^{\text{III}}-\text{Fe}^{\text{II}}$ respectively, i.e., it contains Fe^{3+} and $[\text{Fe}^{\text{II}}(\text{CN})_6]^{4-}$, which was established by the CN stretching frequency in the IR spectrum and confirmed by Mössbauer spectroscopy;⁹⁷ Fe^{III} is high spin and can have H_2O attached, whereas the Fe^{II} is low-spin. While the composition in detail of the PB solids is extraordinarily preparation-sensitive, the major classification of extreme cases delineates “insoluble” PB (*i*-PB) $\text{Fe}^{3+}[\text{Fe}^{3+}\{\text{Fe}^{\text{II}}(\text{CN})_6\}^{4-}]_3$, and “soluble” PB (*s*-PB), $\text{K}^+\text{Fe}^{3+}[\{\text{Fe}^{\text{II}}(\text{CN})_6\}^{4-}]$. All forms of PB are in fact highly insoluble in water ($K_{\text{sp}} \sim 10^{-40}$), the “solubility” in the latter case being an illusion caused by its easy dispersion as colloidal particles, forming a blue suspension in water which looks like a true solution.

The $\text{Fe}^{3+}[\text{Fe}^{\text{II}}(\text{CN})_6]^{4-}$ chromophore falls into Group II of the Robin–Day mixed-valence classification, the blue intervalence CT band on analysis of the intensity indicating $\sim 1\%$ delocalization of the transferable electron in the ground state (i.e., before any optical CT).⁹⁸ X-ray powder diffraction patterns for *s*-PB indicate a face-centered cubic lattice, with the high-spin Fe^{III} and low-spin Fe^{II} ions coordinated octahedrally by the *N*-terminus and *C*-terminus (respectively) of cyanide ligands, with K^+ ions occupying interstitial sites.⁹⁹ In *i*-PB, Mössbauer spectroscopy confirms the interstitial ions to be Fe^{3+} .⁹⁷ Single-crystal X-ray diffraction patterns indicate, however, a primitive cubic lattice, where 1/4 of the Fe^{II} sites are vacant.¹⁰⁰ This proposed structure contains no interstitial ions, with 1/4 of the Fe^{III} centers being coordinated by 6 *N*-bound cyanide ligands, the remainder by 4 *N*-bound cyanides, and every Fe^{II} center surrounded by 6 *C*-bound cyanide ligands. The Fe^{II} vacancies are randomly distributed, and occupied by water molecules which complete the octahedral coordination about Fe^{III} . The widespread assumption of Ludi's model¹⁰⁰ for *i*-PB may be questioned in view of the probably substantial differences between the (slowly grown) single crystals and the more usual polycrystalline forms arising from rapid growth.

(ii) Preparation of Prussian blue thin films

PB thin films are generally prepared by the original method based on electrochemical deposition,⁹¹ although electroless deposition, and sacrificial anode (SA) methods¹⁰¹ have been described. Thus, PB films can be electrochemically deposited onto a variety of inert electrode substrates by electroreduction of solutions containing iron(III) and hexacyanoferrate(III) ions. PB electrodeposition has been studied by numerous techniques. Voltammetry^{102–104} and galvanostatic studies¹⁰⁵ have shown that reduction of iron(III)hexacyanoferrate(III) is the principal electron transfer process in PB electrodeposition. This brown/yellow soluble complex is present in solutions containing iron(III) and hexacyanoferrate(III) ions as a result of the equilibrium in Equation (9):

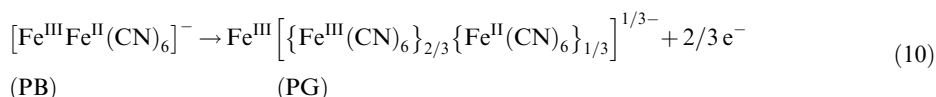


Chronoabsorptometric studies¹⁰⁶ for galvanostatic PB electrodeposition onto ITO electrodes have shown that the absorbance due to the CT band of the growing PB film is proportional to the charge passed. Quartz crystal microbalance measurements for potentiostatic PB electrodeposition onto gold have revealed that the mass gain per unit area is proportional to the charge passed.¹⁰⁷ Ellipsometric measurements for potentiostatic PB electrodeposition onto platinum showed that the level of hydration was around 34 H₂O per PB unit cell.¹⁰⁸ Changes in the ellipsometric parameters during PB electrodeposition revealed growth of a single homogeneous film for the first 80 seconds, followed by growth of a second, outer, more porous film on top of the relatively compact inner film. Chronoamperometric measurements (over a scale of several seconds) supported by scanning electron microscopy (SEM) for the electrodeposition of PB onto ITO and platinum by electroreduction from iron(III) hexacyanoferrate(III)-containing solutions have been performed.¹⁰⁹ Variation of electrode potential, supporting electrolyte, and concentrations of electroactive species have established a three-stage electrodeposition mechanism. In the first growth phase the surface becomes uniformly covered as small PB nuclei form and grow on electrode substrate sites. In the second growth phase there is an increase in rate towards maximal roughness, as the electroactive area increases by formation and three-dimensional growth of PB nuclei attached to the PB interface formed in the initial stage. In the final growth phase, diffusion of locally depleted electroactive species to the now three-dimensional PB interface plays an increasingly dominant role and limits electron transfer resulting in a fall in growth rate.

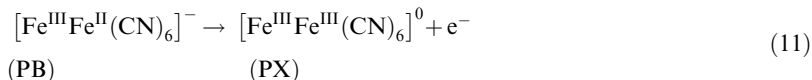
More recently, a new method of assembling multilayers of PB on surfaces has been described.¹¹⁰ In contrast to the familiar process of self-assembly, which is spontaneous and leads to single monolayers, directed assembly is driven by the experimenter and leads to extended multilayers. In a proof-of-concept experiment, the generation of multilayers of Prussian blue (and the mixed Fe^{III}/Ru^{II} analog ruthenium purple) on gold surfaces by exposing them alternately to positively charged ferric cations and [Fe(CN)₆]⁴⁻ or [Ru(CN)₆]⁴⁻ anions has been demonstrated.¹¹⁰

(iii) *Electrochemistry, in situ spectroscopy, and characterization of Prussian blue thin films*

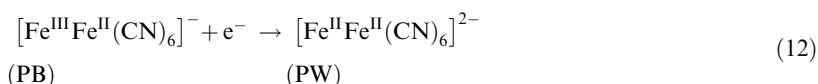
Electrodeposited PB films may be partially oxidized^{102–104} to Prussian green (PG), a species historically also known as Berlin green (Equation (10)):



where the fractions 2/3 and 1/3 are illustrative rather than precise. Thus, although in bulk form PG is believed to have a fixed composition with the anion composition shown above, it has been demonstrated that there is a continuous composition range in thin films from PB, via the partially oxidized PG form, to the fully oxidized all-Fe^{III} form Prussian brown (PX).¹⁰⁴ PX appears brown as a bulk solid, brown/yellow in solution, and golden yellow as a particularly pure form that is prepared on electro-oxidation of thin-film PB (Equation (11)).^{103,104}



Reduction of PB yields Prussian white (PW), also known as Everitt's salt, which appears colorless as a thin film (Equation (12)):



For all redox reactions above there is concomitant counter-ion movement into or out of the films to maintain overall electroneutrality.

Whilst *s*-PB, *i*-PB, PG, and PW are all insoluble in water, PX is slightly soluble in its pure (golden yellow) form (indeed, the electrodeposition technique depends on the solubility of the [Fe^{III}Fe^{III}(CN)₆]⁰ complex). This implies a positive potential limit of about +0.9 V for a high write-erase efficiency in contact with water. Although practical ECDs based on PB have primarily exploited the PB–PW transition, this does not rule out the prospect of four-color PB

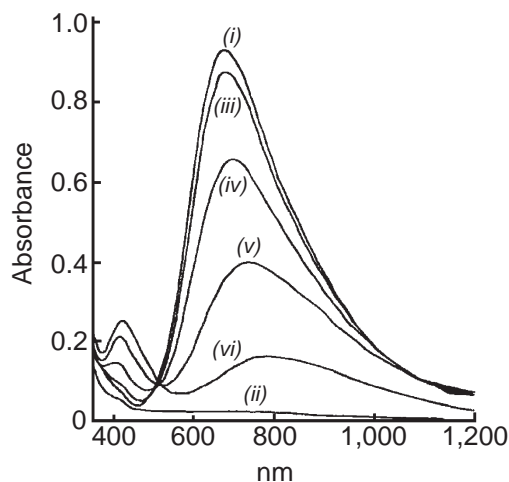
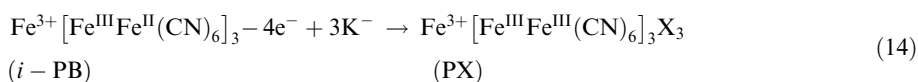
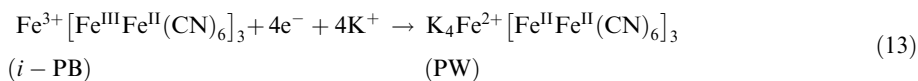


Figure 1 Spectra of iron hexacyanoferrate films on ITO-coated glass at various potentials [(i) +0.50 (PB, blue), (ii) -0.20 (PW, transparent), (iii) +0.80 (PG, green), (iv) +0.85 (PG, green), (v) +0.90 (PG, green), and (vi) +1.20 V (PX, yellow) (potentials vs. SCE)] with $0.2 \text{ mol dm}^{-3} \text{ KCl} + 0.01 \text{ mol dm}^{-3} \text{ HCl}$ as supporting electrolyte (reproduced by permission of the Royal Society of Chemistry from *J. Chem. Soc., Dalton Trans.* 1984, 2059–2061.)

polyelectrochromic ECDs, as other solvent systems may not dissolve PX. The spectra of the yellow, green, blue, and clear (“white”) forms of PB and its redox variants are shown in Figure 1, together with spectra of two intermediate states between the blue and the green forms.

The yellow absorption band corresponds with that of $[\text{Fe}^{\text{III}}\text{Fe}^{\text{III}}(\text{CN})_6]^0$ in solution, both maxima being at 425 nm and coinciding with the (weaker) $[\text{Fe}^{\text{III}}(\text{CN})_6]^{3-}$ absorption maximum. On increase from +0.50 V to more oxidizing potentials, the original 690 nm PB peak continuously shifts to longer wavelengths with diminishing absorption, while the peak at 425 nm steadily increases, owing to the increasing $[\text{Fe}^{\text{III}}\text{Fe}^{\text{III}}(\text{CN})_6]^0$ absorption. The reduction of PB to PW is, by contrast, abrupt, with transformation to all PW or all PB without pause, depending on the applied potential. The broad voltammetric peak for PB–PX in contrast with the sharp PB–PW transition emphasizes the range of compositions involved. This difference in behavior, supported by ellipsometric measurements,¹⁰⁸ indicates continuous mixed-valence compositions over the blue-to-yellow range in contrast with the (presumably immiscible) PB and PW, which clearly transform one into the other without intermediacy of composition.

The identity as *s*-PB or *i*-PB of the initially electrodeposited PB has been debated in the literature.^{104,111–115} Based on changes that take place in the intervalence CT band on redox cycling, it has been postulated that *i*-PB is first formed, followed by a transformation to *s*-PB on potential cycling.¹⁰⁴ Further evidence for this is provided by the difference in the voltammetric response for the PB–PW transition between the first cycle and all succeeding cycles, suggesting structural reorganization of the film during the first cycle.¹⁰³ On soaking *s*-PB films in saturated FeCl_3 solutions, partial reversion of the absorbance maximum and broadening of the spectrum, approaching the values observed for *i*-PB, is found.¹⁰⁴ Itaya and Uchida,¹¹¹ however, claim that the film is always *i*-PB, their argument being based on the ratio of charge passed on oxidation to PX to that passed on reduction to PW, which was 0.708 rather than 1.00; that is, Equations (13) and (14) are applicable:



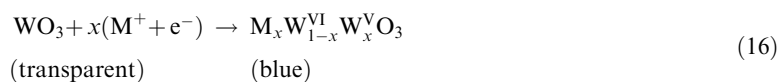
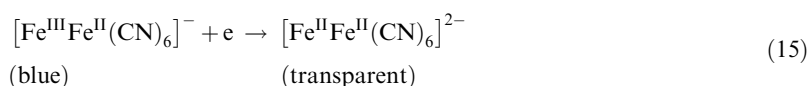
Emrich *et al.*¹¹² using X-ray photoelectron spectroscopy (XPS) data, and Lundgren and Murray,¹¹³ using CV, EDAX, XPS, elemental analytical, and spectroelectrochemical measurements, both confirmed *i*-PB as the initially deposited form with a gradual transformation to *s*-PB on potential cycling. Other support for the *i*-PB to *s*-PB transformation comes from an

ellipsometric study by Beckstead *et al.*¹¹⁴ who found that the PB film, after the first and subsequent cycles for the PB–PW transition, developed optical properties which differed from the original PB film. Results from *in situ* Fourier-transform infrared spectroscopy also demonstrated an *i*-PB to *s*-PB transformation on repeated reductive cycling.¹¹⁵ Quartz crystal microbalance mass change measurements on voltammetrically scanned PB films reinforce the theory of lattice reorganization during the initial film reduction.¹⁰⁷ Whilst PB film stability is frequently discussed in the preceding papers, Stilwell *et al.*¹¹⁶ have studied in detail the factors that influence the cycle stability of PB films. They found that electrolyte pH was the overwhelming factor in film stability; cycle numbers in excess of 100,000 were easily achieved in solutions of pH 2–3. Concurrent with this increase in stability at lower pH was a considerable increase in switching rate; films grown from chloride-containing solutions were found to be slightly more stable, in terms of cycle life, compared to those grown from chloride-free solutions.

(iv) Prussian blue electrochromic devices

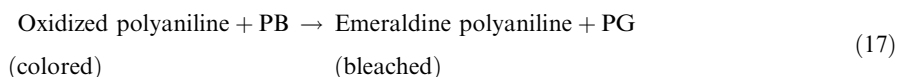
Early PB-based ECDs employed PB as the sole electrochromic material. Examples include a seven-segment display using PB-modified SnO₂ working and counter electrodes at 1 mm separation,¹¹⁷ and an ITO|PB-Nafion[®]|ITO solid-state device.^{118,119} For the solid-state system, device fabrication involved chemical (rather than electrochemical) formation of the PB, by immersion of a membrane of the solid polymer electrolyte Nafion[®] (a sulfonated polytetrafluoroethane polymer) in aqueous solutions of FeCl₂, then K₃Fe(CN)₆. The resulting PB-containing Nafion[®] composite film was sandwiched between the two ITO plates. The construction and optical behavior of an ECD utilizing a single film of PB, without addition of a conventional electrolyte, has also been described.¹²⁰ In the design, a film of PB is sandwiched between two optically transparent electrodes (OTEs). Upon application of an appropriate potential across the film, oxidation occurs near the positive electrode and reduction near the negative electrode to yield PX and PW respectively. The conversion of the outer portions of the film results in a net bleaching of the device. The functioning of the device relies on the fact that PB can be bleached both anodically (to the yellow state) and cathodically (to a transparent state), and that it is a mixed conductor through which potassium cations can move to provide charge compensation required for the electrochromic redox reactions.

Since PB and WO₃² are respectively anodically and cathodically coloring electrochromic materials, they can be used together in a single device^{121–125} so that their electrochromic reactions are complementary (Equation (15)):



In an example of the construction of such a device, thin films of these materials are deposited on OTEs that are separated by a layer of a transparent ionic conductor such as KCF₃SO₃ in poly(ethylene oxide).¹²⁵ The films can be colored simultaneously (giving deep blue) when a sufficient voltage is applied between them such that the WO₃ electrode is the cathode and the PB electrode the anode. Conversely, the colored films can be bleached to transparency when the polarity is reversed, returning the ECD to a transparent state.

Numerous workers^{126–132} have combined PB with the conducting polymer polyaniline in complementary ECDs that exhibit deep blue-to-light green electrochromism. Electrochromic compatibility is obtained by combining the colored oxidized state of the polymer¹ with the blue PB, and the bleached reduced state of the polymer with PG (Equation (17)):



Jelle and Hagen^{129,130,132,133} have recently developed an electrochromic window for solar modulation using PB, polyaniline, and WO₃. They took advantage of the symbiotic relationship between polyaniline and PB, and incorporated PB together with polyaniline and WO₃ in a

complete solid-state electrochromic window. The total device comprised Glass | ITO | polyaniline | PB | polyAMPS | WO₃ | ITO | Glass. Compared with their earlier results with a polyaniline/WO₃ window, Jelle and Hagen were able to block off much more of the light by inclusion of PB within the polyaniline matrix, while still regaining about the same transparency during the bleaching of the window.

Kashiwazaki⁶⁷ has fabricated a complementary ECD using plasma-polymerized ytterbium bis(phthalocyanine) (*pp*-Yb(Pc)₂) and PB films on ITO with an aqueous solution of 4 M KCl as electrolyte. Blue-to-green electrochromicity was achieved in a two-electrode cell by complementing the green-to-blue color transition (on reduction) of the *pp*-Yb(Pc)₂ film with the blue (PB)-to-colorless (PW) transition (oxidation) of the PB. A three-color display (blue, green, and red) was fabricated in a three-electrode cell in which a third electrode (ITO) was electrically connected to the PB electrode. A reduction reaction at the third electrode, as an additional counter electrode, provides adequate oxidation of the *pp*-Yb(Pc)₂ electrode, resulting in the red coloration of the *pp*-Yb(Pc)₂ film.

(v) Prussian blue analogs

PB analogs (other polynuclear transition metal hexacyanometallates⁹⁴⁻⁹⁶) that have been reported as thin films are surveyed in this section.

Bulk ruthenium purple [RP; ferric ruthenocyanide, iron(III) hexacyanoruthenate(II)] is synthesized via precipitation from solutions of the appropriate iron and hexacyanoruthenate salts. The visible absorption spectrum of a colloidal suspension of bulk synthesized RP with potassium as counter cation confirms the Fe³⁺/[Ru(CN)₆]⁴⁻ combination as the chromophore.¹³⁴ The X-ray powder pattern with iron(III) as counter cation gives a lattice constant of 10.42 Å as compared to 10.19 Å for the PB analog.¹³⁴ However, although no single-crystal studies have been made, RP could have a disordered structure similar to that reported for single-crystal PB.¹³⁵ The potassium and ammonium salts give cubic powder patterns similar to their PB analogs.¹³⁶

RP films have been prepared by electroreduction of the soluble ferric hexacyanoruthenate(III) complex either potentiostatically,¹³⁷ galvanostatically,¹³⁸ or using a copper wire as sacrificial anode.¹³⁷ The visible absorption spectrum of RP prepared in the presence of excess potassium ion showed a broad CT band, as for bulk synthesized RP, with a maximum at approximately 550 nm.¹³⁷ RP films can be reversibly reduced to the colorless iron(II) hexacyanoruthenate(II) form, although partial electro-oxidation to the Prussian green analog is not observed. A large background oxidation current is observed in chloride-containing electrolyte, suggesting electrocatalytic activity of RP for either oxygen or chlorine evolution.¹³⁸

Vanadium hexacyanoferrate (VHCF) films have been prepared on Pt or fluorine-doped tin oxide (FTO) electrodes by potential cycling from a solution containing Na₃VO₄ and K₃Fe(CN)₆ in 3.6 M H₂SO₄.^{139,140} Carpenter *et al.*¹³⁹ by correlation with CVs for solutions containing only one of the individual electroactive ions, have proposed that electrodeposition involves the reduction of the dioxovanadium ion VO₂⁺ (the stable form of vanadium(V) under these acidic conditions), followed by precipitation with ferricyanide ion. While the reduction of the ferricyanide ion in solution probably also occurs when the electrode is swept to more negative potentials, this reduction does not appear to be critical to film formation, since VHCF films can be successfully deposited by potential cycling over a range positive of that required for ferricyanide reduction. No evidence was obtained for the formation of a vanadium-ferricyanide-type complex analogous to ferric ferricyanide, the visible absorption spectrum of the deposition solution being a simple summation of spectra from the single-component solutions. While VHCF films are visually electrochromic, switching from green in the oxidized state to yellow in the reduced state, Carpenter *et al.* show that most of the electrochromic modulation occurs in the UV region.¹³⁹ From electrochemical data and XPS they conclude that the electrochromicity involves only the iron centers in the film. The vanadium ions, found to be present predominantly in the +4 oxidation state, are not redox active under these conditions.

Nickel hexacyanoferrate (NiHCF) films can be prepared by electrochemical oxidation of nickel electrodes in the presence of hexacyanoferrate(III) ions,¹⁴¹ or by voltammetric cycling of inert substrate electrodes in solutions containing nickel(II) and hexacyanoferrate(III) ions.¹⁴² NiHCF films do not possess low-energy intervalent CT bands, however, when deposited on ITO they are observed to reversibly switch from yellow to colorless on electroreduction.¹⁴³

A more dramatic color change can be observed by substitution of two iron-bound cyanides by a suitable bidentate ligand.¹⁴⁴ Thus, 2,2'-bipyridine can be indirectly attached to the nickel

electrode via a cyano-iron complex. When 2,2'-bipyridine is employed as the chelating agent, the complex $[\text{Fe}^{\text{II}}(\text{CN})_4(\text{bipy})]^{2-}$ is formed, which takes on an intense red color associated with a MLCT absorption band centered at 480 nm. This optical transition is sensitive to both the iron oxidation state, only being present in the Fe^{II} form of the complex, and the environment of the cyanide nitrogen lone pair. Reaction of the complex with Ni^{2+} , either under bulk conditions or at a nickel electrode surface, generates a bright-red material. By analogy with the parent iron complex this red color is associated with the $(d\pi)\text{Fe}^{\text{II}} \rightarrow (\pi^*)\text{bipy}$ CT transition. For bulk samples, chemical oxidation to the Fe^{III} state yields a light-orange material, while modified electrodes can be reversibly cycled between the intensely red and clear forms, a process which correlates well with the observed CV response.¹⁴⁴

Copper hexacyanoferrate (CuHCF) films can be prepared voltammetrically by electroplating a thin film of copper on glassy carbon (GC) or ITO electrodes in the presence of ferrocyanide ions.^{145–148} Films are deposited by first cycling between +0.40 V and +0.05 V in a solution of cupric nitrate in aqueous KClO_4 . Copper is then deposited on the electrode by stepping the potential from +0.03 to -0.50 V, and subsequently removed (stripped) by linearly scanning the potential from -0.50 to +0.50 V. The deposition and removal sequence is repeated until a reproducible CV was obtained during the stripping procedure. The CuHCF film is then formed by stepping the electrode potential in the presence of cupric ion from +0.03 V to -0.50 V followed by injection of an aliquot of $\text{K}_4\text{Fe}(\text{CN})_6$ solution (a red/brown ferrocyanide sol is formed immediately) into the cell. The CuHCF film formation mechanism has not been elucidated but the co-deposition of copper is important in the formation of stable films. Films formed by galvanostatic or potentiostatic methods from solutions of cupric ion and ferricyanide ion showed noticeable deterioration within a few CV scans. The co-deposition procedure provides a fresh copper surface for film adhesion and the resulting films are able to withstand $\sim 1,000$ voltammetric cycles. Such scanning of a CuHCF film in 0.5 M K_2SO_4 gave a well-defined reversible couple at +0.69 V, characteristic of an adsorbed species. CuHCF films exhibit red/brown-to-yellow electrochromicity.¹⁴⁵ For the reduced film, a broad visible absorption band associated with the iron-to-copper CT in cupric ferrocyanide was observed ($\lambda_{\text{max}} = 490$ nm, $\lambda_{\text{max}} = 2 \times 10^3 \text{ dm}^3 \text{ mol}^{-1} \text{ cm}^{-1}$). This band was absent in the spectrum of the oxidized film, the yellow color arising from the $\text{CN}^- \rightarrow \text{Fe}^{\text{III}}$ CT band at 420 nm for the ferricyanide species.

The preparation of electrochromic palladium hexacyanoferrate films by simple immersion for at least one hour, or potential cycling of conducting substrates (Ir, Pd, Au, Pt, GC), in a mixed solution of PdCl_2 and $\text{K}_3\text{Fe}(\text{CN})_6$ has been reported.¹⁴⁹ The resulting modified electrodes gave broad CV responses, assigned to $\text{Fe}^{\text{III/II}}(\text{CN})_6$, the Pd^{II} sites being electroinactive. Films were orange at >1.0 V, yellow/green at <0.2 V.

Indium hexacyanoferrate films^{150–153} have been grown by potential cycling in a mixed solution containing InCl_3 and $\text{K}_3\text{Fe}(\text{CN})_6$. The electrodeposition occurs during the negative scans as sparingly soluble deposits of In^{3+} with $[\text{Fe}(\text{CN})_6]^{4-}$ were formed.¹⁵⁰ The resulting films are electrochromic, being white when reduced and yellow when oxidized.¹⁵³

Thin films of cadmium hexacyanoferrate,¹⁵⁴ (reversibly white to colorless on reduction¹⁴³) cobalt hexacyanoferrate,¹⁵⁵ (reversibly green/brown to dark green on reduction¹⁴³) manganese hexacyanoferrate,¹⁵⁶ (reversibly pale yellow to colorless on reduction¹⁴³) osmium(IV) hexacyanoruthenate,¹⁵⁷ ruthenium hexacyanoferrate,¹⁵⁸ silver hexacyanoferrate,⁹² titanium hexacyanoferrate,¹⁵⁹ (reversibly brown to pale yellow on reduction¹⁴³) copper heptacyanonitrosylferrate,¹⁶⁰ ferric carbonylpentacyanoferrate,⁹² ferric pentacyanonitroferrate,⁹² Ag^{I} -“crosslinked” nickel hexacyanoferrate¹⁶¹ (reversibly yellow to white on reduction¹⁴³) chromium hexacyanoferrate¹⁶² (reversibly blue to pale blue/gray on reduction¹⁴³), molybdenum hexacyanoferrate¹⁶³ (pink to red on reduction¹⁴³), rhenium hexacyanoferrate¹⁴³ (pale yellow to colorless on reduction¹⁴³), rhodium hexacyanoferrate¹⁴³ (pale yellow to colorless on reduction¹⁴³), and platinum hexacyanoferrate¹⁶⁴ (pale blue to colorless on reduction¹⁴³) have also been studied.

Glassy carbon electrodes have been modified with films of mixed metal hexacyanoferrates.¹⁵⁶ CVs of PB/nickel-hexacyanoferrate and PB/manganese-hexacyanoferrate films show electroactivity of both metal hexacyanoferrate components in each mixture. The authors suggest that the mixed metal hexacyanoferrates have a structure in which some of the outer sphere iron centers in the PB lattice are replaced by Ni^{2+} or Mn^{2+} , rather than being a co-deposited mixture of PB and nickel or manganese hexacyanoferrate. Although film colors are not reported, it seems likely that variation of metal hexacyanoferrate and electrodeposition solution composition would allow color choice in the resulting polyelectrochromic systems. The approach seems general, with PB/metal hexacyanoferrate (metal = Co, Cu, In, Cr, Ru) modified electrodes also being successfully prepared.

9.13.1.3.4 Near-infrared region electrochromic systems

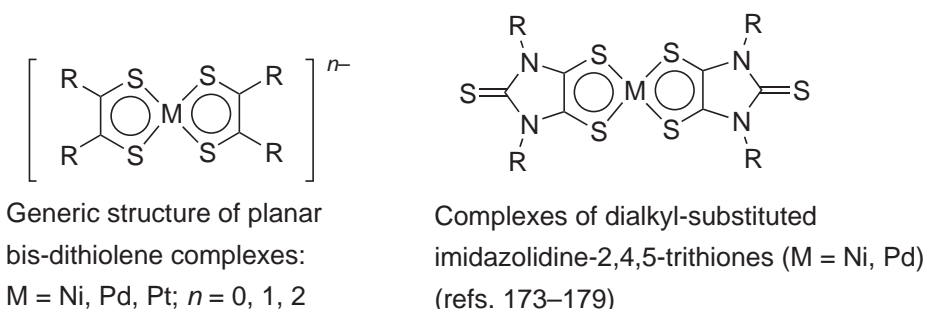
(i) Significance of the near-infrared region

The compounds and materials described so far have been of interest for their electrochromism in the visible region of the spectrum, a property which is of obvious interest for use in display devices. Electrochromism in the near-infrared (NIR) region of the spectrum (ca. 800–2,000 nm) is an area which has also attracted much recent interest⁹ because of the considerable technological importance of this region of the spectrum. NIR radiation finds use in applications as diverse as optical data storage (see later in this chapter); medicine, where photodynamic therapy exploits the relative transparency of living tissue to NIR radiation around 800 nm (see Chapter 9.22); and telecommunications, where fiber-optic signal transmission through silica fibers exploits the “windows of transparency” of silica in the 1,300–1,550 nm region. NIR radiation is also felt as radiant heat, so NIR-absorbing or reflecting materials could have use in “smart” windows which allow control of the environment inside buildings; and the fact that much of the solar emission spectrum is in the NIR region means that effective light-harvesting compounds for use in solar cells need to capture NIR as well as visible light (see Chapter 9.16).

Many molecules with strong NIR absorptions have been investigated, often with a view to examining their performance as dyes in optical data storage media.^{165–167} The majority of these are highly conjugated organic molecules which are not redox active. A minority, however, are based on transition metal components and it is generally these which have the redox activity necessary for electrochromic behavior and which are discussed in the following sections. One such set of complexes has already been discussed; spectral modulation in the NIR region has been reported for a variety of $[\text{Ru}(\text{bipy})_3]^{2+}$ derivatives, whose reduced forms contain ligand radical anions which show intense, low-energy electronic transitions. Since these are also electrochromic in the visible region, they were discussed earlier in Section 9.13.1.3.1(i).¹⁷ NIR electrochromic materials based on doped metal oxides¹⁶⁸ and conducting polymeric films¹⁶⁹ are also extensively studied but are outside the scope of this review.

(ii) Planar dithiolene complexes of Ni, Pd, and Pt

One of the earliest series of metal complexes which showed strong, redox-dependent near-IR absorptions is the well-known set of square-planar bis-dithiolene complexes of Ni, Pd, and Pt (Scheme 4). Extensive delocalization between metal and ligand orbitals in these “non-innocent” systems means that assignment of oxidation states is problematic, but does result in intense electronic transitions. These complexes have two reversible redox processes connecting the neutral, monoanionic, and dianionic species.



Scheme 4

The structures and redox properties of these complexes have been extensively reviewed,^{170,171} of interest here is the presence of an intense NIR transition in the neutral and mono-anionic forms, but not the dianionic forms, i.e., the complexes are polyelectrochromic. The positions of the NIR absorptions are highly sensitive to the substituents on the dithiolene ligands. A large number of substituted dithiolene ligands has been prepared and used to prepare complexes of Ni, Pd, and Pt which show comparable electrochromic properties with absorption maxima at wavelengths up to ca. 1,400 nm and extinction coefficients up to ca. $40,000 \text{ dm}^3 \text{ mol}^{-1} \text{ cm}^{-1}$ (see refs. 170,171 for an extensive listing).

The main application of the strong NIR absorbance of these complexes, pioneered by Müller-Westerhoff and coworkers, is for use in the neutral state as dyes to induce Q-switching of NIR lasers such as the Nd–YAG (1,064 nm), iodine (1,310 nm), and erbium (1,540 nm) lasers. This relies on a combination of very high absorbance at the laser wavelengths, an appropriate excited state lifetime following excitation, and good long-term thermal and photochemical stability. The use of a range of metal dithiolene complexes in this respect was reviewed in the first edition of CCC¹⁷¹ (and elsewhere).¹⁷² Since these reviews, however, the strong NIR absorptions of these complexes have continued to attract attention. A new series of neutral, planar dithiolenes of Ni and Pd has been prepared based on the ligands $[\text{R}_2\text{timdt}]^-$ which contain the dialkyl-substituted imidazolidine-2,4,5-trithione core (Scheme 4).^{173–179} In these ligands the peripheral ring system ensures that the electron-donating *N* substituents are coplanar with the dithiolene unit, maximizing the electronic effect which shifts the NIR absorptions of the $[\text{M}(\text{R}_2\text{timdt})_2]$ complexes to lower energy than found in the “parent” dithiolene complexes. The result is that the NIR absorption maximum occurs at around 1,000 nm and has a remarkably high extinction coefficient (up to $80,000 \text{ dm}^3 \text{ mol}^{-1} \text{ cm}^{-1}$). The high thermal and photochemical stabilities of these complexes make them excellent candidates for Q-switching of the 1,064 nm Nd–YAG laser. In addition, one-electron reduction to the monoanionic species $[\text{M}(\text{R}_2\text{timdt})_2]^-$ results in a shift of the NIR absorption maximum to ca. 1,400 nm, so there is also potential for exploiting their electrochromism.¹⁷⁹

(iii) Mixed-valence dinuclear complexes of ruthenium

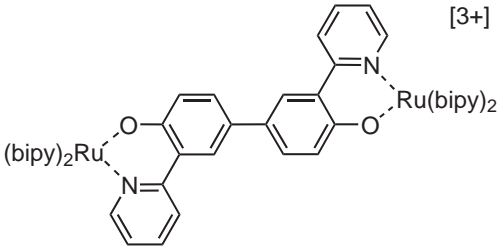
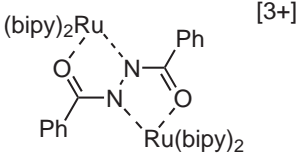
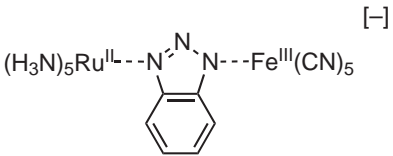
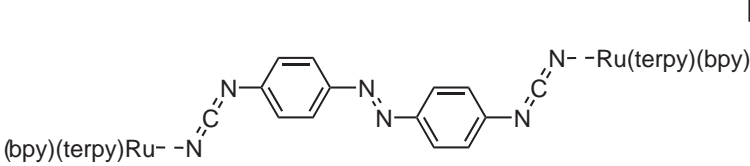
Another well-known class of metal complexes showing NIR electrochromism is the extensive series of dinuclear mixed-valence complexes based principally on ruthenium-ammine or ruthenium-polypyridine components, in which a strong electronic coupling between the metal centers makes a stable $\text{Ru}^{\text{II}}-\text{Ru}^{\text{III}}$ mixed-valence state possible. Such complexes generally show a $\text{Ru}^{\text{II}} \rightarrow \text{Ru}^{\text{III}}$ inter-valence charge-transfer (IVCT) transition which is absent in both the $\text{Ru}^{\text{II}}-\text{Ru}^{\text{II}}$ and $\text{Ru}^{\text{III}}-\text{Ru}^{\text{III}}$ forms. These complexes have primarily been of interest because the characteristics of the IVCT transition provide quantitative information on the magnitude of the electronic coupling between the metal centers, and is accordingly an excellent diagnostic tool. Nevertheless, the position and intensity of the IVCT transition in some cases mean that complexes of this sort could be exploited for their optical properties. Mixed-valence dinuclear complexes of this type are described in Volume 7; however Table 2 shows a small, representative selection of recent examples which show electrochromic behavior (in terms of the intensity of the IVCT transitions) typical of this class of complex.^{180–183} The main purpose of this selection is to draw the reader’s attention to the fact that these complexes which, as a class, are so familiar in a different context could be equally valuable for their electrochromic properties. Of course, the field is not limited to ruthenium complexes, although these have been the most extensively studied because of their synthetic convenience and ideal electrochemical properties; analogous complexes of other metals have also been prepared and could be equally effective NIR electrochromic dyes. (See Note Added in Proof.)

(iv) Tris(pyrazolyl)borato–molybdenum complexes

In the last few years McCleverty, Ward, and co-workers have reported the NIR electrochromic behavior of a series of mononuclear and dinuclear complexes containing the oxo- Mo^{V} core unit $[\text{Mo}(\text{Tp}^*)(\text{O})\text{Cl}(\text{OAr})]$, where “Ar” denotes a phenyl or naphthyl ring system [$\text{Tp}^* = \text{hydrotris}(3,5\text{-dimethylpyrazolyl})\text{borate}$].^{184–189} Mononuclear complexes of this type undergo reversible $\text{Mo}^{\text{IV}}/\text{Mo}^{\text{V}}$ and $\text{Mo}^{\text{V}}/\text{Mo}^{\text{VI}}$ redox processes with all three oxidation states accessible at modest potentials. Whilst reduction to the Mo^{IV} state results in unremarkable changes in the electronic spectrum, oxidation to Mo^{VI} results in the appearance of a low-energy phenolate- (or naphtholate)-to- Mo^{VI} LMCT process.^{184,185}

In mononuclear complexes these transitions are at the low energy end of the visible region and of moderate intensity: for $[\text{Mo}(\text{Tp}^*)(\text{O})\text{Cl}(\text{OPh})]$, for example, the LMCT transition is at 681 nm with $\epsilon = 13,000 \text{ dm}^3 \text{ mol}^{-1} \text{ cm}^{-1}$.¹⁸⁵ However, in many dinuclear complexes of the type $[\{\text{Mo}(\text{Tp}^*)(\text{O})\text{Cl}\}_2(\mu\text{-OC}_6\text{H}_4\text{EC}_6\text{H}_4\text{O})]$, in which two oxo- Mo^{V} fragments are connected by a bis-phenolate bridging ligand in which a conjugated spacer E separates the two phenyl rings,

Table 2 Examples of mixed-valence dinuclear complexes showing NIR electrochromism.

	$\lambda = 2,000 \text{ nm}$ $\epsilon = 14,000 \text{ dm}^3 \text{ mol}^{-1} \text{ cm}^{-1}$ (ref. 180)
	$\lambda = 1,600 \text{ nm}$ $\epsilon = 11,700 \text{ dm}^3 \text{ mol}^{-1} \text{ cm}^{-1}$ (ref. 181)
	$\lambda = 1,210 \text{ nm}$ $\epsilon = 3,900 \text{ dm}^3 \text{ mol}^{-1} \text{ cm}^{-1}$ (ref. 182)
	$\lambda = 1,920 \text{ nm}$ $\epsilon = 10,000 \text{ dm}^3 \text{ mol}^{-1} \text{ cm}^{-1}$ (ref. 183)

the NIR electrochromism is much stronger. In these complexes an electronic interaction between the two metals results in a separation of the two $\text{Mo}^{\text{V}}/\text{Mo}^{\text{VI}}$ couples, such that the complexes can be oxidized from the $\text{Mo}^{\text{V}}-\text{Mo}^{\text{V}}$ state to $\text{Mo}^{\text{V}}-\text{Mo}^{\text{VI}}$ and then $\text{Mo}^{\text{VI}}-\text{Mo}^{\text{VI}}$ in two distinct steps. The redox and magnetic properties of these complexes are discussed in detail in Chapter 2.58. The important point here is that in the oxidized forms, containing one or two Mo^{VI} centers, the LMCT transitions are at lower energy and of much higher intensity than in the mononuclear complexes (Figure 2 gives a representative example).^{185–187} Depending on the nature of the group E in the bridging ligand the absorption maxima can span the range 800–1,500 nm, with extinction coefficients of up to $50,000 \text{ dm}^3 \text{ mol}^{-1} \text{ cm}^{-1}$ (Table 3).^{185–187}

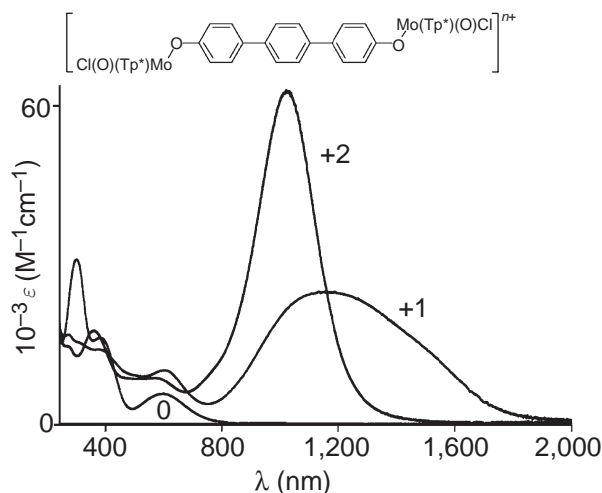
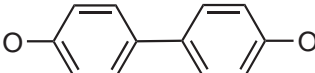
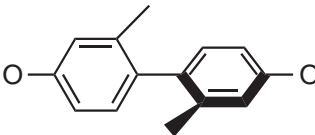

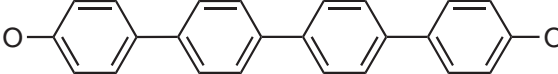
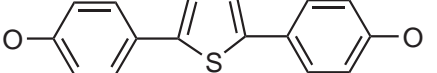
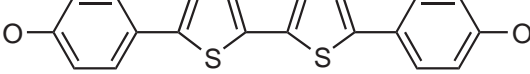
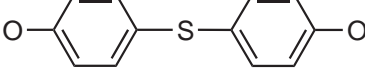
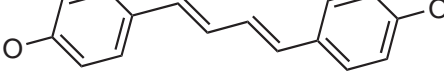
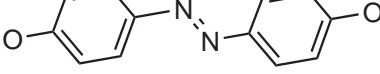



Figure 2 Electrochromic behavior of $[\{\text{Mo}(\text{Tp}^*)(\text{O})\text{Cl}\}_2(\mu\text{-OC}_6\text{H}_4\text{-C}_6\text{H}_4\text{-C}_6\text{H}_4\text{O})]^{n+}$ in the oxidation states $\text{Mo}^{\text{V}}-\text{Mo}^{\text{V}}$ ($n=0$), $\text{Mo}^{\text{V}}-\text{Mo}^{\text{VI}}$ ($n=1$), $\text{Mo}^{\text{VI}}-\text{Mo}^{\text{VI}}$ ($n=2$). Spectra were measured at 243 K in CH_2Cl_2 .¹⁸⁵

A prototypical device to illustrate the possible use of these complexes for modulation of NIR radiation has been described.¹⁸⁸ A thin-film cell was prepared containing a solution of an oxo-Mo^V dinuclear complex and base electrolyte between transparent, conducting glass slides. The complex used has the spacer E = bithienyl between the two phenolate termini (sixth entry in Table 3); this complex develops an LMCT transition (centered at 1,360 nm, with $\epsilon = 30,000 \text{ dm}^3 \text{ mol}^{-1} \text{ cm}^{-1}$) on one-electron oxidation to the Mo^V-Mo^{VI} state, which is completely absent in the Mo^V-Mo^V state. Application of an alternating potential, stepping between +1.5 V and 0 V for a few seconds each, resulted in fast switching on/off of the NIR absorbance reversibly over several thousand cycles. A larger cell was used to show how a steady increase in the applied potential of the solution, which resulted in a larger proportion of the material being oxidized, allowed the intensity of a 1,300 nm laser to be attenuated reversibly and controllably over a dynamic range of 50 dB (a factor of ca. 10^5): the cell accordingly acts as a NIR “variable optical attenuator”.¹⁸⁸ The disadvantage of this prototype is that, being solution-based, switching is relatively slow compared to thin films or solid state devices, but the optical properties of these complexes show great promise for further development.

Some nitrosyl-Mo^I complexes of the form [Mo(Tp*)(NO)Cl(py-R)] (where py-R is a substituted pyridine) also undergo moderate NIR electrochromism on reversible reduction to the Mo⁰ state. In these complexes reduction of the metal center results in appearance of a Mo⁰ \rightarrow py(π^*) MLCT

Table 3 Principal low-energy absorption maxima of dinuclear complexes $\{[\text{Mo}(\text{Tp}^*)(\text{O})\text{Cl}]_2 (\mu\text{-L})^{n+}$ in their oxidized forms ($n = 1, 2$).

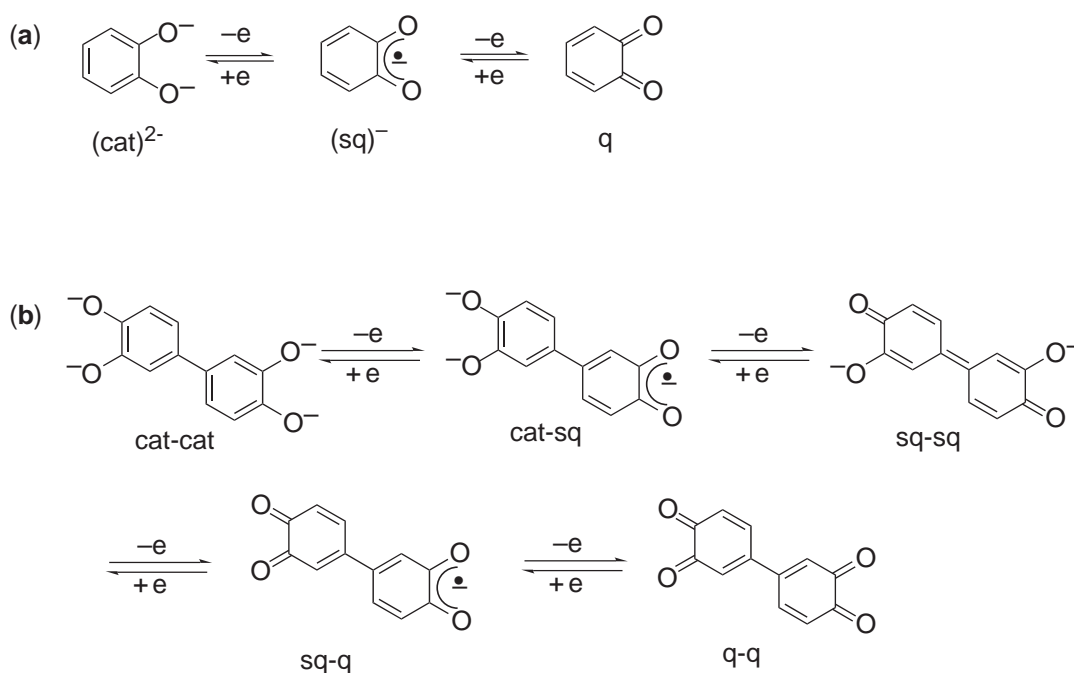
Bridging ligand <i>L</i>	λ_{max} , nm ($10^{-3} \epsilon$, $\text{dm}^3 \text{ mol}^{-1} \text{ cm}^{-1}$)	
	Mo ^V -Mo ^{VI}	Mo ^{VI} -Mo ^{VI}
	1,096 (50)	1,017 (48)
	1,245 (19)	832 (32)
	1,131 (25)	1,016 (62)
	1,047 (24)	1,033 (50)
	1,197 (35)	684 (54)
	1,360 (30)	(not stable)
	900 (10)	900 (20)
	1,210 (41)	(not stable)
	1,268 (35)	409 (38)
	1,554 (23)	978 (37)

transition at the red end of the spectrum (for $R = 4\text{-CH}^n\text{Bu}_2$, $\lambda_{\text{max}} = 830 \text{ nm}$ with $\epsilon = 12,000 \text{ dm}^3 \text{ mol}^{-1} \text{ cm}^{-1}$). However, when the pyridyl ligand contains an electron-withdrawing substituent meta to the N atom ($R = 3\text{-acetyl}$ or 3-benzoyl) an additional MLCT transition at much longer wavelength develops ($\lambda_{\text{max}} = 1,274$ and $1,514 \text{ nm}$, respectively, with $\epsilon = \text{ca. } 2,400 \text{ dm}^3 \text{ mol}^{-1} \text{ cm}^{-1}$ in each case).¹⁸⁹

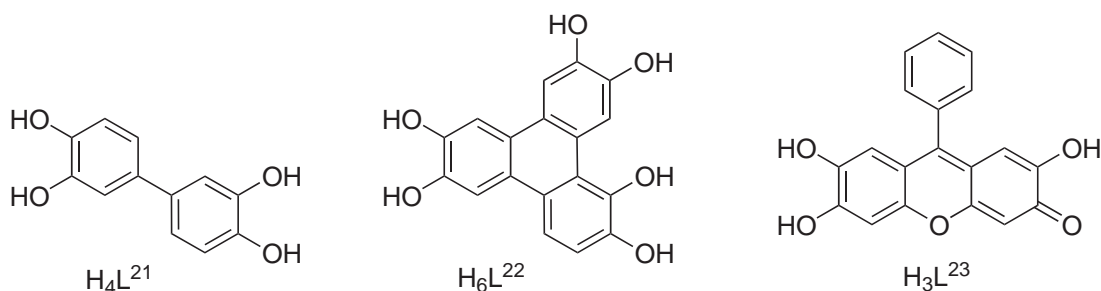
(v) Ruthenium and osmium dioxolene complexes

Lever and co-workers described in 1986 how the mononuclear complex $[\text{Ru}(\text{bipy})_2(\text{cat})]$, which has no NIR absorptions, undergoes two reversible oxidations which are ligand-centered cat/sq and sq/q couples (where “cat,” “sq,” and “q” are abbreviations for catecholate, 1,2-benzosemiquinone monoanion, and 1,2-benzoquinone respectively); see Scheme 5, showing ligand-based redox activity of (a) the catecholate/semiquinone/quinone series; (b) $[\text{L}^{21}]^{n-}$ ($n = 4-0$).¹⁹⁰ In the two oxidized forms the presence of a “hole” in the dioxolene ligand results in appearance of $\text{Ru}^{\text{II}} \rightarrow \text{sq}$ and $\text{Ru}^{\text{II}} \rightarrow \text{q}$ MLCT transitions, the former at 890 nm and the latter at 640 nm with intensities of ca. $10^4 \text{ dm}^3 \text{ mol}^{-1} \text{ cm}^{-1}$. The cat/sq and sq/q couples accordingly result in modest NIR electrochromic behavior (see structures $\text{L}^{21}\text{--L}^{23}$).

As with the oxo- Mo^{V} complexes mentioned in the previous section, the NIR transitions become far more impressive when two or more of these chromophores are linked by a conjugated bridging ligand, as in $[\{\text{Ru}(\text{bipy})_2\}_2(\mu\text{-L}^{21})]^{n+}$ ($n = 0-4$), which exhibits a five-membered redox chain, with reversible



Scheme 5



conversions between the fully reduced (bis-catecholate) and fully oxidized (bis-quinone) states all centered on the bridging ligand (Scheme 5b). In the state $n=2$, the NIR absorption is at 1,080 nm with $\epsilon = 37,000 \text{ dm}^3 \text{ mol}^{-1} \text{ cm}^{-1}$; this disappears in the fully reduced form and moves into the visible region in the fully oxidized form.¹⁹¹ Likewise, the trinuclear complex $[\{\text{Ru}(\text{bipy})_2\}_3(\mu\text{-L}^{22})]^{n+}$ ($n=3-6$) exists in four stable redox states based on redox interconversions of the bridging ligand (from sq-sq-sq to q-q-q; Figure 3).¹⁹² Thus, the complexes are polyelectrochromic, with a large number of stable oxidation states accessible in which the intense NIR MLCT transitions involving the oxidized forms of the bridging ligand are redox-dependent; an example is shown in Figure 3. In this (typical) example, the NIR transitions vary in wavelength between 759 and 1,170 nm over these four oxidation states, with intensities of up to $70,000 \text{ dm}^3 \text{ mol}^{-1} \text{ cm}^{-1}$. Other poly-dioxolene bridging ligands such as $[\text{L}^{23}]^{3-}$ have been investigated and their $\{\text{Ru}(\text{bipy})_2\}_2^{2+}$ complexes show comparable poly-electrochromic behavior in the NIR region.^{193,194} The analogous complexes with osmium have also been characterized and, despite the differences in formal oxidation state assignment of the components (e.g., Os^{III} -catecholate instead of Ru^{II} -semiquinone) also show similar NIR electrochromic behavior over several oxidation states.¹⁹⁵ Incorporation of these complexes into films or conducting solids, for faster switching, has yet to be described. (See Note Added in Proof.)

9.13.2 METAL COMPLEXES AS DYES FOR OPTICAL DATA STORAGE

9.13.2.1 Background

Optical Data Storage (ODS) concerns systems that use light for the recording and/or retrieval of information. This is not a new concept if one considers that the origins of the technology were founded in the first experiments in photography.¹⁹⁶ However, the fundamental principles of ODS were determined in the late 1960s, with much of the developmental work carried out at the Philips Research Laboratories, but it was the development of diode lasers in the late 1970s which was the breakthrough for commercialization of this technology.¹⁹⁷ Lasers enable the production of a beam with a power of several mW that can be focused to a spot of sub-micron size, thus facilitating huge data storage capacity at a very low cost per bit.^{196,197}

ODS technology exists in a wide range of formats including tape and fiche, and systems based on holographic imaging, but the formats which have achieved greatest commercial success are those based on direct bit data storage on disk media (Table 4),¹⁹⁶ and it is these formats which will be briefly discussed here. It can be seen that there are three main categories of ODS—Read Only, Write Once, and Rewriteable media. Each of these will be considered in more detail in Section 9.13.2.2.

ODS has several advantages over more traditional forms of data storage. Laser resolution permits the storage of data in a highly efficient areal manner, leading to a large data storage capacity, similar to a magnetic hard drive, but optical disks are also removable. In addition, the reading of information is a non-contact process, and, as a consequence, thousands of re-reads are possible without loss of data quality due to surface wear effects, in direct contrast to gramophone or magnetic tape recordings. Also of significance in the commercial success of this technology is the low cost for the media and hardware.^{196,197}

9.13.2.2 Optical Data Storage Categories

9.13.2.2.1 Read only media

Read Only media include the CD (Compact Disk), both Audio and CD-ROM (Read Only Memory) formats, and the more recently introduced DVD (Digital Versatile Disk) and DVD-ROM formats. DVD formats have a much higher data capacity than a CD-ROM, with the capacity depending on whether one or two recording layers are used. These read-only (i.e., pre-recorded) media are largely the domain of entertainment and software distribution and publishing.¹⁹⁶

The Compact Disk Digital Audio (CD-DA) was successfully introduced into the market in the early 1980s. It was designed to store at least one hour of high-quality stereo sound using digital techniques. Philips and Sony worked jointly on the specification for CD Audio, known as the *Red Book*. The use of compact disks was subsequently extended to the storage of computer data, with

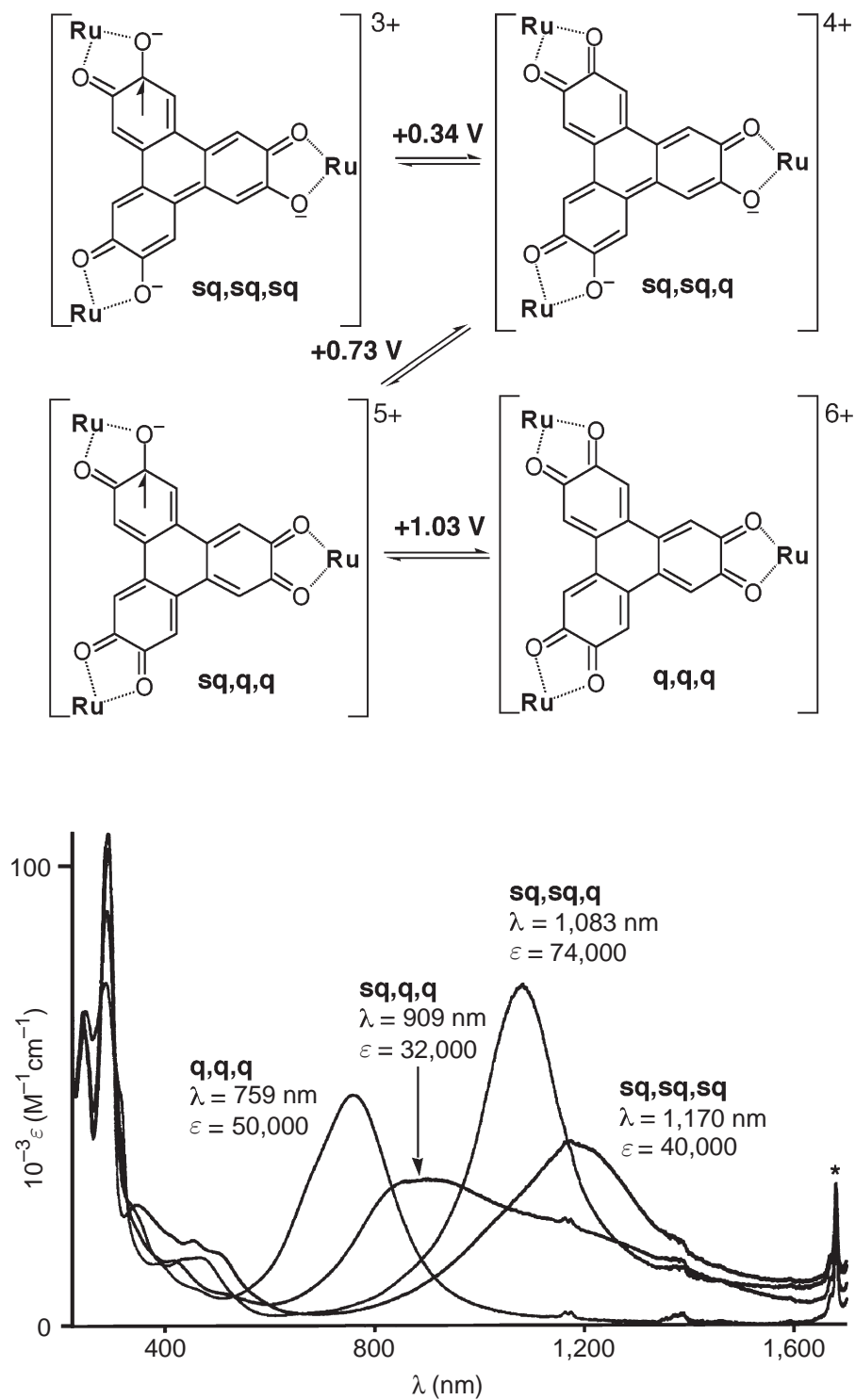


Figure 3 Ligand-centered redox interconversions of $[\{\text{Ru}(\text{bipy})_2\}_3(\mu\text{-L}^{22})]^{n+}$ ($n=3-6$) (potentials vs. SCE), and the resulting electrochromic behavior. Spectra were measured at 243 K in MeCN.¹⁹²

Table 4 Main optical data storage categories.

Type	Read only	Write once		Rewriteable	
Formats	CD CD-ROM	CD-R	WORM (various formats)	MO various formats	Phase Change CD-RW
	DVD DVD-ROM	DVD-R			DVD-RAM DVD-RW
Recording medium	—	Organic and Metal-organic dyes	Dyes/Te alloys	Rare earth- transition metal alloys	Group V,VI chalcogenides

the release of the Compact Disk-Read Only Memory (CD-ROM) in the mid-1980s, of *Yellow Book* specification.

CDs are 12 cm in diameter and 1.2 mm thick. They have a multi-layer structure as shown in Figure 4.

The pits are generally embossed into the substrate (polycarbonate or polymethylmethacrylate) layer by an injection-molding process, and are used to indicate whether a data bit is “0” or “1.” An aluminum or silver layer provides a reflective surface, and is protected from corrosion and damage by a radiation-cured acrylate (lacquer) layer, onto which a label is usually printed.¹⁹⁷

CD players use infrared light-emitting diode lasers (780 nm) to read the data from the pits. Light from the laser beam is scattered when it scans a pit, which is detected by a slight drop in the intensity of the reflected beam. This changing pattern of light is detected and decoded by the electronics of the player into the original audio or computer data signal.

DVD technology provides an optical storage system with a much larger capacity than the CD, for read-only, recordable, and rewriteable applications. Indeed, DVDs have the same physical dimension as CDs but comprise two substrates, of 0.6 mm thickness each, bonded together. This format provides several possible configurations of data layers (single/dual layer, and single/double sided), thus moving from 2D storage towards 3D storage. Each configuration is designed to provide additional storage capacity. This translates to up to 4.7 GB read-only capacity per layer, with a maximum of 8.5 GB per side. Another important feature is that new DVD players and DVD-ROM drives use red lasers at 650 nm and 635 nm (compared to CD players and CD-ROM drives which use infrared lasers at 780 nm). Wavelength is one of the parameters responsible for beam diameter, which translates into smaller and denser bits and therefore a higher information storage capacity. Also important for smaller and denser bits is the Numerical Aperture (NA), which is 0.6 for DVD compared to 0.45 for CD. A comparison between some of the physical parameters of CD and DVD disks is presented in Table 5. Table 6 outlines the common DVD formats. DVD-5 to DVD-18 all store prerecorded data (like CDs) which cannot be altered.

DVD-5 disks are single-sided, single-layer disks, with a capacity of 4.7 GB. They are constructed from two 0.6 mm substrates, one metallized and with data, the other blank, bonded together (Figure 5). Labels can be added, as for a CD. It can be seen that the basic structure is similar to that of a CD, but the major differences are the smaller spot size due to the use of a red laser, smaller bits, and tighter tracks, all resulting in an increased data storage capacity (approximately seven times that of a CD). A two-hour film requires about 4 GB of storage.¹⁹⁶

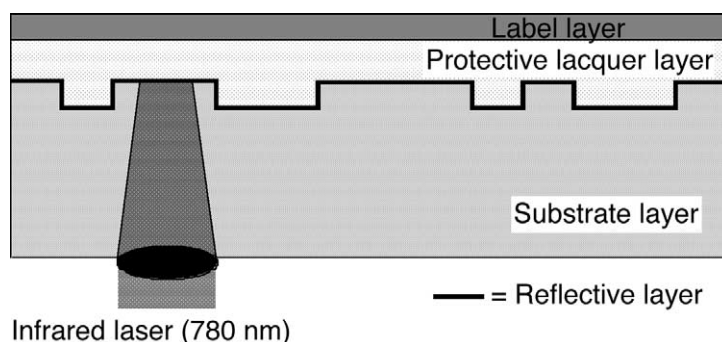
**Figure 4** Schematic representation of the structure of a standard compact disk.

Table 5 A comparison of some of the physical parameters of CD and DVD disks.

	CD	DVD
No. of sides	1	1 or 2
No. of layers per side	1	1 or 2
Capacity/GB*	ca. 0.7	4.7–17
Track pitch/microns	1.6	0.74
Minimum pit length/microns	0.83	0.4
Laser wavelength/nm	780	650 or 635
Numerical aperture	0.45	0.6

*1 GB (Gigabyte) = 10^9 bytes

Table 6 Common DVD formats.

DVD/CD Format	Media structure		Capacity (GB)
	No. sides	No. layers per side	
CD	1	1	ca. 0.7
DVD-5	1	1	4.7
DVD-9	1	2	8.54
DVD-10	2	1	9.4
DVD-18	2	2	17.08
DVD-R	1 or 2	1	4.7 or 9.4
DVD-RAM	1 or 2	1	4.7 or 9.4

The similarity between DVD and CD construction decreases with the next configuration, DVD-9, which uses two layers to store information, requiring two laser beams (but on the same side of the disk) to retrieve the data. These disks are single-sided, double-layer disks with 8.54 GB capacity due to their 3D storage. They comprise one semi-reflective substrate layer, which enables the second beam to reach the second layer which is fully metallized and hence fully reflective. The DVD-10 and DVD-18 formats use a double-sided disk design—a further improvement on CD design—and therefore contain up to four layers. Like a CD, these DVD configurations are all pre-recorded and therefore do not require the dyes that are used for data storage in the user-writable formats such as CD-R and DVD-R.

9.13.2.2.2 Write-once recordable media: CD-R and DVD-R

A viable real-time recording disk medium was developed in the mid 1980s, which became known as WORM (Write Once Read Many). However, there was no common standard for the medium, hence media produced by different manufacturers were incompatible, each requiring its own unique hardware. It is therefore not surprising that growth in this area was restricted and prices remained high.¹⁹⁶ This is in direct contrast to the industry-wide standards which helped lead to the successful introduction of CD technology.

CD-R disks are recordable disks that enable data to be written either once only, or in sessions on a multisession disk, allowing data to be updated and/or added to until the disk is full. However, the data on a CD-R disk cannot be erased or rewritten, hence CD-R disks are Write Once media, and are ideally suited to long-term data storage.

CD-R was something of a surprise invention as, in the late 1980s, most of the major manufacturers in the optical memory area were commercializing the non-standard and relatively expensive WORM media, while focusing their research and development efforts on erasable optical storage. It was also believed that a writable CD-Audio/CD-ROM-compatible medium was not feasible, due to the high reflectivity needed to meet the CD standard as defined by the *Red and Orange Books*.¹⁹⁶

A breakthrough came in 1988 when Hamada *et al.* demonstrated that a dye layer with a relatively low optical absorbance and high reflectance at the recording wavelength could be interposed between the substrate and reflecting layer of a CD-ROM type structure, and, with appropriate optimization of the optical properties, this would record and reproduce in accordance

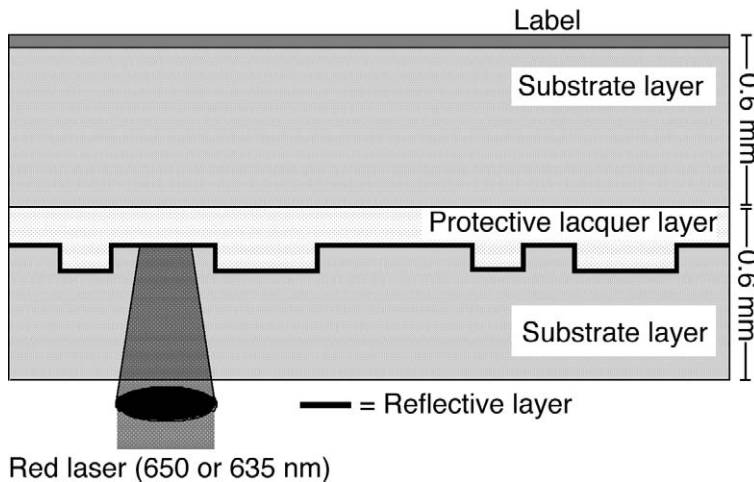


Figure 5 Schematic representation of the structure of a DVD-5 disk.

with the Philips/Sony compact disk standard and could therefore be read on a CD-ROM or CD-audio drive.^{198,199} Compatibility of CD-R media with the existing CD drives was assured by publication of the Standards in the *Orange Book* (Part 2). As CD drive prices fell through the 1990s, CD-R became a commercial success. It is the nature of this dye, which usually consists of a metal coordination complex based on highly conjugated ligands, which has a significant absorption maximum at or close to the wavelength of the laser, that is the focus of interest in this article.

The structure of a CD-R disk is accordingly slightly different from that of a CD because of this additional dye layer between the substrate and the reflective layer (Figure 6). The substrate contains a molded spiral pre-groove, enabling a tracking signal to be generated which guides the incident laser beam and improves the modulation of the recorded signal.

The molded disk containing the spiral pre-groove is made from a special grade of pure, dried polycarbonate, and is produced by injection molding. The dye formulation is dispensed onto the substrate by spin coating, after which a thin reflective layer (of gold or silver—due to their high reflectivity at the recording wavelength) is applied by sputtering. A protective UV-curable lacquer coating is also applied by spin coating, and finally, a hard coat and/or label can be added by screen printing.¹⁹⁹

A CD-R drive is different from a standard CD-ROM drive since the laser can be used at different power levels. The highest level is used to burn the pits on the disk surface, whereas the lowest level reads the data without any damage to the surface of the disk. The laser beam, modulated by the recording signal, is focused on the groove, and heats and subsequently melts the recording dye layer to form pits by which the binary data is stored. This mechanism is discussed in more detail in Section 9.13.2.3.2.

Recordable DVD formats are derived from those of CD, CD-R, and CD-RW, and consist of DVD, DVD-R (analogous to CD-R), DVD-ROM, DVD-RW, and an additional random-access, rewriteable-format DVD-RAM.¹⁹⁹ DVD-R is a recordable (dye-polymer) write-once format, with

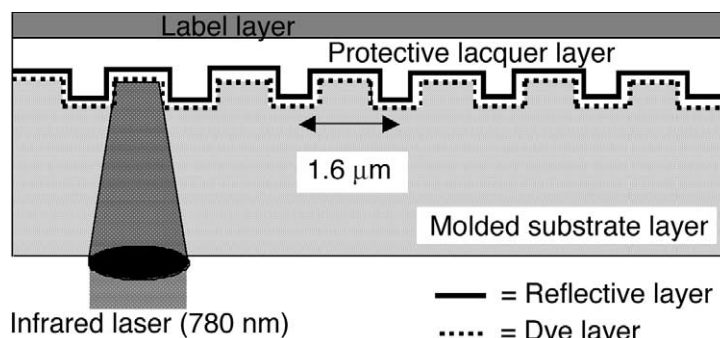


Figure 6 Schematic representation of the structure of a CD-R disk.

a capacity of up to 4.7 GB per side (Table 6). DVD-R media function on a similar principle to that of CD-R. The laser burns marks in a special dye layer causing localized changes in reflectivity. The shorter-wavelength laser required for DVD-R (630–655 nm, rather than 780 nm for CD-R) requires different dyes from those used in CD-R disks.

9.13.2.2.3 Rewriteable media

The rewriteable formats CD-RW and DVD-RW, which are becoming more popular, work in a fundamentally different way. The write-once media CD-R and DVD-R store the information as a series of holes in a dye layer; once the dye has been burnt away the process cannot, of course, be reversed. Rewriteable formats, in contrast, use in the recording layer materials which can undergo reversible phase changes, e.g., Ag–In–Sb–Te in CD-RW disks. The operation of a CD-RW drive is more complex than CD-R because it has to operate at three different power levels. The highest level is used for data recording, causing melting of the phase-change material, which rapidly cools to its recorded (amorphous) phase. The medium power level is used for erasure via annealing; the material in the recording layer heats and cools more gradually, resulting in the formation of the erased (crystalline) phase. The lowest level of laser power is used for data reading, without damaging the disk surface. The older magneto-optic (MO) storage media use a similar principle, except that the information is stored magnetically and read optically.¹⁹⁷ None of these rewriteable formats use dye molecules in the way that CD-R and DVD-R media do and they will not be discussed further.

9.13.2.3 Optical Data Storage on Write-once Media

9.13.2.3.1 Heat-mode recording

The mechanism of WORM recording (and indeed *all* optical disk media to date, including rewriteable media) is dependent on the heat generated by a focused laser beam, which impinges on an absorbing medium. The energy is transmitted to the absorbing medium much faster than the heat generated can be dissipated by thermal conduction. The subsequent rise in temperature depends on (i) laser pulse duration, power, and spot size; (ii) the absorption properties of the recording layer; and (iii) the thermal conductivity of the medium.¹⁹⁶

Heat dissipation occurs primarily by conduction, therefore organic materials having low thermal conductivities typically need less laser power for recording than other materials. Indeed, it has been found that a writing energy of just 0.1 nanojoule per square micron can give rise to a temperature rise sufficient to melt many plastics and dyes.¹⁹⁶

Upon irradiation, the dye molecules may form either excited singlet or triplet states (depending upon their structure), and, in the absence of photochemical reactions, may decay either radiatively or non-radiatively. Internal conversion is the predominant non-radiative process, i.e. the exchange of energy without change of spin state via a downward cascading process through vibrationally excited states, typically occurring in less than a few nanoseconds. Non-radiative energy loss may also be achieved by intersystem crossing. However, this process is less likely, and is strongly dependent on the electronic structure of the molecule. Intersystem crossing from a triplet to a singlet state occurs slowly, taking typically 0.01 to 1 seconds for purely organic dyes in the absence of a metal ion. In both processes, successively lower vibrational energy levels are occupied giving rise to heat production.¹⁹⁶

In addition to heat emission, radiative decay processes may also occur, in which light is emitted due to a transition from the lowest excited singlet or triplet state to the ground state (fluorescence or phosphorescence). In order to effect rapid and efficient conversion of optical energy (the laser) to heat, dyes which exhibit low fluorescence and in which excitation primarily involves the singlet states are the most suitable for heat-mode recording.¹⁹⁶

There are two thermal processes which can occur following the non-radiative decay, depending upon the heat generated: either melting, viscous flow and rapid cooling; or, at higher temperatures, evaporation or ablation, which result in the formation of a pit. If the recording material is reflective, the reflectivity will decrease in the exposed area and the signal will be detected as a change in intensity as the readout beam travels across the edge of the pit. As a consequence, well-defined pit edges are imperative in order to achieve high contrast and therefore low error rates.

The phenomenon of thin-film interference leads to an optimum condition for the film thickness in order to achieve the greatest change in the reflectivity of the medium. Subsequently, control of film thickness and uniformity across the disk are important factors in the practical implementation of this technology.¹⁹⁶

9.13.2.3.2 *CD-R: Recording mechanism*

The thickness of the all-important dye layer is carefully selected to achieve an absorbance of laser energy high enough to generate the heat necessary for heat-mode recording, whilst still allowing at least 60–65% of the incident light to be reflected back to the detector from the metal layer having passed twice through the dye layer. Typically, about 15–17% of the incident laser radiation is absorbed by the dye layer, and the temperature rise induced by the recording laser pulse is approximately 250–300 °C.²⁰⁰ This is substantially lower than the temperature achieved in typical WORM media (which are chosen to have very high optical absorption), but it is above the glass transition temperature of the substrate and the decomposition temperature of most organic dyes.^{196,199}

The subsequent thermal processes²⁰¹ give rise to diffusion of the polycarbonate substrate into the dye layer, decomposition of the dye, and mechanical deformation of the film due to thermal contraction. Each of these processes can contribute to a reduction in the optical path length of the low-intensity readout beam. The optics within the detector are designed such that phase differences due to the optical path length differences cause the light intensity falling on the detector to be reduced when the beam passes over a recorded “mark”.¹⁹⁶

The rate of dye decomposition should be negligible at exposure energies up to several thousand times the energy absorbed during the read process and increase rapidly thereafter. Dye compositions which exhibit this type of threshold behavior must have relatively high photochemical and thermal stability and decompose by a free radical process above the melting point of the substrate.¹⁹⁹

The recording modulation amplitude of all typical heat mode recording media depends on the recording layer possessing a high reflectivity at the record/read wavelength. The notion of a dye with a high reflectivity may seem a strange concept, but there is a fundamental relationship between the real part of the refractive index (n) and optical absorption, such that dyes with high extinction coefficients capable of forming stable films can exhibit a high refractive index at certain wavelengths depending on the position and shape of the absorption bands and the strength of the intermolecular interaction which occurs in the solid state. For CD-R and DVD-R recording, the wavelength dependence of the reflectivity and absorption is very important, as is the combination of low but finite absorbance and high reflection caused by a high refractive index.¹⁹⁹

9.13.2.3.3 *Brief history of development of dyes for optical data storage*

Much of the ground-breaking research on dyes for optical recording media was carried out in the 1970s and 1980s, and, at that time, the emphasis was on WORM media.¹⁹⁶ There are many classes of dyes which are potentially suitable for WORM media and excellent reviews of the patent and scientific literature have been published.^{166,202}

However, only a few compounds with good photo-stability, which absorb in the 750–850 nm range, have achieved commercial significance, and these belong to the polymethine, porphine, or triphenylmethane classes. In particular, phthalocyanine and naphthalocyanines, and cyanine dyes based on indole, benzindole, and benzthiazoles are the most widely used, mainly as a result of the ease with which their properties can be modified, and the relatively low cost of producing pure materials. These compounds can also be readily deposited onto a variety of substrates via spin coating from a solution, this being the method of lowest cost in producing uniform thin films. By the mid-1980s dyes began to replace the more expensive, toxic, and relatively unstable semi-metals such as tellurium alloys as the materials of choice. Due to the commercial impact of the use of GaAlAs diode lasers, virtually all dyes used commercially for WORM must have a high absorbance in the 780–850 nm region. The pioneering work on WORM dyes has provided a substantial resource for the selection of dyes suitable for CD-R and DVD-R.¹⁹⁶

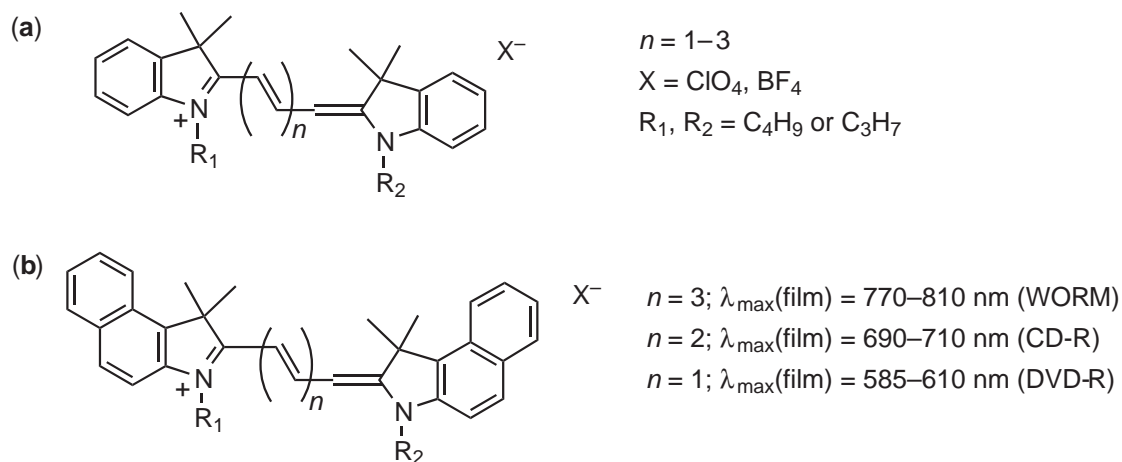
9.13.2.3.4 Specific requirements for dyes for optical disk recording

The following properties are generally required for all heat-mode optical recording applications:

- Appropriate absorbance and reflectivity of the solid film at the recording wavelength;
- Good oxidative and hydrolytic stability;
- Good solubility and solution stability in a suitable solvent for spin coating;
- Capacity to form uniform and stable solid films;
- Non-toxicity;
- Reasonable cost with significant potential for reduction as volume increases.¹⁹⁶

For WORM media, the film absorbance and reflectivity should both be high in the 775–830 nm range. For CD-R media the reflectivity should be high and the absorbance small but finite from 775 to 830 nm. For DVD-R, the requirements are the same as for CD-R, except that the critical wavelength range is 630–650 nm.¹⁹⁶

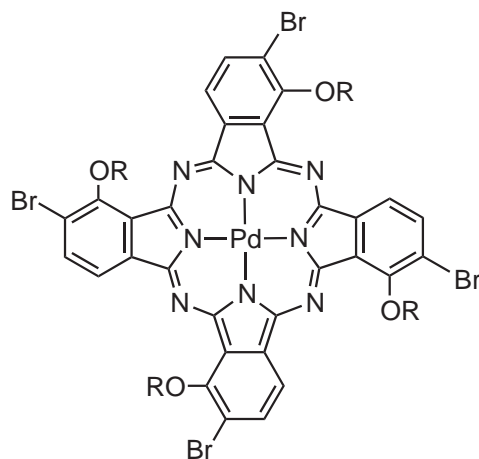
It is unsurprising that dyes that have become widely used in CD-R production fall into the same categories as those used for WORM media. As can be seen, most of the requirements are similar, except for the optical absorbance at the recording wavelength, which must be lower for CD-R than for WORM. Additionally, thicker films are generally used in CD-R, and the dye solubility in the solvent for spin coating must be higher. Classes of dye which have been found to be most suitable for CD-R are indole and benzindole–cyanine dyes (Scheme 6) and phthalocyanines (Scheme 2), which are the most widely used for mass production of CD-R media.^{196,199}



Scheme 6

The indole- and benzindole–cyanine dyes illustrated in Scheme 6 are used by many major manufacturers in optical disk recording applications. These types of dye tend to be more light-stable than many other readily synthesized polymethine dyes. To increase the photostability, the dyes are used in combination with various types of stabilizers such as nickel dithiolato complexes and selected tertiary aromatic amine compounds.¹⁹⁹ The application of cyanine dyes for optical storage media was primarily developed in Japan²⁰³ and several dyes and compatible stabilizers are commercially available in pure form from Japanese suppliers.¹⁹⁹

Phthalocyanine-based dyes are especially useful for CD-R, as the chromophore absorption band falls in the desirable spectral range, and they are noted for excellent photostability. Unlike cyanine dyes, phthalocyanines tend to have very poor solubility, particularly in solvents such as alcohols and aliphatic hydrocarbons (which do not attack polycarbonate and are therefore used for spin coating). Therefore, the main barrier to the wider use of these dyes is the relatively high cost of synthesizing soluble derivatives. Suitable modifications to the Pc core which have been developed, notably by Mitsui Toatsu, are shown in Scheme 7. The bulky R groups reduce undesirable molecular association (which in turn lower the extinction coefficient and hence reflectivity), whereas partial bromination allows fine-tuning of the film absorbance and reflectivity. The metal atom influences the position of the absorption band, the photostability, and the efficiency of the radiationless transition from the excited state.¹⁹⁹ This material is marketed by Ciba as Supergreen.²⁰⁴



Scheme 7

There are no clear advantages in terms of functional performance between the two classes of dyes, except that phthalocyanines are generally more light stable but tend to be more expensive to synthesize and modify. Phthalocyanine dyes are not suitable for DVD-R media, since the main chromophore cannot readily be modified to produce a sufficiently large hypsochromic shift. Other dyes potentially suitable for DVD-R include metal azo complexes, quinophthalones, and diphenylmethanes. The cyanine dyes are particularly useful as they can be readily modified to tailor the optical absorbance requirements for all current optical disk recording applications.¹⁹⁹

9.13.2.3.5 Phthalocyanines and related compounds

Unsubstituted naphthalocyanine and phthalocyanine complexes (Schemes 2 and 3) are pigments with broad absorption bands between 650 and 690 nm. The addition of sterically bulky pendant groups, e.g., siloxy, aryl, or alkyl ether or thioether moieties, gives rise to a bathochromic shift into the infrared region, and increases the solubility by hindering the ability of the macrocycles to form close molecular associations.¹⁹⁷ Phthalocyanines are useful as dyes for ODS as they have high absorption coefficients ($\epsilon > 10^5 \text{ dm}^3 \text{ mol}^{-1} \text{ cm}^{-1}$), they are thermally stable, they exhibit virtually no toxicity, they show exceptional stability towards atmospheric effects, and they may be applied to the substrate by sublimation, or, with appropriate substitution, by spin coating. Their absorption properties arise from the rigid, internal 18 π -electron system.¹⁶⁶

Vanadyl phthalocyanine (VOPc) was investigated for early use in ODS, and the findings were reported in 1981. At the time, high-power injection lasers (working in the 780–890 nm region) were used, and films of tellurium provided the recording medium (the principle of mark generation was by laser ablation of the metal). It was perceived that organic or metal–organic dyes had several advantages over metal layers, such as their chemical stability, insolubility in water, small heat conduction and enthalpy of melting per volume of dyes, the possibility of being spin coated, and their ability to be used in different types of anti-reflection layer structures.²⁰⁵

Thin films of VOPc were prepared by vapor deposition in vacuum on polymethylmethacrylate (PMMA) substrates, and the suitability for high-density optical storage of single, double, and triple layer structures containing such a film was investigated. Laser exposure was typically performed using a Krypton laser (799 nm). It was concluded that if VOPc was used in combination with a tellurium film, some reduction in power relative to single tellurium films could be achieved.²⁰⁵ The optical recording performance of vacuum-sublimed thin films of VOPc, and the tetra-pentyloxy (VOTPPc) and tetra-nonyloxy (VOTNPc) derivatives, have been investigated.²⁰⁶ The introduction of a vanadyl group in the phthalocyanine ring results in a red shift of the absorption wavelength, giving rise to a rather broad absorption region (580 to 850 nm) which matched the wavelength of semiconductor lasers and several other lasers in the visible to NIR region. A comparison of the optical writing characteristics of VOPc, VOTPPc, and VOTNPc indicated that a larger reflectivity contrast could be obtained at lower laser power and pulse width for a single layer of VOPc film. In addition, the morphology of the recording layer before and

after laser irradiation indicated that a sharp contrast was produced between laser-irradiated spots and the other regions, and both the static and dynamic optical recording tests demonstrated that VOPc could be used as a good WORM material.²⁰⁶

Phthalocyanine dyes with various central metal atoms and different substituents, which showed improved spectroscopic properties to match the output of a GaAs diode laser, were reported; smooth thin films were prepared by spin coating.²⁰⁷ Solvent-vapor induced crystallization of VO{Pc(OC₃H₇)₄} [Pc(OC₃H₇)₄ = tetra(propoxy)-phthalocyanine] was also studied. It was found that VO{Pc(OC₃H₇)₄} primarily deposited on a glass substrate in an amorphous form, but could be changed to a crystalline form by exposure to suitable solvent vapor. The polymorphs of VO{Pc(OC₃H₇)₄} were studied by a number of techniques, and the optical recording performances of the thin films were also reported.²⁰⁷

Thin films of the free-base phthalocyanine (H₂Pc) for use in optical recording were reported in 1985.²⁰⁸ H₂Pc was found to be thermally, hydrolytically, and oxidatively stable, and in all cases the writing mechanisms were found to be dependent on the sublimation of H₂Pc. Several recording structures, which took advantage of the sublimation property of H₂Pc, were demonstrated including pit-forming and bubble-forming media. These H₂Pc-based optical recording structures showed very high optical contrast and low writing threshold energies. In addition, very thin films (50–75 Å) of H₂Pc were incorporated into a tellurium-based medium, which significantly enhanced the writing contrast observed in that medium.²⁰⁸

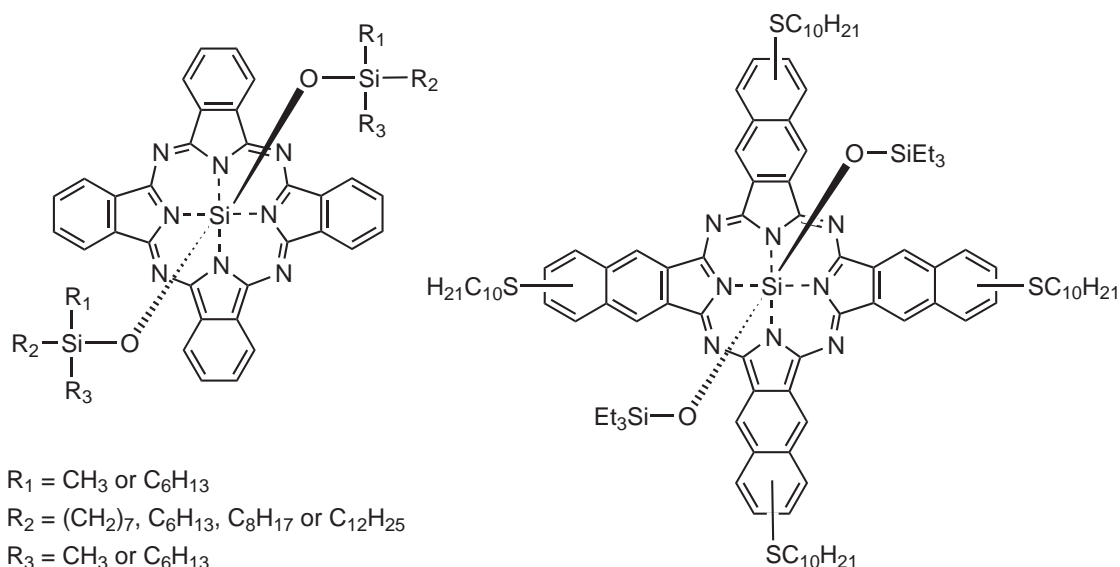
Copper phthalocyanine (CuPc) has also been investigated for use in ODS systems. In 1984, an optical disk medium comprising a multilayer film of tellurium and copper phthalocyanine was reported.²⁰⁹ The medium had high sensitivity, high carrier-to-noise ratio, and was stable. A trilayer medium, with CuPc between tellurium layers, showed 1.7 times better sensitivity than tellurium alone, with the same carrier-to-noise ratio. In addition, it was discovered that a fourth layer of CuPc could act as a protective overcoat against humidity, with only a small reduction in sensitivity (still 1.4 times better than tellurium alone).²⁰⁹ In 1994, CuPc was proposed as a potential ODS medium at short laser wavelength.²¹⁰ The optical writing characteristics of single-layer CuPc film and a CuPc film covered by a reflective layer were reported and analyzed.²¹¹ It was concluded that there was a relatively large absorption between 550 and 750 nm for a vacuum-sublimed CuPc film. The optical writing characteristics of a single CuPc film, and also of a CuPc film covered by a reflective layer (performed on a static optical recording tester) demonstrated that relatively high reflectivity contrast before and after laser irradiation could be achieved, indicating its suitability for application as a WORM material in ODS.²¹¹ It has also been reported that the dynamic optical recording test of a CuPc film covered by a reflective layer on a 5.25" glass substrate illustrated that the carrier-to-noise ratio of the disk was greater than 43 dB, again indicating promising potential of CuPc as a practical WORM medium.²¹²

Phase transitions of magnesium phthalocyanine (MgPc) and its application to optical recording of the Direct Reading After Writing (DRAW) type were investigated.²¹³ The maximum absorption of thin films of the x₁ form of MgPc, obtained from the treatment of a vacuum-deposited film with various halogenated solvents, shifted from 820 nm to 690 nm upon heat treatment above 110 °C. The spectral change was found to be based on a phase transition from the x₁ form to the α form through an intermediate phase. A coated film of x₁-type associates of MgPc, dispersed in a polymer matrix, was obtained from a solution of MgPc in chloroform and a polymer such as PMMA and poly(ethylene-co-vinyl acetate). The associated MgPc molecules were found to dissociate into monomers, depending on the polymer matrix, and to be dispersed homogeneously in the matrix after heat treatment. Irradiation (830 nm) of the vacuum-deposited film and coated film of x₁ type gave rise to an increase in transmittance, suggesting the possible application as an optical recording medium.²¹³ The near-IR absorption of MgPc complexes has been interpreted in terms of exciton coupling effects.²¹⁴

LB films of tetra-(*neo*-pentoxy)-phthalocyanine zinc (ZnTNPPc) and tetra-nonyl-phthalocyanine copper were reported.²¹⁵ Their structures, optical properties, and temperature dependencies were investigated. Static optical recording tests with a HeNe laser on the LB films demonstrated that the derivatives were useful for phase change-type (erasable) data storage media.²¹⁵ LB films of ZnTNPPc undergo two phase changes when treated at different temperatures.²¹⁶ The monomer dominates and the molecules are not uniformly oriented as deposited in the films. Once the films are heated to between 363 and 433 K, the dimer becomes dominant. A well-ordered structure in the LB film can be obtained, with the ZnTNPPc molecules arranged such that the phthalocyanine rings are perpendicular to the substrate surface. This phase change results in a decrease in the absorption coefficient at 680 nm, an increase at 620 nm, and the refractive index decreases. Upon heating at 573 K, a reorganization of the molecules in the ZnTNPPc LB film occurs; the

phthalocyanine rings reorient parallel to the substrate surface, and the monomer, with an ordered structure, becomes dominant. During this phase-change process, the absorption coefficient at 680 nm increases, that at 620 nm decreases, the strong peak moves from 620 to 700 nm, and the refractive index rises. Similar phase changes occur after the ZnTNPPc LB film undergoes laser energy treatment; the reflectance properties undergo related changes. The transformation from disordered monomer to ordered dimer occurs initially as the laser energy is slightly increased, with an associated reduction in reflectance, and a negative reflectivity contrast is obtained. As the laser energy is further increased, the transformation between the ordered dimer and ordered monomer occurs, and the reflectance increases until a positive saturation reflectivity contrast is reached. The writing, reading, and erasing are performed by laser irradiation in the ZnTNPPc LB film, and the initial results suggest that such films may be used as a new type of erasable optical storage medium.²¹⁶ Thin films of ZnTNPPc were more recently prepared by spin coating and vacuum sublimation.²¹⁷ The absorption spectra and X-ray diffraction of both types of thin film were measured at various temperature after annealing at various temperatures. Phase changes were found in the ZnTNPPc spin-coated film, but the evaporated thin film showed hardly any changes.²¹⁷

Silicon phthalocyanine-based dyes have also been studied for use in ODS. The synthesis, structural and conformational analysis, and chemical properties of some silicon phthalocyanine-based dyes (Scheme 8) were recently reported.²¹⁸



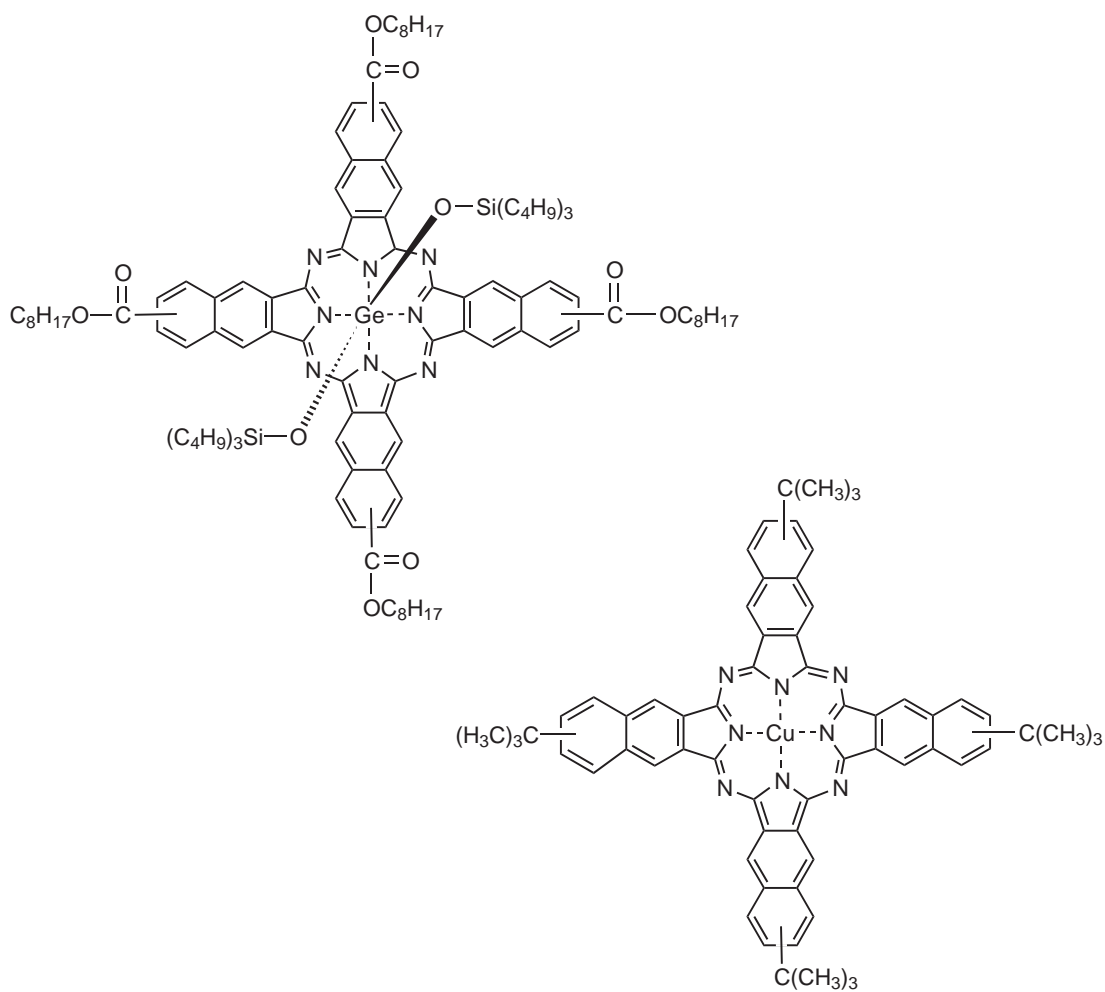
Scheme 8

A number of these dyes were applied, mixed with a polymer for the control of the aggregation state, to CD-R and DVD-R recording systems. The aggregation state in the recording layer was controlled by choosing the set of axial substituents (Scheme 8; R^1 , R^2 , and R^3). The interaction between the phthalocyanine dyes and the polymers was dependent on the length of the axial substituents; or, more carbon atoms in the alkyl group were found to be necessary for the axial substituents to mix with the polymers.²¹⁸

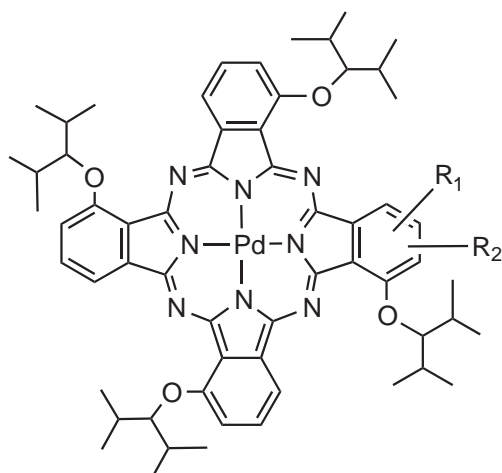
A novel rewriteable optical disk comprising a Si-naphthalocyanine dye (Scheme 8) and the conductive polymer polythiophene as the recording layer has been reported. The complex refractive index of the recording material changed reversibly, depending upon the aggregation states of the naphthalocyanine, induced by a conformational change of the polythiophene matrix. It was reported that the polythiophene/naphthalocyanine optical disk could be played back on conventional CD players, even after 10 cycles of rewriting.²¹⁹

Two naphthalocyanine derivatives (Scheme 9) were mixed together to improve read-out stability in a write-once optical storage system.²²⁰ The Ge derivative has a bulky structure with large side chains on the central atom, whilst the Cu derivative has a flat structure. The stability of the medium under 1 mW laser irradiation for read-out was improved 100-fold compared to that of a single-component system.²²⁰

The new phthalocyanine derivatives in Scheme 10 have recently been reported to be capable of recording high-quality signals at higher speeds.²²¹



Scheme 9



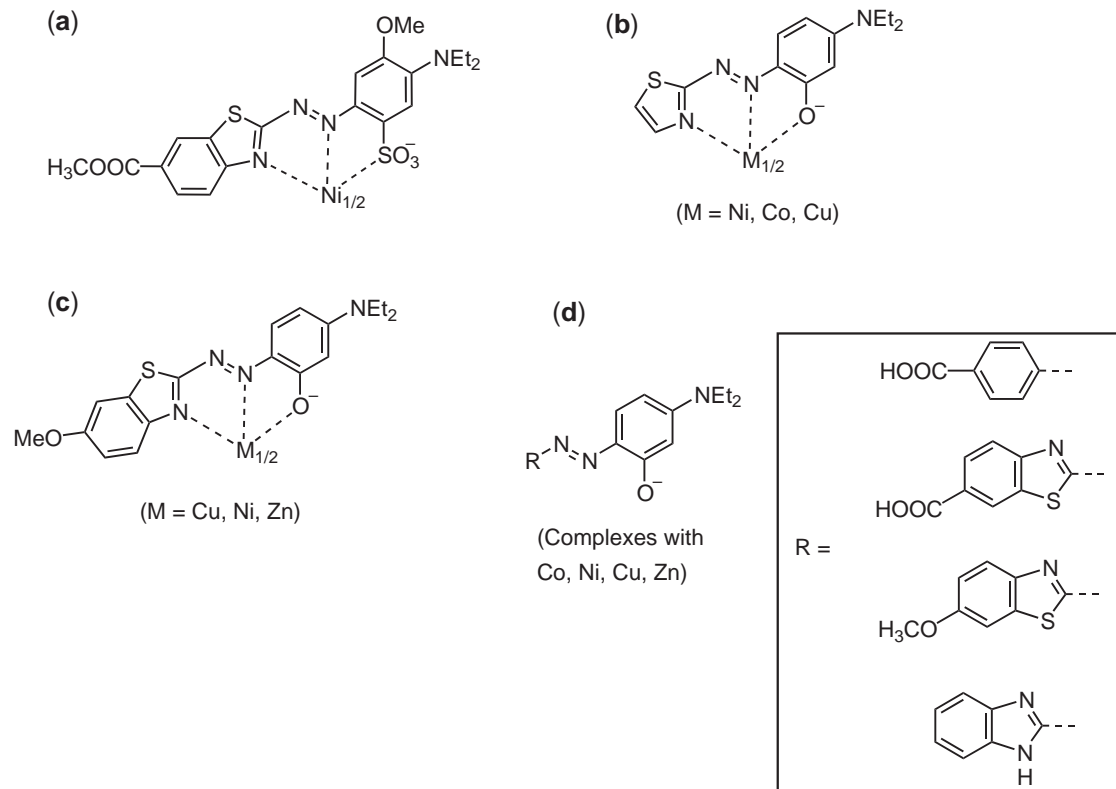
Scheme 10

It should be noted that the patent literature describes a vast number of phthalocyanine derivatives for use as CD-R dyes along the lines already described, with almost every conceivable combination of central metal, axial groups on the central metal, and peripheral substituents on the ligand; however, the difference between real and proposed molecules is not obvious, and experimental information and optical performance data is sketchy at best.

9.13.2.3.6 *Metal complexes of azo dyes*

The development of semiconductor diode lasers with wavelengths shorter than those used for CD-based systems means that there is a need for dyes which can exploit these wavelengths (635–650 nm) to obtain higher-density data storage, as in DVD media. Azo metal-chelate dyes can have absorption maxima in the appropriate region, and, coupled with their excellent light resistance and durability, are possible candidates for use in this respect. However, their recording and readability characteristics need to be improved.

Chelation of a metal to the azo and other groups in the azo dye gives rise to an improvement in the fastness of the metallized azo dye (see Chapter 9.12). A series of metallized thiazolyl-azo dyes with a hydroxy substituent ortho to the azo linkage, to provide a chelating ligand structure (Scheme 11), were subsequently prepared and evaluated and show promise as dyes for ODS.^{222,223} The complexes in Scheme 11c were also evaluated for use as DVD-R dyes; the Zn^{II} complex was felt to be the most promising candidate due to its good solubility, thermal stability, and a suitable absorption at 635 nm.²²⁴ The complexes in Scheme 11d were prepared in an attempt to obtain a high refractive index and good thermal stability for the dye; a variety of substituents R (benzoic acid, 6-methoxybenzothiazole, benzothiazole-6-carboxylic acid, and benzimidazole) were evaluated.²²⁵ The free dyes were reacted with metal ions such as Ni²⁺, Cu²⁺, Zn²⁺, and Co²⁺; the Zn²⁺ complex with R = 6-methoxybenzothiazole gave rise to a good absorption at 635 nm, thermal stability up to 300 °C, and a high refractive index of about 2.08.



Scheme 11

9.13.2.4 Future Developments

Several series of organic and metal–organic materials for optical data storage have been studied in recent years, but only the phthalocyanine and cyanine dyes for CD-R media have reached practical application.²²⁶

To increase the storage density, the tracking pitch and mark length both need to be reduced. In the region of far field optical recording, the diameter of the focused spot is proportional to λ/NA , where λ is writing and reading laser wavelength, and NA is the optical numerical aperture of the focusing lens. The practical approach to minimize the mark length is thus to decrease λ and to increase NA. After the decrease in laser wavelength from 780–800 nm (CD technology) to 630–650 nm (DVD technology), the next step is to use 400–500 nm (blue–green) lasers; development of dyes for these, as well as for current DVD-R technology, will require materials that are sensitive (to the laser, for reading and writing information), have long-term stability for archival storage, and have good recording performance at the appropriate wavelengths. Research is currently focusing on HD-DVD (430–500 nm) and SHD (200–350 nm).²²⁶

For archival storage, optical media are preferred to magnetic media because of longer lifetimes. As a consequence, long-term thermal and light stability is essential for new dye materials. Candidate materials can be divided into three approximate groups:

- Low stability—organic compounds with unsaturated carbon–hydrogen bonds, e.g., cyanines;
- Moderate stability—benzenoid organic compounds such as anthraquinones or compounds with unsaturated nitrogen bonds, such as azo-dyes;
- High stability—metallo-organic compounds such as porphyrin, phthalocyanine, metallized dyes, metallo-organic complexes.²²⁶

In general, coordination complexes and “metallized” dyes exhibit higher photochemical stability than purely organic molecules so it is clear that coordination chemistry has a major role to play in the future development of ODS media.

NOTE ADDED IN PROOF

Since this article was submitted, two examples have been published of ruthenium complexes incorporated into thin films which show near-infrared electrochromism with fast switching times (of the order of 1 second). One is a trinuclear Ru(II) complex which shows a typical inter-valence charge transfer transition at 1,550 nm in the mixed-valence Ru(II)-Ru(III) forms (see Section 9.13.1.3.4(iii)). The complex has pendant hydroxyl groups which react with a tri-isocyanate to give a crosslinked polymer which was deposited on an ITO substrate. Good electrochromic switching of 1,550 nm radiation was maintained over several thousand redox cycles.²²⁷ The second example consists of a mononuclear [Ru(bipy)₂(cat)] derivative (see Section 9.13.1.3.4(v)) bearing carboxylate substituents which anchor it to a nanocrystalline Sb-doped tin oxide surface; redox cycling of the catecholate/semiquinone couple results in electrochromic switching of the film at 940 nm as the Ru(II) → sq MLCT transition appears and disappears.²²⁸

9.13.3 REFERENCES

1. Monk, P. M. S.; Mortimer, R. J.; Rosseinsky, D. R. *Electrochromism: Fundamentals and Applications* 1995, 5VCH: Weinheim.
2. Granqvist, C. G. *Handbook of Inorganic Electrochromic Materials* 1995, Elsevier: Amsterdam.
3. Green, M. *Chem. Ind.* **1996**, 641–644.
4. Leventis, N. Electrochromic devices. In *McGraw-Hill Encyclopedia of science and Technology*, 8th ed. McGraw-Hill: New York, 1997; Vol. 6, pp 153–156.
5. Mortimer, R. J. *Chem. Soc. Rev.* **1997**, 26, 147–156.
6. Mortimer, R. J. *Electrochim. Acta* **1999**, 44, 2971–2981.
7. Rosseinsky, D. R.; Mortimer, R. J. *Adv. Mater.* **2001**, 13, 783–793.
8. Rauh, R. D. *Electrochim. Acta* **1999**, 44, 3165–3176.
9. Ward, M. D.; McCleverty, J. A. *J. Chem. Soc., Dalton Trans.* **2002**, 275–288.
10. Colley, R. A.; Budd, P. M.; Owen, J. R.; Balderson, S. *Polym. Int.* **2000**, 49, 371–376.
11. Grätzel, M. *Nature* **2001**, 409, 575–576.
12. Cummins, D.; Boschloo, G.; Ryan, M.; Corr, D.; Nagaraja Rao, S.; Fitzmaurice, D. *J. Phys. Chem. B* **2000**, 104, 11449–11459.
13. Zhang, S. S.; Qui, X. P.; Chou, W. H.; Liu, Q. G.; Lang, L. L.; Xing, B. Q. *Solid State Ionics* **1992**, 52, 287–289.

14. Juris, A.; Balzani, V.; Barigelletti, F.; Campagna, S.; Belser, P.; von Zelewsky, A. *Coord. Chem. Rev.* **1988**, *84*, 85–277.
15. Pichot, F.; Beck, J. H.; Elliott, C. M. *J. Phys. Chem. A* **1999**, *103*, 6263–6267.
16. Elliott, C. M.; Redepenning, J. G. *J. Electroanal. Chem.* **1986**, *197*, 219–232.
17. Elliott, C. M. *J. Chem. Soc., Chem. Commun.* **1980**, 261–262.
18. Elliott, C. M.; Hershenhart, E. J. *J. Am. Chem. Soc.* **1982**, *104*, 7519–7526.
19. Mortimer, R. J. *Dynamic processes in polymer modified electrodes. In Research in Chemical Kinetics*; Compton, R. G., Hancock G., Eds.; Elsevier: Amsterdam, 1994; Vol. 2, pp 261–311.
20. Ellis, C. D.; Margerum, L. D.; Murray, R. W.; Meyer, T. J. *Inorg. Chem.* **1983**, *22*, 1283–1291.
21. Horwitz, C. P.; Zuo, Q. *Inorg. Chem.* **1992**, *31*, 1607–1613.
22. Hanabusa, K.; Nakamura, A.; Koyama, T.; Shirai, H. *Polym. Int.* **1994**, *35*, 231–238.
23. Zhang, H.-T.; Subramanian, P.; Fussa-Rydal, O.; Bebel, J. C.; Hupp, J. T. *Sol. Energy Mater. Sol. Cells* **1992**, *25*, 315–325.
24. Beer, P. D.; Kocian, O.; Mortimer, R. J.; Ridgway, C.; Stradiotto, N. R. *J. Electroanal. Chem.* **1996**, *408*, 61–66.
25. Beer, P. D.; Kocian, O.; Mortimer, R. J. *J. Chem. Soc., Dalton Trans.* **1990**, 3283–3288.
26. Beer, P. D.; Kocian, O.; Mortimer, R. J.; Ridgway, C. *J. Chem. Soc., Faraday Trans.* **1993**, *89*, 333–338.
27. Beer, P. D.; Kocian, O.; Mortimer, R. J.; Ridgway, C. *J. Chem. Soc., Dalton Trans.* **1993**, 2629–2638.
28. Leasure, R. M.; Ou, W.; Moss, J. A.; Linton, R. W.; Meyer, T. J. *Chem. Mater.* **1996**, *8*, 264–273.
29. Mashiko, T.; Dolphin, D. Porphyrins, hydrophorphyrins, azaporphyrins, phthalocyanines, corroles, corrins and related macrocycles. In *Comprehensive Coordination Chemistry*; Wilkinson, G., Gillard, R. D., McCleverty, J. A., Eds.; Pergamon: Oxford, 1987, Vol. 2, Chapter 21.1.
30. Leznoff, C. C.; Lever, A. B. P., Eds. *Phthalocyanines: Properties and Applications*. Wiley: New York, Vol. 1 (1989); Vol. 2 (1993); Vol. 3 (1993); Vol. 4 (1996).
31. Passard, M.; Blanc, J. P.; Maleysson, C. *Thin Solid Films* **1995**, *271*, 8–14.
32. Moskalev, P. N.; Kirin, I. S. *Russ. J. Inorg. Chem.* **1970**, *15*, 7.
33. Collins, G. C. S.; Schiffrin, D. J. *J. Electroanal. Chem.* **1982**, *139*, 335–369.
34. Collins, G. C. S.; Schiffrin, D. J. *J. Electrochem. Soc.* **1985**, *132*, 1835–1842.
35. Nicholson, M. M.; Pizzarello, F. A. *J. Electrochem. Soc.* **1979**, *126*, 1490–1495.
36. Nicholson, M. M.; Pizzarello, F. A. *J. Electrochem. Soc.* **1980**, *127*, 821–827.
37. Nicholson, M. M.; Pizzarello, F. A. *J. Electrochem. Soc.* **1980**, *127*, 2617–2620.
38. Nicholson, M. M.; Pizzarello, F. A. *J. Electrochem. Soc.* **1981**, *128*, 1740–1743.
39. Pizzarello, F. A.; Nicholson, M. M. *J. Electrochem. Soc.* **1981**, *128*, 1288–1290.
40. Nicholson, M. M. *Ind. Eng. Chem., Prod. Res. Dev.* **1982**, *21*, 261–266.
41. Chang, A. T.; Marchon, J. C. *Inorg. Chim. Acta* **1981**, *53*, L241–L243.
42. Moskalev, P. N.; Shapkin, G. N. *Sov. Electrochem.* **1978**, *14*, 486–488.
43. Sammells, A. F.; Pujare, N. U. *J. Electrochem. Soc.* **1986**, *133*, 1065–1066.
44. Moskalev, P. N.; Shapkin, G. N.; Darovskikh, A. N. *Russ. J. Inorg. Chem.* **1979**, *24*, 188.
45. Green, J. M.; Faulkner, L. R. *J. Am. Chem. Soc.* **1983**, *105*, 2950–2955.
46. Kohno, Y.; Masui, M.; Ono, K.; Wada, T.; Takeuchi, M. *Jpn. J. Appl. Phys.* **1992**, *31*, L252–L253.
47. Silver, J.; Lukes, P.; Hey, P.; Ahmet, M. T. *J. Mater. Chem.* **1992**, *2*, 841–847.
48. Starke, M.; Androsche, I.; Hamann, C. *Phys. Status Solidi A* **1990**, *120*, K95–K99.
49. Silver, J.; Billingham, J.; Barber, D. J. In *The First Pacific Rim International Conference on Advanced Materials and Processing*; Shi, C., Li, H., Scott, A., Eds.; The Minerals, Metals and Materials Society, 1992.
50. Silver, J.; Lukes, P.; Houlton, A.; Howe, S.; Hey, P.; Ahmet, M. T. *J. Mater. Chem.* **1992**, *2*, 849–855.
51. Kahl, J. L.; Faulkner, L. R.; Dwarakanath, K.; Tackikawa, H. *J. Am. Chem. Soc.* **1986**, *108*, 5438–5440.
52. Silver, J.; Lukes, P.; Hey, P.; Ahmet, M. T. *J. Mater. Chem.* **1991**, *1*, 881–888.
53. Corbeau, P.; Riou, M. T.; Clarisse, C.; Bardin, M.; Plichon, V. *J. Electroanal. Chem.* **1989**, *274*, 107–115.
54. Petty, M.; Lovett, D. R.; Miller, J.; Silver, J. *J. Mater. Chem.* **1991**, *1*, 971–976.
55. Lukas, B.; Lovett, D. R.; Silver, J. *Thin Solid Films* **1992**, *210/211*, 213–215.
56. Muto, J.; Kusayanagi, K. *Phys. Status Solidi A* **1991**, *126*, K129–K132.
57. Silver, J.; Lukes, P.; Howe, S. D.; Howlin, B. *J. Mater. Chem.* **1991**, *1*, 29–35.
58. Frampton, C. S.; O'Connor, J. M.; Peterson, J.; Silver, J. *Displays* **1988**, *9*, 174–178.
59. Walton, D.; Ely, B.; Elliott, G. *J. Electrochem. Soc.* **1981**, *128*, 2479–2484.
60. Irvine, J. T. S.; Eiggins, B. R.; Grimshaw, J. J. *J. Electroanal. Chem.* **1989**, *271*, 161–172.
61. Leznoff, C. C.; Lam, H.; Marcuccio, S. M.; Nevin, W. A.; Janda, P.; Kobayashi, N.; Lever, A. B. P. *J. Chem. Soc., Chem. Commun.* **1987**, 699–701.
62. Nevin, W. A.; Hempstead, M. R.; Liu, W.; Leznoff, C. C.; Lever, A. B. P. *Inorg. Chem.* **1987**, *26*, 570–577.
63. Nevin, W. A.; Liu, W.; Greenberg, S.; Hempstead, M. R.; Marcuccio, S. M.; Melnik, M.; Leznoff, C. C.; Lever, A. B. P. *Inorg. Chem.* **1987**, *26*, 891–899.
64. Nevin, W. A.; Liu, W.; Lever, A. B. P. *Can. J. Chem.* **1987**, *65*, 855–858.
65. Nevin, W. A.; Liu, W.; Melnik, M.; Lever, A. B. P. *J. Electroanal. Chem.* **1986**, *213*, 217–234.
66. Yamana, M.; Kanda, K.; Kashiwazaki, N.; Yamamoto, M.; Nakano, T.; Walton, C. *Jpn. J. Appl. Phys.* **1989**, *28*, L1592–L1594.
67. Kashiwazaki, N. *Solar Energy Mater. Solar Cells* **1992**, *25*, 349–359.
68. Kashiwazaki, N. *Jpn. J. Appl. Phys.* **1992**, *31*, 1892–1896.
69. Moore, D. J.; Guarr, T. F. *J. Electroanal. Chem.* **1991**, *314*, 313–321.
70. Li, H. F.; Guarr, T. F. *J. Electroanal. Chem.* **1991**, *297*, 169–183.
71. Kimura, S.; Horai, T.; Hanabusa, K.; Shirai, H. *Chem. Letts.* **1997**, *7*, 653–654.
72. Besbes, S.; Plichon, V.; Simon, J.; Vaxiviere, J. *J. Electroanal. Chem.* **1987**, *237*, 61–68.
73. Jones, R.; Krier, A.; Davidson, K. *Thin Solid Films* **1997**, *298*, 228–236.
74. Granito, C.; Goldenberg, L. M.; Bryce, M. R.; Monkman, A. P.; Troisi, L.; Pasimeni, L.; Petty, M. C. *Langmuir* **1996**, *12*, 472–476.
75. Rodriguez-Méndez, M. L.; Souto, J.; de Saja, J. A.; Aroca, R. *J. Mater. Chem.* **1995**, *5*, 639–642.
76. Schlettwein, D.; Kaneko, M.; Yamada, A.; Wöhrle, D.; Jaeger, N. I. *J. Phys. Chem.* **1991**, *95*, 1748–1755.

77. Yanagi, H.; Toriida, M. *J. Electrochem. Soc.* **1994**, *141*, 64–70.
78. Guyon, F.; Pondaven, A.; L'Her, M. *J. Chem. Soc., Chem. Commun.* **1994**, 1125–1126.
79. Yamada, Y.; Kashiwazaki, N.; Yamamoto, M.; Nakano, T. *Displays* **1988**, *9*, 190–198.
80. Ng, D. K. P.; Jiang, J. *Chem. Soc. Rev.* **1997**, *26*, 433–442.
81. Silver, J.; Sosa-Sanchez, J. L.; Frampton, C. S. *Inorg. Chem.* **1988**, *37*, 411–417.
82. Dodd, J. W.; Hush, N. S. *J. Chem. Soc.* **1964**, 4607–4612.
83. Closs, G. L.; Closs, L. E. *J. Am. Chem. Soc.* **1963**, *85*, 818–819.
84. Felton, R. H.; Linschitz, H. *J. Am. Chem. Soc.* **1966**, *88*, 1112–1116.
85. Fajer, J.; Borg, D. C.; Forman, A.; Dolphin, D.; Felton, R. H. *J. Am. Chem. Soc.* **1970**, *92*, 3451–3459.
86. Fajer, R. H.; Dolphin, D.; Borg, D. C.; Fajer, J. *J. Am. Chem. Soc.* **1969**, *91*, 196–198.
87. Aziz, A.; Narasimhan, K. L.; Periasamy, N.; Maiti, N. C. *Philos. Mag. B-Phys. Condens. Matter Stat. Mech. Electron. Opt. Magn. Prop.* **1999**, *79*, 993–1004.
88. Diesbach (1704) cited in Gmelin, Handbuch der Anorganischen Chemie, Vol. 59, Teil B.
89. Fukuda, K. In *Pigment Handbook*, Lewis, P. A., Ed., 2nd. ed., Wiley Interscience, New York, 1986, Vol. 1, p 357.
90. Color Index 3rd. ed., Vol. 4, Society of Dyers and Colourists, Bradford, England, 1971, p 4673.
91. Neff, V. D. *J. Electrochem. Soc.* **1978**, *125*, 886–887.
92. Itaya, K.; Uchida, I.; Neff, V. D. *Acc. Chem. Res.* **1986**, *19*, 162–168 and Chapter 6 of ref. 1.
93. Karyakin, A. A. *Electroanalysis* **2001**, *13*, 813–819.
94. Chadwick, B. M.; Sharpe, A. G. *Adv. Inorg. Chem. Radiochem.* **1966**, *8*, 83–176.
95. Sharpe, A. G. *The Chemistry of Cyano Complexes of the Transition Metals* 1976, Academic Press: New York.
96. Dunbar, K. R.; Heintz, R. A. Chemistry of Transition Metal Cyanide Compounds: Modern Perspectives. In *Progress in Inorganic Chemistry*, Karlin, K. D., Ed.; J. Wiley: New York, 1997, Vol. 45, pp 283–391.
97. Bonnette, Jr., A. K.; Allen, J. F. *Inorg. Chem.* **1971**, *10*, 1613–1616.
98. Mayoh, B.; Day, P. *J. Chem. Soc., Dalton Trans.* **1974**, 846–852.
99. Keggins, J. F.; Miles, F. D. *Nature (London)* **1936**, *137*, 577–578.
100. Buser, H. J.; Schwarzenbach, D.; Petter, W.; Ludi, A. *Inorg. Chem.* **1977**, *16*, 2704–2710.
101. Ellis, D.; Eckhoff, M.; Neff, V. D. *J. Phys. Chem.* **1981**, *85*, 1225–1231.
102. Goncalves, R. M. C.; Kellawi, H.; Rosseinsky, D. R. *J. Chem. Soc., Dalton Trans.* **1983**, 991–994.
103. Mortimer, R. J.; Rosseinsky, D. R. *J. Electroanal. Chem.* **1983**, *151*, 133–147.
104. Mortimer, R. J.; Rosseinsky, D. R. *J. Chem. Soc., Dalton Trans.* **1984**, 2059–2061.
105. Itaya, K.; Ataka, T.; Toshima, S. *J. Am. Chem. Soc.* **1982**, *104*, 4767–4772.
106. Cheng, G. J.; Dong, S. J. *Electrochim. Acta* **1987**, *32*, 1561–1565.
107. Feldman, B. J.; Melroy, O. R. *J. Electroanal. Chem.* **1987**, *234*, 213–227.
108. Hamnett, A.; Higgins, S.; Mortimer, R. J.; Rosseinsky, D. R. *J. Electroanal. Chem.* **1988**, *255*, 315–324.
109. Mortimer, R. J.; Rosseinsky, D. R.; Glidle, A. *Solar Energy Mater. Solar Cells* **1992**, *25*, 211–223.
110. Millward, R. C.; Madden, C. E.; Sutherland, I.; Mortimer, R. J.; Fletcher, S.; Marken, F. *Chem. Commun* **2001**, 1994–1995.
111. Itaya, K.; Uchida, I. *Inorg. Chem.* **1986**, *25*, 389–392.
112. Emrich, R. J.; Traynor, L.; Gambogi, W.; Buhks, E. *J. Vac. Sci. Technol. A* **1987**, *5*, 1307–1310.
113. Lundgren, C. A.; Murray, R. W. *Inorg. Chem.* **1988**, *27*, 933–939.
114. Beckstead, D. J.; De Smet, D. J.; Ord, J. L. *J. Electrochem. Soc.* **1989**, *136*, 1927–1932.
115. Christensen, P. A.; Hamnett, A.; Higgins, S. J. *J. Chem. Soc., Dalton Trans.* **1990**, 2233–2238.
116. Stilwell, D. E.; Park, K. W.; Miles, M. H. *J. Appl. Electrochem.* **1992**, *22*, 325–331.
117. Itaya, K.; Shibayama, K.; Akahoshi, H.; Toshima, S. *J. Appl. Phys.* **1982**, *53*, 804–805.
118. Honda, K.; Ochiai, J.; Hayashi, H. *J. Chem. Soc., Chem. Commun.* **1986**, 168–170.
119. Honda, K.; Kuwana, A. *J. Electrochem. Soc.* **1986**, *133*, 853–854.
120. Carpenter, M. K.; Conell, R. S. *J. Electrochem. Soc.* **1990**, *137*, 2464–2467.
121. Honda, K.; Fujita, M.; Ishida, H.; Yamamoto, R.; Ohgaki, K. *J. Electrochem. Soc.* **1988**, *135*, 3151–3151.
122. Habib, M. A.; Maheswari, S. P.; Carpenter, M. K. *J. Appl. Electrochem.* **1991**, *21*, 203–207.
123. Habib, M. A.; Maheswari, S. P. *J. Electrochem. Soc.* **1992**, *139*, 2155–2157.
124. Béraud, J.-G.; Deroo, D. *Solar Energy Mater. Solar Cells* **1993**, *31*, 263–275.
125. Ho, K. C. *Electrochim. Acta* **1999**, *44*, 3227–3235.
126. Duek, E. A. R.; De Paoli, M.-A.; Mastragostino, M. *Adv. Mater.* **1992**, *4*, 287–291.
127. Duek, E. A. R.; De Paoli, M.-A.; Mastragostino, M. *Adv. Mater.* **1993**, *5*, 650–652.
128. Morita, M. *J. Appl. Poly. Sci.* **1994**, *52*, 711–719.
129. Jelle, B. P.; Hagen, G.; Nodland, S. *Electrochim. Acta* **1993**, *38*, 1497–1500.
130. Jelle, B. P.; Hagen, G. *J. Electrochem. Soc.* **1993**, *140*, 3560–3564.
131. Leventis, N.; Chung, Y. C. *J. Electrochem. Soc.* **1990**, *137*, 3321–3322.
132. Jelle, B. P.; Hagen, G. *J. Appl. Chem.* **1999**, *29*, 1103–1110.
133. Jelle, B. P.; Hagen, G. *Solar Energy Mater. Solar Cells* **1999**, *58*, 277–286.
134. Robin, M. B. *Inorg. Chem.* **1962**, *1*, 337–342.
135. Inoue, H.; Yanagisawa, S. *J. Inorg. Nucl. Chem.* **1974**, *36*, 1409–1411.
136. Wilde, R. E.; Ghosh, S. N.; Marshall, B. J. *Inorg. Chem.* **1970**, *9*, 2512–2516.
137. Rajan, K. P.; Neff, V. D. *J. Phys. Chem.* **1982**, *86*, 4361–4368.
138. Itaya, K.; Ataka, T.; Toshima, S. *J. Am. Chem. Soc.* **1982**, *104*, 3751–3752.
139. Carpenter, M. K.; Conell, R. S.; Simko, S. J. *Inorg. Chem.* **1990**, *29*, 845–850.
140. Dong, S. J.; Li, F. B. *J. Electroanal. Chem.* **1987**, *217*, 49–63.
141. Bocarsly, A. B.; Sinha, S. *J. Electroanal. Chem.* **1982**, *137*, 157–162.
142. Joseph, J.; Gomathi, H.; Rao, G. P. *Electrochim Acta* **1991**, *36*, 1537–1541.
143. Dillingham, J. L. PhD Thesis. Loughborough University, 1999.
144. Sinha, S.; Humphrey, B. D.; Fu, E.; Bocarsly, A. B. *J. Electroanal. Chem.* **1984**, *162*, 351–357.
145. Siperko, L. M.; Kuwana, T. *J. Electrochem. Soc.* **1983**, *130*, 396–402.
146. Siperko, L. M.; Kuwana, T. *J. Electrochem. Soc.* **1986**, *133*, 2439–2440.

147. Siperko, L. M.; Kuwana, T. *Electrochim. Acta* **1987**, *32*, 765–771.
148. Siperko, L. M.; Kuwana, T. *J. Vac. Sci. Technol. A* **1987**, *5*, 1303–1306.
149. Jiang, M.; Zhao, Z. F. *J. Electroanal. Chem.* **1990**, *292*, 281–287.
150. Kulesza, P. J.; Faszynska, M. *J. Electroanal. Chem.* **1988**, *252*, 461–466.
151. Kulesza, P. J.; Faszynska, M. *Electrochim. Acta* **1989**, *34*, 1749–1753.
152. Dong, S. J.; Jin, Z. *Electrochim. Acta* **1989**, *34*, 963–968.
153. Jin, Z.; Dong, S. J. *Electrochim. Acta* **1990**, *35*, 1057–1060.
154. Luangdilok, C. H.; Arent, D. J.; Bocarsly, A. B.; Wood, R. *Langmuir* **1992**, *8*, 650–657.
155. Joseph, J.; Gomathi, H.; Prabhakar Rao, G. *J. Electroanal. Chem.* **1991**, *304*, 263–269.
156. Bharathi, S.; Joseph, J.; Jeyakumar, D.; Prabhakara Rao, G. *J. Electroanal. Chem.* **1991**, *319*, 341–345.
157. Cox, J. A.; Das, B. K. *J. Electroanal. Chem.* **1987**, *233*, 87–98.
158. Kulesza, P. J. *J. Electroanal. Chem.* **1987**, *220*, 295–309.
159. Jiang, M.; Zhou, X. Y.; Zhao, Z. F. *J. Electroanal. Chem.* **1990**, *292*, 289–296.
160. Gao, Z.; Zhang, Y.; Tian, M.; Zhao, Z. *J. Electroanal. Chem.* **1993**, *358*, 161–176.
161. Kulesza, P. J.; Jedral, T.; Galus, Z. *Electrochim. Acta* **1989**, *34*, 851–853.
162. Jiang, M.; Zhou, X.; Zhao, Z. *J. Electroanal. Chem.* **1990**, *287*, 389–394.
163. Dong, S.; Jin, Z. *J. Electroanal. Chem.* **1988**, *256*, 193–198.
164. Liu, S. Q.; Li, H. L.; Jiang, M.; Li, P. B. *J. Electroanal. Chem.* **1997**, *426*, 27–30.
165. Fabian, J.; Nakazumi, H.; Matsuoka, M. *Chem. Rev.* **1992**, *92*, 1197–1226.
166. Emmelius, M.; Pawlowski, G.; Vollmann, H. W. *Angew. Chem. Int. Ed. Engl.* **1989**, *28*, 1445–1471.
167. Fabian, J.; Zahradnik, R. *Angew. Chem. Int. Ed. Engl.* **1989**, *28*, 677–694.
168. Franke, E. B.; Trimble, C. L.; Hale, J. S.; Schubert, M.; Woollam, J. A. *J. Appl. Phys.* **2000**, *88*, 5777–5784.
169. Schwendeman, I.; Hwang, J.; Welsh, D. M.; Tanner, D. B.; Reynolds, J. R. *Adv. Mater.* **2001**, *13*, 634–637.
170. McCleverty, J. A. *Prog. Inorg. Chem.* **1968**, *10*, 49–221.
171. Mueller-Westerhoff, U. T.; Vance, B. Dithiolenes and related species. In *Comprehensive Coordination Chemistry*; Wilkinson, G., Gillard, R. D., McCleverty, J. A., Eds.; Pergamon: Oxford, 1987, Vol. 2, pp 595–631.
172. Mueller-Westerhoff, U. T.; Vance, B.; Yoon, D. I. *Tetrahedron* **1991**, *47*, 909–932.
173. Bigoli, F.; Deplano, P.; Devillanova, F. A.; Lippolis, V.; Lukes, P. J.; Mercuri, M. L.; Pellinghelli, M. A.; Trogu, E. F. *J. Chem. Soc., Chem. Commun.* **1995**, 371–372.
174. Bigoli, F.; Deplano, P.; Mercuri, M. L.; Pellinghelli, M. A.; Pintus, G.; Trogu, E. F.; Zonedda, G.; Wang, H. H.; Williams, J. M. *Inorg. Chim. Acta* **1998**, *273*, 175–183.
175. Bigoli, F.; Deplano, P.; Devillanova, F. A.; Ferraro, J. R.; Lippolis, V.; Lukes, P. J.; Mercuri, M. L.; Pellinghelli, M. A.; Trogu, E. F.; Williams, J. M. *Inorg. Chem.* **1997**, *36*, 1218–1226.
176. Arca, M.; Demartin, F.; Devillanova, F. A.; Garau, A.; Isaia, F.; Lelj, F.; Lippolis, V.; Pedraglio, S.; Verani, G. *J. Chem. Soc., Dalton Trans.* **1998**, 3731–3736.
177. Aragoni, M. C.; Arca, M.; Demartin, F.; Devillanova, F. A.; Garau, A.; Isaia, F.; Lelj, F.; Lippolis, V.; Verani, G. *J. Am. Chem. Soc.* **1999**, *121*, 7098–7107.
178. Bigoli, F.; Cassoux, P.; Deplano, P.; Mercuri, M. L.; Pellinghelli, M. A.; Pintus, G.; Serpe, A.; Trogu, E. F. *J. Chem. Soc., Dalton Trans.* **2000**, 4639–4644.
179. Deplano, P.; Mercuri, M. L.; Pintus, G.; Trogu, E. F. *Comments Inorg. Chem.* **2001**, *22*, 353–374.
180. Laye, R. H.; Couchman, S. M.; Ward, M. D. *Inorg. Chem.* **2001**, *40*, 4089–4092.
181. Kasack, V.; Kaim, W.; Binder, H.; Jordanov, J.; Roth, E. *Inorg. Chem.* **1995**, *34*, 1924–1933.
182. Rocha, R. C.; Toma, H. E. *Can. J. Chem.* **2001**, *79*, 145–156.
183. Mosher, P. J.; Yap, G. P. A.; Crutchley, R. J. *Inorg. Chem.* **2001**, *40*, 1189–1195.
184. Lee, S.-M.; Marcaccio, M.; McCleverty, J. A.; Ward, M. D. *Chem. Mater.* **1998**, *10*, 3272–3274.
185. Harden, N. C.; Humphrey, E. R.; Jeffrey, J. C.; Lee, S.-M.; Marcaccio, M.; McCleverty, J. A.; Rees, L. H.; Ward, M. D. *J. Chem. Soc., Dalton Trans.* **1999**, 2417–2426.
186. Bayly, S. R.; Humphrey, E. R.; de Chair, H.; Paredes, C. G.; Bell, Z. R.; Jeffrey, J. C.; McCleverty, J. A.; Ward, M. D.; Totti, F.; Gatteschi, D.; Courric, S.; Steele, B. R.; Scretttas, C. G. *J. Chem. Soc., Dalton Trans.* **2001**, 1401–1414.
187. McDonagh, A. M.; Ward, M. D.; McCleverty, J. A. *New J. Chem.* **2001**, *25*, 1236–1243.
188. McDonagh, A. M.; Bayly, S. R.; Riley, D. J.; Ward, M. D.; McCleverty, J. A.; Cowin, M. A.; Morgan, C. N.; Varrazza, R.; Penty, R. V.; White, I. H. *Chem. Mater.* **2000**, *12*, 2523–2524.
189. Kowallick, R.; Jones, A. N.; Reeves, Z. R.; Jeffrey, J. C.; McCleverty, J. A.; Ward, M. D. *New J. Chem.* **1999**, *23*, 915–921.
190. Haga, M.; Dodsworth, E. S.; Lever, A. B. P. *Inorg. Chem.* **1986**, *25*, 447–453.
191. Joulié, L. F.; Schatz, E.; Ward, M. D.; Weber, F.; Yellowlees, L. J. *J. Chem. Soc., Dalton Trans.* **1994**, 799–804.
192. Barthram, A. M.; Cleary, R. L.; Kowallick, R.; Ward, M. D. *Chem. Commun.* **1998**, 2695–2696.
193. Barthram, A. M.; Ward, M. D. *New J. Chem.* **2000**, *24*, 501–504.
194. Barthram, A. M.; Cleary, R. L.; Jeffrey, J. C.; Couchman, S. M.; Ward, M. D. *Inorg. Chim. Acta* **1998**, *267*, 1–5.
195. Barthram, A. M.; Reeves, Z. R.; Jeffrey, J. C.; Ward, M. D. *J. Chem. Soc., Dalton Trans.* **2000**, 3162–3169.
196. Hurditch, R. *Adv. Color Sci. Technol.* **2001**, *4*, 33–40.
197. Hunt, P. A. Optical Data-Storage Systems. In *Chemistry and Technology of Printing and Imaging Systems*; Gregory, P., Ed.; Blackie: London, 1996.
198. Hamada, E.; Shin, Y.; Ishiguro, T. *Proc. SPIE* **1989**, *1078*, 80.
199. Hurditch, R. Dyes for Optical Storage Disc Media. *Chemichromics '99*, New Orleans, Jan 27–29, 1999.
200. Novotny, V.; Alexandru, L. *J. Appl. Phys.* **1979**, *50*, 1215–1221.
201. Holtslag, A. H. M.; McCord, E. F.; Werumeus Buning, G. H. *Jpn. J. Appl. Phys.* **1992**, *31*, 484.
202. Kuder, J. E. Proc. SPIE 40th Annual Conference, 1987, May 17–22.
203. Matsui, F. Optical Recording Systems. In *Infrared Absorbing Dyes*, Matsuoka, M., Ed., Plenum, 1990. Chapter 10.
204. Ciba, *Supergreen Product Dossier*, Issue 2.0, November 1999.
205. Kivits, P.; de Bont, R.; van der Veen, J. *J. Appl. Phys.* **1981**, *A26*, 101–105.
206. Gu, D.; Chen, Q.; Shu, J.; Tang, X.; Gan, F.; Shen, S.; Liu, K.; Xu, H. *Thin Solid Films* **1995**, *257*, 88–93.

207. Shen, S.; Liu, K.; Huijun, X.; Gu, D.; Tang, F.; Chen, Q. Spectroscopic properties of phthalocyanine dyes for optical recording medium. *Proc. SPIE* Vol. 2931, 73–77. Fourth International Symposium on Optical Storage (ISOS '96), Gan, F.X., Ed.
208. Dautartas, M. F.; Suh, S. Y.; Forrest, S. R.; Kaplan, M. L.; Lovinger, A. J.; Schmidt, P. H. *Appl. Phys. A* **1985**, *36*, 71–79.
209. Goto, Y.; Koshino, N.; Itoh, K.-I. *Fujitsu Sci. Tech. J.* **1984**, *20*, 411–429.
210. Gu, D.; Chen, Q.; Gan, F. Optical Data Recording Using Copper Phthalocyanine in Short-Wavelength Region. *Proc. SPIE* Vol. 2273, 226–233, Ultrahigh and High-Speed Photography, Videography, and Photonics '94, Kyrala, G. A., Snyder, D.R. Eds.
211. Chen, Q.; Gu, D.; Shu, J.; Tang, X.; Gan, F. *Mater. Sci. Eng.* **1994**, *B25*, 171–174.
212. Chen, Q.; Gu, D.; Gan, F. *Solid-State Electron.* **1994**, *37*, 1768–1770.
213. Daidoh, T.; Matsuzawa, H.; Iwata, K. *Nippon Kagaku Kaishi* **1988**, *7*, 1090–1097.
214. Endo, A.; Matsumoto, S.; Mizuguchi, J. *J. Phys. Chem. A* **1999**, *103*, 8193–8199.
215. Fuxi, G.; Tao, L. Optical properties and recording characteristics of phthalocyanine-derivative LB films. *Proc. SPIE* Vol. 2053, 95–105. Optical Storage: Third International Symposium, Fuxi, G. Ed.
216. Tao, L.; Fuxi, G. *Appl. Opt.* **1994**, *33*, 3760–3763.
217. Yin, J.; Gu, D.; Tang, F.; Tang, X.; Gan, F. Comparison of two types of phthalocyanine thin films. *Proc. SPIE, Optical Storage Technology*, Xu, D.; Ogawa, S., Eds.; **1998**, *3562*, 174–178.
218. Sasa, N.; Okada, K.; Nakamura, K.; Okada, S. *J. Mol. Struct.* **1998**, *446*, 163–178.
219. Tomiyama, T.; Watanabe, I.; Kuwano, A.; Habiro, K.; Takane, N.; Yamada, M. *Appl. Opt.* **1995**, *34*, 8201–8208.
220. Kobayashi, S.; Iwasaki, K.; Sasaki, H.; Oh-Hara, S.; Nishizawa, M.; Katayose, M. *Jpn. J. Appl. Phys.* **1990**, *30(1B)*, L114–L116.
221. Verhoeven, J.A. Th., Mischke, W.S. Developments in CD-R. *Proc SPIE 2001* Vol. 4085, 298–305. Fifth International Symposium on Optical Storage (ISOS 2000), Gan, F., Hou, L. Eds.
222. Wang, S.; Shen, S.; Xu, H.; Gu, D.; Yin, J.; Tang, X. *Dyes Pigments.* **1999**, *42*, 173–177.
223. Wang, S.; Shen, S.; Xu, H.; Gu, D.; Yin, J.; Dong, X. *Mater. Sci. Engineering.* **2001**, *B79*, 45–48.
224. Park, H. Y.; Lee, N. H.; Je, J. T.; Min, K. S.; Young, J. H.; Kim, E.-R.; Lee, H. *Mol. Cryst. Liq. Cryst.* **2001**, *371*, 305–308.
225. Park, H.; Kim, E.-R.; Kim, D. J.; Lee, H. *Bull. Chem. Soc. Jpn.* **2002**, *75*, 2067–2070.
226. Gan, F. *Chin. Sci. Bull.* **2000**, *45*, 572–576.
227. Qi, Y.; Desjardins, P.; Wang, Z. Y. Novel near-infrared active dinuclear ruthenium complex materials: effects of substituents on optical attenuation. *J. Opt. A: Pure Appl. Optics* **2002**, *4*, S273–S277.
228. García-Cañadas, J. Meacham, A. P. Peter, L. M. Ward, M. D. Electrochromic switching in the visible and near IR with a Ru-dioxolene complex adsorbed on to a nanocrystalline SnO₂ electrode. *Electrochem. Commun.* **2003**, *5*, 416–420.

9.14

Nonlinear Optical Properties of Metal Complexes

B. J. COE

University of Manchester, UK

9.14.1	INTRODUCTION	621
9.14.1.1	General Context and Scope of this Review	621
9.14.1.2	The Origins of NLO Behavior in Molecular Materials	621
9.14.1.3	Requirements for NLO Activity	623
9.14.1.4	Measurement of NLO Properties	623
9.14.1.5	Why are Metal Complexes of Interest?	626
9.14.2	COORDINATION COMPLEXES WITH NLO PROPERTIES	627
9.14.2.1	Complexes of Nonchelating Pyridyl Ligands	627
9.14.2.2	Complexes of Chelating Pyridyl Ligands	632
9.14.2.3	Complexes of Porphyrin and Related Ligands	638
9.14.2.4	Complexes of Phthalocyanine and Naphthalocyanine Ligands	643
9.14.2.5	Complexes of Schiff Base Ligands	650
9.14.2.6	Complexes of Thiocyanate Ligands	655
9.14.2.7	Complexes of 1,2-Dithiolene and Related Ligands	656
9.14.2.8	Cluster Complexes	659
9.14.2.9	Miscellaneous Complexes	667
9.14.3	CONCLUSIONS	673
9.14.4	REFERENCES	675

9.14.1 INTRODUCTION

9.14.1.1 General Context and Scope of this Review

Materials that exhibit nonlinear optical (NLO) behavior are useful because they allow manipulation of the fundamental properties of laser light beams, and are hence of great technological importance in areas such as optical data processing and storage. The most readily understood amongst NLO effects are frequency doubling or tripling (second- or third-harmonic generation (SHG/THG), respectively), but various other more esoteric NLO phenomena are also potentially useful. Inorganic crystalline salts such as lithium niobate (LiNbO_3), ammonium dihydrogen phosphate ($\text{NH}_4\text{H}_2\text{PO}_4$, ADP), or potassium dihydrogen phosphate (KH_2PO_4 , KDP) and semiconductors like gallium arsenide (GaAs) are already widely used in commercial NLO devices,¹⁻³ but the applicability of such materials is limited. The requirements of emerging optoelectronic and photonic technologies have stimulated much research into the NLO properties of various molecular organic materials.⁴⁻⁷ Such compounds offer a number of potential advantages over the conventional inorganic materials for advanced applications. For example, the NLO responses of molecules often exceed those of purely inorganic substances, and molecular electronic properties can be finely

controlled by using directed synthetic chemistry. Furthermore, the fabrication of device structures may be facilitated by the ready availability of organic matrices such as polymer films.

Within the research field of molecular NLO materials, increasing attention is being paid to metal complexes (mostly of the d-transition elements) which offer possibilities for combination of NLO effects with other molecular electronic properties.⁸⁻²¹ This review aims to provide a reasonably comprehensive survey of the quadratic (second-order) and cubic (third-order) NLO properties of metal coordination complexes up to mid-2002. The intention is to give an overview of the diverse types of complexes that have been studied, with the primary emphasis on molecular structures rather than the detailed physical properties. The following are excluded: (i) studies lacking NLO data, merely reporting complexes that are expected to display NLO effects; (ii) compounds showing NLO activity which contain metal complexes that are present in a purely passive role, e.g., as counterions with active organic chromophores; (iii) the patent literature; (iv) complexes of σ -acetylide or η^n -hydrocarbon ligands, except in cases of multinuclear complexes that contain other nonorganometallic centers; (v) fullerene complexes. However, complexes in which the only direct metal-carbon bonds are to CO or CN^- ligands are considered, and a small number featuring a single metal-carbon bond are also included because they contain otherwise nonorganometallic coordination shells. Because the preparation of metal complexes with NLO activity is usually focused on ligand design, the complexes are generally classified according to their ligands, rather than their metal ions or their specific NLO properties. In order to avoid unnecessary duplication of background material previously covered by many authors, this introduction is as brief as possible.

9.14.1.2 The Origins of NLO Behavior in Molecular Materials

Although detailed discussion of the origins of NLO effects in molecules and molecular materials is unnecessary here, a brief general and simplified explanation is appropriate. Parametric molecular NLO responses do not involve any interchange of light energy with the medium (i.e., no population of actual excited states is necessary), but arise from subtle interactions between polarizable electron density (largely consisting of π electrons) and the unusually strong alternating electric field of a laser light beam. The resulting *induced polarization response*, P (dipole moment per unit volume), of a molecule can be expressed as a function of the applied electric field, E , according to the following power series expansion.

$$P = \alpha E + \beta E^2 + \gamma E^3 + \dots \quad (1)$$

With “normal” values of E , the quadratic and cubic terms in Equation (1) can be neglected, and only linear optical behavior such as refraction is observed. The coefficient α is known as the *linear molecular polarizability* and is related to the refractive index of the bulk material. However, under conditions where E approaches the magnitude of atomic field strengths, such as in a laser beam, the βE^2 and γE^3 terms in Equation (1) become significant and it is these components of the polarization response which give rise to quadratic and cubic NLO effects, respectively. The coefficients β and γ are termed the *first* and *second molecular hyperpolarizabilities*, respectively. At the molecular level, the phenomena of SHG and THG can be thought of as the electromagnetic radiation produced by corresponding induced dipole moments oscillating at two- and three-times the incident laser frequency.

When considering molecular materials, Equation (1) translates into its macroscopic equivalent

$$P = \chi^{(1)}E + \chi^{(2)}E^2 + \chi^{(3)}E^3 + \dots \quad (2)$$

where the coefficients $\chi^{(2)}$ and $\chi^{(3)}$ are the bulk NLO susceptibilities which can lead to a wide variety of phenomena, depending on factors such as the exact nature of the input frequencies. The complex coefficients β and $\chi^{(2)}$ are third-rank tensors, whilst γ and $\chi^{(3)}$ are fourth-rank tensors, so all of these parameters actually comprise a number of components which may sometimes be quoted as β_{zzz} , $\chi^{(3)}_{xyyx}$, etc. although only the dominant components are usually given. It is also worth noting that all of these NLO coefficients can have either positive or negative signs, but usually only their magnitudes are quoted.

Quadratic NLO effects arising from β and $\chi^{(2)}$ include SHG, the electro-optic (EO, Pockels) effect and frequency mixing (parametric amplification). SHG is actually just a special case of a three-wave

mixing process in which both input frequencies are the same. The term *phase-matching* refers to a situation when the fundamental and second-harmonic SH beams emerge from the material in phase, hence avoiding undesirable destructive interference. The EO effect involves changes in refractive index induced by an applied electric field, and can be exploited in devices such as optical switches and modulators. Quadratic NLO phenomena are better understood and are also of greater immediate practical utility than their cubic counterparts. Although almost all of the studies to date concerning the quadratic NLO behavior of coordination complexes have involved only SHG or (solution) harmonic scattering, the results imply that such materials may also display EO or other effects.

Cubic NLO effects arising from γ and $\chi^{(3)}$ include THG, optical phase conjugation, and the optical Kerr effect (OKE), which involves intensity-dependent refractive indices, and is hence envisioned as providing the basis of all-optical information processing. Optical limiting (OL) materials show high transmission at normal light intensities, but become almost opaque under very bright illumination, ideally limiting the transmitted light intensity to a maximum value. They are hence of great interest for the protection of sensitive photodetectors (including eyes) from very bright light sources. Because the response speed is crucial, OL materials that rely on cubic or pseudo-cubic NLO effects (e.g., nonlinear absorption or refraction) are particularly attractive for practical applications.^{22,23}

The predominant mechanism by which metal complexes achieve OL is known as reverse saturable absorption (RSA), which involves a sequential two-photon process and can generally be adequately explained using a four-state model. The ground state (S_0) is initially excited to a singlet state (S_1) which undergoes intersystem crossing (ISC) to a triplet state (T_1) and then absorbs a second photon to reach a higher triplet state (T_2). If the transition $T_1 \rightarrow T_2$ has a larger absorption cross section σ than $S_0 \rightarrow S_1$, then RSA occurs, dramatically attenuating transmission through the material. RSA becomes more pronounced as both the ratio $\sigma(T_1 \rightarrow T_2)/\sigma(S_0 \rightarrow S_1)$ and the lifetime of T_1 increase. Because ISC rates are enhanced by the presence of heavy atoms, due to increased spin-orbit coupling, metal complexes are especially well-suited to exhibit rapid and efficient RSA. As its name indicates, RSA is the opposite of saturable absorption (SA), in which an increase in transmission is observed at high illumination levels.²⁴

9.14.1.3 Requirements for NLO Activity

Most molecules that possess large β values contain an electron donor group (D) connected to an electron acceptor group (A) by a π -conjugated polarizable bridge. The linear optical properties of such dipolar, polarizable (D- π -A) molecules are characterized by low-energy, D \rightarrow A intramolecular charge-transfer (ICT) excitations. It has been discovered that octupolar molecules which possess zero ground state dipole moments can also show large β values.²⁵ For a centrosymmetric molecule, β is necessarily equal to 0, but no symmetry restrictions exist for γ . Although the primary requirement for large γ values is simply an extensive π -conjugated system, factors such as molecular asymmetry and 2-D conjugation are also important for enhancing cubic NLO responses.²⁶

For a bulk material, the extent of potentially useful NLO activity depends not only on molecular structure, but also on the macroscopic ordering of the component molecules, i.e., the crystal-packing arrangement or the ordering within a thin-film or other material. As at the microscopic level, a nonzero $\chi^{(2)}$ value can only be exhibited by a noncentrosymmetric material, but no special symmetry requirements apply to $\chi^{(3)}$. The creation of materials for quadratic NLO effects is hence especially challenging because it necessitates both the molecular engineering of suitable structures and their incorporation into appropriate bulk arrangements. Whilst modern synthetic chemistry allows a high degree of control over molecular structures, current ability to predetermine macroscopic structures (e.g., by crystal engineering) is rather limited. By contrast, although the design criteria for $\chi^{(3)}$ materials are less well defined, all substances exhibit some degree of cubic NLO activity. The challenge in this area is hence primarily to prepare molecules with NLO responses sufficiently large for practical applications.²⁶

9.14.1.4 Measurement of NLO Properties

The initial stages in the development of novel molecular NLO materials are the synthesis of molecules with large β and/or γ values and their incorporation into materials with substantial $\chi^{(2)}$ and/or $\chi^{(3)}$ coefficients. Although many additional factors must be considered for practical device

applications (e.g., thermal and photochemical stability, processability, etc.) the NLO properties of molecules and molecular materials can be adequately described here by reference to values of β , γ , $\chi^{(2)}$, and $\chi^{(3)}$. Each of these parameters can be measured by using various experimental techniques. In most such measurements, the effects of resonance must always be considered; β , γ , $\chi^{(2)}$, and $\chi^{(3)}$ are all wavelength dependent, being strongly resonance enhanced whenever the fundamental or harmonic frequencies are close to an electronic excitation. Although large NLO responses are required, any significant absorption of light is obviously highly undesirable for most applications of NLO materials. This aspect has led to the use of the expression “transparency/efficiency trade-off” when discussing the merit of such materials.

For studies of quadratic NLO properties, $\chi^{(2)}$ values are obtained from solid-state SHG measurements, and the eponymous Kurtz powder test is often used to screen materials for activity.²⁷ This technique most often involves collection of the 532 nm SH light produced following irradiation with a near-infrared 1,064 nm Nd³⁺:YAG laser, and SHG efficiencies may be quoted with respect to quartz, ADP, KDP, urea, or other reference samples. Urea is the most commonly used standard for organic compounds, and the relative 1,064 nm SHG activities are: quartz (0.0025); ADP \approx KDP (ca. 0.04); LiNbO₃ (1.5).²⁷ Different laser fundamentals (e.g., 1,907 nm) may be used with materials which absorb strongly around 532 nm. It is important to remember that the Kurtz powder test is only semiquantitative, the results being affected by various factors including particle sizes. Furthermore, a lack of SHG often merely indicates the adoption of a centrosymmetric crystal structure by a molecule which may nevertheless on its own possess a significant β value. Powder SHG testing is hence not useful for establishing structure–activity correlations (SACs).

Molecular β values are normally determined in solution. Until relatively recently, the only reliable method for doing so was the electric-field-induced SHG (EFISHG) technique.^{28–30} SHG cannot be observed from an isotropic solution, so poling with a strong external electric field is used to induce the constituent molecules to adopt a partially ordered macroscopic structure from which SHG can be obtained. Analysis of the SH light produced on irradiation with a suitable laser beam affords the vectorial projection of β along the molecular dipole axis. Since the early 1990s the versatile hyper-Rayleigh scattering (HRS) technique has also become widely available.^{31–33} This approach depends on the fact that microscopic anisotropy within a solution of molecules with quadratic NLO activity can produce incoherent SH scattering which can be analyzed to afford different directional components of β . The HRS technique has certain advantages over EFISHG, e.g., it does not require knowledge of molecular dipole moments (μ) and is applicable to charged and octupolar compounds which are not amenable to EFISHG study. Although a lack of discrimination between HRS and multi-photon fluorescence can complicate the derivation of reliable β values for certain compounds, this potential problem can be circumvented.³⁴

The results from EFISHG or HRS experiments can be corrected for resonance enhancement by using a simple theoretical two-state model (TSM, Equations (3) and (4)),^{35,36} which is reasonably valid for dipolar molecules in which β is primarily associated with a single ICT excitation:

$$\beta = \beta_0 \frac{E_{\max}^2}{\left[1 - (2E_f)^2 (E_{\max}^2)^{-1}\right] \left[(E_{\max})^2 - E_f^2\right]} \quad (3)$$

$$\beta_0 = \frac{3\Delta\mu_{12}(\mu_{12})^2}{2(E_{\max})^2} \quad (4)$$

E_f is the fundamental laser energy, E_{\max} is the energy of maximal absorption, $\Delta\mu_{12}$ is the dipole moment change for ICT excitation, and μ_{12} is the transition dipole moment. The application of Equation (3) to β values measured with a 1,064 nm laser (β_{1064}), or at any other chosen wavelength, affords β_0 , the *static* or *zero-frequency first hyperpolarizability*, which provides an estimate of the “intrinsic” molecular hyperpolarizability, in the absence of any resonance effects. For octupolar chromophores, a related three-state model can be used.³⁷ The complications of resonance enhancement are often minimized in EFISHG studies by using a 1,907 nm laser, but HRS is not well suited to working at such low wavelengths because the SH scattering effect becomes very weak. However, a 1,907 nm HRS technique was developed in the late 1990s.³⁸ β_0 values are particularly useful when considering potential practical applications of molecular quadratic

NLO materials which necessitate operation at “off-resonance” wavelengths, generally in the NIR region ca. 1,000–1,500 nm.

Two other techniques have also been occasionally used for estimating β , both of which involve the measurement of $\Delta\mu_{12}$ values and the assumption that the TSM applies to the chromophore in question. The first of these is the so-called solvatochromic (SC) method which uses solvent-induced shifts in the ICT maximum energy to derive $\Delta\mu_{12}$.^{39–41} This approach is based on several approximations and is hence of rather variable reliability, but has the advantage of being experimentally undemanding.^{39–41} The β values obtained by using Equations (3) and (4) may be denoted β_{CT} because their derivation assumes that the NLO response is dominated by a CT transition. Stark (electroabsorption) spectroscopy is a more sophisticated technique, which affords $\Delta\mu_{12}$ by analyzing the effects of an applied electric field on the shapes of absorption bands (which correspond with ICT transitions for NLO purposes).^{42,43} However, the use of Stark spectroscopy to derive β values has to date been restricted to a very few studies. When using data from either SC or Stark studies to calculate β_0 values, it should be noted that alternatives to Equation (4) are also available, which will change the resulting values by a factor of either 0.5 or 2.⁴⁴

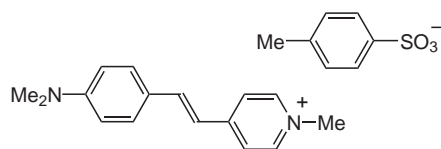
For studies of cubic NLO properties, values of $\chi^{(3)}$ and γ are usually obtained from THG^{45–48} or degenerate four-wave mixing (DFWM) experiments.^{49–52} EFISHG may also be used to determine γ . THG studies simply involve measurement of the light produced at the third harmonic (TH), but are often complicated by the fact that many NLO materials absorb strongly in the TH region, even when using a 1,907 nm fundamental which gives a TH at 636 nm. DFWM involves three laser beams of the same frequency interacting in a material to produce a fourth degenerate beam, the intensity of which allows determination of $\chi^{(3)}$. DFWM may hence circumvent the effects of resonance, but has the additional aspect that vibrational and orientational mechanisms can contribute substantially to the observed optical nonlinearity. In contrast, only the electronic hyperpolarizability is fast enough to be probed by THG measurements. Hence, THG-derived γ values are generally considerably smaller than those determined via DFWM, and are more useful for deriving SACs for the purely electronic part of γ , i.e., the only part of interest for potential practical applications. Polarization and time-dependent DFWM measurements can be used to distinguish the electronic (parametric) part of γ from other (nonparametric) components, but several experimental subtleties must be considered if this is to be achieved reliably. It is important to remember that $\chi^{(3)}$ values which are most often determined for solutions will always be concentration dependent.

Another experimental method that has become popular for characterization of cubic NLO materials is the relatively simple, but highly sensitive Z-scan technique which measures the phase change induced in a single laser beam on propagation through a material.^{53–55} The sample is moved along the propagation path (z) of a focused Gaussian beam whilst its transmittance is measured through a finite aperture in the far field, and the sign and magnitude of the nonlinear refractive index n_2 are deduced from the resulting transmittance curve (Z-scan). If the value of n_2 is positive, then the material has a tendency to shrink a laser pulse and is termed “self-focusing” (SF), whilst a negative n_2 characterizes “self-defocusing” (SDF) behavior. Although the ultrafast, electronic n_2 arises from the real part of $\chi^{(3)}$, published n_2 values often include, and indeed may be dominated by, nonparametric (thermal) contributions. In cases where nonlinear refraction is accompanied by nonlinear absorption, the nonlinear absorption coefficient α_2 can be determined by performing a second Z-scan with the aperture removed. Effective $\chi^{(3)}$ and γ values can also be determined via this method, but must be interpreted with great care in terms of their actual origins which may be largely thermal effects.

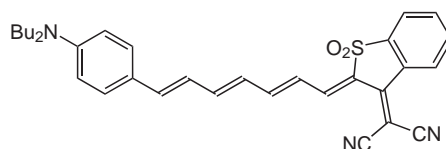
Ultrafast, time-resolved OKE measurements (which involve another type of four-wave mixing process) may also occasionally be used to determine $\chi^{(3)}$ and γ values.^{56,57} In each of the THG, DFWM, Z-scan, and OKE techniques, γ is derived from the measured $\chi^{(3)}$ values by using the solute number density of the solution. In a few cases, $\chi^{(3)}$ values have also been determined by using Stark spectroscopy. It should be remembered that comparisons of γ or $\chi^{(3)}$ values obtained using different techniques with different experimental conditions are generally of little utility.

OL behavior is assessed simply by monitoring the transmission of a (usually solution) sample as a function of the incoming laser fluence measured in joules per square centimeter (rather than intensity in watts per square centimeter).^{22,23} Limiting thresholds F_{th} , defined as the incident fluence at which the actual transmittance falls to 50% of the corresponding linear transmittance, are then commonly quoted. Since excited-state absorption processes generally determine the OL properties of molecules, the excited-state structure and dynamics are often studied in detail. The laser pulse width is an important consideration in the study of OL effects. Compounds (1–5)^{58–62} are representative non-metal-containing compounds with especially large NLO and/or OL

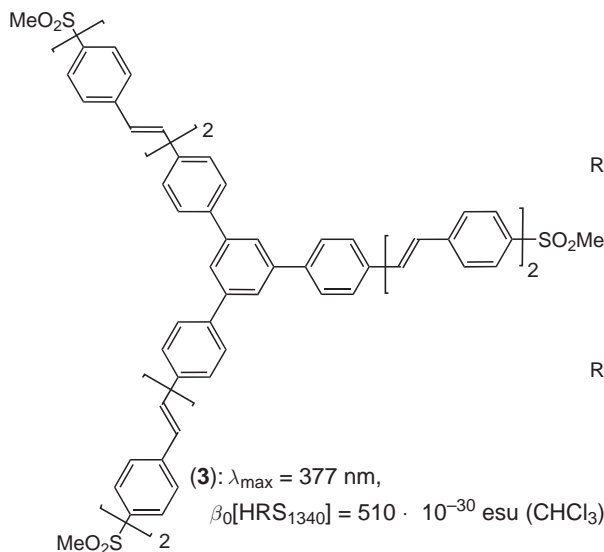
activities, given for purposes of comparison with the data included in the following sections. Note that in all cases here, the wavelength quoted for a particular NLO measurement refers to the fundamental, rather than the SH or TH.



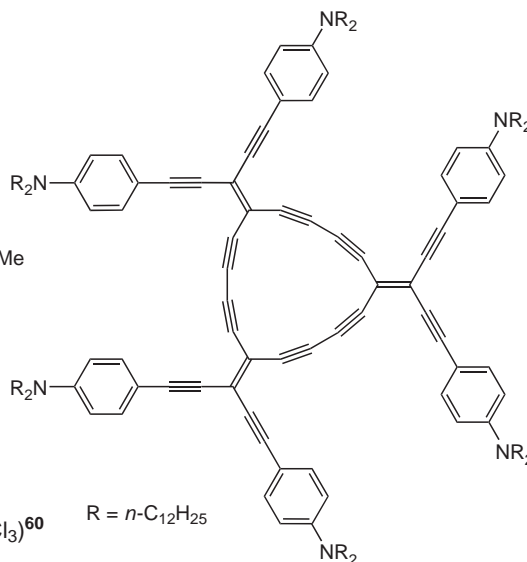
(1): $\text{SHG}_{1907} = 1,000 \cdot \text{urea}^{58}$



(2): $\lambda_{\text{max}} = 826 \text{ nm}$, $\beta_0[\text{EFISHG}_{1907}] = 1,470 \cdot 10^{-30} \text{ esu (CHCl}_3)^{59}$

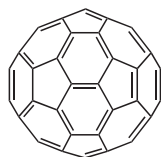


(3): $\lambda_{\text{max}} = 377 \text{ nm}$,
 $\beta_0[\text{HRS}_{1340}] = 510 \cdot 10^{-30} \text{ esu (CHCl}_3)^{60}$



$R = n\text{-C}_{12}\text{H}_{25}$

(4): $\gamma[\text{THG}_{2100}] = 4.3 \cdot 10^{-32} \text{ esu}$,
 $\chi^{(3)} = 7.6 \cdot 10^{-11} \text{ esu (CHCl}_3)^{26}$



(5) (C_{60}): $\lambda[\text{Z-scan}_{497}] = 2.3 \cdot 10^{-32} \text{ esu (0.5 ps pulses, toluene)}^{61}$
 $F_{\text{th}} (\text{J cm}^{-2}, 532 \text{ nm, toluene}):$
 1.6 (8 ns pulses), 0.3 (30 ps pulses)⁶²

9.14.1.5 Why are Metal Complexes of Interest?

The reasons for studying the NLO properties of metal complexes have been expounded in numerous previous reviews,⁸⁻²¹ so will be only briefly outlined here. Coordinated metal centers often engage in π -bonding, both with organic ligating groups and with each other, meaning that they can be involved in various strongly allowed ICT processes, i.e., metal-to-ligand CT (MLCT), ligand-to-metal CT (LMCT), or metal-to-metal/intervalence CT (MM/IVCT). They can also participate in less directional $\pi \rightarrow \pi^*$ electronic excitation processes. As in purely organic chromophores, the existence of such transitions is often associated with large molecular NLO responses. Furthermore, their unparalleled diversity of both structural and electronic properties renders metal complexes especially attractive for the molecular engineering of novel NLO materials.

The early forays by synthetic coordination/organometallic chemists into the NLO arena were most likely motivated largely by academic curiosity, and the optimistic belief that anything that purely organic compounds can do, metal complexes can do better and with added multifunctionality. Whether this hope has proven to be well founded will become clearer as this review unfolds,

and with the continuing passage of time. Whilst the cynical observer may pose the question “Why bother to put metals into molecular NLO chromophores?,” the simple response “Why not?” is not without merit (although less so now than in the past). The ever-increasing need for the metallo-organic chemistry community to justify their existence by creating materials that are not just interesting but also useful has obviously been another significant driving force. Because the multidisciplinary chain of development from a new molecule with interesting properties to a functioning NLO device is inevitably long and convoluted, the majority of studies to date in this field have focused on chromophore design and the elucidation of molecular SACs. Whilst this is clearly a scientifically rewarding endeavor, a greater emphasis on the properties of bulk materials will be necessary if continued progress is to be made. Hence, future studies in this field will become increasingly driven by the specific, stringent requirements of device applications, rather than pure academic curiosity.

9.14.2 COORDINATION COMPLEXES WITH NLO PROPERTIES

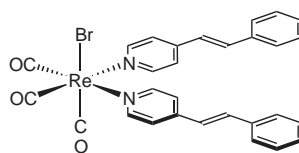
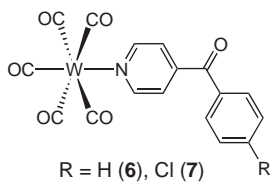
9.14.2.1 Complexes of Nonchelating Pyridyl Ligands

The earliest NLO studies involving metal pyridyl complexes were reported by Frazier *et al.* in 1986 who investigated the SHG properties of various group 6 metal pyridyl carbonyls.⁶³ Although most of the complexes tested show little or no activity, (6) and (7) have respective SHG efficiencies of 0.2 and 1.0 times ADP using a 1,064 nm laser.⁶³ Shortly after, Calabrese and Tam reported SHG from the Re^I complex (8).⁶⁴ Subsequent studies by Eaton and Tam *et al.*^{65,66} describe the preparation of inclusion compounds of various metal complexes with thiourea or tris-*ortho*-thymotide. Unfortunately, none of the complexes [W(CO)₅L] (L = pyridine, py, or a 4-substituted py) produce SHG-active materials.^{65,66}

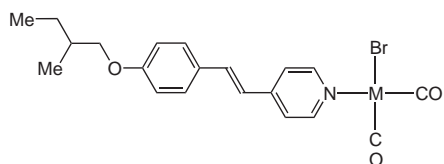
Following these early solid-state investigations, 1,907 nm EFISHG studies by Tam and co-workers on several complexes [W(CO)₅L] (L = py or a 4-substituted py) quote β values similar to that of 4-nitroaniline (ca. 10×10^{-30} esu) and sensitive to the nature of the pyridyl substituent.^{67–69} These results were quickly followed by ZINDO/SCI-SOS calculations on the same series of complexes by Kanis *et al.*⁷⁰ the first time that MO theory had been used to describe the quadratic NLO responses of metal complexes. The results of these calculations agree reasonably well with the EFISHG data, and indicate that the modest β responses can be traced to relatively small $\Delta\mu_{12}$ values.⁷⁰ Lacroix *et al.* obtained low 1,064 nm SHG activities by corona poling films of poly (4-vinylpyridine) and of two other related polymers functionalized with {W(CO)₅} centers.⁷¹

The EFISHG technique has also been applied to some pyridyl carbonyls of Rh^I or Ir^I by Bruce *et al.*^{72,73} These complexes (e.g., (9) and (10)) contain stilbazole ligands bearing resolved 2-methylbutyloxy substituents, incorporated with the aim of encouraging noncentrosymmetric crystal packing structures. The observed 1.5- to 3-fold enhancements of β of the free stilbazole on complexation are attributable to the σ -electron-withdrawing abilities of the metal centers.^{72,73}

Bimetallic complexes containing pyridyl carbonyl centers with ruthenium σ -acetylide⁷⁴ or ferrocenyl (Fc)^{75,76} electron donor groups have also been investigated by using 1,064 nm HRS. For example, complexes (11–15) show relatively large β responses.^{74,75} Although these studies do indicate that coordination of the pyridyl nitrogen increases β when compared with free *trans*-[1-Fc-2-(4-pyridyl)ethylene],^{75,76} their ability to afford further NLO SACs is limited because reliable β_0 values can not be obtained for Fc complexes due to inapplicability of the TSM. The related trimetallic complex (16), together with the monometallic (17) have also been studied via HRS at different wavelengths.⁷⁷ Comparisons of the resulting β values with calculated data indicate that the Re^I carbonyl bromide center is rather less effective at increasing the electron-accepting ability of a pyridyl group when compared with an *N*-methyl substituent.⁷⁷ Various bimetallics with Fc or tetra/octa-methyl-Fc electron donor groups linked via pyridyl functions to electron-deficient {Mo^{II}(NO)Tp*X}⁺ [Tp* = tris(3,5-dimethylpyrazolyl)borate; X = Cl/I] or {W(CO)₅} centers have been studied by Malaun *et al.*⁷⁸ Although the measured HRS data are extensively resonance enhanced and the derived β_0 values should be treated with extra caution for these Fc derivatives (e.g., (18) and (19)), the β trends imply the following conclusions: (i) methylation of a Fc unit increases its electron donor abilities, and (ii) the electron-accepting abilities of the {Mo^{II}(NO)Tp*Cl}⁺ and {W(CO)₅} moieties appear to be similar.⁷⁸ Furthermore, chemical oxidation of the octamethyl-Fc group in (18) produces a ca. 40% decrease in β_{1064} ,⁷⁸ indicating a mechanism for redox-induced switching of NLO responses.

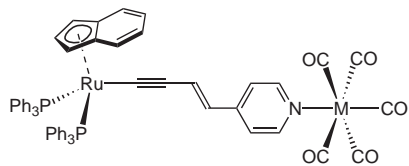


(8): $\text{SHG}_{1064} = 0.1 \cdot \text{urea}^{64}$



M = Rh (9): $\beta_{1907}[\text{EFISHG}] = 24 \cdot 10^{-30} \text{esu} (\text{CHCl}_3)$

M = Ir (10): $\beta_{1907}[\text{EFISHG}] = 56 \cdot 10^{-30} \text{esu} (\text{acetone})^{72,73}$

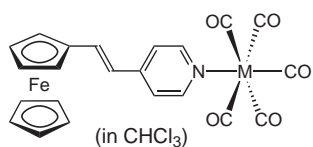


M = Cr (11): $\lambda_{\text{max}} = 451 \text{ nm}$,

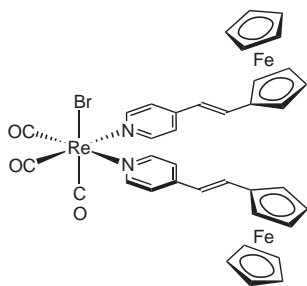
$\beta_0 [\text{HRS}] = 60 \cdot 10^{-30} \text{esu} (\text{CH}_2\text{Cl}_2)$

M = W (12): $\lambda_{\text{max}} = 462 \text{ nm}$,

$\beta_0 [\text{HRS}] = 71 \cdot 10^{-30} \text{esu} (\text{CH}_2\text{Cl}_2)^{74}$

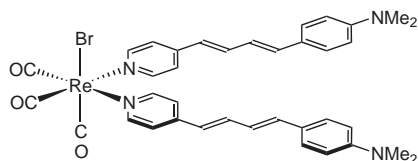


No.	M	λ_{max} (nm)	$\beta_{1064}[\text{HRS}] (10^{-30} \text{esu})^{75}$
(13)	Cr	401	63
(14)	Mo	487	95
(15)	W	491	101



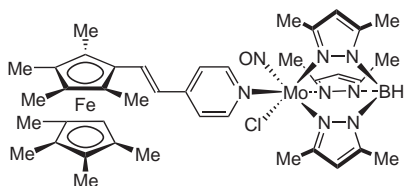
(16): $\lambda_{\text{max}} = 501 \text{ nm} (\text{CH}_2\text{Cl}_2)$,

$\beta_{1300}[\text{HRS}] = 24 \cdot 10^{-30} \text{esu} (\text{CHCl}_3)^{77}$



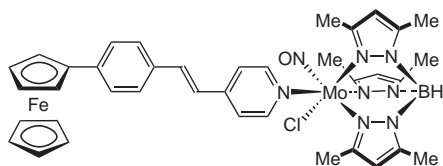
(17): $\lambda_{\text{max}} = 438 \text{ nm} (\text{CH}_2\text{Cl}_2)$,

$\beta_{1500}[\text{HRS}] = 208 \cdot 10^{-30} \text{esu} (\text{CHCl}_3)^{77}$



(18): $\lambda_{\text{max}} = 555 \text{ nm}$,

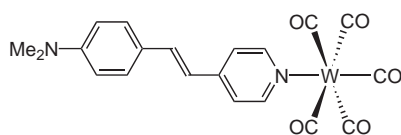
$\beta_{1064}[\text{HRS}] = 205 \cdot 10^{-30} \text{esu} (\text{CH}_2\text{Cl}_2)^{78}$



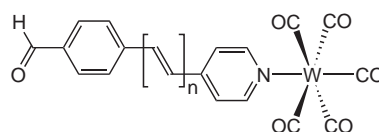
(19): $\lambda_{\text{max}} = 495 \text{ nm}$,

$\beta_{1064}[\text{HRS}] = 166 \cdot 10^{-30} \text{esu} (\text{CH}_2\text{Cl}_2)^{78}$

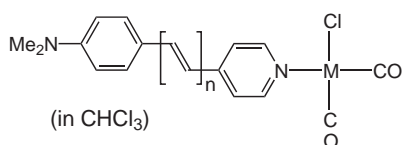
Continued, detailed ZINDO/SCI-SOS β calculations by Kanis *et al.* on $\{M(CO)_5\}$ ($M = Cr/W$) pyridyl complexes afford several important conclusions:⁷⁹ (i) excellent agreement with EFISHG data is found in many cases (e.g., **(20)**), but is generally better for monoaryl systems, (ii) coordination enhances the β responses of the free pyridines, and (iii) the complexes obey the TSM, but their β values are limited by relatively small oscillator strengths for their associated CT transitions which arise from poor metal-ligand π -coupling and offset the β -enhancing effects of relatively large $\Delta\mu_{12}$ and low E_{max} values. In all of the monoaryl complexes, the NLO responses are primarily determined by MLCT excitations and are hence greatly influenced by the pyridyl 4-substituents.⁷⁹ However, the very nature of the CT transition that dominates the NLO response in the stilbazole complexes depends on the phenylene 4-substituent (R).⁷⁹ When R is the electron-donating $-NMe_2$, β is dominated by an intraligand CT (ILCT) transition, with the metal center functioning primarily as an inductive electron acceptor.⁷⁹ By contrast, if R is an electron-accepting group such as $-NO_2$, then an MLCT excitation is most important in determining the NLO response.⁷⁹ However, the primary acceptor in such complexes is the pyridyl ring.⁷⁹ Hence, the β responses of such stilbazole complexes are much less affected by 4-substituents than those of their monoaryl counterparts.⁷⁹ Furthermore, extension of the conjugation length in the series **(21)**–**(24)**



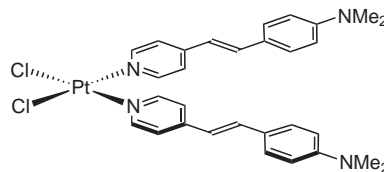
(20): $\beta_{1064}[\text{EFISHG}] = 61 \cdot 10^{-30}$ esu (1,4-dioxane),
 $\beta[\text{ZINDO}] = 66 \cdot 10^{-30}$ esu⁷⁹



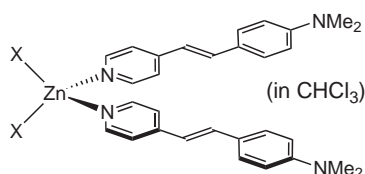
No.	n	$\beta[\text{ZINDO}] (10^{-30} \text{ esu})$ ⁷⁹
(21)	0	-29
(22)	1	-45
(23)	2	-29
(24)	3	-22



No.	M	n	λ_{max} (nm)	$\beta_{1340}[\text{EFISHG}] (10^{-30} \text{ esu})$ ⁸⁰
(25)	Rh	1	421	111
(26)	Rh	2	442	131
(27)	Ir	1	431	128
(28)	Ir	2	449	135



(29): $\lambda_{max} = 375$ nm,
 $\beta_{1340}[\text{EFISHG}] = 41 \cdot 10^{-30}$ esu (CHCl_3)⁸¹

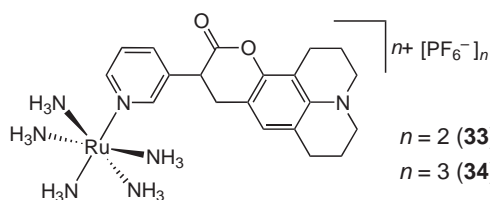


No.	X	λ_{max} (nm)	$\beta_{1340} [\text{EFISHG}] (10^{-30} \text{ esu})$ ⁸¹
(30)	MeCO_2^-	376	48
(31)	Cl^-	410	84
(32)	CF_3CO_2^-	420	97

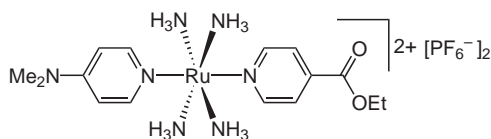
does not lead to a continual, dramatic increase in β , in marked contrast to the behavior of related purely organic NLO chromophores.⁷⁹

EFISHG studies by Roberto *et al.* show that coordination of pyridines with the 4-substituents-NMe₂, -*t*-Bu, -H, -COMe, or -CN to square planar *cis*-{M^I(CO)₂Cl} (M = Rh/Ir) or octahedral *fac*-{Os^{II}(CO)₃Cl₂} centers increases β by up to ca. 100-fold when compared with the free pyridines.^{80,81} These studies provide further experimental confirmation for the hypothesis of Kanis *et al.*⁷⁹ concerning the ambivalent acceptor/donor role of pyridyl-coordinated metal carbonyl centers. Roberto *et al.* have also investigated more extended complexes such as (25)–(28)⁸⁰; note that these contain electron-donating 4-NMe₂ groups and hence conjugation extension does increase β (albeit modestly). In contrast to the carbonyl complexes, no β enhancement on stilbazole complexation occurs in (29), and of the tetrahedral Zn^{II} complexes (30)–(32), only the chloride and trifluoroacetate show β increases over the free ligand.⁸¹ The β_{CT} values estimated from SC studies for (29) and (30) differ greatly from the corresponding EFISHG β_{1340} values due to noncoincidence of the dipole moment axes and the ILCT transition directions.⁸¹

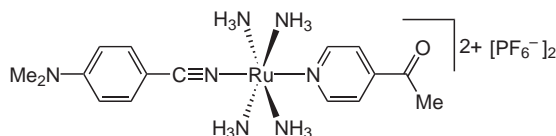
Coe and co-workers have reported a number of studies on the NLO properties of ruthenium ammine complex salts of pyridyl ligands, focusing on the establishment of SACs for β values derived via 1,064 nm HRS.^{82–91} Data for (33) and (34) show that β_0 of the dye coumarin-510 (33×10^{-30} esu from EFISHG in CHCl₃) is largely unaffected by complexation, attributable to weak coumarin-metal π -electronic coupling arising from the 3-substitution at the pyridyl ring.⁸² Systematic studies with various salts *trans*-[Ru^{II}(NH₃)₄(L^D)(L^A)](PF₆)_n (L^D = an electron-rich ligand; L^A = an electron-deficient ligand; *n* = 2 or 3)^{83–89} yield the following conclusions: (i) such



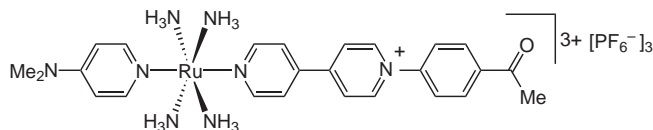
$n = 2$ (33): $\lambda_{\max} = 430$ nm, $\beta_0[\text{HRS}] = 35 \cdot 10^{-30}$ esu (MeCN)
 $n = 3$ (34): $\lambda_{\max} = 438$ nm, $\beta_0[\text{HRS}] = 37 \cdot 10^{-30}$ esu (MeCN)⁸²



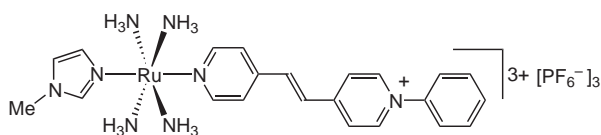
(35): $\lambda_{\max} = 500$ nm,
 $\beta_0[\text{HRS}] = 27 \cdot 10^{-30}$ esu (MeCN)⁸³



(36): $\lambda_{\max} = 472$ nm,
 $\beta_0[\text{HRS}] = 53 \cdot 10^{-30}$ esu (MeCN)⁸³



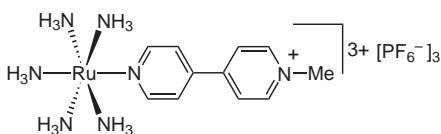
(37): $\lambda_{\max} = 688$ nm,
 $\beta_0[\text{HRS}] = 410 \cdot 10^{-30}$ esu (MeCN)⁸⁵



(38): $\lambda_{\max} = 638$ nm,
 $\beta_0[\text{HRS}] = 310 \cdot 10^{-30}$ esu (MeCN)⁸⁶

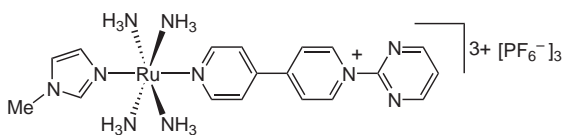
complexes possess large β_0 values which are associated with intense, low-energy $\text{Ru}^{\text{II}} \rightarrow \text{L}^{\text{A}}$ MLCT excitations, (ii) the β_0 responses of complexes containing three or more aryl rings (e.g., (37) and (38)) are very pronounced and considerably larger than those of related species with only 2 aryl rings (e.g., (35) and (36)), and (iii) the MLCT E_{max} and β_0 values can be finely tuned by ligand-based changes, in reasonable agreement with the TSM. Perhaps the most interesting result to emerge from these studies is the observation that the MLCT absorptions and β_0 responses of certain complexes (e.g., (39)) can be reversibly and very effectively (10–20-fold) attenuated by $\text{Ru}^{\text{III/II}}$ redox using chemical reagents.^{87–91} This first clear demonstration of redox-induced switching of NLO responses provides a novel justification for including transition metal centers in molecules with large β_0 values.

The most recent advances reported by Coe *et al.* involve detailed Stark spectroscopic studies carried out in butyronitrile glasses at 77 K which serve to verify and rationalize the HRS results obtained previously.⁹² These data confirm that *N*-arylation enhances β_0 , the latter effect being most significant in the 4,4'-bipyridinium-based complexes. Increases in β_0 are generally associated with decreases in E_{max} and increases in both μ_{12} and $\Delta\mu_{12}$, and insertion of a *trans*-CH=CH bridge into the 4,4'-bipyridinium unit of L^{A} enhances β_0 by up to 50%. ZINDO/SCI-SOS calculations on the $\{\text{Ru}^{\text{II}}(\text{NH}_3)_5\}^{2+}$ complexes do not accurately reproduce E_{max} or β_0 , but they do predict the dipole properties reasonably well. The agreement between $\beta_0[\text{Stark}]$ values calculated according to the TSM equation $\beta_0 = 3\Delta\mu(\mu_{12})^2/(E_{\text{max}})^2$ and the $\beta_0[\text{HRS}]$ data (e.g., for (39) and (40)) is mostly good.⁹² Furthermore, quantitative comparisons with purely organic compounds show that a pyridyl-coordinated $\{\text{Ru}^{\text{II}}(\text{NH}_3)_5\}^{2+}$ center is more effective than a -NMe₂ group as a π -electron donor.⁹³ This arises because the higher HOMO energy of the Ru^{II} center more than offsets the superior π -orbital overlap in analogous purely organic chromophores.⁹³ Lin *et al.* have reported the results of MO calculations on some of the complexes described by Coe and colleagues.⁹⁴ The TDDFT method gives reasonably good agreement with the $\beta_0[\text{HRS}]$ values (e.g., $\beta_{\text{xxx}} = 31 \times 10^{-30}$ esu for (35) and $\beta_{\text{xxx}} = 326 \times 10^{-30}$ esu for (37) at 1,064 nm), and is more reliable than the *ab initio* HF approach in treating such complexes.⁹⁴



$$\text{(39): } \beta_0[\text{HRS}] = 123 \cdot 10^{-30} \text{ esu (MeCN),}^{85}$$

$$\beta_0[\text{Stark}] = 120 \cdot 10^{-30} \text{ esu (BuCN)}^{92}$$

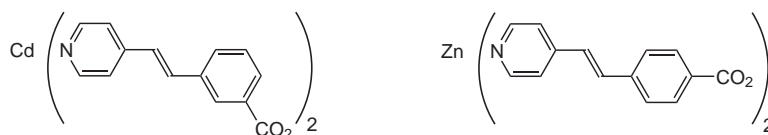


$$\text{(40): } \beta_0[\text{HRS}] = 336 \cdot 10^{-30} \text{ esu (MeCN),}^{86}$$

$$\beta_0[\text{Stark}] = 323 \cdot 10^{-30} \text{ esu (BuCN)}^{92}$$

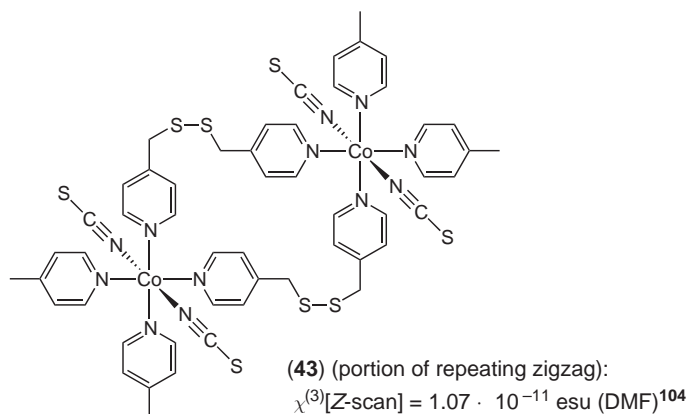
The only report describing the cubic NLO properties of Ru amines is a theoretical study of linear, mixed-valence $\text{Ru}^{\text{III/II}}$ complexes comprising pyrazine-bridged *trans*- $\{\text{Ru}(\text{NH}_3)_4\}^{n+}$ ($n = 2$ or 3) centers with $\{\text{Ru}(\text{NH}_3)_5\}^{n+}$ ($n = 2$ or 3) termini.⁹⁵ The $\chi^{(3)}$ values, computed exactly through a linear algebraic method (avoiding the SOS bottleneck), are remarkably high for these “Creutz-Taube” oligomeric chain complexes.⁹⁵

A number of reports concerning the NLO properties of coordination polymers with bridging pyridyl ligands have appeared.^{96–107} Lin and co-workers have studied various Zn^{II} or Cd^{II} complexes of pyridyl ligands with $-\text{CO}_2^-$ substituents which form unusual 2- or 3-D network structures.^{96–102} These compounds combine complete visible transparency with high thermal stability and can exhibit large powder SHG efficiencies. For example, (41) forms a 2-D rhombohedral grid structure, with each Cd^{II} center coordinated by two *cis*-pyridyl ligands and two chelating $-\text{CO}_2^-$ groups to give a highly distorted octahedron in the noncentrosymmetric space group (NCSG) *Fdd2*.^{96,102} By contrast, (42) adopts a 3-D diamondoid structure with tetrahedral connectivity (NCSG *C2*) featuring two types of Zn^{II} center, one resembling the Cd^{II} centers in (41), and the other having a tetrahedral coordination with two monodentate $-\text{CO}_2^-$ groups.¹⁰⁰ $[\text{Cd}^{\text{II}}_2(4,4'\text{-bipy})_2(\text{H}_2\text{O})_3(\text{SO}_4)_2] \cdot 3\text{H}_2\text{O}$ also crystallizes in *C2*, with a 3-D, interwoven network in which 4,4'-bipy-bridged linear chains are connected via μ_2 - and μ_3 -sulfate ions and H-bonded water molecules, but gives only relatively weak SHG from 1,064 nm (ca. 0.01 times urea).¹⁰³



(41): $\text{SHG}_{1064} = 800\text{--}1,000 \cdot \text{quartz}$
(ca. 2 · urea)^{96,102}

(42): $\text{SHG}_{1064} = 400 \cdot \text{quartz}$
(ca. 1 · urea)¹⁰⁰



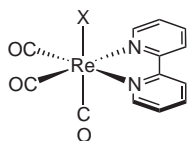
Hou and colleagues have used 532 nm Z-scan measurements to investigate several coordination polymers.^{104–107} $[\text{Mn}^{\text{II}}(\text{SO}_4)(4,4'\text{-bipy})(\text{H}_2\text{O})_2]_n$ and $[\text{Mn}^{\text{II}}(\text{N}_3)_2(4,4'\text{-bipy})]_n$ have 3-D network structures in the solid-state and show strong SF effects, with respective $\chi^{(3)}$ values of $5.0 \times 10^{-12} \text{ esu}$ and $1.2 \times 10^{-11} \text{ esu}$ in DMF.¹⁰⁵ By contrast, $[\text{Co}^{\text{II}}(\text{NCS})_2(\text{bpms})_2]_n$ (43) (bpms = 1,2-bis(4-pyridylmethyl)disulfenyl) crystallizes in 1-D double zigzag chains which stack to form a layered structure.¹⁰⁴ Layered solid-state structures are also adopted by the polymers $[\text{Pb}^{\text{II}}(\text{NCS})_2(\text{bpe})]_n$ (bpe = 1,2-bis(4-pyridyl)ethane),¹⁰⁶ $[\text{Mn}^{\text{II}}(\text{N}_3)_2(\text{bpp})_2]_n$, and $\{[\text{Mn}^{\text{II}}(\text{NCS})_2(\text{bpp})_2] \cdot 0.25\text{H}_2\text{O}\}_n$ (bbp = 1,3-bis(4-pyridyl)propane),¹⁰⁷ which all exhibit strong SF in DMF, the latter having an n_2 value of $2.6 \times 10^{-11} \text{ cm}^2 \text{ W}^{-1} \text{ M}^{-1}$.

9.14.2.2 Complexes of Chelating Pyridyl Ligands

The early solid-state NLO studies carried out by Calabrese and Tam included 7 complexes of the 2,2'-bipy ligand.⁶⁴ These materials (e.g., (44–47)) show moderate SHG activities, and complex (2) crystallizes in the NCSG $P2_1$.⁶⁴ Bourgault *et al.* used 1,340 nm EFISHG to investigate a number of Re^{I} complexes related to (44) and (45), together with some tetrahedral complexes of Zn^{II} and Hg^{II} with the same electron donor-substituted 2,2'-bipy ligands.^{108,109} The NLO responses of such complexes are associated with intense UV–visible ILCT excitations which are red-shifted on complexation, and the β_0 values of the complexes are hence larger than those of their free ligands.¹⁰⁹ Correlations between β_0 and the nature of the electron donor group and the metal center can be made in accord with the TSM. For example, the β_0 of (48) is larger than that of (49) because $-\text{NBU}_2$ is a stronger electron donor than $-\text{OOct}$, and (50) has a greater β_0 than (51) due to the stronger Lewis acidity of Zn^{II} compared with Hg^{II} .¹⁰⁹ The β responses of these Re^{I} complexes may be decreased by the presence of MLCT excitations which oppose the ILCT processes.¹⁰⁹

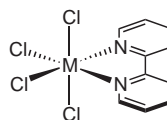
Roberto *et al.* have also applied EFISHG and detailed SC studies to tetrahedral complexes (e.g., (52) and (53)) of 1,10-phenanthroline (phen) ligands 5-substituted with electron donor groups.⁸¹ Increases of free ligand β responses occur on complexation to Zn^{II} but not to Cd^{II} , attributable to the greater Lewis acidity of the former ion.⁸¹ The β enhancement factors on coordination of these phen pro-ligands are considerably smaller than those found for the 2,2'-bipy pro-ligands of Bourgault *et al.*^{108,109} This result can be traced to the larger β values of the phen pro-ligands, arising from their greater rigidity when compared with related 2,2'-bipy molecules which only become fully planar on coordination.⁸¹ Good agreement between EFISHG β_{1340} and

SC β_{CT} values indicates that the ILCT transitions coincide with the dipole moment axes in complexes such as (52) and (53).⁸¹



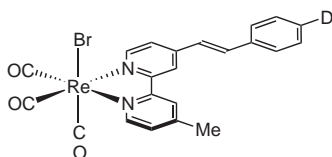
X = Cl⁻ (44): SHG₁₀₆₄ = 1.6–3 · urea

X = CF₃SO₃⁻ (45): SHG₁₀₆₄ = 1.7–2 · urea⁶⁴



M = Pd (46): SHG₁₀₆₄ = 0.1 · urea

M = Pt (47): SHG₁₀₆₄ = 1.2 · urea⁶⁴

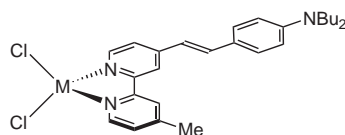


R = NBu₂ (48): λ_{max} = 475 nm (CH₂Cl₂),

β_0 [EFISHG] = 31 · 10⁻³⁰ esu (CHCl₃)

R = OOOct (49): λ_{max} = 367 nm (CH₂Cl₂),

β_0 [EFISHG] = 7 · 10⁻³⁰ esu (CHCl₃)¹⁰⁹

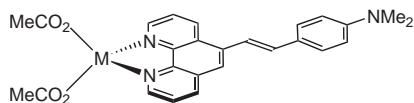


M = Zn (50): λ_{max} = 460 nm (CH₂Cl₂),

β_0 [EFISHG] = 71 · 10⁻³⁰ esu (CHCl₃)

M = Hg (51): λ_{max} = 442 nm (CH₂Cl₂),

β_0 [EFISHG] = 32 · 10⁻³⁰ esu (CHCl₃)¹⁰⁹



M = Zn (52): λ_{max} = 419 nm, β_{1340} [SC] = 71 · 10⁻³⁰ esu,

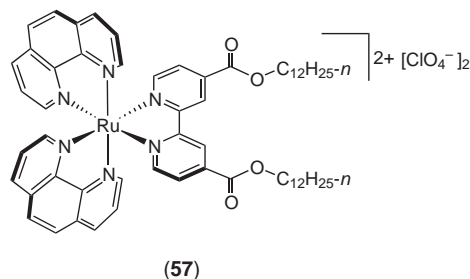
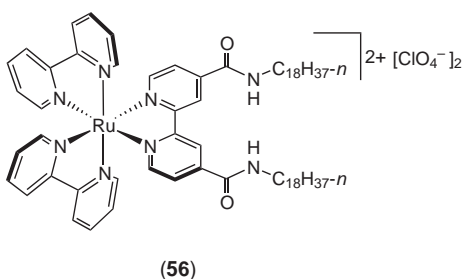
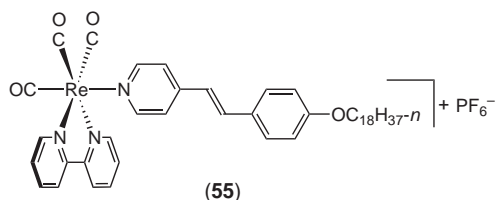
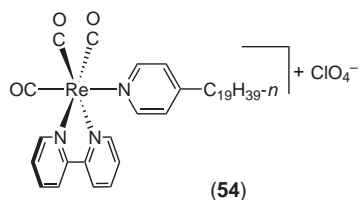
β_{1340} [EFISHG] = 77 · 10⁻³⁰ esu (CHCl₃)

M = Cd (53): λ_{max} = 411 nm, β_{1340} [SC] = 43 · 10⁻³⁰ esu,

β_{1340} [EFISHG] = 46 · 10⁻³⁰ esu (CHCl₃)⁸¹

Bulk NLO studies on luminescent *fac*-{Re^I(CO)₃(α -diimine)}⁺ complexes by Yam and co-workers note SHG from surfactant derivatives such as (54) and (55) deposited in Langmuir–Blodgett (LB) thin films.^{110–112} For example, the 532 nm SHG from LB films of the stilbazole derivative (55) is ca. 50% more intense than that from films of the structurally related purely organic salt *trans*-*N*-methyl-4-[2-(4-octadecyloxyphenyl)ethenyl]pyridinium iodide.¹¹²

The quadratic NLO properties of derivatives of the celebrated complex [Ru^{II}(2,2'-bipy)₃]²⁺ (RTB) have been studied relatively intensively, e.g., by Sakaguchi and colleagues.^{113–118} Initial reports describe SHG from amphiphilic complexes (e.g., (56)) in alternate Y-type LB films¹¹³ and in crystalline powders.¹¹⁴ The β_{1064} of (56) is estimated at 70 × 10⁻³⁰ esu,¹¹³ and it was suggested that the β response of RTB is increased by the presence of two amide substituents.¹¹⁴ Subsequent studies have focused on rapid photoinduced modulation of the SHG from LB films of (56).^{115–118} Irradiation at 378 nm causes the SHG signal from a 590 nm dye laser to decrease by 30% in less than 2 ps and return to almost its initial value within several hundred picoseconds.¹¹⁷ A similar phenomenon is observed with 355 nm or 460 nm excitation and a 1,064 nm probe beam.^{115,116,118} A quantitative correlation between the SHG time-profile and the luminescence decay of the MLCT excited state indicates that these SHG switching effects are due to the change in β on MLCT excitation.^{115–118} Ultrathin PVC films impregnated with (56) also exhibit SHG.¹¹⁹ The bis-phen complex (57) has very recently been incorporated as a probe of macroscopic structures into hybrid LB multilayers of the clay mineral saponite.¹²⁰ The observation of SHG from a 1,064 nm laser, which is enhanced when using the resolved Λ enantiomer of (57) rather than the racemate, demonstrates the utility of the novel fabrication technique for preparing noncentrosymmetric ultrathin films.¹²⁰

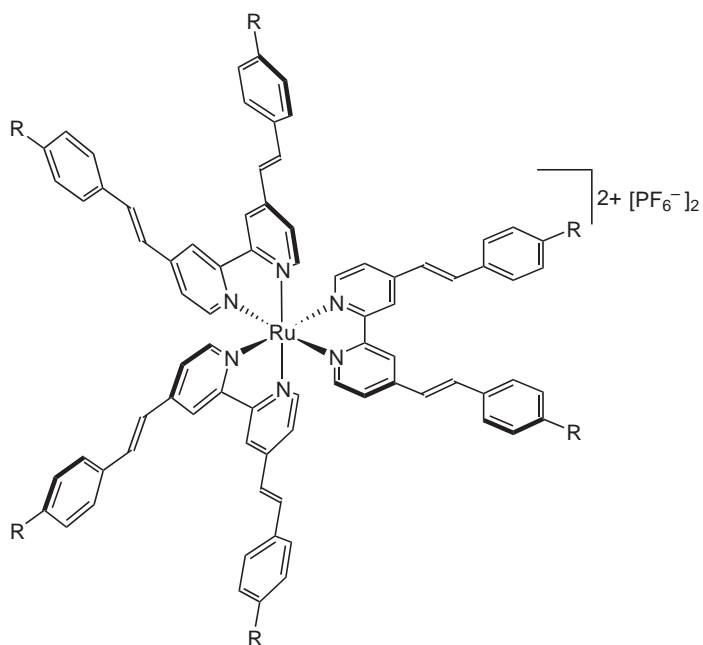


Attention was originally drawn to the octupolar nature of D_3 tris-chelates by Zyss *et al.* who used HRS and a three-state model to obtain β_0 values of 53×10^{-30} esu and 47×10^{-30} esu for the salts [RTB]Br₂ and [Ru^{II}(phen)₃]Cl₂, respectively.¹²¹ Although Persoons *et al.* found rather smaller β_0 values for these complexes, they did demonstrate that Ru^{II} \rightarrow Ru^{III} chemical oxidation causes decreases in β .¹²² By using 1340 nm HRS, Dhenaut *et al.* subsequently reported an extremely large β_0 value for a RTB derivative bearing electron-donating styryl substituents (58).¹²³ However, it has been suggested that this β_0 value is overestimated due to contributions from two-photon luminescence,¹²⁴ and more recent studies have accordingly given a smaller (although still large) β_0 of 380×10^{-30} esu for (58).¹²⁵ Although the RTB unit is itself octupolar, Vance and Hupp have used polarized HRS and Stark spectroscopic measurements to show that the β response of the complex salt (59) is better described as arising from multiple degenerate dipolar CT transitions, rather than an octupolar transition.¹²⁶ Furthermore, the dominant transitions are ILCT excitations which are red-shifted on coordination to Ru^{II} and oppose the MLCT transitions.^{125,126}

In further 1,320 nm HRS studies with compounds related to (58) and (59), Le Bozec and co-workers have also investigated the effects of varying the donor substituents and the metal center.^{18,125} Although the relatively complicated electronic structures of such tris-(α -diimine) complexes of Ru^{II} and Fe^{II} obscure the establishment of clear SACs, the smaller β_0 of (60) corresponds with a higher ILCT energy when compared with (58).^{18,125} This difference can be traced to the weaker electron-donating ability of an alkoxy compared with a dialkylamino group.¹²⁵ Also, the more electron-rich Fe^{II} center in (61) causes blue-shifting of the ILCT absorption and red-shifting of the MLCT band when compared with (58),^{18,125} and both of these changes can logically be linked with the observed decrease in β . Analogues of (58) containing Zn^{II} (62) or Hg^{II} (63) centers show only ILCT absorptions and the interpretation of their NLO properties is hence more straightforward.¹²⁵ (63) has a higher ILCT energy and a lower β_0 than (62) because Zn^{II} is a more effective Lewis acid than Hg^{II}.¹²⁵ It is noteworthy that (62) exhibits a similar β_0 to (58), but offers wider visible transparency.¹²⁵

In encouraging steps towards the preparation of useful NLO materials, Le Bozec and colleagues have recently incorporated the chromophoric units of (58) and (59) into macromolecular structures. HRS shows that a highly thermally stable polyimide derivative of (58) has a β_{1910} value of $1,300 \times 10^{-30}$ esu (in CH₂Cl₂), which is several times larger than that of the monomeric complex.¹²⁷ Also, a dendrimeric species containing 7 units derived from (59) exhibits a β_{1910} of $1,900 \times 10^{-30}$ esu (in CH₂Cl₂).¹²⁸ The greater β response of this heptamer when compared with the linear polymer containing an average of 14 chromophores is attributable to quasi-optimized octupolar ordering in the former structure.¹²⁸

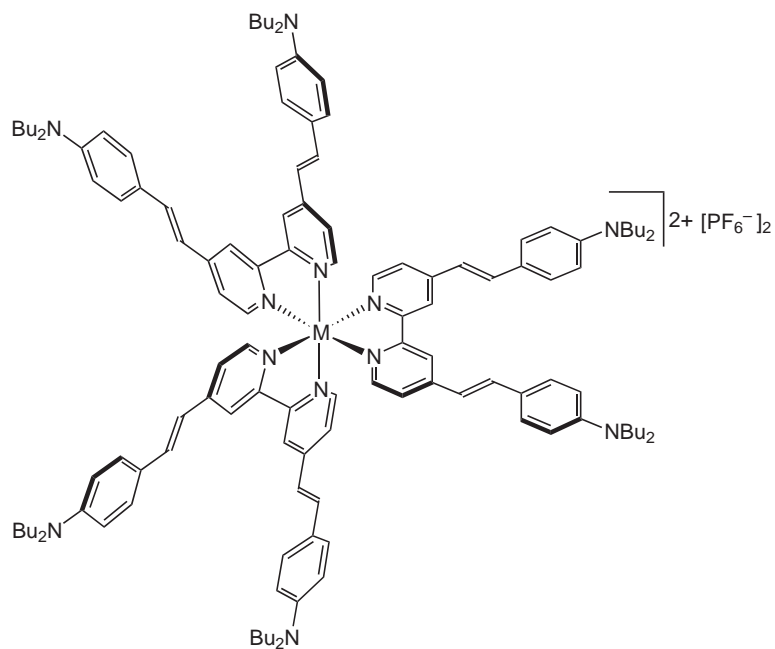
Besides tris-chelates such as (58)–(63), Le Bozec and co-workers have also studied several tetrahedral complexes of 4,4'-disubstituted 2,2'-bipy ligands.^{129–131} 1,340 nm EFISHG was applied



R = NBu₂ (**58**): $\lambda_{\max} = 513 \text{ nm}$ (CH₂Cl₂), $\beta_0[\text{HRS}] = 2,200 \cdot 10^{-30} \text{ esu}$ (CHCl₃)¹²³

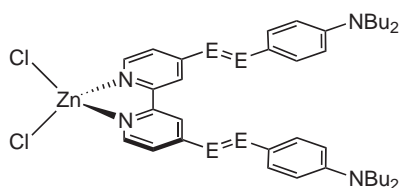
R = NEt₂ (**59**): $\beta_0[\text{Stark}] = 300 \cdot 10^{-30} \text{ esu}$ (BuCN/2-MeTHF)¹²⁶

R = OOct (**60**): $\lambda_{\max} = 382 \text{ nm}$ (CH₂Cl₂), $\beta_0[\text{HRS}] = 298 \cdot 10^{-30} \text{ esu}$ (CHCl₃)¹²⁵



No.	M	λ_{\max} (nm) (CH ₂ Cl ₂)	$\beta_0[\text{HRS}]$ (10 ⁻³⁰ esu) (CHCl ₃) ¹²⁵
(61)	Fe	467	113
(62)	Zn	473	398
(63)	Hg	438	256

to dipolar Zn^{II} systems (e.g., (64) and (65)),¹²⁹ whilst octupolar Cu^I salts (e.g., (66))¹³⁰ were investigated by 1,340 nm HRS. The latter are rare examples of nondipolar tetrahedral metal-based NLO chromophores which show relatively good transparency/efficiency trade-off characteristics.¹³⁰ (67) has also been studied by 1,907 nm HRS, and its NLO properties compared with those of (64) ($\beta_0 = 62 \times 10^{-30}$ esu from 1,340 nm EFISHG) and (62) ($\beta_0 = 241 \times 10^{-30}$ esu).¹³¹ The β_0 values increase monotonically with the number of coordinated 2,2'-bipy ligands, as the chromophore structure changes from dipolar to D_{2d} and then D_3 octupolar.¹³¹ Furthermore, the larger β_0 and lower ILCT energy of (67) compared with (66) are consistent with the greater Lewis acidity of Zn^{II} vs. Cu^I and also the absence of an MLCT transition in (67).¹³¹ The salt $[\Delta-Zn^{II}(2,2'-bipy)_3][Zn^{II}L_4]$ (L = 2-chloro-4-nitrophenolate) shows SHG activity of 5 times urea at 1,064 nm.¹³² Although this compound contains two octupolar ions, only the tetrahedral anions contribute to the observed SHG, and the presence of the resolved chiral cations encourages the adoption of the NCSG C2.¹³²

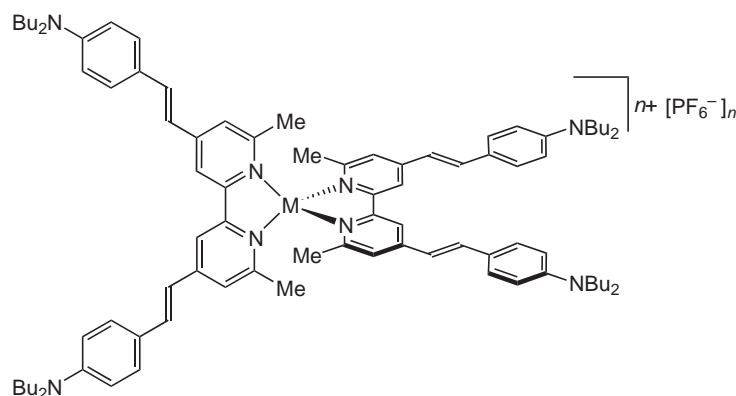


E = CH (64): $\lambda_{max} = 455$ nm (CH_2Cl_2),

μ, β_0 [EFISHG] = $660 \cdot 10^{-48}$ esu ($CHCl_3$)

E = N (65): $\lambda_{max} = 516$ nm (CH_2Cl_2),

μ, β_0 [EFISHG] = $700 \cdot 10^{-48}$ esu ($CHCl_3$)¹²⁹

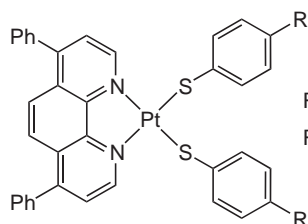


M = Cu, $n = 1$ (66): $\lambda_{max} = 424$ nm (CH_2Cl_2), β_0 [HRS] = $78 \cdot 10^{-30}$ esu ($CHCl_3$)¹³⁰

M = Zn, $n = 2$ (67): $\lambda_{max} = 529$ nm, β_0 [HRS] = $157 \cdot 10^{-30}$ esu (CH_2Cl_2)¹³¹

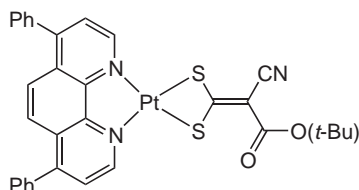
Only two studies have described the quadratic NLO properties of square planar complexes of α -diimines.^{133,134} Cummings *et al.* used 1,907 nm EFISHG to study a series of α -diimine/dithiolate complexes of Ni^{II} , Pd^{II} , or Pt^{II} and found that the low energy CT transitions and β_0 values appear to correlate, in accord with the TSM.¹³³ For example, the complex (68) has a lower CT energy and a larger β_0 when compared with (69) because $-NH_2$ is a stronger electron donor than $-OMe$.¹³³ The electron-accepting substituents on the dithiolate ligand in (70) further raise the CT energy and decrease β_0 .¹³³ The lowest energy (and hence β dominating) CT bands in such complexes are termed "CT to diimine" because the HOMOs comprise mixtures of metal and thiolate orbital character, whilst the LUMOs are diimine π^* orbitals.¹³³ In complexes such as (70), metal \rightarrow dithiolate MLCT excitations oppose the "CT to diimine" processes.¹³³ The tetrahedral Zn^{II} complex (71) was also included in this study and is noteworthy not for its modest β_0 value, but for the origin of this response which is a ligand-to-ligand (dithiolate \rightarrow diimine) CT (LLCT) excitation. The electronic role of the metal in such a case is hence minimal.¹³³ Base *et al.* have also used 1,907 nm EFISHG to show that square planar Pt^{II} complexes such as (72) obey the TSM and exhibit solvent-dependent β_0 values.¹³⁴

The cubic NLO properties of Ru^{II} tris(α -diimine) complexes have been investigated only relatively recently by Ji and co-workers using 540 nm Z-scan; all of the complexes studied exhibit both NLO absorption and SDF behavior.¹³⁵⁻¹³⁸ The large $\chi^{(3)}$ and γ values of complexes such as (73) depend on the position of the $-NO_2$ group in the order 4- > 2- > 3-.¹³⁵ Also, the NLO responses decrease on deprotonation of the imidazolyl nitrogens (although this effect is only

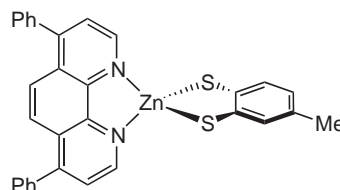


R = NH₂ (**68**): $\lambda_{\max} = 517$ nm, $\beta_0[\text{EFISHG}] = -26 \cdot 10^{-30}$ esu (CH₂Cl₂)

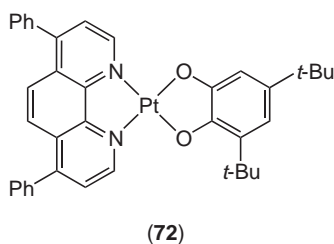
R = OMe (**69**): $\lambda_{\max} = 503$ nm, $\beta_0[\text{EFISHG}] = -21 \cdot 10^{-30}$ esu (CH₂Cl₂)¹³³



(**70**): $\lambda_{\max} = 457$ nm,
 $\beta_0[\text{EFISHG}] = -11 \cdot 10^{-30}$ esu (CH₂Cl₂)¹³³



(**71**): $\lambda_{\max} = 440$ nm,
 $\beta_0[\text{EFISHG}] = -4 \cdot 10^{-30}$ esu (CH₂Cl₂)¹³³



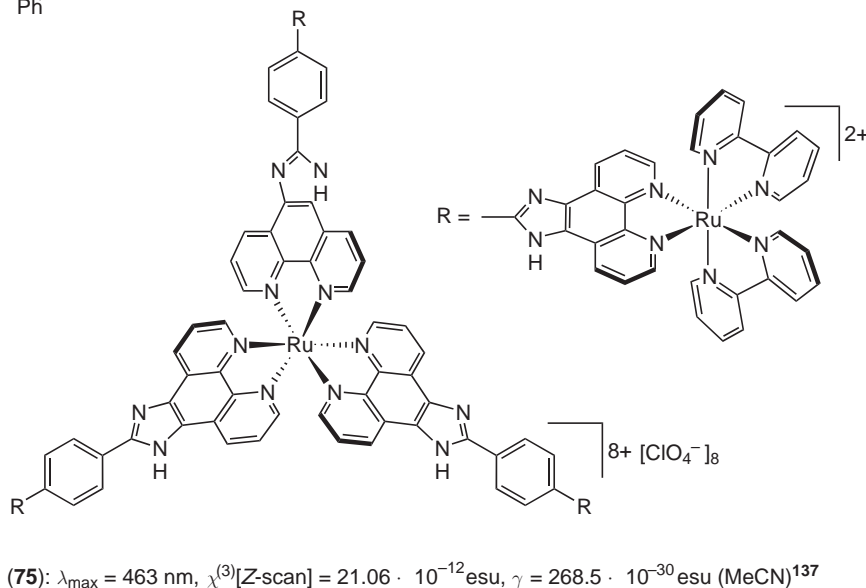
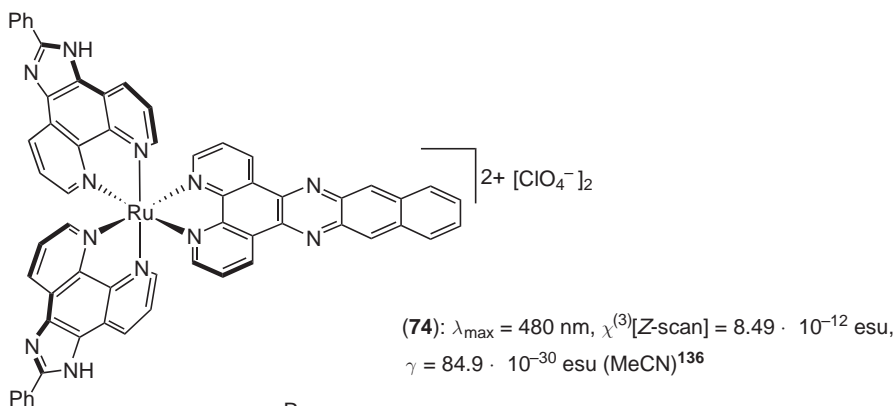
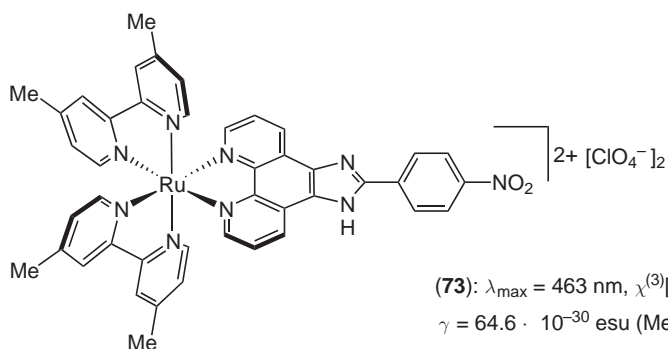
Solvent	λ_{\max} (nm)	$\mu\beta_0[\text{EFISHG}]$ (10^{-48} esu) ¹³⁴
Toluene	717	-523
CHCl ₃	657	-635
CH ₂ Cl ₂	621	-669
DMSO	601	-597

statistically significant for (**73**)), an effect attributable to the resulting decreased π -acceptor capacity of the phen-derived ligand.¹³⁵ Studies with (**74**) and related salts show that the γ values decrease as the π -system is shortened by the sequential removal of aryl rings from the hexacyclic benzo[*i*]dipyrido[3,2-*a*:2',3'-*c*]phenazine ligand (the phen analogue of (**74**) has $\gamma = 47.8 \times 10^{-30}$ esu).¹³⁶ The tetranuclear species (**75**) has larger $\chi^{(3)}$ and γ values than its mono- or dinuclear counterparts.¹³⁷ These parameters scale with the number of metal centers (e.g., $\gamma = 73.4 \times 10^{-30}$ esu for the mononuclear complex), indicating an additive contribution of the individual chromophores to the NLO responses.¹³⁷ The salts [Ru^{II}(2,2'-bipy)_{3-n}(PIP)_{*n*}][ClO₄]₂ (PIP = 2-phenylimidazo[4,5-*f*][1,10]phenanthroline) have γ values in the range 4.15 – 4.86×10^{-29} esu (in DMF), which increase with *n*.¹³⁸

Okubo *et al.* have used Stark spectroscopy to study the unusual trinuclear complex salt (**76**) which has pseudo D_{3h} symmetry and contains tetrahedral Cu^I centers and a symmetrical hexazatriphenylene-derived radical anionic ligand.¹³⁹ The $\chi^{(3)}$ responses of PMMA thin films doped with (**76**) are enhanced by an intense, broad MLCT transition which has a maximal absorbance in the NIR region.¹³⁹

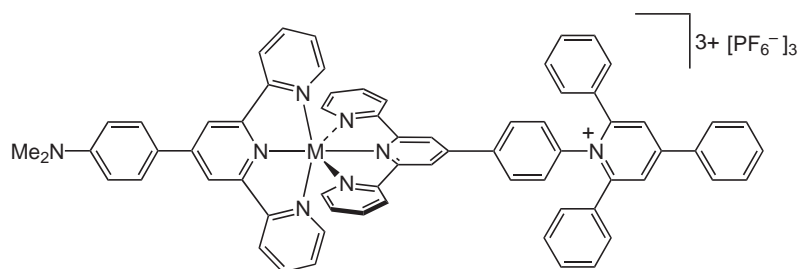
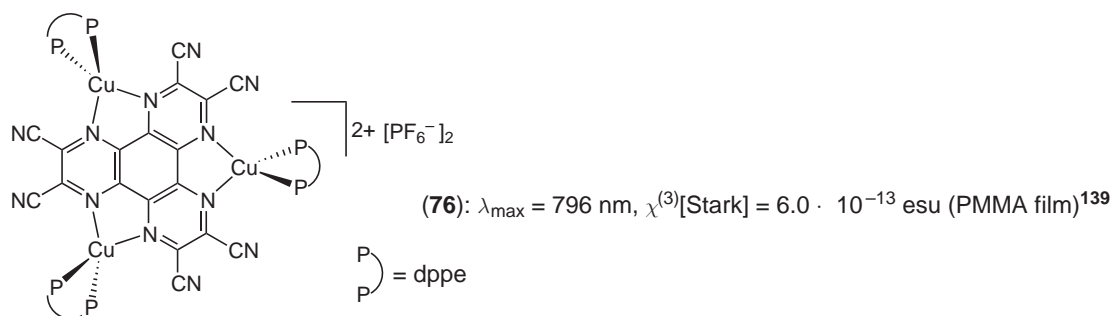
Given the extensive NLO studies carried out with Ru^{II} tris(α -diimine) derivatives, it is perhaps surprising that only a single investigation involving related complexes of tridentate ligands has been reported to date.¹⁴⁰ Konstantaki *et al.* have used 532 nm Z-scan to study several bis-(2,2':6',2''-terpyridyl)-based complexes of Ru^{II} and Os^{II}, and found very large cubic NLO responses for compounds such as (**77**) and (**78**).¹⁴⁰ Furthermore, when excited with 10 ns laser pulses, the Ru^{II} complexes exhibit RSA, whilst the Os^{II} analogues show SA for low incident intensities that turns into RSA above an intensity threshold which depends on the solution concentrations. In contrast, with faster (500 fs) laser excitation, all of the complexes show only SA.¹⁴⁰ Roberto *et al.* have very recently reported the first NLO studies on mono-(2,2':6',2''-terpyridyl) complexes, applying 1,340 nm EFISHG to complexes of 4'-(4-dibutylaminophenyl)-2,2':6',2''-terpyridyl with several different metal centers.¹⁴¹ The β values are enhanced in all cases

when compared with the free ligand, being positive for trigonal bipyramidal Zn^{II} complexes, but negative with octahedral Ru^{III} and Ir^{III} centers.¹⁴¹



9.14.2.3 Complexes of Porphyrin and Related Ligands

LeCours *et al.* reported extremely large quadratic NLO responses for the asymmetrically substituted metalloporphyrin (MP) derivatives (**79**) and (**80**) determined via HRS.¹⁴² These complexes show intense Soret (B) $\pi \rightarrow \pi^*$ bands at $\lambda_{\text{max}} = \text{ca. } 460 \text{ nm}$ as well as lower energy Q-type $\pi \rightarrow \pi^*$ absorptions in the range 650–700 nm.¹⁴² The β response for the Cu^{II} complex (**79**) shows a marked wavelength dependence, whilst its Zn^{II} analogue (**80**) has essentially identical β_{830} and β_{1064} values.¹⁴² Using the Soret band and the TSM, the estimated minimum β_0 value for (**80**) of



$$\text{M} = \text{Ru} \text{ (77): } \gamma [\text{Z-scan}] = 228 \cdot 10^{-30} \text{ esu}$$

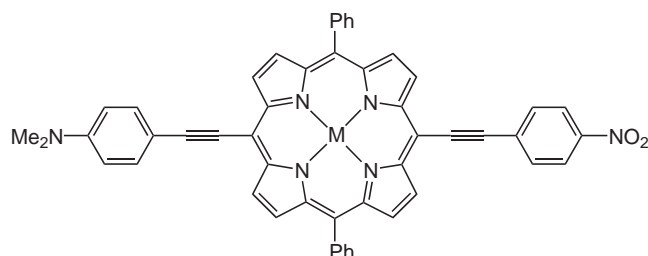
$$\text{M} = \text{Os} \text{ (78): } \gamma [\text{Z-scan}] = 203 \cdot 10^{-30} \text{ esu (MeCN)}^{140}$$

800×10^{-30} esu is the largest yet observed for a metal complex and competes favorably with the best known purely organic NLO chromophores.¹⁴² Although ZINDO/SCI-SOS calculations carried out by Priyadarshy *et al.* verify the experimentally determined large β of (80), they do not account for the observed wavelength independence.¹⁴³ The theory also predicts a small contribution of the cumulenonic resonance structure to the ground state of (80).¹⁴³ Subsequent Stark spectroscopic experiments with (80) show that large $\Delta\mu_{12}$ values accompany excitations of x -polarized B and Q transitions, and the single largest contributor to β is the $B_x(1,0)$ transition.¹⁴⁴ These studies yield a β_0 value of 335×10^{-30} esu, and show that the apparent wavelength independence of β at 830 nm and 1,064 nm is only coincidental.¹⁴⁴

1,064 nm HRS studies on a series of MPs (e.g., (81) and (82)) show that metallation significantly enhances β compared with the free-base porphyrins, with a greater influence being exerted by the open shell Cu^{II} (d^9) than the closed shell Zn^{II} (d^{10}).¹⁴⁵ Also, the β responses of the Zn^{II} complexes can be described by the TSM, but a large number of excited states seem to contribute to β in the Cu^{II} analogues.¹⁴⁵ Compared with the arylolethynyl derivatives (79) and (80), the NLO responses of *meso*-tetraaryl-MPs such as (81) and (82) are limited by relatively weak donor-acceptor coupling. The sandwich complex $[\text{Zr}^{\text{IV}}(\text{OEP})(\text{OETAP})]$ (OEP = octaethylporphyrin; OETAP = octaethyltetraazaporphyrin) has been studied by 1,907 nm EFISHG.¹⁴⁶ Using the Q band at 434 nm gives a TSM β_0 of -62×10^{-30} esu (in CHCl_3), and it has been suggested that strong metal-mediated π -coupling between two macrocycles offers a new approach to the construction of high β MP-based molecules.¹⁴⁶

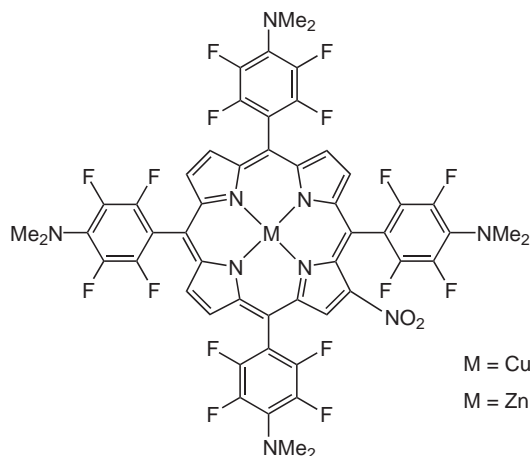
On account of their particularly extensive delocalized π -systems, MPs have received comparatively more attention for their cubic, as opposed to quadratic, NLO properties. From the viewpoint of practical applications, such complexes (and also metallophthalocyanines and other closely related compounds) are of major interest for OL due to their tendency to exhibit RSA behavior. These materials are particularly well suited in this regard because they often exhibit strongly absorbing, long-lived triplet excited states as well as reasonably wide transparency windows over the visible region of interest between the intense B- and Q-bands.

Blau and co-workers first reported observations of RSA in toluene solutions of Zn^{II} or Co^{II} *meso*-tetraphenylporphyrins with 80 ps pulses at 532 nm,¹⁴⁷ and also proposed a theoretical mechanistic description for the cubic NLO properties of these complexes.¹⁴⁸ RSA in Fe^{II} *meso*-tetraphenylporphyrin was later described by Fei *et al.*¹⁴⁹ Other early 532 nm DFWM studies^{150–152} involve complexes of tetrabenzoporphyrins which were found in THF to display $\chi^{(3)}$ values



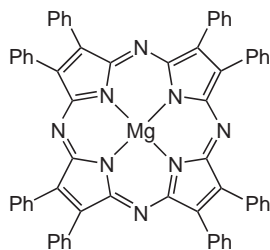
M = Cu (**79**): β_{830} [HRS] = $4374 \cdot 10^{-30}$ esu, β_{1064} [HRS] = $1501 \cdot 10^{-30}$ esu (CHCl₃)

M = Zn (**80**): β_{830} [HRS] = $5142 \cdot 10^{-30}$ esu, β_{1064} [HRS] = $4933 \cdot 10^{-30}$ esu (CHCl₃)¹⁴²



M = Cu (**81**): β_{1064} [HRS] = $118 \cdot 10^{-30}$ esu

M = Zn (**82**): β_{1064} [HRS] = $92 \cdot 10^{-30}$ esu (CH₂Cl₂)¹⁴⁵



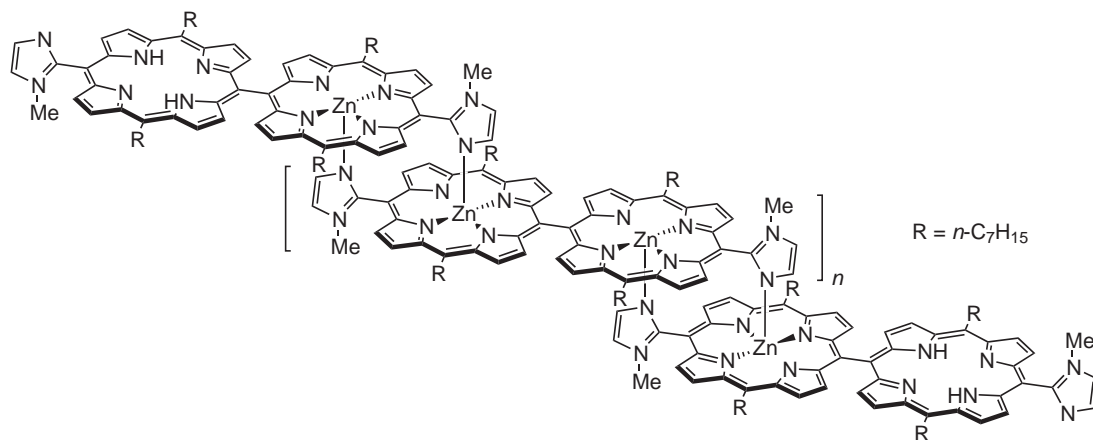
(**83**): $\chi_{xxxx}^{(3)}$ [DFWM] = $1.17 \cdot 10^{-11}$ esu,
 $\chi_{yyyy}^{(3)}$ [DFWM] = $0.303 \cdot 10^{-11}$ esu (PMMA film)¹⁵⁸

4–5 orders of magnitude larger than that of CS₂ (five of the complexes of Zn^{II} show $\chi^{(3)}$ in the range $1.2\text{--}2.8 \times 10^{-8}$ esu).¹⁵⁰ 532 nm Z-scan has also been applied to Zn^{II} tetrabenzoporphyrin, affording excited-state cross sections and other parameters.¹⁵³ A combination of time-resolved DFWM with incoherent light and Z-scan measurements has been used to investigate the excited-state dynamics of several Zn^{II} *meso*-tetraarylporphyrins and also Co^{II} and Ni^{II} *meso*-tetraarylporphyrins, and excited-state and ground-state relaxation times were calculated based on a theoretical formalism.¹⁵⁴ Chen *et al.* used ps transient absorption studies on a series of *meso*-tetraaryl-tetrabenzoporphyrins (including Pt^{II} complexes) to confirm that RSA is the dominant OL mechanism, the results agreeing well with a five-state model.¹⁵⁵ In the expectation that the incorporation of further heavy atoms should enhance the RSA properties of MPs, nonlinear absorption measurements have been carried out on some octabromo-*meso*-tetraphenyl-MPs.¹⁵⁶ The performance of the Zn^{II} complex is comparable with that of In^{III} phthalocyanines.¹⁵⁶

A $\chi^{(3)}$ value of 2.6×10^{-12} esu for spin-coated films of [Mn^{III}Cl(OEP)] was determined by 1,907 nm THG measurements.¹⁵⁷ Thin PMMA films incorporating the Mg^{II} tetraazaporphyrin complex (**83**) have also been studied by DFWM in the phase conjugate geometry, allowing the derivation of different $\chi^{(3)}$ components.¹⁵⁸ The dynamics of the NLO response were also measured, with the film of (**83**) exhibiting both a sub-ps response and a more slowly decaying

response (10 ps–1 ns) owing to excited-state population.¹⁵⁸ 532 nm DFWM has been applied to benzene solutions of a series of mesogenic 5,10,15,20-tetrakis (4-pentadecylphenyl)MPs, affording $\chi^{(3)}$ values of ca. 10^{-11} esu for Co^{II} , Ni^{II} , Cu^{II} , Zn^{II} , and $\{\text{V}^{\text{IV}}(\text{O})\}^{2+}$ complexes.¹⁵⁹

In order to create molecules with even larger conjugated π -systems, oligomeric MPs have also been studied. Two series of Zn^{II} porphyrin oligomers featuring direct *meso-meso* or 1,4-phenylene bridges have been investigated by using *Z*-scan at 640 and 1,064 nm, and γ increases predictably with the number of MP units.¹⁶⁰ Ogawa *et al.* have exploited axial Zn^{II} -imidazolyl interactions to form a series of self-assembled oligomeric Zn^{II} porphyrins including (84)–(86).¹⁶¹ 800 nm fs time-resolved OKE measurements yield very large off-resonant cubic optical nonlinearities, with γ showing a marked tendency to increase with the chain length.¹⁶¹ Furthermore, the terminal free-base porphyrins are necessary to enhance the cubic NLO responses in such assemblies.¹⁶¹



No.	<i>n</i>	$\gamma_{\text{yyyy}}[\text{OKE}]$ (10^{-32} esu)	$\chi_{\text{yyyy}}^{(3)}[\text{OKE}]$ (10^{-15} esu) ¹⁶¹
(84)	1	180	50
(85)	2	950	165
(86)	3	1,300	163

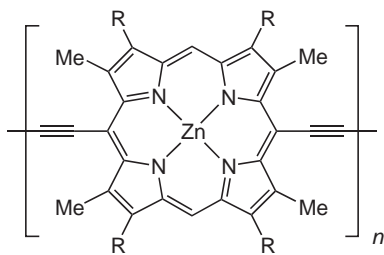
Anderson and co-workers have carried out detailed investigations into the cubic NLO properties of (mostly oligomeric) MPs,^{162–174} and this work has been reviewed.¹⁷⁵ Stark spectroscopic studies with thin films of Zn^{II} porphyrin polymers containing acetylenic bridges^{162–164} afford a peak resonant $\chi^{(3)}$ of 7.2×10^{-8} esu at 850 nm for (87). This response is an order of magnitude larger than those of simple conjugated organic polymers.^{163,164} Further studies on (87) and related MPs have included a battery of techniques including fs transient-photoinduced transmission spectroscopy,¹⁶⁵ RSA measurements,¹⁶⁶ DFWM experiments,^{167,168} *Z*-scan studies¹⁶⁹ and ZINDO/MRDCI calculations.¹⁷⁰ It is particularly noteworthy that the off-resonant $\chi^{(3)}$ value of 2.1×10^{-9} esu obtained for thin films of (87) by using 1,064 nm DFWM is still very large.¹⁶⁸ Indeed, the γ per macrocycle (γ/n) of (87) is approximately 10^3 times greater than that of the corresponding monomer, indicating that inter-porphyrin conjugation plays an important role in enhancing the optical nonlinearity.¹⁶⁸ The latter is in accord with the ZINDO/MRDCI calculations which infer a sizable cumulemic contribution in the excited-state of the dimeric complex.¹⁷⁰ Detailed 1,064 nm DFWM studies show that γ/n increases by nearly 100-fold between the monomer and dimer, then rises linearly at least up to the pentamer.¹⁶⁷

The major focus of the work by Anderson and colleagues has latterly been on attempts to derive molecular SACs for the OL behavior of Zn^{II} and various group 13 and 14 MPs.^{171–174} OL measurements at 532 nm on a range of mononuclear complexes reveal a strong dependence on the metal atom and peripheral substitution. The σ_e/σ_g ratios (σ_e = (triplet) excited-state absorption cross-section and σ_g = ground-state absorption cross-section) determined for complexes (88)–(90) are the largest such values ever reported for macrocyclic dyes, suggesting that these compounds are strong candidates for practical applications.¹⁷⁴ Other researchers have also studied the cubic NLO properties of *meso*-tetra-alkynyl Zn^{II} porphyrins by using the *Z*-scan method,¹⁷⁶ and OL measurements.¹⁷⁷ The OL potential of various other MPs has also been considered,^{178–180} and

γ values of ca. 10^{-30} esu have been calculated for Zn^{II} *meso*-tetraarylbenzoporphyrins by using the PM3 method.¹⁸¹

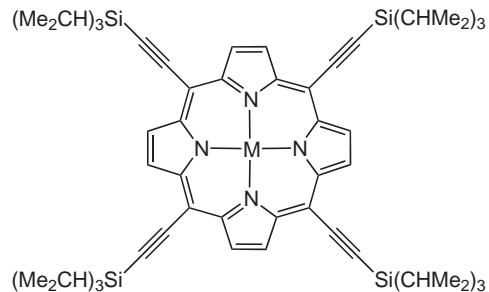
With the intention of identifying new OL materials, Sun and co-workers have studied the cubic NLO properties of a number of porphyrin-like metal complexes (mostly of Cd^{II}) in which one of the pyrrole rings is replaced with an aryl or vinyl group (so-called *texaphyrins*).^{182–189} Initial 1,064 nm DFWM results show that the complex salts **(91)** and **(92)** exhibit very large cubic NLO responses.¹⁸² Subsequent measurements at 532 nm have included a range of related complexes,^{183–189} and most of these display very strong RSA for ns laser pulses. The dynamics of the NLO responses have been investigated,^{183,184} and the RSA explained by using a five-state model.¹⁸⁴ A σ_e of $7.0 \times 10^{-17} \text{ cm}^2$ and a nonlinear refractive cross section of $1.7 \times 10^{-17} \text{ cm}^2$ were obtained for one Cd^{II} compound from a theoretical simulation and Z-scan results.¹⁸⁸ The complex salt **(93)** has one of the largest γ values for an off-resonant cubic NLO material, and measurements of different $\chi^{(3)}$ tensor components indicate that the nonlinearities of such complexes are predominantly electronic in origin with 40 ps laser pulses.¹⁸⁹ The twofold increase in γ compared with **(91)** ($\gamma = 4.8 \times 10^{-31}$ esu at 532 nm) is due to the more extensive conjugation in the benzophenone unit.¹⁸⁹ **(93)** shows strong RSA with 5 ns laser pulses with a F_{th} of ca. 1 mJ cm^{-2} , but exhibits a transformation from RSA to SA behavior at high fluence when using ps pulses.¹⁸⁹

Torres and co-workers have investigated the cubic NLO properties of various metallotriazole-*le*hemiporphyrazines.^{190–194} Early THG studies at 1,340 nm and 1,907 nm with $CHCl_3$ solutions show that metal ions with partially filled d-shells enhance γ when compared to the uncomplexed macrocycles.^{190,191} However, later 1,064 nm THG studies with LB films of some Co^{II} complexes indicate that metallation has no significant effects on the NLO responses.¹⁹² More recently,

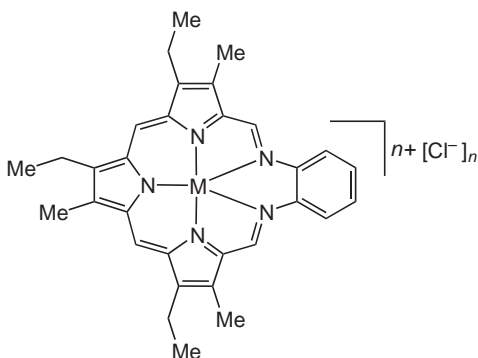


(87) ($n = 10–15$; end groups unknown)

R = $(CH_2)_2CO_2(CH_2)_2CHMe(CH_2)_3CHMe_2$

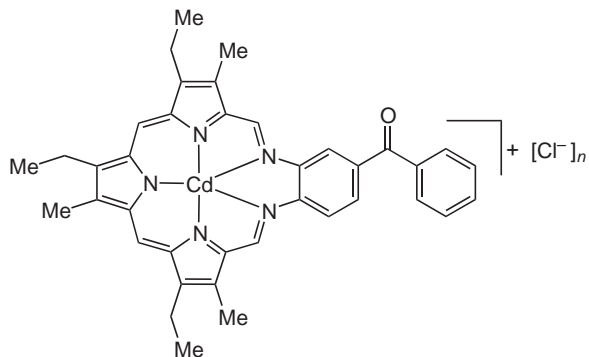


No.	M	$\sigma_e/\sigma_g(CH_2Cl_2)^{174}$
(88)	InCl	48
(89)	TlCl	46
(90)	Pb	45



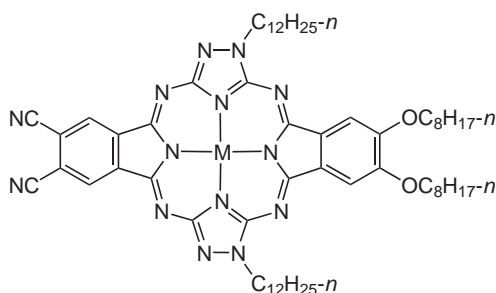
M = Cd **(91)**: $n = 1$, γ [DFWM] = $1.2 \cdot 10^{-31}$ esu (MeOH)

M = Gd **(92)**: $n = 2$, γ [DFWM] = $1.0 \cdot 10^{-31}$ esu (MeOH)¹⁸²

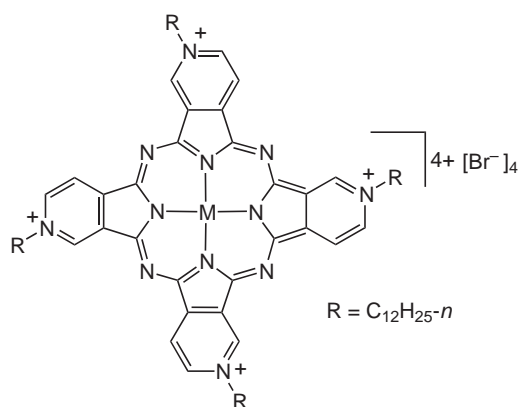


(93): γ [DFWM] = $9.7 \cdot 10^{-31}$ esu (MeOH)¹⁸⁹

532 nm Z-scan results with complexes such as (94)–(96) reveal very large γ values, with a clear dependance on the metal center, and (95) and (96) also show RSA.¹⁹⁴ Thin films of the metallotetrapyrrolineporphyrazines (97)–(99) have also been studied by 1,064 nm THG experiments.¹⁹⁵ The $\chi^{(3)}$ values of LB films of (97)–(99) are essentially independent of the film thicknesses, whilst spin-coated PMMA samples show strong THG enhancements, attributable to molecular aggregation, on increasing the concentration of the solutions used to prepare the samples.¹⁹⁵ THG dispersion measurements on spin-coated thin films of the complex *trans*-dihydroxy-1,6,11,16-tetra(*tert*-butyl)porphyrazine Ge^{IV} have been reported by Nalwa *et al.*¹⁹⁶ The maximum $\chi^{(3)}$ value of 1.3×10^{-11} esu with a 1,650 nm fundamental is associated with a three-photon resonance.¹⁹⁶



No.	M	γ [Z-scan] (10^{-30} esu) (toluene) ¹⁹⁴
(94)	Co	1.3
(95)	Cu	66
(96)	Zn	31



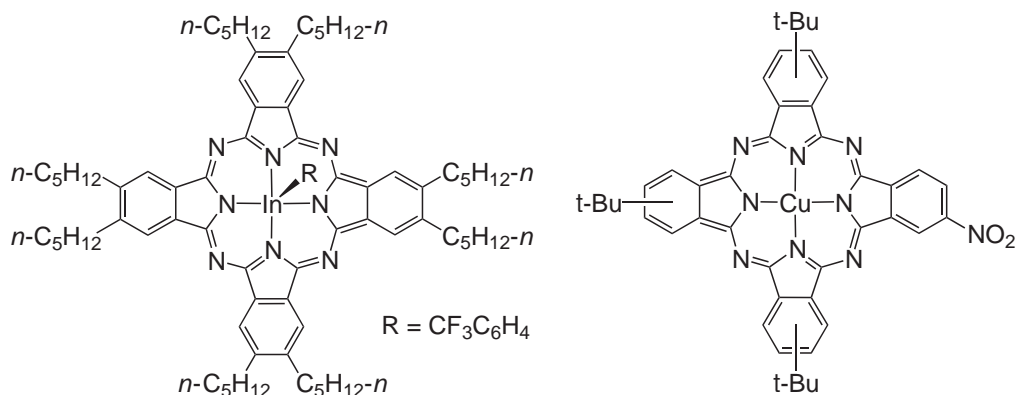
No.	M	$\chi^{(3)}$ [THG] (10^{-14} esu) (LB film) ¹⁹⁵
(97)	Co	108
(98)	Ni	96
(99)	Cu	94

9.14.2.4 Complexes of Phthalocyanine and Naphthalocyanine Ligands

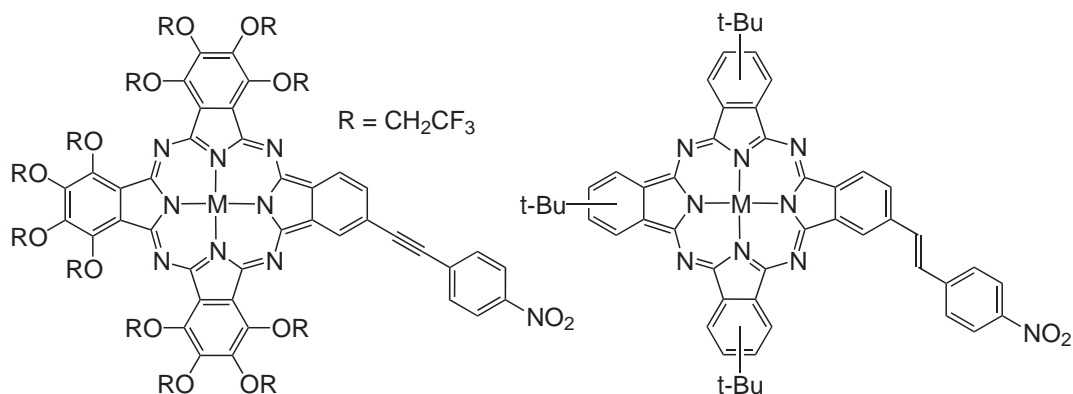
The NLO properties of metallophthalocyanines (MPcs) and metallo-2,3-naphthalocyanines (MNPCs) have been extensively studied, primarily due to their OL potential. This area has been reviewed,^{197–200} and although citations are near-comprehensive, discussion here will be limited to selected highlights and more recent developments.

The first report of the NLO properties of MPcs appeared in 1987, when Ho *et al.* described THG from thin polycrystalline films of $[\text{M}^{\text{III}}\text{PcX}]$ ($\text{M} = \text{Al}, \text{Ga}; \text{X} = \text{Cl}, \text{F}$).²⁰¹ Soon after, 532 nm OL measurements were made on solutions of several MPcs and MNPCs,²⁰² and off-resonant $\chi^{(3)}$ values were determined for Pt^{II} and Pb^{II} tetrakis(cumylphenoxy)Pcs via 1,064 nm DFWM.²⁰³ Metallation greatly enhances the cubic responses; for example, $\chi^{(3)}_{\text{xxxx}}$ for the Pt^{II} complex is ca. 45 times that of the free ligand.²⁰³ Following these early experiments, many groups have investigated the NLO properties of MPcs. Although these studies have considered predominantly cubic effects, there have been a number of reports of SHG from MPcs.^{204–224} Perhaps surprisingly, many of these materials comprise thin films of centrosymmetric molecules, such as $[\text{Ni}^{\text{II}} \{\text{tetrakis(cumylphenoxy)Pc}\}]$,²⁰⁵ and $[\text{Cu}^{\text{II}}\text{Pc}]$.^{206,208,209,218} In the former case, the noncentrosymmetry arises from random orientations of the substituent groups,²⁰⁵ whilst several explanations may explain the origins of SHG from other centrosymmetric MPcs. Of these, an electric quadrupole mechanism seems to be the favored theory,^{211,212,214,218} and this is supported by measurements on films grown by the molecular beam epitaxy (MBE) technique.²¹³ Due to its square pyramidal coordination geometry, $[\text{V}^{\text{IV}}\text{OPc}]$ is noncentrosymmetric and SHG has been observed from MBE-grown thin films of this complex^{207,215} and of $[\text{Ti}^{\text{IV}}\text{OPc}]$.²¹⁵ Films of $[\text{V}^{\text{IV}}\text{OPc}]$ and $[\text{Ti}^{\text{IV}}\text{OPc}]$ on

glass substrates also show fairly strong SHG.²¹⁸ DFT calculations reinforce the suggestion that the resonant NLO processes in such complexes are attributable to electric quadrupole transitions at SH frequencies.²¹⁵ 1,064 nm EFISHG has been applied to three axially substituted In^{III} Pcs, e.g., (**100**) (the data were analyzed with a TSM corresponding to the Q-band), and $\chi^{(2)}$ values were also determined for spin-coated thin films of these complexes dissolved in PMMA.²²¹ (**100**) has the largest β and $\chi^{(2)}$ values, when compared with its analogues containing axial chloride or phenyl ligands.²²¹



(**100**): $\beta_0[\text{EFISHG}] = 35 \cdot 10^{-30} \text{ esu (CHCl}_3\text{)}^{221}$ (**101**): $\chi^{(2)}[\text{SHG}] = 1.63 \cdot 10^{-5} \text{ esu (LB film)}^{210}$



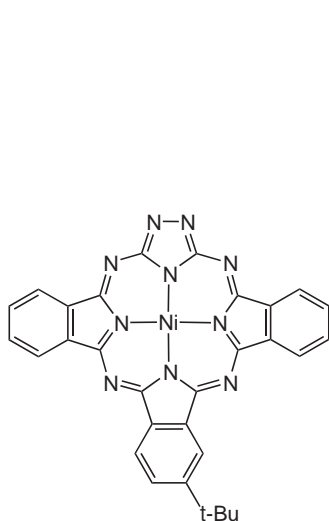
M = Zn (**102**), V=O (**103**)

No.	M	$\beta_0[\text{EFISHG}] (10^{-30} \text{ esu})$ (CHCl ₃) ²²⁰
(104)	Co	28
(105)	Ni	40
(106)	Cu	44

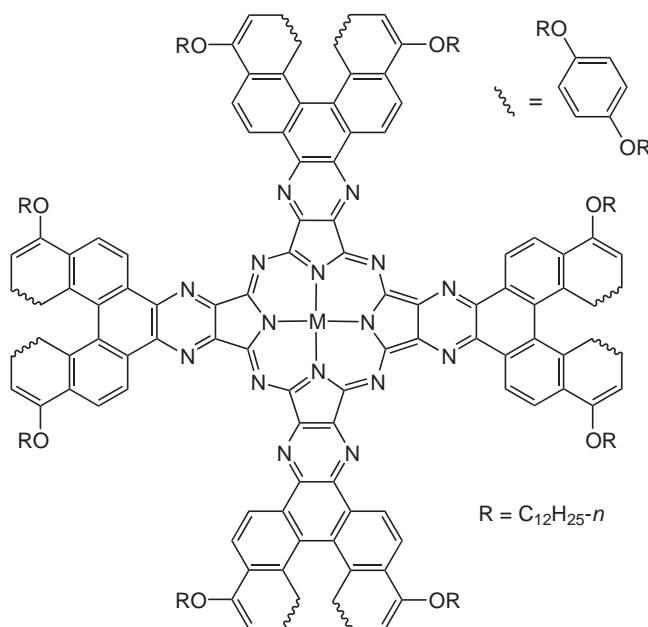
Ultrathin films of a fluoro-bridged aluminum Pc polymer give SHG,²⁰⁴ and asymmetrically-substituted MPcs have also been investigated.^{210,216,217,219,220} Alternating LB films of the Cu^{II} complex (**101**) show a quadratic dependance of the SHG intensity with the number of layers, and a $\chi^{(2)}$ enhancement of ca. 10^3 compared with the free ligand.²¹⁰ Spin-coated thin PMMA films doped with complexes such as (**102**) and (**103**) also give SHG at 532 nm after electric poling at 110 °C for 30 min.^{216,217} Related MPcs such as (**104**)–(**106**) have also been studied by using 1,907 nm EFISHG^{219,220} with a TSM including the Q-band energies.²²⁰ The observed trend of

increasing β_0 in the sequence $\text{Co}^{\text{II}} < \text{Ni}^{\text{II}} < \text{Cu}^{\text{II}}$ correlates with the magnitude of the ground state dipole moments and with the metal ion polarizabilities.²²⁰

Preliminary 1,064 nm EFISHG results for a series of Co^{II} , Ni^{II} , or Cu^{II} triazole-Pcs have been reported.²²² More recently, Rojo *et al.* have investigated the quadratic NLO responses of three noncentrosymmetric triazole-MPCs, by using 1,340 nm HRS and 1,907 nm EFISHG.²²³ These complexes (e.g., **(107)**) have β values of ca. 10^{-28} esu, and the ratio $(\beta[\text{EFISHG}])^2/(\beta[\text{HRS}])^2$ markedly decreases if the donor strength of the substituents on the isoindole rings (opposite to the triazole unit) is increased.²²³ This phenomenon is attributable to corresponding changes in the perpendicular/parallel components of the transition dipole moments.²²³ Fox *et al.* have described interesting molecules **(108)** and **(109)** in which Cu^{II} and Ni^{II} octaaza-Pc cores are fused to four nonracemic [7]helicenes.²²⁴ MM3 calculations indicate that **(108)** and **(109)** stack in chiral superstructures with a core-to-core distance of ca. 3.4 Å.²²⁴ Although symmetric, these complexes give large $\chi^{(2)}$ responses in LB films due to the chirality of their bulk structures.²²⁴



(107): $\beta_{1907}[\text{EFISHG}] = -103 \cdot 10^{-30}$ esu,
 $\beta_{1340}[\text{HRS}] = 110 \cdot 10^{-30}$ esu (CHCl_3)²²³



M = Cu **(108)**: $\chi_{xyz}^{(2)}[\text{SHG}] = 5.73 \cdot 10^{-8}$ esu (LB film)

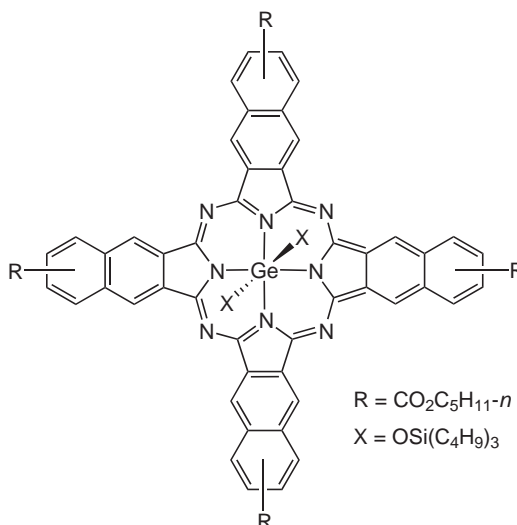
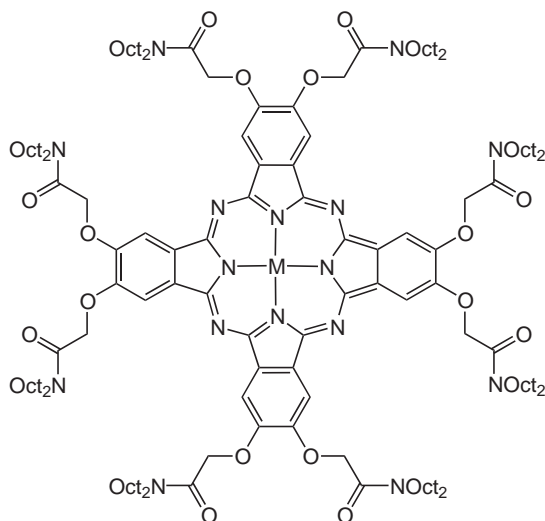
M = Ni **(109)**: $\chi_{xyz}^{(2)}[\text{SHG}] = 4.54 \cdot 10^{-8}$ esu (LB film)²²⁴

Many studies dealing with the cubic NLO properties of MPCs have been reported since 1990, and these will be discussed only briefly here, focusing on the research of the following leaders in this field: Agullo-Lopez,^{220,225–232} Nalwa,^{196,233–239} Perry,^{240–248} Shirk,^{249–265} Hanack,^{239,264–271} Wada,^{272–284} Heflin,^{285–290} Yamashita,^{291–297} and Fang.^{298–302}

Agullo-Lopez and co-workers have used 1,346 nm THG and 1,064 nm EFISHG studies on CHCl_3 solutions of **(110–112)** to obtain both real and imaginary parts of γ from the TH concentration dependences.²²⁵ Whilst the THG data show no significant γ increases on metallation, the EFISHG results do show clear enhancements, particularly for Co^{II} .²²⁵ The THG data are satisfactorily analyzed in terms of a four-state model including two one-photon allowed states (corresponding to the Q and B bands), and the γ enhancements shown by EFISHG are attributable to one-photon resonance with $d-d$ transitions at ca. 1,000 nm.²²⁵ 1,064 nm Z-scan studies with ps pulses on **(112)** confirm that the nonlinear absorption process is dominated by RSA.²³¹ $\chi^{(3)}$ values at 1,064 nm and 1,907 nm have been measured for sol-gel films containing $\text{Cu}^{\text{II}}\text{Pc}$ at several concentrations in the range 10^{-4} – 10^{-5} M.²²⁸ Samples containing 10^{-4} M of $[\text{Cu}^{\text{II}}\text{Pc}]$ and treated by annealing at 200 °C have $\chi^{(3)}$ values up to 2.6 times larger than those of the sol-gel host.²²⁸

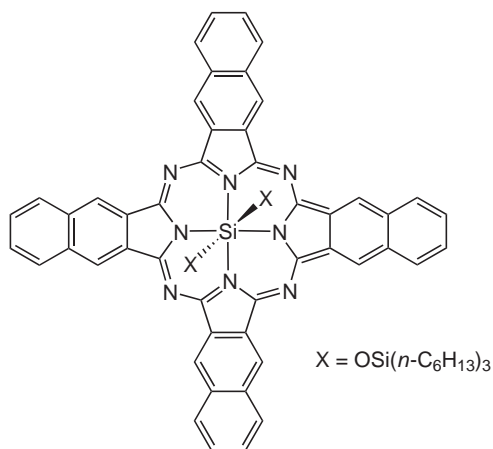
Nalwa and colleagues have reported THG from various MPCs and MNPCs, including different crystalline forms of $[\text{Ti}^{\text{IV}}\text{OPc}]$.²³⁴ The measured $\chi^{(3)}$ values for the amorphous material and three polymorphs vary significantly depending on the crystal structures and measurement wavelengths,

the largest $\chi^{(3)}$ of 1.59×10^{-10} esu being for α -[Ti^{IV}OPc] with a 2,430 nm fundamental.²³⁴ The different NLO susceptibilities of the polymorphs are attributable to crystal-packing induced variations in the intermolecular interactions.²³⁴ [V^{IV}O{(CO₂C₅H_{11-n})₄NPc}] has a maximum $\chi^{(3)}$ of 8.6×10^{-11} esu at 2,100 nm,^{235,236} more than 10 times larger than those of its Cu^{II}, Zn^{II}, Pd^{II}, or Ni^{II} analogues.²³⁵ Studies on the wavelength dependence of $\chi^{(3)}$ in spin-coated thin films of a range of MNPcs show that Si^{IV} complexes have the largest susceptibilities (ca. 10^{-10} esu at 1,500 nm), DFWM measurements on one derivative giving a $\chi^{(3)}$ of 5.0×10^{-7} esu at 800 nm, enhanced by one-photon resonance near the Q-band.²³⁸ A THG comparison between related Ge^{IV} porphyrine,¹⁹⁶ Pc and NPc (**113**)²³⁸ complexes in thin films shows progressive red-shifting of the Q-bands and increasing $\chi^{(3)}$ with sequential benzo substitution from the porphyrine to NPc due to increased π -conjugation.²³⁹

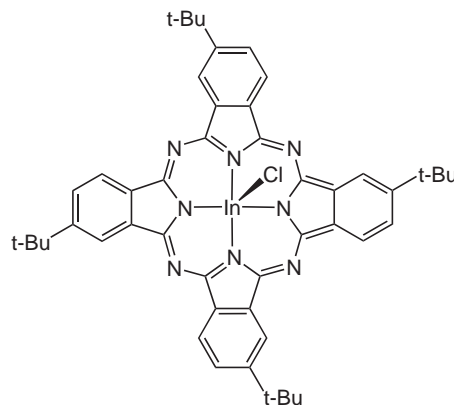


No.	M	γ [THG] (10^{-32} esu)	γ [EFISHG] (10^{-32} esu) ²²⁵
(110)	Co	4.48	4.39
(111)	Ni	3.18	2.47
(112)	Cu	2.45	3.94

(113): $\chi^{(3)}$ [THG] = $18.6 \cdot 10^{-12}$ esu (thin film)²³⁸



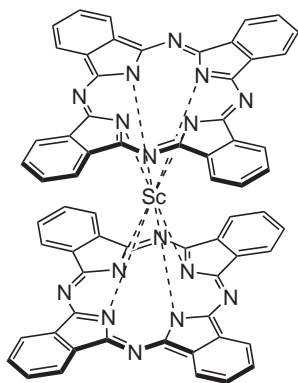
(114): $\sigma_e/\sigma_g = 55$ (toluene)²⁴¹



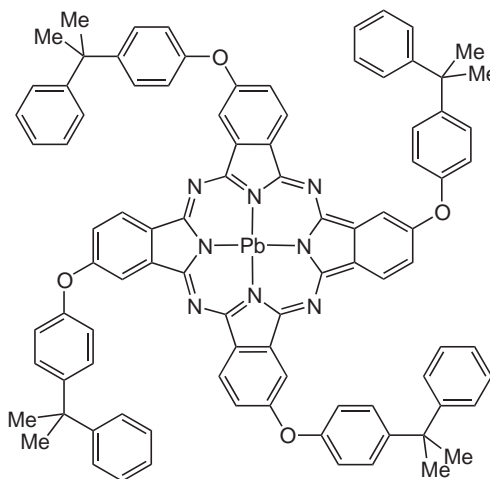
(115)

Perry and co-workers have focused on the OL properties of MPcs. The σ_e and the associated nonlinear refractive cross-section for solutions of the now commonly used benchmark Si^{IV} optical limiter (**114**) were measured using ps pulses at 532 nm.²⁴¹ RSA is the dominant nonlinear absorption process, and the observed nonlinear refraction is also due to real population excitation.²⁴¹ Subsequent studies reveal that MPcs with heavy ions, such as In^{III} , Sn^{IV} , and Pb^{II} show almost twofold enhancements in the ratios σ_e/σ_g compared with those containing lighter ions, such as Al^{III} and Si^{IV} .²⁴³ Hence, increases in OL efficiencies arise from excited triplet-state absorption.²⁴³ Homogeneous solutions of heavy-metal Pcs, with an f/8 optical geometry and at 30% linear transmission, limit 8 ns, 532 nm pulses to $\leq 3 \mu\text{J}$ (the energy for 50% probability of eye damage) for incident energies of $\leq 800 \mu\text{J}$.²⁴³ Of particular note is the report that an inhomogeneous solution distribution of the In^{III} complex (**115**) along the beam path substantially enhances the RSA, affording an optical limiter with a 70% linear transmission which can attenuate 8 ns, 532 nm pulses by factors of as much as 540.²⁴⁶ Such a level of performance approaches the characteristics necessary for a practical OL device.

Shirk and colleagues have also largely focused on the OL potential of heavy-metal Pcs. A series of bis(Pc) sandwich complexes (and some of their anions) containing Sc^{III} (**116**), Y^{III} or several lanthanide ions Ln^{III} have large γ values from 1,064 nm DFWM.²⁵¹ Such complexes contain an unpaired electron residing on the Pc rings, and are hence mixed-valence species. For the neutral complexes, the observed γ values vary with the metal ion by a factor of 3, and increase as the IVCT transition approaches resonance.²⁵¹ Studies with Pb^{II} complexes, especially (**117**), indicate that such compounds hold considerable promise for OL applications.^{253,261} More recently, Shirk, Hanack, and co-workers have used various techniques including Z-scan and time-resolved DFWM to confirm that the ns nonlinear absorption and OL behavior of monoaxially chloro- and aryl-substituted In^{III} Pcs are dominated by strong RSA from orientationally averaged triplet states.²⁶⁴ The F_{th} and transmission at high fluences for an optical limiter based on [4-(trifluoromethyl)phenyl]phenyl- In^{III} (t-Bu)₄Pc are both much lower than those reported previously for In^{III} Pcs.²⁶⁴ Furthermore, the optical properties of the In^{III} Pc moiety are surprisingly insensitive to axial ligand changes.²⁶⁴ Reviews discussing OL by In^{III} Pcs/NPcs and Ti^{IV} Pcs have appeared.^{265,266}



(**116**): $\lambda_{\text{max}} = 1,190 \text{ nm}$,
 $\gamma [\text{DFWM}] = 48 \cdot 10^{-32} \text{ esu} (\text{CHCl}_3)^{251}$

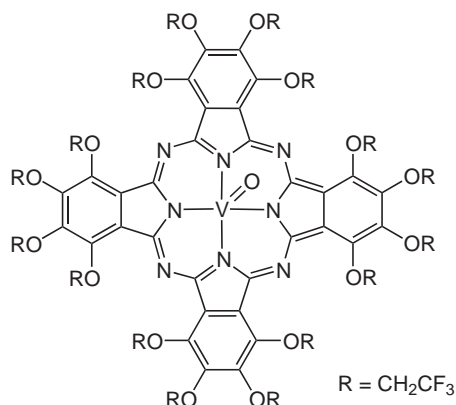
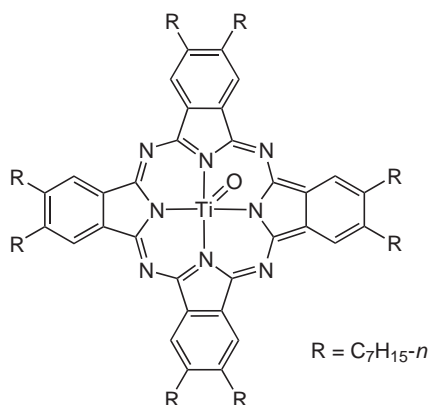


(**117**)

Hanack and co-workers have been involved in several other studies on the cubic NLO properties of MPcs, and an early review also covered MPs.²⁶⁷ 1,064 nm DFWM and THG studies on spin-cast films of soluble $[\text{Ru}^{\text{II}}(\text{t-Bu})_4\text{Pc}]$ oligomers with 4-diisocyanobenzene bridges have been reported.²⁶⁸ The DFWM wavelength was varied over the complete range of the Q-band, showing the dispersion of $\chi^{(3)}$ to a maximum value of $11.5 \times 10^{-8} \text{ esu}$.²⁶⁸ The optical properties of this oligomer are primarily determined by the planar MPc units (which show SA), due to weak axial electronic coupling.²⁶⁸ Z-scan and time-resolved DFWM studies on highly soluble Ni^{II} , Pd^{II} , and Pt^{II} Pcs reveal SA behavior and fast ground-state recovery times in the ps regime.²⁶⁹ ZINDO calculations on $\text{Ti}^{\text{IV}}\text{O}$ Pcs predict that peripheral substituents strongly affect the molecular

electronic properties, including the state dipole moments and Q-band absorption wavelengths, whilst Z-scan studies around the Q-bands show that complexes such as **(118)** exhibit both RSA and SA, depending on the wavelength.²⁷⁰ These combined theoretical and experimental results show that the opto-electronic properties are effectively tuned by peripheral substitutions.²⁷⁰

Wada and co-workers have pursued THG studies on various types of thin film containing V^{IV}O or Ti^{IV}O Pcs, the $\chi^{(3)}$ responses of which are greatly influenced by molecular packing arrangements. More recently, Stark spectroscopy was used to derive $\chi^{(3)}$ for films of these and other MPcs.^{281,283,284} Hence, $\chi^{(3)}$ values have been measured for PMMA thin films doped with Ni^{II} or Pb^{II} (t-Bu)₄Pcs.²⁸¹ and also for **(119)**, its Zn^{II} analogue, and [V^{IV}O{(EtO)₁₆Pc}].²⁸³ Interestingly, these (2,2,2-trifluoroethoxy)-substituted complexes do not show aggregation (which is generally deleterious for OL purposes due to increased triplet state decay), even in the condensed state.²⁸³ Solutions of **(119)** have also been studied by using fs OKE in the region 770–850 nm, showing a broad near-resonant enhancement of γ .²⁸² The anisotropy of the sub-ps transient absorption changes and Stark responses of various MPcs in PMMA show evidence for wavelength-dependent 1-D character (due to coplanar intermolecular interactions) and 2-D character (due to cofacial interactions).²⁸⁴



(118): γ [Z-scan] = $4.13 \cdot 10^{-29}$ esu,
 $\chi^{(3)}$ [Z-scan] = $6.93 \cdot 10^{-11}$ esu (650 nm, toluene)²⁷⁰

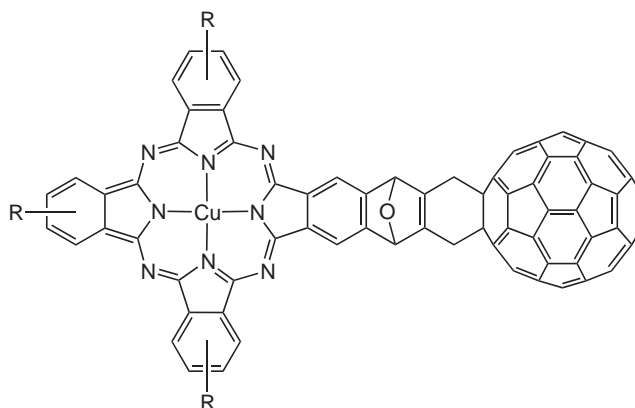
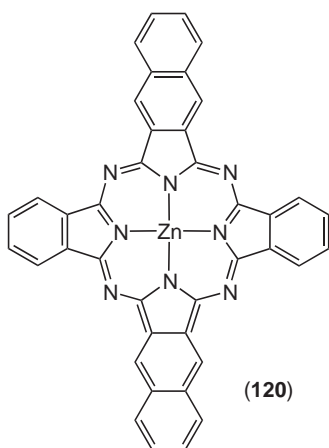
(119)

Heflin and colleagues have used solution 1,907 nm THG experiments to obtain a γ value of -31.4×10^{-34} esu for a Si^{IV} NPC closely related to **(114)**.²⁸⁷ A general enhancement mechanism for NLO processes originating from real population of electronic excited-states has been discussed, with a $>10^2$ enhancement of nonresonant THG from an optically pumped singlet state being observed for a Si^{IV} NPC.²⁸⁹ OL dispersion measurements with a Si^{IV} NPC and [Al^{III}CIPc] over the range 543–651 nm show that these complexes become less-effective limiters at the longer wavelengths where their σ_g values are large.²⁹⁰

Yamashita and co-workers have focused on THG studies of various MPc thin films formed by organic molecular beam deposition (OMBD) on polished sapphire surfaces. Early reports quoted a maximum $\chi^{(3)}$ value of 3×10^{-10} esu, on highly ordered Ti^{IV}OPc films grown on top of ordered films of the less symmetric [Zn^{II}-(dibenzo[b,t]Pc)] **(120)**.^{291,292} The $\chi^{(3)}$ values for the nonplanar complexes [Ti^{IV}OPc] and [V^{IV}OPc] are larger than those for planar [Cu^{II}Pc] and [Zn^{II}Pc] in both amorphous and crystalline films.^{293,294} Other studies involve OMBD-grown films of V^{IV}OPc, V^{IV}O(dibenzoPc), and V^{IV}ONPc and evaporated films of [Sn^{II}Pc] which also has a pyramidal molecular shape.^{295,297} The $\chi^{(3)}$ values of triclinic OMBD-grown films of [Mo^{IV}OPc] and [Sn^{II}Pc] are slightly smaller than those found previously for similar [Ti^{IV}OPc] or [V^{IV}OPc] films, but still about an order of magnitude larger than those of planar MPcs.²⁹⁶ The THG properties of thin films of [V^{IV}OPc] have also been extensively investigated by Fang and colleagues. With a 1,200 nm laser, a film grown epitaxially on KBr has a $\chi^{(3)}$ value of 2.87×10^{-10} esu, about 7.7 times that of a polycrystalline film grown on fused silica.³⁰² This enhancement of $\chi^{(3)}$ is associated with

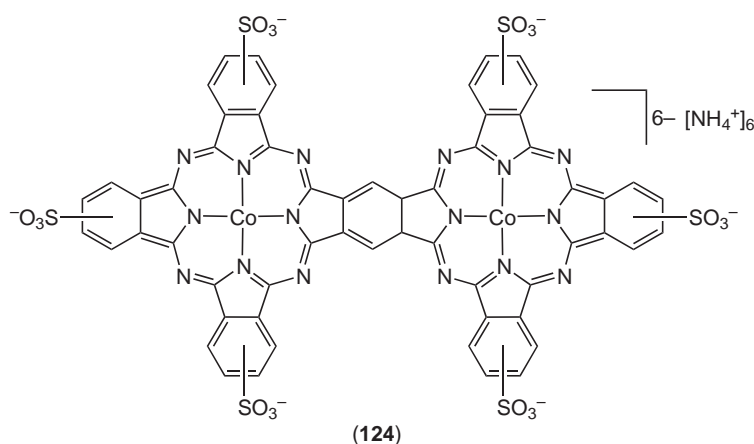
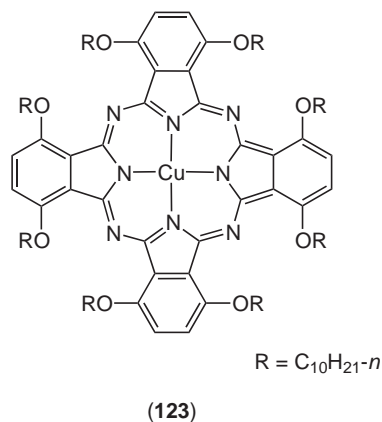
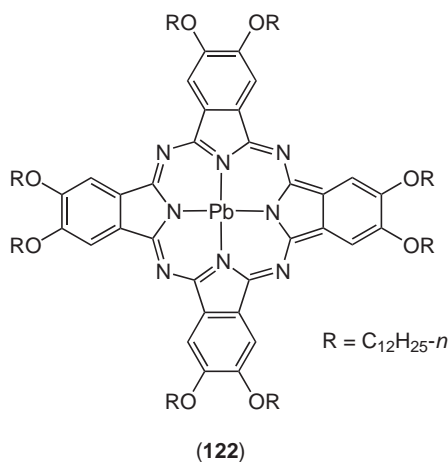
intermolecular π - π interactions arising from the optimized orientation of the Pc units in the condensed phase.³⁰² These interactions give rise to an additional two-photon resonance which does not appear in the polycrystalline films.³⁰¹

Many other reports on the cubic NLO and OL properties of MPcs have appeared.^{158,303-333} These include 532 nm Z-scan measurements on Ln^{III} bis(Pcs),³¹² and several studies on MPcs doped into gel matrices.³¹⁵⁻³¹⁸ Huang *et al.* have used fs OKE experiments to determine γ for a Pc-C₆₀ Diels-Alder adduct (**121**) at 830 nm.³²⁵ The cubic NLO response of (**121**) is considerably enhanced compared with those of its component fragments due to Pc \rightarrow C₆₀ CT, evidence for which is obtained from UV-visible spectroscopy and cyclic voltammetry.³²⁵ 800 nm fs OKE studies indicate that the $\chi^{(3)}$ responses of vapor-deposited thin films of [Cu^IPc] or [Mg^{II}Pc] (13 and 5.6×10^{-11} esu, respectively) are at least 10 times larger than that of metal-free Pc.³²⁶ These enhancements are attributable to conjugation of metal *d*-orbitals in the case of [Cu^IPc], but pyramidalization in [Mg^{II}Pc].³²⁶ Pump-probe experiments show that [Cu^IPc] exhibits RSA, whereas [Mg^{II}Pc] displays SA behavior.³²⁶ The OL properties of bis{2,3,9,10,16,17,23,24-(OC₅H₁₁)₈Pc} sandwich complexes of Eu^{III} or Gd^{III} have been studied using 10 ns 532 nm pulses in CHCl₃.³²⁷ The 20% superior OL performance of the Eu^{III} complex goes against expectations based on atomic weights, but is attributable to stronger π - π interactions arising from the smaller ionic radius of Gd^{III}.³²⁷



(121) (R unspecified): γ [OKE] = $5.4 \cdot 10^{-31}$ esu (toluene)³²⁵

The Pb^{II} complex (**122**) exhibits OL which is about 10 times more effective than that of C₆₀ in toluene solution with 8 ns 532 nm pulses, and good agreement between experiment and theory indicates that RSA is the main OL mechanism.³²⁸ ZINDO/SDCI-SOS calculations on [Mg^{II}Pc] and [Ni^{II}Pc] show that the γ values are always larger in the first excited singlet state compared with the ground-state, and afford insights into the excited-state enhancement mechanism for NLO processes.³³⁰ Similar calculations have been reported for polymorphs of [Ti^{IV}OPc],³³² and the resulting nonresonant $\chi^{(3)}$ values are in agreement with the available experimental data,²³⁴ decreasing in the order α -[Ti^{IV}OPc] > γ -[Ti^{IV}OPc] > β -[Ti^{IV}OPc]. Nonlinear transmission measurements at 532 nm have been carried out on a series of 1,4,8,11,15,18,22,25-octa-(decyloxy) MPcs (e.g., (**123**)), and the data analyzed using two models.³³¹ The importance of ISC rates in influencing the RSA behavior is shown by using a five-state model, and a simple model based only on the effective excited-state absorption cross sections shows that (**123**) gives the strongest RSA.³³¹ Z-scan at 532 nm with 8 ns pulses has been applied to self-assembled, ultrathin composite films containing both the polyoxometalate anion [PMo₁₂O₄₀]³⁻ and the binuclear complex (**124**).³³³ Introduction of the anions causes a change from RSA to SA behavior, and also enhances $\chi^{(3)}$ (from 0.92×10^{-12} esu to 4.21×10^{-12} esu) when compared with films containing (**124**) alone.³³³



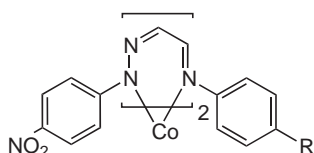
9.14.2.5 Complexes of Schiff Base Ligands

The first study of NLO effects in nonpolymeric Schiff base complexes was reported by Thami *et al.* in 1992.³³⁴ The Co^{II} complexes ((125) and (126)) of two electron donor/acceptor-substituted hydrazone imine glyoxal derivatives have distorted tetrahedral coordination geometries with approximate C_2 symmetry.³³⁴ Although their β values are larger than those calculated from the tensorial addition of the β coefficients of the free ligands, the electronic origins of these enhancement effects are unclear.³³⁴

A number of quadratic NLO studies involving Schiff base complexes have been carried out by Di Bella, working in collaboration with Lacroix and/or Marks and co-workers.^{335–340} In all such compounds, complexation increases β when compared with the free Schiff base. The results of EFISHG measurements and ZINDO/SCI-SOS calculations on several donor–acceptor bis(salicylidiminato)-Ni^{II} complexes (e.g., (127)) are in good agreement and show that the β responses are dominated by MLCT excitations.^{335,339} The metal centers in such complexes template the formation of noncentrosymmetric molecular structures, impart high thermal stability to the chelate rings, and both “switch on” and enhance the β responses.³³⁹ EFISHG and ZINDO/SCI-SOS studies on the series (128)–(130) also afford good agreement between experiment and theory and show that replacement of diamagnetic d^8 Ni^{II} with paramagnetic d^9 Cu^{II} or d^7 Co^{II} ions causes large increases in β .^{336,337} The TSM applies to (129) (with the MLCT band at $\lambda_{max} = 480$ nm in $CHCl_3$), but not to (128) or (130) in which the β values are increased by contributions from additional MLCT states.^{336,337}

Although the metal electronic configuration exerts a profound influence on β in (128)–(130), the situation is rather different if the ligands bear strong electron donor/acceptor substituents. For example, in (131) and (132) the β responses are dominated by two ILCT excitations with the

metals acting primarily as bridging centers which facilitate the CT processes; the TSM hence does not apply to such complexes.³³⁸ Different molecular and electronic structures are likely to apply in the d^{10} Zn^{II} complex (**133**), including the possibility of LLCT excitations contributing to the large β value.³³⁸ In order to encourage related complex chromophores to crystallize noncentrosymmetrically, a chiral ligand has been prepared.³⁴⁰ The paramagnetic, square based pyramidal Mn^{III} complex (**134**) crystallizes in the NCSG $P2_12_12_1$ and gives relatively high SHG activity, whilst the low SHG efficiency of its square planar Ni^{II} counterpart arises from effective dipole cancellation within the NCSG $P2_1$.³⁴⁰ Furthermore, the more intense and lower energy CT absorptions of (**134**) suggest that this compound may exhibit a larger β value than its Ni^{II} analogue.³⁴⁰ A review of these studies by Di Bella and colleagues, including brief discussion of complexes incorporated into main-chain copolymers, has appeared.³⁴¹

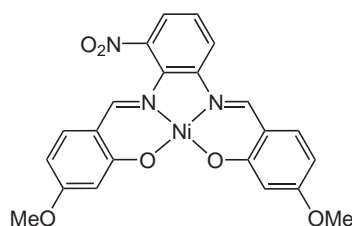


R = OMe (**125**):

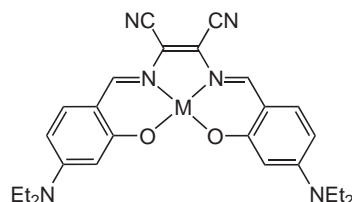
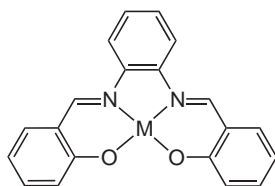
β_{1907} [EFISHG] = $25 \cdot 10^{-30}$ esu (1,4-dioxane),
 $30 \cdot 10^{-30}$ esu (CHCl₃)

R = NMe₂ (**126**):

β_{1907} [EFISHG] = $70 \cdot 10^{-30}$ esu (1,4-dioxane),
 $100 \cdot 10^{-30}$ esu (CHCl₃)³³⁴



(**127**): β_{1340} [EFISHG] = $-55 \cdot 10^{-30}$ esu (CHCl₃)^{335,339}



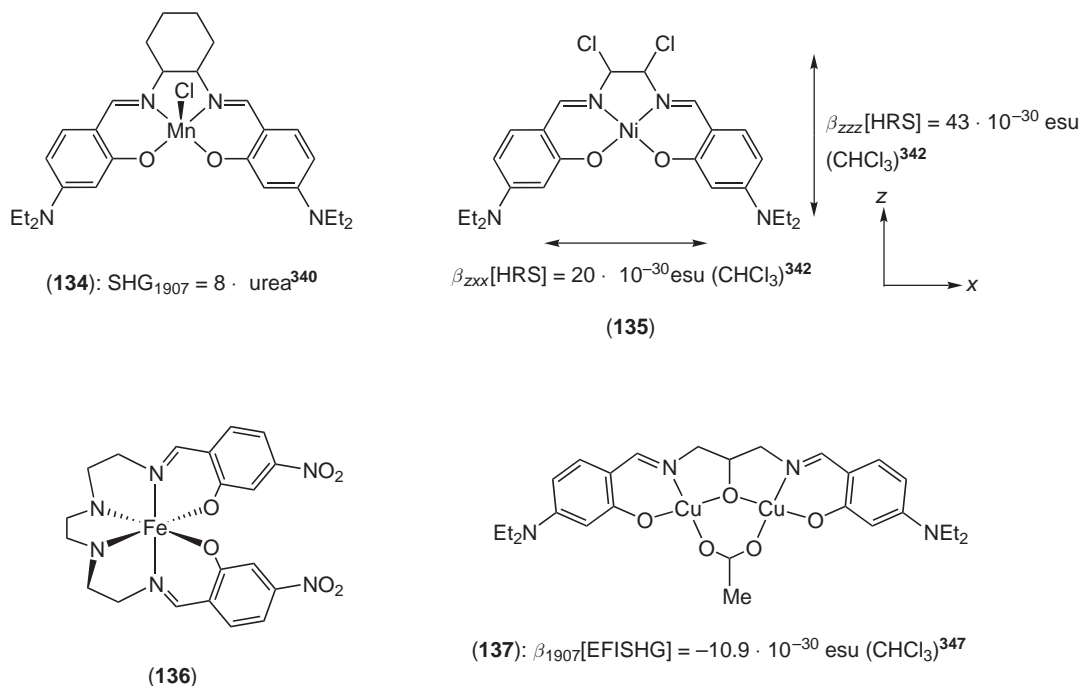
No.	M	β_{1340} [EFISHG] (10^{-30} esu) (CHCl ₃) ^{336,337}
(128)	Co	-170
(129)	Ni	-21
(130)	Cu	-50

No.	M	β_{1340} [EFISHG] (10^{-30} esu) (CHCl ₃) ³³⁸
(131)	Ni	235
(132)	Cu	200
(133)	Zn	400

More recently, a combination of 1340 nm HRS experiments and ZINDO/SCI-SOS calculations has been used to investigate the 2-D character of the β response in (**135**).³⁴² Such complexes exhibit various low-energy CT states, and z -polarized excitations (parallel to the molecular dipole axis) contribute to the diagonal β_{zzz} tensor, whilst perpendicular x -polarized transitions contribute to the off-diagonal, β_{zxx} , and β_{xzx} tensors.³⁴² These conclusions are corroborated by further ZINDO/SCI-SOS analyses on a range of known and hypothetical Ni^{II} donor-acceptor substituted Schiff base complexes.³⁴³

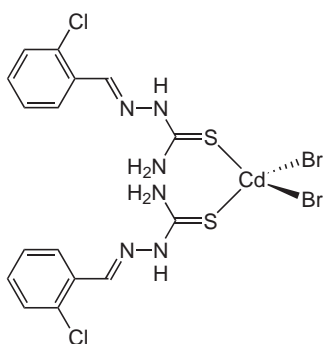
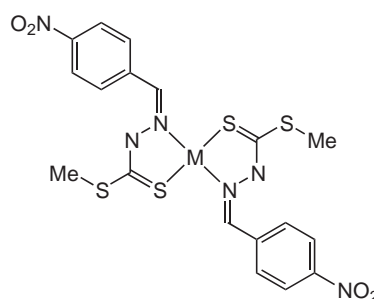
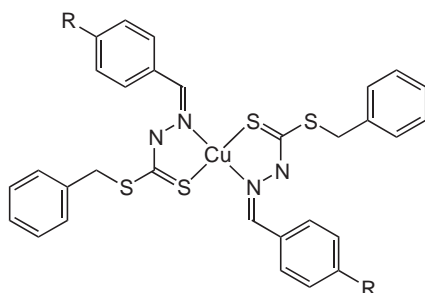
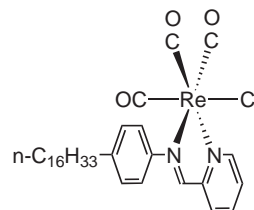
Similar complexes have also been further investigated independently by Lacroix and co-workers.³⁴⁴⁻³⁴⁷ 1,907 nm EFISHG shows that a Ni^{II} complex related to (**131**) in which the *cis*-1,2-dicyanovinyl unit is replaced by a 3,4-dinitro-1,2-phenylene bridge has an off-resonance $\mu\beta$ value of $1,530 \times 10^{-48}$ cm⁵ esu⁻¹, the largest molecular quadratic NLO response amongst such complexes.³⁴⁴ Although this complex crystallizes centrosymmetrically, doped and poled polyhydroxystyrene thin films give SHG.³⁴⁴ A chiral complex related to (**131**), but derived from (1*R*,2*R*)-(+)-1,2-diphenylethylenediamine, crystallizes in $P2_1$ and exhibits a powder SHG efficiency of 13 times

urea at 1,907 nm.³⁴⁵ The large difference in SHG activity between this complex and the Ni^{II} analogue of (134)³⁴⁰ is attributable to the steric effects of the mutually *trans* disposed phenyl substituents.³⁴⁵ ZINDO/SCI-SOS and DFT calculations based on variable temperature crystallographic data show that the thermally induced high-spin $S=2$ to low-spin $S=0$ transition in the Fe^{II} complex (136) causes β to increase by about 25%, mainly due to concomitant geometry modifications.³⁴⁶ 1,907 nm EFISHG studies show that the β response of the almost visibly transparent, binuclear pseudo-square planar Cu^{II} complex (137) is almost twice that of a related mononuclear species, an observation which is satisfactorily explained by qualitative ZINDO/SCI-SOS calculations.³⁴⁷



Tian and co-workers have studied various complexes of chelating Schiff base ligands containing coordinating thiocarbonyl groups.^{348–359} The colorless, tetrahedral Cd^{II} complex (138) crystallizes in the NCSG *Cc* and shows strong SHG activity, whereas the analogous iodide complex crystallizes centrosymmetrically and is hence SHG inactive.³⁴⁸ Intermolecular Cd–I contacts in the latter generate a distorted trigonal bipyramidal coordination geometry.³⁴⁸ Tetrahedral Zn^{II} halides related to (138), but with 4-methoxyphenyl groups in place of the 2-chlorophenyl substituents have also been studied.^{359,360} The chloride and bromide complexes both adopt the NCSG *Aba2*, with 1,064 nm SHG efficiencies of 7.6 and 13.2 times urea, respectively.³⁵⁹ MNDO-PM3 calculations predict that the iodide complex has a larger β value (-10.1×10^{-30} esu) than its chloride or bromide counterparts, but the former compound is SHG inactive, crystallizing in the CSG *P2₁/c*.³⁵⁹ 532 nm *Z*-scan experiments yielded $\chi^{(3)}$ values for the square planar Ni^{II} or Cu^{II} complexes (139) and (140).³⁴⁹ Further reports have described 450 nm DFWM and *Z*-scan studies on Ni^{II}, Cu^{II}, and Zn^{II} complexes of related ligands,^{350–355} including (141) and (142).³⁵⁰ DFWM has also been used to investigate trinuclear bis-complexes of the ligands *S*-*R*-*N'*-(ferrocenyl-1-methylmethylidene) dithiocarbazate (R = Me, Bz).^{356–358} The larger $\chi^{(3)}$ values of the square planar Ni^{II} or Pd^{II} complexes when compared with their tetrahedral Cu^{II} counterparts correspond with more effective interligand electronic coupling, as shown electrochemically.^{357,358}

The NLO properties of Schiff base complexes have also been studied by several other research groups.^{111,361–372} Monolayer LB films of the luminescent Re^I complex (143) give strong SHG from a 1,064 nm laser, comparison with a quartz crystal reference allowing estimates of β and $\chi^{(2)}$ to be calculated.¹¹¹ 532 nm DFWM studies on Ni^{II} or Cu^{II} complexes of *N,N'*-ethylenebis(salicylaldimine) (SALEN) and similar ligands show large complexation-induced enhancements of γ , reaching a maximum value of 2.6×10^{-29} esu.³⁶¹ [Ni^{II}(SALEN)] and also the Ni^{II} or Cu^{II} complexes of a related ligand derived from acetylacetonone have been studied using wavelength-tunable DFWM experiments in the region 550–600 nm, and *Z*-scan.³⁶² Chiang *et al.* observed

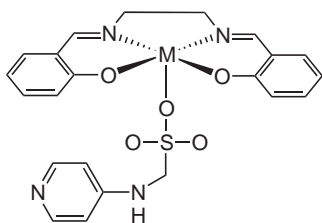
(138): $\text{SHG}_{1064} = 22 \cdot \text{urea}^{348}$ M = Ni (139): $\chi^{(3)}[\text{Z-scan}] = 7.35 \cdot 10^{-13} \text{ esu (DMF)}$ M = Cu (140): $\chi^{(3)}[\text{Z-scan}] = 7.03 \cdot 10^{-13} \text{ esu (DMF)}^{349}$ R = OMe (141): $\chi^{(3)}[\text{DFWM}] = 12.5 \cdot 10^{-13} \text{ esu (DMF)}$ M = NMe₂ (142): $\chi^{(3)}[\text{DFWM}] = 13.8 \cdot 10^{-13} \text{ esu (DMF)}^{350}$ (143): $b_{1064}[\text{SHG}] = 54 \cdot 10^{-30}$
 $\chi^{(2)} = 1.8 \cdot 10^{-7} \text{ esu (LB film)}^{111}$

weak SHG from (144) and (145), which are likely to adopt polymeric structures in the solid state due to bridging by the axial pyridyl sulfonate ligand.³⁶³ A series of octahedral Fe^{III}(SALEN) complexes give similarly small SHG responses, the most active (146) adopting the NCSG *P*6₅, with the complex units arranged helically.³⁶⁴ The NLO responses of such complexes may arise from CT transitions involving both the SALEN and py ligands.³⁶⁴ Poled, spin-coated films of a soluble main-chain polyurethane containing a Zn^{II} Schiff base complex also give weak SHG from a 1,064 nm laser.³⁶⁵

1,340 nm EFISHG has been applied to a series of mono- and binuclear square planar Pd^{II} or Pt^{II} complexes such as (147).³⁶⁶ Although for (147), complexation produces a red-shift in the ILCT absorption, together with a small increase in β_0 when compared with the sum of those for two free ligands, corresponding β_0 enhancements are only found in complexes with the strongly electron-donating -NBU₂ group attached to the cyclometallated ring.³⁶⁶ Replacement of Pd^{II} with Pt^{II} affords no clear trend in the β_0 values.³⁶⁶ You and co-workers have carried out OL and Z-scan measurements on several square planar complexes of Schiff base ligands derived from *S*-benzyl dithiocarbamate.^{367,368,372} At 532 nm, the *S*-benzyl analogue of (140) has F_{th} values of ca. 1 J cm^{-2} and 1.4 J cm^{-2} using 7 ns and 35 ps pulses, respectively (in CH₂Cl₂).³⁶⁷ The Pd^{II} complex (148) shows SDF and has a F_{th} of 0.9 J cm^{-2} with ps pulses, whereas its Cu^{II} and Ni^{II} analogues have larger thresholds of ca. 2 J cm^{-2} under the same conditions (in CH₂Cl₂).³⁶⁸

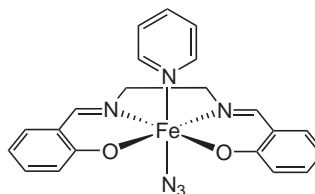
The SHG activities of several binuclear chiral Schiff base complexes related to (134) have been measured, e.g., (149) which contains square pyramidal Zn^{II} centers and crystallizes in *P*2₁.³⁶⁹ A salt of a related Fe^{III} complex also shows modest SHG activity, whereas similar Cu^{II} and Ni^{II} compounds adopt CSGs and hence show no bulk NLO effects.³⁶⁹ HRS studies by Gaudry *et al.* with a series of high-spin octahedral M^{II} (M = Mn, Fe, Co, Ni, Zn) complexes show that the Mn^{II} compounds (e.g., (150)) with five unpaired electrons have the largest β values.³⁷⁰ Furthermore, β decreases with the number of unpaired electrons, suggesting that the well-studied, thermally induced spin transition may be used to switch the NLO responses in complexes such as the Fe^{II} analogue of (150).³⁷⁰ Tetrahedral Zn^{II} complexes (e.g., (151)) of chiral ligands derived from

(*R*)-(+)-1-phenylethylamine show large 1,064 nm SHG responses (ca. 10–100 times urea; actual efficiencies not given), combined with good visible transparency.³⁷¹

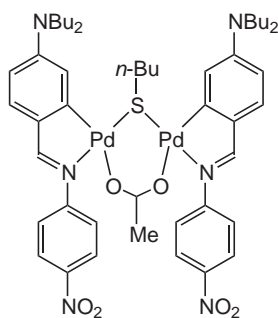


M = Cr (**144**): SHG₁₉₀₇ = 0.18 · urea

M = Mn (**145**): SHG₁₉₀₇ = 0.012 · urea³⁶³

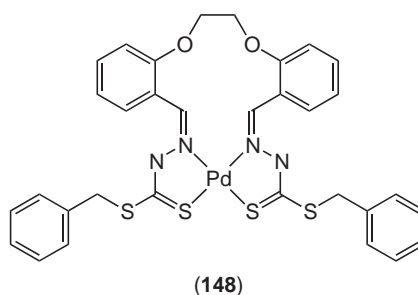


(**146**): SHG₁₀₆₄ = 2.0 · urea³⁶⁴

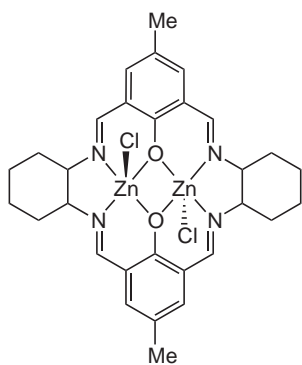


(**147**): λ_{max} = 466 nm,

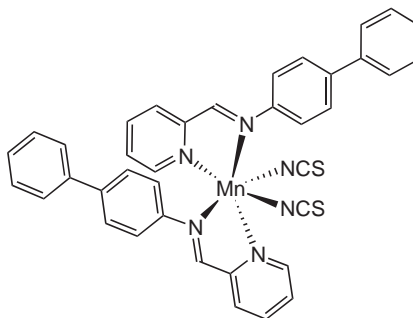
β₀[EFISHG] = 87 · 10⁻³⁰ esu (CHCl₃)³⁶⁶



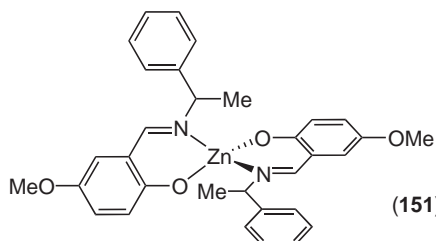
(**148**)



(**149**): SHG₁₀₆₄ = 0.90 · urea³⁶⁹



(**150**): β₁₀₆₄[HRS] = 175 · 10⁻³⁰ esu (MeCN)³⁷⁰



(**151**): Λ configuration, NCSG C2³⁷¹

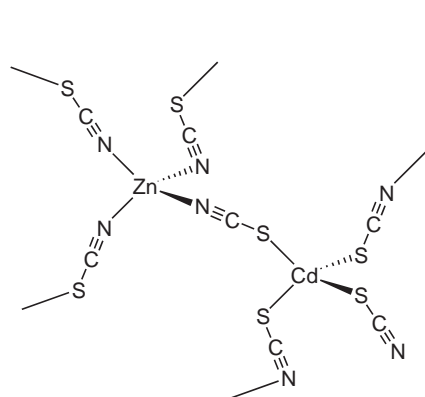
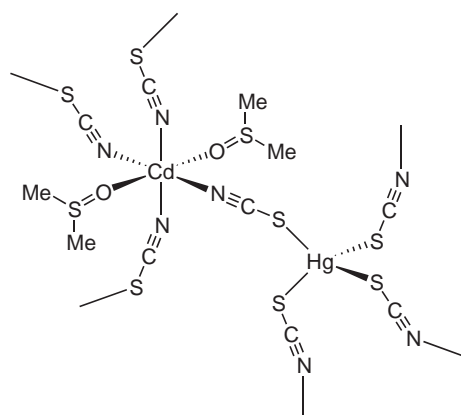
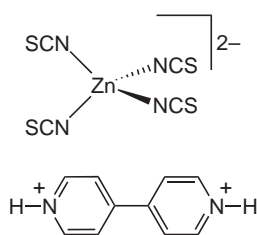
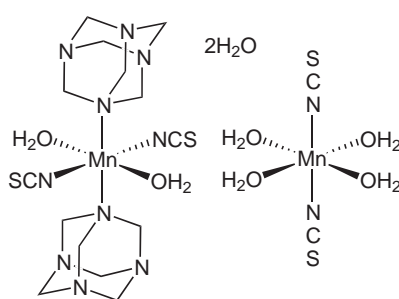
9.14.2.6 Complexes of Thiocyanate Ligands

The first coordination complexes to be studied for their NLO properties were the colorless bimetallics $[\text{Cd}^{\text{II}}\text{Hg}^{\text{II}}(\text{SCN})_4]$ (CMTC) and $[\text{Zn}^{\text{II}}\text{Hg}^{\text{II}}(\text{SCN})_4]$ (ZMTC), single crystals of which were found by Bergman *et al.* to exhibit efficient and phase-matchable SHG.³⁷³ This early discovery has stimulated considerable research into these and related $\text{AB}(\text{SCN})_4$ -type materials, much of which has been carried out by Wang and co-workers.^{374–385} $[\text{Fe}^{\text{II}}\text{Hg}^{\text{II}}(\text{SCN})_4]$ crystallizes in the NCSG $\overline{14}$ with distorted tetrahedral coordination geometries and $\text{Fe}^{\text{II}}-\text{NCS}-\text{Hg}^{\text{II}}$ linkages forming an infinite 3-D network, and has a 1,064 nm SHG activity of 0.6 times urea.³⁷⁴ $[\text{Zn}^{\text{II}}\text{Cd}^{\text{II}}(\text{SCN})_4]$ (**152**, ZCTC) is essentially isostructural with $[\text{Fe}^{\text{II}}\text{Hg}^{\text{II}}(\text{SCN})_4]$, having $\text{Zn}^{\text{II}}-\text{NCS}-\text{Cd}^{\text{II}}$ units, but has a much higher powder SHG efficiency.³⁷⁵ Furthermore, ZCTC exhibits larger SHG activity and also a higher energy transparency cut-off (290 nm) when compared with CMTC (SHG ca. 10 times urea; cut-off at 380 nm) or ZMTC.³⁷⁵ These attractive features have justified further studies on ZCTC, involving the growth of large, high-quality single crystals by slow solvent evaporation.³⁷⁹ Relatively efficient, high energy SHG at 380 nm and 404 nm has been achieved by frequency doubling of Ti:sapphire and GaAlAs diode lasers, respectively.^{380,383,385} Various other physical parameters relevant to NLO device applications, including EO coefficients, have also been measured for ZCTC.³⁸⁵ A combination of good thermal stability³⁸¹ with a relatively high optical damage threshold³⁸⁵ makes ZCTC a promising material for UV SHG. Comparative studies confirm that ZCTC is more attractive than the related complexes CMTC, ZMTC, or $[\text{Mn}^{\text{II}}\text{Hg}^{\text{II}}(\text{SCN})_4]$ (MMTC) for such applications.³⁸¹

Wang and colleagues have also studied a material related to CMTC but containing DMSO ligands (**153**), forming an infinite 3-D network, but with Cd^{II} in a pseudo-octahedral coordination environment.^{376,377,384} (**153**) shows higher SHG activity than CMTC, with a blue-shifted transparency cut-off of 360 nm, and large single crystals of high optical quality (NCSG $P2_12_12_1$) can be grown more readily by temperature lowering.^{376,377,384} The Mn^{II} analogue of (**153**), $[\text{Mn}^{\text{II}}\text{Hg}^{\text{II}}(\text{SCN})_4(\text{DMSO})_2]$, gives a powder SHG efficiency of ca. 23 times urea with a transparency cut-off of 375 nm, and is superior to the previously studied MMTC as a candidate for blue-violet SHG.³⁸² The compound $[\text{Mn}^{\text{II}}\text{Hg}^{\text{II}}(\text{SCN})_4(\text{H}_2\text{O})_2]$ as its bis(*N,N*-dimethylacetamide) solvate crystallizes in the NCSG $\overline{P4}$ with an infinite 2-D network structure, and gives a relatively low powder SHG similar to that of KDP.³⁷⁸ The high-energy SHG properties of CMTC^{386–388} and MMTC^{389,390} have also been studied by other workers. As expected, both of these materials are isostructural with ZCTC.^{386,389}

The NLO properties of various other thiocyanate complexes have been reported.^{391–397} Tao and co-workers have measured EO coefficients for the thiosemicarbazide complex $[\text{Cd}^{\text{II}}(\text{NH}_2\text{NHCSNH}_2)(\text{SCN})_2]$ which crystallizes in $P2_12_12_1$,^{391,392} and have found that $[\text{Zn}^{\text{II}}(\text{SCN})_2(\text{H}_2\text{O})_2]$ adopts the same NCSG with a very high energy UV cut-off of 270 nm.³⁹³ The salt (**154**) crystallizes in the NCSG $P2_12_12$ with the tetrahedral anions connected via weak $\text{S}\cdots\text{S}$ contacts and H-bonded to the bipyridinium dications to form a 2-D network.³⁹⁴ The Mn^{II} analogue is isostructural with (**154**), but shows SHG activity which is 100 times lower.³⁹⁴ The glycol monomethyl ether complex $[\text{Cd}^{\text{II}}\text{Hg}^{\text{II}}(\text{SCN})_4(\text{HOC}_2\text{H}_4\text{OMe})]$ crystallizes in the NCSG $Pca2_1$ with a similar SHG activity to CMTC, but a blue-shifted absorption cut-off (366 nm).³⁹⁵ Extensive H-bonding causes the Mn^{II} hexamethylenetetramine compound (**155**) to adopt a centrosymmetric supramolecular 3-D structure which exhibits a $\chi^{(3)}$ value of 3.41×10^{-12} esu in DMF.³⁹⁶ $[\text{Fe}^{\text{III}}(\text{SCN})_6](\text{H}-4,4'\text{-bipy})(\text{H}_2-4,4'\text{-bipy})(4,4'\text{-bipy})$ contains octahedral, N-coordinated anions which H-bond with the bipy and protonated bipy molecules to give another supramolecular 3-D network.³⁹⁷ 532 nm *Z*-scan in DMF shows that this material has a $\chi^{(3)}$ value of 1.06×10^{-10} esu.³⁹⁷

Zhang, Teo, and co-workers have carried out SHG screening on several visibly transparent Cd^{II} thiocyanate coordination polymers in which the relative alignment of the 1-D zig-zag $[\text{Cd}^{\text{II}}(\text{SCN})_3^-]_{\infty}$ chains is cation-mediated.^{398–402} The compound $[\text{18C6K}][\text{Cd}^{\text{II}}(\text{SCN})_3]$ (18C6 = 18-crown-6) crystallizes in the NCSG $Cmc2_1$ with parallel chains and gives SHG from 1,064 nm of 200 times quartz.³⁹⁸ By contrast, in $[(18\text{C6})_2\text{Na}_2(\text{H}_2\text{O})_2]_{1/2}[\text{Cd}^{\text{II}}(\text{SCN})_3]$ ³⁹⁸ and $[(12\text{C4})_2\text{Na}][\text{Cd}^{\text{II}}(\text{SCN})_3]$ ³⁹⁹ (12C4 = 12-crown-4), the chains are aligned antiparallel (CSG $P2_1/n$) and neither compound is SHG active. Similar effects are observed in related salts of tetraalkylammonium cations; $[\text{NET}_4][\text{Cd}^{\text{II}}(\text{XCN})_3]$ crystallize in the NCSG $Cmc2_1$ and exhibit SHG of 1.5 ($\text{X} = \text{S}$) and 3 ($\text{X} = \text{Se}$) times KDP, whereas the analogous NMe_4^+ salts are SHG inactive, despite adopting the NCSG $Pna2_1$.⁴⁰¹ The salt $[(\text{DB24C8})\text{Na}][\text{Cd}^{\text{II}}(\text{SCN})_3]$ (DB24C8 = dibenzo-24-crown-8) contains unusual linear $[\text{Cd}^{\text{II}}(\text{SCN})_3^-]_{\infty}$ chains and is SHG inactive, crystallizing in the CSG $C2/c$.⁴⁰²

(152) (ZCTC): $\text{SHG}_{1064} = 52 \cdot \text{urea}^{375}$ (153): $\text{SHG}_{1064} = 15 \cdot \text{urea}^{384}$ (154): $\text{SHG}_{1064} = 0.21 \cdot \text{urea}^{394}$ 

(155)

9.14.2.7 Complexes of 1,2-Dithiolene and Related Ligands

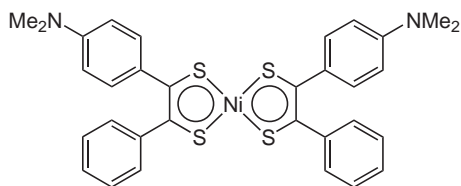
Because their high degree of electronic delocalization leads to intense $\pi \rightarrow \pi^*$ absorptions in the NIR region (see Chapter 9.13), complexes of 1,2-dithiolene (DT) and related ligands have attracted considerable attention for their (largely cubic) NLO properties. The complex (156) (a.k.a. BDN) is a highly photochemically stable, saturable absorber and has hence found extensive applications in laser Q-switching. The cubic NLO properties of (156) have been studied by DFWM^{148,403–407} and more recently, Z-scan.⁴⁰⁸ Time-resolved DFWM has been applied to square planar Co, Ni, Cu, or Pt complexes of 1,2-benzenedithiolate (BDT) or 1,2-aminobenzenethiolate ligands by Lindle and co-workers.^{409,410}

Winter, Underhill, and co-workers have published extensively on the cubic NLO properties of complexes of DT and related ligands,^{411–422} particularly those containing formally “Ni^{II}” centers. For example, time-resolved 1,064 nm DFWM was used to obtain resonantly enhanced $\chi^{(3)}$ values for group 10 complexes such as (157).^{411–415} The smaller $\chi^{(3)}$ of (157) compared with (156) is largely due to resonance effects since the absorption maximum of (157) is somewhat removed from the laser fundamental. However, figures of merit derived from measurements of n_2 and linear and two-photon absorption (TPA) coefficients show that low optical losses render complexes such as (157) superior to (156)⁴¹³ for potential all-optical switching applications.^{411–414}

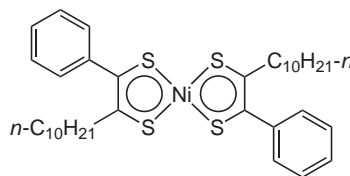
Having established the promise held by Ni^{II} DTs as cubic NLO chromophores,^{416,417} several subsequent reports by Winter and/or Underhill and colleagues describe studies with such complexes doped into easily processable PMMA thin films.^{418–426} Initial Z-scan results show that at high doping concentrations, TPA increases more rapidly with concentration than does n_2 , decreasing the $\chi^{(3)}$ response and hence limiting the maximum usable chromophore concentration.⁴¹⁸ 1,064 nm DFWM studies on PMMA films containing (158) show that an increase in n_2 is

offset by an increase in the linear absorption coefficient α_1 , leading to a lower figure of merit W compared with the solution ($W = \Delta n_{\text{sat}}/\alpha_1\lambda$, where Δn_{sat} is the maximum change in refractive index, which is the product of n_2 and the damage intensity, and λ is the operational wavelength).⁴¹⁹ However, the NLO performance of these films is still encouraging when compared with other organic materials,⁴¹⁹ and improved W values greater than 2 have subsequently been achieved.⁴²¹

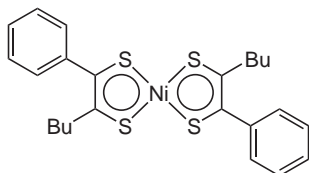
Papadopoulos and colleagues have used the CHF-PT-EB-CNDO method to calculate off-resonance γ values for Ni^{II} and Pd^{II} DTs.^{425–427} Calculations on Ni^{II}(DT)₂ and some of its methylated derivatives afford the following conclusions: (i) a satisfactory treatment requires the use of 3d orbitals on sulfur; (ii) the γ value of Ni^{II}(DT)₂ is ca. 1.6 times larger than that of tetrathiafulvalene in which the nickel is replaced by a C=C bridge; (iii) the γ value of its *trans*-dimethyl derivative is ca. 2.5 times larger than that of Ni^{II}(DT)₂ itself.⁴²⁵ Hypothetical binuclear complexes such as (159) have very large γ values, that of (159) being ca. 2.2 times that of Ni^{II}(DT)₂,⁴²⁶ and a similar enhancement occurs for the Pd^{II} analogues.⁴²⁷ Craig and Williams have also carried out CNDO calculations of γ on Ni^{II} bis(DT/BDT) complexes,⁴²⁸ and have considered the $\chi^{(3)}$ enhancing effects of -NO₂ and -NH₂ substituents in Ni^{II}(BDT)₂ complexes.⁴²⁹ Trohalaki *et al.* have reported the results of *ab initio* calculations on the effects on γ of phenyl torsion angles in Ni^{II}(1-Ph-DT)₂.⁴³⁰



(156): $\lambda_{\text{max}} = 1064$ nm,
 $\chi^{(3)}$ [DFWM] = $7.59 \cdot 10^{-11}$ esu (CH₂Cl₂)⁴¹³

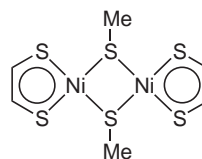


(157): $\lambda_{\text{max}} = 800$ nm,
 $\chi^{(3)}$ [DFWM] = $9.74 \cdot 10^{-13}$ esu (CH₂Cl₂)⁴¹³



(158)

$n_2 = 2.4 \cdot 10^{-11}$ cm² kW⁻¹, $\alpha = 0.06$ cm⁻¹, $W = 3.8$ (CH₂Cl₂)
 $n_2 = 2.1 \cdot 10^{-9}$ cm² kW⁻¹, $\alpha = 5.70$ cm⁻¹, $W = 1.2$ (PMMA film)⁴¹⁹

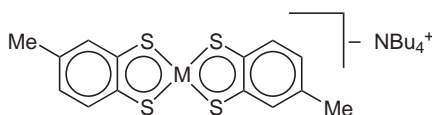


(159): γ [MO] = $4.37 \cdot 10^{-34}$ esu⁴²⁶

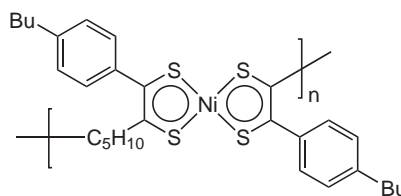
Underhill and co-workers have reported further studies on the cubic NLO properties of complexes of DT and related ligands.^{431–440} Highlights include PMMA thin films containing the BDT salts (160) and (161) ((160) has a n_2/ϕ value, where ϕ is the TPA coefficient, in excess of the device threshold of 2π)⁴³¹ and sol-gels doped with DT complexes.⁴³² Because aggregation is likely to be responsible for the TPA increases which limit the maximum usable chromophore concentration of monomeric complexes, oligomeric species such as (162) have been studied.^{433,436} 1,064 nm DFWM gives encouraging results, particularly with respect to the figure of merit ratio n_2/ϕ (by contrast, PMMA films containing (158) at similar concentrations, have respective W and n_2/ϕ values of 0.3 and 1.4).⁴³⁶ Salts of the ligands 1,3-dithiol-2-thione-4,5-dithiolate (e.g., (163) and (164)) or 1,2-mercaptophenolate and also neutral complexes of 3,5-di-*tert*-butyl-1,2-benzoquinone have been studied by 1,064 nm DFWM⁴³⁴ and THG measurements.⁴³⁹ As expected, the resulting THG γ values are lower than those from DFWM by several orders of magnitude.⁴³⁹ Dispersion measurements in the region 1,065–1,480 nm show that (163) has a maximum γ of 20×10^{-33} esu at ca. 1,325 nm, red-shifted by 172 nm from the NIR absorption maximum, and (164) has an estimated maximum γ of more than 2.5 times that of (163).⁴³⁹ The γ values of these

compounds appear to be strongly influenced by several resonances (one-, two-, and three-photon).⁴³⁹ A detailed THG study of (**158**) reveals that the NLO responses of such complexes are dominated by thermal mechanisms, with only relatively small electronic contributions.⁴⁴⁰

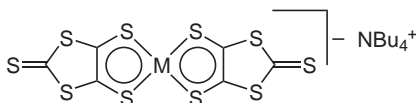
With the aim of producing electrically conducting NLO materials, 532 nm DFWM with 200 ps pulses has been used to determine $\chi^{(3)}$ values for several Ni complexes (e.g., (**165**)) of DT ligands featuring six- or seven-membered disulfur heterocycles fused to the chelating unit.⁴⁴¹ Wang *et al.* have used the fs OKE technique at 830 nm to determine the nonresonant cubic NLO response of the Au^{III} complex salt (**166**) which is capable of forming electrically conductive LB films.⁴⁴² Time-resolved 1,064 nm DFWM studies using the near-counter-propagating geometry by Kuebler and Denning with (**158**) show that population gratings (periodic refractive index changes) make a substantial contribution to the DFWM signals.⁴⁴³ Since such long-lived gratings may not be detected using the retro-reflection configuration used by Winter, Underhill, and co-workers, the cubic NLO figures of merit reported previously for such complexes are probably artificially high.⁴⁴³



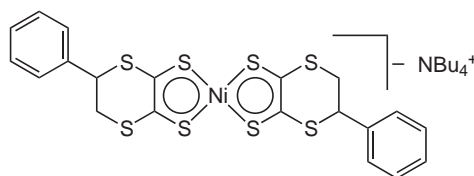
M = Ni (**160**); M = Pt (**161**)



(**162**): $n_2 = -4.6 \cdot 10^{-9} \text{ cm}^2 \text{ kW}^{-1}$, $\alpha = 240 \text{ cm}^{-1}$,
 $W = 0.5$, $n_2/\phi = 4.3$ (PMMA film)⁴³⁶



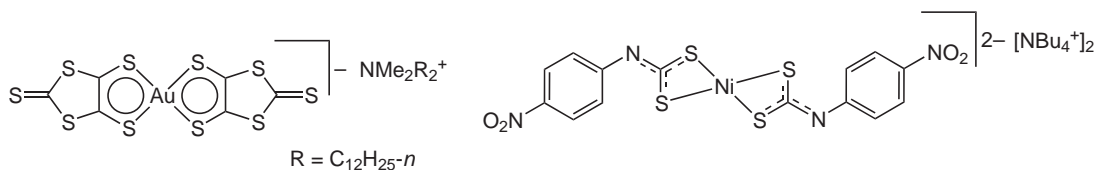
M = Ni (**163**): γ [THG] = $0.75 \cdot 10^{-33} \text{ esu}$ (CH_2Cl_2),⁴³⁹
 γ [DFWM] = $4,890 \cdot 10^{-33} \text{ esu}$ (PMMA film)⁴³⁴
M = Pd (**164**): γ [THG] = $3.1 \cdot 10^{-33} \text{ esu}$ (CH_2Cl_2),⁴³⁹
 γ [DFWM] = $1,360 \cdot 10^{-33} \text{ esu}$ (PMMA film)⁴³⁴



(**165**): $\lambda_{\text{max}} = 1,172 \text{ nm}$,
 $\chi^{(3)}$ [DFWM] = $1.6 \cdot 10^{-11} \text{ esu}$ (MeCN)⁴⁴¹

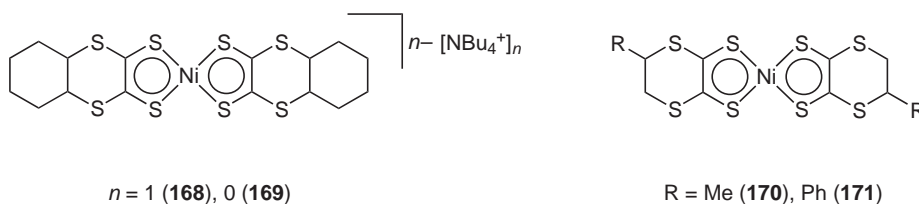
Several other THG studies have been carried out with DT complexes.^{444–448} Solution measurements at 1,064 nm and 1,907 nm give γ values in the range 10^{-32} – 10^{-33} esu ,⁴⁴⁵ whilst PMMA films doped with Ni^{III} or Au^{III} complexes related to (**160**) have γ values below 10^{-33} esu at 1,064 nm.⁴⁴⁶ The intense NIR transitions of the Ni^{III} complexes do not seem to contribute to their THG responses, since the Au^{III} complexes lack such absorptions, but have similar γ values compared with their Ni^{III} analogues.⁴⁴⁶ Other THG dispersion studies confirm that no correlation exists between the cubic NLO response and the NIR transition in such complexes.⁴⁴⁷ The effects of aryl substituents on the THG from evaporated thin films of Ni^{II} or Pt^{II} bis(DT)s have also been investigated.⁴⁴⁸ Schougaard *et al.* have carried out THG studies on PMMA films containing centrosymmetric Ni^{II} bis(*N*-phenyldithiocarbamato) complexes such as (**167**).^{449–451} Analogous complexes with -H, -OMe, or -CN groups in place of the -NO₂ substituents have CT bands blue-shifted by ca. 100 nm together with smaller γ values, and the γ response of (**167**) at 1,907 nm is 50 times larger than the sum of those for two 4-nitroaniline molecules.⁴⁴⁹ The Pd^{II} or Pt^{II} analogues of (**167**) with 4-NH₂ instead of the -NO₂ substituents have been studied by 450 nm DFWM with 20 ns pulses, affording $\chi^{(3)}$ values of ca. $6 \times 10^{-12} \text{ esu}$.³⁶⁰ These responses are larger than those of the corresponding neutral dithiocarbamato complexes, a result attributable to decreased delocalization in the latter.³⁶⁰

Two redox states of one complex, (168) and (169), exhibit very similar respective F_{th} values of ca. 0.6 J cm^{-2} and 0.7 J cm^{-2} with 32 ps pulses at 532 nm (in benzene).⁴⁵² A 532 nm OL study of the two neutral complexes (170) and (171) using ns and ps pulses has also been reported.^{453–455} Low F_{th} values of ca. 0.3 J cm^{-2} are observed with ps pulses in benzene, and both ps time-resolved pump-probe and Z-scan measurements reveal that RSA and nonlinear refraction are responsible for the OL behavior.^{453–455} Because (170) and (171) are transparent in the region 400–900 nm, their OL responses should cover a wider range than those of fullerenes and MPCs.^{453–455} Dai *et al.* have applied ps 532 nm DFWM to the tetrahedral Zn^{II} or Cd^{II} complexes (172) and (173), the modest γ responses of which are resonance enhanced by the $n \rightarrow \pi^*$ transition at 512 nm.⁴⁵⁶ The dimeric square pyramidal Zn^{II} complex (174) exhibits a broad $n \rightarrow \pi^*$ absorption with $\lambda_{\text{max}} = 497 \text{ nm}$ in DMF and is shown by 532 nm Z-scan to exhibit SF behavior.⁴⁵⁷



(166): γ [OKE] = $2.2 \cdot 10^{-32}$ esu (acetone)⁴⁴²

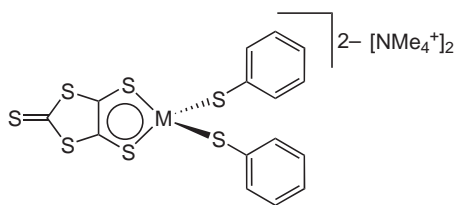
(167): $\lambda_{\text{max}} = 541 \text{ nm}$, γ [THG] = $1.4 \cdot 10^{-33}$ esu (1064 nm),
 γ [THG] = $2.0 \cdot 10^{-33}$ esu (1,907 nm) (PMMA film)⁴⁴⁹



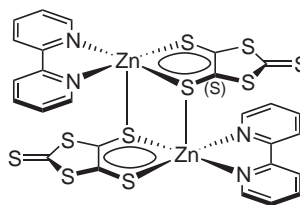
Several reports have also considered the quadratic NLO properties of DT complexes.^{458–461} Chen *et al.* have used NIR absorption data and SC $\Delta\mu_{12}$ values to estimate β_0 according to the TSM for various Ni^{II} or Pt^{II} mixed α -diimine/DT complexes,^{458,459} and also for several asymmetrically substituted bis(DT)s (e.g., (175) and (176)).⁴⁶⁰ Dipole analyses indicate that the NIR transition in (175) is primarily LLCT in nature, whereas that of (176) has only limited CT character.⁴⁶⁰ The complex (177) has a red-shifted LLCT absorption and a considerably larger β_0 value than (175).⁴⁶¹ The μ_{12} for the NIR band of (177) is also somewhat larger than that of (175), but the two complexes have very similar $\Delta\mu_{12}$ values.⁴⁶¹

9.14.2.8 Cluster Complexes

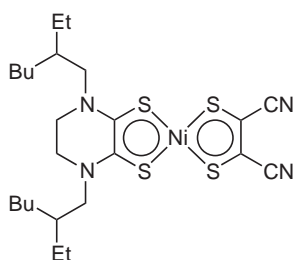
The first reports of the NLO properties of cluster complexes described RSA and OL behavior in the tetrahedral carbonyl clusters $[\text{HFeCo}_3(\text{CO})_{12}]$, $[\text{NET}_4][\text{FeCo}_3(\text{CO})_{12}]$ and $[\text{HFeCo}_3(\text{CO})_{10}(\text{PR}_3)_2]$ ($R = \text{Me/Ph}$; phosphines coordinated to Co).^{462–464} Data obtained from CH_2Cl_2 solutions with 8 ns pulses at 532 nm indicate that the OL properties are unaffected by the counterion, but depend on the ligand substitution.^{463,464} Shi *et al.* subsequently reported that MeCN solutions of the cubic heterothiometallic cluster salts (178) and (179) show superior OL capabilities with 532 nm, 7 ns pulses when compared with C_{60} (the best molecular OL material known at the time).⁴⁶⁵ The F_{th} values of 0.6 J cm^{-2} and 0.5 J cm^{-2} for (178) and (179), respectively, are about a third that of C_{60} .⁴⁶⁵ Z-scan and pump-probe results confirm that the OL derives from RSA, and the slightly lower F_{th} for (179) compared with (178) is attributable to heavy atom effects.⁴⁶⁵ Unfortunately, the potential of (178) and (179) for real OL applications is limited by their low optical damage thresholds.⁴⁶⁵ Other studies on the closely similar compounds $[\text{NBu}_4]_3[\text{W}^{\text{VI}}\text{S}_4\text{M}^{\text{I}}_3\text{Br}_4]$ ($M = \text{Cu/Ag}$) show that the OL performance improves on replacement of Cu by Ag, again attributable to heavy atom effects, but neither of these salts are as effective as (178) or (179).⁴⁶⁶ The compound (180), which consists of two nest-shaped cluster units, exhibits a still higher limiting threshold of 2 J cm^{-2} .⁴⁶⁷



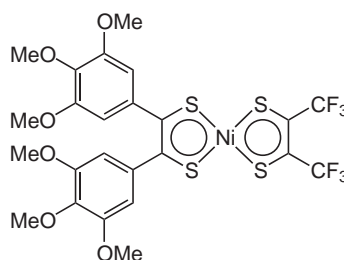
M = Zn (**172**): γ [DFWM] = $2.80 \cdot 10^{-30}$ esu (acetone)
 M = Cd (**173**): γ [DFWM] = $2.63 \cdot 10^{-30}$ esu (acetone)⁴⁵⁶



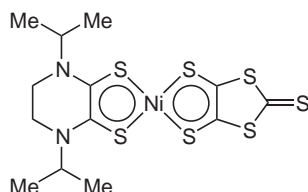
(**174**): $n_2 = 9.2 \cdot 10^{-10}$ cm² W⁻¹ M⁻¹,
 $\chi^{(3)}$ [Z-scan] = $1.0 \cdot 10^{-12}$ esu (DMF)⁴⁵⁷



(**175**): $\lambda_{\max} = 829$ nm,
 β_0 [SC] = $-37 \cdot 10^{-30}$ esu (CHCl₃)⁴⁶⁰



(**176**): $\lambda_{\max} = 842$ nm,
 β_0 [SC] = $5 \cdot 10^{-30}$ esu (CHCl₃)⁴⁶⁰

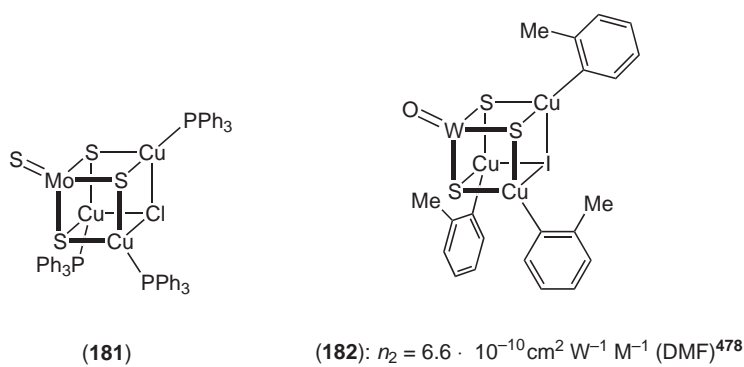
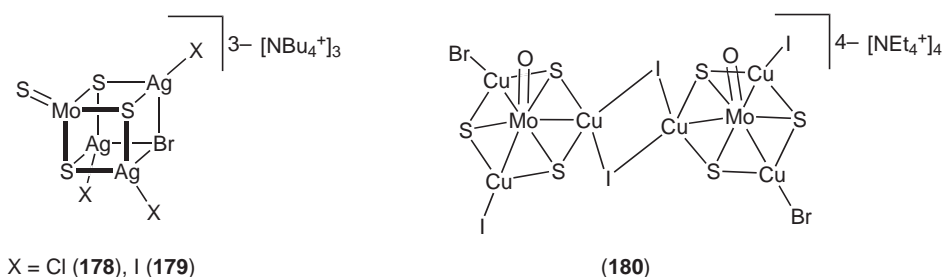


(**177**): $\lambda_{\max} = 965$ nm,
 β_0 [SC] = $-130 \cdot 10^{-30}$ esu (CHCl₃)⁴⁶¹

Following these early studies, an extensive, but somewhat fragmented literature has emerged concerning the cubic NLO and OL properties of clusters with a wide variety of topologies. These include cubic,^{468–484} incomplete cubic,^{485–491} “butterfly,”^{492–497} “flywheel,”⁴⁹⁸ hexagonal prismatic,^{499–502} “nest,”^{472,503–511} dodecanuclear,⁵¹² pentanuclear planar,^{513–527} supracage,^{528,529} linear,^{530–532} and polymeric species.^{533–538} Such complexes are typically colored, with visible absorption bands of variable energies and intensities. Unfortunately, scope for making quantitative comparisons is somewhat restricted by variations in the choice of physical parameters reported. Selected highlights of these investigations, all of which involve ca. 10 ns pulses at 532 nm unless otherwise stated, are briefly discussed below.

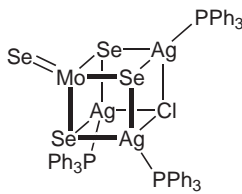
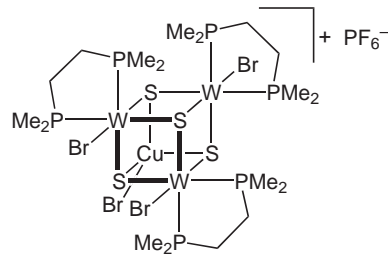
Further NLO studies on the trianionic cubic cluster salts, (**178**), (**179**), [NBu₄]₃[W^{VI}S₄M^I₃Br₄] (M = Cu/Ag),^{468,469} and the similar [NBu₄]₃[Mo^{VI}S₄Ag^I₃Br₄]⁴⁷⁰ and [NBu₄]₃[Mo^{VI}OS₃Cu^I₃-BrI₃]⁴⁷¹ have been reported by Shi and co-workers. More recent experiments with cubic clusters have focused almost exclusively on neutral Mo/W-Cu/Ag compounds, including several tetrathio species capped with PPh₃ ligands.^{472,473} However, such complexes (e.g., (**181**)) show essentially negligible OL properties.⁴⁷² This markedly different behavior when compared with their anionic counterparts is attributable to RSA being much less efficient in the neutral clusters due to larger HOMO-LUMO gaps and smaller μ_{12} and σ_e values.⁴⁷² Even so, other neutral clusters [M^{VI}OS₃-Cu^I₃I(2-pic)₃] (M = Mo/W; pic = picoline) and [Mo^{VI}OS₃Cu^I₃Br(2-pic)₃] do show strong OL.^{474–478} In DMF, (**182**) has a very low F_{th} of only 0.1 J cm⁻² and a large σ_e/σ_g ratio of 8.0 which is about twice that of C₆₀.^{474,475} Interestingly, (**182**) shows SF, whereas the isostructural [Mo^{VI}OS₃-Cu^I₃X(2-pic)₃] (X = Br/I) show SDF (for X = Br, $n_2 = -6.1 \times 10^{-11}$ cm² W⁻¹ M⁻¹).^{475,478} Furthermore, the nonlinear refractive behavior of [Mo^{VI}OS₃Cu^I₃I(2-pic)₃] becomes SF when excited with shorter 40 ps pulses, a phenomenon attributable to the larger refraction volume η of the initially

populated singlet state which can not undergo significant ISC to the triplet state of smaller η within the pulse duration.⁴⁷⁷

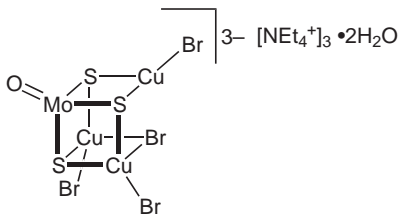
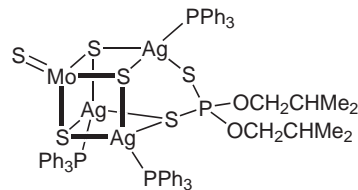


Recent NLO experiments with neutral cubic clusters have involved heteroselenometallic complexes $[\text{M}^{\text{VI}}\text{Se}_4\text{M}'^{\text{I}}_3(\text{PPh}_3)_3\text{Cl}]$ ($\text{M} = \text{Mo}/\text{W}$, $\text{M}' = \text{Cu}/\text{Ag}$) and $[\text{Mo}^{\text{VI}}\text{Se}_4\text{Cu}^{\text{I}}_3(\text{PPh}_3)_3\text{Br}]$.^{479–483} (183) has a F_{th} of 0.8 J cm^{-2} , and DFWM measurements made below this threshold show that the $\chi^{(3)}$ value is much smaller than that of C_{60} , despite the better OL performance of the cluster, indicating that the OL behavior is dominated by nonlinear scattering (rather than cubic NLO effects) at high fluence.⁴⁸⁰ Under identical conditions, the Cu analogue of (183) has a higher F_{th} of 1.8 J cm^{-2} , due to heavy atom effects.⁴⁸² The W analogue of (183) shows SF and a very large σ_e/σ_g ratio of 20 (for a singlet excited state) when excited with 40 ps pulses in DMF.⁴⁸³ Three salts of monocationic cubic clusters, $[\text{M}^{\text{IV}}\text{S}_4\text{Cu}^{\text{I}}\text{X}_4(\text{dmpe})_3]\text{PF}_6$ ($\text{M} = \text{Mo}$, $\text{X} = \text{Cl}/\text{Br}$; $\text{M} = \text{W}$, $\text{X} = \text{Br}$; dmpe = 1,2-bis(dimethylphosphino)ethane), also exhibit OL, with a σ_e/σ_g ratio of 6.0 for (184) with 40 ns pulses at 523 nm in MeCN.⁴⁸⁴

The isostructural salts $[\text{NEt}_4]_3[\text{M}^{\text{VI}}\text{OS}_3\text{Cu}^{\text{I}}_3\text{Br}_4] \cdot 2\text{H}_2\text{O}$ ($\text{M} = \text{Mo}/\text{W}$) and $[\text{NEt}_4]_3[\text{W}^{\text{VI}}\text{OS}_3\text{Cu}^{\text{I}}_3\text{I}_4] \cdot \text{H}_2\text{O}$ contain incomplete cubic clusters, and Z-scan shows that these compounds (e.g., (185)) all have large α_2 values in MeCN.^{485–487} Furthermore, (185) is strongly SDF, whilst its W analogue is strongly SF ($n_2 = 1.2 \times 10^{-9} \text{ cm}^2 \text{ W}^{-1} \text{ M}^{-1}$), these nonlinear refractive properties being more pronounced than those of the related cubic cluster compounds such as $[\text{NBu}_4]_3[\text{M}^{\text{VI}}\text{S}_4\text{Cu}^{\text{I}}_3\text{Br}_4]$ ($\text{M} = \text{Mo}/\text{W}$).^{485–487} Several neutral incomplete cubic clusters containing triply-bridging bidentate O,O'-dialkyl dithiophosphate and capping PPh_3 ligands also show cubic NLO behavior (e.g., (186)).^{488–490} The presence of the dithiophosphate ligands greatly increases the solubility in common nonpolar organic solvents, a property designed to facilitate incorporation of the clusters into polymer matrices, and (186) has a F_{th} value of 0.8 J cm^{-2} in CH_2Cl_2 .⁴⁸⁸ $[\text{Mo}^{\text{VI}}\text{OS}_3\text{Cu}^{\text{I}}_3(\text{PPh}_3)_3(\text{MeCO}_2)]$ also exhibits NLO effects and has a similar molecular structure to (186), but with the acetate ligand only doubly bridging.⁴⁹¹ Salts of monocationic incomplete cubic clusters (e.g., (187)) have large σ_e/σ_g ratios in the range 5.3–6.2 and lower F_{th} values in MeCN when compared with the cubic cluster compounds to which they act as synthetic precursors.⁴⁸⁴

(183): $\chi^{(3)}$ [DFWM] = $7.0 \cdot 10^{-12}$ esu (CH₂Cl₂)⁴⁸⁰

(184)

(185): $n_2 = -1.2 \cdot 10^{-9}$ cm² W⁻¹ M⁻¹,
 $\alpha_2 = 8.4 \cdot 10^{-6}$ cm W⁻¹ M⁻¹,
 $\chi^{(3)}$ [Z-scan] = $5.4 \cdot 10^{-10}$ esu (MeCN)⁴⁸⁵

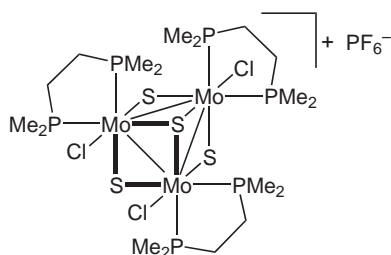
(186)

PPh₃-capped “butterfly” clusters (e.g., (188)) exhibit relatively weak nonlinear absorption but strong SF, the opposite of the combination of NLO properties found in related cubic species, [M^{VI}OS₃M^I₃X₄]³⁻ (M = Mo/W; M^I = Cu/Ag; X = Cl/Br/I).^{492,493} Very similar “butterfly” clusters with capping py or 2-(diphenylphosphino)pyridine ligands have also been studied.^{494,495} The “butterfly” iron carbonyl cluster (189) and a cyclopentaannulated derivative thereof have F_{th} values of ca. 1 J cm⁻², with γ responses similar to those of the incomplete cubic clusters [W^{VI}OS₃Cu^I₃I₄]³⁻ (X = Br, $\gamma = 1.6 \times 10^{-28}$ esu; X = I, $\gamma = 2.8 \times 10^{-29}$ esu),^{486,487} but superior photostabilities.⁴⁹⁶ The complex [W^{VI}₂S₈Ag^I₄(dppm)₃] (dppm = 1,2-bis(diphenylphosphino)-methane) has a cyclic structure with two W^{VI}S₄Ag^I₂ “butterflies” linked by dppm bridges, but shows only modest cubic NLO properties.⁴⁹⁷ In contrast, [Mo^{VI}S₄Cu^I₃(dppm)₃]BF₄·2H₂O contains a “flywheel” Mo^{VI}S₄Cu^I₃ cluster, corresponding to a Mo^{VI}S₄Cu^I₂ “butterfly” with an extra bridging Cu^I ion, and has large n_2 and γ values of -5.5×10^{-10} cm² W⁻¹ M⁻¹ and 2.8×10^{-29} esu, respectively, in DMF.⁴⁹⁸

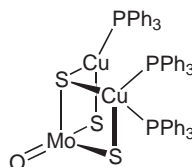
The neutral cluster [W^{VI}₂S₈Ag^I₄(AsPh₃)₄] has a hexagonal prismatic topology which can be viewed as two fused W^{VI}S₄Ag^I₂(AsPh₃)₂ “butterflies,” with a large $\chi^{(3)}$ value of 1.7×10^{-10} esu in MeCN.⁴⁹⁹ The isostructural complex (190) shows an impressive OL response which is 10 times larger than that of C₆₀.⁵⁰⁰ Furthermore, (190) is almost transparent in the visible region and its OL performance is irradiance independent between 532 nm and 700 nm, unlike C₆₀ or MPcs.⁵⁰⁰ Comparative ps OL studies with (190) and carbon black suspensions indicate that the nonlinear mechanisms are the same for the two materials, i.e., primarily due to scattering and absorption by microplasmas formed after thermionic emission from heated carbon particles/clusters, augmented by scattering from subsequently created bubbles.^{501,502}

DFWM and Z-scan measurements show that the “nest” cluster salts (191)^{503–505} and [NBu₄]₂[Mo^{VI}OS₃Cu^I₃BrCl₂]^{505,506} exhibit strong OL. Such dianionic *nido* clusters can be derived from the related trianionic cubic (*closo*) species (e.g., [Mo^{VI}OS₃Cu^I₃BrCl₃]³⁻) simply by removal of a halide vertex. However, this structural modification causes a distinct change in the nonlinear refractive behavior from weak SF to strong SDF.^{503–505} By using the number density calculated from crystallographic data, a solid-state $\chi^{(3)}$ value of 1×10^{-8} esu is obtained for (191).⁵⁰³ The twin-“nest” cluster compound [NEt₄]₄[Mo^{VI}₂O₂S₈Cu^I₆I₆] is isostructural with (180) and has linear and NLO properties similar to those of (191) and [NBu₄]₂[Mo^{VI}OS₃Cu^I₃BrCl₂] ($n_2 = -3 \times 10^{-10}$ cm² W⁻¹ M⁻¹, $\alpha_2 = 2 \times 10^{-5}$ cm W⁻¹ M⁻¹).⁵⁰⁷ The neutral “nest” cluster (192) has a large γ value,

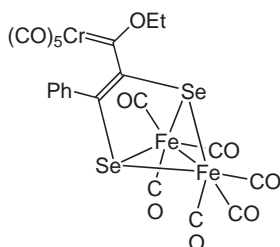
with very strong NLO absorption and SDF, and its W analogue behaves similarly.⁵⁰⁸ However, the corresponding iodide compounds have smaller α_2 and n_2 values, with the W complex showing SF behavior.⁵⁰⁹ Two salts of related cationic “nest” clusters, $[M^{VI}OS_3Cu^I_3(4-pic)_6]Br$ ($M = Mo/W$), show strong NLO absorption and SF with F_{th} values of 0.18 ($M = Mo$) and 0.15 ($M = W$) $J\text{cm}^{-2}$, but smaller γ values (ca. 10^{-31} esu) when compared with neutral clusters such as (192) (in DMF).⁵¹⁰ Salts of these same cationic clusters with $[M^{VI}_2O_7]^{2-}$ ($M = Mo/W$) or BF_4^- counteranions show larger F_{th} values of 0.20–0.45 $J\text{cm}^{-2}$ in MeCN, these being lower for the W compounds than their Mo analogues and also lower for the polyoxometalate salts.⁵¹¹ The dodecanuclear cluster compound (193), can be thought of as comprising four fused “nests,” and shows large NLO coefficients in DMF.⁵¹²



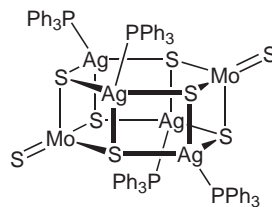
(187)



(188): $n_2 = 6.8 \cdot 10^{-9} \text{cm}^2 \text{W}^{-1} \text{M}^{-1}$,
 $\chi^{(3)}[\text{Z-scan}] = 1.2 \cdot 10^{-10} \text{esu}$,
 $\gamma = 9.8 \cdot 10^{-28} \text{esu (MeCN)}$ ⁴⁹³



(189): $\gamma [\text{Z-scan}] = 8.5 \cdot 10^{-29} \text{esu (n-hexane)}$ ⁴⁹⁶

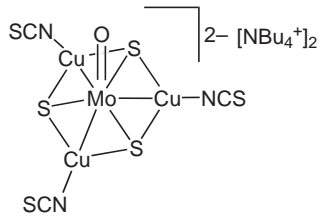


(190): $n_2 = 1.2 \cdot 10^{-8} \text{cm}^2 \text{W}^{-1} \text{M}^{-1}$,
 $\alpha_2 = 1.0 \cdot 10^{-3} \text{cm W}^{-1} \text{M}^{-1} (\text{acetone})$ ⁴⁹⁹

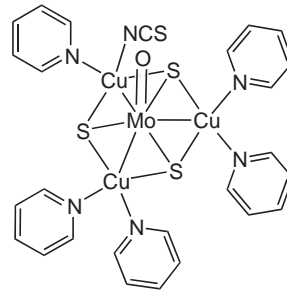
Low *et al.* first described the NLO properties of a pentanuclear planar “open” heterothio-metallic cluster, with a F_{th} value of 0.3 $J\text{cm}^{-2}$ for compound (194) in DMF.⁵¹³ This OL threshold was amongst the lowest known at the time, and (194) also possesses higher photostability than the previously studied cubic or hexagonal prismatic clusters.⁵¹³ (194) and its Mo analogue have very similar α_2 and n_2 values, and crystal structures show that the four edges of the tetrahedral $[M^{VI}S_4]^{2-}$ cores coordinate to four Cu^I ions, giving pseudo D_{2h} $[M^{VI}S_4Cu^I_4]^{2+}$ units with the five metal ions nearly coplanar.⁵¹⁴ A family of six halide-containing clusters $[M^{VI}S_4Cu^I_4X_2(py)_6]$ ($M = Mo/W$; $X = Cl/Br/I$), structurally very similar to (194), has also been extensively studied with both ns and ps pulses.^{515–523} $[W^{VI}S_4Cu^I_4I_2(py)_6]$ has a γ value of 6.9×10^{-30} esu and a $\chi^{(3)}$ of 6.2×10^{-9} esu with 8 ns pulses in DMF,⁵²² and this cluster also has both the lowest F_{th} value (0.07 $J\text{cm}^{-2}$) and the largest σ_e/σ_g ratio (28) of the six related compounds.⁵²³ Interestingly, the OL properties of these clusters with 40 ps pulses are very similar to those observed using 8 ns pulses, and their F_{th} values are lower than that of C_{60} (0.30 $J\text{cm}^{-2}$) even on an ultrafast timescale.⁵²³

The anionic pentanuclear planar cluster salt (195) and its Mo analogue^{521,524} have higher F_{th} values and smaller σ_e/σ_g ratios when compared with their neutral counterparts,^{521,523} but their OL properties are slightly improved under 40 ps, as opposed to 8 ns, excitation.⁵²³ $[NEt_4]_2[Mo^{VI}S_4Cu^I_4(SCN)_4(2-pic)_4]$ shows a pulse-width-dependent SF/SDF transformation, rationalized in terms of singlet/triplet excited-state populations.⁵²⁵ The dithiocarbamate-capped heteroseleno-metallic cluster salt $[NEt_4]_2[W^{VI}Se_4Cu^I_4(Me_2NCS_2)_4]$ has a F_{th} value of 1.1 $J\text{cm}^{-2}$, whilst the related tetranuclear “T-frame” compound $[NEt_4]_2[W^{VI}Se_4Cu^I_3(Me_2NCS_2)_3]$ has a considerably

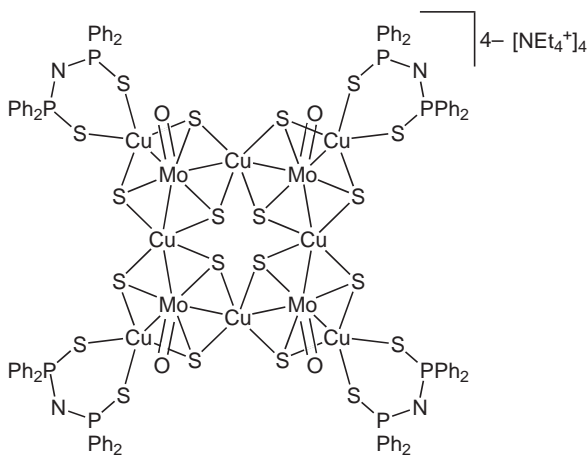
higher F_{th} of 6.0 J cm^{-2} in DMF.⁵²⁶ The salt $[\text{W}^{\text{VI}}\text{S}_4\text{Ag}^{\text{I}}_3(\text{dppm})_4]\text{PF}_6$ also contains a “T-frame” cluster and shows only modest cubic NLO effects in MeCN.⁴⁹⁷ A salt of a dicationic pentanuclear planar cluster (**196**) has a low F_{th} of 0.30 J cm^{-2} in MeCN.⁵²⁷



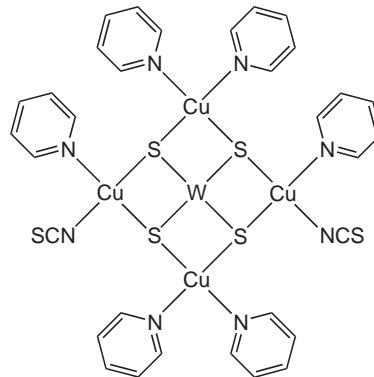
(191): γ [DFWM] = $4.8 \cdot 10^{-29} \text{ esu (MeCN)}$ ⁵⁰³



(192): $n_2 = -3.4 \cdot 10^{-8} \text{ cm}^2 \text{ W}^{-1} \text{ M}^{-1}$,
 $\alpha_2 = 2.4 \cdot 10^{-3} \text{ cm W}^{-1} \text{ M}^{-1}$,
 γ [Z-scan] = $5.8 \cdot 10^{-27} \text{ esu (DMF)}$ ⁵⁰⁸

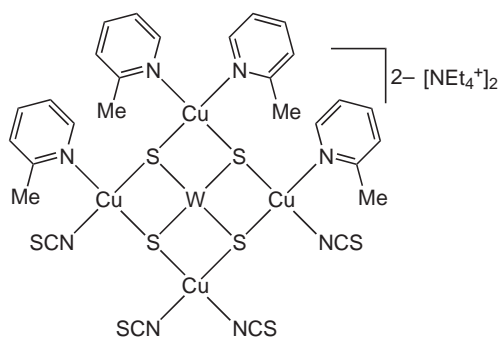


(193): $n_2 = -1.7 \cdot 10^{-10} \text{ cm}^2 \text{ W}^{-1} \text{ M}^{-1}$,
 $\alpha_2 = 1.0 \cdot 10^{-5} \text{ cm W}^{-1} \text{ M}^{-1}(\text{DMF})$ ⁵¹²



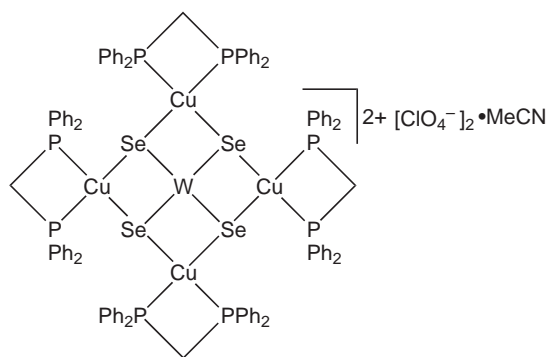
(194): $n_2 = -4.3 \cdot 10^{-10} \text{ cm}^2 \text{ W}^{-1} \text{ M}^{-1}$,
 $\alpha_2 = 4.3 \cdot 10^{-5} \text{ cm W}^{-1} \text{ M}^{-1}(\text{DMF})$ ⁵¹⁴

By analogy with the crystallographically characterized $[\text{NBu}_4]_4[\text{Mo}^{\text{VI}}_8\text{Cu}^{\text{I}}_{12}\text{S}_{32}]$, the compound $[\text{NBu}_4]_4[\text{Mo}^{\text{VI}}_8\text{Cu}^{\text{I}}_{12}\text{O}_8\text{S}_{24}]$ (**197**) contains a “supracage” structure with pseudotetrahedrally coordinated metal ions bridged by μ_2 -/ μ_3 -/ μ_4 -S ions, and significant Mo–Cu interactions.⁵²⁸ Based on DFWM and Z-scan results, (**197**) exhibits a very high extrapolated solid-state $\chi^{(3)}$ value of $3 \times 10^{-6} \text{ esu}$, and is amongst the largest metallic clusters investigated for their cubic NLO properties.⁵²⁸ The dispersion behavior of the SDF effect and the OL properties of (**197**) have also been described.⁵²⁹ The cluster (**198**) and its Mo analogue, which contain linearly arranged pseudotetrahedral $[\text{W}^{\text{VI}}\text{S}_4]^{2-}$ ($\text{M} = \text{Mo}/\text{W}$) ions and distorted trigonal planar gold ions, show large cubic NLO responses.⁵³⁰ Under the same conditions, the isostructural $[\text{W}^{\text{VI}}\text{Se}_4\text{Au}^{\text{I}}_2(\text{PPh}_3)_2]$ has α_2 and n_2 values very similar to those of (**198**) and gives a F_{th} of 1.3 J cm^{-2} .⁵³¹ The complexes $[\text{W}^{\text{VI}}\text{Se}_4\text{M}^{\text{I}}_2(\text{PPh}_3)_3]$, which contain both trigonal and tetrahedral M centers, have smaller NLO coefficients and F_{th} values of 3.0 ($\text{M} = \text{Cu}$) and 1.4 ($\text{M} = \text{Ag}$) J cm^{-2} .⁵³¹ In contrast, the heterotrimetallic 1,1'-bis(diphenylphosphino)ferrocene-capped linear cluster (**199**) has a considerably lower F_{th} of 0.35 J cm^{-2} .⁵³²

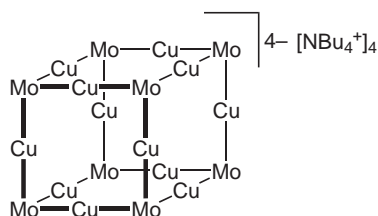


(195) (DMF): $F_{th} = 0.30$, $\sigma_e/\sigma_g = 4.6$ (8 ns pulses)

$F_{th} = 0.23$, $\sigma_e/\sigma_g = 9.0$ (40 ps pulses)⁵²³



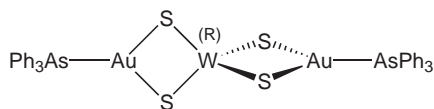
(196)



(197) (O and S ions omitted):

γ [Z-scan] = $5.7 \cdot 10^{-28}$ esu,⁵²⁸

$n_2 = -2.3 \cdot 10^{-9}$ cm² W⁻¹ M⁻¹ (MeCN)⁵²⁹



(198): $n_2 = 1.9 \cdot 10^{-9}$ cm² W⁻¹ M⁻¹,

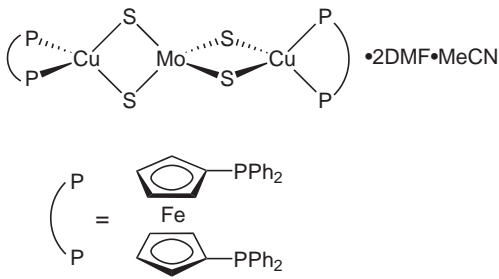
$\alpha_2 = 1.3 \cdot 10^{-4}$ cm W⁻¹ M⁻¹,

γ [Z-scan] = $6.5 \cdot 10^{-29}$ esu (CH₂Cl₂)⁵³⁰

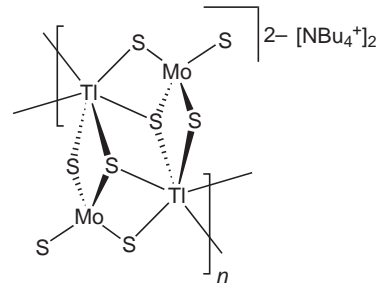
The first report of cubic NLO effects in polymeric cluster complexes concerned $[\text{NBu}_4][\text{M}^{\text{VI}}\text{S}_4\text{-TI}^{\text{I}}]$ ($\text{M} = \text{Mo}$ (**200**) or W) which contain linear chains of $[\text{M}^{\text{VI}}\text{S}_4]^{2-}$ tetrahedra connected by TI^{I} ions.⁵³³ These compounds show strong SF, but the effective magnitudes of their NLO coefficients are limited by poor solubility.⁵³³ $[\text{Mo}^{\text{VI}}\text{S}_4\text{Cu}^{\text{I}}_6\text{I}_4(\text{py})_4]_n$ contains $[\text{Mo}^{\text{VI}}\text{S}_4]^{2-}$ tetrahedra enveloped by a distorted octahedron comprising axial trigonal planar Cu^{I} and equatorial tetrahedral $\text{Cu}^{\text{I}}(\mu_2\text{-I})\text{py}$ centers in a 2-D network.⁵³⁴ Z-scan experiments in DMSO reveal that this compound is strongly SF ($n_2 = -3.8 \times 10^{-9}$ cm² W⁻¹ M⁻¹) and also the first cluster polymer found to exhibit OL with a F_{th} value of 0.6 J cm^{-2} .⁵³⁴ A 1-D cyanide-bridged polymer of the “nest” $[\text{Mo}^{\text{VI}}\text{OS}_3\text{Cu}^{\text{I}}_3]^+$ has large NLO coefficients in MeCN,⁵³⁵ and a 2-D 4,4'-bipy-bridged polymer of the same cluster unit gives a F_{th} of 0.4 J cm^{-2} in DMF, which is much lower than those of related monomeric or dimeric clusters.⁵³⁶ The salt $\{[\text{La}^{\text{III}}(\text{DMSO})_8][\text{W}^{\text{VI}}_3\text{Se}_{12}\text{Ag}^{\text{I}}_3]\}_n$ contains anionic 1-D helical chains comprised of “butterfly” clusters and has a F_{th} value of 0.7 J cm^{-2} (in DMF), whilst the 3-D cross-framework compound $\{[\text{NEt}_4]_2[\text{W}^{\text{VI}}\text{Se}_4\text{Cu}^{\text{I}}_4(\text{CN})_4]\}_n$ which contains pentanuclear planar clusters has an improved F_{th} of 0.2 J cm^{-2} .⁵³⁷ The thiometallic analogues of the latter (**201**) and (**202**) also show very strong cubic NLO effects,⁵³⁸ but the OL thresholds of such materials are higher than those of the neutral monomeric planar clusters.⁵²³

Studies on the cubic NLO properties of Mo/W-S/Se-Cu/Ag clusters have been reviewed,^{539–541} and some related species which contain pseudo-square planar Pd^{II} centers instead of $\text{Cu}^{\text{I}}/\text{Ag}^{\text{I}}$ have also been investigated.^{542–545} However, such complexes, e.g., the hexanuclear “windmill” cluster (**203**),⁵⁴⁵ typically show inferior NLO and OL performances when compared with their group 11 counterparts. A number of other, essentially organometallic, carbonyl-containing clusters have also been studied by Kumar, Mathur, and co-workers.^{546–549} These complexes have γ values similar to, or larger than, those of the best Mo/W-S/Se-Cu/Ag clusters, combined with superior photostabilities. Furthermore, unusually low OL thresholds have been reported for one complex (**204**) using 35 ps pulses,⁵⁴⁶ but other related clusters such as $[\text{Cp}_2\text{Mo}_2\text{Fe}_2 \text{STe}(\text{CO})_7]$ ($\text{Cp} =$ cyclopentadienyl) have more normal F_{th} values of “less than 1 J cm^{-2} ” under ns excitation.⁵⁴⁹

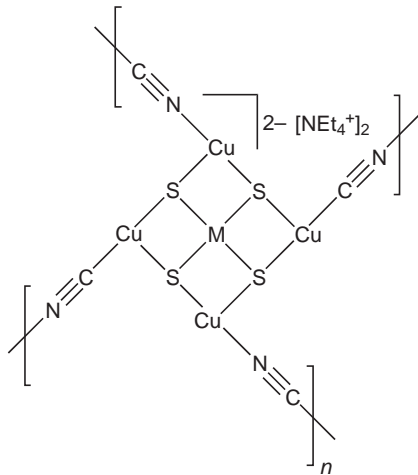
DFT calculations have afforded a relatively large β_{xxx} value of 28.5×10^{-30} esu at 1,064 nm for the compound $[\text{NET}_4][\text{CoFe}_2(\text{CO})_8\text{S}(\text{PPh}_3)]$ which contains a tetrahedral CoFe_2S cluster.⁵⁵⁰



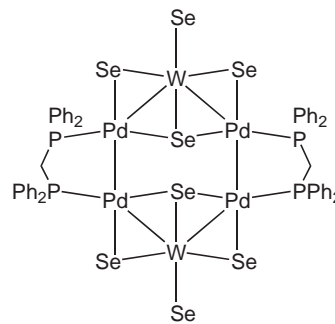
(199): $n_2 = -1.04 \cdot 10^{-9} \text{ cm}^2 \text{ W}^{-1} \text{ M}^{-1}$,
 $\alpha_2 = 1.2 \cdot 10^{-3} \text{ cm W}^{-1} \text{ M}^{-1} (\text{DMF})$ ⁵³²



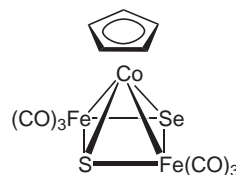
(200): $n_2 = 6.1 \cdot 10^{-7} \text{ cm}^2 \text{ W}^{-1} \text{ M}^{-1}$,
 $\alpha_2 = 4.3 \cdot 10^{-2} \text{ cm W}^{-1} \text{ M}^{-1} (\text{MeCN})$ ⁵³³



M = Mo (201): $F_{\text{th}} = 0.28 \text{ J cm}^{-2}$,
 $\chi^{(3)}[\text{Z-scan}] = 4.58 \cdot 10^{-9} \text{ esu}$
 M = W (202): $F_{\text{th}} = 0.15 \text{ J cm}^{-2}$,
 $\chi^{(3)}[\text{Z-scan}] = 5.12 \cdot 10^{-9} \text{ esu (DMF)}$ ⁵³⁸



(203): $n_2 = -3.7 \cdot 10^{-10} \text{ cm}^2 \text{ W}^{-1} \text{ M}^{-1}$,
 $\alpha_2 = 5.9 \cdot 10^{-5} \text{ cm W}^{-1} \text{ M}^{-1}$,
 $F_{\text{th}} = 3.1 \text{ J cm}^{-2} (\text{DMF})$ ⁵⁴⁵



(204): $F_{\text{th}} = 2.1 \text{ mJ cm}^{-2}$
 $(n\text{-hexane})$ ⁵⁴⁶

Z-scan studies on the homometallic, thiophenolate-containing cluster salts $[\text{NMe}_4]_2[\text{Cu}^I_4(\text{SPh})_6]$ and $[\text{NMe}_4]_2[\text{Ag}^I_6(\text{SPh})_8]$ show that these compounds combine relatively large γ , α_2 , and n_2 values with increased visible transparencies when compared with heterometallic clusters.⁵⁵¹ The OL properties of neutral homometallic Ag clusters of thiophenolate or selenophenolate ligands have also been studied.^{552–554} The complex $[\text{Ag}^I_8(2,4,6\text{-i-Pr}_3\text{C}_6\text{H}_2\text{Se})_8]$ has a distorted Ag^I_8 hexagonal bipyramidal core and a F_{th} value of 0.2 J cm^{-2} ,^{552,553} whilst $[\text{Ag}^I_{10}(2,4,6\text{-i-Pr}_3\text{C}_6\text{H}_2\text{S})_{10}] \cdot 2\text{CHCl}_3 \cdot \text{EtOH}$ contains a folded 20-membered ring of alternating Ag and S ions and has a much higher F_{th} of 2.6 J cm^{-2} , which is about 5 times that of C_{60} under the same conditions.⁵⁵⁴ Zhang *et al.* have observed efficient OL from a polyicosahedral cluster $[\text{Ag}_{20}\text{Cl}_{14}\text{Au}_{18}(\text{PPh}_3)_{12}]$, PMMA-doped thin films giving a four-fold efficiency increase over ethanol solutions.⁵⁵⁵

Several studies have addressed the cubic NLO properties of salts of heteropolymolybdate/tungstate cluster anions.^{360,557–561} The tetraanion in $\alpha\text{-H}_4\text{SiW}_{12}\text{O}_{40} \cdot 4\text{HMPA} \cdot 2\text{H}_2\text{O}$ (HMPA = hexamethylphosphoramide) has a Keggin structure which has idealized T_d point symmetry

and comprises four trigonal groups of edge-shared WO_6 octahedra, each group sharing corners with its neighbors and with the enclosed central SiO_4 tetrahedron.⁵⁵⁶ This pale yellow compound adopts the NCSG $P2_1$ and gives relatively weak powder SHG from a 1,064 nm laser of 0.7 times KDP.⁵⁵⁶ Z-scan experiments with 200 ps pulses show that the cubic NLO properties are dominated by nonlinear refraction, with a n_2 value of $1.11 \times 10^{-10} \text{ cm}^2 \text{ W}^{-1} \text{ M}^{-1}$ leading to $\chi^{(3)} = 2.63 \times 10^{-11}$ esu in MeCN.⁵⁵⁶ Heteropoly acids readily form salts with organic bases which can show visible/NIR CT excitations from the organic cation to the inorganic anion. A number of such salts based on Keggin ions with central B, Si, Ge, or P atoms and the protonated organic electron donors quinolin-8-ol, phen, or *N*-methylpyrrolidone (NMP) have been studied by Z-scan and also exhibit SHG from 1,064 nm,^{360,557–561} e.g., that of $[\text{NMPH}]_5[\text{BW}_{12}\text{O}_{40}] \cdot 2\text{H}_2\text{O}$ is 1.1 times KDP.³⁶⁰ Compounds with lacunary Keggin structures derived by the removal of MO_6 octahedra have lower symmetries than their parent structures and accordingly exhibit larger SHG activities.⁵⁶² For example, $[\text{Na}_{10}\text{SiW}_9\text{O}_{34}] \cdot 18\text{H}_2\text{O}$ gives a 1,064 nm SHG efficiency of 10.2 times KDP, and has a transmission cut-off at 300 nm, allowing SHG well into the UV.⁵⁶²

9.14.2.9 Miscellaneous Complexes

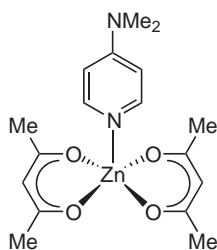
Besides thiocyanates, many other studies have concerned the quadratic NLO properties of colorless complexes of the group 12 metals.^{563–587} The tetrahedral complex $[\text{Zn}^{\text{II}}(\text{MNPO})_2\text{Br}_2]$ (MNPO = 3-methyl-4-nitropyridine-*N*-oxide) is SHG inactive (CSG $P\bar{1}$),⁵⁶³ but the thiourea-containing $[\text{Zn}^{\text{II}}(\text{SO}_4)\{\text{S}=\text{C}(\text{NH}_2)_2\}_3]$ crystallizes in the NCSG $Pca2_1$ and shows SHG from 1,064 nm of similar intensity to that of KDP.⁵⁶⁴ EO coefficients have also been measured for crystals of the latter compound⁵⁶⁵ and of its deuterated analogue.⁵⁶⁶ In the square pyramidal complex (205), electrostatic interactions and weak intermolecular H-bonds lead to a perfect parallel alignment of the dipoles in the NCSG $Fdd2$.⁵⁶⁷

The tetrahedral thiosemicarbazide complex $[\text{Cd}^{\text{II}}\text{Cl}_2\{\text{NH}_2\text{C}(\text{S})\text{NHNH}_2\}] \cdot \text{H}_2\text{O}$ crystallizes in the NCSG Cc and a 2 mm thick crystal gives a 1,064 nm SHG conversion efficiency of ca. 30%, which is 14 times that of KDP with the same thickness.^{568,569} The six independent quadratic NLO coefficients (d) have been determined for this material.⁵⁷⁰ The closely related $[\text{Cd}^{\text{II}}\text{Cl}_2\{\text{NH}_2\text{C}(\text{O})\text{NHNH}_2\}]$ crystallizes in the NCSG $Pna2_1$ and also shows quadratic NLO effects.⁵⁷¹ The allylthiourea compound (206)^{572,573} and its chloride analogue^{574–576} both adopt the NCSG $R3c$ and show significant quadratic NLO activities; EO coefficients have been determined for the chloride complex.⁵⁷⁷ $[\text{Cd}^{\text{II}}\text{Cl}_2(\text{NPO})_2]$ (NPO = 4-nitropyridine-*N*-oxide) crystallizes in the NCSG $Fdd2$ with a transparency cut-off at ca. 420 nm and 1,064 nm SHG activity of ca. 8 times urea.⁵⁷⁸ The Hg^{II} analogue of (206)^{579,580} and its chloride counterpart^{581,582} both crystallize in $R3c$ and show 1,064 nm SHG activities of ca. 3 times urea. The NLO properties of these allylthiourea^{583,584} and other complexes⁵⁸⁵ of the group 12 metals have been reviewed. The xanthate complex $[\text{Cd}^{\text{II}}(\text{EtOCS}_2)_2]$ is also SHG active,⁵⁸⁶ and the salt $\text{NH}_4[\text{Cd}^{\text{II}}(3,3'\text{-azodibenzoate})_2] \cdot \text{H}_2\text{NMe}_2$ forms a polymeric diamondoid network with tetragonal antiprismatic Cd^{II} centers, giving a 1,064 nm SHG activity of 1.2 times urea.⁵⁸⁷

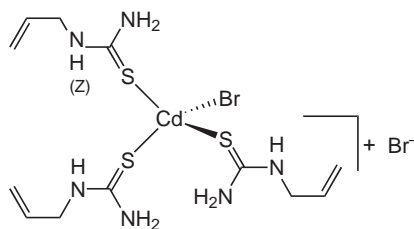
Mingos and co-workers have reported that a number of square planar Rh^{I} or Pd^{II} complex salts of pentane-2,4-dionato ligands (e.g., (207)) exhibit significant SHG, despite crystallizing in $P\bar{1}$.^{588,589} This unusual observation is attributable to either co-crystallization of more than one polymorph or the large (inevitably noncentrosymmetric) surface effects associated with fine powders.^{588,589} A range of octahedral Sn^{IV} -tris(catecholato) compounds also show moderate SHG activities at 1,064 nm and 1,907 nm, e.g., (208) which again crystallizes centrosymmetrically (in $Pbca$).⁵⁹⁰ The glutamate complex $[\text{Cu}^{\text{II}}\{\text{O}_2\text{C}(\text{H}_2\text{N})\text{CHC}_2\text{H}_4\text{CO}_2\}]$ is also SHG active.⁵⁹¹ Barberá *et al.* have carried out 1,380 nm EFISHG measurements on a series of thermotropic liquid crystalline square planar Rh^{I} or Ir^{I} complexes of β -diketonate or pyrazole ligands, but found only relatively small $\mu\beta_0$ values (e.g., for (209)).⁵⁹²

In a very early study of metal complexes with NLO properties, the binuclear Ru^{III} complexes (210) and (211) were considered for SHG of a 1,064 nm laser in LB film waveguides.⁵⁹³ It was anticipated that phase-matching could be achieved due to anomalous dispersion arising from the intense CT absorptions at ca. 800 nm, but unfortunately the materials are insufficiently photostable for such an application.⁵⁹³ Laidlaw *et al.* reported extremely large β values for two mixed-valence bimetallic Ru complexes (e.g., (212)) which possess intense low energy IVCT transitions.⁵⁹⁴ However, these 1,064 nm HRS-derived data were subsequently found to be heavily overestimated due to a factor of 6 error in the solvent reference β ,⁵⁹⁵ giving results which are more consistent with the relatively short conjugated pathlengths of the complexes. In such complexes, the electron-accepting d^5 Ru^{III} center is stabilized

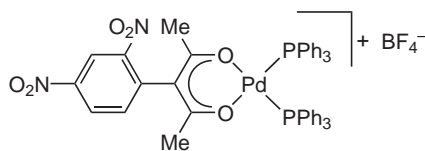
by strongly basic ammine ligands, whilst the electron-donating d^6 Ru^{II} is stabilized by π -accepting cyanides. β_0 values for **(212)** have also been calculated based on the TSM with $\beta_0 = 3\Delta\mu_{12}(\mu_{12})^2 / (E_{\text{max}})^2$. Laidlaw *et al.* obtained $\beta_0 = 41 \times 10^{-30}$ esu by using a $\Delta\mu_{12}$ value calculated for transfer of 1 electron over the geometric $\text{Ru}^{\text{II}}-\text{Ru}^{\text{III}}$ distance,⁵⁹⁵ whereas Vance *et al.* used a $\Delta\mu_{12}$ derived from Stark spectroscopy to afford a β_0 value of 28×10^{-30} esu.⁵⁹⁶ The discrepancy between the latter and the HRS-derived value may be due to errors in the HRS experiments incurred by working near to resonance.⁵⁹⁶ Another 1,064 nm HRS study with Ru pentaammine complexes involved the salts **(213)** and **(214)** which contain the laser dye coumarin 523.⁸² The significant increase in β_0 for **(214)** over that of the free dye derived via EFISHG in CHCl_3 is attributable to the inductive electron-withdrawing influence of the Ru^{III} center.⁸²



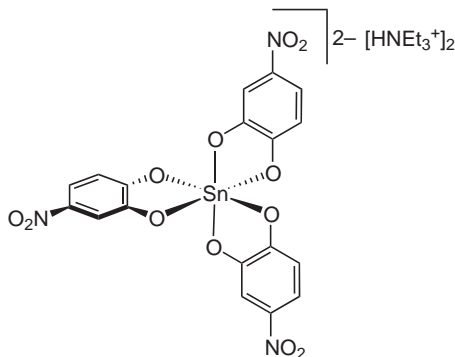
(205): $\text{SHG}_{1064} = \text{ca. } 1 \cdot \text{urea}$,
 $\beta_0[\text{AM1/TDHF}] = 4.4 \cdot 10^{-30}$ esu⁵⁶⁷



(206): $\text{SHG}_{1064} = 12.5 \cdot \text{KDP (ca. } 0.5 \cdot \text{urea)}$ ⁵⁷³

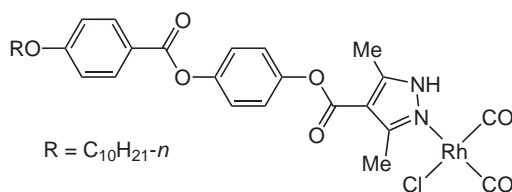


(207): $\text{SHG}_{1064} = 0.73 \cdot \text{urea}$ ^{588, 589}

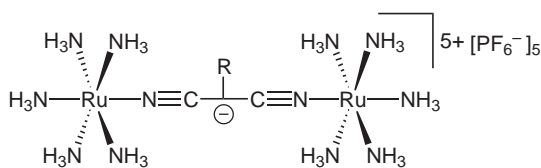


(208): $\text{SHG}_{1064} = 1.33 \cdot \text{urea}$, $\text{SHG}_{1907} = 0.44 \cdot \text{urea}$ ⁵⁹⁰

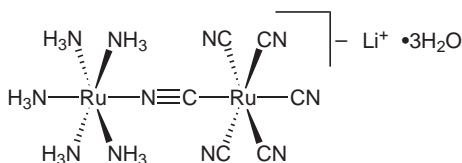
Coe *et al.* have reported very high 1,907 nm SHG activities in a number of strongly colored metal mononitrosyl complexes containing Fc electron donor groups (e.g., **(215)**–**(218)**).^{597–600} Complexes **(215)** and **(216)** crystallize isostructurally in the NCSG $P2_1$ with a “herring-bone” packing featuring dipole alignment which is almost ideal for phase-matching of SHG.^{598,599} Although these complexes were prepared as racemates, spontaneous resolution of the chiral octahedral metal centers occurs on crystallization.^{598,599} Furthermore, the Fc groups play a crucial steric role in influencing the bulk NLO activities because analogous complexes containing -OMe or -NMe₂ substituents all show no SHG.^{599,600} The NCSG $Pca2_1$ is found for one complex, but complete dipole cancellation occurs nevertheless.⁶⁰⁰ Although powder SHG activities are only semiquantitative, the W complexes always give significantly lower SHG than their Mo analogues.^{598–600} This observation is consistent with electrochemical data which show that a $\{\text{W}^{\text{II}}\text{Cl}(\text{Tp}^*)(\text{NO})\}^+$ center is less electron-withdrawing than its Mo counterpart.^{598–600} Related complexes with only a single aryl ring between the Fc and metal nitrosyl groups show only relatively weak SHG, the largest being found for **(219)**.⁶⁰¹



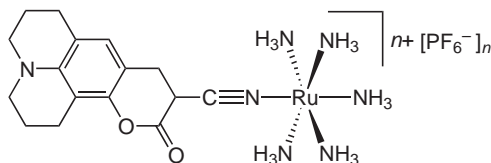
(209): $\lambda_{\max} = 339$ nm,
 $\mu\beta_0[\text{EFISHG}] = 18 \cdot 10^{-48}$ esu (1,4-dioxane)⁵⁹²



R = H (210), t-Bu (211)



(212): $\lambda_{\max} = 700$ nm,
 $\beta_0[\text{HRS}] = 81 \cdot 10^{-30}$ esu (H_2O)⁵⁹⁵



$n = 2$ (213): $\lambda_{\max} = 498$ nm, $\beta_0[\text{HRS}] = 41 \cdot 10^{-30}$ esu (MeCN)

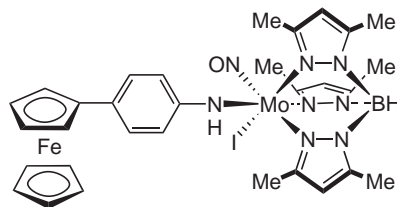
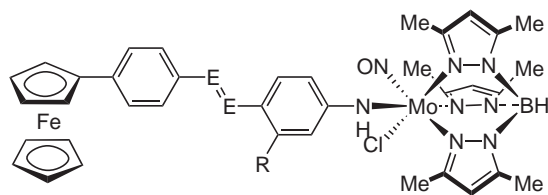
$n = 3$ (214): $\lambda_{\max} = 460$ nm, $\beta_0[\text{HRS}] = 49 \cdot 10^{-30}$ esu (MeCN)⁸²

Malaun *et al.* have used 1,064 nm HRS to determine β values for some of the complexes previously studied by Coe *et al.* together with some other related compounds.⁷⁸ Unfortunately, extensive resonance enhancement at 532 nm and the inadequacy of the TSM for Fc chromophores serve to limit the conclusions which can be drawn from these studies.⁷⁸ Nevertheless, it is apparent that β is increased by the following molecular structural changes: (i) replacement of a bromide or chloride ligand with an iodide; (ii) extension of the conjugated bridge (see data for (220)–(225)).⁷⁸ Furthermore, nondegenerate six-wave mixing experiments show that chemical reduction of (223) with cobaltocene causes β to decrease by a factor of ca. 0.25, indicating that the molecular NLO responses of such complexes can be switched by reduction of the electron-accepting metal nitrosyl centers.⁷⁸ Reis *et al.* have carried out *ab initio* MO calculations on the complex (226) (previously reported by Coe *et al.*),⁶⁰⁰ together with the related purely organic chromophore 4,4'-(dimethylamino)nitrostilbene (DANS).⁶⁰² Although the nature of the treatment renders the absolute results uncertain, the average β and γ values of (226) are smaller than, or at most of similar magnitude to, those of DANS.⁶⁰²

Agulló-López and co-workers have reported several investigations into the bulk NLO properties of bimetallic Mo complexes similar to (215)–(219) in CHCl_3 solutions and in poled, spin-coated PMMA thin films.^{603–606} 1,064 nm SHG measurements on these films afford the three nonzero components of the quadratic susceptibility tensor, $\chi^{(2)}_{31}$, $\chi^{(2)}_{15}$, and $\chi^{(2)}_{33}$, the first (off-diagonal) of these always being the largest, and corresponding β values are estimated from these data, assuming thermal equilibrium under the poling field.^{603,605,606} These results were discussed on the basis of a low energy CT transition having a component perpendicular to the permanent dipole moment.^{603,605,606} As expected, the $\chi^{(2)}$ values are largest for complexes with diaryl, as opposed to monoaryl, conjugated bridges,^{603,606} and “straight” complexes (e.g., (227)) have larger quadratic NLO responses than their “bent” analogues (e.g., (228)).^{605,606} These studies also show that $\chi^{(2)}$ values are larger for diazobenzene vs. stilbene bridges,^{603,606} and that the $\{\text{Mo}(\text{NO})\}^{3+}$ center is a weaker electron acceptor than a $-\text{NO}_2$ group.^{603,605,606} The results of THG experiments at 1,064 and 1,907 nm reveal all of the same trends for $\chi^{(3)}$ and γ values, except that the cubic NLO responses are larger for the complexes when compared with their $-\text{NO}_2$ analogues, especially for the “straight” chromophores.^{604,606}

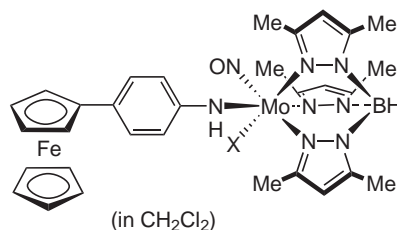
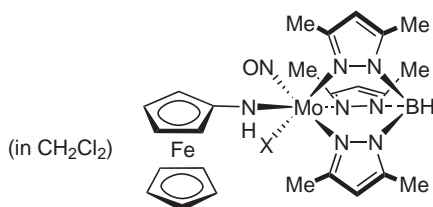
Balavoine and co-workers have also studied the quadratic NLO properties of bimetallic complexes containing Fc electron donor groups ((229) and (230)) by using EFISHG at 1,340 nm and 1,907 nm.⁶⁰⁷ Complexation of Fc-oxazolynyl ligands to square planar Pd^{II} centers causes ca. three-fold enhancements in β , presumably due to the inductive electron-withdrawing effect of the Pd^{II} ions.⁶⁰⁷ The Ni^{II} and Pt^{II} analogues of (229) and (230), as well as related species having additional $\text{C}\equiv\text{C}$ or $\text{CH}=\text{CH}$ units between the Fc and Pd^{II} centers, also show larger β values than the free ligands, but the nature of the square planar metal center does not greatly influence the NLO

response.^{608,609} A copolymer of one bimetallic complex with methyl methacrylate shows SHG activity at 1,064 nm,⁶⁰⁸ and these Fc complexes were predictably found not to obey the TSM.⁶⁰⁹



(219): SHG₁₉₀₇ = 1.15 · urea⁶⁰¹

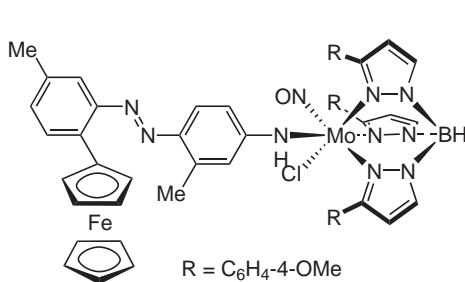
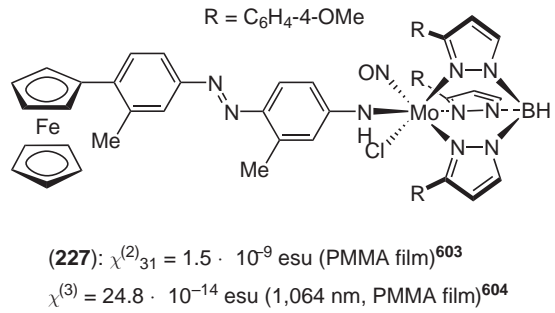
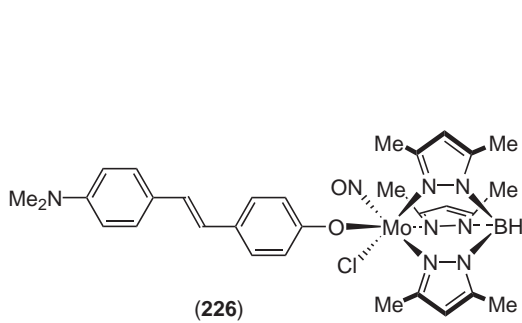
No.	M	E	R	SHG ₁₉₀₇ (· urea)
(215)	Mo	N	Me	50 ⁵⁹⁹
(216)	W	N	Me	8 ⁵⁹⁹
(217)	Mo	CH	H	35 ⁶⁰⁰
(218)	W	CH	H	8 ⁶⁰⁰



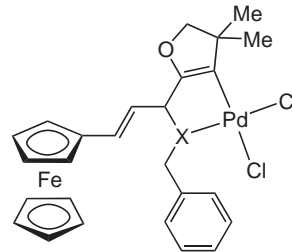
No.	X	λ_{\max} (nm)	β_{1064} [HRS] (10^{-30} esu) ⁷⁸
(220)	Cl	737	119
(221)	Br	753	135
(222)	I	764	197

No.	X	λ_{\max} (nm)	β_{1064} [HRS] (10^{-30} esu) ⁷⁸
(223)	Cl	596	297
(224)	Br	609	289
(225)	I	627	431

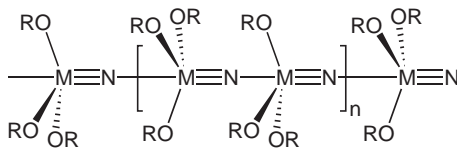
Pollagi *et al.* reported SHG activity for the colorless 1-D nitrido coordination polymers (231)–(233) which feature distorted trigonal bipyramidal W^{VI} or Mo^{VI} centers.⁶¹⁰ These compounds crystallize noncentrosymmetrically (NCSG $P6_3cm$ for (231) and $P6_3$ for (232)) with parallel dipole alignment, and their relatively weak quadratic NLO activities are attributable to limited π -conjugation along the chains.⁶¹⁰ Electrochemically synthesized magnetic thin films of $(\text{Fe}^{\text{II}}_x\text{-Cr}^{\text{II}}_{1-x})_{1.5}[\text{Cr}^{\text{III}}(\text{CN})_6] \cdot 7.5\text{H}_2\text{O}$ show SHG from a 775 nm laser, but powdered samples are inactive.⁶¹¹ Such “Prussian blue” analogues normally form centrosymmetric structures, but the introduction of Fe^{II} ions may cause lattice distortions which become aligned perpendicular to the film plane on electrocrystallization.⁶¹¹ Below the magnetic ordering temperature, the SHG intensity increases with increasing magnetization, indicating that magnetic ordering enhances $\chi^{(2)}$.⁶¹¹ The strongly luminescent, 2-D sheet coordination polymer $\{[\text{Eu}^{\text{III}}(\text{cda})_3(\text{H}_2\text{O})_3] \cdot \text{H}_2\text{O}\}_\infty$ ((234); cda = carbamoyldicyanomethanide anion) crystallizes in the NCSG Cc and combines a high SHG activity with good visible transparency.⁶¹² Houbrechts *et al.* found that complexation of an azacrown ether by addition of an excess of Na^I, K^I, or Ba^{II} thiocyanates produces small blue-shifts in the ICT absorption accompanied by decreases of 25–35% in β (e.g., for (235)).⁶¹³



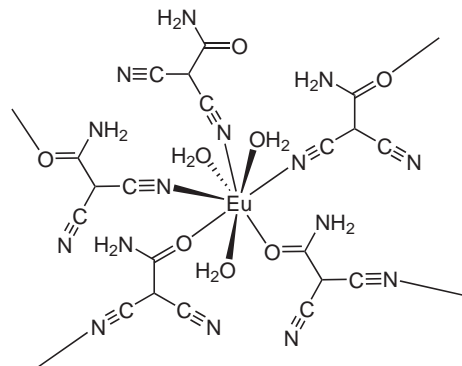
(228): $\chi^{(2)}_{31} = 0.4 \cdot 10^{-9}$ esu (PMMA film)⁶⁰⁵
 $\chi^{(3)} = 15.2 \cdot 10^{-14}$ esu (1,064 nm, PMMA film)⁶⁰⁴



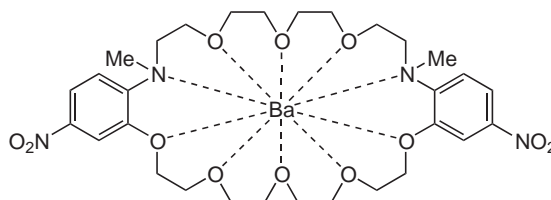
X = S (229): $\lambda_{\max} = 530$ nm,
 $\beta_{1340}[\text{EFISHG}] = 12.2 \cdot 10^{-30}$ esu (CHCl₃)
 X = SO (230): $\lambda_{\max} = 559$ nm,
 $\beta_{1340}[\text{EFISHG}] = 30.2 \cdot 10^{-30}$ esu (CHCl₃)⁶⁰⁷



No.	M	R	SHG ₁₀₆₄ (\cdot urea) ⁶¹⁰
(231)	W	t-Bu	0.20
(232)	Mo	t-Bu	0.25
(233)	Mo	CM ₂ CF ₃	0.35



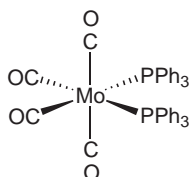
(234) (portion of network):
 SHG₁₀₆₄ = 16.8 \cdot urea⁶¹²



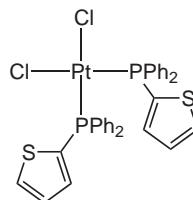
(235): $\lambda_{\max} = 393$ nm, $\beta_{1064}[\text{HRS}] = 24 \cdot 10^{-30}$ esu (MeCN)⁶¹³

The cubic NLO properties of a number of simple carbonyl complexes of phosphine or arsine ligands have been studied.^{614–620} 532 nm DFWM and Z-scan experiments with a series of Mo complexes (e.g., (236)) reveal relatively large values of $\chi^{(3)}$ and γ , with a close correlation between the number of delocalized π electrons and the magnitude of γ .^{614–616} Square planar Pd^{II} and Pt^{II} phosphine complexes (e.g., (237)) also exhibit cubic NLO effects, but the dependance of these properties on the molecular structure is not as pronounced as in the octahedral Mo carbonyls.^{615,617} Detailed DFWM studies on CH₂Cl₂ solutions of (236) show that exposure to air/O₂ causes large increases in $\chi^{(3)}$ with time which cease on addition of excess PPh₃.⁶¹⁸ THF solutions behave differently in that the $\chi^{(3)}$ increases do not stop on addition of PPh₃.⁶¹⁸ CH₂Cl₂ solutions of analogous complexes of AsPh₃ or PPh₂(2-naphthalenyl) behave similarly to those of (236), but the $\chi^{(3)}$ values of solutions of *cis*-[Mo{P(OPh)₃}₂(CO)₄] remain constant.⁶¹⁹ These studies indicate that the large γ value previously reported for (236) is actually due to oxidation which occurs following PPh₃ dissociation.⁶¹⁹ The addition of excess PPh₃ to a solution of (236) before exposure to O₂ gives a much smaller γ value of 1.8×10^{-33} esu.⁶¹⁹ Further studies on oxidized and PPh₃-stabilized CH₂Cl₂ solutions of (236) with 6 ns, 532 nm pulses reveal strong nonlinear absorption/refraction and OL behavior.⁶²⁰

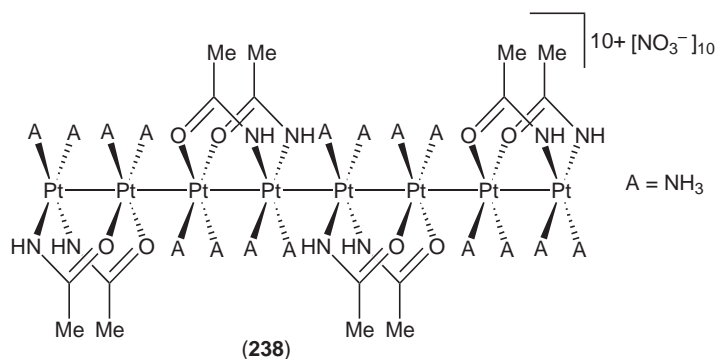
1,064 nm DFWM has also been applied to various square planar (mostly group 10) complexes of chelating, dianionic N-donor ligands derived from 2-aminobenzenethiol,⁶²¹ 3,4-toluenediamine,⁶²² 3,4-benzophenonediamine,⁶²² diaminomaleonitrile,⁶²³ or 1,2-phenylenediamine.⁶²³ The $\chi^{(3)}$ values of such systems are comparable to those of S-donor DT complexes (see Section 9.14.2.7). THG measurements on composite thin films of linear Pt ammine complexes and polyvinylalcohol have allowed the estimation of $\chi^{(3)}$ values.⁶²⁴ Predictably, the octanuclear acetamidato-bridged complex in (238) has an enhanced cubic NLO response when compared with its 2,2-dimethylpropanamidato tetranuclear counterpart, [Pt^{III}(Pt^{II})₃{*t*-BuC(O)NH}₄(NH₃)₈] [CF₃SO₃]₅.⁶²⁴ Transparent sol-gel films of the latter compound, which appears to exist in several valence states and may oligomerize at higher concentrations in alumina matrices, have $\chi^{(3)}$ values in the range ca. $1\text{--}5 \times 10^{-13}$ esu.^{625,626}



(236): γ [DFWM] = $1.7 \cdot 10^{-31}$ esu (THF)⁶¹⁵



(237): γ [DFWM] = $1.9 \cdot 10^{-31}$ esu (CH₂Cl₂)⁶¹⁵

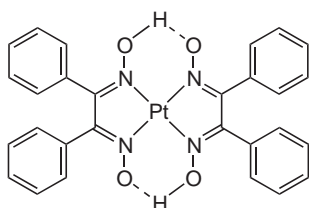


(238)

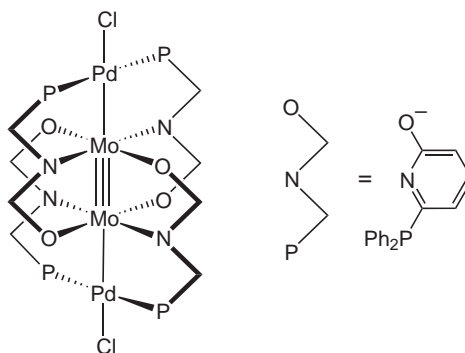
Kamata and co-workers have carried out a number of investigations into the cubic NLO properties of vacuum-deposited thin films of square planar d^8 group 10 complexes of dimethylglyoximate (DMGH) and related ligands.^{627–639} In the solid-state, such complexes adopt linear columnar chain structures with strong metal–metal d -orbital interactions that give rise to $d_z^2 \rightarrow p_z$ transitions in the visible region which are associated with large $\chi^{(3)}$ values. 1500–2100 nm THG experiments show that the Pt^{II} complexes have the largest $\chi^{(3)}$ values,⁶²⁷ and these can be reversibly controlled by chemically disrupting the Pt–Pt interactions.⁶²⁸ The intense $5d_z^2 \rightarrow 6p_z$ absorption at 690 nm of

[Pt^{II}(DMGH)₂] is almost completely bleached on treatment with I₂ vapor (with the color changing from blue to yellow), and this is accompanied by a ca. 100-fold decrease in $\chi^{(3)}$.⁶²⁸ Removal of the I₂ by heating restores both the visible absorption and the NLO response.⁶²⁸ Interestingly, the complex (239) exists as two different crystalline phases; the $5d_{z^2} \rightarrow 6p_z$ λ_{\max} values are 550 nm and 730 nm for the red and (metastable) green forms, respectively.⁶²⁹ The considerably larger $\chi^{(3)}$ of the latter is attributable to shortening of the Pt–Pt distance,⁶²⁹ and the inverse correlation between this parameter and the bulk cubic NLO response has subsequently been investigated in more detail in related complexes.⁶³⁶ Other studies have involved CNDO/SDCI calculations,⁶³⁰ tuning of λ_{\max} values by alloying,^{631,632} and doping with Cl₂/Br₂ which causes ca. 100-fold increases in $\chi^{(3)}$ for [Ni^{II}(DMGH)₂].^{633,634} The surface plasmon resonance method has been used to measure n_2 values at 1,064 nm, that for [Pt^{II}(DMGH)₂] ($-1.9 \times 10^{-10} \text{ cm}^2 \text{ W}^{-1}$) being about 10 times those of [Ni^{II}(DMGH)₂] or [Pd^{II}(DMGH)₂],⁶³⁷ and degenerate 500–600 nm pump-probe^{635,639} and Z-scan⁶³⁸ studies have also been carried out.

Mashima *et al.* were the first to describe the cubic NLO properties of complexes containing metal–metal multiple bonds, using 532 nm DFWM with ps pulses to study several di- and tetranuclear 6-diphenylphosphino-2-pyridonate complexes (e.g., (240)).⁶⁴⁰ They also carried out 790 nm fs OKE measurements on (240), and on the basis of the agreement in magnitude with the DFWM results, suggested that the large γ response is largely nonresonant (i.e., due to instantaneous electronic polarization).⁶⁴⁰ Pate *et al.* have since applied ps DFWM at 1,064 nm to several metal–metal multiply bonded dinuclear Mo or W complexes (e.g., (241)) which shows almost complete visible transparency.⁶⁴¹ When using cross-polarized excitation beams ($x\gamma yx$ configuration), negligible instantaneous electronic polarizations are observed, but using similarly polarized beams ($y\gamma yy$ configuration) gives significant effective γ values, which are attributable to the formation of bulk thermal excitation gratings.⁶⁴¹ This conclusion is supported by time-dependent DFWM measurements, suggesting that the previously reported large γ values for complexes such as (240) are due to resonant contributions in the $y\gamma yy$ configuration.⁶⁴¹



(239): $\chi^{(3)}$ [THG] = ca. 10^{-12} esu (red film),
ca. 10^{-11} esu (green film)⁶²⁹



(240): λ_{\max} = 640 nm, γ [DFWM] = $1.5 \cdot 10^{-30}$ esu (CH₂Cl₂)⁶⁴⁰



(241): γ [DFWM] = $1.3 \cdot 10^{-32}$ esu (CH₂Cl₂)⁶⁴¹

9.14.3 CONCLUSIONS

As this review has demonstrated, the study of metal complexes with NLO properties has produced a very large body of published work, representing a truly global scientific enterprise. Indeed, the number of citations would have been considerably larger if purely organometallic complexes had also been included. Although it seems that activity in this area has now passed its peak purely in terms of volume, this is arguably not the case when studies are judged in terms of their quality and/or significance. For quadratic NLO materials, there has been a logical and

continual refinement in the approach from SHG powder test screening (which has at times been of an almost random nature), to focused systematic studies aimed at establishing detailed molecular SACs for β_0 responses. Although some of the conclusions emerging from such investigations have simply reinforced trends previously found with purely organic chromophores, new insights have also emerged. A particularly good example of such novelty is the pseudo-octupolar chromophores based on tris(α -diimine) cores with metal ions including Zn^{II} and Ru^{II} (e.g., (58))¹²³ which have no parallels in metal-free systems. It can realistically be expected that continued experimentation will afford further new, and perhaps unexpected, conclusions. Examples of types of chromophore that beg to be more fully explored include extended binuclear mixed-valence complexes, polymetallic metal–metal bonded chains and the rich diversity of octupolar structures.

A number of complex chromophores are now known which display β_0 values larger than most purely organic compounds, and the gains achieved by incorporating metal centers are particularly impressive when considering molecular sizes. For example, the β_0 values for Ru^{II}-pyridinium salts such as (37)⁸⁵ are several times larger than those of organic chromophores of similar dimensions. Furthermore, the magnitudes of these NLO responses have been confirmed by two independent experimental techniques (HRS and Stark spectroscopy) as well as by TD-DFT calculations. Although metal centers can act as very strong electron donor or acceptor groups, it has become apparent that relatively poor orbital overlap between heavy metal ions and organic ligands acts to decrease the β_0 values which can be achieved. Nevertheless, it is certainly true that the quadratic NLO responses of metal complexes have yet to reach the stage of optimization at the molecular level. In common with purely organic chromophores, the metal complexes that show the largest β_0 values are all relatively strongly colored, precluding any applications involving visible lasers. However, this does not necessarily rule out applications for such chromophores in which only NIR frequencies are involved, such as EO modulation. In any case, several of the 3-D network thiocyanate complexes such as ZTC (152) combine visible transparency with impressive activities for SHG into the UV region.³⁷⁵ For quadratic NLO materials, the realization of molecule-based devices now hinges more on considerations such as stability, because sufficiently large NLO responses have been achieved in many cases. Multifunctionality is very likely a key selling point of metal complexes in this area, and the more recent literature has featured a growing focus on aspects such as switchability of NLO responses.⁹¹

The situation regarding cubic NLO materials is generally less well defined, both for metal complexes and also for their purely organic counterparts. Driven largely by the tantalizing potential for using the optical intensity dependence of refractive indices as the basis of all-optical information processing, research into cubic NLO phenomena has not suffered from a lack of effort. However, the creation of potentially useful molecules has been hindered by a paucity of clear design guidelines, in contrast to the quadratic NLO field. Although it has been suggested that conjugated organic compounds with cubic NLO responses sufficiently large for practical applications may not be realisable, advances in chromophore design have given cause for hope. The area in which cubic NLO materials, and especially those containing metals, currently seem best suited to enter the marketplace is OL devices. Because efficient OL behavior is most often attributable to RSA, and the presence of heavy atoms is advantageous for achieving the appropriate excited state structures and dynamics, MPcs and cluster complexes are currently amongst the most promising materials for potential OL applications.^{174,523} Although further work remains to be done in terms of chromophore optimization (solubility, stability, etc.), the creation and study of bulk OL materials involving for example sol–gel or polymer matrices is increasingly of interest.

Finally, although it might be considered disappointing that no NLO devices based on metal complexes have yet reached the stage of commercialization, it should be remembered that almost all of the references cited herein have appeared in the years since the original (CCC, 1987) was published. The field of molecular NLO materials may be reaching maturity, at least in some respects, but the fact that it has not yet delivered on its potential in terms of real-world applications need not cause undue concern just yet. The realization of working devices is a major challenge and will hinge to a large extent on efficient communication and interaction between synthetic chemists, physicists, electronic engineers, etc. Without such collaborative efforts, many potentially useful materials will remain just that. At the very least, the quest for novel metal-containing molecular NLO materials has stimulated much interesting scientific study and greatly added to our knowledge and understanding of the electronic and photonic properties of metal complexes.

9.14.4 REFERENCES

1. Harper, P.; Wherrett, B., Eds. *Nonlinear Optics* 1977, Academic Press: New York.
2. Shen, Y. R. *The Principles of Nonlinear Optics* 1984, Wiley: New York.
3. Saleh, B. E. A.; Teich, M. C. *Fundamentals of Photonics* 1991, Wiley: New York.
4. Chemla, D. S.; Zyss, J., Eds. *Nonlinear Optical Properties of Organic Molecules and Crystals*; Academic Press: Orlando, FL, 1987, Vols. 1 and 2.
5. Zyss, J. *Molecular Nonlinear Optics: Materials, Physics and Devices* 1994, Academic Press: Boston.
6. Bosshard, Ch.; Sutter, K.; Prêtre, Ph.; Hulliger, J.; Flörsheimer, M.; Kaatz, P.; Günter, P. *Organic Nonlinear Optical Materials (Advances in Nonlinear Optics, Vol. 1)* Gordon & Breach: Amsterdam, 1995.
7. Nalwa, H. S.; Miyata, S., Eds. *Nonlinear Optics of Organic Molecules and Polymers* 1997, CRC Press: Boca Raton, FL.
8. Nalwa, H. S. *Appl. Organomet. Chem.* **1991**, *5*, 349–377.
9. Marder, S. R. Metal-containing Materials for Nonlinear Optics. In *Inorganic Materials*, 2nd ed.; Bruce, D. W., O'Hare, D., Eds.; Wiley: Chichester, UK, 1992, pp 121–169.
10. Kanis, D. R.; Ratner, M. A.; Marks, T. J. *Chem. Rev.* **1994**, *94*, 195–242.
11. Long, N. J. *Angew. Chem., Int. Ed. Engl.* **1995**, *34*, 21–38.
12. Whittall, I. R.; McDonagh, A. M.; Humphrey, M. G.; Samoc, M. *Adv. Organomet. Chem.* **1998**, *42*, 291–362.
13. Whittall, I. R.; McDonagh, A. M.; Humphrey, M. G.; Samoc, M. *Adv. Organomet. Chem.* **1998**, *43*, 349–405.
14. Qin, J.; Liu, D.; Dai, C.; Chen, C.; Wu, B.; Yang, C.; Zhan, C. *Coord. Chem. Rev.* **1999**, *188*, 23–34.
15. Heck, J.; Dabek, S.; Meyer-Friedrichsen, T.; Wong, H. *Coord. Chem. Rev.* **1999**, *190–192*, 1217–1254.
16. Gray, G. M.; Lawson, C. M. Structure–Property Relationships in Transition Metal-organic Third-order Nonlinear Optical Materials. In *Optoelectronic Properties of Inorganic Compounds*; Roundhill, D. M., Fackler, J. P., Jr., Eds.; Plenum: New York, 1999; pp 1–27.
17. Shi, S. Nonlinear Optical Properties of Inorganic Clusters. In *Optoelectronic Properties of Inorganic Compounds*; Roundhill, D. M.; Fackler, J. P., Jr., Eds.; Plenum: New York, 1999, pp 55–105.
18. Le Bozec, H.; Renouard, T. *Eur. J. Inorg. Chem.* **2000**, 229–239.
19. Barlow, S.; Marder, S. R. *Chem. Commun.* **2000**, 1555–1562.
20. Lacroix, P. G. *Eur. J. Inorg. Chem.* **2001**, 339–348.
21. Di Bella, S. *Chem. Soc. Rev.* **2001**, *30*, 355–366.
22. Tutt, L. W.; Boggess, T. F. *Prog. Quantum Electron.* **1993**, *17*, 299–338.
23. Van Stryland, E. W.; Hagan, D. J.; Xia, T.; Said, A. A. Application of Nonlinear Optics to Passive Optical Limiting. In *Nonlinear Optics of Organic Molecules and Polymers*; Nalwa, H. S.; Miyata, S., Eds.; CRC Press: Boca Raton, FL 1997, pp 841–860.
24. Hercher, M. *Appl. Opt.* **1967**, *6*, 947–954.
25. Zyss, J.; Ledoux, I. *Chem. Rev.* **1994**, *94*, 77–105.
26. Tykewinski, R. R.; Gubler, U.; Martin, R. E.; Diederich, F.; Bosshard, C.; Günter, P. *J. Phys. Chem. B* **1998**, *102*, 4451–4465.
27. Kurtz, S. K.; Perry, T. T. *J. Appl. Phys.* **1968**, *39*, 3798–3813.
28. Levine, B. F.; Bethea, C. G. *Appl. Phys. Lett.* **1974**, *24*, 445–447.
29. Levine, B. F.; Bethea, C. G. *J. Chem. Phys.* **1975**, *63*, 2666–2682.
30. Singer, K. D.; Garito, A. F. *J. Chem. Phys.* **1981**, *75*, 3572–3580.
31. Terhune, R. W.; Maker, P. D.; Savage, C. M. *Phys. Rev. Lett.* **1965**, *14*, 681–684.
32. Clays, K.; Persoons, A. *Rev. Sci. Instrum.* **1992**, *63*, 3285–3289.
33. Hendrickx, E.; Clays, K.; Persoons, A. *Acc. Chem. Res.* **1998**, *31*, 675–683.
34. Olbrechts, G.; Strobbe, R.; Clays, K.; Persoons, A. *Rev. Sci. Instrum.* **1998**, *69*, 2233–2241.
35. Oudar, J. L.; Chemla, D. S. *J. Chem. Phys.* **1977**, *66*, 2664–2668.
36. Oudar, J. L. *J. Chem. Phys.* **1977**, *67*, 446–457.
37. Joffe, M.; Yaron, D.; Silbey, J.; Zyss, J. *J. Chem. Phys.* **1992**, *97*, 5607–5615.
38. Pauley, M. A.; Wang, C. H. *Rev. Sci. Instrum.* **1999**, *70*, 1277–1284.
39. Paley, M. S.; Harris, J. M.; Looser, H.; Baumert, J. C.; Bjorklund, G. C.; Jundt, D.; Twieg, R. J. *J. Org. Chem.* **1989**, *54*, 3774–3778.
40. Bosshard, C.; Knöpfle, G.; Prêtre, P.; Günter, P. *J. Appl. Phys.* **1992**, *71*, 1594–1605.
41. Bruni, S.; Cariati, E.; Cariati, F.; Porta, F. A.; Quici, S.; Roberto, D. *Spectrochim. Acta, Pt. A* **2001**, *57*, 1417–1426.
42. Liptay, W. Dipole Moments and Polarizabilities of Molecules in Excited Electronic States. In *Excited States*, Vol. 1; Lim, E. C., Ed.; Academic Press: New York, 1974, Vol. 1, pp 129–229.
43. Bublitz, G. U.; Boxer, S. G. *Annu. Rev. Phys. Chem.* **1997**, *48*, 213–242.
44. Willetts, A.; Rice, J. E.; Burland, D. M.; Shelton, D. P. *J. Chem. Phys.* **1992**, *97*, 7590–7599.
45. Hermann, J. P.; Ricard, D.; Ducuing, J. *Appl. Phys. Lett.* **1973**, *23*, 178–180.
46. Kajzar, F.; Messier, J. *Phys. Rev. A* **1985**, *32*, 2352–2363.
47. Kajzar, F.; Messier, J. *Rev. Sci. Instrum.* **1987**, *58*, 2081–2085.
48. Perry, J. W. Nonlinear Optical Properties of Molecules and Materials. In *Materials for Nonlinear Optics: Chemical Perspectives*; Marder, S. R.; Sohn, J. D.; Stucky, G. D., Eds.; ACS Symposium Series 455; American Chemical Society: Washington, DC, 1991, pp 67–88.
49. Yariv, A. *IEEE J. Quantum Electron.* **1978**, *QE14*, 650–660.
50. Steel, D. G.; Lind, R. C.; Lam, J. F. *Phys. Rev. A* **1981**, *23*, 2513–2524.
51. Lind, R. C.; Steel, D. G.; Dunning, G. J. *Opt. Eng.* **1982**, *21*, 190–198.
52. Biaggio, I. *Phys. Rev. A* **2001**, *64*, 063813/1–13.
53. Sheik-Bahae, M.; Said, A. A.; van Stryland, E. W. *Opt. Lett.* **1989**, *14*, 955–957.
54. Sheik-Bahae, M.; Said, A. A.; Wei, T. H.; Hagan, D. J.; van Stryland, E. W. *IEEE J. Quantum Electron.* **1990**, *26*, 760–769.
55. van Stryland, E. W.; Sheik-Bahae, M. *Opt. Eng.* **1998**, *60*, 655–692.
56. McMorow, D.; Lotshaw, W. T.; Kenney-Wallace, G. A. *IEEE J. Quantum Electron.* **1988**, *QE-24*, 443–454.
57. Righini, R. *Science* **1993**, *262*, 1386–1390.

58. Marder, S. R.; Perry, J. W.; Schaefer, W. P. *Science* **1989**, *245*, 626–628.
59. Blanchard-Desce, M.; Alain, V.; Bedworth, P. V.; Marder, S. R.; Fort, A.; Runser, C.; Barzoukas, M.; Lebus, S.; Wortmann, R. *Chem. Eur. J.* **1997**, *3*, 1091–1104.
60. Brunel, J.; Ledoux, I.; Zyss, J.; Blanchard-Desce, M. *Chem. Commun.* **2001**, 923–924.
61. Couris, S.; Koudoumas, E.; Dong, F.; Leach, S. *J. Phys. B* **1996**, *29*, 5033–5041.
62. McLean, D. G.; Sutherland, R. L.; Brant, M. C.; Brandelik, D. M.; Fleitz, P. A.; Pottenger, T. *Opt. Lett.* **1993**, *18*, 858–860.
63. Frazier, C. C.; Harvey, M. A.; Cockerham, M. P.; Hand, H. M.; Chauchard, E. A.; Lee, C. H. *J. Phys. Chem.* **1986**, *90*, 5703–5706.
64. Calabrese, J. C.; Tam, W. *Chem. Phys. Lett.* **1987**, *133*, 244–245.
65. Eaton, D. F.; Anderson, A. G.; Tam, W.; Wang, Y. *J. Am. Chem. Soc.* **1987**, *109*, 1886–1888.
66. Tam, W.; Eaton, D. F.; Calabrese, J. C.; Williams, I. D.; Wang, Y.; Anderson, A. G. *Chem. Mater.* **1989**, *1*, 128–140.
67. Cheng, L.-T.; Tam, W.; Eaton, D. F. *Organometallics* **1990**, *9*, 2856–2857.
68. Cheng, L.-T.; Tam, W.; Meredith, G. R. *Mol. Cryst. Liq. Cryst.* **1990**, *189*, 137–153.
69. Tam, W.; Cheng, L.-T.; Bierlein, J. D.; Cheng, L. K.; Wang, Y.; Feiring, A. E.; Meredith, G. R.; Eaton, D. F.; Calabrese, J. C.; Rikken, G. L. J. A. Donor- and Acceptor-substituted Organic and Organometallic Compounds. Second-order Nonlinear Optical Properties. In *Materials for Nonlinear Optics: Chemical Perspectives*; Marder, S. R.; Sohn, J. D.; Stucky, G. D., Eds.; ACS Symposium Series 455; American Chemical Society: Washington, DC, 1991; pp 158–169.
70. Kanis, D. R.; Ratner, M. A.; Marks, T. J. *J. Am. Chem. Soc.* **1990**, *112*, 8203–8204.
71. Lacroix, P. G.; Lin, W.; Wong, G. K. *Chem. Mater.* **1995**, *7*, 1293–1298.
72. Bruce, D. W.; Thornton, A. *Mol. Cryst. Liq. Cryst.* **1993**, *231*, 253–256.
73. Bruce, D. W. *Adv. Inorg. Chem.* **2001**, *52*, 151–204.
74. Houbrechts, S.; Clays, K.; Persoons, A.; Cadierno, V.; Pilar Gamasa, M.; Gimeno, J. *Organometallics* **1996**, *15*, 5266–5268.
75. Mata, J.; Uriel, S.; Peris, E.; Llusar, R.; Houbrechts, S.; Persoons, A. *J. Organomet. Chem.* **1998**, *562*, 197–202.
76. Lee, I. S.; Lee, S. S.; Cheung, Y. K.; Kim, D.; Song, N. W. *Inorg. Chim. Acta* **1998**, *279*, 243–248.
77. Briel, O.; Sünkel, K.; Krossing, I.; Nöth, H.; Schmäzlin, E.; Meerholz, K.; Bräuchle, C.; Beck, W. *Eur. J. Inorg. Chem.* **1999**, 483–490.
78. Malaun, M.; Kowallick, R.; McDonagh, A. M.; Marcaccio, M.; Paul, R. L.; Asselberghs, I.; Clays, K.; Persoons, A.; Bildstein, B.; Fiorini, C.; Nunzi, J.-M.; Ward, M. D.; McCleverty, J. A. *J. Chem. Soc., Dalton Trans.* **2001**, 3025–3038.
79. Kanis, D. R.; Lacroix, P. G.; Ratner, M. A.; Marks, T. J. *J. Am. Chem. Soc.* **1994**, *116*, 10089–10102.
80. Roberto, D.; Ugo, R.; Bruni, S.; Cariati, E.; Cariati, F.; Fantucci, P.; Invernizzi, I.; Quici, S.; Ledoux, I.; Zyss, J. *Organometallics* **2000**, *19*, 1775–1788.
81. Roberto, D.; Ugo, R.; Tessore, F.; Lucenti, E.; Quici, S.; Vezza, S.; Fantucci, P.; Invernizzi, I.; Bruni, S.; Ledoux-Rak, I.; Zyss, J. *Organometallics* **2002**, *21*, 161–170.
82. Coe, B. J.; Chadwick, G.; Houbrechts, S.; Persoons, A. *J. Chem. Soc., Dalton Trans.* **1997**, 1705–1711.
83. Coe, B. J.; Chamberlain, M. C.; Essex-Lopresti, J. P.; Gaines, S.; Jeffery, J. C.; Houbrechts, S.; Persoons, A. *Inorg. Chem.* **1997**, *36*, 3284–3292.
84. Coe, B. J.; Essex-Lopresti, J. P.; Harris, J. A.; Houbrechts, S.; Persoons, A. *Chem. Commun.* **1997**, 1645–1646.
85. Coe, B. J.; Harris, J. A.; Harrington, L. J.; Jeffery, J. C.; Rees, L. H.; Houbrechts, S.; Persoons, A. *Inorg. Chem.* **1998**, *37*, 3391–3399.
86. Coe, B. J.; Harris, J. A.; Asselberghs, I.; Persoons, A.; Jeffery, J. C.; Rees, L. H.; Gelbrich, T.; Hursthouse, M. B. *J. Chem. Soc., Dalton Trans.* **1999**, 3617–3625.
87. Houbrechts, S.; Asselberghs, I.; Persoons, A.; Coe, B. J.; Harris, J. A.; Harrington, L. J.; Essex-Lopresti, J. P. *Mol. Cryst. Liq. Cryst. Sci. Technol., Sect. B: Nonlinear Opt.* **1999**, *22*, 161–164.
88. Houbrechts, S.; Asselberghs, I.; Persoons, A.; Coe, B. J.; Harris, J. A.; Harrington, L. J.; Chamberlain, M. C.; Essex-Lopresti, J. P.; Gaines, S. *Proc. SPIE-Int. Soc. Opt. Eng.* **1999**, *3796*, 209–218.
89. Asselberghs, I.; Houbrechts, S.; Persoons, A.; Coe, B. J.; Harris, J. A. *Synth. Met.* **2001**, *124*, 205–207.
90. Coe, B. J.; Houbrechts, S.; Asselberghs, I.; Persoons, A. *Angew. Chem., Int. Ed. Engl.* **1999**, *38*, 366–369.
91. Coe, B. J. *Chem. Eur. J.* **1999**, *5*, 2464–2471.
92. Coe, B. J.; Harris, J. A.; Brunshwig, B. S. *J. Phys. Chem. A* **2002**, *106*, 897–905.
93. Coe, B. J.; Harris, J. A.; Clays, K.; Persoons, A.; Wostyn, K.; Brunshwig, B. S. *Chem. Commun.* **2001**, 1548–1549.
94. Lin, C.-S.; Wu, K.-C.; Snijders, J. G.; Sa, R.-J.; Chen, X.-H. *Acta Chim. Sinica* **2002**, *60*, 664–668.
95. Ferretti, A.; Lami, A.; Villani, G. *J. Phys. Chem. A* **1997**, *101*, 9439–9444.
96. Lin, W.-B.; Evans, O. R.; Xiong, R.-G.; Wang, Z. *J. Am. Chem. Soc.* **1998**, *120*, 13272–13273.
97. Lin, W.-B.; Wang, Z.; Ma, L. *J. Am. Chem. Soc.* **1999**, *121*, 11249–11250.
98. Evans, O. R.; Xiong, R.-G.; Wang, Z.-Y.; Wong, G. K.; Lin, W. *Angew. Chem., Int. Ed. Engl.* **1999**, *38*, 536–538.
99. Evans, O. R.; Wang, Z.-Y.; Lin, W. *Chem. Commun.* **1999**, 1903–1904.
100. Lin, W.-B.; Ma, L.; Evans, O. R. *Chem. Commun.* **2000**, 2263–2264.
101. Evans, O. R.; Lin, W. *Chem. Mater.* **2001**, *13*, 2705–2712.
102. Evans, O. R.; Lin, W. *Chem. Mater.* **2001**, *13*, 3009–3017.
103. Huang, S. D.; Xiong, R.-G.; Han, J.; Weiner, B. R. *Inorg. Chim. Acta* **1999**, *294*, 95–98.
104. Hou, H.-W.; Song, Y.-L.; Fan, Y.-T.; Zhang, L.-P.; Du, C.-X.; Zhu, Y. *Inorg. Chim. Acta* **2001**, *316*, 140–144.
105. Hou, H.-W.; Wei, Y.-L.; Fan, Y.-T.; Du, C.-X.; Zhu, Y.; Song, Y.-L.; Niu, Y.-Y.; Xin, X.-Q. *Inorg. Chim. Acta* **2001**, *319*, 212–218.
106. Niu, Y.-Y.; Hou, H.-W.; Li, F.; Zheng, H.-G.; Song, Y.-L.; Fun, H.-K.; Xin, X.-Q. *Chin. J. Inorg. Chem.* **2001**, *17*, 533–537.
107. Hou, H.-W.; Wei, Y.-L.; Song, Y.-L.; Zhu, Y.; Li, L.-K.; Fan, Y.-T. *J. Mater. Chem.* **2002**, *12*, 838–843.
108. Bourgault, M.; Mountassir, C.; Le Bozec, H.; Ledoux, I.; Pucetti, G.; Zyss, J. *J. Chem. Soc., Chem. Commun.* **1993**, 1623–1624.
109. Bourgault, M.; Baum, K.; Le Bozec, H.; Pucetti, G.; Ledoux, I.; Zyss, J. *New J. Chem.* **1998**, 517–522.

110. Yam, V. W.-W.; Lau, V. C.-Y.; Wang, K.-Z.; Cheung, K.-K.; Huang, C.-H. *J. Mater. Chem.* **1998**, *8*, 89–97.
111. Yam, V. W.-W.; Wang, K.-Z.; Wang, C.-R.; Yang, Y.; Cheung, K.-K. *Organometallics* **1998**, *17*, 2440–2446.
112. Yam, V. W.-W.; Yang, Y.; Yang, H.-P.; Cheung, K.-K. *Organometallics* **1999**, *18*, 5252–5258.
113. Sakaguchi, H.; Nakamura, H.; Nagamura, T.; Ogawa, T.; Matsuo, T. *Chem. Lett.* **1989**, 1715–1718.
114. Sakaguchi, H.; Nagamura, T.; Matsuo, T. *Appl. Organomet. Chem.* **1991**, *5*, 257–260.
115. Sakaguchi, H.; Nagamura, T.; Matsuo, T. *Jpn. J. Appl. Phys., Part 2* **1991**, *30*, L377–L379.
116. Nagamura, T.; Sakaguchi, H.; Matsuo, T. *Thin Solid Films* **1992**, *210–211*, 160–162.
117. Sakaguchi, H.; Gomez-Jahn, L. A.; Prichard, M.; Penner, T. L.; Whitten, D. G.; Nagamura, T. *J. Phys. Chem.* **1993**, *97*, 1474–1476.
118. Sakaguchi, H.; Nagamura, T.; Penner, T. L.; Whitten, D. G. *Thin Solid Films* **1994**, *244*, 947–950.
119. Matsuo, T.; Nakamura, H.; Nakao, T.; Kawazu, M. *Chem. Lett.* **1992**, 2363–2366.
120. Umemura, Y.; Yamagishi, A.; Schoonheydt, R.; Persoons, A.; De Schryver, F. J. *Am. Chem. Soc.* **2002**, *124*, 992–997.
121. Zyss, J.; Dhenaut, C.; Chauvan, T.; Ledoux, I. *Chem. Phys. Lett.* **1993**, *206*, 409–414.
122. Persoons, A.; Clays, K.; Kauranen, M.; Hendrickx, E.; Put, E.; Bijmens, W. *Synth. Met.* **1994**, *67*, 31–38.
123. Dhenaut, C.; Ledoux, I.; Samuel, I. D. W.; Zyss, J.; Bourgault, M.; Le Bozec, H. *Nature* **1995**, *374*, 339–342.
124. Morrison, I. D.; Denning, R. G.; Laidlaw, W. M.; Stammers, M. A. *Rev. Sci. Instrum.* **1996**, *67*, 1445–1453.
125. Le Bozec, H.; Renouard, T.; Bourgault, M.; Dhenaut, C.; Brasselet, S.; Ledoux, I.; Zyss, J. *Synth. Met.* **2001**, *124*, 185–189.
126. Vance, F. W.; Hupp, J. T. *J. Am. Chem. Soc.* **1999**, *121*, 4047–4053.
127. Le Bouder, T.; Maury, O.; Le Bozec, H.; Ledoux, I.; Zyss, J. *Chem. Commun.* **2001**, 2430–2431.
128. Le Bozec, H.; Le Bouder, T.; Maury, O.; Bondon, A.; Ledoux, I.; Deveau, S.; Zyss, J. *Adv. Mater.* **2001**, *13*, 1677–1681.
129. Hilton, A.; Renouard, T.; Maury, O.; Le Bozec, H.; Ledoux, I.; Zyss, J. *Chem. Commun.* **1999**, 2521–2522.
130. Renouard, T.; Le Bozec, H.; Brasselet, S.; Ledoux, I.; Zyss, J. *Chem. Commun.* **1999**, 871–872.
131. Senechal, K.; Maury, O.; Le Bozec, H.; Ledoux, I.; Zyss, J. *J. Am. Chem. Soc.* **2002**, *124*, 4560–4561.
132. Evans, C. C.; Masse, R.; Nicoud, J.-F.; Bagieu-Beucher, M. *J. Mater. Chem.* **2000**, *10*, 1419–1423.
133. Cummings, S. D.; Cheng, L.-T.; Eisenberg, R. *Chem. Mater.* **1997**, *9*, 440–450.
134. Base, K.; Tierney, M. T.; Fort, A.; Muller, J.; Grinstaff, M. W. *Inorg. Chem.* **1999**, *38*, 287–289.
135. Chao, H.; Li, R.-H.; Ye, B.-H.; Li, H.; Feng, X.-L.; Cai, J.-W.; Zhou, J.-Y.; Ji, L.-N. *J. Chem. Soc., Dalton Trans.* **1999**, 3711–3717.
136. Jiang, C.-W.; Chao, H.; Li, R.-H.; Li, H.; Ji, L.-N. *Polyhedron* **2001**, *20*, 2187–2193.
137. Chao, H.; Li, R.-H.; Jiang, C.-W.; Li, H.; Ji, L.-N.; Li, X.-Y. *J. Chem. Soc., Dalton Trans.* **2001**, 1920–1926.
138. Jiang, C.-W.; Chao, H.; Li, R.-H.; Li, H.; Ji, L.-N. *Transition Met. Chem.* **2002**, *27*, 520–525.
139. Okubo, T.; Kitagawa, S.; Masaoka, S.; Furukawa, S.; Kondo, M.; Noh, T.; Isoshima, T.; Wada, T.; Sasabe, H. *Mol. Cryst. Liq. Cryst. Sci. Technol., Sect. B: Nonlinear Opt.* **2000**, *24*, 129–132.
140. Konstantaki, M.; Koudoumas, E.; Couris, S.; Laine, P.; Amouyal, E.; Leach, S. *J. Phys. Chem. B* **2001**, *105*, 10797–10804.
141. Roberto, D.; Tessore, F.; Ugo, R.; Bruni, S.; Manfredi, A.; Quici, S. *Chem. Commun.* **2002**, 846–847.
142. LeCours, S. M.; Guan, H.-W.; DiMagno, S. G.; Wang, C. H.; Therien, M. J. *J. Am. Chem. Soc.* **1996**, *118*, 1497–1503.
143. Priyadarshy, S.; Therien, M. J.; Beratan, D. N. *J. Am. Chem. Soc.* **1996**, *118*, 1504–1510.
144. Karki, L.; Vance, F. W.; Hupp, J. T.; LeCours, S. M.; Therien, M. J. *J. Am. Chem. Soc.* **1998**, *120*, 2606–2611.
145. Sen, A.; Ray, P. C.; Das, P. K.; Krishnan, V. *J. Phys. Chem.* **1996**, *100*, 19611–19613.
146. Collman, J. P.; Kendall, J. L.; Chen, J. L.; Eberspacher, T. A.; Moylan, C. R. *Inorg. Chem.* **1997**, *36*, 5603–5608.
147. Blau, W.; Byrne, H.; Dennis, W. M.; Kelly, J. M. *Opt. Commun.* **1985**, *56*, 25–29.
148. Maloney, C.; Byrne, H.; Dennis, W. M.; Blau, W.; Kelly, J. M. *Chem. Phys.* **1988**, *121*, 21–39.
149. Fei, H.-S.; Han, L.; Ai, X.-C.; Yin, R.; Shen, J.-C. *Chin. Sci. Bull.* **1992**, *37*, 298–301.
150. Rao, D. V. G. L. N.; Aranda, F. J.; Roach, J. F.; Remy, D. E. *Appl. Phys. Lett.* **1991**, *58*, 1241–1243.
151. Guha, S.; Kang, K.; Porter, P.; Roach, J. F.; Remy, D. E.; Aranda, F. J.; Rao, D. V. G. L. N. *Opt. Lett.* **1992**, *17*, 264–266.
152. Rao, D. V. G. L. N.; Aranda, F. J.; Remy, D. E.; Roach, J. F. *Int. J. Nonlinear Opt. Phys.* **1994**, *3*, 511–529.
153. Miller, M. J.; Mott, A. G.; Wood, G. L. *Proc. SPIE-Int. Soc. Opt. Eng.* **1996**, *2853*, 2–11.
154. Narayana Rao, D.; Venugopal Rao, S.; Aranda, F. J.; Rao, D. V. G. L. N.; Nakashima, M.; Akkara, J. A. *J. Opt. Soc. Am. B* **1997**, *14*, 2710–2715.
155. Chen, P.-L.; Tomov, I. V.; Dvornikov, A. S.; Nakashima, M.; Roach, J. F.; Alabran, D. M.; Rentzepis, P. M. *J. Phys. Chem.* **1996**, *100*, 17507–17512.
156. Su, W.; Cooper, T. M.; Brant, M. C. *Chem. Mater.* **1998**, *10*, 1212–1213.
157. Hosoda, M.; Wada, T.; Garito, A. F.; Sasabe, H. *Jpn. J. Appl. Phys., Part 2* **1992**, *31*, L249–L251.
158. Norwood, R. A.; Sounik, J. R. *Appl. Phys. Lett.* **1992**, *60*, 295–297.
159. Sakaguchi, T.; Shimizu, Y.; Miya, M.; Fukumi, T.; Ohta, K.; Nagata, A. *Chem. Lett.* **1992**, 281–284.
160. Terazima, M.; Shimizu, H.; Osuka, A. *J. Appl. Phys.* **1997**, *81*, 2946–2951.
161. Ogawa, K.; Zhang, T.-Q.; Yoshihara, K.; Kobuke, Y. *J. Am. Chem. Soc.* **2002**, *124*, 22–23.
162. Martin, S. J.; Bradley, D. D. C.; Anderson, H. L. *Mol. Cryst. Liq. Cryst. Sci. Technol., Sect. A* **1994**, *256*, 649–655.
163. Martin, S. J.; Anderson, H. L.; Bradley, D. D. C. *Adv. Mater. Opt. Electron.* **1994**, *4*, 277–283.
164. Anderson, H. L.; Martin, S. J.; Bradley, D. D. C. *Angew. Chem., Int. Ed. Engl.* **1994**, *33*, 655–657.
165. O’Keefe, G. E.; Denton, G. J.; Harvey, E. J.; Phillips, R. T.; Friend, R. H.; Anderson, H. L. *J. Chem. Phys.* **1996**, *104*, 805–811.
166. McEwan, K. J.; Robertson, J. M.; Wylie, A. P.; Anderson, H. L. *Mater. Res. Soc. Symp. Proc.* **1997**, *479*, 29–40.
167. Thorne, J. R. G.; Kuebler, S. M.; Denning, R. G.; Blake, I. M.; Taylor, P. N.; Anderson, H. L. *Chem. Phys.* **1999**, *248*, 181–193.
168. Kuebler, S. M.; Denning, R. G.; Anderson, H. L. *J. Am. Chem. Soc.* **2000**, *122*, 339–347.
169. Screen, T. E. O.; Lawton, K. B.; Wilson, G. S.; Dolney, N.; Ispasoiu, R.; Goodson, T., III; Martin, S. J.; Bradley, D. D. C.; Anderson, H. L. *J. Mater. Chem.* **2001**, *11*, 312–320.

170. Beljonne, D.; O'Keefe, G. E.; Hamer, P. J.; Friend, R. H.; Anderson, H. L.; Bredas, J. L. *J. Chem. Phys.* **1997**, *106*, 9439–9460.
171. Qureshi, F. M.; Martin, S. J.; Long, X.; Bradley, D. D. C.; Henari, F. Z.; Blau, W. J.; Smith, E. C.; Wang, C. H.; Kar, A. K.; Anderson, H. L. *Chem. Phys.* **1998**, *231*, 87–94.
172. McEwan, K. J.; Bourhill, G.; Robertson, J. M.; Anderson, H. L. *J. Nonlinear Opt. Phys. Mater.* **2000**, *9*, 451–468.
173. McEwan, K. J.; Robertson, J. M.; Anderson, H. L. *Mater. Res. Soc. Symp. Proc.* **2000**, *597*, 395–406.
174. Krivokapic, A.; Anderson, H. L.; Bourhill, G.; Ives, R.; Clark, S.; McEwan, K. J. *Adv. Mater.* **2001**, *13*, 652–656.
175. Anderson, H. L. *Chem. Commun.* **1999**, 2323–2330.
176. Henari, F. Z.; Blau, W. J.; Milgrom, L. R.; Yahioğlu, G.; Phillips, D.; Lacey, J. A. *Chem. Phys. Lett.* **1997**, *267*, 229–233.
177. Tang, N.; Su, W.; Krein, D. M.; McLean, D. G.; Brant, M. C.; Fleitz, P. A.; Brandelik, D. M.; Sutherland, R. L.; Cooper, T. M. *Mater. Res. Soc. Symp. Proc.* **1997**, *479*, 47–52.
178. Tang, N.; Su, W.; Cooper, T.; Adams, W.; Brandelik, D.; Brant, M.; McLean, D.; Sutherland, R. *Proc. SPIE-Int. Soc. Opt. Eng.* **1996**, *2853*, 149–157.
179. Su, W.; Cooper, T. M.; Tang, N.; Krein, D.; Jiang, H.; Brandelik, D.; Fleitz, P.; Brant, M. C.; Mclean, D. G. *Mater. Res. Soc. Symp. Proc.* **1997**, *479*, 313–318.
180. Su, W.; Cooper, T. M.; Nguyen, K.; Brant, M. C.; Brandelik, D.; McLean, D. G. *Proc. SPIE-Int. Soc. Opt. Eng.* **1998**, *3472*, 136–143.
181. Zhang, Y.; You, X.-Z. *J. Chem. Res. (S)* **1999**, 156–157.
182. Gong, Q.-H.; Wang, Y.; Yang, S.-C.; Xia, Z.-J.; Zou, Y. H.; Sun, W.-F.; Dong, S.-M.; Wang, D.-Y. *J. Phys. D: Appl. Phys.* **1994**, *27*, 911–913.
183. Si, J.-H.; Yang, M.; Wang, Y.-X.; Zhang, L.; Li, C.-F.; Wang, D.-Y.; Dong, S.-M.; Sun, W.-F. *Appl. Phys. Lett.* **1994**, *64*, 3083–3085.
184. Si, J.-H.; Wang, Y.-G.; Zhao, J.; Ye, P.-X.; Wang, D.-Y.; Sun, W.-F.; Dong, S.-M. *Appl. Phys. Lett.* **1995**, *67*, 1975–1977.
185. Sun, W.-F.; Byeon, C. C.; McKerns, M. M.; Gray, G. M.; Wang, D.-Y.; Lawson, C. M. *Proc. SPIE-Int. Soc. Opt. Eng.* **1998**, *3472*, 127–134.
186. Sun, W.-F.; Byeon, C. C.; McKerns, M. M.; Lawson, C. M.; Gray, G. M.; Wang, D.-Y. *Appl. Phys. Lett.* **1998**, *73*, 1167–1169. [Erratum: *Appl. Phys. Lett.* **1998**, *73*, 2218].
187. Sun, W.-F.; Byeon, C. C.; Lawson, C. M.; Gray, G. M.; Wang, D.-Y. *Appl. Phys. Lett.* **1999**, *74*, 3254–3256.
188. Sun, W.-F.; Byeon, C. C.; McKerns, M. M.; Lawson, C. M.; Dong, S.-M.; Wang, D.-Y.; Gray, G. M. *Proc. SPIE-Int. Soc. Opt. Eng.* **1999**, *3798*, 107–116.
189. Sun, W.-F.; Byeon, C. C.; Lawson, C. M.; Gray, G. M.; Wang, D.-Y. *Appl. Phys. Lett.* **2000**, *77*, 1759–1761.
190. Diaz-Garcia, M. A.; Ledoux, I.; Fernandez-Lazaro, F.; Sastre, A.; Torres, T.; Agullo-Lopez, F.; Zyss, J. *J. Phys. Chem.* **1994**, *98*, 4495–4497.
191. Diaz-Garcia, M. A.; Ledoux, I.; Fernandez-Lazaro, F.; Sastre, A.; Torres, T.; Agullo-Lopez, F.; Zyss, J. *Mol. Cryst. Liq. Cryst. Sci. Technol., Sect. B: Nonlinear Opt.* **1995**, *10*, 101–108.
192. Fernandez-Lazaro, F.; Diaz-Garcia, M. A.; Sastre, A.; Delhaes, P.; Mingotaud, C.; Agullo-Lopez, F.; Torres, T. *Synth. Met.* **1998**, *93*, 213–218.
193. Fernandez-Lazaro, F.; Torres, T.; Hauschel, B.; Hanack, M. *Chem. Rev.* **1998**, *98*, 563–575.
194. de la Torre, G.; Gray, D.; Blau, W.; Torres, T. *Synth. Met.* **2001**, *121*, 1481–1482.
195. Nicolau, M.; Rojo, G.; Torres, T.; Agullo-Lopez, F. *J. Porphyrins Phthalocyanines* **1999**, *3*, 703–711.
196. Nalwa, H. S.; Engel, M. K.; Hanack, M.; Pawlowski, G. *Appl. Phys. Lett.* **1997**, *71*, 2070–2072.
197. Nalwa, H. S.; Shirk, J. S. Nonlinear Optical Properties of Metallophthalocyanines. In *Phthalocyanines: Properties and Applications*; Leznoff, C. C.; Lever, A. B. P. Eds.; VCH: New York, 1996; Vol. 4, pp 79–181.
198. Shirk, J. S. *Phthalocyanines* **1996**, *4*, 79–181.
199. de la Torre, G.; Torres, T.; Agullo-Lopez, F. *Adv. Mater.* **1997**, *9*, 265–269.
200. de la Torre, G.; Vazquez, P.; Agullo-Lopez, F.; Torres, T. *J. Mater. Chem.* **1998**, *8*, 1671–1683.
201. Ho, Z. Z.; Ju, C. Y.; Hetherington, W. M. III. *J. Appl. Phys.* **1987**, *62*, 716–718.
202. Coulter, D. R.; Miskowski, V. M.; Perry, J. W.; Wei, T.-H.; Van Stryland, E. W.; Hagan, D. J. *Proc. SPIE-Int. Soc. Opt. Eng.* **1989**, *1105*, 42–51.
203. Shirk, J. S.; Lindle, J. R.; Bartoli, F. J.; Hoffman, C. A.; Kafafi, Z. H.; Snow, A. W. *Appl. Phys. Lett.* **1989**, *55*, 1287–1288.
204. Hoshi, H.; Nakamura, N.; Maruyama, Y. *J. Appl. Phys.* **1991**, *70*, 7244–7248.
205. Neuman, R. D.; Shah, P.; Akki, U. *Opt. Lett.* **1992**, *17*, 798–800.
206. Kumagai, K.; Muzutani, G.; Tsukioka, H.; Yamauchi, T.; Ushioda, S. *Phys. Rev. B: Condens. Matter* **1993**, *48*, 14488–14495.
207. Hoshi, H.; Hamamoto, K.; Yamada, T.; Ishikawa, K.; Takezoe, H.; Fukuda, A.; Fang, S.-L.; Kohama, K.; Maruyama, Y. *Jpn. J. Appl. Phys., Part 2* **1994**, *33*, L1555–L1558.
208. Yamada, T.; Hoshi, H.; Ishikawa, K.; Takezoe, H.; Fukuda, A. *Jpn. J. Appl. Phys., Part 2* **1995**, *34*, L299–L302.
209. Hoshi, H.; Yamada, T.; Kajikawa, K.; Ishikawa, K.; Takezoe, H.; Fukuda, A. *Mol. Cryst. Liq. Cryst. Sci. Technol., Sect. A* **1995**, *267*, 1–6.
210. Liu, Y.-Q.; Xu, Y.; Zhu, D.-B.; Zhao, X.-S. *Thin Solid Films* **1996**, *289*, 282–285.
211. Yamada, T.; Hoshi, H.; Ishikawa, K.; Takezoe, H.; Fukuda, A. *Mol. Cryst. Liq. Cryst. Sci. Technol., Sect. B: Nonlinear Opt.* **1996**, *15*, 131–138.
212. Yamada, T.; Manaka, T.; Hoshi, H.; Ishikawa, K.; Takezoe, H.; Fukuda, A. *Mol. Cryst. Liq. Cryst. Sci. Technol., Sect. B: Nonlinear Opt.* **1996**, *15*, 193–196.
213. Hoshi, H.; Yamada, T.; Ishikawa, K.; Takezoe, H.; Fukuda, A. *Phys. Rev. B: Condens. Matter* **1996**, *53*, 12663–12665.
214. Yamada, T.; Hoshi, H.; Manaka, T.; Ishikawa, K.; Takezoe, H.; Fukuda, A. *Phys. Rev. B: Condens. Matter* **1996**, *53*, R13314–R13317.
215. Hoshi, H.; Yamada, T.; Ishikawa, K.; Takezoe, H.; Fukuda, A. *J. Chem. Phys.* **1997**, *107*, 1687–1691.
216. Tian, M.-Q.; Wada, T.; Kimura, H.; Sasabe, H. *Mol. Cryst. Liq. Cryst. Sci. Technol., Sect. A* **1997**, *294*, 271–274.

217. Tian, M.-Q.; Wada, T.; Kimura-Suda, H.; Sasabe, H. *J. Mater. Chem.* **1997**, *7*, 861–863.
218. Yamada, T.; Manaka, T.; Hoshi, H.; Ishikawa, K.; Takezoe, H. *J. Porphyrins Phthalocyanines* **1998**, *2*, 133–137.
219. Torres, T.; de la Torre, G.; Garcia-Ruiz, J. *Eur. J. Org. Chem.* **1999**, 2323–2326.
220. Rojo, G.; de la Torre, G.; Garcia-Ruiz, J.; Ledoux, I.; Torres, T.; Zyss, J.; Agullo-Lopez, F. *Chem. Phys.* **1999**, *245*, 27–34.
221. Rojo, G.; Martin, G.; Agullo-Lopez, F.; Torres, T.; Heckmann, H.; Hanack, M. *J. Phys. Chem. B* **2000**, *104*, 7066–7070.
222. Cabezon, B.; Fernandez-Lazaro, F.; Martinez-Diaz, M. V.; Rodriguez-Morgade, S.; Sastre, A.; Torres, T. *Synth. Met.* **1995**, *71*, 2289–2290.
223. Rojo, G.; Agullo-Lopez, F.; Cabezon, B.; Torres, T.; Brasselet, S.; Ledoux, I.; Zyss, J. *J. Phys. Chem. B* **2000**, *104*, 4295–4299.
224. Fox, J. M.; Katz, T. J.; Van Elshocht, S.; Verbiest, T.; Kauranen, M.; Persoons, A.; Thongpanchang, T.; Krauss, T.; Brus, L. *J. Am. Chem. Soc.* **1999**, *121*, 3453–3459.
225. Diaz-Garcia, M. A.; Ledoux, I.; Duro, J. A.; Torres, T.; Agullo-Lopez, F.; Zyss, J. *J. Phys. Chem.* **1994**, *98*, 8761–8764.
226. Diaz-Garcia, M. A.; Agullo-Lopez, F.; Torruellas, W. E.; Stegeman, G. I. *Chem. Phys. Lett.* **1995**, *235*, 535–540.
227. Diaz-Garcia, M. A.; Agullo-Lopez, F.; Hutchings, M. G.; Gordon, P. F.; Kajzar, F. *Mol. Cryst. Liq. Cryst. Sci. Technol., Sect. B: Nonlinear Opt.* **1995**, *14*, 169–174.
228. Litran, R.; Blanco, E.; Ramirez-del-Solar, M.; Hierro, A.; Diaz-Garcia, M. A.; Garcia-Cabanes, A.; Agullo-Lopez, F. *Synth. Met.* **1996**, *83*, 273–276.
229. Diaz-Garcia, M. A.; Cabrera, J. M.; Agullo-Lopez, F.; Duro, J. A.; de la Torre, G.; Torres, T.; Fernandez-Lazaro, F.; Delhaes, P.; Mingotaud, C. *Appl. Phys. Lett.* **1996**, *69*, 293–295 (Erratum p 1495).
230. Diaz-Garcia, M. A.; Fernandez-Lazaro, F.; de la Torre, G.; Maya, E. M.; Vazquez, P.; Agullo-Lopez, F.; Torres, T. *Synth. Met.* **1997**, *84*, 923–924.
231. Diaz-Garcia, M. A.; Dogariu, A.; Hagan, D. J.; Van Stryland, E. W. *Chem. Phys. Lett.* **1997**, *266*, 86–90.
232. Diaz-Garcia, M. A.; Rojo, G.; Agullo-Lopez, F. *Proc. SPIE-Int. Soc. Opt. Eng.* **1998**, *3473*, 91–100.
233. Nalwa, H. S.; Kobayashi, S.; Kakuta, A. *Mol. Cryst. Liq. Cryst. Sci. Technol., Sect. B* **1993**, *6*, 169–179.
234. Nalwa, H. S.; Saito, T.; Kakuta, A.; Iwayanagi, T. *J. Phys. Chem.* **1993**, *97*, 10515–17.
235. Nalwa, H. S.; Kakuta, A.; Mukoh, A. *Chem. Phys. Lett.* **1993**, *203*, 109–113.
236. Nalwa, H. S.; Kakuta, A.; Mukoh, A. *J. Phys. Chem.* **1993**, *97*, 1097–1100.
237. Nalwa, H. S.; Kakuta, A. *Thin Solid Films* **1995**, *254*, 218–223.
238. Nalwa, H. S.; Kobayashi, S. *J. Porphyrins Phthalocyanines* **1998**, *2*, 21–30.
239. Nalwa, H. S.; Hanack, M.; Pawlowski, G.; Engel, M. K. *Chem. Phys.* **1999**, *245*, 17–26.
240. Perry, J. W.; Khundkar, L. R.; Coulter, D. R.; Alvarez, D.; Marder, S. R.; Wei, T. H.; Sence, M. J.; Van Stryland, E. W.; Hagan, D. J. Excited State Absorption and Optical Limiting in Solutions of Metallophthalocyanines. In *Organic Molecules for Nonlinear Optics and Photonics*; Messier, J., Kajzar, F., Prasad, P., Eds.; NATO ASI Series E, Vol. 194; Kluwer: Boston: 1991; pp 369–382.
241. Wei, T. H.; Hagan, D. J.; Sence, M. J.; Van Stryland, E. W.; Perry, J. W.; Coulter, D. R. *Appl. Phys. B* **1992**, *54*, 46–51.
242. Mansour, K.; Alvarez, D., Jr.; Perry, K. J.; Choong, I.; Marder, S. R.; Perry, J. W. *Proc. SPIE-Int. Soc. Opt. Eng.* **1993**, *1853*, 132–141.
243. Perry, J. W.; Mansour, K.; Marder, S. R.; Perry, K. J.; Alvarez, D. Jr.; Choong, I. *Opt. Lett.* **1994**, *19*, 625–627.
244. Perry, J. W.; Mansour, K.; Miles, P.; Chen, C. T.; Marder, S. R.; Kwag, G.; Kenney, M. *Polym. Mater. Sci. Eng.* **1995**, *72*, 222–223.
245. Perry, J. W.; Mansour, K.; Marder, S. R.; Chen, C.-T.; Miles, P.; Kenney, M. E.; Kwag, G. *Mater. Res. Soc. Symp. Proc.* **1995**, *374*, 257–265.
246. Perry, J. W.; Mansour, K.; Lee, I.-Y. S.; Wu, X.-L.; Bedworth, P. V.; Chen, C.-T.; Ng, D.; Marder, S. R.; Miles, P.; Wada, T.; Tian, M.-Q.; Sasabe, H. *Science* **1996**, *273*, 1533–1536.
247. Cumpston, B. H.; Mansour, K.; Heikal, A. A.; Perry, J. W. *Mater. Res. Soc. Symp. Proc.* **1997**, *479*, 89–95.
248. Perry, J. W. Organic and Metal-containing Reverse Saturable Absorbers for Optical Limiters. In *Nonlinear Optics of Organic Molecules and Polymers*; Nalwa, H. S.; Miyata, S., Eds; CRC: Boca Raton FL: 1997; pp 813–840.
249. Shirk, J. S.; Lindle, J. R.; Bartoli, F. J.; Kafafi, Z. H.; Snow, A. W. Nonlinear Optical Properties of Substituted Phthalocyanines. In *Materials for Nonlinear Optics: Chemical Perspectives*; Marder, S. R., Sohn, J. D., Stucky, G. D., Eds.; ACS Symposium Series 455; American Chemical Society: Washington, DC: 1991; pp 626–634.
250. Shirk, J. S.; Lindle, J. R.; Bartoli, F. J.; Kafafi, Z. H.; Snow, A. W.; Boyle, M. E. *Int. J. Nonlinear Opt. Phys.* **1992**, *1*, 699–726.
251. Shirk, J. S.; Lindle, J. R.; Bartoli, F. J.; Boyle, M. E. *J. Phys. Chem.* **1992**, *96*, 5847–5852.
252. Shirk, J. S.; Lindle, J. R.; Flom, S. R.; Bartoli, F. J.; Snow, A. W. *Mater. Res. Soc. Symp. Proc.* **1992**, *247*, 197–201.
253. Shirk, J. S.; Pong, R. G. S.; Bartoli, F. J.; Snow, A. W. *Appl. Phys. Lett.* **1993**, *63*, 1880–1882.
254. Flom, S. R.; Pong, R. G. S.; Shirk, J. S.; George, R. D.; Snow, A. W. *Polym. Prepr. (Am. Chem. Soc., Div. Polym. Chem.)* **1994**, *35*, 240–241.
255. George, R. D.; Snow, A. W.; Shirk, J. S.; Flom, S. R.; Pong, R. G. S. *Polym. Prepr. (Am. Chem. Soc., Div. Polym. Chem.)* **1994**, *35*, 236–237.
256. Flom, S. R.; Shirk, J. S.; Pong, R. G. S.; Lindle, J. R.; Bartoli, F. J.; Boyle, M. E.; Adkins, J. D.; Snow, A. W. *Proc. SPIE-Int. Soc. Opt. Eng.* **1994**, *2143*, 229–238.
257. Shirk, J. S.; Flom, S. R.; Lindle, J. R.; Bartoli, F. J.; Snow, A. W.; Boyle, M. E. *Mater. Res. Soc. Symp. Proc.* **1994**, *328*, 661–666.
258. George, R. D.; Snow, A. W.; Shirk, J. S.; Flom, S. R.; Pong, R. G. S. *Mater. Res. Soc. Symp. Proc.* **1995**, *374*, 275–280.
259. Shirk, J. S.; Pong, R. G. S.; Flom, S. R.; Boyle, M. E.; Snow, A. W. *Mater. Res. Soc. Symp. Proc.* **1995**, *374*, 201–209.
260. Bartoli, F. J.; Lindle, J. R.; Shirk, J. S.; Flom, S. R.; Snow, A. W.; Boyle, M. E. *Mol. Cryst. Liq. Cryst. Sci. Technol., Sect. B* **1995**, *10*, 161–166.

261. Shirk, J. S.; Pong, R. G. S.; Flom, S. R.; Bartoli, F. J.; Boyle, M. E.; Snow, A. W. *Pure Appl. Opt.* **1996**, *5*, 701–707.
262. Flom, S. R.; Pong, R. G. S.; Shirk, J. S.; Bartoli, F. J.; Cozzens, R. F.; Boyle, M. E.; Snow, A. W. *Mater. Res. Soc. Symp. Proc.* **1997**, *479*, 23–28.
263. Pong, R. G. S.; Shirk, J. S.; Flom, S. R.; Snow, A. W. *Mater. Res. Soc. Symp. Proc.* **1997**, *479*, 53–58.
264. Shirk, J. S.; Pong, R. G. S.; Flom, S. R.; Heckmann, H.; Hanack, M. *J. Phys. Chem. A* **2000**, *104*, 1438–1449.
265. Hanack, M.; Schneider, T.; Barthel, M.; Shirk, J. S.; Flom, S. R.; Pong, R. G. S. *Coord. Chem. Rev.* **2001**, *219–221*, 235–258.
266. Dini, D.; Barthel, M.; Hanack, M. *Eur. J. Org. Chem.* **2001**, 3759–3769.
267. Schultz, H.; Lehmann, H.; Rein, M.; Hanack, M. *Struct. Bonding* **1991**, *74*, 41–146.
268. Grund, A.; Kaltbeitzel, A.; Mathy, A.; Schwarz, R.; Bubeck, C.; Vermehren, P.; Hanack, M. *J. Phys. Chem.* **1992**, *96*, 7450–7454.
269. Henari, F. Z.; Callaghan, J.; Blau, W. J.; Haisch, P.; Hanack, M. *Pure Appl. Opt.* **1997**, *6*, 741–748.
270. Henari, F.; Davey, A.; Blau, W.; Haisch, P.; Hanack, M. *J. Porphyrins Phthalocyanines* **1999**, *3*, 331–338.
271. Claessens, C. G.; Blau, W. J.; Cook, M.; Hanack, M.; Nolte, R. J. M.; Torres, T.; Wohrle, D. *Monatsh. Chem.* **2001**, *132*, 3–11.
272. Hosoda, M.; Wada, T.; Yamada, A.; Garito, A. F.; Sasabe, H. *Mater. Res. Soc. Symp. Proc.* **1990**, *175*, 89–94.
273. Hosoda, M.; Wada, T.; Yamada, A.; Garito, A. F.; Sasabe, H. *Proc. SPIE-Int. Soc. Opt. Eng.* **1990**, *1337*, 99–104.
274. Wada, T.; Hosoda, M.; Garito, A. F.; Sasabe, H.; Terasaki, A.; Kobayashi, T.; Tada, H.; Koma, A. *Proc. SPIE-Int. Soc. Opt. Eng.* **1991**, *1560*, 162–171.
275. Hosoda, M.; Wada, T.; Yamada, A.; Garito, A. F.; Sasabe, H. *Jpn. J. Appl. Phys., Part 1* **1991**, *30*, 1715–1719.
276. Hosoda, M.; Wada, T.; Yamada, A.; Garito, A. F.; Sasabe, H. *Jpn. J. Appl. Phys., Part 2* **1991**, *30*, L1486–L1488.
277. Hosoda, M.; Wada, T.; Garito, A. F.; Sasabe, H. *Mater. Res. Soc. Symp. Proc.* **1992**, *247*, 105–110.
278. Hosoda, M.; Wada, T.; Yamada, A.; Garito, A. F.; Sasabe, H. *Mol. Cryst. Liq. Cryst. Sci. Technol., Sect. B* **1992**, *3*, 183–191.
279. Hosoda, M.; Wada, T.; Yamamoto, T.; Kaneko, A.; Garito, A. F.; Sasabe, H. *Jpn. J. Appl. Phys., Part 1* **1992**, *31*, 1071–1075.
280. Wada, T.; Sasabe, H. *Proc. SPIE-Int. Soc. Opt. Eng.* **1994**, *2143*, 164–171.
281. Yanagi, S.; Wada, T.; Sasabe, H.; Sasaki, K. *Mol. Cryst. Liq. Cryst. Sci. Technol., Sect. B: Nonlinear Opt.* **1996**, *15*, 267–270.
282. Gong, Q.-H.; Isoshima, T.; Tian, M. Q.; Wada, T.; Sasabe, H. *Chin. Phys. Lett.* **1997**, *14*, 96–99.
283. Tian, M.-Q.; Yanagi, S.; Sasaki, K.; Wada, T.; Sasabe, H. *J. Opt. Soc. Am. B* **1998**, *15*, 846–853.
284. Isoshima, T.; Watanabe, H.; Ishizaki, K.; Wada, T.; Sasabe, H. *Proc. SPIE-Int. Soc. Opt. Eng.* **1999**, *3796*, 49–60.
285. Wu, J. W.; Heflin, J. R.; Norwood, R. A.; Wong, K. Y.; Zamani-Khamiri, O.; Garito, A. F.; Kalyanaraman, P.; Sounik, J. *J. Opt. Soc. Am. B: Opt. Phys.* **1989**, *6*, 707–720.
286. Wang, N. Q.; Cai, Y. M.; Heflin, J. R.; Wu, J. W.; Rodenberger, D. C.; Garito, A. F. *Proc. SPIE-Int. Soc. Opt. Eng.* **1990**, *1328*, 100–107.
287. Wang, N. Q.; Cai, Y. M.; Heflin, J. R.; Garito, A. F. *Mol. Cryst. Liq. Cryst.* **1990**, *189*, 39–48.
288. Wang, N. Q.; Cai, Y. M.; Heflin, J. R.; Wu, J. W.; Rodenberger, D. C.; Garito, A. F. *Polymer* **1991**, *32*, 1752–1755.
289. Heflin, J. R.; Zhou, Q. L.; Rodenberger, D. C.; Cai, Y. M.; Garito, A. F. *Mater. Res. Soc. Symp. Proc.* **1992**, *247*, 3–15.
290. Heflin, J. R.; Wang, S.; Marciu, D.; Freeland, J. W.; Jenkins, B. *Polym. Prepr. (Am. Chem. Soc., Div. Polym. Chem.)* **1994**, *35*, 238–239.
291. Maruno, T.; Yamashita, A.; Hayashi, T.; Kanbara, H.; Konami, H.; Hatano, M.; Shiratori, Y.; Ohhira, K. *Mol. Cryst. Liq. Cryst. Sci. Technol., Sect. B* **1994**, *7*, 207–211.
292. Hayashi, T.; Maruno, T.; Yamashita, A.; Folsch, S.; Kanbara, H.; Konami, H.; Hatano, M. *Jpn. J. Appl. Phys., Part 1* **1995**, *34*, 3884–3888.
293. Kanbara, H.; Maruno, T.; Yamashita, A.; Matsumoto, S.; Hayashi, T.; Konami, H.; Tanaka, N. *J. Appl. Phys.* **1996**, *80*, 3674–3682.
294. Yamashita, A.; Hayashi, T. *Adv. Mater.* **1996**, *8*, 791–799.
295. Yamashita, M.; Wajiki, A.; Tako, T.; Morinaga, A.; Mito, A.; Sakamoto, M.; Isobe, T. *Mol. Cryst. Liq. Cryst. Sci. Technol., Sect. A* **1996**, *280*, 33–38.
296. Yamashita, A.; Matsumoto, S.; Sakata, S.; Hayashi, T.; Kanbara, H. *J. Phys. Chem. B* **1998**, *102*, 5165–5167.
297. Yamashita, A.; Matsumoto, S.; Sakata, S.; Hayashi, T.; Kanbara, H. *Opt. Commun.* **1998**, *145*, 141–144.
298. Hoshi, H.; Kohama, K.; Fang, S.-L.; Maruyama, Y. *Appl. Phys. Lett.* **1993**, *62*, 3080–3081.
299. Fang, S.-L.; Kohama, K.; Hoshi, H.; Maruyama, Y. *Jpn. J. Appl. Phys., Part 2* **1993**, *32*, L1418–L1420.
300. Fang, S.-L.; Kohama, K.; Hoshi, H.; Maruyama, Y. *Chem. Phys. Lett.* **1995**, *234*, 343–347.
301. Fang, S.-L.; Hoshi, H.; Kohama, K.; Maruyama, Y. *J. Phys. Chem.* **1996**, *100*, 4104–4110.
302. Fang, S.-L.; Tada, H.; Mashiko, S. *Appl. Phys. Lett.* **1996**, *69*, 767–769.
303. Chollet, P. A.; Kajzar, F. *Proc. SPIE-Int. Soc. Opt. Eng.* **1990**, *1273*, 87–98.
304. Casstevens, M. K.; Samoc, M.; Pfeleger, J.; Prasad, P. N. *J. Chem. Phys.* **1990**, *92*, 2019–2024.
305. Matsuda, H.; Okada, S.; Masaki, A.; Nakanishi, H.; Suda, Y.; Shigehara, K.; Yamada, A. *Proc. SPIE-Int. Soc. Opt. Eng.* **1990**, *1337*, 105–113.
306. Garito, A. F.; Wu, J. W.; Lipscomb, G. F.; Lytel, R. *Mater. Res. Soc. Symp. Proc.* **1990**, *173*, 467–486.
307. Tajalli, H.; Jiang, J. P.; Murray, J. T.; Armstrong, N. R.; Schmidt, A.; Chandross, M.; Mazumdar, S.; Peyghambarian, N. *Appl. Phys. Lett.* **1995**, *67*, 1639–1641.
308. Brunel, M.; Canva, M.; Brun, A.; Chaput, F.; Malier, L.; Boilot, J.-P. *Mater. Res. Soc. Symp. Proc.* **1995**, *374*, 281–286.
309. Kolinsky, P. V.; Hall, S. R.; Venner, M. R. W.; Croxall, D. F.; Welford, K.; Swatton, S. *Mater. Res. Soc. Symp. Proc.* **1995**, *374*, 195–199.
310. Welford, K. R.; Swatton, S. N. R.; Hughes, S.; Till, S. J.; Spruce, G.; Hollins, R. C.; Wherrett, B. S. *Mater. Res. Soc. Symp. Proc.* **1995**, *374*, 239–256.
311. Wen, T.-C.; Jen, S.-J.; Liu, H.-W.; Hwang, L.-C.; Lian, I.-D. *J. Chin. Chem. Soc.* **1996**, *43*, 123–132.
312. Wen, T. C.; Lian, I. D. *Synth. Met.* **1996**, *83*, 111–116.

313. Si, J.-H.; Wang, Y.-G.; Zhao, J.; Zou, B.-S.; Ye, P.-X.; Qiu, L.; Shen, Y.-Q.; Cai, Z.-G.; Zhou, J.-Y. *Opt. Lett.* **1996**, *21*, 357–359.
314. Dentan, V.; Feneyrou, P.; Soyer, F.; Vergnolle, M.; Le Barny, P.; Robin, Ph. *Mater. Res. Soc. Symp. Proc.* **1997**, *479*, 261–267.
315. Ramos, R.; Petersen, P. M.; Johansen, P. M.; Lindvold, L.; Ramirez, M.; Blanco, E. *J. Appl. Phys.* **1997**, *81*, 7728–7733.
316. Brunel, M.; Chaput, F.; Vinogradov, S. A.; Campagne, B.; Canva, M.; Boilot, J.-P.; Brun, A. *Mater. Res. Soc. Symp. Proc.* **1997**, *479*, 97–102.
317. Acosta, A.; Sarkisov, S. S.; Wilkosz, A.; Leyderman, A.; Venkateswarlu, P. *Proc. SPIE-Int. Soc. Opt. Eng.* **1997**, *3136*, 246–256.
318. Jiang, H.; Su, W.-J.; Brant, M.; Tomlin, D.; Bunning, T. J. *Mater. Res. Soc. Symp. Proc.* **1997**, *479*, 129–134.
319. Hughes, S.; Spruce, G.; Wherrett, B. S.; Kobayashi, T. *J. Appl. Phys.* **1997**, *81*, 5905–5912.
320. Sanghadasa, M.; Wu, B.; Clark, R. D.; Guo, H.-S.; Penn, B. G. *Proc. SPIE-Int. Soc. Opt. Eng.* **1997**, *3147*, 185–195.
321. Hughes, S.; Spruce, G.; Burzler, J. M.; Rangel-Rojo, R.; Wherrett, B. S. *J. Opt. Soc. Am. B* **1997**, *14*, 400–404.
322. Li, C.-F.; Zhang, L.; Yang, M.; Wang, H.; Wang, Y.-X. *Phys. Rev. A* **1994**, *49*, 1149–1157.
323. Sanghadasa, M.; Sung, C. C.; Shin, I.-S.; Penn, B. G.; Clark, R. D.; Guo, H.-S.; Martinez, A. *Proc. SPIE-Int. Soc. Opt. Eng.* **1998**, *3472*, 116–126.
324. Kumar, G. R.; Philip, R.; Ravikanth, M.; Mathur, P.; Ghosh, S. G. *Proc. Int. Conf. Lasers* **1999**, 21st, 770–776.
325. Huang, W.-T.; Wang, S.-F.; Liang, R.-S.; Gong, Q.-H.; Qiu, W.-F.; Liu, Y.-Q.; Zhu, D.-B. *Chem. Phys. Lett.* **2000**, *324*, 354–358.
326. Ma, G.; Guo, L.; Mi, J.; Liu, Y.; Qian, S.; Pan, D.; Huang, Y. *Solid State Commun.* **2001**, *118*, 633–638.
327. Wang, X.; Liu, C.-L.; Gong, Q.-H.; Huang, Y.; Huang, C.-H. *Opt. Commun.* **2001**, *197*, 83–87.
328. Qu, S.-L.; Chen, Y.; Wang, Y.-X.; Song, Y.-L.; Liu, S.-T.; Zhao, X.-L.; Wang, D.-Y. *Mater. Lett.* **2001**, *51*, 534–538.
329. de la Torre, G.; Nicolau, M.; Torres, T. Phthalocyanines: Synthesis, Supramolecular Organization, and Physical Properties. In *Supramolecular Photosensitive and Electroactive Materials*; Nalwa, H. S., Ed., Academic Press: San Diego 2001; pp 1–111.
330. Cheng, W.-D.; Wu, D.-S.; Zhang, H.; Chen, J.-T. *J. Phys. Chem. B* **2001**, *105*, 11221–11226.
331. Sanghadasa, M.; Shin, I.-S.; Clark, R. D.; Guo, H.-S.; Penn, B. G. *J. Appl. Phys.* **2001**, *90*, 31–37.
332. Wu, D.-S.; Cheng, W.-D.; Zhang, H.; Chen, J.-T. *Chem. Phys. Lett.* **2002**, *351*, 486–494.
333. Xu, L.; Wang, E.; Li, Z.; Kurth, D. G.; Du, X.-G.; Zhang, H.-Y.; Qin, C. *New J. Chem.* **2002**, *26*, 782–786.
334. Thami, T.; Bassoul, P.; Petit, M. A.; Simon, J.; Fort, A.; Barzoukas, M.; Villaeys, A. *J. Am. Chem. Soc.* **1992**, *114*, 915–921.
335. Di Bella, S.; Fragalà, I.; Ledoux, I.; Diaz-Garcia, M. A.; Lacroix, P. G.; Marks, T. J. *Chem. Mater.* **1994**, *6*, 881–883.
336. Di Bella, S.; Fragalà, I.; Ledoux, I.; Marks, T. J. *J. Am. Chem. Soc.* **1995**, *117*, 9481–9485.
337. Di Bella, S.; Fragalà, I.; Marks, T. J.; Ratner, M. A. *J. Am. Chem. Soc.* **1996**, *118*, 12747–12751.
338. Lacroix, P. G.; Di Bella, S.; Ledoux, I. *Chem. Mater.* **1996**, *8*, 541–545.
339. Di Bella, S.; Fragalà, I.; Ledoux, I.; Diaz-Garcia, M. A.; Marks, T. J. *J. Am. Chem. Soc.* **1997**, *119*, 9550–9557.
340. Lenoble, G.; Lacroix, P. G.; Daran, J. C.; Di Bella, S.; Nakatani, K. *Inorg. Chem.* **1998**, *37*, 2158–2165.
341. Di Bella, S.; Fragalà, I. *Synth. Met.* **2000**, *115*, 191–196.
342. Di Bella, S.; Fragalà, I.; Ledoux, I.; Zyss, J. *Chem. Eur. J.* **2001**, *7*, 3738–3743.
343. Di Bella, S.; Fragalà, I. *New J. Chem.* **2002**, *26*, 285–290.
344. Averseng, F.; Lacroix, P. G.; Malfant, I.; Lenoble, G.; Cassoux, P.; Nakatani, K.; Maltey-Fanton, I.; Delaire, J. A.; Aukauloo, A. *Chem. Mater.* **1999**, *11*, 995–1002.
345. Averseng, F.; Lacroix, P. G.; Malfant, I.; Dahan, F.; Nakatani, K. *J. Mater. Chem.* **2000**, *10*, 1013–1018.
346. Averseng, F.; Lepetit, C.; Lacroix, P. G.; Tuchagues, J. P. *Chem. Mater.* **2000**, *12*, 2225–2229.
347. Averseng, F.; Lacroix, P. G.; Malfant, I.; Périssé, N.; Lepetit, C.; Nakatani, K. *Inorg. Chem.* **2001**, *40*, 3797–3804.
348. Tian, Y.-P.; Duan, C.-Y.; Zhao, C.-Y.; You, X.-Z.; Mak, T. C. W.; Zhang, Z.-Y. *Inorg. Chem.* **1997**, *36*, 1247–1252.
349. Duan, C.-Y.; Tian, Y.-P.; You, X.-Z.; Mak, T. C. W. *Polyhedron* **1997**, *16*, 4097–4103.
350. Tian, Y.-P.; Duan, C.-Y.; You, X.-Z.; Mak, T. C. W.; Luo, Q.; Zhou, J.-Y. *Transition Met. Chem.* **1998**, *23*, 17–20.
351. Tian, Y.-P.; Wu, J.-Y.; Xie, F.-X.; Ni, S.-S. *Chin. Chem. Lett.* **1998**, *9*, 215–217.
352. Zhang, S.-Y.; Tian, Y.-P.; Zhang, Y.-H.; Xie, F.-X.; Duan, C.-Y. *Chin. Chem. Lett.* **1998**, *9*, 599–602.
353. Xie, F.-X.; Tian, Y.-P.; Ni, S.-S. *Chin. Chem. Lett.* **1998**, *9*, 691–693.
354. Duan, C.-Y.; Tian, Y.-P.; Lu, Z.-L.; You, X.-Z.; Mak, T. C. W. *J. Coord. Chem.* **1998**, *46*, 59–70.
355. Wu, J.-Y.; Tian, Y.-P.; Zhang, Y.-H.; Duan, C.-Y.; Xie, F.-X.; Ni, S.-S. *Huaxue Xuebao* **1999**, *57*, 202–209.
356. Wu, J.-Y.; Tian, Y.-P.; Xie, F.-X.; Ni, S.-S. *Chin. Chem. Lett.* **1999**, *10*, 251–254.
357. Wu, J.-Y.; Tian, Y.-P.; Xie, F.-X.; Ni, S.-S. *Chem. Res. Chin. Univ.* **1999**, *15*, 218–225.
358. Tian, Y.-P.; Lu, Z.-L.; You, X.-Z.; Luo, B.-S.; Chen, L.-R. *Huaxue Xuebao* **1999**, *57*, 1068–1074.
359. Tian, Y.-P.; Yu, W.-T.; Zhao, C.-Y.; Jiang, M.-H.; Cai, Z.-G.; Fun, H. K. *Polyhedron* **2002**, *21*, 1217–1222.
360. You, X.-Z. *J. Photochem. Photobiol. A: Chemistry* **1997**, *106*, 85–90.
361. Gale, D. C.; Lawson, C. M.; Zhai, T.; Gray, G. M. *Proc. SPIE-Int. Soc. Opt. Eng.* **1994**, 2229, 41–47.
362. Fleurov, V. B.; Lawson, C. M.; Gale, D. C.; Gray, G. M. *Proc. SPIE-Int. Soc. Opt. Eng.* **1996**, 2853, 20–27.
363. Chiang, W.; Thompson, M. E.; Van Engen, D. Synthesis and Nonlinear Optical Properties of Inorganic Co-ordination Polymers. In *Organic Materials for Nonlinear Optics II*; Hann, R. A., Bloor, D., Eds.; Royal Society of Chemistry: London, 1991; pp 210–216.
364. Chiang, W.; Van Engen, D.; Thompson, M. E. *Polyhedron* **1996**, *15*, 2369–2376.
365. Tao, X. T.; Suzuki, H.; Watanabe, T.; Lee, S. H.; Miyata, S.; Sasabe, H. *Appl. Phys. Lett.* **1997**, *70*, 1503–1505.
366. Buey, J.; Coco, S.; Diez, L.; Espinet, P.; Martín-Alvarez, J. M.; Miguel, J. A.; Garcia-Granda, S.; Tesouro, A.; Ledoux, I.; Zyss, J. *Organometallics* **1998**, *17*, 1750–1755.
367. Zhu, X.-H.; Chen, X.-F.; Zhang, Y.; You, X.-Z.; Tan, W.-L.; Ji, W. *Chem. Lett.* **1999**, 1211–1212.
368. Zhu, X.-H.; Chen, X.-F.; Zhang, Y.; You, X.-Z.; Tan, W.-L.; Ji, W.; Vittal, J. J.; Tan, G.-K.; Kennard, C. H. L. *New J. Chem.* **2000**, *24*, 419–423.
369. Korupoju, S. R.; Mangayarkarasi, N.; Ameerunisha, S.; Valente, E. J.; Zacharias, P. S. *J. Chem. Soc., Dalton Trans.* **2000**, 2845–2852.

370. Gaudry, J.-B.; Capes, L.; Langot, P.; Marcen, S.; Kollmannsberger, M.; Lavastre, O.; Freysz, E.; Letard, J.-F.; Kahn, O. *Chem. Phys. Lett.* **2000**, *324*, 321–329.
371. Evans, C.; Luneau, D. *J. Chem. Soc., Dalton Trans.* **2002**, 83–86.
372. Zhou, J.-H.; Wang, Y.-X.; Chen, X.-T.; Song, Y.-L.; Weng, L.-H.; You, X.-Z. *Chin. J. Inorg. Chem.* **2002**, *18*, 533–536.
373. Bergman, J. G., Jr.; McFee, J. H.; Crane, G. R. *Mater. Res. Bull.* **1970**, *5*, 913–917.
374. Yan, Y.-X.; Fang, Q.; Yu, W.-T.; Tian, Y.-P.; Yuan, D.-R.; Wang, X.-Q.; Meng, F.-Q.; Cai, Z.-G.; Zhang, L.-Z. *Chin. Chem. Lett.* **1998**, *9*, 1125–1128.
375. Wang, X.-Q.; Xu, D.; Yuan, D.-R.; Tian, Y.-P.; Yu, W.-T.; Sun, S.-Y.; Yang, Z.-H.; Fang, Q.; Lu, M.-K.; Yan, Y.-X.; Meng, F.-Q.; Guo, S.-Y.; Zhang, G.-H.; Jiang, M.-H. *Mater. Res. Bull.* **1999**, *34*, 2003–2011.
376. Guo, S.-Y.; Yuan, D.-R.; Xu, D.; Zhang, G.-H.; Sun, S.-Y.; Meng, F.-Q.; Wang, X.-Q.; Jiang, X.-N.; Jiang, M.-H.; Sun, D.-L.; Yu, X.-L. *Prog. Cryst. Growth Charact. Mater.* **2000**, *40*, 75–79.
377. Guo, S.-Y.; Xu, D.; Lu, M.-K.; Yuan, D.-R.; Yang, Z.-H.; Zhang, G.-H.; Sun, S.-Y.; Wang, X.-Q.; Zhou, M.; Jiang, M.-H. *Prog. Cryst. Growth Charact. Mater.* **2000**, *40*, 111–114.
378. Wang, X.-Q.; Yu, W.-T.; Xu, D.; Lu, M.-K.; Yuan, D.-R.; Liu, J.-R.; Lu, G.-T. *Acta Crystallogr.* **2000**, *C56*, 1305–1307.
379. Wang, X.-Q.; Xu, D.; Lu, M.-K.; Yuan, D.-R.; Zhang, G.-H.; Xu, S.-X.; Guo, S.-Y.; Jiang, X.-N.; Liu, J.-R.; Song, C.-F.; Ren, Q.; Huang, J.; Tian, Y.-P. *Mater. Res. Bull.* **2001**, *36*, 1287–1299.
380. Zhang, G.-H.; Xu, D.; Lu, M.-K.; Yuan, D.-R.; Wang, X.-Q.; Meng, F.-Q.; Guo, S.-Y.; Ren, Q.; Jiang, M.-H. *Opt. Laser Technol.* **2001**, *33*, 121–124.
381. Wang, X.-Q.; Xu, D.; Lu, M.-K.; Yuan, D.-R.; Zhang, G.-H.; Meng, F.-Q.; Guo, S.-Y.; Zhou, M.; Liu, J.-R.; Li, X.-R. *Cryst. Res. Technol.* **2001**, *36*, 73–84.
382. Wang, X.-Q.; Xu, D.; Lu, M.-K.; Yuan, D.-R.; Xu, S.-X.; Guo, S.-Y.; Zhang, G.-H.; Liu, J.-R. *J. Cryst. Growth* **2001**, *224*, 284–293.
383. Zhang, G.-H.; Xu, D.; Lu, M.-K.; Yuan, D.-R.; Wang, X.-Q.; Meng, F.-Q.; Guo, S.-Y.; Ren, Q. *Guangxue Xuebao* **2001**, *21*, 305–308.
384. Guo, S.-Y.; Xu, D.; Yang, P.; Yu, W.-T.; Lu, M.-K.; Yuan, D.-R.; Yang, Z.-H.; Zhang, G.-H.; Sun, S.-Y.; Wang, X.-Q.; Zhou, M.; Jiang, M.-H. *Cryst. Res. Technol.* **2001**, *36*, 609–614.
385. Wang, X.-Q.; Xu, D.; Lu, M.-K.; Yuan, D.-R.; Yin, X.; Zhang, G.-H.; Xu, S.-X.; Lu, G.-W.; Song, C.-F.; Guo, S.-Y.; Liu, J.-R.; Zhou, G.-Y.; Wang, D.; Yang, Z.-H.; Zhao, X.; Ren, Q.; Zhao, J.-Q.; Liu, W.-L. *Chem. Phys. Lett.* **2001**, *346*, 393–406.
386. Yuan, D.-R.; Xu, D.; Liu, M.-G.; Qi, F.; Yu, W.-T.; Hou, W.-B.; Bing, Y.-H.; Sun, S.-Y.; Jiang, M.-H. *Appl. Phys. Lett.* **1997**, *70*, 544–546.
387. Wang, C.-Q. Q.; Chow, Y.-T.; Gambling, W. A.; Yuan, D.-R.; Xu, D.; Zhang, G.-H.; Liu, M.-G.; Jiang, M.-H. *Opt. Laser Technol.* **1998**, *30*, 291–293.
388. Zhang, G.-H.; Liu, M.-G.; Xu, D.; Yuan, D.-R.; Sheng, W.-D.; Yao, J.-Q. *J. Mater. Sci. Lett.* **2000**, *19*, 1255–1257.
389. Yan, Y.-X.; Fang, Q.; Yuan, D.-R.; Tian, Y.-P.; Liu, Z.; Wang, X.-M.; Jiang, M.-H.; Williams, D.; Siu, A.; Cai, Z.-G. *Chin. Chem. Lett.* **1999**, *10*, 257–260.
390. Yan, Y.-X.; Fang, Q.; Yu, W.-T.; Yuan, D.-R.; Tian, Y.-P.; Williams, I. D.; Cai, X.-G. *Huaxue Xuebao* **1999**, *57*, 1257–1261.
391. Tao, X.-T.; Zhang, N.; Yuan, D.-R.; Xu, D.; Yu, W.-T.; Jiang, M.-H. *Proc. SPIE-Int. Soc. Opt. Eng.* **1990**, *1337*, 385–389.
392. Yin, X.; Tao, X.-T. *Rengong Jingti Xuebao* **1991**, *20*, 193–197.
393. Tao, X.-T.; Zhang, N.; Yuan, D.-R.; Yu, W.-T.; Jiang, M.-H. *Rengong Jingti Xuebao* **1991**, *20*, 113–116.
394. Chen, H.-J.; Zhang, L.-Z.; Cai, Z.-G.; Yang, G.; Chen, X.-M. *J. Chem. Soc., Dalton Trans.* **2000**, 2463–2466.
395. Zhou, M.; Guo, S.-Y.; Xu, D. *Rengong Jingti Xuebao* **2000**, *29*, 325–328.
396. Meng, X.-R.; Li, L.-K.; Song, Y.-W.; Zhu, Y.; Du, C.-X.; Fan, Y.-T.; Hou, H.-W. *Huaxue Xuebao* **2001**, *59*, 1277–1282.
397. Wei, Y.-L.; Zhu, Y.; Song, Y.-L.; Hou, H.-W.; Fan, Y.-T. *Inorg. Chem. Commun.* **2002**, *5*, 166–170.
398. Zhang, H.; Wang, X.-M.; Teo, B. K. *J. Am. Chem. Soc.* **1996**, *118*, 11813–11821.
399. Zhang, H.; Wang, X.-M.; Zhang, K.; Teo, B. K. *Inorg. Chem.* **1998**, *37*, 3490–3496.
400. Zhang, H.; Wang, X.-M.; Zhang, K.; Teo, B. K. *Coord. Chem. Rev.* **1999**, *183*, 157–195.
401. Zhang, H.; Zelmon, D. E.; Price, G. E.; Teo, B. K. *Inorg. Chem.* **2000**, *39*, 1868–1873.
402. Zhang, H.; Wang, X.-M.; Zelmon, D. E.; Teo, B. K. *Inorg. Chem.* **2001**, *40*, 1501–1507.
403. Moses, E. I.; Wu, F. Y. *Opt. Lett.* **1980**, *5*, 64–66.
404. Guo, Y.-L.; Yao, M.-Y.; Pang, S.-M. *IEEE J. Quantum Electron.* **1984**, *QE-20*(4), 328–331.
405. Guo, Y.-L.; Yao, M.-Y.; Pang, S.-M. *Kexue Tongbao* **1984**, *29*, 731–734.
406. Wu, C.-K.; Wang, Z.-Y. *Guangxue Xuebao* **1984**, *4*, 918–923.
407. Maloney, C.; Blau, W. *J. Opt. Soc. Am. B: Opt. Phys.* **1987**, *4*, 1035–1039.
408. Li, H.-P.; Ogusu, K. *Jpn. J. Appl. Phys., Part 1* **1998**, *37*, 5572–5577.
409. Lindle, J. R.; Weisbecker, C. S.; Bartoli, F. J.; Pong, R. G. S.; Kafafi, Z. H. *Mater. Res. Soc. Symp. Proc.* **1992**, *247*, 277–282.
410. Kafafi, Z. H.; Lindle, J. R.; Flom, S. R.; Pong, R. G. S.; Weisbecker, C. S.; Claussen, R. C.; Bartoli, F. J. *Proc. SPIE-Int. Soc. Opt. Eng.* **1992**, *1626*, 440–449.
411. Oliver, S. N.; Winter, C. S.; Rush, J. D.; Underhill, A. E.; Hill, C. *Proc. SPIE-Int. Soc. Opt. Eng.* **1990**, *1337*, 81–88.
412. Winter, C. S.; Oliver, S. N.; Rush, J. D.; Manning, R. J.; Hill, C.; Underhill, A. *ACS Symp. Ser.* **1991**, *455*, 616–625.
413. Winter, C. S.; Hill, C. A. S.; Underhill, A. E. *Appl. Phys. Lett.* **1991**, *58*, 107–109.
414. Winter, C. S.; Oliver, S. N.; Rush, J. D.; Hill, C. A. S.; Underhill, A. E. Third-order Optical Nonlinearities in Metal Dithiolate Complexes. In *Organic Molecules for Nonlinear Optics and Photonics*; Messier, J., Kajzar, F., Prasad, P., Eds.; NATO ASI Series E, 194; Kluwer: Boston, 1991; pp 383–390.
415. Hill, C. A. S.; Underhill, A. E.; Winter, C. S.; Oliver, S. N.; Rush, J. D. Resonance Enhanced Third-order Nonlinearities in Metal Dithiolenes. In *Organic Materials for Nonlinear Optics II*; Hann, R. A., Bloor, D., Eds.; Royal Society of Chemistry: London, 1991, pp 217–222.

416. Oliver, S. A.; Winter, C. *Adv. Mater.* **1992**, *4*, 119–121.
417. Hill, C. A. S.; Underhill, A. E.; Charlton, A.; Winter, C. S.; Oliver, S. N.; Rush, J. D. *Proc. SPIE-Int. Soc. Opt. Eng.* **1993**, *1775*, 43–53.
418. Winter, C. S.; Manning, R. J.; Oliver, S. N.; Hill, C. A. S. *Opt. Commun.* **1992**, *90*, 139–143.
419. Winter, C. S.; Oliver, S. N.; Rush, J. D.; Hill, C. A. S.; Underhill, A. E. *J. Appl. Phys.* **1992**, *71*, 512–514.
420. Winter, C. S.; Oliver, S. N.; Hill, C. A. S. *Mater. Res. Soc. Symp. Proc.* **1992**, *247*, 99–104.
421. Winter, C. S.; Oliver, S. N.; Manning, R. J.; Rush, J. D.; Hill, C. A. S.; Underhill, A. E. *J. Mater. Chem.* **1992**, *2*, 443–447.
422. Underhill, A. E.; Hill, C. A. S. *Mol. Cryst. Liq. Cryst. Sci. Technol., Sect. A* **1992**, *217*, 7–12.
423. Winter, C. S.; Oliver, S. N.; Rush, J. D.; Hill, C. A. S.; Underhill, A. E. *Mol. Cryst. Liq. Cryst. Sci. Technol., Sect. A* **1993**, *235*, 181–189.
424. Oliver, S. N.; Winter, C. S.; Manning, R. J.; Rush, J. D.; Hill, C.; Underhill, A. E. *Proc. SPIE-Int. Soc. Opt. Eng.* **1993**, *1775*, 110–120.
425. Papadopoulos, M. G.; Waite, J.; Winter, C. S.; Oliver, S. N. *Inorg. Chem.* **1993**, *32*, 277–280.
426. Waite, J.; Papadopoulos, M. G.; Oliver, S. N.; Winter, C. S. *Mol. Cryst. Liq. Cryst. Sci. Technol., Sect. B* **1994**, *6*, 297–303.
427. Papadopoulos, M. G.; Waite, J. *Opt. Mater.* **1994**, *3*, 145–150.
428. Craig, B. I.; Williams, G. R. J. *Adv. Mater. Opt. Electron.* **1992**, *1*, 221–228.
429. Craig, B. I.; Williams, G. R. J. *Appl. Phys. B* **1993**, *56*, 331–334.
430. Trohalaki, S.; Zellmer, R. J.; Pachter, R. *Mater. Res. Soc. Symp. Proc.* **1997**, *479*, 325–329.
431. Kershaw, S. V.; Oliver, S. N.; Manning, R. J.; Rush, J. D.; Hill, C. A.; Underhill, A. E.; Charlton, A. *Proc. SPIE-Int. Soc. Opt. Eng.* **1993**, *2025*, 388–399.
432. Gall, G. J.; King, T. A.; Oliver, S. N.; Capozzi, C. A.; Seddon, A. B.; Hill, C. A. S.; Underhill, A. E. *Proc. SPIE-Int. Soc. Opt. Eng.* **1994**, *2288*, 372–381.
433. Hill, C. A. S.; Charlton, A.; Underhill, A. E.; Oliver, S. N.; Kershaw, S.; Manning, R. J.; Ainslie, B. J. *J. Mater. Chem.* **1994**, *4*, 1233–1237.
434. Dhindsa, A. S.; Underhill, A. E.; Oliver, S. N.; Kershaw, S. V. *Proc. SPIE-Int. Soc. Opt. Eng.* **1995**, *2531*, 350–359.
435. Oliver, S. N.; Kershaw, S. V.; Underhill, A. E.; Hill, C. A. S.; Charlton, A. *Mol. Cryst. Liq. Cryst. Sci. Technol., Sect. B: Nonlinear Opt.* **1995**, *10*, 87–99.
436. Underhill, A. E.; Hill, C. A. S.; Charlton, A.; Oliver, S.; Kershaw, S. *Synth. Met.* **1995**, *71*, 1703–1704.
437. Hill, C. A. S.; Charlton, A.; Underhill, A. E.; Abdul Malik, K. M.; Hursthouse, M. B.; Karaulov, A. I.; Oliver, S. N.; Kershaw, S. V. *J. Chem. Soc., Dalton Trans.* **1995**, 587–594.
438. Wenseleers, W.; Goovaerts, E.; Dhindsa, A. S.; Underhill, A. E. *Chem. Phys. Lett.* **1996**, *254*, 410–414.
439. Geisler, T.; Pedersen, K.; Underhill, A. E.; Dhindsa, A. S.; Greve, D. R.; Bjørnholm, T.; Petersen, J. C. *J. Phys. Chem. B* **1997**, *101*, 10625–10630.
440. Martin, S. J.; Bradley, D. D. C.; Long, X.; Qureshi, F.; Dhindsa, A. S.; Underhill, A. E.; Jakobsen, C.; Petersen, J. C.; Geisler, T.; Blau, W.; Davey, A. P.; Gray, D.; Henari, F. Z. *Mol. Cryst. Liq. Cryst. Sci. Technol., Sect. B: Nonlinear Opt.* **1997**, *18*, 41–55.
441. Zuo, J.-L.; Yao, T.-M.; You, F.; You, X.-Z.; Fun, H.-K.; Yip, B.-C. *J. Mater. Chem.* **1996**, *6*, 1633–1637.
442. Wang, S.-F.; Huang, W.-T.; Zhang, T.-Q.; Yang, H.; Gong, Q.-H.; Okuma, Y.; Horikiri, M.; Miura, Y. F. *Appl. Phys. Lett.* **1999**, *75*, 1845–1847.
443. Kuebler, S. M.; Denning, R. G. *Chem. Phys. Lett.* **1996**, *250*, 120–127.
444. Fukaya, T.; Mizuno, M.; Murata, S.; Mito, A. *Proc. SPIE-Int. Soc. Opt. Eng.* **1992**, *1626*, 135–139.
445. Diaz-Garcia, M. A.; Agullo-Lopez, F.; Hutchings, M. G.; Gordon, P. F.; Kajzar, F. *Proc. SPIE-Int. Soc. Opt. Eng.* **1994**, *2285*, 227–235.
446. Bjørnholm, T.; Geisler, T.; Petersen, J. C.; Greve, D. R.; Schioedt, N. C. *Mol. Cryst. Liq. Cryst. Sci. Technol., Sect. B: Nonlinear Opt.* **1995**, *10*, 129–137.
447. Geisler, T.; Pedersen, K.; Petersen, J. C. Third-harmonic Generation in Substituted Oligo-phenylene Vinylenes and Organic Square Planar Nickel Complexes. In *Notions and Perspectives of Nonlinear Optics*; Keller, O., Eds.; World Scientific: Singapore, 1996; pp 580–585.
448. Ushijima, H.; Kawasaki, T.; Kamata, T.; Kodzasa, T.; Matsuda, H.; Fukaya, T.; Fujii, Y.; Mizukami, F. *Mol. Cryst. Liq. Cryst. Sci. Technol., Sect. A* **1996**, *286*, 597–602.
449. Schougaard, S. B.; Greve, D. R.; Geisler, T.; Petersen, J. C.; Bjørnholm, T. *Synth. Met.* **1997**, *86*, 2179–2180.
450. Greve, D. R.; Schougaard, S. B.; Geisler, T.; Petersen, J. C.; Bjørnholm, T. *Adv. Mater.* **1997**, *9*, 1113–1116.
451. Bjørnholm, T. *Israel J. Chem.* **1997**, *36*, 349–356.
452. Bai, J.-F.; Zuo, J.-L.; Tan, W.-L.; Ji, W.; Shen, Z.; Fun, H.-K.; Chinnakali, K.; Abdul Razak, I.; You, X.-Z.; Che, C.-M. *J. Mater. Chem.* **1999**, *9*, 2419–2423.
453. Tan, W.-L.; Ji, W.; Zuo, J.-L.; Bai, J.-F.; You, X.-Z.; Lim, J.-H.; Yang, S. S.; Hagan, D. J.; Van Stryland, E. W. *Proc. SPIE-Int. Soc. Opt. Eng.* **1999**, *3899*, 475–482.
454. Tan, W. L.; Ji, W.; Zuo, J. L.; Bai, J. F.; You, X. Z.; Lim, J. H.; Yang, S. S.; Hagan, D. J.; Van Stryland, E. W. *Mater. Res. Soc. Symp. Proc.* **2000**, *597*, 413–418.
455. Tan, W.-L.; Ji, W.; Zuo, J.-L.; Bai, J.-F.; You, X.-Z.; Lim, J.-H.; Yang, S.; Hagan, D. J.; Van Stryland, E. W. *Appl. Phys. B* **2000**, *70*, 809–812.
456. Dai, J.; Bian, G.-Q.; Wang, X.; Xu, Q.-F.; Zhou, M.-Y.; Munakata, M.; Maekawa, M.; Tong, M.-H.; Sun, Z.-R.; Zeng, H.-P. *J. Am. Chem. Soc.* **2000**, *122*, 11007–11008.
457. Liu, C.-M.; Zhang, D.-Q.; Song, Y.-L.; Zhan, C.-L.; Li, Y.-L.; Zhu, D.-B. *Eur. J. Inorg. Chem.* **2002**, 1591–1594.
458. Chen, C.-T.; Liao, S.-Y.; Lin, K.-J.; Lai, L.-L. *Mater. Res. Soc. Symp. Proc.* **1998**, *488*, 165–170.
459. Chen, C.-T.; Liao, S.-Y.; Lin, K.-J.; Lin, T.-Y. J.; Lai, L.-L.; Chen, C.-H. *Mol. Cryst. Liq. Cryst. Sci. Technol., Sect. B: Nonlinear Opt.* **1999**, *22*, 35–38.
460. Chen, C.-T.; Liao, S.-Y.; Lin, K.-J.; Lai, L.-L. *Adv. Mater.* **1998**, *10*, 334–338.
461. Bigoli, F.; Chen, C.-T.; Wu, W.-C.; Deplano, P.; Mercuri, M. L.; Pellinghelli, M. A.; Pilia, L.; Pintus, G.; Serpe, A.; Trogu, E. F. *Chem. Commun.* **2001**, 2246–2247.
462. McCahon, S. W.; Tutt, L. W.; Klein, M. B.; Valley, G. C. *Proc. SPIE-Int. Soc. Opt. Eng.* **1990**, *1307*, 304–314.

463. Tutt, L. W.; McCahon, S. W.; Klein, M. B. *Proc. SPIE-Int. Soc. Opt. Eng.* **1990**, *1307*, 315–326.
464. Tutt, L. W.; McCahon, S. W. *Opt. Lett.* **1990**, *15*, 700–702.
465. Shi, S.; Ji, W.; Tang, S. H.; Lang, J.-P.; Xin, X.-Q. *J. Am. Chem. Soc.* **1994**, *116*, 3615–3616.
466. Shi, S.; Ji, W.; Lang, J. P.; Xin, X.-Q. *J. Phys. Chem.* **1994**, *98*, 3570–3572.
467. Hou, H.-W.; Xin, X.-Q.; Liu, J.; Chen, M.-Q.; Shu, S. *J. Chem. Soc., Dalton Trans.* **1994**, 3211–3214.
468. Ji, W.; Du, H.-J.; Tang, S.-H.; Shi, S. *J. Opt. Soc. Am. B* **1995**, *12*, 876–881.
469. Shi, S.; Ji, W.; Xin, X.-Q. *Mater. Res. Soc. Symp. Proc.* **1995**, *374*, 363–368.
470. Ji, W.; Du, H.-J.; Tang, S.-H.; Shi, S.; Lang, J.-P.; Xin, X.-Q. *Singapore J. Phys.* **1995**, *11*, 55–64.
471. Hoggard, P. E.; Hou, H.-W.; Xin, X.-Q.; Shi, S. *Chem. Mater.* **1996**, *8*, 2218–2222.
472. Shi, S.; Lin, Z.; Mo, Y.; Xin, X.-Q. *J. Phys. Chem.* **1996**, *100*, 10696–10700.
473. Long, D.-L.; Shi, S.; Mei, Y.-H.; Xin, X.-Q. *Chin. Sci. Bull.* **1997**, *42*, 1184–1189.
474. Song, Y.-L.; Zhang, C.; Wang, Y.-X.; Fang, G.-Y.; Duan, C.-Y.; Liu, S.-T.; Xin, X.-Q.; Ye, H.-G. *Opt. Commun.* **1999**, *168*, 131–134.
475. Song, Y.-L.; Zhang, C.; Wang, Y.-X.; Fang, G.-Y.; Jin, G.-S.; Zhang, X.-R.; Liu, S.-T.; Chen, L.-X.; Xin, X.-Q. *Opt. Commun.* **2000**, *186*, 105–110.
476. Fang, G.-Y.; Song, Y.-L.; Wang, Y.-X.; Zhang, X.-R.; Xin, X.-Q.; Zhang, C.; Li, C.-F. *Guangxue Xuebao* **2001**, *21*, 541–544.
477. Song, Y.-L.; Wang, Y.-X.; Zhang, C.; Fang, G.-Y.; Qu, S.; Xin, X.-Q. *Opt. Commun.* **2001**, *192*, 273–276.
478. Zhang, C.; Song, Y.-L.; Kühn, F. E.; Wang, Y.-X.; Fun, H.-K.; Xin, X.-Q.; Herrmann, W. A. *New J. Chem.* **2002**, *26*, 58–65.
479. Xiong, Y.-N.; Zhang, Q.-F.; Xin, X.-Q.; Ji, W. *Proc. SPIE-Int. Soc. Opt. Eng.* **1999**, 3899, 483–488.
480. Xiong, Y.-N.; Ji, W.; Zhang, Q.-F.; Xin, X.-Q. *J. Appl. Phys.* **2000**, *88*, 1225–1229.
481. Zhang, Q.-F.; Zhang, C.; Song, Y.-L.; Xin, X.-Q. *J. Mol. Struct.* **2000**, *525*, 79–86.
482. Zhang, Q.-F.; Xiong, Y.-N.; Lai, T.-S.; Ji, W.; Xin, X.-Q. *J. Phys. Chem. B* **2000**, *104*, 3446–3449.
483. Song, Y.-L.; Qu, S.-L.; Wang, Y.-X.; Zhang, Q.-F.; Xin, X.-Q. *Chem. Phys. Lett.* **2001**, *338*, 108–112.
484. Feliz, M.; Garriga, J. M.; Llusar, R.; Uriel, S.; Humphrey, M. G.; Lucas, N. T.; Samoc, M.; Luther-Davies, B. *Inorg. Chem.* **2001**, *40*, 6132–6138.
485. Shi, S.; Chen, Z.-G.; Hou, H.-W.; Xin, X.-Q.; Yu, K.-B. *Chem. Mater.* **1995**, *7*, 1519–1524.
486. Chen, Z.-R.; Hou, H.-W.; Xin, X.-Q.; Yu, K.-B.; Shi, S. *J. Phys. Chem.* **1995**, *99*, 8717–8721.
487. Hou, H.-W.; Liang, B.; Xin, X.-Q.; Yu, K.-B.; Ge, P.; Ji, W.; Shi, S. *J. Chem. Soc., Faraday Trans.* **1996**, *92*, 2343–2346.
488. Long, D.-L.; Shi, S.; Xin, X.-Q.; Luo, B.-S.; Chen, L.-R.; Huang, X.-Y.; Kang, B.-S. *J. Chem. Soc., Dalton Trans.* **1996**, 2617–2622.
489. Wu, X.-T.; Wang, Q.-M.; Shi, S. *Polyhedron* **1996**, *16*, 945–948.
490. Zheng, H.-G.; Tan, W.-L.; Low, M. K. L.; Ji, W.; Long, D.-L.; Wong, W.-T.; Yu, K.-B.; Xin, X.-Q. *Polyhedron* **1999**, *18*, 3115–3121.
491. Zeng, D.-X.; Ji, W.; Wong, W.-T.; Wong, W.-Y.; Xin, X.-Q. *Inorg. Chim. Acta* **1998**, *279*, 172–177.
492. Shi, S.; Xin, X.-Q. *Mater. Res. Soc. Symp. Proc.* **1995**, *374*, 151–157.
493. Shi, S.; Hou, H.-W.; Xin, X.-Q. *J. Phys. Chem.* **1995**, *99*, 4050–4053.
494. Hou, H.-W.; Xin, X.-Q.; Song, L.-Q.; Fan, Y.-T. *Huaxue Xuebao* **2000**, *58*, 283–286.
495. Niu, Y.-Y.; Zheng, H.-G.; Cai, Y.; Xin, X.-Q.; Song, Y.-L. *Huaxue Xuebao* **2001**, *59*, 1435–1441.
496. Philip, R.; Kumar, G. R.; Mathur, P.; Ghosh, S. *Chem. Phys. Lett.* **1999**, *313*, 719–724.
497. Yu, H.; Xu, Q.-F.; Sun, Z.-R.; Ji, S.-J.; Chen, J.-X.; Liu, Q.; Lang, J.-P.; Tatsumi, K. *Chem. Commun.* **2001**, 2614–2615.
498. Tan, W.-L.; Zheng, H.-G.; Jin, Q.-H.; Jin, G.-C.; Ji, W.; Long, D.-L. Xin, X.-Q. *Polyhedron* **2000**, *19*, 1545–1549.
499. Sakane, G.; Shibahare, T.; Hou, H.-W.; Xin, X.-Q.; Shi, S. *Inorg. Chem.* **1995**, *34*, 4785–4789.
500. Ji, W.; Shi, S.; Du, H.-J.; Ge, P.; Tang, S.-H.; Xin, X.-Q. *J. Phys. Chem.* **1995**, *99*, 17297–17301.
501. Xia, T.; Dogariu, A.; Mansour, K.; Hagan, D. J.; Said, A. A.; Van Stryland, E. W.; Shi, S. *Proc. SPIE-Int. Soc. Opt. Eng.* **1996**, 2853, 142–148.
502. Xia, T.; Dogariu, A.; Mansour, K.; Hagan, D. J.; Said, A. A.; Van Stryland, E. W.; Shi, S. *J. Opt. Soc. Am. B* **1998**, *15*, 1497–1501.
503. Shi, S.; Ji, W.; Xie, W.; Chong, T.-C.; Zeng, H.-C.; Lang, J.-P.; Xin, X.-Q. *Mater. Chem. Phys.* **1995**, *39*, 298–303.
504. Ji, W.; Ge, P.; Xie, W.; Tang, S. H.; Shi, S. *J. Lumin.* **1995**, *66–67*, 115–119.
505. Shi, S.; Xin, X.-Q.; Ji, W.; Xie, W. *Mater. Res. Soc. Symp. Proc.* **1995**, *374*, 311–317.
506. Hou, H.-W.; Ye, X.-G.; Xin, X.-Q.; Liu, J.; Chen, M.-Q.; Shi, S. *Chem. Mater.* **1995**, *7*, 472–476.
507. Hou, H.-W.; Long, D.-L.; Xin, X.-Q.; Huang, X.-X.; Kang, B.-S.; Ge, P.; Ji, W.; Shi, S. *Inorg. Chem.* **1996**, *35*, 5363–5367.
508. Hou, H.-W.; Ang, H. G.; Ang, S. G.; Fan, Y.-T.; Low, M. K. M.; Ji, W.; Lee, Y. W. *Phys. Chem. Chem. Phys.* **1999**, *1*, 3145–3149.
509. Ge, P.; Tang, S.-H.; Ji, W.; Shi, S.; Hou, H.-W.; Long, D.-L.; Xin, X.-Q.; Lu, S.-F.; Wu, Q.-J. *J. Phys. Chem. B* **1997**, *101*, 27–31.
510. Zhang, C.; Song, Y.-L.; Xu, Y.; Jin, G.-C.; Fang, G.-Y.; Wang, Y.-X.; Fun, H.-K.; Xin, X.-Q. *Inorg. Chim. Acta* **2000**, *311*, 25–32.
511. Zhang, C.; Song, Y.-L.; Kühn, F. E.; Xu, Y.; Xin, X.-Q.; Fun, H.-K.; Herrmann, W. A. *Eur. J. Inorg. Chem.* **2002**, 55–64.
512. Niu, X.-Y.; Song, Y.-L.; Zheng, H.-G.; Long, D.-L.; Fun, H.-K.; Xin, X.-Q. *New J. Chem.* **2001**, *25*, 945–948.
513. Low, M. K. M.; Hou, H.-W.; Zheng, H.-G.; Wong, W.-T.; Jin, G.-X.; Xin, X.-Q.; Ji, W. *Chem. Commun.* **1998**, 505–506.
514. Zheng, H.-G.; Tan, W.-L.; Ji, W.; Leung, W.-H.; Williams, I. D.; Long, D.-L.; Huang, J.-S.; Xin, X.-Q. *Inorg. Chim. Acta* **1999**, *294*, 73–78.
515. Song, Y.-L.; Zhang, C.; Zhao, X.-L.; Wang, Y.-X.; Fang, G.-Y.; Jin, G.-C.; Qu, S.-L.; Wu, S.-P.; Xin, X.-Q.; Ye, H.-G. *Chem. Lett.* **2000**, *9*, 1076–1077.

516. Song, Y.-L.; Zhang, C.; Wang, Y.-X.; Fang, G.-Y.; Jin, G.-C.; Chang, C.; Liu, S.-T.; Xin, X.-Q.; Ye, H.-G. *Chem. Phys. Lett.* **2000**, *326*, 341–343.
517. Hou, H.-W.; Fan, Y.-T.; Ang, H. G.; Low, M. K. M.; Ji, W.; Lee, Y. W. *Indian J. Chem.* **2000**, *39A*, 534–536.
518. Song, Y.-L.; Zhang, C.; Wang, Y.-X.; Fang, G.-Y.; Jin, G.-C.; Zhan, X.-R.; Liu, S.-T.; Chen, L.-X.; Xin, X.-Q. *Mater. Lett.* **2000**, *46*, 49–52.
519. Fang, G.-Y.; Song, Y.-L.; Wang, Y.-X.; Zhang, X.-R.; Li, C.-F.; Zhang, C.; Xin, X.-Q. *Opt. Commun.* **2000**, *181*, 97–100.
520. Song, Y.-L.; Zhang, C.; Wang, Y.-X.; Fang, G.-Y.; Jin, G.-C.; Liu, S.-T.; Chen, L.-X.; Xin, X.-Q. *Opt. Mater.* **2000**, *15*, 187–190.
521. Zhang, C.; Song, Y.-L.; Fung, B. M.; Xue, Z.-L.; Xin, X.-Q. *Chem. Commun.* **2001**, 843–844.
522. Zhang, C.; Song, Y.-L.; Kühn, F. E.; Wang, Y.-X.; Fun, H.-K.; Xin, X.-Q. *J. Mater. Chem.* **2002**, *12*, 239–248.
523. Zhang, C.; Song, Y.-L.; Kühn, F. E.; Wang, Y.-X.; Xin, X.-Q.; Herrmann, W. A. *Adv. Mater.* **2002**, *14*, 818–822.
524. Zhang, C.; Song, Y.-L.; Jin, G.-C.; Fang, G.-Y.; Wang, Y.-X.; Raj, S. S. S.; Fun, H.-K.; Xin, X.-Q. *J. Chem. Soc., Dalton Trans.* **2000**, 1317–1323.
525. Song, Y.-L.; Zhang, C.; Chen, G.-P.; Fang, G.-Y.; Wang, Y.-X.; Xin, X.-Q. *J. Opt. A: Pure Appl. Opt.* **2002**, *4*, 199–201.
526. Zhang, Q.-F.; Bao, M.-T.; Hong, M.-C.; Cao, R.; Song, Y.-L.; Xin, X.-Q. *J. Chem. Soc., Dalton Trans.* **2000**, 605–610 (Additions and Corrections: *J. Chem. Soc., Dalton Trans.* **2000**, 4702).
527. Zhang, Q.-F.; Raj, S. S. S.; Fun, H.-K.; Xin, X.-Q. *Chem. Lett.* **1999**, 619–620.
528. Shi, S.; Ji, W.; Xin, X.-Q. *J. Phys. Chem.* **1995**, *99*, 894–898.
529. Ji, W.; Xie, W.; Tang, S. H.; Shi, S. *Mater. Chem. Phys.* **1996**, *43*, 45–51.
530. Zheng, H.-G.; Ji, W.; Low, M. L. K.; Sakane, G.; Shibahara, T.; Xin, X.-Q. *J. Chem. Soc., Dalton Trans.* **1997**, 2357–2361.
531. Zhang, Q.-F.; Leung, W.-H.; Song, Y.-L.; Hong, M.-C.; Kennard, C. H. L.; Xin, X.-Q. *New J. Chem.* **2001**, *25*, 465–470.
532. Niu, Y.-Y.; Chen, T.-N.; Liu, S.-X.; Song, Y.-L.; Wang, Y.-X.; Xue, Z.-L.; Xin, X.-Q. *J. Chem. Soc., Dalton Trans.* **2002**, 1980–1984.
533. Lang, J.-P.; Tatsumi, K.; Kawaguchi, H.; Lu, J.-M.; Ge, P.; Ji, W.; Shi, S. *Inorg. Chem.* **1996**, *35*, 7924–7927.
534. Hou, H.-W.; Fan, Y.-T.; Du, C.-X.; Zhu, Y.; Wang, W.-L.; Xin, X.-Q.; Low, M. K. M.; Ji, W.; Ang, H. G. *Chem. Commun.* **1999**, 647–648.
535. Hou, H.-W.; Zheng, H.-G.; Ang, H. G.; Fan, Y.-T.; Low, M. K. M.; Zhu, Y.; Wang, W.-L.; Xin, X.-Q.; Ji, W.; Wong, W.-T. *J. Chem. Soc., Dalton Trans.* **1999**, 2953–2957.
536. Zhang, Q.-F.; Niu, Y.-Y.; Leung, W.-H.; Song, Y.-L.; Williams, I. D.; Xin, X.-Q. *Chem. Commun.* **2001**, 1126–1127.
537. Zhang, Q.-F.; Leung, W.-H.; Xin, X.-Q.; Fun, H.-K. *Inorg. Chem.* **2000**, *39*, 417–426.
538. Zhang, C.; Song, Y.-L.; Xu, Y.; Fun, H.-K.; Fang, G.-Y.; Wang, Y.-X.; Xin, X.-Q. *J. Chem. Soc., Dalton Trans.* **2000**, 2823–2829.
539. Long, D.-L.; Shi, S.; Hou, H.-W.; Tao, R.-D.; Xin, X.-Q. *Chin. J. Inorg. Chem.* **1996**, *12*, 225–233.
540. Hou, H.-W.; Xin, X.-Q.; Shi, S. *Coord. Chem. Rev.* **1996**, *153*, 25–56.
541. Zhang, C.; Jin, G.-C.; Xin, X.-Q. *Chin. J. Inorg. Chem.* **2000**, *16*, 229–240.
542. Long, D.-L.; Wong, W.-T.; Shi, S.; Xin, X.-Q.; Huang, J.-S. *J. Chem. Soc., Dalton Trans.* **1997**, 4361–4366.
543. Zheng, H. G.; Leung, W.-H.; Tan, W.-L.; Long, D.-L.; Ji, W.; Chen, J.-T.; Xin, F.-B.; Xin, X.-Q. *J. Chem. Soc., Dalton Trans.* **2000**, 2145–2149.
544. Zheng, H.-G.; Tan, W.-L.; Jin, G.-C.; Ji, W.; Jin, Q.-H.; Huang, X.-Y.; Xin, X.-Q. *Inorg. Chim. Acta* **2000**, *305*, 14–18.
545. Zhang, Q.-F.; Song, Y.-L.; Wong, W.-Y.; Leung, W.-H.; Xin, X.-Q. *J. Chem. Soc., Dalton Trans.* **2002**, 1963–1968.
546. Banerjee, S.; Kumar, G. R.; Mathur, P.; Sekar, P. *Chem. Commun.* **1997**, 299–300.
547. Mathur, P.; Ghose, S.; Hossain, Md. M.; Satyanarayana, C. V. V.; Banerjee, S.; Kumar, G. R.; Hitchcock, P. B.; Nixon, J. F. *Organometallics* **1997**, *16*, 3815–3818.
548. Mathur, P.; Ghose, S.; Hossain, Md. M.; Satyanarayana, C. V. V.; Chadha, R. K.; Banerjee, S.; Kumar, G. R. *J. Organomet. Chem.* **1998**, *568*, 197–204.
549. Philip, R.; Kumar, G. R.; Mathur, P.; Ghose, S. *Opt. Commun.* **2000**, *178*, 469–475.
550. Zhuang, B.-T.; Sun, H.-F.; He, L.-J.; Zhou, Z.-F.; Lin, C.-S.; Wu, K.-C.; Huang, Z.-X. *J. Organomet. Chem.* **2002**, *655*, 233–238.
551. Shi, S.; Zhang, X.; Shi, X. F. *J. Phys. Chem.* **1995**, *99*, 14911–14914.
552. Tang, K.-L.; Jin, X.-L.; Yan, H.; Xie, X.-J.; Liu, C.-L.; Gong, Q.-H. *J. Chem. Soc., Dalton Trans.* **2001**, 1374–1377.
553. Liu, C.-L.; Wang, X.; Gong, Q.-H.; Tang, K.-L.; Jin, X.-L.; Yan, H.; Cui, P. *Adv. Mater.* **2001**, *13*, 1687–1690.
554. Jin, X.-L.; Xie, X.-J.; Qian, H.; Tang, K. L.; Liu, C.-L.; Wang, X.; Gong, Q.-H. *Chem. Commun.* **2002**, 600–601.
555. Zhang, H.; Zelmon, D. E.; Deng, L.; Liu, H.-K.; Teo, B. K. *J. Am. Chem. Soc.* **2001**, *123*, 11300–11301.
556. Niu, J.-Y.; You, X.-Z.; Duan, C.-Y.; Fun, H.-K.; Zhou, Z.-Y. *Inorg. Chem.* **1996**, *35*, 4211–4217.
557. Zhou, Y.-S.; Wang, E.-B.; Peng, J.; Liu, J.; Hu, C.-W.; Huang, R.-D.; You, X.-Z. *Polyhedron* **1999**, *18*, 1419–1423.
558. Niu, J.-Y.; Wang, J.-P.; Chen, Y. *Chin. J. Inorg. Chem.* **1999**, *15*, 401–404.
559. Niu, J.-Y.; Wang, J.-P.; Bo, Y.; Dang, D.-B.; Yu, L. *Chin. J. Inorg. Chem.* **1999**, *15*, 773–778.
560. Niu, J.-Y.; Wang, J.-P.; Bo, Y.; Dang, D.-B.; Yu, L. *Yingyong Huaxue* **2000**, *17*, 134–137.
561. Niu, J.-Y.; Wang, J.-P.; Bo, Y.; Dang, D.-B.; Yu, L. *Yingyong Huaxue* **2000**, *17*, 589–592.
562. Murakami, H.; Kozeki, T.; Suzuki, Y.; Ono, S.; Ohtake, H.; Sarukura, N.; Ishikawa, E.; Yamase, T. *Appl. Phys. Lett.* **2001**, *79*, 3564–3566.
563. Li, S.-X.; Wang, Z.-M.; Chen, J.-Z.; Su, W.-Y. *Chin. Chem. Lett.* **1992**, *3*, 397–398.
564. Marcy, H. O.; Warren, L. F.; Webb, M. S.; Ebberts, C. A.; Velsko, S. P.; Kennedy, G. C.; Catella, G. C. *Appl. Opt.* **1992**, *31*, 5051–5060.
565. Ramabadran, U. B.; Zelmon, D. E.; Kennedy, G. C. *Appl. Phys. Lett.* **1992**, *60*, 2589–2591.
566. Ramabadran, U. B.; McPherson, A. L.; Zelmon, D. E. *J. Appl. Phys.* **1994**, *76*, 1150–1154.
567. Anthony, S. P.; Radhakrishnan, T. P. *Chem. Commun.* **2001**, 931–932.
568. Tao, X.-T.; Jiang, M.-H.; Xu, D.; Shao, Z.-S. *Rengong Jingti* **1987**, *16*, 28–32.

569. Tao, X.-T.; Jiang, M.-H.; Xu, D.; Shao, Z.-S. *Kexue Tongbao (Foreign Lang. Ed.)* **1988**, *33*, 651–654.
570. Dou, S.-X.; Jiang, M.-H.; Shao, Z.-S.; Tao, X.-T. *Appl. Phys. Lett.* **1989**, *54*, 1101–1105.
571. Wang, B. G. *Cryst. Res. Technol.* **1996**, *31*, 421–428.
572. Yuan, D.-R.; Zhang, N.; Yu, W.-T.; Xu, D.; Tao, X.-T.; Jiang, M.-H. *Zhongguo Jiguang* **1990**, *17*, 332–335.
573. Yuan, D.-R.; Zhang, N.; Yu, W.-T.; Xu, D.; Tao, X.-T.; Jiang, M.-H. *Proc. SPIE-Int. Soc. Opt. Eng.* **1990**, *1337*, 394–397.
574. Zhang, N.; Jiang, M.-H.; Yuan, D.-R.; Xu, D.; Tao, X.-T. *Chin. Phys. Lett.* **1989**, *6*, 280–283.
575. Zhang, N.; Jiang, M.-H.; Yuan, D.-R.; Xu, D.; Shao, Z.-S.; Tao, X.-T. *Proc. SPIE-Int. Soc. Opt. Eng.* **1990**, *1337*, 390–393.
576. Zhang, N.; Jiang, M.-H.; Yuan, D.-R.; Xu, D.; Tao, X.-T.; Shao, Z.-S. *J. Cryst. Growth* **1990**, *102*, 581–584.
577. Ramabadrán, U. B.; Vuppaladhadiam, R.; Small, D.; Zelmon, D. E.; Kennedy, G. C. *Appl. Opt.* **1996**, *35*, 903–906.
578. Xu, D.; Liu, M.-G.; Hou, W.-B.; Yuan, D.-R.; Jian, M.-H.; Ren, Q.; Chai, B. H. C. *Mater. Res. Bull.* **1994**, *29*, 73–79.
579. Hou, W.-B.; Yuan, D.-R.; Xu, D.; Zhang, N.; Yu, W.-T.; Liu, M.-G.; Tao, X.-T.; Sun, S.-Y.; Jiang, M.-H. *J. Cryst. Growth* **1993**, *133*, 71–74.
580. Hou, W. B.; Jiang, M. H.; Ruan, D. R.; Xu, D.; Zhang, N.; Liu, M. G.; Tao, X. T. *Mater. Res. Bull.* **1993**, *28*, 645–653.
581. Yuan, D.-R.; Zhang, N.; Tao, X.-T.; Xu, D.; Jiang, M.-H. *Chin. Phys. Lett.* **1990**, *7*, 334–336.
582. Yuan, D.-R.; Zhang, N.; Tao, X.-T.; Xu, D.; Jiang, M.-H.; Shao, Z.-S. *Chin. Sci. Bull.* **1991**, *36*, 1401–1404.
583. Yuan, D.-R.; Zhang, N.; Tao, X.-T.; Xu, D.; Jiang, M.-H. *Rengong Jingti Xuebao* **1989**, *18*, 267–273.
584. Yuan, D.-R.; Zhang, N.; Tao, X.-T.; Xu, D.; Yu, W.-T.; Shao, Z.-S.; Jiang, M.-H. *Guangxue Xuebao* **1993**, *13*, 456–460.
585. Hu, S.-Z.; Huang, Y.-Q.; Li, S.-X.; Lin, F.; Chen, J.-Z.; Dong, M.-B.; Yang, Y.-C.; Wu, W.-S. *Jiegou Huaxue* **1995**, *14*, 476–481.
586. Zelmon, D. E.; Gebeyehu, Z.; Tomlin, D.; Cooper, T. M. *Mater. Res. Soc. Symp. Proc.* **1998**, *519*, 395–400.
587. Chen, Z.-F.; Xiong, R.-G.; Abrahams, B. F.; You, X.-Z.; Che, C.-M. *J. Chem. Soc., Dalton Trans.* **2001**, 2453–2455.
588. Lamberth, C.; Murphy, D. M.; Mingos, D. M. P. Second Harmonic Generation Properties of Some Coordination Compounds Based on Pentadionate and Polyene Ligands. In *Organic Materials for Nonlinear Optics II*; Hann, R. A., Bloor, D., Eds.; Royal Society of Chemistry: London, 1991; pp 183–189.
589. Copley, R. C. B.; Lamberth, C.; Machell, J.; Mingos, D. M. P.; Murphy, D. M.; Powell, H. *J. Mater. Chem.* **1991**, *1*, 583–589.
590. Lamberth, C.; Machell, J. C.; Mingos, D. M. P.; Stolberg, T. L. *J. Mater. Chem.* **1991**, *1*, 775–780.
591. Cooper, T. M.; Cline, S. M.; Zelmon, D. E.; Vuppaladhadiam, R.; Das Gupta, S.; Ramabadrán, U. B. *Mater. Res. Soc. Symp. Proc.* **1996**, *435*, 655–659.
592. Barberá, J.; Elduque, A.; Giménez, R.; Lahoz, F. J.; López, J. A.; Oro, L. A.; Serrano, J. L.; Villacampa, B.; Villalba, J. *Inorg. Chem.* **1999**, *38*, 3085–3092.
593. Cahill, P. A. *Mater. Res. Soc. Symp. Proc.* **1988**, *109*, 319–322.
594. Laidlaw, W. M.; Denning, R. G.; Verbiest, T.; Chauchard, E.; Persoons, A. *Nature* **1993**, *363*, 58–60.
595. Laidlaw, W. M.; Denning, R. G.; Verbiest, T.; Chauchard, E.; Persoons, A. *Proc. SPIE, Int. Soc. Opt. Eng.* **1994**, *2143*, 14–19.
596. Vance, F. W.; Karki, L.; Reigle, J. K.; Hupp, J. T.; Ratner, M. A. *J. Phys. Chem. A* **1998**, *102*, 8320–8324.
597. Coe, B. J.; Jones, C. J.; McCleverty, J. A.; Bloor, D.; Kolinsky, P. V.; Jones, R. J. *J. Chem. Soc., Chem. Commun.* **1989**, 1485–1487.
598. Coe, B. J.; Kurek, S. S.; Rowley, N. M.; Foulon, J.-D.; Hamor, T. A.; Harman, M. E.; Hursthouse, M. B.; Jones, C. J.; McCleverty, J. A.; Bloor, D. *Chemtronics* **1991**, *5*, 23–28.
599. Coe, B. J.; Foulon, J.-D.; Hamor, T. A.; Jones, C. J.; McCleverty, J. A.; Bloor, D.; Cross, G. H.; Axon, T. L. *J. Chem. Soc., Dalton Trans.* **1994**, 3427–3439 (additions/corrections, *J. Chem. Soc., Dalton Trans.* **1995**, 153).
600. Coe, B. J.; Hamor, T. A.; Jones, C. J.; McCleverty, J. A.; Bloor, D.; Cross, G. H.; Axon, T. L. *J. Chem. Soc., Dalton Trans.* **1995**, 673–684.
601. Coe, B. J.; Jones, C. J.; McCleverty, J. A.; Bloor, D.; Kolinsky, P. V.; Jones, R. J. *Polyhedron* **1994**, *13*, 2107–2115.
602. Reis, H.; Raptis, S. G.; Papadopoulos, M. G. *Phys. Chem. Chem. Phys.* **2001**, *3*, 3901–3905.
603. Lopez-Garabito, C.; Campo, J. A.; Heras, J. V.; Cano, M.; Rojo, G.; Agullo-Lopez, F. *J. Phys. Chem. B* **1998**, *102*, 10698–10706.
604. Rojo, G.; Agullo-Lopez, F.; Campo, J. A.; Heras, J. V.; Cano, M. *J. Phys. Chem. B* **1999**, *103*, 11016–11020.
605. Campo, J. A.; Cano, M.; Heras, J. V.; Lopez-Garabito, C.; Pinilla, E.; Torres, R.; Rojo, G.; Agullo-Lopez, F. *J. Mater. Chem.* **1999**, *9*, 899–907.
606. Rojo, G.; Agullo-Lopez, F.; Campo, J. A.; Cano, M.; Lagunas, M. C.; Heras, J. V. *Synth. Met.* **2001**, *124*, 201–203.
607. Doisneau, G.; Balavoine, G.; Fillebeen-Khan, T.; Clinet, J. C.; Delaire, J.; Ledoux, I.; Loucif, R.; Puccetti, G. *J. Organomet. Chem.* **1991**, *421*, 299–304.
608. Loucif-Saïbi, R.; Delaire, J. A.; Bonazzola, L.; Doisneau, G.; Balavoine, G.; Fillebeen-Khan, T.; Ledoux, I. *Mol. Eng.* **1992**, *2*, 221–231.
609. Loucif-Saïbi, R.; Delaire, J. A.; Bonazzola, L.; Doisneau, G.; Balavoine, G.; Fillebeen-Khan, T.; Ledoux, I.; Puccetti, G. *Chem. Phys.* **1992**, *167*, 369–375.
610. Pollagi, T. P.; Stoner, T. C.; Dallinger, R. F.; Gilbert, T. M.; Hopkins, M. D. *J. Am. Chem. Soc.* **1991**, *113*, 703–704.
611. Ikeda, K.; Ohkoshi, S.-I.; Hashimoto, K. *Chem. Phys. Lett.* **2001**, *349*, 371–375.
612. Shi, J.-M.; Xu, W.; Liu, Q.-Y.; Liu, F.-L.; Huang, Z.-L.; Lei, H.; Yu, W.-T.; Fang, Q. *Chem. Commun.* **2002**, 756–757.
613. Houbrechts, S.; Kubo, Y.; Tozawa, T.; Tokita, S.; Wada, T.; Sasabe, H. *Angew. Chem., Int. Ed. Engl.* **2000**, *39*, 3859–3862.
614. Zhai, T.; Lawson, C. M.; Burgess, G. E.; Lewis, M. L.; Gale, D. C.; Gray, G. M. *Opt. Lett.* **1994**, *19*, 871–873.
615. Zhai, T.; Lawson, C. M.; Gale, D. C.; Gray, G. M. *Opt. Mater.* **1995**, *4*, 455–460.
616. Lawson, C. M.; Zhai, T.; Gale, D. C.; Gray, G. M. *Mater. Res. Soc. Symp. Proc.* **1995**, *374*, 287–292.
617. Gale, D. C.; Gray, G. M.; Lawson, C. M. *Proc. SPIE-Int. Soc. Opt. Eng.* **1997**, *3146*, 54–60.

618. Sun, W.; Byeon, C. C.; McKerns, M. M.; Lawson, C. M.; Dunn, J. M.; Hariharasarma, M.; Gray, G. M. *Proc. SPIE-Int. Soc. Opt. Eng.* **1998**, *3472*, 108–115.
619. Sun, W.; Byeon, C. C.; McKerns, M. M.; Lawson, C. M.; Dunn, J. M.; Hariharasarma, M.; Gray, G. M. *Opt. Mater.* **1998**, *11*, 87–93.
620. Sun, W.; Lawson, C. M.; Gray, G. M. *Opt. Commun.* **2000**, *180*, 361–366.
621. Kafafi, Z. H.; Lindle, J. R.; Weisbecker, C. S.; Bartoli, F. J.; Shirk, J. S.; Yoon, T. H.; Kim, O.-K. *Chem. Phys. Lett.* **1991**, *179*, 79–84.
622. Dhindsa, A. S.; Underhill, A. E.; Oliver, S.; Kershaw, S. *J. Mater. Chem.* **1995**, *5*, 261–264.
623. Dhindsa, A. S.; Underhill, A. E.; Oliver, S.; Kershaw, S. *Mol. Cryst. Liq. Cryst. Sci. Technol., Sect. B: Nonlinear Opt.* **1995**, *10*, 115–121.
624. Kodzasa, T.; Kamata, T.; Ushijima, H.; Matsuda, H.; Fukaya, T.; Mizukami, F.; Matsunami, J.; Nagai, Y.; Matsumoto, K. *Mol. Cryst. Liq. Cryst. Sci. Technol., Sect. A* **1996**, *286*, 603–608.
625. Kodzasa, T.; Kamata, T.; Matsuda, H.; Fukaya, T.; Mizukami, F.; Matsunami, J.; Nagai, Y.; Matsumoto, K. *Mol. Cryst. Liq. Cryst. Sci. Technol., Sect. A* **1995**, *267*, 123–128.
626. Kodzasa, T.; Kamata, T.; Matsuda, H.; Fukaya, T.; Mizukami, F.; Matsunami, J.; Nagai, Y.; Matsumoto, K. *J. Sol-Gel Sci. Tech.* **1997**, *8*, 1029–1033.
627. Kamata, T.; Fukaya, T.; Mizuno, M.; Matsuda, H.; Mizukami, F. *Chem. Phys. Lett.* **1994**, *221*, 194–198.
628. Kamata, T.; Fukaya, T.; Matsuda, H.; Mizukami, F. *Appl. Phys. Lett.* **1994**, *65*, 1343–1345.
629. Kamata, T.; Fukaya, T.; Matsuda, H.; Mizukami, F.; Tachiya, M.; Ishikawa, R.; Uchida, T. *J. Phys. Chem.* **1995**, *99*, 13239–13246.
630. Fukaya, T.; Kamata, T.; Mizuno, M. *Synth. Met.* **1995**, *71*, 1693–1694.
631. Kamata, T.; Fukaya, T.; Kodzasa, T.; Matsuda, H.; Mizukami, F. *Synth. Met.* **1995**, *71*, 1725–1726.
632. Kamata, T.; Fukaya, T.; Kodzasa, T.; Matsuda, H.; Mizukami, F. *Mol. Cryst. Liq. Cryst. Sci. Technol., Sect. A* **1995**, *267*, 117–122.
633. Kamata, T.; Kubota, S.; Fukaya, T.; Matsuda, H.; Mizukami, F.; Uchida, T. *Jpn. J. Appl. Phys., Part 2* **1995**, *34*, L1274–L1277.
634. Kamata, T.; Kambayashi, H.; Kubota, S.; Fukaya, T.; Matsuda, H.; Mizukami, F.; Uchida, T. *Mol. Cryst. Liq. Cryst. Sci. Technol., Sect. B: Nonlinear Opt.* **1996**, *15*, 255–258.
635. Van Keuren, E.; Matsuda, H.; Kamata, T.; Fukaya, T.; Mizukami, F. *Mol. Cryst. Liq. Cryst. Sci. Technol., Sect. B: Nonlinear Opt.* **1996**, *15*, 279–282.
636. Kamata, T.; Curran, S.; Roth, S.; Fukaya, T.; Matsuda, H.; Mizukami, F. *Synth. Met.* **1996**, *83*, 267–271.
637. Fukaya, T.; Nezu, Y.; Kamata, T.; Uchida, T. *Mol. Cryst. Liq. Cryst. Sci. Technol., Sect. A* **1996**, *286*, 609–614.
638. Yamada, S.; Van Keuren, E.; Matsuda, H.; Kamata, T.; Fukaya, T.; Mizukami, F.; Smith, E. C.; Kar, A. K.; Wherrett, B. S. *Mol. Cryst. Liq. Cryst. Sci. Technol., Sect. A* **1997**, *295*, 299–302.
639. Van Keuren, E.; Matsuda, H.; Kamata, T.; Fukaya, T.; Mizukami, F. *Synth. Met.* **1997**, *86*, 2149–2150.
640. Mashima, K.; Tanaka, M.; Kaneda, Y.; Fukumoto, A.; Mizomoto, H.; Tani, K.; Nakano, H.; Nakamura, A.; Sakaguchi, T.; Kamada, K.; Ohta, K. *Chem. Lett.* **1997**, 411–412.
641. Pate, B. D.; Thorne, J. R. G.; Click, D. R.; Chisholm, M. H.; Denning, R. G. *Inorg. Chem.* **2002**, *41*, 1975–1978.

9.15

Metal Compounds as Phosphors

J. SILVER

University of Greenwich, London, UK

9.15.1	INTRODUCTION	689
9.15.1.1	History of Phosphors and Past Uses	690
9.15.2	CURRENT USES OF PHOSPHORS	691
9.15.3	DISPLAY TECHNOLOGIES USING PHOSPHORS	691
9.15.3.1	Cathode Ray Tube Displays	691
9.15.3.2	Electroluminescent Displays	692
9.15.3.3	Vacuum Fluorescent Displays	696
9.15.3.4	Field Emission Displays	696
9.15.3.5	Plasma Displays	697
9.15.4	PHOSPHOR SYNTHESIS	697
9.15.4.1	Traditional Solid-state Synthesis	698
9.15.4.2	Hydrothermal and Related Methods	698
9.15.4.2.1	<i>Homogeneous precipitation</i>	698
9.15.4.2.2	<i>Sol-gel methods</i>	701
9.15.4.2.3	<i>Microemulsion methods</i>	701
9.15.4.3	Other Solution-based Techniques	702
9.15.4.3.1	<i>Combinatorial methods</i>	702
9.15.4.3.2	<i>Solution-coating methods</i>	702
9.15.4.4	Vapor-phase Methods	702
9.15.4.4.1	<i>Chemical vapor deposition</i>	702
9.15.4.4.2	<i>Molecular beam epitaxy and its derivatives</i>	702
9.15.4.4.3	<i>RF magnetron sputtering</i>	703
9.15.4.4.4	<i>Electron beam evaporation</i>	703
9.15.4.4.5	<i>Pulsed laser decomposition</i>	703
9.15.4.4.6	<i>Ion implantation</i>	703
9.15.4.4.7	<i>Aerosol spray pyrolysis</i>	704
9.15.4.4.8	<i>Charged liquid cluster beam methods</i>	704
9.15.5	ORGANO-ELECTROLUMINESCENT DEVICES	704
9.15.5.1	Coordination Compounds as Organo-electroluminescent Devices	704
9.15.5.1.1	<i>Group II metal complexes</i>	704
9.15.5.1.2	<i>Tris(8-hydroxyquinolato)aluminum and related complexes</i>	705
9.15.5.1.3	<i>Lanthanide β-diketonate complexes</i>	707
9.15.5.1.4	<i>Other metal complexes</i>	708
9.15.5.2	Novel Organo-electroluminescent Devices/Inorganic Devices	709
9.15.5.3	Problems with Organo-electroluminescent Devices	709
9.15.6	LIGHT-EMITTING DIODES	709
9.15.7	ANTI-STOKES PHOSPHORS	709
9.15.8	QUANTUM CUTTERS	710
9.15.8.1	Novel Inorganic-Based Luminous Materials	711
9.15.9	PHOSPHORESCENT PAINTS	711
9.15.10	PHOTONICS	711
9.15.11	THE FUTURE	712
9.15.12	REFERENCES	712

9.15.1 INTRODUCTION

The phenomenon where the formation of an electronically excited state of a material (by the application of external energy) is followed by the emission of the excitation energy as light is called *luminescence*. This is usually subdivided into two categories; fluorescence is (short-lived) emission from a singlet excited state, and phosphorescence refers to (longer-lived) emission from a triplet excited state. For the purposes of the inorganic materials discussed in this chapter, more relaxed (historical) definitions are used. Light emission from a material during the time it is exposed to exciting radiation is referred to as *fluorescence*; this was the term introduced to denote the imperceptible short after-glow of the mineral fluorite (CaF_2) following its excitation.¹ In contrast, if the after-glow is detectable by eye after the end of the excitation it is called *phosphorescence*;¹ the word *phosphor* means “light bearer” in Greek, and the term was introduced around the seventeenth century to refer to light-emitting stones.

The phosphors described in this chapter are usually based on metal oxide, metal oxysulfide, and metal sulfide lattices, which act as hosts for light-emitting centers that are doped into them. This is denoted by, for example, ZnS:Pb (meaning a trace of Pb doped into a ZnS host lattice) or $\text{LiGdF}_4:\text{Er}^{3+},\text{Tb}^{3+}$ (meaning a mixture of Er^{3+} and Tb^{3+} ions doped into a LiGdF_4 host lattice).

As such, these materials do not fit the strict definition of coordination compounds. However, in their synthesis, whether from calcining solids or by homogeneous precipitation, the precursors can invariably be described as coordination compounds. In the solid-state reactions, diffusion (often involving some or much melting) and flux growth (liquid or vapor phase) involves activator cations being part of a coordination complex. In solution preparations of precursors, the activators are always present as coordination complexes. Vapor-phase deposition methods such as metal organic chemical vapor deposition (MOCVD) or radio frequency magnetron sputtering use coordination compounds either directly (in the former) or transitorily (in the latter). The various host phosphor lattices are often chosen for the coordination geometries they can impose on the guest activator ions. The incorporation of these cations is often carried out by pre-coating host lattices with solutions of coordination compounds of the activators, followed by annealing to destroy the compounds and allow the cations to diffuse into the host crystals.

This chapter covers both traditional and more recent synthetic methods of preparing phosphors. It is important to note that as phosphors are used in all types of display, and are, therefore, an important part of a multibillion-dollar industry; research and development is always ongoing to improve light output and, therefore, ease of viewing. The same is also true in the use of phosphors for lighting.

It is worth summarizing at this point the different excitation methods used for phosphors that will be referred to throughout this chapter. There are three types: photoluminescence (PL) which is based on initial excitation by absorption of light, cathodoluminescence (CL) which is based on bombardment with a beam of electrons, as in a cathode ray tube (CRT); and electroluminescence (EL) which is based on application of an electric field (either a.c. or d.c.) across the phosphor.

9.15.1.1 History of Phosphors and Past Uses

The recorded history of phosphors begins in the seventeenth century when Vincentius Casciarola, an alchemist from Bologna in Italy, found a heavy crystalline stone near a Volcano.¹ He fired the stone in a charcoal oven hoping to convert it to a noble metal. Although he was not successful in transforming the elements in the stone, he found that after sintering it emitted red light in the dark if previously exposed to sunlight. The stone is now called the “Bolognian stone” and from modern insights it appears to have been barite (BaSO_4) which, when fired, became BaS, now known as a host lattice for phosphors. Before the discovery of this stone, there is a reference to the preparation of phosphorescent paint from seashells (by grinding them with a rock from a volcano) that is ascribed to people living in what is now Japan.² This is recorded in a tenth century Chinese document (Song dynasty) written by Xiang-Shan Ye-Lu.³

Scientific research in the field of phosphors is almost 140 years old. In 1866, the young French chemist Theodore Sidot prepared, by a sublimation method, tiny ZnS crystals that manifested phosphorescence in the dark.⁴ After the experiment was repeated and confirmed it was presented in a note to the Academy of Sciences of Paris; the note was then published by Becquerel.⁵ From present knowledge of phosphors it seems likely that Sidot’s ZnS contained a small quantity of copper as an impurity, and was the precursor for ZnS-type phosphors.

In the late nineteenth century and early twentieth century, Lenard *et al.* in Germany carried out systematic research on phosphors. They prepared phosphors based on alkaline earth sulfides and selenides, and also on ZnS, and studied their luminescence. In these studies, they laid down the fundamentals of phosphor research.⁶ Other significant contributions included those of H. W. Leverenz and colleagues at the Radio Corporation of America (RCA)¹ laboratories who investigated many phosphors for use in television tubes which led to detailed work being carried out on ZnS-type phosphors.⁷

9.15.2 CURRENT USES OF PHOSPHORS

The understanding of phosphors and solid-state luminescence has matured to the point at which relatively rational design and preparation of new light-emitting materials can be achieved. This has resulted from advances in solid-state physics and optical spectroscopy coupled to the development of new chemical synthesis techniques. This has led to the rapid development of phosphors as important industrial/technological materials. Examples of the occurrence of phosphors in everyday use include:

- CRTs for televisions and computer display monitors
- CRTs in radar
- Plasma televisions (photoluminescent devices)
- Electroluminescent displays
- Emergency lighting systems based on electroluminescent devices
- Lighting in fluorescent and phosphorescent lamps
- Intensifying screens (for X rays and in industrial nondestructive testing)
- Infrared up-conversion phosphors
- Luminous paints
- Marking systems (security uses on currency, etc.)
- Stamps printed with phosphor-containing inks
- Application of near-IR phosphors for optical fiber amplifiers

In addition, luminescent materials are also essential to other modern technologies based on the exploitation and manipulation of light. Such uses include modern lasers, inorganic light-emitting diodes (LEDs), and organic LEDs (OLEDs), which often include inorganic coordination compounds as part of the light-emitting layers.

9.15.3 DISPLAY TECHNOLOGIES USING PHOSPHORS

Phosphors are finely designed and highly engineered inorganic materials, and specific phosphors must be developed for each application. This is a point often overlooked in the development of a new display, and it can cause the technology to fail. It is usually not possible to use phosphors developed for one technology in a different application because the electron voltage or photon energy used to excite the phosphors for particular display technologies may be very different. The specific phosphors used in a range of electronic displays, with emphasis on more recent developments, will now be reviewed. These displays are each finding niches in the marketplace along with liquid crystal displays. Of the five reviewed here, the oldest and most important is still the CRT, which still represents nearly 50% in dollar or yen terms of the display industry. It is worth noting that the main reason for the wish to replace the CRT is not because of its efficiency (it is still the most efficient technology by far), but the wish to make thinner and larger displays. The bulk and weight of large CRTs are their main drawback.

9.15.3.1 Cathode Ray Tube Displays

The entire CRT industry is based on the quality and reproducibility of the phosphors used. As stated earlier the phosphors used for the different kinds of CRT displays are constantly being researched and improved. For high-definition television screens the phosphors must be prepared with great control over powder morphology and particle size (see [Section 9.15.4.2.1](#)).

Phosphors for CRTs are predominantly based on zinc and cadmium sulfides. Selected CRT phosphors are listed in Table 1 which also includes their precursors, their “P-numbers”, and their uses. (The system used to classify CRT phosphors came from JEDEC, the former Joint Electronic Device Engineering Council, now JT- Committee on Phosphor and Optical Characteristics within the Electronic Industries Association. JEDEC established the original code for these phosphors in terms of “P-numbers”.⁸ Many manufacturers of CRTs use these when specifying phosphor screen characteristics.) Although the precursors are tabulated, the mole ratios used in the syntheses are not.

9.15.3.2 Electroluminescent Displays

High-field EL was discovered by Destiau in 1936.⁹ He observed light emission when a high voltage (a.c.) was applied to ZnS powder, dispersed in castor oil, sandwiched between two electrodes. Over the last 50 years since the development of transparent conducting films, a.c. powder EL devices have been used widely, particularly for emergency lighting in aircraft and for display (advertising purposes). The first d.c. powder EL device was fabricated by coating a ZnS phosphor with copper ions.¹⁰

Phosphor host materials for EL applications must have the following properties:¹¹

- (i) A bandgap large enough to emit visible light without absorption
- (ii) The possibility of producing an electron avalanche when excited by a high electric field ($\sim 10^6$ V cm⁻¹)
- (iii) Lattices that can accept suitable light-emitting dopants

Such host II–VI compounds are ZnS, ZnSe, SrS, and CaS;^{12–16} ZnS is now the most widely used host material.

The luminescent centers require a range of properties that include a large cross-section for the collision excitation to occur, an ionic radius and valency to fit the lattice and be stable under the applied high electronic fields, and the capability to display high luminous efficiency when excited.¹¹ Metal ions suitable for EL devices include Mn²⁺, Tb³⁺, Sm³⁺, Tm³⁺, Pr³⁺, Eu²⁺, and Ce³⁺.^{12–17} ZnS lattices doped with Mn²⁺ (yellow–orange emission at ca. 585 nm) have proved to be one of the best phosphors for EL devices.

In a.c. EL cells routine use is made of dielectric insulators often based on amorphous oxides (e.g., Al₂O₃, SiO₂, TiO₂, or Ta₂O₇) or ferroelectric materials such as BaTiO₃, SrTiO₃, and PbTiO₃.¹⁸ However, a novel low-cost binder for flexible a.c. powder EL panels has recently been found which eliminates the need for insulating layers.¹⁹ This binder is prepared from long-chain organic molecules cross-linked by metal ions such as Si, B, and Ti added in the form of alkoxides, and the phosphor powder is covered with this polymer.¹⁹

Efficient IR-emitting phosphors excited by a direct current electroluminescence (DCEL) device were first reported in 1969.²⁰ Sixty/40 CdS/ZnS doped with 10⁻⁴ g g⁻¹ Cu was shown to be an efficient converting phosphor giving a maximum output at 900 nm.²⁰ The near-IR emission of thin-film electroluminescence (TFEL) devices containing ZnS:Er (at 980 nm), ZnS:Nd (at 900 nm), and ZnS:Tm (at 805 nm) have been reported.²¹

The light-emission characteristics of a white-light-emitting EL device with a doubly doped ZnS:Pr,Ce,F phosphor layer have been described. It was observed that optimization of the co-doping of Ce enhances the emission characteristics compared to an EL device with a singly doped ZnS:Pr,F layer.²² An electrical characterization of Ce-doped ZnS:TbOF EL thin films has been reported; Ce doping was seen to improve the radiative emission efficiency leading to improved performance of Ce co-doped film.²³

Using a stack phosphor consisting of the newly developed SrS:Cu,Ag blue-emitting phosphor and ZnS:Mn, it has been shown that it is possible to produce TFEL displays that emit a true white color (e.g., Commission Internationale de l’Eclairage (CIE) coordinates $x \sim 0.40$, $y \sim 0.40$).²⁴ A comprehensive study of the influence of the growth technique, flux, co-activator, and charge compensation element selection in optimizing the performance of SrS:Cu thin film EL phosphors has been reported. It was shown that low temperature (<400 °C) elemental evaporation followed by a post-growth sulfur anneal dramatically enhances the performance of SrS:Cu thin film electroluminescent phosphors.²⁵ A process for doping Cu into SrS for thin-film EL devices has been reported recently.²⁶ The process involves the evaporation of dopant-containing material onto undoped SrS thin films and the rapid thermal annealing of the films. SrS:Cu,Na, (emitting

Table 1 CRT phosphors.

<i>JEDEC No.</i>	<i>Phosphor composition</i>	<i>Precursor</i>	<i>Use</i>
P-1	$Zn_2SiO_4:Mn^{2+}(Pb^{2+})^*$	ZnO, SiO ₂ , MnCO ₃ , (PbF ₂) [*]	Green-emitting (525 nm) phosphor for display (CRT)
P-2	ZnS:Cu	ZnS, CuS, MgCl ₂ , NaCl	Green-emitting (520 nm) phosphor long decay for radar
P-3	Zn ₂ BeSiO ₄ :Mn ²⁺	ZnO, BeO, SiO ₂ , MnCO ₃ , PbF ₂	Due to its composition now obsolete – used in earlier CRTs
P-4	ZnS:Ag ⁺ + ZnCdS ₂ :Ag ⁺	ZnS, (Zn _{0.834} -Ag _{0.166})S, MgCl ₂ , LiSO ₄ ZnS, (Zn _{0.68} -Ag _{0.32})S, CdS MgCl ₂ , LiSO ₄	Blue and yellow-emitting phosphor mix for the white in black and white television
P-5	CaWO ₄ :W	CaCO ₃ , WO ₃ , NaCl, PbCO ₃ .	Deep blue emitter, CRTs
P-11	ZnS:Ag ⁺ :Ni ²⁺	ZnS(Zn _{0.987} -Ag _{0.010} -Ni _{0.003})S ₂	Used in oscilloscopes where emission matched response curve of the then available photographic films. Blue-emitting phosphor.
P-12	(ZnMg)F ₂ :Mn ²⁺	ZnF ₂ ·4H ₂ O, MgF ₂ , MnF ₂	Radar tubes where moderate decay was desirable. Orange-emitting phosphor (588 nm)
P-15	ZnO:Zn	ZnO (reducing atmosphere)	Used originally in a flying spot scanner is applicable for any CRT requiring a highly visible screen and a fast decay. Green-emitting phosphor (515 nm).
P-16	Ca ₂ MgSi ₂ O ₇ :Ce	CaCO ₃ , 3MgCO ₃ ·Mg(OH) ₂ ·3H ₂ O, SiO ₂ , Ce(NO ₃) ₃ ·6H ₂ O	Flying spot scanners and other devices where a very fast decay is desired. UV emitting phosphor (380 nm).

Table 1 continued

<i>JEDEC No.</i>	<i>Phosphor composition</i>	<i>Precursor</i>	<i>Use</i>
P-19	KMgF ₃ :Mn ²⁺	KF, MgF ₂ , MnF ₂	(Orange emission, 585 nm) Radar CRT's
P-20	ZnCdS ₂ :Ag ⁺	ZnS, (Zn _{0.715} .Ag _{0.285})S ₂	Display tubes, phosphor is used for standard of comparison. Greenish-yellow emission (555 nm)
P-22	ZnS:Ag ⁺ + ZnCdS ₂ :Ag ⁺ + Y ₂ O ₃ :Eu ³⁺	Mix of phosphors, each phosphor prepared and applied separately. ZnS, (Zn _{0.88} .Ag _{0.12})S ₂ , MgCl ₂ LiSO ₄ ZnS, (Zn _{0.715} .Ag _{0.285})S ₂ , CdS MgCl ₂ .NaCl Y ₂ O ₃ :Eu _{0.65} , S	Color television (blue, green, and red emitters)
P-31	ZnS:Cu:Ni ²⁺	ZnS, (Zn _{0.88} Cu _{0.12})S ₂ , (Zn _{0.933} .Ni _{0.067})S ₂ MgCl ₂ , NaCl, BaCl ₂	Display screens including computer screens. Main emission peak at 554 nm. Ni ²⁺ is present to lower decay time
P-32	CaMg(SiO ₃) ₂ :Ti + ZnCdS ₂ :Cu	CaCO ₃ .3MgCO ₃ .Mg(OH) ₂ .3H ₂ O, TiO ₂ , H ₂ SiO ₃ , NH ₄ Cl, (NH ₄) ₂ SO ₄ ZnS, (Zn _{0.68} .Cu _{0.32})S, CdS, MgCl ₂ LiSO ₄	Cascade screen used primarily in military radar (made up of blue and yellow-emitting phosphors).
P-33	(K,Na)MgF ₃ :Mn	KF, MgF ₂ , MnF ₂ , NaF	Display screen. Orange emission at 588 nm
P-36	ZnCdS ₂ :Ag.Ni	ZnS, CdS, (Zn _{0.715} .Ag _{0.285})S ₂ , (Zn _{0.933} .Ni _{0.067})S ₂ , MgCl ₂ , NaCl, BaCl ₂	Fast decay screens for display. Yellow-green emission at 552 nm
P-37	ZnS:Ag:Ni	ZnS, CdS, (Zn _{0.715} .Ag _{0.285})S ₂ , (Zn _{0.933} .Ni _{0.067})S ₂ , MgCl ₂ , NaCl, BaCl ₂	Fast decay screens for display. Blue emission at 466 nm

P-38	MgZnF ₂ :Mn ²⁺	MgF ₂ , ZnF ₂ ·4H ₂ O, MnF ₂	Long decay time phosphor for use in radar. Orange emission at 575 nm
P-39	ZnSiO ₄ :Mn:As ³⁺	ZnO, SiO ₂ , MnCO ₃ , PbF ₂ , As ₂ O ₃	Long decay time phosphor for use in radar applications. Green emission at 525 nm. As ³⁺ added to promote longer decay
P-40	ZnCdS ₂ :Ag + ZnCdS ₂ :Cu	ZnS, CdS, (Zn _{0.834} Ag _{0.166})S, MgCl ₂ LiSO ₄ ZnS, (Zn _{0.834} Ag _{0.166})S, MgCl ₂ , LiSO ₄	“Penetration-phosphor screen”. Blue and yellow-green-emitting phosphors
P-43	Gd ₂ O ₃ :S:Tb ³⁺	Gd ₂ O ₃ :Tb _{0.075} , S	Green emitting (544 nm) phosphor for display screens and color televisions at high current densities better than other green phosphors
P-44	La ₂ O ₃ :S:Tb ³⁺	La ₂ O ₃ , Tb ₄ O ₇ , S	Green emitting (547 nm) phosphor for display screens and color television, not quite as bright as Gd ₂ O ₃ :Tb ³⁺
P-45	Y ₂ O ₃ :S:Tb ³⁺	Y ₂ O ₃ , Tb ₄ O ₇ , S	This phosphor has many emission lines in the blue, green, and red areas of the electromagnetic spectrum; screens made from it have a whitish appearance
P-46	Y ₃ Al ₅ O ₁₂ :Ce ³⁺	(Y _{0.988} , Ce _{0.012}) ₂ (C ₂ O ₄) ₃ ·3H ₂ O, Al ₂ O ₃	Yellow-emitting (526 nm) phosphor; decay time in nanoseconds
P-47	Y ₂ SiO ₅ :Ce ³⁺	Y ₂ O ₃ :Ce _{0.055} , H ₂ SiO ₃	Deep blue-emitting (centered at 415 nm) phosphor screen used wherever a very fast decay is needed, such as flying spot scanners
P-52	Y ₂ SiO ₅ :Tb	Y ₂ O ₃ :Tb _{0.075} , H ₂ SiO ₃	Projection color television tubes where high brightness maintenance is critical

* not always added.

green), SrS:Cu,Ag,Cl (emitting blue), and SrS:Ca,Cl (emitting greenish–blue) phosphors have been prepared using this methodology.²⁶

9.15.3.3 Vacuum Fluorescent Displays

Vacuum fluorescent displays (VFD) have been used since 1970. At the start they were in the form of single-digit round tubes, then multidigit tubes were developed, followed by flat multidigit panels.²⁷ These devices are now used in a wide range of applications, including audio and video equipment, home electronics, office equipment, and in road vehicles.²⁸

VFD tubes operate by the same principle as CRTs but use low-energy electrons (10–100 V) to excite the phosphor. The electrons are emitted from a cathode (wire) and are accelerated and controlled so that they bombard a phosphor-coated anode, causing the phosphor to emit light. ZnO:Zn (green-emitting) phosphors were used in early VFD devices, but as the application range expanded, demand developed for multicolored displays.²⁹

The influence of chemical modification of the surface of red, green, and blue phosphors on their low-voltage CL properties has been reported.³⁰ A series of VFDs has been prepared using ZnO:Zn, (Zn,Cd)S:Ag,In, ZnS:Cu,Al, ZnS:Ag,Cl, and Y₂O₂S:Eu phosphors. The surfaces were modified using a range of transparent wide band oxides such as SiO₂, WO₃, MoO₃, V₂O₅, TiO₂, and SnO₂ whose concentrations were varied from 0.05 to a few wt.%.³⁰ It was found that the CL efficiency, as well as chemical resistance and the service life of the phosphors, was increased by using low-energy electrons for excitation. The chief cause of the effect is claimed to be the formation of electrical fields in the surface layers, which facilitate migration of nonequilibrium carriers deep into the grain to less defective bulk layers with a high probability of radiative recombination.³⁰

As low-energy electron excitation is used, the phosphors need to have some conductivity.²⁹ One way of achieving this is to mix conductive materials (In₂O₃, SnO₂, and ZnO) with the high-resistance phosphors used in CRTs or color television screens (ZnS:Cu,Al (green), Y₂O₂S:Eu³⁺ (red), and ZnS:AgCl (blue)) to make a phosphor with a low resistance.³¹ Another way to achieve a phosphor with the desired properties is to use an inherently low-resistance phosphor; an example of this is (Zn_{1-x}Cd_x)S:Ag ($x = 0.75$), a red-emitting phosphor which is doped with Al (6×10^{-3} at. mol⁻¹).³²

9.15.3.4 Field Emission Displays

Field emission displays are VFDs that use field emission cathodes as the electron source. The cathodes can be molybdenum microtips,^{33–35} carbon films,^{36,37} carbon nanotubes,^{38–46} diamond tips,⁴⁷ or other nanoscale-emitting materials.⁴⁸ Niobium silicide applied as a protective layer on silicon tip field emission arrays has been claimed to improve the emission efficiency and stability.⁴⁹ ZnO:Zn is used in monochrome field emission device (FED) displays but its disadvantage is that it saturates at over 200 V.²⁹

Various forms of carbon material such as graphite, diamond, carbon nanotubes (fibers), and amorphous carbon-containing, diamond-like carbon have been compared and analyzed for their potential application in the fields of flat panel displays and lighting elements.⁴⁸

In order to achieve high brightness at low voltages in FEDs, beam currents higher than those normally applied to conventional CRTs are necessary, and this has led to breakdown of the material. Degradation of ZnS and Y₂O₂S:Eu³⁺ FED phosphors excited by an electron beam has been shown to result from electron-stimulated surface chemical reactions.⁵⁰ For example, ZnO was produced on the surface of ZnS, resulting in a surface “dead layer”, but O point defects in the near surface region also reduce the CL intensity.⁵⁰ The CL degradation of the commercial phosphor powder Y₂O₂S:Eu³⁺ was shown to be dependent on the surface loss of S and the conversion of the near-surface region to a luminescent Y₂O₃:Eu³⁺ phase.⁵¹ The near surface was converted from Y₂O₂S:Eu³⁺ to Y₂O₃:Eu³⁺ by electron beam-stimulated reactions involving oxygen-containing gas species and surface S.⁵¹ Sulfide phosphors also degrade because of volatilization of the surface sulfur and its dispersal into the vacuum causing contamination of the cathode materials and limiting electron emissions.^{52–55} To circumvent the problems encountered with metal sulfide phosphors, metal oxide analogs have been intensely studied.⁵⁶ Such materials include (Zn,Mg)O:Zn (blue), ZnGa₂O₄:Mn²⁺ (green), and CaTiO₃:Pr³⁺ (red). Metal oxide

phosphors have much greater stability than metal sulfide lattices, but are usually less efficient emitters at low voltage.

Another blue phosphor that has received attention for FED is $\text{YNbO}_4:\text{Bi}$ ⁵⁷ (emits at 440 nm). The bismuth-activated niobate phosphor system appears to be a promising candidate as a low voltage saturated blue phosphor.^{57,58} A saturated blue phosphor has also been produced by Ta replacement of Nb in the $\text{YNbO}_4:\text{Bi}$ lattice but it is less efficient.⁵⁸ The phosphor has been optimized in $\text{Y}_{1-x}\text{Bi}_x\text{NbO}_4$ ($x=0.005$) for low-voltage applications.⁵⁷ The luminance behavior of YNbO_4 and $\text{YNbO}_4:\text{Bi}$ have been investigated under UV and low-voltage electron excitations and interpreted with first-principle calculations.^{59,60} The calculations confirm that the charge transfer gap is between the Nb 4*d* and O 2*p* of the host YNbO_4 . For Bi-doped YNbO_4 the calculated partial density of states (PDOS) indicates that Bi 6*s* and O 2*p* PDOS are overlapped.^{59,60} The results are in broad agreement with the simple electronic band structure model put forward earlier; it was also demonstrated that the nature (symmetry) of the chemical environment of the Bi^{3+} is important for the influence of the cation on the luminescent properties.⁵⁷

A blue-emitting phosphor from the $\text{ZnO-Ga}_2\text{O}_3\text{-Li}_2\text{O}$ system has been developed for FED applications.⁶¹ $(\text{Li}_{0.5}\text{G}_{0.5})_{0.5}\text{Zn}_{0.5}\text{Ga}_2\text{O}_4$ was shown to have a CL efficiency up to 0.2 Lm W^{-1} in the voltage range 100–600 V. Although the intrinsic efficiency of this blue-emitting phosphor was found to be lower than ZnS:Ag,Cl , the good resistance to saturation of the oxide phosphor may make it more desirable for low-voltage FEDs operating at high current densities.⁶¹

Bright, well-saturated red, green, and blue CL has been produced in ZnGa_2O_4 thin films deposited by RF sputtering and implanted with Eu, Mn, and Ga ions. Luminescence in these phosphors was found to be critically dependent on post-implantation annealing conditions and substrate texture.⁶² It has been suggested that thin film deposition of a single layer of ZnGa_2O_4 with red, green, blue (RGB) luminescence centers introduced in this way may be a possible solution to FED fabrication.⁶²

A family of bright phosphors based on alkaline-earth gallates has been reported. Ce-doped SrGa_2O_4 has bright greenish-blue PL and CL; the emission spectra exhibit the characteristic Ce^{3+} double peaks.⁶³ $\text{BaGa}_2\text{O}_4:\text{Ce}$ has a very bright yellow-orange CL emission (560 nm). It is claimed that the two phosphors prepared from their precursors by high-temperature sintering are viable candidates for application in FEDs.⁶³

9.15.3.5 Plasma Displays

Plasma displays are based on the use of lamp phosphors which have been investigated for over 60 years. Optimization for plasma display panels (PDPs) has only taken place in the last few years and there is much room for improvement.

$\text{BaAl}_{12}\text{O}_{19}:\text{Mn}$ is the green phosphor preferred for PDPs.⁶⁴ However, a novel synthesis of bright green $\text{Ce}_{1-x}\text{Tb}_x\text{MgAl}_{11}\text{O}_{19}$ (CAT) phosphors suitable for plasma displays has also been described.⁶⁵ $\text{BaMgAl}_{10}\text{O}_{17}:\text{Eu}^{2+}$ is the blue phosphor of choice used for PDPs, although it is known to deteriorate during the manufacturing process and in operation.^{66,67} There is, however, no alternative yet available, and much research effort is directed at preventing this degradation.^{67–72} The red phosphor⁷³ used in PDPs is $\text{Y}_{0.65}\text{Gd}_{0.35}\text{BO}_3:\text{Eu}^{3+}$, which is efficient but its emission is too orange. $\text{Y}_2\text{O}_3:\text{Eu}^{3+}$ and $\text{Y(V,P)O}_4:\text{Eu}^{3+}$ would improve the color, but at the cost of efficiency. There is, as yet, no material comparable to $\text{Y}_2\text{O}_2\text{S}:\text{Eu}^{3+}$ (which is the red phosphor of choice for CRTs) for PDPs.

9.15.4 PHOSPHOR SYNTHESIS

The synthesis of inorganic phosphors has been the subject of intensive research for over 80 years. Much of the work has been carried out in industry and is not in the public domain. Accordingly, the literature on the manufacturing methods for industrial phosphors tend to be confined to specialist books rather than research journals, and for this reason the reader is referred to the well-known texts by Ropp^{8,74} which contain preparative details. Almost all were synthesized by solid-state reactions between very pure inorganic compounds at high temperature. It is impossible in the space available to discuss every aspect of synthesis from its inception to present-day, so priority has been given to discoveries and developments appearing in the last 5–10 years, and

significant reviews are cited where appropriate. The structures of most host lattices used for phosphors have been described and correlated by Wells⁷⁵ and others,⁷⁶ and the host lattice will, of course, determine the coordination environment of the dopant guest which can influence its emission behavior. Thus, zinc orthosilicate Zn_2SiO_4 contains ZnII ions in distorted tetrahedral O-donor sites; substitution of these by MnII ions results in green emission which has been attributed to the spin-forbidden ${}^4\text{T}_1({}^4\text{G}) \rightarrow {}^6\text{A}_1({}^6\text{S})$ $d-d$ transition of the Mn^{2+} ions.^{77,78} The influence of different site geometries for the dopant can be seen in the emission spectrum of $\text{SrY}_2\text{O}_4:\text{Eu}^{3+}$, which manifests two kinds of Eu^{3+} emission bands that are assigned to Eu^{3+} ions in the Sr site and the Y site.⁷⁹

The general properties of luminescent materials have been discussed in several texts.^{8,74,80,81} The most important lamp phosphors are listed in Table 2, together with their precursors used and some uses. Full synthetic details of most phosphors can be found elsewhere^{8,74} but an outline of traditional and newer methods is given below.

9.15.4.1 Traditional Solid-state Synthesis

The first step involves blending the compound which will act as the host lattice with the dopant (and/or co-dopant) and the fluxes, the mixture then being fired in an unreactive container. The dopant, usually in the form of a simple salt, can be added either during or after the firing of the host. The fired product is usually sintered and then crushed, milled, and sorted to remove the coarse particles. In some syntheses the product may then undergo surface treatments, and some or all of these processes may be carried out several times.

The host lattices are frequently prepared from ZnS , $\text{Zn}_{1-x}\text{Cd}_x\text{S}_2$, alkaline earth carbonates, MHPO_4 ($\text{M} = \text{Ca}$, Sr , or Ba), and $\text{MNH}_4\text{PO}_4 \cdot \text{H}_2\text{O}$ ($\text{M} = \text{Cd}$ or Mn).⁸ The general (industrial method) of preparation involves precipitation of the phosphor itself, or an intermediate, from solutions of pure cationic and anionic precursors. The purity of all materials used is vital, and impurities must not be present at levels great than 1.0 ppm. Impurities, which are detrimental to phosphor quality and are usually referred to as “killers”,⁷⁴ may include M^{2+} ($\text{M} = \text{Fe}$, Co , Ni , Cu , Pd , and Pt), M^{3+} ($\text{M} = \text{Ti}$, V , Cr , Fe , Ru , Zr , Nb , Mo , Rh , Hf , Ta , and W), and M^{4+} ($\text{M} = \text{Os}$, Ir , and Re). Such cations are usually removed by precipitation or sequestration by selective chelation on solutions before processing.⁸

A selection of important phosphors, together with their precursors and uses is given in Table 2. Those compounds based on oxide hosts are generally prepared from suitable metal and nonmetal oxides although, occasionally, fluoride salts have been used.⁸² Sulfides may be obtained by solid-state metatheses using, for example, sodium sulfide⁸⁶ (e.g., the Eu-doped strontium thiogallate phosphors $\text{Sr}_{1-x}\text{Eu}_x\text{Ga}_2\text{S}_4$) or by thermolysis of zinc and related sulfides. Nitride phosphors may be prepared by reaction of metal powders with Si_3N_4 (e.g., phosphors based on $\text{Mg}_x\text{Zn}_{1-x}\text{SiN}_2$ doped with Eu and Tb, which were evaluated as part of a program to develop phosphors for flat panel display applications).^{87,88}

The main drawbacks of solid-state techniques are that (i) the distribution of the dopant in the host lattice may not be even since the precursors are not mixed on the atomic scale, and (ii) particle growth cannot be easily controlled and so milling and sieving is necessary.

9.15.4.2 Hydrothermal and Related Methods

9.15.4.2.1 Homogeneous precipitation

Homogeneous precipitation of phosphors from solution affords the possibility of mixing the dopant into the host lattice at the atomic level without depending on high temperature diffusion. This provides more effective control over stoichiometry in the product. It also affords control over phosphor morphology which, for example, has facilitated the generation of spherical particles which will pack well in small pixel areas for high-definition display screens.⁸⁹⁻⁹⁹ In addition, the size of the final phosphor particle can be controlled by manipulating solution conditions in the precipitation process.¹⁰¹⁻¹⁰³ Nanocrystalline phosphors are believed to have more perfect lattices¹⁰⁴ and thus fewer bulk defects compared to conventional micron size phosphor particles. Emission studies of, for example, $\text{ZnS}:\text{Mn}^{2+}$ indicate that the intrinsic

Table 2 Commercially important phosphors.

<i>Phosphor (name or formula)</i>	<i>Precursors</i>	<i>Uses</i>
Calcium halophosphates, $\text{Ca}_5(\text{F,Cl})(\text{PO}_4)_3$	CaHPO_4 , CaCO_3 , CaF_2 , NH_4Cl , Sb_2O_3 , MnCO_3	White phosphors for fluorescent coating in low-pressure fluorescent lamps
$\text{Sr}_2\text{P}_2\text{O}_7\text{:Sn}^{2+}$	CaHPO_4 , SrHPO_4 , SnO , $(\text{NH}_4)_2\text{HPO}_4$, NH_4Cl	Blue-emitting phosphor used in blends with halophosphate phosphors for specific lamp colors
$(\text{SrMg})_3(\text{PO}_4)_2\text{:Sn}^{2+}$	SrHPO_4 , SrCO_3 , 3MgCO_3 , $\text{Mg}(\text{OH})_2 \cdot 3\text{H}_2\text{O}$, CaCO_3 , SnO	Deep red-emitting phosphor used in blends with halo phosphate phosphors for specific lamp colors
$(\text{SrZn})_3(\text{PO}_4)_2\text{:Sn}^{2+}$	SrHPO_4 , SrCO_3 , ZnO , Al_2O_3 , SnO	Used as red-emitting phosphor in high-pressure mercury vapor lamps
$\text{Zn}_2\text{SiO}_4\text{:Mn}^{2+}$	ZnO , SiO_2 , MnCO_3 , PbF_2	Green-emitting phosphor used in blends for specific lamp colors
$\text{Ca}_3\text{SiO}_3\text{:Pb}^{2+}\text{:Mn}^{2+}$	CaCO_3 , SiO_2 , PbF_2 , MnCO_3	Orange-emitting phosphor can be made redder. It was used in fluorescent lamps
$\text{MgWO}_4\text{:W}$	3MgCO_3 , $\text{Mg}(\text{OH})_2 \cdot 3\text{H}_2\text{O}$, WO_3	Blue-green emission used in white blends for fluorescent lamps
$\text{CaWO}_4\text{:Pb}^{2+}$	$\text{CaSO}_4 \cdot 2\text{H}_2\text{O}$, WO_3 , $\text{Pb}(\text{NO}_3)_2$	Blue emission used in blends for fluorescent lamps
$\text{Ba}_2\text{P}_2\text{O}_7\text{:Ti}$	BaHPO_4 , BaF_2 , TiO_2 , AlF_3 , BaO_2 , $(\text{NH}_4)_2\text{HPO}_4$	Broad emission centered at 494 nm used in many blends for fluorescent lamps
$\text{CdBO}_3\text{:Mn}^{2+}$	CdCO_3 , H_3BO_3 , MnCO_3	Red-emitting phosphor used in early fluorescent lamps now obsolete because of Cd disposal problem
$\text{Cd}_5\text{Cl}(\text{PO}_4)_3\text{:Mn}^{2+}$	$\text{CdNH}_4\text{PO}_4 \cdot 2\text{H}_2\text{O}$, CdO_2 , $\text{MnNH}_4\text{PO}_4 \cdot \text{H}_2\text{O}$, CdCl_2	Red-emitting phosphor used in white blends for fluorescent lamps
$\text{Mg}_4\text{FGeO}_6\text{:Mn}^{4+}$	3MgCO_3 , $\text{Mg}(\text{OH})_2 \cdot 3\text{H}_2\text{O}$, MgF_2 , GeO_2 , MnCO_3	Red-emitting phosphor used in both high pressure mercury vapor (HPMV) and fluorescent lamps
$\text{Mg}_5\text{As}_2\text{O}_{11}\text{:Mn}^{4+}$	3MgCO_3 , $\text{Mg}(\text{OH})_2 \cdot 3\text{H}_2\text{O}$, As_2O_3 , MnCO_3	Red-emitting phosphor now obsolete in USA (because of disposal of arsenic). Still used in Europe
$\text{Y}_2\text{O}_3\text{:Eu}^{3+}$	$(\text{Y, Eu})_2(\text{C}_2\text{O}_4)_3$	In fluorescent lamps but originally developed as a red-emitting phosphor for color televisions in 1959. ⁸²

Table 2 continued

<i>Phosphor (name or formula)</i>	<i>Precursors</i>	<i>Uses</i>
$YVO_4:Eu^{3+}$	$(Y, Eu)_2(C_2O_4)_3, V_2O_5$	Red-emitting phosphor used in blends with halophosphate phosphors for specific lamp colors. ⁸³
$YVO_4:Dy^{3+}$	Y_2O_3, Dy_2O_3	Can be used for calibration of optical equipment for quantum efficiency measurements. ⁸⁴
$Sr_5Cl(PO_4)_3:Eu^{2+}$	$SrHPO_4, SrCO_3, SrCl_2, Eu_2O_3$	Blue-emitting phosphor for high brightness fluorescent lamp (U-shaped)
$BaMg_2Al_{16}O_{27}:Eu^{2+}$	$3MgCO_3, Mg(OH)_2 \cdot 3H_2O, BaCO_3, Al_2O_3, EuCO_3$	Blue-emitting phosphor for high brightness fluorescent lamp (U-shaped), and as blue for plasma television
$SrMg_2Al_{18}O_{39}:Eu^{2+}$	$3MgCO_3, Mg(OH)_2 \cdot 3H_2O, SrCO_3, Al_2O_3, Eu_2O_3$	Another blue-emitting phosphor for high brightness fluorescent lamp
$Mg_3Al_{11}O_{19}:Ce^{3+}; Tb^{3+}$	$3MgCO_3, Mg(OH)_2 \cdot 3H_2O, Al_2O_3, Tb_4O_7, CeO_2$	Green emitting phosphor for high-output miniature fluorescent lamps
$BaSi_2O_5:Pb^{2+}$	$BaCO_3, SiO_2, PbF_2$	“Black light” lamps for plant growth. Emission at 355 nm
$(Ba, Sr)_2(Mg, Zn)Si_2O_7:Pb^{2+}$	$Ba(NO_3)_2, BaF_2, SrCO_3, ZnO, CaCO_3, 3MgCO_3, Mg(OH)_2 \cdot 3H_2O, SiO_2, PbO$	“Black light” lamps. Emission around 362 nm
$Y_3Al_5O_{11}:Ce^{3+}$	$Y_2(C_2O_4)_3 \cdot 3H_2O, Al_2O_3, CeCO_3$	Yellow-emitting phosphor. High-pressure mercury vapor lamps and high-output miniature lamps
$Sr_2P_2O_7:Eu^{2+}$	$SrHPO_4, EuCO_3, (NH_4)_2HPO_4$	Emission of this phosphor is near to the UV (420 nm). Lamps for photocopy machines
$YMg_2Al_{11}O_{19}:Ce^{3+}$	$3MgCO_3, Mg(OH)_2 \cdot 3H_2O, Y_2O_3, Al_2O_3, CeCO_3$	“Suntan” lamp for medical use phosphor emits in the near-UV (340 nm)
$MgGa_2O_4:Mn^{2+}$	$3MgCO_3, Mg(OH)_2 \cdot 3H_2O, Ga_2O_3, MnCO_3$	Green-emitting phosphor used in fluorescent lamps for photocopy purposes
$Sr_3(PO_4)_2:Eu^{2+}$	$SrHPO_4, SrCO_3, EuCO_3$	Blue-emitting phosphor used in photocopy lamps

luminescence efficiency of the doped phosphors can be drastically improved if the particle size is reduced to nanodimensions; in addition, lifetime shortening is reported.^{105–107}

One successful technique involves the addition of urea to metal salts in aqueous solution under conditions of pH which facilitate the decomposition of the urea and precipitation of metal hydroxycarbonates.^{89–100} This has led, for example, to the preparation of spherical particles of $\text{Y}_2\text{O}_3:\text{Eu}$ particles of 100, 200, 300, 400, and 500 nm dimensions having a size distribution that can be controlled to within 5%.^{92–97} $\text{Gd}_2\text{O}_3:\text{Eu}$ has been prepared similarly, giving particles of sizes between 70 nm and 250 nm.¹⁰⁸

Precipitation methods have also been developed for the preparation of metal sulfide and selenides.^{109–113} There are two general methods. The first involves treatment of aqueous metal salts, with or without added dopant, with hydrazine hydrate and either sulfur or selenium. This method has afforded metal chalcogenide phosphors such as $\text{ZnS}:\text{Ag}$, ZnSe , $\text{Zn}(\text{S},\text{Se})$, CdS , $\text{ZnS}:\text{Cu}$, $\text{ZnS}:\text{Cu},\text{Al},\text{Au}$,¹¹¹ $(\text{Zn},\text{Cd})\text{S}:\text{Cu}$, and $\text{Zn}(\text{S},\text{Se}):\text{Cu}$;^{109–111} this method was also extended to the synthesis of ternary metallo-sulfide phosphors such as $\text{Sr}_{0.97}\text{Ga}_2\text{S}_4:\text{Eu}_{0.03}$, $\text{Sr}_{0.985}\text{Ga}_2\text{S}_4:\text{Ce}_{0.015}$, $\text{Zn}_{0.98}\text{Ga}_2\text{S}_4:\text{Mn}_{0.02}$, $\text{Ca}_{0.8}\text{Ga}_2\text{S}_4:\text{Eu}_{0.2}$, and $\text{Ba}_2\text{Zn}_{0.985}\text{S}_3:\text{Mn}_{0.015}$.¹¹² The second method involves effecting decomposition of thiourea dioxide in aqueous solution at elevated temperatures in the presence of metal acetates, and has been used to prepare ZnS phosphors.¹¹³ The advantage of these new methods is that the elaborate techniques necessary for the removal of toxic gases or vapors (H_2S and CS_2) common in solid-state reactions are no longer required.¹⁰⁹

Precipitation may also be employed in solvents other than water. For example, nanocrystals of $\text{ZnS}:\text{Tb}$ could be prepared by a coprecipitation was effected by addition of aqueous sodium sulfide to $\text{Tb}(\text{NO}_3)_3$ and zinc acetate dissolved in methanol.¹¹⁴ $\text{ZnS}:\text{TbF}_3$ and $\text{ZnS}:\text{Eu}$ were prepared similarly. The photoluminescent intensities of the nanocrystals of $\text{ZnS}:\text{Tb}$ and $\text{ZnS}:\text{Eu}$ prepared in this way were 2.5 and 2.8 times stronger than those of bulk (conventionally prepared) phosphors, and these nanocrystals have been proposed for FED, EL, PDP, and CRT applications.¹¹⁴

Fine spherical $\text{Y}_2\text{O}_2\text{S}:\text{Eu}^{3+}$ has been from yttrium isopropoxide and europium chloride dissolved in absolute isopropyl alcohol, hydrolysis and precipitation being effected by water. Introduction of sulfur was achieved by grinding and firing the calcined product with sodium thiosulfate pentahydrate.¹¹⁵ Nanoparticles of ZnO-based phosphors have been prepared from aqueous propanol solutions of $\text{Zn}(\text{ClO}_4)_2$ containing sodium hexametaphosphate as capping agent.¹¹⁶ ZnS -based phosphors can be prepared similarly in basic aqueous methanolic solutions using trioctylphosphine oxide as capping agent and sulfide ions.¹¹⁶

9.15.4.2.2 Sol-gel methods

$\text{Zn}_2\text{SiO}_4:\text{Mn}^{2+}$ phosphors doped with $\text{Al}^{3+} + \text{Li}^+$ and $\text{Ga}^{3+} + \text{Li}^+$ ions were prepared by sol-gel methods using zinc acetate, ethanol, HNO_3 , and nitrates of Ga^{3+} and Al^{3+} . Lithium was introduced as the acetate or hydroxide, whereas Mn metal powder was dispersed in the host lattice by dry mixing into the calcined xerogel powders. The precursors were then reacted hydrothermally at 700 °C and 100 MPa.¹¹⁷ Other phosphors which have been produced by sol-gel techniques include $\text{Y}_2\text{SiO}_5:\text{Tb}^{3+}$,¹¹⁸ Li-doped $\text{Gd}_2\text{O}_3:\text{Eu}^{3+}$, $\text{Y}_2\text{O}_3:\text{M}^{3+}$, $\text{Y}_2\text{SiO}_5:\text{M}^{3+}$, and $\text{Y}_3\text{Al}_5\text{O}_{12}:\text{M}^{3+}$ (where $\text{M}^{3+} = \text{Eu}^{3+}$ or Tb^{3+}).^{119,120} Silica glass ceramics containing nanoparticles of TiO_2 doped with Er^{3+} and Yb^{3+} for up-conversion emission (anti-Stokes emission, see below) have also been prepared by sol-gel methods.¹²¹ The addition of titanium is believed to improve the chemical durability of the material and to increase the glass transition temperature.¹²²

The green CL-phosphors $\text{Y}_3\text{Ga}_5\text{O}_{12}:\text{Tb}^{3+}$, $\text{Y}_3\text{Al}_3\text{Ga}_2\text{O}_{12}:\text{Tb}^{3+}$, and $\text{Gd}_3\text{Ga}_5\text{O}_{12}:\text{Tb}^{3+}$, which are isostructural with yttrium aluminum garnet ($\text{Y}_3\text{Al}_5\text{O}_{12}$), were obtained as fine-grained crystalline powders following hydrothermal treatment of amorphous gels obtained by aqueous precipitation of Y, Gd, Al, Ga, and Tb salts.¹²³ Process parameters were identified that gave submicron powders without grinding making the method attractive for preparing such phosphors for FEDs and head-up displays.

9.15.4.2.3 Microemulsion methods

$\text{Y}_2\text{O}_3:\text{Eu}$ nanoparticles for potential use in FEDs have been prepared in nonionic reverse microemulsions.¹²⁴ The particles were synthesized by the reaction between aqueous yttrium nitrate, europium nitrate, and ammonium hydroxide, by bulk precipitation in the reverse microemulsion

composed of NP-5/NP-9, cyclohexane, and water. Compared with material prepared by the bulk precipitation method, the particles prepared by this technique showed a narrower size distribution, spherical shape, smaller size (20–30 nm), higher crystallinity, and stronger PL.¹²⁴

9.15.4.3 Other Solution-based Techniques

9.15.4.3.1 Combinatorial methods

The red phosphors $Y(\text{As}, \text{Nb}, \text{P}, \text{V})\text{O}_4:\text{Eu}^{3+}$ have been synthesized by combinatorial chemical methods.¹²⁵ The precursors, as oxides, were dissolved in weak acids and the required amount of each solution was injected by a computer-programmed system into a ceramic container. The solutions were evaporated, the container and residue pulverized and fired, and the PL performance of the calcined powders monitored. The apex compounds were $Y_{0.9}\text{PO}_4:\text{Eu}_{0.1}^{3+}$, $Y_{0.9}(\text{P}_{0.9}\text{V}_{0.1})\text{O}_4:\text{Eu}_{0.1}^{3+}$, and $Y_{0.9}(\text{P}_{0.9}\text{Nb}_{0.1})\text{O}_4:\text{Eu}_{0.1}^{3+}$, the maximum luminescence being observed with $Y_{0.9}(\text{P}_{0.92}\text{V}_{0.03}\text{Nb}_{0.05})\text{O}_4:\text{Eu}_{0.1}^{3+}$.¹²⁵ Eu and Tb-activated phosphors in the system $\text{MO}-\text{Gd}_2\text{O}_3-\text{Al}_2\text{O}_3$ ($\text{M} = \text{Ca}$ and Sr) have been prepared by polymeric-complex combinatorial chemical screening.¹²⁶ The technique is claimed as a powerful means of increasing the rate of synthesizing and screening new phosphors, though only “candidate” phosphors based on $\text{Gd}_{1-x-y-z}\text{Eu}_x\text{Ca}$ (or Sr) $_y\text{Al}_2\text{O}_8$ for red-emitting, $\text{Ca}_{0.3}\text{Eu}_x\text{Al}_{0.7}\text{O}_8$ for blue-emitting, and $\text{Sr}_{0.25}\text{Eu}_x\text{Al}_{0.75}\text{O}_8$, $\text{Ca}_{0.25}\text{Gd}_{0.25-x}\text{Tb}_x\text{Al}_{0.5}\text{O}_8$, $\text{Ca}_{0.65}\text{Tb}_x\text{Al}_{0.35}\text{O}_8$, $\text{Gd}_{0.4-x}\text{Al}_{0.6}\text{Tb}_x\text{O}_8$, $\text{Gd}_{0.7-x}\text{Al}_{0.3}\text{Tb}_x\text{O}_8$, and $\text{Sr}_{0.05}\text{Tb}_x\text{Al}_{0.95}\text{O}_8$ for the green-emitting phosphors were found.¹²⁶

9.15.4.3.2 Solution-coating methods

EL devices can be made using solution coating techniques which eliminate the need for vacuum processes.¹²⁷ Thin films of $\text{ZnGa}_2\text{O}_4:\text{Mn}^{2+}$ and $\text{Ga}_2\text{O}_3:\text{Mn}$ could be deposited on BaTiO_3 ceramic sheets by dip coating from the pentanedionato complexes $[\text{Zn}(\text{C}_5\text{H}_7\text{O}_2)_2]$, $[\text{Ga}(\text{C}_5\text{H}_7\text{O}_2)_3]$, and MnCl_2 dissolved in methanol or ethanol at 25 °C. The coated ceramic sheets were then heated at 500–950 °C for 30 s.¹²⁷

9.15.4.4 Vapor-phase Methods

9.15.4.4.1 Chemical vapor deposition

In chemical vapor deposition (CVD or MOCVD), a film of the desired material is prepared by evaporation of volatile precursor molecules which then decompose to give a film deposited on the substrate. The ordering in the film as it grows is dictated by the surface ordering of the substrate, hence the deposition is “epitaxial”. The necessary decomposition of the precursor molecules can take place either on the surface of the substrate or in the gas phase close to it.

This technique has been used to make thin and thick films of $\text{ZnS}:\text{Mn}$ phosphors for TFEL.^{128–144} Precursors include dimethyl zinc,^{128–130,136–141} $[\text{Mn}(\text{CO})_3(\text{Cp}')]$ ($\text{Cp}' = \text{methylcyclopentadienyl}$),^{130,141} methyl zinc dialkyl-dithiocarbamates,¹⁴² metal-organic tetramethylheptanedionate (thd) powders,¹⁴⁴ and zinc dithiophosphinates $[\text{Zn}(\text{S}_2\text{PR}_2)_2]$.¹⁴³ Among the phosphors prepared by this general method are $\text{CaGa}_2\text{S}_4:\text{Ce}$ ¹⁴⁵ and $\text{SrGa}_2\text{S}_4:\text{Ce}$.¹⁴⁶ Thin films of $\text{CaGa}_\alpha\text{S}_\beta:\text{Ce}$ films were prepared using $[\text{Ca}(\text{thd})_2]$, $\text{Ga}(\text{C}_2\text{H}_5)_3$, H_2S , and $[\text{Ce}(\text{thd})_4]$ as precursors,¹⁴⁷ and $\text{SrS}:\text{Ce}$ TFEL devices were prepared by MOCVD methods from $\text{Sr}(\text{thd})_2$, $\text{Ce}(\text{thd})_4$, and H_2S as precursors.¹⁴⁸

9.15.4.4.2 Molecular beam epitaxy and its derivatives

In molecular beam epitaxy (MBE), the constituent elements of the desired film in the form of “molecular beams” are deposited epitaxially onto a heated crystalline substrate. These molecular beams are typically from thermally evaporated elemental sources (e.g., evaporation of elemental As produces molecules of As_2 , As_3 , and As_4). A refinement of this is atomic layer epitaxy (ALE) (also known as atomic layer deposition, ALD) in which the substrate is exposed alternately to two

(or more) precursors, allowing the film to be grown with remarkable control, one layer of atoms at a time. In contrast to CVD (see above), these methods do not involve chemical decomposition of the vapor-phase precursor.

SrGa₂S₄:M (where M = Ce or Eu) thin films were grown in a MBE system from Sr metal, GaS₃ and CeCl₃ or EuCl₃.¹⁴⁹ The films manifested small grain size and high CL efficiency and were suitable for high-resolution emissive displays such as FEDs.

High luminosity blue-emitting films of CaS:Pb have been prepared by ALE using [Ca(thd)₂], Pb(C₂H₅)₄, and H₂S as precursors,¹⁵⁰ the emission intensity being strongly dependent on the Pb concentration, the growth parameters (e.g., temperature), and the precursors.¹⁵¹ ALE has been used to make ZnS:Mn for use in EL displays. Sources for zinc include ZnEt₂,^{152,153} ZnCl₂,¹⁵⁴ Zn(CH₃COO)₂,¹⁵⁴ and Zn₄O(CH₃COO)₆,¹⁵⁴ and the manganese may be introduced via [Mn(thd)₃],^{152,153} [Mn(Cp)₂],¹⁵³ or [Mn(CO)₃(MeCp)].¹⁵³ EL devices using ZnS:Tb(O,Cl) EL employed ZnS, Tb(thd)₃ and H₂S as precursors.¹⁵⁵ Films of SrS:Ce, for use as TFEL devices were prepared using [Sr(thd)₂], [Ce(thd)₄], and H₂S as precursors.¹⁵⁶

9.15.4.4.3 RF magnetron sputtering

In RF magnetron sputtering a “target” is bombarded with fast-moving ions which are generated by an electrical discharge in an inert gas (typically, argon) and directed onto the surface by a strong magnetic field. Momentum transfer results in atoms or molecules from the target being vaporized, and then deposited in the substrate. The advantage of this method is that, because it is a “cold” technique, it can be used to prepare films of a wide variety of conducting or insulating materials on many types of substrate. It is also cheaper and faster than MBE, although it lacks the remarkable control that MBE offers.

RF magnetron sputtering has been used either to introduce dopants into host lattices, or to coat surfaces with preformed phosphors. The former method has been used for doping a variety of gallium oxide and oxyanions (e.g., Ga₂O₃, MGa₂O₄, MGa₂O₄, M₃Ga₄O₉, M₃Ga₂O₆, and MGa₄O₇ where M = Ca, Sr, or Ba) with Eu, Tb, Pr, or Dy,¹⁵⁷ and in making some forms of Mg_{0.5}Zn_{0.5}SiN₂:Eu⁸⁷ and Mg_xZn_{1-x}SiN₂.⁸⁸ The latter technique was useful for sputtering manganese-doped ZnS onto Si substrates,¹⁵⁸ for depositing thin films of lanthanide-doped alkaline earth thiogallates Ca_{1-x}Sr_xGa₂S₄:Ln phosphors onto ceramic substrates,¹⁵⁹ and for depositing thin films of Y₂O₃:Mn onto BaTiO₃ ceramic sheets.¹⁶⁰

Zn₂GeO₄:Mn films deposited by RF-magnetron sputtering were investigated as a potential green-emitting phosphor for TFEL devices.^{161,162} Y₄GeO₈:Mn, Y₂GeO₅:Mn, and Y₂Ge₂O₇:Mn phosphor thin films were deposited onto thick ceramic sheets by RF sputtering using (Y₂O₃-GeO₂):Mn phosphor targets.¹⁶³ High-luminance yellow emissions were obtained in TFEL devices, and it was concluded that the new oxides are very promising as host materials for EL phosphors.¹⁶³

9.15.4.4.4 Electron beam evaporation

Films of SrS:HoF₃, useful as white EL devices, were deposited by electron beam evaporation of SrS pellets and HoF₃ powder.¹⁶⁴

9.15.4.4.5 Pulsed laser decomposition

Eu³⁺-activated Y₂O₃ phosphor films have been grown *in situ* on silicon- and diamond-coated silicon substrates using this technique.¹⁶⁵ Thin films of the silicate phosphors CaSiO₃:Mn,Pb (red emitting), ZnSiO₄:Mn (green emitting), and Y₂SiO₃:Ce (blue emitting) have also been prepared by this method; a good correlation was found between photoluminescence intensity, and film crystallinity and surface morphology.¹⁶⁶

9.15.4.4.6 Ion implantation

Ion-implanted ZnGa₂O₄ thin films have been produced on flexible organic (polyimide) substrates.¹⁶⁷ Preliminary CL results indicate brightness levels comparable to similar films on

glass. Green CL was achieved by implanting Mn ions into sputter-deposited ZnGa_2O_4 films, followed by a “low” temperature (450 °C) anneal.¹⁶⁷

9.15.4.4.7 Aerosol spray pyrolysis

This method uses a solution of the desired metal ion precursors that is passed through a nozzle using a carrier gas to produce small droplets. These droplets are passed through a high-temperature furnace which transforms their contents into spherical metal oxide particles. Phosphors prepared by such methods include $\text{Y}_2\text{O}_3:\text{Eu}^{3+}$,^{168–170} $\text{BaMgAl}_{10}\text{O}_{17}:\text{Eu}^{2+}$,¹⁷¹ $\text{Zn}(\text{Ga}_{1-x}\text{Al}_x)_2\text{O}_4:\text{Mn}$,¹⁷² $\text{ZnGa}_2\text{O}_4:\text{Mn}$,¹⁷³ and $\text{Gd}_2\text{O}_3:\text{Eu}$.¹⁰⁸ Thin films of $\text{ZnO}:\text{Zn}$,¹⁷⁴ $\text{Y}_2\text{O}_3:\text{Eu}$,¹⁷⁴ and the blue emitter $\text{YNbO}_4:\text{Bi}$ ¹⁷⁵ have also been prepared by this method. $\text{Gd}_2\text{O}_3:\text{Eu}$ phosphor particles of spherical and filled morphology have been prepared by spray pyrolysis.¹⁰⁸ A typical preparation of $\text{Zn}_2\text{SiO}_4:\text{Mn}$ particles involved solutions of tetraethylorthosilicate, zinc acetate, and manganese acetate as precursors, and used nitric acid to control pH. The technique is also useful for developing particles with controlled morphology, and films from colloidal suspensions.^{170,176–178}

9.15.4.4.8 Charged liquid cluster beam methods

Deposition of Mn-doped Zn_2SiO_4 for PDPs has been achieved using a charged liquid cluster beam (CLCB) technique.¹⁷⁹ This methodology is inherently suited to the fabrication of uniform, conformal coatings of controlled chemical compositions and stoichiometries. The technique utilizes nanometer-scale charged drops of liquid precursors for thin-film deposition and makes use of atomic scale mixing present in these liquids to achieve a film of uniform stoichiometry. The morphology and PL intensity of films of $(\text{Zn}_{1-x}\text{Mn}_x)_2\text{SiO}_4$ prepared by the CLCB technique were dependent on the deposition conditions.¹⁷⁹

9.15.5 ORGANO-ELECTROLUMINESCENT DEVICES

The fabrication of a *tris*(8-hydroxyquinolino)aluminum (AlQ_3)-based multilayer thin film device by Tang *et al.* in 1987^{180,181} stimulated the search for new types of electroluminescent materials based on organic compounds. The group of materials which are based on organic, organometallic, and coordination compounds is known collectively as organo-electroluminescent devices (OLEDs). OLEDs are already in use in camcorders and as backlights because of their high luminous efficiencies, operational stabilities, ease of fabrication, and the ability to prepare different samples whose emission wavelengths cover the whole visible region.^{182–184} Current initiatives aim to develop OLEDs as diffuse light emitters for domestic and commercial use.

To date, most small molecule-based OLEDs are prepared by vapor deposition of the metal-organic light-emitting molecules. Such molecules must, therefore, be thermally stable, highly fluorescent (in the solid state), form thin films on vacuum deposition, and be capable of transporting electrons. These properties limit the number of metal coordination compounds that can be used in OLED fabrication.

Coordination compounds used in OLEDs frequently contain metal ions from Groups 2 or 13. Of these, Be^{2+} and Zn^{2+} (both with a coordination number of four), and Al^{3+} (coordination number of six), are the most important; examples are discussed in the following sections.

9.15.5.1 Coordination Compounds as Organo-electroluminescent Devices

9.15.5.1.1 Group II metal complexes

Bis(10-hydroxybenzo[*h*]quinolino)beryllium, $[\text{Be}(\text{bq})_2]$, Figure 1(a) is a green emitter,¹⁸⁵ whereas *bis*[2-(2-hydroxyphenyl)benzothiazolato]zinc ($\text{Zn}(\text{BTZ})_2$, Figure 1(b)) emits a broad greenish-white band.¹⁸⁶ $\text{Be}(\text{PBI})_2$ is a blue emitter (PBI is *o*-[(*N*-phenyl)-2-benzimidazolyl]phenolate; see Figure 1(c)).¹⁸⁷

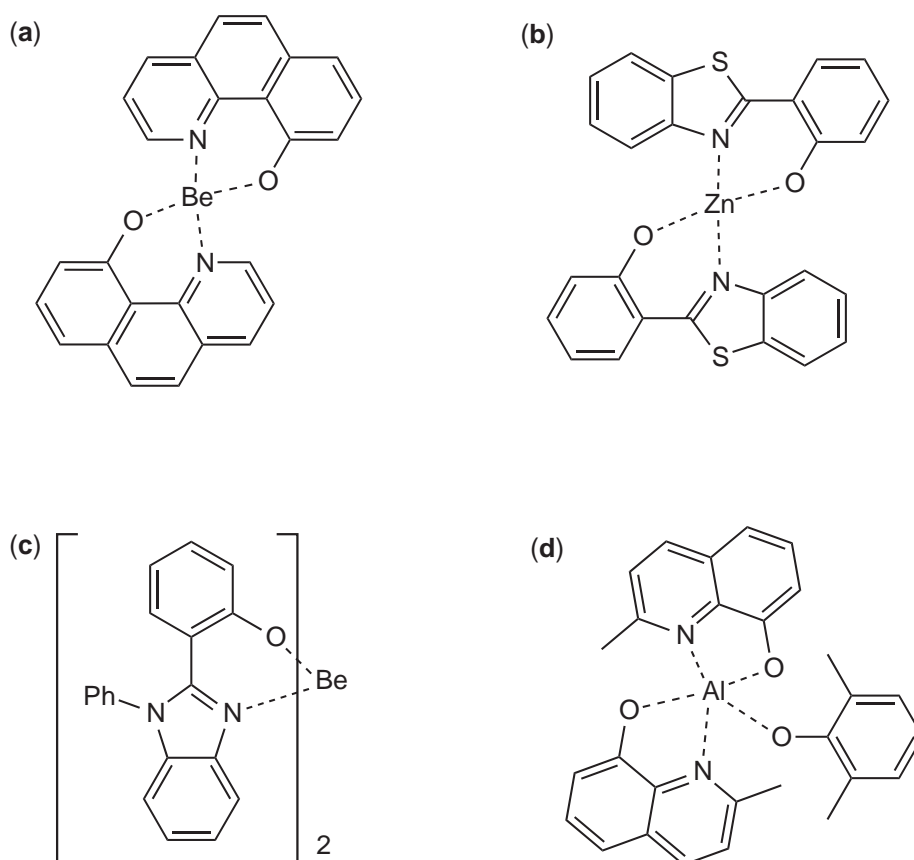


Figure 1 Structures of some metal complex phosphors: (a) $[\text{Be}(\text{bq})_2]$,¹⁸⁴ (b) $[\text{Zn}(\text{BTZ})_2]$,¹⁸⁵ (c) $[\text{Be}(\text{PBI})_2]$,¹⁸⁶ and (d) $[\text{Al}(\text{Q}')_2(2,6\text{-dimethylphenolate})]$.¹⁸⁶

9.15.5.1.2 Tris(8-hydroxyquinolato)aluminum and related complexes

The discovery of the use of AlQ_3 as an electron-transport-emitting layer is undoubtedly the most significant achievement in the research that led to the development of stable OLEDs.^{180,181} It is very stable and can be sublimed without decomposition at 350°C ,¹⁸⁸ and its thin-film PL quantum efficiency at room temperature is about 32%, independent of film thickness between 10 nm and 1,350 nm.¹⁸⁹

A typical multilayer thin film OLED is made up of several active layers sandwiched between a cathode (often Mg/Ag) and an indium-doped tin oxide (ITO) glass anode. The cathode is covered by the electron transport layer which may be AlQ_3 . An emitting layer, doped with a fluorescent dye (which can be AlQ_3 itself or some other coordination compound), is added, followed by the hole transport layer which is typically α -naphthylphenylbiphenyl amine. An additional layer, copper phthalocyanine is often inserted between the hole transport layer and the ITO electrode to facilitate hole injection.

The AlQ_3 layer in the OLED structure is responsible for broadband green EL emission. Other colors can be produced by introducing various fluorescent molecules into the emitting layer (as dopants) or by replacing the emitting layers with these molecules. The preferred method for controlling the EL colors is by doping a guest molecule into the AlQ_3 host-emitting layer.¹⁸¹ The guest molecule emits at its characteristic wavelength either by direct excitation or via energy transfer from the host. The doped AlQ_3 layers have been shown to have a better than three-fold increase in efficiency than the undoped layers.¹⁹⁰

Some useful general rules which seem to account for the fluorescent properties of metal coordination complexes of 8-hydroxyquinoline have been proposed.^{191,192} These are:

- (i) Complexes containing paramagnetic metal ions (such as Cr^{3+}) are essentially nonfluorescent (due to a high rate of intersystem crossing from the excited singlet to the triplet state)

- (ii) Fluorescence decreases with increasing atomic number of the metal ion – this is also caused by an increase in the rate of intersystem crossing, and is known as the “heavy atom effect”, as shown by the relative fluorescence intensities for the series $\text{AlQ}_3 > \text{GaQ}_3 > \text{InQ}_3$
- (iii) When the covalent nature of the metal–ligand bonding (primarily metal–nitrogen) is increased, the emission is at longer wavelength. In contrast, more ionic metal–ligand bonding results in a blue shift; e.g., MgQ_2 emits at 500 nm, whereas ZnQ_2 emits at 557 nm.¹⁸⁷

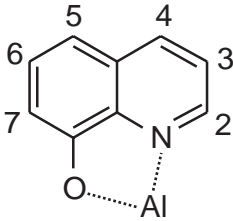
AlQ_3 layers in OLEDs continue to be a focus of attention as their stability and light-emitting properties still leave room for improvement.^{193,194} From predictions made by molecular modeling,¹⁹⁵ substitution of an electron-withdrawing substituent at C-5 or C-7 of the hydroxyquinolate ligand (see Figure in Table 3 for the numbering scheme) causes a blue shift of the absorption spectrum of AlQ_3 , whereas an electron-withdrawing group at the C-4 or C-2 position results in a red shift.¹⁸⁷ Moreover, if the substituents are electron donating, the direction of the spectral shifts will reverse. This is illustrated in Table 3 in which the PL properties of several substituted AlQ_3 complexes are compared with those of the parent complex in solution or in the solid. Table 3 reveals that the blue shift caused by an electron acceptor group at C-5 (such as CN)¹⁹⁶ is small compared to the donating effect at C-4 (e.g., Me). This result is also in keeping with a ZINDO semi-empirical MO calculation.¹⁹⁶

As a blue EL emitter is necessary for full-color displays, efforts have been made to shift the emission of AlQ_3 .¹⁹⁷ Although the emission from *tris*(4-methyl-8-hydroxyquinolinato)-aluminum(III) is blue shifted with respect to that from AlQ_3 , it occurs at about 515 nm which is not suitable for use as the blue emitter in a display system. Methyl substitution at the C-2 position, to give 8-hydroxy-2-methylquinolate (Q') might be desirable, but formation of AlQ'_3 is sterically inhibited. Attempts to isolate this complex resulted only in the formation of the unstable $[(\text{Q}'\text{Al})_2\text{O}]$ which emits at 490 nm.¹⁹⁸ Formation of $[\text{Q}'_2\text{Al-R}]$, where R is an anionic phenolate or an aryl carboxylate ligand, has led to more stable species with suitable blue emissions.¹⁹⁹ When R is sterically bulky, as in 2,6-dimethylphenolate (see Figure 1(d)) the Al^{3+} is shielded from nucleophilic attack and the complex is more stable.¹⁸⁷

Other attempts have been made to design ligands that alter the $\pi-\pi^*$ transition of Q without distorting the overall molecular shape of AlQ_3 . Incorporation of a “heteroatom” into the 8-hydroxyquinoline ring system seemed to be the most promising and, indeed, complexes of 5-hydroxyquinoxaline, AlX_3 ,¹⁹⁵ generated a PL emission at 580 nm, red shifted by ca. 50 nm relative to AlQ_3 . This bathochromic shift, which was predicted by ZINDO calculations, has been ascribed to the intrinsic electron-withdrawing nature of the nitrogen atom which replaces the CH at the four position of the hydroxyquinolate ligand.¹⁸⁷ A blue shift of ca. 90 nm compared to AlQ_3 (to 440 nm) has been by replacing the CH group at the five position of the quinolate ligand by a nitrogen atom, generating $\text{Al}(\text{NQ})_3$.²⁰⁰ Single crystal X-ray diffraction studies of both AlQ_3 and $\text{Al}(\text{NQ})_3$ showed that they have virtually identical molecular shapes with the Al–O and Al–N bond lengths of $(1.84 \pm 0.02 \text{ \AA})$ and $(2.04 \pm 0.02 \text{ \AA})$, respectively.²⁰¹

$[\text{Al}(\text{PBI})_3]$ (c.f. the BeII analogue mentioned above and in Figure 1(c)) is also a stable complex which can be thermally evaporated and also emits in the blue region of the spectrum.¹⁸⁷

Table 3 Photoluminescence properties of substituted AlQ_3 complexes.

	Substituent group and literature reference	λ_{max} (nm)
	5-CN ¹⁹⁵	525
	5-H ¹⁸¹	528
	5-Cl ¹⁸⁸	530
	5-F ¹⁹⁴	543
	5-Me ¹⁸⁶	559
	4-Me ¹⁸⁶	515
	Ligand numbering scheme	7-n-Pr ¹⁸⁰

9.15.5.1.3 Lanthanide β -diketonate complexes

Vacuum-deposited thin films of lanthanide β -diketonate complexes are useful in OLEDs.²⁰² The complexes $[\text{Eu}(\text{TTFA})_3(\text{phen})]$,^{202,203} $[\text{Tb}(\text{ACAC})_3(\text{phen})]$ (ACAC = acetylacetonate), and $[\text{Dy}(\text{BTFA})_3(\text{phen})]$ were prepared for this purpose, and their structures are shown in Figure 2(a)–(c). EL devices with molecular beam-deposited Eu and Tb emitter layers based on these complexes manifest nearly monochromatic red (613 nm) and green (543 nm) emission, respectively. The potential of a Dy complex for white light devices was also demonstrated.²⁰² In addition to their very narrow emission bands, one of the principal reasons to use lanthanide coordination complexes as emitters in OLEDs is their potentially high internal quantum efficiencies. This occurs because the luminescence of lanthanide coordination compounds is based on intramolecular energy transfer from the triplet excited state of the chelating ligand to the $4f$ states of the metal ions. The result is that the theoretical internal quantum efficiency is, in principle, not limited. In contrast, organic molecules produce emission from $\pi \rightarrow \pi^*$ transitions resulting in broad bandwidths (160–200 nm) and spin statistic estimations indicate that internal quantum efficiencies are limited to about 25%.

The pentanedionates $[\text{Tb}(\text{ACAC})_3]$ and $[\text{Tb}(\text{ACAC})_3(\text{phen})]$ have both been shown to generate green emission in OLEDs.²⁰⁴ OLEDs containing $[\text{Eu}(\text{DBM})_3(\text{phen})]$ or $[\text{Eu}(\text{DBM})_3(\text{bath})]$ (Figure 2(d) and (e)) generate red emission whereas $[\text{Tb}(\text{ACAC})_3(\text{phen})]$ is a green emitter.²⁰⁵ EL at 980 nm has been demonstrated using *tris*(8-hydroxyquinolino)-ytterbium(III) (YbQ_3),²⁰⁶ while

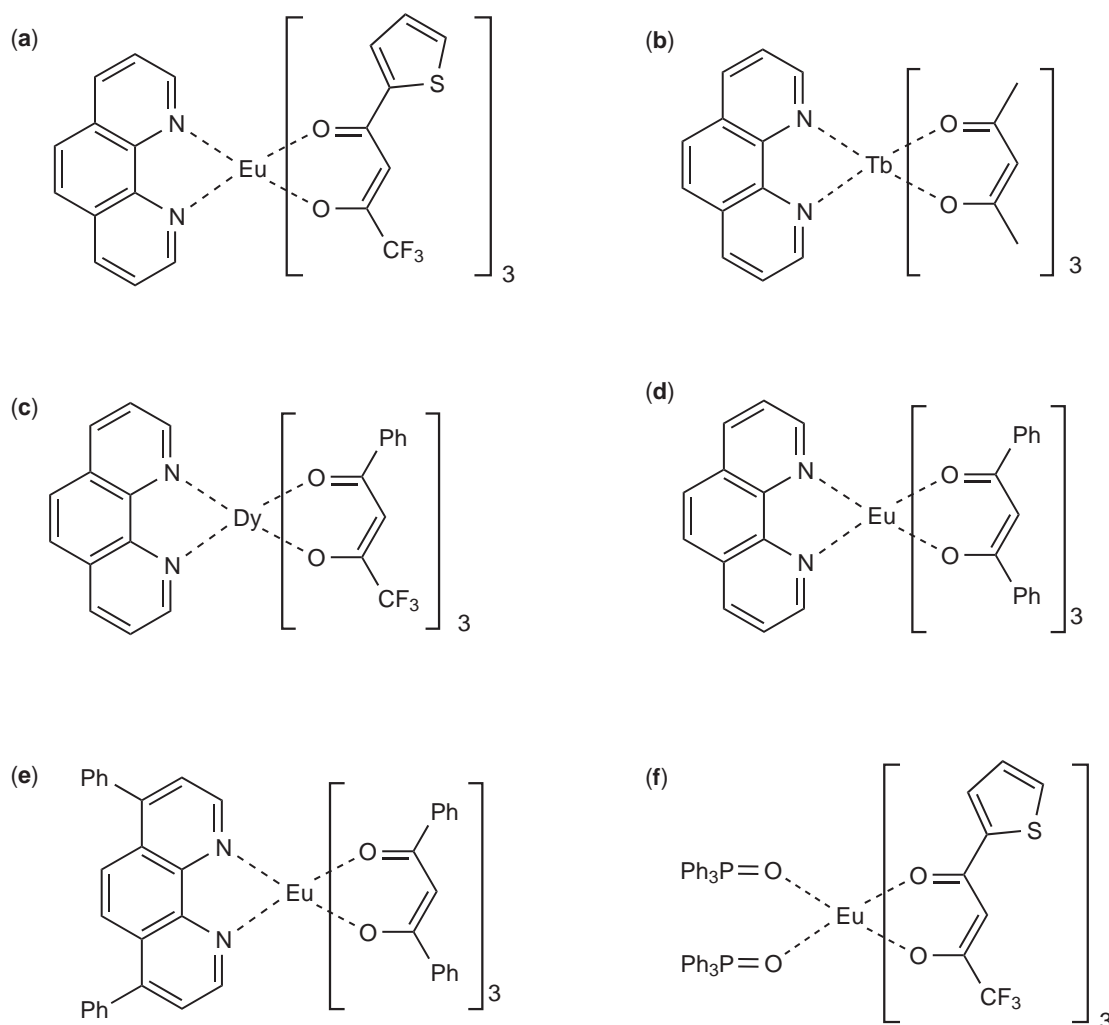


Figure 2 Structures of some lanthanide complex phosphors: (a) $[\text{Eu}(\text{TTFA})_3(\text{phen})]$, (b) $[\text{Tb}(\text{ACAC})_3(\text{phen})]$, (c) $[\text{Dy}(\text{BTFA})_3(\text{phen})]$, (d) $[\text{Eu}(\text{DBM})_3(\text{phen})]$, (e) $[\text{Eu}(\text{DBM})_3(\text{bath})]$ and (f) $[\text{Eu}(\text{TTFA})_3(\text{TPPO})_2]$ (see Section 9.15.5.1.3).

ErQ₃ gives both PL and EL emission at 1,500 nm.^{207–209} Red light (614 nm) is emitted by [Eu(TTFA)₃(phen)] (Figure 2(a)) doped in a poly(*N*-vinylcarbazole) layer.²¹⁰ The complex [Eu(TTFA)₃(TPPO)₂] (TPPO = triphenylphosphine oxide, see Figure 2(f)) emits in the red when incorporated in OLEDs,^{211,212} behavior which is enhanced when the material is heat treated.²⁰⁴ Near-IR EL and PL emission was observed from blends of poly(*p*-phenylene-vinylene) with [Yb(TPP)(ACAC)] and [Er(TPP)(ACAC)] (H₂TPP is 5,10,15,20-tetraphenylporphyrin) by both EL and PL.²¹³

9.15.5.1.4 Other metal complexes

The *ortho*-metalated complex *fac*-{Ir[C₆H₄(2-py)]₃} (the ligand is the C–N coordinated anion of 2-phenylpyridine, Figure 3(a)) has been shown to undergo triplet emission when incorporated into OLEDs (PL emission is at 510–515 nm).^{214–217} Compared to phosphors such as 2,3,7,8,12,13,17,18-octaethylporphinato-platinum(II) (Pt(OEP)),²¹⁸ (see next paragraph), these Ir^{III} complexes manifest both high internal quantum efficiencies and relatively short triplet lifetimes. The shorter lifetimes are advantageous as they minimize triplet annihilation, thereby reducing losses at high current densities.²¹⁹ A number of other iridium(III) complexes based on cyclometalated ligands exhibit high efficiency electrophosphorescence in OLEDs when doped into hosts having wide energy gaps.²²⁰ Examples include [(btp)₂Ir(ACAC)] (btp = 2-(2'-benzo[4,5-*a*]thienyl)pyridinato-*N*,C³; Figure 3(b)), an efficient red phosphor (λ_{max} = 616 nm), and [(dfpp)₂Ir(pic)] (dfpp = 4,6-difluorophenyl-pyridinato-*N*,C^{2'}; Figure 3(c)), which has a blue emission at 470 nm.²²⁰ Numerous phosphorescent complexes of the type [Ir(N-C)₂(ACAC)] (where N-C denotes an anionic, cyclometalated, *N*,*C*-donor bidentate ligand) were evaluated as phosphors for OLEDs, and have emission maxima spanning a wide range (yellow, green, and red) according to the nature of the cyclometalating ligand (e.g., see Figure 3(d)).^{220,221}

Red electrophosphorescent devices employing exciton blocking have been demonstrated.²²² These devices contained the luminescent dye [Pt(OEP)], doped into a 4,4'-*N*, *N'*-dicarbazolebi-

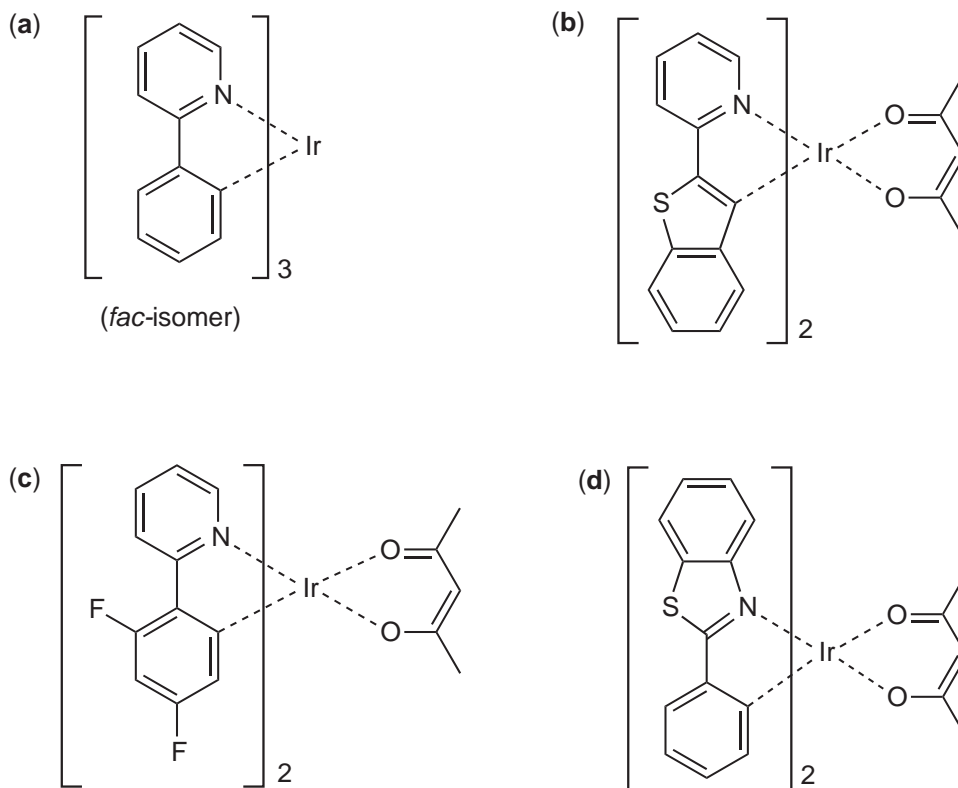


Figure 3 Structures of some Ir^{III} complex phosphors based on cyclometalating N,C-donor ligands (see Section 9.15.5.1.4).

phenyl (CBP) host. Because of weak overlap between excitonic states in [Pt(OEP)] and CBP, efficiency losses due to nonradiative recombinations are low.²²²

9.15.5.2 Novel Organo-electroluminescent Devices/Inorganic Devices

A novel EL device in which UV light at 350 nm emitted by a poly(dimethylsilane) layer is converted by phosphors into visible light emission has been described.²²³ The phosphors used were $\text{Y}_2\text{O}_2\text{S}:\text{Eu}$, $\text{ZnS}:\text{Cu,Al}$, and $\text{ZnS}:\text{Ag,Al}$ for red, green, and blue, respectively, and the result is a full color LED.²²³ LEDs based on polymer/inorganic heterostructures have also been described.²²⁴ Poly[(2,5-didodecyloxy)-1,4-phenylenevinylene]/ZnO:Zn interfaces have been studied and show far superior brightness and luminous efficiency in comparison with single polymer diodes. The EL spectrum of the bilayer device shifts continuously as the applied voltage increases; the shift is ascribed to the superposition of emission from the polymer layer and the inorganic layer.²²⁴

9.15.5.3 Problems with Organo-electroluminescent Devices

The OLED technology, though advancing rapidly, still has some unresolved technical issues. These include: differential aging of the three different emissive colors (for full color display), patterning for full color, and high-temperature performance.²²⁵ The problem of degradation of OLEDs has been receiving continuous attention; moisture has been shown to cause dark spots,^{226,227} and an excess of "holes" in the AlQ_3 layer results in rapid decay of the luminescence.²²⁸ Cu^{II} -phthalocyanine has been introduced to control "hole" entry.²²⁸

9.15.6 LIGHT-EMITTING DIODES

Much progress has been achieved in LEDs since the 1980s. They have become much more efficient and are now the point light sources of choice. Recent technological progresses in the color conversion by suitable phosphors has brought solid-state lighting nearer to reality.²²⁹

The mechanism of acceptor-compensation, which prevents low-resistivity *p*-type GaN and AlGaIn from being prepared, has been elucidated.²³⁰ For Mg-doped *p*-type GaN, the Mg acceptors are deactivated by atomic hydrogen which originates from the NH_3 gas used as a source of nitrogen during GaN growth. After growth, thermal annealing in an N_2 atmosphere was shown to reactivate the Mg acceptors.²³⁰ Blue-emitting GaInN/AlGaIn LEDs exhibiting high brightness were made on the basis of these results, and luminous intensities of over 2 candelas have been demonstrated.²³⁰⁻²³² A range of blue/green GaInN single-quantum-well LEDs with a narrow spectrum width have been developed and are now commercially available.^{233,234} High-power LEDs based on GaN/InGaIn prepared by MOCVD process have been described.²²⁹ Garnet phosphors have been investigated for the preparation of white LEDs.²³⁵ A series $(\text{Gd}_x\text{Y}_{1-x})_3\text{Al}_5\text{O}_{12}:\text{Ce}^{3+}$ (with varying Gd content x) has been investigated at constant Ce concentrations as well as with varied dopant concentration.²³⁵ Good ZnS films have been grown on Si substrates; the material shows promise as a blue LED.²³⁶

9.15.7 ANTI-STOKES PHOSPHORS

An anti-Stokes (or up-converting) phosphor is one which takes multiple photons of lower energy and converts them to one photon of higher energy. The principle was first suggested in 1959.²³⁷ Up-conversion materials are currently used in the detection of light from laser diodes²³⁸ and in optical fiber-based telecommunications.²³⁹ A significant improvement in up-conversion efficiencies was realized by incorporating the near-IR-emitting Yb^{3+} ion as a sensitizer and utilizing energy transfers between lanthanide ions for the up-conversion.²⁴⁰ Among the materials now used are $\text{Y}_{0.78}(\text{Yb}_{0.20}\text{Er}_{0.02})\text{F}_3$,²⁴¹ $\text{NaY}_{0.69}(\text{Yb}_{0.30}\text{Er}_{0.01})\text{F}_4$,²⁴¹ $\text{BaY}_{1.34}(\text{Yb}_{0.60}\text{Er}_{0.06})\text{F}_3$,²⁴² and $\text{Y}_{0.65}(\text{Yb}_{0.35}\text{Tm}_{0.001})\text{F}_3$.²⁴¹ The fluoride species (particularly as glasses) have been used in many applications and have a number of advantages over other materials.²⁴³ However, it has now been established that chloride systems such as $\text{BaCl}_2[(\text{ErCl}_3)_{0.25}(\text{BaCl}_2)_{0.75}]$ ²⁴⁴⁻²⁴⁶ are more suitable hosts than fluorides for Er^{3+} ions, although moisture sensitivity of these compounds

requires protection procedures.²⁴⁷ The Er^{3+} ion is particularly useful in doped fiber amplifier applications since it can provide significant optical gain in the 1,530–1,570 nm low-loss window of fibers.²⁴⁸

Possible future applications of up-converting phosphors include (i) three-dimensional displays,^{249–251} (ii) fiber optic amplifiers (referred to above) that operate at 1.55, 1.46, and 1.31 μm ,^{239,251–255} (iii) up-conversion lasers,²⁵⁰ and (iv) remote sensing thermometers for high-temperature applications (utilizing the temperature dependence of optical properties of, for example, cubic $\text{Y}_2\text{O}_3:\text{Er}^{3+}$).^{256–258}

It was relatively recently reported that the absorption cross-section (or oscillator strength) of the ${}^4\text{I}_{15/2} \rightarrow {}^4\text{F}_{9/2}$ transition of Er^{3+} is larger than those of the IR ${}^4\text{I}_{15/2} \rightarrow {}^4\text{I}_{11/2}$ and ${}^4\text{I}_{15/2} \rightarrow {}^4\text{I}_{9/2}$ IR transitions.²⁴⁷ For this reason red light excitation (in the 620–650 nm range) results in more efficient pumping compared to that possible with 974 nm or 800 nm light.²⁵⁶ This finding was confirmed by studies on Er^{3+} luminescence from cubic $\text{Y}_2\text{O}_3:\text{Er}^{3+}$ materials,^{256,257} which included temperature-dependent studies.²⁵⁷ The temperature dependence of the anti-Stokes properties of cubic $\text{Y}_2\text{O}_3:\text{Er}^{3+}$ were also studied.⁹⁷ All the emission features exhibited a marked thermal dependence, decreasing in intensity as the temperature was lowered. It was shown that the Er^{3+} ions were thermally excited to a low lying level ca. $1,300\text{ cm}^{-1}$ above the ground state.⁹⁷ Subsequent absorption of a 632.8 nm photon by the thermally excited Er^{3+} ion promoted it to its ${}^5\text{D}_0$ level; thus, the up-conversion was obtained only because the thermal energy (phonon energy) coupled to the vibrational levels and this was added to the red laser energy of 632.8 nm to reach the ${}^5\text{D}_0$ level.⁹⁷ Er^{3+} and Yb^{3+} -doped TiO_2 nanoparticles in silicon glass ceramics have also been shown to manifest up-conversion properties,¹²¹ and such oxide glasses containing microscopic crystals (10–30 nm in diameter) are being evaluated for three-dimensional imaging.²⁵⁹

LiNbO_3 is a technologically important material with potential applications in telecommunications. A number of papers have appeared that discuss up-conversion processes in $\text{LiNbO}_3:\text{Er}$, and some of the more recent ones are included here. A comprehensive spectroscopic study of an $\text{LiNbO}_3:\text{Er}$ wafer (Er^{3+} concentration = $3.7 \times 10^{19}\text{ cm}^{-3}$) at low temperature has been reported which aimed at the characterization of the Er^{3+} defect site and the exploration of the up-converted luminescence. It was found that excited state absorption and energy transfer between excited Er^{3+} ions are the important mechanisms for up-conversion.²⁶⁰ Er -doped LiNbO_3 single crystal fibers have been grown, and the near-IR to visible up-conversion process in these fibers has been studied. Multiple sites for Er^{3+} were found to exist in the fiber samples; they fall into two groups which were related to the substitution of either Li or Nb by Er.²⁶¹ Green emission was displayed from pure trigonal phase $\text{LiNbO}_3:\text{Er}^{3+}$ upon excitation with two near-IR wavelengths (993 and 800 nm). In contrast, on excitation at 331 nm and 399 nm, bright green photoluminescent emission occurs at 543 nm.²⁶²

Efficient up-conversion luminescence from $\text{YNbO}_4:\text{Er}^{3+}$ has also been observed.²⁶³ Studies on up-conversion phosphors using red laser light excitation have been reported for $\text{Cs}_2\text{NaYCl}_4:\text{Tm}^{3+},\text{Mo}$;²⁶⁴ $\text{Cs}_2\text{ZrCl}_6:\text{Tm}^{3+},\text{Re}$;²⁶⁴ and also for $\text{Tm}^{3+},\text{Er}^{3+}$ co-doped into tellurite glass.²⁶⁵ In recent years up-conversion in Ho^{3+} has also been studied in $\text{Y}_3\text{Al}_5\text{O}_{12}$ ^{266,267} and YAlO_3 ²⁶⁶ using continuous-wave (c.w.) 580–590 nm excitation. Intense UV and blue up-conversion fluorescence in Tm^{3+} -doped fluoroindate glasses has been reported. The intense up-conversion and high thermal stability of these fluoroindate glasses indicate a real possibility for the realization of a UV and blue up-conversion laser.²⁶⁸

9.15.8 QUANTUM CUTTERS

This is a relatively new concept and can be thought of as the opposite to multiphoton up-conversion. Recently interest in the luminescence spectroscopy of lanthanide ions in the vacuum UV (VUV) region of the electromagnetic spectrum has steadily increased, because of a perceived need for new phosphors with high quantum efficiencies under VUV excitation. If efficient phosphors for quantum cutting could be achieved, then not only would they have applications for PDPs but also for everyday lighting. These phosphors must also display good stability in the plasma environments (necessary for VUV) used in mercury-free lamps and PDPs. Such phosphors, therefore, require three attributes: high efficiency, good stability, and an optimum VUV absorption. For such applications (e.g., in Xe discharge) the resonance line is at 147 nm and the excimer band at 173 nm. The drawback is that the power efficiency is rather low due to the large Stokes shift that arises from the conversion of one VUV photon ($>8\text{ eV}$) to one visible

photon ($\sim 1.6\text{--}3.2\text{ eV}$), and the probability that energy transfer is also relatively small because of strong absorption by the oxide host lattice. To address these problems two different approaches have been used. The first makes use of a concept called “quantum cutting”, based on utilizing two or more rare-earth element ions through down conversion in large bandgap materials.^{269,270} The second approach involves the use of a sensitizer together with the emitting ions or dopants in a fluoride host (necessary, as such hosts are transparent in the VUV region of the spectrum). The sensitizer is required to absorb the VUV radiation and transfer the energy efficiently to the dopants.

Several papers have debated the best way to accomplish quantum splitting in utilizing a cascade emission starting from the 1S_0 level of Pr^{3+} .^{271,272} One important requirement for a cascade to occur is that the lowest level of the $4f5d$ configuration must be located above the 1S_0 level; however, for most compounds this is not the case. To find a possible host lattice, the relationship between the $5d$ -level energy and the host crystal must be understood, and accordingly a large amount of fundamental spectroscopic data has been gathered on the energy of the lowest level of the $4f^{n-1}5d$ configuration of trivalent lanthanides in inorganic materials.^{273–275} The results of this work are now being used to predict the quantum splitting phenomenon of Pr^{3+} in various lattices²⁷¹ such as BaSiF_6 ,²⁷² BaSO_4 ,²⁷² and $\text{LaZr}_3\text{F}_{15}$ ²⁷² in the quest for finding efficient materials.

The second approach uses multilanthanide-doped fluoride phosphors for VUV excitation.²⁷⁵ Enhancement of Gd^{3+} 311 nm emission ($^6P_J - ^8S_{7/2}$) in a YF_3 host can be achieved by the addition of Pr. As it is thought that the energy transfer from this level to other $4f$ levels in suitable activators such as Eu and Tb may produce efficient VUV phosphors, a survey of suitable activators for such energy transfer from the 6P_J level of Gd is currently in progress.²⁷⁶ The feasibility of quantum cutting has been demonstrated in $\text{LiGdF}_4:\text{Eu}^{3+}$ and $\text{LiGdF}_4:\text{Er}^{3+},\text{Tb}^{3+}$, with the highest efficiency being achieved in the former.²⁷⁷

9.15.8.1 Novel Inorganic-Based Luminous Materials

The use of doped and undoped silica aerogels as multifunctional host materials for fluorescent dyes and other luminescent materials for display and imaging applications has been reported.²⁷⁸ Results have been presented on the PL spectra of undoped silica aerogels and aerogels doped with Er^{3+} , rhodamine, and fluorescein.²⁷⁸

Improvement of contrast and brightness by using crystal pigment phosphor screens has been reported.²⁷⁹ This has been achieved by preparing phosphors coated with five times as much pigment as those currently used. Ultramarine and Co-blue ($\text{CuO-Al}_2\text{O}_3$) were used as blue pigments, and for red pigments iron oxide (Fe_2O_3), cadmium red (CdS-CdSe), and chrome vermilion ($\text{PbCrO}_4\text{-PbMoO}_4\text{-PbSO}_4$) were used.²⁷⁹

9.15.9 PHOSPHORESCENT PAINTS

These are prepared by mixing a phosphor (particle size around $10\text{--}30\ \mu\text{m}$) with a transparent (to the excitation and emission wavelengths) synthetic varnish. Traditionally $\text{ZnS}:\text{Cu}$ phosphor was used for this purpose, but over the last few years much better oxide-based phosphors have appeared in the marketplace.

One such material is $\text{SrAl}_2\text{O}_4:\text{Eu}^{2+},\text{Dy}^{3+}$ which, like $\text{ZnS}:\text{Cu}$, can be excited by 365 nm light, resulting in a broad green emission peak at 520 nm.²⁸⁰ $\text{Sr}_2\text{MgSi}_2\text{O}_7:\text{Eu}^{2+},\text{Dy}^{3+}$ has been reported recently as a new phosphor with a long blue after-glow.²⁸¹ These kinds of phosphor also find use embedded in plastics for undersea equipment and divers (for recognition purposes), as well for external “after dark” markings.

9.15.10 PHOTONICS

Lanthanide-doped inverse photonic crystals have been reported.²⁸² The lattices were prepared by infilling self-assembled polystyrene sphere templates with a mixture of zirconium alkoxide and europium at $450\ ^\circ\text{C}$, the polystyrene spheres were burnt out leaving hollow spheres of air, and the infilled material was converted to $\text{ZrO}_2:\text{Eu}^{3+}$. The PL properties of the resulting photonic lattice were reported.²⁸² The possibility of including phosphors into photonic lattices could lead to many

new applications in the control and manipulation of light emission. Prior to this work, optical probes inside photonic crystals have been reviewed.²⁸³ Reference to unpublished results mentions the use of ErCl_3 solution to coat the inside of photonic SiO_2 lattices and subsequent oxidation and annealing to incorporate Er^{3+} in the structure.²⁸³

9.15.11 THE FUTURE

The future for the use of coordination compounds in phosphors looks very bright indeed. Man's need to illuminate his surroundings, transfer information, and display that information efficiently can only mean an ever more demanding and growing marketplace for materials that emit light. Coordination compounds are, and will remain, in widespread use as both precursors in phosphor synthesis and as major constituents in small molecule OLEDs.

9.15.12 REFERENCES

- Shionoya, S. Introduction. In *Phosphor Handbook*; Shionoya, S.; Yen, W. M., Eds.; CRC Press: New York, 1998, Chapter 1, pp 3–34.
- Harvey, E. E. *A History of Luminescence from the Earliest Times until 1900*. Am. Phil. Soc: Philadelphia, 1957, 1–692.
- Nakajima, S.; Tamatani, M. History of Phosphor Technology and Industry. In *Phosphor Handbook*; Shionoya, S.; Yen, W. M., Eds.; CRC Press: New York, 1998, Chapter 18, p 847.
- Arpiarian, N. In *The Century of the Discovery of Luminescent Zinc Sulfide*, Proceedings of the International Conference of Luminescence, Budapest, Hungary, 1966; Szigeti, G., Ed.; Akadémia Kiado: Budapest, 1968, p 903.
- Becquerel, E. C. *R. Acad. Sci.* LX111, **1866**, 188.
- Lenard, P. E. A.; Schmidt, F.; Tomaschek, R. Phosphoreszenz and Fluoreszenz. In *Handbuch der Experimentalphysik*, Bd. 23, 1.u.2. Teil. Akademie Verlagsgesellschaft: Leipzig, 1928 (German), pp 745–1038.
- Leverenz, H. W. *An Introduction to Luminescence of Solids*, Wiley: New York, 1950, pp 1–569.
- Ropp, R. C. *The Chemistry of Artificial Lighting Devices*, Elsevier: Amsterdam, 1993; pp 1–664.
- Destriau, G. *J. Chim. Phys.* **1936**, 33, 587–625.
- Vecht, A.; Werring, N. J.; Smith, P. J. F. *Br. J. Appl. Phys.* **1968**, 1, 134–136.
- Yoshida, M.; Mikami, A.; Inoguchi, T. Electroluminescence Materials. In *Phosphor Handbook*; Shionoya, S.; Yen, W. M., Eds.; CRC Press: New York, 1998, Chapter 9, pp 581–600.
- Tanaka, K.; Mikami, A.; Ogura, T.; Taniguchi, K.; Yoshida, M.; Nakajima, S. *Appl. Phys. Lett.* **1986**, 48, 1730–1732.
- Ono, Y. A.; Fuyama, M.; Onisawa, K.; Tamura, K.; Ando, M., *J. Appl. Phys.* **1989**, 66, 5564–5571.
- Ogura, T.; Mikami, A.; Tanaka, K.; Taniguchi, K.; Yoshida, M.; Nakajima, S. *Appl. Phys. Lett.* **1986**, 48, 1570–1571.
- Okamoto, K.; Yoshimi, T.; Nakamura, K.; Kobayashi, T.; Sato, S.; Miura, S. *Jpn. J. Appl. Phys.* **1989**, 28, 1378–1384.
- Vecht, A. In *Digest; 1980 SID Int. Symp. Society for Information Display 1980*, 110–111.
- Chase, E. W.; Hoppelwhite, R. T.; Keupka, D. C.; Kalonf, D. *J. Appl. Phys.* **1969**, 40, 2512–2519.
- Marello, V.; Onton, A. *IEEE Trans. Electron Dev.* **1980**, 27, 1767.
- Davies, D. A.; Vecht, A.; Silver, J.; Titler, P.; Morton, D. C. *SID'01 Digest*, **2001**, 32, 395–397.
- Werring, N. J.; Vecht, A.; Fletcher, J. W. *Br. J. Appl. Phys.* **1969**, 2, 509–513.
- Davidson, M. R.; Glass, W.; Kale, A.; Holloway, P.; Sun, S.-S.; Bowen, M. In *Extended Abstracts of the First International Conference on the Science and Technology of Emissive Displays and Lighting*, San Diego, CA, Nov 12–14, 2001; 99–101.
- Lee, Y. H.; Song, M. H.; Ju, B. K.; Hahn, T. S.; Oh, M.; Shin, D. K. *SID'96 Digest 1996*, 27, 478–481.
- Kim, P.; Davidson, M. R.; Holloway, P. H. *Extended Abstracts of the First International Conference on the Science and Technology of Emissive Displays and Lighting*, San Diego, CA, Nov 12–14, 2001; 155–158.
- Sun, S. S.; Bowen, M. S.; Daniel, J. L.; Moehnke, S.; Hodges, A.; Tuengo, R. T.; Pearson, S.; Philips, J.; Simonsen, L.; King, C. N. *SID'99 Digest 1999*, 30, 1146–1149.
- Summers, C. T.; Tong, W.; Wagner, B. K.; Menkara, H. *SID'00 Digest 2000*, 31, 7–9.
- Baukol, B. A.; Wager, J. F.; Moehnke, S. *SID'00 Digest 2000*, 31, 656–657.
- Morimoto, K. *Denshi Tenbou* **1974**, 11–19, 34–38 (in Japanese).
- Morimoto, K.; Pykosz, T. L. Trend in Vacuum Fluorescent Display. In *Electronic Display and Information Systems and On-board Electronics*, 820264, **1982**, 69, p 103.
- Morimoto, K. Phosphors for Vacuum Fluorescent Displays and Field Emission Displays. In *Phosphor Handbook*. Shionoya, S.; Yen, W. M., Eds.; CRC Press: New York, 1998, Chapter 8, pp 561–580.
- Bukesov, S. A.; Nikishon, N. V.; Dmitrienko, A. O.; Shmakov, S. L.; Kim, J. M. *SID'98 Digest 1998*, 29, 585–588.
- Kagami, A.; Mimura, Y.; Narita, K.; Kanda, K. In *Development of Low Energy Cathode Ray Phosphors*, Tech. Digest, Jpn. Soc. Prom. Sci. 125th Committee, 90th Meeting, Proceedings number 340, 1979, 13–20. (in Japanese).
- Morimoto, K. *Tech. Digest, Phosphor Res. Soc.* 189th Meeting, 1982, 19–35. (in Japanese).
- Jung, J.-H.; Park, G. S. *SID'01 Digest 2001*, 32, 84–87.
- Chalamala, B. R.; Reuss, R. H. *SID'01 Digest 2001*, 32, 89–91.
- Choi, J. H.; Lee, H. W.; Park, Y. J.; Seung, N. C.; Kim, J. W.; Jung, S. Y.; Suk, H. K.; Eun, S. C.; Jung, J. E.; Park, N. S.; Lee, N. S.; You, J. H.; Kim, J. M. *SID'00 Digest 2000*, 31, 420–423.
- Kastalsky, A.; Shokhor, S.; Hou, J.; Naar, S.; Abanshin, N.; Gorfinkel, B. *SID'01 Digest 2001*, 32, 201–203.
- Ko, C. G.; Ju, B. K.; Lee, Y. H.; Oh, M. H.; Park, J. H. *SID'96 Digest 1996*, 27, 463–466.
- Lee, Y.-H.; Jang, Y.-T.; Choi, C.-H.; Ju, B.-K.; Oh, M.-H. *SID'01 Digest 2001*, 32, 309–311.

39. Yotani, J.; Uemura, S.; Nagasako, T.; Kerachi, H.; Yasmada, H.; Ezaki, T.; Saito, Y.; Zhoo, Y.; Yumura, M. *SID'01 Digest* **2001**, 32, 312–315.
40. Lee, C.-H.; Chang, Y.-Y.; Sheu, J. R.; Ho, J.-C.; Lia, J.-H.; Cheng, H.-C.; Hsipo, M.-C.; Han, C.-X.; Huang, S.-M.; Wang, W.-C. *SID'01 Digest* **2001**, 32, 316–319.
41. Kim, J. M.; Lee, N. S.; Chung, D. S.; Park, S. H.; Jin, Y. W.; Kang, J. H.; Choi, Y. S.; Kim, H. Y.; Yun, M. J.; Park, S.; Han, I. T.; Kim, J. W.; Jung, J. E.; You, J. H.; Lee, C. G.; Jo, S. H.; Choi, K. S.; Chi, E. J.; Lee, S. J.; Park, H. G. *SID'01 Digest* **2001**, 32, 304–307.
42. Chung, S. J.; Kim, H. S.; Jang, J.; Lim, S. H.; Lee, C. H.; Moon, B. Y. *SID'01 Digest* **2001**, 32, 92–95.
43. Uemura, S.; Yotani, J.; Agasako, T.; Saito, Y.; Yumura, M. *SD'00 Digest* **2000**, 31, 320–323.
44. Choi, W. B.; Lee, N. S.; Yi, W. K.; Jin, Y. W.; Choi, Y. S.; Han, I. T.; Chung, D. S.; Kim, H. Y.; Kang, J. H.; Lee, Y. J.; Yun, M. J.; Park, S. H.; Yu, S.; Jang, J. E.; You, J. H.; Kim, J. M. *SID'00 Digest* **2000**, 31, 324–327.
45. Chuang, F. Y.; Lee, C.-C.; Lim, J.-D.; Liao, J.-H.; Cheng, H.-C.; Han, C.-X.; Kwo, J.-L.; Wang, W. C. *SID'00 Digest* **2000**, 31, 329–331.
46. Chung, S. J.; Lim, S. H.; Jang, J. *SID'00 Digest* **2000**, 31, 666–669.
47. Kim, S.-J.; Ju, B. K.; Lee, Y.-H.; Park, B. S.; Baik, Y.-J.; Oh, M. H.; Lim, S.-K. *SID'96 Digest* **1996**, 27, 459–462.
48. Thuesen, L. H.; Yaniv, Z. In *Extended Abstracts of the First International Conference on the Science and Technology of Emissive Displays and Lighting*, San Diego, CA, Nov 12–14 2001; 13–16.
49. Park, J. S.; Lee, S.; Ju, K.; Oh, M. H.; Jang, J.; Jeon, D. *SID'99 Digest* **1999**, 30, 576–579.
50. Holloway, P. H.; Trotter, T. A.; Sebastian, J.; Jones, S.; Zhang, X.-M.; Bang, J.-S.; Abrams, B.; Thomes, W. J.; Kim, T.-J. In *Extended Abstracts of the Third International Conference on the Science and Technology of Display Phosphors*, Huntington Beach, CA, Nov 3–5, 1997; 7–10.
51. Trotter, T.; Krishnamoorthy, V.; Zhang, X.-M.; Peterson, R.; Holloway, P. *Extended Abstracts of the Third International Conference on the Science and Technology of Display Phosphors*, Huntington Beach, CA, Nov 3–5, 1997; 321–324.
52. Reuss, R. H.; Chalamala, B. R. *SID'01 Digest* **2001**, 32, 81–83.
53. Itoh, S.; Kimizuka, T.; Tonegawa, T. *J. Electrochem. Soc.* **1989**, 136, 1819–1923.
54. Lee, H. W.; Cha, S. N.; Choi, J. H.; Park, Y. J.; Kim, J. W.; Jung, J. E.; Lee, N. S.; Jin, Y. W.; Jung, B. H.; Jang, J. E.; Lee, E. S.; Kang, S. H.; You, J. H.; Kim, J. M.; Park, G. S.; Chee, J. K.; Hong, J. R. *SID'00 Digest* **2000**, 31, 674–677.
55. Itoh, S.; Toki, H.; Kataoka, F.; Sato, Y.; Tamura, K.; Kagawa, Y. *IEICE Trans. Electron.* **1999**, E52-C, 1808–1813.
56. Chadha, S. S.; Smith, D. W.; Vecht, A.; Gibbons, C. S. *SID'94 Digest* **1994**, 25, 51–54.
57. Jing, X.; Gibbons, C.; Nicholas, D.; Silver, J.; Vecht, A.; Frampton, C. S. *J. Mater. Chem.* **1999**, 9, 2913–2918.
58. Vecht, A.; Charlesworth, D.; Smith, D. W. *SID'97 Digest* **1997**, 28, 588–590.
59. Chang, H.; Lee, S. K.; Park, H. D.; Han, C. H. *SID'00 Digest* **2000**, 31, 662–664.
60. Han, C. H.; Kim, H. J.; Chang, H.; Lee, S. K.; Park, H. D. *J. Electrochem. Soc.* **2000**, 147, 2800–2804.
61. Dimitrienko, A. O.; Nikishin, N. V.; Dmitrienko, V. P.; Bukesov, S. A.; Kim, J. M. *SID'98 Digest* **1998**, 29, 581–584.
62. Kalkhoran, N. M.; Halverson, W. D.; Vakerlis, G. D. *SID'96 Digest* **1996**, 27, 474–477.
63. Nakua, A.; Kitai, A. H.; Xiao, T. *SID'98 Digest* **1998**, 29, 1048–1051.
64. Bacalski, C. F.; Cherry, M. A.; Hirata, G. A.; McKittrick, J. M. *Extended Abstracts of the Third International Conference on the Science and Technology of Display Phosphors*, Huntington Beach, CA, Nov 3–5, 1997 143–145.
65. Ravichandran, D.; Ravindranathan, P.; Roy, R.; White, W. B. *Extended Abstracts of the Third International Conference on the Science and Technology of Display Phosphors*, Huntington Beach, CA, Nov 3–5, 1997; 137–141.
66. Zhang, S.; Uchiike, H. *Proceedings 7th IDW'00* November, 2000, 865–868.
67. Shiiki, M.; Okazzaki, C.; Komatsu, M.; Iwanaga, S.; Furukawa, T.; Suzuki, T.; Suzuki, K. *Proceedings 5th IDW' 1998*, 859–860 (Late-newspaper PH2-7).
68. Ushirozawa, M. *SID'00 Digest* **2000**, 31, 224–227.
69. Zhang, S.; Yokota, K.; Onishi, H.; Fujii, H.; Uchiike, H.; Hirakawa, T. *SID'00 Digest* **2000**, 31, 683–685.
70. Kishima, N. *Display and Imaging* **1999**, 7, 225–234 (in Japanese).
71. Tadaki, S.; Inoue, K.; Fukuta, S.; Ishimoto, M.; Betsui, K.; Iwase, N. *SID'01 Digest* **2001**, 32, 418–421.
72. Zhang, S.; Kobubu, M.; Fujii, H.; Uchiike, H. *SID'01 Digest* **2001**, 32, 414–417.
73. Kojima, T. Phosphors for Plasma Display, In *Phosphor Handbook*; Shionoya, S.; Yen, W. M. Eds.; CRC Press: New York, 1998, Chapter 10, p 632.
74. Ropp, R. C. *Luminescence and the Solid State*, Elsevier: Amsterdam, 1991, pp 1–453.
75. Wells, A. F. *Structural Inorganic Chemistry*, 4th ed.; Clarendon Press: Oxford, 1975, pp 1–1095.
76. Leskela, M.; Ninisto, L.; Inorganic Complex Compounds I In *Handbook on the Physics and Chemistry of Rare Earths*. Gschneidner, K. A., Jr.; Eyring, L. Eds.; Elsevier: 1986, Chapter 56, 203–334.
77. Perkins, H. H. K.; Sienko, M. J. *J. Chem. Phys.* **1967**, 46, 2398–2401.
78. Palumbo, D. T.; Brown, J. J. *J. Electrochem. Soc.* **1970**, 117, 1184–1189.
79. Park, S.-J.; Park, C.-H.; Yu, B.-Y.; Bae, H.-S.; Kim, C.-H.; Pyum, C.-H. *J. Electrochem. Soc.* **1999**, 146, 3903–3906.
80. Garlick, G. F. J. *Luminescent Materials*. Clarendon Press: Oxford, 1949, pp 1–254.
81. Shinoya, S.; Yen, W. M. Eds.; *Phosphor Handbook*. CRC Press: London, 1998, pp 1–921.
82. Ropp, R. C. Method for Preparing Rare Earth Oxide Phosphors. U.S. Patent 3,449,25, Nov 27, 1968.
83. Ropp, R. C.; Carroll, B. J. *Inorg. Nucl. Chem* **1977**, 39, 1303–1307.
84. Ropp, R. C.; Carroll, B. *Inorg. Chem.* **1975**, 14, 2199–2202.
85. Sohn, K.-S.; Choi, Y.-G.; Park, H. D. *J. Electrochem. Soc.* **2000**, 147, 3552–3558.
86. Sastry, I. S. R.; Bacalski, C. F.; McKittrick, J. J. *Electrochem. Soc.* **1999**, 146, 4316–4319.
87. Lee, S. S.; Chang, C. K.; Lim, S. *SID'96 Digest* **1996**, 27, 471–473.
88. Lee, S. S.; Lim, S.; Oh, M. H.; Chang, H. *SID'97 Digest* **1997**, 28, 576–579.
89. Nishisu, Y.; Kobayashi, M. Particulate Fluorescent Material from $(Y_{1-x}Eu_x)_2O_3$ and its Method of Preparation. U. S. Patent 5,413,736, 30 Sept 1994.
90. Her, Y. S.; Matijevec, E.; Wilcox, W. R. *J. Mater. Res.* **1992**, 7, 2269–2272.
91. Jiang, Y. D.; Wang, Z. L.; Zhang, F.; Paics, H. G.; Summers, C. J. *J. Mater. Res.* **1998**, 13, 2950–2955.
92. Vecht, A.; Jing, X.; Gibbons, C.; Ireland, T.; Davies, D.; Marsh, P.; Newport, A. *SID'98 Digest* **1998**, 29, 1043–1047.

93. Vecht, A.; Gibbons, C.; Davies, D.; Jiang, X.; Marsh, P.; Ireland, T.; Silver, J.; Newport, A.; Barber, D. *J. Vac. Sci. Technol. B* **1999**, *17*, 750–757.
94. Jing, X.; Ireland, T.; Gibbons, C.; Barber, D. J.; Silver, J.; Vecht, A.; Fern, G.; Trowga, P.; Morton, D. C. *J. Electrochem. Soc.* **1999**, *146*, 4654–4658.
95. Martinez-Rubio, M. I.; Ireland, T. G.; Silver, J.; Fern, G.; Gibbons, C.; Vecht, A. *Electrochem. Solid St.* **2000**, *3*, 446–449.
96. Vecht, A.; Martinez-Rubio, M. I.; Ireland, T. G.; Silver, J.; Fern, G.; Gibbons, C. *SID'00 Digest* **2000**, *31*, 15–17.
97. Silver, J.; Martinez-Rubio, M. I.; Ireland, T. G.; Fern, G.; Withnall, R. *J. Phys. Chem. B* **2001**, *105*, 9107–9112.
98. Martinez-Rubio, M. I.; Ireland, T. G.; Fern, G.; Snowden, M. J.; Silver, J. *Langmuir* **2001**, *17*, 7145–7149.
99. Martinez-Rubio, M. I.; Ireland, T. G.; Fern, G.; Silver, J.; Snowden, M. J. *J. Electrochem. Soc.* **2002**, *149*, H53–H58.
100. Ma, D.; Liu, X.; Pei, Y.; Cao, L. *SID'97 Digest* **1997**, *28*, 423–426.
101. Williams, R.; Yocum, P. N.; Stofko, F. S. *J. Colloid Interf. Sci.* **1985**, *106*, 388–398.
102. Cooper, J. A.; Paris, H. G.; Stock, S. R.; Yeng, S.; Summers, C. J.; Hill, D. N. *J. SID* **1998**, *6*, 163–166.
103. Ireland, T. G.; Silver, J.; Gibbons, C.; Vecht, A. *Electrochem. Solid St.* **1999**, *2*, 52–54.
104. Hines, M. A.; Guyot-Sionnest, P. *J. Phys. Chem.* **1996**, *100*, 468–471.
105. Gallagher, D.; Heady, W. E.; Racz, J. M.; Bhargava, R. N. *J. Mater. Res.* **1995**, *10*, 870–876.
106. Bhargava, R. N.; Gallagher, D.; Hong, X.; Nurmikkol, A. *Phys. Rev. Lett.* **1994**, *72*, 416–419.
107. Bhargava, B. N.; Gallagher, D.; Welker, T. *J. Lumin.* **1994**, *60–61*, 275–280.
108. Kang, Y. C.; Roh, H. S.; Seung, B. P. *J. Electrochem. Soc.* **2000**, *147*, 1601–1603.
109. Vecht, A.; Davies, D. A.; Smith, D. *Mater. Res. Innovat.* **1998**, *2*, 176–180.
110. Davies, A.; Vecht, A.; Rose, J. A.; Marsh, P. J.; Gibbons, C. S.; Silver, J.; Morton, D.; Blomquist, S.; Ravihandren, R. *SID'99 Digest* **1999**, *30*, 1018–1021.
111. Davies, D. A.; Vecht, A.; Silver, J.; Marsh, P. J.; Rose, J. A. *J. Electrochem. Soc.* **2000**, *147*, 765–771.
112. Marsh, P. J.; Davies, D. A.; Silver, J.; Smith, D. W.; Withnall, R.; Vecht, A. *J. Electrochem. Soc.* **2001**, *148*, D89–D93.
113. Davies, D. A.; Silver, J.; Vecht, A.; Marsh, P. J.; Rose, J. A. *J. Electrochem. Soc.* **2001**, *148*, H143–H148.
114. Ihara, M.; Igarashi, T.; Kusanoki, T.; Ohno, K. *SID'99 Digest* **1999**, *30*, 1026–1029.
115. Kottaisamy, M.; Horikawa, K.; Kominami, H.; Aoki, T.; Azuma, N.; Nakamura, T.; Nakanishi, Y.; Hatanaka, Y. *J. Electrochem. Soc.* **2000**, *147*, 1612–1616.
116. Wakefield, G.; Dobson, P. J. *Extended Abstracts of the Third International Conference on the Science and Technology of Display Phosphors*, Huntington Beach, CA, Nov 3–5, 1997; 299–302.
117. Li, Q. H.; Komarnej, S.; White, W. B.; Roy, R. *Extended Abstracts of the International Conference on the Science and Technology of Display Phosphors*, Huntington Beach, CA, Nov 3–5, 1997; 21–23.
118. Popovich, N. V.; Soschin, N. P.; Galactionou, S. S.; Popova, M. N.; Pogrebisskaya, O. P. *Extended Abstracts of the First International Conference on Science and Technology of Emissive Displays and Lighting*, San Diego, CA, Nov 12–14, 2001; 231–234.
119. Park, J.-C.; Moon, H.-K.; Kim, D.-K.; Byeon, S.-H.; Kim, B.-C.; Suh, K.-S. *SID'00 Digest* **2000**, *31*, 686–689.
120. Ravichandran, D.; Roy, R.; White, W. B. *J. SID* **1997**, *5*, 107–110.
121. Newport, A.; Fern, G. R.; Ireland, T.; Withnall, R.; Silver, J.; Vecht, A. *J. Mater. Chem.* **2001**, *11*, 1447–1451.
122. Bausa, L. E.; Garcia Sole, J.; Duran, A.; Fernandez Navarro, J. M. *J. Non-cryst. Solids* **1991**, *127*, 267–272.
123. Phillips, M. L. F.; Walko, R. J.; Shea, L. E. *SID'96 Digest* **1996**, *27*, 121–124.
124. Lee, M. H.; Oh, S. G.; Yi, S. C.; Seo, D. S.; Hong, J. P.; Kim, C. O.; Yoo, J. S. *J. Electrochem. Soc.* **2000**, *147*, 3139–3142.
125. Sohn, K.-S.; Zeon, I. W.; Park, H. D. *Extended Abstracts of the First International Conference on Science and Technology of Emissive Displays and Lighting*, San Diego, CA, Nov 12–14 2001; 139–142.
126. Kim, C. H.; Park, S. M.; Jeong, Y. S.; Park, J. K.; Park, H. D.; Park, J. T. *Extended Abstracts of the First International Conference on Science and Technology of Emissive Displays and Lighting*, San Diego, CA, Nov 12–14, 2001; 43–48.
127. Minam, T.; Sakagami, Y.; Miyata, T. *Extended Abstracts of the Third International Conference on the Science and Technology of Display Phosphors*, Huntington Beach, CA, Nov 3–5, 1997, 37–40.
128. Manasevit, H.; Simpson, W. *J. Electrochem. Soc.* **1971**, *118*, 644–647.
129. Wright, P. J.; Cockayne, B. *J. Cryst. Growth* **1982**, *59*, 148–154.
130. Wright, P. J.; Cockayne, B.; Cattell, A. F.; Dean, P. J.; Pitt, A. D.; Blackmore, G. M. *J. Cryst. Growth* **1982**, *59*, 155–160.
131. Cattell, A. F.; Cockayne, B.; Dexter, K.; Kirton, J.; Wright, P. J. *IEEE Trans. Electron. Devices* **1983**, *30*, 471–475.
132. Cockayne, B.; Wright, P. J.; Armstrong, A. J.; Jones, A. C.; Orrell, E. D. *J. Cryst. Growth* **1988**, *91*, 57–62.
133. Takata, S.; Minami, T.; Miyata, T.; Nanto, H. *J. Cryst. Growth* **1988**, *86*, 257–262.
134. Fujita, S.; Isemura, M.; Sakamoto, T.; Yoshimura, N. *J. Cryst. Growth* **1988**, *86*, 263–267.
135. Cockayne, B.; Wright, P. J.; Skolnick, M. S.; Pitt, A. D.; Williams, J. D.; Ng, T. L. *J. Cryst. Growth* **1985**, *72*, 17–22.
136. Yoshiwaya, A.; Yamaga, S.; Tanaka, K. *Jpn. J. Appl. Phys.* **1984**, *23*, L388–L390.
137. Hirabayashi, K.; Kogure, D. *Jpn. J. Appl. Phys.* **1985**, *5*, 1484–1487.
138. Hirabayashi, K.; Kozawaguchi, H. *Jpn. J. Appl. Phys.* **1986**, *25*, L379–L381.
139. Hirabayashi, K.; Kozawaguchi, H. *Jpn. J. Appl. Phys.* **1986**, *25*, 711–713.
140. Hirabayashi, K.; Kozawaguchi, H.; Tsujiyama, B. *Jpn. J. Appl. Phys.* **1987**, *26*, 1472–1476.
141. Hirabayashi, K.; Kozawaguchi, H.; Tsujiyama, B. *Kenkyu Jitsuyoko Hokoku* **1987**, *36*, 829–835.
142. Vecht, A. Methods of Producing Thin Films. U.K. Patent 2,049,636, Dec 31, 1980.
143. Katahasi, Y.; Yuki, R.; Sugiura, M.; Motojima, S.; Sugiya, K. *J. Cryst. Growth* **1980**, *5*, 491–497.
144. Hiskes, R.; DiCarolis, S. A.; Mueller-Mach, R.; Mazzi, V.; Nauka, K.; Mueller, J. *SID* **1997**, *5*, 93–97.
145. Moss, T. S.; Smith, D. C.; Samuels, J. A.; Dye, R. C.; DelaRosa, M. J.; Schaus, C. F. *J. SID* **1997**, *5*, 103–106.
146. Chakhovstov, A. G.; Hunt, C. E.; Yang, T.; Wagner, B. K.; Summers, C. J.; Malinowski, M. E.; Felner, T. E. *J. SID* **1998**, *6*, 185–189.
147. Kato, A.; Katayama, M.; Mizutani, A.; Ito, N.; Hattori, T. *J. SID* **1998**, *6*, 5–8.

148. Moss, T. S.; Dye, R. C.; Tuenge, R. T. *Extended Abstracts of the Third International Conference on the Science and Technology of Display Phosphors*, Huntington Beach, CA, Nov 3–5, 1997; 117–120.
149. Tanaka, K.; Okamoto, S.; Izumi, Y.; Kominami, H.; Nakanishi, Y.; Du, X.; Yoshikawa, A. *Extended Abstracts of the First International Conference on Science and Technology of Emissive Displays and Lighting*, San Diego, CA, Nov 12–14, 2001; 235–238.
150. Kim, Y. S.; Park, S.-H. K.; Cho, K.-I.; Yun, S. J. *SID'01 Digest* **2001**, 32, 763–765.
151. Yun, S. J.; Kim, Y. S.; Kang, J. S.; Park, K.; Cho, K.; Ma, D. S. *SID'99 Digest* **1999**, 30, 1142–1145.
152. Vlasenko, N. A.; Kononets, Ya. F.; Beletskii, A. I.; Denisova, Z. L.; Kopytko, Yu. F.; Soininen, E. L.; Tornqvist, R. O.; Vasama, K. M. *Extended Abstracts of the Third International Conference on the Science and Technology of Display Phosphors*, Huntington Beach, CA, Nov 3–5, 1997; 53–56.
153. Soininen, E. L.; Harkonen, G.; Vasama, K. *Extended Abstracts of the Third International Conference on the Science and Technology of Display Phosphors*, Huntington Beach, CA, Nov 3–5, 1997; 105–108.
154. Soenen, B.; Visschere, P.; Ihanus, J.; Ritala, M.; Leskela, M. *Extended Abstracts of the Third International Conference on the Science and Technology of Display Phosphors*, Huntington Beach, CA, Nov 3–5, 1997; 49–52.
155. Yun, S. J.; Nan, S.-D.; Kang, J.-S.; Nam, K.-S.; Pank, H.-M. *Extended Abstracts of the Third International Conference on the Science and Technology of Display Phosphors*, Huntington Beach, CA, Nov 3–5, 1997; 167–170.
156. Vlasenko, N. A.; Beletskii, A. I.; Denisova, Z. L.; Kononets, Ya. F. *Extended Abstracts of the Third International Conference on the Science and Technology of Display Phosphors*, Huntington Beach, CA, Nov 3–5, 1997; 77–80.
157. Kitai, A. H.; Xiao, T.; Liu, G.; Li, J. H. *SID'97 Digest* **1997**, 28, 419–422.
158. Cranton, W. M.; Thomas, C. B.; Stevens, R. *SID'97 Digest* **1997**, 28, 966–969.
159. Liu, G.; Lobban, K.; Bailey, P. *SID'98 Digest* **1998**, 29, 648–651.
160. Minami, T.; Shirai, T.; Kobayashi, Y.; Miyata, T.; Yamazaki, M. *Extended Abstracts of the First International Conference on Science and Technology of Emissive Displays and Lighting*, San Diego, CA, Nov 12–14, 2001; 107–110.
161. Lewis, J. S.; Holloway, P. H. *J. Electrochem. Soc.* **2000**, 147, 3148–3150.
162. Bender, J. P.; Wager, J. F.; Kissick, J.; Clark, B. L.; Keszler, D. A. *Extended Abstracts of the First International Conference on Science and Technology of Emissive Displays and Lighting*, San Diego, CA, Nov 12–14, 2001; 103–106.
163. Minami, T.; Kobayashi, Y.; Miyata, T.; Yamazaki, M. *Extended Abstracts of the First International Conference on Science and Technology of Emissive Displays and Lighting*, San Diego, CA, Nov 12–14, 2001; 169–172.
164. Zhao, L. J.; Li, C. H.; Zheng, C. W.; Zhong, G. Z.; Fan, X. W.; Liu, J. H. *Extended Abstracts of the Third International Conference on the Science and Technology of Display Phosphors*, Huntington Beach, CA, Nov 3–5, 1997; 199–202.
165. Cho, K. G.; Kumar, D.; Jones, S. L.; Lee, P. G.; Holloway, P. H.; Singh, R. K. *J. Electrochem. Soc.* **1998**, 145, 3456–3462.
166. Sun, X. W.; Kwok, H. S. *SID'98 Digest* **1998**, 29, 608–611.
167. Kalkhoran, N. M.; Vernon, S. M.; Trivedi, D. A.; Halverson, W. D.; Pathange, B.; Davidson, M.; Holloway, P. *SID'97 Digest* **1997**, 28, 623–626.
168. Xu, C.; Watkins, B. A.; Jing, X.; Trowga, P.; Gibbons, C. S.; Vecht, A. *Appl. Phys. Lett.* **1997**, 71, 1643–1645.
169. Sievers, R. E.; Milewski, P. D.; Xu, C. Y.; Watkins, B. A. *Extended Abstracts of the Third International Conference on the Science and Technology of Display Phosphors*, Huntington Beach, CA, Nov 3–5, 1997; 303–306.
170. Cho, S. H.; Koon, S. H.; Yoo, J. S.; Oh, C. W.; Lee, J. D.; Hong, K. J.; Koon, S. J. *J. Electrochem. Soc.* **2000**, 147, 3143–3147.
171. Yoo, J.-S.; Jeon, B. S.; Hong, G. Y.; Yoo, Y. K. *SID'01 Digest* **2001**, 32, 750–753.
172. Hong, G. Y.; Yoo, Y. K.; Yoo, J. S. *SID'01 Digest* **2001**, 32, 754–757.
173. Cho, S. H.; Yoo, J. S.; Lee, J. D.; Choi, J. S.; Park, S. B. *Extended Abstracts of the Third International Conference on the Science and Technology of Display Phosphors*, Huntington Beach, CA, Nov 3–5, 1997; 307–310.
174. Gibbons, C. S.; Vecht, A.; Smith, D. W. *J. SID* **1997**, 5, 151–155.
175. Gibbons, C. S.; Vecht, A.; Smith, D. W.; Jing, X. *J. SID* **1998**, 6, 191–193.
176. Roh, H. S.; Kang, Y. C.; Park, S. B. *Extended Abstracts of the First International Conference on Science and Technology of Emissive Displays and Lighting*, San Diego, CA, Nov 12–14, 2001; 29–31.
177. Kang, Y. C.; Park, S. B. *J. Electrochem. Soc.* **2000**, 147, 799–802.
178. Golego, N.; Studenikin, S. A.; Cocivera, M. *J. Electrochem. Soc.* **2000**, 147, 1993–1996.
179. Kim, K.; Cich, M.; Choi, H.; Hwang, S. T. *SID'98 Digest* **1998**, 29, 605–607.
180. Tang, C. W.; Van Slyke, S. A. *Appl. Phys. Lett.* **1987**, 51, 913–915.
181. Tang, C. W.; Van Slyke, S. A.; Chen, C. H. *J. Appl. Phys.* **1989**, 65, 3610–3616.
182. Van Slyke, S. A.; Chen, C. H.; Tang, C. W. *Appl. Phys. Lett.* **1996**, 69, 2160–2162.
183. Tang, C. W. *SID 96 Digest* **1996**, 27, 181–184.
184. Hosokawa, C.; Eida, M.; Matsuura, M.; Fukuoka, K.; Nakamura, H.; Kusumoto, T. *SID'97 Digest* **1997**, 28, 1073–1076.
185. Hamada, Y.; Sano, T.; Shibata, K.; Kuroki, K. *Jpn. J. Appl. Phys.* **1995**, 34, L824–L826.
186. Hamada, Y.; Sano, T.; Fujii, H.; Nishio, Y.; Takahashi, H.; Shibata, K. *Jpn. J. Appl. Phys.* **1996**, 35, L1339–L1341.
187. Chen, C. H.; Shi, J. *Coord. Chem. Rev.* **1998**, 171, 161–174.
188. Naito, K. *Chem. Mater.* **1994**, 6, 2343–2350.
189. Garbuzov, D. Z.; Bulovic, V.; Burrows, P. E.; Forrest, S. R. *Chem. Phys. Lett.* **1996**, 249, 433–437.
190. Wakimoto, T.; Murayama, R.; Nakada, H.; Imai, K. *Polym. Prepr. Jpn.* **1991**, 40, 3600.
191. Bhatnagar, D. C.; Forster, L. S. *Spectrochim. Acta* **1965**, 21, 1803–1807.
192. Ballardini, R.; Varani, G.; Indelli, M. T.; Scandola, F. *Inorg. Chem.* **1986**, 25, 3858–3865.
193. Troadec, D.; Veriot, G.; Antony, R.; Moliton, A. *Synth. Met.* **2001**, 124, 49–51.
194. Jiang, S.-Y.; Zhang, Z.-L.; Zheng, X.-Y.; Wu, Y.-Z.; Xu, S.-H. *Thin Solid Films* **2001**, 401, 251–254.
195. Van Slyke, S. A.; Bryan, P. S.; Lovecchio, F. V. Blue Emitting Internal Junction Organic Electroluminescent Device (II). U.S. Patent 5,150,006, Sept 22, 1992.
196. Burrows, P. E.; Shen, Z.; Bulovic, V.; McCarty, D. M.; Forrest, S. R.; Cronin, J. A.; Thompson, M. E. *J. Appl. Phys.* **1996**, 79, 7991–8006.
197. Matsumura, M.; Tokalin, H.; Edia, M.; Hosokawa, C.; Hironaka, Y.; Kusumoto, T. *Asia Display 95* **1996**, S11, 269.

198. Van Slyke, S. A. Blue Emitting Internal Junction Organic Electroluminescent Device. U.S. Patent 5,151,629 Sept 29, 1992.
199. Bryan, P. S.; Lovecchio, F. V.; Van Slyke, S. A. Mixed Liquid 8-quinolino Aluminum Chelate Liminophore. U.S. Patent 5,141,671, Aug 25, 1992.
200. Eck, T. D.; Wehry, E. L.; Hercules, D. M. *J. Inorg. Nucl. Chem.* **1966**, *28*, 2439–2441.
201. Shi, J.; Tang, C. W.; Chen, C. H. *55th Annual Device Research Conference Digest* **1997**, 154.
202. Dirr, S.; Johannes, H.-H.; Schobel, J.; Ammermann, D.; Bohler, A.; Kowalsky, W.; Grahn, W. *SID'97 Digest* **1997**, *28*, 778–781.
203. Campos, R. A.; Kovalev, I. P.; Guo, Y.; Wakili, N.; Skotheim, T. *J. Appl. Phys.* **1996**, *80*, 7144–7150.
204. Li, W.; Yu, J.; San, G.; Yu, Y.; Zhao, Y.; Tsutsui, T. *J. SID* **1998**, *6*, 133–135.
205. Li, W.; Hong, Z.; Liang, C.; Zhao, D.; Sun, G.; Liu, X.; Liu, Y.; Peng, J. *Extended Abstracts of the Third International Conference on the Science and Technology of Display Phosphors*, Huntington Beach, CA, Nov 3–5, 1997; 219–221.
206. Khreis, O. M.; Gillin, W. P.; Somerton, M.; Curry, R. *J. Org. Electron.* **2001**, *2*, 45–51.
207. Gillin, W. P.; Curry, R. *J. Appl. Phys. Lett.* **1999**, *74*, 798–799.
208. Curry, R. J.; Gillin, W. P. *Synth. Met.* **2000**, *111*, 35–38.
209. Curry, R. J.; Gillin, W. P.; Knights, A.; Gwilliam, R. *Opt. Mater.* **2001**, *17*, 161–163.
210. Ohmori, Y.; Kajji, H.; Sawatani, T.; Ueta, H.; Yoshino, K. *Thin Solid Films* **2001**, *393*, 407–411.
211. Qian, G.; Wang, M. *MRS Bull.* **2001**, *26*, 2289–2299.
212. Melby, L. R.; Rose, N. J.; Abramson, E.; Caris, J. C. *J. Am. Chem. Soc.* **1964**, *86*, 5117–5125.
213. Shim, J.; Reynolds, J.; Boncella, J.; Schanze, K.; Foley, T.; Harrison, B.; Bouguettaya, M.; Ramakrishnan, S.; Holloway, P. H. *Extended Abstracts of the First International Conference on Science and Technology of Emissive Displays and Lighting*, San Diego, CA, Nov 12–14, 2001; 69–71.
214. Tsutsui, T.; Yang, M.-J.; Yahiro, M.; Nakamura, K.; Watanabe, T.; Tsuji, T.; Fukuda, Y.; Wakimoto, T.; Miyaguchi, S. *Jpn. J. Appl. Phys.* **1999**, *38*, L1502–L1504.
215. Baldo, M. A.; Lamansky, S.; Burrows, P. E.; Thompson, M. E.; Forrest, S. R. *Appl. Phys. Lett.* **1999**, *75*, 4–6.
216. Watanabe, T.; Nakamura, K.; Kawami, S.; Fukuda, Y.; Tsuji, T.; Wakimoto, T.; Miyaguchi, R.; Yahiro, M.; Yang, M. J.; Tsutsui, T. *Synth. Met.* **2001**, *122*, 203–207.
217. Adachi, C.; Baldo, M. A.; Forest, S. R.; Thompson, M. E. *Appl. Phys. Lett.* **2000**, *77*, 904–906.
218. Baldo, M. A.; O'Brien, D. F.; You, Y.; Shoustikov, A.; Sibley, S.; Thompson, M. E.; Forrest, S. R. *Nature* **1998**, *395*, 151–154.
219. Baldo, M. A.; Adachi, C.; Andrade, B. D.; Forrest, S. R.; Lamansky, S.; Thompson, M. E. *Extended Abstracts of the Sixth International Conference on the Science and Technology of Display Phosphors*, San Diego, CA, Nov 6–8, 2000; 3–6.
220. Adachi, C.; Kwong, R. C.; Baldo, M. A.; Thompson, M. E.; Forrest, S. R. *Extended Abstracts of the First International Conference on Science and Technology of Emissive Displays and Lighting*, San Diego, CA, Nov 12–14, 2001; 115–116.
221. Lamansky, S.; Djurovich, P.; Murphy, D.; Abdel-Razzaq, F.; Lee, H.-E.; Adachi, C.; Burrows, P. E.; Forrest, S. R.; Thompson, M. E. *J. Am. Chem. Soc.* **2001**, *123*, 4304–4312.
222. O'Brien, D. F.; Baldo, M. A.; Thompson, M. E.; Forrest, S. R. *Appl. Phys. Lett.* **1999**, *74*, 442–444.
223. Forsythe, E. W.; Campbell, A. J. *SID'01 Semin.* **2001**, *M.10*, 1–57.
224. McElvain, J.; Antoniadis, H.; Hueschen, M. R.; Miller, J. N.; Roitman, D. M.; Sheats, J. R.; Moon, R. L. *J. Appl. Phys.* **1996**, *80*, 6002–6007.
225. Hattori, R.; He, Y.; Kanicki, J.; Sugano, T.; Fujiki, T. *SID'98 Digest* **1998**, *29*, 663–666.
226. Tan, H. S.; Yao, J. W.; Chen, L. C.; Wang, W. J.; Xie, H. Q.; Gao, G. H. *SID'98 Digest* **1998**, *29*, 667–670.
227. Burrows, P. E.; Bulovic, V.; Forrest, S. R.; Sapochak, L. S.; McCarty, D. M.; Thompson, M. E. *Appl. Phys. Lett.* **1994**, *65*, 2922–2924.
228. Aziz, H.; Popovic, Z. D.; Hu, N. X.; Hor, A.-M.; Xu, G. *Science* **1999**, *283*, 1900–1902.
229. Mueller, G. O. *Extended Abstracts of the First International Conference on Science and Technology of Emissive Displays and Lighting*, San Diego, CA, Nov 12–14, 2001; 11.
230. Nakamura, S.; Iwasa, N.; Senoh, M.; Mukai, T. *Jpn. J. Appl. Phys.* **1992**, *31*, 1258–1266.
231. Nakamura, S.; Mukai, T.; Senoh, M. *Appl. Phys. Lett.* **1994**, *64*, 1687–1689.
232. Nakamura, S.; Mukai, T.; Senoh, M. *J. Appl. Phys.* **1994**, *76*, 8189–8191.
233. Nakamura, S.; Senoh, M.; Iwasa, N.; Nagahama, S. *Jpn. J. Appl. Phys. Lett.* **1995**, *34*, L797–L799.
234. Nakamura, S.; Senoh, M.; Iwasa, N.; Nagahama, S.; Yamada, T.; Mukai, T. *Jpn. J. Appl. Phys. Lett.* **1995**, *34*, L1332–L1335.
235. Mueller-Mach, R.; Mueller, G. O.; Trottier, T. *Extended Abstracts of the First International Conference on Science and Technology of Emissive Displays and Lighting*, San Diego, CA, Nov 12–14, 2001; 49–52.
236. Liu, C. H.; Yokoyama, M.; Su, Y. K.; Lee, N. C. *J. SID* **1997**, *5*, 99–102.
237. Bloembergen, N. *Phys. Res. Lett.* **1959**, *2*, 84–85.
238. Auzel, F.; Santacruz, P. A.; Desa, G. F. *Rev. Phys. Appl.* **1985**, *20*, 273–281.
239. Allain, J. Y.; Monerie, M.; Poignant, H. *Electron. Lett.* **1992**, *28*, 111–113.
240. Auzel, F. C. *R. Acad. Sci. B. Phys.* **1966**, *262*, 1016–1019.
241. Johnson, L. F.; Geusic, J. E.; Guggenheim, H. I.; Kushida, T.; Singh, S.; Van Uitert, L. *Appl. Phys. Lett.* **1969**, *15*, 48–50.
242. Mita, Y. *Appl. Phys. Lett.* **1981**, *39*, 587–589.
243. Auzel, F.; Santa-Cruz, P. de Sa, G. F. *Rev. Phys. Appl.* **1985**, *20*, 273–281.
244. Ohwaki, J.; Wang, Y. *Jpn. J. Appl. Phys.* **1994**, *33*, L334–L337.
245. Ohwaki, J.; Wang, Y. *Jpn. J. Appl. Phys.* **1992**, *31*, L1481–L1483.
246. Wang, Y.; Ohwaki, J. *J. Appl. Phys.* **1993**, *74*, 1272–1278.
247. Xu, W.; Dai, S.; Toth, L. M.; Del Cul, G. D.; Peterson, J. D. *J. Phys. Chem.* **1995**, *99*, 4447–4450.
248. Desurvire, E. *Erbium-doped Amplifiers. Principles and Applications*, Wiley: New York, 1994; pp 1–770 (see particularly Chapter 4).
249. Dejneka, M. J. *MRS Bull.* **1998**, *23*, 57–62.

250. Downing, E.Hesselink, L.Ralson, J.MacFarlane, R. *Science* **1996**, 273, 1185–1189.
251. Dejneka, M. J. *J. Non-cryst. Solids* **1998**, 239, 149–155.
252. Massicott, J. F.; Briereyly, M. C.Wyatt, M. C.Davey, S. T.Szebesta, D. *Electron. Lett.* **1993**, 29, 2119–2120.
253. Dejneka, M. J.; Samson, B. *MRS Bull.* **1999**, 24, 39–45.
254. Tick, P. A.; Borelli, N. F.; Cornelius, L. K.; Newhouse, M. A. *J. Appl. Phys.* **1995**, 78, 6367–6374.
255. Ainslie, B. J.; Davey, S. T.; Szebesta, D.; Williams, J. R.; Moore, M. W.Whitley, T.Wyatt, R. *J. Non-cryst. Solids* **1995**, 184, 225–228.
256. Silver, J.; Martinez-Rubio, M. I.; Ireland, T. G.; Fern, G. R.Withnall, R. *J. Phys. Chem. B* **2001**, 105, 948–953.
257. Silver, J.Martinez-Rubio, M. I.Ireland, T. G.Withnall, R. *J. Phys. Chem. B* **2001**, 105, 7200–7204.
258. Suggested by Thomas, Prof. C.B. of Nottingham Trent University (UK) in talks with the author.
259. Ballato, J.; Lewis III, J. S.; Holloway, P. *MRS Bull.* **1999**, 24, 51–56.
260. Witte, O.; Stolz, H.; von der Osten, W. *J. Phys. D. Appl. Phys.* **1996**, 29, 561–568.
261. Jia, W.; Lim, K. S.; Liu, H.; Wang, Y.; Ju, J. J.; Yun, S. I.Fernandez, F. E.Yen, W. M. *J. Lumin.* **1996**, 66–67, 190–197.
262. Chang, S. D.Kam, C. H.Zhou, Y.Lam, Y. L.Chan, Y. C.Buddhudu, S. *Mater. Lett.* **2000**, 45, 19–22.
263. Silver, J.; Marsh, P. J.; Withnall, R.; Fern, G. R. *Extended Abstracts of the First International Conference on Science and Technology of Emissive Displays and Lighting*, San Diego, CA, Nov 12–14, 2001; 147–150.
264. Kirk, A. D.; Furer, N.; Guidel, H. U. *J. Lumin.* **1996**, 68, 77–89.
265. Tanabe, S.; Suzuki, K.; Soga, N.; Hanada, T. *J. Lumin.* **1995**, 65, 247–255.
266. Malinowski, M.; Wnuk, A.; Frukacz, Z.Chadeyron, G.Mahiou, R.Guy, S.Joubert, M. F. *J. Alloy Compd* **2001**, 323–324, 731–735.
267. Shaw, L. B.; Chang, R. S.Djeu, N. *Phys. Rev. B* **1994**, 50, 6609–6619.
268. Kishimoto, S.; Hirao, K. *J. Appl. Phys.* **1999**, 80, 1965–1969.
269. Wegh, R. T.; Donker, H.; Meijerink, A.Lamminmaki, R. J.Holsa, J. *Phys. Rev. B* **1997**, 56, 13841–13848.
270. Wegh, R. T.van Loef, E. V. D.Meijerink, A. *J. Lumin.* **2000**, 90, 111–122.
271. Dorenbos, P.; van der Kolk, E.; van Eijk, C. W. E. *Extended Abstracts of the Sixth International Conference on the Science and Technology of Display Phosphors*, San Diego, CA, Nov 6–8, 2000; 25–28.
272. van der Kolk, E.; Dorenbos, P.; van Eijk, C. W. E. *Extended Abstracts of the Sixth International Conference on the Science and Technology of Display Phosphors*, San Diego, CA, Nov 6–8, 2000; 33–36.
273. Dorenbos, P. *J. Lumin.* **2000**, 91, 91–106.
274. Dorenbos, P. *J. Lumin.* **2000**, 91, 155–176.
275. Juestel, T.; Mayr, W.; Schmidt, J.; Wiechert, D. U. *Extended Abstracts of the First International Conference on Science and Technology of Emissive Displays and Lighting*, San Diego, CA, Nov 12–14, 2001; 21–23.
276. Daud, A.; Kunimoto, T.; Olmi, K.; Tanaka, S.; Kobayashiu, H. *Extended Abstracts of the Sixth International Conference on the Science and Technology of Display Phosphors*, San Diego, CA, Nov 6–8, 2000; 29–32.
277. Wegh, R. T.; Donker, H.van Loef, E. V. D.Oskam, K. D.Meijerink, A. *J. Lumin.* **1998**, 87–89, 1017–1019.
278. Cahill-Glauser, S. A.; Lee, H. W. H. *SID'97 Digest* **1997**, 28, 580–583.
279. Kawasaki, M.; Tani, N.; Onishi, R. *SID'98 Digest* **1998**, 28, 266–269.
280. Katsumata, T.; Nabaie, T.; Sasajima, K.; Komuro, S.; Morikawa, T. *J. Electrochem. Soc.* **1997**, 144, L243–L245.
281. Lin, Y.Tang, Z.Zhang, Z.Wang, X.Zhang, J. *J. Mater. Sci. Lett.* **2000**, 20, 1505–1506.
282. Silver, J.; Martinez-Rubio, M. I.; Ireland, T. G.; Fern, G. R.; Withnall, R. *Extended Abstracts of the First International Conference on Science and Technology of Emissive Displays and Lighting*, San Diego, CA, Nov 12–14, 2001; 151–154.
283. Vos, W. L.; Polman, A. *MRS Bull.* **2001**, 26, 642–646.

9.16

Conversion and Storage of Solar Energy using Dye-sensitized Nanocrystalline TiO₂ Cells

MD. K. NAZEERUDDIN and M. GRÄTZEL

Institute of Molecular and Biological Chemistry, Lausanne, Switzerland

9.16.1	CONCEPTS AND DEFINITIONS	720
9.16.1.1	Overview	720
9.16.1.2	Dye-sensitized Solar Cell	721
9.16.1.3	Dye-sensitized Solar Cell Fabrication	721
9.16.1.4	Operating Principles of the Dye-sensitized Solar Cell	721
9.16.1.5	Incident Photon-to-current Efficiency	723
9.16.1.6	Open-circuit Photovoltage	723
9.16.1.7	Fill Factor	723
9.16.1.8	Power Conversion Efficiency	724
9.16.1.9	Solar Radiation and Air Mass	724
9.16.1.10	Photophysical Properties of Metal Complexes	724
9.16.2	SEMICONDUCTOR FILMS	725
9.16.2.1.1	<i>Preparation of Mesoscopic TiO₂ Colloids</i>	725
9.16.2.1.2	<i>Preparation of Films</i>	726
9.16.3	MOLECULAR SENSITIZERS	727
9.16.3.1	Requirements of the Sensitizers	727
9.16.3.2	Tuning of MLCT Transitions	728
9.16.3.3	Spectral Tuning in “Push–Pull” Type Complexes	728
9.16.3.4	Osmium Complexes	733
9.16.3.5	MLCT Transitions in Geometrical Isomers	733
9.16.3.6	Sensitizers Containing Functionalized Hybrid Tetradentate Ligands	733
9.16.3.7	Hydrophobic Sensitizers	735
9.16.3.8	Near IR Sensitizers	737
9.16.4	SURFACE CHELATION AND ELECTRON INJECTION	740
9.16.4.1	Surface Chelation	740
9.16.4.2	X-ray Diffraction, X-ray Photoelectron Spectroscopy, and XAFS Spectroscopy Study	741
9.16.4.3	Acid-base Equilibria of <i>cis</i> -Dithiocyanato- <i>bis</i> (2,2'-bipyridine-4,4'-dicarboxylate) Ruthenium(II)	742
9.16.4.4	ATR-FTIR Studies of Sensitizer Adsorption on TiO ₂ Oxide Surface	742
9.16.4.5	Effect of Protons Carried by the Sensitizer on the Performance	743
9.16.4.6	Comparison of IPCE Values Obtained with Various Sensitizers	744
9.16.4.7	Electron Injection Kinetics	746
9.16.5	REDOX MEDIATORS	747
9.16.5.1	New Redox Couples	747
9.16.5.2	Solid Electrolytes/Hole-transport Materials	748
9.16.6	ENERGY CONVERSION AND STORAGE	749
9.16.6.1	Water Splitting by Visible Light using a Tandem cell	749
9.16.7	SYNTHESIS AND CHARACTERIZATION OF COMPLEXES	750
9.16.7.1	Synthetic Strategies for Ruthenium Complexes	750
9.16.7.2	Purification	752

9.16.1 CONCEPTS AND DEFINITIONS

9.16.1.1 Overview

It is clear that the world's conventional energy supplies (oil, natural gas, and coal) have a limited lifetime as our major source of energy and the current forecasts suggest that alternatives will have to make a major contribution in the near future. Nuclear power was once regarded as a solution for the problem of depleting fossil fuels and increasing energy demands, but the sincere worries about the storage of the nuclear waste have led scientists to search for renewable sources of energy. Most renewable energy sources must rely on a net input of energy into the earth and since the sun is our only external energy source, harnessing its energy (which is clean) is the main objective of all alternative energy strategies.

The solar emission spectrum has a maximum at 500 nm and extends into the IR and the UV regions of the electromagnetic spectrum. A standard intensity spectrum for light incident on the earth's surface is shown in Figure 1. Absorption by ozone, H₂O, and CO₂ removes a large proportion of the UV and the IR region of the sun's energy leaving the visible region, which reaches the surface of the earth. The energy of less than 10 min of sunshine on the planet Earth is equal to the total yearly human energy consumption. Therefore, if we could harvest a fraction of the solar energy reaching the Earth, we would solve many energy supply and environmental problems associated with reliance on fossil fuels.

Ideally, all photons with a wavelength of about 900 nm or shorter should be harvested and converted to electric current. This limit is derived from thermodynamic considerations showing that the conversion efficiency of any single-junction photovoltaic solar converter peaks at approximately 33% near the threshold energy of 1.4 eV.^{1,2} There are numerous ways to convert the solar radiation directly into electrical power or chemical fuel. The silicon solar cell is the most efficient in this respect. Nevertheless, the capital cost of such devices is not attractive for large-scale applications.

One attractive strategy, discussed in this chapter, is the development of systems that mimic photosynthesis in the conversion and storage of solar energy. A way to successfully trap solar radiation is by a sensitizer molecule (analogous to the light-absorbing chlorophyll molecule found in nature) anchored to a rough titania surface. The past decade has witnessed a great triumph for dye-sensitized solar cell technology in various laboratories, because of its low cost and high efficiencies. Several groups have obtained 8–10% solar energy conversion efficiency using dye-sensitized nanocrystalline TiO₂ solar cells.^{3–23}

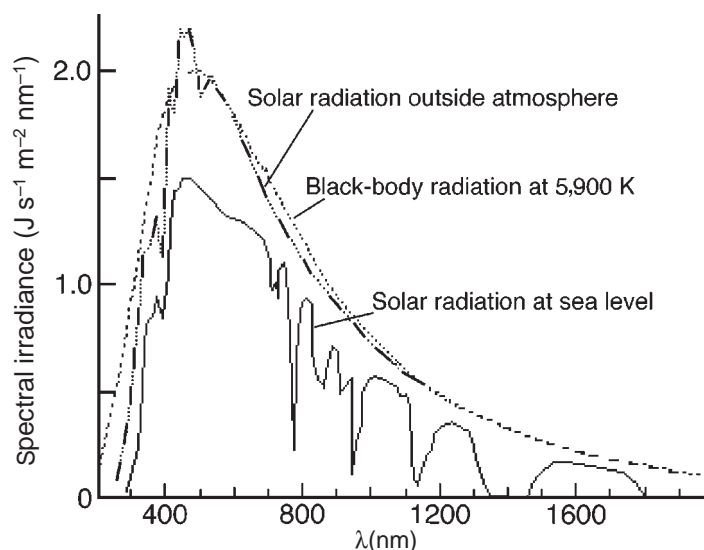


Figure 1 Spectral irradiance of the sun at mean Earth–Sun separation.

9.16.1.2 Dye-sensitized Solar Cell

The dye-sensitized solar cell technology developed at the École Polytechnique Fédérale de Lausanne (EPFL) contains broadly five components: (i) a conductive mechanical support, (ii) a semiconductor film, (iii) a sensitizer, (iv) an electrolyte containing the I^-/I_3^- redox couple, and (v) a counter electrode with a platinum catalyst. The total efficiency of the cell depends on optimization and compatibility of each of these components.²⁴ A cross-section of the dye-sensitized solar cell is shown in Figure 2. To a large extent, the nanocrystalline semiconductor film technology (see Section 9.16.2) and the dye spectral response are mainly responsible for the high efficiency. The high surface area and the thickness of the semiconductor film yields a high optical density for the adsorbed dye, resulting in efficient light harvesting.²⁵

The sensitizers display a crucial role in harvesting of sunlight. To trap solar radiation efficiently in the visible and the near IR region of the solar spectrum requires engineering of sensitizers at a molecular level (see Section 9.16.3).²⁶ The electrochemical and photophysical properties of the ground and the excited states of the sensitizer have a significant influence on the charge transfer (CT) dynamics at the semiconductor interface (see Section 9.16.4). The open-circuit potential of the cell depends on the redox couple, which shuttles between the sensitizer and the counter electrode (for details see Section 9.16.5).

9.16.1.3 Dye-sensitized Solar Cell Fabrication

Briefly, we describe here various steps involved in the preparation of dye-sensitized solar cell. The nanocrystalline TiO₂ films were prepared by depositing TiO₂ colloids on a transparent fluorine-doped tin oxide-conducting glass using either screen printing or by the doctor blade technique.^{27,28} The films are then dried in air and fired at 450 °C. The hot electrodes ($\approx 80^\circ\text{C}$) are immersed into the dye solution, which is usually prepared in ethanol ($2\text{--}5 \times 10^{-4}\text{ M}$). The deposited dye film is used as a working electrode. A sandwich cell is prepared with a second piece of conducting glass coated with chemically deposited platinum from 0.05 M hexachloroplatinic acid. This platinum-coated counter electrode and the dye-coated TiO₂ film are then put together with a thin transparent film of Surlyn polymer frame (DuPont). The sandwiched electrodes are tightly held and then heat is applied (130°C) around the Surlyn frame to seal the two electrodes. A thin layer of electrolyte containing the I_3^-/I^- redox couple in methoxyacetonitrile is introduced into the interelectrode space from the counter electrode side through predrilled holes. The drilled holes are sealed with a microscope cover slide and Surlyn to avoid leakage of the electrolyte solution. A module of a solar cell based on a dye-sensitized TiO₂ nanocrystalline film is shown in Figure 3.

9.16.1.4 Operating Principles of the Dye-sensitized Solar Cell

The details of the operating principles of the dye-sensitized solar cell are given in Figure 4. Photoexcitation of the metal-to-ligand charge transfer (MLCT) of the adsorbed sensitizer (Equation (1)) leads to injection of electrons into the conduction band of the oxide (Equation (2)). The oxidized dye is subsequently reduced by electron donation from an electrolyte containing the iodide/triiodide redox system (Equation (3)). The injected electron flows through the semiconductor network to arrive at the back contact and then through the external load to the counter electrode. At the counter electrode, reduction of triiodide in turn regenerates iodide (Equation (4))

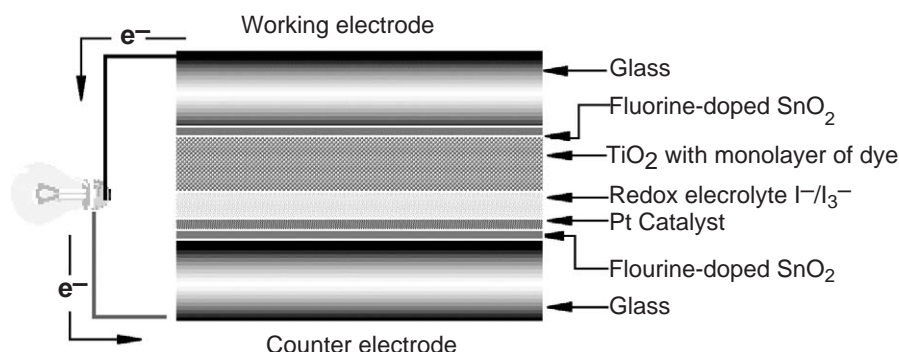


Figure 2 Schematic representation of the cross-section of a dye-sensitized solar cell.

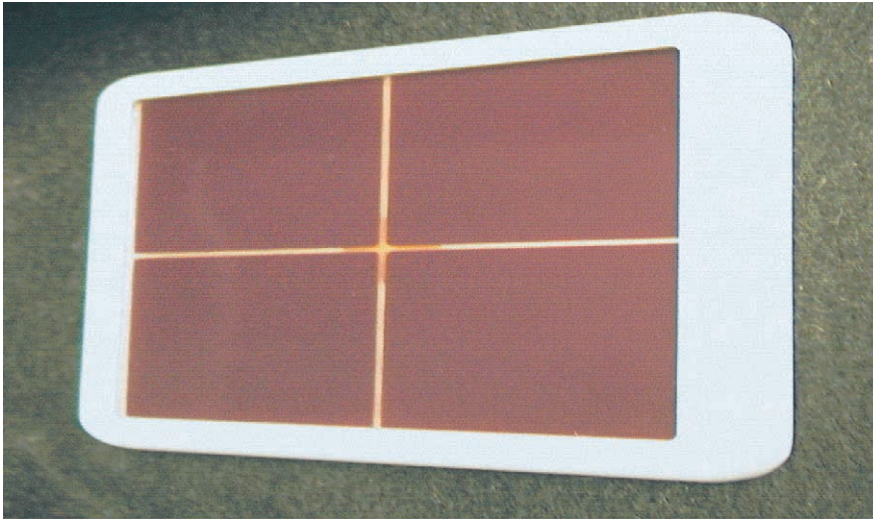


Figure 3 A module of a photoelectrochemical solar cell based on a dye-sensitized TiO₂ nanocrystalline film.

through the donation of electrons from the external circuit, which completes the circuit. With a closed external circuit and under illumination, the device then constitutes a photovoltaic energy conversion system, which is regenerative and stable. However, there are undesirable side reactions: the injected electrons may recombine either with oxidized sensitizer (Equation (5)), or with the oxidized redox couple at the TiO₂ surface (Equation (6)), resulting in losses in the cell efficiency. For a net forward current under study state illumination, the processes of Equations (2) and (3) must be kinetically more favorable than Equations (5) and (6):

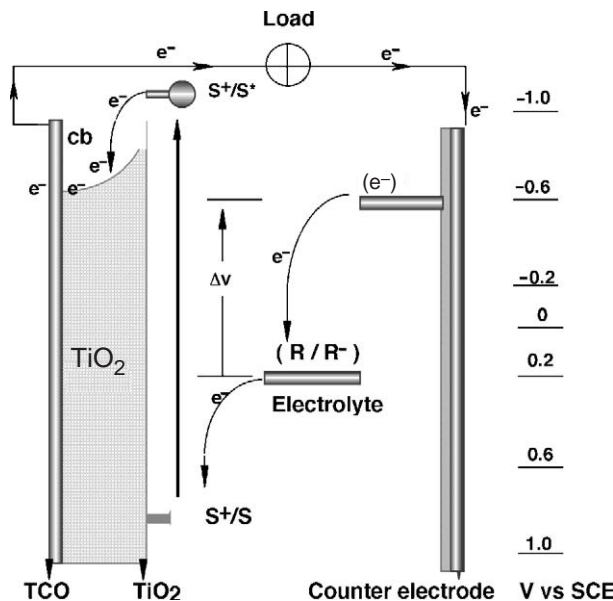
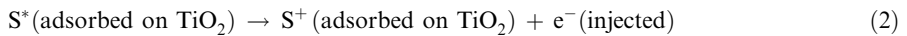
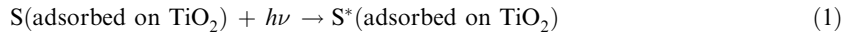
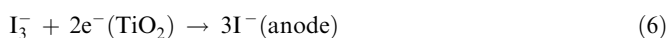
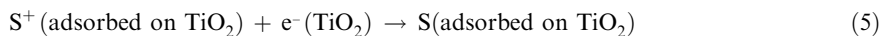
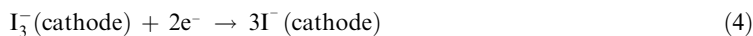
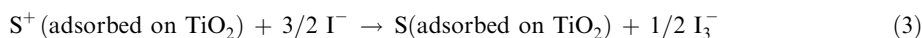


Figure 4 Operating principles and energy level diagram of a dye-sensitized solar cell. S/S⁺/S* = Sensitizer in the ground, oxidized and excited state, respectively. R/R⁻ = redox mediator (I₃⁻/I⁻).



9.16.1.5 Incident Photon-to-current Efficiency

The incident monochromatic photon-to-current conversion efficiency (IPCE), also called *external quantum efficiency*, is defined as the number of electrons generated by light in the external circuit divided by the number of incident photons as a function of excitation wavelength. It is expressed in Equation (7).²⁹ In most cases, the photoaction spectrum overlaps with the absorption spectrum of the sensitizer adsorbed on the semiconductor surface. A high IPCE is a prerequisite for high-power photovoltaic applications, which depends on the sensitizer photon absorption, excited state electron injection, and electron transport to the terminals:

$$\text{IPCE} = \frac{(1.25 \times 10^3) \times \text{photocurrent density}[\text{mA cm}^{-2}]}{\text{wavelength}[\text{nm}] \times \text{photon flux}[\text{W m}^{-2}]} \quad (7)$$

9.16.1.6 Open-circuit Photovoltage

The origin of the open-circuit potential (V_{oc}) in dye-sensitized solar cells is the subject of much discussion. However, grossly it can be determined by the energy difference between the Fermi level of the solid under illumination, and the Nernst potential of the redox couple in the electrolyte (Figure 4). The experimentally observed open-circuit potential for various sensitizers is smaller than the difference between the conduction band and the redox couple, probably due to the competition between electron transfer and charge recombination pathways. The decrease in the rate constants for triiodide reduction (k_{et}) at the photoanode should lead to a decrease in the dark current and thereby an increase in the open-circuit voltage of the cell. For regenerative photoelectrochemical systems, Equation (8) holds, where I_{inj} is the flux of charge resulting from sensitized injection and n_{cb} is the concentration of electrons at the TiO₂ surface:

$$V_{oc} = \frac{kT}{e} \ln \left(\frac{I_{inj}}{n_{cb} k_{et} [I_3^-]} \right) \quad (8)$$

Knowledge of the rates and mechanisms of these competing reactions are vital for the design of efficient sensitizers and thereby improvement of the solar devices.^{14,30,31} Surface modifications also influence significantly the open-circuit potential. For example, treatment of dye-coated electrodes with a base such as ammonia or *tert*-butyl pyridine increases the open-circuit potential by 200–300 mV, due to a band edge shift coupled with reduced charge recombination dynamics. Alternatively, treatment of the TiO₂ electrodes with small cations such as Li⁺ or H⁺ decreases the open-circuit potential substantially. This dependence has been attributed to the influence of such ions on the energetics of the TiO₂ conduction band (a relative negative shift of the conduction band edge occurs, induced by the adsorption of these cations onto the surface) and, therefore, on the energetics of electron injection.³²

9.16.1.7 Fill Factor

The fill factor is obtained by dividing the product of current and voltage measured at the power point by the product of short-circuit current and the open-circuit voltage. The power point is the maximum product of the cell voltage and the photocurrent obtained on the I - V plot (see Section 9.16.4.5). The open-circuit voltage is the potential of the illuminated electrode, where the short-circuit current (I_{sc}) is zero.

9.16.1.8 Power Conversion Efficiency

The overall conversion efficiency (η) of the dye-sensitized solar cell is determined by the photocurrent density (i_{ph}) measured at short circuit, V_{oc} , the fill factor (ff) of the cell, and the intensity of the incident light (I_s) as shown in Equation (9).

$$\eta_{\text{global}} = \frac{i_{\text{ph}} V_{\text{oc}} \text{ff}}{I_s} \quad (9)$$

9.16.1.9 Solar Radiation and Air Mass

Specific solar radiation conditions are defined by the *air mass* (AM) value. The spectral distribution and total flux of radiation outside the Earth's atmosphere, similar to the radiation of a black body of 5,900 K, has been defined as AM-0. The AM-1 and AM-1.5 are defined as the path length of the solar light relative to a vertical position of the Sun above the terrestrial absorber, which is at the equator when the incidence of sunlight is vertical (90°) and 41.8°, respectively. The AM-1.5 conditions are achieved when the solar flux is 982 W m². However, for convenience purpose the flux of the standardized AM-1.5 spectrum has been corrected to 1,000 W m².

9.16.1.10 Photophysical Properties of Metal Complexes

The photophysics and photochemistry of polypyridyl complexes of ruthenium can be understood with the aid of the energy diagram shown in Figure 5. In these complexes there are three possible excited states: (i) metal centered (MC), which are due to promotion of an electron from t_{2g} to e_g orbitals; (ii) ligand centered (LC), that are π - π^* transitions; and (iii) CT excited states, which are either MLCT or ligand-to-metal CT (LMCT). An electronic transition from metal t_{2g} orbitals to empty ligand orbitals without a spin change (a singlet-singlet transition) occurs; these (allowed) transitions are characterized by large extinction coefficients. The transitions in which a spin-state change from singlet (ground state) to triplet (excited state) occurs are "forbidden" and, hence, usually associated with a small extinction coefficient. However, the excited singlet-state may also undergo a spin flip, resulting in an excited triplet state. This process is called *intersystem crossing* (ISC). The possible de-excitation processes can be radiative or nonradiative. The radiative decay of singlet and triplet excited states to a singlet ground state are termed *fluorescence* and *phosphorescence*, respectively.

The intense colors in 2,2'-bipyridyl complexes of iron(II), ruthenium(II), and osmium(II) are due to excitation of an electron from metal t_{2g} orbitals to an empty, low-lying π^* orbital of a conjugated 2,2' bipyridyl ligand. The photoexcitation of this MLCT excited state can lead to emission as the excited state collapses back to the ground state. However, not all complexes are

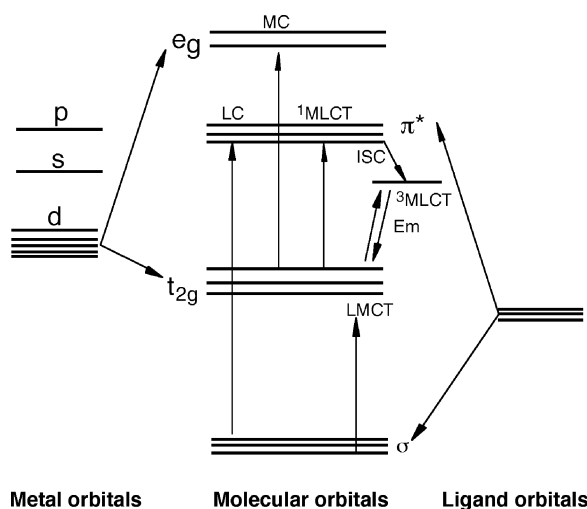
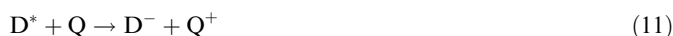


Figure 5 Schematic presentation of a molecular orbital diagram for an octahedral d⁶ metal complex involving 2,2'-bipyridyl-type ligands, in which various possible transitions are indicated.

luminescent because of the different competing deactivation pathways, many of which are non-radiative; a discussion of this subject is beyond the scope of this chapter. The interested reader can refer to a number of publications on this subject.^{33–37} The other potential deactivation pathways for the excited state of the dye are donation of an electron (called *oxidative quenching*, Equation (10)), the capture of an electron (*reductive quenching*, Equation (11)), or transfer of its energy to other molecules or solvent (Equation (12)):



The excited state redox potential of a sensitizer plays an important role in the electron transfer process. An approximate value of the excited state redox potential can be extracted from the potentials of the ground state couples and the zero-zero excitation energy (E_{0-0}) according to Equations (13) and (14). The zero-zero energy can be obtained from the 77 K emission spectrum of the sensitizer:³⁸

$$E(S^*/S^-) = E(S/S^-) + E_{0-0} \quad (13)$$

$$E(S^+/S^*) = E(S^+/S) - E_{0-0} \quad (14)$$

9.16.2 SEMICONDUCTOR FILMS

9.16.2.1.1 Preparation of Mesoscopic TiO₂ Colloids

The favored semiconductor material is titanium dioxide because of its abundance, low cost and nontoxicity. This last characteristic promotes its use in healthcare products and paints. As mentioned in the introduction, the efficiency of the solar cell depends to a large extent on the nanocrystalline semiconductor films; the high surface area of these films yields a high dye loading and, therefore, high optical density, resulting in efficient light absorption. The nanoporous structure permits surface coverage of the dye to be sufficiently high for total absorption of the incident light, necessary for efficient solar energy conversion, since the area available for monomolecular distribution of adsorbate is 2–3 orders of magnitude higher than the geometric area of the substrate.

The original substrate structure used for our early photosensitization experiments was a fractal surface derived by hydrolysis of an organo-titanium compound, but this has since been replaced with a nanostructured layer deposited from a colloidal suspension of TiO₂. This evidently provides for a much more reproducible and controlled high surface area nanotexture. Further, since it is compatible with screen-printing technology, it anticipates future production requirements. While commercially available titania powders produced by a pyrolysis route from a chloride precursor have been successfully employed, the present optimized material is the result of a hydrothermal technique, described by Brooks *et al.*³⁹ A specific advantage of the procedure is the ease of control of the particle size, and hence, of the nanostructure and porosity of the resultant semiconductor substrate. Figure 6 shows the relevant flow diagram and the reaction steps involved in the sol–gel preparation of the films. The procedure involves the hydrolysis of the titanium alkoxide precursor producing an amorphous precipitate followed by peptization in acid or alkaline aqueous conditions to produce a sol, which is subjected to hydrothermal Ostwald ripening in an autoclave. The resulting crystallites of TiO₂ consist either of anatase, or of a mixture of anatase and rutile, depending on the reaction conditions.

The temperature of the hydrothermal treatment has a decisive influence on the particle size. The standard sol, treated for about 12 h at 230 °C in the autoclave, has an average particle diameter of 15 nm. Figure 7 shows a scanning microscope picture of a TiO₂ film deposited on transparent conducting glass by screen-printing from a concentrated solution of such particles. Each particle is a single crystal exposing predominantly surface planes with (101) direction. The formation of the latter face is favored by its low surface energy. The autoclaving temperature has an effect on pore size distribution. The maximum shift to larger pore diameters with increasing temperature reflects enhanced particle growth. For the 230 °C sol the most frequent pore size is about 10 nm.

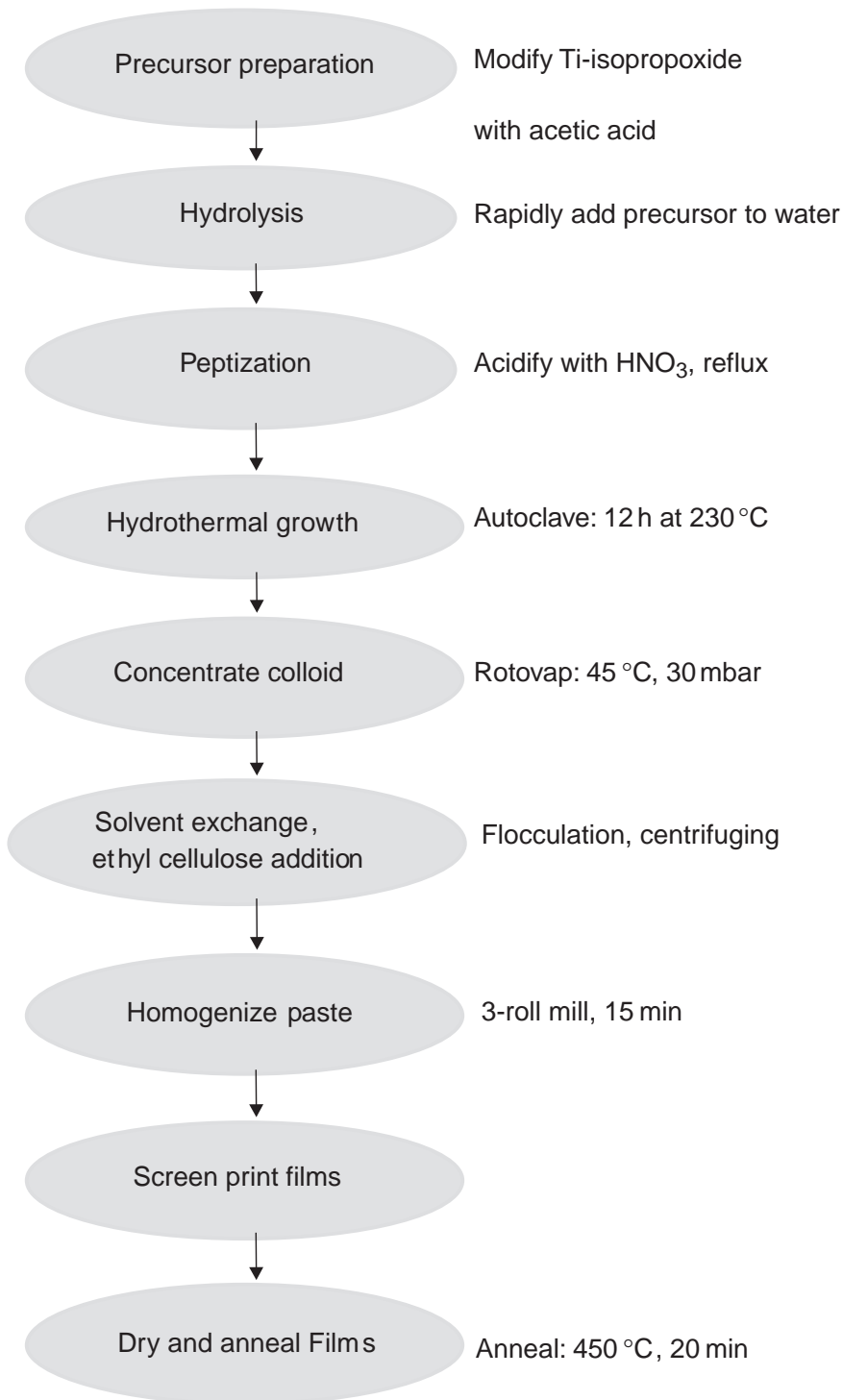


Figure 6 A flow diagram showing the reaction steps involved in the sol-gel preparation of TiO₂ colloids and films.

9.16.2.1.2 Preparation of Films

The TiO₂ paste is deposited onto a sheet of glass using a screen-printing technique. The glass is coated with a fluorine-doped stannic oxide layer for conductivity, and has a resistance of 8–10 Ω cm⁻². The TiO₂ screen-printed layer is dried in air at 100 °C for 15 min followed by another 15 min at 150 °C. For the final processing, the layers were heated using a titanium hot plate (Bioblock Scientific) to 325 °C at

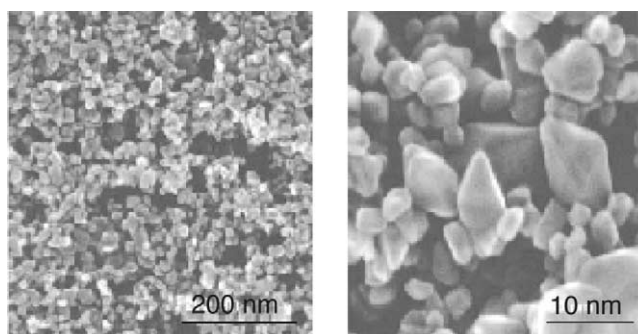


Figure 7 SEM image of the surface of a mesoporous film prepared from colloidal TiO₂.

a rate of 30 °C min⁻¹ and kept at this temperature for 5 min. Then, the temperature was raised to 375 °C at a rate of 10 °C min⁻¹ and held there for 5 min. Finally the layers were fired to 450 °C at a rate of 15 °C min⁻¹, under flowing oxygen and left at this temperature for 20 min, before cooling to room temperature. The film thickness is 13–18 μm. The heated electrodes were impregnated with a 0.05 M titanium tetrachloride solution (65 μl cm⁻²) in a water-saturated desiccator for 30 min at 70 °C and washed with distilled water.⁴⁰ The TiO₂ layers were again fired at 450 °C for 20 min and allowed to cool to 100 °C before plunging into a dye solution.

A striking and unexpected behavior of the mesoporous TiO₂ films prepared by the sol-gel method is that the high surface roughness does not promote charge carrier loss by recombination. The reason for this behavior is that the electron and the positive charge find themselves, femtoseconds after light excitation of the dye, on opposite sides of the liquid-solid interface. The carrier loss mechanisms (charge recombination) are comparatively slow. The loss of a photoexcited electron from the semiconductor should be regarded as a recapture (by an oxidized dye species), or as a redox capture (when the electron reacts directly with an ion in the electrolyte). Either occurs on a millisecond time scale, i.e., relatively slowly.

9.16.3 MOLECULAR SENSITIZERS

9.16.3.1 Requirements of the Sensitizers

The optimal sensitizer for the dye-sensitized solar cell should be panchromatic, i.e., it should absorb visible light of all colors. Ideally, all photons at wavelengths shorter than a threshold of about 920 nm (see Section 9.16.1.1) should be harvested and converted to electric current.^{1,2} In addition, the sensitizer should fulfill several other demanding conditions:

- (i) It must be firmly grafted onto the semiconductor oxide surface, and inject electrons into the conduction band with a quantum yield of unity.
- (ii) The excited state of the dye must be higher in energy than the conduction band edge of the semiconductor, in order to inject electrons quantitatively.
- (iii) The ground state redox potential of the dye should be sufficiently high that it can be regenerated rapidly via electron donation from the electrolyte or a hole conductor.
- (iv) The extinction coefficient of the dye should be high over the whole absorption spectrum to absorb most of the incident light.
- (v) The dye should be soluble in some solvent for adsorption on TiO₂ surface, and should not be desorbed by the electrolyte solution.
- (vi) It should be stable enough to sustain at least 10⁸ redox turnovers under illumination, corresponding to about 20 years of exposure to natural sunlight.

Molecular engineering of ruthenium complexes that can act as panchromatic CT sensitizers for TiO₂-based solar cells presents a challenging task as several requirements have to be fulfilled by the dye, which are very difficult to be met simultaneously. The lowest unoccupied molecular orbitals (LUMOs) and the highest occupied molecular orbitals (HOMOs) have to be maintained at levels where photo-induced electron transfer into the TiO₂ conduction band and regeneration

of the dye by iodide can take place with practically 100% yield. This restricts greatly the options available to accomplish the desired red shift of the MLCT transitions to about 900 nm (necessary to optimize absorption of solar radiation).

The spectral and redox properties of ruthenium(II) polypyridyl complexes can be tuned in two ways: firstly, by introducing a ligand with a low-lying π^* molecular orbital; and secondly, by destabilization of the metal t_{2g} orbital through the introduction of a strong donor ligand. Meyer and co-workers have used these strategies to tune considerably the MLCT transitions in ruthenium complexes.⁴¹ Heteroleptic complexes containing bidentate ligands with low-lying π^* orbitals, together with others having strong sigma-donating properties, show impressive panchromatic absorption properties.⁴¹ However, the extension of the spectral response into the near IR was gained at the expense of shifting the LUMO orbital to lower levels from where charge injection into the TiO₂ conduction band can no longer occur.⁹

Near IR absorption by the dye can also be achieved by upward shifting of the Ru t_{2g} (HOMO) levels. However, it turns out that the mere introduction of strong sigma donor ligands into the complex often does not lead to the desired spectral result, as both the HOMO and LUMO are displaced in the same direction. Furthermore, the HOMO position can not be varied freely as the redox potential of the dye must be maintained sufficiently positive to ensure rapid regeneration of the dye by electron donation from iodide following charge injection into the TiO₂.

Based on extensive screening of hundreds of ruthenium complexes, it was discovered that the sensitizer's excited state oxidation potential should be negative of at least -0.9 V vs. SCE, in order to inject electrons efficiently into the TiO₂ conduction band. The ground state oxidation potential should be about 0.5 V vs. SCE, in order to be regenerated rapidly via electron donation from the electrolyte (iodide/triiodide redox system) or a hole conductor. A significant decrease in electron injection efficiencies will occur if the excited and ground state redox potentials are lower than these values.

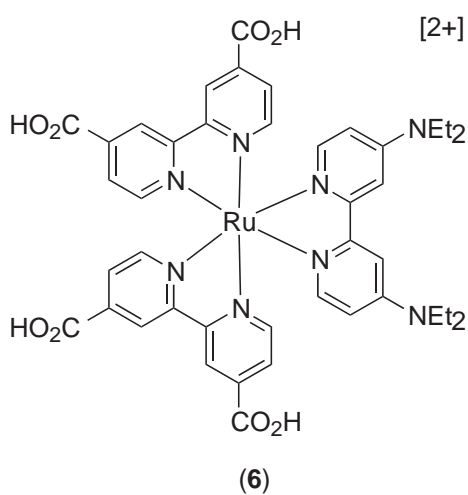
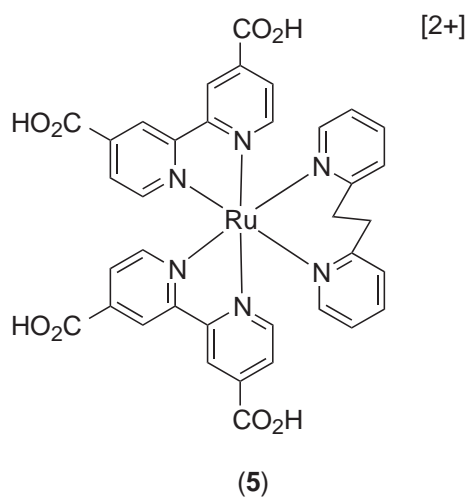
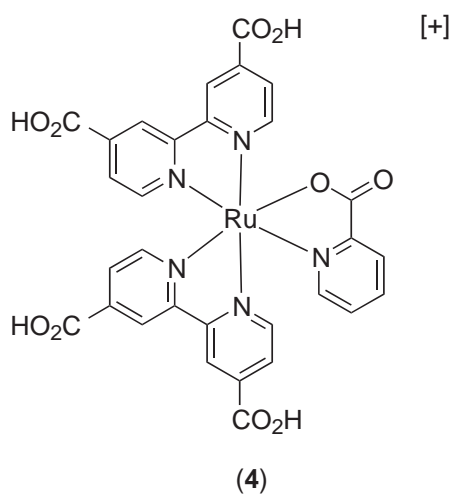
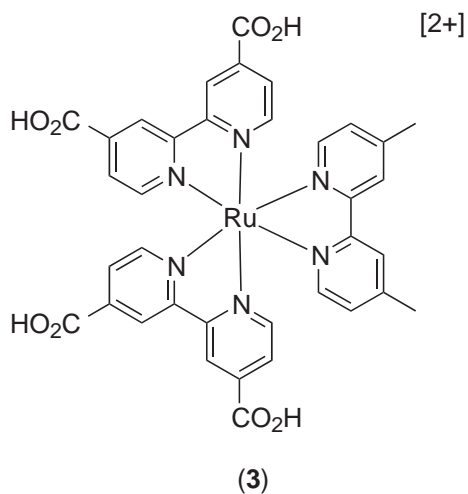
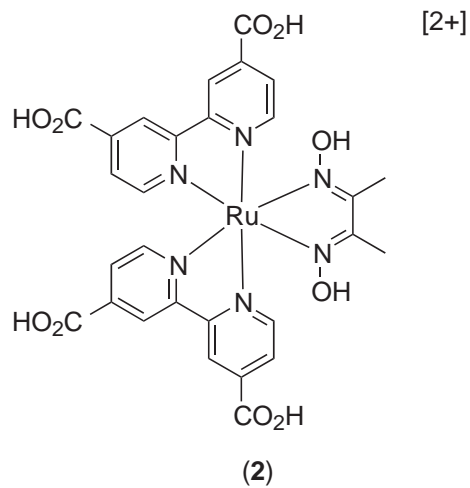
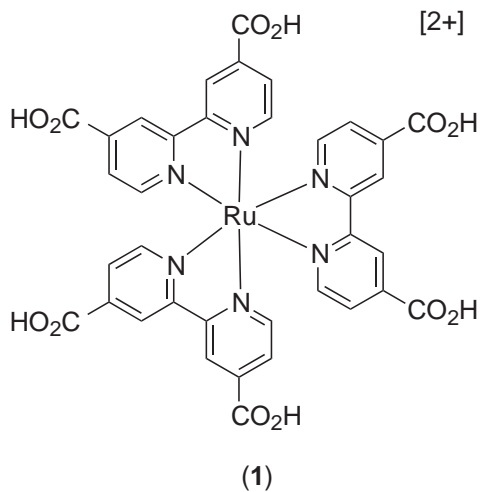
9.16.3.2 Tuning of MLCT Transitions

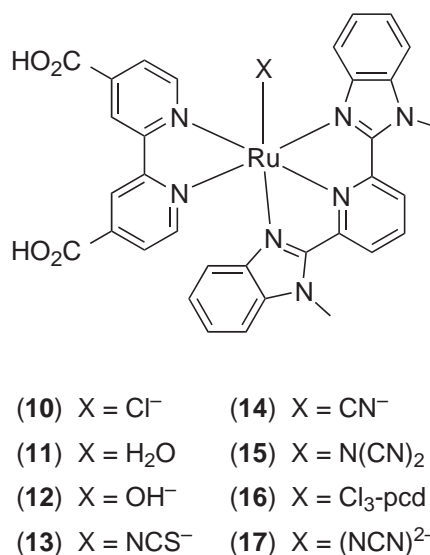
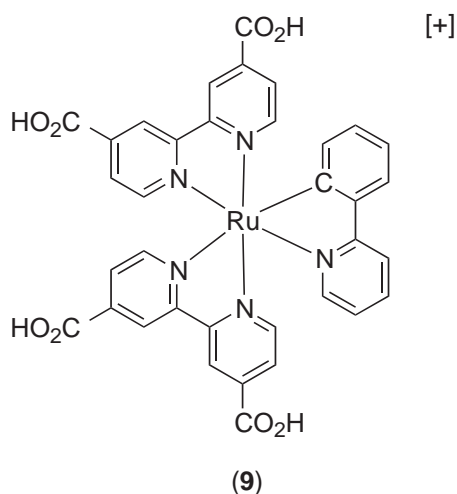
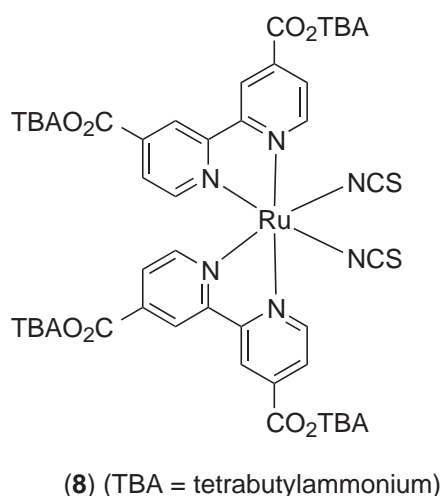
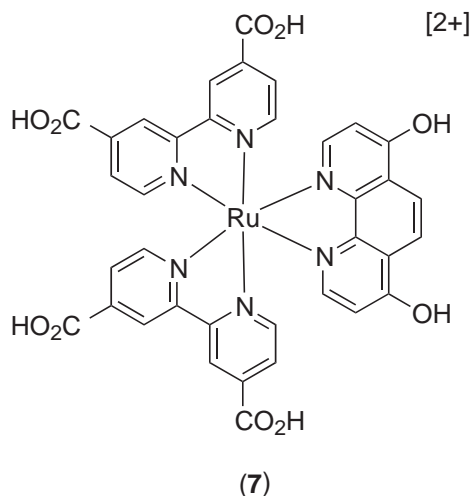
To illustrate aspects of the tuning of the MLCT transitions in ruthenium polypyridyl complexes, let us begin by considering the well-known ruthenium *tris*-bipyridine complex (**1**). This complex shows a strong absorption band in the visible region at 466 nm, due to a CT transition from metal t_{2g} (HOMO) orbitals to π^* (LUMO) orbitals of the ligand. The Ru^{II/III} oxidation potential is at 1.3 V, and the ligand-based reduction potential is at -1.5 V vs. SCE.³⁵ From detailed spectroscopic and electrochemical studies, it has been concluded that these oxidation and reduction potentials are good indicators of the energy levels of the HOMO and LUMO.⁴² The energy between the metal t_{2g} orbitals and π^* orbitals can be reduced either by raising the energy of the t_{2g} or by decreasing the energy of the π^* orbitals with donor or acceptor ligands, respectively (Figure 8). In the following sections we will be discussing the ways to tune HOMO and LUMO energy levels by introducing various ligands.

9.16.3.3 Spectral Tuning in “Push–Pull” Type Complexes

The lowest energy MLCT transition of ruthenium polypyridyl complexes of the type (**1**) can be lowered so that it absorbs more in the red region of the visible spectrum, by substituting one of the bidentate ligands with a donor (“pushing”) ligand. The remaining two electron-withdrawing bidentate ligands act as “pulling” ligands. A list of complexes ((**1**)–(**9**)) is shown where the absorption maxima of the complexes are tuned from 466 nm to 560 nm by introducing different donor ligands. The oxidation potential in these complexes was tuned from 1.3 V to 0.3 V vs. SCE, going from (**1**) to (**9**). Thus, the energy of the HOMO is varied over a range of 1 eV in this series of complexes.⁴³

It is interesting to note the magnitude of the spectral shift for the lowest energy CT transition that is ≈ 0.5 eV, and the shift in the oxidation potential ≈ 1 eV. This shows clearly that the HOMO tuning is not all translated into the spectral shift of the complex. The apparent 0.5 eV discrepancy is due to the increase in energy of the π^* orbitals of the “pulling” ligands, caused by the “pushing” ligands.⁴³





The other interesting class of compounds ((10)–(20)) contains donor and acceptor groups in the same ligand, for example 2,6-*bis*(1-methylbenzimidazol-2'-yl)pyridine. This hybrid ligand, which contains donor (benzimidazol-2'-yl) and acceptor (pyridyl) groups, was tuned further by introducing different substituents on the benzimidazol-2'-yl group. The complexes containing these ligands show intense UV absorption bands at 362 and 346 nm due to the intraligand π – π^* transition of 2,6-*bis*(1-methylbenzimidazol-2'-yl)pyridine; this acts as a UV filter and/or a converter of UV light to visible light in dye-sensitized solar cells.

The MLCT bands of these complexes are broad and red shifted by approximately 140 nm compared to (1). The lowest-energy MLCT transitions within this series were shifted from 486 nm to 608 nm, and the HOMO level varied over an extent of 0.45 eV vs. SCE.⁴⁴ The energy of the MLCT transition in these complexes decreases with the decrease in the π acceptor strength of the ancillary ligand, that is, CN⁻ > NCS⁻ > H₂O > NCN²⁻ > Cl⁻. The red shift of the absorption maxima in complexes (19) and (20), containing 4,4'-dicarboxy-2,2'-biquinoline (dcbiq) instead of 4,4'-dicarboxy-2,2'-bipyridine (dcbpy) as acceptor ligand, is due to the low energy of the π^* orbitals of 4,4'-dicarboxy-2,2'-biquinoline. The resonance Raman spectra of these complexes for excitation at 568 nm show predominantly bands associated with the dcbpy and dcbiq ligands indicating that the lowest excited state is a ruthenium to dcbpy or dcbiq MLCT state.^{44–46}

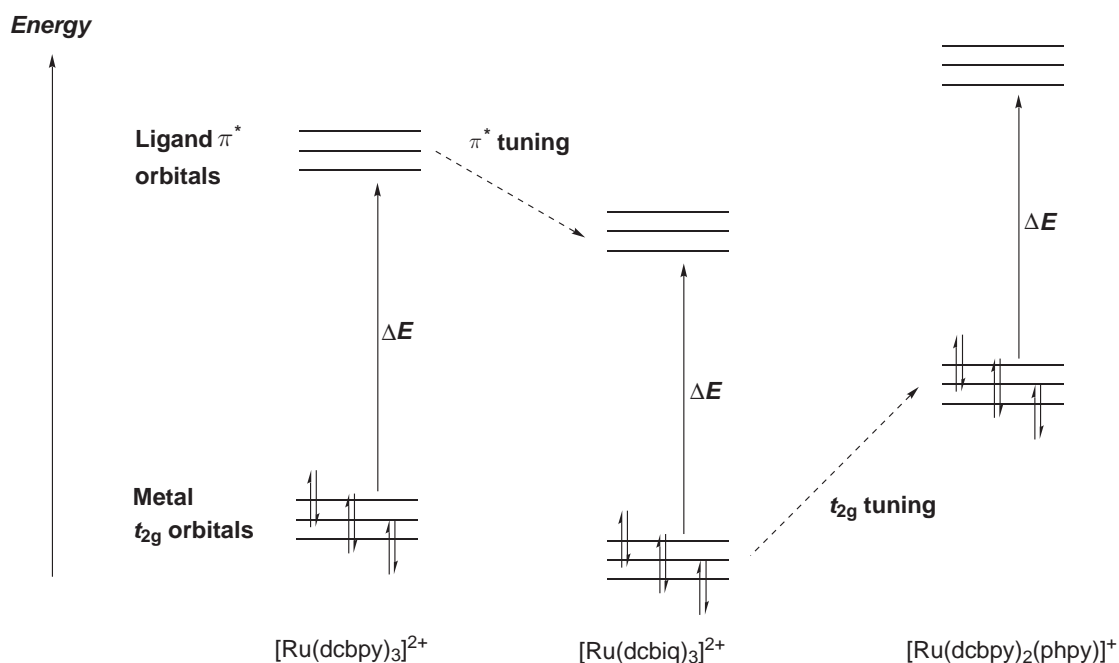
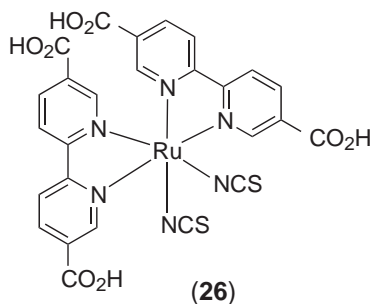
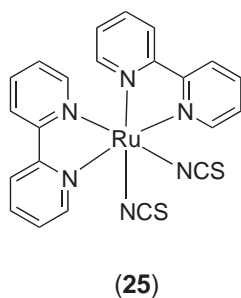
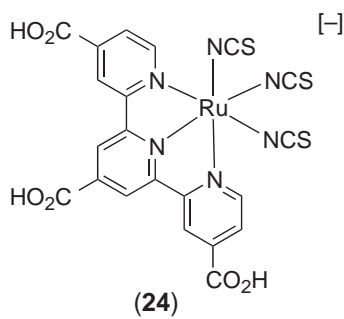
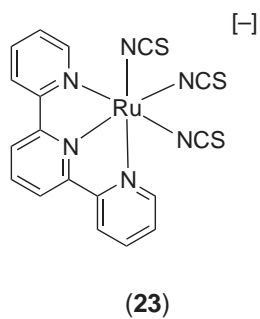
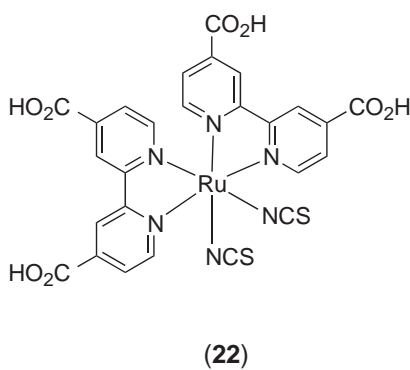
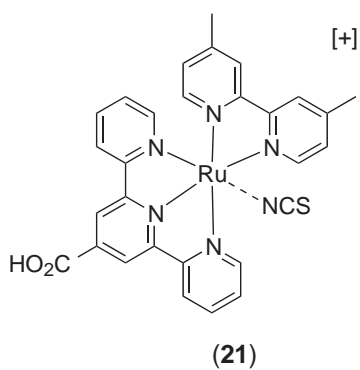
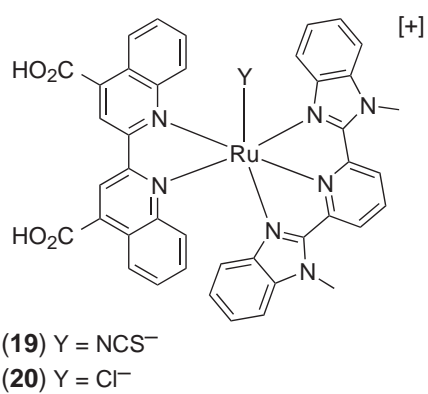
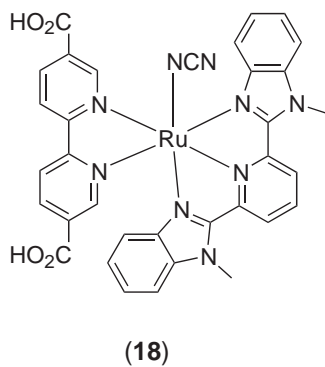


Figure 8 Tuning of HOMO (t_{2g}) and LUMO (π^*) orbital energy in various ruthenium polypyridyl complexes (Hphpy = 2-phenylpyridine).

The spectral properties of ruthenium polypyridyl complexes can also be tuned by introducing nonchromophoric donor ligands such as NCS^- , which destabilizes the metal t_{2g} orbitals. A comparison of the visible absorption spectra of complexes ((**21**)–(**24**)), where the number of nonchromophoric ligands is varied from one to three, shows that the most intense MLCT transition maxima are at 500, 535, 570, and 620 nm, respectively. The 70 nm red shift in complex (**23**) compared to complex (**21**) is due to an increase in the energy of the metal t_{2g} orbitals caused by introducing the nonchromophoric ligands. Complex (**24**) shows an absorption maximum at 620 nm, and the 50 nm red shift of complex (**24**) compared to complex (**23**) reflects the extent of decrease in the LUMO energy, due to substitution of three carboxylic acid groups at the 4,4',4''-positions of 2,2':6',2''-terpyridine compared to unsubstituted terpyridine.^{29,47,48}

In an effort to tune further the spectral responses of the ruthenium complexes containing polypyridyl ligands, several groups have explored the influence of the position of the carboxylic acid substituents.^{49–51} Comparison of complexes ((**25**)–(**28**)) shows the extent HOMO and LUMO tuning. The lowest MLCT absorption maximum of complex (**25**) is at 510 nm in ethanol. By substituting two carboxylic acid groups at the 4,4'-positions of the 2,2'-bipyridine ligands in (**22**), the MLCT maximum was red-shifted to 535 nm. However, on substitution at the 5,5' positions of 2,2'-bipyridine in (**26**), the absorption maximum shifted further into the red (580 nm). In contrast, the MLCT maximum was blue shifted (500 nm) by substituting at the 6,6' positions of 2,2'-bipyridine, in (**27**). The enhanced red response of complexes containing the 5,5'-dicarboxylic acid-2,2'-bipyridine ligand is due to a decrease in the energy of the π^* orbitals, which makes them attractive as sensitizers for nanocrystalline TiO₂ films. Bigozzi and co-workers found that the IPCE of complexes having the 5,5'-dicarboxylic acid-2,2'-bipyridine ligands were lower than the analogous complexes that contain 4,4'-dicarboxylic acid-2,2'-bipyridine.⁴⁹ They rationalized the low efficiency of these sensitizers containing 5,5'-dicarboxylic acid-2,2'-bipyridine ligands in terms of low excited state redox potentials.

In search of new sensitizers that absorb strongly in the visible region of the spectrum, Arakawa and co-workers have developed several sensitizers based on 1,10-phenanthroline ligands. Among these new compounds, (**29**) and (**30**) are noteworthy; they show an intense and broad MLCT absorption band at 525 nm in ethanol. The energy levels of the LUMO and HOMO for (**29**) were estimated to be -1.02 and 0.89 eV vs. SCE, respectively, which are slightly more positive than those of the sensitizer (**22**). These sensitizers, when anchored onto a TiO₂ surface, yield more than 85% photon to electron injection efficiencies.^{8,52,53}



9.16.3.4 Osmium Complexes

Although there are a large number of osmium polypyridyl complexes, very few have been used as sensitizers in dye-sensitized solar cells. Osmium complexes have several advantages compared to their ruthenium analogues: in particular, osmium has a stronger ligand field splitting compared to ruthenium, and the spin-orbit coupling leads to excellent response in the red region by enhancing the intensity of the “forbidden” singlet-triplet MLCT transitions.⁵⁴ Heimer *et al.* found that the complex (31) is extremely stable under irradiation in a homogeneous aqueous solution compared to the analogous ruthenium complex.⁵⁵ The greater photostability for osmium is consistent with a stronger crystal field splitting of the metal *d*-orbitals, which inhibits efficient population of *d-d* excited states. Lewis and co-workers have developed osmium-based sensitizers (31) and (32), and found nearly 80% incident monochromatic photon-to-current conversion efficiencies.⁵⁶

9.16.3.5 MLCT Transitions in Geometrical Isomers

Isomerization is another approach for tuning the spectral properties of metal complexes.^{57–59} The UV–vis absorption spectrum of the *trans*-dichloro complex (35) in DMF solution shows at least three MLCT absorption bands in the visible region at 690, 592, and 440 nm. Alternatively, the *cis*-dichloro complex (33) in DMF solution shows only two distinct broadbands in the visible region at 590 and 434 nm, assigned as MLCT transitions. The lowest energy MLCT band in the *trans*-complexes ((35)–(37)) is significantly red shifted compared to that in the corresponding *cis*-complexes ((22), (33), (34)) (Figure 9). This red shift is due to stabilization of the LUMO of the dcby ligand in the *trans* species relative to the *cis* species. The red shift (108 nm) of the lowest energy MLCT absorption of the *trans*-dichloro complex (35) compared to that of the *trans*-dithiocyanato complex (37) is due to the strong σ -donor property of the Cl[−] ligand compared to NCS[−]. The chloride ligands cause destabilization of the metal *t*_{2g} orbitals, raising them in energy closer to the ligand π^* orbitals, resulting in lower energy MLCT transitions.

9.16.3.6 Sensitizers Containing Functionalized Hybrid Tetradentate Ligands

The main drawback of the *trans* complexes discussed above is their thermal and photo-induced isomerization back to the *cis* configuration. In an effort to stabilize the *trans* configuration of an octahedral ruthenium complex, and integrate the concepts of donor and acceptor ligands in a single complex, Renouard *et al.* have developed functionalized hybrid tetradentate ligands and their ruthenium complexes ((38)–(47)).⁶⁰ In these complexes the donor units of the tetradentate ligand (benzimidazole in (38) and (39) and *tert*-butylpyridine in (40) and (41)) tune the metal *t*_{2g} orbital energies, and the acceptor units (methoxycarbonyl) tune the π^* molecular orbital energies. The use of a tetradentate ligand will inhibit the *trans*- to *cis*-isomerization process. The axial coordination sites are used further to fine-tune the spectral and redox properties, and to stabilize the hole that is being generated on the metal, after injection of an electron into the conduction band.

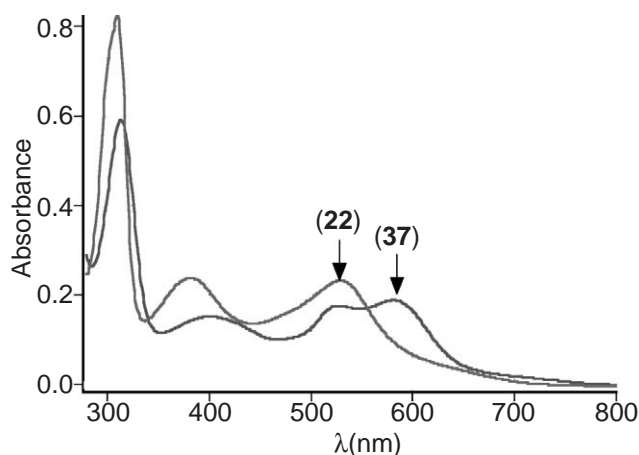
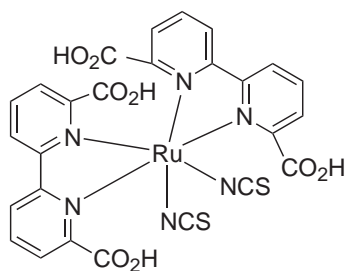
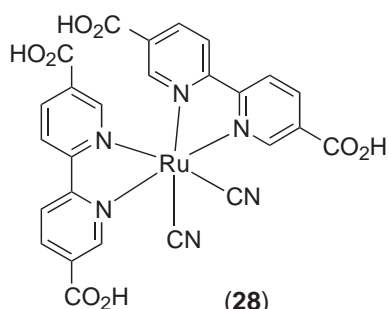


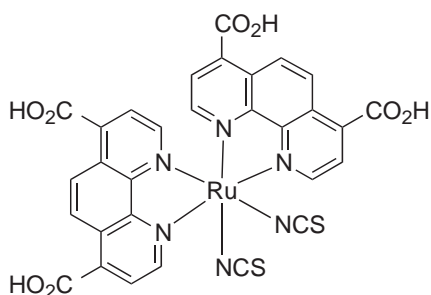
Figure 9 UV–visible absorption spectra of the complexes (22) and (37) in ethanol solution at room temperature.



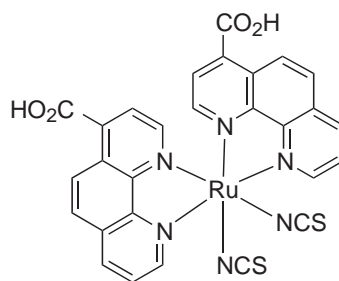
(27)



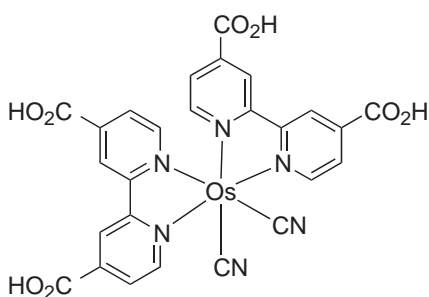
(28)



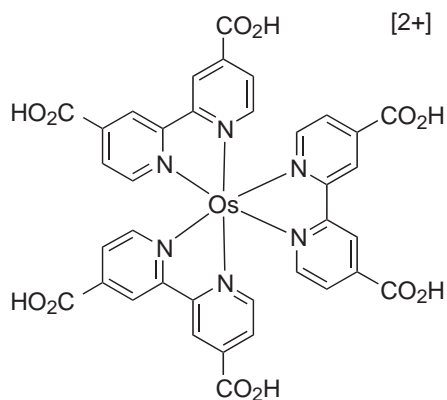
(29)



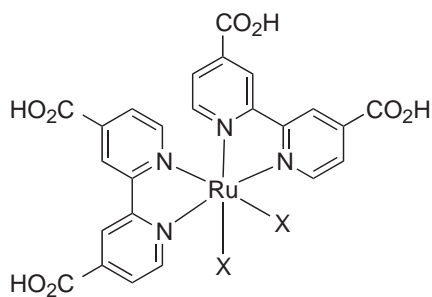
(30)



(31)

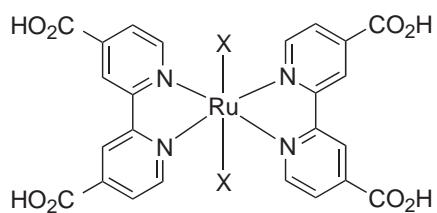


(32)



(33) X = Cl⁻

(34) X = H₂O



(35) X = Cl⁻

(36) X = H₂O

(37) X = NCS⁻

The *trans*-dichloro and dithiocyanate complexes show MLCT transitions in the entire visible and near IR region. The lowest energy MLCT transition band of the *trans*-dichloro complexes is around 700 nm in DMF solution, and the complexes show weak and broad emission signals above 950 nm. The absorption and emission maxima of the *trans*-dithiocyanate complexes are blue shifted compared to its *trans*-dichloro analogues due to the strong π acceptor property of the NCS⁻ ligands compared to Cl⁻, which is consistent with the electrochemical properties of these complexes.

The Ru^{III/II} redox potentials of the thiocyanate complexes were more positive (by ≈ 350 mV) than those of the corresponding dichloro complexes. This is in good agreement with the Ligand Electrochemical Parameters scale, according to which the potential of the Ru^{III/II} couple in the thiocyanate complex should be ~ 340 mV more positive than in the analogous dichloride complex.⁶¹ The $i_{\text{ox}}/i_{\text{red}}$ peak current is substantially greater than unity due to the oxidation of the thiocyanate ligand subsequent to the oxidation of the ruthenium(II) center.

The electronic spectrum of (**38**) was calculated by intermediate neglect of differential overlay (INDO/S) and compared with the experimental data. Geometry optimization of (**38**) produced a structure with C₂-point group symmetry. The three HOMOs (HOMO, HOMO-1, and HOMO-2) for complex (**38**) are mostly formed from 4d(Ru) orbitals and their contribution ranges from 52% to 84%. The d_{yz} Ru orbital is directed toward the tetradentate ligand and coupled to the π -orbitals of the ligand, and is thereby delocalized to a greater extent than the other $d(t_{2g})$ orbitals. The LUMOs are almost entirely localized on the ligand (Figure 10). Extensive π -back-donation between metal 4d and ligand π^* orbitals is observed. Complex (**45**) when anchored on a TiO₂ layer shows an IPCE of 75%, yielding a current density of 18 mA cm⁻² under standard AM 1.5 sunlight.⁶⁰

9.16.3.7 Hydrophobic Sensitizers

An important aspect of dye-sensitized solar cells is water-induced desorption of the sensitizer from the surface. Extensive efforts have been made to overcome this problem by introducing hydrophobic properties in the ligands. Complexes that contain hydrophobic ligands ((**48**)–(**53**)) have several advantages compared to *cis*-dithiocyanato-*bis*-(2,2'-bipyridyl-4,4'-dicarboxylate)ruthenium(II) (**22**):

- (i) The ground state pK_a is higher due to acceptor and donor properties of the 4, 4'-dicarboxylic acid and the hydrophobic ligand, respectively.
- (ii) The dye uptake onto the TiO₂ surface is enhanced significantly, because of the increased ground state pK_a , and the decreased charge on the complex (only two ionizable carboxylic acid units instead of four).
- (iii) The long aliphatic chains interact laterally and decrease the back electron transfer to the oxidized redox couple (see Section 9.16.4.5).
- (iv) The hydrophobicity of the ligand increases the stability of solar cell towards water-induced desorption.

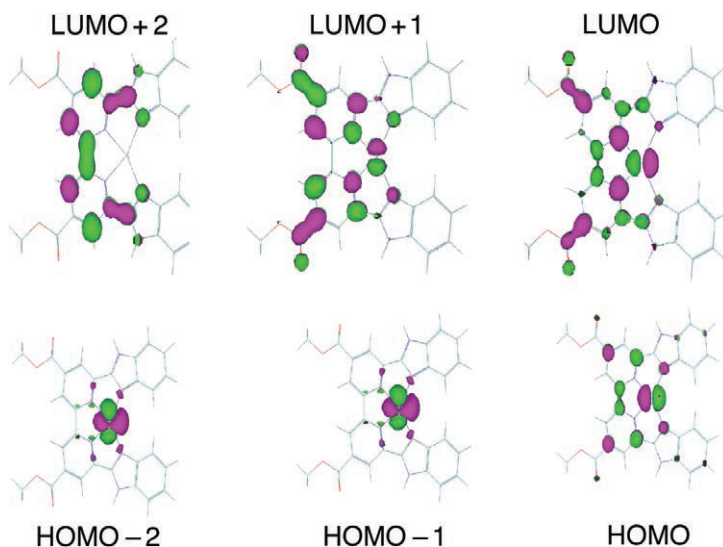
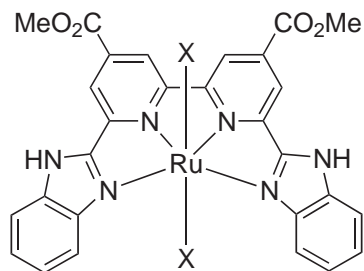
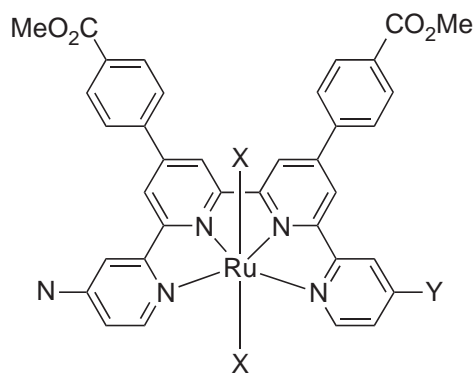


Figure 10 Pictures of the frontier orbitals of the complex (**38**).



(38) X = Cl⁻

(39) X = NCS⁻

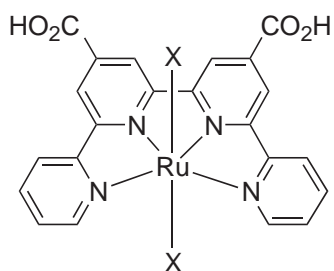


(40) X = Cl⁻, Y = ^tBu

(41) X = NCS⁻, Y = ^tBu

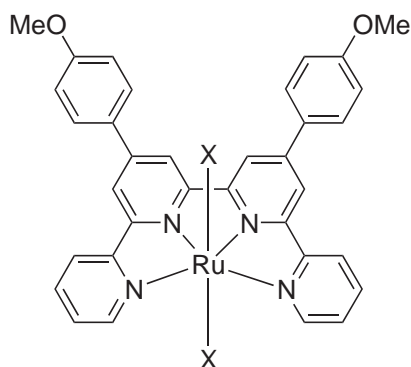
(42) X = Cl⁻, Y = H

(43) X = NCS⁻, Y = H



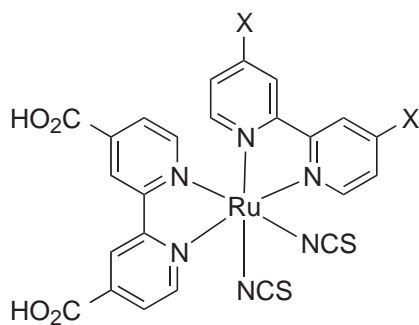
(44) X = Cl⁻

(45) X = NCS⁻



(46) X = Cl⁻

(47) X = NCS⁻



(48) X = Me

(49) X = ^tBu

(50) X = C₆H₁₃

(51) X = C₉H₁₉

(52) X = C₁₃H₂₇

(53) X = C₁₆H₃₃

The photocurrent action spectra of these complexes show broad features covering a large part of visible spectrum, and display a maximum at around 550 nm, where the incident monochromatic IPCE exceeds 85%. These hydrophobic complexes show excellent stability towards water-induced desorption when used as CT photosensitizers in nanocrystalline TiO₂-based solar cells.⁶²

The rate of electron transport in dye-sensitized solar cells is a major element of the overall efficiency of the cells. The electrons injected into the conduction band from the excited state of the dye can traverse the TiO₂ network and can be collected at the transparent conducting glass, or can react either with oxidized dye molecules or with the oxidized redox couple (recombination). The reaction of injected electrons in the conduction band with the oxidized redox mediator (I₃⁻) gives undesirable dark currents, reducing significantly the charge-collection efficiency, and thereby decreasing the total efficiency of the cell (Figure 11).

Several groups have tried to reduce the recombination reaction by using sophisticated device architecture such as composite metal oxides with different band gaps as the semiconductor.^{63,64} Gregg *et al.* have examined surface passivation by deposition of insulating polymers.⁶⁵ We have used additional spacer units between the dye and the TiO₂ surface to reduce the recombination reaction, but with little success (Nazeeruddin *et al.* personal observations). Nevertheless, by using TiO₂ films containing hydrophobic sensitizers that contains long aliphatic chains ((50)–(53)) the recombination reaction was suppressed considerably. The most likely explanation for the reduced dark current is that the long chains of the sensitizer interact laterally to form an aliphatic network as shown in Scheme 1, thereby preventing triiodide from reaching the TiO₂ surface.

9.16.3.8 Near IR Sensitizers

Phthalocyanines possess intense absorption bands in the near-IR region and are known for their excellent stability, rendering them attractive for photovoltaic applications.⁶⁶ They have been repeatedly tested in the past as sensitizers of wide band gap oxide semiconductors but gave poor incident photon-to-electric current conversion yields of under 1%, which is insufficient for solar cell applications.^{67–70} One of the reasons for such low efficiencies is aggregation of the dye on the TiO₂ surface. This association often leads to undesirable photophysical properties, such as self-quenching and excited state annihilation. However, the advantage of this class of complexes is the near-IR response, which is very strong with extinction coefficients of close to 50,000 M⁻¹ cm⁻¹ at 650 nm, compared to the ruthenium polypyridyl complexes, which have much smaller extinction coefficients at this wavelength.

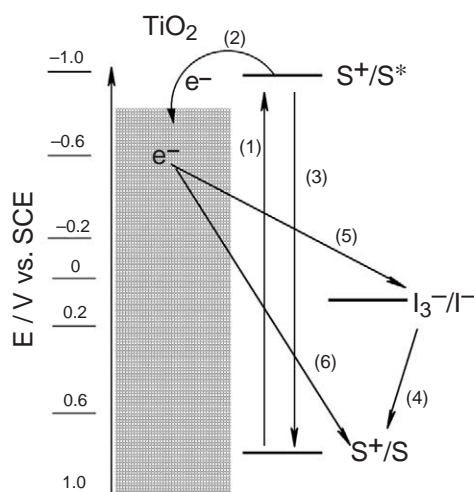
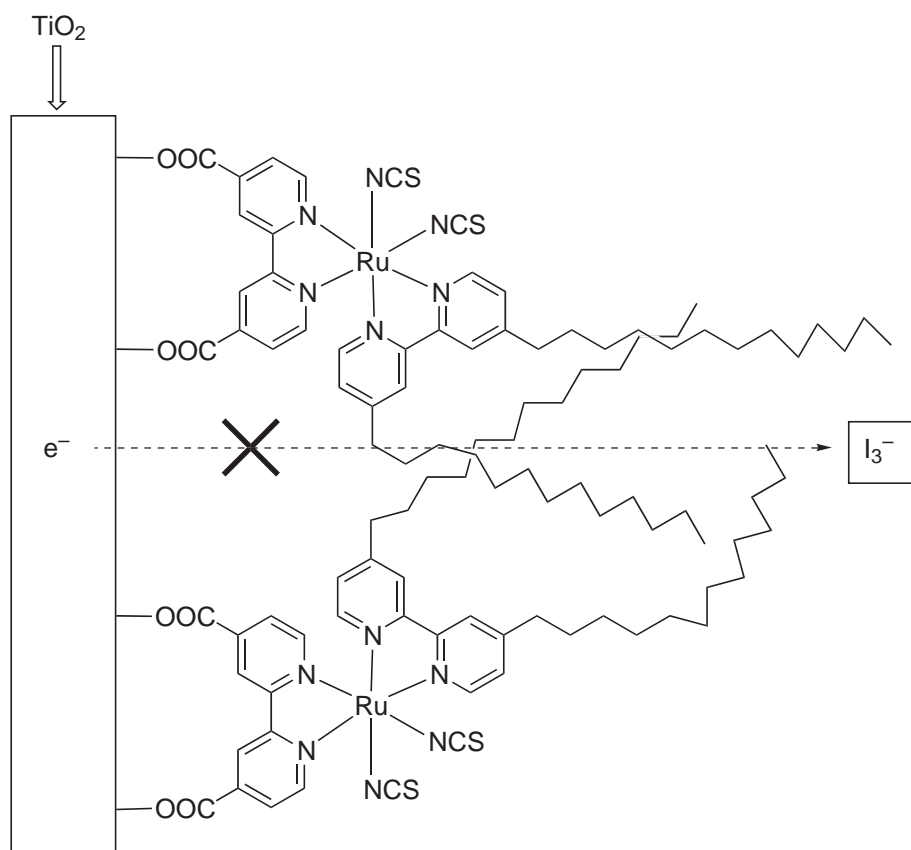


Figure 11 Illustration of the interfacial CT processes in a nanocrystalline dye-sensitized solar cell. S / S⁺/S* represent the sensitizer in the ground, oxidized and excited state, respectively. Visible light absorption by the sensitizer (1) leads to an excited state, followed by electron injection (2) onto the conduction band of TiO₂. The oxidized sensitizer (3) is reduced by the I⁻/I₃⁻ redox couple (4). The injected electrons into the conduction band may react either with the oxidized redox couple (5) or with an oxidized dye molecule (6).



Scheme 1

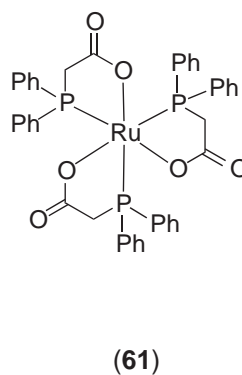
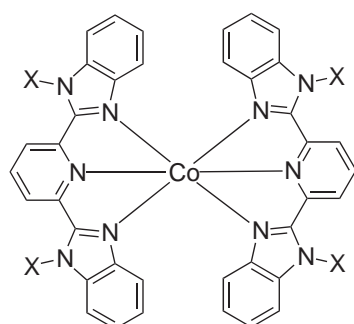
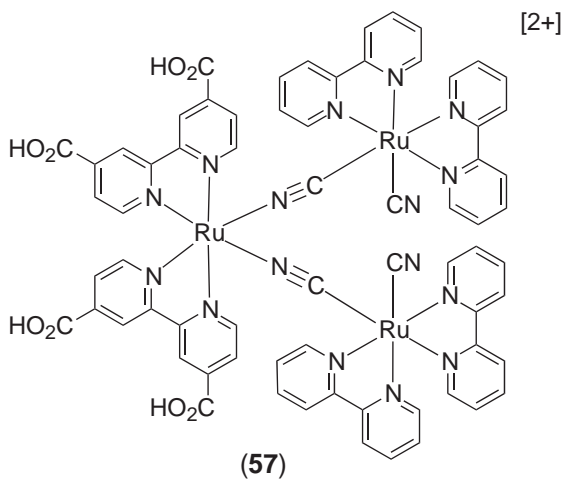
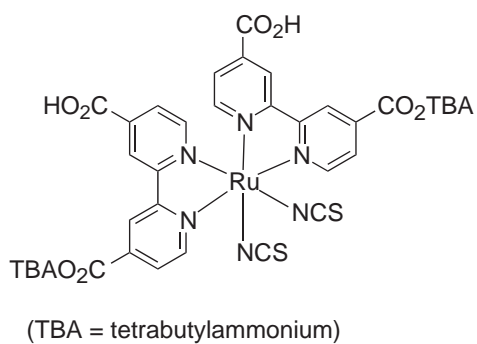
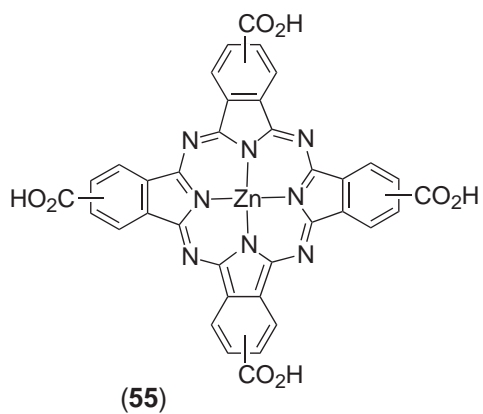
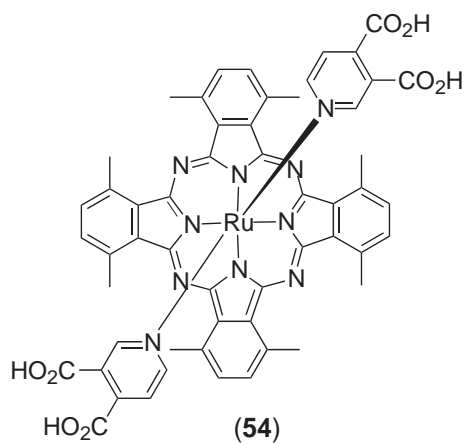
(i) Ruthenium phthalocyanines

The ruthenium phthalocyanine complex (**54**) shows a visible absorption band at 650 nm (ϵ 49,000 M⁻¹ cm⁻¹) and a phosphorescence band at 895 nm. The triplet state lifetime is 474 ns under anaerobic conditions. The emission is entirely quenched when complex (**54**) is adsorbed onto a nanocrystalline TiO₂ film. The very efficient quenching of the emission of (**54**) was found to be due to the electron injection from the excited singlet/triplet state of the phthalocyanine into the conduction band of the TiO₂.⁷¹ The photocurrent action spectrum, where the IPCE value is plotted as a function of wavelength, shows 60% IPCE with a maximum at around 660 nm (Figure 12). These are by far the highest conversion efficiencies obtained with phthalocyanine-type sensitizers.

It is fascinating to note that this class of dye injects electrons efficiently into the conduction band of TiO₂, despite the fact that the orbitals of the axial pyridine ligands (bearing the carboxylate anchors) do not participate in the phthalocyanine-based π - π^* excitation which is responsible for the 650 nm absorption band. This phenomenon shows that the electronic coupling of the excited state of the dye to the Ti (3d) conduction band manifold is strong enough through this axial mode of attachment to render charge injection very efficient. These results establish a new pathway for grafting dyes to oxide surfaces through axially attached pyridine ligands.

(ii) Phthalocyanines containing 3d metals

Several zinc(II) and aluminum(III) phthalocyanine derivatives substituted with carboxylic acid and sulfonic acid groups were anchored to nanocrystalline TiO₂ films and tested for their photovoltaic behavior.^{72,73} Interestingly, zinc(II)-2,9,16,23-tetracarboxyphthalocyanine (**55**) exhibited 45% monochromatic current conversion efficiency at 700 nm. It is shown that electron injection to TiO₂ occurs from the excited singlet state of the phthalocyanine derivatives. The



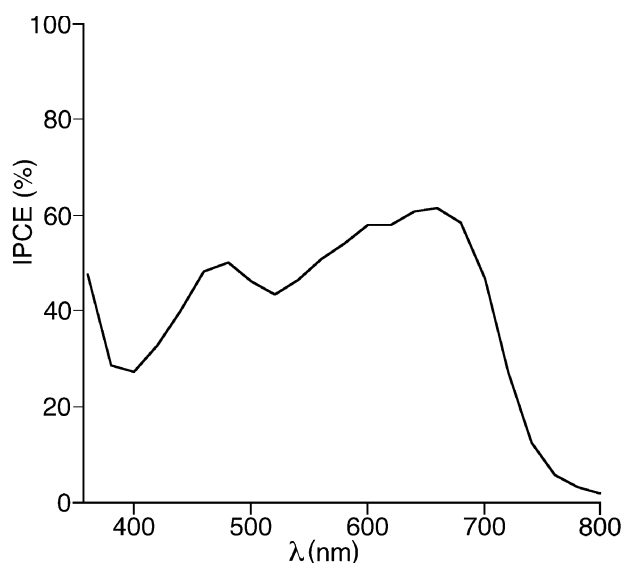


Figure 12 Photocurrent action spectra of nanocrystalline TiO₂ films sensitized by *bis*(3,4-dicarboxypyridine) Ru^{II} (1,4,8,11,15,18,22,25-octamethyl-phthalocyanin) (**54**). The incident photon to current conversion efficiency is plotted as a function of wavelength.

inherent problem of aggregation in this class of compounds is reduced considerably by introducing 4-*tert*-butylpyridine and 3 α ,7 α -dihydroxy-5 β -cholic acid (cheno) into the dye solution. The added 4-*tert*-butylpyridine probably coordinates to the metal in the axial position and thereby prevents aggregation of the dye molecules.

This type of sensitizer opens up new avenues for improving the near-IR response of dye-sensitized solar cells. In addition, important applications can be foreseen for the development of photovoltaic windows transmitting part of the visible light. Such devices would remain transparent to the eye, while absorbing enough solar energy photons in the near IR to render efficiencies acceptable for practical applications.

9.16.4 SURFACE CHELATION AND ELECTRON INJECTION

9.16.4.1 Surface Chelation

The peripheral functional groups such as carboxylates serve as grafting agents to anchor the dye molecules to the oxide surface of the TiO₂ films. The grafting of polypyridyl complexes onto the oxide surface, which allows for electronic communication between the complex and the substrate, is an important feature of dye-sensitized solar cells. Several ruthenium complexes, incorporating a wide variety of anchoring groups such as carboxylic acid, catechol, and phosphonic acid substituents on pyridine ligands have been described;^{23,74–79} these groups all bind effectively to nanocrystalline TiO₂ films to immobilize the sensitizer. To achieve a high quantum yield for electron injection from the excited state of the dye, the dye ideally needs to be in intimate contact with the semiconductor surface. The ruthenium complexes that have carboxylic acid and phosphonic acid groups show electron transfer efficiencies of close to 100%, which indicates a close overlap of the ligand π^* orbitals and the titanium 3d orbitals.

The interaction between the adsorbed sensitizer and the semiconductor surface has been investigated using resonance Raman and FTIR spectroscopy. The carboxylic acid functional groups could adsorb on the surface using a unidentate, a bidentate, or a bridging mode (or a combination of these). Yanagida and co-workers concluded that the sensitizer *cis*-dithiocyanato-*bis*(2,2'-bipyridine-4,4'-dicarboxylate)ruthenium(II) (**22**) binds to the surface using an ester-like C-type linkage.⁸⁰ Finnie *et al.* reported that sensitizer (**22**) anchors onto the surface of TiO₂ in a bidentate or bridging mode, using two carboxylate groups per dye.⁸¹ However, Fillinger and Parkinson studied the adsorption behavior of sensitizer (**22**) onto the TiO₂ surface, and found that the *initial* binding involves one carboxylate, with subsequent additional binding of two or more carboxylate groups to the surface.⁸²

Shklover *et al.* have reported the crystal structure and molecular modeling of the sensitizer (**22**) with different anchoring types onto the TiO₂ anatase surface.⁸³ In their modeling the initial attachment of the dye is a single A-type bond (Figure 13). The main feature of this type of anchoring is the great rotational freedom of the molecule, which leads to immediate capture of another neighboring Ti atom resulting in anchoring B- and C-type interactions (Figure 13). When the sensitizer (**22**) anchors onto the TiO₂ surface using both carboxylic acid groups of the same bipyridyl ligand, this results in two-bond anchoring of type D. Like the transition from A- to B-type, the B-type anchoring mode can be followed by thermal rotation around the axis to give E- and F-type linkages, involving two of the four carboxylate groups of the dye. The carboxylate group either bridges two adjacent rows of titanium ions through bidentate coordination, or interacts with surface hydroxyl groups through hydrogen bonds. The two remaining carboxylic acid groups retain their protons. Thermodynamically the E- and F-type binding modes are the most favorable. The attenuated total reflection (ATR-FTIR) data discussed in Section 9.16.4.4 using the sensitizer (**22**) and its different protonated forms are consistent with F-type anchoring, in which the sensitizer adsorbs onto the surface of TiO₂ in a bridging bidentate manner, using the two carboxylate groups which are *trans* to the NCS ligands.

9.16.4.2 X-ray Diffraction, X-ray Photoelectron Spectroscopy, and XAFS Spectroscopy Study

Zubavichus *et al.* have characterized nanocrystalline anatase films supported on a conducting glass and sensitized with the complexes (**22**) and (**24**) using out-of-plane X-ray diffraction, X-ray photoelectron spectroscopy (XPS), and Ti K-edge X-ray absorption fine spectroscopy (XAFS) (XANES and EXAFS) methods.⁸⁴ Their data indicate that the sensitizers most probably form a monolayer at the surface of anatase nanoparticles. Anchoring of the sensitizer onto the TiO₂ surface leads to a stronger distortion of the local environment of Ti atoms in anatase nanoparticles. X-ray diffraction patterns from a surface layer for solar cell prototypes with a “blank” TiO₂ nanocrystalline film, and for TiO₂ films anchored with (**22**) and (**24**), show broadened anatase reflections corresponding to the average nanocrystallite dimensions of ≈ 12.5 nm. No evidence of a

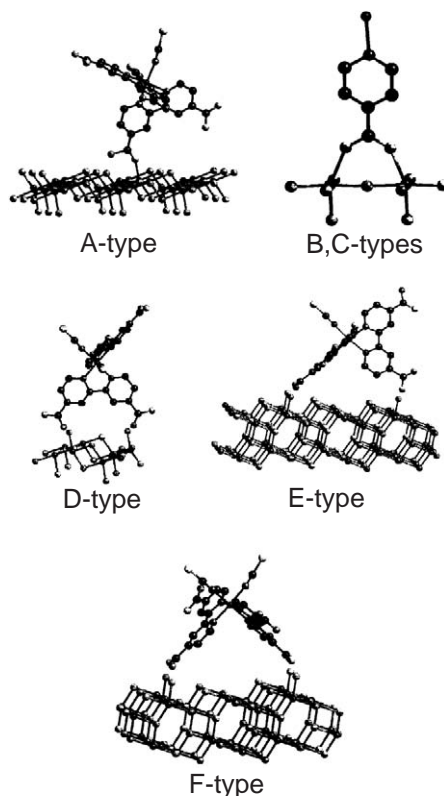
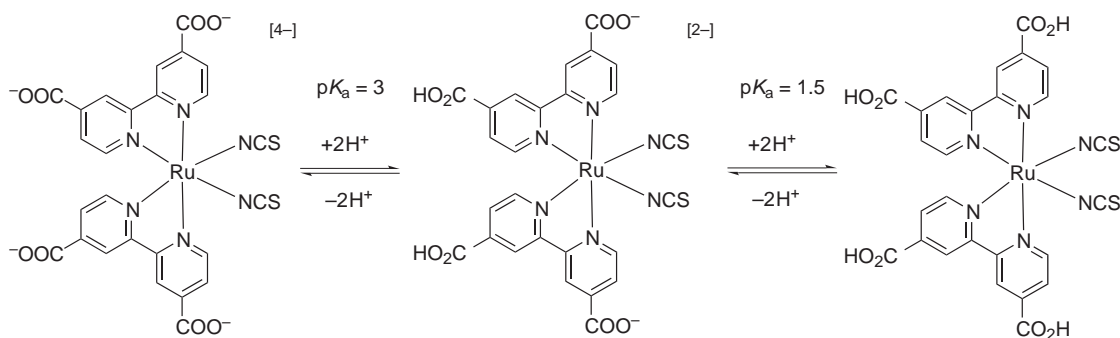


Figure 13 Possible anchoring modes for sensitizer (**22**) on a TiO₂ surface using carboxylate functional groups.

separated bulk dye phase was obtained indicating that the dye is adsorbed onto the surface in an ordered manner. Using XPS data they were able to determine the stoichiometry of the anchored sensitizer to the titanium (Ru per Ti) as 1:100 and show a dominance of the anatase O 1s band that agrees with the model of a monomolecular coating.

9.16.4.3 Acid-base Equilibria of *cis*-Dithiocyanato-*bis*(2,2'-bipyridine-4,4'-dicarboxylate) Ruthenium(II)

Understanding of the binding nature of sensitizers onto the TiO₂ surface requires detailed knowledge of the pK_a values of the anchoring groups on the sensitizer. Here we discuss the pK_a values of the sensitizer (**22**) and the implications of this on the adsorption studies. The ground state pK_a values of (**22**) were determined from the relationship between the change in the optical density at a given wavelength, or in the position of the MLCT maximum, with pH.³² The plot of λ_{\max} change vs. pH for (**22**) shows the expected sigmoidal shape, with the pH at the inflection point giving two ground state pK_a values of 3 and 1.5 ± 0.1 . In complex (**22**) there are two 4,4'-dicarboxy-2,2'-bipyridine ligands which could give four separate acid-base equilibria, if the dissociation of protons is stepwise. Alternatively, if the dissociation were simultaneous one would expect one equilibrium constant. The two separate equilibria in the complex (**22**), suggests that the pyridyl subunits are nonequivalent. Scheme 2 presents the simplified two-step equilibrium for the complex (**22**).



Scheme 2

The complex (**24**) has three carboxylic groups on the 4,4',4'' positions of the terpyridine ligand and shows a ground state pK_a value of 3.3 ± 0.1 due to concurrent dissociation of two protons coming from the peripheral pyridines. This value is similar to the ground state pK_a values observed for the complex (**22**). However, there is a second inflection point at pH = 5 which is due to the second protonation/deprotonation process pK_{a2} coming from the central pyridine, which is *trans* to the thiocyanate ligand.⁴⁰

9.16.4.4 ATR-FTIR Studies of Sensitizer Adsorption on TiO₂ Oxide Surface

The difference in binding properties of the complexes containing carboxylic acid anchoring groups may stem from the differences in the pK_a values of the complexes. To understand the anchoring mode of sensitizers (**22**), (**8**), and (**56**), which contain four, zero, and two protons, respectively, were studied using IR spectroscopy. The IR spectra of these three complexes as a solid and as an adsorbed film onto TiO₂ were recorded in the region 4,000–500 cm⁻¹. Figures 14 and 15 show a comparison of the solid state ATR-FTIR spectra of the three free and adsorbed complexes. The IR spectrum of complex (**22**) as a solid sample shows a broad band at 1,709 cm⁻¹ due to the carboxylic acid groups. However, the complex that contains two protons (**56**) shows bands at 1,709 and 1,610 cm⁻¹ due to carboxylic acid and carboxylate groups, respectively. The symmetric stretch of the carboxylate group was observed at 1,362 cm⁻¹. The intense peak at 1,225 cm⁻¹ in both complexes is due to the $\nu(\text{C}-\text{O})$ stretch. The $\nu(\text{NC})$ of the thiocyanate ligand band was observed at 2,098 cm⁻¹. The bands at 2,873, 2,931, and 2,960 cm⁻¹ are due to $\nu(\text{C}-\text{H})$ of tetrabutylammonium groups. In contrast the FTIR spectrum of complex (**8**) shows bands due

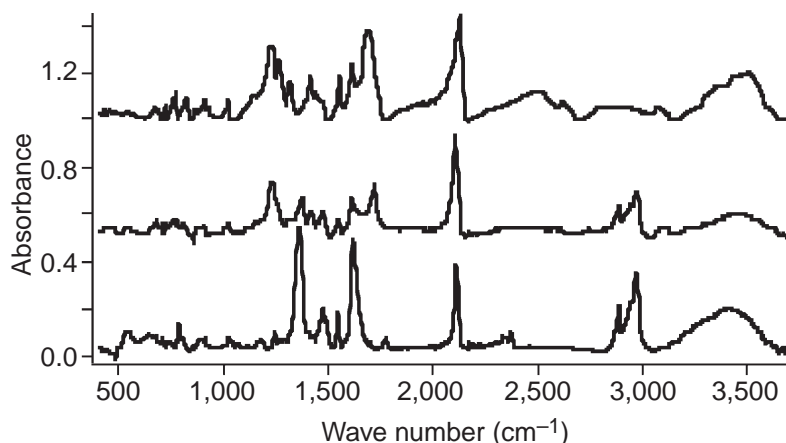


Figure 14 Comparison of the solid state (dry powder) ATR-FTIR spectra of the complexes (8) bottom, (56) middle, and (22) top.

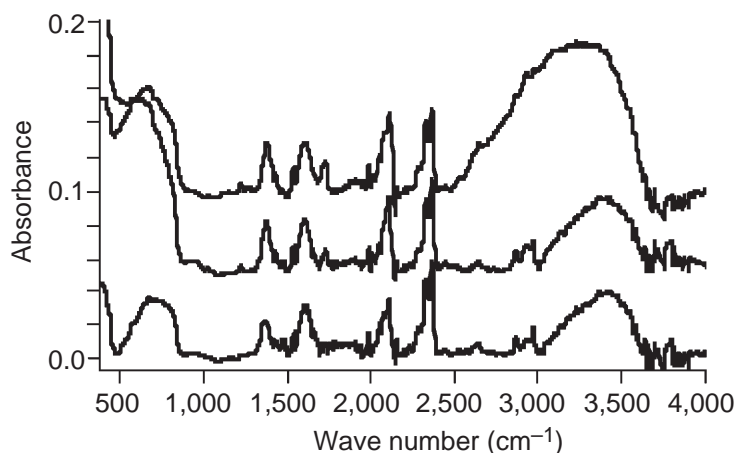


Figure 15 Comparison of the ATR-FTIR spectra of complexes adsorbed on TiO₂: (8) bottom, (56) middle, and (22) top.

to the carboxylate groups at $1,623\text{ cm}^{-1}$ ($-\text{CO}_2^-_{\text{as}}$), $1,345\text{ cm}^{-1}$ ($-\text{CO}_2^-_{\text{s}}$), and the thiocyanate at $2,105\text{ cm}^{-1}$.⁸³

The IR spectrum of complex (22) adsorbed onto a TiO₂ surface shows the presence of characteristic bands due to NCS, carboxylic acid, and carboxylate groups. The presence of both carboxylic acid and carboxylate groups indicates that complex (22) is not fully deprotonated on the TiO₂ surface. Alternatively, complex (8) shows the presence of only carboxylate groups, confirming the absence of an ester linkage between the complex and the TiO₂. The complex (56) contains two protons on the carboxylic acid groups *trans* to the NCS ligands, and two carboxylate groups which are *trans* to each other. When complex (56) attaches to a TiO₂ surface it could adsorb using either the carboxylic acid or the carboxylate groups (or both). The FTIR spectra show the presence of mainly carboxylate groups, indicating that the complex is being adsorbed on the surface using the two groups that are *trans* to the NCS ligands (F-type in Figure 13). The difference between the symmetric and asymmetric bands in the free and the adsorbed state suggest that the adsorption of these dyes on the surface of TiO₂ is bidentate chelation rather than physisorption. The FTIR data show a compelling evidence for Shklover's theoretical model of the dye adsorption on TiO₂ surface (Nazeeruddin *et al.*, personal observations).

9.16.4.5 Effect of Protons Carried by the Sensitizer on the Performance

In order to obtain high conversion efficiencies, optimization of the short-circuit photocurrent and open-circuit potential of the solar cell are essential. The conduction band of the TiO₂ is known to have

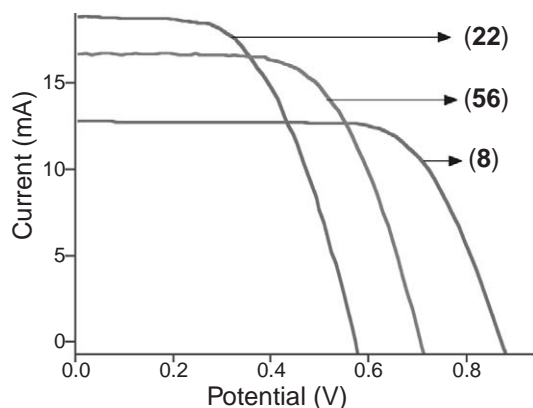


Figure 16 Photocurrent-voltage characteristics of nanocrystalline TiO₂ films sensitized by the complexes (22), (56), and (8), measured under AM 1.5 sun using 1 cm² TiO₂ electrodes with I⁻/I₃⁻ redox couple in methoxyacetonitrile.

a Nernstian dependence on pH.^{85,86} The fully protonated sensitizer (22) upon adsorption transfers most of its protons to the TiO₂ surface, charging it positively. The electric field associated with the surface dipole generated in this fashion enhances the adsorption of the anionic ruthenium complex and assists electron injection from the excited state of the sensitizer into the TiO₂ conduction band, giving higher photocurrents (18–19 mA cm⁻²). However, the open-circuit potential (0.6 V) is lower due to the positive shift of the conduction band edge induced by the surface protonation.

In contrast, sensitizer (8), which has no ionizable protons, shows a higher open-circuit potential (0.9 V) compared to complex (22), due to the relative negative shift of the conduction band edge induced by the adsorption of the anionic complex. As a consequence the short-circuit photocurrent is lower (12–13 mA cm⁻²). Thus, there should be an optimal degree of protonation of the sensitizer in order to optimize both the short-circuit photocurrent and the open-circuit potential, which both affect the power conversion efficiency of the cell. The photovoltaic performance of (56) (which carries two ionizable protons) shows a current of 17 mA cm⁻² and a potential of 0.73 V.³² Figure 16 shows photocurrent–voltage characteristics obtained with a monolayer of the complexes (22), (8), and (56), coated on TiO₂ films and measured under AM 1.5 sun using 1 cm² TiO₂ electrodes with the I⁻/I₃⁻ redox couple in methoxyacetonitrile.

9.16.4.6 Comparison of IPCE Values Obtained with Various Sensitizers

Figure 17 shows the photocurrent action spectrum of a dye-sensitized solar cell with various sensitizers. The broad feature covers the entire visible spectrum and extending into the near IR region up to 920 nm for complex (24); the IPCE value in the plateau region is about 80% for this complex. Taking the light losses in the conducting glass into account, the efficiency of electric current generation is practically 95% over a broad wavelength range extending from 400 nm to 700 nm. The overlap integral of the absorption spectrum with the standard global AM 1.5 solar emission spectrum for complex (24) yields a photocurrent density of 20.5 mA cm⁻². The open-circuit potential is 0.72 V and the fill factor is 0.7. These results were confirmed at the National Renewable Energy Laboratory (NREL, Golden, CO, USA) (Figure 18). The complexes (1) and (22) under similar conditions show IPCE values of 70–80% in the plateau region. Although the IPCE values for (1) and (22) are comparable with that of (24), the total integrated current was significantly lower due to the blue shift in the spectral response of the later complexes (i.e., they could not harvest the red part of the solar spectrum).

The photocurrent value obtained using sensitizer (24) anchored on TiO₂ is a lower limit, because the surface concentration of (24) is lower (0.42 molecules nm⁻²) than the maximum values found for complex (22), in spite of the larger molecular size of the latter complex. The question then arises as to what causes the lower dye loading of complex (24) compared to (22) on the TiO₂ surface. Two specific types of interaction in complex (24) can significantly affect the monolayer packing. Strong hydrogen bonds between complex anions, and their electrostatic interactions within the monolayer, are the first factor to consider. Electrostatic forces are long-range and isotropic, therefore, their influence on the short-range order in the absorbed layer

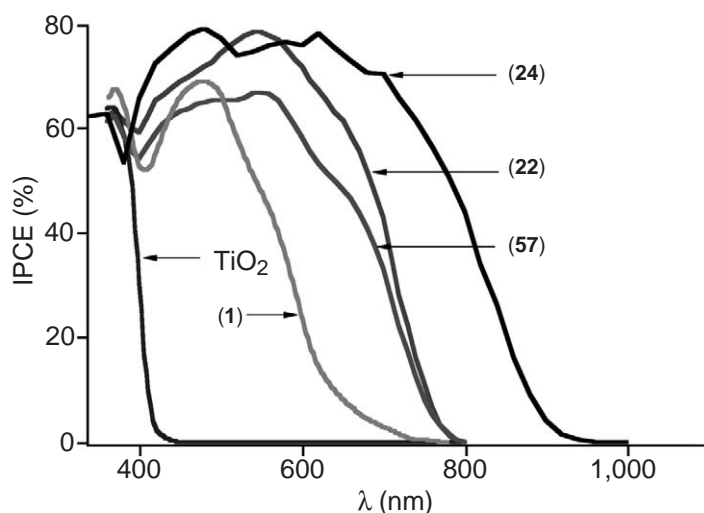


Figure 17 Photocurrent action spectra of bare nanocrystalline TiO₂ film, and the sensitizers (1), (22), (24), and (57) adsorbed on TiO₂ films. The incident photon to current conversion efficiency is plotted as a function of wavelength.

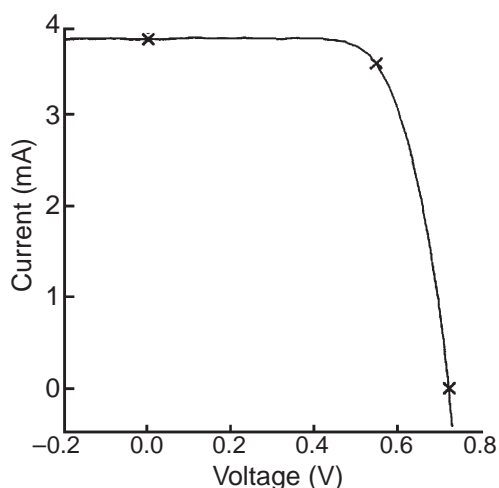


Figure 18 Photocurrent-voltage characteristics of the complex (24) measured at National Renewable Energy Laboratory (NREL). Pertinent data are as follows. Temperature, 298 K; area of cell, 0.1863 cm²; irradiance, 1,000 W m⁻²; V_{oc} = 0.721 V; I_{max} = 3.552 mA; J_{sc} = 20.53 mA cm⁻²; fill factor = 70.41%; V_{max} = 0.5465 V; I_{sc} = 3.824 mA; P_{max} = 1.941 mW; efficiency = 10.4%.

cannot be substantial, considering that the layer formation proceeds in the presence of cations. In contrast, the directional character of hydrogen bonds is rather strict, and strong hydrogen-bonding interactions can only occur within a narrow range of intermolecular distances, e.g., 2.4–2.8 Å for the O···O spacings in an OH···O interaction. Hence, hydrogen bonds may have a strong influence on the molecular packing. Figure 19 shows the crystal structure of complex (24), which displays strong O—H···O hydrogen bonds leading to 2-dimensional sheets along the [111] direction of the crystal. The second possible reason for low dye uptake may be slow surface diffusion. Whatever the reason, the (001) surfaces of TiO₂ have space to accommodate more of complex (24), and it should be possible to increase the dye coverage (which is rather low at present) to improve further the efficiency of the solar cell.

The cyano-bridged trinuclear complex [RuL₂{Ru(bpy)₂(CN)₂}₂]²⁺ (57) (L = 2,2'-bipyridine-4,4'-dicarboxylic acid) has been found to be an excellent photosensitizer for spectral sensitization of TiO₂. Amongst the possible MLCT excited states associated with the three metal centers, the lowest energy one is based on the central unit carrying the ligand dc bpy. When coated on a TiO₂-electrode, the complex anchors through the carboxylate substituents of this central unit. Photons

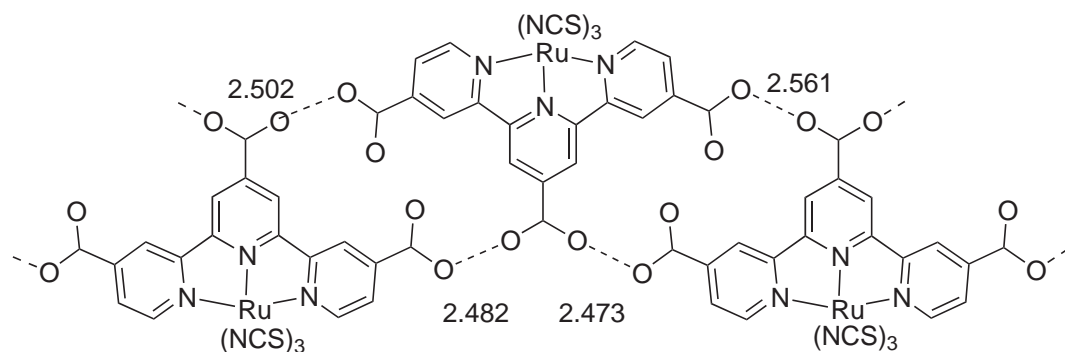


Figure 19 Sketch of the O—H···O hydrogen bonding present in the crystal structure of (**24**); H atoms on the carboxylic acid units are not shown. Nonbonded O···O separations are given in Å.

absorbed by the peripheral units, whose MLCT states are higher in energy than those of the central unit, efficiently transfer their excitation energy to this central unit, accounting for the excellent performance of the dye. However, the total efficiency of a solar cell based on the trinuclear complex (**57**) was lower than one based on the mononuclear complex (**24**).^{87,88} The most likely reason for such behavior is the porosity of the TiO₂ semiconductor substrate, which allows the mononuclear complex free access into the small pores, in contrast to the bulkier polynuclear complex. This shows that the ideal sensitizer should be as small as possible and absorb as much visible light as possible, in order to achieve high currents and thereby high energy-conversion efficiency.

9.16.4.7 Electron Injection Kinetics

The adsorbed sensitizers in the excited state inject an electron into the conduction band of the semiconductor substrate, provided that the excited state oxidation potential is above that of the conduction band. The excitation of the sensitizer involves transfer of an electron from the metal t_{2g} orbital to the π^* orbital of the ligand, and the photo-excited sensitizer can inject an electron from a singlet or a triplet electronically excited state, or from a vibrationally “hot” excited state. The electrochemical and photophysical properties of both the ground and the excited states of the dye play an important role in the CT dynamics at the semiconductor interface.

Several groups have investigated the dynamics of charge injection, recombination, and regeneration, using sensitizer (**22**) and a range of different spectroscopic techniques. Durrant and co-workers performed ultrafast interfacial electron injection studies of the complex (**22**) adsorbed on TiO₂ surface in 1:1 ethylene carbonate–propylene carbonate solvent.⁸⁹ Using time-resolved absorption spectroscopy, they were able to observe both the oxidized sensitizer and the electron in TiO₂ conduction band. They found that the injection process is ultrafast and multiphasic with 100 fs (35%), 1.3 ps (22%), and 13 ps (43%) components. However, the electron injection kinetics observed for sensitizer (**56**) were found to be significantly slower than for sensitizer (**22**): half lives for electron injection are observed to be 0.4 and 12 ps with (**22**) and (**56**), respectively, indicating a significant influence from the counterions carried by the sensitizers.⁹⁰

Willig and co-workers used near-IR spectroscopy to measure the excited state electron transfer process for sensitizer (**22**) adsorbed on TiO₂, and found that the electron injection occurred in <25 fs.⁹¹ Lian and co-workers have also reported the femtosecond mid-IR properties of sensitizer (**22**) adsorbed on TiO₂. In this region, the thiocyanate ligands show characteristic asymmetric and symmetric stretches for the ground and the excited states, which leads to direct monitoring of injected electrons onto the conduction band.⁵ Careful examination at different wavelengths and time scales yielded complex electron transfer kinetics with injection times of 50 fs (84%) and 1.7 ps (16%). The origin of such complicated electron transfer kinetic behavior could be the adsorption of dye molecules on different surface sites, coupled with various different anchoring modes of the sensitizer (**22**). Moser *et al.* have reported direct spectroscopic evidence for electron injection from “hot” vibrational states using semiconductors and dyes having different conduction band levels and excited state oxidation potentials, respectively.⁹² They employed time-resolved absorption spectroscopy to monitor the injection yields of the sensitizer (**22**) adsorbed on Nb₂O₅ and ZrO₂, which show clear wavelength dependence. Measurements carried out under identical conditions using the sensitizer (**22**)

adsorbed on TiO₂ electrodes gave an injection quantum yield close to unity which was independent of the excitation wavelength.

Schnadt *et al.* have showed experimental evidence for sub-3-fs CT from a 4,4'-dicarboxy-2,2'-bipyridine ligand of (**22**) adsorbed onto TiO₂, using resonant photoemission spectroscopy (PES).⁹³ The PES technique show significant improvement in time resolution compared to time resolved laser techniques. Their results are direct confirmation that the electronic coupling between the dye and the TiO₂ surface is sufficiently strong to suppress other competing processes. Therefore it is clear that the photoexcitation of the MLCT of the adsorbed sensitizer (**22**) leads to injection of electrons into the TiO₂ conduction band in the femtosecond time frame. However, the back electron transfer (i.e., transfer of an electron from the conduction band to the oxidized dye) occurs on a time scale between microseconds and milliseconds. The orders of magnitude difference between the forward and back electron transfer rates is the key to high injection efficiency. The possible reasons for such an enormous difference between the forward and back electron transfer rates are as follows. In the MLCT excited state of the sensitizer, an electron is promoted from metal *d*-orbitals to the π^* -orbital of a ligand, which is intimately involved in overlapping with titanium 3*d* orbitals and, therefore, fast electron injection occurs. The slow back electron transfer, in contrast, is due to the dynamics of trapping and detrapping of electrons in the conduction band, where the electrons spend a large fraction of their transit time at interband trap sites. However, the origin of trap sites has not been well understood. The other reason for slow back electron transfer is that the reaction lies deep in the inverted Marcus region, where the rate of the CT process is expected to decrease with increasing driving force. In dye-sensitized nanocrystalline TiO₂ solar cells, after electron injection into the conduction band of TiO₂ the positive charge is formally localized on the ruthenium atom. However, the HOMO in complex (**22**) actually has a significant contribution from the π orbitals of the NCS ligands, in addition to the expected Ru(*t_{2g}*) character. Therefore, some of the positive charge on the metal center following charge injection is delocalized onto the coordinated NCS ligands. This charge separation, due significant transfer of electron density from the coordinated NCS ligands to the oxidized metal center, may also contribute towards reducing the back electron transfer. Results from *ab initio* and DFT calculations on complex (**22**) agree with this hypothesis.⁹⁴

Apart from recapture of the injected electrons by the oxidized dye, there are additional loss channels in dye-sensitized solar cells, which involve reduction of triiodide ions in the electrolyte, resulting in dark currents. The TiO₂ layer is an interconnected network of nanoparticles with a porous structure. The functionalized dyes penetrate through the porous network and adsorb over TiO₂ the surface. However, if the pore size is too small for the dye to penetrate, that part of the surface may still be exposed to the redox mediator whose size is smaller than the dye. Under these circumstances, the redox mediator can collect the injected electron from the TiO₂ conduction band, resulting in a dark current (Equation (6)), which can be measured from intensity-modulated experiments and the dark current of the photovoltaic cell. Such dark currents reduce the maximum cell voltage obtainable, and thereby the total efficiency.

The interception of the oxidized dye by the electron donor in the electrolyte (i.e., iodide) occurs within 10 ns. The rate of the reaction leading to the regeneration of the dye ground state was found to depend strongly on the nature and the concentration of the cations present in the solution. Small cations such as Li⁺, Mg²⁺, and La³⁺ can intercalate into the oxide surface, thereby favoring fast oxidation of iodide by the oxidized state of the sensitizer.

9.16.5 REDOX MEDIATORS

9.16.5.1 New Redox Couples

The total efficiency of the solar cell depends on the current, voltage, and the fill factor of the cell as shown in Equation (9). Many groups have focused on the development of new sensitizers, which exhibit a visible spectral response that matches the solar spectrum.^{8,9,20,22,55,56,87} The open-circuit photovoltage is one of the key factors that determined the cell efficiency, and this is determined by the energy difference between the Fermi level of the semiconductor under illumination and the Nernst potential of the redox couple in the electrolyte (Figure 4). However, the experimentally observed open-circuit potential using various sensitizers is smaller than the difference between the conduction band and the redox couple due to differences in recombination rates.

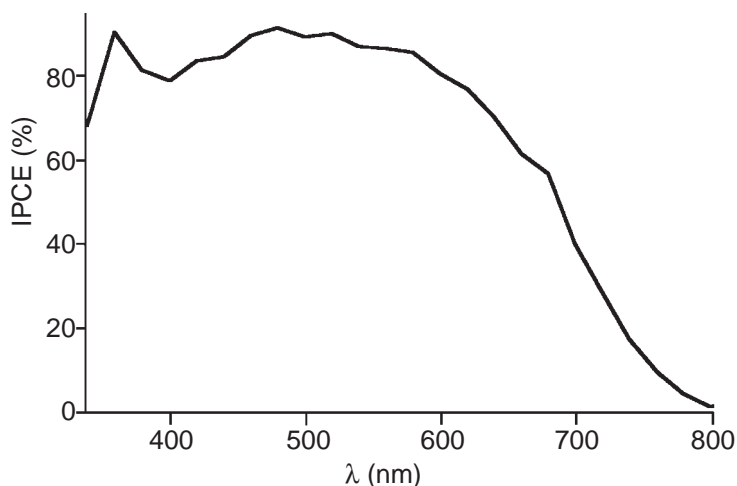


Figure 20 Incident photon to current conversion efficiency of a nanocrystalline TiO₂ cell sensitized by dye (51) using the complex (59) as a redox mediator.

Using the tri-iodide/iodide redox couple and the sensitizers (22) and (56), several groups have reported up to 8–10% solar cell efficiency where the potential mismatch between the sensitizer and the redox couple is around 0.5 V vs. SCE. If one develops a suitable redox couple that decreases the potential difference between the sensitizer and the redox couple, then the cell efficiency could increase by 30%, i.e., from the present value of 10% up to 13%. Towards this goal, Oskam *et al.* have employed pseudohalogens in place of the triiodide/iodide redox couples, where the equilibrium potential is 0.43 V more positive than that of the iodide/iodide redox couple.¹⁷ Yamada and co-workers have used cobalt *tris*-phenanthroline complexes as electron relays (based on the Co^{II/III} couple) in dye-sensitized solar cells.⁹⁵

Of course, the design and the development of new redox couples for solar cell applications is a challenging task because it has to meet several critical requirements:

- (i) The components of the redox pair should be highly soluble in organic solvents.
- (ii) They should be stable in both the reduced and oxidized forms, and able to undergo millions of turnovers.
- (iii) The components should be as nearly transparent as possible in the visible region (very low molar extinction coefficient).

Towards this goal the new redox couples ((58)–(61)) have been prepared. These complexes meet all of the above stringent requirements and rival the iodide/triiodide redox couple in dye-sensitized solar cells. The imidazole and pyridine groups in complex (58) stabilize the oxidized and the reduced state of the metal, respectively. The long aliphatic substituents on the imidazole group allow the complexes to dissolve in polar and nonpolar organic solvents. The molar extinction coefficient of these complexes is low, typically in the range 250–350 M⁻¹ cm⁻¹, allowing most of the visible light to pass through the electrolyte to the light-harvesting dye. For the first time photovoltaic cells incorporating the relay (59) have yielded IPCE values of 85% (Figure 20). In contrast, the electrolyte that contains relay (61) yielded 40% IPCE.⁹⁶

9.16.5.2 Solid Electrolytes/Hole-transport Materials

A crucial factor for industrial development of the solar cell is its stability. Several studies have shown good endurance of the various components under accelerated illumination tests. The main problem of the dye-sensitized solar cell is finding a suitable sealing method that can resist the organic solvents containing the redox electrolyte to give long-term stability. A possible solution would be replacement of the liquid electrolyte by a solid electrolyte such as hole-transporting material, in which charge can carry by hopping. However, the key requirement is rapid regeneration of the dye cation and slow recombination with electrons in the porous film. Several approaches have been made to realize these goals. Bach *et al.* have successfully introduced

the concept of a solid *p*-type semiconductor (heterojunction), with the amorphous organic hole-transport material 2,2',7,7'-tetrakis(*N,N*-dip-methoxyphenyl-amine)-9,9'-spirobifluorene.⁹⁷ This hole-conducting material allows the regeneration of the sensitizer molecules after electron injection due to its hole transport properties. However, the IPCE values obtained using complex (22) as a CT sensitizer and the spirobifluorene as a hole-conducting material were significantly lower than those obtained using the redox electrolyte based on iodide/triiodide.

The low efficiencies could be due to lack of intimate contact (interface) between the sensitizer (which is hydrophilic) and the spirobifluorene (which is hydrophobic). Moreover, the surface charge also plays a significant role in the regeneration of the dye by the electrolyte.⁹⁸ In an effort to reduce the charge of the sensitizer and improve the interfacial properties between the surface-bound sensitizer and the spirobifluorene hole-carrier, amphiphilic heteroleptic ruthenium(II) complexes ((48)–(53)) have been used as sensitizers. These complexes show excellent stability and good interfacial properties with hole-transport materials, resulting in improved efficiencies for the solar cells.

Kumara *et al.* have developed a solid-state dye-sensitized solar cell based on CuI as hole conductors, which gave an energy conversion efficiency of 3%.²¹ Nonetheless, the short-circuit photocurrent and the open-circuit voltage both decreased due to formation of large crystals that decreased the contact between the dyed TiO₂ surface and the CuI crystallites. However, by addition of a small quantity of 1-methyl-3-ethylimidazolium thiocyanate in the hole-conducting CuI solution, they dramatically improved the stability of the solar cell. O'Regan *et al.* have developed *p*-type CuSCN, which upon electrodeposition into dye-sensitized ZnO films resulted in *n-p* heterojunctions. The efficiency of charge separation and collection in such a device has been reported to be 100%, resulting in an overall power conversion efficiency of 1.5%.⁹⁹

9.16.6 ENERGY CONVERSION AND STORAGE

9.16.6.1 Water Splitting by Visible Light using a Tandem cell

Since solar energy cannot be utilized on demand like oil and coal, the energy must be stored. One exciting solution would be splitting of water into hydrogen and oxygen using a dye-sensitized solar cell. Solar hydrogen production from water has a number of advantages: water is highly abundant and is regenerated on burning hydrogen, so that no raw material is consumed and no pollution is generated. Hydrogen has a very high fuel value, and is easily stored, transported, and used.

Conversion of solar energy into storable fuels such as hydrogen in an economic way is both a challenge and a dream. Direct photoelectrolysis of water is not possible because of its lack of light absorption. A number of approaches have been tried to overcome the obstacles for the direct splitting of water.¹⁰⁰ One successful approach to this challenging task is the design of a tandem device based on two superimposed cells with complementary light absorption in the visible range. The final goal is to achieve the reaction (Equation (15)), which requires energy of 1.23 eV, corresponding to a wavelength of 1,000 nm.¹⁰¹ Thus, in theory most of the solar energy available in the visible spectrum could be used for this process:



This section describes a tandem device that consists of two photosystems connected in series (by analogy with natural photosynthesis, Figure 21). The cell on the left consists of a thin film of nanocrystalline tungsten trioxide which absorbs the blue part of the solar spectrum. Tungsten trioxide is so far the only known oxide semiconductor that is capable of producing oxygen with a high quantum yield using visible light. On the right is the dye-sensitized TiO₂ solar cell, absorbing the green and red part of the spectrum. The valence band holes created (Equation (16)) by band gap excitation of the WO₃ serve to oxidize water to oxygen (Equation (17)), while the conduction band electrons are fed into the second photosystem composed of the dye-sensitized nanocrystalline TiO₂ film. The second photosystem is placed directly behind the WO₃ film, capturing that part of the incident light which is transmitted through the WO₃ electrode. The photovoltage generated by the second photosystem enables the generation of hydrogen by the conduction band electrons (Equation (18)). Figure 17 presents the conversion efficiency of incident monochromatic light to electric current achieved with the sensitized TiO₂ films for several ruthenium complexes. Very high efficiency of current generation, exceeding 85%, is obtained. When corrected for the

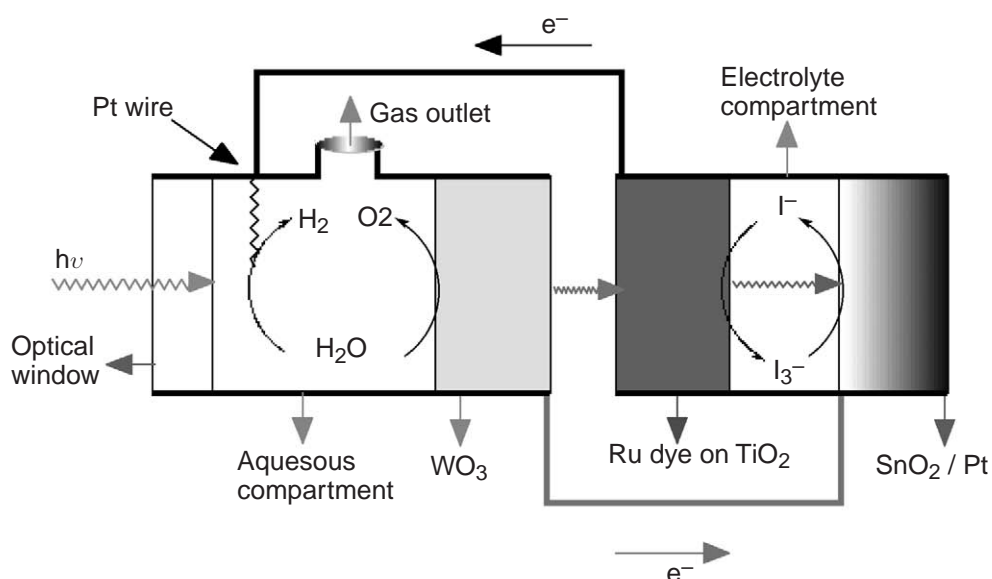


Figure 21 Circuit diagram of a tandem cell for water photolysis.

inevitable reflection and absorption losses in the conducting glass serving to support the nanocrystalline film, the yield is practically 100%:



The energy level diagram for this tandem device is shown in [Figure 22](#). There is a close analogy to the photosynthetic Z-scheme (named for the shape of the flow diagram) operative in the light reaction in green plants in which the two photosystems are connected in series, one affording oxidation of water to oxygen and the other generating the NADPH used in CO₂ fixation. A photograph of the working tandem device, based on the thin film of polycrystalline tungsten trioxide and the dye-sensitized nanocrystalline TiO₂ film, is shown in [Figure 23](#). The overall conversion efficiency of this tandem device is 5% for the photocleavage of water into hydrogen and oxygen under AM 1.5 solar irradiation.

9.16.7 SYNTHESIS AND CHARACTERIZATION OF COMPLEXES

9.16.7.1 Synthetic Strategies for Ruthenium Complexes

Dwyer and co-workers used K₄[Ru₂Cl₁₀O] as a starting material for synthesis of homoleptic ruthenium complexes in weakly acidic aqueous solution with an appropriate ligand.¹⁰² Wilkinson's group used ruthenium blue solutions for synthesis of variety of complexes.¹⁰³ Several groups have used RuCl₃·3H₂O as a starting material in DMF for synthesis of [RuL₃]²⁺, [RuL₂L']²⁺, and [RuL₂(X)₂]-type complexes.³⁷ The advantage of DMF as a solvent is that it provides high refluxing temperature and at the same time acts as a reducing agent for the ruthenium(III) starting material. The groups of Kelly, Meyer, Vos, and Deacon have used the polymeric starting complex [Ru(CO)₂Cl₂]_n for stepwise synthesis of heteroleptic complexes containing different ligands.^{41,104,105} Recently, we have reported a new synthetic procedure for heteroleptic complexes starting from the complex [Ru(Cl)₂(DMSO)₄].¹⁰⁶ However, the reported procedures for synthesis of heteroleptic complexes involve several steps, resulting very low yields and mixture of isomers. Subsequently, Meyer's group has developed a one-pot synthesis for *tris*-heteroleptic complexes using [Ru(Cl)₂(DMSO)₄] as starting material by successive addition of various ligands in a specific order from electron accepting to electron donating.¹⁰⁷ Again, the method seems very convenient

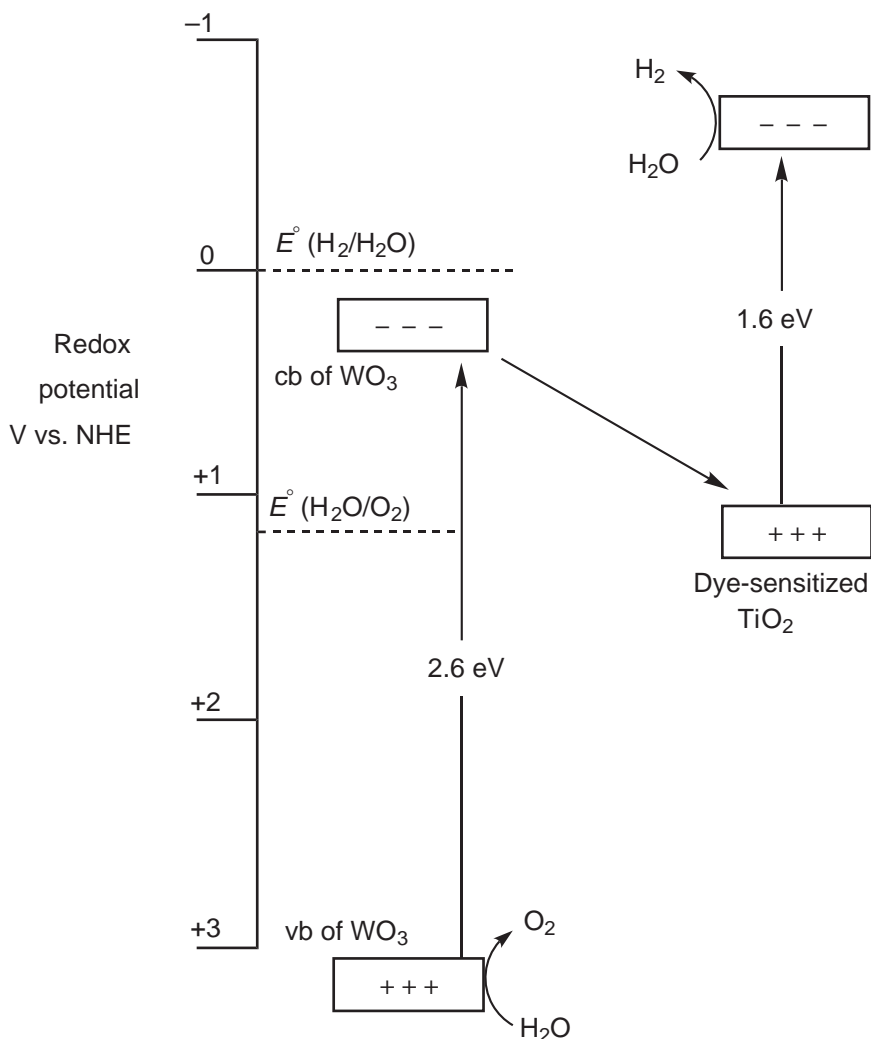


Figure 22 The energy level diagram (Z-scheme) for photocatalytic water decomposition by a tandem cell.

but the separation of the required *tris*-heteroleptic complex from a mixture of various products that forms due to ligand scrambling is a daunting task. To overcome the problem of ligand scrambling during the synthesis, the authors have developed a novel and a reproducible synthetic route that leads to the heteroleptic ruthenium complex in high yields.

Scheme 3 shows the details of the synthetic strategy adopted for the preparation of heteroleptic *cis*- and *trans*-complexes. Reaction of dichloro(*p*-cymene)ruthenium(II) dimer in ethanol solution at reflux temperature with 4,4'-dicarboxy-2,2'-bipyridine (L) resulted the pure mononuclear complex $[\text{Ru}(\text{cymene})\text{CIL}]\text{Cl}$. In this step, the coordination of substituted bipyridine ligand to the ruthenium center takes place with cleavage of the doubly chloride-bridged structure of the dimeric starting material. The presence of three pyridine proton environments in the NMR spectrum is consistent with the symmetry seen in the solid-state crystal structure (**Figure 24**).

The heteroleptic dichloro complexes were prepared by reacting the mononuclear complex $[\text{Ru}(\text{cymene})\text{CIL}]\text{Cl}$ with one equivalent of substituted bipyridine ligand (L') in DMF under reduced light at 150 °C. It is interesting to note that the displacement of the cymene ligand from the coordination sphere of ruthenium metal by a substituted bipyridine ligand takes place efficiently in organic solvents such as ethanol and DMF even in the dark at 80 °C without any scrambling (Nazeeruddin and Graetzel, personal observations). The UV-vis spectral properties of the complexes $[\text{Ru}(\text{L})(\text{L}')\text{Cl}_2]$ prepared in this way are identical to those of the same complexes prepared from $[\text{RuCl}_2(\text{DMSO})_4]$ as starting material. This clearly shows that the chloride ligand, which is outside the coordination sphere in the cymene complex $[\text{Ru}(\text{cymene})\text{CIL}]\text{Cl}$, ends up back in the metal the coordination sphere. The chloride ligands from $[\text{Ru}(\text{L})(\text{L}')\text{Cl}_2]$ can then be

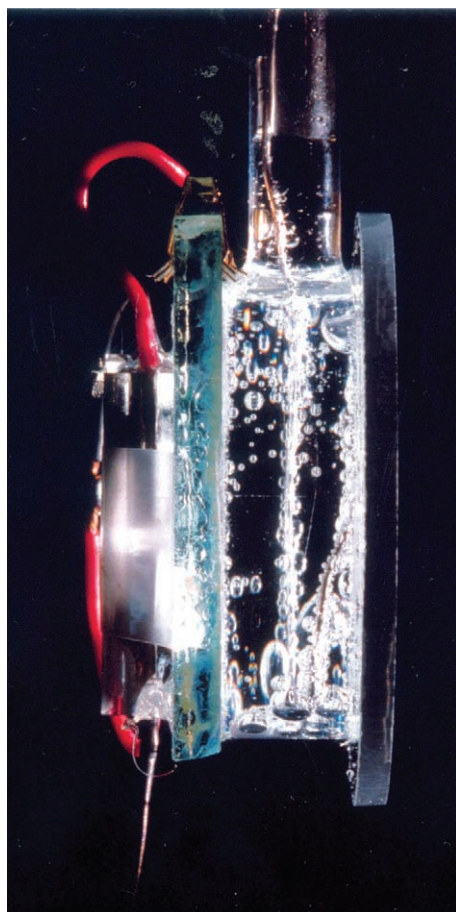


Figure 23 Photograph of a working tandem device based on a thin film of polycrystalline tungsten trioxide and a dye-sensitized nanocrystalline TiO₂ film.

replaced by reacting the complex with a 30-fold excess of pseudohalogens such as NCS⁻, CN⁻ and NCO⁻ to obtain the complexes [Ru(L)(L')(NCS)₂], [Ru(L)(L')(CN)₂] and [Ru(L)(L')(NCO)₂], respectively (Nazeeruddin and Graetzel, personal observation).

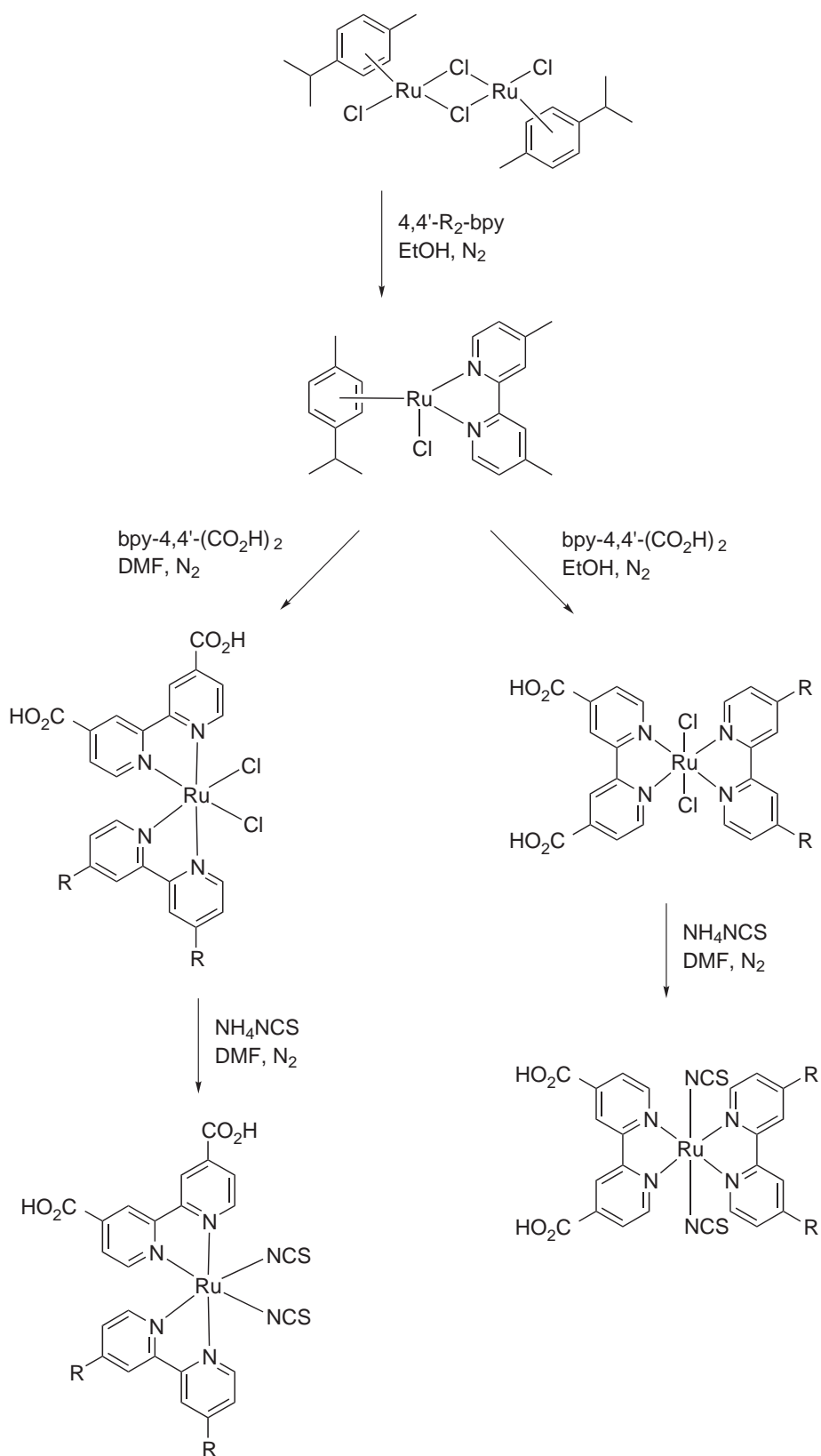
9.16.7.2 Purification

Purity is an indispensable requirement of any sensitizer in a dye-sensitized solar cell. While well worked out procedures exist for the efficient purification of metal complexes, we found that the isolation of the complexes at their isoelectric point, followed by column purification using Sephadex LH-20 gel, resulted in analytically pure samples.

9.16.7.3 Characterization

The most commonly used methods for characterization of ruthenium sensitizers are elemental analysis, NMR, IR, Raman, UV-vis, and luminescence spectroscopy; and cyclic voltammetry, HPLC, and X-ray crystallography.

The ¹H NMR spectra are useful for “finger printing” the stereochemistry in solution. This is illustrated for number of *cis*- and *trans*-complexes containing bpy ligands.⁵⁷ The proton de-coupled ¹³C NMR spectral data are particularly useful in complexes that contain ambidentate ligands such as NCS⁻ for determining the mode of its coordination. NCS ligand coordination to ruthenium metal through the sulfur atom shields the carbon atom much more than the coordination through the nitrogen atom, due to increased π-back bonding to the 3*d* orbitals of sulfur.



Scheme 3

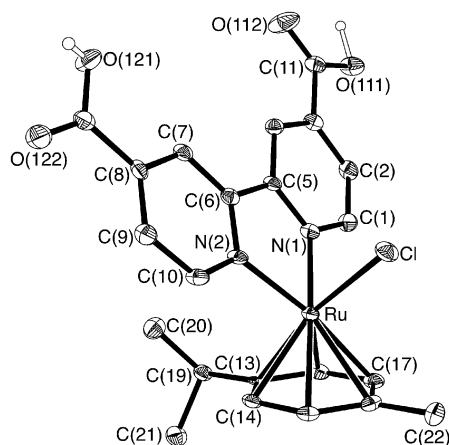


Figure 24 A view of the molecular structure of [Ru(4,4'-dicarboxy-2,2'-bipyridine)Cl(cymene)]Cl showing the symmetrical orientation of 4,4'-dicarboxy-2,2'-bipyridine ligand in relation to the cymene group.

Therefore, sulfur coordination of NCS ligand to ruthenium shows a carbon resonance at around 120–125 ppm, compared to the nitrogen coordination of NCS ligand, where the ¹³C resonance is in the region of 130–145 ppm.⁴⁶

IR and Raman spectroscopy are important structural probes in molecules which contain functional groups such as carboxylic acid, carboxylate, and NCS⁻. These groups have characteristic frequencies, which are used for identifying structural information. Resonance Raman spectroscopy is often used for identification of the lowest energy MLCT transitions in complexes.¹⁰⁸ For [RuL₃]²⁺-type complexes (where L = 2,2'-bipyridine), the data are interpreted as revealing the electronic transition that has the excited state electron localized on one of the three equivalent ligands. Generally, for mixed ligand complexes the excited electron density is localized on the more easily reducible ligand. However, if the ligands have similar LUMO energies, the Raman spectra show a mixture of excited states.¹⁰⁹ In mixed ligand complexes, it is useful to know which of the coordinating ligands is intimately involved in the lowest MLCT process, and there have been a number of such studies on mixed-ligand ruthenium-polypyridyl complexes.^{110,111} The homoleptic complexes can be used to establish the marker bands, and then subsequently this information can be used to establish the nature of the lowest energy excited state in the mixed-ligand complexes.

Electronic absorption spectra provide the most convenient way to monitor the formation of metal complexes during the synthesis. Although the spectra do not identify the structure of the complex, one can distinguish fundamental types of electronic transition: (i) intraligand, (ii) CT transitions (MLCT or LMCT), and (iii) MC. The intensity of the appropriate absorption bands is routinely used to identify the extent of formation of the desired complex during reflux. Figure 25 shows comparison of the three sensitizers (22), (24), and (43) which absorb in the visible and near-IR region, which also underscore the concept of tunability of HOMO and LUMO energy levels in ruthenium complexes.

Luminescence spectroscopy is one of the most sensitive techniques for identification of impurities in dyes. The most commonly observed impurities in *bis*-bipyridyl complexes of the type [RuL₂X₂] are the homoleptic *tris*-bipyridyl species [RuL₃]²⁺. Since the emission quantum yields of the [RuL₃]²⁺ complexes are significantly higher than those of the [RuL₂X₂] complexes, one can identify the homoleptic impurities at a level of less than 1%. This does depend, however, on the relative quantum yields, and position of the emission spectral maxima, for the complexes and impurities involved.

Cyclic voltammetry is an excellent tool to explore electrochemical reactions and to extract thermodynamic as well as kinetic information. Cyclic voltammetric data of complexes in solution show waves corresponding to successive oxidation and reduction processes. In the localized orbital approximation of ruthenium(II) polypyridyl complexes, these processes are viewed as MC and LC, respectively. Electrochemical and luminescence data are useful for calculating excited state redox potentials of sensitizers, an important piece of information from the point of view of determining whether charge injection into TiO₂ is favorable.

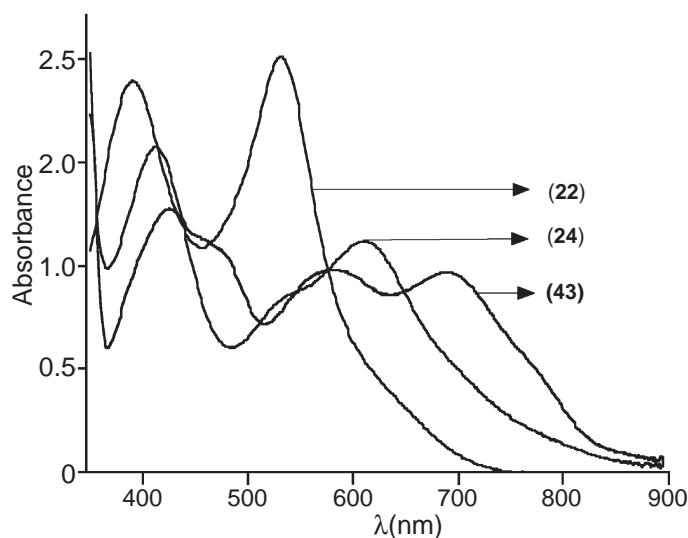


Figure 25 Comparison of the UV-visible absorption spectra of complexes (22), (24), and (43) in ethanol solution at room temperature.

Identification of trace amounts of impurities and/or isomers by these techniques is a rather exhausting task. We and others find that the HPLC method is more useful for identifying linkage isomer impurities (e.g., involving N- or S-bound thiocyanate).^{32,112}

9.16.8 CONCLUSIONS AND PERSPECTIVES

In this chapter, we have illustrated the working principle of the dye-sensitized solar cell and details of its components. A wide range of complexes has been discussed to emphasize the concept of tunability of their photophysical, redox, and spectral properties. It has been shown how careful design of the sensitizers is necessary, to obtain an enhanced spectral response across the visible and near IR region. This is accomplished using various ligands which are judiciously selected, both to optimize the optical properties of the sensitizer, and to afford efficient electron-injection into the semiconductor. Amphiphilic ruthenium(II) sensitizers that yield incident photon-to-current conversion efficiency values about 60% in a heterojunction solar cell due to an enhanced interface between the sensitizer and the hole conductor were illustrated. In addition, ideas for development of new redox mediators, which can decrease the potential difference mismatch between the sensitizer and the electrolyte redox couple, have been discussed. Among the several applications for dye-sensitized solar cells, a specific example of a “tandem device” for generation of hydrogen (fuel) from water is illustrated.

The dye-sensitized solar cell has a great future for applications that include windows to generate electricity, electrochromic materials, batteries, panels for building integration, automobile roofs, displays, toys, solar-powered clothes, etc. The coordination chemist does have a unique role to play in the “molecular engineering” of suitable sensitizers that absorb the entire visible and near-IR region of the solar spectrum, and of the associated redox partners which need to be transparent in the visible region. We believe that the further development of panchromatic sensitizers with optimized redox couples could yield cell efficiencies beyond 15%, which would expand our ability to better harvest the sun’s energy and decrease our dependency on fossil fuels. There are several approaches for modifying the sensitizers and the redox couples that are at present under scrutiny.

ACKNOWLEDGEMENTS

We thank Dr R. Humphry-Baker for his time and valuable discussions. Financial support from the Swiss Federal Office for Energy (OFEN), the US Air Force Research Office under Contract Number F61775-00-C0003 and the Institute for Applied Photovoltaics (INAP, Gelsenkirchen, Germany) is greatly appreciated.

9.16.9 REFERENCES

1. Haught, A. F. *J. Sol. Ener. Engin.* **1984**, *106*, 3.
2. De Vos, A. *Endoreversible Thermodynamics of Solar Energy Conversion*, Chapter 6, Oxford Science Publishers, Oxford, 1992.
3. McConnell, R. D. *Ren. Sust. Energ. Rev.* **2002**, *6*, 273–295.
4. Grätzel, M. *Prog. Photovoltaics* **2000**, *8*, 171–185.
5. Asbury, J. B.; Ellingson, R. J.; Ghosh, H. N.; Ferrere, S.; Nozik, A. J.; Lian, T. *J. Phys. Chem. B* **1999**, *103*, 3110–3119.
6. Ellingson, R. J.; Asbury, J. B.; Ferrere, S.; Ghosh, H. N.; Sprague, J. R.; Lian, T.; Nozik, A. J. *J. Phys. Chem. B* **1998**, *102*, 6455–6458.
7. van de Lagemaat, J.; Frank, A. J. *J. Phys. Chem. B* **2001**, *105*, 11194–11205.
8. Hara, K.; Horieuchi, H.; Katoh, R.; Singh, L. P.; Sugihara, H.; Sayama, K.; Murata, S.; Tachiya, M.; Arakawa, H. *J. Phys. Chem. B* **2002**, *106*, 374–379.
9. Islam, A.; Sugihara, H.; Singh, L. K.; Hara, K.; Katoh, R.; Nagawa, Y.; Yanagida, M.; Takahashi, Y.; Murata, S.; Arakawa, H. *Inorg. Chim. Acta* **2001**, *322*, 7–16.
10. Kubo, W.; Kitamura, T.; Hanabusa, K.; Wada, Y.; Yanagida, S. *Chem. Commun.* **2002**, 374–375.
11. Kambe, S.; Nakade, S.; Kitamura, T.; Wada, Y.; Yanagida, S. *J. Phys. Chem. B* **2002**, *106*, 2967–2972.
12. Boschloo, G.; Lindstrom, H.; Magnusson, E.; Holmberg, A.; Hagfeldt, A. *Photochem. Photobiol.* **2002**, *148*, 11–15.
13. Hagfeldt, A.; Grätzel, M. *Acc. Chem. Res.* **2000**, *33*, 269–277.
14. Ferber, J.; Luther, J. *J. Phys. Chem. B* **2001**, *105*, 4895–4903.
15. Heimer, T. A.; Heilweil, J.; Bignozzi, C. A.; Meyer, G. J. *J. Phys. Chem. A* **2000**, *104*, 4256–4262.
16. Nogueira, A. F.; Durrant, J. R.; De Paoli, M.-A. *J. Advanced Materials* **2001**, *13*, 826–830.
17. Oskam, G.; Bergeron, B. V.; Meyer, G. J.; Searson, P. C. *J. Phys. Chem. B* **2001**, *105*, 6867–6873.
18. Kuciauskas, D.; Freund, M. S.; Gray, H.; Winkler, J. R.; Lewis, N. S. *J. Phys. Chem. B* **2001**, *105*, 392–403.
19. De Paoli, M.-A.; Machado, D. A.; Nogueira, A. F.; Longo, V. *Electrochim. Acta* **2001**, *46*, 4243–4249.
20. Hou, Y.-J.; Xie, P.-H.; Zjing, B.-W.; Cao, Y.; Xiao, X.-R.; Wang, W.-B. *Inorg. Chem.* **1999**, *38*, 6320–6322.
21. Kumara, G. R. A.; Konno, A.; Shiratsuchi, K.; Tsukahara, J.; Tennakone, K. *Chem. Mater.* **2002**, *14*, 954–955.
22. Lees, A. C.; Kleverlaan, C. J.; Bignozzi, C. A.; Vos, J. G. *Inorg. Chem.* **2001**, *40*, 5343–5349.
23. Lemon, B.; Hupp, J. T. *J. Phys. Chem. B* **1999**, *103*, 3797–3799.
24. Hagfeldt, A.; Grätzel, M. *Chem. Rev.* **1995**, *95*, 49–68.
25. Rothenberger, G.; Comte, P.; Grätzel, M. *Sol. Energ. Mat. Sol. C.* **1999**, *58*, 321–326.
26. Nazeeruddin, M. K.; Graetzel, M. Dyes for Semiconductor Sensitization. In *Encyclopedia of Electrochemistry: Semiconductor Electrodes and Photoelectrochemistry*, Vol. 6: Licht, S., Ed.; Wiley-VCH: 2002; Darmstadt, pp 407–431.
27. Barbe, C. J.; Arendse, V.; Comte, P.; Jirousek, M.; Lenzmann, F.; Shklover, V.; Grätzel, M. *J. Am. Ceram. Soc.* **1997**, *80*, 3157–3171.
28. Burnside, S. D.; Shklover, V.; Barbe, C. J.; Comte, P.; Arendse, F.; Brooks, K.; Grätzel, M. *Chem. Mater.* **1998**, *10*, 2419–2425.
29. Nazeeruddin, M. K.; Kay, A.; Rodicio, I.; Humphry-Baker, R.; Muller, E.; Liska, P.; Vlachopoulos, N.; Grätzel, M. *J. Am. Chem. Soc.* **1993**, *115*, 6382–6390.
30. van de Lagemaat, J.; Frank, A. J. *J. Phys. Chem. B* **2000**, *104*, 4292–4294.
31. Cahen, D.; Hodes, G.; Grätzel, M.; Guilemole, J. F.; Riess, I. *J. Phys. Chem. B* **2000**, *104*, 2053–2059.
32. Nazeeruddin, M. K.; Zakeeruddin, S. M.; Humphry-Baker, R.; Jirousek, M.; Liska, P.; Vlachopoulos, N.; Shklover, V.; Fischer, C. H.; Grätzel, M. *Inorg. Chem.* **1999**, *38*, 6298–6305.
33. Crosby, G. A. *Acc. Chem. Res.* **1975**, *8*, 231–238.
34. Meyer, T. J. *Acc. Chem. Res.* **1978**, *11*, 94–100.
35. Juris, A.; Balzani, V.; Barigelletti, F.; Campagna, S.; Belser, P.; von Zelewsky, A. *Coord. Chem. Rev.* **1988**, *84*, 85–277.
36. Kalyanasundaram, K. *Coord. Chem. Rev.* **1982**, *46*, 159–244.
37. Krause, R. *Struct. Bond.* **1987**, *67*, 1–52.
38. Ernst, S.; Kaim, W. *Inorg. Chem.* **1989**, *28*, 1520–1528.
39. Brooks, K. G.; Burnside, S. D.; Shklover, V.; Comte, P.; Arendse, F.; McEvoy, A. J.; Grätzel, M. In *Am. Ceram. Soc.; Kumta, P. N., Ed.; Indianapolis*, 2000, p 115.
40. Nazeeruddin, M. K.; Pechy, P.; Renouard, T.; Zakeeruddin, S. M.; Humphry-Baker, R.; Comte, P.; Liska, P.; Le, C.; Costa, E.; Shklover, V.; Spiccia, L.; Deacon, G. B.; Bignozzi, C. A.; Graetzel, M. *J. Am. Chem. Soc.* **2001**, *123*, 1613–1629.
41. Anderson, P. A.; Strouse, G. F.; Treadway, J. A.; Keene, F. R.; Meyer, T. J. *Inorg. Chem.* **1994**, *33*, 3863–3864.
42. Balzani, V.; Juris, A.; Venturi, M.; Campagna, S.; Serroni, S. *Chem. Rev.* **1996**, *96*, 759–833.
43. Kalyanasundaram, K.; Nazeeruddin, M. K. *Chem. Phys. Lett.* **1992**, *193*, 292–297.
44. Nazeeruddin, M. K.; Muller, E.; Humphry-Baker, R.; Vlachopoulos, N.; Grätzel, M. *J. Chem. Soc. Dalton Trans.* **1997**, 4571–4578.
45. Ruile, S.; Kohle, O.; Pechy, P.; Grätzel, M. *Inorg. Chim. Acta* **1997**, *261*, 129–140.
46. Kohle, O.; Ruile, S.; Grätzel, M. *Inorg. Chem.* **1996**, *35*, 4779–4787.
47. Zakeeruddin, S. M.; Nazeeruddin, M. K.; Pechy, P.; Rotzinger, F. P.; Humphry-Baker, R.; Kalyanasundaram, K.; Grätzel, M. *Inorg. Chem.* **1997**, *36*, 5937–5946.
48. Nazeeruddin, M. K.; Pechy, P.; Grätzel, M. *Chem. Commun.* **1997**, 1705–1706.
49. Argazzi, R.; Bignozzi, C. A.; Heimer, T. A.; Castellano, F. N.; Meyer, G. J. *Inorg. Chem.* **1994**, *33*, 5741–5749.
50. Xie, P.-H.; Hou, Y. J.; Zhang, B. W.; Cao, Y.; Wu, F.; Tian, W.-J.; Shen, J. C. *J. Chem. Soc., Dalton Trans.* **1999**, 4217–4221.
51. Nazeeruddin, M. K.; Humphry-Baker, R.; Pechy, P.; Rotzinger, F. P.; Grätzel, M. In *10th International Conference on Photochemical Conversion and Storage of Solar Energy*; Interlaken, Switzerland, July 24–29, 1994, p 201.
52. Hara, S.; Sugihara, H.; Tachibana, Y.; Islam, A.; Yanagida, M.; Sayama, K.; Arakawa, H. *Langmuir* **2001**, *17*, 5992–5999.

53. Yanagida, M.; Sing, L. P.; Sayama, K.; Hara, K.; Katoh, R.; Islam, A.; Sugihara, H.; Arakawa, H.; Nazeeruddin, M. K.; Grätzel, M. *J. Chem. Soc., Dalton Trans.* **2000**, 2817–2821.
54. Kober, E. M.; Meyer, T. J. *Inorg. Chem.* **1983**, *22*, 1614–1616.
55. Heimer, T. A.; Bignozzi, C. A.; Meyer, G. J. *J. Phys. Chem.* **1993**, *97*, 11987–11994.
56. Sauvè, G.; Cass, M. E.; Doig, S. J.; Laueremann, I.; Pomykal, K.; Lewis, N. S. *J. Phys. Chem.* **2000**, *104*, 3488–3491.
57. Nazeeruddin, M. K.; Zakeeruddin, S. M.; Humphry-Baker, R.; Gorelsky, S. I.; Lever, A. B. P.; Grätzel, M. *Coord. Chem. Rev.* **2000**, *208*, 213–225.
58. Masood, M. A.; Sullivan, B. P.; Hodges, D. J. *Inorg. Chem.* **1994**, *33*, 4611–4612.
59. Durham, B.; Wilson, S. R.; Hodges, D. J.; Meyer, T. J. *J. Am. Chem. Soc.* **1980**, *102*, 600–607.
60. Renouard, T.; Fallahpour, R.-A.; Nazeeruddin, M. K.; Humphry-Baker, R.; Gorelsky, S. I.; Lever, A. B. P.; Grätzel, M. *Inorg. Chem.* **2002**, *41*, 367–378.
61. Lever, A. B. P. *Inorg. Chem.* **1990**, *29*, 1271–1285.
62. Zakeeruddin, S. M.; Nazeeruddin, M. K.; Humphry-Baker, R.; Pe'chy, P.; Quagliotto, P.; Barolo, C.; Viscardi, G.; Graetzel, M. *Langmuir* **2002**, *18*, 952–954.
63. Tennakone, K.; Kumara, G. R. R. A.; Kottegoda, I. R. M.; Perera, V. P. S. *Chem. Commun.* **1999**, 15–16.
64. Chandrasekharan, N.; Kamat, P. V. *J. Phys. Chem. B* **2000**, *104*, 10851–10857.
65. Gregg, B. A.; Pichot, F.; Ferrere, S.; Fields, C. L. *J. Phys. Chem. B* **2001**, *105*, 1422–1429.
66. Wöhrle, D.; Meissner, D. *Adv. Mater.* **1991**, *3*, 129–138.
67. Jaeger, C. D.; Fan, F. F.; Bard, A. J. *J. Am. Chem. Soc.* **1980**, *102*, 2592–2598.
68. Giraudeau, A.; Ren, F.; Fan, F.; Bard, A. J. *J. Am. Chem. Soc.* **1980**, *102*, 5137–5142.
69. Jaeger, C. D.; Far, Fu-Ren, F.; Bard, A. J. *J. Am. Chem. Soc.* **1980**, *102*, 2592–2598.
70. Yanagi, H.; Chen, S.; Lee, P. A.; Nebesny, K. W.; Armstrong, N. R.; Fujishima, A. *J. Phys. Chem.* **1996**, *100*, 5447–5451.
71. Nazeeruddin, M. K.; Humphry-Baker, R.; Murrer, B. A.; Grätzel, M. *J. Chem. Soc., Chem. Commun.* **1998**, 719–720.
72. He, J.; Benko, G.; Korodi, F.; Polivka, T.; Lomoth, R.; Åkermark, B.; Sun, L.; Hagfeldt, A.; Sundstrom, V. *J. Am. Chem. Soc.* **2002**, *124*, 4922–4932.
73. Nazeeruddin, M. K.; Humphry-Baker, R.; Graetzel, M.; Wöhrle, D.; Schnurpfeil, G.; Schneider, G.; Hirth, A.; Trombach, N. *J. Porphyrins Phthalocyanines* **1999**, *3*, 230–237.
74. Kalyanasundaram, K.; Grätzel, M. *Coord. Chem. Rev.* **1998**, *77*, 347–414.
75. Bignozzi, C. A.; Aragazzi, R.; Kleverlaan, C. J. *Chem. Soc. Rev.* **2000**, *29*, 87–96.
76. Trammell, S. A.; Moss, J. A.; Yang, J. C.; Nakhle, B. M.; Slate, C. A.; Odobel, F.; Sykora, M.; Erickson, B. W.; Meyer, T. J. *Inorg. Chem.* **1999**, *38*, 3665–3669.
77. Will, G.; Boschloo, G.; Nagaraja Rao, S.; Fitzmaurice, D. *J. Phys. Chem. B* **1999**, *103*, 8067–8079.
78. Jing, B.; Zhang, H.; Zhang, M.; Lu, Z.; Shen, T. *J. Mater. Chem.* **1998**, *8*, 2055–2060.
79. Rice, C. R.; Ward, M. D.; Nazeeruddin, M. K.; Grätzel, M. *New J. Chem.* **2000**, *24*, 651–652.
80. Murakoshi, K.; Kano, G.; Wada, Y.; Yanagida, S.; Miyazaki, H.; Matsumoto, M.; Murasawa, S. *J. Electroanal. Chem.* **1995**, *396*, 27–34.
81. Finnie, K. S.; Bartlett, J. R.; Woolfrey, J. L. *Langmuir* **1998**, *14*, 2744–2749.
82. Fillinger, A.; Parkinson, B. A. *J. Electrochem. Soc.* **1999**, *146*, 4559–4564.
83. Shklover, V.; Ovehinnikov, Y. E.; Braginsky, L. S.; Zakeeruddin, S. M.; Grätzel, M. *Chem. Mater.* **1998**, *10*, 2533–2541.
84. Zubavichus, Y. V.; Slovokhotov, Y. L.; Nazeeruddin, M. K.; Zakeeruddin, S. M.; Grätzel, M.; Shklover, V. *Chem. Mater.* **2002**, *14*, 3556–3563.
85. Yan, S. G.; Hupp, J. T. *J. Phys. Chem.* **1996**, *100*, 6867–6870.
86. Qu, P.; Meyer, G. J. *Langmuir* **2001**, *17*, 6720–6728.
87. Scandola, F.; Indelli, M. T.; Chiorboli, C.; Bignozzi, C. A. *Top. Curr. Chem.* **1990**, *158*, 73–149.
88. Nazeeruddin, M. K.; Liska, P.; Moser, J.; Vlachopoulos, N.; Grätzel, M. *Helv. Chim. Acta* **1990**, *73*, 1788–1803.
89. Haque, S. A.; Tachibana, Y.; Klug, D. R.; Durrant, J. R. *J. Phys. Chem. B* **1998**, *102*, 1745–1749.
90. Tachibana, Y.; Nazeeruddin, M. K.; Graetzel, M.; Klug, D. R.; Durrant, J. R. *Chem. Phys.* **2002**, *285*, 127–132.
91. Willig, F.; Burnfeindt, B.; Schwarzbürg, K.; Hannappel, T.; Stock, W. *Proc. Indian Acad. Sci. (Chem. Sci.)* **1997**, *109*, 415–428.
92. Moser, J.-E.; Graetzel, M. *Chimia* **1998**, *52*, 160–163.
93. Schnadt, J.; Brühwiler, P. A.; Patthey, L.; O'Shea, J. N.; Södergren, S.; Odelius, M.; Ahuja, R.; Karls, O.; Bässler, M.; Persson, P.; Siegbahn, H.; Lunell, S.; Martensson, N. *Nature* **2002**, *418*, 620–623.
94. Rensmo, H.; Lunell, H.; Siegbahn, S. *J. Photochem. Photobiol.* **1998**, *114*, 117–124.
95. Wen, C.; Ishikawa, K.; Kishima, M.; Yamada, K. *Sol. Energ. Mat. Sol. C* **2000**, *61*, 339–351.
96. Nusbaumer, H.; Moser, J. E.; Zakeeruddin, S. M.; Nazeeruddin, M. K.; Graetzel, M. *J. Phys. Chem. B* **2001**, *105*, 10464–10465.
97. Bach, U.; Lupo, D.; Comte, P.; Moser, J.-E.; Weissörtel, F.; Salbeck, J.; Spreitzer, H.; Grätzel, M. *Nature* **1998**, *395*, 583–585.
98. Pelet, S.; Moser, J. E.; Graetzel, M. *J. Phys. Chem. B* **2000**, *104*, 1791–1795.
99. O'Regan, B.; Schwartz, D. T.; Zakeeruddin, S. M.; Grätzel, M. *Adv. Mater.* **2000**, *12*, 1263–1267.
100. Licht, S. *J. Phys. Chem. B* **2001**, *105*, 6281–6294.
101. Infelta, P. P. *J. Photochemistry* **1982**, *20*, 181–196.
102. Dwyer, F. P.; Humpolett, J. E.; Nyholm, R. S. *J. Proc. Roy. Soc. N. S. Wales* **1946**, *80*, 212.
103. Rose, D.; Wilkinson, G. *J. Chem. Soc. A* **1970**, 1791–1795.
104. Clear, J. M.; Kelly, J. M.; O'Connell, C. M.; Vos, J. G.; Cardin, C. J.; Costa, S. R.; Edwards, A. J. *J. Chem. Soc., Chem. Commun.* **1980**, 750–751.
105. Black, D. S. C.; Deacon, G. B.; Thomas, N. C. *Inorg. Chim. Acta* **1982**, *65*, L75–L76.
106. Zakeeruddin, S. M.; Nazeeruddin, M. K.; Humphry-Baker, R.; Grätzel, M.; Shklover, V. *Inorg. Chem.* **1998**, *37*, 5251–5259.
107. Maxwell, K. A.; Sykora, M.; DeSimone, J. M.; Meyer, T. J. *Inorg. Chem.* **2000**, *39*, 71–75.
108. Nazeeruddin, M. K.; Grätzel, M.; Kalyanasundaram, K.; Girling, R. B.; Hester, R. E. *J. Chem. Soc., Dalton Trans.* **1993**, 323–325.

109. Goff, A. H.-L.; Joiret, S.; Falaras, P. *J. Phys. Chem. B.* **1999**, *103*, 9569–9575.
110. Mabrouk, P. A.; Wrighton, M. S. *Inorg. Chem.* **1986**, *25*, 526–531.
111. Tait, C. D.; Vess, T. M.; DeArmond, M. K.; Hank, K. W.; Wertz, D. W. *J. Chem. Soc. Dalton Trans.* **1987**, 2467–2471.
112. Wang, R.; Vos, J. G.; Schmehl, R. H.; Hage, R. *J. Am. Chem. Soc.* **1992**, *114*, 1964–1970.

9.17

Metal Complexes for Hydrometallurgy and Extraction

P. A. TASKER, P. G. PLIEGER, and L. C. WEST
University of Edinburgh, UK

9.17.1	INTRODUCTION	759
9.17.2	MINERAL PROCESSING	762
9.17.3	LEACHING	763
9.17.3.1	Leaching of Gold and Silver into Basic Media	764
9.17.3.2	Leaching of Gold and Silver into Acidic Media	765
9.17.3.3	Leaching of Base Metals	766
9.17.3.3.1	<i>Leaching of base metals into sulfate media</i>	766
9.17.3.3.2	<i>Leaching of base metals into chloride media</i>	767
9.17.3.3.3	<i>Leaching of base metals into ammoniacal media</i>	768
9.17.4	SEPARATION AND CONCENTRATION	768
9.17.4.1	Solvent Extraction Processes	769
9.17.4.2	Hydroxy-oxime Extractants	770
9.17.4.3	Organophosphorus Acid Extractants	772
9.17.4.4	Carboxylic Acids	772
9.17.4.5	Amine Salt Extractants	774
9.17.4.6	Solvating Extractants	775
9.17.5	BASE METALS	776
9.17.5.1	Copper	776
9.17.5.1.1	<i>Extraction of Cu^{II} from sulfate solutions</i>	776
9.17.5.1.2	<i>Extraction of Cu^{II} from chloride solutions</i>	778
9.17.5.1.3	<i>Extraction of Cu^{II} from ammoniacal solutions</i>	780
9.17.5.1.4	<i>Recovery of Cu^{II} from secondary sources</i>	781
9.17.5.2	Zinc	781
9.17.5.2.1	<i>Extraction of Zn^{II} from sulfate media</i>	782
9.17.5.2.2	<i>Extraction of Zn^{II} from chloride media</i>	783
9.17.5.2.3	<i>Zn/Fe recovery from secondary sources</i>	785
9.17.5.3	Nickel and Cobalt	785
9.17.5.3.1	<i>Co/Ni separation in sulfate solutions</i>	786
9.17.5.3.2	<i>Co/Ni separation in chloride and ammoniacal solutions</i>	788
9.17.6	PRECIOUS METALS	790
9.17.6.1	Au ^I , Au ^{III}	791
9.17.6.2	Ag ^I	793
9.17.6.3	Pt ^{IV} , Pt ^{II}	794
9.17.6.4	Pd ^{II}	796
9.17.7	CONCLUSIONS	797
9.17.8	REFERENCES	797

9.17.1 INTRODUCTION

Extractive metallurgy covers a huge range of mechanical and chemical processes, some of which date back several thousand years.^{1,2} In terms of recovery from primary sources (metal ores) these processes are often broken down into the unit operations: *concentration, separation,*

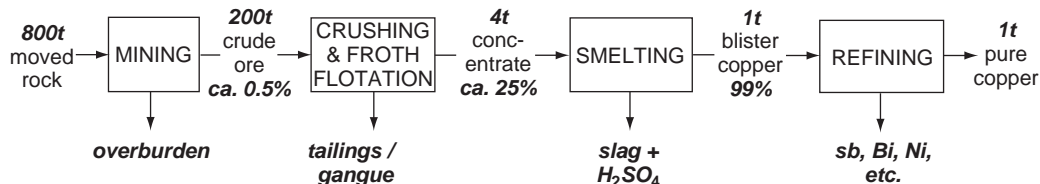


Figure 1 Typical quantities involved in the concentration of copper from sulfide ores.

reduction, and, when a high-purity product is required, additionally *refining*.¹⁻³ The wide range of technologies applied is partly a consequence of the different challenges presented by the *concentrating* operations which need to address precious metals which are often present at $<10^{-3}\%$ in natural deposits and the more abundant metals such as Al and Fe, which can approach 50% metal content. Base metals fall between these extremes; production of 1 ton of electrical grade copper typically requires movement of 800 tons of rock (Figure 1).

In the broadest sense, coordination chemistry is involved in the majority of steps prior to the isolation of a pure metal because the physical properties and relative stabilities of metal compounds relate to the nature and disposition of ligands in the metal coordination spheres. This applies both to *pyrometallurgy*, which “produces metals or intermediate products directly from the ore by use of high-temperature oxidative or reductive processes” and to *hydrometallurgy*, which “involves the processing of an ore by the dissolution, separation, purification, and precipitation of the dissolved metal by the use of aqueous solutions.”⁴

This review will focus on processes which depend on the selection or design of ligands to enhance the effectiveness of the four unit operations listed above. In general, the application of such ligands relates to equilibria involving distribution of a metal between two phases.

Liquid–liquid distributions form the basis of solvent extraction and related processes, and smelting processes.

Liquid–solid distributions are involved in ion-exchange and other adsorption-based separation processes, separation processes based on crystallization or precipitation, flotation processes for ore dressing, and smelting processes.

Examples of the formation of volatile metal compounds or complexes leading to separations based on gas–liquid and gas–solid distribution are much rarer.

Since the last review in *Comprehensive Coordination Chemistry* (CCC, 1987),⁴ R & D activity on the recovery of metals from secondary sources has increased significantly, reflecting economic and environmental requirements to recycle materials and to remove them from process streams prior to discharge of effluents. Integrating recycling processes with those for the generation and use of materials is favored in the “Industrial Ecology” approach, which requires an audit of the materials and energy consumption in a total system.⁵⁻⁸ A systems engineering approach can then be used to minimize the impact of the total system. The relative ease of tracking metal-containing materials in such systems, in contrast to organic compounds, has resulted in these being favored in industrial ecology case studies.⁹

Another factor which has increased the applications of coordination chemistry to extractive metallurgy since the mid-1980s is the emergence of hydrometallurgy as an alternative to pyrometallurgy in the recovery of base metals. The proven robustness of the hydrometallurgical process involving solvent extraction in the nuclear industries¹⁰ and the commercial success of heap leaching/solvent extraction/electrowinning processes for copper¹¹⁻¹⁴ (Section 9.17.5.1) have stimulated the development of new leaching and separation technologies for a wide range of metals. The use of hydrometallurgy to replace or complement pyrometallurgical operations is summarized in Figure 2.

One of the most important roles of coordination chemistry in hydrometallurgical processes is to effect the separation and concentration of the target metal. The design of metal complexing agents with the appropriate “strength” and selectivity to meet the requirements of the front-end of the flowsheet, leaching, and the back-end, reduction to generate pure metal (Figure 3), presents challenging targets for the coordination chemist.

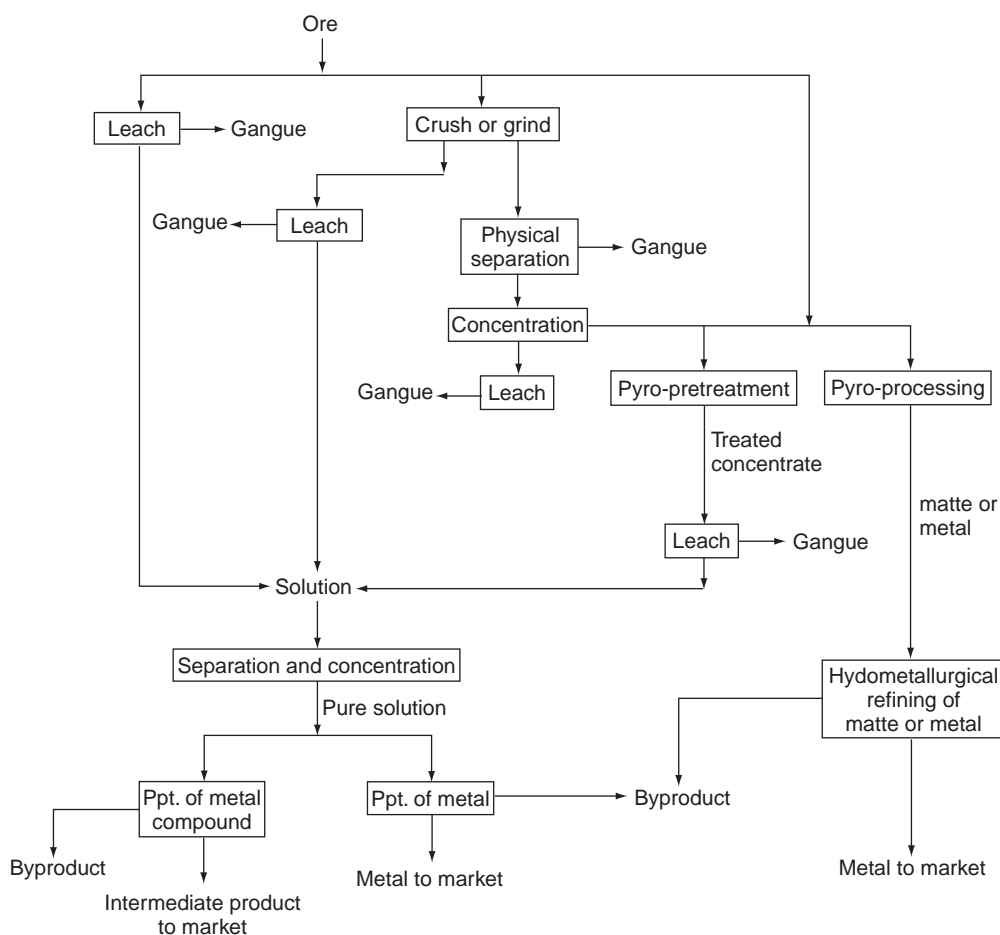


Figure 2 Routes for metal recovery from primary sources involving hydrometallurgy, based on the scheme used in previous review.⁴

In the sections which follow processes based on metal complex formation are described in the order they occur in the flowsheets in Figures 2 and 3, i.e.,

mineral processing,
leaching,
separation and concentration, and
reduction.

The application of these methods is described in some detail for recovery of base metals and platinum group metals in Sections 9.17.5–9.17.6 focusing mainly on solution-based hydrometallurgical operations, largely those involving solvent extraction, because the nature of the metal complexes formed is usually best understood in such systems. NB. Extraction of lanthanides and actinides is not included as this subject is treated separately in Chapters 3.2 and 3.3.

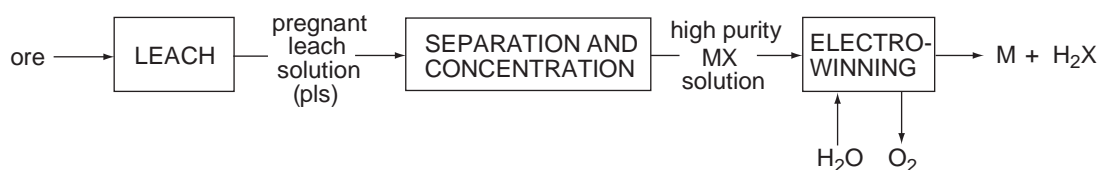


Figure 3 A simplified flowsheet for the hydrometallurgical recovery of base metals using metal complexing agents.

9.17.2 MINERAL PROCESSING

Natural mineral deposits are usually heterogeneous mixtures of solid materials that require crushing and grinding to liberate the minerals containing the metal values. Such operations often represents a sizeable fraction of the total capital and energy costs of metal recovery. One of the potential advantages of hydrometallurgical routes for metal recovery is that it is sometimes possible to carry out heap leaching on ores which have not had to be milled, for example in the recovery of copper from oxidic or transition ores (see Section 9.17.5.1).

Separation of milled solid materials is usually based on differences in their physical properties. Of the various techniques to obtain ore “concentrates,” those of froth flotation and agglomeration exploit differences in surface activities, which in many cases appear to involve the formation of complexes at the surface of the mineral particles. Separation by froth flotation (Figure 4) depends upon conversion of water-wetted (hydrophilic) solids to nonwetted (hydrophobic) ones which are transported in an oil-based froth leaving the undesired materials (gangue) in an aqueous slurry which is drawn off from the bottom of the separator. The selective conversion of the ore particles to hydrophobic materials involves the adsorption of compounds which are usually referred to as “collectors.”⁴

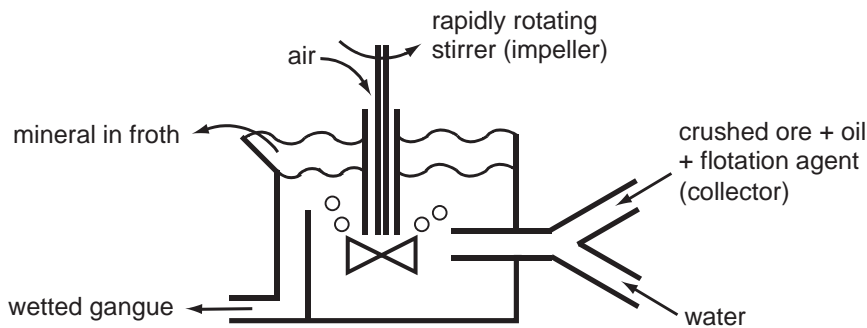


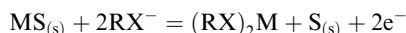
Figure 4 Schematic representation of a froth flotation separator.

Some of the more commonly used types of collector are listed in Table 1. Many of these contain sulfur atoms in their polar “head groups” and are used in the recovery of base metals from their

Table 1 Collectors used in mineral flotation.

Thiols	Alkyl thiocarbonates	Alkyl dithiocarbonates (xanthates)	Alkyl thionocarbamates
RSH	$\text{RO}-\text{C}(=\text{O})-\text{S}^-$	$\text{RO}-\text{C}(=\text{S})-\text{S}^-$	$\text{RO}-\text{C}(=\text{S})-\text{N}^-(\text{R})$
Mercapto-benzothiazolates	Dialkyl-dithiophosphates	Dialkyl(aryl)-monothiophosphates	Fatty carboxylates
	$\text{RO}-\text{P}(=\text{S})(\text{S}^-)-\text{RO}$	$\text{RO}-\text{P}(=\text{O})(\text{S}^-)-\text{RO}$	$\text{R}-\text{C}(=\text{O})-\text{O}^-$
Hydroxamates	<i>N</i> -alkyl- <i>N'</i> -alkoxy-carbonylthioureates		
$\text{R}-\text{C}(=\text{O})-\text{N}(\text{H})-\text{O}^-$	$\text{ROCO}-\text{N}(\text{H})-\text{C}(=\text{S})-\text{N}^-(\text{R})$		

sulfidic ores. They are effective under oxidizing conditions and it is proposed that chemisorption is involved in bonding with the formation of metal–sulfur and/or sulfur–sulfur bonds.⁴ The modes of chemisorption depend on the redox properties of the collector, and mechanisms resulting in the liberation of elemental sulfur from the surface of sulfidic ores are proposed.¹⁵



Details of the structures of complexes formed at the surface of the ore particles are difficult to obtain,¹⁶ but it is noteworthy that the majority of the collectors used have ligating head groups which are capable of forming polynuclear complexes. Bidentate groups that would form five- or six-membered chelate rings are more rarely used. The stability of such complexes is likely to favor removal of metal atoms from the surface, transferring them to the liquid phase rather than surface ligation, which is needed to generate hydrophobic particles.

Several reviews on ore processing by flotation are available.^{17–21} In addition to providing details of the chemistry of collectors they describe the use of activators and depressants. The former usually convert the surfaces of an ore particle which does not bind strongly to conventional collectors to one that does. The addition of Cu^{2+} ions to enhance the flotability of minerals such as sphalerite, a zinc sulfide, has been exploited for some time.⁴ Formation of a surface layer of CuS has been assumed to account for this, but the mechanisms and selectivities of such processes continue to be investigated.^{18,22,23}

Depressants are used to make materials less floatable, and again have been used for some time.^{4,18} A recent example is the use of phosphoric acid to depress the flotation of a sedimentary phosphate ore, enhancing the selectivity of recovery of calcite and silica.²⁴ Natural and synthetic polymers have also been used as depressants.²⁰

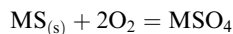
Several of the ligating functions in the collectors shown in Table 1 are also present in compounds which are used in metal-surface engineering, e.g., the dialkyldithiophosphates are anti-wear agents in lubricants.²⁵ This emphasizes the need for a better understanding of ligand design features to achieve strong and selective binding to surfaces of lightly oxidized metals or to minerals if a more rational approach is to be used to the development of new “actives” for mineral processing and surface engineering.

9.17.3 LEACHING

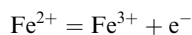
Leaching is the primary process in hydrometallurgy whereby the metal values of a solid metal-bearing material are transferred into an aqueous solution by the action of a lixiviant. Typically, leaching is applied to ores, spent catalysts, pyrometallurgically derived intermediates, metal scraps, and by-products from metal refining. Processes generally fall into two categories, those in which the formal oxidation state of the metal remains unchanged and those where dissolution is accompanied by a redox process.

In addition to water molecules the coordination chemistry of leaching generally involves simple inorganic anionic ligands, ammonia, or acetonitrile. Many of the well-established processes (see Table 2) were considered in CCC (1987),⁴ and are also described in a recent comprehensive text on hydrometallurgy.²

Bioleaching, particularly of sulfidic ores, has received much attention since the early 1980s. The conditions needed and mechanisms for such processes have been reviewed. Microbial processes involve complete oxidation of sulfide to sulfate, e.g.,



This is often accompanied by oxidation of metals, particularly iron,



which is important (see below) because the ferric ion is very effective in oxidative leaching of both simple and complex sulfides:²⁶

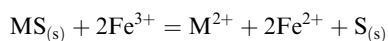


Table 2 Metals recovered by leaching and types of ligands employed.

<i>Metal</i>	<i>Ligand</i>	<i>Metal</i>	<i>Ligand</i>
Al	OH ⁻ , Cl ⁻	Zr, Nb, Mo, Hf, Ta, W	Cl ⁻ , OH ⁻
Ti	Cl ⁻	Ru, Rh, Pd, Os, Ir, Pt	Cl ⁻
Cr	SO ₄ ²⁻ , Cl ⁻	Ag	NH ₃ , CN ⁻ , CH ₃ CN, Cl ⁻
Mn	SO ₄ ²⁻	Au	CN ⁻ , (NH ₂)CS, S ₂ O ₃ ²⁻ , SCN ⁻ , Cl ⁻
Fe	SO ₄ ²⁻ , Cl ⁻	Sn	OH ⁻ , Cl ⁻
Co	SO ₄ ²⁻ , Cl ⁻ , NH ₃	Sb	Cl ⁻
Ni	SO ₄ ²⁻ , Cl ⁻ , NH ₃	Pb	OH ⁻ , Cl ⁻ , CH ₃ CO ₂ ⁻
Cu	SO ₄ ²⁻ , Cl ⁻ , NH ₃ , CH ₃ CN	Lanthanides	SO ₄ ²⁻
Zn, Cd	SO ₄ ²⁻	U	SO ₄ ²⁻ , CO ₃ ²⁻
Se, Te	Cl ⁻		

Source:^{2,4}

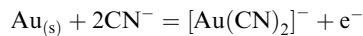
There are some examples of commercially successful bioleaching operations for copper, uranium, and gold,²⁷ but the full potential of microbial processes is likely only to be realized by better understanding and integration of the reactions involved and the engineering needed.²⁶ The regeneration of Fe^{III} salts as above is important in heap leaching operations; see, for example, Section 9.17.3.3.1. Microbial leaching of metals from sulfidic minerals has been practiced for many years without the realization that microorganisms are involved.²⁸

In both bio- and “inorganic”-leaching processes, metal complex formation at the surface of mineral particles being leached is often accompanied by catalytic redox reactions which labilize the metal ions, leading to complicated reaction sequences. An understanding of these is important for the design and operation of processes which minimize the formation of toxic by-products, are selective and achieve a high recovery of the desired metal, operate at a reasonable rate and produce pregnant leach solutions suitable for downstream processing. In the sections which follow the chemistry of leaching processes is described where the efficacy of the process is dependent on strong, selective, and rapid complex formation and where a knowledge of the composition of streams is important for understanding the downstream “separation and concentration” steps which involve coordination chemistry (Sections 9.17.5–9.17.6).

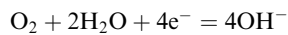
9.17.3.1 Leaching of Gold and Silver into Basic Media

It has been more than a hundred years since MacArthur and Forrest developed a process for the leaching of gold based upon the use of an alkaline cyanide solution.²⁹ Despite the toxicity of cyanide solutions this is still the most widely used process for both Ag and Au, and has been extensively reviewed.^{30–32}

The dissolution of gold in its native form by cyanidation involves oxidation to Au^I,

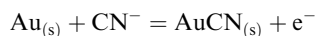


coupled to the reduction of dioxygen,



and depends on the formation of very stable aurocyanide complexes.³³ The formation of these complexes is a complicated process; 35 equilibria have been proposed in a model system to account for their generation at a rotating gold electrode.³⁴

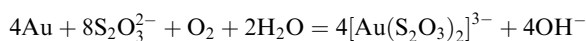
Species, including cyanide, that bind strongly to the surfaces of gold-bearing materials result in passivation and, when high-purity cyanide solutions are used, gold dissolution is negligible,³⁵ consistent with a two-step mechanism. AuCN_(s) is formed rapidly at the gold surface, and a subsequent rate-determining step involves the addition of a second ligand, followed by the dissolution of Au(CN)₂⁻



The low solubility of $\text{AuCN}_{(s)}$ is thought to be a consequence of a polymeric structure based on linear chains, $-\text{Au-CN-Au-CN}-$, which lie parallel to one another with a close-packed arrangement of gold atoms in which each is in contact with six nearest neighbors.³⁶ The addition of cyanide and dissolution of $[\text{Au}(\text{CN})_2]^-$ is believed to take place at the chain ends. This process is enhanced by the presence of Ag^{2+} or other ions such as Pb^{2+} (see below) normally present in the gold-bearing ores.

Sulfide is a well-known passivating species, and recently Jeffrey *et al.* using a rotating electrochemical quartz micro-balance, suggested that $\text{Au}_2\text{S}_{(s)}$ is formed at surfaces.³² This passivity has led to a preference for recovering gold from oxidic matrices rather than refractory ores which have sulfidic matrices, but since the majority of gold deposits available for exploitation in the twenty-first century are refractory ores, methods are needed to improve leaching. Lead acetate has traditionally been used to enhance gold leaching,^{30,32,35,37} but the origins of this are not fully understood. In the absence of sulfide the addition of as little as a few ppb of Pb^{2+} results in a large increase in the rate of dissolution of pure gold into high-purity cyanide solution.³⁵ This is believed to result from cementation of Pb on the gold surface, providing cyanide ions better access to $\text{AuCN}_{(s)}$ "chain ends" (see above).³⁵ The binding of hydroxyl ions to the ends of AuCN chains accounts^{38,39} for the decrease in rates of cyanidation when the process is carried out at a $\text{pH} > 12$.⁴⁰

The toxicity of cyanide has led to the development of alternative lixiviants for gold and silver; see also Sections 9.17.3.2 and 9.17.3.3. Thiosulfate is potentially a cheaper reagent for use in alkaline or near-neutral solutions in the presence of a mild oxidant such as dioxygen,⁴¹⁻⁴⁸

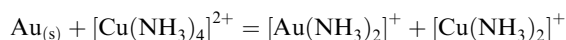


Alkaline conditions must be used to prevent the decomposition of thiosulfate. The resulting pregnant leach solutions also contain the monothiosulfato complex, $[\text{Au}(\text{S}_2\text{O}_3)]^-$.⁴⁹

Dissolution is depressed by the build-up of sulfur-containing coatings on the ore particles.⁵⁰⁻⁵² The presence of ammonia and Cu^{2+} ions in the leach solution appears to overcome this problem and greatly enhances dissolution.^{43,48,52}

The coordination chemistry of such an ammonia-thiosulfate-copper-gold system is complicated. Its interpretation must take into account the influence of ligands on the $\text{Cu}^{2+}/\text{Cu}^+$ and Au^+/Au redox couples and the occurrence of oxidative decomposition reactions of thiosulfate involving the formation of tetrathionate and other compounds.⁵³ Extensive thermodynamic calculations and E^θ -pH diagrams under typical leaching conditions have been used to clarify which species predominate⁵⁴ and mechanistic studies^{51,55,56} have provided a greater understanding of reaction pathways.

It is believed that copper acts as the oxidant in these systems, effecting the dissolution of gold as an ammine complex,



which then transfers the Au^{I} ion to thiosulfato ligands.

The ammonia stabilizes Cu^{II} relative to Cu^{I} allowing it to be regenerated in the presence of air,⁵² and although the reduction of Cu^{II} by thiosulfate is normally rapid in a pure aqueous solution, in the presence of ammonia in these systems it proceeds much more slowly,⁴³



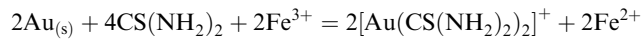
Reagent losses of this type need to be minimized if the technology is to achieve wide application.

9.17.3.2 Leaching of Gold and Silver into Acidic Media

Sulfidic matrices often require an oxidative pre-treatment prior to leaching the gold (see above). Bio-oxidative processes to achieve this usually generate acidic aqueous phases which must be neutralized prior to cyanidation. To avoid this neutralization step, lixiviants such as thiourea have been considered, which can be used in acidic media.⁵⁷⁻⁶⁷ The thiourea-based processes have a

much lower environmental impact than conventional cyanidation and are claimed to show greater selectivity and faster kinetics of gold dissolution.

Stable cationic complexes of Au^I are formed with thiourea in acidic solutions in the presence of oxidants such as Fe^{III} or hydrogen peroxide,⁶⁸

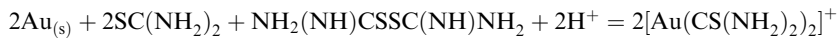


Lacoste-Bouchet *et al.*⁶⁶ have shown that acidic thiourea is a more selective leachant for gold over copper than alkaline cyanide solutions.

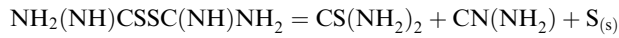
Oxidation of thiourea occurs fairly rapidly with H₂O₂ but more slowly with Fe^{III},⁶⁹



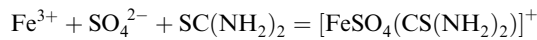
The resulting formamidine disulphide acts as a gold oxidant,⁶⁰



regenerating thiourea, but is not stable in acidic solutions and decomposes irreversibly, producing elemental sulfur and cyanamide:

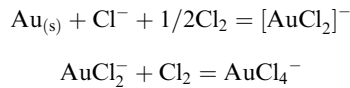


Thiourea can also be lost from the system by the formation of stable iron sulfate complexes,^{63,66}



Such reagent losses need to be minimized to ensure that thiourea leaching finds widespread use.

Leaching with chlorine in acidic media proceeds via a Au^I intermediate;



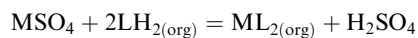
faster than traditional cyanidation.⁷⁰⁻⁷⁴ The Cl₂ can be generated *in situ* from the reaction of chloride and hypochlorite salts, and can be operated as part of the oxidative treatment of the ores.⁷⁰

9.17.3.3 Leaching of Base Metals

A review of processes for leaching of base metals from their ores has appeared recently.² Recent developments involving the generation and composition of sulfate-, chloride-, or ammonia-based streams which are used to feed solvent extraction processes are considered briefly below.

9.17.3.3.1 Leaching of base metals into sulfate media

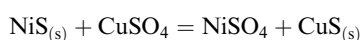
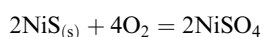
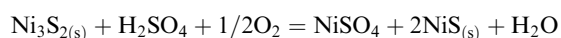
Sulfate process streams are commonly used in metal recovery because they are readily derived by leaching with sulfuric acid or by oxidation of sulfidic ores. Metal recovery from such streams rarely involves the formation of metal sulfate complexes because the sulfate ion is a weak ligand for base metal cations and consequently acidic ion exchange extractants are commonly employed (see Section 9.17.5), which generate sulfuric acid which can be returned to the leaching stage,



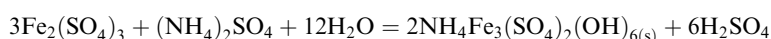
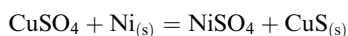
Following the success of the Moa Bay plant in Cuba where commercial acid pressure leaching of limonitic ores has been practiced since the 1950s,⁷⁵⁻⁸⁰ there has been a large amount of work undertaken on high-pressure acid leaching of lateritic ores⁸¹⁻⁸⁸ which represents nearly 70% of the

world's Ni reserves and also represents a major resource for cobalt.⁸⁹ Until recently, these oxidic ores have remained largely unexploited due to the absence of appropriate technology, but as they are located close to the surface they can be mined at a significantly lower cost than sulfidic ores from which the majority of nickel is presently extracted. The investment in the pressure leaching of lateritic nickel ores has been based on the increased confidence gained by the growing number of successful pressure oxidation plants brought on stream for gold and zinc recovery.^{72,90-97} Apart from bringing pressure technology into the mainstream, these plants have produced a pool of engineering and equipment designing expertise, which can be applied to laterites projects. More than 90% of the Ni and Co in laterite ores (1.0–1.6% nickel) can be leached by sulfuric acid at $\geq 240^\circ\text{C}$ and 0.2–1.1 MPa, typically producing relatively dilute leach solutions containing 3–6 g L⁻¹ of nickel and around 40 g L⁻¹ H₂SO₄.⁹⁸ The processes are relatively selective for nickel and cobalt over iron and the content of the latter can be further reduced by precipitation as Fe^{III}oxyhydroxides on raising the pH.

Oxidative pressure acid leaching is also applied to copper–nickel mattes. Nickel recoveries of >99% are obtained when leaching is carried out at 135–160 °C at oxygen partial pressures of 140–350 kPa,



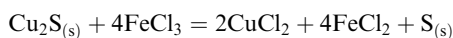
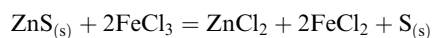
giving a solution depleted in both iron and copper with respect to the matte. Further purification can be achieved by addition of Ni metal and ammonium sulfate, which leads to precipitation of CuS and jarosite,



Heap leaching of copper oxides and transition ores and acid/neutral leaching of zinc calcine are well-established processes to generate the feed solutions for the hydrometallurgical recovery of these metals.²

9.17.3.3.2 Leaching of base metals into chloride media

Different approaches are needed for the dissolution of oxides, silicates, and sulfides.² Generally, the processes dealing with sulfides require oxidizing conditions, and much work has been described^{99,100} aimed at generating sulfur as a by-product using reactions such as

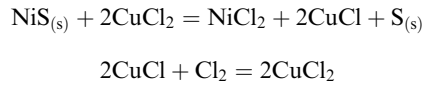


The resulting mixed-metal feeds can be processed using solvent extractants and the processes—see, for example, Figure 6 (Section 9.17.5.1.2)—often involve electrowinning of the metals from chloride solutions, providing chlorine for regeneration of the ferric chlorine leachant,

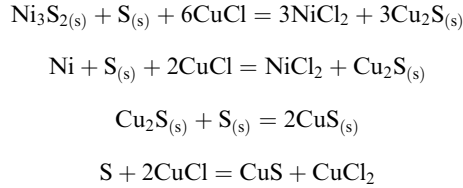


In the Falconbridge process, copper-containing nickel mattes produced by preliminary pyrometallurgical processing of ore concentrates (see Figure 2) are oxidized by chlorine in reactions in which Cu^{II} is responsible for electron transfer to the metal.





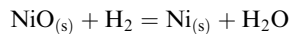
The sulfur liberated is involved in a complicated sequence of reactions which lead to almost complete removal of copper from the matte as very insoluble $\text{CuS}_{(s)}$.^{101–103}



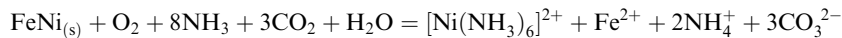
Société Le Nickel (SLN) employ similar chemistry at their operations to treat mattes obtained from the pyrometallurgical treatment of Ni-bearing oxidic laterite ores.¹⁰⁴ It has demonstrated at laboratory scale that Ni-containing lateritic ores may be directly leached into HCl acid solution without pyrometallurgical pre-concentration at atmospheric pressure and relatively low temperature (ca. 70 °C).¹⁰⁵

9.17.3.3 Leaching of base metals into ammoniacal media

Ammoniacal leaching is typically applied to oxidic nickel-bearing materials that have been subjected to a “reductive roast,” which converts the cobalt and nickel present to their metallic form (or as ferro-alloys) and most of the iron to Fe^{II} .^{106,107}

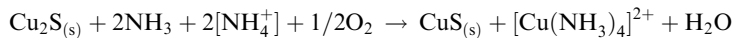


The resulting calcine is leached with an ammonia/ammonium carbonate solution,



Good separation from iron is achieved by formation of solutions of stable Ni^{II} and Co^{II} ammine complexes, whilst any Fe^{II} leached is oxidized and precipitates as Fe^{III} oxyhydroxides.

Ammoniacal leaching of chalcocite ores^{108–110} generates two Cu streams, an enriched ore—covellite—which can be treated in a conventional smelter, and a fairly concentrated aqueous solution (ca. 5 M, pH 8.5–10) containing ammine complexes,



which can be conveniently treated by solvent extraction (see Section 9.17.5.1.3).

9.17.4 SEPARATION AND CONCENTRATION

Some of the types of equilibria involved in the unit operations *separation* and *concentration* are listed in the introduction, Section 9.17.1. Those which depend most on coordination chemistry, and for which details of metal complex formation are best understood, are associated with hydrometallurgy. Once the metal values have been transferred to an aqueous solution, the separation from other metals and concentration can be achieved by one of the following processes.³

- (i) Selective crystallization, e.g., removal of PbCl_2 from the chlorometallate complexes of other base metals (see Section 9.17.3.3.2).
- (ii) Selective precipitation, e.g., the sequential separation of CuS and ZnS , followed by co-precipitation of CoS and NiS is achieved in the Outokumpu process by the generation of H_2S *in situ* resulting from addition of pyrite to an acidic solution of the mixed metal chlorides.

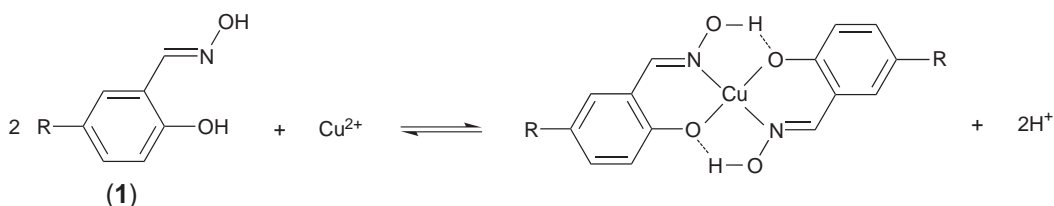
- (iii) Selective reduction, e.g., cementation of copper by addition of scrap iron to aqueous solutions of Cu^{II} salts, $\text{Cu}^{2+} + \text{Fe}_{(\text{s})} = \text{Cu}_{(\text{s})} + \text{Fe}^{2+}$.
- (iv) Selective adsorption of ions or complexes onto solid materials, e.g., cyanogold(I) complexes onto activated carbon (see Section 9.17.6.1) or the uptake of lanthanides on ion exchange resins.
- (v) Selective transfer of ions or complexes into water-immiscible phases, e.g., the solvent extraction of uranyl nitrate into tri-butyl phosphate.

The choice between the use of solid-state supported extractants and solvent extraction is often made on the basis of the concentration of the desired metal in the aqueous feed. Solvent extraction is usually not effective for treating very dilute feeds because an impracticably large volume of the aqueous phase must be contacted with an organic extractant to achieve concentration of the materials across the circuit. However, solvent extraction is preferred for treating moderately concentrated feeds because most ion-exchange resins and related materials have relatively low metal capacities and very large quantities of resin are required. In this review we will focus on reagents used in solvent extraction because, in the main, the nature of the complexes formed are better understood.

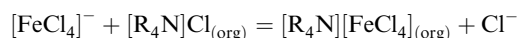
9.17.4.1 Solvent Extraction Processes

This technology lends itself to continuous, rather than batch, processing and has been proven robust since first applied for the extraction of uranium in the early 1940s.¹⁰ The types of extractant used can be classified according to the types of reactions involved in phase transfer.¹¹¹

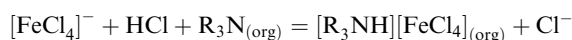
- (i) *Extraction by cation exchange* is characterized by the formation of an electrically neutral metal complex in which the extracted metal cation has displaced another cation (most commonly a proton) from the complexing agents. When the extraction involves the release of a proton, as with copper recovery by the phenolic oximes (**1**), the equilibrium is dependent on the pH of the aqueous phase, and the pH associated with 50% loading of the extractant (the $\text{pH}_{1/2}$) is often used to indicate the “strength” of an extractant at a stated concentration, and for a defined composition of aqueous feed.



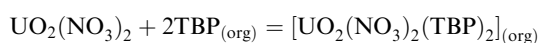
- (ii) *Extraction by anion exchange* involves the transfer of an anionic metal complex from the aqueous phase, displacing an ion from the organic solvent. Such reactions are commonly used for transport of chlorometallate complexes, e.g.,



Often, the cationic component of the ion pair is generated by the protonation of an organic base, e.g.,



- (iii) *Extraction by solvation* is characterized by the displacement of some or all of the water molecules in the coordination sphere of a metal cation or its complexes by neutral organic donors, typically ethers, ketones, or neutral phosphorus(V) molecules containing $\text{P}=\text{O}$ units, e.g., the extraction of uranium(VI) from nitrate solutions by tri-*n*-butyl phosphate (TBP).



- (iv) *Extraction by physical distribution* involves the transfer of a discrete molecular entity from the aqueous phase to an inert solvent. Such a situation arises only for solutes which are only weakly solvated and very few examples exist in extractive metallurgy.⁴

Whilst this classification is useful in giving an indication of the types of chemical changes which occur at the metal centers, it oversimplifies the situation in many cases. For example, changes in the solvation spheres of anionic species in both (ii) and (iii) are also very important in defining the free energies of extraction.¹¹² Frequently, acidic ligands used as cation exchangers are also present in the second coordination sphere in an undissociated form, acting as solvating extractants in species such as $[\text{ML}_2 \cdot 2\text{LH}]$, etc. (see below).

Recently, reagents have been used which operate as both cation and anion exchangers, providing binding sites in organic solvents for both components of a metal salt, either by mixing extractants (binary systems)¹¹³ or by using ditopic ligands.^{114,115}

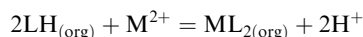
The sections below review the coordination chemistry of the most important classes of extractants used commercially. Particular attention is paid to the importance of secondary bonding between extractant components. This facilitates the assembly of ligating packages which match the coordination requirements of particular metal cations or their complexes and enhances both the selectivity and “strength” of extraction. Hydrogen bonding between ligands—e.g., esters of phosphorus(V) acids (see Section 9.17.4.3)—is particularly prevalent in the hydrocarbon solvents commonly used in industrial processes.

9.17.4.2 Hydroxy-oxime Extractants

The history and chemistry of the hydroxy-oxime extractants which were originally developed for Cu recovery has been extensively reviewed.^{11,13,14} Szymanowski's book¹⁴ provides comprehensive cover of the literature prior to 1993 and assigns chemical structures to reagents which in most metallurgy texts are referred to only by codes provided by reagent suppliers. An updated version of this information is provided in Table 3.

All commercial activity is currently based on the phenolic-oximes. A convenient Mg-catalyzed process for the manufacture of parent salicylaldehydes has been developed.¹¹⁶

Extraction equilibria based on the “pH-swing” process



have been extensively investigated.¹⁴ Reagents can be selected or combined to meet the “extractant strength” requirements of different Cu-recovery circuits—see Section 9.17.5.1. Ketoximes are slightly weaker extractants than aldioximes and operate efficiently when the leach liquor is relatively warm and the pH is ca. 1.8 or above.¹³ The aldioximes are stronger and thus are used in modified formulations for recovery at low temperatures and pH.¹³ The extent to which interligand H-bonding influences the stability of complexes in the organic phase, and hence the selectivity and efficiency of extraction, provides a good example of how supramolecular chemistry can be exploited in hydrometallurgy, allowing quite simple, inexpensive reagents to provide organized donor sets in nonpolar solvents. Such effects are also of great importance in selecting the appropriate carboxylic acid or organophosphorus acid extractants—see below.

In the solid state, H-bonding between the oxime OH groups and phenolate oxygen atoms *within* a complex unit is almost invariably observed,¹¹⁷ leading to *pseudo*-macrocyclic complexes (as in (2)) with VO^{2+} , CoNO^{2+} , Ni^{2+} , Cu^{2+} , Zn^{2+} , or Pd^{2+} . In the complexes which have planar donor sets, i.e., those of Ni^{II} , Cu^{II} , and Pd^{II} , the “goodness-of-fit” of the metal is dependent on the size of the cavity prescribed by the *pseudo*-macrocycle.¹¹⁷ The *pseudo*-macrocyclic structure is also present in the solid state forms of some free ligands (e.g., (3))¹¹⁷ and is retained in solution.^{118,119} Although the dimeric forms of the free ligands are not planar¹¹⁷ and have a step conformation to reduce repulsion between the central phenolic protons, they are partially preorganized for complex formation and the dimers should be considered in modeling extraction equilibria,^{118,120}

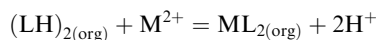
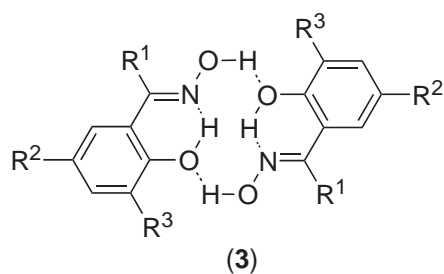
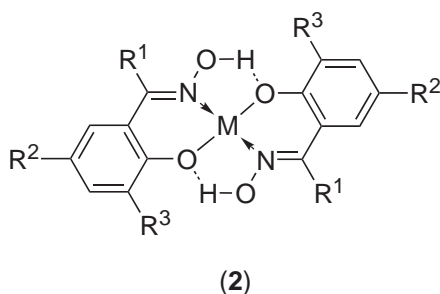


Table 3 The commercial^a names and structures^b of commonly used reagents containing hydroxyoximes.

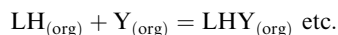
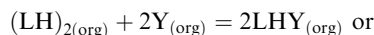
R^1	R^2	R^3	Reagents containing phenolic oximes
H	C ₉ H ₁₉	H	P1, P50, P5100, P5200, P5300, P5050, M5615, M5397, M5640 (Acorga)
C ₆ H ₅ CH ₂	C ₉ H ₁₉	H	P17 (Acorga)
CH ₃	C ₉ H ₁₉	H	SME529 (Shell), LIX84 LIX84-I LIX84-R(Cognis), LIX984 (Cognis as 1:1 mixtures with LIX860)
C ₆ H ₅	C ₁₂ H ₂₅	H	LIX64 (Cognis)
C ₆ H ₅	C ₉ H ₁₉	H	HS-LIX 65N (Cognis), LIX 65N (General Mills), HS-LIX64N (Cognis in 44:1 mixture with LIX63), LIX 64N (General Mills in 44:1 mixture with LIX63)
C ₆ H ₅	C ₉ H ₁₉	Cl	LIX70, LIX71 (in mixture with LIX 65N), LIX73 (in mixture with LIX 64N) (General Mills)
H	C ₁₂ H ₂₅	H	LIX860, LIX622, LIX6022, LIX864 (as mixture with LIX 64N), LIX865 (as mixture with LIX65N)(Cognis)
Reagents containing α -hydroxyoximes			
R^1	R^2		
2-Ethyl-pentyl	2-ethyl-pentyl		LIX63 (Cognis), LIX 64N (General Mills in 1:44 mixture with LIX 65N), HS-LIX 64N (Cognis in 1:44 mixture with LIX 65N)

Source:¹⁴

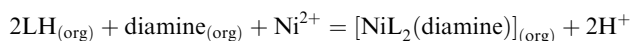
^a Details of some of the modifiers and other additives in these formulated reagents are available in references 14 and 118. ^b The R^2 substituents on the phenolic oximes are usually multiply branched alkyl groups containing mixtures of isomers.



Interactions of the monomeric, dimeric, or other forms of the extractant with a modifier (Y) are also important in interpreting extraction equilibria,^{118,120} e.g.,

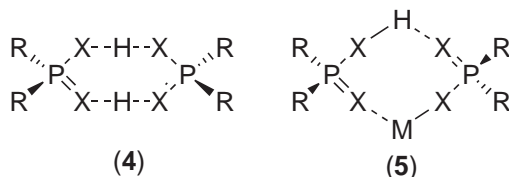


where the modifier competes with metal cations for the donor functionalities. Work in this area has been reviewed^{14,118} and the importance of the preorganized dimer, particularly in saturated hydrocarbon solutions, in the recovery of copper has been established.¹²⁰ The head-to-tail *pseudo*-macrocyclic structure is preserved in *cis*-octahedral Ni^{II} complexes formed in the presence of α,ω -diamines,¹²¹



9.17.4.3 Organophosphorus Acid Extractants

All the commonly used extractants of this type are phosphorus(V) acid derivatives containing at least one P–OH or P–SH group (Table 4). The coordination chemistry is greatly influenced by the formation of strong ligand–ligand H-bonds in solvents of low polarity. The eight-membered rings in dimers (4) are preserved when metal complexes (5) are formed in the presence of excess extractant.⁴



The bite angle defined by such eight-membered *pseudo*-chelate rings favors tetrahedral coordination geometry¹²² and consequently selectivity for first transition series metal dications does not follow the Irving–Williams¹²³ order. Zn^{II} is more strongly extracted by D2EHPA than other first transition series M²⁺ ions (see also Section 9.17.5.2), and Co^{II} can be selectively extracted from solutions containing Ni^{II} salts by the sulfur-donor extractants Cyanex 301 and Cyanex 302 (see Section 9.17.3).

For divalent metals which readily form tetrahedral complexes and for trivalent metals which show a preference for octahedral donor sets, neutral D2EHPA complexes are formed with 4:1 and 6:1 ligand:metal stoichiometries respectively,



which allows the eight-membered chelate rings to be preserved. For *divalent* octahedral metal ions the formation of charge neutral complexes is achieved with an equatorial arrangement of two eight-membered chelate rings and two neutral axial donors, either LH monomers or L₂H₂ dimers.⁴

Although the lanthanide cations most commonly give complexes with coordination numbers of 8 or 9, the [ML₃(LH)₃] species predominate on extraction with phosphorus(V) acids and it has been suggested that the bulk of the L···LH chelate ring favors a lower coordination number.⁴ The phosphorus(V) acids are very effective reagents for the extraction and separation of lanthanides.¹²⁴ (See chapter 3.2).

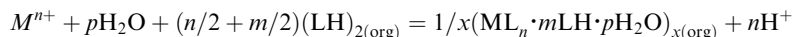
9.17.4.4 Carboxylic Acids

Whilst carboxylic acids are readily available and inexpensive, they are relatively weak extractants and have not found much use in the recovery of base metals until recently when Versatic 10 has been piloted for the separation of Ni from Mn and Mg (Section 9.17.5.4). As with the phosphorus(V) acid extractants, the propensity for association leads to substantial levels of solvation of caboxylato

Table 4 The commercial names and structures of phosphorus(V) acid extractants.

Structure	R	Reagents
$\begin{array}{c} \text{OH} \\ \\ \text{RO}-\text{P}-\text{OH} \\ \\ \text{O} \end{array}$ <p>(phosphoric)</p>	$\text{CH}_2\text{CH}(\text{C}_2\text{H}_5)\text{C}_4\text{H}_9^n$ $\text{C}_{18}\text{H}_{37}^{\text{iso}}$	MEHPA, SBX50
$\begin{array}{c} \text{OH} \\ \\ \text{RO}-\text{P}-\text{OR} \\ \\ \text{O} \end{array}$ <p>(phosphoric)</p>	$\text{CH}_2\text{CH}(\text{C}_2\text{H}_5)\text{C}_4\text{H}_9^n$ $\text{C}_{10}\text{H}_{21}^{\text{iso}}$ $\text{C}_{18}\text{H}_{37}^{\text{iso}}$	D2EHPA, DP-8R, Hostarex PA216 P204 DP10-R TR-63
$\begin{array}{c} \text{OH} \\ \\ \text{RO}-\text{P}-\text{OR} \\ \\ \text{S} \end{array}$ <p>(mono-thio phosphoric)</p>	$\text{CH}_2\text{CH}(\text{C}_2\text{H}_5)\text{C}_4\text{H}_9^n$	Hoe F 3787
$\begin{array}{c} \text{S} \\ \\ \text{RO}-\text{P}-\text{OR} \\ \\ \text{S} \end{array}$ <p>(di-thio phosphoric)</p>	$\text{CH}_2\text{CH}(\text{C}_2\text{H}_5)\text{C}_4\text{H}_9^n$	DEHTPA
$\begin{array}{c} \text{OH} \\ \\ \text{R}-\text{P}-\text{OR} \\ \\ \text{O} \end{array}$ <p>(phosphonic)</p>	$\text{CH}_2\text{CH}(\text{C}_2\text{H}_5)\text{C}_4\text{H}_9^n$	PC-88A, SME, YP-AC, 4050-MOOP, Ionquest 801
$\begin{array}{c} \text{OH} \\ \\ \text{R}-\text{P}-\text{R} \\ \\ \text{O} \end{array}$ <p>(phosphinic)</p>	$\text{CH}_2\text{CH}(\text{CH}_3)\text{CH}_2\text{C}_4\text{H}_9^t$ $\text{CH}_2\text{CH}(\text{C}_2\text{H}_5)\text{CH}_2\text{C}_4\text{H}_9^n$	Cyanex 272 PIA-8
$\begin{array}{c} \text{OH} \\ \\ \text{R}-\text{P}-\text{R} \\ \\ \text{S} \end{array}$ <p>(mono-thio phosphinic)</p>	$\text{CH}_2\text{CH}(\text{CH}_3)\text{CH}_2\text{C}_4\text{H}_9^t$	Cyanex 302
$\begin{array}{c} \text{SH} \\ \\ \text{R}-\text{P}-\text{R} \\ \\ \text{S} \end{array}$ <p>(di-thio phosphinic)</p>	$\text{CH}_2\text{CH}(\text{CH}_3)\text{CH}_2\text{C}_4\text{H}_9^t$	Cyanex 301
$\begin{array}{c} \text{H} \\ \\ \text{R}-\text{P}-\text{N}-\text{P}-\text{R} \\ \quad \quad \\ \text{S} \quad \text{N} \quad \text{S} \end{array}$	R = aryl or aryloxy	DS 5968, DS 6001

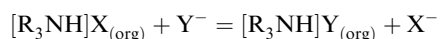
complexes by neutral carboxylic acid molecules and to the formation of polynuclear complexes. Extraction can be represented by the general equation:



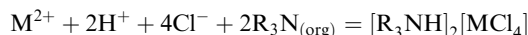
With copper, for example, monomeric $[\text{CuL}_2]$, $[\text{CuL}_2 \cdot \text{LH}]$, $[\text{CuL}_2 \cdot 2\text{LH}]$, $[\text{CuL}_2 \cdot 4\text{LH}]$, and dinuclear $[\text{CuL}_2]_2$, $[(\text{CuL}_2 \cdot \text{LH})_2]$, $[(\text{CuL}_2 \cdot 2\text{LH})_2]$ species have all been observed.¹²⁵

9.17.4.5 Amine Salt Extractants

The applications of hydrophobic amine salts (see Table 5) as anion exchange extractants to recover a diverse range of metals in the form of anionic, usually chloro, complexes was reviewed⁴ in CCC (1987). The order of preference shown by this class of extractants for simple inorganic anions



follows the sequence $\text{ClO}_4^- > \text{NCS}^- > \text{I}^- > \text{NO}_3^- > \text{Br}^- > \text{Cl}^- > \text{SO}_4^{2-} > \text{F}^-$ and represents the readiness by which such anions leave the aqueous phase.^{126,127} Large anions with more diffuse charge are less favorably hydrated and consequently are more readily accommodated in the organic phase as ion-pairs. Similar principles account for the favorable transport of simple chloro metallates from acidic chloride streams

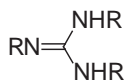


and are exemplified in processes in Sections 9.17.5 and 9.17.6. This type of extraction mechanism is particularly important for substitution-inert metal ions, where replacement of inner-sphere ligands by cation exchange reagents occurs so slowly that impracticably long contact times would be required in solvent extraction.

An understanding of the interactions in ion-pairs, e.g., a combination of electrostatic and hydrogen bonding in species such as $[\text{R}_3\text{NH}]_2[\text{MCl}_4]$, is needed for a more rational design of anion exchange extractants, and is timely considering the recent extension of supramolecular chemistry to the design of anion receptors.¹²⁸⁻¹³⁰ The trialkylguanidinium salts, LIX 79,¹³¹⁻¹³³ (see Table 5) represent an example of a class of extractant which is likely to recognize the outer coordination sphere of an anionic metal complex (see also Section 9.17.6.1).

Table 5 Commercially available anion exchange extractants.

Class	Commercial name	Substituents ^a
Primary	Primene 81R	<i>t</i> -C ₁₂ -C ₁₄
	Primene JMT	C ₁₂ -C ₁₄
Secondary	Adogen 283, Adogen 283D	di- <i>i</i> -octyl
	ditridecylamine, HOE 2652	di-tridecyl
	Amberlite LA-1	Undefined
	Amberlite LA-2	Undefined
Tertiary	Alamine 336, Adogen 364	tri-C ₈ -C ₁₀
	Adogen 381, Alamine 330, TIOA	tri- <i>i</i> -octyl
Quarternary	Adogen 364, Aliquat 336	methyl, tri-C ₈ -C ₁₀
Other(guanidine)	LIX 79	Undefined



^a Commercial anion exchange extractants are often complex, poorly defined mixtures. Information is given where available from Chemical Abstracts.

9.17.4.6 Solvating Extractants

A diverse range of neutral organic molecules has been used to stabilize or to enhance the solubilities of neutral metal-containing entities in an organic phase. Some examples of commercial significance are listed in Table 6. When used alone they efficiently transport metal salts across a circuit. An example is the use of tributyl phosphate (TBP) in recovery of uranyl nitrate,

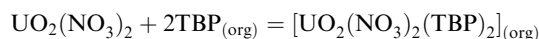
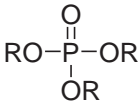
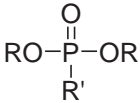
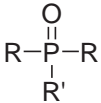
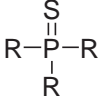
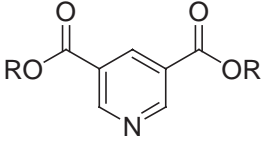
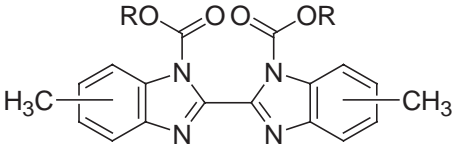
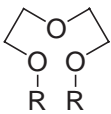
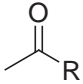


Table 6 The structures of some neutral (solvating) extractants.

Structure	R	R'	Reagent
	C ₄ H ₉ ⁿ C ₈ H ₁₇		TBP TOPO, Hostarex PX 324, Cyanex 921 ^a VP-AC 4046, DBBP
	C ₄ H ₉ ⁿ C ₂ H ₅ C ₂ H ₅	C ₄ H ₉ ⁿ C ₅ H ₁₁ C ₁₂ H ₂₃	VP-AC 4014, DPPP DEDP, VP-A1 4059
	C ₈ H ₁₇ ⁿ	C ₄ H ₉ ^{sec}	Hostarex 320
	C ₄ H ₉ ⁱ		Cyanex 471
	C ₁₀ H ₂₁ ⁱ		CLX50
	C ₁₃ H ₂₇		ZNX50
	C ₄ H ₉ ⁿ		Butex
	C ₄ H ₉ ⁱ		MIBK
RSR	C ₈ H ₁₇ ⁿ C ₆ H ₁₃ ⁿ		HOE F 3440, SFI-6

^a Cyanex 923 contains a mixture of *n*-octyl and *n*-hexyl groups and Cyanex 925 a mixture of normal and branched octyl groups.

They are also used in combination with other cation exchange reagents as synergistic extractants, often stabilizing the resulting complex by completing the metal coordination sphere. An example is the addition of TBP to thienoyltrifluoroacetone, HTTA, which enhances the extraction of Am^{III} or lanthanide ions by formation of neutral complexes of general formula $[\text{M}(\text{tta})_3(\text{TBP})_n]$.^{134,135}

9.17.5 BASE METALS

9.17.5.1 Copper

The application of solvent extraction to copper recovery has been a major growth area since the last review of this series.^{11,13} Almost 30% of world production in 2000 involved the use of sulfuric acid heap leaching, solvent extraction, and electrowinning, far exceeding earlier predictions.¹³⁶

9.17.5.1.1 Extraction of Cu^{II} from sulfate solutions

The commercial success of this technology is based on the very good materials balance which applies when processing oxidic ores, using the phenolic oxime “pH-swing” extractants (Section 9.17.3) in conjunction with a conventional electrolysis process. The reactions involved in the flowsheet are listed in Figure 5. The relatively “strong” phenolic oxime reagents ensure that high recovery is possible from pregnant leach solutions which can have pH values as low as 1.5.¹³ Acid released on extraction is re-used in leaching and the acid needed for stripping is generated by the electrolysis process. The “strength” of a formulated reagent can be tuned to meet the requirements of a particular feed solution, e.g., it can be reduced by selecting a ketoxime over an aldoxime or by the addition of modifiers, see Section 9.17.4.2.

The reagent suppliers provide loading and stripping isotherm data, which allow metallurgists to select appropriate reagents and to design circuits with the appropriate numbers and configurations of extraction and stripping stages.¹³⁷

The key separation achieved by the phenolic oxime reagents is copper from iron, which is often present in comparable or higher concentrations in pregnant leach solutions. The intrinsic selectivity for Cu over Fe shown by both the aldoxime and ketoxime extractants is high,¹⁴ and in practice in formulated reagents depends markedly^{138,139} on the nature of the modifiers used (see Section 9.17.4.2). Entrainment of droplets of the aqueous feed solutions into the kerosene solution of the extractant¹⁴⁰ often represents the main route for transfer of iron across the flowsheet into the electrowinning tankhouse. Keeping the Fe concentration in the electrolyte down to a level which ensures good current efficiencies is usually achieved by taking a bleed from the tankhouse and returning this to the leachant.¹³⁹ An alternative approach is to purify the electrolyte, “polishing” to remove Fe to a very low level using the “Diphonix” resin which shows a remarkably high selectivity for Fe^{III} over Cu^{II} .¹⁴¹ This avoids the loss of acid and beneficial additives from the tankhouse. The iron

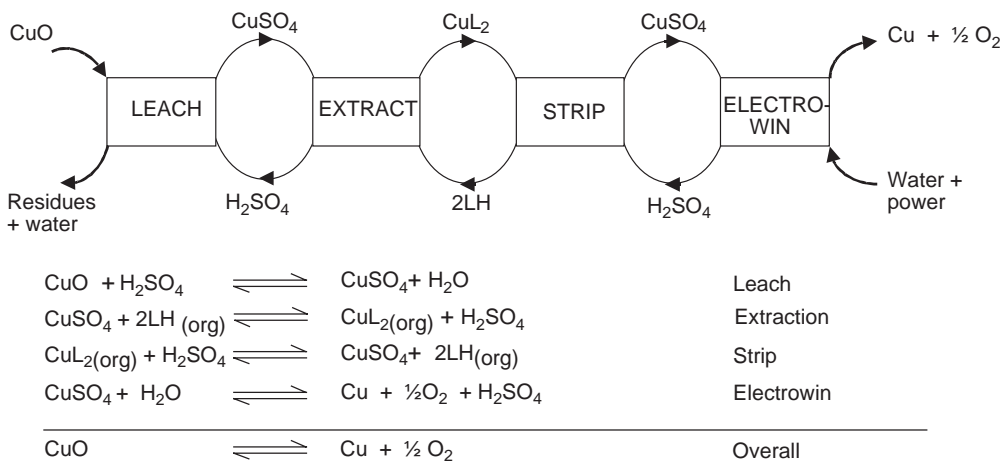
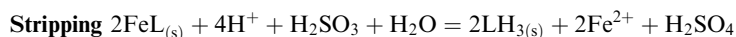
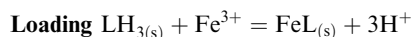
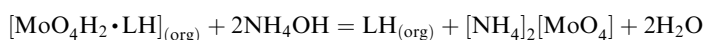


Figure 5 A simplified flowsheet and materials balance for the recovery of copper from oxidic and transition ores by heap leaching, solvent extraction and electrowinning.

can be released from the resin by reductive stripping with sulfurous acid because Fe^{II} binds much more weakly to the bisphosphonic acid chelating units in the resin, $\text{LH}_{3(\text{s})}$.¹⁴¹

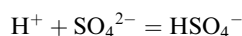


Co-extraction of Mo and Cu is potentially a problem with certain feed solutions,¹⁴ and again selectivities are very dependent on the nature of modifiers present in formulated reagents.¹⁴² The Mo species extracted have not been fully characterized, but may include a neutral dioxo complex, $[\text{MoO}_2\text{L}_2]$, which can be assumed to have an $\text{N}_2\text{O}_2^{2-}$ donor set similar to that in the Cu^{II} complex, and molybdate complexes solvated by neutral phenolic oxime ligands such as $[\text{MoO}_4\text{H}_2\cdot\text{LH}]$.¹⁴³ Formation of solvated forms of molybdic acid is supported by evidence that extraction is favorable at very low pH values and that the complexes are readily stripped by aqueous ammonia to produce ammonium molybdate,¹⁴⁴



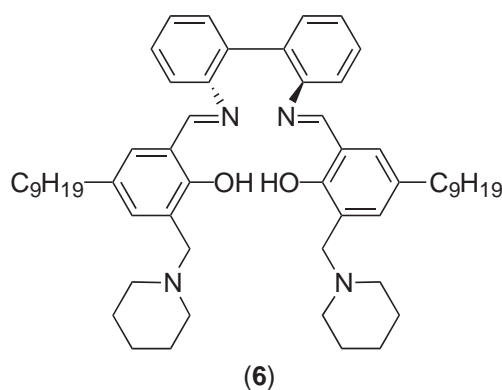
Formation of polynuclear complexes by phenolic oximes is also possible with such oxo-metal species in high oxidation states, e.g., $[(\text{C}_4\text{H}_9)_4\text{N}][\text{Mo}_2\text{O}_5(\text{sal}\cdot 2\text{H})]$, which has both a μ_2 -oxo-bridge between the two metal centers and two Mo–N–O–Mo oximinato bridges formed by the doubly deprotonated salicylaldoxime ligands, sal-2H.¹⁴⁵

Commissioning new oxime extraction plants has been driven by major developments in leaching technologies—Section 9.17.3—which allow mixed oxide/sulfidic and sulfidic ores to be processed. When such leach processes do not consume sulfuric acid there is potentially a problem of acid build-up in the front end of this circuit because 1.54 g of H_2SO_4 is generated per g of copper extracted.¹⁴⁶ This release of acid is also a problem with very high tenor feeds because the extraction equilibrium shown in Figure 5 is depressed. In practice it has been shown¹⁴⁶ that the extraction isotherms are not as adversely effected as might be expected, presumably due to the buffering effects of very high concentrations of sulfate which reduce the activity of proton,



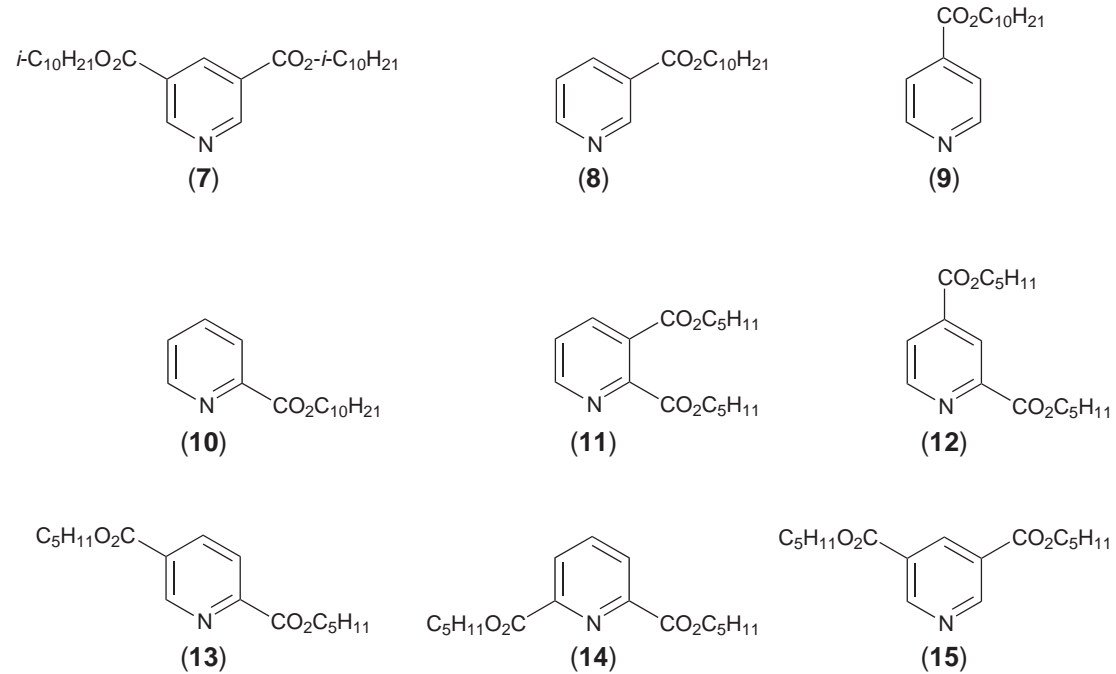
A creative approach has been proposed¹⁴⁶ to deal with the acid generated from copper extraction from high tenor feeds by using it for heap leaching of another ore which has a high content of basic materials. This is planned for the acidic raffinate from Cu extraction from the 65 g L^{-1} pregnant leach solution from HPAL of the Konkola Deeps sulfide deposit, using it to leach the Chingola refractory ore and thus generate a conventional low tenor feed (5 g L^{-1} Cu) for a separate solvent extraction process. The electrolytes from both SX processes are to be combined for electrowinning.¹⁴⁶

An alternative strategy to treat feed solutions from leaching processes which do not consume acid is to use extractants which transport metal *salts* rather than metal ions.¹⁴⁷ The ditopic ligands based on functionalized salicylaldimines described in Section 9.17.4.1 are strong extractants forming well-characterized 1:1:1 complexes, LCuSO_4 .¹¹⁵ The copper-binding site has to be “detuned,” e.g., by introduction of a 2,2'-biphenylene bridge as in (6), which disfavors formation of a planar $\text{N}_2\text{O}_2^{2-}$ donor set, to allow the copper to be acid-stripped.



9.17.5.1.2 Extraction of Cu^{II} from chloride solutions

Oxidative leaching of sulfidic ores with ferric chloride generates elemental sulfur, avoiding the liberation of SO_2 and produces (Section 9.17.3.3.2) pregnant leach solutions with high concentrations of FeCl_2 , FeCl_3 , CuCl_2 , and other metal chlorides. In the CUPREX process¹⁴⁸ extraction with a neutral ligand L such as CLX50, (7), transports CuCl_2 across a circuit with a good materials balance (see Figure 6).



The extraction equilibrium in the CUPREX process is dependent on the activity of Cl^- in the feed solutions which in turn is dependent on the stability of chlorometallate complexes $[\text{MCl}_x]^{2-x}$ and $[\text{MCl}_x]^{3-x}$ for the di- and tri-valent metals present^{149,150}, rather than the simple stoichiometry represented by the equation shown in Figure 6.^{151,152}

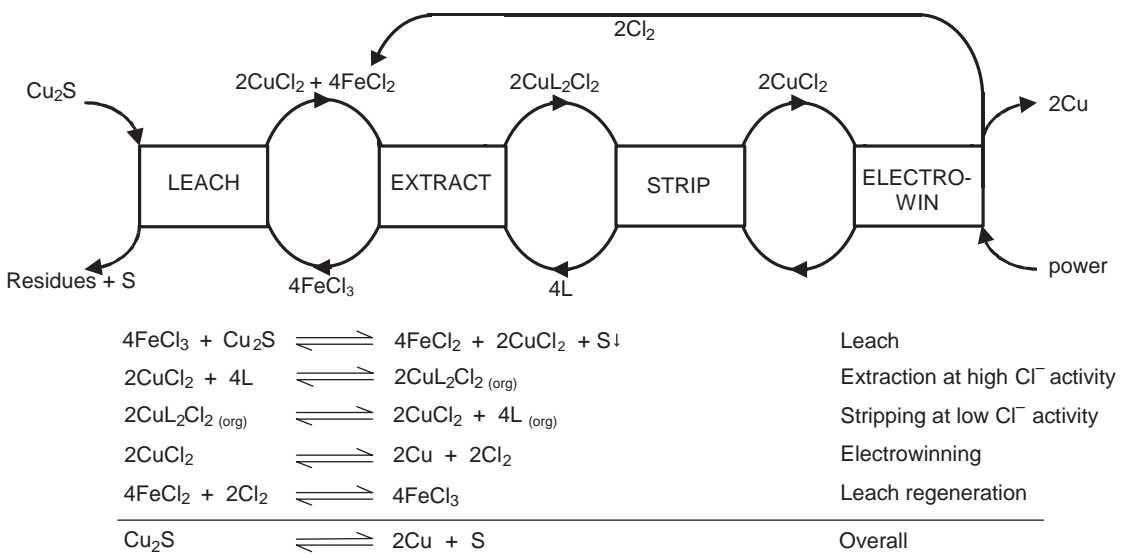
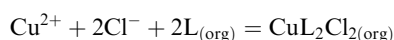
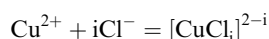


Figure 6 A simplified flowsheet and materials balance for the recovery of copper from sulfidic ores by chloride leaching, solvent extraction and electrowinning, using for example reagents such as 7.

Systematic studies^{150,153} with CLX50, (7), decyl esters of pyridine monocarboxylic acids (8)–(10), and dipentyl esters of pyridine dicarboxylic acids (11)–(15) showed that extraction of Cu^{II} is strongly dependent on the activity of water and the total concentration of ionic and molecular species in the aqueous phase. For the monoesters, copper distribution is dependent on



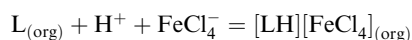
and



but more complicated behavior is observed for CLX50 in kerosene. The monoester model ligands (8)–(10) form neutral complexes, [CuL₂Cl₂], which appear to be too stable to strip effectively with hot water.¹⁴⁹ The diesters (11)–(15) are weaker extractants and readily water-stripped. There are marked differences in the strengths of these extractants and the dependence of Cu extraction on chloride concentration which are not easily accounted for in terms of steric factors associated with the location of the carboxylate groups. ESR spectra suggest that similar complexes are formed, with the exception of the 2,6-dicarboxylate (14), which exhibits a hyperfine splitting not found in complexes of the other ligands.¹⁵³

As Cu^{II} is substitution-labile,¹⁵⁴ the rates of mass transfer are dependent on interfacial processes, which have been shown¹⁵⁵ to be fast for both loading and stripping in conventional contactors, but possibly too slow in stripping for the industrial application of columns.

The low activity of water in these feed solutions ensures that activity of proton is high in acidic solutions. In addition to the problem this creates with regard to the corrosiveness, there is a tendency for even the very weakly basic pyridine nitrogen in CLX50 (7) to become protonated by aqueous feeds with high acidity allowing extraction of Fe^{III} by an ion-pairing mechanism,

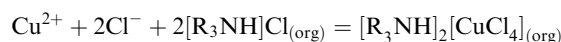
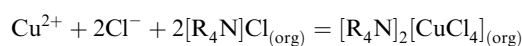
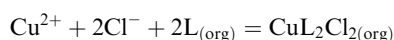


which reduces the otherwise very high Cu/Fe selectivity.

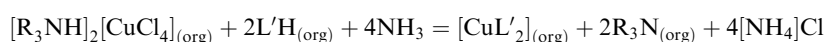
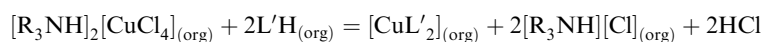
The phenolic oxime reagents (Section 9.17.4.2) have also been used to recover copper from chloride leach solutions,¹⁵⁶



but the high proton activity in these feeds limits the efficiency of these processes and steps have to be taken to adjust and control pH.^{148,157} A creative solution to this problem is to use a mixture of a “pH-swing” extractant (Equation (1)) and either a solvating or an ion-pairing (Section 9.17.4.6) extractant. The approach has been reviewed recently.^{157,158} On contacting the aqueous feed the majority of the copper extracted is transferred to the organic phase by the solvating or the ion-pairing reagents by reactions such as,

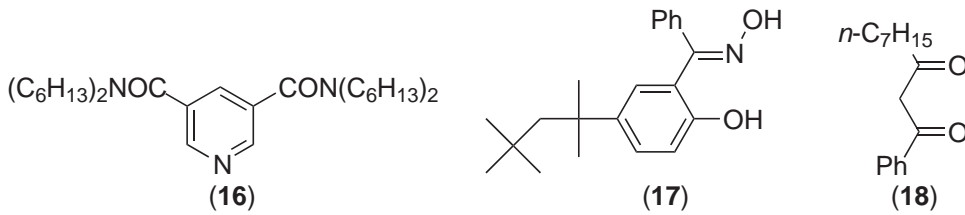


Scrubbing the loaded organic phase with water or ammonia removes HCl, transferring the copper to the “pH-swing” extractant, e.g., as in,



which then can be stripped with sulfuric acid to give a sulfate electrolyte for conventional electrowinning.¹⁵⁹ Examples of this approach include combinations of Alamine336 and LIX 54

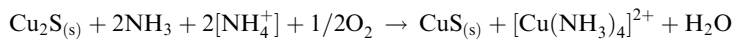
(18) for extraction and separation of Cu and Zn,^{160–163} CLX50 and LIX 54 for recovery of Cu from >2 M chloride solutions,¹⁵⁷ (16) and (17) for recovery of Cu from dilute chloride solutions phase,¹⁶⁴ or (16) and (18).¹⁵⁷



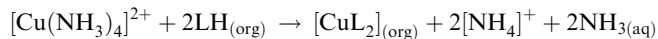
There has been much development of processes to electrowin Cu from chloride media,¹⁶⁵ but to date no major plants using the solvent extraction coupled with electrowinning from chloride media have been commissioned.

9.17.5.1.3 Extraction of Cu^{II} from ammoniacal solutions

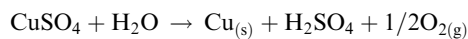
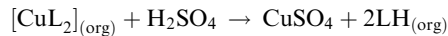
Ammoniacal leaching of chalcocite ores^{108,109,166,167} generates two Cu streams, an enriched ore, covellite, which can be treated in a conventional smelter, and a fairly concentrated aqueous solution (ca. 5 M, pH 8.5–10) containing ammine complexes,



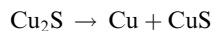
Solvent extraction with a weakly acidic reagent,



regenerates the leachant. Stripping with sulfuric acid and conventional electrowinning of the copper regenerates the extractant without consumption of acid,

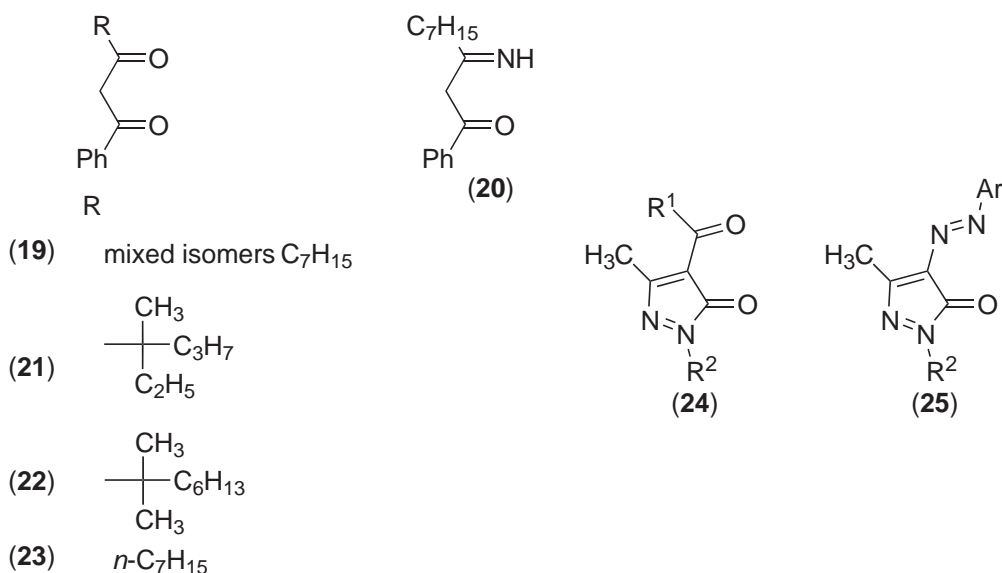


giving the materials balance;



The pH of the lixiviant and the leach conditions are such that very little of the iron present in the ores and only small quantities of other transition metals are transferred to the pregnant leach solution, which typically has a composition of ca. 280 g L⁻¹ Cu, 440 mg L⁻¹ Zn, <1 mg L⁻¹ Fe, Mn, and $\ll 1$ mg l⁻¹ Ni.¹⁰⁸ Consequently, the Cu extractant is not required to show very high selectivity over iron or high “strength” because the extraction equilibrium is effectively buffered by $[\text{NH}_4^+]/\text{NH}_3$. The diketone extractant LIX 54, (19), with a mixture of isomeric forms of the heptyl group, provides appropriate “strength” and selectivity, performing well in a small continuous SX-plant,¹⁰⁹ but is prone to chemical degradation, forming the ketimine (20) exclusively at the octanoyl carbon atom in the presence of high levels of NH_3 at 45 °C.^{168,169} Reagents with sterically hindered acyl groups as in XI-N54 and XI-57 (21,22) or the n-heptyl analog (23) show much greater resistance to chemical degradation and better strip kinetics than LIX 54.^{168,170}

Acylpyrazolones (24) also form neutral β -diketonate-type complexes suitable for extraction of a range of metals into organic solvents and have been considered¹⁷¹ as alternatives to LIX 54 for use in ammoniacal leach circuits. Although they are stronger extractants than LIX 54,^{4,172} the low solubility of their metal complexes has limited their usefulness in Cu recovery.¹⁷¹ The structurally related diazopyrazolones (25) have $\text{pH}_{1/2}$ values, ca. 3.7, and their chemical stability on contact with ammoniacal feeds meets the requirements of the flowsheet outlined above, but their very intense colors may restrict their use as commercial extractants.^{173,174} The bulk of the arylazo



group in these ligands leads to significant deviations from planarity of the N₂O₂²⁻ donor sets, accounting for their weakness in comparison with the phenolic oximes (Section 9.17.4.2).¹⁷⁴

Ni and Cu in ammoniacal feeds can be effectively separated by quantitative co-extraction with the phenolic oxime LIX 84 (Section 9.17.4.2) followed by selectively stripping of the more weakly bound Ni with dilute sulfuric acid.^{169,175}

9.17.5.1.4 Recovery of Cu^{II} from secondary sources

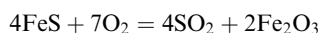
The diverse range of applications of copper in different alloys and products presents challenging problems for recycling.^{9,176} Many of the recycling processes to recover copper from mixtures with other metals are based on hydrometallurgy using sulfate, chloride, or ammoniacal streams. Copper can be selectively extracted using phenolic oximes^{169,176–180} or diketones,^{169,176,179} even when the aqueous feed contains Cu-complexing agents which have been used in etching processes to generate the waste stream. Where the small volumes of copper recovered by solvent extraction in such plants do not justify the capital investment of an electrowinning plant the strip solution can be evaporated to generate a copper salt.

9.17.5.2 Zinc

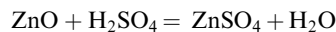
Approximately 80% of Zn production involves hydrometallurgy, in which roasted sulfide concentrates are dissolved in sulfuric acid.¹⁸¹ Currently, the major separation steps involve the precipitation of other metals from the sulfate stream (Figure 7).^{181,182} The precipitation of iron is achieved by raising the pH with calcine, the mixture of zinc/iron oxides from roasting, producing large volumes of iron oxy-hydroxide materials, the disposal of which presents major challenges.^{183–185}



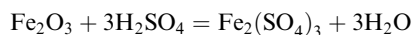
and



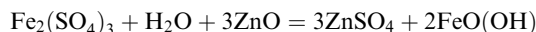
Acid leach:



and



Neutral leach/iron precipitation:



Electrowinning:

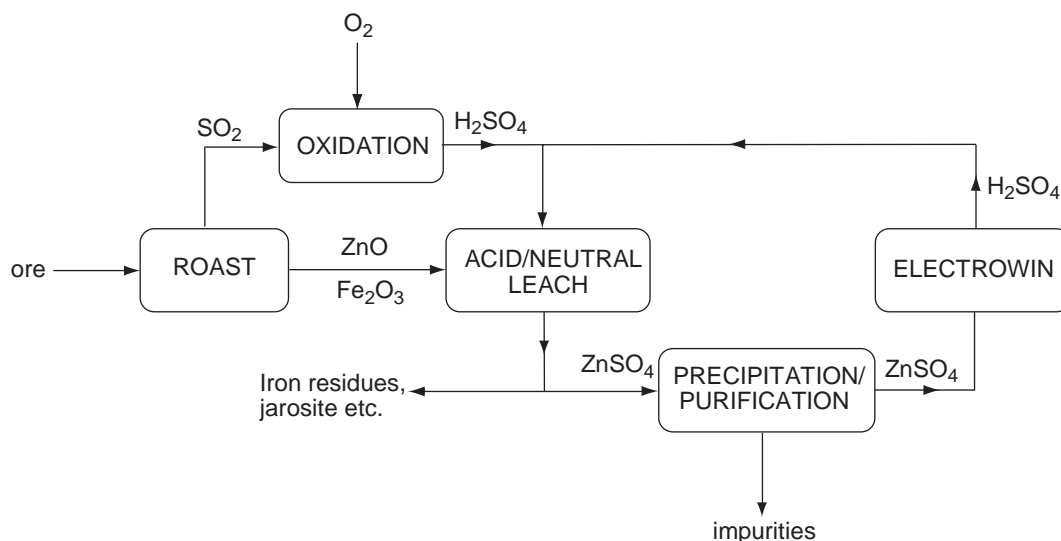
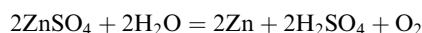
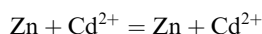
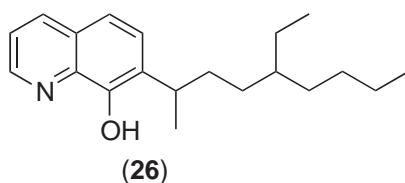


Figure 7 An outline of the flowsheet for zinc production by the conventional roast/neutral-leach/electrowinning circuit.

Zinc electrowinning requires high electrolyte purity.¹⁸⁶ Cementation with powdered zinc to remove heavy metals such as Cd, Hg, and Pb, and other precipitation techniques are most



commonly employed. In some plants germanium is recovered from the electrolyte with 8-hydroxyquinoline reagents such as Kelex 100 (**26**).^{184,187–189}



9.17.5.2.1 Extraction of Zn^{II} from sulfate media

The use of D2EHPA to purify and concentrate ZnSO_4 electrolytes from which the majority of the iron has been removed by precipitation has received much attention, forming the basis of the ZINCEX processes.^{165,190} These processes have been developed to treat a range of primary and

Table 7 Metal loading^a (mg l⁻¹) of a 0.3 M solution of DS5869^b

Metals extracted	Zn	Cd	Cu	Hg	As
	6400	110	105	100	99
	Bi	Pb			
	65	12			
Metals rejected	Fe	Ge	Sn	As	In
	1	4	4	<5	<5
	Ca	Mg	Mn	Co	Ni
	<1	<1	<1	<1	<1

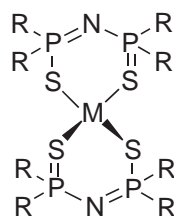
Source:¹⁹⁶

^a After contacting with an equal volume of an aqueous solution (pH 2.0) containing 10.7 g L⁻¹ Zn, 4.1 g L⁻¹ Fe^{III}, and ca. 100 mg L⁻¹ of the other metals. ^b See Table 4 for structure.

secondary materials,^{190–193} including sulfides via pressure leaching.¹⁹⁰ D2EHPA shows a good selectivity for Zn over the most common impurities in these sulfate streams, Mn, Co, Ni, Cu, Mg, and Cd, see Section 9.17.4.3.^{4,194}

Anglo America's Skorpion project¹⁹⁵ which uses the ZINCEX process will be the first major application of solvent extraction for Zn recovery from primary sources, involving a capital investment of \$454 million in southern Namibia. The use of the pH-swing extractant D2EHPA coupled with the scrubbing of Zn-loaded organic solutions ensures that chloride and fluoride ions originating from minerals associated with the zinc silicate ore are not carried forward to the Zn electrolyte. Any iron which has not precipitated following neutralization of the pregnant leach solution is strongly extracted by D2EHPA and the resulting Fe^{III} complexes are not stripped under the conditions used to generate the Zn electrolyte. To ensure that the recycled extractant is not eventually poisoned a bleed is treated with 6 M HCl, regenerating D2EHPA and producing FeCl₃ as a waste stream.¹⁹⁵

As a consequence of D2EHPA's high affinity for Fe^{III} the commercial success of the ZINCEX-based processes for Zn recovery depends on removal of almost all the iron from feed solutions prior to solvent extraction of the zinc. An alternative strategy is to develop a pH-swing extractant with a high Zn^{II}/Fe^{III} selectivity which would be used in a circuit analogous to the well-proven commercial operations for copper (Section 9.17.5.1.1) to treat oxidic ores by sulfuric acid leaching, solvent extraction, and electrowinning. The DS5869 reagent (27) (Table 4), which contains a tetra-substituted bisdithiophosphoramidate, shows a remarkable discrimination for Zn^{II} over most of the other metal ions in the first transition series.¹⁹⁶ The bulky substituents at the phosphorus atoms disfavor formation of a planar arrangement of the S₄²⁻ donors or formation of neutral 3:1 complexes such as [FeL₃]_{org} with transition metals.



(27)

The soft S₂⁻ donor sets presented by these bidentate ligands lead to very strong binding of heavy metals (Table 7) which are not stripped by sulfuric acid, ensuring that these deleterious elements do not transfer to the Zn electrolyte.¹⁹⁶ However, co-extraction of copper is accompanied by reduction to Cu^I which has proved very difficult to strip to regenerate the reagent and will lead to poisoning of the extractant unless all traces of copper are removed from the feed solution.

9.17.5.2.2 Extraction of Zn^{II} from chloride media

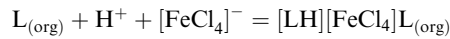
Selective extraction of zinc from chloride solutions is required for recovery from primary sources via new sulfide ore leaching technology (Section 9.17.3.3.2) and from secondary sources

Table 8 Selectivity of loading^a of ZNX50.

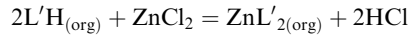
Metal	Zn	Fe	Cu	Pb	Cd	Sb
Aqueous feed	50 g L ⁻¹	110 g L ⁻¹	25 mg L ⁻¹	1.5 g L ⁻¹	25 mg L ⁻¹	25 mg L ⁻¹
Loaded organic	15 g L ⁻¹	6 mg L ⁻¹	15 mg L ⁻¹	<5 mg L ⁻¹	<5 mg L ⁻¹	<5 mg L ⁻¹

Source:¹⁹⁷^a Of a 0.3 M solution in Escaid after contact with an equal volume of a simulated chloride pregnant leach solution.

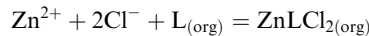
which arise from the production and use of galvanized steel such as pickle liquors. The potential advantages of Zn recovery directly from chloride leaching of sulfidic ores¹⁸⁷ are similar to those described in Section 9.17.5.1 for Cu recovery. The use of phosphate triesters to transfer Zn in the form of neutral [ZnCl₂L₂] complexes has not proved successful because they show poor selectivity over Fe^{III}.¹⁸⁷ The bis-benzimidazole reagent ZNX50 (Table 6) was developed to show high Zn^{II}/Fe^{III} selectivity.¹⁹⁷ The very weakly basic nitrogen atoms ensure that the reagent is not easily protonated, limiting transfer of iron by a competing ion-pairing mechanism



even in relatively acidic feed solutions, see Table 8.^{187,197} A study of the concentration dependence of Zn extraction by ZNX50 suggests that a dinuclear complex, [Zn₂Cl₄L₂], is formed in the organic phase.¹⁹⁷ The high activity of proton in concentrated chloride solutions limits the efficiency of acidic, pH-swing, extractants (see also Section 9.17.5.1.2),



The use of a combination of a pH-swing extractant, L'H, and a solvating extractant, L, in flowsheets similar to that outlined in Figure 8 has been proposed by several groups to transport zinc from chloride to sulfate media.^{160,163,187,198-200} An advantage of this approach is that stripping the zinc into a sulfate medium allows conventional electrowinning processes to be used. The zinc is transferred from the aqueous feed mainly by the solvating (or ion pairing) extractants,



Scrubbing this loaded organic solution with aqueous ammonia triggers the transfer of the zinc to the acidic extractant L'H,



from which it can be stripped with sulfuric acid,

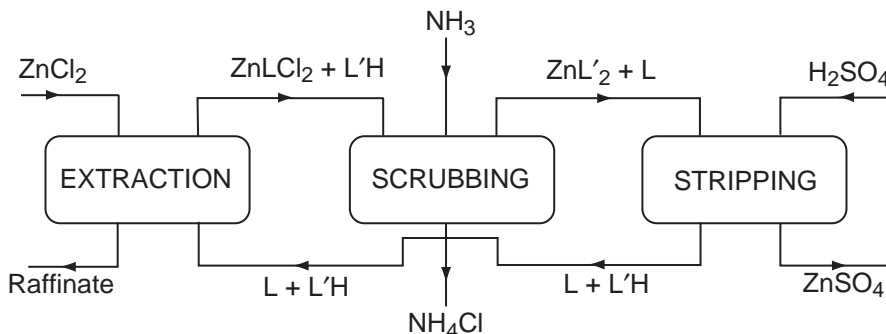
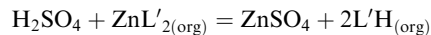
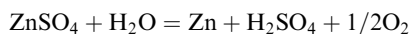
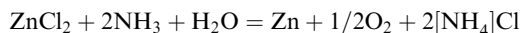


Figure 8 An outline flowsheet to transport zinc from chloride to sulfate media using a mixture of an acidic (pH-swing) extractant L'H and a solvating extractant L.¹⁸⁷

and electrowon in the conventional manner,



The ammonia scrubbing of loaded anion exchange extractants, e.g., $[\text{R}_3\text{NH}]_2[\text{ZnCl}_4]_{(\text{org})}$, proceeds similarly (see also Section 9.17.5.1.2), and thus in each case the mixed extractant system achieves the overall process,



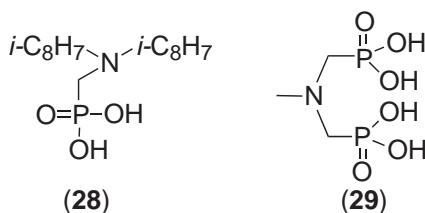
In the systems reported, the β -diketone reagent LIX54 has been used as the acidic extractant with either ZNX50 as a solvating extractant¹⁹⁹ or Alamine 336 as an anion exchange extractant.¹⁸⁷ Aliquat 336 has been used alone to extract Zn^{II} and Cd^{II} from chloride streams.²⁰⁰ The Zn/Cd selectivity depends on whether the chloride or thiocyanate form of the extractant $[\text{R}_4\text{N}]\text{X}$ is used, which is rationalized on the basis of the different types of thiocyanate complexes formed by zinc and cadmium.

9.17.5.2.3 Zn/Fe recovery from secondary sources

The increased use of galvanized steel has required the development of technology to separate and recycle zinc and iron.¹⁹⁵ Electric arc furnace (EAF) dusts contain significant quantities of zinc, together with heavy metals, most commonly lead and cadmium, and halides which make them difficult to process in both pyro- and hydro-metallurgical primary zinc recovery plants.^{195,202,203} Variations of the ZINCEX process using D2EHPA as a Zn extractant have been tested in a number of locations.¹⁹⁰ Other reagents proven in primary metal recovery have also been evaluated, e.g., Cyanex 301 for recovery from spent batteries¹⁹⁵ and ZNX50 from EAF dusts.¹⁹⁵ Despite the need for new technology to effect the Zn/Fe separation and the recycling of zinc, the relatively low value of the two metals places great pressure on keeping the costs of processes down and commissioning of large new plants has been slow.

The use or safe disposal of the iron residues from zinc production (see Figure 7) presents a major technical problem.²⁰⁴ The use of chelating aminomethylene phosphonic acid extractants such as (28) and (29) to recover iron from these residues has been proposed.²⁰⁵ These give much higher $\text{Fe}^{\text{III}}/\text{Zn}^{\text{II}}$ selectivity than D2EHPA but are more difficult to strip. A reductive-stripping process is proposed.^{187,205}

As in primary recovery the slow introduction of new technology to recover zinc, which nearly always requires a separation from iron, appears to be related to the relatively low market value of this metal.¹⁸⁷



9.17.5.3 Nickel and Cobalt

The decade 1990–2000 has seen a large volume of research on the application of solvent extraction of nickel,^{175,206–226} responding to the development of protocols for the high-pressure acid leaching (HPAL) in horizontal agitated autoclaves of nickel and cobalt into solution from lateritic ores^{81–88} which have followed the success of the Moa Bay plant in Cuba where commercial acid pressure leaching of limonitic ores has been practiced since the 1950s.^{75–78,80,227} Nearly 70% of the world's Ni reserves are in the form of nickeliferous lateritic ores, which also represent a major resource for cobalt. Until recently these oxidic ores have remained largely unexploited due to the absence of appropriate technology, but as they are located close to the surface they can be mined at a significantly lower cost than sulfidic ores from which the majority of nickel is presently extracted. The investment in the pressure leaching of lateritic nickel ores has been based on the

increased confidence gained by the growing number of successful pressure oxidation plants brought on stream for gold and zinc recovery.^{72,90–97}

Apart from bringing pressure technology into the mainstream, these plants have produced a pool of engineering and equipment designing expertise, which can be applied to laterites projects.

More than 90% of the nickel and cobalt in laterite ores (1.0–1.6% nickel) can readily be leached by sulfuric acid at $\geq 240^\circ\text{C}$, typically producing large volumes of relatively dilute leach solution containing $3\text{--}6\text{ g L}^{-1}$ of nickel and around $40\text{ g L}^{-1}\text{ H}_2\text{SO}_4$.⁹⁸ In addition to nickel and cobalt these leach solutions contain Al, Cr, Ca, Cu, Fe, Mg, Mn, Na, Si, and Zn.⁸⁹ The design of reagents and protocols for the separation and concentration of metal values in these streams has depended heavily on differences in the coordination chemistry of the components.

9.17.5.3.1 Co/Ni separation in sulfate solutions

The most extensively investigated reagents for the recovery of nickel and cobalt from acidic media have been the organophosphorus acids.^{220,222,228–234} The commercial and systematic names and the structures of the ligands used have been collected in the table presented earlier (Table 4).

The use of di(2-ethylhexyl)phosphoric acid (D2EHPA) to separate Co from Ni and other metals has been the subject of many fundamental investigations and was reviewed in CCC (1987).⁴ Important features for Ni/Co recovery are that D2EHPA exists in organic solvents of low polarity, such as kerosene, in the form of cyclic hydrogen-bonded dimers, and that in the presence of excess extractant these cyclic structures persist upon complexation with different degrees of protonation. The ease of extraction of the divalent metals of the first transition series follows the sequence $\text{Zn} > \text{Cr} > \text{Mn} > \text{Cu} > \text{Fe} > \text{Co} > \text{Ni} \approx \text{V}$. This sequence largely reflects the ease with which the respective metal ions adopt the tetrahedral geometry favored by the bulky dimerized D2EHPA ligands.

D2EHPA is thus a poor extractant for nickel as this shows a preference for a *pseudo*-octahedral structure in which two axial ligands are either fully protonated extractant molecules, fully protonated extractant dimers, or water molecules depending on extractant concentration, and four equatorial sites are occupied by deprotonated isolated D2EHPA molecules.

For cobalt it is proposed that both tetrahedral and octahedral forms exist in equilibrium. The entropy contribution arising from the dissociation of the octahedral cobalt complex to give the tetrahedral form has been exploited industrially to enhance the separation of cobalt from nickel by performing the separation at elevated temperatures.²³⁵ At high metal loading when the metal-to-extractant ratio approaches the limiting 1:2 stoichiometry it has been proposed that polymeric complexes form in which the PO_2^- units act as a bridging ligand. The stepwise change in viscosity observed upon high metal loading in working systems employing D2EHPA (and other phosphorus acid reagents) has often been attributed to the formation of such polymeric complexes.⁴

More recently, reagents containing phosphonic acid, phosphinic acid, and thio-phosphinic acids have been the subjects of considerable attention.^{122,222,230,236–243} These exhibit a greater selectivity for cobalt over nickel than D2EHPA. In a manner analogous to that of D2EHPA, they are believed to exist in the hydrogen-bonded dimerized form in low-polarity solvents. The first of this new generation of ligands to be developed and exploited for Co/Ni recovery was 2-ethylhexyl phosphonic acid (referred to here as PC-88A but also marketed as Ionquest 801).^{213,222,225,231,244–246} The enhanced selectivity of PC-88A for cobalt has been attributed to the destabilization of the octahedral nickel complex resulting from the greater steric bulk of the ligand caused by having an alkyl group attached directly to the phosphorus atom.

The phosphinic acid reagent Cyanex 272 exhibits even greater selectivity for cobalt. It is currently used in several commercial operations and has been the subject of much fundamental research.^{226,230–234,236–238,241,246–253} The further destabilization of the octahedral nickel complex has been ascribed to steric crowding arising from replacing all alkoxy groups with alkyl groups at the phosphorus atom.²⁵⁴ Cyanex 272 and di(1,3,3-trimethylbutyl)phosphoric acid (Figure 9) have selectivity factors $K_{\text{ex}}(\text{Co/Ni})$ of 3.8×10^2 and 3.7, respectively.²⁵⁴ The steric bulk of the alkoxy groups on the phosphorus atom in the latter is presumed to be similar to that of the alkyl group in Cyanex 272 because although the oxygen atom carries no hydrogen substituents, the P–O bond length (on average 162 pm) is significantly shorter than the P–C bond (on average 185 pm). These observations led Zhu¹²² to investigate the steric and electronic effects arising from variation in substituents in the commercial reagents D2EHPA, PC-88A, and Cyanex 272 (Table 9) using molecular mechanics and molecular orbital calculations. The predominant structural parameter

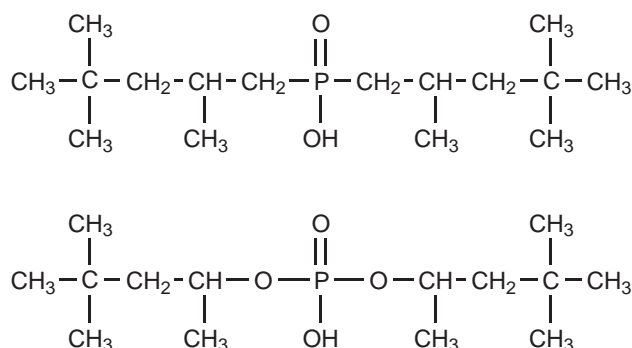


Figure 9 The structures of Cyanex 272 and di(1,3,3-trimethylbutyl)phosphoric acid.

defining the preference for formation of tetrahedral over octahedral complexes was the angle between the alkyl/alkoxy substituents, R and R', and the phosphorus atom.

Table 9 Calculated R–P–R' angles and dihedral angles between the RPR' and OPO' planes in D2EHPA, PC-88A, and Cyanex 272.

Extractant	Substituent		R–P–R'(degree)	Dihedral angle (degree)
	R	R'		
D2EHPA	oxy-2-ethylhexyl	oxy-2-ethylhexyl	104.7	90.2
PC-88A	oxy-2-ethylhexyl	2-ethylhexyl	115.7	91.2
Cyanex 272	2,4,4-trimethylpentyl	2,4,4-trimethylpentyl	120.1	89.5

Replacing alkoxy with alkyl groups results in an increase in the R–P–R', bond angle. This larger bond angle in the phosphinic acid (Cyanex 272) will lead to greater steric hindrance between the equatorial and axial ligands in an octahedral complex, but is assumed to have less effect upon a tetrahedral complex and is thus consistent with the observed increased selectivity for cobalt over nickel along the sequence D2EHPA, PC-88A, Cyanex 272.

The electron density of the oxygen atoms of the reagents also plays a role in determining their strength/selectivity (Table 10).¹²² The calculated point charges on the oxygen donor atoms follows the order D2EHPA < PC-88A < Cyanex 272, consistent with the increasing pK_a along the series and decreased extraction constants for both metals. This decrease is greater for nickel, leading to a larger Co/Ni separation factor along the sequence D2EHPA, PC-88A, Cyanex 272. This same order is expected as a result of the increasing repulsion between the oxygen donor atoms which will lead to a preference for the formation of species of lower coordination number (i.e., tetrahedral vs. octahedral) to minimize electronic repulsion.

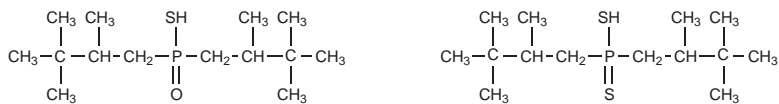
Table 10 Values of pK_a 's, extraction constants, separation factors, and calculated point charges in D2EHPA, PC-88A, and Cyanex 272.

Extractant	pK_a	$K_{ex(Co)}$	$K_{ex(Ni)}$	$K_{ex(Co/Ni)}$	Point Charge (q)		
					P	O	O'
D2EHPA	3.57	5.50×10^{-6}	1.10×10^{-6}	5	0.161	–0.345	–0.772
PC-88A	4.10	1.07×10^{-6}	1.51×10^{-8}	71	0.028	–0.367	–0.794
Cyanex 272	5.05	1.66×10^{-7}	2.00×10^{-10}	830	0.092	–0.393	–0.814

Source:¹²²

Phosphorus acids containing P–S bonds in which the sulfur atom acts as the metal ligating atom also received much attention.^{243,252,255–261} The commercially available reagents bis(2,4,4-trimethylpentyl)phosphinothioic acid (Cyanex 302) and bis(2,4,4-trimethylpentyl)dithiophosphinic

acid (Cyanex 301) are analogs of Cyanex 272 in which one or both oxygen atoms, respectively, have been replaced by sulfur [Table 4](#).



Like Cyanex 272 they exhibit a preference for Co^{II} over Ni^{II} , but are much “stronger” reagents, extracting cobalt at a pH of 1–2, in comparison to the P–O-containing phosphoric, phosphonic, and phosphinic acids, which typically extract in the pH range of 4.5–6.^{252,256,258,262,263} This enhanced strength can be ascribed to the presence of the softer sulfur donors which are preferred by tetrahedral forms of the metals. One of the major disadvantages of the thio-phosphinic acids is their tendency to form organo-phosphorus disulfides in the presence of oxidizing species such as Fe^{III} , Co^{III} , or O_2 . In the commercial processes using Cyanex 301 for Co/Ni separation this problem is overcome by the incorporation of an extractant recovery stage in which partially oxidized reagent is regenerated via reduction with H_2 formed from the reaction of metallic zinc with H_2SO_4 .²⁶⁴

Because the organophosphorus reagents DE2HPA, PC-88A, and Cyanex 272 are selective for Ca^{II} and Mg^{II} over Ni^{II} , this precludes their use for nickel recovery from laterite HPAL solutions where these metals are often present at close to saturation levels.²²⁶ The tertiary carboxylic acids represent a source of potential extractants that are inexpensive, readily soluble in kerosene, and chemically stable. However, they have rarely been applied in commercial applications because they show appreciable solubility in aqueous media and poor selectivity.⁸⁹ Recently, the reagent Versatic 10 (predominately C_{10} mono-carboxylic acids, see [Section 9.17.4.4](#)) has been extensively tested as it shows selectivity for Ni^{II} over Ca^{II} and Mg^{II} at low pH.^{226,241} It is not selective for Co^{II} over Ni^{II} , the difference between $\text{pH}_{1/2}$ values being <0.2 pH units. Consequently, it can only be used when cobalt has been removed from the process stream or when a mixed Co/Ni salt is the desired product.^{226,241,265}

The stoichiometry of Versatic 10 Ni extraction has been the subject of much investigation. Distribution data for the extraction of nickel from aqueous solution is consistent with the generalized equilibrium.^{266,267}



At low Ni-loading the monomeric species $\text{NiA}_2 \cdot 4\text{HA}$ predominates, whereas at higher nickel loadings the dimeric complex $[\text{NiA}_2 \cdot 2\text{HA}]_2$ is the major species.²⁶⁶ The amount of water extracted at first increases with Ni loading to give a ratio of H_2O :nickel of about 2 with $\text{Ni} < 9 \text{ g L}^{-1}$, and at higher loadings this ratio decreases to 1.²⁶⁶ The significant water solubility of Versatic 10 at the moderately high pH values required for efficient nickel extraction poses significant difficulties in commercial use. In continuous trials it was found that 50% of the total Versatic 10 inventory was lost in 75 hours, necessitating the incorporation of an additional step in the circuit to recover the reagent from raffinate.²²⁶

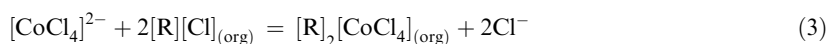
The H_2SO_4 liberated on Ni extraction must be neutralized in order to maintain an efficient equilibrium position in [Equation \(2\)](#). “Pre-neutralizing” Versatic 10 by contacting with a solution of aqueous ammonia prior to Ni extraction much enhances recovery.^{266,268,269} Pre-neutralization, or saponification, also eliminates the need for pH control in the mixer. Partial (ca. 50%) pre-neutralization of an iso-octane solution of Versatic 10 with saturated aqueous ammonia results in the formation of a single-phase system. Loading of the pre-neutralized extractant proceeds very quickly as the rate of exchange between the amphiphilic aggregates of the microemulsion and the bulk water is extremely fast and at high nickel loadings the system reverts to two phases in which the organic solution is loaded with nickel, free of ammonia and contains little water.²⁶⁹

9.17.5.3.2 Co/Ni separation in chloride and ammoniacal solutions

Effective protocols have also been developed for the extraction of nickel and cobalt from chloride and ammoniacal process streams derived from leaching sulfidic ores or mattes.^{103,175,214,224,270–279}

The greater thermodynamic stability of the Co^{II} chloroanionic complexes such as $[\text{CoCl}_4]^{2-}$ over analogous Ni^{II} species has been exploited to effect the separation of nickel and cobalt via an

anion exchange mechanism from acidic solutions of high chloride activity (Co extraction occurs when $[\text{Cl}^-] > 3.0 \text{ M}$).^{103,279}

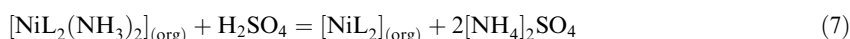
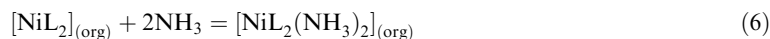
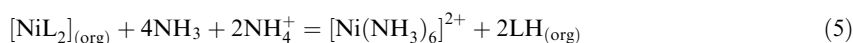
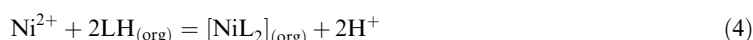


The anionic exchange reagents commonly employed in these processes are tris-alkyl ammonium cations, generally dissolved in an aromatic diluent such as xylene. Tris-isooctylamine has been used at Falconbridge Nikkelverk in Kristiansand, Norway for the purification of solutions derived from HCl leaching of Ni—Cu matte for over 30 years.¹⁰³

It is essential in processes which employ such reagents to effect Co/Ni separation that metals such as Fe^{III} , Cu^{II} , and Zn^{II} that also form stable chloro-metallate complexes are removed prior to Co extraction.^{103,280}

Hydrochloric acid is a very effective lixiviant for nickel/cobalt laterites.^{243,256,281} Unlike H_2SO_4 , almost complete Ni recovery is achievable without the application of high pressure and temperatures²⁴³ and has a significant advantage in terms of energy consumption. However, unlike the solutions obtained from the HCl leaching of Co/Ni intermediates described previously, these solutions contain substantial amounts of magnesium. Thus, while it is possible to use anion exchange reagents to recover the cobalt from such solutions (e.g., as in Equation (3)), other types of reagents are needed to separate the nickel from magnesium. Studies using Cyanex 301, Cyanex 302, and Versatic 10 have shown that the carboxylic acid Versatic 10 is most effective.^{243,256} Cyanex 301 exhibits good selectivity of Ni/Mg extraction from chloride media, but the kinetics of Ni loading are poor and stripping of Ni-loaded solutions requires HCl of concentrations approaching 10 mol L^{-1} . Stripping from Ni-loaded Cyanex 301 and related alkylphosphorodithioic acids can be somewhat improved by addition of octan-1-ol to the organic phase.²⁴³ Cyanex 302, a weaker Ni extractant from chloride, shows better kinetic characteristics of loading and stripping, but unfortunately it lacks the specificity to achieve Ni/Mg separation.²⁴³

Ammoniacal leaching has been used for some time to process nickel- and cobalt-containing materials from a wide range of sources under oxidative conditions,^{106,175,212,219,224,274,282,283} generating solutions containing Co^{III} -ammine complexes. The inert nature of $[\text{Co}(\text{NH}_3)_6]^{3+}$ forms the basis for the separation of nickel and cobalt, using conventional contact times. Phenolic oximes of the type shown in Table 3 extract very little Co^{III} .^{175,271,276,277} The pH dependence of Ni loading has a characteristic bell shape with maximum uptake in the pH range ca. 5–9.^{224,272,273,277} At high pH the formation of stable ammine complexes in the aqueous phase reduces Ni loading of the oxime reagent. Investigations of the stoichiometry of loading suggest that the predominant species is the diamagnetic planar bis-oxime complex $[\text{NiL}_2]$, but there is also a possibility that this co-exists with the high-spin, *pseudo*-octahedral species $[\text{NiL}_2(\text{NH}_3)_2]$ at higher pH values (Equation (6)).

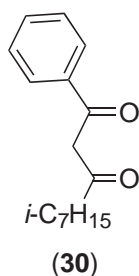


This use of phenolic oximes to achieve the separation of Ni^{II} from Co^{III} also results in the complete rejection of Zn^{II} , Cd^{II} , and Mg^{II} , a distinct advantage over the organo-phosphorus reagents discussed above. Any copper present in the feed will be co-extracted with the nickel but it is possible to acid strip the nickel selectively at moderately high pH and then recover the copper at much lower pH. The equilibration times for Ni loading or stripping are significantly longer than those for copper, often involving contact times of up to 10 minutes. Whilst this order is consistent with the relative labilities of the hydrated divalent metal cations,¹⁵⁴ both are sufficiently labile that it implies that rates are determined by interfacial or organic phase reactions.

A problem encountered with the use of the phenolic oximes in Ni recovery from ammoniacal solution is the co-extraction of ammonia that must be removed prior to generating the electrolyte for

reduction to the metal. Scrubbing of ammonia may be achieved by contacting the ammonia-loaded reagent with a dilute acid solution (Equation (7)). Conditions must be controlled carefully to avoid Ni loss into the wash stream by the standard acid strip reaction (Equation (8)). It has been shown²⁷² that the hydrocarbon solutions of metal-free phenolic oximes also load ammonia. Adducts of salicylaldoximes with α,ω -diamines with 2:1 stoichiometries have been characterized in the solid state.¹²¹

The β -diketone LIX-54 (30) shows a similar dependence of Ni-loading on pH to the phenolic oximes with Ni-uptake decreasing at pH > 9, attributable to the formation of nickel ammine complexes in the aqueous phase. The stoichiometry of the extraction reaction can be represented by the general equilibrium shown in Equation (4).^{214,270} Equilibrium is reached in both stripping and extraction within 10 minutes. Extraction of nickel by LIX-54 has been found to be slightly exothermic ($\Delta H^\circ = -44.8 \text{ kJ mol}^{-1}$) and stripping very slightly endothermic ($\Delta H^\circ = 10.9 \text{ kJ mol}^{-1}$).²⁷⁰ The advantage of β -diketones as Ni extractants from ammoniacal media is that neither the reagent nor its nickel complex transfer ammonia into the organic phase. The absence of NH_3 bound to nickel in such complexes has been confirmed via IR spectroscopy.²¹⁴



Very good extraction of Co^{II} from Ni^{II} can be achieved using the amido-bis-thiophosphoryl extractant DS6001 (see Table 4). After the removal of Zn^{II} or Cu^{II} from the feed solution, Co^{II} can be selectively extracted at pH 3–4 and then Ni^{II} at pH 4–6 in the presence of a range of metal cations commonly obtained in HPAL solutions from laterites.²⁸⁴ The affinity of this reagent for the divalent cations, $\text{Zn}^{\text{II}} > \text{Co}^{\text{II}} > \text{Ni}^{\text{II}}$, accords with its ability to present a soft S_4^{2-} tetrahedral donor set (see also Section 9.17.4.3).

9.17.6 PRECIOUS METALS

The greatly increased use of the precious metals (Pt, Pd, Rh, Ir, Ru, Os), Ag, and Au in applications from jewellery to electronic devices, exhaust control catalysts to dental materials has stimulated considerable research into their recovery.^{285–289} A typical flowsheet for the solvent extraction of the PGMs (Figure 10) involves pressure or heap leaching in chloride media under conditions which generate a pregnant leach solution devoid of base metals, but containing a myriad of chloro complexes. The volatile osmium and ruthenium species OsO_4 and RuO_4 are removed by distillation and the remaining PGMs are subjected to various solvent-extraction steps until only rhodium is present, which is then separated by precipitation. Many extractants have been tested and some have been put into commercial operations to recover Au, Pd, Pt, and Ir in flowsheets of the type shown in Figure 10.^{290,291}

Most modern hydrometallurgical installations rely heavily on solvent-extraction technologies, especially in refining high-grade metals.²⁹¹ The design of new extractants (Section 9.17.4) must pay particular attention to the type of aqueous media used, usually chloride, bromide, or thiocyanate. Soft-base donor ligands such as the organo-sulfur compounds have been much studied,^{292–295} and some researchers have addressed problems of the kinetic inertness of many of these metals by lowering oxidation states—see Section 9.17.6.3.²⁹⁶

The commercial extractants currently used fall into the following categories:²⁹⁷ α -hydroxy-ketoximes, phenolic-oximes,²⁹⁸ dialkylsulfides, esters of pyridine mono and di-carboxylic acids,^{299–301} alkyl derivatives of 8-hydroxyquinoline,^{79,302,303} trialkylamines,^{304,305} alkyl derivatives of aniline,³⁰⁶ aliphatic ethers, and ketones.^{307–309}

Many of the reagents developed initially for the recovery of base or radioactive metals have also been investigated as potential PGM extractants, e.g., phosphine oxides,^{310–313} dialkylsulfoxides,³¹⁴ dialkyl- and diphenyl-thioureas,^{296,315–317} thiopicolinamides,³¹⁸ thiobenzanilide,³¹⁹ phosphate diesters,³²⁰ tetra-thioethers,³²¹ dialkylthietanes,^{322–324} amino acids such as dialkylglycine,³²⁵ dialkylsuccinamic acid,³²⁶

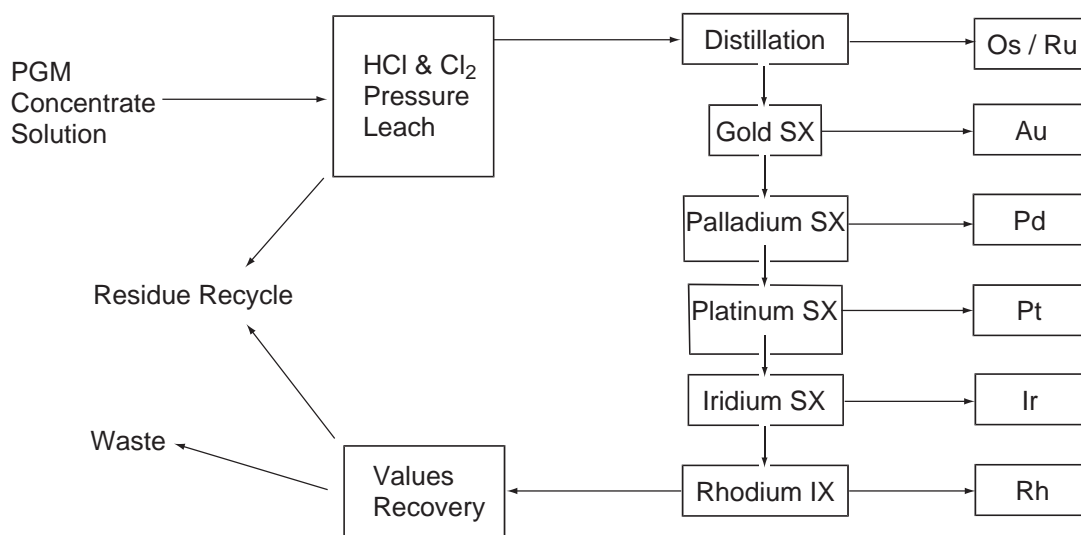


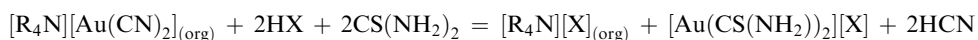
Figure 10 A typical solvent extraction flowsheet for PGM refining.^{290,291}

and most recently, calixarenes.^{327–329} Several extractants have been designed for special applications, such as fluorinated amides for use in CO₂.³³⁰ A review by Yordanov and Roundhill deals with PGM-recovery by chelate and macrocyclic ligands,³²⁹ and Wisniewski and Szymanowski have surveyed the use of existing commercial extractants in the flowsheets for the INCO, Matthey, and Lonhro PGM-recovery processes.²⁹⁷ The following sections consider the recovery of individual precious metals.

9.17.6.1 Au^I, Au^{III}

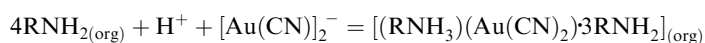
Gold is conventionally recovered by leaching ores or recycled materials with alkaline cyanide solutions in the presence of oxygen. The gold, as [Au(CN)₂][−] or [Au(CN)₄][−], in the pls is concentrated by zinc cementation (Merill–Crowe), carbon absorption (carbon-in-pulp or CIP), or via ion exchangers and then electrowon.^{4,331} Advances in hydrometallurgy and the imposition of increasingly stringent environmental controls have prompted research into solvent extraction as an alternative technology for concentration and separation.

Quaternary ammonium salts were first used as extractants from alkaline solutions.^{4,332,333} Aliquat 336, Adogen 481, and Adogen 483 (Table 5) have been tested in plant feasibility studies conducted by Riveros.³³⁴ The advantages of these reagents (good selectivity, fast kinetics, high loading capacity, low water solubility, and good phase separation) were outweighed by the proposed stripping protocols which involved acidic solutions of thiourea, which generate hydrogen cyanide, or via incineration of the gold-loaded extractant.

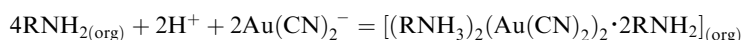


The affinity of [Au(CN)₂][−] for primary, secondary, and tertiary amines is very low at pH values typical for cyanide feed solutions, but in 1983 Mooiman *et al.* showed that the addition of solvating phosphorus(V) oxides enhanced extraction at higher pH.^{335,336} During the course of this work it was discovered that TBP and DBBP (see Table 6) could themselves extract gold.³³⁷ This led to subsequent investigations on phosphates and phosphorus oxides.³³³

Caravaca *et al.*^{338,339} evaluated the primary amines Primene 81R, Primene JMT (Table 5), and tridecylamine and concluded that for Primene 81R and tridecylamine the extraction occurs via,

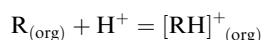


i.e., by a combination of anion exchange and solvation effects. The stoichiometry of the assembly is different for Primene JMT,

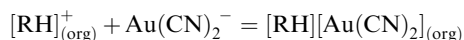


Selectivity over other metalocyno species was poor, decreasing in the order tridecylamine > Primene 81R > Primene JMT. The best extraction conditions proved to involve neutral or slightly elevated pH.³³⁹ The addition of Cyanex 921, Cyanex 923, or TBP (Table 6) allowed extractions to be performed under more alkaline conditions and improved the selectivity over other metals.³³⁸

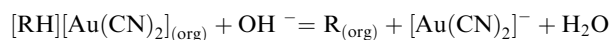
In the late 1980s Henkel Coporation¹³¹ developed a series of dialkylguanidine derivatives (**31**) for the recovery of Au and Ag from low-grade cyanide liquors. The dialkylguanidinium cation [RH]⁺ functions as an anion exchange extractant whose concentration is controlled by the pH swing:



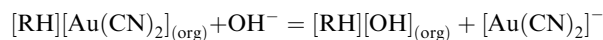
At pH ≤ 10.5 the guanidine is protonated and phase transport of [Au(CN)₂]⁻ is favored,



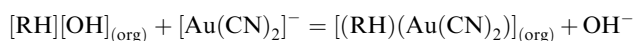
Increasing the pH to ≥ 13.5 favors deprotonation of the guanidinium reagent and Au(CN)₂⁻ is released,



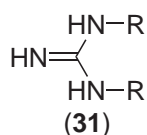
Early tests using *N,N'*-bis(2-ethylhexyl)guanidine resulted in excellent selectivity for gold, but it was found that longer-chain alkyl groups were needed to prevent losses of the reagent to the aqueous phase.³⁴⁰ Another problem encountered was the transport of hydroxide during Au stripping,



which is then released into the aqueous feed solution when the reagent is recycled,



The consequent increase in pH of the feed solution significantly reduces the efficiency of Au extraction.



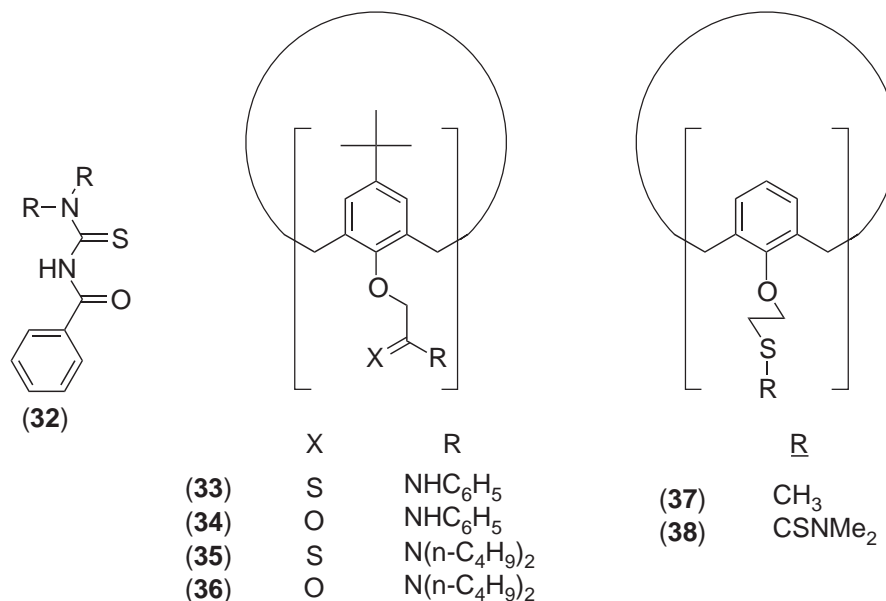
Hydroxide transfer was reduced to undetectable levels by varying the composition of the organic phase,³⁴⁰ and the LIX 79 reagents, trialkylguanidines of unspecified composition (Table 5), have been subsequently commercialized. Working trials at two gold mines revealed the selectivity of LIX 79 to be Au > Zn > Ag > Ni > Cu > Fe. Addition of 50 g L⁻¹ of tridecanol was needed to prevent formation of a third phase. Reduced metal loading of LIX 79 when cyanide concentrations in the feed solution are increased has been ascribed to ligand competition and formation of more highly charged cyano complexes in the aqueous phase.^{341,342} Extraction of gold has been undertaken using LIX 79 in liquid membranes^{343,344} and robust hollow-fiber membranes³⁴⁵ as alternatives to solvent extraction for recovery from dilute feeds. A similar study, for recovery from acidic chloride media, has used Cyanex 923 as the carrier in liquid membranes.³⁴⁶

The development of more benign alternatives to cyanide for gold-leaching (see Section 9.17.3.1) such as thiourea, thiocyanate, or thiosulfate, which form stable complexes in water has prompted research to identify suitable solvent extractants from these media. Cyanex 301, 302, 272, Ionquest 801, LIX 26, MEHPA, DEHPA, Alamine 300 (Table 5) have been evaluated as extractants for gold or silver from acidic thiourea solutions.³⁴⁷ Whilst the efficacy of Cyanex 301 and 302 was unaffected by the presence of thiourea in the aqueous feed, the loading of the other extractants is severely depressed. Formation of solvated complexes of gold and of an inner-sphere complex of silver has been proposed.³⁴⁷

Oxidative leaching with ammonium thiosulfate (Section 9.17.3.1) generates solutions containing a mixture of the mono- and di-thiosulfato complexes, [Au(S₂O₃)]⁻ and [Au(S₂O₃)₂]³⁻. Gold can

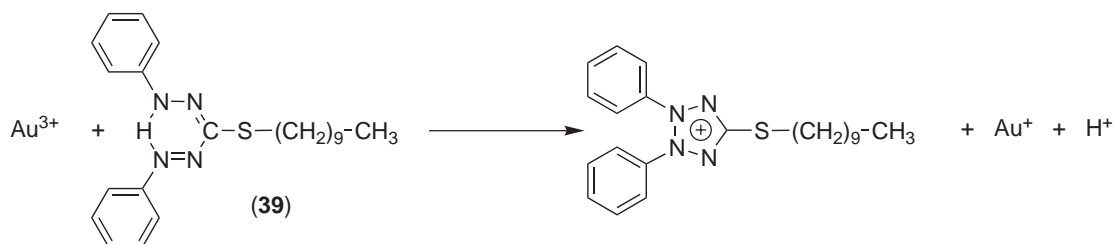
be recovered selectively from such solutions using mixtures of an amine extractant with a solvating extractant such as TBP or a trialkyl amine oxide.^{348–351}

There has been a renewed interest in recovery of gold from chloride media containing both Au^I and Au^{III} chloro-complexes. Vest *et al.*³⁵² and Salvadó *et al.*³⁵³ independently evaluated various substituted benzoylthioureas (**32**) as Au^{III} extractants.^{352,353} Good kinetic selectivity is reported for Au^{III} and Pd^{II} over the other PGMs, based on the higher lability of their chloro complexes.³⁵²



Chloroform solutions of calixarenes (**33–38**)^{293,354} show high affinity for Au^{III} and good selectivity over Fe^{III} in some cases.²⁹³ Spectroscopic data indicate that complex formation with thioethoxy calix[4]arenes involves formation of inner-sphere complexes with Au–S bonds.³⁵⁴

Extraction of gold from acidic chloride media by *S*-decylthiozone (**39**) is associated with oxidation of the extractant to the 2H-tetrazolium cation. Reductive stripping results in the regeneration of the extractant and precipitation of Au⁰ as a black powder.³⁵⁵



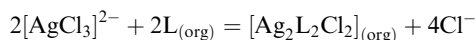
Relatively little has been reported on solvating extractants for recovery from chloride media³⁵⁶ since BUTEX (see Table 6) was used by INCO in the 1970s,³⁵⁷ and subsequently MIBK by Johnson Matthey and Anglo.³⁵⁸ Recently, 2-ethylhexanol has been shown to have a higher Au capacity, a higher selectivity over other metals, and to be more easily stripped than other alcohols tested previously.³⁵⁶ The MinataurTM process³⁵⁹ uses a solvating extractant of undisclosed composition to effect a very efficient separation from other metals present in the cathode sludge obtained from conventional CIP/electrowinning.^{360,361}

9.17.6.2 Ag^I

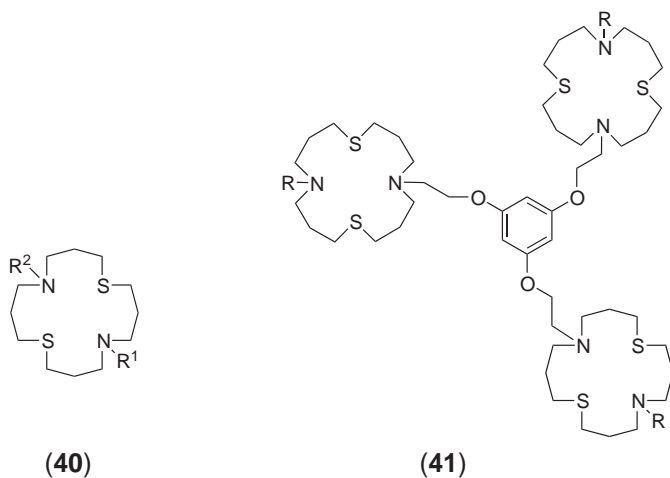
The extractive metallurgy of silver involves a wide range of processes reflecting the diverse sources of this element. It is recovered in significant quantities from sulfidic ores or as a high-value by-product from zinc/lead, copper, nickel, tin, and gold production, mainly by pyrometallurgy.¹⁸² The coordination chemistry involved in hydrometallurgical recovery is generally based on

leachants similar to those for gold (see above), but there has not been widespread use of selective complexing agents in separation, concentration, and refinement operations.¹⁸² Solvent-extraction processes have received more attention in recovery from secondary sources such as photographic fixing solutions.³⁶² The working system chosen by the majority of investigators usually comprises a nitrate feed and a chloroform organic phase which is attractive for the experimentalist, as investigation of complex formation and extraction by NMR is straightforward. Two comprehensive reviews have recently been published^{363,364} providing a survey of the literature up to 2000. Since then more than 50 further papers have been published, many involving the use of extractants in membranes or on solid supports. The extractants reported are predominantly based on macrocyclic ligands, examples include calixarenes with pendent sulfur or nitrogen donors³⁶⁵⁻³⁷¹ and crown ethers.³⁷²⁻³⁷⁴ Sulfur-containing macrocycles³⁷⁵⁻³⁷⁸ show remarkably high selectivity for Ag^{I} over base metal cations.

Both the mono- and tri-nucleating ligands (**40**) and (**41**) transport Ag^{I} exclusively from a feed solution containing Co^{II} , Ni^{II} , Cu^{II} , Zn^{II} , Ag^{I} , Pb^{II} , and Cd^{II} .³⁷⁵ The relative ease of separation of silver from base metals by traditional processes,¹⁸² and its decreasing value relative to the PGMs make it likely that extractants based on expensive ligands are unlikely to be commercialized in the near future. The much simpler solvating extractants tri-*n*-butyl- and tri-*n*-octyl-phosphine sulfide have been shown to give high recoveries of Ag^{I} from concentrated chloride media after stripping with thiosulfate.³⁷⁹ Selectivities are lower than for tri-*iso*-butyl-phosphine sulfide, the active ingredient of Cyanex 471X. Analysis of the concentration dependencies of extraction equilibria indicate³⁷⁹ that the less-hindered *n*-alkyl derivatives form a dinuclear Ag^{I} complex in the organic phase,

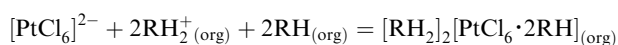
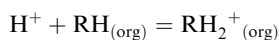


although the Cyanex 471X ligand has been claimed to give a mononuclear complex, $[\text{AgL}_2\text{Cl}]$.³⁸⁰

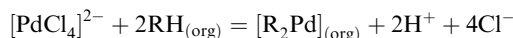


9.17.6.3 Pt^{IV} , Pt^{II}

The refining of platinum is technically more challenging than gold or silver due to the lack of easily implemented electrorefining steps. The separation from other PGMs is most commonly approached by dissolution of concentrates into HCl solutions (Figure 10). Options for extraction are limited by the very slow rates of ligand exchange shown by the chlorometallates, only Pd^{II} being sufficiently labile for the recovery by processes based on inner-sphere complex formation to be of practical use.⁴ The nature of the solvating or ion-pairing extractants currently in use in commercial operations is shrouded in secrecy, but a wide range of reagent types have been tested, and Wisniewski and Szymanowski give a useful summary²⁹⁷ of extractants used prior to 1996. The 8-hydroxyquinoline reagents (Kelex100), (**26**), on contact with acidic solutions containing $[\text{PtCl}_6]^{2-}$ are readily protonated and transfer³⁸¹ platinum to an organic solution as a solvated ion pair,

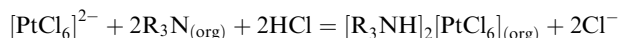
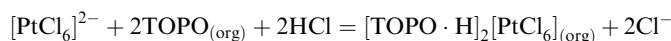
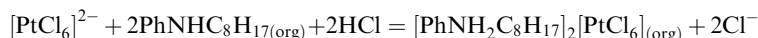


Inner sphere complexes are formed with Pd^{II},



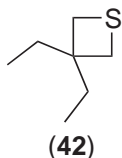
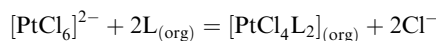
and, at low concentrations of HCl the extraction of Pd^{II} is favored. Pt^{IV} can be selectively stripped into water at pH 1.5–2.0, and then the Pd^{II} recovered with 6–8 M HCl or by reduction with hydrogen.²⁹⁷

Quantitative extraction of Pt^{IV} by *n*-octylaniline affords a method of separation from Fe^{III}, Co^{II}, Ni^{II}, and Cu^{II} in hydrochloric acid.³⁰⁶ A similar ion-pairing mechanism accounts for extraction by TOPO^{305,310} and Alamine 304³⁰⁴ (see Tables 5 and 6 for reagent structures):

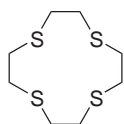


It has been shown that upper-rim substitution of some dithiocarbamoyl-derivatized calix[4]arenes affects selectivity of Pt^{IV} extraction.^{327,329} Some selectivity over Pb^{II}, Hg^{II}, and Pt^{II} has been achieved by the introduction of 2-pyridyl-*N*-oxide groups on the lower rim, but Sn^{II}, Ag^I, Pd^{II}, and Au^{III} were still extracted to a greater extent.³²⁸

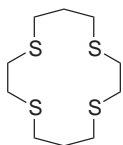
An inner-sphere complex (42) is formed when toluene solutions of 3,3-diethylthietane are contacted with solutions of Pt^{IV} in hydrochloric acid, but extraction is slow.³²²



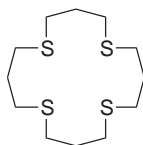
The kinetic inertness of $[\text{PtCl}_6]^{2-}$ in solvent extraction reactions can be dramatically altered by the addition of SnCl₂.^{79,285} After a 10-minute contact time, negligible quantities of Pt^{IV} are extracted from 0.1 to 12 M HCl solutions by thiobenzanilide in chloroform, whereas almost quantitative recovery is recorded after the addition of a slight excess of SnCl₂.³¹⁹ Reduction of Pt^{IV} to Pt^{II} and formation of mixed Pt/Sn complexes are thought to be responsible. Extraction of Pt^{II} from chloride solutions by the macrocyclic tetrathioethers (43)–(45) is very slow, but is considerably enhanced by the addition of thiourea.³²¹



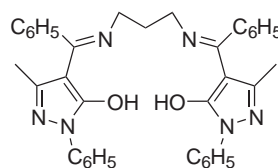
(43)



(44)



(45)



(46)

König, Schuster, and others have demonstrated that by controlling the pH of the aqueous phase, *N*-benzoyl-*N,N'*-dialkylthioureas can be used to separate Pt^{II}, Pd^{II}, Ru^{III}, Rh^{III}, Os^{III}, and Ir^{III} from base-metal chlorides.^{382–385} Extraction of Pt^{IV} by *N*-acyl-*N'*-alkylthiourea and *N*-acyl-*N,N'*-dialkylthiourea reagents is substantially accelerated by addition of SnCl₂ and is accompanied by reduction to Pt^{II}.²⁹⁶ Ring opening of the OS⁻ chelate rings and *cis/trans*-isomerization of the resulting dichloroPt^{II} complexes has been shown to be dependent on HCl concentration by ¹H and ¹⁹⁵Pt NMR spectroscopy.^{317,386} The coordination chemistry of this class of reagent and formation of other types of isomer based on *E/Z* arrangements of the *N,N'*-dialkyl groups and *cis/trans*-arrangements (Figure 11) of the bis-chelates has been reviewed.³⁸⁷

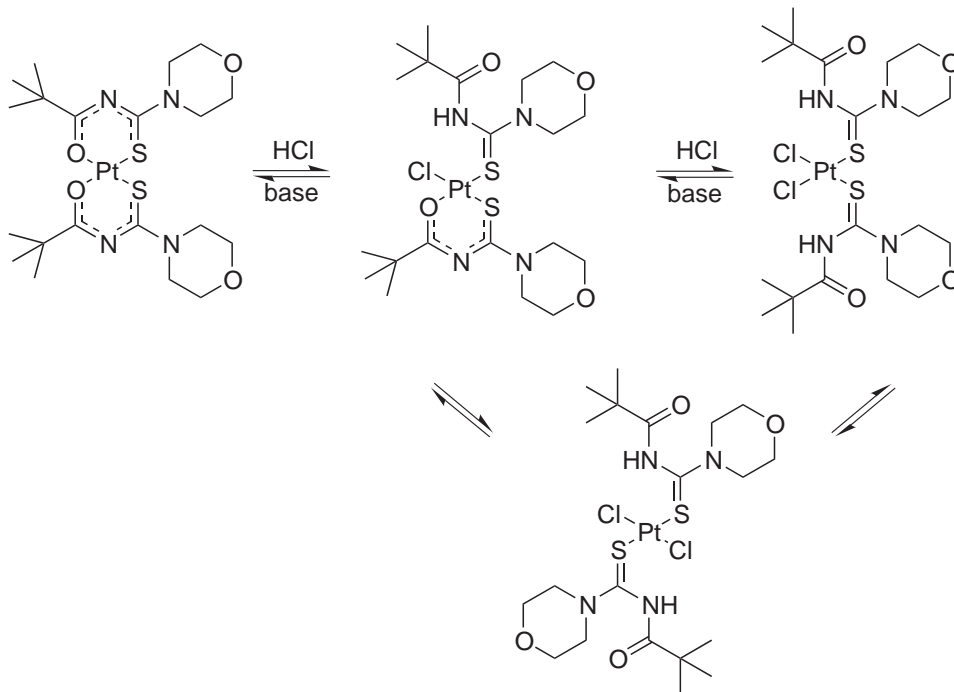
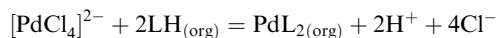


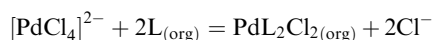
Figure 11 Interconversion of Pt^{II} complexes of *N-t*-pentanoyl-*N'*-morpholiniothiourea.³⁸⁶

9.17.6.4 Pd^{II}

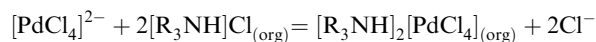
The development of new technology for extraction and recycling of palladium has been stimulated by its increasing use in automobile catalysts, which now consume ca. 55% of world production. A range of options for extraction from acidic media and for separation from other PGMs is possible because Pd^{II} is relatively substitution-labile. This allows cationic exchange, e.g.,



or solvating reagents



to be used to effect separation from platinum.³⁸⁸ The thermodynamic stability of chloropalladate(II) complexes also allows recovery using anion exchange reagents, e.g.,



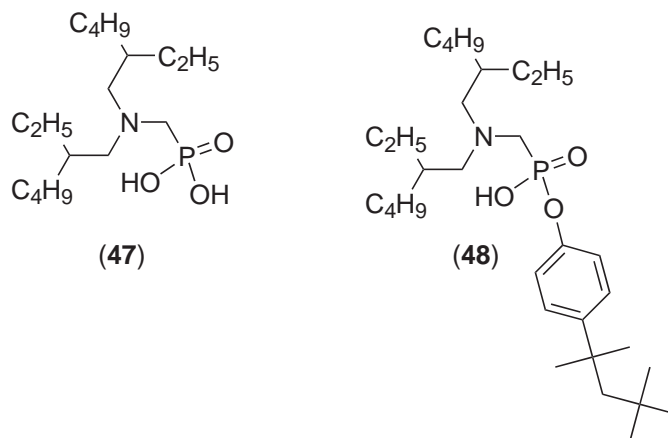
but achieving good selectivity of extraction by the anion exchange route is a challenging problem. The lower charge density of the Pt^{IV} complex $[\text{PtCl}_6]^{2-}$ leads to this being preferentially extracted with reagents having lower charge density on the cation, e.g., quaternary alkyl ammonium or phosphonium salts. This Pt/Pd selectivity is reduced when there are substantial quantities of the dinuclear complex $[\text{Pd}_2\text{Cl}_6]^{2-}$ in the feed solution.³⁸⁸

Alkylammonium reagents have also been shown to act as phase transfer catalysts when used in conjunction with cation exchange reagents such as Kelex 100 or solvating extractants such as di-octylsulfide. It has been suggested³⁸⁹ that formation of the inner-sphere complexes occurs in the bulk organic phase following transport of chloropalladate complexes across the interface in ion pairs with $[\text{R}_4\text{N}]^+$. A similar approach has been reported by Belova *et al.*³⁹⁰ who have used alkylammonium salts of di(2-ethylhexyl)dithiophosphoric acid (DEHPTA, see Table 4), but in this case the extracted species, $[\text{R}_4\text{N}][\text{PdCl}_2\text{L}]$, contain mononanionic Pd^{II} complexes with one deprotonated DEHPTA ligand in the inner coordination sphere, except when the reagent is in large excess, when $[\text{PdL}_2]$ is formed.³⁹⁰ Similar results are obtained with D2EHPTA.³⁹¹

A number of chelating cation exchangers have been used as extractants. The modes of complex formation by acylthioureas (**32**) are described in Section 9.17.6.3.^{382–385} Their use has been extended to membrane systems for the recovery of Pd.³⁹² The use of Kelex 100²⁹⁷ and of hydroxyoximes^{14,297} (Table 3) has been reviewed and methods for improving rates of phase transfer have been surveyed by Szymanowski.¹⁴

The quadridentate ligand (**46**), LH₂, has been used to extract palladium from solutions containing platinum. Equilibrium studies indicated that a mono-deprotonated form of the ligand is involved,³⁹³ giving [PdCl(LH)].

The dialkylaminomethyl phosphonates, (**47**) and (**48**), could function as either a cation exchanger using its phosphonate group or as an anion exchanger using a protonated form of the amino group. Equilibrium studies suggest formation of a mono-chloro complex containing one deprotonated and three neutral solvating ligands.³⁹⁴



Whilst many solvating ligands have been studied, the dialkyl sulfide reagents (see Table 6) remain the most important commercially.²⁹⁷

9.17.7 CONCLUSIONS

Since the publication of the *CCC* (1987) the expanding use of hydrometallurgical methods for the recovery of base and precious metals has provided a major stimulus for applying coordination chemistry to leaching, separation, and concentration operations. This large volume of research and development work has not resulted in the commercialization of many new classes of metal extractants, and instead “playing new tricks with old reagents”³⁹⁵ has been very much a feature. The development of any new extractant by a specialty chemical company is most likely to succeed when there is collaboration with metal producers at the outset to define the design requirements and to ensure the reagent supplier receives reward for the value of improvements in the metal recovery process. Playing “new tricks with old reagents” should include synergistic combinations of extractants resulting from ligand assembly processes that in future should exploit design principles emerging from supramolecular chemistry.

9.17.8 REFERENCES

- Habashi, F.; *Handbook of Extractive Metallurgy*; Wiley-VCH Verlag GmbH; Weinheim, 1997.
- Burkin, A. R. *Chemical Hydrometallurgy—Theory and Principles*; 1st ed.; Imperial College: London, 2001.
- Swaddle, T. W.; Editor. *Inorganic Chemistry: An Industrial and Environmental Perspective*; Academic Press: San Diego, 1996.
- Nicol, M. J.; Fleming, C. A.; Preston, J. S. Application to Extractive Metallurgy. In *Comprehensive Coordination Chemistry*; Wilkinson, G., Gillard, R. D., McCleverty, J. A., Eds.; Pergamon: Oxford, U.K., 1987, Volume 6, pp 779–842.
- Ehrenfeld, J. R. Industrial ecology: coming of age. *Env. Sci Technol.* **2002**, *36*, 280A–285A.
- Shooter, D.; Ong, J. H.; Preston, A.; Ehrenfeld, J. R. Treatment of reactive wastes at hazardous waste landfills. Little, Arthur D., Inc., Cambridge, MA, 1983.
- Graedel, T. E. The evolution of industrial ecology. *Env. Sci Technol.* **2000**, *34*, 28A–31A.
- Richards, D. J. *The Industrial Green Game: Implications for Environmental Design and Management*; National Academic Press: Washington, DC, 1997.

9. Frosch, R. A.; Clark, W. C.; Crawford, J.; Sagar, A.; Tschang, F. T.; Webber, A. The industrial ecology of metals: A reconnaissance. *Philos. Trans. R. Soc. Lond. Ser. A-Math. Phys. Eng. Sci.* **1997**, 355, 1335–1347.
10. Singh, H.; Gupta, C. K. Solvent extraction in production and processing of uranium and thorium. *Min. Process. Extractive Metall. Rev.* **2000**, 21, 307–349.
11. Davenport, W. G. Copper 99-Cobre 99 International conference, Phoenix, 1999; pp 55–79.
12. Avecia “Continued evolution of copper SX reagents,” Avecia, Blackley, 2000–2001.
13. Kordosky, G. A. International Solvent Extraction Conference, Cape Town, South Africa, Mar. 17–21, 2002; pp 853–862.
14. Szymanowski, J. *Hydroxyoximes and Copper Hydrometallurgy*. CRC Press: Boca Raton, 1993.
15. Yoon, R. H.; Basilio, C. I. *Publ. Australas. Inst. Min. Metall.* **1993**; 611–617.
16. Persson, I. Adsorption of Ions and Molecules to Solid Surfaces in Connection with Flotation of Sulfide Minerals. *J. Coord. Chem.* **1994**, 32, 261–342.
17. Hodouin, D.; Jamsa-Jounela, S. L.; Carvalho, M. T.; Bergh, L. State of the art and challenges in mineral processing control. *Control Eng. Practice* **2001**, 9, 995–1005.
18. Allan, G. C.; Woodcock, J. T. A review of the flotation of native gold and electrum. *Min. Eng.* **2001**, 14, 931–962.
19. Rao, G. V.; Sastri, S. R. S. Plant scale studies to enhance the recoveries of Cu, Ni & Mo at by-product recovery plant of UCIL, Jaduguda. *Metall. Mater. Proc.* **1998**, 10, 135–143.
20. Nagaraj, D. R. Development of new flotation chemicals. *Trans. Indian Inst. Met.* **1997**, 50, 355–363.
21. Fuerstenau, M. C.; Han, K. N. Flotation of sulfides. *Extr. Metall. Copper, Nickel Cobalt, Proc. Paul E. Queneau Int. Symp.* **1993**, 1, 669–687.
22. Dichmann, T. K.; Finch, J. A. The role of copper ions in sphalerite–pyrite flotation selectivity. *Miner. Eng.* **2001**, 14, 217–225.
23. Fan, X.; Rowson, N. A. The effect of Pb(NO₃)₂ on ilmenite flotation. *Miner. Eng.* **2000**, 13, 205–215.
24. Abdel-Khalek, N. A. Evaluation of flotation strategies for sedimentary phosphates with siliceous and carbonates gangues. *Miner. Eng.* **2000**, 13, 789–793.
25. Barnes, A. M.; Bartle, K. D.; Thibon, V. R. A. A review of zinc dialkyldithiophosphates (ZDDPS): characterisation and role in the lubricating oil. *Tribol. Int.* **2001**, 34, 389–395.
26. Suzuki, I. Microbial leaching of metals from sulfide minerals. *Biotechnol. Adv.* **2001**, 19, 119–132.
27. Bosecker, K. Bioleaching: Metal solubilization by microorganisms. *Fems Microbiol. Rev.* **1997**, 20, 591–604.
28. Torma, A. E. The role of *Thiobacillus ferrooxidans* in hydrometallurgical processes. *Advances in Biochemical Engineering* **1977**, 6, 1–37.
29. MacArthur, J. S.; Forrest, W. *British Patent 14174* Britain, 1888.
30. Deschenes, G.; Lastra, R.; Brown, J. R.; Jin, S.; May, O.; Ghali, E. Effect of lead nitrate on cyanidation of gold ores: Progress on the study of the mechanisms. *Miner. Eng.* **2000**, 13, 1263–1279.
31. Zhang, Y.; Fang, Z. H.; Muhammed, M. On the solution chemistry of cyanidation of gold and silver bearing sulphide ores. A critical evaluation of thermo dynamic calculations. *Hydrometallurgy* **1997**, 46, 251–269.
32. Jeffrey, M. I.; Breuer, P. L. The cyanide leaching of gold in solutions containing sulfide. *Miner. Eng.* **2000**, 13, 1097–1106.
33. Smith, R. M.; Martell, A. E. *Critical Stability Constants, Vol. 4: Inorganic Complexes*, Plenum, New York, N.Y. 1976.
34. Lapidus, G. Unsteady-state model for gold cyanidation on a rotating disk. *Hydrometallurgy* **1995**, 39, 251–263.
35. Jeffrey, M. I.; Ritchie, I. M. The leaching and electro chemistry of gold in high-purity cyanide solutions. *J. Electrochem. Soc.* **2001**, 148, D29–D36.
36. Bowmaker, G. A.; Kennedy, B. J.; Reid, J. C. Crystal structures of AuCN and AgCN and vibrational spectroscopic studies of AuCN, AgCN, and CuCN. *Inorg. Chem.* **1998**, 37, 3968–3974.
37. Tshilombo, A. F.; Sandenbergh, R. F. An electro chemical study of the effect of lead and sulphide ions on the dissolution rate of gold in alkaline cyanide solutions. *Hydrometallurgy* **2001**, 60, 55–67.
38. Kirk, D. W.; Foulkes, F. R.; Graydon, W. F. Gold passivation in aqueous alkaline cyanide. *J. Electrochem. Soc.* **1980**, 127, 1962–1969.
39. Kirk, D. W.; Foulkes, F. R.; Graydon, W. F. The electrochemical formation of gold(I) hydroxide on gold in aqueous potassium hydroxide. *J. Electrochem. Soc.* **1980**, 127, 1069–1076.
40. Kameda, M. Fundamental studies on solution of gold in cyanide solutions. III. Effects of alkalis lead acetate and some impurities contained in foul cyanide solutions. *Sci. Repts. Res. Insts. Tohoku Univ.* **1949**, 1, 435–444.
41. Ficeriova, J.; Balaz, P.; Boldizarova, E.; Jelen, S. Thiosulfate leaching of gold from a mechanically activated Cu-Pb-Zn concentrate. *Hydrometallurgy* **2002**, 67, 37–43.
42. Breuer, P. L.; Jeffrey, M. I. Thiosulfate leaching kinetics of gold in the presence of copper and ammonia. *Miner. Eng.* **2000**, 13, 1071–1081.
43. Aylmore, M. G.; Muir, D. M. Thiosulfate leaching of gold—A review. *Miner. Eng.* **2001**, 14, 135–174.
44. Molleman, E.; Dreisinger, D. The treatment of copper–gold ores by ammonium thiosulfate leaching. *Hydrometallurgy* **2002**, 66, 1–21.
45. Chu, C. K.; Breuer, P. L.; Jeffrey, M. I. The impact of thiosulfate oxidation products on the oxidation of gold in ammonia thiosulfate solutions. *Miner. Eng.* **2003**, 16, 265–271.
46. Schmitz, P. A.; Duyvesteyn, S.; Johnson, W. P.; Enloe, L.; McMullen, J. Ammoniacal thiosulfate and sodium cyanide leaching of preg-robbed Goldstrike ore carbonaceous matter. *Hydrometallurgy* **2001**, 60, 25–40.
47. Abbruzzese, C.; Fornari, P.; Massidda, R.; Veglio, F. Thiosulfate leaching for gold hydrometallurgy. *Hydrometallurgy* **1995**, 39, 265–276.
48. Breuer, P. L.; Jeffrey, M. I. Copper catalysed oxidation of thiosulfate by oxygen in gold leach solutions. *Miner. Eng.* **2003**, 16, 21–30.
49. Bailar, J. C. *et al.* editors *Comprehensive Inorganic Chemistry*, Vol. 5, Pergamon, Elmsford, N.Y. 1973.
50. Pedraza, A. M.; Villegas, I.; Freund, P. L.; Chornik, B. Electro oxidation of thiosulfate ion on gold. Study by means of cyclic voltammetry and Auger electron spectroscopy. *J. Electroanal. Chem. Inter. Electrochem.* **1988**, 250, 443–449.
51. Tao, J.; Jin, C.; Shi, X. Electrochemistry and mechanism of leaching gold with ammoniacal thiosulfate. *Publ. Australas. Inst. Min. and Metall.* **1993**, 3/93, 1141–1146.

52. Chen, J.; Deng, T.; Zhu, G.; Zhao, J. Leaching and recovery of gold in thiosulfate-based system. A research summary at ICM. *Trans. Indian Inst. Met.* **1996**, *49*, 841–849.
53. Byerley, J. J.; Fouda, S. A.; Rempel, G. L. Oxidation of thiosulfate in aqueous ammonia by copper(II) oxygen complexes. *Inorg. Nucl. Chem. Lett.* **1973**, *9*, 879–883.
54. Zipperian, D.; Raghavan, S.; Wilson, J. P. Gold and silver extraction by ammoniacal thiosulfate leaching from a rhyolite ore. *Hydrometallurgy* **1988**, *19*, 361–375.
55. Wan, R. Y. Importance of solution chemistry for thiosulfate leaching of gold. *Publ. Australas. Inst. Min. and Metall.* **1997**, *2/97*, 159–162.
56. Gong, Q.; Hu, J.; Cao, C. Kinetics of gold leaching from sulfide gold concentrates with thiosulfate solution. *Trans. Nonferrous Met. Soc. China* **1993**, *3*, 30–36.
57. Murthy, D. S. R.; Kumar, V.; Rao, K. V. Extraction of gold from an Indian low-grade refractory gold ore through physical beneficiation and thiourea leaching. *Hydrometallurgy* **2003**, *68*, 125–130.
58. Tremblay, L.; Deschenes, G.; Ghali, E.; McMullen, J.; Lanouette, M. Gold recovery from a sulfide bearing gold ore by percolation leaching with thiourea. *Int. J. Miner. Process.* **1996**, *48*, 225–244.
59. Ubaldini, S.; Fornari, P.; Massidda, R.; Abbruzzese, C. An innovative thiourea gold leaching process. *Hydrometallurgy* **1998**, *48*, 113–124.
60. Urbanski, T. S.; Fornari, P.; Abbruzzese, C. Gold electrowinning from aqueous-alcoholic thiourea solutions. *Hydrometallurgy* **2000**, *55*, 137–152.
61. Orgul, S.; Atalay, U. Reaction chemistry of gold leaching in thiourea solution for a Turkish gold ore. *Hydrometallurgy* **2002**, *67*, 71–77.
62. Gonen, N. Leaching of finely disseminated gold ore with cyanide and thiourea solutions. *Hydrometallurgy* **2003**, *69*, 169–176.
63. Kai, T.; Hagiwara, T.; Haseba, H.; Takahashi, T. Reduction of thiourea consumption in gold extraction by acid thiourea solutions. *Ind. Eng. Chem. Res.* **1997**, *36*, 2757–2759.
64. Almeida, M. F.; Amarante, M. A. Leaching of a silver-bearing sulfide by-product with cyanide thiourea and chloride solutions. *Miner. Eng.* **1995**, *8*, 257–271.
65. Murthy, D. S. R.; Prasad, P. M. Leaching of gold and silver from Miller Process dress through non-cyanide leachants. *Hydrometallurgy* **1996**, *42*, 27–33.
66. Lacoste-Bouchet, P.; Deschenes, G.; Ghali, E. Thiourea leaching of a copper–gold ore using statistical design. *Hydrometallurgy* **1998**, *47*, 189–203.
67. Sankaran, R. N.; Yadava, R. S.; Sen, D. B.; Kulshrestha, S. C.; Mohanty, K. B.; Singh, J. Leachable U and Au in an Indian schistose quartzite. *Hydrometallurgy* **1996**, *43*, 387–389.
68. Groenewald, T. The dissolution of gold in acidic solutions of thiourea. *Hydrometallurgy* **1976**, *1*, 277–290.
69. Piga, L.; Abbruzzese, C.; Fornari, P.; Massidda, R.; Ubaldini, S. Thiourea leaching of a siliceous Au–Ag bearing ore using a four-factor composite design. *Proceedings of the International Mineral Processing Congress, 19th, San Francisco* **1995**, *4*, 43–46.
70. Pangum, L. S.; Browner, R. E. Pressure chloride leaching of a refractory gold ore. *Miner. Eng.* **1996**, *9*, 547–556.
71. Donmez, B.; Ekinici, Z.; Celik, C.; Colak, S. Optimization of the chlorination of gold in decopperized anodes lime in aqueous medium. *Hydrometallurgy* **1999**, *52*, 81–90.
72. Puvvada, G. V. K.; Murthy, D. S. R. Selective precious metals leaching from a chalcopyrite concentrate using chloride/hypochlorite media. *Hydrometallurgy* **2000**, *58*, 185–191.
73. Vinals, J.; Nunez, C.; Herrerros, O. Kinetics of the aqueous chlorination of gold in suspended particles. *Hydrometallurgy* **1995**, *38*, 125–148.
74. Hait, J.; Jana, R. K.; Kumar, V.; Sanyal, S. K. Some studies on sulfuric acid leaching of anodes lime with additives. *Ind. Eng. Chem. Res.* **2002**, *41*, 6593–6599.
75. Carlson, E. T.; Simons, C. S. Acid leaching of Moa Bay's nickel. *J. Metals* **1960**, *12*, 206–213.
76. Chalkley, M. E.; Toirac, I. L. The acid pressure leach process for nickel and cobalt laterite. Part I: review of operations at Moa. *Hydrometallurgy and Refining of Nickel and Cobalt, Annual Hydrometallurgy Meeting of CIM, 27th, Sudbury, Ont., Aug. 17–20, 1997*, 341–353.
77. Das, G. K.; Acharya, S.; Anand, S.; Das, R. P. Acid pressure leaching of nickel-containing chromite over burden in the presence of additives. *Hydrometallurgy* **1995**, *39*, 117–128.
78. Roy, T. K. New process for recovering Ni and Co from lateritic ores. *Ind. Eng. Chem.* **1961**, *53*, 559–566.
79. Benguerel, E.; Demopoulos, G. P. Formation and extraction of Rh–Sn–Cl complexes with an alkylated 8-hydroxyquinoline. *J. Chem. Technol. Biotechnol.* **1998**, *72*, 183–189.
80. Wilson, F. The Moa Bay Port Nickel project. *Mining Eng.* **1958**, *10*, 563–565.
81. Johnson, J. A.; McDonald, R. G.; Whittington, B. I.; Quan, L. P.; Muir, D. M. Process water salinity effects in the pressure leaching of Cawse nickel laterite ores. *Chloride Metallurgy 2002: Practice and Theory of Chloride/Metal Interaction, Annual Hydrometallurgy Meeting, 32nd, Montreal, QC, Canada, Oct. 19–23, 2002*, *1*, 339–354.
82. Georgiou, D.; Papangelakis, V. G. Sulfuric acid pressure leaching of alimonitic laterite: chemistry and kinetics. *Hydrometallurgy* **1998**, *49*, 23–46.
83. Krause, E.; Singhal, A.; Blakey, B. C.; Papangelakis, V. G.; Georgiou, D. Sulfuric acid leaching of nickeliferous laterites. *Hydrometallurgy and Refining of Nickel and Cobalt, Annual Hydrometallurgy Meeting of CIM, 27th, Sudbury, Ont., Aug. 17–20, 1997*, 441–458.
84. Mayze, R. Nickel laterite processing in Western Australia. *Copper, Cobalt, Nickel and Zinc Recovery, Conference, Victoria Falls, Zimbabwe, July 16–18, 2001*, F1–F12.
85. Papangelakis, V. G.; Georgiou, D.; Rubisov, D. H. Control of iron during the sulfuric acid pressure leaching of limonitic laterites. *Iron Control and Disposal, Proceedings of the International Symposium on Iron Control in Hydrometallurgy, 2nd, Ottawa, Oct. 20–23, 1996*, 263–274.
86. Rubisov, D. H.; Papangelakis, V. G. Sulfuric acid pressure leaching of laterites—prediction of metal solubilities and speciation analysis at temperature. *EPD Congress 1999, Proceedings of Sessions and Symposia held at the TMS Annual Meeting, San Diego, Feb. 28–Mar. 4, 1999*, 535–546.
87. Rubisov, D. H.; Papangelakis, V. G. Sulphuric acid pressure leaching of laterites—a comprehensive model of a continuous autoclave. *Hydrometallurgy* **2000**, *58*, 89–101.

88. Rubisov, D. H.; Krowinkel, J. M.; Papangelakis, V. G. Sulphuric acid pressure leaching of laterites—universal kinetics of nickel dissolution for limonites and limonitic/saprolitic blends. *Hydrometallurgy* **2000**, *58*, 1–11.
89. Ritcey, G. M. Process options using solvent extraction for the processing of laterites. *Publ. Australas. Inst. Min. and Metall.* **1996**, *6/96*, 251–258.
90. Bruckard, W. J.; Sparrow, G. J.; Woodcock, J. T. Gold and silver extraction from Hellyer lead-zinc flotation middlings using pressure oxidation and thiourea leaching. *Hydrometallurgy* **1993**, *33*, 17–41.
91. Fraser, K. S.; Walton, R. H.; Wells, J. A. Processing of refractory gold ores. *Miner. Eng.* **1991**, *4*, 1029–1041.
92. Harvey, T. J.; Yen, W. T.; Paterson, J. G. Selective zinc extraction from complex copper-zinc sulfide concentrates by pressure oxidation. *Miner. Eng.* **1992**, *5*, 975–992.
93. Harvey, T. J.; Yen, W. T.; Paterson, J. G. A kinetic investigation into the pressure oxidation of sphalerite from a complex concentrate. *Miner. Eng.* **1993**, *6*, 949–967.
94. Holtum, D. A.; Murray, D. M. Bacterial heap leaching of refractory gold sulfide ores. *Miner. Eng.* **1994**, *7*, 619–631.
95. Labrooy, S. R.; Linge, H. G.; Walker, G. S. Review of gold extraction from ores. *Miner. Eng.* **1994**, *7*, 1213–1241.
96. Nyavor, K.; Egiebor, N. O. Application of pressure oxidation pretreatment to a double-refractory gold concentrate. *CIM Bull.* **1992**, *85*, 84–96.
97. Ozberk, E.; Jankola, W. A.; Vecchiarelli, M.; Krysa, B. D. Commercial operations of the Sherritt zinc pressure leach process. *Hydrometallurgy* **1995**, *39*, 49–52.
98. Kyle, J. H. Pressure acid leaching of Australian nickel/cobalt laterites. *Publ. Australas. Inst. Min. and Metall.* **1996**, *6/96*, 245–250.
99. Kobayashi, M.; Dutrizac, J. E.; Toguri, J. M. A critical review of the ferric chloride leaching of galena. *Can. Metall. Q.* **1990**, *29*, 201–211.
100. Dutrizac, J. E. The leaching of sulfide minerals in chloride media. *Hydrometallurgy* **1992**, *29*, 1–45.
101. Stensholt, E. O.; Dotterud, O. M.; Henriksen, E. E.; Ramsdal, P. O.; Stalesen, F.; Thune, E. Development and practice of the Falconbridge chlorine leach process. *CIM Bull.* **2001**, *94*, 101–104.
102. Stensholt, E. O.; Zachariassen, H.; Lund, J. H.; Thornhill, P. G. Recent improvements in the Falconbridge nickel refinery. *Extr. Metall. Nickel Cobalt, Proc. Symp. 117th TMS Annu. Meet.* **1988**, 403–412.
103. Thornhill, P. G.; Wigstol, E.; Van Weert, G. Falconbridge matte leach process. *J. Metals* **1971**, *23*, 13–18.
104. Lenoir, P.; Van Peteghem, A.; Feneau, C. Extractive metallurgy of cobalt. *Proc. Int. Conf. Cobalt: Metall. Uses* **1981**, *1*, 51–62.
105. Mukherjee, A. D.; Sen, R.; Mondal, A. Freibergite from polymetallic sulphide deposits of the Delhi–Aravalli belt Rajasthan. *J. Geol. Soc. India* **1998**, *52*, 543–547.
106. Jana, R. K.; Pandey, B. D. Premchand Ammoniacal leaching of roast reduced deep-sea manganese nodules. *Hydrometallurgy* **1999**, *53*, 45–56.
107. Pandey, B. D.; Bagchi, D.; Kumar, V. Co extraction—selective stripping for the recovery of nickel and copper from the leach liquor of ocean nodules. *Can. J. Chem. Eng.* **1994**, *72*, 631–636.
108. Duyvesteyn, W. P. C.; Sabacky, B. J. Ammonia Leaching Process for Escondida Copper Concentrates (Reprinted from Extractive Metallurgy of Copper, Nickel, and Cobalt. Vol. 1, 1993). *Trans. Inst. Min. Metall. Sect. C-Miner. Process. Extr. Metall.* **1995**, *104*, C125–C140.
109. Duyvesteyn, W. P. C.; Sabacky, B. J. The Escondida process for copper concentrates. *Extr. Metall. Copper, Nickel Cobalt, Proc. Paul E. Queneau Int. Symp.* **1993**, *1*, 881–910.
110. Duyvesteyn, W. P. C.; Sabacky, B. J. Ammonia leaching process for Escondida copper concentrates. *Transactions of the Institution of Mining and Metallurgy, Section C: Mineral Processing and Extractive Metallurgy* **1995**, *104*, C125–C140.
111. Poole, C.; Beeson, S. A. Separation of KCl values from Canadian sylvinitic and carnallite potash ores by selective flocculation. *CIM Bull.* **2000**, *93*, 81–85.
112. Baes, C. F., Jr.; Moyer, B. A. Solubility parameters and the distribution of ions to nonaqueous solvents. *J. Phys. Chem. B* **1997**, *101*, 6566–6574.
113. Kholkin, A. I.; Belova, V. V.; Pashkov, G. L.; Fleitlikh, I. Y.; Sergeev, V. V. Solvent binary extraction. *J. Mol. Liq.* **1999**, *82*, 131–146.
114. Kirkovits, G. J.; Shriver, J. A.; Gale, P. A.; Sessler, J. L. Synthetic ditopic receptors. *J. Incl. Phenom. Macrocycl. Chem.* **2001**, *41*, 69–75.
115. Coxall, R. A.; Lindoy, L. F.; Miller, H. A.; Parkin, A.; Parsons, S.; Tasker, P. A.; White, D. J. Solvent extraction of metal sulfates by zwitterionic forms of ditopic ligands. *Dalton* **2003**, 55–64.
116. Aldred, R.; Johnston, R.; Levin, D.; Neilan, J. Magnesium-mediated ortho-specific formylation and formaldoximation of phenols. *J. Chem. Soc., Perkin Trans. 1* **1994**, 1823–1831.
117. Smith, A. G.; Tasker, P. A.; White, D. J. *Coord. Chem. Rev.* **2003**, *241*, 61–85.
118. Szymanowski, J. Physicochemical modification of extractants. *Crit. Rev. Anal. Chem.* **1995**, *25*, 143–194.
119. Szymanowski, J.; Mittal, B. K. L.; Lindman, B., Eds., *Surfactants in Solution*, Plenum Press: New York, **1989**.
120. Russell, J. H.; Rickel, R. L. Modeling copper extraction from acidic solutions using P5100, PT5050, and LIX84. *Solvent Extr. Ion Exch.* **1990**, *8*, 855–873.
121. Hultgren, V. M.; Atkinson, I. M.; Beddoes, R. L.; Collison, D.; Garner, C. D.; Helliwell, M.; Lindoy, L. F.; Tasker, P. A. Formation of folded complexes retaining intramolecular H-bonding in the extraction of nickel(II) by phenolic oxime and aliphatic diamine ligands. *Chem. Commun.* **2001**, 573–574.
122. Zhu, T. A structure parameter characterizing the steric effect of organophosphorous acid extractants. *International Solvent Extraction Conference, Cape Town, South Africa, Mar. 17–21, 2002*, 203–207.
123. Irving, H. M.; Williams, R. J. P. Stability of transition metal complexes. *J. Chem. Soc.* **1953**, 3192–3210.
124. Alguacil, F. J.; Rodriguez, F. Separation processes in rare earths. *Rev. Metal.* **1997**, *33*, 187–196.
125. Yamada, H.; Tanaka, M. Solvent extraction of metal carboxylates. *Adv. Inorg. Chem. Radiochem.* **1985**, *29*, 143–68.
126. Eyal, A. M.; Kogan, L.; Bressler, E. Extraction of metal salts by mixtures of water-immiscible amines and organic acids (acid-base couple extractants) .2. Theoretical treatment and analysis. *Ind. Eng. Chem. Res.* **1994**, *33*, 1076–1085.
127. Eyal, A. M.; Baniel, A. M. Recovery and concentration of strong mineral acids from dilute solutions through LLX. I: Review of parameters for adjusting extractant properties and analysis of process options. *Solvent Extr. Ion Exch.* **1991**, *9*, 195–210.
128. Gale, P. A. Anion receptor chemistry: highlights from 1999. *Coord. Chem. Rev.* **2001**, *213*, 79–128.

129. Gale, P. A. Anion coordination and anion-directed assembly: highlights from 1997 and 1998. *Coord. Chem. Rev.* **2000**, *199*, 181–233.
130. Christoffels, L. A. J.; de Jong, F.; Reinhoudt, D. N.; Sivelli, S.; Gazzola, L.; Casnati, A.; Ungaro, R. Facilitated transport of hydrophilic salts by mixtures of anion and cation carriers and by ditopic carriers. *J. Am. Chem. Soc.* **1999**, *121*, 10142–10151.
131. Lin, W. L.; Mattison, P. L.; Virnig, M. J. In *Brit. UK Pat. Appl.*; (Henkel Corp., Japan). Gb, 1987.
132. Virnig, M. J.; Mackenzie, J. M. W.; Adamson, C. The use of guanidine-based extractants for the recovery of gold. *Symposium Series—South African Institute of Mining and Metallurgy* **1996**, *S16*, 151–156.
133. Pabby, A. K.; Melgosa, A.; Haddad, R.; Sastre, A. M. Hollow fiber membrane-based non-dispersive extraction of silver(I) from alkaline cyanide media using LIX 79. *International Solvent Extraction Conference, Cape Town, South Africa, Mar. 17–21, 2002*, 699–705.
134. Pai, S. A.; Lohithakshan, K. V.; Mithapara, P. D.; Aggarwal, S. K. Solvent extraction of uranium(VI) plutonium(VI) and americium(III) with HTTA/HPMBP using mono- and bi-functional neutral donors: Synergism and thermodynamics. *J. Radioanal. Nucl. Chem.* **2000**, *245*, 623–628.
135. Pai, S. A.; Lohithakshan, K. V.; Mithapara, P. D.; Aggarwal, S. K. Thermodynamics of synergistic extraction of americium(III) with HTTA using DHDECMP (bi-functional) and TBP (mono-functional). *Radiochim. Acta* **1998**, *81*, 189–193.
136. Biswas, A. K.; Davenport, W. G. *International Series in Materials Science and Technology, Vol. 20: Extractive Metallurgy of Copper*, Pergamon, Oxford, Engl. 1976.
137. Cramer, K.; Morrison, J.; Moore, T.; Kentish, S. Using Avecia's Minchem copper solvent extraction process modelling program for education. *EPD Congress 2002 and Fundamentals of Advanced Materials for Energy Conversion, Proceedings of Sessions and Symposia held during the TMS Annual Meeting, Seattle, WA, United States, Feb. 17–21, 2002*, 715–721.
138. Dalton, R. F.; Severs, K. J. Advances in solvent extraction for copper by optimized use of modifiers. *Min. Lat. Am., Pap. Min. Lat. Am./Min. Latinoam. Conf.* **1986**, 67–75.
139. Cupertino, D. C.; Charlton, M. H.; Buttar, D.; Swart, R. M.; Maes, C. J. A study of copper/iron separation in modern solvent extraction plants. *Proceedings of the COPPER 99-COBRE 99 International Conference, 4th, Phoenix, Oct. 10–13, 1999*, *4*, 263–276.
140. Spasic, A. M.; Djokovic, N. N.; Babic, M. D.; Marinko, M. M.; Jovanovic, G. N. Performance of demulsions: Entrainment problems in solvent extraction. *Chem. Eng. Sci.* **1997**, *52*, 657–675.
141. Gula, M. J.; Dreisinger, D. B.; Montijo, J. C.; Young, S. K. In *Iron Control and Disposal*; Dutrizac, J. E., Harris, G. B., Ed.; Canadian Institute of Mining, Metallurgy and Petroleum: Montreal, 1996.
142. Seward, G. W.; Dalton, R. F. *Reagents in the Mineral Industry*; IMM: London, 1984.
143. Sernetz, F. G.; Mulhaupt, R.; Fokken, S.; Okuda, J. Copolymerization of ethene with styrene using methylaluminoxane-activated bis(phenolate) complexes. *Macromolecules* **1997**, *30*, 1562–1569.
144. Sastre, A. M.; Alguacil, F. J. Co-extraction and selective stripping of copper(II) and molybdenum(VI) using LIX622. *Chem. Eng. J.* **2001**, *81*, 109–112.
145. Liu, S.; Zhu, H.; Zubieta, J. Reactions of polyoxomolybdates with oximes. The crystal and molecular structures of $[(C_4H_9)_4N]_2[Mo_2O_5\{C_6H_4(O)CHNO\}_2] \cdot CH_2Cl_2$ and $[(C_4H_9)_4N]_2[Mo_2O_4\{C_6H_5CH(O)C(NO)C_6H_4\}_2]$. *Polyhedron* **1989**, *8*, 2473–2480.
146. Sole, K. C. Solvent extraction of copper from high concentration pressure acid leach liquors. *International Solvent Extraction Conference, Cape Town, South Africa, Mar. 17–21, 2002*, 1033–1038.
147. Tasker, P. A.; White, D. J. In *PCT Int. Appl.*; (The University Court of the University of Edinburgh, UK). Wo, 2000.
148. Dalton, R. F.; Diaz, G.; Price, R.; Zunkel, A. D. The cuprex metal extraction process—recovering copper from sulfide ores. *JOM-J. Miner. Met. Mater. Soc.* **1991**, *43*, 51–56.
149. Szymanowski, J. Copper hydrometallurgy and extraction from chloride media. *J. Radioanal. Nucl. Chem.-Artic.* **1996**, *208*, 183–194.
150. Cote, G.; Jakubiak, A.; Bauer, D.; Szymanowski, J.; Mokili, B.; Poitrenaud, C. Modeling of extraction equilibrium for copper(II) extraction by pyridinecarboxylic acid esters from concentrated chloride solutions at constant water activity and constant total concentration of ionic or molecular species dissolved in the aqueous solution. *Solvent Extr. Ion Exch.* **1994**, *12*, 99–120.
151. Soldenhoff, K. H. Solvent extraction of copper(II) from chloride solutions by some pyridine carboxylate esters. *Solvent Extr. Ion Exch.* **1987**, *5*, 833–851.
152. Dalton, R. F.; Price, R.; Hermana, E.; Hoffmann, B. In *Separation Process in Hydrometallurgy*; Davies, G. A., Ed.; Ellis Horwood Ltd: Chichester, 1987.
153. Jakubiak, A.; Szymanowski, J.; Cote, G. Extraction of copper(II) from chloride solutions by pyridinedicarboxylates. *Value Adding through Solvent Extraction, [Papers presented at ISEC'96], Melbourne, Mar. 19–23, 1996*, *1*, 517–522.
154. Purcell, K. F.; Kotz, J. C. *Inorganic Chemistry*; W. B. Saunders Company, 1977.
155. Bart, H. J.; Dalton, R. F.; Hillisch, W.; Hughes, M. A.; Slater, M. J. ACORGA CLX50—a novel reagent for solvent extraction of copper—a kinetics study. *Value Adding through Solvent Extraction, [Papers presented at ISEC'96], Melbourne, Mar. 19–23, 1996*, *2*, 845–850.
156. Meadows, N. E.; Valenti, M. The BHAS copper–lead matte treatment plant. *Publ. Australas. Inst. Min. and Metall.* **1989**, *6/89*, 153–157.
157. Kyuchoukov, G.; Szymanowski, J. Extraction of copper(II) and zinc(II) from chloride media with mixed extractants. *J. Radioanal. Nucl. Chem.* **2000**, *246*, 675–682.
158. Hataye, I.; Suganuma, H.; Shimizu, I. Mutual separation of Po-210 Bi-210 and Pb-210 with solvent extraction using copper dithizonate- CCl_4 and Dithizone- CCl_4 solutions. *J. Radioanal. Nucl. Chem.* **1991**, *148*, 101–105.
159. Fletcher, A. W.; Sudderth, R. B.; Olafson, S. M. Combining sulfate electrowinning with chloride leaching. *JOM-J. Miner. Met. Mater. Soc.* **1991**, *43*, 56–59.
160. Kyuchoukov, G.; Mishonov, I. On the extraction of copper and zinc from chloride media with mixed extractant. *Solvent Extr. Res. Dev. Jpn.* **1999**, *6*, 1–11.

161. Kyuchoukov, G.; Mihaylov, Y. A novel method for recovery of copper from hydrochloric acid solutions. *Hydrometallurgy* **1991**, *27*, 361–369.
162. Kyuchoukov, G.; Mishonov, I. A new extractant mixture for recovery of copper from hydrochloric etching solution. *Solvent Extr. Ion Exch.* **1993**, *11*, 555–567.
163. Mishonov, I.; Kyuchoukov, G. Separation of copper and zinc during their transfer from hydrochloric acid to sulfuric acid medium using a mixed extractant. *Hydrometallurgy* **1996**, *41*, 89–98.
164. Borowiak-Resterna, A. Extraction of copper(II) from acid chloride solutions by N-dodecyl- and N,N-dihexylpyridinecarboxamides. *Solvent Extr. Ion Exch.* **1999**, *17*, 133–148.
165. Tecnicas Reunidas, S. A. Hydrometallurgy and Electrochemistry, Technological Package. R&D Division, 1999.
166. Herreros, O.; Quiroz, R.; Manzano, E.; Bou, C.; Vinals, J. Copper extraction from reverberatory and flash furnace slags by chlorine leaching. *Hydrometallurgy* **1998**, *49*, 87–101.
167. Bouvier, C.; Cote, G.; Cierpiszewski, R.; Szymanowski, J. Influence of salting-out effects temperature and the chemical structure of the extractant on the rate of copper(II) extraction from chloride media with dialkyl pyridine dicarboxylates. *Solvent Extr. Ion Exch.* **1998**, *16*, 1465–1492.
168. Kordosky, G. A.; Virnig, M. J.; Mattison, P. Beta-diketone copper extractants: structure and stability. *International Solvent Extraction Conference, Cape Town, South Africa, Mar. 17–21, 2002*, 360–365.
169. Sudderth, R. B. Randol Copper Hydromet Roundtable, 2000; pp 203–214.
170. Virnig, M. J.; Kordosky, G. A. In *PCT Int. Appl.*; (Henkel Corporation, USA). Wo, 1997.
171. Mickler, W.; Uhlemann, E. Liquid-Liquid extraction of copper from ammoniacal solution with 4-acylpyrazol-5-ones. *Sep. Sci. Technol.* **1993**, *28*, 1913–1921.
172. Mickler, W.; Reich, A.; Uhlemann, E. Extraction of iron(II) and iron(III) with 4-acyl-5-pyrazolones in comparison with long-chain 1-phenyl-1,3-(cyclo)alkanediones. *Sep. Sci. Technol.* **1998**, *33*, 425–435.
173. Campbell, J.; Cupertino, D. C.; Emeleus, L. C.; Harris, S. G.; Owens, S.; Parsons, S.; Swart, R. M.; Tasker, P. A.; Tinkler, O. S.; White, D. J. Diazopyrazolones as solvent extractants for copper from ammonia leach solutions. *International Solvent Extraction Conference, Cape Town, South Africa, Mar. 17–21, 2002*, 347–352.
174. Emeleus, L. C.; Cupertino, D. C.; Harris, S. G.; Owens, S.; Parsons, S.; Swart, R. M.; Tasker, P. A.; White, D. J. Diazopyrazolones as weak solvent extractants for copper from ammonia leach solutions. *J. Chem. Soc., Dalton Trans.* **2001**, 1239–1245.
175. Parija, C.; Sarma, P. Separation of nickel and copper from ammoniacal solutions through co-extraction and selective stripping using LIX84 as the extractant. *Hydrometallurgy* **2000**, *54*, 195–204.
176. Queneau, P. B.; Gruber, R. W. The U.S. production of copper chemicals from secondary and byproduct sources. *JOM-J. Miner. Met. Mater. Soc.* **1997**, *49*, 34–37, 49.
177. Mahmoud, M. H. H.; Barakat, M. A. Utilization of spent copper-pickle liquor for recovery of metal values. *Renew. Energy* **2001**, *23*, 651–662.
178. Barakat, M. A.; Mahmoud, M. H. H. Recovery of metal values from car-radiator scrap. *Sep. Sci. Technol.* **2000**, *35*, 2359–2374.
179. Kehl, R.; Schwab, W. In *Ger. Offen.*; (Henkel Kгаа, Germany). De, 1996.
180. Rabah, M. A. Recovery of iron and copper from spent HCl used to clean up dirty car radiators. *Hydrometallurgy* **2000**, *56*, 75–92.
181. Palencia Perez, I.; Dutrizac, J. E. The effect of the iron content of sphalerite on its rate of dissolution in ferric sulfate and ferric chloride media. *Hydrometallurgy* **1991**, *26*, 211–232.
182. Habashi, F. *Handbook of Extractive Metallurgy*; Wiley-VCH Verlag GMBH: Weinheim, 1997.
183. Peacey, J. G.; Hancock, P. J. Review of pyrometallurgical processes for treating iron residues from electrolytic zinc plants. *Iron Control and Disposal, Proceedings of the International Symposium on Iron Control in Hydrometallurgy, 2nd, Ottawa, Oct. 20–23, 1996*, 17–35.
184. Chen, S.; Li, X.; Huang, H. Winning germanium from zinc sulfate solution by solvent extraction. *Hydrometallurgy, Proceedings of the International Conference, 3rd, Kunming, China, Nov. 3–5, 1998*, 509–512.
185. Rosato, L. I.; Agnew, M. J. Iron disposal options at Canadian electrolytic zinc. *Iron Control and Disposal, Proceedings of the International Symposium on Iron Control in Hydrometallurgy, 2nd, Ottawa, Oct. 20–23, 1996*, 77–89.
186. Ritcey, G. M.; Ashbrook, A. W. *Process Metallurgy, Vol. 1: Solvent Extraction: Principles and Applications to Process Metallurgy, Pt. 2*, Elsevier, Amsterdam, Netherlands, 1979.
187. Cote, G. Hydrometallurgy of strategic metals. *Solvent Extr. Ion Exch.* **2000**, *18*, 703–727.
188. Harbuck, D. D.; Judd, J. C.; Behunin, D. V. Germanium solvent extraction from sulfuric acid solutions (and co-extraction of germanium and gallium). *Solvent Extr. Ion Exch.* **1991**, *9*, 383–401.
189. Penner, L. R.; Russell, J. H.; Campbell, M. J. Solvent Extraction in Process Industries. Proc. ISEC'93, London, 1993; p 1391.
190. Martin, D.; Diaz, G.; Garcia, M. A.; Sanchez, F. Extending zinc production possibilities through solvent extraction. *International Solvent Extraction Conference, Cape Town, South Africa, Mar. 17–21, 2002*, 1045–1051.
191. Martin, D.; Falgueras, J.; Garcia, M. A.; Spanish Pat.: Spain, 1997.
192. Garcia, M. A.; Mejias, A.; Martin, D.; Diaz, G. Upcoming zinc mine projects: the key for success is ZINCEX solvent extraction. *Lead-Zinc 2000, Proceedings of the Lead-Zinc 2000 Symposium, Pittsburgh, PA, United States, Oct. 22–25, 2000*, 751–761.
193. Martin, D.; Garcia, M. A.; Diaz, G. International Symposium on Recycling and Reuse of Used Tyres, Dundee, UK, 2001; pp 141–148.
194. Sole, K. C.; Cole, P. M. Purification of nickel by solvent extraction. *Ion Exch. Solvent Extr.* **2002**, *15*, 143–195.
195. Cole, P. M.; Sole, K. C. Solvent extraction in the primary and secondary processing of zinc. *International Solvent Extraction Conference, Cape Town, South Africa, Mar. 17–21, 2002*, 863–870.
196. Cupertino, D. C.; Dalton, R. F.; Seward, G. W.; Townson, B.; Harris, G. B.; Tasker, P. A. Iron control in zinc circuits; the role of highly selective zinc extractants. *Iron Control and Disposal, Proceedings of the International Symposium on Iron Control in Hydrometallurgy, 2nd, Ottawa, Oct. 20–23, 1996*, 369–379.
197. Dalton, R. F.; Burgess, A. In *Solvent extraction in the process industries*; Logsdail, D. H., Slater, M. J., Eds., Elsevier Applied Science: London 1993; Vol. 3.

198. Kyuchoukov, G.; Jakubiak, A.; Szymanowski, J.; Cote, G. Extraction of zinc(II) from highly concentrated chloride solutions by KELEX 100. *Solvent Extr. Res. Dev. Jpn.* **1998**, *5*, 172–188.
199. Jakubiak, A.; Cote, G.; Szymanowski, J. Extraction of zinc(II) from chloride media with a mixture of ACORGA ZNX50 and LIX54. *Solvent Extr. Res. Dev. Jpn.* **1999**, *6*, 24–32.
200. Sudderth, R. B.; Fletcher, A. W.; Olafson, S. M. *PCT Int. Appl.*; (Henkel Corp., USA) Wo, 1991.
201. Rubisov, D. H.; Papangelakis, V. G. The effect of acidity “at temperature” on the morphology of precipitates and scale during sulphuric acid pressure leaching of laterites. *CIM Bull.* **2000**, *93*, 131–137.
202. Xia, D. K.; Pickles, C. A. Caustic roasting and leaching of electric arc furnace dust. *Can. Metall. Q.* **1999**, *38*, 175–186.
203. McElroy, R. O.; Murray, W. Developments in the Terra Gaia process for the treatment of EAF dust. *Iron Control and Disposal, Proceedings of the International Symposium on Iron Control in Hydrometallurgy, 2nd, Ottawa, Oct. 20–23, 1996*, 505–517.
204. *Iron Control and Disposal, Proceedings of the International Symposium on Iron Control in Hydrometallurgy, 2nd, Ottawa, Oct. 20–23, 1996*.
205. Delmas, F.; Nogueira, C. A.; Ehle, M.; Oppenlander, K.; Koch, R. O.; Lemmert, F.; Plazanet, C.; Weigel, V.; Ujma, K. H.; Ketels, E. In *Iron Control and Disposal*; Dutrizac, J. E., Harris, G. B., Eds.; Canadian Institute of Mining, Metallurgy and Petroleum: Montreal, 1996.
206. Tozawa, K. Recent Trend of Nickel Extractive Metallurgy. *Tetsu To Hagane-J. Iron Steel Inst. Jpn.* **1993**, *79*, 1–11.
207. Preston, J. S.; du Preez, A. C. Separation of nickel and calcium by solvent extraction using mixtures of carboxylic acids and alkylpyridines. *Hydrometallurgy* **2000**, *58*, 239–250.
208. Preston, J. S.; du Preez, A. C. Solvent extraction of nickel from acidic solutions using synergistic mixtures containing pyridinecarboxylate esters. 3. Systems based on arylsulphonic acids. *J. Chem. Technol. Biotechnol.* **1998**, *71*, 43–50.
209. Preston, J. S.; duPreez, A. C. The solvent extraction of nickel from acidic solutions using synergistic mixtures containing pyridinecarboxylate esters. 2. Systems based on alkylsalicylic acids. *J. Chem. Technol. Biotechnol.* **1996**, *66*, 293–299.
210. Preston, J. S.; duPreez, A. C. Solvent extraction of nickel from acidic solutions using synergistic mixtures containing pyridinecarboxylate esters. 1. Systems based on organophosphorus acids. *J. Chem. Technol. Biotechnol.* **1996**, *66*, 86–94.
211. Preston, J. S.; Dupreez, A. C. Synergistic effects in the solvent-extraction of some divalent metals by mixtures of Versatic-10 acid and pyridinecarboxylate esters. *J. Chem. Technol. Biotechnol.* **1994**, *61*, 159–165.
212. Virnig, M. J.; Mackenzie, J. M. W.; Wolfe, G. A.; Boley, B. D. Nickel laterite processing: Recovery of nickel from ammoniacal leach liquors. *Miner. Metall. Process.* **2001**, *18*, 18–24.
213. Reddy, B. R.; Parija, C.; Sarma, P. Processing of solutions containing nickel and ammonium sulphate through solvent extraction using PC-88A. *Hydrometallurgy* **1999**, *53*, 11–17.
214. Alguacil, F. J.; Alonso, M.; Lopez, F. A. J. Influence of ammonium salts on solvent extraction of nickel using LIX 54. *Chem. Eng. Jpn.* **2001**, *34*, 83–86.
215. Itagaki, M.; Fukushima, H.; Inoue, H.; Watanabe, K. Electrochemical impedance spectroscopy study on the solvent extraction mechanism of Ni(II) at the water 1,2-dichloroethane interface. *J. Electroanal. Chem.* **2001**, *504*, 96–103.
216. Suyama, T.; Awakura, Y.; Hirato, T.; Konto, M.; Majima, H. Extraction and stripping characteristics of Ni(II) with di(2-ethylhexyl)phosphoric acid under a high electrostatic field. *Mater. Trans. JIM* **1993**, *34*, 37–42.
217. Saitoh, T.; Yamazaki, Y.; Kamidate, T.; Watanabe, H.; Haraguchi, K. Steric effect of alkyl substituent on the extraction of nickel(II) and cobalt(II) by N-alkylcarbonyl substituted N-phenylhydroxylamines. *Anal. Sci.* **1992**, *8*, 767–771.
218. Qian, D.; Wang, K. Y.; Cai, C. L.; Pan, C. Y.; Tang, Y. G.; Jiang, J. Z. Separation of nickel, cobalt and copper by solvent extraction with P204. *Trans. Nonferrous Met. Soc. China* **2001**, *11*, 803–805.
219. Wang, K. Y.; Niu, C. W.; Qian, D.; Liu, J. H.; Chen, X. Y.; Lai, D. Y. Separation of cobalt and nickel by non-equilibrium solvent extraction. *J. Cent. South Univ. Technol.* **2001**, *8*, 50–53.
220. Cheng, C. Y. Purification of synthetic laterite leach solution by solvent extraction using D2EHPA. *Hydrometallurgy* **2000**, *56*, 369–386.
221. Zhu, T. Structure of organophosphorus acid extractants and their steric effect. *Chin. J. Inorg. Chem.* **2000**, *16*, 305–309.
222. Devi, N. B.; Nathsarma, K. C.; Chakravorty, V. Sodium salts of D2EHPA, PC-88A and Cyanex-272 and their mixtures as extractants for nickel(II). *Scand. J. Metall.* **1994**, *23*, 194–200.
223. Juang, R. S.; Jiang, J. D. Recovery of nickel from a simulated electroplating rinse solution by solvent extraction and liquid surfactant membrane. *J. Membr. Sci.* **1995**, *100*, 163–170.
224. Alguacil, F. J.; Cobo, A. Separation of copper and nickel from ammoniacal ammonium carbonate solutions using ACORGA PT5050. *Sep. Sci. Technol.* **1998**, *33*, 2257–2264.
225. Jayachandran, J.; Dhadke, P. M. Solvent extraction separation of cobalt(II) with 2-ethylhexyl phosphonic acid mono-2-ethylhexyl ester (PC-88A). *Chem. Anal.* **1999**, *44*, 157–165.
226. Soldenhoff, K.; Hayward, N.; Wilkins, D. EPD Congress 1998, Proceedings of Sessions and Symposia held at the TMS Annual Meeting, San Antonio, Feb. 16–19, **1998**; pp 153–165.
227. Simons, C. S. Materials selection and design problems in a nickel-cobalt extraction plant. *Corrosion* **1959**, *95–98*.
228. Dreisinger, D. B.; Cooper, W. C. The Kinetics of Zinc, Ion exchange characteristics of palladium from nitric acid solution by anion exchangers. *Solvent Extr. Ion Exch.* **1989**, *7*, 335–360.
229. Devi, N. B.; Nathsarma, K. C.; Chakravorty, V. Sodium salts of D2EHPA, PC-88A and Cyanex-272 and their mixtures as extractants for cobalt(II). *Hydrometallurgy* **1994**, *34*, 331–342.
230. Golding, J. A.; Xun, F.; Zhao, S. Z.; Hu, Z. S.; Sui, S. P.; Hao, J. M. Extraction of nickel from aqueous sulfate-solution into bis(2,2,4-trimethylpentyl) phosphinic acid, Cyanex 272(Tm)-Equilibrium and kinetic studies. *Solvent Extr. Ion Exch.* **1993**, *11*, 91–118.
231. Lindell, E.; Jaaskelainen, E.; Paatero, E.; Nyman, B. Effect of reversed micelles in Co/Ni separation by Cyanex 272. *Hydrometallurgy* **2000**, *56*, 337–357.

232. Sarangi, K.; Reddy, B. R.; Das, R. P. Extraction studies of cobalt (II) and nickel (II) from chloride solutions using Na-cyanex 272. Separation of Co(II)/Ni(II) by the sodium salts of D2EHPA, PC88A and Cyanex 272 and their mixtures. *Hydrometallurgy* **1999**, *52*, 253–265.
233. Reddy, B. R.; Sarma, P. Separation and recovery of cobalt and nickel from sulfate solutions of Indian Ocean nodules using Cyanex 272. *Miner. Metall. Process.* **2001**, *18*, 172–176.
234. Hubicka, Z.; Hubicka, H. Studies on the extraction process of nickel(II) sulphate purification using Cyanex 272. *Hydrometallurgy* **1996**, *40*, 65–76.
235. Preston, J. S. Solvent extraction of cobalt and nickel by organophosphorus acids. I. Comparison of phosphoric, phosphonic, and phosphinic acid systems. *Hydrometallurgy* **1982**, *9*, 115–133.
236. Xun, F.; Golding, J. A. Solvent extraction of cobalt and nickel in bis(2,4,4-trimethylpentyl)phosphinic acid, Cyanex-272. *Solvent Extr. Ion Exch.* **1987**, *5*, 205–226.
237. Nagel, V.; Gilmore, M.; Scott, S. Bateman pulsed column pilot-plant campaign to extract cobalt from the nickel electrolyte stream at Anglo Platinum's base metal refinery. International Solvent Extraction Conference, Cape Town, South Africa, Mar. 17–21, **2002**, pp 970–975.
238. Bhaskara Sarma, P. V. R.; Reddy, B. R. Liquid–liquid extraction of nickel at macro-level concentration from sulphate/chloride solutions using phosphoric acid based extractants. *Miner. Eng.* **2002**, *15*, 461–464.
239. Daudinot, A. M.; Liranza, E. G. Cobalt-nickel separation by solvent extraction in Cuba. *International Solvent Extraction Conference, Cape Town, South Africa, Mar. 17–21, 2002*, 964–969.
240. Liranza, E. G.; Daudinot, A. M.; Martinez, R. V.; Barzaga, B. R. Separation of cobalt and nickel by solvent extraction from sulfate liquors obtained by acid leaching of a product from the caron process. *International Solvent Extraction Conference, Cape Town, South Africa, Mar. 17–21, 2002*, 952–957.
241. Feather, A.; Bouwer, W.; Swarts, A.; Nagel, V. Pilot-plant solvent extraction of cobalt and nickel for Avmin's Nkomati project. *International Solvent Extraction Conference, Cape Town, South Africa, Mar. 17–21, 2002*, 946–951.
242. Cote, G.; Bauer, D. In Metal complexes with organothiophosphorus ligands and extraction phenomena. *Rev. Inorg. Chem* **1989**; Vol. 10, 121–144.
243. Gibson, R. W.; Rice, N. M. Hydrometallurgy and refining of nickel and cobalt, Annual Hydrometallurgy Meeting of CIM, 27th, Sudbury, Ont., Aug. 17–20, 1997; pp 247–261.
244. Nogueira, C. A.; Delmas, F. New flowsheet for the recovery of cadmium, cobalt and nickel from spent Ni-Cd batteries by solvent extraction. *Hydrometallurgy* **1999**, *52*, 267–287.
245. Thakur, N. V.; Mishra, S. L. Separation of Co, Ni and Cu by solvent extraction using di-(2-ethylhexyl) phosphonic acid, PC 88A. *Hydrometallurgy* **1998**, *48*, 277–289.
246. Zhang, P. W.; Inoue, K.; Tsuyama, H. Recovery of metal values from spent hydrodesulfurization catalysts by liquid-liquid extraction. *Energy Fuels* **1995**, *9*, 231–239.
247. Cole, P. M. The introduction of solvent-extraction steps during upgrading of a cobalt refinery. *Hydrometallurgy* **2002**, *64*, 69–77.
248. Feather, A. M.; Cole, P. M. The separation of cobalt from nickel ammonium sulfate solution by solvent extraction. *Value Adding through Solvent Extraction, [Papers presented at ISEC'96], Melbourne, Mar. 19–23, 1996*, *1*, 511–516.
249. Gandhi, M. N.; Deorkar, N. V.; Khopkar, S. M. Solvent extraction separation of cobalt(II) from nickel and other metals with Cyanex-272. *Talanta* **1993**, *40*, 1535–1539.
250. Maljkovic, D.; Lenhard, Z. The effect of organophosphoric extractant concentration and initial phase volume ratio on cobalt(II) and nickel(II) extraction. *International Solvent Extraction Conference, Cape Town, South Africa, Mar. 17–21, 2002*, 982–987.
251. Martinez, R. V.; Liranza, E. G.; Barzaga, B. R.; Daudinot, A. M. Cobalt recovery by solvent extraction from acid leach solutions of Caron's process mixed Ni/Co sulfide. *Hydrometallurgy and Refining of Nickel and Cobalt, Annual Hydrometallurgy Meeting of CIM, 27th, Sudbury, Ont., Aug. 17–20, 1997*, 293–304.
252. Tait, B. K. Cobalt Nickel Separation—the extraction of cobalt(II) and nickel(II) by Cyanex-301, Cyanex-302 and Cyanex-272. *Hydrometallurgy* **1993**, *32*, 365–372.
253. Zhang, P. W.; Yokoyama, T.; Itabashi, O.; Wakui, Y.; Suzuki, T. M.; Inoue, K. Recovery of metal values from spent nickel-metal hydride rechargeable batteries. *J. Power Sources* **1999**, *77*, 116–122.
254. Danesi, P. R.; Reichley-Yinger, L.; Mason, G.; Kaplan, L.; Horwitz, E. P.; Diamond, H. Selectivity structure trends in the extraction of cobalt(II) and nickel(II) by dialkyl phosphoric, alkyl alkylphosphonic, and dialkylphosphinic acids. *Solvent Extr. Ion Exch.* **1985**, *3*, 435–452.
255. Almela, A.; Elizalde, M. P. Interactions of metal extractant reagents. Part VIII. Comparative aggregation equilibria of Cyanex 302 and Cyanex 301 in heptane. *Anal. Proc.* **1995**, *32*, 145–147.
256. Rice, N. M.; Gibson, R. W. Solvent extraction with Cyanex 301 and 302 for the upgrading of chloride leach liquors from lateritic nickel ores. *Value Adding through Solvent Extraction, [Papers presented at ISEC'96], Melbourne, Mar. 19–23, 1996*, *1*, 715–720.
257. Shinde, P. S.; Dhadke, P. M. Solvent extraction separation of Cu(II) and Ni(II) with bis(2,4,4-trimethylpentyl)dithiophosphinic acid (Cyanex 301). *Indian J. Chem. Technol.* **1996**, *3*, 367–370.
258. Singh, R.; Khwaja, A. R.; Gupta, B.; Tandon, S. N. Extraction and separation of nickel(II) using bis(2,4,4-trimethylpentyl) dithiophosphinic acid (Cyanex 301) and its recovery from spent catalyst and electroplating bath residue. *Solvent Extr. Ion Exch.* **1999**, *17*, 367–390.
259. Sole, K. C.; Hiskey, J. B. Solvent-extraction characteristics of thiosubstituted organophosphinic acid extractants. *Hydrometallurgy* **1992**, *30*, 345–365.
260. Sole, K. C.; Hiskey, J. B.; Ferguson, T. L. An assessment of the long-term stabilities of Cyanex 302 and Cyanex 301 in sulfuric and nitric acids. *Solvent Extr. Ion Exch.* **1993**, *11*, 783–796.
261. Sze, Y. K. P.; Lam, J. K. S. A study of a solvent extraction method for the treatment of spent electrolyte solutions generated in nickel–cadmium (Ni–Cd) battery manufacturing. *Environ. Technol.* **1999**, *20*, 943–951.
262. Menoyo, B.; Elizalde, M. P. Extraction of cobalt(II) by Cyanex 301. *Solvent Extr. Ion Exch.* **1997**, *15*, 563–576.
263. Ocana, N.; Alguacil, F. J. Cobalt–manganese separation: The extraction of cobalt(II) from manganese sulphate solutions by Cyanex 301. *J. Chem. Technol. Biotechnol.* **1998**, *73*, 211–216.
264. Mihaylov, I.; Krause, E.; Colton, D. F.; Okita, Y.; Duterque, J. P.; Perraud, J. L. The development of a novel hydrometallurgical process for nickel and cobalt recovery from Goro laterite ore. *CIM Bull.* **2000**, *93*, 124–130.

265. Cole, P. M.; Feather, A. M. Proceedings of the Copper 95—Cobre 95 International Conference, Santiago, Nov. 26–29, 1995; pp 607–616.
266. Jaaskelainen, E.; Paatero, E. Characterisation of organic phase species in the extraction of nickel by pre-neutralised Versatic 10. *Hydrometallurgy* **2000**, *55*, 181–200.
267. Preston, J. S. Solvent extraction of metals by carboxylic acids. *Hydrometallurgy* **1985**, *14*, 171–188.
268. Jaaskelainen, E.; Paatero, E. Extraction of nickel using saponified Versatic 10. *Value Adding through Solvent Extraction, [Papers presented at ISEC'96], Melbourne, Mar. 19–23, 1996*, *1*, 421–426.
269. Jaaskelainen, E.; Paatero, E. Properties of the ammonium form of Versatic 10 in a liquid-liquid extraction system. *Hydrometallurgy* **1999**, *51*, 47–71.
270. Alguacil, F. J.; Cobo, A. Solvent extraction equilibrium of nickel with LIX 54. *Hydrometallurgy* **1998**, *48*, 291–299.
271. Parija, C.; Reddy, B. R.; Sarma, P. Recovery of nickel from solutions containing ammonium sulphate using LIX 84-I. *Hydrometallurgy* **1998**, *49*, 255–261.
272. Bhaskara Sarma, P. V. R.; Nathsarma, K. C. Extraction of nickel from ammoniacal solutions using LIX 87QN. *Hydrometallurgy* **1996**, *42*, 83–91.
273. Alguacil, F. J.; Cobo, A. Extraction of nickel from ammoniacal ammonium carbonate solutions using Acorga M5640 in Iberfluid. *Hydrometallurgy* **1998**, *50*, 143–151.
274. Alguacil, F. J.; Cobo, A. Solvent extraction with LIX 973N for the selective separation of copper and nickel. *J. Chem. Technol. Biotechnol.* **1999**, *74*, 467–471.
275. Tanaka, M.; Kobayashi, M.; Seki, T. Recovery of nickel from spent electroless nickel plating baths by solvent extraction. *International Solvent Extraction Conference, Cape Town, South Africa, Mar. 17–21, 2002*, 787–792.
276. Rodriguez de San Miguel, E.; Aguilar, J. C.; Bernal, J. P.; Ballinas, M. L.; Rodriguez, M. T. J.; de Gyves, J.; Schimmel, K. Extraction of Cu(II), Fe(III), Ga(III), Ni(II), In(III), Co(II), Zn(II) and Pb(II) with LIX 984 dissolved in n-heptane. *Hydrometallurgy* **1997**, *47*, 19–30.
277. Sandhibigraha, A.; Bhaskara Sarma, P. V. R. Coextraction and selective stripping of copper and nickel using LIX87QN. *Hydrometallurgy* **1997**, *45*, 211–219.
278. Zhang, P. W.; Inoue, K.; Yoshizuka, K.; Tsuyama, H. Extraction and selective stripping of molybdenum(VI) and vanadium(IV) from sulfuric acid solution containing aluminum(III), cobalt(II), nickel(II) and iron(III) by LIX 63 in Exxsol D80. *Hydrometallurgy* **1996**, *41*, 45–53.
279. Suetsuna, A.; Iio, T.; Niihama, E.; Takahashi, N. In *Ger. Offen.*; (Sumitomo Metal Mining Co., Ltd., Japan). De, 1975.
280. Ono, N.; Itasako, S.; Fukui, I. Sumitomo's cobalt refining process. *Proc. Int. Conf. Cobalt: Metall. Uses* **1981**, *1*, 63–71.
281. Rice, N. M.; Strong, L. W. Leaching of lateritic nickel ores in hydrochloric acid. *Can. Metall. Q.* **1974**, *13*, 485–493.
282. Saha, A. K.; Khan, Z. H.; Akerkar, D. D. Extraction of nickel from Indian low-grade siliceous ore. *Trans. Inst. Min. Metall. Sect. C-Miner. Process. Extr. Metall.* **1992**, *101*, C52–C56.
283. Kumar, V.; Jana, R. K.; Pandey, B. D.; Jha, D.; Nayak, A. K.; Bagchi, D.; Akerkar, D. D. Recovery of copper, nickel and cobalt from ammoniacal leach liquors obtained by direct ammonia leaching of sea nodules. *Trans. Indian Inst. Met.* **1987**, *40*, 64–70.
284. Cupertino, D. C.; Campbell, J.; Lawson, J. R.; Stocks, J. A.; Dalton, R. F. In *PCT Int. Appl.*; (Zeneca Limited, UK; Cupertino, Domenico Carlo; Campbell, John; Lawson, John Robert; Stocks, Julie Ann; Dalton, Raymond Frederick). Wo, 1997.
285. Alam, M. S.; Inoue, K. Extraction of rhodium from other platinum group metals with Kelex 100 from chloride media containing tin. *Hydrometallurgy* **1997**, *46*, 373–382.
286. Kim, C.-H.; Woo, S. I.; Jeon, S. H. Recovery of platinum-group metals from recycled automotive catalytic converters by carbochlorination. *Ind. Eng. Chem. Res.* **2000**, *39*, 1185–1192.
287. Mhaske, A. A.; Dhadke, P. M. Extraction separation studies of Rh, Pt and Pd using Cyanex 921 in toluene—a possible application to recovery from spent catalysts. *Hydrometallurgy* **2001**, *61*, 143–150.
288. Lee, S. H.; Kim, K. R.; Jung, C. H.; Chung, H. Ion exchange characteristics of palladium from nitric acid solution by anion exchangers. *Korean J. Chem. Eng.* **1999**, *16*, 571–575.
289. Kramer, J.; Driessen, W. L.; Koch, K. R.; Reedijk, J. Highly selective extraction of platinum group metals with silica-based (poly)amine ion exchanges applied to industrial metal refinery effluents. *Hydrometallurgy* **2002**, *64*, 59–68.
290. Cramer, L. A. The extractive metallurgy of South Africa's platinum ores. *JOM-J. Miner. Met. Mater. Soc.* **2001**, *53*, 14–18.
291. Mooiman, M. B.; Kinneberg, D. J.; Simpson, L. W.; Cettou, P.; Ramoni, P. High-purity precious metals. *Value-Addition Metallurgy, Proceedings of an International Symposium, San Antonio, Feb. 16–19, 1998*, 141–163.
292. Paiva, A. P. Solvent Extraction for the 21st Century, Proceedings of ISEC '99, Barcelona, Spain, July 11–16, 1999, 2001; pp 399–404.
293. Belhamel, K.; Dzung, N. T. K.; Benamor, M.; Ludwig, R. International Solvent Extraction Conference, Cape Town, South Africa, Mar. 17–21, 2002; pp 307–312.
294. Tanaka, M.; Nakamura, M.; Ikeda, K.; Ando, H.; Shibutani, Y.; Yajima, S.; Kimura, K. Synthesis and metal-ion binding properties of monoazathiocrown ethers. *J. Org. Chem.* **2001**, *66*, 7008–7012.
295. Jung, J. H.; Yoon, I.; Park, K. J.; Lee, S. S.; Choi, K. S.; Park, S. B. Solvent extraction of silver(I) over lead(II) by oxygen-sulfur mixed donor podands. *Microchem. J.* **1999**, *63*, 100–108.
296. Vest, P.; Schuster, M.; König, K. H. Influence of tin(II) chloride on the solvent-extraction of platinum group metals with N,N-di-normal-hexyl-N'-benzoylthiourea. *Fresenius J. Anal. Chem.* **1991**, *339*, 142–144.
297. Wisniewski, M.; Szymanowski, J. Industrial applications of noble metals' extraction. *Pol. J. Appl. Chem.* **1996**, *40*, 17–26.
298. Kopyrin, A. A.; Balamsov, G. F. Using new ion-exchange materials in the hydrometallurgy of rhenium. *Russ. Metall.* **1998**, 31–35.
299. Wisniewski, M. Palladium(II) extraction by pyridinecarboxylic acid esters. *J. Radioanal. Nucl. Chem.* **2000**, *246*, 693–696.
300. Wisniewski, M.; Jakubiak, A.; Szymanowski, J. Interfacial activity and rate of palladium(II) extraction with decyl pyridine monocarboxylates. *J. Chem. Technol. Biotechnol.* **1995**, *63*, 209–214.

301. Burgess, A.; Dalton, R. F. Solvent extraction of palladium by pyridine carboxylic esters. *Process Metallurgy* **1992**, pp 1087–1092.
302. Yan, G. L.; Alstad, J. Hydrometall. '94, Pap. Int. Symp., 1994; p 701–707.
303. Demopoulos, G. P.; Benguerel, E.; Harris, G. B. Recovery of rhodium from aqueous solutions by extraction with hydroxyquinoline. (McGill University, Can.). US, 1993. 33pp. Application US 91–793638.
304. Alguacil, F. J.; Cobo, A.; Coedo, A. G.; Dorado, M. T.; Sastre, A. Extraction of platinum(IV) from hydrochloric acid solutions by amine alamine 304 in xylene. Estimation of the interaction coefficient between PtCl_6^{2-} and H^+ . *Hydrometallurgy* **1997**, *44*, 203–212.
305. Hasegawa, Y.; Kobayashi, I.; Yoshimoto, S. Extraction of palladium(II) and platinum(IV) as chlorocomplex acids into basic organic solvents. *Solvent Extr. Ion Exch.* **1991**, *9*, 759–768.
306. Lokhande, T. N.; Anuse, M. A.; Chavan, M. B. Extraction and separation studies of platinum(IV) with N-n-octylaniline. *Talanta* **1998**, *47*, 823–832.
307. Nogaeva, K. A.; Imanakunov, V. I.; Linichenko, T. V.; Mamytova, A. A.; Kozhonov, A. K. Gold extraction from industrial wastes. *Ekho Nauki* **1997**, 77–79.
308. Liu, M.; Zhang, S.; Sun, S. The industrial practice of utilizing dibutyl carbitol in solvent extraction of gold. *Kuangye Gongcheng* **1995**, *15*, 37–40.
309. Hill, J. W.; Lear, T. A. Recovery of gold from electronic scrap. *Journal of Chemical Education* **1988**, *65*, 802.
310. Inoue, K.; Nagamatsu, I.; Baba, Y.; Yoshizuka, K. Solvent extraction of platinum(IV) by trioctylphosphine oxide. *Solvent Extr. Ion Exch.* **1989**, *7*, 1111–1119.
311. Hasegawa, Y.; Kobayashi, I.; Okuda, A. Solvent-extraction behavior of platinum(IV) and palladium(II) as chlorocomplex acids with trioctylphosphine oxide. *Anal. Sci.* **1991**, *7*, 377–381.
312. Duché, S. N.; Dhadke, P. M. Comparative study of the determination of platinum by extraction with Cyanex 923 and Cyanex 471X from bromide media. *J. Chem. Technol. Biotechnol.* **2001**, *76*, 1227–1234.
313. Mhaske, A.; Dhadke, P. Liquid–liquid extraction and separation of rhodium(III) from other platinum group metals with Cyanex 925. *Sep. Sci. Technol.* **2001**, *36*, 3253–3265.
314. Preston, J. S.; du Preez, A. C. Solvent extraction of platinum-group metals from hydrochloric acid solutions by dialkyl sulphoxides. *Solvent Extr. Ion Exch.* **2002**, *20*, 359–374.
315. Koch, K. R.; Sacht, C.; Grimmbacher, T.; Bourne, S. New Ligands for the platinum-group metals: deceptively simple coordination chemistry of N-acyl-N'-alkyl and N-acyl-N',N'-dialkyl-thioureas. *S. Afr. J. Chem.* **1995**, *48*, 71–77.
316. Albazi, S. J.; Freiser, H. Kinetic-studies of the solvent-extraction of platinum(II) with diphenylthiourea. *Solvent Extr. Ion Exch.* **1988**, *6*, 1067–1079.
317. Koch, K. R.; Grimmbacher, T.; Sacht, C. A H-1 and Pt-195 NMR study of the protonation mediated interconversion of mono-(S) versus bidentate (S,O) coordination of Pt(II) by N-acyl-N',N'-dialkylthioureas. *Polyhedron* **1998**, *17*, 267–274.
318. Rukhadze, E. G.; Shkil, A. N.; Zolotov, Y. A. Solvent-extraction of platinum and silver by n-substituted alpha-thiopicolinamide derivatives. *J. Anal. Chem. USSR* **1989**, *44*, 1026–1029.
319. Shkil, A. N.; Zolotov, Y. A. Solvent-extraction of platinum with thiobenzanilide-separation of platinum from copper. *J. Anal. Chem. USSR* **1988**, *43*, 1188–1193.
320. Sherikar, A. V.; Phalke, P. N.; Dhadke, P. M. Solvent extraction and separation studies of platinum using bis(2-ethylhexyl) hydrogen phosphate. *Bull. Chem. Soc. Jpn.* **1997**, *70*, 805–808.
321. Saito, K.; Taninaka, I.; Yamamoto, Y.; Murakami, S.; Muromatsu, A. Liquid-liquid extraction of platinum(II) with cyclic tetraethioethers. *Talanta* **2000**, *51*, 913–919.
322. Inoue, K.; Koba, M.; Yoshizuka, K.; Tazaki, M. Solvent-extraction of platinum(IV) with a novel sulfur-containing extracting reagent. *Solvent Extr. Ion Exch.* **1994**, *12*, 55–67.
323. Koba, M.; Yoshizuka, K.; Inoue, K. *Proceedings of Symposium on Solvent Extraction, Solvent extraction of palladium and platinum with a new type of sulfur-containing extractant*; 1991, pp 133–40.
324. Inoue, K.; Yoshizuka, K.; Baba, Y.; Tazaki, M. In *Jpn. Kokai Tokkyo Koho*; (Tanaka Kikinzoku Kogyo K. K., Japan). Jp, 1991.
325. Inoue, K.; Yoshizuka, K.; Baba, Y.; Wada, F.; Matsuda, T. Solvent extraction of palladium(II) and platinum(IV) from aqueous chloride media with n,n-dioctylglycine. *Hydrometallurgy* **1990**, *25*, 271–279.
326. Yoshizuka, K.; Baba, Y.; Inoue, K.; Wada, F.; Matsuda, T. Solvent-extraction of palladium(II) and platinum(IV) with n,n-dioctylsuccinamic acid from aqueous chloride media. *Bull. Chem. Soc. Jpn.* **1990**, *63*, 221–226.
327. Yordanov, A. T.; Mague, J. T.; Roundhill, D. M. Solvent extraction of divalent palladium and platinum from aqueous solutions of their chloro complexes using an N,N-dimethyldithiocarbamoylthoxy substituted calix 4 arene. *Inorg. Chim. Acta* **1995**, *240*, 441–446.
328. Yordanov, A. T.; Roundhill, D. M. Extraction of platinum from aqueous solution into chloroform using a 2-pyridylthio-N-oxide derivatized calix[4]arene as phase transfer reagent. *Inorg. Chim. Acta* **1997**, *264*, 309–311.
329. Yordanov, A. T.; Roundhill, D. M. Solution extraction of transition and post-transition heavy and precious metals by chelate and macrocyclic ligands. *Coord. Chem. Rev.* **1998**, *170*, 93–124.
330. Powell, C. J.; Beckman, E. J. Design of ligands for the extraction of PtCl_6^{2-} in introduction to liquid CO_2 . *Ind. Eng. Chem. Res.* **2001**, *40*, 2897–2903.
331. Marsden, J.; House, I. *The Chemistry of Gold Extraction*; Ellis Horwood Limited: Chichester, 1992.
332. Plaksin, I. N.; Laskorin, B. N.; Shvirin, G. N. Liquid extraction of complex gold and silver cyanides from cyanide solutions. *Tsvetnye Metally* **1961**, *34*, 20–23.
333. Gang, M. A.; Wenfei, Y.; Jing, C.; Chunhua, Y.; Nai, S.; Jinguang, W. U.; Guangxian, X. Progress in gold solvent extraction. *Prog. Nat. Sci.* **2000**, *10*, 881–886.
334. Riveros, P. A. Studies on the solvent extraction of gold from cyanide media. *Hydrometallurgy* **1990**, *24*, 135–156.
335. Miller, J. D.; Mooiman, M. B. A review of new developments in amine solvent-extraction systems for hydrometallurgy. *Sep. Sci. Technol.* **1984**, *19*, 895–909.
336. Mooiman, M. B.; Miller, J. D. The chemistry of gold solvent extraction from cyanide solution using modified amines. *Hydrometallurgy* **1986**, *16*, 245–261.
337. Mooiman, M. B.; Miller, J. D. The chemistry of gold solvent extraction from alkaline cyanide solution by solvating extractants. *Hydrometallurgy* **1991**, *27*, 29–46.

338. Caravaca, C.; Alguacil, F. J.; Sastre, A.; Martinez, M. Extraction of gold(I) cyanide by the primary amine tridecylamine. *Hydrometallurgy* **1996**, *40*, 89–97.
339. Caravaca, C.; Alguacil, F. J.; Sastre, A. The use of primary amines in gold(I) extraction from cyanide solutions. *Hydrometallurgy* **1996**, *40*, 263–275.
340. Kordosky, G. A.; Sierakoski, J. M.; Virnig, M. J.; Mattison, P. L. Gold solvent extraction from typical cyanide leach solutions. *Hydrometallurgy* **1992**, *30*, 291–305.
341. Virnig, M. J.; Wolfe, G. A. LIX 79—a new liquid ion exchange reagent for gold and silver. *Value Adding through Solvent Extraction, [Papers presented at ISEC'96], Melbourne, Mar. 19-23, 1996*, *1*, 311–316.
342. Sastre, A. M.; Madi, A.; Cortina, J. L.; Alguacil, F. J. Solvent extraction of gold by LIX 79: experimental equilibrium study. *J. Chem. Technol. Biotechnol.* **1999**, *74*, 310–314.
343. Sastre, A. M.; Madi, A.; Alguacil, F. J. Solvent extraction of $\text{Au}(\text{CN})_2^-$ and application to facilitated supported liquid membrane transport. *Hydrometallurgy* **2000**, *54*, 171–184.
344. Sastre, A. M.; Madi, A.; Alguacil, F. J. Facilitated supported liquid-membrane transport of gold(I) using LIX 79 in cumene. *J. Membr. Sci.* **2000**, *166*, 213–219.
345. Kumar, A.; Haddad, R.; Benzal, G.; Sastre, A. M. Dispersion-free solvent extraction and stripping of gold cyanide with LIX79 using hollow fiber contactors: Optimization and modeling. *Ind. Eng. Chem. Res.* **2002**, *41*, 613–623.
346. Alguacil, F. J.; Coedo, A. G.; Dorado, M. T.; Padilla, I. Phosphine oxide mediate transport: modelling of mass transfer in supported liquid membrane transport of gold(III) using Cyanex 923. *Chem. Eng. Sci.* **2001**, *56*, 3115–3122.
347. Dzul Erosa, M. S.; Mendoza, R. N.; Medina, T. I. S.; Lavine, G. L.; Avila-Rodriguez, M. Recovery of Ag and Au from Aqueous Thiourea solutions by liquid-liquid extraction. *International Solvent Extraction Conference, Cape Town, South Africa, Mar. 17-21, 2002*, 902–907.
348. Zhao, J.; Wu, Z. C.; Chen, J. C. Gold extraction from thiosulfate solutions using mixed amines. *Solvent Extr. Ion Exch.* **1998**, *16*, 1407–1420.
349. Zhao, J.; Wu, Z. H.; Chen, J. Y. Extraction of gold from thiosulfate solutions using amine mixed with neutral donor reagents. *Hydrometallurgy* **1998**, *48*, 133–144.
350. Zhao, J.; Wu, Z. C.; Chen, J. Y. Solvent extraction of gold in thiosulfate solutions with amines. *Solvent Extr. Ion Exch.* **1998**, *16*, 527–543.
351. Zhao, J.; Wu, Z. C.; Chen, J. Y. Separation of gold from other metals in thiosulfate solutions by solvent extraction. *Sep. Sci. Technol.* **1999**, *34*, 2061–2068.
352. Vest, P.; Schuster, M.; Konig, K. H. Solvent extraction of gold with N-substituted benzoylthioureas. *Fresenius J. Anal. Chem.* **1991**, *341*, 566–568.
353. Dominguez, M.; Antico, E.; Beyer, L.; Aguirre, A.; Garcia-Granda, S.; Salvado, V. Liquid-liquid extraction of palladium(II) and gold(III) with N-benzoyl-N',N'-diethylthiourea and the synthesis of a palladium benzoylthiourea complex. *Polyhedron* **2002**, *21*, 1429–1437.
354. Yordanov, A. T.; Roundhill, D. M. Electronic absorption spectroscopy for the investigation of the solution binding of gold, palladium, mercury and silver salts to the lower rim substituted calix[4]arenes 25,26,27,28-(2-N,N-dimethyl-dithiocarbamoylthioxy)calix[4]arene and 25,26,27,28-(2-methylthioethoxy)calix[4]arene. *Inorg. Chim. Acta* **1998**, *270*, 216–220.
355. Sanchez-Loredo, M. G.; Grote, M. Solvent extraction and hydrochemical preparation of gold powders with dithizone derivatives. *International Solvent Extraction Conference, Cape Town, South Africa, Mar. 17–21, 2002*, 934–939.
356. Grant, R. A.; Drake, V. A. The application of solvent extraction to the refining of gold. *International Solvent Extraction Conference, Cape Town, South Africa, Mar. 17–21, 2002*, 940–945.
357. Rimmer, B. F. Refining of gold from precious metal concentrates by liquid-liquid extraction. *Chemistry & Industry (London, United Kingdom)* **1974**, 63–66.
358. Cleare, M. J.; Grant, R. A.; Charlesworth, P. Separation of the platinum-group metals by use of selective solvent extraction techniques. *Extr. Metall. '81, Pap. Symp.* **1981**, 34–41.
359. Feather, A.; Sole, K. C.; Bryson, L. J. Gold refining by solvent extraction—the Minataur™ process. *J. S. Afr. Inst. Min. Metall.* **1997**, *97*, 169–173.
360. Sole, K. C.; Feather, A.; Watt, J.; Bryson, L. J.; Sorensen, P. F. Commercialisation of the Minataur process: commissioning of Harmony gold refinery. *EPD Congress 1998, Proceedings of Sessions and Symposia held at the TMS Annual Meeting, San Antonio, Feb. 16–19, 1998*, 175–186.
361. Feather, A.; Bouwer, W.; O'Connell, R.; le Roux, J. Commissioning of the new Harmony gold refinery. *International Solvent Extraction Conference, Cape Town, South Africa, Mar. 17–21, 2002*, 922–927.
362. Mendoza, C. S.; Kamata, S. Silver extraction for pollution control of photographic fixing solution with tetramethylthiuram disulfide. *Bull. Chem. Soc. Jpn.* **1996**, *69*, 3499–3504.
363. Paiva, A. P. Review of recent solvent extraction studies for recovery of silver from aqueous solutions. *Solvent Extr. Ion Exch.* **2000**, *18*, 223–271.
364. Paiva, A. P. Solvent extraction and related studies on silver recovery from aqueous solutions. *Sep. Sci. Technol.* **1993**, *28*, 947–1008.
365. Ohto, K.; Higuchi, H.; Inoue, K. Solvent extraction of silver with pyridino calix-4-arenes. *Solvent Extr. Res. Dev.-Jpn.* **2001**, *8*, 37–46.
366. Liu, Y.; Zhao, B. T.; Wang, H.; Chen, Q. F.; Zhang, H. Y. Molecular design of calixarene 5. Syntheses and cation selectivities of novel Schiff's base p-tert-butylcalix-4-arenes. *Chin. J. Chem.* **2001**, *19*, 291–295.
367. Ohto, K.; Murakami, E.; Shinohara, T.; Shiratsuchi, K.; Inoue, K.; Iwasaki, M. Selective extraction of silver(I) over palladium(II) with ketonic derivatives of calixarenes from highly concentrated nitric acid. *Anal. Chim. Acta* **1997**, *341*, 275–283.
368. Ohto, K.; Yamaga, H.; Murakami, E.; Inoue, K. Specific extraction behavior of amide derivative of calix-4-arene for silver (I) and gold (III) ions from highly acidic chloride media. *Talanta* **1997**, *44*, 1123–1130.
369. Regnouf-de-Vains, J. B.; Dalbavie, J. O.; Lamartine, R.; Fenet, B. Quantitative solvent extraction from neutral aqueous nitrate media of silver(I) against lead(II) with a new calix-4-arene-based bipyridine podand. *Tetrahedron Lett.* **2001**, *42*, 2681–2684.

370. Memon, S.; Yilmaz, M. Liquid-liquid extraction of alkali and transition metal cations by two bisalix[4]arenes. *Sep. Sci. Technol.* **2000**, *35*, 457–467.
371. Yamato, T.; Zhang, F.; Kumamaru, K.; Yamamoto, H. Synthesis, conformational studies and inclusion properties of tetrakis(2-pyridinylmethoxy)thiacalix[4]arenes. *J. Incl. Phenom. Macrocycl. Chem.* **2002**, *42*, 51–60.
372. van de Water, L. G. A.; ten Hoonte, F.; Driessen, W. L.; Reedijk, J.; Sherrington, D. C. Selective extraction of metal ions by azathiacrown ether-modified polar polymers. *Inorg. Chim. Acta* **2000**, *303*, 77–85.
373. van de Water, L. G. A.; Driessen, W. L.; Reedijk, J.; Sherrington, D. C. Metal-ion extraction by immobilised aza crown ethers. *Eur. J. Inorg. Chem.* **2002**, 221–229.
374. Shamsipur, M.; Mashhadizadeh, M. H. Highly efficient and selective membrane transport of silver(I) using hexathia-18-crown-6 as a specific ion carrier. *Sep. Purif. Technol.* **2000**, *20*, 147–153.
375. Chartres, J. D.; Groth, A. M.; Lindoy, L. F.; Meehan, G. V. Metal ion recognition. Selective interaction of silver(I) with tri-linked N₂S₂-donor macrocycles and their single-ring analogues. *J. Chem. Soc.-Dalton Trans.* **2002**, 371–376.
376. Lee, B. L.; Lee, Y. H.; Yoon, I.; Jung, J. H.; Park, K. M.; Lee, S. S. Cyclic and acyclic S₂O₂ donor-type ionophores. Ion-pair extraction and transport of Ag(I) picrate, and X-ray confirmation of existence of the ion-pair complex. *Microchem J.* **2001**, *68*, 241–250.
377. Lee, S. S.; Yoon, I.; Park, K.-M.; Jung, J. H.; Lindoy, L. F.; Nezhadali, A.; Rounaghi, G. Competitive bulk membrane transport and solvent extraction of transition and post transition metal ions using mixed-donor acyclic ligands as ionophores. *J. Chem. Soc.-Dalton Trans.* **2002**, 2180–2184.
378. Kim, J.; Ahn, T.-H.; Lee, M.; Leong, A. J.; Lindoy, L. F.; Rumbel, B. R.; Skelton, B. W.; Strixner, T.; Wei, G.; White, A. H. Metal ion recognition. The interaction of cobalt(II), nickel(II), copper(II), zinc(II), cadmium(II), silver(I) and lead(II) with N-benzylated macrocycles incorporating O₂N₂-, O₃N₂- and O₂N₃-donor sets. *J. Chem. Soc.-Dalton Trans.* **2002**, 3993–3998.
379. Capela, R. S.; Paiva, A. P. Extraction of silver from concentrated chloride solutions: use of tri-n-butyl- and tri-n-octylphosphine sulfides. *International Solvent Extraction Conference, Cape Town, South Africa, Mar. 17–21, 2002*, 335–340.
380. Abe, Y.; Flett, D. S. Solvent extraction of silver from chloride solutions by Cyanex 471X. *Process Metallurgy* **1992**, *7B*, 1127–1132.
381. Dziwinski, E.; Cote, G.; Bauer, D.; Szymanowski, J. Composition of Kelex(R)-100, Kelex(R)-100s and Kelex(R)-108—a discussion on the role of impurities. *Hydrometallurgy* **1995**, *37*, 243–250.
382. Vest, P.; Schuster, M.; Koenig, K. H. Solvent extraction of platinum metals with N-mono- and N,N-disubstituted benzoylthioureas. *Fresenius' Z. Anal. Chem.* **1989**, *335*, 759–763.
383. Schuster, M. Selective complexing agents for the trace enrichment of platinum metals. *Fresenius' J. Anal. Chem.* **1992**, *342*, 791–794.
384. Koenig, K. H.; Schuster, M.; Steinbrech, B.; Schneeweis, G.; Schlodder, R. N,N-Dialkyl-N'-benzoylthioureas as reagents for selective extractions for the separation and enrichment of platinum-group metals. *Fresenius' Z. Anal. Chem.* **1985**, *321*, 457–460.
385. Merdivan, M.; Aygun, R. S.; Kulcu, N. Solvent extraction of platinum group metals with N,N-diethyl-N'-benzoylthiourea. *Ann. Chim.* **2000**, *90*, 407–412.
386. Koch, K. R.; Miller, J.; Westra, A. N. On the liquid-liquid extraction of Pt(IV/II) from hydrochloric acid by N-Acyl(aryl)-N', N'-dialkylthioureas: a multinuclear (1H, 13C and 195Pt) NMR speciation study of the extracted complexes. *International Solvent Extraction Conference, Cape Town, South Africa, Mar. 17–21, 2002*, 327–334.
387. Koch, K. R. New chemistry with old ligands: N-alkyl- and N,N-dialkyl-N'-acyl(aryl)thioureas in co-ordination, analytical and process chemistry of the platinum group metals. *Coord. Chem. Rev.* **2001**, *216*, 473–488.
388. du Preez, J. G. H.; Hosten, E. C.; Knoetze, S. E. Separation of palladium from platinum. *International Solvent Extraction Conference, Cape Town, South Africa, Mar. 17–21, 2002*, 319–326.
389. Al-Bazi, S. J.; Freiser, H. Phase-transfer catalysts in extraction kinetics: palladium extraction by dioctyl sulfide and KELEX 100. *Inorg. Chem.* **1989**, *28*, 417–420.
390. Belova, V. V.; Kholkin, A. I.; Jidkova, T. I. Solvent extraction of palladium from chloride solutions by alkylammonium di(2-ethylhexyl)dithiophosphates. *Solvent Extr. Ion Exch.* **1999**, *17*, 1473–1491.
391. Belova, V. V.; Jidkova, T. I.; Kholkin, A. I.; Brenno, Y. Y.; Jidkov, L. L. Extraction of chlorocomplexes of Pt and Pd by diamines and their salts with organic acids. *International Solvent Extraction Conference, Cape Town, South Africa, Mar. 17–21, 2002*, 916–921.
392. Antico, E.; Masana, A.; Hidalgo, M.; Salvado, V.; Valiente, M. New sulfur-containing reagents as carriers for the separation of palladium by solid supported liquid membranes. *Hydrometallurgy* **1994**, *35*, 343–352.
393. Ouyang, J. M. Solvent extraction of palladium(II) with a Schiff base and separation of palladium from Pd(II)-Pt(VI) mixture. *Solvent Extr. Ion Exch.* **1999**, *17*, 1255–1270.
394. Ohto, K.; Nagata, J.; Honda, S.; Yoshizuka, K.; Inoue, K.; Baba, Y. Solvent extraction of precious metals with an organoaminophosphonate. *Solvent Extr. Ion Exch.* **1997**, *15*, 115–130.
395. Flett, D. S. New reagents or new ways with old reagents. *J. Chem. Technol. Biotechnol.* **1999**, *74*, 99–105.

9.18

Metal Complexes as Drugs and Chemotherapeutic Agents

N. FARRELL

Virginia Commonwealth University, Richmond, VA, USA

9.18.1	INTRODUCTION	809
9.18.1.1	Biological Assays	810
9.18.2	PLATINUM COMPLEXES AS THERAPEUTIC AGENTS	812
9.18.2.1	Clinically Used Anticancer Agents. <i>Cis</i> -platinum Compounds	812
9.18.2.2	Platinum Compounds in Clinical Trials	817
9.18.2.2.1	<i>AMD473 (ZDO-473)</i>	817
9.18.2.2.2	<i>JM-216 (Satraplatin)</i>	818
9.18.2.2.3	<i>Poly (di and tri)-nuclear platinum complexes</i>	819
9.18.2.2.4	<i>Transplatinum compounds</i>	823
9.18.3	NONPLATINUM ANTICANCER AGENTS	825
9.18.3.1	Ruthenium Complexes	825
9.18.3.2	Arsenic Trioxide	826
9.18.3.3	The Mitochondrion as Target. Gold–phosphane Complexes	827
9.18.3.4	Manganese-based Superoxide Dismutase Mimics	827
9.18.3.5	Titanium Compounds	829
9.18.3.6	Gallium Nitrate	830
9.18.4	ANTIBACTERIAL AGENTS	830
9.18.4.1	Silver and Mercury Salts	830
9.18.4.2	Bismuth-containing Antiulcer Drugs	831
9.18.4.3	Metal-containing Drugs as Antiparasitic Agents	831
9.18.5	PHARMACODYNAMIC USES OF METAL COMPLEX DRUGS	832
9.18.5.1	Lithium Carbonate	832
9.18.5.2	Vanadium Complexes in Diabetes	833
9.18.5.3	Gold Compounds as Antiarthritic Agents	833
9.18.5.4	Nitric Oxide in Physiology and Medicine	834
9.18.5.5	Lanthanum Carbonate	834
9.18.6	REFERENCES	834

9.18.1 INTRODUCTION

The medicinal uses and applications of metals and metal complexes are of increasing clinical and commercial importance. Monographs and major reviews, as well as dedicated volumes, testify to the growing importance of the discipline.^{1–11} Relevant reviews are to be found throughout annual series, for example *Metal Ions in Biological Systems*¹² and *Coordination Chemistry Reviews*.¹³ The field of inorganic chemistry in medicine may usefully be divided into two main categories: firstly, ligands as drugs which target metal ions in some form, whether free or protein-bound; and secondly, metal-based drugs and imaging agents where the central metal ion is usually the key feature of the mechanism of action.¹⁴ This latter class may also be conveniently expanded to include those radionuclides used in radioimmunoimaging and radioimmunotherapy (Chapter 9.20). A reasonable estimate of the commercial importance is approaching US\$5 billion annually

for the whole field. A list of clinically used chelating agents may be found in most pharmacopoeia,¹⁵ while new chelating agents continue to be sought.^{15,16} The use of chelating agents in the treatment of Wilson's disease is a good example of how medical problems due to free metal ion (Cu^{II}) toxicity may be ameliorated by chelating agents.¹⁷ The extensive work on matrix metalloproteinases likewise represents a case study in design of small organic ligands as drugs to inactivate a metalloenzyme.^{18,19} Overexpression of these zinc-containing enzymes is associated with several diseases including arthritis and cancer, so inhibition of the zinc active site is a reasonable drug development strategy. Indeed, enzymatic zinc is an attractive target because of the diversity of its structural and catalytic roles in enzymes.^{20,21} This chapter is restricted to the uses of well-defined inorganic compounds as drugs and chemotherapeutic agents. Current uses and prospective uses, as well as those of essentially historical relevance, are covered. An important distinction to be made is between drugs as chemotherapeutic agents, whose function is to kill cells, and drugs acting by a pharmacodynamic mechanism—whose action must be essentially reversible and/or short-lived.²²

9.18.1.1 Biological Assays

Most therapeutic agents and drugs will first be tested in tissue culture on a suitable model system. For prospective anticancer drugs, for example, *in vitro* data obtained by proliferation or colony formation assays give useful initial information on the cytotoxicity of the agents. The preponderance of human tumor tissues now available with well-defined genetic makeup and detailed information of up- or downregulation of critical genes now means that the relevance of murine (mouse-derived) tumor models such as P388 and L1210 leukemias is somewhat diminished, although useful for preliminary data and also for historical and comparative purposes. *In vivo* assays also rely initially on the murine models for determination of pharmacokinetic properties, but the use of human tumor xenografts, while significantly more expensive than murine models, is also considered more relevant to the real situation. In evaluating true drug efficacy, attention must also be paid to routes of administration: a method where drug is delivered intraperitoneally to a tumor growing in the intraperitoneal cavity (ip/ip) is common but not as relevant to a clinical situation as intravenous administration to a tumor growing subcutaneously (sc/iv). The term “antitumor activity” should be reserved for data obtained on tumor regression in animals and not used for cytotoxicity data obtained from tissue cultures.

Phase I clinical trials assess safety and dose-limiting toxicity of prospective drugs and may be achieved with a relatively small number of patients. phase II clinical trials usually assess single-agent efficacy in defined diseases, i.e., ovarian cancer or relapsed ovarian cancer etc.; they generally involve many patients and may take a significant amount of time before statistically useful data are obtained. phase III studies may assess efficacy in combination regimens, as the chemotherapy of most cancers is treated in this manner. An overview of the drug development and approval process is available through web sites of agencies such as the US Food and Drug Administration²³ and the National Cancer Institute Developmental Therapeutics program.²⁴

The application of inorganic compounds to medicine requires detailed examination of the fundamental aqueous chemistry of the proposed drug, including its pharmacokinetics, the metabolic fate in blood and intracellularly, and the effects of the drug on the target of choice. Coordination and organometallic complexes present a wide variety of coordination spheres, ligand designs, oxidation states, and redox potentials, giving the ability to systematically alter the kinetic and thermodynamic properties of the complexes toward biological receptors. The toxicology of inorganic compounds in medicinal use, especially those containing the heavy metals, confronts the “stigma” of heavy metal toxicity; but therapeutic windows are rigorously defined to minimize such side effects—the usefulness of any drug is a balance between its toxicity and activity.

The toxicity of a compound may derive from its metabolism and unwanted “random” protein interactions. Human serum albumin is of fundamental importance in the transport of drugs, metabolites, endogenous ligands, and metal ions.²⁵ The crystal structure, combined with physical and biophysical studies, allows visualization of likely binding sites of many potential inorganic drugs.²⁶ Abundant cysteine-rich small peptides, especially glutathione (GSH) (Figure 1a), and proteins such as metallothionein²⁷ represent detoxifying but also deactivating pathways for inorganic drugs. A further source of metal ion/protein interactions is provided by transferrin, whose natural iron-binding site is accessible to many metal ions of similar radius and charge including Ru^{2+} , Ga^{3+} , and Al^{3+} .²⁸

The nature of the target to be attacked by any drug obviously depends on the specific application. Many cytotoxic metal complexes target DNA because of its importance in replication and cell viability. Coordination compounds offer many binding modes to polynucleotides, including outer-sphere noncovalent binding, metal coordination to nucleobase and phosphate backbone

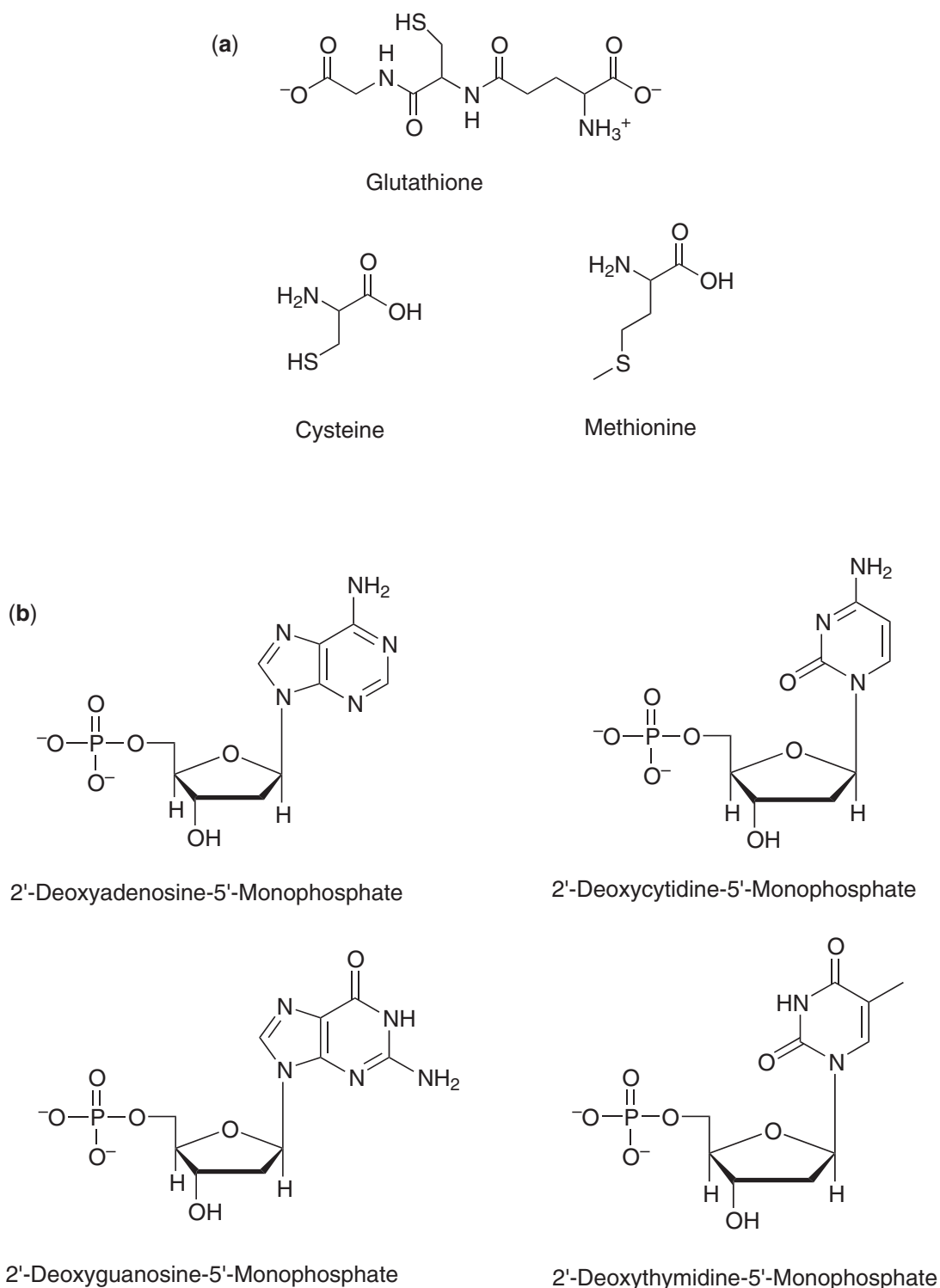


Figure 1 (a) Structures of common sulfur-based amino acids and tripeptides. (b) Structures of nucleic acid monophosphates capable of metal binding.

sites, as well as strand cleavage induced by oxidation using redox-active metal centers. The purine and pyrimidine mononucleotide building blocks are depicted in [Figure 1b](#). The later transition metals such as platinum and ruthenium favor binding to electron-rich nitrogens on the bases, especially guanine N7. Titanium and early metals may display a mixture of nucleobase and

Table 1 Medical and prospective medical uses of inorganic compounds.^a

Element	Compound	Uses	Trade names/comments
<i>Approved agents (mostly US or worldwide):</i>			
Li	Li ₂ CO ₃	Manic depression	Camcolit; Cibalith-S; Lithane (of many)
Fe	[Fe(NO)(CN) ₅] ²⁻	Vasodilation	Nipride. For acute shock. NO release
Ga	Ga(NO ₃) ₃	Hypercalcemia of malignancy	Ganite. Possible anticancer agent. In clinical trials for use in lymphomas
As	As ₂ O ₃	Anticancer agent	Trisenox. Use in acute promyelocytic leukemia
Ag	AgNO ₃	Disinfectant	Neonatal conjunctivitis
	Ag(sulfadiazene)	Antibacterial	Flamazone; Silvadene; treatment of burns. 1% cream
Sb	Sb ^{III} (tartarate)	Antiparasitic, leishmaniasis	Tartar Emetic Stibophen; Astiban
Pt	<i>cis</i> -[Pt(amine) ₂ X ₂]	Anticancer agents	Platinol; Paraplatin; Eloxatine Testicular, ovarian, colon cancers
Au	Au(PET ₃)(acetylthioglucose)	Rheumatoid arthritis	Ridaura. Orally active
Bi	Bi(sugar) polymers	Antiulcer; antacid	Pepto-Bismol; Ranitidine Bismutrex; De-Nol
Hg	Hg-organic compounds	Antibacterial	Thiomersal; mercurochrome (amongst many)
		Antifungal	Slow release of Hg ²⁺
<i>Agents in clinical trials:</i>			
Pt	Polynuclear Pt ^{IV} species	Anticancer agents	BBR3464, Satraplatin, AMD-473 Expands spectrum of activity of cisplatin; overcomes resistance; oral activity?
Mn	Mn chelates	Anticancer agents	SOD mimics
Ru	<i>trans</i> -[RuCl ₄ (Me ₂ SO)(Im)] ⁻	Anticancer agent	NAMI-A; antiangiogenic?
V	VO(maltate) ₂	Type II diabetes	BMOV; insulin mimetic
Ln	Ln(CO ₃) ₃	Hyperphosphatemia	Fosrenol; phosphate binder

^a Principal uses as medicinal agents. Other "trivial" or topical uses as ointments; antacids and skin desiccants for individual elements (especially Zn, Mg, and Al) may be found throughout.¹⁴

phosphate backbone binding. The accessibility of different oxidation states of metals such as Fe, Cu, Co, Ru, Mn, etc. may allow for redox chemistry resulting in strand breakage. Noteworthy in this respect is the anticancer antibiotic bleomycin, whose mode of action on target DNA is strand scission mediated by Fe binding to the drug.^{29,30}

Cytotoxic agents reduce the proliferation of a tumor but lack of selectivity between normal and malignant tissue may render many agents of little clinical utility. Drug discovery in general has been transformed by rapid advances in the understanding of the cell's molecular biology coupled with information sciences.³¹ Cancer treatment strategies especially have evolved in favor of agents targeted toward specific pathways, notably those involved in cell signaling.³² A challenge for the medicinal inorganic chemist is the placement of coordination chemistry within this new paradigm. This section reviews both established and evolving approaches to uses of inorganic-based drugs with emphasis on the most recent literature. The major clinical application and promising preclinical areas are summarized in Table 1.

9.18.2 PLATINUM COMPLEXES AS THERAPEUTIC AGENTS

9.18.2.1 Clinically Used Anticancer Agents. *Cis*-platinum Compounds

Cisplatin, (*cis*-[PtCl₂(NH₃)₂]), also known as *cis*-DDP (**1**, Figure 2) is perhaps the best known example of a small molecule metal-containing drug. The clinically used platinum complexes are shown in Figure 2. The history of the discovery and development of cisplatin remains a remarkable scientific story.³³ Its use and effectiveness in cancer chemotherapy since the entry into the clinic in the late 1970s has been thoroughly documented.³⁴⁻³⁶ Cisplatin is cited for treatment of

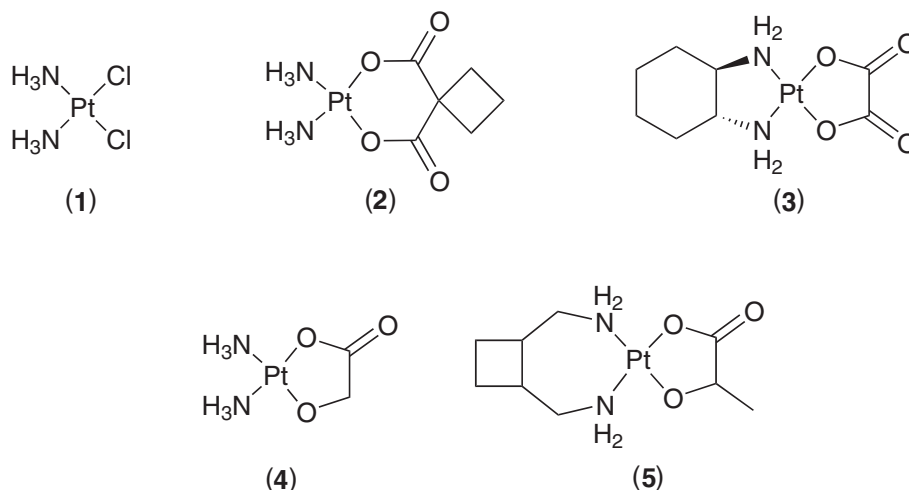


Figure 2 Structures of the clinically used platinum anticancer agents.

germ-cell cancers, gestational trophoblastic tumors, epithelial ovarian cancer, and small cell lung cancer as well as for palliation of bladder, cervical, nasopharyngeal, esophageal, and head and neck cancers.^{37–39} The use of cisplatin (usually as a principal component of combination regimens) has rendered at least one cancer, testicular cancer, curable and is significant in treatment of ovarian and bladder cancers. Typical doses range from 20 mg/m² to 100 mg/m², usually for up to five consecutive days. Despite this success, there is still a limited range of tumors sensitive to cisplatin intervention—some cancers are inherently resistant.^{40,41} A further disadvantage is the onset of clinical (acquired) resistance after treatment with the drug. The side effects of cisplatin treatment are severe and include the dose-limiting nephrotoxicity, neurotoxicity, ototoxicity, and emetogenesis. The “second-generation” compounds based on the cisplatin structure were developed in attempts to improve toxicity and/or expand the range of useful anticancer activity. Carboplatin (2) entered the clinic in 1998, principally in response to the necessity to reduce the toxic side effects of the parent drug. Despite this lower toxicity, carboplatin is essentially active in the same set of tumors as cisplatin and a broader spectrum of activity is not indicated.⁴² For some tumors, cisplatin appears to be therapeutically more effective than carboplatin (germ cell tumors, head and neck, and bladder) whereas for lung cancer and ovarian cancer effectiveness is comparable.⁴³ The choice of the most appropriate analog is a function of the cancer being treated, treatment intention (palliative or curative), and other component drugs used in combination.

Since the advent of cisplatin in the clinic, the consistent goals for drug development have been improvement of toxicity profile, circumvention of resistance, and expansion of the tumors sensitive to treatment by cisplatin. The importance of circumventing resistance was recognized very early on and reports of the activity of complexes containing 1,2-diaminocyclohexane (dach) in murine L1210 resistant to cisplatin date back to 1978.⁴⁴ After approval and use in Europe for a number of years, oxaliplatin (3) was finally granted approval for use in the US in August 2002 for colorectal cancer in combination with 5-fluorouracil (5-FU).^{45,46} Little information is available on nedaplatin (4) and lobaplatin (5), which have been approved for use in Japan and China, respectively.

DNA is accepted to be the cellular target of cisplatin. The natural sequence of scientific understanding has developed from a detailed structural understanding of the cisplatin–DNA interaction to the biological consequences of these adducts. In this respect, the field has also kept pace with the understanding of cellular cancer biology over the same period. Thus, it is not the DNA adduct *per se* but the downstream effects of protein recognition and cell signaling events that are the ultimate causes of cell death. In essence, the two major pathways a cell must take upon receiving an “insult” such as a chemotherapeutic drug, or indeed a mutagenic lesion in any fashion, are (i) to repair the damage, or (ii) or initiate the pathway to apoptosis (programmed cell death). The factors that affect cisplatin cytotoxicity, whether in sensitive or resistant cells, are summarized in Figure 3. DNA damage by chemotherapeutic agents is in many cases mediated through the p53 pathway.⁴⁷ Cisplatin damage to DNA stimulates apoptosis via a p53-dependent pathway, although in some cell lines or tumor types a p53-independent pathway has been observed.^{48,49}

Resistance to cisplatin is multifactorial and has been shown to be due to a combination of decreased cellular accumulation of cisplatin, increased efflux of platinum from the cell,

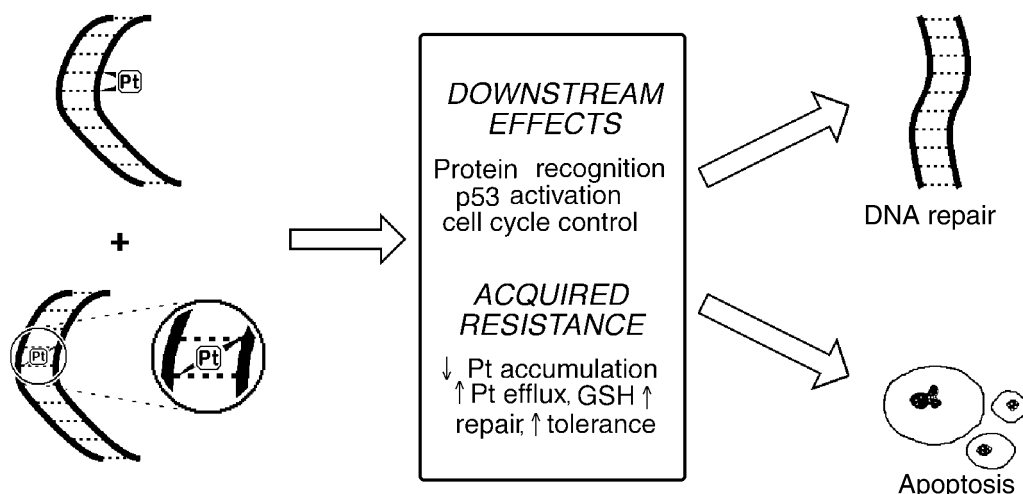


Figure 3 A general scheme for cellular response to platinum-induced DNA damage.

increased cytoplasmic detoxification (through increased levels of cellular thiols such as GSH), or enhanced repair/tolerance of platinum-DNA adducts.^{50,51} Cellular accumulation of cisplatin is a much more complicated process than previously thought—both active and passive diffusion pathways are now thought to exist.⁵² The establishment of resistant cell lines with characterized and calibrated mechanisms of action has aided greatly in advancing a molecular approach to overcoming resistance.^{53,54} Coupled with this understanding has been the necessity to understand the fate or metabolism of cisplatin in the biological milieu and explain the pharmacokinetic profile of the drug. For the purposes of this review, the major outlines of the biological understanding will be reviewed with reference to key understandings and most recent comprehensive reviews.

The rate-limiting step in DNA binding is aquation of the Pt—Cl bonds. The major products of the aquation of cisplatin are the mono- and bis-aqua species $cis-[Pt(NH_3)_2(H_2O)Cl]^+$ and $cis-[Pt(NH_3)_2(H_2O)_2]^{2+}$, respectively (Figure 4).

Deprotonation gives inert hydroxo species, which may also form dinuclear and trinuclear hydroxo-bridged species in concentrated solution. Calculation of the pK_a of the coordinated water molecules coupled with equilibrium constants for both aquation and deprotonation reactions allows calculation of speciation in biological medium.^{55,56} The compound, and its direct structural analogs, form adducts between neighboring guanine residues on DNA, forming d(GG) 1,2-intrastrand and d(GC) interstrand cross-links, shown schematically in (Figure 5). Minor lesions, which have consequently received somewhat less attention, are 1,2-intrastrand cross-links formed between an adenine and a guanine in a d(AG) adduct as well as a 1,3-intrastrand cross-link where two platinated guanines are separated by one base pair—d(GNG).

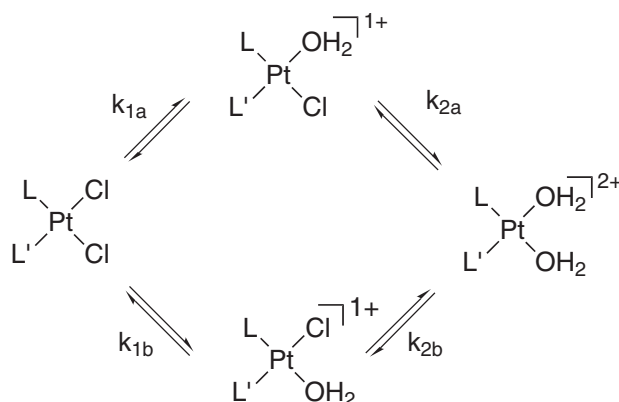


Figure 4 Hydrolysis scheme for cisplatin-based anticancer agents. Where $L=L'=NH_3$ cisplatin is indicated. When $L=NH_3$ and $L'=2$ -picoline or cha the rates of aquation of the *trans*-chloride ligands are different.

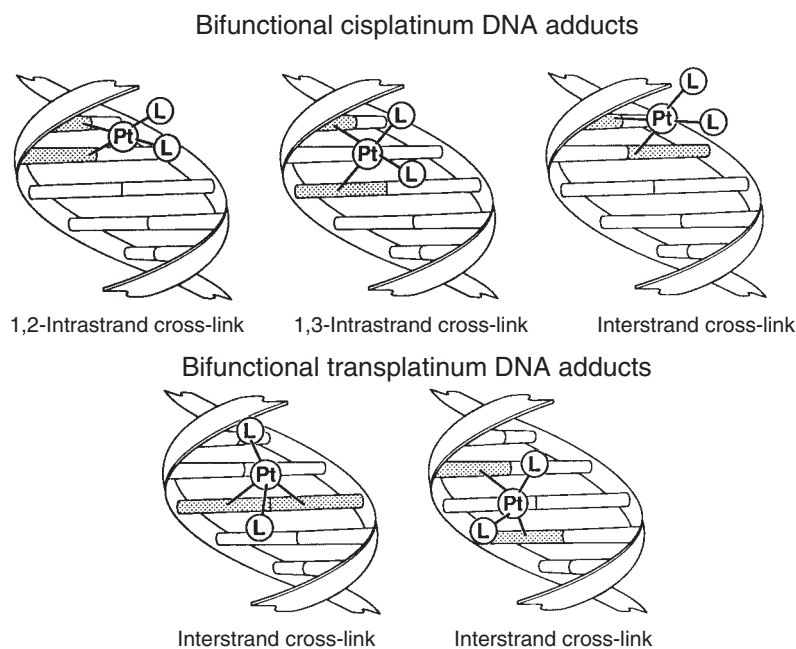


Figure 5 Schematic depiction of cross-links formed by both *cis*- and *trans*-platin.

The application of $\{^1\text{H}, ^{15}\text{N}\}$ HSQC NMR techniques has proven to be very informative in elucidating detailed kinetic parameters for both aquation and DNA-binding processes. Platinated DNA may be observed at low (μM) concentrations because only ^1H and ^{15}N resonances derived from platinum am(m)ine species are seen and the ^{15}N shifts are strongly influenced by the *trans* ligand.^{57,58} The mono-aquated species is the most likely reactant with DNA, although evidence has also been put forward for the importance of the *cis*- $[\text{Pt}(\text{NH}_3)_2(\text{H}_2\text{O})_2]^{2+}$ species in this regard.⁵⁹ The hydrolysis of carboplatin involves the displacement of the chelating cyclobutane-1,1-dicarboxylate from the coordination sphere and is unsurprisingly very slow. In the presence of acid, the process resembles the successive displacement of two monodentate carboxylates.⁶⁰ In keeping with the kinetic inertness of carboplatin, significantly higher doses are required for both equivalent levels of DNA platination compared to cisplatin and also to generate equitoxic and equivalent antitumor effects—clinical doses are 800–900 mg/m².³⁶ The benefit, of course, is reduced nephrotoxicity as the drug may be excreted essentially intact.

The well-known affinity for sulfur binding of Pt^{II} has led to detailed study of interactions with GSH, metallothionein, and human serum albumin.^{61,62} Interestingly, direct substitution of the Pt–Cl bonds by sulfur donors such as cysteine and GSH, without the necessity for prior aquation, is indicated from kinetic studies.^{63,64} Eventually, binding of the thiolate also results in displacement of the ammonia ligands by chelation of the tripeptide moiety.⁶⁵ Novel binding modes involving *N*-ligation from deprotonated amide bonds as well as sulfur have been deduced from the reaction of $[\text{PtCl}_2(\text{en})]$ (where en = ethylene 1,2 diamine) and GSH.⁶⁶ Platinum-thiolate species $[\text{Pt}-\text{RS}^-]$ display a great tendency to form dinuclear bridging structures $\{\text{Pt}-\mu(\text{RS})-\text{Pt}\}$ as the bound thiolate is even more nucleophilic than free ligand.⁶⁷ The crystal structure of $[\text{Pt}_2(\mu-N\text{-acetylcysteine})_2(2,2'\text{-bipyridine})_2]$ confirms the bridging propensity of thiolate.⁶⁸ Methionine metabolites such as $[\text{Pt}(\text{Met}-S,N)_2]$ have been identified from the urine of cisplatin-treated patients, emphasizing the importance of this amino acid in the biotransformation of the drug.⁶⁹ The mechanism of formation has been studied—the metabolite exists predominantly as the *cis* isomer (*cis:trans* = 87:13).⁷⁰ Methionine interactions with carboplatin and the formation of a stable ring-opened species may provide a chemical understanding of the activation of this inert drug.⁷¹ A combination of 2D NMR techniques, chemical modification of the protein, and gel filtration chromatography identified the dominant binding site on Human Serum Albumin (HSA) as involving methionine rather than the expected Cys-34.⁶² The propensity of platinum binding to sulfur has also led to use of sulfur compounds as rescue agents in cisplatin toxicity.⁶³ In these cases, a balance must be found between overcoming toxicity and reduction of antitumor efficacy through competitive binding.

The binding of Pt to DNA is irreversible and is kinetically controlled. Platinum may be removed from DNA by strong nucleophiles such as CN^- . NMR methods have also provided new insight into

the kinetics and mechanism of DNA binding by cisplatin and other mononuclear analogs. The sequence dependence on the rate constants for monofunctional and bifunctional adduct formation have been cataloged.⁷² The structural consequences of bifunctional binding for the major intrastrand and interstrand adducts have now been elucidated in great detail (Figure 6).⁷³

The requirement to bind two adjacent guanines on the same strand of DNA to form the intrastrand adduct, whilst maintaining the square-planar geometry of Pt^{II}, places considerable steric restraints on the final structure. Molecular and biological studies have confirmed that the principal effect of bifunctional intrastrand binding to DNA is a bending of the helical axis toward the major groove—exact measurements of bending angle vary to some extent with technique but a typical value of approximately 30–35° is often quoted from gel electrophoresis studies.⁷² The high resolution X-ray crystal structure of the 1,2-intrastrand adduct in the sequence d(CCTCTG*G*TCTCC)_d(GGAGACCAGAGG) shows the helix bending of approximately 50° toward the major groove.⁷⁵ The DNA is a mixture of conformations—B-form on the 3'-side of the adduct and the more condensed A-form on the 5'-side. In agreement with the possibility that the A-form is induced by crystal packing forces or the concentrations of cations in the crystallization procedure, the DNA remains in the B-form in solution.⁷⁶ The d(ApG) adduct appears to be similarly kinked.⁷⁷ Spectroscopic (especially NMR) studies on the sequence dependence of the adduct have been reviewed.^{72,78,79} Carboplatin, as might be expected, gives the same adducts on DNA as cisplatin since loss of the dicarboxylate produces the same *cis*-{Pt(NH₃)₂}²⁺ moiety. Interestingly, the crystal structure of the oxaliplatin adduct of the same dodecanucleotide shows the overall geometry to be very similar to the cisplatin case, with a bending of approximately 30° toward the major groove. The enantiomerically pure (*R,R*)-dach ligand results in a hydrogen bond between the pseudoequatorial NH hydrogen and the O-6 atom of the 3-guanine, emphasizing the importance of chirality in mediating biological properties.⁸⁰ These results confirm the findings that the oxaliplatin-induced damage of cellular DNA and its consequences are very similar to those of cisplatin.^{81,82}

The interstrand cross-link also induces DNA bending.⁷² X-ray and NMR studies on this adduct show that platinum is located in the minor groove and the cytosines of the d(GC) base pair involved in interstrand cross-link formation are “flipped out” of the helix stack and a localized “Z-form” DNA is observed.^{83–85} This is a highly unusual structure and very distorting—implications for differential repair of the two adducts have been addressed. Alternatively, the interstrand cross-link of the antitumor inactive *trans*-DDP is formed between a guanine (G) and its complementary cytosine (C) on the same base pair.^{86,87} *trans*-DDP is sterically incapable of producing 1,2-intrastrand adducts and this feature has been cited as a dominant structural reason for its lack of antitumor efficacy. It is clear that the structural distortions induced on the DNA are very different and likely to induce distinctly different biological consequences.

Cisplatin-adducted DNA is recognized by a host of proteins.^{52,72,73,88,89,90} Two general classes of protein may be identified—those that specifically recognize the platinated sites as a first step in their repair, and those that bind to such sites because of structural similarity to the protein's natural binding sites. DNA repair occurs primarily through the nucleotide excision repair pathway and proteins of the first class include the human excision repair complex, mismatch repair proteins, XPA, and RPA (single stranded binding proteins involved in DNA replication and repair) proteins. DNA damage induced by cisplatin is recognized by proteins containing the

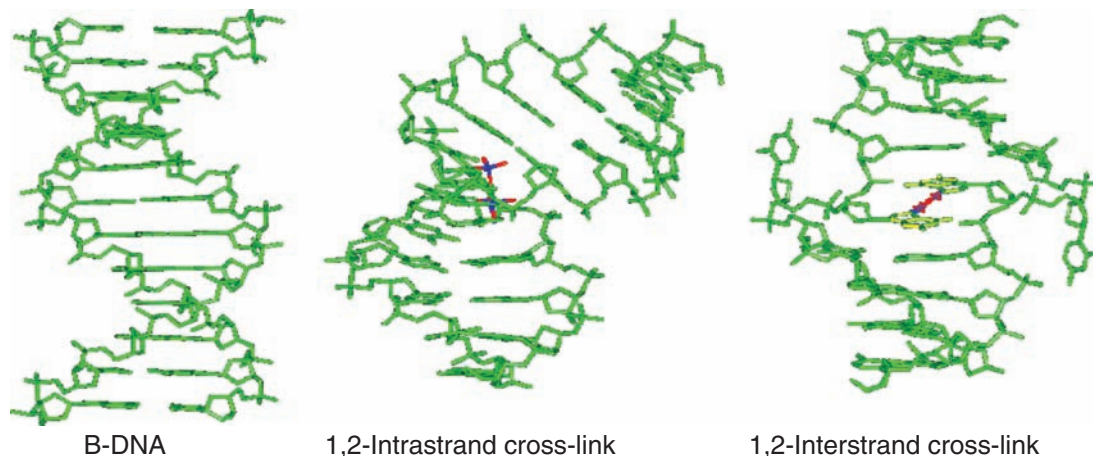


Figure 6 Structures of the major cisplatin/DNA adducts.

so-called high mobility group (HMG) domain motif. The exact function of these nuclear but extrachromosomal DNA binding proteins is still a matter of debate but they bind strongly to unusual noncanonical DNA structures, such as cruciform DNA.⁹¹ A common feature of all HMG domain proteins is their ability to bend DNA. Several HMG domain proteins recognize cisplatin-DNA adducts but not those of the clinically ineffective adducts of *trans*-DDP or the monofunctional $[\text{PtCl}(\text{dien})]^+$ (where dien = diethylenetriamine). This preferential recognition has led to the suggestion that proteins with high binding affinity for cisplatin-damaged DNA may shield the polynucleotide from cellular repair. The structural characterization of the recognition motifs of HMG protein and cisplatin-adducted DNA give insight into the molecular details of protein recognition.⁹² Domain A of the structure-specific HMG-domain protein, HMG1, binds to the widened minor groove of a 16-base pair DNA duplex containing a site-specific 1,2-GG intrastrand cross-link. The DNA in the protein complex is bent significantly further than in the Pt-DNA adduct alone, and a phenylalanine moiety intercalates into a hydrophobic notch created at the platinated d(GpG)-binding site. The importance of an intercalating protein residue such as phenylalanine in forming the bend and in contributing to the affinity toward platinated DNA was confirmed by site-directed mutagenesis where removal of the intercalating moiety reduced binding affinity.⁹³

9.18.2.2 Platinum Compounds in Clinical Trials

The need for new agents in cancer chemotherapy is apparent from the inability to predictably cure or induce remissions in common tumors such as breast, lung, colon, or prostate cancer. New cytotoxic agents building on our experience and knowledge of the current armamentarium continue to play an important role in the clinical management of cancer. Approximately 28 direct structural analogs of cisplatin entered clinical trials but most have been abandoned through a combination of unacceptable toxicity profile and/or lack of improved or expanded anticancer efficacy.³⁸ For new, direct structural analogs of cisplatin to find clinical use exceptional properties would need to be found.³⁸ Currently, there are three principal drugs ((6)–(8); Figure 7) in clinical trials—the approaches to their development represent examples of steric control of reactivity, control of oxidation state and ligand lipophilicity aimed at producing orally active agents, and manipulation of new structures to produce structurally new DNA adducts.

9.18.2.2.1 AMD473 (ZDO-473)

As understanding of the mechanisms of platinum resistance has increased, more rationally designed platinum derivatives have been synthesized. One approach has been to insert steric

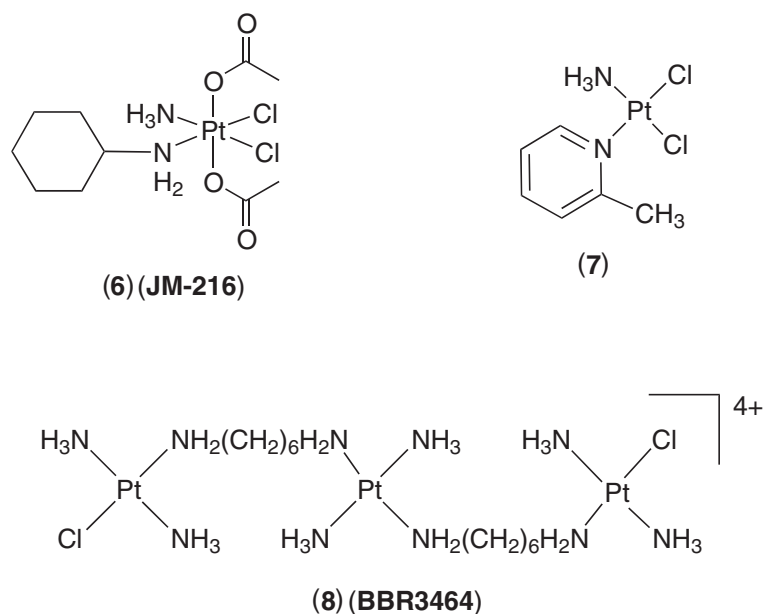


Figure 7 Platinum-based drugs in clinical trials.

bulk at the platinum center to retard the kinetics of substitution in comparison to cisplatin.^{94,95} AMD473 (*cis*-[PtCl₂(NH₃)(2-methylpyridine)], also known as ZDO-473 (7)) (AnorMED; <http://www.anormed.com>) is a molecule that was designed specifically to circumvent thiol-mediated drug resistance by sterically hindering its reaction with GSH while retaining the ability to form cytotoxic adducts with DNA.⁹⁶ GSH competes for platinum binding and may diminish DNA platination, thus reducing cytotoxicity. The rate of aquation of AMD473 is 2–3 times slower than that of cisplatin,⁹⁷ and interstrand cross-link formation is much slower. The DNA binding is similar to cisplatin, and the complex forms a highly stereoselective adduct on DNA, but not for reactions with mono- and dinucleotides.⁹⁸ In cell lines with previously determined mechanisms of cell resistance, AMD473 showed little cross-resistance compared with cisplatin or carboplatin. This partial or complete circumvention of acquired platinum drug resistance makes this a promising compound for clinical development. It is currently undergoing phase II trials where it has shown linear pharmacokinetics and evidence of antitumor activity in ovarian cancer patients. It has a manageable side effect profile; the dose-limiting toxicity was a reversible, dose-dependent thrombocytopenia. Nonhematological toxicities (nausea, vomiting, and metallic taste) were mild. No nephrotoxicity, peripheral neurotoxicity, or ototoxicity has been observed.⁹⁹

9.18.2.2.2 JM-216 (*Satraplatin*)

Another avenue in platinum chemistry is to manipulate chemical and biological properties through oxidation number. Indeed, the early Rosenberg studies recognized the Pt^{IV} complex *cis*-[PtCl₄(NH₃)₂] as an active anticancer agent.³³ A number of Pt^{IV} compounds have since undergone clinical trials—including *cis*-[PtCl₄(1,2-dach)], known as tetraplatin, and *cis,cis,cis*-[PtCl₂(OH)₂(PrⁱNH₂)₂], known as CHIP or Iproplatin. These compounds have been abandoned because of either undesirable side effects or lack of a significantly enhanced therapeutic range compared to cisplatin.³⁸ Potential oral activity of JM-216 (6) is achieved by carboxylation of the Pt-OH groups as well as replacement of one NH₃ group by the more lipophilic cyclohexylamine (cha). Interestingly, *trans*-Pt^{IV} compounds were also tested because their kinetic inertness give more reasonable *in vivo* activity than their analogous Pt^{II} compounds (see Section 9.18.2.2.4).¹⁰⁰ The cytotoxicity is dependent on the reduction potential of the Pt^{IV} compound, allowing suitable modification of pharmacokinetic parameters.¹⁰¹ Biological reducing agents, however, such as GSH, reduce Pt^{IV} readily.^{102,103} The general synthetic scheme for JM-216 is shown in Figure 8¹⁰⁴ In practice use of I⁻ in the first step to give *cis*-[PtCl(I)(NH₃)(cha)] (mixture of isomers) followed by conversion to the dichloride greatly facilitates synthesis.

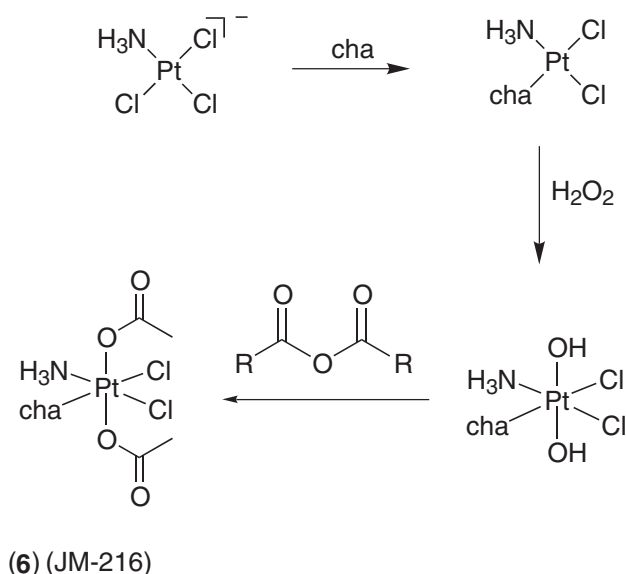


Figure 8 Preparation of JM-216.

Despite the reputed inertness of Pt^{IV} compounds, JM-216 undergoes rapid biotransformation in human red blood cells.¹⁰⁵ The Pt^{II} complex *cis*-[PtCl₂(NH₃)(cha)] is the major metabolite.¹⁰⁶ The consequences of DNA binding are again similar to those of cisplatin, as expected from the general similarity of the *cis*-dichlorodiam(m)ineplatinum structure.¹⁰⁷ An interesting difference between the cha and pyridine groups is that in the former case stereoisomers are seen in the 1,2-intrastrand adduct—the cha group may reside either on the 3' or 5' end of the duplex. The cytotoxicity of both the Pt^{II} and Pt^{IV} compounds has been examined extensively. The compound was well tolerated orally.^{108,109} Interest has recently been revived in this agent.

9.18.2.2.3 Poly (di and tri)-nuclear platinum complexes

All direct structural analogs of cisplatin produce a very similar array of adducts on target DNA and it is, therefore, not surprising that they induce similar biological consequences. This latter consideration led to the hypothesis that development of platinum compounds structurally dissimilar to cisplatin may, by virtue of formation of different types of Pt-DNA adducts, lead to compounds with a spectrum of clinical activity genuinely complementary to the parent drug.^{110–113} In terms of cellular biology, the cell signals (structure and conformation of Pt-DNA adducts as outlined in Figure 3) must be altered to produce different cell signaling and protein recognition and induction effects downstream of the platination event, which may be eventually reflected in an altered pattern of antitumor activity. Polynuclear (dinuclear and trinuclear) bifunctional DNA-binding agents are amongst the best studied of these nonclassical structures. The class as a whole represents a second, distinctly new structural group of platinum-based anticancer agents. The first example of this class to advance to clinical trials is BBR3464 ((8), Figure 7).

The dinuclear structure is extremely flexible and capable of producing a wide series of compounds differing in functionality (bifunctional to tetrafunctional DNA-binding), geometry (leaving chloride groups *cis* or *trans* to diamine bridge), as exemplified in Figure 9.¹¹⁴ Further systematic variations on nonleaving groups in the Pt coordination spheres (NH₃ or a planar group such as pyridine or quinoline) and linker (flexible, variable chain length) are also possible.¹¹⁵

The patterns of DNA modification induced by the various structural motifs have been examined and further related to cytotoxicity and antitumor activity.^{116,117} The necessity to concentrate on a limited number of compounds identified the 1,1/t,t series (see Figure 9 for explanation of this nomenclature) as having the most promising pattern of antitumor activity and DNA-binding. Linker modifications have produced most success in terms of enhanced cytotoxicity. The presence of charge and hydrogen bonding capacity within the central linker (either in the form of a tetraamineplatinum moiety, or a charged polyamine linker such as spermidine or spermine), Figure 9b, produces very potent compounds significantly more cytotoxic than the “simple” dinuclear species. Their biological activity varies with chain length and charge, although the overall profile is similar.

(i) BBR3464. A trinuclear platinum clinical agent

The first polynuclear drug to enter clinical trials (in June 1998), and the first platinum drug not based on the cisplatin structure, is the trinuclear compound denominated BBR3464 ((15), Figure 9b). The structure, derived from general structures of trinuclear systems¹¹⁸ is notable for the presence of the central Pt, which contributes to DNA affinity only through electrostatic and hydrogen bonding interactions. The 4+ charge, the presence of at least two Pt coordination units capable of binding to DNA, and the consequences of such DNA binding are remarkable departures from the cisplatin structural paradigm.

In tissue culture, BBR3464 is cytotoxic at 10–100-fold lower molar concentrations than cisplatin and displays activity in cisplatin-resistant cell lines.¹¹⁹ The profile of antitumor efficacy mirrors its unique structure and is characterized by activity in human tumor (e.g., ovarian) xenografts resistant to cisplatin and alkylating agents.¹²⁰ Importantly, BBR3464 also consistently displays high antitumor activity in human tumor xenografts characterized as mutant p53.¹²¹ These tumors are historically insensitive to drug intervention. This important feature suggests that the new agent may find utility in the over 60% of cancer cases where mutant p53 status is indicated. Consistently, cytotoxicity displayed in mutant cell lines would suggest an ability to by-pass this pathway. In agreement, transfection of p53 into p53-null SAOS osteosarcoma cells resulted in a marked reduction in cellular

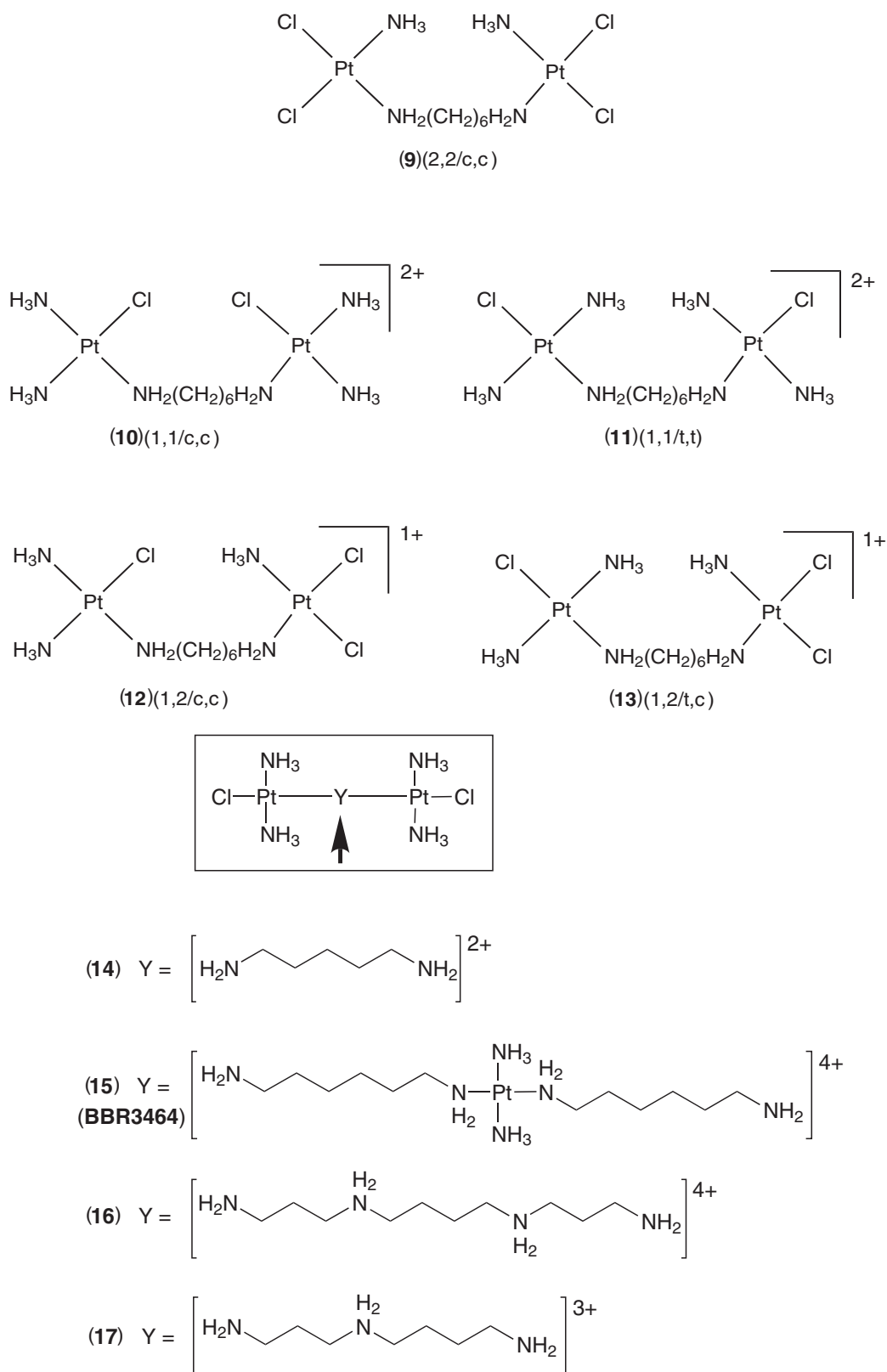


Figure 9 (a) Variation of structures of dinuclear platinum complexes depending on the coordination sphere of the platinum. The structural notation describes the number of chloride ligands at each platinum center, followed by the position of the leaving group at each site (*cis* or *trans*) with respect to the N atom of the bridging diamine. (b) Variation of linker diamine within one class of dinuclear complexes producing both the trinuclear structure and polyamine-bridged species.

sensitivity to BBR3464 but only a slight sensitization to cisplatin. In addition, in contrast to cisplatin, the triplatinum complex was a very effective inducer of apoptosis in a lung carcinoma cell line carrying mutant p53. Cell cycle analysis showed a dose-dependent G₂/M arrest by BBR3464.¹²²

In phase I clinical trials 47 patients, all of whom had previously failed standard treatments for solid tumors, received the drug in the UK, Italy, and Switzerland on three different schedules.^{123,124} Dose-limiting toxicities have been defined as bone marrow depression and diarrhea. The latter is treatable with loperamide. Signs of biological activity were seen. Notably one patient with metastatic pancreatic cancer showed a partial response (for 4 months) and two further patients, one with metastatic melanoma and one with bronchoalveolar carcinoma, also showed partial responses. In a phase I trial in combination with 5-FU, a partial response in breast cancer was observed.¹²⁵ Furthermore, a reduction in tumor marker levels was observed in two patients, one with ovarian cancer, and one with colon cancer. Phase II studies have shown partial responses in cisplatin-resistant ovarian and nonsmall-cell lung cancer.^{126,127} The indications are that the profile of clinical activity is different and complementary to the mononuclear platinum agents.

Cellular pharmacology studies showed enhanced cellular uptake of the charged polynuclear platinum compounds in comparison to cisplatin.^{128,129} This in itself is very surprising given that the “classical” structure–activity paradigms for platinum agents require complex neutrality. The enhanced uptake is not sufficient to explain, by itself, the increased cytotoxicity of BBR3464. Formation of BBR3464-induced interstrand cross-links in L1210/0 (murine leukemia) and U2-OS (human osteosarcoma) cells peaks at the earliest time points observed. Their persistence over time and very slow removal suggests that they are not good substrates for DNA repair. The cellular response of HCT116 (human colon tumor) mismatch repair-deficient cells was consistent with a lack of influence of mismatch repair status on BBR3464 cytotoxicity.¹²¹

(ii) DNA binding of polynuclear platinum compounds

The polynuclear platinum compounds stand in vivid contrast to mononuclear platinum complexes because the predominant DNA lesions are long-range inter- and intrastrand cross-links where the sites of platination may be separated by up to four base pairs. The consequent structural and conformational changes in DNA are also distinct.

(iii) Aquation of dinuclear and trinuclear platinum agents

The hydrolysis profile of platinum complexes with monofunctional [Pt(amine)₃Cl] coordination spheres (e.g., mononuclear complexes such as [PtCl(dien)]⁺ or [PtCl(NH₃)₃]⁺ and the 1,1/t,t and 1,1/c,c dinuclear compounds of (Figure 9) differs from that of cisplatin.¹³⁰ The aquation rate constant is comparable, but the reverse chloride anation rate constant is much higher so that the equilibrium favors the chloro form.¹³¹ For the dinuclear diaqua complex [*trans*-Pt(H₂O)(NH₃)₂]₂μ-(H₂N(CH₂)₆NH₂)⁴⁺ the pK_a of the aqua ligands (pK_a 5.62) is much lower than in *cis*-[PtCl(H₂O)(NH₃)₂]⁺ (pK_a 6.41). For the trinuclear compound BBR3464 the aquation rate constant is comparable to the dinuclear analog, but the chloride anation rate constant is lower so that there is a significantly greater percentage of aquated species (~30%) present at equilibrium. The pK_a of 5.62 for the aqua ligands is identical to the dinuclear case. Based on the calculated equilibrium and dissociation constants, and assuming physiological pH (7.2), the maximum tolerated dose (MTD) of BBR3464 in patients corresponds to 1.8 × 10⁻⁸ M and at an intracellular chloride concentration of 22.7 mM the drug will be 98.7% in the dichloro form at equilibrium. In blood plasma, at a [Cl⁻] of 103 mM only 0.3% of the total is aquated.¹³²

(iv) Reactions with oligonucleotides

Global DNA binding of polynuclear platinum compounds is characterized by very rapid binding, a high level of DNA–DNA interstrand cross-links, unwinding of supercoiled plasmid DNA typical of bifunctional DNA binding, and a sequence specificity different from that of cisplatin.^{133,134} Strong sequence preference for single dG or d(GG) sites was found and molecular modeling suggested various possible adducts including 1,4-(G,G) and 1,6-(G,G) interstrand and 1,5-(G,G) intrastrand cross-links, which were similar in energy (Figure 10).

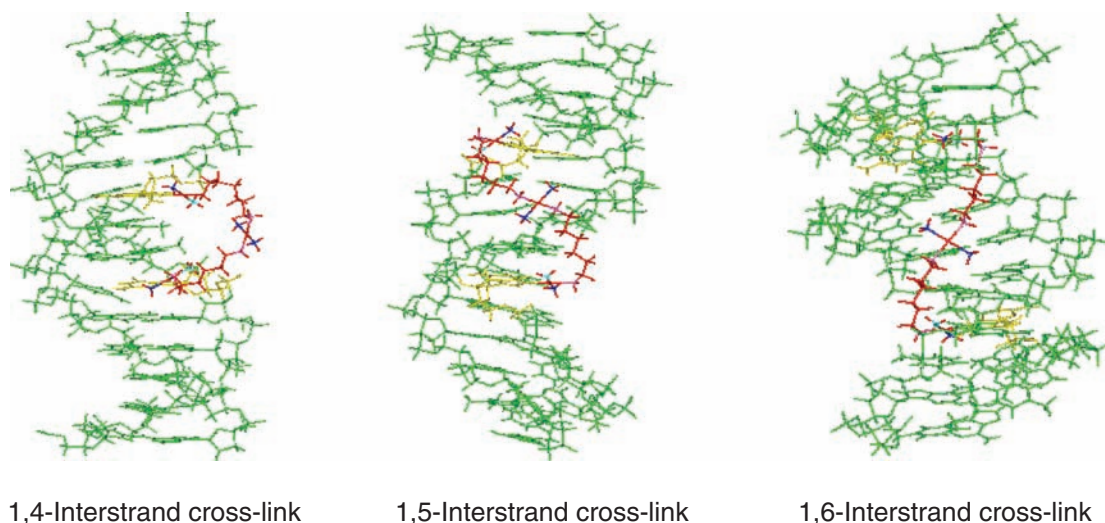


Figure 10 Structures from molecular modeling of the major DNA adducts of BBR3464.

Due to the charged nature of polynuclear platinum complexes, ranging from 2+ to 4+, it is not surprising that binding to DNA occurs significantly more rapidly than for cisplatin. The binding of polyamine-bridged dinuclear compounds is even faster than BBR3464, suggesting strong preassociation or electrostatic binding prior to covalent attachment. Conformational changes characteristic of the B \rightarrow A and B \rightarrow Z transitions have been observed in poly(dG)·poly(dC) and poly(dG-dC)·poly(dG-dC) modified by all polynuclear platinum compounds.^{135–138} Ethidium bromide binding favors the B-form of DNA, and intercalation into Z-DNA induced by NaCl or [Co(NH₃)₆]³⁺ results in reversal to the B-form.¹³⁹ In contrast, intercalation into A- and Z-form DNA induced by dinuclear or trinuclear platinum compounds is inhibited indicating that the conformational changes are essentially irreversible. The ability to maintain unusual DNA conformations in solution is a unique characteristic of polynuclear platinum compounds. Induced A-like conformations *in vivo* are theorized to be control mechanisms for DNA binding proteins like transcription factors.¹⁴⁰ The biological function of Z-DNA is still not clearly defined;¹⁴¹ but Z-DNA is known to form in the wake of RNA polymerase as DNA is transcribed.¹⁴³ The conformational “locking” into either A- or Z-form by polynuclear platinum compounds is likely to have profound effects on DNA function. Antibodies raised to cisplatin-DNA adducts do not recognize DNA adducts of dinuclear or trinuclear compounds.

An interesting and potentially important finding is that BBR3464 is preferentially bound to single-stranded rather than double-stranded DNA.¹⁴³ Comparison of single-stranded DNA, RNA, and duplex DNA indicated that the reaction of BBR3464 with single-stranded DNA and RNA was faster than with duplex DNA, and produced more drug–DNA and drug–RNA adducts. BBR3464 binding to different nucleic acid conformations raises the possibility that the adducts of single-stranded DNA and RNA may play a role in the different antitumor efficacies as compared with cisplatin. Single-stranded DNA is present during transcription, replication, recombination, and repair and is recognized by various single-stranded DNA binding proteins.

The kinetics of the reaction of the self-complementary 12-mer duplex d(5'-A₁T₂ATGTA₇CA-TAT-3')₂ with ¹⁵N labeled [trans-PtCl(NH₃)₂]₂μ-(H₂N(CH₂)₆NH₂)⁴⁺ and BBR3464 indicated the formation of 1,4-interstrand cross-links.^{144,145} Initial preassociation or electrostatic binding to DNA is observed in both cases, as deduced by chemical shift changes in presence of DNA immediately upon mixing. The time scale of the NMR experiment makes the weak preassociation of cisplatin difficult to observe, although it may be observed with techniques such as quartz crystal microbalance and mass spectrometry. The former system permits direct, real time detection of interactions between platinum complexes and surface immobilized oligonucleotides (in this case 5'-GGGAAGGATGGCGCACGCTG-3').¹⁴⁶ The closure rates to form bifunctional adducts are significantly faster than the rate of closure to form a 1,2 GG intrastrand cross-link by *cis*-[Pt(H₂O)₂(NH₃)₂]²⁺. For the dinuclear compound, consideration of the ¹H {Guanine H(8)} and ¹⁵N shifts of the interstrand cross-link showed that an initially formed conformer converts into another nonreversible final product conformer.

The 1,4-interstrand cross-link of BBR3464 with the self-complementary 5'-(ATGTACAT)₂-3' has been characterized and analyzed by MS and CD, UV and NMR spectroscopy.¹⁴⁷ The alternating purine–pyrimidine sequence mimics the structural requirements for Z-DNA. NMR analysis of the adduct shows the strong H8/H1' intraresidue cross-peaks for the platinated guanine residues, consistent with a *syn* conformation of the nucleoside. More interestingly, a strong H8/H1' intraresidue cross-peak for the A7 resonance is also consistent with a *syn* conformation for this base which is usually not observed for adenine residues and bases not directly involved in the cross-link in oligonucleotides. Within the sequence covered by the cross-link, the bases appear to be a mixture of *syn* and *anti* and Watson-Crick hydrogen bonding is maintained. The central platinum unit resides in the minor groove. The observation of an altered conformation (Adenine N7 *syn*) outside the binding site is unique and suggests the possibility of delocalized lesions beyond the binding site. In contrast, long-range interstrand cross-linking agents such as CC-1065 and Bizelesin do not show conformational changes beyond the environment of the binding sequence.^{148–150} These unusual cooperative effects are unique to this class of anticancer drug and are the first demonstration of cooperative effects in solution for an anticancer drug.

(v) *Site-specific intrastrand and interstrand cross-links of BBR3464. Bending, protein recognition and nucleotide excision repair*

Oligonucleotide duplexes containing various site-specific intra- and interstrand cross-links formed by both dinuclear [*trans*-PtCl(NH₃)₂]₂μ-(H₂N(CH₂)_nNH₂)]²⁺ and trinuclear compounds have been prepared. The 1,2-intrastrand cross-link with one Pt unit each attached to two adjacent guanines is formally the structural analog of the most prominent adduct formed by cisplatin. The dinuclear intrastrand adducts distorted the DNA conformation in a way different from those seen for adducts of cisplatin.^{151–153} Bending induced in DNA by dinuclear interstrand cross-links is not directed, and at approximately 10–12° is much less than that of cisplatin, as was duplex unwinding (9° vs. 13°, respectively). As a result, gel retardation assays revealed only very weak recognition of DNA adducts by HMG1 protein.¹⁵⁴ For BBR3464 intrastrand site-specific adducts were also prepared which create a local conformational distortion but without a stable curvature.¹⁵⁵ Again, no recognition by HMG1domA and HMG1domB proteins was evident and it is clear that the intrastrand DNA adducts of BBR3464 may present a block to DNA or RNA polymerases but are not a substrate for recognition by HMG-domain proteins.

In general, DNA interstrand cross-links could be even more effective lesions than intrastrand adducts in terminating DNA or RNA synthesis in tumor cells and thus could be even more likely candidates for the genotoxic lesion relevant to antitumor effects of BBR3464.¹⁵⁶ In addition, the interstrand cross-links pose a special challenge to repair enzymes because they involve both strands of DNA and cannot be repaired using the information in the complementary strand for resynthesis.¹⁵⁷ Unlike the intrastrand adduct, the interstrand cross-link is a poor substrate for nucleotide excision repair. These results validate the finding that overexpressing the human nucleotide excision repair complex (ERCC1) was not detrimental to the cellular sensitivity of BBR3464 in two ovarian cancer cell lines.¹⁵⁸

These findings in sum suggest that these structurally distinct compounds produce a profile of DNA damage that is quite distinct from that of cisplatin. Lack of recognition by proteins which bind avidly to cisplatin-damaged DNA suggest that the mediation of antitumor properties of polynuclear platinum compounds by cisplatin-like processes is unlikely. Thus, the structural paradigm for antitumor activity based on the cisplatin structure is no longer valid—clinically useful compounds may arise from study of new structures. Following this work, new dinuclear compounds based on heterocycle azole and 4,4'-dipyrazolylmethane bridges have also been described ((18)–(20), Figure 11).^{159–161} These agents again give a different spectrum of activity to the dinuclear complexes with flexible diamine linkers.

9.18.2.2.4 *Transplatinum compounds*

The earliest “structure–activity” relationships indicated that the transplatinum geometry is inactive—significantly higher doses must be given before any therapeutic effect is seen. In 1991, it was reported that alteration of amine structure and the introduction of sterically hindered amines produced cytotoxicity similar to that of cisplatin.¹⁶² The first examples used planar amines and a variety of *trans*-[PtCl₂(L)(L')] compounds have been synthesized and evaluated ((21)–(26), Figure 12).¹⁶³

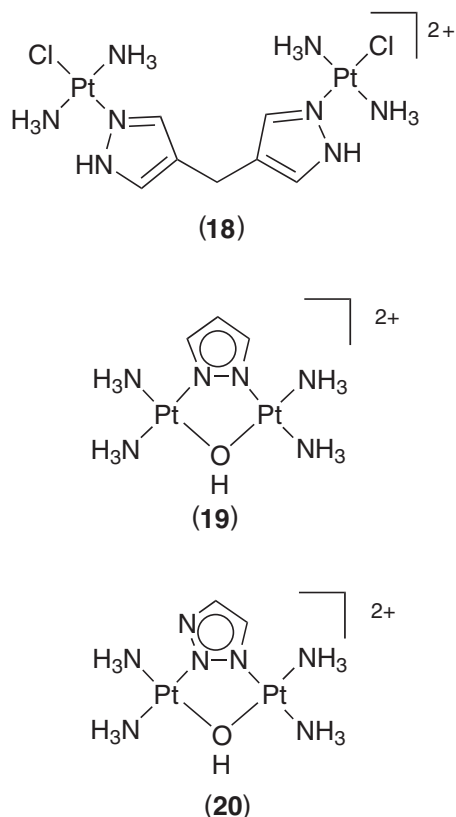


Figure 11 Dinuclear platinum compounds based on heterocycle bridges.

In general, the cytotoxicity of these compounds was equivalent to cisplatin, and they maintained their activity in cisplatin-resistant cells. In many cases the activity of a *trans* complex was actually comparable to that of the *cis* isomer.¹⁶⁴ Later these general observations were confirmed for a range of complexes in the *trans* geometry; examples of carrier ligands now include cha, iminoethers, piperazine, and piperidine, as well as sterically hindered primary amines such as isopropylamine.^{165–169} While their *in vitro* cytotoxicity is clearly comparable with cisplatin, no exceptionally active compounds *in vivo* have been prepared. This fact may reflect some pharmacokinetic problems still associated with the *trans* geometry. While most emphasis on the differences between *cis*- and *trans*-platin has centered on the structures of their DNA adducts, the different chemistry of the complexes themselves may also be important. This point is emphasized by the enhanced antitumor activity of the Pt^{IV} compound (27) over its cytotoxic but antitumor inactive Pt^{II} analog, *trans*-[PtCl₂(NH₃)(cha)].¹⁷⁰ Solubility is still a major issue in the *trans* complexes; the use of N,O-chelates in complexes such as [PtCl(NH₃)(*N,O*-pyridine-2-acetate)] (compound (28), in which the two N atoms are mutually *trans*) may solve this problem.¹⁷¹ Nevertheless, formally one may consider that *trans*-platinum complexes do indeed show *in vivo* antitumor activity.

In the case of complexes such as (21) and (23) which have an extended planar ligand, a significantly higher proportion of interstrand cross-links in DNA is formed in comparison to either *cis*- or *trans*-platin.¹⁷² The steric effects of these planar ligands result in the formation of structurally unique 1,2-interstrand cross-links like those formed by cisplatin, a unique example of how steric effects may alter a nonactive lesion into an active one (Figure 13).^{173,174} Model studies predicted this outcome by preparation of the monofunctional models *trans*-[PtCl(9-ethylguanine)(NH₃)(quinoline)] and comparison of substitution rates of the Pt—Cl bond by G or C mononucleotides.^{175,176} Interestingly, the iminoether compound (25) appears to form predominantly monofunctional adducts with DNA.¹⁷⁷

The DNA binding of *trans*-platinum complexes is thus quite rich and varied. The cellular effects of such adduct formation also appear to be significantly different from those of cisplatin.

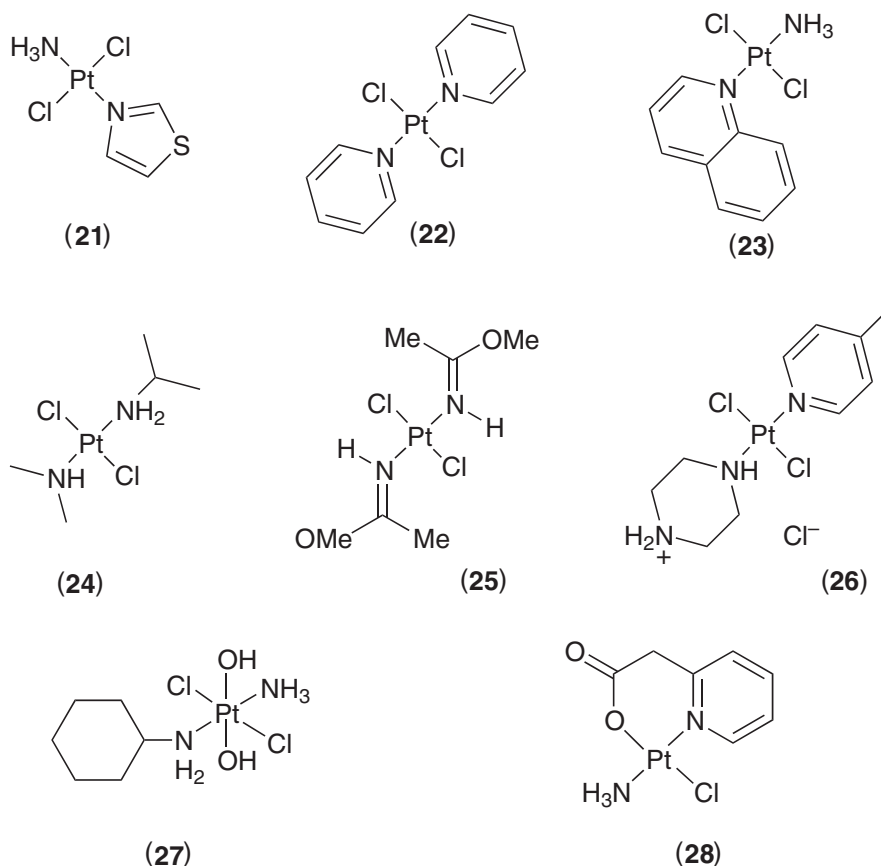


Figure 12 *Trans*-platinum compounds as potential anticancer compounds.

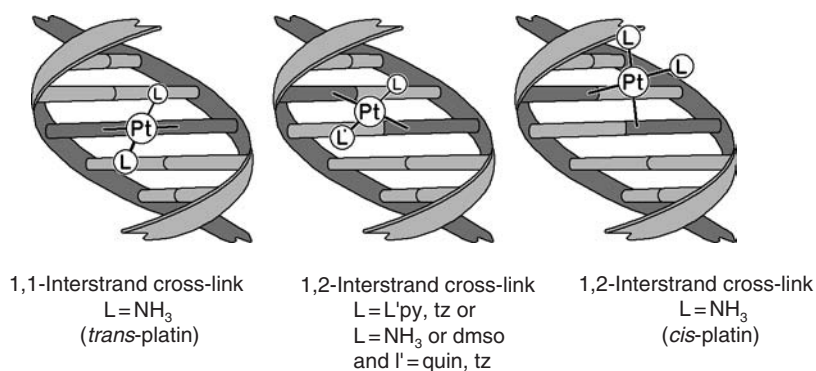


Figure 13 Interstrand cross-links formed by sterically hindered *trans*-platinum compounds.

Optimization of the pharmacokinetic profile of *trans*-platinum compounds may eventually produce a clinically effective agent.

9.18.3 NONPLATINUM ANTICANCER AGENTS

9.18.3.1 Ruthenium Complexes

In the early development of analogs of the platinum compounds, complexes with “windows of reactivity” similar to the platinum complexes were examined extensively. Whereas direct Ni and Pd analogs of Pt complexes are too kinetically reactive to be of use as drugs, Ir and Os ammine

compounds are in general too inert. Ruthenium and rhodium have produced compounds with the greatest promise, although no direct analogs have yet advanced to the clinic. In ruthenium ammine complexes of the general series $[\text{RuCl}_n(\text{NH}_3)_{6-n}]^{z+}$ (where $n = 3, 4,$ or 5), *fac*- $[\text{RuCl}_3(\text{NH}_3)_3]$ showed good activity but was not sufficiently water soluble for extensive testing.^{178,179} Ruthenium-ammine compounds have a rich DNA chemistry which has been described by Clarke. The guanine N7 site is the preferred binding site for the aqua species $[\text{Ru}(\text{H}_2\text{O})(\text{NH}_3)_5]^{2+}$, but metal migration may occur to other nucleobases.¹⁸⁰ GSH modulates DNA binding of Ru-ammine complexes: GSH reduction of the Ru^{III} compound $[\text{ClRu}(\text{NH}_3)_5]^{2+}$ to the Ru^{II} state enhances its DNA binding, but at $[\text{GSH}]/[\text{Ru}]$ ratios >1 DNA binding is inhibited through eventual formation of $[(\text{GS})(\text{NH}_3)_5\text{Ru}^{\text{III}}]$. Covalent binding of *trans*- $[(\text{H}_2\text{O})(\text{py})\text{Ru}(\text{NH}_3)_4]^{2+}$ to DNA occurs specifically at guanine N7.¹⁸¹ The pyridine ligand further stabilizes the Ru^{II} oxidation state, which may lead to disproportionation of the generated Ru^{III} species to Ru^{II} and Ru^{IV} species.¹⁸² Oxidative damage to DNA through base-catalyzed air oxidation of guanine occurs in the presence of $\{\text{Ru}^{\text{III}}(\text{NH}_3)_5\}$ -bound DNA. These and other aspects have been reviewed thoroughly.

A wide variety of Ru-based complexes, including carboxylate-bridged di- and trinuclear complexes, exhibit antitumor activity in animal models. The imidazole complexes *trans*- $[\text{RuCl}_4(\text{L})_2]^-$ (where L = imidazole, indazole) have good antitumor activity.^{183,184} Transferrin and serum albumin may act as transporters of the metal complexes in blood, and DNA is considered the ultimate target.¹⁸⁵ Modification of the structural motif of the DMSO complexes *cis/trans*- $[\text{RuCl}_2(\text{DMSO})_4]$ with imidazole ligands has led to an interesting clinical candidate, NAMI-A ((29), Figure 14).¹⁸⁶ The mechanism of action of this compound is not related to DNA binding; rather, it is an antimetastatic agent.¹⁸⁷ Metastasis (the process whereby tumor growth occurs distant from the original or primary tumor site) is intimately linked with angiogenesis, the dynamic process that involves new blood vessel formation. Inhibition of angiogenesis is an attractive approach to antitumor (antimetastatic) therapy.¹⁸⁸ NAMI-A is active against lung metastasis *in vivo* and tumor cell invasion *in vitro*.^{189–191}

The molecular details by which NAMI-A exerts antimetastatic effects *in vivo* have not been definitely determined, and may occur by multiple mechanisms. The solution chemistry of NAMI-A involves both loss of Cl and DMSO. Interestingly, the antimetastatic activity is retained under a wide variety of experimental conditions producing solvolyzed intermediates.¹⁹² The exact nature of the active species may be difficult to resolve.

A noteworthy addition to Ru-DNA chemistry is the inhibition of topoisomerase II by the arene-Ru complex $[\text{RuCl}_2(\text{DMSO})(\eta^6\text{-C}_6\text{H}_6)]$.¹⁹³ Further variations on the arene theme produce cytotoxic compounds of formula $[(\text{arene})\text{Ru}(\text{en})\text{Cl}]^+$.^{194,195} The crystal structure of the 9-ethylguanine adduct $[(\text{arene})\text{Ru}(\text{en})(9\text{-EtG})]^{2+}$ shows interesting stacking between the arene and guanine rings.

9.18.3.2 Arsenic Trioxide

Platinum complexes are cytotoxic agents yet the paradigm in cancer chemotherapy has moved to a more targeted approach, with special emphasis on signaling pathways. In this respect a remarkable story is that of arsenic trioxide, As_2O_3 (Trisenox, Cell Therapeutics Inc, Seattle, USA) which was approved by the FDA in September 2000 for treatment of acute promyelocytic leukemia (APL) in patients who have relapsed or are refractory to retinoid and anthracycline chemotherapy. An estimated 1,500 new cases of APL are diagnosed yearly in the US, of which an

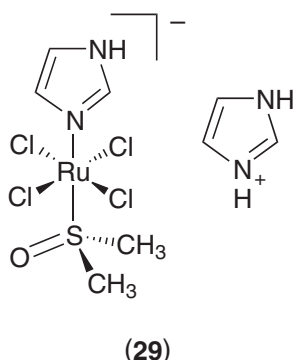


Figure 14 Structure of a potential ruthenium-based antimetastatic agent, NAMI-A.

estimated 400 patients will not respond to, or will relapse from, first-line therapy. The approval of arsenic trioxide as a chemotherapeutic agent invokes the pioneering work of Ehrlich and the development of Salvarsan for use in syphilis—the foundation stone for the science of chemotherapy. The use of chelating agents in medicine may even be traced to a collaboration between Werner (the father of coordination chemistry) and Ehrlich (the father of chemotherapy) to find less toxic arsenic compounds for the treatment of syphilis.¹⁵ Arsenic has been used therapeutically for more than 2,000 years and was used in the 1930s for treatment of chronic myelogenous leukemia until supplanted by newer chemotherapies.^{196,197} The past, present, and future of medicinal arsenic has been described as a story of “use, dishonor, and redemption”. Recent interest in arsenic trioxide initially arose through Chinese reports of its efficacy and use.¹⁹⁸ The recommended dose is $0.15 \text{ mg kg}^{-1} \text{ d}^{-1}$ until remission.¹⁹⁹ Side effects are cardiotoxicity, skin rashes, and hyperglycemia.²⁰⁰

Arsenic trioxide apparently affects numerous intracellular signal transduction pathways and causes many alterations in cellular function. Thus, the mechanisms of cell death induced by arsenic trioxide are multiple: induction of apoptosis, inhibition of proliferation, and even inhibition of angiogenesis have all been reported.²⁰¹ In cellular studies, arsenic trioxide inhibits glutathione peroxidase, possibly through generation of arsenic–GSH conjugates, and increases cellular hydrogen peroxide content.²⁰² Consistent with a general role in redox processes, ascorbic acid enhances arsenic trioxide-induced apoptosis of lymphoma cells but not of normal bone marrow cells, by increasing cellular H_2O_2 content.²⁰³ Arsenic trioxide sensitivity is associated with low levels of GSH in cancer cells.²⁰⁴ Apoptosis is apparent when cells are treated with low concentrations of the drug; this effect is associated with the collapse of mitochondrial transmembrane potentials in a thiol-dependent manner.²⁰⁵ The combined effects have led to the suggestion that arsenic trioxide may be situated as a novel mitochondriotoxic anticancer agent.²⁰⁶ Membrane potential decreases and membrane permeability increases as a result of arsenic treatment, resulting in the release of messenger molecules for the degradation phase of apoptosis.

9.18.3.3 The Mitochondrion as Target. Gold–phosphane Complexes

Apoptosis is important in tissue homeostasis; inhibition of apoptosis may contribute to transformation of cells and/or chemotherapy resistance. The apoptosis factors leading to cell death are mitochondrion-regulated. Mitochondria contribute to the regulation of energy production, metabolism, and redox status as well as apoptosis.²⁰⁷ The integral role of the mitochondrion in programmed cell death is by now well recognized and means that the mitochondrion is a suitable target for drug intervention.²⁰⁸ Mitochondrial DNA is also an attractive target because it is significantly more sensitive to covalent damage than nuclear DNA, because of the lack of protective histones and a limited capacity for repair. The pioneering work of Chen showed that enhanced mitochondrial membrane potential is a prevalent cancer cell phenotype;²⁰⁹ lipophilic cations accumulate inside mitochondria as a consequence of the higher membrane potentials.²⁰⁷ Treatment strategies directed at novel cellular targets but which are differentiated between normal and tumor cells are attractive approaches to selective tumor cell killing.

The gold–phosphane complexes (30)–(33) (Figure 15) are examples of lipophilic cations which may also have a role in mitochondrial toxicity.^{210,211} Whereas the role of gold salts in antiarthritis therapy is intimately related to thiol binding, the tetrahedral diphosphane compounds are much less reactive toward thiols.^{212,213} The lipophilic cation $[\text{Au}(\text{dppe})_2]^+$ (where dppe = 2-bis(diphenylphosphino)ethane) showed potent *in vitro* cytotoxicity with evidence of antimitochondrial function²¹⁴ but hepatotoxicity attributed to alterations in mitochondrial function curtailed clinical trials. The solution chemistry of gold–diphosphane compounds is rich and the interchange between mononuclear and dinuclear phosphane-bridged species has been extensively examined.⁵⁷ Substitution of the phenyl groups by 2-pyridyl groups provides an opportunity to investigate systematically the relationship of drug activity to lipophilicity.^{215,216} Compounds that are highly active *in vitro* may be obtained. Alteration of the lipophilicity greatly affected cellular uptake and binding to plasma proteins. Alterations in lipophilicity also affect host toxicity, allowing the opportunity for optimization of pharmacokinetic properties.

9.18.3.4 Manganese-based Superoxide Dismutase Mimics

A significant amount of the O_2 metabolized by the human organism is converted to the highly reactive superoxide radical anion $\text{O}_2^{\bullet-}$. Endogenous overproduction of $\text{O}_2^{\bullet-}$ may cause considerable

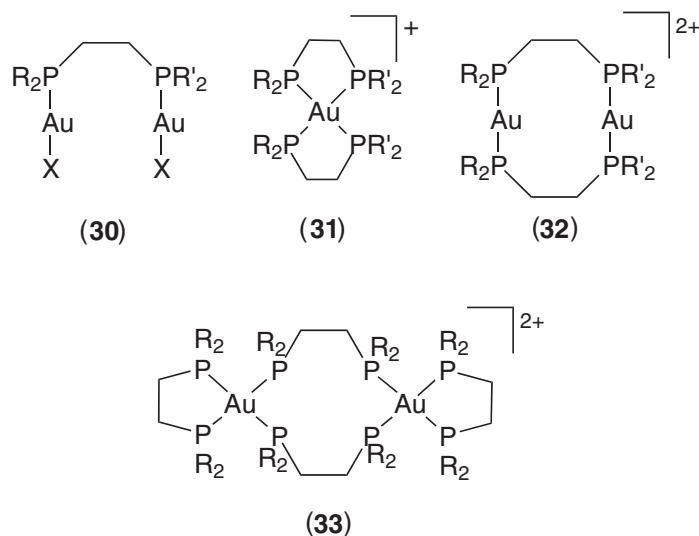
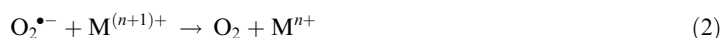
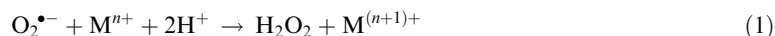


Figure 15 Structures of Au-phosphane compounds as potential mitochondrial poisons.

damage to biological systems. Superoxide has been shown to be a mediator of reperfusion diseases, such as those occurring after a stroke, and has been shown to be associated with development of inflammatory processes and also in the initiation of neurological disorders such as Parkinson's disease.²¹⁷ The enzyme superoxide dismutase (SOD), either as the manganese-containing MnSOD (present in the mitochondrion) or the dinuclear Cu/Zn-SOD (present in the cytosol and extracellular space), performs the role of superoxide detoxification in normal cells and tissue:²¹⁸



Overall:



Attempts to use the enzyme itself as a therapeutic agent have been partially successful in animals, but not in humans.²¹⁹ Pharmacokinetic problems, including delivery problems and the short half-life in the blood, are major obstacles to use of the enzyme in humans. Cu/Zn-SOD preparations (trade names Palosein, Orotein) are used to treat inflammatory diseases in dogs and horses. Small molecule mimics of natural enzymes such as SOD (dubbed *synzymes* for *synthetic enzymes*) may effect similar chemistry and thus be useful in treating disease states brought on by an imbalance in superoxide. The considerations for successful application of this strategy are many: a compound must possess high chemical stability, SOD-like activity, specificity under biological conditions, low toxicity, and favorable biodistribution. Manganese chelate compounds such as (34) and (35), especially those based on cyclam (1,4,8,11-tetraazacyclotetradecane) and *N,N'*-bis(salicylaldehyde) ethylenediamine (salen), have shown considerable promise in this regard (Figure 16).^{220–222} Rational design has produced an optimal structure M40403 (35) which is a leading clinical candidate.^{223,224} This pyridine-based macrocycle has been used as a cancer co-therapy with interleukin-2 (IL-2), an immune-stimulating cytokine drug that is approved for use in metastatic melanoma and renal cell carcinoma. As usual, the utility of IL-2 is limited by side effects, notably hypotension, and hospitalization is necessary for many patients. Preclinical studies have shown that M40403 enhances the efficacy of IL-2. A phase I, double-blind, placebo-controlled clinical trial of M40403 administered intravenously to 36 normal, healthy human subjects showed no dose-limiting side effects. A phase II clinical trial is planned to assess the effectiveness of M40403 as co-therapy with IL-2 in patients with advanced skin and end-stage kidney cancers (<http://www.metaphore.com>). Interestingly,

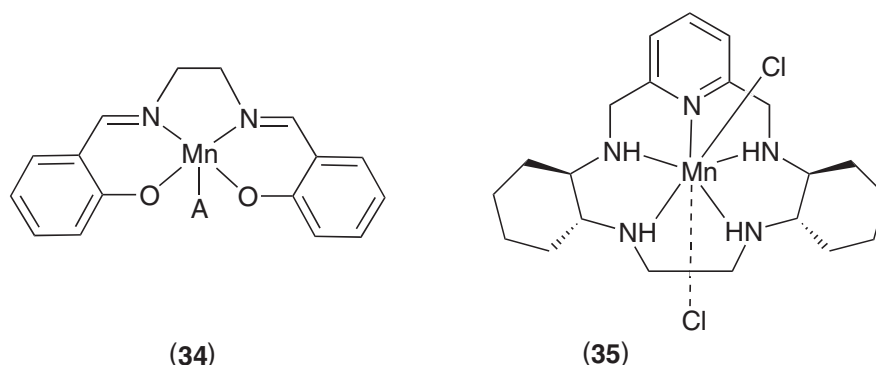


Figure 16 Manganese compounds as SOD mimics.

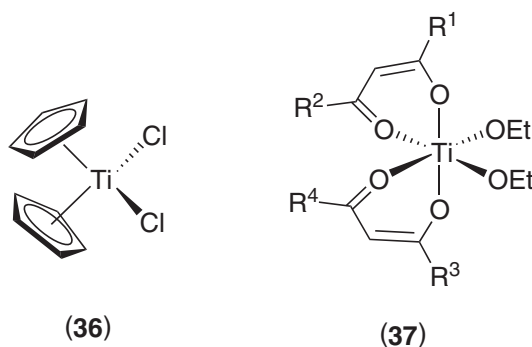
there is some indication that the salen-based compounds may involve catalase rather than SOD activity (Equation 4):



9.18.3.5 Titanium Compounds

Two titanium compounds have had clinical trials in Germany. The titanocene compound $[\text{TiCl}_2\text{Cp}_2]$ ((36); known as MTK4) and budotitane (37), a β -diketonate derivative, are structurally quite different compounds (Figure 17). Little information is available on the mode of action of budotitane which is formulated in a mixture of glycols and water because of a lack of aqueous solubility.²²⁵ Budotitane exists as a mixture of three *cis* isomers (37a–c) in thermal equilibrium, so that no isomerically pure species have been isolated.²²⁶ Hydrolysis of the ethoxy groups is rapid—the formulation slows this down and prevents formation of oligomeric oxo-bridged complexes. The MTD of budotitane was 230 mg m^{-2} and the dose-limiting toxicity was cardiac arrhythmia.²²⁷ The poorly defined aqueous properties and lack of details on the mechanism of action do not bode well for this drug.

The phase I clinical trial of $[\text{TiCl}_2\text{Cp}_2]$ indicated a MTD of 315 mg m^{-2} for a single intravenous infusion, and 185 mg m^{-2} weekly.²²⁸ The dose-limiting toxicity was nephrotoxicity.²²⁹ A phase II trial in renal cell cancer concluded that no advantage was gained by use of $[\text{TiCl}_2\text{Cp}_2]$.²³⁰ Modifications on the basic $[\text{TiCl}_2\text{Cp}_2]$ structure have included metal modification, Cp and leaving group (Cl) substitution, as well as use of ionic metallocenes for improving aqueous solubility.²³¹



a: $\text{R}^1 = \text{R}^3 = \text{Me}$; $\text{R}^2 = \text{R}^4 = \text{Ph}$

b: $\text{R}^1 = \text{R}^3 = \text{Ph}$; $\text{R}^2 = \text{R}^4 = \text{Me}$

c: $\text{R}^1 = \text{R}^4 = \text{Me}$; $\text{R}^2 = \text{R}^3 = \text{Ph}$

Figure 17 Titanium anticancer agents that have undergone clinical trials.

DNA is purportedly the target of $[\text{TiCl}_2\text{Cp}_2]$. The somewhat naïve early assertion that it could act in a manner similar to cisplatin because of the similarity in $\text{Cl}\cdots\text{Cl}$ distances has never been upheld experimentally.^{232,233} Instead the aqueous chemistry of $[\text{TiCl}_2\text{Cp}_2]$ is dominated by loss of the Cp ring as well as hydrolysis of the Ti—Cl bonds. DNA interactions at pH 7 are very weak and the adducts when formed do not suppress DNA-processing enzymes so there is doubt as to whether DNA is the locus of action for these drugs. Ti—DNA interactions are dominated by interaction with the phosphodiester backbone. Other biological effects observed for $[\text{TiCl}_2\text{Cp}_2]$ include inhibition of protein kinase C and DNA topoisomerase II activity, as well as inhibition of collagenase type IV activity, suggesting some antimetastatic behavior. Titanium may also replace iron in transferrin, allowing a possible uptake mechanism into tumor cells.²³⁴

9.18.3.6 Gallium Nitrate

The principal, approved use of $\text{Ga}(\text{NO}_3)_3$ (Ganite, gallium nitrate) is in treating hypercalcemia of malignancy, by reducing the elevated Ca^{2+} in blood.²³⁵ This disorder is often associated with bone cancers and is an acute-care condition in which rapid bone loss leads to life-threatening levels of blood calcium. Gallium reduces the rate of bone loss by inhibition of the action of osteoclasts, which produce acid onto the bone surface dissolving mineral and protein components. Inhibition of this “proton” pump is thus a well-defined mechanism of action for gallium. Relatively low levels ($200 \text{ mg m}^{-2} \text{ day}^{-1}$) are effective. At therapeutic doses, it has few side effects and is well tolerated. Most recent attention has focused on the activity of gallium nitrate against malignancies, especially non-Hodgkin’s lymphoma, non-squamous cell carcinoma of the cervix, and bladder cancer. Clinical trials under the auspices of Genta (<http://www.genta.com>) will evaluate its efficacy on patients with low- or intermediate-grade non-Hodgkin’s lymphoma who have failed prior chemotherapy. The results of phase II trials in non-small-cell lung cancer and prostate cancer have also been reported.^{236,237}

Gallium compounds may be designed to deliver the Ga^{3+} cation more effectively or selectively. Combination with bisphosphonates has been suggested to improve oral availability of gallium. Chelating agents such as 8-hydroxyquinoline,²³⁸ thiosemicarbazones²³⁹ and pyridoxal isonicotinoyl hydrazone (Ga-PIH)²⁴⁰ give well-defined Ga^{III} complexes.

9.18.4 ANTIBACTERIAL AGENTS

9.18.4.1 Silver and Mercury Salts

Silver and mercury salts have a long history of use as antibacterial agents.^{241–243} The use of mercurochrome ((40), Figure 18) as a topical disinfectant is now discouraged. Silver sulfadiazene (38) finds use for treatment of severe burns; the polymeric material slowly releases the antibacterial Ag^+ ion. Silver nitrate is still used in many countries to prevent ophthalmic disease in newborn children.²⁴⁴ The mechanism of action of Ag and Hg is through slow release of the active metal ion—inhibition of thiol function in bacterial cell walls gives a rationale for the specificity of bacteriocidal action.

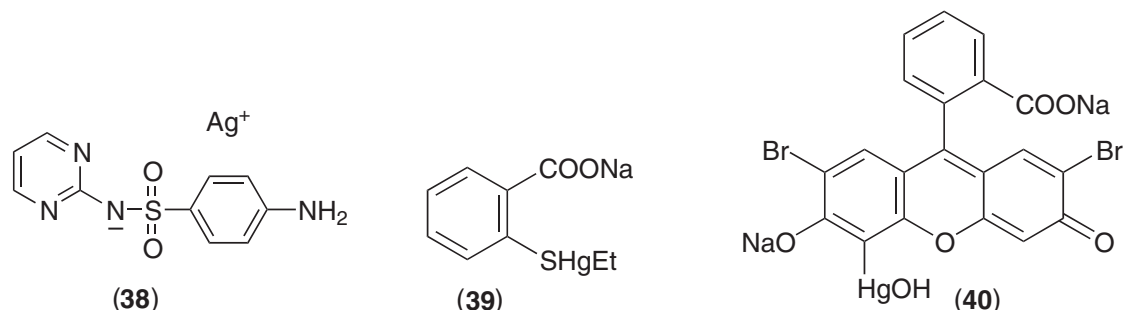


Figure 18 Silver- and mercury-based antibacterial agents.

9.18.4.2 Bismuth-containing Antiulcer Drugs

Bismuth compounds have been used for their antacid and astringent properties in a variety of gastrointestinal disorders.^{245,246} The effectiveness of bismuth is due to its bacteriocidal action against the Gram-negative bacterium, *Helicobacter pylori*. Usually the bismuth preparations are obtained by mixing an inorganic salt with a sugar-like carrier (see Figure 19). Commonly used agents are colloidal bismuth subcitrate (CBS), and bismuth subsalicylate (BSS). The mechanism of action is complex and includes inhibition of protein and cell wall synthesis, membrane function, and ATP synthesis. The most notable salts are tripotassiumdicitratobismuth, bismuth salicylate, Pepto-Bismol (BSS), and De-Nol (CBS; (41)). The “sub” designation most likely arose from stoichiometry of oxygen to bismuth. The combination of ranitidine (a histamine H₂-receptor antagonist) and bismuth citrate is marketed as Ranitidine Bismutrex for the management of peptic ulcer and ulcers associated with *H. pylori*.²⁴⁷

Much progress has been made on the coordination chemistry of these preparations. Detailed molecular characterization is obviously of primary importance in understanding chemical and biochemical function. Bi^{III} is highly acidic in aqueous medium and the oxygen-rich nature of the sugar carrier ligands leads to formation of di- and polynuclear-bridged complexes, based on the typical dinuclear unit (41) shown in Figure 19.^{248–251} The nature of the ranitidine/bismuth citrate adduct has been examined and second coordination sphere effects were noted for the organic amine.²⁵² Methylthiosalicylate has also been used instead of salicylate, and discrete complexes (e.g., (42)) have been comprehensively characterized.^{253,254} Bismuth (III) remarkably forms stable complexes with GSH²⁵⁵ and transferrin.²⁵⁶ The latter observation may be correlated with the high acidity of the Bi^{III} ion.

9.18.4.3 Metal-containing Drugs as Antiparasitic Agents

There remains an urgent need for new effective antiparasitic agents, an area of drug development that has languished because of poor economic return. The spread of resistance to chloroquine (an antimalaria treatment) is one reason for attention to be paid to this area, as well as the sheer numbers of people affected. Antimony compounds (43) and (44) (Figure 20) are used to treat

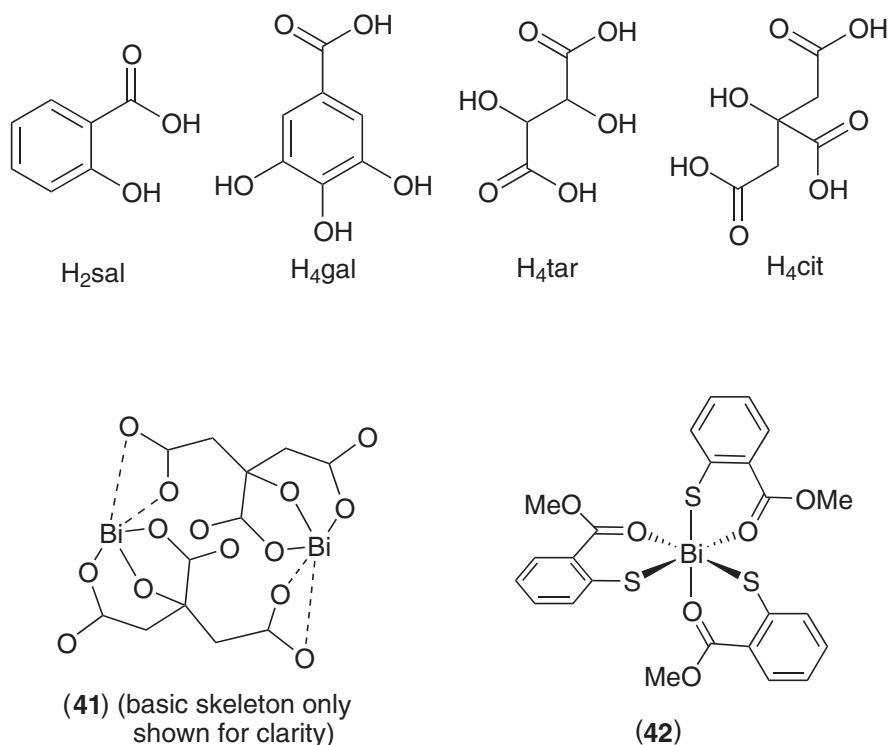


Figure 19 Bismuth antiulcer drugs—the sugars used to produce the usually polymeric structures are shown in the top panel.

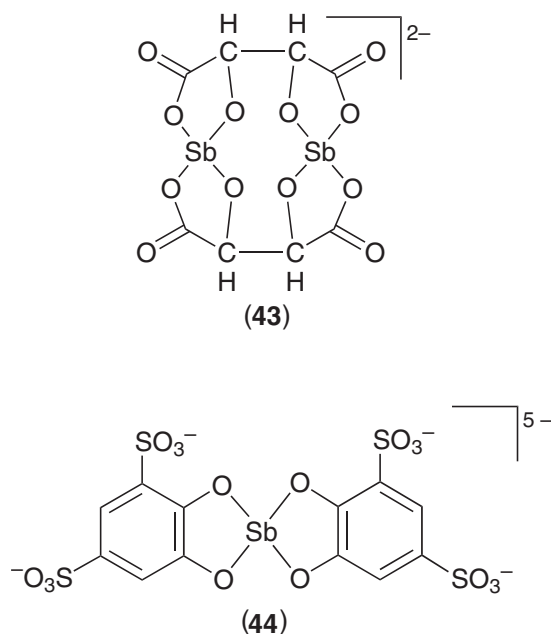


Figure 20 Antimony-based antiparasitic agents.

leishmaniasis (H. Sun, personal communication). Another approach is to complex metal ions to known antiparasitic agents in attempts to gain selective uptake or selective action of the metal–drug conjugate. Gold and ruthenium complexes of chloroquine and clotrimazole have been described ((45) and (46), Figure 21).^{257–260} In favorable cases, some of these compounds show good activity—the chloroquine complexes being useful even in chloroquine-resistant cases.

9.18.5 PHARMACODYNAMIC USES OF METAL COMPLEX DRUGS

9.18.5.1 Lithium Carbonate

The clinical value of lithium has been recognized since 1949. Lithium carbonate is used in manic depressive psychoses for the treatment of recurrent mood changes.^{261,262} Mood stability may only occur after months rather than weeks. The drug is administered orally in doses up to 2 g day⁻¹ (30 mmol day⁻¹). The serum Li concentration should be in the range of 0.4–0.8 mmol l⁻¹.

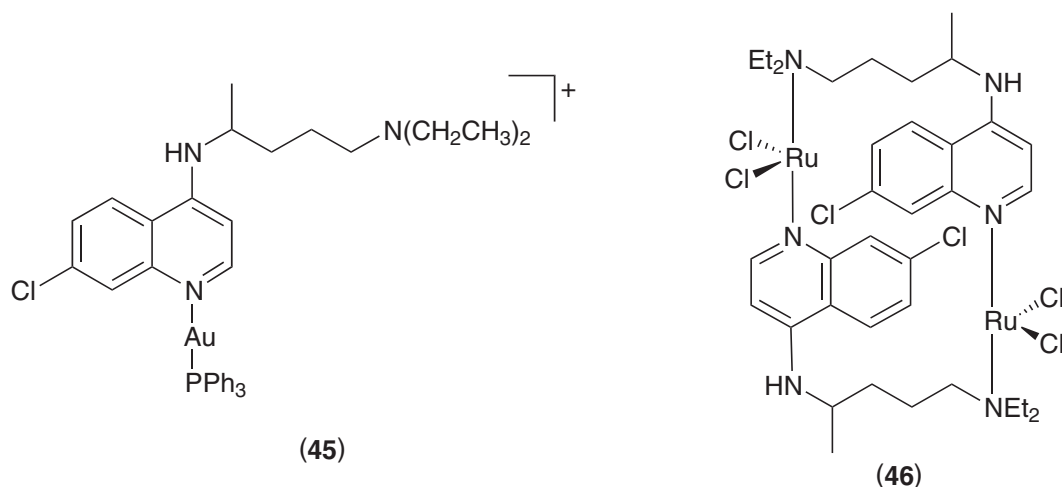


Figure 21 Gold and ruthenium complexes of antiparasitic agents.

The development of lithium-specific electrodes has assisted greatly in monitoring patient compliance. The toxicity profile of lithium carbonate is now well established and the drug is safely administered and well tolerated. It is of limited use in other psychiatric disorders such as pathological aggression, although additional benefit may also include a reduction in actual or attempted suicide.

Newer uses have appeared in the treatment of viral diseases including AIDS, alteration of the immune response, and cancer. The lithium salt of γ -linolenic acid (LiGLA) has a significant anticancer effect against certain cancers. The neurochemical basis for lithium action is difficult to define. Lithium carbonate induces a wide range of intra- and extracellular changes—most emphasis has been naturally on the similarities with Na/K/Ca/Mg ions. Lithium selectively interferes with the inositol lipid cycle, representing a unified hypothesis of action. The biochemistry, distribution, and cellular localization of lithium has been extensively documented.

9.18.5.2 Vanadium Complexes in Diabetes

The role of vanadium in biological systems in general is of increasing interest.²⁶³ The discovery of the insulin-like properties of vanadate ions spurred research into the clinical use of vanadium compounds as insulin mimics.²⁶⁴ Inadequate glucose metabolism, either through absence of endogenously secreted insulin or insulin resistance, leads to diabetes mellitus. The potential of insulin-mimetic compounds as drugs lies in their oral administration—insulin, as a small protein, is not orally active. The vanadate (V) ion is effective upon oral administration, and an obvious strategy to enhance the pharmacokinetic characteristics and the efficacy of the insulin-mimetic response is complexation of vanadate with suitable biologically compatible ligands.^{265,266}

Insulin binding to the extracellular side of cell membranes initiates the “insulin cascade”, a series of phosphorylation/dephosphorylation steps. A postulated mechanism for vanadium is substitution of vanadate for phosphate in the transition state structure of protein tyrosine phosphatases (PTP).^{267,268} In normal physiological conditions, the attainable oxidation states of vanadium are V^{III}, V^{IV} and V^V. Relevant species in solution are vanadate, (a mixture of $\text{HVO}_4^{2-}/\text{H}_2\text{VO}_4^-$) and vanadyl VO^{2+} . Vanadyl is not a strong inhibitor of PTPs, suggesting other potential mechanisms for insulin mimesis for this cation.

Both V^{IV} and V^V coordination compounds have been tested as insulin mimics. The preponderance of V^{IV} compounds contain the $\text{V}=\text{O}(\text{L-L})_2$ motif (e.g., (47) and (48), Figure 22) and complexes containing a variety of O,O; N,O; N,S; and S,S bidentate ligands L-L have been synthesized and tested. Control of lability and ligand displacement are important criteria for drug design in terms of delivery of the biologically active vanadate. Clinical trials have focused to date on sodium orthovanadate and the bis(maltolato)oxovanadium(IV) compound (BMOV) (47). The speciation and aqueous chemistry of BMOV have been described.²⁶⁶

9.18.5.3 Gold Compounds as Antiarthritic Agents

Gold salts have had a long history of use in rheumatoid arthritis.^{269,270} The development of orally active auranofin (also known as Ridaura; (50), Figure 23) was a major improvement over the early “injectable gold” preparations which were polymeric (e.g., (51)–(53)). However, use has declined with the popularity of nonsteroidal antiinflammatory drugs (NSAIDs) such as indomethacin; a recent estimate of the commercial value for auranofin was \$6 million. The mechanism

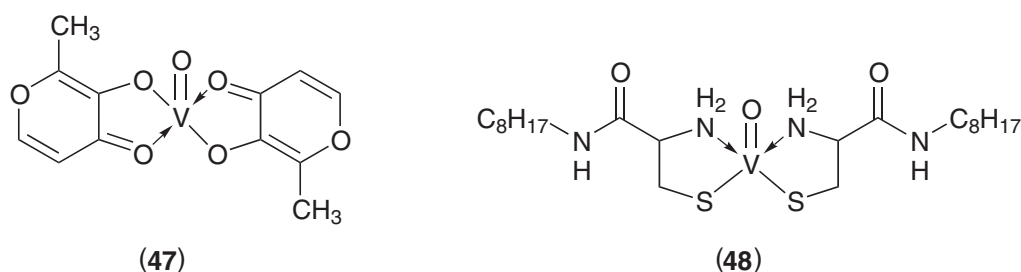
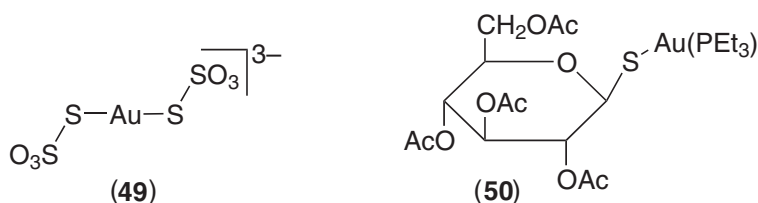


Figure 22 Vanadium compounds in treatment of diabetes.



Polymeric $[\text{AuRS}]_n$ compounds:

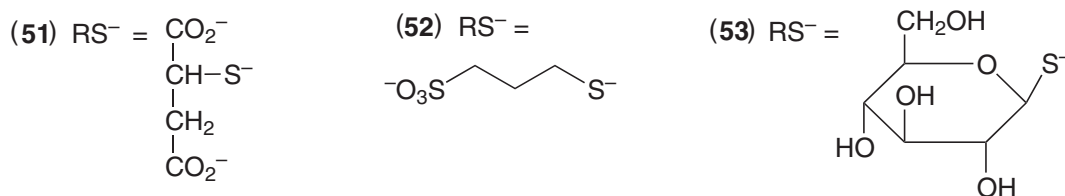


Figure 23 Au antiarthritis compounds.

of action is postulated to occur through thiolate exchange reactions.²⁷¹ The structures of the polymeric gold compounds have been described in detail. An interesting feature of gold metabolism is the production of $[\text{Au}(\text{CN})_2]^-$ ²⁶⁹ as a metabolite of the gold-thiol compounds.

9.18.5.4 Nitric Oxide in Physiology and Medicine

An intriguing aspect of the role of metal complexes in medicine is the role of NO.^{272,273} The nitroprusside ion, $[\text{Fe}(\text{NO})(\text{CN})_5]^{2-}$ is a vasodilator used in emergency situations to treat hypertensive patients in operating theaters.^{274,275} The complex is 30–100 times more potent than simple nitrites. The mechanism is considered to be release of NO, an understanding prompted by the emergence of NO as a prominent cell signaling molecule.²⁷³ Related to the biology of NO is production of peroxynitrite ONOO^- through reaction of NO with O_2^- . In this regard, production of peroxynitrite may play a role in many pathological conditions.^{276,277} Water-soluble porphyrins and texaphyrins may catalytically react with ONOO^- and may have clinical utility in peroxynitrite scavenging.

9.18.5.5 Lanthanum Carbonate

Patients with end-stage renal disease hyperphosphatemia ineffectively filter excess phosphate that enters the body in the normal diet.²⁷⁸ Elevated phosphate produces the bone disorder renal osteodystrophy. Skeletal deformity may occur, possibly associated with cardiovascular disease. Calcium deposits may further build up around the body and in blood vessels creating further health risks. The use of lanthanum carbonate is being promoted as an alternative to aluminum-based therapies.^{279,280} Systemic absorption, and cost have produced a clinical candidate, Fosrenol (AnorMED), an intriguing use of a lanthanide compound in therapy.

9.18.6 REFERENCES

1. Farrell, N. P. *Transition Metal Complexes as Drugs and Chemotherapeutic Agents*; James, B. R.; Ugo, R., Ed.; Reidel-Kluwer Academic Press: Dordrecht, 1989; Vol. 11.
2. Farrell, N. P. *The Uses of Inorganic Chemistry in Medicine*; The Royal Society of Chemistry: Cambridge, 1999.
3. Orvig, C.; Abrams, M. J. *Chem. Rev.* **1999**, *99*, 2201–2204.
4. Guo, Z.; Sadler, P. J. *Angew Chem., Int. Ed. Engl.* **1999**, *38*, 1512–1531.

5. Keppler, B. *Metal Complexes in Cancer Chemotherapy*; VCH: Basel, 1993.
6. Clarke, M. J. *Progress in Clinical Biochemistry and Medicine*, 1989; Vol. 10.
7. Fricker, S. P., Ed.; *Metal Complexes in Cancer Therapy*. Chapman and Hall: London, 1994; Vol. 1, p 215.
8. Berthon, G. *Handbook of Metal-ligand Interactions in Biological Fluids*; Marcel-Dekker Inc.: New York, 1995; Vol. 1 and 2.
9. Clarke, M. J.; Sadler, P. J., Eds.; *Metallopharmaceuticals I: DNA Interactions*; Springer-Verlag: Berlin 1999; Vol. 1, p 199.
10. Sadler, P. J. *Adv. Inorg. Chem.* **1999**, *49*, 183–306.
11. Roat, R. M. *Bioinorganic Chemistry: A Short Course*, Wiley Interscience, Hoboken, New Jersey, 2002.
12. Sigel, H.; Sigel, A., Eds., *Metal Ions in Biological Systems*; Marcel Dekker: New York 1995; Vol. 31.
13. Lever, A. B. P. Ed., *Coord. Chem. Rev.* **2003**, Vol. 232 Aspects of Biomedical Inorganic Chemistry. Elsevier Press.
14. Reynolds, J. E. F. Ed., *Martindale The Extra Pharmacopoeia*, 31sted.; The Royal Pharmaceutical Society; London, 1996. Martindales Pharmacopoeia.
15. Andersen, O. *Chem. Rev.* **1999**, *99*, 2683–2710.
16. Liu, Z. D.; Hider, R.C. *Coord. Chem. Rev.* **2002**, *232*, 151–172.
17. Sarkar, B. *Chem. Rev.* **1999**, *99*, 2535–2544.
18. Whittaker, M.; Floyd, C. D.; Brown, P.; Gearing, A. J. *Chem. Rev.* **1999**, *99*, 2735–2776.
19. Parks, W. C.; Mecham, R.; Mecham, R. P. *Matrix Metalloproteinases*; Academic Press, 1998.
20. Vallee, B. L.; Auld, D. S.; *Acc. Chem. Res.* **1993**, *26*, 543–551. Jolles, P.; Jornvall, H., Eds.; Verlag: Basel, 1995, p 259.
21. Rein, A.; Henderson, L. E.; Levin, J. G. *Trends Biochem. Sci.* **1998**, *23*, 297–301.
22. Albert, A. *Selective Toxicity*, 6th ed.; Wiley: New York, 1979.
23. Food and Drug Administration: <http://www.fda.gov> *United States Food and Drug Administration*; Vol. 2002.
24. National Cancer Institute: <http://nci.nih.gov/dtp.cfm> *NCI-DTP*; Vol. 2002.
25. Bertucci, C.; Domenici, E. *Curr. Med. Chem.* **2002**, *9*, 1463–1481.
26. He, X. M.; Carter, D. C. *Nature* **1992**, *358*, 209–215.
27. Chan, J.; Huang, Z.; Merrifield, M. E.; Salgado, M. T.; Stillman, M. J. Studies of metal binding reactions in metallothioneins by spectroscopic, molecular biology, and molecular modeling techniques. *Coord. Chem. Rev.* **2002**, *233*, 319–339.
28. Sun, H.; Li, H.; Sadler, P. J. *Chem. Rev.* **1999**, *99*, 2817–2842.
29. Petering, D.; Xiao, J.; Nyayapati, S.; Fulmer, P.; Antholine, W. *Oxidation Damage by Bleomycin, Adriamycin and Other Cytotoxic Agents that Require Iron or Copper*; Farrell, N., Ed.; The Royal Society of Chemistry: Cambridge, 1999, pp 135–157.
30. Claussen, C. A.; Long, E. C. *Chem. Rev.* **1999**, *99*, 2797–2816.
31. Weinstein, J. N.; Myers, T. G.; O'Connor, P. M.; Friend, S. H.; Fornace, A. J., Jr.; Kohn, K. W.; Fojo, T.; Bates, S. E.; Rubinstein, L. V.; Anderson, N. L.; Buolamwini, J. K.; van Osdol, W. W.; Monks, A. P.; Scudiero, D. A.; Sausville, E. A.; Zaharevitz, D. W.; Bunow, B.; Viswanadhan, V. N.; Johnson, G. S.; Wittes, R. E.; Paull, K. D. *Science* **1997**, *275*, 343–349.
32. Boyle, F. T.; Costello, G. F. *Chem. Soc. Rev.* **1998**, *27*, 251–261.
33. Rosenberg, B. Platinum Complexes for the Treatment of Cancer. Why the Search goes on. In *Cisplatin: Chemistry and Biochemistry of a Leading Anticancer Drug*; Lippert, B., Ed.; Wiley-VCH: New York, 1999 pp 3–30.
34. Lippert, B., Ed. *Cisplatin: Chemistry and Biochemistry of a Leading Anticancer Drug*; Wiley-VCH: New York, 1999.
35. Kelland, L. R.; Farrell, N. P. *Platinum-based Drugs in Cancer Therapy*; Humana Press, Totowa, New Jersey, 2000.
36. Wong, E.; Giandomenico, C. M. *Chem. Rev.* **1999**, *99*, 2451–2466.
37. Weiss, R. B.; Christian, M. C. *Drugs* **1993**, *46*, 360–377.
38. Lebwahl, D.; Canetta, R. *Eur. J. Cancer* **1998**, *34*, 1522–1534.
39. O'Dwyer, P. J.; Johnson, S. W.; Hamilton, T. C. Cisplatin and Its Analogues. In *Cancer Principles and Practice of Oncology* 5th ed.; DeVita, V. T., Hellman, S.; Rosenberg, S. A., Eds.; Lippincott-Raven: Philadelphia, 1997; Vol. 2, pp 418–431.
40. O'Dwyer, P. J.; Stevenson, J. P.; Johnson, S. W. Clinical Status of Cisplatin, Carboplatin, and Other Platinum-based Antitumor Drugs. In *Cisplatin: Chemistry and Biochemistry of a Leading Anticancer Drug*; Lippert, B., Ed.; Wiley-VCH: New York 1999, pp 31–72.
41. Highley, M. S.; Calvert, A. H. *Clinical Experience with Cisplatin and Carboplatin*; Kelland, L. R.; Farrell, N. P., Eds.; Humana Press: Totowa NJ, 2000, pp 89–113.
42. Christian, M. C. *Semin. Oncol.* **1992**, *19*, 720.
43. Lokich, J.; Anderson, N. *Ann. Oncol.* **1998**, *9*, 13–21.
44. Burcheranal, J. H.; Kalaher, K.; Dew, K. *Biochimie* **1978**, *60*, 961.
45. Macdonald, J. S.; Astrow, A. B. *Semin. Oncol.* **2001**, *28*, 30–40.
46. Pelley, R. J. *Curr. Oncol. Rep.* **2001**, *3*, 147–155.
47. Ruley, H. E. *Important Adv. Oncol.* **1996**, *10*, 37–56.
48. Eastman, A. The Mechanism of Action of Cisplatin: From Adducts to Apoptosis. In *Cisplatin: Chemistry and Biochemistry of a Leading Anticancer Drug*; Lippert, B., Ed.; Wiley-VCH: Weinheim, 1999, pp 111–134.
49. Gonzalez, V. M.; Fuytes, M. A.; Alonso, C.; Perez, J. M. *Mol. Pharmacol.* **2001**, *59*, 657–663.
50. Kartalou, M.; Essigmann, J. M. *Mutat. Res.* **2001**, *478*, 23–43.
51. Perez, R. P. *Eur. J. Cancer* **1998**, *34*, 1535–1542.
52. Kartalou, M.; Essigmann, J. M. *Mutat. Res.* **2001**, *478*, 1–21.
53. Harrap, K. R.; Jones, M.; Siracky, J.; Pollard, L. A.; Kelland, L. R. *Ann. Oncol.* **1990**, *1*, 65–76.
54. Loh, S. Y.; Mistry, P.; Kelland, L. R.; Abel, G.; Harrap, K. R. *Br. J. Cancer* **1992**, *66*, 1109–1115.
55. Berners-Price, S. J.; Appleton, T. G. The Chemistry of Cisplatin in Aqueous Solution; In *Platinum-Based Drugs in Cancer Therapy*. Kelland, L. R.; Farrell, N., Eds.; Humana Press: Totowa, NJ, 2000.
56. Miller, S. E.; House, D. A. *Inorg. Chim. Acta* **1991**, *187*, 125–132.
57. Berners-Price, S. J.; Sadler, P. J. *Coord. Chem. Rev.* **1996**, *151*, 1–40.
58. Appleton, T. G.; Hall, J. R.; Ralph, S. F. *Inorg. Chem.* **1985**, *24*, 4685–4693.
59. Kozelka, J.; Legendre, F.; Reeder, F.; Chottard, J. *Coord. Chem. Rev.* **1999**, *190–192*, 61–82.

60. Canovese, L.; Cattalini, L.; Chessa, G.; Tobe, M. L. *J. Chem. Soc. Dalton Trans.* **1988**, 2135–2140.
61. Esposito, B. P.; Najjar, R. *Coord. Chem. Rev.* **2002**, *232*, 137–150.
62. Ivanov, A. I.; Christodoulou, J.; Parkinson, J. A.; Barnham, K. J.; Tucker, A.; Woodrow, J.; Sadler, P. J. *J. Biol. Chem.* **1998**, *273*, 14721–14730.
63. Reedijk, J. *Chem. Rev.* **1999**, *99*, 2499–2510.
64. Djuran, M. I.; Lempers, E. L. M.; Reedijk, J. *Inorg. Chem.* **1991**, *30*, 2648–2652.
65. Appleton, T. G.; Connor, J. W.; Hall, J. R.; Prenzler, P. D. *Inorg. Chem.* **1989**, *28*, 2030–2037.
66. Murdoch, P. d. S.; Kratochwil, N. A.; Parkinson, J. A.; Patriarca, M.; Sadler, P. J. *Angew. Chem., Int. Ed. Engl.* **1999**, *38*, 1949–2951.
67. Lempers, E. L. M.; Inagaki, K.; Reedijk, J. *Inorg. Chim. Acta* **1988**, *152*, 201–207.
68. Mitchell, K. A.; Strevler, K. C.; Jensen, C. M. *Inorg. Chem.* **1993**, *32*, 2608–2609.
69. Alden, W. W.; Repta, A. J. *Chem. Biol. Interact.* **1984**, *48*, 121–124.
70. Murdoch, P. d. S.; Ranford, J. D.; Sadler, P. J.; Berners-Price, S. J. *Inorg. Chem.* **1993**, *32*, 2249–2255.
71. Barnham, K. J.; Djuran, M. I.; Murdoch, P. d. S.; Ranford, J. D.; Sadler, P. J. *Inorg. Chem.* **1996**, *35*, 1065–1072.
72. Hambley, T. W. *J. Chem. Soc., Dalton Trans.* **2001**, 2711–2718.
73. Cohen, S. M.; Lippard, S. J. *Prog. Nucleic Acid Res. Mol. Biol.* **2001**, *67*, 93–130.
74. Brabec, V. *DNA Modifications by Antitumor Platinum and Ruthenium Compounds: Their Recognition and Repair*; Academic Press: Amsterdam, 2002; Vol. 71 pp 2–45.
75. Takahara, P. M.; Rosenzweig, A. C.; Frederick, C. A.; Lippard, S. J. *Nature* **1995**, *377*, 649–652.
76. Gelasco, A.; Lippard, S. J. *Biochemistry* **1998**, *37*, 9230–9239.
77. Schwartz, A.; Marrot, L.; Leng, M. *Biochemistry* **1989**, *28*, 7975–7979.
78. Gelasco, A.; Lippard, S. J. Anticancer Activity of Cisplatin and Related Complexes; In *Metallopharmaceuticals I: DNA Interactions*. Clarke, M. J.; Sadler, P. J., Eds.; Springer-Verlag: Berlin, 1999; Vol. 1, pp 1–44.
79. Marzilli, L. G.; Saad, J. S.; Kuklenyik, Z.; Keating, K. A.; Xu, Y. *J. Am. Chem. Soc.* **2001**, *123*, 2764–2770.
80. Spingler, B.; Whittington, D. A.; Lippard, S. J. *Inorg. Chem.* **2001**, *40*, 5596–5602.
81. Mani, S.; Graham, M. A.; Bregman, D. B.; Ivy, P.; Chaney, S. G. *Cancer Invest.* **2002**, *20*, 246–263.
82. Woynarowski, J. M.; Faivre, S.; Herzig, M. C.; Arnett, B.; Chapman, W. G.; Trevino, A. V.; Raymond, E.; Chaney, S. G.; Vaisman, A.; Varchenko, M.; Juniewicz, P. E. *Mol. Pharmacol.* **2000**, *58*, 920–927.
83. Coste, F.; Malinge, J. M.; Serre, L.; Shepard, W.; Roth, M.; Leng, M.; Zelwer, C. *Nucleic Acids Res.* **1999**, *27*, 1837–1846.
84. Coste, F.; Shepard, W.; Zelwer, C. *Acta Crystallogr. D* **2002**, *58*, 431–440.
85. Huang, H.; Zhu, L.; Reid, B. R.; Drobný, G. P.; Hopkins, P. B. *Science* **1995**, *270*, 1842–1845.
86. Paquet, F.; Perez, C.; Leng, M.; Lancelot, G.; Malinge, J. M. *J. Biomol. Struct. Dyn.* **1996**, *14*, 67–77.
87. Brabec, V.; Leng, M. *Proc. Natl. Acad. Sci. USA* **1993**, *90*, 5345–5349.
88. Chu, G. *J. Biol. Chem.* **1994**, *269*, 787–790.
89. Zlatanova, J.; Yaneva, J.; Leuba, S. H. *Faseb J.* **1998**, *12*, 791–799.
90. Patrick, S. M.; Turchi, J. J. *Biochemistry* **1998**, *37*, 8808–8815.
91. Thomas, J. O. *Biochem. Soc. Trans.* **2001**, *29*, 395–401.
92. Ohndorf, U. M.; Rould, M. A.; He, Q.; Pabo, C. O.; Lippard, S. J. *Nature* **1999**, *399*, 708–712.
93. He, Q.; Ohndorf, U. M.; Lippard, S. J. *Biochemistry* **2000**, *39*, 14426–14435.
94. Holford, J.; Sharp, S. Y.; Murrer, B. A.; Abrams, M.; Kelland, L. R. *Br. J. Cancer* **1998**, *77*, 366–373.
95. Raynaud, F. I.; Boxall, F. E.; Goddard, P. M.; Valenti, M.; Jones, M.; Murrer, B. A.; Abrams, M.; Kelland, L. R. *Clin. Cancer Res.* **1997**, *3*, 2063–2074.
96. Holford, J.; Raynaud, F.; Murrer, B. A.; Grimaldi, K.; Hartley, J. A.; Abrams, M.; Kelland, L. R., *Anticancer Drug Des.* **1998**, *13*, 1–18.
97. Chen, Y.; Guo, Z.; Parsons, S.; Sadler, P. J. *Chem. Eur. J.* **1998**, *4*, 672–676.
98. Chen, Y.; Parkinson, J. A.; Guo, Z.; Brown, T.; Sadler, P. J. *Angew. Chem., Int. Ed.* **1999**, *38*, 2060–2063.
99. Trigo, J. M.; Beale, P.; Judson, I. R.; Raynaud, F.; Rees, C.; Milan, D.; Wolf, L.; Walker, R.; Hanwell, J.; Giandomenico, C. *ASCO* **1999**, 648.
100. Mellish, K. J.; Barnard, C. F.; Murrer, B. A.; Kelland, L. R. *Int. J. Cancer* **1995**, *62*, 717–723.
101. Hall, M. D.; Hambley, T. W. *Coord. Chem. Rev.* **2002**, *232*, 49–67.
102. Lemma, K.; Sargeson, A. M.; Elding, L. I. *J. Chem. Soc., Dalton Trans.* **2000**, 1167–1172.
103. Lemma, K.; Berglund, J.; Farrell, N.; Elding, L. I. *J. Biol. Inorg. Chem.* **2000**, *5*, 300–306.
104. Giandomenico, C. M.; Abrams, M. J.; Murrer, B. A.; Vollano, J. F.; Rheinheimer, M. I.; Wyer, S. B.; Bossard, G. E.; Higgins, III, J. D. *Inorg. Chem.* **1998**, *34*, 1015–1021.
105. Carr, J. L.; Tingle, M. D.; McKeage, M. J. *Cancer Chemother. Pharmacol.* **2002**, *50*, 9–15.
106. Raynaud, F. I.; Mistry, P.; Donaghue, A.; Poon, G. K.; Kelland, L. R.; Barnard, C. F.; Murrer, B. A.; Harrap, K. R. *Cancer Chemother. Pharmacol.* **1996**, *38*, 155–162.
107. Hartwig, J. F.; Lippard, S. J. *J. Am. Chem. Soc.* **1992**, *114*, 5646–5654.
108. Kurata, T.; Tamura, T.; Sasaki, Y.; Fujii, H.; Negoro, S.; Fukuoka, M.; Saijo, N. *Jpn J. Clin. Oncol.* **2000**, *30*, 377–384.
109. Kelland, L. R. *Exp. Opin. Invest. Drugs* **2000**, *9*, 1373–1382.
110. Farrell, N.; Qu, Y.; Hacker, M. P. *J. Med. Chem.* **1990**, *33*, 2179–2184.
111. Farrell, N. *Comm. Inorg. Chem.* **1995**, *16*, 373–389.
112. Farrell, N. DNA Binding of Dinuclear Platinum Complexes; In *Advances in DNA Sequence Specific Agents*. Vol. 2 Hurley, L. H.; Chaires, J. B., Eds.; JAI Press, 1996, pp 187–216.
113. Farrell, N. *Cancer Invest.* **1993**, *11*, 578–589.
114. Qu, Y.; Rauter, H.; Soares Fontes, A. P.; Bandarage, R.; Kelland, L. R.; Farrell, N. *J. Med. Chem.* **2000**, *43*, 3189–3192.
115. Farrell, N. P.; Qu, Y.; Bierbach, U.; Valsecchi, M.; Menta, E. Structure–activity Relationships within Di- and Trinuclear Platinum Phase I Clinical Agents; In *Cisplatin: Chemistry and Biochemistry of a Leading Anticancer Drug*; Lippert, B., Ed.; Verlag, 1999, pp 479–496.
116. Farrell, N.; Spinelli, S. Dinuclear and Trinuclear Platinum Anticancer Agents; In *Uses of Inorganic Chemistry in Medicine*, Farrell, N., Ed.; The Royal Society of Chemistry: Cambridge, 1999, pp 124–134.

117. Farrell, N. P. Polynuclear Charged Platinum Compounds as a New Class of Anticancer Agents: Toward a New Paradigm; In *Platinum-Based Drugs in Cancer Therapy*, Kelland, L. R. and Farrell, N. P., Ed.; Humana Press, 2000, pp 321–338.
118. Qu, Y.; Appleton, T. G.; Hoeschele, J. D.; Farrell, N. *Inorg. Chem.* **1993**, *32*, 2591.
119. Manzotti, C.; Pratesi, G.; Menta, E.; Di Domenico, R.; Cavalletti, E.; Fiebig, H. H.; Kelland, L. R.; Farrell, N.; Polizzi, D.; Supino, R.; Pezzoni, G.; Zunino, F. *Clin. Cancer Res.* **2000**, *6*, 2626–2634.
120. Pratesi, G.; Perego, P.; Polizzi, D.; Righetti, S. C.; Supino, R.; Caserini, C.; Manzotti, C.; Giuliani, F. C.; Pezzoni, G.; Tognella, S.; Spinelli, S.; Farrell, N.; Zunino, F. *Br. J. Cancer* **1999**, *80*, 1912–1919.
121. Perego, P.; Caserini, C.; Gatti, L.; Carenini, N.; Romanelli, S.; Supino, R.; Colangelo, D.; Viano, I.; Leone, R.; Spinelli, S.; Pezzoni, G.; Manzotti, C.; Farrell, N.; Zunino, F. *Mol. Pharmacol.* **1999**, *55*, 528–534.
122. Orlandi, L.; Colella, G.; Bearzatto, A.; Abolafio, G.; Manzotti, C.; Daidone, M. G.; Zaffaroni, N., *Eur. J. Cancer* **2001**, *37*, 649–659.
123. Calvert, P. M.; Highley, M. S.; Hughes, A. N.; Plummer, E. R.; Azzabi, A. S. T.; Verrill, M. W.; Camboni, M. G.; Verdi, E.; Bernareggi, A.; Zuchetti, M.; Robinson, A. M.; Carmichael, J.; Calvert, A. H. *Clin. Cancer Res.* **1999**, *5*, 3796s.
124. Sessa, C.; Capri, G.; Gianni, L.; Peccatori, F.; Grasselli, G.; Bauer, J.; Zuchetti, M.; Vigano, L.; Gatti, A.; Minoia, C.; Liati, P.; Van den Bosch, S.; Bernareggi, A.; Camboni, G.; Marsoni, S. *Ann. Oncol.* **2000**, *11*, 977–983.
125. Gourley, C.; Cassidy, J.; Bisset, D.; Camboni, G.; Boyle, D.; Jodrell, D. *Proc. AACR* **2002**, 2760.
126. Calvert, A. H.; Thomas, H.; Colombo, N.; Gore, M.; Earl, H.; Sena, L.; Camboni, G.; Liati, P.; Sessa, C. *European Journal of Cancer* **2001**, *37* (supp6) Poster Discussion 965. *Phase II Clinical Study of BBR3464, a Novel, Bifunctional Platinum Analogue, in Patients with Advanced Ovarian Cancer*, 2001.
127. Scagliotti, G.; Crino, L.; de Marinis, F.; Tonato, M.; Selvaggi, G.; Massoni, F.; Maestri, A.; Gatti, B.; Camboni, G. *European Journal of Cancer* **2001**, *37* (Supp6) Poster 182. *Phase II Trial of BBR3464, a Novel, Bifunctional Platinum Analogue, in Advanced but Favourable Out-come, Non Small Cell Lung Cancer Patients*, 2001.
128. Roberts, J. D.; Peroutka, J.; Farrell, N. *J. Inorg. Biochem.* **1999**, *77*, 51–57.
129. Perego, P.; Gatti, L.; Caserini, C.; Supino, R.; Colangelo, D.; Leone, R.; Spinelli, S.; Farrell, N.; Zunino, F. *J. Inorg. Biochem.* **1999**, *77*, 59–64.
130. Guo, Z.; Chen, Y.; Zang, E.; Sadler, P. J. *J. Chem. Soc., Dalton Trans.* **1997**, 4107–4111.
131. Davies, M. S.; Cox, J.; Berners-Price, S.; Barklage, W.; Qu, Y.; Farrell, N. *Inorg. Chem.* **2000**, *39*, 1710–1715.
132. Davies, M. S.; Thomas, D. S.; Hegmans, A.; Berners-Price, S. J.; Farrell, N. *Inorg. Chem.* **2002**, *41*, 1101–1109.
133. McGregor, T. D.; Hegmans, A.; Kasparkova, J.; Neplechova, K.; Novakova, O.; Penazova, H.; Vrana, O.; Brabec, V.; Farrell, N. *J. Biol. Inorg. Chem.* **2002**, *7*, 397–404.
134. Brabec, V.; Kasparkova, J.; Vrana, O.; Novakova, O.; Cox, J. W.; Qu, Y.; Farrell, N. *Biochemistry* **1999**, *38*, 6781–6790.
135. Johnson, A.; Qu, Y.; Van Houten, B.; Farrell, N. *Nucleic Acids Res.* **1992**, *20*, 1697–1703.
136. Wu, P. K.; Kharatishvili, M.; Qu, Y.; Farrell, N. *J. Inorg. Biochem.* **1996**, *63*, 9–18.
137. McGregor, T. D.; Balcarova, Z.; Qu, Y.; Tran, M. C.; Zaludova, R.; Brabec, V.; Farrell, N. *J. Inorg. Biochem.* **1999**, *77*, 43–46.
138. McGregor, T. D.; Bousfield, W.; Qu, Y.; Farrell, N. *J. Inorg. Biochem.* **2002**, *91*, 212–219.
139. Walker, G. T.; Stone, M. P.; Krugh, T. R. *Biochemistry* **1985**, *24*, 7462–7471.
140. Kim, Y.; Geiger, J. H.; Hahn, S.; Sigler, P. B. *Nature* **1993**, *365*, 512–520.
141. Herbert, A.; Rich, A. *J. Biol. Chem.* **1996**, *271*, 11595–11598.
142. Gohlke, C.; Murchie, A. I.; Lilley, D. M.; Clegg, R. M. *Proc. Natl. Acad. Sci. USA* **1994**, *91*, 11660–11664.
143. Kloster, M. B.; Hannis, J. C.; Muddiman, D. C.; Farrell, N. *Biochemistry* **1999**, *38*, 14731–14737.
144. Cox, J. W.; Berners-Price, S. J.; Davies, M. S.; Qu, Y.; Farrell, N. *J. Am. Chem. Soc.* **2001**, *123*, 1316–1326.
145. Davies, M. S.; Thomas, D. S.; Hegmans, A.; Berners-Price, S. J.; Qu, Y.; Farrell, N. A Comparison of the kinetics of formation of 1,4-interstrand crosslinks by the trinuclear clinical agent BBR3464: Preassociation and evidence of conformational flexibility *J. Am. Chem. Soc.* submitted for publication.
146. Wang, Y.; Farrell, N.; Burgess, J. D. *J. Am. Chem. Soc.* **2001**, *123*, 5576–5577.
147. Qu, Y.; Scarsdale, N. J.; Tran, M. C.; Farrell, N. Cooperative effects in long-range 1,4 DNA-DNA interstrand crosslinks formed by polynuclear platinum complexes: an unexpected syn-orientation of adenine bases outside the binding sites. *J. Biol. Inorg. Chem.* **2003**, *8*, 19–28.
148. Rajski, S. R.; Williams, R. M. *Chem. Rev.* **1998**, *98*, 2723–2796.
149. Thompson, A. S.; Hurley, L. H. *J. Mol. Biol.* **1995**, *252*, 86–101.
150. Seaman, F. C.; Chu, J.; Hurley, L. *J. Am. Chem. Soc.* **1996**, *118*, 5383–5395.
151. Qu, Y.; Bloemink, M. J.; Reedijk, J.; Hambley, T. W.; Farrell, N. *J. Am. Chem. Soc.* **1996**, *118*, 9307.
152. Kasparkova, J.; Novakova, O.; Vrana, O.; Farrell, N.; Brabec, V. *Biochemistry* **1999**, *38*, 10997–11005.
153. Kasparkova, J.; Mellish, K. J.; Qu, Y.; Brabec, V.; Farrell, N. *Biochemistry* **1996**, *35*, 16705–16713.
154. Kasparkova, J.; Farrell, N.; Brabec, V. *J. Biol. Chem.* **2000**, *275*, 15789–15798.
155. Zehnulova, J.; Kasparkova, J.; Farrell, N.; Brabec, V. *J. Biol. Chem.* **2001**, *276*, 22191–22199.
156. Kasparkova, J.; Zehnulova, J.; Farrell, N.; Brabec, V. DNA interstrand crosslinks of novel antitumor trinuclear platinum complex BBR. Conformation, recognition by HMG-domain proteins and nucleotide excision repair. *J. Biol. Chem.* **2002**, *277*, 48076–48086.
157. Sancar, A. *Annu. Rev. Biochem.* **1996**, *65*, 43–81.
158. Servidei, T.; Ferlini, C.; Riccardi, A.; Meco, D.; Scambia, G.; Segni, G.; Manzotti, C.; Riccardi, R. *Eur. J. Cancer* **2001**, *37*, 930–938.
159. Wheate, N. J.; Webster, L. K.; Brodie, C. R.; Collins, J. G. *Anticancer Drug Des.* **2000**, *15*, 313–322.
160. Komeda, S.; Lutz, M.; Spek, A. L.; Chikuma, M.; Reedijk, J. *Inorg. Chem.* **2000**, *39*, 4230–4236.
161. Komeda, S.; Lutz, M.; Spek, A. L.; Yamanaka, Y.; Sato, T.; Chikuma, M.; Reedijk, J. *J. Am. Chem. Soc.* **2002**, *124*, 4738–4746.
162. Farrell, N.; Ha, T. T.; Souchard, J. P.; Wimmer, F. L.; Cros, S.; Johnson, N. P. *J. Med. Chem.* **1989**, *32*, 2240–2241.
163. Van Beusichem, M.; Farrell, N. *Inorg. Chem.* **1992**, *31*, 634.
164. Farrell, N.; Kelland, L. R.; Roberts, J. D.; Van Beusichem, M. *Cancer Res.* **1992**, *52*, 5065–5072.

165. Natile, G.; Coluccia, M. Trans-platinum Compounds in Cancer Therapy: A Largely Unexplored Strategy for Identifying Novel Antitumor Platinum Drugs; In *Metallopharmaceuticals I: DNA Interactions*, Clarke, M. J.; Sadler, P. J., Eds.; Springer-Verlag: Berlin, 1999; Vol. 1, pp 73–98.
166. Natile, G.; Coluccia, M. *Coord Chem. Rev.* **2001**, *216*, 383–410.
167. Perez, J. M.; Montero, E. I.; Gonzalez, A. M.; Solans, X.; Font-Bardia, M.; Fuertes, M. A.; Alonso, C.; Navarro-Ranninger, C. *J. Med. Chem.* **2000**, *43*, 2411–2418.
168. Montero, E. I.; Diaz, S.; Gonzalez-Vadillo, A. M.; Perez, J. M.; Alonso, C.; Navarro-Ranninger, C. *J. Med. Chem.* **1999**, *42*, 4264–4268.
169. Khazanov, E.; Barenholz, Y.; Gibson, D.; Najraeh, Y. Novel apoptosis-including trans-platinum piperidine and piperazine derivatives: Synthesis and biological characterization. *J. Med. Chem.* **2002**, *45*, 5189–5195.
170. Farrell, N. *Met. Ions Biol. Sys.* **1996**, *32*, 603–634.
171. Bierbach, U.; Sabat, M.; Farrell, N. *Inorg. Chem.* **2000**, *39*, 1882–1890.
172. Zou, Y.; Van Houten, B.; Farrell, N. *Biochemistry* **1993**, *32*, 9632–9638.
173. Brabec, V.; Nephlechova, K.; Kasparkova, J.; Farrell, N. *J. Biol. Inorg. Chem.* **2000**, *5*, 364–368.
174. Bierbach, U.; Qu, Y.; Hambley, T. W.; Peroutka, J.; Nguyen, H. L.; Doedee, M.; Farrell, N. *Inorg. Chem.* **1999**, *38*, 3535–3542.
175. Bierbach, U.; Farrell, N. *Inorg. Chem.* **1997**, *36*, 3657–3665.
176. Bierbach, U.; Farrell, N. *J. Biol. Inorg. Chem.* **1998**, *3*, 570.
177. Zaludova, R.; Zakovska, A.; Kasparkova, J.; Balcarova, Z.; Vrana, O.; Coluccia, M.; Natile, G.; Brabec, V. *Mol. Pharmacol.* **1997**, *52*, 354–361.
178. Clarke, M. J.; Zhu, F.; Frasca, D. R. *Chem. Rev.* **1999**, *99*, 2511–2534.
179. Clarke, M. J. *Ruthenium Chemistry Pertaining to the Design of Anticancer Agents; Progress in Clinical Biochemistry and Medicine*; Springer-Verlag: Berlin, 1989; Vol. 10, pp 25–40.
180. Frasca, D. R.; Clarke, M. J. *J. Am. Chem. Soc.* **1999**, *121*, 8523–8532.
181. Zhao, M.; Clarke, M. J. *J. Biol. Inorg. Chem.* **1999**, *4*, 318–324.
182. LaChance-Galang, K.; Zhao, M.; Clarke, M. J. *Inorg. Chem.* **1996**, *35*, 6021–6026.
183. Keppler, B. K.; Friesen, C.; Moritz, H. G.; Vongerichten, H.; Vogel, E. *Struct. Bonding* **1991**, *78*, 97–127.
184. Pieper, T.; Borsky, K.; Keppler, B. K. Non-platinum Antitumor Compounds; In *Metallopharmaceuticals I: DNA Interactions*, Clarke, M. J.; Sadler, P. J., Eds.; Springer-Verlag: Berlin, 1999; Vol.1, pp 171–199.
185. Kratz, F.; Hartmann, M.; Keppler, B.; Messori, L. *J. Biol. Chem.* **1994**, *269*, 2581–2588.
186. Sava, G.; Alessio, E.; Bergamo, A.; Mestroni, G. Sulfoxide Ruthenium Complexes: Non Toxic Tools for the Selective Treatment of Solid Tumor Metastases; In *Metallopharmaceuticals I: DNA Interactions*, Clarke, M. J. and Sadler, P. J., Ed.; Springer-Verlag: Berlin, 1999; Vol.1, pp 143–170.
187. Sanna, B.; Debidda, M.; Pintus, G.; Tadolini, B.; Posadino, A. M.; Bennardini, F.; Sava, G.; Ventura, C. *Arch. Biochem. Biophys.* **2002**, *403*, 209–218.
188. Cherrington, J. M.; Strawn, L. M.; Shawver, L. K. *Adv. Cancer Res.* **2000**, *79*, 1–38.
189. Sava, G.; Clerici, K.; Capozzi, I.; Cocchietto, M.; Gagliardi, R.; Alessio, E.; Mestroni, G.; Perbellini, A. *Anticancer Drugs* **1999**, *10*, 129–138.
190. Bergamo, A.; Gagliardi, R.; Scarcia, V.; Furlani, A.; Alessio, E.; Mestroni, G.; Sava, G. *J. Pharmacol. Exp. Ther.* **1999**, *289*, 559–564.
191. Zorzet, S.; Bergamo, A.; Cocchietto, M.; Sorc, A.; Gava, B.; Alessio, E.; Iengo, E.; Sava, G. *J. Pharmacol. Exp. Ther.* **2000**, *295*, 927–933.
192. Sava, G.; Bergamo, A.; Zorzet, S.; Gava, B.; Casarsa, C.; Cocchietto, M.; Furlani, A.; Scarcia, V.; Serli, B.; Iengo, E.; Alessio, E.; Mestroni, G. *Eur. J. Cancer* **2002**, *38*, 427–435.
193. Gopal, Y. N.; Jayaraju, D.; Kondapi, A. K. *Biochemistry* **1999**, *38*, 4382–4388.
194. Chen, H.; Parkinson, J. A.; Parsons, S.; Coxall, R. A.; Gould, R. O.; Sadler, P. J. *J. Am. Chem. Soc.* **2002**, *124*, 3064–3082.
195. Morris, R. E.; Aird, R. E.; Murdoch Pdel, S.; Chen, H.; Cummings, J.; Hughes, N. D.; Parsons, S.; Parkin, A.; Boyd, G.; Jodrell, D. I.; Sadler, P. J. *J. Med. Chem.* **2001**, *44*, 3616–3621.
196. Antman, K. H. *Oncologist* **2001**, *6*, 1–2.
197. Waxman, S.; Anderson, K. C. *Oncologist* **2001**, *6*, 3–10.
198. Shen, Z. X.; Chen, G. Q.; Ni, J. H.; Li, X. S.; Xiong, S. M.; Qiu, Q. Y.; Zhu, J.; Tang, W.; Sun, G. L.; Yang, K. Q.; Chen, Y.; Zhou, L.; Fang, Z. W.; Wang, Y. T.; Ma, J.; Zhang, P.; Zhang, T. D.; Chen, S. J.; Chen, Z.; Wang, Z. Y. *Blood* **1997**, *89*, 3354–3360.
199. Novick, S. C.; Warrell, R. P., Jr. *Semin. Oncol.* **2000**, *27*, 495–501.
200. Rust, D. M.; Soignet, S. L. *Oncologist* **2001**, *6*, 29–32.
201. Miller, W. H., Jr.; Schipper, H. M.; Lee, J. S.; Singer, J.; Waxman, S. *Cancer Res.* **2002**, *62*, 3893–3903.
202. Jing, Y.; Dai, J.; Chalmers-Redman, R. M.; Tatton, W. G.; Waxman, S. *Blood* **1999**, *94*, 2102–2111.
203. Dai, J.; Weinberg, R. S.; Waxman, S.; Jing, Y. *Blood* **1999**, *93*, 268–277.
204. Yang, C. H.; Kuo, M. L.; Chen, J. C.; Chen, Y. C. *Br. J. Cancer* **1999**, *81*, 796–799.
205. Zhang, T. D.; Chen, G. Q.; Wang, Z. G.; Wang, Z. Y.; Chen, S. J.; Chen, Z. *Oncogene* **2001**, *20*, 7146–7153.
206. Kroemer, G.; de The, H. *J. Natl. Cancer Inst.* **1999**, *91*, 743–745.
207. Preston, T. J.; Abadi, A.; Wilson, L.; Singh, G. *Adv. Drug Deliv. Rev.* **2001**, *49*, 45–61.
208. Costantini, P.; Jacotot, E.; Decaudin, D.; Kroemer, G. *J. Natl. Cancer Inst.* **2000**, *92*, 1042–1053.
209. Koya, K.; Li, Y.; Wang, H.; Ukai, T.; Tatsuta, N.; Kawakami, M.; Shishido; Chen, L. B. *Cancer Res.* **1996**, *56*, 538–543.
210. McKeage, M.J.; Maharaj, L.; Berners-Price, S. J. *Coord. Chem. Rev.* **2002**, *232*, 127–135.
211. Berners-Price, S. J.; Bowen, R. J.; Galettis, P.; Healy, P. C.; McKeage, M. J. *Coord. Chem. Rev.* **1999**, *185–186*, 823–836.
212. Berners-Price, S.; Jarrett, P.; Sadler, P. *Inorg. Chem.* **1987**, *26*, 3074–3077.
213. Shaw, C. F. *Chem. Rev.* **1999**, *99*, 2589–2600.
214. Berners-Price, S. J.; Girard, G. R.; Hill, D. T.; Sutton, B. M.; Jarrett, P. S.; Faucette, L. F.; Johnson, R. K.; Mirabelli, C. K.; Sadler, P. J. *J. Med. Chem.* **1990**, *33*, 1386–1392.

215. McKeage, M. J.; Berners-Price, S. J.; Galettis, P.; Bowen, R. J.; Brouwer, W.; Ding, L.; Zhuang, L.; Baguley, B. C. *Cancer Chemother. Pharmacol.* **2000**, *46*, 343–350.
216. Berners-Price, S.; Bowen, R.; Hambley, T.; Healy, P. *J. Chem. Soc., Dalton Trans.* **1999**, *8*, 1337–1346.
217. Riley, D. P. *Chem. Rev.* **1999**, *99*, 2573–2588.
218. McCord, J. M.; Fridovich, I. *J. Biol. Chem.* **1969**, *244*, 6049–6055.
219. Kramer, R. *Angew Chem., Int. Ed.* **2000**, *39*, 4469–4470.
220. Weiss, R.; Riley, D. Therapeutic Aspects of Manganese(II)-based Superoxide Dismutase Mimics; In *Uses of Inorganic Chemistry in Medicine*, Farrell, N., Ed.; The Royal Society of Chemistry: Cambridge, 1999, pp 77–92.
221. Doctrow, S. R.; Huffman, K.; Marcus, C. B.; Musleh, W.; Bruce, A.; Baudry, M.; Malfroy, B. *Adv. Pharmacol.* **1997**, *38*, 247–269.
222. Melov, S.; Ravenscroft, J.; Malik, S.; Gill, M. S.; Walker, D. W.; Clayton, P. E.; Wallace, D. C.; Malfroy, B.; Doctrow, S. R.; Lithgow, G. J. *Science* **2000**, *289*, 1567–1569.
223. Salvemini, D.; Wang, Z. Q.; Zweier, J. L.; Samouilov, A.; Macarthur, H.; Misko, T. P.; Currie, M. G.; Cuzzocrea, S.; Sikorski, J. A.; Riley, D. P. *Science* **1999**, *286*, 304–306.
224. Aston, K.; Rath, N.; Naik, A.; Slomczynska, U.; Schall, O. F.; Riley, D. P. *Inorg. Chem.* **2001**, *40*, 1779–1789.
225. Melendez, E. *Crit. Rev. Oncol. Hematol.* **2002**, *42*, 309–315.
226. Comba, P.; Jakob, H.; Nuber, B.; Keppler, B. K. *Inorg. Chem.* **1994**, *33*, 3396–3400.
227. Schilling, T.; Keppler, K. B.; Heim, M. E.; Niebch, G.; Dietzfelbinger, H.; Rastetter, J.; Hanauske, A. R. *Invest. New Drugs* **1996**, *13*, 327–332.
228. Christodoulou, C. V.; Ferry, D. R.; Fyfe, D. W.; Young, A.; Doran, J.; Sheehan, T. M.; Eliopoulos, A.; Hale, K.; Baumgart, J.; Sass, G.; Kerr, D. J. *J. Clin. Oncol.* **1998**, *16*, 2761–2769.
229. Korfel, A.; Scheulen, M. E.; Schmoll, H. J.; Grundel, O.; Harstrick, A.; Knoche, M.; Fels, L. M.; Skorzec, M.; Bach, F.; Baumgart, J.; Sass, G.; Seeber, S.; Thiel, E.; Berdel, W. E. *Clin. Cancer Res.* **1998**, *4*, 2701–2708.
230. Lummen, G.; Sperling, H.; Luboldt, H.; Otto, T.; Rubben, H. *Cancer Chemother. Pharmacol.* **1998**, *42*, 415–417.
231. Harding, M. M.; Mokdsi, G. *Curr. Med. Chem.* **2000**, *7*, 1289–1303.
232. Kuo, L. Y.; Liu, A. H.; Marks, T. J. *Met. Ions Biol. Syst.* **1996**, *33*, 53–85.
233. Harding, M. M.; Mokdsi, G.; Lucas, W. *Inorg. Chem.* **1998**, *37*, 2432–2437.
234. Sun, H.; Li, H.; Weir, R. A.; Sadler, P. J. *Angew Chem., Int. Ed. Engl.* **1998**, *37*, 1577–1579.
235. Apseloff, G. *Am. J. Ther.* **1999**, *6*, 327–339.
236. Webster, L. K.; Olver, I. N.; Stokes, K. H.; Sephton, R. G.; Hillcoat, B. L.; Bishop, J. F. *Cancer Chemother. Pharmacol.* **2000**, *45*, 55–58.
237. Senderowicz, A. M.; Reid, R.; Headlee, D.; Abornathy, T.; Horti, J.; Lush, R. M.; Reed, E.; Figg, W. D.; Sausville, E. A. *Urol. Int.* **1999**, *63*, 120–125.
238. Coltery, P.; Lechenault, F.; Cazabat, A.; Juvin, E.; Khassanova, L.; Evangelou, A.; Keppler, B. *Anticancer Res.* **2000**, *20*, 955–958.
239. Arion, V. B.; Jakupec, M. A.; Galanski, M.; Unfried, P.; Keppler, B. K. *J. Inorg. Biochem.* **2002**, *91*, 298–305.
240. Knorr, G. M.; Chitambar, C. R. *Anticancer Res.* **1998**, *18*, 1733–1737.
241. Grier, N. Mercurials—Inorganic and Organic. In *Mercurials—Inorganic and Organics (Disinfection, Sterilization and Preservation.)*, Block, S. S., Ed.; Lea and Fabringer, 1983, pp 346–374.
242. Grier, N. Silver and Its Compounds. In *Mercurials—Inorganic and Organics (Disinfection, Sterilization and Preservation.)*, Block, S. S., Ed.; Lea and Fabringer, 1983, pp 375–389.
243. Gupta, A.; Matsui, K.; Lo, J. F.; Silver, S. *Nat. Med.* **1999**, *5*, 183–188.
244. Clement, J. L.; Jarrett, P. S. *Met. Based Drugs* **1994**, *1*, 467–782.
245. Briand, G. G.; Burford, N. *Chem. Rev.* **1999**, *99*, 2601–2658.
246. Reglinski, J. *Chemistry of Arsenic, Antimony, and Bismuth*; Blackie Academic & Professional: London 1998.
247. Briand, N. *Adv. Inorg. Chem.* **2002**, *50*, 285–357.
248. Asato, E.; Driessen, W. L.; de Graaff, R. A. G.; Hulsbergen, F. B.; Reedijk, J. *Inorg. Chem.* **1991**, *30*, 4210–4218.
249. Asato, E.; Katsura, K.; Mikuriya, M.; Fujii, T.; Reedijk, J. *Inorg. Chem.* **1993**, *32*, 5322–5329.
250. Asato, E.; Katsura, K.; Mikuriya, M.; Turpeinen, U.; Mutikainen, I.; Reedijk, J. *Inorg. Chem.* **1995**, *34*, 2447–2454.
251. Sadler, P. J.; Li, H.; Sun, H. *Coord. Chem. Rev.* **1999**, *185–186*, 689–709.
252. Sadler, P. J.; Sun, H. *J. Chem. Soc., Dalton Trans.* **1995**, 1395–1401.
253. Burford, N.; Eelman, M. D.; Cameron, T. S. *Chem. Commun. (Camb)* **2002**, 1402–1403.
254. Whitmire, K. *J. Chem. Soc. Chem. Commun.* **2002**, 2834–2835.
255. Sadler, P. J.; Sun, H. Z.; Li, H. Y. *Chem. Eur. J.* **1996**, *2*, 701–708.
256. Sun, H.; Li, H.; Mason, A. B.; Woodworth, R. C.; Sadler, P. J. *Biochem. J.* **1999**, *337*, 105–111.
257. Navarro, M.; Perez, H.; Sanchez-Delgado, R. A. *J. Med. Chem.* **1997**, *40*, 1937–1939.
258. Navarro, M.; Cisneros-Fajardo, E. J.; Lehmann, T.; Sanchez-Delgado, R. A.; Atencio, R.; Silva, P.; Lira, R.; Urbina, J. A. *Inorg. Chem.* **2001**, *40*, 6879–6884.
259. Sanchez-Delgado, R. A.; Lazard, K.; Rincon, L.; Urbina, J. A. *J. Med. Chem.* **1993**, *36*, 2041–2043.
260. Sanchez-Delgado, R. A.; Navarro, M.; Perez, H.; Urbina, J. A. *J. Med. Chem.* **1996**, *39*, 1095–1099.
261. Birch, N. *Biomedical Uses of Lithium*; Farrell, N., Ed.; The Royal Society of Chemistry: Cambridge, 1999, pp 11–21.
262. Birch, N. *J. Chem. Rev.* **1999**, *99*, 2659–2682.
263. Orvig, C.; Thompson, K. H.; Battell, M.; McNeill, J. H. Metal Ions in Biological Systems: Vanadium and its Role in Life; In *Metal Ions in Biological Systems*, Sigel, H.; Sigel, A.; Eds.; Marcel Dekker: New York, 1995; Vol. 31, p 575.
264. Blondel, O.; Simon, J.; Chevalier, B.; Portha, B. *Am. J. Physiol.* **1990**, *258*, E459–E467.
265. Thompson, K. H.; McNeill, J. H.; Orvig, C. *Chem. Rev.* **1999**, *99*, 2561–2572.
266. Orvig, C.; Thompson, K.; Cam, M.; McNeil, J. Vanadium Compounds as Possible Insulin Modifiers; In *Uses of Inorganic Chemistry in Medicine*, Farrell, N. Ed.; The Royal Society of Chemistry: Cambridge, 1999, pp 93–108.
267. Huyer, G.; Liu, S.; Kelly, J.; Moffat, J.; Payette, P.; Kennedy, B.; Tsaprailis, G.; Gresser, M. J.; Ramachandran, C. *J. Biol. Chem.* **1997**, *272*, 843–851.
268. Elberg, G.; He, Z.; Li, J.; Sekar, N.; Shechter, Y. *Diabetes* **1997**, *46*, 1684–1690.
269. Shaw, C. Gold Complexes with Anti-arthritis, Anti-tumour and Anti-HIV Activity; In *Uses of Inorganic Chemistry in Medicine*, Farrell, N., Ed.; The Royal Society of Chemistry: Cambridge, 1999, pp 26–57.

270. Snyder, R. M.; Mirabelli, C. K.; Crooke, S. T. *Semin. Arthritis Rheum.* **1987**, *17*, 71–80.
271. Rudkowski, R.; Graham, G. G.; Champion, G. D.; Ziegler, J. B. *Biochem. Pharmacol.* **1990**, *39*, 1687–1695.
272. Butler, A.; Rhodes, P. Nitric Oxide in Physiology and Medicine; In *Uses of Inorganic Chemistry in Medicine*, Farrell, N., Ed.; The Royal Society of Chemistry: Cambridge, 1999, pp 58–76.
273. Clarke, M. J.; Gaul, J. B. *Struct. Bonding* **1993**, *81*, 147–181.
274. Butler, A. R.; Williams, D. L. H. *Chem. Soc. Rev.* **1993**, *22*, 233–241.
275. Groves, J. T. *Curr. Opin. Chem. Biol.* **1999**, *3*, 226–235.
276. Shimanovich, R.; Groves, J. T. *Arch. Biochem. Biophys.* **2001**, *387*, 307–317.
277. Shimanovich, R.; Hannah, S.; Lynch, V.; Gerasimchuk, N.; Mody, T. D.; Magda, D.; Sessler, J.; Groves, J. T. *J. Am. Chem. Soc.* **2001**, *123*, 3613–3614.
278. Hergesell, O.; Ritz, E. *Kidney Int.* **1999**, *73*, S42–S45.
279. Hutchison, A. J. *Perit. Dial. Int.* **1999**, *19*, S408–S412.
280. Hergesell, O.; Ritz, E., Phosphate binders on iron basis: a new perspective? *Kidney Int. Suppl.* **1999**, *73*, S42–45.

9.19

Metal Complexes as MRI Contrast Enhancement Agents

É. TÓTH, L. HELM, and A. E. MERBACH

École Polytechnique Fédérale de Lausanne, Switzerland

9.19.1	INTRODUCTION	841
9.19.2	RELAXIVITY OF Gd ^{III} COMPLEXES	843
9.19.2.1	Inner-sphere Proton Relaxivity	845
9.19.2.1.1	<i>Hydration number and Gd–H distance</i>	847
9.19.2.1.2	<i>Water/proton exchange</i>	847
9.19.2.1.3	<i>Rotation</i>	851
9.19.2.1.4	<i>Electron spin relaxation</i>	851
9.19.2.2	Outer and Second-sphere Relaxation	853
9.19.2.3	NMRD Profiles	853
9.19.3	TOXICITY OF Gd ^{III} COMPLEXES: THERMODYNAMIC STABILITY AND KINETIC INERTNESS	853
9.19.3.1	Complex Stability Constants	854
9.19.3.2	Blood Plasma Models	856
9.19.3.3	Kinetic Inertness of Gd ^{III} Complexes	857
9.19.4	BLOOD POOL AGENTS	857
9.19.4.1	Covalently Bound Macromolecular Agents	858
9.19.4.1.1	<i>Gd^{III} chelates covalently bound to proteins</i>	858
9.19.4.1.2	<i>Linear polymers</i>	858
9.19.4.1.3	<i>Dendrimers</i>	859
9.19.4.1.4	<i>Dextran derivatives</i>	861
9.19.4.1.5	<i>Micelles and liposomes</i>	861
9.19.4.2	Noncovalently Bound Macromolecular Agents	862
9.19.5	SMART CONTRAST AGENTS	866
9.19.5.1	pH-sensitive Agents	866
9.19.5.2	Temperature-sensitive Agents	870
9.19.5.3	Contrast Agents Sensitive to Partial Oxygen Pressure	871
9.19.5.4	Enzymatically Responsive Contrast Agents	871
9.19.5.5	Contrast Agents Responsive to Metal Ion Concentration	873
9.19.6	CHEMICAL EXCHANGE SATURATION (CEST) CONTRAST AGENTS	874
9.19.7	TARGETING CONTRAST AGENTS	875
9.19.8	REFERENCES	877

9.19.1 INTRODUCTION

Since the early 1990s, magnetic resonance imaging (MRI) has evolved into one of the most powerful techniques in medical diagnostics. In 2001, around 40 million MRI examinations were conducted in the world. MR images are always based on proton magnetic resonance. The contrast of the images is a function of three main factors: the proton density, and the longitudinal and transverse relaxation times, T_1 and T_2 , of the proton spins. The variation in proton density between different tissues is relatively small; thus images based solely on the difference in proton density would have poor contrast. Proton spin relaxation times differ substantially from one

tissue to the other, therefore T_1 - or T_2 -weighted images display a good contrast and provide valuable diagnostic information (images recorded with pulse sequences that emphasize changes in $1/T_1$ or $1/T_2$ are called T_1 - or T_2 -weighted images, respectively). In earlier times, MRI was considered as a noninvasive medical diagnostic modality that could produce high-quality images without the use of a contrast agent. However, it was rapidly realized that contrast enhancement by paramagnetic substances can be very beneficial, and now the use of contrast agents has become an integral part of MRI for many applications (Figure 1).

Today, around 30–40% of all medical MR images are generated with the use of a contrast medium. This number is expected to increase substantially with the development of new agents and new applications.

MRI contrast agents work by reducing T_1 and/or T_2 relaxation times of protons (mainly of water solvent protons) in the target tissue.^{1–3} MRI agents are unique among all pharmaceuticals in that they are catalysts: catalysts for water proton relaxation.⁴ They are commonly described as T_1 - or T_2 -agents depending on whether the relative reduction in relaxation times caused by the agent is greater for the longitudinal (T_1) or transverse (T_2) relaxation. Signal intensity increases with increasing $1/T_1$ (a bright spot on T_1 -weighted images) and decreases with increasing $1/T_2$ (decreased brightness on T_2 -weighted images). Given that proton $T_1 \gg T_2$ for most tissues, usually the relative effect of the contrast agent on T_1 is much larger than on T_2 . In MRI practice, T_1 agents are strongly favored, since a positive contrast is more easily detected than a negative

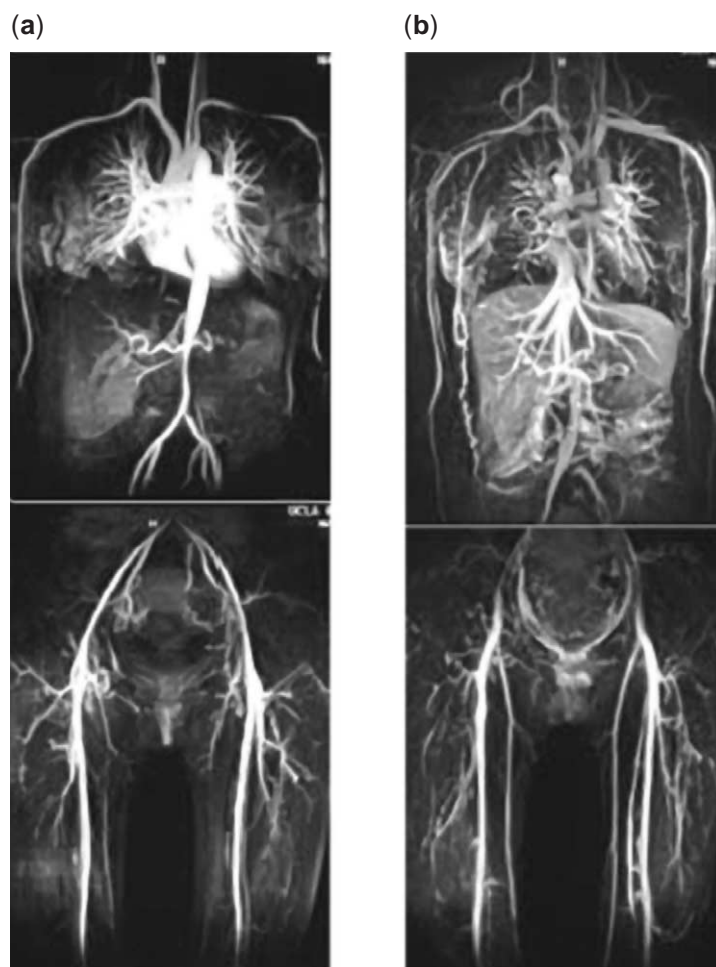


Figure 1 Images obtained by magnetic resonance angiography, using the Gd^{III} -based contrast agent Gadodiamide. The first images show the arteries and were obtained right after injection of the contrast agent (arterial phase). Following a delay of 30 seconds after arterial phase, the scan was repeated to obtain images of both arteries and veins. Upon subtraction of arterial phase images (a) from steady state images, venous phase images (b) were obtained (reproduced by permission of Magnetic Moments, LLC, from www.magneticmoments.com).

one. Gadolinium(III) complexes, which belong to the family of T_1 agents, are by far the most widely used contrast media in clinical practice. The choice of Gd^{III} is explained by the seven unpaired electrons, which make it the most paramagnetic stable metal ion, and by its relatively slow electronic relaxation, originating from a symmetric S-state. The free gadolinium ion, Gd^{3+} , however, cannot be injected into the blood, as it can induce toxicity in many ways. Gd^{3+} has a tendency to form hydroxo complexes and precipitate at physiological pH; it can also bind to donor groups of proteins, replace other metal ions in enzymes or, due to its similar size to Ca^{2+} , it may interfere in Ca^{2+} -regulated signal transmission processes. In order to circumvent toxicity, Gd^{3+} is complexed with appropriate multidentate ligands, preferentially poly(amino carboxylates). Poly(amino carboxylate) ligands ensure a high thermodynamic stability and kinetic inertness under physiological conditions for the lanthanide chelate. As a result, the Gd^{III} complex remains intact throughout its stay in the body and is excreted before any dissociation to free metal and ligand occurs. The first Gd^{III} complex approved for MRI contrast agent applications was $[\text{Gd}(\text{DTPA})(\text{H}_2\text{O})]^{2-}$ in 1988. This was soon followed by the kinetically more inert, macrocyclic $[\text{Gd}(\text{DOTA})(\text{H}_2\text{O})]^-$ and later by Gd^{III} complexes of DTPA or DOTA derivatives (Scheme 1).

In addition to Gd^{III} complexes, one Mn^{II} compound, Mn^{II} DPDP, has been approved for medical application (DPDP = *N,N'*-dipyridoxylethylenediamine-*N,N'*-diacetate 5,5'-bis(phosphate)). Mn^{II} DPDP is a weak chelate that dissociates *in vivo* to give free manganese(II), which is taken up by hepatocytes.⁵ The complexation of Mn^{II} by the ligand facilitates a slower release of manganese. Apart from these paramagnetic metal complexes, different formulations of small iron particles have also been commercialized as MRI contrast media.⁶ Since the majority of the current contrast agent applications in MRI involve Gd^{III} complexes, we focus here only on Gd^{III} -based agents. Several reviews and monographs have been published on this topic in the late 1990s and early 2000s.¹⁻³

In this chapter we discuss first proton relaxivity, the parameter that directly translates to the effectiveness of an MRI contrast agent, and all the factors that influence proton relaxivity for Gd^{III} complexes. Then we will address the main physico-chemical aspects of *in vivo* stability of Gd^{III} -based agents, such as thermodynamic and kinetic stability. The second part of the chapter will be devoted to new-generation MRI contrast media, such as macromolecular agents for imaging the blood pool, and “smart” contrast agents that are capable of reporting on the physico-chemical environment in tissues; and finally we will discuss the possibility of targeting in MRI.

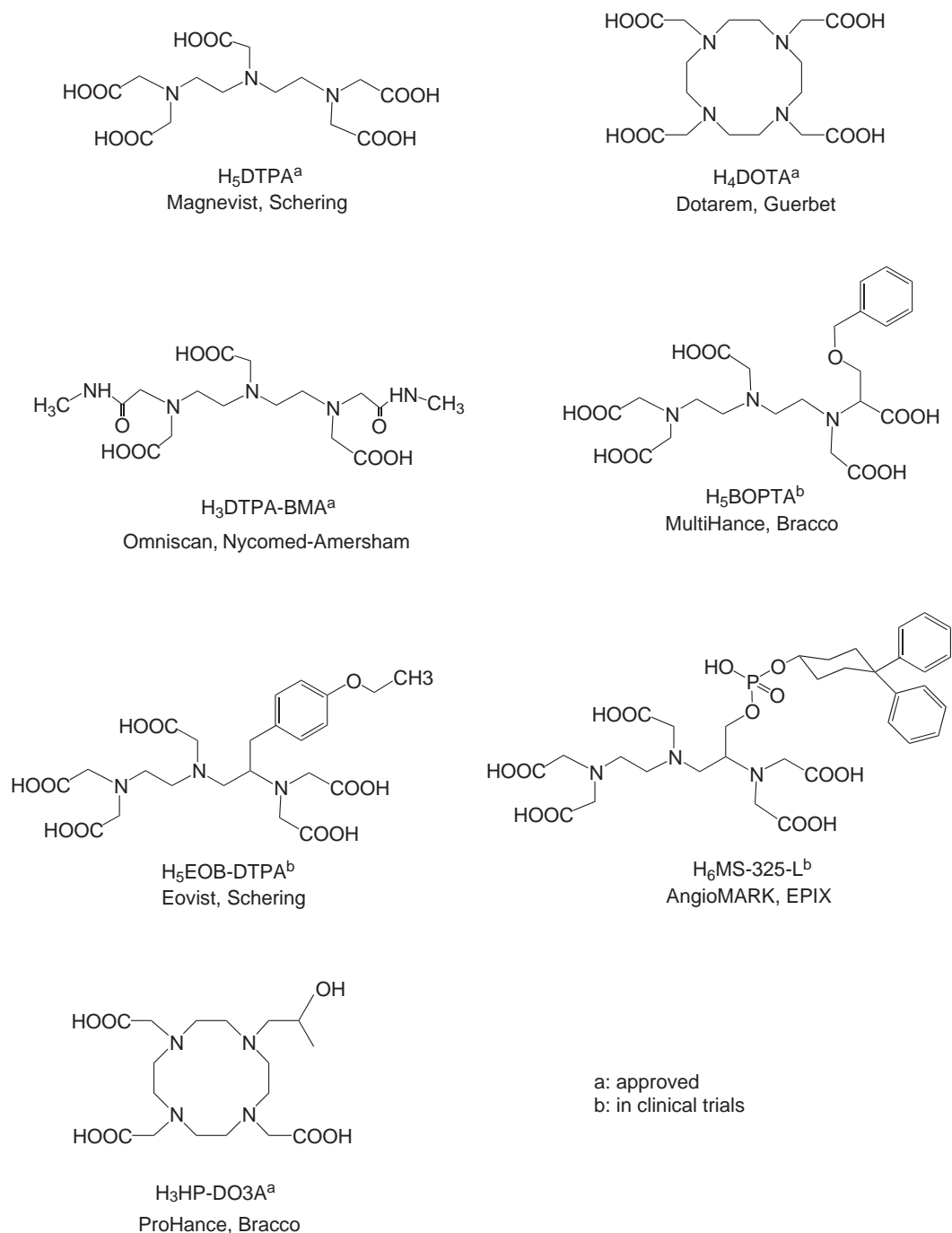
9.19.2 RELAXIVITY OF Gd^{III} COMPLEXES

The efficiency of a Gd^{III} chelate as a contrast agent in MRI is measured by its ability to increase the relaxation rate of the surrounding (bulk) water protons. The paramagnetic proton relaxation rate enhancement induced by the Gd^{III} chelate, and normalized by its concentration, is called proton relaxivity. Given the preponderance of T_1 agents in practice, proton relaxivity generally refers to longitudinal relaxation (r_1) (Equation (1)):

$$\frac{1}{T_{\text{obs}}} = \frac{1}{T_{\text{ld}}} + \frac{1}{T_{\text{lp}}} = \frac{1}{T_{\text{ld}}} + r_1 [\text{Gd}] \quad (1)$$

The observed proton relaxation rate, $1/T_{\text{obs}}$, is the sum of a diamagnetic contribution, $1/T_{\text{ld}}$, and the paramagnetic relaxation rate enhancement, $1/T_{\text{lp}}$, this latter being linearly proportional to the concentration of the paramagnetic species, $[\text{Gd}]$. In Equation (1), the concentration is usually given in mmol L^{-1} , thus the unity of proton relaxivity, r_1 , is $\text{mM}^{-1} \text{s}^{-1}$.

The general theory of solvent nuclear relaxation in the presence of paramagnetic substances was described by Bloembergen, Solomon, and others.⁷⁻¹² The paramagnetic relaxation of the water protons originates from the dipole–dipole interactions between the proton nuclear spins and the fluctuating local magnetic field caused by the Gd^{III} unpaired electron spins. For Gd^{III} complexes, the proton relaxivity has two main contributions: (i) Inner-sphere relaxivity arises from protons on the inner-sphere water molecule(s), directly bound to the metal ion. The paramagnetic effect is then transmitted to the bulk water via the exchange of these protons, or of the entire water molecules to which they are attached. (ii) Bulk solvent molecules experience a paramagnetic effect also when they diffuse near the paramagnetic complex. The effect of this random translational diffusion is defined as outer-sphere relaxation. The separation of inner- and



Scheme 1

outer-sphere terms is thus based on the intra- and intermolecular nature of the interaction, respectively. On the other hand, the separation is also useful in explaining the observed proton relaxivities in terms of existing theories (see below). Water molecules may be also bound via hydrogen bonds to the ligand (e.g., to carboxylates or phosphonates) or to the inner-sphere water. These give rise to a “second-sphere” relaxivity term, described by the same theory as the inner-sphere term, and which, in certain cases, represents a nonnegligible contribution to the overall relaxivity. However, owing to difficulties in separating the outer- and second-sphere contributions, the latter is often neglected, or simply taken into account in the outer-sphere term. Figure 2 shows inner-, second-, and outer-sphere water molecules in a typical Gd^{III} chelate.

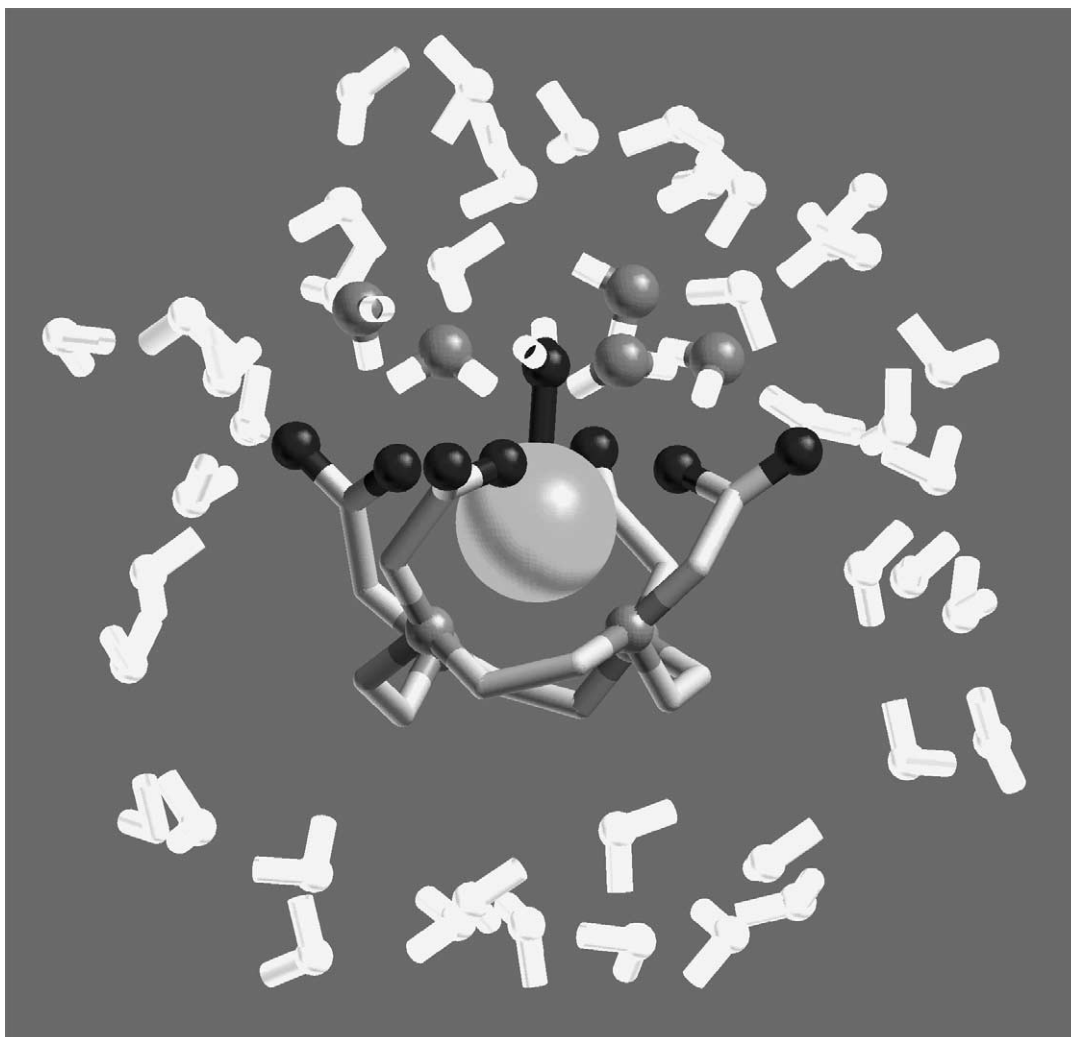


Figure 2 The molecular dynamics simulation picture of $[\text{Gd}(\text{DOTA})(\text{H}_2\text{O})]^-$ in aqueous solution shows the inner sphere water, directly bound to the metal (its oxygen is dark); the second sphere water molecules, bound to the carboxylates of the ligand through hydrogen bridges (their oxygens are gray); and outer sphere or bulk water molecules without preferential orientation (in white).

The contributions of the inner- and outer-sphere relaxation mechanisms to the overall relaxivity are split roughly 50–50% for currently used, low molecular weight, Gd^{III} -based contrast agents (at imaging magnetic fields). The inner-sphere term can be substantially improved by optimization of the influencing parameters, and then becomes preponderant for the new-generation contrast agents with high proton relaxivity.

9.19.2.1 Inner-sphere Proton Relaxivity

The longitudinal inner-sphere relaxation rate, $1/T_1$, of bulk water protons is given by Equation (2):¹³

$$\left(\frac{1}{T_1}\right)^{\text{IS}} = \frac{cq}{55.5} \frac{1}{T_{1\text{m}} + \tau_{\text{m}}} = P_{\text{m}} \frac{1}{T_{1\text{m}} + \tau_{\text{m}}} \quad (2)$$

where c is the molal concentration, q is the number of bound water nuclei per Gd (hydration number), P_{m} is the mole fraction of the bound water nuclei, τ_{m} is the lifetime of a water molecule in the inner sphere (equal to the reciprocal water/proton exchange rate, $1/k_{\text{ex}}$), and $1/T_{1\text{m}}$ is the

relaxation rate in the bound water. The longitudinal relaxation of bound water protons originates from the magnetic field dependent dipole–dipole mechanism, modulated by the reorientation of the molecule, the electron spin relaxation and the water/proton exchange. The relaxation rate is expressed by the modified Solomon–Bloembergen equation:

$$\frac{1}{T_{1m}} = \frac{2}{15} \frac{\gamma_I^2 g^2 \mu_B^2}{r_{GdH}^6} S(S+1) \left(\frac{\mu_0}{4\pi}\right)^2 \left[7 \frac{\tau_{e2}}{1 + \omega_s^2 \tau_{c2}^2} + 3 \frac{\tau_{c1}}{1 + \omega_I^2 \tau_{c1}^2} \right] \quad (3)$$

Here, γ_I is the nuclear gyromagnetic ratio, g is the electron g-factor, μ_B is the Bohr magneton, r_{GdH} is the electron spin–proton distance, and ω_I and ω_s are the nuclear and electron Larmor frequencies, respectively ($\omega = \gamma B$, where B is the magnetic field). The correlation times, τ_{ci} , are defined as $1/\tau_{ci} = 1/\tau_R + 1/T_{ie} + 1/\tau_m$ ($i = 1, 2$), where τ_R is the rotational correlation time, and T_{1e} and T_{2e} are the longitudinal and transverse electron spin relaxation times of Gd^{III} . The electronic relaxation rates, interpreted in terms of zero-field splitting (ZFS) interactions, also depend on the magnetic field (Bloembergen–Morgan theory of paramagnetic electron spin relaxation, valid if $\tau_v^2 \Delta^2 \ll 1$):¹⁴

$$\left(\frac{1}{T_{1e}}\right) = \frac{1}{25} \Delta^2 \tau_v \{4S(S+1) - 3\} \left(\frac{1}{1 + \omega_s^2 \tau_v^2} + \frac{4}{1 + 4\omega_s^2 \tau_v^2}\right) \quad (4)$$

$$\left(\frac{1}{T_{2e}}\right) = \frac{1}{50} \Delta^2 \tau_v \{4S(S+1) - 3\} \left(\frac{5}{1 + \omega_s^2 \tau_v^2} + \frac{2}{1 + 4\omega_s^2 \tau_v^2} + 3\right) \quad (5)$$

In Equations 4 and 5, Δ^2 is the mean square ZFS energy and τ_v is the correlation time for the modulation of the ZFS, resulting from the transient distortions of the complex. The combination of Equations (3)–(5) constitutes a complete theory to relate the paramagnetic relaxation rate enhancement to microscopic properties (Solomon–Bloembergen–Morgan (SBM) theory).^{15,16}

It is clear from the above equations that numerous parameters (proton exchange rate, $k_{ex} = 1/\tau_m$; rotational correlation time, τ_R ; electronic relaxation times, $1/T_{1,2e}$; Gd–proton distance, r_{GdH} ; hydration number, q); all influence the inner-sphere proton relaxivity. Simulated proton relaxivity curves, like that in Figure 3, are often used to visualize better the effect of the

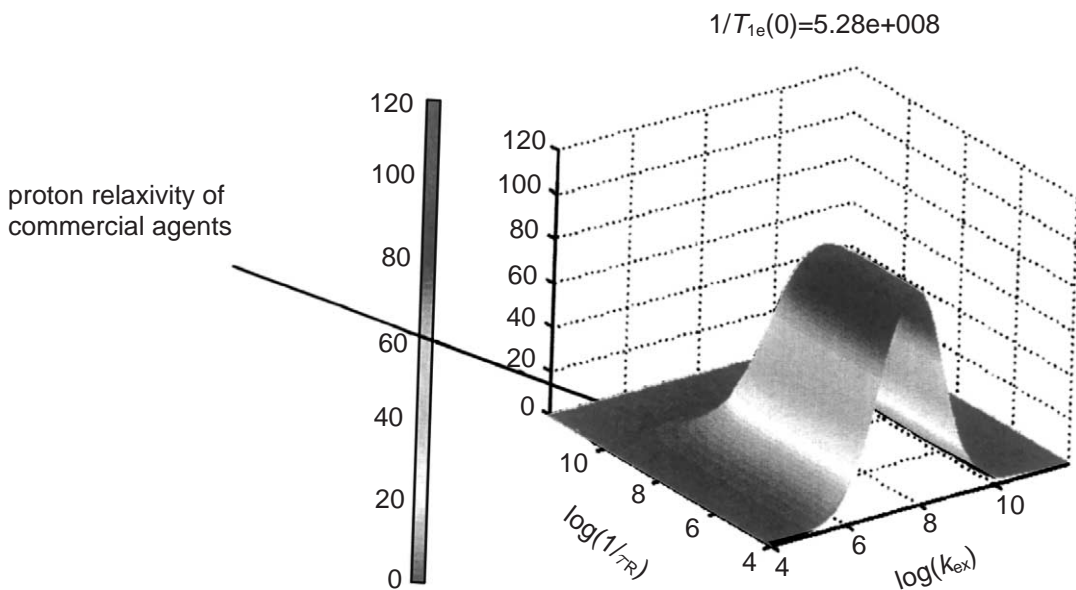


Figure 3 Effect of the water exchange rate, k_{ex} , and the rotational correlation time, τ_R , on inner-sphere proton relaxivity. The plot was simulated for a particular value of the longitudinal electron spin relaxation rate, $1/T_{1e} = 5.28 \times 10^8 \text{ s}^{-1}$. The marketed contrast agents all have relaxivities around $4\text{--}5 \text{ mM}^{-1} \text{ s}^{-1}$ in contrast to the theoretically attainable values over $100 \text{ mM}^{-1} \text{ s}^{-1}$, and this is mainly due to their fast rotation and slow water exchange.

influencing parameters. Their important message is that the rotational correlation time, proton exchange, and electronic relaxation rates, as the most significant variables, have to be simultaneously optimized in order to attain maximum relaxivities.

9.19.2.1.1 Hydration number and Gd–H distance

The hydration state of lanthanide(III) chelates can be assessed by different techniques. Luminescence studies are widely used for Eu^{III} and Tb^{III} chelates (see Chapter 9.21).^{17,18} ^{17}O NMR chemical shift measurements in solution of lanthanide(III) (most often Dy or Gd) complexes can also give information on q .¹⁹ These techniques in the context of MRI contrast agent research have been reviewed in 2001.¹

All Gd^{III} chelates approved for use as MRI contrast agents are nine-coordinate, with one inner-sphere water molecule. As the inner-sphere relaxivity is linearly proportional to the hydration number q , increasing q would result in increased relaxivities (Equation (2)). Unfortunately, so far no Gd^{III} complex with more than one inner-sphere water molecule has been found stable enough for medical use. Furthermore, in a biological fluid containing small coordinating ligands (carbonate, phosphate, citrate), such compounds would have a strong tendency to form ternary complexes, which would erase any relaxivity advantage *in vivo*.

The Gd–H distance, r_{GdH} , which enters at the inverse sixth power into the expression of inner-sphere relaxivity, is a difficult parameter to obtain experimentally. It is generally estimated on the basis of Gd–coordinated water oxygen distances, determined by solid-state X-ray analysis. Solid-state distances are good estimates of the aqueous solution state, as was experimentally proven by an X-ray absorption fine-structure study on $[\text{Gd}(\text{DOTA})(\text{H}_2\text{O})]^-$ and $[\text{Gd}(\text{DTPA})(\text{H}_2\text{O})]^{2-}$, which gave identical values for the Gd–O distances for both complexes in solid and solution states.²⁰

9.19.2.1.2 Water/proton exchange

The proton exchange rate, k_{ex} , has a dual role in determining relaxivity. It governs the chemical exchange between the inner sphere and the bulk (Equation (2)), and it also enters the overall correlation time, τ_{c} , that modulates the relaxation of inner-sphere protons (Equation (3)). Proton exchange can occur either via the exchange of the water molecules or independently (or both). For current Gd^{III} -based contrast agents, inner-sphere protons exchange only via water exchange, at least at physiological pH. Nevertheless, in certain Gd^{III} complexes proton exchange can proceed considerably faster than water exchange.^{21,22}

Since the introduction of MRI contrast agents, water exchange has been studied on numerous Gd^{III} complexes by ^{17}O NMR spectroscopy. Variable-temperature ^{17}O transverse relaxation rate measurements provide the rate of the water exchange, whereas the mechanism can be assessed by determining the activation volume, ΔV^\ddagger , from variable pressure ^{17}O T_2 measurements.²³ A dissociative **D** mechanism is characterized by a large positive ΔV^\ddagger , whereas an associative **A** mechanism is described by a large negative ΔV^\ddagger . Between these two extremes, the bond breaking and bond making both contribute to ΔV^\ddagger , resulting in a continuum of interchange **I** mechanisms. On either side of **I** are the **I_d** and **I_a** mechanisms, which are characterized by positive and negative ΔV^\ddagger values corresponding to a greater or smaller bond-breaking contribution.²³ The technique of ^{17}O NMR spectroscopy has been described in detail.²⁴

All medically used Gd^{III} chelates have similar water-exchange rates. However, other Gd^{III} complexes might have considerably slower (e.g., positively charged DOTA–amide derivatives) or faster ($\text{Gd}(\text{H}_2\text{O})_8^{3+}$) water exchange. Overall, water exchange rates on Gd^{III} span 4–5 orders of magnitude. Table 1 shows water-exchange rates and activation volumes for selected Gd^{III} complexes.

In the early days of contrast agent applications, it had been assumed that the water exchange rate in Gd^{III} complexes is at least as fast as in $[\text{Gd}(\text{H}_2\text{O})_8]^{3+}$. However, contrary to transition metal complexes, where chelation of other ligands labilizes the remaining water molecules, in Gd^{III} complexes the water exchange is slower compared to $[\text{Gd}(\text{H}_2\text{O})_8]^{3+}$. In addition to the decrease in water-exchange rate on complexation of other ligands, the mechanism also changes from associative for $[\text{Gd}(\text{H}_2\text{O})_8]^{3+}$ (negative activation volume) to dissociative or dissociative interchange for the nine-coordinate Gd^{III} poly(amino carboxylates) (positive activation volumes) (Table 1). Several factors should be considered to rationalize these differences between the eight-coordinate aqua ion and the nine-coordinate complexes. The rate and the mechanism of water exchange are closely related to the inner-sphere solution structure of the complexes. In $[\text{Gd}(\text{H}_2\text{O})_8]^{3+}$, the rearrangement of the flexible eight-coordinate inner sphere to reach the

Table 1 Water-exchange rates and activation volumes determined on small molecular weight Gd^{III} chelates by ¹⁷O NMR.

Ligand	coordinating unit	q	k_{ex}^{298} (10 ⁶ s ⁻¹)	ΔV^{\ddagger} (cm ³ mol ⁻¹)	Mechanism	References
aqua		8	804	-3.3	A	44
DTPA	DTPA	1	3.30	+12.5	D	32
BOPTA	DTPA	1	3.45			60
EOB-DTPA	DTPA	1	3.60	+12.3	D	31
MP-2269	DTPA	1	4.20		D	39
DTPA-BMA	DTPA-bisamide	1	0.45	+7.3	D	32
DOTA	DOTA	1	4.1	+10.5	D	32
DO3A	DO3A	1.9	11			204
DOTASA	DOTA+COO ⁻	1	6.3		I _d -D	35
DO3A-bz-NO ₂	DOTA-monoamide	1	1.6	+7.7	D	34
DOTAM	DOTA-tetraamide	1	0.053			46,47
EGTA		1	31	+10.5	D	40
PDTA		2	102	-1.5	I _a	44
TTAHA		2	8.6	+2.9	I _d	41
taci		2	11.0	-12.7	A	45

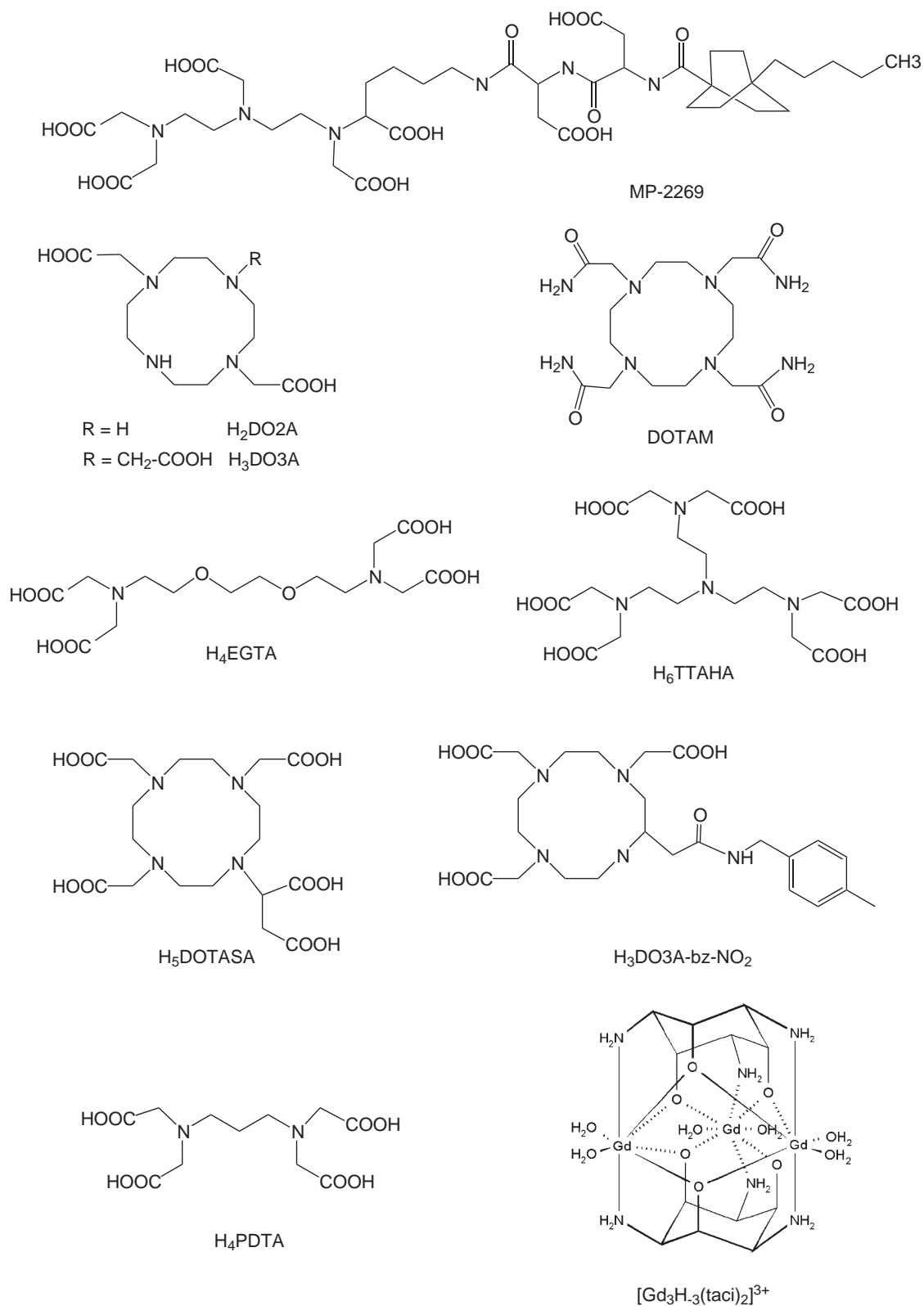
nine-coordinate transition state is easy. The first coordination sphere of the poly(amino carboxylate) complexes is more rigid, which does not favor rearrangement needed to reach the transition state. Moreover, for many of these complexes, only the coordination number of nine exists all through the series.²⁵⁻²⁷ The eight-coordinate transition state is relatively unstable; thus a high activation energy is needed to reach the transition state in a dissociative process. Furthermore, the large charge density of the trivalent ion is a favorable factor in associatively activated water exchange for [Gd(H₂O)₈]³⁺, but it is rather unfavorable in a dissociative process.

Several amide derivatives of [Gd(DTPA)(H₂O)]²⁻ and [Gd(DOTA)(H₂O)]⁻ have been tested as contrast agents, mainly with the aim of decreasing the osmotic load on intravenous injection. All amide derivatives have lower water-exchange rates than the parent carboxylate complexes.²⁸⁻³⁴ This decrease is in part explained by the reduced steric crowding around the metal ion in amide complexes as compared to carboxylates, due to longer metal-coordinated oxygen distances. Steric crowding is important in dissociatively activated exchange: a tightly coordinating ligand pushes harder on the water molecule to leave, thus favoring the dissociative activation step. Charge effects are also significant, since a higher negative charge favors the dissociation of the water molecule and accelerates the exchange. Several examples of comparison between structurally similar, but differently charged, complexes have been reported.^{35,36} Recently, DTPA derivatives with an elongated carbon backbone were synthesized, and the water exchange on their Gd^{III} complexes was found to be much faster than on [Gd(DTPA)(H₂O)]²⁻ itself.³⁷ This result shows again the importance of steric crowding in dissociative water exchange.

The water exchange rate is hardly affected by substituents which do not directly interfere in the inner coordination sphere. Different bisamide DTPA derivatives have similar exchange rates.²⁸⁻³⁰ Substituents on the carbon backbone of DTPA also have little influence on the water-exchange kinetics.^{31,38,39}

Among non-DTPA- or non-DOTA-type complexes, [Gd(EGTA)(H₂O)]⁻,⁴⁰ the tripod [Gd(HTTAHA)(H₂O)₂]²⁻,⁴¹ or some pyridine-based macrocycles^{42,43} have relatively high water-exchange rates (see Scheme 2 for structures). Several eight-coordinate complexes, such as [Gd(PDTA)(H₂O)₂]⁻,⁴⁴ or the trimer [Gd₃(H₃taci)₂(H₂O)₆]³⁺,⁴⁵ also undergo fast water exchange with a strong associative character.

DOTA-type complexes exist in two diastereomeric forms (**m** and **M**; Figure 4) which may have remarkably different water-exchange rates.⁴⁶⁻⁴⁹ In a ¹⁷O and ¹H NMR study performed on the Eu^{III} complexes of DOTA-tetraamides in acetonitrile-water solvent, the NMR signals of the coordinated water molecules could be detected for both isomers, and the water-exchange rates for each isomer were measured individually. (In general, the bound water signal for Ln^{III} poly(amino carboxylates) is not observed, because of the fast exchange, and for Gd^{III} complexes, because of the slow electronic relaxation.) The water-exchange rates for the diastereomeric (**m** and **M**) isomers were found to be independent of the ligand (within the family of the DOTA-like tetraamides studied).⁵⁰ Therefore, the overall water exchange depends only on the **m**/**M** isomeric



Scheme 2

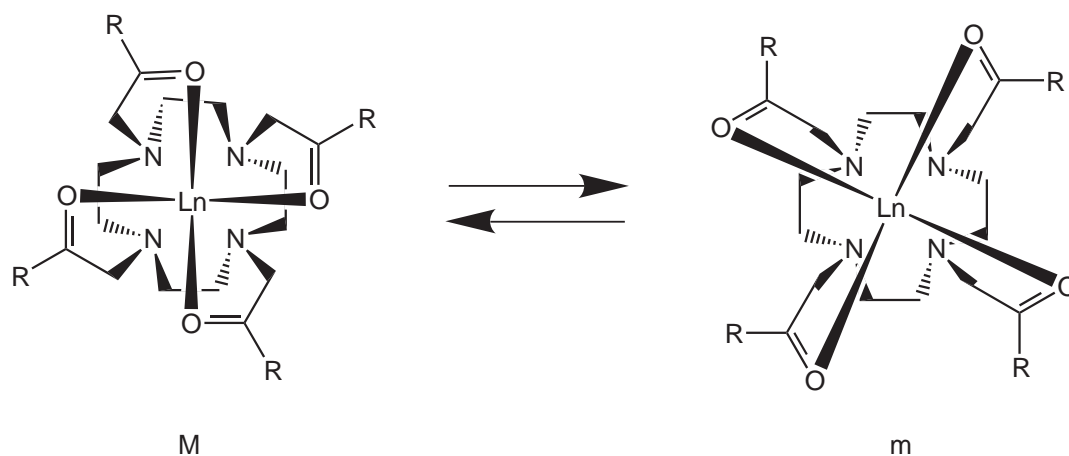


Figure 4 Two diastereoisomeric isomers of DOTA-type Ln^{III} complexes.

ratio. Synthetic modifications of the DOTA-type ligand that favor the fast exchanging **m** isomer could ensure faster overall water exchange on potential Gd^{III} -based MRI contrast agents.

Water exchange was also studied on several macromolecular Gd^{III} chelates (Table 2). The rate and mechanism have been found to be similar for different generations (generations 3–5) of PAMAM dendrimers functionalized with the same Gd^{III} DO3A–monoamide chelate, and for the monomer Gd^{III} DO3A–monoamide complex itself.³⁴ This was the first experimental evidence that the attachment of a Gd^{III} chelate to a dendrimer did not significantly influence the water-exchange kinetics. Similar results have been obtained for “Gadomer 17,” another dendrimeric Gd^{III} chelate.⁵¹ Linear copolymers of $\text{Gd}(\text{DTPA-bisamide})$ or $\text{Gd}(\text{EGTA-bisamide})$ units with poly(ethylene glycol) (PEG) or polyalkyl $(-\text{CH}_2)_n-$; $n = 6, 10,$ and 12) spacers also had water-exchange kinetics similar to that of the corresponding monomer chelate.^{52–54} Similarly, the micellization of amphiphilic Gd –DOTA derivatives in aqueous solutions does not affect the water exchange.^{55,56} Noncovalent binding to a protein, however, can have an influence. Owing to the interaction between the Gd^{III} chelate and the protein, the access to the water binding site can be limited, and consequently, the rate of water exchange significantly reduced.^{42,57,58} On the other hand, if the distance is relatively large between the metal- and the protein-binding site of the ligand, water exchange is not affected by protein binding.³⁹

Although for Gd^{III} complexes currently used as contrast agents at physiological pH, all proton exchange occurs via exchange of the inner-sphere water molecules, H^+ - or OH^- catalyzed prototropic exchange has been observed and found important with respect to the water exchange for several other Gd^{III} chelates.^{21,22,38,59} The overall proton-exchange rate is expressed then as:

$$k = k_{\text{ex}}^{\text{H}_2\text{O}} + k^{\text{H}}[\text{H}^+] + k^{\text{OH}}[\text{OH}^-] \quad (6)$$

Table 2 Water exchange rates and activation volumes measured on macromolecular Gd^{III} chelates and on the corresponding monomer units by ^{17}O NMR.

	Complex	k_{ex}^{298} (10^6 s^{-1})	ΔV^\ddagger ($\text{cm}^3 \text{ mol}^{-1}$)	References
Dendrimers	$[\text{G}_3(\text{N}\{\text{CS}\}\text{N-bz-Gd}\{\text{DO3A}\}\{\text{H}_2\text{O}\})_{23}]$	1.0	+3.1	34
	$[\text{G}_4(\text{N}\{\text{CS}\}\text{N-bz-Gd}\{\text{DO3A}\}\{\text{H}_2\text{O}\})_{30}]$	1.3		34
	$[\text{G}_5(\text{N}\{\text{CS}\}\text{N-bz-Gd}\{\text{DO3A}\}\{\text{H}_2\text{O}\})_{52}]$	1.5		34
	Gadomer 17	1.0		51
Monomer unit	$[\text{Gd}(\text{DO3A-bz-NO}_2)(\text{H}_2\text{O})]$	1.6	+7.7	34
Linear polymers	$[\text{Gd}(\text{DTPA-BA})(\text{H}_2\text{O})(\text{CH}_2)_n]_x$ $n = 6$	0.43	+9.6	53
	$[\text{Gd}(\text{DTPA-BA})(\text{H}_2\text{O})(\text{CH}_2)_n]_x$ $n = 10$	0.66		53
	$[\text{Gd}(\text{DTPA-BA})(\text{H}_2\text{O})(\text{CH}_2)_n]_x$ $n = 12$	0.50		53
	$[\text{Gd}(\text{DTPA-BA})(\text{H}_2\text{O})\text{-PEG}]_x$	0.48	+9.2	52
Monomer unit	$[\text{Gd}(\text{DTPA-BMA})(\text{H}_2\text{O})]$	0.45	+7.3	32

where $k_{\text{ex}}^{\text{H}_2\text{O}}$ is the water-exchange rate, and k^{H} and k^{OH} are the rate constants for the acid- and base-catalyzed prototropic exchange, respectively.⁶⁰ k^{H} and k^{OH} can be obtained from pH-dependent proton relaxivity measurements,²¹ if the water-exchange rate is known from ^{17}O NMR. Since water exchange on Gd-based MRI contrast agents is lower than the optimal value to attain high proton relaxivities, much effort is being made to accelerate proton exchange at physiological pH by displacing the domain of H^+ or OH^- catalysis.

9.19.2.1.3 Rotation

For low molecular weight Gd^{III} chelates, it is mainly fast rotation that limits proton relaxivity (Figure 3). In order to circumvent this problem, Gd^{III} poly(aminocarboxylates) have been linked via either covalent or noncovalent interactions to different macromolecules.

Several experimental methods exist to estimate rotational correlation times, τ_{R} . Most of the values for Gd^{III} complexes have been obtained from proton relaxivity measurements. However, as numerous factors influence relaxivity, this technique gives often ambiguous results; thus independent measurements of τ_{R} are needed. For spherical molecules, the Debye–Stokes equation can give an estimation of τ_{R} . ^{17}O longitudinal relaxation rates measured in solutions of Gd^{III} complexes are dependent on the rotation and have been widely used to assess the rotational correlation time. The impact of the internal motion of the bound water molecule on proton relaxivity has also been investigated.^{61,62} An NMR study on $[\text{Ln}(\text{DOTAM})(\text{H}_2\text{O})]^{3+}$ and $[\text{Ln}(\text{DOTA})(\text{H}_2\text{O})]^-$ ($\text{Ln} = \text{Gd}, \text{Eu}, \text{Tb}$) showed that τ_{R} of the $\text{Ln}-\text{H}_{\text{water}}$ vector is about 65% of the overall correlation time, which itself is close to the τ_{R} of the $\text{Ln}-\text{O}_{\text{water}}$ vector. A molecular dynamics simulation of $[\text{Gd}(\text{EGTA})(\text{H}_2\text{O})]^-$ gave a similar result: τ_{R} of the $\text{Gd}-\text{O}_{\text{water}}$ vector is $\sim 40\%$ longer than that of the $\text{Gd}-\text{H}_{\text{water}}$ vector. Furthermore, it confirmed that the overall rotational correlation time of the complex is close (within 5%) to the reorientational correlation time of the $\text{Gd}-\text{O}_{\text{water}}$ vector. The internal rotation of the coordinated water could have negative consequences on the water proton relaxivity. However, it appears that for the new generation of macromolecular contrast agents, the cutback in relaxivity due to such internal motions of the bound water molecule would not exceed 10%.

Rotational correlation times can be also obtained from ^{13}C or deuterium relaxation measurements on a diamagnetic analogue (Y^{III} , La^{III} , or Lu^{III}).^{29,63–65} The disadvantage of this technique is the low ^{13}C or ^2D sensitivity at natural abundance. Furthermore, these methods do not measure directly the rotation of the metal-coordinated water vector, which is important for relaxivity. EPR spectroscopy has also been used to study rotation on vanadyl (VO^{2+}) analogues of Gd^{III} chelates,^{66–69} making use of the motion-sensitive EPR line shape of the vanadyl unit. Rotational correlation times of selected Gd^{III} chelates are shown in Table 3.

In comparison to low molecular weight complexes, macromolecules have longer rotational correlation times. However, the increase in τ_{R} and thus in relaxivity is often less than expected on the basis of the molecular weight, due to the internal flexibility of the macromolecule. For instance, the rotational correlation time, and correspondingly the proton relaxivity of certain linear polymers, was found to be independent of the molecular weight, which shows that segmental motions dominate their rotational correlation time.^{70,71} In other cases, the flexibility of the linker group between the Gd^{III} chelate and the macromolecule is responsible for the low effective rotational correlation time, and consequently low relaxivity.³⁹

The rotational motion of different types of macromolecular Gd^{III} compounds has been assessed by the model-free Lipari–Szabo approach,^{72,73} using longitudinal ^{17}O relaxation rates.^{51,53,54} This technique allows the separation of a rapid, local motion of the Gd^{III} chelate—which lies in the extreme narrowing limit—from a slower, global motion of the whole macromolecule. A generalized order parameter, S , is also calculated, which characterizes the degree of spatial restriction of the local motion with respect to the global motion.

9.19.2.1.4 Electron spin relaxation

Electronic relaxation is a crucial and difficult issue in the analysis of proton relaxivity data. The difficulty resides, on the one hand, in the lack of a theory valid in all real conditions, and on the other hand in the technical problems of independent and direct determination of electronic relaxation parameters. Proton relaxivity is essentially influenced by the longitudinal electron spin relaxation time, $T_{1\text{e}}$, of Gd^{III} . This decay is too fast to be assessed by commonly available techniques, though very recently $T_{1\text{e}}$ values have been directly measured.⁷⁴ Nevertheless,

Table 3 Comparison of rotational correlation times and proton relaxivities for low molecular weight and macromolecular Gd^{III} complexes.

	Ligand	τ_R^{298} (ps)	M_w	$r_1 / (mM^{-1}s^{-1})$ 20 MHz; 37 °C	References
Monomers	Aqua	41 ^a	301		32
	DTPA	58 ^a	563	4.02	32
		103 ^b			205
	EOB-DTPA	84 ^c	696	5.3	63
		93 ^d			
		178 ^b			
	BOPTA	88 ^c	683	4.39	206
	DTPA-BMA	66 ^a	587	3.96	32
		167 ^b			
	MP-2269	139 ^a	1069	5.64	55
DOTA	77 ^a	575	3.83	32	
	90 ^b				
Linear polymers	[DTPA-BA-PEG] _x	232 ^a	20.2 kDa	6.31	52
	[DTPA-BA(CH ₂) _n] _x <i>n</i> = 6	801 ^b	19.4 kDa	9.8	53
	[DTPA-BA(CH ₂) _n] _x <i>n</i> = 10	$\tau_g = 2900^{b,e}$ $\tau_l = 460^f$	10.3 kDa	15.4	53
	[DTPA-BA(CH ₂) _n] _x <i>n</i> = 12	$\tau_g = 4400^{b,e}$ $\tau_l = 480^f$	15.7 kDa	19.6	53
Dendrimers	[G3(N{CS}N-bz- {DO3A}) ₂₃]	580 ^b	22.1 kDa	14.6	34
	[G4(N{CS}N-bz- {DO3A}) ₃₀]	700 ^b	37.4 kDa	15.9	34
	[G5(N{CS}N-bz- {DO3A}) ₅₂]	870 ^b	61.8 kDa	18.7	34
Protein Bound	MS-325-HSA	3–4000, 10000 ^c	69 kDa	48.9	57,156
		6–7000 ^d			57
	MP-2269-BSA	1000 ^c	66 kDa	24.5	55

^a From simultaneous analysis of NMRD and ¹⁷O T₁ data. ^b From ¹⁷O T₁ data. ^c From NMRD. ^d From ²D NMR. ^e Global rotational correlation time of the whole molecule (Lipari-Szabo treatment). ^f Local rotational correlation time of the Gd-O_{water} vector (Lipari-Szabo treatment).

transverse electronic relaxation times, T_{2e} , measurable by EPR, may allow estimation of T_{1e} within the framework of a given model.

The basic theory of electron spin relaxation of Gd^{III} complexes, proposed by Hudson and Lewis, uses a transient ZFS as the main relaxation mechanism.⁷⁵ The transverse relaxation is described by four relaxation times, due to the superposition of four transitions with different intensities. For complexes of cubic symmetry, Bloembergen and Morgan developed an approximate theory which led to the equations generally used in the context of electronic relaxation of Gd^{III} complexes.¹¹ A similar approximate treatment was used by Powell *et al.* to describe temperature and magnetic field dependence of T_{2e} .⁷⁶ In order to explain ¹⁷O transverse relaxation rates, dependent on electronic relaxation, it was necessary to include an additional relaxation mechanism due to spin rotation. Novel approaches also account for the dynamic frequency shift, which is a small displacement in the transition frequencies, often neglected.^{77–79} In the early 2000s, Rast *et al.* developed a refined model of electronic relaxation of the *S* states of metal complexes in solution.^{80–81} Besides the usual transient crystal ZFS caused by vibration, intramolecular rearrangement, and collision, this model includes a contribution of the static crystal field surrounding the Gd^{III} which is modulated by random rotation of the complex. The approach is able to provide a complete and satisfactory description of the full EPR line shapes over a wide range of magnetic fields and temperatures, without supposing any spin rotation contribution. It also allows a calculation of longitudinal electronic relaxation rates relevant to nuclear magnetic relaxation. A limitation of the model is the Redfield's approximation used in the line shape calculation, which may be inadequate for slowly rotating complexes and at very low magnetic fields. Therefore, it has been extended beyond the electronic Redfield limit using Monte

Carlo simulations.⁸² The application of this theory in a combined analysis of ¹⁷O NMR, ¹H NMRD, and EPR data is not straightforward and needs EPR spectra over a wide frequency and temperature range.⁸³ Therefore, the common Bloembergen–Morgan theory will probably be applied in the future to generate electron spin relaxation rates, though one should be aware of its limitations and refrain from discussing the resulting electronic parameters τ_v and Δ^2 .

9.19.2.2 Outer and Second-sphere Relaxation

Outer-sphere relaxation arises from the dipolar intermolecular interaction between the water proton nuclear spins and the gadolinium electron spin whose fluctuations are governed by random translational motion of the molecules.⁸⁴ The outer-sphere relaxation rate depends on several parameters, such as the closest approach of the solvent water protons and the Gd^{III} complex, their relative diffusion coefficient, and the electron spin relaxation rate.^{85–87} Freed and others^{88–90} developed an analytical expression for the outer-sphere longitudinal relaxation rate, $(1/T_1)^{OS}$, for the simplest case of a force-free model. The force-free model is only a rough approximation for the interaction of outer-sphere water molecules with Gd^{III} complexes. Phosphonate or carboxylate groups of the ligand are capable of tightly binding water molecules which cannot be treated any more using only translational diffusion. Aime⁹¹ and Botta⁹² proposed adding a second-sphere contribution (r_1^{2nd}) to the overall proton relaxivity in such cases:

$$r_1 = r_1^{IS} + r_1^{2nd} + r_1^{OS} \quad (7)$$

where r_1^{IS} is the inner sphere relaxivity and r_1^{OS} represents the contribution from water molecules diffusing in the proximity of the paramagnetic complex. r_1^{2nd} can be calculated with equations similar to those applied for first-sphere relaxation. A more realistic model should consider that several distinct binding sites, characterized with different binding modes, exchange rates, and Gd–H distances, can be present on the chelating ligand. Clearly, this approach is not easily realizable, thus the second-sphere contribution is usually included in the outer-sphere term.

9.19.2.3 NMRD Profiles

MRI contrast agents are often characterized by water proton relaxivities, r_1 , measured as a function of the Larmor frequency or magnetic field on a logarithmic scale (nuclear magnetic relaxation dispersion or NMRD profiles, Figure 5). Proton relaxivities at low field (below 1 MHz) can provide very useful information; however, they are difficult to measure owing to low sensitivity. This prompted the development of a special experimental technique using fast cycling of the magnetic field.^{93–95}

Figure 5 shows typical NMRD profiles of low molecular weight Gd^{III} complexes such as the commercialized [Gd(DTPA)(H₂O)]²⁻ or [Gd(DOTA)(H₂O)]⁻. For these small complexes, relaxivity is limited by fast rotation, especially at imaging fields (>10 MHz). The difference in low-field relaxivities reflects the slower electronic relaxation of the symmetric [Gd(DOTA)(H₂O)]⁻, which has no further influence at higher fields. The inner- and outer-sphere relaxivity terms contribute more or less to the same extent to the overall effect. Consequently, by doubling the inner-sphere contribution by using a bishydrated chelate such as [Gd(HTTAHA)(H₂O)₂]²⁻, the overall relaxivity is increased by 50% (Figure 5).

Macromolecular Gd^{III} chelates are widely investigated as potential MRI contrast agents. In addition to the potential increase in relaxivity because of their slower rotation, they have an extended lifetime in the blood pool, allowing for magnetic resonance angiography (MRA) applications. When the rotation of the Gd^{III} chelate is substantially slowed down, the typical “high-field” peak around 20–60 MHz is observed in the NMRD profile (Figure 6).

9.19.3 TOXICITY OF Gd^{III} COMPLEXES: THERMODYNAMIC STABILITY AND KINETIC INERTNESS

The Gd^{III} chelates, when used as contrast agents, are administered intravenously and distribute through the extracellular and intravascular spaces. Typical doses of the currently used, low molecular

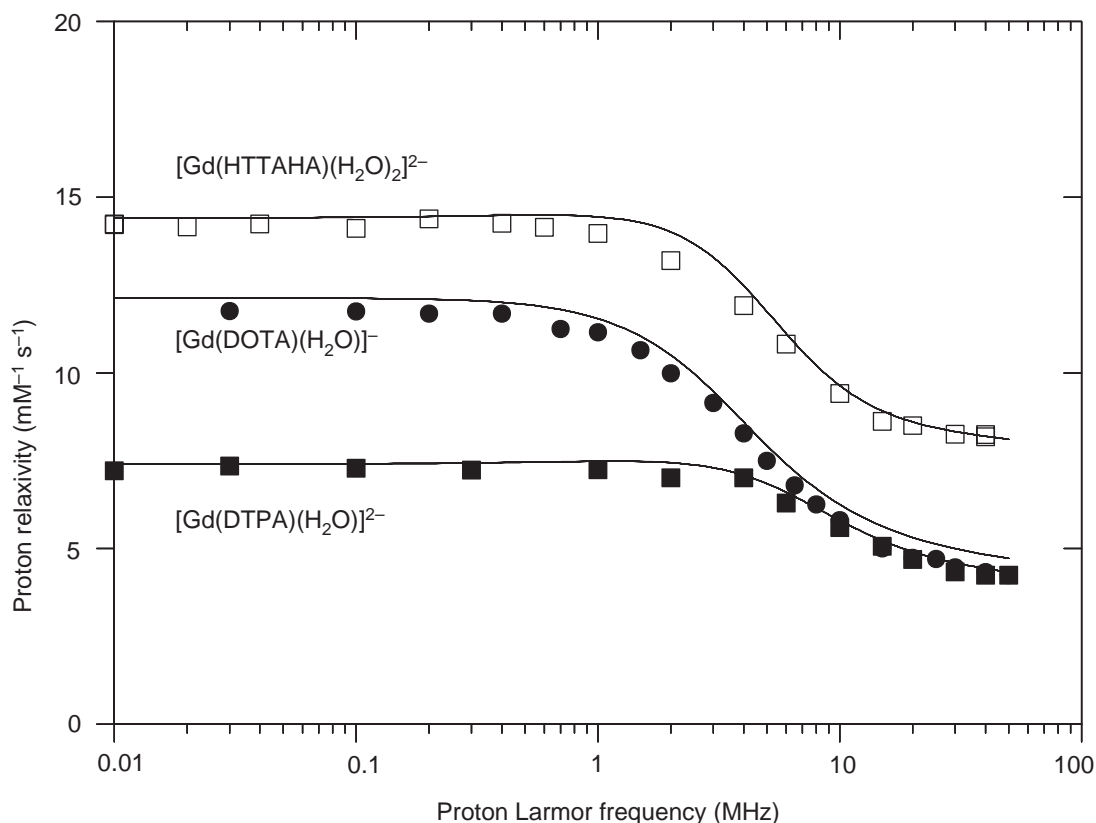


Figure 5 Typical NMRD curves of monomer Gd^{III} complexes with one ($[\text{Gd}(\text{DOTA})(\text{H}_2\text{O})]^-$ and $[\text{Gd}(\text{DTPA})(\text{H}_2\text{O})]^{2-}$) and with two inner-sphere water molecules ($[\text{Gd}(\text{HTTAHA})(\text{H}_2\text{O})_2]^{2-}$).

weight complexes are $0.1\text{--}0.3 \text{ mmol kg}^{-1}$ of body weight, with a Gd^{III} concentration of the injected solution of about 0.5 M . This high concentration requires high water solubility of the agent, and may represent a high osmolality as compared with blood. The osmolality is more important for the negatively charged complexes such as $[\text{Gd}(\text{DTPA})(\text{H}_2\text{O})]^{2-}$ or $[\text{Gd}(\text{DOTA})(\text{H}_2\text{O})]^-$ ($1.96 \text{ osmol kg}^{-1}$ and $1.35 \text{ osmol kg}^{-1}$, respectively, compared with $0.3 \text{ osmol kg}^{-1}$ for blood plasma). The medical formulations of $[\text{Gd}(\text{DTPA})(\text{H}_2\text{O})]^{2-}$ and $[\text{Gd}(\text{DOTA})(\text{H}_2\text{O})]^-$ are *N*-methylglucamine (NMG, also called meglumine, MEG) salts. However, even this relatively high osmotic load is much lower than that associated with ionic X-ray contrast agents, therefore the argument for low osmolality represents only a general principle that agents should be as close to the physiological as possible.⁹⁶ Nevertheless, the majority of new-generation contrast agents are neutral.

In addition to high water solubility and low osmolality, the Gd^{III} complex must stay intact in the body and not dissociate to free metal ion and ligand, both toxic alone (LD_{50} values for free Gd^{3+} and for uncomplexed ligands are in the range $0.1\text{--}0.2 \text{ mmol kg}^{-1}$).^{97–99} Upon complexation, the LD_{50} increases dramatically (e.g., 6 mmol kg^{-1} for $\text{NMG}_2[\text{Gd}(\text{DTPA})]$; 12 mmol kg^{-1} for the neutral complex, $\text{Gd}(\text{HP-DO3A})$). The most important criteria for safe *in vivo* application thus include high thermodynamic stability and kinetic inertness. Since the chemical bonds in lanthanide complexes are predominantly of an ionic nature, stable chelates form only with multidentate ligands. The ligands used in practice are octadentate, and all eight donor atoms are coordinated to the metal ion (Scheme 1).

9.19.3.1 Complex Stability Constants

The thermodynamic stability of an ML complex is expressed by the equilibrium constant of the formation reaction, K_{ML} , called the stability constant:

$$K_{\text{ML}} = \frac{[\text{ML}]}{[\text{M}][\text{L}]} \quad (8)$$

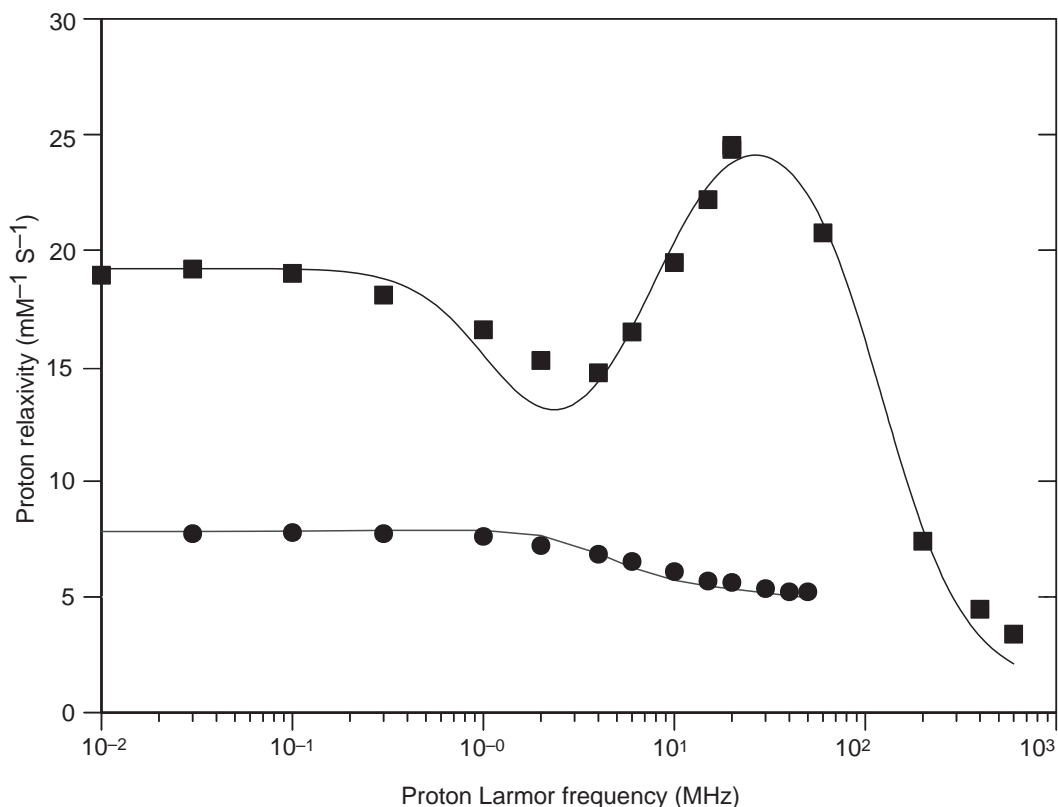
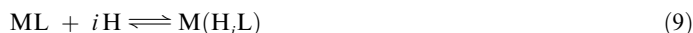


Figure 6 Effect of the increased rotational correlation time on the proton relaxivity of MP2269, a Gd^{III} chelate capable of noncovalent protein binding (Scheme 2). The lower NMRD curve was measured in water, whereas the upper curve was obtained in a 10% w/v bovine serum albumin solution in which the chelate is completely bound to the protein. The rotational correlation times calculated are $\tau_R = 105$ ps in the non-bound state, and $\tau_R = 1,000$ ps in the protein-bound state ($t = 35^\circ\text{C}$). For this chelate, the water exchange rate remains unchanged on protein binding.³⁹

where $[\text{M}]$, $[\text{L}]$, and $[\text{ML}]$ are the equilibrium concentrations of metal ion, deprotonated ligand, and complex, respectively (charges are omitted for simplicity). Complexes formed with multi-dentate ligands can be protonated at low pH, which has also to be taken into account:



This protonation equilibrium is characterized by the protonation constant of the complex:

$$K_{\text{MH}_i\text{L}} = \frac{[\text{M}(\text{H}_i\text{L})]}{[\text{M}(\text{H}_{i-1}\text{L})][\text{H}^+]} \quad (10)$$

The protonation constants of the ligand, K_i , are also necessary for the calculation of the complex stability constant, K_{ML} :

$$K_i = \frac{[\text{H}_i\text{L}]}{[\text{H}_{i-1}\text{L}][\text{H}^+]} \quad (11)$$

Complex stability constants are most often determined by pH-potentiometric titration of the ligand in the presence and absence of the metal ion.¹⁰⁰ This method works well when equilibrium is reached rapidly (within a few minutes), which is usually the case for linear ligands. For macrocyclic compounds, such as DOTA and its derivatives, complex formation is very slow, especially for low pH values where the formation is not complete, therefore a batch method is

Table 4 Stability constants, $\log K_{ML}$, for selected complexes.

	Gd^{3+}	Ca^{2+}	Zn^{2+}	Cu^{2+}	$\log (K_{GdL}/K_{ZnL})$	References
DTPA	22.46	10.75	18.29	21.38	4.17	207
EOB-DTPA	23.46	11.74				208
BOPTA	22.59					206
DTPA-BMA	16.85	7.17	12.04	13.03	4.81	101
DOTA	24.6	16.70	21.05	22.72	3.55	209,210
DO3A	21.0	11.35	19.26	22.87	1.74	210
HP-DO3A	23.8	14.83	19.37	22.84	4.43	210

used instead of direct titration.^{101,102} A large body of stability constant data on MRI relevant Gd^{III} complexes has been gathered in the early 2000s,¹⁰³ of which only a few representative examples are presented in Table 4.

9.19.3.2 Blood Plasma Models

The correlation between complex stability and *in vivo* toxicity has always been an important question in contrast agent development. Conditional stability constants were often correlated to the selectivity of a given ligand for Gd^{III} over endogenous metals, such as Zn^{2+} or Cu^{2+} ,¹⁰⁴ and therefore they are widely used to compare the behavior of different complexes at physiological pH. Body fluids are very complex systems from the coordination chemistry point of view. The free metal ion, the free ligand, or the complex itself can participate in many side reactions. Among these, the most important are the protonation of the free ligand, its interaction with endogenous metal ions (Mg^{2+} , Ca^{2+} , Zn^{2+} , Cu^{2+} , etc.), the complexation of free Gd^{3+} by many different biological ligands (citrate, phosphate, bicarbonate, transferrin, oxalic acid, etc.), and the interaction of the Gd^{III} complex with protons or with small ligands like carbonate, phosphate, or dicarboxylic acids to form ternary complexes. All of these significant side reactions can be incorporated into a conditional stability constant, K^* , which is related to the thermodynamic stability constant, K_{ML} .¹⁰⁵ If the protonation and stability constants of all the complexes involved are known, K^* can be calculated and the concentration of the “free” paramagnetic metal ion evaluated. This “free” metal concentration is considered important and is generally assumed to be related to toxicity. Sometimes only ligand protonation and competition between Gd^{3+} and endogenous metal ions are taken into account, and the conditional stability constant defined in this way is called the selectivity constant.¹⁰⁴ The order of the selectivity constants determined for different complexes was found to follow the order of experimental LD_{50} values. This illustrates the importance of selectivity of the ligand for Gd^{3+} over endogenous metals, particularly free Zn^{2+} , since its concentration is the largest.

For the simulation of coordination equilibria in the blood plasma, several models have been proposed in the literature. May *et al.*¹⁰⁶ included seven metal ions (Mg^{2+} , Ca^{2+} , Mn^{2+} , Fe^{3+} , Cu^{2+} , Zn^{2+} , and Pb^{2+}) and forty low molecular weight ligands (amino acids, dicarboxylic acids, carbonate, phosphate, citrate, lactate, salicylate, etc.) in a complex equilibrium involving about 5,000 binary and ternary complexes. Starting from this model, Jackson *et al.* estimated species distribution in the presence of $[Gd(DTPA)]^{2-}$. Cacheris *et al.*¹⁰⁴ used a simplified plasma model to calculate the amount of Gd^{3+} released from $[Gd(DTPA)]^{2-}$, $Gd(DTPA-BMA)$, and $[Gd(EDTA)]^-$. Their model included competition amongst Gd^{3+} , H^+ , Ca^{2+} , Cu^{2+} , and Zn^{2+} for the ligand, as well as competitive binding of citrate, amino acids, and albumin for all ions. At a typical dose of 0.1 mmol kg^{-1} , the Gd^{3+} released was estimated in the range of $1-10 \times 10^{-6} \text{ M}$, depending on the ligand. The released Gd^{3+} was predicted to be largely coordinated by citrate and only negligibly by amino acids or albumin. Based on a very simple model, Brücher *et al.* also concluded that citrate coordination of the free Gd^{3+} , liberated from $[Gd(DTPA)]^{2-}$ by Zn^{2+} transmetalation occurred.¹⁰⁷ Experimental biodistribution studies in humans or animals generally indicate little Gd^{3+} displacement from the contrast agent. For instance, animal experiments using radioactively labeled Gd complexes showed around only 1% Gd retention after 7–14 days; the retention was somewhat higher for $Gd(DTPA-BMA)$ than for other linear compounds, and it was very low for all macrocyclic chelates.^{108,109}

In practice, some contrast agent formulations also include a small amount of the corresponding Ca^{II} chelate ($\sim 5\%$) which acts as a sacrificial complex to pre-empt displacement of Gd^{III} from GdL by adventitious Zn^{2+} . As a result, the LD_{50} value for $\text{Gd}(\text{DTPA}-\text{BMA})$ increased from $14.8 \text{ mmol kg}^{-1}$ to $38.2 \text{ mmol kg}^{-1}$ upon addition of the adjuvant Ca^{II} complex.¹⁰³

9.19.3.3 Kinetic Inertness of Gd^{III} Complexes

The competitive equilibria based on the different plasma models cannot solely explain the *in vivo* behaviour of Gd^{III} complexes. The excretion of low molecular weight Gd^{III} chelates from the body is very rapid (e.g., $t_{1/2} = 1.6 \text{ h}$ for $[\text{Gd}(\text{DTPA})]^{2-}$),¹¹⁰ whereas the dissociation and transmetallation of the Gd^{III} complexes is relatively slow. Therefore, the system is far from equilibrium and kinetic factors could substantially change the predicted amount of free Gd^{3+} .

The kinetic stability of the Gd^{III} complex depends on exchange reactions that take place in plasma. The most important one is probably the displacement of Gd^{3+} by the endogenous metals Cu^{2+} and Zn^{2+} . This can occur via the direct attack of the endogenous metal on GdL, or via the proton-assisted dissociation of the complex, followed by the fast recombination of the ligand with the endogenous metal ion. Ligand-exchange reactions between GdL and ligands present in the blood plasma are usually considered to be of low probability.

In a qualitative approach to assess the kinetic stability of GdL complexes, the extent of complex dissociation was measured in the presence of excess phosphate and carbonate.¹¹¹ Macrocyclic complexes, like $[\text{Gd}(\text{DOTA})]^{-}$, were found to be kinetically inert, whereas $[\text{Gd}(\text{DTPA})]^{2-}$ dissociated by 20–25% in the presence of Zn^{2+} or Cu^{2+} (formation of GdPO_4). The dissociation of several Gd^{III} complexes has been studied in highly acidic solutions.^{112–117} Complexes with macrocyclic ligands dissociate much more slowly than those formed with linear chelators. The rate constants which characterize the dissociation of the Gd^{III} chelates and which are used to compare the kinetic stabilities are about 10^3 times lower for macrocyclic DOTA derivative complexes than for the linear DTPA family. In addition to the rate, the mechanism of dissociation is also considerably different for macrocyclic and linear complexes. The high inertness of DOTA-type chelates is usually interpreted in terms of the rigidity of the 12-membered macrocyclic ring. As a consequence, $[\text{Gd}(\text{DOTA})]^{-}$ is stable even at as low a pH as that in the stomach, and therefore it is suitable for oral use as a gastrointestinal contrast agent.¹¹⁸ Functional groups with donor atoms of lower basicity (e.g., amide, phosphinate, or phosphonate ester) result in significantly lower thermodynamic stability constants, whereas the kinetic inertness of the complexes is practically undiminished. For DTPA-type chelates, substituents attached to the diethylenetriamine backbone increase the kinetic stability of the Gd^{III} complex.¹¹⁹ The dissociation kinetics of linear and macrocyclic Gd^{III} complexes was reviewed in the early 2000s.^{103,120}

In conclusion, Gd^{III} complexes currently used as MRI contrast agents can be considered as safe drugs, due to their high thermodynamic stability and kinetic inertness, as well as to efficient excretion from the body. For the new-generation macromolecular contrast agents, kinetic inertness will become a more significant issue, since they have prolonged clearance time, increasing the possibility of *in vivo* dissociation. The results of kinetic studies indicate that kinetic stabilities can be increased through the use of more rigid ligands. Therefore it is probable that macrocyclic or rigidified linear ligands will have to be used when macromolecular agents are synthesized.

9.19.4 BLOOD POOL AGENTS

Typical low molecular weight agents, such as $[\text{Gd}(\text{DTPA})]^{2-}$ or $[\text{Gd}(\text{DOTA})]^{-}$, rapidly equilibrate after injection between the intravascular and interstitial spaces in the body. Macromolecular agents of a substantially higher molecular weight ($>20 \text{ kDa}$) remain largely intravascular for an extended period of time; thus they can act as specific markers of the blood pool, without increasing the signal from the interstitial or intracellular compartments. The plasma concentration remains relatively stable for the time of the examination, as the elimination, primarily renal, first requires the degradation of the macromolecule. Under these conditions, the enhancement of the images of the various tissues will mainly depend on the blood volume. Thus highly vascular tissues such as kidneys, liver, lung, and myocardium show the greatest enhancement, whereas brain and skeletal muscle, having lower blood volumes, display a lower enhancement. In clinical practice, there is a strong need for noninvasive detection of vascular abnormalities by MRA, as a

large number of diseases result in modification of the vasculature. One example is abnormal angiogenesis (blood vessel growth) associated with tumor development. The detection of haemorrhage, embolism, or arteriosclerosis would also be desirable. MRA could represent a low-cost, attractive alternative to standard X-ray angiography, which is potentially dangerous as it requires the rapid injection of large amounts of iodinated X-ray contrast agents through long catheters introduced to the site of interest.²

In addition to angiographic applications, the synthesis of macromolecular contrast agents for MRI is also prompted by efforts to increase proton relaxivity. In contrast to small chelates, rotation is largely slowed down for these high molecular weight compounds, resulting in increased relaxivity. Thus, macromolecular Gd^{III} chelates, endowed with enhanced relaxivity, are expected to be exceptionally dose-effective agents. The attainment of such high efficiency per Gd can allow specific applications such as targeting. The number of paramagnetic centers needed for the visualization of receptors on the surface of cells could be substantially reduced by using high relaxivity agents.

Several approaches have been tested to increase the molecular weight of contrast agents. Generally, two main groups of macromolecular agents are distinguished, based on the covalent or noncovalent nature of the binding between the monomeric agent and the macromolecule. Covalent binding may involve the conjugation of functionalized Gd^{III} chelates to polymers, dendrimers, or biological molecules. One major drawback of covalently bound conjugates is their metabolic fate. On the other hand, these multimeric derivatives appear to be a possible way to deliver a high number of paramagnetic complexes at a given site of interest.

The noncovalent approach is based on the use of complexes containing suitable moieties which are able to recognize specific proteins, primarily human serum albumin (HSA). When the targeting protein is confined in the blood, the adduct between the serum albumin and the functionalized complex may function as a blood pool agent. Due to the reversible nature of binding between the protein and the paramagnetic chelate, these adducts maintain excretory pathways typical of small complexes which, from the pharmacological point of view, favors them over covalently bound macromolecules.

9.19.4.1 Covalently Bound Macromolecular Agents

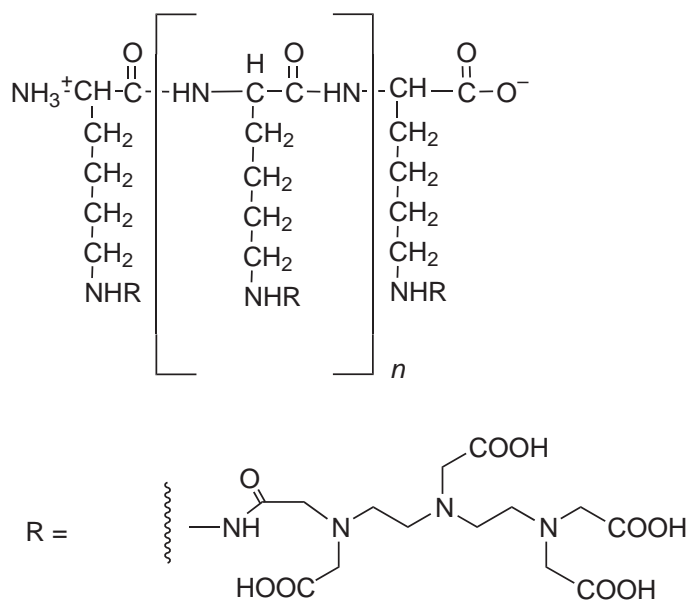
9.19.4.1.1 Gd^{III} chelates covalently bound to proteins

This method represents one of the first attempts towards macromolecular agents.^{121–123} As many as 60–90 [Gd(DTPA)]²⁻ or [Gd(DOTA)]⁻ chelates were first linked to a polylysine chain, then covalently conjugated to a HSA molecule.¹²⁴ The increase in relaxivity per Gd, as compared with the monomeric chelate, was remarkable (two- to threefold), though far from optimal. However, the development of these albumin conjugates was abandoned at an early stage, since their synthesis is not easily controlled, and there are also toxicity concerns due to the retention of gadolinium observed in the bones and liver.¹²⁵

9.19.4.1.2 Linear polymers

Gd^{III} chelates have been attached to linear polymers as side groups or incorporated into the polymer chain itself to form copolymers. The first group is typically represented by polylysine derivatives, where the Gd^{III} poly(aminocarboxylate) can be easily conjugated to the ϵ -amino group of the lysine backbone^{70,71,124–127} (Scheme 3). The relaxivities of these agents are much lower than expected on the basis of their increased molecular weight, and more particularly, they often do not change with the molecular weight of the polymer. As an example, Gd(DTPA)-loaded polylysine chains of molecular weight between 36 kDa and 480 kDa all had relaxivities of 10.4–11.9 mM⁻¹ s⁻¹.⁷⁰ Similarly, the relaxivities of PEG-modified polylysine chains with [Gd(DTPA-monoamide)]⁻ chelates were constant (6.0 mM⁻¹ s⁻¹ at 20 MHz, 37 °C) for molecular weights of 10.8–83.4 kDa.⁷¹ This was explained by the highly flexible nature of the polylysine backbone and of the Gd^{III}-containing sidechain.

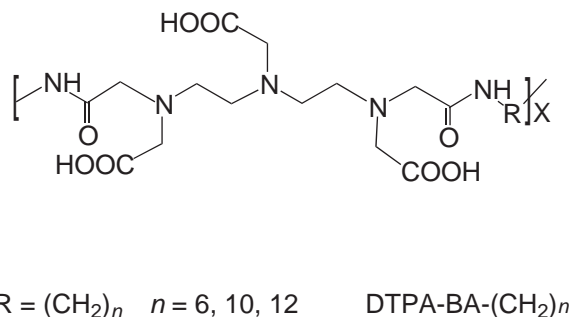
Gd(DTPA-bisamide)-PEG copolymers⁵² are also flexible, which explains their low relaxivity. A combined ¹⁷O NMR, EPR, and NMRD study performed on [Gd(DTPA-BA)-PEG]_x concluded that the effective rotational correlation time in the long polymer chain is not higher than that of the same Gd^{III} monomer unit, Gd(DTPA-BMA) restricted to rotate around a single axis (τ_R for the polymer equals three times the τ_R for the monomer).⁵² An interesting feature of this



compound is that its relaxivity is practically independent of temperature, which makes it a good standard to calibrate MRI signal intensities and T_1 values. Provided that the T_1 of the standard is not so long that the temperature dependence of the solvent makes a significant contribution, the T_1 of the standard will not change with positioning from the patient, when large ranges in temperature (body temperature to room temperature) are possible. This temperature independence is the consequence of the interplay between the different temperature behavior of rotation and water exchange.⁵² Considerably higher proton relaxivities have been found for DTPA–bisamide copolymers, $[\text{Gd}(\text{DTPA-BA})-(\text{CH}_2)_n]_x$ ($n = 6, 10, \text{ and } 12$), containing hydrophobic sections in the polymer (Scheme 4; Table 3).⁵³ The intramolecular micellar aggregates that form in solution are the origin of the high relaxivities.

9.19.4.1.3 Dendrimers

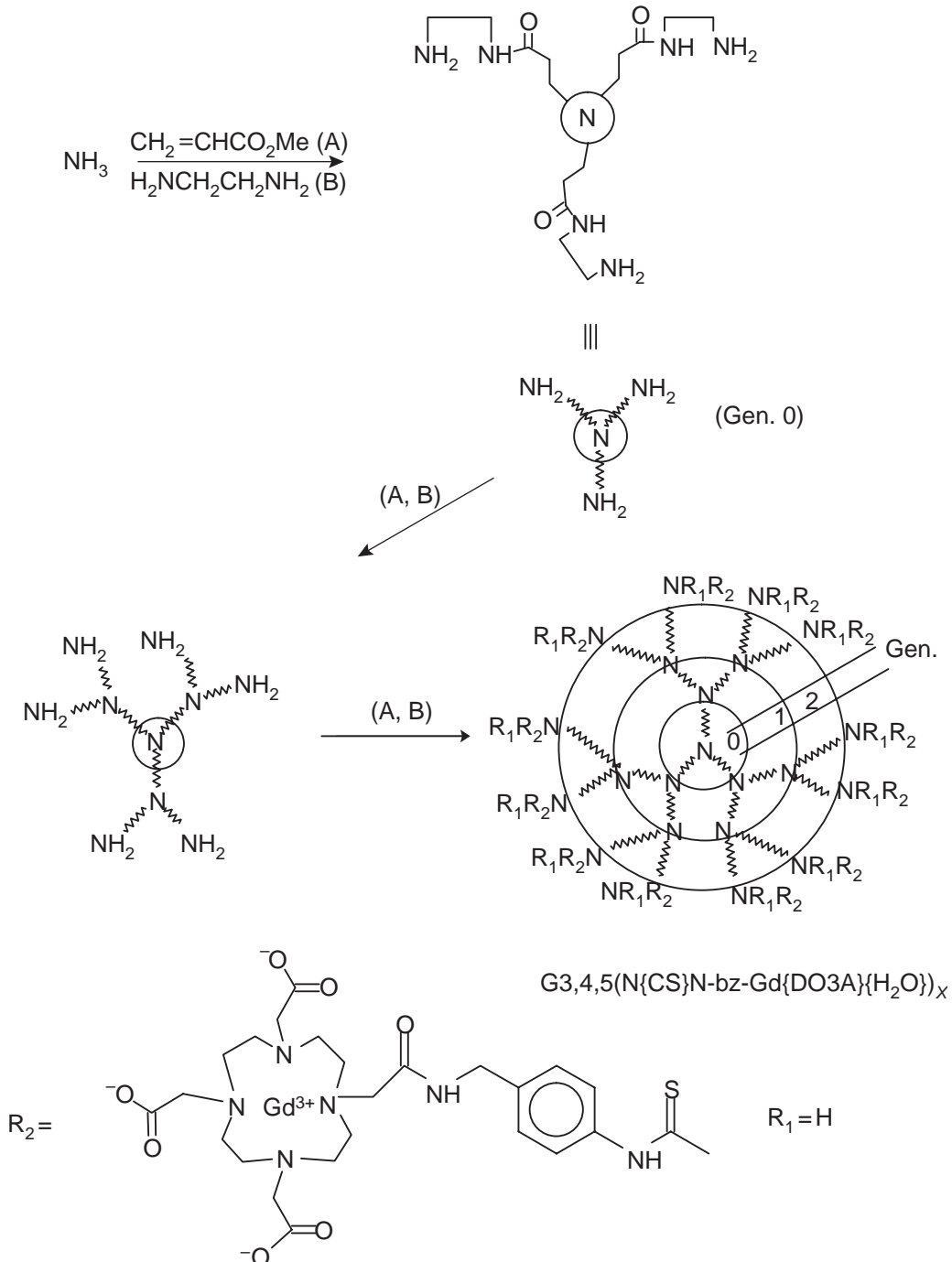
In contrast to linear polymers, dendrimers in general are more rigid, monodisperse, and often have a quasi-spherical or spherical three-dimensional structure.¹²⁸ They are synthesized in repetitive reaction steps starting from a small core molecule, leading to consecutive generations. The surface groups, whose number increases substantially with increasing generation, can be used for the conjugation of Gd^{III} chelates (Schemes 5 and 6). This method has made possible the



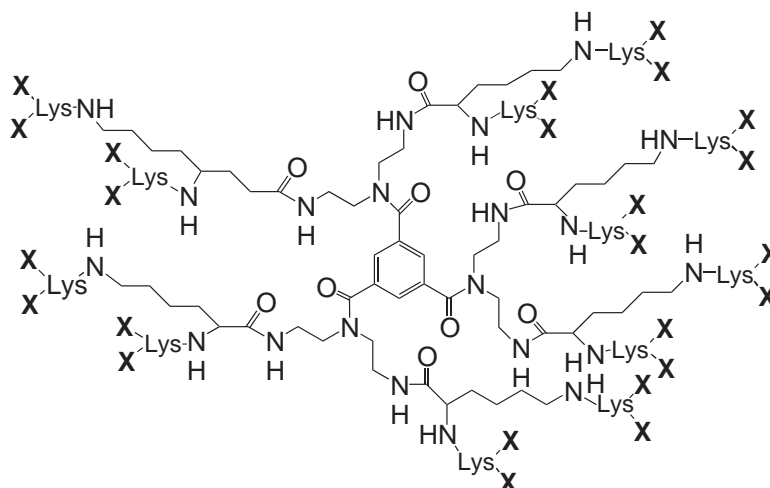
Scheme 4

accumulation of as many as 1,860 gadolinium chelates within one molecule, as reported for a generation-10 PAMAM (polyamidoamine) dendrimer.¹²⁹ As for their proton relaxivity, an important issue is the correct choice of the linking group between the macromolecule and the Gd^{III} complex. This has to be rigid enough for the slow rotation of the rigid dendrimer molecule to be transmitted to the surface chelate itself. Relaxivities of up to $36 \text{ mM}^{-1} \text{ s}^{-1}$ (20 MHz; 23 °C) have been reported for dendrimeric Gd^{III} complexes.¹²⁹

PAMAM dendrimers of different generations have been loaded with DOTA-type^{129,130} or DTPA-type^{131–133} chelates, most often using the p-NCS–benzyl linker. For these types of



Scheme 5



Scheme 6

dendrimer-based Gd^{III} complexes, the relaxivity was increasing with each generation before reaching a plateau for the high-generation compounds (above generation 7, e.g., for $[\text{Gd}(\text{p-NCS-bz-DOTA})]^-$ -loaded dendrimers). The NMRD profiles show typical high field peaks around 20 MHz, characteristic of slow rotation. The relaxivities for the high-generation dendrimers ($G = 5\text{--}10$) decrease as the temperature decreases, indicating that slow water exchange limits relaxivity. Slow water exchange and fast internal motions were found to be responsible for the limited relaxivities for $\text{Gd}(\text{DOTA-monoamide})$ functionalized PAMAM dendrimers,³⁴ as well as for Gadomer 17, a lysine-based dendrimer with a 1,3,5-tricarboxylic acid core and 24 Gd^{III} chelates on the surface (Scheme 6).^{51,134,135} These results indicate that high molecular weight complexes like these dendrimers have rotational correlation times that are long enough for the water exchange to influence the overall relaxivity. Therefore, apart from slowing down rotation, a further improvement in the efficiency of the contrast agents can be achieved only with higher water-exchange rates.

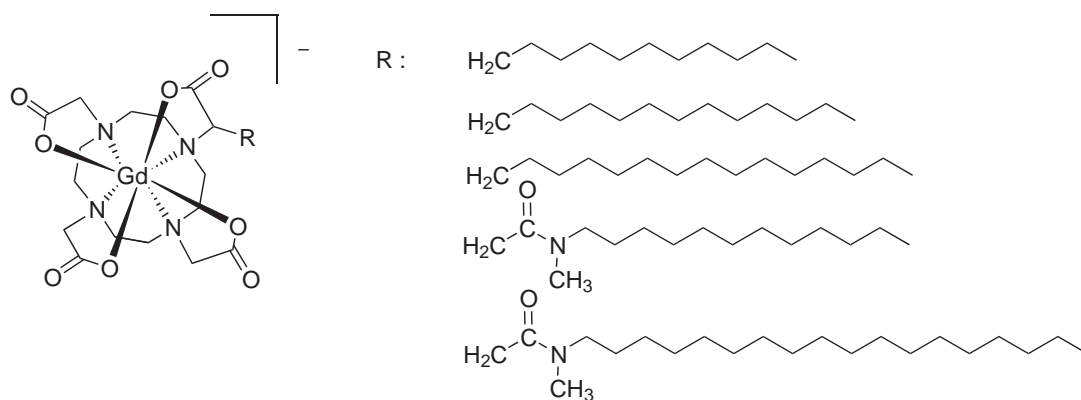
9.19.4.1.4 Dextran derivatives

Dextrans are also attractive as macromolecular carriers of paramagnetic chelates because of their hydrophilicity, the different available molecular weights with narrow polydispersity, and the versatility of activation methods applicable. Several DTPA- or DOTA-loaded carboxymethyl dextran (CMD) derivatives have been prepared and tested in blood pool MRI.^{136–139} The relaxivities reported for these compounds are, however, relatively moderate.

9.19.4.1.5 Micelles and liposomes

Amphiphilic Gd^{III} chelates, capable of micellar self-organization, were also investigated as potential blood pool agents. The micelle size and rigidity, both important in attaining high relaxivities for such compounds, can be regulated by the structure of the monomers. Gd^{III} complexes of DOTA derivatives having an alkyl side chain with different length and different linkage to the macrocycle had relaxivities around $r_1 = 18\text{--}20 \text{ mM}^{-1} \text{ s}^{-1}$ (25°C , 20 MHz) which are comparable to those attained with macromolecular systems (Scheme 7).^{55,56,140} Furthermore, with the micellar approach one could avoid the problems of slow elimination from the body that are often encountered with polymeric systems. Micelles are also known to mimic the phospholipid structure of the membranes, and hence could be candidates as hepatocyte-specific agents.

Liposomal contrast agents have also been proposed in recent years. Liposomes are vesicles built from a double layer of lipids encapsulating an aqueous cavity. Their ability to transport substances, either in the lipid bilayer or in the internal aqueous phase, makes them a versatile delivery



Scheme 7

system for different drugs. Liposomes can be made large enough to be retained in the circulation after injection and thus can function as blood pool agents. Different approaches exist to prepare paramagnetic liposomes: the metal chelate can be encapsulated within the aqueous phase of the liposome, covalently attached to the liposome surface, or incorporated into the membrane. Iron, manganese, or gadolinium chelates have been entrapped in liposomes.^{141,142} The size and membrane-water permeability of the liposome were found to be the most important factors influencing relaxivity, as both affect the rate of water exchange between the interior and exterior of the liposome.¹⁴³ The direct incorporation of the paramagnetic chelate into the lipid bilayer via a long hydrophobic side chain would allow for better immobilization of the chelate. This, in addition to the more open access from the bulk to the water-binding site to maintain fast water exchange, could lead to higher proton relaxivity. Recently, amphiphilic polychelating polymers have been used for loading liposomes with $[\text{Gd}(\text{DTPA})]^{2-}$.¹⁴⁴ The advantage here is that one phospholipid anchor can carry a polymer molecule with multiple chelating side groups on the liposome surface, i.e., it can carry an increased number of metals. One major problem associated with liposomes is that they can easily disrupt, though surface modification can improve their stability.¹⁴⁵ Despite the intensive research, no liposomal contrast agent has so far found an application.

9.19.4.2 Noncovalently Bound Macromolecular Agents

The toxicological problems often associated with the covalently bound conjugates (slow elimination and immune response) can be overcome by the use of noncovalently bound adducts formed between the paramagnetic chelate and a protein. Noncovalent binding is the basis of the “receptor-induced magnetization enhancement” (RIME) concept as defined by Lauffer.^{2,146} In this approach, a contrast agent is targeted to a particular protein or receptor molecule. The binding causes an increased concentration and retention of the Gd^{III} complex in the area of the receptor molecule (Figure 7). Owing to an equilibrium between the protein-bound and the free state of the chelate, these agents will be excreted via the usual pathway of low molecular weight compounds, though during a longer period of time. Given the highest abundance of serum albumin in the blood ($\sim 0.67 \text{ mM}$; 4.5% of the plasma),¹⁴⁷ most of the work has been directed towards noncovalent binding of Gd, or other metallic complexes, to HSA.¹⁴⁸ HSA is a large, globular protein of $M_w = 67 \text{ kDa}$. Its structure, and in particular the various binding sites, are well characterized.¹⁴⁷ For example, it is well established that the presence of hydrophobic residues, as well as negative electrical charges, is a basic requirement for strongly binding a substrate to serum albumin.¹⁴⁷ All these data constitute a good starting point for developing protein-bound MRI contrast agents. Beside serum albumin, β -cyclodextrin has also been proposed as a macromolecular carrier of Gd^{III} chelates through noncovalent binding.^{38,149–152} However, the relaxivity gain achieved by cyclodextrin binding is rather limited as compared to protein-bound systems.

Both the retention time of the paramagnetic complex in the vasculature and the relaxivity increase resulting from the slower rotation of the macromolecular adduct will depend on the

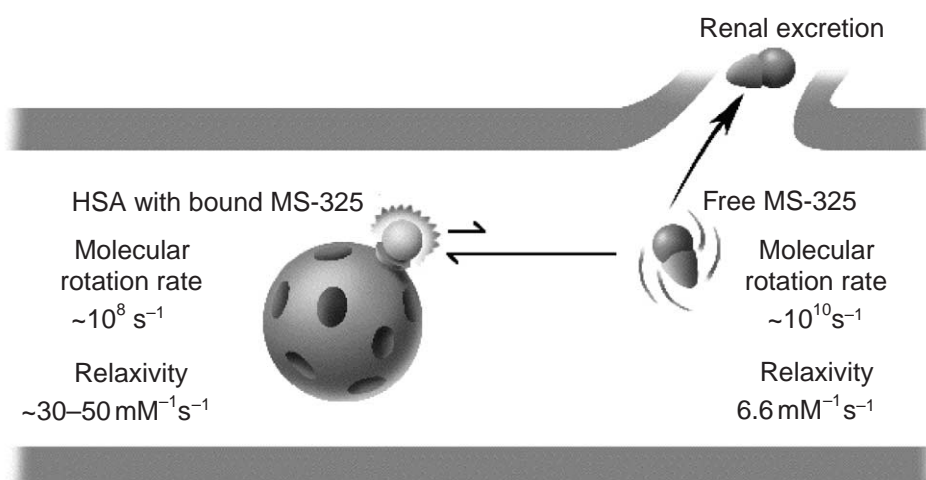
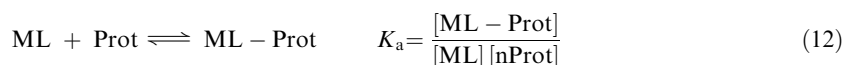


Figure 7 Receptor-induced magnetization enhancement mechanism. The contrast agent consists of two parts: the Gd^{III} chelate and the protein-binding moiety. Within the bloodstream, the agent binds to the protein. The bound form is in equilibrium with the small amount of free form, which can be renally excreted steadily over time. The bound form has high relaxivity by virtue of its slow rotation (reproduced by permission of the American Chemical Society from *Chem. Rev.*, **1999**, 99, 2293).

binding affinity of the chelate to the protein. Therefore, strong protein binding is a prerequisite for such agents. Principally, three techniques are applied to assess the degree of protein binding for paramagnetic chelates. Equilibrium dialysis and ultrafiltration are general separative methods.¹⁵³ The third, nonseparative technique takes advantage of the difference in the water proton relaxation-rate enhancement induced by the bound and unbound states of the paramagnetic chelate (Proton Relaxation Enhancement, PRE method); thus it is specific to paramagnetic substrate binding.¹⁵⁴ The majority of the affinity constants in the context of MRI have been obtained by PRE. In addition to the association constant and the number of binding sites on the protein, this approach also gives access to the relaxivity of the protein-bound Gd^{III} chelate.

If the binding between the paramagnetic chelate, ML, and the protein, Prot, involves a single class of equivalent binding sites, the equilibrium is characterized by the association constant, K_a :

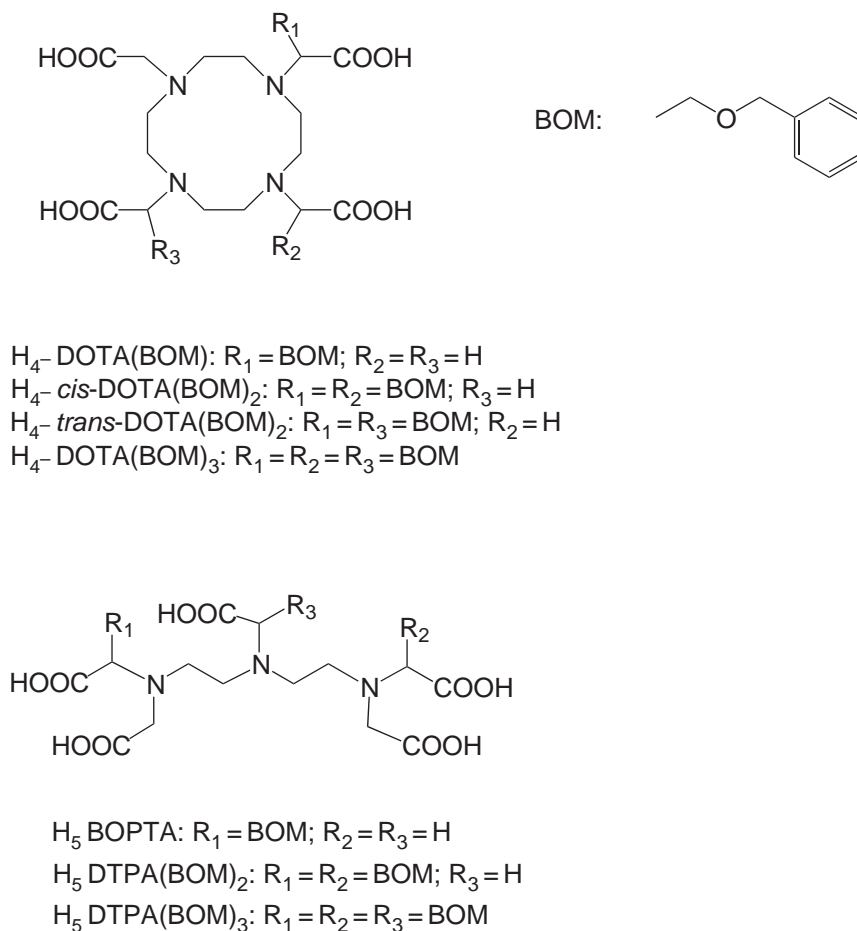


where $[\text{nProt}]$ is the concentration of the equivalent and independent binding sites on the protein. In an aqueous solution containing the protein and the metal complex, the observed proton relaxivity will be the sum of the relaxivities due to the unbound and the bound chelate:

$$r_1 = r_{1,\text{free}}[\text{ML}] + r_{1,\text{bound}}[\text{ML} - \text{Prot}] \quad (13)$$

where $r_{1,\text{free}}$ and $r_{1,\text{bound}}$ are the relaxivities of the unbound and bound substrate, respectively. The combination of Equations (12) and (13) allows correlation of the measured relaxivity, r_1 , to the binding parameters K_a and n .¹⁴⁸ In general, the experimental procedure consists of carrying out two distinct titrations: first titrating the paramagnetic substrate of a given concentration with the protein (called E-titration), then titrating the protein of a given concentration with the substrate (M-titration). The E-titration provides a good estimation of the relaxivity of the metal chelate bound to the highest affinity binding site of the protein, whereas K_a and n are more precisely determined from the M-titration. In actual cases, the analysis often becomes complicated when the binding is too weak, or when weaker binding sites coexist with the high affinity ones. Despite these difficulties, the PRE method proved useful in many examples. Comparison of the results obtained by PRE and by separative techniques for the same systems showed generally good agreement.^{63,155} In some cases the PRE could even provide an estimation of weak association constants which were not accessible by the other approaches.

The effect of the hydrophobicity of the paramagnetic complex on the affinity towards serum albumin has been studied by comparing the K_a values for a series of Gd^{III} complexes bearing an



Scheme 8

increasing number of lipophilic residues (Scheme 8).¹⁵⁶ The parent $[\text{Gd}(\text{DOTA})]^-$ complex, possessing one negative charge, showed a negligible relaxivity increase in the presence of HSA. Among the substituted $\text{Gd}(\text{DOTA})$ complexes, the relaxivity gain in the presence of HSA owing to the formation of the macromolecular adduct was the most significant for the tri-substituted $[\text{Gd}\{\text{DOTA}(\text{BOM})_3\}]^-$, suggesting the highest affinity for this compound to the protein. Indeed, the K_a value obtained for $[\text{Gd}\{\text{DOTA}(\text{BOM})_3\}]^-$ ($K_a = 1.7 \times 10^3 \text{ M}^{-1}$) is almost one order of magnitude higher than those for the *cis*- and *trans*-isomers of $[\text{Gd}\{\text{DOTA}(\text{BOM})_2\}]^-$ ($K_a = 3.2$ and $3.6 \times 10^2 \text{ M}^{-1}$, respectively), whereas for the monosubstituted $[\text{Gd}\{\text{DOTA}(\text{BOM})\}]^-$ only a weak interaction is detectable ($K_a < 1 \times 10^2 \text{ M}^{-1}$; 25°C , $\text{pH} = 7.4$; $n = 2$ equivalent binding sites). The number and the location of the protein binding sites involved have been assessed by using competitor probes like ibuprofen and warfarin, which strongly bind at well-known regions of the HSA.¹⁴⁷ It was found that $[\text{Gd}\{\text{DOTA}(\text{BOM})_3\}]^-$ occupies the same two equivalent binding sites as the competitors studied. The importance of hydrophobic binding is further confirmed by the temperature dependence of the association constant, which points to an entropically driven process, as expected for hydrophobic interactions.

The effect of the negative charge, the second important factor in HSA binding, has been proved in a study of a series of $\text{Gd}(\text{DTPA})$ derivatives bearing the same hydrophobic residue, but with an additional negative charge as compared with the macrocyclic $\text{DOTA}(\text{BOM})_x$ derivatives (Scheme 8). The more negatively charged, DTPA-type chelates have almost one order of magnitude higher affinity constants than the corresponding macrocyclic ones.¹⁴⁸

During the late 1990s, a number of hydrophobic residues were tested with the aim of strong binding of the metal chelate to HSA.^{39,63,157,158} Some examples of ligands able to bind plasma proteins are BOPTA, EOB-DTPA, MS-325 or MP2269 (Schemes 1 and 2). The most promising results were obtained with MS-325, which became the first Gd^{III} -based contrast agent for

angiographic applications to proceed to human trials.¹⁵⁷ The binding of MS-325 to HSA is induced by a bulky hydrophobic residue consisting of two phenyl rings attached to a cyclohexyl moiety linked, through a negatively charged phosphate group, to one of the two ethylenediamine sides of the DTPA backbone.^{57,58,157} The affinity of MS-325 for HSA is moderate, at typical circulating blood concentrations of 0.1 mM, 88% of the complex is noncovalently bound to the protein.¹⁵⁹

The conjugation of Gd^{III} chelates with plasma proteins results in a strong enhancement of the longitudinal relaxation rate of the water protons. For instance, binding of MS-325 to HSA causes a dramatic increase in the relaxivity of the molecule (ninefold at 20 MHz; Figure 8), which is primarily the result of a 60- to 100-fold increase in the rotational correlation time of the molecule upon protein binding.¹⁵⁹ In addition to slow rotation, there are two other favorable factors: an increased outer-sphere relaxivity and a slower electron spin relaxation. The outer-sphere contribution to the observed relaxivity in the protein-bound chelate has been evaluated by using a related compound, a TTHA derivative (TTHA = triethylene-tetramine-hexaacetate), which has no water molecule in the inner sphere. It was found that the outer-sphere relaxivity increases by a factor of 2–4 upon protein binding, which may be due to the presence of long-lived (~1 ns) water molecule(s) in the second coordination sphere. This effect has been observed for other Gd^{III} chelates without inner-sphere water as well.^{42,160} The electronic relaxation rate, $1/T_{1e}$, also slows

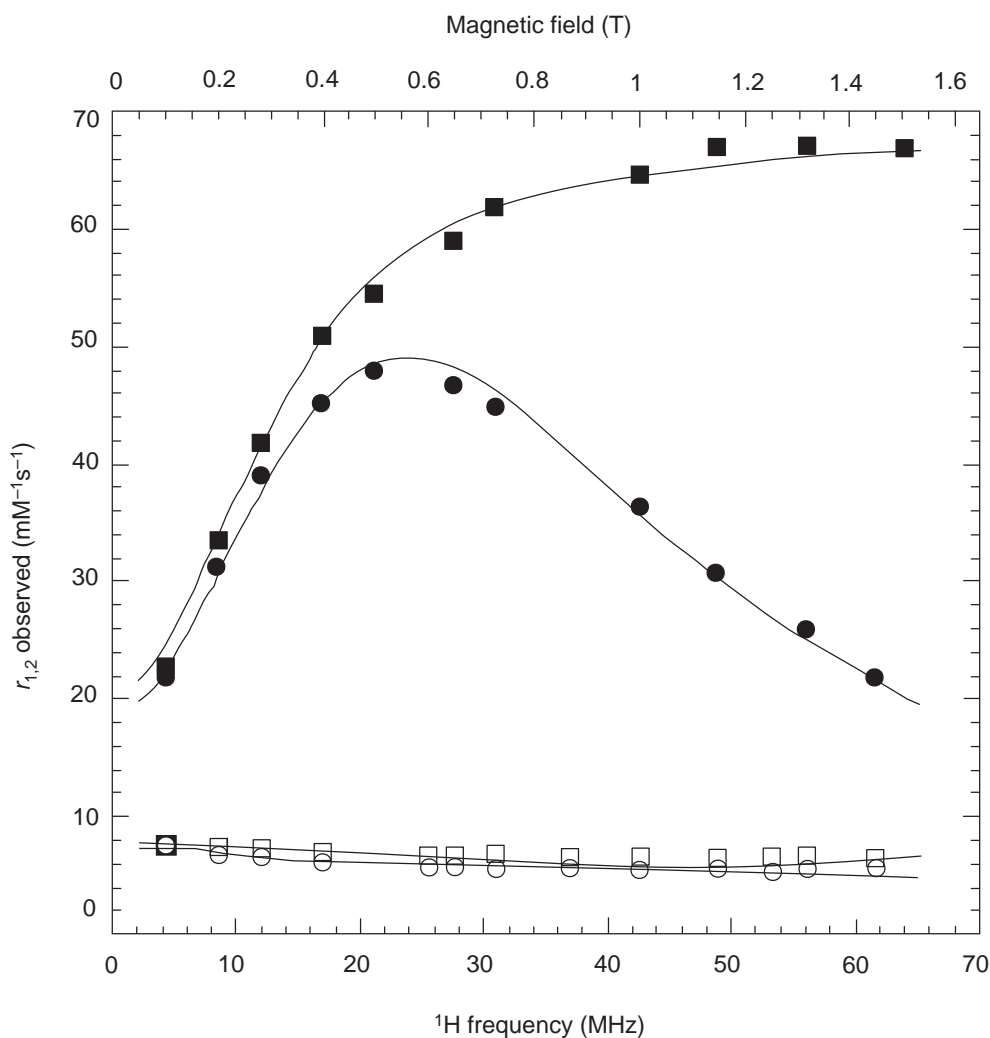


Figure 8 Observed longitudinal (r_1^{obs} , circles) and transverse (r_2^{obs} , squares) relaxivity for 0.1 mM MS-325 in the presence (filled symbols) and in the absence (open symbols) of 22.5% (w/v) HSA at 37°C, phosphate-buffered saline, pH 7.4 (reproduced by permission of the American Chemical Society from *J. Am. Chem. Soc.*, **2002**, *124*, 3152).

down upon binding, which is an unexpected benefit. On the other hand, the water exchange is slowed down, which limits the amount of relaxation enhancement observed.¹⁵⁹

Aime *et al.* studied albumin binding of DO3A derivatives, in the hope of taking advantage of the presence of two fast-exchanging, inner-sphere water molecules.¹⁵⁸ Upon interaction with HSA, the expected relaxation enhancement is not observed, as the two inner-sphere water molecules are displaced by donor atoms (likely to be carboxylates) on the protein. Based on all available examples, protein-bound Gd^{III} chelates can be classified into three categories based on their water-exchange behavior: (i) Systems where the exchange rate of the coordinated water is not influenced by protein binding. These are chelates with one inner-sphere water, and a rigid and bulky linkage to the protein to avoid direct contact of the coordination cage with the protein surface, like MP2269.³⁹ (ii) Systems where the geometry of the binding mode gives rise to an overall encumbrance along the water-exchange pathway. This was observed for a tri-negatively charged complex whose tight, electrostatic interaction with HSA blocks the water binding site and considerably diminishes the exchange rate.⁴² (iii) Systems where donor atoms of the protein replace the inner-sphere water molecules of the Gd^{III} chelate, such as for DO3A derivatives.¹⁵⁸

An interesting feature of binding to serum albumin is stereospecificity.¹⁴⁷ An example among metal complexes is [Gd(EOB-DTPA)]²⁻, where the S-enantiomer binds the protein about three times more strongly than the R-form (nK_a of $6.8 \times 10^2 \text{ M}^{-1}$ and $2.0 \times 10^2 \text{ M}^{-1}$, respectively, at 37°C).¹⁴⁸ Lauffer *et al.* investigated the HSA binding of two diastereoisomers (*rac*- and *meso*-) of [Fe(EHPG)]⁻ and found that the two diastereoisomers bind to different sites of the protein (EHPG = ethylenebis(*o*-hydroxyphenylglycine)).¹⁵⁵

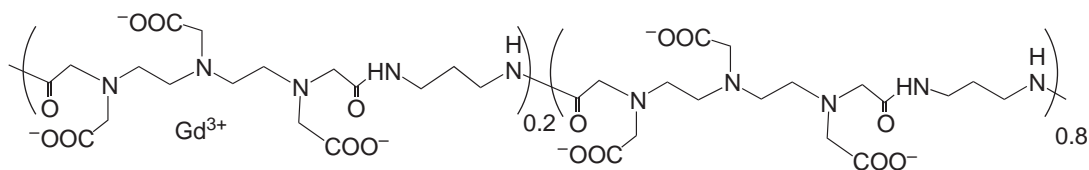
9.19.5 SMART CONTRAST AGENTS

Over the last few years, much effort has been directed towards the development of paramagnetic contrast agents which are reporters of the biochemical environment.¹⁶¹ The main characteristic of this new class of drugs, called “responsive” or “smart” contrast agents, is that their proton relaxivity depends on some variable of the given tissue. The relaxivity difference of the agent for different values of the biochemical parameter in question should be large enough to be detected on the MR images. It is well known that in the presence of pathology, physiological parameters may be altered. Therefore, contrast materials that can visualize pathology based on alterations of physiological parameters would be invaluable in medical diagnostics (see Chapter 9.21). The most important biochemical variables to be monitored involve pH, temperature, partial oxygen pressure, or the concentration of enzymes and metal ions. These contrast agents should ideally function as “off-on” switches, i.e., the MR efficacy being markedly enhanced at given values of pH, temperature, etc.

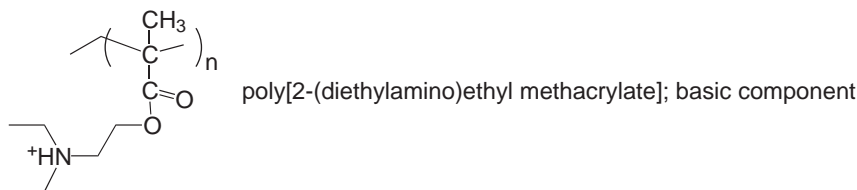
9.19.5.1 pH-sensitive Agents

It has been reported that the pH in solid human tumors is approximately 0.4 units lower than in healthy tissues.¹⁶² This pH decrease is attributed to the extensive production of lactic acid within tumor cells. The traditionally used, invasive technique of measuring *in vivo* extracellular pH with microelectrodes is not suited to studying pH variations over small distances, which is of interest for tumor characterization. Magnetic resonance spectroscopy, using shift reagents with extracellular distribution, has been proposed to measure extracellular pH; however, low resolution limits its use.¹⁶³ Concerning pH-sensitive MRI contrast agents, pH changes may have an effect on different parameters which, in turn, will influence proton relaxivity. Such pH-dependent parameters involve the hydration state, the protonation of the ligand or of the coordinated water molecules, or, for polymeric agents, the structure of the macromolecule.

The first paramagnetic complex with pH-dependent relaxivity was reported and proposed as a pH-sensitive contrast agent as early as 1987.¹⁶⁴ The longitudinal water proton relaxation rates measured in a solution of Fe^{III}-*meso*-tetra(4-sulfonatophenyl)porphine (Fe(TPPS4)) were found to increase over the pH range from 7.75 to 5.75. The relaxivity increase was attributed to a pH-dependent equilibrium between the high-spin ($S = 5/2$) Fe(TPPS4) monomer at low pH and the antiferromagnetically coupled μ -oxo-dimer [O-(FeTPPS4)₂] at high pH.



poly[(GdDTPA)(1,3-propanediamide)]; acidic component



poly[2-(diethylamino)ethyl methacrylate]; basic component

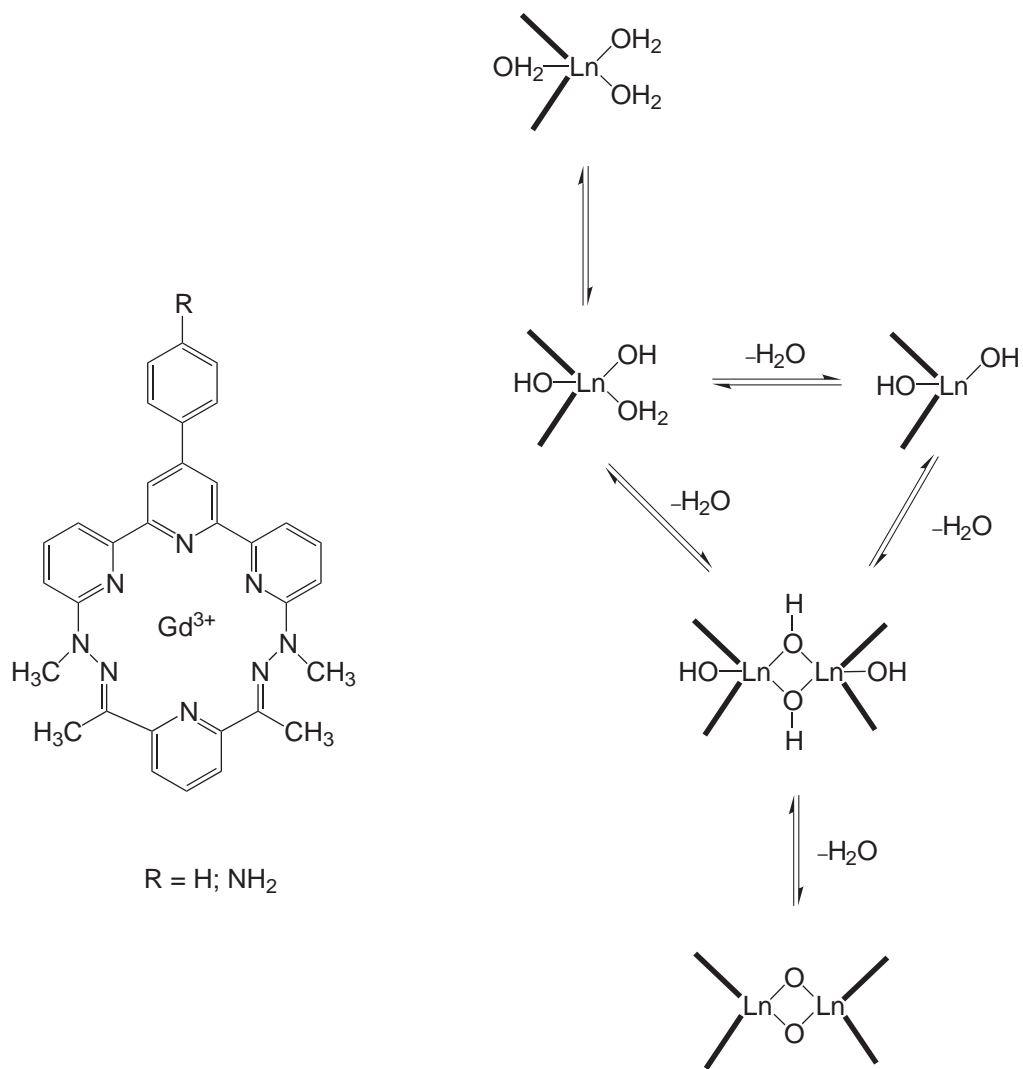
Scheme 9

Mikawa *et al.* reported pH-dependent relaxivity for a polyionic Gd^{III} complex composed of a couple of weakly acidic and basic polymers (Scheme 9).^{165,166} The acidic component is a poly-Gd(DTPA) chelate with additional, noncomplexing DTPA units. Depending on the pH, the noncoordinating carboxylates are progressively deprotonated, resulting in an excess negative charge which can then be neutralized with poly(2-(diethylamino)ethyl)methacrylate, a positively charged polycation. The complex formation between the oppositely charged polyions is accompanied by the release of water molecules when the overall charge is neutral, which, consequently, results in the relaxivity decrease observed between pH 5 and 7. At pH values higher than 8, the positively charged polyamine is deprotonated and neutralized, which causes the dissociation of the polyionic complex. This permits again the access of water molecules to the gadolinium center to allow for an increased relaxivity. The pH responsivity of the system varies with the composition of the polyionic complex (mixing ratio of the polycation and polyanion), allowing modulation of the pH sensibility.

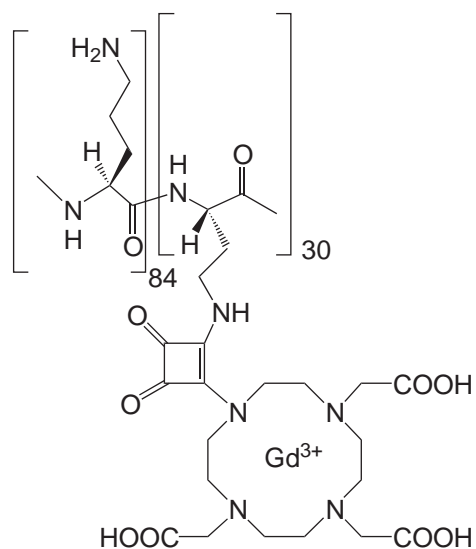
A strong decrease in relaxivity (from $12.8 \text{ mM}^{-1} \text{ s}^{-1}$ to $2 \text{ mM}^{-1} \text{ s}^{-1}$) between pH 6 and 11 has been reported for a positively charged macrocyclic Gd^{III} complex (Scheme 10), which was explained by the successive deprotonation of the coordinated water molecules.¹⁶⁷ Luminescence lifetime measurements of a Yb^{III} analogue proved that the complex possesses three bound waters at pH 5.5. Above pH 11, a di-oxo-bridged dimer is formed that has no more bound water or OH groups.

pH can be assayed by designing systems whose molecular mobility is a function of pH. Indeed, structural changes occurring upon protonation are responsible for the pH-dependent relaxivity observed for the paramagnetic macromolecular complex $[\text{Gd}(\text{DO3ASQ})]_{30}\text{-Orn}_{114}$ (Scheme 11).¹⁶⁸ The concept that is exploited to produce a pH-sensitive agent is based on the rotational limitation of the relaxivity at imaging magnetic fields. The structure of poly(amino acids) such as polylysine or polyornithine strongly depends on pH. At acidic pH, the repulsion among positively charged amino groups induces a highly flexible structure, whereas at basic pH intra-chain hydrogen bonds give rise to a highly rigid, α -helical structure. This pH-dependent structural change results in a continuous and linear relaxivity increase from $24 \text{ mM}^{-1} \text{ s}^{-1}$ to $32 \text{ mM}^{-1} \text{ s}^{-1}$ in the pH range 3–9.

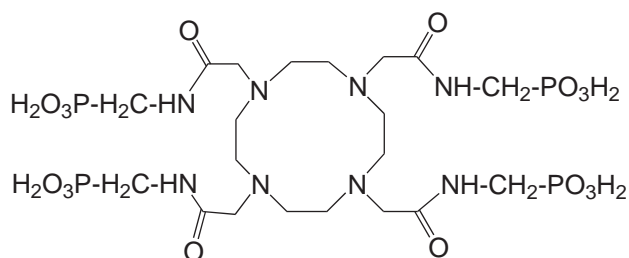
An unusual pH dependence has been reported for the Gd^{III} complex of a tetraamide-based ligand with extended noncoordinating phosphonate side chains (Scheme 12).^{169,170} The relaxivity increases from pH 4 to 6, followed by a decrease until pH 8.5, then from pH 10.5 it increases again. The system, as well as isostructural lanthanide complexes, was characterized by various techniques such as ^{31}P and ^{17}O NMR and fluorescence measurements. The pH dependence could be attributed to protonation equilibria of the noncoordinating phosphonate groups, which can



Scheme 10



Scheme 11



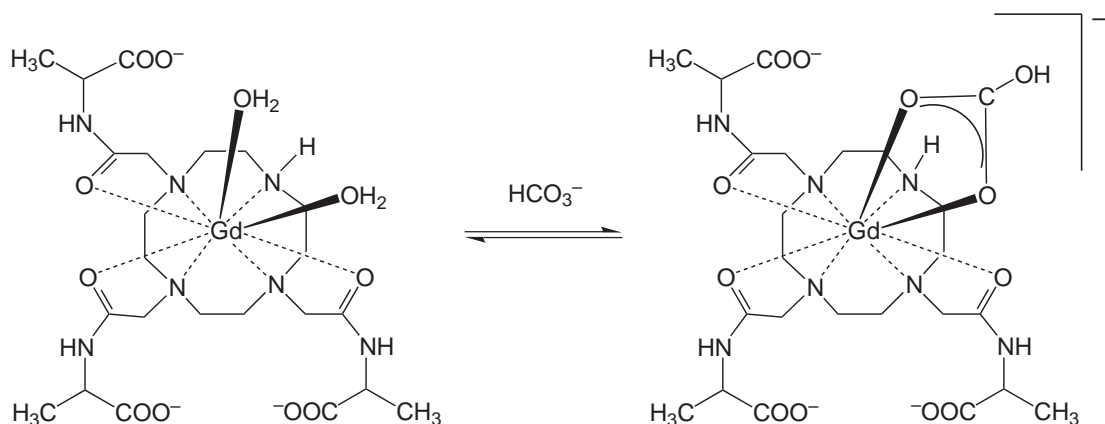
Scheme 12

catalyze proton exchange by providing an efficient hydrogen-bond network. Despite the slow water-molecule exchange, the prototropic exchange on the Gd^{III} complex at pH 6 appears to be near optimal for maximizing water proton relaxivity.

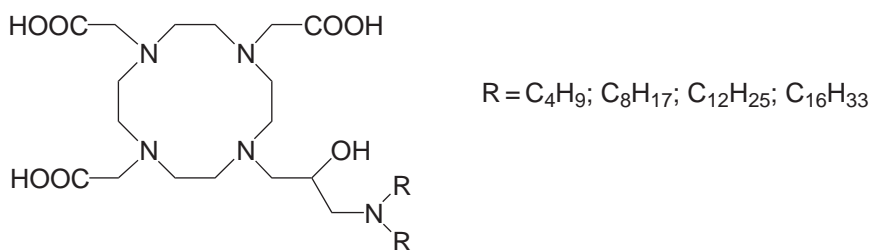
Another approach towards pH-responsive contrast agents is based on the pH-dependent ternary complex formation between hydrogencarbonate and the Gd^{III} complex of a heptadentate macrocyclic ligand (Scheme 13).⁵⁹ The Gd^{III} complex has two inner-sphere water molecules, which can be replaced by the bidentate hydrogencarbonate or carbonate ion, resulting in a relaxivity decrease (from $7.5 \text{ mM}^{-1} \text{ s}^{-1}$ to $1.9 \text{ mM}^{-1} \text{ s}^{-1}$). The relaxivity observed for this complex in the presence of hydrogencarbonate is sensitive to pH in the range 6–8, where the reversible binding occurs. Such a system offers a means of studying the concentration of HCO_3^- in solution as well. The luminescence behavior of the corresponding Eu^{III} complex in the presence of hydrogencarbonate also reflects the ternary complex formation, and can be used as a pH-dependent luminescence probe.

Amphiphilic Gd^{III} -DO3A derivatives, containing a tertiary amino group in the side chain, were also reported to have pH-dependent relaxivities (Scheme 14).¹⁷¹ At low pH (3–6), the relaxivity is $7.9 \text{ mM}^{-1} \text{ s}^{-1}$, then reaches a value of $19.1 \text{ mM}^{-1} \text{ s}^{-1}$ at pH 8. This large increase is attributed to the formation of colloidal aggregates, due to the higher lipophilicity of the deprotonated (neutral) complex at higher pH compared with the protonated (positively charged) species at lower pH.

pH-sensitive paramagnetic liposomes have also been proposed as potential *in vivo* pH meters, therefore as tumor markers in MRI.¹⁷² pH-sensitive liposomes in general are currently evaluated as delivery vehicles in several therapeutic concepts. Such liposomes become unstable and leaky under weakly acidic conditions.¹⁷³ $\text{Gd}(\text{DTPA-BMA})$ was encapsulated within saturated dipalmitoyl phosphatidyl ethanolamine/palmitic acid liposomes. At physiological pH and above, the relaxivity of this system is significantly lowered compared with that of the nonliposomal Gd^{III} chelate, which is explained by the water-exchange limitation of the relaxation process. Lowering the pH below physiological value (e.g., pH in tumors), gives a sharp, six- to sevenfold relaxivity increase, due to liposome destabilization and subsequent leakage of the entrapped $\text{Gd}(\text{DTPA-BMA})$ (Figure 9).



Scheme 13



Scheme 14

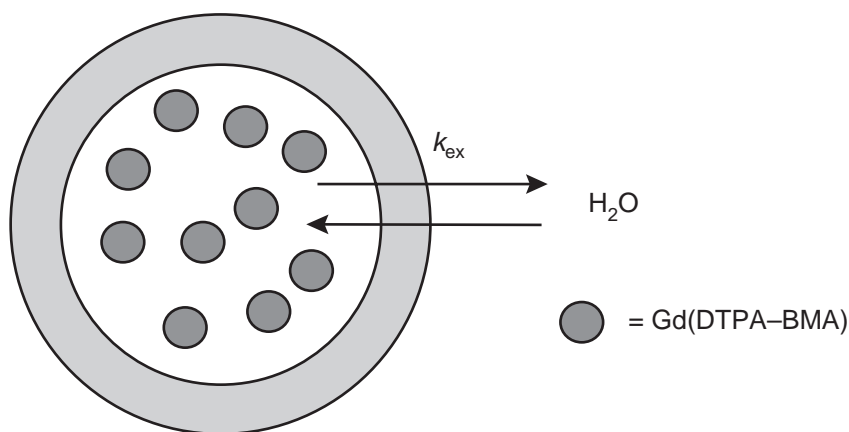


Figure 9 pH-sensitive paramagnetic liposomes: at physiological pH and above, Gd(DTPA–BMA) is entrapped in the liposome and the relaxivity is low due to the low water exchange rate (k_{ex}) through the liposome membrane. At lower pH, the liposome is disrupted and the relaxivity increases.¹⁷²

9.19.5.2 Temperature-sensitive Agents

As most biochemical reaction cascades are exothermic, the spatial temperature distribution within a living organism directly reflects local metabolic activity. Potential applications of an *in vivo* thermometer could be detection and localization of tumors, inflammations, or infraction. In addition, hyperthermia treatment of malignant tumors also requires an accurate temperature control in the range 41–45 °C. For this purpose, Fossheim *et al.* tested thermosensitive, liposome-encapsulated Gd^{III} chelates whose temperature response is linked to the phase transition properties of the liposome carrier.¹⁷⁴ At ambient temperature, the relaxivity of the liposomal Gd(DTPA–BMA) is exchange limited, because of the slow water exchange between the liposome interior and exterior. A sharp, marked increase in relaxivity occurs as the temperature reaches and exceeds the gel-to-liquid crystalline phase transition temperature of the liposome (42 °C), due to the marked increase in transmembrane water permeability, yielding fast exchange conditions. With an appropriate choice of the liposome composition, the transition temperature can be fine-tuned for the specific application.

Magnetic resonance spectroscopy has also been proposed for temperature measurements. Roth *et al.* have reported the *in vivo* applicability of a Pr^{III} methoxyethyl–DO3A derivative, for which the ¹H chemical shift of the methoxy proton was found to change linearly with temperature within the range relevant to clinical application.¹⁷⁵ Since the frequency difference between the methoxy protons and the protons of the water tissue was relatively large (24 ppm), the interference of the strong water signal could be avoided by suppression, using standard techniques. Aime *et al.* also found a strong temperature dependence of the ¹H chemical shift of a methyl group in a macrocyclic Yb^{III} chelate (–0.42 ppm °C^{–1}).¹⁷⁶ Lanthanide complexes of cyclen derivatives with phenylphosphinic pendant arms have been also proposed as temperature-sensitive probes for ¹H or ³¹P magnetic resonance spectroscopy.¹⁷⁷

9.19.5.3 Contrast Agents Sensitive to Partial Oxygen Pressure

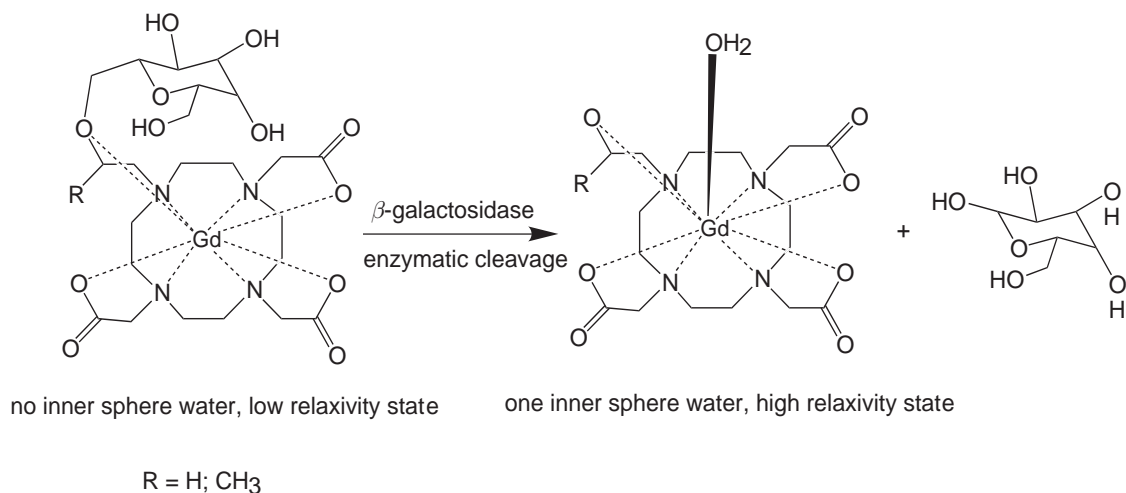
The partial oxygen pressure, pO_2 , is particularly significant in metabolic processes of cells, and its variation from normal values often indicates pathologies (ischemic diseases, strokes, tumors). Accurate and localized measurements of the oxygen concentration are also desirable for differentiation between venous and arterial blood, or for cerebral mapping of task activation. In the past, invasive methods were used involving oxygen-sensitive electrodes which had to be placed directly in the blood or tissue and could only offer pO_2 from a few body points.

The simplest design of a pO_2 -responsive, MRI contrast agent is based on metal complexes whose metal ion can be reduced or oxidized depending on the biological environment, with the two oxidation forms having different relaxation properties. The two redox states influence the proton relaxation of the surrounding protons to a different extent, resulting in different image intensities. The first example reported for such a system is the Mn^{III}/Mn^{II} -TPPS4 complex (tpps = 5,10,15,20-tetrakis-(p-sulfonatophenyl)porphinate).¹⁷⁸ The Mn^{II} form of the complex can be oxidized to Mn^{III} by oxygen. Although the two redox states have similar relaxivity values at MRI-relevant frequencies, their relaxation mechanisms are different. For the reduced Mn^{II} state, fast rotation limits proton relaxivity, whereas for the oxidized Mn^{III} form, electronic relaxation is limitative. As a consequence, the formation of a slowly tumbling adduct, e.g., with poly- β -cyclodextrine, will considerably increase the relaxivity of the reduced form, but does not affect that of the Mn^{III} complex. This gives rise to a remarkable relaxivity difference between the Mn^{II} - and Mn^{III} -(TPPS4)-(poly- β -cyclodextrine) conjugates. Indeed, the relaxivity observed in a Mn (TPPS4)-(poly- β -cyclodextrine) solution was dependent on the partial oxygen pressure.

The Eu^{III}/Eu^{II} system could also be a candidate, since Eu^{II} has seven unpaired electrons in an 8S ground state and is isolectronic with Gd^{III} . Thus the Gd^{III} and Eu^{II} complexes are expected to have similar proton relaxivities, whereas Eu^{III} is a very poor relaxing agent. A potential application of Eu^{III}/Eu^{II} complexes as redox-responsive MRI probes requires the control of both the redox and thermodynamic stability of the complex in the lower oxidation state. From this perspective, several Eu^{II} complexes have been investigated in the late 1990s and early 2000s.^{179–182}

9.19.5.4 Enzymatically Responsive Contrast Agents

MRI can offer an alternative to light microscopy in studying biological structure, function, and development of intact cells and tissues. A great advantage of MRI over optical microscopy techniques is that it allows *in vivo* imaging of deep tissues, whereas optical microscopy is limited by light scattering to cells within 100 μm of the surface. In order to exploit the power of MRI for biological studies, appropriate contrast agents, capable of reporting on enzymatic activity, gene expression, etc., have to be developed. The first enzymatically responsive MRI contrast agent was reported by Meade *et al.* in 1997.¹⁸³ This Gd (DOTA) derivative contains a galactopyranose residue, which is positioned at the ninth coordination site of Gd^{III} , thus preventing the coordination of an inner-sphere water molecule (Scheme 15). Consequently, this form has a low, outer-sphere-only relaxivity. Exposure of the chelate to the enzyme β -galactosidase irreversibly removes the galactopyranose from the chelator ligand, and by opening the access of water molecules into the first coordination sphere, it causes a transition from the low to the high relaxivity state. The enzymatic cleavage of the galactopyranose residue gives rise to a 20% increase in proton relaxivity and it could be visualized by *in vitro* MR images. The galactopyranosyl moiety can be further rigidified by addition of a methyl group to the linker (Scheme 15). This restricts the rotation of the galactopyranose blocking group, reduces the water access to the first coordination sphere of the Gd^{III} , and thus further decreases the relaxivity of the inactive state.¹⁸⁴ In this case, the enzymatic cleavage results in a threefold relaxivity increase, which makes the agent adequate for *in vivo* imaging. Indeed, it has been used for *in vivo* MRI visualization of β -galactosidase expression, a commonly used marker gene, in *Xenopus laevis* embryos.¹⁸⁴ The contrast agent was injected into both cells, and messenger RNA for β -galactosidase into one of the cells of the embryo at the two-cell stage. As the first mitosis roughly separates the future left and right sides of the embryo, these injections introduce the contrast medium to both sides of the embryo, whereas β -galactosidase will be expressed on one side of the animal. Each embryo contains cells in which the contrast agent is enzymatically cleaved and activated, and other cells with the contrast agent in nonactive form. On the MR images the left and right side of the embryo, representing the two types of cells, could be clearly distinguished. This method is very promising for *in vivo* mapping of gene expression in developmental biology and gene therapy.

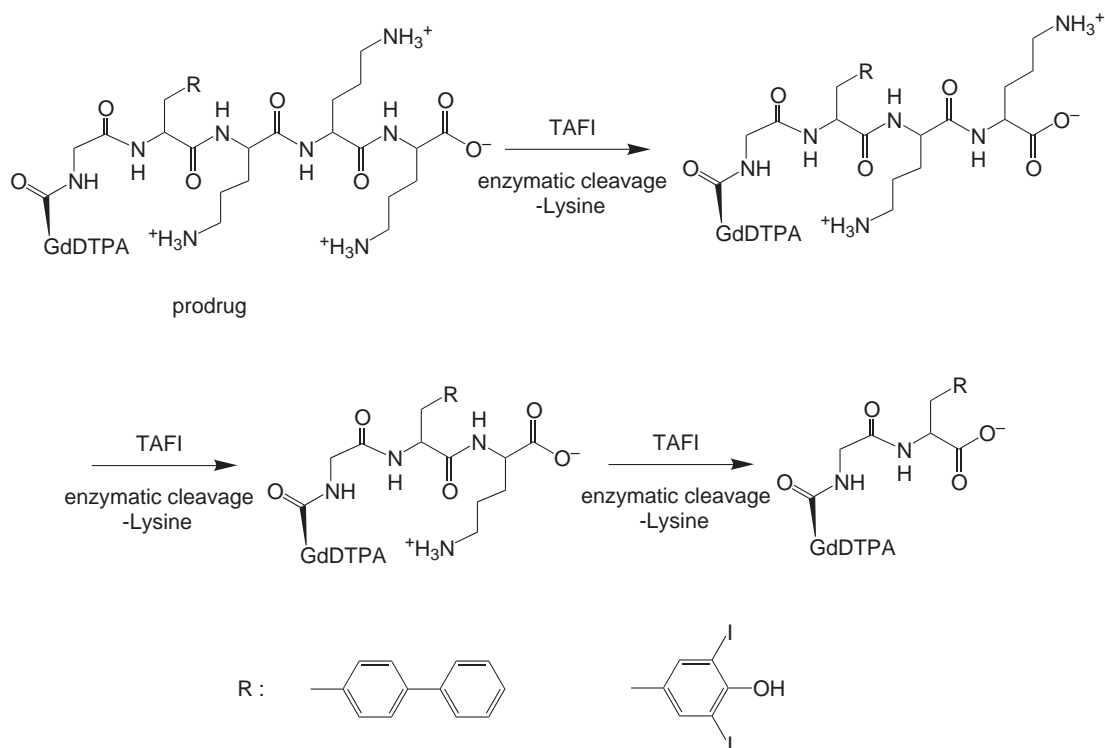


Scheme 15

Another strategy was used by Anelli *et al.* to detect carbonic anhydrase, a zinc enzyme present in various tissues in variable amounts.¹⁸⁵ [Gd(DTPA)]²⁻ was functionalized with sulfonamide (SA), which is known to be a specific inhibitor of carbonic anhydrase. The functionalized contrast agent, Gd(DTPA-SA), is able to specifically react with carbonic anhydrase, therefore targeting the enzyme and any enzyme-rich tissue. The interaction between the Gd^{III} complex and the enzyme is strong enough to ensure a remarkable increase in relaxivity as compared to the free chelate, due to the slow rotation of the macromolecular adduct (MW = 30 kDa; $r_1 = \sim 5 \text{ mM}^{-1} \text{ s}^{-1}$ and $\sim 27 \text{ mM}^{-1} \text{ s}^{-1}$ for the free and for the enzyme-conjugated chelate, respectively, at 20 MHz, 25 °C). The agent does not appreciably interact with any soluble macromolecule in serum, and the amount of carbonic anhydrase present on the outer erythrocyte membranes is too small (though detectable) to block this reagent in the blood pool. Therefore, Gd(DTPA-SA) is a potential candidate for *in vivo* tests for specificity in various tissues outside the blood pool.

McMurry *et al.* tested an approach which relies upon the enzymatic transformation of a prodrug-Gd^{III} complex, with poor affinity to HSA and concomitant low relaxivity, to a species with improved HSA affinity and enhanced relaxivity.¹⁸⁶ The conversion involves enzymatic removal from the Gd^{III} complex of a masking group that inhibits HSA binding. The prodrugs shown in Scheme 16 were designed to be cleaved by a human enzyme carboxypeptidase B, the thrombin-activatable fibrinolysis inhibitor (TAFI), implicated in thrombotic disease. The prodrugs (or pro-RIME contrast agents, according to the Receptor Induced Magnetization Enhancement concept)^{2,146} are composed of four moieties: (i) a masking group consisting of three lysine residues; (ii) an HSA binding group; (iii) a glycine linker; and (iv) the signal generation group, Gd(DTPA). The trilycine masking group was selected because charged groups have generally poor HSA affinity, whereas the aryl residues are expected to bind strongly to HSA and enhance the agent's relaxivity when unmasked by TAFI turnover. Indeed, the relaxivity measured in a 4.5% (w/v) HSA solution, following cleavage of the lysine residues with physiological concentrations of TAFI, showed more than 100% increase as compared with the prodrug itself (20 MHz; 37 °C). This study demonstrated the feasibility of using MRI to detect, with an efficient contrast agent, an enzyme associated with a disease state. Such bioactivation of the MRI agent allows the detection of targets present at submicromolar concentrations. The same pro-RIME principle has been applied for the detection of alkaline phosphatase.¹⁸⁷

Another strategy, developed by Bogdanov *et al.*, is based on the enzyme-mediated polymerization of paramagnetic substrates into oligomers of higher relaxivity.¹⁸⁸ The substrates consist of a Gd^{III} chelate covalently bound to phenols, which then serve as electron donors during enzymatic hydrogen peroxide reduction by peroxidase. The converted monomers undergo rapid condensation into paramagnetic oligomers, leading to a threefold increase in relaxivity due to increased rotational correlation time. This method allowed imaging of nanomolar amounts of the oxidoreductase enzyme.



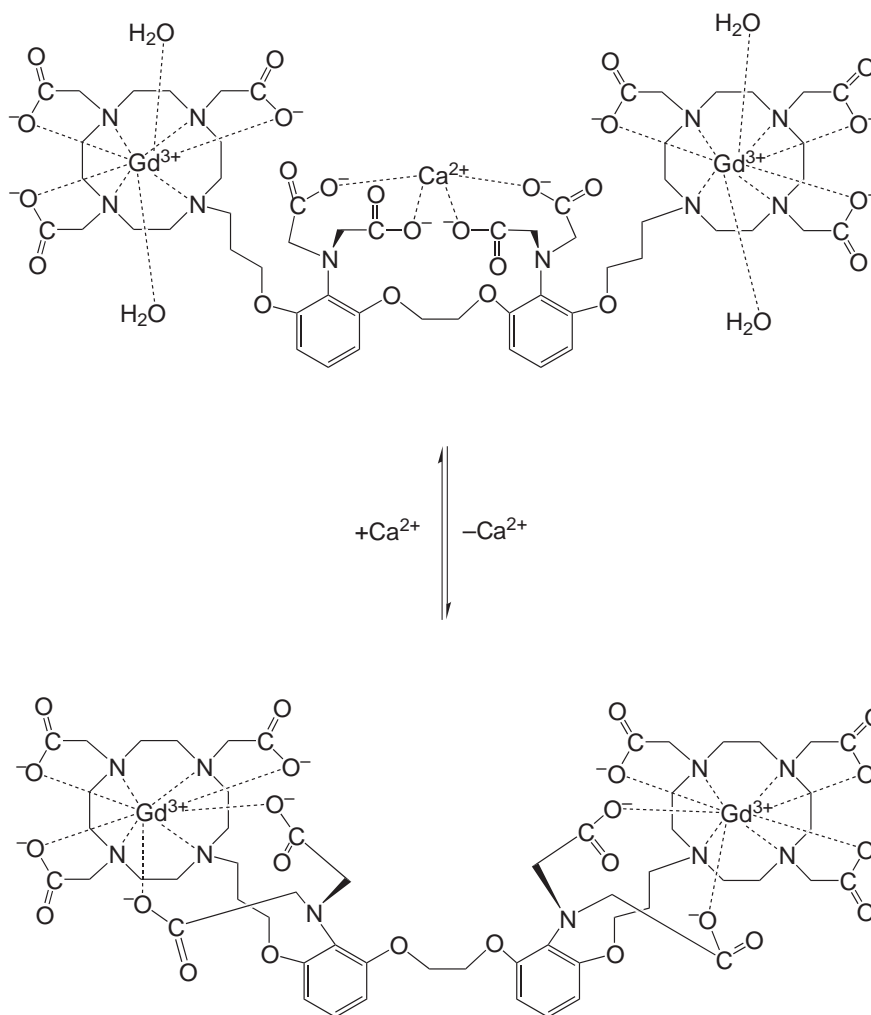
Scheme 16

9.19.5.5 Contrast Agents Responsive to Metal Ion Concentration

Several metal ions play a crucial role in biological processes, whereas some others are toxic. Alteration of the metal concentration in the body can often be correlated to disease states. The necessity for *in vivo* determination of metal ion concentration and distribution has prompted research to develop appropriate metal-responsive MRI contrast agents.

Ca^{2+} is an important intracellular secondary messenger of signal transduction. Changes in the cytosolic concentration of Ca^{2+} trigger changes in cellular metabolism and are responsible for cell signalling and regulation. Meade *et al.* reported a dimeric Gd(DO3A)-derivative contrast agent, $[\text{Gd}_2(\text{DOPTA})]^{4-}$, whose proton relaxivity is selectively modulated by Ca^{2+} concentration (Scheme 17).¹⁸⁹ Gd(DOPTA) has a Ca^{2+} dissociation constant of $0.96 \mu\text{M}$, and the relaxivity of the complex increases approximately 80% when Ca^{2+} is added to a Ca^{2+} -free solution (from $3.26 \text{ mM}^{-1} \text{ s}^{-1}$ to $5.76 \text{ mM}^{-1} \text{ s}^{-1}$; 500 MHz, 25°C). The central part of the DOPTA ligand is able to bind Ca^{2+} with high selectivity over other metals (e.g., Mg^{2+}). In the absence of Ca^{2+} , the aromatic iminoacetates of the central part interact through ionic attractions with the Gd^{III} , coordinated by the macrocycle. In this state, the access of bulk water to the paramagnetic metal ion is blocked, so the relaxivity is low. In the presence of Ca^{2+} , the aromatic iminoacetates will rearrange to bind Ca^{2+} , thereby allowing water to bind to Gd^{III} and, as a consequence, the relaxivity increases. The effect of $[\text{Ca}^{2+}]$ on relaxivity is most striking in the calcium concentration range $0.1\text{--}10 \mu\text{M}$, and then levels off at higher concentrations.

Another essential metal ion in biological systems is iron. MRI contrast agents have been also designed whose relaxivity is iron concentration dependent.^{161,190} One example is Gd(PhenHDO3A) (Scheme 18) which, similarly to the previously discussed Gd(DOPTA), features two complexing units of totally different natures. The macrocyclic binding site forms highly stable lanthanide chelates, while the phenanthroline-like unit is a good complexing agent for Fe^{II} . The Gd(PhenHDO3A) chelate spontaneously associates with Fe^{II} to form a tris-complex of high molecular weight, giving rise to more than a threefold relaxivity increase (from $3.7 \text{ mM}^{-1} \text{ s}^{-1}$ to $12.2 \text{ mM}^{-1} \text{ s}^{-1}$; 20 MHz, 37°C). Another family of iron-sensitive contrast agents uses a *tris*-hydroxamate moiety for iron(III) complexation (Scheme 18).¹⁶¹ In the presence of Fe^{III} , the

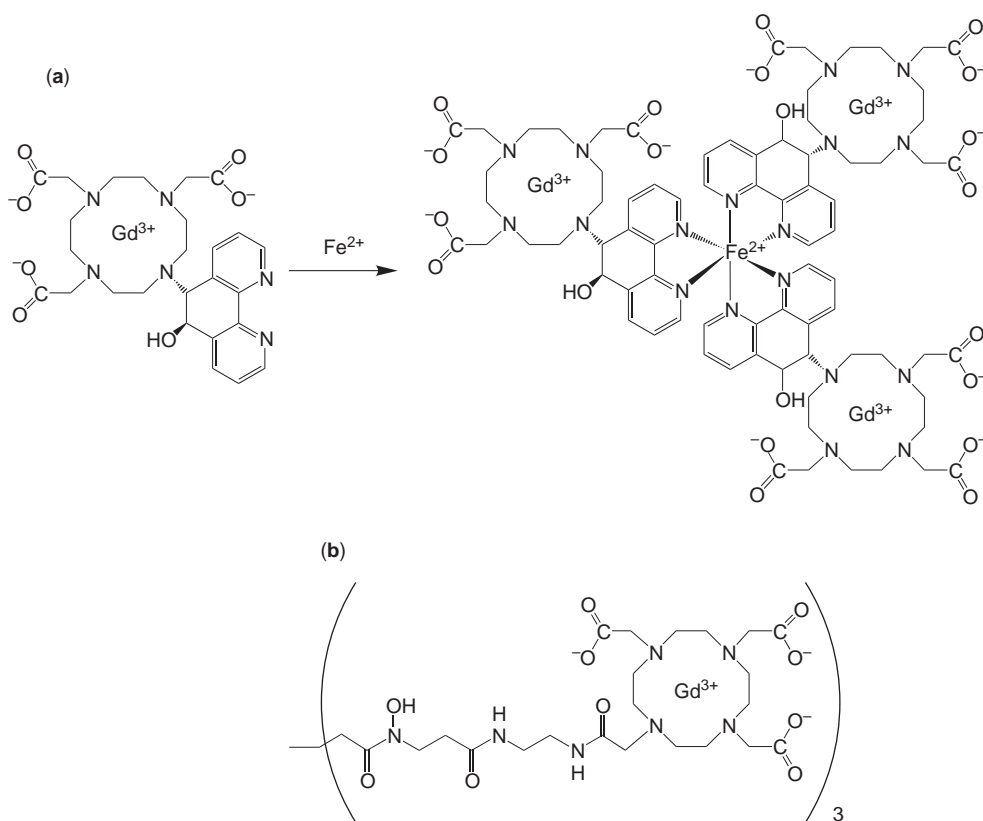


Scheme 17

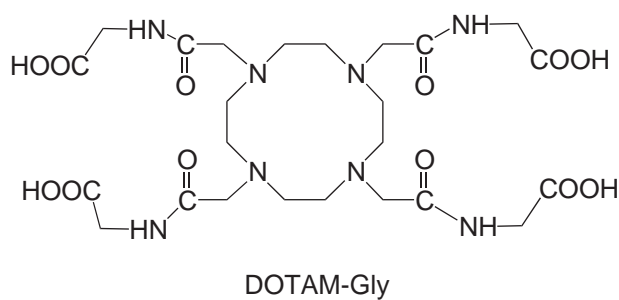
rotation of the Gd^{III} chelating part is largely restricted and, as a consequence, the relaxivity is increased by 57% (from $5.4 \text{ mM}^{-1} \text{ s}^{-1}$ to $8.5 \text{ mM}^{-1} \text{ s}^{-1}$; 20 MHz).

9.19.6 CHEMICAL EXCHANGE SATURATION (CEST) CONTRAST AGENTS

Chemicals containing mobile protons may also act as T_2 agents through the reduction of the water proton relaxation time via exchange processes. A remarkable improvement of the efficacy of such T_2 -reducing contrast agents has been shown when a proper RF irradiating field is applied at the resonance frequency of the exchangeable protons. This results in a net decrease of the bulk water signal intensity due to a saturation transfer effect. Balaban, who carried out a lot of work in this field, named this contrast-enhancing procedure “chemical exchange saturation transfer” (CEST).¹⁹¹ A good contrast agent for CEST application has to possess mobile protons, whose exchange rate with water is as high as possible before their broadening makes the RF irradiation ineffectual. Roughly, this condition occurs when the exchange rate approaches the separation (in Hz) between the chemical shift values of the two exchanging sites.¹⁹² Therefore, larger chemical shift differences enable the exploitation of faster exchange, thus resulting in an enhanced CEST effect. Zhang *et al.* showed that a particularly useful source of highly shifted exchangeable protons can be provided by the slowly exchanging water protons bound to a paramagnetic Eu^{III} chelate.¹⁹³ Another possibility is to take advantage of the highly shifted exchangeable amide protons of the ligand. The Yb complex of the tetraglycineamide derivative of DOTA, DOTAM–Gly



Scheme 18



Scheme 19

(Scheme 19), displays interesting CEST properties when its amide NH resonance is irradiated.¹⁹² As the exchange rate of the amide protons is base catalyzed, the complex proves to be an efficient pH-sensitive probe in the 5.5–8.2 pH range.

9.19.7 TARGETING CONTRAST AGENTS

Targeting contrast agents are able to recognize specific target molecules. Antibodies, or other tissue-specific molecules, may be combined with paramagnetic probes to provide disease-specific MRI agents. For instance, tumor enhancement could be achieved by targeting receptors on the tumor cell surface. Targeted MRI could also be beneficial in gene therapy to follow gene delivery and expression. The main difficulty in MRI targeting lies in the delivery of a sufficient quantity of the paramagnetic substance to the targeted site, given the relatively low sensitivity of the magnetic resonance imaging technique. In case of receptor targeting, biological constraints are limitative, as

pointed out by Nunn *et al.*¹⁹⁴ These constraints are the very low concentration of receptors (10^{-9} – 10^{-13} mol g⁻¹ of tissue) and the biological implications of saturating receptors. The limitation is reduced by increasing the relaxivity of the contrast agent, either by greater intrinsic relaxivity or by attaching many paramagnetic centers to the targeting molecule. Estimations for the minimal detectable concentration of the contrast agent vary from 5×10^{-7} mol g⁻¹ for the low molecular weight Gd(HP-DO3A)(H₂O) ($r_1 = 3.7$ mM⁻¹ s⁻¹) to 1.9×10^{-10} mol g⁻¹ for a sixth-generation, Gd(DTPA)-loaded dendrimer ($r_1 = 5,800$ mM⁻¹ s⁻¹ per dendrimer), or 1.6×10^{-11} mol g⁻¹ for superparamagnetic iron oxide particles ($r_2 = 72,000$ mM⁻¹ s⁻¹ per particle).¹⁶¹ For the macromolecular or particle contrast agents, the lowest detectable concentration is already in the range of the receptor concentration (10^{-9} – 10^{-13} mol g⁻¹), and indeed, some of them have been found applicable for receptor imaging. Despite the difficulties involved in targeting of MRI contrast agents, several promising reports and reviews^{2,161,195,196} have been published. Here we will present only a few strategies from the vast and very diverse field of targeting.

Monoclonal antibodies can be grown against a variety of receptor sites and thus represent an important area in the targeting of therapeutic or diagnostic drugs in general, including MRI contrast agents. The affinity of the antibody must be retained after labeling, which often limits the number of paramagnetic probes that can be attached to the polypeptide chain. From the early days of MRI applications, efforts have been made to mark monoclonal antibodies with paramagnetic probes, often without success in terms of contrast enhancement on real images. Among the more recent studies, Curtet *et al.* conjugated as many as 24–28 [Gd(DTPA)]²⁻ or [Gd(DOTA)]⁻ units per antibody, while retaining the 80–85% of the immunoreactivity.¹⁹⁷ The accumulation of the conjugates was rather slow on the tumor site, however, allowing for a tumor enhancement in half of the tested mice.

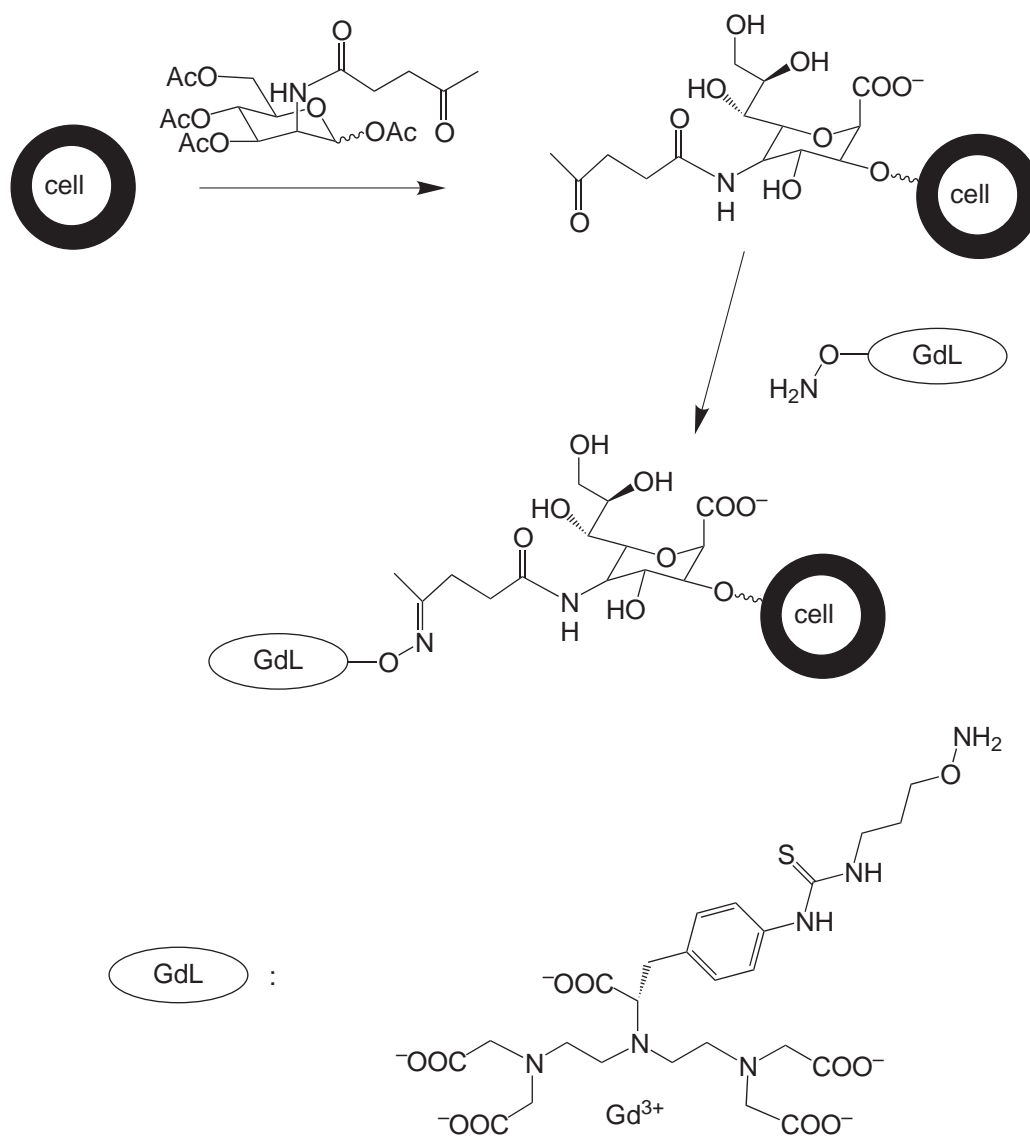
Monoclonal antibodies were also loaded with large particles, with the aim of ensuring high relaxivity. For instance, Anderson *et al.* targeted the $\alpha_v\beta_3$ receptor by using biotinylated Gd(DTPA)-perfluorocarbon nanoparticles coupled to biotinylated anti- $\alpha_v\beta_3$ monoclonal antibody via avidin.¹⁹⁸ The $\alpha_v\beta_3$ receptor is expressed on growing angiogenic vessels, therefore its visualization by MRI would help to directly indicate tumor growth. The avidin-biotin coupling approach used here is quite general and has often been proposed for delivering diagnostic agents to the targeted site.¹⁹⁹

One important drawback of using antibodies to deliver the paramagnetic center is the slow accumulation of these high molecular weight species on the target site, which may take as long as weeks. Therefore, suitable low molecular weight species capable of finding the target site are continually sought. Among the numerous imaginable approaches, one interesting route was recently proposed by Lemieux *et al.*²⁰⁰ It exploits the fact that tumor cell surfaces exhibit abnormal glycosylation. As a consequence, the overexpression of sialic acid has been correlated with the malignant and metastatic form of certain types of cancer. Their approach is based on the unnatural substrate tolerance of the enzymes in the sialoside biosynthetic pathway, which allows the metabolic conversion of peracetylated *N*-levulinoylmannosamine. Not normally resident on cell surfaces, the ketone group introduced in this way provides a unique chemical target for aminoxy- or hydrazide-functionalized paramagnetic contrast agent (Gd(DTPA)) probes (Scheme 20). As the ketone expression on the treated cells reflects the sialic acid level, the contrast agent will be delivered to the cancerous cell surfaces. By using Eu(DTPA) instead of the Gd analog, they managed to quantify by fluorescence the contrast agent loading on the tumor cells. This corresponded to around 10–20 μ M concentration, which could allow MRI enhancement of the targeted cancerous cells.

Wiener and co-workers used folic acid-conjugated Gd(DTPA)-PAMAM dendrimers for visualizing the high-affinity folate receptor, overexpressed in many tumors.²⁰¹ The contrast agent accumulated in the cells, resulting in a remarkable contrast enhancement on T_1 -weighted images.

Cell labeling, and more particularly accumulation of the paramagnetic probe on the target site, can be achieved by taking advantage of internalization of the probe within the cell via cell uptake processes. In addition to several examples of tumor cell targeting, this approach may open the way towards the visualization of gene expression and gene delivery.²⁰²

In order to avoid difficulties associated with receptor targeting, Aime *et al.* proposed another route for seeking accumulation at tumor cells.²⁰³ Their idea is based on the observation that positively charged polyamino acids selectively bind to tumors having a larger net negative charge on the cell surface than normal cells. They prepared Gd^{III} chelates containing on their external surface pendant phosphonate and carboxylate groups, which promote electrostatic interaction with the positively charged groups of polyornithine and polyarginine. The interaction, which depends on the acidity of the solution, is maximal at neutral pH. Due to the slow rotation of the macromolecular adduct, it also results in a remarkable relaxivity increase. This noncovalent approach appears to have several



Scheme 20

advantages over paramagnetic probes covalently conjugated to targeting molecules. It allows an easy route for delivery and accumulation of the contrast agent through the separate administration of the polyamino acid first and then the Gd^{III} chelate (pre-targeting approach). Once the polyamino acid is accumulated on the tumor cell surface and the excess is excreted rapidly (which decreases toxicity), the paramagnetic chelate can be administered whose high affinity for the polyamino acid will allow its specific recognition. This method also overcomes the problems associated with the limited accessibility of the targeting sites to large conjugates.

9.19.8 REFERENCES

1. Tóth, É.; Merbach, A. E., Eds. *The Chemistry of Contrast Agents in Medical Magnetic Resonance Imaging*; Wiley: Chichester, UK, 2001.
2. Caravan, P.; Ellison, J. J.; McMurry, T. J.; Lauffer, R. B. *Chem. Rev.* **1999**, *99*, 2293–2352.
3. *Contrast Agents I. Magnetic Resonance Imaging*; Krause, W., Ed.; Topics in Current Chemistry; Springer-Verlag: Berlin, 2002; Vol. 221.
4. Tweedle, M. F. *J. Am. Chem. Soc.* **2002**, *124*, 884–885.
5. Gallez, B.; Bacic, G.; Swartz, H. M. *Magn. Reson. Med.* **1996**, *35*, 14–19.

6. Muller, R. N.; Roch, A.; Colet, J.-M.; Ouakssim, A.; Gillis, P. Particulate Magnetic Contrast Agents. In *The Chemistry of Contrast Agents in Medical Magnetic Resonance Imaging*; Tóth, E., Merbach, A. E., Eds.; Wiley: Chichester, UK, 2001. pp 417–435.
7. Bloembergen, N.; Purcell, E. M.; Pound, R. V. *Phys. Rev.* **1948**, *73*, 678–712.
8. Solomon, I. *Phys. Rev.* **1955**, *99*, 559–565.
9. Solomon, I.; Bloembergen, N. *J. Chem. Phys.* **1956**, *25*, 261–266.
10. Bloembergen, N. *J. Chem. Phys.* **1957**, *27*, 572–573.
11. Bloembergen, N.; Morgan, L. O. *J. Chem. Phys.* **1961**, *34*, 842–850.
12. Connick, R. E.; Fiat, D. *J. Chem. Phys.* **1966**, *44*, 4103–4107.
13. Luz, Z.; Meiboom, S. *J. Chem. Phys.* **1964**, *40*, 2686–2692.
14. McLachlan, A. D. *Proc. R. Soc. London* **1964**, *A280*, 271–288.
15. Kowalewski, J.; Nordenskiöld, L.; Benetis, N.; Westlund, P.-O. *Progr. NMR Spectrosc.* **1985**, *17*, 141–185.
16. Kowalewski, J. In Grant, D. M., Harris, R. K., Eds; *Encyclopedia of NMR*; Wiley, Chichester, UK, 1996; pp 3456–3462.
17. Horrocks, W.D., Jr.; Sudnick, D. R. *J. Am. Chem. Soc.* **1979**, *101*, 334–340.
18. Parker, D.; Williams, J. A. G. *J. Chem. Soc. Dalton Trans.* **1996**, 3613–3628.
19. Alpoim, M. C.; Urbano, A. M.; Geraldès, C. F. G. C.; Peters, J. A. *J. Chem. Soc. Dalton Trans.* **1992**, 463–467.
20. Bénazeth, S.; Purans, J.; Chalbot, M. C.; Mguyen-van-Duong, M. K.; Nicolas, L.; Keller, F.; Gaudemer, A. *Inorg. Chem.* **1998**, *37*, 3667–3674.
21. Aime, S.; Barge, A.; Botta, M.; Parker, D.; De Sousa, A. S. *J. Am. Chem. Soc.* **1997**, *119*, 4767–4768.
22. Aime, S.; Botta, M.; Fasano, M.; Paoletti, S.; Terreno, E. *Chem. Eur. J.* **1997**, *3*, 1499–1504.
23. Lincoln, S. F.; Merbach, A. E. *Adv. Inorg. Chem.* **1995**, *42*, 1–87.
24. Tóth, E.; Helm, L.; Merbach, A. E. Relaxivity of Gadolinium(III) Complexes: Theory and Mechanism. In *The Chemistry of Contrast Agents in Medical Magnetic Resonance Imaging*; Tóth, E., Merbach, A. E., Eds.; Wiley: Chichester, UK, 2001. pp 45–119.
25. Peters, J. A. *Inorg. Chem.* **1988**, *27*, 4686–4691.
26. Rizkalla, E. M.; Choppin, G. R.; Cacheris, W. *Inorg. Chem.* **1993**, *32*, 582–586.
27. Geraldès, C. F. G. C.; Sherry, A. D.; Cacheris, W. P.; Kuan, K.-T.; Brown, R. D. III.; Koenig, S. H.; Spiller, M. *Magn. Res. Med.* **1988**, *8*, 191–199.
28. Gonzalez, G.; Powell, D. H.; Tissières, V.; Merbach, A. E. *J. Phys. Chem.* **1994**, *98*, 53–59.
29. Lammers, H.; Maton, F.; Pubanz, D.; Van Laren, M. W.; Van Bekkum, H.; Merbach, A. E.; Muller, R. N.; Peters, J. A. *Inorg. Chem.* **1997**, *36*, 2527–2538.
30. Tóth, É.; Connac, F.; Helm, L.; Adzamlı, K.; Merbach, A. E. *Eur. J. Inorg. Chem.* **1998**, 2017–2021.
31. Tóth, É.; Burai, L.; Brücher, E.; Merbach, A. E. *J. Chem. Soc. Dalton Trans.* **1997**, 1587–1594.
32. Powell, H. D.; Ni Dhubhghaill, O. M.; Pubanz, D.; Helm, L.; Lebedev, Y.; Schlaepfer, W.; Merbach, A. E. *J. Am. Chem. Soc.* **1996**, *118*, 9333–9346.
33. Tóth, É.; Vauthey, S.; Pubanz, D.; Merbach, A. E. *Inorg. Chem.* **1996**, *35*, 3375–3379.
34. Tóth, É.; Pubanz, D.; Vauthey, S.; Helm, L.; Merbach, A. E. *Chem. Eur. J.* **1996**, *2*, 209–217.
35. André, J. P.; Maecke, H. R.; Tóth, É.; Merbach, A. E. *J. Biol. Inorg. Chem.* **1999**, *4*, 341–347.
36. Szilágyi, E.; Tóth, É.; Brücher, E.; Merbach, A. E. *J. Chem. Soc. Dalton Trans.* **1999**, 2481–2486.
37. Cheng, T.-H.; Wang, Y.-M.; Lin, K.-T.; Liu, G.-C. *J. Chem. Soc. Dalton Trans.* **2001**, 3357–3366.
38. Aime, S.; Crich, S. G.; Gianolio, E.; Terreno, E.; Beltrami, A.; Uggeri, F. *Eur. J. Inorg. Chem.* **1998**, 1283–1289.
39. Tóth, É.; Connac, F.; Helm, L.; Adzamlı, K.; Merbach, A. E. *J. Biol. Inorg. Chem.* **1998**, *3*, 606–613.
40. Aime, S.; Barge, A.; Borel, A.; Botta, M.; Chemerisov, S.; Merbach, A. E.; Muller, R. N.; Pubanz, D. *Inorg. Chem.* **1997**, *36*, 5104–5112.
41. Ruloff, R.; Muller, R. N.; Pubanz, D.; Merbach, A. E. *Inorg. Chim. Acta.* **1998**, 275–276, 15–23.
42. Aime, S.; Botta, M.; Crich, S. G.; Giovenzana, G.; Pagliarin, R.; Piccinini, M.; Sisti, M.; Terreno, E. *J. Biol. Inorg. Chem.* **1997**, *2*, 470–479.
43. Aime, S.; Botta, M.; Crich, S. G.; Giovenzana, G.; Pagliarin, R.; Sisti, M.; Terreno, E. *Magn. Res. Chem.* **1998**, *36*, S200–S208.
44. Micskei, K.; Powell, D. H.; Helm, L.; Brücher, E.; Merbach, A. E. *Magn. Res. Chem.* **1993**, *31*, 1011–1020.
45. Tóth, É.; Helm, L.; Merbach, A. E.; Hedinger, R.; Hegetschweiler, K.; Jánosy, A. *Inorg. Chem.* **1998**, *37*, 4104–4113.
46. Aime, S.; Barge, A.; Bruce, J. I.; Botta, M.; Howard, J. A. K.; Moloney, J. M.; Parker, D.; De Sousa, A. S.; Woods, M. J. *Am. Chem. Soc.* **1999**, *121*, 5762–5771.
47. Dunand, A. F.; Aime, S.; Merbach, A. E. *J. Am. Chem. Soc.* **2000**, *122*, 1506–1512.
48. Woods, M.; Aime, S.; Botta, M.; Howard, J. A. K.; Moloney, J. M.; Navet, M.; Parker, D.; Port, M.; Rousseaux, O. *J. Am. Chem. Soc.* **2000**, *122*, 9781–9792.
49. Zhang, S.; Kovács, Z.; Burgess, S.; Aime, S.; Terreno, E.; Sherry, A. D. *Chem. Eur. J.* **2001**, *7*, 288–296.
50. Dunand, A. F.; Dickins, R. S.; Parker, D.; Merbach, A. E. *Chem. Eur. J.* **2001**, *7*, 5160–5167.
51. Nicolle, G. M.; Tóth, É.; Schmitt-Willich, H.; Radüchel, B.; Merbach, A. E. *Chem. Eur. J.* **2002**, *15*, 1040–1048.
52. Tóth, É.; van Uffelen, I.; Helm, L.; Merbach, A. E.; Ladd, D.; Briley-Saebo, K.; Kellar, K. E. *Magn. Res. Chem.* **1998**, *36*, S125–S134.
53. Tóth, É.; Helm, L.; Kellar, K. E.; Merbach, A. E. *Chem. Eur. J.* **1999**, *5*, 1202–1211.
54. Dunand, F. A.; Tóth, É.; Hollister, R.; Merbach, A. E. *J. Biol. Inorg. Chem.* **2001**, *6*, 247–245.
55. André, J. P.; Tóth, É.; Fischer, H.; Seelig, A.; Maecke, H. R.; Merbach, A. E. *Chem. Eur. J.* **1999**, *5*, 2977–2983.
56. Nicolle, G. M.; Tóth, É.; Eisenwiener, K.-P.; Maecke, H.; Merbach, A. E. *J. Biol. Inorg. Chem.* **2002**, 757–769.
57. Muller, R. N.; Radüchel, B.; Laurent, S.; Platzek, J.; Pierart, C.; Mareski, P.; Vander Elst, L. *Eur. J. Inorg. Chem.* **1999**, 1949–1955.
58. Aime, S.; Chiaussa, M.; Digilio, G.; Gianolio, E.; Terreno, E. *J. Biol. Inorg. Chem.* **1999**, *4*, 766–774.
59. Aime, S.; Barge, A.; Botta, M.; Howard, J. A. K.; Katakı, R.; Lowe, M. P.; Moloney, J. M.; Parker, D.; de Sousa, A. S. *Chem. Commun.* **1999**, 1047–1048.
60. Aime, S.; Botta, M.; Fasano, M.; Terreno, E. *Accounts of Chem. Res.* **1999**, *32*, 941–949.
61. Dunand, F. A.; Borel, A.; Merbach, A. E. *J. Am. Chem. Soc.* **2002**, *124*, 710–716.

62. Yerly, F.; Hardcastle, K. I.; Helm, L.; Aime, S.; Botta, M.; Merbach, A. E. *Chem. Eur. J.* **2002**, *8*, 1031–1039.
63. Vander Elst, L.; Maton, F.; Laurent, S.; Seghi, F.; Chapelle, F.; Muller, R. N. *Magn. Reson. Med.* **1997**, *38*, 604–614.
64. Aime, S.; Nano, R. *Invest. Radiol.* **1988**, *23*, S264–S266.
65. Vander Elst, L.; Laurent, S.; Muller, R. N. *Invest. Radiol.* **1998**, *33*, 828–834.
66. Chen, J. W.; Auteri, F. P.; Budil, D. E.; Belford, R. L.; Clarkson, R. B. *J. Phys. Chem.* **1994**, *98*, 13452–13459.
67. Chen, J. W.; Clarkson, R. B.; Belford, R. L. *J. Phys. Chem.* **1996**, *100*, 8093–810.
68. Wiener, E. C.; Auteri, F. P.; Chen, J. W.; Brechbiel, M. W.; Gansow, O. A.; Schneider, D. S.; Clarkson, R. B.; Lauterbur, P. C. *J. Am. Chem. Soc.* **1996**, *118*, 7774–7782.
69. Chen, J. W.; Belford, R. L.; Clarkson, R. B. *J. Phys. Chem. A.* **1998**, *102*, 2117–2130.
70. Vexler, V. S.; Clement, O.; Schmitt-Willich, H.; Brasch, R. C. *J. Magn. Res. Imaging* **1994**, *4*, 381–388.
71. Desser, T. S.; Rubin, D. L.; Muller, H. H.; Qing, F.; Khodor, S.; Zanazzi, G.; Young, S. U.; Ladd, D. L.; Wellons, J. A.; Kellar, K. E.; Toner, J. L.; Snow, R. A. *J. Magn. Res. Imaging* **1994**, *4*, 467–472.
72. Lipari, G.; Szabo, A. *J. Am. Chem. Soc.* **1982**, *104*, 4546–4559.
73. Lipari, G.; Szabo, A. *J. Am. Chem. Soc.* **1982**, *104*, 4559–4570.
74. Atsarkin, V. A.; Demidov, V. V.; Vasneva, G. A.; Odintsov, B. M.; Belford, R. L.; Radüchel, B.; Clarkson, R. B. *J. Phys. Chem.* **2001**, *105*, 9323–9327.
75. Hudson, A.; Lewis, L. W. E. *Trans. Faraday Soc.* **1970**, *66*, 1297–1301.
76. Powell, D. H.; Merbach, A. E.; González, G.; Brücher, E.; Micskei, K.; Ottaviani, M. F.; Köhler, K.; von Zelewsky, A.; Grinberg, O. Y.; Lebedev, Y. S. *Helv. Chim. Acta* **1993**, *76*, 1–18.
77. Strandberg, E.; Westlund, P.-O. *J. Magn. Res.* **1996**, *122*, 179–191.
78. Borel, A.; Tóth, É.; Helm, L.; Jánossy, A.; Merbach, A. E. *Phys. Chem. Chem. Phys.* **2000**, *2*, 1311–1317.
79. Clarkson, R. B.; Smirnov, A. I.; Smirnova, T. I.; Kang, H.; Belford, R. L.; Earle, K.; Freed, J. H. *Mol. Phys.* **1998**, *96*, 1325–1332.
80. Rast, S.; Fries, H. P.; Belorizky, E. *J. Chem. Phys.* **2000**, *113*, 8724–8735.
81. Rast, S.; Borel, A.; Helm, L.; Belorizky, E.; Fries, H. P.; Merbach, A. E. *J. Am. Chem. Soc.* **2001**, *123*, 2637–2644.
82. Rast, S.; Fries, H. P.; Belorizky, E.; Borel, A.; Helm, L.; Merbach, A. E. *J. Chem. Phys.* **2001**, *115*, 7554–7563.
83. Borel, A.; Yerly, F.; Helm, L.; Merbach, A. E. *J. Am. Chem. Soc.* **2002**, *124*, 2042–2048.
84. McConnell, J. *The Theory of Nuclear Magnetic Relaxation in Liquids* **1987**, Cambridge University Press: Cambridge.
85. Abragam, A. *The Principles of Nuclear Magnetism* **1961**, Oxford University: Oxford.
86. Fries, P. H.; Belorizky, E. *J. Phys. (Paris)* **1978**, *39*, 1263–1265.
87. Albrand, J. P.; Taieb, M. C.; Fries, P. H.; Belorizky, E. *J. Chem. Phys.* **1983**, *78*, 5809–5815.
88. Hwang, L.-P.; Freed, J. H. *J. Chem. Phys.* **1975**, *63*, 4017–4025.
89. Freed, J. H. *J. Chem. Phys.* **1978**, *68*, 4034–4037.
90. Polnaszek, C. F.; Bryant, R. G. *J. Chem. Phys.* **1984**, *81*, 4038–4045.
91. Aime, S.; Botta, M.; Crich, S. G.; Giovenzana, G.; Pagliarin, R.; Piccinini, M.; Sisti, M.; Terreno, E. *J. Biol. Inorg. Chem.* **1997**, *2*, 470–479.
92. Botta, M. *Eur. J. Inorg. Chem.* **2000**, 399–407.
93. Noack, F. *Prog. Nucl. Magn. Reson. Spectrosc.* **1986**, *18*, 171–276.
94. Koenig, S. H.; Brown, R. D. *Prog. Nucl. Magn. Reson. Spectrosc.* **1990**, *22*, 487–567.
95. Kimmich, R. *NMR Tomography, Diffusometry, Relaxometry* **1997**, Springer: Berlin.
96. Dawson, P. Gadolinium Chelates: Chemistry. In *Textbook of Contrast Media*; Dawson, P.; Cosgrove, D. O.; Grainger, R. G., Eds.; Isis Medical Media: Oxford, 1999; p 295.
97. Tweedle, M. F. Relaxation Agents in NMR Imaging. In *Lanthanide Probes in Life, Chemical and Earth Sciences: Theory and Practice*; Bünzli, J.-C. G., Choppin, G. R., Eds.; Amsterdam: Elsevier, 1989; p 127.
98. Weinmann, R. J.; Laniado, M.; Muetzel, W. *Physiol. Chem. Phys. Med. NMR* **1984**, *16*, 167–172.
99. Chang, C. A. *Eur. J. Solid State Inorg. Chem.* **1991**, *28*, 237–244.
100. Beck, M. T.; Nagypál, I. *Chemistry of Complex Equilibria* **1990**, Ellis Horwood: Chichester, UK.
101. Burai, L.; Fabian, I.; Kiraly, R.; Szilagy, E.; Brücher, E. *J. Chem. Soc. Dalton Trans.* **1998**, 243–248.
102. Clarke, E. T.; Martell, A. E. *Inorg. Chim. Acta* **1991**, *190*, 27–36.
103. Brücher, E.; Sherry, A. D. Stability and Toxicity of Contrast Agents. In *The Chemistry of Contrast Agents in Medical Magnetic Resonance Imaging*; Tóth, E., Merbach, A. E., Eds.; Wiley: Chichester, UK, 2001; pp. 243–279.
104. Cacheris, W. P.; Quay, S. C.; Rocklage, S. M. *Magnetic Resonance Imaging* **1990**, *8*, 467–481.
105. Ringbom, A., Ed.; *Complexation in Analytical Chemistry*. Interscience Publishers: New York, 1963.
106. May, P. M.; Linder, P. W.; Williams, D. R. *J. Chem. Soc. Dalton Trans.* **1977**, 588–595.
107. Sarka, L.; Burai, L.; Brücher, E. *Chem. Eur. J.* **2000**, *6*, 719–724.
108. Wedeking, P.; Kumar, K.; Tweedle, M. F. *Magnetic Resonance Imaging* **1992**, *10*, 641–648.
109. Tweedle, M. F.; Wedeking, P.; Kumar, K. *Invest. Radiol.* **1995**, *30*, 372–380.
110. Weinmann, R. J.; Laniado, M.; Muetzel, W. *Physiol. Chem. Phys. Med. NMR* **1984**, *16*, 167–172.
111. Magerstadt, M.; Gansow, O. A.; Brechbiel, M. W.; Colcher, D.; Baltzer, L.; Knop, R. H.; Girton, M. E.; Naegel, M. *Magn. Reson. Med.* **1986**, *3*, 808–812.
112. Wedeking, P.; Kumar, K.; Tweedle, M. F. *Magnetic Resonance Imaging* **1992**, *10*, 641–648.
113. Tweedle, M. F.; Hagan, J. J.; Kumar, K.; Mantha, S.; Chang, C. A. *Magnetic Resonance Imaging* **1991**, *9*, 409–445.
114. Broan, C. J.; Cox, J. P. L.; Craig, A. S.; Katakya, R.; Parker, D.; Ferguson, G.; Harrison, A.; Randall, A. M. *J. Chem. Soc. Perkin Trans.* **1991**, *2*, 87–99.
115. Lazar, I.; Sherry, A. D.; Ramasamy, R.; Brücher, E.; Kiraly, R. *Inorg. Chem.* **1991**, *30*, 5016–5019.
116. Harrison, A.; Royle, L.; Walker, C.; Pereira, C.; Parker, D.; Pulukkody, K.; Norman, T. J. *Magnetic Resonance Imaging* **1993**, *11*, 761–770.
117. Pulukkody, K. P.; Norman, T. J.; Parker, D.; Royle, L.; Broan, C. J. *J. Chem. Soc. Perkin Trans.* **1993**, 605–620.
118. Schwizer, W.; Fraser, R.; Maেকে, H.; Siebold, K.; Funk, R.; Fried, M. *Magn. Reson. Med.* **1994**, *31*, 388–393.
119. McMurry, T. J.; Pippin, C. G.; Wu, C.; Deal, K. A.; Brechbiel, M. W.; Mirzadek, S.; Gansow, O. A. *J. Med. Chem.* **1998**, *41*, 3546–3549.
120. Brücher, E. Kinetic Stabilities of Gadolinium(III) Chelates used as MRI Contrast Agents. In *Contrast Agents I. Magnetic Resonance Imaging*; Krause, W., Ed.; Topics in Current Chemistry; Springer: Berlin, 2002; Vol. 221, p 104.

121. Lauffer, R. B.; Brady, T. J. *J. Magnetic Resonance Imaging* **1985**, *3*, 11–16.
122. Schmiedl, U.; Ogan, M.; Paaanen, H.; Marotti, M.; Crooks, L. E.; Brito, A. C.; Brasch, R. C. *Radiology* **1987**, *162*, 205–210.
123. Sherry, A. D.; Cacheris, W. P.; Kuan, K. T. *Magn. Reson. Med.* **1988**, *8*, 180–190.
124. Sieving, P. F.; Watson, A. D.; Rocklage, S. M. *Bioconjugate Chem.* **1990**, *1*, 65–71.
125. Clarkson, R. B. Blood-Pool MRI Contrast Agents: Properties and Characterization. In *Contrast Agents I. Magnetic Resonance Imaging*; Krause, W., Ed.; Topics in Current Chemistry, Springer: Berlin, 2002; Vol. 221, p 202.
126. Schuhmann-Giampieri, G.; Schmitt-Willich, H.; Frenzel, T.; Press, W. R.; Weinmann, H. J. *Invest. Radiol.* **1991**, *26*, 969–974.
127. Aime, S.; Botta, M.; Crich, S. G.; Giovenzana, G.; Palmisano, G.; Sisti, M. *Bioconjugate Chem.* **1999**, *10*, 192–199.
128. Zeng, F.; Zimmerman, S. C. *Chem. Rev.* **1997**, *97*, 1681–1712.
129. Bryant, L. H., Jr.; Brechbiel, M. W.; Wu, C.; Bulte, J. W. M.; Herynek, V.; Frank, J. A. *J. Magnetic Resonance Imaging* **1999**, *9*, 348–352.
130. Margerum, L. D.; Campion, B. K.; Koo, M.; Shargill, N.; Lai, J.-J.; Marumoto, A.; Sontum, P. C. *J. Alloys Compds.* **1997**, *249*, 185–190.
131. Wiener, E. C.; Brechbiel, M. W.; Brothers, H.; Magin, R. L.; Gansow, O. A.; Tomalia, D. A.; Lauterbur, P. C. *Magn. Reson. Med.* **1994**, *31*, 1–8.
132. Tacke, J.; Adam, G.; Claben, H.; Muhler, A.; Prescher, A.; Gunther, R. W. *Magnetic Resonance Imaging* **1997**, *7*, 678–682.
133. Roberts, H. C.; Saeed, M.; Roberts, T. P. L.; Muhler, A.; Shames, D. M.; Mann, J. S.; Stiskal, M.; Demsar, F.; Brasch, R. C. *Magnetic Resonance Imaging* **1997**, *7*, 331–338.
134. Dong, Q.; Hurst, D. R.; Weinmann, H. J.; Chenevert, T. L.; Londy, F. J.; Prince, M. R. *Invest. Radiol.* **1998**, *33*, 699–708.
135. Schmitt-Willich, H.; Platzek, J.; Radüchel, B.; Ebert, W.; Franzel, T.; Misselwitz, B.; Weinmann, H.-J. *Abstracts of the 1st Dendrimer Symposium*, Deckence Frankfurt am Main, Germany, 3–5 Oct. 1999; p 25.
136. Corot, C.; Schaefer, M.; Beaute, S.; Bourrinet, P.; Zehaf, S.; Benize, V.; Sabatou, M.; Meyer, D. *Acta Radiologica, Suppl.* **1997**, *412*, 91–99.
137. Casali, C.; Janier, M.; Canet, E.; Obadia, J. F.; Benderbous, S.; Corot, C.; Revel, D. *Academic Radiology* **1998**, *5 Suppl. 1*, S214–S218.
138. Meyer, D.; Schaefer, M.; Bouillot, A.; Beaute, S.; Chambon, C. *Invest. Radiology* **1991**, *26*, S50–S52.
139. Rebizak, R.; Schaefer, M.; Dellacherie, E. *Eur. J. Pharm. Sci.* **1999**, *7*, 243–248.
140. Gløgård, C.; Hovland, R.; Fosshem, S. L.; Aasen, A. J.; Klaveness, J. *J. Chem. Soc. Perkin Trans. 2* **2000**, 1047–1052.
141. Unger, E. C.; Fritz, T.; Wu, G. *Liposome Res.* **1994**, *4*, 811–834.
142. Fosshem, S. L.; Colet, J. M.; Mansson, S.; Fahlvik, A. K.; Muller, R. N.; Klaveness, J. *Invest. Radiol.* **1998**, *33*, 810–821.
143. Fosshem, S. L.; Fahlvik, A. K.; Klaveness, J.; Muller, R. N. *Magnetic Resonance Imaging* **1999**, *17*, 83–99.
144. Weissig, V.; Babich, J.; Torchilin, V. *Colloids Surf. B.* **2000**, *18*, 293–299.
145. Woodle, M. C.; Newman, M. S.; Cohen, J. A. *J. Drug Targeting*, **1994**, *2*, 397–403.
146. Lauffer, R. B. *Magn. Reson. Med.* **1991**, *22*, 339–392.
147. Peters, T. J. *All About Albumin: Biochemistry, Genetics and Medical Applications* **1996**, Academic Press: San Diego, CA.
148. Aime, S.; Fasano, M.; Terreno, E.; Botta, M. Protein-bound Metal Chelates. In *The Chemistry of Contrast Agents in Medical Magnetic Resonance Imaging*; Tóth, E., Merbach, A. E., Eds.; Wiley, Chichester, UK, 2001; pp 193–241.
149. Aime, S.; Botta, M.; Panero, M.; Grandi, M.; Uggeri, F. *Magn. Reson. Chem.* **1991**, *29*, 923–927.
150. Aime, S.; Botta, M.; Parker, D.; Williams, J. A. G. *J. Chem. Soc. Dalton Trans.* **1995**, 2259–2266.
151. Aime, S.; Botta, M.; Ermondi, G.; Terreno, E.; Anelli, P. L.; Fedeli, F.; Uggeri, G. *Inorg. Chem.* **1996**, *35*, 2726–2736.
152. Aime, S.; Benetollo, F.; Bombieri, G.; Colla, S.; Fasano, M.; Paoletti, S. *Inorg. Chim. Acta* **1997**, *254*, 63–70.
153. Wright, J. D.; Boudinot, F. D.; Ujhelyi, M. R. *Clin. Pharmacokinetics*. **1996**, *30*, 445–462.
154. Dwek, R. A. *Nuclear Magnetic Resonance in Biochemistry: Application to Enzyme Systems*; Clarendon Press: Oxford, UK, 1973; p 174.
155. Larsen, S. K.; Jenkins, B. G.; Memon, N. G.; Lauffer, R. B. *Inorg. Chem.* **1990**, *29*, 1147–1152.
156. Aime, S.; Botta, M.; Fasano, M.; Crich, G. S.; Terreno, E. *J. Biol. Inorg. Chem.* **1996**, *1*, 312–318.
157. Lauffer, R. B.; Parmalee, D. J.; Dunham, S. U.; Ouellet, H. S.; Dolan, R. P.; Witte, S.; McMurry, T. J.; Walowitch, R. C. *Radiology* **1998**, *207*, 529–538.
158. Aime, S.; Gianolio, E.; Terreno, E.; Giovenzana, G. B.; Pagliarin, R.; Sisti, M.; Palmisano, G.; Botta, M.; Lowe, M. P.; Parker, D. *J. Biol. Inorg. Chem.* **2000**, *5*, 488–497.
159. Caravan, P.; Cloutier, N. J.; Greenfield, M. T.; McDermid, S. A.; Dunham, S. U.; Bulte, J. W. M.; Amedio, J. C., Jr.; Looby, R. J.; Supkowski, R. M.; DeW Horrocks, W. Jr.; McMurry, T. J.; Lauffer, R. B. *J. Am. Chem. Soc.* **2002**, *124*, 3152–3162.
160. Aime, S.; Batsanov, A. S.; Botta, M.; Howard, J. A. K.; Parker, D.; Senanayake, K.; Williams, G. *Inorg. Chem.* **1994**, *33*, 4696–4706.
161. Jacques, V.; Desreux, J. F. New Classes of MRI Contrast Agents. In *Contrast Agents I. Magnetic Resonance Imaging*; Krause, W., Ed.; Topics in Current Chemistry; Springer: Berlin, 2002; Vol. 221.
162. Tannock, I. F.; Rotin, D. *Cancer Res.* **1989**, *49*, 4373–4384.
163. Van Sluis, R.; Bhujwala, Z. M.; Raghunand, N.; Ballesteros, P.; Alvarez, J.; Cardan, S.; Galons, J.-P.; Gillies, R. J. *Magn. Reson. Med.* **1999**, *41*, 743–750.
164. Helsen, J. A.; Curtis, J. C.; Hearshen, D.; Smith, M. B.; Welch, K. M. A. *Magn. Reson. Med.* **1987**, *5*, 302–305.
165. Mikawa, M.; Miwa, N.; Brautigam, M.; Akaike, T.; Maruyama, A. *Chem. Lett.* **1998**, 693–694.
166. Mikawa, M.; Miwa, N.; Brautigam, M.; Akaike, T.; Maruyama, A. *J. Biomed. Mater. Res.* **2000**, *49*, 390–395.
167. Hall, J.; Haner, R.; Aime, S.; Botta, M.; Faulkner, S.; Parker, D.; de Sousa, A. S. *New J. Chem.* **1998**, 627–631.
168. Aime, S.; Botta, M.; Crich, S. G.; Giovenzana, G.; Palmisano, G.; Sisti, M. *Chem. Commun.* **1999**, 1577–1578.
169. Zhang, S.; Wu, K.; Sherry, A. D. *Angew. Chem. Int. Ed. Engl.* **1999**, *38*, 3192–3194.

170. Zhang, S.; Wu, K.; Sherry, A. D. *Invest. Radiol.* **2001**, *36*, 82–86.
171. Hovland, R.; Gløgård, C.; Aasen, A. J.; Klaveness, J. *J. Chem. Soc., Perkin Trans. 2*, **2001**, 929–933.
172. Løtting, K.-E.; Fossheim, S.; Skurtveit, R.; Bjørnerud, A.; Klaveness, J. *Magnetic Resonance Imaging* **2001**, *19*, 731–738.
173. Litzinger, D. C.; Huang, L. *Biochim. Biophys. Acta* **1992**, *11–13*, 201–227.
174. Fossheim, S. L.; Il'yasov, K. A.; Hennig, J.; Bjørnerud, A. *Acad. Radiol.* **2000**, *7*, 1107–1115.
175. Roth, K.; Bartholomae, G.; Bauer, H.; Frenzel, T.; Kossler, S.; Platzek, J.; Radüchel, B.; Weinmann, H.-J. *Angew. Chem. Int. Ed. Engl.* **1996**, *35*, 655–657.
176. Aime, S.; Botta, M.; Fasano, M.; Terreno, E.; Kinchesh, P.; Calabi, L.; Paleari, L. *Magn. Reson. Med.* **1996**, *35*, 648–651.
177. Rohovec, J.; Lukeš, I.; Hermann, P. *New J. Chem.* **1999**, *23*, 1129–1132.
178. Aime, S.; Botta, M.; Gianolio, E.; Terreno, E. *Angew. Chem. Int. Ed.* **2000**, *39*, 747–750.
179. Caravan, P.; Tóth, E.; Rockenbauer, A.; Merbach, A. E. *J. Am. Chem. Soc.* **1999**, *121*, 10403–10409.
180. Seibig, S.; Tóth, E.; Merbach, A. E. *J. Am. Chem. Soc.* **2000**, *122*, 5822–5830.
181. Burai, L.; Tóth, E.; Seibig, S.; Scopelliti, R.; Merbach, A. E. *Chem. Eur. J.* **2000**, *6*, 3761–3769.
182. Tóth, E.; Burai, L.; Merbach, A. E. *Coord. Chem. Rev.* **2001**, *216–217*, 363–382.
183. Moats, R. A.; Fraser, S. E.; Meade, T. J. *Angew. Chem. Int. Ed. Engl.* **1997**, *36*, 726–728.
184. Louie, A. Y.; Hüber, M. M.; Ahresn, E. T.; Rothbächer, U.; Moats, R.; Jacobs, R. E.; Fraser, S. E.; Meade, T. J. *Nature Biotechnol.* **2000**, *18*, 321–325.
185. Anelli, P. L.; Bertini, I.; Fragai, M.; Lattuada, L.; Luchinat, C.; Parigi, G. *Eur. J. Inorg. Chem.* **2000**, 625–630.
186. Nivorozhkin, A. L.; Kolodziej, A. F.; Caravan, P.; Greenfield, M. T.; Lauffer, R. B.; McMurry, T. J. *Angew. Chem. Int. Ed. Engl.* **2001**, *40*, 2903–2906.
187. Lauffer, R. B.; McMurry, T. J.; Dunham, S. O.; Scott, D. M.; Parmelee, D. J.; Dumas, S. WO Patent 9,736,619, 1997.
188. Bogdanov, A.; Matuszewski, L.; Bremer, C.; Petrovsky, A.; Weissleder, R. *Molecular Imaging* **2002**, *1*, 16–23.
189. Li, W.; Fraser, S. E.; Meade, T. J. *J. Am. Chem. Soc.* **1999**, *121*, 1413–1414.
190. Comblin, V.; Gilsoul, D.; Hermann, M.; Humblet, V.; Jacques, V.; Mesbahi, M.; Sauvage, C.; Desreux, J. F. *Coord. Chem. Rev.* **1999**, *185–186*, 451–470.
191. Ward, K. M.; Aletras, A. H.; Balaban, R. S. *J. Magn. Res.* **2000**, *143*, 79–87.
192. Aime, S.; Barge, A.; Castelli, D. D.; Fedeli, F.; Mortillaro, A.; Nielsen, F. U. Terreno, E. *Magn. Reson. Med.* **2002**, *47*, 639–648.
193. Zhang, S.; Winter, P.; Wu, K.; Sherry, A. D. *J. Am. Chem. Soc.* **2001**, *123*, 1517–1518.
194. Nunn, A. D.; Linder, K. E.; Tweedle, M. F. *Q. J. Nucl. Med.* **1997**, *41*, 155–162.
195. Okuhata, Y. *Adv. Drug Delivery Rev.* **1999**, *37*, 121–137.
196. Tilcock, C. *Adv. Drug Delivery Rev.* **1999**, *37*, 33–51.
197. Curtet, C.; Maton, F.; Havet, T.; Slinkin, M.; Mishra, A.; Chatal, J. F.; Muller, R. N. *Invest. Radiol.* **1998**, *33*, 752–761.
198. Anderson, S. A.; Rader, R. K.; Westlin, W. F.; Null, C.; Jackson, D.; Lanza, G. M.; Wickline, S. A.; Kotyk, J. J. *Magn. Reson. Med.* **2000**, *44*, 433–439.
199. Sakahara, H.; Saga, T. *Adv. Drug Delivery Rev.* **1999**, *37*, 89–101.
200. Lemieux, G. A.; Yarema, K. J.; Jacobs, C. L.; Bertozzi, C. R. *J. Am. Chem. Soc.* **1999**, *121*, 4278–4279.
201. Konda, S. D.; Aref, M.; Brechbiel, M.; Wiener, E. C. *Invest. Radiol.* **2000**, *35*, 50–57.
202. Kayyem, J. F.; Kumar, R. M.; Fraser, S. E.; Meade, T. J. *Chem. Biol.* **1995**, *2*, 615–620.
203. Aime, A.; Botta, M.; Garino, E.; Crich, S. G.; Giovenzana, G.; Pagliarini, R.; Palmisano, G.; Sisti, M. *Chem. Eur. J.* **2000**, *6*, 2609–2617.
204. Tóth, E.; Ni Dhubhghaill, O. M.; Besson, G.; Helm, L.; Merbach, A. E. *Magn. Res. Chem.* **1999**, *37*, 701–708.
205. Micskei, K.; Helm, L.; Brücher, E.; Merbach, A. E. *Inorg. Chem.* **1993**, *32*, 3844–3850.
206. Uggeri, F.; Aime, S.; Anelli, P. L.; Botta, M.; Brochetta, M.; de Haen, C.; Ermondi, G.; Grandi, M.; Paoli, P. *Inorg. Chem.* **1995**, *34*, 633–642.
207. Martell, A. E.; Smith, R. M.; Motekaitis, R. J. *NIST Critical Stability Constants of Metal Complexes 1993*, NIST Standard Reference Data: Gaithersburg, MD.
208. Schmitt-Willich, H.; Brehm, M.; Ewers, C. L. J.; Michl, G.; Müller-Fahrnow, A.; Petrov, O.; Platzek, J.; Radüchel, B.; Sülzle, D. *Inorg. Chem.* **1999**, *38*, 1134–1144.
209. Cacheris, W. P.; Nickle, S. K.; Sherry, A. D. *Inorg. Chem.* **1987**, *26*, 958–960.
210. Powell, K. J. *IUPAC Stability Constants*. Academic Software, Yorkshire, UK, **1999**.

9.20

Radioactive Metals in Imaging and Therapy

S. Z. LEVER, J. D. LYDON, C. S. CUTLER, and S. S. JURISSON
University of Missouri, Columbia, MO, USA

9.20.1	INTRODUCTION	883
9.20.1.1	Diagnostic Imaging	884
9.20.1.2	Radiotherapy	885
9.20.1.3	Nuclear and Physical Properties Needed for Imaging and Therapy	886
9.20.2	RADIONUCLIDE PRODUCTION	887
9.20.2.1	Cyclotron- or Accelerator-produced Radionuclides	887
9.20.2.1.1	<i>Gallium</i>	887
9.20.2.1.2	<i>Copper</i>	887
9.20.2.1.3	<i>Tin</i>	888
9.20.2.1.4	<i>Rubidium</i>	888
9.20.2.1.5	<i>Thallium</i>	888
9.20.2.2	Reactor-produced Radionuclides	888
9.20.2.2.1	<i>Strontium</i>	888
9.20.2.2.2	<i>Yttrium</i>	888
9.20.2.2.3	<i>Radiolanthanides</i>	888
9.20.2.2.4	<i>Rhodium</i>	889
9.20.2.2.5	<i>Gold</i>	890
9.20.2.2.6	<i>Scandium</i>	890
9.20.2.2.7	<i>Actinium</i>	890
9.20.2.2.8	<i>Lead and Bismuth</i>	890
9.20.3	PHARMACEUTICAL APPLICATIONS OF RADIONUCLIDES	891
9.20.3.1.1	<i>Gallium, Indium, and Yttrium</i>	891
9.20.3.1.2	<i>Copper</i>	894
9.20.3.1.3	<i>Radiolanthanides</i>	897
9.20.3.1.4	<i>Rhodium</i>	902
9.20.3.1.5	<i>Gold</i>	902
9.20.3.1.6	<i>Scandium</i>	903
9.20.3.1.7	<i>Tin</i>	903
9.20.3.1.8	<i>Thallium</i>	903
9.20.3.1.9	<i>Rubidium</i>	904
9.20.3.1.10	<i>Strontium</i>	904
9.20.3.1.11	<i>Actinium</i>	904
9.20.3.1.12	<i>Bismuth and Lead</i>	905
9.20.4	SUMMARY	906
9.20.5	REFERENCES	906

9.20.1 INTRODUCTION

Metals continue to play an important role in radiopharmaceuticals for diagnostic and therapeutic applications in nuclear medicine. Radiopharmaceuticals are drugs that contain a radionuclide and are used for imaging if the radionuclide is a photon emitter (gamma (γ) or positron (β^+)) or for

therapy if the radionuclide is a particle emitter (alpha (α), beta (β^-) or Auger/conversion e^-). The number of radiometals with nuclear properties suitable for nuclear medicine applications is quite large, making radiometals important both to existing radiopharmaceuticals and to those under investigation (Table 1). The most widely used radiometal in diagnostic imaging is ^{99m}Tc , with its virtually ideal nuclear properties (6 h half-life, 140 keV γ emission) and convenient availability from a molybdenum-based ($^{99}\text{Mo}/^{99m}\text{Tc}$) generator. ^{99m}Tc has been used routinely in nuclear medicine for imaging since the early 1970s. Although technetium-based radiopharmaceuticals will not be covered in this chapter (see instead Chapter 5.2), they deserve mention for their role in driving nuclear medicine imaging and in the realization of the importance of metals for radiopharmaceuticals. Several reviews on the chemistry and radiopharmaceutical applications of ^{99m}Tc have been published since 1990.^{6–13}

9.20.1.1 Diagnostic Imaging

Diagnostic imaging requires that a radiopharmaceutical localize at a particular site after systemic administration and emit penetrating radiation that can be detected outside of the body, i.e., either gamma or positron emission. Gamma-ray emission is the basis of single photon emission computed tomography (SPECT), which is used routinely in nuclear medicine for imaging radiopharmaceuticals based on ^{99m}Tc , ^{111}In , or $^{123}\text{I}/^{131}\text{I}$. Positron emission results in the production of two 511 keV annihilation photons that are emitted at an angle of 180° (with respect to each

Table 1 Radionuclide properties.^{1–5}

Radionuclide	Maximum particle emission (%)	Gamma emission (%)	Half-life
^{47}Sc	0.600 MeV β^-	159.4 keV (68%)	3.345 days
^{60}Cu	3.92 MeV β^+ (93%) EC Decay (7%)	1332 keV (88%) 1792 keV (45.4%) 826 keV (21.7%)	23.7 min
^{61}Cu	1.215 MeV β^+ (62%) EC Decay (38%)	511 keV (184.8%) 656 keV (10.1%) 511 keV (122.9%) 283 keV (12.8%)	3.35 h
^{62}Cu	2.926 MeV β^+ (97.8%) EC Decay (2.2%)	511 keV (196%)	9.74 min
^{64}Cu	0.653 MeV β^+ (19%) EC Decay (41%)	511 keV (38.6%)	12.7 h
^{67}Cu	0.579 MeV β^- (40%) 0.577 MeV β^-	184.6 keV (46.7%) 93.3 keV (16.6%) 91.3 keV (7.3%)	2.58 days
^{66}Ga	4.153 MeV β^+ (57%) EC Decay (43%)	2752 keV (23.5%) 1039 keV (38.4%) 834 keV (6.1%)	9.49 h
^{67}Ga	EC Decay	511 keV (117.3%) 393.5 keV (4.2%) 300 keV (15.3%) 184.6 keV (20.8%) 93 keV (38.6%)	3.2612 days
^{68}Ga	1.899 MeV β^+ (90%) EC Decay (10%)	1077 keV (3.3%) 511 keV (176%)	67.63 min
^{82}Rb	3.35 MeV β^+ (96%) EC Decay (4%)	777 keV (13.8%) 511 keV (190%)	1.273 min
^{89}Sr	1.488 MeV β^-	909 keV (0.095%)	50.53 days
^{86}Y	3.15 MeV β^+ (34%) EC Decay (66%)	1921 keV (20.8%) 1854 keV (17.2%) 1153 keV (30.54%) 1077 keV (82.5%) 777 keV (22.45%) 703 keV (15.4%)	14.74 h

Table 1 continued

Radionuclide	Maximum particle emission (%)	Gamma emission (%)	Half-life
⁸⁷ Y	EC Decay	485 keV (92.2%)	3.346 days
⁹⁰ Y	2.28 MeV β^-	none	64.1 h
^{99m} Tc	IT	140 keV (89.3%)	6.01 h
¹⁰⁵ Rh	0.566 MeV β^-	319 keV (19.6%)	35.36 h
¹⁰⁹ Pd	1.028 MeV β^-	88 keV (3.7%)	13.427 h
¹¹¹ Ag	1.0368 MeV β^-	342 keV (6%)	7.45 days
¹¹¹ In	EC Decay	245 keV (94%) 171 keV (91%)	2.83 days
^{114m} In	IT	190 keV (17.7%)	49.5 days
^{115m} In	IT (95%) 150.83 MeV β^- (5%)	336 keV (46.1%)	4.486 h
^{117m} Sn	IT	156 keV (2.1%) 158.6 keV (86.3%)	13.6 days
¹⁴⁹ Pm	1.072 MeV β^- (95.9%)	286 keV (3.1%)	53.08 h
¹⁵³ Sm	0.808 MeV β^-	103 keV (28.3%)	46.27 h
¹⁶⁶ Dy	0.4035 MeV β^-	82.5 keV (13%)	81.6 h
¹⁶⁶ Ho	1.8545 MeV β^-	80.6 keV (6.2%)	26.83 h
¹⁷⁷ Lu	0.498 MeV β^-	208 keV (11%) 113 keV (6.6%)	6.64 days
¹⁸⁸ Re	2.12 MeV β^-	155 keV (15%)	16.98 h
¹⁹⁸ Au	0.96 MeV β^-	412 keV (95.6%)	2.694 days
¹⁹⁹ Au	0.4526 MeV β^-	208 keV (9.1%) 158 keV (40%)	3.139 days
²⁰¹ Tl	EC decay	80 keV (16.9%) 135 keV (3.7%)	73.1 h
²¹² Pb	0.5737 MeV β^-	238.6 keV (43.1%)	10.64 h
²¹² Bi	2.25 MeV β^- (55.5%) 8.784 MeV α (Po-212)	727 keV (11.8%)	60.55 min
²¹³ Bi	1.426 MeV β^- (97.9%) 5.87 MeV α (2.1%) 8.375 MeV α (Po-213)	440 keV (27.3%)	45.6 min
²²⁵ Ac	5.83 MeV α 6.34 MeV α (Fr-221) 7.067 MeV α (At-217) 1.426 MeV β^- (Bi-213)	99 keV (5.8%)	10 days

other), and forms the basis of positron emission tomography (PET). The most widely used PET radiopharmaceutical is F-18 fluorodeoxyglucose (FDG) for imaging glucose metabolism. Radio-metal positron emitters under investigation include ⁶²Cu, ⁶⁴Cu, and ⁶⁸Ga.

9.20.1.2 Radiotherapy

Radiotherapy, in general, targets cancer cells (tumors) for cell destruction. Radiotherapy requires that the particle emission from the radionuclide have a decay energy that is deposited over a short range in tissue. Alpha, beta, and Auger/conversion electron emitters are currently under investigation. Alpha particles are helium nuclei emitted by the radionuclide on decay. The relatively high mass of the α particle makes its range quite short (several cell diameters) and its ionization very intense. Examples of radiometal α emitters are ²¹²Bi, ²¹³Bi, and ²²⁵Ac. Beta emitters have received the most attention for use in therapeutic applications. Beta particles are negatively charged electrons emitted by the nucleus on decay (splitting of a neutron). Beta particles can approach the speed of light on emission, and thus their range in tissue is greater than that observed for α particles, with the actual range dependent on the β^- particle energy. Energy deposition by the β^- particle is most intense at the end of its path. Intense radiometal β^- particle emitters under investigation for potential radiotherapy include ⁹⁰Y, ¹⁶⁶Ho, ¹⁷⁷Lu, ¹⁸⁶Re, and ¹⁸⁸Re. Auger electrons have a very short range in tissue, and thus the Auger electron emitters must localize in the cell nucleus to be effective in damaging the DNA, making them very difficult to incorporate into a viable radiopharmaceutical. The critical issue when using particle emitters in radiotherapy

is the selective and specific delivery of the radiolabeled molecule to the target cancer cells, while sparing normal tissue from the effects of the radiation. Because of the potential damage to normal tissues by the particle emitters, this issue is much more critical for therapeutic radiopharmaceuticals than for diagnostic radiopharmaceuticals. Much effort has been and continues to be spent on the development of site-specific molecules for delivering the radiopharmaceutical to its target.

9.20.1.3 Nuclear and Physical Properties Needed for Imaging and Therapy

The nuclear and physical properties that make a radionuclide suitable for nuclear medicine applications include the half-life of the decay process, type and energy of the emission(s), specific activity, availability, and cost. Diagnostic imaging relies on detection of the radiation that penetrates the body by instrumentation external to the patient. This requires the emission of photons of energies greater than 35 keV, but more practically greater than about 80 keV.¹⁴ In order to be viable, the gamma or positron emitters should have a short half-life (less than a day), and decay to a relatively stable daughter without any accompanying α or β^- particle emission. The half-life must be sufficiently long to span the time needed to synthesize and purify the radiopharmaceutical, inject the drug into the patient, localize and image the desired area with the available SPECT or PET instrumentation. In practice, gamma-ray energies from 80 to 350 keV are necessary, while those from 100 to 200 keV are optimal for instrumentation currently used in nuclear medicine departments. Special PET instrumentation is required for imaging the two 511 keV annihilation photons emitted during positron decay. The use of coincidence circuitry to image the annihilation photons makes the resolution obtained with PET imaging significantly better than that with SPECT imaging.

Radiotherapy generally involves cell destruction, requiring some form of particle emission on decay and a half-life between 1 and 10 days. The choice of a particular therapeutic application determines the type of particle emission (α , β , or Auger e^-), and the energy and half-life of the radionuclide to be used. Considerations include time for delivery of the radiopharmaceutical to its *in vivo* target, location of the target (tumor surface, tumor cell cytoplasm, tumor cell nucleus) and size of the tumor. The reader is directed to a number of reviews on this subject.^{15–22}

The cost and availability of a radionuclide are almost as important as its nuclear properties. In general, nuclear reactors normally produce β^- -emitting radionuclides through neutron capture reactions, whereas cyclotrons or linear accelerators are used to produce β^+ -emitters by charged particle reactions. The development of parent–daughter generator systems has increased the suitability and availability of some radionuclides that would otherwise not have achieved widespread use. Parent–daughter generators are systems in which a longer-lived parent radionuclide decays to a shorter-lived daughter that is eluted from a chromatographic column. A prime example of such a system is the $^{99}\text{Mo}/^{99\text{m}}\text{Tc}$ generator that yields the 6-h half-life, 140 keV γ -emitting $^{99\text{m}}\text{Tc}$, now the mainstay of diagnostic nuclear medicine. $^{99\text{m}}\text{Tc}$ pertechnetate (TcO_4^-) is eluted daily from a generator containing its parent, 66 h ^{99}Mo , for a constant supply of $^{99\text{m}}\text{Tc}$. Another generator system approved by the United States Food and Drug Administration (FDA) for clinical use is the $^{82}\text{Sr}/^{82}\text{Rb}$ system, which is a direct-infusion generator allowing the use of ^{82}Rb that has a 76-second half-life for myocardial imaging.^{20,21} Other generator systems with potential clinical utility include $^{188}\text{W}/^{188}\text{Re}$,^{22,23} $^{115}\text{Cd}/^{115\text{m}}\text{In}$,²⁴ $^{90}\text{Sr}/^{90}\text{Y}$,^{25,26} $^{68}\text{Ge}/^{68}\text{Ga}$,^{27,28} and $^{62}\text{Zn}/^{62}\text{Cu}$.^{29–32}

This chapter focuses on the use of radiometals in diagnostic and therapeutic radiopharmaceuticals, discussing only those applications of radiometals for use in formulating drugs for systemic injection. It does not address external beam radiotherapy applications, radioactive seed implants for brachytherapy applications, or radioactive microspheres. Furthermore, the focus will be on the chemical aspects of metal coordination, and biological data will be presented as supporting documentation regarding the success of the coordination chemistry. The presentation of extensive biological or clinical data is outside the scope of this chapter.

Excellent reviews have been written on the topic of chelating agents, radiolabeling, and receptor targeting. Because this research area, by definition, is a multi-disciplinary area, these topics are usually treated to some degree in any of these review articles.^{33–36}

A number of radiometals have nuclear properties suitable for diagnostic and/or therapeutic applications. The radiometals that form the basis of current radiopharmaceuticals, and those with nuclear properties most suitable for diagnostic or therapeutic applications, are discussed in terms of their chemistry, nuclear properties, and potential pharmaceutical applications. Two clearly

important radiometals, ^{99m}Tc (diagnostic) and ^{188}Re (therapeutic), are not discussed in this chapter as they are covered in depth elsewhere in this series, in the chapters on the respective elements in Volume 4.

9.20.2 RADIONUCLIDE PRODUCTION

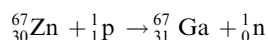
The production of the various metallic radionuclides with utility to either diagnosis or treatment are described, separated by route of production (either cyclotron/accelerator or reactor).

9.20.2.1 Cyclotron- or Accelerator-produced Radionuclides

Cyclotrons and accelerators are sources of charged particles (i.e., protons, deuterons, α particles, etc.), and the radionuclides produced are generally proton rich and decay by positron emission and/or electron capture. A positive ion beam is eventually extracted from the cyclotron, regardless of whether positive or negative ions were accelerated. The isotope of interest is separated from the target for use in chemical syntheses. Accelerator- or cyclotron-produced radioisotopes tend to be the most expensive as only one radionuclide is produced at a time.

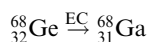
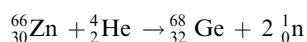
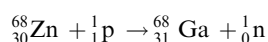
9.20.2.1.1 Gallium

^{67}Ga has nuclear properties that make it potentially useful for diagnostic imaging applications. ^{67}Ga has a 3.26-day half-life and decays by both electron capture and positron emission. ^{67}Ga is produced at a cyclotron or accelerator by proton irradiation of a ^{67}Zn target. The ^{67}Ga is then separated from the ^{67}Zn target:



^{68}Ga is a positron emitter with a 1.13-h half-life, and it is potentially useful for diagnostic imaging applications. There are two methods of production for ^{68}Ga , namely through a (p, n) reaction on ^{68}Zn and from the decay of ^{68}Ge . The most useful form of ^{68}Ga , however, is from a $^{68}\text{Ge}/^{68}\text{Ga}$ generator.^{37,38} This fact is particularly true because of the short half-life of ^{68}Ga . The two methods of production are shown below.

(a) Direct production:

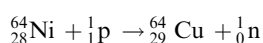


(b) Generator route:

The ^{68}Ge decays to ^{68}Ga by electron capture with a half-life of 270.8 days. The long half-life of ^{68}Ge makes this generator system for producing ^{68}Ga useful for quite some time, since the ^{68}Ga daughter is in secular equilibrium with the ^{68}Ge parent.

9.20.2.1.2 Copper

^{64}Cu is produced via a proton reaction on enriched ^{64}Ni , followed by separation from the ^{64}Ni target:



^{64}Cu is unusual in that it undergoes three types of decay: β^- , electron capture and β^+ leading to particulate emissions for therapy and gamma rays for imaging.

9.20.2.1.3 Tin

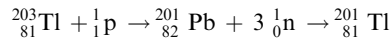
$^{117\text{m}}\text{Sn}$ decays by isomeric transition to ^{117}Sn ground-state emitting 156 (2.1%) and 159 (86.3%) keV γ photons, and a high abundance of conversion electrons (111.5% per decay) and Auger electrons (281% per decay), making this radionuclide useful for therapeutic applications.^{4,39} $^{117\text{m}}\text{Sn}$ has a 14-day half-life and is produced via $^{121}\text{Sb}(p,2p3n)$ or $^{123}\text{Sb}(p,2p5n)$ reactions.³⁹

9.20.2.1.4 Rubidium

^{82}Rb has a half-life of 1.27 min and decays by β^+ emission, making it suitable for PET imaging. It is available from a $^{82}\text{Sr}/^{82}\text{Rb}$ direct infusion generator where the 25.36-day half-life ^{82}Sr is in secular equilibrium with its daughter ^{82}Rb . The ^{82}Sr parent is produced at an accelerator via $^{85}\text{Rb}(p,4n)^{82}\text{Sr}$.

9.20.2.1.5 Thallium

^{201}Tl is produced by proton irradiation of an enriched ^{203}Tl target to yield ^{201}Pb ($t_{1/2} = 9.4$ h), which then decays by positron emission and electron capture to ^{201}Tl :

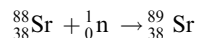


9.20.2.2 Reactor-produced Radionuclides

Reactors are sources of neutrons, and thus most reactor-produced radionuclides are neutron-rich β^- emitters. Reactor-produced radionuclides are of relatively low specific activity if the target nucleus is the same element as the product radionuclide, because the target and the product cannot then be chemically separated.

9.20.2.2.1 Strontium

^{89}Sr has a half-life of 50.53 days and emits a 1.488 MeV β^- particle on decay, suitable for radiotherapy applications. ^{89}Sr is produced from ^{88}Sr via an (n, γ) reaction.



This yields ^{89}Sr in low specific activity; however, this is sufficient for use as a pain palliation agent in metastatic bone disease.

9.20.2.2.2 Yttrium

^{90}Y emits a 2.28 MeV β^- particle with a half-life of 64.1 h and is suitable for radiotherapy applications. ^{90}Y is available from a $^{90}\text{Sr}/^{90}\text{Y}$ generator system. The ^{90}Sr is produced as a fission product.

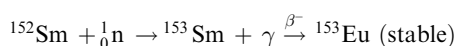
9.20.2.2.3 Radiolanthanides

Many factors must be considered when choosing a therapeutic isotope, and the ideal isotope for one treatment modality may not be the same for another. As a group, radiolanthanides show

great versatility in the production of radiopharmaceuticals. They can be produced inexpensively, in large quantities, and a variety of β^- -emitting radiolanthanides (e.g., ^{149}Pm , ^{166}Ho and ^{177}Lu) can be produced in high-flux reactors. In addition, all of the radiolanthanides listed in Table 1 have low-abundance gamma emissions suitable for estimating dosimetry as well as tracking the radiopharmaceuticals *in vivo*. Thus, the radiolanthanides comprise a family of radionuclides that, through the use of appropriate carrier molecules, can be matched to tumor size, and uptake and clearance times.

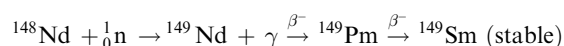
Lanthanide radioisotopes are typically produced in a reactor by *direct* neutron activation (n, γ) reactions. For instance, ^{166}Ho is produced by direct irradiation of ^{165}Ho . Production by this route normally results in a low-specific-activity radioisotope, as only a small portion of the overall target material is converted to the desired radioisotope. Only 0.31% of the ^{165}Ho atoms are converted to ^{166}Ho , resulting in a specific activity that is too low for use in receptor targeting agents. However, there are a few cases in which the neutron absorption cross-sections of the target material are sufficiently high to yield high-specific-activity radionuclides. An example of this is ^{177}Lu , in which up to 28% of the ^{176}Lu target is converted to ^{177}Lu at the end of irradiation.

The thermal neutron production product, ^{153}Sm , is used in the formulation of Quadramet[®], a US FDA-approved radiopharmaceutical for pain palliation in metastatic bone disease. It is produced by an (n, γ) reaction on ^{152}Sm :



The ^{153}Sm produced has low specific activity because it is heavily outnumbered by and cannot be chemically separated from the ^{152}Sm target.

Indirect production results when a target undergoes an (n, γ) reaction followed by β^- decay to the desired product. As noted in the previous paragraph, ^{177}Lu can be produced by direct (n, γ) irradiation of ^{176}Lu , with about 28% of the ^{176}Lu being converted to ^{177}Lu . The direct method also produces the long-lived impurity $^{177\text{m}}\text{Lu}$ (half-life = 160 days) in small quantities. Higher specific activities of ^{177}Lu can be achieved using an indirect irradiation method from ^{176}Yb . Direct irradiation of ^{176}Yb produces ^{177}Yb (half-life = 1.9 h), which β^- decays to form ^{177}Lu , and this route produces much less of the undesirable long-lived $^{177\text{m}}\text{Lu}$. Subsequent chemical separation of the ^{177}Lu from the Yb target results in high-specific-activity ^{177}Lu that is suitable for radiotherapy. The chemical separation requirement for the indirect production of radionuclides greatly increases the amount of time, complexity, and ultimately the expense of the radionuclide. The University of Missouri Research Reactor (MURR) has been investigating the production of high-specific-activity ^{149}Pm , ^{166}Ho , and ^{177}Lu by single and double neutron capture reactions on ^{148}Nd , ^{164}Dy , and ^{176}Yb to produce high-specific-activity radiolanthanides necessary for developing receptor-targeted radiotherapeutic agents. An example of this is the thermal neutron production of ^{149}Pm from an enriched ^{148}Nd target:



Because Pm and Nd are different elements, they can be separated to generate high-specific-activity ^{149}Pm (where virtually all of the Pm atoms are ^{149}Pm and the Nd target has been chemically removed).

Several methods have been used to separate the lanthanides chemically: solvent extraction, ion exchange chromatography, HPLC using α -hydroxyisobutyric acid and, in limited cases, selective reduction of a particular metal cation.^{40–43} The use of di(2-ethylhexyl)orthophosphoric acid (HDEHP) for the separation of various rare-earth elements via solvent extraction has also been reported.^{44–46} This separation method is based on the strong tendency of Ln^{3+} ions to form complexes with various anions (i.e., Cl^- or NO_3^-) and their wide range of affinities for complexation to dialkyl orthophosphoric acid. When the HDEHP is attached to a solid phase resin, the lanthanides can be selected with various concentrations of acid in order of size, with the smallest ion being the most highly retained.

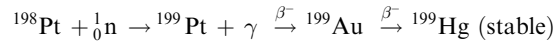
9.20.2.2.4 Rhodium

^{105}Rh is a β^- emitting radionuclide suitable for therapeutic applications. It has a 35.4-h half-life and emits 0.566 MeV and 0.248 MeV β^- particles and a 319 keV gamma photon. It is a reactor-produced radionuclide that is also potentially available from the separation of fission products in

spent reactor fuel. Troutner first suggested ^{105}Rh for use as a therapeutic radionuclide because of its nuclear properties and the high specific activity attainable with this radionuclide.⁴⁷ ^{105}Rh is produced by thermal neutron irradiation of ^{104}Rh to make ^{105}Ru , which decays with a 4.4-h half-life to ^{105}Rh . The ^{105}Rh is separated from the Ru target, first by oxidation to RuO_4 and then distillation of the RuO_4 into an HCl trap, leaving the ^{105}Rh in an oxidation state of +3. The ^{105}Rh is then heated with dilute HCl giving a solution of Rh^{III} -chloride.⁴⁸

9.20.2.2.5 Gold

^{199}Au has a half-life of 3.14 days and emits β^- particles with energies of 0.453 MeV, 0.292 MeV, and 0.250 MeV with accompanying gamma photons of 158.4 keV and 208.2 keV. It is potentially available in high specific activity through thermal neutron irradiation of a ^{198}Pt target:



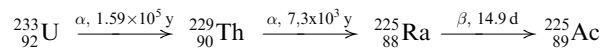
The ^{199}Pt produced from thermal neutron irradiation of ^{198}Pt decays with a 30.8-min half-life to ^{199}Au . After allowing for this decay, the ^{199}Au is separated readily from the Pt target using anion exchange to separate $[\text{AuCl}_4]^-$ from $[\text{PtCl}_4]^{2-}$.⁴⁹

9.20.2.2.6 Scandium

^{47}Sc has a 3.35-day half-life, emits medium-energy β^- particles (0.601 (32%) and 0.441 (68%) MeV) and a 159 keV γ photon in 68% abundance on decay. ^{47}Sc is produced in no-carrier-added quantities by an (n, p) reaction on $^{47}\text{TiO}_2$ targets, followed by cation exchange separation using Dowex AG 50W-X4 resin with HCl/HF as the eluent.^{50,51}

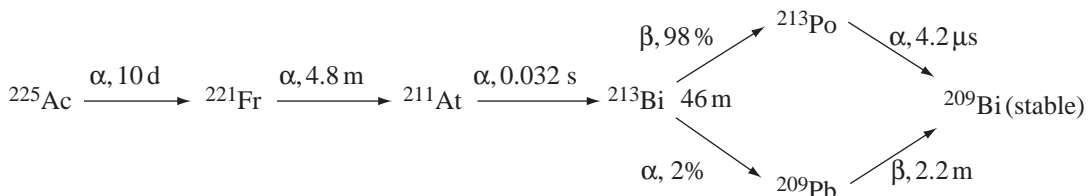
9.20.2.2.7 Actinium

^{225}Ac is available from the decay of ^{229}Th , which is present in old samples of ^{233}U . The decay scheme for generating ^{225}Ac is as follows:

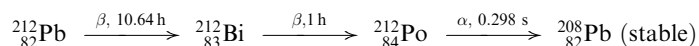


^{225}Ac is considered an attractive option as an α emitter because it decays through a chain to the stable ground state daughter, ^{209}Bi , by emitting four α particles and two β^- particles and about 28 MeV of energy to the surrounding media with a half-life of 10 days.⁵²

9.20.2.2.8 Lead and Bismuth



^{212}Pb is a β^- -emitting radionuclide with a half-life of 10.64 h. It is the parent radionuclide of the α -emitting ^{212}Bi . The decay scheme is shown below:



^{212}Pb is available from $^{224}\text{Ra}/^{212}\text{Pb}$ generator.^{53–56}

^{212}Bi and ^{213}Bi are considered to be two potential radiometal α emitters suitable for radiotherapy applications. The production modes for ^{212}Bi and ^{213}Bi have been recently reviewed.^{57,58} ^{212}Bi is the daughter of ^{212}Pb discussed above, and is available from the same generator system ($^{224}\text{Ra}/^{212}\text{Pb}$).^{54–56} ^{212}Bi is a member of the ^{232}Th decay series. ^{213}Bi is available from an ^{225}Ac generator system, as described above, and is a member of the now-extinct ^{237}Np decay series, of which ^{233}U is a member.^{59,60}

9.20.3 PHARMACEUTICAL APPLICATIONS OF RADIONUCLIDES

Directing radiometal-labeled molecules to their *in vivo* target sites is quite challenging. The exact choice of chelate is dependant on the ultimate therapeutic use. There are typically three ways of selectively delivering a radiometal to the intended target site: by natural affinity of the radiometal for the target site, such as pertechnetate for the thyroid; by labeled small-molecule delivery in which the overall properties of the metal-chelated complex such as charge, lipophilicity, and size determine its selectivity for the target site; or by the use of bifunctional chelating agents (BFCAs) to attach the radiometal to a biological molecule with proven affinity for the desired target site, such as peptides and monoclonal antibodies.

The most common mode of targeting is through the use of BFCAs, multidentate ligands that complex the radiometal at one site and are covalently bonded to a targeting biomolecule at another site.⁶¹ The targeting biomolecule often consists of a specific receptor-binding molecule, a specific antibody or antibody fragment, a hormone specific for a receptor, or some other biological molecule with a very specific target. The bifunctional chelate must form a complex with the radiometal that is kinetically inert *in vivo* so that the radiometal is delivered to its target site in the body. The bifunctional chelate complex must not significantly alter the biological targeting properties of the biomolecule to which it is appended. The requirements for the bifunctional chelate are obviously metal dependent, and the specific chelates are discussed below with the radiometals.

Pretargeting is a strategy to circumvent the slow uptake of radiolabeled antibodies. In pretargeting, an antibody, modified with a streptavidin moiety, is injected and permitted to reach the *in vivo* target.^{62–65} In the second stage of the strategy, a biotin molecule, which is known to have great affinity for the streptavidin, is modified to incorporate an appropriate bifunctional chelate and a corresponding imaging or therapeutic radionuclide. Because the biotin–chelate combination is a relatively small molecule, it leaves the circulation quickly and accumulates wherever the antibody is located. Material that does not bind to the streptavidin portion of the antibody is quickly excreted from the body. The sum total of this strategy is specific uptake at the targeted site with minimal non-specific binding and high tumor dose to the patient. This approach, in theory, can be applied to any metal/chelate combination. Clinical studies using this “three-step” approach to therapy have been reported.^{66–68}

Published papers since the first volume of this series appeared have centered on the coordination chemistry of a simple chelate with a metal, or when the chelate has been conjugated to a biological target. In the former case, results are helpful but limited; the real potential for a chelate depends on the success achieved when the chelate is attached to a biological target. In the latter case, biological targets within this time frame have included antibodies, antibody fragments, and peptide molecules. Thus, the scientific studies are quite diverse.

For the radiometals discussed in this chapter, nitrogen and oxygen most often serve as the coordinating atoms. Sulfur has been utilized less often as a coordinating atom. Polyfunctional constrained, open-chain ligands or macrocyclic ligands afford the greatest stability for the resulting complexes. The chelates utilized are discussed with the particular radiometal, as they are generally metal specific.

9.20.3.1.1 Gallium, Indium, and Yttrium

In general, chelants for these metals must be polycordinate, having at least three coordinating atoms for gallium and increased numbers (i.e., 4–7) for indium and yttrium. Gallium complexes can be challenged *in vivo* by either hydrolysis or transchelation by transferrin. Tripodal ligands, where an apical nitrogen serves as one of the coordinating atoms, have been the subject of numerous coordination studies with gallium. Tris-(2-mercaptobenzyl)amine, when coordinated

with ^{68}Ga , exhibited *in vitro* stability in rat serum (95% intact) up to two hours, and passive diffusion across the blood-brain-barrier in a *Nemestrina macaque* (3.9% ID/organ at 1 min).⁶⁹ A polydentate tripodal Schiff-base ligand, derived from triethylenetetramine (tren) and 5-bromosalicylaldehyde, was studied by Figuet and co-workers in the coordination of gallium.⁷⁰ This ligand does not exhibit imine hydrolysis in complexation studies, and crystallographic analysis supports participation of the phenolic groups in coordination to the metal.

The gallium and indium complexes of novel bis(thiosemicarbazones) have been investigated.^{71–73} Initial publications indicated a more complex stoichiometry where X-ray crystal structures suggested either dinuclear or trinuclear complexes. Whereas these complexes are quite interesting, they are less likely to result in useful nuclear medicine radiopharmaceuticals. The bis(thiosemicarbazones) are quite useful as ligands for copper, and are discussed in more detail (*vide infra*).

The Orvig group has been conducting an exploration of the coordination chemistry of gallium and indium with hexadentate amine ligands containing pendant pyridyl and phenolate groups.^{74–77} The use of these ligands has not been extended into the biological arena as yet.

N,N'-bis(2-hydroxybenzyl)-ethylenediamine-*N,N'*-diacetic acid (HBED) and *N*-hydroxybenzyl-ethylenediamine-*N,N,N'*-triacetic acid (HBET) are multidentate ligands investigated for coordination with gallium and indium (Figure 1).⁷⁸ HBED, with its two phenolate donor groups, led to increased stability constants over HBET.

Investigation of the coordination of tetradentate N_2S_2 ligands has been reported for gallium and indium.⁷⁹ This type of chelate had previously been incorporated into many technetium complexes for biomedical applications.

^{90}Y does not have an accompanying gamma emission that can be used to follow its biodistribution *in vivo*; thus, ^{111}In has been used quite often in imaging studies as a surrogate for ^{90}Y for distribution, as well as dosimetry estimates. Because there is no direct correspondence between the results, ^{86}Y has been developed as an imaging isotope. Clearly, there are advantages in using ^{86}Y to provide valuable *in vivo* data; however, currently, it is much less available and its short half-life precludes long-term studies. Some studies are exploring the use of high doses of ^{111}In as therapeutic agents, relying on the Auger electron emission during its decay.

Open-chain ligands were the first evaluated for complexation studies with indium and yttrium. The use of diethylenetriaminepentaacetic acid (DTPA) anhydride permitted early evaluation of labeled chelate-conjugates (Figure 2).⁸⁰ The use of this activated chelating agent was quite popular, until the drawbacks associated with its crosslinking of proteins became apparent.

A peptide linker-chelate analog, glycyl-tyrosyl-lysine-*N*- ϵ -DTPA (GYK-DTPA), was incorporated onto B72.3 antibody and labeled with ^{111}In and ^{90}Y .^{81,82} *In vitro* and *in vivo* evaluations in dogs were conducted. Results indicated that the ^{111}In chelate was stable *in vivo*; however, the ^{90}Y version showed a biphasic decay pattern. The covalent bond between the peptide and DTPA precluded use of one of the coordinating arms that is necessary to coordinate ^{90}Y in a stable fashion.

DTPA has also been used in the peptide-based ^{111}In -DTPA-octreotide. Octreotide is a shortened peptide analog of somatostatin designed to be more stable *in vivo*. Radiolabeling of octreotide for diagnostic imaging applications with radioisotopes for PET or SPECT has been investigated,

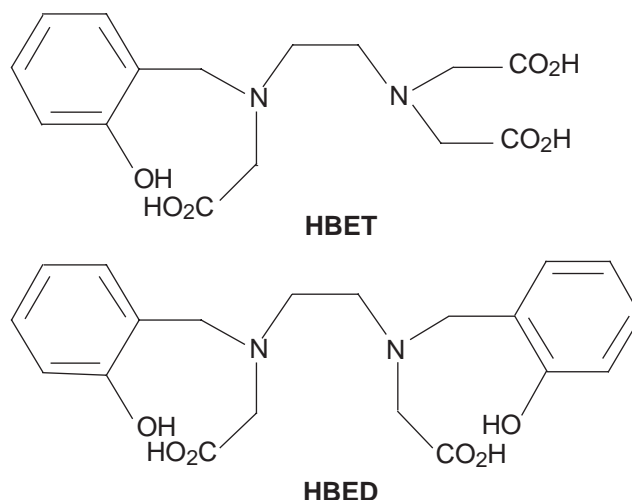
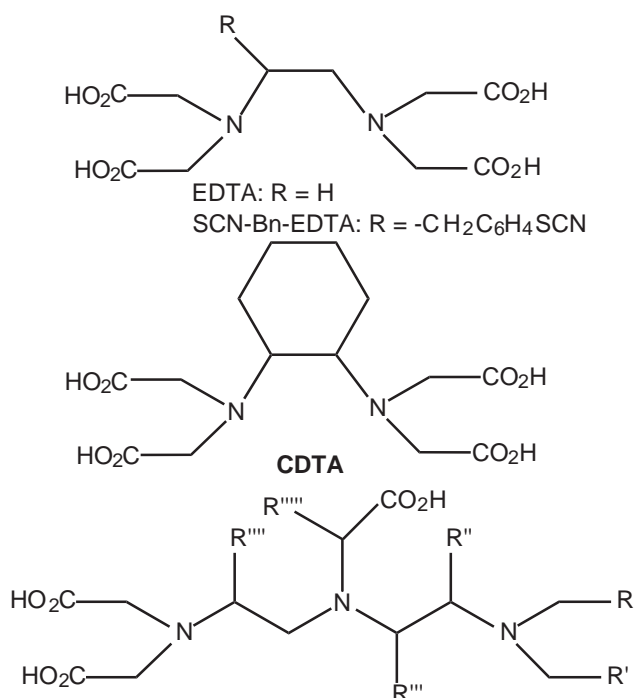


Figure 1 Multidentate ligands for gallium and indium.



DTPA: $R = R' = \text{CO}_2\text{H}$; $R'' = R''' = R'''' = R''''' = \text{H}$

CM-DTPA: $R = R' = \text{CO}_2\text{H}$; $R'' = R''' = R'''' = \text{H}$; $R''''' = -\text{CH}_2\text{CO}_2\text{H}$

CA-DTPA: $R, R' = -\text{CO}-\text{O}-\text{OC}-$; $R'' = R''' = R'''' = R''''' = \text{H}$

MA-DTPA: $R = \text{CONH}_2$; $R' = \text{CO}_2\text{H}$; $R'' = R''' = R'''' = R''''' = \text{H}$

1B4MDTPA: $R = R' = \text{CO}_2\text{H}$; $R'' = \text{CH}_3$; $R''' = R'''' = \text{H}$; $R''''' = -\text{CH}_2\text{C}_6\text{H}_4\text{NO}_2$

p-SCN-Bz-6-Me: $R = R' = \text{CO}_2\text{H}$; $R'' = \text{CH}_3$; $R''' = R'''' = \text{H}$; $R''''' = -\text{CH}_2\text{C}_6\text{H}_4\text{SCN}$

Nitro-MX-DTPA: $R = R' = R'' = \text{CO}_2\text{H}$; $R''' = R'''' = \text{H}$; $R''''' = -\text{CH}_2\text{C}_6\text{H}_4\text{NO}_2$

CITC-DTPA, MX-DTPA: $R = R' = R'' = \text{CO}_2\text{H}$; $R''' = R'''' = \text{H}$; $R''''' = -\text{CH}_2\text{C}_6\text{H}_4\text{SCN}$

Nitro-CHX-DTPA: $R = R' = \text{CO}_2\text{H}$; $R'''' = \text{H}$; $R'', R''' = -\text{CH}_2\text{CH}_2\text{CH}_2\text{CH}_2-$; $R''''' = -\text{C}_6\text{H}_5\text{NO}_2$

Figure 2 Acyclic polyaminocarboxylate ligands.

and successful results have been obtained for the *in vivo* imaging of somatostatin receptor-positive tumors.⁸³⁻⁸⁷ Neuroendocrine tumors, which express a high concentration of somatostatin receptors, can be identified by ^{111}In -DTPA-octreotide, which can help in the staging of these cancers.⁸⁸ After extensive validation, the ^{111}In -DTPA-octreotide material was approved for clinical use by the US FDA and marketed as Octreoscan[®].⁸⁸

Due to the clinical availability of Octreoscan[®], the first peptide-based receptor-imaging radiopharmaceutical, there has been much interest in the development of a complimentary therapeutic radiopharmaceutical.⁸⁹

Simple DTPA chelates labeled with ^{90}Y are not sufficiently stable *in vivo*. This instability leads to accretion of the metal ion in bone; such unwanted accumulation results in undesirable irradiation of the bone marrow.⁹⁰

In order to maintain the coordinating capability of the nitrogen atoms in the polyaminocarboxylates, the site of incorporation of the activated linking arm was moved to the ethylene backbone. This resulted in synthetic strategies that were more complicated and challenging. In addition to modifying the site of attachment for the linking moiety, rigid open-chain ligands were designed and evaluated. The goal in designing these ligands was to decrease their flexibility, so

that the ligand might act more as a claw. At the same time, however, the ligand would still be more flexible than a macrocyclic ligand, allowing for more favorable kinetics.

A ligand that appears to yield sufficiently stable complexes with ^{90}Y is the “constrained” DTPA analogue, methyl-benzylisothiocyanato-diethylenetriaminepentaacetic acid (MX-DTPA) (Figure 2), originally developed by Gansow and Brechbiel at the US National Institutes of Health.^{91,92} This chelating agent is the ligand used in the preparation of Zevalin.[®] Zevalin[®] is a treatment for refractory non-Hodgkin’s lymphoma,⁹³ and was approved for use in the USA in early 2002. This was the first approval for a radioimmunotherapeutic agent. A recent publication⁹⁴ utilized the isothiocyanobenzyl-EDTA (SCN-Bn-EDTA) (Figure 2) chelating agent as a means to introduce ^{90}Y into phosphorothioate antisense oligonucleotides as a potential targeted radionuclide therapeutic agent for malignant tumors.

Extending the homology of the DTPA ligand has been studied by the synthesis of triethylenetetraamine-*N,N,N',N'',N''',N''''*-hexaacetic acid (TTHA) and TTHA-bis(butanamide) for the complexation of gallium and indium (Figure 3).⁹⁵ The amide analog showed decreased stability with these metals in comparison to the full acid structure. The free acid was also determined to have the best stability for gallium, and the authors suggest that it may prove useful in biological studies.

There has been intense investigation of macrocyclic ligands including the nine-membered rings 1,4,7-triazacyclononane-1,4,7-triacetic acid (NOTA, 9N3) where the linking moiety contains the maleimide group,^{95,96} the isothiocyanato group,^{97,98} or the cyanato group as the reactive portion (Figure 4).⁹⁹ Without a doubt, however, “DOTA,” 1,4,7,10-tetraazacyclododecane *N,N',N'',N'''*-tetraacetic acid, has been the most studied macrocyclic chelating agent for indium, yttrium, and a number of other metals described in this chapter (Figure 5).¹⁰⁰⁻¹⁰² ^{90}Y -DOTA-octreotide has been synthesized as a more stable analog to the ^{90}Y -DTPA-octreotide.^{103,104}

9.20.3.1.2 Copper

Two distinct classes of ligand have been investigated for the complexation of copper: the poly-functional bis(thiosemicarbazones) and the macrocyclic ligands exemplified by 1,4,8,11-tetraaza-

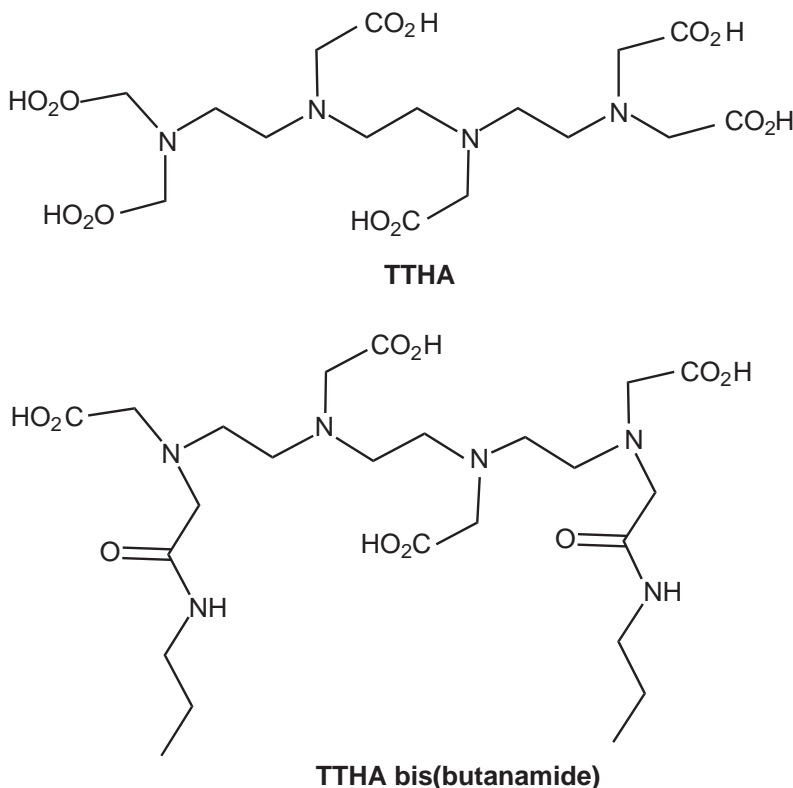
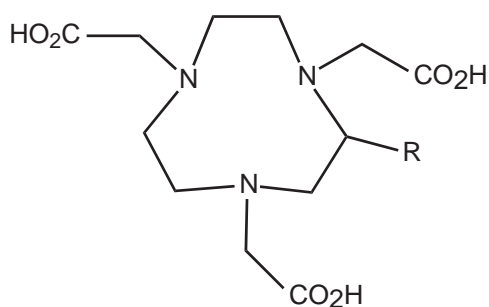


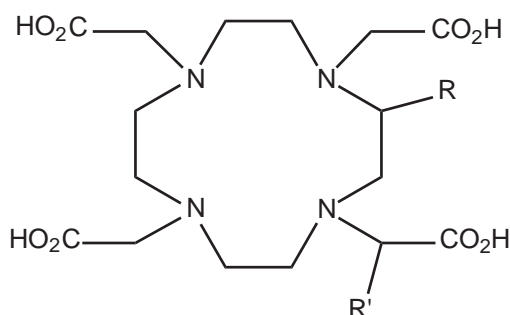
Figure 3 Expanded acyclic polyaminocarboxylates ligands for Ga^{III} and In^{III} .



NOTA: R = H

C-NOTA: R = *p*-SCN-Bz

Figure 4 NOTA analogues.



DOTA: R = R' = H

nitro-DOTA: R = -CH₂C₆H₄NO₂; R' = H

***p*-NCS-Bz-DOTA** R = -CH₂C₆H₄NCS; R' = H

nitro-PA-DOTA: R = H; R' = -CH₂CH₂C₆H₄NO₂

PA-DOTA: R = H; R' = -CH₂CH₂C₆H₄NH₂

Figure 5 DOTA and derivatives.

cyclotetradecane-*N,N',N'',N'''*-tetraacetic acid (TETA) (Figure 6). The two most prominent bis(thiosemicarbazones) are pyruvaldehyde bis-(*N*4-methylthiosemicarbazone) (PTSM)^{105–109} and diacetyl-bis(*N*4-methylthiosemicarbazone) (ATSM) (Figure 7).^{110,111} These ligands have been labeled with copper and evaluated *in vivo* and display cell uptake that is either non-hypoxia driven (Cu–PTSM) or hypoxia selective (Cu–ATSM). Labeling of PTSM by copper results in a neutral lipophilic complex that is rapidly taken up by the cells, and the Cu^{II} is reduced to Cu^I by intracellular thiols (probably glutathione). The PTSM ligand cannot stabilize Cu^I, and the Cu^I then dissociates and becomes bound to intracellular proteins. This agent has been evaluated as a possible blood flow tracer but its high lipophilicity results in high liver uptake and slow clearance, making it less than ideal. Cu–ATSM differs from Cu–PTSM by the addition of a single methyl group on the ligand backbone. This simple change results in a 100 mV lowering of the reduction potential of Cu–ATSM. Cu–PTSM is reduced in both normoxic and hypoxic tissue, whereas the Cu–ATSM is only reduced in hypoxic tissue.^{109–111} Hypoxia imaging agents using radioisotopes of copper offer the potential of therapy for hypoxic regions of solid tumors.

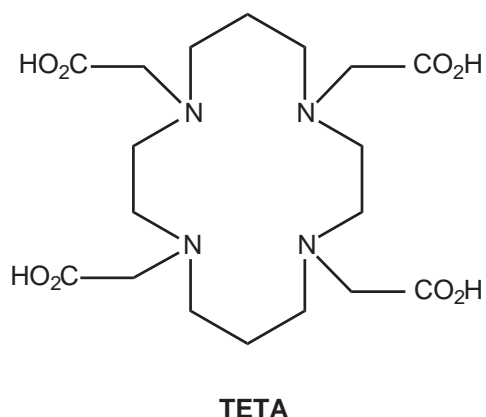


Figure 6 TETA ligand for Cu^{II} .

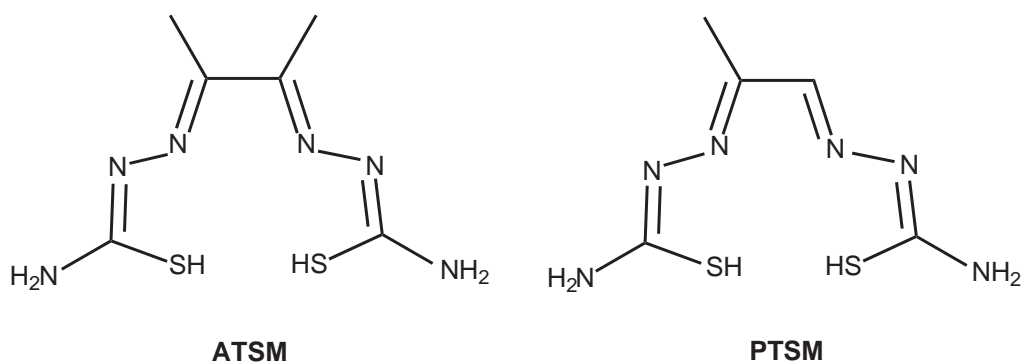


Figure 7 Bis(thiosemicarbazone) ligands for Cu^{II} .

The macrocyclic ligands utilized for incorporation of copper generally contain four nitrogens separated by ethylene or propylene groups. The overall size of the macrocycle, thus, extends to fourteen atoms in the case of 4-[(1,4,8,11-tetraazacyclotetradec-1-yl)methyl]benzoic acid (PCBA) (Figure 8).¹¹²

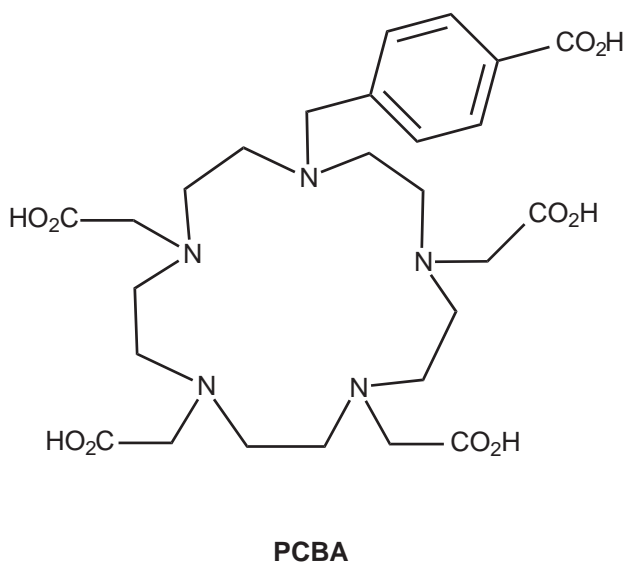


Figure 8 PCBA ligand for Cu^{II} .

A new hexaazamacrobicyclic cage ligand, 1-*N*-(4-aminobenzyl)-3,6,10,13,16,19-hexaazabicyclo[6.6.6]icosane-1,8-diamine (SarAr) is a sarcophagine (sar) type cage compound¹¹³ evaluated for its potential in complexing copper. These macrobicyclic ligands are designed to confer greater *in vivo* stability. The parent caged ligand, 1,3,6,10,13,16,19-hexaazabicyclo[6.6.6]icosane, when complexed with ⁶⁷Cu, lost less than 2% of the label in competition with blood plasma over 174 h (Figure 9).

A number of novel dioxo variants of the tetraazamacrocycles have been synthesized and stability constants were measured with Cu²⁺.¹¹⁴ A few of these were further evaluated as chelating agents with ⁶⁴Cu.¹¹⁵ Structural differences included ring size (from 12 to 14) and placement of the oxo groups. Of the six variations synthesized, only one, 1,4,8,11-tetraazacyclotetradecane-3,9-dione(14N4O2-3,9), readily formed a complex (Figure 9).

One macrocyclic ligand, TETA, has been intensely studied as a chelant of copper.¹¹⁶⁻¹²⁰ After extensive evaluation, experimental results are consistent with *in vivo* transchelation of ⁶⁴Cu from TETA-octreotide to superoxide dismutase (SOD) in rat liver.¹¹² These results were subsequently confirmed by utilizing a SOD specific assay.¹²¹ They suggest that more stable chelates than TETA are needed for copper. A preliminary report on cross-bridged tetraamine ligands was published in 1996.¹²² Since that time, a number of basic studies have been conducted; however, it remains to be seen whether these ligands exhibit sufficient biological stability.

9.20.3.1.3 Radiolanthanides

The 15 lanthanide elements exhibit analogous chemical behavior due to similarities in charge, ionic radii, and coordination chemistry, with the most common oxidation state being +3. In aqueous media, the lanthanides are considered to be hard acids which are stabilized by multidentate chelates with “hard” oxygen and nitrogen donor atoms. The size of the lanthanides decreases with increasing atomic number due to the lanthanide contraction. Their coordination numbers range from 7 to 10, with 8 and 9 being the most common. The ionic character of lanthanide bonding requires multidentate chelates in order to form complexes with high thermodynamic stability and kinetic inertness to prevent precipitation and transmetalation to proteins containing metal binding sites such as transferrin (see Chapter 9.19).

When not complexed, lanthanide ions have a high affinity for bone *in vivo* because they act as calcium ion mimics. Because the lanthanides undergo hydrolysis above a pH of 4, they readily form radiocolloids when not complexed, and are then taken up by the liver. This bone and liver uptake results in non-specific radiation doses to non-target (normal) tissues and organs and is undesirable.⁹¹ The polyaminocarboxylate class of ligands are considered to be the optimal choice for the basis of BFCAs for the +3 metal cations, including the lanthanides. It is essential that the

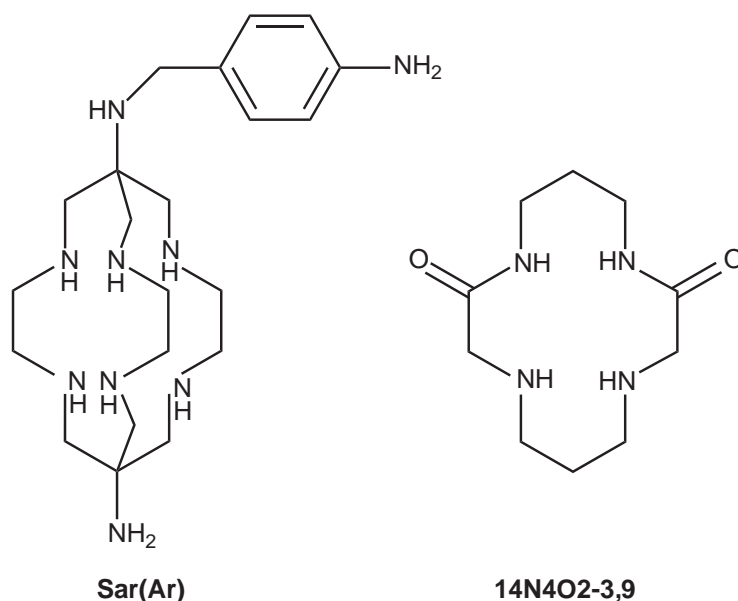


Figure 9 Macrocylic ligands for Cu^{II}.

BFCA used for the radiolanthanides forms a kinetically stable complex *in vivo* to minimize toxicity to non-target tissues.¹²³ Aminocarboxylates such as diethylenetriaminepentaacetic acid (DTPA) and ethylenediaminetetraacetic acid (EDTA) have been used to stably bind and selectively deliver radiometals, particularly ¹¹¹In, to their target site (Figure 2).^{91,124} This stability results from the multidenticity of these chelates. DTPA forms complexes of high thermodynamic stability with lanthanides.¹²⁵ However, ligands of this type can lose chelating stability *in vivo* if one of the appended arms necessary for metal coordination is covalently linked to the peptide or protein, because of their tendency to undergo acid- or cation-promoted decomplexation *in vivo*.¹²⁶ When the radiolanthanide is lost from the chelate, the radionuclide can be taken up by serum proteins, bone tissue, liver, and/or the gastrointestinal mucosa, all of which are undesirable effects with some being potentially lethal.¹²⁶ The lanthanides form complexes with distorted tricapped trigonal prism geometries with DTPA analogs.³⁵ A major advantage of using these ligands is their fast labeling kinetics, and a variety of derivatives have been synthesized for the radiolabeling of peptides.^{91,123,127–129} Brechbiel and co-workers have synthesized and evaluated a series of backbone-modified DTPA ligands that contain a *p*-isothiocyanatobenzyl group.^{91,128}

A recent study by Li *et al.* evaluated the *in vitro* and *in vivo* stability of a series of aminocarboxylates including EDTA, 1,2-cyclohexanediaminetetraacetic acid (CDTA), DTPA, the monoamide derivative of DTPA (MA-DTPA), and DOTA labeled with ¹⁷⁷Lu, ¹⁵³Sm, and ¹⁴⁰La (Figures 2 and 5).¹³⁰ The following order of stability was observed for each metal tested: Ln-DOTA > Ln-DTPA > Ln-MA-DTPA > Ln-CDTA ~ Ln-EDTA. The results showed an increase in stability in going from the acyclic ligand EDTA to the more preorganized ligand CDTA and from DTPA to DOTA, with the highest stability observed for DOTA. In preorganization the ligand is restricted in movement to a conformation that more closely resembles that of the complexed ligand, typically resulting in higher thermodynamic stability and kinetic inertness of the resultant metal complex. In addition, an increase in stability was observed in going from the larger early lanthanides to the smaller later lanthanides. This was attributed to the smaller lanthanide, ¹⁷⁷Lu, having all or more of its coordination site requirements filled compared to the larger lanthanides. Similar results were reported by Stimmel and Kull comparing ¹⁵³Sm- and ¹⁷⁷Lu-labeled acyclic aminocarboxylates such as nitro-CHX-DTPA, nitro-MX-DTPA, DTPA, and a novel terpyridine acyclic chelator, 6,6''-bis[*N,N,N''',N''*-tetra(carboxymethyl)aminomethyl]-4'-(3-amino-4-methoxyphenyl)-2,2',6',2''-terpyridine (TMT-amine) (Figure 2) with polycyclic aminocarboxylates (nitro-DOTA, nitro-PA-DOTA) (Figure 5).¹³¹ The macrocyclic aminocarboxylates require more time and higher ratios of ligand:metal (2:1) than the acyclic ligands (1:1). The macrocyclic ligands were very stable over physiological pH ranges, down to 4.0, but dissociation at pH 2.0 was observed for all the macrocycles. The smaller ¹⁷⁷Lu was more stable than the larger ¹⁵³Sm except for the nitro-PA-DOTA ligand in which the ¹⁵³Sm and ¹⁷⁷Lu stabilities were observed to be similar. For the acyclic ligands, nitro-CHX-DTPA exhibited the highest stability of all the chelates at the examined pH values, and this was attributed to the rigidity of this chelator. The following stability was observed for the ¹⁵³Sm-labeled chelates in human serum: nitro-MX-DTPA > nitro-PA-DOTA > DTPA > nitro-DOTA > nitro-CHX-DTPA. For ¹⁷⁷Lu the complexes with macrocycles were the most stable in human serum followed by those with the acyclic ligands: nitro-DOTA > nitro-PA-DOTA > TMT-amine > nitro-MX-DTPA > nitro-CHX-DTPA > DTPA.

The macrocyclic effect provided by polyazamacrocyclic polycarboxylate ligands generally results in more kinetically inert metal complexes than observed with their acyclic analogs.^{100,132} Many compounds have been designed around the macrocyclic skeleton 1,4,7,10-tetraazacyclododecane. For example, DOTA forms kinetically stable complexes with a variety of radiometals, even under the most stringent conditions.¹³⁰ These macrocyclic ligands provide a degree of rigidity to their metal complexes, resulting in a higher degree of kinetic inertness *in vivo*.⁶¹ Lanthanide complexes tend to be nine coordinate and thus the DOTA ligand fills eight of the coordination sites with four amine-nitrogen and four carboxylate-oxygen atoms arranged in a square antiprismatic geometry, and a monodentate water capping the face of the four carboxylate-oxygen donors.^{35,133–138}

The high *in vivo* stability of DOTA complexes makes it a desirable ligand framework for BFCAs relative to acyclic analogs; however, complex formation with DOTA and its analogs can be slow. The slow kinetics of complex formation with DOTA-type ligands does not pose problems with nuclides such as ¹⁷⁷Lu ($t_{1/2} = 6.64$ d); however, improved reaction conditions may need to be developed for the shorter half-life radioisotopes such as ¹⁵³Sm ($t_{1/2} = 1.93$ d) and ¹⁶⁶Ho ($t_{1/2} = 1.12$ d).^{61,139}

There are several methods used to conjugate DOTA and other polyaminocarboxylate ligands to biomolecules.^{140,141} The simplest method, commonly used in solid-phase peptide synthesis, is the

formation of an amide bond between one of the carboxylate arms of DOTA (Figure 5) and a primary amine present on the biomolecule generating DO3A-amide. In the case of a monoclonal antibody (MAb), the DOTA is normally attached via the ϵ -amino moiety of a lysine residue, and in the case of peptides, it is typically attached through the primary amine group of the terminal amino acid. Some thought needs to be given to the point of chelate attachment to ensure it does not interfere with the binding or receptor affinity of the biomolecule. A major disadvantage of this method is the loss of one of the carboxylate chelating groups, which results in an overall reduction in stability especially in the case of large metals such as the lanthanides.

Mäcke recently introduced a monoreactive DOTA prochelator (4,7,10-tricarboxymethyl-*tert*-butyl ester *N,N',N'',N'''*-tetraazacyclododecane-1-acetate), which was coupled to Tyr³-Lys⁵ (BOC)-octreotide via solid-phase peptide synthesis. A one-step deprotection reaction generated the bioactive compound DOTATOC in about 65% yield.¹⁴² The ⁹⁰Y and ¹⁷⁷Lu DOTATOC complexes have shown promise for the treatment of neuroendocrine tumors in early clinical trials.^{143,144}

Another method for generating a BFCA from DOTA is through a linking group attached to one of the carbon atoms of the cyclen backbone or to a methylene carbon atom of one of the carboxylate arms. An example of the latter approach is α -[2-(4-amino-phenyl)ethyl]-1,4,7,10-tetraazacyclododecane-*N,N',N'',N'''*-tetraacetic acid (PA-DOTA) in which an aminophenyl group is covalently bonded to the methylene carbon of a carboxylate arm; this BFCA has been used for labeling Mab and F(ab')₂ fragments (Figure 5).^{140,145} Attachment of the aromatic isothiocyanate group to the ligand backbone, as in the case of 2-(4-isothiocyanatobenzyl)-1,4,7,10-tetraazacyclotetradecane-*N,N',N'',N'''*-tetraacetic acid (*p*-NCS-Bz-DOTA), is an example of the former approach and has been used to attach metals to biomolecules (Figure 5).^{132,141} Here again the chelate is attached to the biomolecule by formation of a thiourea bond with a primary amine, however, in this case the four nitrogen groups and the four carboxylate chelating arms remain available for chelation to the metal. There are various other linkers such as maleimides, aldehydes, ketones, and anhydrides that have been used to conjugate chelates to biomolecules.^{139,146-148} An important consideration in choosing which chelate or linker should be used for a given metal or biological molecule is its effect on biological behavior. Changes in metal coordination, size, charge, and lipophilicity affect the pharmacodynamics. Labeling the same chelated biomolecule with different radiometals can result in very different tissue uptake and clearance ratios. For example, the above-mentioned DOTATOC (a DOTA-chelated somatostatin analog) exhibits different kidney and tumor uptake and clearance ratios when labeled with ⁶⁷Ga, ¹¹¹In, or ⁹⁰Y, all +3 metal ions.^{33,142} The ⁶⁷Ga compound exhibited faster kidney clearance and higher tumor uptake than either the ¹¹¹In- or ⁹⁰Y-labeled DOTATOC.^{33,142} The result is attributed to the change in the coordination geometry of ⁶⁷Ga, which results in a different dipole moment and solvation chemistry, and, more importantly relative to In³⁺ and Y³⁺, results in a free carboxylate group. This additional negative charge (i.e., the free carboxylate group) may result in the faster clearance of the ⁶⁷Ga agent through the kidneys.^{33,142}

This difference has also been observed for a DOTA-labeled J591 antibody labeled with ⁹⁰Y and ¹⁷⁷Lu, which are currently being evaluated in humans.¹⁴⁸⁻¹⁵⁰ A comparison of the biodistribution of ⁹⁰Y-, ¹¹¹In-, and ¹⁷⁷Lu-labeled DOTA-J591 in nude mice bearing the LNCap tumor showed that the uptake and clearance rates of these agents differed in the bone, kidney, spleen, liver, and gastrointestinal tract.¹⁴⁸⁻¹⁵⁰ No differences were observed in the muscle and tumor uptake of these three agents until day 6 for the In/Lu pair ($p = 0.03$). A higher bone uptake was observed for the ⁹⁰Y-labeled agent that increased to day 6, while the ¹⁷⁷Lu agent had a lower initial bone uptake, which decreased over time. In this case, using ¹¹¹In to predict the behavior of ⁹⁰Y results in an overestimation of the liver, spleen, and lower GI tract doses and an underestimation of the kidney dose. The differences are due to different routes of metabolism for the ¹¹¹In-labeled antibody compared to the ⁹⁰Y- and ¹⁷⁷Lu-labeled antibodies. This has significant implications as ¹¹¹In is generally used as a surrogate imaging agent for prediction of ⁹⁰Y biodistribution and dosimetry. Due to the large variability noticed for patients undergoing therapy, it is necessary to perform an initial imaging study to determine biodistribution and uptake values. An imaging study comparing the predicted estimated dose of ⁹⁰Y with ¹¹¹In and the PET tracer ⁸⁶Y was performed on the DOTA-labeled somatostatin analog DOTATOC.¹⁵¹ Using ¹¹¹In to predict the dose from ⁹⁰Y resulted in a 23-86% underestimation of the actual dose to the tumor. The ⁸⁶Y agent most accurately reflected the biodistribution of the ⁹⁰Y agent. These results stress that the use of a radionuclide with an imageable gamma emission for predicting patient dose or the use of another radioisotope of the same metal for therapy with an imageable gamma emission for dosimetry determination is essential.

¹⁵³Sm complexes with phosphonate ligands were found to target actively growing bone (i.e., tumors; fractures).¹⁵² Several ¹⁵³Sm phosphonate complexes were synthesized and evaluated in

chemical and biological systems to optimize bone uptake and biological clearance.^{153,154} In an early study in the evolution of the radiopharmaceutical now known as Quadramet[®], the biodistributions of the ^{99m}Tc, ¹¹¹In, and ¹⁵³Sm complexes with ethylenediaminetetramethylenediphosphonic acid (EDTMP) were determined in rats. All were found to clear blood predominantly by bone and liver uptake (Figure 10). Bone uptake was greatest for the ¹⁵³Sm complex.¹⁵⁵ In 1998, a double-blind placebo-controlled clinical trial was carried out with ¹⁵³Sm-EDTMP proving its value as an agent for bone cancer pain palliation.¹⁵⁶

These evaluations showed that there was a correlation between skeletal uptake and the stability constant of the complexes; the stability constant needed to be high enough to prevent the ¹⁵³Sm from hydrolyzing or transchelating in the blood.¹⁵³ Although all of the polyaminophosphonates labeled with ¹⁵³Sm exhibited bone uptake, ¹⁵³Sm complexed to EDTMP exhibited the highest bone uptake with the fastest blood clearance.¹⁵² The main route of excretion for the ¹⁵³Sm-EDTMP not taken up by the skeleton was through the kidneys.¹⁵² ¹⁵³Sm-EDTMP or Quadramet[®] was approved for clinical use in 1997 by the US FDA.

Based on their work with ¹⁵³Sm-EDTMP, researchers at Dow Chemical Company went on to develop another therapeutic agent to treat patients with multiple myeloma. The agent required a high-energy β^- particle to ablate the diseased bone marrow, but a short enough half-life to allow for the bone marrow transplant that must occur within 7–14 days post treatment. A radiolanthanide analog of ¹⁵³Sm-EDTMP, namely ¹⁶⁶Ho-EDTMP, was evaluated to ablate bone marrow since it emits a more energetic β^- particle (1.8 MeV) and decays in a shorter time frame (26.8 h) than ¹⁵³Sm. A comparison of ¹⁵³Sm and ¹⁶⁶Ho-EDTMP in a baboon model showed ¹⁶⁶Ho-EDTMP to be inferior for pharmacokinetics, biodistribution, and bone localization.¹⁵⁷ Subsequently, a ¹⁶⁶Ho complex of a bone-seeking amino bisphosphonate chelate (APD) was evaluated. Thermodynamic K_f 's were measured and speciation calculated relative to Sm- and Ho-EDTMP. Subsequent animal studies showed that Ho-APD accumulated in the liver.¹⁵⁸ It was concluded that a chelate with a higher thermodynamic stability was necessary to ensure that the fraction of complex that did not localize in the bone would quickly clear out of the body via the kidneys. The diphosphonate ligand 1,4,7,10-tetraazacyclododecane-*N,N',N'',N'''*-tetra methylenephosphonic acid (DOTMP) was chosen due to its high binding constant for lanthanides (Figure 10). This agent has undergone phase I and II clinical trials, and complete responses in about 60% of those treated have been observed.¹⁵⁹

The biodistribution of a number of no-carrier-added (nca; i.e., high specific activity) radiolanthanides (¹⁴¹Ce, ¹⁴⁵Sm, ¹⁴⁹Gd, and ¹⁶⁷Tm) in tumor-bearing mice were examined as a function

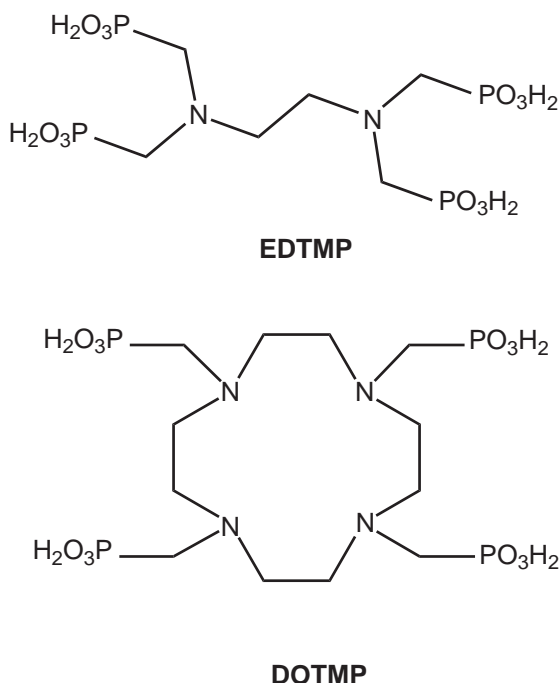


Figure 10 Polyaminophosphonate ligands.

of the concentration of co-injected EDTMP. Tumor/liver ratios were found to be dependent on Ln radii, consistent with the known trend of EDTMP complex stabilities.¹⁶⁰

Two new hexadentate BFCA ligands, modeled on EDTMP, incorporating phosphonate groups on a semi-rigid backbone and a terminal isothiocyanate group for coupling were synthesized. Efficacy was demonstrated by preliminary ¹⁵³Sm labeling tests.¹⁶¹

Pharmacokinetics and biodistribution in grafted mice were compared for Mab OC125, whole or as the F(ab')₂ fragment, labeled with ¹⁵³Sm-DTPA and ¹⁵³Sm-CITC-DTPA. The latter conjugate was found to have more favorable *in vivo* properties although high renal uptake was noted.¹⁶² Dadachova and co-workers¹⁶³ reported on the labeling of Mabs conjugated to the BFCA CHX-DTPA (2-(*p*-isothiocyanatobenzyl)-cyclohexyl-DTPA) with high-specific-activity ¹⁶⁶Ho produced from a ¹⁶⁶Dy/¹⁶⁶Ho generator. The complexes were stable when challenged with transferrin.¹⁶³ The somatostatin analog Tyr³-octreotate was extended to ¹⁵³Sm with labeling of CMDTPA-Tyr³-octreotate. High receptor affinity was demonstrated and biodistribution in tumor-bearing rats showed high tumor uptake and favorable clearance properties (Figure 2).¹⁶⁴

Two new amino carboxylate BFCA macrocycles were synthesized, labeled with ¹¹¹In and ¹⁵³Sm, and *in vitro* stabilities were assessed. These ligands were structural variants of DOTA with one carboxymethylene arm replaced by an ethyl amine.¹⁶⁵

Lutetium-177 has been used in a series of clinical trials, typically bound to a biological target with a DOTA-based chelator. Researchers at Dow Chemical Company reported that the use of lysine facilitated clearance of ¹⁷⁷Lu-DOTA Fab conjugates through the kidneys.¹⁶⁶ In a phase I trial, a ¹⁷⁷Lu-labeled PA-DOTA antibody conjugate administered intraperitoneally was shown to localize in ovarian tumors.¹⁶⁷ In follow-up phase I/II trials, marrow suppression was found to be dose limiting.

In some clever strategies employed for radioimmunotherapy,¹⁶⁸ genetically engineered Mabs and gene transfer were utilized to increase receptor numbers prior to the use of radiolabeled peptide. ¹³¹I- and ¹⁷⁷Lu-labeled Mabs evaluated (injected intraperitoneally) in nude mice with human colon cancer xenografts showed increased tumor uptake.¹⁶⁹ The first clinical trials using ¹⁷⁷Lu for radiotherapy were reported in 1995.¹⁷⁰ The murine monoclonal antibody CC49 was linked to PA-DOTA, which had been labeled with ¹⁷⁷Lu.¹⁷¹ Two clinical trials were performed, one in which the radiopharmaceutical was injected intravenously and a second in which the drug was administered intraperitoneally. In the clinical trial using intravenously administered agent, unexpected hematological toxicity was observed due to the undesirable accumulation and long retention of ¹⁷⁷Lu in the bone marrow. In the second trial, using intraperitoneally administered agent, no detectable bone marrow localization was observed and only mild marrow suppression was observed. The maximum tolerated dose was not reached in the second trial. Of the eight patients treated, one patient had a 75% reduction in tumor mass after therapy, one patient maintained stable disease, while six patients progressed. The results indicate that intraperitoneal administration of ¹⁷⁷Lu-PA-DOTA-CC49 can lead to antitumor activity with minimal side effects. It is not known why the different routes of administration led to differences in marrow localization. In a recent phase I trial, combination therapy with ¹⁷⁷Lu-labeled PA-DOTA conjugated antibody (CC49), Interferon and Taxol was evaluated.¹⁷² A ¹⁷⁷Lu-labeled DOTA Mab conjugate was evaluated in a non-small-cell lung carcinoma nude mouse model. They found high tumor uptake and biodistribution similar to the ⁸⁸Y analog.¹⁷³

The success of Octreoscan[®] has led to a search for an analogous therapeutic radiopharmaceutical.^{88,118,144,174,175} DOTATOC labeled with ⁹⁰Y was shown to target somatostatin-receptor-positive tumors with less renal uptake than Octreoscan[®].¹⁴² During clinical trials of ⁹⁰Y-labeled DOTATOC, kidney toxicity was encountered which limited the dose that could be delivered to the tumor.¹⁷⁶ In order to minimize or eliminate kidney toxicity, investigators began searching for alternative radionuclides that could be bound successfully to DOTA, but having a lower β^- energy than ⁹⁰Y. The lower β^- energy would have a lower penetration and result in lower kidney toxicity. Previous dosimetry studies performed in animals and humans support this approach.^{145,170,177,178}

¹⁷⁷Lu-DOTA-Tyr³-octreotate (Lu-177-DOTATATE) was studied in a therapy model using somatostatin-positive tumor-bearing rats. The agent showed better tumor localization than ⁸⁸Y and ¹¹¹In analogs and better cure rates were observed. The ¹⁷⁷Lu octreotate outperformed its octreotide analog.¹⁷⁹ Toxicity and dosimetry of ¹⁷⁷Lu-DOTA-Tyr³-octreotate were evaluated in normal and pancreatic tumor-bearing mice and low toxicity was observed.^{180,181} In a clinical trial against somatostatin-positive tumors, ¹⁷⁷Lu-DOTA-Tyr³-octreotate was compared to ¹¹¹In-DOTA-Tyr³-octreotide. Increased tumor doses were seen for the ¹⁷⁷Lu conjugate while clearance rates were similar for the two agents.¹⁸²

Lutetium-177 has a lower β^- energy than ⁹⁰Y (0.5 MeV vs. 2.28 MeV) and is stably bound by DOTA-type chelators. An additional advantage with ¹⁷⁷Lu is the imageable gamma emission

(11%, 208 keV) that can be used for dosimetry and biodistribution studies. The use of ^{177}Lu labeled to a somatostatin analog, octreotate, was initially evaluated in a rat tumor model and shown to have high therapeutic potential.^{181,182} Based on these results this agent is currently being evaluated in human clinical trials and initial results suggest a range of responses from tumor shrinkage (8/26) to stable disease (14/26) to partial remission (1/26) to tumor progression (3/26).¹⁸³ The therapeutic index obtained for the ^{177}Lu -labeled DOTATATE, shown to have better clearance and tumor uptake, is double that observed for the analogous ^{90}Y agent.¹⁸⁴ In addition, it has been shown that ^{177}Lu is more effective in treating metastases than ^{90}Y .^{185,186} The higher β^- energy of ^{90}Y , and therefore longer path length, results in the energy being deposited outside of the metastasis in normal tissue.

^{177}Lu -EDTMP was evaluated as a bone pain palliation agent and found in animal studies (rabbits) to be comparable to ^{153}Sm -EDTMP.¹⁸⁷

Recently, researchers have built on the discovery of a class of novel ^{188}Re cyclized peptides that exhibit high melanoma tumor uptake and good pharmacokinetics by designing analogs containing non-radioactive rhenium and an appended DOTA BFCA to act as a carrier for radiolanthanides.¹⁸⁸

9.20.3.1.4 Rhodium

The nuclear properties of ^{105}Rh and the kinetic inertness of low-spin, d^6 Rh^{III} complexes make this radionuclide attractive for therapeutic applications. Early studies involved complexes with N and O donor ligands, such as amine-oxime,^{189,190} amine-phenol,¹⁹¹ amine,¹⁹² and porphyrin¹⁹³ ligands. However, these ligands require harsh complexation reactions and often do not generate high yield products, although the resultant ^{105}Rh complexes are stable and kinetically inert.

Thioether-containing tetradentate ligands have been complexed with ^{105}Rh and evaluated for their utility as potential radiotherapeutic agents. The macrocyclic S_4 -ane ligand, 1,5,9,13-tetrathiacyclohexadecane-3,11-diol ([16]ane S_4 -diol),¹⁹⁴ and the linear S_4 chelates (2,5,8,11-tetrathiadodecane-1,12-dicarboxylic acid, 2,5,9,12-tetrathiatridecane-1,13-dicarboxylic acid, 1,14-diphenyl-2,6,9,13-tetrathiatetradecane and 2,6,10,14-tetrathiapentadecane-1,15-dicarboxylic acid) with varying backbone lengths (222, 232, 323, and 333)^{195,196} were found to form octahedral Rh^{III} complexes of the *cis* and/or *trans* geometry, depending on the chelate ring size (Figure 11). The ^{105}Rh complexes with these tetrathioether chelates were readily formed in high yields (>95%) at pH 4–5 and 80 °C for 1 h.^{194,196} Various tetradentate N- and/or S-containing tetradentate macrocyclic ligands were complexed with ^{105}Rh and evaluated *in vitro* for stability and *in vivo* for their biodistribution patterns.^{197,198} The more thioether donors present on the ligand in these N and/or S ligands, the higher the complexation yield with ^{105}Rh . A pentadentate N_3S_2 bicyclic macrocyclic ligand, 4,10-dithia-1,7,13-triazabicyclo[11.3.3]nonadecane, was found to complex ^{105}Rh in greater than 98% yield at pH 5 and 80 °C for 1 h (Figure 11). The X-ray crystal structure of the non-radioactive analog showed the Rh^{III} complex to have the form $[\text{RhCl}(\text{N}_3\text{S}_2)]\text{Cl}_2$, with the secondary amine *trans* to the chloride ligand.¹⁹⁹

9.20.3.1.5 Gold

Although ^{199}Au has nuclear properties suitable for radiotherapeutic applications, it has not been pursued extensively. Au^{III} is unstable to reduction, making it difficult to work with, especially at the radiotracer level. Au^{III} readily undergoes hydrolysis reactions, and the resulting Au^{III} or Au^{I} complexes formed at the macroscopic level often precipitate as sparingly soluble $[\text{AuCl}_4]^-$, $[\text{AuCl}_2]^-$, or mixed $[\text{AuCl}_4]^-/[\text{AuCl}_2]^-$ salts that are difficult to characterize. The direct radiolabeling of antibodies with ^{199}Au has been reported. It appears that ^{199}Au labels as clusters of gold bound to the antibody.^{49,200} The radiochemistry of Au^{III} complexes with tetradentate Schiff-base ligands (sal₂en and sal₂pn) (Figure 12) was investigated and efficient synthesis was demonstrated from $[\text{Bu}_4\text{N}](^{198/199}\text{AuCl}_4)$ in the presence of NH_4PF_6 at 40 °C in a dichloromethane/ethanol solution.²⁰¹ Radiochemical yields of 95–100% were observed for the formation of $[\text{Au}(\text{sal}_2\text{pn})\text{PF}_6]$.¹⁹⁸ ^{198}Au complexes with water-soluble phosphines (THP, HMPE, and HMPB) were evaluated *in vitro* for stability and *in vivo* in rats (Figure 12).²⁰² These ^{198}Au complexes were found to be stable in aqueous solution to cysteine challenge. These complexes previously had been characterized on the macroscopic level with non-radioactive gold and found to generate gold(I) complexes having a tetrahedral geometry.^{203,204}

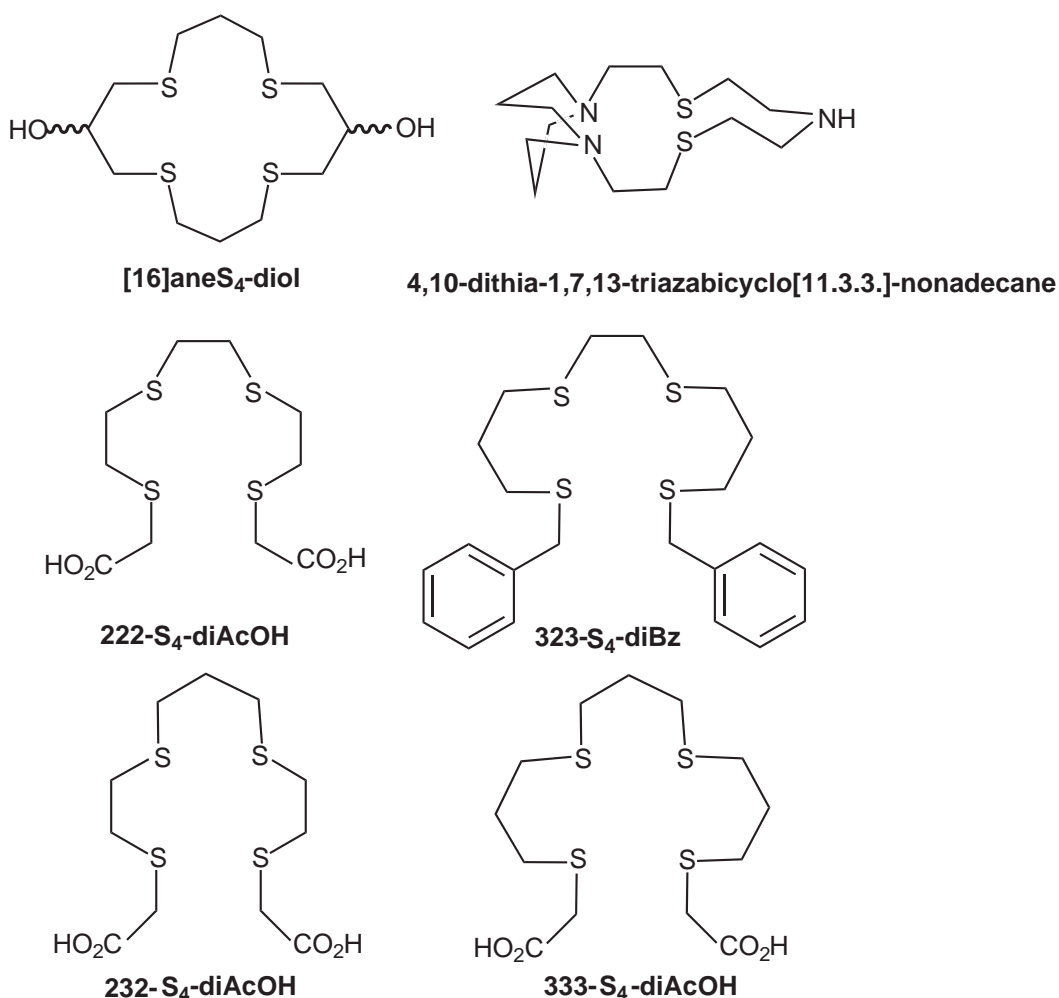


Figure 11 Ligands for Rh^{III}.

9.20.3.1.6 Scandium

⁴⁷Sc, with nuclear properties similar to those of ⁶⁷Cu, has been proposed as a potential replacement for ⁶⁷Cu by Mausner and co-workers.²⁰⁵ The anti-CEA F(ab')₂ MAb has been labeled with ⁴⁷Sc using four different chelating agents, namely, DOTA-NHS, 2-(*p*-SCN-Bz)-6-Me-DTPA, 4-isothiocyanatocyclohexyl EDTA, and the conventional DTPA anhydride method.^{50,51} The DOTA chelate was found to form the most stable complex.

9.20.3.1.7 Tin

^{117m}Sn, as the Sn⁴⁺ ion, and complexed with DTPA has been developed as a potential therapeutic agent for the alleviation of pain associated with metastatic bone cancer.^{206–213} The high abundance of short-range conversion and Auger electrons is useful for pain palliation and spares bone marrow from irradiation.²⁰⁷

9.20.3.1.8 Thallium

²⁰¹Tl, as the thallos ion (Tl⁺), has been used for imaging heart function under stress and rest conditions since about 1975. The thallos ion distributes in viable heart muscle as a potassium ion mimic, through the Na⁺-K⁺ ATPase pump. Clinical images with ²⁰¹Tl show the infarcted regions of the heart as “cold” spots or without radioactivity. ²⁰¹Tl decays by electron capture with a

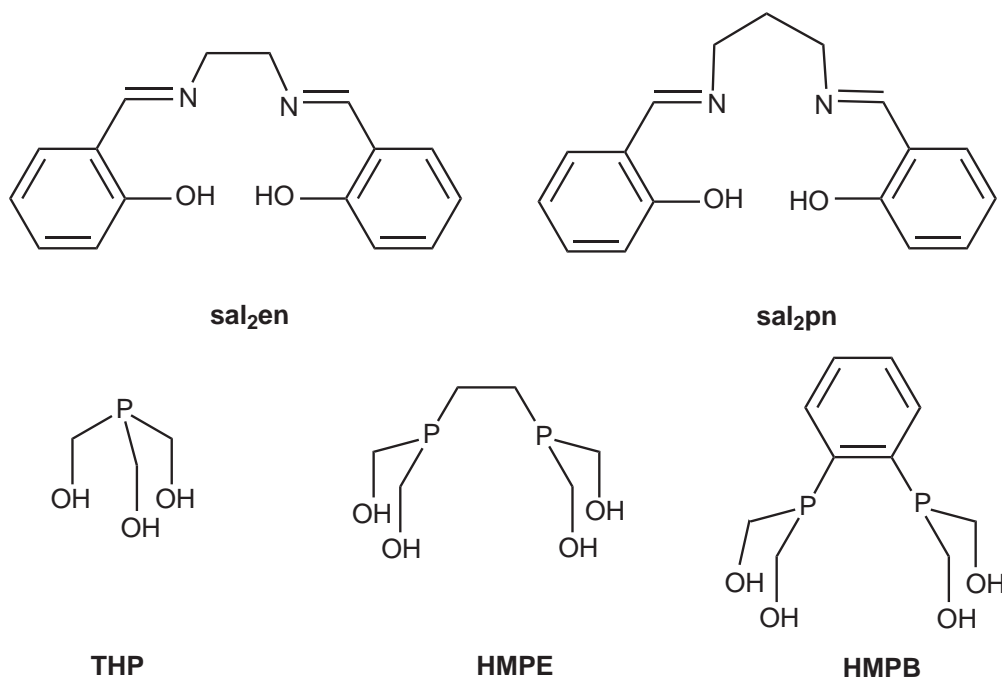


Figure 12 Ligands for Au^I and Au^{III}.

3.039-day half-life and the emission of 65–83 keV X-rays. Both the half-life and emissions are less than ideal for imaging applications.

9.20.3.1.9 Rubidium

⁸²Rb, as the rubidium ion (Rb⁺), is a potassium ion mimic and can be used to image viable myocardium. The development of an infusion generator makes this very-short-half-life (76 s) positron-emitting radionuclide useful.^{20,21}

9.20.3.1.10 Strontium

⁸⁹Sr, as the strontium ion (Sr²⁺), is used for pain palliation in patients with metastatic bone disease. The strontium ion is a calcium ion mimic, being taken up in metabolically active bone such as cancer. ⁸⁹Sr is a therapeutic radionuclide with a half-life of 50.53 days, emitting a 1.49 MeV β⁻ particle on decay. Several recent reviews discuss the use of radionuclides and their complexes as pain palliation agents in metastatic bone disease.^{18,212–215}

9.20.3.1.11 Actinium

The chemistry of Ac³⁺ is expected to be analogous to that of yttrium and the lanthanides, although its ionic radius is larger (~1.14 Å). Thus, the chelates that have been investigated for complexing ²²⁵Ac are the polyaminocarboxylates such as EDTA, DTPA, DOTA, PEPA ([¹⁵]aneN₅ analog of DOTA), HEHA ([¹⁸]aneN₆ analog of DOTA), and derivatives of these chelates (Figure 13).^{52,216,217} One study has compared EDTMP complexes of the radiolanthanides and ²²⁵Ac in tumor-bearing mice with respect to bone uptake and EDTMP concentration.¹⁶⁰ However, no real conclusions regarding ²²⁵Ac-EDTMP complexes can be made. Brechbiel and co-workers evaluated a number of linear and macrocyclic polyaminocarboxylate ligands as potential chelates for forming stable ²²⁵Ac complexes, using both *in vitro* and *in vivo* animal studies for evaluation. They evaluated the expanded-ring DOTA analogs, PEPA and HEHA, believing the size of the Ac³⁺ ion warranted a larger and higher denticity chelate. They found that the linear chelates (EDTA, CHX-DTPA) were not good ligands for ²²⁵Ac because high liver and bone

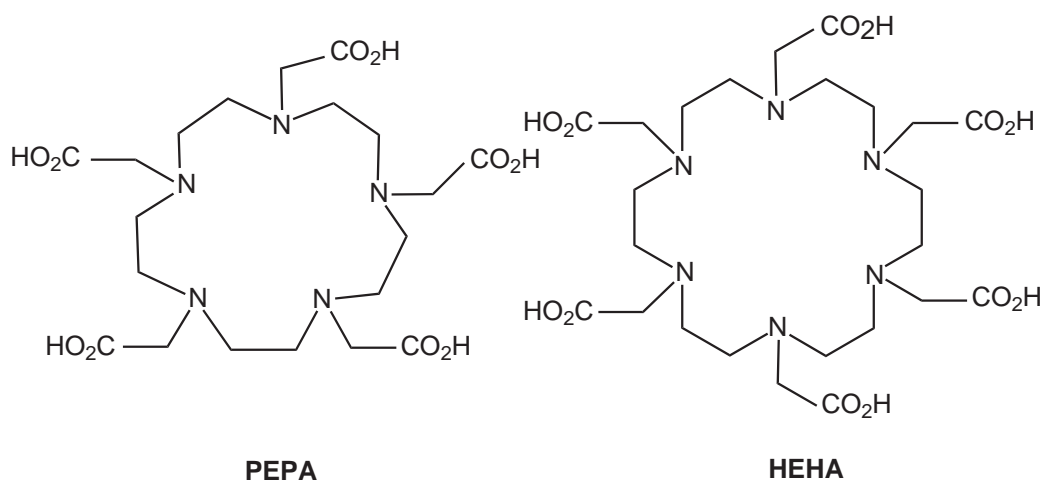


Figure 13 Macrocyclic polyaminocarboxylate ligands for Ac^{III} .

uptake were observed in mice at all time points.^{216,217} The macrocyclic chelates were better. The ^{225}Ac complex with DOTA was significantly more stable than observed for the linear analogs, and its complex with HEHA showed very good stability ($<0.3\%$ ID/g in liver and $<0.03\%$ ID/g in bone at all time points). The PEPA chelate, however, did not exhibit *in vivo* stability ($>15\%$ ID/g in liver at all time points).^{216,217} Conjugation of the HEHA chelate to antibodies, and evaluation of the ^{225}Ac -labeled MAb showed that they were not stable *in vitro* in serum at 37°C , having decreased to $<50\%$ radiochemical yield after 24 h.²¹⁸ Scheinberg and co-workers have evaluated DOTA-conjugated antibodies labeled with ^{225}Ac .⁵² The *in vitro* serum stability of these ^{225}Ac MAb conjugates was very good, with less than 5% loss of the ^{225}Ac label over 15 days at 37°C . The *in vivo* studies in tumor-bearing mice showed a dose response and increased survival times compared to the control animals after administration of ^{225}Ac -DOTA-Mab.⁵² The authors suggest that the “ ^{225}Ac nanogenerator,” referring to the generation of several daughter emissions in addition to the ^{225}Ac α emission, may be a very efficacious approach to targeted radiotherapy.⁵²

9.20.3.1.12 Bismuth and Lead

Since ^{212}Pb is the parent radionuclide of ^{212}Bi , it has been used as a means of delivering ^{212}Bi to cancer cells. The ^{212}Pb is complexed to an appropriate chelate (generally a DOTA analog) and then injected into animals to deliver the ^{212}Bi complex, which is generated on decay of ^{212}Pb . Gansow and co-workers have demonstrated that ^{206}Bi - and ^{203}Pb -labeled DOTA immunoconjugates are each separately stable *in vivo*.^{219,220} However, when ^{212}Pb complexed to DOTA was injected into animals as a means of delivering ^{212}Bi -DOTA, Mirzadeh and co-workers reported that 36% of the ^{212}Bi was released from ^{212}Pb -DOTA on β^- decay of the ^{212}Pb .²²¹ Horak and co-workers investigated the use of the immunoconjugate ^{212}Pb -DOTA-AE1 for treating ovarian tumors in mice after an intraperitoneal injection (*i.p.* injection).²²² The investigators did not carry out biodistribution studies with the ^{212}Pb -DOTA-AE1 immunoconjugate, only dose-toxicity studies in tumor-bearing mice, and they determined that this agent did not possess the properties necessary for successful radiotherapy applications (i.e., combination of chelate, antibody, tumor model, tumor size were not ideal).²²² The dithiol chelating agents, 2,3-dimercapto-1-propanesulfonic acid (DMPS) and *meso*-2,3-dimercaptosuccinic acid (DMSA), were evaluated as potential adjuvants for ^{212}Pb or ^{212}Bi immunoconjugates to address the issue of the stability of these radiometal chelate-immunoconjugates.²²³ In this study, mice were injected with $^{205/206}\text{Bi}$ acetate following two days of oral supplementation of DMPS or DMSA. The mice were then maintained on the chelating agent for three days following intraperitoneal injection of the radionuclide. The conclusion from the study was that DMPS deserved further investigation as an adjuvant for ^{212}Pb and ^{212}Bi radioimmunotherapy since it was effective at clearing $^{205/206}\text{Bi}$ through the kidneys, and the bone uptake was significantly reduced.²²³

The oxidation state +3 of bismuth is of primary interest for radiotherapy applications. As such, various polyaminocarboxylate ligands have been investigated as chelates for ^{212}Bi and ^{213}Bi .

Recent reviews of the use of ^{212}Bi and ^{213}Bi in radiotherapy have been published.^{224–231} The DOTA chelate, conjugated to appropriate biomolecules for delivery to the tumor sites, appears to be the most appropriate chelate for $^{212/213}\text{Bi}$, although some researchers are having success with the sterically hindered DTPA analog, CHX-DTPA (Figure 2).²³¹ Numerous studies have utilized an analog of DOTA conjugated to an antibody or peptide for targeted radioimmunotherapy.^{232–237} The linear polyaminocarboxylate ligands generally do not form sufficiently stable complexes for *in vivo* applications. The DOTMP ligand has been complexed with ^{212}Bi and $^{212}\text{Pb}/^{212}\text{Bi}$, and evaluated for utility in targeting bone metastases.²³⁸ The ^{212}Bi –DOTMP showed the same biodistribution in mice as did ^{14}C -labeled DOTMP, indicating that the ^{212}Bi was not released from the chelate *in vivo* (Figure 10). It also showed a similar biodistribution to ^{153}Sm –EDTMP, the currently approved radiopharmaceutical for pain palliation associated with metastatic bone disease.²³⁹ The primary non-target organs receiving radiation doses from $^{212/213}\text{Bi}$ that has been released from its chelate are the kidneys and the bone.^{223,239} Targeted radiotherapy with the high linear energy transfer (LET) α particles of ^{212}Bi and ^{213}Bi seems to be most useful for small and circulating tumor cells, since the short range of the α particles is most effective in these cases.

9.20.4 SUMMARY

A variety of radiometals have potential utility in either diagnostic or therapeutic nuclear medicine. The development of kinetically stable complexes with the radiometals is of very high importance, since loss of the radiometal *in vivo* results in radiation doses to non-target (normal) tissues. The advances in molecular biology and from the “genome project” will continue to make better tumor targeting agents available. Incorporating the appropriate radiometal and chelate to these targeting agents will continue to be a challenge, since their incorporation (conjugation) can lead to reduced biological activity of the targeting agent. There is no “ideal” radionuclide for therapeutic applications because it will be dependent on the biological targeting vector, the tumor characteristics, and the resultant radiometal complex formed. The *in vivo* biology of the agent will determine its ultimate utility.

ACKNOWLEDGMENTS

The authors would like to thank Dr. Michael J. Welch of Washington University in St. Louis, USA and Dr. Gary J. Ehrhardt of the University of Missouri Research Reactor, University of Missouri–Columbia, USA for excellent technical assistance in the compilation of Table 1.

9.20.5 REFERENCES

- Browne, E.; Dairiki, J. M.; Doeblner, R. E.; Shihab-Eldin, A. A.; Jardine, L. J.; Tuli, J. K.; Buyrn, A. B. *Table of Isotopes*, 7th ed.; Lederer, C. M., Shirley, V. S., Eds.; Wiley: New York, 1978.
- Erdtmann, G.; Soyka, W. *The Gamma Rays of the Radionuclides* **1978**, Verlag Chemie: Weinheim, Germany.
- Walker, F. W.; Parrington, J. R.; Feiner, F. Nuclides and Isotopes. In *Chart of the Nuclides*, 14th ed.; GE Nuclear Energy, General Electric Company, Nuclear Energy Operations, 175 Curtner Avenue, M/C 397, San Jose, CA, 95125 (USA), Revised 1989.
- Weber, D. A.; Eckerman, L.; Dillman, L. T.; Ryman, J. C. *MIRD: Radionuclide Data and Decay Schemes* **1989**, Society of Nuclear Medicine: New York.
- Firestone, R. B. *Table of the Isotopes*. Shirley, V. S., Ed., Baglin, C. M.; Chu, S. Y. F.; Zipkin, J.; Asst., Eds. Wiley: New York, 1996.
- Jurisson, S.; Berning, D.; Jia, W.; Ma, D. *Chem. Rev.* **1993**, *93*, 1137–1156.
- Schwochau, K. *Angew. Chem., Int. Ed. Engl.* **1994**, *33*, 2258–2267.
- Jones, A. G. *Radiochim. Acta* **1995**, *70/71*, 289–297.
- Maecke, H. R.; Eisenhut, M. Technetium complexes as radiopharmaceuticals. In *Metal–Ligand Interactions in Biological Fluids*, Berthon, G., Ed., Dekker: New York, 1995.
- Dilworth, J. R.; Parrott, S. J. *Developments in Nuclear Medicine*. **1996**, *30* (Current Directions in Radiopharmaceutical Research and Development), 1–29.
- Hom, R. K.; Katzenellenbogen, J. A. *Nucl. Med. Biol.* **1997**, *24*, 485–498.
- Jurisson, S. S.; Lydon, J. D. *Chem. Rev.* **1999**, *99*, 2205–2218.
- Liu, S.; Edwards, D. S. *J. Med. Chem.* **1999**, *99*, 2235–2268.
- Saha, G. P. *Fundamentals of Nuclear Pharmacy*, 2nd ed.; Springer-Verlag: New York, 1984.
- Spencer, R. P. *Nucl. Med. Biol.* **1986**, *13*, 461–463.
- Volkert, W. A.; Deutsch, E. A. *Adv. Met. Med.* **1993**, *1*, 115–153.
- Heeg, M. J.; Jurisson, S. S. *Acc. Chem. Res.* **1999**, *32*, 1053–1060.
- Volkert, W. A.; Hoffman, T. J. *Chem. Rev.* **1999**, *99*, 2269–2292.

19. Ercan, M. T.; Caglar, M. *Curr. Pharmac. Des.* **2000**, *6*, 1085–1121.
20. Yano, Y.; Cahoon, J. L.; Budinger, T. F. *J. Nucl. Med.* **1981**, *22*, 1006–1010.
21. Gould, K. L. *Cardiovasc. Intervent. Radiol.* **1989**, *12*, 245–251.
22. Schaab, K. M.; Ketring, A. R.; Ehrhardt, G. J.; Stringham, L. M.; Hammar, R. J. *J. Nucl. Med.* **1991**, *32*, 1040.
23. Liscic, E.; Mirzadeh, S.; Callahan, A. P.; Knapp, F. F., Jr. *J. Nucl. Med.* **1991**, *32*, 945 (abstract).
24. Ehrhardt, G. J.; Volkert, W. A.; Goeckeler, W. F.; Kapsch, D. N. *J. Nucl. Med.* **1983**, *24*, 349.
25. Chinol, M.; Hnatowich, D. J. *J. Nucl. Med.* **1987**, *28*, 1465–1470.
26. Wike, J. S.; Guyer, C. E.; Ramey, D. W.; Phillips, B. P. *Intl. J. Appl. Radiat. Isot.* **1990**, *41*, 861–865.
27. Hnatowich, D. J. *Int. J. Appl. Radiat. Isot.* **1977**, *28*, 169–181.
28. Green, M. A.; Welch, M. J. *J. Nucl. Med. Biol.* **1989**, *16*, 435–448.
29. Mathias, C. J.; Welch, M. J.; Raichle, M. E.; Mintun, M. A.; Lich, L. L.; McGuire, A. H.; Zinn, K. R.; John, E. K.; Green, M. A. *J. Nucl. Med.* **1990**, *31*, 351.
30. Green, M. A.; Mathias, C. J.; Welch, M. J.; McGuire, A. H.; Perry, D.; Fernandez-Rubio, F.; Perlmutter, J. S.; Raichle, M. E.; Bergmann, S. R. *J. Nucl. Med.* **1990**, *31*, 1989.
31. Fujibayashi, Y. M. K.; Yonekura, Y.; Konishi, J.; Yokoyama, A. *J. Nucl. Med.* **1996**, *30*, 1838.
32. Matsumoto, K. F. Y.; Konishi, J.; Yokoyama, A. *Radioisotopes* **1990**, *39*, 482.
33. Heppeler, A.; Froidevaux, S.; Eberle, A. N.; Maecke, H. R. *Curr. Med. Chem.* **2000**, *7*, 971–994.
34. Behr, T. M.; Behe, M.; Lohr, M.; Sgouros, G.; Angerstein, C.; Wehrmann, E.; Nebendahl, K.; Becker, W. *Eur. J. Nucl. Med.* **2000**, *27*, 753–765.
35. Liu, S.; Edwards, D. S. *Bioconjugate Chem.* **2001**, *12*, 7–34.
36. Anderson, C. J.; Welch, M. J. *Chem. Rev.* **1999**, *99*, 2219–2234.
37. Ehrhardt, G. J.; Welch, M. J. *J. Nucl. Med.* **1978**, *19*, 925–929.
38. Ehrhardt, G. J.; Symes, S.; Guimon, R. K.; Zinn, K. R. *Nucl. Sci. Eng.* **1992**, *110*, 369–373.
39. Mausner, L. F.; Mirzadeh, S.; Ward, T. E. *Radiation Effects* **1986**, *94*, 59–63.
40. Campbell, D. O. *J. Inorg. Nucl. Chem.* **1973**, *35*, 3911–3919.
41. Sisson, D. H.; Mode, V. A.; Campbell, D. O. *J. Chromatography* **1972**, *5799*, 129–135.
42. Lawless, F. R.; Wahlgren, M. A. *J. Radioanalyt. Chem.* **1970**, *5*, 11–20.
43. Lebedev, N. A.; Novgorodov, A. F.; Misiak, R.; Brockmann, J.; Rosch, F. *Appl. Radiat. Isot.* **2000**, *53*, 421–425.
44. Horwitz, E. P.; Bloomquist, C. A. A. *J. Inorg. Nucl. Chem.* **1975**, *17*, 425–434.
45. Horwitz, E. P.; Bloomquist, C. C. A.; Henderson, D. A.; Nelson, D. J. *J. Inorg. Nucl. Chem.* **1969**, *31*, 3255–3271.
46. Pin, C.; Zaldueni, J. F. S. *Analytical Chim. Acta* **1997**, *339*, 79–89.
47. Grazman, B.; Troutner, D. E. *Radiat. Isot.* **1988**, *39*, 257–260.
48. Jia, W.; Ma, D.; Volkert, E. W.; Ketring, A. R.; Ehrhardt, G. J.; Jurisson, S. S. *Platinum Met. Rev.* **2000**, *44*, 50–55.
49. Kolsky, K. L.; Mausner, L. F. *Appl. Radiat. Isot.* **1993**, *44*, 553–560.
50. Kolsky, K. L.; Joshi, V.; Mausner, L. F.; Srivastava, S. C. *Appl. Radiat. Isot.* **1998**, *49*, 1541–1549.
51. Pietrelli, L.; Mausner, L. F.; Kolsky, K. L. *J. Radioanal. Nucl. Chem.* **1992**, *157*, 335–345.
52. McDevitt, M. R.; Ma, D.; Lai, L. T.; Simon, J.; Borchardt, P.; Frank, R. K.; Wu, K.; Pellegrini, V.; Curcio, M. J.; Miederer, M.; Bander, N. H.; Scheinberg, D. A. *Science* **2001**, *294*, 1537–1540.
53. Atcher, R. W.; Hines John, J.; Friedman, A. M. *J. Radioanal. Nucl. Chem.* **1987**, *117*, 155–162.
54. Atcher, R. W.; Friedman, A. M.; Hines, J. J. *Appl. Radiat. Isot.* **1988**, *39*, 283–286.
55. Hassfjell, S. P.; Hoff, P. *Appl. Radiat. Isot.* **1994**, *45*, 1021–1025.
56. Hassfjell, S. B.; Brechbiel, M. W. *Chem. Rev.* **2001**, *101*, 2019–2036.
57. Lambrecht, R. M.; Tomiyoshi, K.; Sekine, T. *Radiochim. Acta* **1997**, *77*, 103–123.
58. Mirzadeh, S. *Appl. Radiat. Isot.* **1998**, *49*, 345–349.
59. Wu, C.; Brechbiel, M. W.; Gansow, O. A. *Radiochim. Acta* **1997**, *79*, 141–144.
60. Ma, D.; McDevitt, M. R.; Finn, R. D.; Scheinberg, D. A. *Appl. Radiat. Isot.* **2001**, *55*, 667–678.
61. Jang, Y. H.; Blanco, M.; Dasgupta, S.; Keire, D. A.; Shively, J. E.; Goddard, W. A.; III. *J. Am. Chem. Soc.* **1999**, *121*, 6142–6151.
62. Renn, O.; Goodwin, D. A.; Studer, M.; Moran, J. K.; Jacques, V.; Meares, C. F. *J. Controlled Release* **1996**, *39*, 239–249.
63. Goodwin, D. A.; Meares, C. F. *Cancer* **1997**, *80*, 2675–2680.
64. Chinol, M.; Paganelli, G.; Sudati, F.; Meares, C.; Fazio, F. *Nucl. Med. Commun.* **1997**, *18*, 176–182.
65. Axworthy, D. B.; Reno, J. M.; Hylarides, M. D.; Mallett, R. W.; Theodore, L. J.; Gustavson, L. M.; Su, F. M.; Hobson, L. J.; Beaumier, P. L.; Fritzbeg, A. R. *Proc. Natl. Acad. Sci.* **2000**, *97*, 1802–1807.
66. Paganelli, G.; Grana, C.; Chinol, M.; Cremonesi, M.; De Cicco, D.; De Braud, F.; Robertson, C.; Zurrida, S.; Casadio, C.; Zoboli, S.; Siccardi, A. G.; Veronesi, U. *Eur. J. Nucl. Med.* **1999**, *26*, 348–357.
67. Paganelli, G.; Orecchia, R.; Jereczek-Fossa, B.; Grana, C.; Cremonesi, M.; De Braud, F.; Tradati, N.; Chinol, M. *Eur. J. Nucl. Med.* **1998**, *25*, 1336–1339.
68. Cremonesi, M.; Ferrari, M.; Chinol, M.; Stabin, M. G.; Grana, C.; Prisco, G.; Robertson, C.; Tosi, G.; Paganelli, G. *Eur. J. Nucl. Med.* **1999**, *26*, 110–120.
69. Cutler, C. S.; Giron, M. C.; Reichert, D. E.; Snyder, A. Z.; Herrero, P.; Anderson, C. J.; Quarless, D. A.; Koch, S. A.; Welch, M. J. *J. Nucl. Med. Biol.* **1999**, *26*, 305–316.
70. Fiquet, M.; Averbuch-Pouchot, M. T.; du Moulinet d'Hardemare, A.; Jarjayes, O. *Eur. J. Inorg. Chem.* **2001**, 2089–2096.
71. Paek, C.; Kang, S. O.; Ko, J.; Carroll, P. J. *Organometallics* **1997**, *16*, 4755–4758.
72. Paek, C.; Kang, S. O.; Ko, J.; Carroll, P. J. *Organometallics* **1997**, *16*, 1503–1506.
73. Paek, C.; Kang, S. O.; Ko, J.; Carroll, P. J. *Organometallics* **1997**, *16*, 2110–2115.
74. Liu, S.; Wong, E.; Rettig, S. J.; Orvig, C. *Inorg. Chem.* **1993**, *32*, 4268–4276.
75. Caravan, P.; Rettig, S. J.; Orvig, C. *Inorg. Chem.* **1997**, *36*, 1306–1315.
76. Wong, E.; Liu, S.; Lugger, T.; Hahn, F. E.; Orvig, C. *Inorg. Chem.* **1995**, *34*, 93–101.
77. Wong, E.; Liu, S.; Rettig, S. J.; Orvig, C. *Inorg. Chem.* **1995**, *34*, 3057–3064.
78. Ma, R.; Motekaitis, R. J.; Martell, A. E. *Inorg. Chim. Acta.* **1995**, *233*, 137–143.
79. Benoist, E.; Gestin, J.-F.; Blanchard, P.; Jubault, M.; Quintard, J.-P. *Transition Met. Chem.* **1999**, *24*, 42–48.

80. Hnatowich, D. J.; Lane, W. W.; Childs, R. L. *Int. J. Appl. Radiat. Isot.* **1982**, *33*, 327–332.
81. Quadri, S. M.; Shao, Y.; Blum, J. E.; Lechner, P. K.; Williams, J. R.; Vriesendorp, H. M. *Nucl. Med. Biol.* **1993**, *20*, 559–570.
82. Vriesendorp, H. M.; Shao, Y.; Blum, J. E.; Quadri, S. M.; Williams, J. R. *Nucl. Med. Biol.* **1993**, *20*, 571–578.
83. Bakker, W. H.; Albert, R.; Bruns, C.; Breeman, W. A.; Hofland, L. J.; Marbach, P.; Pless, J.; Pralet, D.; Stolz, B.; Koper, J. W.; Lamberts, S. W. J.; Visser, T. J.; Krenning, E. P. *Life Sci.* **1991**, *49*, 1583–1591.
84. Breeman, W. A.; Hofland, L. J.; Bakker, W. H.; van der Pluijm, M.; van Koetsveld, P. M.; de Jong, M.; Setyono-Han, B.; Kwekkeboom, D. J.; Visser, T. J.; Lamberts, S. W. *Eur. J. Nucl. Med.* **1993**, *20*, 1089–1094.
85. Maina, T.; Stolz, B.; Albert, B.; Bruns, C.; Koch, P.; Maecke, H. *Eur. J. Nucl. Med.* **1994**, *21*, 437–444.
86. Anderson, C. J.; Pajeau, T. S.; Edwards, W. B.; Sherman, E. L. C.; Rogers, B. E.; Welch, M. J. *J. Nucl. Med.* **1995**, *36*, 2315–2325.
87. Wester, W. H.; Brockman, J.; Rosch, F.; Wutz, W.; Herzog, H.; Smith-Jones, P.; Stolz, B.; Bruns, C.; Stöcklin, G. *Nucl. Med. Biol.* **1997**, *24*, 275–286.
88. Krenning, E. P.; Kwekkeboom, D. J.; Bakker, W. H.; Breeman, W. A. P.; Kooij, P. P.; Oei, H. Y.; van Hagen, M.; Postema, P. T.; de Jong, M.; Reubi, J. C.; Visser, T. J.; Reijs, A. E. M.; Hofland, L. J.; Koper, J. W.; Lamberts, S. W. J. *Eur. J. Nucl. Med.* **1993**, *20*, 716–731.
89. Smith-Jones, P. M.; Stolz, B.; Albert, R.; Ruser, G.; Mäcke, H.; Briner, U.; Tolcsvai, L.; Weckbecker, G.; Bruns, C. *J. Labelled Compd. Radiopharm.* **1995**, *37*, 499–501.
90. Maraveyas, A.; Snook, D.; Hird, V.; Kosmas, C.; Meares, C. F.; Lambert, H. E.; Epenetos, A. A. *Cancer* **1994**, *73*, 1067–1075.
91. Brechbiel, M. W.; Gansow, O. A. *Bioconjugate Chem.* **1991**, *2*, 187–194.
92. Mirzadeh, S.; Brechbiel, M. W.; Archer, B.; Gansow, O. A. *Bioconjugate Chem.* **1990**, *1*, 59–65.
93. Wiseman, G. A.; White, C. A.; Stabin, M.; Dunn, W. L.; Erwin, W.; Dahlbom, M.; Raubitschek, A.; Karvelis, K.; Schultheiss, T.; Witzig, T. E.; Belanger, R.; Spies, S.; Silverman, D. H. S.; Berlfein, J. R.; Ding, E.; Grillo-Lopez, A. J. *Eur. J. Nucl. Med.* **2000**, *27*, 766–777.
94. Watanabe, N.; Sawai, H.; Endo, K.; Shinozuka, K.; Ozaki, H.; Tanada, S.; Murata, H.; Sasaki, Y. *Nucl. Med. Biol.* **1999**, *26*, 239–243.
95. Achour, B.; Costa, J.; Delgado, R.; Garrigues, E.; Geraldès, C. F. G. C.; Korber, N.; Nepveu, F.; Prata, M. I. *Inorg. Chem.* **1998**, *37*, 2729–2740.
96. Turner, A.; King, D. J.; Farnsworth, A. P. H.; Rhind, S. K.; Pedley, R. B.; Boden, J.; Boden, R.; Millican, T. A.; Millar, K.; Boyce, B.; Beeley, N. R. A.; Eaton, M. A. W.; Parker, D. *Br. J. Cancer* **1994**, *70*, 35–41.
97. McMurry, T. J.; Brechbiel, M. W.; Kumar, K.; Gansow, O. A. *Bioconjugate Chem.* **1992**, *3*, 108–117.
98. Lee, J.; Garmestani, K.; Wu, C.; Brechbiel, M. W.; Chang, J. K.; Choi, C. W.; Gansow, O. A.; Carrasquillo, J. A.; Paik, C. H. *Nucl. Med. Biol.* **1997**, *24*, 225–230.
99. Brechbiel, M. W.; McMurry, T. J.; Gansow, O. A. *Tetrahedron Lett.* **1993**, *34*, 3691–3694.
100. Li, M.; Meares, C. F.; Zhong, G.-R.; Miers, L.; Xiong, C. Y.; Denardo, S. J. *Bioconjugate Chem.* **1994**, *5*, 101–104.
101. Chen, J. Q.; Chen, Z.; Owen, N. K.; Hoffman, T. J.; Miao, Y.; Jurisson, S. S.; Quinn, T. P. *J. Nucl. Med.* **2001**, *42*, 1847–1855.
102. de Jong, M.; Bakker, W. H.; Krenning, E. P.; Breeman, W. A. P.; Vanderpluijm, M. E.; Bernard, B. F.; Visser, T. J.; Jermann, E.; Behe, M.; Powell, P.; Mäcke, H. R. *Eur. J. Nucl. Med.* **1997**, *24*, 368–371.
103. Stolz, B.; Smith-Jones, P. M.; Weckbecker, G.; Albert, R.; Knecht, H.; Haller, R.; Tolcsvai, L.; Hofman, G.; Pollehn, K.; Bruns, C. *J. Nucl. Med.* **1997**, *38*, 18P (abstract).
104. Otte, A.; Mueller-Brand, J.; Goetze, M.; Hermann, R.; Nitzsche, H. R.; Mäcke, H. R. *J. Nucl. Med.* **1998**, *39*, 70P (abstract).
105. Darling, J. L. J.; Lewis, J. S.; Mullen, G. E. D.; Rae, M. T.; Zweit, J.; Blower, P. J. *Eur. J. Nucl. Med.* **1998**, *25*, 788–792.
106. Young, H.; Carnochan, P.; Zweit, J.; Babich, J.; Cherry, S.; Ott, R. *Eur. J. Nucl. Med.* **1994**, *21*, 336–341.
107. Wada, K.; Fujibayashi, Y.; Taniuchi, H.; Tajima, N.; Tamaki, N.; Konishi, J.; Yokoyama, A. *Nucl. Med. Biol.* **1994**, *21*, 613–617.
108. Green, M. A.; Matthias, C. J.; Welch, M. J.; McGuire, A. H.; Perry, D.; Fernandez-Rubio, F.; Perlmutter, J. S.; Raichie, M. E.; Bergmann, S. R. *J. Nucl. Med.* **1990**, *31*, 1989–1996.
109. Taniuchi, H.; Fujibayashi, Y.; Okazawa, H.; Yonekura, Y.; Konishi, J. *Biol. Pharm. Bull.* **1995**, *18*, 1126–1129.
110. Fujibayashi, Y.; Cutler, C. S.; Anderson, C. J.; McCarthy, D. W.; Jones, L. A.; Sharp, T.; Yonekura, Y.; Welch, M. J. *Nucl. Med. Biol.* **1999**, *26*, 117–121.
111. Fujibayashi, Y.; Taniuchi, H.; Yonekura, Y.; Ohtani, H.; Konishi, J.; Yokoyama, A. *J. Nucl. Med.* **1997**, *38*, 1115–1160.
112. Rogers, B. E.; Anderson, C. J.; Connett, J. M.; Guo, L. W.; Edwards, W. B.; Sherman, E. L. C.; Zinn, K. R.; Welch, M. J. *Bioconjugate Chem.* **1996**, *7*, 511–522.
113. Di Bartolo, N. M.; Sargeson, A. M.; Donlevy, T. M.; Smith, S. V. *J. Chem. Soc. Dalton Trans.* **2001**, 2303–2309.
114. Motekaitis, R. J.; Sun, Y.; Martell, A. E.; Welch, M. J. *Can. J. Chem.* **1999**, *77*, 614–623.
115. Cutler, C. S.; Wuest, M.; Anderson, C. J.; Reichert, D. E.; Sun, Y. Z.; Martell, A. E.; Welch, M. J. *Nucl. Med. Biol.* **2000**, *27*, 375–380.
116. Kukis, D. L.; Li, M.; Meares, C. F. *Inorg. Chem.* **1993**, *32*, 3981–3982.
117. Motekaitis, R. J.; Sherry, A. D.; Martell, A. E.; Welch, M. J. *Nucl. Med. Biol.* **1998**, *25*, 523–530.
118. Lewis, J. S.; Lewis, M. R.; Cutler, P. D.; Srinivasan, A.; Schmidt, M. A.; Schwarz, S. W.; Morris, M. M.; Miller, J. P.; Anderson, C. J. *Clin. Cancer Res.* **1999**, *5*, 3608–3616.
119. Lewis, J. S.; Srinivasan, A.; Schmidt, M. A.; Anderson, C. J. *Nucl. Med. Biol.* **1999**, *26*, 267–273.
120. Anderson, C. J.; Dehdashti, F.; Cutler, P. D.; Schwarz, S. W.; Laforest, R.; Bass, L. A.; Lewis, J. A.; McCarthy, D. W. *J. Nucl. Med.* **2001**, *42*, 213–221.
121. Bass, L. A.; Wang, M.; Welch, M. J.; Anderson, C. J. *Bioconjugate Chem.* **2000**, *11*, 527–532.
122. Weisman, G. R.; Wong, E. H.; Hill, D. C.; Rogers, M. E.; Reed, D. P. *J. Chem. Soc. Chem. Commun.* **1996**, 947–948.
123. Ugur, O.; Kostakoglu, L.; Hui, E. T.; Fisher, D. R.; Garmestani, K.; Gansow, O. A.; Cheung, N.-K. V.; Larson, S. M. *Nucl. Med. Biol.* **1996**, *23*, 1–8.
124. Brechbiel, M. W.; Gansow, O. A.; Atcher, R. W.; Schlom, J.; Esteban, J.; Simpson, D. E.; Colcher, D. *Inorg. Chem.* **1986**, *25*, 2772–2781.

125. Martell, A. E.; Smith, R. M. (1989). *Critical Stability Constants* **1989**, Plenum: New York, Vol. 6.
126. Broan, C. J.; Jankowski, K. J.; Katakay, R.; Parker, D. *J. Chem. Soc. Chem. Commun.* **1990**, 1738–1739.
127. Keana, J. F. W.; Mann, J. S. *J. Org. Chem.* **1990**, *55*, 2868–2871.
128. Roselli, M.; Schlom, J.; Gansow, O. A. M.; Brechbiel, M. W.; Mirzadeh, S.; Pippin, C. G.; Milenic, D. E.; Colcher, D. *Nucl. Med. Biol.* **1991**, *18*, 389–394.
129. Cummins, C. H.; Rutter, E. W., Jr.; Fordyce, W. A. *Bioconjugate Chem.* **1999**, *2*, 180–186.
130. Li, W. P.; Ma, D. S.; Higginbotham, C. A.; Hoffman, T.; Ketrting, A. R.; Cutler, C. S.; Jurisson, S. S. *Nucl. Med. Biol.* **2001**, *28*, 145–154.
131. Stimmel, J. B.; Kull, F. C. *Nucl. Med. Biol.* **1998**, *25*, 117–125.
132. Moi, M. K.; Meares, C. F. *J. Am. Chem. Soc.* **1988**, *110*, 6266–6267.
133. Kang, S. I.; Rangathan, R. S.; Emswiler, J. E.; Kumar, K.; Gougoutas, J. Z.; Malley, M. F.; Tweedle, M. F. *Inorg. Chem.* **1993**, *32*, 2912–2918.
134. Howard, J. A. K.; Kemwright, A. A.; Maloney, J. M.; Parker, D.; Port, M.; Navet, M.; Rousseau, O.; Woods, M. *Chem. Commun.* **1998**, 1381–1382.
135. Spirlet, M. R.; Rebizant, J.; Desreux, J. F.; Loncin, M.-F. *Inorg. Chem.* **1984**, *23*, 359–363.
136. Chang, C. A.; Francesconi, L. C.; Malley, M. F.; Kumar, K.; Gougoutas, J. Z.; Tweedle, M. F. *Inorg. Chem.* **1993**, *32*, 3501–3508.
137. Desreux, J. F. *Inorg. Chem.* **1980**, *19*, 1319–1324.
138. Aime, S.; Botte, M.; Ermondi, G. *Inorg. Chem.* **1992**, *31*, 4291–4299.
139. Lewis, M. R.; Raubitschek, A.; Shively, J. E. *Bioconjugate Chem.* **1994**, *5*, 565–576.
140. Schott, M. E.; Schlom, J.; Siler, K.; Milenic, D. E.; Eggenesperger, D.; Colcher, D.; Cheng, R.; Kruper, W. J., Jr.; Fordyce, W.; Goeckeler, W. *Cancer* **1994**, *73*, 993–998.
141. McMurry, T. J.; Brechbiel, M.; Wu, C.; Gansow, O. A. *Bioconjugate Chem.* **1993**, *4*, 236–245.
142. Heppeler, A.; Froidevaux, S.; Mäcke, H. R.; Jermann, E.; Béhé, M.; Powell, P.; Hennig, M. *Chem. Eur. J.* **1999**, *5*, 1974–1981.
143. Otte, A.; Jermann, E.; Behe, M.; Goetze, M.; Bucher, H. C.; Roser, H. W.; Heppeler, A.; Mueller-Brand, J.; Maecke, H. R. *Eur. J. Nucl. Med.* **1997**, *24*, 792–795.
144. de Jong, M.; Breeman, W. A. P.; Bernard, B. F.; Bakker, W. H.; Srinivasan, A.; Schmidt, M. A.; Erion, J.; Bugaj, J.; Krenning, E. P. *Nucl. Med. Commun.* **2000**, *21*, 569.
145. Schlom, J.; Siler, K.; Milenic, D. E.; Eggenesperger, D.; Colcher, D.; Miller, L. S.; Houchens, D.; Cheng, R.; Kaplan, D.; Goeckeler, W. *Cancer Res.* **1991**, *21*, 2889–2896.
146. Sherry, A. D.; Brown, R. D. III; Gerales, C. F. G. C.; Koenig, S. H.; Kuan, K.-T.; Spiller, M. *Inorg. Chem.* **1989**, *28*, 620–622.
147. Sieving, P. F.; Watson, A.; Rocklage, S. M. *Bioconjugate Chem.* **1990**, *1*, 65–72.
148. Kuji, I.; Vallabhajosula, S.; Smith-Jones, P. M.; Kostakoglu, L.; Goldsmith, S. J.; Bander, N. H. *J. Nucl. Med.* **2001**, *42*, 249(abstract).
149. Smith-Jones, P. M.; Navarro, V.; St. Omer, S.; Bander, N. H. *J. Nucl. Med.* **2001**, *42*, 151 (abstract).
150. Smith-Jones, P. M.; Omer, S. S.; Navarro, V.; Bander, N. H.; Goldsmith, S. J.; Vallabhajosula, S. *J. Nucl. Med.* **2001**, *42*, 241.
151. Forster, G. J.; Engelbach, M. J.; Brockmann, J.; Reber, H. J.; Buchholz, H. G.; Maecke, H. R.; Rosch, F. R.; Herzog, H. R.; Bartenstein, P. R. *Eur. J. Nucl. Med.* **2001**, *28*, 1743–1750.
152. Goeckeler, W. F.; Edwards, B.; Volkert, W. A.; Troutner, D. E.; Holmes, R. A.; Simon, J.; Wilson, D. *J. Nucl. Med.* **1987**, *28*, 495–504.
153. Volkert, W. A.; Simon, J.; Ketrting, A. R.; Holmes, R. A.; Lattimer, L. C.; Corwin, L. A. *Drugs of the Future* **1989**, *14*, 799–811.
154. Simon, J.; Wilson, D. A.; Baughman, S. A.; McMillan, K.; Leggett, D.; Goeckeler, W. F.; Stringham, L.; Volkert, W. A. *Proc. VII Intl. Symp. Radiopharm. Chem.* **1988**, *7*, 359–361.
155. Láznicek, M.; Láznicková, A.; Budsky, F.; Prokop, J.; Kopicka, K. *Appl. Radiat. Isot.* **1994**, *45*, 949–953.
156. Serafini, A. N.; Houston, S. J.; Resche, I.; Quick, D. P.; Grund, F. M.; Ell, P. J.; Bertrand, A.; Ahmann, F. R.; Orihuela, E.; Reid, R. H.; Lerski, R. A.; Collier, B. D.; McKillop, J. H.; Purnell, G. L.; Pecking, A. P.; Thomas, F. D.; Harrison, K. A. *J. Clin. Oncol.* **1998**, *16*, 1574–1581.
157. Louw, W. K. A.; Dormehl, I. C.; Vanrensburg, A. J.; Hugo, N.; Alberts, A. S.; Forsyth, O. E.; Beverley, G.; Sweetlove, M. A.; Marais, J.; Lötter, M. G. Vanaswegen, A. *Nucl. Med. Biol.* **1996**, *23*, 935–940.
158. Zeevaart, J. R.; Jarvis, N. V.; Louw, W. K. A.; Jackson, G. E.; Cukrowski, I.; Mouton, C. J. *J. Inorg. Biochem.* **1999**, *73*, 265–272.
159. Giralt, S.; Williams, P.; Maloney, D.; Holmberg, L.; Lilleby, K.; Champlin, R.; Bensinger, W.; Eary, J.; McCullough, S.; Wendt, R.; Podoloff, D.; Ha, C.; Bryan, J. K.; Thielke, K. In Proceedings from the VII International Multiple Myeloma Workshop, Stockholm, Sweden September 1–5, 1999. O33.
160. Beyer, G. J.; Offord, R.; Kunzi, G.; Aleksandrova, Y.; Ravn, U.; Jahn, S.; Barker, J.; Tengblad, O.; Lindroos, M. *Nucl. Med. Biol.* **1997**, *24*, 367–372.
161. Loussouarn, A.; Duflos, M.; Benoist, E.; Chatal, J.-F.; Lebaud, G.; Gestin, J. F. *J. Chem. Soc. Perkin Trans.* **1998**, *1*, 237–241.
162. Kraeber-Bodéré, F.; Mishra, A.; Thédrez, P.; Faivre-Chauvet, A.; Bardiès, M.; Imai, S.; Leboterff, J.; Chatal, J.-F. *Eur. J. Nucl. Med.* **1996**, *23*, 560–567.
163. Dadachova, E.; Mirzadeh, S.; Smith, S. V.; Knapp, F. F., Jr.; Hetherington, E. L. *Appl. Radiat. Isot.* **1997**, *48*, 477–481.
164. Bugaj, J. E.; Erion, J. L.; Johnson, M. A.; Schmidt, M. A.; Srinivasan, A. *Nucl. Med. Biol.* **2001**, *28*, 327–334.
165. Mishra, A. K.; Gestin, J. F.; Benoist, E.; Faivre-chauvet, A.; Chatal, J. F. *New Journal of Chemistry* **1996**, *20*, 585–588.
166. DePalatis, L. R.; Frazier, K. A.; Cheng, R. C.; Kotite, N. J. *Cancer Res.* **1995**, *55*, 5288–5295.
167. C. D.; Wheeler, R. H.; Liu, T. P.; Grizzle, W. E.; Schlom, J.; LoBuglio, A. F. *J. Nucl. Med.* **1996**, *37*, 1491–1496.
168. Alvarez, R. D.; Partridge, E. E.; Khazaeli, M. B.; Plott, G.; Austin, M.; Kilgore, L.; Russell, C. D.; Liu, T. P.; Grizzle, W. E.; Schlom, J.; LoBuglio, A. F.; Meredith, R. F. *Gynecologic Oncology* **1997**, *65*, 94–101.
169. Buchsbaum, D. J.; Rogers, B. E.; Khazaeli, M. B.; Mayo, M. S.; Milenic, D. E.; Kashmiri, S. V. S.; Anderson, C. J.; Chappell, L. L.; Brechbiel, M. W.; Curiel, D. T. *Clin. Cancer Res.* **1999**, *5*, 3048s–3055s.

170. Mulligan, T.; Carrasquillo, J. A.; Chung, Y.; Milenic, D. E.; Schlom, J.; Feuerstein, I.; Paik, C.; Perentesis, P.; Reynolds, J.; Curt, G.; Goeckeler, W.; Fordyce, W.; Cheng, R.; Riseberg, D.; Cowan, K.; O'Shaughnessy, J. *Clin. Cancer Res.* **1995**, *1*, 1447–1454.
171. Kufe, D. W.; Hayes, D. F.; Abe, M.; Ohno, T.; Schlom, J. *In vitro Diagnosis of Human Tumors using Monoclonal Antibodies*. Kupchik, H. C., Ed., Marcel Dekker: New York, 1988.
172. Meredith, R. F.; Alvarez, R. D.; Partridge, E. E.; Khazaeli, M. B.; Lin, C. Y.; Macey, D. J.; Austin, J. M.; Kilgore, L. C.; Grizzle, W. E.; Schlom, J.; LoBuglio, A. F. *Cancer Biother. Radiopharm.* **2001**, *16*, 305–315.
173. Stein, R.; Govindan, S. V.; Chen, S.; Reed, L.; Richel, H.; Griffiths, G. L.; Hansen, H. J.; Goldenberg, D. M. *J. Nucl. Med.* **2001**, *42*, 967–974.
174. Krenning, E. P.; Kooij, P. P.; Bakker, W. H.; Breeman, W. A.; Postema, P. T.; Kwekkeboom, D. J.; Oei, H. Y.; de Jong, M.; Visser, T. J.; Reijns, A. E.; Lamberts, S. W. J. *Ann. N Y Acad. Sci.* **1994**, *733*, 496–506.
175. de Jong, M.; Breeman, W. A.; Bernard, B. F.; Rolleman, E. J.; Hofland, L. J.; Visser, T. J.; Setyono-Han, B.; Bakker, W. H.; van der Pluijm, M. E.; Krenning, E. P. *Eur. J. Nucl. Med.* **1995**, *22*, 608–616.
176. Paganelli, G.; Zoboli, S.; Cremonesi, M.; Macke, H. R.; Chinol, M. *Cancer Biother. Radiopharm.* **1999**, *14*, 477–483.
177. Schrier, D. M.; Stemmer, S. M.; Johnson, T.; Kasliwal, R.; Lear, J.; Matthes, S.; Taffs, S.; Dufton, C.; Glenn, S. D.; Butchko, G.; Ceriani, R. L.; Rovira, D.; Bunn, P.; Shpall, E. J.; Bearman, S. I.; Purdy, M.; Cagnoni, P.; Jones, R. B. *Cancer Res. (Suppl.)*. **1995**, *55*, 5921s–5924s.
178. Stewart, J. S.; Hird, V.; Snook, D.; Sullivan, M.; Myers, M. J.; Epenetos, A. A. *Int. J. Cancer* **1988**, *3*(Suppl.), 71–76.
179. Kwekkeboom, D. J.; Bakker, W. H.; Kooij, P. P. M.; Konijnenberg, M. W.; Srinivasan, A.; Erion, J. L.; Schmidt, M. A.; Bugaj, J. L.; de Jong, M.; Krenning, E. P. *Eur. J. Nucl. Med.* **2001**, *28*, 1319–1325.
180. Lewis, J. S.; Wang, M.; Laforest, R.; Wang, F.; Erion, J. L.; Bugaj, J. E.; Srinivasan, A.; Anderson, C. J. *Int. J. Cancer* **2001**, *94*, 873–877.
181. Erion, J. L.; Bugaj, J. E.; Schmidt, M. A.; Wilhelm, R. R.; Srinivasan, A. *J. Nucl. Med.* **1999**, *40*, 223P (abstract).
182. de Jong, M.; Breeman, W. A. P.; Bernard, B. F.; Bakker, W. H.; Schaar, M.; van Gameren, A.; Bugaj, J. E.; Erion, J.; Schmidt, M.; Srinivasan, A.; Krenning, E. P. *Int. J. Cancer* **2001** *92*, 628–633.
183. Kwekkeboom, D. J.; Kam, B. L.; Bakker, W. H.; Kooij, P. P.; Srinivasan, A.; Erion, J. L.; Bugaj, J. E.; Schmidt, M. A.; De Jong, M.; Krenning, E. P. *J. Nucl. Med.* **2001**, *42*, 37 (abstract).
184. Smith, M. C.; Liu, J.; Chen, T. L.; Schran, H.; Yeh, C. M.; Jamar, F.; Valkema, R.; Bakker, W.; Kvols, L.; Krenning, E.; Pauwels, S. *Digestion* **2000**, *62*, 69–72(Suppl 1).
185. Capello, A.; Krenning, E. P.; Bernard, H. F.; Breeman, W. A.; Van Den Aardweg, G.; De Jong, M. *J. Nucl. Med.* **2001**, *42*, 125 (Abstract).
186. de Jong, M.; Breeman, W. A.; Bernard, H. F.; Van Gameren, A.; Van Harskamp, E.; Bakker, W. H.; Bugaj, J. E.; Erion, J. E.; Krenning, E. P. *J. Nucl. Med.* **42** (5125)..
187. Solá, G. A. R.; Arguelles, M. G.; Bottazzini, D. L.; Furnari, J. C.; Parada, I. G.; Rojo, A.; Ruiz, H. V. *Radiochim. Acta* **2000**, *88*, 157–161.
188. Chen, J. Q.; Cheng, Z.; Owen, N. K.; Hoffman, T. J.; Miao, Y. B.; Jurisson, S. S.; Quinn, T. P. *J. Nucl. Med.* **2001**, *42*, 1847–1855.
189. Efe, E. G.; Pillai, M. R. A.; Schlemper, E. O.; Troutner, D. E. *Polyhedron*. **1991**, *10*, 1617–1624.
190. Venkatesh, M.; Schlemper, E. O.; Jurisson, S. S.; Ketring, A. R.; Volkert, W. A.; Corlija, M. *Radiochim. Acta.* **1999**, *85*, 157–163.
191. Pillai, M. R. A.; John, C. S.; Troutner, D. E. *Bioconjugate Chem.* **1990**, *2*, 191–197.
192. Pillai, M. R. A.; Lo, J. M.; John, C. S.; Troutner, D. E. *Nucl. Med. Biol.* **1990**, *17*, 419–426.
193. Pillai, M. R. A.; Lo, J. M.; Troutner, D. E. *Appl. Radiat. Isot.* **1990**, *41*, 69–73.
194. Venkatesh, M.; Goswami, N.; Volkert, W. A.; Schlemper, E. O.; Ketring, A. R.; Barnes, C. L.; Jurisson, S. *Nucl. Med. Biol.* **1996**, *23*, 33–40.
195. Goswami, N. A.; Alberto, R.; Barnes, C. L.; Jurisson, S. *Inorg. Chem.* **1996**, *35*, 7546–7555.
196. Goswami, N.; Higginbotham, C.; Volkert, W.; Alberto, R.; Nef, W.; Jurisson, S. *Nucl. Med. Biol.* **1999**, *26*, 951–957.
197. Li, N.; Eberlein, C. M.; Volkert, W. A.; Ochrymowycz, L.; Barnes, C.; Ketring, A. R. *Radiochimica Acta.* **1996**, *75*, 83–95.
198. Li, N.; Struttman, M.; Higginbotham, C.; Grall, A. J.; Skerlj, J. F.; Vollano, J. F.; Bridger, S. A.; Ochrymowycz, L. A.; Ketring, A. R.; Abrams, M. J.; Volkert, W. A. *Nucl. Med. Biol.* **1997**, *24*, 85–92.
199. Goodman, D. C. Reibenspies, J. H.; Goswami, N.; Jurisson, S.; Darensbourg, M. Y. *J. Am. Chem. Soc.* **1997**, *119*, 4955–4963.
200. Anderson, P.; Vaughan, A. T. M.; Varley, N. R. *Nucl. Med. Biol.* **1988**, *15*, 293–297.
201. Barnholtz, S. L.; Lydon, J. D.; Huang, G.; Venkatesh, M.; Barnes, C. L.; Ketring, A. R.; Jurisson, S. S. *Inorg. Chem.* **2001**, *40*, 972–976.
202. Berning, D. E.; Katti, K. V.; Volkert, W. A.; Higginbotham, C. J.; Ketring, A. R. *Nucl. Med. Biol.* **1998**, *25*, 577–583.
203. Berning, D. E.; Katti, K. V.; Barnes, C. L.; Volkert, W. A. *Chem. Ber.* **1997**, *130*, 907–911.
204. Berning, D. E.; Katti, K. V.; Barnes, C. L.; Volkert, W. A.; Ketring, A. R. *Inorg. Chem.* **1997**, *36*, 2765–2769.
205. Mausner, L. F.; Kolsky, K. L.; Joshi, V.; Sweet, M. P.; Meinken, G. E.; Srivastava, S. C. In *Scandium-47: A replacement for Cu-67 in nuclear medicine therapy with beta/gamma emitters*, Isotope Production and Applications in the 21st Century, Proceedings of the International Conference on Isotopes, Vancouver, BC, Canada, 1999; Stevenson, N. R., Ed.; World Scientific Publishing: Singapore, 1999.
206. Swailem, F. M.; Krishnamurthy, G. T.; Srivastava, S. C.; Aguirre, M. L.; Ellerson, D. L.; Walsh, T. K.; Simpson, L. *Nucl. Med. Biol.* **1998**, *25*, 279–287.
207. Srivastava, S. C.; Atkins, H. L.; Krishnamurthy, G. T.; Zanzi, I.; Silberstein, E. B.; Meinken, G.; Mausner, L. F.; Swailem, F.; D'alessandro, T.; Cabahug, C. J.; Lau, Y.; Park, T.; Madajewicz, S. *Clin. Cancer Res.* **1998**, *4*, 61–68.
208. Oster, Z. H.; Som, P.; Srivastava, S. C.; Fairchild, R. G.; Meinken, G. E.; Tillman, D. Y.; Sacker, D. F.; Richards, P.; Atkins, H. L.; Brill, A. B. *Int. J. Nucl. Med. Biol.* **1985**, *12*, 175–184.
209. Bishayee, A.; Rao, D. V.; Srivastava, S. C.; Bouchet, L. G.; Bolch, W. E.; Howell, R. W. *J. Nucl. Med.* **2000**, *41*, 2043–2050.
210. Krishnamurthy, G. T.; Swailem, F. M.; Srivastava, S. C.; Atkins, H. L.; Simpson, L. J.; Walsh, T. K.; Ahmann, F. R.; Meinken, G. E.; Shah, J. H. *J. Nucl. Med.* **1997**, *38*, 230–237.

211. Srivastava, S. C.; Meinken, G. E.; Richards, P.; Som, P.; Oster, Z.; Atkins, H. L.; Brill, A. B.; Knapp, F. F., Jr.; Butler, T. A. *Int. J. Nucl. Med. Biol.* **1985**, *12*, 167–174.
212. Silberstein, E. B. *Seminars Radiat. Oncol.* **2000**, *10*, 240–249.
213. Lewington, V. J. *Phys. Med. Biol.* **1996**, *41*, 2027–2042.
214. McEwan, A. J. B. *Cancer Biother. Radiopharm.* **1998**, *13*, 413–426.
215. De Ligny, C. L.; Gelsema, W. J.; Tji, T. G.; Huigen, Y. M.; Vink, H. A. *Nucl. Med. Biol.* **1990**, *17*, 161–179.
216. Deal, K. A.; Davis, I. A.; Mirzadeh, S.; Kennel, S. J.; Brechbiel, M. W. *J. Med. Chem.* **1999**, *42*, 2988–2992.
217. Davis, I. A.; Glowienka, K. A.; Boll, R. A.; Deal, K. A.; Brechbiel, M. W.; Stabin, M.; Bochsler, P. N.; Mirzadeh, S.; Kennel, S. J. *Nucl. Med. Biol.* **1999**, *26*, 581–589.
218. Chappell, L. L.; Deal, K. A.; Dadachova, E.; Brechbiel, M. *Bioconjugate Chem.* **2000**, *11*, 510–519.
219. Gansow, O. A.; Brechbiel, M. W.; Pippin, C. G.; McMurray, T. J.; Lambrecht, R.; Colcher, D.; Schlom, J.; Roselli, M.; Strand, M.; Huneke, R. B.; Ruegg, C. L. *Antibody, Immunoconjugates, Radiopharm.* **1991**, *4*, 413–425.
220. Ruegg, C. L.; Anderson-Berg, W. T.; Brechbiel, M. W.; Mirzadeh, S.; Gansow, O. A.; Strand, M. *Cancer Research* **1990**, *50*, 4221–4226.
221. Mirzadeh, S.; Kumar, K.; Gansow, O. A. *Radiochim. Acta* **1993**, *60*, 1–10.
222. Horak, E.; Hartmann, F.; Garmestani, K.; Wu, C.; Brechbiel, M.; Gansow, O. A.; Landolfi, N. F.; Waldmann, T. A. *J. Nucl. Med.* **1997**, *38*, 1944–1950.
223. Jones, S. B.; Tiffany, L. J.; Garmestani, K.; Gansow, O. A.; Kozak, R. W. *Nucl. Med. Biol.* **1996**, *23*, 105–113.
224. Macklis, R. M.; Kinsey, B. M.; Kassis, A. I.; Ferrara, J. L.; Atcher, R. W.; Hines, J. J.; Coleman, C. N.; Adelstein, S. J.; Burakoff, S. J. *Science* **1988**, *240*, 1024–1026.
225. Macklis, R. M.; Kaplan, W. D.; Ferrara, J. L.; Atcher, R. W.; Hines, J. J.; Burakoff, S. J.; Coleman, C. N. *Int. J. Radiat. Oncol. Biol. Phys.* **1989**, *16*, 1377–1387.
226. Gansow, O. A. *Nucl. Med. Biol.* **1991**, *18*, 369–381.
227. Vaidyanathan, G.; Zalutsky, M. R. *Phys. Med. Biol.* **1996**, *41*, 1915–1931.
228. Zalutsky, M. R.; Bigner, D. D. *Acta Oncol.* **1996**, *35*, 373–379.
229. McDevitt, M. R.; Sgouros, G.; Finn, R. D.; Humm, J. L.; Jurcic, J. G.; Larson, S. M.; Scheinberg, D. A. *Eur. J. Nucl. Med.* **1998**, *25*, 1341–1351.
230. Hassfjell, S. *Appl. Radiat. Isot.* **1**, *55*, 433–439.
231. Imam, S. K. *Int. J. Radiat. Oncol. Biol. Phys.* **2001**, *51*, 271–278.
232. Kennel, S. J.; Mirzadeh, S. *Nucl. Med. Biol.* **1998**, *25*, 241–246.
233. Kennel, S. J.; Stabin, M.; Yoriyaz, H.; Brechbiel, M.; Mirzadeh, S. *Nucl. Med. Biol.* **1999**, *26*, 149–157.
234. Adams, G. P.; Shaller, C. C.; Chappell, L. L.; Wu, C.; Horak, E. M.; Simmons, H. H.; Litwin, S.; Marks, J. D.; Weiner, L. M.; Brechbiel, M. W. *Nucl. Med. Biol.* **2000**, *27*, 339–346.
235. Sgouros, G.; Ballangrud, A. M.; Jurcic, J. G.; McDevitt, M. R.; Humm, J. L.; Erdi, Y. E.; Mehta, B. M.; Finn, R. D.; Larson, S. M.; Scheinberg, D. A. *J. Nucl. Med.* **1999**, *40*, 1935–1946.
236. McDevitt, M. R.; Finn, R. D.; Ma, D.; Larson, S. M.; Scheinberg, D. A. *J. Nucl. Med.* **1999**, *40*, 1722–1727.
237. Whitlock, J. L.; Roeske, J. C.; Dietz, M. L.; Straus, C. M.; Hines, J. J.; Horwitz, E. P.; Reba, R. C.; Rotmensch, J. *Ind. Eng. Chem. Res.* **2000**, *39*, 3135–3139.
238. Hassfjell, S. P.; Bruland, O. S.; Hoff, P. *Nucl. Med. Biol.* **24**(3), 231–237.
239. Zidenberg-Cherr, S.; Parks, N. J.; Keen, C. L. *Radiat. Res.* **1987**, *111*, 119–129.

9.21

Fluorescent Complexes for Biomedical Applications

S. FAULKNER and J. L. MATTHEWS

University of Manchester, UK

9.21.1	INTRODUCTION AND SCOPE	913
9.21.2	PHYSICAL BACKGROUND TO LUMINESCENCE	914
9.21.3	ORGANIC MOLECULES AS LUMINESCENT PROBES FOR METAL IONS	914
9.21.4	LANTHANIDE COMPLEXES AS PROBES: BASIC PHOTOPHYSICAL PROPERTIES	917
9.21.4.1	Long-lived Luminescence and Time-gating	918
9.21.4.2	Sensitization of Luminescence: Energy Transfer	919
9.21.4.2.1	Triplet-mediated energy transfer	921
9.21.4.2.2	Energy transfer mediated by LMCT	922
9.21.4.3	Solvent Effects on Lanthanide Luminescence	923
9.21.4.4	Long-wavelength Sensitization and Near-IR Luminescence	924
9.21.5	LANTHANIDE COMPLEXES IN BIOLOGICAL ASSAYS	927
9.21.5.1	Background	927
9.21.5.2	The DELFIA Assay	930
9.21.5.3	The CYBERFLUOR Assay	931
9.21.5.4	Enzyme-amplified Lanthanide Luminescence (EALL)	934
9.21.5.5	Homogeneous Assays: DEFRET	934
9.21.5.6	Assays with Near-IR Luminescent Lanthanides	935
9.21.5.7	Use of Other Metal Ions in Assays	936
9.21.6	LANTHANIDE COMPLEXES FOR IMAGING	936
9.21.7	RESPONSIVE LANTHANIDE COMPLEXES AS SENSORS	939
9.21.8	CONCLUSIONS	941
9.21.9	REFERENCES	941

9.21.1 INTRODUCTION AND SCOPE

Imaging and assay do not, at first sight, fall into the realm of coordination chemistry. This is emphatically not the case, and this chapter covers the applications of metal complexes for both imaging and assay applications. The techniques described here all rely on the emission of light by a probe molecule, which acts as a reporter group *in vitro* or *in vivo*. Such probes are non-invasive, in that they cause minimal perturbation to the system under study, and have the potential for very high sensitivity. In this chapter, we will concentrate first on the uses of (usually organic) molecules whose luminescence is modified by binding to a metal ion, and which accordingly act as sensors for these metal ions which are normally present in the biological sample. Secondly, we will review the uses of metal complexes as probes and tags in their own right. In these cases the metal in the complex is not native to the biological sample, but is part of a luminescent complex which is being used for imaging or assaying some other feature of the sample.

9.21.2 PHYSICAL BACKGROUND TO LUMINESCENCE

It is worth beginning by defining the terms used in this chapter. When a molecule or supra-molecular assembly absorbs a photon it enters an excited state which can have a variety of fates, as illustrated by simple organic chromophores. Such molecules usually have a singlet ground state (S_0). Absorption of energy promotes an electron to give the first excited singlet state (S_1). The Jablonskii diagram in Figure 1 shows each of the processes available to this excited singlet state, after relaxation to the lowest-energy vibrational level within the S_1 state. Fluorescence occurs when a photon is emitted as a result of the spin-allowed relaxation back to the ground state (the $S_1 \rightarrow S_0$ transition). The energy of the photon corresponds to the energy difference between the excited state and the acceptor level of the ground state. This process is in competition with other deactivation processes, not all of which result in the emission of light. Those which do not are called non-radiative processes, and can involve the interaction of the excited state with surrounding molecules, or with the high-energy vibrational levels of the ground state. Intersystem crossing to the triplet state (T_1) is a formally spin-disallowed process which can nevertheless occur, particularly where heavy atoms or $n \rightarrow \pi^*$ transitions result in spin-orbit coupling. Emission from the triplet state to the ground state ($T_1 \rightarrow S_0$) is known as phosphorescence, and is much longer lived than fluorescence as the transition is spin-forbidden. The term phosphorescence is also often loosely used to describe long-lived luminescence in general. The relative efficiency of luminescent processes is given by their quantum yield (defined as the ratio of the number of photons emitted to the number of photons absorbed).

9.21.3 ORGANIC MOLECULES AS LUMINESCENT PROBES FOR METAL IONS

The story of fluorescent probes begins in the mid 1970s, with the development of fluorescent probes for calcium ions. This represents an early example of interdisciplinarity at the interface between chemistry and biology, and provides an excellent starting point for this review. Most of the seminal work in this area was carried out by Roger Tsien and his co-workers, who founded two related disciplines on either side of the chemistry/biology interface, and who made two significant breakthroughs in molecular biology: namely the development of effective fluorescent probes for calcium¹ and cAMP.² The latter of these is outside the scope of this chapter, so we concentrate on the former, particularly as it represents the first case in which a fluorescent sensor was designed to operate in aqueous systems and *in vivo*.

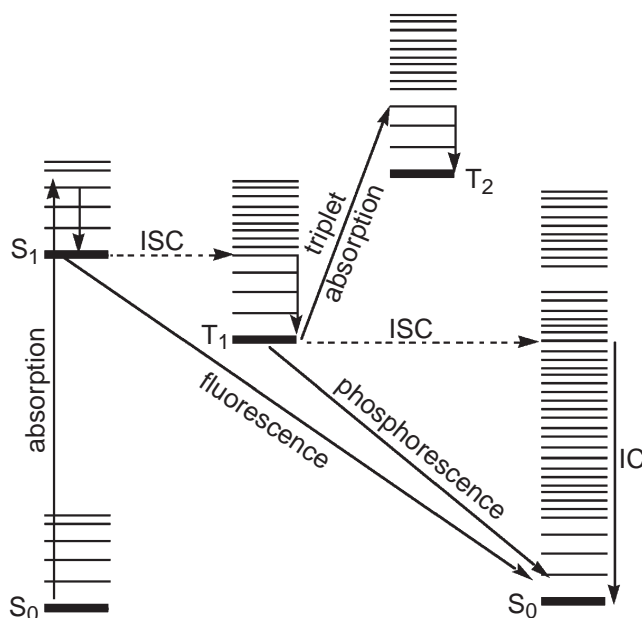


Figure 1 Jablonskii diagram illustrating the energy levels and photophysical processes for an aromatic chromophore (ISC = inter-system crossing; IC = internal conversion).

Calcium plays a critical role in many biological processes, including muscle action. As such, a method of monitoring the calcium concentration is a useful tool for physiologists. The problem is particularly challenging in several respects. First, the resting concentration of calcium ions in cells is much less than that of magnesium ions (which may compete for binding to a luminescent ligand). Secondly, changes in concentration occur rapidly, requiring millisecond-timescale response times and equally high resolution in the time-resolved luminescence measurements which will yield the calcium concentration. Thus, it is necessary that the probe has (i) high selectivity for one ion over competing analytes, and (ii) rapid kinetics for binding and release of the analyte ion. These criteria apply to all ion sensors, and the case of calcium can easily be extended to other elements.

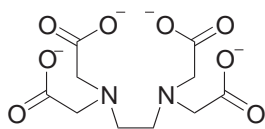
That said, calcium has been selected for its biological function with good reason, not least because it undergoes very rapid exchange of ligating groups (close to the diffusion limit). The binding of calcium by amino-carboxylate derived ligands such as EDTA (**1**) and EGTA (**2**) had also been long been established when Tsien began his investigations.^{3,4} Both ligands are based on an acyclic backbone, and EGTA offers sufficient selectivity for calcium over magnesium to be useful as a calcium buffer.⁵ However, at physiological pH, the amino groups in these amino acid-derived ligands are almost always protonated, meaning that very high concentrations would be required to bind the calcium ions.⁶ Tsien realized that conjugation of these amines with aromatic rings would change their pK_a to the point where they would not be protonated at physiological pH (7.4). The resulting ligand BAPTA (**3**), is ideal for use as a calcium buffer.⁶ However, its fluorescence properties render it unsuitable for use as a probe. It has a relatively low quantum yield; its absorption and emission maxima are at too short a wavelength for use *in vivo*, where biological chromophores like tryptophan and tyrosine also absorb and emit light; and the difference in energy between the absorption and emission maxima (the Stokes shift) is small, making it difficult to separate the signals. For widespread application a fluorescent probe should allow the use of standard non-quartz optics (i.e., it should absorb and emit light at wavelengths longer than 340 nm) and should exhibit the largest possible Stokes shift, while maintaining high-emission quantum yields for both the bound and free species.⁷

Tsien developed two ligands, INDO-1 (**4**) and FURA-2 (**5**), which go some way towards fulfilling these goals, both of which show a change in their fluorescence properties when bound to calcium ions.⁸ These ligands are highly selective for calcium ions over the other common metal ions. There is an eight-coordinate EGTA-like binding site which binds to the metal ion, attached to a conjugated chromophoric system which absorbs light in the near UV ($\lambda_{max} = 330$ nm). The amine moiety can act as an electron donor in this system while the carboxylate group at the bottom of the molecule can act as an electron acceptor, increasing the wavelength at which absorption occurs by reducing the energy gap between the HOMO and the LUMO. As with BAPTA, the aromatic parts of the molecule make the amines less basic, reducing protonation at physiological pH. This enhances the affinity for metal ions *in vivo*, since there is no competition with bound protons. The acyclic nature of these ligands helps them to equilibrate with local metal ion concentrations without difficulty since they are flexible, and since alkaline earth ions exchange ligands and solvent molecules at a rate close to the diffusion limit (many times faster than any physiological process).

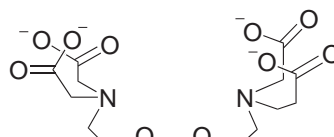
The amine lone pairs at the metal binding site are conjugated with the chromophoric unit; the extent of this conjugation depends on whether or not they are involved in ligation to a metal ion. Coordination of the N atoms to a metal ion will therefore affect the photophysical properties of the system. In the case of INDO-1, little change is observed in the absorption spectrum following metal ion binding, but the emission maximum is shifted considerably. This may be taken to indicate that the excited state is perturbed by metal binding, while the ground state is less affected.

Changes in absorption and emission wavelengths therefore arise as the result of perturbations to the chromophore.⁹ In the metal-free state, the N lone pair acts as a good electron donor, stabilizing the excited state of the chromophore and giving rise to a long-wavelength emission. When a metal ion binds to the ligand, the lone pair is intimately involved in the binding to the metal and becomes a less effective donor, making formation of the charge-transfer excited state more difficult; accordingly, the emission shifts to shorter wavelength. It is important to remember that both the free and bound forms of the ligand contribute to the overall luminescence intensity at each point. Since these contributions can be quantified, it is possible to calculate the calcium concentration.

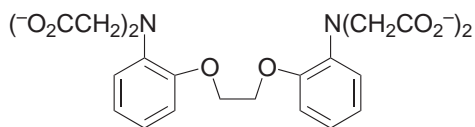
The main drawback to the INDO-1 system is autofluorescence from the sample, arising from competitive excitation of biological chromophores. If the ligand has another fault, it is that it binds so strongly to calcium that it might buffer the metal ion concentration under certain



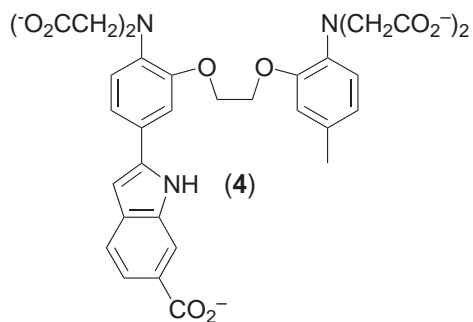
(1)



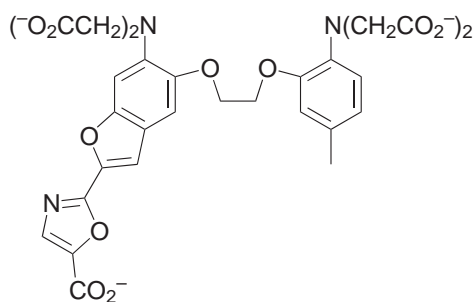
(2)



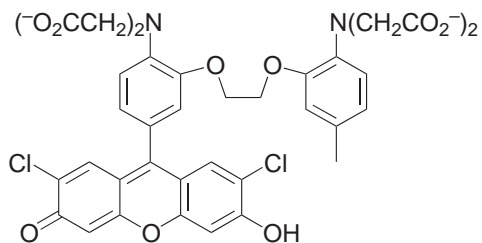
(3)



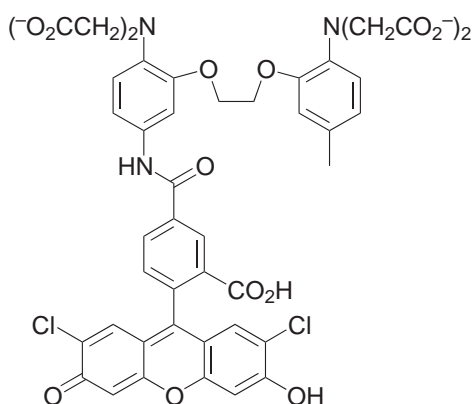
(4)



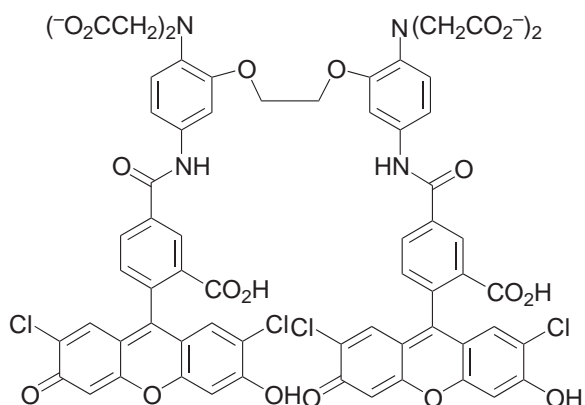
(5)



(6)



(7)



(8)

circumstances and not respond fast to changes in concentration. This has never been proved to occur, and would be difficult to circumvent without losing the selectivity over other ions which is so desirable, so most biologists seem not to worry too much about it.

It is a tribute to the rightness of the original concept that INDO-1 and FURA-2 remain in many ways the most effective molecules for luminescent sensing of calcium ions. Initially, INDO-1 was used more frequently, due to the ease with which the two emission wavelengths (from metal-free and metal-bound forms) could be monitored. Since their synthesis was reported the original paper has been cited nearly 14,000 times. In addition to the original probes, which need to be introduced into cells using invasive techniques such as patch-clamping, cell-permeant variants bearing acetoxymethyl (AM) ester substituents have become available.¹⁰ Having entered the cell, these are hydrolyzed by intracellular enzymes to liberate the free ligand, and have achieved very wide usage.

A slightly modified approach has been used to make calcium probes which operate at longer wavelengths. In these, changes in intramolecular photo-induced electron transfer (PET) on metal–ion binding is used as the basis for the luminescent sensor. Fluo-3 (**6**) and Calcium Green 1 and 2 (**7**, **8**) all contain a chromophore linked to the BAPTA binding site.^{11–13} In the absence of calcium, amine chromophore PET quenches the fluorescence from these probes. Metal binding inhibits PET because the amine lone pairs are now stabilized by coordination to a metal ion, giving enhanced fluorescence. These probe molecules operate at much longer wavelengths than INDO-1 and FURA-2. However, they do not exhibit wavelength *shifts* upon binding, but instead show a change in luminescence *intensity*, meaning that ratiometric techniques need to be used with reference to an external standard before concentrations can be quantified.¹⁴

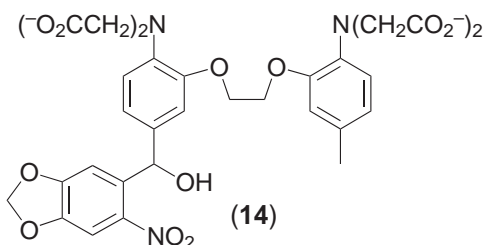
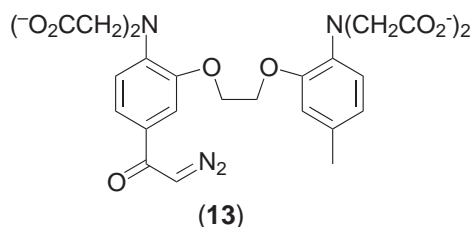
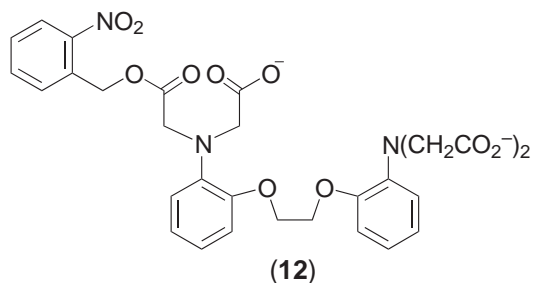
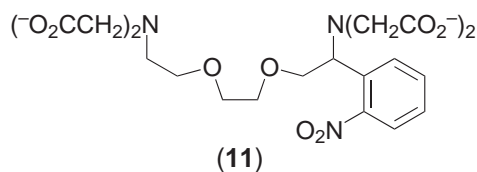
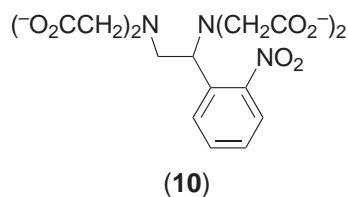
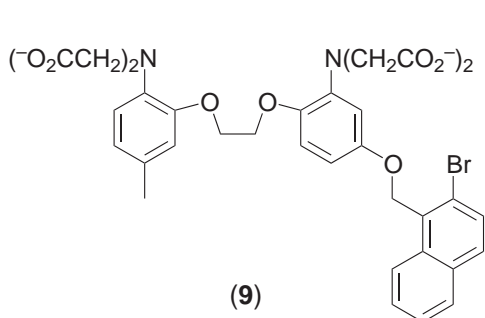
De Silva and co-workers have also investigated the theme of PET-based sensors for calcium ions (and indeed for many other ions) in fluorophore–spacer–acceptor assemblies.^{15–19} This approach has been extended to the preparation of phosphorescent systems such as (**9**), in which the bromonaphthalene chromophore can be protected by binding inside a cyclodextrin cavity. Luminescence from the bromonaphthalene unit is switched on by metal–ion binding at the aminocarboxylate site, but only as long as (i) there is no O₂ present (an effective quencher of organic triplet excited states), and (ii) the bromonaphthalene unit is protected from collisional deactivation by encapsulating it within a cyclodextrin ‘sheath’.²⁰ This sensitivity of the luminescence to a combination of several external factors (presence or absence of a metal ion; presence or absence of O₂; presence or absence of cyclodextrin) means that such molecules have the ability to act as ‘molecular logic gates’, with a positive (luminescent) readout for assembly (**9**) signalling the presence of both a metal ion and cyclodextrin and the absence of O₂.

Before leaving calcium it is worth mentioning the use of photolabile chelators to engineer rapid changes in calcium ion concentration. Kaplan *et al.* showed that DM-nitrophen (an EDTA analog bearing an *o*-nitrobenzyl group on the central diamine unit; (**10**)) undergoes rapid photolysis to cleave the metal binding site, leading to release of sequestered metal ion.²¹ This strategy permits a very large change in binding constant to be accomplished almost instantaneously. However, the EDTA-like binding fragment has limited selectivity, and synthesis of the calcium-specific analog (**11**) is much more challenging.²² Tsien *et al.* investigated the possibility of using nitrobenzyl esters as photolabile systems in which the binding constant increases after photolysis. Indeed, they observed that the binding constant of ligand (**12**) (the mono-nitrobenzyl ester of (**3**)) is lower than that of unprotected (**3**).²³ However, photolysis (to remove the ester group blocking the binding site) proved relatively ineffective in aqueous media, leading them to adopt an alternative strategy. DIAZO-2 (**13**) and NITR-5 (**14**) represent alternative strategies for photo-induced uptake and release respectively.^{23–25} These rely on relatively remote, photosensitive substituents to cause changes in the electron-donating abilities of the amine and oxygen atoms bound to the aromatic ring on BAPTA after a chemical conversion induced by photolysis. In (**13**), for example, photochemical conversion of the diazoacetyl group to an electron-donating carboxymethyl group resulted in a 30-fold increase in the binding constant for calcium ions. Since the binding site exists throughout, the changes observed tend to be very much smaller than with systems in which the entire binding site is either unmasked or cleaved by photolysis.

Calcium sensors are merely representative of a much wider class of ion sensors, albeit probably the best understood. Fluorescent probes have now been developed for a wide range of metal ions of biological interest,²⁶ particularly sodium,²⁷ potassium,²⁸ magnesium,²⁹ and zinc.³⁰

9.21.4 LANTHANIDE COMPLEXES AS PROBES: BASIC PHOTOPHYSICAL PROPERTIES

Having thus illustrated the use of organic ligands as fluorescent sensors, we will now consider the applications of the photophysical properties of coordination compounds themselves. All the



systems described above rely on reversible coordination of metal ions, typically with rapidly established equilibria; thus, the kinetic instability needed for time-resolved observation of rapid ion transients needs to be combined with high thermodynamic stability of the target complex (desirable to prevent competition from interferent anions). The circumstances associated with the use of pre-formed coordination complexes as probes are rather different. Many of the ions used are non-endogenous or toxic, and can therefore act as interferents in their own right. To overcome this problem, it is desirable to be able to form kinetically inert complexes. For the purposes of this chapter, the lanthanide series is of particular interest, though these considerations also apply in the *d*-block. In the case of lanthanides, the low penetration of *f*-orbitals and hard character of the ions mean that the ligands used for these applications tend to be challenging to prepare. However, the widespread commercial use of lanthanide-containing MRI contrast agents (see Chapter 9.19) has ensured that there is a broad base of expertise when it comes to preparing suitable ligands for these applications. Before considering the ligands and complexes themselves, it is worth considering the nature and potential benefit of the applications envisaged, and the spectroscopic properties of the lanthanides themselves.

9.21.4.1 Long-lived Luminescence and Time-gating

While fluorescent imaging techniques offer very high sensitivity, there remains the problem of background noise arising from fluorescence from the sample itself (autofluorescence).³¹ There are two strategies to overcome this: (i) two-photon excitation,³² and (ii) the use of phosphorescent

species whose emission is longer-lived than that of the sample. We will concentrate here on the latter strategy, since two-photon experiments—although they can be carried out with conventional probes—require very high pulse energies to excite the molecule *via* a virtual state, making the experiment destructive.

Autofluorescent species have luminescence lifetimes significantly less than 10 ns: the longer lifetimes required for probes in such systems are the preserve of either metal complexes or phosphorescent organic species. However, phosphorescence is not usually observed for organic chromophores, since the triplet state is easily quenched by interaction with molecular oxygen.³³ In biological systems, where dissolved oxygen is (obviously) abundant, purely organic phosphorescent probes are therefore not suitable. Thus, metal complexes are the molecules of choice for use as long-lifetime luminescent probes in biological systems.

Long luminescence lifetimes can be separated from short ones by time-gating techniques, as shown in Figure 2. By switching on the detector a fixed time, t_d , after the excitation pulse, at which time the autofluorescence has decayed away, the signal from the probe can be detected free of background interference from the sample, which greatly improves the signal-to-noise ratio compared to a conventional fluorescence experiment. Time-gating techniques have been used for a wide variety of metal complexes, particularly ruthenium complexes,³⁴ but the technique has really blossomed with the lanthanides.

9.21.4.2 Sensitization of Luminescence: Energy Transfer

In recent years, lanthanide ions have been put forward as suitable molecules for a wide range of applications in solution, including magnetic resonance imaging^{35–37} and time resolved-luminescent assay (*vide infra*). These applications have rejuvenated interest in the fundamental properties of the lanthanides since they have called for the development of new systems and the better understanding of old ones. This section deals with the development of lanthanide luminescence in solution and concentrates on sensitized luminescence from lanthanide complexes; that is, luminescence in which the metal ion enters its excited state by energy transfer from another chromophore, rather than by direct excitation. There have been a number of significant developments in recent years which merit the discussion of the properties of luminescent lanthanides in depth. These include the renewal of interest in near-IR luminescence and in the use of time-resolved methods to probe energy transfer and solvation around the metal center. We will begin by dealing with concepts that can be taken in general across the lanthanides.

All lanthanides with partly filled 4*f* shells have been shown to be luminescent.^{38–42} They all have sharp, quasi-atomic emission spectra as a result of the poor penetration of the *f*-orbitals with which transitions are associated. Figure 3 shows the energies of the *f*-centered states of some of the lanthanide ions, with emissive states marked with a*. It may be seen that nearly all of the emissive states are significantly higher in energy than the state immediately below them. Thus, luminescence occurs when there is a large energy gap between the states involved, which reduces the likelihood of non-radiative deactivation of the emissive state within the manifold of lanthanide-centered states; smaller energy gaps are more likely to match vibrational modes of the molecule, which provide a route for non-radiative deactivation. The exception to this is the ⁵D₁ state of europium, which has been shown to be emissive,^{43–45} although it has a much shorter lifetime than the lower ⁵D₀ state since radiationless deactivation to the lower-lying state is facile. It may be that other intermediate states of the lanthanides are also emissive, though they have not been reported as such.

The other notable feature of the optical spectroscopy of the lanthanide ions is that their absorption bands generally have very low extinction coefficients, because *f*–*f* transitions are

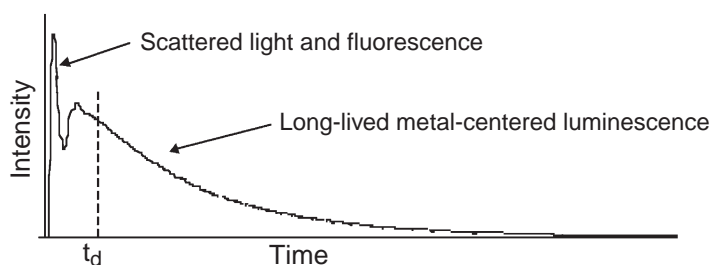


Figure 2 Time-gating as a way of separating short-lived luminescence from long-lived luminescence.

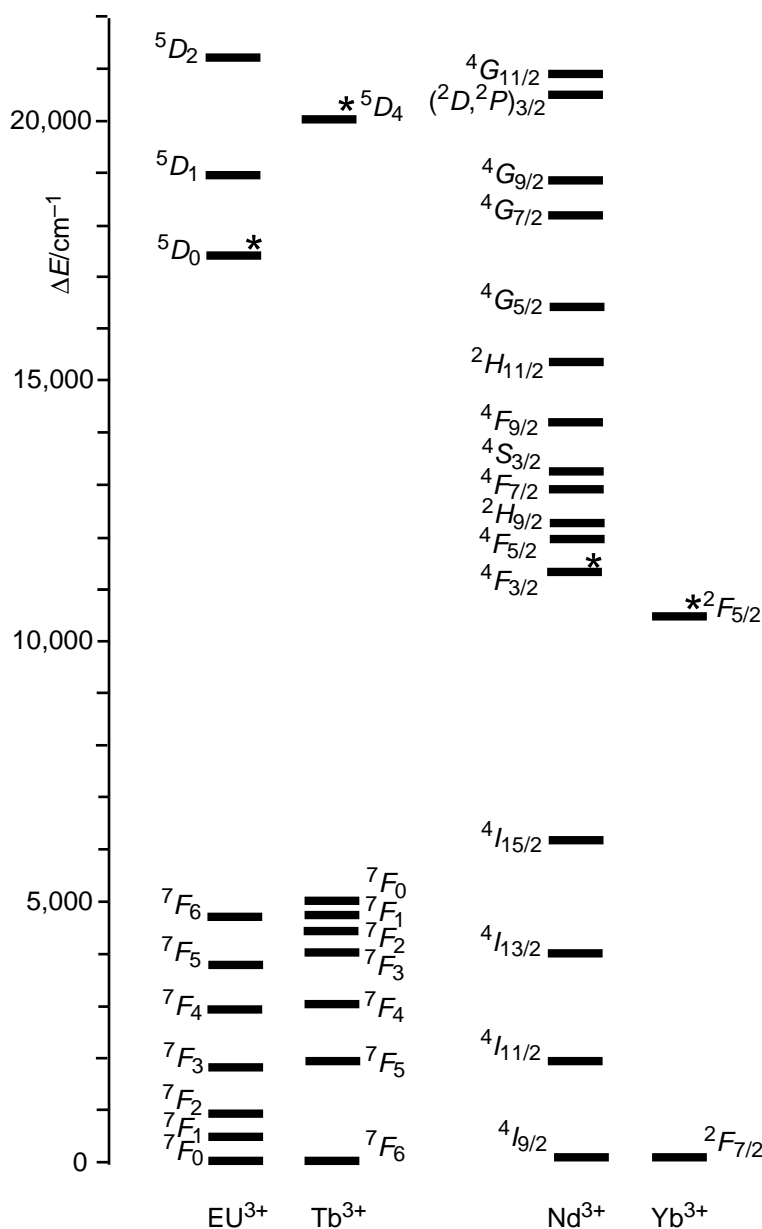


Figure 3 Energy level diagram for selected luminescent lanthanide ions.

Laporte forbidden. This means that direct excitation of the metal center is inefficient, requiring either a high concentration of the metal or excitation with very intense (laser) light,⁴⁶ thereby negating some of the advantages which might otherwise be associated with the technique. This difficulty can be overcome by the simple expedient of incorporating an aromatic chromophore into the structure of a ligand bound to the metal center.^{47,48} This provides a means by which energy can be absorbed by the complex as a whole, using the fully allowed $\pi-\pi^*$ transition of this chromophore. Energy transfer then occurs from the excited state of the aromatic unit to the metal center, as illustrated by the cartoon in Figure 4. This energy transfer means that the absorption cross-section of the overall complex is enhanced, while retaining the long lifetime associated with the metal. It does, of course, require that the ligand-centered excited state (the energy donor) is higher in energy than the lanthanide acceptor state. Transfer of energy from the chromophore to the lanthanide can vary in efficiency depending on the nature of both the chromophore and the lanthanide. Ideally, energy transfer should have a quantum yield of 1 to optimize the efficiency of other processes but in fact this is never the case.

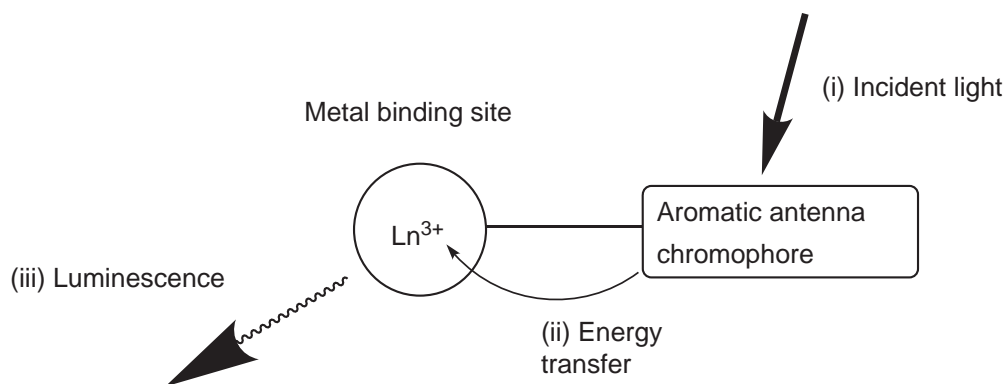


Figure 4 Cartoon illustrating sensitized emission from a lanthanide ion.

The exact mechanism of energy transfer can vary from one complex to another, and is still the subject of some debate. The possibilities are discussed in the following sections.

9.21.4.2.1 Triplet-mediated energy transfer

The most common form of energy transfer is mediated by the triplet state of the aromatic chromophore, [Figure 5](#).^{49–51} Although initial excitation generates the S_1 state of the chromophore, fast inter-system crossing (facilitated by the high spin–orbit coupling of the lanthanides) converts this to the T_1 state, which acts as the energy donor to the metal ion. In such cases, the intermediacy of the triplet state can be probed by transient triplet–triplet absorption spectroscopy. This technique is essentially a variant on the laser flash photolysis experiment: a laser pulse is used to generate the excited state of the chromophore while the sample is continuously illuminated at right angles to the incident beam. Observation of the T_1 – T_2 absorption band demonstrates the presence of the T_1 state of the chromophore and allows its decay to be observed over time. The rate constant for the decay of the T_1 – T_2 absorption band may be compared with the rise time of the metal-centered luminescence. Such processes are commonplace among the lanthanides and have been observed for a range of ligands and metal ions.

The mechanism by which energy is transferred from the T_1 state of the aromatic chromophore to the metal is more controversial. Two mechanisms have been proposed, namely Förster and Dexter energy transfer. Förster energy transfer⁵² involves overlap between the energy levels of the ligand T_1 state and the metal center; more specifically, there must be a non-zero overlap between the emission spectrum of the energy donor (the ligand T_1 state) and the absorption spectrum of the energy acceptor (the lanthanide ion). Energy transfer occurs through space and as such the efficiency of the process is expected to exhibit a dependence on r^{-6} , where r is the chromophore–metal separation. Förster energy transfer is strictly restricted to dipole–dipole interactions, but

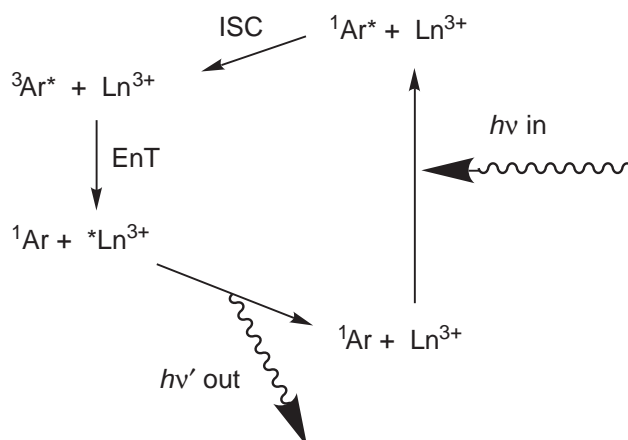


Figure 5 Triplet-mediated ligand-to-metal energy transfer in lanthanide complexes.

has been widely applied to the interaction between triplet states and lanthanide ions. Dexter energy transfer,⁵⁷ in contrast, is a double electron exchange between donor and acceptor, and involves a through-bond orbital coupling between the donor (chromophore) and the acceptor (lanthanide) components. Such a process requires that the efficiency of energy transfer should be dependent upon e^{-r} .

A variety of methods has been used to probe the energy transfer process. These include the obvious approach of using the same chromophore and lanthanide while varying the spacing between the donor and the acceptor. Though this may sound trivial, the synthesis of such systems is fraught with difficulty since it is important that the spacer between the metal and the chromophore defines the geometry precisely.⁵³ Otherwise, the determination of r becomes so difficult as to render the technique of little use. One example of the synthetic approach to this problem is that of Parker and co-workers, who developed a series of ligands incorporating the phenanthridine chromophore, in which the distance from the phenanthridinium chromophore to the Eu^{III} ion varies from 2.5 to ca. 8.2 Å.⁵³ These complexes do not provide sufficient data to confirm either energy-transfer mechanism unambiguously, but seem to agree with an r^{-6} dependence of phenanthridine $\rightarrow \text{Eu}^{\text{III}}$ energy-transfer for, except where the phenanthridine lone pair is coordinated directly to the metal center and appears to have an anomalously high quantum yield.

An alternative approach is that adopted by Horrocks and co-workers, where the aromatic residues in metal-binding proteins are used as sensitizers. Since the distance between the metal and the donor is effectively fixed, this provides a rigid scaffold for the experiment, and the absence of a directly conjugated pathway between the metals means that Förster (through space) energy transfer can be assumed. The r^{-6} distance-dependence of this means that the extent of sensitized emission from the lanthanide ion provides information on the spatial relationship between the metal-ion binding site (lanthanide ions often bind at Ca^{2+} sites) and nearby aromatic residues.^{58–60}

9.21.4.2.2 Energy transfer mediated by LMCT

An alternative energy-transfer mechanism may also be valid for some lanthanide ions, when electron transfer from the (excited) ligand to the metal is thermodynamically possible. Transfer of a “hot” electron from the excited state of the chromophore would give rise to an excited M^{2+} species. Subsequent back electron transfer could then generate the M^{3+} center in its excited state, as shown in Figure 6. There is little practical evidence for energy transfer occurring by this method, though it is thermodynamically feasible for the majority of ytterbium(III) complexes.^{61–64} Yb^{3+} has only one, relatively low energy, excited state (see Figure 3) as a result of the single hole in the f shell. This almost-complete f shell is also responsible for the relative ease of generation of Yb^{2+} . Many sensitizing triplet states have negligible spectral overlap with the absorption spectrum of Yb^{3+} , making triplet-mediated energy transfer slow and inefficient, and ineffective at competing with LMCT sensitization. For many Yb^{3+} complexes, just such a situation applies. In these cases, it is often impossible to observe any intermediate ligand-centered triplet state; nonetheless, energy transfer is still rapid and occurs within the envelope of the laser pulse. Such negative evidence does not preclude the existence of a triplet state, but does lend some credence to the hypothesis of an alternative LMCT-mediated process.

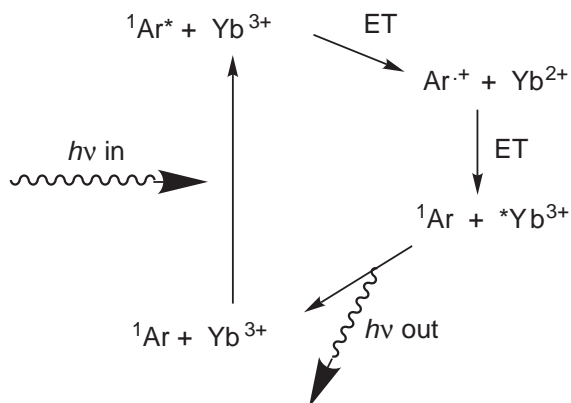


Figure 6 LMCT-mediated energy transfer in an ytterbium complex.

There are other cases in which triplet-mediated energy transfer might compete with LMCT-mediated energy transfer, particularly where the metal ion is either europium or samarium. In these cases, the redox potentials of the metal ions are such that LMCT is feasible, although the LMCT state will be lower in energy than the emissive state of the metal, precluding luminescence.⁶⁵

9.21.4.3 Solvent Effects on Lanthanide Luminescence

Significant non-radiative quenching of excited states of lanthanide ions occurs in protic solvents as a result of the spectral overlap of the emissive state of the metal center with vibrational harmonics of the O–H oscillators in the solvent.³⁸ When deuterated solvents are used, the lower energy of the O–D oscillation compared to O–H means that the excited state of the metal interacts with a higher harmonic in the O–D vibrational manifold. As a result, overlap between the metal-centered and solvent-centered wavefunctions is reduced, in accordance with the Franck–Condon principle, and the likelihood of quenching is accordingly reduced. This means that observed lifetimes for luminescence are longer in deuterated solvents than in their protic analogs. Horrocks and co-workers pointed out that, for a given complex in aqueous solution, the change in lifetime on moving from H₂O to D₂O can be related to the hydration state of the metal.^{66–68} Since the rate constants for deactivation of the excited state of the metal ion are additive, the observed rate constant for luminescence can be represented by Equation (1):

$$k_{\text{obs}} = \sum_i k_i \quad (1)$$

Changing the solvent does not influence most pathways, only those involving the solvent, while the magnitude of the change in the solvent rate constants should be proportional to the number of close-diffusing water molecules, q , so

$$q \propto (k_{\text{H}_2\text{O}} - k_{\text{D}_2\text{O}}) \quad (2)$$

or

$$q \propto (1/\tau_{\text{H}_2\text{O}} - 1/\tau_{\text{D}_2\text{O}}) \quad (3)$$

Thus,

$$q = A_{\text{Ln}}(k_{\text{H}_2\text{O}} - k_{\text{D}_2\text{O}}) \quad (4)$$

or

$$q = A_{\text{Ln}}(1/\tau_{\text{H}_2\text{O}} - 1/\tau_{\text{D}_2\text{O}}) \quad (5)$$

where A_{Ln} is an experimentally determined coefficient calculated from crystal structure values of q . On this basis the calculation of provides a good model for establishing solution state hydration numbers. Available A_{Ln} factors for lanthanides according to this model in aqueous solution are found in Table 1 (values for Nd are not included as they are highly sensitive to the presence of C–H oscillators also, which precludes use of this simple model; *vide infra*).^{40,66–72} These have been modified by various workers for use in other protic solvents, particularly alcohols, where the A

Table 1 A and B factors for some common luminescent lanthanides (for Equations (4) and (7)).

Equation	$q = A(k_{\text{H}} - k_{\text{D}})$		$q = A(k_{\text{H}} - k_{\text{D}} - B)$	
	A		A	B
<i>Aqueous systems</i>				
Eu ^{3+a}	1.05 ms		1.2 ms	(0.25 + 0.075 x) ms ⁻¹
Tb ³⁺	4.2 ms		5 ms	0.06 ms ⁻¹
Yb ³⁺	0.9 μ s		1.0 μ s	0.1 μ s ⁻¹
<i>Alcoholic systems</i>				
Eu ^{3+a}	2.1 ms		2.4 ms	(0.125 + 0.0375 x) ms ⁻¹
Tb ³⁺	8.4 ms		10 ms	0.03 ms ⁻¹
Yb ³⁺	2.0 μ s		2.0 μ s	0.05 μ s ⁻¹

^a The Parker treatment of europium requires that account is taken of x , the number of exchangeable N–H oscillators.

factors are doubled to take account of the fact that the number of close-diffusing oscillators will be halved by the change of close-diffusing molecule (i.e., only one O–H oscillator per alcohol molecule compared to two in water).

These approaches provide an effective means of estimating the solvation number, but provide little more than an estimate. Horrocks originally suggested that the fact that Equation (5) rarely produces an integral value of q was suggestive of a large error. Such errors are more significant for certain complexes than for others. For instance, the complex (15) has four N–H oscillators which exchange in D₂O solution, ensuring that their effect will differ with the degree of deuteration of the solvent. Parker and co-workers began by making a minor modification to Equation (5) to account for such oscillators.⁷³

It is also necessary to take account of outer sphere contributions to the quenching of the metal-centered excited state. The nature of the outer sphere will vary from one complex to another, depending on the size, charge, and shape of the complex. However, it is possible to correct for a “generalized” outer sphere contribution for each lanthanide giving a new equation for q which can be expressed in several ways:⁷⁴

$$q = A'_{Ln}(\Delta k_{\text{corr}}) \quad (6)$$

or

$$q = A'_{Ln}(k_{\text{H}_2\text{O}} - k_{\text{D}_2\text{O}} - B) \quad (7)$$

or

$$q = A'_{Ln}(k_{\text{H}_2\text{O}} - k_{\text{D}_2\text{O}}) - C \quad (8)$$

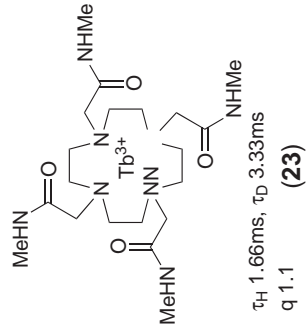
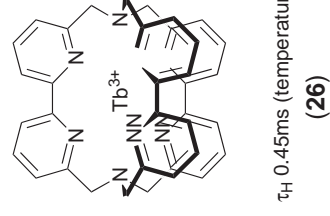
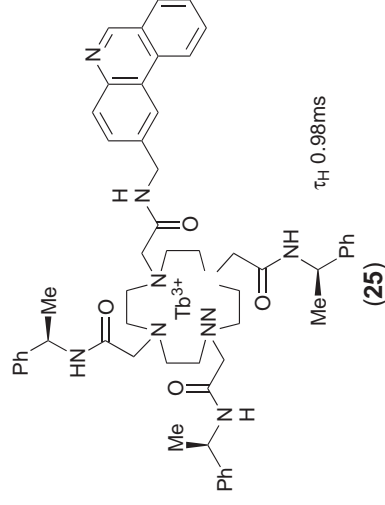
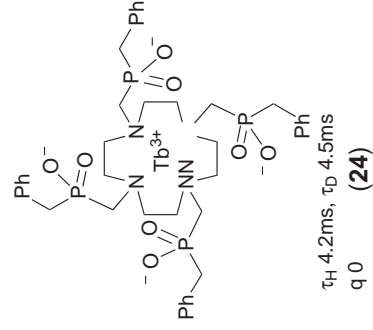
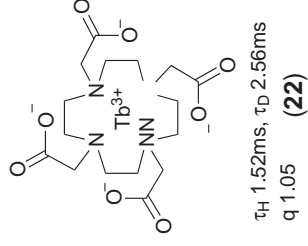
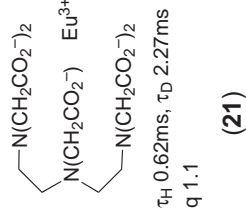
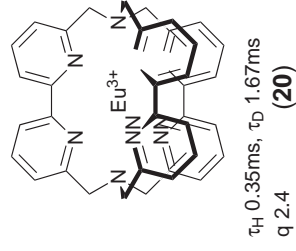
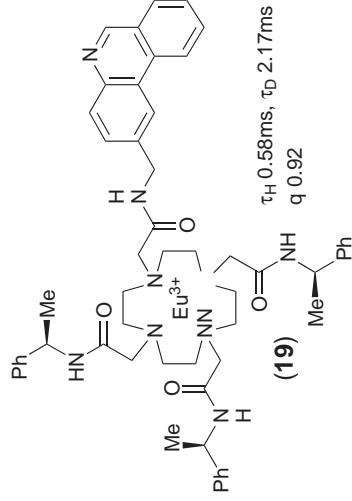
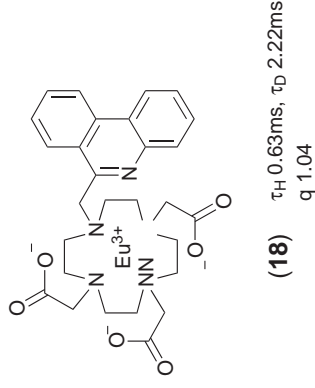
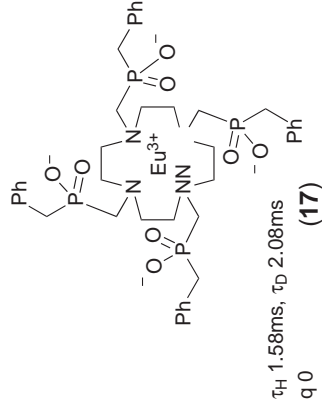
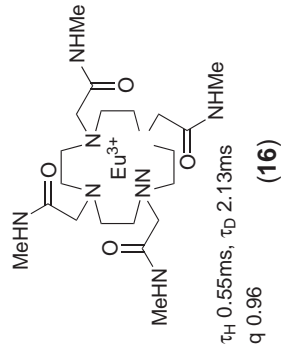
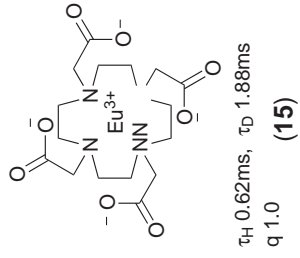
Values of A'_{Ln} and B are shown in Table 1.^{74–76} It is worth noting that both A_{Ln} and A'_{Ln} have dimensions of time, while B has dimensions of reciprocal time and C is dimensionless. It is usual to give A factors the units which correspond to the most convenient units of measuring lifetimes.

This approximation works very well for most lanthanide complexes, in that changes in structure tend to be relatively insignificant compared to the effect of solvent so far as their effect on luminescence is concerned.^{53,74–85} Figure 7 shows luminescence lifetimes and calculated inner sphere q values for a wide range of terbium, europium, and ytterbium complexes (15)–(35). It may be seen that the q values are still non-integral. This does not necessarily represent an error, since it can be seen as representing different distances for the closest approach of solvent to the metal. Thus, the closest-diffusing water molecules will have a greater effect than those which are constrained to lie further from the metal center. Horrocks has also proposed an alternative set of factors for europium complexes with three or more coordinated water molecules.^{86,87}

A more significant error appears to arise for neodymium complexes where the A'_{Nd} factor tends to work well for aminocarboxylate complexes, but breaks down completely for other types of complex, such as the Lehn cryptand (complex (29) in Figure 7), giving calculated inner sphere hydration numbers which are far too low.⁷⁵ This results from the fact that neodymium has a high density of metal-centered excited states,^{40,42} giving rise to quenching of excited states through the C–H vibrational manifold as well as through the N–H and O–H manifolds. In the cases where Equations (6–8) break down, there are comparatively few C–H oscillators close to the metal center, leading to less efficient non-radiative quenching and increased lifetime and quantum yield for the luminescence. It would be possible to account for the effects of C–H oscillators more accurately, but this would require taking into account the distance of each individual C–H oscillator from the metal center, which becomes unnecessarily complicated.

9.21.4.4 Long-wavelength Sensitization and Near-IR Luminescence

Until very recently, studies of the use of luminescent lanthanide complexes as biological probes concentrated on the use of terbium and europium complexes. These have emission lines in the visible region of the spectrum, and have long-lived (millisecond timescale) metal-centered emission. The first examples to be studied in detail were complexes of the Lehn cryptand (complexes (20) and (26) in Figure 7),^{48,50,88} whose luminescence properties have also been applied to bioassay (*vide infra*). In this case, the europium and terbium ions both have two water molecules



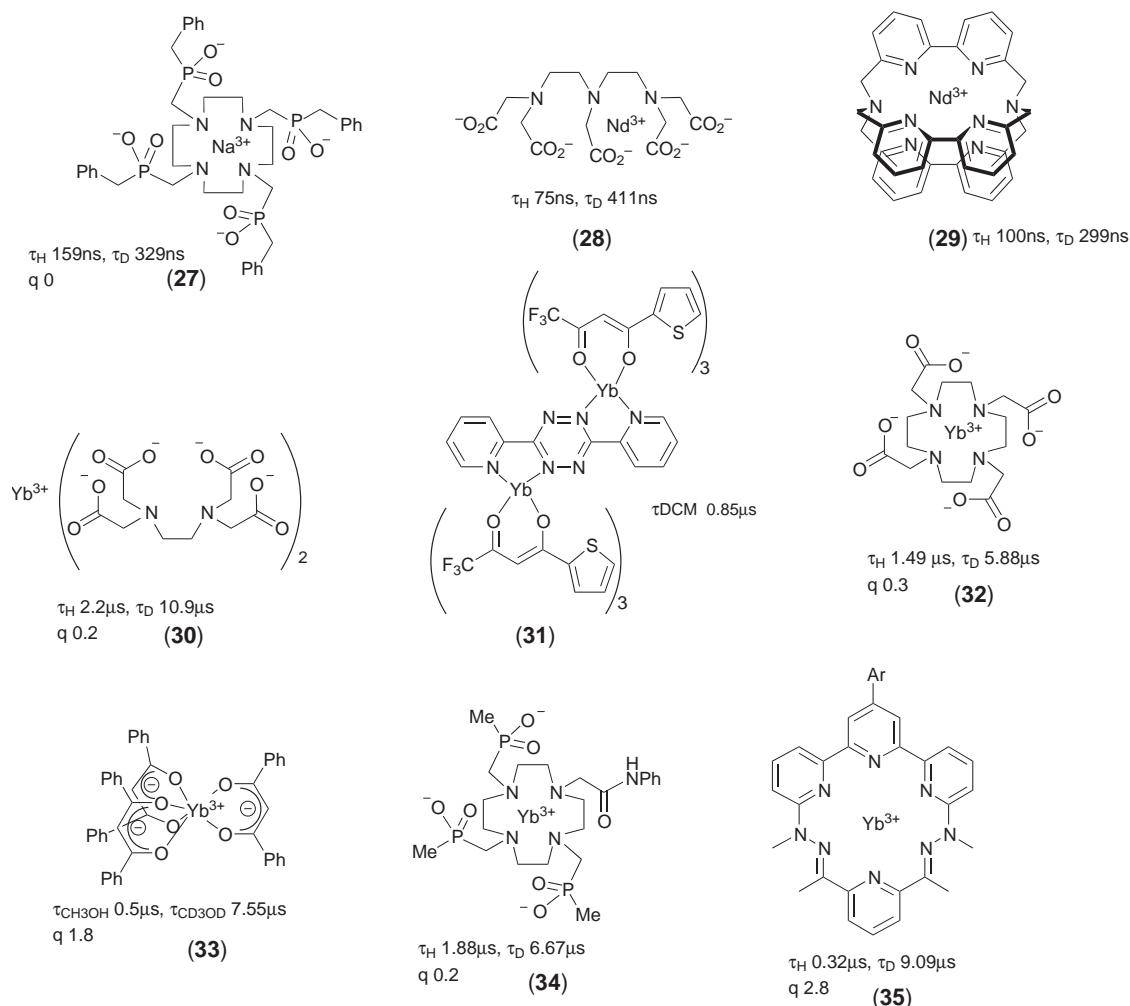
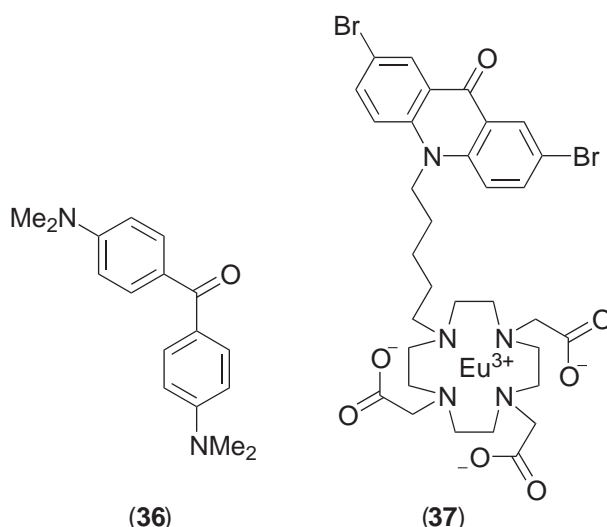


Figure 7 Luminescent lanthanide complexes with representative luminescence lifetimes, and hydration states (derived from luminescence measurements) where appropriate.

bound to the metal center in addition to the N atoms of the cryptand, and energy transfer from the bipyridyl chromophores provides an effective route to sensitized emission.

The choice of chromophore in europium and terbium complexes is limited by the large energy gap between the emissive state and the ground state. With terbium, the energy gap of $20,300\text{ cm}^{-1}$ is inconsistent with sensitization by all but relatively simple chromophores, which have high-energy triplet states; more extended chromophores such as naphthalene have triplet states close in energy to the terbium excited state,⁸⁹ making energy transfer reversible and sensitive to temperature and the concentration of dissolved oxygen. For europium (energy gap $17,500\text{ cm}^{-1}$), a wider range of chromophores with lower energy excited states can be used, but long-wavelength sensitization is difficult. The best examples (e.g. (36)–(37)) use chromophores with small differences between the energy of the triplet and singlet states, particularly aryl ketones, which have high triplet yields.^{90–93} Some of these systems can exhibit sensitized emission from europium upon excitation above 400 nm, but these represent the realistic limit of long-wavelength sensitization combined with visible emission.

The quest for lanthanide-based agents for luminescent imaging has meant that considerable importance has been attached to long-wavelength sensitization, using excitation at a wavelength outside the range of biological absorption and emission. Recently, considerable interest has centered on the use of lanthanide complexes which emit light in the near-IR region.^{40–43,49,60–64,71,72,75,76,94–101} Particular attention has been paid to solution-state luminescence from complexes of neodymium, ytterbium, and erbium. Since the emissive states of these systems are much lower



in energy than the analogous states in europium and terbium complexes, longer wavelength sensitization becomes relatively trivial. A range of ligands ((38)–(43)) suitable for excitation of these ions using visible light are shown in Figure 8;^{41,94–96,102,103} see also structure (31) in Figure 7. The ruthenium complex (42) is of particular interest, exhibiting energy transfer from the MLCT state of the ruthenium complex (excited at 450 nm) to the lanthanide center;¹⁰³ this illustrates how d-block complexes (with their wide range of absorption maxima) can be used as antenna groups for sensitization of near-IR emission from an attached lanthanide ion.

However, there is a trade-off in using near-IR emissive lanthanides, in that luminescence lifetimes are shorter, and quantum yields lower, compared to complexes of Tb and Eu. This arises because the near-IR emissive lanthanides are quenched by lower harmonics of the O–H oscillator, increasing the Franck–Condon overlap with the metal excited state. For neodymium, matters are further complicated by the manifold of available metal-centered excited states, which leads to particularly effective quenching by C–H oscillators. Thus, complexes in which there are few C–H oscillators close to the metal are desirable if the luminescence lifetime is to be optimized (e.g. 44).^{76,97–101}

Complexes such as those described above provide the bedrock of applied studies using these complexes, which we will now describe in detail.

9.21.5 LANTHANIDE COMPLEXES IN BIOLOGICAL ASSAYS

9.21.5.1 Background

As has been mentioned, the long-lived luminescence from lanthanide ions allows time-gated techniques to be used to separate the signal from the short-lived fluorescent background of biological samples. This is particularly important for time-resolved immunoassay work, where detection of ultra-trace concentrations is critical for effective assay and screening. Traditional immunoassay has used radiotracers to provide tags to study the interaction between an antibody and an antigen (Figure 9 shows the basic principles of such an assay).¹⁰⁴ While offering very high sensitivity (particularly when using scintillants to signal radioactive decay events), concerns about the use of radioisotopes have led to a search for less controversial probes. Fluorescent probes have begun to replace radioisotopes in many conventional bioassays.¹⁰⁵ In this case, it is not simply a question of locating a luminescent tag, but rather of relying on combined recognition events (Figure 10) coupled with energy transfer between two chromophores by fluorescent resonant energy transfer (FRET).¹⁰⁶ However, the sensitivity of this technique is limited by autofluorescence from biological backgrounds.

Assays based on luminescent lanthanide ions were developed initially in the 1970s, when instrumentation became available which could distinguish long-lived luminescence from a short-lived background. Leif and co-workers reported the first attempts to use lanthanide complexes (in this case europium complexes with 1,10-phenanthroline and β -diketonates, i.e., [Eu(phen)(diketonate)₃]) as tags for antibodies.¹⁰⁷ These proved kinetically unstable in the pH regime required

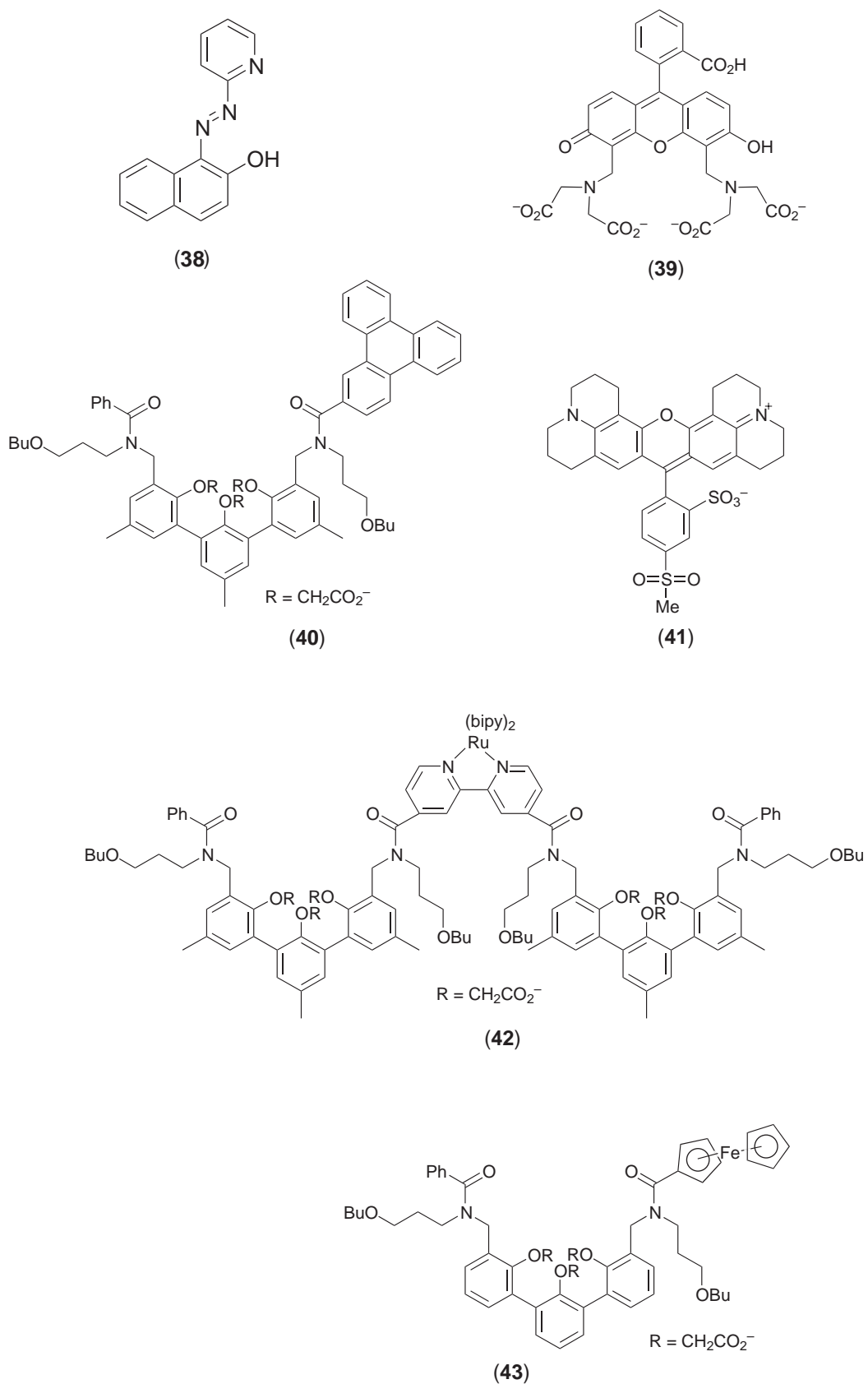
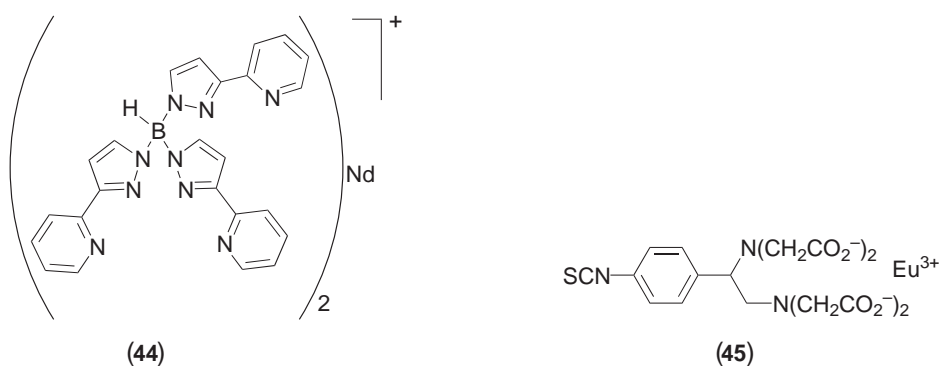


Figure 8 Sensitizers of near-IR lanthanide luminescence that are effective in the visible region of the spectrum.



for bioassay, but did show long-lived, metal-centered luminescence. They suggested that the ideal lanthanide probe complex should have the following characteristics:

- (i) a high extinction coefficient for the sensitizing chromophore;
- (ii) relatively long wavelength absorption (certainly >300 nm and ideally >340 nm, to permit the use of glass instead of quartz optics);
- (iii) kinetic stability on the timescale of the experiment; and
- (iv) functional groups which permit attachment to an antibody, without impairing immunoreactivity or binding to the surface of the vessel used for study.

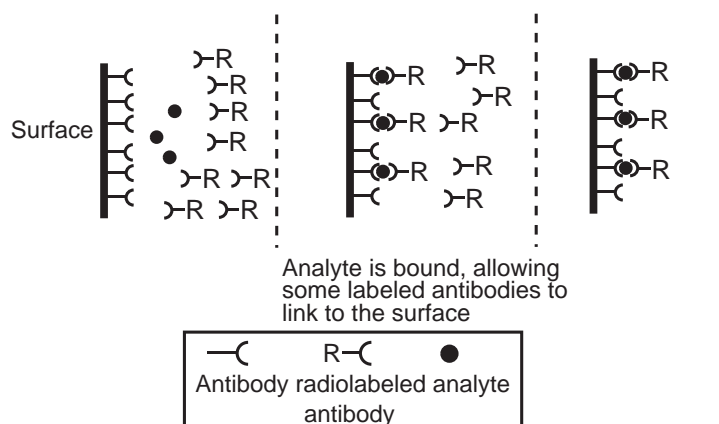


Figure 9 Representation of a typical radioimmunoassay.

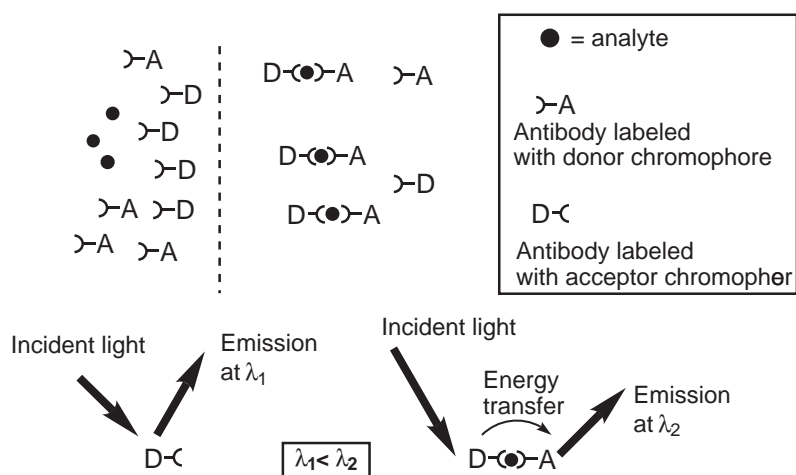


Figure 10 Representation of a typical FRET-based assay.

9.21.5.2 The DELFIA Assay

The DELFIA assay, the first effective lanthanide-based immunoassay, was developed and commercialized by the early 1980s.^{108–112} DELFIA (Dissociation Enhanced Lanthanide Fluoro-ImmunoAssay) is a heterogeneous assay which uses a lanthanide complex based on aminocarboxylate ligands such as EDTA, EGTA, or DTPA, linked to the antibody by reaction of appended isothiocyanate groups (e.g., complex (45)) with nucleophilic residues, particularly amines, on the protein surface (Figure 11).

These ligands are useful in two respects. First, they bind tightly to the lanthanide ion at physiological pH, meaning that dissociation on the experimental timescale is not likely to be a problem. Secondly, the flexible ligand framework allows the europium to be removed and coordinated to when the assay is to be “developed”. Figure 11 also shows the assay itself. A multi-well plate coated with unlabeled antibody is allowed to react with the antigen. A known quantity of the lanthanide-conjugated antibody is then added, and the mixture incubated. When the target antigen is present it acts to link the lanthanide-conjugated antibody to the surface of the plate, *via* the antigen which is itself bound to the surface-bound, unlabeled antibody. Washing the plate removes any uncomplexed antibody, meaning that the remainder can be used to quantify the amount of europium present (and hence the concentration of the target antigen). This is achieved by lowering the pH to less than 4, causing the amino groups in the ligand to become protonated, releasing the metal. The mixture is then treated with an aryl diketonate, forming a complex from which water is excluded. This complex contains a good chromophore, so sensitized luminescence is now possible, and the concentration of lanthanide ion can be determined from the luminescence intensity. The nature of this assay means that care should be taken to exclude other lanthanides from the reaction mixture.

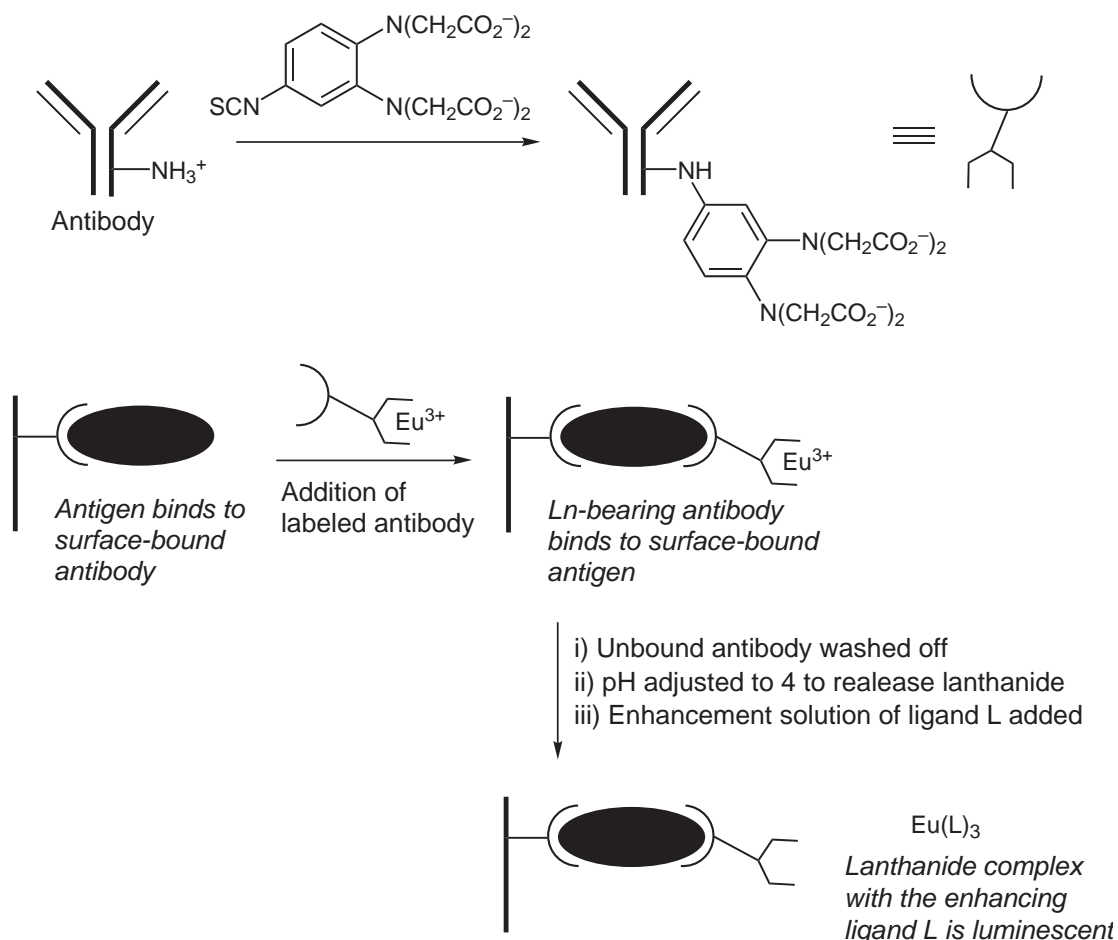


Figure 11 Representation of a typical DELFIA assay.

DELFLIA assays have been applied to a wide variety of systems including protein¹¹³ and hormone¹¹⁴ assays, Hapten assays,¹¹⁵ virus antigen assays,¹¹⁶ and DNA hybridization assays.¹¹⁷ In this last case, some functionalization of the DNA is required, either with biotin (which can then react with europium-appended streptavidin, prepared using the same route as that described for antibody functionalization),¹¹⁷ or by direct linkage to a lanthanide binding site. Direct linkage is commonly carried out by amination of DNA followed by functionalization with a lanthanide-binding ligand, and then a “conventional” DELFLIA assay. The necessary DNA amination can either be carried out by oligonucleotide synthesis involving unnatural bases,¹¹⁸ or by transamination of whole DNA strands.¹¹⁹ The former approach has certain advantages, in that multiple labeling reduces hybridization efficiency.

A variation on the theme of conventional assay uses both lanthanide-labeled and biotin-labeled single strands to form split probes for sequence of target strands (Figure 12).¹²⁰ When both of these bind to DNA, the complex binds (via the biotin residue) to a surface functionalized with streptavidin, immobilizing the europium and allowing assay to be carried out. This approach is already very sensitive to DNA sequence, since both sequences must match to permit immobilization of the lanthanide, but can be made even more sensitive by using PCR (the polymerase chain reaction) to enhance the concentration of DNA strands. In this way, initial concentrations corresponding to as few as four million molecules can be detected. This compares very favorably with radioimmunoassay detection limits.

9.21.5.3 The CYBERFLUOR Assay

The cyberfluor assay (Figure 13) differs from DELFLIA in that the immunoreagent contains no metal. In this case, the reagent incorporates a chromophoric ligand, typically 4,7-bis(chlorosulfonylmethyl)-1,10-phenanthroline-2,9-dicarboxylic acid (BCPDA, (46), in Figure 13).¹²¹ This ligand forms relatively stable complexes with lanthanide ions; the europium complex is luminescent both on a solid support and in aqueous solution, and can react directly with antibodies by reaction of surface groups with the chlorosulfonyl units.

Diamandis and co-workers have used BCPDA to develop a universal detection system based on CYBERFLUOR principles.¹²² Once again, we see the use of the interaction between streptavidin and biotin, though in this case, the way in which it is employed makes the detection system very widely applicable. Here, the early stages of the assay are the same as those described for DELFLIA, in that the antigen binds to a solid-supported antibody. The mixture is then incubated with a biotinylated antibody, ensuring that biotin binds to the surface only when there is antigen already bound. This biotin can then be used to immobilize streptavidin molecules which have been functionalized with BCPDA. Such an approach allows multiple labeling with europium complexes and circumvents the problem of background lanthanide concentrations. However,

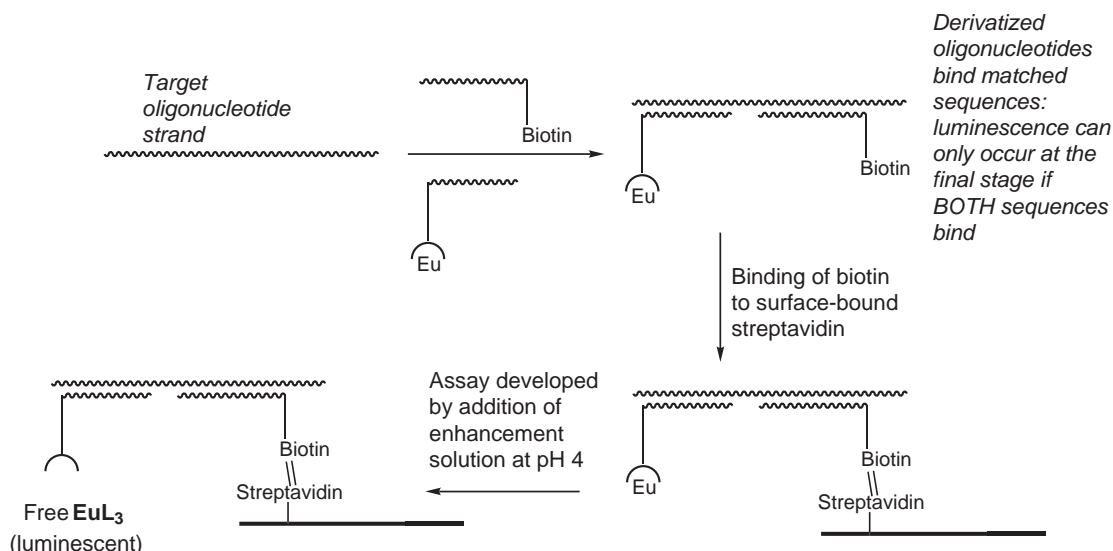


Figure 12 Split-probe oligonucleotide sequencing using DELFLIA.

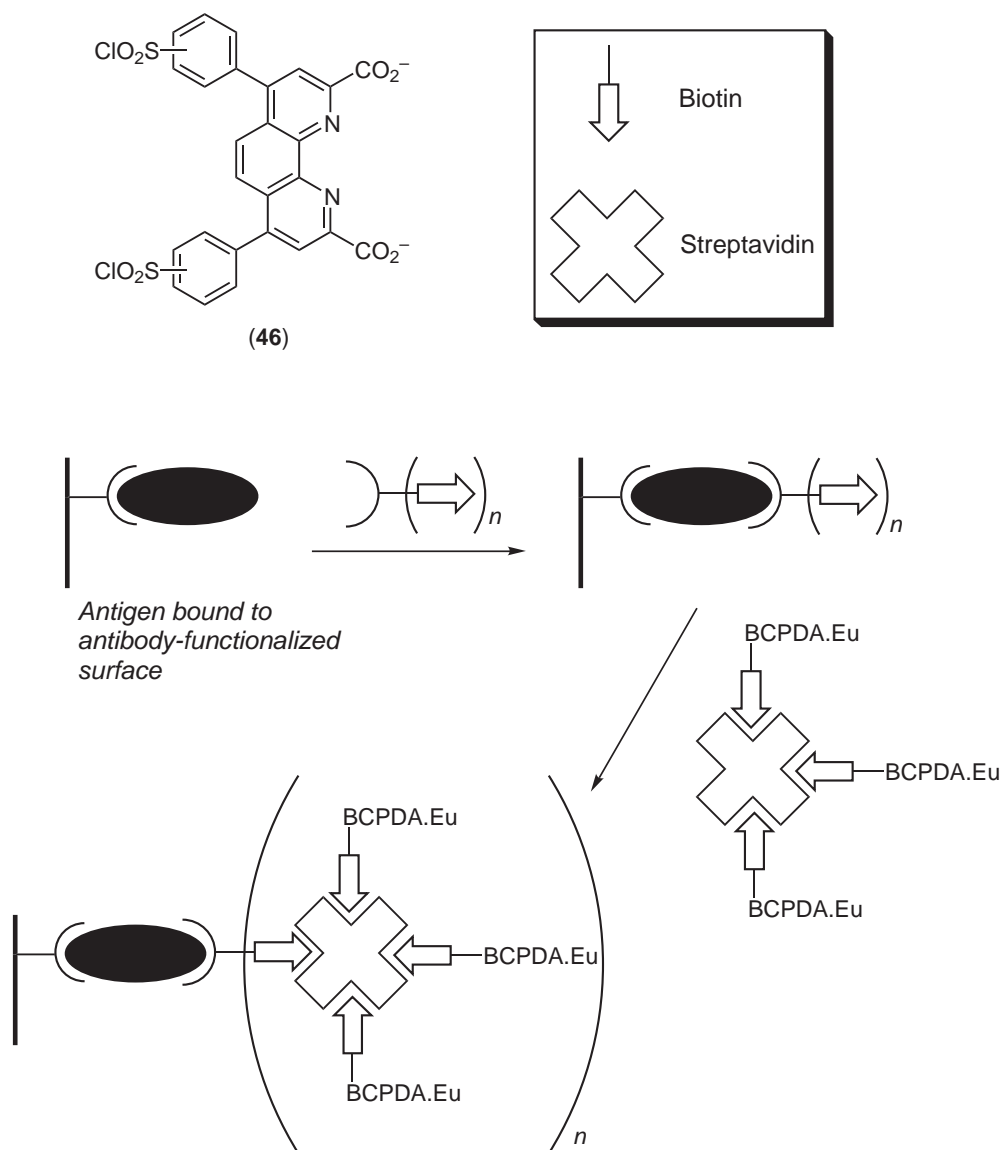


Figure 13 Representation of the CYBERFLUOR assay.

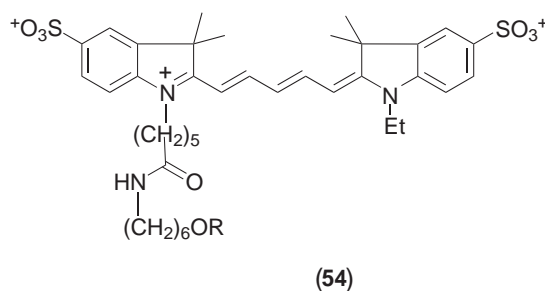
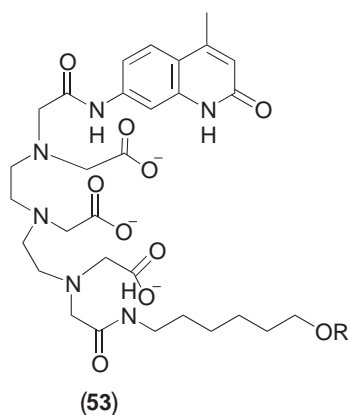
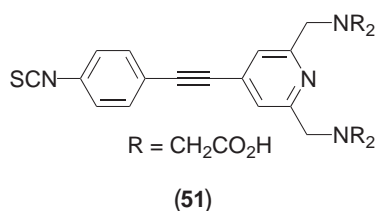
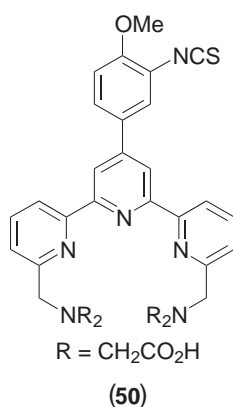
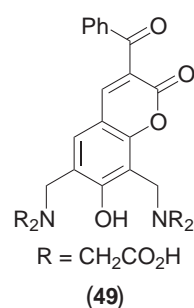
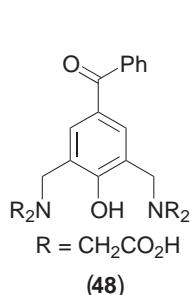
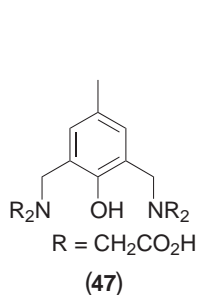
BCPDA is a tetradentate ligand, and forms 1:1 complexes in these conditions. The metal ion is thus coordinatively unsaturated, and also binds a number of water molecules, which can lead to non-radiative quenching of the metal-centered excited state (*vide supra*). These must be removed by drying to achieve optimal luminescence intensity. This form of assay is, in fact, slightly less sensitive than DELFIA.

A number of routes have been used to improve sensitivity in these assays. The simplest involves incorporating more lanthanide ions. For instance, the thyroglobulin conjugate of streptavidin can be labeled with up to 150 BCPDA molecules per conjugate without loss of affinity for biotin (compared to 14 molecules for direct reaction of BCPDA with biotin).¹²³ Further sensitivity enhancements can be achieved by incubating the BCPDA-labeled thyroglobulin–streptavidin conjugate with BCPDA-labeled thyroglobulin at pH 6.¹²⁴ This results in the formation of a macromolecular complex of around 3,000 kDa, offering considerable enhancements compared to the monomeric conjugate.

Other workers have sought to increase the sensitivity by improving the binding ligand. A whole series of assays have been developed using HXTA derivatives (47). These complexes bind strongly to lanthanide ions (forming M_2L_2 complexes in solution)^{125,126} and sensitize lanthanide-centered luminescence. Triplet-mediated energy transfer can be optimized by incorporating aryl ketones into the structure (e.g. (48));¹²⁷ such systems have near-unity triplet quantum

efficiencies for energy transfer due to the high quantum efficiency of the $n-\pi^*$ transition. While the terbium complexes from such systems tend to be highly emissive, the europium complexes tend to have very weak emission as a result of effective quenching by LMCT from the phenol chromophore. Higher luminescence quantum yields for europium are obtained with the coumarin system (49), which is less susceptible to oxidation and therefore does not participate in LMCT quenching.¹²⁸

Terpyridyl derived systems (e.g., (50)) overcome many of the difficulties associated with HXTA systems, and are more compatible with europium.¹²⁹ The molecule shown has an isothiocyanate group, which allows facile conjugation to antibody surfaces. Such systems give very good detection limits, down to around 10^{-16} M.¹³⁰ Bis-phenanthroline macrocycles and bipyridyl cryptates both offer alternatives. The DELFIA and CYBERFLUOR approaches have been combined in chelating agent (51),¹³¹ which combines a metal complex site, a chromophore, and a functional group for linking to antibodies.



9.21.5.4 Enzyme-amplified Lanthanide Luminescence (EALL)

Assays can also be based on changes to chelating ability induced by enzyme action. In these cases, an antibody-bound enzyme is used to amplify the original signal (Figure 14).¹³² The basis of the assay is broadly the same as the heterogeneous assays described above, but the bound enzyme catalyzes the conversion of a molecule unlikely to bind to lanthanide ions into one that will bind effectively. One of the best examples is the use of the salicyl phosphate ((52), in Figure 14), which is converted to salicylate by the bound alkaline phosphatase enzyme.¹³³ Addition of $[\text{Tb}(\text{EDTA})]^-$ gives a ternary complex in which the salicylate chromophore binds to the $[\text{Tb}(\text{EDTA})]^-$ unit, with water being largely excluded from the binding site. This allows a large excess of lanthanide to be used to develop the assay, because unbound $[\text{Tb}(\text{EDTA})]^-$ contains no chromophore and will not be luminescent. This gives much lower limits of detection than would otherwise be obtained. Studies on fluorogenic groups have shown a wide range of enzyme substrates which can be used for such assays, particularly using phosphatases¹³⁴ and β -galactosidase.¹³⁵

9.21.5.5 Homogeneous Assays: DEFRET

Most of the assays described above are heterogeneous (i.e., they require separation of components at some stage). Homogeneous assays with lanthanide ions have the potential to offer much higher throughput rates, since separation steps can be eliminated. Such assays commonly rely on the use of resonance (Förster) energy transfer from a donor to an acceptor chromophore; in such systems, lanthanide complexes can be used as either donors or acceptors. Since lanthanide ions have longer luminescence lifetimes than most other fluorophores, such assays are referred to as DEFRET (delayed fluorescence resonance energy transfer) to distinguish them from conventional FRET processes.¹³⁶ Furthermore, the possibilities for time-gating the luminescence signal still apply, allowing rejection of background autofluorescence.

Lanthanide ions have been used as DEFRET acceptors in split probes for DNA sequence such as shown in Figure 15.¹³⁷ When using europium and terbium complexes, the choice of chromophores is rather restricted, owing to the high-energy emissive states associated with these ions (*vide supra*). In this case, the donor chromophore is a salicylic acid unit appended to an

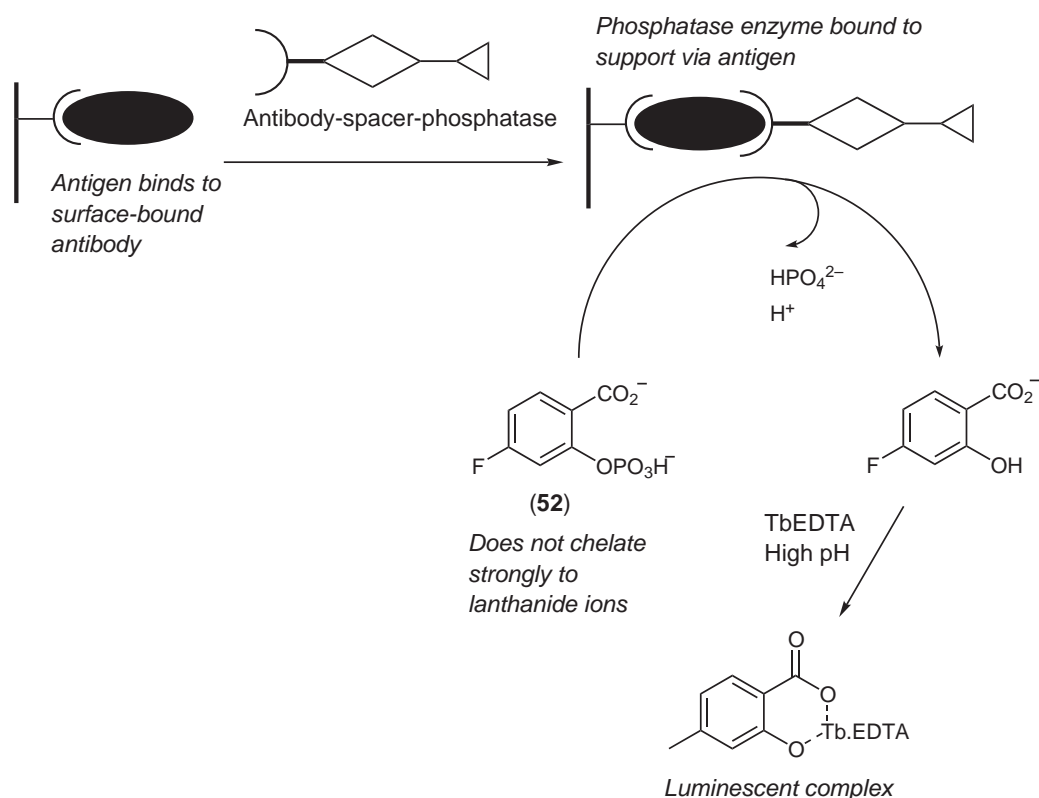


Figure 14 Representation of an EALL assay.

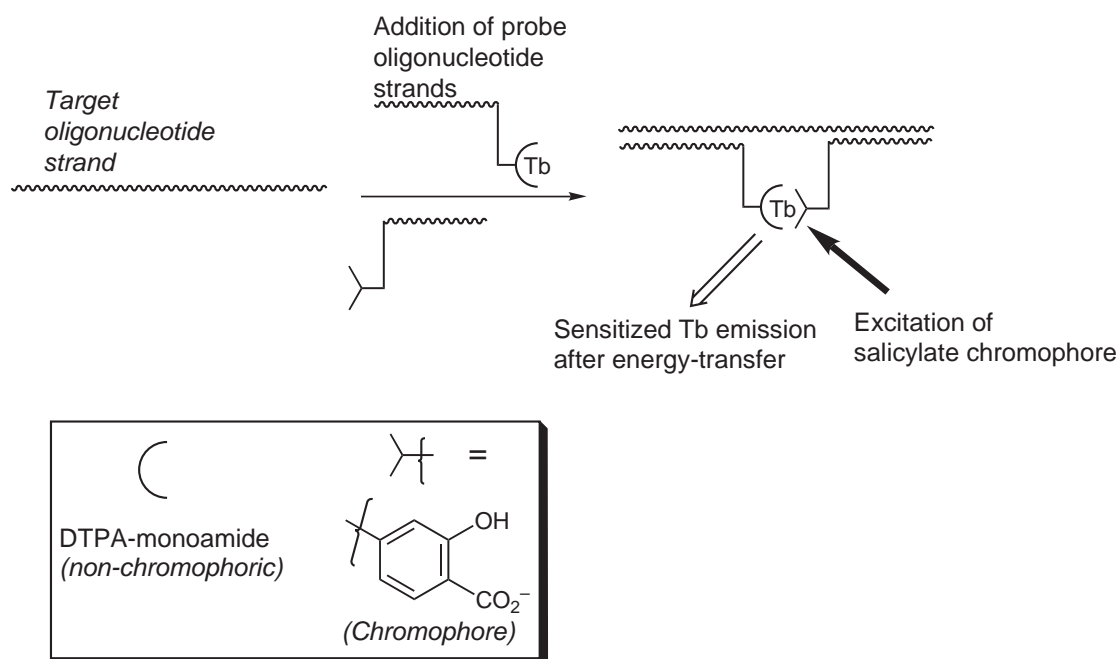


Figure 15 Split-probe oligonucleotide sequencing using DEFRET.

oligonucleotide, while the lanthanide energy acceptor is bound to a DTPA-based oligonucleotide conjugate. Signals are only obtained as a result of sensitized luminescence when the donor and acceptor are held in close proximity by matched base pairing of both fragments with a target oligonucleotide strand.

Lanthanides also have potential as DEFRET energy donors. Selvin *et al.* have reported the use of carbostyryl-124 complexes (**53**) with europium and terbium as sensitizers for cyanine dyes (e.g., **54**) in a variety of immunoassays and DNA hybridization assays.^{138–140} The advantage of this is that the long lifetime of the lanthanide excited state means that it can transfer its excitation energy to the acceptor over a long distance (up to 100 Å); sensitized emission from the acceptor, which occurs at a wavelength where there is minimal interference from residual lanthanide emission, is then measured.

Europium complexes of the Lehn cryptand (**20** in Figure 7) have similarly been deployed to great effect as energy donor chromophores for use with cyanine acceptors¹⁴¹ and other systems,¹⁴² while Amersham have commercialized the use of the terpyridyl derived system (**50**) as a DEFRET donor for use with cyanine dyes as part of their LeadSeeker package for high-throughput drug discovery.

A rather different approach to homogenous assay has been pioneered by Sammes and co-workers (Figure 16).^{143–145} They utilized the lanthanide binding properties of a 1,10-phenanthroline dicarboxylate ligand to which is attached a phenanthridinium group, which intercalates to double-stranded DNA. This molecule accordingly provides both a chromophore and a test for base pairing and sequence recognition. The second component of the assay is an oligonucleotide conjugate with an aminocarboxylate-based (non-chromophoric) lanthanide complex. Luminescence can only occur when the oligonucleotide/lanthanide conjugate is bound to the target single-stranded oligonucleotide to give a double-stranded sequence, *and* the phenanthridinium unit is intercalated to this in a suitable position to allow the phenanthroline dicarboxylate to coordinatively saturate the lanthanide and act as a sensitizer. Since the intercalator is non site-specific, it can move until it finds an appropriate site for binding. This means that all the recognition element is built into a single oligonucleotide; while convenient, this necessitates the use of oligonucleotides with more base pairs than would be required with split probe techniques if the response is to be trusted.

9.21.5.6 Assays with Near-IR Luminescent Lanthanides

Traditionally, lanthanide-based assays have used ions which emit light in the visible region of the spectrum. Europium has been favored over other alternatives since it has a long luminescence

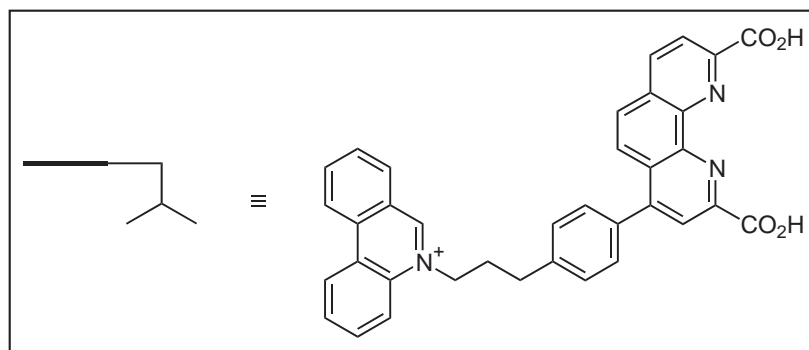
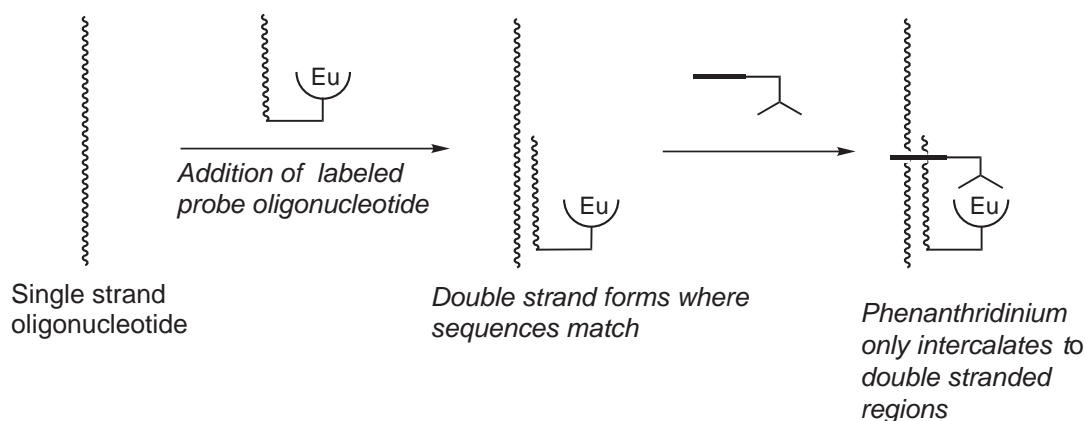


Figure 16 Recognition of double-stranded DNA using a phenanthridinium probe.

lifetime and a relatively low energy for the emissive state, maximizing the choice of chromophores which can be used as sensitizers. These factors compensate for the relatively low quantum yields of europium complexes (where non-radiative quenching through the LMCT state is commonplace). The advent of near-IR luminescent systems has had some impact on this area, and lanthanide bioassays have recently been extended into the near-IR, using ytterbium complexes instead of europium and terbium.¹⁴⁶ The equipment required here is much more specialized, since the emission occurs outside the range of detection by conventional photomultiplier tubes and CCDs, and since the lifetimes are shorter, but this is balanced by the fact that emission occurs outside the regions of the near IR commonly associated with absorption of radiation by water.

9.21.5.7 Use of Other Metal Ions in Assays

Long-lived luminescence is not confined to lanthanide complexes; MLCT emission from a range of transition metal complexes is also long lived. From the point of view of assay, interest has centered on ruthenium(II) pyridyl and polypyridyl complexes, particularly systems containing 1,10-phenanthroline. These complexes, which display orange luminescence, function as tags in the same way as do many lanthanide complexes, and have been used in hybridization assays to achieve 10^{-18} M detection limits for DNA by conjugation with amine-modified oligonucleotides¹⁴⁷ or direct linkage of the complex to the oligonucleotide by use of appropriate functional groups.¹⁴⁸

9.21.6 LANTHANIDE COMPLEXES FOR IMAGING

Luminescent imaging with lanthanide complexes can allow spatial resolution based on techniques developed for assay. It can also be applied to high-resolution microscopy, using luminescent lanthanide complexes to provide information about the location and concentration of target substrates. Simple time-gated luminescence imaging requires an experimental set-up like that shown in Figure 17.¹⁴⁸ Here, a time-gated image intensifier synchronized with the laser pulse is

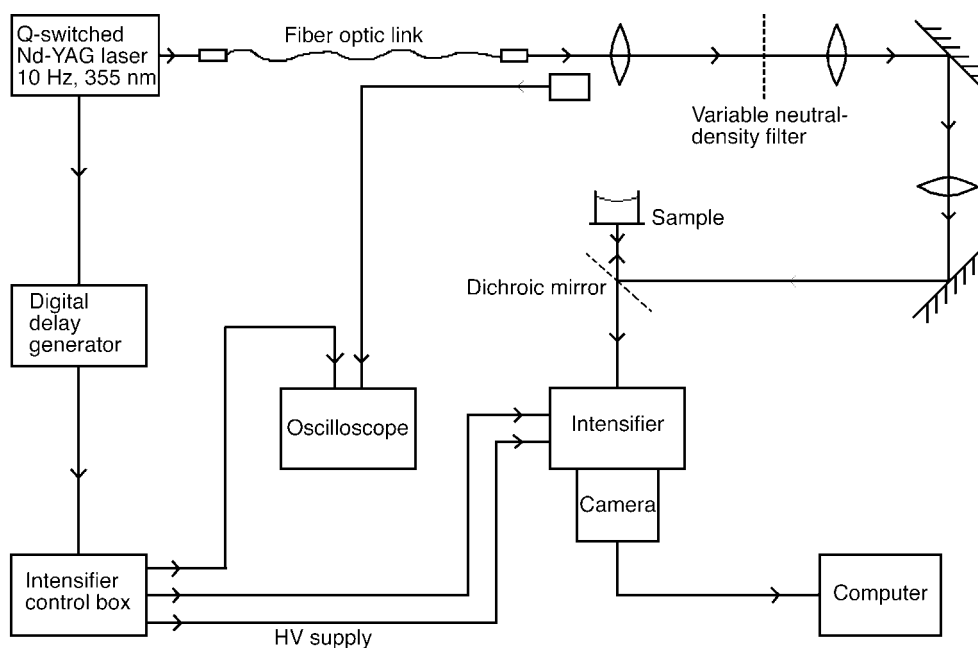


Figure 17 Experimental setup for time-resolved luminescence microscopy with lanthanide ions.

used to control the time domain over which measurements are made, while a CCD camera is used to monitor the emission. When the image intensifier is switched off or set to give a zero time delay, the CCD will record a fluorescence image. However, when a time gate is applied, the CCD only records signals which have not decayed away. Examples of this kind of luminescence microscopy are increasingly common.¹⁵⁰⁻¹⁵⁸ For example, in Figure 18, three particles are

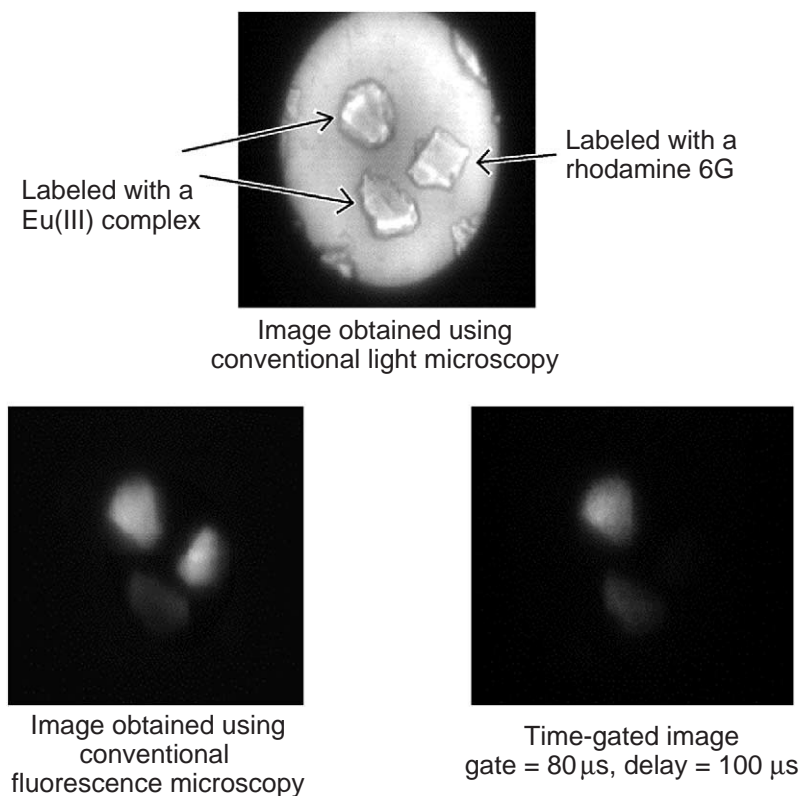


Figure 18 Differentiating lanthanide-labeled particles from rhodamine-labeled particles by luminescence microscopy.

shown. The two on the left are labeled with a europium complex (**19**), while that on the right is labeled with rhodamine 6G, which absorbs and emits light at the same wavelengths as the europium complex (355 and 617 nm, respectively). The particles are indistinguishable when studied by conventional transmission microscopy, while fluorescence microscopy without a time gate can only give information about loading (and incidentally demonstrate the “worst case” problems associated with background fluorescence, since the labels cannot be distinguished). However, when a time gate is applied, the only observed signals correspond to luminescence from the lanthanide complex since fluorescence from the rhodamine 6G has already decayed. This is amply illustrated by the absence of any signal corresponding to the rhodamine-labeled particle.

Such intensity-based imaging essentially provides an extension to conventional luminescence microscopy. However, luminescence microscopy of lanthanides can yield significantly more information, particularly when it is realized that the luminescence lifetimes of lanthanide ions can be controlled by controlling the inner sphere hydration state, while their emission lines are very sharp, allowing different species to be identified with comparative ease. Taking the issue of luminescence lifetimes first, lifetime mapping¹⁴⁹ can provide useful information about the nature of a species in a given location. Essentially, the rate of decay of each pixel in an image can be monitored to provide spatial information relating to the luminescence lifetime. At its simplest, this can be a tool to provide contrast. However it also offers the potential to study the localization of more than one complex at once. Figure 19 shows the use of this technique to distinguish two particles, one labeled with a terbium complex with an eight-coordinate ligand (DOTA, see structure (**22**)) and the other labeled with a complex of a related seven-coordinate ligand (missing one acetate arm).¹⁵⁹ As can be seen, the lifetimes of the luminescence from the two particles are different.

In a similar manner, the luminescence from two complexes containing different lanthanides can also be separated. In the example shown in Figure 20,¹⁵⁹ the terbium complex (**55**) and the europium complex (**20**) both absorb light in similar areas of the spectrum, making them amenable to laser excitation. However, their emission spectra are different. The emission at 545 nm is solely ascribable to terbium, while that at 690 nm is solely due to europium. Use of interference filters between the microscope and the CCD camera allows the signals to be separated effectively, obtaining two images corresponding to the presence of each of the two ions. In principle, these

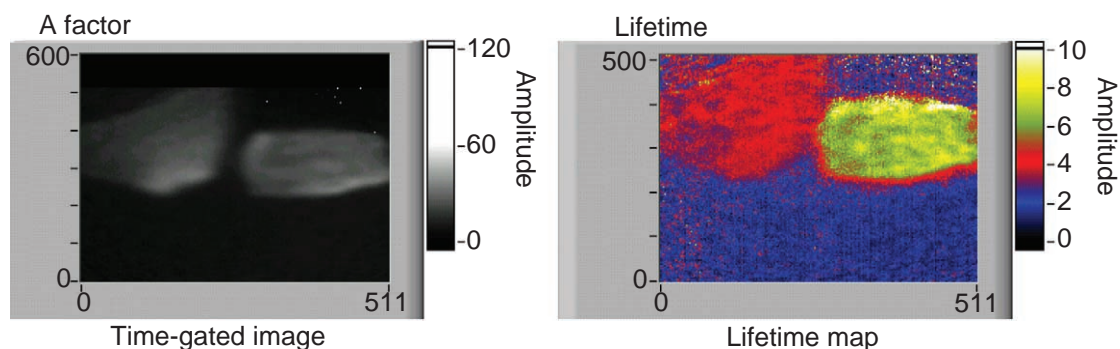


Figure 19 Differentiation of lanthanide-labeled particles by lifetime mapping.

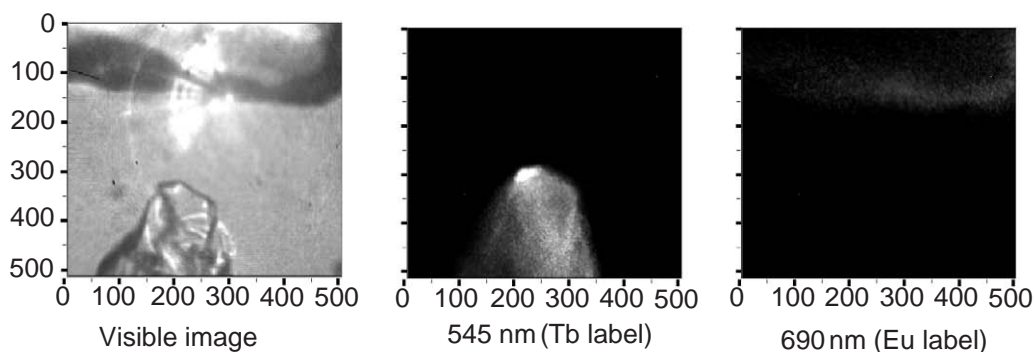
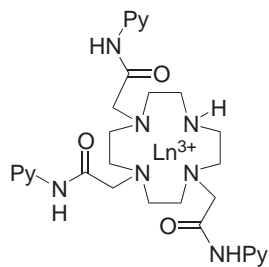
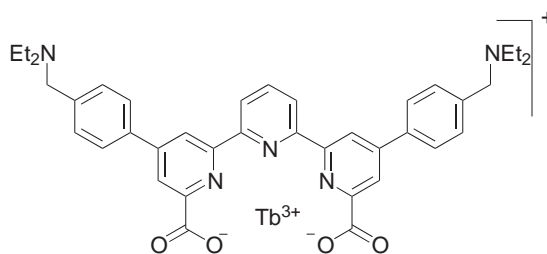


Figure 20 Differentiation of lanthanide-labeled particles by wavelength selection.

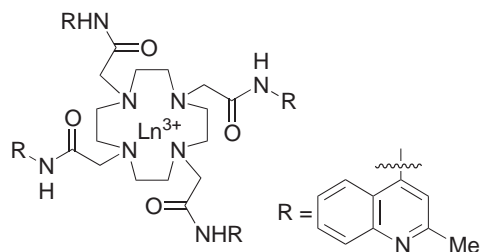
two techniques can be combined to allow multiple addressing of signals from a variety of complexes, with potential application to both high-throughput screening and security encoding, as well as to parallel monitoring of the concentrations of a variety of different analytes.



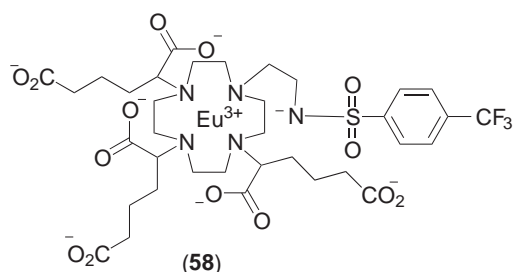
(55)



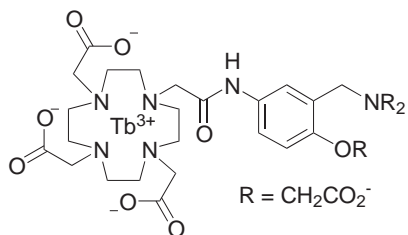
(56)



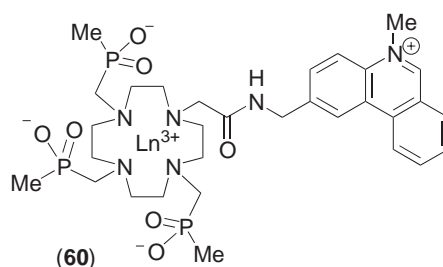
(57)



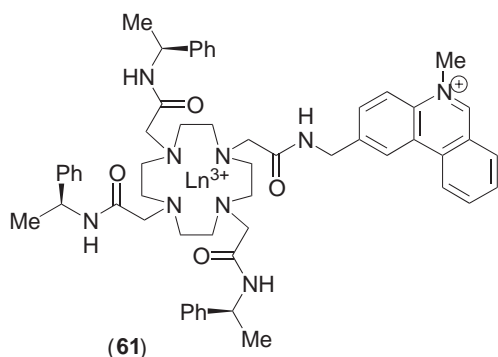
(58)



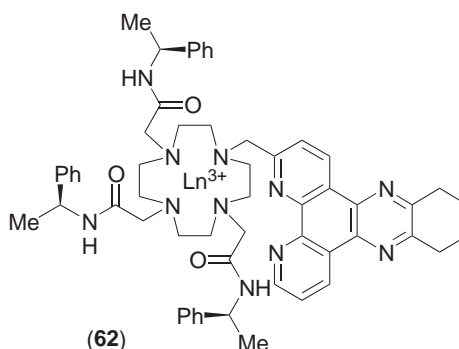
(59)



(60)



(61)



(62)

9.21.7 RESPONSIVE LANTHANIDE COMPLEXES AS SENSORS

Up to this point, we have discussed the use of metal complexes in assay and imaging. It remains to consider how they can be used as sensors analogous to those described at the beginning of this chapter.

The photophysical properties of lanthanide ions are influenced by their local environment, the nature of the quenching pathways available to the excited states of sensitizing chromophores, and the presence of any available quenchers (as we have seen when discussing bioassay). All of these factors can be exploited for the sensing of external species.

pH sensors are by far the most common type of lanthanide-based luminescent sensor. In some cases, these operate by perturbation of the excited singlet state of the sensitizing chromophore. In amine-containing systems, photo-induced electron transfer can be inhibited by protonation of the amine, leading to switching on of the luminescence signal.^{160–164} For instance, in the terpyridyl complex (**56**), the inhibition of PET within the ligand following protonation leads to changes in the luminescence intensity. A slightly different process is at work in the phenanthridyl- and quinolinyl-appended complexes (**19**) and (**57**), where the metal is directly involved in photoelectron transfer.^{161,162} In this case PET from the free amine to the excited Eu^{III} center is inhibited by protonation, leading to a decrease in non-radiative quenching of the ligand triplet state, and a concomitant increase in metal-centered luminescence intensity. Such complexes have been incorporated into sol-gel systems and used as sensors.

The analogous terbium complex (**25**) also acts as a pH sensor, albeit in a slightly different way. In this case, the changes in luminescence are the result of changes in the triplet energy of the ligand on protonation. The triplet energy of the (protonated) phenanthridinium moiety (the dominant species at low pH) is close to that of the emissive $^5\text{D}_4$ state of terbium.⁵¹ As a result, back energy transfer becomes possible and the energy transfer process is reversible at low pH, meaning that quenching of triplet by dissolved oxygen leads to reductions in the metal-centered emission intensity. At higher pH values, the triplet energy of the (non-protonated) phenanthridine moiety precludes back energy transfer, and the metal-centered emission is more intense. Thus, the terbium complex can not only act as a pH sensor, but can also be used to monitor oxygen concentrations in the low pH domain.

The europium complex (**58**) acts in a different way.¹⁶³ In this case, the changes to the inner sphere hydration are responsible for changes to the luminescence intensity and lifetime. At low pH, the sulfonamide group is protonated, and cannot act as a donor, allowing two water molecules to approach the metal center. As the pH is raised, deprotonation of the ligand gives rise to coordination of the sulfonamide nitrogen atom and displacement of bound water. Since the luminescence of lanthanide ions is quenched by the proximate O–H oscillators of bound water molecules, the emission intensity and luminescence lifetime are greater at high pH than at low pH. Similar behavior is shown by (**35**), where three water molecules can bind to the metal at low pH. As the pH is increased, the structure of the molecule changes, and luminescence lifetime measurements indicate that there are no bound O–H oscillators in aqueous solution. This has been explained by oxo-bridged dimer formation.

Cation sensors require the presence of an additional binding site for the substrate cation. For instance, the Zn^{2+} sensor (**59**) acts by incorporation of Zn^{2+} ions into a separate aminocarboxylate binding pocket.¹⁶⁴ This perturbs intermolecular PET, and gives rise to enhancement of the luminescence intensity.

Anion concentrations can also be monitored through lanthanide luminescence. Once again, a wide range of pathways can be responsible for luminescence quenching. For instance, complex (**60**) with a pendant phenanthridinium group exhibits halide ion-dependent luminescence properties as a result of collisional quenching of the phenanthridinium-centered singlet state by halide ions.¹⁶⁵

The binding of more complex ions is best observed as a result of displacement of water from the metal center by other donor ligands. The simplest of these are ions such as bicarbonate^{166,167} and phosphate.¹⁶⁸ A range of seven-coordinate (i.e., coordinatively unsaturated) complexes have been synthesized which bind strongly to such ions,^{169,170} and signal binding by an increase in luminescence lifetime and signal intensity after expulsion of water from the primary coordination sphere. Such systems can also act as sensors for other ions of biological interest such as citrate and lactate,¹⁷¹ where the larger chelate rings involved in complex formation lead to stronger binding of the anion. The sensitivity of such sensors can be improved when studying ions which contain a chromophore, by using a coordinatively unsaturated complex which contains no aryl groups (e.g., a polyamino-carboxylate complex) which forms a ternary complex with an anion containing a suitable sensitizing chromophore, such as tetrathiafulvalene carboxylate,¹⁷² or salicylate.¹⁷³ This approach is particularly effective with ytterbium complexes, where the metal center cannot be sensitized directly in the UV or visible regions of the spectrum as there are no f – f transitions in these regions. This means that the form with no bound anion is non-luminescent, while the anion-bound form can luminesce effectively.

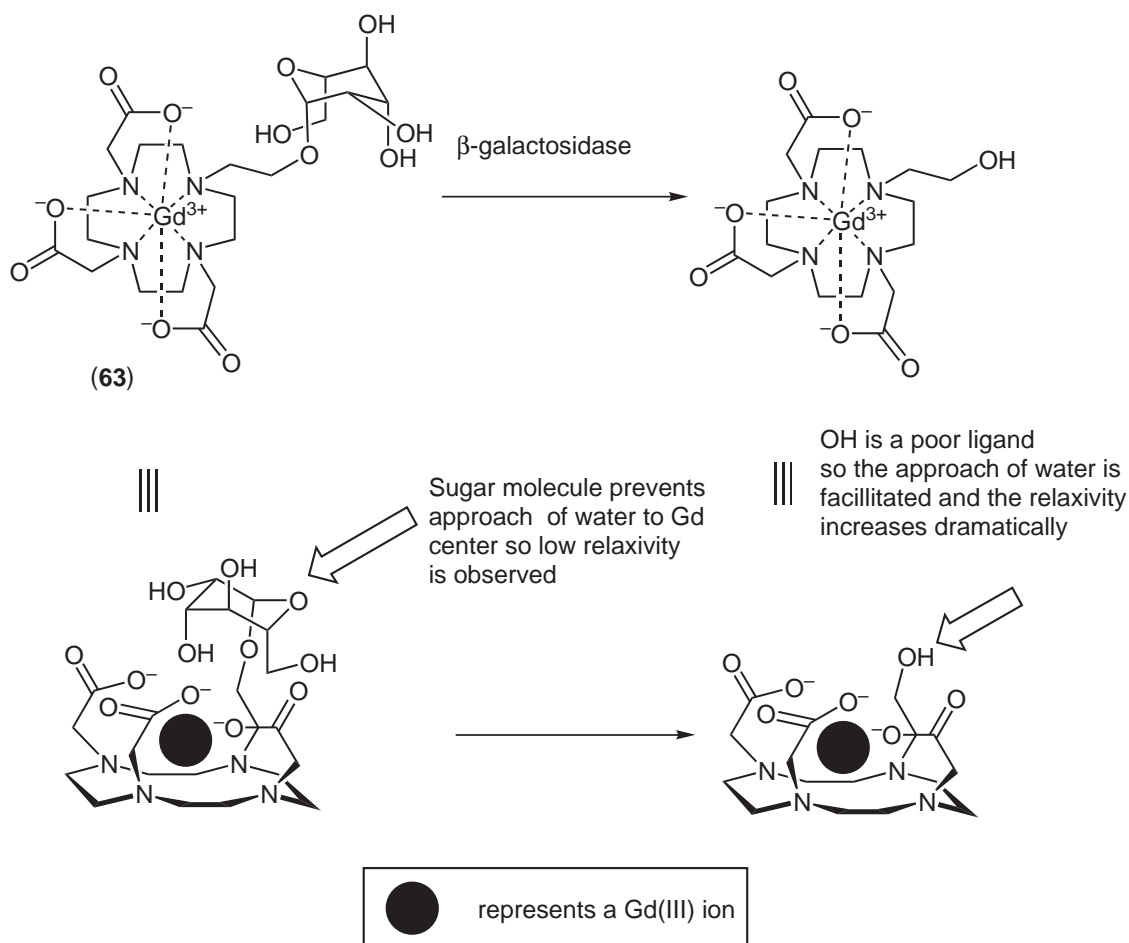


Figure 21 Galactosidase-mediated changes to the inner-sphere coordination environment of a lanthanide complex

DNA binding by lanthanide complexes can also be reflected in their luminescence properties. The pendant phenanthridinium unit of complex (61) binds to DNA in GC-rich areas, leading to non-radiative charge transfer quenching of the phenanthridinium excited state, thereby reducing the intensity of the emission.¹⁷⁴ Complex (62), with a pendant tetraaza-triphenylene group, exhibits similar properties.¹⁷⁵ Enzyme-activated changes in hydration state can also be used as a probe of enzyme action. The galactose-appended molecule (63) (in Figure 21) undergoes galactosidase-mediated hydrolysis to yield a product with increased solvation at the metal center; although this is a Gd^{III} complex and therefore non-luminescent, the same principle causes changes in luminescence with, e.g., Tb^{III}.¹⁷⁶

9.21.8 CONCLUSIONS

Since the early 1970s, coordination chemistry and photochemistry have combined to allow development of a wide range of responsive metal complexes. These allow non-invasive monitoring of metal ion concentrations. Time-resolved measurements are particularly powerful, since they allow detection of very small amounts of substrate and have optimal signal-to-noise ratios. Nonetheless, much remains to be done using the tools which these early studies have provided, particularly with reference to the development of effective sensor systems for a range of ions by time-resolved techniques.

9.21.9 REFERENCES

1. Tsien, R. Y. Fluorescent and photochemical probes of dynamic biochemical signals inside living cells. In: *Fluorescent Chemosensors for Ion and Molecule Recognition*. ACS symposium series 538, 1993.
2. Adams, S. R.; Harootunian, A. T.; Buechler, Y. J.; Taylor, S. S.; Tsien, R. Y. *Nature* **1991**, 349, 694.

3. Schwarzenbach, G.; Ackerman, H. *Helv. Chim. Acta* **1947**, *30*, 1798.
4. Holloway, J. H.; Reilly, C. N. *Anal. Chem.* **1960**, *32*, 249.
5. Martell, A. E.; Smith, R. M. *Critical Stability Constants*, Vol. 1, Plenum, 1974.
6. Tsien, R. Y. *Biochemistry* **1980**, 2396.
7. Czarnik, A. W. *Chem. Biol.* **1995**, *2*, 423.
8. Gryniewicz, G.; Poenie, M.; Tsien, R. Y. *J. Biol. Chem.* **1985**, *260*, 3440.
9. Szmajkowski, H.; Lacombe, J. R. Lifetime-based Sensing Using Phase-Modulation Fluorometry. In: *Fluorescent Chemosensor for Ion and Molecule Recognition*. ACS Symposium Series 538, 1993.
10. Luckhoff, A. *Cell Calcium* **1986**, *7*, 233.
11. Minta, A.; Kao, J. P. Y.; Tsien, R. Y. *J. Biol. Chem.* **1989**, *264*, 8171.
12. Eberhard, M.; Erne, P. *Biochem. Biophys. Res. Commun.* **1991**, *180*, 209.
13. Thomas, A. P. *Methods Toxicol.* **1994**, *1*, 287.
14. Kao, J. P. Y.; Harootyan, A. T.; Tsien, R. Y. *J. Biol. Chem.* **1989**, *264*, 8179.
15. de Silva, A. P.; Gunaratne, H. Q. N.; Gunnlaugsson, T.; Huxley, A. J. M.; McCoy, C. P.; Rademacher, J. T.; Rice, T. E. *Chem. Rev.* **1997**, *97*, 1515.
16. de Silva, A. P.; Fox, D. B.; Huxley, A. J. M.; Moody, T. S. *Coord. Chem. Rev.* **2000**, *205*, 41.
17. Brown, G. J.; de Silva, A. P.; Pagliari, S. *Chem. Commun.* **2002**, 2461.
18. de Silva, A. P.; McClenaghan, N. D. *J. Am. Chem. Soc.* **2000**, *122*, 3965.
19. de Silva, A. P.; Gunaratne, H. Q. N.; Gunnlaugsson, T.; Nieuwenhuizen, M. *Chem. Commun.* **1996**, 1967.
20. de Silva, A. P.; Dixon, I. M.; Gunaratne, H. Q. N.; Gunnlaugsson, T.; Maxwell, P. R. S.; Rice, T. E. *J. Am. Chem. Soc.* **1999**, *121*, 1393.
21. Grell, E.; Lewitzki, E.; Ruf, H.; Bamberg, E.; Ellies-Davies, G. C. R.; Kaplan, J. H.; De Weer, P. *Cell. Mol. Biol.* **1989**, *35*, 515.
22. Ellis-Davies, G. C.; Kaplan, J. H. *Proc. Natl. Acad. Sci. USA* **1994**, *91*, 187.
23. Adams, S. R.; Kao, J. P. Y.; Tsien, R. Y. *J. Am. Chem. Soc.* **1989**, *111*, 7957.
24. Mulligan, I. P.; Ashley, C. C. *FEBS Lett.* **1989**, *255*, 196.
25. Adams, S. R.; Tsien, R. Y. *Annu. Rev. Physiol.* **1993**, *55*, 755.
26. Zhang, J.; Campbell, R. E.; Ting, A. Y.; Tsien, R. Y. *Nature Reviews Molecular Cell. Biology* **2002**, *3*, 906.
27. Minta, A.; Tsien, R. Y. *J. Biol. Chem.* **1989**, *264*, 19449.
28. Meuwis, K.; Boens, N.; De Schryver, F. C.; Gallay, J.; Vincent, M. *Biophys. J.* **1995**, *68*, 2469.
29. Raju, B.; Murphy, E.; Levy, L. A.; Hall, R. D.; London, R. E. *Am. J. Physiol.* **1989**, *256*, C540.
30. Gee, K. R.; Zhou, Z.-L.; Ton-That, D.; Sensi, S. L.; Weiss, J. H. *Cell Calcium* **2002**, *31*, 245.
31. Cullender, C. J. *Microsc.* **1994**, *176*, 281.
32. So, P. T. C.; Dong, C. Y.; Masters, B. R.; Berland, K. M. *Ann. Rev. Biomed. Eng.* **2000**, *2*, 399.
33. Turro, N. J. *Modern Molecular Photochemistry*, University Science Books, 1991.
34. Xu, X. H. N.; Jeffers, R. B.; Gao, J. S.; Logan, B. *Analyst* **2001**, *126*, 1285.
35. Lauffer, R. B. *Chem. Rev.* **1987**, *87*, 901.
36. Caravan, P.; Ellison, J. J.; McMurry, T. J.; Lauffer, R. B. *Chem. Rev.* **1999**, *99*, 2293.
37. Aime, S.; Botta, M.; Fasano, M.; Terreno, E. *Chem. Soc. Rev.* **1998**, *27*, 19.
38. Stein, G.; Wurzburg, E. *J. Chem. Phys.* **1975**, *62*, 208.
39. Lories, J.; Caro, P.; Brun, P.; Babusiaux, A. *Comptes Rendus Seances Acad. Sci., Ser. C: Sci. Chim.* **1972**, *275*, 977.
40. Beeby, A.; Faulkner, S. *Chem. Phys. Lett.* **1997**, *266*, 116.
41. Beeby, A.; Dickins, R. S.; Faulkner, S.; Parker, D.; Williams, J. A. G. *Chem. Commun.* **1997**, 1401.
42. Werts, M. H. V.; Hofstraat, J. W.; Geurts, F. A. J.; Verhoeven, J. W. *Chem. Phys. Lett.* **1997**, *276*, 196.
43. Beitz, J. V. *J. Alloys Comp.* **1994**, *207*, 41.
44. Beeby, A.; Bushby, L. M.; Maffeo, D.; Williams, J. A. G. *J. Chem. Soc. Perkin Trans. 2* **2001**, 1281.
45. Abdelkader, A.; ElKholi, M. M. *J. Mater. Sci.* **1992**, *27*, 2887.
46. Feng, A. L.; Panek, M.; Horrocks, W. D.; Uhlenbeck, O. C. *Chem. Biol.* **1999**, *6*, 801.
47. Breen, P. J.; Hild, E. K.; Horrocks, W. D. *Biochemistry* **1985**, *24*, 4991.
48. Sabbatini, N.; Guardigli, M.; Lehn, J. M. *Coord. Chem. Rev.* **1993**, *123*, 201.
49. Klink, S. I.; Grave, L.; Reinhoudt, D. N.; van Veggel, F. C. J. M.; Werts, M. H. V.; Guerts, F. A. J.; Hofstraat, J. W. *J. Phys. Chem. A* **2000**, *104*, 5457.
50. Alpha, B.; Ballardini, R.; Balzani, V.; Lehn, J. M.; Perathoner, S.; Sabbatini, N. *Photochem. Photobiol.* **1990**, *52*, 299.
51. Beeby, A.; Faulkner, S.; Parker, D.; Williams, J. A. G. *J. Chem. Soc. Perkin Trans. 2* **2001**, 1268.
52. Förster, T. *Ann. Phys. (Leipzig)* **1948**, *2*, 55.
53. Clarkson, I. M.; Beeby, A.; Bruce, J. I.; Govenlock, L. J.; Lowe, M. P.; Matthieu, C. E.; Parker, D.; Senanayake, K. *New J. Chem.* **2000**, *24*, 377.
54. Förster, T. *Discuss. Faraday Soc.* **1959**, *27*, 7.
55. Chaudhuri, D.; Horrocks, W. D.; Amburgey, J. C.; Weber, D. J. *Biochemistry* **1997**, *36*, 9674.
56. Bruno, J.; Horrocks, W. D.; Zauhar, R. J. *Biochemistry* **1992**, *31*, 7016.
57. Barigelli, F.; Flamigni, L.; Balzani, V.; Collin, J.-P.; Sauvage, J.-P.; Sour, A.; Constable, E. C.; Cargill Thompson, A. M. W. *Coord. Chem. Rev.* **1994**, *132*, 209.
58. Burroughs, S. E.; Horrocks, W. D.; Ren, H.; Klee, C. B. *Biochemistry* **1994**, *33*, 10428.
59. Cronce, D. T.; Horrocks, W. D. *Biochemistry* **1992**, *31*, 7963.
60. Horrocks, W. D. *Methods Enzymol.* **1993**, *226*, 495C.
61. Horrocks, W. D.; Bolender, J. P.; Smith, W. D.; Supkowski, R. M. *J. Am. Chem. Soc.* **1997**, *119*, 5972.
62. Supkowski, R. M.; Bolender, J. P.; Smith, W. D.; Reynolds, L. E. L.; Horrocks, W. D. *Coord. Chem. Rev.* **1999**, *186*, 307.
63. Beeby, A.; Faulkner, S.; Williams, J. A. G. *J. Chem. Soc. Dalton Trans.* **2002**, 1918.
64. Faulkner, S.; Burton-Pye, B. P.; Khan, T.; Martin, L. R.; Wray, S. D.; Skabara, P. J. *Chem. Commun.* **2002**, 1668.
65. Villata, L. S.; Wolcan, E.; Feliz, M. R.; Capparelli, A. L. *J. Phys. Chem. A* **1999**, *103*, 5661.
66. Horrocks, W. D.; Sudnick, D. R. *J. Am. Chem. Soc.* **1979**, *101*, 334.
67. Horrocks, W. D.; Sudnick, D. R. *Acc. Chem. Res.* **1979**, *14*, 384.

68. Holz, R. C.; Meister, G. E.; Horrocks, W. D. *Inorg. Chem.* **1990**, *29*, 5183.
69. Wolbers, M. P. O.; van Veggel, F. C. J. M.; Snellink-Ruel, B. H. M.; Hofstraat, W.; Guerts, F. A. J.; Reinhoudt, D. N. *J. Chem. Soc. Perkin Trans. 2* **1998**, 2141.
70. Wolbers, M. P. O.; van Veggel, F. C. J. M.; Snellink-Ruel, B. H. M.; Hofstraat, W.; Guerts, F. A. J.; Reinhoudt, D. N. *J. Am. Chem. Soc.* **1997**, *119*, 138.
71. Beeby, A.; Dickins, R. S.; Faulkner, S.; Parker, D.; Williams, J. A. G. *J. Fluoresc.* **1999**, 45.
72. Hall, J.; Hamer, R.; Aime, S.; Botta, M.; Faulkner, S.; Parker, D.; deSousa, A. S. *New J. Chem.* **1998**, *22*, 627.
73. Dickins, R. S.; Parker, D.; de Sousa, A. S.; Williams, J. A. G. *Chem. Commun.* **1996**, 697.
74. Beeby, A.; Clarkson, I. M.; Dickins, R. S.; Faulkner, S.; Parker, D.; de Sousa, A. S.; Williams, J. A. G. *J. Chem. Soc. Perkin Trans. 2* **1999**, 493.
75. Faulkner, S.; Beeby, A.; Carrie, M.-C.; Dadabhoy, A.; Kenwright, A. M.; Sammes, P. G. *Inorg. Chem. Commun.* **2001**, *4*, 187.
76. Beeby, A.; Burton-Pye, B. P.; Faulkner, S.; Motson, G. R.; Jeffery, J. C.; McCleverty, J. A.; Ward, M. D. *J. Chem. Soc. Dalton Trans.* **2002**, 1923.
77. Li, C.; Wong, W. T. *Chem. Commun.* **2002**, 2034.
78. Galaup, C.; Azema, J.; Tisnes, P.; Picard, C.; Ramos, P.; Juanes, O.; Brunet, E.; Rodriguez-Ubis, J. C. *Inorg. Chim. Acta* **2002**, *85*, 1613.
79. Werts, M. H. V.; Jukes, R. T. F.; Verhoeven, J. W. *Phys. Chem. Chem. Phys.* **2002**, 1548.
80. Zucchi, G.; Ferrand, A. C.; Scopelliti, R.; Bunzli, J. C. G. *Inorg. Chem.* **2002**, *41*, 2459.
81. Michels, J. J.; Huskens, J.; Reinhoudt, D. N. *J. Am. Chem. Soc.* **2002**, *124*, 2056.
82. Messeri, D.; Lowe, M. P.; Parker, D.; Botta, M. *Chem. Commun.* **2001**, 2742.
83. Hebbink, G. A.; Reinhoudt, D. N.; van Veggel, F. C. J. M. *Eur. J. Org. Chem.* **2001**, 4101.
84. Cooper, M. E.; Sammes, P. G. *J. Chem. Soc. Perkin Trans. 2* **2000**, 1695.
85. Greenbaum, N. L.; Mundoma, C.; Peterman, D. R. *Biochemistry* **2001**, *40*, 1124.
86. Supkowski, R. M.; Horrocks, W. D. *Inorg. Chem.* **1999**, *38*, 5616.
87. Supkowski, R. M.; Horrocks, W. D. *Inorg. Chim. Acta* **2002**, *340*, 44.
88. Alpha, B.; Lehn, J. M.; Mathis, G. *Angew. Chem. Int. Ed. Engl.* **1987**, *26*, 266.
89. Beeby, A.; Parker, D.; Williams, J. A. G. *J. Chem. Soc. Perkin Trans. 2* **1996**, 1565.
90. Werts, M. H. V.; Duin, M. A.; Hofstraat, J. W.; Verhoeven, J. W. *Chem. Commun.* **1999**, 799.
91. Dadabhoy, A.; Faulkner, S.; Sammes, P. G. *J. Chem. Soc. Perkin Trans. 2* **2000**, 2359.
92. Dadabhoy, A.; Faulkner, S.; Sammes, P. G. *J. Chem. Soc. Perkin Trans. 2* **2002**, 348.
93. Bretonniere, Y.; Cann, M. J.; Parker, D.; Slater, R. *Chem. Commun.* **2002**, 1930.
94. Klink, S. I.; Hebbink, G. A.; Grave, L.; Peters, F. G. A.; van Veggel, F. C. J. M.; Reinhoudt, D. N.; Hofstraat, J. W. *Eur. J. Org. Chem.* **2000**, 1923.
95. Hebbink, G. A.; Klink, S. I.; Grave, L.; Alink, P. G. B. O.; van Veggel, F. C. J. M. *ChemPhysChem* **2002**, *3*, 1014.
96. Hebbink, G. A.; Klink, S. I.; Alink, P. G. B. O.; van Veggel, F. C. J. M. *Inorg. Chim. Acta* **2001**, *317*, 114.
97. Hasegawa, Y.; Ohkubo, T.; Sogabe, K.; Kawamura, Y.; Wada, Y.; Nakashima, N.; Yanagida, S. *Angew. Chem. Int. Ed.* **2000**, *39*, 357.
98. Kawamura, Y.; Wada, Y.; Hasegawa, Y.; Iwamuro, M.; Kitamura, T. *Appl. Phys. Lett.* **1999**, *74*, 3245.
99. Hasegawa, Y.; Iwamuro, M.; Murakoshi, K.; Wada, Y.; Arakawa, R.; Yamanaka, T.; Nakashima, N.; Yanagida, S. *Bull. Chem. Soc. Jpn.* **1998**, *71*, 2573.
100. Iwamuro, M.; Hasegawa, Y.; Wada, Y.; Murakoshi, Nakashima N.; Yamanaka, T.; Yanagida, S. *J. Lumin.* **1998**, *79*, 29.
101. Yanagida, S.; Hasegawa, Y.; Murakoshi, K.; Wada, Y.; Nakashima, N.; Yamanaka, T. *Coord. Chem. Rev.* **1998**, *171*, 461.
102. Klink, S. I.; Keizer, H.; Hofstraat, J. W.; van Veggel, F. C. J. M. *Synth. Met.* **2002**, *127*, 213.
103. Klink, S. I.; Keizer, H.; van Veggel, F. C. J. M. *Angew. Chem., Int. Ed. Engl.* **2000**, *39*, 4319.
104. Beeby, A.; Dickins, R. S.; FitzGerald, S.; Govenlock, L. J.; Parker, D.; Williams, J. A. G. *Chem. Commun.* **2000**, 1183.
105. Chard, T. An introduction to radioimmunoassay and related techniques. Elsevier, 1995.
106. Hemilla, I. A. Applications of fluorescence in immunoassays. Wiley Interscience, 1991.
107. Didenko, V. V. *Biotechniques* **2001**, *31*, 1106.
108. Leif, R. C.; Clay, S. P.; Gratzner, H. G.; Haines, H. G.; Vallarino, L. M.; Weidner, I. Proceedings of the International Conference on the automation of Uterine Cancer Cytology, eds. G. L. Weid, G. F. Bahr and P. H. Bartels, Chicago 1976, pp 313.
109. Wallac Laboratories, Turku, Finland. European Patent, EP0064484, 1982.
110. Soini, E.; Lovgren, T. *Crit. Rev. Anal. Chem.* **1987**, *18*, 105.
111. Hemmila, I.; Mukkala, V. M. *Crit. Rev. Clin. Lab. Sci.* **2001**, *38*, 441.
112. Lee, Y. C. *Anal. Biochem.* **2001**, *297*, 123.
113. Peuralahti, J.; Hakala, H.; Mukkala, V. M.; Loman, K.; Hurskainen, P.; Mulari, O.; Hovinen, J. *Bioconjugate. Chem.* **2002**, *13*, 870.
114. Thuren, T.; Vitaren, J. A.; Lalla, M.; Kinnunen, P. K. *Clin. Chem.* **1985**, *31*, 714.
115. Taimela, E.; Aalto, E.; Koskinen, P.; Irjala, K. *Clin. Chem.* **1993**, *39*, 679.
116. Siitari, H.; Hemmila, I.; Lovgren, T.; Soini, E. *Nature* **1983**, *301*, 258.
117. Dahlen, P.; Hurskainen, P.; Lovgren, T. *Nonisotopic DNA probe techniques* **1992**, 263.
118. Sund, C.; Ylikoski, J.; Hurskainen, P.; Kwiatkowski, M. *Nucleosides and Nucleotides* **1988**, *7*, 655.
119. Hurskainen, P.; Dahlen, P.; Ylikowski, J.; Siitara, M.; Lovgren, T. *Nucleic Acids Res.* **1991**, *19*, 1057.
120. Dahlen, P.; Iitia, A.; Skagius, G.; Frostell, A.; Nunn, M.; Kwiatkowski, M. *J. Clin. Microbiol.* **1991**, *29*, 798.
121. Evangelista, R. A.; Polak, A. European Patent, EP0171978, 1986.
122. Diamandis, E. P.; Morton, R. C. *J. Immunol Methods* **1988**, *112*, 43.
123. Diamandis, E. P.; Morton, R. C.; Reichstein, E.; Khosravi, M. J. *Anal. Chem.* **1989**, *61*, 48.
124. Diamandis, E. P.; Morton, R. C. *Anal. Chem.* **1990**, *62*, 1841.
125. Mukkala, V. M.; Helenius, M.; Hemmila, I.; Kankare, J.; Takalo, H. *Helv. Chim. Acta* **1993**, *76*, 1361.

126. Latva, M.; Maekinen, P.; Kulmala, S.; Haapakka, K. *J. Chem. Soc. Faraday Trans.* **1996**, *92*, 3321.
127. Ala-Kleme, T.; Haapakka, K.; Latva, M. *J. Alloys Comp.* **1998**, *275–277*, 911.
128. Hinshaw, J. C.; Toner, J. L.; Reynolds, G. A. Eur. Pat. Appl. EP 68875, 1983.
129. Hinshaw, J. C.; Toner, J. L.; Reynolds, G. A. US Patent, US 4637988, 1987.
130. Hinshaw, J. C.; Toner, J. L.; Reynolds, G. A. US Patents, US 4670572, 1987; US 4837169, 1989, US 4859777, 1989.
131. Kankare, J. PCT world patent, WO 92/16839, 1992.
132. Gudgin-Dickson, E. F.; Pollak, A.; Diamandis, E. P. *J. Photochem. Photobiol. B; Biol.* **1995**, *27*, 2.
133. Evangelista, R. A.; Pollak, A.; Gudgin-Templeton, E. F. *Anal. Biochem.* **1991**, *197*, 213.
134. Christopoulos, T.; Diamandis, E. P. *Anal. Chem.* **1992**, *64*, 342.
135. Evangelista, R. A.; Templeton, E. F.; Pollak, A. PCT Int. Appl. (1991), WO 9108490.
136. Sammes, P. G.; Yahgliou, G. *Nat. Product. Rep.* **1996**, *1*.
137. Oser, A.; Valet, G. *Angew. Chem. Int. Ed. Engl.* **1990**, *29*, 1167.
138. Selvin, P. R.; Rana, T. M.; Hearst, J. E. *J. Am. Chem. Soc.* **1994**, *116*, 6029.
139. Selvin, P. R. *IEE J. Sel. Top. Quantum Electron.* **1997**, *3*, 1119.
140. Selvin, P. R. *Ann. Rev. Biophys. Biomol. Struct.* **2002**, *31*, 275.
141. Mathis, G. *Clin. Chem.* **1993**, *39*, 1953.
142. Mathis, G. *Clin. Chem.* **1995**, *41*, 1391.
143. Coates, J.; Sammes, P. G.; Yagliou, G.; West, R. M.; Garman, A. J. *J. Chem. Soc., Chem. Commun.* **1994**, 2311.
144. Coates, J.; Sammes, P. G.; West, R. M. *J. Chem. Soc. Chem. Commun.* **1995**, 1107.
145. Sammes, P. G.; Shek, L.; Watmore, D. *Chem. Commun.* **2000**, 1625.
146. Werts, M. H. V.; Woudenberge, R. H.; Emmerink, P. G.; van Gassel, R.; Hofstraat, J. W.; Verhoeven, J. W. *Angew. Chem., Int. Ed.* **2000**, *39*, 4542.
147. Banwarth, W.; Schmidt, D.; Stallard, R. L.; Hornung, C.; Knorr, R.; Muller, F. *Helv. Chim. Acta* **1988**, *71*, 2085.
148. Jenkins, Y.; Barton, J. K. *J. Am. Chem. Soc.* **1992**, *114*, 8736.
149. Clarkson, I. M.; Faulkner, S.; Botchway, S.; Parker, D.; Parker, A. W. *J. Photochem. Photobiol. B. Biol.* **2000**, *57*, 83.
150. Charbonniere, L.; Ziessel, R.; Guardigli, M.; Roda, A.; Sabbatini, N.; Cesario, M. *J. Am. Chem. Soc.* **2001**, *123*, 2436.
151. Vereb, G.; Jares-Erijman, E.; Selvin, P. R.; Jovin, T. M. *Biophys. J.* **1998**, *74*, 2210.
152. Seveus, L.; Vaisala, M.; Syrjanen, S.; Sandberg, M.; Kuusisto, A.; Harju, R.; Salo, J.; Hemmila, I.; Kojola, H.; Soini, E. *Cytometry* **1992**, *13*, 329.
153. Connally, R.; Veal, D.; Piper, J. *FEMS Microbiol. Ecol.* **2002**, *41*, 239.
154. Soini, A. E.; Seveus, L.; Meltola, N. J.; Papkovsky, D. B.; Soini, E. *Microsc. Res. Tech.* **2002**, *58*, 125.
155. Lacowicz, J. R.; Piszczek, G.; Maliwal, B. P.; Gryczynski, I. *Chem. Phys. Chem.* **2001**, *2*, 247.
156. Phimphivong, S.; Kolchens, S.; Edmison, P. L.; Saavedra, S. S. *Anal. Chim. Acta* **1995**, *307*, 403.
157. Marriott, G.; Heidecker, M.; Diamandis, E. P.; Yan-Marriott, Y. *Biophys. J.* **1994**, *67*, 957.
158. Beverloo, H. B.; Van Schadewijk, A.; Bonnet, J.; van der Geest, R.; Runia, R.; Verwoerd, N. P.; Vrolijk, J.; Ploem, J. S.; Tanke, H. J. *Cytometry* **1992**, *13*, 561.
159. Aarons, R. J.; Burton-Pye, B. P.; Faulkner, S.; Botchway, S. W.; Parker, A. W.; Topley, S.; Beeby, A.; Snaith, J. S.; Ashraf, A.; Notta, J. *CLF Ann. Rep.* **2001/2002**, 130.
160. de Silva, A. P.; Gunaratne, H. Q. N.; Rice, T. E. *Angew. Chem. Int. Ed. Engl.* **1996**, *35*, 2116.
161. Parker, D.; Senanayake, K.; Williams, J. A. G. *J. Chem. Soc. Perkin Trans. 2* **1998**, 2129.
162. Gunnlaugsson, T.; Parker, D. *Chem. Commun.* **1998**, 511.
163. Lowe, M. P.; Parker, D. *Chem. Commun.* **2000**, 708.
164. Gunnlaugsson, T.; MacDonall, D. A.; Parker, D. *J. Am. Chem. Soc.* **2001**, *123*, 12866.
165. Parker, D.; Senanayake, K.; Williams, J. A. G. *Chem. Commun.* **1997**, 1777.
166. Aime, S.; Barge, A.; Botta, M.; Howard, J. A. K.; Katakly, R.; Lowe, M. P.; Moloney, J. M.; Parker, D.; de Sousa, A. S. *Chem. Commun.* **1999**, 1047.
167. Bruce, J. I.; Dickins, R. S.; Govenlock, L. J.; Gunnlaugsson, T.; Lopinski, S.; Lowe, M. P.; Parker, D.; Peacock, R. D.; Perry, J. J. B.; Aime, S.; Botta, M. *J. Am. Chem. Soc.* **2000**, *122*, 9674.
168. Aime, S.; Gianolio, E.; Terreno, E.; Giovenza, G. B.; Pagliarini, R.; Sisti, M.; Palmisano, G.; Botta, M.; Lowe, M. P.; Parker, D. *J. Biol. Inorg. Chem.* **2000**, *5*, 488.
169. Parker, D.; Dickins, R. S.; Puschmann, H.; Crossland, C.; Howard, J. A. K. *Chem. Rev.* **2002**, *102*, 1977.
170. Parker, D. *Coord. Chem. Rev.* **2000**, *205*, 109.
171. Dickins, R. S.; Aime, S.; Batsanov, A. S.; Beeby, A.; Botta, M.; Bruce, J. I.; Howard, J. A. K.; Love, C. S.; Parker, D.; Peacock, R. D.; Puschman, H. *J. Am. Chem. Soc.* **2002**, *124*, 12697.
172. Faulkner, S.; Burton-Pye, B. P.; Khan, T.; Martin, L. R.; Wray, S. D.; Skabara, P. J. *Chem. Commun.* **2002**, 1668.
173. Gunnlaugsson, T.; Harte, A. J.; Leonard, J. P.; Nieuwenhuyzen, M. *Chem. Commun.* **2002**, 2134.
174. Bobba, G.; Kean, S. D.; Parker, D.; Beeby, A.; Baker, G. *J. Chem. Soc. Perkin Trans. 2* **2001**, 1738.
175. Bobba, G.; Frias, J. C.; Parker, D. *Chem. Commun.* **2002**, 890.
176. Moats, R. A.; Fraser, S. E.; Meade, T. J. *Angew. Chem., Int. Ed. Engl.* **1997**, *36*, 726.

9.22

Metal Complexes for Photodynamic Therapy

R. BONNETT

Queen Mary, University of London, UK

9.22.1	INTRODUCTION	946
9.22.2	PHOTODYNAMIC THERAPY	947
9.22.2.1	The Photodynamic Effect and Photodynamic Therapy	947
9.22.2.2	Mechanistic Aspects	947
9.22.2.3	Haematoporphyrin Derivative	950
9.22.3	DESIGN FEATURES FOR A GOOD PHOTSENSITIZER FOR PDT	950
9.22.4	PHOTOSENSITIZERS IN CLINICAL USE	953
9.22.5	COORDINATION COMPLEXES AS PDT SENSITIZERS: SOME GENERAL CONSIDERATIONS	955
9.22.5.1	Synthesis of Metalloporphyrins and Metallophthalocyanines	955
9.22.5.1.1	<i>Metalation of the preformed ligand</i>	955
9.22.5.1.2	<i>Transmetalation</i>	956
9.22.5.1.3	<i>Template synthesis</i>	956
9.22.5.2	Metal Complex Stability	956
9.22.5.3	Structural Variation	959
9.22.5.4	Solubility	959
9.22.5.5	Disaggregation	960
9.22.5.6	Spectroscopic Properties	961
9.22.5.7	Redox Properties	964
9.22.5.8	Drug Delivery Systems	966
9.22.6	COMPLEXES OF GROUP 2	967
9.22.6.1	Magnesium	967
9.22.7	COMPLEXES OF GROUP 3	970
9.22.7.1	Lanthanides	970
9.22.8	COMPLEXES OF GROUP 7	972
9.22.8.1	Manganese	972
9.22.8.2	Technetium	972
9.22.9	COMPLEXES OF GROUP 8	972
9.22.9.1	Ruthenium	972
9.22.10	COMPLEXES OF GROUP 10	973
9.22.10.1	Nickel	973
9.22.10.2	Palladium	975
9.22.10.3	Platinum	977
9.22.11	COMPLEXES OF GROUP 11	977
9.22.11.1	Copper	977
9.22.11.2	Gold	979
9.22.12	COMPLEXES OF GROUP 12	979
9.22.12.1	Zinc	979
9.22.12.1.1	<i>Porphyrin complexes</i>	979
9.22.12.1.2	<i>Zinc chlorins and bacteriochlorins</i>	980
9.22.12.1.3	<i>Zinc phthalocyanines</i>	981
9.22.12.1.4	<i>Zinc naphthalocyanines</i>	984
9.22.12.1.5	<i>Other zinc complexes</i>	985
9.22.12.2	Cadmium	985
9.22.13	COMPLEXES OF GROUP 13	986

9.22.13.1	Boron	986
9.22.13.2	Aluminum	987
9.22.13.3	Gallium	990
9.22.13.4	Indium	991
9.22.14	COMPLEXES OF GROUP 14	991
9.22.14.1	Silicon	991
9.22.14.2	Germanium	992
9.22.14.3	Tin	993
9.22.15	CONCLUSIONS	994
9.22.16	REFERENCES	995

9.22.1 INTRODUCTION

Phototherapy may be defined as the use of light in the treatment of disease. The light referred to in this definition is electromagnetic radiation in the visible and adjacent ultraviolet and infrared regions; electromagnetic radiation at high energies (ionizing radiation, X radiation) is not included. Additionally, applications of high-intensity laser sources, albeit in the visible or near infrared regions, are also not included, since it is photochemical—rather than thermal or photo-mechanical—applications of electromagnetic radiation that are of interest here. The subject has an extensive and fascinating history, which has been reviewed.^{1–4}

The forms of phototherapy in common use include: (i) the phototherapy of jaundice (neonatal hyperbilirubinemia) in the newborn, and especially in the prematurely born;⁵ (ii) the treatment of psoriasis using light in the UV-A range (320–400 nm) and an administered photosensitizer, such as 8-methoxypsoralen;⁶ (iii) the treatment of the wet form of age-related macular degeneration with a photosensitizer such as a benzoporphyrin derivative (VISUDYNE[®]), and a laser light source;⁷ and (iv) the treatment of certain cancers with a photosensitizer such as a porphyrin derivative, and red light.⁸

Mechanistically, these processes are diverse. Thus, the phototherapy of neonatal hyperbilirubinemia requires irradiation at about 450 nm (the absorption maximum of bilirubin, which is responsible for the colour of jaundice), but no additional drug. The treatment of psoriasis requires light plus an administered drug, and is often called “photochemotherapy.” The treatment of cancer with red light requires a photosensitizing drug *and* oxygen, and is termed “photodynamic therapy” (PDT). The logic of this classification can be illustrated in a Venn diagram, as shown in Figure 1.

Two other aspects may be mentioned at the outset. First, fluorescent substances which accumulate preferentially in tumors (e.g., some porphyrins) may be used in diagnosis, since under appropriate irradiation (usually weak irradiation in the UV) the tumor tissue will be revealed by the fluorescence of the added substance. This is not a photodynamic effect, and is generally

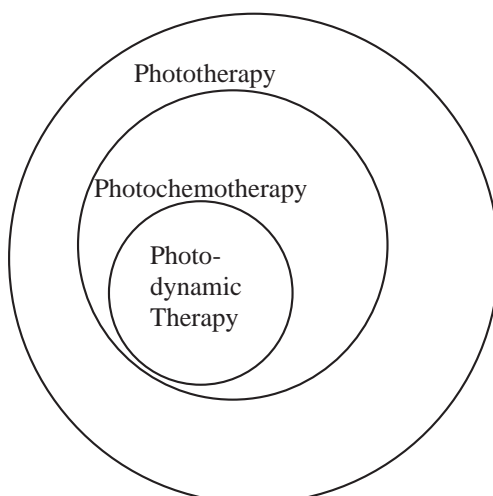


Figure 1 Subdivisions of phototherapy, illustrated by a Venn diagram.

termed “photodiagnosis” (PD). Second, chromophoric substances (usually with very strong absorption in the far red) which have very short excited-state lifetimes, because of the particular metal that they carry, do not act as photodynamic agents: their excitation energy is rapidly transformed into heat, and if they are preferentially localized in tumor tissue, the tumor may be destroyed thermally. Such agents are currently being developed: the topic is referred to as “photothermal therapy” (PTT).

For numerical values in what follows, estimated errors are generally not quoted. Usually, for wavelengths the values are about ± 1 nm; for molecular absorption coefficients and quantum yields, about $\pm 10\%$. For details, see the original references.

9.22.2 PHOTODYNAMIC THERAPY

Photodynamic therapy is based on a phenomenon known as photodynamic action, or the photodynamic effect, which are terms used to describe the damage to living tissue caused by certain photosensitizers in the presence of visible light and oxygen. Again, there is an extensive historical record, which has been reviewed several times during the 1990s.^{4,9–15}

9.22.2.1 The Photodynamic Effect and Photodynamic Therapy

The photodynamic effect was discovered in 1900 by Raab, who showed that paramecia were not much affected by being placed in dilute solutions of acridine in the dark, but were killed when such suspensions were exposed to light.¹⁶ There was initially a considerable effort to develop these findings, but after a few years the topic seems somehow to have lost its attractiveness, and clinical reports became infrequent.

Thus, although some early clinical studies appeared to be promising (e.g., treatment of basal cell carcinoma of the lip using topical eosin as the photosensitizer¹⁷), real progress did not occur until the 1960s and 1970s, when two important observations were made.

First, it was shown that when a porphyrin preparation called “haematoporphyrin derivative” (HpD) was injected into a tumor-bearing mammal, the porphyrin localized with some degree of selectivity in the tumor tissue. Since the porphyrin could be visualized by its red fluorescence under low-intensity UV light (366 nm), this offered a novel method of determining the outline of the tumor.¹⁸ That led to the photodiagnostic application of such drugs, which in 2002 is still being actively investigated.

Second, it was shown that, if the porphyrin-containing tumor so produced was irradiated with a visible (or red) light source of moderate intensity, the photodynamic effect came into operation, and photonecrosis of the tumor ensued.¹⁹ Subsequent studies, particularly by Dougherty and his colleagues,²⁰ demonstrated the clinical promise of the technique.

The selectivity (albeit often rather low) of the photosensitizer for tumor tissue, the directional properties of light, and the potency of some of the new photosensitizers (“second generation” with respect to haematoporphyrin derivative) combine to give an approach which is becoming increasingly attractive as an addition to the methods available to the oncologist for the management and treatment of cancer. The most common methodology of treatment is summarized schematically in Figure 2. The sensitizer is injected intravenously, and the patient is kept in subdued light (the drug–light interval, DLI, 3–96 h) until the drug has attained a distribution optimal for selective tumor damage. The tumor is then irradiated with a measured light dose: this is usually given at the absorption maximum of the sensitizer in the red region, and varies, of course, with the structure of the photosensitizer,²¹ with a range of 5–250 J cm⁻², giving treatment times of 50–2,500 s (for a fluence rate of 100 mW cm⁻²). After treatment, while the normal tissue around the damaged/destroyed tumor is healing, the patient may again be advised to stay in subdued light to avoid the possibility of inadvertent photodamage to normal tissue.

9.22.2.2 Mechanistic Aspects

At a macroscopic biological level, the damage to tissue is related to the concentration of photosensitizer and dioxygen in the tissues being irradiated, and to the light flux: the key mechanistic questions here are—in which compartment does the photosensitizer accumulate,

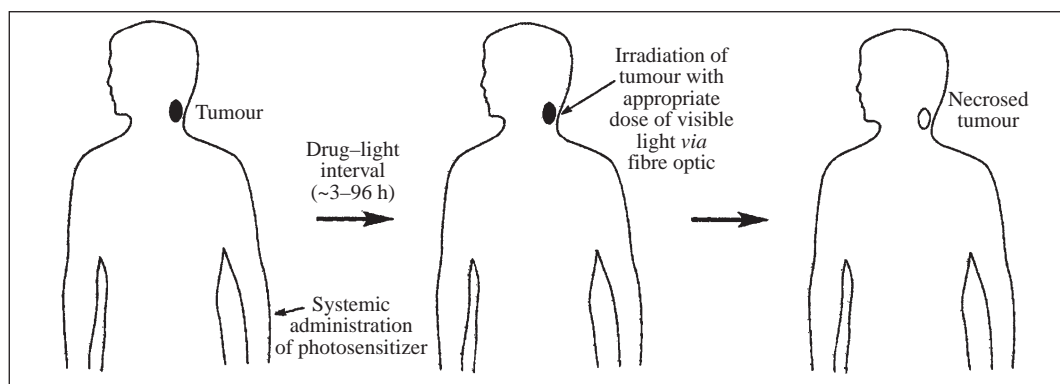
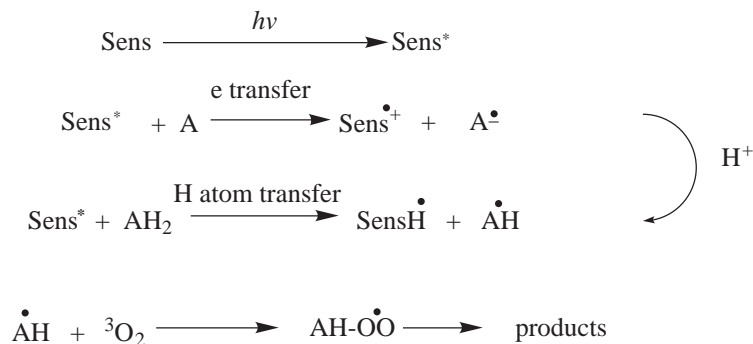


Figure 2 Schematic of tumor phototherapy using a sensitizing drug (photodynamic therapy) (reproduced by permission of the Royal Society of Chemistry from *Chem. Soc. Rev.*, 1995, 24, 19–33.)

and how long does it stay there? Depending on the structure of the photosensitizer, the principal target at the macroscopic level may be, for example, the liver, the tumor, or the skin; and at a cellular level, the plasma membrane, lysosomes, or mitochondria.^{22,23} Subsequent cell death may result from cell necrosis, or from apoptosis, a process of programmed cell death stimulated here by photodynamic sensitization. Specific protein targets have been identified with some sensitizers (e.g., Bcl-2 with Pc 4; see Section 9.22.14.1).

At a molecular level, two mechanistic routes for photosensitized oxidation with dioxygen are usually recognized, termed type I and type II.

The type I mechanism is a radical process, and involves the excited state of the photosensitizer in electron-transfer processes, as indicated in Scheme 1. The reactions there are essentially photochemically stimulated autoxidation processes.



Superoxide variant



followed by Fenton chemistry

Scheme 1

The type II reaction is not a radical process (at least, not initially), but involves energy transfer from the excited triplet of the photosensitizer to ground-state triplet dioxygen to generate singlet oxygen (${}^1\Delta_g$), which is the reactive (toxic) species, as shown in Scheme 2. For a porphyrin sensitizer, the origin of the two reaction types can be summarized with a modified Jablonski diagram, as shown in Figure 3.

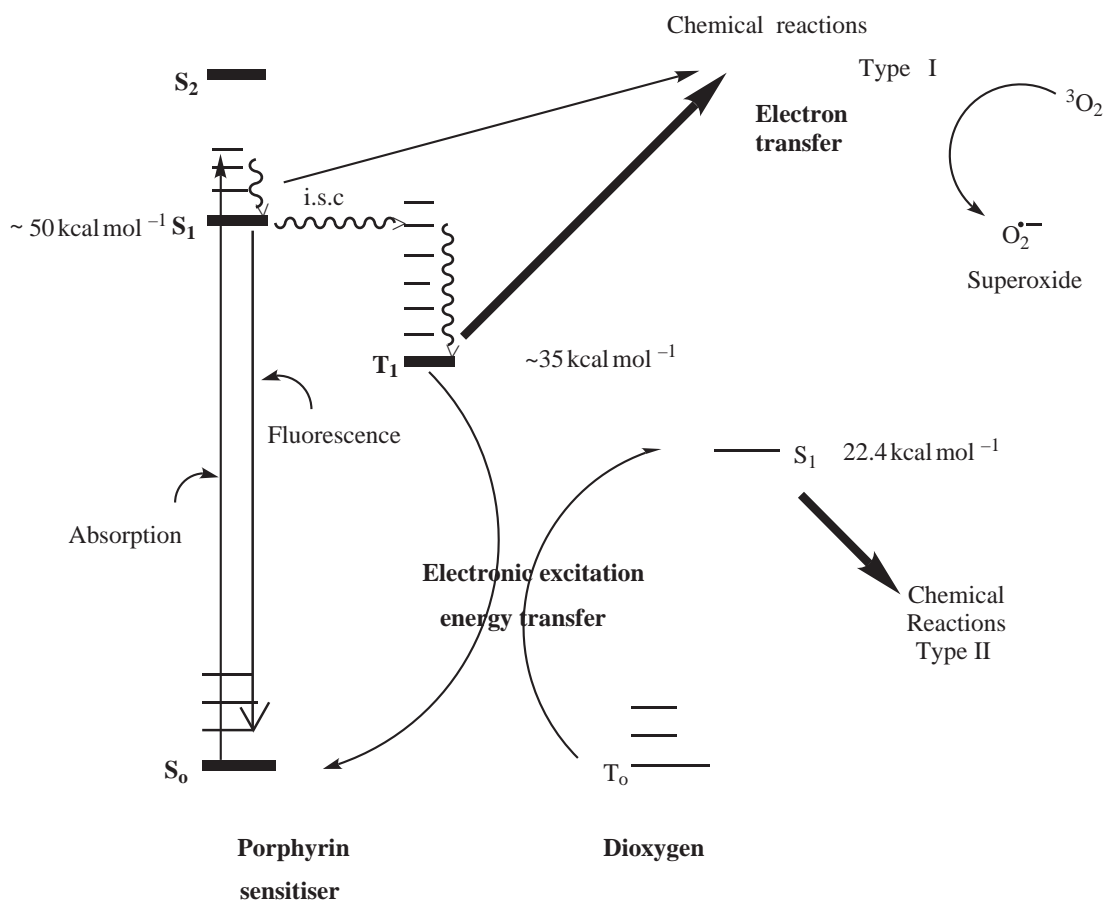
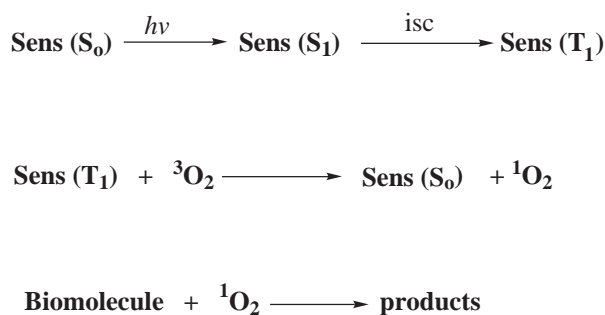
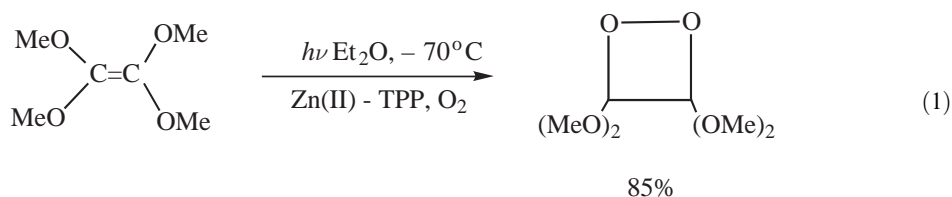


Figure 3 Type I and type II photooxidation processes with a porphyrin sensitizer illustrated with a modified Jablonski diagram. (S_0 = ground singlet state, S_1 = first excited singlet state, S_2 = second excited singlet state, T_0 = ground triplet state, T_1 = first excited triplet state, i.s.c. = intersystem crossing.)



Scheme 2

In the photodynamic effect and photodynamic therapy, it is generally considered that the type II process predominates. Certainly a number of second-generation photosensitizers have been developed with this idea in mind. In chemical systems it is relatively easy to show the involvement of singlet oxygen and, indeed, a photosensitizer such as zinc(II) tetraphenylporphyrin, oxygen, and light can be used to generate singlet oxygen in efficient chemical syntheses requiring that reagent, as illustrated in Equation (1):²⁴



However, in biological systems it is difficult to demonstrate the participation of singlet oxygen, presumably because it is so readily mopped up by a variety of biomolecules present in living tissue. Nevertheless, the current and reasonable consensus is that type II reactions predominate in photodynamic therapy, with type I reactions playing an important but secondary role. It is pertinent to note that singlet oxygen reacts readily with unsaturated lipids and certain α -amino acid side chains (e.g., tryptophan, tyrosine) in proteins: these are important components of biomembranes surrounding the cell and encapsulating its internal structures, and damage to these is thought to be a principal cause of cell death.

9.22.2.3 Haematoporphyrin Derivative

As mentioned above, the first photosensitizer to be applied to the photodynamic therapy of cancer was haematoporphyrin derivative (HpD). It is prepared by treating haematoporphyrin (**1**) with 5% H_2SO_4 -HOAc for 15 min at room temperature, followed by precipitation with water, and then basification. As has been described elsewhere,^{25,26} this procedure gives a very complex mixture, which comprises a number of monomeric porphyrins together with oligomers derived from them with covalent ether, ester and carbon-carbon internuclear linkages. The putative structural detail of the oligomeric components is illustrated schematically in Figure 4. The oligomeric fractions hold the main PDT activity and, commercially, the monomeric fraction is chromatographically removed to give a residual oligomeric mixture with (in its principal manifestation) the proprietary name of PHOTOFRIN[®], which has regulatory approval for the treatment of various cancers. There appears to have been little PDT development of metal complexes of HpD itself, although a fluorescent emission observed *in vivo* after treating tumor tissue with HpD has been attributed to the adventitious formation of zinc(II) complexes.²⁷ (Porphyrins are avid ligands and, for example, give rise to zinc and copper complexes on merely being manipulated with tap water). Radiolabelling of HpD with a metal in the N_4 cavity has been reported (e.g., ^{54}Mn , $^{99\text{c}}\text{Tc}$, refs. 28, 29 respectively) in attempts to detect tumors by scintillography by making use of the tumor-selective properties of HpD.

HpD and its commercial variants, although effective agents for tumor photonecrosis and the first drugs in the field, have a number of disadvantages. First, although the starting material, haematoporphyrin (**1**), is readily available from blood, it is a sensitive compound (two benzylic functions) and commercial samples are usually impure. Second, while the preparation of HpD is experimentally simple, the product is a very complex mixture, even when the porphyrin monomers are removed. Attempts to isolate a single, highly active oligomer have not succeeded. Third, in light absorption HpD possesses a band at about 625 nm in the red region, and this is where visible irradiation is carried out (see Section 9.22.3). However, this is the weakest of the four visible bands (typical etio-type spectrum), and this has to be made up for by larger photosensitizer doses and larger light doses, and/or protracted irradiation times. Fourth, in clinical use it tends to cause some photosensitization of normal tissue over some weeks, i.e., it is not selective enough.

9.22.3 DESIGN FEATURES FOR A GOOD PHOTSENSITIZER FOR PDT

The preferred features in a good ("second-generation")³⁰ photosensitizer for PDT may be summarized as follows:

- (i) A single achiral substance, available conveniently in good yield as a pure compound; and a stable substance (good shelf life).
- (ii) Little or no toxicity in the dark.

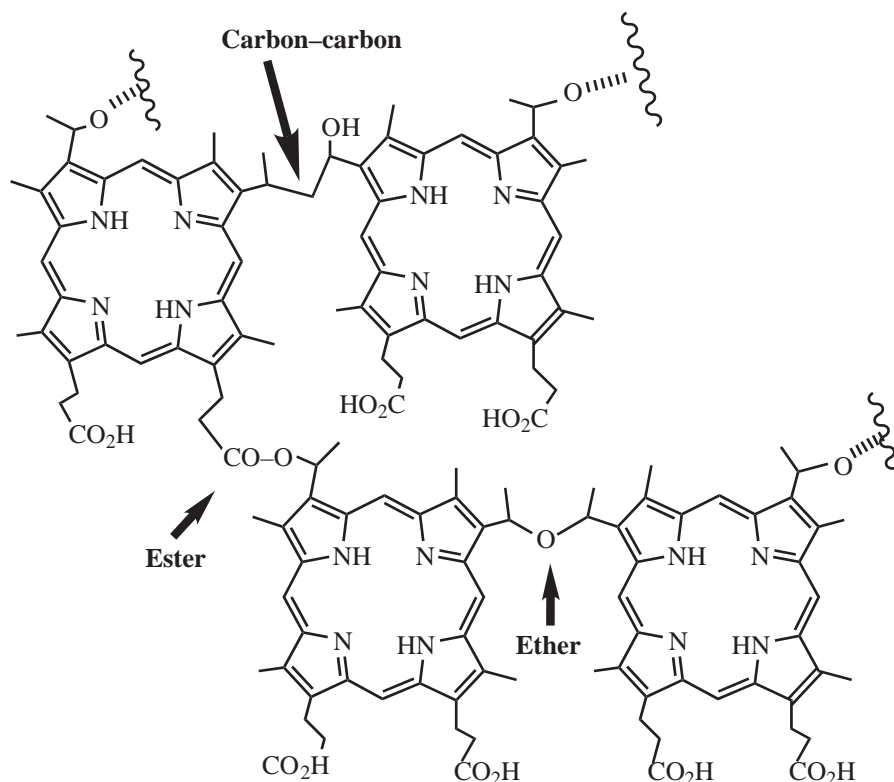


Figure 4 Schematic representation of the structural features of the HpD oligomer (drawn as a tetramer), showing ether, ester and carbon-carbon internuclear bonds.

- (iii) The substance to show appropriate pharmacokinetic behaviour, which means being able to localize with some degree of selectivity in tumor tissue with respect to normal tissue, and not to suffer long-term retention in any tissue. This criterion, which rests on solution chemistry, has been, and continues to be, the most difficult to meet. Amphiphilic character seems to confer advantage, but several researchers have chosen to work with hydrophobic compounds (e.g., zinc(II) phthalocyanine) and to administer them with special delivery systems (see Section 9.22.5.8).
- (iv) For photodiagnostic applications, it is fluorescence that is being observed, so the fluorescence quantum yield, Φ_f , is important. For photonecrosis following a singlet oxygen mechanism (Scheme 2, Figure 3) a high Φ_f value is deleterious, since it is the lifetime and quantum yield Φ_T of the triplet that is important. In order to excite triplet oxygen to the first excited singlet $^1\Delta_g$ state, it is necessary for the photosensitizer to possess a triplet energy greater than or about $22.4 \text{ kcal mol}^{-1}$ (94 kJ mol^{-1}), which is the excitation energy of singlet oxygen. Overall, it is the singlet oxygen quantum yield, Φ_Δ , that is the key parameter, and many porphyrin molecules show high values for this. Thus, haematoporphyrin (**1**) in aqueous methanol has $\Phi_T = 0.83$,³¹ and $\Phi_\Delta = 0.53$ (ethanol, air).³² 5,10,15,20-Tetraphenylporphyrin (**2**) has values of $\Phi_T = 0.67$ and $\Phi_\Delta = 0.63$ in benzene under air.³³ It is such high values, coupled with fluorescent properties and (generally) low dark toxicity, that seems to have been responsible for the predominance of porphyrin-type sensitizers in PDT.
- (v) Absorption, preferably strong, in the red region is highly desirable. This arises because human tissue strongly absorbs visible light in the region below about 620 nm, due in large part to the absorption of haemoglobin/myoglobin. Because living tissue is compartmentalized and membrane-rich, there is also a considerable amount of light scattering, and this too becomes increasingly important as we move to higher energies. Hence a photosensitizer with strong absorption in the red region is desirable if the aim is to have effective electronic excitation in a biological milieu.

The situation is illustrated in Figure 5, which shows (dotted line) the transmittance of a piece of human tissue (0.7 cm thick) over the visible range, together with the absorption spectra of

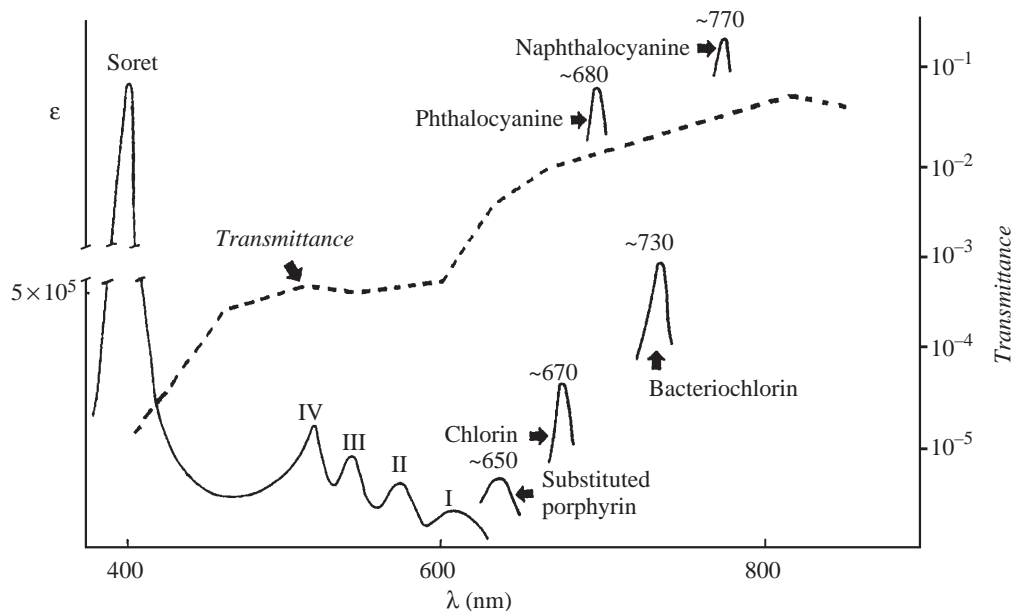
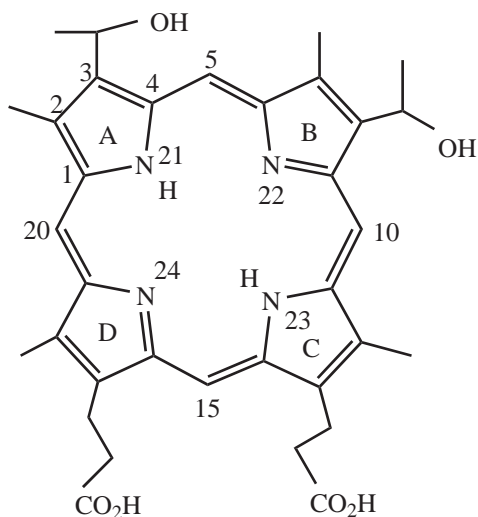
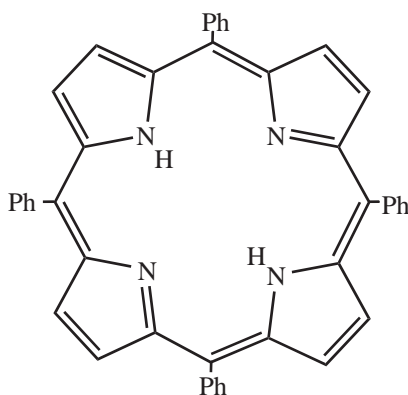


Figure 5 Schematic representation of absorbance of porphyrin compounds in relation to tissue transmittance at various wavelengths (see text). The lowest energy band (Band I) is shown in each case, apart from the porphyrin spectrum (etio type shown) on the left. The transmittance curve refers to a fold of human scrotal sac 0.7 cm thick (Wan, S.; Parrish, J. A.; Anderson, R. R.; Madden, M. *Photochem. Photobiol.* **1981**, *34*, 679–681). The broad feature at ca. 500–600 nm is ascribed to haemoglobin (reproduced by permission of the Royal Society of Chemistry from *Chem. Soc. Rev.* **1995**, *24*, 19–33).

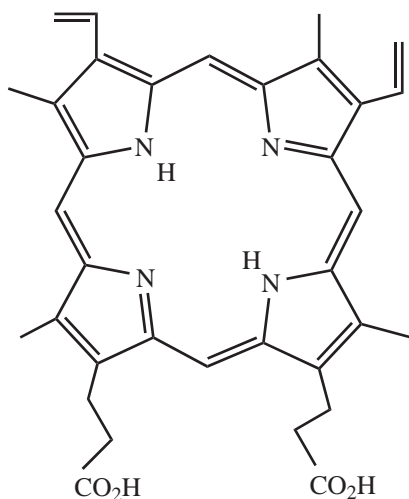
haematoporphyrin (**1**) (continuous curve on the left of the field: protoporphyrin (**3**) has a similar spectrum) and some sensitizers of the second-generation type (shown only as individual absorption peaks). The preferred range for λ_{\max} for the sensitizer is probably about 650–800 nm, since at much above the upper value the absorption of water begins to cut in; and in any case the triplet energy of the sensitizer is in danger of falling below $22.4 \text{ kcal mol}^{-1}$, so that energy transfer to triplet oxygen can no longer occur efficiently.



(1) Haematoporphyrin



(2) 5,10,15,20-Tetraphenyl porphyrin (TPP)



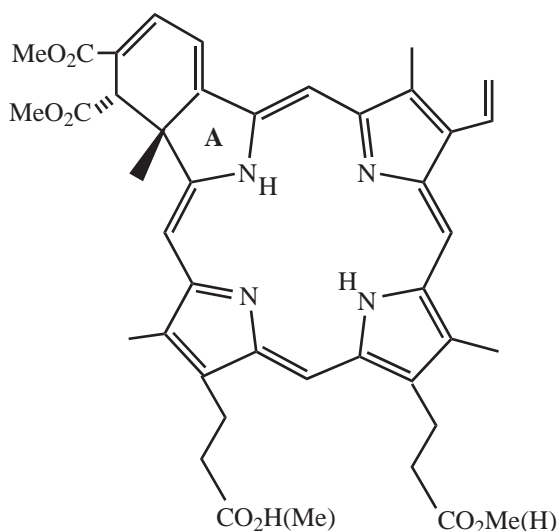
(3) Protoporphyrin

(4) δ -ALA

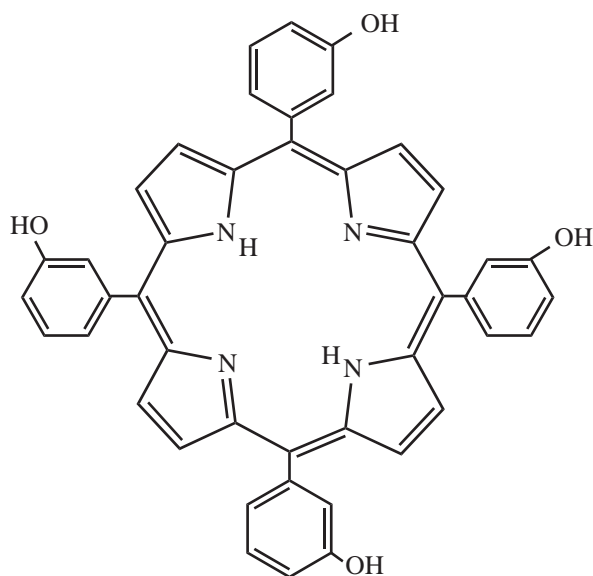
9.22.4 PHOTOSENSITIZERS IN CLINICAL USE

Over the recent past, these criteria, and especially the last of them, have been applied to the bringing forward of new PDT drugs. Those photosensitizers which have so far (June 2002) been approved by regulatory agencies are as follows:

- (i) PHOTOFRIN[®] This has been described briefly above. It was the first sensitizer to receive regulatory approval (in Canada in 1993, for papilloma of the bladder). Subsequently, it has received regulatory approvals in Japan, the USA, and some European countries for various cancers such as those of the lung, esophagus, and stomach, including palliative applications.³⁴
- (ii) LEVULAN[®] The drug referred to here is δ -aminolevulinic acid (ALA, (4)). This is a colorless substance, and not a photosensitizer, but a pro-drug. It is an intermediate in the biosynthesis of protoporphyrin (3), which is itself on the route to haem. When ALA (4) is administered (topically, intravenously, or by mouth) a sequence of enzymatic reactions takes over and converts it, after several steps, to protoporphyrin (3), which, when generated *in situ* in this way, is an effective photodynamic sensitizer. As a PDT pro-drug, δ -aminolevulinic acid is capable of destroying superficial lesions (e.g., basal cell carcinoma, squamous cell carcinoma),^{35,36} providing that they are of limited thickness. It also has potential as a photodiagnostic agent.
- (iii) VISUDYNE[®] Benzoporphyrin derivative (benzoporphyrin derivative mono acid ring A adduct, BPDMA, (5)) was originally developed as a tumor photosensitizer, and has also been examined as a photodynamic treatment for psoriasis.^{37,38} However, it has recently found application (and regulatory approval) for the management of the wet form of age-related macular degeneration, for which there was earlier no satisfactory treatment available. Benzoporphyrin derivative (5) is prepared from protoporphyrin (3) (itself ex-haemoglobin/blood) in a three-stage synthesis (from the dimethyl ester of protoporphyrin).^{39,40} Unlike the compounds mentioned previously, compound (5) is a chlorin (a 2,3-dihydroporphyrin) and has a strong absorption band characteristic of chlorins in the red region (λ_{max} MeOH 686 nm, ϵ 34,000 M⁻¹ cm⁻¹) and a high singlet oxygen quantum yield (Φ_{Δ} = 0.76, MeOH).⁴¹
- (iv) FOSCAN[®] 5,10,15,20-tetrakis(*m*-hydroxyphenyl)chlorin, m-THPC, (6) is available via a three-stage synthesis from simple starting materials (pyrrole and *m*-methoxybenzaldehyde).^{42,43} It has λ_{max} = 650 nm, ϵ = 29,600 M⁻¹ cm⁻¹ (MeOH) and Φ_{Δ} = 0.43 (MeOH, air).⁴⁴ It shows remarkable potency, typical drug doses being ca. 0.15 mg kg⁻¹, with photon doses of 5–20 J cm⁻², so that at a fluence rate of 100 mW cm⁻², treatment times are 50–200s. This compound has so far not been approved in the USA, but received regulatory approval in Europe in 2001 for the treatment of head and neck cancer.⁴⁵



- (5) Benzoporphyrin derivative, monoacid, ring A adduct
BPD, VERTEPORFIN, VISUDYNE

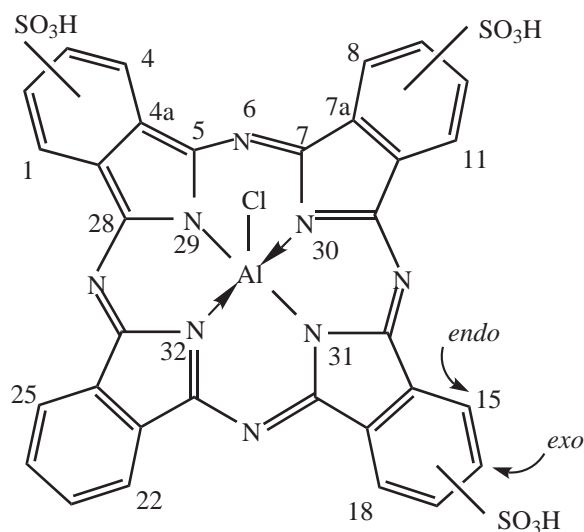


- (6) 5,10,15,20-Tetrakis(*m*-hydroxyphenyl)
chlorin, *m*-THPC, FOSCAN

It will not be lost on the reader that, while PHOTOFRIN[®] and compounds (3), (5) and (6) contain no metal, they would be expected to be excellent ligands. Are metal complexes useful as PDT photosensitizers? Indeed, they are, and may be expected in the future to become more important. The rest of this chapter is about this aspect: it will emphasize metal complex formation and properties in relation to PDT. The synthesis of ligands, while of crucial importance, will not usually be treated here in detail, but leading references to relevant synthetic organic chemistry will be provided. The synthesis of porphyrins and related compounds has been considered in several monographs and reviews (porphyrins,^{46,47} phthalocyanines⁴⁸).

In fact, one metal complex has already had considerable clinical application in PDT, although its regulatory approval status is not clear at present. The photosensitizer has the trade name PHOTOSENS and may be represented by structure (7). It is prepared by the direct sulfonation of chloroaluminum(III)-phthalocyanine, and the isolated material appears to contain a mixture of

the di- and trisulfonic acids. This preparation is water soluble, and has the very intense absorption peak in the red typical of metallophthalocyanines ($\lambda_{\max} \sim 680 \text{ nm}$, $\epsilon \sim 10^5 \text{ M}^{-1} \text{ cm}^{-1}$). The components can be separated by HPLC.⁴⁹ From 1994 onwards, Stranadko and his colleagues in Moscow have reported the extensive use of this photosensitizer in the treatment of skin, breast, and oropharyngeal cancer.⁵⁰ Thus, in the period 1994–1997, 134 patients with various cancers (mainly of the skin) were treated with PHOTOSENS: 70 were judged to show complete response, and 57 partial response.



(7) ClAlPcS₃

9.22.5 COORDINATION COMPLEXES AS PDT SENSITIZERS: SOME GENERAL CONSIDERATIONS

It is clear from the examples given in the previous section that metal complexation is not an essential requirement for a clinically useful sensitizer in PDT. Nonetheless, the presence of a coordinated metal ion may confer advantages, and these advantages and related matters will now be rehearsed.

9.22.5.1 Synthesis of Metalloporphyrins and Metallophthalocyanines

At the outset it is to be observed that these metal complexes, although they need to be circum-spectly handled, are user-friendly substances, and are usually readily obtained. The preparation of metalloporphyrins and metallophthalocyanines is accomplished in three ways, as described below.

9.22.5.1.1 Metalation of the preformed ligand

This is the most common route, the reagent being a metal compound/solvent combination. Typical conditions call for the metal salt (e.g., acetate) in a buffer system (e.g., NaOAc/AcOH) and a co-solvent such as chloroform. Generally the reaction mixture is refluxed until the metal complex spectrum (see Section 9.22.5.6 and Table 4) is fully developed. Metal acetylacetonates and metal phenoxides have also been employed. The topic has been reviewed in detail by Buchler,⁵¹ who has also summarized the history and classification of metal complexes of this series, and the mechanisms of metalation.⁵²

9.22.5.1.2 Transmetalation

This reaction has been observed for porphyrins, and used to establish relative stabilities.^{51,53} It is of practical use in the preparation of metal complexes, e.g., metallophthalocyanines by metal exchange with dilithium(I) phthalocyanine.⁵⁴

9.22.5.1.3 Template synthesis

This is the common route to metallophthalocyanines: the principal variants of this reductive cyclotetramerization are outlined in Figure 6. This 4×1 route has also sometimes been used in the synthesis of metalloporphyrins having a D_{4h} pattern of peripheral substitution. Thus, copper(II)-octamethylporphyrin is obtained in 20% yield on refluxing 2-dimethylamino-3,4-dimethylpyrrole 4-carboxylic acid (**8**) with copper(II) acetate in methanol.⁵⁵ In another example, heating 1,3,4,7-tetramethylisoindole (**9**) with copper(II) acetate in a sealed tube, followed by extraction with pyridine, gives 81% of bis(pyridine) magnesium(II)-octamethyltetrabenzoporphyrin (**10**).⁵⁶

9.22.5.2 Metal Complex Stability

The typical metalloporphyrins and metallophthalocyanines have in general very high thermodynamic stabilities. However, because it is difficult to establish conditions under which the

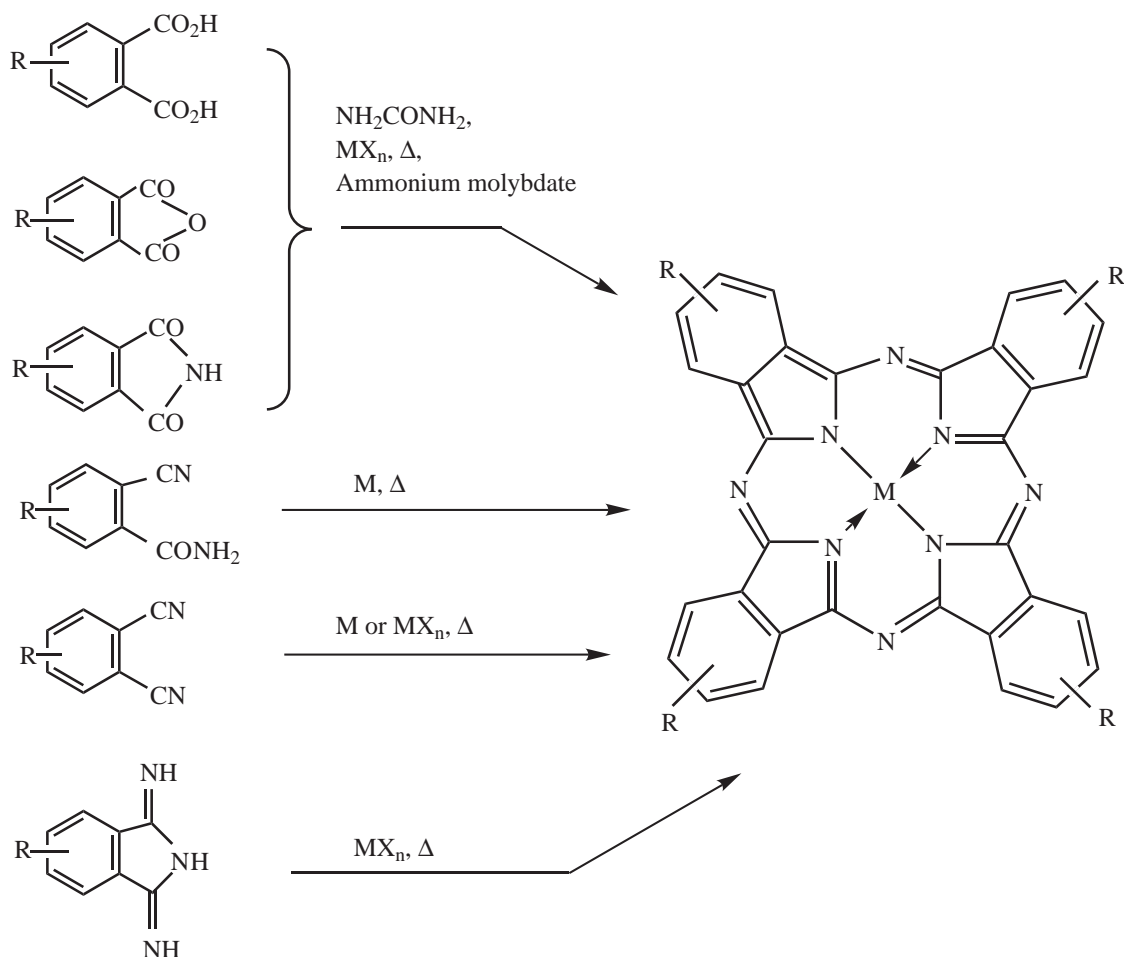
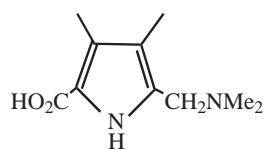
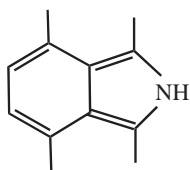


Figure 6 An outline of synthetic routes to metallophthalocyanines. The syntheses are often carried out in a melt, or in the presence of a high boiling solvent, such as 1,3,4-trichlorobenzene, or under other conditions eg LiOR, $\text{Me}_2\text{NCH}_2\text{CH}_2\text{OH}$; see later examples (Figures 8, 10, 12, 13).

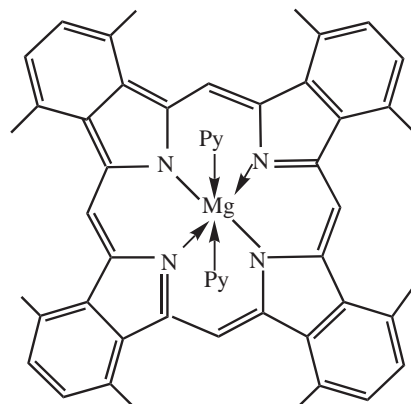
components of Equation (2) are in true and measurable equilibrium, direct measurements of stability constants have been lacking.⁵⁷ An estimate^{58,59} has been made for the stability constant, K_s , of zinc(II) mesoporphyrin dimethyl ester (**11**) (Equation (3)). The value was estimated as 10^{29} for a solution, presumably a micellar solution, in 0.25% cetylammmonium bromide at room temperature, but confirmatory determinations appear to be absent. It is clear, however, that K_s is very large.⁵⁷



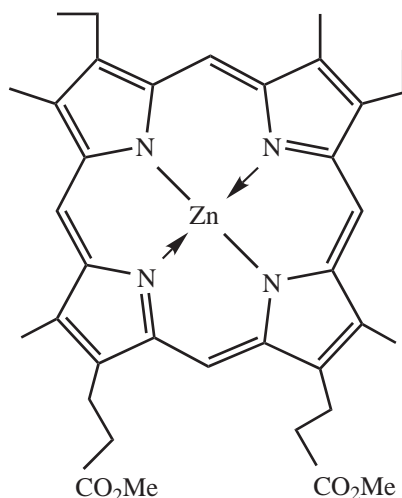
(8)



(9)



(10)



(11) Zinc(II) mesoporphyrin dimethyl ester



$$K_s = \frac{[\text{Zn(II) mesoporphyrin-dme}]}{[\text{Zn}^{++}][\text{mesoporphyrin-dme}^{--}]} \quad (3)$$

The ease of demetalation under acidic conditions is of considerable practical importance, and is an everyday concern for those working in this field. Laboratory practice has built up over the decades: it was codified by Falk⁶⁰ and Phillips,^{58,59} as shown in Table 1.

Phillips^{58,59} gives the order of decreasing stability of metalloporphyrins as: $\text{Pt}^{\text{II}} > \text{Pd}^{\text{II}} > \text{Ni}^{\text{II}} > \text{Co}^{\text{II}} > \text{Ag}^{\text{II}} > \text{Cu}^{\text{II}} > \text{Zn}^{\text{II}} > \text{Mg}^{\text{II}} > \text{Cd}^{\text{II}} > \text{Sn}^{\text{II}} > \text{Li}^{\text{I}} > \text{Na}^{\text{I}} > \text{Ba}^{\text{II}} > \text{K}^{\text{I}} > \text{Ag}^{\text{I}}$.

Table 1 Demetalation of metalloporphyrins under acidic conditions.^{52,58–60}

Stability class	Reagent 25 °C, 2 h	Examples
V	H ₂ O/CH ₂ Cl ₂	Na ^I , Ba ^{II}
IV	HOAc	Mg ^{II} , Cd ^{II}
III	HCl/H ₂ O/CH ₂ Cl ₂	Fe ^{II} , Zn ^{II}
II	H ₂ SO ₄	Cu ^{II} , Ni ^{II} , Fe ^{III}
I ^a	H ₂ SO ₄	Sn ^{IV} , Al ^{III}

^a Little or no demetalation.

There have been several comments and criticisms of this sequence.^{51,52,57} Buchler^{51,52} has suggested a “stability index,” S_i :

$$S_i = 100\chi \frac{Z}{r_i} \quad (4)$$

where χ is the Pauling electronegativity of the central metal, and r_i is the effective ionic radius (pm) of the metal ion with oxidation number Z and appropriate coordination number and spin state. In this approach, the electronegativity, χ , is held to represent the covalent bonding capacity of the metal (which becomes especially important as back bonding increases, e.g., in Pt), while the charge to radius ratio Z/r_i makes allowance for the electrostatic contribution to bonding. Thus metalloporphyrins, such as Sn^{IV}, with high values of Z and χ and small r_i are very stable; while metalloporphyrins, such as Cd^{II}, with relatively low values of Z and χ and large r_i , have low stability (i.e., kinetic stability in acidic medium). As the periods are descended, ionic radius begins to take on a steric aspect, as the ions (e.g., Ba^{II}, Pb^{II}) become too large to fit comfortably into the coordination hole.

Table 2 summarizes these data for metal complexes of the porphyrin series which appear at present to be most relevant to PDT. Apart from the platinum(II) example, there is a reasonable correlation between this empirical S_i and stability class within each oxidation number.

In general, for a particular metal state, metallophthalocyanines are more difficult to demetallate than are metalloporphyrins (the central hole is marginally smaller in the phthalocyanine ligand). Thus, copper(II) phthalocyanine, dissolved in concentrated sulfuric acid, is precipitated unchanged when the solution is poured into ice/water. However, metallochlorins are demetallated more readily than the corresponding metalloporphyrins (basicity: chlorin < porphyrin).

Table 2 Buchler's stability index S_i and stability classes for metallo-octaalkylporphyrins.

Z	M	χ	r_1 (pm)	S_i	Stability class
2	Pd	2.20	[64]	6.88	I
	Ni	1.91	[60]	6.37	II
	Cu	1.90	[62]	6.12	II
	Pt	2.28	(78)	5.85	II(I?)
	Zn	1.65	74	4.46	III
	Mg	1.31	72	3.64	IV
	Cd	1.69	95	3.56	IV
3	Ru	2.2	68	9.71	I
	Al	1.61	53	9.11	I
	Ga	1.81	62	8.76	II
	In	1.78	79	6.76	III
4	Si	1.90	40	19.00	I
	Ge	2.01	54	14.89	I
	Sn	1.96	69	11.36	I

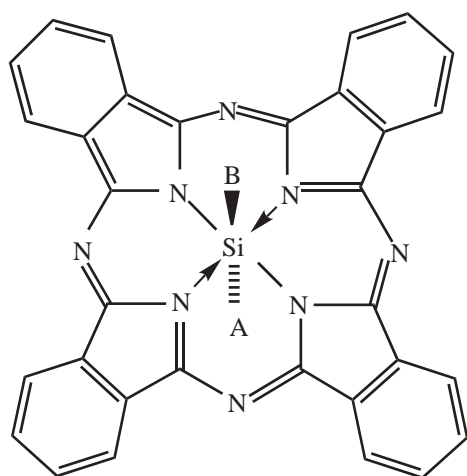
Source: Buchler⁵¹ r_1 for CN + 6. [r_1] for CN = 4. () estimated r_1 .

9.22.5.3 Structural Variation

Pharmaceutical discoveries are principally made by thoughtful structural variation on a lead compound which has been found, by chance or design, to have a certain amount of the desired activity. It is clear that with metalloporphyrins, there are additional structural variations to be had. In the first place, it is possible to vary the metal. It was realized at an early stage that inserting and varying the metal would modify PDT activity.⁶¹ The possibility also exists of structural changes in axial ligands in those metalloporphyrins which possess them. This structural variation occurs in the space immediately above and below the macrocycle, which is a space not readily accessible to controlled variation in metal-free compounds of this series.

An interesting example is provided by the observation that Chinese hamster cells grown in culture with chloroaluminum(III)-phthalocyanine as sensitizer are protected from photodamage in the presence of fluoride ions. It is supposed that the active photosensitizer in this case is (HO)Al^{III}Pc·H₂O, and that in the presence of excess fluoride ions it is converted into the axial fluoride complex, which is presumably less active.⁶² The same sensitizer, when reacted with poly(ethyleneglycol) (MW ~ 2000) or with poly(vinyl alcohol) (MW 13,000–23,000) gives products with these species as axial ligands, which products are water soluble. In *in vivo* bioassays against the EMT-6 mammary tumor, these preparations caused complete regression in 75–100% of the animals when irradiated (DLI = 24 h) at a light dose of 400 J cm⁻² (650–700 nm) and a drug dose of 0.25 μmol kg⁻¹.⁶³ In the animals which were not regarded as cured, the poly(vinyl alcohol) conjugate produced the largest delay in tumor growth. In comparison with chloroaluminum(III)-phthalocyanine and the poly(ethyleneglycol) conjugate, the poly(vinyl alcohol) conjugate showed the longest plasma half-life, and the highest tumor/skin and tumor/muscle concentration ratios.⁶³

The three examples in the previous paragraph lack precise structural definition, for one reason or another, but the silicon(IV) phthalocyanine derivatives described by Kenney and his colleagues are well-defined single substances.^{64–66} The synthesis of a typical example is shown in Figure 7⁶⁵ Four compounds with differing axial ligands are displayed at (12)–(15). Table 3 summarizes some photophysical and photobiological data for these compounds. It is evident that the nature of the axial ligand has an appreciable influence on the results obtained. All of these compounds were as least as effective as PHOTFRIN[®] in PDT studies in animal models, and showed much less skin photosensitization.⁶⁶



	A	B
(12)	HO	OSiMe ₂ (CH ₂) ₃ NMe ₂
(13)	HO	OSiMe ₂ (CH ₂) ₃ NEt(CH ₂) ₂ NMe ₂
(14)	OSiMe ₂ (CH ₂) ₃ NMe ₂	as A
(15)	OSiMe ₂ (CH ₂) ₃ NEt(CH ₂) ₂ NMe ₂	as A

9.22.5.4 Solubility

It may seem curious to make specific mention of this matter, but in a biological context, it is crucial. The nuclei of porphyrins and related systems are hydrophobic: it appears to be generally desirable that the photosensitizer has some degree of intermediate polarity (i.e., amphiphilic properties; Section 9.22.3) and the incorporation of a metal, such as zinc(II), which can take on an axial ligand (e.g., H₂O in aqueous media, or RNH₂ in a biological fluid), or magnesium(II), which can take on two, is expected to enhance solubility in hydroxylic solvents, and shift the

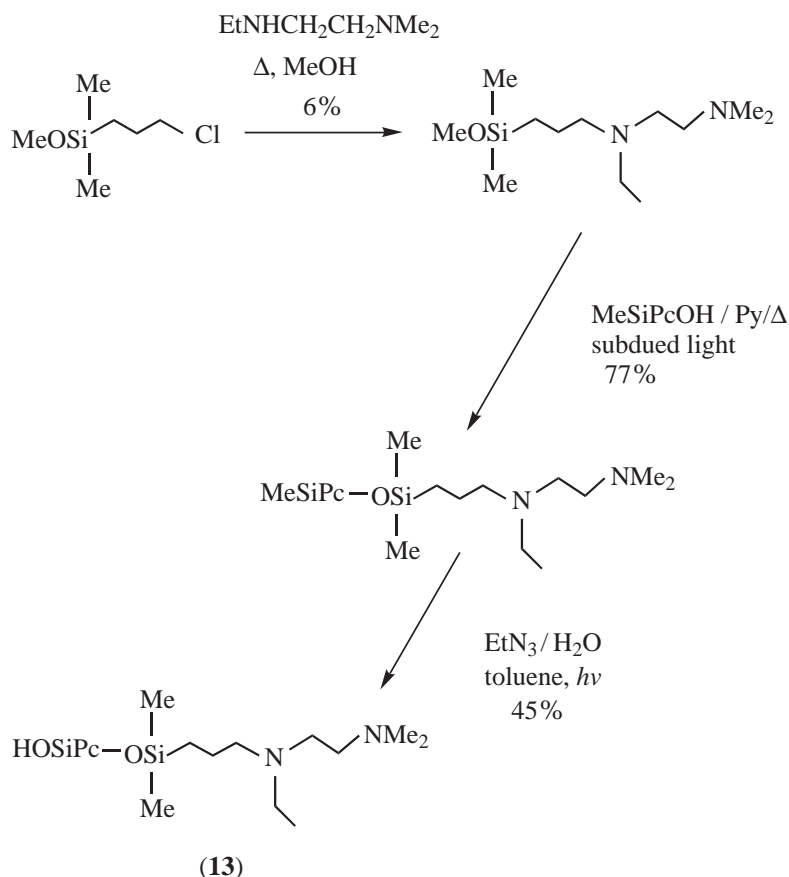


Figure 7 Synthesis of a silicon(IV) phthalocyanine with defined polar axial ligands.⁶⁵ Pc = phthalocyanine nucleus; the centrally coordinated atom (here Si) immediately precedes the Pc acronym.

Table 3 Photophysical and photobiological properties of silicon(IV) phthalocyanine derivatives with various axial ligands.⁶⁵

Compound	Triplet lifetime ^b (μs)	Relative Φ_{Δ}	Compound levels in V79 cells ^c (nmol/10 ⁶ cells kJ m ⁻²)	Fluence for 90% kill of V79 cells ^d (kJ m ⁻²)
(12) (Pc 4) ^a	113	0.43	0.72 \pm 0.06	3.8
(13) (Pc 10) ^a	139	0.50	0.56 \pm 0.09	5.8
(14) (Pc 12) ^a	160	0.32	2.11 \pm 0.60	3.8
(15) (Pc 18) ^a	188	0.20	0.33 \pm 0.03	10.3

^a Laboratory code, used in publications. ^b In acetonitrile. ^c Uptake from a 1.0 μM solution of the sensitizer. ^d Photosensitizer concentration 0.5 μM .

partition coefficient in favour of the aqueous phase. Thus, on reversed-phase HPLC separation, zinc(II) haematoporphyrin emerges from the column before haematoporphyrin (1) itself;²⁷ and zinc(II) tetrakis(*p*-carboxyphenyl)porphyrin is more soluble in water than is the free base.⁶⁷

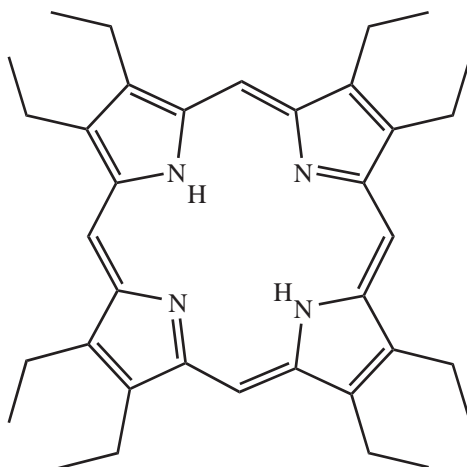
9.22.5.5 Disaggregation

Compounds of the porphyrin series, like other aromatic compounds, have a strong tendency to aggregate in solution. In general, aggregation is favoured by increased concentration and by an increased proportion of the poor solvent in a mixed solvent system.^{67–70} The aggregate shows reduced fluorescence and reduced PDT activity with respect to the monomer.⁷¹

In structural terms, aggregation of porphyrin rings usually results from π - π and π - σ electronic interactions between parallel plates;⁶⁹ however, if a coordinated metal is present, and it has axial ligands, then the aromatic systems cannot come close together, and so aggregation is inhibited and PDT activity is expected to be enhanced.⁷²

9.22.5.6 Spectroscopic Properties

The absorption and emission spectra of the porphyrins and related compounds change significantly on metal complex formation, especially in the visible (Q-band) region.⁷³ On complexation, the symmetry of the porphyrin chromophore changes from D_{2h} to D_{4h} , and the absorption in the visible region becomes simpler.⁷³ Thus, octaethylporphyrin (**16**) has four bands in the visible (Q-band) region, Table 4, whereas its Al^{III} , Zn^{II} , Co^{II} , Co^{III} , Pd^{II} , and Pt^{II} complexes have only two. As far as the desirability of absorption in the red is concerned, this result is somewhat disadvantageous from a PDT standpoint since, as Table 4 shows, the peak at lowest energy moves, albeit hyperchromically, to shorter wavelengths (generally <600 nm) in the spectrum of the metal complex. Phthalocyanine shows similar behaviour,⁷⁹ the free base showing two strong absorption peaks at about 680 nm, while the divalent metal complexes show only one intense peak in that region.



(16)

For the photodiagnostic use of these compounds, a high quantum yield of fluorescence, Φ_f , is desirable. The metal complexes of the common first-row transition metals are not suitable, because they show very low Φ_f values. On the other hand, porphyrin complexes of d^0 and d^{10} elements show appreciable fluorescence, although generally less than that of the metal-free compounds, presumably because of the heavy-atom effect (e.g., TPP \rightarrow ZnTPP, Table 5). The further operation of the heavy-atom effect, which increases the rate of intersystem crossing (k_{isc}) by

Table 4 Absorption spectra (500–700 nm) of octaethylporphyrin (**16**) and some of its metal complexes.

Compound	Solvent	λ_{max} ($\epsilon_{\text{max}} \text{ M}^{-1} \text{ cm}^{-1}$)					References	
		IV	β	III	II	α		
Octaethyl porphyrin (OEP, 16)	PhH	498 (14,500)		532 (10,800)	568 (6,800)		622 (5,800)	74
$\text{HOAl}^{\text{III}}\text{OEP}$	PhH		533(11,700)			572(22,900)		75
$\text{Co}^{\text{II}}\text{OEP}$	CHCl_3		518(10,300)			551(21,700)		76
$\text{PyCo}^{\text{III}}\text{OEP}$	CHCl_3		529(10,900)			561(11,500)		76
$\text{Zn}^{\text{II}}\text{OEP}$	Dioxan		536(18,200)			572(24,500)		77
$\text{Pd}^{\text{II}}\text{OEP}$	PhH		515(14,500)			548(58,900)		78
$\text{Pt}^{\text{II}}\text{OEP}$	PhH		503(12,600)			536(56,200)		78

Table 5 Effect of metallation, and further substitution, on the emission spectra of tetraphenylporphyrin (**2**).

Compound ^a	Solvent	Φ_f	Φ_p/Φ_f	Φ_p	References
TPP (2)	PhH	0.13 ^b			80
ZnTPP	PhH	0.033 ^b	0.32 ^c		80
Zn(<i>To</i> -FPP)	PhH	0.033 ^b	0.60 ^c		80
Zn(<i>To</i> -ClPP)	PhH	0.038 ^b	1.32 ^c		80
Zn(<i>To</i> -BrPP)	PhH	0.0004 ^b	52 ^c		80
PdTPP	d,e	0.00015 ^d		0.2 ^e	73,81
PtTPP	d,e	–		0.45 ^e	81

^a (*To*-FPP) = 5,10,15,20-tetrakis(*o*-fluorophenyl)porphyrin and so on. ^b Under nitrogen at room temperature. ^c At 77 K in methylcyclohexane/isopentane. ^d In methyl methacrylate at room temperature. ^e In ether : isopentane : dimethylformamide : ethanol = 12:10:6:1 at 77 K.

spin-orbit coupling to generate the triplet (Table 6), is seen in the series of *ortho*-halogenated ZnTPP derivatives (Table 5), with the Φ_p/Φ_f ratio increasing along the sequence *o*-H to *o*-Br.^{73,80}

With respect to the properties of the first excited triplet state of the sensitizer, which is required in cases of singlet oxygen involvement, it is the triplet lifetime and energy, and the efficiency of energy transfer to dioxygen, that are important. As we have seen (Section 9.22.3), these factors may be summarized in the singlet oxygen quantum yield Φ_Δ . Some illustrative values of this parameter in relation to the coordinated metal ion are given in Table 7, which shows data for complexes of tetraphenylporphyrin (**2**), of the dimethyl ester of haematoporphyrin (**1**), and of phthalocyanine sulfonic acids (cf. (7)). It can be seen that, for a singlet oxygen mechanism, complexes of common first-row transition metals are not appropriate: such metal ions with partially filled *d* shells (e.g., Mn^{III}, Ni^{II}, and Cu^{II} in Table 7) offer alternative pathways for rapid deactivation of the excited state; k_{isc} increases, and singlet and triplet lifetimes are decreased. Hence both Φ_f and Φ_Δ are usually very low. However, complexes of *d*⁰ (Mg, Al) and *d*¹⁰ (Zn, Cd) configurations have moderate to high values of Φ_Δ , as do complexes of some of the heavier elements (e.g., Pd, Pt). Indeed, apart from those cases where the excited states have available an efficient deactivation pathway (e.g., by the presence of a partially filled *d* shell), the heavy atom facilitates intersystem crossing (Tables 5 and 6), and the metal complexes often have higher Φ_Δ than the parent free base. For example, for complexes of 5,10,15,20-tetrakis(*p*-methoxyphenyl)porphyrin ((**17**), M = 2H), the Φ_Δ values measured in tetrahydrofuran were 0.73 for the zinc(II) and cadmium(II) complexes, 0.65 for the free base, and ~0.00 for the copper(II) complex. The phototoxicities against a laryngeal carcinoma cell line, using liposomal preparations of the photosensitizers, were: M = Cu <<< M = 2H < M = Zn ~ M = Cd.⁹¹

There have been occasional reports of metal complexes that are effective PDT photosensitizers, but where the singlet oxygen quantum yield is low or zero. The copper(II) benzo-chlorin iminium salt ((**18**), M = Cu^{II}) is such a case.^{92–95} The absorption spectrum of this compound is markedly solvent sensitive, with λ_{max} 752 nm in dichloromethane, 723 nm in serum, and 720 nm in a lipid emulsion. In spite of being a salt, this substance is not water soluble, and requires a delivery agent (a lipid emulsion). It shows PDT activity against cultures of radiation-induced fibrosarcoma (RIF) cells and in *in vivo* experiments (mammary adenocarcinoma, mouse). Although Φ_Δ appears to be close to zero, oxygen is still required. An electron-transfer mechanism is suggested, since the photosensitized lipid peroxidation in erythrocyte membranes is reduced in the presence of superoxide dismutase and of catalase. With a 24 h drug–light interval (DLI) the bioactivity of the zinc(II) complex ((**18**), M = Zn) is greater than that of the copper(II) complex ((**18**), M = Cu),

Table 6 Rates of intersystem crossing, k_{isc} , for some metallophthalocyanines in 1-chloronaphthalene at 298 K.

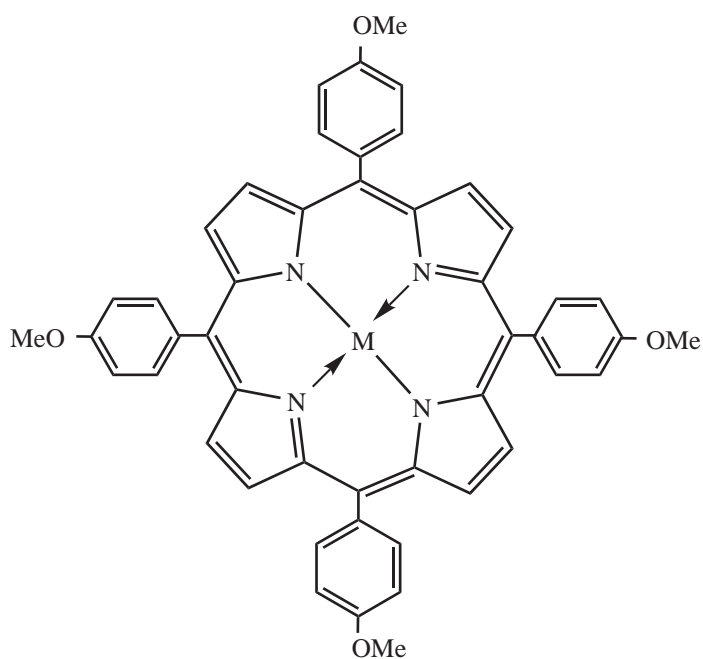
Compound	Φ_f	Φ_T	k_{isc} (10 ⁹ s ⁻¹)
ClAl ^{III} Pc	0.58 ± 0.04	0.4 ± 0.08	0.059
ClGa ^{III} Pc	0.31 ± 0.03	0.7 ± 0.10	0.18
ClIn ^{III} Pc	0.031 ± 0.004	0.9 ± 0.21	2.4

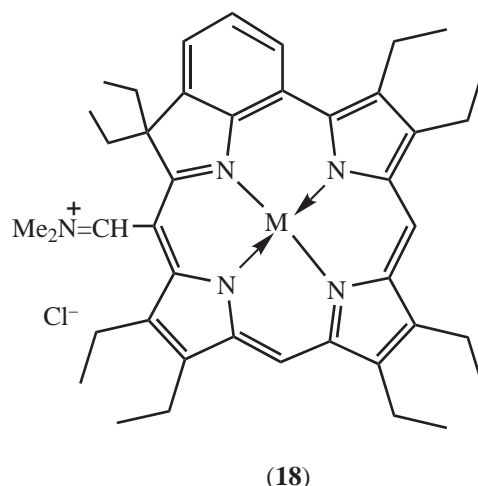
Source: Brannon and Magde.⁸²

Table 7 Singlet oxygen quantum yields Φ_{Δ} .

Compound	Solvent	[O ₂]	Φ_{Δ}	References
Tetraphenylporphyrin, TPP (2) complexes				
TPP(2)	PhH	air	0.66	83
ClAl ^{III} TPP	CCl ₄	air	0.90	84
XMn ^{III} TPP	CCl ₄	air	<0.01	84
Ni ^{II} TPP	CCl ₄	air	<0.01	84
Cu ^{II} TPP	CCl ₄	air	<0.01	84
Zn ^{II} TPP	PhH	air	0.72	83
Cd ^{II} TPP	PhMe	1.1 × 10 ⁻³	0.98	85
Cl ₂ Sn ^{IV} TPP	CCl ₄	air	0.55	84
Haematoporphyrin dimethyl ester ((1) as dme) complexes				
Hp dme	PhH	O ₂	0.50	86
XMn ^{III} Hp	H ₂ O	air	<0.001	87
Ni ^{II} Hp dme	DMF	O ₂	0.02	88
Pd ^{II} Hp dme	DMF	O ₂	0.38	88
Pt ^{II} Hp dme	DMF	O ₂	0.24	88
Phthalocyanine sulfonic acid (PcS _n) complexes				
PcS _n	H ₂ O	air	0.14	89
ClAl ^{III} PcS ₃ (7)	D ₂ O	O ₂	0.34	90
VO ^{IV} PcS _n	H ₂ O	air	0	89
Cu ^{II} PcS _n	H ₂ O	air	0	89
Zn ^{II} PcS ₃	D ₂ O	O ₂	0.36	90
ClGa ^{III} PcS ₄	H ₂ O/MeOH	O ₂	0.57	71

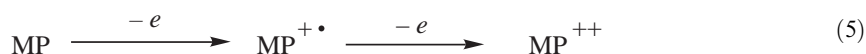
presumably because a singlet oxygen mechanism can now operate. Interestingly, the metal-free compound ((**18**), M = 2H), shows no PDT effect *in vivo* with a DLI of 24 h, but a PDT effect was found when the DLI was reduced to 3 h (at which point the metal complexes were essentially inactive), illustrating the profound effect that metallation can have on pharmacokinetic behaviour.⁹⁵

**(17)**



9.22.5.7 Redox Properties

The one-electron oxidation of the ring of a metalloporphyrin to give the radical cation (Equation (5)) is very sensitive to the nature of the metal ion present.



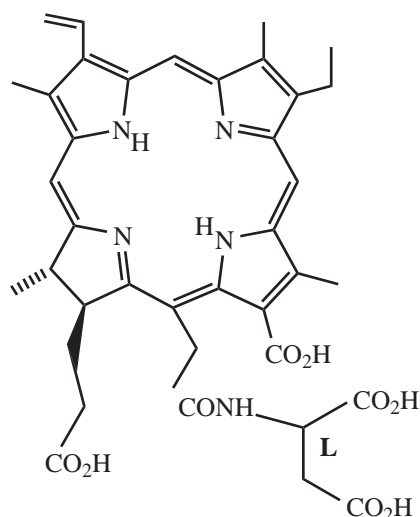
A prime example of this is the crucial ease of such oxidation in the magnesium(II) complex of the chlorin system present in chlorophyll during photosynthesis. Table 8 shows the half-wave potentials for the first ring oxidation of some metalloporphyrins, the examples chosen being based on 5,10,15,20-tetraphenyl porphyrin, TPP (2) and on 1,2,7,8,12,13,17,18-octaethylporphyrin, OEP (16).

The effects in evidence are complex. There is clearly an electrostatic effect due to the central positive charge [$E_{1/2} \text{M}^{\text{IV}} > \text{M}^{\text{III}} > \text{M}^{\text{II}}$]. Nonetheless, Sn^{IV} , Ge^{IV} , Fe^{III} , and Pt^{II} complexes are more difficult to oxidize than are the metal-free porphyrins; while in contrast the Zn^{II} , Cd^{II} , and

Table 8 First half-wave potentials for ring oxidation of various tetraphenylporphyrin and octaethylporphyrin derivatives^a

Compound	$E_{1/2}$ in volts vs. SCE
TPP	0.95
Mg^{II} TPP	0.54
Cu^{II} TPP	0.90
Zn^{II} TPP	0.71
Cd^{II} TPP	0.63
Pd^{II} TPP	1.02
OEP	0.81
Mg^{II} OEP	0.54
$(\text{HO})_2\text{Si}$ OEP	0.92
Cu^{II} OEP	0.79
Zn^{II} OEP	0.63
$(\text{HO})\text{Ga}^{\text{III}}$ OEP	1.01
$(\text{HO})_2\text{Ge}^{\text{IV}}$ OEP	1.09
$(\text{CO})\text{Ru}^{\text{II}}$ OEP	0.64
$(\text{HO})_2\text{Sn}^{\text{IV}}$ OEP	>1.4

Source: Felton.^{96a} In acetonitrile or butyronitrile with supporting electrolyte.

(19) Monoaspartylchlorin-*e*₆

(especially) the Mg^{II} complexes, in spite of their formal dipositive charge, are more readily oxidized than are the metal-free systems.

The first half-wave potentials in Table 8 have a bearing on shelf life: for example, other things being equal, Sn^{IV} complexes are expected to be much more stable towards aerial oxidation in solution in the dark than are Mg^{II} complexes.

The values in Table 8 also have a bearing on photobleaching. Photobleaching occurs when the chromophore is altered or destroyed during irradiation, and can proceed by either an oxidative or a reductive pathway. In PDT it appears that the oxidative pathway predominates and, indeed, singlet oxygen or other reactive oxygen species are thought to be responsible for the photobleaching in many cases.⁹⁷ At first sight, it might be thought that photobleaching would be a disadvantage in PDT, since the photosensitizer, the precursor of the active agent, is being destroyed. However, it might be possible to take advantage of this photobleaching⁹⁸ by arranging matters so that, with a photobleachable sensitizer, effective photodamage to the tumor can be done; whereas in a longer time frame, with ambient light intensities, the (lower) levels of sensitizer in surrounding normal tissue can quickly be brought below the threshold required for photodamage, thereby effectively increasing the selectivity of the drug. Some metal-free photosensitizers are readily photobleached (e.g., naphthalocyanines, bacteriochlorins),⁹⁷ and it is evident from Table 8 that coordination with certain metals (e.g., Mg^{II}, Zn^{II}) might be expected to enhance the susceptibility to photobleaching. This is demonstrated in Table 9, which shows the photobleaching quantum yields for monoaspartylchlorin-*e*₆ (19) (which has the acronym MACE, and which is being developed for market as a PDT sensitizer under the designation Npe6) and two of its metal complexes. In accord with general expectations based on Table 8, the Sn^{IV} complex is photobleached very slowly, but the Zn^{II} complex is photobleached 24 times more rapidly than the free base.⁹⁹

Table 9 Quantum yields of photobleaching Φ_{pb} of monoaspartylchlorin-*e*₆ derivatives. (5 μ M in 100 mM phosphate buffer, pH 7, 0.22 mM O₂)

Compound	Φ_{pb}
Monoaspartylchlorin <i>e</i> ₆ (MACE, (19))	8.2×10^{-4}
Zn ^{II} -monoaspartylchlorin <i>e</i> ₆	1.9×10^{-2}
Sn ^{II} -monoaspartylchlorin <i>e</i> ₆	5.7×10^{-6}

Source: Spikes and Bommer.⁹⁹

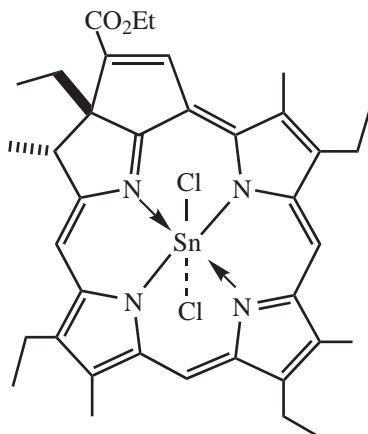
9.22.5.8 Drug Delivery Systems

For systemic administration, the photosensitizer usually has to be delivered into the bloodstream by intravenous injection. Since the photosensitizer is a solid, this means that a solution or a stable suspension has to be provided. Metal complexes of the basic porphyrin and phthalocyanine nuclei are insoluble in water, so that some effort has to be made to render the system water soluble, or at least amphiphilic, by placing various substituents (e.g., SO_3H , CO_2H , OH , NR_3^+ , polyether, aminoacid, sugar) on the periphery of the molecule. The aromatic character of the ligand offers a suitable opportunity for such substitutions to be made. Examples will appear frequently in the following sections.

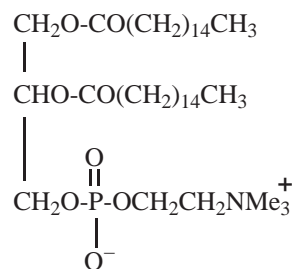
However, some researchers have preferred to develop hydrophobic sensitizers; and, indeed, it needs to be recognized that some degree of hydrophobicity is advantageous to facilitate the penetration of biological membranes. In these cases a delivery vehicle is required, and this must be biocompatible, and provide a suspension which is stable up to the point at which the natural transport system (e.g., albumin or lipoprotein or both) takes over.

Amongst the delivery systems, the following have been most frequently used:

- (i) Emulsifying agents, especially neutral, detergent-like molecules such as Tween 80 (polyoxyethylene sorbitan monooleate) and Cremophor EL ("Cremophor", ethoxylated castor oil).
- (ii) Cyclodextrins. The diameter of base of the hydrophobic cone of γ -cyclodextrin is about 8.5 Å, and is large enough to form an inclusion complex with all or part of a photosensitizer molecule. Such a complex of dichlorotin(IV)-etiopurpurin (**20**) caused greater photodamage in cell culture than that observed using ethanol as solvent.¹⁰⁰



(20) Dichlorotin(IV) - etiopurpurin



(21) Dipalmitoylphosphatidylcholine (DPPC)

- (iii) Liposomes are prepared from synthetic phospholipids (such as dipalmitoylphosphatidylcholine, DPPC (**21**)), palmitoyloleoylphosphatidylcholine, POPC, and dioleoylphosphatidylserine, DOPS) by ultrasonication. Liposomal delivery has been used, for example, with zinc(II) phthalocyanine.¹⁰¹ Sometimes, however, aqueous organic solvents have been appropriate, e.g., 10% DMSO in PBS for distribution studies with tritiated benzoporphyrin derivative (**5**).¹⁰²
- (iv) Biodegradable nanospheres (150–250 nm in diameter) based on a cyanoacrylate polymer and encapsulating phthalocyanines and naphthalocyanines have been described,¹⁰³ although they do not seem to have found widespread application.
- (v) Lipoproteins in blood are the natural carriers of injected hydrophobic drugs. They can be obtained from serum, and fractionated by centrifugation into very low density (VLDL), low density (LDL), and high density (HDL) lipoprotein, which have themselves been used as delivery vehicles. For example, injections of benzoporphyrin derivative (**5**) with LDL or HDL fractions showed increased activity *in vivo* with a DLI of 3 h: with an 8 h interval, only the LDL delivery system was effective.¹⁰⁴

9.22.6 COMPLEXES OF GROUP 2

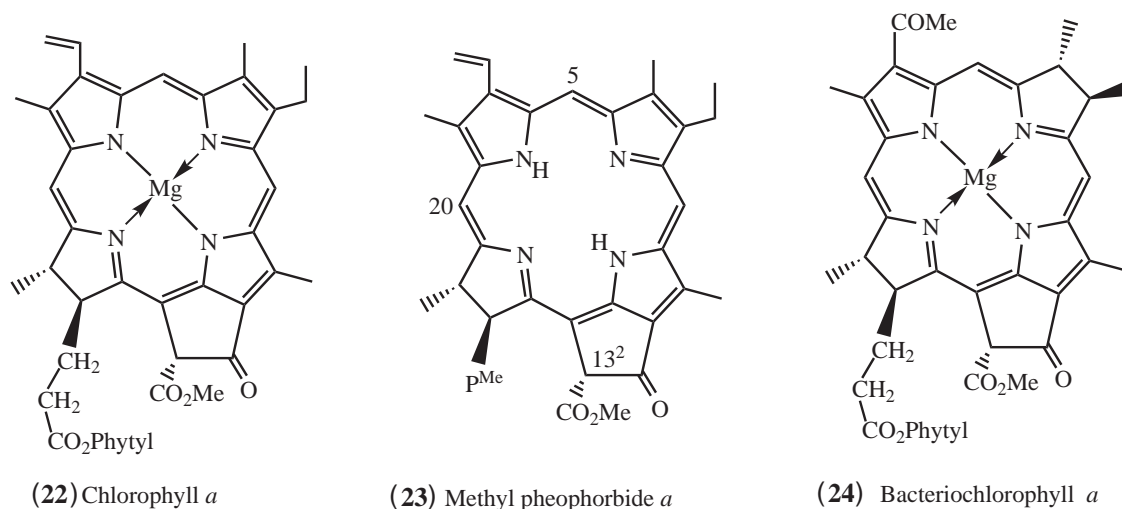
Because of their decomposition in aqueous media (Table 1), complexes of group 1 metals have not been developed for PDT applications.

9.22.6.1 Magnesium

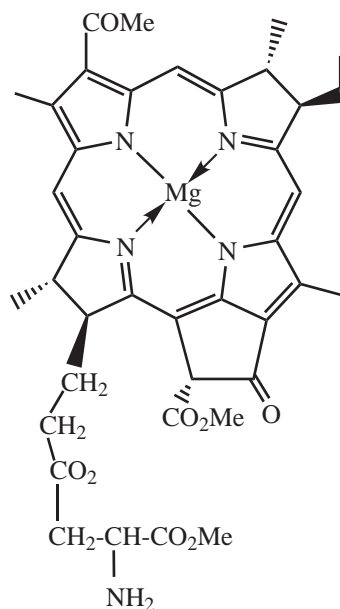
The magnesium(II) complexes have been relatively little studied as PDT sensitizers, probably because they are rather sensitive to demetalation under mildly acidic conditions (Table 1) and to oxidation (Table 8).

There are two sources—natural products and synthesis. Chlorophylls and bacteriochlorophylls may be extracted from higher plant material and photosynthetic bacteria, respectively. Most higher plant material contains both chlorophyll *a* and chlorophyll *b*, but certain algae, e.g., *Spirulina maximum*, contain only chlorophyll *a* (**22**), so using it as a starting point avoids a tedious and difficult separation.^{105,106} Because of the sensitivity and waxy nature of the product, the phytyl group is usually replaced by methyl, and the magnesium is removed, to give methyl pheophorbide *a* (**23**); subsequent manipulation leads to other chlorins and purpurins.¹⁰⁷

Bacteriochlorophyll *a* (**24**) may be isolated from purple photosynthetic bacteria, such as *Rhodobacter capsulata*, by extraction with dioxan.^{108–110} It has been examined as a PDT sensitizer against SMT-F (spontaneous mammary carcinoma, fast growing) and RIF (radiation-induced fibrosarcoma) tumors. With light treatment at 750–780 nm (**24**) has λ_{\max} 780 nm in CH₂Cl₂–MeOH) and a DLI of 2 h, tumor cures were observed in 80% of mice after 90 days, but selectivity was poor.¹¹¹ Like chlorophyll *a*, bacteriochlorophyll *a* is a very lipophilic substance, and needed neutral detergent for injection (1% Tween 80). During light treatment, bacteriochlorophyll *a* ($\Phi_{\Delta}=0.6$) was shown by HPLC to be rapidly degraded to bacteriopheophytin *a* (**24**, for Mg read 2H, $\Phi_{\Delta}=0.73$) and other products.^{111,112}

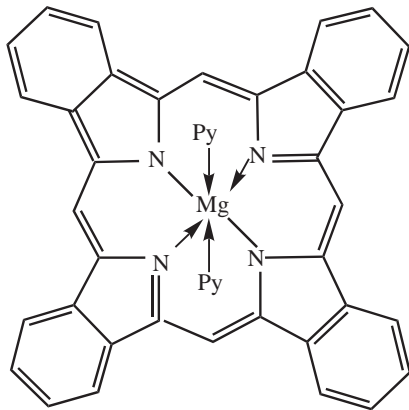


Enzymatic transesterification of (**24**) with L-serine methyl ester gives the methyl ester of seryl bacteriochlorophyllide *a* (Bchl-ser) (**25**), which is water soluble.¹¹³ The analogous chlorophyll *a* conjugate (Chl-ser) has also been made, and in animal model experiments clearance times of 16 h (BChl-ser) and 72 h (Chl-ser) were observed, with significantly longer retention in melanoma tissue.¹¹³ BChl-ser has λ_{\max} (MeOH) 770 nm ($\epsilon = 59,000 \text{ M}^{-1} \text{ cm}^{-1}$); [(PBS) $\epsilon = 42,000 \text{ M}^{-1} \text{ cm}^{-1}$] and $\Phi_{\text{f}} = 0.11$ (MeOH).¹¹⁴ This drug was administered in a different way from the norm. Using a large dose (20 mg kg^{-1}), and immediate irradiation (i.e., no DLI for equilibration) with a fluence of $108\text{--}180 \text{ J cm}^{-2}$ at 580–750 nm, melanotic tumors suffered major photoinduced vascular damage, with a cure rate reported as over 80%.¹¹⁵

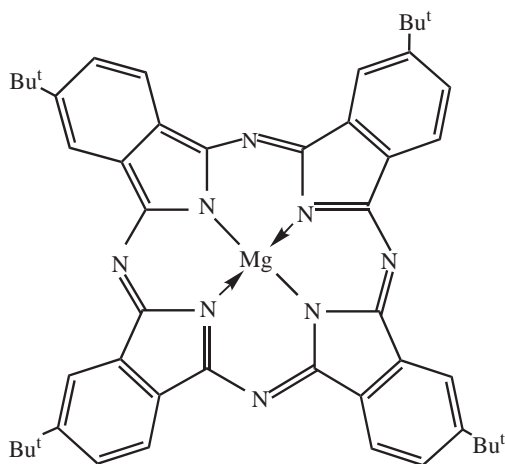
(25) Methyl ester of serylbacteriochlorophyllide *a*

In an attempt to increase specificity by introducing a targeting feature in the structure (such drugs with an additional targeting feature are sometimes referred to as “third-generation photosensitizers” in this area), bacteriochlorophyllide *a* has also been conjugated with rabbit immunoglobulin G. The purpose here is to use PDT in a microbicidal way, since the conjugate, (BChl)-IgG, binds with high specificity to protein A residues on the cell wall surface of *Staphylococcus aureus*. (BChl)-IgG was found to be 30 times more effective (per cell-bound molecule) than the (nontargeted) BChl-ser in the photokilling of *S. aureus*.¹¹⁶

Amongst the synthetic magnesium(II) complexes, a comparison of bis(pyridine)magnesium(II)-tetrabenzoporphyrin (**26**) with bis(pyridine)magnesium(II)-octamethyltetrabenzoporphyrin (**10**) *in vitro* (HeLa cells), and *in vivo* using liposomal delivery, showed that while (**26**) was more effective than (**10**) in cell kill, (**10**) had the greater tumor selectivity ([tumor]/[muscle] = 36.0 after 24 h). Zinc(II) tetrabenzoporphyrin also showed promising activity; nickel(II) tetrabenzoporphyrin derivatives were inactive.¹¹⁷



(26) Bis(pyridine)magnesium(II) tetrabenzoporphyrin

(27) Mg(II) tetra-(*t*-butyl)phthalocyanine (isomers)

The photophysical properties of magnesium(II) tetra(*t*-butyl)phthalocyanine (**27**) have been studied in solution, in micelles and in liposomes: cation radical formation (CBr₄ as electron acceptor) has been detected with UV excitation, or by a two-photon excitation using a pulsed laser in the “therapeutic window” at 670 nm.¹¹⁸ The Mg^{II} complex of octa(*tri*-*i*-propylsilylethynyl)tetra[6,7]quinoxalinoporphyrazine (**28**) has been prepared as a potential PDT sensitizer. The synthesis is shown in Figure 8. Compound (**28**) has λ_{\max} 770 nm ($\epsilon = 512,000 \text{ M}^{-1} \text{ cm}^{-1}$), $\Phi_f = 0.46$ and $\Phi_{\Delta} = 0.19$ (all in THF, under air).¹¹⁹

The photooxidation of magnesium(II) porphyrins leads to cleavage of the macroring, with the generation of bilinone derivatives.^{120–122}

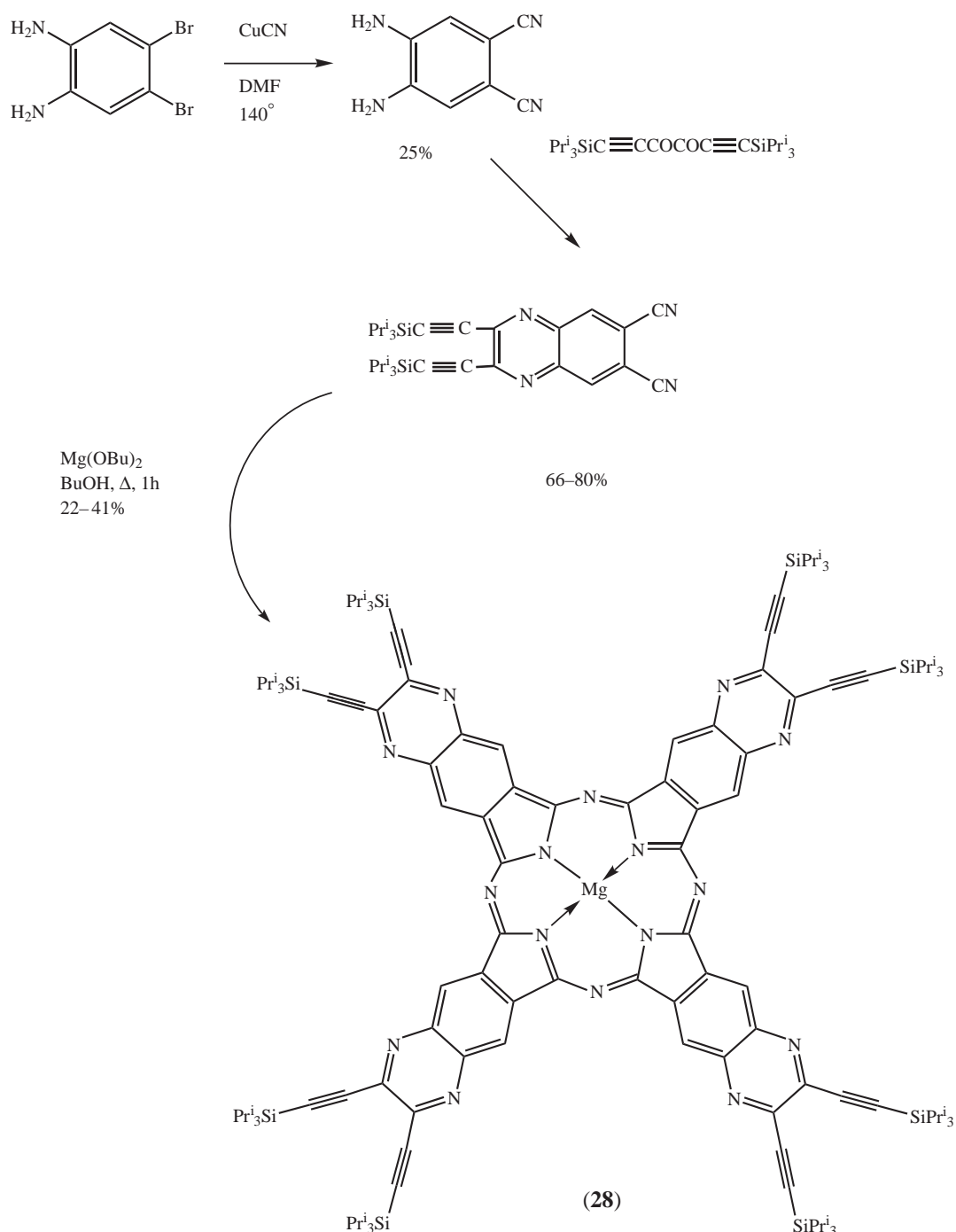
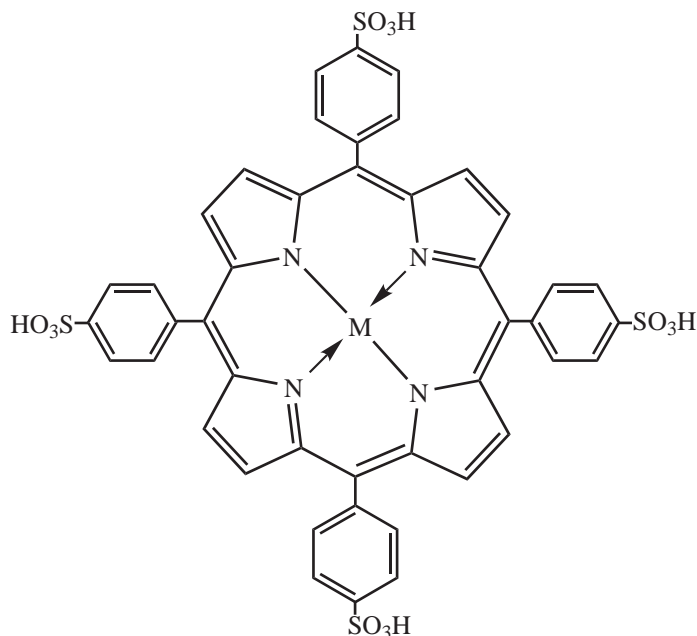


Figure 8 Synthesis of magnesium(II) octa(*tri*-*i*-propylsilylethynyl)tetra[6,7]quinoxalinoporphyrazine (**28**).¹¹⁹

9.22.7 COMPLEXES OF GROUP 3

9.22.7.1 Lanthanides

Structures of the complexes of porphyrins with the lanthanide metals are largely determined by the large effective ionic radii of the M^{III} ions, e.g., La^{III} 127 pm for CN = 10, Gd^{III} 111 pm for CN = 9, and Lu^{III} 98 pm for CN = 8¹²³ (cf. Table 2, where the largest r_i value quoted (Cd^{II}) is 95 pm). In these complexes the central hole cannot accommodate the metal ion in the N_4 plane, and ligand : metal stoichiometries of 2:1 or 3:2 frequently result.^{124,125} In those cases where 1:1 stoichiometry is found, the metal ion is considerably displaced from the N_4 plane (e.g., 92 pm for Lu^{III} in $(Me_3Si)_2CHLu(OEP)$).¹²⁶ Such complexes lack stability: for example, gadolinium(III)-TPPS₄ ((29), $M = Gd$) is demetalated by EDTA.¹²⁷



(29) MTPPS₄

Since the later 1990s there has been increasing interest in expanded macrocyclic systems capable of firmly binding larger cations.¹²⁸ The texaphyrins provide an extensively studied example.^{129–131} These compounds are synthesized by the condensation of a 1,14-diformyltripyrane, such as (30), with an *o*-phenylenediamine derivative (Figure 9). The condensation product (31) is a bis-azomethine, but is not through-conjugated (λ_{max} 369 nm) and so does not have macrocyclic aromaticity. But on refluxing with lutetium(III) acetate in methanol in air, complexation/dehydrogenation occurs, and the lutetium(III) diacetate derivative (32), which does have an aromatic ligand, is isolated. Complexes with other peripheral substitution patterns, and of other metals (including all the lanthanides except Pm) have been prepared in an analogous manner.^{130–134} X-ray analysis shows that (for an eight-coordinate Lu^{III} analogue of (32) with axial nitrate and MeOH ligands) the metal ion is about 27 pm out of the mean N_5 plane.¹³⁵ For a related Gd^{III} complex, the metal is displaced 60 pm out of plane, and is nine-coordinate:¹³⁵ while for a La^{III} complex the metal ion is ten-coordinate, and is now displaced 91 pm from the mean N_5 plane.¹³⁵ These displacements parallel the ionic radii quoted above, and show the effect of the increased size of the coordination cavity with respect to that of the porphyrin.

The lutetium(III) texaphyrin (32) is water soluble, although aggregation occurs at concentrations $>3 \mu M$.¹³⁶ In methanol, λ_{max} is 732 nm ($42,000 M^{-1} cm^{-1}$),¹³⁰ and in 5% aqueous Tween 20 it is 730 nm ($49,000 M^{-1} cm^{-1}$).¹³⁶ Low Φ_{Δ} values (0.11) are quoted in water (probably due to aggregation),¹³⁶ but higher values are observed in the presence of detergent (0.38 in 5% Tween 20).¹³⁶

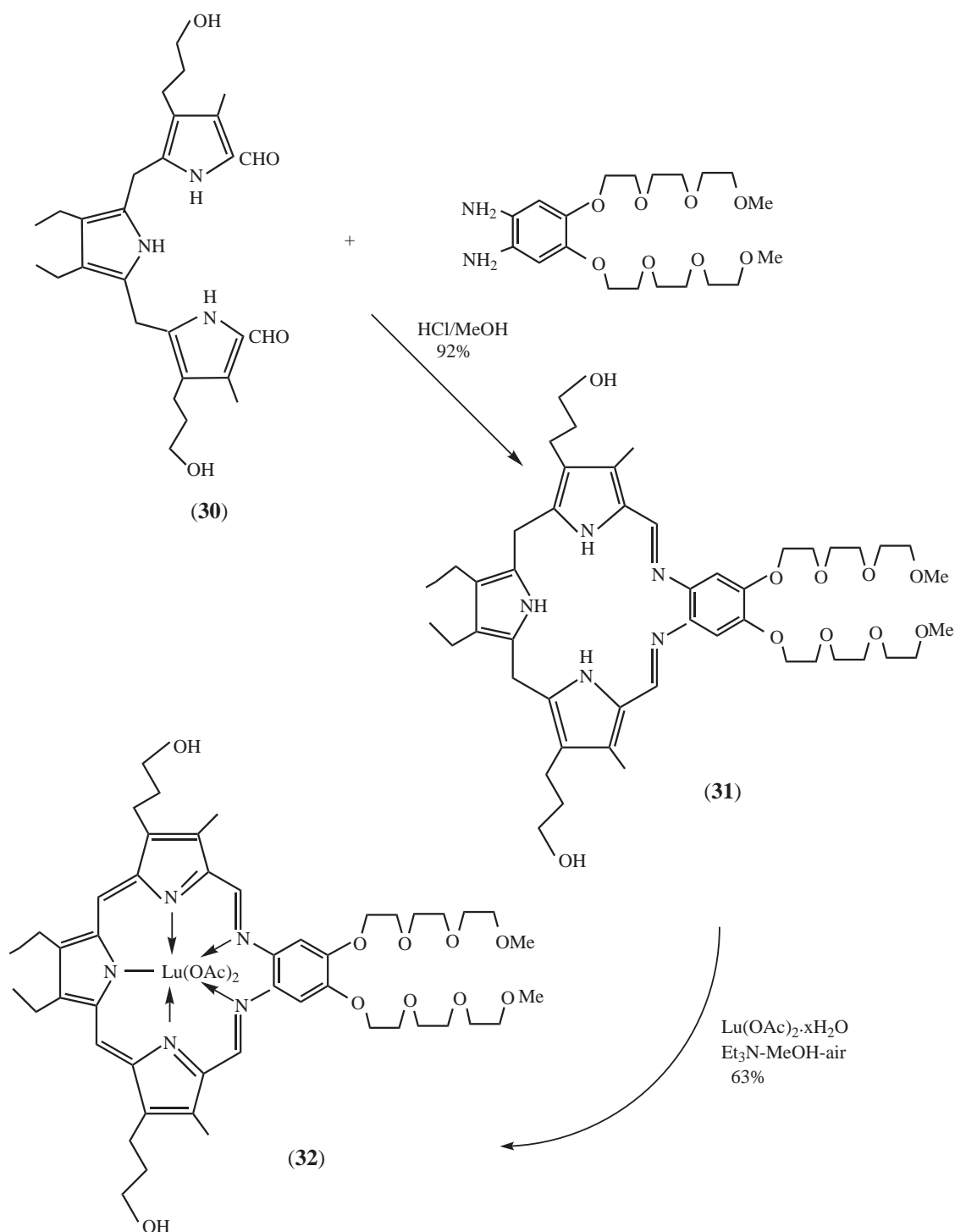


Figure 9 Synthesis of a lutetium(III) texaphyrin derivative illustrated by the synthesis of (32) (trade name “motexafin lutetium”).^{131,135}

In spite of the heavy atom, compound (32) is sufficiently fluorescent for this to be used as an analytical tool to examine localization and pharmacokinetics. In EMT-6 murine tumors, (32) localizes initially on lysosomes, with selectivity for tumor over surrounding normal tissue, and with evidence for apoptotic cell kill.¹³⁷ Fluorescence studies using a hamster cheek pouch model show a maximum emission in 2–3 h, with selectivity for the tumor ($\times 1.5$ over normal tissue): after 24 h the photosensitizer is no longer detectable.¹³⁸ Lutetium texaphyrin (32) has been compared

Table 10 Φ_{Δ} values versus *in vivo* bioactivity.¹³⁶

Compound (32) for Lu read	Φ_{Δ} ^a	Cure rate ^b
Y ^{III}	0.29	30%
Cd ^{II}	0.30	no data
In ^{III}	0.24	no data
Gd ^{III}	0.17	0%
Lu ^{III}	0.38	100%

^a in 5% aqueous Tween 20 irradiated at 730 nm. ^b EMT-6 mammary tumor implants: % cure after 40 days.

with other sensitizers (including AlPcS₄) using the chorioallantoic membrane assay.¹³⁹ It is an effective photohaemolytic agent for erythrocytes.¹⁴⁰ Animal experiments have shown it to be effective, selective, and rapidly acting in tumor PDT. Thus, tumor-bearing animals were treated with 10 $\mu\text{mol kg}^{-1}$ of (**32**) and irradiated at 732 nm with 150 J cm⁻²: when the DLI was 3 h, 100% cure was seen, but when the DLI was 24 h, no cures were observed, although tumor growth was inhibited.¹³⁰

Compound (**32**) is currently being developed for the clinical treatment of cancer, of atherosclerotic vascular disease, and of age-related macular degeneration, all of which are PDT applications.^{132,133} Photodiagnostic applications also appear to be in view.¹⁴¹

An interesting (partial) comparison can be made between Φ_{Δ} values and *in vivo* bioassay results in this series (Table 10).¹³⁶ All the complexes in Table 10 are diamagnetic, with the exception of Gd^{III}, and it is perhaps surprising that this gives an appreciable singlet oxygen quantum yield. It has been suggested¹³⁶ that the lack of more efficient quenching of the triplet state of the Gd^{III} complex, which contrasts with what is observed with the first-row transition metals (cf. Table 7), is due to the *f*⁷ configuration of Gd^{III} for which there is an absence of those intermediate energy levels which facilitate radiationless deactivation. In any event, the Gd^{III} complex is ineffective as a PDT agent in the *in vivo* assay.

However, the highly paramagnetic nature (4*f*⁷) of Gd^{III}, and the ability of these metal complexes to localize with some selectivity in tumors, has suggested other possible applications in medicine. The Gd^{III} analogue of (**32**) has received attention as a potential and stable MRI contrast agent (see Chapter 9.19)¹³¹ (the Gd^{III} porphyrins being easily demetalated),¹²⁷ and as a potentiator of X-radiation.^{132,133}

9.22.8 COMPLEXES OF GROUP 7

9.22.8.1 Manganese

Manganese(III) porphyrin compounds (*d*⁴) are paramagnetic with very short triplet lifetimes and very low Φ_{Δ} values. They have found application as potential contrast agents for MRI.^{142,143} Manganese(III)-TPPS₄ ((**29**), M = Mn^{III}) was found to be a reagent of choice. It remained stable in human plasma for 9 days, whereas Gd^{III}TPPS₄ ((**29**), M = Gd) suffered demetalation.¹⁴² Manganese(III) porphyrins have also been examined as nonphotosensitizing transport systems to deliver covalently attached radiosensitizer moieties to tumors,¹⁴⁴ and similarly to transport peripherally coordinated radionuclides (^{99m}Tc, ¹¹¹In, refs. 145, 146 respectively) to tumors.

9.22.8.2 Technetium

Coordinated ^{99m}Tc has featured in attempts to follow the distribution and tumor uptake of the water-soluble sensitizers PcS₄¹⁴⁷ and 5,10,15,20-tetrakis[3,4-bis(carboxymethyleneoxy)phenyl]porphyrin,¹⁴⁸ and of haematoporphyrin.²⁹

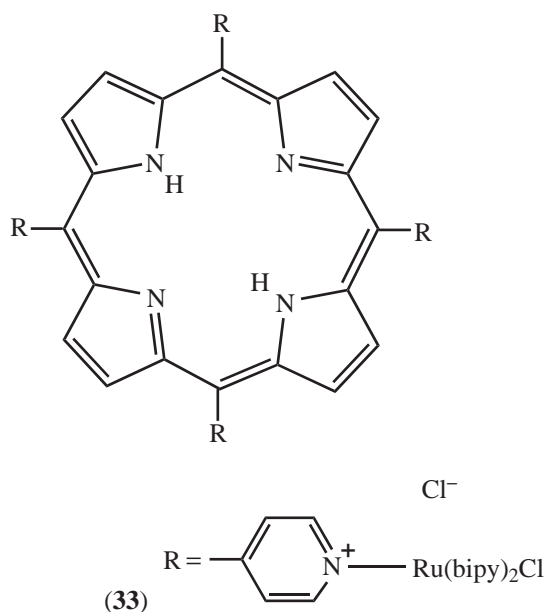
9.22.9 COMPLEXES OF GROUP 8

9.22.9.1 Ruthenium

It has been known for many years that ruthenium(II) complexes of non-macrocyclic ligands photogenerate singlet oxygen. Thus, in 1973 it was observed for [Ru^{II}(phen)₂(CN)₂] that singlet

oxygen production was a significant pathway for the deactivation of the charge-transfer triplet excited state.¹⁴⁹ Tris(2,2'-bipyridyl)ruthenium(II) dichloride sensitizes the formation of singlet oxygen in aqueous aerated solution with $\Phi_{\Delta} = 0.18$, and electron transfer is negligible. However, electron transfer becomes important when the photosensitizer is adsorbed on colloidal tin oxide doped with antimony.¹⁵⁰

Reaction of 5,10,15,20-tetra(4-pyridyl)porphyrin with dichloro-bis(2,2'-bipyridyl)ruthenium(II) gives the tetra-ruthenated porphyrin formulated as (33).¹⁵¹ Porphyrins with cationic substituents at the *meso* positions are known to have a high affinity for DNA.^{152,153} Photosensitized oxidation of 2'-deoxyguanosine using (33) as the sensitizer gave predominantly the products which are regarded as typical of a type II oxidation.¹⁵⁴ However, three ruthenium(II) complexes of porphyrins having peripheral cationic (R_3N^{+}) and anionic (SO_3^- , CO_2^-) groups were inactive as photocytotoxic agents *in vivo*.¹⁵⁵



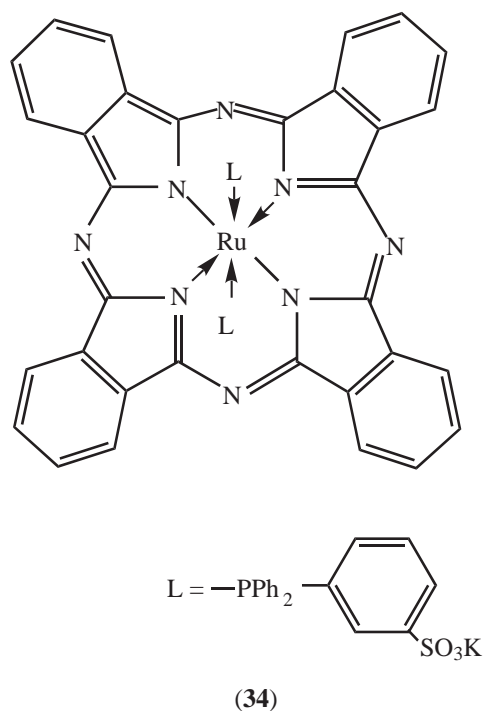
Some macrocyclic complexes of ruthenium have been examined as PDT sensitizers. The ruthenium phthalocyanine system has been made water soluble by attaching as axial ligands two solubilizing groups, such as triphenylphosphine monosulfonate, as in (34).¹⁵⁶ In water, this shows λ_{\max} 650 nm ($88,000 \text{ M}^{-1} \text{ cm}^{-1}$): this is a broad band, which does not change up to $c. = 10^{-4} \text{ M}$, suggesting that aggregation is not occurring. Nevertheless, Φ_{Δ} in D_2O is < 0.01 , although in methanol the value is 0.3. This looks like aggregation quenching, but the authors argue that the lower solubility of oxygen in water (compared to methanol) is responsible, and suggest an electron-transfer mechanism in water. *In vitro* and *in vivo* experiments demonstrated that (34) had a PDT activity comparable with that of Photofrin and much greater than that of $ClAlPcS_{3-4}$.¹⁵⁷

Analogous ruthenium(II) naphthalocyanines have been prepared as PDT sensitizers. Figure 10 shows a representative example of the synthetic route leading to (35).¹⁵⁸ Again, solubility could be modulated by changing the axial ligands. Compound (35) has λ_{\max} 728 nm ($250,000 \text{ M}^{-1} \text{ cm}^{-1}$) in water. These complexes do not fluoresce, and are much more susceptible to photobleaching than the corresponding phthalocyanines. They show biological activity against HeLa cells in culture.¹⁵⁸

9.22.10 COMPLEXES OF GROUP 10

9.22.10.1 Nickel

Nickel(II) coordination is useful in stabilizing the macrocycle during synthetic manipulations at the periphery (e.g., Section 9.22.14.3, Figure 15), but nickel(II) complexes of porphyrin-type macrocycles (square planar, d^8 , diamagnetic) are not PDT sensitizers (e.g., nickel(II) octaethyl-dihydropurpurin *in vivo*, no tumor necrosis; corresponding Zn^{II} and Cl_2Sn^{IV} complexes examined in the same system, compounds active).¹⁵⁹ Comparisons across small series of metal complexes show



that nickel(II) macrocycles are poor generators of reactive oxygen species. Thus, for metallo octa-2[2(2-methoxyethoxy)ethoxy]ethoxy-phthalocyanines the observed Φ_{Δ} values in benzene were 2H, 0.13; Ni, 0.0; Zn, 0.20; Pb, 0.25.¹⁶⁰ Neither singlet oxygen nor superoxide formation was found on irradiation of a variety of nickel (and cobalt) complexes.¹⁶¹ In the photooxidation of tryptophan using PcS₄ complexes as photosensitizers,¹⁶² the nickel complex was inactive (as were Co, Fe, VO, and Cr complexes). The relative rates of tryptophan photooxidation with effective metal complexes were: ClGa, 100; ClAl, 65; Zn, 20; Cu, 11; Mg, 8; Mn, 7; 2H, 5. These values may well hide different aggregation effects, but demonstrate that some metal complexes may show considerably more activity than the free base,⁶¹ although the activity of Cu^{II} is unexpected.

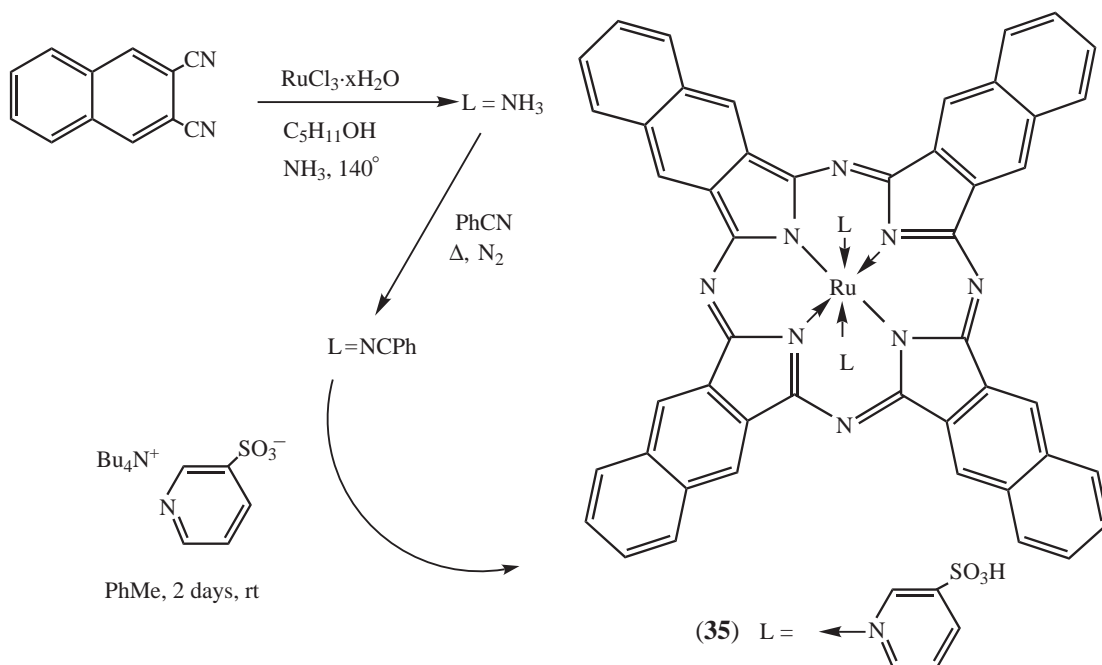
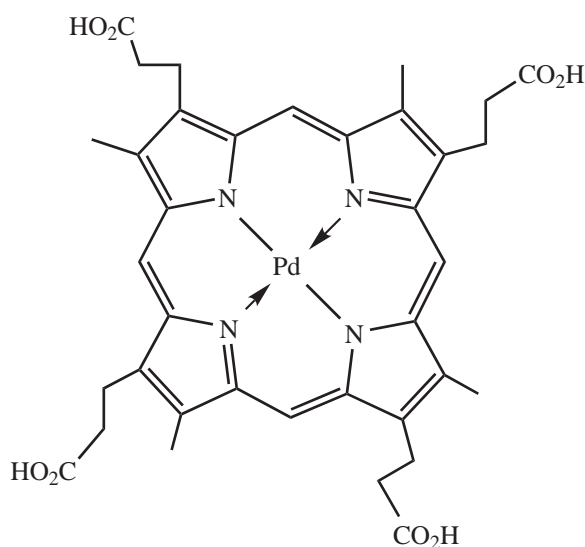


Figure 10 Synthesis of axially substituted ruthenium(II) 2,3-naphthalocyanines. Compounds with a variety of hydrophilic axial ligands have been characterized.¹⁵⁸

It appears to the author that the *in vivo* testing of metal complexes of first-row transition metals for classical photochemical PDT activity is no longer defensible. However, a recent development actually benefits from complexes of metals with low Φ_{Δ} values. Termed “photothermal sensitization,” it relies on thermal effects (chemical and mechanical) generated at high laser fluence rates. Nickel(II) 1,6,10,15,19,24,28,33-octabutoxynaphthalocyanine ($\lambda_{\max}(\text{THF}) = 850 \text{ nm}$, $\epsilon = 280,000 \text{ M}^{-1} \text{ cm}^{-1}$) administered in liposomes to amelanotic melanoma cells, followed by irradiation at 850 nm using a pulsed laser source (30 ns pulses, 10 Hz, 200 mJ per pulse) causes efficient cell death.¹⁶³

9.22.10.2 Palladium

Palladium(II) porphyrin complexes fluoresce weakly, but show phosphorescence, often in solution at room temperature, the intensity increasing with protein binding.¹⁶⁴ This property has been used as the basis for an immunoassay with palladium(II) coproporphyrin-I (**36**) as a phosphorescent label.¹⁶⁵ (**36**) covalently linked to a heptadecadeoxyribonucleotide has selective action in photo-modification of a 34-mer oligodeoxynucleotide embodying a complementary region (selective oxidation of deoxyguanosine 17).^{166,167}

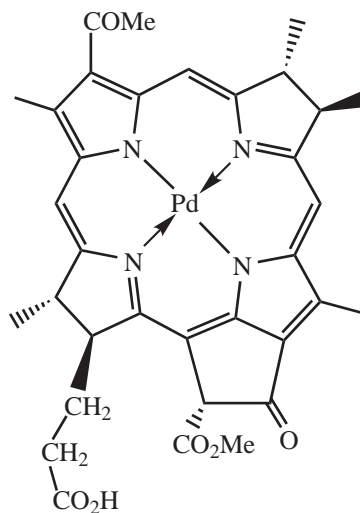


(**36**) Palladium(II) coproporphyrin-I

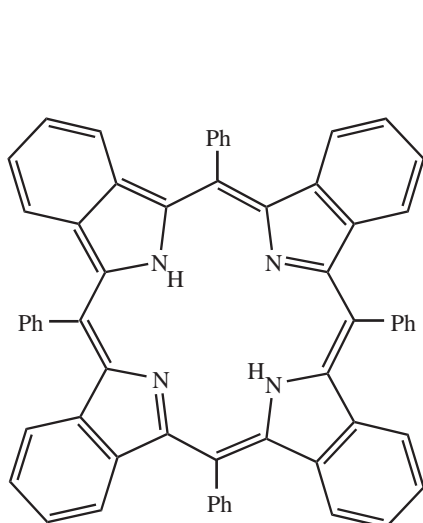
A series of *meso*-substituted palladium(II) porphyrins had low Φ_f (ca. 10^{-4} in toluene), low Φ_p (ca. 10^{-4} in N_2 -flushed toluene at 225 K), moderate Φ_{Δ} (ca. 0.2 in DPPC liposomes in D_2O), but showed no photokilling of T-cell lymphoma cells, the photosensitizer being provided in liposomes or in DMSO.¹⁶⁸ Quenching of excited states appears to be particularly sensitive to aggregation.¹⁶⁹ As expected on the basis of relative oxidation potentials (e.g., Table 8), the palladium(II) complexes are much more resistant to photobleaching than are the zinc(II) and magnesium(II) complexes.^{111,112} A series of patents has been filed describing the application of palladium(II) complexes of chlorophyll- and bacteriochlorophyll-derived macrocycles in tumor PDT and photodiagnosis, and in photomicrobicidal applications.¹⁷⁰ Thus, palladium(II)-bacteriopheophorbide *a* ((**37**), “TOOKAD”) is non-selective, but is rapidly cleared *in vivo*. Photodamage is primarily to the tumor vasculature. The use of a minimal DLI, and interstitial and superficial light delivery, results in hemorrhagic necrosis and atrophy in prostate tissue: while C6 rat glioma implants are treatable with some control of metastasis.¹⁷¹

A series of closely related palladium(II) complexes of TPP ((**2**), as Pd^{II} complex), *meso*-tetraphenyltetrabenzoporphyrin (TPTBP, (**38**), as Pd^{II} complex) and *meso*-tetraphenyltetranaphthoporphyrin (TPTNP, (**39**), as Pd^{II} complex) have been synthesized and compared with analogous complexes of Zn^{II} , Lu^{III} , Y^{III} , Sn^{IV} , and Pb^{IV} .^{173–175} Some photophysical properties of the palladium(II) complexes are recorded in Table 11, where comparison is made with the properties of the corresponding zinc(II) complexes (Section 9.22.12.1).^{176,177} For the palladium(II) *meso*-tetraphenyltetranaphthoporphyrin ((**39**), as Pd^{II} complex) the triplet energy is less than that

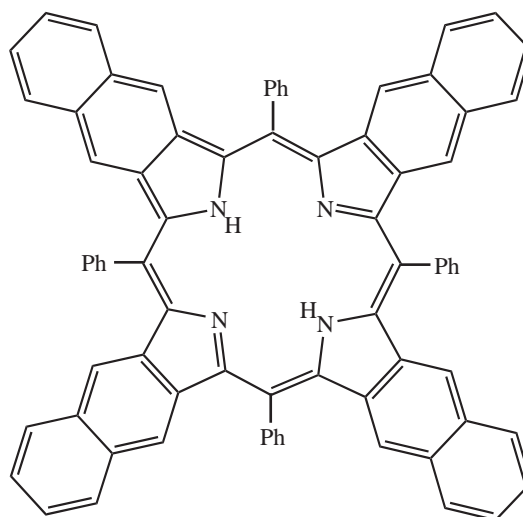
required to generate singlet oxygen. These compounds have been examined as phosphorescent probes for oxygen measurements and for imaging tissue oxygen.^{173-175,178} The tetrasulfonic acid derivative of TPTBP (**38**) as its palladium(II) complex exerts a photodynamic effect on cultures of *Aspergillus fumigatis*.¹⁷⁹



(37)



(38) TPTBP



(39) TPTNP

The palladium(II) phthalocyanines are satisfactory singlet oxygen generators. Thus, Φ_{Δ} values for tetra-*t*-butylphthalocyanine (**27**), with stated replacement for Mg) are 2H, 0.22; Zn, 0.34; Pd, 0.54, i.e., increasing in line with the heavy atom effect.¹⁸⁰ For palladium(II) tetra-*t*-butylphthalocyanine (**27**), Pd instead of Mg) in benzene at 290 K, $\Phi_{\text{F}}=0.048$ and $\Phi_{\text{T}}=0.49$.¹⁸⁰ However, palladium(II) 2,3-dihydroxy-9,16,23-tri-*t*-butylphthalocyanine was synthesized by a mixed condensation (1:9 mix of appropriate dinitriles) as a likely amphiphilic sensitizer, but did not show bioactivity in an enzyme assay, possibly because of aggregation.¹⁸⁰

In a benzene solution of the palladium(II) complex of 1,6,10,15,19,24,28,33-octabutoxynaphthalocyanine (**40**), energy transfer from singlet oxygen to the metal complex occurs to produce the triplet state of the metal complex which phosphoresces in fluid solution, suggesting that such compounds might be useful as emission probes for singlet oxygen determination.¹⁸¹ Applications in photothermal therapy also appear to be promising.^{182,183} Complex (**40**) also

Table 11 Some photophysical parameters of palladium(II) complexes with increasing aromatic annelation compared with those of the corresponding zinc(II) complexes.¹⁷⁶

Parameter	Palladium(II)			Zinc(II) complexes		
	TPP (2)	TPTBP (38)	TPTNP (39)	TPP (2)	TPTBP (38)	TPTNP (39)
1. α -band (Q, 00) (nm)	554	629	707	603	658	712
2. Soret band (B, 00) (nm)	418	445	462	430	474	481
3. $T_1 \rightarrow T_n$, (nm)	475	530	615	475	550	585
4. ϕ_T	0.92	n.d.	0.58	0.84	0.94	0.56
5. τ_T , (μ s)	>310	143	65	406	148	180
6. Fluorescence λ_{\max} , (nm)	565	649	741	620	676	725
7. ϕ_i^a	~ 0.0004	~ 0.0003	~ 0.0003	0.029	0.0067	0.024
8. Phosphorescence λ_{\max} , (nm) (rt, pyridine)	705	797	900	n.d.	n.d.	n.d.
9. E_T (kJ mol ⁻¹) [kcal mol ⁻¹]	177[42.3]	153[36.6]	86.8[20.7]			

Source: Rogers, J. E.; Su, W.; Vinogradov, S. A.; Fleitz, P. A.; McLean, D. G. In Abstracts, 30th Annual meeting American Society of Photobiology, Quebec City, Canada, July 13–17, 2002; Hastings, J. W., Program Chair; Abstract 233, p 79. Rogers, J. E. personal communication. Solvent: pyridine. ^a deoxygenated pyridine.

undergoes a competing reversible addition of oxygen when irradiated with an argon ion laser, the oxygen adding in a Diels–Alder fashion to form a metastable endoperoxide.¹⁸¹ With palladium(II) tetraanthraporphyrine (41) the reaction is even more clear-cut: in this case on irradiation at >690 nm the tetraendoperoxide (42) has been isolated (Figure 11), and intermediate mono-, di-, and tri-adducts have been detected.^{184,185} Compound (41) has λ_{\max} 846 nm ($\epsilon = 230,000 \text{ M}^{-1} \text{ cm}^{-1}$) in benzene: weak fluorescence occurs at 858 nm and phosphorescence at 1345 nm. This corresponds to an E_T value of 21.3 kcal mol⁻¹ for (41), i.e., slightly below the excitation energy of singlet oxygen ($T_0 \rightarrow {}^1\Delta_g$, 22.4 kcal mol⁻¹), and presumably as a result Φ_Δ is rather low (>0.14).¹⁸⁵ The tetraendoperoxide (42) has the chromophore of a palladium(II) phthalocyanine (λ_{\max} 662 nm). The reaction is reversible both photochemically and thermally. Excitation into the B band using a nitrogen laser (337 nm) causes stepwise ejection of oxygen (presumably singlet oxygen from S_2). On two-photon deoxygenation with irradiation in the red (664 nm) using very short pulses (fs), dioxygen is generated mainly in higher excited singlet states.^{186,187} This reversible reaction has been suggested¹⁸⁸ as an alternative way of generating singlet oxygen in tissue, but the practicability of the idea remains to be proved. The thermal reversion (42) \rightarrow (41) is accompanied by some homolysis of the O–O bond.¹⁸⁷

9.22.10.3 Platinum

Like the palladium(II) complexes, the platinum(II) porphyrins show appreciable phosphorescence even in aqueous media at room temperature: in one study,¹⁶⁹ singlet oxygen quantum yields ranged from 0.1 to 0.9 and were strongly influenced by dimerization/aggregation. Platinum(II) 5,10,15,20-tetrakis(*p*-carboxyphenyl)porphyrin and platinum(II)coproporphyrin-I ((36): for Pd read Pt) have been studied as phosphorescent labels of antibodies for use in time-resolved microscopy.¹⁸⁹

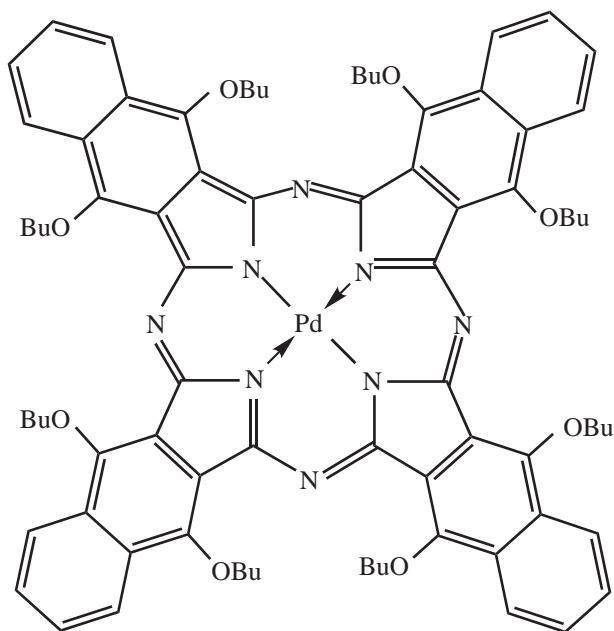
Bioassays of a considerable number of drugs embodying a combination of porphyrin and cis-platin moieties in the same molecule have led to compound (43): *in vitro* and *in vivo* studies on this compound showed a phototoxicity which was additive to the cytotoxic effect of the platinum moiety.^{190–193}

9.22.11 COMPLEXES OF GROUP 11

9.22.11.1 Copper

An early account¹⁹⁴ describes an attempt to use ⁶⁴Cu complexes of haematoporphyrin, protoporphyrin, uroporphyrin, and coproporphyrin to detect tumors; preferential localization in tumors was not observed. It needs to be recognized that metalation can change solution

properties so much that the biolocalization properties of the ligand may not be reproduced in the metal complex.



(40)

As with other first-row transition metals, copper complexes are not expected to be satisfactory singlet oxygen photogenerators, because of the rapid deactivation of excited states in the presence of partially filled *d*-orbitals. The exceptional case of the copper(II) benzochlorin iminium salt ((18), M = Cu) has already been referred to (Section 9.22.5.6): this showed bioactivity, although the nickel(II) complex ((18), M = Ni^{II}) was inactive.¹⁹⁵

Photothermal sensitization has been mentioned briefly with regard to nickel(II) octabutoxy-naphthalocyanine (Section 9.22.10.1). A similar phenomenon has been observed with copper(II) haematoporphyrin ((1), Cu for 2H).¹⁹⁶ This substance is accumulated by amelanotic melanoma cells. When the impregnated cells were subjected to light from a quartz-halogen lamp cell survival was not affected (i.e., no PDT effect), but intense pulsed laser irradiation (532 nm, Q-switched

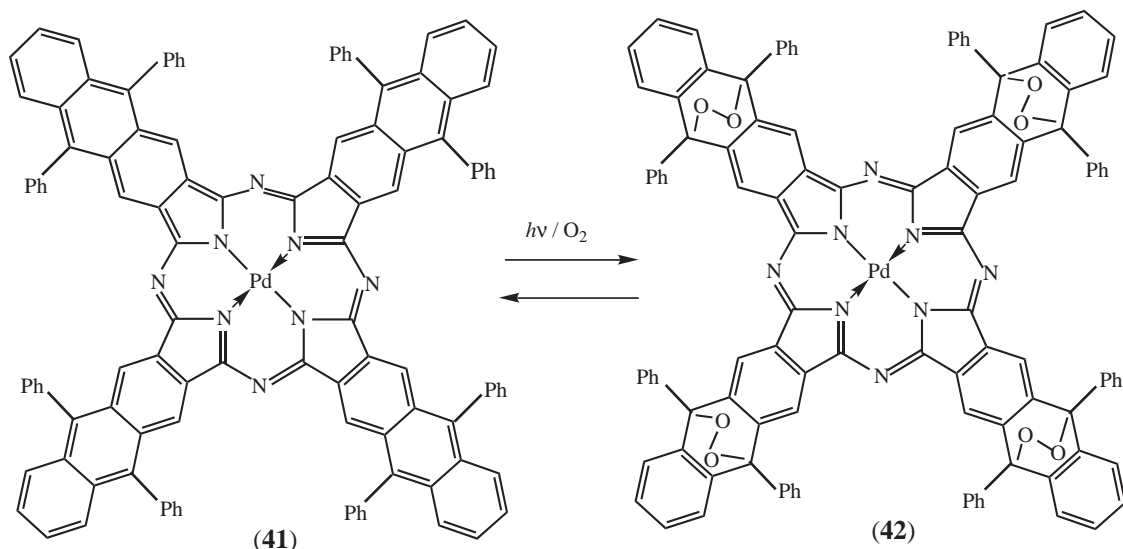
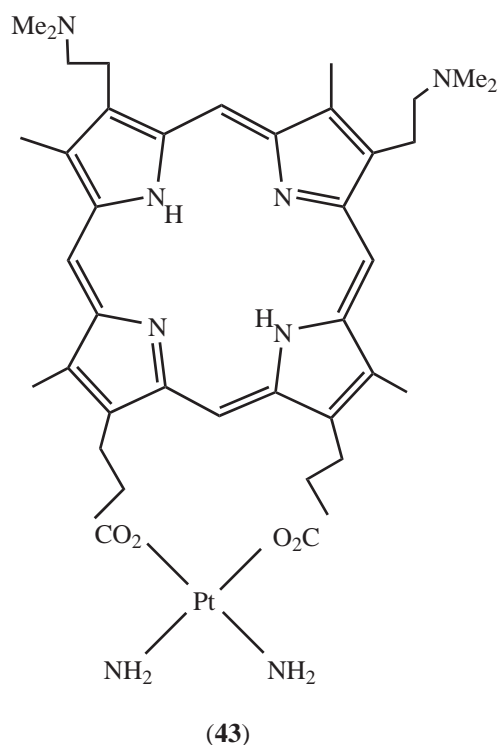


Figure 11 Reversible formation of octaphenyltetraanthraporphyrazine tetraendoperoxide (42).^{185,186}

Nd: YAG laser, 10 ns pulses, 10 Hz) caused cell death, presumably because of localized heating and/or mechanical effects.



9.22.11.2 Gold

The gold complex of MACE ((19) as gold complex, referred to as AuNPe6) has been studied as a photodiagnostic agent using synchrotron radiation to detect small (<1 mm diameter) solid tumors in peripheral lung tissue.¹⁹⁷ The dose of AuNPe6 was 20 mg kg⁻¹, and the best image was obtained 5 h after administration.

9.22.12 COMPLEXES OF GROUP 12

Having traversed more than halfway across the periodic table, we now come to the most significant examples. The next three Groups provide the main players for PDT, and zinc is probably the chief amongst these.

9.22.12.1 Zinc

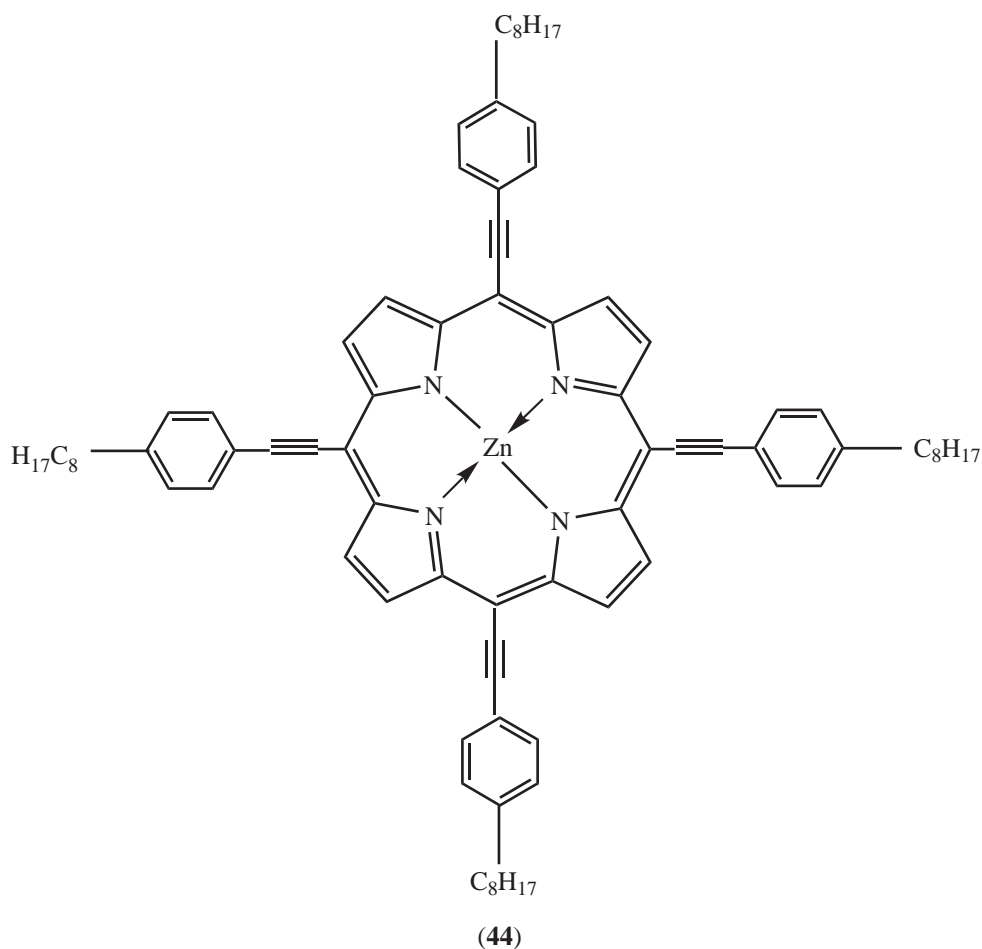
9.22.12.1.1 Porphyrin complexes

Zinc(II) protoporphyrin ((3), Zn^{II} complex) has been detected by fluorimetry in erythrocytes in cases of lead intoxication.¹⁹⁸ Kinetic studies on the photooxidation of methionine to give the corresponding sulfoxide in the presence of haematoporphyrin (1) and its metal complexes showed that the rate of reaction decreased in the sequence 2H, Mg^{II}, Zn^{II} \gg Cu^{II}, Fe^{II}, and a singlet oxygen mechanism was favoured.¹⁹⁹ Haematoporphyrin (1) and its zinc(II) complex are aggregated to some degree in aqueous media: incorporation into Triton micelles caused disaggregation, and an increase in Φ_T and the photooxidation rate of both tryptophan and histidine.²⁰⁰ Human carcinoma *in situ* cells (NH1K 3025) accumulate HpD and haematoporphyrin better than they accumulate the corresponding zinc complexes; the photosensitizing efficiency of the zinc

complexes was reported to be about half that of the free base compounds in this system.²⁷ The bis-cysteine adduct of protoporphyrin (termed porphyrin *c* because of its structural relationship to cytochrome *c*) gives a zinc(II) chelate: the free base has a larger Φ_{Δ} value than the zinc complex; there is no prolonged cutaneous photosensitivity with either compound.²⁰¹

Zinc(II) coproporphyrin-III ("Zincphyrin") has a similar effect to HpD in the photosensitization of melanoma-bearing mice, but is less phototoxic than HpD.²⁰² Zinc(II) complexes based on 5,15-diphenylporphyrin,²⁰³ *meso*-tetraphenylethynylporphyrin ester²⁰⁴ and thiobarbituric acid derivatives of octaethylporphyrin-5-acraldehyde²⁰⁵ have been described possessing strong absorption bands in the red region with PDT targets in view. Thus, the zinc(II) tetraethynylporphyrin derivative (**44**) has $\lambda_{\max} \sim 675$ nm, and solutions are green (rather than purple) in colour.²⁰⁴

The zinc(II) complexes of *meso*-tetraphenyltetrabenzoporphyrin (**38**) and of *meso*-tetraphenyl-tetranaphthoporphyrin (**39**) have been prepared.^{173–175} Some photophysical properties of this interesting series are given in Table 11¹⁷⁶ Photooxidation of zinc(II) porphyrins causes cleavage of the macrocycle with formation of bilinone derivatives.^{122,206,207}

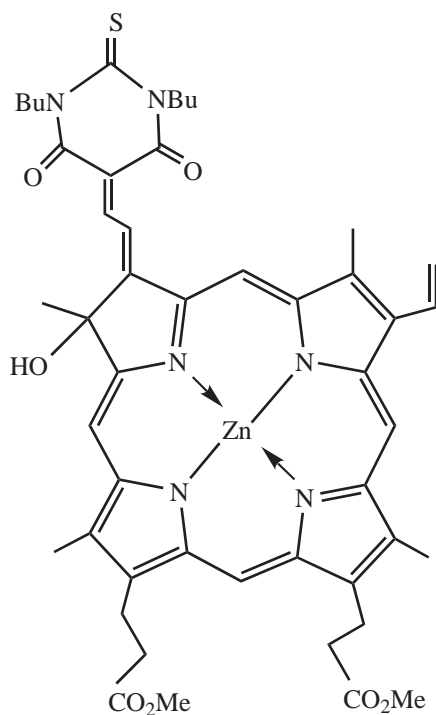


9.22.12.1.2 Zinc chlorins and bacteriochlorins

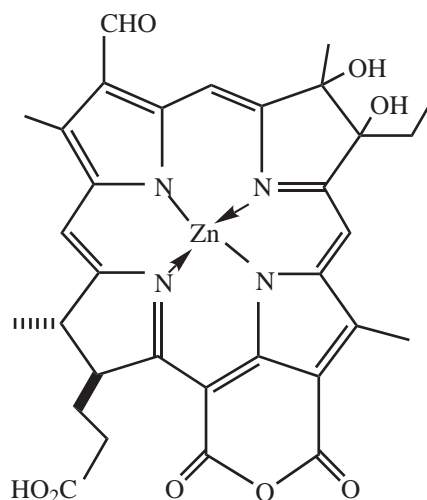
Zinc(II) etiopurpurin ((**20**): for Cl_2Sn read Zn) has PDT activity in bioassays *in vivo*, but is less effective than the Sn^{IV} complex (**20**).^{159,208,209}

Several zinc complexes possessing strong absorption in the red region have been described. Photoporphyrin A condenses with 1,3-dibutyl-2-thiobarbituric acid in the presence of pyrrolidine to give a conjugated chlorin, whose zinc(II) complex (**45**) has λ_{\max} 800 nm.²⁰⁵ Zinc(II) 3-desvinyl-3-formylpurpurin (**18**) undergoes osmylation regioselectively at the C7–C8 double

bond to give the bacteriochlorindiol (**46**), which has λ_{\max} 828 nm.²¹⁰ Photophysical data have been reported for a lipophilic chlorin and its zinc(II) and (MeO)₂Sn^{IV} complexes.²¹¹



(45)



(46)

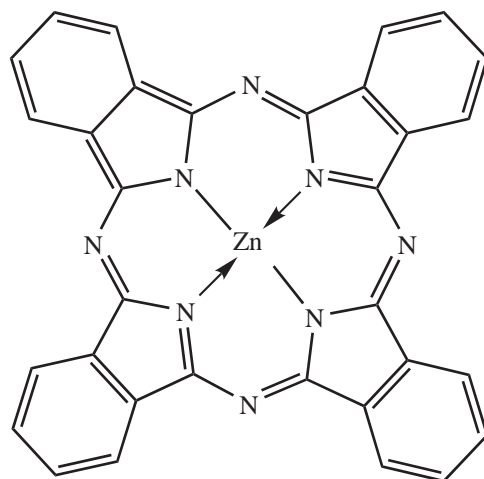
Tumor cells impregnated with zinc(II) benzochlorin iminium salt [(**18**), M = Zn^{II}] undergo a change in fluorescence (λ_{em} 770 nm \rightarrow 640 nm) with (presumed) product formation, and migration of the fluorescent substance from cytoplasm to nucleus.²¹² Photooxidation of zinc(II) chlorins leads to the formyl-dihydrobilinone system resulting from the cleavage of the macrocycle.^{120,121,213} Remarkably, the photocleavage reactions of the zinc and cadmium complexes of pyropheophorbide *a* methyl ester ((**23**), CO₂Me at 13² replaced by H) take different pathways—the zinc(II) complex is cleaved at the C-20 bridge, whereas the cadmium(II) complex is cleaved at the C-5 bridge.²¹⁴

9.22.12.1.3 Zinc phthalocyanines

Zinc(II) phthalocyanine (**47**) is a commercial product and is an effective PDT photosensitizer. However, it is virtually insoluble in water and a delivery system is essential (e.g., liposomes,^{215–218} serum albumin²¹⁹). In ethanol, Φ_{Δ} is ~ 0.4 , and this value increases in DPPC liposomes.^{220,221} Spin-trapping experiments with 5,5-dimethyl-1-pyrroline-1-oxide indicate that a type I mechanism contributes to activity in liposomes.^{220,221} In animal experiments with tumor-bearing mice the sensitizer is rapidly transferred to serum lipoproteins, and transported by them: it is cleared from the serum in a biphasic process, about 60% being eliminated with a half-life of ~ 9 h, the rest much more slowly (suggesting the possibility of long-term sensitization). After 18–24 h the tumor : muscle ratio is ~ 7.5 .²¹⁶ Pharmacokinetic studies based on fluorescence have been made in relation to tumor treatment²²² and to the prevention of intimal hyperplasia and restenosis in angioplasty.²²³

At the cellular level, the photohemolysis of erythrocytes is sensitized by (**47**).²²⁴ In tumor cell cultures, both apoptosis and necrosis are detected. With a short (2 h) DLI, necrosis (loss of membrane integrity) is the main route for cell death, but with a 24 h interval, apoptosis predominates. In both cases, (**47**) is mainly localized in the Golgi apparatus.^{225,226} At the molecular level, singlet oxygen generation using (**47**) in liposomes has been followed by measuring the formation of the 6β -hydroperoxide (rather than the less stable 5α -hydroperoxide) of

cholesterol;²²⁷ photodamage to microtubules, actin, α -actinin, and keratin has been measured in HeLa cells.²²⁸



(47)

The photobleaching of (47) (and XAlPcS_2 and XAlPcS_4) in mouse skin *in vivo* deviates from first order kinetics.²²⁹ Photobleaching of zinc(II) tetra-(*t*-butyl)-phthalocyanine in methanol containing 1% pyridine flushed with air gives fragments, including 4-(*t*-butyl)-phthalonitrile and 4-(*t*-butyl)-phthalimide.²³⁰

Because of the acute solubility problems with (47), there has been much effort with solubilizing substituents. The use of lithium metal in 1-octanol to generate phthalocyanines at room temperature and in good yield represents a significant advance on the synthetic side, and has been illustrated by the synthesis of substituted zinc(II), magnesium(II), and metal-free phthalocyanines.²³¹ Zinc(II) 2-hydroxy-, 2,3-dihydroxy-, 2,9-dihydroxy-, and 2,9,16-trihydroxy- phthalocyanines have been prepared using this route: *in vivo* bioassay shows that the zinc(II) 2,9-dihydroxyphthalocyanine complex is the most effective PDT agent of this series.^{232,233} Synthesis of zinc(II) 1,8,15,22-tetrahydroxyphthalocyanine as a single isomer has been reported using the mild Li/1-octanol method.²³² For example, the reductive cyclotetramerization of 3-methoxyphthalonitrile with lithium in 1-octanol at 40–50 °C, followed by metalation (zinc acetate), gave a single isomer (zinc(II) 1,8,15,22-tetramethoxyphthalocyanine) in 50% yield. At higher temperatures a mixture of isomers results. Other derivatives studied for PDT activity include zinc(II) 2,9,16,23-tetrakis(4-oxy-*N*-methylpiperidiny) phthalocyanine (presumed isomers),²³⁵ zinc(II) 2,9,16,23-tetrakis(2,2,2-trifluoroethoxy)phthalocyanine (presumed isomers),²³⁶ and an extensive series of 2,3,9,10,16,17,23,24-octasubstituted zinc(II) phthalocyanines.²³⁷

Octaalkylphthalocyanines with the alkyl groups at the 1,4,8,11,15,18,22,25- positions have been synthesized as their zinc(II) complexes for PDT studies.²³⁸ Tumor localizing and tumor photosensitizing properties have been presented for the octapentyl²³⁹ and octadecyl²⁴⁰ compounds. Zinc(II) tetrakis(ω -hydroxyalkyl)phthalocyanines have been prepared and tested *in vivo*, the tetrakis(3-hydroxypropyl) compound being the most active.²⁴¹

Halogenated zinc(II) phthalocyanines are less effective against melanocytes than is the unsubstituted (47) in the delivery systems employed (Cremophor, lecithin preparations).²⁴² The effects of halogenation and aggregation on the photosensitizing properties of (47) have been reported.²⁴³ Zinc(II) tetracarboxyfluorophthalocyanine (mixed isomers) is soluble in water, and is more effective as a PDT agent *in vitro* (HeLa cells) than is zinc(II) perfluorophthalocyanine.²⁴⁴ Zinc(II) perfluoro-2,3,9,10,16,17,23,24-octa-(*i*-propyl)phthalocyanine (48) (synthesis: Figure 12) is (remarkably) a planar structure (X-ray analysis, crystallizes with two acetone molecules as axial ligands). Against EMT-6 mammary tumors in mice, (48) administered in Cremophor was more effective than zinc(II) perfluorophthalocyanine.²⁴⁵

The most studied of the water-soluble metallophthalocyanines (Zn, Al, Ga) are the sulfonic acids. These are prepared by cyclotetramerization of 4-sulfophthalic acid or its derivatives (Figure 6),^{246,247} or by the direct sulfonation (oleum) of the metallophthalocyanine.²⁴⁸ The latter method gives complex mixtures, since direct sulfonation occurs at both *exo* and *endo* positions. These mixtures may be separated by chromatographic methods (usually reverse-phase HPLC). Thus

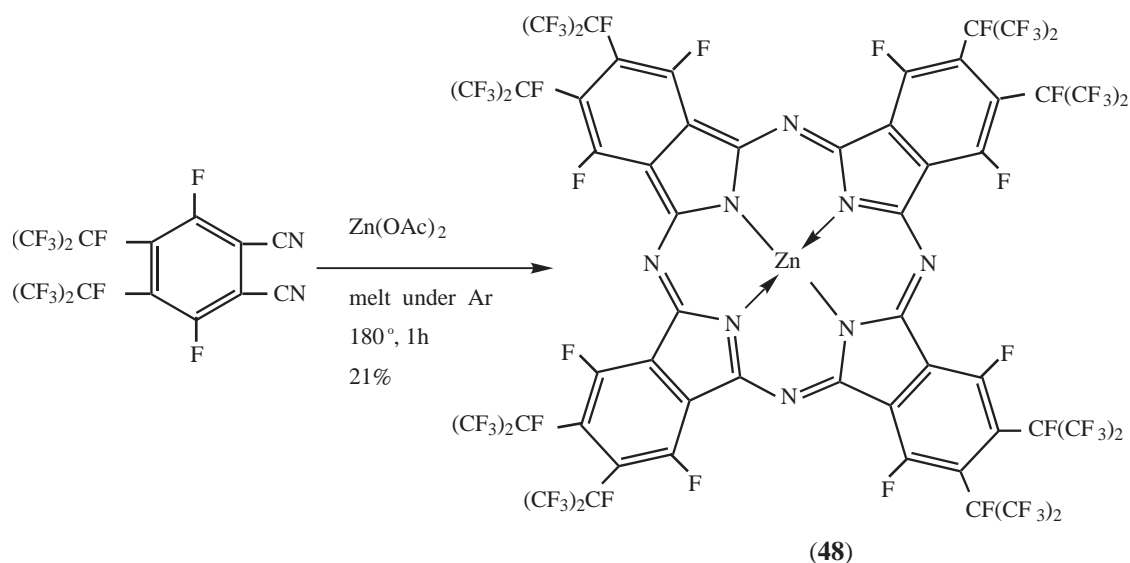


Figure 12 Synthesis of zinc(II) perfluoro-2,3,9,10,16,17,23,24-octaisopropylphthalocyanine (48).²⁴⁵

treatment of (47) with oleum at 50 °C for 30 min gives a mixture of mono- and di-sulfonic acid derivatives.²⁴⁸ The number of sulfonic acid groups present may be determined by chemical/spectroscopic methods and confirmed by oxidation (e.g., ceric ammonium nitrate) to give phthalimide and 4-sulphophthalimide, again estimated by HPLC.^{248,249}

Mixed condensation of 4-sulphophthalic acid with other substituted phthalic acids (typically >200 °C, metal salt, urea, ammonium molybdate catalyst: Figure 6) again gives mixtures.^{246–248} Routes which lead predominantly to monosulfonic acids of zinc(II) phthalocyanine and related compounds have been described.^{247,250}

A completely different approach uses the ring enlargement of the haloboron(III)-subphthalocyanines, a group of compounds discovered by Meller and Ossko in 1972.²⁵¹ For example (Figure 13), treatment of 4-(chlorosulfonyl)phthalonitrile with boron tribromide in chlorobenzene gives the cyclic aromatic system (49), a haloboron(III) subphthalocyanine. It appears that, in some cases at least, treatment of this compound with a diiminoisoindoline of a different substitution pattern (e.g., (50)) in the presence of zinc(II) acetate induces a remarkable and clean ring insertion with the generation of the unsymmetrically substituted phthalocyanine system, in the particular case shown in Figure 13 by the trisulfonic acid (51).^{252,253} This insertion reaction has sometimes been observed to give rise to by-products: that it is found here to be a clear-cut process is attributed to the low temperatures employed and to the stabilizing effect of the electron-withdrawing sulfonic functions.^{252,253} *In vivo* testing of a series of compounds made in this way showed that the zinc(II) t-butyl-naphtho (trisulfobenzo) compound (51) gave the best results against tumors: its absorption in the red (λ_{\max} = 678, 706 nm) and its water solubility make it an attractive PDT candidate.^{252,253}

The number and position of the sulfonic acid substituents in zinc(II) phthalocyanine have an appreciable effect on bioactivity. Partial sulfonation gives the greatest activity, and the S_{2a} derivatives (two sulfonic acid substituents on adjacent benzene rings) appear to be the most active.^{254,255} While this can be readily understood in general terms of developing amphiphilic character (Section 9.22.3), the detailed mechanism responsible for this result is not yet clear. The aggregation of zinc(II) sulphonic acid derivatives in solution and in tissue has been studied in relation to PDT.²⁵⁶

A series of zinc(II) phthalocyanines with other sorts of solubilizing groups in *exo* or *endo* positions (carboxyalkyl, carboxyalkoxy, amino acid) has been synthesized and subjected to preliminary *in vitro* assays.²⁵⁷ Interestingly, the seryl derivative zinc(II) 2,9,16,23-tetrakis(1-carboxy-2-hydroxyethylaminocarbonyl)phthalocyanine proved to be cytotoxic (i.e., toxic in the dark) which is not so commonly observed with macrocyclic systems.

Several studies have been reported on the biological mechanisms of zinc(II) phthalocyanines as photosensitizers. *In vitro* studies (mouse RIF-1 cells) on zinc(II) phthalocyanines differing in overall charge (tetrapyrrolium quaternary salt; tetrasulfonic acid; tetrasulfonamide derivative:

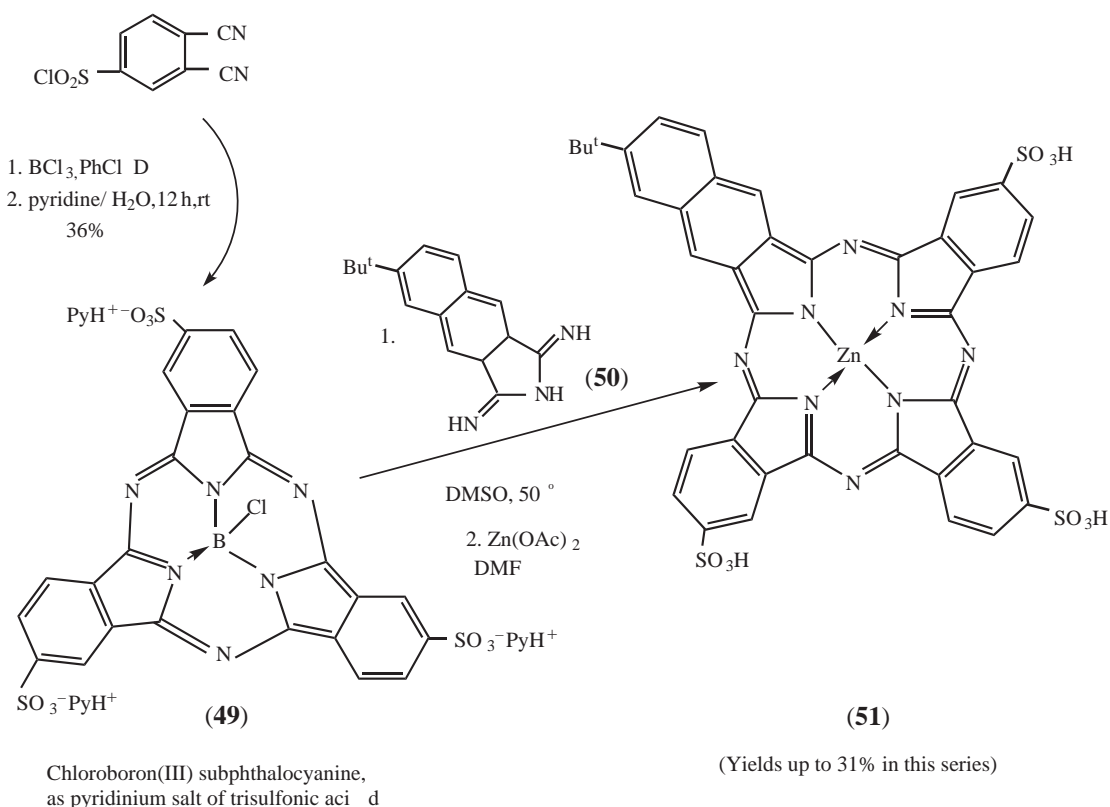


Figure 13 Ring expansion of a haloboron(III) subphthalocyanine (49) to give an unsymmetrically substituted phthalocyanine, here the zinc(II) benzonaphthoporphyrazine (51).^{252,253} As usual, the product is expected to be a mixture of positional isomers.

i.e., respectively, cationic, anionic, and neutral at biological pH) show that in this system the relative sensitizer uptake and cell kill decrease in the order cationic \gg neutral $>$ anionic. For ionic sensitizers the initial localization was in the lysosomes, but the neutral compound was more diffusely spread. On irradiation, the ionic drugs rapidly shifted to different sites, as determined by fluorescence.^{258,259} Cationic zinc(II) phthalocyanines with lipophilic side chains selectively photosensitize mitochondria in HeLa cells.²⁶⁰ Comparisons of (47) with its *endo* octapentyl and octadecyl derivatives *in vivo* showed that (47) was the most effective in delaying tumor regrowth after irradiation: random necrosis was the main pathway, but apoptosis was detected and became more important as the chain length of the alkyl group increased.²⁶¹

Zinc(II) phthalocyanines with quaternary pyridinium salt substituents are effective photobactericides for both Gram +ve (*Enterococcus seriolicida*) and Gram -ve (*Escherichia coli*; *Pseudomonas aeruginosa*) bacteria.²⁶²

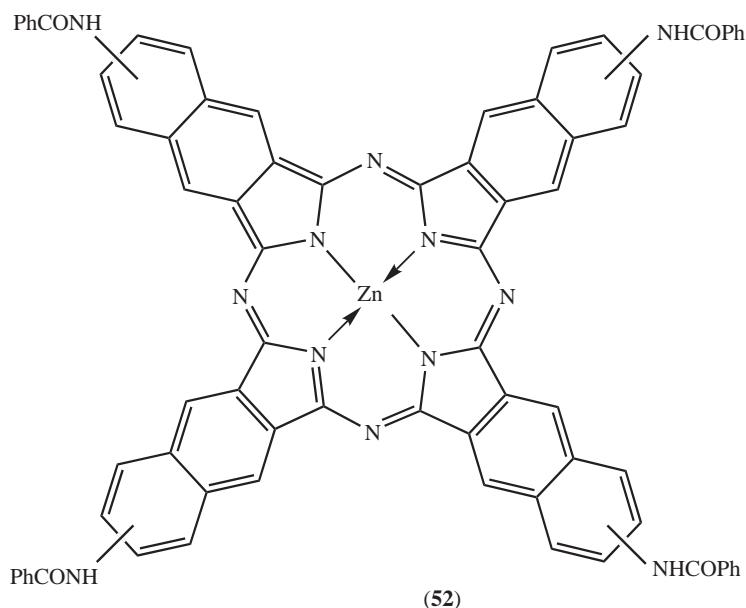
Ring systems intermediate between phthalocyanines and naphthalocyanines are known:^{263,264} (51) is such a compound. They are most simply called benzonaphthoporphyrazines, and various zinc(II) complexes with cationic (*N*-methylpyridinium-3-oxo) substituents have λ_{\max} in the range 680–750 nm in solution or in Cremophor micelles, and show promise in bioassays *in vivo*.²⁶⁴

The photobleaching kinetics for the zinc(II) complexes of several substituted phthalocyanines and analogues under a variety of conditions (e.g., aqueous media,^{265–267} organic solvents,^{230,235,265,266} polymer-bound²⁶⁶) have been reported.

9.22.12.1.4 Zinc naphthalocyanines

Early experiments with zinc(II) (and aluminum(III)) naphthalocyanine were not very promising, although the lower sulfonic acids did show some PDT activity.^{268,269} The chromophore is of

interest since it has intense absorption at about 780 nm ($\epsilon_{\max} > 10^5 \text{ M}^{-1} \text{ cm}^{-1}$), which provides an opportunity to promote PDT in pigmented cells, such as occur in melanoma. The compounds are readily photobleached,^{265,267,270} which might be turned to practical advantage.⁹⁷ Φ_{Δ} is about 0.15.²⁷¹ Synthesis and *in vivo* bioassay of a range of substituted zinc(II) naphthalocyanines has led to the selection of the tetrabenzamido derivative (**52**) (λ_{\max} (DMF) 772 nm, Φ_{Δ} 0.33) as the most promising of the compounds tested.^{270–273} The effect of fluence rate on the PDT of B16-pigmented melanoma transplants has been observed using (**52**) delivered in liposomes: best results were obtained with a fluence rate of 380 mW cm^{-2} at 774 nm.²⁷⁴ Against Lewis lung carcinoma implants in mice, apoptotic processes became more apparent at higher fluence rates.²⁷⁵



9.22.12.1.5 Other zinc complexes

The effect of peripheral substituents on absorption spectrum and *in vitro* PDT activity has been studied for the zinc(II) porphyrine (5,10,15,20-tetraazaporphyrin) system.^{276,277} Water-soluble zinc(II) polyazaphthalocyanines have been synthesized for PDT applications.^{278,279} A zinc(II) bis(dimethylamino)porphyrine is photooxidised to give the zinc(II)-*seco*-porphyrine, the reaction being autocatalytic.²⁸⁰ The zinc(II)-complex of a hexaalkyltexaphyrin chloride has λ_{\max} (MeOH) 732 nm and Φ_{Δ} 0.61,²⁸¹ but the system does not appear to have been developed for PDT.

9.22.12.2 Cadmium

Because of its ionic size, cadmium(II) does not fit well into the coordination site of the porphyrin nucleus (N-centre distance ~ 200 pm), and the complexes are readily demetalated (stability group IV, Tables 1 and 2). The complexes can be prepared, of course, but zinc(II) compounds have been overwhelmingly favored for PDT purposes.

The cadmium(II) complex of pyropheophorbide *a* methyl ester ((**23**) with ^{13}C - CO_2Me removed) photooxidises with cleavage of the macroring at the C-5 bridge. The reaction involves a single molecule of dioxygen, which is taken as evidence for a singlet oxygen $2\pi + 2\pi$ addition to give a dioxetane intermediate.²⁸²

The expanded cavity of the texaphyrin nucleus can accommodate the cadmium(II) ion more effectively. In the crystal of the bis-pyridinecadmium(II) hexaalkyltexaphyrin system, the cadmium atom lies in the plane of the near-planar texaphyrin nucleus: the average Cd–ring N bond length is 235 pm, while the average bond length to the nitrogen atoms of the axial pyridine ligands is 246 pm.²⁸³ With favorable photophysical characteristics (λ_{\max} (5% Tween 20) 730 nm, $\epsilon = 49,000 \text{ M}^{-1} \text{ cm}^{-1}$, Φ_{Δ} 0.30)^{136,281} the CdX–texaphyrin system would appear to be an attractive

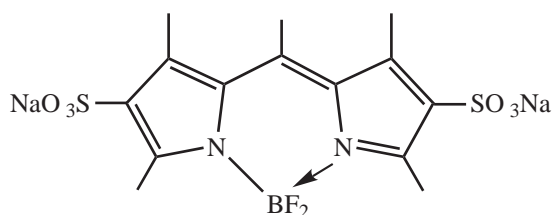
PDT candidate. Indeed, it is effective against human leukemia cells,^{128,284} and as a photobactericide.^{128,285,286} However, concerns about solubility and cadmium toxicity led to a discontinuation of biological work,¹²⁸ and in any case the cadmium(II) complex was soon overtaken as a PDT sensitizer by the lutetium(III) derivative (**32**) (Section 9.22.7.1).

The rates of photooxidation of metallotetrazabenzoporphyrins in pyridine decrease in the sequence $\text{Cd}^{\text{II}} > \text{Mg}^{\text{II}} > \text{Zn}^{\text{II}} > 2\text{H}$.²⁸⁷

9.22.13 COMPLEXES OF GROUP 13

9.22.13.1 Boron

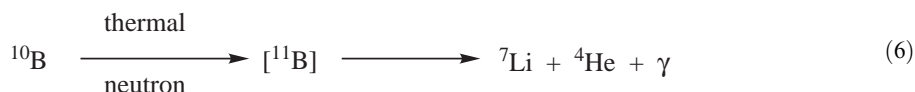
Difluoroboron(III) complexes of pyrromethene systems have been proposed as PDT agents. Thus, preliminary studies on difluoroboron(III) 1,3,5,7,9-pentamethylpyrromethene 2,8-disulfonic acid disodium salt (**53**), developed as a laser dye, show PDT activity *in vitro* against ovarian adenocarcinoma cells.²⁸⁸ This compound had $\lambda_{\text{max}} \sim 500 \text{ nm}$ ($\epsilon \sim 100,000 \text{ M}^{-1} \text{ cm}^{-1}$) in ethanol, and shows some photostability in water.



(53)

With the 5-azapyrromethene system, aryl substitution shifts the absorption band to a position much more suitable for PDT. The tetraaryl-5-azapyrromethene (**54**) (synthesis: Figure 14)²⁸⁹ gives the difluoroboron(III) complex (**55**), which has $\lambda_{\text{max}} (\text{CHCl}_3)$ 650 nm, ϵ 79,000 $\text{M}^{-1} \text{ cm}^{-1}$, and a fluorescence maximum of 672 nm, Φ_f 0.34. In water/Cremophor emulsions it has λ_{max} 658 nm, and with this delivery system it is taken up by the cytoplasm of HeLa cells.²⁹⁰ Bromination of (**54**) gives the dibromo compound (**56**), which analogously forms the difluoroboron(III) complex (**57**). Because of the heavy-atom effect, (**57**) is much less fluorescent (Φ_f 0.012) than is (**55**), but is a much more effective photogenerator of singlet oxygen (as determined by comparative photooxidations of 1,3-diphenylisobenzofuran). Chromophoric properties can be adjusted by substitution in the phenyl groups. Thus the 1,9-di(*p*-methoxyphenyl) analogue of (**55**) has $\lambda_{\text{max}} (\text{CHCl}_3)$ 688 nm ($\epsilon = 85,000 \text{ M}^{-1} \text{ cm}^{-1}$).²⁹⁰ Although at an early stage, this series has intriguing novelty and appears to have promising PDT potential.

Porphyrins have been used as tumor-localizing agents in the related area of boron neutron capture therapy (BNCT). The basis of this process is the irradiation of ^{10}B with thermal neutrons to give an excited ^{11}B atom, which breaks down to give ^4He and ^7Li (Equation (6)). These energetic and damaging particles are shortlived and short range and, *in vivo*, can destroy the immediately surrounding tissue (e.g., tumor tissue). Heavily boronated compounds are needed, and this is achieved by attaching carborane units. The topic has been reviewed,^{291–294} and the patent literature is very active.^{295,296} Two *meso*-tetra[*nido*-carboranylmethyl]phenyl porphyrins and their zinc(II) complexes have been studied *in vitro*: they have low cytotoxicities. The free-base compounds are thought to have the greater promise because they have a higher percentage of boron.²⁹⁷



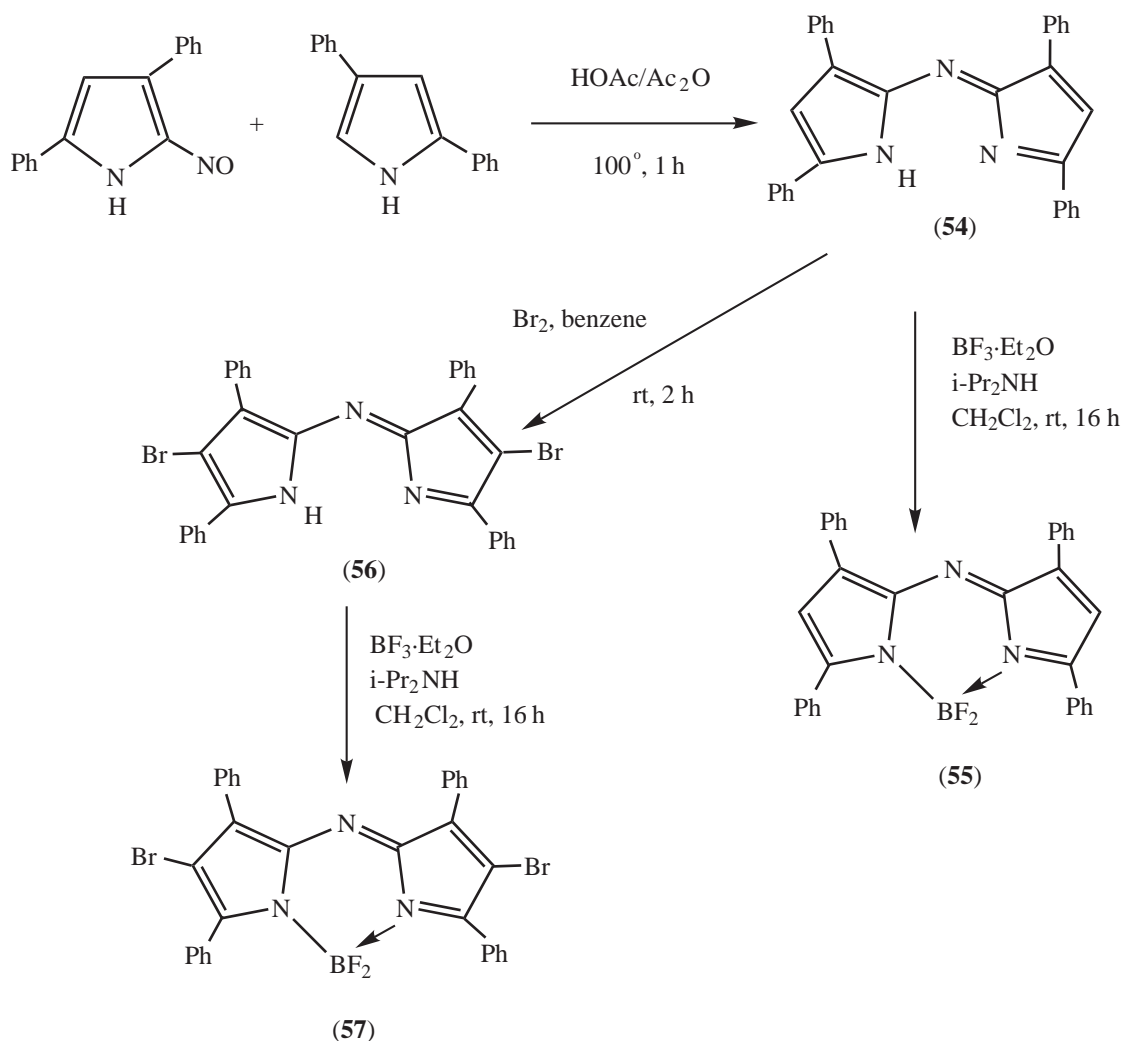


Figure 14 Syntheses of difluoroboron(III) complexes of arylpyrromethenes.²⁹⁰

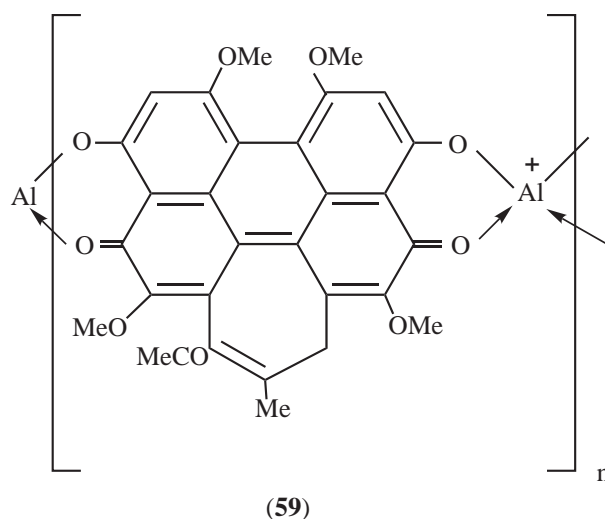
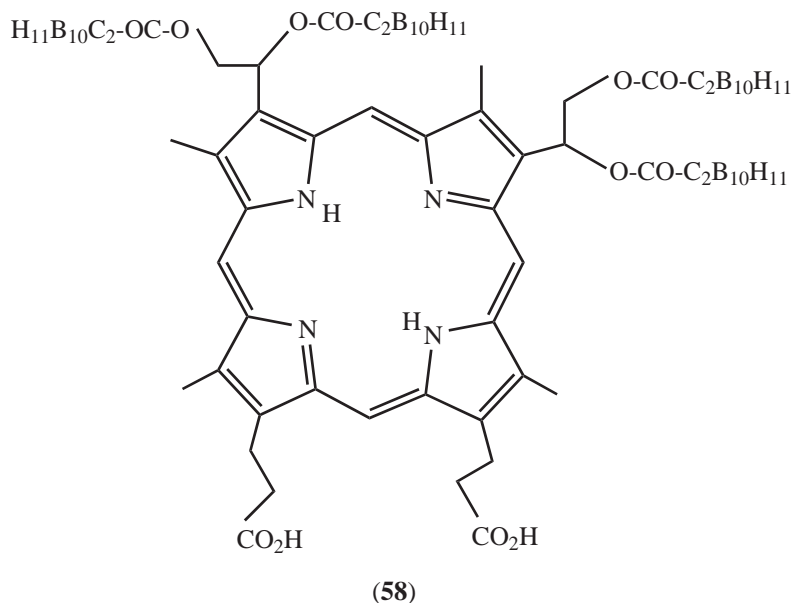
BNCT sensitizers are designed with neutron capture in mind, but those that are porphyrin/phthalocyanine-based may show PDT activity. An example is the disodium (or dipotassium) salt of the tetrakis-carborane ester (**58**) derived from 3,8-bis(1,2-dihydroxyethyl)deuteroporphyrin.²⁹⁸ This is water soluble and tumor selective, showing high tumor/normal brain ratios.²⁹⁹ Photo-physical properties are similar to other water-soluble porphyrins: in rat glioma cells, specific localization in mitochondria is observed.³⁰⁰

9.22.13.2 Aluminum

Although the majority of metal complexes developed for PDT have porphyrin-style ligands, there are exceptions (e.g., compounds (**53**) and (**54**) to (**57**)). The aluminum(III) complex of hypocrellin B (**59**) provides another example. Compound (**59**) is an oligomeric system where *n* is about 9: the material is water soluble, has λ_{\max} (DMSO) 614 nm, and generates both superoxide and singlet oxygen on irradiation (Φ_{Δ} in DMSO estimated at 0.23).³⁰¹

The photodynamic effect of chloroaluminum(III) phthalocyanine ((**47**), with ClAl in place of Zn), a commercial product, was reported by Ben-Hur and Rosenthal.³⁰² The photosensitizer was delivered in ethanol to cultures of Chinese hamster fibroblasts. After equilibration (16 h), exposure to visible light (fluence rate 64 W m⁻²) of a suspension in PBS for 2 min gave a 3 log kill. Lack of water solubility is a problem, and for *in vivo* PDT of EMT-6 mammary tumors in mice a Cremophor emulsion was employed.³⁰³ The compound was a more effective PDT sensitizer than

its sulfonated derivatives (see below) in this system: vascular disruption was significant in causing tumor damage.³⁰³ A synergistic interaction with hyperthermia has been observed *in vitro* using chloroaluminum(III) phthalocyanine as the sensitizer.³⁰⁴ Photokilling of the yeast *Kluyveromyces marxianus* has been attributed to a photodynamically induced inhibition of protein synthesis.³⁰⁵ Studies have been made on the destruction (apoptosis vs. necrosis) of leukemia cells^{306,307} and on the detection of atherosclerotic plaques,³⁰⁸ using this sensitizer.



The axial chloride ligand of ClAlPc is readily replaced by hydroxide ($\text{H}_2\text{O}-\text{NH}_3-\text{Py}$, 4h, Δ), and other axial ligands can then be attached (e.g., trihexylsiloxy-, cholesteryloxydiphenylsiloxy-). In *in vitro* assays (M6 melanocytes) these compounds (lecithin or Cremophor delivery) were more effective PDT agents than ClAlPc.²⁴¹

Solubilization of the aluminum(III) complexes has been most commonly effected by sulfonation. As with the zinc(II) phthalocyanines (Section 9.22.12.1.3) sulfonic acid groups have been introduced by ring synthesis using 4-sulfophthalic acid or, more commonly, by direct sulfonation of chloroaluminum(III) phthalocyanine.^{254,309,310} Separation of mono-, di-, tri- and tetra-sulfonic acid fractions requires reverse-phase HPLC.^{49,310} The four fractions are still mixtures of regioisomers: as before, the disulfonic acids are distinguished as S_{2a} for substitution on adjacent benzene rings, and as S_{2o} for substitution on opposite benzene rings. The structures of the 16 disulfonic acid regioisomers have been drawn out,³¹¹ but not one of them appears to have been

characterized as a single entity. As with the zinc analogues (Section 9.22.12.1.3) the disulfonic acids, and especially the S_{2a} compounds, exhibit the best PDT properties.^{254,310} In spite of earlier reports,^{254,312} the presence of a coordinated metal ion (e.g., Al^{III}) in these sulfonic acids is not essential for PDT activity.^{162,313,314}

Studies on $XAlPcS_2$ fractions are the most extensive: the results need to be interpreted carefully, since different preparations may be expected to have different compositions. Often the axial ligand is not stated: in any case, if it is chloride it would be expected to be gradually replaced by OH in aqueous media, and so where there is doubt it is represented here by X. Quantification methods (*in situ* fluorescence vs. chemical extraction from tissues) have been compared.³¹⁵ For $XAlPcS_{2a}$ in DPPC liposomes both Φ_{Δ} and Φ_T decrease with photosensitizer concentration, but aggregation is not observed in the concentration range studied (0.76–2.2 μM).³¹⁶ In mouse cancer cells no transient other than the photosensitizer triplet state was detected, suggesting that type I photooxidation processes are not involved (this is in contrast to microbial systems where a transient radical anion is detected).^{317,318} Fluorescence imaging of the development of tumors in different host tissues in the mouse has been reported.³¹⁹

In tumor-bearing animals photosensitized with $XAlPcS_{2a}$, direct tumor cell damage rather than vascular disruption is principally responsible for tumor destruction.^{320–323} δ -Aminolaevulinic acid (4) is more selective than $XAlPcS_2$ for the treatment of dysplastic mucosa in an animal model.³²⁴ Peptides containing the Arg-Gly-Asp sequence protect cancer cells (2 cell lines studied) from apoptotic death with $XAlPcS_{2a}$ as photosensitizer.³²⁵ Fluorescence lifetimes³²⁶ and microbicidal effects^{311,327,328} have been studied for $XAlPcS_2$ in various bacteria (Gram +ve and Gram –ve) and yeasts.

With $XAlPcS_3$, selective photonecrosis of colonic tumors induced with dimethylhydrazine was observed with low drug doses (0.5 $mg\ kg^{-1}$), but selectivity over normal tissue disappeared at 5 $mg\ kg^{-1}$.³²⁹ The use of this material (in the form of PHOTOLENS as a mixture of di- and trisulfonic acids (7)) in extensive clinical treatments in Moscow has been referred to in Section 9.22.4.

In spite of having lower activity than the disulfonic acids, the tetrasulfonic acid, $XAlPcS_4$, has attracted some attention, possibly because it is commercially available, or is available in one synthetic step from 4-sulfophthalic acid. Erythrocyte lysis, virus inactivation and the photooxidation of reduced glutathione and histidine were all enhanced (for a given fluence) when the fluence rate was at a lower (100 $W\ m^{-2}$) rather than a higher (500 $W\ m^{-2}$) value.³³⁰ A comparison of several features important in PDT activity (e.g., uptake by cancer cells, tumor/skin concentration ratio, localization, partition coefficient, photokill *in vitro*, relative Φ_{Δ}) put $ClAlPcS_4$ behind tetrakis(*m*-hydroxyphenyl)porphyrin, but ahead of Photofrin and chlorin e_6 .^{331,332} During irradiation of cultures of rat bladder epithelial cells with $XAlPcS_4$, a transient elevation of calcium concentration was observed, especially in the nuclei, followed by a more sustained increase: interestingly, stimulation of cell growth was noticed at very low light doses.³³³ Increases in intracellular calcium ion concentrations seem to be associated with PDT and apoptosis.³³⁴ Repeated photodynamic treatments of human cancer cell lines to a 1–10% survival level using $XAlPcS_4$ as sensitizer has led to cell cultures which are up to 2.6 times more resistant to PDT than normal.³³⁵ $XAlPcS_4$ has been used as the photosensitizer in studies of laser photo-occlusion of choroidal neovascularization.³³⁶ There has been considerable activity aimed at improved targeting of $XAlPcS_4$ using conjugation (e.g., to monoclonal antibodies,^{337–339} low-density lipoproteins,³⁴⁰ and other proteins^{341,342}) and liposomal systems³⁴³ (“third-generation” sensitizers). The synthesis of monosulfonamides (tetrasulfonyl chloride + 1 mol. aliphatic amine + quenching) gives amphiphilic compounds with improved PDT activity: the most promising compound of those tested had a C_{12} aliphatic chain.³⁴⁴

Biological studies comparing PDT features of the various sulfonic acid fractions have been prominent.^{345–348} Curiously, it appears that cellular incorporation is better for mixtures of different sulfonated fractions, or for mixtures of regioisomers, than it is for the “pure” compounds, which tend to aggregate more easily.³⁴⁹ The fluorescence of $XAlPcS_2$ and $XAlPcS_4$ in the skin of mice increased over the first few minutes of irradiation, suggesting initial lysosomal localization followed by lysosome rupture and release of the dye.³⁵⁰ Subcellular sites of photodynamic action were studied in a human melanoma cell line:³⁵¹ $AlPcS_1$ and $AlPcS_2$ damaged membrane systems (e.g., plasma membrane, mitochondria, endoplasmic reticulum) while $AlPcS_3$ / $AlPcS_4$ destroyed the lysosomes.

With mice bearing mammary carcinoma implants, $XAlPcS_2$ concentrations in the tumor peaked at 2–24 h after injection, while $XAlPcS_4$ peaked at 1–2 h. With a DLI of 24 h and a drug dose of 10 $mg\ kg^{-1}$, the sequence of PDT activities was $XAlPcS_2 > XAlPcS_4 > Photofrin > XAlPcS_1$.³⁵²

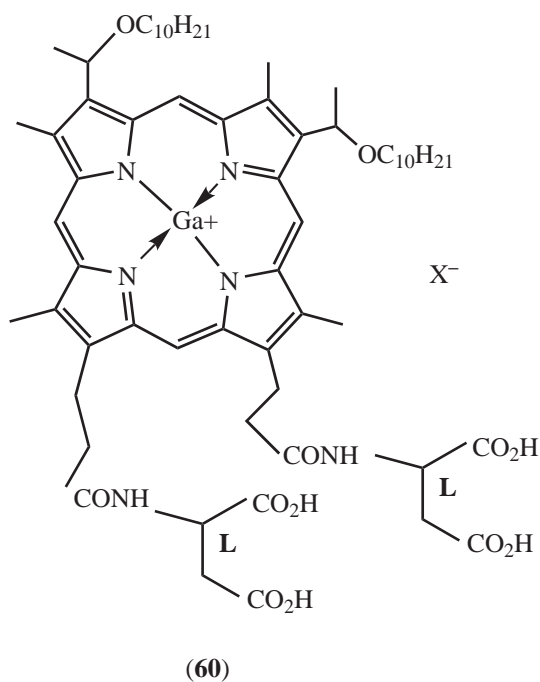
A series of aluminum(III) naphthalocyanines of potential value as PDT sensitizers has been synthesized. Thus, treatment of 2,3-dicyanonaphthalene with aluminum(III) chloride in refluxing quinoline for 2 h gave 48% of ClAl(NPc) .^{353,354} Hydrolysis gave HOAl(NPc) , from which tri-alkylsiloxy derivatives could be made.³⁵⁴ Although nonenveloped viruses were resistant, various enveloped viruses were inactivated with aluminum(III) complexes of benzonaphthoporphyrine sulphonic acids as sensitizers.³⁵⁵

The photobleaching of $\text{XAlPcS}_{\sim 3}$ has been studied in water and in aqueous methanol.^{270,356,357} The rate increased in the presence of human serum albumin.³⁵⁶ Under the same conditions, $\text{XAlNPcS}_{\sim 3}$ in aqueous methanol was bleached about a thousand times more rapidly.²⁷⁰

9.22.13.3 Gallium

Gallium(III) forms stable (class II, Table 2) porphyrin complexes and has a filled *d* shell; nonetheless, relatively few PDT photosensitizers have made use of complexes of this metal.

Japanese workers have developed a series of gallium(III) porphyrins, for example the complex (60), for which the code ATX-70 is frequently used in publications.³⁵⁸ This series seems to have been thought of in terms of sonosensitization,^{358,359} but is also referred to with respect to photosensitization.³⁶⁰ Compound (60) accumulated in murine tumors (maximum concentration at 2–6 h), although it was still detected in normal tissue at 6 h.³⁶⁰ The combined effect of high-energy shock waves, cisplatin, and (60) has been reported to inhibit tumor growth *in vivo*.³⁶¹ A related gallium(III) porphyrin (code Ga-C10-P) in combination with irradiation at 525 nm (LED source) markedly inhibits the proliferation of leukemia cell line K562.³⁶²



Sulfonation of gallium(III) phthalocyanines, as with zinc(II) and aluminum(III) complexes (Sections 9.22.12.1.3 and 9.22.13.2, respectively), is carried out by direct sulfonation, or by condensation (including crossed condensation) of appropriate phthalic acid/4-sulfophthalic acid mixtures with gallium salts.^{248,255,309,363} The relative yields of the components have been tabulated for both processes for gallium, aluminum, and zinc complexes.²⁴⁸ The mono- and di-sulfonic acids were photoactive, but the tri- and tetra-acids were not, against V-79 Chinese hamster cells *in vitro*.³⁶³ Amongst the disulfonic acids, the most hydrophobic (presumed to be XGaPcS_{2a}) was the most active; XAlPcS_2 was slightly more active than XGaPcS_2 .³⁶³ *In vivo* (mammary tumor implant) the lower sulfonated fraction of gallium(III) phthalocyanine had an activity similar to that of Photofrin.²⁵⁴ The cerium complex (S_2) was even more active, but also caused serious photodamage to normal tissue.²⁵⁴

Gallium(III) naphthalocyanines (e.g., trihexylsiloxygallium(III) naphthalocyanine, λ_{\max} (PhH) 795 nm) have been prepared for PDT applications.³⁵⁴

9.22.13.4 Indium

Metalloporphyrin systems have been used to transport peripherally coordinated ¹¹¹In for tumor localization purposes (Section 9.22.8.1).¹⁴⁶ The ¹¹¹In complex of HpD has been described.³⁶⁴

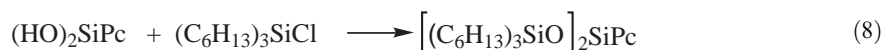
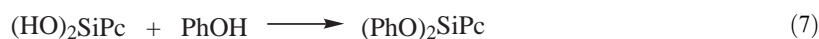
9.22.14 COMPLEXES OF GROUP 14

9.22.14.1 Silicon

Most activity here has been with the phthalocyanine and naphthalocyanine complexes.

The X₂silicon(IV) phthalocyanines are octahedral complexes and have already been met in Section 9.22.5.3 where they were used to illustrate variation in axial ligands.^{64–66} Syntheses have been described in detail with full characterization, including elemental analyses,^{64,65,365} an example is given in Figure 7. Table 3 summarizes some photophysical and photobiological properties of four compounds (referred to in the literature by the codes Pc4, Pc10, Pc12 and Pc18) for which the structures are given at (12), (13), (14), and (15), respectively.

The dichlorosilicon(IV) phthalocyanines are important intermediates, and may be obtained by the reaction of phthalonitrile with silicon tetrachloride or hexachlorodisiloxane in quinoline; 1,3-diiminoisindoline and *o*-cyanobenzamide may also serve as precursors (cf. Figure 6).^{365,366} Hydrolysis of Cl₂SiPc (e.g., with pyridine/NH₃/H₂O) gives (HO)₂SiPc, which on subsequent ligand exchange or ligand reaction allows a variety of axial ligands to be put in place (Equations (7), (8)).^{365,367}



A considerable number of compounds with alkoxy (aryloxy) and trialkylsiloxy ligands (including some embodying cholesteryl units)³⁶⁸ have been made in this way.

The silicon(IV) phthalocyanines are robust: the silicon is not removed in sulfuric acid. They have strong absorption in the red (λ_{\max} ca. 670 nm), have satisfactory Φ_{Δ} values, and generally appear promising as PDT agents.³⁶⁹ They show encouraging activity in bioassays *in vitro* and *in vivo*.³⁷⁰ Thus, [(C₆H₁₃)₃SiO]₂SiPc and Cl₂SiPc photosensitize amelanotic human melanoma cells: in this comparison, PDT activity is highest with the trihexylsiloxy derivative using lecithin liposomes for delivery.³⁷¹ In comparative studies against leukemia cell lines, XAIPc showed the highest photoactivity, but Cl₂SiPc and the trihexylsiloxy compound showed significant photokill; bis(triphenylsiloxy)silicon(IV) phthalocyanine and nickel(II) phthalocyanine were inactive.³⁷² With Lewis lung carcinoma implants in mice, both DPPC liposomes and Cremophor were effective delivery agents for bis(2-methoxyethoxy)silicon(IV) phthalocyanine. Interestingly, the Cremophor emulsion caused higher accumulation and retention of the sensitizer in the brain.³⁷³

Comparative studies,^{65,66} both *in vitro* and *in vivo*, on the series of silicon(IV) phthalocyanines made by Kenney and his colleagues resulted in the selection of compound (12) {[3-dimethylaminopropyl]dimethylsiloxy}hydroxysilicon(IV) phthalocyanine, [Me₂(CH₂)₃SiMe₂O](HO)SiPc}, and several studies have been devoted to the biological chemistry of this substance. Since it is not water soluble, it has been delivered using Cremophor/ethanol/saline mixtures or in a polar aprotic organic solvent such as DMF or DMSO. Inhibitors of cutaneous sensitization have been sought.³⁷⁴ *In vivo* photoactivity has been demonstrated against RIF tumor implants,³⁷⁵ chemical carcinogen-induced skin tumors,³⁷⁶ and ovarian carcinoma xenografts,³⁷⁷ in each case with evidence of early apoptosis. Irradiation of mouse lymphoma cells with (12) causes increased production of ceramide,³⁷⁸ which appears to be linked to PDT-induced apoptosis and phototoxicity. Cell binding of (12) occurs preferentially in the mitochondria and Golgi apparatus; little goes to the plasma membrane or nucleus.³⁷⁹ At the molecular level, one of the immediate

phototargets of (12) appears to be the anti-apoptotic mitochondrial protein designated Bcl-2: this protein is spared, and apoptosis is inhibited, in the presence of histidine, regarded as acting as a scavenger of singlet oxygen.^{380,381} Other protein targets are involved, and the overall result is interpreted in terms of the release of cytochrome *c* from the mitochondrion into the cytosol, where it activates a series of proteases (caspases) leading to apoptosis.^{380,381} Sensitizer (12), labelled at the *N*-methyl group with ¹⁴C, has been used to show that the peripheral benzodiazepine receptor (a protein of the outer mitochondrial membrane)³⁸² is less relevant in this case.³⁸³

The silicon(IV) phthalocyanine (12) is also effective in the photoinactivation of the parasite *Plasmodium falciparum*³⁸⁴ and various enveloped viruses in red blood cell concentrates.^{385–387} Other silicon (and aluminum) phthalocyanines have been evaluated for the photoinactivation of viruses: cationic derivatives appear to be most effective.³⁸⁸

The absorption spectra of the silicon(IV) naphthalocyanines follows the pattern already seen with the analogous zinc(II) (Section 9.22.12.1.4) and aluminum(III) (Section 9.22.13.2) derivatives;³⁵⁴ the red band is shifted about 100 nm further to the red, with intensification. Bis(trihexylsiloxy)silicon(IV) naphthalocyanine has $\lambda_{\max}(\text{PhH}) = 776 \text{ nm}$ ($\epsilon = 650,000 \text{ M}^{-1} \text{ cm}^{-1}$) and Φ_{Δ} 0.35 (oxygen-saturated benzene).³⁸⁹ The solution is fluorescent (main emission at $\sim 780 \text{ nm}$, τ_f 2.85 ns): the triplet energy (ca. 22 k cal mol⁻¹) is a little less than the energy of the first singlet state of dioxygen, and the process (Equation (9)) is reversible (cf. compounds (40) and (41), Section 9.22.10.2).



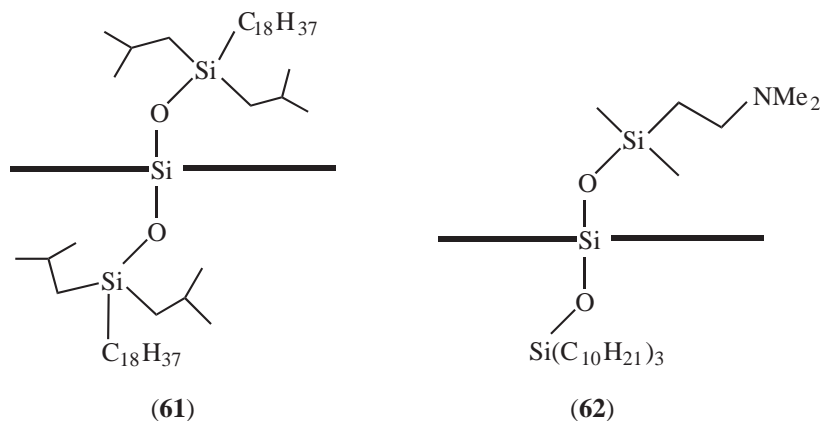
Silicon(IV) naphthalocyanines with various axial ligands are available by syntheses analogous to those used with the phthalocyanine complexes (above).^{353,365,390,391} Pharmacokinetic, and tissue distribution and delivery, studies have revealed good tumor/muscle ratios for bis-(di-(*i*-butyl)octadecylsiloxy)silicon(IV) naphthalocyanine (61);³⁹² in *in vitro* studies with melanotic and amelanotic melanoma cells, the activity of this compound was exceeded by that of compound (62) with a basic center in one of the axial ligands.³⁹³ The spectra of the melanotic cells showed that at 776 nm the melanin absorbs only 10% of the incident radiation under the conditions employed. Irradiation of a pigmented melanoma transplant with a single 650 mJ pulse at 1064 nm from a Nd-YAG laser caused instant bleaching of the tissue.³⁹⁴ Administration of (61) (1 mg kg⁻¹) followed by the 1064 nm pulse, followed immediately by the PDT irradiation (774 nm, 300 mW cm⁻², 520 J cm⁻²), resulted in a much improved delay in tumor growth (16 days) compared to PDT without the Nd-YAG laser pulse (6 days). In another series of four silicon(IV) naphthalocyanine derivatives, limited cellular toxicity was detected *in vitro*, although the compounds had appreciable Φ_{Δ} values,³⁹⁵ and showed some activity *in vivo*.³⁹⁶ Bis(2-methoxyethoxy)silicon(IV) naphthalocyanine (0.5 mg kg⁻¹) was delivered in a Cremophor formulation to animals bearing Lewis lung carcinoma or pigmented melanoma implants.³⁹¹ Photosensitizer concentrations peaked at 24 h, but with markedly higher levels in the Lewis lung carcinoma (0.70 $\mu\text{g g}^{-1}$) than in the melanoma (0.15 $\mu\text{g g}^{-1}$). On PDT, the Lewis lung carcinoma responded well, but the melanoma did not. Although melanoma remains a difficult target for PDT, it still seems that the best chance will reside with far-red absorbing photosensitizers, such as the naphthalocyanines.

9.22.14.2 Germanium

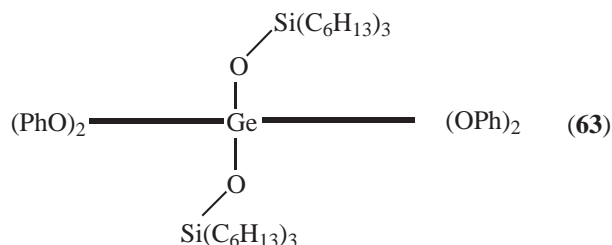
Germanium(IV) forms well-defined porphyrin complexes, but they have not been accorded much attention in the PDT field.

Some phthalocyanines have been examined. Treatment of phthalocyanine with germanium(IV) tetrachloride gives Cl₂GePc in 50% yield; aqueous ammoniacal pyridine gives (HO)₂GePc, which undergoes reactions at axial positions similar to those of the silicon derivatives (Equations (7), (8)).^{397,398} Germanium (IV) phthalocyanines with various axial ligands have been prepared in this way;^{397,399} they have $\lambda_{\max} \sim 675 \text{ nm}$, fluoresce, and have high Φ_{Δ} values.³⁹⁹ These compounds showed some tumor selectivity, although they were less selective than zinc(II) phthalocyanine (liposomal delivery). Nonetheless, they were effective PDT sensitizers *in vivo*.⁴⁰⁰ The tumor-localizing properties of germanium(IV)-octabutoxypthalocyanine have been reported. The axial ligands employed were bis(triethylsiloxy) and bis(trihexylsiloxy), and liposomal or Cremophor delivery was required. Cremophor-supported photosensitizer was cleared from the bloodstream

at a much slower rate than when liposomal (DPPC) delivery was used: however, Cremophor led to enhanced sensitizer uptake by tumor tissue.^{401,402}



Bis(trihexylsiloxy)germanium(IV)-tetraphenoxynaphthalocyanine (**63**) has been prepared by standard methods. It has λ_{\max} (cyclohexane) 779 nm ($\epsilon=616,000 \text{ M}^{-1} \text{ cm}^{-1}$).⁴⁰³



(In structures **(61)**–**(63)** the horizontal bar represents naphthalocyanine viewed along the edge of the macrocycle)

9.22.14.3 Tin

Tin protoporphyrin, when administered in conjunction with UVA irradiation, has been reported to be of possible benefit in the treatment of psoriasis.⁴⁰⁴

One tin complex, dichlorotin(IV)-etiopurpurin (**20**), code name SnEt2, has been under commercial development as a PDT photosensitizer.⁴⁰⁵ The synthesis has unusual features, and is shown in Figure 15.^{159,406,407} Etioporphyrin I, protected as its nickel(II) complex (**64**), is subjected to Vilsmeier–Haack formylation, followed by a Wittig reaction to give the acrylic ester which, after demetallation, provides the key intermediate (**65**). Heated in acetic acid under an inert atmosphere this undergoes equilibration with the cyclized product (**66**), in a reaction of a type discovered by Woodward in his synthesis of chlorophyll *a*.⁴⁰⁸ Metallation with tin(II) chloride in acetic acid is accompanied by adventitious oxidation to give the $\text{Cl}_2\text{Sn}^{\text{IV}}$ complex (**20**). The overall yield is good. Tin etiopurpurin (**20**) belongs to the chlorin class, and has λ_{\max} (CH_2Cl_2) 659 nm ($\epsilon 30,300 \text{ M}^{-1} \text{ cm}^{-1}$), and Φ_{Δ} 0.6. It is a lipophilic compound, and requires a delivery agent (such as Cremophor). Studies related to prostate cancer have been published,⁴⁰⁹ and the compound has been in a Phase III trial against wet age-related macular degeneration.⁴⁰⁵ Photodamage of murine leukemia cells by SnEt2 (**20**),^{410,411} involves localization in lysosomes and mitochondria, and apoptosis occurs at an early stage; with a related tin(IV) purpurin

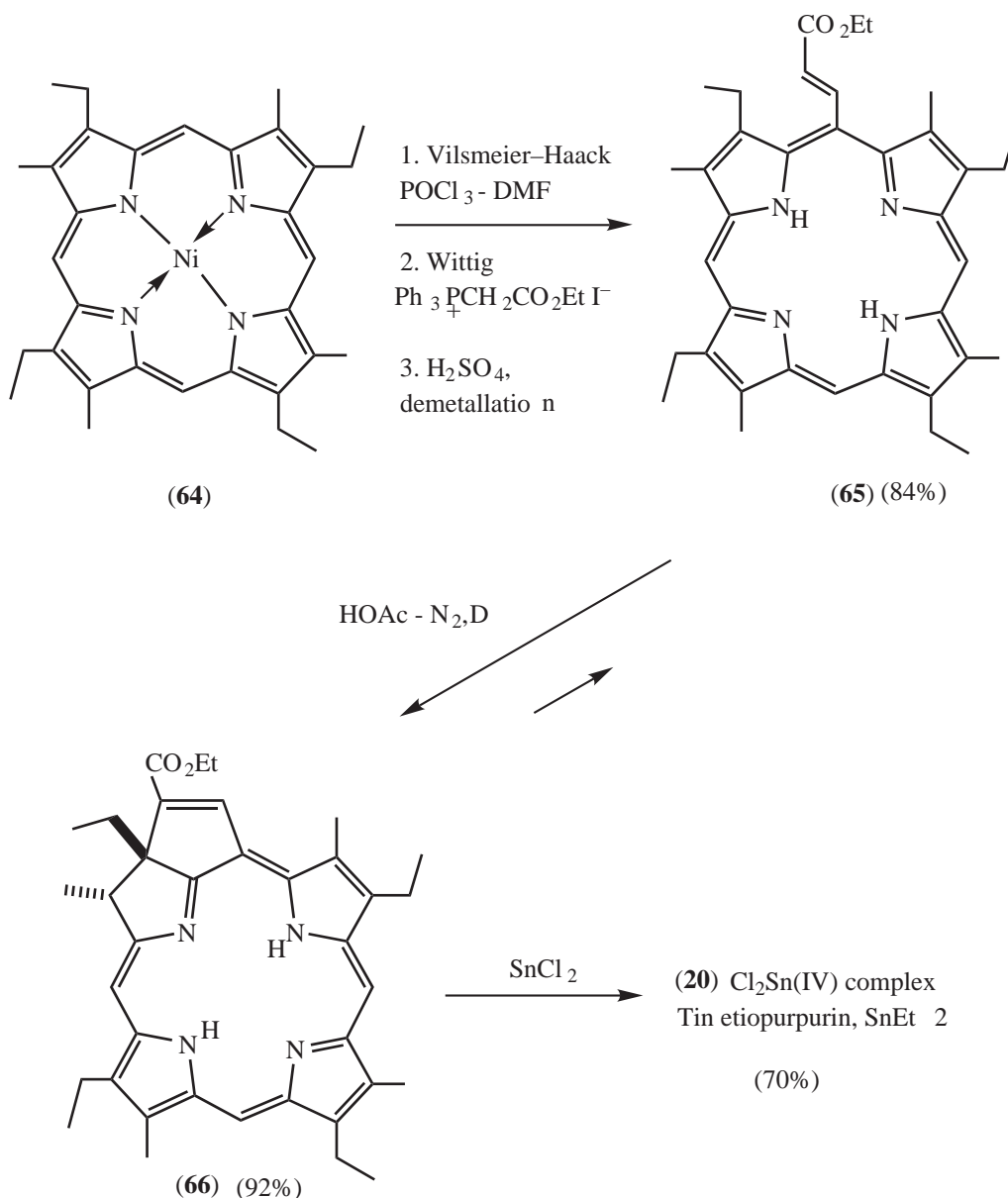


Figure 15 Synthesis of dichlorotin(IV) etiopurpurin (SnEt_2) (20) from nickel(II) etioporphyrin I (64).^{159,406,407}

amidine derivative, which targets lysosomes, mitochondria and cell membranes, the apoptotic response was delayed.⁴¹¹

During studies on the effect of solvent on spectroscopic properties, photobleaching of (20) was observed.⁴¹² In addition to true photobleaching, a photoproduct which fluoresces at 625 nm was produced in ethyl acetate solution.

A series of tin(IV) naphthalocyanines has been prepared.³⁵⁴ Bis(trihexylsiloxy) tin(IV) naphthalocyanine has λ_{max} 788 nm in benzene.

9.22.15 CONCLUSIONS

- A considerable effort has gone into the study of metal complexes for PDT applications in the last quarter of the twentieth century; much of this has been devoted to complexes of porphyrins and phthalocyanines and their relatives. A metal complex has not yet received regulatory approval (as of June 2002), but sulfonated aluminum phthalocyanine is in

- regular clinical use in Russia, and tin purpurin and lutetium texaphyrin derivatives are in advanced clinical trials.
- (ii) Groups 12, 13 and 14 have provided the metals for the most promising photosensitizing complexes. Most work has been done with zinc, aluminum, and silicon complexes (porphyrins, phthalocyanines, naphthalocyanines), but with macrocycles which have larger coordination cavities (e.g., texaphyrins) metals with larger ionic radii (e.g., cadmium, lutetium), are appropriate. If a metal-free system is discovered with PDT potential, it certainly seems prudent to examine zinc and aluminum complexes. Since the zinc complex is expected to have a lower redox potential, and the aluminum a higher one, than the free base, this provides considerable variation in structure and reactivity, e.g., with respect to ease of photobleaching.
 - (iii) Silicon complexes are particularly interesting, since they offer the possibility of axial ligand variation (well explored), as well as variation of substituents on the macrocycle (which seems to have been less well explored so far). These variations are important, not because they affect the photophysical properties very much, but because they can change the solution physical chemistry of the sensitizer, particularly water solubility and partition coefficient.
 - (iv) Complexes of first-row transition metals in general are unlikely to emerge as useful PDT agents, because excited-state lifetimes and singlet oxygen quantum yields are so low. It now seems unreasonable to the author to test these compounds *in vivo* for PDT. However, some of these compounds, if they are suitably selective, may find application as the emerging area of photothermal therapy (PTT) develops.
 - (v) Palladium complexes are attracting increasing interest.
 - (vi) The target diseases for PDT are widening. In addition to the original objective of tumor treatment, the potential targets now include, for example, atherosclerosis, prevention of restenosis, wound healing, psoriasis, ophthalmological and dermatological conditions, and a range of photomicrobicidal applications. It seems that PDT now has a momentum which will ensure that it will continue to expand into new areas over the next few years.

ACKNOWLEDGMENTS

I would like to acknowledge the permission that I have received from Dr. Joy E Rogers (AFRL, USA) and Dr. Donal O'Shea (Dublin), and their colleagues, to include reference to some of their work before publication. Mrs. Lesley Lambert is thanked for her contributions to the typing, and Dr. Paul Bonnett is thanked for his much-needed help with the computer.

9.22.16 REFERENCES

1. Finsen, N. R. *Phototherapy*; Sequeira, J. H., Transl.; Arnold: London, 1901.
2. Regan, J. D.; Parrish, J. A., Eds.; *The Science of Photomedicine*; Plenum: New York, 1982.
3. Lim, H. W.; Soter, N. A., Ed.; *Clinical Photomedicine*; Marcel Dekker: New York, 1993.
4. Bonnett, R. *Rev. Contemporary Pharmacother.* **1999**, *10*, 1–17.
5. McDonagh, A. F.; Lightner, D. A. *Pediatrics* **1985**, *75*, 443–455.
6. Parrish, J. A.; Fitzpatrick, T. B.; Tanenbaum, L.; Pathak, M. A. *New Engl. J. Med.* **1974**, *291*, 1207–1222.
7. Boehncke, W.-H. *Current Opin. Anti-inflammatory Immunomodulatory Invest. Drugs* **1999**, *1*, 338–352.
8. Dougherty, T. J.; Gomer, C. J.; Henderson, B. W.; Jori, G.; Kessel, D.; Korbek, M.; Moan, J.; Peng, Q. *J. Natl. Cancer Inst.* **1998**, *90*, 889–905.
9. Blum, H. F. *Photodynamic Action and Diseases Caused by Light*, American Chemical Society Monograph Series No. 85; Reinhold: New York, 1941.
10. Daniel, M. D.; Hill, J. S. *Austral. N. Z. J. Surg.* **1991**, *61*, 340–348.
11. Dougherty, T. J.; Henderson, B. W.; Schwartz, S.; Winkelman, J. W.; Lipson, R. L. *Historical Perspectives*; Henderson, B. W.; Dougherty, T. J.; Eds.; *Photodynamic Therapy: Basic Principles and Clinical Applications*; Dekker: New York, 1992, 1–15.
12. Kick, G.; Messer, G.; Plewig, G. *Hautarzt* **1996**, *47*, 644–649.
13. Bonnett, R. *Chem. Soc. Rev.* **1995**, *24*, 19–33.
14. Bonnett, R. *Chemical Aspects of Photodynamic Therapy*; Gordon Breach Science: Amsterdam, 2000.
15. Ackroyd, R.; Kelty, C.; Brown, N.; Reed, M. *Photochem. Photobiol.* **2001**, *74*, 656–669.
16. Raab, O. *Z. Biol.* **1900**, *39*, 524–546.
17. Jesionek, A.; von Tappeiner, H. *Arch. Klin. Med.* **1905**, *82*, 223–227.
18. Lipson, R. L.; Baldes, E. J.; Olsen, A. M. *J. Natl. Cancer Inst.* **1961**, *26*, 1–11.
19. Diamond, I.; Granelli, S.; McDonagh, A. F.; Nielsen, S.; Wilson, C. B.; Jaenicke, R. *Lancet* **1972**, *ii*, 1175–1177.

20. Dougherty, T. J.; Kaufman, J. E.; Goldfarb, A.; Weishaupt, K. R.; Boyle, D.; Mittelman, A. *Cancer Res.* **1978**, *38*, 2628–2635.
21. Milgrom, L.; MacRobert, S. *Chem. Br.* **1998**, *34*(5), 45–52.
22. Bonnett, R. *Chemical Aspects of Photodynamic Therapy*; Gordon Breach Science: Amsterdam, 2000, pp 70–87.
23. Boyle, R. W.; Dolphin, D. *Photochem. Photobiol.* **1996**, *64*, 469–485.
24. Mazur, S.; Foote, C. S. *J. Am. Chem. Soc.* **1970**, *92*, 3225–3226.
25. Sternberg, E.; Dolphin, D. *Curr. Med. Chem.* **1996**, *3*, 239–272.
26. Bonnett, R. *Chemical Aspects of Photodynamic Therapy*; Gordon Breach Science: Amsterdam, 2000, pp 115–128.
27. Sommer, S.; Rimington, C.; Moan, J. *FEBS Letters* **1984**, *172*, 267–271.
28. Crone-Escanye, M. C.; Anghileri, L. J.; Robert, J. *J. Nucl. Med. Allied Sci.* **1988**, *32*, 237–241.
29. Wong, D. W.; Mandal, A.; Reese, I. C.; Brown, J.; Siegler, R. *Int. J. Nucl. Med. Biol.* **1983**, *10*, 211–218.
30. Kreimer-Birnbaum, M. *Semin. Hematol.* **1989**, *26*, 157–173.
31. Reddi, E.; Jori, G.; Rodgers, M. A. J.; Spikes, J. D. *Photochem. Photobiol.* **1983**, *38*, 639–645.
32. Redmond, R. W.; Heihoff, K.; Braslavsky, S. E.; Truscott, T. G. *Photochem. Photobiol.* **1987**, *45*, 209–213.
33. Bonnett, R.; McGarvey, D. J.; Harriman, A.; Land, E. J.; Truscott, T. G.; Winfield, U.-J. *Photochem. Photobiol.* **1988**, *48*, 271–276.
34. In 2000 the commercial interests in this photosensitizer were acquired by Axcan Pharma (Mont-Saint-Hilaire, Quebec, Canada). www.axcan.com.
35. Peng, Q.; Warloe, T.; Berg, K.; Moan, J.; Kongshaug, M.; Giercksky, K.-E.; Nesland, J. M. *Cancer* **1997**, *79*, 2282–2308.
36. LEVULAN[®] was approved by the FDA in 1999 for the treatment of actinic keratosis, a precancerous condition of the skin caused by excessive light exposure. The compound has been commercialized by DUSA Pharmaceuticals Inc, Wilmington, MA. www.DUSApharma.com.
37. This photosensitizer and application have been commercialized jointly by QLT Inc. (Vancouver, Canada) and Novartis Ophthalmics (Bulach, Switzerland). FDA approval for the ophthalmological application was accorded in 2000. www.visudyne.com and www.qltinc.com.
38. For an appreciation in clinical and commercial terms, see Boehncke, W.-H. *Current Opinion Anti-Inflamm. Immunomod. Invest. Drugs* **1999**, *1*, 338–352.
39. Pangka, V. S.; Morgan, A. R.; Dolphin, D. *J. Org. Chem.* **1986**, *51*, 1094–1100.
40. Sternberg, E. D.; Dolphin, D.; Brückner, C. *Tetrahedron* **1998**, *54*, 4151–4202.
41. Aveline, B.; Hasan, T.; Redmond, R. W. *Photochem. Photobiol.* **1994**, *59*, 328–335.
42. Bonnett, R.; Ioannou, S.; White, R. D.; Winfield, U.-J.; Berenbaum, M. C. *Photobiochem. Photobiophys. Suppl.* **1987**, *45–56*.
43. Bonnett, R.; White, R. D.; Winfield, U.-J.; Berenbaum, M. C. *Biochem. J.* **1989**, *261*, 277–280.
44. Bonnett, R.; Charlesworth, P.; Djelal, B. D.; Foley, S.; McGarvey, D. J.; Truscott, T. G. *J. Chem. Soc., Perkin Trans.* **1999**, *2*, 325–328.
45. FOSCAN[®] was developed by Scotia Pharmaceuticals Ltd (Stirling, UK); the commercial interest in it was acquired in 2002 by Biolitec AG (Jena, Germany). www.biolitec.com.
46. Kadish, K. M.; Smith, K. M.; Guillard, R., Ed., *The Porphyrin Handbook: Vol. 1, Synthesis and Organic Chemistry*; Academic Press: San Diego, CA, 2000.
47. Shanmugathasan, S.; Edwards, C.; Boyle, R. W. *Tetrahedron* **2000**, *56*, 1025–1046.
48. Leznoff, C. C. Synthesis of metal-free phthalocyanines. In *Phthalocyanines Properties and Applications*; Leznoff, C. C., Lever, A. B. P., Eds., VCH: New York, 1989, Vol. 1, pp 1–54.
49. Ambroz, M.; Beeby, A.; MacRobert, A. J.; Simpson, M. S. C.; Svendsen, R. K.; Phillips, D. J. *Photochem. Photobiol. B: Biol.* **1991**, *9*, 87–95.
50. Stranadko, E. F.; Skobelkin, O. K.; Vorozhtsov, G. N.; Mironov, A. F.; Beshleul, S. E.; Markitchev, N. A.; Riabov, M. V. *Proc. SPIE* **1997**, *3191*, 253–262.
51. Buchler, J. W. Static coordination chemistry of metalloporphyrins. In *Porphyrins and Metalloporphyrins*, Smith, K. M., Ed.; Elsevier: Amsterdam, 1975, pp 157–231.
52. Buchler, J. W. Synthesis and properties of metalloporphyrins. In *The Porphyrins*; Dolphin, D., Ed., Academic Press: New York, 1978, Vol. I, pp 389–483.
53. Grant, C.; Hambright, P. *J. Am. Chem. Soc.* **1969**, *91*, 4195–4198.
54. Barrett, P. A.; Frye, D. A.; Linstead, R. P. *J. Chem. Soc.* **1938**, 1157–1163.
55. Badger, G. M.; Ward, A. D. *Aust. J. Chem.* **1964**, *17*, 649–660.
56. Bender, C. O.; Bonnett, R.; Smith, R. G. *J. Chem. Soc. C* **1970**, 1251–1257.
57. Berezin, B. D. *Coordination Compounds of Porphyrins and Phthalocyanines*; Vopian, V. G. Wiley: Chichester: UK, 1981, 189–208.
58. Phillips, J. N. *Rev. Pure Appl. Chem.* **1960**, *10*, 35–60.
59. Dempsey, B.; Lowe, M. B.; Phillips, J. N. In *Haematin Enzymes*, Falk, J. E., Lemberg, R., Morton, R. K., Eds.; Pergamon: London, 1961, p 29.
60. Falk, J. E. *Porphyrins and Metalloporphyrins*; Elsevier: Amsterdam, 1964, pp 33–34.
61. Winkelman, J. *Experientia* **1967**, *23*, 949–950.
62. Ben-Hur, E.; Clay, M. E.; Vicioso, E. F.; Antunez, A. R.; Rihter, B. D.; Kenney, M. E.; Oleinick, N. L. *Photochem. Photobiol.* **1992**, *55*, 231–237.
63. Brasseur, N.; Ouellet, R.; La Madeleine, C.; van Lier, J. E. *Br. J. Cancer* **1999**, *80*, 1533–1541.
64. Oleinick, N. L.; Antunez, A. R.; Clay, M. E.; Rihter, B. D.; Kenney, M. E. *Photochem. Photobiol.* **1993**, *57*, 242–247.
65. He, J.; Larkin, H. E.; Li, Y.-S.; Rihter, B. D.; Zaidi, S. I. A.; Rodgers, M. A. J.; Mukhtar, H.; Kenney, M. E.; Oleinick, N. L. *Photochem. Photobiol.* **1997**, *65*, 581–586.
66. Anderson, C. Y.; Freye, K.; Tubesing, K. A.; Li, Y.-S.; Kenney, M. E.; Mukhtar, H.; Elmets, C. A. *Photochem. Photobiol.* **1998**, *67*, 332–336.
67. Kalyanasundaram, K.; Neumann-Spallart, M. *J. Phys. Chem.* **1982**, *86*, 5163–5169.
68. White, W. I. Aggregation of porphyrins and metalloporphyrins. In *The Porphyrins*; Dolphin, D., Ed., Academic Press: New York, 1978, Vol. V, pp 303–339.

69. Hunter, C. A.; Sanders, J. K. M. *J. Am. Chem. Soc.* **1990**, *112*, 5525–5534.
70. Bonnett, R.; Djelal, B. D.; Nguyen, A. J. *Porphyryns Phthalocyanines* **2001**, *5*, 652–661.
71. Wagner, J. R.; Ali, H.; Langlois, R.; Brasseur, N.; van Lier, J. E. *Photochem. Photobiol.* **1987**, *45*, 587–594.
72. MacRobert, A. J.; Phillips, D. *Chem. Ind.* **1992**, 17–20.
73. For a review of absorption and emission spectroscopy of porphyrins and metalloporphyrins, see Gouterman, M. Optical spectra and electronic structure of porphyrins and related rings. In *The Porphyrins*; Dolphin, D., Ed., Academic Press: New York 1978, Vol. III, pp 1–165.
74. Eisner, U.; Lichtarowitz, A.; Linstead, R. P. *J. Chem. Soc.* **1957**, 733–739.
75. Buchler, J. W.; Eikermann, G.; Puppe, L.; Rohbock, K.; Schneehage, H. H.; Weck, D. *Liebigs Ann. Chem.* **1971**, *745*, 135–151.
76. Bonnett, R.; Dimsdale, M. J. *J. Chem. Soc., Perkin Trans. 1* **1972**, 2540–2548.
77. Buchler, J. W.; Puppe, L. *Liebigs Ann. Chem.* **1970**, *740*, 142–163.
78. Buchler, J. W.; Puppe, L. *Liebigs Ann. Chem.* **1974**, 1046–1062.
79. Stillman, M. J.; Nyokong, T. Absorption and magnetic circular dichroism properties of phthalocyanines. Part 1: Complexes of the dianion Pc(-2). In *Phthalocyanine Properties and Application*; Leznoff, C. C., Lever, A. B. P., Eds., VCH: New York, 1989, Vol. 1, 133–289.
80. Quimby, D. J.; Longo, F. R. *J. Am. Chem. Soc.* **1975**, *97*, 5111–5117.
81. Eastwood, D.; Gouterman, M. *J. Mol. Spectros.* **1970**, *35*, 359–375.
82. Brannon, J. H.; Magde, D. *J. Am. Chem. Soc.* **1980**, *102*, 62–65.
83. Average values from Wilkinson, F.; Helman, W. P.; Ross, A. B. *J. Phys. Chem. Ref. Data* **1993**, *22*, 113–262.
84. Venediktov, E. A.; Krasnovsky, A. A., Jr. *Zh. Prikl. Spektrosk.* **1982**, *36*, 152–154.
85. Dzhagorov, B. M.; Salokhiddinov, K. I.; Egorova, G. D.; Gurinovich, G. P. *Russ. J. Phys. Chem.* **1987**, *61*, 1281–1283.
86. Keene, J. P.; Kessel, D.; Land, E. J.; Redmond, R. W.; Truscott, T. G. *Photochem. Photobiol.* **1986**, *43*, 117–120.
87. Vrlhac, J. B.; Gaudemer, A.; Kraljic, I. *Nouv. J. Chim.* **1984**, *8*, 401–406.
88. Kamath, S. S.; Shukla, S.; Srivastava, T. S. *Bull. Chem. Soc. Jpn.* **1991**, *64*, 1351–1358.
89. Rosenthal, I.; Krishna, C. M.; Riesz, P.; Ben-Hur, E. *Radiat. Res.* **1986**, *107*, 136–142.
90. Davila, J.; Harriman, A. *Photochem. Photobiol.* **1990**, *51*, 9–19.
91. Milanesio, M. E.; Alvarez, M. G.; Yslas, E. I.; Borsarelli, C. D.; Silber, J. J.; Rivarola, V.; Durantini, E. N. *Photochem. Photobiol.* **2001**, *74*, 14–21.
92. Morgan, A. R.; Gupta, S. *Tetrahedron Lett.* **1994**, *35*, 5347–5350.
93. Hampton, J. A.; Skalkos, D.; Taylor, P. M.; Selman, S. H. *Photochem. Photobiol.* **1993**, *58*, 100–105.
94. Skalkos, D.; Hampton, J. A.; Keck, R. W.; Wagoner, M.; Selman, S. H. *Photochem. Photobiol.* **1994**, *59*, 175–181.
95. Garbo, G. M.; Fingar, V. H.; Weiman, T. J.; Noakes, E. B. III; Haydon, P. S.; Cerrito, P. B.; Kessel, D. H.; Morgan, A. R. *Photochem. Photobiol.* **1998**, *68*, 561–568.
96. Felton, R. H. Primary redox reactions of metalloporphyrins. In *The Porphyrins*; Dolphin, D., Ed.; Academic Press: New York, 1978, Vol. V, pp 53–125.
97. Bonnett, R.; Martinez, G. *Tetrahedron* **2001**, *57*, 9513–9547.
98. Mang, T. S.; Dougherty, T. J.; Potter, W. R.; Boyle, D. G.; Jones, S.; Moan, J. *Photochem. Photobiol.* **1987**, *45*, 501–506.
99. Spikes, J. D.; Bommer, J. C. *Photochem. Photobiol.* **1993**, *58*, 346–350.
100. Kessel, D.; Morgan, A.; Garbo, G. M. *Photochem. Photobiol.* **1991**, *54*, 193–196.
101. Isele, U.; Schieweck, K.; Kessler, R.; van Hoogevest, P.; Capraro, H.-G. *J. Pharm. Sci.* **1995**, *84*, 166–173.
102. Richter, A. M.; Cerruti-Sola, S.; Sternberg, E. D.; Dolphin, D.; Levy, J. G. *J. Photochem. Photobiol. B: Biol.* **1990**, *5*, 231–244.
103. Labib, A.; Lenaerts, V.; Chouinard, F.; Leroux, J. C.; Ouellet, R.; van Lier, J. E. *Pharm. Res.* **1991**, *8*, 1027–1031.
104. Allison, B. A.; Waterfield, E.; Richter, A. M.; Levy, J. G. *Photochem. Photobiol.* **1991**, *54*, 709–715.
105. Smith, K. M.; Goff, D. A.; Simpson, D. J. *J. Am. Chem. Soc.* **1985**, *107*, 4946–4954.
106. Ma, L.; Dolphin, D. *Tetrahedron* **1996**, *52*, 849–860.
107. Bonnett, R. *Chem. Soc. Rev.* **1995**, *24*, 184.
108. Mironov, A. F.; Efremov, A. V. Recovery and Purification of Bacteriochlorophyll a from Purple Bacteria. Russ. Patent RU 2,144,085, 2000; *Chem. Abstr.* **2001**, *135*, 18611.
109. Mironov, A. F.; Kozyrev, A. N.; Perepyolkin, P. Y. *Proc. SPIE* **1994**, *2078*, 186–192.
110. Mironov, A. F. *Proc. SPIE* **1995**, *2625*, 23–32.
111. Henderson, B. W.; Sumlin, A. B.; Owczarczak, B. L.; Dougherty, T. J. *J. Photochem. Photobiol. B: Biol.* **1991**, *10*, 303–313.
112. Fiedor, J.; Fiedor, L.; Kammhuber, N.; Scherz, A.; Scheer, H. *Photochem. Photobiol.* **2002**, *76*, 145–152.
113. Rosenbach-Belkin, V.; Chen, L.; Fiedor, L.; Tregub, I.; Pavlitsky, F.; Brumfeld, V.; Salomon, Y.; Scherz, A. *Photochem. Photobiol.* **1996**, *64*, 174–181.
114. Eichwurzel, I.; Stiel, H.; Teuchner, K.; Leupold, D.; Scheer, H.; Salomon, Y.; Scherz, A. *Photochem. Photobiol.* **2000**, *72*, 204–209.
115. Zilberstein, J.; Schreiber, S.; Bloemers, M. C. W. M.; Bendel, P.; Neeman, M.; Schechtman, E.; Kohen, F.; Scherz, A.; Salomon, Y. *Photochem. Photobiol.* **2001**, *73*, 257–266.
116. Gross, S.; Brandis, A.; Chen, L.; Rosenbach-Belkin, V.; Roehrs, S.; Scherz, A.; Salomon, Y. *Photochem. Photobiol.* **1997**, *66*, 872–878.
117. Valles, M. A.; Biolo, R.; Bonnett, R.; Canete, L.; Gomez, A. M.; Jori, G.; Juarranz, A.; McManus, K. A.; Okolo, K. T.; Soncin, M.; Villaneuva, A. *Proc. SPIE* **1996**, *2625*, 11–22.
118. Stiel, H.; Teuchner, K.; Paul, A.; Freyer, W.; Leupold, D. *J. Photochem. Photobiol. A: Chem.* **1994**, *80*, 289–298.
119. Mitzel, F.; FitzGerald, S.; Beeby, A.; Faust, R. *Chem. Commun.* **2001**, 2596–2597.
120. Fuhrhop, J.-H.; Mauzerall, D. *Photochem. Photobiol.* **1971**, *13*, 453–458.
121. Fuhrhop, J.-H.; Wasser, P. K. W.; Subramanian, J.; Schrader, U. *Liebigs Ann. Chem.* **1974**, 1450–1466.
122. Cavaleiro, J. A. S.; Neves, M. G. P. S.; Hewlins, M. J. E.; Jackson, A. H. *J. Chem. Soc., Perkin Trans. 1* **1990**, 1937–1943.

123. Shannon, A. D. *Acta Cryst.* **1976**, *A32*, 751–767.
124. Buchler, J. W.; De Cian, A.; Fischer, J.; Kihn-Botulinski, M.; Paulus, H.; Weiss, R. *J. Am. Chem. Soc.* **1986**, *108*, 3652–3659.
125. Buchler, J. W.; Löffler, J.; Wicholas, M. *Inorg. Chem.* **1992**, *31*, 524–526.
126. Schaverien, C. J.; Orpen, A. G. *Inorg. Chem.* **1991**, *30*, 4968–4978.
127. Hambright, P.; Adams, C.; Vernon, K. *Inorg. Chem.* **1988**, *27*, 1660–1662.
128. Sessler, J. L.; Weghorn, S. J. *Expanded, Contracted and Isomeric Porphyrins*; Pergamon: Oxford, 1997, pp 385–503.
129. Sessler, J. L.; Johnson, M. R.; Lynch, V. J. *Org. Chem.* **1987**, *52*, 4394–4397.
130. Young, S. W.; Woodburn, K. W.; Wright, M.; Mody, T. D.; Fan, Q.; Sessler, J. L.; Dow, W. C.; Miller, R. A. *Photochem. Photobiol.* **1996**, *63*, 892–897.
131. Sessler, J. L.; Hemmi, G.; Mody, T. L.; Murai, T.; Burrell, A.; Young, S. W. *Acc. Chem. Res.* **1994**, *27*, 43–50.
132. Mody, T. D.; Sessler, J. L. *J. Porphyrins Phthalocyanines* **2001**, *5*, 134–142. The texaphyrin drugs are being developed by Pharmacyclics Inc., Sunnyvale, CA. Motexafin lutetium **32** is being formulated under three proprietary names: LUTRIN[®] for cancer; ANTRIN[®] for atherosclerotic lesions; and OPTRIN[®] for ophthalmological applications.
133. Motexafin gadolinium is being developed under the name XCYTRIN[®] for the enhancement of X-radiation. www.pyc.com.
134. Sessler, J. L.; Mody, T. D.; Lynch, V. J. *Am. Chem. Soc.* **1993**, *115*, 3346–3347.
135. Sessler, J. L.; Mody, T. D.; Hemmi, G. W.; Lynch, V. *Inorg. Chem.* **1993**, *32*, 3175–3187.
136. Grossweiner, L. I.; Bilgin, M. D.; Berdusis, P.; Mody, T. D. *Photochem. Photobiol.* **1999**, *70*, 138–145.
137. Woodburn, K. W.; Fan, Q.; Miles, D. R.; Kessel, D.; Luo, Y.; Young, S. W. *Photochem. Photobiol.* **1997**, *65*, 410–415.
138. Zellweger, M.; Radu, A.; Monnier, P.; van den Bergh, H.; Wagnières, G. *J. Photochem. Photobiol. B: Biol.* **2000**, *55*, 56–62.
139. Hammer-Wilson, M. J.; Akian, L.; Espinosa, J.; Kimel, S.; Berns, M. W. *J. Photochem. Photobiol. B: Biol.* **1999**, *53*, 44–52.
140. Bilgin, M. D.; Al-Akhras, M.-A.; Khalili, M.; Hemmati, H.; Grossweiner, L. I. *Photochem. Photobiol.* **2000**, *72*, 121–127.
141. Mody, T. D.; Sessler, J. L. *Perspec. Supramol. Chem.* **1999**, *4*, 245–294.
142. Lyon, R. C.; Faustino, P. J.; Cohen, J. S.; Katz, A.; Mornex, F.; Colcher, D.; Baglin, C.; Koenig, S. H.; Hambright, P. *Magn. Reson. Med.* **1987**, *4*, 24–33.
143. Takehara, Y.; Sakahara, H.; Masunaga, H.; Isogai, S.; Kodaira, N.; Takeda, H.; Saga, T.; Nakajima, S.; Sakata, I. *Br. J. Cancer* **2001**, *84*, 1681–1685.
144. Nakajima, S.; Shigemitsu, N.; Murakami, N.; Aburano, T.; Sakata, I.; Maruyama, I.; Inoue, M.; Takemura, T. *Anti-Cancer Drugs* **1997**, *8*, 386–390.
145. Nakajima, S.; Takemura, T.; Sakata, I. *Cancer Lett.* **1995**, *92*, 113–118.
146. Nakajima, S.; Yamauchi, H.; Sakata, I.; Hayashi, H.; Yamazaki, K.; Maeda, T.; Kubo, Y.; Samejima, N.; Takemura, T. *Nucl. Med. Biol.* **1993**, *20*, 231–237.
147. Rousseau, J.; Autenreith, D.; van Lier, J. E. *Int. J. Appl. Radiat. Isot.* **1983**, *34*, 571–579.
148. Subbarayan, M.; Shetty, S. J.; Srivastava, T. S.; Noronha, O. P. D.; Samuel, A. M. *J. Porphyrins Phthalocyanines* **2001**, *5*, 824–828.
149. Demas, J. N.; Diemente, D.; Harris, E. W. *J. Am. Chem. Soc.* **1973**, *95*, 6864–6865.
150. Wessels, J. M.; Foote, C. S.; Ford, W. E.; Rodgers, M. A. J. *Photochem. Photobiol.* **1997**, *65*, 96–102.
151. Onuki, J.; Ribas, A. V.; Medeiros, M. H. G.; Araki, K.; Toma, H. E.; Catalani, L. H.; Di Mascio, P. *Photochem. Photobiol.* **1996**, *63*, 272–277.
152. Fiel, R. J.; Howard, J. C.; Mark, E. H.; Datta Gupta, N. *Nucl. Acids Res.* **1979**, *6*, 3093–3118.
153. Armitage, B. *Chem. Rev.* **1998**, *98*, 1171–1200.
154. Ravanat, J.-L.; Cadet, J.; Araki, K.; Toma, H. E.; Medeiros, M. H. G.; Di Mascio, P. *Photochem. Photobiol.* **1998**, *68*, 698–702.
155. Hartmann, M.; Robert, A.; Duarte, V.; Keppler, B. K.; Meunier, B. *J. Biol. Inorg. Chem.* **1997**, *2*, 427–432.
156. Bossard, G. E.; Abrams, M. J.; Darkes, M. C.; Vollano, J. F.; Brooks, R. C. *Inorg. Chem.* **1995**, *34*, 1524–1527.
157. Charlesworth, P.; Truscott, T. G.; Brooks, R. C.; Wilson, B. C. *J. Photochem. Photobiol. B: Biol.* **1994**, *26*, 277–282.
158. Vollano, J. F.; Bossard, G. E.; Martellucci, S. A.; Darkes, M. C.; Abrams, M. J.; Brooks, R. C. *J. Photochem. Photobiol. B: Biol.* **1997**, *37*, 230–235.
159. Morgan, A. R.; Garbo, G. M.; Keck, R. W.; Selman, S. H. *Cancer Res.* **1988**, *48*, 194–198.
160. Foley, S.; Jones, G.; Liuzzi, R.; McGarvey, D. J.; Perry, M. H.; Truscott, T. G. *J. Chem. Soc., Perkin Trans. 2* **1997**, 1725–1730.
161. Maillard, P.; Krausz, P.; Gianotti, C.; Gaspard, S. *J. Organomet. Chem.* **1980**, *197*, 285–290.
162. Langlois, R.; Ali, H.; Brasseur, N.; Wagner, J. R.; van Lier, J. E. *Photochem. Photobiol.* **1986**, *44*, 117–123.
163. Busetti, A.; Soncin, M.; Reddi, E.; Rodgers, M. A. J.; Kenney, M. E.; Jori, G. *J. Photochem. Photobiol. B: Biol.* **1999**, *53*, 103–109.
164. Losev, A. P.; Knukshto, V. N.; Zhuravkin, I. N. *Proc. SPIE* **1994**, *2133*, 254–259.
165. Mantrova, E. Y.; Demcheva, M. V.; Savitsky, A. P. *Anal. Biochem.* **1994**, *219*, 109–114.
166. Fedorova, O. S.; Savitskii, A. P.; Shoikhet, K. G.; Ponomarev, G. V. *FEBS Lett.* **1990**, *259*, 335–337.
167. Yuan, W.; Jin, W.-J.; Dong, C. *Chem. Abstr.* **2001**, *135*, 192336.
168. Wiehe, A.; Stolberg, H.; Runge, S.; Paul, A.; Senge, M. O.; Röder, B. *J. Porphyrins Phthalocyanines* **2001**, *5*, 853–860.
169. Borisov, S. M.; Vasilev, V. V. *Zhur. Fiz. Khim.* **2001**, *75*, 2057–2062. (*Chem. Abstr.* 2002, *136*, 332666).
170. eg Scheer, H.; Kammhuber, N.; Scherz, A.; Brandis, A.; Salomon, Y. Synthesis and photodynamic activity of chlorophyll and bacteriochlorophyll esters. PCT Int. Appl. WO 01 40,232, 2001; (*Chem. Abstr.* 2001, *135*, 19494).
171. Huang, Z.; Chen, Q.; Stolberg, H.; Rutzel, F.; Luck, D.; Brun, P.-H.; Wilson, B.; Scherz, A.; Salomon, Y. In Abstracts, 30th Annual Meeting, American Society of Photobiology, Quebec City, Canada, July 13-17, 2002; Hastings, J. W., Program Chair; Abstract 102, p 35.
172. Schreiber, S.; Gross, S.; Brandis, A.; Harmelin, A.; Rosenbach-Belkin, V.; Scherz, A.; Salomon, Y. *Int. J. Cancer* **2002**, *99*, 279–285.

173. Vinogradov, S. A.; Wilson, D. F. *J. Chem. Soc., Perkin Trans. 2* **1995**, 103–111.
174. Finikova, O.; Cheprakov, A.; Beletskaya, I.; Vinogradov, S. A. *Chem. Commun.* **2001**, 261–262.
175. Vinogradov, S. A.; Wilson, D. F. *Adv. Exper. Med. Biol.* **1997**, *411*, 597–603.
176. Rogers, J. E.; Su, W.; Vinogradov, S. A.; Fleitz, P. A.; McLean, D. G. In Abstracts, 30th Annual Meeting, American Society of Photobiology, Quebec City, Canada, July 13–17, 2002; Hastings, J. W., Program Chair; Abstract 233, p 79.
177. Rogers, J. E., personal communication.
178. Vinogradov, S. A.; Wilson, D. F. Porphyrin compounds for imaging tissue oxygen. US Patent 6,363,175 B1, 2002.
179. Friedberg, J. S.; Skema, C.; Baum, E. D.; Burdick, J.; Vinogradov, S. A.; Wilson, D. F.; Horan, A. D.; Nachamkin, I. *J. Antimicrob. Chemother.* **2001**, *48*, 105–107.
180. Lawrence, D. S.; Whitten, D. G. *Photochem. Photobiol.* **1996**, *64*, 923–935.
181. Rihter, B. D.; Kenney, M. E.; Ford, W. E.; Rodgers, M. A. *J. Am. Chem. Soc.* **1993**, *115*, 8146–8152.
182. Bucking, M.; Gudgin Dickson, E. F.; Farahani, M.; Fischer, F.; Holmes, D.; Jori, G.; Kennedy, J. C.; Kenney, M. E.; Peng, X.; Pottier, R. H.; Weagle, G. *J. Photochem. Photobiol. B: Biol.* **2000**, *58*, 87–93.
183. Diddens, H.; Pottier, R. H. In Abstracts, 9th International Conference on Laser Applications in Life Sciences, Vilnius, Lithuania, 7–11 July, 2002; Juodka, B., Piskarskas, A., Conference Chairs; Abstract I6, p 45.
184. Freyer, W.; Flatau, S. *Tetrahedron Lett.* **1996**, *37*, 5083–5086.
185. Freyer, W.; Leupold, D. *J. Photochem. Photobiol. A: Chem.* **1997**, *105*, 153–158.
186. Freyer, W.; Stiel, H.; Hild, M.; Teuchner, K.; Leupold, D. *Photochem. Photobiol.* **1997**, *66*, 596–604.
187. Freyer, W.; Hild, M.; Stiel, H.; Leupold, D. *J. Inf. Recording* **1998**, *24*, 95–100.
188. Freyer, W.; Leupold, D. *J. Photochem. Photobiol. B: Biol.* **1995**, *30*, 77–78.
189. de Haas, R. R.; van Gijlswijk, R. P. M.; van der Tol, E. B.; Zijlmans, H. J. M. A. A.; Bakker-Schut, T.; Bonnett, J.; Verwoed, N. P.; Tanke, H. J. *J. Histochem. Cytochem.* **1997**, *45*, 1279–1292.
190. Brunner, H.; Maiterth, F.; Trettinger, B. *Chem. Ber.* **1994**, *127*, 2141–2149.
191. Brunner, H.; Obermeier, H. *Angew. Chem., Int. Ed. Engl.* **1994**, *33*, 2214–2215.
192. Brunner, H.; Obermeier, H.; Szeimies, R.-M. *Chem. Ber.* **1995**, *128*, 173–181.
193. Lottner, C.; Bart, K.-C.; Bernhardt, G.; Brunner, H. *J. Med. Chem.* **2002**, *45*, 2064–2078.
194. Bases, R.; Brodie, S. S.; Rubinfeld, S. *Cancer* **1958**, *11*, 259–263.
195. Skalkos, D.; Hampton, J. A. *Med. Chem. Res.* **1992**, *2*, 276–281.
196. Soncin, M.; Busetti, A.; Fusi, F.; Jori, G.; Rodgers, M. A. *J. Photochem. Photobiol.* **1999**, *69*, 708–712.
197. Tsuchida, T.; Usuda, J.; Okunaha, T.; Furakawa, K.; Kinoshita, K. In Abstracts, 30th Annual Meeting, American Society of Photobiology, Quebec City, Canada, July 13–17, 2002; Hastings, J. W., Program Chair; Abstract 37, p 12.
198. Lamola, A. A.; Piomelli, S.; Poh-Fitzpatrick, M. B.; Yamane, T.; Harber, L. C. *J. Clin. Invest.* **1975**, *56*, 1528–1535.
199. Cuzzo, G.; Gennari, G.; Jori, G.; Spikes, J. D. *Photochem. Photobiol.* **1977**, *25*, 389–395.
200. Lambert, C. R.; Reddi, E.; Spikes, J. D.; Rodgers, M. A. J.; Jori, G. *Photochem. Photobiol.* **1986**, *44*, 595–601.
201. Ghiggino, K. P.; Bennett, L. E.; Henderson, R. W. *Photochem. Photobiol.* **1988**, *47*, 65–72.
202. Toriya, M.; Yamamoto, M.; Saeki, K.; Fujii, Y.; Matsumoto, K. *Biosci. Biotechnol. Biochem.* **2001**, *65*, 363–370 (*Chem. Abstr.* 2001, *134*, 337676).
203. Boyle, R. W.; Johnson, C. K.; Dolphin, D. *J. Chem. Soc., Chem. Commun.* **1995**, 527–528.
204. Lacey, J. A.; Phillips, D.; Milgrom, L. R.; Yahsioglu, G.; Rees, R. D. *Photochem. Photobiol.* **1998**, *67*, 97–100.
205. Robinson, B. C.; Morgan, A. R. *Tetrahedron Lett.* **1993**, *34*, 3711–3714.
206. Smith, K. M.; Brown, S. B.; Troxler, R. F.; Lai, J.-J. *Photochem. Photobiol.* **1982**, *36*, 147–152.
207. Besecke, S.; Fuhrhop, J.-H. *Angew. Chem. Intl. Edn. Engl.* **1974**, *13*, 150–151.
208. Morgan, A. R.; Garbo, G. M.; Kreimer-Birnbaum, M.; Keck, R. W.; Chaudhuri, K.; Selman, S. H. *Cancer Res.* **1987**, *47*, 496–498.
209. Morgan, A. R.; Kreimer-Birnbaum, M.; Garbo, G. M.; Keck, R. W.; Selman, S. H. *Proc. SPIE* **1987**, *847*, 29–35.
210. Kozyrev, A. N.; Dougherty, T. J.; Pandey, R. K. *Tetrahedron Lett.* **1996**, *37*, 3781–3784.
211. Grewer, C.; Schermann, G.; Schmidt, R.; Völcker, A.; Brauer, H.-D.; Meier, A.; Montforts, F.-P. *J. Photochem. Photobiol. B: Biol.* **1991**, *11*, 285–293.
212. Amit, I.; Malik, Z.; Kessel, D. *Photochem. Photobiol.* **1999**, *69*, 700–702.
213. Smith, K. M.; Bisset, G. M. F.; Bushell, M. J. *Bioorg. Chem.* **1980**, *9*, 1–26.
214. Iturraspe, J.; Gossauer, A. *Helv. Chim. Acta* **1991**, *74*, 1713–1717.
215. Love, W. G.; Duk, S.; Biolo, R.; Jori, G.; Taylor, P. W. *Photochem. Photobiol.* **1996**, *63*, 656–661.
216. Polo, L.; Bianco, G.; Reddi, E.; Jori, G. *Int. J. Biochem. Cell Biol.* **1995**, *27*, 1249–1255.
217. Reddi, E.; Castro, G. L.; Biolo, R.; Jori, G. *Br. J. Cancer* **1987**, *56*, 597–600.
218. Valduga, G.; Pifferi, A.; Taroni, P.; Valentini, G.; Reddi, E.; Cubeddu, R.; Jori, G. *J. Photochem. Photobiol. B: Biol.* **1999**, *49*, 198–203.
219. Laroque, C.; Pelegrin, A.; van Lier, J. E. *Br. J. Cancer* **1996**, *74*, 1886–1890.
220. Valduga, G.; Nonell, S.; Reddi, E.; Jori, G.; Braslavsky, S. E. *Photochem. Photobiol.* **1988**, *48*, 1–5.
221. Hadjur, C.; Wagnieres, G.; Ihringer, F.; Monnier, P.; van den Bergh, H. *J. Photochem. Photobiol. B: Biol.* **1997**, *38*, 196–202.
222. van Leengoed, H. L. L. M.; Cuomo, V.; Versteeg, A. A. C.; van der Veen, N.; Jori, G.; Star, W. M. *Br. J. Cancer* **1994**, *69*, 840–845.
223. Visona, A.; Angelini, A.; Gobbo, S.; Bonanome, A.; Thiene, G.; Pagnan, A.; Tonello, D.; Bonandini, E.; Jori, G. *J. Photochem. Photobiol. B: Biol.* **2000**, *57*, 94–101.
224. Zavadnik, I. B.; Zavadnik, L. B.; Bryszewska, M. J. *J. Photochem. Photobiol. B: Biol.* **2002**, *67*, 1–10.
225. Fabris, C.; Valduga, G.; Miotto, G.; Borsetto, L.; Jori, G.; Garbisa, S.; Reddi, E. *Cancer Res.* **2001**, *61*, 7495–7500.
226. Villaneuva, A.; Dominguez, V.; Polo, S.; Vendrell, V. D.; Sanz, C.; Canete, M.; Juarranz, A.; Stockert, J. C. *Oncol. Res.* **1999**, *11*, 447–453.
227. Fu, Y.; Sima, P. D.; Kanofsky, J. R. *Photochem. Photobiol.* **1996**, *63*, 468–476.
228. Juarranz, A.; Espada, J.; Stockert, J. C.; Villaneuva, A.; Polo, S.; Dominguez, V.; Canete, M. *Photochem. Photobiol.* **2001**, *73*, 283–289.
229. Moan, J.; Iani, V.; Ma, L. W.; Peng, Q. *Proc. SPIE* **1996**, *2625*, 187–193.
230. Bonnett, R.; Martinez, G. *J. Porphyrins Phthalocyanines* **2000**, *4*, 544–550.

231. Leznoff, C.; D'Ascanio, A. M.; Yildiz, S. Z. *J. Porphyrins Phthalocyanines* **2000**, *4*, 103–111.
232. Hu, M.; Brasseur, N.; Yildiz, S. Z.; van Lier, J. E.; Leznoff, C. C. *J. Med. Chem.* **1998**, *41*, 1789–1802.
233. Rosenthal, I.; Ben-Hur, E.; Greenberg, S.; Concepcion-Lam, A.; Drew, D. M.; Leznoff, C. C. *Photochem. Photobiol.* **1987**, *46*, 959–963.
234. Ben-Hur, E.; Rosenthal, I.; Leznoff, C. C. *J. Photochem. Photobiol. B: Biol.* **1988**, *2*, 243–252.
235. Kassab, K.; Fabris, C.; DeFilippis, M. P.; Dei, D.; Fantetti, L.; Roncucci, G.; Reddi, E.; Jori, G. *J. Photochem. Photobiol. B: Biol.* **2000**, *55*, 128–137.
236. Gao, L.; Qian, X.; Zhang, L.; Zhang, Y. *J. Photochem. Photobiol. B: Biol.* **2001**, *65*, 35–38.
237. Maree, S. E.; Nyokong, T. *J. Porphyrins Phthalocyanines* **2001**, *5*, 782–792.
238. Cook, M. J.; Chambrier, I.; Cracknell, S. J.; Mayes, D. A.; Russell, D. A. *Photochem. Photobiol.* **1995**, *62*, 542–545.
239. Fabris, C.; Ometto, C.; Milanese, C.; Jori, G.; Cook, M. J.; Russell, D. A. *J. Photochem. Photobiol. B: Biol.* **1997**, *39*, 279–284.
240. Ometto, C.; Fabris, C.; Milanese, C.; Jori, G.; Cook, M. J.; Russell, D. A. *Br. J. Cancer* **1996**, *74*, 1891–1899.
241. Boyle, R. W.; Leznoff, C. C.; van Lier, J. E. *Br. J. Cancer* **1993**, *67*, 1177–1181.
242. Decreau, R.; Richard, M.-J.; Julliard, M. *J. Porphyrins Phthalocyanines* **2001**, *5*, 390–396.
243. Zhang, X.; Xu, H. *J. Chem. Soc., Faraday Trans.* **1993**, *89*, 3347–3351.
244. Oda, K.; Ogura, S.-I.; Okura, I. *J. Photochem. Photobiol. B: Biol.* **2000**, *59*, 20–25.
245. Bench, B. A.; Beveridge, A.; Sharman, W. M.; Diebold, G. J.; van Lier, J. E.; Gorun, S. M. *Angew. Chem., Int. Ed. Engl.* **2002**, *41*, 748–750.
246. Weber, J. H.; Busch, D. H. *Inorg. Chem.* **1965**, *4*, 469–471.
247. Li, Z.; van Lier, J. E.; Leznoff, C. C. *Can. J. Chem.* **1999**, *77*, 138–145.
248. Ali, H.; Langlois, R.; Wagner, J. R.; Brasseur, N.; Paquette, B.; van Lier, J. E. *Photochem. Photobiol.* **1988**, *47*, 713–717.
249. Bishop, S. M.; Khoo, B. J.; MacRobert, A. J.; Simpson, M. S. C.; Phillips, D.; Beeby, A. *J. Chromatogr.* **1993**, *646*, 345–350.
250. Kudrevich, S. V.; Ali, H.; van Lier, J. E. *J. Chem. Soc., Perkin Trans. 1* **1994**, 2767–2774.
251. Mellor, A.; Ossko, O. *Monatsh. Chem.* **1972**, *103*, 150–155.
252. Kudrevich, S.; Gilbert, S.; van Lier, J. E. *J. Org. Chem.* **1996**, *61*, 5706–5707.
253. Kudrevich, S.; Brasseur, N.; La Madeleine, C.; Gilbert, S.; van Lier, J. E. *J. Med. Chem.* **1997**, *40*, 3897–3904.
254. Brasseur, N.; Ali, H.; Langlois, R.; Wagner, J. R.; Rousseau, J.; van Lier, J. E. *Photochem. Photobiol.* **1987**, *45*, 581–586.
255. Margaron, P.; Grégoire, M.-J.; Scasnar, V.; Ali, H.; van Lier, J. E. *Photochem. Photobiol.* **1996**, *63*, 217–223.
256. Tabata, K.; Fukushima, K.; Oda, K.; Okura, I. *J. Porphyrins Phthalocyanines* **2000**, *4*, 278–284.
257. Drechsler, U.; Pfaff, M.; Hanack, M. *Eur. J. Org. Chem.* **1999**, 3441–3453.
258. Wood, S. R.; Holroyd, J. A.; Brown, S. B. *Photochem. Photobiol.* **1997**, *65*, 397–402.
259. Ball, D. J.; Mayhew, S.; Wood, S. R.; Griffiths, J.; Vernon, D. I.; Brown, S. B. *Photochem. Photobiol.* **1999**, *69*, 390–396.
260. Dummin, H.; Cernay, T.; Zimmermann, H. *J. Photochem. Photobiol. B: Biol.* **1997**, *37*, 219–229.
261. Jori, G.; Fabris, C. *J. Photochem. Photobiol. B: Biol.* **1998**, *43*, 181–185.
262. Minnock, A.; Vernon, D. I.; Schofield, J.; Griffiths, J.; Howard Parrish, J.; Brown, S. B. *J. Photochem. Photobiol. B: Biol.* **1996**, *32*, 159–164.
263. Gaspard, S.; Margaron, P.; Tempête, C.; Thi, T. H. T. *J. Photochem. Photobiol. B: Biol.* **1990**, *4*, 419–423.
264. Peeva, M.; Shopova, M.; Michelsen, U.; Wöhrle, D.; Petrov, G.; Diddens, H. *J. Porphyrins Phthalocyanines* **2001**, *5*, 645–651.
265. Sobbi, A. K.; Wöhrle, D.; Schlettwein, D. *J. Chem. Soc., Perkin Trans. 2* **1993**, 481–488.
266. Gu, Z.-W.; Spikes, J. D.; Kopeckova, P.; Kopecek, J. *Collect. Czech. Chem. Commun.* **1993**, *58*, 2321–2336.
267. Spikes, J. D.; van Lier, J. E.; Bommer, J. C. *J. Photochem. Photobiol. A: Chem.* **1995**, *91*, 193–198.
268. Margaron, P.; Tempête, C.; Dendane, Y.-M.; Gaspard, S.; Gianotti, C.; Werner, G.-H. *C. R. Acad. Sci. Paris* **1989**, *309(II)*, 1159–1164.
269. Yates, N. C.; Moan, J.; Western, A. *J. Photochem. Photobiol. B: Biol.* **1990**, *4*, 379–390.
270. McCubbin, I.; Phillips, D. *J. Photochem.* **1986**, *34*, 187–195.
271. Wöhrle, D.; Shopova, M.; Müller, S.; Milev, A. D.; Mantareva, V. N.; Krastev, K. K. *J. Photochem. Photobiol. B: Biol.* **1993**, *21*, 155–165.
272. Shopova, M.; Wöhrle, D.; Stoichkova, N.; Milev, A.; Mantareva, V.; Müller, S.; Kassabov, K.; Georgiev, K. *J. Photochem. Photobiol. B: Biol.* **1994**, *23*, 35–42.
273. Müller, S.; Mantareva, V.; Stoichkova, N.; Kliesch, H.; Sobbi, A.; Wöhrle, D.; Shopova, M. *J. Photochem. Photobiol. B: Biol.* **1996**, *35*, 167–174.
274. Michailov, N.; Peeva, M.; Angelov, I.; Wöhrle, D.; Müller, S.; Jori, G.; Ricchelli, F.; Shopova, M. *J. Photochem. Photobiol. B: Biol.* **1997**, *37*, 154–157.
275. Shopova, M.; Peeva, M.; Stoichkova, N.; Jori, G.; Wöhrle, D.; Petrov, G. *J. Porphyrins Phthalocyanines* **2001**, *5*, 798–802.
276. Morgan, A. R.; Petousis, N. H.; van Lier, J. E. *Eur. J. Med. Chem.* **1997**, *32*, 21–26.
277. Morgan, A. R.; Garbo, G. M.; Krivak, T.; Mastroianni, M.; Petousis, N. H.; St. Clair, T.; Weisenberger, M.; van Lier, J. E. *Proc. SPIE* **1991**, *1426*, 350–355.
278. Kudrevich, S. V.; Galpern, M. G.; van Lier, J. E. *Synthesis* **1994**, 779–781.
279. Kudrevich, S. V.; van Lier, J. E. *Coord. Chem. Rev.* **1996**, *156*, 163–182.
280. Montalban, A. G.; Meunier, H. G.; Ostler, R. B.; Barrett, A. G. M.; Hoffman, B. M.; Rumbles, G. *J. Phys. Chem. A* **1999**, *103*, 4352–4358.
281. Harriman, A.; Maiya, B. G.; Murai, T.; Hemmi, G.; Sessler, J. L.; Mallouk, T. E. *J. Chem. Soc., Chem. Commun.* **1989**, 314–316.
282. Curty, C.; Engel, N.; Iturraspe, J.; Gossauer, A. *Photochem. Photobiol.* **1995**, *61*, 552–556.
283. Sessler, J. L.; Murai, T.; Lynch, V.; Cyr, M. *J. Am. Chem. Soc.* **1988**, *110*, 5586–5588.

284. Sessler, J. L.; Hemmi, G.; Maiya, B. G.; Harriman, A.; Judy, M. L.; Boriak, R.; Matthews, J. L.; Ehrenberg, B.; Malik, Z.; Nitzan, Y.; Rück, A. *Proc. SPIE* **1991**, *1426*, 318–329.
285. Ehrenberg, B.; Roitman, L.; Lavi, A.; Nitzan, Y.; Malik, Z.; Sessler, J. L. *Proc. SPIE* **1994**, *2325*, 68–79.
286. Ehrenberg, B.; Malik, Z.; Nitzan, Y.; Ladan, H.; Johnson, F. M.; Hemmi, G.; Sessler, J. L. *Lasers Med. Sci.* **1993**, *8*, 197–203.
287. Venediktov, E. A.; Kitaev, V. I.; Berezin, B. D. *Russ. J. Phys. Chem.* **1987**, *61*, 1278–1280. (Transl. from *Zhur. Fiz. Khim.* **1987**, *61*, 2445–2449).
288. Morgan, L. R.; Chaudhuri, A.; Gillen, L. E.; Boyer, J. H.; Wolford, L. T. *Proc. SPIE* **1990**, *1203*, 253–265.
289. Rogers, M. A. T. *J. Chem. Soc.* **1943**, 590–596.
290. Killoran, J.; Allen, L.; Gallagher, J. F.; Gallagher, W. M.; O'Shea, D. F. *Chem. Commun.* **2002**, 1862–1863.
291. Solway, A. H.; Tjarks, W.; Barnum, B. A.; Rong, F.-C.; Barth, R. F.; Codogni, I. M.; Wilson, J. G. *Chem. Rev.* **1998**, *98*, 1515–1562.
292. Bregadze, V. I.; Sivaev, I. G.; Gabel, D.; Wöhrle, D. *J. Porphyrins Phthalocyanines* **2001**, *5*, 767–781.
293. For full spectroscopic characterization of some carborane derivatives of TPP, see Vicente, M. G. H.; Sheety, S. J.; Wickramasinghe, A.; Smith, K. M. *Tetrahedron Lett.* **2000**, *41*, 7623–7627. (TPP derivatives with up to 44% B).
294. For X-ray crystal structure see Vicente, M. G. H.; Nurco, D. J.; Sheety, S. J.; Medforth, C. J.; Smith, K. M. *Chem. Commun.* **2001**, 483–484.
295. Sessler, J. L.; Allen, W. E.; Kral, V. A. Preparation of highly boronated derivatives of expanded porphyrins (texaphyrins) for potential use in boron neutron capture therapy and related applications. US Patent 5,955,586, 1999; *Chem. Abstr.* **1999**, *131*, 222611.
296. Vicente, M. G. H.; Shetty, S. J.; Jaquinod, L.; Smith, K. M. Porphyrin-based neutron capture agents for cancer therapy. PCT Int. Patent Appl. WO 01 85,736, 2001; *Chem. Abstr.* **2001**, *135*, 365996.
297. Vicente, M. G. H.; Edwards, B. F.; Shetty, S. J.; Hou, Y.; Boggan, J. E. *Bioorg. Med. Chem.* **2002**, *10*, 481–492.
298. Kahl, S. B.; Koo, M.-S. *J. Chem. Soc., Chem. Commun.* **1990**, *24*, 1769–1771.
299. Hill, J. S.; Kahl, S. B.; Kaye, A. H.; Stylli, S. S.; Koo, M.-S.; Gonzales, M. F.; Vardaxis, N. J.; Johnson, C. I. *Proc. Natl. Acad. Sci. USA* **1992**, *89*, 1785–1789.
300. Spizzirri, P. G.; Hill, J. S.; Kahl, S. B.; Ghigginio, K. P. *Photochem. Photobiol.* **1996**, *64*, 975–983.
301. Ma, J.; Zhao, J.; Jiang, L. *New J. Chem.* **2001**, *25*, 847–852.
302. Ben-Hur, E.; Rosenthal, I. *Int. J. Radiat. Biol.* **1985**, *47*, 145–147.
303. Chan, W.-S.; Brasseur, N.; La Madeleine, C.; van Lier, J. E. *Eur. J. Cancer* **1997**, *33*, 1855–1859.
304. Rasch, M. H.; Tijssen, K.; van Steveninck, J.; Dubbelman, T. M. A. R. *Photochem. Photobiol.* **1996**, *64*, 586–593.
305. Paardekooper, M.; van Gompel, A. E.; van Steveninck, J.; van den Broek, P. J. A. *Photochem. Photobiol.* **1995**, *62*, 561–567.
306. Luo, Y.; Kessel, D. *Photochem. Photobiol.* **1997**, *66*, 479–483.
307. Daziano, J.-P.; Humeau, L.; Henry, M.; Mannoni, P.; Chanon, M.; Chabannon, C.; Julliard, M. *J. Photochem. Photobiol. B: Biol.* **1998**, *43*, 128–135.
308. Corbani, E. A.; Rodrigues, K. C.; Hage, R.; Duarte, J.; Silveira, L. Jr.; Villaverde, A. B.; Zangaro, R. A.; Pacheco, M. T. T. *Proc. SPIE* **2001**, *4244*, 434–441.
309. Linstead, R. P.; Weiss, F. T. *J. Chem. Soc.* **1950**, 2975–2981.
310. Paquette, B.; Ali, H.; Langlois, R.; van Lier, J. E. *Photochem. Photobiol.* **1988**, *47*, 215–220.
311. Phillips, D. *Prog. Reaction Kinetics* **1997**, *22*, 175–300.
312. Evensen, J. F.; Moan, J. *Photochem. Photobiol.* **1987**, *46*, 859–865.
313. Brasseur, N.; Ali, H.; Autenreith, D.; Langlois, R.; van Lier, J. E. *Photochem. Photobiol.* **1985**, *42*, 515–521.
314. Feofanov, A.; Grichine, A.; Karmakova, T.; Kazachkina, N.; Pecherskih, E.; Yakubovskaya, R.; Luk'yanets, E.; Derkacheva, V.; Egret-Charlier, M.; Vigny, P. *Photochem. Photobiol.* **2002**, *75*, 527–533.
315. Lee, C. C.; Pouge, B. W.; Strawbridge, R. R.; Moodie, K. L.; Bartholomew, L. R.; Burke, G. C.; Hoopes, P. J. *Photochem. Photobiol.* **2001**, *74*, 453–460.
316. Dhami, S.; Rumbles, G.; MacRobert, A. J.; Phillips, D. *Photochem. Photobiol.* **1997**, *65*, 85–90.
317. Oldham, T. C.; Phillips, D. *J. Photochem. Photobiol. B: Biol.* **2000**, *55*, 16–19.
318. Oldham, T. C.; Phillips, D. *J. Phys. Chem. B* **1999**, *103*, 9333–9349.
319. Cubeddu, R.; Pifferi, A.; Taroni, P.; Torricelli, A.; Valentini, G.; Comelli, D.; D'Andrea, C.; Angelini, V.; Canti, G. *Photochem. Photobiol.* **2000**, *72*, 690–695.
320. Peng, Q.; Moan, J.; Nesland, J. M.; Rimmington, C. *Int. J. Cancer* **1990**, *46*, 719–726.
321. Margaron, P.; Madanas, P.; Ouellet, R.; van Lier, J. E. *J. Chim. Phys.-Chim. Biol.* **1994**, *91*, 1219–1222.
322. Margaron, P.; Madanas, P.; Ouellet, R.; van Lier, J. E. *Anticancer Res.* **1996**, *16*, 613–620.
323. Chan, W.-S.; Brasseur, N.; La Madeleine, C.; van Lier, J. E. *Anticancer Res.* **1996**, *16*, 1887–1892.
324. Loh, C. S.; Bedwell, J.; MacRobert, A. J.; Krasner, N.; Phillips, D.; Bown, S. G. *Br. J. Cancer* **1992**, *66*, 452–462.
325. Allen, C. M.; Sharman, W. M.; La Madeleine, C.; van Lier, J. E.; Weber, J. M. *Photochem. Photobiol. Sci.* **2002**, *1*, 246–254.
326. Lacey, J. A.; Phillips, D. *Photochem. Photobiol. Sci.* **2002**, *1*, 378–383.
327. Wilson, M.; Burns, T.; Pratten, T. *J. Antimicrob. Chemother.* **1996**, *37*, 377–381.
328. Lacey, J. A.; Phillips, D. *J. Photochem. Photobiol. A: Chem.* **2001**, *142*, 145–150.
329. Barr, H.; Tralau, C. J.; Boulos, P. B.; MacRobert, A. J.; Krasner, N.; Phillips, D.; Bown, S. G. *Gastroenterology* **1990**, *98*, 1532–1537.
330. Moor, A. C. E.; Lagerberg, J. W. M.; Tijssen, K.; Foley, S.; Truscott, T. G.; Kochevar, I. E.; Brand, A.; Dubbelman, T. M. A. R.; van Steveninck, J. *Photochem. Photobiol.* **1997**, *66*, 860–865.
331. Moan, J.; Peng, Q.; Evensen, J. F.; Berg, K.; Western, A.; Rimmington, C. *Photochem. Photobiol.* **1987**, *46*, 713–721.
332. Peng, Q.; Nesland, J. M.; Moan, J.; Evensen, J. F.; Kongshaug, M.; Rimmington, C. *Int. J. Cancer* **1990**, *45*, 972–979.
333. Rück, A.; Heckelsmiller, K.; Kaufmann, R.; Grossman, N.; Haseroth, E.; Akgün, N. *Photochem. Photobiol.* **2000**, *72*, 210–216.
334. Agarwal, M. L.; Larkin, H. E.; Zaidi, S. J. A.; Mukhtar, H.; Oleinick, N. L. *Cancer Res.* **1993**, *53*, 5897–5902.
335. Singh, G.; Espiritu, M.; Shen, X. Y.; Hanlon, J. G.; Rainbow, A. J. *Photochem. Photobiol.* **2001**, *73*, 651–656.

336. Nishiwaki, H.; Zeimer, R.; Goldberg, M. F.; D'Anna, S. A.; Viores, S. A.; Grebe, R. *Photochem. Photobiol.* **2002**, *75*, 149–158.
337. Savitsky, A. P.; Lopatin, K. V.; Golubeva, N. A.; Poroshina, M. Y.; Chernyaeva, E. B.; Stepanova, N. V.; Solovieva, L. I.; Lukyanets, E. A. *J. Photochem. Photobiol. B: Biol.* **1992**, *13*, 327–333.
338. Carcenac, M.; Larroque, C.; Langlois, R.; van Lier, J. E.; Artus, J.-C.; Pèlerin, A. *Photochem. Photobiol.* **1999**, *70*, 930–936.
339. Vrouwenraets, M. B.; Visser, G. W. M.; Stigter, M.; Oppelaar, H.; Snow, G. B.; van Dongen, G. A. M. S. *Cancer Res.* **2001**, *61*, 1970–1975.
340. Urizzi, P.; Allen, C. M.; Langlois, R.; Ouellet, R.; La Madeleine, C.; van Lier, J. E. *J. Porphyrins Phthalocyanines* **2001**, *5*, 154–160.
341. Brasseur, N.; Langlois, R.; La Madeleine, C.; Ouellet, R.; van Lier, J. E. *Photochem. Photobiol.* **1999**, *69*, 345–352.
342. Allen, C. M.; Sharman, W. M.; La Madeleine, C.; Weber, J. M.; Langlois, R.; Ouellet, R.; van Lier, J. E. *Photochem. Photobiol.* **1999**, *70*, 512–523.
343. Qualls, M. M.; Thompson, D. H. *Int. J. Cancer* **2001**, *93*, 384–392.
344. Allen, C. M.; Langlois, R.; Sharman, W. M.; La Madeleine, C.; van Lier, J. E. *Photochem. Photobiol.* **2002**, *76*, 208–216.
345. Farrell, T. J.; Wilson, B. C.; Patterson, M. S.; Olivo, M. C. *Photochem. Photobiol.* **1998**, *68*, 394–399.
346. Edrei, R.; Kimel, S. *J. Photochem. Photobiol. B: Biol.* **1999**, *50*, 197–203.
347. Rokitskaya, T. I.; Block, M.; Antonenko, Y. N.; Kotova, E. A.; Pohl, P. *Biophys. J.* **2000**, *78* 2572–2580.
348. Korbelik, M. J. *Photochem. Photobiol. B: Biol.* **1993**, *20*, 173–181.
349. Edrei, R.; Gottfried, V.; van Lier, J. E.; Kimel, S. *J. Porphyrins Phthalocyanines* **1998**, *2*, 191–199.
350. Moan, J.; Iani, V.; Ma, L. W. *J. Photochem. Photobiol. B: Biol.* **1998**, *42*, 100–103.
351. Peng, Q.; Nesland, J. M.; Madslie, K.; Danielsen, H. E.; Moan, J. *Proc. SPIE* **1996**, *2628*, 102–113.
352. Peng, Q.; Moan, J. *Br. J. Cancer* **1995**, *72*, 565–574.
353. Mikhalenko, S. A.; Luk'yanets, E. A. *J. Gen. Chem. USSR* **1969**, *39*, 2495–2498. (Transl. from *Zhur. Obshch. Khim.* **1969**, *39*, 2554–2558).
354. Ford, W. E.; Rodgers, M. A. J.; Schechtman, L. A.; Sounik, J. R.; Rihter, B. D.; Kenney, M. E. *Inorg. Chem.* **1992**, *31*, 3371–3377.
355. Smetana, Z.; Mendelson, E.; Manor, J.; van Lier, J. E.; Ben-Hur, E.; Salzberg, S.; Malik, Z. *J. Photochem. Photobiol. B: Biol.* **1994**, *22*, 37–43.
356. Kogan, B. Y.; Butenin, A. V.; Kaliya, O. L.; Luk'yanets, E. A. *Proc. SPIE* **1996**, *2924*, 69–74.
357. Roberts, W. G.; Smith, K. M.; McCullough, J. L.; Berns, M. W. *Photochem. Photobiol.* **1989**, *49*, 431–438.
358. Maruyama, M.; Asano, T.; Uematsu, T.; Nakagohri, T.; Hasegawa, M.; Miyauchi, H.; Iwashita, C.; Tsuchiya, Y.; Isono, K. *Jpn. J. Cancer Res.* **1995**, *86*, 800–801.
359. Yumita, N.; Sasaki, K.; Umemura, S.; Nishigaki, R. *Jpn. J. Cancer Res.* **1996**, *87*, 310–316.
360. Sasaki, K.; Yumita, N.; Nishigaki, R.; Sakata, I.; Nakajima, S.; Umemura, S.-I. *Jpn. J. Cancer Res.* **2001**, *92*, 989–995.
361. Maruyama, M.; Asano, T.; Nakagohri, T.; Uematsu, T.; Hasegawa, M.; Miyauchi, H.; Iwashita, C.; Isono, K. *Anti-Cancer Res.* **1999**, *19*, 1989–1994.
362. Kamano, H.; Okamoto, K.; Sakata, I.; Kubota, Y.; Tanaka, T. *Transplant. Proc.* **2000**, *32*, 2442–2443.
363. Brasseur, N.; Ali, H.; Langlois, R.; van Lier, J. E. *Photochem. Photobiol.* **1987**, *46*, 739–744.
364. Lavallee, D. K.; Fawwaz, R. *Nucl. Med. Biol.* **1986**, *13*, 639–641.
365. Wheeler, B. L.; Nagasubramanian, G.; Bard, A. J.; Schechtman, L. A.; Dininny, D. R.; Kenney, M. E. *J. Am. Chem. Soc.* **1984**, *106*, 7404–7410.
366. Lowery, M. K.; Starshak, A. J.; Esposito, J. N.; Krueger, P. C.; Kenney, M. E. *Inorg. Chem.* **1965**, *4*, 128.
367. Joyner, R. D.; Kenney, M. E. *Inorg. Chem.* **1962**, *1*, 236–238.
368. Decreau, R. D.; Chanon, M.; Julliard, M. *Synlett* **1998**, 375–376.
369. Wöhrle, D.; Shopova, M.; Moser, J. G.; Kliesch, H.; Michelsen, U.; Müller, S.; Weitemyer, A. *Makromol. Symp.* **1996**, *105*, 127–138.
370. Zaidi, S. I. A.; Agarwal, R.; Eichler, G.; Rihter, B. D.; Kenney, M. E.; Mukhtar, H. *Photochem. Photobiol.* **1993**, *58*, 204–210.
371. Decreau, R.; Richard, M. J.; Verrando, P.; Chanon, M.; Julliard, M. *J. Photochem. Photobiol. B: Biol.* **1999**, *48*, 48–56.
372. Daziano, J.-P.; Steenken, S.; Chabannon, C.; Mannoni, P.; Chanon, M.; Julliard, M. *Photochem. Photobiol.* **1996**, *64*, 712–719.
373. Wöhrle, D.; Muller, S.; Shopova, M.; Mantareva, V.; Spassova, G.; Vietri, F.; Ricchelli, F.; Jori, G. *Photochem. Photobiol. B: Biol.* **1999**, *50*, 124–128.
374. Anderson, C.; Hrabovsky, S.; McKinley, Y.; Tubesing, K.; Tang, H.-P.; Dunbar, R.; Mukhtar, H.; Elmets, C. A. *Photochem. Photobiol.* **1997**, *65*, 895–901.
375. Zaidi, S. I. A.; Oleinick, N. L.; Zaim, M. T.; Mukhtar, H. *Photochem. Photobiol.* **1993**, *58*, 771–776.
376. Agarwal, R.; Korman, N. J.; Mohan, R. R.; Feyes, D. K.; Jawed, S.; Zaim, M. T.; Mukhtar, H. *Photochem. Photobiol.* **1996**, *63*, 547–552.
377. Colussi, V. C.; Feyes, D. K.; Mulvihill, J. W.; Li, Y.-S.; Kenney, M. E.; Elmets, C. A.; Oleinick, N. L.; Mukhtar, H. *Photochem. Photobiol.* **1999**, *69*, 236–241.
378. Separovic, D.; Mann, K. J.; Oleinick, N. L. *Photochem. Photobiol.* **1998**, *68*, 101–109.
379. Trivedi, N. S.; Wang, H.-W.; Nieminen, A.-L.; Oleinick, N. L.; Izatt, J. A. *Photochem. Photobiol.* **2000**, *71*, 634–639.
380. Xue, L.-Y.; Chiu, S.-M.; Oleinick, N. L. *Oncogene* **2001**, *20*, 3420–3427.
381. Useda, J.; Chiu, S.-M.; Azizuddin, K.; Xue, L.-Y.; Lam, M.; Nieminen, A.-L.; Oleinick, N. L. *Photochem. Photobiol.* **2002**, *76*, 217–223.
382. Verma, A.; Facchina, S. L.; Hirsch, D. J.; Song, S. Y.; Dillahey, L. F.; Williams, J. R.; Snyder, S. H. *Mol. Med.* **1998**, *4*, 40–45.
383. Morris, R. L.; Varnes, M. E.; Kenney, M. E.; Li, Y.-S.; Azizuddin, K.; McEnery, M. W.; Oleinick, N. L. *Photochem. Photobiol.* **2002**, *75*, 652–661.

384. Zhao, X.-J.; Lustigman, S.; Kenney, M. E.; Ben-Hur, E. *Photochem. Photobiol.* **1997**, *66*, 282–287.
385. Ben-Hur, E.; Zuk, M. M.; Chin, S.; Banerjee, D.; Kenney, M. E.; Horowitz, B. *Photochem. Photobiol.* **1995**, *62*, 575–579.
386. Zmudska, B. Z.; Strickland, A. G.; Beer, J. Z.; Ben-Hur, E. *Photochem. Photobiol.* **1997**, *65*, 461–464.
387. Ben-Hur, E.; Chan, W. S.; Yim, Z.; Zuk, M. M.; Dayal, V.; Roth, N.; Heldman, E.; Lazo, A.; Valeri, C. R.; Horowitz, B. *Dev. Biol.* **2000**, *102*, 149–155.
388. Rywkin, S.; Ben-Hur, E.; Malik, Z.; Prince, A. M.; Li, Y.-S.; Kenney, M. E.; Oleinick, N. L.; Horowitz, B. *Photochem. Photobiol.* **1994**, *60*, 165–170.
389. Firey, P. A.; Rodgers, M. A. J. *Photochem. Photobiol.* **1987**, *45*, 535–538.
390. Brasseur, N.; Nguyen, T.-L.; Langlois, R.; Ouellet, R.; Marengo, S.; Houde, D.; van Lier, J. E. *J. Med. Chem.* **1994**, *37*, 415–420.
391. Mantareva, V.; Shopova, M.; Spassova, G.; Wöhrle, D.; Muller, S.; Jori, G.; Richelli, F. *J. Photochem. Photobiol. B: Biol.* **1997**, *40*, 258–262.
392. Zuk, M. M.; Rihter, B. D.; Kenney, M. E.; Rodgers, M. A. J.; Kreimer-Birnbaum, M. *Photochem. Photobiol.* **1994**, *59*, 66–72. *Photochem. Photobiol.* **1996**, *63*, 132–140.
393. Soncin, M.; Buseti, A.; Biolo, R.; Jori, G.; Kwag, G.; Li, Y.-S.; Kenney, M. E.; Rodgers, M. A. J. *J. Photochem. Photobiol. B: Biol.* **1998**, *42*, 202–210.
394. Buseti, A.; Soncin, M.; Jori, G.; Kenney, M. E.; Rodgers, M. A. J. *Photochem. Photobiol.* **1998**, *68*, 377–381.
395. Marengo, S.; Houde, D.; Brasseur, N.; Nguyen, T. L.; Ouellet, R.; van Lier, J. E. *J. Chim. Phys. Phys.-Chim. Biol.* **1994**, *91*, 1211–1218.
396. Brasseur, N.; Nguyen, T. L.; Langlois, R.; Ouellet, R.; Marengo, S.; Houde, D.; van Lier, J. E. *J. Chim. Phys. Phys.-Chim. Biol.* **1994**, *91*, 1011–1017.
397. Joyner, R. D.; Kenney, M. E. *J. Am. Chem. Soc.* **1960**, *82*, 5790–5791.
398. Joyner, R. D.; Linck, R. G.; Esposito, J. N.; Kenney, M. E. *J. Inorg. Nucl. Chem.* **1962**, *24*, 299–302.
399. Capraro, H. G.; Schieweck, K.; Hilfiker, R.; Ochsner, M.; Isele, U.; van Hoogevest, P.; Naef, R.; Baumann, M. *Proc. SPIE* **1994**, *2078*, 158–164.
400. Schieweck, K.; Capraro, H. G.; Isele, U.; Batt, E.; Ochsner, M.; van Hoogevest, P.; Love, W. G. *Proc. SPIE* **1994**, *2078*, 165–170.
401. Cuomo, V.; Jori, G.; Rihter, B.; Kenney, M. E.; Rodgers, M. A. J. *Br. J. Cancer* **1991**, *64*, 93–95.
402. Soncin, M.; Polo, L.; Reddi, E.; Jori, G.; Kenney, M. E.; Cheng, G.; Rodgers, M. A. J. *Cancer Lett. (Shannon)* **1995**, *89*, 101–106.
403. Sounik, J. R.; Rihter, B. D.; Ford, W. E.; Rodgers, M. A. J.; Kenney, M. E. *Proc. SPIE* **1991**, *1426*, 340–348.
404. Emtestam, L.; Berglund, L.; Angelin, B.; Drummond, G. S.; Kappas, A. *Lancet* **1989**, 1231–1233.
405. This substance has been developed by Miravant Medical Technologies, Santa Barbara, California. www.miravant.com.
406. Morgan, A. R.; Tertel, N. C. *J. Org. Chem.* **1986**, *51*, 1347–1350.
407. Morgan, A. R.; Rampersaud, A.; Garbo, G. M.; Keck, R. W.; Selman, S. H. *J. Med. Chem.* **1989**, *32*, 904–908.
408. Woodward, R. B.; Ayer, W. A.; Beaton, J. M.; Bickelhaupt, F.; Bonnett, R.; Buchschacher, P.; Closs, G. L.; Dutler, H.; Hannah, J.; Hauck, F. P.; Ito, S.; Langemann, A.; Le Goff, E.; Leimgruber, W.; Lwowski, W.; Sauer, J.; Valenta, Z.; Volz, H. *Tetrahedron* **1990**, *46*, 7599–7659.
409. Selman, S. H.; Keck, R. W.; Kondo, S.; Albrecht, D. *Proc. SPIE* **1999**, *3590*, 142–150.
410. Luo, Y.; Chang, C. K.; Kessel, D. *Photochem. Photobiol.* **1996**, *63*, 528–534.
411. Kessel, D.; Luo, Y.; Deng, Y.; Chang, C. K. *Photochem. Photobiol.* **1997**, *65*, 422–426.
412. Sekher, P.; Garbo, G. M. *J. Photochem. Photobiol. B: Biol.* **1993**, *20*, 117–125.

9.23

Coordination Complexes as Precursors for Semiconductor Films and Nanoparticles

P. O'BRIEN and N. L. PICKETT

University of Manchester, UK

9.23.1	INTRODUCTION	1006
9.23.1.1	Compound Semiconductors	1006
9.23.1.2	III–V Materials	1008
9.23.1.3	II–VI Materials	1008
9.23.1.4	Thin Films from Vapor-phase Deposition Techniques	1008
9.23.1.5	Precursor Volatility by Molecular Design	1011
9.23.1.6	New Delivery Approaches	1011
9.23.1.7	Related Deposition Techniques	1012
9.23.2	COORDINATION CHEMISTRY METHODS USED FOR PURIFICATION OF METAL ALKYL PRECURSORS: “ADDUCT PURIFICATION”	1012
9.23.2.1	Purification of Group 12 Metal Alkyls	1015
9.23.2.2	Purification of Group 13 Metal Alkyls	1017
9.23.2.3	Modified Adduct Purification Techniques	1019
9.23.3	PRECURSORS FOR FABRICATION OF II–VI THIN FILMS	1020
9.23.3.1	New Group 12 Precursors	1021
9.23.3.2	New Group 16 Precursors	1021
9.23.4	PRECURSORS FOR FABRICATION OF III–V THIN FILMS	1021
9.23.4.1	Aluminum Compounds	1022
9.23.4.2	Gallium Compounds	1023
9.23.4.3	Indium Compounds	1024
9.23.4.4	Nitrogen Compounds	1026
9.23.4.5	Phosphorus Compounds	1027
9.23.4.6	Antimony Compounds	1027
9.23.4.7	Arsenic Compounds	1027
9.23.5	SINGLE-MOLECULE APPROACH TO THE DEPOSITION OF COMPOUND SEMICONDUCTING MATERIALS BY MOCVD	1029
9.23.5.1	Single-molecule Precursors for II–VI Materials	1029
9.23.5.1.1	<i>Dialkyldichalcogenocarbamate compounds</i>	1029
9.23.5.1.2	<i>Asymmetric dialkyldichalcogenocarbamate precursors</i>	1031
9.23.5.1.3	<i>Lewis base adducts of bis(dialkyldithiocarbamate) compounds</i>	1031
9.23.5.1.4	<i>Mixed alkyl/dichalcogenocarbamate complexes</i>	1032
9.23.5.1.5	<i>Mixed alkyl/dichalcogenocarbamate complexes as precursors for ternary materials</i>	1033
9.23.5.1.6	<i>Monothiocarbamate and monothiocarboxylate compounds</i>	1033
9.23.5.1.7	<i>Other chalcogenide-based compounds</i>	1034
9.23.5.1.8	<i>Chalcogenide-based compounds with high volatility</i>	1034
9.23.5.1.9	<i>Thiophosphinates and related compounds</i>	1037
9.23.5.2	Single-molecule Precursors for III–V Compounds	1037
9.23.5.2.1	<i>Dimeric precursor compounds</i>	1039
9.23.5.2.2	<i>Monomeric precursor compounds</i>	1039
9.23.5.2.3	<i>Trimeric precursor compounds</i>	1040

9.23.5.3	Nitride Films from Single-molecule Precursors	1040
9.23.5.3.1	Group 13 azides as single-molecule precursors for nitrides	1041
9.23.5.4	III–VI Materials from Single-molecule Precursors	1044
9.23.5.5	IV–VI Materials from Single-molecule Precursors	1047
9.23.5.6	CuInS ₂ and Related Ternary Semiconductors	1047
9.23.6	PREPARATION OF NANODIMENSIONAL MATERIALS USING SINGLE-MOLECULE PRECURSORS	1048
9.23.6.1	Semiconductor Nanoparticles “Quantum Dots”	1048
9.23.6.2	Methods of Preparation of Semiconductor Nanoparticles	1049
9.23.6.3	Semiconductor Nanoparticles Produced from Single-molecule Precursors	1051
9.23.6.3.1	II–VI particles	1051
9.23.6.3.2	III–V particles	1053
9.23.6.3.3	II–V particles	1056
9.23.6.3.4	III–VI particles	1056
9.23.7	REFERENCES	1056

9.23.1 INTRODUCTION

In order to appreciate the need for precursor chemistry it is necessary to have some understanding of the kinds of functional devices that are manufactured by the modern electronics industry.¹ Solid-state lasers represent some of the more commonly available electronic devices and illustrate well the range of different inorganic materials required within one device. Solid-state lasers (Figure 1) are complex structures involving two- and three-dimensional fabrication of thin layers of different materials.² In preparing such devices there is a need for a number of materials with different electrical properties; for instance, along with layers of semiconductor materials, metalization (e.g., Au) may be needed to make electrical contacts, insulators (e.g., [CaFe₂]_n) are often required, and stable boundary layers to prevent interdiffusion may be needed (e.g., silicides).

9.23.1.1 Compound Semiconductors

Semiconductors are materials that contain a relatively small number of current carriers compared to conductors such as metals. Intrinsic semiconductors are materials in which electrons can be excited across a forbidden zone (bandgap) so that there are carriers in both the valence (holes, *p*-type) and conduction (electrons, *n*-type) bands. The crucial difference between a semiconductor and an insulator is the magnitude of the energy separation between the bands, called the bandgap (E_g). In the majority of useful semiconducting materials this is of the order of 1 eV; some common semiconductors are listed in Table 1.

At absolute zero semiconductors behave as insulators as there is insufficient thermal energy to promote electrons to the conduction band. In metals the bands overlap forming a continuum, which leads to high electron mobility and thus high conductivity. The biggest difference between the properties of metals and semiconductors is that for metals conductivity decreases with temperature, essentially because the scattering of carrier electrons within the material increases with temperature. However, in semiconductors, although scattering will still increase with temperature, the most important effect is the promotion of electrons to the conduction band; thus conductivity in general *increases* with temperature.

The majority of important semiconducting materials are isoelectronic with elemental silicon. Important semiconductor materials include the III–V (13–15) materials such as GaAs or InP, and II–VI (12–16) materials such as CdS or ZnSe (Table 1). These compound semiconductors are most often formed by combining elements displaced on either side of silicon by one place (i.e., III = Ga or In and V = N or As for a III–V material) or two places (i.e., II = Zn or Cd and VI = S or Se for a II–VI material) in the periodic table. Other materials are of specialist importance, especially ternary materials such as CuInE₂ (E = S and Se), which find applications in solar cell technologies, as do materials of III–VI composition such as In_xS_y, although their properties are often complicated by the potential for the formation of a wide range of similar phases.

One important feature of compound semiconductors is that their bands span a much wider range than that of elemental silicon and can therefore cover a wider range of the electromagnetic spectrum, in particular the visible region. Compound semiconductors are also more often “direct,” i.e., there is conservation of the wave vector for optical transitions, leading to allowed

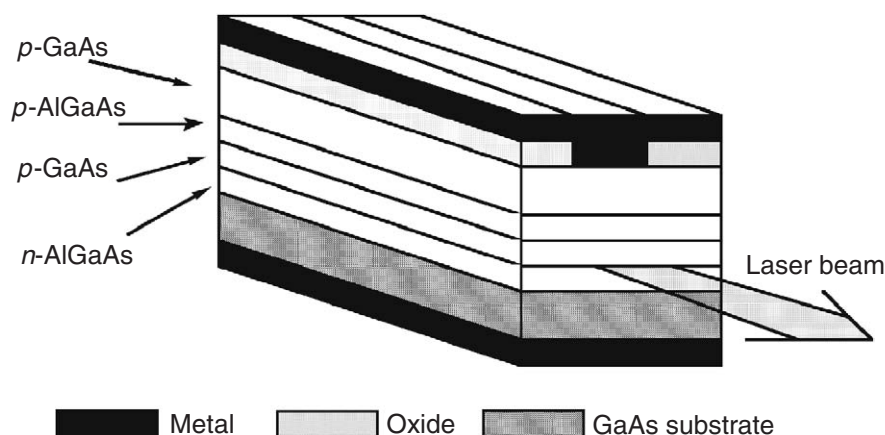


Figure 1 Stripe geometry laser in which the oxide layer isolates all but the stripe contact (stripe widths are usually in the region of 3–30 μm).

Table 1 Properties of some common compound semiconductors.

Compound	Band gap ^a (eV)	Type ^b	Structure	Lattice spacing (Å)	Applications
Si	1.11	i	Diamond	5.43	Integrated circuits, power electronics
Ge	0.67	i	Diamond	5.66	
III–V materials					
GaP	2.25	i	Zinc blende	5.450	LED
GaAs	1.43	d	Zinc blende	5.653	High-speed integrated circuits, displays
GaSb	0.69	d		6.095	Thermal imaging devices
InP	1.28	d	Zinc blende	5.8687	Transistor devices
InAs	0.36	d	Zinc blende	6.058	
InSb	0.17	d		6.4787	
II–VI materials					
CdS	2.53	d	Wurtzite	<i>a</i> : 4.136; <i>c</i> : 6.713	Photovoltaic cells
CdSe	1.74	d	Wurtzite	<i>a</i> : 4.299; <i>c</i> : 7.010	Photovoltaic cells
CdTe	1.50	d	Zinc blende	6.477	Photovoltaic cells, electrooptic modulators
ZnS	3.8	d	Wurtzite	<i>a</i> : 3.814; <i>c</i> : 6.257	Phosphors, infrared windows
ZnS	3.6	d	Zinc blende	5.406	
ZnSe	2.58	d	Zinc blende	5.667	Infrared windows, LEDs
ZnTe	2.28	d	Zinc blende	6.101	
IV–VI materials					
PbS	0.37	d	NaCl	5.936	Infrared sensors
PbSe	0.26	d	NaCl	6.124	Infrared sensors
PbTe	0.29	d	NaCl	6.460	Infrared sensors

^a At 300 K. ^b d, direct; i, indirect.

transitions with large absorption coefficients. (This contrasts with semiconductors where the lowest electronic transition between the valence and conduction bands is formally forbidden; these are said to have “indirect” bandgaps and normally have small absorption coefficients.) The most important semiconducting materials are probably those obtained by intentional doping, i.e., substituting into the correct lattice site an element containing one less electron which acts as

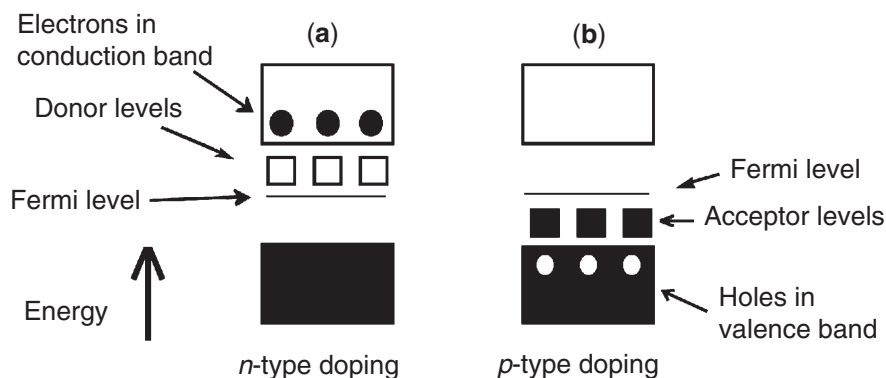


Figure 2 Schematic representation of how doping can lead to (a) *n*-type and (b) *p*-type semiconductors. Note that the exact position of the Fermi level is temperature-dependent.

an acceptor (an *n*-type dopant, such as N in ZnSe, or Zn or Cd in GaAs) or one extra electron which acts as a donor (a *p*-type dopant, such as S or Se in GaAs). Figures 2a and 2b show simple bandgap diagrams for *n*- and *p*-type materials, respectively.

9.23.1.2 III–V Materials

The applications of III–V materials represent a fairly well-developed area of technology. Most applications of such semiconductors are in the area of optoelectronics; there are many commercial processes for the manufacture of light-emitting diodes (LEDs) and solid-state lasers.³ Gallium arsenide solar cells are commonly used to power satellites. Development of LED and laser technologies for the blue end of the electromagnetic spectrum using gallium nitride is in progress at a number of research institutes and commercial corporations. The majority of III–V materials are direct bandgap materials; switching in these is faster than in indirect materials such as silicon. Complete device technologies based on direct bandgap materials has led to the production of devices faster than the equivalent ones fabricated from silicon—such as is needed in many wireless devices and applications.

9.23.1.3 II–VI Materials

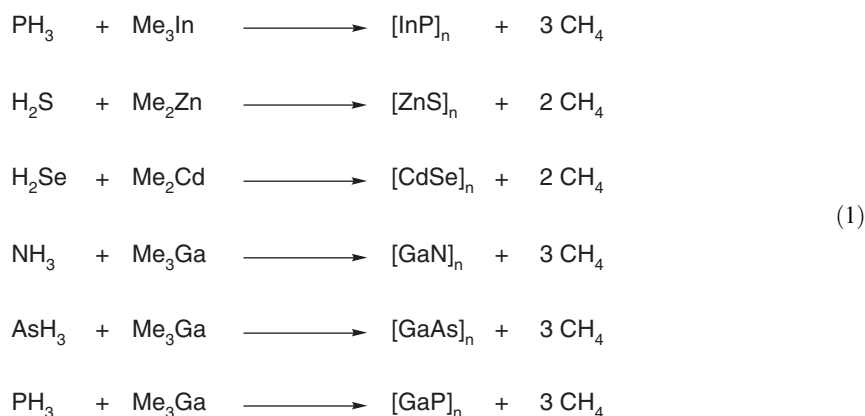
The wide-bandgap, direct-transition nature of II–VI materials is similar to that of the III–V materials, but the bandgap energies are in general larger and more suited to applications in optical and optoelectronic devices. II–VI compounds have generally been limited to simple applications as in optical coatings, gratings, or photoconductors. However, heteroepitaxial technologies have started to be developed and advances in chemical vapor deposition (CVD) techniques may open up new device fabrication methods for new applications. The principal II–VI compounds have structures closely related to that of ZnS and there is the possibility of growing both cubic and hexagonal phases during the deposition of thin layers. II–VI compounds are potentially important materials for the emission, detection, and modulation of light in the visible and near-UV region.^{4–6}

9.23.1.4 Thin Films from Vapor-phase Deposition Techniques

The fabrication of very thin layers of semiconducting materials was pioneered by Manasevit⁷ and involves the reaction of volatile chemical precursor species above, or at, the surface of a substrate, leading to the deposition of a solid phase. This is generally termed CVD, or—if a metal-containing species is involved—metal organic CVD (MOCVD). Metalorganic vapor-phase epitaxy (MOVPE), is a less general term and involves the use of organometallic precursors for growth of epitaxial single-crystal films, which have the same orientation as the single-crystal substrate on which the film is grown. Low-pressure MOVPE (LP-MOVPE) and photoassisted MOVPE (PA-MOVPE) are examples of process modifications which may be important in the growth of

compound semiconductor layers under more convenient reaction conditions, using simpler and cheaper chemical precursors. These terms are often used inaccurately in the literature; one reason for this perhaps being the interdisciplinary nature of the work, crossing the interface between materials science and conventional chemistry.

Ideally, an optimal deposition system will involve precursors, probably consisting of a sophisticated mixture of organometallic compounds, or a designed single-molecular species containing all the elements required within the material to be grown. These should decompose at a solid–vapor interface, to generate a solid phase. A full understanding of the factors controlling the growth of solid thin films in such systems will include: the design and characterization of precursor molecules; the study of the absorption of the precursor at an interface (i.e., on the substrates); an appreciation of the deposition mechanisms in the gas and solid phases, and at the substrate; and an understanding of the desorption of by-products. The overall chemical reactions involved are complex but may be represented in oversimplified ways, e.g., as shown in Equations (1).



The process of layer deposition is represented schematically in Figure 3 and can be summarized as follows:

- Mass transport of precursors in the bulk gas flow to the deposition zone (1).
- Gas-phase reaction in the stationary gas-phase boundary layer above the substrate (2).
- Mass transport of precursors through the boundary layer to the growth surface (3), on the substrate.
- Absorption of precursor on the substrate or growing film surface (4).
- Surface diffusion of the precursor to growth site (5).
- Surface chemical reaction leading to precursor deposition and film growth (6).
- Desorption of by-products (7).
- Mass transport of by-products (precursor ligands) into gas flow and out of reactor (8).

The mechanisms of the deposition process will be of crucial importance in determining the quality of the grown layers and when growth is optimal, with epitaxial layers grown, the process

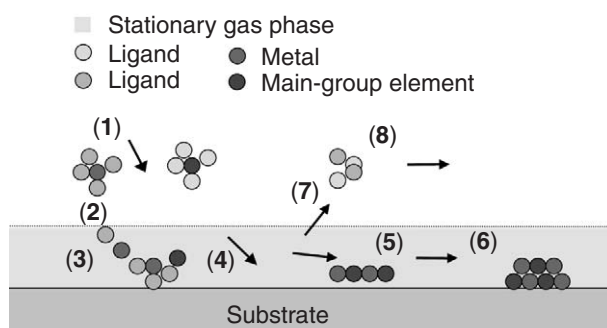


Figure 3 Outline of the stages involved in the chemical vapor deposition of precursors on a substrate.

must involve a surface-controlled reaction. The surface chemistry of such systems is under intense study and is beyond the scope of this chapter.⁸

Features common to all CVD reactors include: source evaporators with an associated gas handling system to control input gases and gas-phase precursor concentrations, a reactor cell with a susceptor heated by either radio frequency or infrared radiation, and an exhaust system to remove waste products (which may include a vacuum pump for low-pressure operations). Substrate temperatures can vary from less than 200 °C to temperatures in excess of 1000 °C, depending on the nature of the material layer and precursor used. Schematic diagrams of some simple CVD reactors are shown in Figure 4.

For a compound to be used as a successful precursor there are a number of criteria it must satisfy, including, for semiconductor thin films, the need for high purity. Of particular importance is the exclusion of extrinsic impurities acquired during precursor synthesis, especially if they can act as dopants.⁹ Other requirements include the need for compounds that decompose cleanly on the surface of a substrate without the incorporation of unwanted intrinsic impurities arising from elements present within the ligands used in the precursors (e.g., carbon from an alkyl group or fluoride from a substituted β -diketonate derivative). Other important criteria are that the compounds should have moderate vapor pressures, should volatilize quantitatively on heating, and should be stable for an adequate period of time in the gas phase at the volatilization temperature, but should decompose cleanly at the temperature of the substrate (this may only be a little higher than the temperature required to volatilize the precursor).¹⁰

Conventionally gases or volatile liquids are used as precursors. For gases, phosphine (PH₃), hydrogen sulfide (H₂S), and hydrogen selenide (H₂Se) are used to grow phosphide, sulfide, and selenide thin films, respectively. The conventional method is to use a cylinder containing the correct composition of the precursor(s) gases in conjunction with a thermal mass flow controller (MFC), to control the vapor-phase concentration.¹¹ The main criteria for successful and reproducible use are that the inlet pressure is greater than ca. 50 torr, the operating temperature at the mass flow controller is less than 60 °C, and the flow rate is greater than 0.1 scfm (standard cubic centimeters).

Conventionally, since the time of the original CVD work by Manasevit,⁷ group 12 (Zn, Cd) and 13 (Ga, In) precursors used were volatile, usually organometallic metal alkyl compounds (see later). The delivery of these volatile and sometimes pyrophoric liquid precursors has been dominated by the use of so-called “bubblers.” Typically, these are passivated stainless steel Dreschler bottles (Figure 5) containing the precursor. The precursor is delivered to the CVD reactor by entrainment with a carrier gas, which is fed through the liquid and ideally should become fully saturated with the precursor on passage through the bubbler. There are few problems with the use of moderately volatile liquids, i.e., those with equilibrium vapor pressures roughly in the range 5–30 torr at room temperature. There are, however, problems when using materials with very low or high vapor pressures and with the use of solids. To overcome these difficulties, liquids with low vapor pressures can be heated, using oil baths or thermal tape wrapped around the bubbler, which increases the equilibrium vapor pressure within the bubbler. However, there are two problems in using this technique. First, to prevent condensation of the precursor in other cooler parts of the CVD system it may become necessary to heat the entire

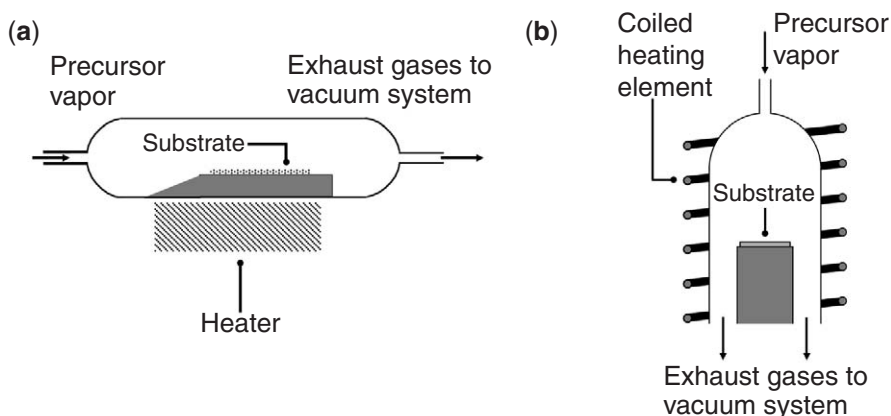


Figure 4 (a) Cold-wall CVD reactor with parallel vapor flow; (b) hot-wall CVD reactor with perpendicular vapor flow.

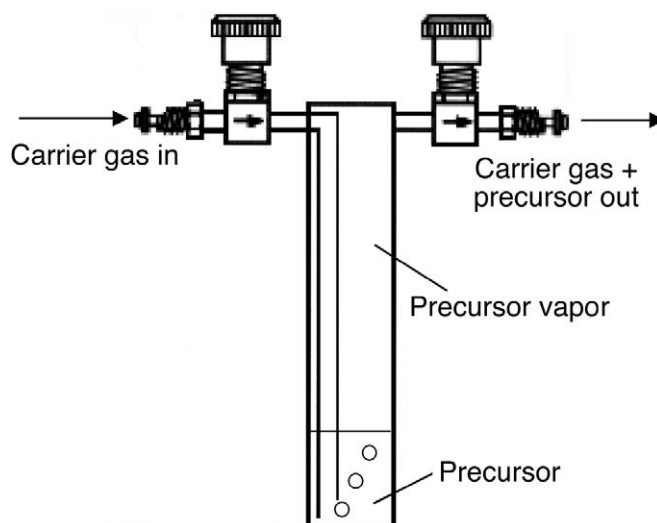


Figure 5 Dreschler bottle “bubbler” (made from passivated stainless steel).

network of feed lines upstream of the reactor chamber. Second, for delivery to be successful the precursors must have long-term stability at the elevated temperature employed. Precursors that are extremely volatile, having high vapor pressures, can also be difficult to control and in such cases it may be necessary to cool the bubbler. Solid precursors such as Me_3In have also been used. Most solid precursors have very low volatilities and thus suffer similar problems to those of low volatility liquid precursors in that the entire CVD system may have to be heated. Additionally, the surface area of solids in contact with the entraining gas may be insufficient for equilibrium to be established on passage of the carrier gas. Moreover, as the solid sublimates there will be a variation in the surface area leading to a variation in the rate of mass transport over time. Thus, for solids it is more difficult for equilibrium to be established under dynamic gas flow conditions within a bubbler. When using this CVD approach, therefore, only compounds with some degree of volatility can be considered as precursors.

Although a compound may be volatile, it may not necessarily lead to clean deposition. Since the late 1980s, new approaches to precursor delivery have allowed for a wider range of compounds to be considered as precursors. Compounds with very low or no volatility whatsoever, including many coordination compounds, can now be used as precursors.

9.23.1.5 Precursor Volatility by Molecular Design

A number of approaches whereby the precursor is designed and synthesized with the intention of improved volatility have been employed and include the use of bulky ligands to reduce the degree of intermolecular association. One problem with this strategy is that steric bulk is achieved by the incorporation of a large number of carbon and sometimes silicon atoms, leading in most cases to the incorporation of intrinsic elemental impurities into the thin films. Another method to increase volatility is to complete the coordination sphere about the central metal or main group atom, thus making the center coordinatively saturated, which prevents dimerization and further oligomerization from occurring. A third method is the use of fluorinated ligands, such as fluorinated β -diketones (Figure 6), so as to decrease intermolecular interactions and increase volatility.

9.23.1.6 New Delivery Approaches

A number of new approaches to the way in which precursors are delivered to a substrate have been developed in which the precursor is dispersed into the gas phase without having to be volatile. These new systems each have their own advantages for a particular precursor depending on its physical state. Most of the delivery systems in use can be classified as one of the following: a liquid injection system (LIS), where a precursor is vaporized directly from a neat liquid or solution containing the precursors; a solid delivery system (SDS), where the precursor is vaporized

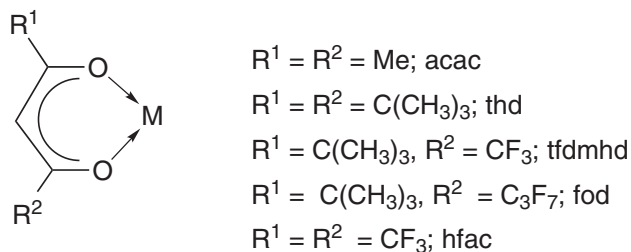


Figure 6 Derivatives of β -diketonates used as CVD precursors.

directly from a solid; or an aerosol-assisted delivery system (AADS), where an aerosol containing the precursor is formed prior to delivery. These methods rely, in principle, on the mechanical delivery of liquid-, solid-, or aerosol-containing precursors to a hot zone where they are (flash) vaporized into a dispersed precipitate in the gas phase, which is then delivered to the substrate via a carrier gas.

These new systems are not accurately encompassed by the true definition of CVD, but will be considered here as they are an important step in the evolution of thin-film deposition techniques. Using these new delivery methods the stability of the precursor, and its reproducible behavior with respect to the method of delivery, is fundamentally more important than its volatility. Moreover, the clean deposition of the precursor and the subsequent low levels of impurities and defects within the final material can now be considered of greater importance than volatility when choosing or designing a precursor compound.

These new techniques allow for the use of much less volatile compounds such as single-source precursors which contain all the elements that are required within the as-grown material. Thus, a much larger number of compounds (including many coordination complexes) can now be employed as precursors. Single-source precursors and nonvolatile coordination compounds potentially possess many advantages over conventional CVD precursors, such as being air and/or moisture insensitive (unlike most metal alkyls) and also having much lower toxicities (mainly due to low volatility).

9.23.1.7 Related Deposition Techniques

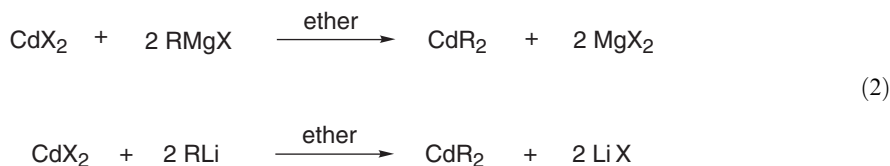
The deposition of a wide range of materials using beams of elemental sources in high-vacuum apparatus (10^{-4} – 10^{-8} torr), essentially by physical methods, is known as molecular beam epitaxy (MBE)^{8,12} and atomic layer epitaxy (ALE). These methods will be mentioned where there is an overlap with CVD techniques, but will not be fully reviewed. (They are mentioned also in Chapter 9.15).

9.23.2 COORDINATION CHEMISTRY METHODS USED FOR PURIFICATION OF METAL ALKYL PRECURSORS: "ADDUCT PURIFICATION"

As mentioned, the conventional approach to CVD is to use a volatile precursor compound. For thin-film compound semiconductors a metal alkyl precursor is often used, such as dialkylzinc/cadmium ($R_2\text{Zn}/\text{Cd}$) compounds as the group 12 source or trialkylindium/gallium ($R_3\text{In}/\text{Ga}$) as the group 13 source ($R = \text{Me}, \text{Et}, \text{Pr}^1$). The growth of high-quality semiconductor layers using CVD techniques requires the metal alkyls to be of ultrahigh purity.⁹ In conventional CVD growth of semiconductors the group 16 (for II–VI) and the group 15 (for III–V) precursors are usually gaseous hydrides, i.e., H_2S for sulfur, H_2Se for selenium, and NH_3 for nitrogen. These can be purified to ultrahigh standards using conventional gas purification methods. The volatile, sometimes pyrophoric group 12 and 13 precursors are somewhat harder to handle and purify.¹³

Metal alkyls can be prepared in a simple manner from the main group halides ($X = \text{Cl}, \text{Br}, \text{I}$) and the appropriate alkyl Grignard reagent (RMgI) or the alkyllithium salt (RLi), as shown for the cadmium alkyls (Equation (2)).¹³ The elimination of impurities from the precursor source is of great importance, as any remaining impurities are invariably carried over into the growing semiconductor layers. Incorporation of impurities, even at levels as low as 10^{15} free carriers per cubic centimeter (one part in ca. 10^7), can drastically affect the electronic properties of the

semiconductor or device in which it is incorporated. For example, alkyl halide impurities in the metal alkyl precursor will be incorporated into the films and can act as unwanted *n*-type dopants. Therefore, the removal from the metal alkyl of even trace amounts of starting material is imperative. The highly reactive, volatile, and sometimes toxic and/or pyrophoric nature of metal alkyls means that conventional methods for liquid purification, such as fractional distillation or low-temperature crystallization, are not feasible on a commercial scale:



The removal of impurities from metal alkyl precursors is achieved by a technique known as “adduct-purification” which can produce metal alkyls containing no impurities above the detection limits of inductively coupled plasma optical emission spectroscopy (ICPOES). This method is also thought safer, and in general gives larger recovery yields, than conventional purification techniques. Adduct purification involves the formation of an adduct between the metal alkyl (a Lewis acid), and a Lewis base. The resulting adduct is isolated from the solvent and solvent-soluble impurities by filtration, and then, after washing, is heated in a static vacuum above its dissociation temperature, when the free metal alkyl distils off and is collected in a cold trap. Thus, volatile impurities can be removed by evacuation of the isolated adduct at temperatures below its dissociation temperature, while nonvolatile impurities along with the free base remain when the adduct is dissociated, as outlined in Figure 7. For this method to be successful the base must have

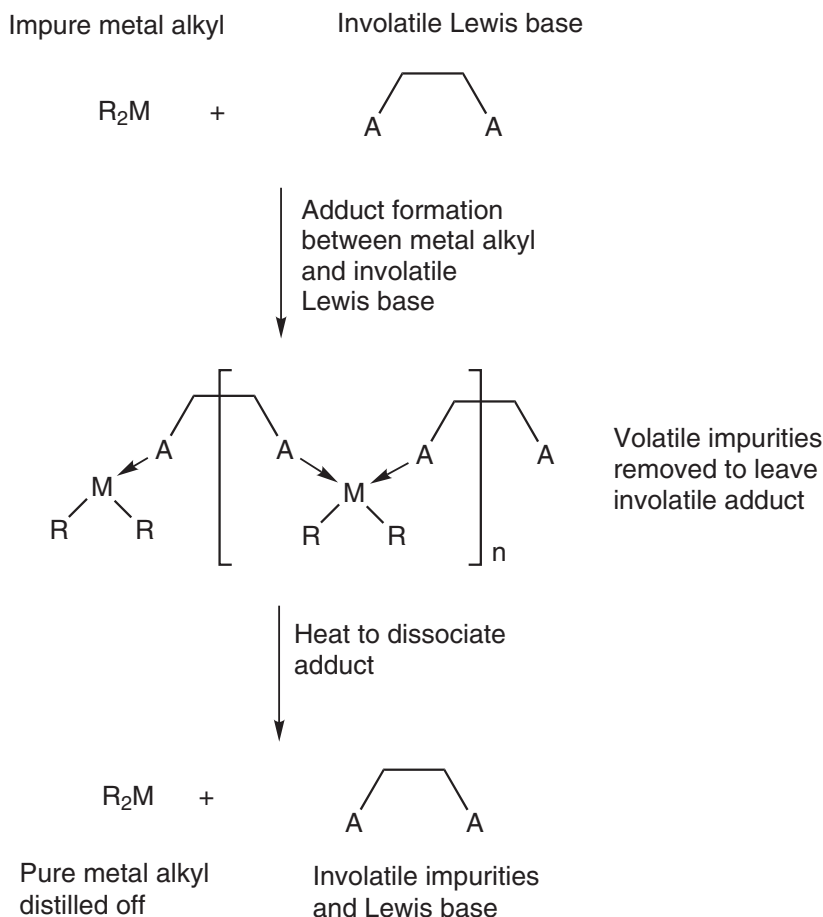


Figure 7 Outline of the “adduct purification” process.

low volatility at the adduct dissociation temperature, but must form a stable crystalline solid adduct which does not sublime under vacuum conditions. In order to avoid contamination of the purified product, it is important that the Lewis base and the resulting adduct both have a significantly lower volatility than the metal alkyl undergoing purification, and that the donor–acceptor adduct bond is sufficiently weak to allow thermal dissociation of the adduct under relatively mild conditions (i.e., at temperatures $<160^\circ\text{C}$). A further crucial requirement is that the donor ligand (Lewis base) used is of ultrahigh purity.

An advantage of the adduct purification method is that it combines chemical purification (forming an adduct) with physical purification when the purified metal alkyl is obtained by distillation, e.g., through a fractionating column.

A variety of donor ligands (Lewis bases) can be used in adduct purification, depending on the relative Lewis acidity and volatility of the metal alkyl in question. For example, group 13 trialkyls have been purified by distillation from high-boiling sterically hindered ethers¹⁴ or from phosphines¹⁵ or amines,¹⁶ while group 12 dialkyls have been purified using adducts with bidentate amines (Figure 8).

It has been established that oxygen contamination within thin films, especially aluminum-containing films such as $\text{Al}_x\text{In}_{(x-1)}\text{As}$, arises from trace amounts of ether (Et_2O) coordinated to the metal alkyl during the synthesis procedure.¹⁷ Moreover, the conventional synthesis uses ethers that cannot be completely removed using the adduct purification approach, especially in the case of aluminum which forms strong dative $\text{Al}-\text{O}$ bonds with oxygen. A new synthesis and adduct procedure has been employed which involves an ether-free synthesis using a trialkylamine, such as NEt_3 , as solvent. The pure base-free precursor is obtained by thermal dissociation of the adducts with poorly volatile tertiary amines.^{18,19}

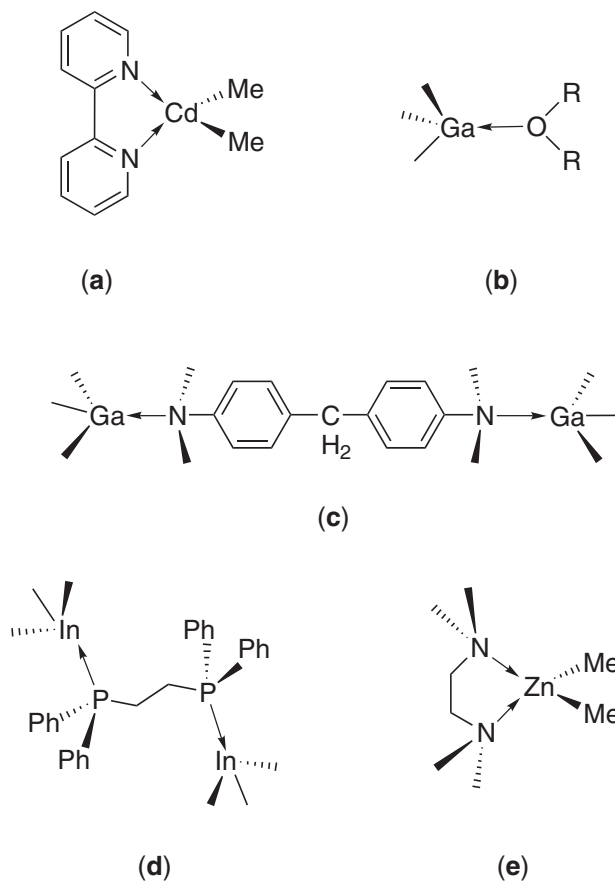


Figure 8 Molecular structures of (a) $[\text{Me}_2\text{Cd}(2,2'\text{-bipy})]$; (b) a generic trimethylgallium etherate; (c) $[\{\text{Me}_3\text{Ga}\}_2(\mu\text{-dppe})]$; (d) $[\{\text{Me}_3\text{In}\}_2(\mu\text{-MBDA})]$ (MBDA = 4,4'-methylene-bis(*N,N'*-dimethylaniline)); (e) $[\text{Me}_2\text{Zn}(\text{TMEDA})]$.

9.23.2.1 Purification of Group 12 Metal Alkyls

Zinc is a class A-type acceptor (a “hard” Lewis acid), and thus forms complexes (or adducts) more readily with oxygen and nitrogen than with heavier donors such as sulfur and phosphorus. However, Me_2Zn forms relatively unstable complexes with simple ethers; the bis-tetrahydrofuran adduct $[\text{Me}_2\text{Zn}(\text{THF})_2]$ is extensively dissociated in dilute benzene solution²⁰ and fully dissociated into its components in the vapor phase.²¹ Chelating diethers (e.g., 1,4-dioxan, 1,4-thioxan) form more stable adducts for which the parent chelating structures are shown in Figure 9, although these have also been shown to be essentially fully dissociated in the gas phase.²² Me_2Zn also forms 1:1 adducts with chelating bidentate nitrogen donors, such as tetramethylethylenediamine (TMEDA; Figure 8).²³

Me_2Zn has been reported to form both 1:1 and 1:2 complexes, $[\text{Me}_2\text{Zn}(\text{NR}_3)]$ and $[\text{Me}_2\text{Zn}(\text{NR}_3)_2]$, with simple trialkylamines. However, in benzene solution the bis-triethylamine adduct $[\text{Me}_2\text{Zn}(\text{NEt}_3)_2]$ has been shown to exist as a mixture of the 1:1 adduct $[\text{Me}_2\text{Zn}(\text{NEt}_3)]$ and free NEt_3 .²⁴ $[\text{Me}_2\text{Zn}(\text{NEt}_3)]$ itself has been shown to be almost fully dissociated in the vapor phase.²² This compound is interesting as it forms a stable 1:1 eutectic which is useful for reproducible precursor delivery. Triazine forms a 1:2 adduct with Me_2Zn (see Figure 9), which is stable and distillable; however, this too is almost fully dissociated in the vapor phase at room temperature.²⁵

For successful adduct purification of group 12 metal alkyls (methyl and ethyl) a number of bidentate nonchelating diamines have been employed as the Lewis base.^{26–29} Decreasing the volatility of the adducts is particularly important in the first step of the purification process. The effectiveness of an amine in this respect can be increased by preventing the bidentate Lewis bases from forming chelate compounds by ensuring the two nitrogen atoms within the same molecule cannot, for geometrical reasons, coordinate to the same metal atom, but have to bridge two metal centers. This leads to the formation of, for example, $[\text{Me}_2\text{Zn}\{(\text{NC}_5\text{H}_4)\text{CH}_2\text{CH}_2\text{CH}_2(\text{C}_5\text{H}_4\text{N})\}]_n$,³⁰ a structure consisting of one-dimensional polymeric chains running parallel to one another, with adjacent metal atoms connected by a bridging 1,3-bis(4-pyridyl) propane ligand (Figure 10). Amines α to an aromatic group or a pyridyl derivative are generally used as these tend to result in greater crystallinity in the adduct complex than do simple alkyl amines. Amines used also include 2,2'-bipyridyl to purify the dialkyls R_2M ($\text{M} = \text{Cd}$, $\text{R} = \text{Me}$, Et ; $\text{M} = \text{Zn}$, $\text{R} = \text{Me}$).^{26,27,31,32}

Other aryl amine compounds used in the purification of group 12 metal alkyls include 4,4'-bipyridyl for Me_2Zn and Me_2Cd ,^{26–28} 1,4-bis(dimethylamino)benzene for Me_2Cd and Et_2Zn ,¹⁴ 4-dimethylaminopyridine in the purification of Me_2Cd and Et_2Zn ,²⁷ and 1,3-bis(4-pyridyl)propane for purification of Me_2Zn and Et_2Zn .^{13,28}

Me_2Zn has been “adduct purified” using aza-crown ether macrocycles, which form adducts of the type $[(\text{Me}_2\text{Zn})_2\{\text{Me}_4\text{-14-ane-N}_4\}]$ and $[(\text{Me}_2\text{Zn})_2\{\text{Me}_6\text{-18-ane-N}_6\}]$ (Figure 11). Both structures consist of molecular units with distorted tetrahedral geometries at the zinc centers. $[(\text{Me}_2\text{Zn})_2\{\text{Me}_4\text{-14-ane-N}_4\}]$ has a Me_2Zn :ligand stoichiometry of 2:1; steric constraints in $[(\text{Me}_2\text{Zn})_2\{\text{Me}_6\text{-18-ane-N}_6\}]$ complex limit the Me_2Zn :ligand ratio also to 2:1 despite the fact that six N-donor atoms are available. It was shown that these adducts thermally dissociate at 120 °C, making them ideal candidates for use in the commercial purification of many metal alkyls by this method (see later).³³

Adducts that have been characterized by single X-ray crystallography include the dimethylzinc complexes with triazine, $[\text{Me}_2\text{Zn}\{(\text{CH}_2\text{NMe})_3\}_2]$,^{23,25} and TMEDA, $[\text{Me}_2\text{Zn}\{\text{Me}_2\text{N}(\text{CH}_2)_2\text{NMe}_2\}]$.²³ Other amine adducts that have been structurally characterized, but not used in

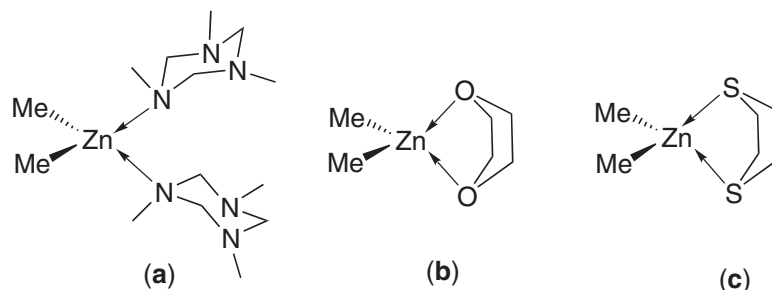


Figure 9 Adducts of dimethylzinc with (a) trimethyltriazine; (b) 1,4-dioxan; (c) 1,4-thioxan.

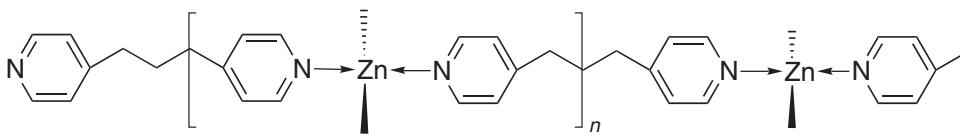


Figure 10 Structure of the polymeric complex $[\text{Me}_2\text{Zn}\{(\text{C}_5\text{H}_4\text{N})\text{CH}_2\text{CH}_2\text{CH}_2(\text{C}_5\text{H}_4\text{N})\}]_n$.

precursor purification, include the TMEDA adduct $[(\text{Me}_3\text{CCH}_2)_2\text{Zn}\{\text{Me}_2\text{N}(\text{CH}_2)_2\text{NMe}_2\}]$,²³ the adduct of Me_2Zn with (–)-sparteine (a naturally occurring tertiary amine),³⁴ and $[\text{Me}_2\text{Zn}(\text{Bu}^t_2\text{-DAB})]$ (where $\text{Bu}^t_2\text{-DAB} = 1,4\text{-di}(t\text{-butyl})\text{-}1,4\text{-diaz}\text{-}1,3\text{-butadiene}$).³⁵

One other class of zinc alkylamine adducts consisting of single molecules involves long-chain organozinc alkyls with a nitrogen donor atom in the δ - or ε -position of the chain, with the alkyl chain coiled back to form an intramolecular Lewis acid–base bond between the zinc center and the nitrogen atom. One such complex to have been structurally characterized is bis{3-(dimethylamino)propyl}zinc, $[\text{Zn}\{(\text{CH}_2)_3\text{NMe}_2\}_2]$,³⁶ Figure 12c. $[\text{Zn}(\text{CF}_3)_2(\text{C}_5\text{H}_5\text{N})_2]$ has also been structurally characterized (Figure 12b).³⁷

Alkyl cadmium compounds are considerably less reactive than those of zinc and are not generally spontaneously flammable in air. They are, however, highly reactive toward substances containing acidic hydrogen (e.g., H_2O , alcohols), readily eliminating hydrocarbons. Although many can be distilled at reduced pressure, thermal decomposition can occur above ca. 150°C and they may become explosive. Therefore, these compounds also are purified using “adduct purification” techniques. Related cadmium alkylamine complexes which have been structurally characterized include $[\text{Me}_2\text{Cd}(\text{TMEDA})]$ and $[(\text{Me}_3\text{CCH}_2)_2\text{Cd}(\text{TMEDA})]$.²³

In line with the relatively “soft” class B acceptor character of $\text{Cd}(\text{II})$, R_2Cd compounds form weaker adducts with nitrogen and oxygen donors than do the corresponding R_2Zn compounds. For instance, while the yellow crystalline adduct between Me_2Zn and 2,2'-bipyridyl is stable, Me_2Cd forms an unstable orange/yellow complex, $[\text{Me}_2\text{Cd}(2,2'\text{-bipy})]$, from which Me_2Cd can be removed by distillation *in vacuo* at room temperature.³⁸ This observation has formed the basis for a range of adduct purification techniques for R_2Cd compounds,³⁹ of which $[\text{Me}_2\text{Cd}(2,2'\text{-bipy})]$ has been structurally characterized (Figure 14).⁴⁰

Coordination complexes between Me_2Cd and chelating ethers such as 1,4-dioxan are largely dissociated into their components in benzene solution;⁴¹ the crystal structure of the 1:1 adduct $[\text{Me}_2\text{Cd}(\text{dioxan})]$ has been reported.⁴² $[\text{Me}_2\text{Cd}(\text{TMEDA})]$ ³⁹ and $[(\text{neopentyl})_2\text{Cd}(\text{TMEDA})]$ ⁴³ have been isolated; at elevated temperatures⁴² they are close to fully dissociated in the vapor phase^{22,41} although an electron diffraction study has been reported for $[\text{Me}_2\text{Cd}(\text{TMEDA})]$ at around 0°C . More stable adducts result between R_2Cd and sulfur and selenium donors, as exemplified by $[\text{Me}_2\text{Cd}(\text{tht})_2]$ (tht = tetrahydrothiophene).

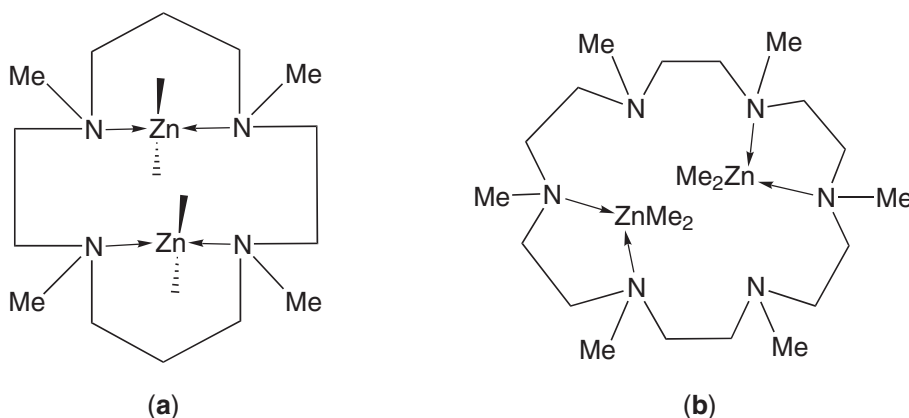


Figure 11 Structures of (a) $[(\text{Me}_2\text{Zn})_2(\text{Me}_4\text{-}14\text{-ane-N}_4)]$; (b) $[(\text{Me}_2\text{Zn})_2(\text{Me}_6\text{-}18\text{-ane-N}_6)]$.

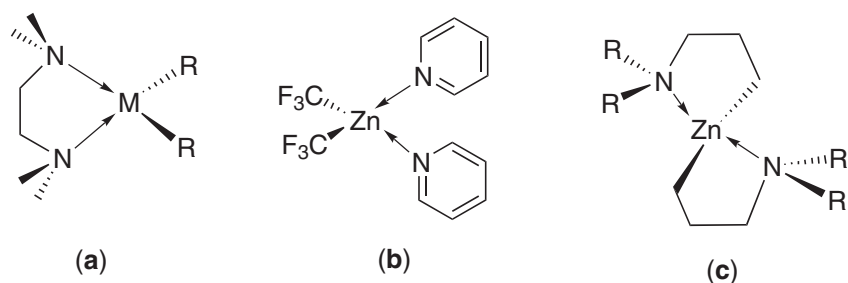


Figure 12 Structures of (a) $[R_2M(TMEDA)]$ ($M = Cd, Zn$; $R = Me, Me_3CCH_2$); (b) $[Zn(CF_3)_2(C_5H_5N)_2]$; (c) $[Zn\{(CH_2)_3NMe_2\}_2]$.

9.23.2.2 Purification of Group 13 Metal Alkyls

The first reported studies into “adduct purification”^{39,44} of the group 13 alkyl compounds involved the use of high boiling point, sterically hindered ethers (e.g., diisopentyl ether, anisole) which form low-volatility adducts with trimethylgallium of the type $[Me_3Ga(OR_2)]$. It was found that noncoordinating hydrocarbons, such as methyl iodide (a residue from the synthesis with $GaCl_3/MeMgI$), and C_2 – C_4 hydrocarbons, could be readily removed by distillation *in vacuo* or at atmospheric pressure through a fractionating column. In addition, trace impurities of Si and Zn, detected by ICP-ES in nonpurified Me_3Ga , were reduced to nondetectable levels by distillation of the Me_3Ga from a $[Me_3Ga(OR_2)]$ adduct.

The bis-chelating tertiary phosphine 1,2-bis(diphenylphosphino)ethane (dppe) proved successful in the purification of Me_3In . Several studies have shown that distillation of Me_3In from its dppe adduct resulted in the removal of Si and Zn impurities; this high-purity Me_3In was used in combination with high-purity PH_3 to grow extremely high-purity InP films by MOVPE.⁴⁵ A range of related adducts has now been prepared between group 13 trialkyls and tertiary phosphines, including $[Me_3M(PPh_3)]$ ($M = Ga, In$), $[Me_3In\{P(2-MeC_6H_4)_3\}]$, $[(R_3M)_2(dppe)]$ ($R = Me, M = Al, Ga, In$; $R = Et, M = Ga, In$; $R = Bu^i, M = Al$), $[(R_3M)_3(triphos)]$ ($M = Al, Ga, In$; triphos = $Ph_2P(CH_2)_2P(Ph)(CH_2)_2PPh_2$), and $[(R_3M)_4(tetraphos)]$ ($M = Al, Ga, In$; tetraphos = $Ph_2P(CH_2)_2P(Ph)(CH_2)_2P(Ph)(CH_2)_2PPh_2$).¹⁴ All of these adducts were shown to liberate the free metal trialkyl on moderate heating ($>80^\circ C$, 10^{-2} torr) (Figure 13).

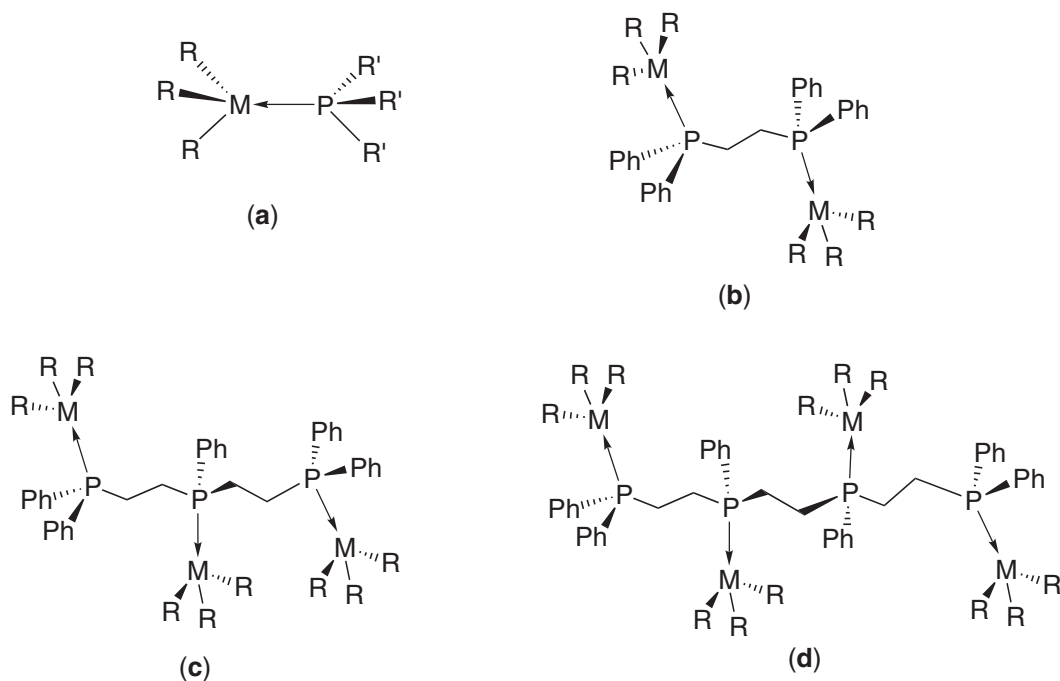


Figure 13 Structures of trialkylmetal adducts with multidentate phosphines: (a) $[R_3M(PR_3)]$ ($M = Ga, In$; $R = \text{alkyl}$); (b) $[(R_3M)_2(\mu\text{-dppe})]$ ($M = Al, Ga, In$); (c) $[(R_3M)_3(\mu^3\text{-triphos})]$ ($M = Al, Ga, In$); (d) $[(R_3M)_4(\mu^4\text{-tetraphos})]$ ($M = Al, Ga, In$).

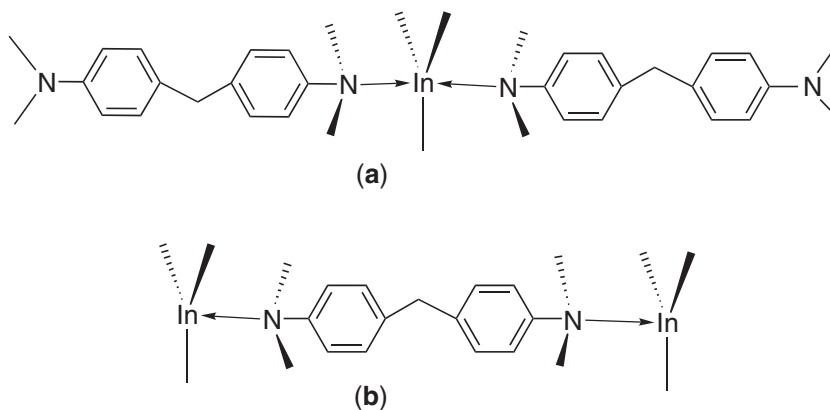


Figure 14 Structures of (a) $[\text{Me}_3\text{In}(\text{MBDA})_2]$; (b) $[(\text{Me}_3\text{In})_2(\text{MBDA})]$.

The group 13 trialkyls Me_3Al , Me_3Ga , Me_3In , and Et_3In have also been purified via adduct formation with 4,4'-methylene-bis(*N,N'*-dimethylaniline) (MBDA).¹⁶ These adducts can have either a 2:1 stoichiometry $[(\text{MR}_3)_2(\text{MBDA})]$ or a 1:2 stoichiometry $[(\text{MR}_3)(\text{MBDA})_2]$, as in the case of $[(\text{Me}_3\text{In})_2(\text{MBDA})]$ and $[(\text{Me}_3\text{In})(\text{MBDA})_2]$ (Figure 14).⁴⁶ In $[(\text{Me}_3\text{In})(\text{MBDA})_2]$ the indium atom has a trigonal bipyramidal five-coordinate geometry coordinating with the N atoms of the two MBDA ligands in the axial positions. The $[(\text{Me}_3\text{In})_2(\text{MBDA})]$ complex consists of discrete molecular units unlike the related (but polymeric) compound $[(\text{InR}_3)\{\text{N}(\text{CH}_2\text{CH}_2)_3\text{N}\}]_n$ (where $\text{N}(\text{CH}_2\text{CH}_2)_3\text{N} = \text{DABCO}$) (Figure 15).⁴⁷

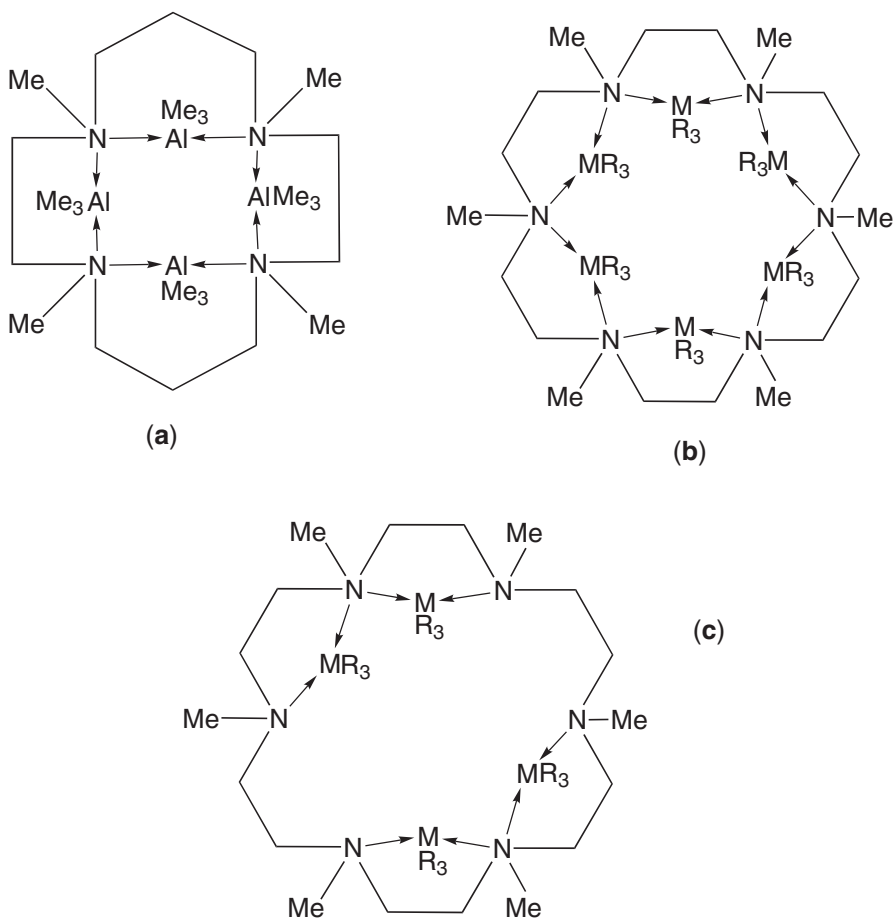


Figure 15 Structures of (a) $[(\text{Me}_3\text{Al})_4(\text{Me}_4\text{-14-ane-N}_4)]$; (b) $[(\text{Et}_3\text{Ga})_6(\text{Me}_6\text{-18-ane-N}_6)]$; (c) $[(\text{R}_3\text{Ga})_4(\text{Me}_6\text{-18-ane-N}_6)]$ (R = Et, Prⁱ).

Table 2 Main classes of conventional precursors used in CVD techniques.

Type of compound	Group	Typical compounds	Uses and comments
Metal alkyls	13	AlR ₃ , GaR ₃ , InR ₃ (R = Me, Et, Pr ⁱ , etc.)	Matrix element sources for III–V alloys
	12	ZnR ₂ , CdR ₂ (R = Me, Et)	Sources for wide-bandgap II–VI and narrow-bandgap II–VI materials; <i>p</i> -type dopants for III–V materials
Main group alkyls	15	NR ₃ , PR ₃ , AsR ₃ (R = Me, Et)	Adducts with metal alkyls or alternative group 15 sources in MOCVD
	15	SbR ₃ (R = Me, Et, Bu ^t , etc.)	Source for Sb-based III–V materials
	16	SR ₂ , SeR ₂ (R = Me, Et, Pr ⁱ)	Sources for wide-bandgap II–VI materials
	16	TeR ₂ (R = Me, Et, Pr ⁱ)	Source for narrow-bandgap II–VI materials/alloys
Main group hydrides	15	PH ₃ , AsH ₃	Conventional group 15 sources in MOCVD
	16	H ₂ S, H ₂ Se, H ₂ Te	Conventional group 16 sources in MOCVD
Metal alkyl adducts	13	R ₃ ML (M = Al, Ga, In; R = Me, Et, Pr ⁱ ; L = NR ₃ , PR ₃)	Safer and less reactive sources for III–V alloys
	13	R ₃ ML (L = R' ₂ O, dppe)	Adduct purification of group 13 metal alkyls
Metal alkyl hydrides	15	(R ₂ AlH) ₂ or ₃ (R = Me, Et), R ₂ AlH(NMe ₃)	Sources for growth of Al-based III–V alloys and Al CVD
Hydrides	15	RAsH ₂ , RPH ₂ (R = Bu ^t , Et), R ₂ AsH	Liquid alternatives to AsH ₃ and PH ₃ in MOCVD
Metal hydride adducts	13	AlH ₃ (NMe ₃), AlH ₃ (NMe ₂ Et), GaH ₃ (NR ₃)	Sources for III–V alloys where carbon must be avoided

Other high molecular weight amines to have been successfully used for adduct purification include the aza-crown macrocycles Me₄-14-ane-N₄ and Me₆-18-ane-N₆.⁴⁸ These reversibly form adducts with indium and gallium alkyls, such as [(Et₃Ga)₄(Me₆-18-ane-N₆)], [(Et₃Ga)₆(Me₆-18-ane-N₆)], [(Prⁱ₃Ga)₄(Me₆-18-ane-N₆)], and [(Prⁱ₃Ga)₄(Me₄-14-ane-N₄)].⁴⁹ Formation of [(Me₃Al)₄(Me₄-14-ane-N₄)] has also been reported.⁵⁰

Table 3 shows some typical effects of “adduct purification” on precursor purity and on the electrical properties of the resulting semiconductor layers grown by MOVPE.

9.23.2.3 Modified Adduct Purification Techniques

A variation of the adduct purification technique has been reported⁵¹ in which Me₃In is reacted with MeLi to form the involatile tetramethylindate salt Li[InMe₄], from which volatile impurities are removed. The Me₃In is recovered by reacting Li[InMe₄] with excess InCl₃. However, a drawback of this process is that impurities may be introduced in the final stage of the process from the halide InCl₃.

Me₃Al has also been purified by distillation of its adduct with high-boiling ethers, such as diphenylether.⁵² Purification of Me₃Al from [Me₃Al(OPh₂)] reduced the Si level to 0.7 ppm, and the Al_{0.3}Ga_{0.7}As film grown using this purified source switched from *n*- to *p*-type in character, due to the incorporation of carbon which was deemed to be an intrinsic impurity from the Me₃Al.

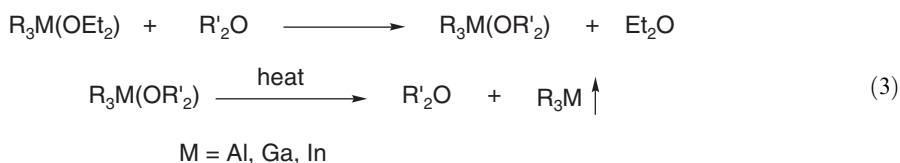
Another variant of the adduct purification technique has been reported by Russian workers involving the formation of volatile adducts between a metal alkyl and diethylether, such as [(Me₃Ga)(OEt₂)], [(Et₃Ga)(OEt₂)], etc. Noncoordinating metallic and organic impurities are readily separated from the organometallic component by fractional distillation. The volatile diethylether is then displaced from the group 13 trialkyl by the addition of a large excess of involatile ether, R'₂O

Table 3 Some typical effects of adduct purification on precursor purity and on the electrical properties of the resulting semiconductor layers grown by MOVPE.

Precursor	Impurities detected by plasma emission (ppm)	Material grown and temperature (°C)	Carrier concentration, $n_{77\text{K}}$ (cm^{-3}) ^a	Mobility, $\mu_{77\text{K}}$ ($\text{cm}^2 \text{V}^{-1} \text{s}^{-1}$) ^a
Me ₃ Ga (nonpurified)	Si 1.2, Zn 2.0	GaAs (650)	1.1% 10^{15}	42,600
Me ₃ Ga (adduct-purified)	Si < 0.03, Zn < 0.2	GaAs (650)	1.4% 10^{14}	137,000
Me ₃ In (nonpurified)	Si 3.0, Mg 0.17	InP (600)	3.4% 10^{15}	37,500
Me ₃ In (dppe-purified)	Si < 0.03, Zn < 0.2	InP (570)	5.0% 10^{13}	305,000
Me ₃ Al (nonpurified)	Si 14	Al _{0.3} Ga _{0.7} As (720)	1.0% 10^{17} (<i>n</i>)	
Me ₃ Al (adduct-purified)	Si < 0.3	Al _{0.3} Ga _{0.7} As (720)	1.0% 10^{16} (<i>p</i>)	

^a Low *n* values and high μ values indicate that the layer is of high purity.

(e.g., diisopentyl ether, diglyme etc.), and the purified metal alkyl is obtained by thermal dissociation of the weak [(R₃M)(OR'₂)] adduct as outlined in Equation (3). However, for aluminum alkyls it has been established that the use of ethers in the synthesis routes can produce Al–ether adducts that are difficult to dissociate and can result in oxygen contamination within the final films:



9.23.3 PRECURSORS FOR FABRICATION OF II–VI THIN FILMS

The growth of Zn–VI materials by CVD techniques has traditionally been carried out using dimethylzinc (Me₂Zn)⁵³ or diethylzinc (Et₂Zn)⁵⁴ in combination with H₂X (X = S, Se, Te). This has been followed by the successful use of other zinc alkyls, which have been specifically designed for use in CVD applications. Although quality thin films of, for example, ZnSe with excellent electrical and optical properties have been obtained,^{55,56} at low substrate temperatures (~300 °C) a severe premature reaction (prereaction) frequently occurs in the gas phase, especially during atmospheric pressure CVD.^{54,57} A similar prereaction occurs with the growth of Cd–VI materials, and again results in the growth of II–VI compound semiconductor thin film layers with low compositional uniformity and poor morphology, with correspondingly poor electrical and optical properties. These premature reactions have been attributed to the facile elimination of alkyl groups from R₂Zn/Cd by the acidic hydrogen atoms of H₂Se or H₂S.⁴¹ An approach to eliminate the prereaction is to modify the Zn/Cd source so that it is no longer susceptible to alkyl elimination when in the presence of the group 16 hydride.^{58,59} The prereactions appeared to be inhibited by the use of Lewis base compounds NR₃ and OR₂. The adducts [Me₂Zn(1,4-dioxan)] and [Me₂Zn(1,4-thioxan)] were investigated as precursors and were shown to reduce the prereaction with H₂Se, while still allowing the growth of ZnSe at low temperature (200–350 °C).⁶⁰ Pyridine also suppresses the prereaction; in the presence of pyridine the prereaction is limited to the growth of gas-phase nanoparticulate material in the range 5–100 nm, instead of a precipitate of micrometer-size material which occurs in its absence (Figure 16).⁶¹

A comprehensive study of the amine complex [(Me₂Zn)(NET₃)] as a precursor for ZnSe and ZnS has been undertaken.^{62–64} There are a number of significant advantages associated with its use.^{65,66} First, the premature reaction with H₂Se or H₂S is much reduced, although it has been claimed that nanoparticulate material is still produced. Second, [(Me₂Zn)(NET₃)] is nonpyrophoric and less susceptible to contamination with oxygen-containing impurities. [(Me₂Zn)(NET₃)] is also much easier to handle and purify than Me₂Zn. Finally, it has been shown that [(Me₂Zn)(NET₃)] forms a eutectic mixture, leading to a more reproducible delivery of the precursor.⁶⁷ Other Me₂Zn–amine adducts also serving to eliminate prereactions include the adduct between

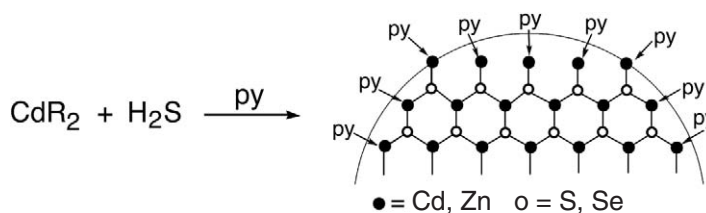


Figure 16 Suppression of the pre-reaction between dialkylcadmium/zinc compounds and hydrogen sulfide/selenide using pyridine.

Me_2Zn and 1,3,5-trimethylhexahydro-1,3,5-triazine⁶³ (Figure 9) and $[(\text{Me}_2\text{Zn})(\text{Me}_2\text{NCH}_2\text{NMe}_2)]$ (Figure 17).⁶³

The addition of pyridine directly into the gas phase also led to a significant reduction of pre-reaction and an improvement in the structural quality of the ZnSe layers, compared with layers grown using Me_2Zn and H_2Se in the absence of pyridine.⁶⁶

9.23.3.1 New Group 12 Precursors

There have been only a few precursors used which are not metal alkyls. Electrostatic spray-assisted vapor deposition (ESAVD) is a variation of the CVD process and involves spraying atomized droplets of a precursor-containing solution across an electric field, initiating decomposition of the precursor in the vapor phase close to the substrate.^{68,69} This method has been used to deposit thin films of ZnS ⁷⁰ on Si(110). ZnS was grown using ZnCl_2 as the Zn source and thiourea (H_2NCSNH_2) as the sulfur source to produce epitaxial ZnS thin films. CdSe thin films were grown from a combination of CdCl_2 and thiourea and gave near-stoichiometric films containing^{68,71} small amounts of oxygen and chlorine impurities, but showing reasonable optical and electrical properties. These results suggest that ESAVD is a cheap alternative to conventional CVD techniques.

9.23.3.2 New Group 16 Precursors

Only a small number of group 16 “nonconventional” precursors have been investigated (Tables 4 and 5). For example, growth of ZnSe, ZnS, and $\text{ZnS}_x\text{Se}_{1-x}$ thin films has been reported using as precursors linear dialkyldiselenides or disulfides such as dimethyldiselenide (Me_2Se_2), diethyldiselenide (Et_2Se_2), and diethyldisulfide (Et_2S_2) which possess unsupported Se—Se and S—S bonds (Figure 18). These precursors, in combination with $[\text{Me}_2\text{Zn}(\text{Et}_3\text{N})]$, were used to prepare the films by atmospheric pressure MOVPE at $<400^\circ\text{C}$ (whereas conventional precursors require temperatures of about 550°C or higher).^{72,73}

9.23.4 PRECURSORS FOR FABRICATION OF III–V THIN FILMS

As described above, the precursors traditionally employed for preparation of III–V films have been group 13 metal alkyls (Me_3Ga , Me_3Al , Me_3In) in combination with the group 15 hydride gases (Table 2). These are available on a commercial scale and have appropriate vapor pressures for both atmospheric pressure and low-pressure applications.

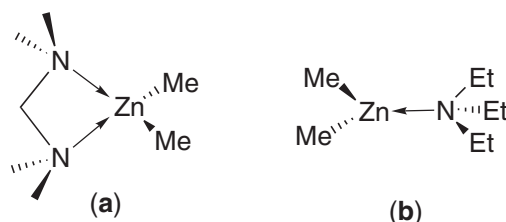


Figure 17 Structures of (a) $[\text{Me}_2\text{Zn}(\text{Me}_2\text{NCH}_2\text{NMe}_2)]$; (b) $[\text{Me}_2\text{Zn}(\text{NEt}_3)]$.

Table 4 Compounds used as sulfur sources in MOCVD.

Precursor	Typical deposition temperature (°C)	Extent of prereaction with R ₂ Zn or R ₂ Cd	Physical properties
H ₂ S	ZnS (250–350)	Severe	Gas
R ₂ S (R = Me, Et)	ZnS (>500)	None	Liquid
Tetrahydrothiophene	ZnS (>500)	None	Liquid
MeSH	ZnS (>450)	None	Gas
Bu ^t SH	ZnS (325–400)	None	Liquid
CH ₃ CH=CHSH	CdS (300–450)	None	Liquid

Table 5 Selected selenium precursors.

Precursor	Vapor pressure (torr)	Comments and temperature	References
H ₂ Se	Gas	280–400 °C/Me ₂ Zn. Toxic gas.	53–55
Me ₂ Se		Severe prereaction with R ₂ Zn >500 °C/R ₂ Zn. Too stable. No prereaction with R ₂ Zn	74
Et ₂ Se	20.5 at 17 °C	450–550 °C/R ₂ Zn. Too stable. No prereaction with R ₂ Zn	75,76
Me(allyl)Se		480–550 °C/R ₂ Zn. Heavy carbon contamination (no prereaction)	77
(Allyl) ₂ Se	3.7 at 20 °C	440–500 °C/Me ₂ Zn(NEt ₃) or R ₂ Zn. Too stable for successful <i>p</i> -doping (no prereaction)	28
Pr ⁱ ₂ Se	8.9 at 20 °C	440–500 °C/Me ₂ Zn(NEt ₃) or R ₂ Zn. Too stable for successful <i>p</i> -doping (no prereaction)	28
Bu ^t ₂ Se	1.3 at 17 °C	330–440 °C/R ₂ Zn or Me ₂ Zn(NEt ₃). Most suited for low-temperature ZnSe growth. Free from prereactions	53,78,79

9.23.4.1 Aluminum Compounds

The use of conventional aluminum precursors R₃Al (R = Me, Et, Prⁿ, Buⁿ; Table 6) can lead, in some cases, to layers that contain significant levels of carbon contamination. This is because of the exceptional strength of the Al—C bond. Et₃Al generally gives less carbon contamination than Me₃Al. This problem has generally been overcome by the removal of alkyl radicals from the growth system using an adduct of AlH₃ (alane) with either trimethylamine [AlH₃(NMe₃)]^{80–82}

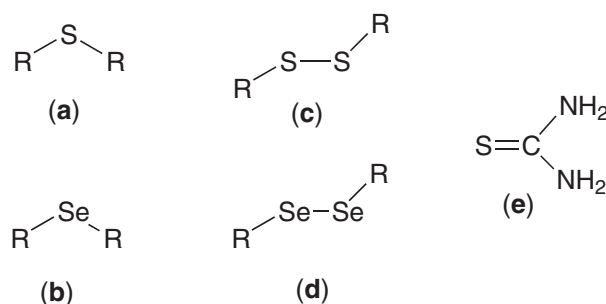
**Figure 18** Structures of (a) dialkylsulfides; (b) dialkylselenides; (c) dialkyldisulfides; (d) dialkyldiselenides; (e) thiourea.

Table 6 Metalorganic Al precursors for MOVPE mostly used for $\text{Al}_x\text{Ga}_{1-x}\text{As}$ studies.

Precursor	Precursor pressure (torr)	Comment	References
$(\text{Me}_3\text{Al})_2$	9 at 20 °C (good)	Pyrophoric liquid	90
$[\text{Me}_3\text{Al}(\text{NMe}_3)]$	0.9 at 24 °C (low)	Nonpyrophoric solid	91
$(\text{Me}_2\text{AlH})_3$	2.4 at 28 °C (adequate)	Pyrophoric liquid	92,93
$[\text{Me}_2\text{AlH}(\text{NMe}_3)]$	1.8 at 20 °C (adequate)	Nonpyrophoric solid	93
$[\text{Me}_2\text{Al}(\text{NMe}_2)]_2$	0.6 at 30 °C (low)	Nonpyrophoric solid	91
$(^t\text{BuAlMe}_2)_2$	0.6 at 20 °C (low)	Pyrophoric liquid	94
$(\text{Et}_3\text{Al})_2$	0.04 at 27 °C; 0.5 at 55 °C (very low)	Pyrophoric liquid	95,96
$[\text{Et}_3\text{Al}(\text{NMe}_3)]$	0.09 at 35 °C (very low)	Nonpyrophoric liquid	91
$[\text{Et}_2\text{AlH}(\text{NMe}_3)]$	0.2 at 30 °C (low)	Nonpyrophoric liquid	93,97
$[\text{AlH}_3(\text{NMe}_3)]$	1.8 at 25 °C (adequate)	Nonpyrophoric solid	50,81,82,98
$[\text{AlH}_3(\text{NMe}_2\text{Et})]$	2 at RT (adequate)	Liquid alane source	83
$[(\text{C}_5\text{H}_{10})\text{Al}(\text{CH}_2)_3\text{NMe}_2]$	0.58 at 30 °C (low)	Non-pyrophoric solid	88
Bu^t_3Al	0.5 at 24 °C (low)	Pyrophoric liquid	99,100

(Figure 19b) or dimethylethylamine $[\text{AlH}_3(\text{NMe}_2\text{Et})]$ (Figure 19c), since neither contains any strong Al—C bonds.^{83–86} Further, $[\text{AlH}_3(\text{NMe}_3)]$ has a greatly reduced tendency to form volatile oxides and has an adequate vapor pressure (1.8 torr at 25 °C). However, these alane-based precursors are relatively unstable and decompose on storing, liberating hydrogen gas.⁸⁷

To reduce oxygen contamination in MOVPE-grown $\text{Al}_x\text{Ga}_{1-x}\text{As}$ films, intramolecularly saturated compounds such as 1,3-dimethylaminopropyl-1-ala-cyclohexane, $[(\text{C}_5\text{H}_{10})\text{Al}(\text{CH}_2)_3\text{NMe}_2]$, have been employed.⁸⁸ This type of precursor displays full coordinative saturation at the aluminum atom, by coordination of the amine group, and is unreactive to oxygen and moisture. Therefore it has less of a tendency than Me_3Al to generate alkoxide impurities, and has been used to grow AlGaAs layers with good luminescent properties.⁸⁸

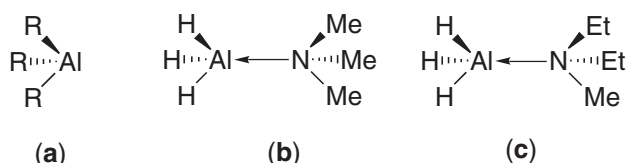
Intramolecular adducts have also been used as gallium and indium precursor complexes; they are synthesized by the alkylation of the group 13 metal trihalide with an appropriate Grignard reagent,⁸⁹ as shown Figure 20.

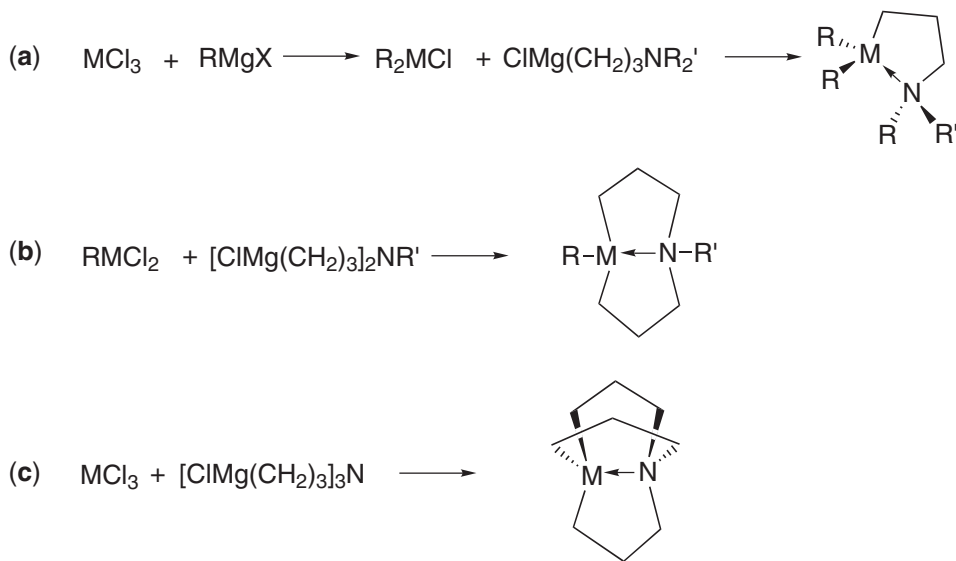
Intramolecular adducts are generally nonpyrophoric and relatively unreactive towards both air and H_2O . However, they generally have a much higher molecular weight than the base-free R_3M compounds ($\text{M} = \text{Al}, \text{Ga}, \text{In}$) and thus have rather low vapor pressures. This has somewhat restricted their widespread use in MOVPE.

9.23.4.2 Gallium Compounds

The conventional gallium-containing precursors have been the alkyl gallium compounds, as listed in Table 7.

To overcome the problem of high reactivity and toxicity, the adduct $[\text{ClEt}_2\text{Ga}(\text{AsEt}_3)]$ was used in conjunction with HPeT_2 as the source for P.¹¹¹ Epitaxial growth of $\text{GaAs}_{1-x}\text{P}_x$ layers on (111)- and (100)-oriented GaAs and Ge were obtained, in the temperature range 500–650 °C.¹¹² GaAs film growth from both $[(\text{C}_6\text{F}_5)_2\text{Me}_2\text{Ga}(\text{AsEt}_3)]$ and $[\{\text{ClEt}_2\text{Ga}(\text{AsEt}_2)\}_2\text{CH}_2]$ has been undertaken with growth in the 600–700 °C and 500–625 °C temperature ranges, respectively.¹¹³ However, in the latter case contamination of the films from the intrinsic Cl atoms is a concern.

**Figure 19** Structures of (a) aluminum trialkyls; (b) $[\text{AlH}_3(\text{NMe}_3)]$; (c) $[\text{AlH}_3(\text{DMEA})]$.



M = Al, Ga, and R, R' = Me, Et

Figure 20 Syntheses and structures of group 13 intramolecular alkyl-amine adducts.

Table 7 Metalorganic Ga precursors used in MOVPE.

Precursor	Vapor pressure (torr)	Comment	References
Me_3Ga	182 at 20 °C (excellent)	Pyrophoric liquid	101–104
Et_3Ga	3.4 at 20 °C (adequate)	Pyrophoric liquid	103,105
Bu^i_3Ga	0.08 at 18 °C (very poor)	Pyrophoric liquid	106
$[\{(\text{CH}_2)_5\text{Ga}\}(\text{CH}_2)_3\text{NMe}_2]$	0.02 at 20 °C (very poor)	Nonpyrophoric solid	107,108
$[\text{H}_3\text{Ga}(\text{HNMe}_2)]$	2 at RT (poor)	Nonpyrophoric	109,110

To reduce the incorporation of carbon, the nonpyrophoric adduct dimethylamine-gallane, $[\text{H}_3\text{Ga}(\text{HNMe}_2)]$ (a liquid at room temperature with a vapor pressure of ~ 2 mbar) has been used in the growth of GaAs and AlGaAs films by low-pressure MOVPE.¹⁰⁹ This is the same strategy used to prevent carbon contamination of Al-containing films. However, $[\text{H}_3\text{Ga}(\text{HNMe}_2)]$ —in common with other amine adducts of gallane¹¹⁰—is unstable, even at room temperature, decomposing to gallium metal. This necessitates low-temperature storage (e.g., -15°C) and renders such adducts difficult to synthesize and purify on an adequate scale. Consequently, GaAs layers grown using $[\text{H}_3\text{Ga}(\text{HNMe}_2)]$ and AsH_3 or H_2AsBu^t exhibited pronounced *n*-type semiconducting behavior.¹⁰⁹

As with the group 12 complexes, the intramolecular adducts are much less reactive to air and moisture than the coordinatively unsaturated compounds R_3Ga ; they are generally nonpyrophoric but suffer from lower volatility. In an effort to find a less hazardous, nonpyrophoric precursor, 1,3-dimethylaminopropyl-1-galla-cyclohexane, $[\text{Me}_2\text{Ga}(\text{CH}_2)_3\text{NMe}_2]$, has been investigated (Figure 20a).^{108,109} Like the analogous aluminum precursor, this exhibits full coordinative saturation at the metal center and is accordingly much less reactive to moisture and oxygen. $[\text{Me}_2\text{Ga}(\text{CH}_2)_3\text{NMe}_2]$ has been used in combination with AsH_3 to grow GaAs of moderate purity ($n_{77\text{k}} = 3 \times 10^{14} \text{ cm}^{-3}$, $\mu_{77\text{k}} = 51,000 \text{ cm}^2 \text{ V}^{-1} \text{ s}^{-1}$) by low-pressure MOVPE.¹⁰⁹ Photoluminescence (PL) data indicated that neither carbon nor nitrogen incorporation had occurred. However, $[\text{Me}_2\text{Ga}(\text{CH}_2)_3\text{NMe}_2]$ has only a very low vapor pressure (0.4 mbar at 20 °C) which is likely to restrict seriously its wider use in CVD.

9.23.4.3 Indium Compounds

The conventional method of CVD growth of In–V thin films is to use indium alkyl precursors (Table 8), preferably Me_3In . However, early problems in the growth of InP and InGaAs were

Table 8 Metalorganic In precursors for MOVPE.

Precursor	Vapor pressure (torr)	Comment	References
Me ₃ In	1.73 at 20 °C	Crystalline solid, pyrophoric, good vapor pressure	45
Et ₃ In	1.2 at 44 °C	Liquid, pyrophoric, low vapor pressure	121
[Me ₃ In(NMe ₃)]	0.76 at 30 °C	Nonpyrophoric, low vapor pressure	118
[Me ₃ In(PEt ₃)]		Nonpyrophoric liquid, low vapor pressure	117
EtInMe ₂	0.85 at 17 °C	Liquid, pyrophoric	122
[Me ₃ In(NPr ⁱ ₂ H)]	0.56 at 30 °C	Nonpyrophoric liquid, low vapor pressure	123
(Me ₂ NC ₃ H ₆)InMe ₂	0.58 at 30 °C	Nonpyrophoric liquid, low vapor pressure	123
Me ₃ In/DMDA ^a	1.75 at 20 °C	Adduct mixture has good vapor pressure	124

^a DMDA = dimethyldodecylamine, (CH₃)₂N(C₁₂H₂₅).

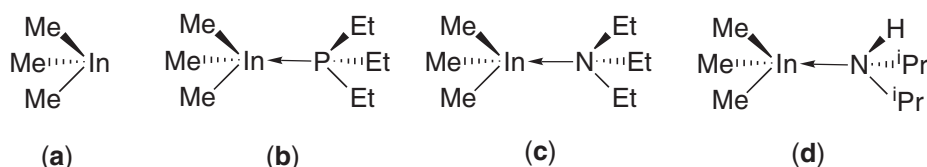
attributed¹¹⁴ to a parasitic reaction (prereaction) between Me₃In and PH₃ or AsH₃, largely due to the relatively weak In—C bond. This reaction had been shown¹¹⁵ previously to occur at room temperature, leading to the formation of the nonvolatile polymer (MeInPH)_n. The extent of prereaction was observed to be variable, being catalyzed by the stainless steel and silica surfaces of the reactor. As with II–VI materials, prereaction can cause variable growth rates and poor morphology resulting in films having inferior electrical properties.¹¹⁵

Adducts such as [Me₃In(PEt₃)] and [Me₃In(NEt₃)] (Figures 21b and 21c) were used as alternatives to Me₃In and other base-free indium alkyls.^{114,116} Adducts were initially formed *in situ* in the gas phase, with the system no longer susceptible to premature reaction with the PH₃ (used as the P source). The dative bond arises from donation of an electron pair from NEt₃ or PEt₃ into an empty *sp*³ hybrid orbital on Me₃In and is the weakest bond in the molecule. This, coupled with the strength of the P—C or N—C bonds, means that the group 15 component of the adduct is not involved in the growth process with little or no carbon being incorporated into the In–V layers.

Subsequently, adducts such as [Me₃In(PEt₃)]¹¹⁷ and [Me₃In(NMe₃)]¹¹⁸ were performed in the laboratory and then used as precursors for InP thin films. As with Lewis base adducts of Al and In, in addition to eliminating prereaction with PH₃ there is the advantage of improved safety (i.e., the adducts are nonpyrophoric) and a potentially greater ease of purification and handling.¹¹⁷ A severe disadvantage, however, is their reduced volatilities compared with Me₃In, which leads to low InP growth rates, necessitating the heating of source and reactor lines upstream of the substrate.¹¹⁸ The most volatile adduct, [Me₃In(NMe₃)] (vapor pressure = 0.76 torr at 30 °C), proved suitable for the growth of relatively high-purity InP at 604 °C.¹¹⁸ Other adducts used include [Me₃In(NHPrⁱ₂)]¹¹⁹ (Figure 21d) and [Et₂InNMe₂], which will be mentioned in the section on single-source precursors.¹²⁰

There have been few alternative indium precursors studied. They include intramolecular adducts such as 1,3-[(dimethylamino)propyl]dimethylindium, [Me₂N(CH₂)₃InMe₂]^{125,126} (Figure 20a; with R,R' = Me).

CVD studies on the volatile, air- and moisture-stable precursor [(hfac)InMe₂] (hfac = 1,1,1,5,5,5-hexafluoro-2,4,-pentanedionate; Figure 22) have been undertaken. [(Hfac)InMe₂] consists of discrete molecules forming weakly associated dimers with the central indium atom having a distorted tetrahedral coordination geometry.¹²⁷ Cu–In alloys were grown using

**Figure 21** Structures of (a) Me₃In and its adducts with (b) PEt₃; (c) NEt₃; (d) HN(Prⁱ)₂.

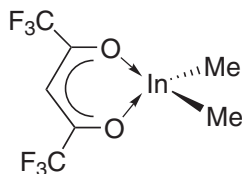


Figure 22 Structure of [(hfac)InMe₂].

[(hfac)InMe₂] and [(hfac)Cu(MHY)] (MHY = 2-methyl-1-hexen-3-yne). Unlike systems using trialkylindium species, no prereaction occurs between these precursors in the gas phase.

9.23.4.4 Nitrogen Compounds

The deposition of III nitride thin films by CVD techniques has traditionally used group 13 alkyls or ammonia as the nitrogen source; however, the high thermal stability of ammonia necessitates the use of high deposition temperatures, sometimes in excess of 1,000 °C. These excessive temperatures in turn can lead to loss of nitrogen or other elements from the as-grown films, resulting in nonstoichiometric film growth.

A number of alternative precursors have been used and include trimethylsilyl azide, Me₃SiN₃ (Figure 23a), used in combination with Me₃Al; films of AlN were grown under atmospheric pressure MOCVD conditions between 300 °C and 450 °C. No silicon contaminants were detected in the as-grown AlN films.¹²⁸

The III–V alloys of MNAs (M = Ga, In) are candidates for long-wavelength laser emission in the optical fiber communications wavelength range (1.3–1.55 μm), and in multijunction solar cell applications.^{129–131} In combination with R₃Ga (R = Me, Et) dimethylhydrazine (Me₂NNH₂; Figure 23c) has been widely used as a liquid source of nitrogen for the growth of Ga_xN_{1-x}As as it requires a lower deposition temperature than ammonia.^{132,133} However, both Me₃Ga and Et₃Ga tend to undergo a prereaction with Me₂NNH₂ forming a nonvolatile, waxy donor–acceptor adduct.^{132,134} The combination of Et₃Ga and Me₂NNH₂ tended to give films with lower carbon contamination.¹³⁵ Me₂NNH₂ has also been used as a substitute for ammonia when growing pure GaN epilayers on a sapphire substrate; both hexagonal¹³⁶ and cubic^{137,138} GaN were observed. A much lower V/III ratio can be employed compared to that used with ammonia, with a ratio of 50:1 giving GaN of good optical quality.¹³⁶

When growing GaInNAs using Me₂NNH₂, high flow rates are required with the as-grown material having a high *p*-type background doping concentration. Therefore, other nitrogen source precursors were investigated and include hydrazine (H₂NNH₂; Figure 23b) which gave significant nitrogen incorporation even at much lower nitrogen/III precursor ratios than that for Me₂NNH₂.¹³⁹ Hydrazine was also shown to be an effective nitrogen source in the growth of pure GaN using MBE,^{140,141} and also in the growth of GaNAs (giving higher nitrogen incorporation for a given nitrogen source/III ratio than obtained with Me₂NNH₂).¹⁴² However, hydrazine is very toxic and under certain conditions the vapor can become highly explosive.

Other alternative nitrogen precursors to be investigated include the amines triethylamine¹⁴³ and *t*-butylamine;^{144,145} however, these were found not to be suitable for GaN deposition. It has been reported that the gaseous amine *n*-propylamine was successfully used to grow GaN in combination with Me₃Ga and ammonia. It was suggested that the presence of *n*-propylamine has a great influence on the deposition process, and on the quality of the crystal structure of the as-grown GaN layers.¹⁴⁶ Moreover, the addition of *n*-propylamine to the conventional Me₃Ga/NH₃ system

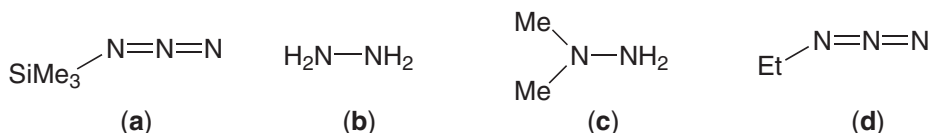


Figure 23 Structures of (a) Me₃SiN₃; (b) hydrazine; (c) dimethylhydrazine; (d) ethylazide.

significantly improved the morphology of the polycrystalline GaN films. However, it was not established whether any of the nitrogen in the GaN film originated from the *n*-propylamine.

Nitrogen doping of ZnSe epilayers was achieved using ethylazide (EtN_3 , Figure 23d), which contains no H—N bonds, as the dopant source, in combination with Et_2Zn and Et_2Se . Although nitrogen was incorporated, hydrogen atoms in the form of N—H units were also found in the as-grown epilayers. By thermally annealing the samples, hydrogen was successfully removed, yielding *p*-type ZnSe layers.¹⁴⁷

9.23.4.5 Phosphorus Compounds

The conventional method of preparation of III–V films containing P is to use a group 13 alkyl in combination with phosphine (PH_3); however, problems in the growth of both InP and InGaAs have been attributed to the prereaction between Me_3In and PH_3 .^{114,117} PH_3 is a highly toxic gas, and therefore alternative P source precursors have been sought and include the trialkylphosphines (with the exception of Me_3P and Et_3P due to their high thermal stability).¹⁴⁸ For adducts such as $[\text{Me}_3\text{In}(\text{PEt}_3)]$ in combination with PH_3 no prereaction is observed.¹¹⁷ $[\text{Me}_3\text{In}(\text{PEt}_3)]$ has no acidic P—H bonds close to the metal and, unlike the PH_3 adduct $[\text{Me}_3\text{In}(\text{PEt}_3)]$, cannot undergo a concerted reductive elimination reaction with loss of methane and subsequent prereaction. However, Et_3P is not consumed in the CVD process when used in combination with PH_3 . Di(*t*-butyl)phosphine (Bu^t_2PH), a volatile liquid with a convenient vapor pressure (264 torr at 25 °C), and *iso*-butylphosphine (Bu^iPH_2) have both successfully been used as alternative precursors.^{149,150} 1,2-Diphosphinoethane ($\text{H}_2\text{PCH}_2\text{CH}_2\text{PH}_2$)¹⁵⁰ has also been used in the growth of both InP and GaInAsP films,¹⁵¹ and gave promising results with low V/III ratios needed. Due to the rather low vapor pressure the lower molecular weight analog diphosphinomethane has also been investigated as a potential phosphorus source,¹⁵² with InP layers successfully grown at temperatures of 580 °C using a low V/III ratio.

Other phosphines investigated include cyanoethylphosphine, benzylphosphine, and cyclopentylphosphine, but all suffered from a prereaction in the presence of metal alkyls.¹⁵³

9.23.4.6 Antimony Compounds

Due to the thermal instabilities of SbH_3 , MeSbH_2 , and Me_2SbH , trimethylantimony (Me_3Sb) is the conventional precursor used to grow antimony-containing materials.^{154,155} In order to reduce the pyrolysis temperature a number of other antimony alkyl compounds have also been investigated and are listed in Table 9.

In a quest to grow good morphology layers below 400 °C antimony sources other than alkyls were investigated and include tris(dimethylamido)antimony, $\text{Sb}(\text{NMe}_2)_3$.¹⁶⁶ GaSb thin films were grown using this over a wide temperature range by the MOMBE method, and produced layers with good surface morphologies.¹⁶⁷ $\text{Sb}(\text{NMe}_2)_3$ was also successfully used to etch various layers using MOMBE.^{168,169}

9.23.4.7 Arsenic Compounds

AsH_3 is the conventional As precursor, but due to its high toxicity and gaseous nature it has been generally replaced with less hazardous alkyl arsines. These tend to have the added advantage of requiring lower deposition temperatures, as listed in Table 10. A number of other mixed alkyl derivatives ($\text{R}_2\text{R}'\text{As}$, $\text{R} \neq \text{R}'$) were investigated but generally gave poor growth results, most likely due to intermolecular alkyl ligand exchange. The most promising results, in the case of GaAs thin films, were obtained using alkyl arsine precursors which contain one or more direct hydrogen–arsenic bonds, with the most successful being *t*-butylarsine, Bu^tAsH_2 .^{103,170,171}

An alternative nitrogen-based As source which is rapidly becoming a viable option in place of the alkyl compounds is tris(dimethylamido)arsine, $(\text{As}(\text{NMe}_2)_3; \text{TDMAA})$ (vapor pressure = 1.35 torr at 20 °C). One of its main advantages is the absence of any prereactions, which was attributed to the shielding of the central As atom by the bulky dimethylamide groups. $\text{As}(\text{NMe}_2)_3$ was initially used in combination with Me_3Ga to grow GaAs layers.¹⁷²

Table 9 Antimony alkyl compounds.

<i>Sb precursor</i>	<i>Vapor pressure (torr)</i>	<i>Minimum achievable growth temperature (alloy grown) (°C)</i>	<i>Comment</i>	<i>References</i>
SbH ₃	Gas	300	Unstable at room temperature, must be generated at the point of use	156
Me ₃ Sb	78 at 20 °C	470 (InSb); 520 (InSb)	Good vapor pressure, but too stable for the growth of <i>n</i> -type InSb and Bi-containing alloys	157
Et ₃ Sb	~1 at 27 °C	410 (InSb)	Only slightly less stable than Me ₃ Sb; no real advantages over Me ₃ Sb	158
Pr ⁱ ₃ Sb	0.7 at 30 °C; 1.6 at 44 °C	300 (InSb)	Low vapor pressure. Allows low-temperature growth but layers have poor morphology	159,160
Pr ⁱ ₂ SbH		275 (InSb)	Allows low-temperature growth but layers have poor morphology	161
(Vinyl) ₃ Sb		>450 (InSb)	Too stable; leads to heavy carbon contamination	162,163
(Allyl) ₃ Sb	0.35 at 30 °C	<400 (InSb)	Low vapor pressure. Unstable at room temperature. Prereacts with Me ₃ In at atmospheric pressure	164
Bu ⁱ SbMe ₂	7.3 at 23 °C	325 (InSb)	Low growth rates. Poor surface morphology in low-temperature layers	165
Sb(NMe ₂) ₃	0.75 at 20 °C	275 (InSb); 450 (GaSb)	Good morphology InSb layers at low temperature. Higher growth efficiency than other Sb precursors. Efficient getter of carbon from growth surface	166,167

Table 10 Arsenic MOVPE precursors.

<i>Precursor</i>	<i>Vapor pressure (torr)</i>	<i>Comment</i>
AsH ₃	Gas	Very toxic gas
Me ₃ As	238 at 20 °C	Liquid, relatively low toxicity
Et ₃ As	5 at 20 °C	Liquid, relatively low toxicity, low vapor pressure
Me ₂ AsH	176 at 20 °C	Liquid
Et ₂ AsH	40 at 20 °C	Liquid, low vapor pressure
Et ₃ As	434 at 20 °C	Liquid
Bu ⁱ AsH ₂	81 at 20 °C	Liquid
PhAsH ₂	1.8 at 20 °C	Liquid, low vapor pressure
As(NMe ₂) ₃	1.4 at 20 °C	Liquid, low vapor pressure
As(CF ₃) ₃		Liquid

9.23.5 SINGLE-MOLECULE APPROACH TO THE DEPOSITION OF COMPOUND SEMICONDUCTING MATERIALS BY MOCVD

In attempts to reduce toxic hazards, eliminate homogeneous prereactions, lower deposition temperatures, and use cheaper precursors there have been considerable efforts directed toward the development of alternative precursors for use in MOCVD.¹⁰ Another approach to using intrinsically less reactive compounds is to use a single-molecule (or “single-source”) precursor, in which all the elements required in the film are present in the one molecular species. The compounds potentially exhibit many or all of the following advantages over conventional MOCVD precursors:

- they are air and moisture stable;
- they are less toxic;
- they overcome the problem of chemical incompatibility between precursors (prereaction is limited), as there is only a single molecule in the supply stream;
- purification of one nonvolatile compound is easier than that of two or more volatile precursors, and hence the chance of incorporation of impurities in the thin films is reduced;
- impurity incorporation into films may be controlled by ligand design;
- low-temperature growth is often possible; and
- they overcome the problem of differences in thermal behavior between precursors.

Initially, the main disadvantage of using single-source precursors was their lack of volatility. However, the advent of ultralow-pressure and vacuum CVD techniques, along with the use of alternative delivery methods which do not rely primarily on precursor volatility, means that many compounds that are essentially nonvolatile can now be considered as potential CVD precursors. A major problem that remains, however, is that of stoichiometry control; a molecular precursor containing two (or more) elements in a specific ratio, as desired within the thin film to be grown, will not necessarily deposit those elements in the same proportions.

Despite the interest in single-source precursors, there are very few commercial applications that use them; however, it seems likely that such compounds will eventually be used for large-scale coverage applications, or in special cases where low-temperature growth is needed and where large areas need to be covered at relatively low cost.

9.23.5.1 Single-molecule Precursors for II–VI Materials

9.23.5.1.1 Dialkyldichalcogenocarbamate compounds

Chalcogenolato complexes, mostly of zinc and cadmium, have been the most studied as viable candidates for single-source precursors for II–VI materials, especially as the lower alkyl derivatives are generally crystalline solids with significant volatility. Further, it is well known that the solid-state pyrolysis of dithiocarbamate complexes, under an inert atmosphere, generally gives the corresponding metal sulfide. However, the stoichiometry and phase of the metal sulfide deposited are strongly dependent on the pyrolysis conditions^{173,174} and the organic ligand within the precursor. Their general formula is $[M(E_2CNRR')_2]$ ($M = \text{Zn, Cd, Te}$; $E = \text{S, Se}$; R and $R' = \text{alkyl}$; Figure 24). The preparation of these precursors follows a simple procedure in which CSe_2 or CS_2 is reacted with an excess of the amine and NaOH or KOH below 0°C to give the dithio/seleno carbamate as the dialkylammonium salt. This compound is then reacted with a stoichiometric

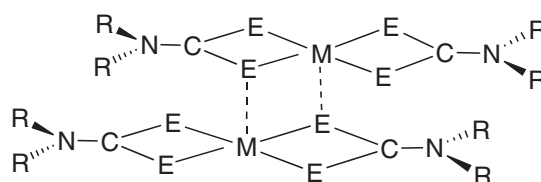
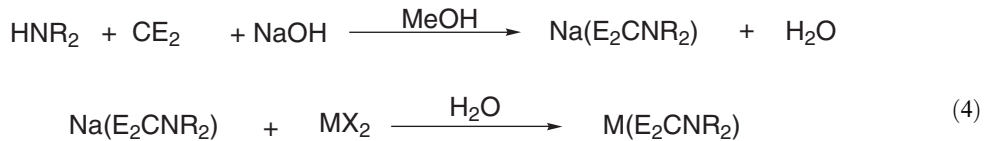


Figure 24 Dimeric structure of dialkyldichalcogenocarbamate compounds $[M(E_2CNR_2)_2]$ ($M = \text{Zn, Cd}$; $E = \text{S, Se}$).

quantity of an aqueous solution of cadmium(II) or zinc(II) halide to give the bis(dialkyldithio-/diselenocarbamato)cadmium(II)/zinc(II) compound (Figure 24, Equation (4)):



M = In or Cd, R = Alkyl or aryl, E = S or Se, X = halide

These complexes generally consist of dimeric units with each metal being five-coordinate, with bridging E atoms (E = S, Se) in each dimer forming a centrosymmetric core consisting of three edge-sharing four-membered rings (Figure 24). (For simplicity the subsequent discussion of these compounds will refer to them by their monomeric formula $[\text{M}(\text{E}_2\text{CNR}'')_2]$ even though in the solid state they are dimers $[\text{M}(\text{E}_2\text{CNR}'')_2]_2$.)

The most extensively studied of these complexes for use in CVD are the diethyldichalcogenocarbamates $[\text{M}(\text{E}_2\text{CNEt}_2)_2]$ (M = Zn, Cd; E = Se, S). These complexes are air-stable solids, and are dimeric in the solid state^{175,176} but monomeric in the vapor phase, as judged from mass spectra. Thin films of CdS, CdSe, ZnS, and ZnSe have been grown by a number of different MOCVD techniques using these complexes as single-source precursors; they are listed in Table 11.

Table 11 Growth of II–VI films from $\text{M}(\text{E}_2\text{CNEt}_2)_2$ (M = Zn, Cd; E = Se, S) precursors.

Compound semiconductor thin films	Method	Comment	References
ZnS, CdS, $\text{Zn}_x\text{Cd}_{1-x}\text{S}$	Low-pressure CVD	Polycrystalline, grown at 370–420 °C, hexagonal phase on glass	177
CdS, ZnS	OMVPE	Heterostructures on CdS, ZnS, CdTe, GaP, GaAs, and glass substrates	178,179
ZnS, CdS, $(\text{Zn}_x\text{Cd}_{1-x})\text{S}$	Hot-wall reactor, under active secondary vacuum	Glass and III–V substrates, growth at 400 °C. ZnS poor-quality films. CdS and $(\text{Zn}_x\text{Cd}_{1-x})\text{S}$ good-quality films. CdS epitaxially growth on (100)-oriented GaAs and InP substrates	180
ZnSe, CdSe	Hot-wall reactor	Deposited elemental selenium	181
ZnS	MOVPE cold-wall horizontal reactor	Epitaxially cubic phase grown on (111)Si growth at 400 °C. Without carrier gas, hexagonal α -ZnS of poor morphology and crystallinity	182
CdS	Low-pressure MOCVD	(10^{-2} torr), He and H_2 carrier gas, SiO_2 , Al_2O_3 , sapphire, (111)Si and (111)InP substrates, growth temperatures >450 °C, polycrystalline films, gave mixture of hexagonal and cubic phase on SiO_2 substrate	183
CdS	Plasma-enhanced MOCVD	Deposition temperature lowered by 200 °C, polycrystalline film of hexagonal phase, contaminated with carbon when grown below 250 °C	184
ZnS or CdS	Ultrasonic spray pyrolysis	Using toluene as solvent, growth temperatures of 460–520 °C, grown on (111)Si, (100)Si, (012) Al_2O_3 , (001) Al_2O_3 , and (100)GaAs substrates. Hexagonal phase when grown on silicon or Al_2O_3 ; epitaxial cubic when grown on GaAs	185

A number of other symmetric dichalcogeno carbamates have been employed in, for example, the deposition of ZnS by a dip-dry method¹⁸⁶ from a chloroform solution containing an equimolar mixture of $[\text{Zn}(\text{S}_2\text{CNBu}_2)_2]$ and the thiolate compound $[\text{EtZn}(\text{SPr}^i)]$. Pyrolysis was carried out at 300 °C under N_2 and the polycrystalline (cubic phase) films were free from oxide contamination.

9.23.5.1.2 Asymmetric dialkyldichalcogenocarbamate precursors

One approach to increasing precursor volatility is to use an asymmetrically substituted carbamate ligand with two different alkyl groups, as in the three compounds $[\text{Zn}\{\text{S}_2\text{CN}(\text{Me})\text{Et}\}_2]$, $[\text{Zn}\{\text{S}_2\text{CN}(\text{Me})\text{Pr}^n\}_2]$, and $[\text{Zn}\{\text{S}_2\text{CN}(\text{Me})\text{Bu}^n\}_2]$ (again, these are dimeric in the solid state).¹⁸⁷ Examples of these that were used successfully in CVD are the sulfur and selenium compounds $[\text{M}\{\text{E}_2\text{CN}(\text{Me})\text{Bu}^n\}_2]$ ($\text{M} = \text{Cd}, \text{Zn}$; $\text{E} = \text{S}, \text{Se}$). For $[\text{Zn}\{\text{S}_2\text{CN}(\text{Me})\text{Bu}^n\}_2]$ ZnS thin films were grown on borosilicate glass in a low-pressure cold-wall MOVCD reactor at substrate temperatures between 450 °C and 490 °C and gave hexagonal-phase films. $[\text{Cd}\{\text{S}_2\text{CN}(\text{Me})\text{Bu}^n\}_2]$, under similar conditions, produced hexagonal-phase films of CdS on glass and InP substrates.¹⁸⁸

In general, the bis(dialkyldithiocarbamate)cadmium(II)/zinc(II) complexes produce good-quality films whether the R groups are the same or different, while the diselenocarbamate the symmetrically substituted ligands (such as diethyldiselenocarbamate) yielded either elemental selenium or selenium-rich films.^{181,189} The bis(dialkyldiselenocarbamate)cadmium(II)/zinc(II) complexes with different R groups, such as $[\text{M}\{\text{Se}_2\text{CN}(\text{Me})\text{Hex}^n\}_2]$ ($\text{M} = \text{Zn}, \text{Cd}$; Figure 25) can be used to deposit stoichiometric ZnSe and CdSe by LP-MOCVD,¹⁸⁹ with source and deposition temperatures in the range 200–250 °C and 400–450 °C.¹⁹⁰ These observations suggest that the R groups determine the mechanistic pathway by which the precursor decomposes. Studies by GC-MS and electron impact mass spectrometry of $[\text{M}\{\text{Se}_2\text{CN}(\text{Me})\text{Hex}^n\}_2]$ ($\text{M} = \text{Zn}, \text{Cd}$), and of the symmetrically substituted analogues $[\text{M}(\text{Se}_2\text{CNET}_2)_2]$ ($\text{M} = \text{Zn}$ or Cd), suggest that selenium-rich films arise from the formation and subsequent decomposition of diethyldiselenide. By changing the combination of alkyl groups from equivalent (diethyl) to different (methyl and *n*-hexyl), the formation of diethyldiselenide is hindered, and thus the formation of selenium during film growth is inhibited.¹⁹⁰

9.23.5.1.3 Lewis base adducts of bis(dialkyldithiocarbamate) compounds

To improve the volatility and stability of $[\text{Cd}(\text{S}_2\text{CNET}_2)_2]$ it was converted to the adduct $[\text{Cd}(\text{S}_2\text{CNET}_2)_2(\text{phen})]$ ($\text{phen} = 1,10\text{-phenanthroline}$). Thin films of CdS were deposited using remote plasma-enhanced chemical vapor deposition (RPECVD) techniques, with films being grown in the temperature range 200–350 °C. The phase and quality of the as-grown films were dependent upon the substrate used, with polycrystalline grains of mixed hexagonal and cubic phases being obtained on fused silica substrates; in contrast only the polycrystalline hexagonal phase was observed on silicon substrates, and the pure cubic phase on InP substrates. Adducts of cadmium or zinc diethyldithiocarbamate have also been prepared with trialkylphosphines and used to deposit binary and ternary chalcogenides.¹⁹¹ A series of Lewis base adducts with bis(dialkyldithiocarbamate) compounds of general formula $[\text{LM}(\text{S}_2\text{CNR}_2)_2]$ ($\text{M} = \text{Zn}, \text{Cd}, \text{Mn}$, $\text{Mn}:\text{Zn}$, or $\text{Zn}:\text{Cd}$; $\text{L} = \text{phen}, 2,2'\text{-bipy}$ or $4,4'\text{-bipy}$) have been prepared and considered for use as

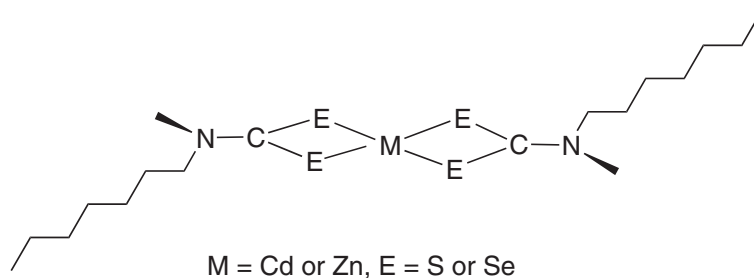


Figure 25 Structure of bis[methyl(*n*-hexyl)dithio-/selenocarbamate]-zinc and -cadmium complexes, $[\text{M}\{\text{E}_2\text{CN}(\text{Me})\text{Hex}^n\}_2]$ ($\text{E} = \text{S}, \text{Se}$; $\text{M} = \text{Zn}, \text{Cd}$).

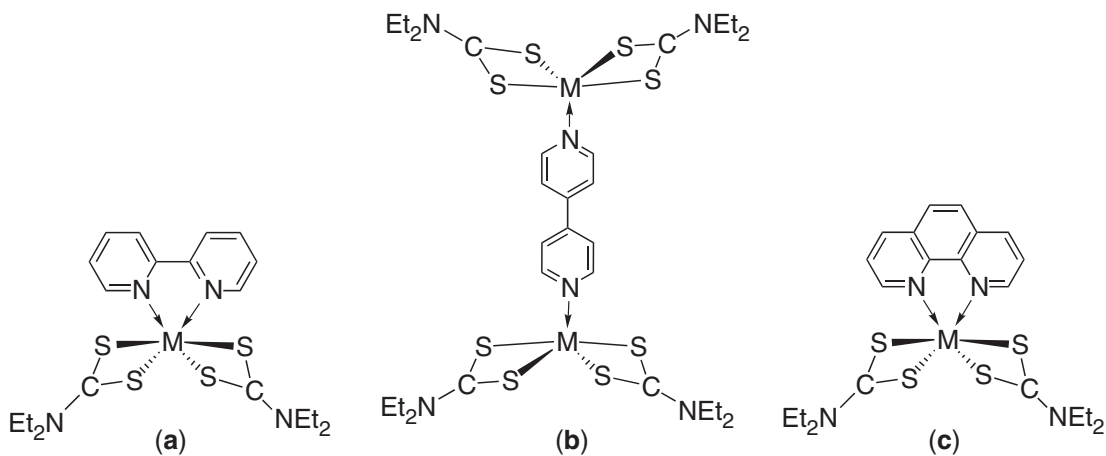
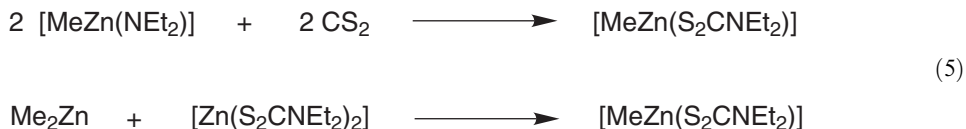


Figure 26 Structures of (a) $[M(S_2CNET_2)_2(2,2'\text{-bipy})]$ ($M = \text{Cd, Zn}$); (b) $\{[M(S_2CNPr^i)_2]_2(\mu\text{-}4,4'\text{-bipy})\}$; (c) $[M(S_2CNET_2)(\text{phen})]$ ($M = \text{Cd, Zn}$).

single-source precursors.^{192,193} The phen adducts $[(\text{phen})M(S_2CNET_2)_2]$ ($M = \text{Zn, Mn, Cd}$) and $[(2,2'\text{-bipy})M(S_2CNET_2)_2]$ ($M = \text{Zn, Cd}$)^{194,195} have been used to grow thin films of the corresponding metal chalcogenide by MOCVD and RPECVD techniques (Figure 26).^{196–199}

9.23.5.1.4 Mixed alkyl/dichalcogenocarbamate complexes

Heteroleptic complexes with both dithio-/diselenocarbamate and alkyl ligands may have the potential to provide lower deposition temperatures as well as increases in precursor volatility.²⁰⁰ These compounds consist of a dichalcogenocarbamate metal complex unit with an additional metal–carbon bond from an alkyl ligand, i.e., the complexes have the general formula $[RM(E_2CNR'_2)]$ ($R, R' = \text{alkyl group}$; $M = \text{Zn, Cd}$; $E = \text{S, Se}$; Figure 27). These compounds were first prepared by Noltes²⁰¹ using an insertion reaction²⁰² or by comproportionation as in Equation (5):^{203–205}



Unless bulky alkyl groups are present the compounds are generally dimeric²⁰² in the solid state with a wide range of compounds having been structurally characterized including:^{203–206} $[RM(E_2CNR'_2)]$ ($R = \text{Me, Et, Bu}^t, \text{Me}_3\text{CCH}_2$; $M = \text{Zn, Cd}$; $E = \text{S, Se}$; $R' = \text{Me, Et}$; Figure 27). The precursors $[RZn(S_2CNET_2)]$ ($R = \text{Me, Me}_3\text{C, and Me}_3\text{CCH}_2$),¹⁹⁸ $[RZn(\text{Se}_2\text{CNET}_2)]$ ($R = \text{Me, Et, Me}_3\text{C, and Me}_3\text{CCH}_2$),^{203,208} and $[MeCd(\text{Se}_2\text{CNET}_2)]$ have all been employed, and in general sublime under mild conditions, 100–150 °C at 10^{-2} torr.²⁰² Low-pressure MOCVD in a hot-wall reactor produced thin films of ZnS, ZnSe, CdSe, and $Zn_{0.5}Cd_{0.5}Se$.

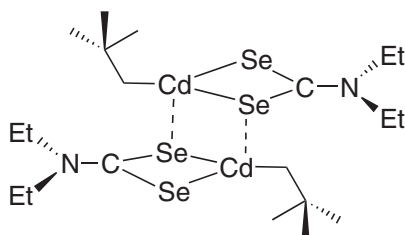


Figure 27 Structure of $[Me_3CCH_2Cd(\text{Se}_2\text{CNET}_2)_2]$.

Table 12 Mixed alkylthio- and diselenocarbamate complexes used to grow ZnSe and CdSe thin layers.

Precursor	Film	Substrate	T_g at 10^{-2} torr (°C)	Growth rate ($\mu\text{m h}^{-1}$)	Characteristic
MeZn(S ₂ CNEt ₂)	Cubic ZnSe ^a	GaAs	400	0.81	Polycrystalline
MeCd(S ₂ CNEt ₂)	CdSe	GaAs	425	0.48	Polycrystalline
MeCd(S ₂ CNEt ₂)	CdS	GaAs	425	0.2	Uneven
NpCd(S ₂ CNEt ₂) ^b	CdS	GaAs	425	0.04	Uneven

^a Determined with RHEED. ^b Np denotes *neo*-pentyl, (CH₃)₃CCH₂.

In a comparative study [(Me)Zn(S₂CNEt₂)], [(Me)Cd(S₂CNEt₂)], [(Me₃CCH₂)Cd(S₂CNEt₂)], and [(Me)Cd(S₂CNEt₂)] were used as precursors to deposit films of the respective metal chalcogenides on both glass and (100)-GaAs.²⁰⁹ It was reported that films of CdS grown at 425 °C from [(Me)Cd(S₂CNEt₂)] were of better quality than those from [(Me₃CCH₂)Cd(S₂CNEt₂)] grown at the same temperature. Both precursors gave films of improved quality at 400 °C. Using [(Me)Cd(S₂CNEt₂)], crystalline films of CdSe were grown on glass and GaAs substrates at temperatures between 280 °C and 425 °C. Some typical results²¹⁰ are summarized in Table 12.

9.23.5.1.5 Mixed alkyl/dichalcogenocarbamate complexes as precursors for ternary materials

An interesting feature of the comproportionation reaction used for the synthesis of these complexes is that it allows the preparation of mixed group 12/group 12 metal species such as methylcadmium-/methylzinc-diethyldiselenocarbamate. These mixed group 12 precursors have proved useful for deposition of thin films of ternary materials of Cd_{0.5}Zn_{0.5}Se. Thus the reaction of Me₂Zn with Cd(S₂CNEt₂)₂ gave [Me₂Cd_{0.5}Zn_{0.5}(S₂CNEt₂)₂]. The mixed aggregate consists of dimeric molecular units, [RM(S₂CNEt₂)₂]₂, similar to those of other alkylmetal dithio- and diselenocarbamates as mentioned above. In the solid state, cadmium and zinc atoms were modeled as randomly occupying the metal sites.²⁰⁴ Many of these mixed-metal complexes have been used to deposit thin films of metal chalcogenides by low-pressure MOCVD (10⁻²–10⁻³ torr); for example, polycrystalline Cd_{0.5}Zn_{0.5}Se layers were deposited on a glass substrate in this manner.

9.23.5.1.6 Monothiocarbamate and monothiocarboxylate compounds

There has also been much interest in the use of monothiocarbamate compounds; for example, thin films of CdS have been grown from [Cd(SOCCNEt₂)₂], in which the cadmium atom is bonded to two *S,O*-bidentate diethylmonothiocarbamate ligands and in a monodentate manner to the oxygen atoms of two further ligands (Figure 28a) from other complex units. The precursor sublimed without decomposition at 10⁻² torr between 200 °C and 250 °C. Films were grown by LP-MOCVD, at substrate temperatures of 300 °C and above,²¹¹ producing polymeric structures in the solid state.²¹²

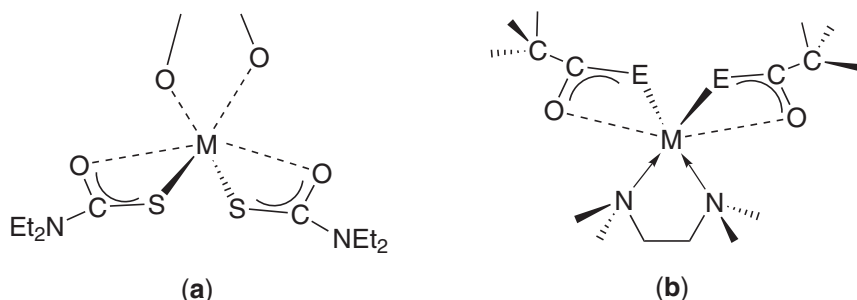


Figure 28 Structures of (a) [Cd{(SOCCMe₃)₂]₂]; (b) [M(SOCCMe₃)₂(TMEDA)] (M = Zn, Cd).

Monothiocarboxylate precursor complexes of the general formula $[M(\text{SOCR})_2(\text{tmeda})]$ ($\text{tmeda} = N,N,N',N'$ -tetramethylethylenediamine; $R = \text{Me}$,²¹³ or Bu^t ²¹⁴) are monomeric complexes in the solid state, with the metal atom in a distorted tetrahedral N_2S_2 coordination environment.²¹³ They have been successfully used to deposit CdS, ZnS, and $\text{Cd}_x\text{Zn}_{1-x}\text{S}$ films using aerosol-assisted liquid delivery CVD (AA-CVD); using AA-CVD from toluene solutions, crystalline films of CdS and ZnS could be grown at temperatures as low as 125 °C. $\text{Cd}_x\text{Zn}_{1-x}\text{S}$ films were also grown at 175 °C from solutions of the precursors mixed in various Cd/Zn ratios. The films were found to be Cd deficient under these deposition conditions, which was attributed to decomposition of the cadmium precursor before the zinc precursor. Better stoichiometric control over film composition was achieved by using feed-rate-limited deposition techniques with $[\text{Zn}(\text{SOCCMe}_3)_2(\text{tmeda})]$ and $[\text{Cd}(\text{SOCCMe}_3)_2(\text{tmeda})]$.²¹⁴

9.23.5.1.7 Other chalcogenide-based compounds

Divalent group 12 compounds with chalcogenate-containing ligands have, in general, polymeric structures with a tetrahedral metal center, and are particularly involatile.²¹⁵ Many such chalcogen-containing complexes have been shown to decompose to the corresponding II–VI material. However, the lack of volatility means that they are not generally useful as precursors using conventional CVD delivery methods. One approach to the volatility problem is the modification of the precursor by forming adducts with Lewis base compounds. A novel series of precursors for the deposition of II–VI materials has been reported by Steigerwald and co-workers²¹⁶, who prepared adducts of the phenyl and Bu^t chalcogens $M(\text{ER})_2$ ($M = \text{Zn}, \text{Cd}, \text{Hg}$; $E = \text{S}, \text{Se}, \text{Te}$) with 1,2-bis(diethylphosphino)ethane (depe). Complexes containing one and two mole equivalents of the bidentate phosphine have been isolated; the 1:2 species are polymeric while the 1:1 complexes are dimers (Figure 29).

These compounds were studied as potential single-source precursors. However, although they gave clean deposition routes to powders of II–VI materials, their nonvolatility means that thin-film growth by conventional CVD techniques was hampered, although it could be improved using new delivery techniques.

Hampden-Smith and co-workers have prepared $[\text{Zn}(\text{SEt})\text{Et}]_{10}$ (Figure 30) by the insertion of sulfur into the Zn–C bond of diethylzinc.²¹⁷ Although this decameric thiolate possesses an arrangement of zinc and sulfur atoms similar to that found in wurtzite, pyrolysis of the material at 250 °C led to predominantly cubic ZnS. Cubic ZnS was also formed when the precursor is used in a spray CVD process.

9.23.5.1.8 Chalcogenide-based compounds with high volatility

To increase precursor volatility, interest focused on using ligands of considerable bulk to reduce the degree of molecular association. This was of limited success, with mercury proving to be an exception. Bradley and Kunchur²¹⁸ reported that $\text{Hg}(\text{SBU}^t)_2$ has only weak intermolecular interactions and occurs as discrete $\text{Hg}(\text{SR})_2$ units even in the solid state. Other attempts to prepare complexes of zinc or cadmium with limited degrees of polymerization have been undertaken.

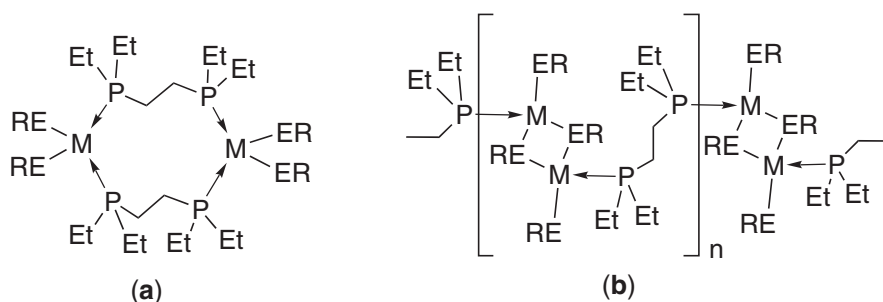


Figure 29 Structures of (a) molecular 1:1 and (b) polymeric 2:1 $M(\text{ER})_2$:depe adducts ($M = \text{Zn}, \text{Cd}, \text{Hg}$; $E = \text{S}, \text{Se}, \text{Te}$; $R = \text{Ph}, \text{Bu}^t$).

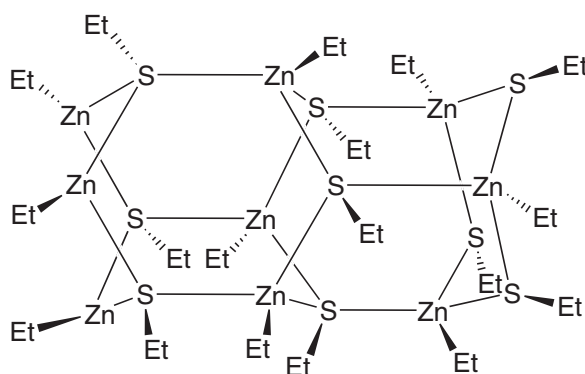


Figure 30 Structure of $[\text{Zn}(\text{SEt})\text{Et}]_{10}$.

Usually, such complexes are prepared using particularly bulky thiolate ligands such as 2,4,6-triisopropylbenzenethiol (tiptH).²¹⁹

Bochmann and co-workers^{220–223} further extended and developed such chemistry and produced a range of precursors for II–VI materials based on the bulky chalcogenolate ligands 2,4,6-tris(*t*-butyl)thiophenolate and 2,4,6-tris(*t*-butyl)selenophenolate. The general preparation method and structures are shown in Figure 31. $[\text{Cd}(\text{EC}_6\text{H}_2\text{Bu}^t_3)_2]$ ($\text{E} = \text{S}, \text{Se}$) are dimeric in the solid state and vapor phase, with two bridging and two terminal Se/S atoms (Figure 32). They sublime under vacuum above 240 °C for S and 220 °C for Se and are thermally stable at these temperatures.

These compounds have been used to deposit thin films of the respective metal sulfides and selenides in preliminary low-pressure growth experiments using LP-MOCVD. One problem with such ligands is that steric bulk is achieved by the use of large numbers of carbon atoms, therefore carbon incorporation into thin films grown from such precursors seems a distinct possibility.^{224,225}

For example, $[\text{Cd}\{\text{SC}_6\text{H}_2-(t\text{-Bu})_3\}_2]$ gave polycrystalline CdS thin films using low-pressure MOCVD techniques at a substrate temperature of 450 °C (0.01 torr). During the deposition, diarylsulfide was detected as a by-product. The mercury analogues readily decompose via a

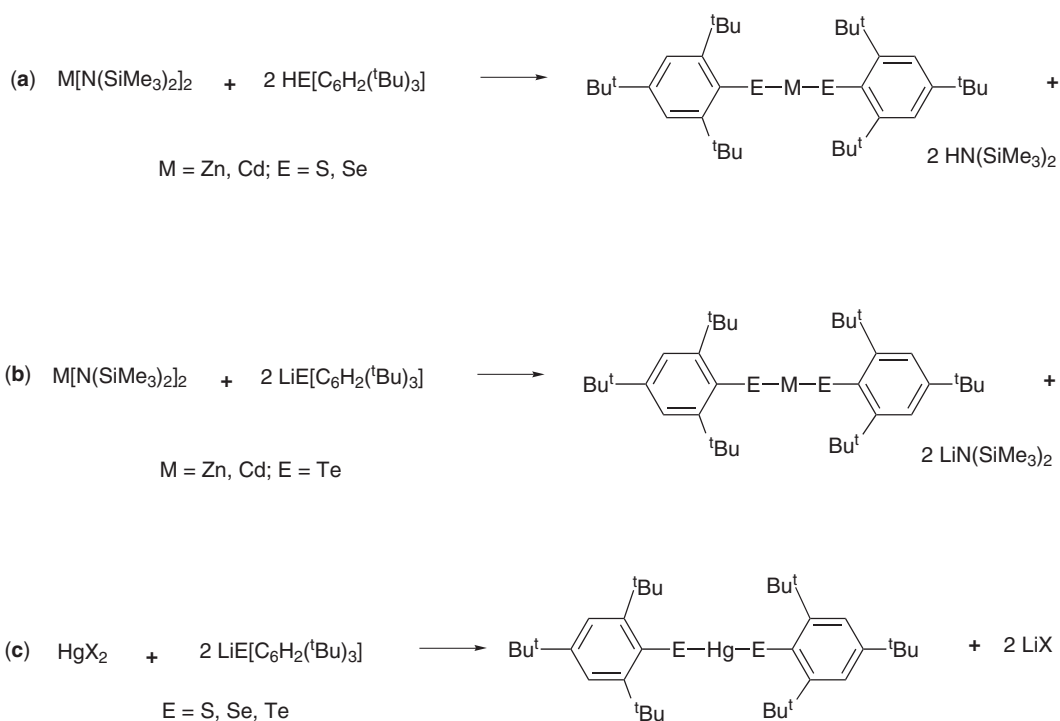


Figure 31 Synthetic routes to $[\text{M}\{\text{EC}_6\text{H}_2(\text{Bu}^t)_3\}_2]$: (a) $\text{M} = \text{Zn}, \text{Cd}; \text{E} = \text{S}, \text{Se}$; (b) $\text{M} = \text{Zn}, \text{Cd}; \text{E} = \text{Te}$; (c) $\text{E} = \text{S}, \text{Se}, \text{Te}$.

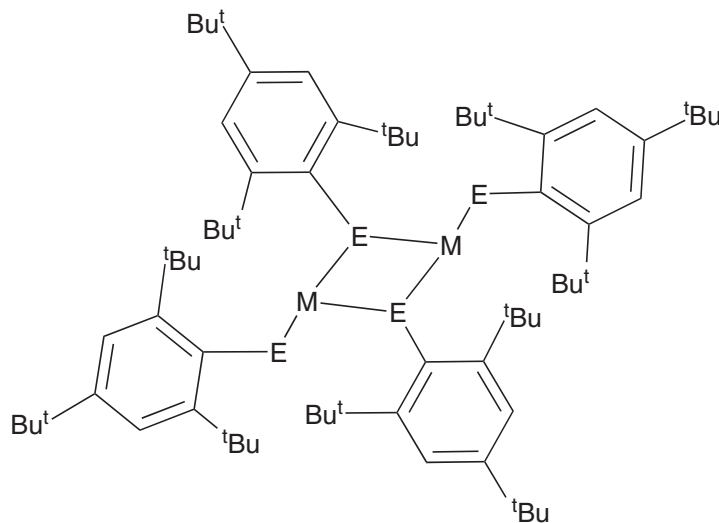
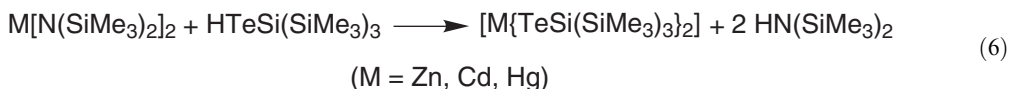


Figure 32 Structure of $[M(ETBu)_2]_2$ ($E = S, Se$; $M = Cd$).

reductive elimination path to form atomic Hg and diaryldichalcogenides, which may indicate that these compounds are more suitable for photoassisted MOCVD rather than thermal CVD.²²²

Another series of precursors designed for increased volatility involves the use of bulky ligands containing silyl groups, such as $[M\{EC(SiMe_3)_3\}_2]$ and $[M\{ESi(SiMe_3)_3\}_2]$ ($M = Zn, Cd, Hg$; $E = S, Se, Te$). In the solid state these form dimers with two bridging and two terminal E atoms (Figure 33) and have been used^{226,227} to deposit a range of chalcogenides. The most detailed work has been reported on the tellurides. Thin films of the tellurides were deposited by LP-MOCVD.²²⁸ The tellurium-containing compound $[HTeSi(SiMe_3)_3]$ has been used in the preparation of metal tellurolates.^{229–231} Its metal complexes are generally prepared as in Equation (6); decomposition to the metal telluride is via an elimination path:



Zinc telluride, ZnTe, was deposited on quartz, silicon, InAs, and GaSb substrates using $Zn[TeSi(SiMe_3)_3]_2$ at temperatures between 250 °C and 350 °C. On InAs (orientation not specified) a cubic ZnTe layer was obtained. Problems of stoichiometry are encountered at temperatures below 325 °C because decomposition of the precursor is incomplete, while at higher temperatures (above 350 °C) the deposited ZnTe decomposes into Zn (which evaporates) and involatile elemental tellurium which remains. The results with the analogous cadmium precursor (1.4 torr, 290 °C) indicate that the CdTe films may be of better stoichiometry than those of ZnTe, with XRD results indicating that on a Si substrate the hexagonal phase is predominantly

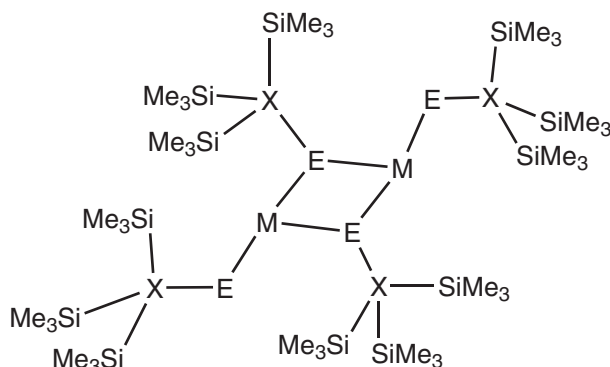


Figure 33 Structure of $[M\{EX(SiMe_3)_3\}_2]_2$ ($M = Zn, Cd, Hg$; $E = S, Se, Te$; $X = C, Si$).

deposited.^{228,231} Deposition studies using $\text{Zn}[\text{SeSi}(\text{SiMe}_3)_3]_2$, $\text{Zn}[\text{SeC}(\text{SiMe}_3)_3]_2$, $\text{Zn}[\text{TeC}(\text{SiMe}_3)_3]_2$, $\text{Zn}[\text{TeC}(\text{SiMe}_3)_3]_2$, $\text{Hg}[\text{SeSi}(\text{SiMe}_3)_3]_2$, and $\text{Hg}[\text{TeC}(\text{SiMe}_3)_3]_2$ gave mixed results.

For even better volatility the fluorinated aryl substituent $\text{C}_6\text{H}_2(\text{CF}_3)_3$ has been employed, as in the cadmium thiolate $[\text{Cd}\{\text{S}(\text{C}_6\text{H}_2(\text{CF}_3)_3)\}_2]$ which sublimates at 160°C under vacuum. When used in deposition the hexagonal phase of CdS was predominant with growth temperatures in the range $425\text{--}475^\circ\text{C}$, with no fluorine incorporation in the CdS films being observed.²³²

9.23.5.1.9 Thiophosphinates and related compounds

Thiophosphinate complexes are another class of chalcogen-containing compounds that may be useful as precursors. Takahashi *et al.*²³³ deposited CdS using the dimethylthiophosphinate $\text{Cd}(\text{S}_2\text{PME}_2)_2$. It was suggested that these complexes would be unsuitable as precursors, a conclusion based solely on their preliminary sublimation data. However, the use of compounds containing the thiophosphinate ligand is in itself undesirable: the deposited CdS shows normally *n*-type conduction (due to nonstoichiometry), and if any phosphorus is incorporated it will act as a *p*-type dopant, leading to a highly compensated semi-insulating material. Subsequently, Evans and Williams²³⁴ demonstrated that highly orientated sulfide films could be grown using the diethylthiophosphinate precursor $[\text{Cd}(\text{Et}_2\text{PS}_2)_2]$ (Figure 34), with no significant phosphorus incorporation. The phosphinochalcogen-amidate complexes $[\text{M}\{(\text{E})\text{NRP}(\text{Bu}^t)_2\}_2]$ ($\text{M} = \text{Zn}, \text{Cd}$; $\text{E} = \text{Se}, \text{Te}$; $\text{R} = \text{Pr}^i, \textit{c}\text{-C}_6\text{H}_{11}$) were also evaluated as single-source precursors for preparation of metal chalcogenide films; in these complexes one S donor of a thiophosphinate is replaced by an NR unit (Figure 34b).²³⁵ The films showed no significant incorporation of nitrogen.

9.23.5.2 Single-molecule Precursors for III–V Compounds

In the mid-1980s it was first realized that compounds of the type $[\text{R}_2\text{M}(\mu\text{-ER}')_2]$ ($\text{M} = \text{Ga}, \text{In}$; $\text{E} = \text{N}, \text{P}$; $\text{R} = \text{aryl or alkyl}$),^{264,265} in which there is a σ -bond between the group 13 and 15 elements giving a central (M_2E_2) core in the solid state (Figure 35), might be effective single-molecule precursors for the thin-film deposition of III–V materials. Some of the most interesting recent *p*-block organometallic chemistry has evolved from attempts to develop alternative precursors for III–V compound semiconductors. Many direct and indirect bandgap III–V semiconducting materials including GaAs, InAs, InP, GaP, and AlAs have now been deposited using such single-source precursors²³⁷ (Table 13).

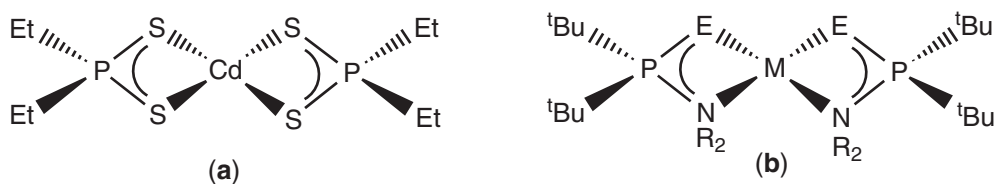


Figure 34 Structures of dithiophosphinate derivatives: (a) $\text{M} = \text{Cd}$, $\text{R} = \text{Et}$; (b) $[\text{M}\{(\text{Bu}^t)_2\text{PE}(\text{NR})\}_2]$ ($\text{M} = \text{Zn}, \text{Cd}$; $\text{E} = \text{Se}, \text{Te}$; $\text{R} = \text{Pr}^i, \textit{c}\text{-C}_6\text{H}_{11}$).

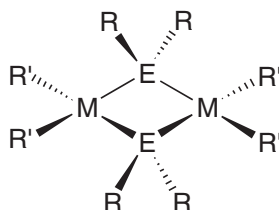


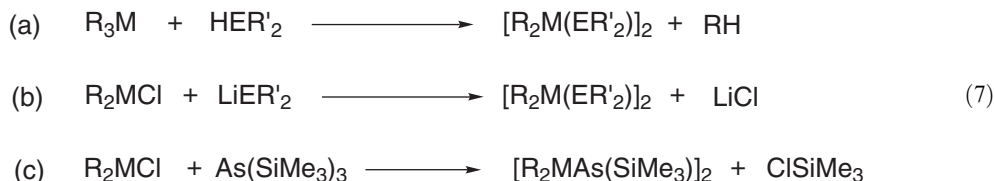
Figure 35 Structure of $[\text{R}_2\text{M}(\mu\text{-ER}')_2]$ ($\text{M} = \text{Ga}, \text{In}$; $\text{E} = \text{N}, \text{P}$; $\text{R} = \text{alkyl}, \text{aryl}$).

Table 13 Some compounds used as single-source precursors for III–V materials.

Compound	References	Compound	References
Dimeric			
[Bu ^t ₂ Ga{P(H)C ₅ H ₉ }] ₂	225	[Me ₂ In(NEt ₂)] ₂	236
[Me ₂ In(PBu ^t ₂)] ₂	236,255, 256,262	[Ph ₂ GaP(SiMe ₃) ₂ Ga(Ph) ₂ Cl]	245
[Et ₂ Al(AsBu ^t ₂)] ₂	254	[(Me ₃ SiCH ₂) ₂ InP(SiMe ₃) ₂] ₂	247
[Bu ^t ₂ Ga{As(SiMe ₃) ₂ }] ₂	246	[Bu ^t GaPAr] ₂	251
[(Me ₃ Si) ₂ Al{P(C ₆ H ₅) ₂ }] ₂	238	[(Me) ₂ Ga(NHBu ^t)] ₂	240
[Et ₂ Al{Sb(SiMe ₃) ₂ }] ₂	263	[Bu ^t ₂ Al{Sb(SiMe ₃) ₂ }] ₂	263
[Bu ⁿ ₂ Ga(AsBu ^t ₂)] ₂	260,261	[Me ₂ Ga(AsBu ^t ₂)] ₂	164, 256–258,264
[Et ₂ Ga(AsBu ^t ₂)] ₂	259		
Trimeric			
[Et ₂ Ga(PEt ₂)] ₃	237	[(Me ₃ CCH ₂)ClGa(PPh ₂)] ₃	248
[Bu ^t ₂ Ga(PH ₂)] ₃	249	[Me ₂ Ga(PPr ^t ₂)] ₃	250
		[Me ₂ In(SbBu ^t ₂)] ₃	
Monomeric			
Bu ^t ₂ Ga(PRR')	252	Ga(AsBu ^t ₂) ₃	264
(R, R' = aryl, silyl)			
Bu ^t ₂ GaN(R)(SiPh ₃)	253		
(R = Bu ^t , 1-adamantyl)			

Although many complexes of this type have appeared in the literature, with many publications emphasizing their potential use as single-source precursors, this section will only address compounds that have actually been used in the deposition of III–V thin films.

These precursors are generally prepared by “alkane elimination” (Equation (7a)); or—especially useful with bulkier substituents—the coupling of metal chlorides with lithium pnictides or silyl arsines (Equation (7b)); or “salt elimination” or “silyl halide elimination” reactions (Equation (7c)):



The first such precursors characterized by single-crystal X-ray crystallography were [R₂Ga(μ-E Bu^t₂)]₂ (R = Me, Buⁿ; E = P, As). The structures have two linked tetrahedra with each metal directly bonded to two alkyl groups and a pnictide and have overall four-coordination at the metal centers (Figure 35). The degree of association of phosphanoalane compounds was studied by Janik *et al.*,²³⁸ who concluded that compounds with small substituents (e.g., H, CH₃, C₂H₅, Cl) tended to form trimeric rings (Figure 36) whereas compounds with larger substituent groups such as aryl and silyl adopted a dimeric structure (Figure 35).

AlN, GaN, and InN are attractive materials for applications such as blue lasers and field emitters; single-source precursors for these of formula [R₂MNR'₂]₂ (R = alkyl, R' = alkyl or H) have been reported.²³⁶ The reaction of alkylamines with group 13 trialkyl metal compounds affords oligomeric or polymeric ring and cage structures of metal amides and imides (see section on nitrides).

The preparation of similar precursors suitable for the deposition of metal nitrides is analogous to the preparations of phosphorus and arsenic compounds. The initial reaction of metal trialkyls MR₃ (M = Al, Ga, In) with amines (NHR'₂) results in the formation of oligomeric amido compounds [R₂MNR'₂]_n (n = 2 or 3) which eliminate alkanes on thermolysis. The incorporation of a proton as a substituent on the pnictide bridging ligand has been examined, and many compounds of the type [R₂MNHR']₂ have been synthesized. The presence of this proton may facilitate β-elimination, allowing lower deposition temperatures to be used.

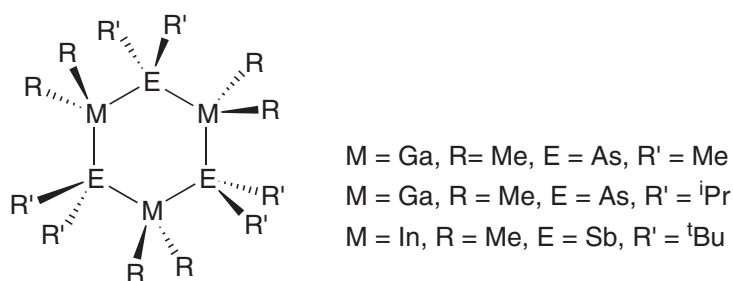


Figure 36 Structures of trimeric compounds $[\text{R}_2\text{M}(\mu\text{-ER}'_2)]_3$ possessing small alkyl substituents.

Some examples of dimeric primary amido compounds include $[\text{Bu}^t_2\text{GaNH}(\text{Ph})]_2$,²³⁹ $[\text{Me}_2\text{GaNH}(\text{Bu}^t)]_2$,²⁴⁰ $[\text{Me}_2\text{GaNH}(\text{Ph})]_2$,²⁴¹ and *trans*- $[(\text{PhMe}_2\text{CCH}_2)_2\text{GaNH}(\text{Pr})]_2$, all with structures similar to that shown in Figure 35.²⁴² Compounds of this type involving secondary amines are well known; two examples are $[(\text{Me}_2\text{N})_2\text{ClGa}]_2$ ²⁴³ and $[\text{Et}_2\text{Al}(\text{NC}_4\text{H}_8\text{S})]_2$ ($\text{NC}_4\text{H}_8\text{S}$ = thiomorphomorpholine)²⁴⁴ which, unusually for N-bridged aluminum compounds, has a butterfly-shaped core.

9.23.5.2.1 Dimeric precursor compounds

$[\text{Me}_2\text{Ga}(\text{AsBu}^t)]_2$ was used in a cold-wall reactor using a low pressure, and temperatures of between 450 °C and 700 °C; with either a neutral (He) or a reducing (H_2) carrier gas, GaAs films with carbon levels of 1000 ppm were obtained.^{255–257} Using CBE techniques, epitaxial (100)-oriented GaAs could be grown. However, high temperatures (475 °C) were necessary to complete the elimination of the hydrocarbon ligands.²⁵⁸ Substitution of Et_3Ga for Me_3Ga is known to lower carbon incorporation, so $[\text{Et}_2\text{Ga}(\mu\text{-AsBu}^t)]_2$ was employed; in the temperature range 400–500 °C GaAs films were grown but, due to the high reactivity of Ga ethyl groups, Ga islands were present.²⁵⁹

Epitaxial GaAs has been grown by UHV-MOCVD²⁶⁰ and using spray pyrolysis techniques with $[\text{Bu}^n_2\text{Ga}(\mu\text{-AsBu}^t)]_2$ as a precursor.²⁶¹ Spray pyrolysis from toluene solutions of $[\text{Bu}^n_2\text{Ga}(\mu\text{-AsBu}^t)]_2$ onto a GaAs substrate at 520–540 °C resulted in (100)-oriented epitaxial films contaminated with both oxygen and carbon.²⁶¹ UHV-MOCVD at 3.5×10^{-8} torr, on a Si substrate, again gave carbon contamination in the GaAs films, which were also arsenic-depleted films.

In two independent studies, InP was grown from the precursor complex $[(\text{CH}_3)_2\text{In}\{\mu\text{-P}(\text{Bu}^t)_2\}]_2$.^{255,256,262} First, Cowley *et al.* employed the use of a cold-wall reactor to deposit InP using H_2 or He as the carrier gas, with substrate temperatures between 450 °C and 700 °C. Using an MBE reactor, Bradley and co-workers found that stoichiometric growth was only possible at 480 °C and only when a simultaneous secondary incident flux of dissociated phosphine was added. Lower growth temperatures resulted in indium-rich deposits.

The Si-containing dimers $[\text{Et}_2\text{Al}\{\text{Sb}(\text{SiMe}_3)_2\}]_2$ and $[\text{Bu}^t_2\text{Al}\{\text{Sb}(\text{SiMe}_3)_2\}]_2$ have been investigated using high-vacuum MOCVD employing a cold-wall reactor; in the absence of a carrier gas deposition of AlSb films was possible. $[\text{Et}_2\text{Al}\{\text{Sb}(\text{SiMe}_3)_2\}]_2$ afforded AlSb films with 1:1 stoichiometry at deposition temperatures of 375–425 °C; temperatures of 425–475 °C were required when $[\text{Bu}^t_2\text{Al}\{\text{Sb}(\text{SiMe}_3)_2\}]_2$ was used as precursor. Higher deposition temperatures resulted in the incorporation of silicon.¹⁷⁰

9.23.5.2.2 Monomeric precursor compounds

The presence of Ga—C σ -bonds in many dimeric precursor complexes was found to affect the quality of the resultant films and the film growth rate; in many cases films obtained from dimers were found to contain significant levels of carbon. Monomer species have also been investigated.

The monomer $\text{Ga}(\text{AsBu}^t)_3$ has been used in a number of deposition studies. In an initial study, films were grown at 480 °C under reduced pressure (5–10 torr) and gave epitaxial films with low carbon incorporation. The nonstoichiometric As:Ga ratio (3:1) in the precursors gave rise to *n*-type films, whereas the films are generally *p*-type when prepared using the dimers mentioned

above.²⁶⁴ A later deposition study using CBE operating at 8×10^{-6} torr gave epitaxial films when grown between 415°C and 590°C, it being noted that the surface smoothness of the as-grown films decreased with increasing temperature. Secondary ion mass spectrometry indicated high levels of Si, O, and C impurities within the films.²⁶⁶ Pyrolysis^{250,265} and temperature-programmed adsorption (TDP)²⁶⁴ studies suggest two modes of decomposition for these precursors; As—C bond hydrolysis to form Bu^t radicals, and H elimination from Bu^tAs moieties, followed by $\cdot\text{CH}_3$ and $\cdot\text{H}$ coupling at Ga to form isobutene and methane.

9.23.5.2.3 Trimeric precursor compounds

Trimeric complexes (Table 13, Figure 36) such as $[\text{Me}_2\text{Ga}(\mu\text{-AsMe}_2)]_3$ and $[\text{Me}_2\text{Ga}(\mu\text{-AsPr}^i)_2]_3$ failed to yield satisfactory thin films of GaAs. Pyrolysis studies suggest that this is because of the facile loss of tetraalkyldiarsine.^{250,265} Films of InSb have been grown on silicon wafers in a hot-wall reactor from the precursor species $[\text{Me}_2\text{In}(\mu\text{-SbBu}^t)_2]_3$ at 450°C, using H_2 (10 torr) as the carrier gas.²⁶⁷

9.23.5.3 Nitride Films from Single-molecule Precursors

The nitrides GaN, AlN, InN, and their ternary alloys such as AlGaN or InGaN now have applications in green/blue and blue LED and semiconductor lasers.²⁶⁸ The conventional method for thin-film deposition is the co-deposition of group 13 metal alkyls with ammonia; however, high temperatures are needed due to the high thermal stability of NH_3 (15% pyrolyzed at 950°C). The current high commercial demand for blue LEDs is leading to interest in using single-source precursors as cheaper and safer alternatives.²⁶⁹ Many studies have been undertaken to use single-source precursors with preformed E—N σ -bonds (E = Ga, In, Al) in attempts to lower the deposition temperature.

Thin films of aluminum nitride, AlN, were deposited at 200–250°C using a combination of $[\text{Al}(\text{NMe}_2)_3]_2$ and NH_3 .²⁷⁰ AlN films were subsequently deposited directly from the parent adduct $[\text{Me}_3\text{Al}(\text{NH}_3)]$ (Figure 37a), without additional NH_3 .²⁷¹ Film growth was carried out at low pressure (65 torr) in the temperature range 400–800°C. Auger electron spectroscopy (AES) showed that the films contained residual oxygen and carbon. The relatively low levels of carbon found in AlN films can be attributed to the efficient removal of methyl radicals by the NH_3 and NH_2 groups present. The general decrease in carbon levels with increasing growth temperatures indicates that this methyl-gathering process is more efficient at high temperature. Using the volatile organoaluminum amide $[\text{Me}_2\text{Al}(\mu\text{-NH}_2)]_3$ (Figure 37b),²⁷² AlN has been grown successfully by LP-CVD in the temperature range 400–800°C. Although the resultant films were shown by AES to contain levels of oxygen, they were essentially free from carbon contamination.

The single-source precursors $[\text{Me}_2\text{Al}(\mu\text{-NHR})]_2$ (R = Prⁱ, Bu^t; Figure 37c) have been used to deposit AlN films by vacuum CVD at substrate temperatures between 377°C and 677°C.²⁷³ The films were shown by X-ray photoelectron spectroscopy (XPS) to contain extremely high levels of carbon (40–50%), which was attributed to the decomposition of methyl groups attached to the Al atom. $[\text{Me}_2\text{Al}(\text{NHBu}^t)]_2$ as precursor was shown to deposit AlN at lower temperatures than

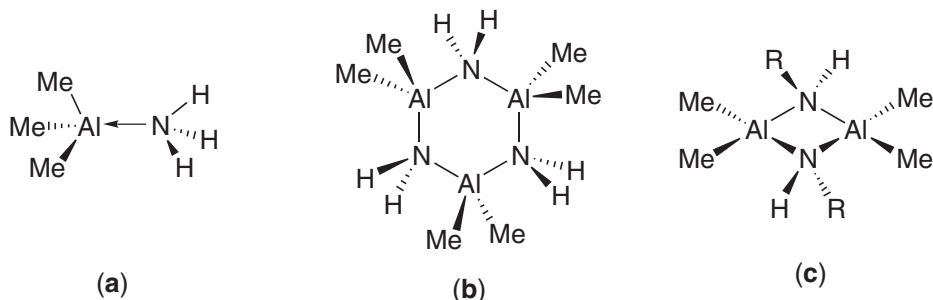
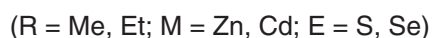
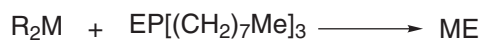
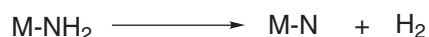
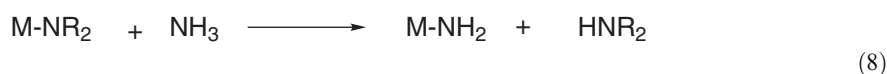


Figure 37 Structures of (a) $[\text{Me}_2\text{Al}(\text{NH}_3)]$; (b) $[\text{Me}_2\text{Al}(\mu\text{-NH}_2)]_3$; (c) $[\text{Me}_2\text{Al}(\mu\text{-NHR})]_2$ (R = Prⁱ, Bu^t).

$[\text{Me}_2\text{Al}(\text{NHPr}^i)]_2$, and led to films with lower levels of carbon contamination. $[\text{Me}_2\text{Al}(\text{NPr}^i)_2]_2$ was used to deposit AlN at 650°C by vacuum CVD although no information on film purity was presented.²⁷⁴ The high carbon levels resulting in Al films grown from single-source precursors of the type $[\text{Me}_2\text{Al}(\text{NHR})]_2$, in contrast to films grown from $[\text{Me}_2\text{Al}(\text{NH}_2)]_3$, can be attributed to the amount of active hydrogen on the nitrogen center, which is required to remove methyl and other alkyl radicals from the growth zone. The hydrazidoalane single-source precursor $[\text{Me}_2\text{Al}\{\text{N}(\text{H})\text{NMe}_2\}]_2$ produced polycrystalline AlN films using CVD at 800°C and at low pressure (6.7×10^{-3} Pa). The ethyl analogue $[\text{Et}_2\text{Al}\{\text{N}(\text{H})\text{NMe}_2\}]_2$, however, produced amorphous films on Si substrates, with Al:N ratios of between 1.2 and 1.4 and high contamination from carbon (15–18%) and oxygen (26–28%).²⁷⁵

GaN films have been deposited on a variety of substrates at 200°C by MOCVD using the nonstoichiometric 3:1 (nitrogen:gallium) precursor $[\text{Ga}(\text{NMe}_2)_3]_2$, although for optimal growth results a further nitrogen source had to be added in the form of NH_3 (to reduce carbon contamination in the as-grown films).²⁷⁶ Analysis by XPS indicated that carbon and oxygen levels in the films were low. These lower levels of C and O as compared with films grown using $[\text{M}(\text{NR}_2)_3]_2$ were attributed to the role²⁷⁶ that NH_3 plays in the removal of carbon-containing radicals via a facile transamination reaction of the type shown in Equation (8):



(9)



Using the gallium complex $[\text{Me}_3\text{Ga}(\text{NH}_3)]$ it did not prove possible to deposit GaN by MOCVD.²⁷¹ At substrate temperatures of $700\text{--}950^\circ\text{C}$, Ga metal was deposited, indicating that the $[\text{Me}_3\text{Ga}(\text{NH}_3)]$ adduct had dissociated into its component parts in the hot zone of the reactor upstream of the substrate. GaN thin films have, however, been deposited at $600\text{--}800^\circ\text{C}$ using $[\text{Et}_3\text{Ga}(\text{NH}_3)]$ in the absence of any added NH_3 .²⁷⁷ In order to achieve acceptable growth rates the sparingly volatile $[\text{Et}_3\text{Ga}(\text{NH}_3)]$ source had to be heated to 70°C . It was suggested that the use of elevated temperatures may have led to source decomposition so that the active precursor to GaN film growth was actually the trimer $[\text{Et}_2\text{Ga}(\text{NH}_2)]_3$ (Figure 36). A later study used $[\text{Et}_2\text{Ga}(\text{NH}_2)]_3$ to prepare highly crystalline GaN films by LP-MOCVD in a cold-walled reactor with growth in the temperature range $500\text{--}700^\circ\text{C}$. With no additional ammonia the films showed 1:1 stoichiometry, but there was carbon and oxygen contamination even under optimal conditions.²⁷⁸

Preliminary studies on the dimeric complex $[\text{Bu}^i(\text{H})\text{Ga}(\mu\text{-NET}_2)]_2$, prepared by the addition of four equivalents of Bu^iLi to the gallium chloride complex $[\text{Cl}_2\text{Ga}(\mu\text{-NET}_2)]_2$, proved to be air stable and produced gallium-rich GaN films at deposition temperatures as low as 250°C using CVD. However, it was necessary to add an external nitrogen source in order to obtain 1:1 GaN films.²⁷⁹

9.23.5.3.1 Group 13 azides as single-molecule precursors for nitrides

There has been much speculation regarding the use of azides as single-source precursors. AlN and GaN have been grown on Si and sapphire substrates by LPCVD using the trimeric dialkylaluminum and dialkylgallium azides $[\text{Et}_2\text{Al}(\text{N}_3)]_3$ ²⁸⁰ and $[\text{Et}_2\text{Ga}(\text{N}_3)]_3$ (Figure 38a).^{280,281} The AlN films were deposited at temperatures in the range $450\text{--}900^\circ\text{C}$ while GaN films were deposited at $400\text{--}600^\circ\text{C}$. GaN films were deposited by LPCVD at 400°C using $[\text{Me}_2\text{Ga}(\text{N}_3)]_m$,²⁸² which were

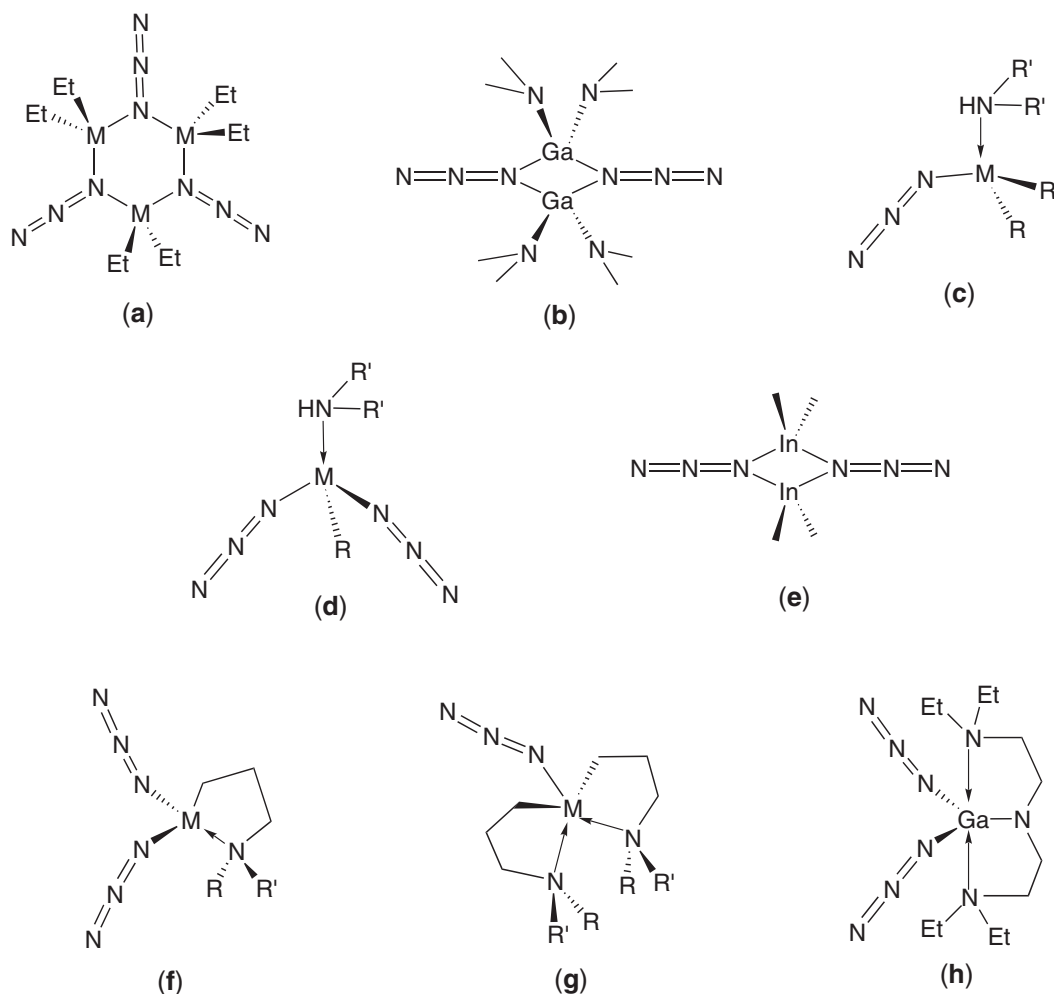


Figure 38 Structures of some group 13 metal-azide complexes: (a) $[\text{Et}_2\text{M}(\text{N}_3)_3]$ ($\text{M} = \text{Al}, \text{Ga}, \text{In}$); (b) $[(\text{Me}_2\text{N})_2\text{Ga}(\text{N}_3)_2]$; (c) $[(\text{N}_3)\text{MR}_2(\text{NHR}')]$; (d) $[(\text{N}_3)_2\text{MR}(\text{NHR}')]$; (e) $[\text{Me}_2\text{In}(\text{N}_3)_2]$; (f) $[(\text{N}_3)_2\text{M}\{(\text{CH}_2)_3\text{NR}_2\}]$; (g) $[(\text{N}_3)\text{M}\{(\text{CH}_2)_3\text{NR}_2\}_2]$; (h) $(\text{N}_3)_2\text{Ga}[\text{N}\{(\text{CH}_2)_2\text{NET}_2\}_2]$ (see Table 14 for more details).

shown to be polymeric in the solid state. It was found²⁸⁰ that the crystalline quality of AlN and GaN films grown from $[\text{Et}_2\text{Al}(\text{N}_3)_3]$ and $[\text{Et}_2\text{Ga}(\text{N}_3)_3]$ was inferior to that of films grown from the separate sources $\text{Et}_3\text{Al}/\text{NH}_3$ and $\text{Et}_3\text{Ga}/\text{NH}_3$, which was attributed to the $[\text{R}_2\text{M}(\text{N}_3)_3]$ species having lower surface diffusion rates than the separate group 13 source and ammonia. The presence of NH_3 was again found to influence significantly film growth, with the addition of a small amount of NH_3 in the gas phase leading to a considerable improvement in the crystalline quality of AlN films deposited.²⁸⁶ It was also found that crystalline GaN could not be deposited from the $[\text{Et}_2\text{Ga}(\text{N}_3)_3]$ sources alone.²⁸¹ Instead, amorphous GaN was deposited at low substrate temperatures,²⁷⁷ it was suggested gas-phase depletion of the Ga precursor inhibited GaN deposition at temperatures greater than 400°C . Again, the addition of a small amount of NH_3 resulted in the growth of higher quality crystalline GaN at temperatures greater than 500°C . It was proposed that NH_3 may act as a donor, blocking the formation of $[\text{Et}_2\text{Ga}(\text{N}_3)_3]$ trimers and reducing the subsequent gas-phase polymerization reactions that would otherwise deplete the $\text{Et}_2\text{Ga}(\text{N}_3)$ monomer concentration.²⁸⁴ The GaN films were grown at 700°C from $[\text{Et}_2\text{Ga}(\text{N}_3)_3]/\text{NH}_3$ and were *n*-type.²⁸⁰ The dimeric single-source precursor $[(\text{Me}_2\text{N})_2\text{Ga}(\text{N}_3)_2]$ (Figure 38b) was used to deposit epitaxial single-crystal films of GaN at 580°C by high-vacuum CVD.²⁸³

A significant problem associated with the use of preformed single-source precursors such as $[(\text{Me}_2\text{N})_2\text{Ga}(\text{N}_3)_2]$, $[\text{Al}(\text{NR}_2)_3]_2$, $[\text{R}_2\text{Al}(\text{NR}_2)]_2$, and $[\text{R}_2\text{M}(\text{N}_3)_3]$ ($\text{M} = \text{Al}, \text{Ga}$) is that being polynuclear species they generally have only very low vapor pressure. Using conventional CVD delivery methods, along with the use of very low pressure vacuum CVD equipment, it is necessary

Table 14 Group 13 azides used as precursors to grow group 13 nitrides.

<i>Compound</i>	<i>Reactor conditions</i>	<i>Comment</i>	<i>References</i>
$[(N_3)_2Ga\{(CH_2)_3NMe_2\}]$; liquid precursor, nonpyrophoric, nonexplo- sive	Horizontal cold-wall CVD	Transparent 1:1 stoichiometric films. Growth temperature 773–1323 K, no additional N source	286
$[(N_3)_2Ga\{N(CH_2CH_2NEt_2)_2\}]$; low volatility	Horizontal hot-wall LP-CVD	Growth temperature 750–950 °C, preferred orientation of crystallites perpendi- cular to <i>c</i> -plane of sapphire substrate, no additional N source	287
$[(N_3)_2Ga\{(CH_2)_3NMe_2\}]$; nonpyrophoric, nonexplo- sive	Horizontal hot-wall LP-CVD	Epitaxial film growth, no additional N source	143
$[(N_3)In\{(CH_2)_3NMe_2\}_2]$; nonpyrophoric	Horizontal hot-wall LP-CVD	Amorphous and polycrystalline film growth at 600–750 °C, no additional N source	143,288,289
$[(N_3)Al\{(CH_2)_3NMe_2\}_2]$; nonpyrophoric, air stable	Horizontal hot-wall LP-CVD	Amorphous and epitaxial film growth, no additional N source	143
$[(N_3)AlMe_2(H_2NBu^t)]$; nonpyrophoric	Horizontal hot-wall LP-CVD	Amorphous and epitaxial film growth at 900 °C, no additional N source	143
$[Me_2In(N_3)]_2$	Vertical cold-wall LP-CVD	Si(100) substrate, 350–450 °C, films N-deficient In:N ~ 1:0.60, polycrystalline hexagonal phase, no carrier gas used	290
$[H_2Ga(N_3)]$; volatile	UHV-CVD	200–800 °C, silicon substrate gave wurtzite-phase GaN, nanocrystalline films with oxygen and carbon incorporation	291
$[Et_2Ga(N_3)(MeNH-NH_2)]$	LP-MOCVD	Si(111) substrate, epitaxial GaN films, low growth temperatures employed, low contamination	292
$[Cl_2Ga(N_3)]$; air sensitive, sublimes at 70–100 °C in vacuum	UHV-CVD	Heteroepitaxial growth on Si and sapphire substrates at 650– 700 °C, 1:1 films, no need for additional N source	293
$[(Me_3Si)(N_3)GaCl]$	UHV-CVD	Reasonable quality GaN at 650 °C	293
$Cl_2Ga(N_3)(NMe_3)$	Cold-wall CVD	1:1 GaN grown at 700 °C on Si and sapphire substrates, chlorine and carbon contamination	293

to heat the source containers and reactor inlet lines in order to achieve acceptable growth rates of the metal nitride films.

There have been many other reports of single-source azido precursors, all aimed at achieving device-quality films using moderate deposition conditions. The azide precursors have the advantages of (i) having preformed Ga—N bonds and (ii) only a limited number of the undesirable Ga—C and N—C bonds which can lead to carbon incorporation into the nitride films.³¹¹ A list of azido-based precursors and deposition conditions is given in Table 14.

9.23.5.4 III–VI Materials from Single-molecule Precursors

The majority of III–VI materials are mid- to wide-bandgap semiconductors, with a direct electronic transition to the conduction band (Table 1). Thin films of III–VI materials have been prepared by various growth techniques and are potential alternatives to II–VI materials in optoelectronic and photovoltaic devices.²¹² In addition to the simple binary compounds, there are important ternary and quaternary phases such as CuInE_2 and $\text{CuIn}_{1-x}\text{Ga}_x\text{E}_2$ ($\text{E} = \text{S}$ or Se), with potential uses in solar cell applications. The approaches that have been taken in developing single-source molecular precursors for III–VI materials are similar to those used for II–VI materials.^{294–296} A wide range of chalcogen-containing ligands has been used to prepare complexes with direct metal–chalcogen bonds. The ligands used include thiolates,^{297,298} selenoates,²⁹⁹ thiocarbonylates,³⁰⁰ dithio- and diselenocarbamates,³⁰¹ and monothiocarbamates.^{302–304} However, there have been relatively few reports of the deposition of III–VI thin films from single-source precursors. For example, the preparation of thin films of $\beta\text{-In}_2\text{S}_3$ by the spray pyrolysis of an aqueous solution of InCl_3 and thiourea in methanol/water was reported.³⁰⁵ The first studies on the deposition of III–VI materials using single-source precursors were carried out by Nomura and co-workers in the late 1980s. Their studies have mainly involved the growth of indium sulfide,^{297,298,306} indium oxide,^{307,308} and the related copper-doped ternary and quaternary materials.^{295,308}

Many of the studies on the preparation of indium sulfide films have been based on the use of volatile alkylindium–alkylthiolate complexes with bulky substituents. Such substituents can lead to an increase in the overall volatility of the precursor. Complexes such as $[(\text{Bu}^t)_2\text{In}(\text{SPr}^n)]$ are liquids, which is an advantage when using conventional CVD techniques.³⁰⁶ The related compound $[(\text{Bu}^t)_2\text{In}(\text{SPr}^t)_2]$, prepared by the reaction of tri-*n*-butylindium and two equivalents of 2-propanethiol, was used to grow films by LP-MOCVD between 300 °C and 400 °C on Si and quartz substrates.²⁹⁸ The films were shown to be tetragonal $\beta\text{-In}_2\text{S}_3$, with a preferred orientation along the (103) plane. Growth at higher temperatures (450 °C) led to the sulfur-deficient phase In_6S_7 . $[(\text{Bu}^t)_2\text{In}(\text{SPr}^n)]$ was also used to prepare sulfur-doped indium oxide thin films by AP-MOCVD.³⁰⁷

As with II–VI and III–V precursors, the molecular design of the precursor can play an important role in the deposition route taken and in determining the nature of the thin films deposited.³⁰⁹ A comparison of the films grown from $[(\text{Bu}^t)_2\text{In}(\text{SBu}^t)]_2$, $[(\text{Me})_2\text{In}(\text{SBu}^t)]_2$, and the bis-thiolate complex $[\text{MeIn}(\text{SBu}^t)_2]$ illustrates the importance of deposition temperature, decomposition mechanism, and the choice of precursor used. At 400 °C the methyl-substituted complex deposited an indium-rich amorphous phase and In_2S_3 , whereas the *t*-butyl-substituted complex deposited highly oriented tetragonal InS . It has been suggested that the stronger In—C bond in

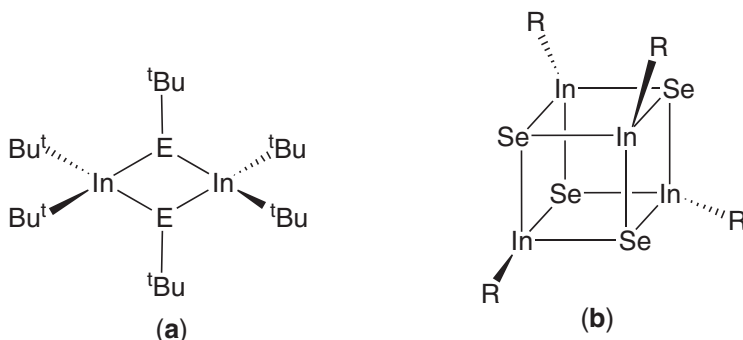


Figure 39 Structures of (a) $[(\text{Bu}^t)_2\text{In}(\text{EBu}^t)]_2$ ($\text{E} = \text{S}, \text{Se}$); (b) $[\text{RInSe}]_4$ ($\text{R} = \text{Bu}^t, \text{CMe}_2\text{Et}$).

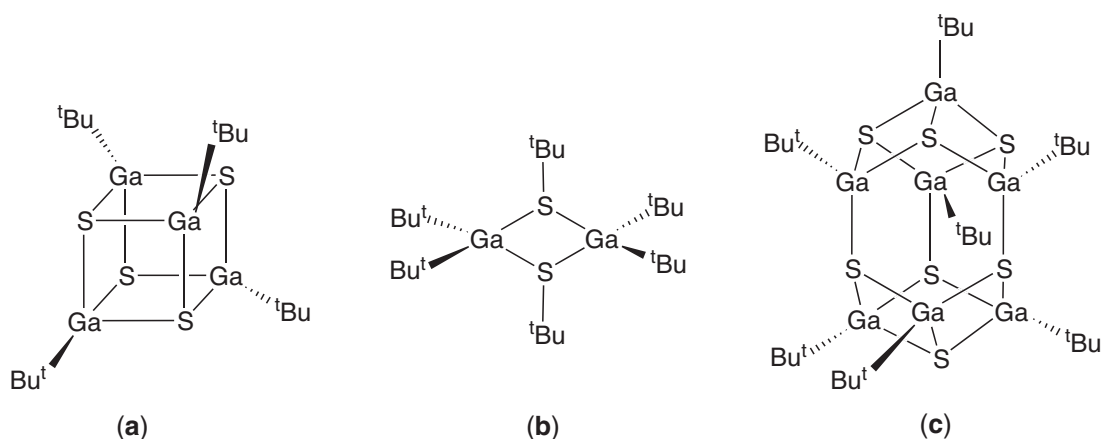


Figure 40 Structures of (a) $[\text{Bu}^t\text{GaS}]_4$; (b) $[\text{Bu}^t_2\text{Ga}(\text{SBu}^t)]_2$; (c) $[\text{Bu}^t\text{GaS}]_7$.

the former results in fragmentation of the precursor upon decomposition, whereas the latter exhibits clean ligand loss. However, the bis-thiolate complex leads to an amorphous phase, although annealing produced crystalline $\beta\text{-In}_2\text{S}_3$. In related studies, indium selenide thin films have been prepared from the analogous selenolate complexes.³¹⁰

Barron and co-workers also prepared a number of dialkylindium selenolates and alkylindium selenides,³¹⁰ and deposited indium selenide films by LP-MOCVD. $[(\text{Bu}^t)_2\text{In}(\text{SeBu}^t)]_2$ (Figure 39a) deposited indium-rich films by LP-MOCVD³¹⁰ at temperatures between 230 °C and 420 °C. $[(\text{Me}_2\text{EtC})\text{InSe}]_4$ (Figure 39b) gave crystalline films of InSe, the film quality being dependent on the growth temperature employed. Gysling and co-workers have also prepared thin films of indium selenide on GaAs (100) from $[(\text{Me})_2\text{In}(\text{SePh})]$ and $[\text{In}(\text{SePh})_3]$ by a spray-assisted MOCVD technique.²⁹⁹ Pyrolysis of $[\text{In}(\text{SePh})_3]$ gave hexagonal films of In_2Se_3 at temperatures of 470–530 °C, whereas the cubic phase is observed at deposition temperatures between 310 °C and 365 °C.

A number of metal chalcogenide complexes with interesting cubane structures $[\text{Bu}^t\text{GaS}]_4$ (Figure 40a), have been prepared by thermolyzing the dimer $[\text{Bu}^t_2\text{Ga}(\mu\text{-SH})]_2$, which was synthesized by the addition of an excess of H_2S to Bu^t_3Ga .^{311,312} The cubane has no direct carbon–sulfur bonds, and is supported by metal–sulfur interactions. $[\text{Bu}^t\text{GaS}]_4$ is air stable and was used to grow GaS by atmospheric pressure MOCVD at 380–400 °C. The GaS films were deposited on both KBr and GaAs (100); on the latter substrate a degree of epitaxial growth was observed, with the films being a novel cubic phase of GaS. It was suggested that the cubic nature of the core structure of the $[\text{Bu}^t\text{GaS}]_4$ precursor is maintained throughout deposition, and leads to the cubic structure observed in the as-deposited GaS. At higher temperatures (>450 °C) there is sulfur loss from the films and an amorphous matrix of gallium resulted. When using the analogous cubane selenide or telluride precursors $[\text{RGa}(\mu_3\text{-E})]_4$ (where E = S, Se, or Te; R = CMe_3 , CETMe_2 , CEt_2Me , or Et_3C),^{313,314} in contrast to the sulfides, the hexagonal phase of GaSe is deposited by AP-MOCVD (~350 °C). Similarly, hexagonal GaTe was deposited by LP-MOCVD at 285–310 °C. There are also examples of cubanes with indium chalcogenides,³¹⁰ however, $[\text{Bu}^t\text{InSe}]_4$ was found to give only indium metal films by LP-MOCVD. The complex $[(\text{Me}_2\text{EtC})\text{InSe}]_4$ (Figure 39b) gave hexagonal InSe in LP-MOCVD, with the best results observed at 290–350 °C.

Barron has also used the dimeric thiolato complex $[(\text{Bu}^t)_2\text{Ga}(\text{SBu}^t)]_2$ (Figure 40b) and the larger heptameric complex $[\text{Bu}^t\text{GaS}]_7$ (Figure 40c) to deposit poorly crystalline hexagonal and amorphous GaS₄ films. Use of $[\text{Ga}(\text{SPR}^t)_2(\mu\text{-SPR}^t)]_2$ as precursor, in a hot-wall horizontal low-pressure CVD reactor, resulted in Ga₂S₃ films at substrate temperatures of 350–610 °C. The phase deposited was dependent on the substrate used, being $\gamma\text{-Ga}_2\text{S}_3$ on glass, $\alpha\text{-Ga}_2\text{S}_3$ on Si(100), and highly oriented $\gamma\text{-Ga}_2\text{S}_3$ on yttria-stabilized zirconia. All films had low carbon and oxygen contamination.³¹⁵

Another series of complexes that have been studied as precursors for the deposition of III–VI thin films are those containing dialkyldithio- and dialkyldiselenocarbamate ligands (as with II–VI materials, discussed above). The tris-dialkyldithiocarbamates of gallium and indium are monomeric solids (Figure 41),¹⁸⁷ with those containing two identical alkyl substituents being of quite low volatility. To improve volatility, asymmetric secondary amines have been employed (R = Me

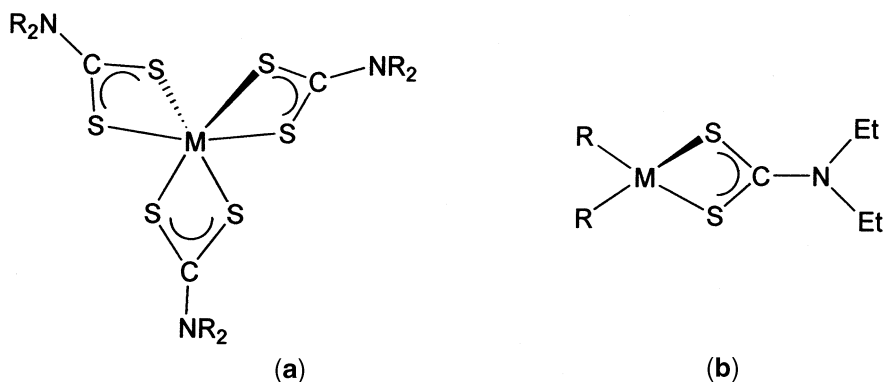


Figure 41 Structures of (a) $[M(S_2CNR_2)_3]$ ($M = \text{Ga, In}$); (b) $[R_2M(S_2CNEt_2)]$ ($R = \text{Me, Et, neo-pentyl}$).

and $R' = \text{Et, Bu}^n, \text{Hex}^n$).³¹⁶ These complexes were used as single-source precursors to grow InS by LP-MOCVD. The compounds volatilized at 250 °C, and growth at temperatures between 450 °C and 500 °C produced cubic $\alpha\text{-In}_2\text{S}_3$ on both glass and InP(111), with the films being strongly orientated in the (111) direction.³⁰¹ The analogous diselenocarbamate $[\text{In}\{\text{Se}_2\text{CN}(\text{Me}^n)\text{Hex}\}_3]$ has also been used to deposit thin films of cubic In_2Se_3 ,³¹⁷ at growth temperatures of 450 °C. The films were deposited on glass substrates with a preferred (111) orientation. The results are similar to those of Arnold and co-workers who prepared cubic In_2Se_3 films from $[\text{In}\{\text{SeC}(\text{SiMe}_3)_3\}_3]$ using a cold-wall vertical reactor.³¹⁸ In a similar way, $\alpha\text{-Ga}_2\text{S}_3$ films have been deposited by LP-MOCVD from the asymmetric precursor $[\text{Ga}\{\text{S}_2\text{CN}(\text{Me}^n)\text{Hex}\}_3]$ at 500 °C on GaAs(111).³¹⁹

A series of mixed alkylindium and gallium diethyldithiocarbamates of formula $[\text{R}_2\text{M}(\text{S}_2\text{CNEt}_2)]$ ($R = \text{Me, Et, neo-pentyl}$; Figure 41b) have been prepared,³²⁰ and were found to be monomeric solids in the case of indium complexes, and liquids at room temperature in the case of gallium. This is different behavior from that observed with the group 12 mixed-alkyl-dithiocarbamate complexes, where a higher degree of association is observed.^{269,307}

$[\text{Me}_2\text{In}(\text{S}_2\text{CNEt}_2)]$, prepared by reaction of Me_3In with $[\text{Zn}(\text{S}_2\text{CNEt}_2)_2]$,³²⁰ was used to deposit indium sulfide films by LP-MOCVD on GaAs(100) substrates at temperatures of 325–425 °C. The alkyl groups present on the indium affect the nature of the as-deposited films; results obtained using $[\text{Et}_2\text{In}(\text{S}_2\text{CNEt}_2)]$ differed from those obtained using either $[\text{Me}_2\text{In}(\text{S}_2\text{CNEt}_2)]$ or $[\text{Np}_2\text{In}(\text{S}_2\text{CNEt}_2)]$ ($\text{Np} = \text{neo-pentyl}$) in that a single-phase, cubic $\beta\text{-In}_2\text{S}_3$ was deposited over the temperature range 325–400 °C. Only the ethyl-substituted compound $[\text{Et}_2\text{In}(\text{S}_2\text{CNEt}_2)]$ contains β -hydrogen atoms, and the elimination of the alkyl fragment may influence the film composition in many ways, such as altering the amount of carbon incorporation. The analogous gallium complex $[\text{Me}_2\text{Ga}(\text{S}_2\text{CNEt}_2)]$ was found to be less successful in the growth of GaS films by LP-MOCVD.³²⁰ When using the $[\text{Bu}^t_2\text{Ga}(\text{S}_2\text{CNR}_2)]$ precursor with $R = \text{Me}$, wurtzite GaS films are produced on GaAs(100); with $R = \text{Et}$, gallium is deposited as well as GaS.³²¹

The monothiocarbamate complexes $[\text{In}(\text{SOCNEt}_2)_3]$,³²³ $[\text{In}(\text{SOCN}^i\text{Pr})_3]$,³⁰³ and $[\text{Ga}(\text{SOCNEt}_2)_3]$ ³⁰⁴ have been used as MOCVD precursors (Figure 42). The films grown from both of the indium precursors were found to be of $\beta\text{-In}_2\text{S}_3$ and, with the diisopropyl compound, deposition occurred at temperatures as low as 300 °C. The gallium monothiocarbamate precursor in contrast deposited films of cubic GaS at 450 °C (comparable to those obtained from

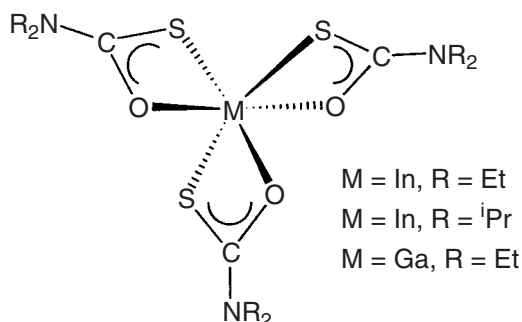


Figure 42 Structure of $[M(\text{SOCNR}_2)_3]$ ($M = \text{In, Ga}$; $R = \text{Et, Pr}^i$).

[Bu¹-GaS]₄),³¹¹ which were sulfur deficient and highly orientated in the (200) direction on the glass substrate.

The deposition of α-In₂S₃ from an indium alkylxanthate, [In(S₂COⁱPr)₃], by LP-MOCVD at temperatures as low as 250 °C has been reported.³²² The reaction of triethylindium, thioacetic acid, and 3,5-dimethylpyridine (dmpy) yields the indium thiocarboxylate salt [Hdmpy]⁺[In(SCOCH₃)₄]⁻, which has been used to deposit tetragonal β-In₂S₃ by AACVD,³⁰⁰ with films of low oxygen and carbon contamination being obtained at substrate temperatures as low as 210 °C. The gallium alkylthiocarboxylate complex [MeGa(SCOCH₃)₂(dmpy)] (dmpy = 3,5-dimethylpyridine) was used in AACVD for the growth of gallium sulfide. This method gave high-purity hexagonal α-Ga₂S₃ at temperatures as low as 290 °C. These results suggest that the indium and gallium thiocarboxylate compounds undergo quantitative elimination of thioacetic anhydride to give the metal sulfide.³²³

9.23.5.5 IV–VI Materials from Single-molecule Precursors

Another interesting class of main group semiconductors are the 14–16 (IV–VI) tin and lead chalcogenides and their ternary alloys, which have narrow bandgaps, making them good candidates for use in mid-IR photodetectors and photovoltaic applications. This has led to interest in the growth of IV–VI materials from single-source precursors, with a number of lead dithiocarbamates, [Pb(S₂CNR₂)₂], used to grow films of PbS. [Pb(S₂CNEt₂)₂] was initially used in a cold-wall reactor using LP-MOCVD at substrate temperatures in the range 424–500 °C.¹⁸⁸ To increase source volatility, the analogue [Pb(S₂CNBuⁿ)₂] was found to deposit PbS films with low carbon contamination on Si(100) and glass (borosilicate) at temperatures in the range 400–600 °C.³²⁴

A number of tin chalcogenide thin film materials have been prepared from single-source precursors such as [Sn{CH(SiMe₃)₂}₂(μ-E)]₂ (E = Se, Te; Figure 43) using a cold-wall LP-CVD reactor. These are mainly mixed-phase films of the tin chalcogenide.^{325,326} A more successful, although preliminary, study using the thiolate/dithiocarbamate compound [(Et₂NCS₂)₂(CyS)₂Sn] (Cy = cyclohexane) deposited SnS₂.³²⁷ Several tin(IV) thiolates have been used in attempts to deposit SnS films; these include [(PhS)₄Sn],³²⁸ [Sn(SCH₂CH₂S)₂],³²⁹ and the tin fluoroalkylthiolate [(CF₃CH₂S)₄Sn]. Using AACVD, SnS films could only be deposited in the presence of the hydrogen sulfide. [(PhS)₄Sn] deposited SnS₂ at growth temperatures of <500 °C, and SnS at temperatures above 500 °C. Again, for both [Sn(SCH₂CH₂S)₂] and [(CF₃CH₂S)₄Sn] films of SnS could only be deposited in the presence of an additional sulfur source, H₂S.

9.23.5.6 CuInS₂ and Related Ternary Semiconductors

The ternary semiconductors CuInS₂ and CuIn₂S₅ have great potential for use in next-generation photovoltaic applications. Nomura used [BuIn(SPr)₂Cu(S₂CNPr)₂] to grow films of CuIn₅S₈ at 350–400 °C using LP-MOCVD methods, while at temperatures above 450 °C In₂S₃ was deposited.^{210,308,330} Thin films of CuInS₂ were successfully deposited at 400 °C using the volatile precursor [(Bu)₂In(SPrⁱ)Cu(S₂CNPrⁱ)].²⁹⁵ Preliminary studies on the two liquid precursors [{P(Buⁿ)₃}₂Cu(μ-SEt)₂In(SEt)₂] (Figure 43a) and [{P(Buⁿ)₃}₂Cu{μ-S(Prⁿ)}₂In{S(Prⁿ)₂}] (Figure 43b) showed them to decompose to CuInS₂ in near-stoichiometric ratios.^{331,332} Using

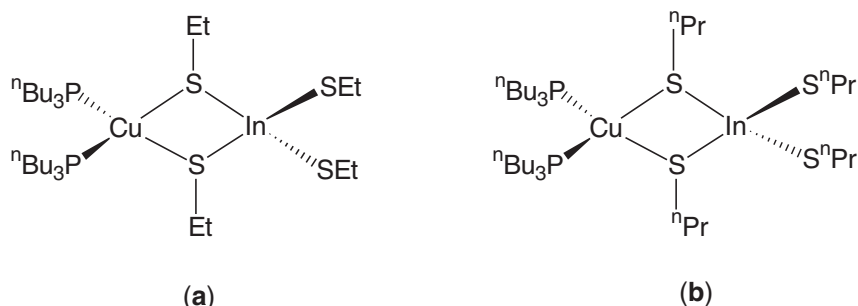


Figure 43 Structures of (a) [(Buⁿ₃P)₂Cu(μ-SEt)₂In(SEt)₂]; (b) [(Buⁿ₃P)₂Cu(μ-SPrⁿ)₂In(SPrⁿ)₂].

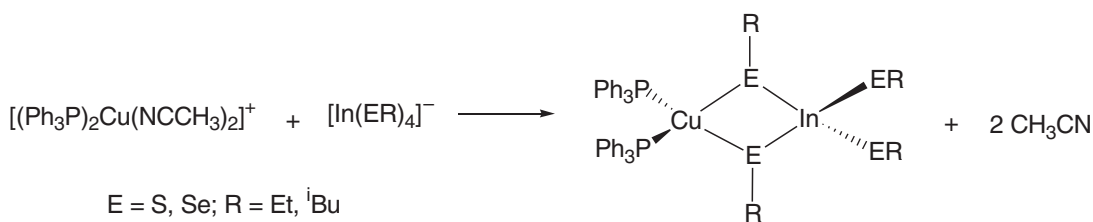


Figure 44 Preparation of $[(\text{Ph}_3\text{P})_2\text{Cu}(\mu\text{-ER})_2\text{In}(\text{ER})_2]$ ($\text{E} = \text{S, Se}; \text{R} = \text{Et, Bu}^i$).

$[(\text{PPh}_3)_2\text{Cu}(\mu\text{-SEt})_2\text{In}(\text{SEt})_2]$ (Figure 44) in a number of studies employing spray CVD techniques, CuInS_2 was deposited on various substrates at temperatures below 400°C with no evidence of phosphorus or carbon incorporation.³³³ The related ternary semiconductor CuInSe_2 was grown using a combination of two chalcogenocarbamate precursors, each containing two of the elements required for the film: $[\text{Cu}\{\text{Se}_2\text{CN}(\text{Me})\text{Hex}\}_2]$ (containing copper and selenium) and $[\text{In}\{\text{Se}_2\text{CN}(\text{Me})\text{Hex}\}_2]$ (containing selenium and indium). This produced good-quality films using LP-MOCVD in the range $400\text{--}450^\circ\text{C}$.³³⁴

The related metastable material ZnIn_2S_4 , which has potential applications as a photoconductor material, was deposited using LP-MOCVD at 400°C from the indium–zinc precursor $[(\text{Et})_2\text{In}(\text{S}_2\text{CNET}_2)\text{Zn}(\text{Et})(\text{S}_2\text{CNET}_2)]$.³³⁵

9.23.6 PREPARATION OF NANODIMENSIONAL MATERIALS USING SINGLE-MOLECULE PRECURSORS

There has been substantial interest in the preparation and characterization of materials consisting of particles with dimensions in the order of $2\text{--}100\text{ nm}$, so-called “nanocrystalline materials.”^{336–343} One factor driving interest in nanoparticle research is the perceived need for the further miniaturization of both optical and electronic devices.^{344,345}

The preparation of nanoparticles can be dated back to the nineteenth century, when Faraday reported the synthesis of colloids of relatively monodispersed gold nanoparticles. However, most research has been concerned with relatively large particles ($\gg 100\text{ nm}$) outside the size range at which interesting effects on the intrinsic properties of semiconductor materials are observed. On a commercial scale most synthetic methods employ “top-down” techniques whereby larger particles are milled down to smaller ones; however, this method cannot produce monodispersed particles in the $2\text{--}50\text{ nm}$ size range. Although some earlier examples appear in the literature,³⁴⁶ subsequent methods have been developed from reproducible “bottom-up” techniques whereby particles are prepared atom by atom, i.e., from molecules to clusters to particles.^{347,348}

9.23.6.1 Semiconductor Nanoparticles “Quantum Dots”

Two fundamental factors, both related to the size of the individual nanocrystal, are responsible for unique properties seen in semiconductor nanoparticles. The first is the large surface-to-volume ratio; as a particle becomes smaller the ratio of the number of surface atoms to those in the interior increases, with greater than a third of all atoms residing on the surface in very small particles. This leads to the surface properties playing an important role in the overall properties of the material. The second factor is the actual size of the particle; with semiconductor nanoparticles there is a change in the electronic properties of the material, the bandgap gradually becoming larger because of quantum confinement effects as the size of the particles decreases. This effect is a consequence of the confinement of an “electron in a box” giving rise to discrete energy levels similar to those in atoms and molecules, rather than a continuous band as in the corresponding bulk semiconductor material. Thus, for a semiconductor nanoparticle, because of the physical parameters, the “electron and hole” produced by the absorption of a photon with energy greater than the first excitonic transition are spatially closer together than in the macrocrystalline material, so that the Coulombic interaction cannot be neglected. Quantum dots have higher kinetic energy than the macrocrystalline material. Consequently, the first excitonic transition

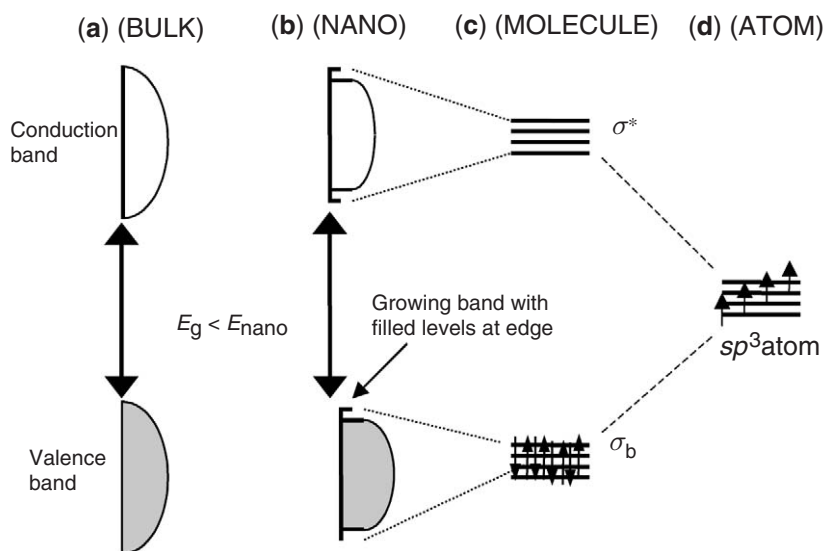


Figure 45 Schematic representation of molecular orbitals: (a) macrocrystalline solid; (b) nanocrystalline material; (c) molecule; (d) hypothetical atom.

(bandgap) increases in energy with decreasing particle diameter (Figure 45). This prediction has since been experimentally confirmed for a wide range of semiconductor nanocrystallites,^{343–346} with a blue shift in the onset of the absorption of light being observed with decreasing particle diameter. Moreover, the valence and conduction bands in nanocrystalline materials consist of discrete sets of electronic levels, and can be viewed as a state of matter between that of molecular (atomic) and bulk material.

The coordination about surface atoms in nanoparticles is incomplete, with highly reactive “dangling bonds” on the surface, which can lead to particle agglomeration. This problem is overcome by passivating (capping) the “bare” surface atoms with protecting groups. The capping or passivating of particles not only prevents particle agglomeration from occurring, it also protects the particle from its surrounding chemical environment, as well as providing electronic stabilization (passivation) to the particles. The capping agent can take one of several forms: a Lewis base compound covalently bound to surface metal atoms; a further layer of a different material epitaxially grown onto the surface of the particle; an organic polymer forming a sheath around the particle; or an organic group bound directly to the surface, as in Figure 46.

Research on semiconductor nanoparticle technology by chemists, materials scientists, and physicists has already led to the fabrication of a number of devices. Initially, Alivisatos and co-workers developed an electroluminescence device from a dispersion of CdSe nanoparticles capped with a conducting polymer³⁴⁹ and then improved on this by replacing the polymer with a layer of CdS, producing a device with efficiency and lifetime increased by factors of 8 and 10, respectively.³⁵⁰ Chemical synthetic methods for the assembly of nanocrystal composites, consisting of II–VI quantum dot–polymer composite materials,³⁵¹ represent one important step towards the fabrication of new functional devices that incorporate quantum dots.

Particle size and the method of nanoparticle preparation (including the capping agent used) determine the physical and electronic properties of the quantum dots produced. This gives chemists the unique ability to change the electronic and chemical properties of a semiconductor material by simply controlling particle size and preparative conditions employed. There are various methods for the preparation of nanoparticles; however, not all methods work well for the preparation of compound semiconductor nanocrystallites.

9.23.6.2 Methods of Preparation of Semiconductor Nanoparticles

Along with compound semiconductor nanoparticles, nanoparticles of many other materials, including metals, metal oxides, carbides, borides, nitrides, silicon, and other elemental

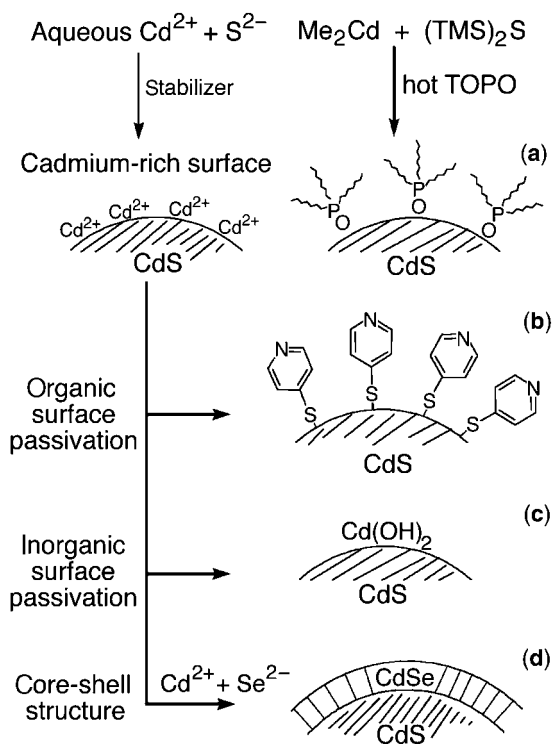


Figure 46 Coordination of molecules or solid-state materials to the surface of a nanoparticle.

semiconductors, have been prepared.^{352–356} The syntheses of elemental nanoparticle semiconductors and metals such as Ag,³⁵⁷ Pd,³⁵⁸ Au,³⁵² and Cu³⁵³ have been the subject of a number of reviews. The preparation and properties of nanocrystalline refractory compounds such as carbides, borides, nitrides, and oxides have been reviewed elsewhere.³⁵⁴

Many synthetic methods for the preparation of nanodispersed material have been reported, several routes applying conventional colloidal chemistry, with others involving the kinetically controlled precipitation of nanocrystallites using organometallic compounds.^{356–343} Controlled precipitation reactions yield dilute suspensions of quasi-monodispersed particles. This synthetic method sometimes involves the use of seeds of very small particles for the subsequent growth of larger ones.^{359,360}

A number of matrices have also been used for the preparation of semiconductor nanoparticles, whereby the particulate material is grown within and subsequently fills the cavities of the host material. These include zeolites,³⁶¹ glasses,³⁶² and molecular sieves,^{363–365} and can be viewed as nanochambers which limit the size to which crystallites can grow. Other synthetic methods include micelles/microemulsions,^{366–369} sol-gels,^{370,371} polymers,^{372–377} and layered solids.³⁷⁸

A powerful method for the preparation of semiconductor nanocrystallites has been described by Murray *et al.*³⁷⁹ using organometallic solutions containing a mixture of metal alkyls (R_2M) and tri-*n*-octylphosphine sulfide/selenide (TOPS/Se) dissolved in tri-*n*-octylphosphine (TOP). The mixture is injected into hot tri-*n*-octylphosphine oxide (TOPO) in the temperature range 120–400 °C, depending on the material being produced. This produces TOPO-capped nanocrystallites of II–VI material. The size of the particles is controlled by the temperature and length of time at which the synthesis is undertaken, with larger particles being obtained at higher temperatures and prolonged reaction times. The combination of tri-*n*-octylphosphine/tri-*n*-octylphosphineoxide (TOP/TOPO) allowed for slow steady growth conditions above 280 °C. The TOPO method has advantages over other synthetic methods, including near monodispersity ($\sigma \sim 5\%$) and scale. Many variants of this method have now appeared in the literature, including modifications to the precursors and capping agent/solution. Some alternative group 12 precursors include (*neo*-pentyl)₂Cd, [(Et₂NCH₂CH₂CH₂)₂Cd], and [Me₂Cd(2,2'-bipy)]³⁸⁰ among many others. For this method to be successful the nucleation step should be separate from particle growth, so as to attain a narrow nanoparticle size distribution. Varying the temperature and time of the reaction controls the particle size.

9.23.6.3 Semiconductor Nanoparticles Produced from Single-molecule Precursors

Many single-molecule complexes containing all the elements required for the as-grown particle have previously been used in the growth of semiconductor thin films using CVD techniques (see earlier sections). However, in some cases the use of these compounds proved problematic because of their low volatility and the lack of stoichiometric control. Single-source precursors have proved useful in the synthesis of nanoparticle materials when a “one-pot” preparative procedure is employed. For rapid particle nucleation followed by slow particle growth to occur, which is essential for a narrow particle size distribution, the synthesis involves the rapid injection of the precursor into a hot solution of a Lewis-basic coordinating solvent (capping agent). This is followed by particle growth at a temperature just below precursor deposition, as the growth reactions are assumed to be heterogeneous taking place on and catalyzed by the surface of the growing nanoparticles. The temperature is then maintained for a period of time. The size of the resulting particles depends on reaction time, temperature, and the ratio of capping agent to precursor used. The resulting solution is cooled, followed by the addition of an excess of a polar solvent (methanol or ethanol) to produce a precipitate of the particles that can be isolated by filtration or centrifugation.

9.23.6.3.1 II–VI particles

Bis(alkyldithio-/selenocarbamates) of Zn(II) and Cd(II) have previously been used in many applications including the rubber industry³⁸¹ and in analysis,³⁸² as well as for single-molecular precursors in the growth of II–VI thin films by CVD, as described earlier.^{181,383} They have also been shown to be good precursors for the preparation of II–VI nanoparticles, in a process that involves their decomposition in a high-boiling donor solvent such as tri-*n*-octylphosphine oxide or 4-ethylpyridine (Figure 47).

Precursors that have been prepared include a number of bis(dialkyldithio-/diselenocarbamato) cadmium(II)/zinc(II) compounds of the type $[M(E_2CNRR')_2]$, ($E = S, Se$) in which the alkyl substituents are the same ($R = R' = Me, Et, Pr, Pr^i$) or different ($R = Me, Et; R' = Hex^n, Bu^n$) with the latter giving cleaner film deposition routes (described in the earlier section for thin-film growth).

The dithiocarbamate complexes ($X = S$) produce good-quality particles, whereas the diethyl-deselenocarbamate complexes ($X = Se, R = R' = Et$) produce either selenium or selenium-rich clusters.¹⁸⁹ However, the diselenocarbamates bearing two different R groups, such as $[Cd\{Se_2CN(Me)Hex^n\}_2]$, afforded good-quality CdSe nanoparticles.¹⁹⁰ These observations were very similar to the results obtained from thin-film growth using the same precursors, and suggest that (as in film growth) the R groups determine the mechanistic pathway by which the precursor decomposes. Promisingly, this route has provided good-quality nanoparticles of both metal sulfides and selenides from appropriate

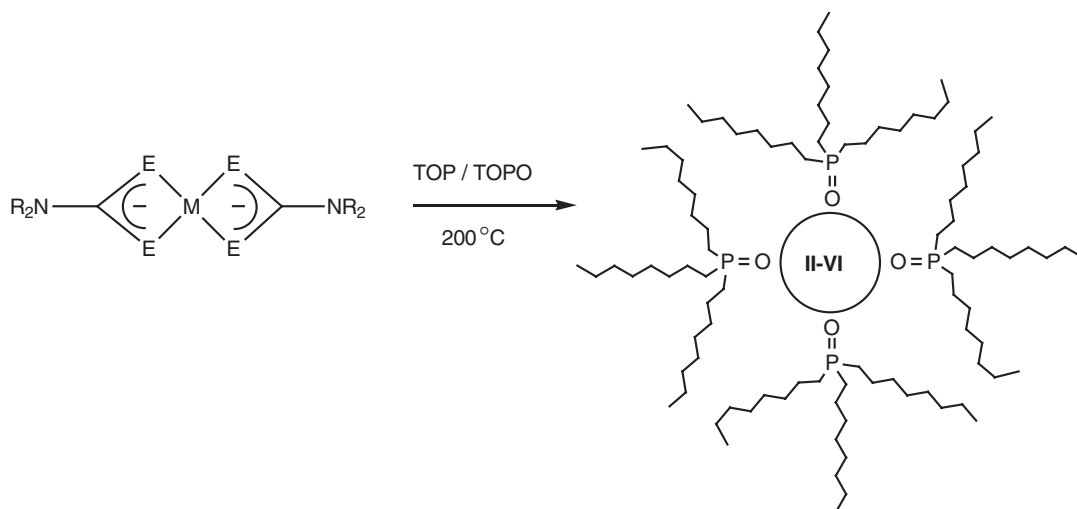


Figure 47 Preparation of TOPO-capped II–VI nanoparticles from bis(dialkyldithio-/selenocarbamato)–cadmium(II)/zinc(II) complexes.

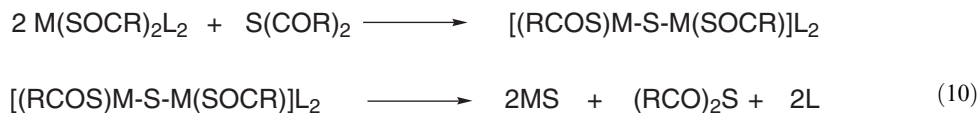
precursors. The heteroleptic alkyl/dithiocarbamate single-molecular precursor [EtZn(Se₂CNEt₂)] has also been used with a high degree of success to produce ZnSe nanoparticles.³⁸⁴

The reaction of CdCl₂ with *N,N'*-bis(thiocarbamoyl)hydrazine gave [Cd{SC(=NH)NH₂}₂Cl₂] which has been used as a single-source precursor. Upon thermolysis in TOPO at 230 °C it produced CdS particles which showed an absorption edge blue shift of 37 nm in relation to that of the bulk material; no chlorine contamination was reported.³⁸⁵

Another concept that has been explored is the synthesis and use of novel bis(dialkyl)dithiocarbamate compound single-molecular precursors that produce self-capped nanoparticles.³⁸⁶ The organic substituents on the precursor should migrate upon thermolysis, and act as the capping agent on the surface of the growing nanoparticle. The cadmium dithiocarbamate [Cd{S₂CNMe(C₁₈H₃₇)₂}₂] was used for nanoparticle synthesis under a dynamic vacuum, as a melt at temperatures in the range 150–300 °C, and produced capped CdS nanoparticles.³⁸⁷

One method to passivate nanoparticles with a robust, nonlabile layer is to grow a second material, e.g., another II–VI material having a wider bandgap and low lattice mismatch, epitaxially on the surface of the particle. This produces a “core–shell particle” such as ZnS grown on the surface of CdSe, or CdS on CdSe. Efforts have been made to prepare CdSe–CdS core–shell nanoparticles using the precursors [Cd{Se₂CNMe(Hexⁿ)₂}₂] as the CdSe “core” source and [Cd{S₂CNMe(Hexⁿ)₂}₂] as the CdS “shell” source.³⁸⁸

Preliminary deposition studies have also been carried out using the group 12 metal thiocarboxylates [M(SOCR)₂(dmpy)₂] (M = Cd, Zn; R = Me, Bu^t; Figure 48). The compounds were prepared from the reaction between either ZnEt₂ or cadmium carbonate with thioacetic and thiopivalic acids. [M(SOCR)₂(dmpy)₂] are monomeric in the solid state with the zinc/cadmium metal centers in a near tetrahedral arrangement and the thiocarboxylate ligands being *S*-monodentate (Figure 48). Heating a solution of [M(SOCR)₂(dmpy)₂] in pyridine or toluene resulted in thiocarboxylic anhydride elimination, as monitored by NMR studies, with the subsequent formation of CdS and ZnS nanocrystals. The proposed deposition route is illustrated in Equation (10). The decomposition of [Cd(SOCR)₂(dmpy)₂] in toluene at 110 °C for 12 h gave 5.0 nm CdS nanoparticles, whereas using pyridine under the same conditions produced 10.0 nm CdS particles. [Zn(SOCR)₂(dmpy)₂] in toluene produced 5.0 nm amorphous particles, whereas the same reaction in pyridine failed to produce any nanoparticulate material:³⁸⁹



Using the related precursor [(2,2′-bipy)Cd(SOCPh)₂] a more comprehensive study was undertaken. Highly monodispersed CdS nanoparticles were formed in an aqueous solution at room temperature using hydrophilic 1-thioglycerol as the capping agent. Particle size was controlled by periodically adding precursor and controlling the concentration of capping agent used, with increasing concentrations of capping agent limiting the particle growth and thus producing smaller particles.³⁹⁰

In an effort to separate particle nucleation from that of particle growth, and thus obtain a narrow size distribution without any further postpreparative separation treatment (such as selective precipitation), single-source molecular inorganic clusters have been employed. The clusters used have discrete units with

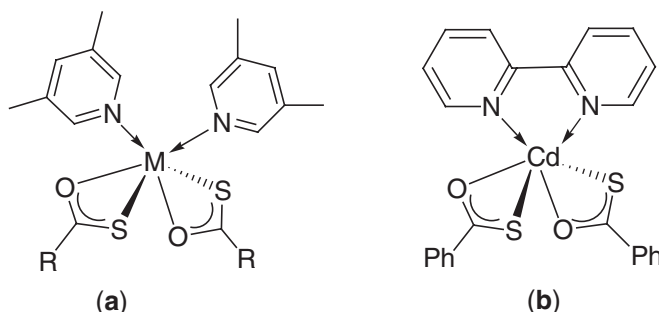


Figure 48 Structures of (a) [M(SOCR)₂(dmpy)₂] (M = Cd, Zn; R = Me, Bu^t); (b) [Cd(SOCPh)₂(2,2′-bipy)].

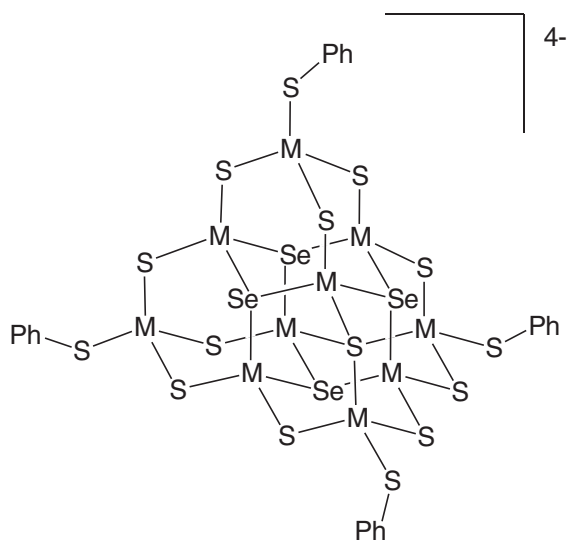
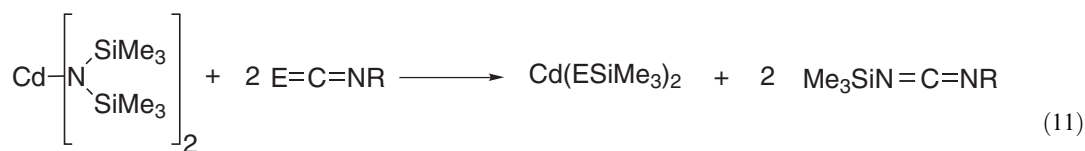


Figure 49 Structure of $[M_{10}Se_4(SPh)_{16}][X]_4$ ($M = Cd, Zn; X^+ = Li^+, Me_3NH^+$).

core structures related to that of the bulk semiconductor materials $[M_{10}Se_4(SPh)_{16}][X]_4$ ($X = Li$ or Me_3NH , $M = Cd$ or Zn) with the structure shown schematically in Figure 49. CdSe particles were grown using $X = Li$ and ZnSe particles were grown using $X = Me_3NH$. Particle growth was carried out in hexadecylamine at 220–240 °C for CdSe, and 220–280 °C for ZnSe. Because of the complete separation of nucleation and growth this method showed a high degree of control over particle size. Once the desired particle size is obtained, as established from UV spectra of aliquots of the reaction solution, the temperature is reduced by ca. 30–40 °C and the mixture left to “size-focus” for 12 h. The average particle size distribution is thereby narrowed due to Ostwald ripening, in a process where small crystallites are less thermodynamically stable than larger ones and thus dissolve more readily into their respective ions. The dissolved ions can then recrystallize on larger crystallites, which are thermodynamically more stable. This method can produce batches of particles with narrow size distributions in the 2.5–9.0 nm range for CdSe and 3.0–5.0 nm range for ZnSe. By post-treating CdSe particles with solutions of Me_2Zn and $(Me_3Si)_2S$, core-shell particles of CdSe–ZnS can be formed with quantum yields enhanced by a factor of >2 (6–20%).³⁹¹

Brus and co-workers produced nanoparticles of CdSe from the pyrolysis of the single-molecular cadmium selenate precursor $[Cd(SePh)_2]$.³⁹² The similar metal(benzylthiolate) compounds $[M(SCH_2C_6H_5)_2]$ ($M = Zn, Cd$) were also used in the solid-state preparation of ZnS and CdS particles and produced mixtures of the hexagonal and cubic phases of the crystallites, with sizes of ~5 nm, on thermolysis between 200 °C and 400 °C under nitrogen.³⁹³ The bis(trialkylsilyl)chalcogenides $[(Me_3SiE)_2Cd]$ ($E = S, Se$), prepared by heterocumulene metathesis as in Equation (11), were used to produce nanoparticles. If the reactions are carried out in TOPO, TOPO-passivated CdE nanoparticles can be obtained although there was little control over particle size:³⁹⁴



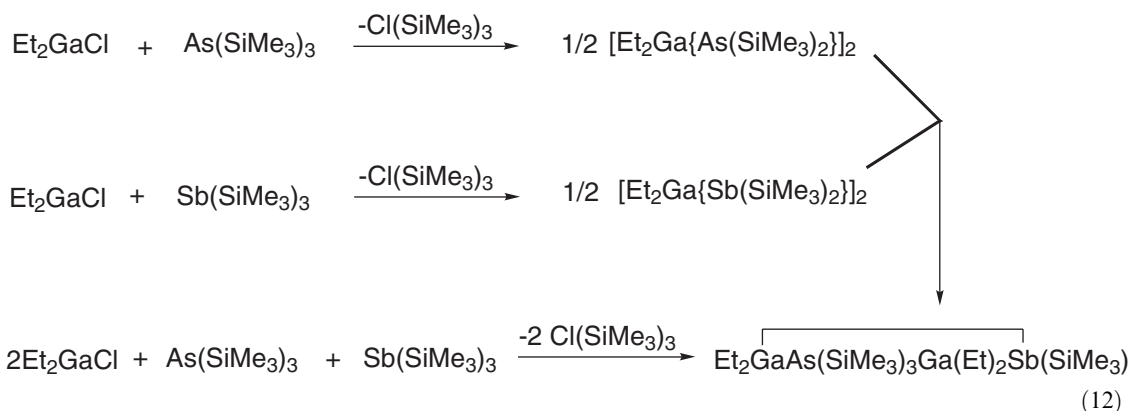
($E = S, R = ^tBu$; $E = Se, R = Cy$)

9.23.6.3.2 III–V particles

The covalent nature of III–V materials causes problems for preparation of highly crystalline nanoparticles and thin films. A single-molecular precursor approach was employed to produce III–V nanoparticles of InP and GaP using the indium/gallium diorganophosphide compounds

$M(\text{PBU}^t)_3$ ($M = \text{Ga}, \text{In}$). The nanoparticles were prepared by dissolving the precursors in 4-ethylpyridine (solvent and capping agent) and refluxing for 7 days.³⁹⁵

Most single-source preparative methods for III–V nanoparticles have been performed in the solid state, which tends to be less controllable, giving particles with less defined structures and large particle size distributions. Wells *et al.* reported the synthesis of GaP nanoparticles from the thermolysis of $[\text{X}_2\text{GaP}(\text{SiMe}_3)_2]_2$ ($\text{X} = \text{Br}, \text{I}$) and from the thermolysis of $[(\text{Cl}_3\text{Ga}_2\text{P})]_n$.³⁹⁶ In a more comprehensive study the two dimeric single-source precursors $[\text{Et}_2\text{GaAs}(\text{SiMe}_3)_2]_2$ and $[\text{Et}_2\text{GaSb}(\text{SiMe}_3)_2]_2$, prepared from Et_2GaCl and $\text{As}(\text{SiMe}_3)_3$ or $\text{Sb}(\text{SiMe}_3)_3$, respectively, were heated to 400°C in the solid state under reduced pressure for 4 h and gave GaAs nanoparticles of 9 nm and 10 nm, respectively. Ternary $\text{GaAs}_x\text{Sb}_{1-x}$ particles (5 nm size) were grown in the solid state from the mixed pnictogen $[\text{Et}_2\text{GaAs}(\text{SiMe}_3)_2\text{Ga}(\text{Et})_2\text{Sb}(\text{SiMe}_3)_2]$ (prepared using a 2:1:1 mole ratio of Et_2GaCl , $\text{As}(\text{SiMe}_3)_3$, and $\text{Sb}(\text{SiMe}_3)_3$, as in Equations (12)).³⁹⁷ The analogous GaP precursor $[\text{Et}_2\text{GaP}(\text{SiMe}_3)_2]_2$ along with the mixed pnictogen compounds $[(\text{Me}_3\text{Si})_2\text{P}\{\mu\text{-GaEt}\}_2\text{As}(\text{SiMe}_3)_2]$ and $[(\text{Me}_3\text{Si})_2\text{P}\{\mu\text{-GaEt}\}_2\text{Sb}(\text{SiMe}_3)_2]$ gave nanoparticles of GaP (6.4 nm), $\text{GaP}_x\text{As}_{1-x}$ (6.7 nm), and $\text{GaP}_x\text{Sb}_{1-x}$ (9.3 nm), respectively. All samples, however, contained carbon contamination:³⁹⁸



The trimeric indium antimonide single-source precursor $[\text{Et}_2\text{InSb}(\text{SiMe}_3)_2]_3$, prepared from Et_2InCl and $\text{Sb}(\text{SiMe}_3)_3$, was shown in a preliminary study to form InSb nanocrystals (average particle size 10 nm) by solid-state thermolysis at 400°C under a static vacuum. However, the particles were contaminated with elemental indium.³⁹⁹

The cyclotrigallazine $[\text{H}_2\text{Ga}(\text{NH}_2)]_3$ was used in conjunction with NH_3 under ammonothermal conditions in an autoclave, with heating at $150\text{--}450^\circ\text{C}$, and produced GaN crystallites with sizes between 3 nm and 7 nm depending on the temperature employed. The GaN product consisted of an inhomogeneous mixture of both the cubic and hexagonal phases, and it was not established if nitrogen from the NH_3 was incorporated into the particles.⁴⁰⁰ The potentially explosive azides $[(\text{R}_3\text{N})\text{Ga}(\text{N}_3)_3]$ ($\text{R} = \text{Me}, \text{Et}$; Figure 50a) prepared from $\text{Na}[\text{Ga}(\text{N}_3)_4]$ and Me_3N or Et_3N gave

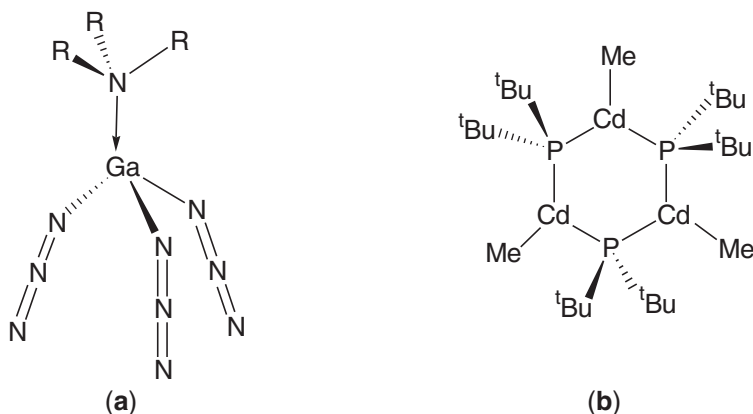


Figure 50 Structures of (a) $[(\text{R}_3\text{N})\text{Ga}(\text{N}_3)_3]$ ($\text{R} = \text{Me}, \text{Et}$); (b) $[\text{MeCd}(\text{PBU}^t)_2]_3$.

Table 15 Single-source precursors used in the preparation of quantum dots.

<i>Semiconductor</i>	<i>Synthetic method</i>	<i>Size range (nm)</i>	<i>References</i>
GaN	Thermolysis of [H ₂ Ga(NH ₂) ₃] in supercritical ammonia	3.0	409
	Thermolysis of [H ₂ Ga(NH ₂) ₃] in supercritical ammonia at 150–450 °C	3–17	400
GaP	[(R ₃ N)Ga(N ₃) ₃] detonation at reduced pressure	2.0–1000	401
	Thermal treatment of [Cl ₂ GaP(SiMe ₃) ₂] ₂ in TOPO + TOP mixture	2.0–6.5	410
	Solid-state thermolysis of [Et ₂ Ga{P(SiMe ₃) ₂ }] ₂ at 425 °C	6.4	398
GaAs	Solid-state thermolysis of [Et ₂ Ga{As(SiMe ₃) ₂ }] ₂ at 400 °C	9.0	397
GaSb	Solid-state thermolysis of [Et ₂ Ga{Sb(SiMe ₃) ₂ }] ₂ at 400 °C	10.0	397
GaAs _x Sb _{1-x}	Solid-state thermolysis of [Et ₂ Ga{As(SiMe ₃) ₂ }Ga(Et) ₂ {Sb(SiMe ₃) ₂ }] at 400 °C	5.0	397
GaP _x As _{1-x}	Solid-state thermolysis of [(Me ₃ Si) ₂ P(μ-GaEt ₂) ₂ As(SiMe ₃) ₂] at 425 °C	6.7	398
GaP _x Sb _{1-x}	Solid-state thermolysis of [(Me ₃ Si) ₂ P(μ-GaEt ₂) ₂ Sb(SiMe ₃) ₂]	9.3	398
InP	Methanolysis of, e.g., [R ₂ In{P(SiMe ₃) ₂ }] ₂		411
InSb	Solid-state thermolysis of [Et ₂ In{Sb(SiMe ₃) ₂ }] ₃ at 400 °C	10.0	399
Cd ₃ P ₂	Thermolysis of (MeCd(PBu ^t) ₂) ₃ in TOPO	3.0	403
	Alcoholysis of [Cd{P(SiPh ₃) ₂ }] ₂	3.0–4.0	412,413
Zn ₃ P ₂	Alcoholysis of [Zn{P(SiPh ₃) ₂ }] ₂	1.5–2.5	412
CdS	Thermolysis of single molecule precursors in TOPO	3.0–7.0	414,415
	Methathesis of [Cd{N(Me ₃ Si) ₂ }] ₂ + SCNR in the presence of TOPO	1.5–2.0	394
	Solid-state thermolysis of [Cd{SSiMe ₃ }] ₂		394
	Thermolysis of [Cd(SCNHNH ₂) ₂ Cl ₂] in TOPO at 230 °C	5.10	385
	Thermolysis of [Cd(SOCR) ₂ (dmpy) ₂] (R = Me, Bu ^t) in toluene or pyridine, 110 °C, 12 h	50.0 (toluene); 100.0 (pyridine)	389
	Room temperature reaction of Cd(SOCR) ₂ (py) in (aq) solutions of 1-thioglycerol	1.7–2.8	390
CdSe	Solution-phase thermolysis of (Cd(SePh) ₂) ₂	3.0	392
	Thermolysis of single-molecule precursors in TOPO	3.0–8.0	414,415,416
	Methathesis of Cd{N(Me ₃ Si) ₂ } + SCNR in the presence of TOPO	1.5–2.0	394
	Solid-state thermolysis Cd(SeSiMe ₃) ₂		394
	Thermolysis of [Cd ₁₀ Se ₄ (SPh) ₁₆][Li] ₄ in hexadecylamine at 220–240 °C	2.5–9.0	391
ZnS	Thermolysis of single-molecule precursors in TOPO		415
	Thermolysis of Zn(SOCR) ₂ (dmpy) ₂ (R = Me, Bu ^t) in toluene at 120 °C	5.0	389
ZnSe	Thermolysis of single-molecule precursors in TOPO	3.5–4.2	415
	Thermolysis of [Zn ₁₀ Se ₄ (SPh) ₁₆][TMA] ₄ in hexadecylamine at 220–280 °C	3.0–5.0	391
CdSe–ZnS core–shell	Thermolysis of [Cd ₁₀ Se ₄ (SPh) ₁₆][Li] ₄ in hexadecylamine at 220–240 °C followed by Me ₂ Zn + (Me ₃ Si) ₂ S at 250 °C		391
PbS	Thermolysis of lead(II) dithiocarbamates in TOP	6.3–2	417
PbSe	Treatment of acetonitrile/aqueous solutions of Pb(CH ₃ CO ₂) ₂ with H ₂ Se in the presence of Nafion	2–20	418

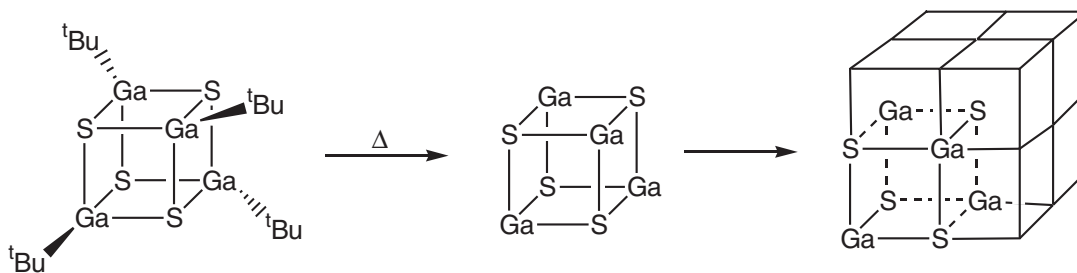


Figure 51 Deposition of $[\text{Bu}^t\text{GaSe}]_4$ to form cubic GaS.

pure hexagonal GaN nanoparticles from a solid-state detonation reaction, but produced particles with a very large size distribution (2–1000 nm). Varying the amount of precursor and amine present, and the pressure of the reaction, allowed limited control over particle size.⁴⁰¹

9.23.6.3.3 II–V particles

Nanoparticles of the II–V material Cd_3P_2 have been prepared using the diorganophosphide precursor $[\text{MeCd}(\text{PBU}^t)_2]_3$ (Figure 50b) in TOPO.^{402,403}

9.23.6.3.4 III–VI particles

III–VI nanoparticles of InS and InSe have been prepared using single-molecular tris(diethyl-dithio-/selenocarbamate) precursors $[\text{In}(\text{S}_2\text{CNEt}_2)_3]$ (to give InS) and $[\text{In}(\text{Se}_2\text{CNEt}_2)_3]$ (to give InSe), and $[\text{In}\{\text{Se}_2\text{CN}(\text{Me})\text{Hex}^n\}_3]$ (also for InSe).^{404,405} As with the synthesis of CuInSe_2 thin films, a combination of the two two-source precursors $[\text{In}\{\text{Se}_2\text{CN}(\text{Me})\text{Hex}^n\}_3]$ and $[\text{Cu}\{\text{Se}_2\text{CN}(\text{Me})\text{Hex}^n\}_2]$ was used to produce nanoparticles of the ternary compound semiconductor CuInSe_2 .^{405,406}

Barron and co-workers have decomposed the Ga–Se and In–Se clusters $[\text{Bu}^t\text{GaSe}]_4$ and $[(\text{EtMe}_2\text{C})\text{InSe}]_4$ in the solid state to produce nanoparticles of GaSe and InSe, respectively.⁴⁰⁷ It has been suggested that the formation of a metastable cubic phase of GaS was a consequence of using the cubane complex $[\text{Bu}^t\text{GaS}]_4$, suggesting that the precursor retained its cubic Ga_4S_4 core upon decomposition. Thus, the molecular structure of the precursor defined the structure of the deposited phase of GaS (Table 15, Figure 51).

9.23.7 REFERENCES

- Grovenor, C. R. M. *Microelectronic Materials*; Adam Hilger: Bristol, UK, 1989.
- Sze, S. M. *Semiconductor Devices: Physics and Technology*; Wiley: Chichester, UK, 1985.
- MacKinnon, A. Physics of Non-tetrahedrally Bonded Ternary Compounds. In *Landolt-Börnstein New Series*, Madelung, O.; von der Ostern, W.; Rössler, U., Eds.; Springer Verlag: Berlin, 1985; Vol. 17h, Chapter 10.1, pp 12–23.
- Nicolau, Y. F.; Dupuy, M.; Brunel, M. *J. Electrochem. Soc.* **1990**, *137*, 2915.
- Marquardt, E.; Optiz, B.; Scholl, M.; Henker, M. *J. Appl. Phys.* **1994**, *75*, 8022.
- Bedenorz, J. G.; Müller, K. A. *Z. Phys. B* **1986**, *64*, 189.
- Manasevit, H. M. *J. Cryst. Growth* **1981**, *55*, 1.
- Davies, G. J.; Andrews, D. A. *Chemtronics* **1988**, *3*, 3.
- Cole-Hamilton, D. J. *Chem. Br.* **1990**, *26*, 852.
- O'Brien, P. *Inorganic Materials*; Bruce, D. W.; O'Hare, D., Eds.; Wiley: Chichester, 1992; Chapter 9, p 500.
- Sullivan, L. A.; Han, B. *Solid State Technol.* **1996**, *39*, 91.
- Liedl, G. L. *Sci. Am.* **1986**, *255*, 105.
- Foster, F.; Cole-Hamilton, D. J. *Inorg. Synth.* **1996**, *31*, 29.
- Jones, A. C.; Holliday, A. K.; Cole-Hamilton, D. J.; Ahmad, M. M.; Gerrard, N. D. *J. Crystl. Growth* **1984**, *68*, 1.
- Bradley, D. C.; Chudzynska, H.; Faktor, M. M.; Frigo, D. M.; Hursthouse, M. B.; Hussain, B.; Smith, L. M. *Polyhedron* **1988**, *7*, 1289.
- Foster, D. F.; Rushworth, S. A.; Cole-Hamilton, D. J.; Jones, A. C.; Stagg, J. P. *Chemtronics* **1988**, *3*, 38.
- Freer, R. W.; Whitaker, T. J.; Martin, T.; Calcott, P. D. J.; Houlton, M.; Lee, D.; Jones, A. C.; Rushworth, S. A. *Adv. Mater.* **1995**, *7*, 478.
- Coward, K. M.; Jones, A. C.; Pemble, M. E.; Rushworth, S. A.; Smith, L. M.; Martin, T. *J. Electron. Mater.* **2000**, *29*, 152.

19. Whitaker, T. J.; Freer, R. W.; Martin, T.; Jones, A. C.; Rushworth, S. A. *J. Electron. Mater.* **1996**, *15*, 1060.
20. Thiele, K. H. *Z. Anorg. Chem.* **1962**, *319*, 183.
21. Elschenbroich, C.; Salzer, A. *Organometallics* **1989**, VCH: New York.
22. Khan, O. F. Z.; O'Brien, P.; Hamilton, P. A.; Walsh, J. R.; Jones, A. C. *Chemtronics* **1989**, *4*, 224.
23. Hursthouse, M. B.; Motevalli, M.; O'Brien, P.; Walsh, J. R.; Jones, A. C. *J. Organomet. Chem.* **1993**, *449*, 1.
24. Thiele, K. H. *Z. Anorg. Chem.* **1963**, *325*, 156.
25. Walsh, J. R.; O'Brien, P.; Hursthouse, M. B.; Motevalli, M.; Jones, A. C. *Mater. Chem.* **1991**, *1*, 139.
26. Jacobs, P. R.; Orrell, E. D.; Mullin, J. B.; Cole-Hamilton, D. J. *Chemtronics* **1986**, *1*, 15.
27. Shenai-Khatkate, D. V.; Orrell, E. D.; Mullin, J. B.; Cupertino, D. C.; Cole-Hamilton, D. J. *J. Cryst. Growth* **1986**, *77*, 27.
28. Foster, D. F.; Patterson, I. L. J.; James, L. D.; Cole-Hamilton, D. J.; Armitage, D. N.; Yates, H. M.; Wright, A. C.; Williams, J. O. *Adv. Mater. Opt. Electron.* **1994**, *3*, 163.
29. Yates, H. M.; Williams, J. O.; Patterson, I. L. J.; Cole-Hamilton, D. J. *J. Cryst. Growth* **1993**, *129*, 215.
30. Pickett, N. L.; Lightfoot, P.; Cole-Hamilton, D. J. *Adv. Mater. Opt. Electron.* **1997**, *7*, 23.
31. Thiele, K.-H.; Rau, H. *Z. Anorg. Allg. Chem.* **1967**, *353*, 127.
32. Noltes, J. G.; Van Den Hurk, J. W. G. *J. Organomet. Chem.* **1965**, *3*, 222.
33. Coward, K. M.; Jones, A. C.; Steiner, A.; Bickley, J. F.; Smith, L. M.; Pemble, M. E. *J. Chem. Soc., Dalton Trans.* **2000**, *3480*, 3482.
34. Motevalli, M.; O'Brien, P.; Robinson, A. J.; Walsh, J. R.; Wyatt, P. B.; Jones, A. C. *J. Organomet. Chem.* **1993**, *461*, 5.
35. Kaupp, M.; Stoll, H.; Preuss, H.; Kaim, W.; Stahl, T.; Van Koten, G.; Wissing, E.; Smeets, W. J. J.; Spek, A. L. *J. Am. Chem. Soc.* **1991**, *113*, 5606.
36. Dekker, J.; Boersma, J.; Fernholt, L.; Haaland, A.; Spek, A. L. *Organometallics* **1987**, *6*, 1202.
37. Behm, J.; Lotz, S. D.; Herrmann, W. A. *Z. Anorg. Allg. Chem.* **1987**, *6*, 1202.
38. Coates, G. E.; Green, S. I. E. *J. Chem. Soc.* **1962**, 3340.
39. Jacobs, P. R.; Orrell, E. D.; Mullin, J. B.; Cole-Hamilton, D. J. *Chemtronics* **1986**, *1*, 15.
40. Almond, M. J.; Beer, M. P.; Drew, M. G. B.; Rice, D. A. *Organometallics* **1991**, *10*, 2072.
41. Coates, G. E. *Organometallic Compounds*, 3rd ed.; Coates, G. E., Green, M. L. H., Wade, K., Eds., Methuen: London 1967; Vol. 1, Chapter 2, pp 141–147.
42. Almond, M. J.; Beer, M. P.; Drew, M. G. B.; Rice, D. A. *Organometallics* **1991**, *10*, 2072.
43. Almond, M. J.; Beer, M. P.; Hagen, K.; Rice, D. A.; Wright, P. J. *J. Mater. Chem.* **1991**, *1*, 1065.
44. Efermov, A. A.; Grinberg, E. E.; Fetisov, Yu. M. USSR Patent 546,617, 1977.
45. Thrush, E. J.; Cureton, C. G.; Trigg, J. M.; Stagg, J. P.; Butler, B. R. *Chemtronics* **1987**, *2*, 62.
46. Coward, K. M.; Jones, A. C.; Brickley, J. K.; Steiner, A.; Smith, L. M.; Ravetz, M. S.; Rushworth, S. A.; Odedra, R.; Roberts, J. S.; Pemble, M. E. *J. Cryst. Growth* **2000**, *221*, 81.
47. Bradley, D. C.; Dawes, H.; Frigo, D. M.; Hursthouse, M. B.; Hussain, B. *J. Organomet. Chem.* **1987**, *325*, 55.
48. Coward, K. M.; Jones, J. C.; Steiner, A.; Bickley, J. F.; Pemble, M. E.; Boag, N. M.; Rushworth, S. A.; Smith, L. M. *J. Mater. Chem.* **2000**, *10*, 1875.
49. Lee, B.; Pennington, W. T.; Robinson, G. H.; Rogers, R. D. *J. Organomet. Chem.* **1999**, *396*, 269.
50. Robinson, G. H.; Zhang, H.; Atwood, J. L. *J. Organomet. Chem.* **1987**, *331*, 153.
51. Reir, F. W.; Wolfram, P.; Schumann, H. *J. Cryst. Growth* **1988**, *93*, 41.
52. Jones, A. C. *Chemtronics* **1989**, *4*, 15.
53. Wright, P. J.; Cockayne, B. *J. Cryst. Growth* **1982**, *59*, 148.
54. Blanconner, P.; Cerdet, M.; Henoc, P.; Jean-Louis, A. M. *Thin Solid Films* **1978**, *55*, 375.
55. Fan, G.; Williams, J. O. *Mater. Lett.* **1985**, *3*, 453.
56. Giapis, K. P.; Lu, D. C.; Jensen, K. F. *Appl. Phys. Lett.* **1989**, *54*, 353.
57. Manasevit, H. M.; Simpson, W. I. *J. Electrochem. Soc.* **1971**, *118*, 644.
58. Wright, P. J.; Cockayne, B.; Williams, A. J.; Jones, A. C.; Orrell, E. D. *J. Cryst. Growth* **1987**, *84*, 552.
59. Jones, A. C.; Wright, P. J.; Cockayne, B. *Chemtronics* **1988**, *3*, 35.
60. Cockayne, B.; Wright, P. J.; Armstrong, A. J.; Jones, A. C.; Orrell, E. D. *J. Cryst. Growth* **1988**, *91*, 57.
61. Pickett, N. L.; Riddell, F. G.; Foster, D. F.; Cole-Hamilton, D. J.; Fryer, J. R. *J. Mater. Chem.* **1997**, *7*, 1855.
62. Wright, P. J.; Parbrook, P. J.; Cockayne, B.; Jones, A. C.; Orrell, E. D.; O'Donnell, K. P.; Henderson, B. *J. Cryst. Growth* **1989**, *94*, 441.
63. Wright, P. J.; Cockayne, B.; Parbrook, P. J.; Jones, A. C.; O'Brien, P.; Walsh, J. R. *J. Cryst. Growth* **1990**, *104*, 601.
64. Lovergine, N.; Longo, M.; Gerardi, C.; Manno, D.; Mancini, A. M.; Vasanelli, L. *J. Cryst. Growth* **1995**, *156*, 45.
65. Briot, O.; Di Blasio, M.; Cloitre, T.; Briot, N.; Bigenwald, P.; Gil, B.; Averous, M.; Aulombard, R. L.; Smith, L. M.; Rushworth, S. A.; Jones, A. C. Materials Research Society Spring Meeting, San Francisco, CA, 1994.
66. Wright, P. J.; Cockayne, B.; Parbrook, P. J.; Oliver, P. E.; Jones, A. C. *J. Cryst. Growth* **1991**, *108*, 525.
67. Griffiths, C. L.; Stafford, A.; Irvine, S. J.; Maung, N.; Jones, A. C.; Smith, L. M.; Rushworth, S. A. *Appl. Phys. Lett.* **1996**, *68*, 1294.
68. Choy, K. L. *Thin Solid Films* **2000**, *359*, 160.
69. Choy, K. L.; Bai, W. British Patent 9525505.5, 1995.
70. Wei, M.; Choy, K. L. *Chem. Vap. Deposition* **2002**, *8*, 15.
71. Choy, K. L.; Su, B. *Thin Solid Films* **2001**, *388*, 9.
72. Prete, P.; Lovergine, N.; Zanotti-Fregonara, C.; Mancini, A. M.; Smith, L. M. S.; Rushworth, A. *J. Cryst. Growth* **2000**, *209*, 279.
73. Prete, P.; Lovergine, N.; Cannoletta, D.; Mancini, A. M.; Mele, G.; Vasapollo, G. *J. Appl. Phys.* **1998**, *84*, 6460.
74. Mitsuhashi, H.; Mitsuishi, I.; Kukimoto, H. *Japan J. Appl. Phys.* **1985**, *24*, 1864.
75. Srithoran, S.; Jones, K. *J. Cryst. Growth* **1984**, *66*, 231.
76. Giapis, K. P.; Jensen, K. F. *J. Cryst. Growth* **1990**, *101*, 111.
77. Kuhn, W. S.; Helbing, R.; Qu'Hen, B.; Gorochoy, O. *J. Cryst. Growth* **1995**, *146*, 580.
78. Fujita, S.; Isemura, M.; Sakamoto, T.; Yoshimura, N. *J. Crystal Growth* **1988**, *86*, 263.
79. Akram, S.; Bhat, I. *J. Cryst. Growth* **1994**, *138*, 105.
80. Roberts, J. S.; Button, C. C.; David, J. P. R.; Jones, A. C.; Rushworth, S. A. *J. Cryst. Growth* **1990**, *104*, 857.

81. Jones, A. C.; Rushworth, S. A. *J. Cryst. Growth* **1990**, *106*, 253.
82. Hobson, W. S.; Harris, T. D.; Abernathy, C. R.; Pearton, S. J. *Appl. Phys. Lett.* **1991**, *58*, 77.
83. Olsthoorn, S. M.; Dressen, F. A. J. M.; Giling, L. J.; Frigo, D. M.; Smith, C. J. *Appl. Phys. Lett.* **1992**, *60*, 82.
84. Wilkie, J. K.; Eyden, G. J. M. V.; Frigo, D. M.; Smit, C. J.; Reuvers, P. J.; Olsthoorn, S. M.; Driessen, F. A. J. M. *Inst. Phys. Conf. Ser.* **1992**, *129*, 115.
85. Hageman, P. R.; Olsthoorn, S. M.; Giling, L. J. *J. Cryst. Growth* **1994**, *142*, 284.
86. Miyashita, M.; Kizuki, H.; Tsugami, M.; Fujii, N.; Mihashi, Y.; Takamiya, S. *J. Cryst. Growth* **1998**, *192*, 79.
87. Wiberg, E.; Amberger, E. *Hydrides of the Elements I-IV*; Elsevier: Amsterdam, 1971; Chapter 5.
88. Molassioti, A.; Moser, M.; Stapor, A.; Scholz, F.; Hostalek, M.; Pohl, L. *Appl. Phys. Lett.* **1988**, *54*, 857.
89. Hostalek, M.; Pohl, L.; Brauers, A.; Balk, P.; Hardtdegen, V. H.; Hovel, A.; Regel, G. K. *Thin Solid Films* **1989**, *174*, 1.
90. Watanabe, N.; Nakanisi, T.; Dapkus, P. D., Eds. *Metalorganic Vapor Phase Epitaxy*, Proceedings of the 4th International Conference (MOVPE-4), Hakone, 1988.
91. Jones, A. C.; Roberts, J. S.; Wright, P. J.; Oliver, P. E.; Cockayne, B. *Chemtronics* **1988**, *3*, 152.
92. Bhat, R.; Koza, M. A.; Chang, C. C.; Schwarz, S. A.; Harris, T. D. *J. Cryst. Growth* **1986**, *77*, 7.
93. Jones, A. C.; Wright, P. J.; Oliver, P. E.; Cockayne, B.; Roberts, J. S. *J. Cryst. Growth* **1990**, *100*, 395.
94. Jones, A. C.; Jacobs, P. R.; Rushworth, S. A.; Roberts, J. S.; Button, C. C.; Wright, P. J.; Oliver, P. E.; Cockayne, B. *J. Cryst. Growth* **1989**, *96*, 769.
95. Kuech, T. F.; Veuhoff, E.; Kuan, T. S.; Deline, V.; Potemski, R. *J. Cryst. Growth* **1986**, *77*, 257.
96. Kobayashi, N.; Makimoto, T. *Japan J. Appl. Phys.* **1985**, *24*, L824.
97. Jones, A. C.; Rushworth, S. A.; Roberts, J. S.; Button, C. C.; David, J. P. R. *Chemtronics* **1989**, *4*, 235.
98. Jones, A. C.; Rusworth, S. A.; Bohlinf, D. A.; Muhr, G. T. *J. Cryst. Growth* **1990**, *106*, 246.
99. Wong, C. A.; Salim, S.; Jensen, K. F.; Jones, A. C. 7th US Workshop on OMVPE, FL, April 1995.
100. Jones, A. C.; Auld, J.; Rushwoth, S. A.; Critchlow, G. W. *J. Cryst. Growth* **1994**, *135*, 285.
101. Dapkus, P. D.; Manasevit, H. M.; Hess, K. L.; Low, T. S.; Stillman, G. E. *J. Cryst. Growth* **1981**, *55*, 10.
102. Nakanisi, T.; Udagawa, T.; Tanaka, A.; Kamai, K. *J. Cryst. Growth* **1981**, *55*, 255.
103. Watkins, S. P.; Haacke, G. *Appl. Phys. Lett.* **1991**, *59*, 2263.
104. Hanna, M. C.; Lu, Z. H.; Oh, E. G.; Mac, E.; Majerfield, A. *J. Cryst. Growth* **1992**, *124*, 443.
105. Shastry, S. K.; Zemon, S.; Lambert, G. *J. Cryst. Growth* **1984**, *68*, 437.
106. Plass, C.; Heinecke, H.; Kayser, O.; Luth, H.; Blak, P. *J. Cryst. Growth* **1988**, *88*, 455.
107. Brauers, A. *J. Cryst. Growth* **1991**, *107*, 281.
108. Pohl, L.; Hostalek, M.; Schumann, H.; Hartmann, U.; Wassermann, W.; Brauers, A.; Regel, G. K.; Hövel, R.; Balk, P.; Scholz, F. *J. Cryst. Growth* **1991**, *107*, 309.
109. Protzmann, H.; Marschner, T.; Zsebok, O.; Stolz, W.; Gobel, E. O.; Dorn, R.; Lorberth, J. *J. Cryst. Growth* **1991**, *115*, 248.
110. Lorberth, J.; Dorn, R.; Wocaldo, S.; Massa, W.; Göbel, E. O.; Marschner, T.; Protzmann, H.; Zsebök, O.; Stolz, W. *Adv. Mater.* **1992**, *4*, 576.
111. Zaouk, A.; Salvetat, E.; Sakaya, J.; Maury, F.; Constant, G. *J. Cryst. Growth* **1981**, *55*, 135.
112. Maury, F.; Constant, G. *J. Cryst. Growth* **1983**, *62*, 568.
113. Maury, F.; Hammadi, A. E.; Constant, G.; Maury, F.; Constant, G. *J. Cryst. Growth* **1984**, *68*, 88.
114. Moss, R. H.; Evans, J. S. *J. Cryst. Growth* **1981**, *55*, 129.
115. Didchenko, R.; Alix, J. E.; Toeniskoettler, R. H. *J. Inorg. Nucl. Chem.* **1960**, *14*, 35.
116. Moss, R. H. *J. Cryst. Growth* **1981**, *68*, 78.
117. Chatterjee, A. K.; Faktor, M. M.; Moss, R. H.; White, E. A. D. *J. Physique* **1982**, *43*, C5-491.
118. Bass, S. J.; Skolnick, M. S.; Chudzynska, H.; Smith, L. *J. Cryst. Growth* **1986**, *75*, 221.
119. Hovel, R.; Brysch, W.; Neumann, H.; Heime, K. *J. Cryst. Growth* **1992**, *124*, 106.
120. Rossetto, G.; Franzheld, R.; Camporese, A.; Favaro, M. L.; Torzo, G.; Ajo, D.; Zanella, P. *J. Cryst. Growth* **1995**, *146*, 511.
121. Manasevit, H. M.; Simpson, W. I. *J. Electrochem. Soc.* **1969**, *116*, 1725.
122. Knauf, J.; Schmitz, D.; Strauch, G.; Jurgensen, H.; Heyen, M.; Melas, A. *J. Cryst. Growth* **1988**, *93*, 34.
123. Scholz, F.; Molassioti, A.; Moser, M.; Northeisen, B.; Streubel, K.; Hostalek, M.; Pohl, L. *J. Cryst. Growth* **1991**, *107*, 365.
124. Frigo, D. M.; van Berkel, W. W.; Maassen, W. A. H.; van Mier James, G. P. M.; Wilke, H.; Gal, A. W. *J. Cryst. Growth* **1992**, *124*, 99.
125. Schumann, H.; Gorlitz, F. H.; Seuf, T. D.; Wasserman, W. *Chem. Ber.* **1992**, *125*, 3.
126. Scholz, F.; Moser, M.; Molassioti, A.; Streubel, K.; Hostalek, M.; Pohl, L. *Inst. Phys. Conf. Ser.* **1990**, *106*, 45.
127. Xu, C.; Baum, T. H.; Guzei, I.; Rheingold, A. L. *Inorg. Chem.* **2000**, *39*, 2008.
128. Auld, J.; Houlton, D. J.; Jones, A. C.; Rushworth, S. A.; Critchlow, G. W. *J. Mater. Chem.* **1994**, *4*, 1245.
129. Choquette, K. D.; Klem, J. F.; Fischer, A. J.; Blum, O.; Allerman, A. A.; Fritz, I. J.; Kurtz, S. R.; Breiland, W. G.; Geib, K. M.; Scott, J. W.; Naone, R. L. *Electron. Lett.* **2000**, *36*, 1388.
130. Steinle, G.; Mederer, F.; Kicherer, M.; Michalzik, R.; Kristen, G.; Egorow, A. Y.; Riechert, H.; Wolf, H. D.; Ebeling, K. *J. Electron. Lett.* **2001**, *37*, 425.
131. Kurtz, S. R.; Allerman, A. A.; Jones, E. D.; Gee, J. M.; Banas, J. J.; Hammons, B. E. *Appl. Phys. Lett.* **1999**, *74*, 729.
132. Lee, R. T.; Stringfellow, G. B. *J. Electron. Mater.* **1999**, *28*, 963.
133. Wei, X.; Wang, G. H.; Zhang, G. Z.; Zhu, X. P.; Ma, X. Y.; Chen, L. H. *J. Cryst. Growth* **2002**, *236*, 516.
134. Lee, W. I.; Huang, T. C.; Guo, J. D.; Feng, M. S. *Appl. Phys. Lett.* **1995**, *67*, 1721.
135. Kurtz, S.; Reedy, R.; Keyes, B.; Barber, G. D.; Geisz, J. F.; Friedman, D. J.; McMahon, W. E.; Olson, J. M. *J. Cryst. Growth* **2002**, *234*, 323.
136. Bourret-Courchesne, E. D.; Yu, K.; Irvine, S. J. C.; Stafford, S.; Rushworth, S. A.; Smith, L. M.; Kanjolia, R. *J. Cryst. Growth* **2000**, *221*, 246.
137. Miyoshi, S.; Onabe, K.; Ohkouchi, N.; Yaguchi, H.; Ito, R.; Fukatsu, S.; Shiraki, Y. *J. Cryst. Growth* **1992**, *124*, 439.
138. Kuwano, N.; Kobayashi, K.; Oki, K.; Miyoshi, S.; Yaguchi, H.; Onabe, K.; Shiraki, Y. *Japan J. Appl. Phys.* **1994**, *33*, 2415.
139. Friedman, D. J.; Norman, A. G.; Geisz, J. F.; Kurtz, S. R. *J. Cryst. Growth* **2000**, *208*, 11.
140. Nikishin, S. A.; Temkin, H.; Antipov, V. G.; Guriev, A. I.; Zubrilov, A. S.; Elyukhin, V. A.; Faleev, N. N.; Kyutt, R. N.; Chin, A. K. *Appl. Phys. Lett.* **1998**, *72*, 2361.

141. Nikishin, S. A.; Antipov, V. G.; Ruvimov, S. S.; Seryogin, G. A.; Temkin, H. *Appl. Phys. Lett.* **1996**, *69*, 3227.
142. Sasaki, M.; Yonemura, S.; Nakayama, T.; Shimoyama, N.; Suemasu, T.; Hasegawa, F. *J. Cryst. Growth* **2000**, *209*, 373.
143. Fischer, R. A.; Miehr, A.; Ambacher, O.; Metzger, T.; Born, E. *J. Cryst. Growth* **1997**, *170*, 139.
144. Beaumont, B.; Vaill, M.; Boufaden, T.; ElJani, B.; Gibart, P. *J. Cryst. Growth* **1997**, *170*, 316.
145. Liu, Z.; Lee, R. T.; Stringfellow, G. B. *J. Cryst. Growth* **1998**, *191*, 1.
146. Liu, Z.-J.; Atakan, B.; Kohse-höinghaus, K. *J. Cryst. Growth* **2000**, *219*, 176.
147. Inoue, K.; Yanashima, K.; Takahashi, T.; Hwang, J. S.; Hara, K.; Munekata, H.; Kukimoto, H. *J. Cryst. Growth* **1996**, *159*, 130.
148. Renz, H.; Benz, K. W.; Weidlen, J. *J. Electron. Mater.* **1981**, *110*, 185.
149. Chen, C. H.; Larsen, C. A.; Stringfellow, G. B.; Brown, D. W.; Roberson, A. J. *J. Cryst. Growth* **1986**, *77*, 11.
150. Ougazzaden, A.; Mellet, P.; Gao, Y.; Rao, K. M. *InP and Related Materials*, Proceedings of the 4th International Conference, Newport, MA, April 1992.
151. Maier, L. *Helv. Chim. Acta* **1966**, *49*, 842.
152. Geiger, M.; Ottenwälder, D.; Scholz, F.; Glanz, M.; Recker, C.; Winterfeld, J.; Schumann, H. *J. Cryst. Growth* **1996**, *169*, 625.
153. Abdul-Ridha, H. H.; Bateman, J. E.; Fan, G. H.; Pemble, M. E.; Povey, I. M. *J. Electrochem. Soc.* **1994**, *141*, 1886.
154. Devgatykh, G. G.; Kedyarkin, V. M.; Zorin, A. D. *Russ. J. Inorg. Chem.* **1969**, *14*, 1055.
155. Beurg, A. B.; Grant, L. R. *J. Am. Chem. Soc.* **1959**, *81*, 1.
156. Siguira, O.; Kameda, H.; Shiina, K.; Matsumars, M. *J. Electron. Mater.* **1988**, *117*, 11.
157. Heywood, S. K.; Martin, R. J.; Mason, N. J.; Nicholson, R. J.; Walker, P. J. *J. Cryst. Growth* **1991**, *107*, 422.
158. Biefeld, R. M.; Wendt, J. R.; Kurtz, S. R. *J. Cryst. Growth* **1991**, *107*, 836.
159. Stauf, G. T.; Gaskill, D. K.; Bottka, N.; Gedridge, N. W. *Appl. Phys. Lett.* **1991**, *58*, 1311.
160. Chen, C. H.; Fang, Z. M.; Stringfellow, G. B.; Gedridge, R. W. *Appl. Phys. Lett.* **1991**, *58*, 2532.
161. Shin, J.; Chui, K.; Stringfellow, G. B.; Gedridge, R. W. *J. Cryst. Growth* **1993**, *132*, 371.
162. Larsen, C. A.; Gedridge, R. W.; Stringfellow, G. B. *Chem. Mater.* **1991**, *3*, 96.
163. Larsen, C. A.; Gedridge, R. W.; Li, S. H.; Stringfellow, G. B. *Mater. Res. Soc. Proc.* **1991**, *204*, 129.
164. Li, S. H.; Larsen, C. A.; Stringfellow, G. B.; Gedridge, R. W. *J. Electron. Mater.* **1991**, *20*, 457.
165. Chen, C. H.; Huang, K. T.; Drobeck, D. L.; Stringfellow, G. B. *J. Cryst. Growth* **1992**, *124*, 142.
166. Shin, J.; Verma, A.; Stringfellow, G. B.; Gedridge, R. W. *J. Cryst. Growth* **1994**, *143*, 15.
167. Shi, J.; Verma, A.; Stringfellow, G. B.; Gedridge, R. W. *J. Cryst. Growth* **1995**, *151*, 1.
168. Yamamoto, K.; Asahi, H. A.; Hidaka, K.; Satoh, J.; Gonda, S. *J. Cryst. Growth* **1998**, *186*, 33.
169. Foord, J. S.; Howard, F. P.; McGrady, G. S.; Davies, G. J. *J. Cryst. Growth* **1998**, *188*, 144.
170. Haacke, G.; Watkins, S. P.; Burkhard, H. *J. Cryst. Growth* **1991**, *107*, 342.
171. Mizuta, M.; Kovata, S.; Iwamoto, T.; Kukimoto, H. *Jpn. J. Appl. Phys* **1984**, *23*, L283.
172. Zimmer, M. H.; Hövel, R.; Brych, W.; Brauers, A.; Balk, P. *J. Cryst. Growth* **1991**, *107*, 348.
173. Sharma, A. K. *Thermochim. Acta* **1986**, *104*, 339.
174. Nomura, R.; Matsuda, H. *Trends Inorg. Chem.* **1991**, *2*, 79.
175. Bonamico, M.; Vacicgo, A.; Zambonelli, L. *Acta Crystallogr.* **1965**, *19*, 898.
176. Bonamico, M.; Dessy, G. *J. Chem. Soc. A* **1971**, 264.
177. Saunders, A.; Vecht, A.; Tyrell, G. *Chem. Abstr.* **1988**, *108*, 66226h.
178. Druz, B. L.; Evtukhov, Y. N.; Rakhlin, M. Y. *Metallorg. Khim.* **1988**, *1*, 645.
179. Druz, B. L.; Dyadenko, A. I.; Evtukhov, Y. N.; Rakhlin, M. Y.; Rodionov, V. E. *Izv. Akad. Nauk. SSSR, Neorg. Mater.* **1990**, *26*, 34.
180. Frigo, D. M.; Khan, O. F. Z.; O'Brien, P. *J. Cryst. Growth* **1989**, *96*, 989.
181. Hursthouse, M. B.; Malik, M. A.; Motevalli, M.; O'Brien, P. *Polyhedron* **1992**, *11*, 45.
182. Nomura, R.; Murai, T.; Toyosaki, T.; Matsuda, H. *Thin Solid Films* **1995**, *271*, 4.
183. Fainer, N. I.; Rumyantsev, Y. M.; Kosinova, M. L.; Kuznetsov, F. A. In Proceedings of the XIV International CVD Conference and EUROCVD11; Allendorf, M. D.; Bernard, C., Eds.; Electrochemical Society: Pennington, NJ, 1997; Vol. 97-25, p 1437.
184. Fainer, N. I.; Kosinova, M. L.; Rumyantsev, Y. M.; Salman, E. G.; Kuznetsov, F. A. *Thin Solid Films* **1996**, *280*, 16.
185. Pike, R. D.; Cui, H.; Kershaw, R.; Dwight, K.; Wold, A.; Blanton, T. N.; Wernberg, A. A.; Gysling, H. J. *Thin Solid Films* **1993**, *224*, 221.
186. Nomura, R.; Konishi, K.; Futenma, S.; Matsuda, H. *Appl. Organomet. Chem.* **1990**, *4*, 607.
187. Motevalli, M.; O'Brien, P.; Walsh, J. R.; Watson, I. M. *Polyhedron* **1996**, *15*, 2801.
188. O'Brien, P.; Walsh, J. R.; Watson, I. M.; Hart, L.; Silva, S. R. P. *J. Cryst. Growth* **1996**, *167*, 133.
189. Chunggaze, M.; McAleese, J.; O'Brien, P.; Otway, D. *J. Chem Commun.* **1998**, 833.
190. Chunggaze, M.; Malik, M. A.; O'Brien, P. *J. Mater. Chem.* **1999**, *9*, 2433.
191. Zeng, D.; Hampden-Smith, M. J.; Alars, T. M.; Rheingold, A. L. *Polyhedron* **1994**, *13*, 2715.
192. Zenskova, S. M.; Berus, E. I.; Glinskaya, L. A.; Klevtsova, R. F.; Gromilov, S. A.; Durasov, V. B.; Larianov, S. V. In Proceedings of the XIII International CVD Conference; Besmann, T. M.; Allendorf, M. D.; Ulrich, R. K., Eds.; Electrochemical Society: Pennington, NJ, 1996; Vol. 96-25, p 267.
193. Zenskova, S. M.; Sysoev, S. V.; Glinskaya, L. A.; Klevtsova, R. F.; Gromilov, S. A.; Larionov, S. V. In Proceedings of the XIV International CVD Conference and EUROCVD11; Allendorf, M. D.; Bernard, C., Eds.; Electrochemical Society: Pennington, NJ, 1997; Vol. 97-25, p 1429.
194. Bessergenev, V. G.; Belyi, V. I.; Rastorguev, A. A.; Ivanova, E. N.; Kovalevskaya, Y. A.; Larionov, S. V.; Zenskova, S. M.; Kirichenko, V. N.; Nodolinnyi, V. A. *Thin Solid Films* **1996**, *279*, 135.
195. Rumyantsev, Y. M.; Fainer, N. I.; Kosinova, M. L.; Ayupov, B. M.; Sysoeva, N. P. *J. Phys. IV* **1999**, *9*, 777.
196. Fainer, N. I.; Rumyantsev, Y. M.; Salmam, E. G.; Kosinova, M. L.; Yurjev, G. S.; Sysoeva, N. P.; Sysoev, S. V.; Maximovskii, E. A.; Golubenko, A. N. *Thin Solid Films* **1996**, *286*, 122.
197. Markunas, R. J.; Hendry, R.; Rudder, R. A. U.S. Patent 5,018,479, August 10, 1989.
198. Markunas, R. J.; Hendry, R.; Rudder, R. A. U.S. Patent 4,870,030, September 24, 1987.
199. Lucovsky, G.; Tsu, D. V. *J. Non-Cryst. Solids* **1979**, *97-98*, 265.
200. Haggata, S. W.; Malik, M. A.; Motevalli, M.; O'Brien, P.; Knowles, J. C. *Chem. Mater.* **1995**, *7*, 716.

201. Noltes, J. G. *Recl. Trav. Chim. Pays-Bas* **1965**, *84*, 126.
202. Hursthouse, M. B.; Malik, M. A.; Motevalli, M.; O'Brien, P. *Organometallics* **1991**, *10*, 730.
203. Malik, M. A.; O'Brien, P. *Chem. Mater.* **1991**, *3*, 999.
204. Hursthouse, M. B.; Malik, M. A.; Motevalli, M.; O'Brien, P. *J. Mater. Chem.* **1992**, *2*, 949.
205. Malik, M. A.; Motevalli, M.; O'Brien, P.; Walsh, J. R. *Organometallics* **1992**, *11*, 3436.
206. Abrahams, I.; Malik, M. A.; Motevalli, M.; O'Brien, P. *J. Organomet. Chem.* **1994**, *465*, 73.
207. Malik, M. A.; Motevalli, M.; Walsh, J. R.; O'Brien, P. *Organometallics* **1992**, *11*, 3136.
208. Malik, M. A.; Saeed, T.; O'Brien, P. *Polyhedron* **1993**, *12*, 1533.
209. Malik, M. A.; O'Brien, P. *Adv. Mater. Opt. Electron.* **1994**, *3*, 171.
210. Nomura, R.; Seki, Y.; Matsuda, H. *Thin Solid Films* **1992**, *209*, 145.
211. Chunggaze, M.; Malik, M. A.; O'Brien, P. *Adv. Mater. Opt. Electron.* **1998**, *7*, 311.
212. Chunggaze, M.; Malik, M. A.; O'Brien, P.; White, A. J. P.; Williams, D. J. *J. Chem. Soc., Dalton Trans.* **1998**, 3839.
213. Nyman, M.; Hampden-Smith, M. J.; Duesler, E. *Chem. Vap. Deposition* **1996**, *2*, 171.
214. Nyman, M.; Jenkins, K.; Hampden-Smith, M. J.; Kodas, T. T.; Duesler, E. N.; Rheingold, A. L.; Liable-Sands, M. L. *Chem. Mater.* **1998**, *10*, 914.
215. Dance, I. G. *Polyhedron* **1986**, *5*, 1037.
216. Brennan, M. J. G.; Siegrist, T.; Carroll, P. J.; Stuczynski, S. M.; Reynders, P.; Burs, L. E.; Steigerwald, M. L. *Chem. Mater.* **1990**, *2*, 403.
217. Zeng, D.; Hampden-Smith, M. J.; Densler, E. N. *Inorg. Chem.* **1994**, *33*, 5376.
218. Bradley, D. C.; Kunchur, D. N. *J. Chem. Phys.* **1964**, *8*, 2258.
219. Blower, P. J.; Dilworth, J. R.; Hutchinson, J. P.; Zubieta, J. A. *J. Chem. Soc., Dalton Trans.* **1985**, 1533.
220. Bochmann, M.; Webb, K.; Harman, M.; Hursthouse, M. B. *Angew. Chem. Int. Engl.* **1990**, *29*, 638.
221. Bochmann, M.; Webb, K. J.; Hursthouse, M. B.; Mazid, M. *J. Chem. Soc., Dalton Trans.* **1991**, 2317.
222. Bochmann, M.; Webb, K. J. *J. Chem. Soc., Dalton Trans.* **1991**, 2325.
223. Bochmann, M.; Bwembya, G. C.; Grinter, R.; Powell, A. K.; Webb, K. J.; Hursthouse, M. B.; Malik, M. A.; Mazid, M. A. *Inorg. Chem.* **1994**, *33*, 2290.
224. Bochmann, M.; Webb, K. J. *Mater. Res. Soc. Symp. Proc.* **1991**, *204*, 149.
225. Bochmann, M.; Webb, K. J.; Hails, J.-E.; Wolverson, D. *Eur. Solid State Inorg. Chem.* **1992**, *29*, 155.
226. Dabbousi, B. O.; Bonasia, P. J.; Arnold, J. *J. Am. Chem. Soc.* **1991**, *113*, 3186.
227. Bonasia, P. J.; Arnold, J. *Inorg. Chem.* **1992**, *31*, 2508.
228. Arnold, J.; Walker, J. M.; Yu, K. M.; Bonasia, P. J.; Seligson, A. L.; Bourret, E. D. *J. Cryst. Growth* **1992**, *124*, 647.
229. Bonasia, P. J.; Gindelberger, D. E.; Dabbousi, B. O.; Arnold, J. *J. Am. Chem. Soc.* **1992**, *114*, 5209.
230. Bonasia, P. J.; Mitchell, G. P.; Hollander, F. J.; Arnold, J. *Inorg. Chem.* **1994**, *33*, 1797.
231. Arnold, J.; Bonasia, P. J. U.S. Patent 5,157,136, October 20, 1992.
232. Park, H. S.; Mokhtari, M.; Roesky, H. W. *Chem. Vap. Deposition* **1996**, *2*, 135.
233. Takahashi, Y.; Yuki, R.; Sugiura, M.; Motojima, S.; Sugiyama, K. *J. Cryst. Growth* **1980**, *50*, 491.
234. Evans, M. A. H.; Williams, J. O. *Thin Solid Films* **1982**, *87*, L1.
235. Bwembya, G. C.; Song, X.; Bochman, M. *Chem. Vap. Deposition* **1995**, *1*, 78.
236. Aitchison, K. A.; Julius Backer-Dirks, J. D.; Bradley, D. C.; Faktor, M. M.; Frigo, D. M.; Hursthouse, M. B.; Hussain, B.; Short, R. L. *J. Organomet. Chem.* **1989**, *366*, 11.
237. Maury, F.; Constant, G. *Polyhedron* **1984**, *3*, 581.
238. Janik, J. F.; Duesler, E. N.; McNamara, W. F.; Westerhausen, M.; Paine, R. T. *Organometallics* **1989**, *8*, 506.
239. Atwood, D. A.; Jones, D. A.; Cowley, A. H. *Polyhedron* **1991**, *10*, 1897.
240. Park, J. T.; Kim, Y.; Kim, J.; Kim, K. *Organometallics* **1992**, *11*, 3320.
241. Waggoner, K. M.; Power, P. P. *J. Am. Chem. Soc.* **1991**, *113*, 3385.
242. Beachley, O. T. Jr.; Noble, M. J.; Churchill, M. R.; Lake, C. H. *Organometallics* **1992**, *11*, 1051.
243. Atwood, D. A.; Cowley, A. H.; Jones, R. A.; Mardones, M. A.; Atwood, J. L.; Bott, S. G. *J. Coord. Chem.* **1992**, *26*, 285.
244. Taghiof, M.; Hendershot, D. G.; Barber, M.; Oliver, J. P. *J. Organomet. Chem.* **1992**, *431*, 271.
245. Wells, R. L.; Aubuchon, S. R.; Self, M. F. *Organometallics* **1992**, *11*, 3370.
246. Wells, R. L.; McPhail, A. T.; Alvanipour, A. *Polyhedron* **1992**, *11*, 839.
247. Wells, R. L.; McPhail, A. T.; Self, M. F. *Organometallics* **1992**, *11*, 221.
248. Beachley, O. T. Jr.; Maloney, J. D.; Rogers, R. D. *J. Organomet. Chem.* **1993**, *449*, 69.
249. Cowley, A. H.; Harris, P. R.; Jones, R. A.; Nunn, C. M. *Organometallics* **1991**, *10*, 652.
250. Cowley, A. H.; Jones, R. A.; Mardones, M. A.; Nunn, C. M. *Organometallics* **1991**, *10*, 1635.
251. Atwood, D. A.; Cowley, A. H.; Jones, R. A.; Mardones, M. A. *J. Am. Chem. Soc.* **1991**, *113*, 7050.
252. Petrie, M. A.; Power, P. P. *J. Chem. Soc., Dalton Trans.* **1993**, 1737.
253. Waggoner, K. M.; Ruhlandt-Senge, K.; Wehmschulte, R. J.; Power, P. P. *Inorg. Chem.* **1993**, *32*, 2557.
254. Heaton, D. E.; Jones, R. A.; Kidd, K. B.; Cowley, A. H.; Nunn, C. M. *Polyhedron* **1988**, *7*, 1901.
255. Cowley, A. H.; Benac, B. L.; Ekerdt, J. G.; Jones, R. A.; Kidd, K. B.; Lee, J. Y.; Miller, J. E. *J. Am. Chem. Soc.* **1988**, *110*, 6248.
256. Cowley, A. H.; Jones, R. A. *Angew. Chem. Int. Ed. Engl.* **1989**, *28*, 1208.
257. Miller, J. E.; Kidd, K. B.; Cowley, A. H.; Jones, R. A.; Ekerdt, J. G.; Gysling, H. J.; Wernberg, A. A.; Blanton, T. N. *Chem. Mater.* **1990**, *2*, 589.
258. Miller, J. E.; Ekerdt, J. G. *Chem. Mater.* **1992**, *4*, 7.
259. Cowley, A. H.; Jones, R. A. *Polyhedron* **1994**, *13*, 1149.
260. Lu, J.-P.; Raj, R.; Wernberg, A. *Thin Solid Films* **1991**, *205*, 236.
261. Wernberg, A. A.; Lawrence, D. J.; Gysling, H. J.; Filo, A. J.; Blanton, T. N. *J. Cryst. Growth* **1993**, *131*, 176.
262. Andrews, D. A.; Davies, G. J.; Bradley, D. C.; Faktor, M. M.; Frigo, D. M.; White, E. A. D. *Semicond. Sci. Technol.* **1988**, *3*, 1053.
263. Park, H. S.; Schulz, S.; Wessel, H.; Roesky, H. W. *Chem. Vap. Deposition* **1999**, *5*, 179.
264. Ekerdt, J. G.; Sun, Y. M.; Jackson, M. S.; Lakhota, V.; Pacheco, K. A.; Koschmieder, S. U.; Cowley, A. H.; Jones, R. A. *J. Cryst. Growth* **1992**, *124*, 158.
265. Miller, J. E.; Mardones, M. A.; Nail, J. W.; Cowley, A. H.; Jones, R. A.; Ekerdt, J. G. *Chem. Mater.* **1992**, *4*, 447.

266. Lakhotia, V.; Heitzinger, J. M.; Cowley, A. H.; Jones, R. A.; Ekerdt, J. G. *Chem. Mater.* **1994**, *6*, 871.
267. Cowley, A. H.; Jones, R. A.; Nunn, C. M.; Westmorland, D. L. *Chem. Mater.* **1990**, *2*, 221.
268. Nakamura, S. *MRS Bull.* **1998**, *23*, 37.
269. Zanella, P.; Rosetto, G. *Chem. Mater.* **1991**, *3*, 225.
270. Gordon, R. G.; Hoffman, D. M.; Riaz, U. *J. Mater. Res.* **1991**, *6*, 5.
271. Rushworth, S. A.; Brown, J. R.; Houlton, D. J.; Jones, A. C.; Roberts, V.; Roberts, J. S.; Critchlow, G. W. *Adv. Mater. Opt. Elect.* **1996**, *6*, 119.
272. Jiang, Z. P.; Interrante, L. V. *Chem. Mater.* **1990**, *2*, 439.
273. Sung, M. M.; Jung, H. D.; Lee, J. K.; Kim, S.; Park, J. T.; Kim, Y. *Bull. Korean Chem. Soc.* **1994**, *15*, 79.
274. Bradley, D. C.; Firgo, D. M.; White, E. A. D. European Pat. Appl. EP 03318, 1979.
275. Kim, Y.; Kim, J. H.; Park, J. E.; Bae, B. J.; Kim, B.; Park, J. T.; Yu, K.-S.; Kim, Y. *Thin Solid Films* **1999**, *339*, 200.
276. Gordon, R. G.; Hoffman, D. M.; Riaz, U. *Mater. Res. Soc. Proc.* **1991**, *204*, 95.
277. Andrews, J. E.; Littlejohn, M. A. *J. Electrochem. Soc.* **1975**, *122*, 1273.
278. Park, H. S.; Waezadas, S. D.; Cowley, A. H.; Roesky, H. W. *Chem. Mater.* **1998**, *10*, 2251.
279. Grocholl, L.; Cullison, S. A.; Wang, J.; Swenson, D. C.; Gillan, E. G. *Inorg. Chem.* **2002**, *41*, 2920.
280. Ho, K. L.; Jensen, K. F.; Hwang, J. W.; Gladfelter, J. W. L.; Evans, J. F. *J. Cryst. Growth* **1991**, *107*, 376.
281. Kouvetakis, J.; Beach, D. B. *Chem. Mater.* **1989**, *1*, 476.
282. Atwood, D. A.; Jones, R. A.; Cowley, A. H.; Atwood, J. L.; Bott, S. G. *J. Organomet. Chem.* **1990**, *C6–C8*, 94.
283. Neumayer, D. A.; Cowley, A. H.; Decken, A.; Jones, R. A.; Lakhotia, L.; Ekerdt, J. G. *J. Am. Chem. Soc.* **1995**, *117*, 5893.
284. Jensen, K. F.; Annapragada, A.; Ho, K. L.; Huh, J. S.; Patnaik, S.; Salim, S. J. *Phys.* **1991**, *IV 1*, C2-243.
285. Bock, H.; Dammal, R. *Angew. Chem.* **1987**, *99*, 518; *Angew. Chem. Int. Ed. Engl.* **1987**, *26*, 504.
286. Devi, A.; Rogge, W.; Wohlfart, A.; Hipler, F.; Becker, H. W.; Fischer, R. A. *Chem. Vap. Deposition* **2000**, *6*, 245.
287. Suuek, H.; Stark, O.; Devi, A.; Pritzkow, H.; Fischer, R. A. *J. Organomet. Chem.* **2000**, *602*, 29.
288. Schäfer, J.; Wolfrum, J.; Fischer, R. A.; Sussek, H. *Chem. Vap. Deposition* **1999**, *5*, 205.
289. Fischer, R. A.; Sussek, H.; Miehr, A.; Pritzkow, H.; Herdtweck, E. *J. Organomet. Chem.* **1997**, *548*, 73.
290. Bae, B.-J.; Park, J. E.; Kim, B.; Park, J. T. *J. Organomet. Chem.* **2000**, *616*, 128.
291. McMurrin, J.; Dai, D.; Balasubramanian, K.; Steffek, C.; Kouvetakis, J.; Hubbard, J. L. *Inorg. Chem.* **1998**, *37*, 6638.
292. Sung, M. M.; Kim, C.; Yoo, S. H.; Kim, C. G.; Kim, Y. *Chem. Vap. Deposition* **2002**, *8*, 50.
293. Kouvetakis, J.; McMurrin, J.; Matsunaga, P.; O'Keeffe, M. *Inorg. Chem.* **1997**, *36*, 1792.
294. MacInnes, A. N.; Power, M. B.; Barron, A. R.; Jenkins, P.; Hepp, A. F. *Appl. Phys. Lett.* **1993**, *62*, 711.
295. Nomura, R.; Sekl, Y.; Matsuda, H. *J. Mater. Chem.* **1992**, *2*, 765.
296. Malik, M. A.; O'Brien, P. *Polyhedron* **1997**, *16*, 3593.
297. Nomura, R.; Fujii, S.; Kanaya, K.; Matsuda, H. *Polyhedron* **1990**, *9*, 361.
298. Nomura, R.; Kanaya, K.; Matsuda, H. *Thin Solid Films* **1991**, *198*, 339.
299. Gysling, H. J.; Wernberg, A. A.; Blanton, T. N. *Chem. Mater.* **1992**, *4*, 900.
300. Shang, G.; Kunze, K.; Hampden-Smith, M. J.; Duesler, E. N. *Adv. Mater., Chem. Vap. Deposition* **1996**, *2*, 242.
301. O'Brien, P.; Otway, D. J.; Walsh, J. R. *Thin Solid Films* **1998**, *315*, 57.
302. Horley, G. A.; Chunggaze, M.; O'Brien, P.; White, A. J. P.; Williams, D. J. *J. Chem. Soc., Dalton Trans.* **1998**, 4205.
303. Horley, G. A.; O'Brien, P.; Park, J.-H.; White, A. J. P.; Williams, D. J. *J. Mater. Chem.* **1999**, *9*, 1289.
304. Horley, A.; Lazell, M. R.; O'Brien, P. *Adv. Mater., Chem. Vap. Deposition* **1999**, *5*, 203.
305. Nomura, R.; Inzawa, S.-J.; Kanaya, K.; Matsuda, H. *Appl. Organomet. Chem.* **1989**, *3*, 195.
306. Nomura, R.; Inzawa, S.-J.; Kanaya, K.; Matsuda, H. *Polyhedron* **1989**, *8*, 763.
307. Nomura, R.; Konishi, K.; Matsuda, H. *J. Electrochem. Soc.* **1991**, *138*, 631.
308. Nomura, R.; Konishi, K.; Matsuda, H. *Chem. Lett.* **1988**, 1849.
309. MacInnes, A. N.; Power, M. B.; Hepp, A. F.; Barron, A. R. *J. Organomet. Chem.* **1993**, *449*, 95.
310. Stoll, S. L.; Bott, S. G.; Barron, A. R. *J. Chem. Soc., Dalton Trans.* **1997**, 1315.
311. MacInnes, A. N.; Power, M. B.; Barron, A. R. *Chem. Mater.* **1992**, *4*, 11.
312. Power, M. B.; Barron, A. R. *J. Chem. Soc., Chem. Commun.* **1991**, 1315.
313. Gillan, E. G.; Barron, A. R. *Chem. Mater.* **1997**, *9*, 3037.
314. Gillan, E. G.; Bott, S. G.; Barron, A. R. *Chem. Mater.* **1997**, *9*, 796.
315. Suh, S.; Hooman, D. M. *Chem. Mater.* **2000**, *12*, 2794.
316. Kemmler, M.; Lazell, M.; O'Brien, P.; Otway, D. J. *Mater. Res. Soc. Symp. Proc.* **2000**, *606*, 147.
317. O'Brien, P.; Otway, D. J.; Walsh, J. R. *Adv. Mater., Chem. Vap. Deposition* **1997**, *3*, 227.
318. Cheon, J.; Arnold, J.; Yu, K.-M.; Bourret, E. D. *Chem. Mater.* **1995**, *7*, 2273.
319. Lazell, M. R.; O'Brien, P.; Otway, D. J.; Park, J.-H. *Chem. Mater.* **1999**, *11*, 3430.
320. Haggata, S. W.; Malik, M. A.; Motevalli, M.; O'Brien, P.; Knowles, J. C. *Chem. Mater.* **1995**, *7*, 716.
321. Keys, A.; Bott, S. G.; Barron, A. R. *Chem. Mater.* **1999**, *11*, 3578.
322. Bessergenev, V. G.; Ivanona, E. V.; Kovalevskaya, Y. A.; Gromilov, S. A.; Kirichenko, V. N.; Larionov, S. V. *Inorg. Mater.* **1996**, *6*, 1639.
323. Shang, G.; Hampden-Smith, M. J.; Duesler, E. N. *J. Chem. Soc., Chem. Commun.* **1996**, 1733.
324. Trindale, T.; O'Brien, P. *Chem. Vap. Deposition* **1997**, *3*, 75.
325. Chuprakov, I. S.; Dahmen, K.-H.; Schneider, J. J.; Hagen, J. *Chem. Mater.* **1998**, *10*, 3467.
326. Chuprakov, I. S.; Dahmen, K.-H. *J. Phys. IV* **1999**, *9*, 313.
327. Barone, G.; Chaplin, T.; Hibbert, T. G.; Kana, A. T.; Mahon, M. F.; Molloy, K. C.; Worsley, I. D.; Parkin, I. P.; Price, L. S. *J. Chem. Soc., Dalton Trans.* **2002**, 1085.
328. Barone, G.; Hibbert, T. G.; Mahon, M. F.; Molloy, K. C.; Price, L. S.; Parkin, I. P.; Hardy, A. M. E.; Field, M. N. *J. Mater. Chem.* **2001**, *11*, 464.
329. Parkin, I. P.; Price, L. S.; Hibbert, T. G.; Molloy, K. C. *J. Mater. Chem.* **2001**, *11*, 1486.
330. Nomura, R.; Matsuda, H. In *Organometallic Chemistry*, Proceedings of the 16th International Conference; Brighton, 1994, p 138.
331. Banger, K. K.; Cowen, J.; Hepp, A. F. *Chem. Mater.* **2001**, *13*, 3827.
332. Hollingsworth, J. A.; Hepp, A. F.; Buhro, W. E. *Chem. Vap. Deposition* **1999**, *5*, 105.

333. Banger, K. K.; Harris, J. D.; Cowen, J.; Hepp, A. F. *Thin Solid Films* **2002**, *390*, 403–404.
334. McAleese, J.; O'Brien, P.; O'tway, D. J. *Chem. Vap. Deposition* **1998**, *4*, 94.
335. Nomura, R.; Matsuda, H.; Miyai, T.; Baba, A. *Thin Solid Films* **1999**, *342*, 108.
336. Henglein, A. *Chem. Rev.* **1989**, *89*, 1861.
337. Steigerwald, M. L.; Brus, L. E. *Acc. Chem. Res.* **1990**, *23*, 183.
338. Bawendi, M. G.; Steigerwald, M. L.; Brus, L. E. *Annu. Rev. Phys. Chem.* **1990**, *41*, 477.
339. Weller, H. *Angew. Chem. Int. Ed. Engl.* **1993**, *32*, 41.
340. Weller, H. *Adv. Mater.* **1993**, *5*, 88.
341. Hagfeldt, A.; Grätzel, M. *Chem. Rev.* **1995**, *95*, 49.
342. Fendler, J. H.; Meldrum, F. C. *Adv. Mater.* **1995**, *7*, 607.
343. Alivisatos, A. P. *J. Phys. Chem.* **1996**, *100*, 13226.
344. Stroschio, J. A.; Eigler, D. M. *Science* **1991**, *254*, 1319.
345. Lieber, C. M.; Liu, J.; Sheehan, P. *Angew. Chem. Int. Ed. Engl.* **1996**, *35*, 687.
346. Berry, C. R. *Phys. Rev.* **1967**, *161*, 848.
347. Matijevic, E. *Annu. Rev. Mater. Sci.* **1985**, *15*, 483.
348. Matijevic, E. *Langmuir* **1986**, *2*, 12.
349. Colvin, V. L.; Schlamp, M. C.; Alivisatos, A. P. *Nature* **1994**, *370*, 354.
350. Schlamp, M. C.; Peng, X. G.; Alivisatos, A. P. *Appl. Phys.* **1997**, *82*, 5837.
351. Lee, J.; Sundar, V. C.; Heine, J. R.; Bawendi, M. G.; Jensen, K. F. *Adv. Mater.* **2000**, *12*, 1103.
352. Brust, M.; Fink, J.; Bethel, D.; Schriffren, D. J.; Kiely, C. J. *Chem. Soc., Chem. Commun.* **1995**, 1655.
353. Tanori, J.; Pileni, M. P. *Adv. Mater.* **1995**, *7*, 862.
354. Andrievskii, R. A. *Russ. Chem. Rev.* **1994**, *63*, 411.
355. Kornowski, A.; Giersig, M.; Vogel, M.; Chemseddine, A.; Weller, H. *Adv. Mater.* **1993**, *5*, 634.
356. Fojtik, A.; Henglein, A. *Chem. Phys. Lett.* **1994**, *221*, 363.
357. Henglein, A.; Mulvaney, P.; Linnert, T. *Faraday Discuss.* **1991**, *92*, 31.
358. Reetz, M. T.; Helbig, W. *J. Am. Chem. Soc.* **1994**, *116*, 7401.
359. Hunter, R. J. *Introduction to Modern Colloid Science*; Oxford University Press: Oxford, UK, 1993.
360. Wilhelmy, D. M.; Matijevic, E. *J. Chem. Soc., Faraday Trans. 1* **1984**, *80*, 563.
361. Wang, Y.; Herron, N. J. *Phys. Chem.* **1987**, *91*, 257.
362. Shinojima, H.; Yumoto, J.; Uesugi, N.; Omi, S.; Asahara, Y. *Appl. Phys. Lett.* **1989**, *55*, 1519.
363. Abe, T.; Tachibana, Y.; Uematsu, T.; Iwamoto, M. *J. Chem. Soc., Chem. Commun.* **1995**, 1617.
364. Brenchley, M. E.; Weller, M. T. *Angew. Chem. Int. Ed. Engl.* **1993**, *32*, 1663.
365. Blasse, G.; Dirksen, C. J.; Brenchley, M. E.; Weller, M. T. *Chem. Phys. Lett.* **1995**, *234*, 177.
366. Watzke, H. J.; Fendler, J. H. *J. Phys. Chem.* **1987**, *91*, 854.
367. Khan-Lodhi, A.; Robinson, B. H.; Towey, T.; Herrmann, C.; Knoche, W.; Thesing, U. In *The Structure, Dynamics and Equilibrium Properties of Colloidal Systems*; Bloor, D. M.; Wyn-Jones, E., Eds.; Kluwer Academic Publishers, 1990; p 373.
368. Towey, T. F.; Khan-Lodi, A.; Robinson, B. H. *J. Chem. Soc., Faraday Trans.* **1990**, *86*, 3757.
369. Korgel, B. A.; Monbouquette, G. *J. Phys. Chem.* **1996**, *100*, 346.
370. Choi, K. M.; Shea, K. J. *J. Phys. Chem.* **1994**, *98*, 3207.
371. Choi, K. M.; Shea, K. J. *J. Am. Chem. Soc.* **1994**, *116*, 9052.
372. Carpenter, J. C.; Lukehart, C. M.; Stock, S. R.; Wittig, J. E. *Chem. Mater.* **1995**, *7*, 201.
373. Wang, Y.; Suna Mahler, A. W.; Kasowski, R. *J. Chem. Phys.* **1987**, *87*, 7315.
374. Gao, M.; Yang, Y.; Yang, B.; Bian, F.; Shen, J. *J. Chem. Soc., Chem. Commun.* **1994**, 2779.
375. Nirmal, M.; Murray, C. B.; Bawendi, M. G. *Phys. Rev. B* **1994**, *50*, 2293.
376. Tassoni, R.; Schrock, R. R. *Chem. Mater.* **1994**, *6*, 744.
377. Moffitt, M.; Eisenberg, A. *Chem. Mater.* **1995**, *7*, 1178.
378. Cassagneau, T.; Hix, G. B.; Jones, D. J.; Maireles-Torres, P.; Rhomari, M.; Roziere, J. *J. Mater. Chem.* **1994**, *4*, 189.
379. Murray, C. B.; Norris, D. J.; Bawendi, M. G. *J. Am. Chem. Soc.* **1993**, *115*, 8706.
380. Hambrock, J.; Birkner, A.; Fisher, R. A. *J. Mater. Chem.* **2001**, *11*, 3197.
381. McCleverty, J. A.; Spender, N.; Bailey, N. A.; Chockleton, S. L. *J. Chem. Soc., Dalton Trans.* **1980**, 1939.
382. Magee, R. J.; Hill, J. O. *Rev. Anal. Chem.* **1985**, *8*, 5.
383. O'Brien, P.; Walsh, J. R.; Watson, I. M.; Motevalli, M.; Henriken, L. *J. Chem. Soc., Dalton Trans.* **1996**, 249.
384. Revaprasadu, N.; Malik, M. A.; O'Brien, P.; Zulu, M. M.; Wakefield, G. *J. Mater. Chem.* **1998**, *8*, 1885.
385. Nair, P. S.; Revaprasadu, N.; Radhakrishnan, T.; Kolawole, G. A. *J. Mater. Chem.* **2001**, *11*, 1555.
386. Abe, K.; Hanada, T.; Yoshida, Y.; Tanigaki, N.; Takiguchi, H.; Nagasawa, H.; Nakamoto, M.; Yamaguchi, T.; Yase, K. *Thin Solid Films* **1998**, *329*, 524.
387. Lazell, M.; O'Brien, P. *Chem. Commun.* **1999**, 2041.
388. Revaprasadu, N.; Malik, M. A.; O'Brien, P.; Wakefield, G. *Chem. Commun.* **1999**, 1573.
389. Nyman, M. D.; Hampden-Smith, M. J.; Duesler, E. N. *Inorg. Chem.* **1997**, *36*, 2218.
390. Zhang, Z.; Chin, W. S.; Vittal, J. *J. Chem. Commun.* (in press).
391. Cumberland, S. L.; Hanif, K. M.; Javier, A.; Khitov, K. A.; Strouse, G. F.; Woessner, S. M.; Yun, C. S. *Chem. Mater.* **2002**, *14*, 1576.
392. Brennan, J. G.; Siegrist, T.; Carrol, P. J.; Stuczynski, S. M.; Brus, L. E.; Steigerwald, M. L. *J. Am. Chem. Soc.* **1989**, *111*, 4141.
393. Boudjouk, P.; Jarabek, B. R.; Simonson, D. L.; Seidler, D. J.; Grier, D. G.; McCarthy, G. J.; Keller, L. P. *Chem. Mater.* **1998**, *10*, 2358.
394. Babcock, J. R.; Zehner, R. W.; Sita, L. R. *Chem. Mater.* **1998**, *10*, 2027.
395. Green, M.; O'Brien, P. *Chem. Commun.* **1998**, 2459.
396. Wells, R. L.; Self, M. F.; McPhail, A. T.; Aubuchon, S. R.; Woudenberg, R. C.; Jasinski, J. P. *Organometallics* **1993**, *12*, 2832.
397. Foos, E. E.; Jouet, R. J.; Wells, R. L.; Rheingold, A. L.; Liable-Sands, L. M. *J. Organomet. Chem.* **1999**, *582*, 45.
398. Jouet, R. J.; Wells, R. L.; Rheingold, A. L.; Incarvito, C. D. *J. Organomet. Chem.* **2000**, *601*, 191.

399. Foos, E. E.; Jouet, R. J.; Wells, R. L.; White, P. S. *J. Organomet. Chem.* **2000**, 598, 182.
400. Jegier, J. A.; McKernan, S.; Purdy, A. P.; Gladfelter, W. L. *Chem. Mater.* **2000**, 12, 1003.
401. Frank, A. C.; Stowasser, F.; Stark, O.; Kwak, H.-T.; Sussek, H.; Rupp, A.; Pritzkow, H.; Ambscher, O.; Giersig, M.; Fischer, R. A. *Adv. Mater. Opt. Electron.* **1998**, 8, 135.
402. Green, M.; O'Brien, P. *Adv. Mater.* **1998**, 10, 527.
403. Green, M.; O'Brien, P. *J. Mater. Chem.* **1999**, 9, 243.
404. Malik, A.; O'Brien, P.; Revaprasada, N. *Adv. Mater.* **1999**, 11, 1441.
405. Revaprasadu, N.; Malik, M. A.; Carstens, J.; O'Brien, P. *J. Mater. Chem.* **1999**, 9, 2885.
406. McAleese, J.; O'Brien, P.; Otway, D. J. *Mater. Res. Soc. Symp. Proc.* **1998**, 485, 157.
407. Stoll, S. L.; Gillan, E. G.; Barron, A. R. *Chem. Vap. Deposition* **1996**, 2, 182.
408. Monteiro, O. C.; Nogueira, H. I. S.; Trindade, T. *Chem. Mater.* **2001**, 13, 2103.
409. Jegier, J. A.; McKernan, S.; Gladfelter, W. L. *Chem. Mater.* **1998**, 10, 2041.
410. Micic, O. I.; Sprague, J. R.; Curtis, C. J.; Jones, K. M.; Machol, J. L.; Nozic, A.; Giessen, J. H.; Fluegel, B.; Mohs, G.; Peyghambarian, N. *J. Phys. Chem.* **1995**, 99, 7754.
411. Douglas, T.; Teopold, K. H. *Inorg. Chem.* **1991**, 30, 594.
412. Buhro, W. E. *Polyhedron* **1994**, 13, 1131.
413. Matchett, M. A.; Viano, A. M.; Adolphi, N. L.; Stoddard, R. D.; Buhro, W. E.; Conradi, M. S.; Gibbons, P. C. *Chem. Mater.* **1992**, 4, 508.
414. Trindade, T.; O'Brien, P.; Zhang, X. *Chem. Mater.* **1997**, 9, 523.
415. Ludolph, B.; Malik, M. A.; O'Brien, P.; Revaprasadu, N. *Chem. Commun.* **1998**, 1849.
416. Trindade, T.; O'Brien, P. *Adv. Mater.* **1996**, 8, 161.
417. Trindade, T.; O'Brien, P.; Zhang, X.; Motevallii, M. *J. Mater. Chem.* **1997**, 7, 1011.
418. Nedeljkovic, J. M.; Nenadovic, M. T.; Micic, O. I.; Nozik, A. J. *J. Phys. Chem.* **1986**, 90, 12.

9.24

Appendix to Volume 9

JON A. McCLEVERTY

University of Bristol, Bristol, UK

and

THOMAS J. MEYER

Los Alamos National University, Los Alamos, New Mexico, USA

This appendix provides access to original chapters from Comprehensive Coordination Chemistry (published in 1987) that are relevant to this volume of Comprehensive Coordination Chemistry II (CCC2) but that are not cited by a specific chapter in CCC2.

For further details please see the end of the Preface under the General Information tab.

PDF 1. Chapter 57 Electrochemical Applications

PDF 2. Chapter 59 Photographic Applications

PDF 3. Chapter 60 Compounds Exhibiting Unusual Electrical Properties

PDF 4. Chapter 66 Other Uses of Coordination Compounds